BNL-98400-2012

RIKEN/RBRC Workshop
Forward Physics at RHIC
July 30 – August 1, 2012

Proceedings of RIKEN BNL Research Center Workshop

Volume 111

RBRC
RIKEN BNL Research Center

DISCLAIMER

This work was prepared as an account of work sponsored by an agency of the United States Government. Neither the United States Government nor any agency thereof, nor any of their employees, nor any of their contractors, subcontractors or their employees, makes any warranty, express or implied, or assumes any legal liability or responsibility for the accuracy, completeness, or any third party's use or the results of such use of any information, apparatus, product, or process disclosed, or represents that its use would not infringe privately owned rights. Reference herein to any specific commercial product, process, or service by trade name, trademark, manufacturer, or otherwise, does not necessarily constitute or imply its endorsement, recommendation, or favoring by the United States Government or any agency thereof or its contractors or subcontractors. The views and opinions of authors expressed herein do not necessarily state or reflect those of the United States Government or any agency thereof.

Notice: This manuscript has been authored by employees of Brookhaven Science Associates, LLC under Contract No. DE-AC02-98CH10886 with the U.S. Department of Energy. The publisher by accepting the manuscript for publication acknowledges that the United States Government retains a non-exclusive, paid-up, irrevocable, world-wide license to publish or reproduce the published form of this manuscript, or allow others to do so, for United States Government purposes.

Preface to the Series

The RIKEN BNL Research Center (RBRC) was established in April 1997 at Brookhaven National Laboratory. It is funded by the "Rikagaku Kenkyusho" (RIKEN, The Institute of Physical and Chemical Research) of Japan. The Memorandum of Understanding between RIKEN and BNL, initiated in 1997, has been renewed in 2002 and again in 2007. The Center is dedicated to the study of strong interactions, including spin physics, lattice QCD, and RHIC physics through the nurturing of a new generation of young physicists.

The RBRC has both a theory and experimental component. The RBRC Theory Group and the RBRC Experimental Group consists of a total of 25-30 researchers. Positions include the following: full time RBRC Fellow, half-time RHIC Physics Fellow, and full-time post-doctoral Research Associate. The RHIC Physics Fellows hold joint appointments with RBRC and other institutions and have tenure track positions at their respective universities or BNL. To date, RBRC has over 85 graduates (Fellows and Post- docs) of which 37 theorists and 19 experimenters have already attained tenure positions at major institutions worldwide.

Beginning in 2001 a new RIKEN Spin Program (RSP) category was implemented at RBRC. These appointments are joint positions of RBRC and RIKEN and include the following positions in theory and experiment: RSP Researchers, RSP Research Associates, and Young Researchers, who are mentored by senior RBRC Scientists. A number of RIKEN Jr. Research Associates and Visiting Scientists also contribute to the physics program at the Center.

RBRC has an active workshop program on strong interaction physics with each workshop focused on a specific physics problem. In most cases all the talks are made available on the RBRC website. In addition, highlights to each speaker's presentation are collected to form proceedings which can therefore be made available within a short time after the workshop. To date there are over one hundred proceeding volumes available.

A 10 teraflops RBRC QCDOC computer funded by RIKEN, Japan, was unveiled at a dedication ceremony at BNL on May 26, 2005. This supercomputer was designed and built by individuals from Columbia University, IBM, BNL, RBRC, and the University of Edinburgh, with the U.S. D.O.E. Office of Science providing infrastructure support at BNL. Physics results were reported at the RBRC QCDOC Symposium following the dedication. QCDSP, a 0.6 teraflops parallel processor, dedicated to lattice QCD, was begun at the Center on February 19, 1998, was completed on August 28, 1998, and was decommissioned in 2006. It was awarded the Gordon Bell Prize for price performance in 1998. QCDOC was decommissioned in May 2012. The next generation computer in this sequence, QCDCQ (600 Teraflops), is currently operational and is expected to produce many more interesting discoveries in the future.

N. P. Samios, Director
August 2012

***Work performed under the auspices of U.S.D.O.E. Contract No. DE-AC02-98CH10886.**

Contents

Presentations

ALBACETE, Javier .....Testing the CGC with RHIC Forward Data

BURTON, Tom .....The STAR Transverse Spin Programme: Present and Future

CHOI, IhnJea.....Sivers Asymmetries in Polarized Drell-Yan Production of Muon Pairs at COMPASS

D'ENTERRIA, David.....Forward Physics at the LHC - Small Seminar Room

DUSLING, Kevin.....Long Range Rapidity Correlations in pp, pA and AA Collisions

FAZIO, Salvatore.....Opportunities for ep Physics at an eRHIC

FISCHER, Wolfram .....RHIC Upgrades

GAMBERG, Leonard .....Sivers and Collins Effect: Single Spin Asymmetries in Photon Production

GIORDANO, Francesca.....Spin Measurements at PHENIX and Future Plans

GROSSE-PERDEKAMP, Matthias...Low x Physics with a Future Forward Upgrade of sPHENIX

HUANG, Jin .....Transverse Spin Physics at Jefferson Lab

JALILIAN-MARIAN, Jamal.....Probing High Energy QCD via Di-hadron Correlations

KANG, Zhongbo.....Sivers Effect of Drell-Yan Production in Small-x Regime

KOIKE, Yuji.....Single Transverse Spin Asymmetry in the Forward and Backward Directions

KOVCHEGOV, Yuri .....Putting Spin on Color Glass

LAMONT, Matt.....EIC e+A Science Programme

LI, Xuan.....Forward Di-hadron Correlations at STAR

QIU, Jianwei.....Transverse Single-spin Asymmetry in pA Collisions

ROGERS, Ted.....QCD Evolution of TMD PDFs

SANDACZ, Andrzej .....COMPASS Transverse Spin Physics Program and Plans for GPD Measurements

STRATMANN, Marco.....Nuclear Parton Densities - Status & Future Avenues

STRIKMAN, Mark .....Looking Forward in p+A at LHC

TUCHIN, Kirill .....Cold Nuclear Matter Effects on Heavy Quark Production

ZHENG, Liang .....Dihadron Correlations at eRHIC and Monte Carlo Development

Agenda

Registered List of Participants

Additional RIKEN BNL Research Center Proceeding Volumes

Testing the CGC with RHIC forward data

Javier L Albacete

Workshop on Forward Physics at RHIC, Jul-30-Aug 1st
Brookhaven National Lab

What the CGC is about : coherence effects in high energy QCD (small-x)

High gluon densities in the projectile/target

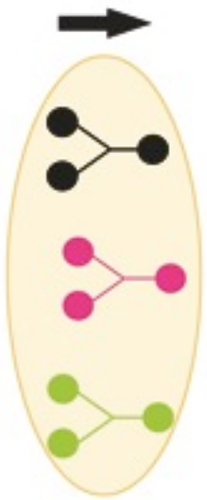

Saturation: gluon self-interactions tame the growth of gluon densities towards small-x

$$\frac{\partial \phi(\mathbf{x}, \mathbf{k_t})}{\partial \ln(\mathbf{x_0}/\mathbf{x})} \approx \mathcal{K} \otimes \phi(\mathbf{x}, \mathbf{k_t}) - \phi(\mathbf{x}, \mathbf{k_t})^{\mathbf{2}}$$

radiation recombination

$$\mathbf{k_t} \lesssim \mathbf{Q_s}(\mathbf{x})$$

Breakdown of independent particle production

$$\mathcal{A}(\mathbf{k} \lesssim \mathbf{Q_s}) \sim \frac{\mathbf{1}}{\mathbf{g}} \qquad \mathbf{g}\mathcal{A} \sim \mathcal{O}(\mathbf{1})$$

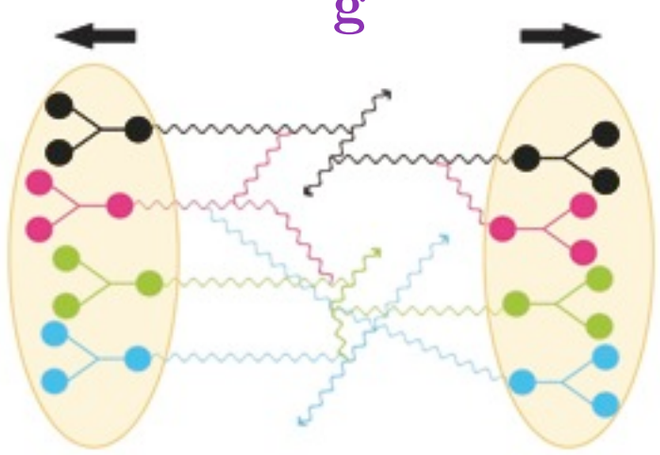

What the CGC is about : coherence effects

High gluon densities in the projectile/target

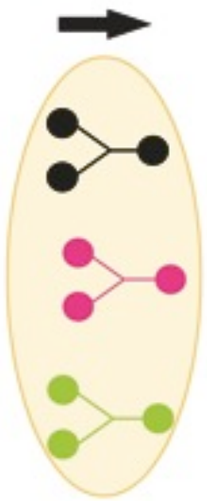

Saturation: gluon self-interactions tame the growth of gluon densities towards small-x

$$\frac{\partial \phi(\mathbf{x}, \mathbf{k_t})}{\partial \ln(\mathbf{x_0}/\mathbf{x})} \approx \mathcal{K} \otimes \phi(\mathbf{x}, \mathbf{k_t}) - \phi(\mathbf{x}, \mathbf{k_t})^2$$

radiation recombination

$$\mathbf{k_t} \lesssim \mathbf{Q_s}(\mathbf{x})$$

Breakdown of independent particle production

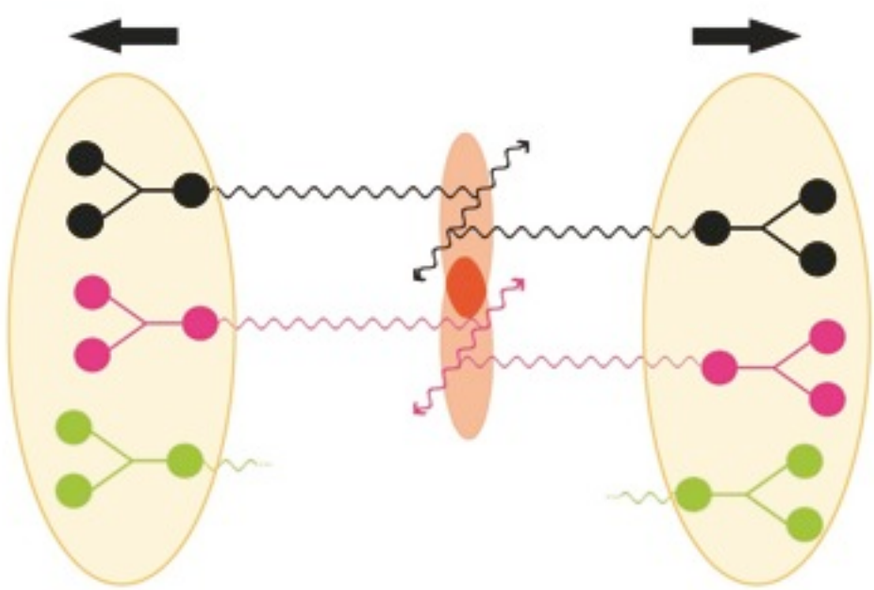

HIC phenomenology

- Nuclear shadowing, String fusion, percolation

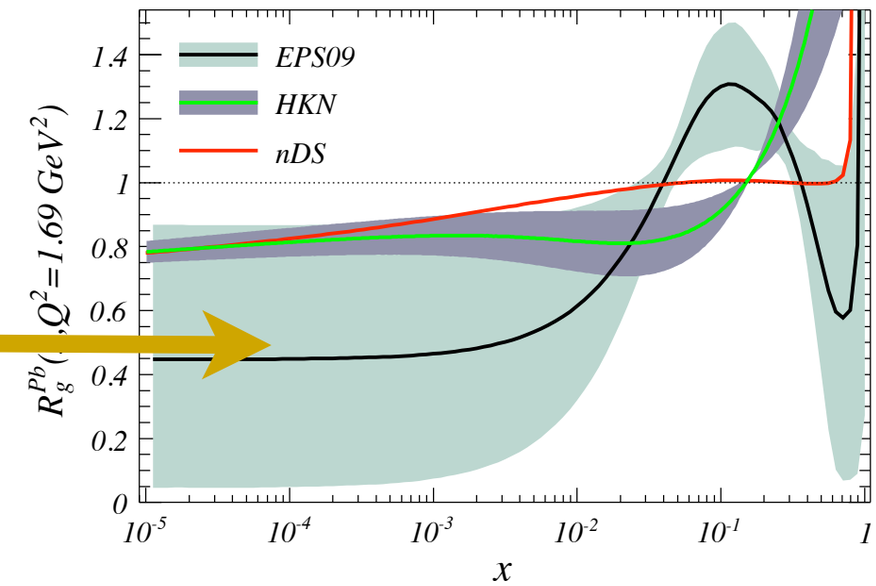

- Resummation of multiple scatterings
- kt-broadening
- Energy dependent cutoff in event generators

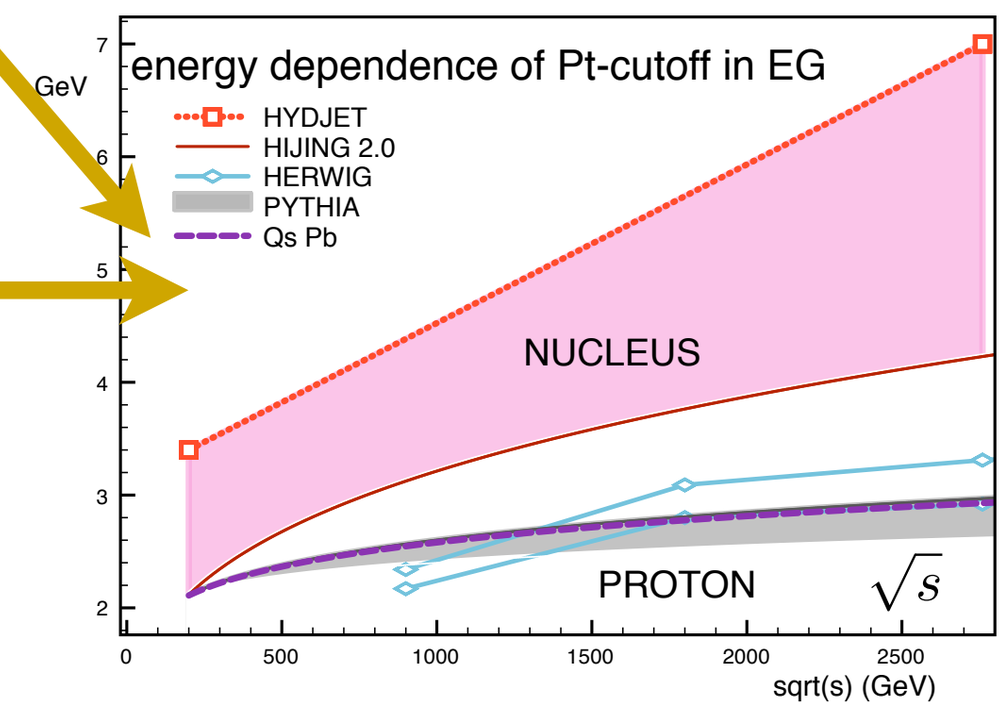

OUTLINE

• Coherence effects are essential for the description of data in HIC collisions (RHIC, LHC)

• The presence of a semi-hard dynamical scale --the saturation scale-- + non-linear dynamics led to semi-quantitative predictions later confirmed by data

- ~ Npart scaling and energy dependence of total multiplicities Kharzeev-Levin-Nardi
- Continuos depletion of nuclear modification factors with increasing hadron rapidity in dA collisions
- Angular decorrelation of hadron pairs produced at forward rapidities in dA collisions, Marquet

JLA-Armesto-Kovner-Salgado-Wiedeman

• Getting quantitative: Is the CGC effective theory (at its present degree of accuracy) the best suited framework to quantify coherence phenomena in HI collisions at RHIC and the LHC?

- Control of missing dynamical effects: are RHIC and LHC energies large enough for the applicability of the CGC?
- Control of higher order terms in the perturbative series
- Do we have enough empiric info (i.e. data) to constrain the NP parameters of the theory?

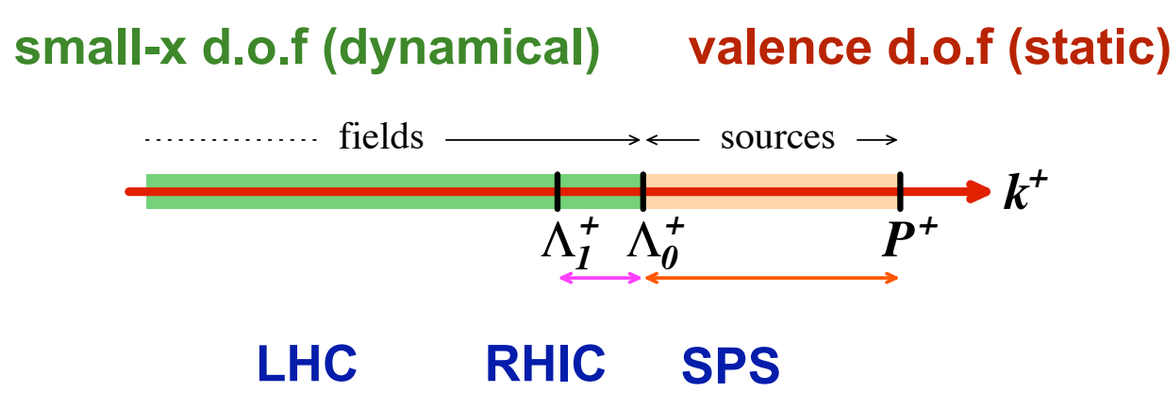

Color Glass Condensate phenomenology tools (in half a slide)

1.- (classical) Ab initio calculation of nuclear structure functions (small-x gluon distributions)

McLerran-Venugopalan model (x_0~0.01). Valid for large nucleus $gA^{1/3}$ >>1

2.- (quantum) Nonlinear renormalization group equations towards small-x

BK-JIMWLK eqns ($x<x_0$~0.01)

$$\frac{\partial\,\phi(x,k)}{\partial\,\ln(1/x)} = \mathcal{K}\otimes\phi(x,k) - \phi^2(x,k) \qquad \frac{\partial\,W[\rho]}{\partial\,Y} = \ldots$$

3.- Production processes

$$\frac{dN^{AB\to X}}{d^3p_1\ldots}\,[\phi(x,k);W_Y[\rho]]$$

CYM,
kt-factorization
hybrid formalism...

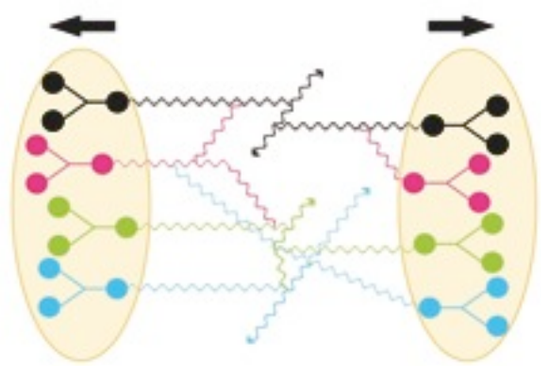

$$\mathcal{A}(\mathbf{k}\lesssim\mathbf{Q_s})\sim\frac{\mathbf{1}}{\mathbf{g}}$$

$$\mathbf{g}\mathcal{A}\sim\mathcal{O}(\mathbf{1})$$

The eikonal (recoil-less) approximation is central in the CGC:

small-x d.o.f (dynamical) **valence d.o.f (static)**

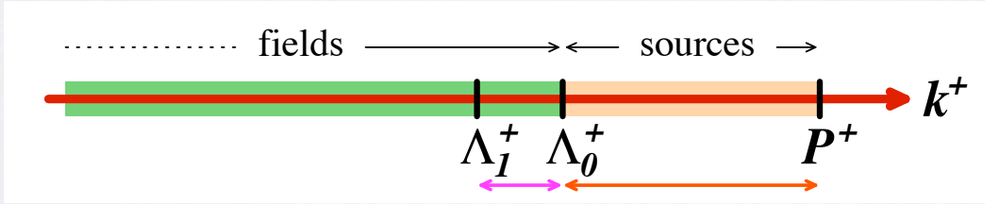

LHC **RHIC** **SPS**

(brief and incomplete) CGC Theory Status: Entering the NLO era

Evolution Equations: $\frac{\partial\,\phi(x,k)}{\partial\,\ln(1/x)} = \mathcal{K}\otimes\phi(x,k) - \phi^2(x,k)$ $\quad \frac{\partial\,W[\rho]}{\partial\,Y} = \ldots$

✓ - Running coupling kernel in BK evolution for the 2-point function Kovchegov Weigert Gardi Balitsky

✗ - Full NLO kernel for BK-JIMWLK [Balitsky Chirilli]

✗ - Analytic [Triantafyllopoulos] and numerical [T. Lappi et.al] solutions of full B-JIMWLK hierarchy for n-point functions

- ...

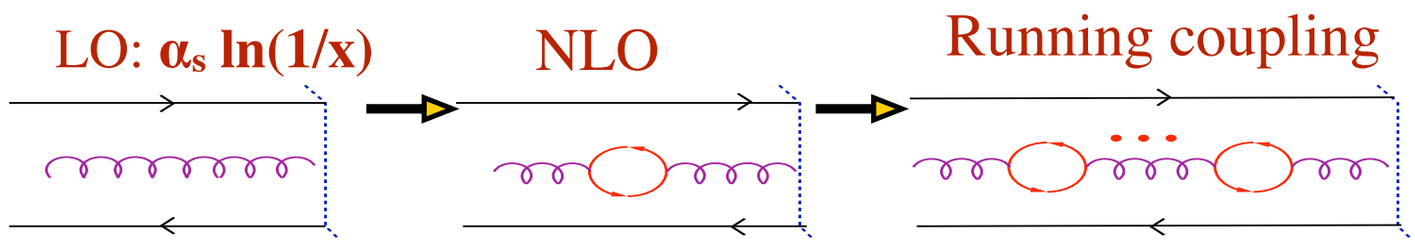

Production processes $\frac{dN^{AB\to X}}{d^3p_1\ldots}[\phi(x,k);W_Y[\rho]]$

✗ - Running coupling and full NLO corrections to kt-factorization [Kovchegov, Horowitz, Balitsky, Chirilli]

✓ - Inelastic terms in the hybrid formalism [Kovner-Altinoluk]

✓ - Hadron-hadron, hadron-photon* correlations

✗ - Factorization of multiparticle production processes at NLO

✗ - DIS NLO photon impact factors [Chirilli]

- ...

Used in phenomenological works? ✓ Yes ✗ No ✓ A bit :)

Data??

Empiric information needed to constrain:

- Non-perturbative parameters: initial conditions for BK-JIMWLK evolution, impact parameter
- K-factors to account for higher order corrections (effectively also for missing high-(x,Q2) contributions, energy-conservation corrections etc)

:)

proton

- Abundant high quality data at small-x
- Good simultaneous description of e+p and p+p data
- Global rcBK fits to constrain gluon distribution

:|

nucleus

- Fewer data at small-x
- LHC Pb+Pb data (difficult...)
- EIC and pPb @ LHC data to come...
- RHIC dAu forward data provides the best testing ground of the CGC

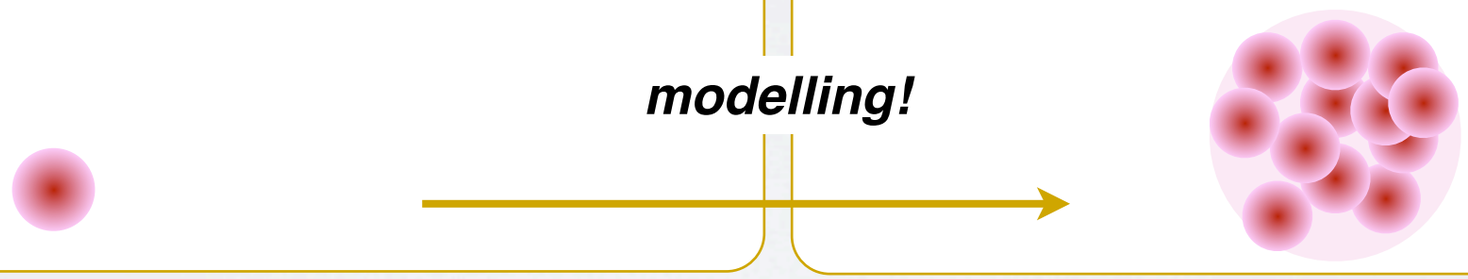

The baseline: proton collisions

1. Global fits to e+p data at small-x

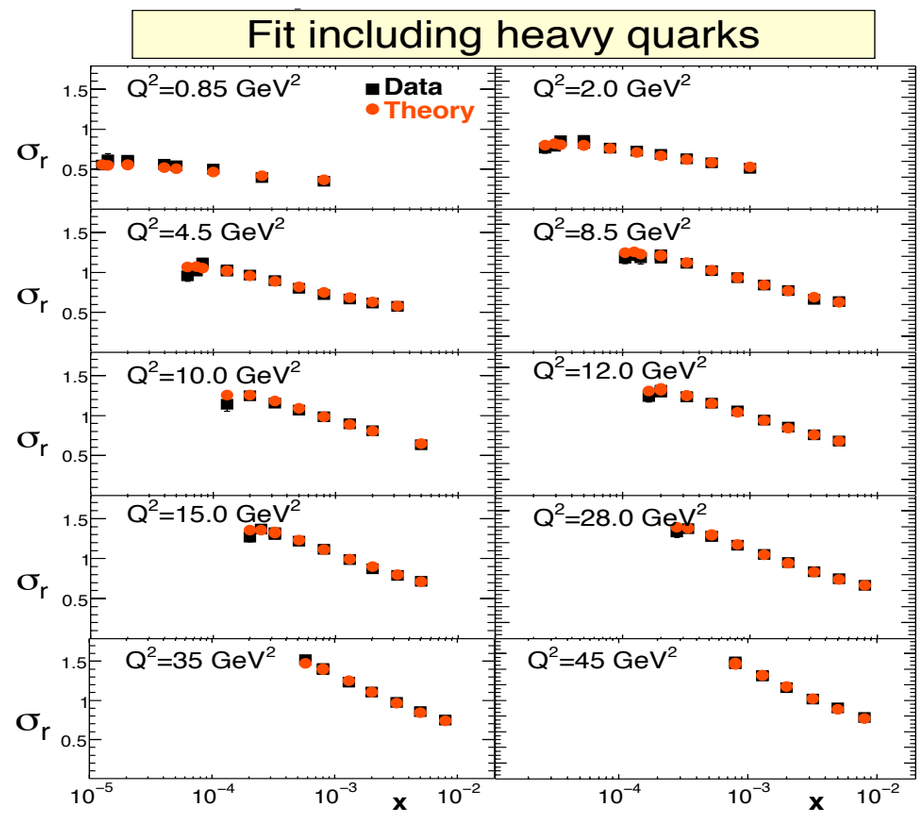

JLA-Armesto-Milhano-Quiroga-Salgado

2. Extract NP fit parameters

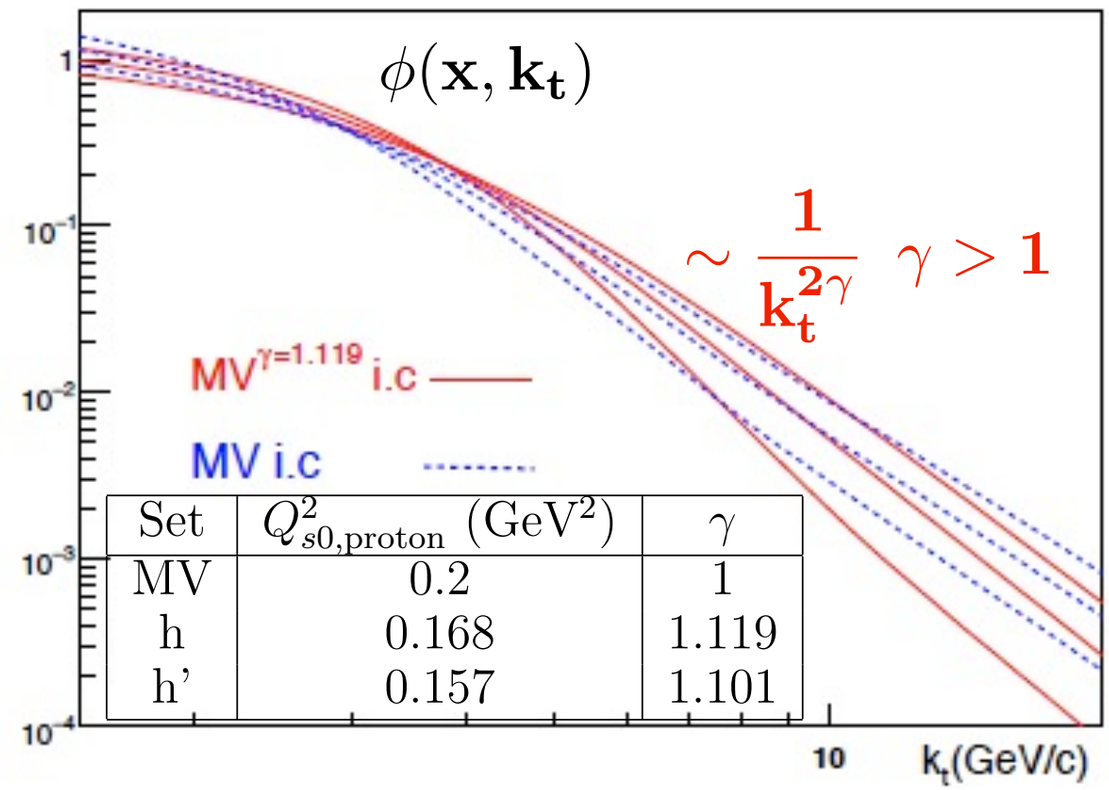

Set	$Q^2_{s0,\mathrm{proton}}$ (GeV^2)	γ
MV	0.2	1
h	0.168	1.119
h'	0.157	1.101

$$\mathcal{N}^{MV}(r, x_0 = 10^{-2}) = 1 - \exp\left[-\left(\frac{r^2\, Q^2_{s0}}{4}\right)^{\gamma} \ln\left(\frac{1}{r\,\Lambda_{QCD}}\right)\right]$$

- Fits to e+p data clearly prefer gamma>1.
- MV (gamma=1) model seems not to work well for protons...
- Possible explanation: subleading in density corrections to the MV model yield gamma> 1 Dumitru & Pereska 11

The baseline: proton collisions

Talk by P. Quiroga

1. Global fits to e+p data at small-x

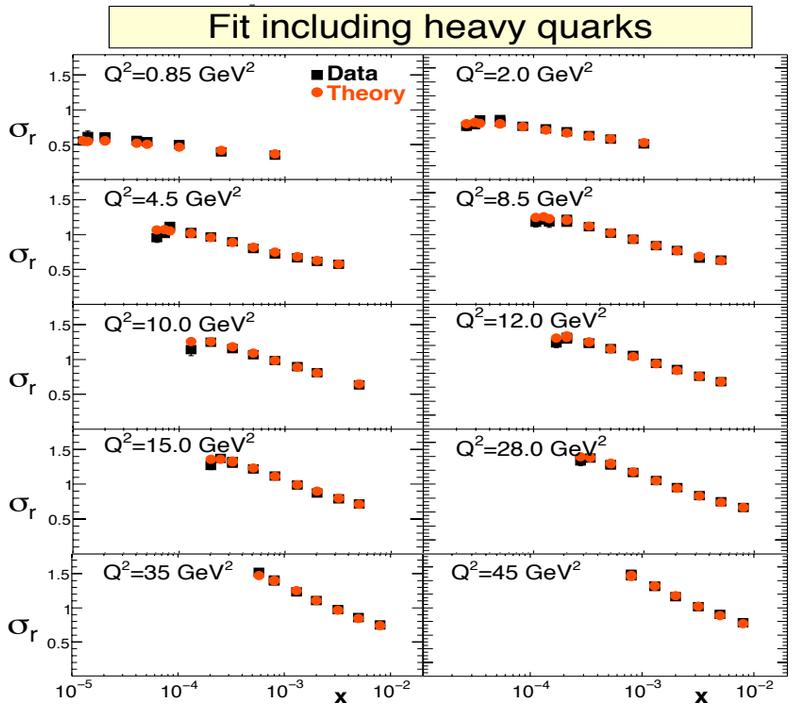

2. Extract NP fit parameters

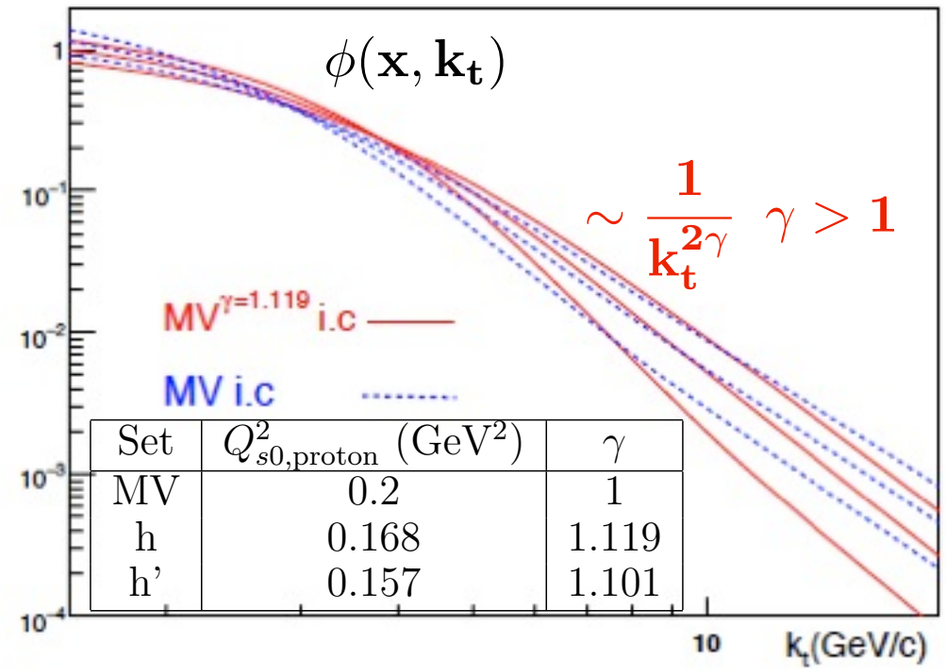

Set	$Q^2_{s0,\mathrm{proton}}$ (GeV^2)	γ
MV	0.2	1
h	0.168	1.119
h'	0.157	1.101

3. Run consistency and stability checks

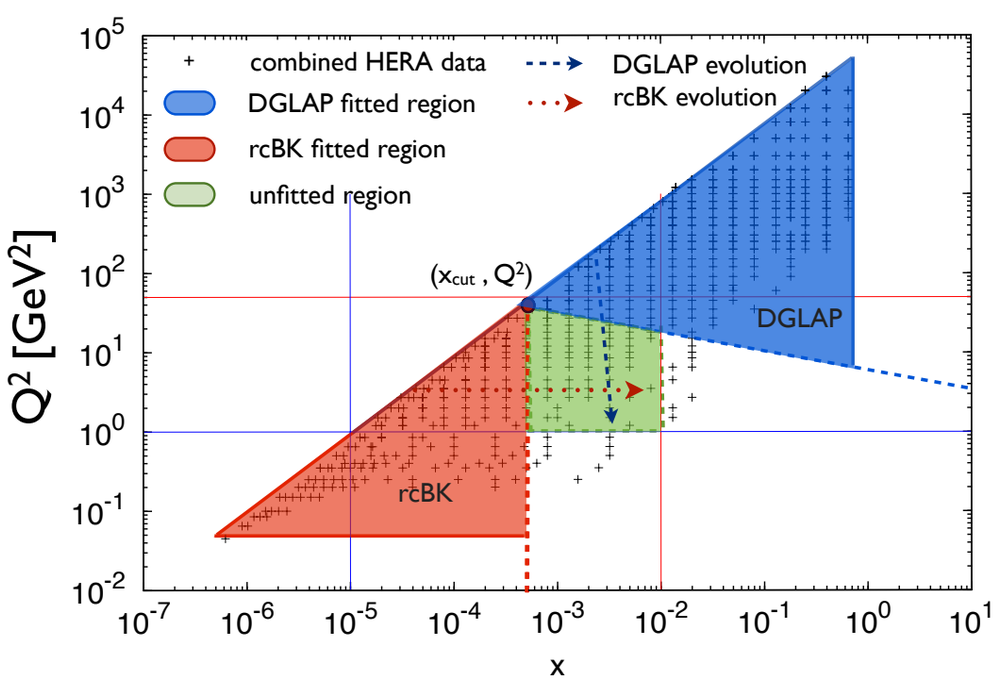

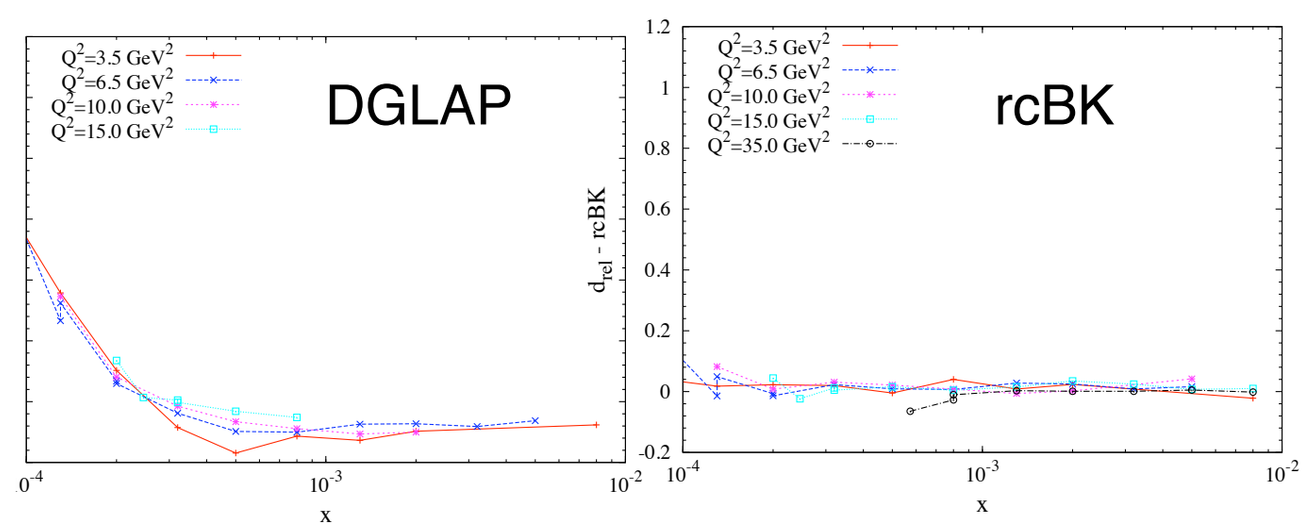

rcBK fits more stable than DGLAP fits at small-x!!!

The baseline: proton collisions

1. Global fits to e+p data at small-x

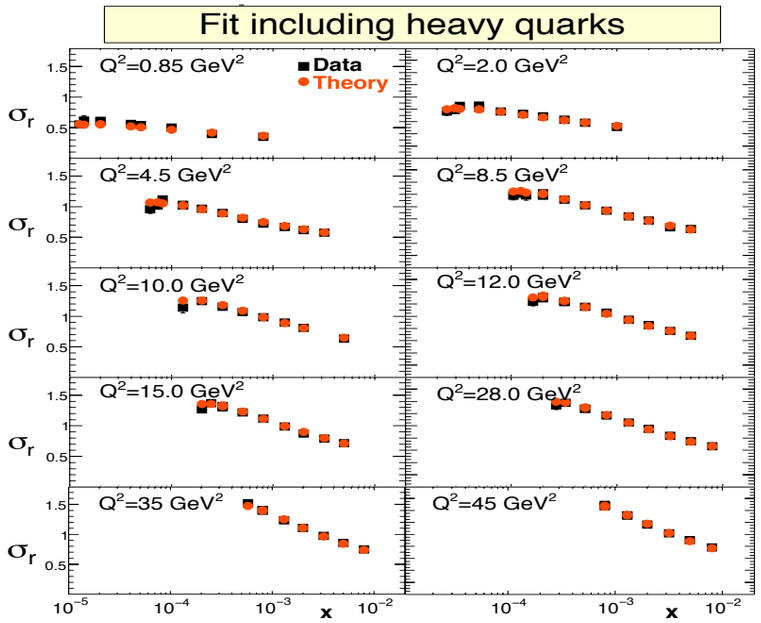

2. Extract NP fit parameters

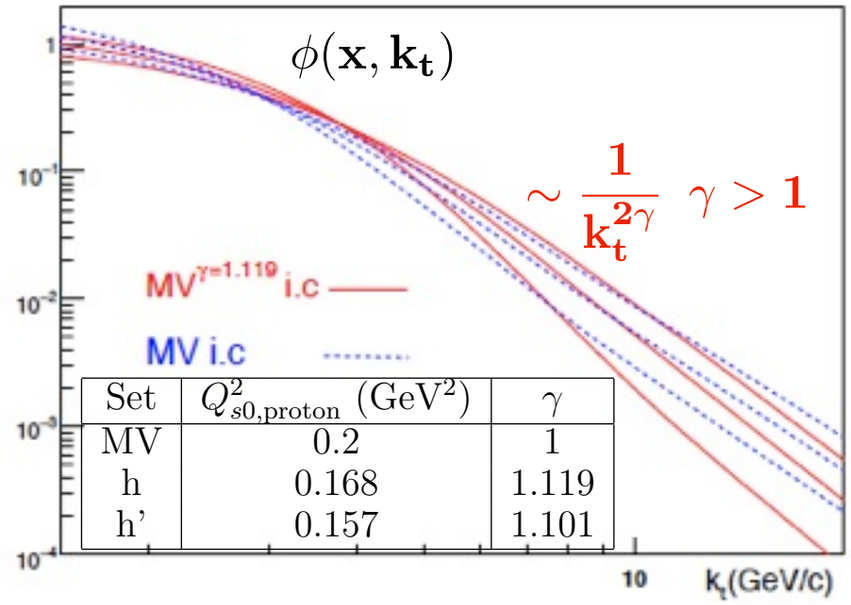

Set	$Q^2_{s0,\mathrm{proton}}$ (GeV^2)	γ
MV	0.2	1
h	0.168	1.119
h'	0.157	1.101

4. Apply gained knowledge in the study of other systems (theory driven extrapolation)

LO kt-factorization: $$\frac{\mathbf{dN^g}}{\mathbf{d\eta d^2p_t}} \sim \mathbf{K}\,\alpha_s(\mathbf{Q_r^2})\,\phi(\mathbf{x_1}, \mathbf{k_t}) \otimes \phi(\mathbf{x_2}, \mathbf{k_t} - \mathbf{pt}) \otimes \mathrm{FF}(Q_f^2)$$

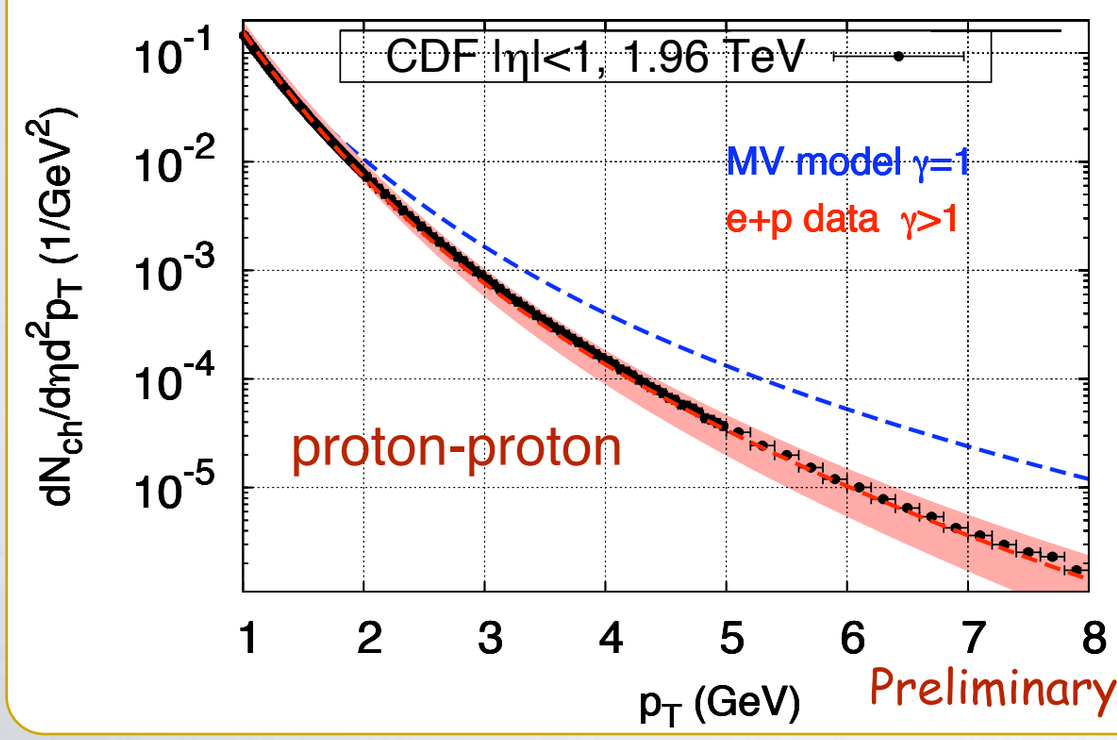

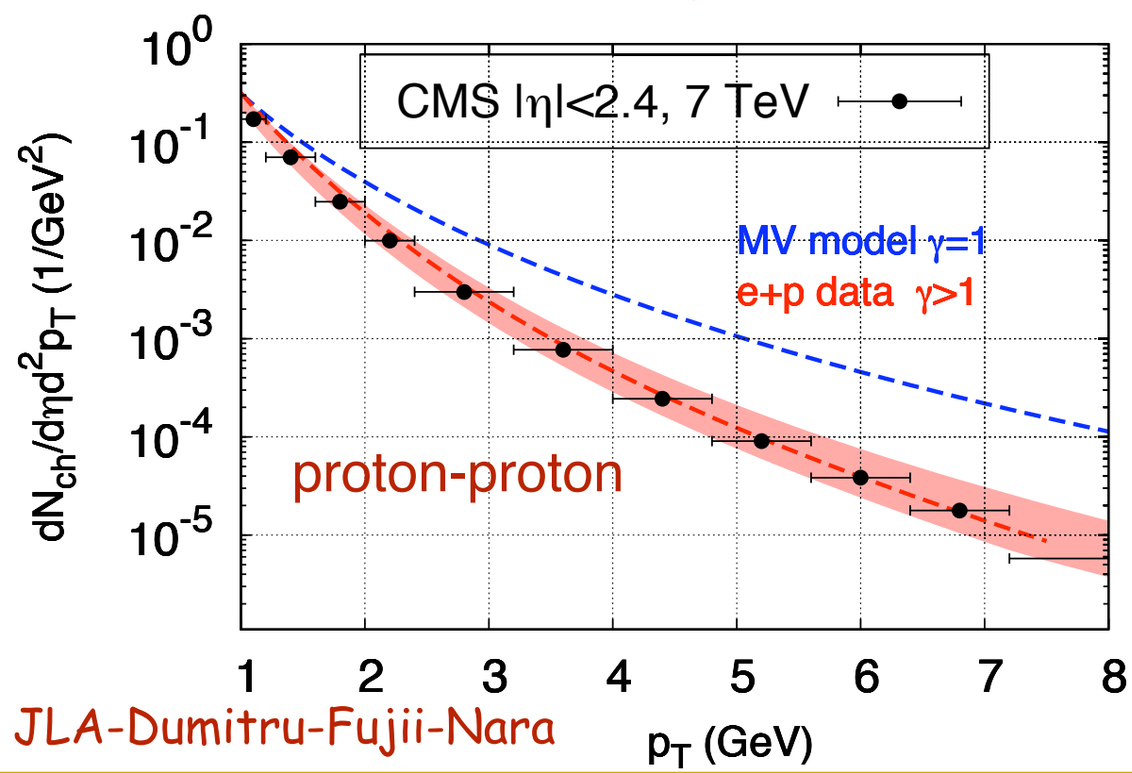

Preliminary results. JLA-Dumitru-Fujii-Nara

Nuclear ugd's and nuclear modification factors

1. Setting up the evolution

$$\phi^{\mathbf{Pb}}(\mathbf{x_0}, \mathbf{k_t}, \mathbf{B}) = \phi^{\mathbf{p}}(\mathbf{x_0}, \mathbf{k_t}; \{\mathbf{Q^2_{s0,p}} \to \mathbf{Q^2_{s0,Pb}}(\mathbf{B})); \gamma\}$$

$$\downarrow$$

$$\phi^{\mathbf{Pb}}(\mathbf{x}, \mathbf{k_t}, \mathbf{B}) = \mathbf{rcBK}[\phi^{\mathbf{Pb}}(\mathbf{x_0}, \mathbf{k_t}, \mathbf{B})]$$

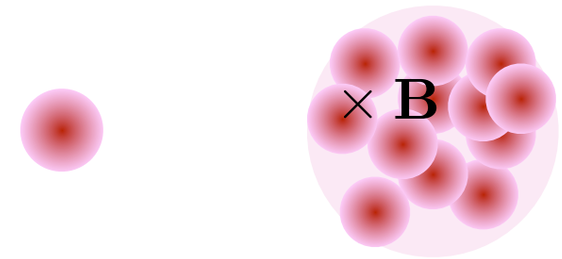

A) Most "natural" option: $\mathbf{Q^2_{s0,Pb}}(\mathbf{B}) = \mathbf{T_A}(\mathbf{B})\, \mathbf{Q^2_{s0,p}}$ $\quad \gamma^{\mathbf{Pb}} = \gamma^{\mathbf{p}}(> \mathbf{1})$

PROBLEM: yields $R_{pPB} > 1$ at high transverse momentum

B) Possible solution $\mathbf{Q^2_{s0,Pb}}(\mathbf{B}) = \mathbf{T_A}(\mathbf{B})^{1/\gamma}\, \mathbf{Q^2_{s0,p}}$ and/or $\gamma^{\mathbf{Pb}} = \mathbf{1}(\mathbf{MV}) + \frac{\#}{\mathbf{A^2/3}}$

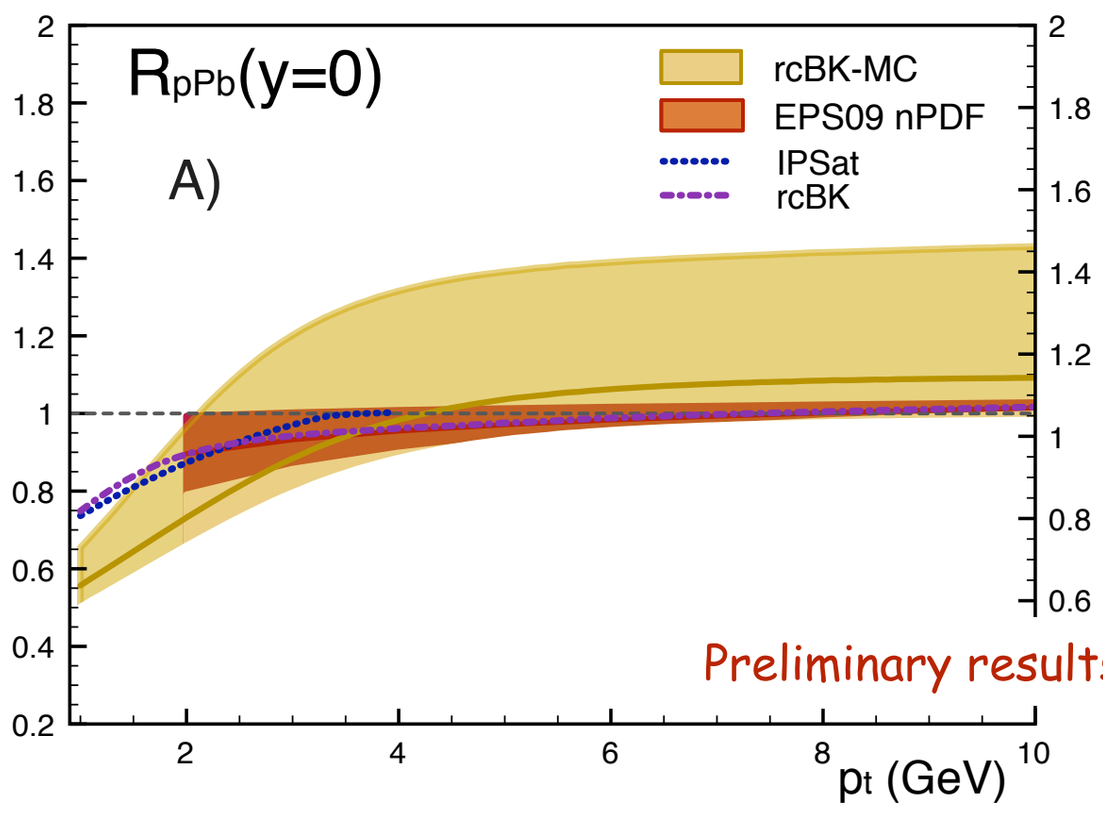

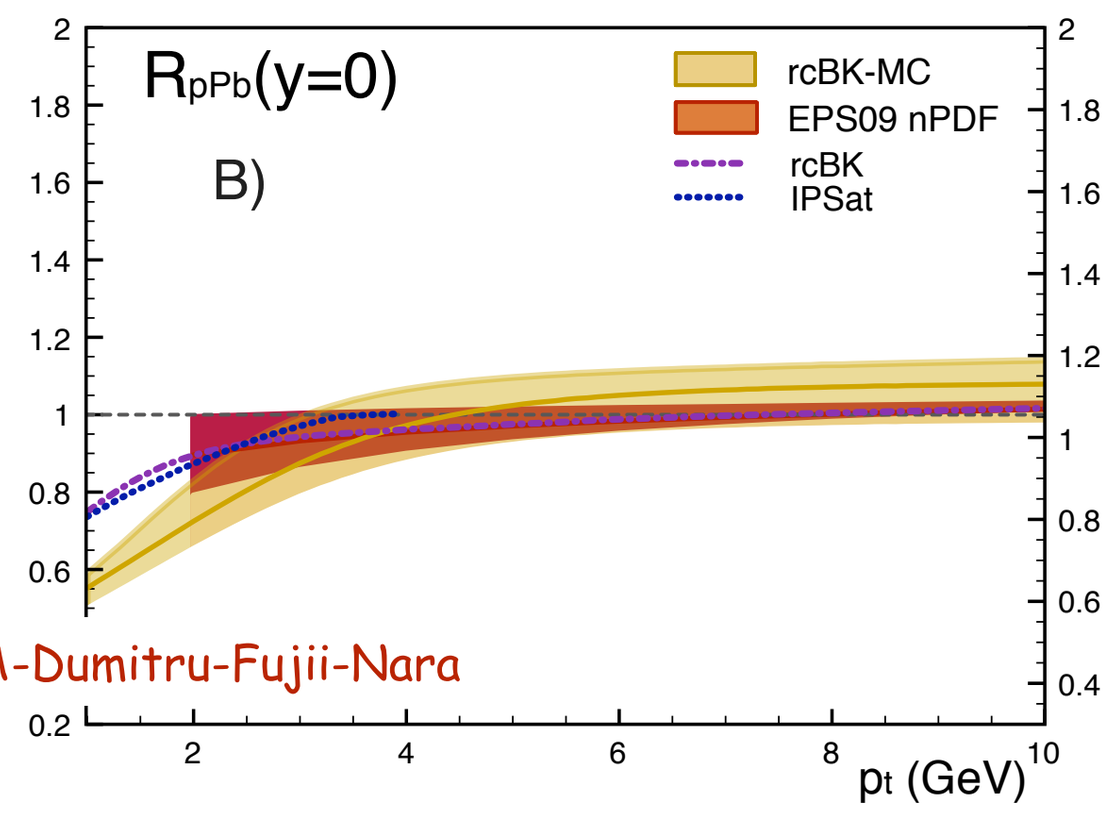

Preliminary results. JLA-Dumitru-Fujii-Nara

Single inclusive forward particle production in p(d)-A collisions

$$R_{pA} = \frac{\frac{dN_{pA}}{dyd^2pd^2b}}{A^{1/3}\frac{dN_{pp}}{dyd^2p\,d^2b}}$$

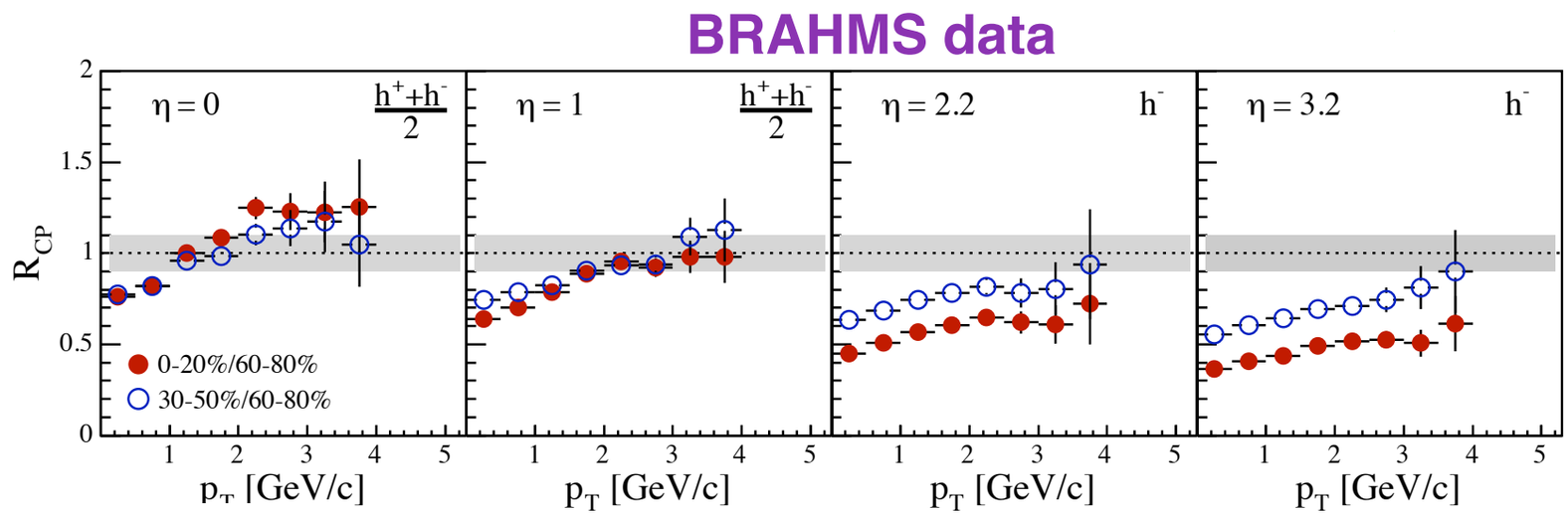

• **CGC**: Forward suppression originates in the dynamical shadowing generated by the quantum non-linear BK-JIMWLK evolution towards small-x

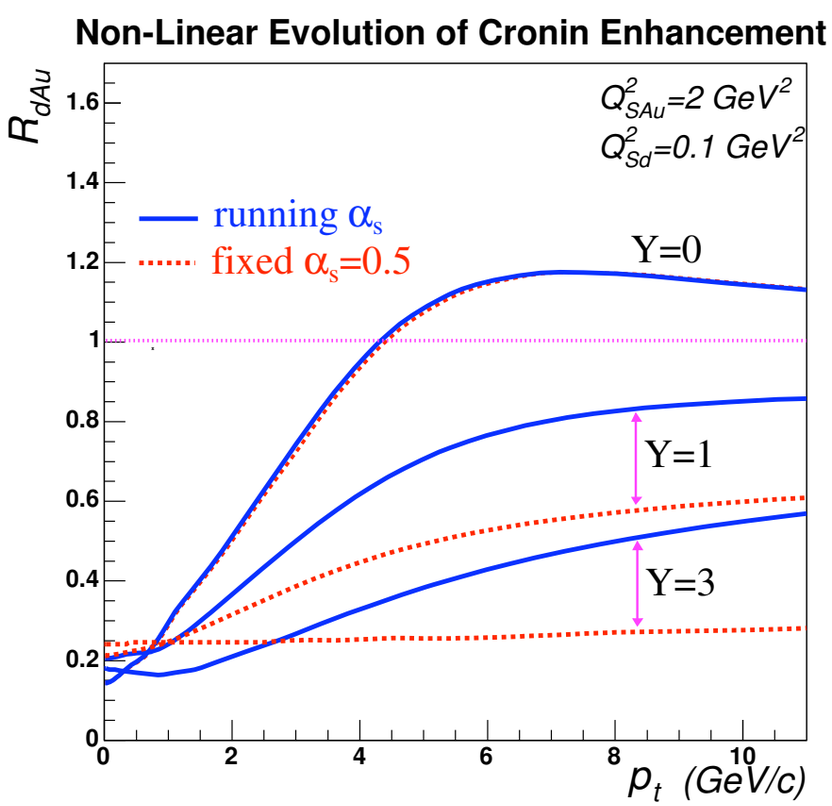

• Alternative: **Energy loss** arising from induced gluon bremstahlung (stronger in nucleus than in proton)

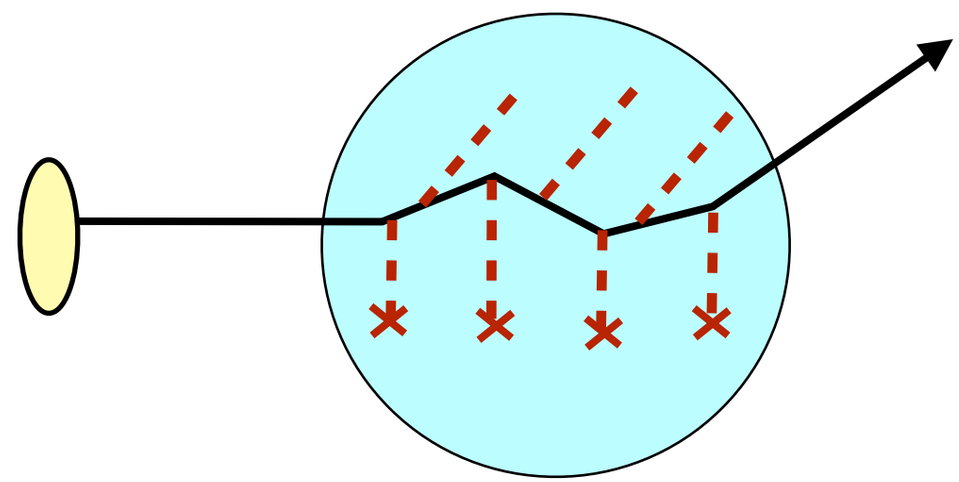

Probability of not losing energy:

$$P(\Delta y) \approx e^{-n_G(\Delta y)} \approx (1 - x_F)^{\#}$$

Kopeliovich et al, Frankfurt Strikman

Single inclusive forward particle production in p(d)-A collisions

Hybrid formalism (Dumitru-Jalilian-Marian):

$$x_{1(2)} \sim \frac{m_t}{\sqrt{s}} \exp(\pm y_h)$$

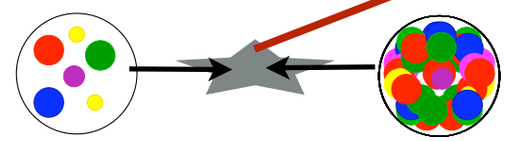

(p_t, y_h>>0)

large-x parton from proj. (pdf)

small-x glue from target (CGC)

$$\frac{dN_h}{dy_h\, d^2p_t} = \frac{K}{(2\pi)^2} \sum_q \int_{x_F}^1 \frac{dz}{z^2} \Big[x_1 f_{q\,/\,p}(x_1, p_t^2)\, \tilde{N}_F\left(x_2, \frac{p_t}{z}\right) D_{h\,/\,q}(z, p_t^2) + x_1 f_{g\,/\,p}(x_1, p_t^2)\, \tilde{N}_A\left(x_2, \frac{p_t}{z}\right) D_{h\,/\,g}(z, p_t^2) \Big]$$

fragmentation

Single inclusive forward particle production in p(d)-A collisions

Hybrid formalism (Dumitru-Jalilian-Marian):

$$x_{1(2)} \sim \frac{m_t}{\sqrt{s}} \exp(\pm y_h)$$

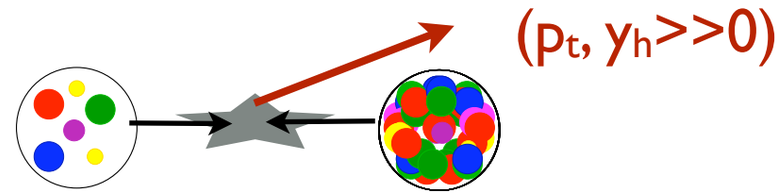

large-x parton from proj. (pdf)

small-x glue from target (CGC)

"elastic" term:

$$\frac{dN_h}{dy_h\, d^2p_t} = \frac{K}{(2\pi)^2} \sum_q \int_{x_F}^1 \frac{dz}{z^2} \Big[x_1 f_{q\,/\,p}(x_1, p_t^2)\, \tilde{N}_F\left(x_2, \frac{p_t}{z}\right) D_{h\,/\,q}(z, p_t^2) \rightarrow \text{fragmentation}$$

$$+\, x_1 f_{g\,/\,p}(x_1, p_t^2)\, \tilde{N}_A\left(x_2, \frac{p_t}{z}\right) D_{h\,/\,g}(z, p_t^2) \Big]$$

+"inelastic" term (Altinoluk-Kovner): (Part of the NLO corrections)

$$+\, \frac{\alpha_s(Q)}{2\pi^2} \int_{x_F}^1 \frac{dz}{z^2} \frac{z^4}{k^4} \int^Q \frac{d^2q}{(2\pi)^2} q^2 \tilde{N}_F(x_2, q) x_1 \int_{x_1}^1 \frac{d\xi}{\xi} \sum_{i,j=q,\bar{q},g} w_{i/j}(\xi) P_{i/j}(\xi) f_j(\frac{x_1}{\xi}, Q^2) D_{h/j}(z, Q^2)$$

Single inclusive forward particle production in p(d)-A collisions

Good description of pp an dAu RHIC forward data using only the “elastic” LO term

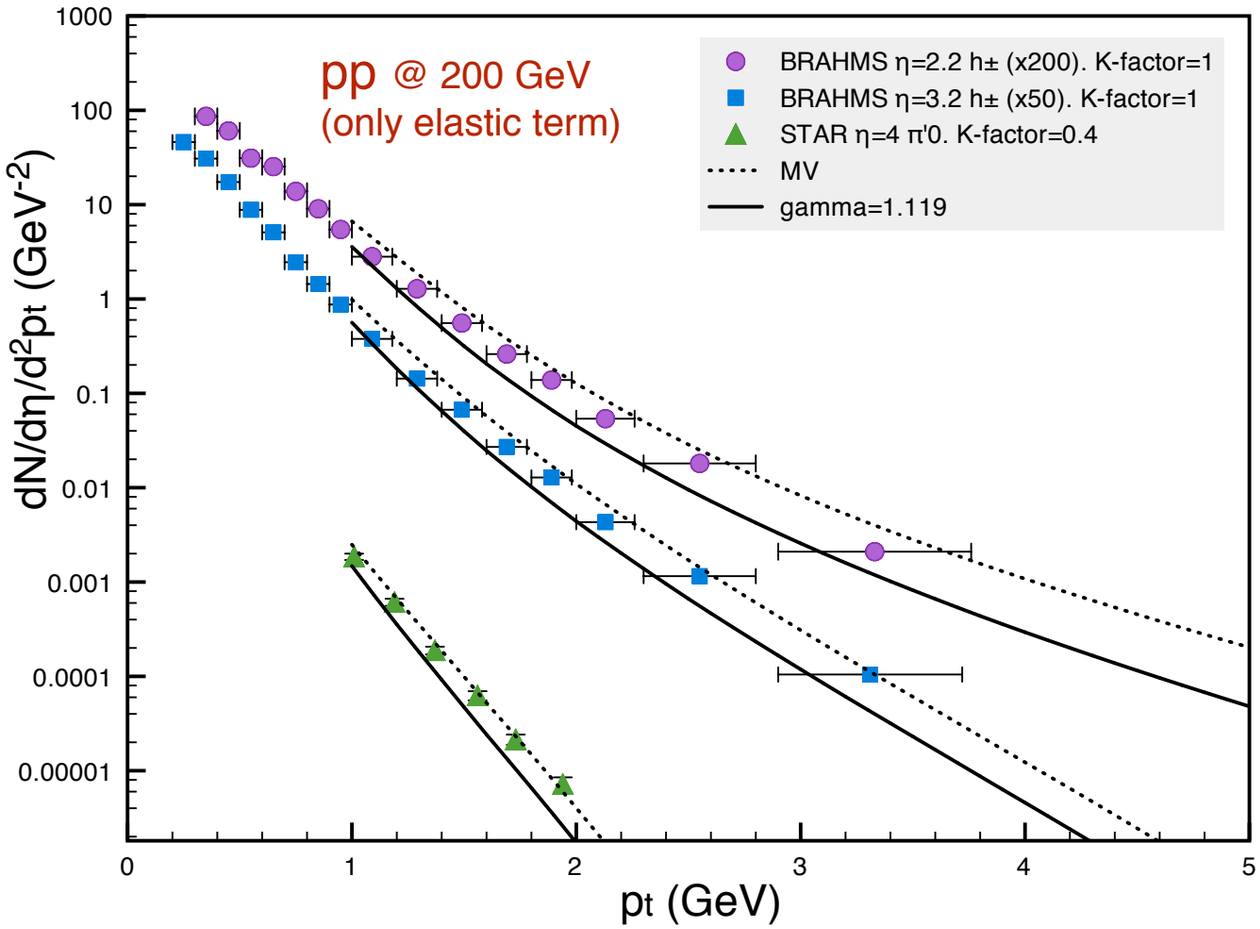

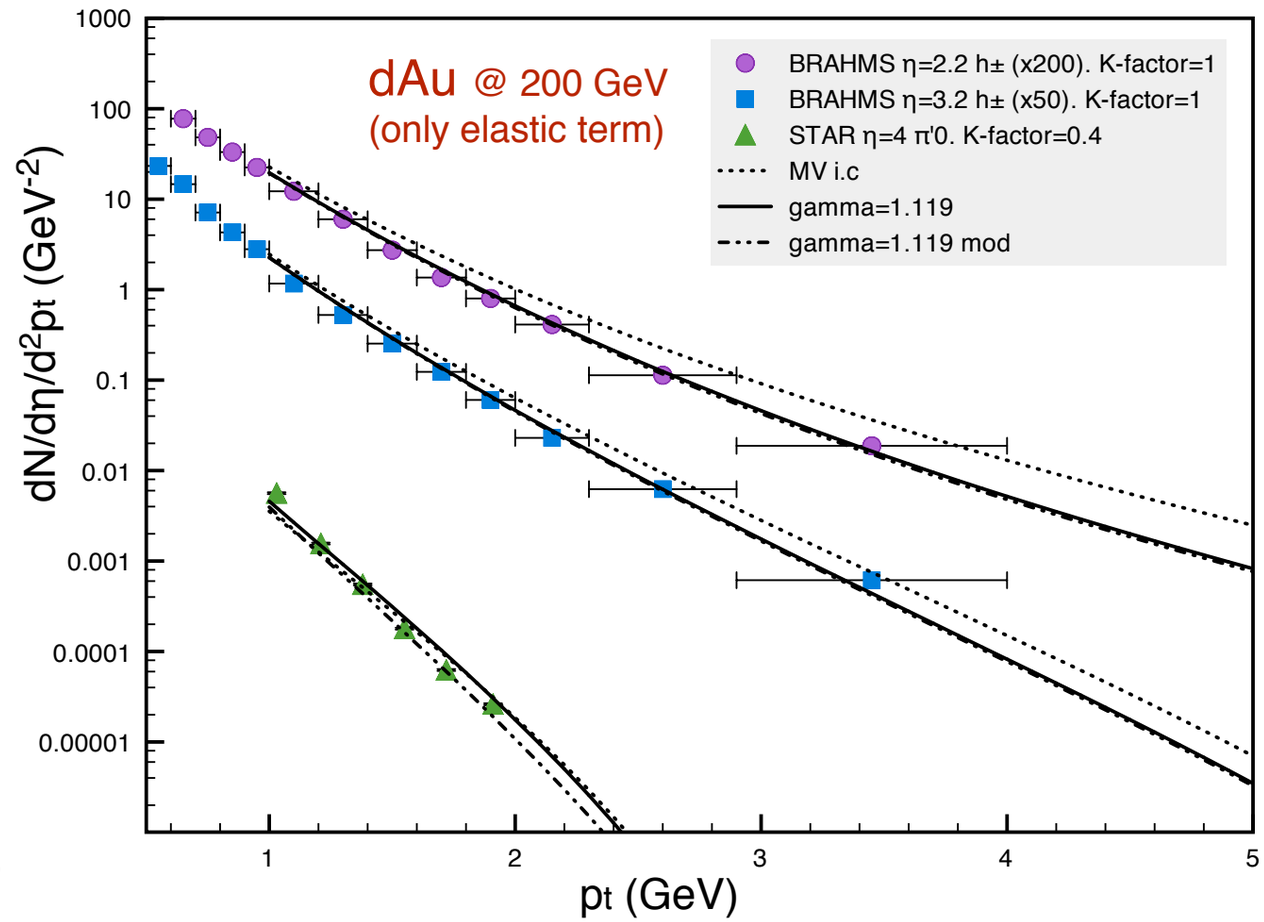

JLA-Marquet '10; JLA-Dumitru-Fujii-Nara (preliminary)

- However, RHIC data do not allow to determine the best i.c. for the nuclear UGD
- K-factor ~ 0.4 needed to describe the most forward pion data

Single inclusive forward particle production in p(d)-A collisions

NLO corrections brought by the “inelastic piece” may be large (preliminary results!!)

JLA-Dumitru-Fujii-Nara (preliminary)

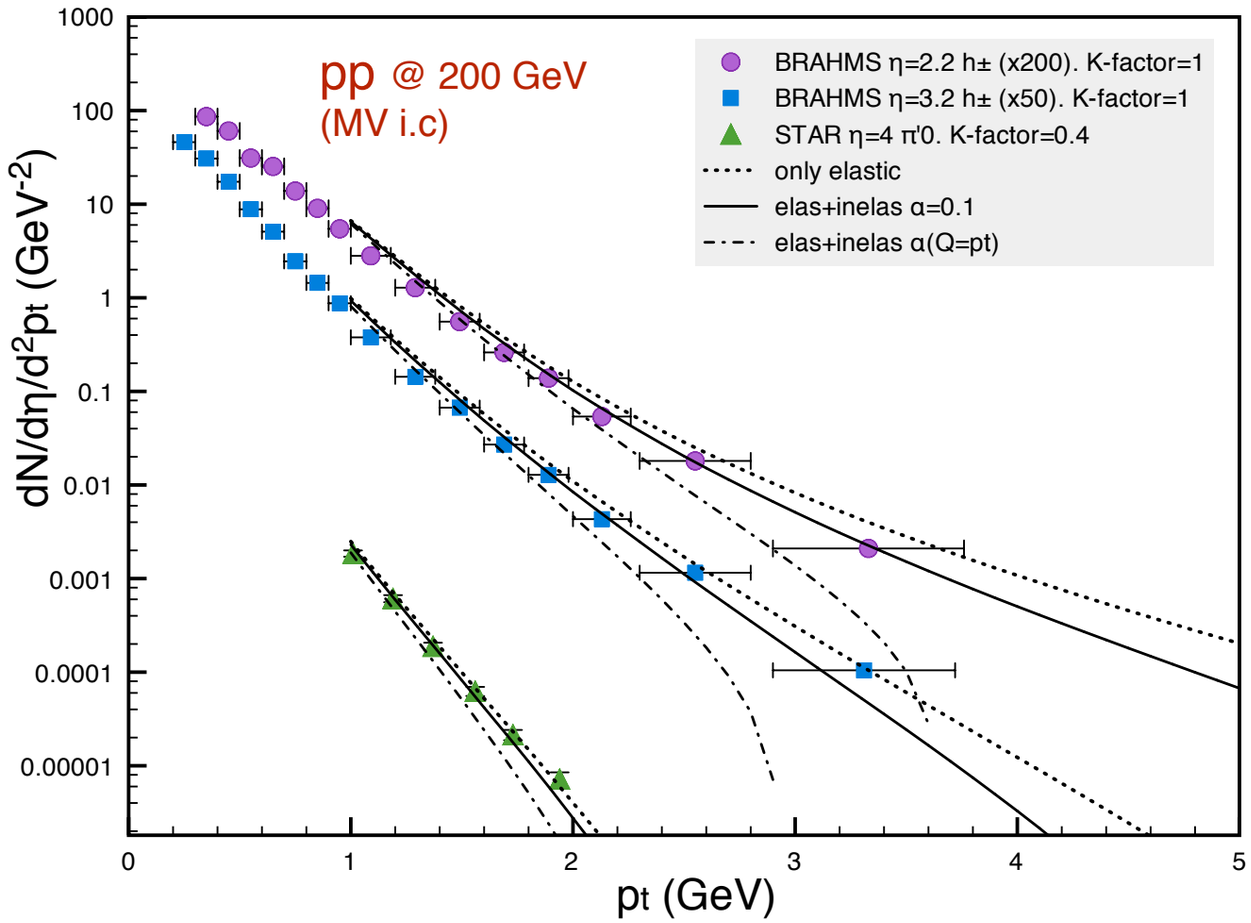

Jalilian-Marian Rezaeian '11

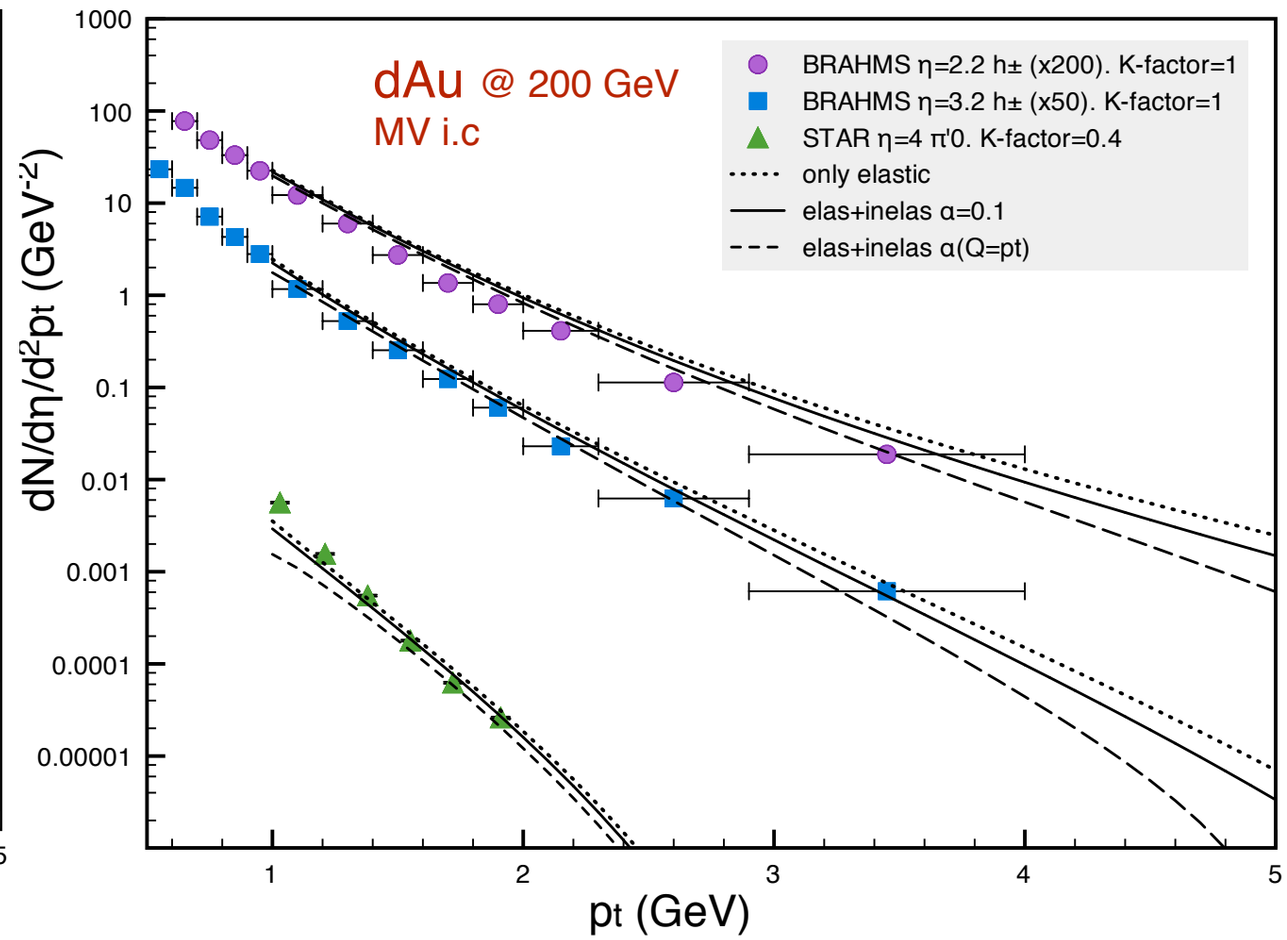

- The inelastic term is negative for all values (y,pt) explored in our work.
- Its relative magnitude wrt the elastic term decreases at small pt or forward rapidities
- Changes in the scale for the running coupling affect significantly its absolute value (NNLO corrections needed?)

LHC: Moving forward: kt-factorization or hybrid?

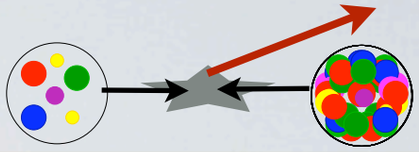

(p_t, y_h>>0)

Yet another issue: Where to switch from kt-factorization to hybrid formalism? $x_{1(2)} \sim \frac{m_t}{\sqrt{s}} \exp(\pm y_h)$

Midrapidity: kt-factorization:

$$\frac{dN^g}{d\eta d^2 p_t} \sim \phi^p(x_1) \otimes \phi^{Pb}(x_2)$$

Forward rapidity: hybrid formalism

$$\frac{dN}{d\eta d^2 p_t} \sim pdf^p(x_1) \otimes \phi^{Pb}(x_2)$$

Preliminary results. JLA-Dumitru-Fujii-Nara

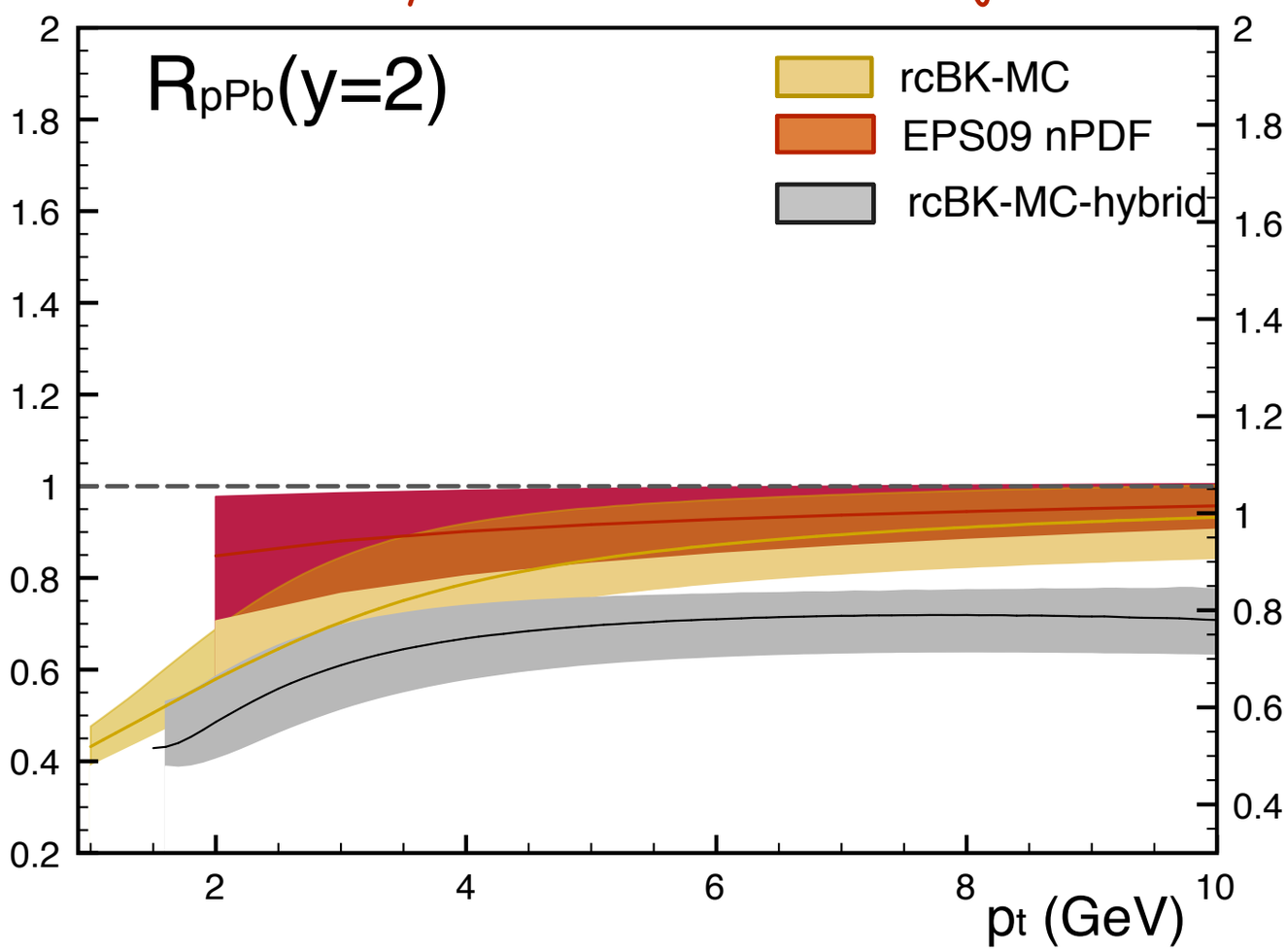

The inclusion of the inelastic term brings closer the hybrid and kt-fact results Jaliian-Marian & Rezaeian

Moving forward: Testing the evolution

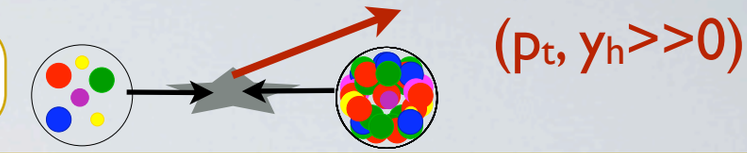

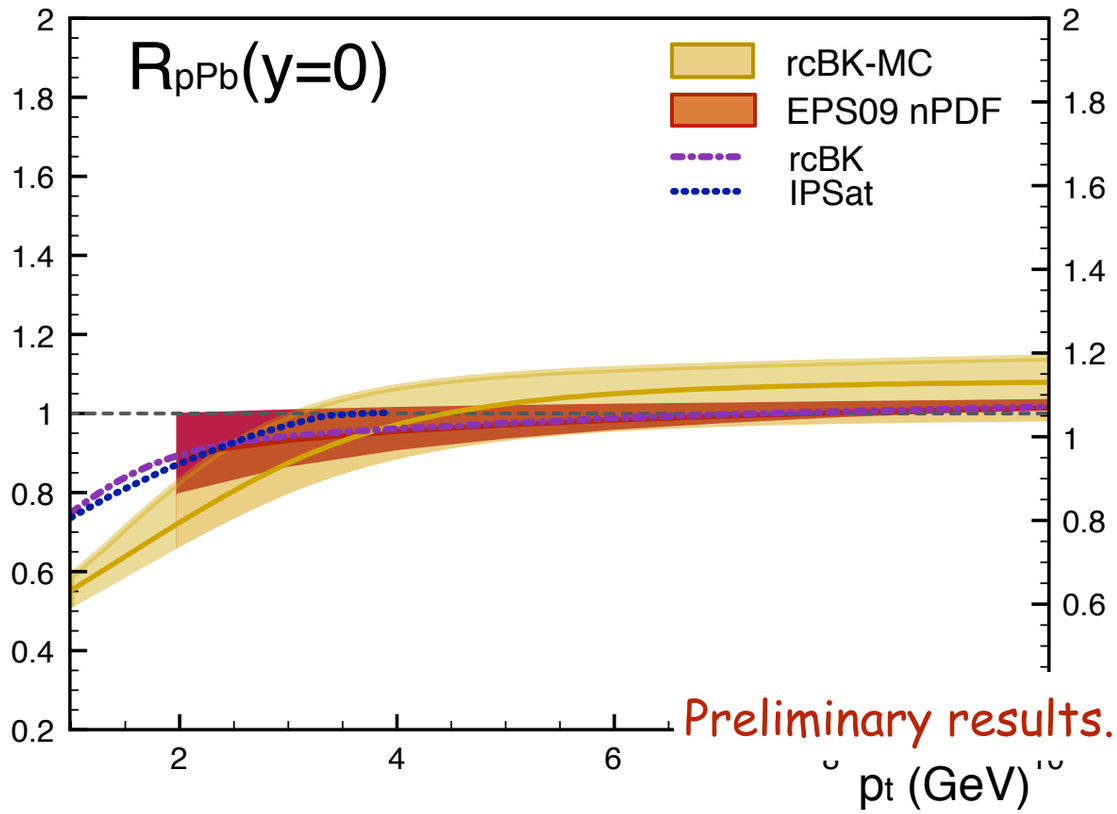

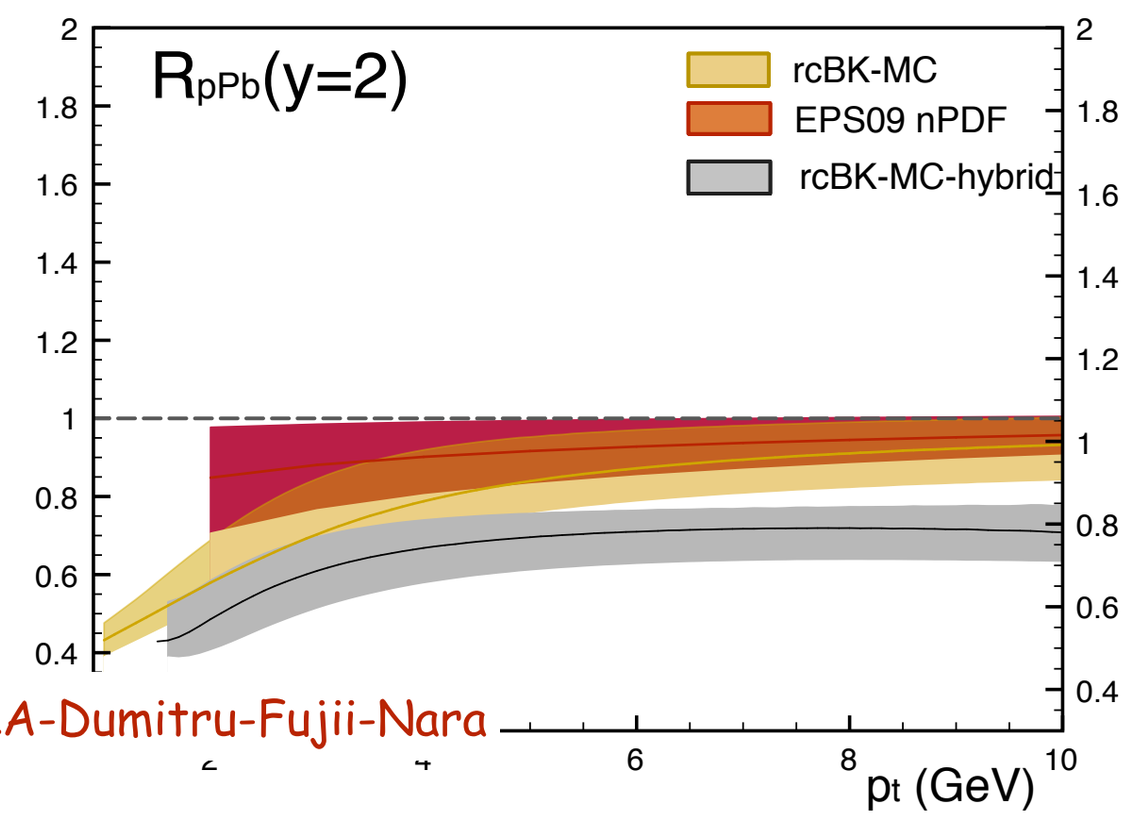

Preliminary results. JLA-Dumitru-Fujii-Nara

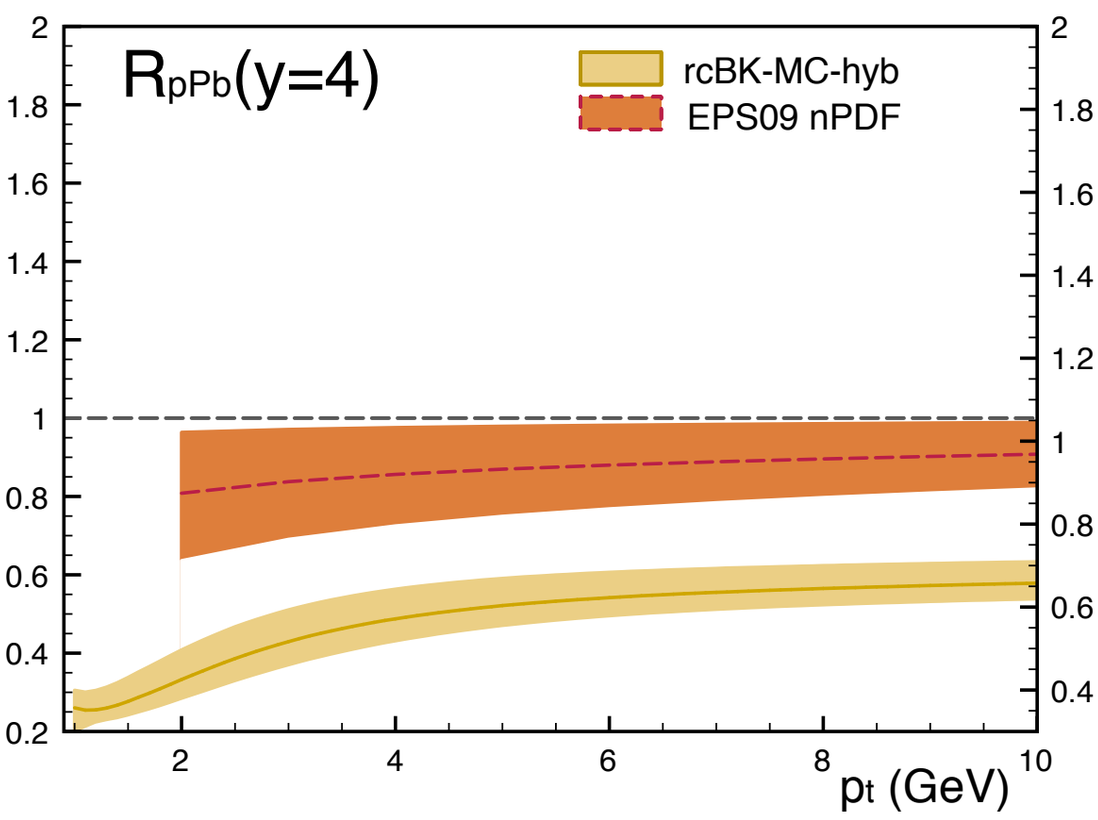

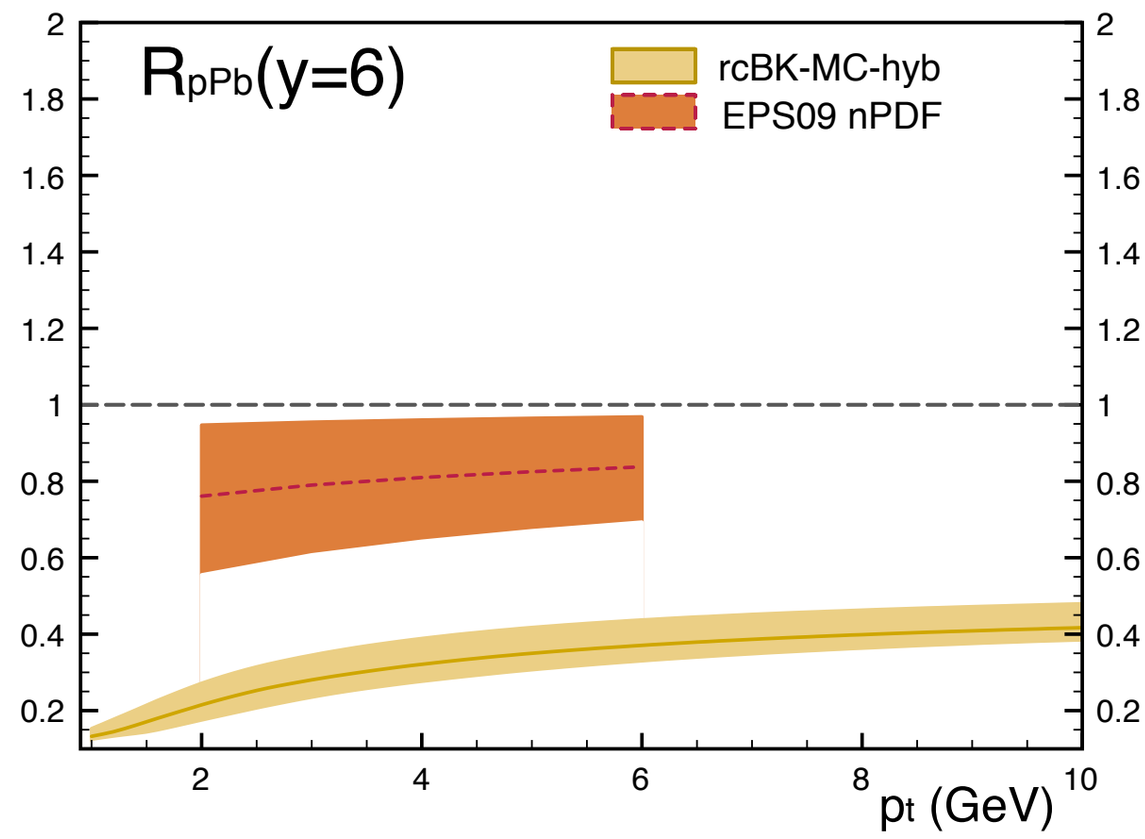

Forward di-hadron angular correlations

Marquet '07, Dominguez et al

CGC description: A quark (gluon) emits a gluon. The pair scatters independently off the target

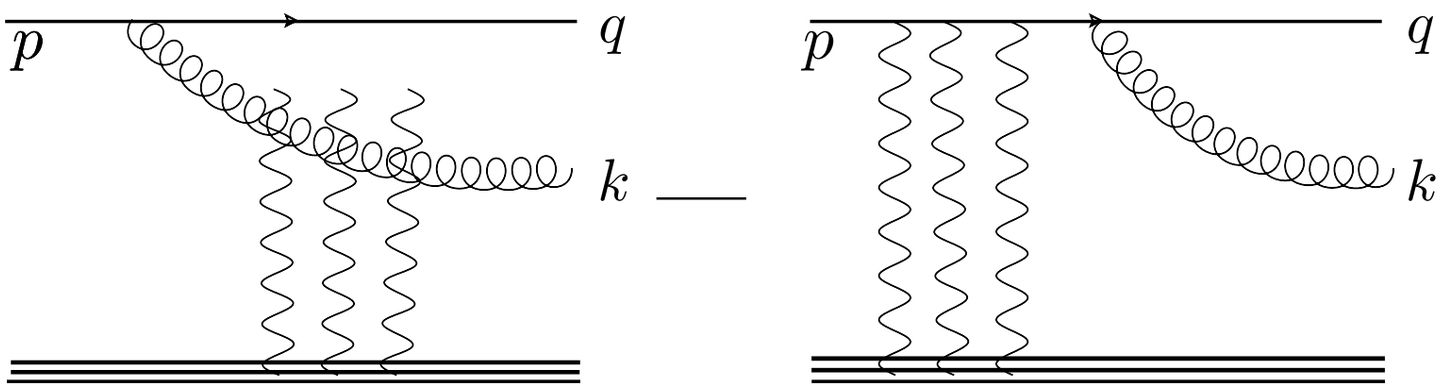

$$x_p = \frac{|k_1|e^{y_1} + |k_2|e^{y_2}}{\sqrt{s}}$$

$$x_A = \frac{|k_1|e^{-y_1} + |k_2|e^{-y_2}}{\sqrt{s}}$$

At small-x, the transverse momentum transfer is controlled by the saturation scale

Angular decorrelation happens if $\mathbf{Q_s^{Pb}(x_A) \sim (k_1, k_2)}$

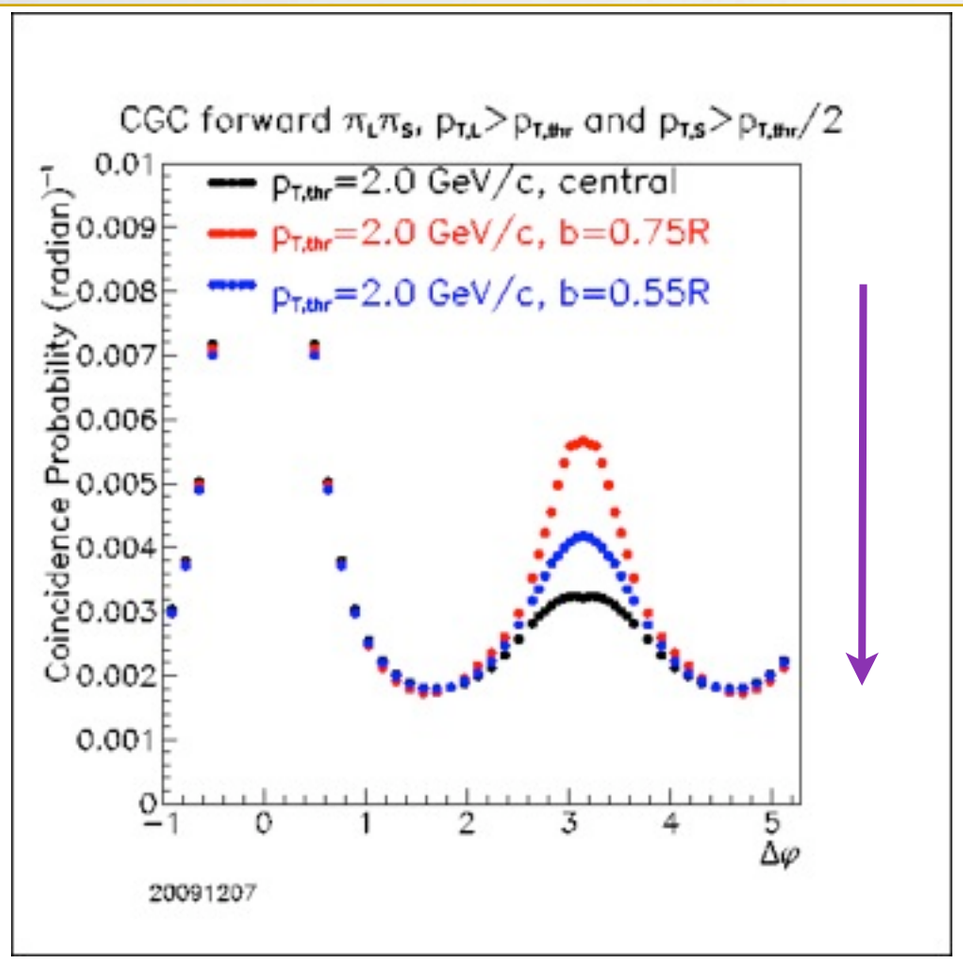

➡ Coincidence probability

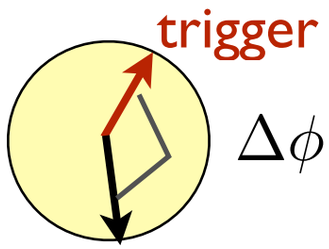

$$CP(\Delta\phi) = \frac{1}{N_{trig}} \frac{dN_{pair}}{d\Delta\phi}$$

Ergo, decorrelation should be stronger with

- Increasing rapidity of the pair
- Increasing collision centrality
- Decreasing hadron momentum

Forward di-hadron angular correlations in RHIC dAu data

central-forward

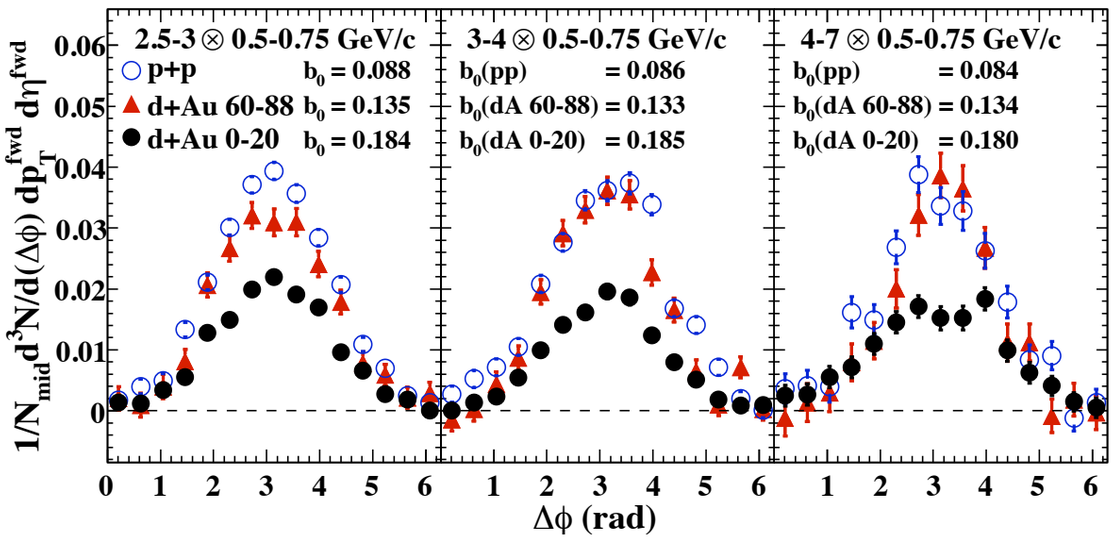

forward-forward

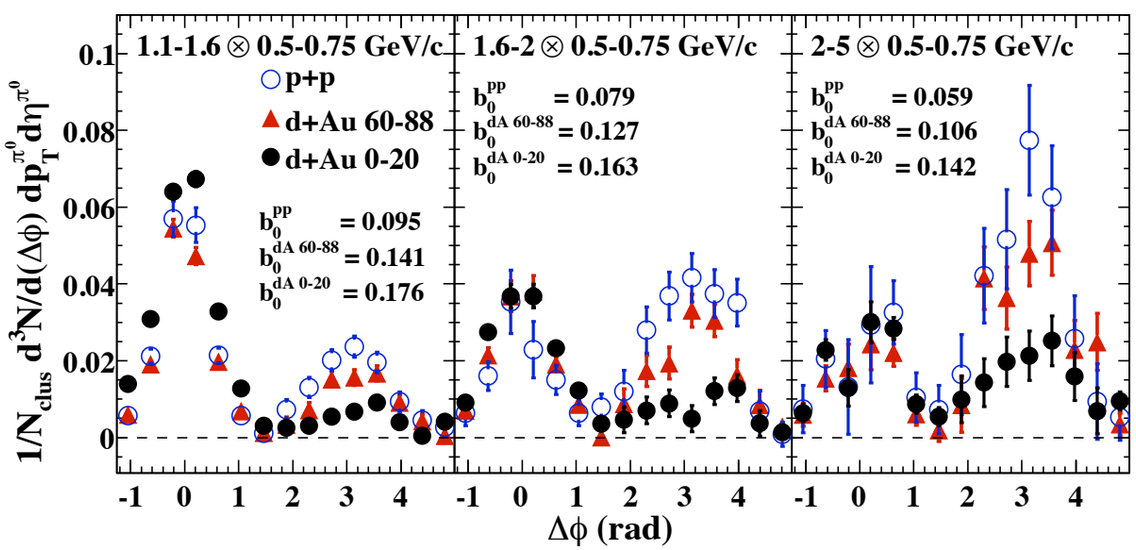

$$J_{dA} = I_{dA} \times R^t_{dA} = \frac{1}{\langle N_{\rm coll}\rangle} \frac{\sigma^{\rm pair}_{dA}/\sigma_{dA}}{\sigma^{\rm pair}_{pp}/\sigma_{pp}}$$

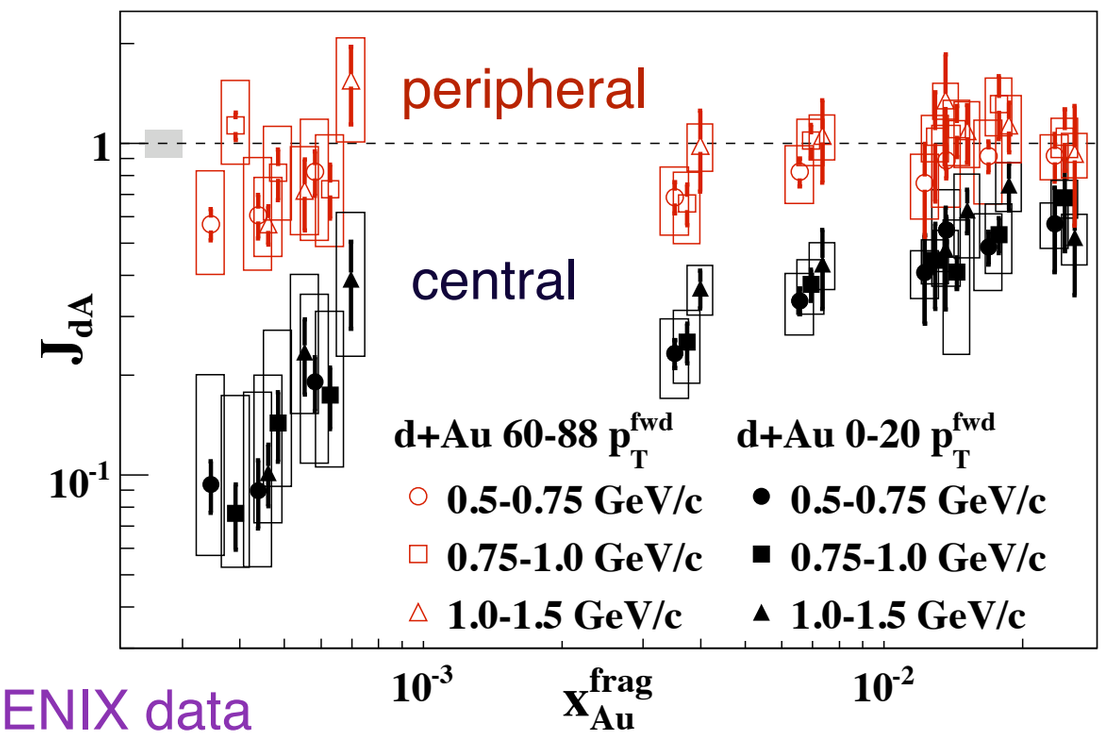

PHENIX data

Observed decorrelation IS stronger with

- Increasing rapidity of the pair
- Increasing collision centrality
- Decreasing hadron momentum

Forward di-hadron angular correlations in RHIC dAu data

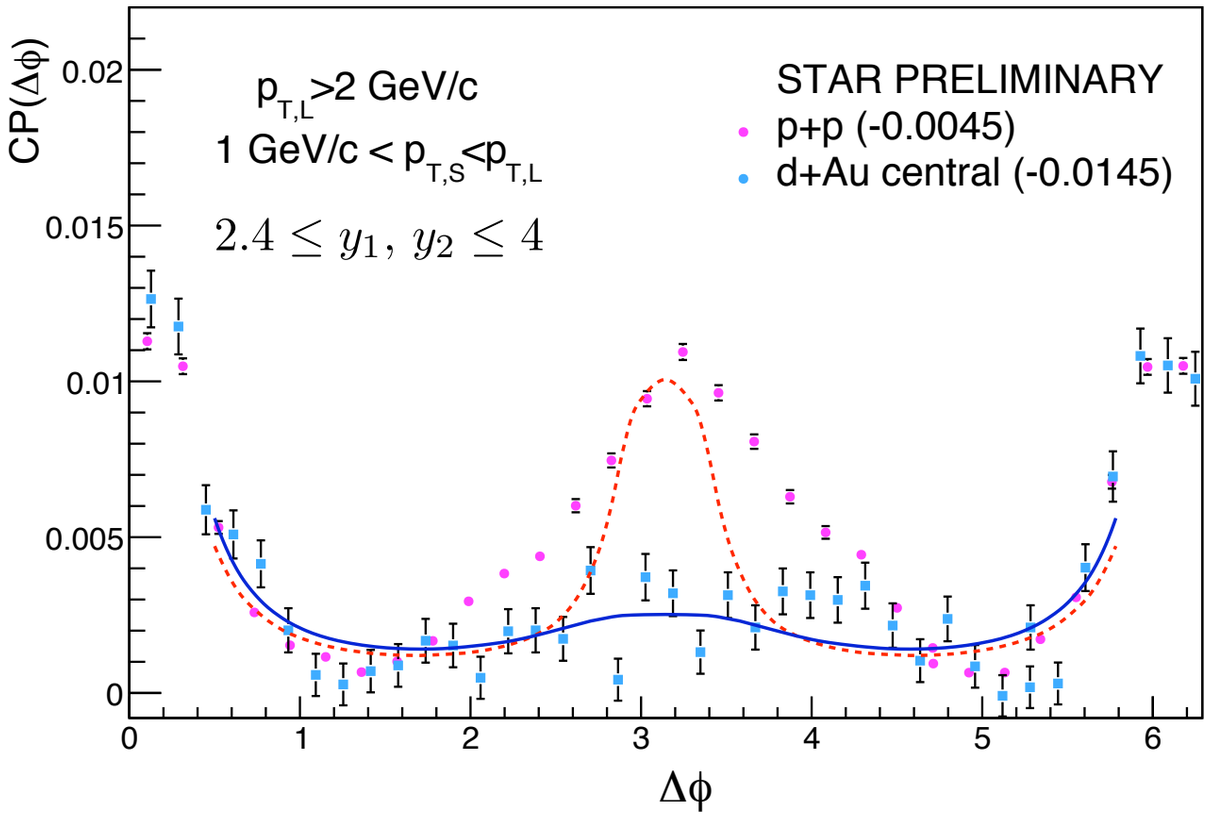

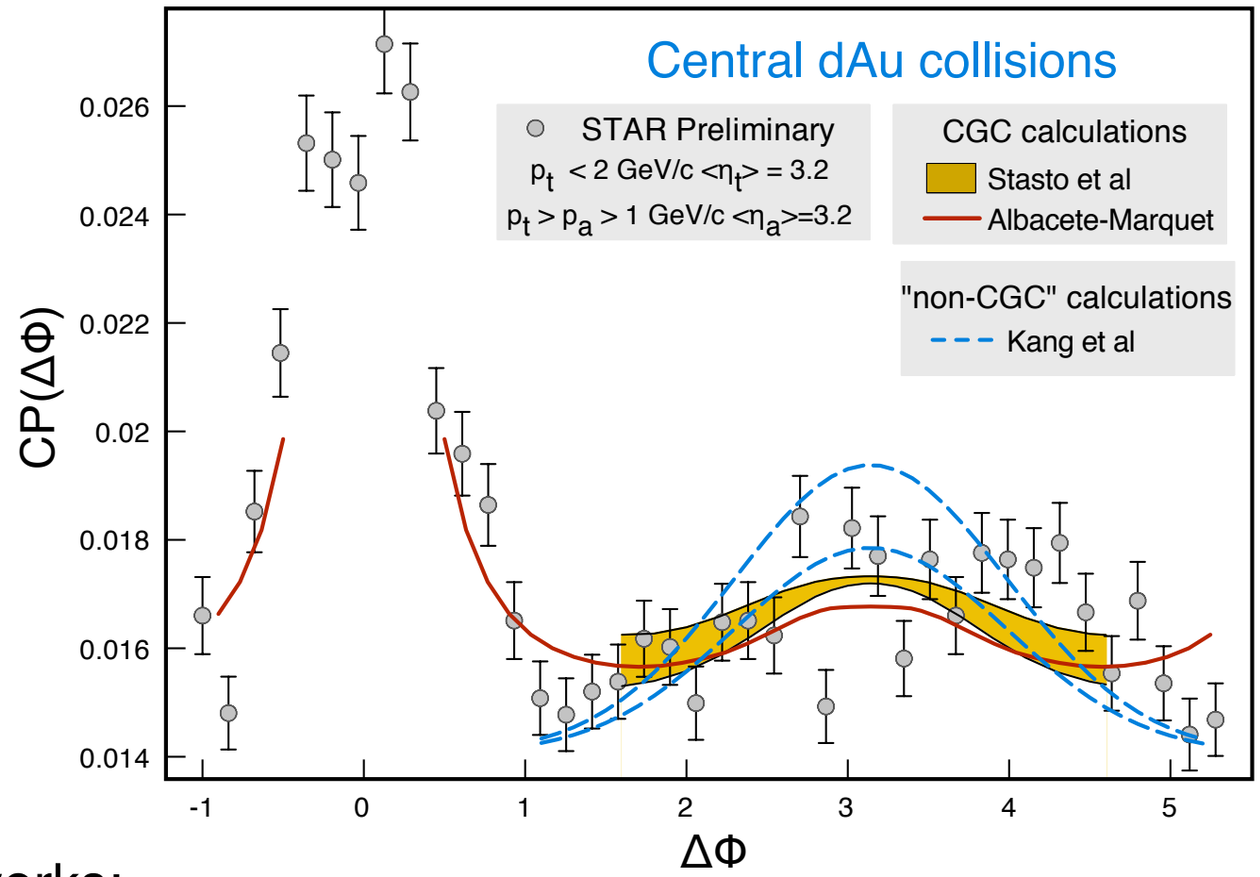

Uncertainties in current CGC phenomenological works:

- Need of a better description of n-point functions.

$$S^{(6)}(b,x,x',b') = Q(b,b',x',x)S(x,x') + \mathcal{O}\left(\frac{1}{N_c^2}\right)$$

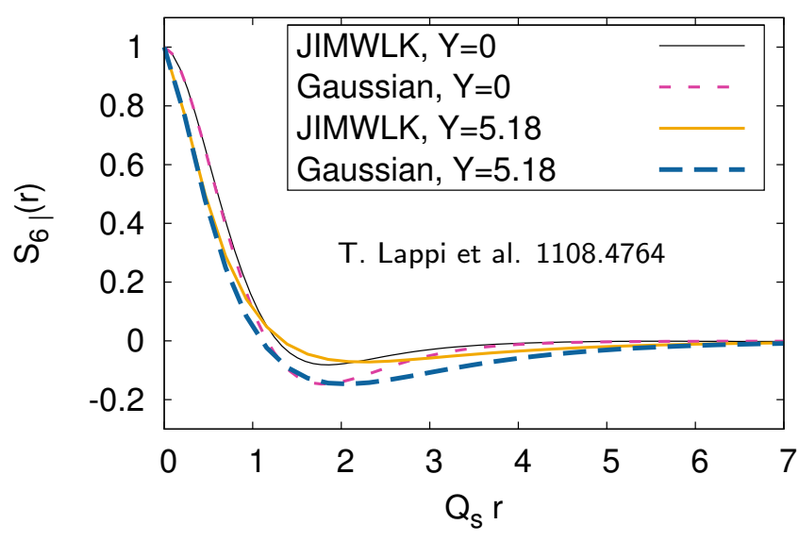

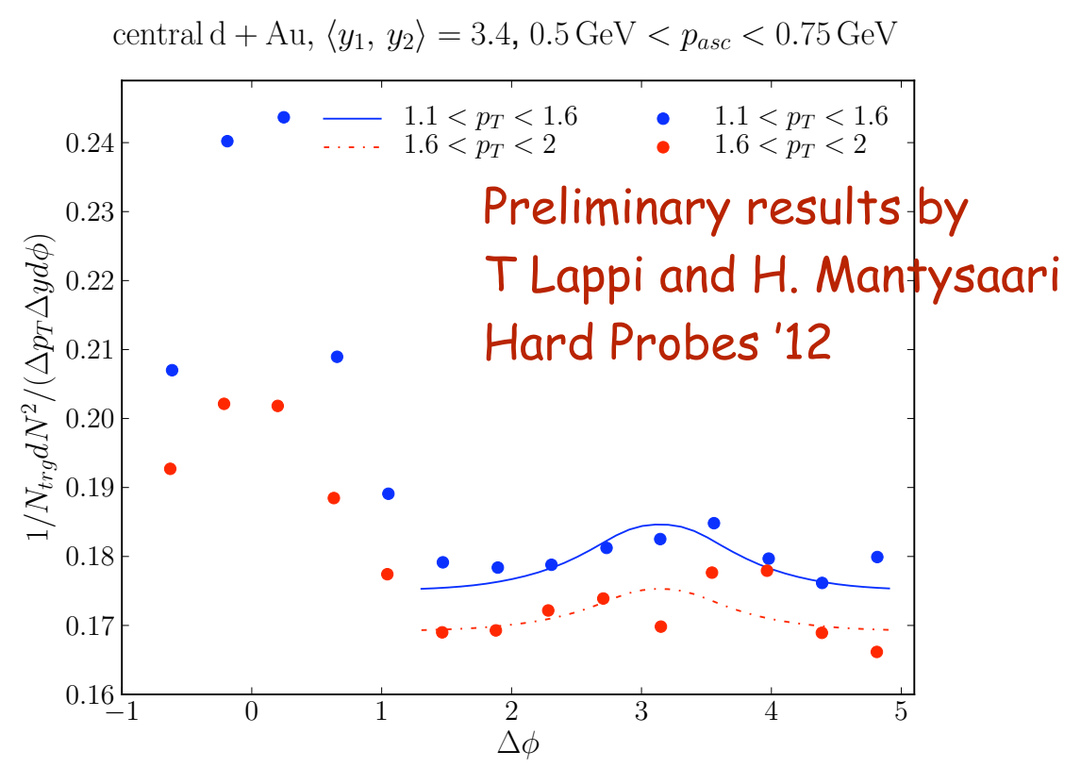

Forward di-hadron angular correlations in RHIC dAu data

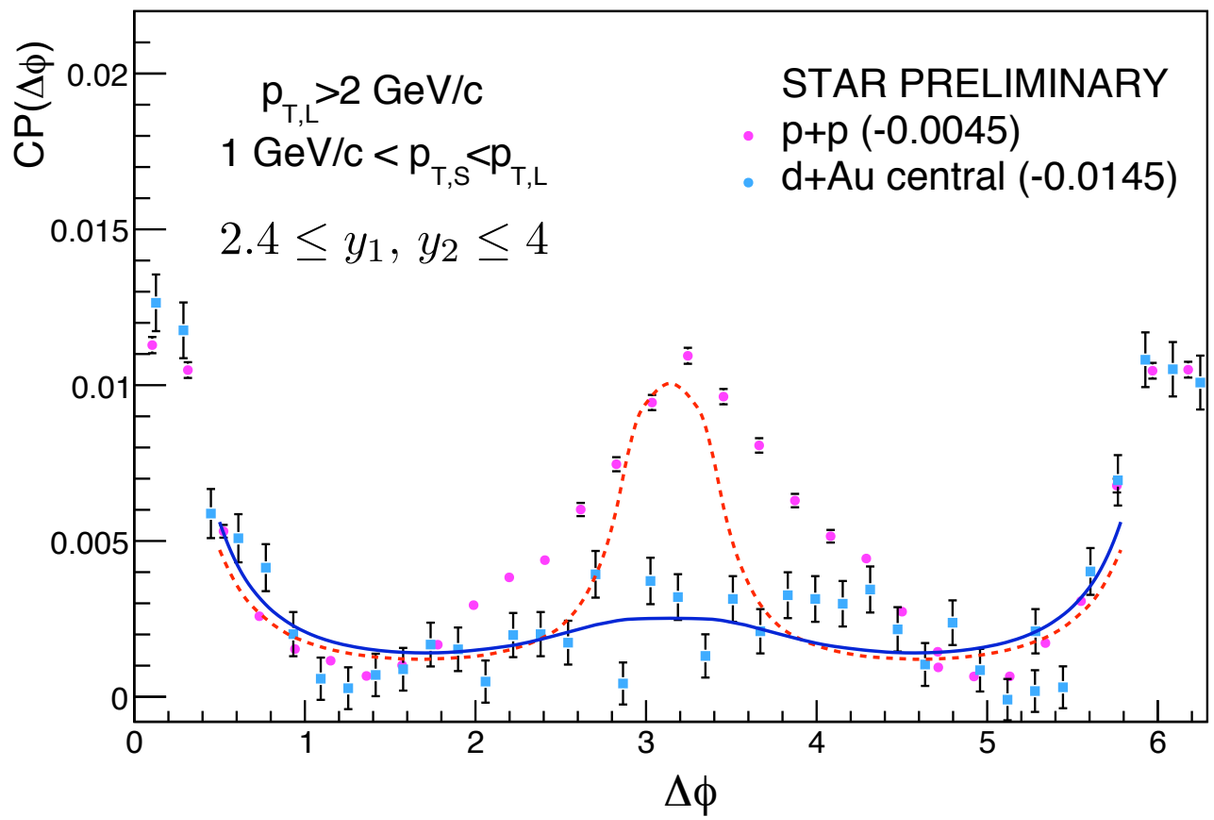

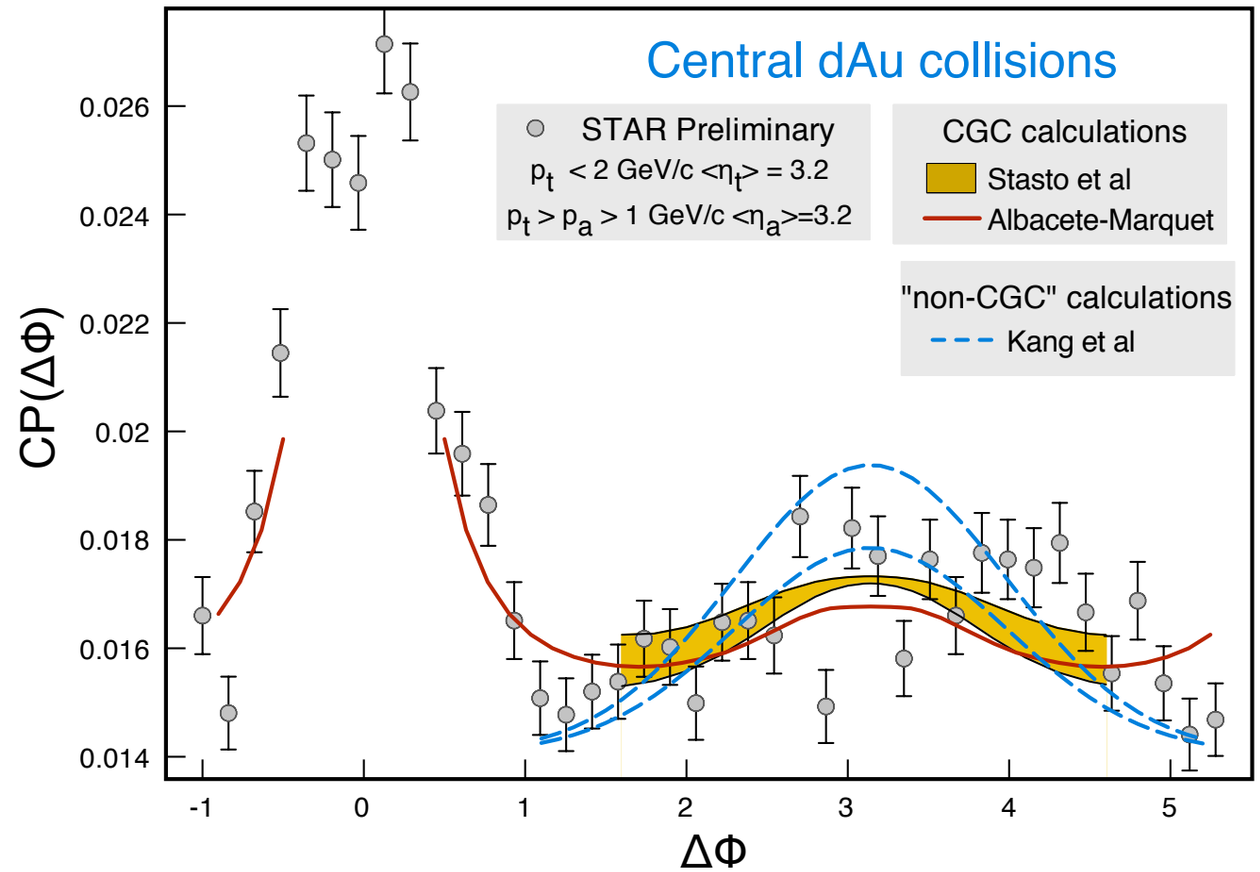

Forward di-hadron angular correlations in RHIC dAu data

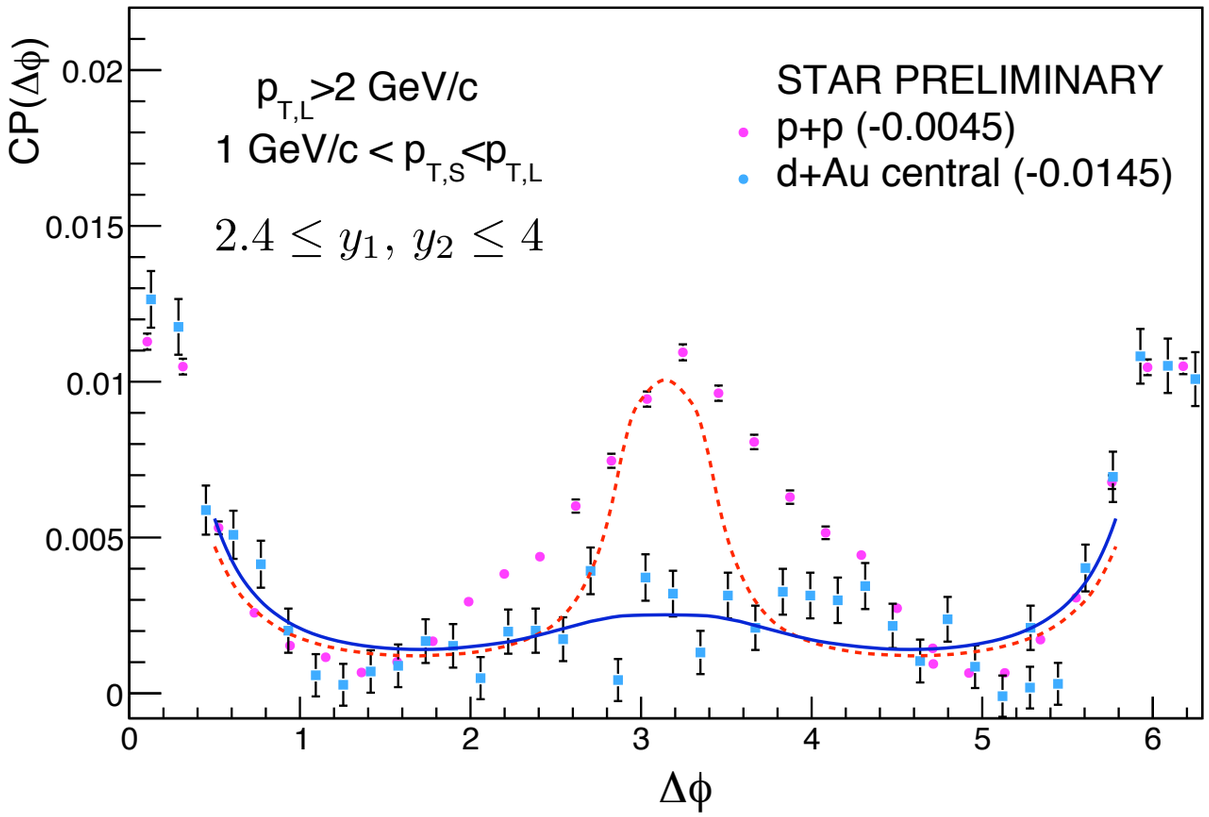

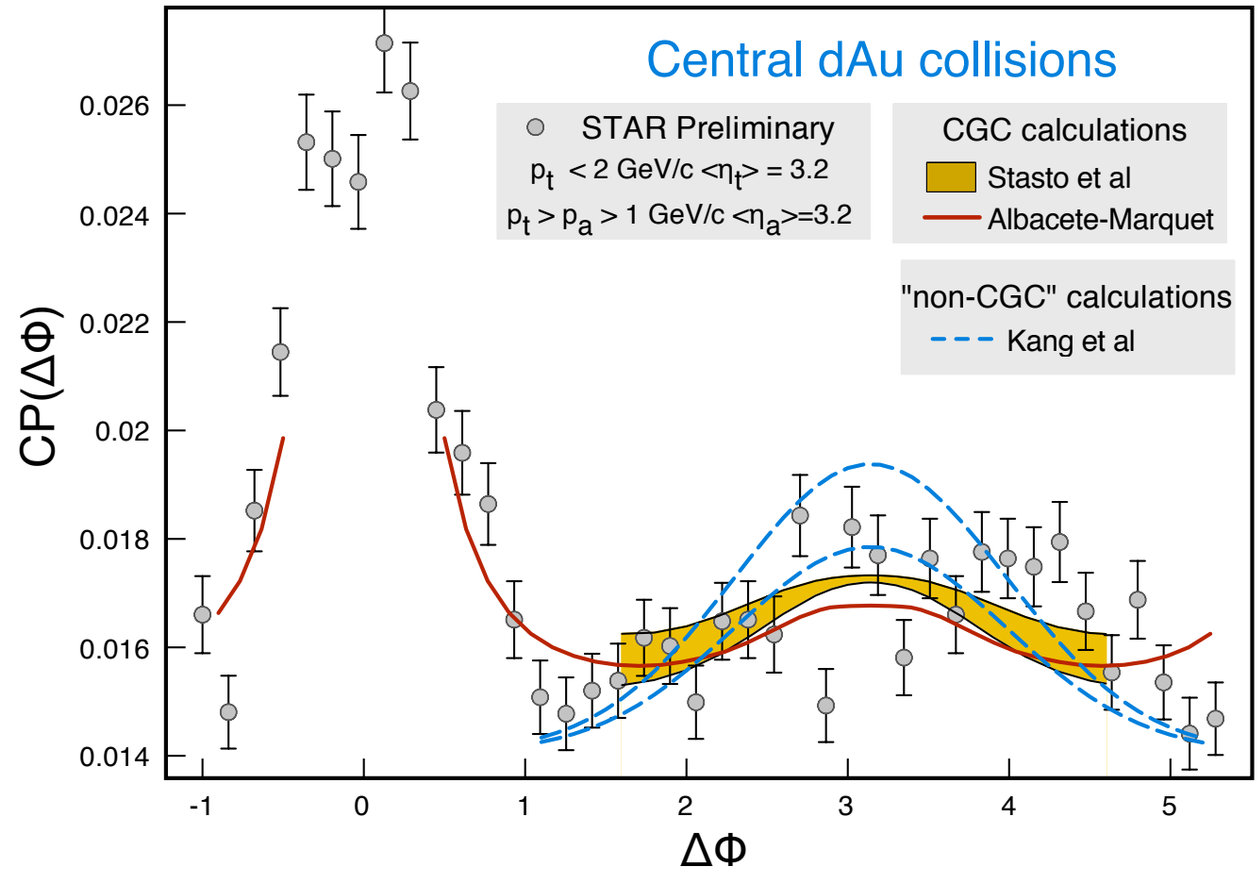

Uncertainties in current CGC phenomenological works:

- Need of a better description of n-point functions.
- Better determination of the pedestal: K-factors in single inclusive production? Role of double parton scattering?

Strikman-Vogelsang

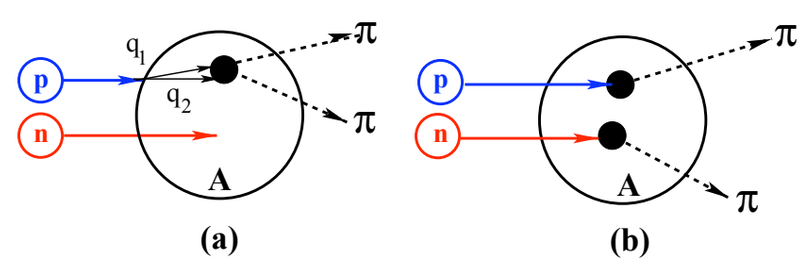

Strikman, Vogelsang, 1009.6123

- Alternative descriptions including resummation of multiple scatterings, nuclear shadowing and cold nuclear matter energy loss seem possible... [Kang et al]

Outlook

- ✔ Important steps have been taken in promoting GCG to an useful quantitative tool
  - Continuos progress on the theoretical side
  - Phenomenological effort to systematically describe data from different systems (e+p, e+A, p+p, d+Au, Aa+Au and Pb+Pb) in an unified framework
- ✔ Observed suppression phenomena in RHIC forward data provide the most compelling evidence for the relevance of CGC effects in presently available data
- ✔ However, RHIC data lies at the limit of applicability of the high-energy CGC formalism. Missing dynamical effects and higher order corrections may modify the interpretation of data
- ✔ More differential studies of data are needed to distinguish the CGC approach from others

Thanks!

Back up

Color Glass Condensate models

charged particles ~ # small-x gluons in the wave functions of the colliding nuclei

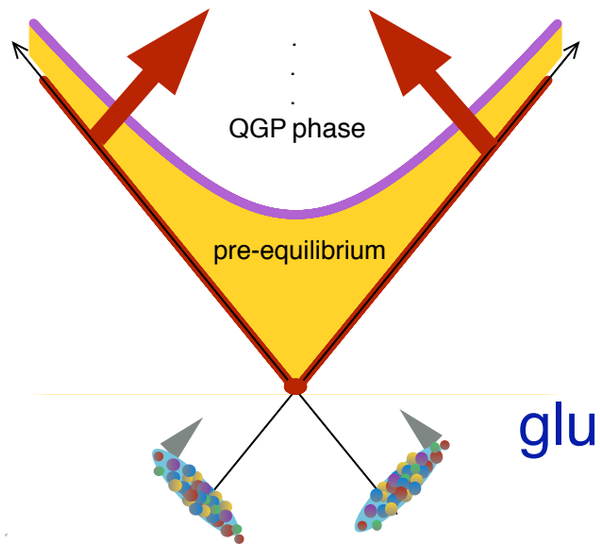

LO kt-factorization:

$$\left.\frac{dN^g}{d\eta\, d^2p_t}\right|_{\eta=0} \propto \frac{1}{p_t^2}\int d^2k_t\, \alpha_s\, \phi(x_1,k_t)\, \phi(x_2,|p_t-kt|)$$

$$\lambda \approx 0.24 \div 0.3$$

gluon-hadron duality:

$$\left.\frac{dN^{ch}}{d\eta}\right|_{\eta=0} = \frac{2}{3}K \left.\frac{dN^g}{d\eta}\right|_{\eta=0} \propto Q_s^2(\sqrt{s},b) \sim \sqrt{s/s_0}^{\,\lambda}\, N_{part}$$

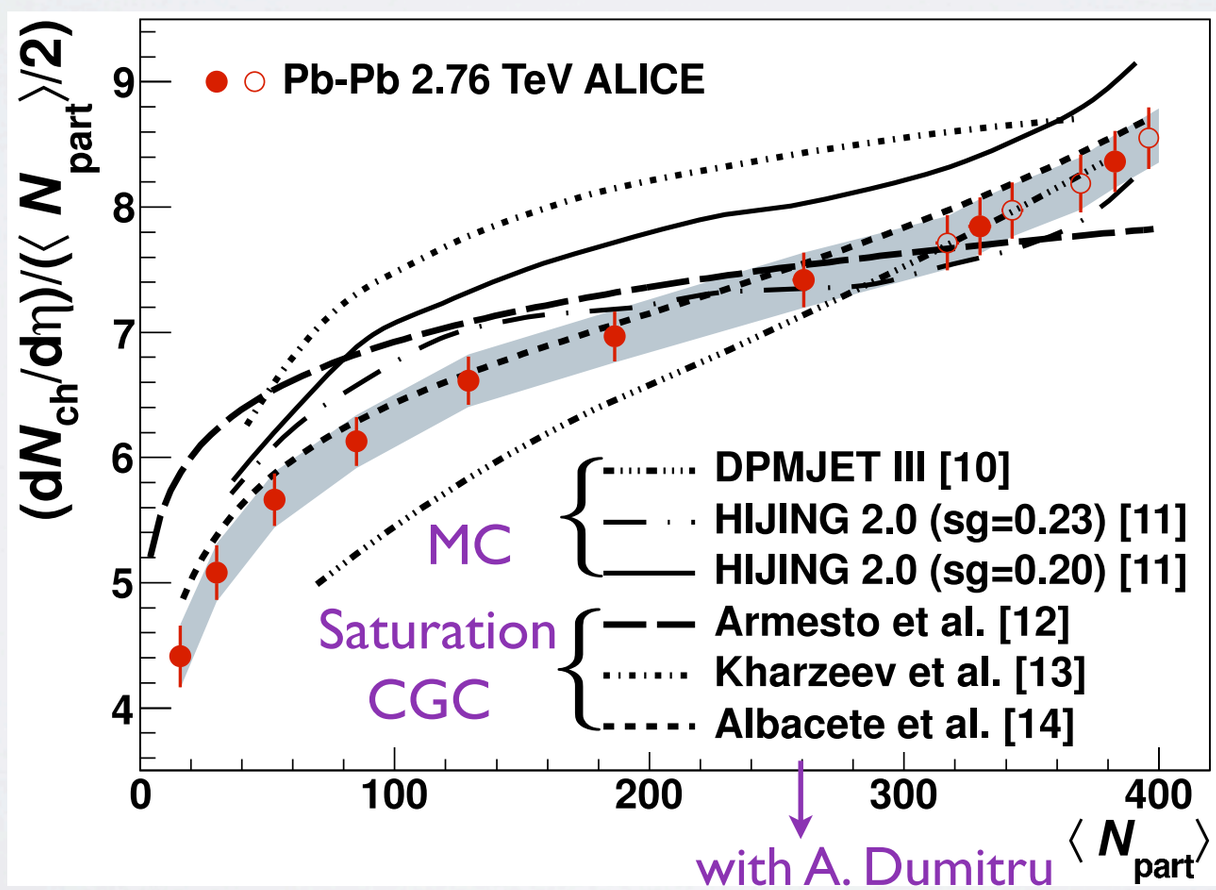

Miscellanea

- CGC gives a very good descriptions of bulk features of multiparticle production

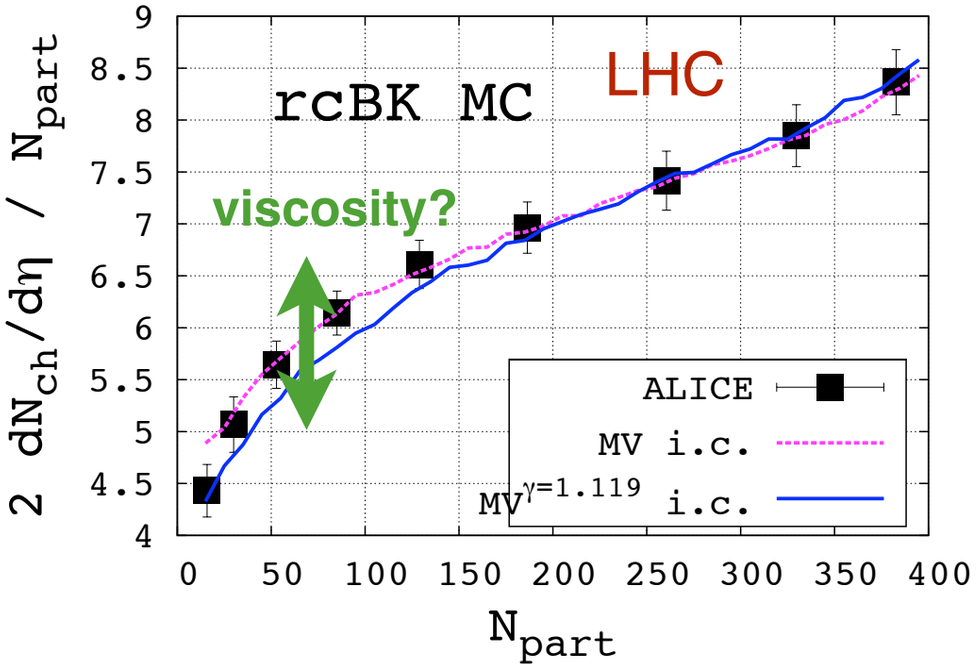

CGC: Non-linear and non-local

Knowledge of the “hard” part of nuclear UGD would further constrain the description of the initial state!

hadron-photon* correlations in pPb collisions at the LHC

- hadron-dilepton pair

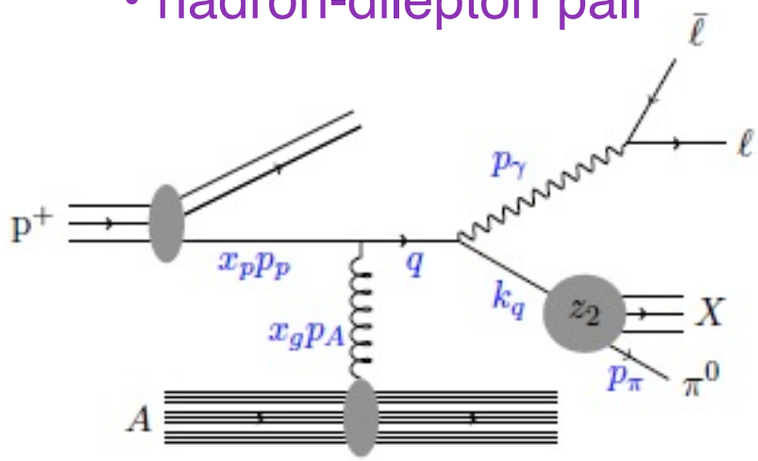

Stasto et al 1204.4861

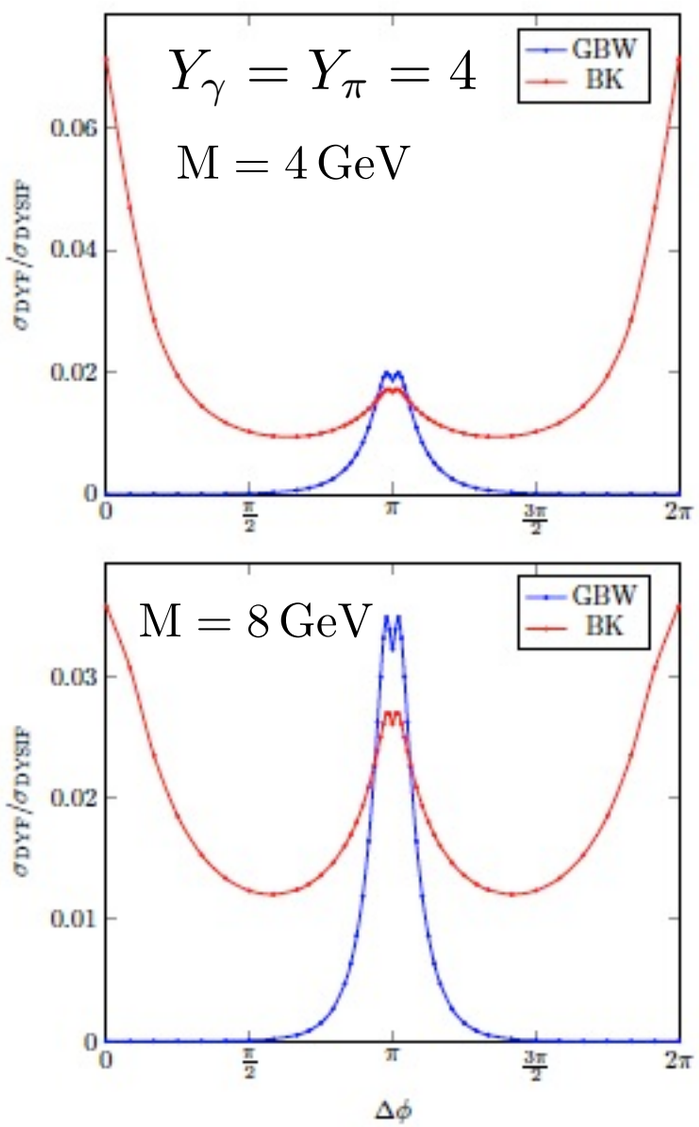

- hadron-photon

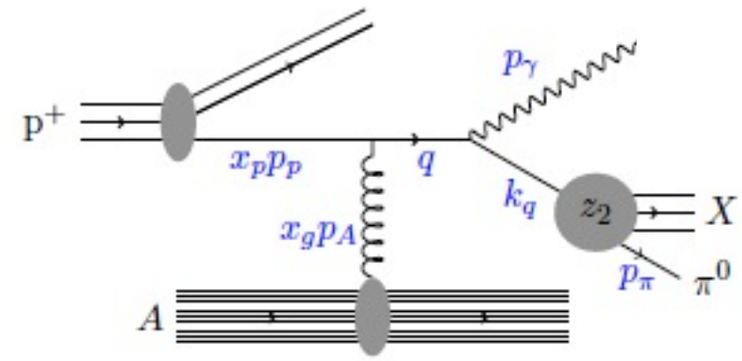

Jalilian-Marian's talk

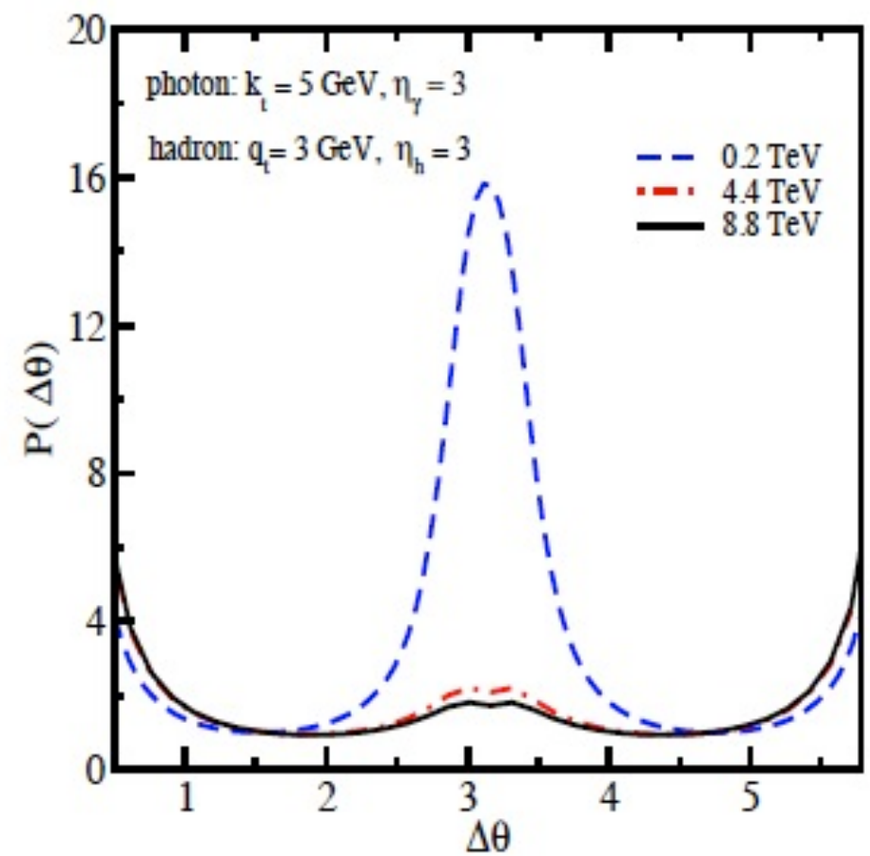

These processes are theoretically cleaner:
Only knowledge of 2-point needed!!

The STAR Transverse Spin Programme

Thomas Burton
RIKEN Forward Physics Workshop
Brookhaven National Lab
31st July 2012

Introduction

- Recent results from STAR transverse spin
- Future: what measurements do we want to make?
  - A_N: Disentagle Sivers, Collins OR other mechanisms
  - A Sivers sign change between DIS and DY?
  - Nucleon structure: flavour decomposition, GPDs
- Upgrade plans - what do we need to add/change?

Past results

Midrapidity: Sivers jet measurement shows no asymmetry

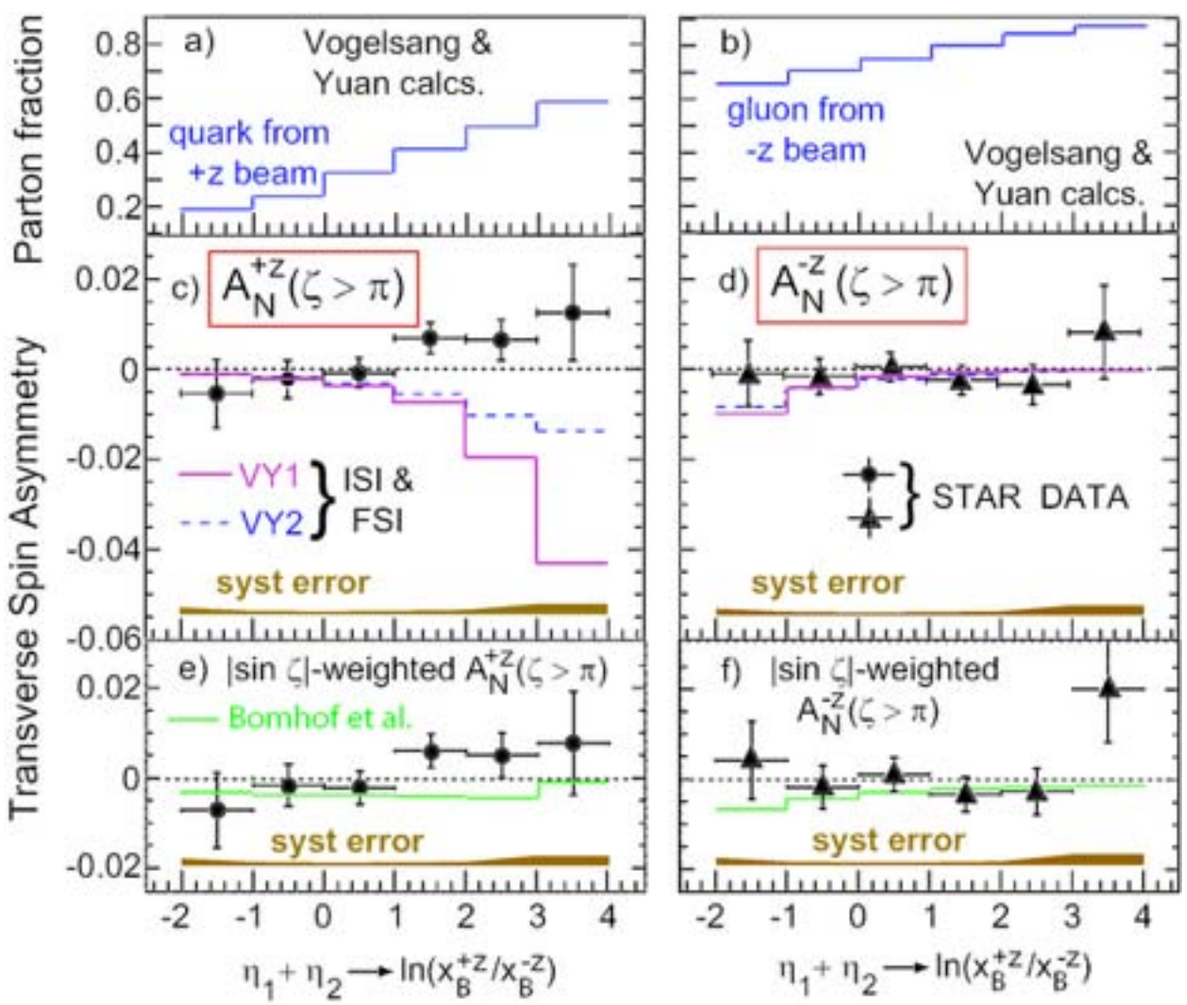

Forward: Large asymmetries in π^0 production

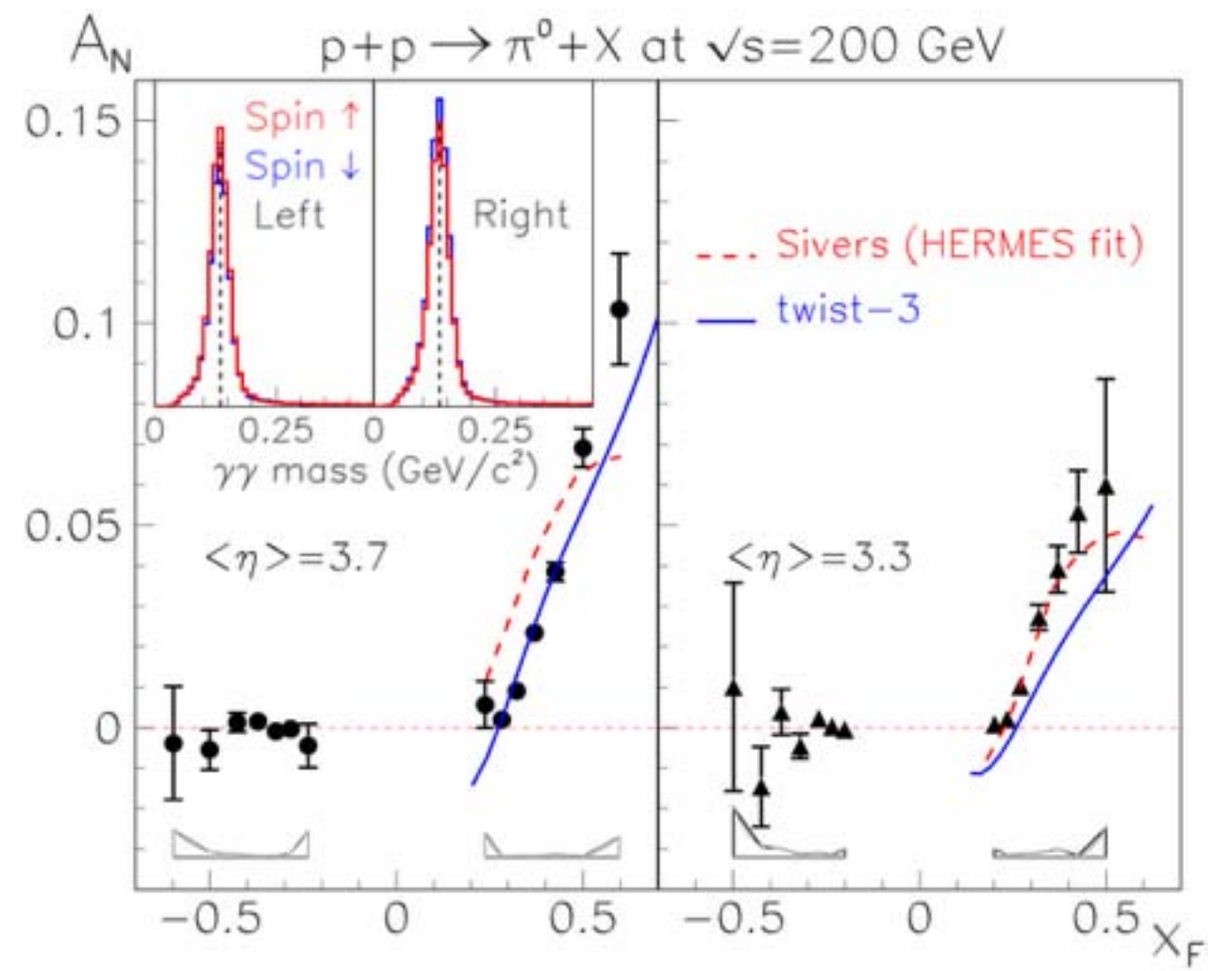

Recent Results

1. **Midrapidity**: transversity and spin-dependent fragmentation
    1. IFF
    2. Collins in jets
2. **Forward**: transverse single-spin asymmetries
    1. π^0/η asymmetries
    2. 2011 π^0

Midrapidity IFF

- **I**nterference **F**ragmentation **F**unction:
  - Spin-dependent dihadron production
- $\sin(\phi_S - \phi_R)$ modulation of hadron pair

asymmetry ∝

transversity ⊗ IFF

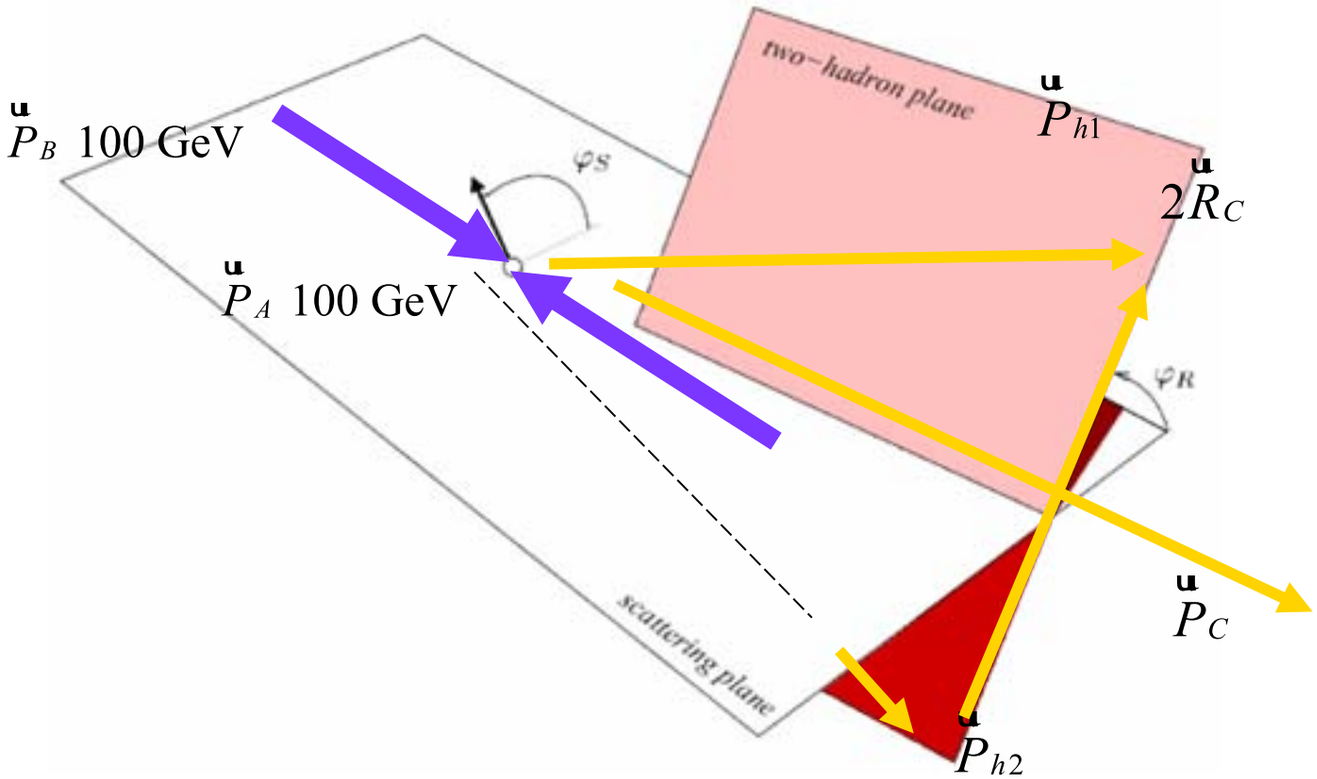

Midrapidity IFF

- Non-zero: **midrapidity transversity**
- More data on the way

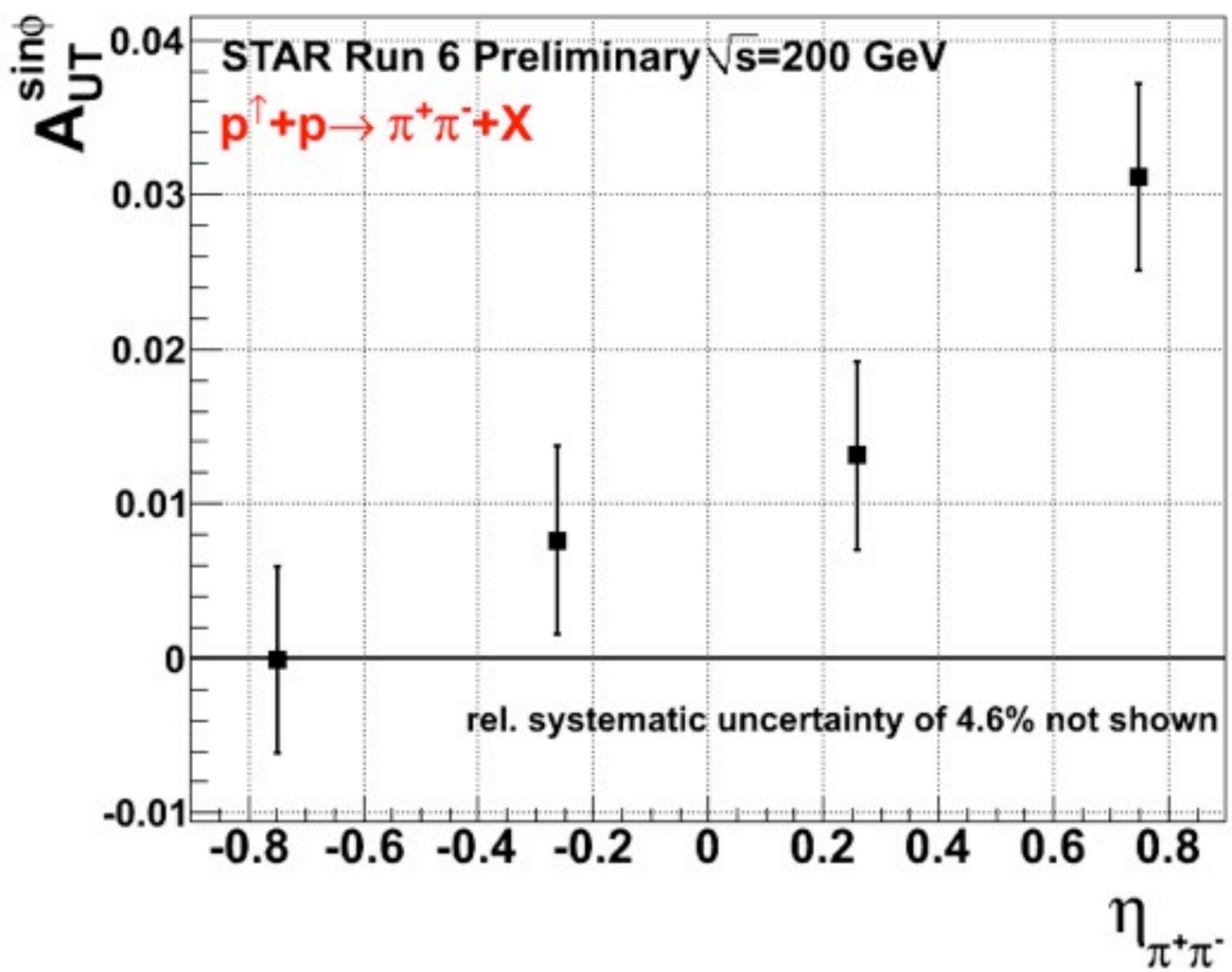

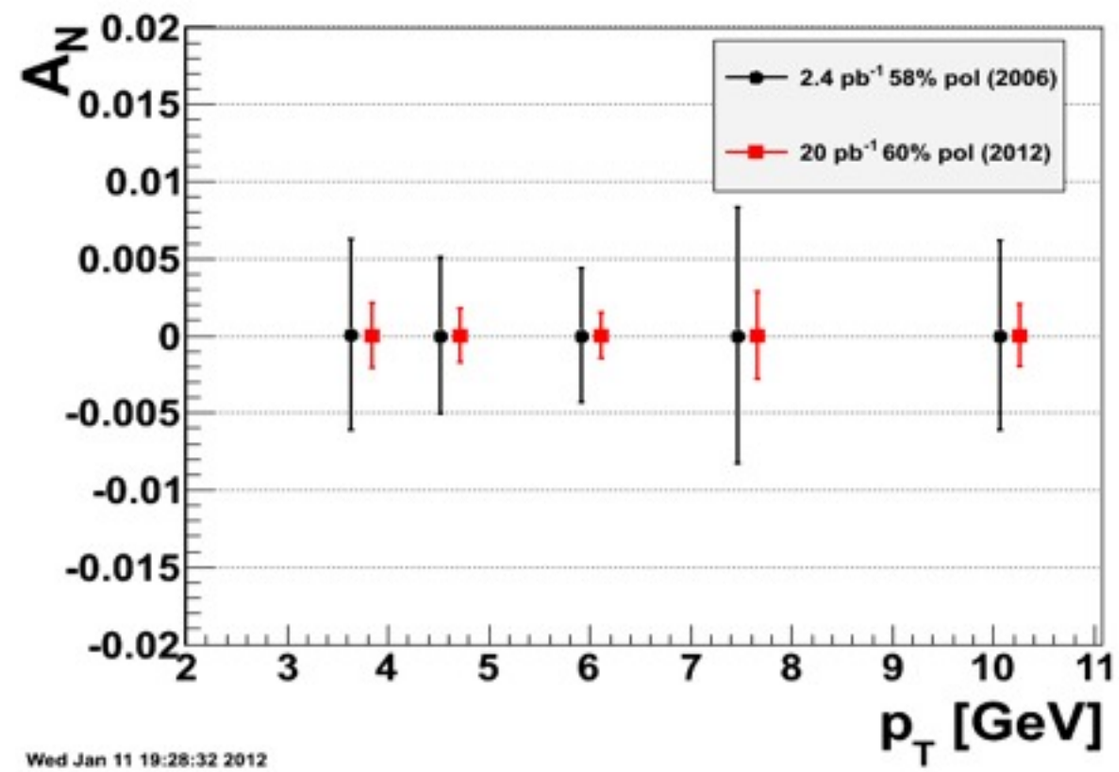

Midrapidity jet Collins

- Measure an azimuthal modulation of π in a jet

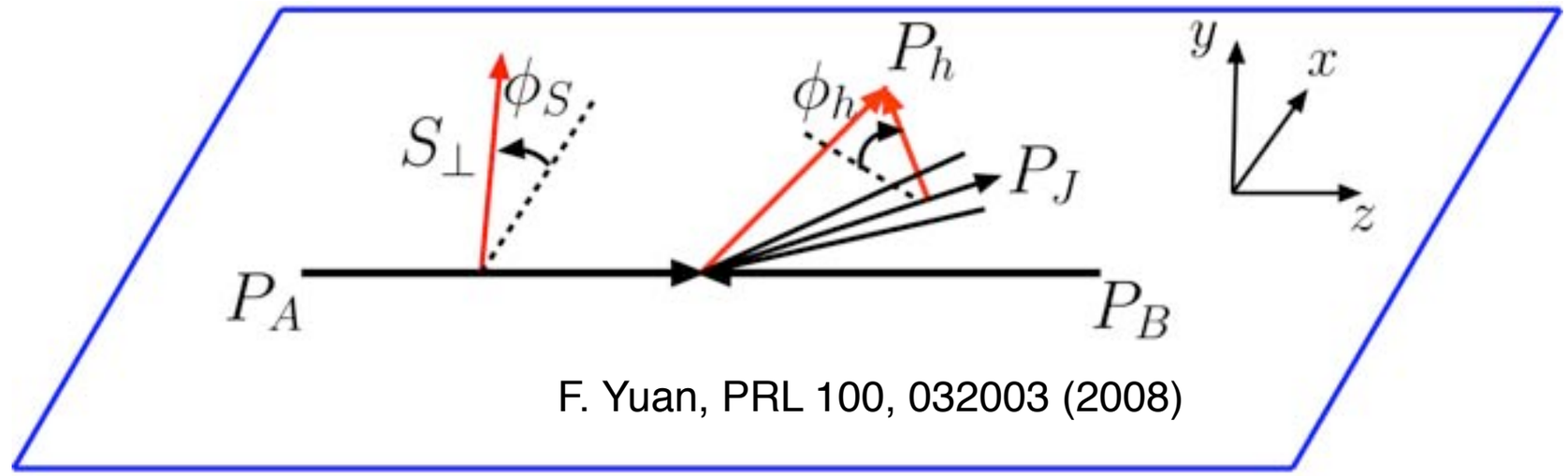

F. Yuan, PRL 100, 032003 (2008)

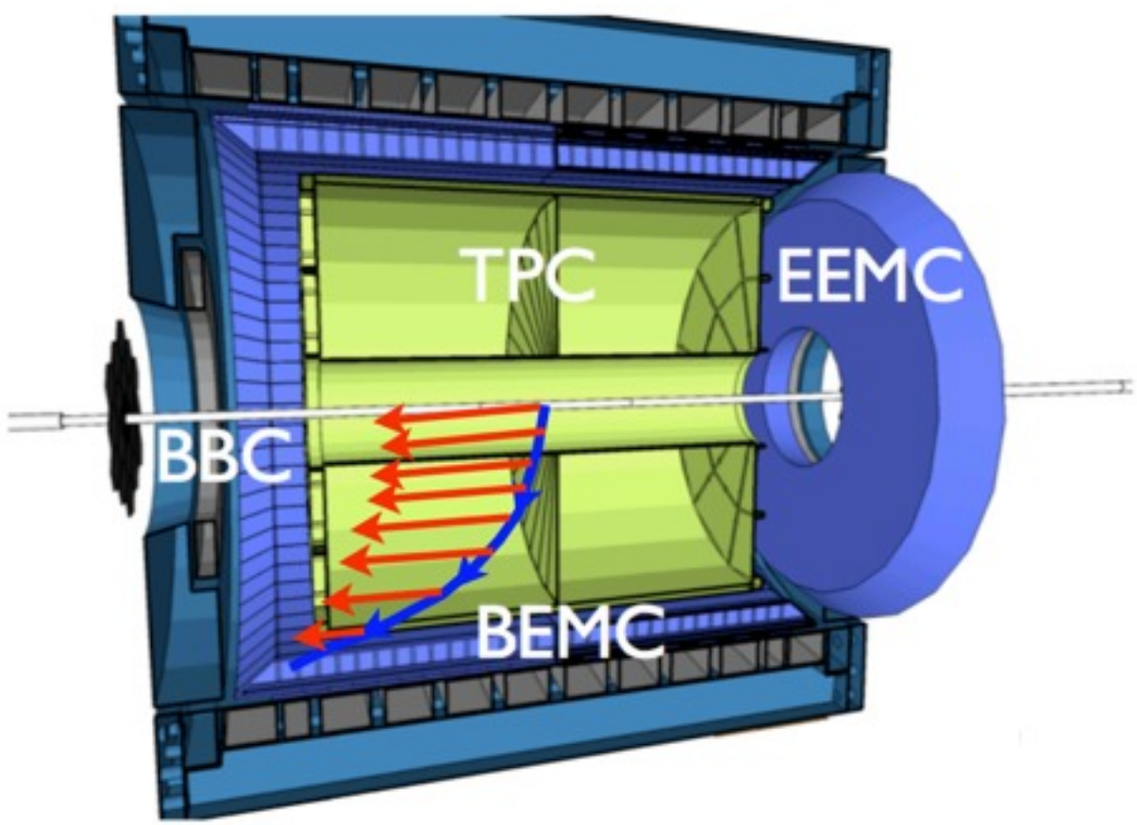

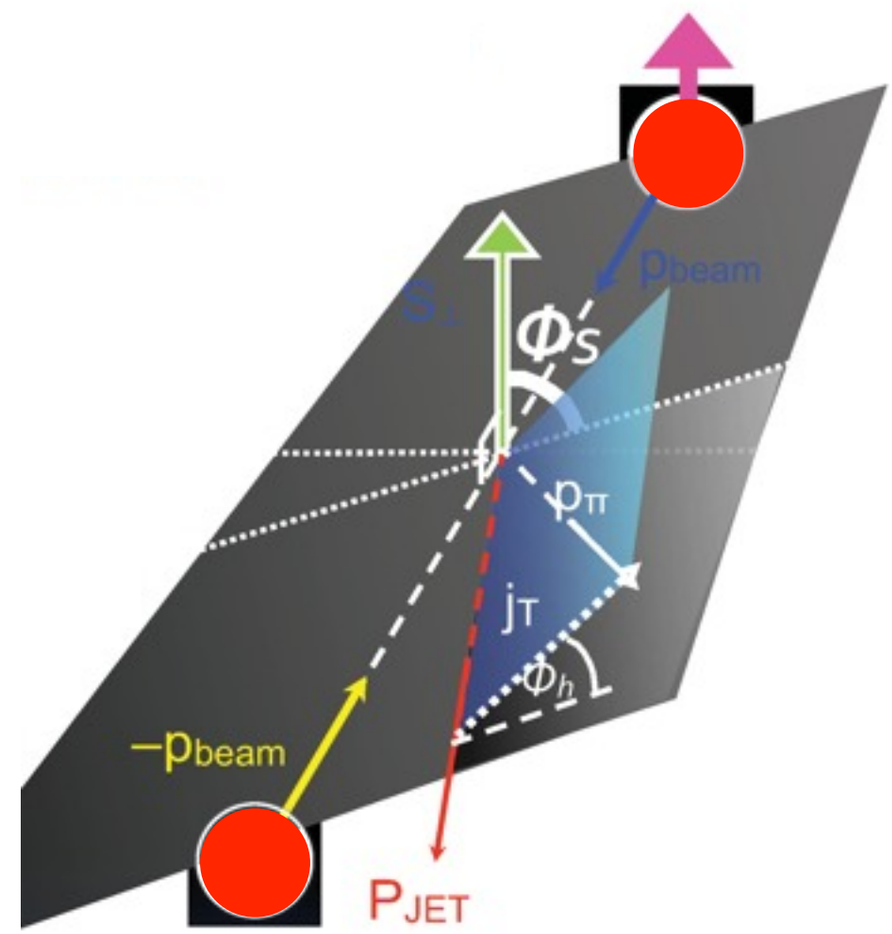

Midrapidity jet Collins

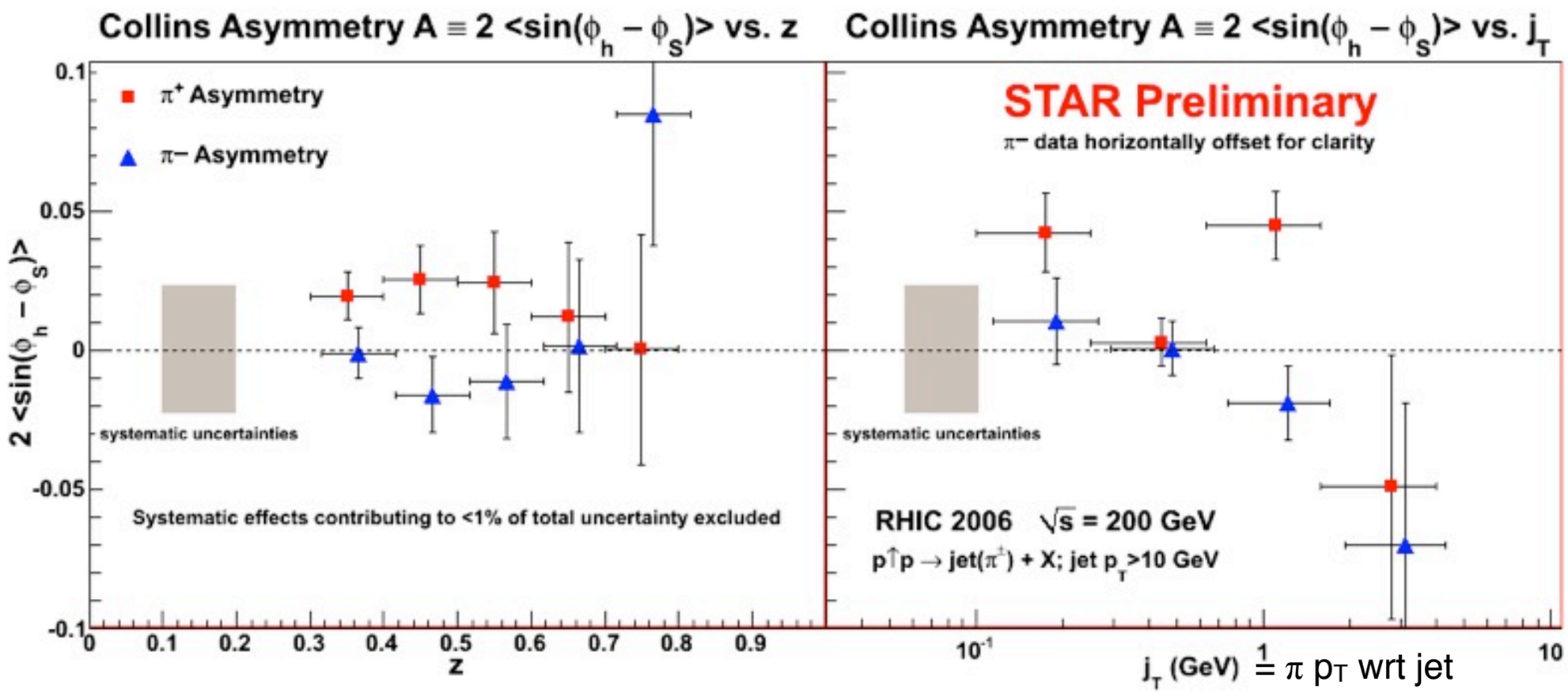

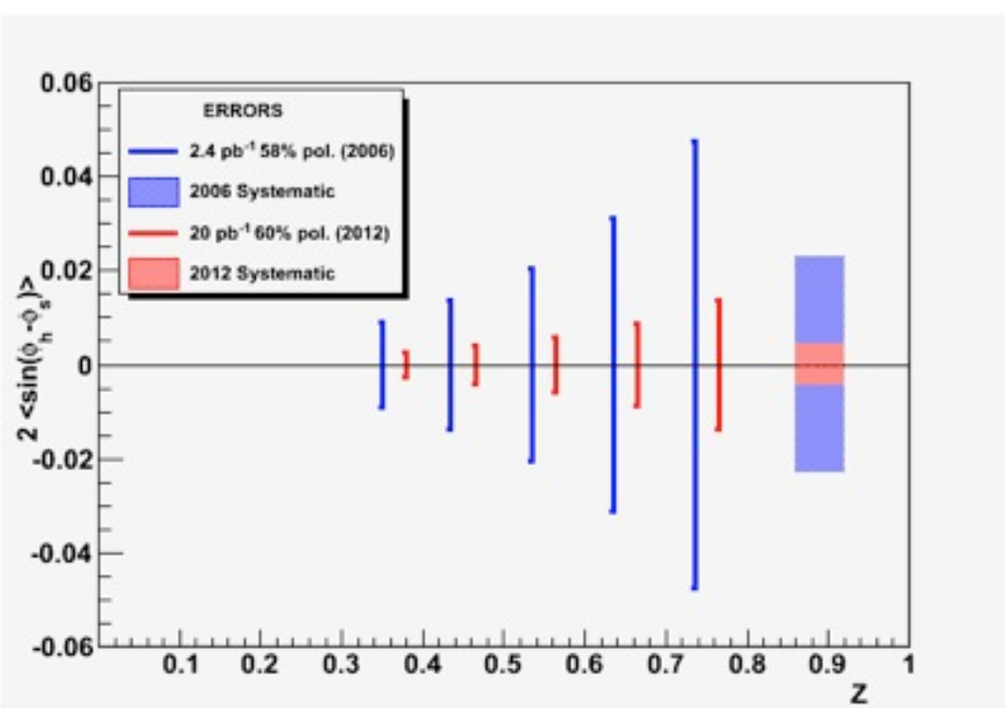

- Sign difference?
- Run 12 data should clarify

Forward π^0/η asymmetry

- π^0/η in forward EM calorimeter (FMS)
- σ described by pQCD
- A_N^η comparable to or greater than π^0
  - Different ff, flavour structure

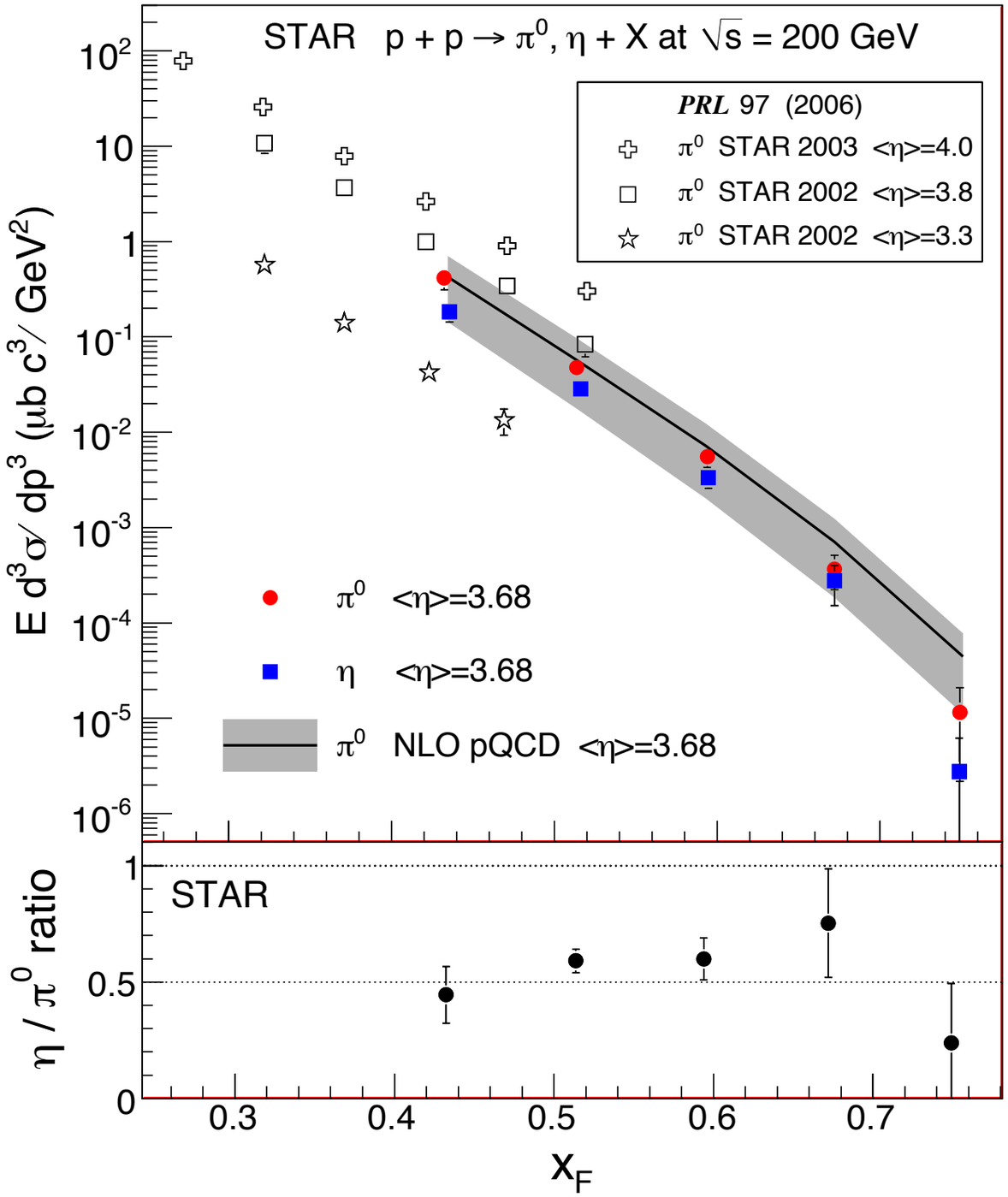

- Len Eun (award-winning thesis!)
  - Thesis: http://arxiv.org/abs/1205.4771
  - Paper submitted to PRDhttp://arxiv.org/pdf/1205.6826v1.pdf

Forward π^0/η asymmetry

- π^0/η in forward EM calorimeter (FMS)
- σ described by pQCD
- A_N^η comparable to or greater than π^0
  - Different ff, flavour structure

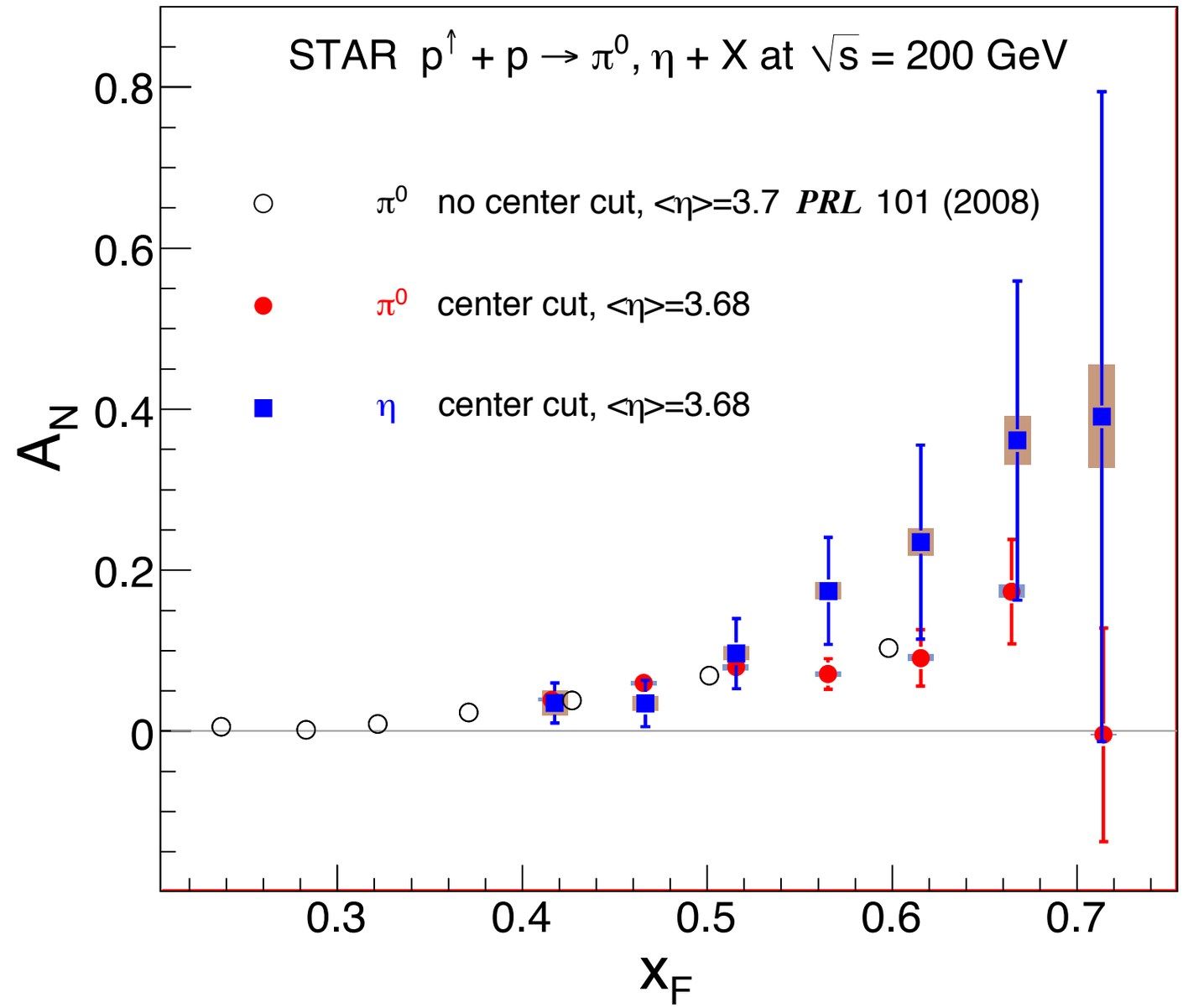

- Len Eun (award-winning thesis!)
  - Thesis: http://arxiv.org/abs/1205.4771
  - Paper submitted to PRDhttp://arxiv.org/pdf/1205.6826v1.pdf

2011 forward pi0

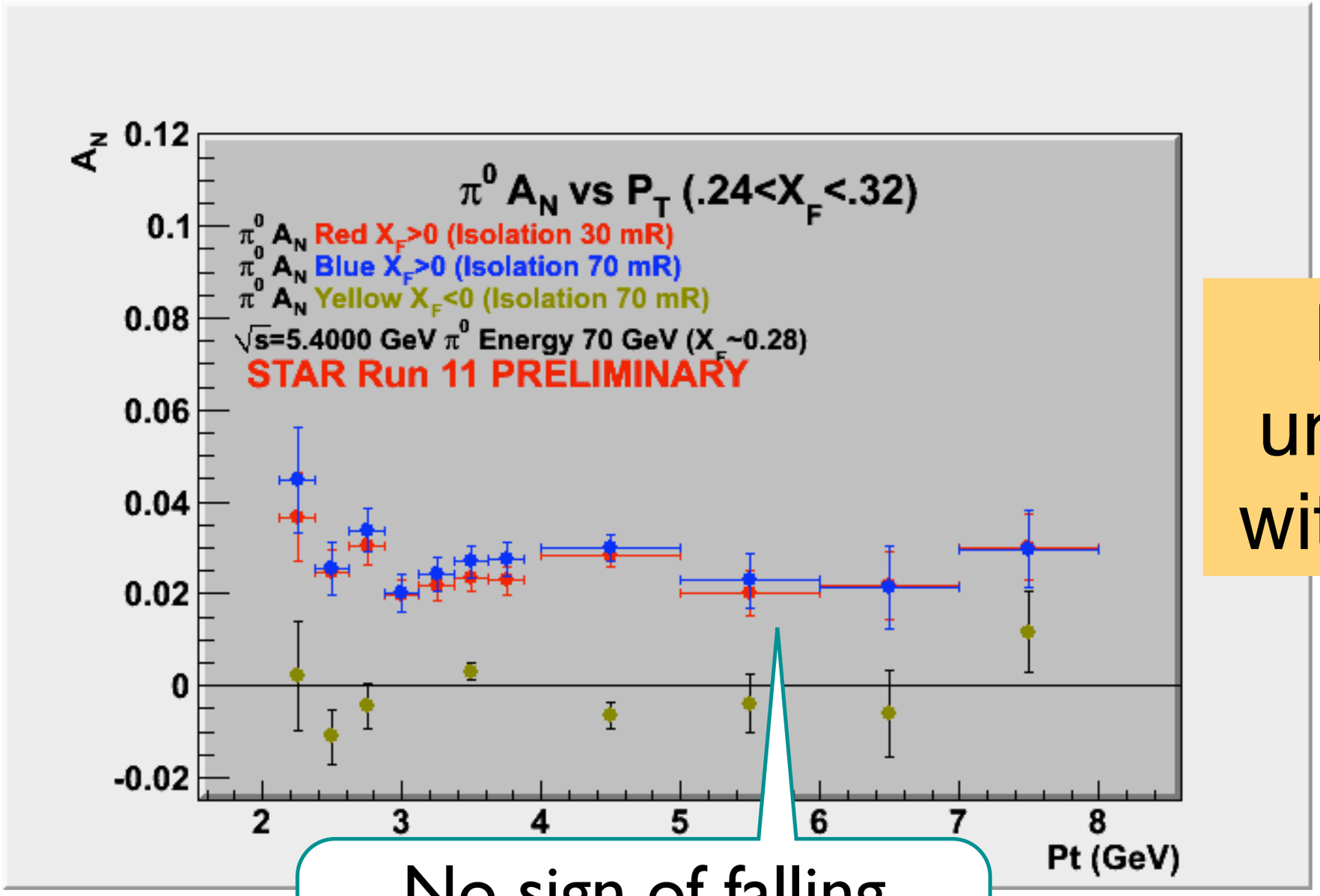

How can we understand this with e.g. Sivers?

No sign of falling with p_T - not what we expect from pQCD

Simple Monte Carlo

- Use weighted PYTHIA

  Weight partons: 1 + (sivers/unpol)*(px/p_T)*(amplitude*spin factor)

  ➡ ϕ modulation in momentum distribution

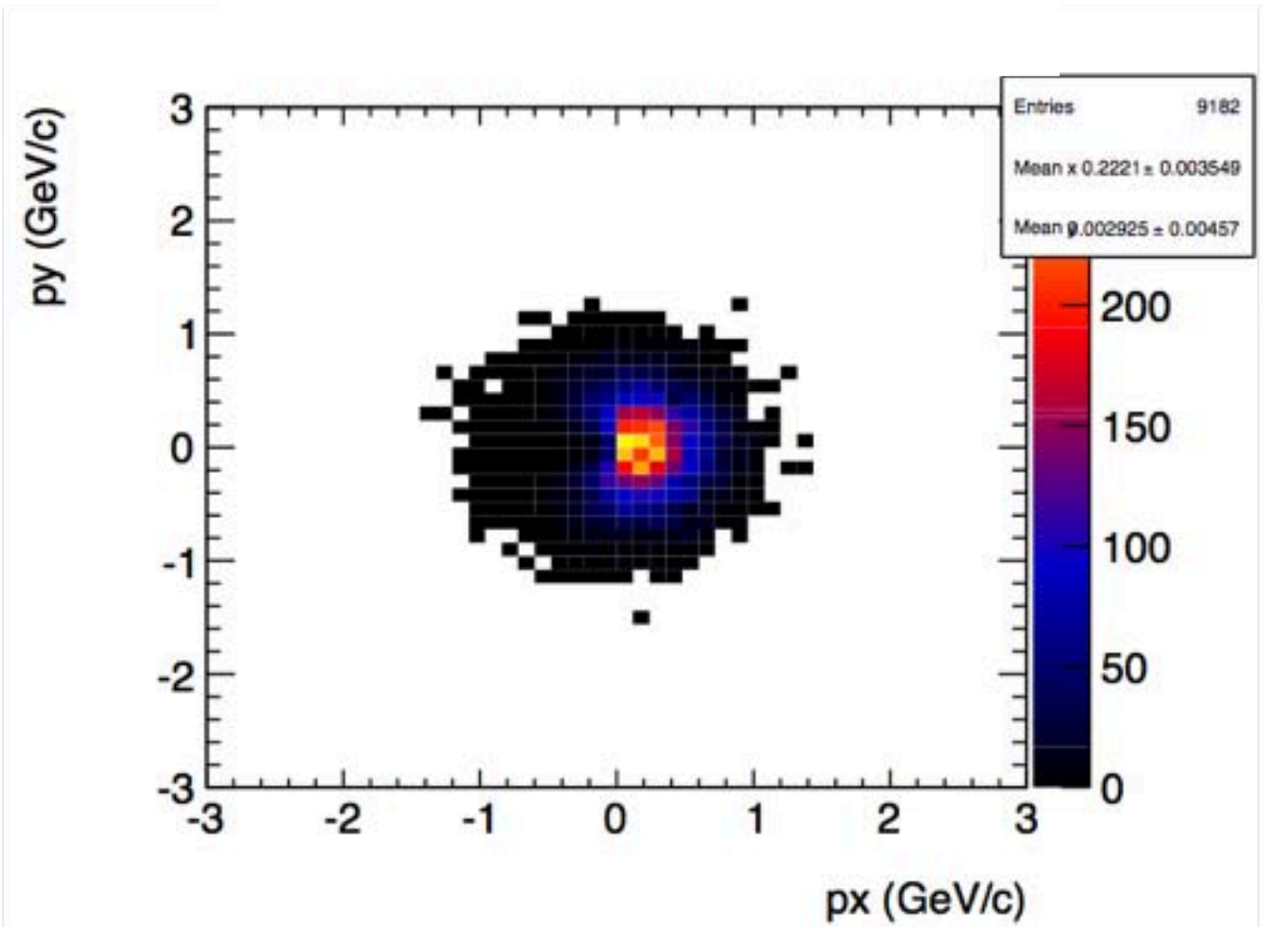

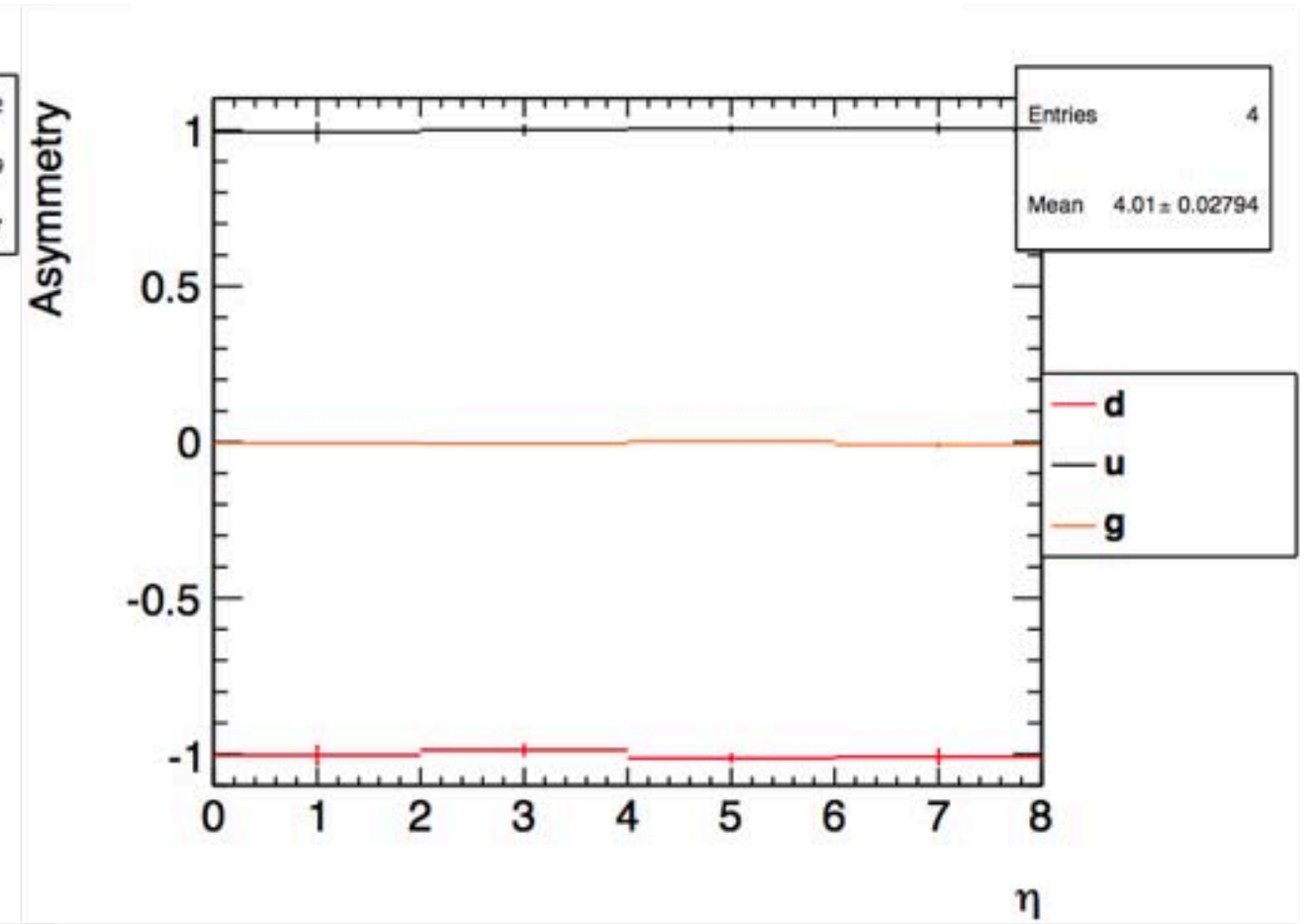

Incident partons: 100% input asymmetry

Simple Monte Carlo

- Use weighted PYTHIA

  Weight partons: 1 + (sivers/unpol)*(px/p_T)*(amplitude*spin factor)

  ➡ ϕ modulation in momentum distribution

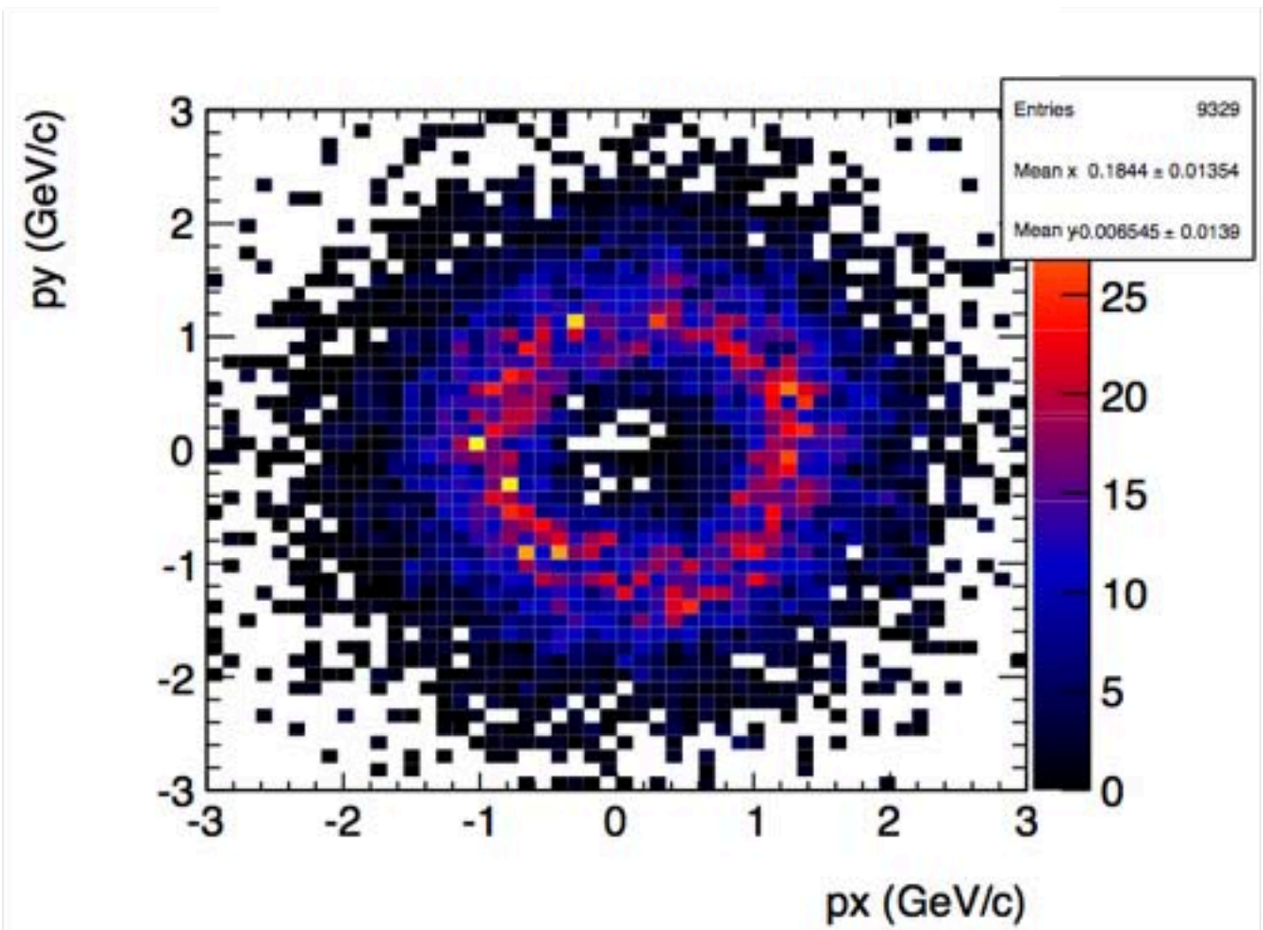

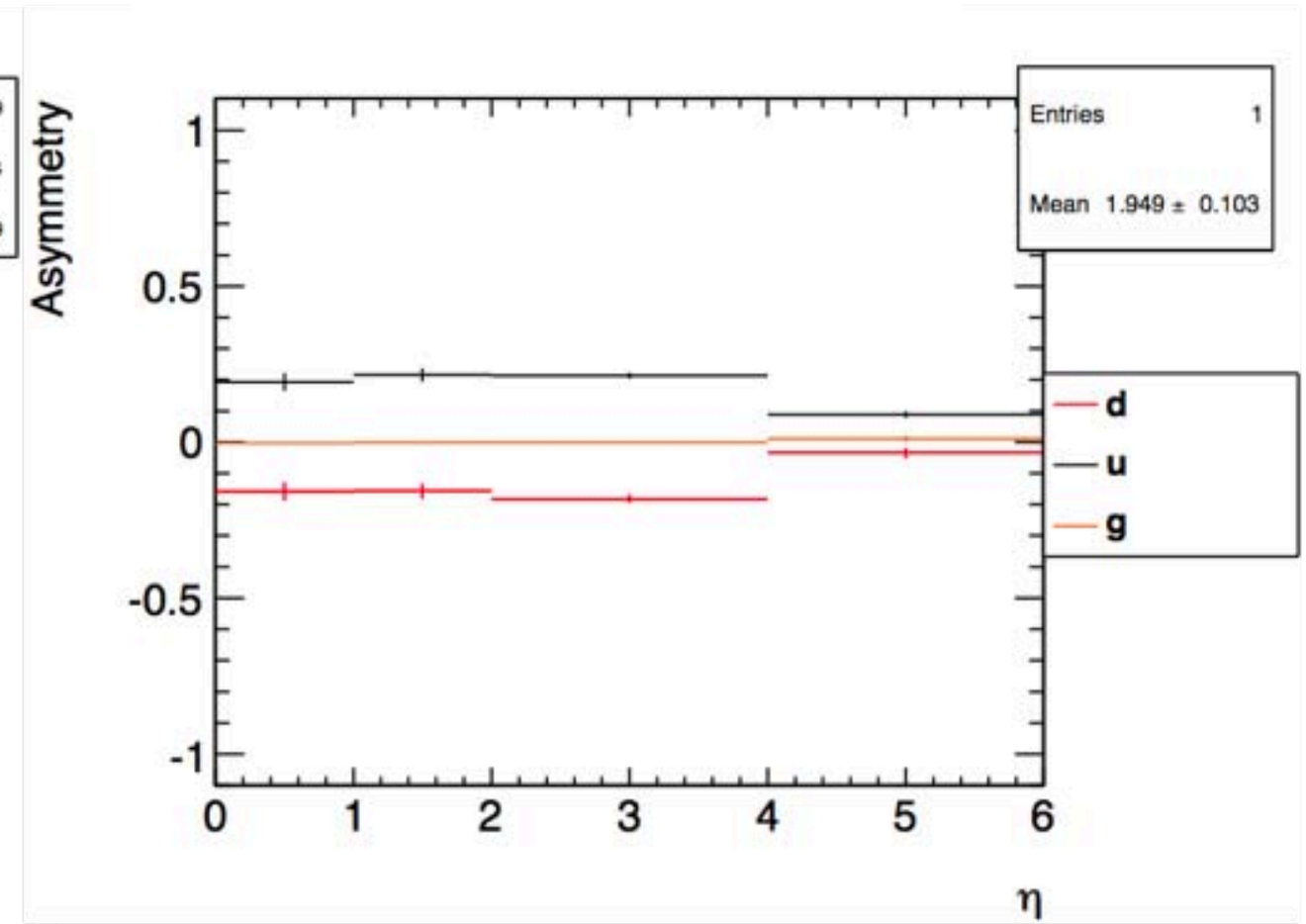

Scattered partons: hard p_T >> intrinsic k_T

→asymmetry watered down

Summary

- Midrapidity: see
  - **transversity** &
  - **spin-dependent fragmentation**
  - Can extend to $\eta < 2$ with FGT + EEMC
- Forward:
  - **Large** asymmetries persist with pT
  - Remains confusing - is it Sivers/twist-3 mechanism? Collins? Something else? All of the above?

Future Directions

- What physics do we want to study?

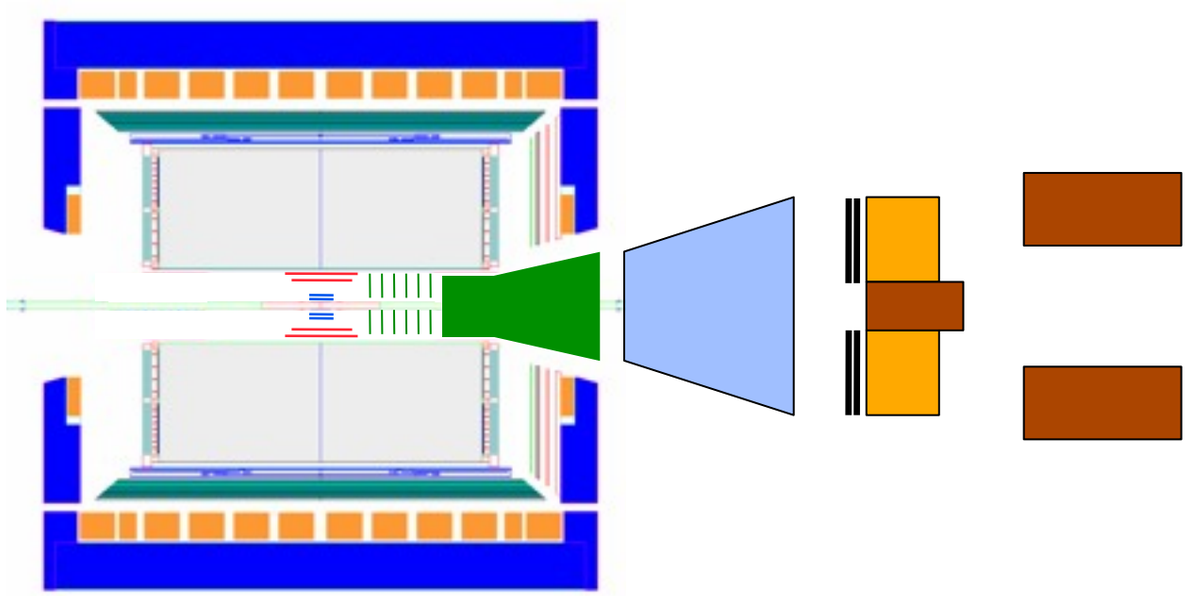

- What upgrades do we need to get there?

Forward jets

- Could we study jets with just extant EMCal?

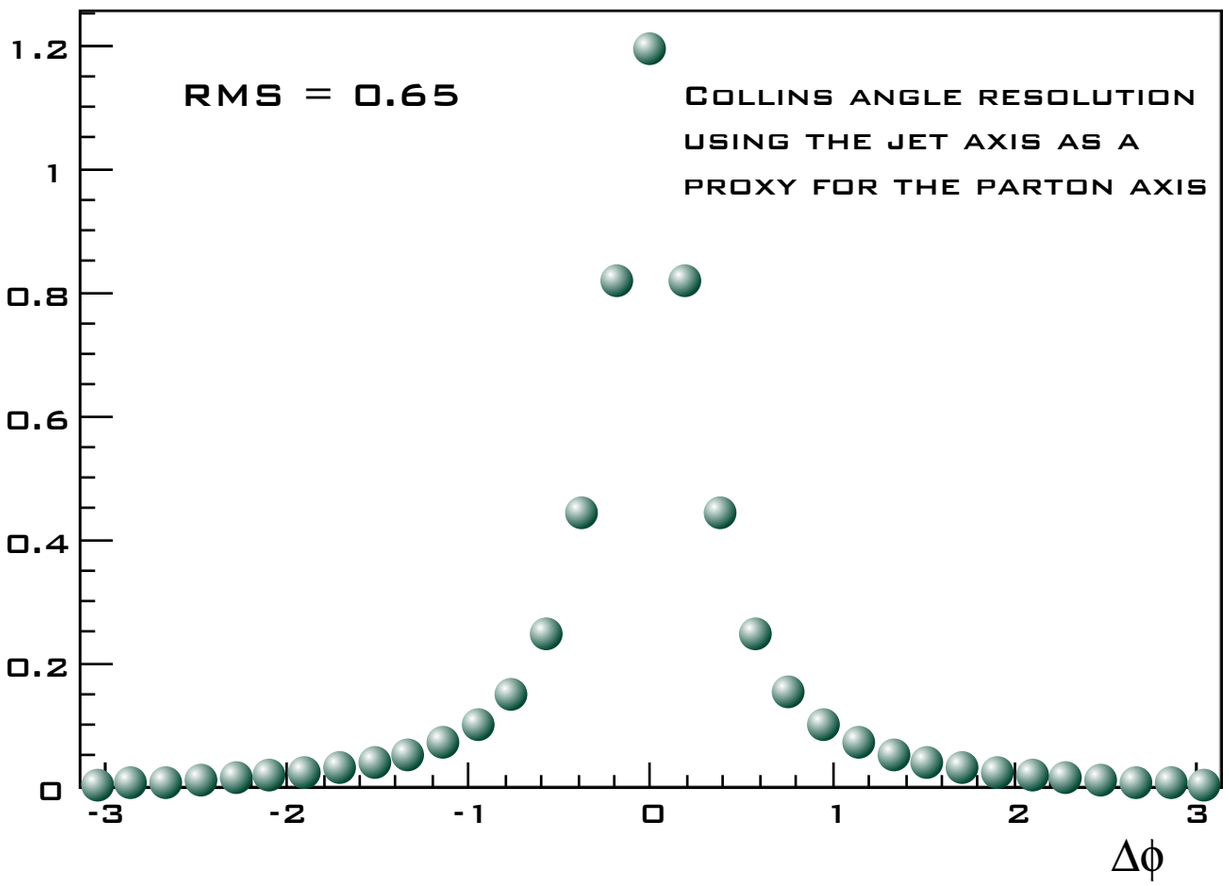

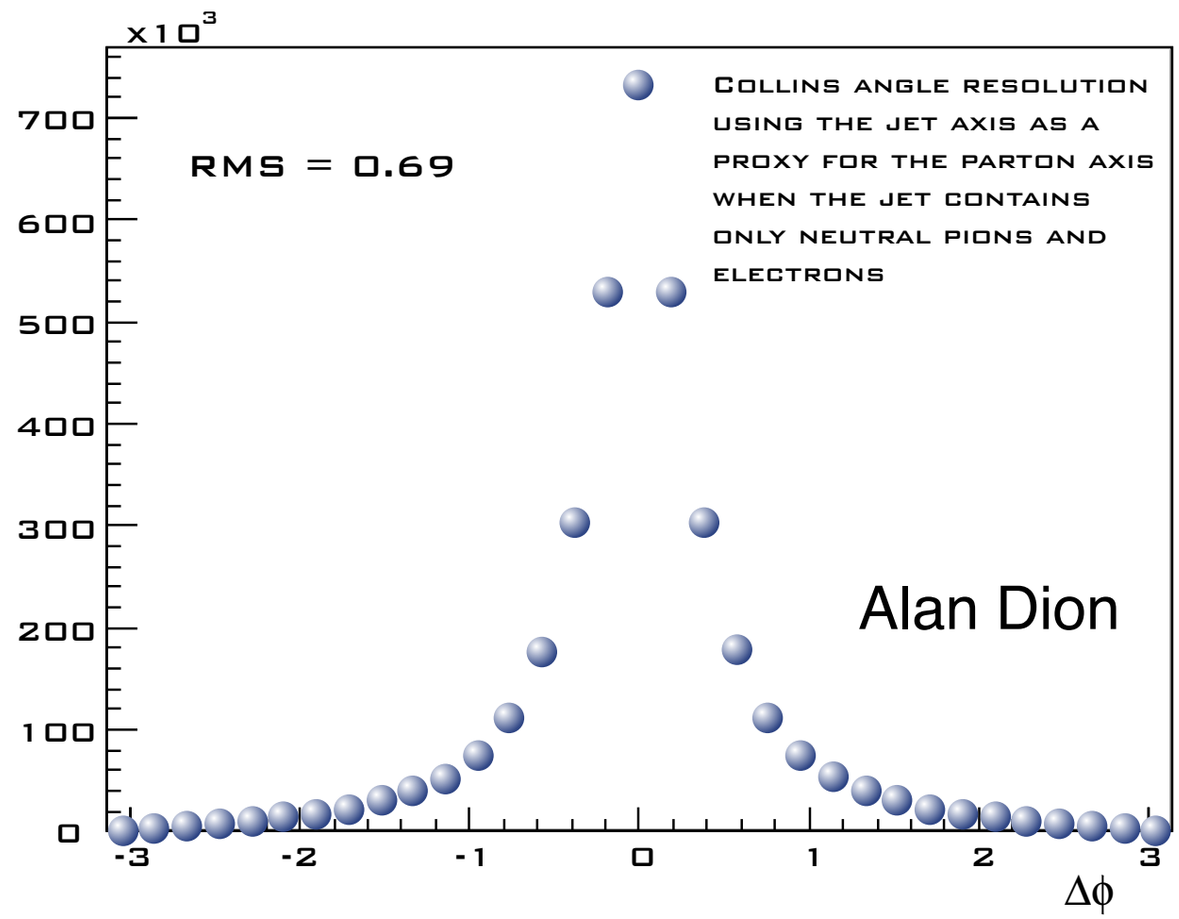

- Bottom line:
  - For just angles: existing EMCal is probably OK
  - For energy/p_T: not enough, need tracking/HCal

Forward Collins

- Large x - essentially unconstrained by SIDIS
- Extend π/jet measurement forward
- Need forward jet capability/PID/tracking

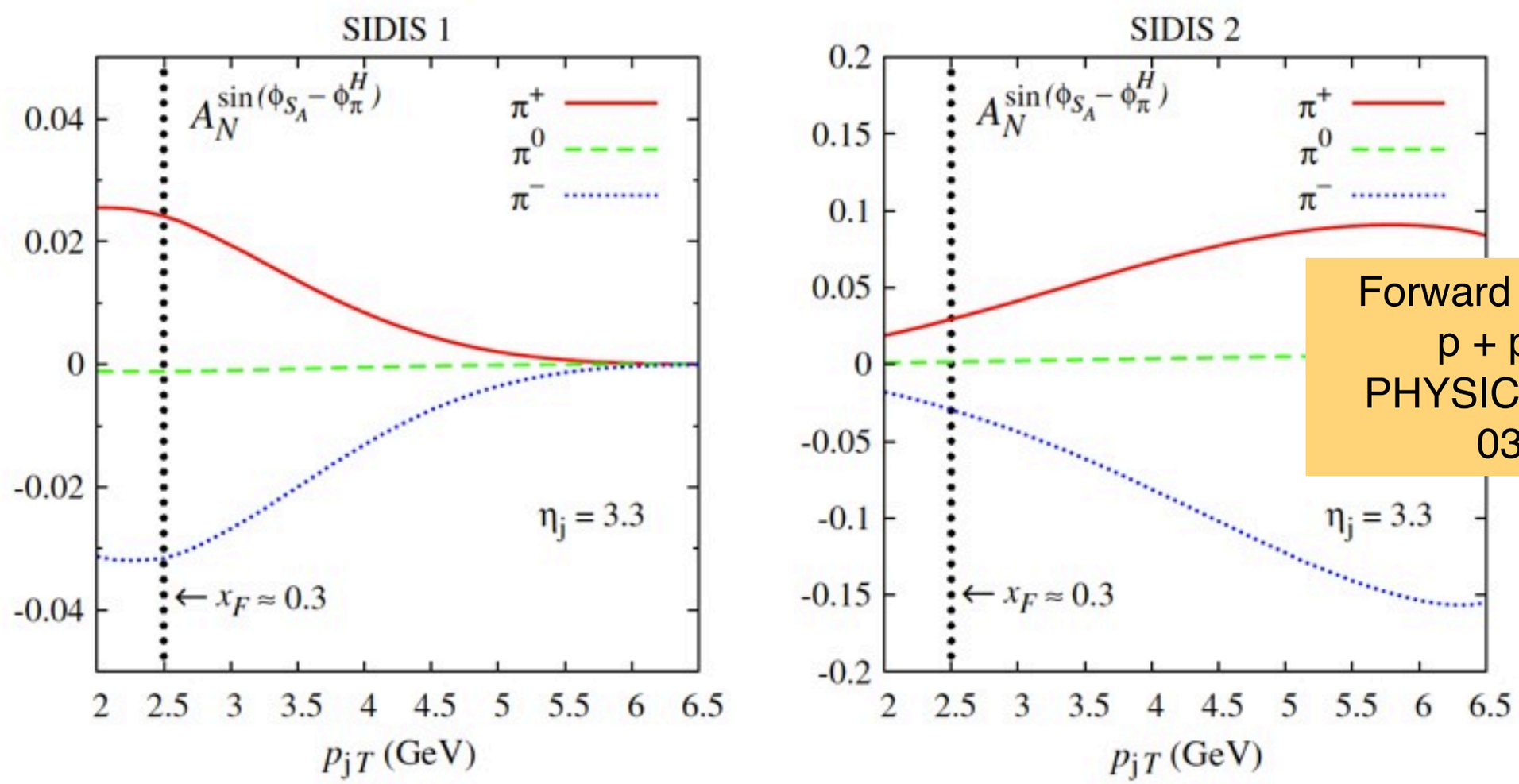

Forward Collins asymmetry
p + p → π + jet + X
PHYSICAL REVIEW D 83, 034021 (2011)

Prompt photons

- Measure isolated γ
- Isolate Sivers: no fragmentation
- Potentially large A_N
- Demands luminosity
- Poor knowledge of forward γ cross section

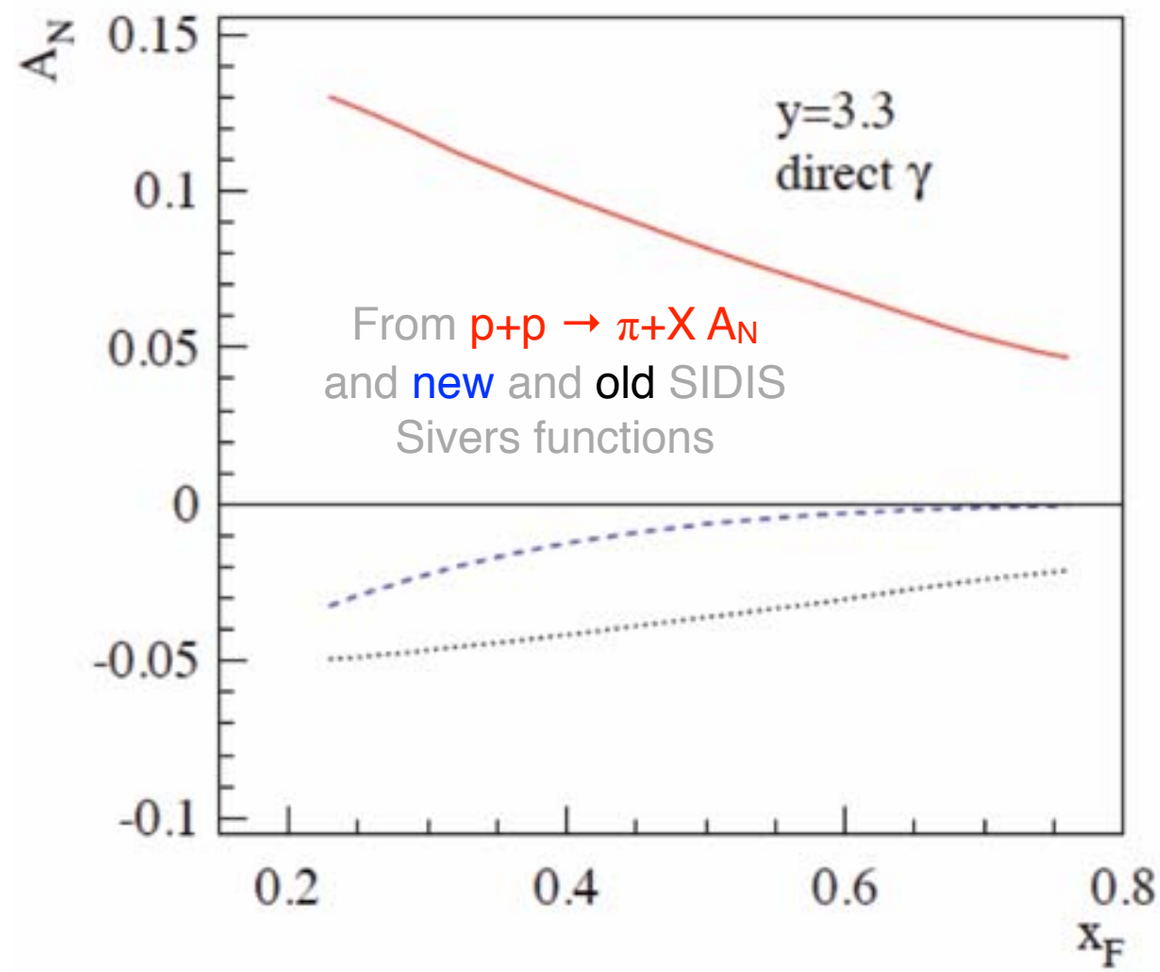

Forward Tracking

6 layers, tracking $1 < \eta < 2$

Commissioned this year

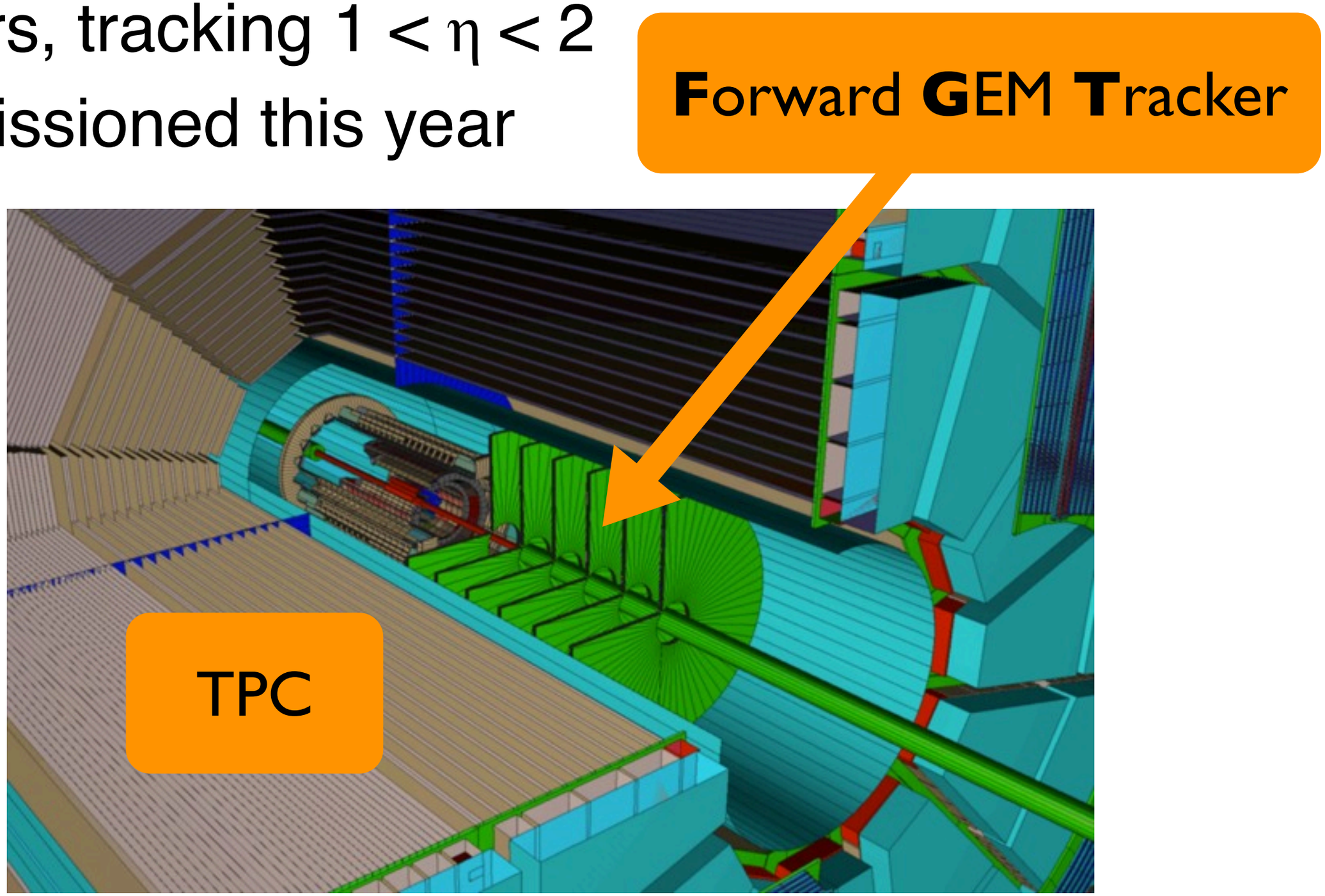

VeryFGT

- Extended tracking
- Based on FGT

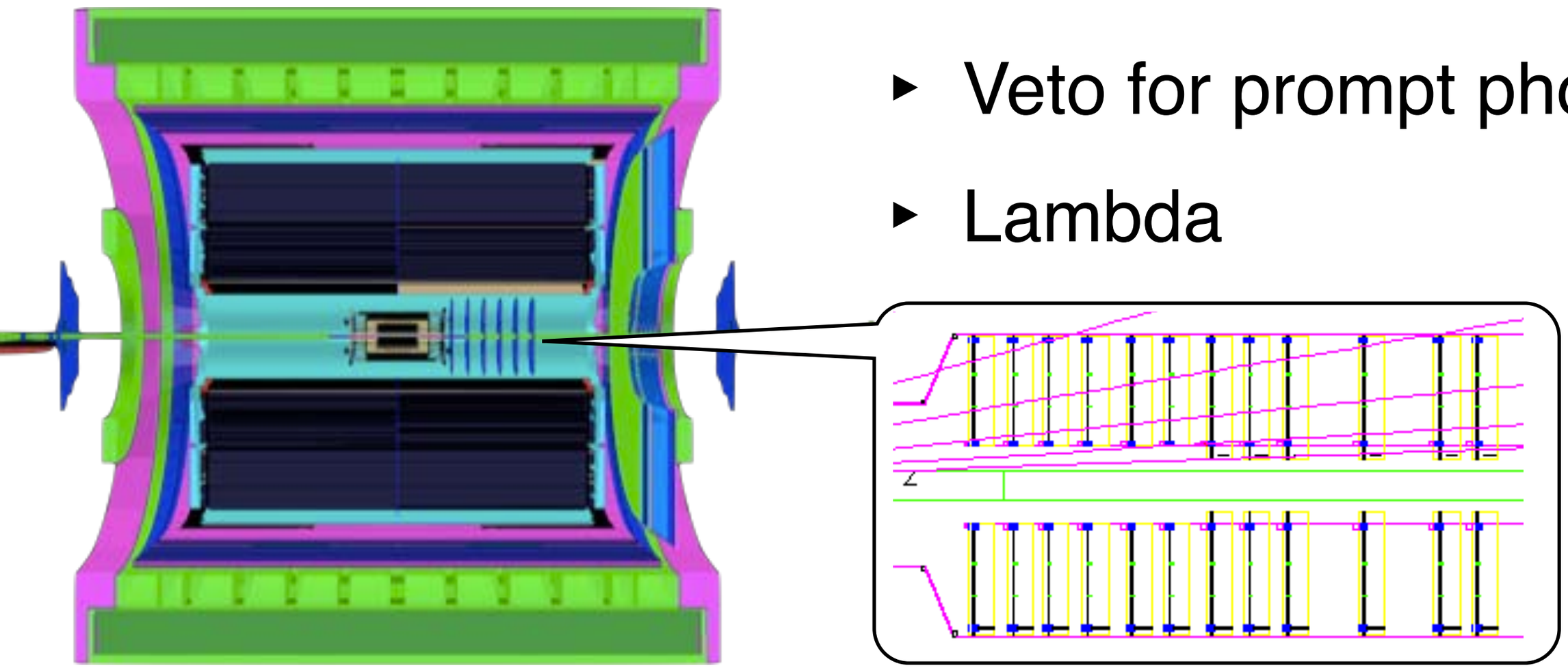

- Enables/enhances:
  - Jets
  - Collins
  - Diffractive
  - Veto for prompt photon
  - Lambda

Sivers sign change

- Drell-Yan vs. DIS:
  - **Fundamental** QCD prediction
  - opposite sign predicted $\text{Sivers}^{DIS} = -\text{Sivers}^{DY}$

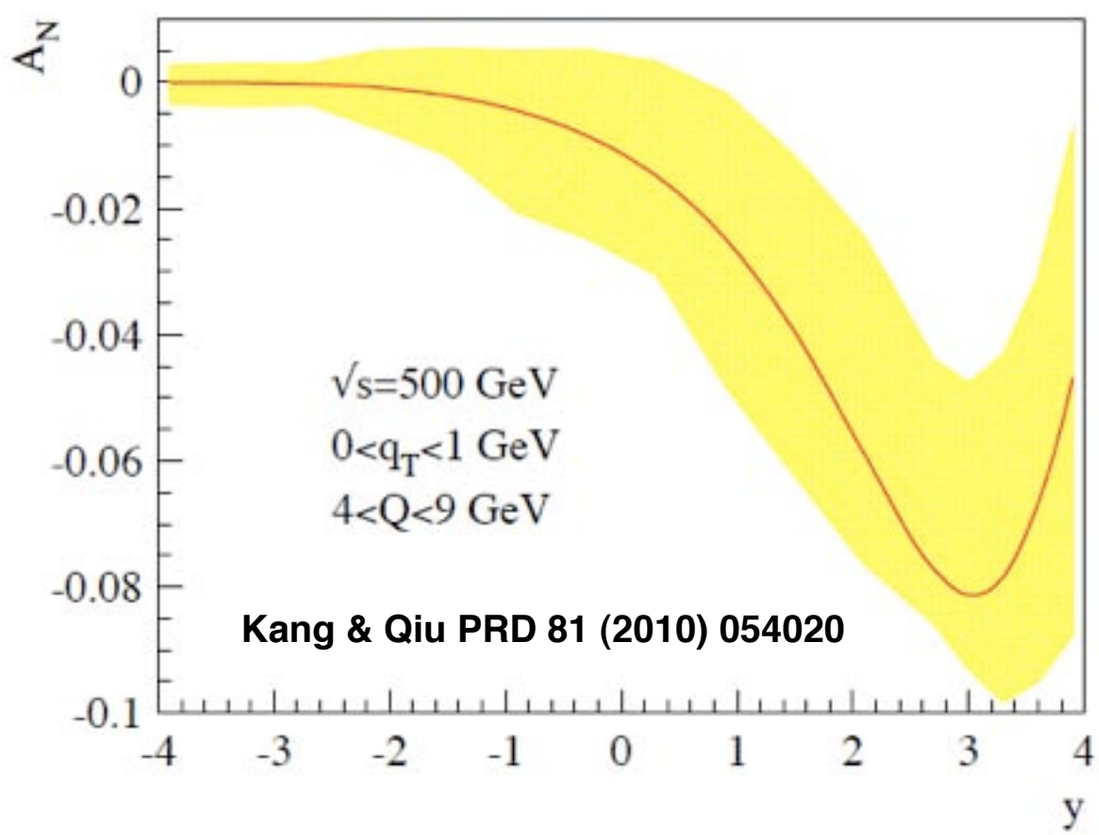

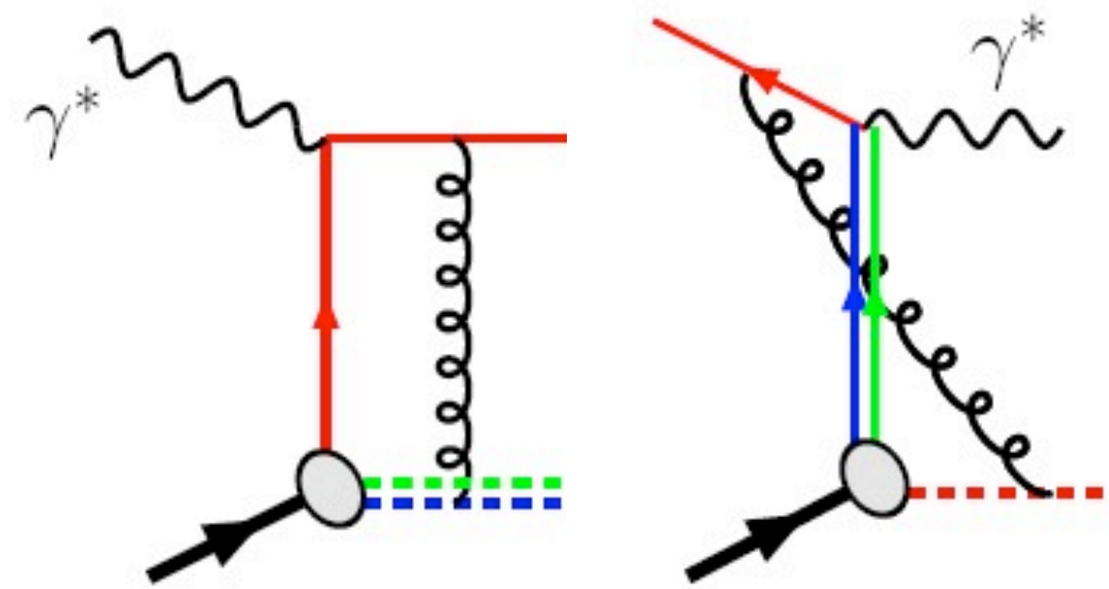

Predicted A_N^{DY} using TMD fit based on HERMES/COMPASS

Drell-Yan backgrounds

QCD

Lower at forward rapidity, large mass

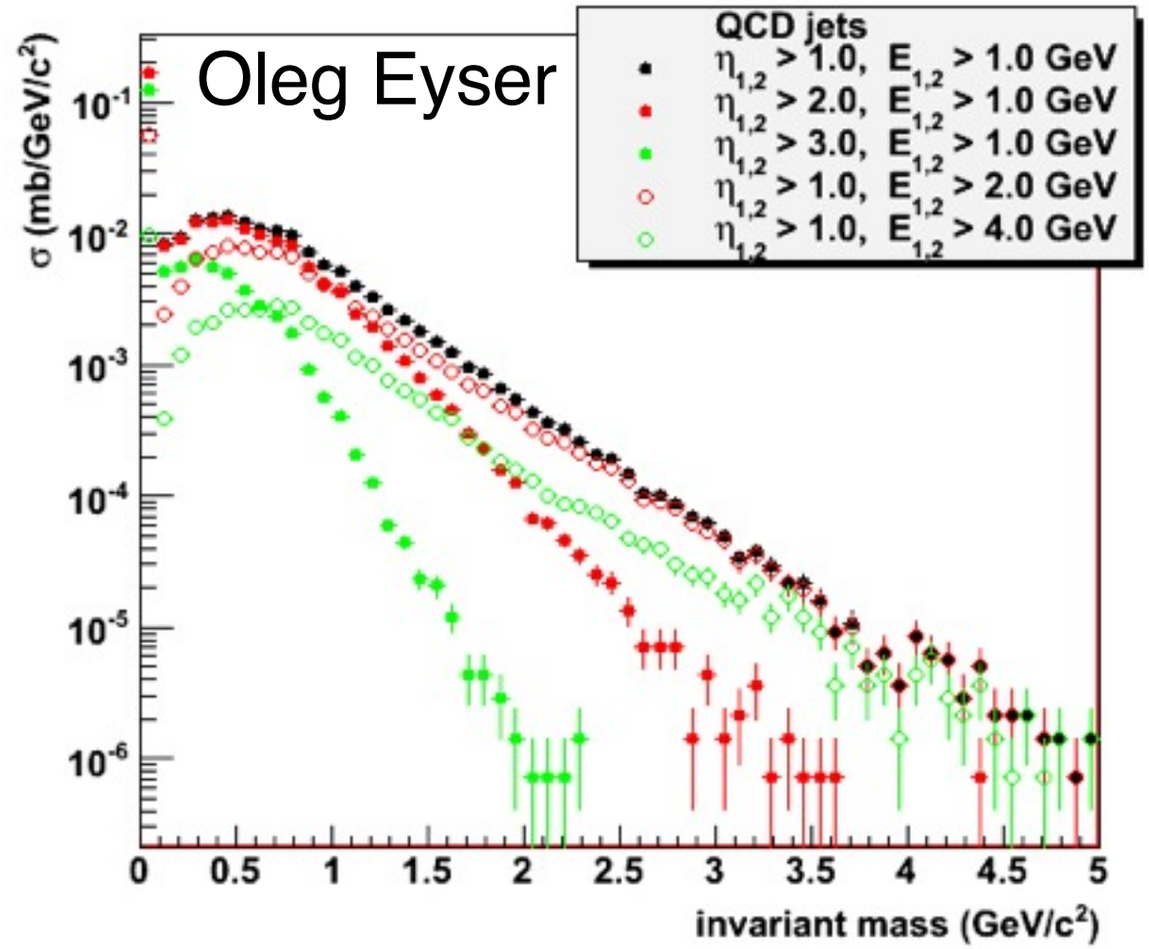

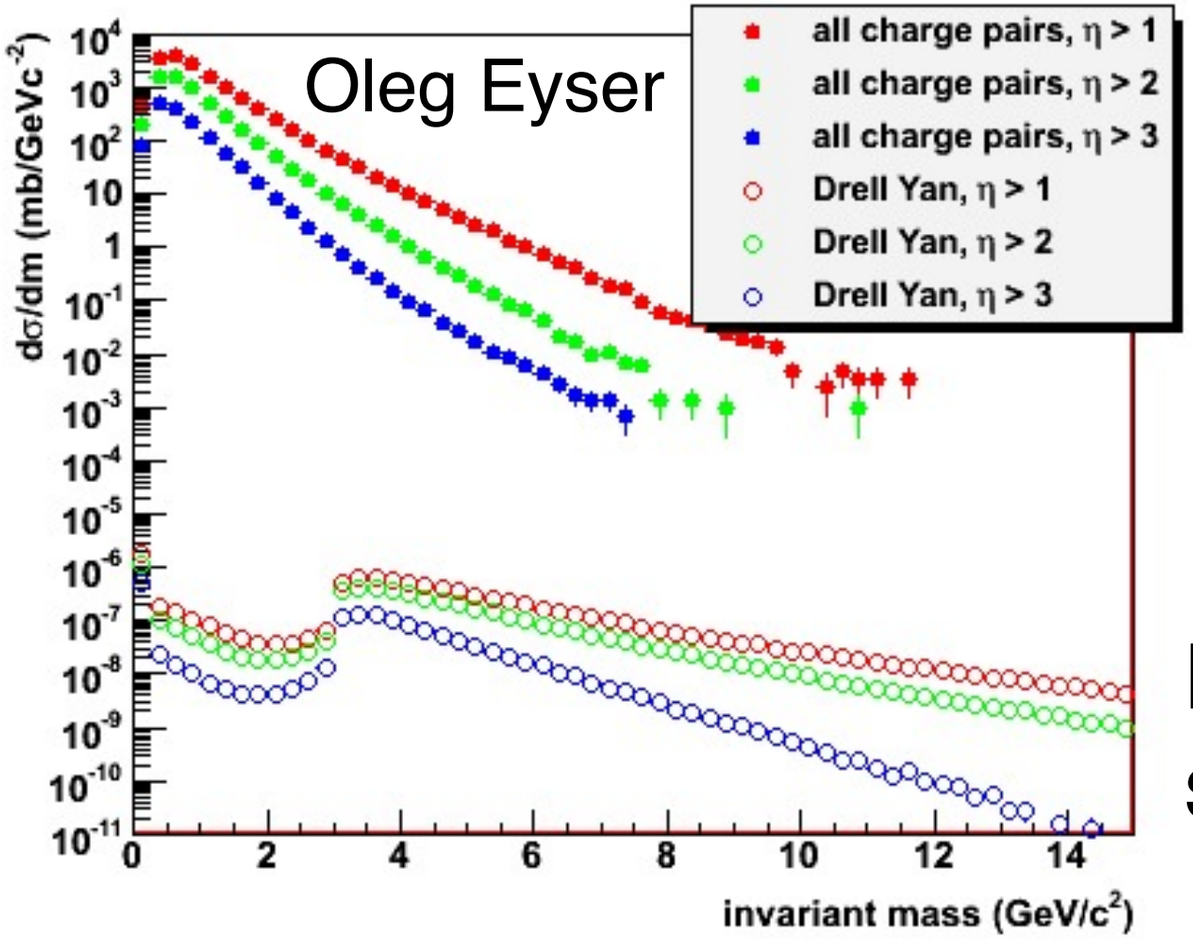

Need ~10^3-10^4 hadron suppression at 500 GeV

Drell-Yan

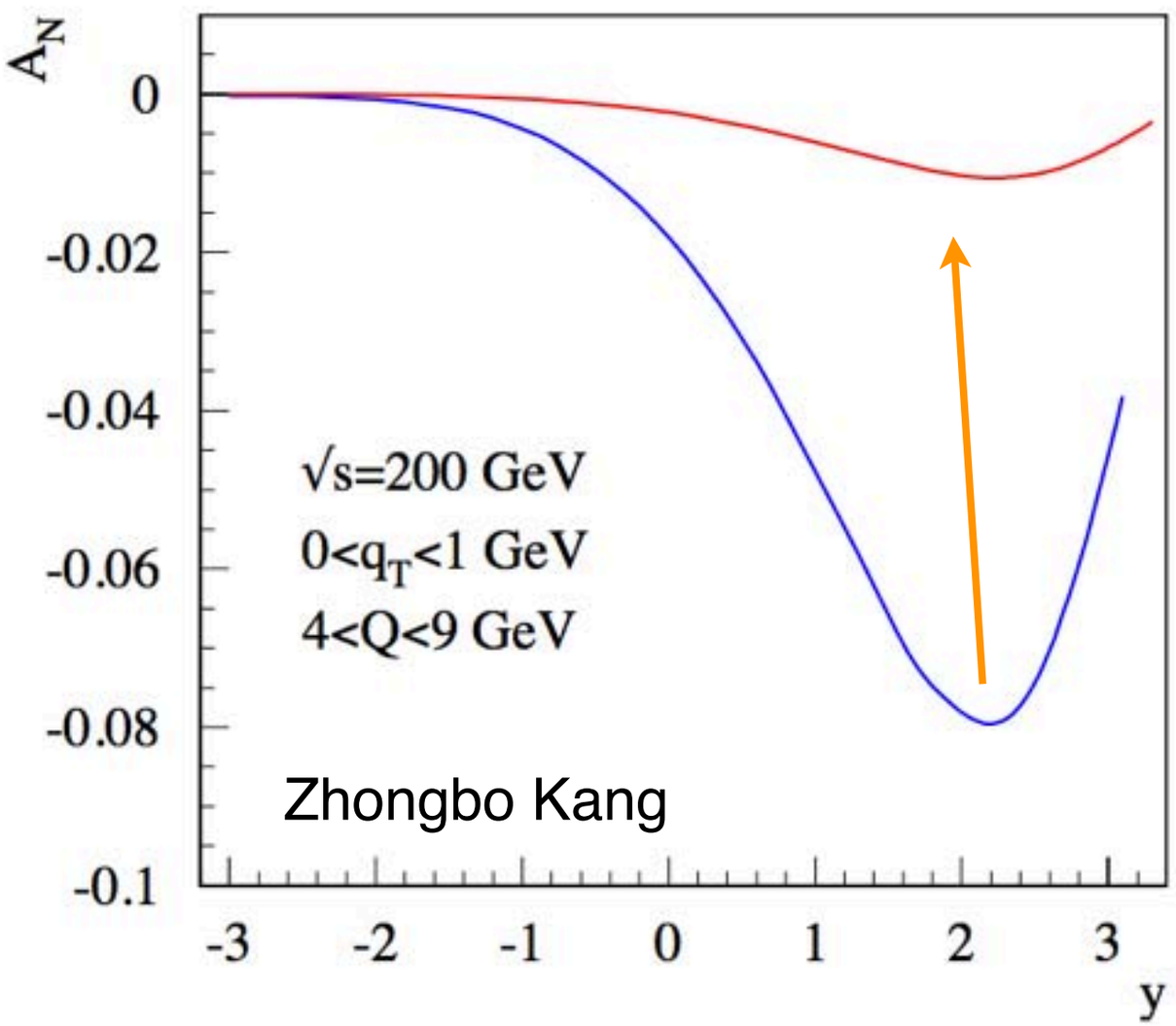

- Using Torino parameterisation:
  - bare parton model
  - evolved

If we account for evolution: is DY asymmetry actually measurable?

Forward calorimeter

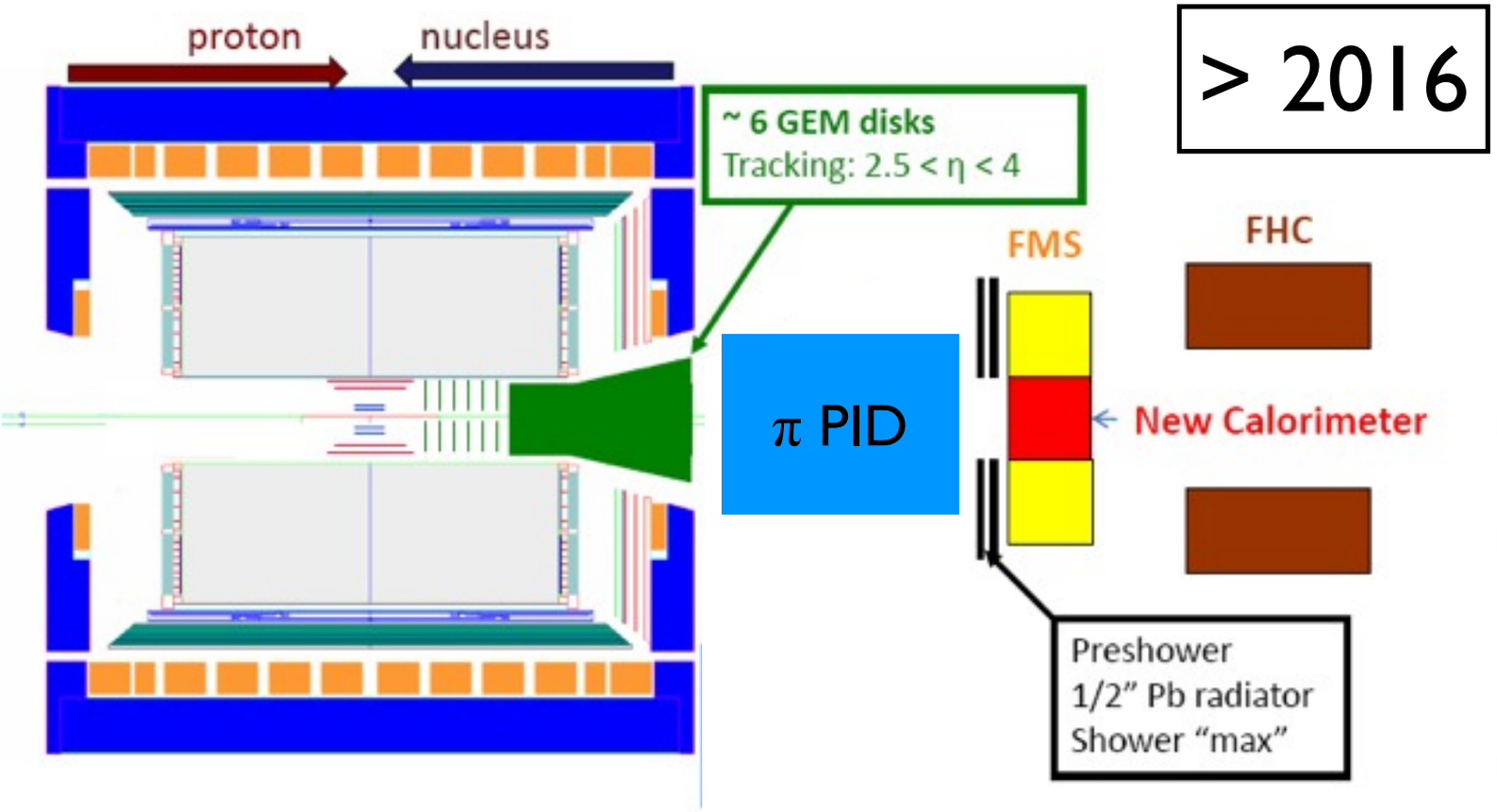

> 2016

Address important forward physics goals

- pp: asymmetries
- pA: saturation

Improved EMCal, add HCal

- π^0 up to 100 GeV
- e/h x1000 at 80GeV

- EMAL: SPACAL(W powder / scin)-type
- HCAL: ZEUS Sc/Pb tile

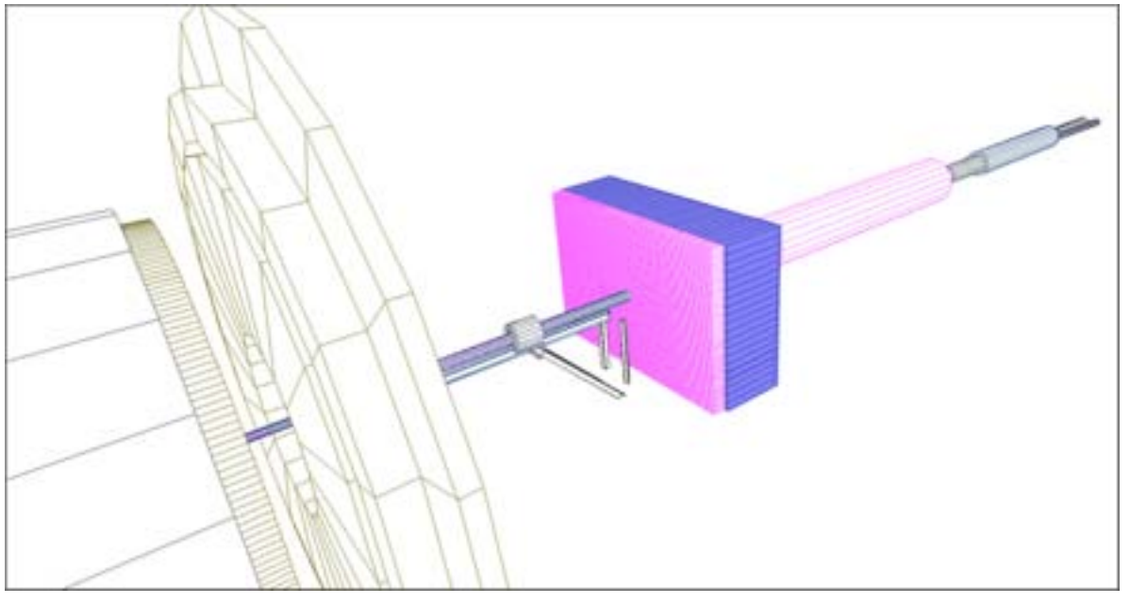

Forward calorimeter

- Geant4:
  - EM 12%/sqrt(E) + 1.5%
  - single hadron 55%/sqrt(E)
  - jets 80%/sqrt(E)
- Test run matches simulation expectation well
- Other details being worked on:
  - readout scheme
  - mechanical design
- compact → EIC

Oleg Tsai
UCLA

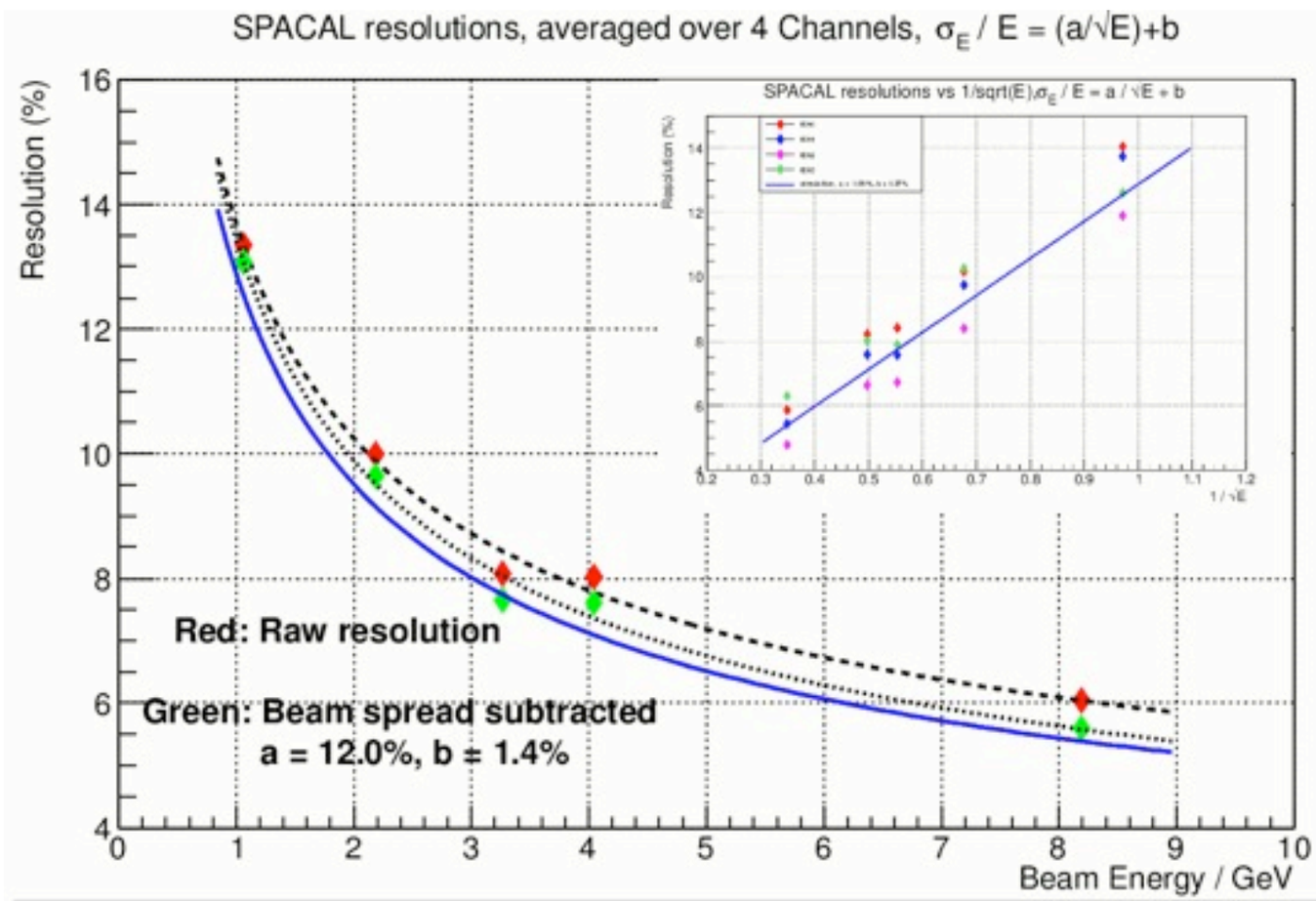

Transverse W

- Can we find the Sivers sign change without measuring Drell-Yan?
  - W production is Drell-Yan-like
  - $\text{Sivers}^{W} = \text{Sivers}^{DY} = -\ \text{Sivers}^{DIS}$
- Actually measure $l^{\pm}$ asymmetry: fraction of W
- Instead:
  - Z: lower statistics but cleaner signal - better channel?
  - Or “reconstruct” W?

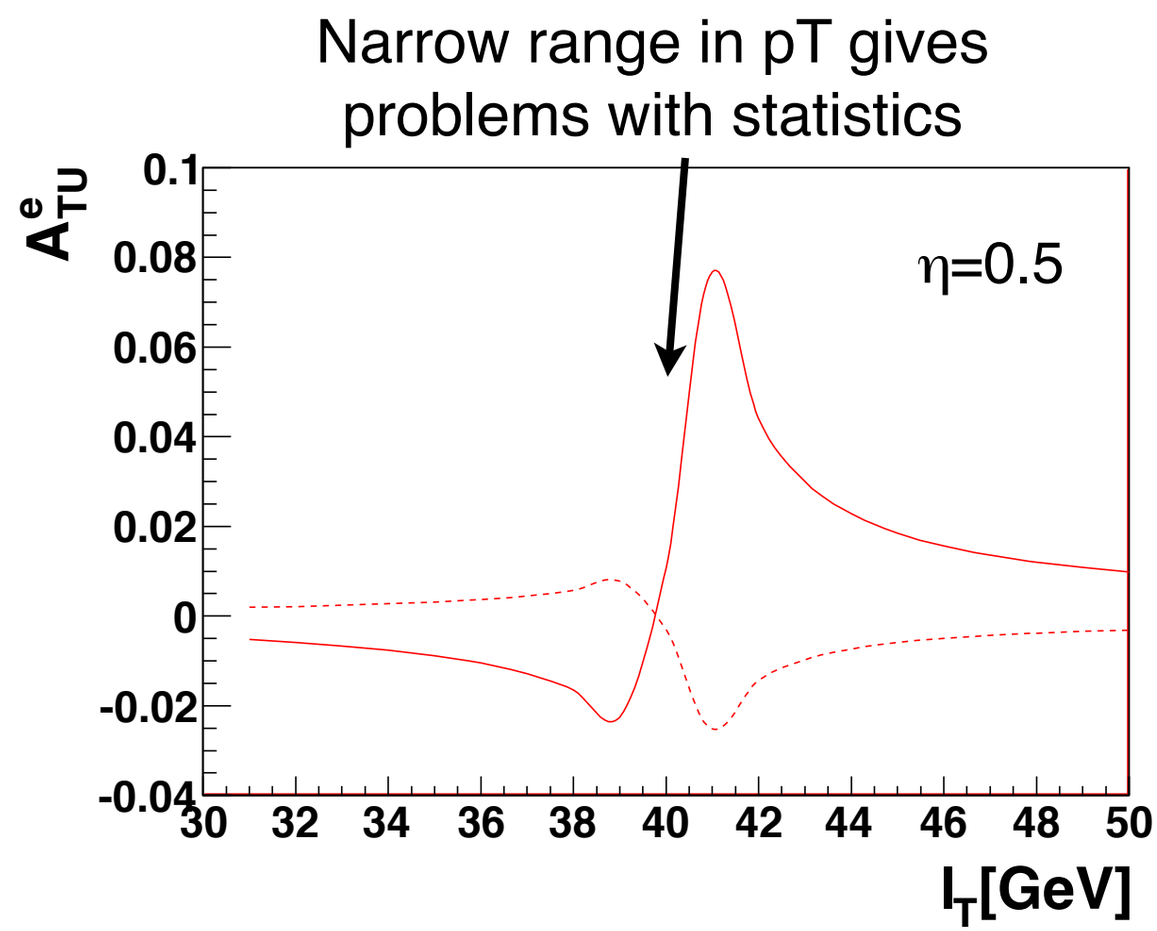

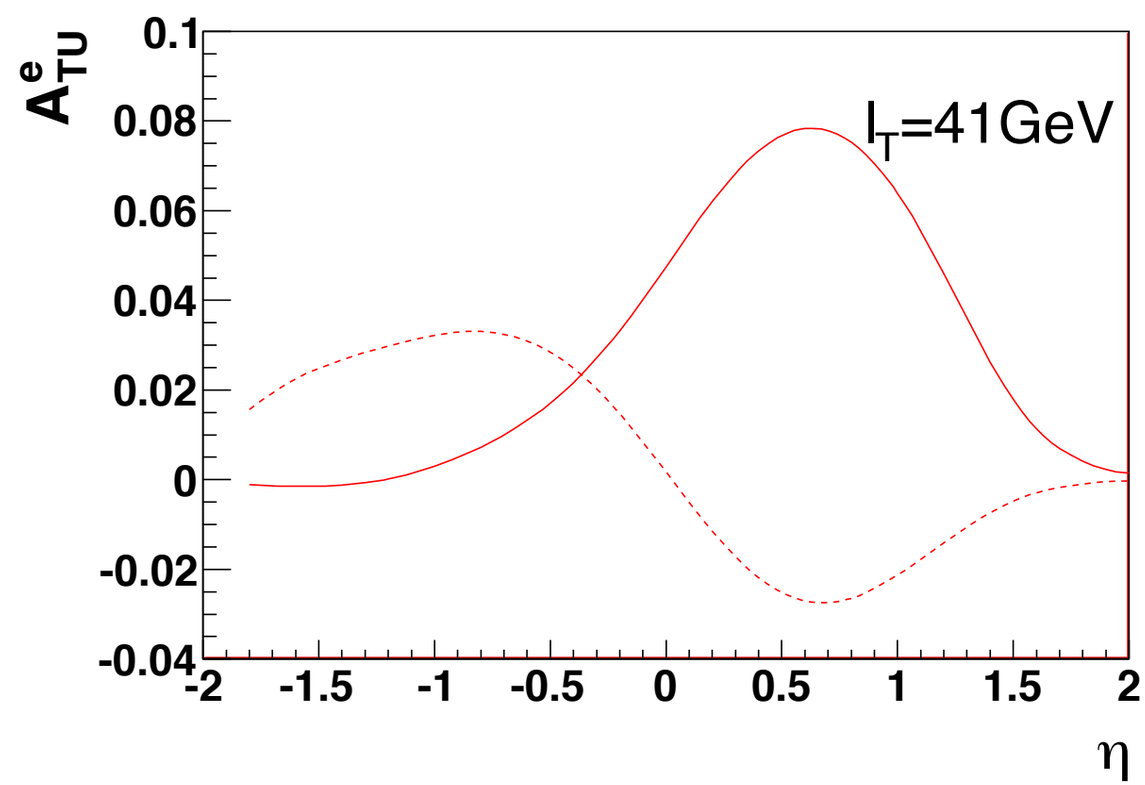

GPDs

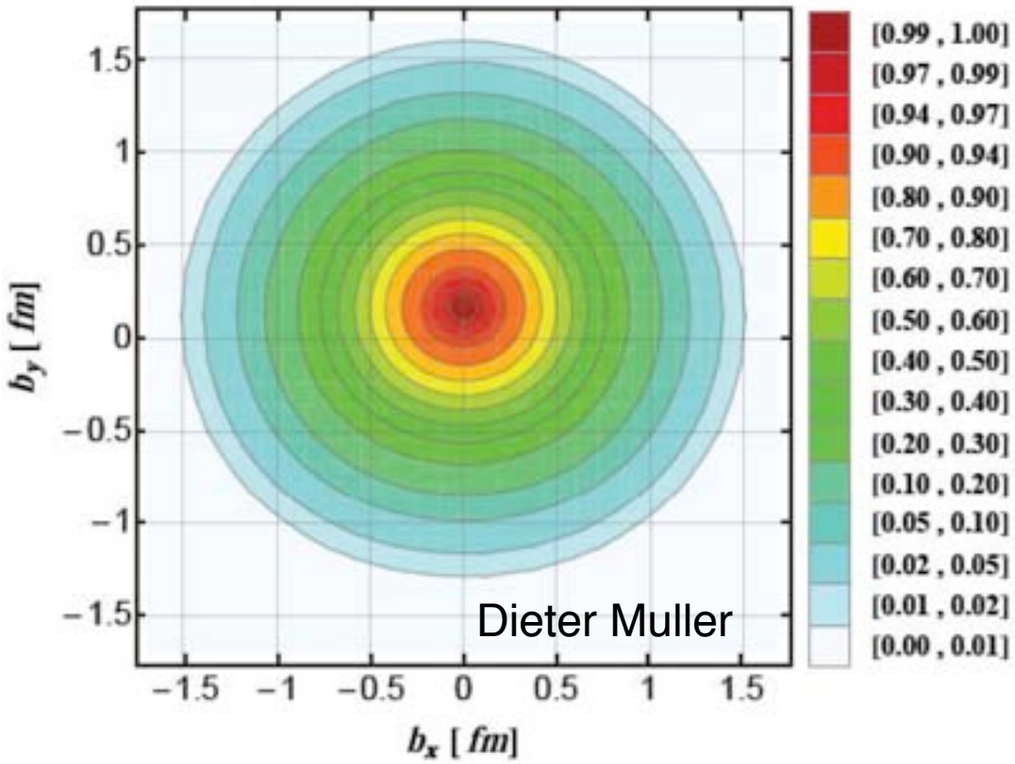

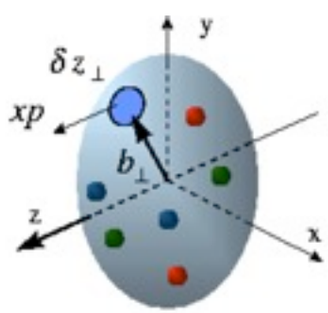

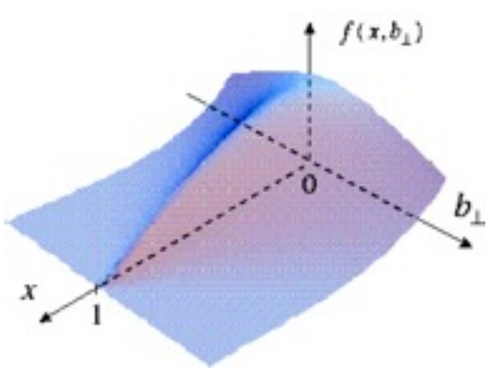

- Functions encoding info beyond 1D momentum structure
  - b distribution of partons
- Measurable via exclusive reactions
- Access to total angular momentum

$$J_q = \frac{1}{2}\int dx\, x\,[H_q(x,0,0) + E_q(x,0,0)]$$

Related to L

GPDs via UPC?

- Single γ exchange low t (large b)
  - pp becomes "γp"
- Pick up proton in Roman Pot
- Need to suppress background
- Access to GPD $E^{q,g}$ if transversely polarised target
  - need E for $J^{q,g}$
- Important precursor to eRHIC GPD programme
- polarised pA would be cool

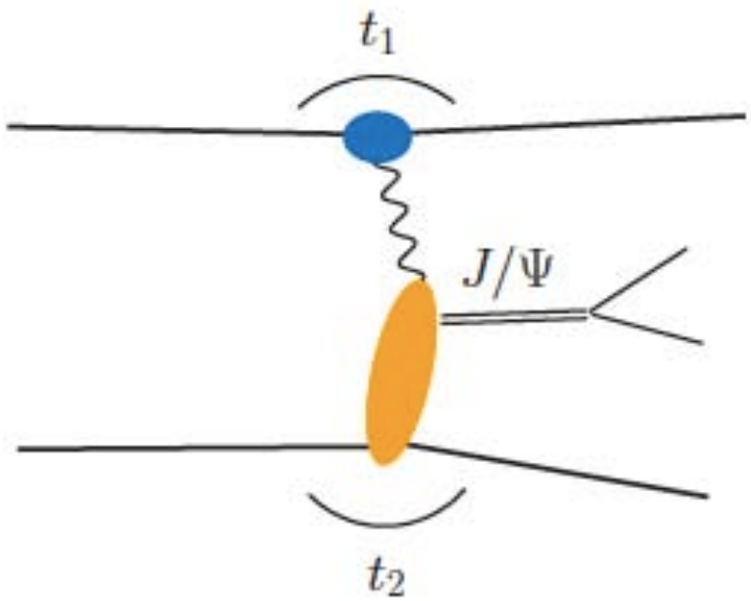

$$A_{UT} \sim \frac{\sqrt{t_0 - t}}{m_p} \frac{\mathrm{Im}(E^* H)}{|H|}$$

Different species probe GPDs of different flavours

ρ^0	**2u+d, 9g/4**
ω	**2u–d, 3g/4**
ϕ	s, **g**
ρ^+	**u–d**
J/ψ	**g**

Roman Pots: Phase II

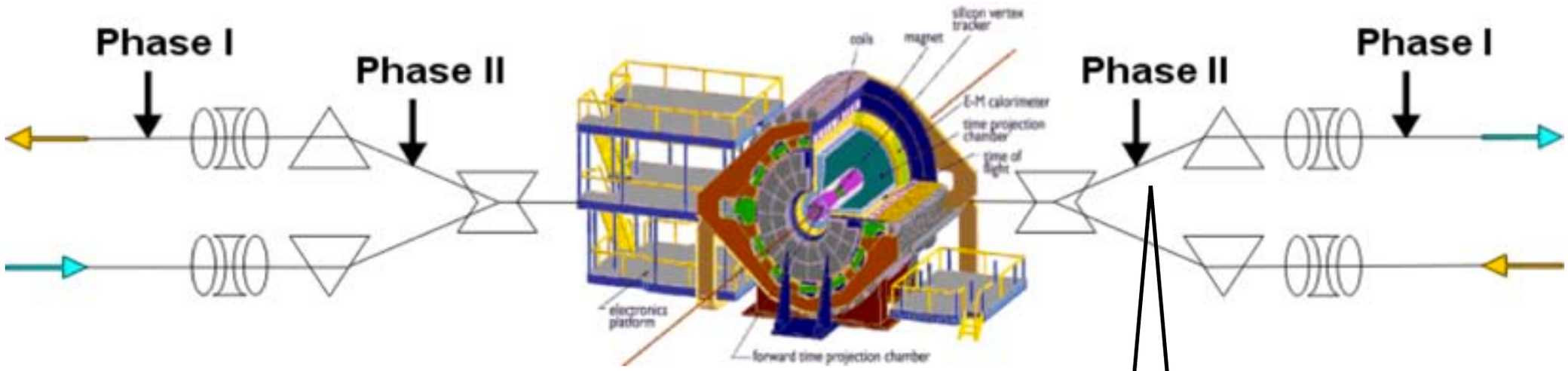

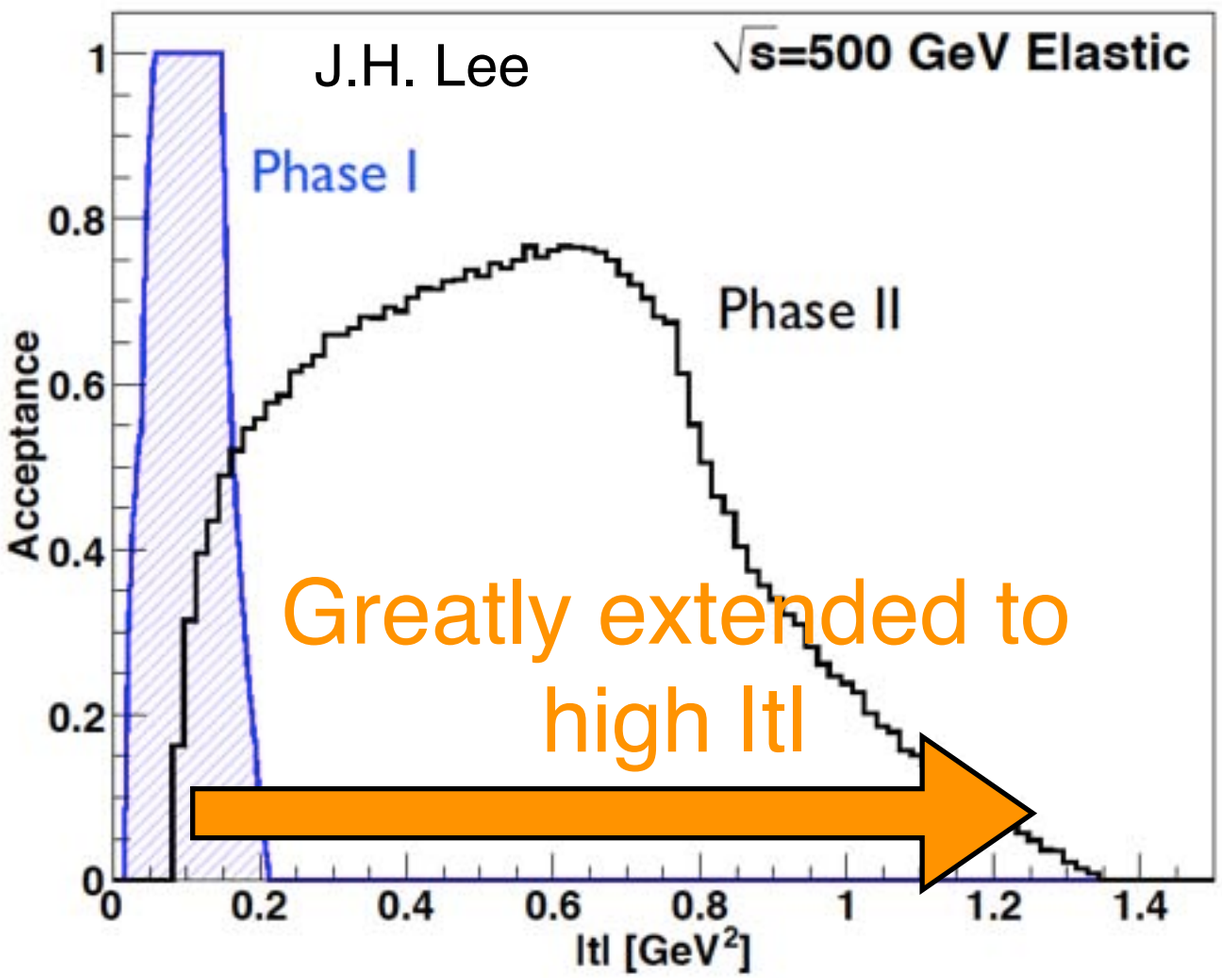

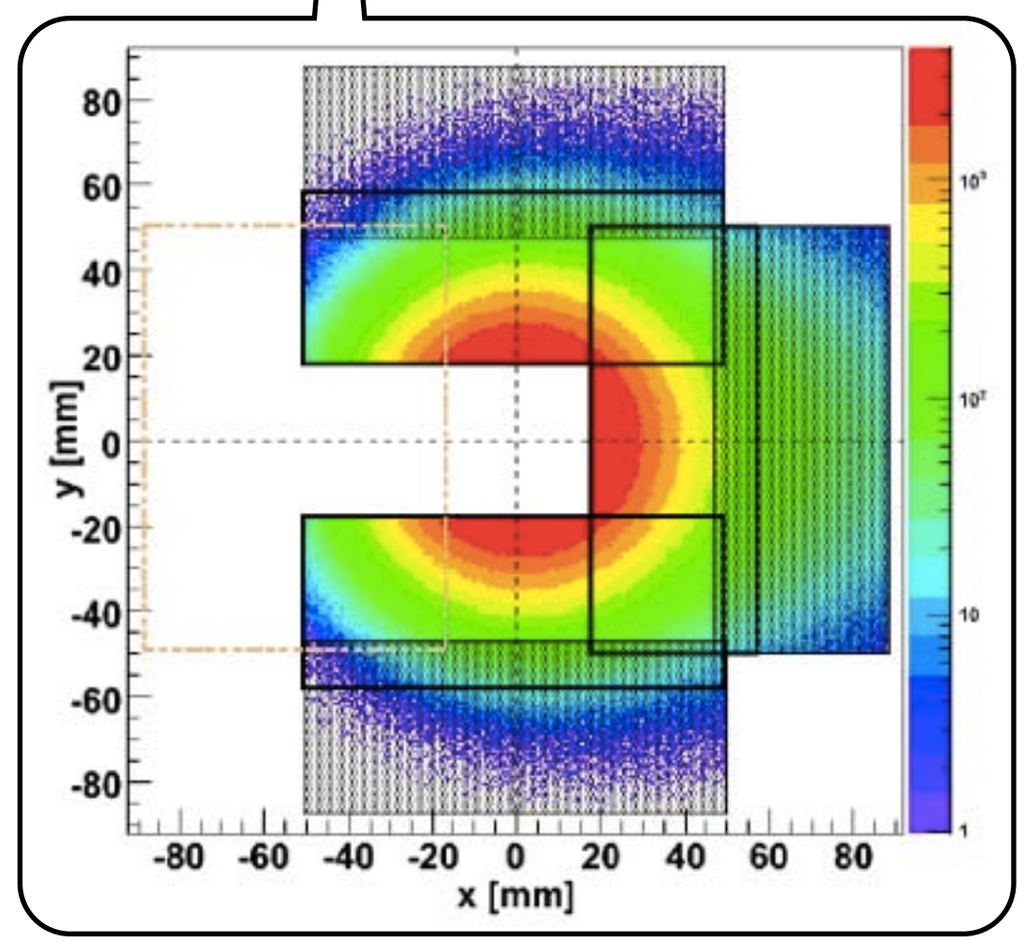

SSA in CGC?

Y. Kovchegov & M. Sievert, arXiv:1201.5890

- Predicts SSA in CGC framework
- Qualitatively matches data:

  1) increases with x_F

  2) non-monotonic function of k_T

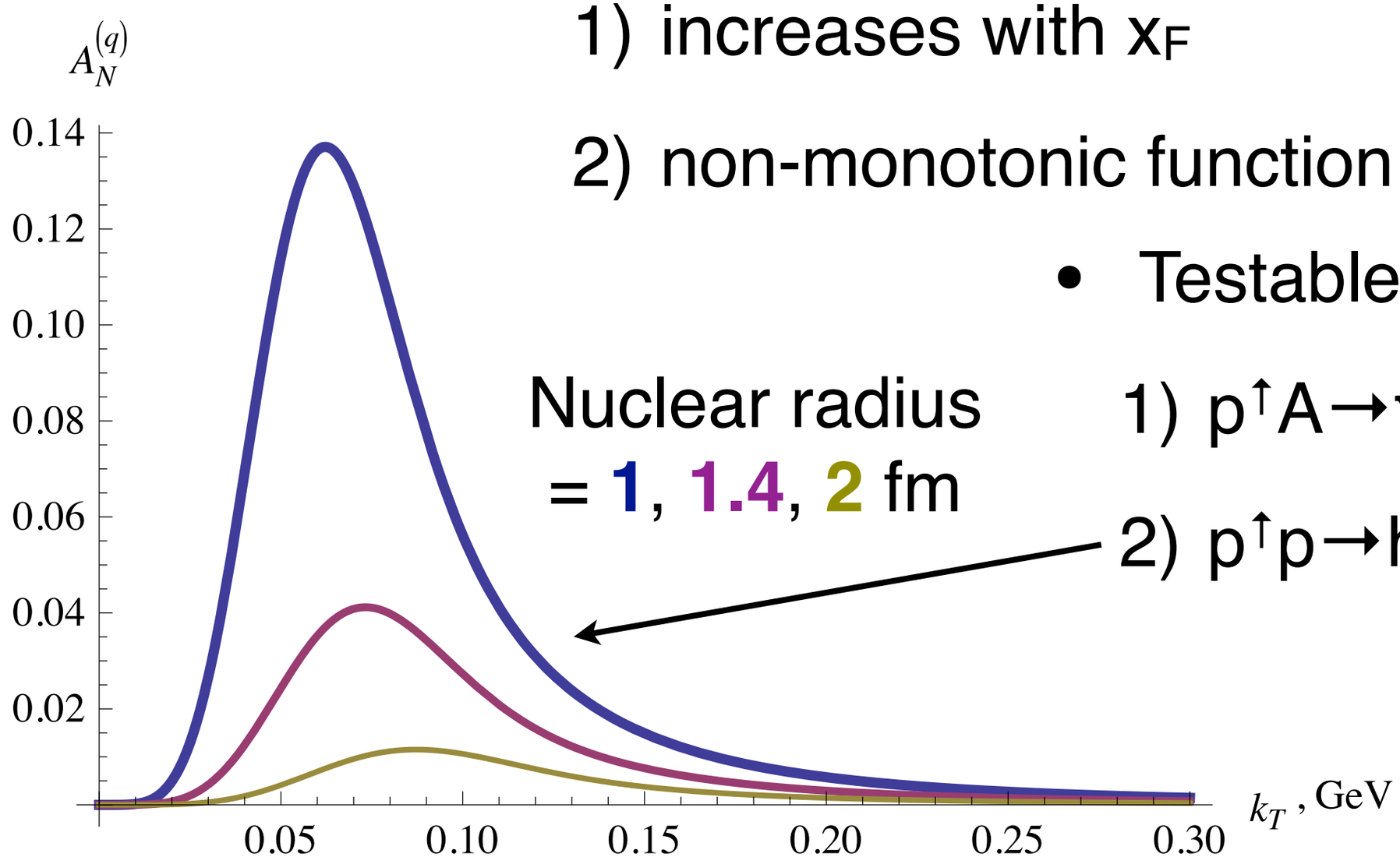

- Testable predictions:

  1) $p^{\uparrow}A \to \gamma X = 0$

  2) $p^{\uparrow}p \to hX > p^{\uparrow}A \to hX$

Polarised He^3

- Extract asymmetries on neutrons
- Lower centre-of-mass energy
  - 250 p → 167 GeV/n He^3
- Need to tag the spectator proton: Roman pots

Large π- asymmetry on neutron predicted

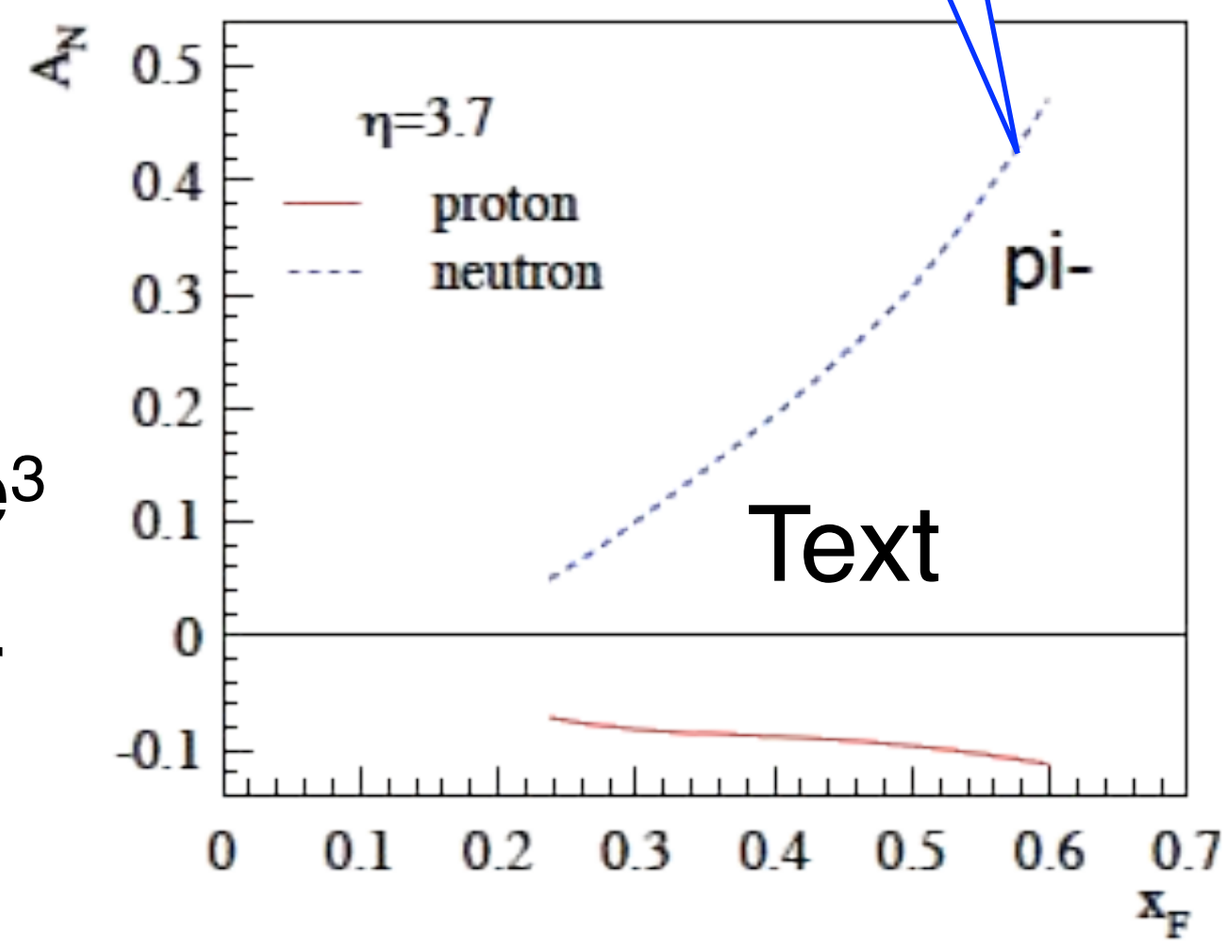

Polarised He^3

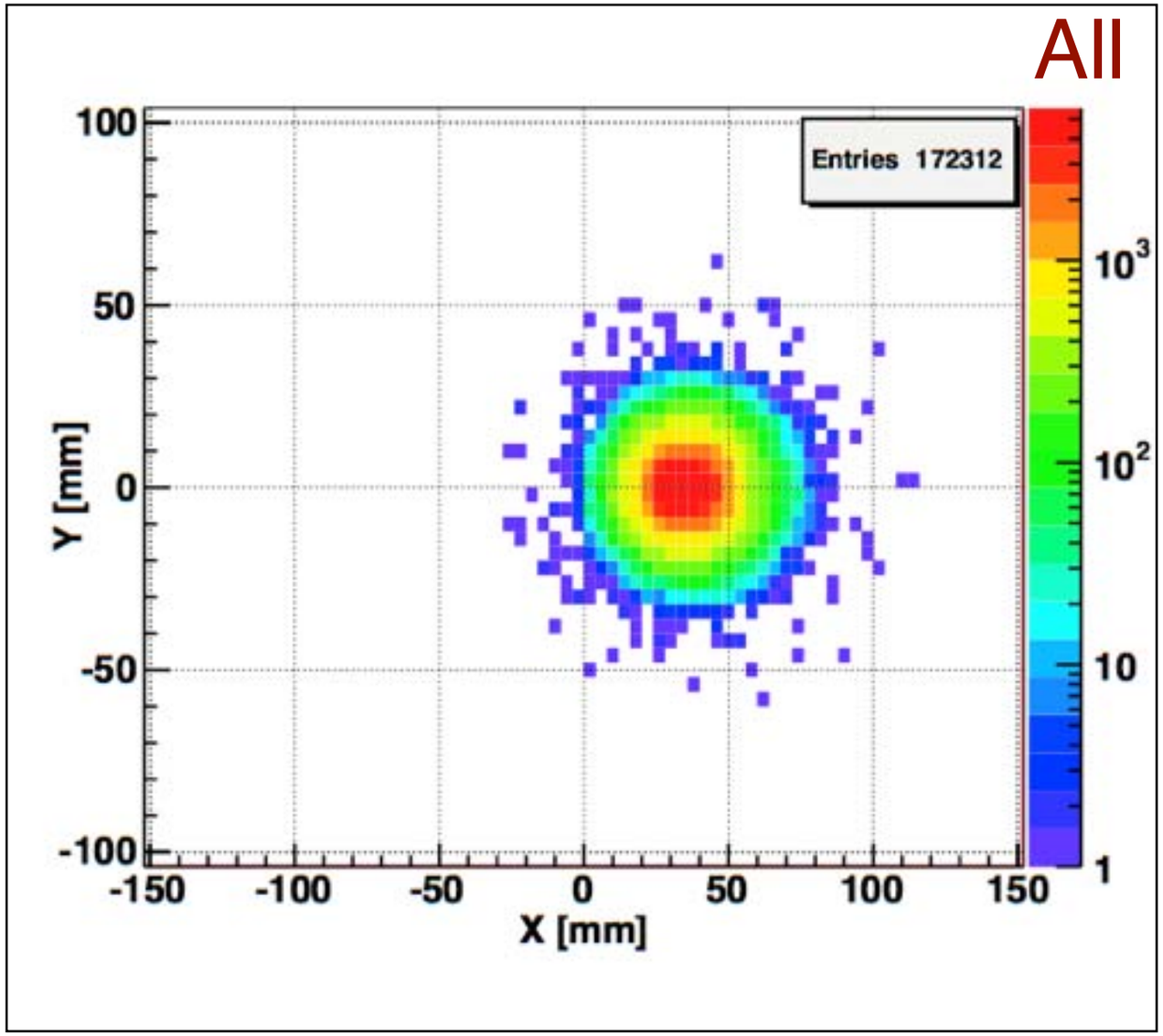

- Spectator proton acceptance with current RHIC optics

Polarised He^3

- Spectator proton acceptance with current RHIC optics

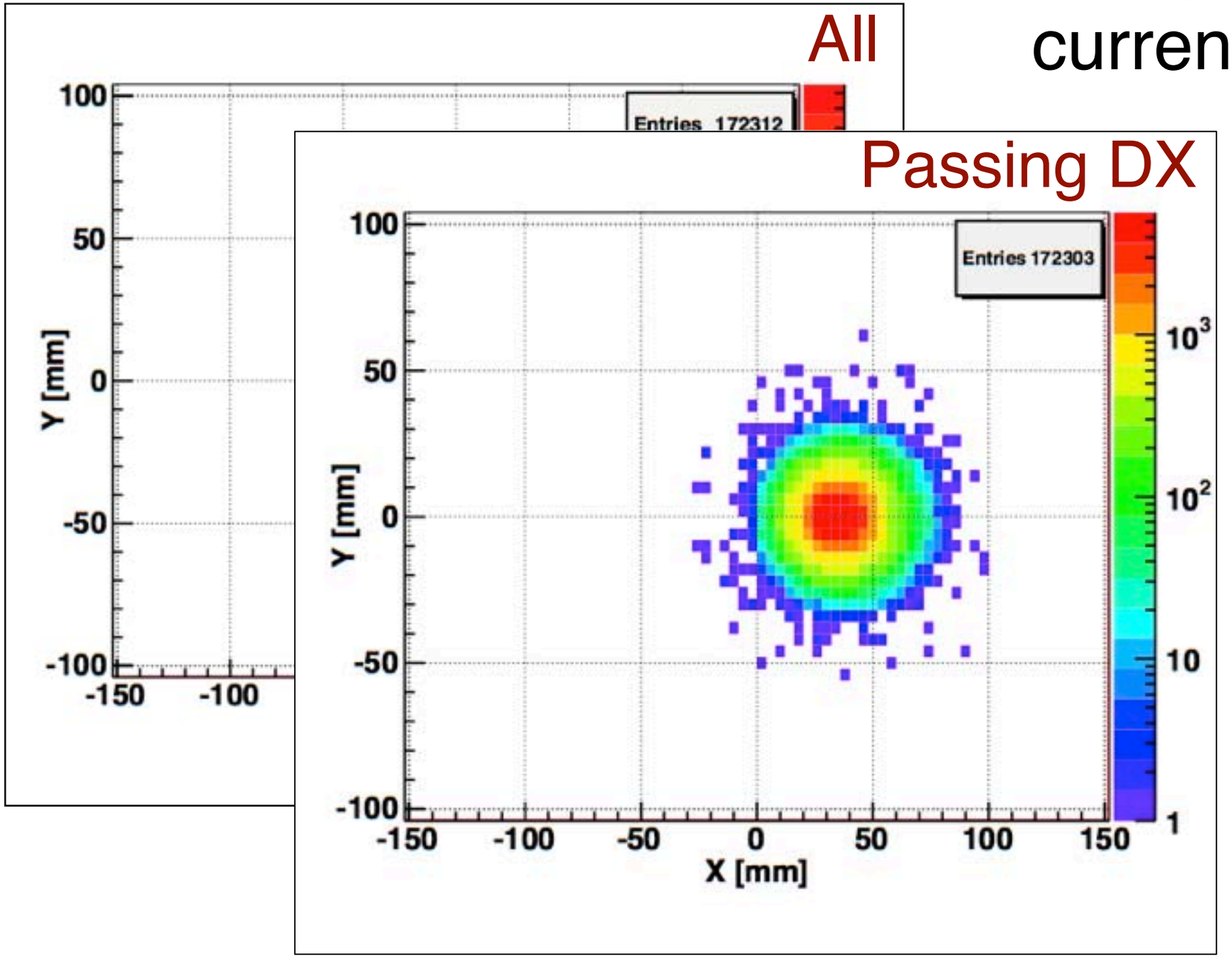

Polarised He^3

- Spectator proton acceptance with current RHIC optics

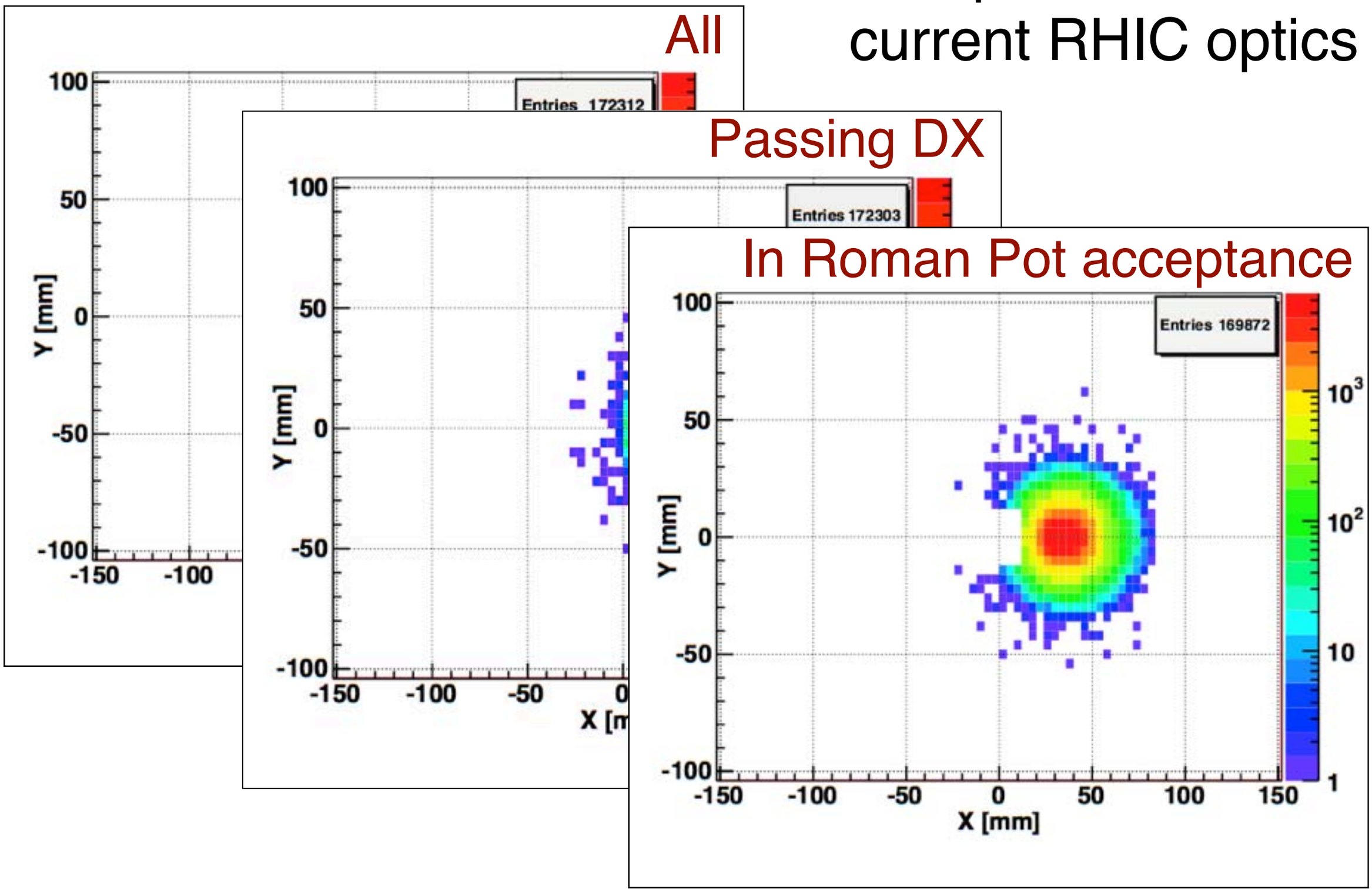

Summary

- Wide range of measurements to mid- and forward rapidity
- Many open questions remain, especially in the forward direction
  - Know the physics we want to measure
  - Are planning the upgrades we need to make those measurements

Sivers Asymmetries in Polarized Drell-Yan Production of Muon Pairs at COMPASS

IhnJea Choi
University of Illinois at Urbana-Champaign
For the COMPASS collaboration

Forward Physics at RHIC (2012)

Outline

- TMD PDFs
- Transverse Polarized Drell-Yan process
- Sivers, Boer Mulders functions from DIS and SIDIS
- DY at COMPASS- acceptance
- DY at COMPASS- feasibility
- Sensitivity projections
- Summary

Quark Structure of Nucleon

At leading twist, spin structure of the nucleon is completely described by 3 independent structure functions

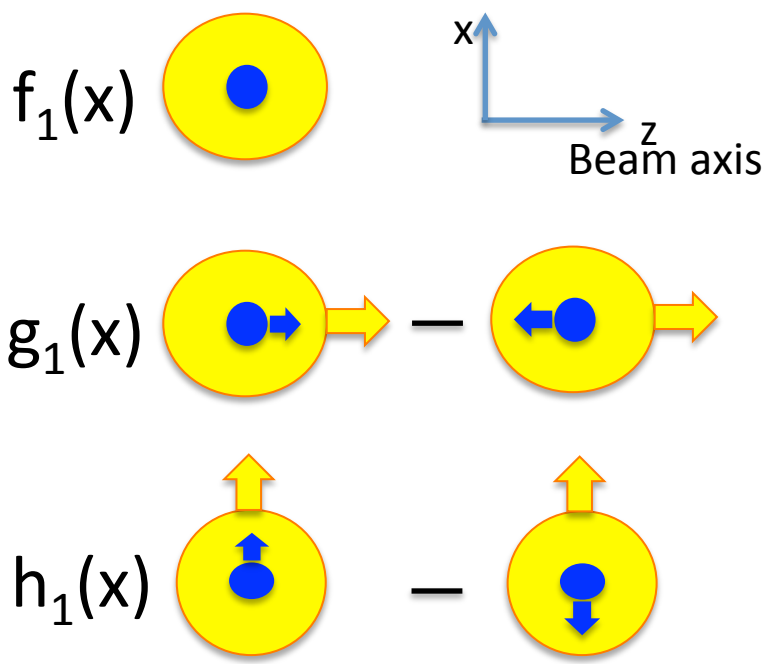

Unpolarized structure function

Helicity structure function

Transversity distribution function

Transvers Momentum Dependent (TMD) PDFs

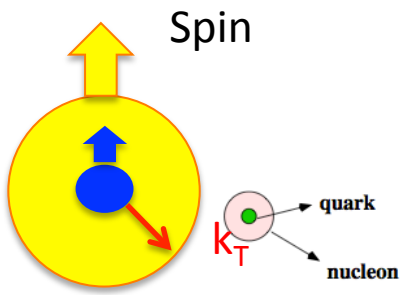

Non-zero quark transvers momentum k_T,
3 independent PDFs(x) ➔ **8 independent PDFs(x,k_T)**

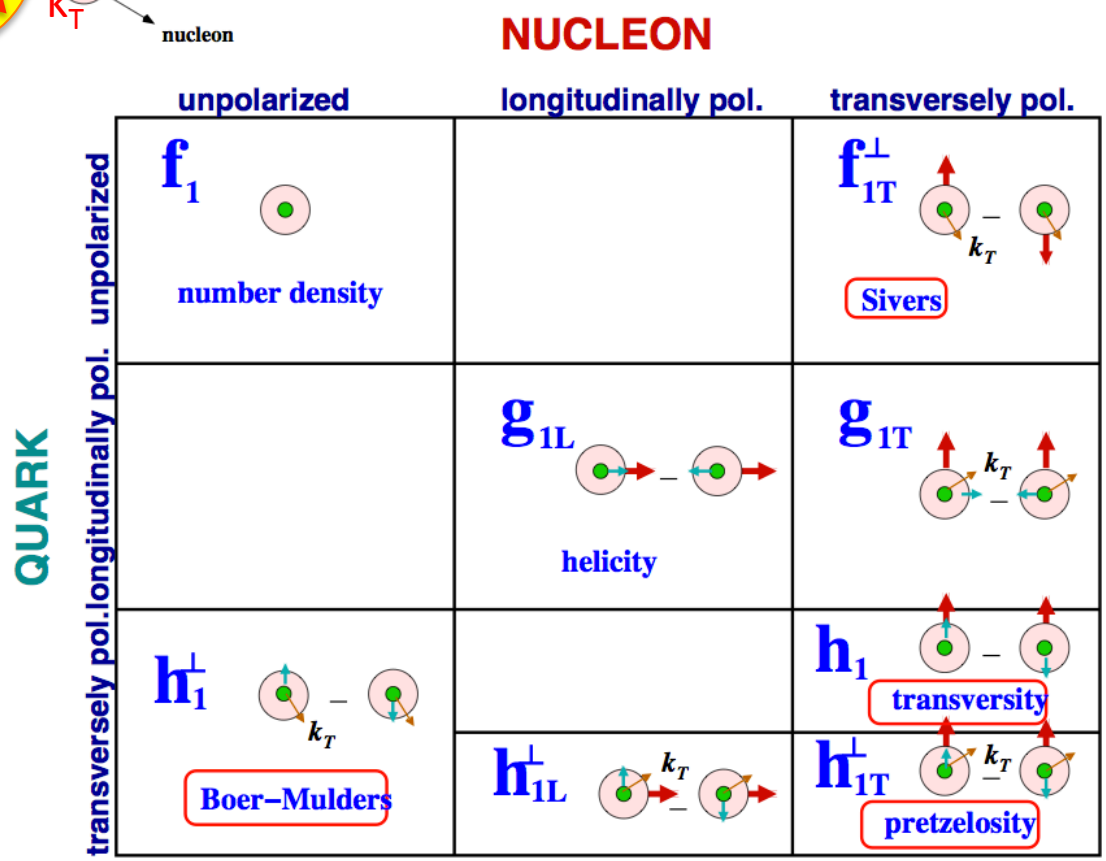

Sivers, Boer-Mulders, Transversity Distributions

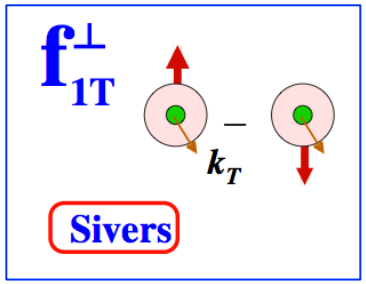

Sivers Function

Influence of the transverse spin of hadron onto their quark transverse momentum distribution

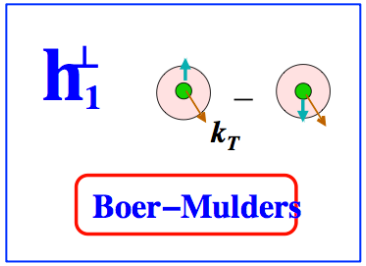

Boer-Mulders Function

Correlation between transverse spin and transverse momentum of the quark in unpolarized nucleon

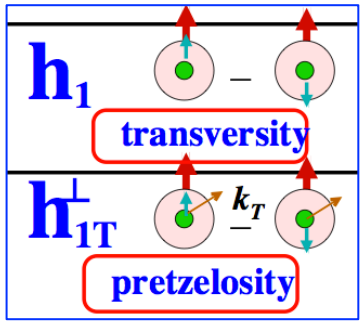

Pretzelosity

Probability to find a quark with Momentum x, k_T and transverse spin s_q in a proton with transverse spin S

Determination of Sivers-, Boer-Mulders-, and Transversity-distributions is very important to understand the partonic spin structure of hadron !

Drell-Yan Process

Drell-Yan process is an excellent tool to study tansversity and k_T-dependent PDFs
Quark and antiquark annihilation process. No fragmentation function
-> Clean signal to access initial parton structure

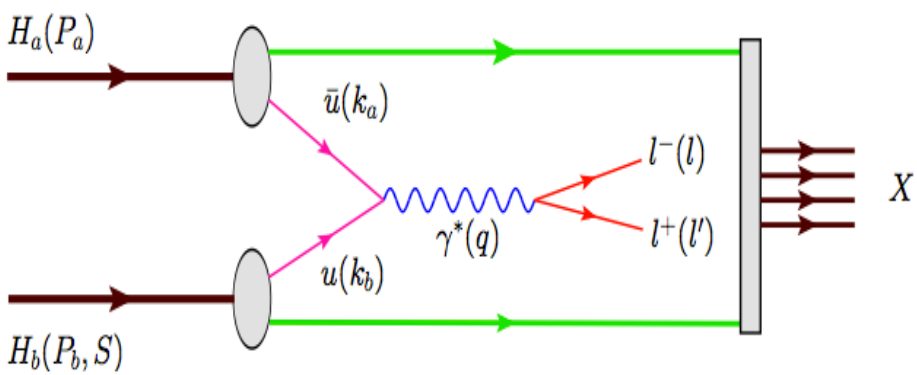

Arnold, Metz and sion Phys. Rev. D79 (2009) 034005

$$H_a(P_a) + H_b(P_b) \rightarrow \gamma^*(q) + X \rightarrow l^-(l) + l^+(l^-)$$

P_a Hadron Beam momentum
P_b = 0, (fixed target)
ι Lepton momenta
S target polarization

If the quarks intrinsic transverse momentum ≠ 0,
The dilepton has also $q_T = k_{Ta} + k_{Tb}$

s	$= (P_a + P_b)^2,$	the total centre-of-mass energy squared,
$x_{a(b)}$	$= q^2/(2P_{a(b)} \cdot q),$	the momentum fraction carried by a parton from $H_{a(b)}$,
x_F	$= x_a - x_b,$	the Feynman variable,
$M^2_{\mu\mu}$	$= Q^2 = q^2 = s\ x_a\ x_b,$	the invariant mass squared of the dimuon.

Definition of azimuthal angles in DY

1) Target rest frame (TF)

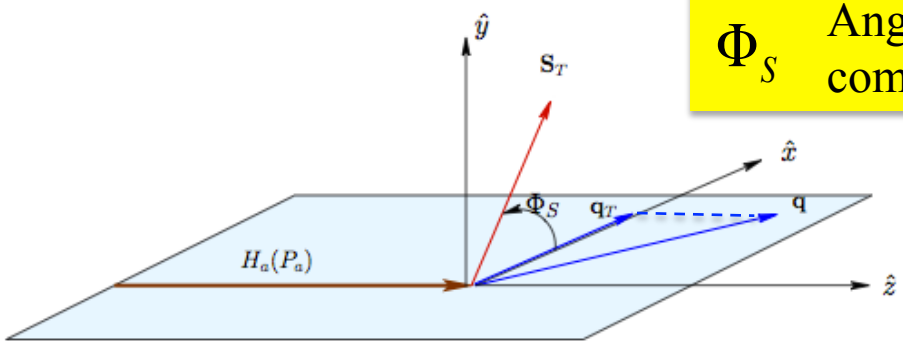

Beam hadron

Φ_S Angle between target spin(S_T) and transverse component of outgoing lepton pair momentum

2) Rest frame of the virtural photon (CF : Collins-Soper frame)

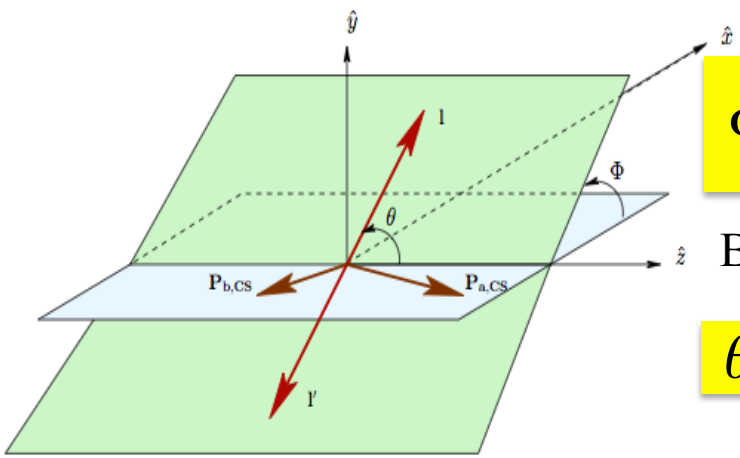

Φ Angle between planes defined by hadron and lepton momenta

Beam hadron

θ Polar angle of lepton pair in the CF frame

Pol. Drell-Yan cross section

DY cross section for transversely polarized nucleon target

$$
\begin{aligned}
\frac{d\sigma}{d^4q\,d\Omega} = & \frac{\alpha_{em}^2}{F\,q^2}\hat{\sigma}_U\Big\{\Big(1 + D_{[\sin 2\theta]}\,A_U^{\cos\phi}\cos\phi + D_{[\sin^2\theta]}\,A_U^{\cos 2\phi}\cos 2\phi\Big) \\
& + S_L\Big(D_{[\sin 2\theta]}\,A_L^{\sin\phi}\sin\phi + D_{[\sin^2\theta]}\,A_L^{\sin 2\phi}\sin 2\phi\Big) \\
& + |\boldsymbol{S}_T|\Big[\Big(D_{[1]}\,A_T^{\sin\phi_S} + D_{[\cos^2\theta]}\,\tilde{A}_T^{\sin\phi_S}\Big)\sin\phi_S \\
& + D_{[\sin 2\theta]}\Big(A_T^{\sin(\phi+\phi_S)}\sin(\phi+\phi_S) + A_T^{\sin(\phi-\phi_S)}\sin(\phi-\phi_S)\Big) \\
& + D_{[\sin^2\theta]}\Big(A_T^{\sin(2\phi+\phi_S)}\sin(2\phi+\phi_S) + A_T^{\sin(2\phi-\phi_S)}\sin(2\phi-\phi_S)\Big)\Big]\Big\}
\end{aligned}
$$

S. Arnold et al.,
Phys. Rev. D79 (2009) 034005.

A. Kotzinian,
COMPASS Note 2010-2,
February 10, 2010,

F: Flux of incoming hadrons, $D_{[]}$ depolarisation factor

At LO QCD

$$
\begin{aligned}
\frac{d\sigma}{d^4q\,d\Omega} \overset{\text{LO}}{=} & \frac{\alpha_{em}^2}{F\,q^2}\hat{\sigma}_U\Big\{\Big(1 + D_{[\sin^2\theta]}\,\boxed{A_U^{\cos 2\phi}}\cos 2\phi\Big) \\
& + |\mathbf{S}_T|\Big[\boxed{A_T^{\sin\phi_S}}\sin\phi_S + D_{[\sin^2\theta]}\Big(\boxed{A_T^{\sin(2\phi+\phi_S)}}\sin(2\phi+\phi_S) \\
& + \boxed{A_T^{\sin(2\phi-\phi_S)}}\sin(2\phi-\phi_S)\Big)\Big]\Big\},
\end{aligned}
$$

DY Asymmetries

DY cross section

$$\frac{d\sigma}{d^4q\,d\Omega} \overset{\text{LO}}{=} \frac{\alpha_{em}^2}{F\,q^2}\hat{\sigma}_U\Big\{\Big(1 + D_{[\sin^2\theta]}\,\boxed{A_U^{\cos 2\phi}}\cos 2\phi\Big)$$
$$+ \quad |\mathbf{S}_T|\Big[\boxed{A_T^{\sin\phi_S}}\sin\phi_S + D_{[\sin^2\theta]}\Big(\boxed{A_T^{\sin(2\phi+\phi_S)}}\sin(2\phi+\phi_S)$$
$$+ \quad \boxed{A_T^{\sin(2\phi-\phi_S)}}\sin(2\phi-\phi_S)\Big)\Big]\Big\},$$

- $A_U^{\cos 2\phi}$ gives access to the Boer–Mulders functions of the incoming hadrons,
- $A_T^{\sin\phi_S}$ to the Sivers function of the target nucleon,
- $A_T^{\sin(2\phi+\phi_S)}$ to the Boer–Mulders function of the beam hadron and to $h_{1T}^{\perp}$, the pretzelosity function of the target nucleon,
- $A_T^{\sin(2\phi-\phi_S)}$ to the Boer–Mulders function of the beam hadron and h_1, the transversity function of the target nucleon.

All these asymmetries(modulations) are expected to be sizable in the valence quark range and can be measured at COMPASS !

Sivers in SIDIS

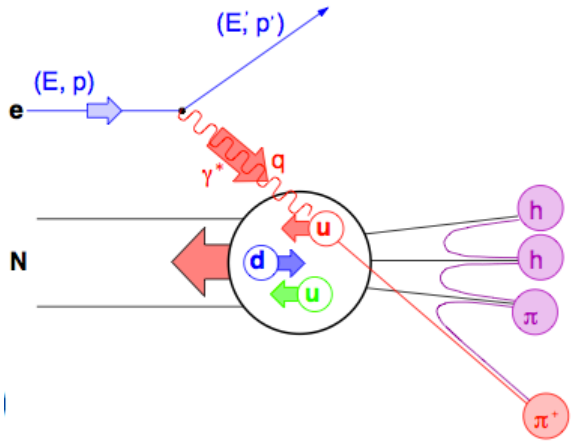

SIDIS Process

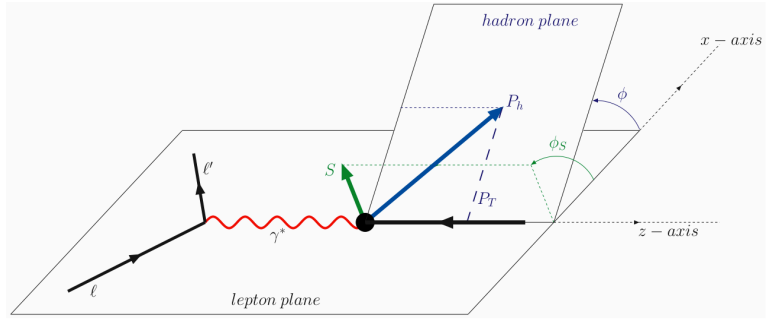

Definition of azimuthal angles
In SIDIS

Sivers from SIDIS $A_{UT}\sin(\phi-\phi_s)$

Lepton and produced hadron used a probe

access to quark k_T and transverse polarization

Convolution of PDFs and fragmentation function(FFs)

Sivers Asymmetries from SIDIS at COMPASS

A positive Sivers asymmetry for positive hadrons
An asymmetry compatible with zero for negative hadrons

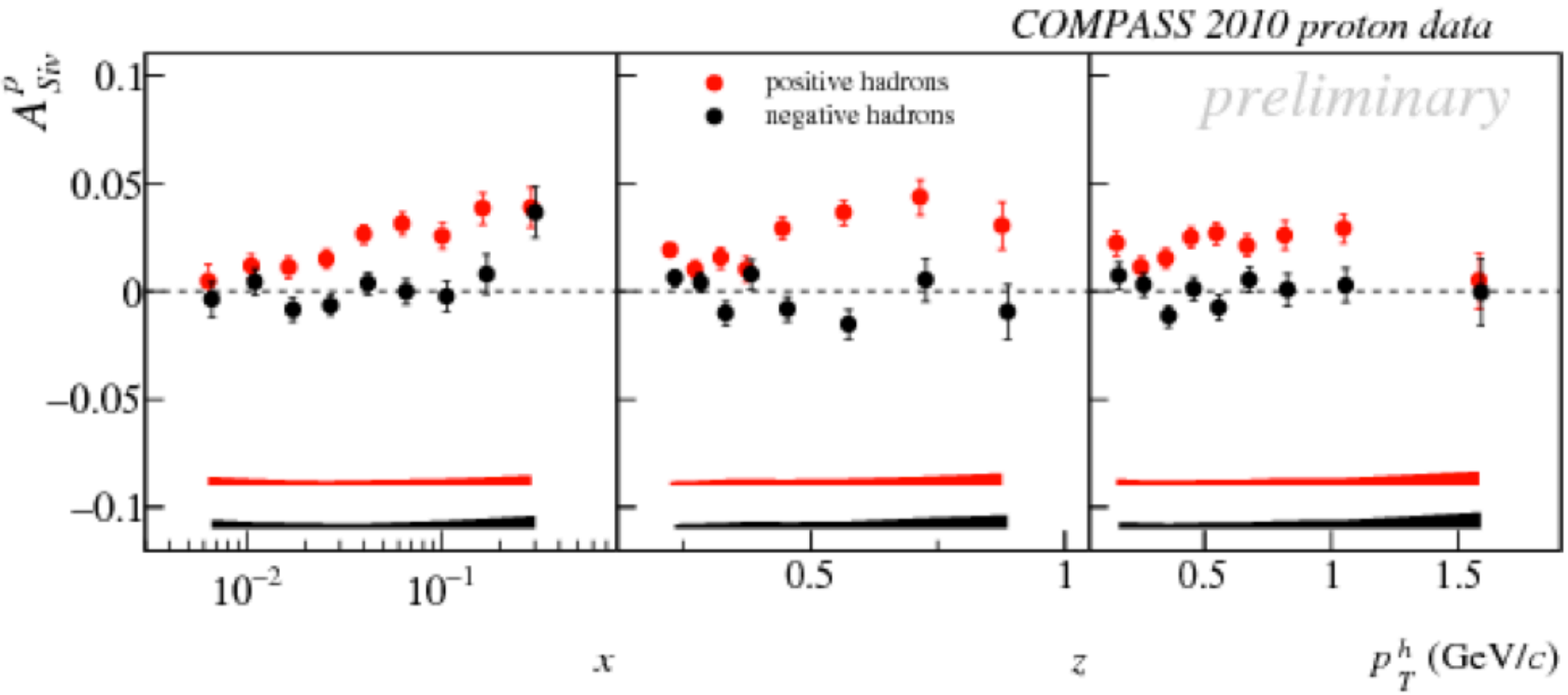

Sivers measurement from SIDIS

Sivers asymmetry measurement from HERMES and COMPSS experiments

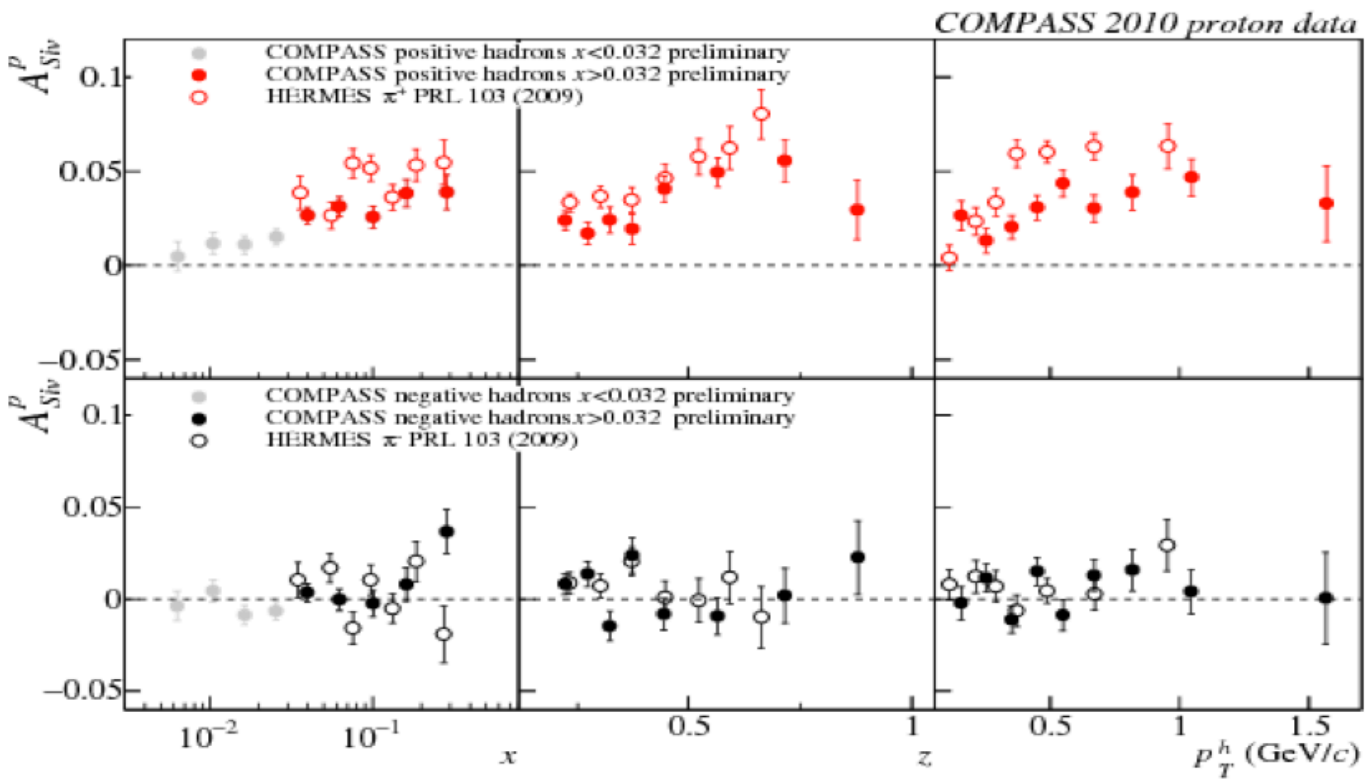

Recent suggestions that difference may be due to TMD evolution: M. Aybat (2011), T. Rogers, A. Prokudin

Sign change of Sivers- and Boer-Mulders Functions between SIDIS and DY

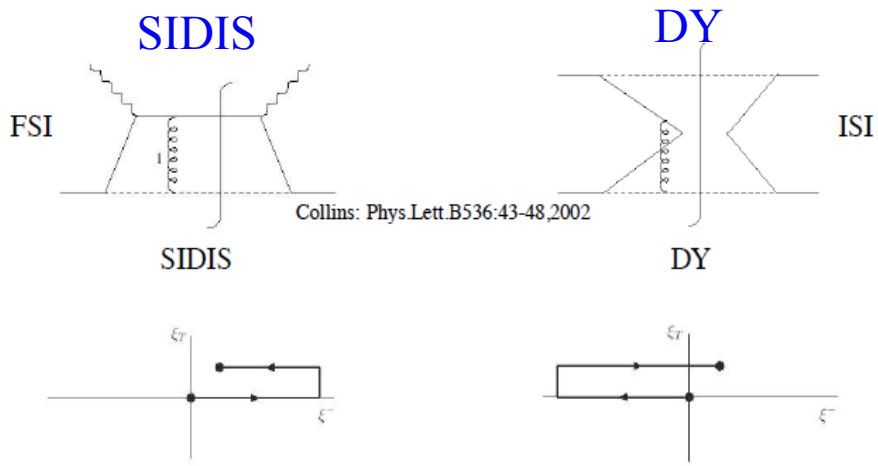

J.C. Collins, Phys. Lett. B536 (2002) 43

Direction of the gauge-link of k_T dependent PDFs is process-dependent and changes its sign between SIDIS and DY

Sivers $$f_{1T}^{\perp}(x,\mathbf{k}_T)\Big|_{SIDIS} = -f_{1T}^{\perp}(x,\mathbf{k}_T)\Big|_{DY}$$

Boer-Mulders $$h_1^{\perp}(x,\mathbf{k}_T)\Big|_{SIDIS} = -h_1^{\perp}(x,\mathbf{k}_T)\Big|_{DY}$$

Unknown !

Need to confirm sign reversal In Pol DY process !

TEST universality of TMD and QCD in non-perturbative regime !

COMPASS

COmmon Muon Proton Apparatus for Structure and Spectroscopy

Fixed target experiment at CERN SPS beam line
Data taking since 2002
Muon and Baryon spectroscopy with high energy muon and hadron beam

The COMPASS Spectrometer

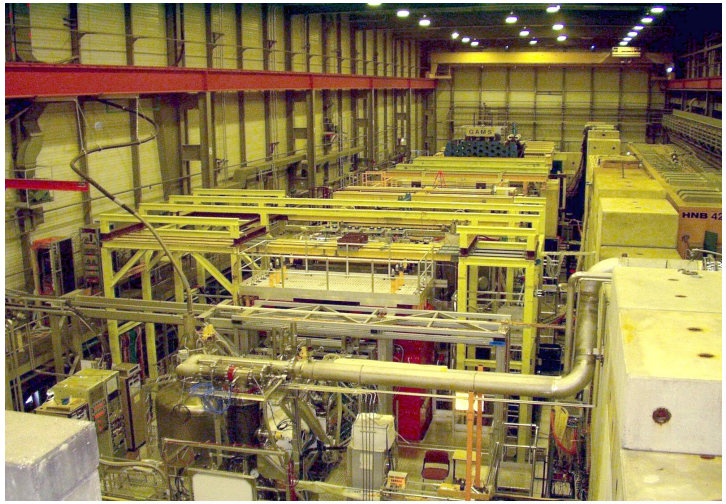

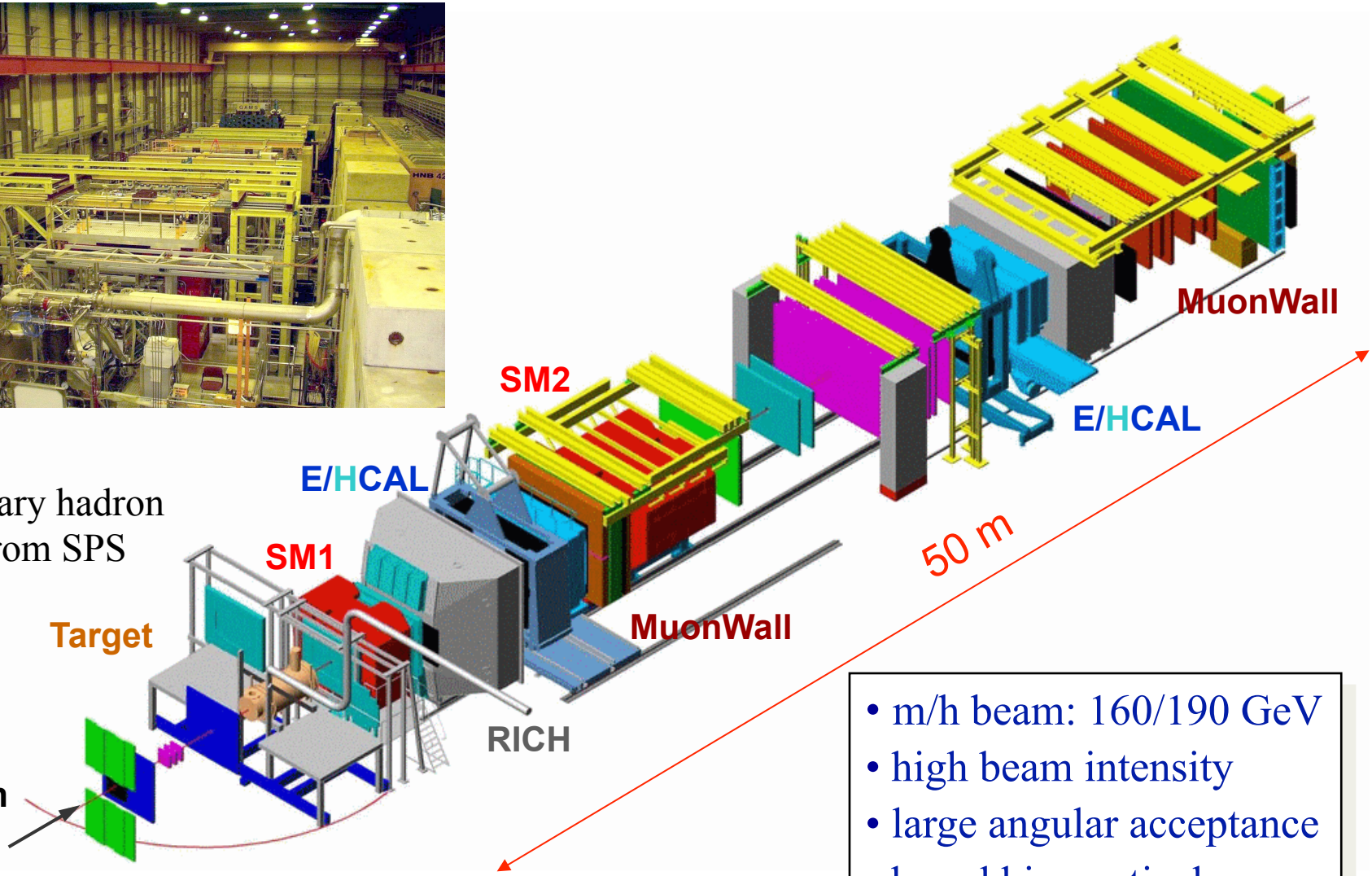

Secondary hadron beam from SPS

- m/h beam: 160/190 GeV
- high beam intensity
- large angular acceptance
- broad kinematical range

Two stage spectrometer in order to cover a large Kinematic range

SIDIS and DY kinematic

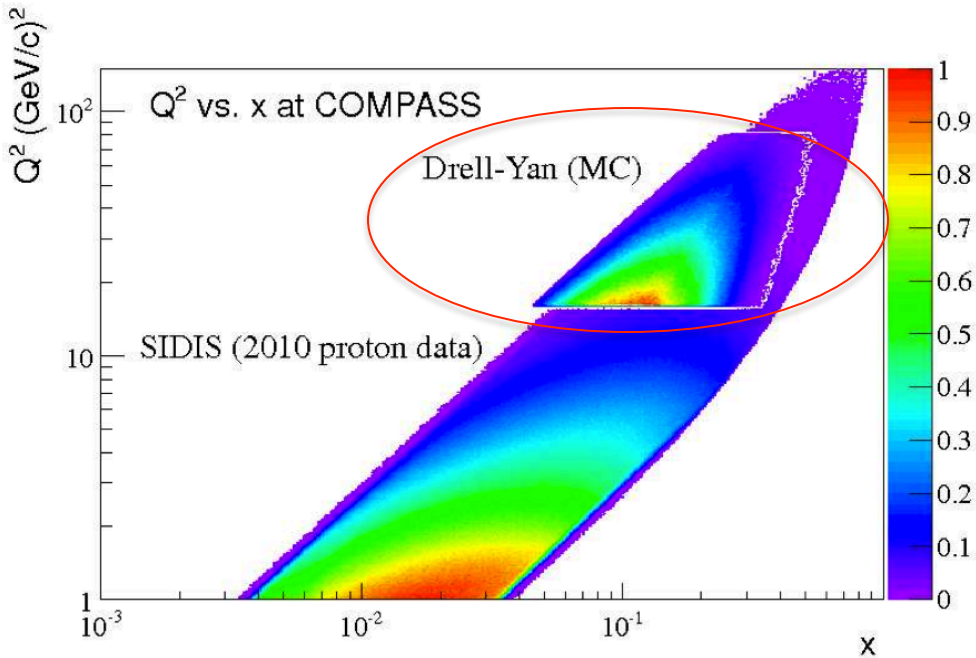

The COMPASS SIDIS and DY experimental measurements have an overlapping kinematic region.

Mean value comparision

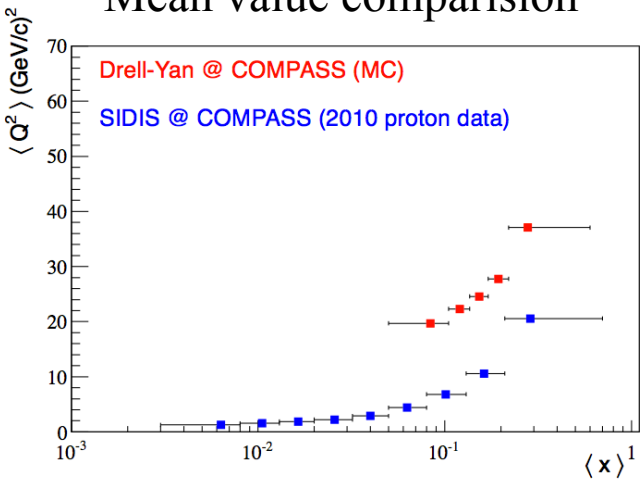

There is overlap in the phase-space accessed by the 2 measurements.
when comparing the TMDs extracted,
the QCD evolution of the TMDs
must be properly taken into account.

π^- beam for Drell-Yan

Choice of beam at COMPASS

$$\pi^-(\bar{u}d) + p\uparrow(uud) \rightarrow \ell^+\ell^- X$$

u-quark and anti-u quark dominant in Drell-Yan process
TMDs are sensitive at valence quark regime

Choice of beam energy PYTHIA, $4 < M_{\mu\mu} < 9$ GeV/c

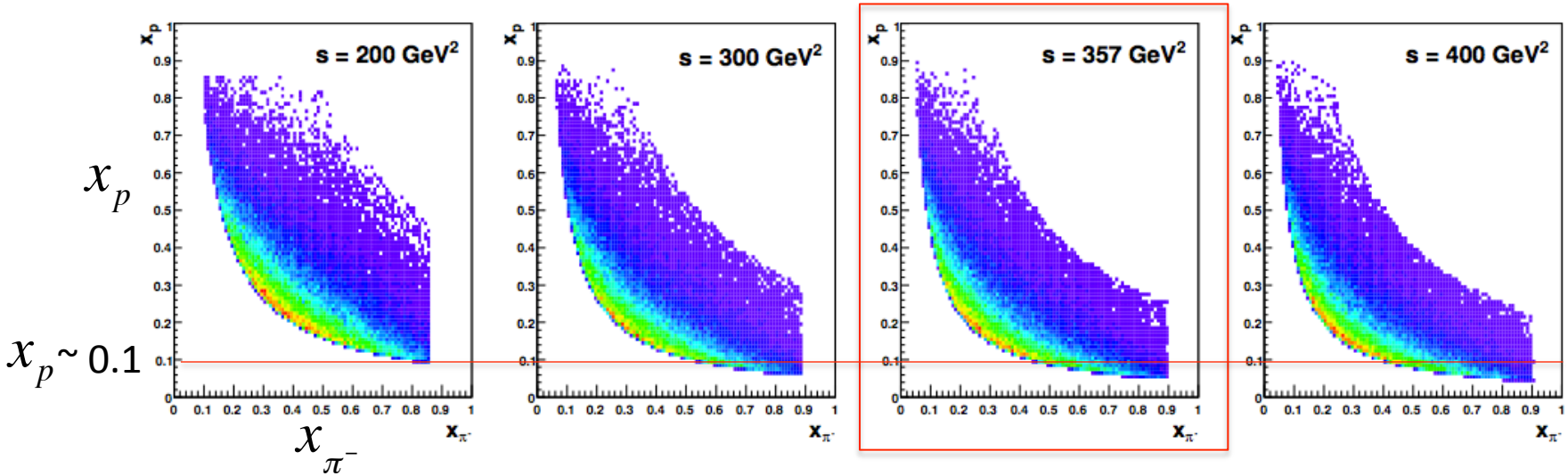

The value s = 357 GeV^2, corresponding to a pion beam momentum of 190 GeV/c, seems to be a good choice. -> As the energy increased, the phase space coverage extends to the low-x non-valence region

DY acceptance at COMPASS (I)

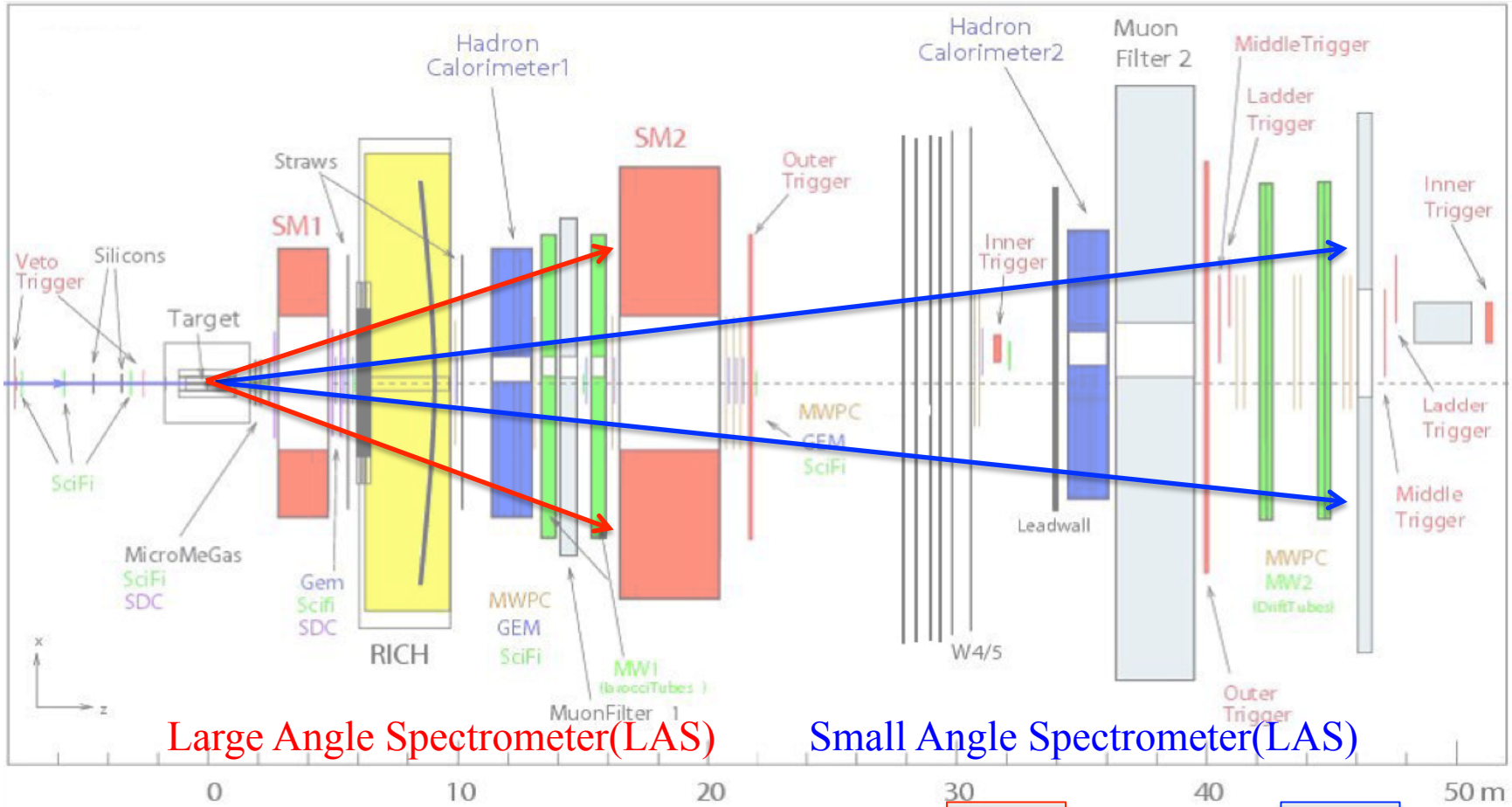

Mass range (GeV/c^2)	Average acceptance (%)	LAS	LAS+SAS	SAS
4–9	35	64	40	4
2–2.5	43	32	54	20

DY acceptance at Compass (II)

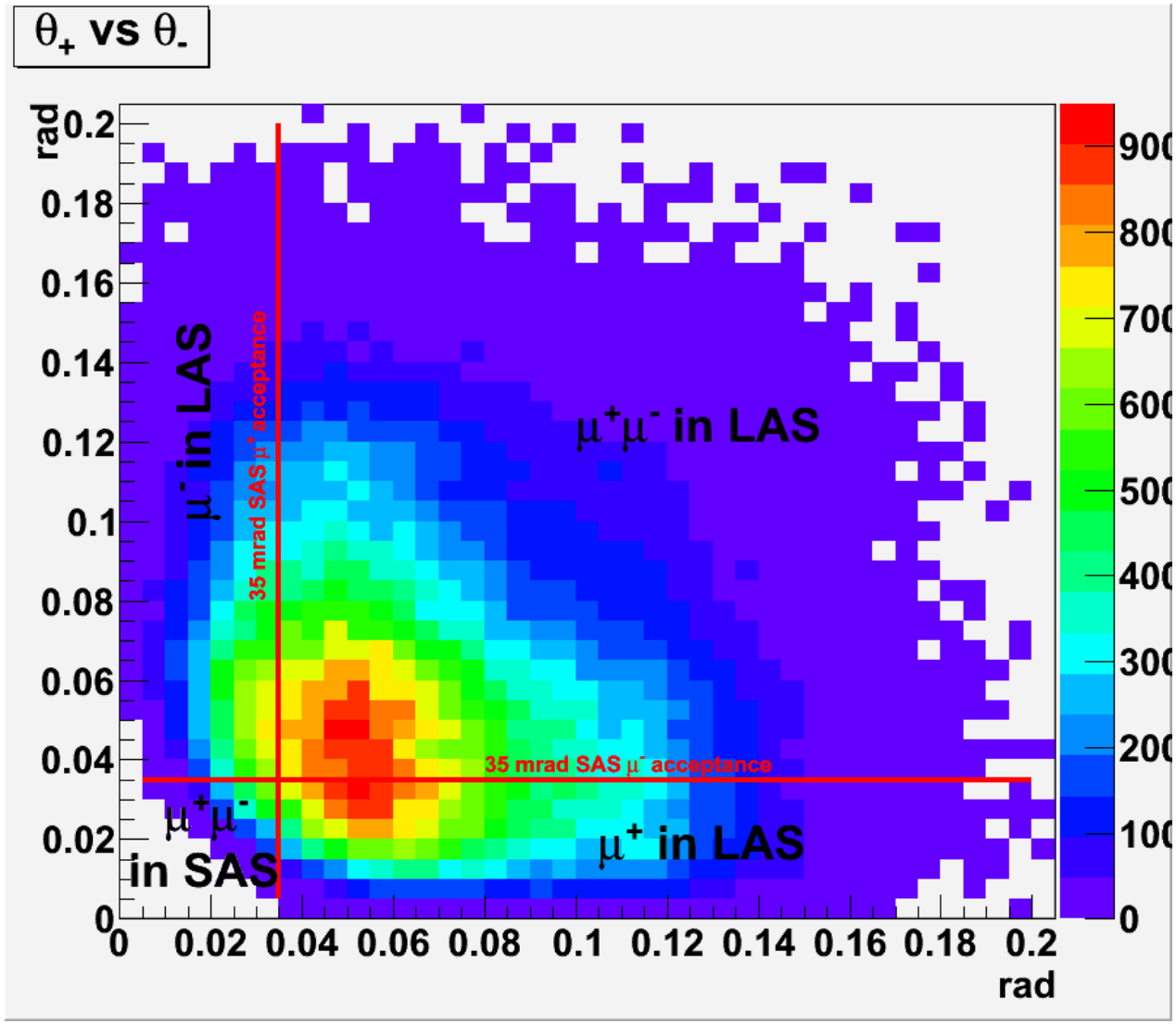

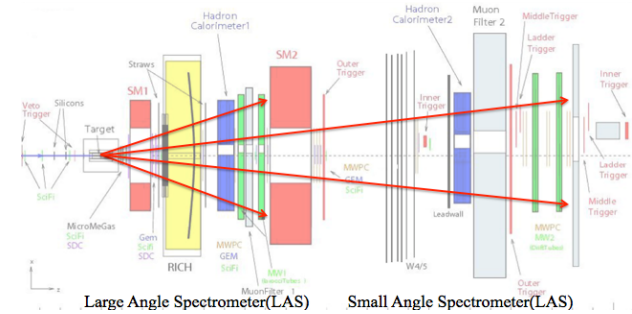

95% of all Drell-Yan muon pairs in the di-muon mass range 4<m<9 GeV/c^2 have at least one muon in the LAS/LAT

DY kinematics $4 < M_{uu} < 9$ GeV/c^2 at COMPASS

M. Anselmino .. Phys.Rev.D79:054010, 2009

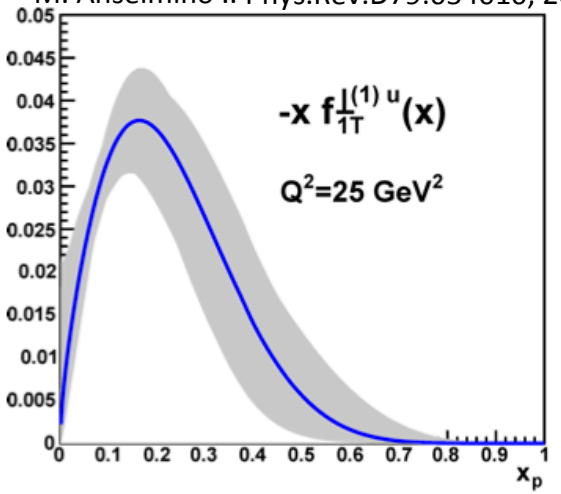

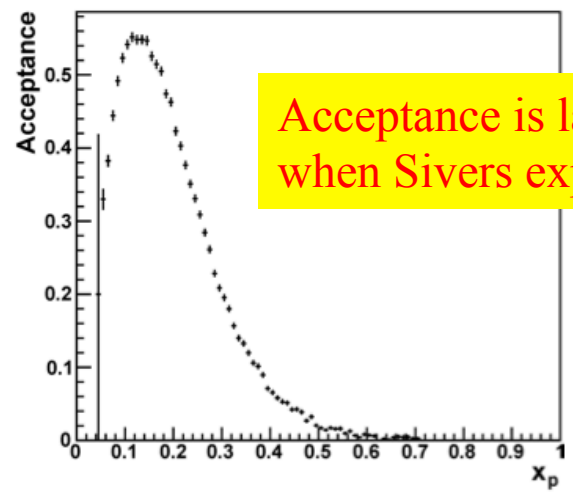

Acceptance is largest
when Sivers expected to be largest

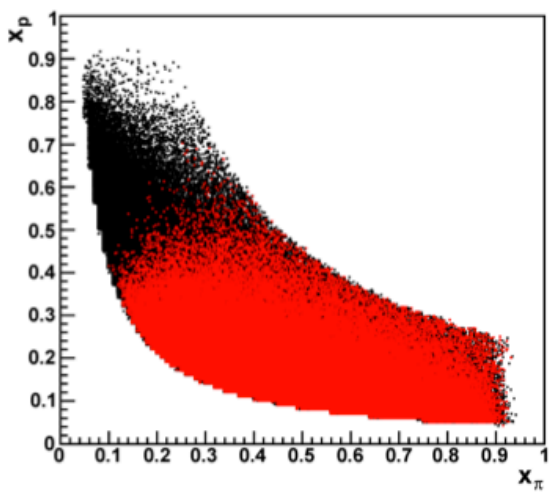

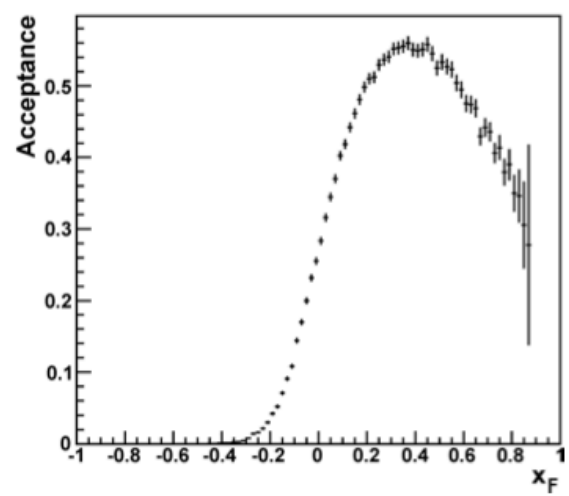

Valence range (x~> 0.1) for both quarks (pure u-ubar annihilation)
PT dimuon about 1GeV/c where TMD effects are dominant

DY kinematics $2 < M_{uu} < 2.5$ GeV/c^2 at COMPASS

M. Anselmino .. Phys.Rev.D79:054010, 2009

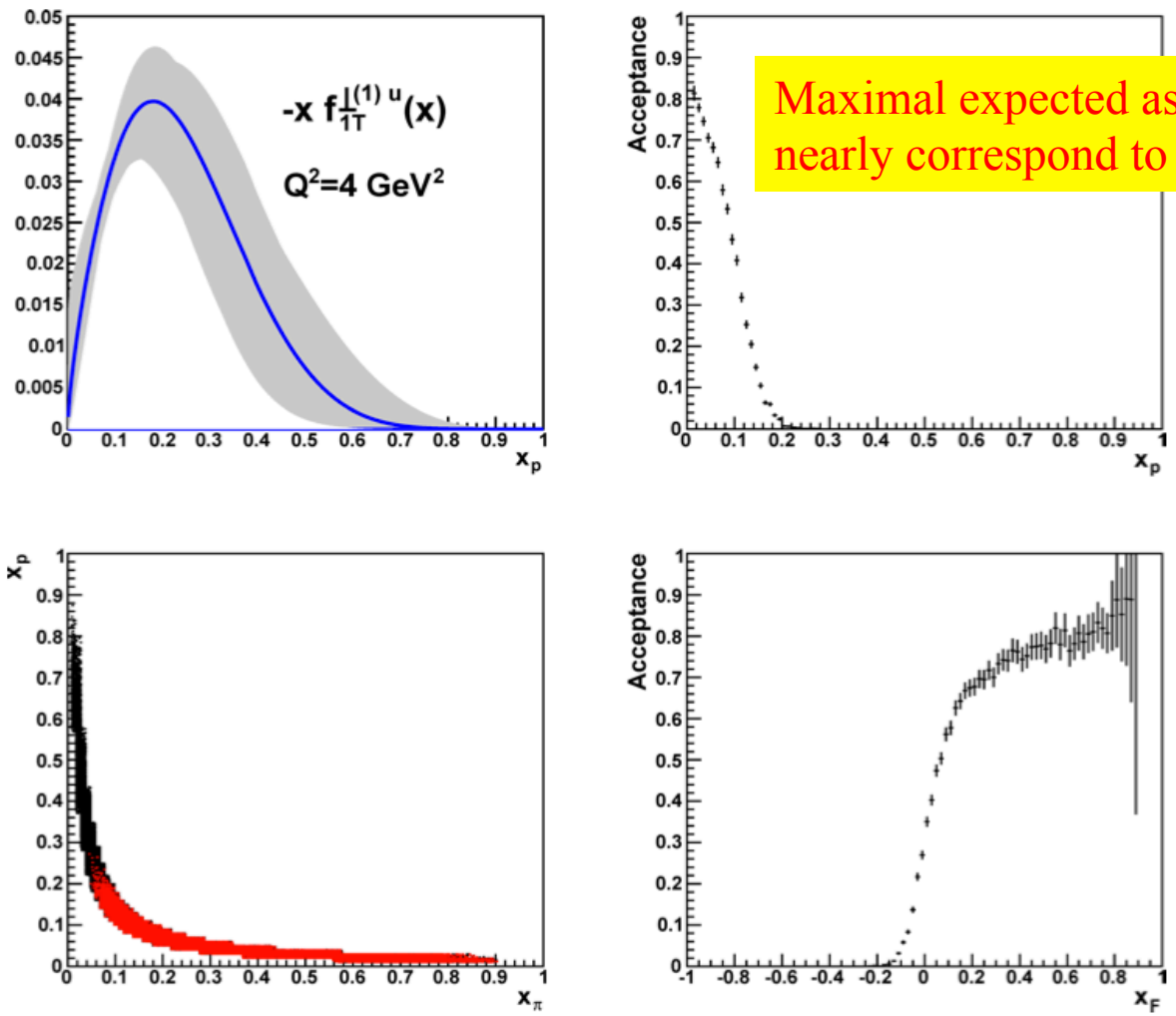

Maximal expected asymmetry value nearly correspond to the maximal acc.

DY feasibility – test setup

Pion induced DY test run, Year 2007, 2008, 2009

π^- 190 GeV/c beam -> u quark anti-uquark dominant DY process
Polarised target simulated by two cylinders of polyetylene (CH_2) -> NH_3
Hadron absorber installed
8 x10^7 pions/spill (spill length 9.6s)

COMPASS Detector

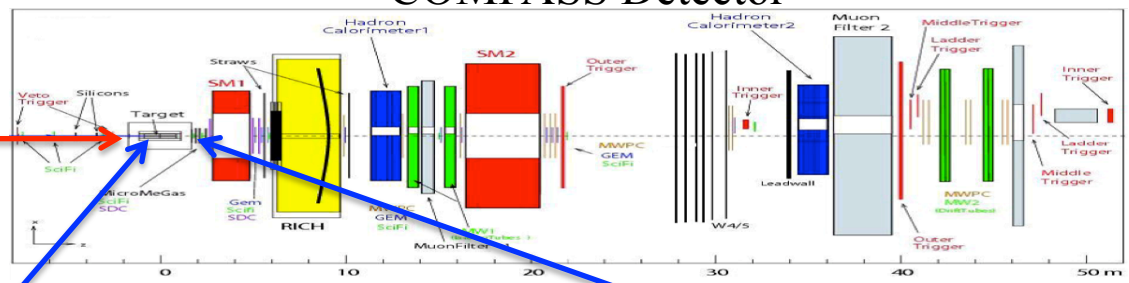

π^- beam

Transvers Pol. target

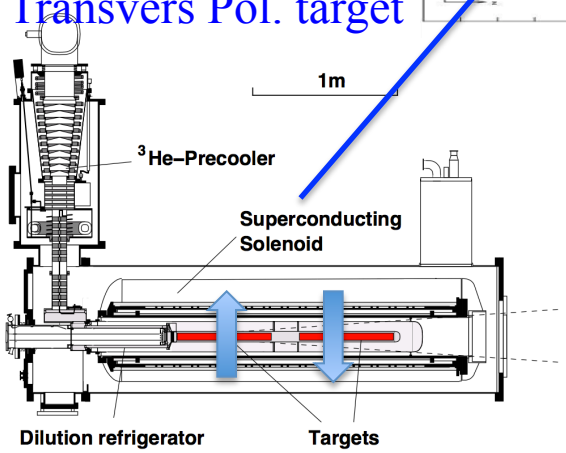

Two 40cm length of Polyethylene(CH_2) separated by 20cm

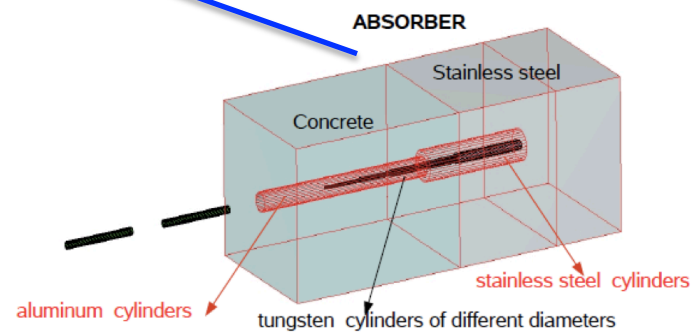

Hadron absorber
Beam plug (stop non-interacting beam)

Muon pairs z-vertex distribution

2009 beam test for DY

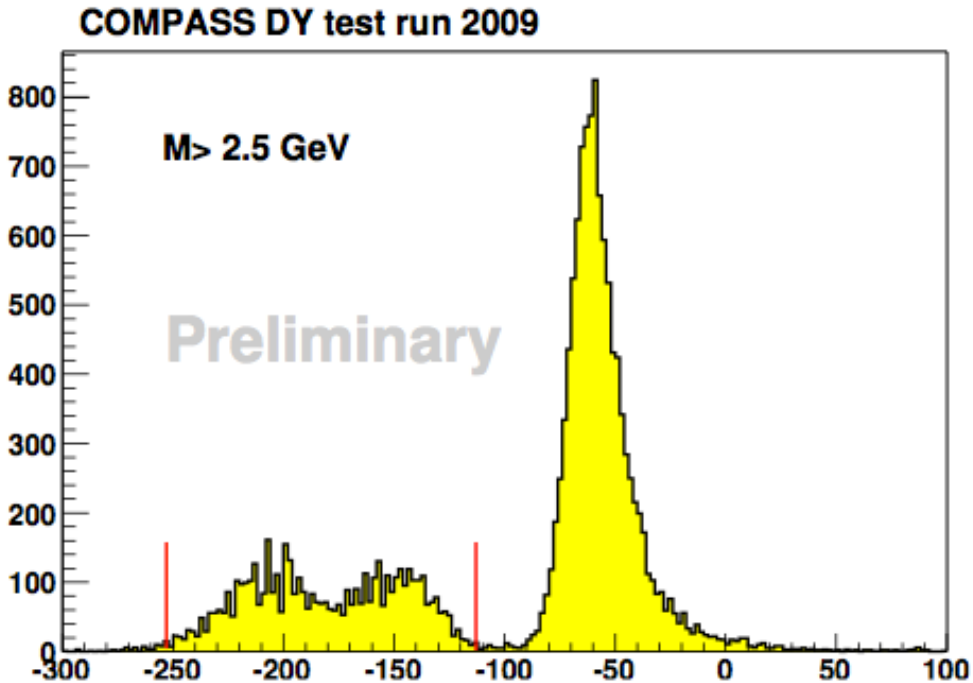

Two CH_2 target cells (40cm + 40cm)
Gap between cells 20cm

Reconstructed z-vertex position visible (Requires improved beam and vertex tracking)

Peak around -50cm is from hadron absorber

DY feasibility (2009 Beam test)

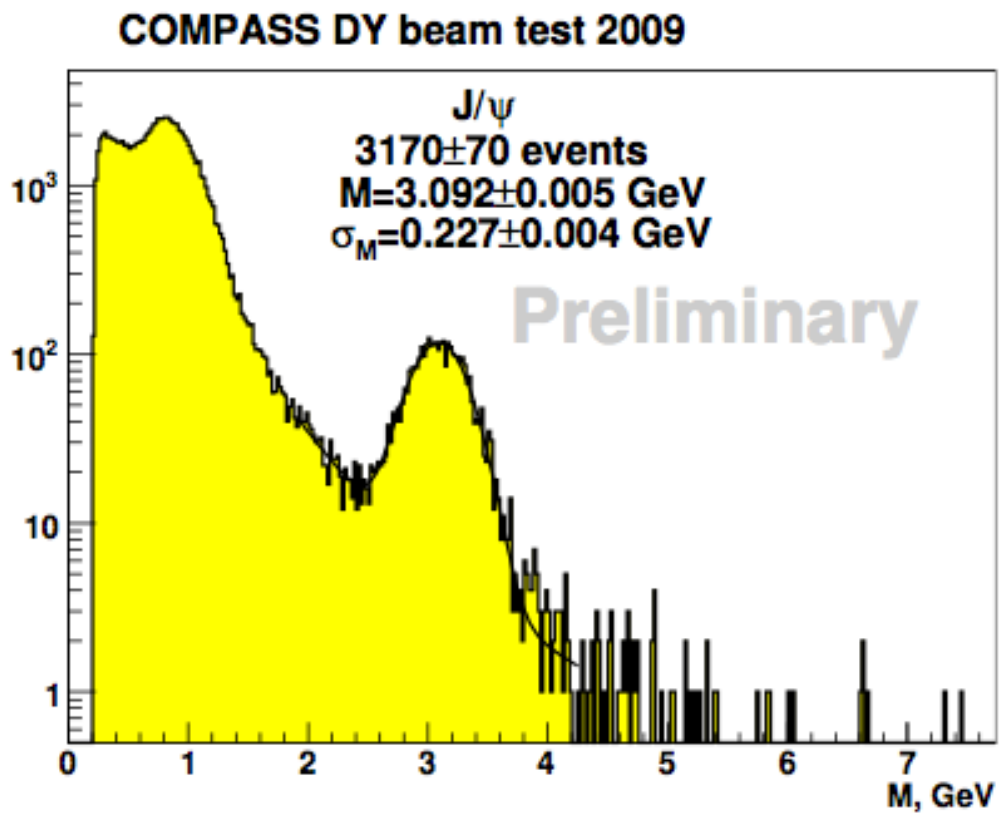

3 days data taking on 2009

	J/Psi	DY ($4<M_{uu}<9$)
Expected	3600+- 600	110+-22
Data	**3170+-70**	**84+-10**

Agreed well with expectation

DY feasibility – p_T, x_F distributions

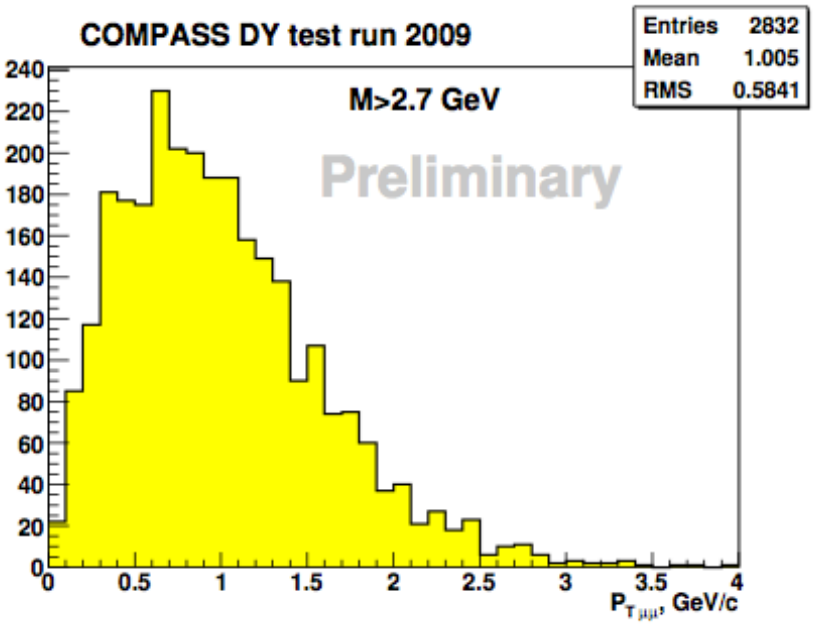

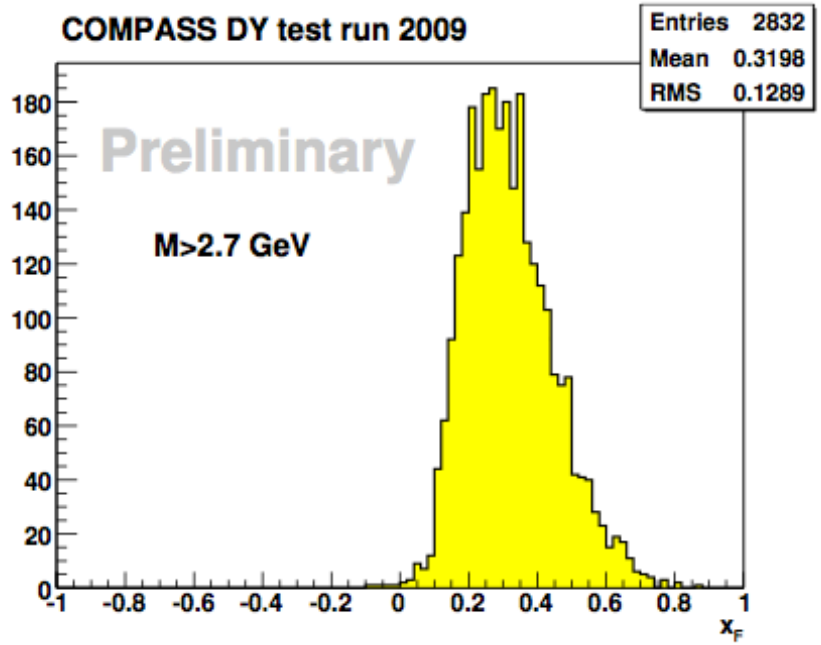

Mean pT ~ 1GeV/C
COMPASS sensitive to TMDs
(TMDs expected to be accessible up to P_T ~ 2GeV/c)

x_p and x_π distributions

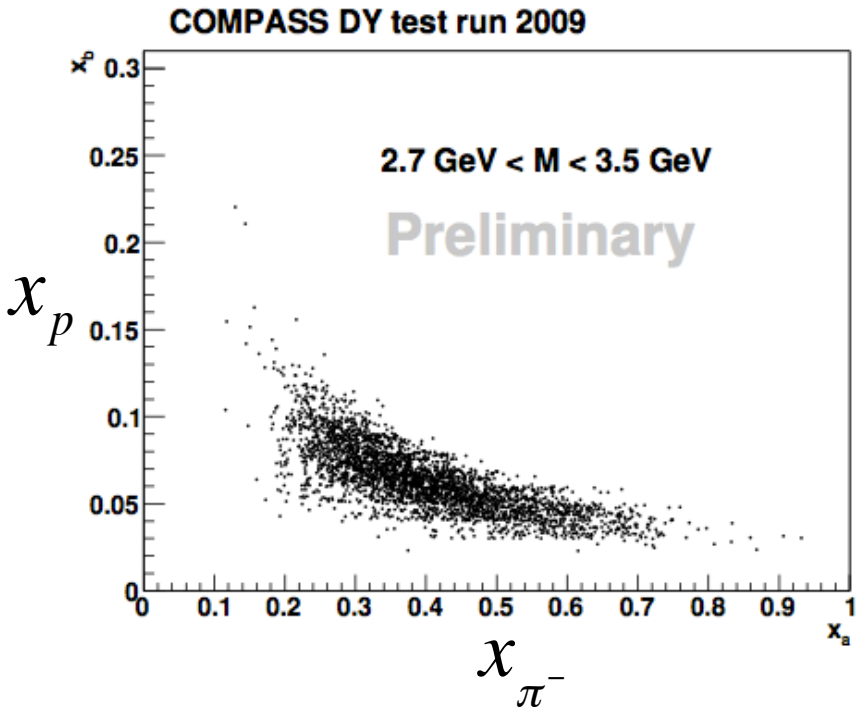

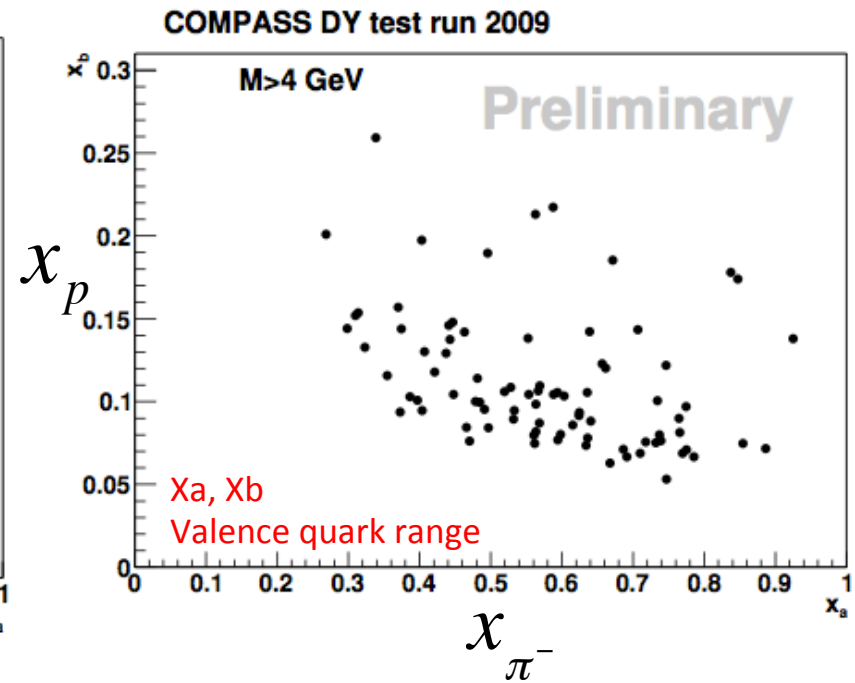

COMPASS Acceptance cover both DY and J/ψ

DY feasibility - Background

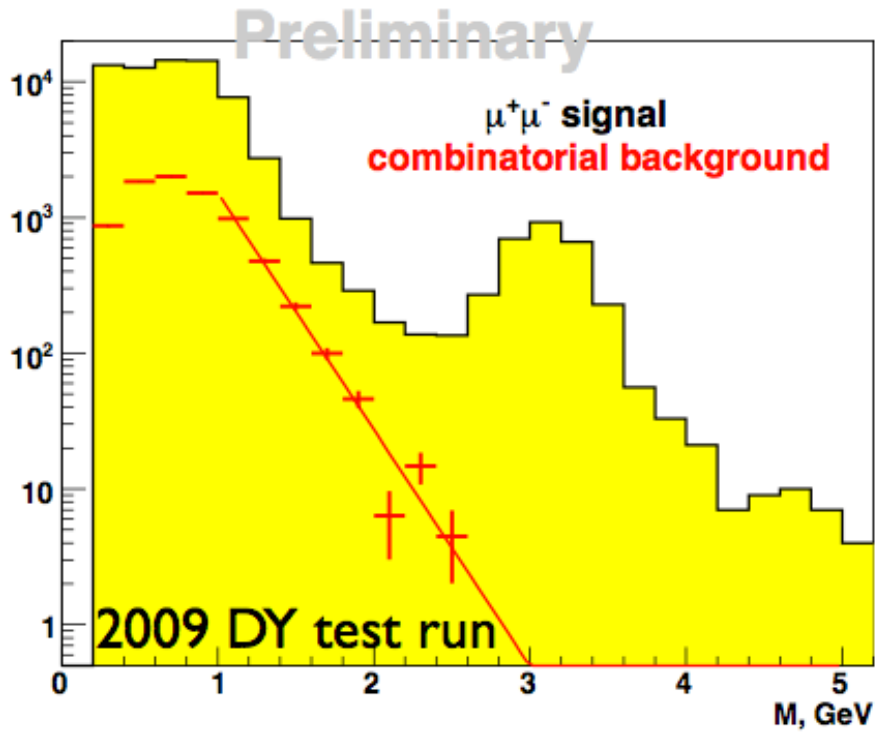

Background

1) Combinatorial muon BG originating from pion and kaon decays
   - controllable by optimizing hadron absorber and beam plug
2) Open-charm semi-leptonic drcays
   - Seen to negligible in simulation Muu>2GeV in PYTHIA
   - Improved by proper muon angular cut

Number of Expected DY events

$$\pi^-(\bar{u}d) + p\uparrow(uud) \rightarrow \ell^+\ell^- X$$

With a beam intensity of $I_{beam} = 6 \times 10^7$ particles/second, $L = 1.2 \times 10^{32}$ $cm^{-2}s^{-1}$

Expect 900/day DY events with $4 < M_{uu} < 9$ GeV/c^2
In 280 days(= 2 years), 250000 events in the DY high mass range
(~ 420000 events if $I_{beam} = 1 \times 10^8$ particles/second)

Expect 4300/day DY events with $2 < M_{uu} < 2.5$ GeV/c^2
In 280 days, 11900000 events in the DY low mass range

Expect 13700/day DY + J/Ψ events with $2.9 < M_{uu} < 3.2$ GeV/c^2
In 280 days, 3845000 events in the DY low mass range

Statistical Error Estimates for Asymmetries

$$\delta A_U^{\cos 2\phi} = 2\sqrt{\frac{2}{N}}; \qquad \delta A_U^{\cos 2\phi} = \frac{1}{fS_T}\sqrt{\frac{2}{N}}; \qquad \delta A_U^{\sin(2\phi \pm \phi_S)} = \frac{2}{fS_T}\sqrt{\frac{2}{N}};$$

Asymmetry	Dimuon mass (GeV/c^2)		
	$2 < M_{\mu\mu} < 2.5$	J/ψ region	$4 < M_{\mu\mu} < 9$
$\delta A_U^{\cos 2\phi}$	0.0020	0.0013	0.0045
$\delta A_T^{\sin \phi_S}$	0.0062	0.0040	0.0142
$\delta A_T^{\sin(2\phi+\phi_S)}$	0.0123	0.008	0.0285
$\delta A_T^{\sin(2\phi-\phi_S)}$	0.0123	0.008	0.0285

DY Statistical Precision (I)

M. Anselmino et all
PRD79(2009)054010

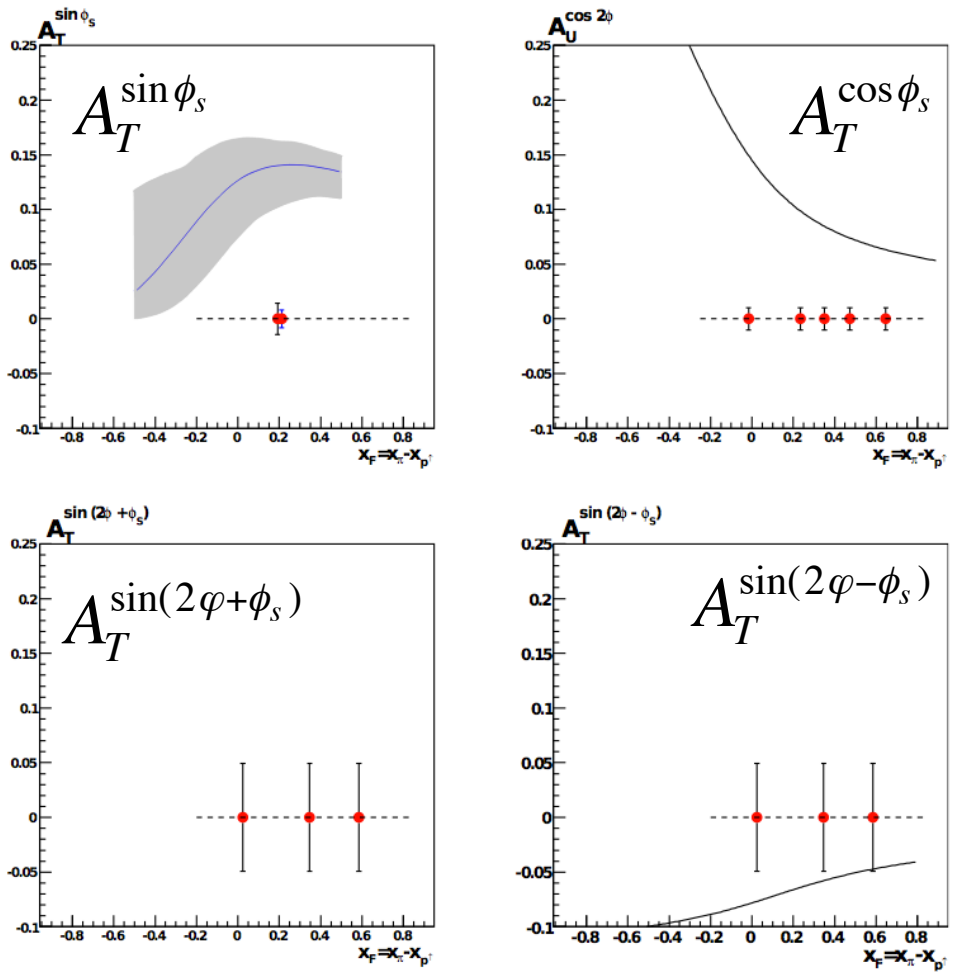

B. Zhang et all
PRD77(2008)054011

A.N. Sissakian et al,
Phys.Part.Nucl.41: 64-100,2010

$4 < M_{\mu\mu} < 9$ GeV/c^2

DY Statistical Precision (II)

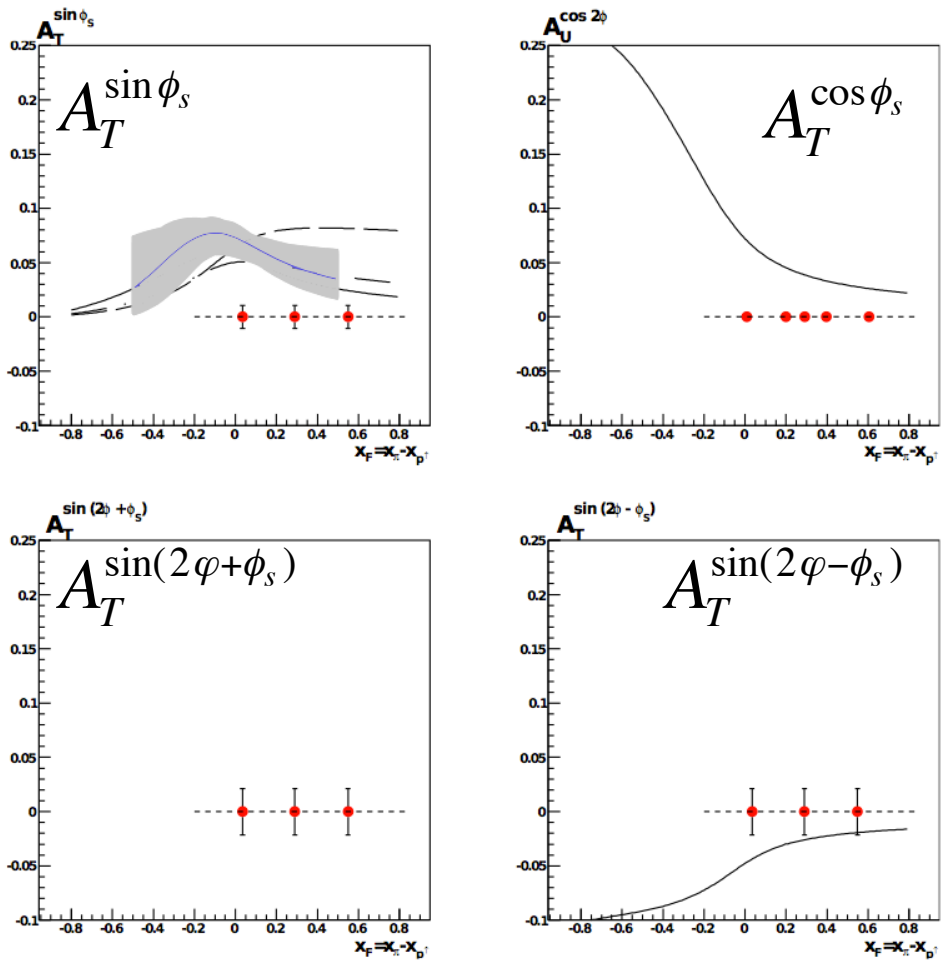

$2 < M_{\mu\mu} < 2.5$ GeV/c^2

J/Ψ Statistical Precision (III)

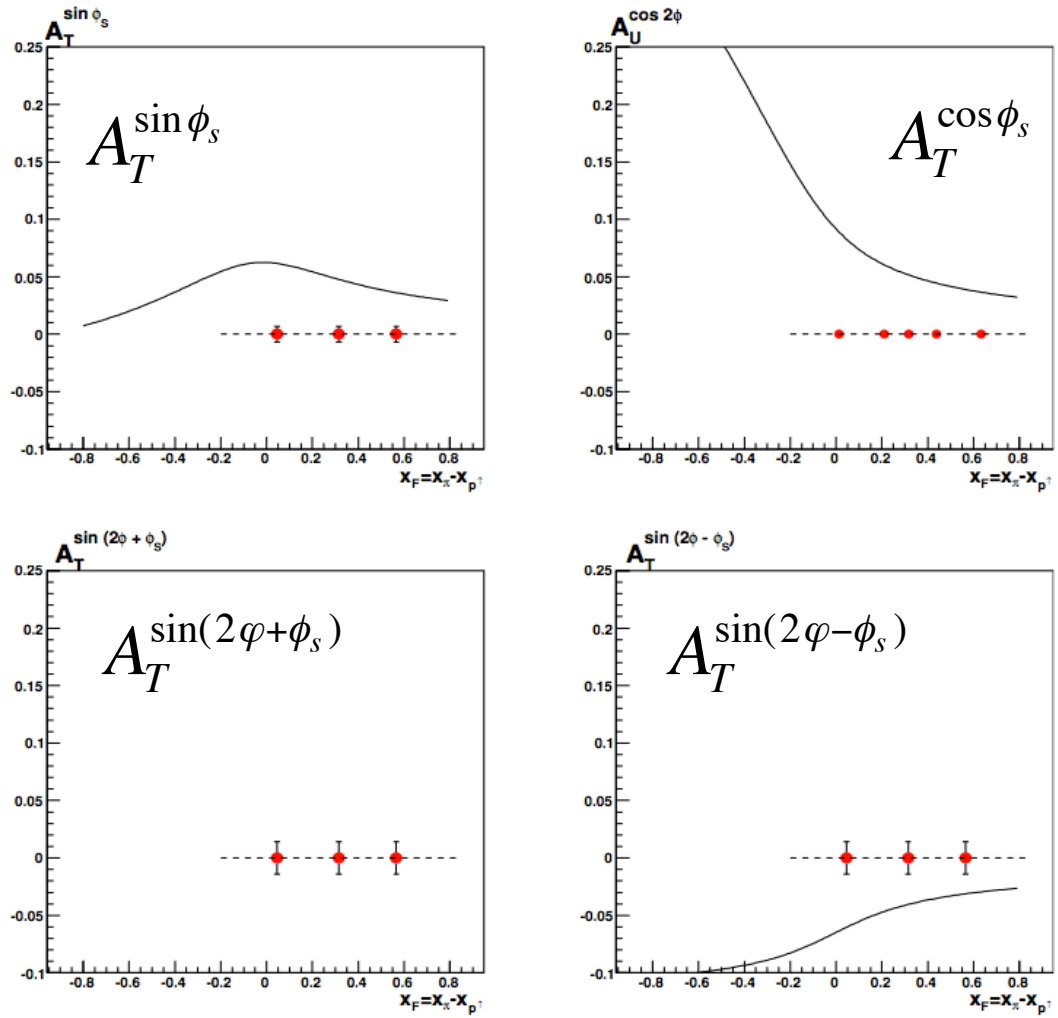

$2.9 < M_{\mu\mu} < 3.2$ GeV/c^2

Detector Upgrades

- COMPASS Polarised target:
  - New target holder (2x55 cm, 20 cm gap)
  - Old/modified Micro-Wave cavity (2 cells target)
  - PT Pump system refurbishing
- COMPASS PT has to be moved by ~2.2 meters upstream in order to release a space for the Hadron Absorber
- Hadron absorber (Alumina Al_2O_3) and beam plug (tungsten)
- Radio-Protection screen (stainless steel & borated polyeth.)
- New SciFi-based beam telescope
- H1 trigger hodoscope modification (central hole size adjustment)
- New vertex detector (SciFi based)
- New Large Area tracking station in the LAS

COMPASS Running until 2016

2014-2016

Tentative schedule

2012	Primakoff	18 weeks
	GPDs	6 weeks
2014	Drell-Yan	
2015	GPDs	
2016	GPDs	

End of 2013 – short DY test very desirable

2013 Long shut down necessary for PT mouvement and installation

→ Agreed upon

Summary

- Sivers asymmetry have been measured in SIDIS at COMPASS and at HERMES.
- COMPASS II will test expected sign change of Sivers and Boer-Mulders PDFs in DY
- Feasibility of Drell-Yan measurement was demonstrated with 2009 test beam
- Expected statistical precision of asymmetry measurement is 1~2%
- The pion induced transverse polarized Drell-Yan measurement will start in 2014

backup

NH_3 + Thin Nuclei Targets

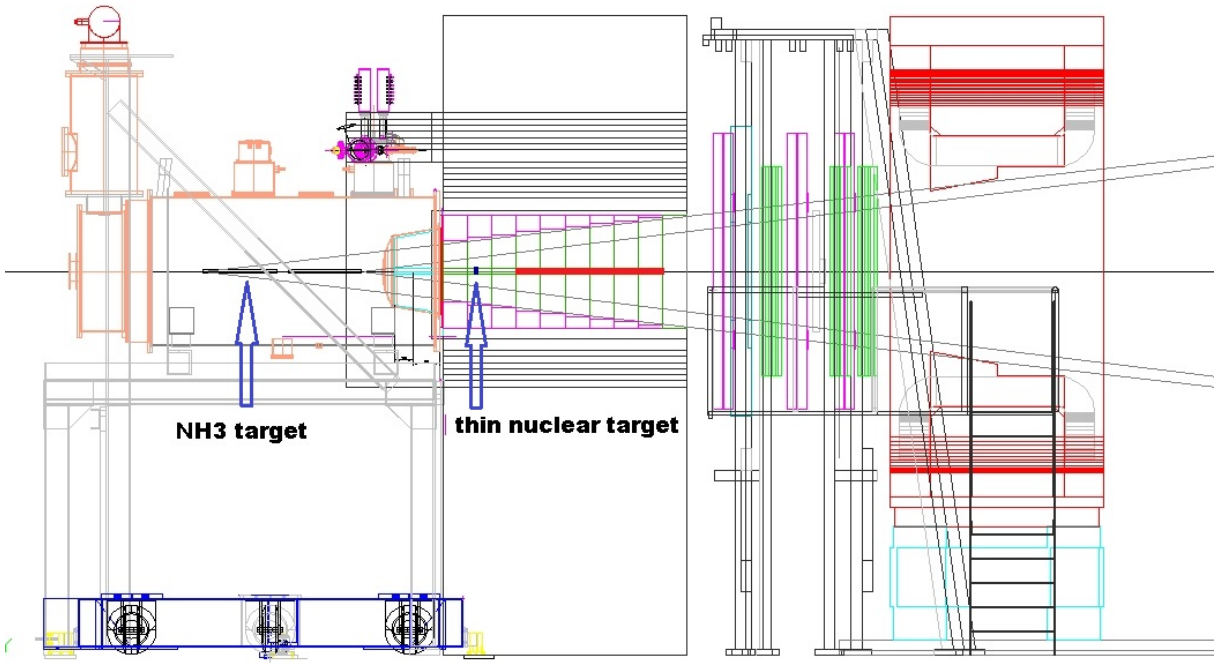

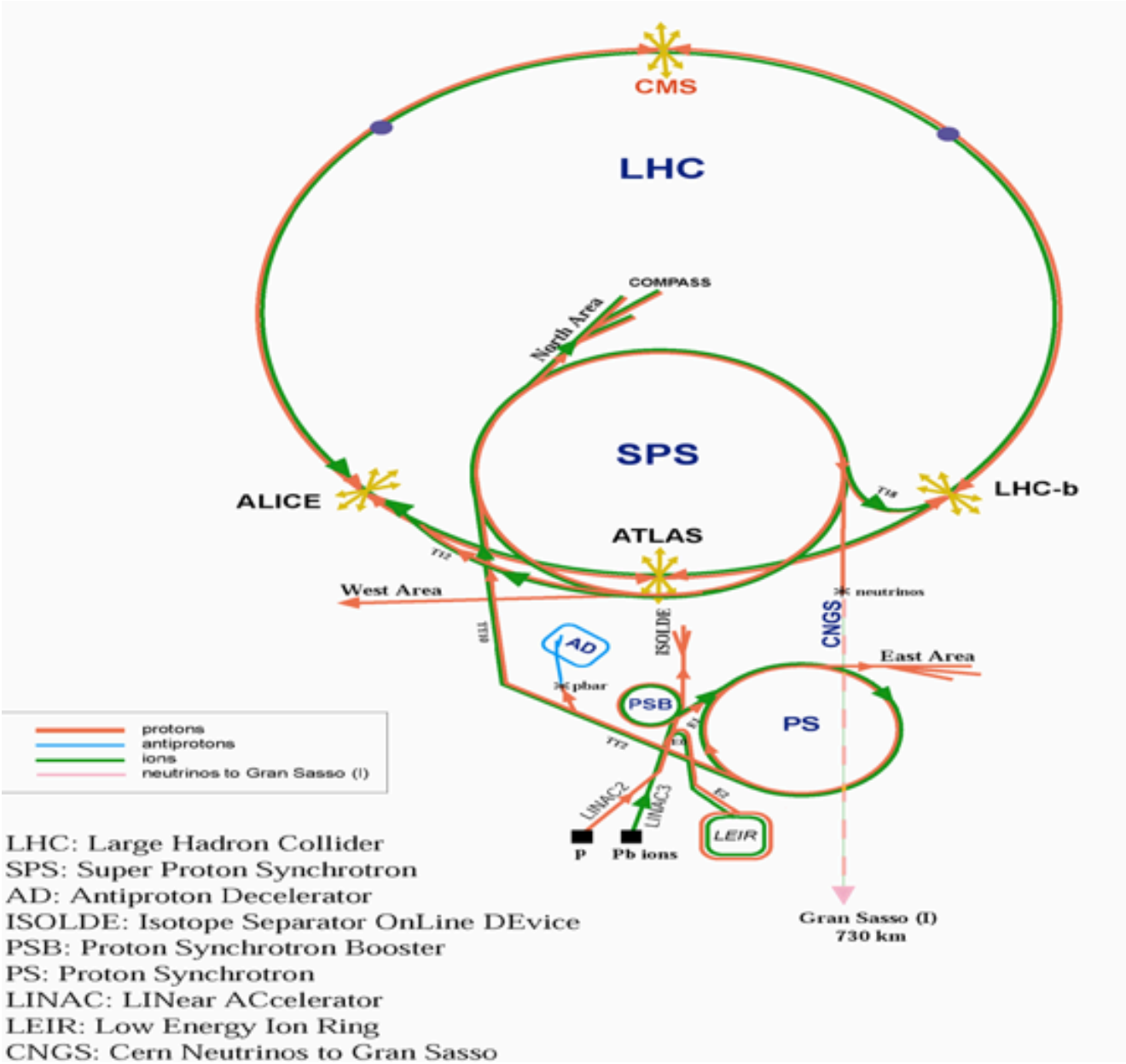
CMS
LHC
COMPASS
North Area
SPS
ALICE
LHC-b
ATLAS
West Area
neutrinos
CNGS
ISOLDE
AD
East Area
pbar
PSB
PS
protons
antiprotons
ions
neutrinos to Gran Sasso (I)
LINAC2
LINAC3
LEIR
P
Pb ions
Gran Sasso (I)
730 km
LHC: Large Hadron Collider
SPS: Super Proton Synchrotron
AD: Antiproton Decelerator
ISOLDE: Isotope Separator OnLine DEvice
PSB: Proton Synchrotron Booster
PS: Proton Synchrotron
LINAC: LINear ACcelerator
LEIR: Low Energy Ion Ring
CNGS: Cern Neutrinos to Gran Sasso

Forward Physics at the LHC

Workshop on Forward Physics at RHIC

RIKEN-BNL Res. Center, 31st July 2012

David d'Enterria

CERN

Overview

(0) Intro. Forward detectors at the LHC

(1) Elastic, inelastic & total x-sections.

(2) Diffractive scattering.

(3) Double Pomeron Exchange & central-exclusive.

(4) Photon-photon collisions.

(5) Low-x QCD.

(6) Beam remnants (UHE cosmic-rays).

LHC experiments: (p_T,η) acceptance

- Particle production at the LHC over $\Delta y = 2 \cdot y_{beam} = 2 \cdot \ln(\sqrt{s})/m_p \sim 20$ units

p-p @ 14 TeV

Particle flow

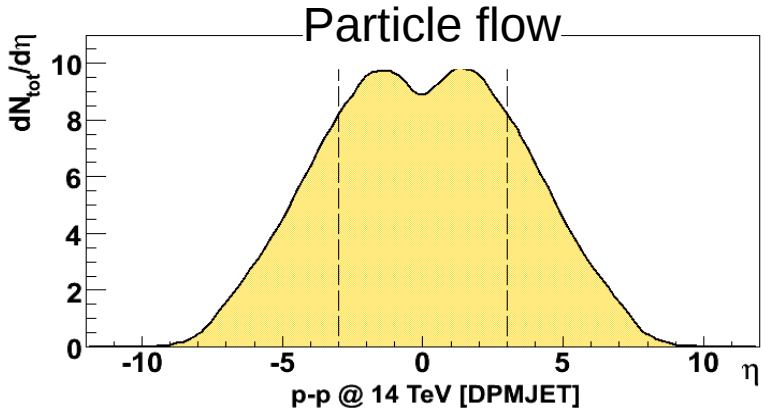

Energy flow

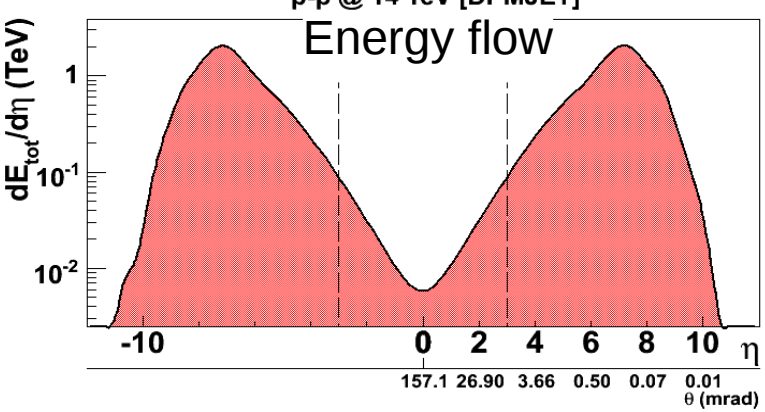

DdE, arXiv:0708.0551

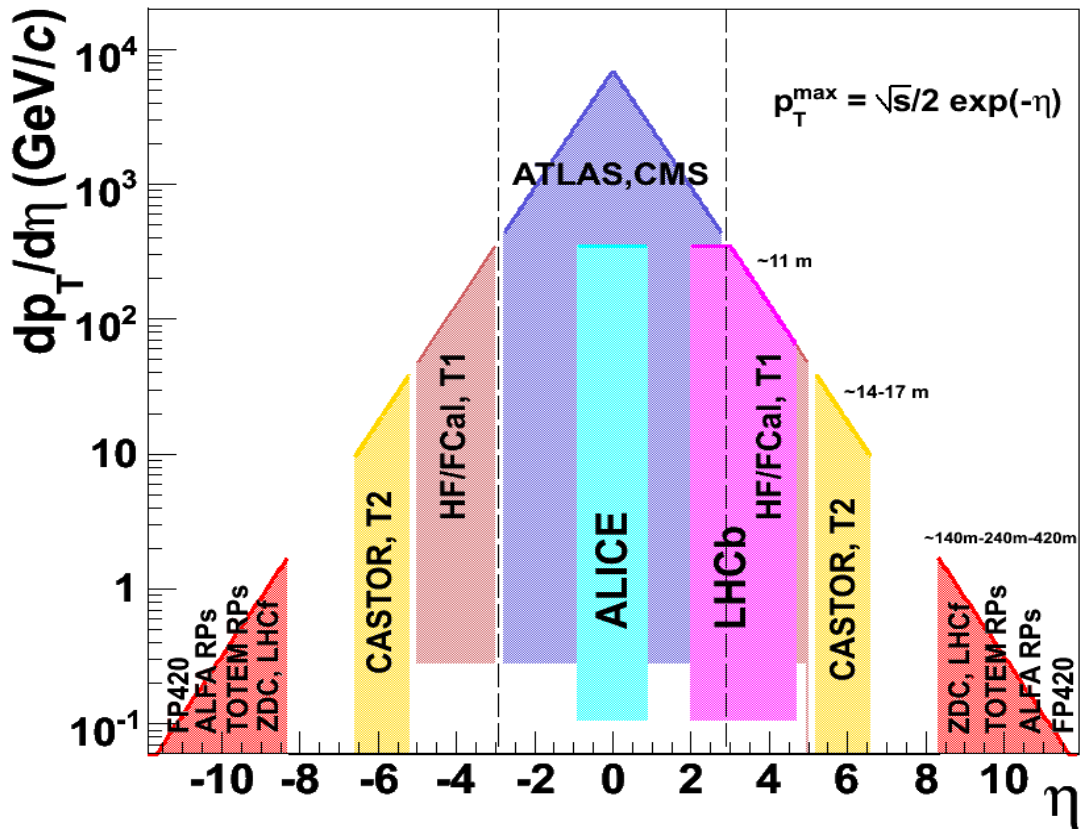

- Most of phase-space covered (1st time in a collider)

LHC experiments: Forward

- Convention (arbitrary): Forward ≡ |η|>3

p-p @ 14 TeV

Particle flow

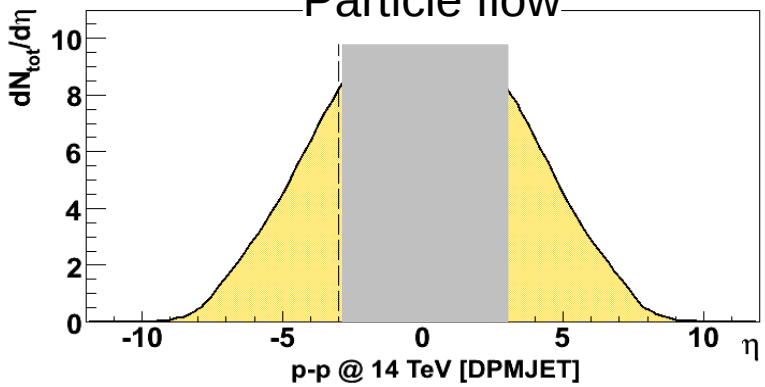

Energy flow

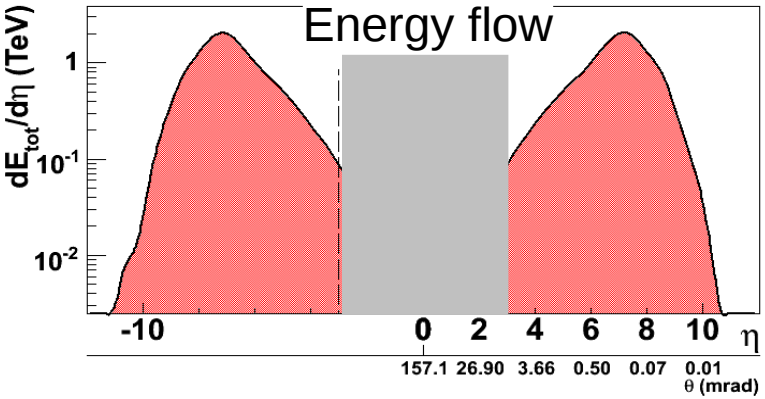

DdE, arXiv:0708.0551

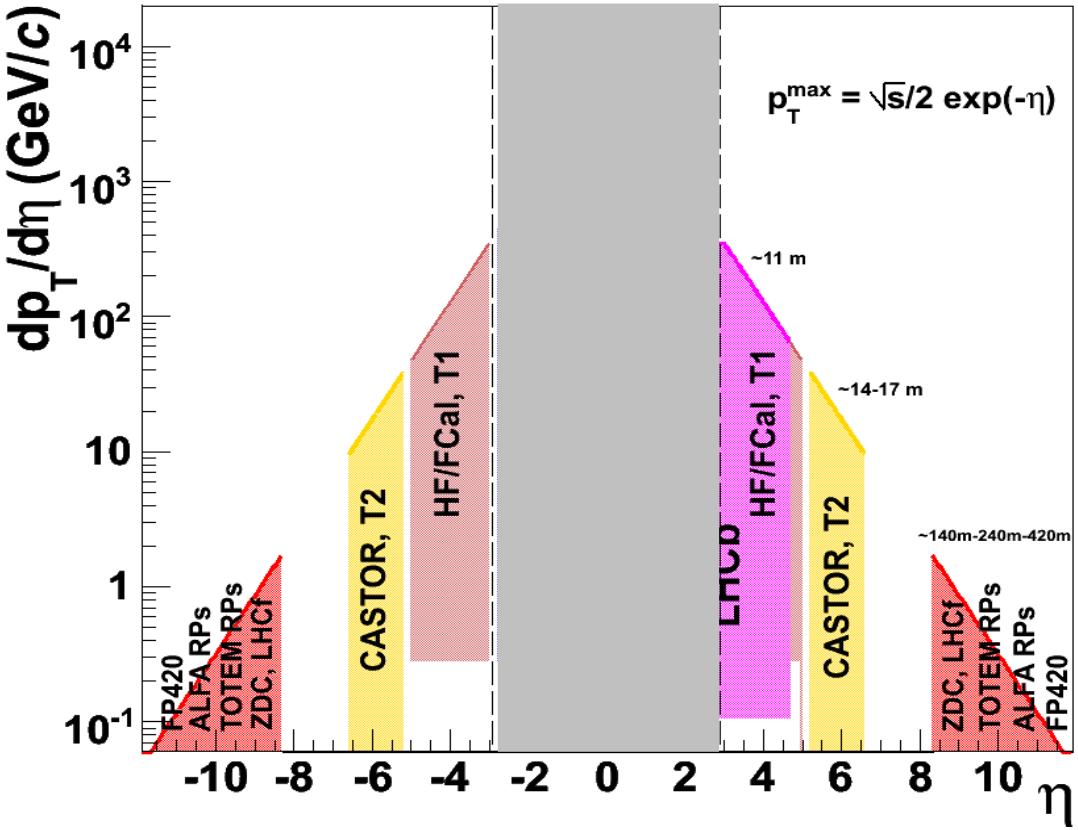

- Disclaimer: Results shown today are for proton-proton at 7 TeV (few forward Pb-Pb results expected for QM'12)

Forward physics: why ?

- Many interesting (mostly color-singlet exchange) scattering processes at the LHC are characterized by forward particle production:

QCD:

Elastic & diffractive:

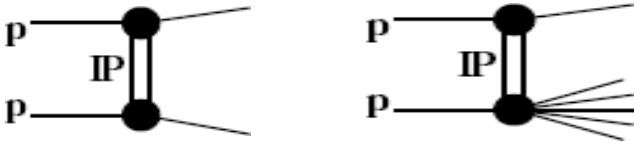

Double-pomeron, central exclusive:

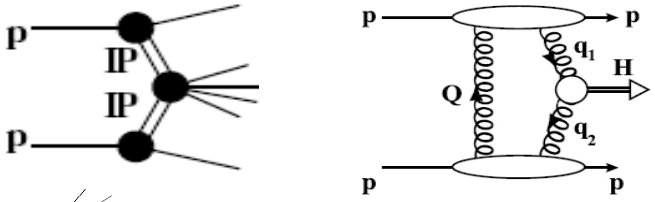

Low-x QCD:

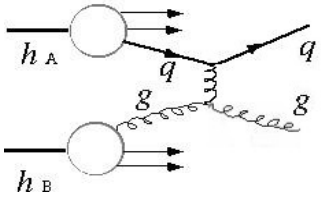

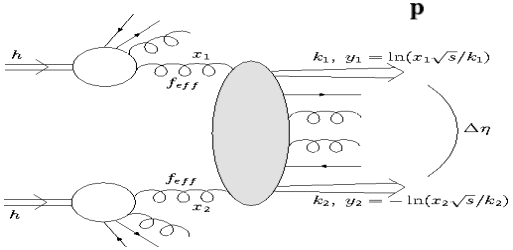

Electro-weak

two-photon, photon-hadron:

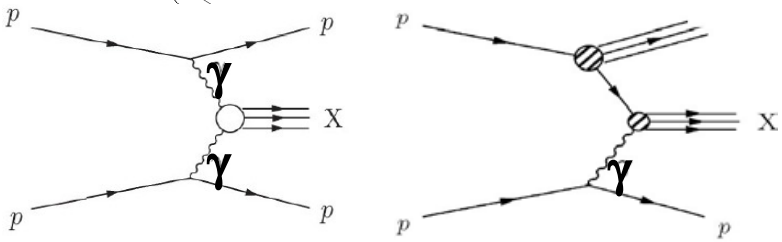

Vector-Boson-Fusion:

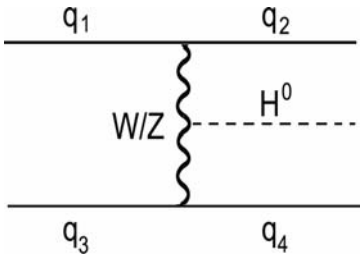

Forward LHC detectors: where ?

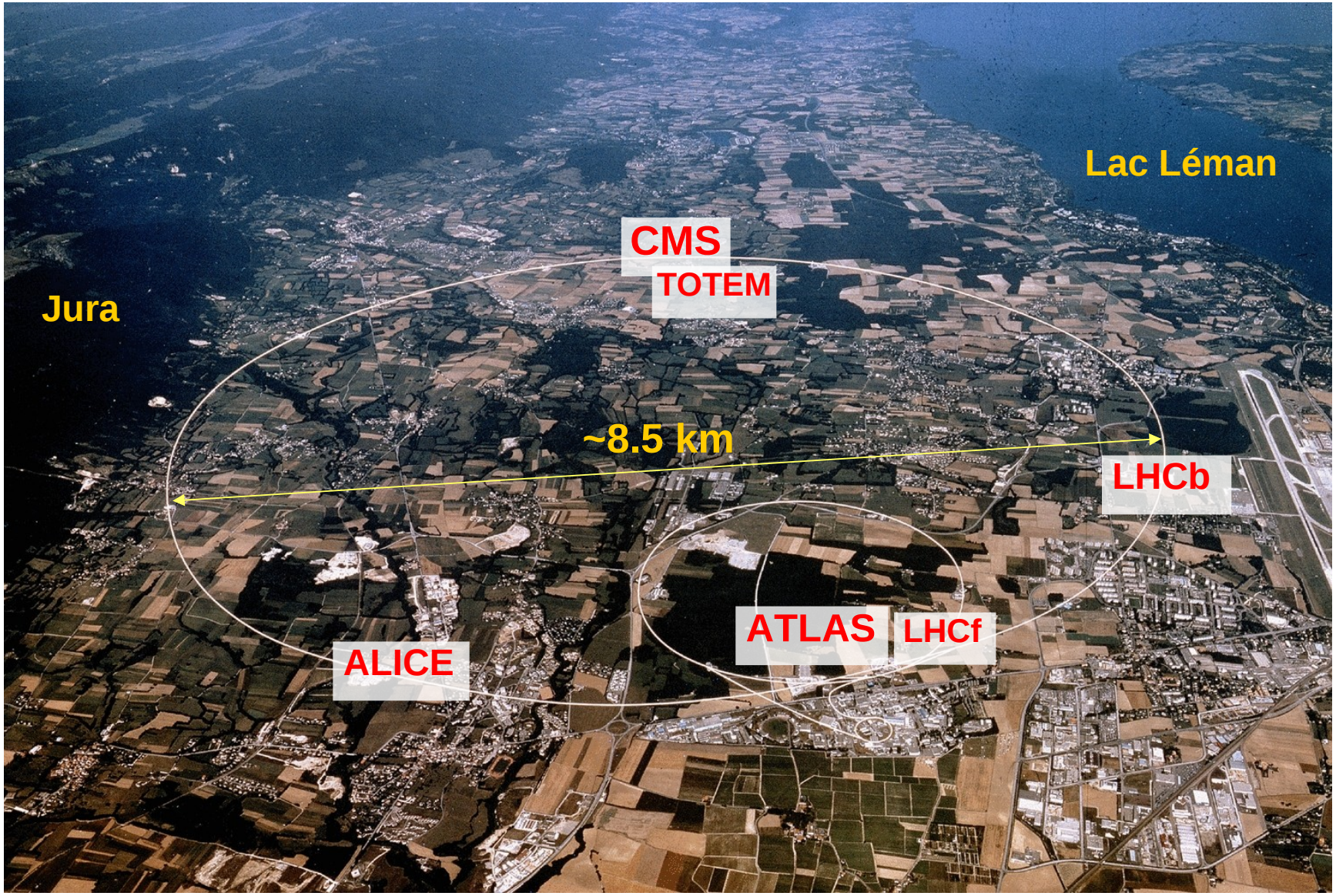

Forward detectors: Atlas & CMS

- Near-beam detectors beyond $|\eta| = \ln \tan(\theta/2) > 3$

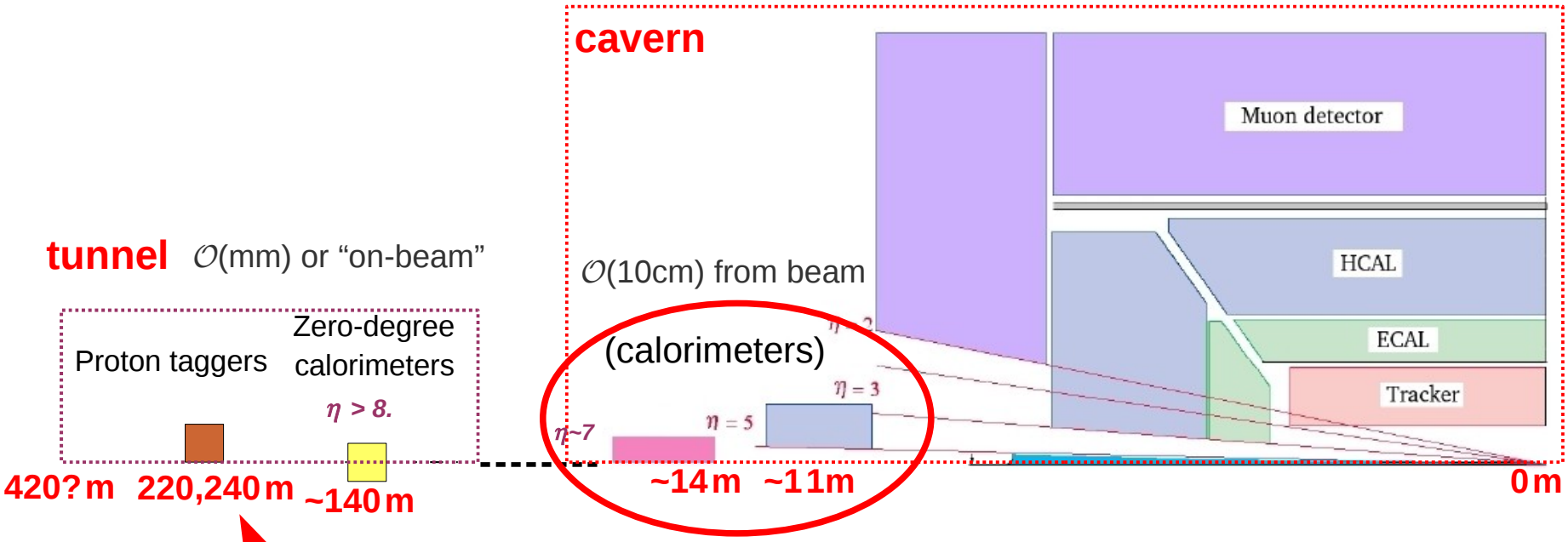

1) p,n tagging devices

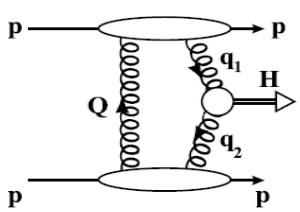

2) Direct particle measurements: fwd. jets, ...

3) Hadron "vetoing" devices: rapidity gaps

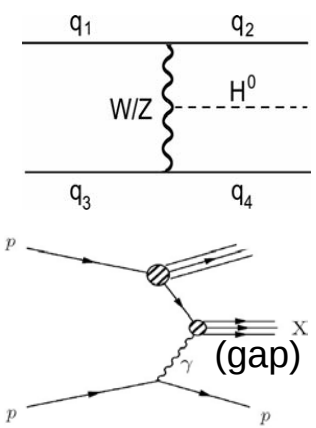

Forward detectors: LHCb & ALICE

- Full LHCb ! Single-arm fwd detector optimized for heavy-flavor reco:

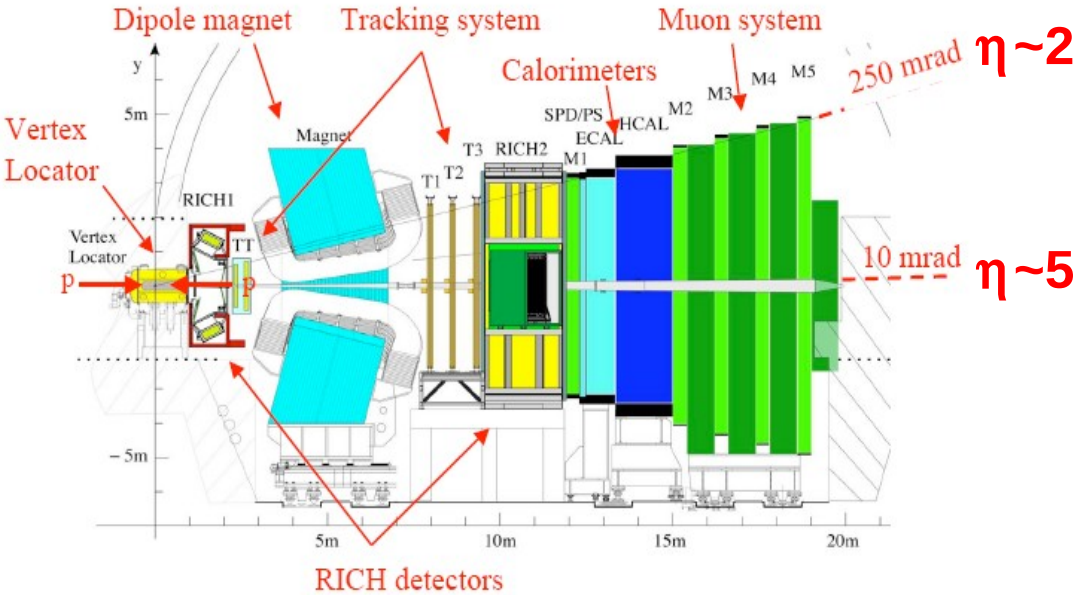

- Particle ID (e, γ, muons, hadron ID), secondary vertexing, ...

- Although so far only few QCD analyses available ...

- Forward muon spectrometer:

  $2.5 < \eta < 4$

  ZDCs also at ±7m,±100m

  $4.8 < |\eta| < 5.7$

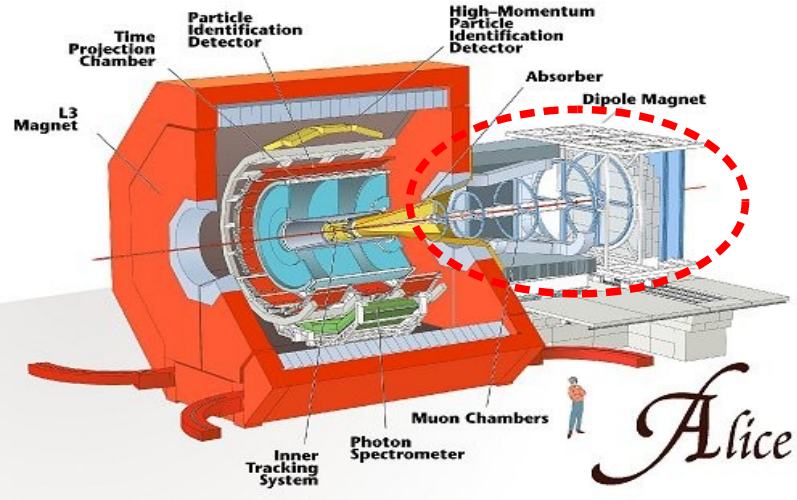

Forward detectors: TOTEM & LHCf

- TOTEM and LHCf: dedicated very-forward experiments

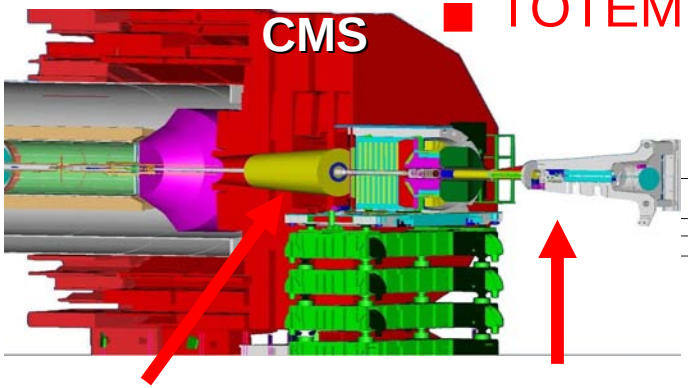

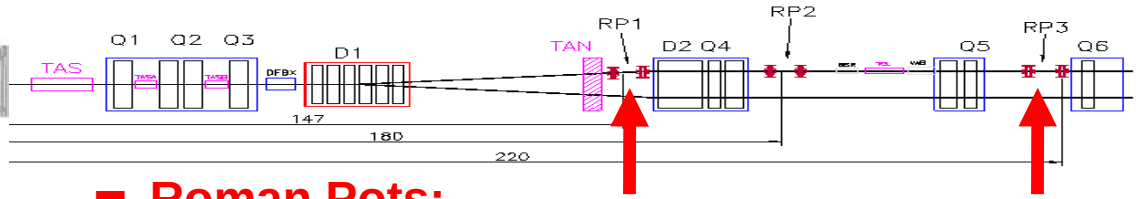

- **Roman Pots:** RPs@147m RPs@220m

- **T1,T2** (±10m,±13m in CMS IP):

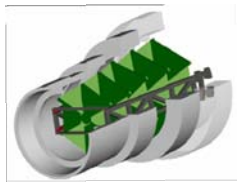

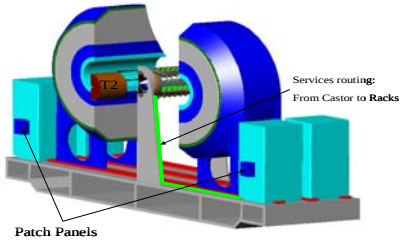

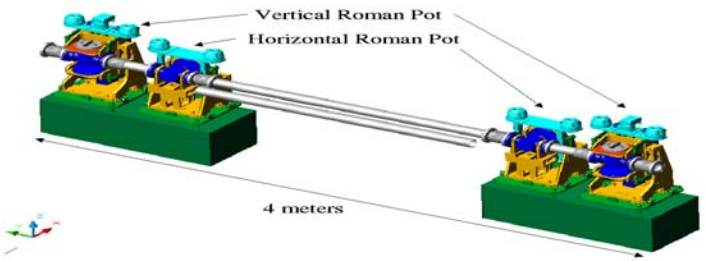

- **LHCf** (±140m in ATLAS tunnel):

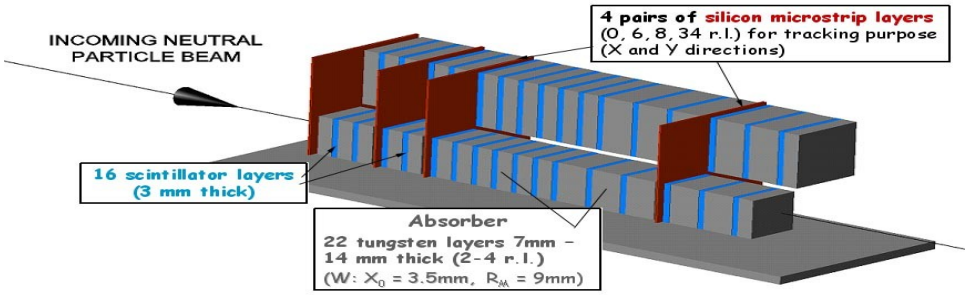

Elastic, inelastic & total cross sections

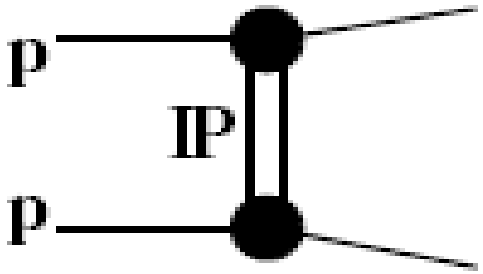

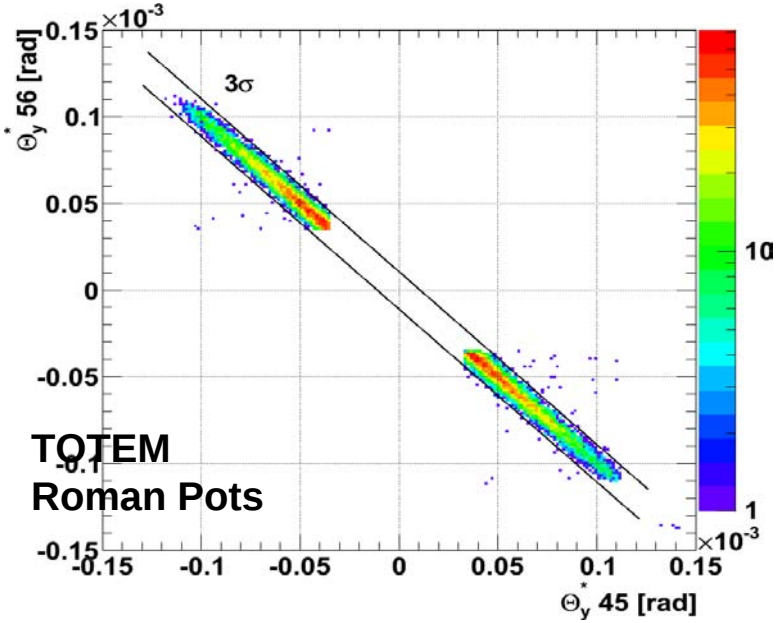

p-p collisions at the LHC

- Hadrons are extended composite objects: Even at asymptotically large c.m. energies, ~40% of hadronic interactions are not "point-like":

pQCD

(1) Perturbative parton-parton collisions

~60%

Regge-Gribov

(2) Diffractive, elastic

~40%

- 1 or 2 protons "intact" + 1 or 2 rapidity gaps:
- No colour flux.
- Colourless exchange with vacuum $J^{PC}=0^{++}$ quantum-numbers: |Pomeron = 2-gluons in colour-singlet state.

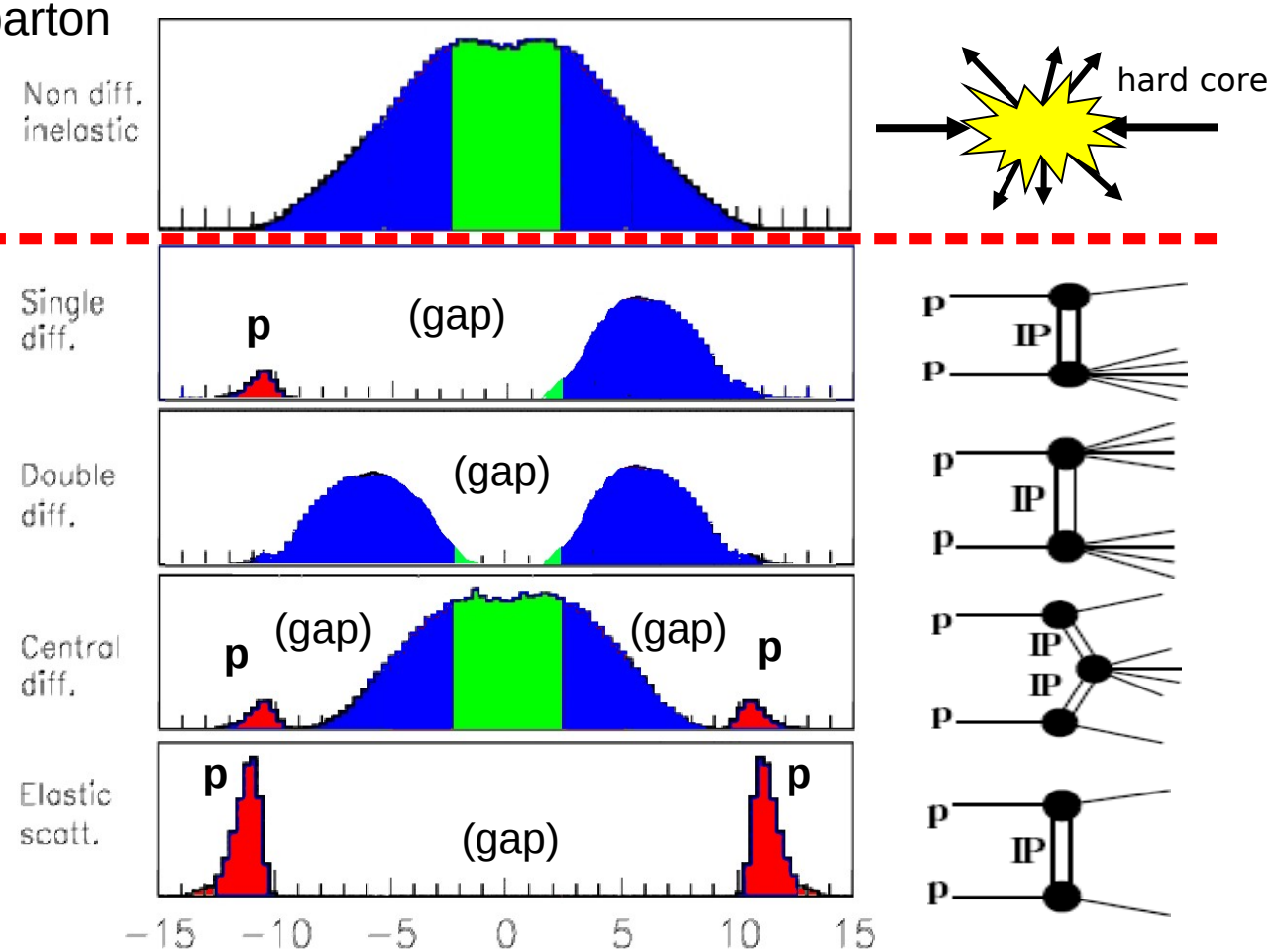

- pQCD (~60 mb) + elastic (~25 mb) + diffractive (~15mb) ~ 100 mb at the LHC.

Total & elastic p-p cross sections

- Non-computable from QCD Lagrangian (maybe lattice ?), but constrained by fundamental QM relations: Froisart bound, optical theorem, dispersion relations.

- LHC p-p x-section predictions:

σ_{tot}(LHC) = 90-120 mb $^{+10}_{-20}$ %.

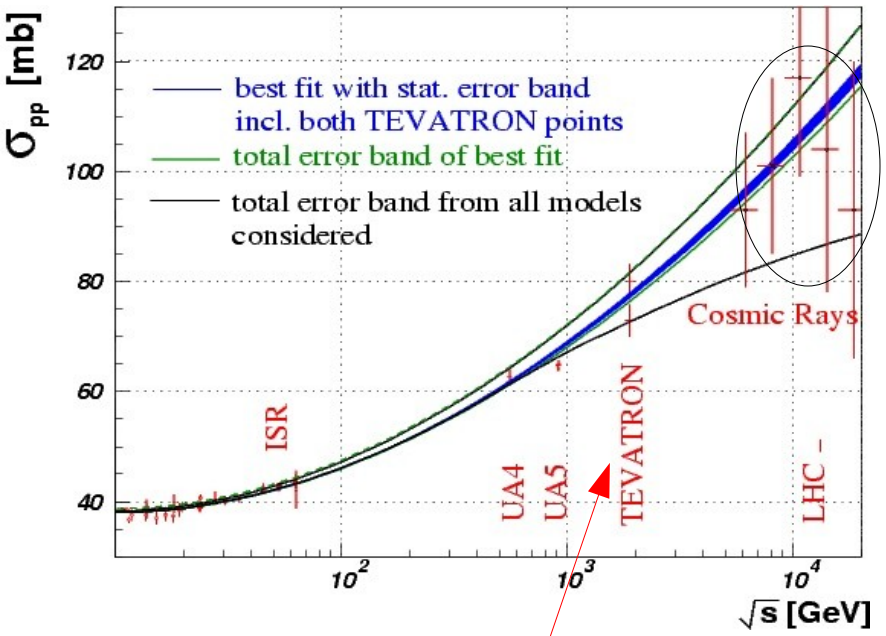

- Pre-LHC model uncertainties driven by E710–CDF 2.6σ disagreement

- Impact on cosmic-ray MCs: Uncertainties of $\sigma_{inel}(E_{lab}\sim10^{19}$ eV) change by factor of ~2 the air-shower maximum fluctuations:

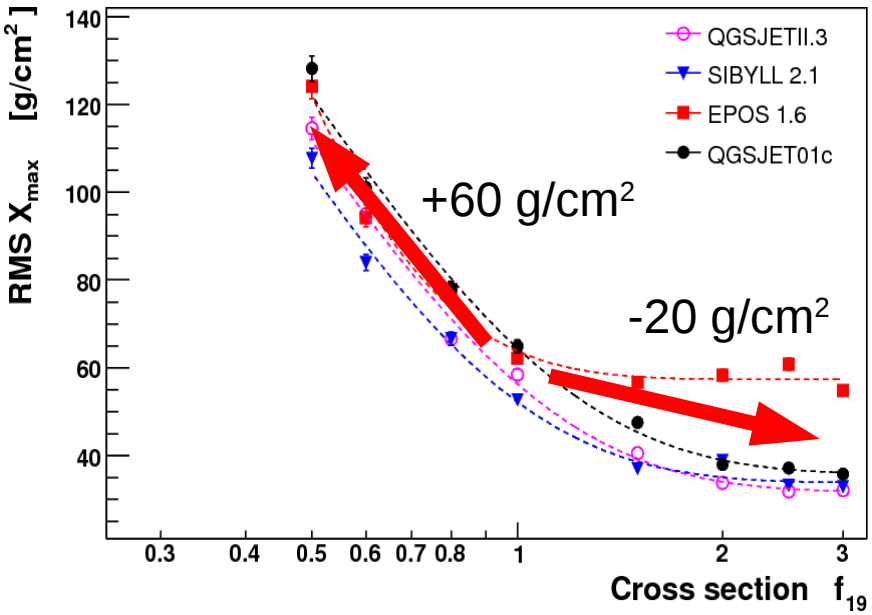

R.Ulrich, R.Engel,M.Unger, PRD83 (2011) 05426

Total & elastic cross sections (TOTEM)

- 3 methods used to measure total x-section:
  - (1) Measure $(dN/dt)_{t=0}$, Lumi (CMS) + ρ_{theor} (COMPETE), optical theorem:
  - (2) Measure N_{el}, N_{inel}, Lumi (TOTEM) :
  - (3) Measure $(dN/dt)_{t=0}$, N_{el}, N_{inel} :

$$\sigma_{TOT}^2 = \frac{16\pi(\hbar c)^2}{1+\rho^2} \cdot \left.\frac{d\sigma_{EL}}{dt}\right|_{t=0}$$

$$\sigma_{tot} = \sigma_{el} + \sigma_{inel}$$

$$\sigma_{tot} = \frac{16\pi}{(1+\rho^2)} \frac{(dN_{el}/dt)_{t=0}}{(N_{el}+N_{inel})}$$

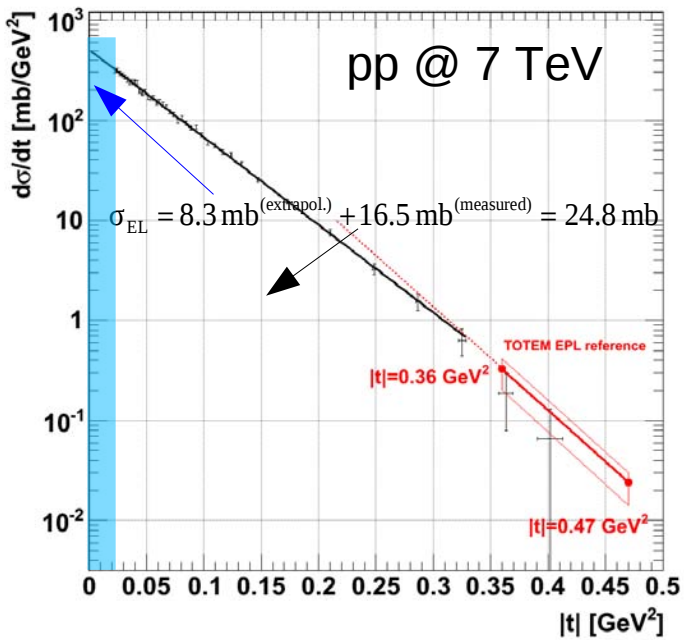

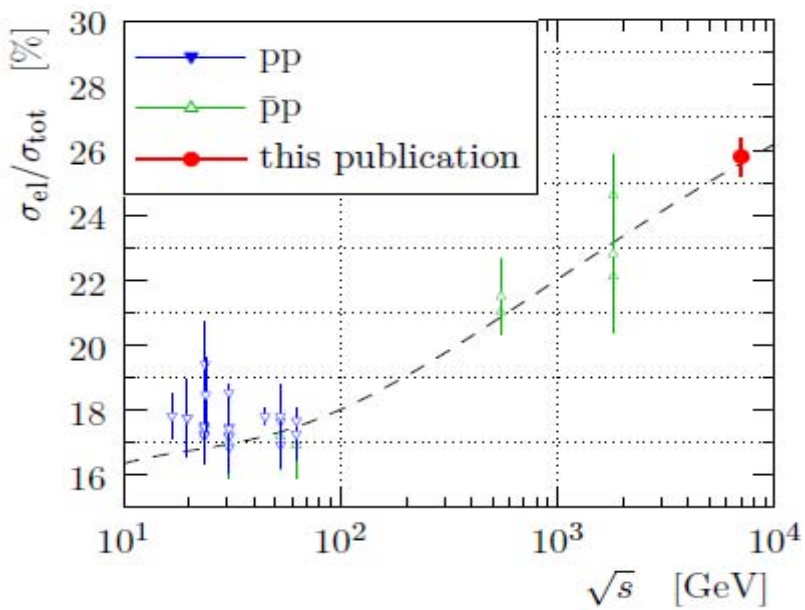

- All methods yield: σ_{tot} ~ 98 mb, σ_{el} ~ 25 mb at 7 TeV. Increase of σ_{el}/σ_{tot}

Differential elastic scattering (TOTEM)

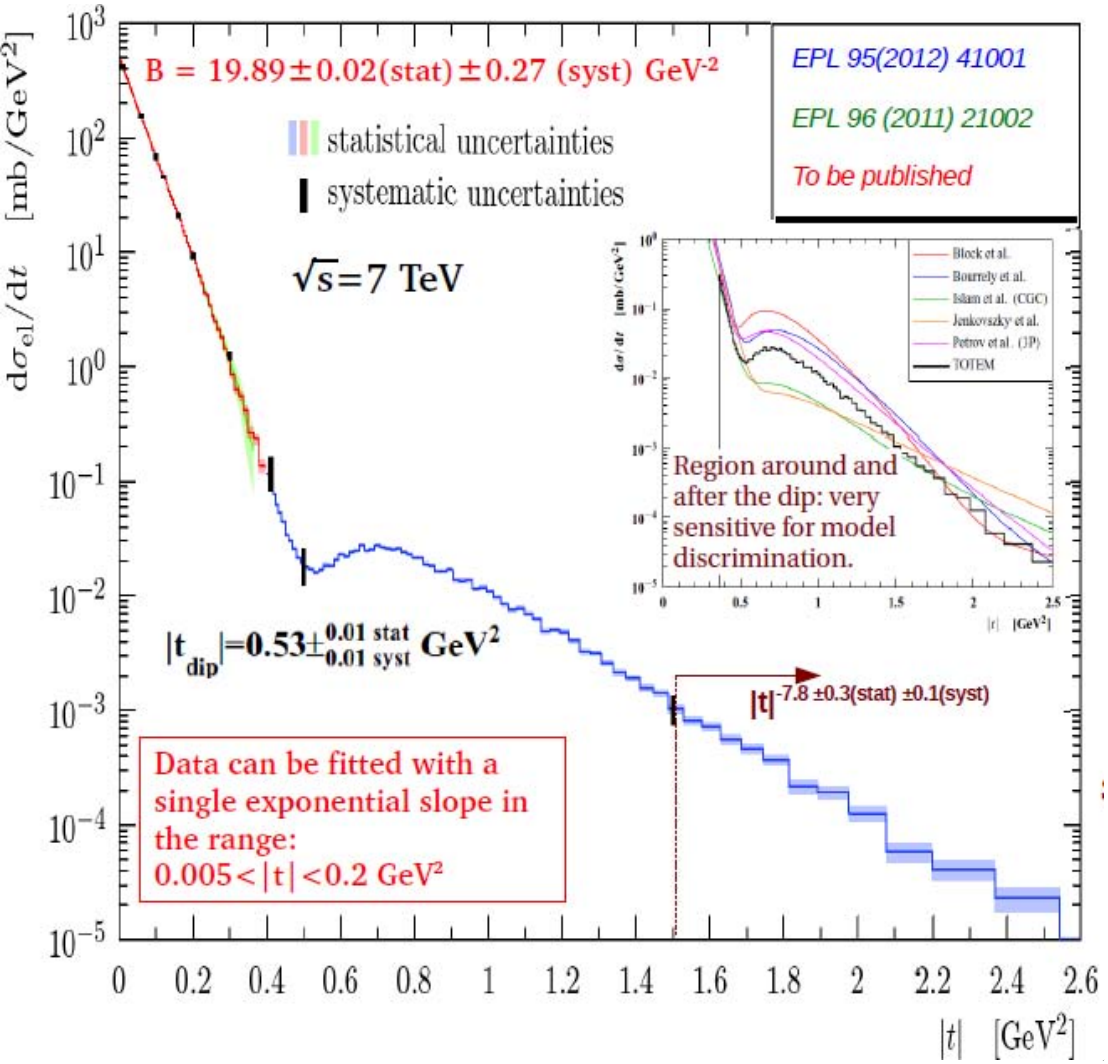

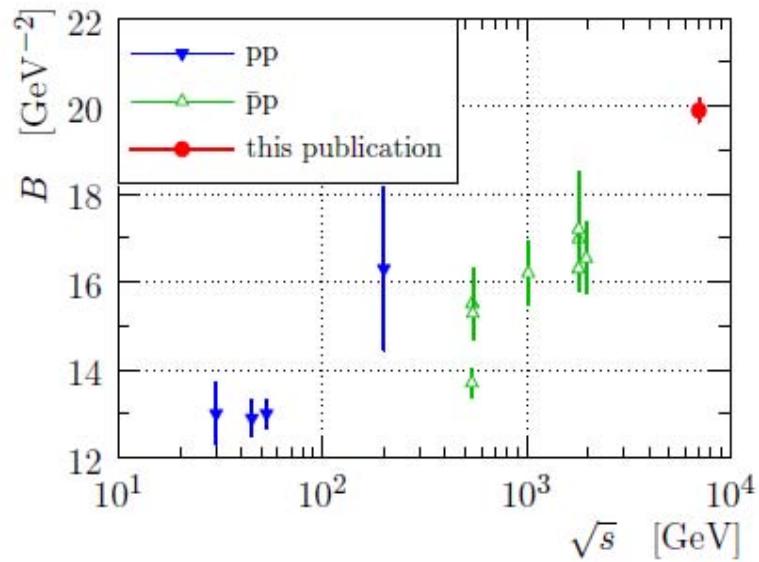

- TOTEM has confirmed :
  - Decrease of inverse expo slope
  - Shrinkage of diffraction peak
  - Decrease of dip t-position
- But so far only partial quantitative agreement with model predictions.

p-p inelastic x-sections (Atlas, CMS, TOTEM)

- Visible inel. x-section $\sigma_{ATLAS,CMS}$~ 60 mb mostly overestimated by MCs:

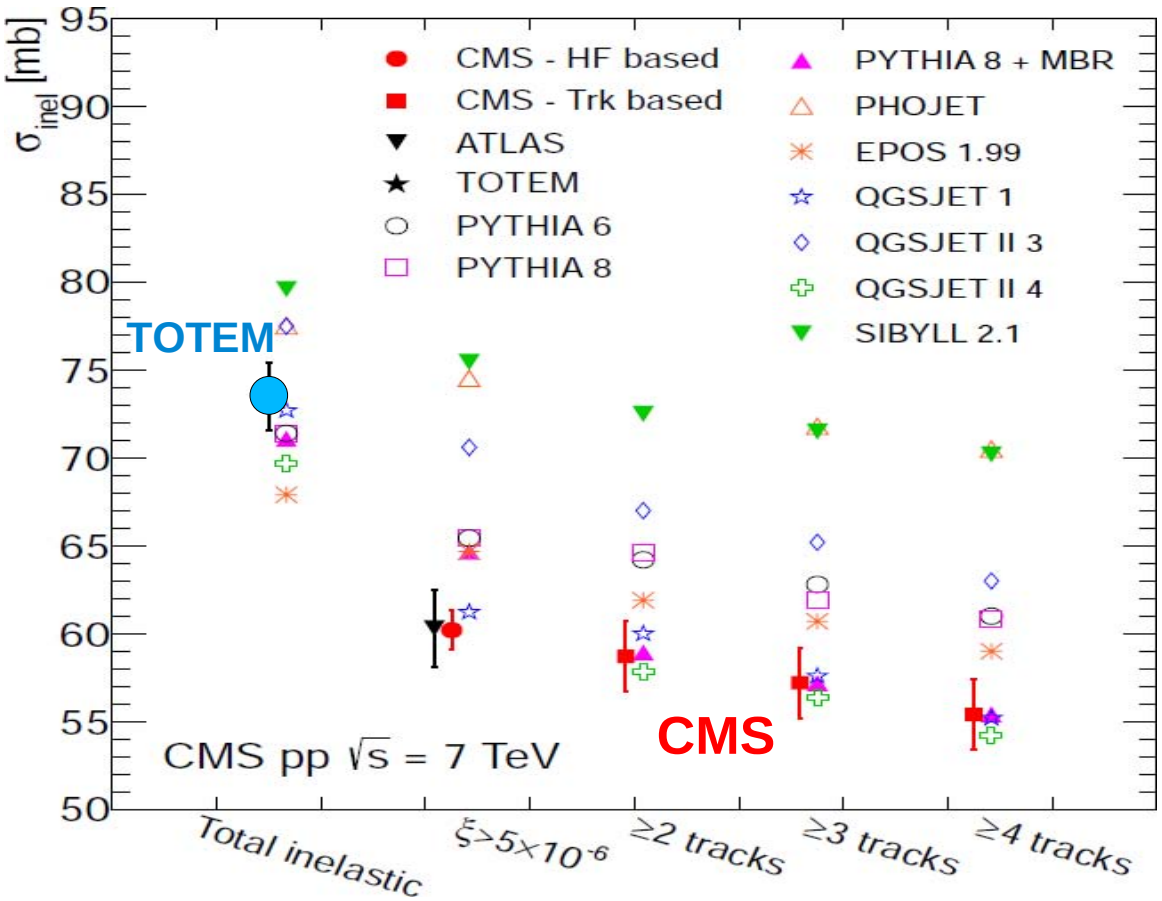

CMS 7-TeV preliminary
PAS-FWD-11-001

- Most models over-/under-estimate high-/low-mass diffraction.
- Increasingly unbiased evt. selection best reproduced by QGSJET01,-II-4

p-p total/elastic/inel. x-sections (TOTEM)

- TOTEM σ_{tot}~ 98 mb falls right on top of COMPETE fit prediction (which goes in between E710–CDF at 1.8 TeV ...)

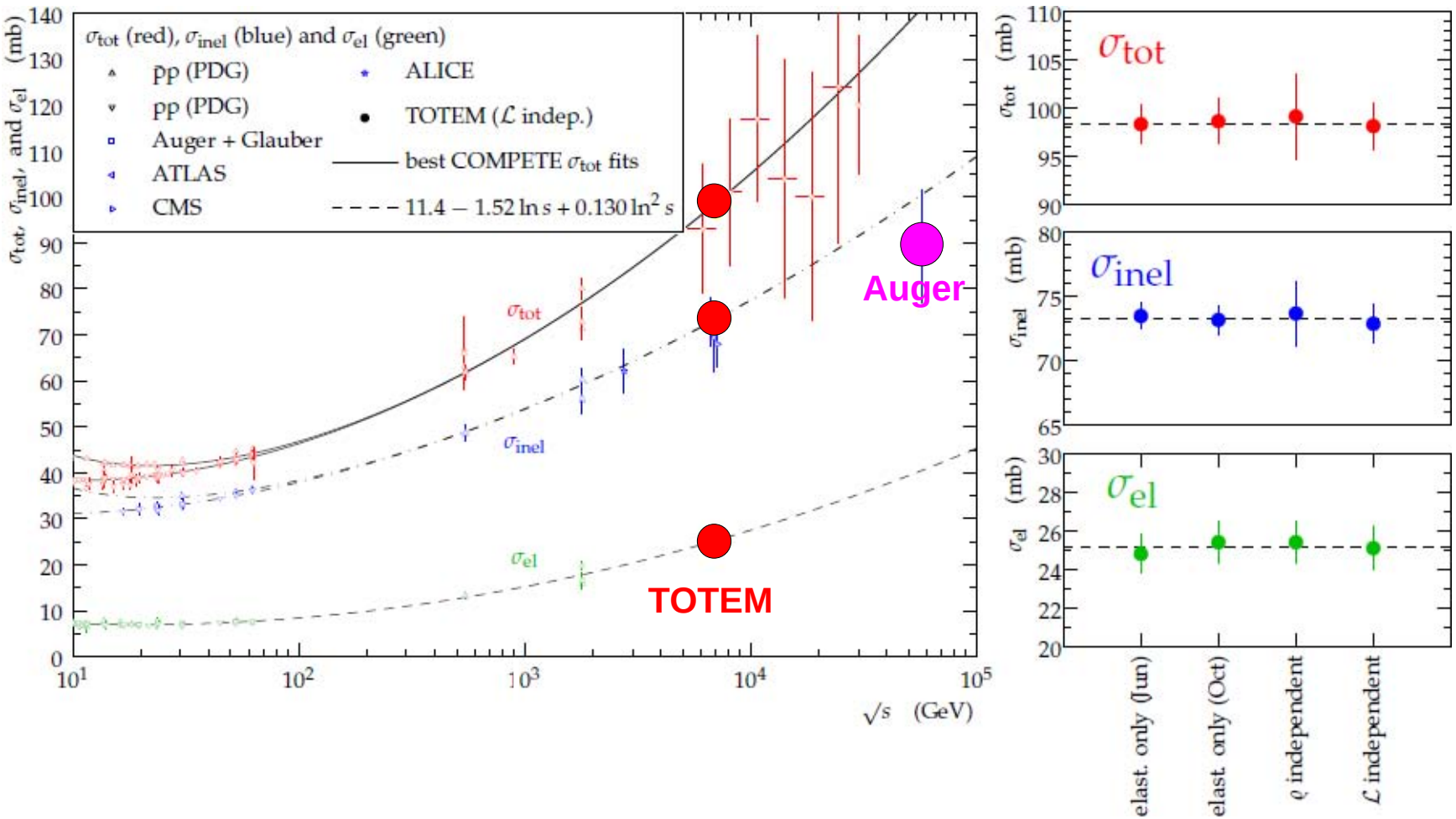

Diffractive scattering

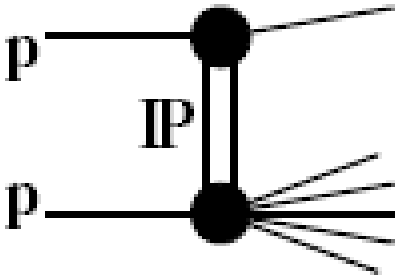

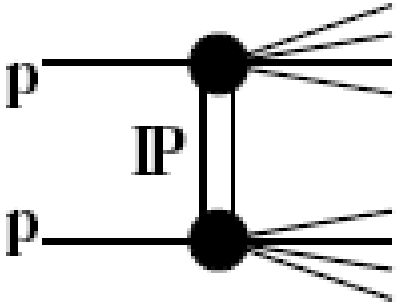

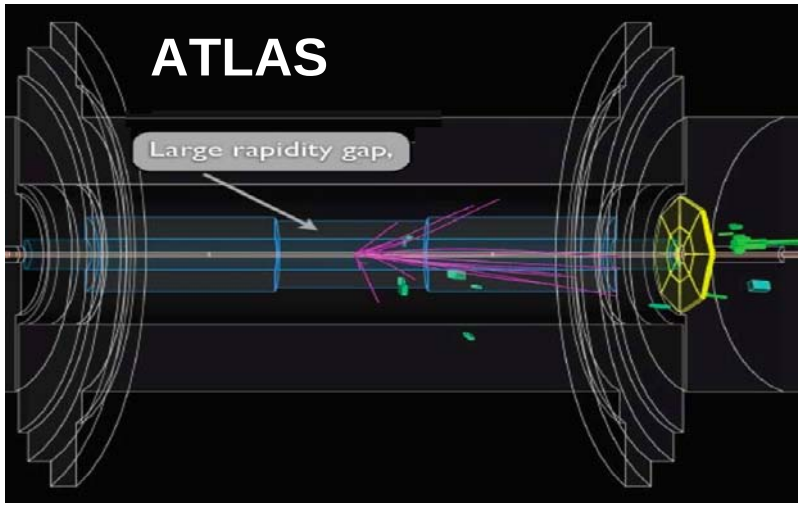

Soft diffraction (ATLAS)

- Inclusive diffractive x-section measurement:

Ratios of single/double-side triggers

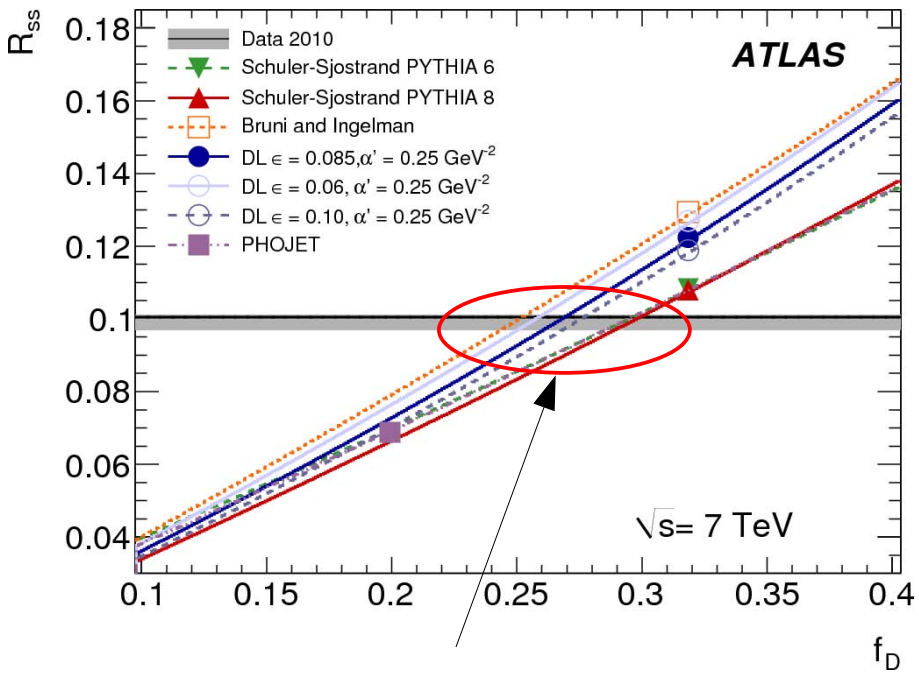

R_{SS} =10.0±0.4% → f_D~25-30%

σ_{diff}~17-21 mb depending on models

- x-section vs. rap-gap:

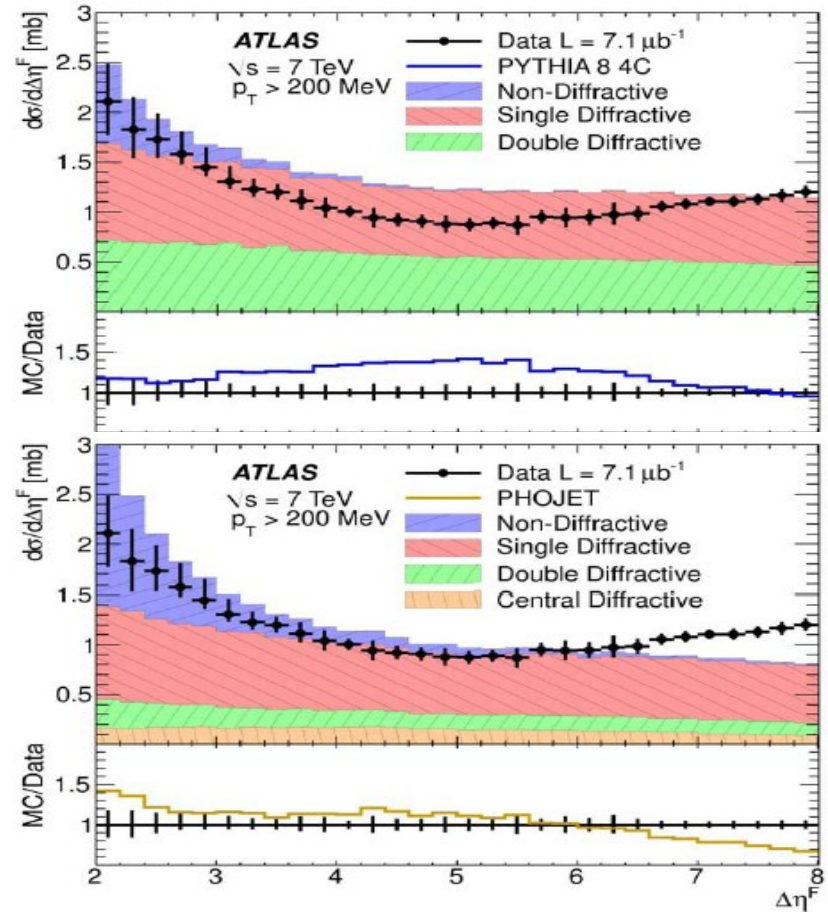

- PHOJET better at large $\Delta\eta_F$ (flat contribution from diffraction)
- PYTHIA (no DPE) better at smaller $\Delta\eta_F$

Non-diffraction dominant (expo decrease)

Hard diffraction

- Hard diffraction calculable using QCD factorization theorem:

$$\sigma_{\text{hard-diffractive}} = \text{dPDF} \otimes \sigma_{\text{parton-parton}} \otimes S_{\text{gap-survival}}$$

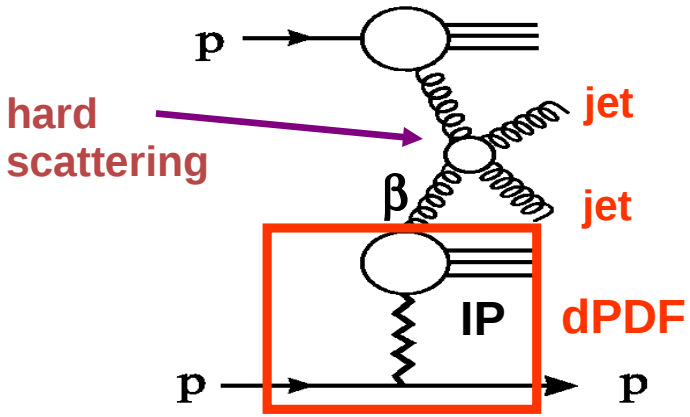

Diffractive PDFs: probability to find a parton of given *x* under condition that proton stays intact (measured at HERA).

- Gap survival S: probability to fill rapidity gap with hadrons from extra rescatterings

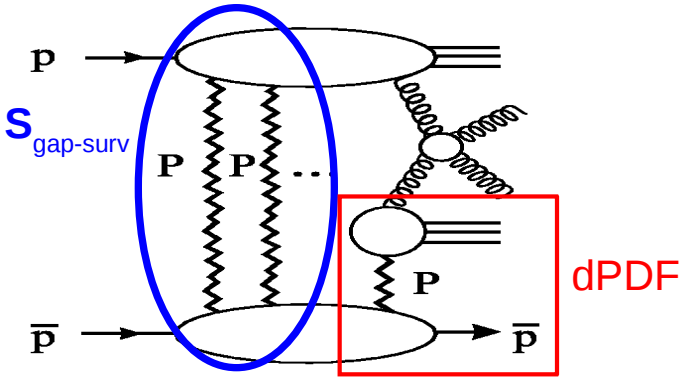

$p\bar{p} \to p\ jj\ X$

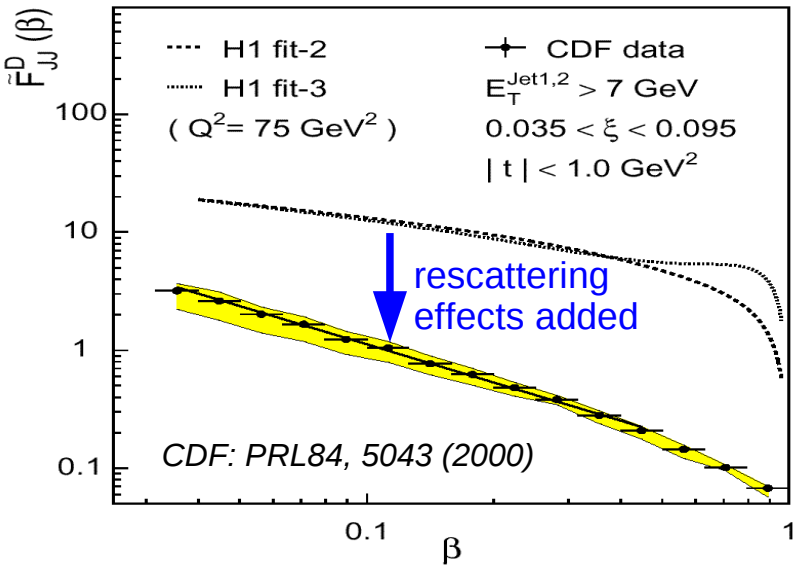

$S_{\text{gap-surv.}}$~10% at Tevatron

Diffractive dijets (CMS)

CMS-FWD-10-004

- Observation of diffractive dijet production:

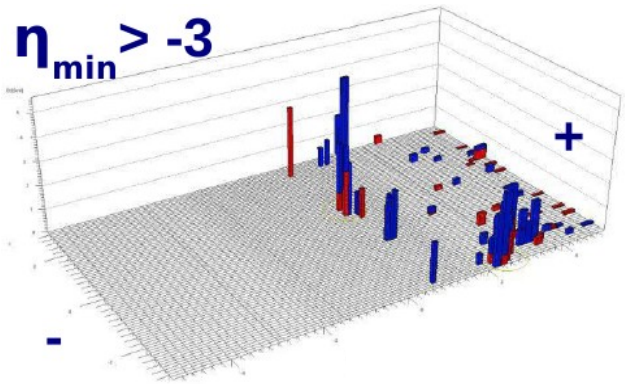

2 jets (anti-k_T, R=0.5) with p_T>20 GeV and |η|<4.4

Dijet distribution binned as a function of:

$$\tilde{\xi}^{\pm} = \frac{\sum (E^i \pm p_z^i)}{\sqrt{s}} \simeq \frac{M_X^2}{s}$$

= proton fractional momentum loss in SD events

ξ reconstructed from all other particles in event.

- Low-ξ region predominantly diffractive:

$$\frac{d\sigma_{jj}}{d\tilde{\xi}} = \frac{N_{jj}^i}{L \cdot \epsilon \cdot A^i \cdot \Delta\tilde{\xi}^i}$$

- Excess of events in low-ξ region wrt. non-diffractive MCs.
- Diffractive MCs x5 above data in lowest-ξ bin interpreted in terms of rap-gap survival probability:
  S=0.12±0.05 (LO), 0.08 ±0.04 (NLO).

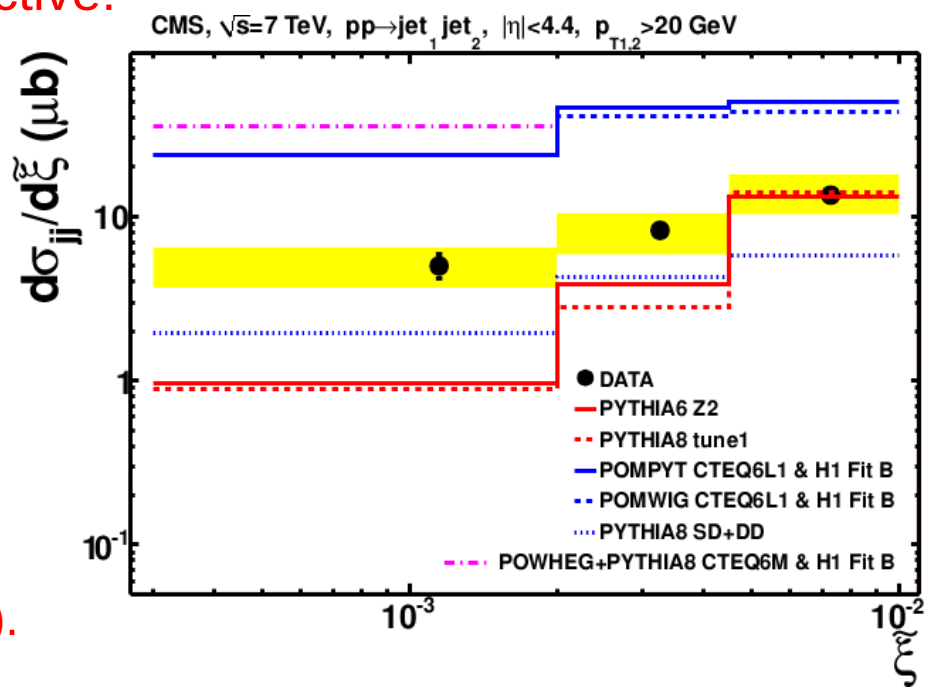

Double-pomeron & central-exclusive

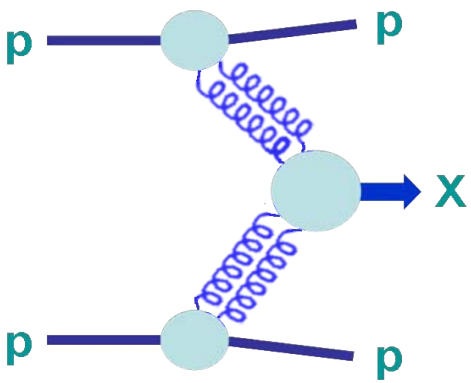

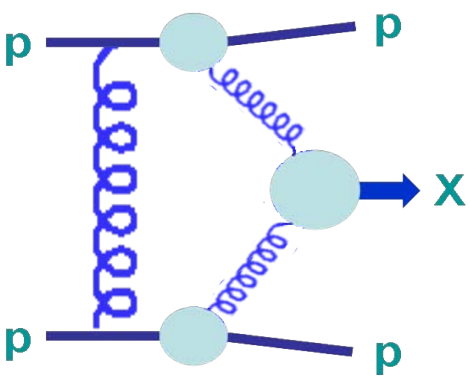

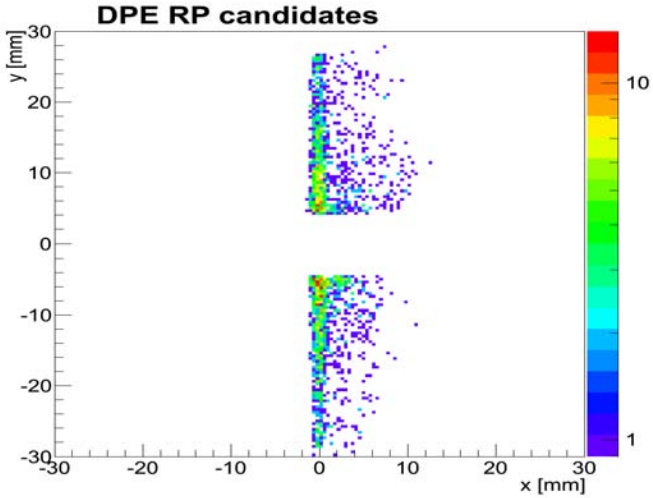

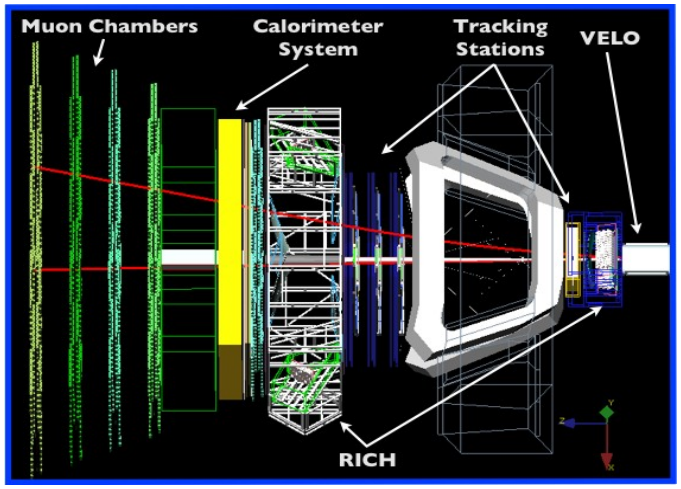

Double pomeron exchange (TOTEM, ALICE)

- First attempts at measuring the inclusive DPE x-section:

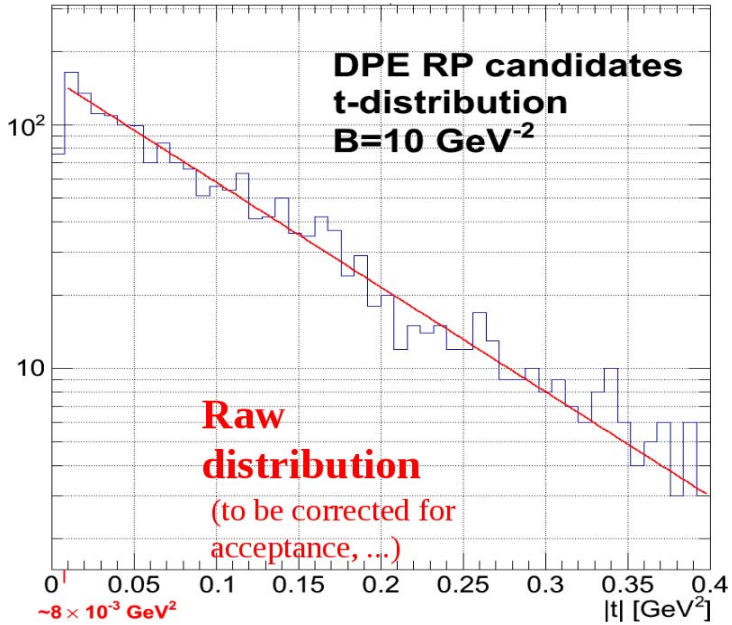

- Enhanced $f_0(980)$ & $f_2(1270)$ production in double-gap events ($\Delta\eta_{gaps}$ = 3, 4):

$J^{PC} = (0,2)^{++}$

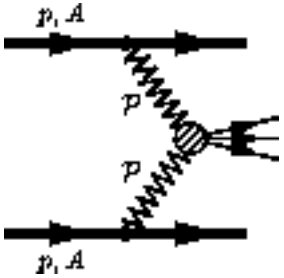

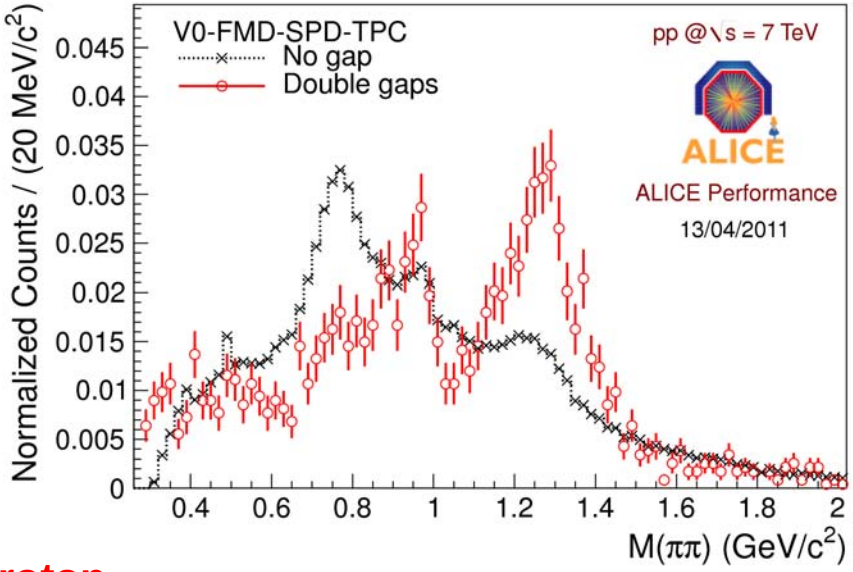

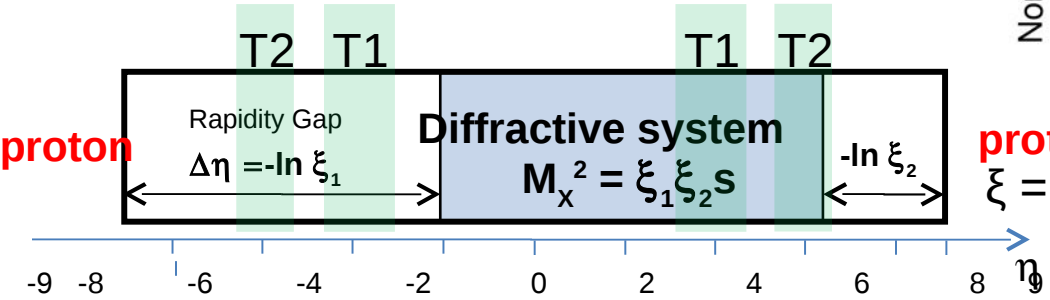

$\xi = \Delta p/p$

Central exclusive production (LHCb, CMS)

CMS PAS-FWD-11-004

- Exclusive χ_c production:

LHCb-CONF-2011-022

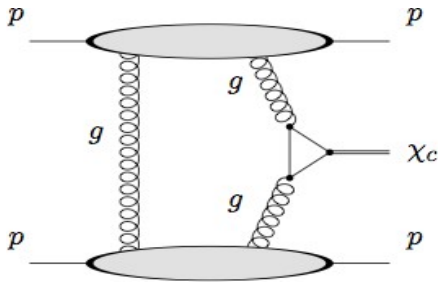

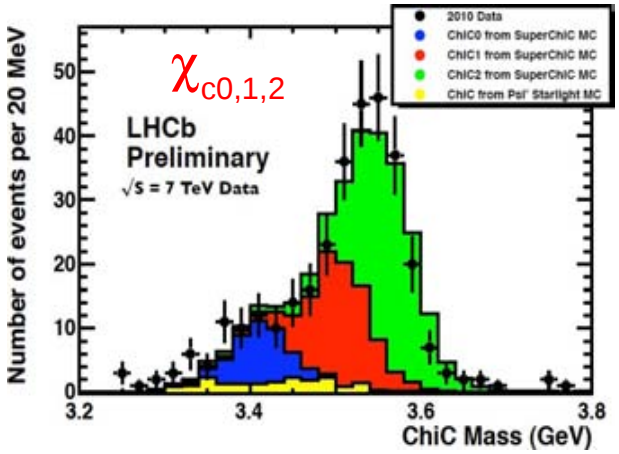

$\chi_c \to J/\Psi\ \gamma$ + nothing else in event

	$\sigma(pp \to pp(J/\psi + \gamma))$ LHCb (pb)	SuperCHIC prediction (pb)
χ_{c0}	9.3 ± 4.5	14
χ_{c1}	16.4 ± 7.1	10
χ_{c2}	28 ± 12.3	3

- Exclusive $\gamma\gamma$ production:

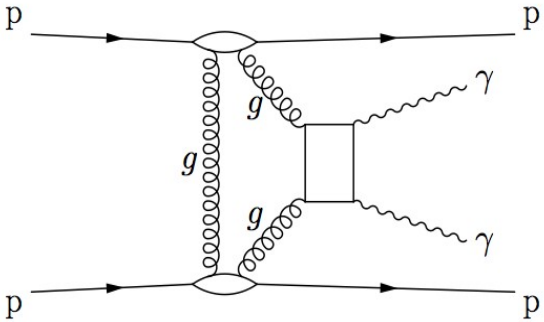

Just 2 EM showers (nothing else to $|\eta| = 5.2$)

No $\gamma\gamma$ candidates found.

Upper limit x-section:

$$\sigma^{E_T(\gamma)>5.5\,\mathrm{GeV},\,|\eta(\gamma)|<2.5}_{\text{exclusive }\gamma\gamma\text{ production}} < 1.30\ \mathrm{pb}$$

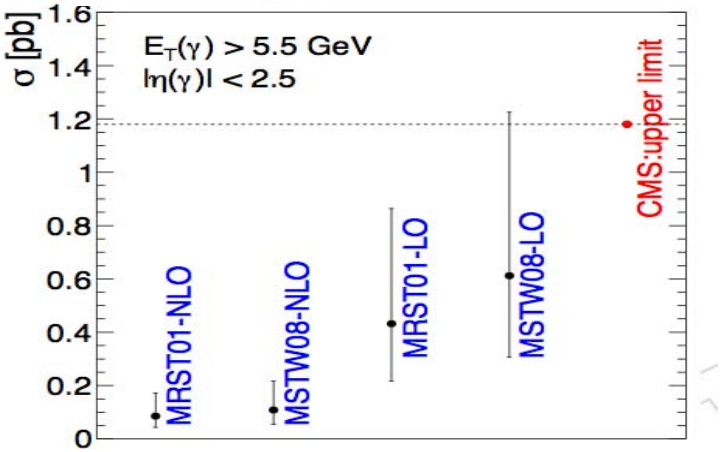

☞ Important constraints for gap-survival probability for CEP Higgs.

Photon-photon collisions

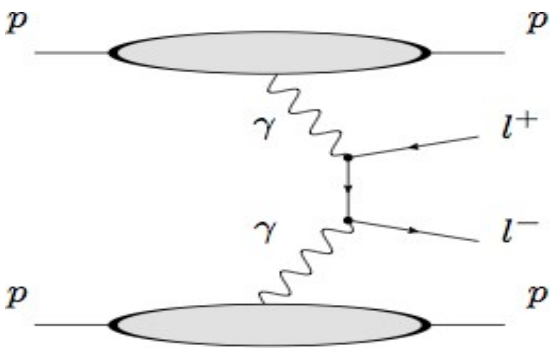

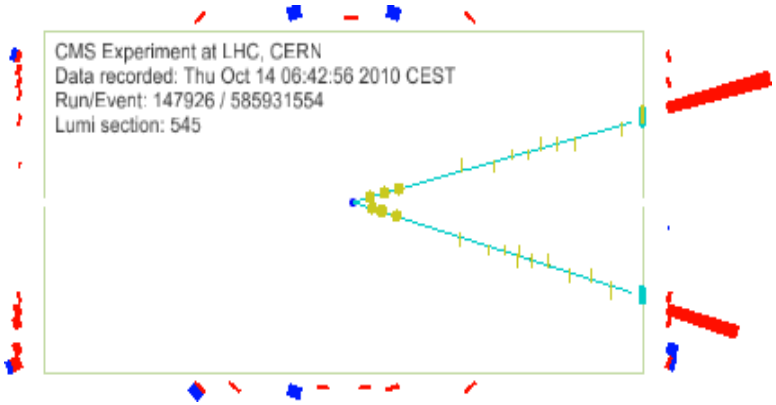

Exclusive γ-γ dimuon production (CMS)

JHEP 01 (2012) 052

- Exclusive dimuons observed in $m_{\mu\mu}$ ~ 11 – 80 GeV (above Υ):

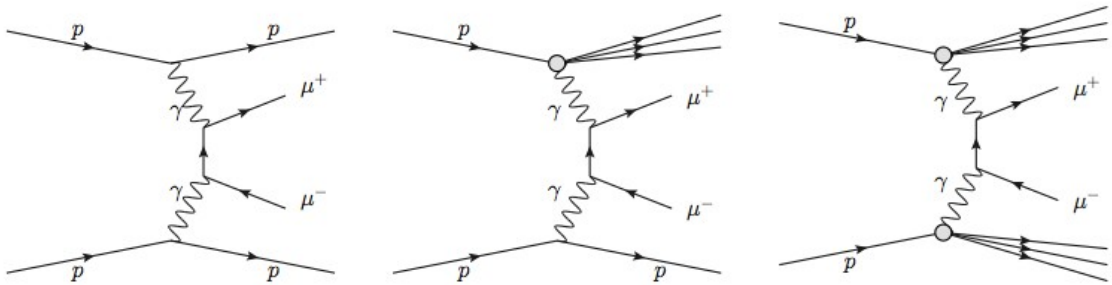

Just 2 muons,
E_T > 5.5 GeV, |η| < 2.1,
nothing else to |η| = 5.2

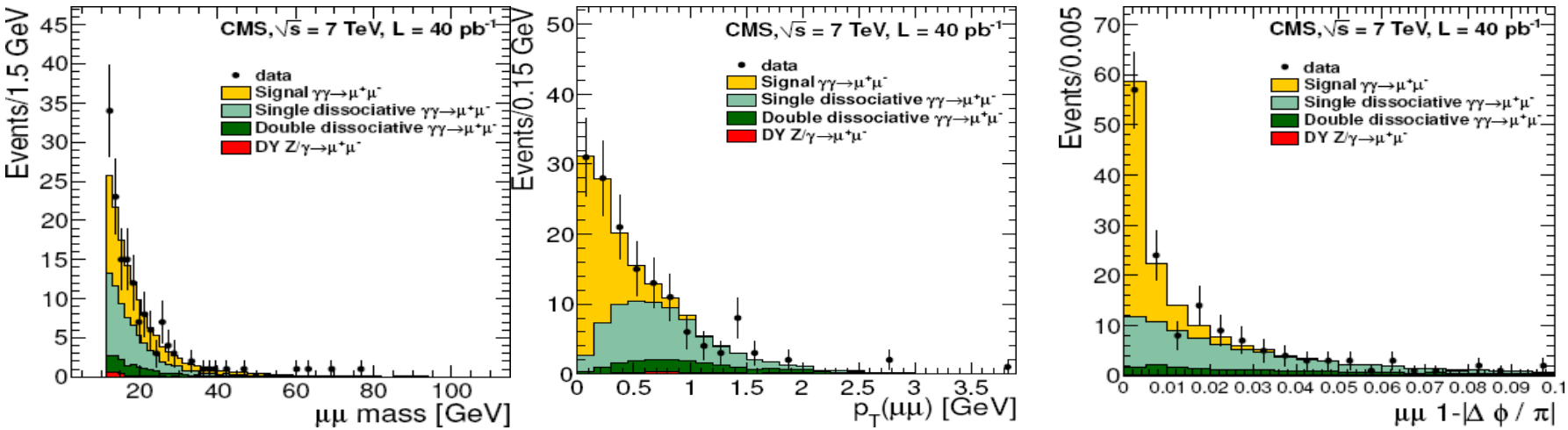

- Pair-p_T very small (peak at ~50 MeV/c). Muons are ~back to back.
- Agreement with LPAIR (QED): pp → γ γ → μμ

Exclusive γ-γ dielectron production (CMS)

CMS PAS-FWD-11-004

- Exclusive dielectrons observed in m_{ee} ~ 11 – 140 GeV (above Υ):

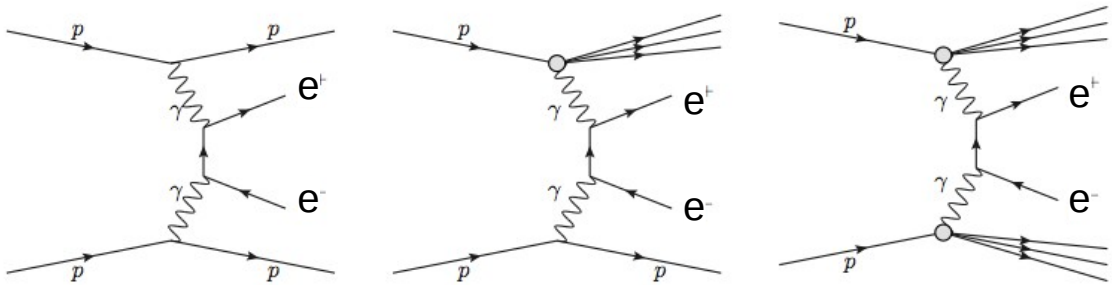

Just 2 EM showers,
E_T > 5.5 GeV, |η| < 2.1,
nothing else to |η| = 5.2

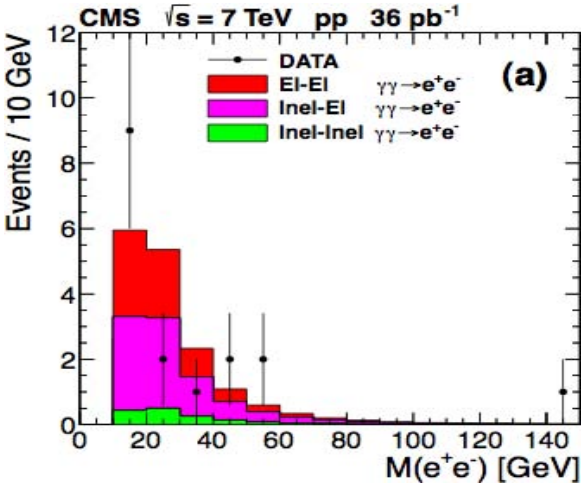

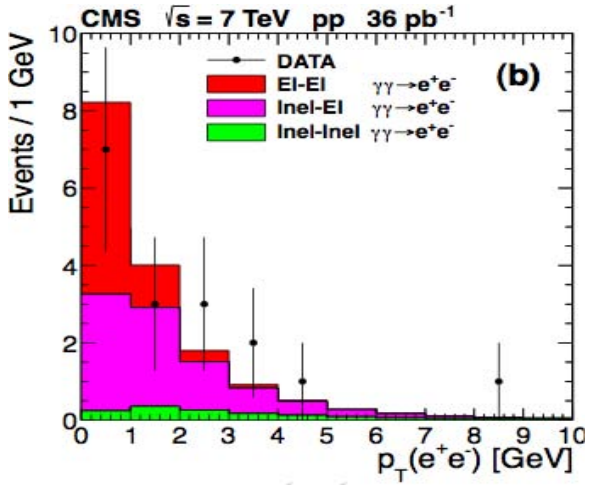

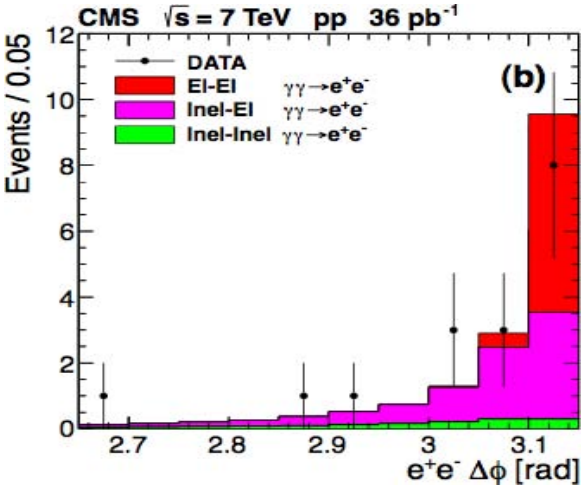

- Pair-p_T very small (peak at ~200 MeV/c). Electrons ~back to back.
- Agreement with LPAIR (QED): pp → γ γ → ee

Low-x QCD

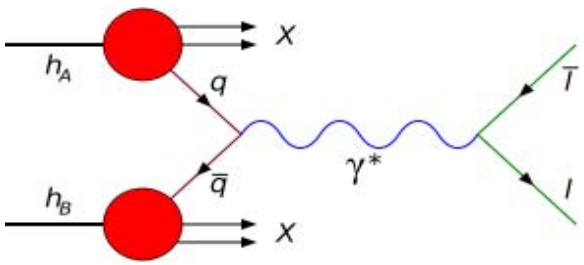
h_A
h_B
x
x
q
$\bar{q}$
γ^*
$\bar{l}$
l

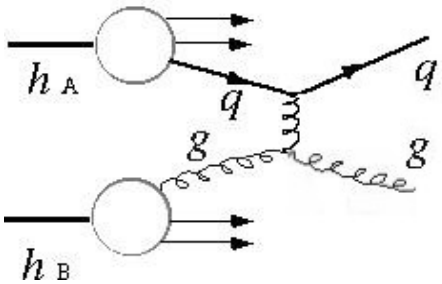
h_A
h_B
q
q
g
g

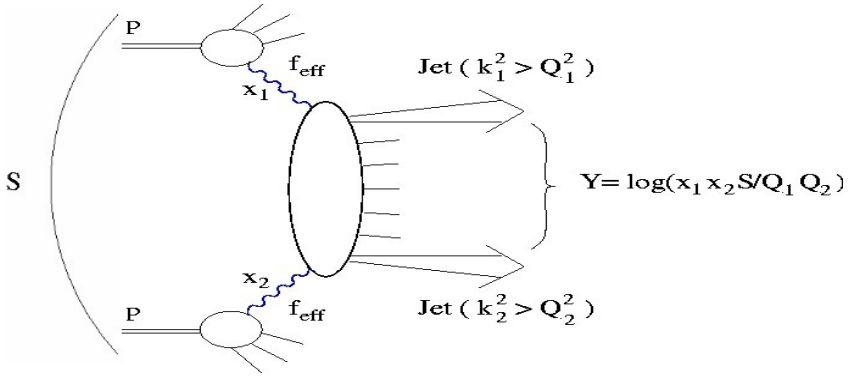
P
P
S
f_{eff}
f_{eff}
x_1
x_2
Jet ($k_1^2 > Q_1^2$)
Jet ($k_2^2 > Q_2^2$)
$Y = \log(x_1 x_2 S/Q_1 Q_2)$

Unitarity of electroweak cross sections

- SM without a Higgs: longitudinal W-W scattering explodes at ~1 TeV

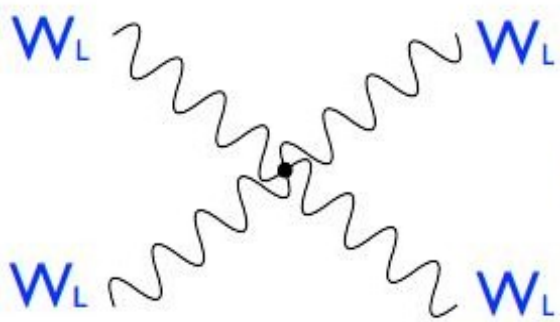

$$\propto \frac{s}{v^2}$$

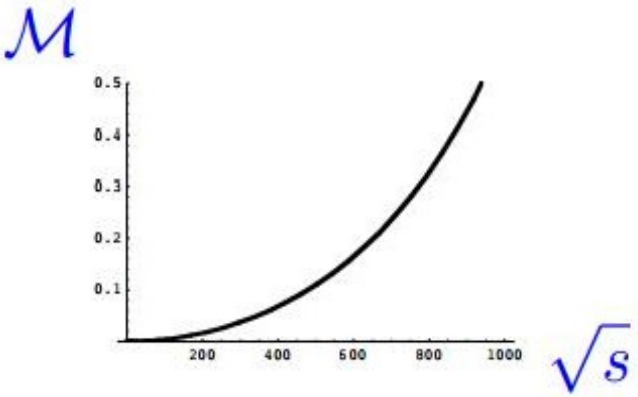

[A.Pomarol, ICHEP'12]

Unitarity is lost at high-energies

- Higgs boson restores finiteness of W-W cross sections:

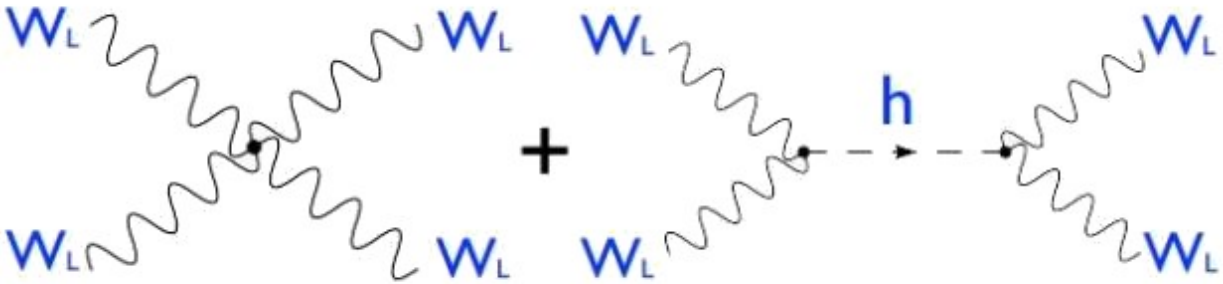

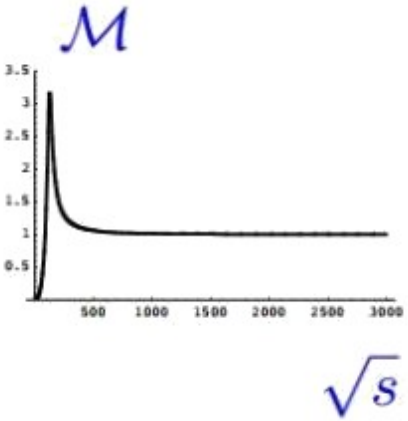

Unitarity of pQCD cross sections

- pQCD (mini)jet production x-section is bigger than total inel p-p x-section for p_{Tmin}~ 5-7 GeV at the LHC !

$$\sigma_{\rm hard}(p_{\perp\rm min}) = \int_{p^2_{\perp\rm min}}^{s/4} \frac{d\sigma}{dp^2_\perp}\, dp^2_\perp$$

... Why this happens ?

- Very high gluon densities at small-x:

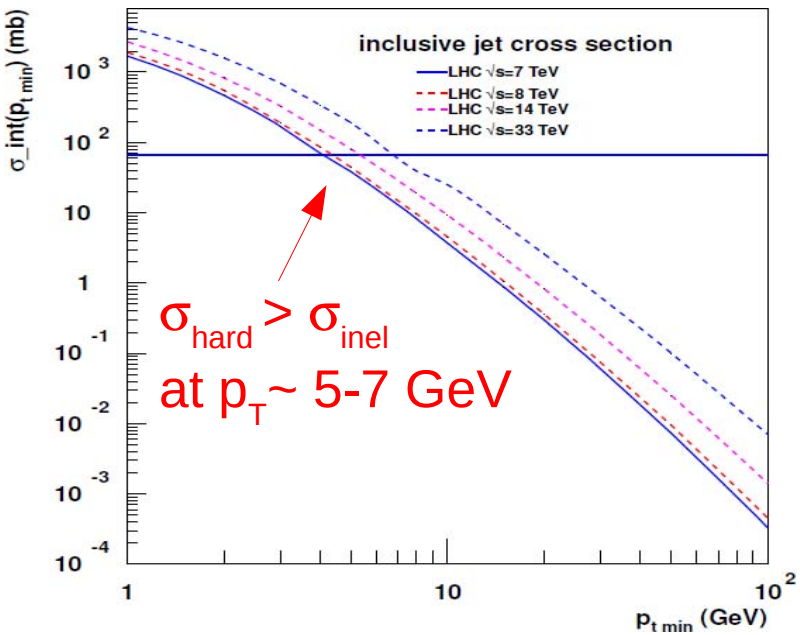

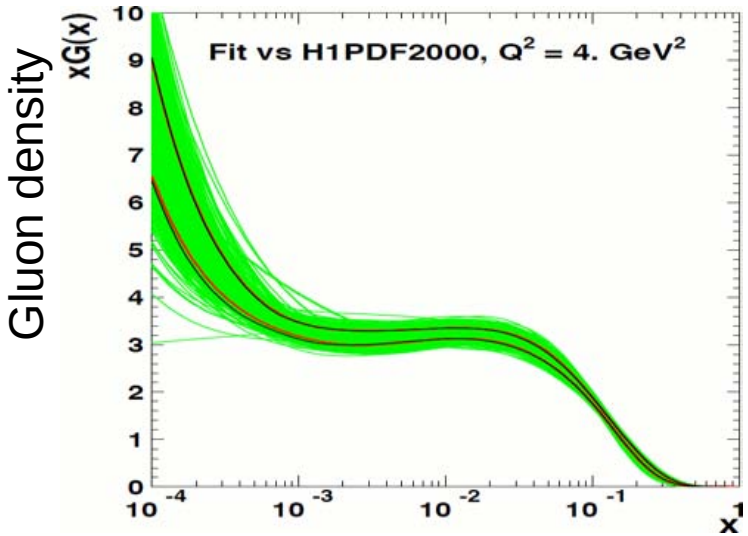

Unitarity of pQCD cross sections

- pQCD (mini)jet production x-section is bigger than total inel p-p x-section for p_{Tmin} ~ 5-7 GeV at the LHC !

$$\sigma_{\rm hard}(p_{\perp\rm min}) = \int_{p^2_{\perp\rm min}}^{s/4} \frac{d\sigma}{dp^2_\perp}\, dp^2_\perp$$

... Why this happens ?

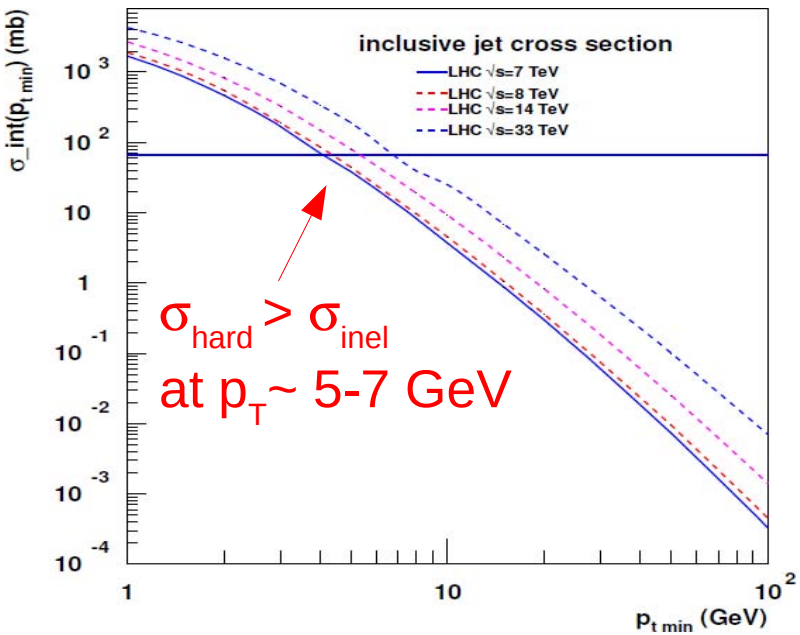

- Very high gluon densities at small-x.
- Solution: Gluon saturation
  - Add non-linear QCD evolution eqs.

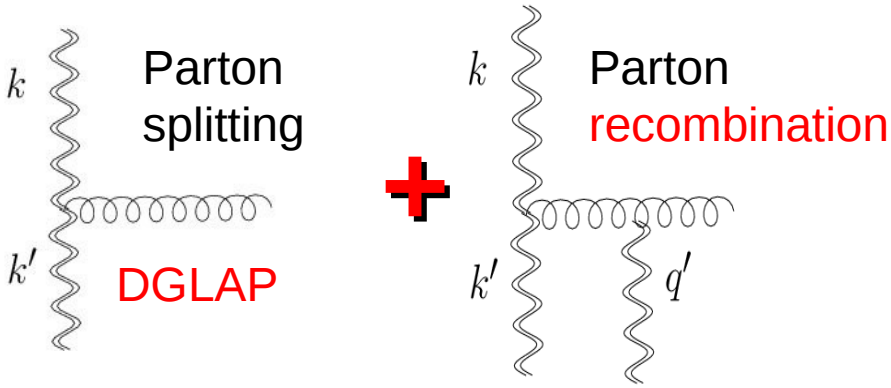

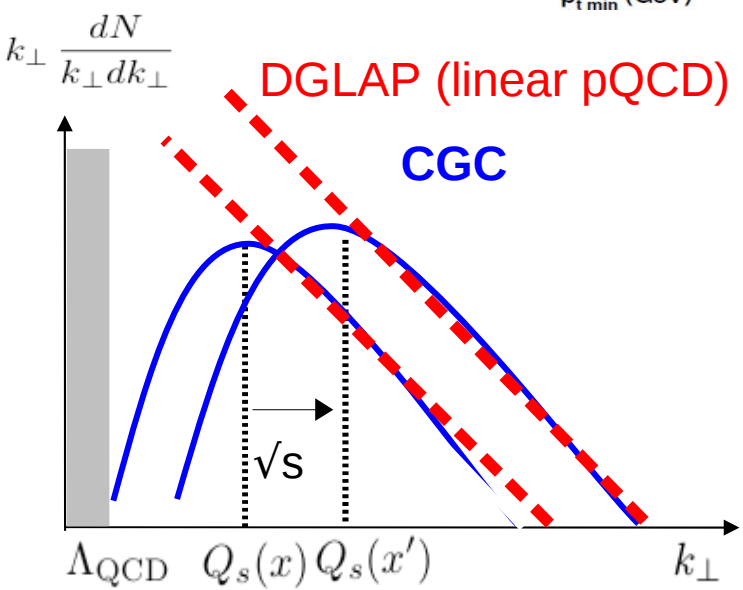

Unitarity of pQCD cross sections

- pQCD (mini)jet production x-section is bigger than total inel p-p x-section for p_{Tmin} ~ 5-7 GeV at the LHC !

$$\sigma_{\rm hard}(p_{\perp\rm min}) = \int_{p^2_{\perp\rm min}}^{s/4} \frac{d\sigma}{dp^2_\perp}\, dp^2_\perp$$

... Why this happens ?

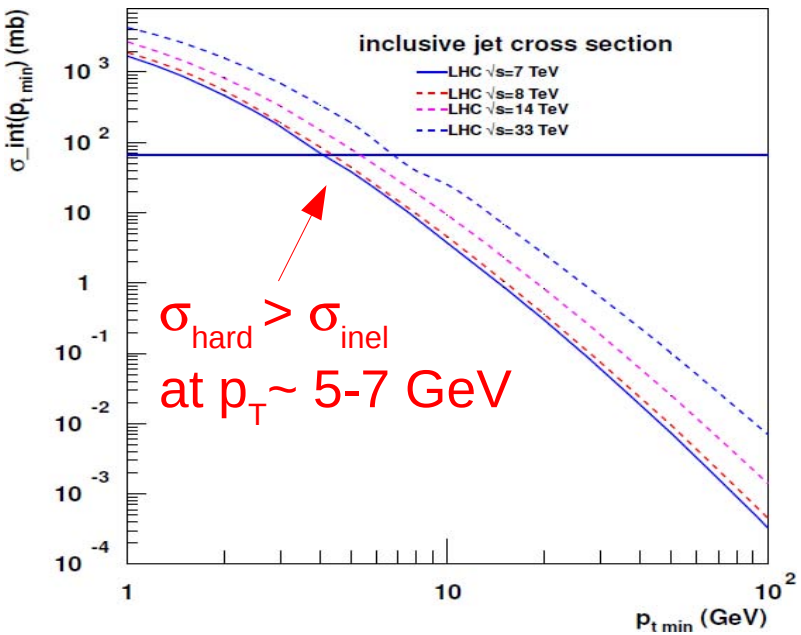

- Very high gluon densities at small-x.
- Solution: Gluon saturation
  - Add non-linear QCD evolution eqs.

collinear factorization assumptions (leading-twist, incoherent parton scatt.) invalid around "saturation scale" Q_s

New effective theory: CGC
New evolution equations: JIMWLK

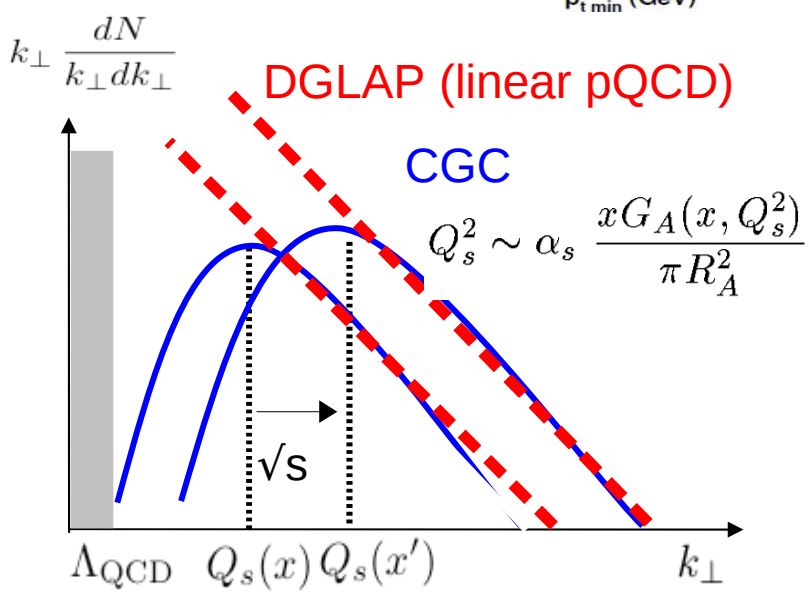

Unitarity of pQCD cross sections

- pQCD (mini)jet production x-section is bigger than total inel p-p x-section for p_{Tmin} ~ 5-7 GeV at the LHC !

$$\sigma_{\rm hard}(p_{\perp\rm min}) = \int_{p^2_{\perp\rm min}}^{s/4} \frac{d\sigma}{dp^2_\perp}\, dp^2_\perp$$

... Why this happens ?

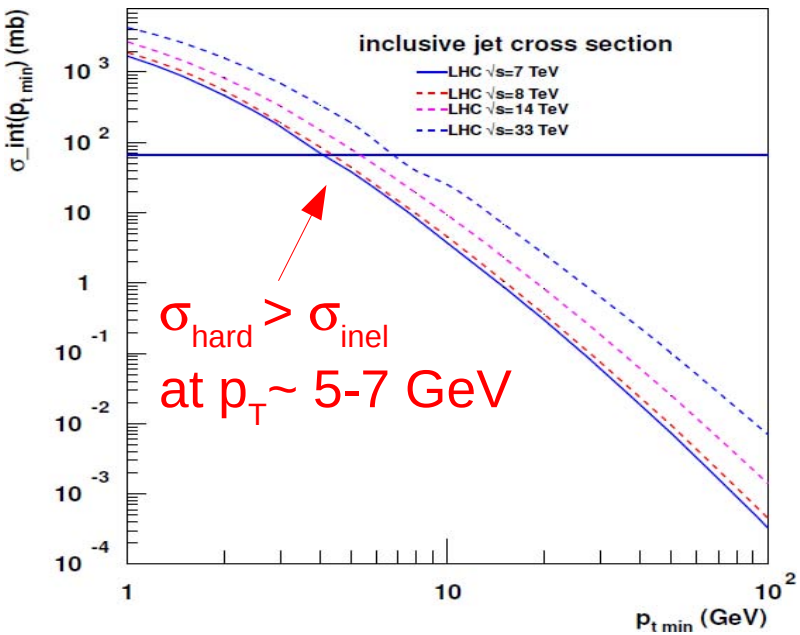

- Very high gluon densities at small-x.
- Solution: Gluon saturation
  - Multi-parton interactions

Interpret ...

$$\langle n \rangle = \frac{\sigma_{\rm hard}(p_{\perp\rm min})}{\sigma_{\rm inel}}$$

= average number of parton–parton scatterings above $p_{\perp\rm min}$ in an event

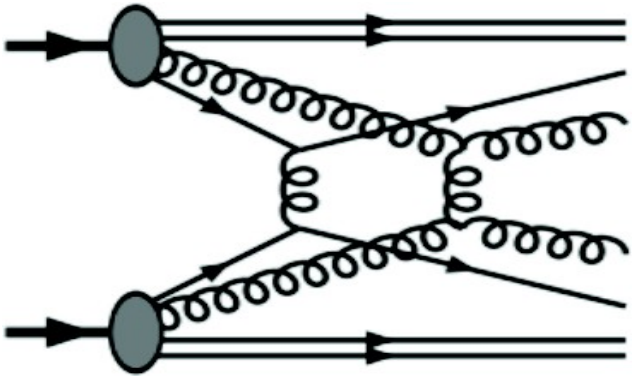

Most collider MCs (PYTHIA, HERWIG) follow this approach

Small-x ⇒ Forward rapidities

- 2 → 2 parton kinematics:

y = 0: $x_1 \sim x_2 \sim x_T = 2p_T/\sqrt{s}$

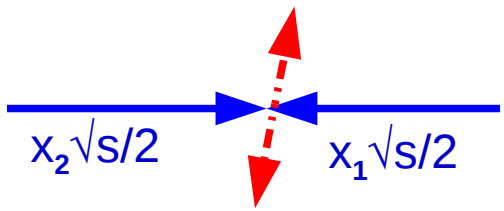

$$x_{1,2}^{2\to 2} = \frac{p_T}{\sqrt{s}}\left(e^{\pm y} + e^{\pm y'}\right) \Rightarrow x_2^{min} = \frac{x_T\, e^{-\eta}}{2 - x_T\, e^{\eta}}$$

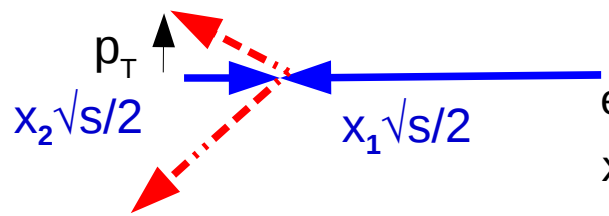

e.g. LHC, p_T = 10 GeV/c

$x_T \sim 10^{-3}$ ($\eta \sim 6$): $x_{min} \sim 10^{-6}$

- 2 → 1 (gluon fusion) CGC kinematics: much lower x reached ($x_2 = x_2^{min}$)

$$x_{1,2}^{2\to 1} = \frac{p_T}{\sqrt{s}}\left(e^{\pm y}\right)$$

Every 2-units of y, x_2 decreases by ~10

CGC: $x(y=4) \sim 10^{-4}$

DGLAP: $x(y=4) \sim 10^{-2}$

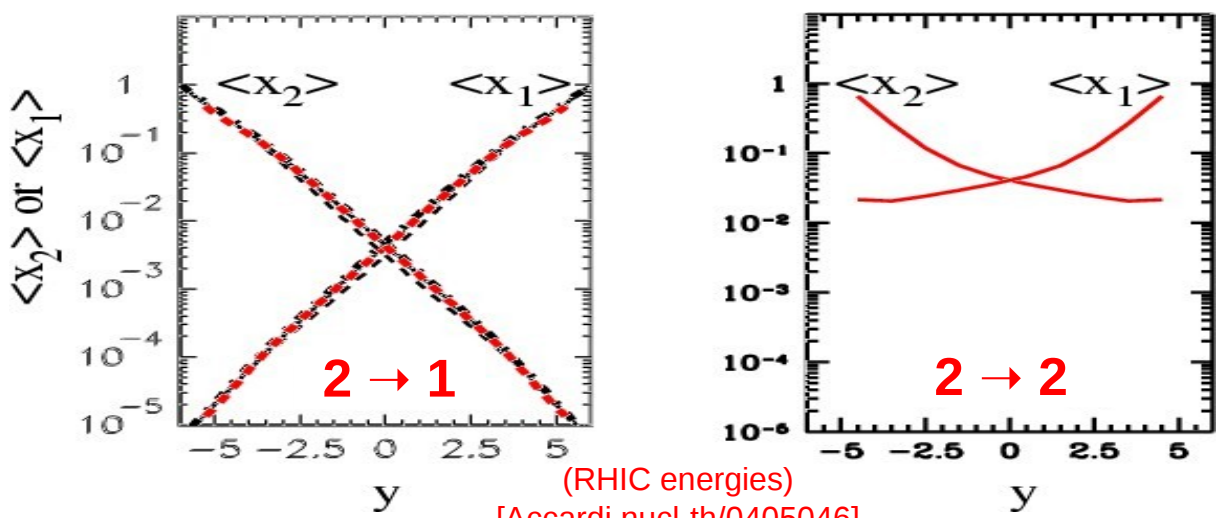

(RHIC energies)
[Accardi,nucl-th/0405046]

Low-*x* studies in p-p at forward η

- At y=0, $x=2p_T/\sqrt{s}\sim10^{-3}$ (probed at HERA,Tevatron). Go fwd. for $x<10^{-4}$
- Very large pQCD cross-sections:

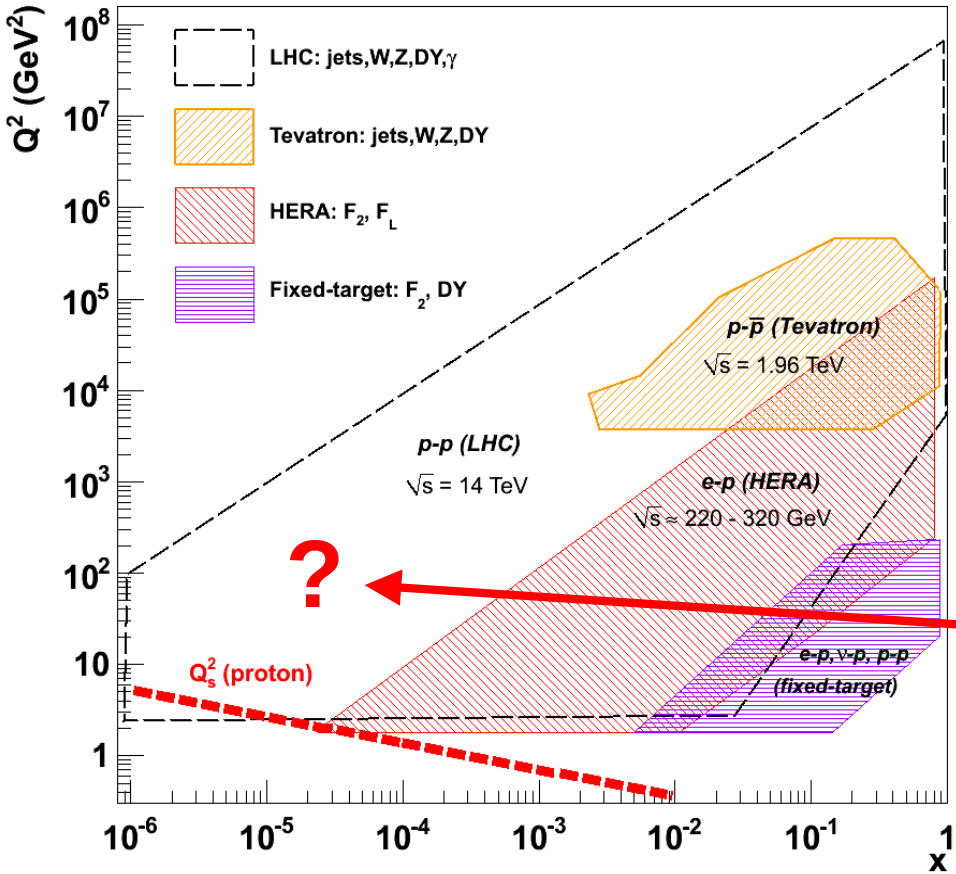

$p(p_1)+p(p_2)\to \text{jet}+\gamma+\text{X}$ Prompt γ

$p(p_1)+p(p_2)\to l\bar{l}+\text{X}$ Drell-Yan

$p(p_1)+p(p_2)\to \text{jet}_1+\text{jet}_2+\text{X}$ Jets

$p(p_1)+p(p_2)\to \text{Q}+\bar{\text{Q}}+\text{X}$ Heavy-Q

$p(p_1)+p(p_2)\to W/Z+\text{X}$ W,Z

Forward rapidities:

(e.g. y~5, M~2.5 GeV)

x down to 10^{-6} !

- But barely touching sat. momentum: $Q_s^2\sim 0.6$ GeV^2 (y=0), 3 GeV^2 (y=5)

Forward Drell-Yan at 2.5 < η < 5 (LHCb)

- Forward DY sensitive to PDFs at $x \sim 10^{-5}, Q^2 = m_{ll}^2$:

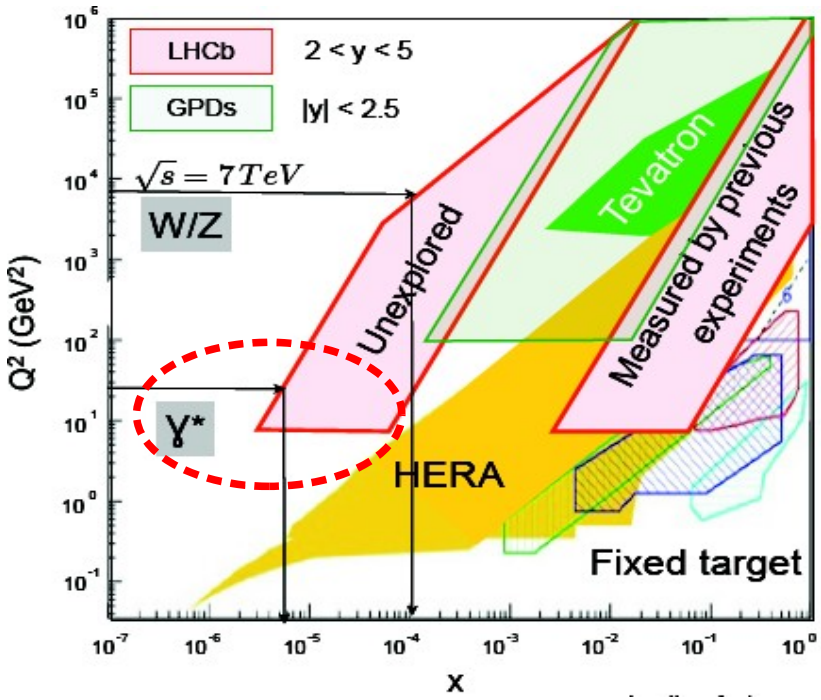

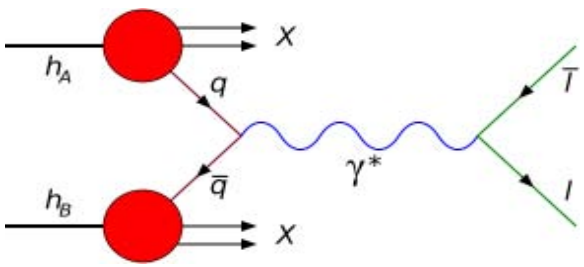

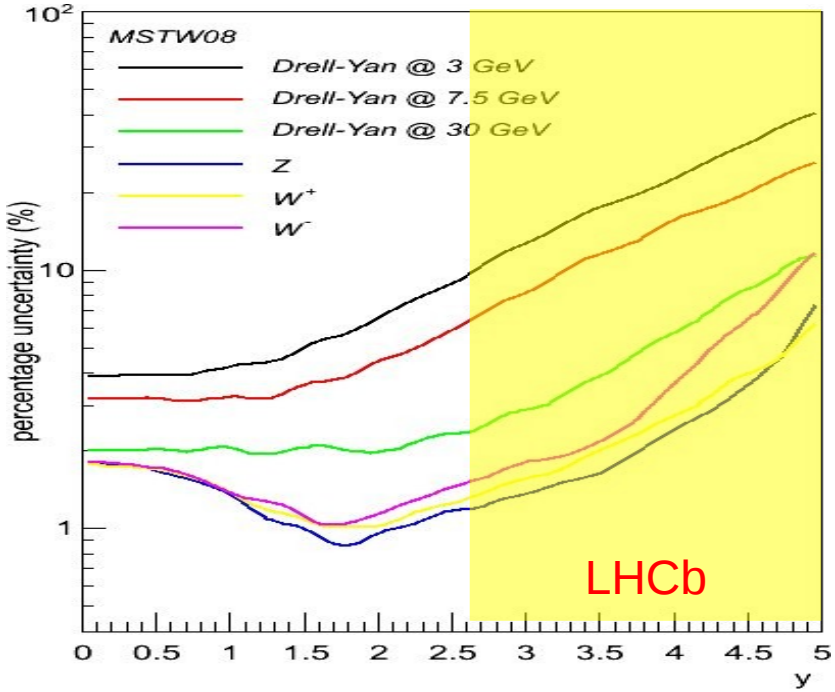

- ~30% PDF uncertainties for low-mass DY NLO x-sections at rapidities y~5:

(parton saturation effects ?)

Forward Drell-Yan at 2.5 < η < 5 (LHCb)

- Forward DY x-section vs $m_{\mu\mu}$ well reproduced by NLO (DGLAP PDFs) from $m_{\mu\mu}$ = 5 – 120 GeV:

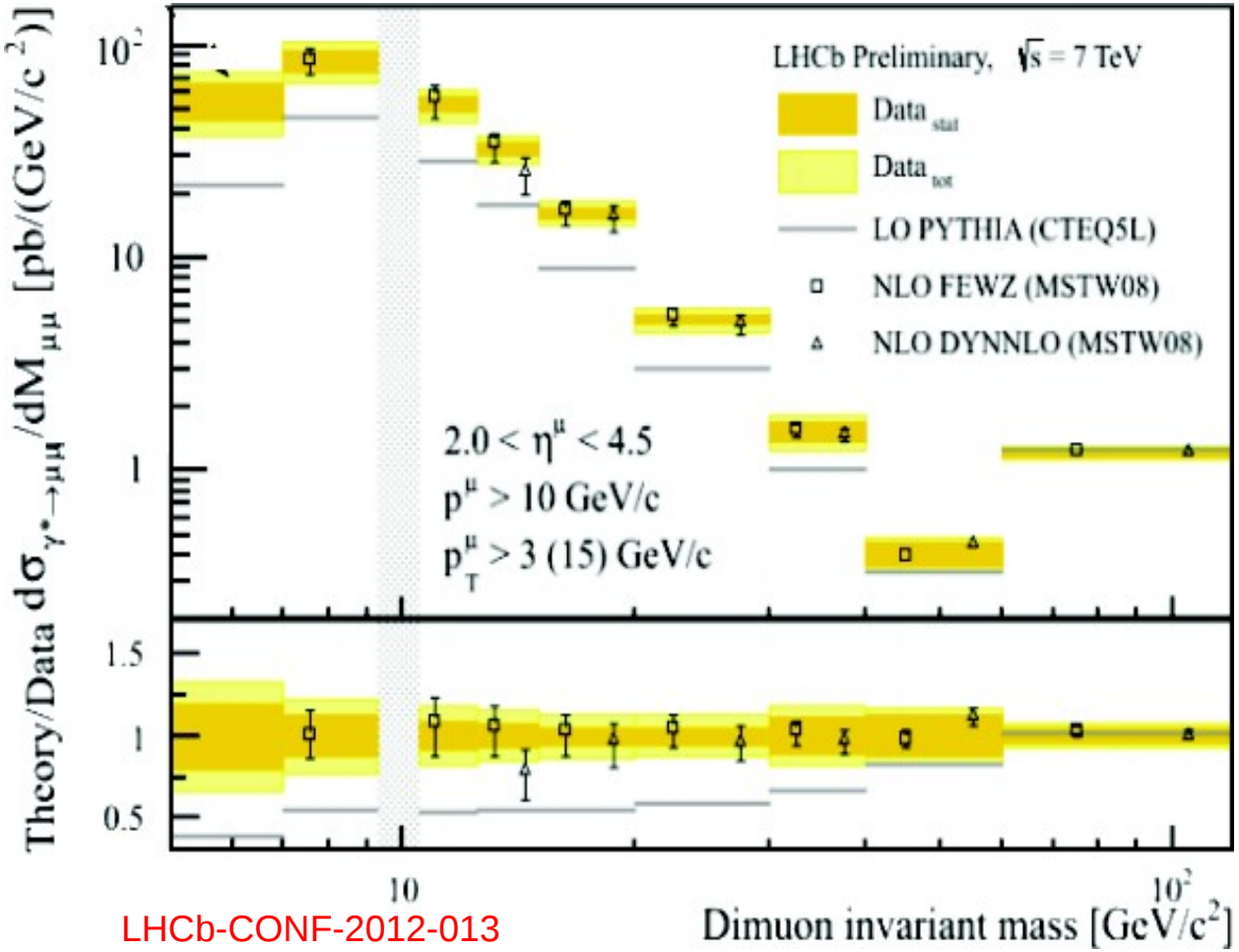

LHCb-CONF-2012-013

muons must have:
p > 10 GeV
p_T > 3 GeV
2 < η < 4.5

(Υ mass excluded)

How well do the data compare to gluon-saturation predictions ?

Forward jets at 3 < |η|< 5 (CMS)

- Forward jets (E_T ~30-140 GeV) sensitive to low-x (and high-x) PDFs:

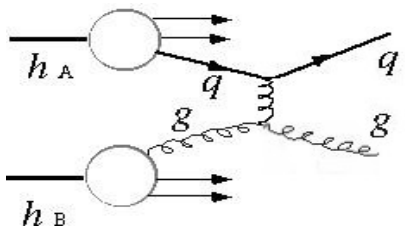

Jets in HF (3<|η|<5) probe: $x_2 \sim 10^{-4}$, $x_1 \sim 0.2$

- Spectrum reproduced by NLO, parton-showers and "BFKL"-MCs:

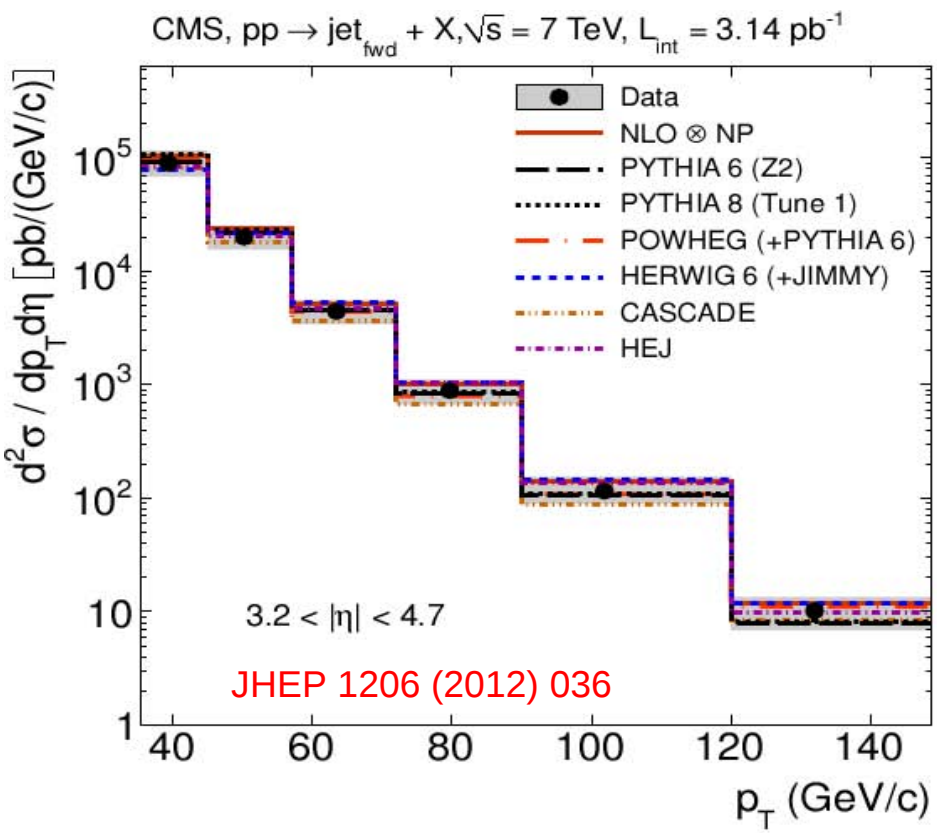

JHEP 1206 (2012) 036

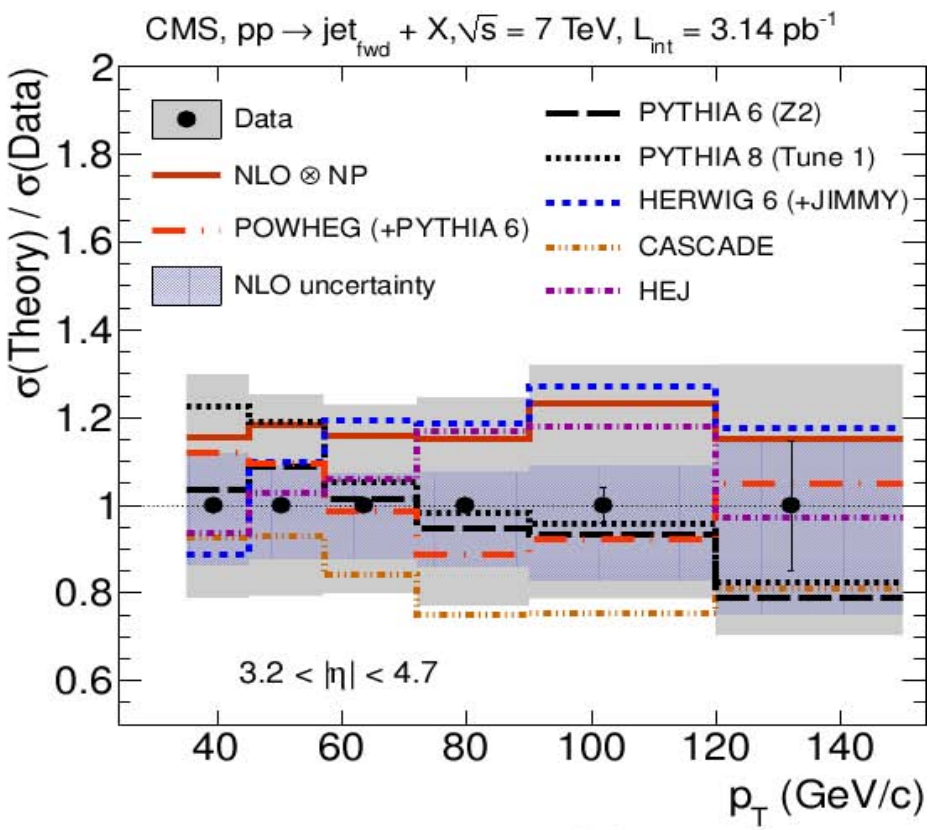

Forward jets at 3 < |η|< 5 (CMS)

- Forward jets (E_T ~30-140 GeV) sensitive to low-x (and high-x) PDFs:

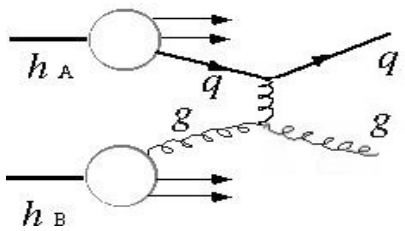

Jets in HF (3<|η|<5) probe: $x_2 \sim 10^{-4}$, $x_1 \sim 0.2$

- Although NLO PDFs tend to be +20% above central data:

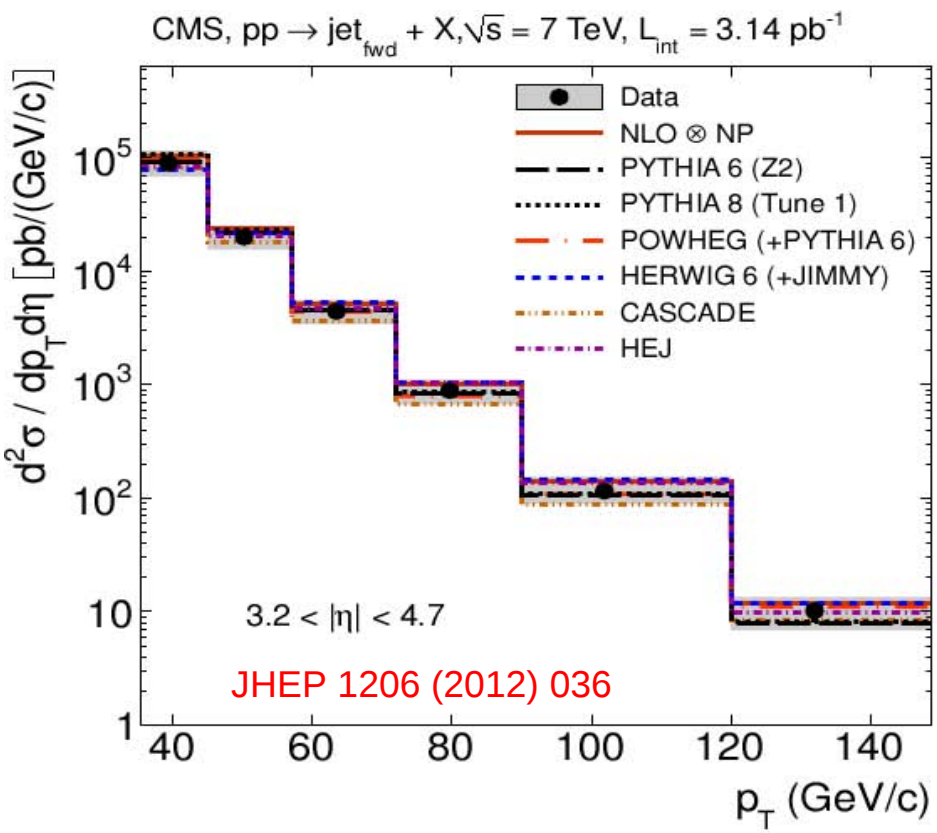

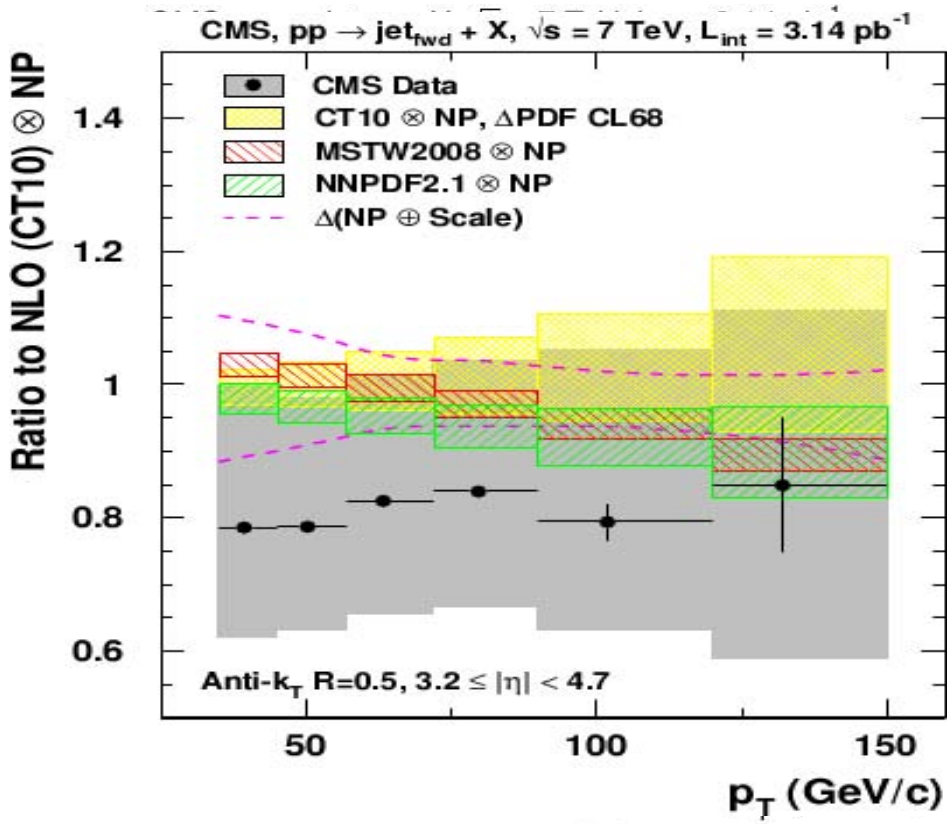

Forward-central dijets (CMS)

- Fwd-cent. dijets with large $\Delta\eta$ separations probe BFKL-type dynamics.
- Ratios model/data for fwd and central jets p_T spectra:

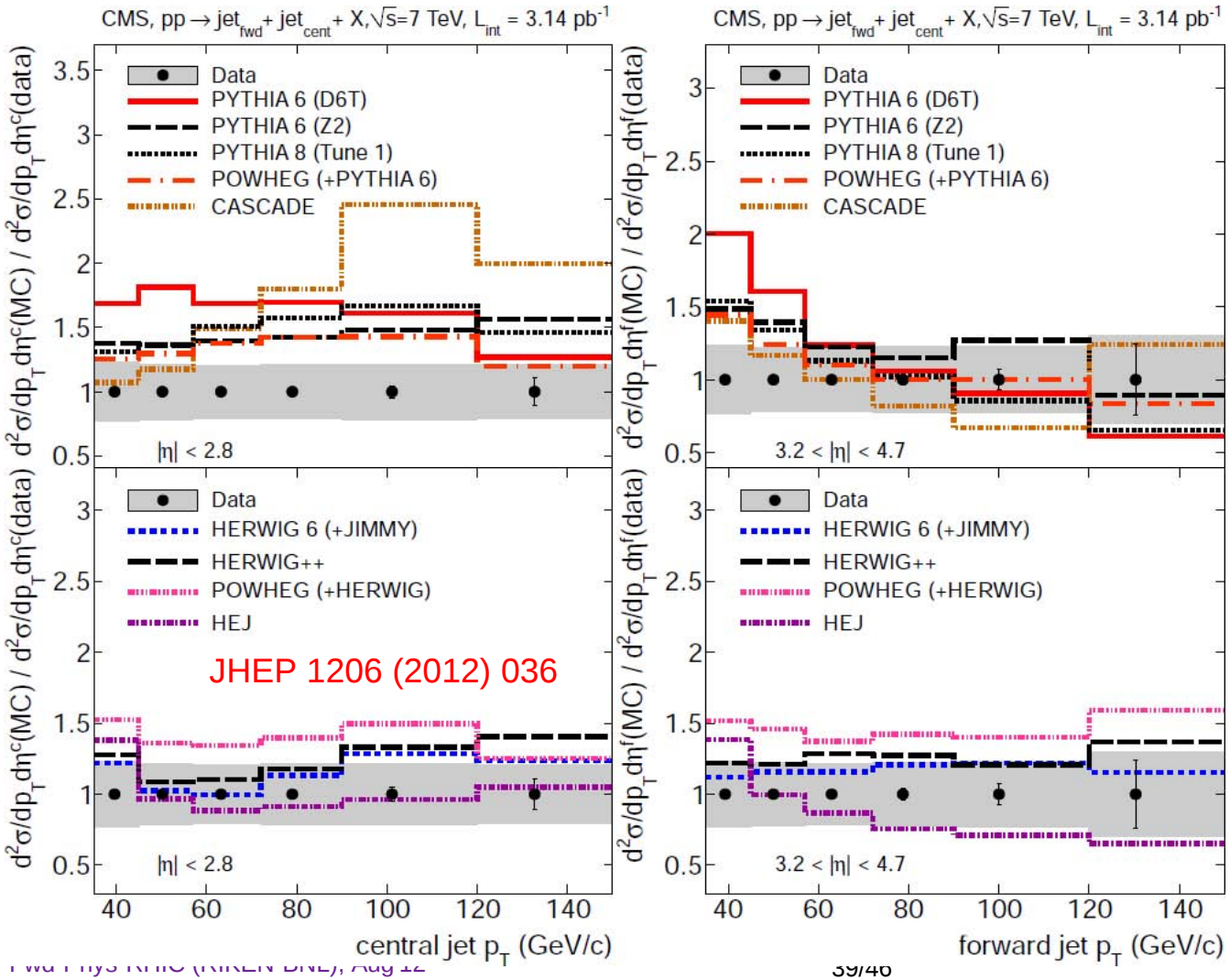

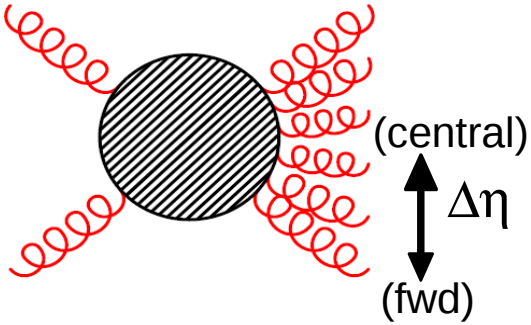

- PYTHIA & NLO overpredict jet spectra specially at low p_T

- HERWIG & models w/ wide-angle radiation (HEJ) show better agreement, but CASCADE (DGLAP+ BFKL) also overshoots.

“Dijet K-factor” vs rapidity separation

- Reconstruct x-sections pair of jets with p_T > 35 GeV over -4.7 < y < 4.7

(1) Inclusive sample: all events with at least 2 jets.
(2) Exclusive sample: exactly 2 jets per event.
(3) “Muller-Navelet” sample: incl. with most fwd-bckwd jets.

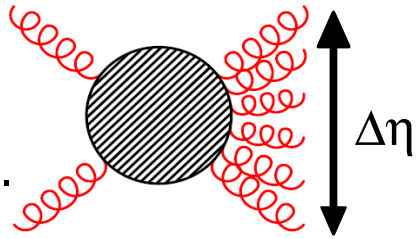

- Compute x-sections as a function of Δy between the jets, take ratios:

$$R_{incl} = \frac{\sigma_{incl}(\text{dijet})}{\sigma_{excl}(\text{dijet})}, R_{MN} = \frac{\sigma_{MN}(\text{dijet})}{\sigma_{excl}(\text{dijet})}$$

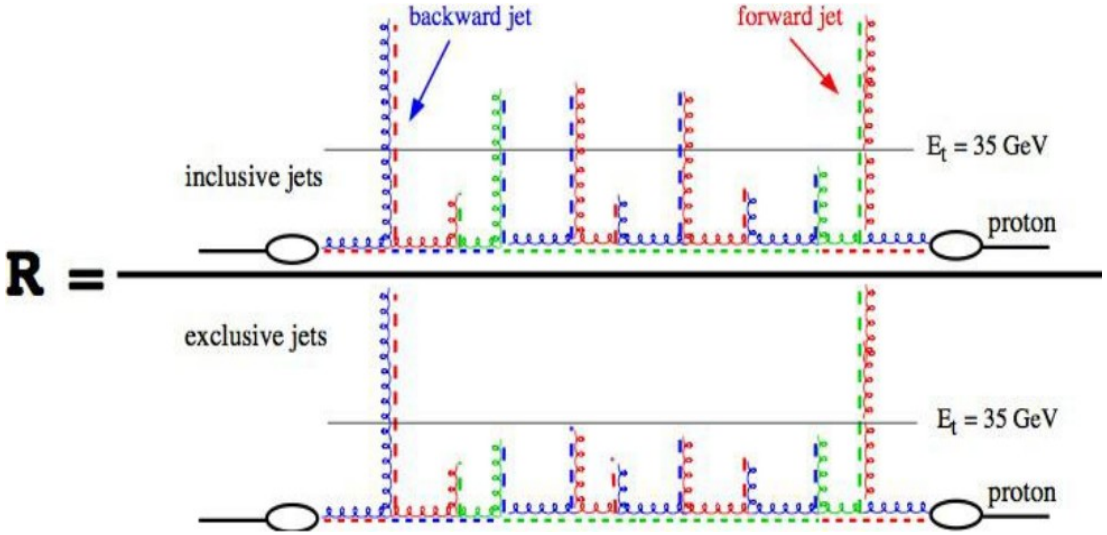

BFKL expectation:
Increased Δy phase space ⇒
Increased rad. probability ⇒
R(Δy) rises with Δy
(up to kinematical limit)

“Dijet K-factor” vs Δy separation (CMS)

- Ratios of x-sections as a function of Δy between the jets:

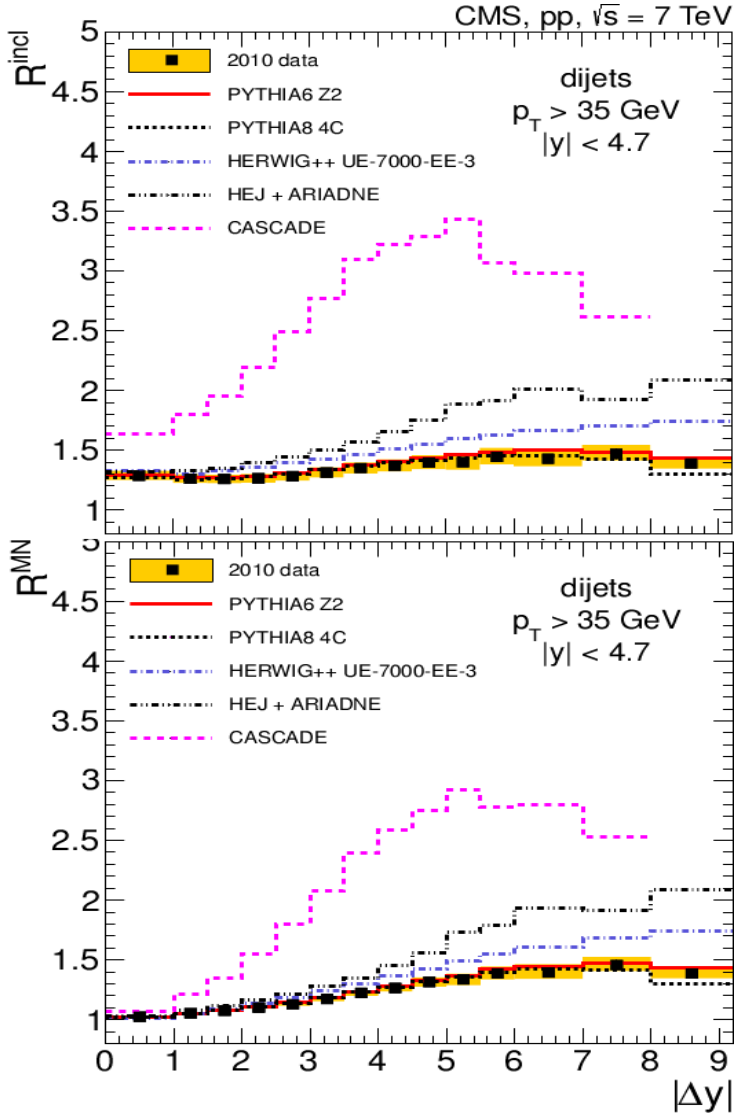

- R rises with |Δy| as expected (drop close to kinematic limit):
  σ(incl.) = 1.2 – 1.4 σ(excl.)
  σ(MN) = 1 – 1.4 σ(excl.)

- PYTHIA: very good agreement w/ data
- HERWIG++ predicts higher R at medium and large Δy.

- HEJ+ARIADNE & CASCADE (BFKL-motivated generators) predict much faster rise of R ...

- Is p_T > 35 GeV too high for searches of non-DGLAP dynamics ?

Hadronic collisions & UHECR

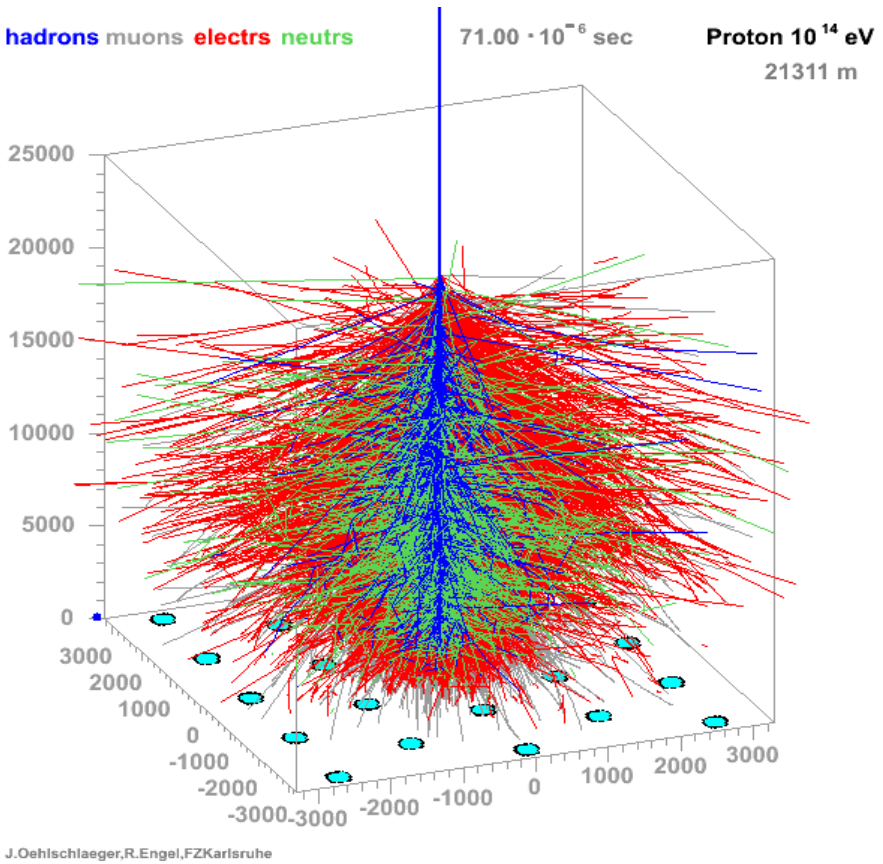

Forward hadrons at |η| = 5.2 – 6.6 (CMS,TOTEM)

- Important influence on cosmic-ray EAS development:
  - Modeling of multi-parton interactions & beam-remnants

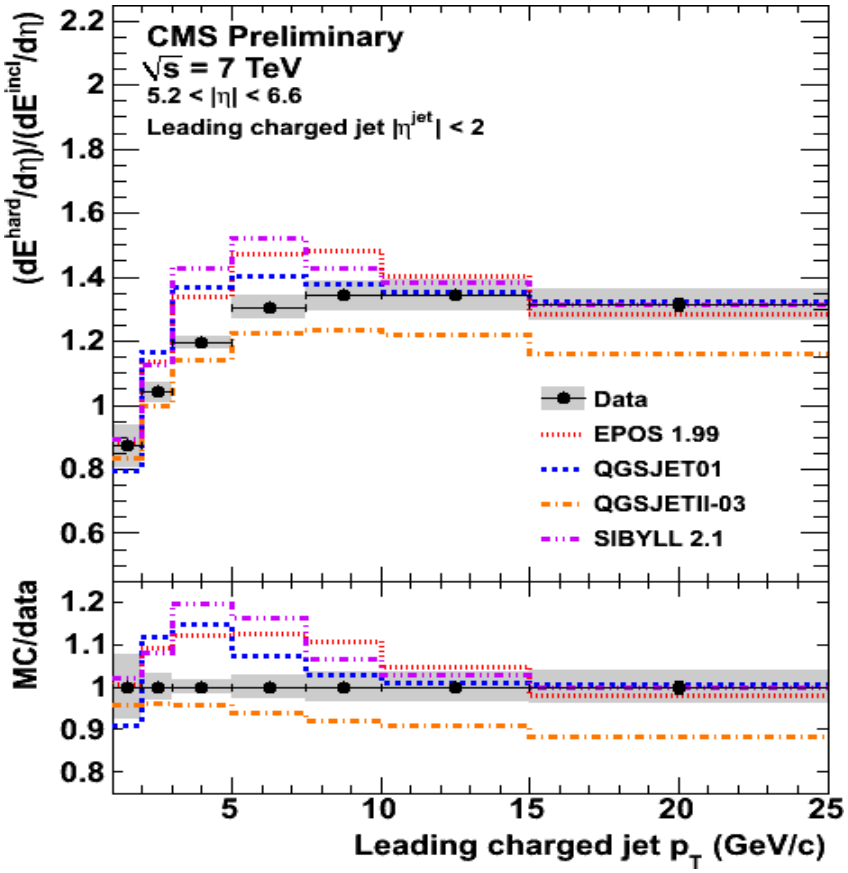

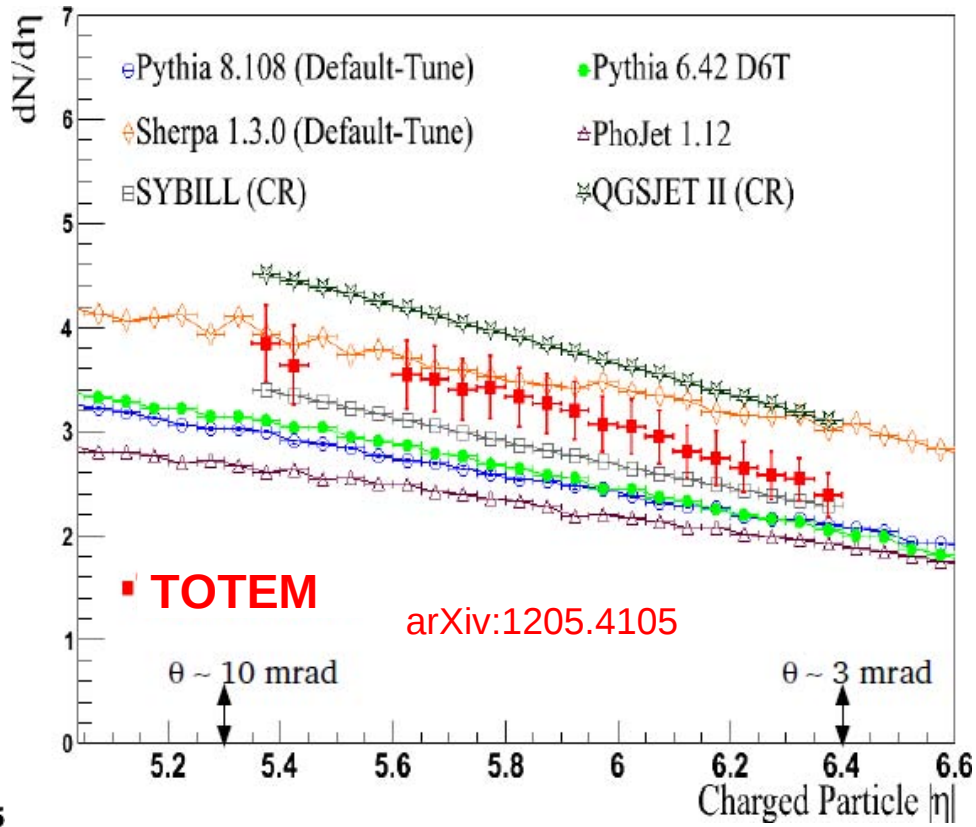

- Good CMS-data vs. CR-model agreement for energy density.
- Collider-MCs do not reproduce well the slope of TOTEM particle density. CR-models better.

(gluon saturation predictions?)

Very forward hadrons at |η| ~ 8. - 11. (LHCf)

- Important influence on cosmic-ray EAS development:
  - leading baryon (inelasticity) & had-to-e.m. energy transfer ($\pi^0 \rightarrow \gamma\gamma$)

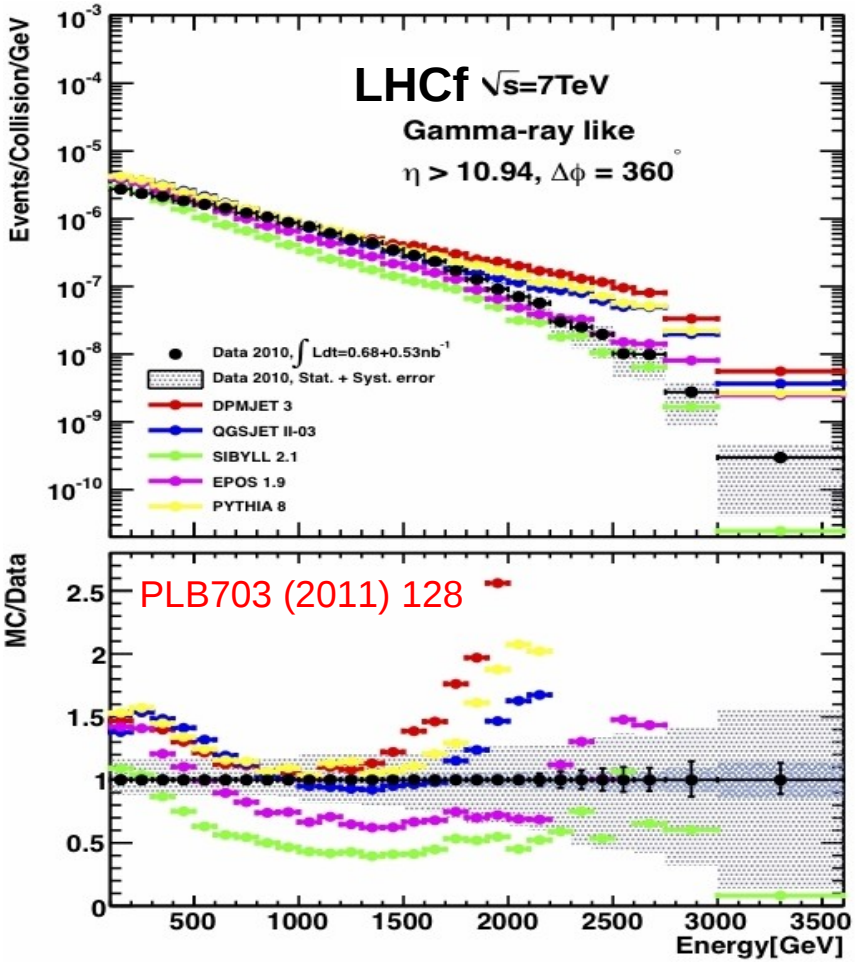

- > ±50% data-model differences for zero degree photon showers.

arXiv:1205.4578

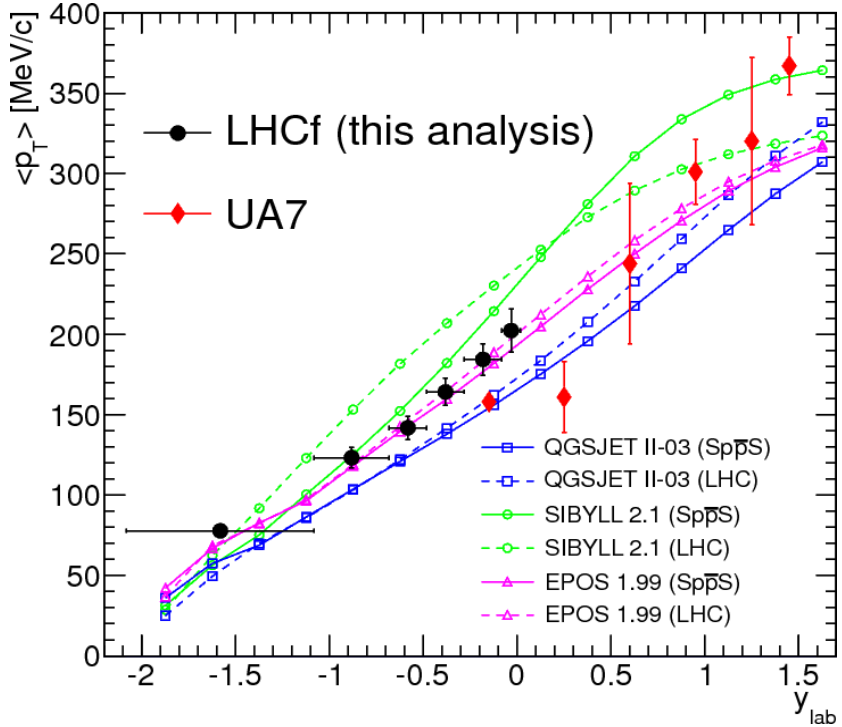

- Mean p_T of zero-degree pions is sqrt(s)-independent. EPOS shows the best overall agreement

Impact on cosmic-ray composition at ~10^{20} eV

- CR hadronic MCs based on Regge-Gribov Field Theory (extended to pQCD regime via "cut Pomerons") retuned to describe new LHC data:

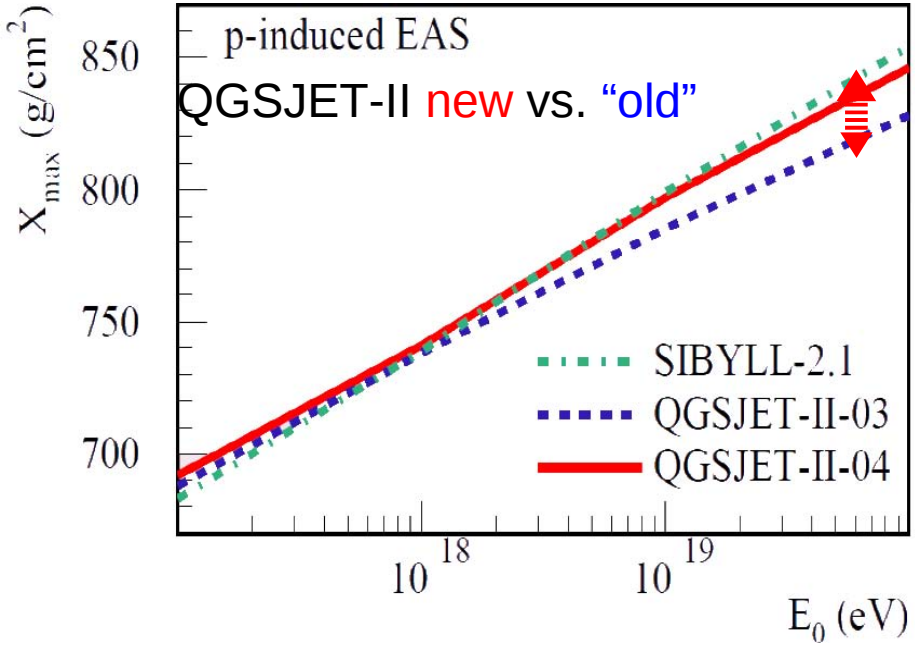

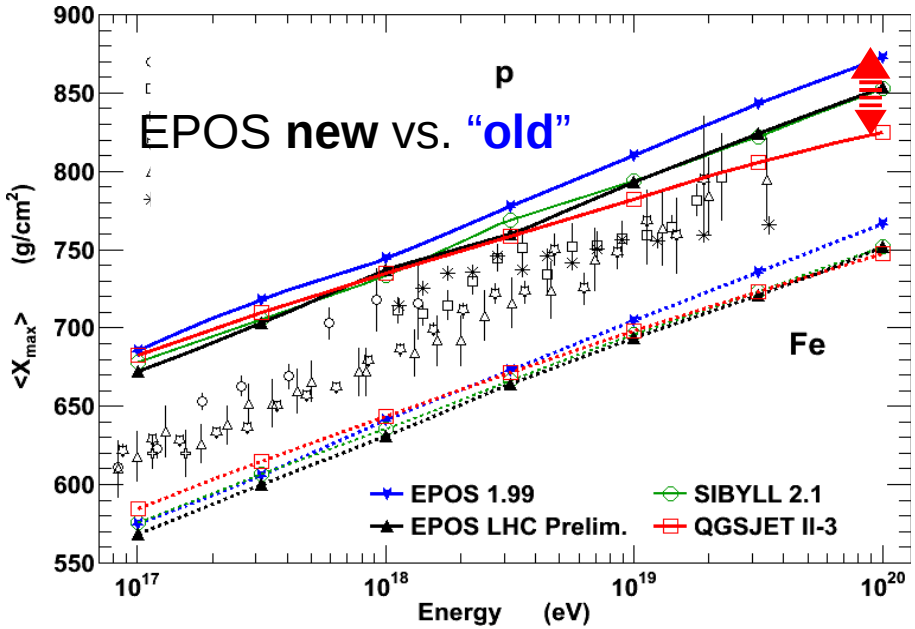

- Consequences:
  - EPOS & QGSJET-II predictions similar now to (older) SIBYLL: change in $<X_{max}>$ (reduced uncertainty ~60 g/cm^2 to ~10 g/cm^2).
  - Composition of CRs closer now to proton (rather than Fe) for all MCs.

Summary

- The LHC is providing a wealth of new forward data open to study !

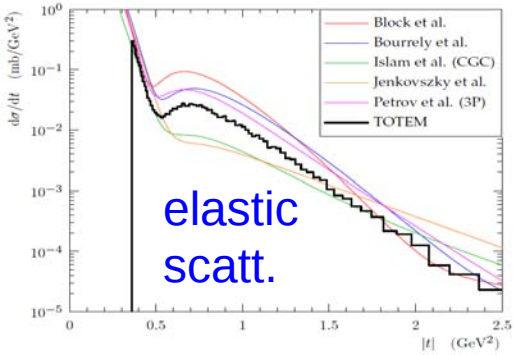

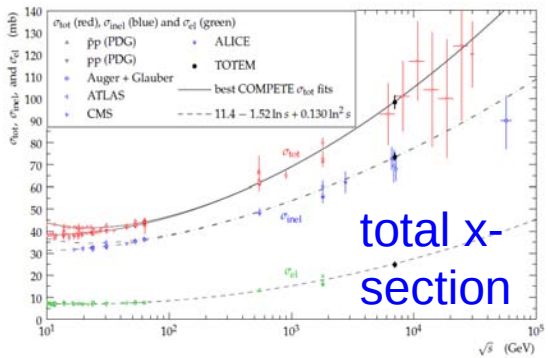

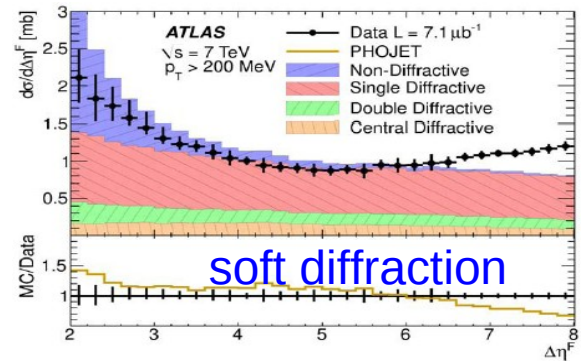

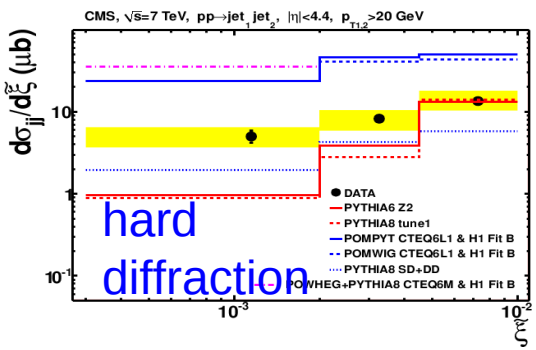

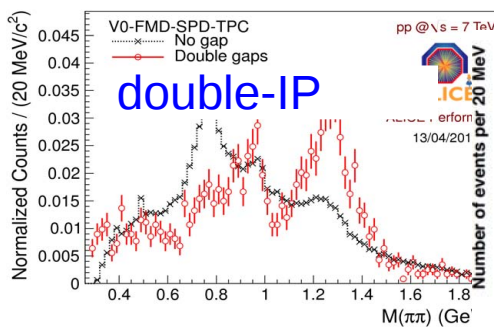

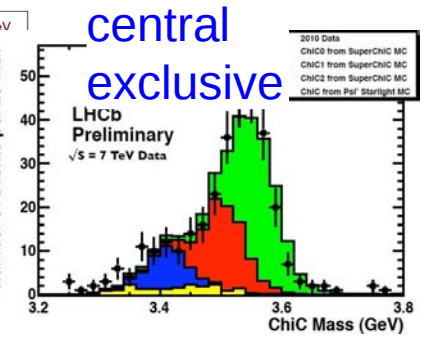

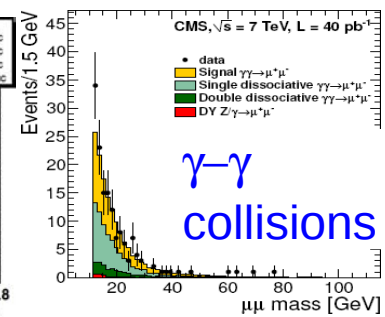

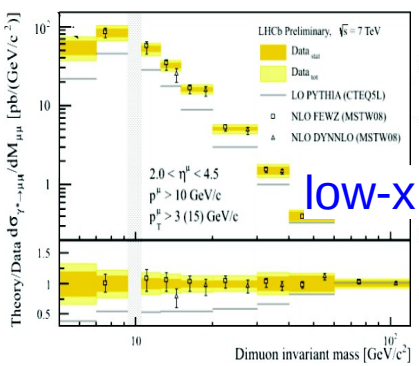

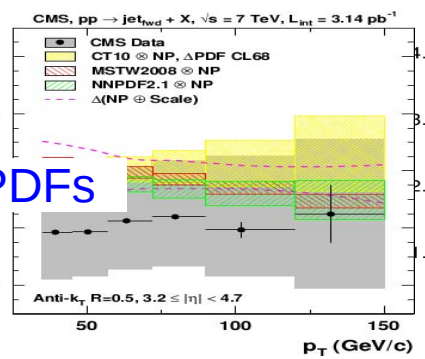

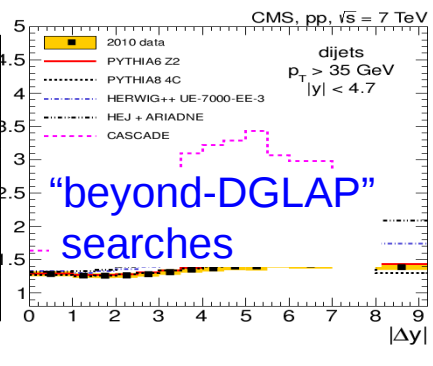

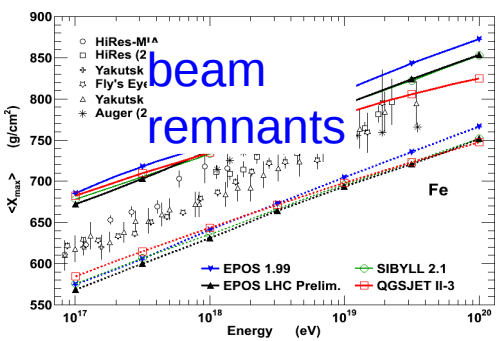

- Exciting experimental/theoretical QCD physics for the years to come!

Backup slides

Low-x dynamics

- Gluons start to overlap at "saturation scale"

$$Q_s^2 \sim \alpha_s \frac{xG_A(x,Q_s^2)}{\pi R_A^2}$$

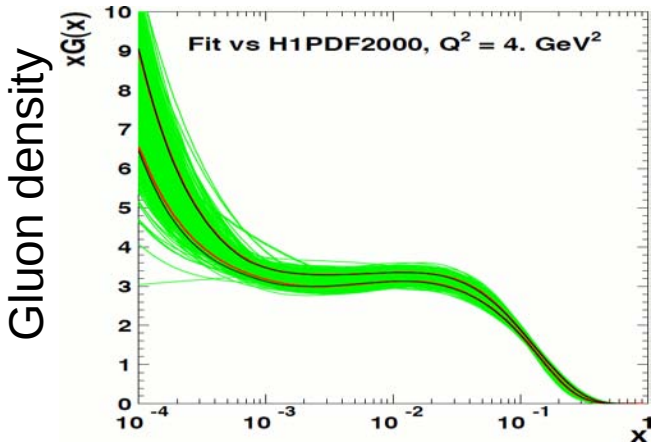

- Asymptotic pQCD g-g x-section peaks at $p_T \sim Q_s(\sqrt{s}) \sim 1\text{-}4$ GeV

$$Q^2_{\rm sat} \propto \log(1/x) \propto \log(\sqrt{s})$$

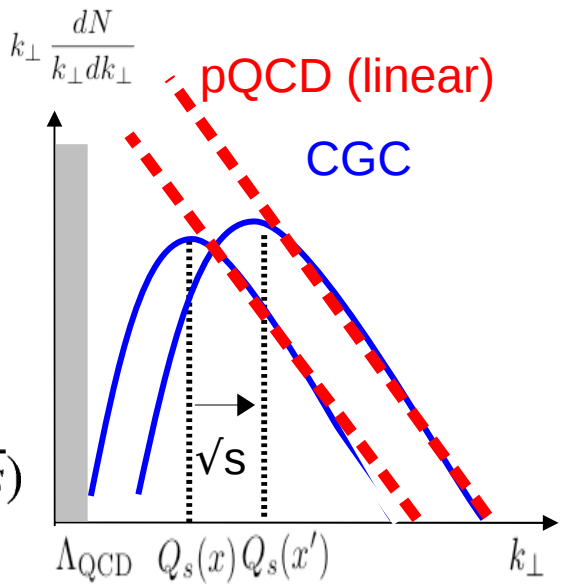

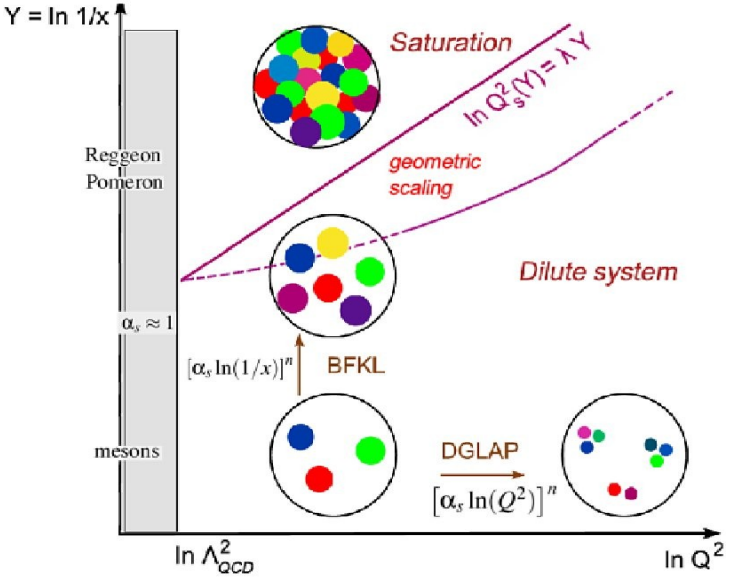

- Hadrons ~ "Color Glass Condensate" below Q_s
- Saturation effects enhanced in nuclei:

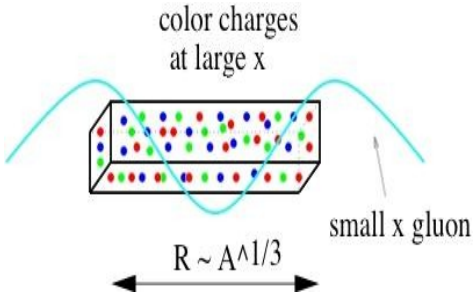

Large # of partons per transverse area

$$Q_s^2 \sim A^{1/3} \sim 6$$

Beyond DGLAP dynamics at the LHC ?

- Fwd-cent. dijets or dijets+central-veto (p-p at 7 TeV) with large $\Delta\eta$ separations access BFKL-type topologies

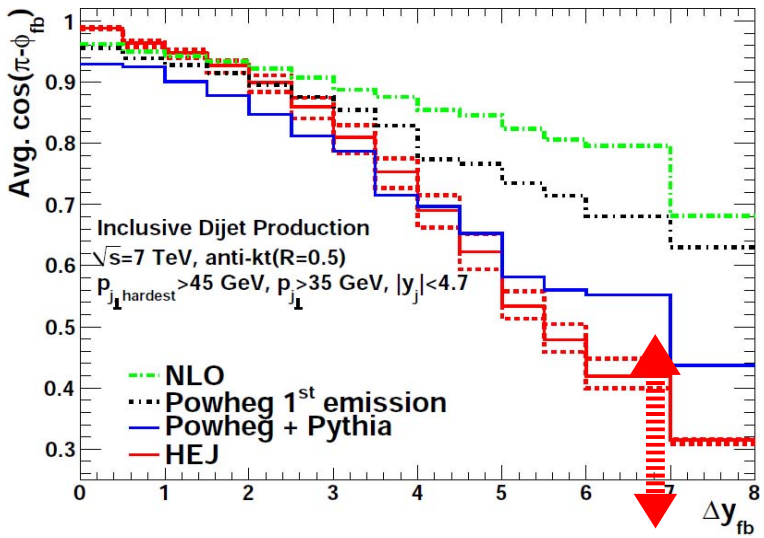

- New observables (Mueller-Navelet dijets) to be studied soon.

Reggeon-Field-Theory hadronic MCs

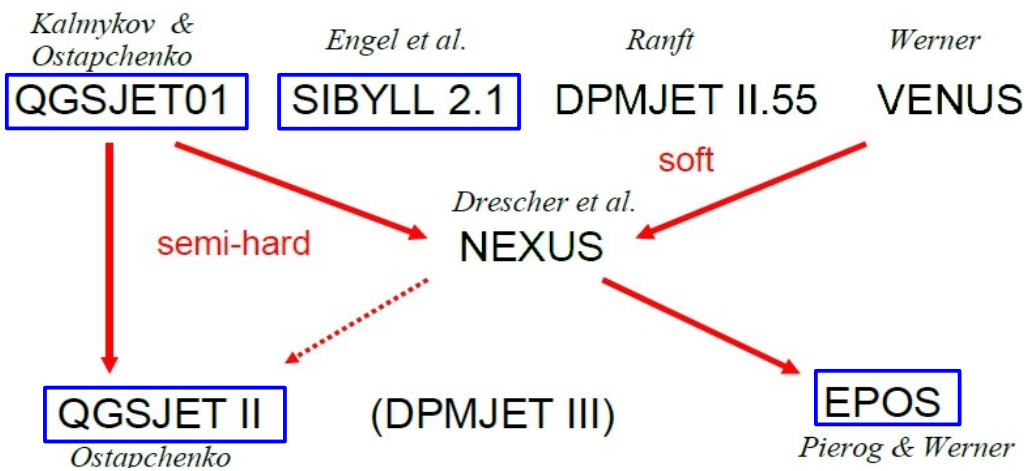

- Soft interactions via Reggeons & Pomerons:
  elastic, diffractive & soft-inelastic scatts. described

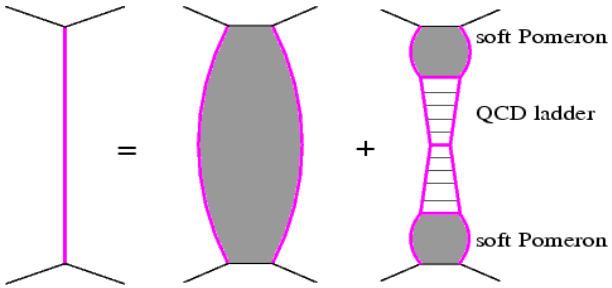

- Perturbative interactions via
  "cut (hard) Pomerons" (≅ LO pQCD)
- Semi-hard dynamics built-in:
  - eikonal (multi)parton ladders (p-A, A-A possible)
  - gluon saturation (via enhanced |P diags)
- Non-perturbative ingredients:
  - string fagmentation (Lund model)
  - beam-remnants
- Model parameters:
  - Tuned with accelerator data.
  - $O(20)$ much less than in std collider MCs

LHC experiments: (p_T,η) acceptance

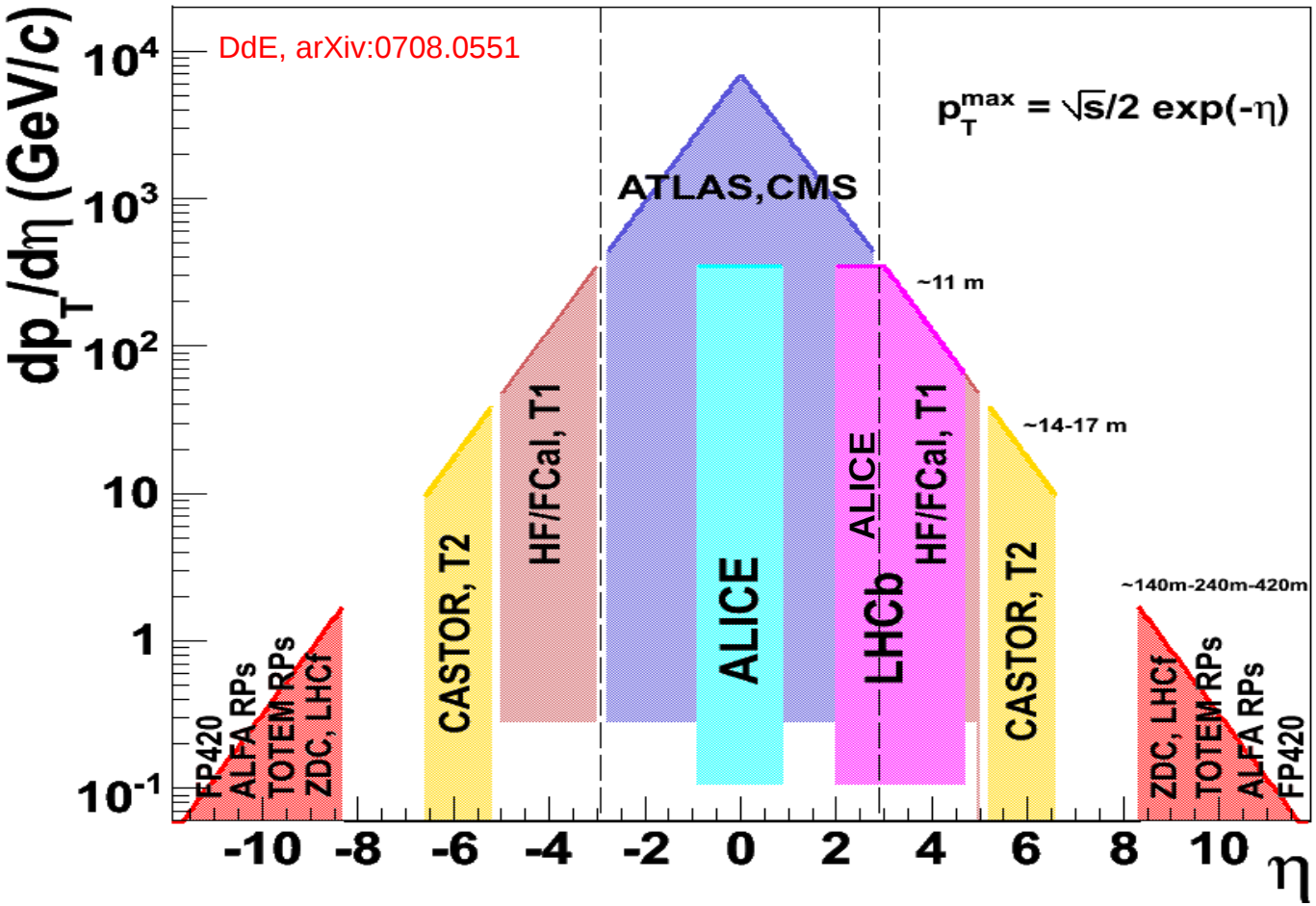

- Detectors cover ~all phase-space (1st time in a collider) !:

  $0 < p_T < (\sqrt{s}/2)e^{-\eta}$, $\Delta\eta \sim 2\times\ln(\sqrt{s})/m_p \sim 20$

Photon-induced collisions

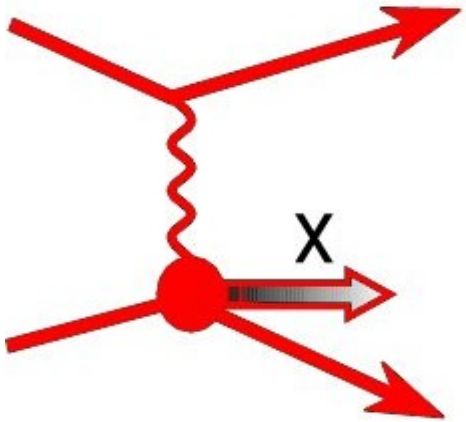

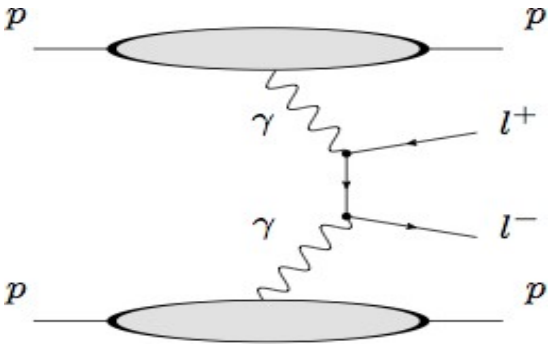

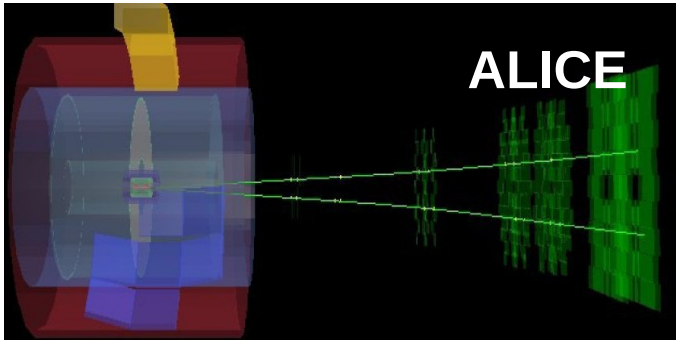

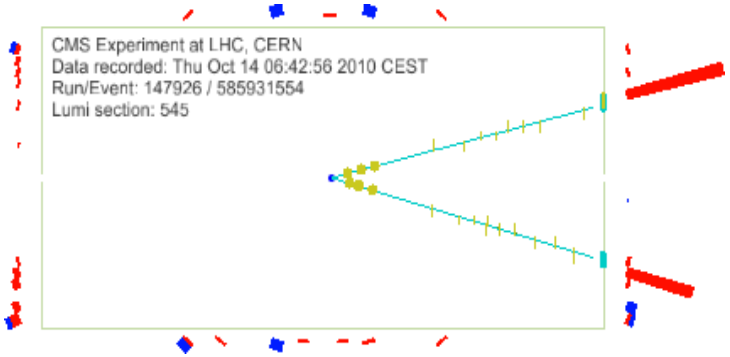

γ-A and γ-γ collisions (LHC)

- Observation of exclusive PbPb → Pb J/Ψ Pb photoproduction:

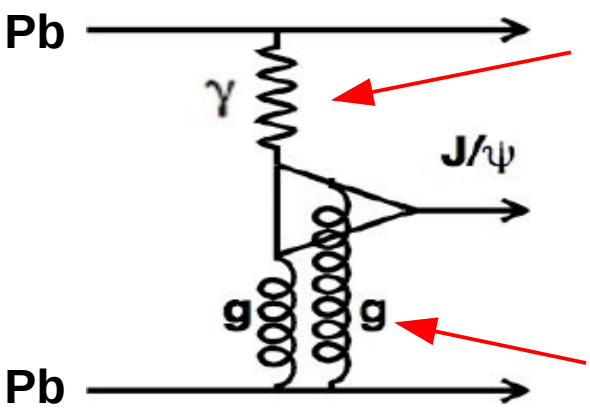

Pb photon fluxes enhanced by Z^2~7000 !

Very sensitive to badly unknown nuclear $xG(x,Q^2)$!

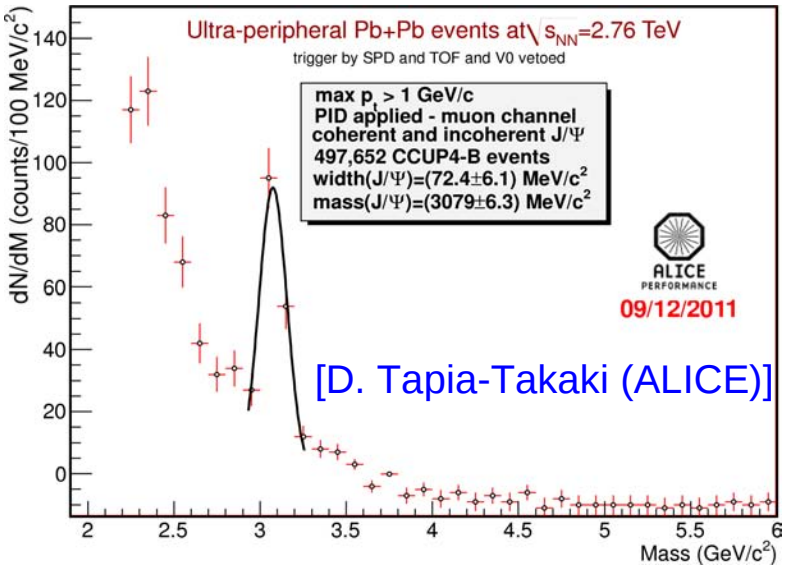

[D. Tapia-Takaki (ALICE)]

- Study of pp → pWWp: 10^4 times larger sensitivity to anomalous QGC

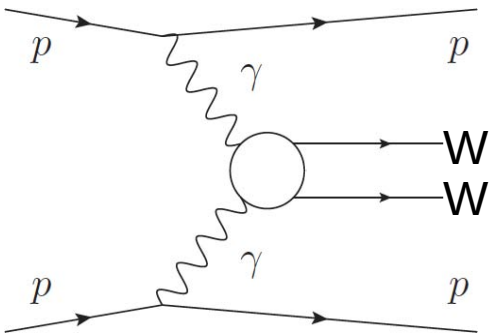

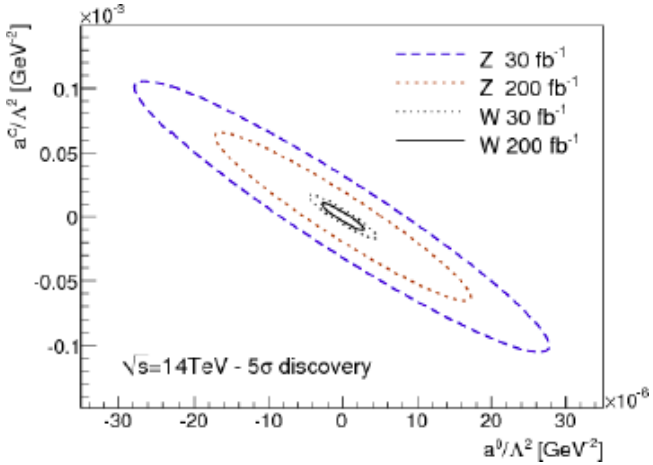

Hard parton-parton scatterings

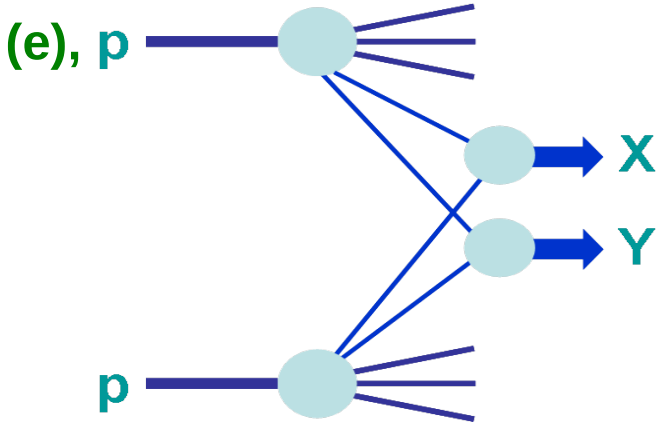

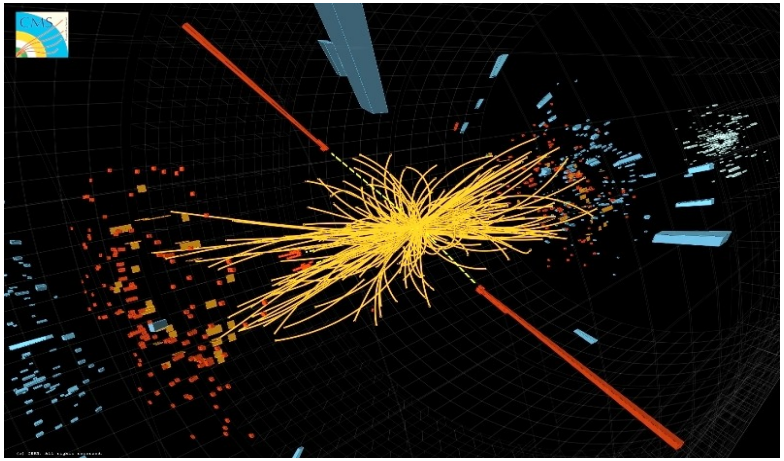

Parton distribution functions (LHC)

- Lots of new <u>data</u> !
  - Medium & large-x gluon:
    precision jets, prompt γ, top pairs.
  - Light-flavors at medium & small x:
    low-mass DY, Z vs y, W asymm.
  - Strangeness & heavy-flavors:
    W+c for s; Z,γ+c for charm; Z+b for bottom.

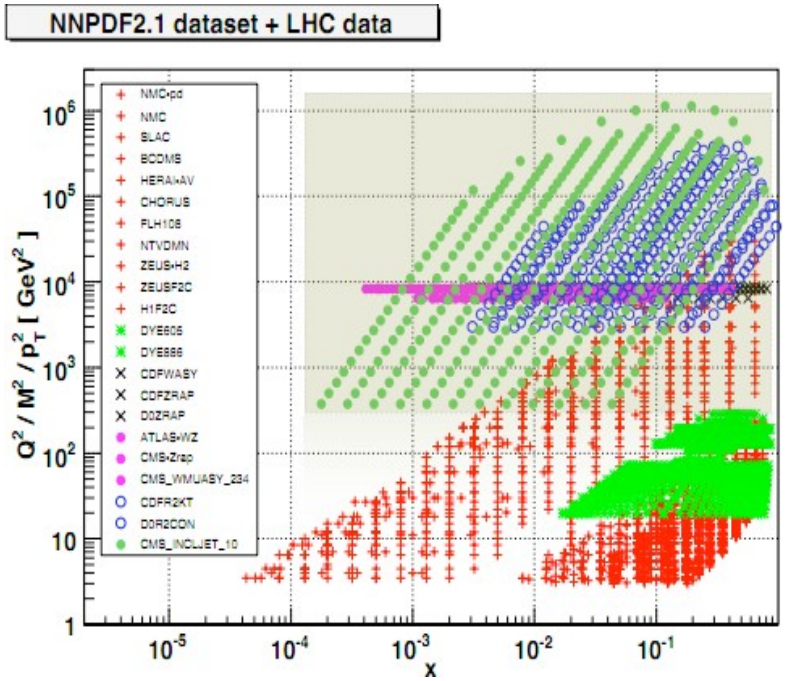

- New fast reweighting techniques (NNPDF2.1) for NLO PDFs:

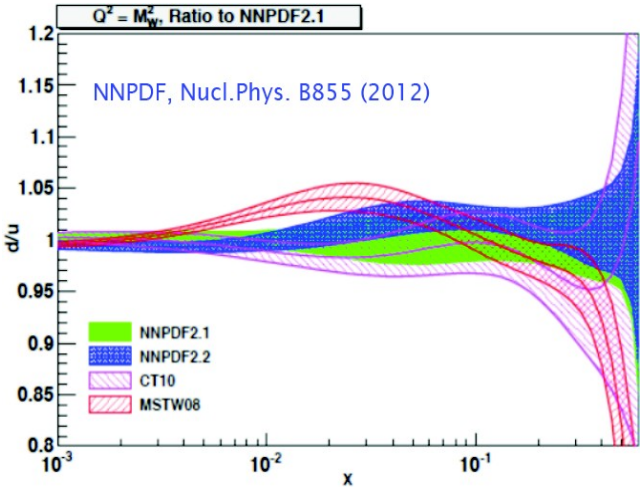

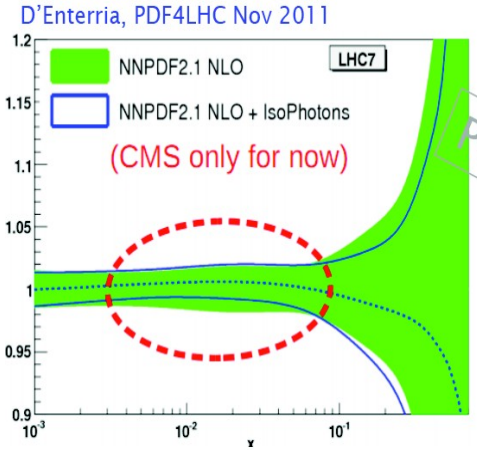

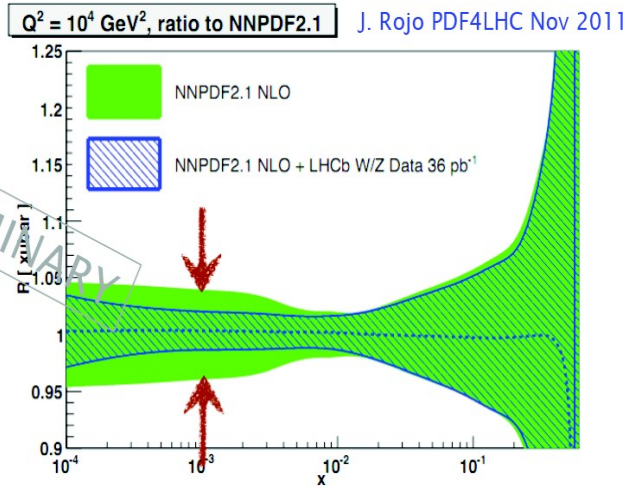

What's the physics “forward” ?

- Non-perturbative limit of QCD:

  elastic, soft diffractive p-p scattering (Regge-Gribov)

- High-energy (low-x) limit of QCD:

  gluon saturation, multi-parton interactions (Color-Glass condensate)

Multi-parton interactions (Atlas/CMS)

- Forward particle / energy flow

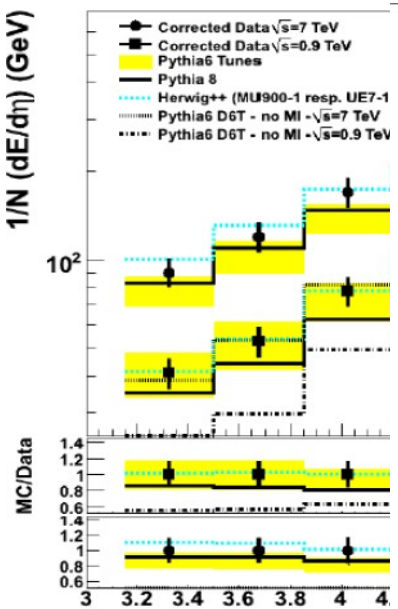

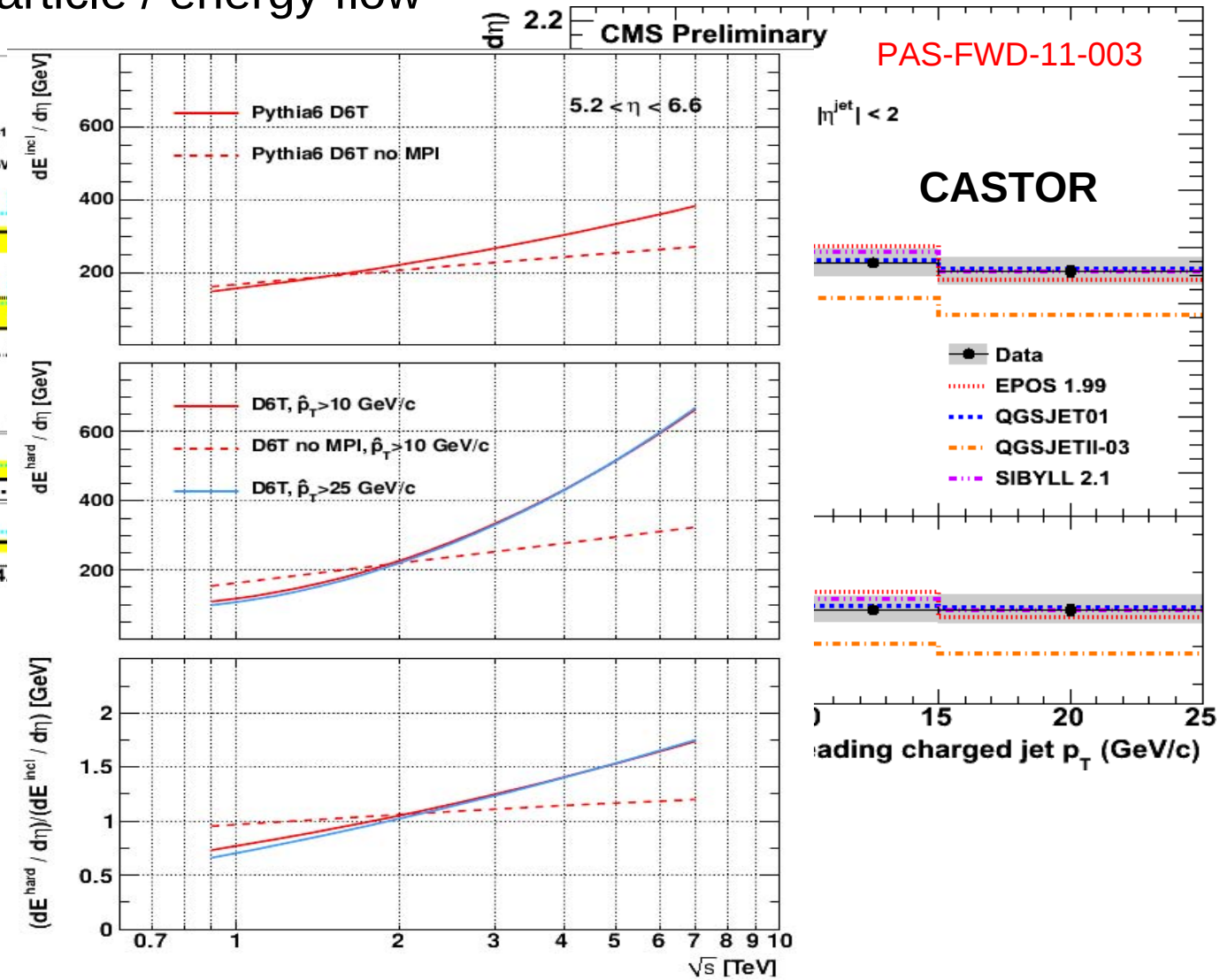

- Forward particle production clearly require MPIs

Double Parton Scattering (LHCb)

- MPI needed but yet no clear-cut proof of double hard parton-parton scattering.
- Maybe first hint on double J/Ψ prod. ?

J.Gaunt,C.Kom,A.Kulesza,W.Stirli
arXiv:1110.1174

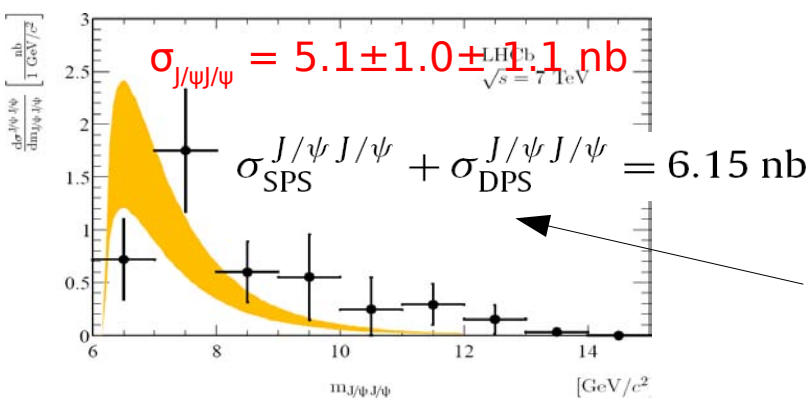

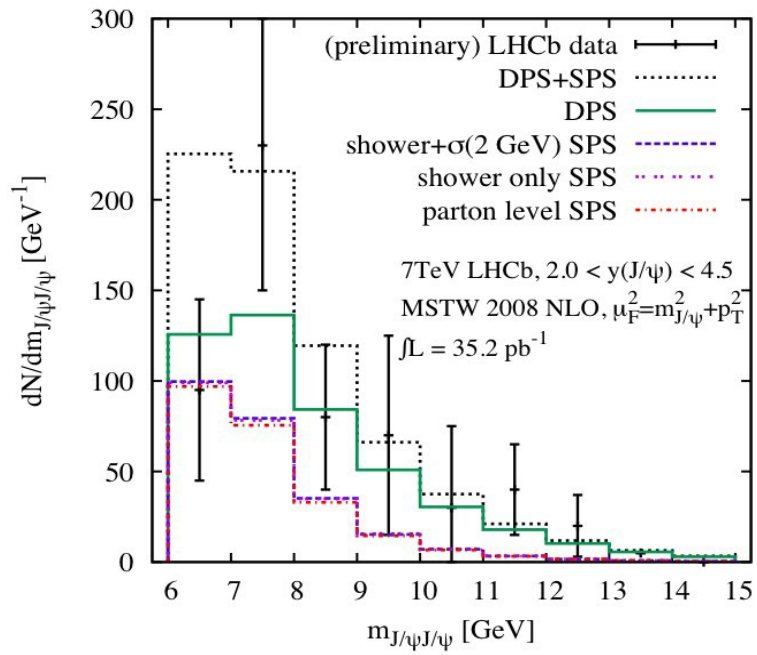

Prospect for a ridge in p+Pb collisions

Kevin Dusling

North Carolina State University
Raleigh, NC 27695

kevin_dusling@ncsu.edu

July 30th, 2012

NC STATE UNIVERSITY

The Ridge

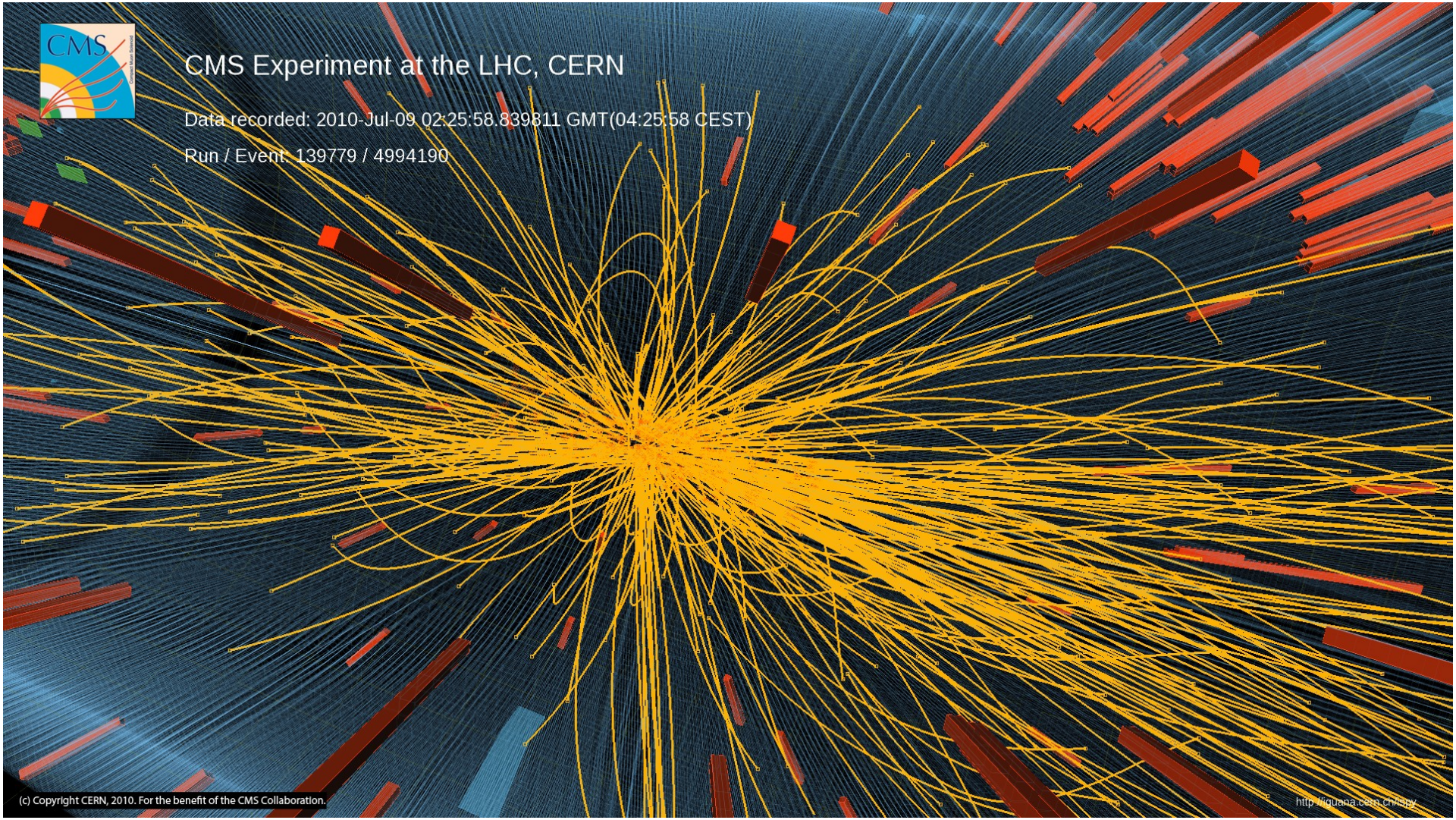

More than 200 charged particles!

The Ridge

CMS $N \geq 110$

$1.0 < p_T[\mathrm{GeV}] < 3.0$

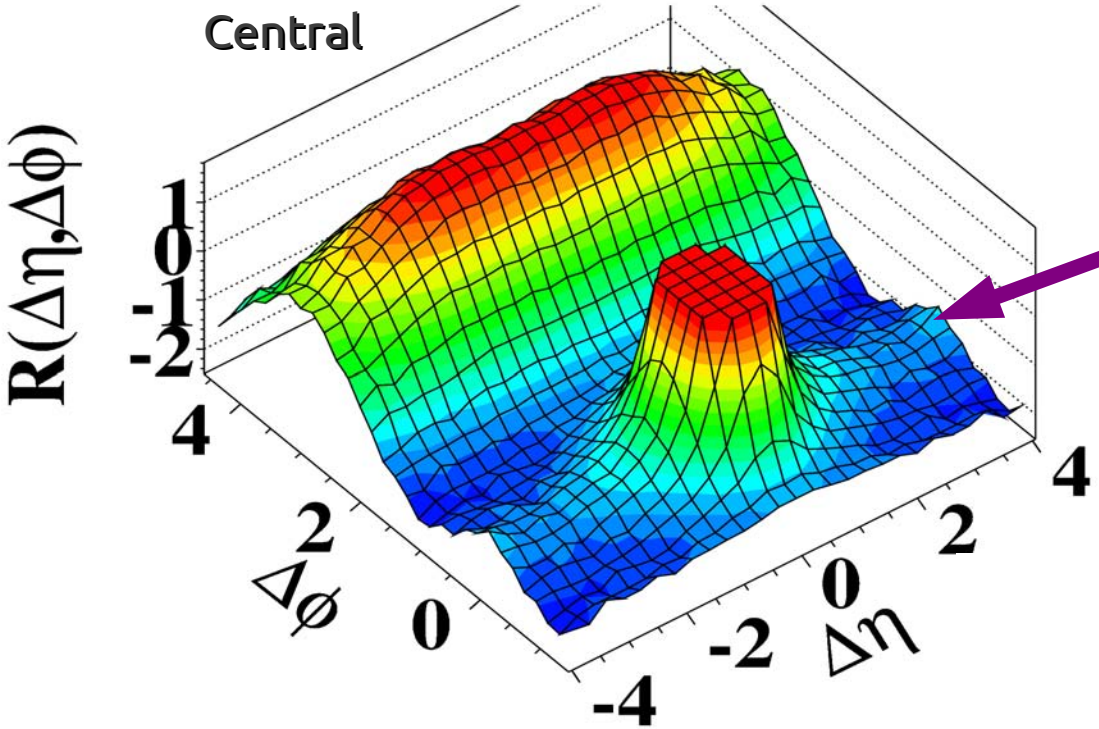

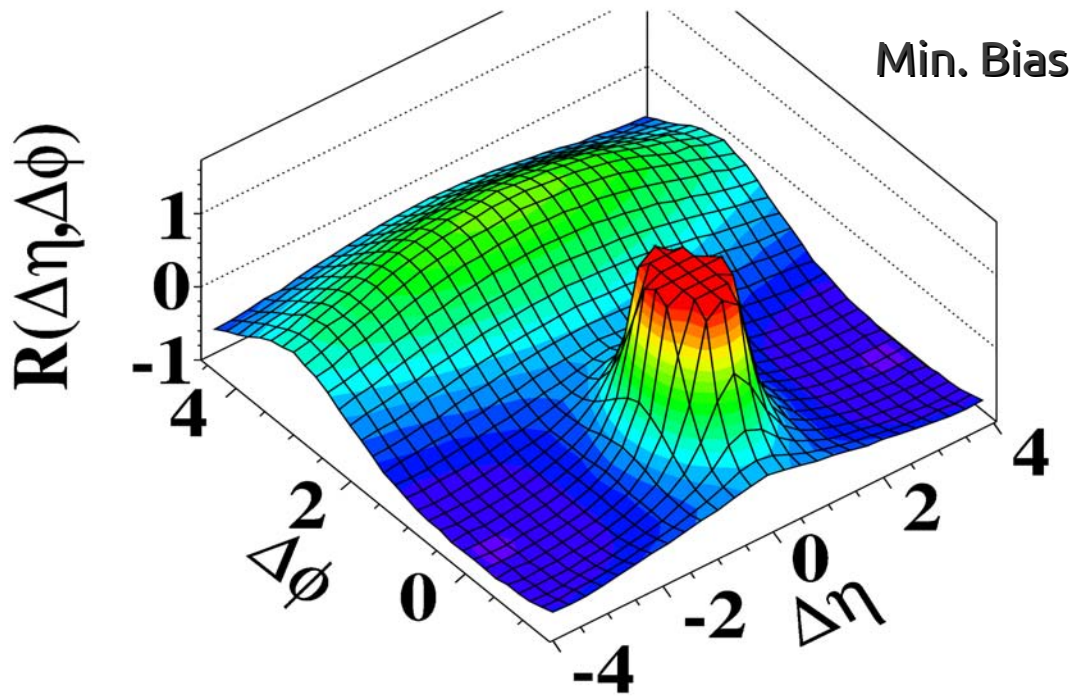

The Ridge

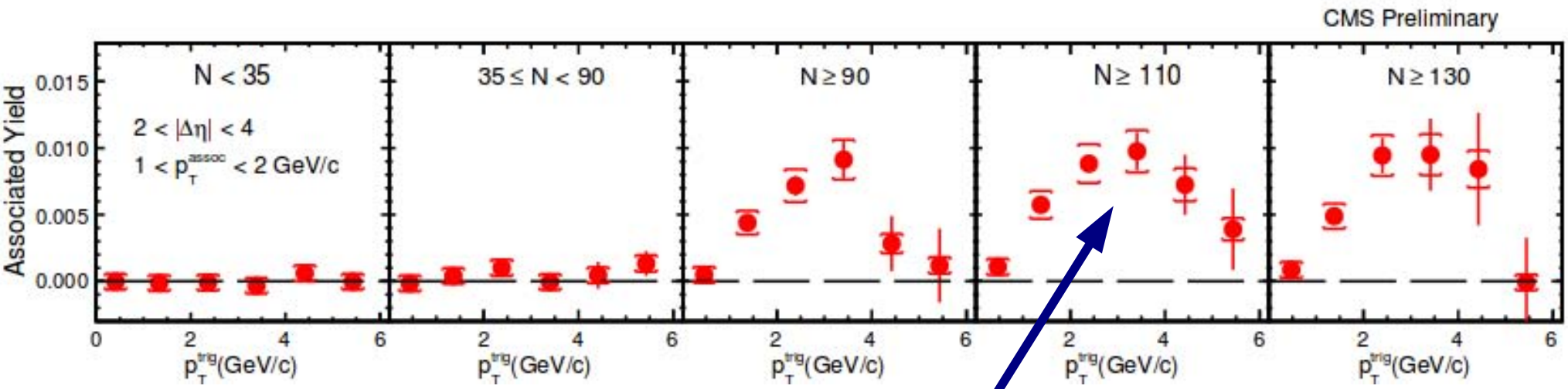

1. There is a clear scale in the data
2. It is semi-hard and will be argued to be Q_s

Multiplicity the same as in Cu+Cu !

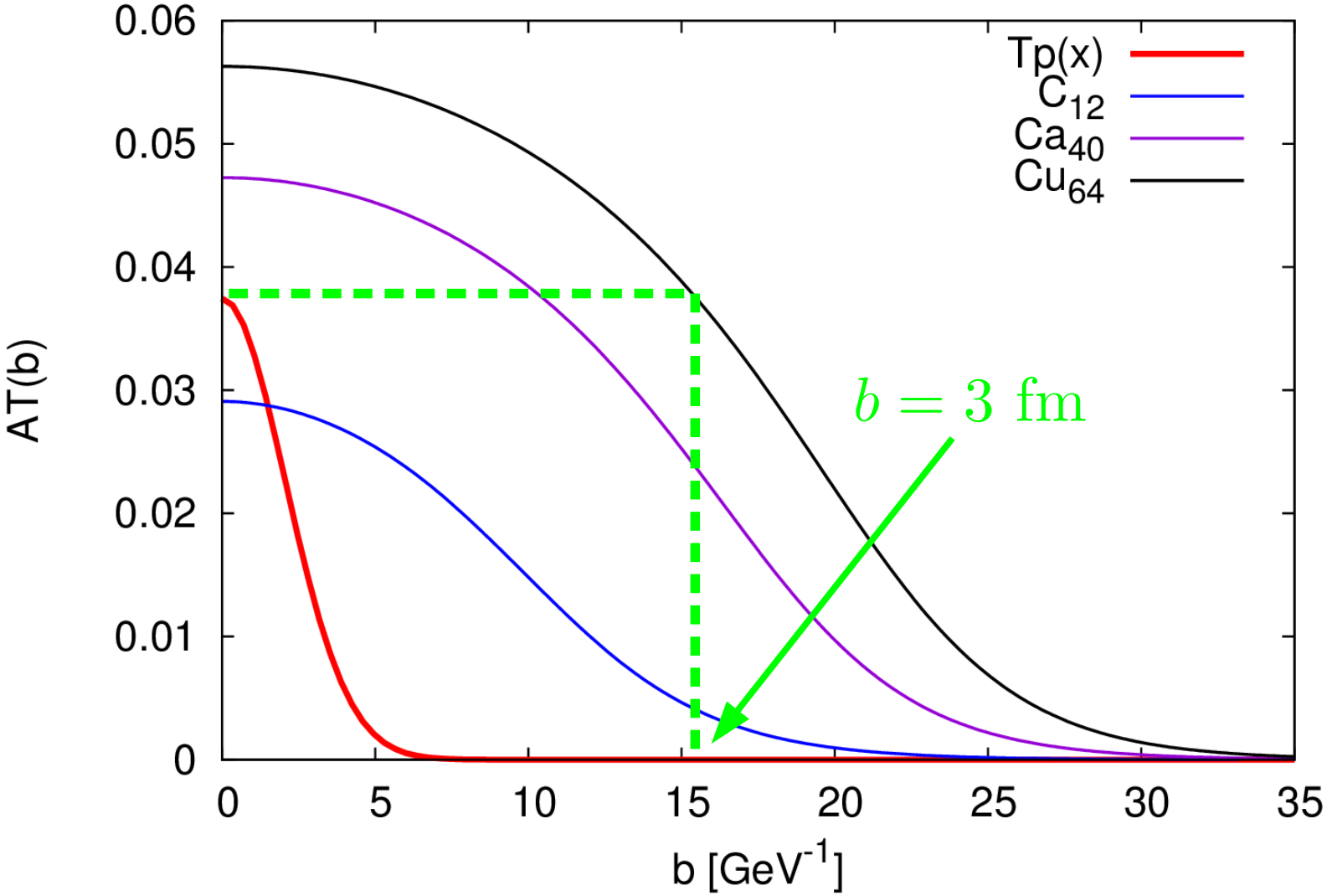

Wave function of the proton

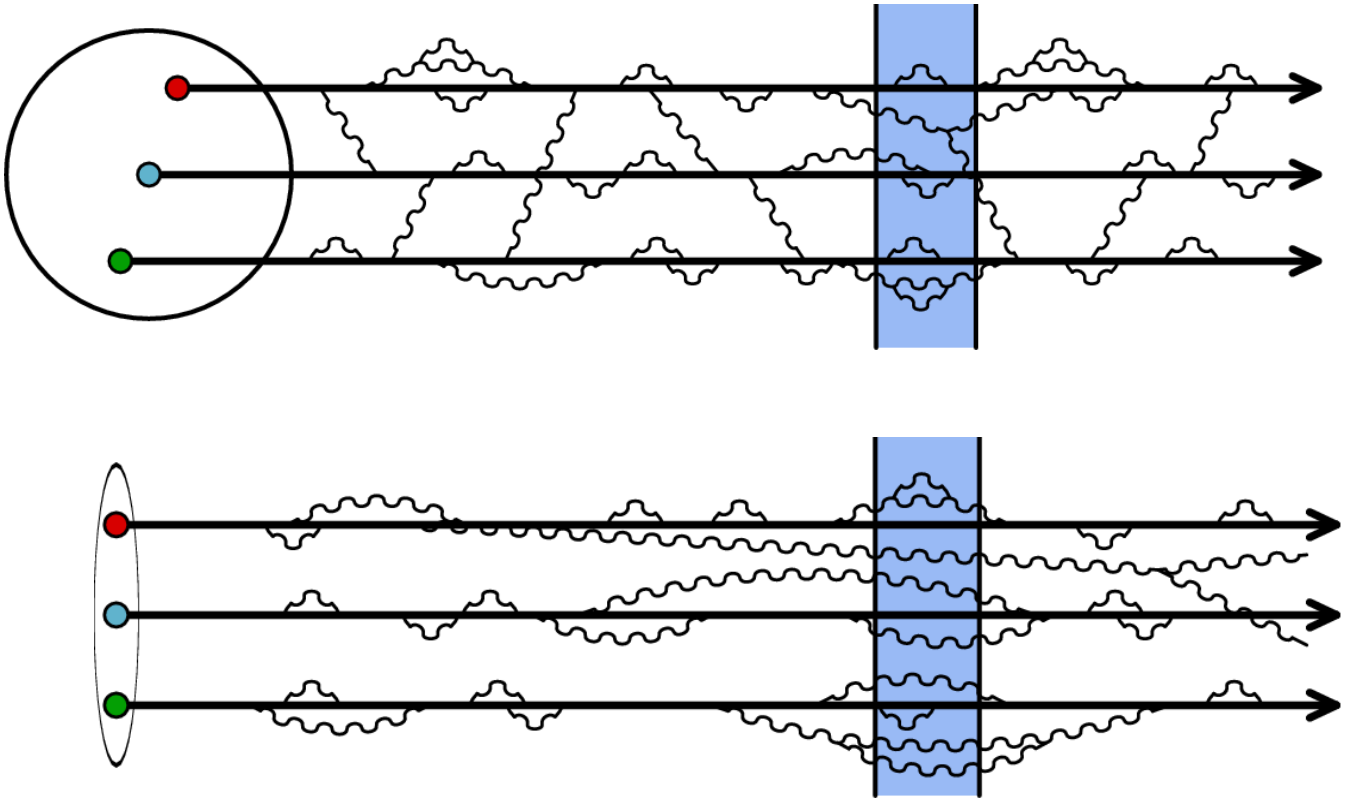

Figure courtesy of Francois Gelis

$$x \sim 10^{-2} \text{ at } \sqrt{s} = 200 \text{ GeV}$$

$$x \sim 10^{-4} \text{ at } \sqrt{s} = 7 \text{ TeV}$$

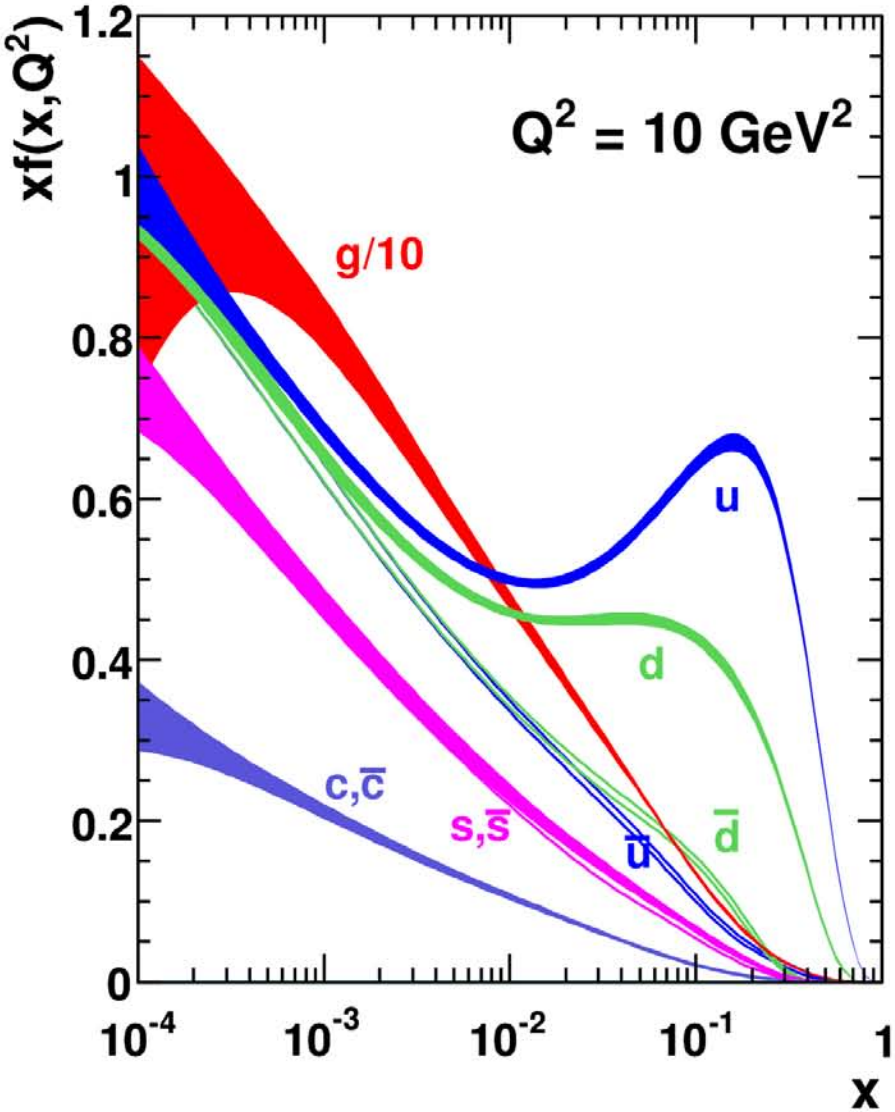

Growth of gluon distribution function at small x is seen experimentally.

Data / figures from: http://mstwpdf.hepforge.org/

The role of STRONG color sources

Diagram:	Min. Bias	Central
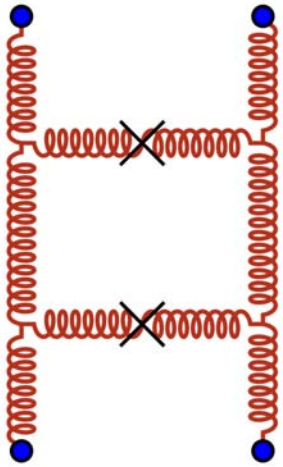	$\mathcal{O}\left(\alpha_s^4\right)$	$\mathcal{O}\left(1\right)$
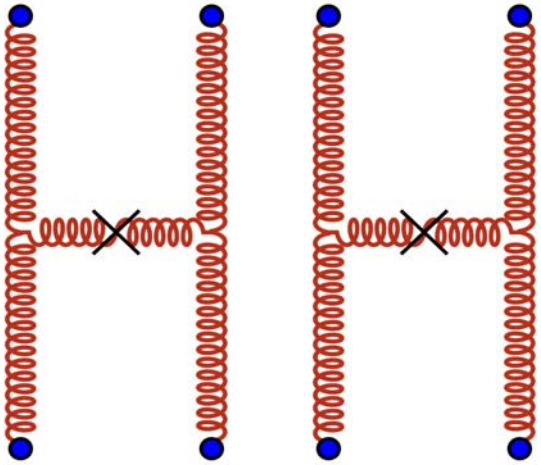	$\mathcal{O}\left(\alpha_s^6\right)$	$\mathcal{O}\left(\alpha_s^{-2}\right)$

High multiplicity are b=0 collisions

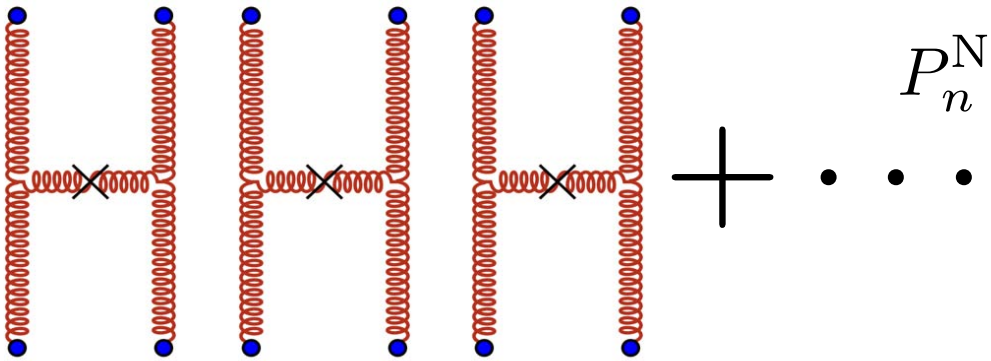

$$P_n^{\mathrm{NB}}(\overline{n},k) = \frac{\Gamma(k+n)}{\Gamma(k)\Gamma(n+1)} \frac{\overline{n}^n k^k}{(\overline{n}+k)^{n+k}}$$

Dumitru, Gelis, McLerran, Venugopalan, NPA810 91-108 (2008).
Dusling, Fernandez-Fraile, Venugopalan NPA828 (2009) 161-177.
Gelis, Lappi, McLerran, NPA828 (2009) 149-160.

$$k = \zeta \frac{\left(N_c^2 - 1\right) S_\perp Q_s^2}{2\pi}$$

$$\zeta = 0.155 \quad [\text{Empirical}]$$

$$\zeta = 0.2 - 1.5 \quad [\text{Lattice}]$$

Emprical: Tribedy, Venugopalan, NPA850 (2011) 136-156.
Lattice (CYM): Lappi, Srednyak, Venugopalan, JHEP01 (2010) 066.
Schenke, Tribedy, Venugopalan, arXiv:1206.6805

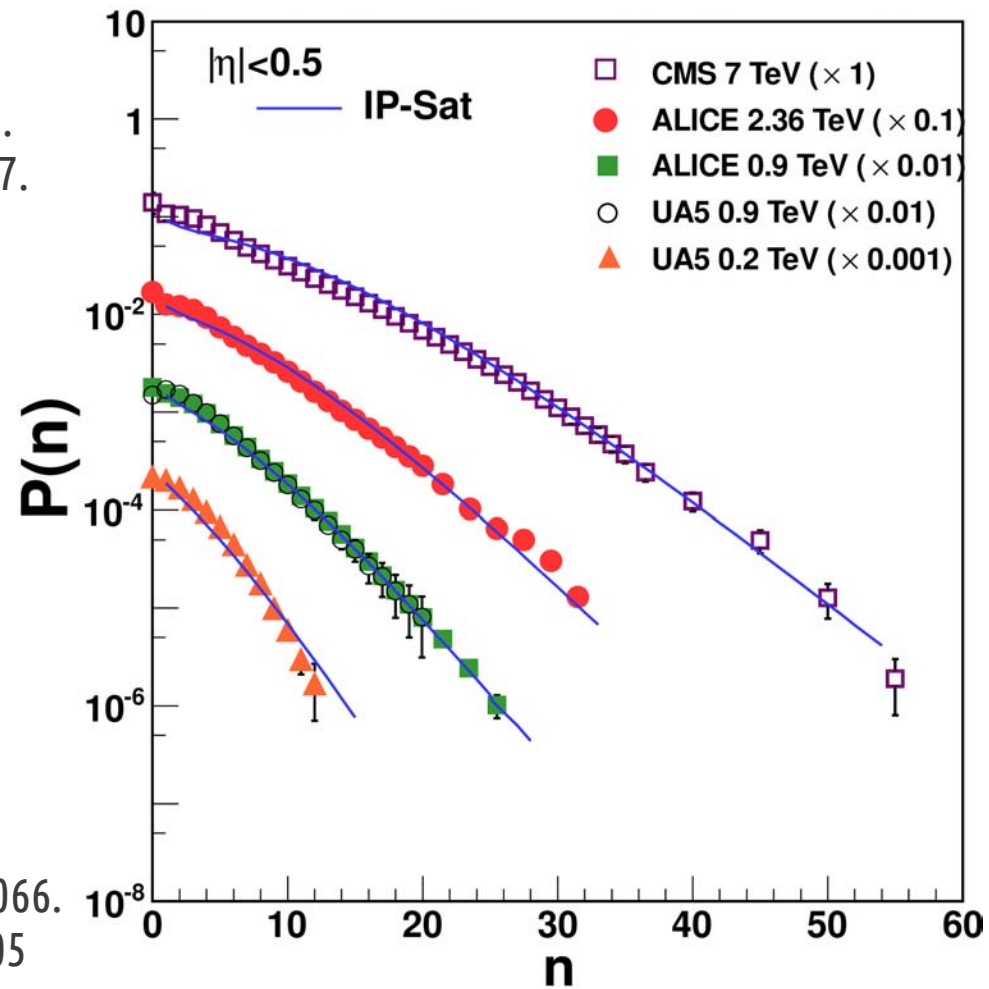

Forward jet structure

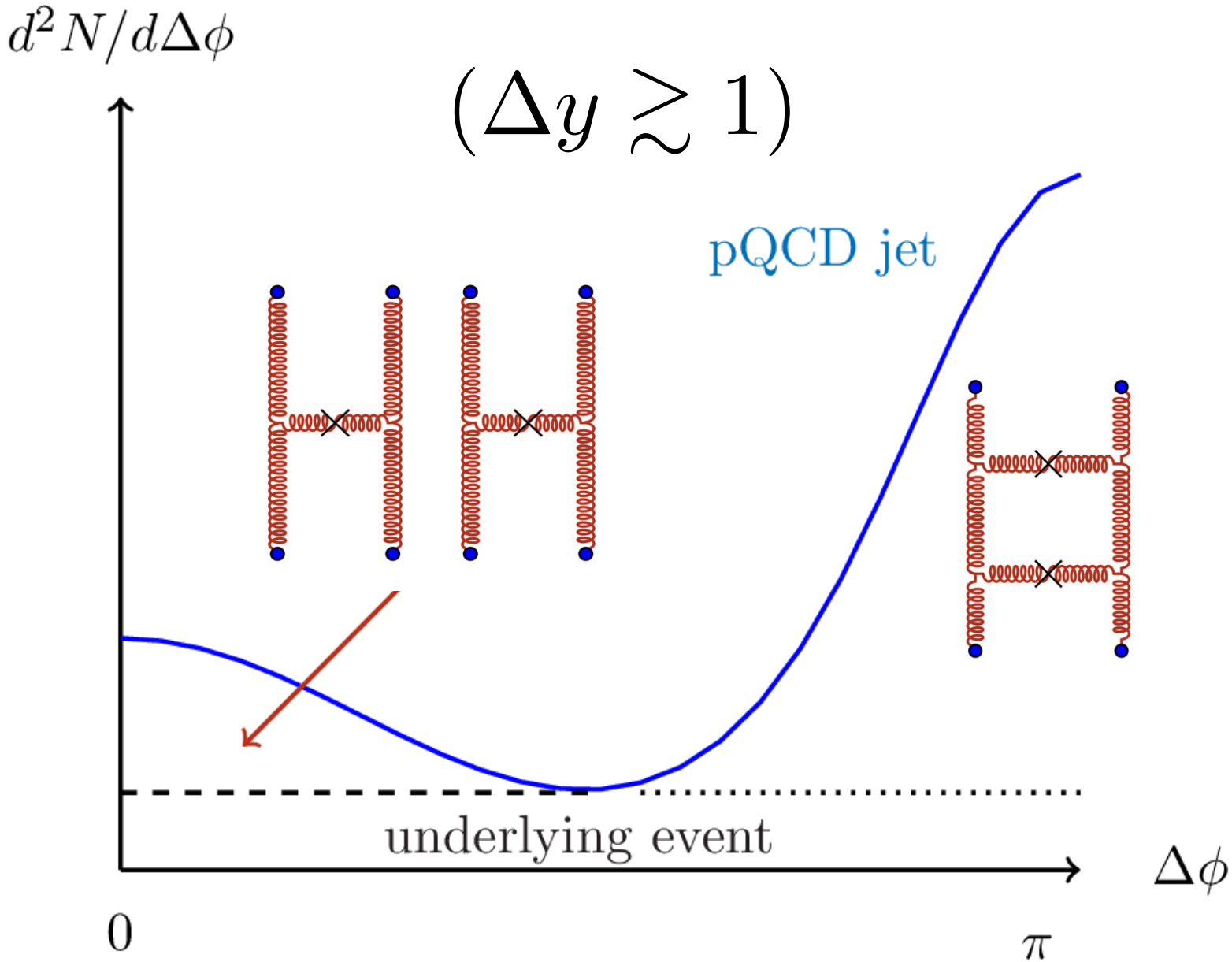

Gluon radiation

As the energy is increased new gluons are emitted with probability

$$\mathrm{d}P_{\mathrm{Brem}} \sim C_R \frac{\alpha_s}{\pi^2} \frac{\mathrm{d}^2 k_\perp}{k_\perp^2} \frac{\mathrm{d}x}{x}$$

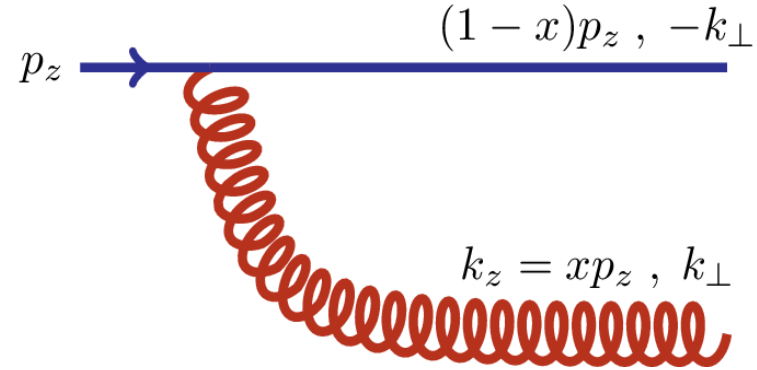

And as long as the density remains low the evolution is linear

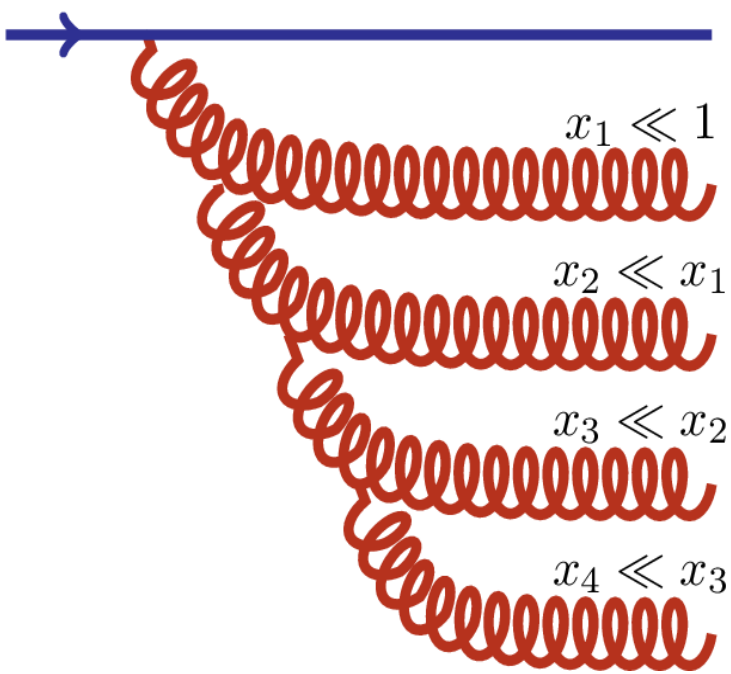

$$\frac{\partial T(\mathbf{r}_\perp, Y)}{\partial Y} = \frac{\alpha_s N_c}{2\pi^2} \int \mathrm{d}\mathbf{r}_1 \frac{\mathbf{r}_\perp^2}{\mathbf{r}_1^2 \left(\mathbf{r}_\perp - \mathbf{r}_1\right)^2} \times$$
$$\left[T(\mathbf{r}_1, Y) + T(\mathbf{r}_\perp - \mathbf{r}_1, Y) - T(\mathbf{r}_\perp, Y)\right]$$

Kuraev, Lipatov, Fadin, Sov.Phys.JETP44 443-450 (1976).
Sov.Phys.JETP45 199-204 (1977).
Balitsky, Lipatov, Sov.J.Nucl.Phys 28 822-829 (1978).

BK Evolution Equation

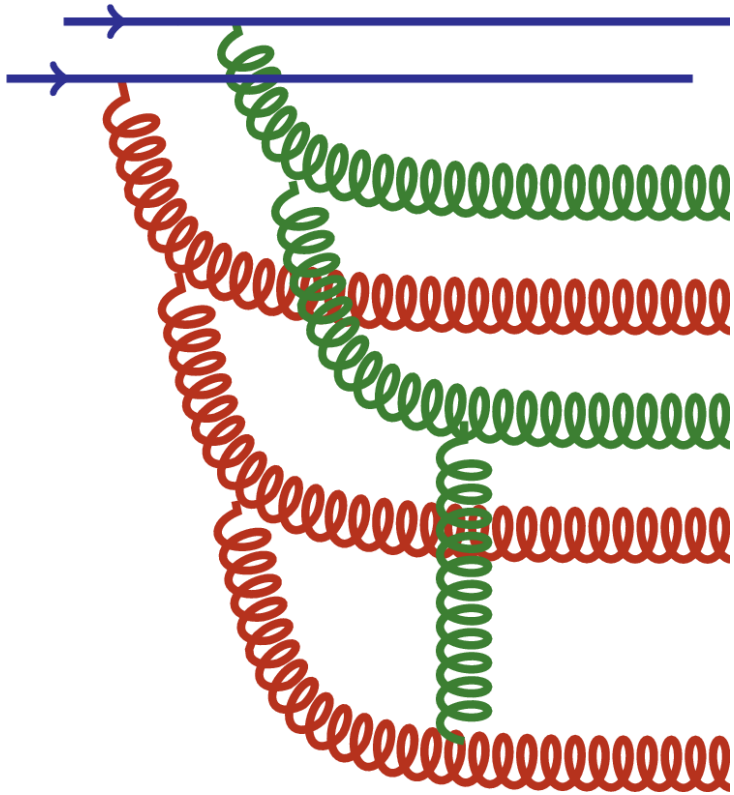

Balitsky, NPB 463, 99 (1996).
Kovchegov, PRD 60, 034008 (1999).

Jalilian-Marian, Kovner, McLerran, Weigert, PRD 55 5414 (1997).
Jalilian-Marian, Kovner, Leonidov, Weigert, NPB 504 415 (1997), PRD 59 014014 (1999).

$$\frac{\partial T(\mathbf{r}_\perp, Y)}{\partial Y} = \frac{\alpha_s N_c}{2\pi^2} \int \mathrm{d}\mathbf{r}_1 \, \frac{\mathbf{r}_\perp^2}{\mathbf{r}_1^2 \left(\mathbf{r}_\perp - \mathbf{r}_1\right)^2} \times$$

$$\left[T(\mathbf{r}_1, Y) + T(\mathbf{r}_\perp - \mathbf{r}_1, Y) - T(\mathbf{r}_\perp, Y) - T(\mathbf{r}_1, Y) T(\mathbf{r}_\perp - \mathbf{r}_1, Y)\right]$$

NLO BK Equation

$$\frac{\partial T(\mathbf{r}_\perp, Y)}{\partial Y} = \int \mathrm{d}\mathbf{r}_1 \mathcal{K}_{\mathrm{Bal.}}(\mathbf{r}_\perp, \mathbf{r}_1, \mathbf{r}_\perp - \mathbf{r}_1) \times$$
$$[T(\mathbf{r}_1, Y) + T(\mathbf{r}_\perp - \mathbf{r}_1, Y) - T(\mathbf{r}_\perp, Y) - T(\mathbf{r}_1, Y) T(\mathbf{r}_\perp - \mathbf{r}_1, Y)]$$

$$\mathcal{K}_{\mathrm{Bal.}}(\mathbf{r}, \mathbf{r}_1, \mathbf{r}_2) = \frac{\alpha_s(\mathbf{r}) N_c}{\pi} \left[\frac{\mathbf{r}^2}{\mathbf{r}_1^2 \mathbf{r}_2^2} + \frac{1}{\mathbf{r}_1^2} \left(\frac{\alpha_s(\mathbf{r}_1^2)}{\alpha_s(\mathbf{r}_2^2)} - 1 \right) + \frac{1}{\mathbf{r}_2^2} \left(\frac{\alpha_s(\mathbf{r}_2^2)}{\alpha_s(\mathbf{r}_1^2)} - 1 \right) \right]$$

Balitsky, Chirilli PRD 77 014019
Kovchegov, Weigert NPA 784 188
Albacete, Kovchegov PRD 75 125021

Deep inelastic scattering on the Proton

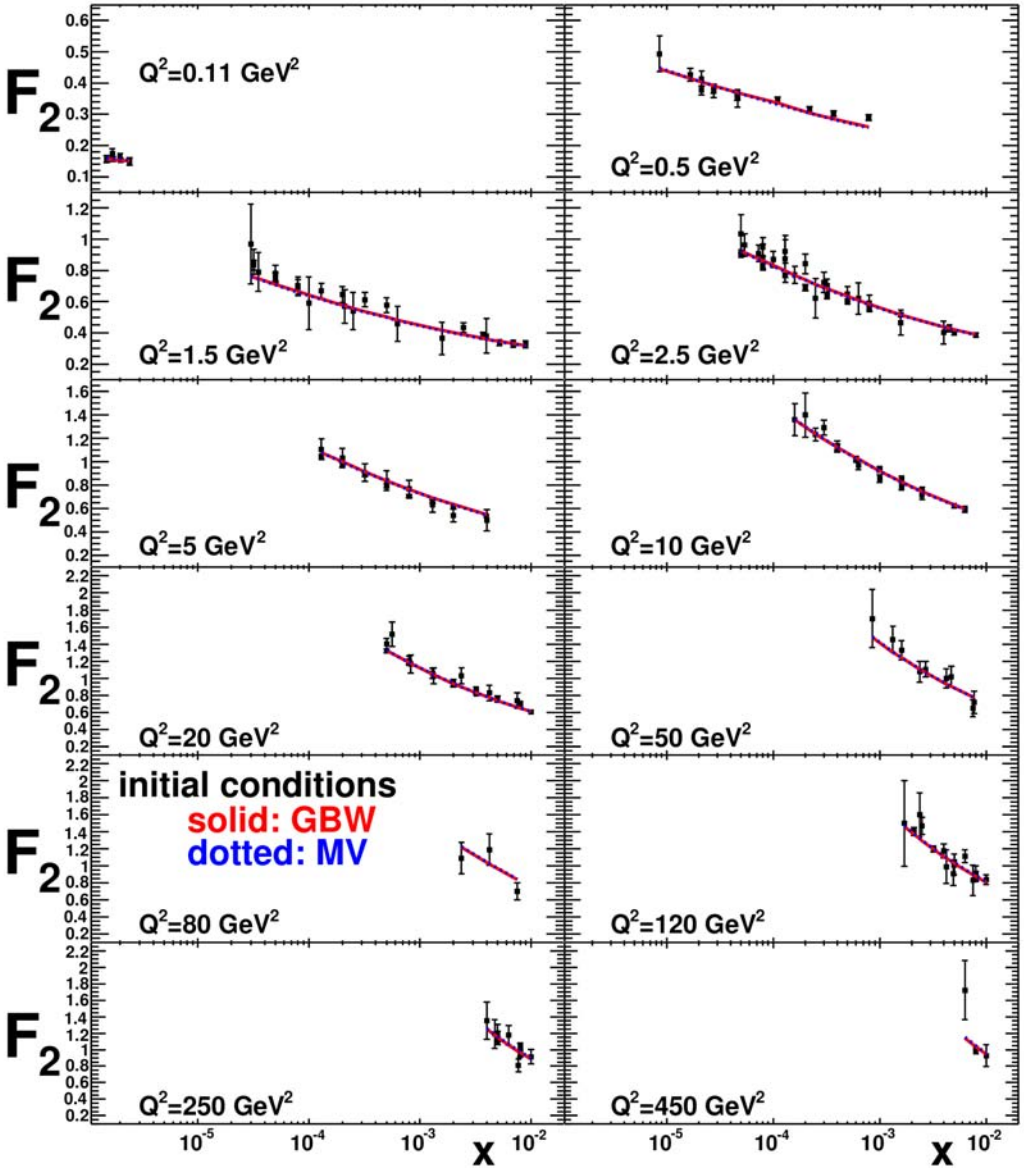

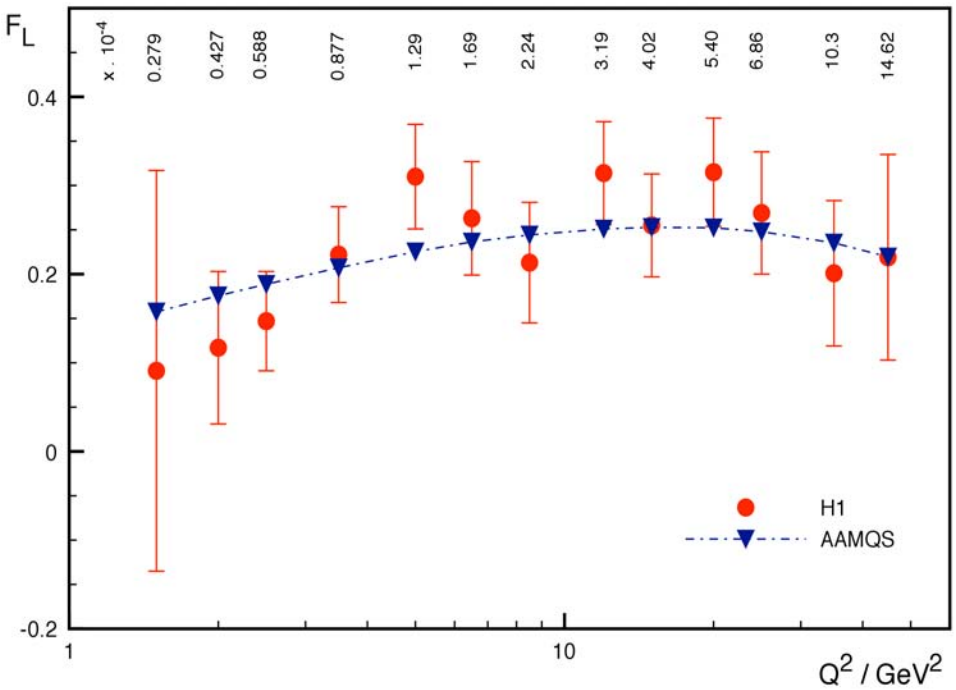

Albacete, Armesto, Milhano, Salgado; PRD80 (2009) 034031.
Quiroga-Arias, Albacete, Armesto, Milhano, Salgado; PRD80 J.Phys.G G38 (2011) 124124.

Unintegrated gluon distribution

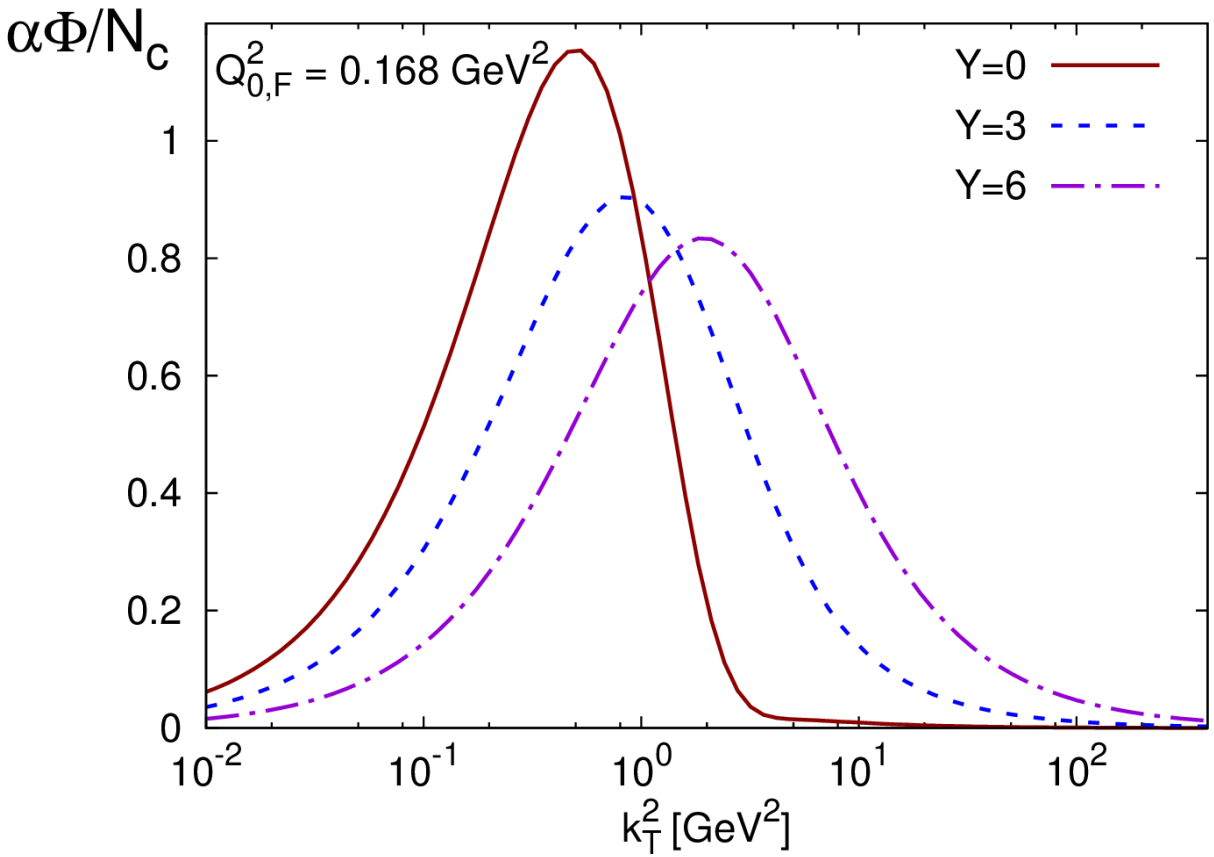

$$\Phi_{A_{1,2}}(x,k_\perp) = \frac{N_c k_\perp^2}{4\,\alpha_s(\mathbf{k}_\perp)} \int \mathrm{d}^2\mathbf{r}_\perp\; J_0(k_\perp r_\perp)\; \left[1 - T_{A_{1,2}}(r_\perp, \ln(1/x))\right]^2$$

k_T factorization: single gluon production

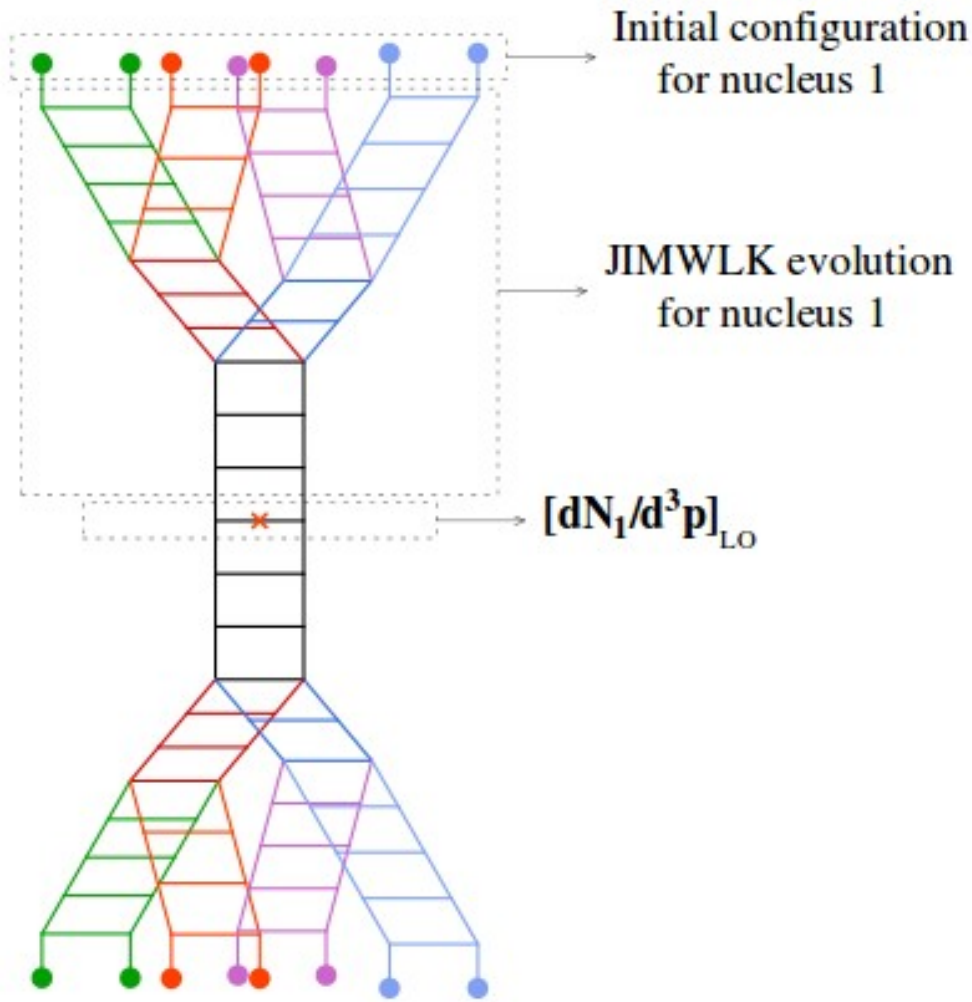

$$\left\langle \frac{\mathrm{d}N_1}{\mathrm{d}^2\mathbf{p}_\perp \mathrm{d}y_p} \right\rangle_{\mathrm{LLog}} = \frac{8\alpha_s(p_\perp)S_\perp}{C_F(2\pi)^4}\frac{1}{\mathbf{p}_\perp^2}\int \frac{\mathrm{d}^2k_\perp}{(2\pi)^2}\Phi_{A_1}(y_p,k_\perp)\Phi_{A_2}(y_p,p_\perp-k_\perp)$$

k_T factorization: double gluon production

$$\left\langle \frac{\mathrm{d}N_2}{\mathrm{d}^2\mathbf{p}_\perp \mathrm{d}y_p \mathrm{d}^2\mathbf{q}_\perp \mathrm{d}y_q} \right\rangle_{\mathrm{LLog}} = \frac{32\alpha_s(\mathbf{p}_\perp)\alpha_s(\mathbf{q}_\perp)}{(2\pi)^{10} N_c C_F^3 \zeta} \frac{1}{\mathbf{p}_\perp^2 \mathbf{q}_\perp^2}$$

$$\begin{aligned}
\times \Bigg\{ & \int \mathrm{d}^2\mathbf{k}_{1\perp} \Phi^2_{A_1}(y_p, \mathbf{k}_{1\perp}) \Phi_{A_2}(y_p, \mathbf{p}_\perp - \mathbf{k}_{1\perp}) \Phi_{A_2}(y_q, \mathbf{q}_\perp + \mathbf{k}_{1\perp}) \\
+ & \int \mathrm{d}^2\mathbf{k}_{1\perp} \Phi^2_{A_1}(y_p, \mathbf{k}_{1\perp}) \Phi_{A_2}(y_p, \mathbf{p}_\perp - \mathbf{k}_{1\perp}) \Phi_{A_2}(y_q, \mathbf{q}_\perp - \mathbf{k}_{1\perp}) \\
+ & \int \mathrm{d}^2\mathbf{k}_{1\perp} \Phi^2_{A_2}(y_q, \mathbf{k}_{1\perp}) \Phi_{A_1}(y_p, \mathbf{p}_\perp - \mathbf{k}_{1\perp}) \Phi_{A_1}(y_q, \mathbf{q}_\perp + \mathbf{k}_{1\perp}) \\
+ & \int \mathrm{d}^2\mathbf{k}_{1\perp} \Phi^2_{A_2}(y_q, \mathbf{k}_{1\perp}) \Phi_{A_1}(y_p, \mathbf{p}_\perp - \mathbf{k}_{1\perp}) \Phi_{A_1}(y_q, \mathbf{q}_\perp - \mathbf{k}_{1\perp}) \Bigg\}
\end{aligned}$$

Gelis, Lappi, Venugopalan, PRD78, 050419 (2008).
PRD78, 054020 (2008).
PRD79, 094017 (2009).
Dusling, Gelis, Lappi, Venugopalan, NPA 836 159-182 (2010).

k_T factorization: double gluon production

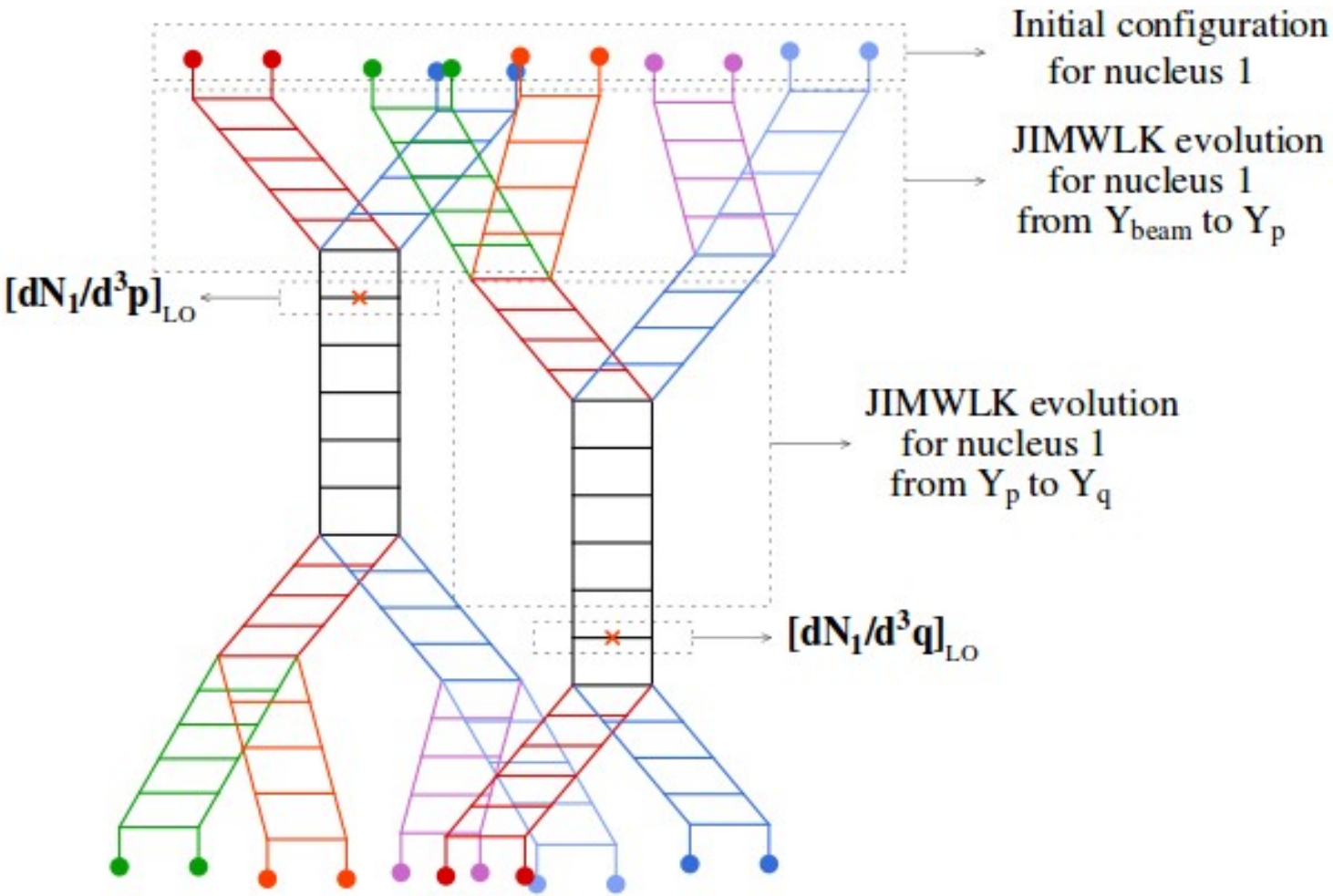

Angular Structure

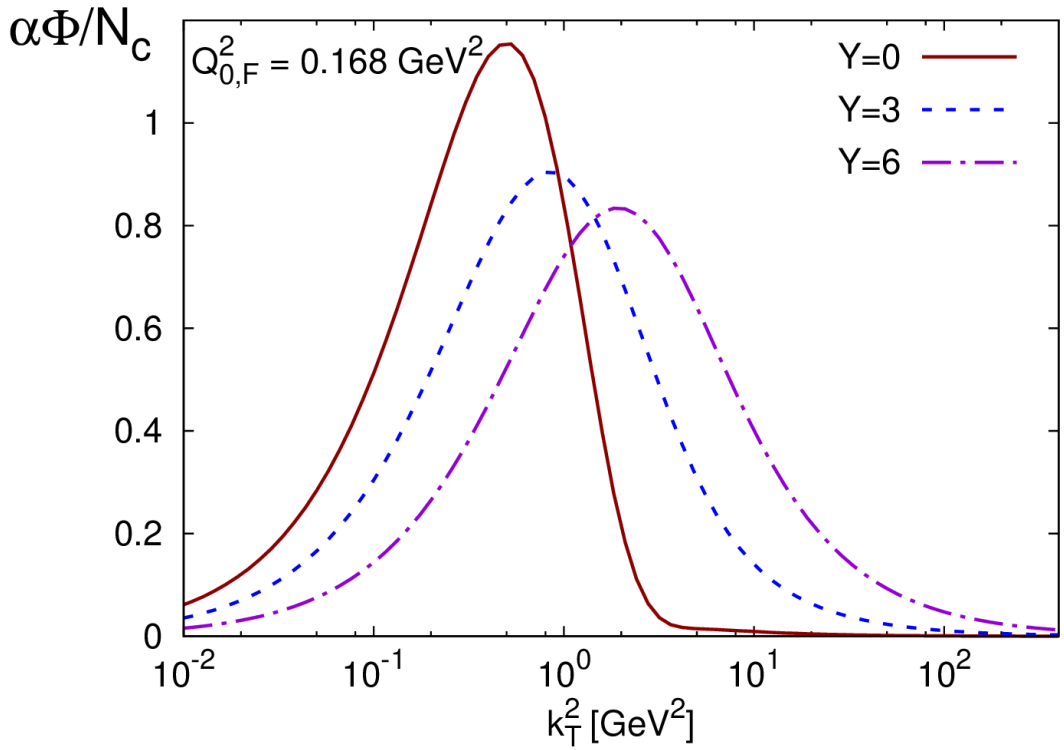

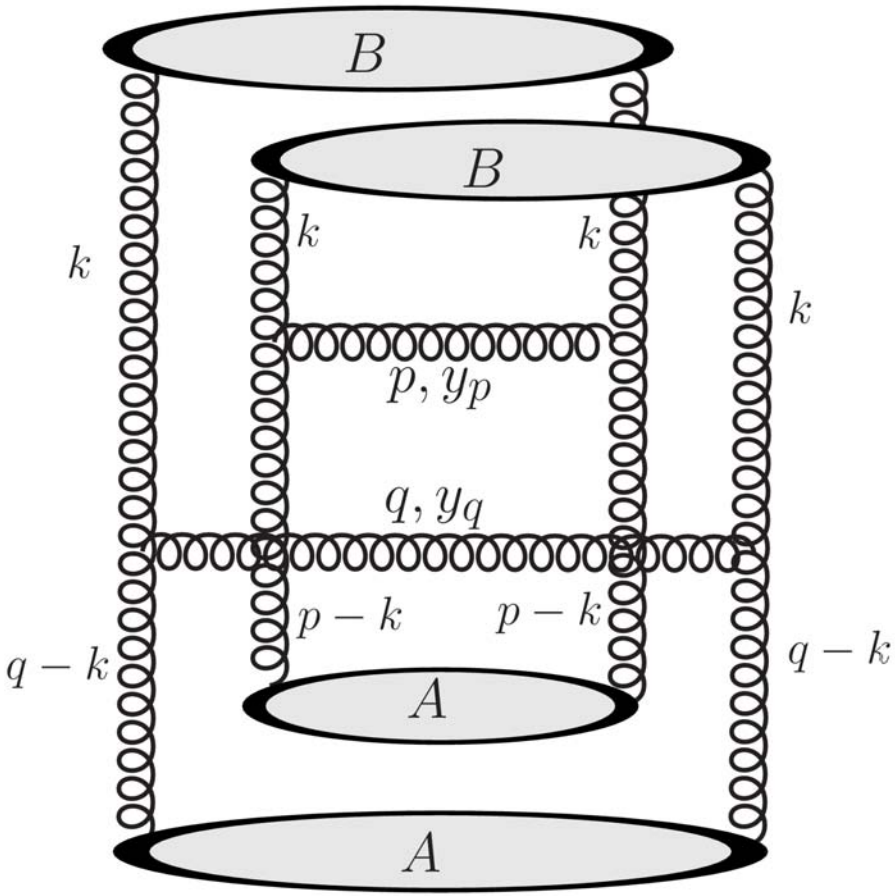

Condition for Ridge (Qualitatively):

$$|\mathbf{k}_\perp| \sim |\mathbf{p}_\perp - \mathbf{k}_\perp| \sim |\mathbf{q}_\perp \pm \mathbf{k}_\perp| \sim Q_s$$

Dumitru, Dusling, Gelis, Lalilian-Marion, Lappi, Venugopalan, PLB 697 12-25 (2011).

Forward jet structure

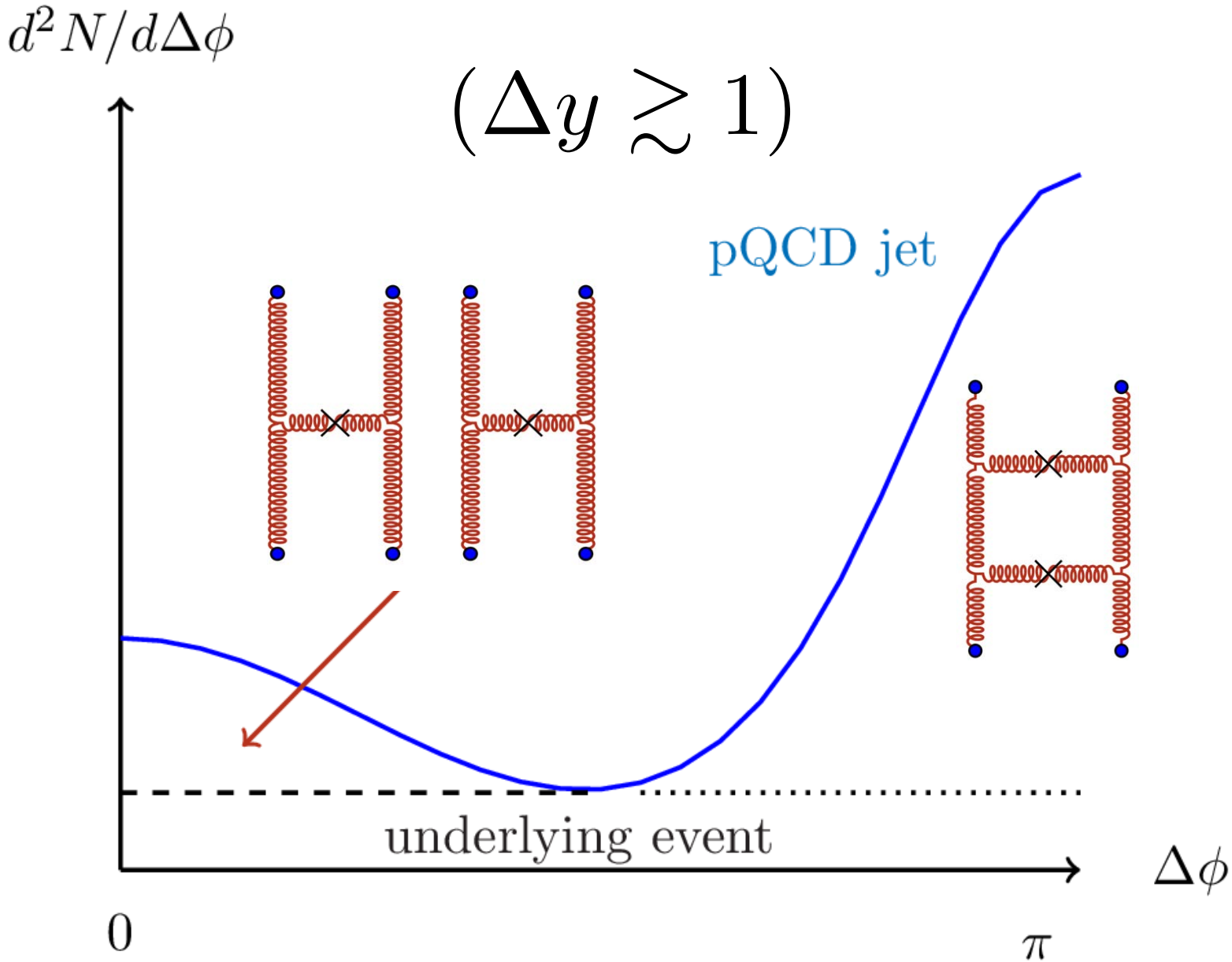

Centrality Dependence

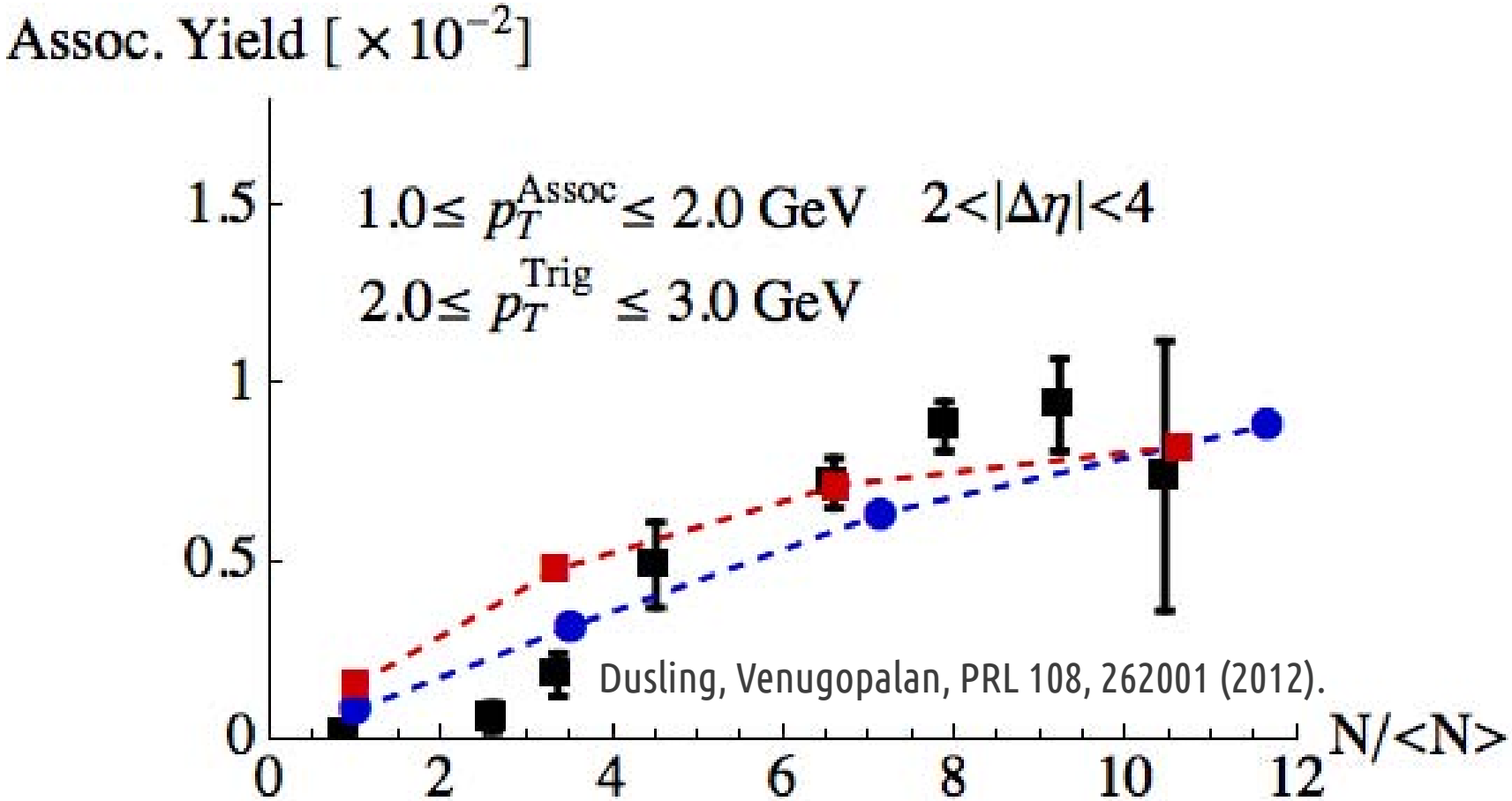

Dusling, Venugopalan, PRL 108, 262001 (2012).

$$Q^2_{0,F}(x_0 = 0.01) = 0.15, 0.3, 0.45, 0.6 \text{ GeV}^2$$

Trigger Dependence

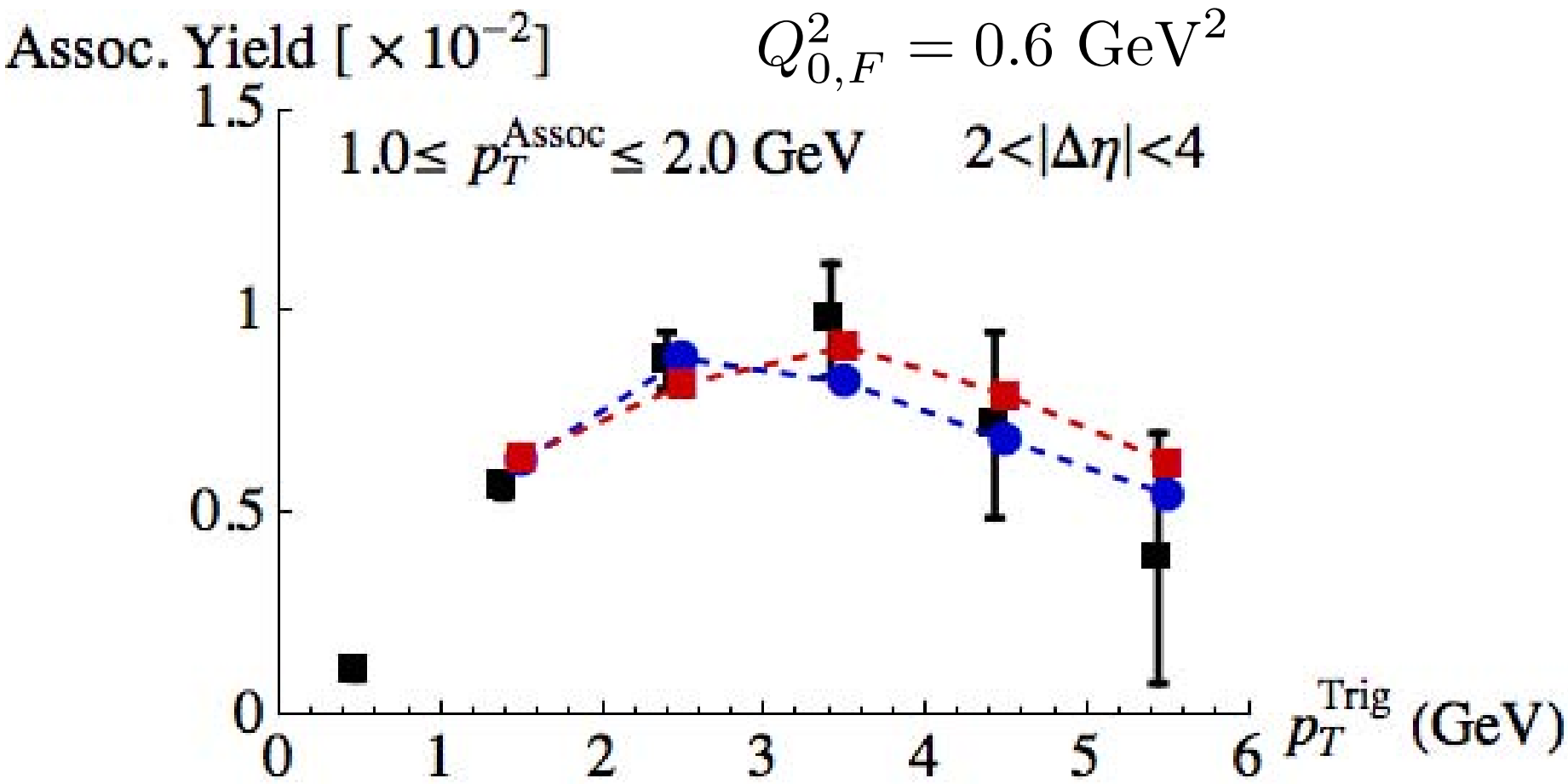

Blast Wave I

$$\frac{d^2N}{d\Delta\phi} = \int_{-\pi}^{\pi} d\Psi \mathcal{J}\left(\Psi, \Delta\phi\right) \frac{d^2N}{d\Delta\tilde{\phi}} \left(\Delta\tilde{\phi}\left(\Psi, \Delta\phi\right)\right)$$

$$2\sin^2\left(\frac{\Delta\tilde{\phi}}{2}\right) =$$

$$\frac{\sqrt{1-\beta^2}\left(1-\cos\left(\Delta\phi\right)\right)}{1-2\beta\cos\Psi\cos\left(\frac{\Delta\phi}{2}\right)+\frac{\beta^2}{2}\left(\cos\left(\Delta\phi\right)+\cos\left(2\Psi\right)\right)} .$$

$$\mathcal{J} = \frac{1-\beta^2}{\left(1-\beta\cos\left(\Psi+\Delta\phi/2\right)\right)\left(1-\beta\cos\left(\Psi-\Delta\phi/2\right)\right)} ,$$

Blast Wave II

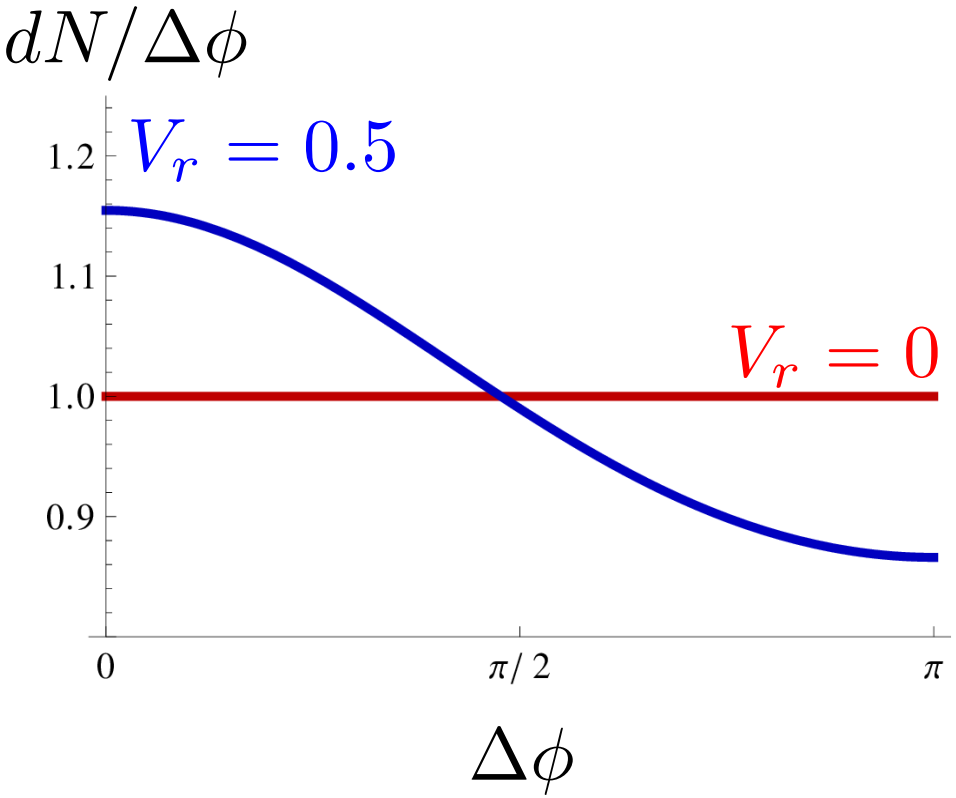

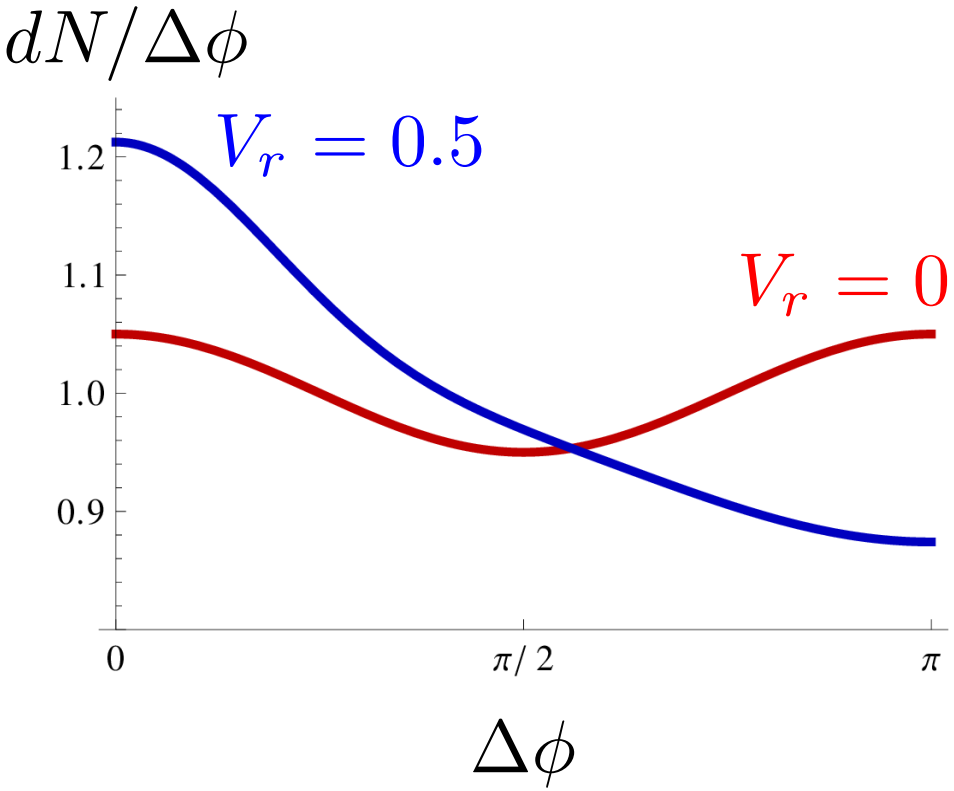

Left: No intrinsic correlation in Δφ followed by radial boost.

Right: Intrinsic azimuthal correlation followed by boost.

Blast wave results

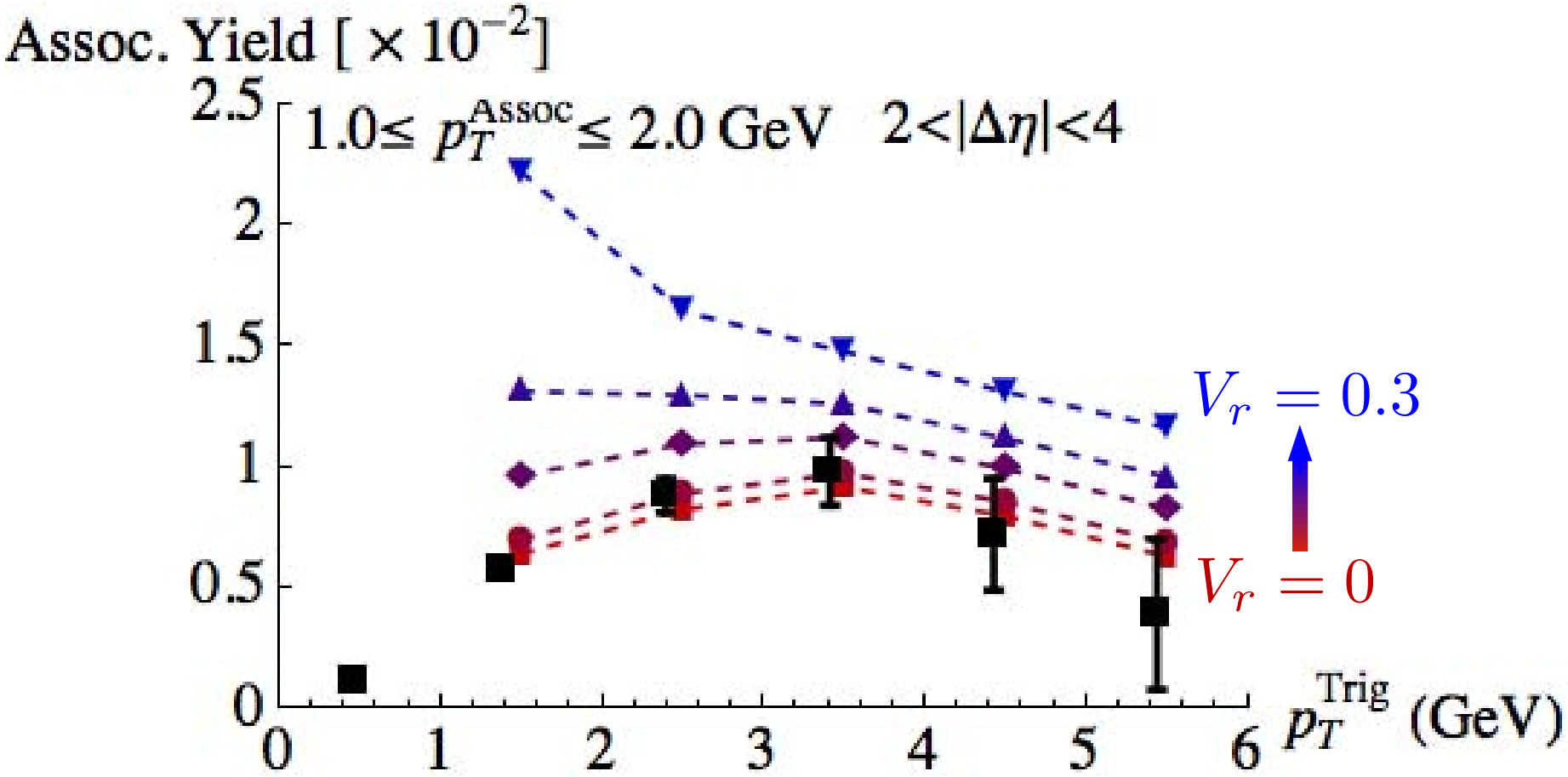

Results for Pb+Pb

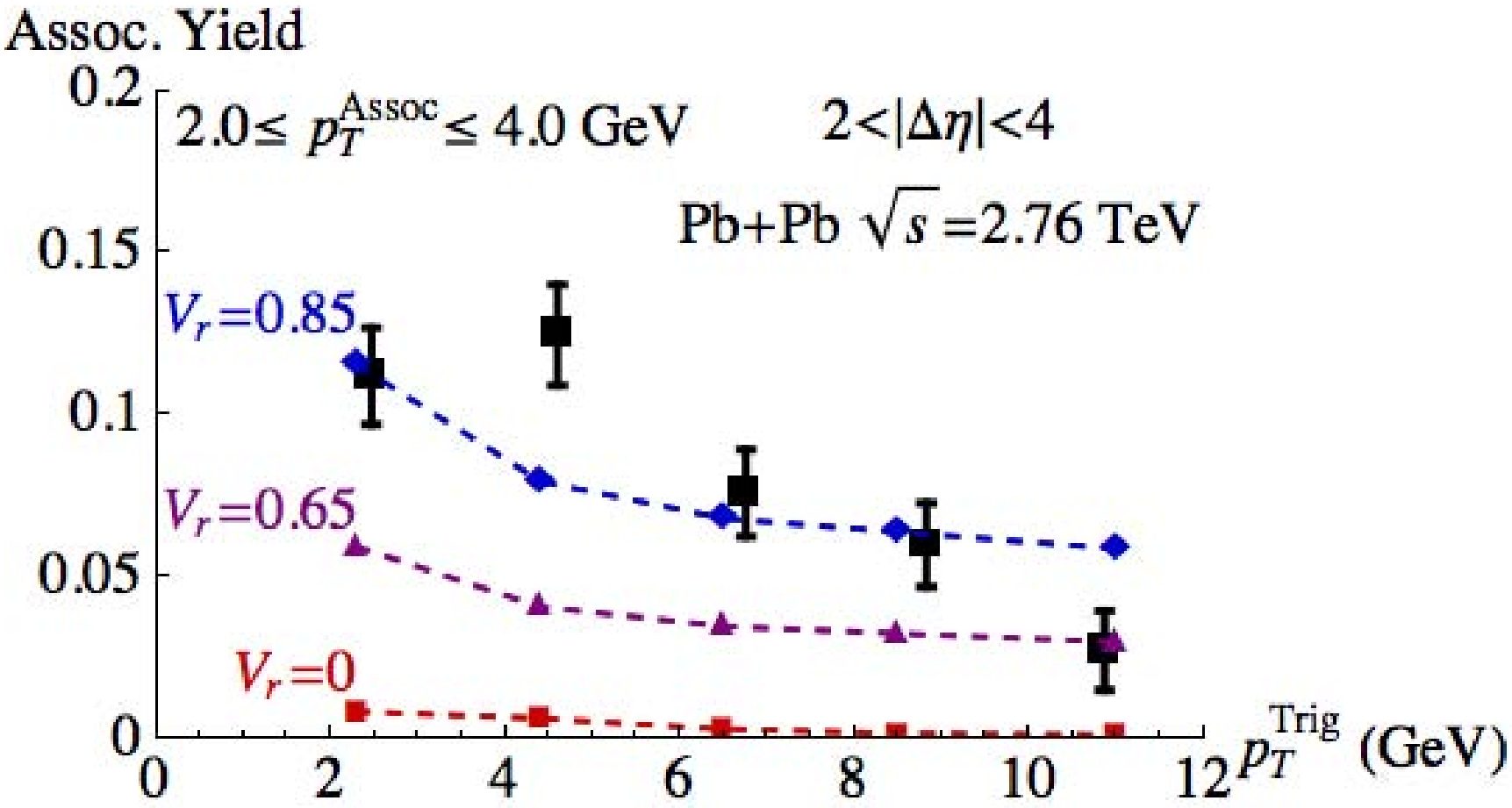

Multiplicity in p+Pb at 5 TeV

$Q^2_{0,\mathrm{Au}} = 0.336, 0.336, 0.504, 0.672, 0.840\ \mathrm{GeV}^2$

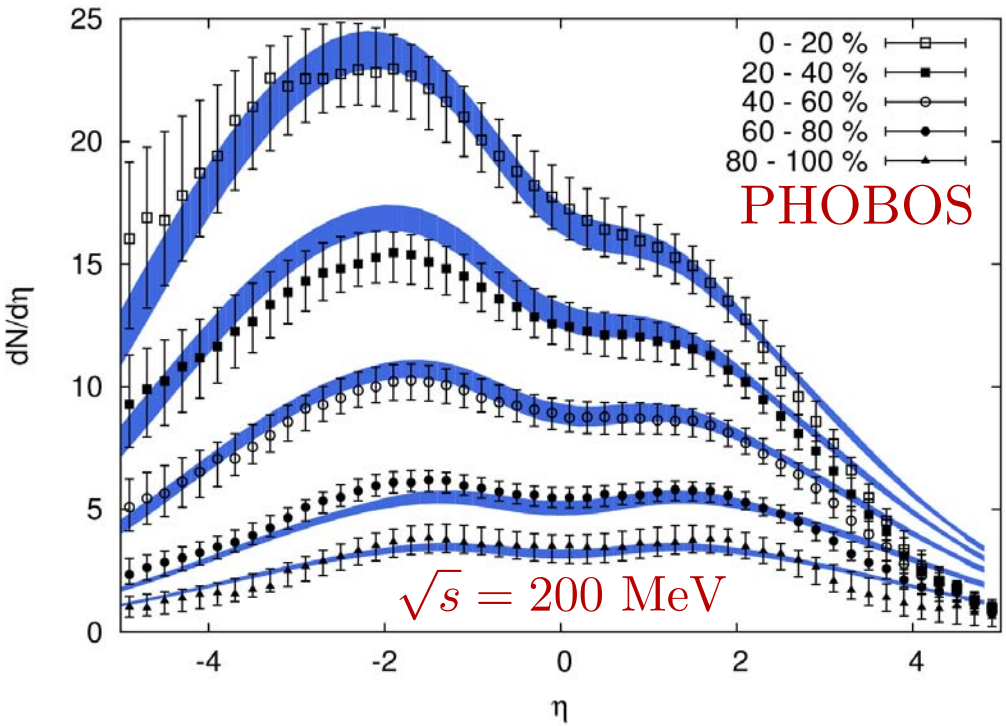

$Q^2_{0,\mathrm{d}} = 0.336\ \mathrm{GeV}^2$

$Q^2_{0,\mathrm{Pb}} = 0.504, 0.672, 0.840, 1.008\ \mathrm{GeV}^2$

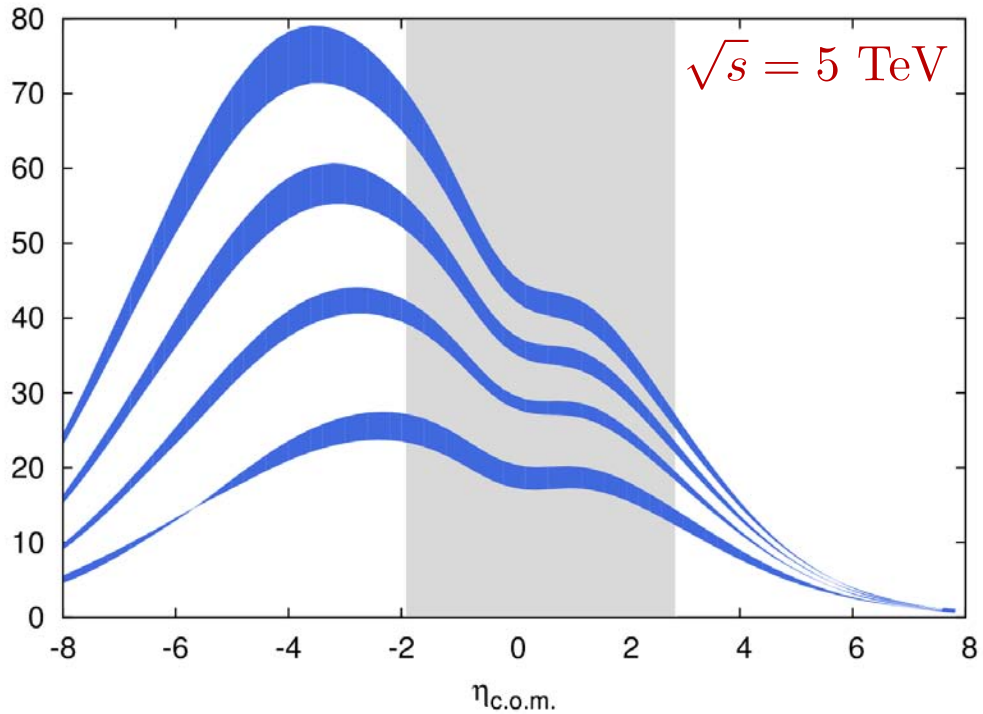

$Q^2_{0,\mathrm{p}} = 0.168\ \mathrm{GeV}^2$

Ridge in p+Pb

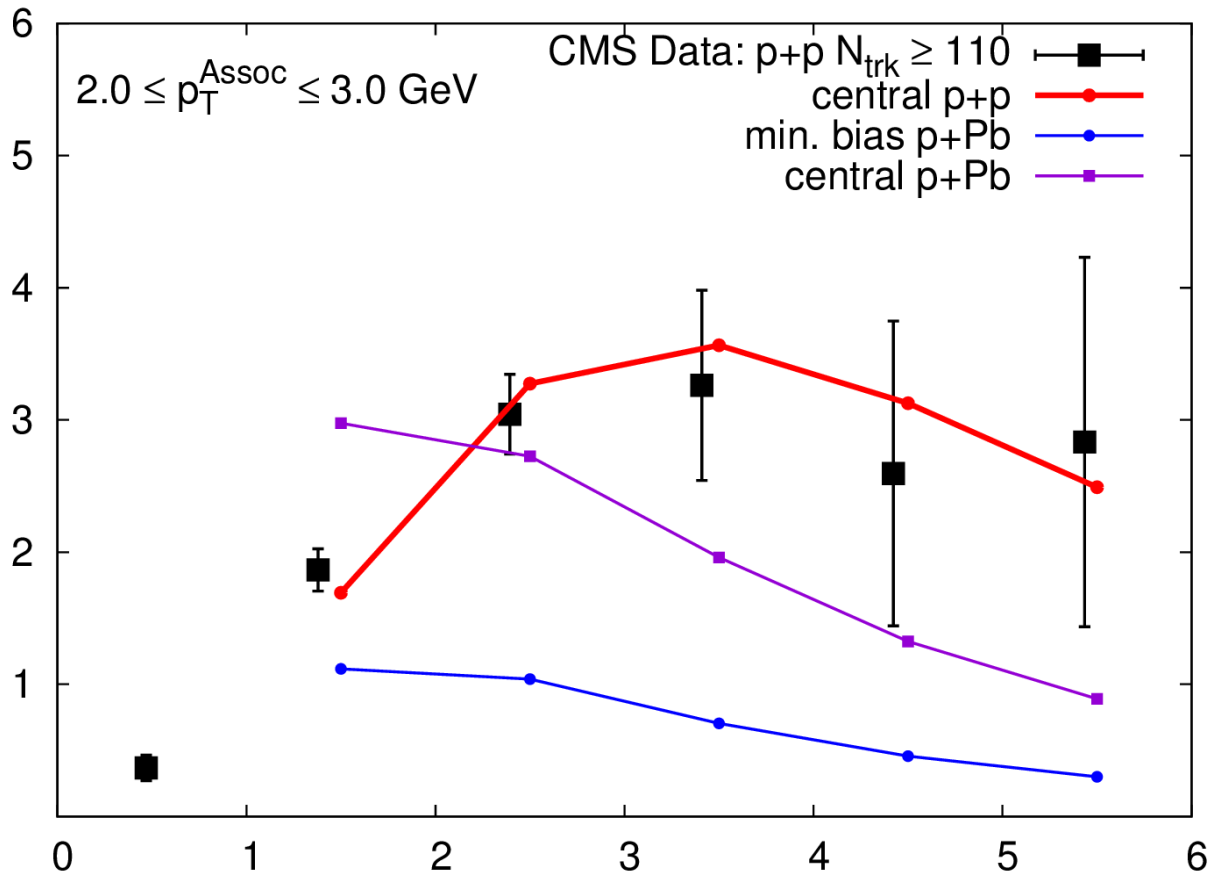

Ridge in p+Pb is smaller than in p+p for CMS acceptance.
Signal will also have to be pulled from a larger background.

Understanding the away-side

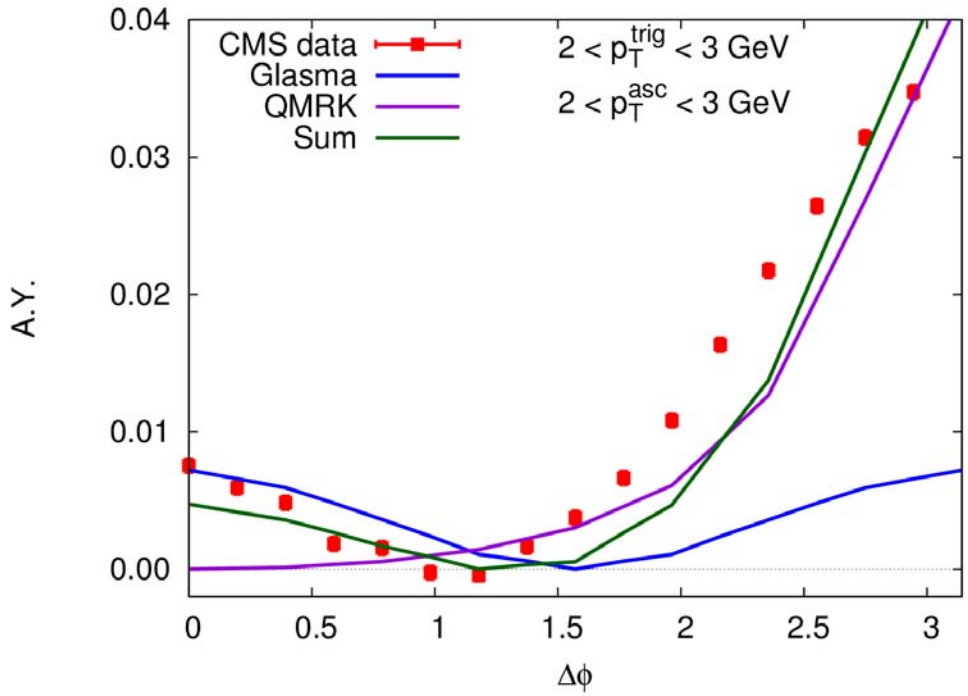

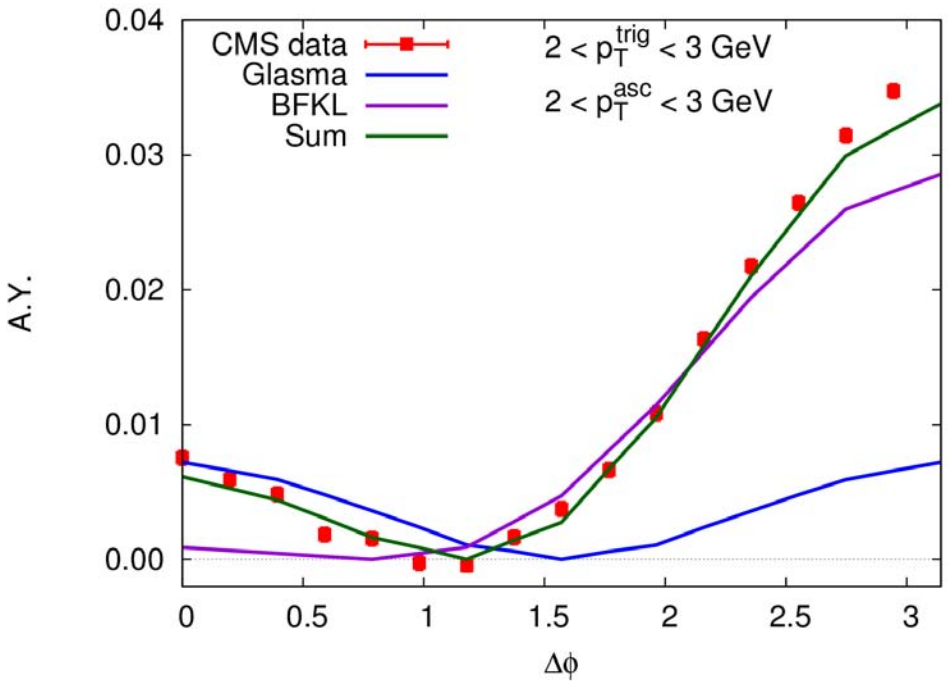

There is a clear need for evolution between the triggered particles
(even for a rapidity gap as small as 2-4 units)

Jet Structure

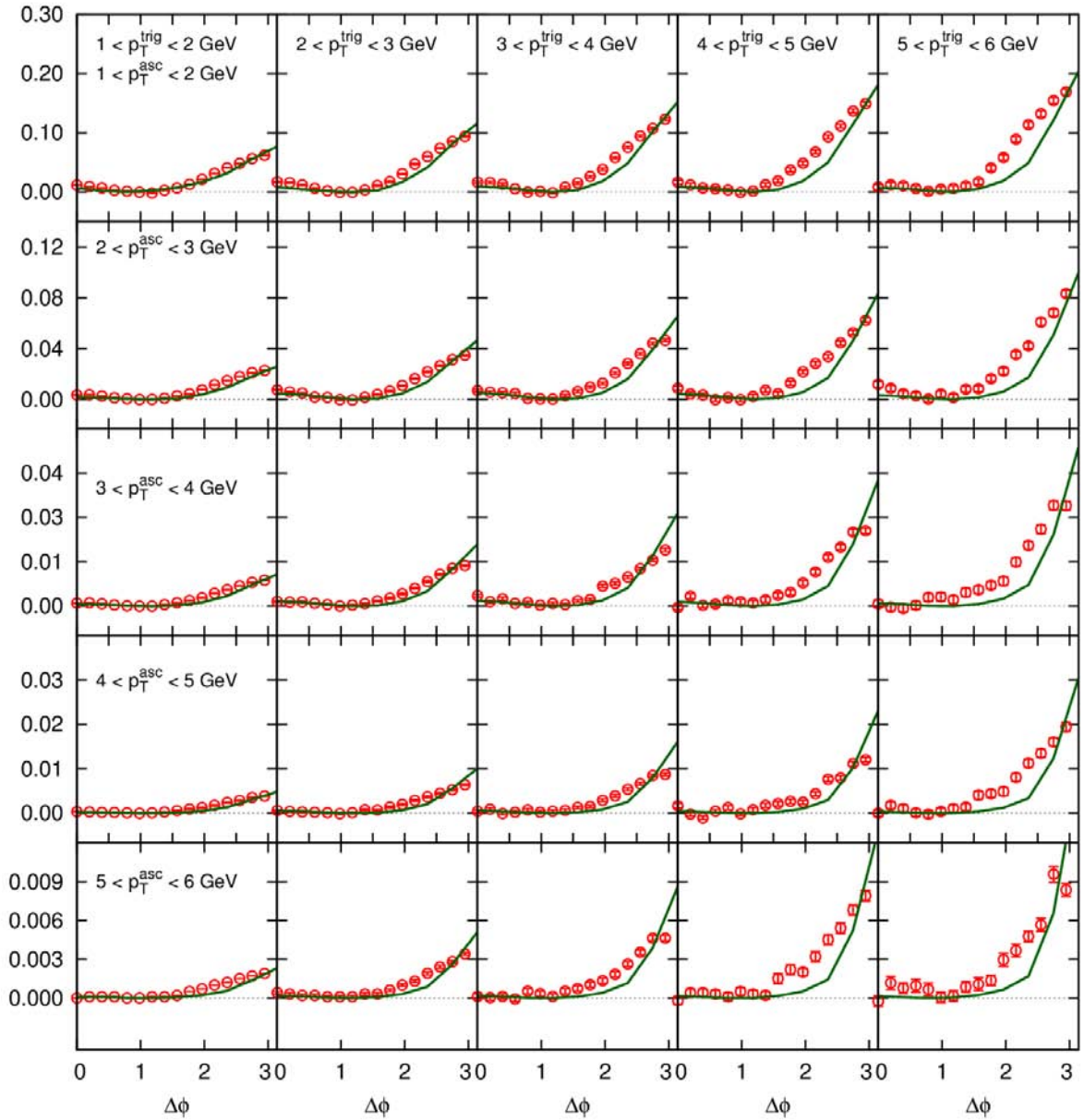

Summary

- Strong color sources lead to α_s^8 enhancement of QCD diagram responsible for near-side enhancement
- Structure of ridge correlation constrains radial flow in p+p
- Radial flow explains identical measurements in Pb+Pb
- Ridge tougher to see in asymmetric collisions

Backup

p+p p_T distribution

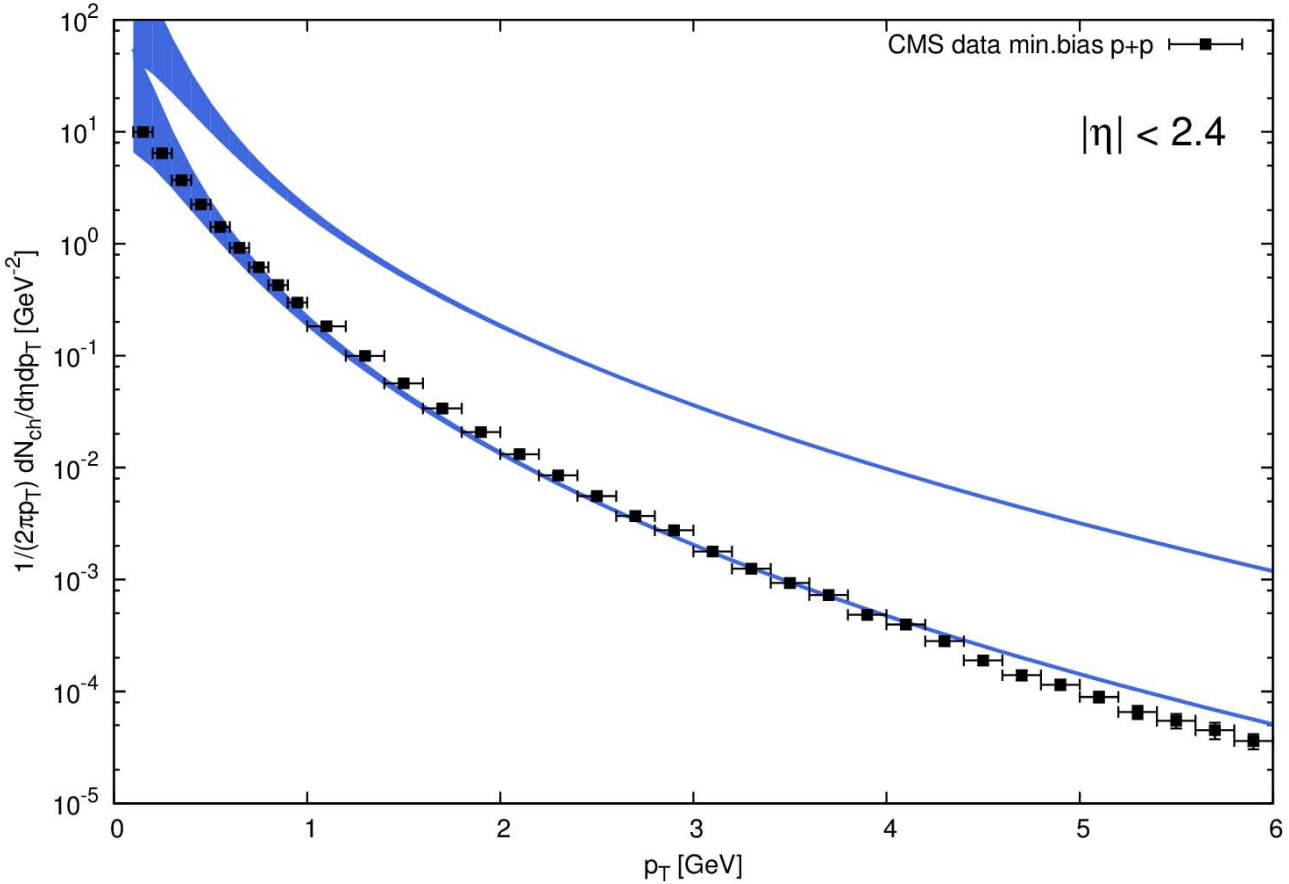

CMS Acceptance

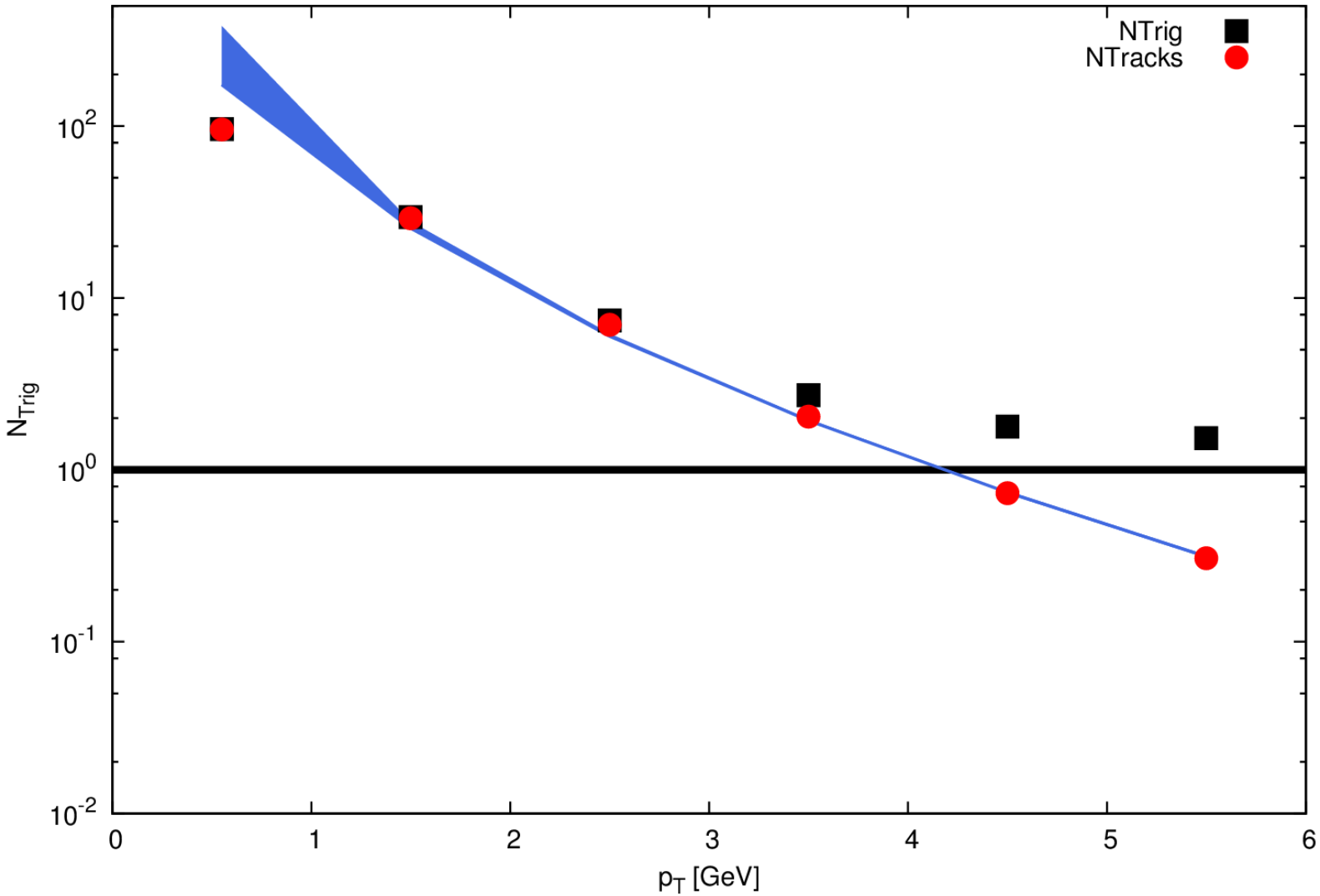

BFKL Formalism

$$\frac{d^2N_{AB}}{d^2\mathbf{p}_\perp d^2\mathbf{q}_\perp dy_p dy_q} = \frac{32N_c\alpha_s(\mathbf{p}_\perp)\alpha_s(\mathbf{q}_\perp)}{(2\pi)^8 C_F}\frac{1}{\mathbf{p}_\perp^2\mathbf{q}_\perp^2}$$
$$\times \int d^2\mathbf{k}_{0\perp}\int d^2\mathbf{k}_{3\perp}\Phi_A(x_1,\mathbf{k}_{0\perp})\Phi_B(x_2,\mathbf{k}_{3\perp})\mathcal{G}(\mathbf{k}_{0\perp}-\mathbf{p}_\perp,\mathbf{k}_{3\perp}+\mathbf{q}_\perp,y_p-y_q)$$

$$\mathcal{G}(a,b,\Delta y) = \frac{1}{(2\pi)^2}\frac{1}{(a^2b^2)^{1/2}}\sum_n e^{in\overline{\phi}}\int_{-\infty}^{+\infty} d\nu\; e^{\omega(\nu,n)\Delta y}e^{i\nu\ln\left(a^2/b^2\right)}$$

$$\omega(\nu,n) = -2\overline{\alpha}_s\mathrm{Re}\left[\Psi\left(\frac{|n|+1}{2}+i\nu\right)-\Psi(1)\right]$$

$$\overline{\alpha}_s \equiv \frac{N_c\alpha_s\left(\sqrt{ab}\right)}{\pi}$$

$$\overline{\phi} \equiv \arccos\left(\frac{a\cdot b}{|a|\;|b|}\right)$$

Possibilities for ep physics at eRHIC

Salvatore Fazio

for the BNL EIC Science Task Force

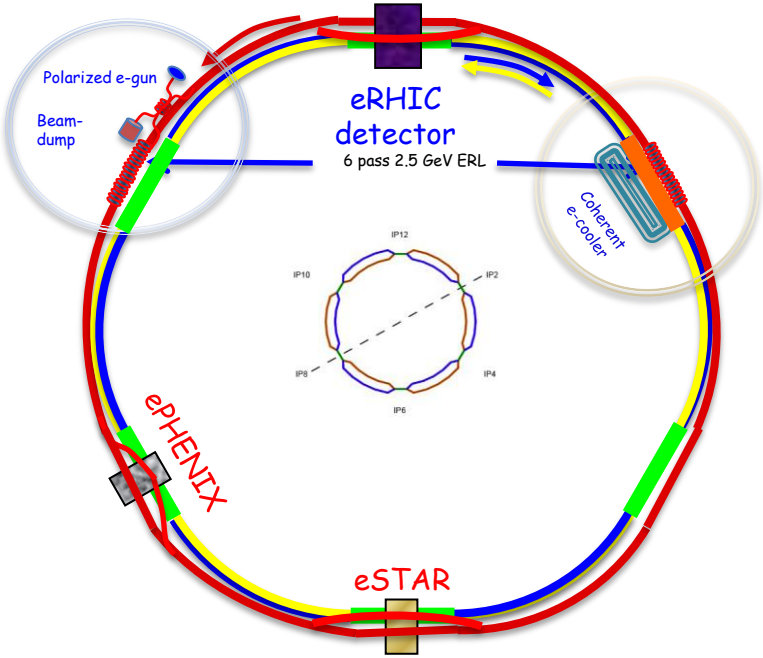

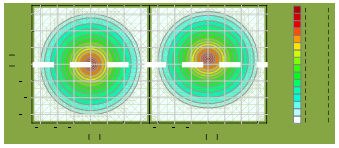

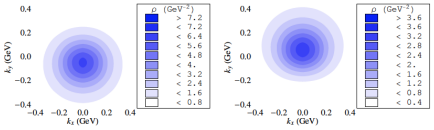

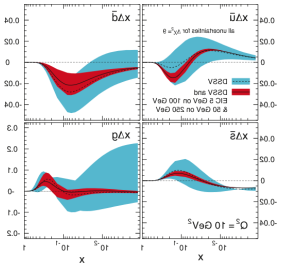

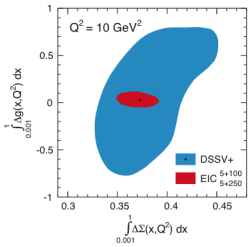

RIKEN Forward Physics

BNL - *August 1, 2012*

Plan of the talk

- The eRHIC accelerator and its dedicated detector
- Spin physics with eRHIC (the impact!)
  - Structure functions
  - Helicity measurements
- Imaging with an eRHIC (the impact!)
  - TMDs
  - GPDs
- Summary

The eRHIC idea

Electron Ion Collider project (EIC) -> 2 options: Brookhaven National Laboratory (eRHIC)

Thomas Jefferson National Laboratory (ELIC)

(Existing)

Electron accelerator
(to be build)

Unpolarized and
polarized leptons
5-20 (30) GeV

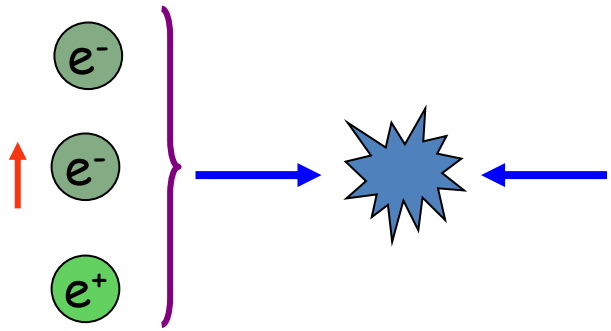

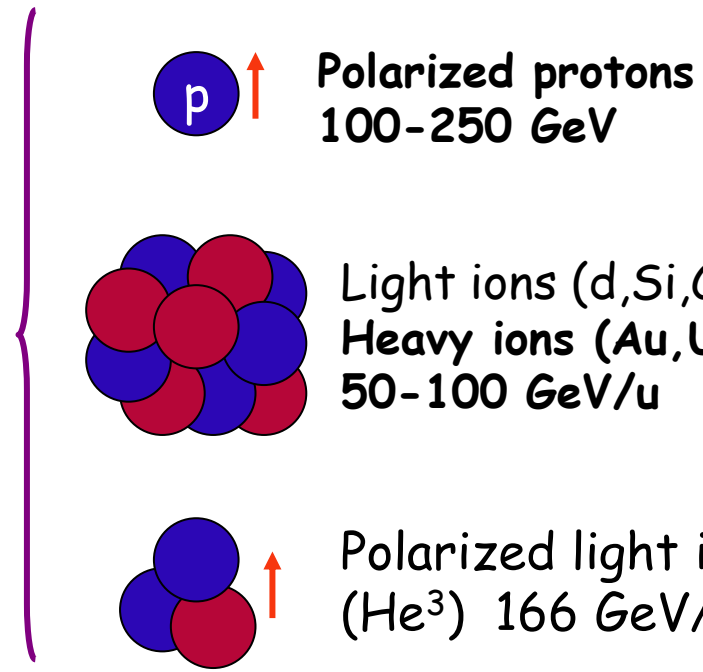

70% e^- beam polarization goal
polarized positrons?

Center mass energy range: $\sqrt{s}$ = (32 for Au) 45 - 140 GeV

Mission: Studying the Physics of Strong Color Fields

The RHIC site @ BNL

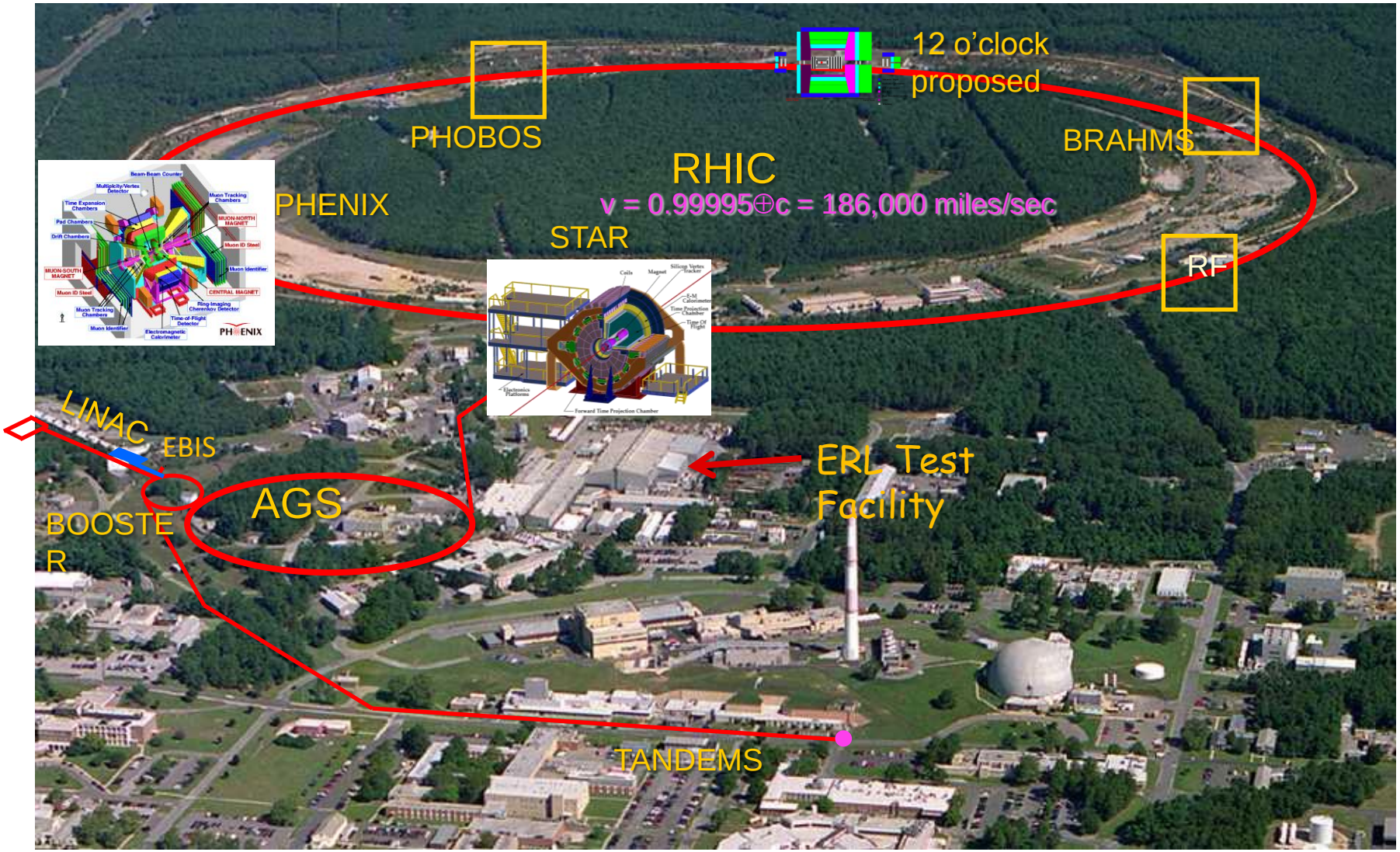

The eRHIC collider

EIC/eRHIC

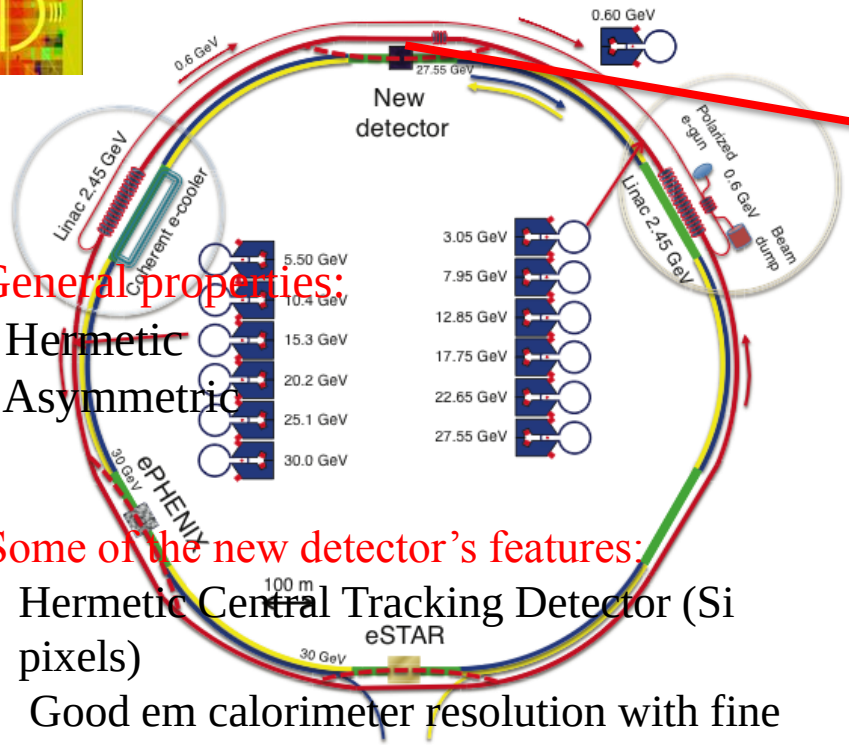

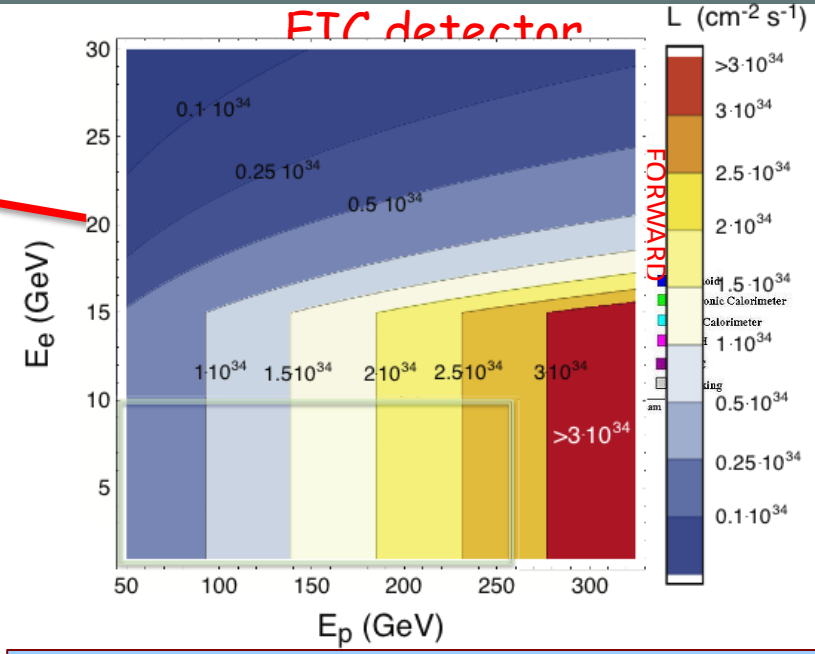

General properties:

- Hermetic
- Asymmetric

Some of the new detector's features:

- Hermetic Central Tracking Detector (Si pixels)
- Good em calorimeter resolution with fine granularity
- Preshower em cal → π^0 background
- Very forward calorimetry
- Roman pots from the early beginning (and with excellent acceptance)

➢ **An electron ring will be built at the RHIC facility**

➢ **The current experiments can be upgraded for ap(A) physics**

➢ **A new dedicated detector will be built**

❑ **Can scan over a wide phase space**

❑ **Very high luminosity**

Important for exclusive DIS:

- **Dedicated forward instrumentation**
- **High tracker coverage**
- **Very High lumi!**

Physics goals

What we aim to do:

eRHIC is designed to investigate the spatial structure quarks and gluons:

- their distributions in position and momentum space
- their orbital angular momenta and polarization

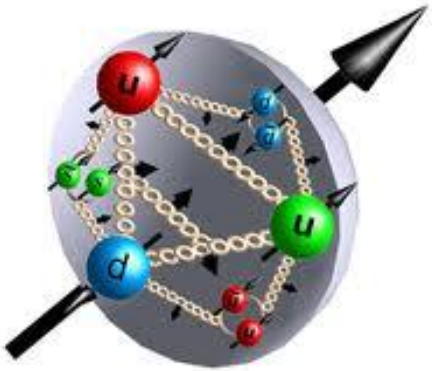

What must be measured:

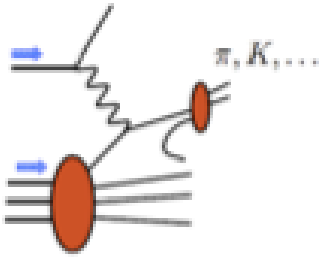

Inclusive (& semi-inclusive) DIS

Longitudinal motion

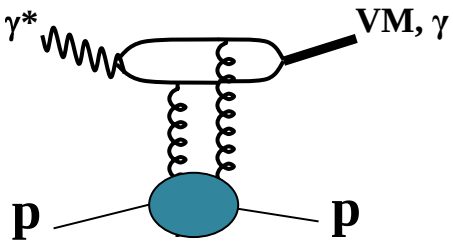

Exclusive diffraction

Transverse space

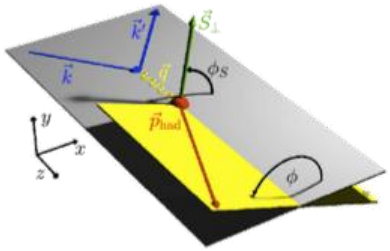

Azimuthal asymmetries

Transverse space and momentum

spin physics

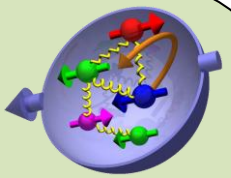

- what is the polarization of gluons at small x where they are most abundant
- what is the flavor decomposition of the polarized sea depending on x

determine quark and gluon contributions to the proton spin

Structure functions

~F_2

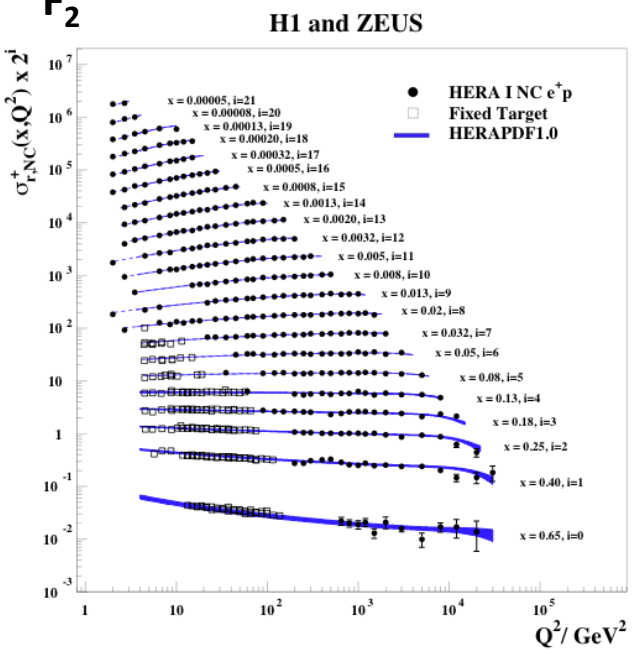

What we Know:

- ✓ Extensive program carried at HERA
- ✓ F_2 precisely measured in a large x range
- ✓ At low-x gluons dominate

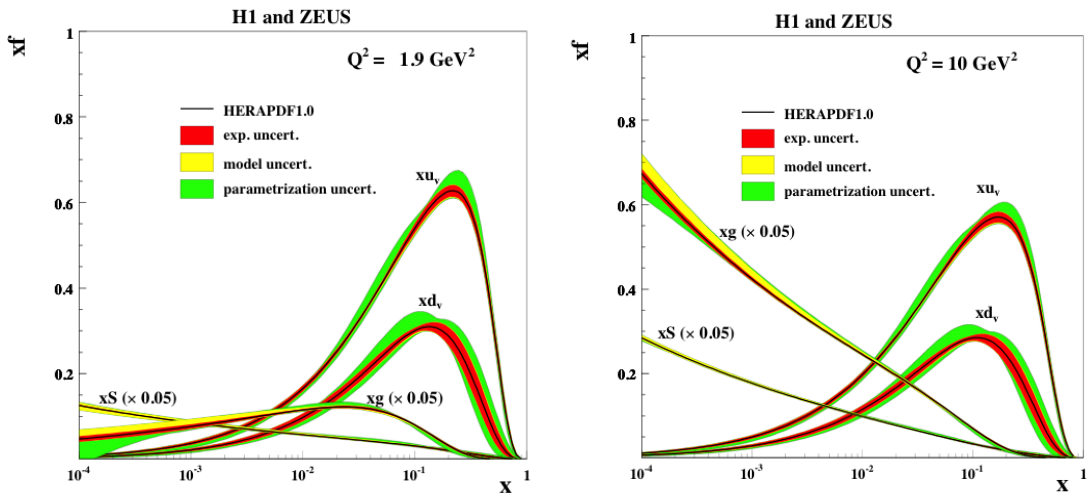

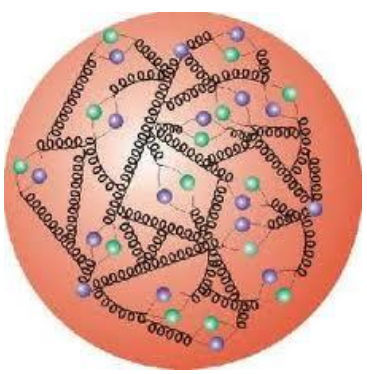

Differential cross section: $$\frac{d\sigma^{e^{\pm}p}}{dx\,dQ^2} = \frac{2\pi\alpha^2 Y_+}{xQ^4}\sigma_r\left(x,Q^2\right)$$

Reduced cross section: $$\sigma_r\left(x,Q^2\right) = F_2\left(x,Q^2\right) - \frac{y^2}{Y^+}F_L\left(x,Q^2\right)$$

F_L

The impact of an eRHIC:

$$F_L(x,Q^2) \sim \alpha_S x G(x,Q^2)$$

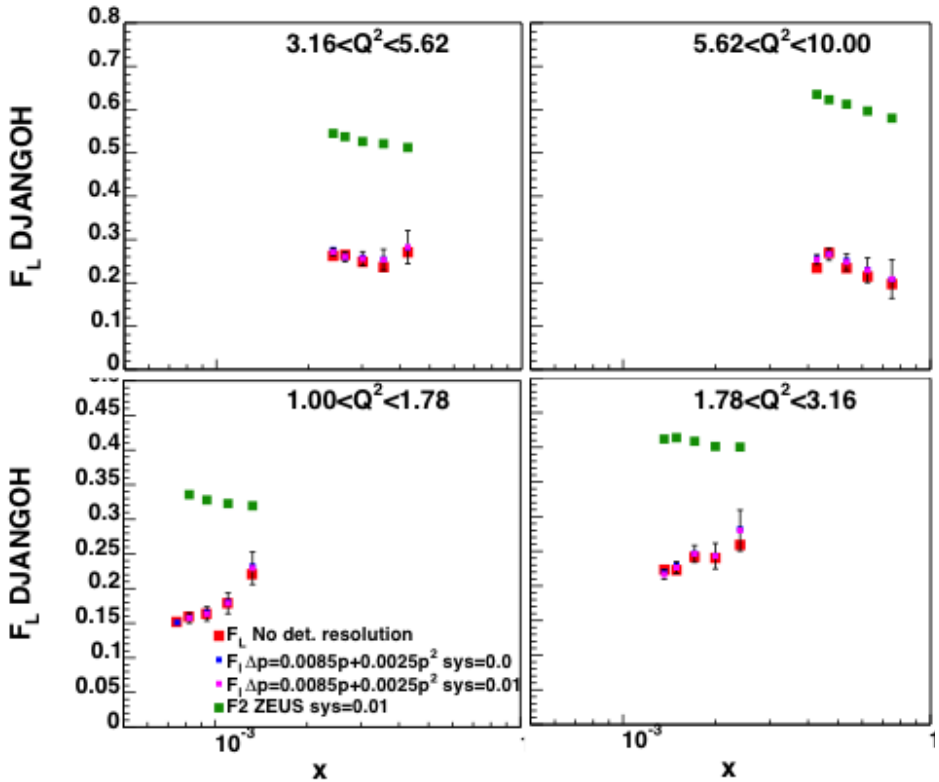

F_L can probe the gluons at low-x and is sensitive to non-linear ("twist") effects

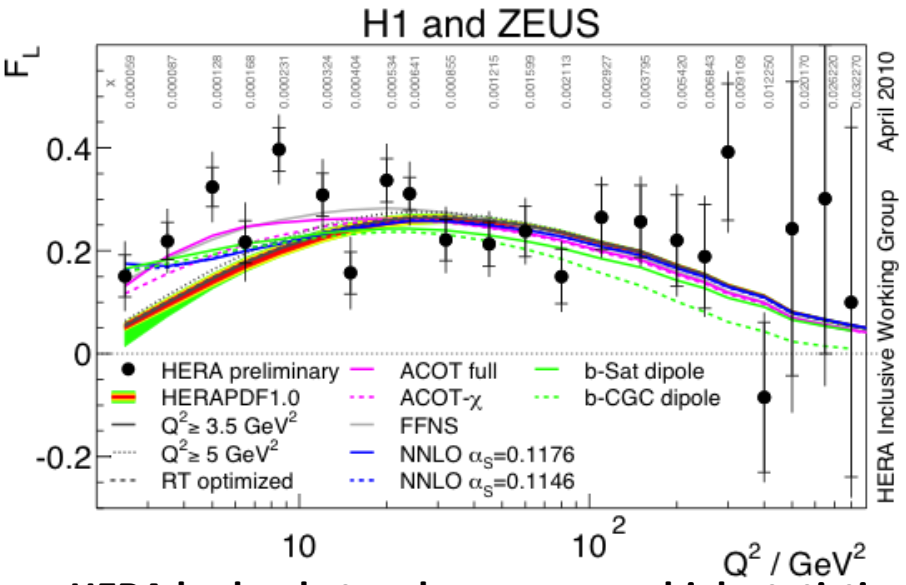

HERA had only two lower-energy high statistics runs -> bad for F_L extraction

Important:

- **The wide rage in beam energy of eRHIC is essential for a precise F_L measurement**
- **F_L can probe the saturation regime in eA (see M. Lamont's talk)**

Proton's helicity structure

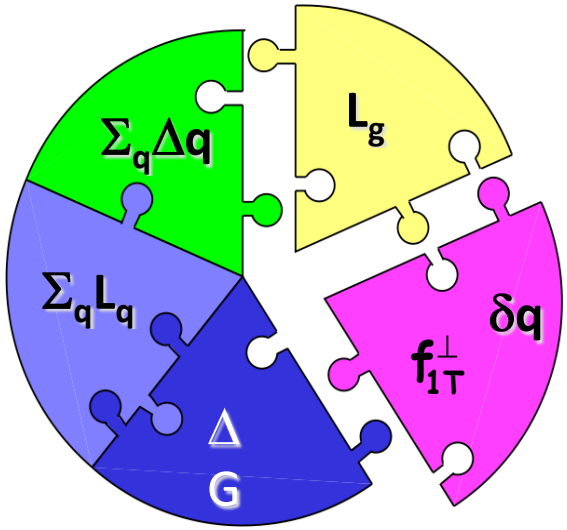

$\Delta g(x,Q^2) = g_{\rightrightarrows}(x,Q^2) - g_{\rightleftarrows}(x,Q^2)$

It is measured in inclusive data via spin asymmetry:

A_{LL} -> Δq

What we Know:

Δg in small at large x (HERMES, COMPAS, RHIC)

Open question:

Δg at small-x still unknown! It is an important ingredient for the proton spin sum role

Impact of an eRHIC:

The x-range will be extended of three orders of magnitude, allowing an extremely precise measurement in the earlier poorly known area

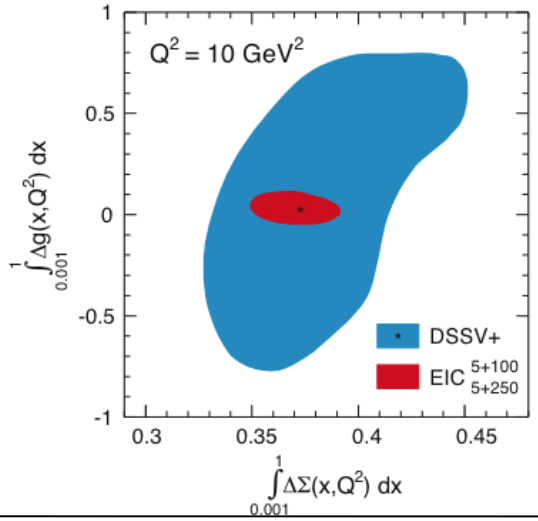

Proton's helicity structure

Current data vs eRHIC phase space

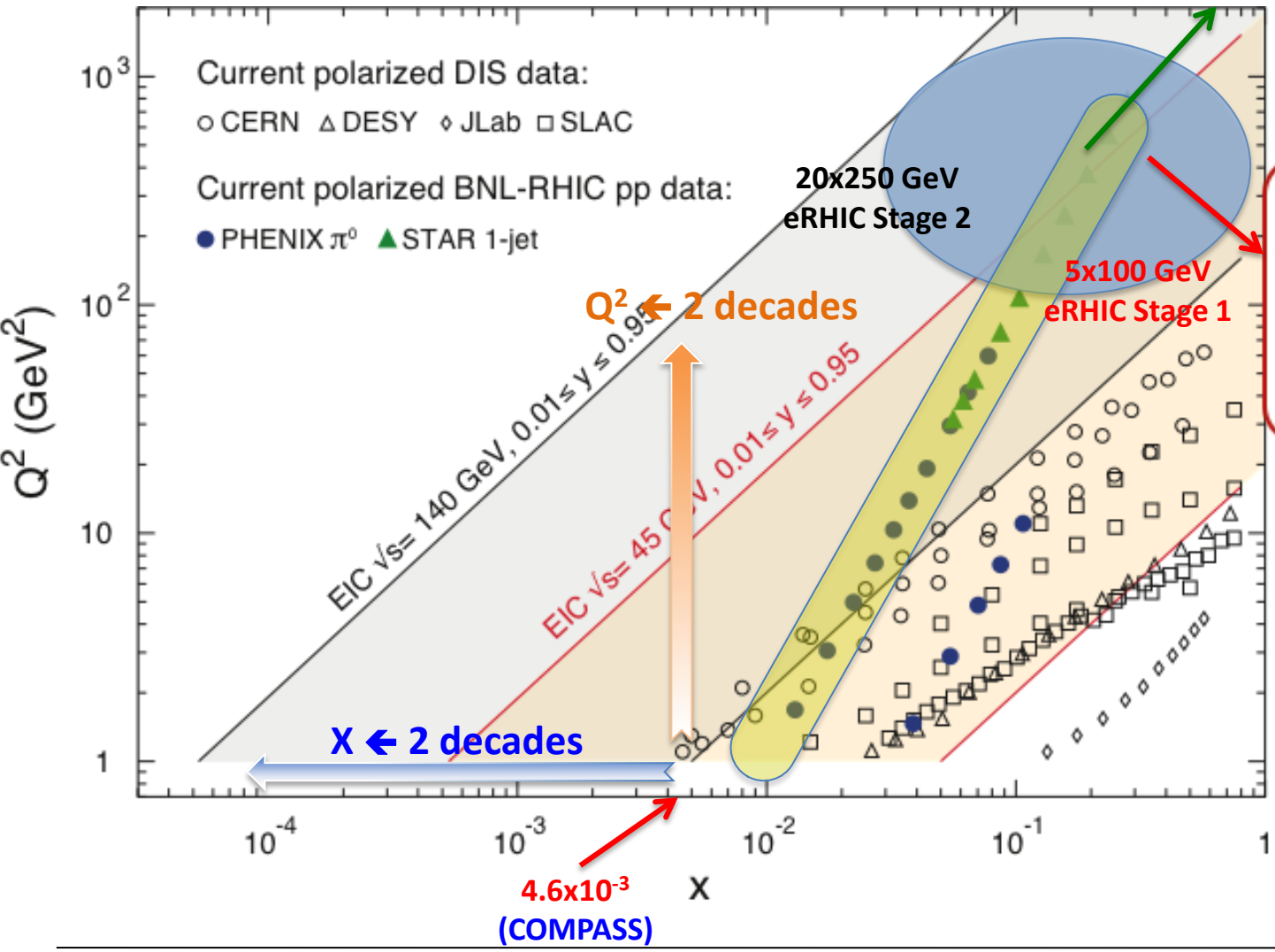

RHIC pp data constraining Δg(x) for ~ 0.05 < x < 0.2

novel electroweak probes
(not accessible at low energies)

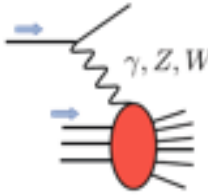

New opportunities for DIS with polarized beams

Proton's helicity structure - Δg

$$\frac{dg_1}{d\log\left(Q^2\right)}$$

g_1 scaling violation

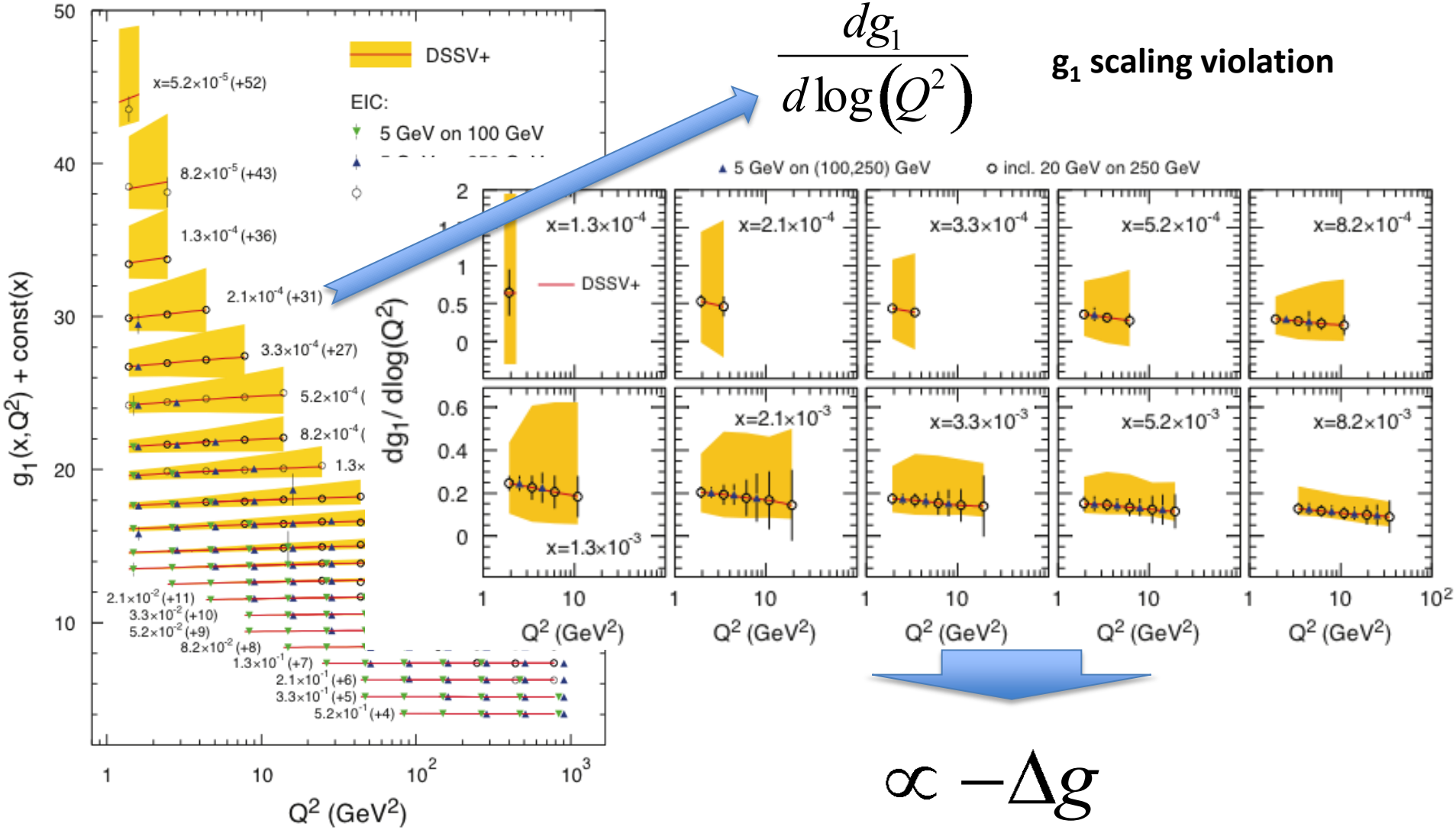

$$\propto -\Delta g$$

Proton's helicity structure

SIDIS data provide detailed flavor separation of sea quark

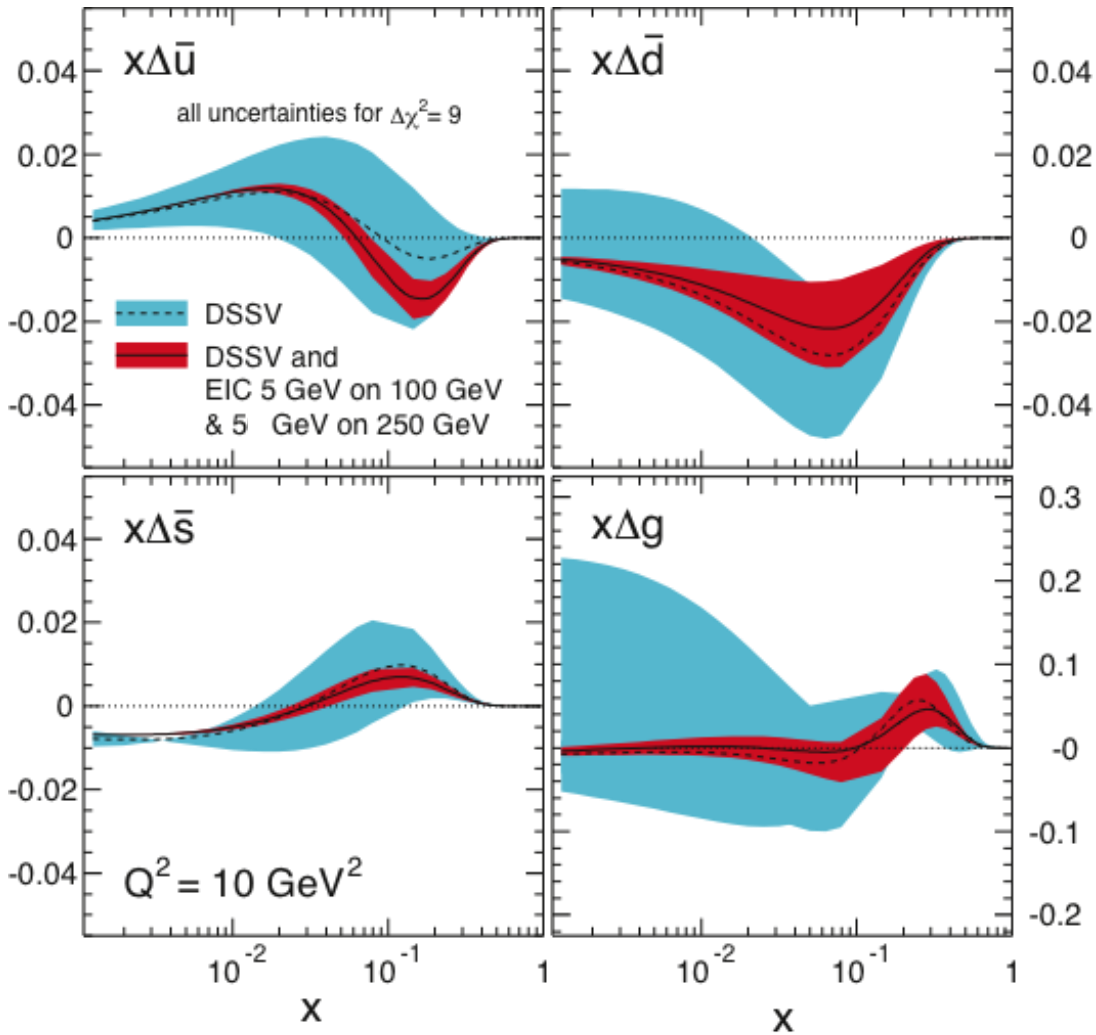

plots includes **only eRHIC stage-1 data**

Detector issues:

- **(SI)DIS @ eRHIC limited by systematics**
  - **rel. lumi, polarimetry, detector performance need to be well under control**
- **QED radiative corrections**

Proton's helicity structure

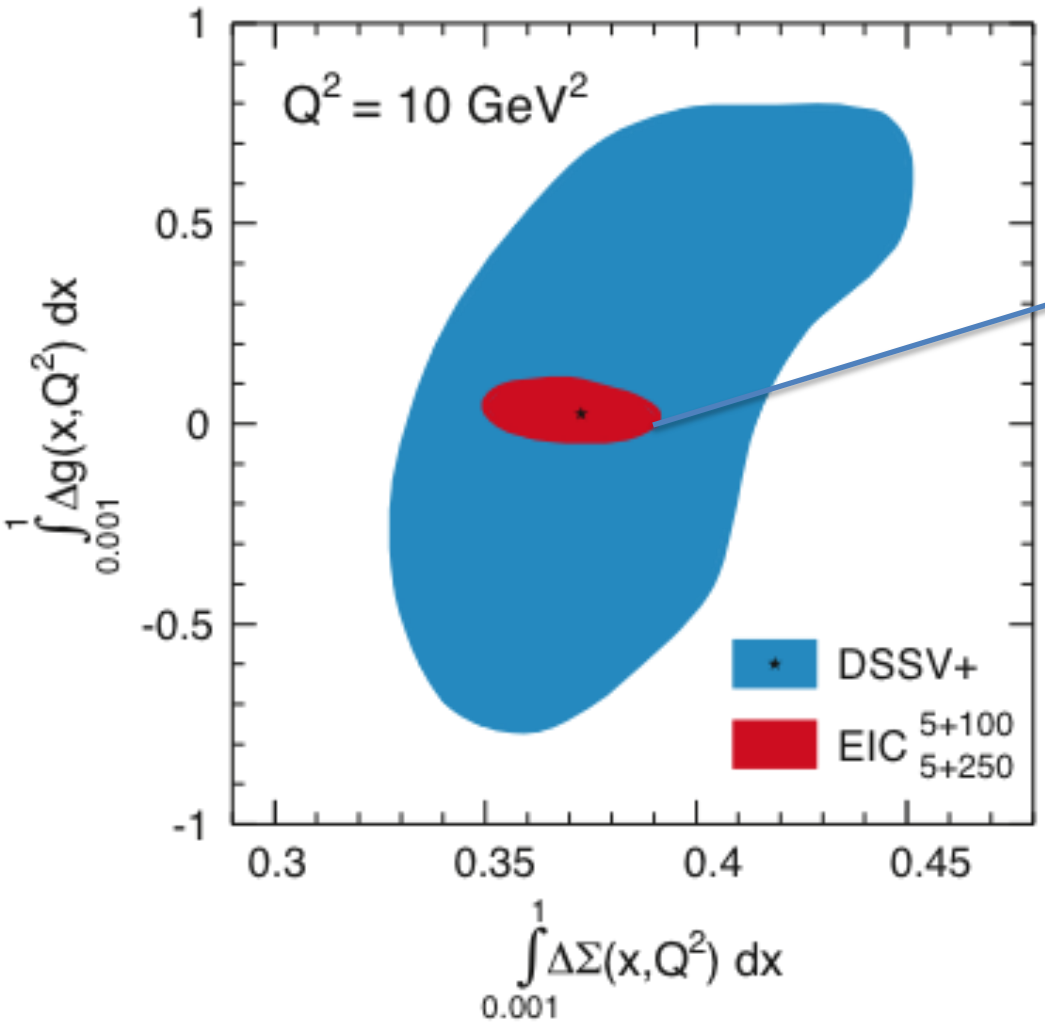

combined correlated uncertainties for ΔΣ and Δg

Statistical errors as low as 5%

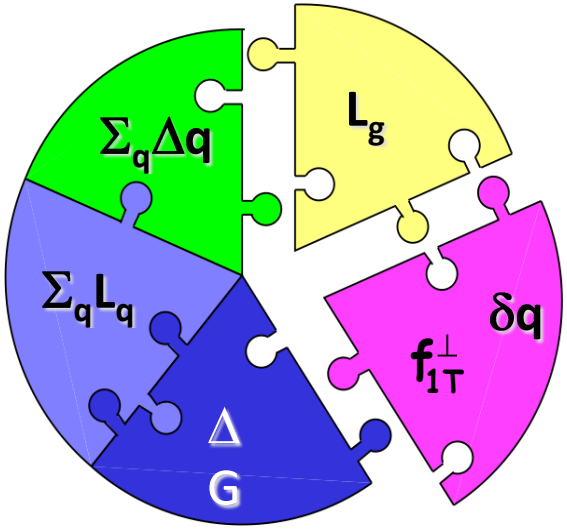

Puzzle complete (mostly) with an eRHIC

eRHIC: the Ultimate 3D experience !!!

Proton imaging

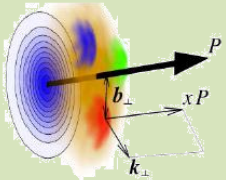

- what is the spatial distribution of quarks and gluons in nucleons/nuclei
- understand deep aspects of gauge theories revealed by k_T dep. distr'n

possible window to orbital angular momentum

(2+1)-Dimensional imaging of the proton

Open questions:

- PDFs do not resolve transverse coordinate or momentum space
- In a fast moving nucleon the longitudinal size squeezes like a `pizza' but transverse size remains about 1 fm

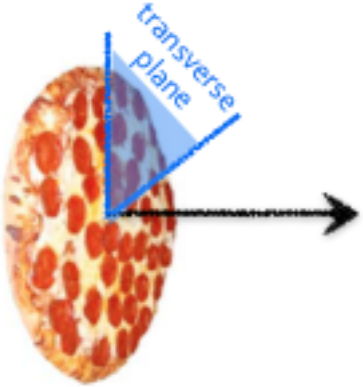

Goal: nucleon tomography!

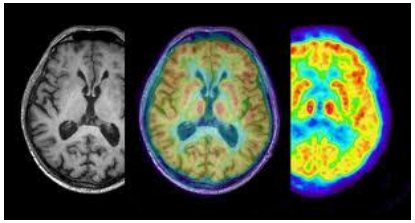

brain

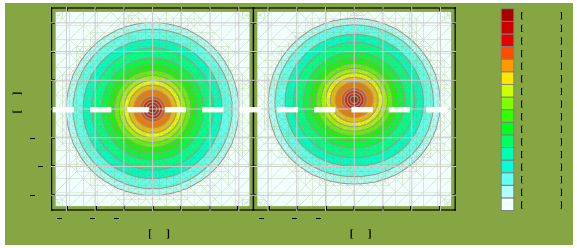

nucleon

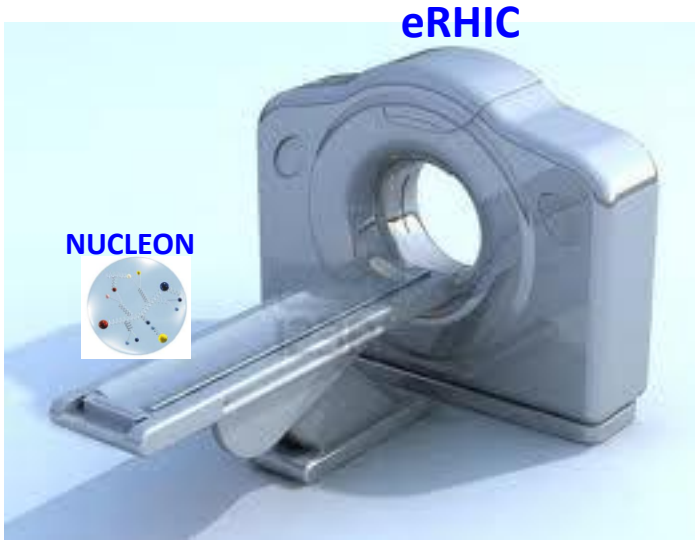

(2+1)-D imaging of the proton

Wigner Distribution

$W(x,r,k_t)$

TMDs

GPDs

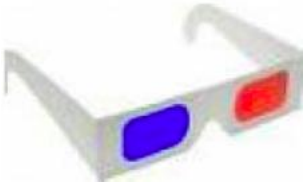

3D picture in momentum space

transverse momentum dependent distributions

$f_1 \rightarrow f_{1T}^{\perp}$

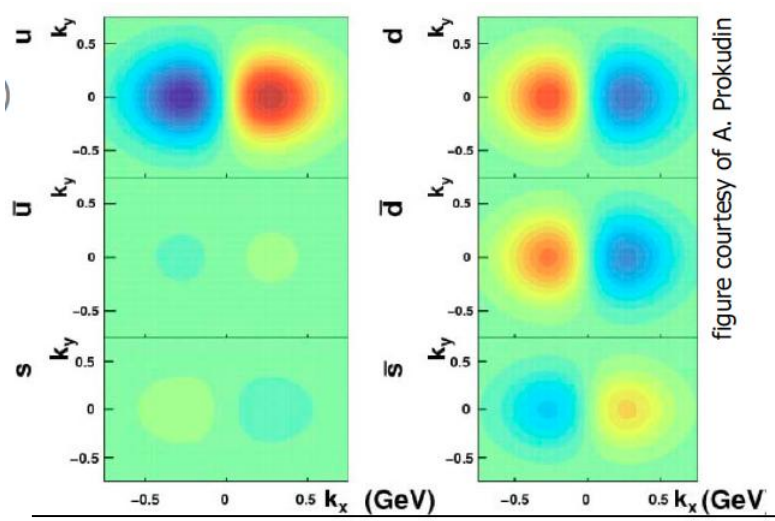

figure courtesy of A. Prokudin

3D picture in coordinate space

generalized parton distributions

→ exclusive reaction like DVCS

Quarks

unpolarised polarised

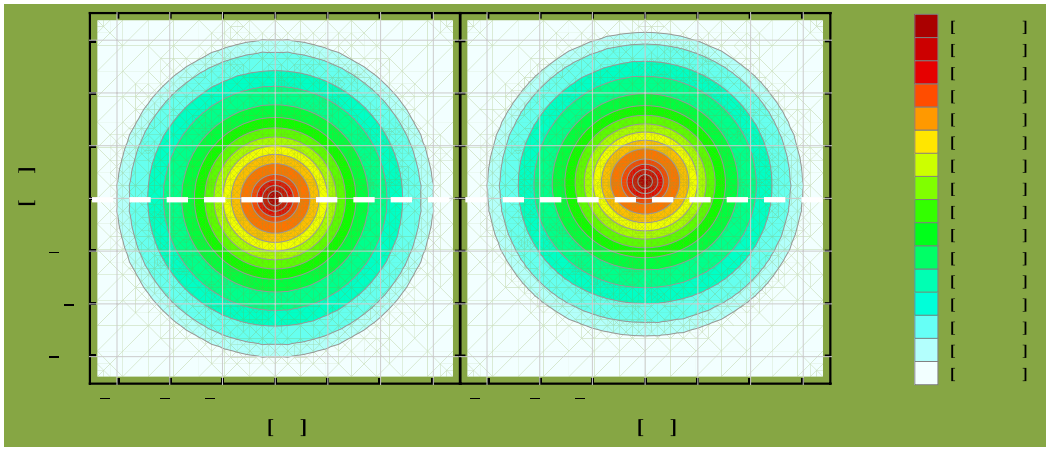

TMDs

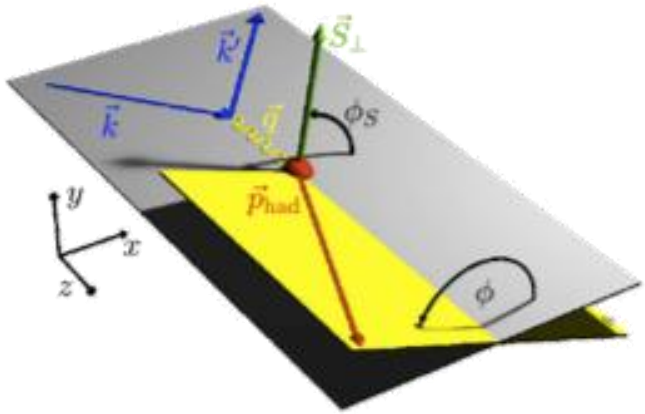

TMDs are PDFs depending on transverse momentum

What we Know:

- ✓ Only **valence quarks** TMDs are extracted so far (fixed target experiments)
- ✓ TMDs factorization applicable for $Q^2 >> p^h_T$

What we want to measure:

$$\frac{d\sigma}{dx\, dQ^2\, dz\, d\phi_S\, d\phi_h\, dp_T^h}$$

- ➢ SI-DIS **6-fold differential cross sections**
- ➢ **Azimuthal asymmetries** and their modulations

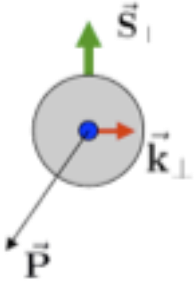

$$f_{q/P^\uparrow}(x, \mathbf{k}_\perp, S) = f_1(x, \mathbf{k}_\perp^2) - \frac{\mathbf{S}\cdot(\hat{\mathbf{P}}\times\mathbf{k}_\perp)}{M} f_{1T}^\perp(x, \mathbf{k}_\perp^2)$$

PDF f_1 ← $\sin(\phi_h - \phi_S)$ → **Sivers function** $f_{1T}^\perp$

- Sensible to spin orbit correlations
- Constrains models on parton orbital motion
- Helps understanding QCD color gauge invariance

TMDs – Sivers function

Measurement of the charm decay

$$\gamma^* N^{\uparrow} \rightarrow D\overline{D} + X$$

- **Suppresses q-g contribution**
- **Requires high luminosity**

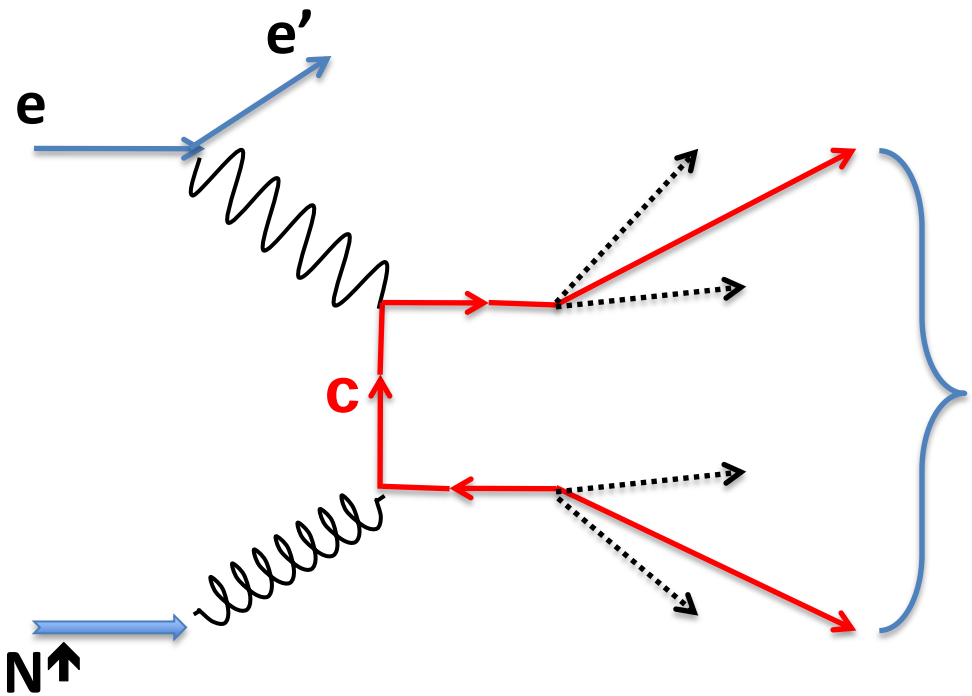

Measure a pair of D mesons

$k_{\perp} = |k_{1T} + k_{2T}|$

Sievers – present and future

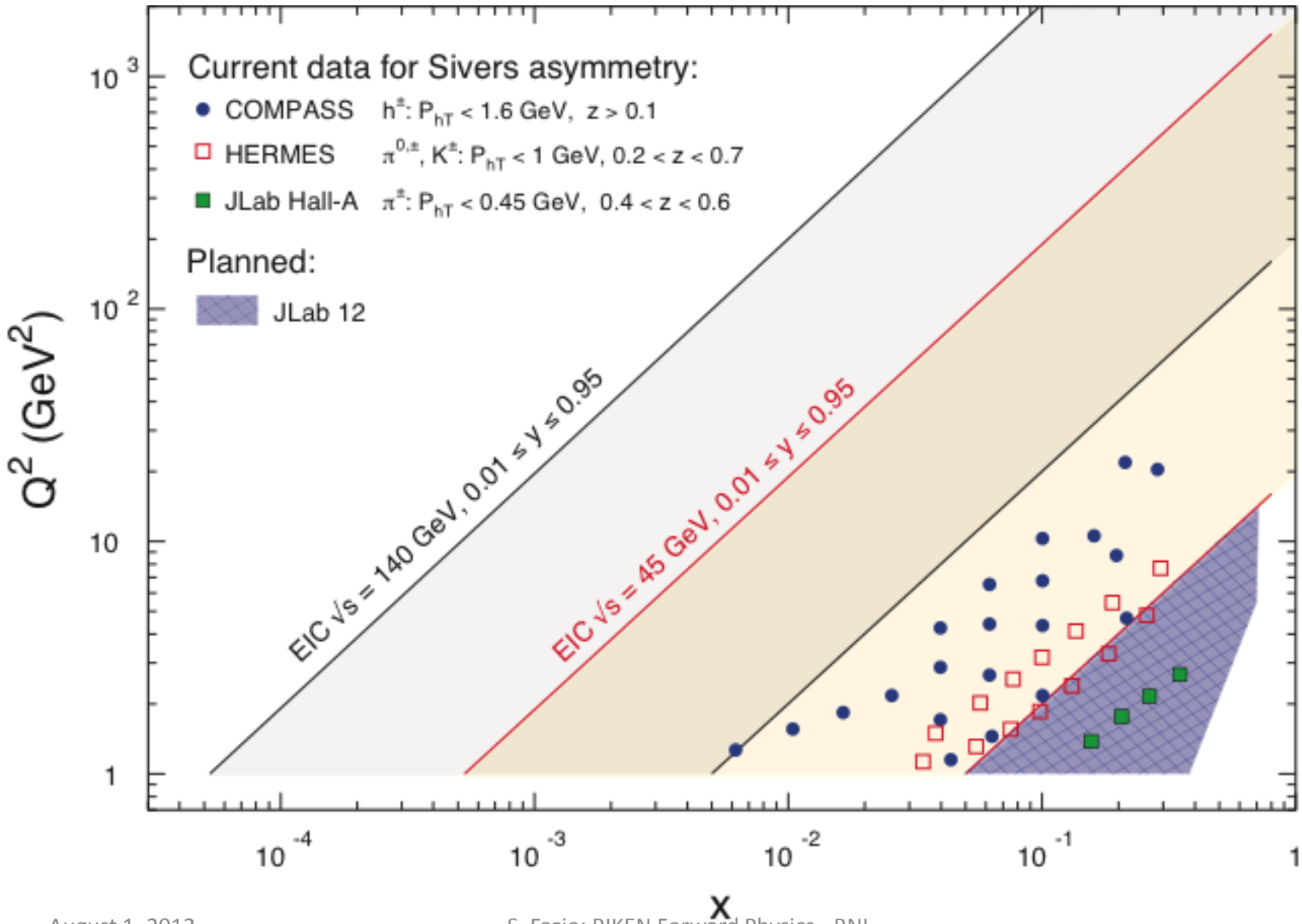

TMDs – Sivers function

T. Burton, F. Yuan, ...

eRHIC impact on sivers

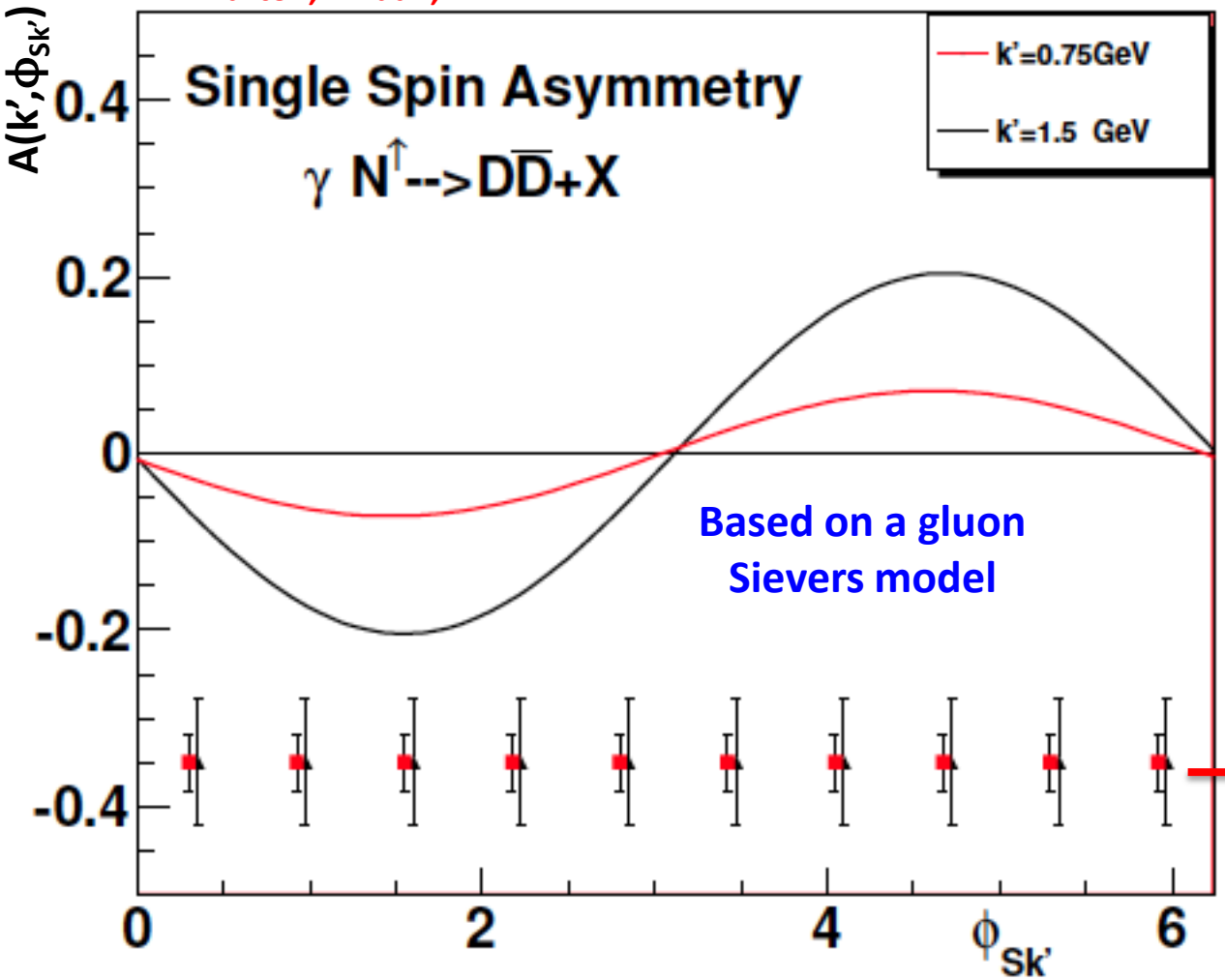

Azimuthal asymmetry which correlates transverse momentum k_T of DD-bar pair with transverse proton spin

Errors assuming 100 fb^{-1}
~8 months @ 50% efficiency

ϕ_{Sk} -> azimuthal angle between the proton spin and k_T of the D-meson

TMDs

eRHIC pseudo data

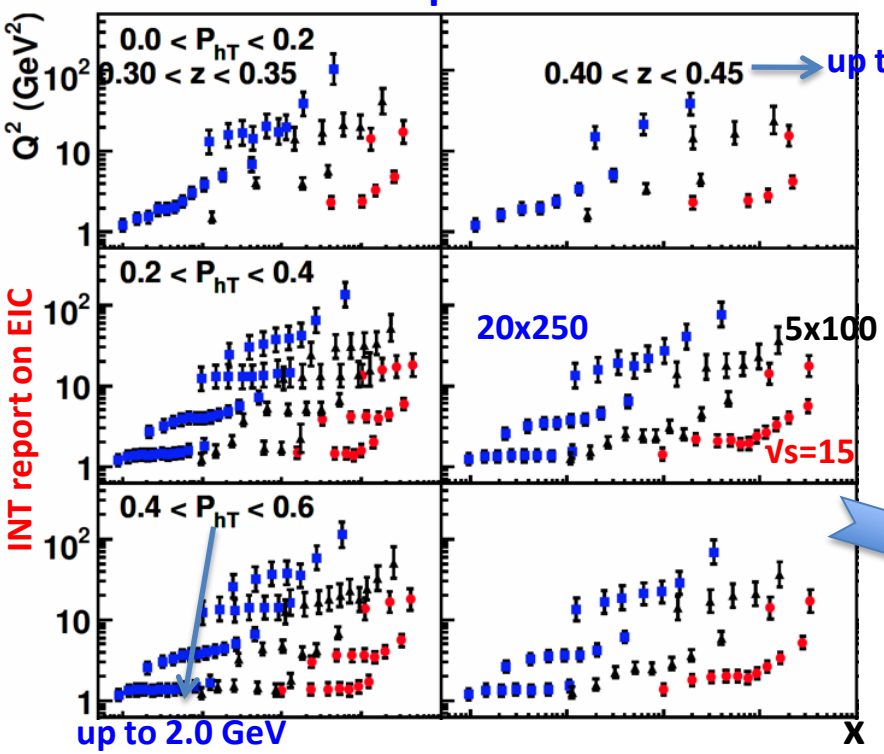

INT report on EIC

Impact of an eRHIC:

eRHIC high lumi → Multidimensional binning in $Q2, x, P^h_T, z, \phi$ is made possible!

Global TMD fit

Stage-1 data

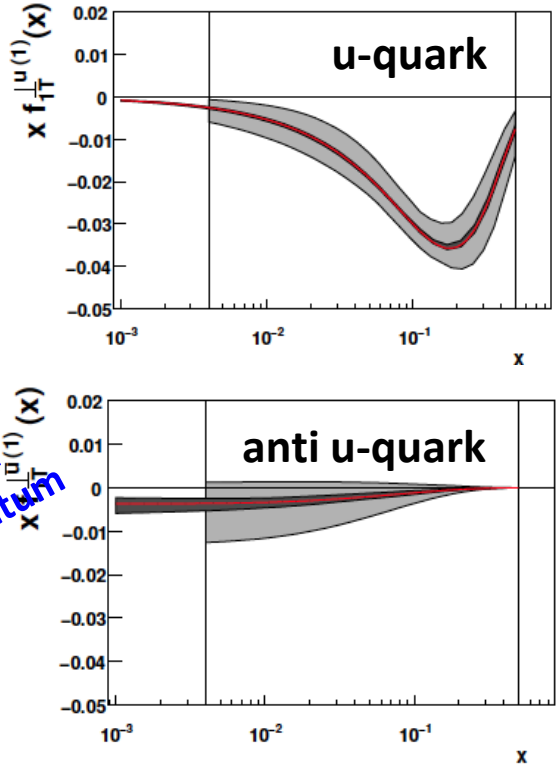

Proton imaging in transverse-momentum space

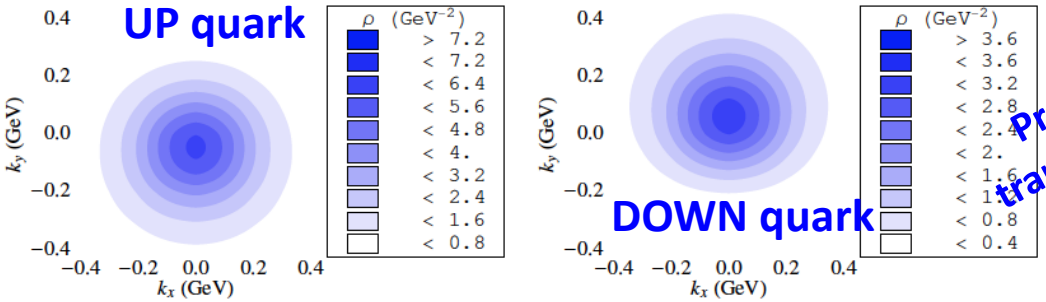

(2+1)-D imaging of the proton

Wigner Distribution

$W(x,r,k_t)$

TMDs

GPDs

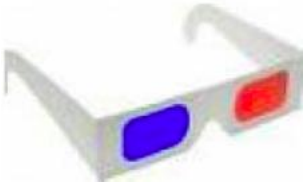

3D picture in momentum space

transverse momentum dependent distributions

$f_1 \rightarrow f_{1T}^{\perp}$

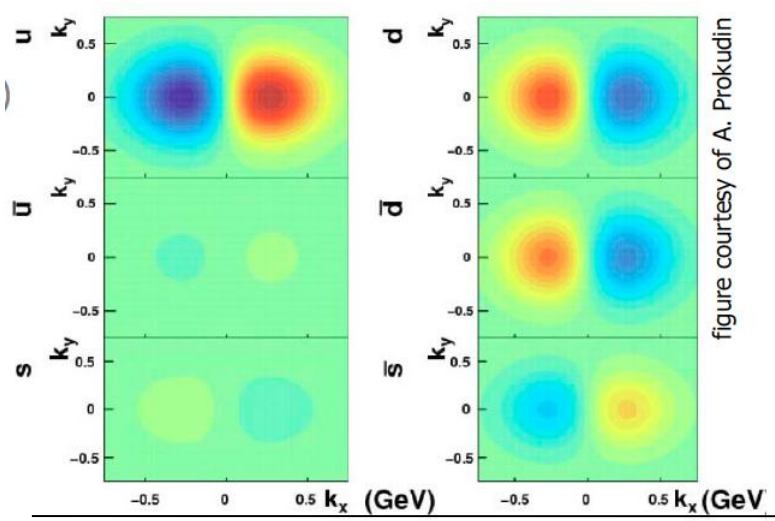

figure courtesy of A. Prokudin

3D picture in coordinate space

generalized parton distributions

→ exclusive reaction like DVCS

Quarks

unpolarised polarised

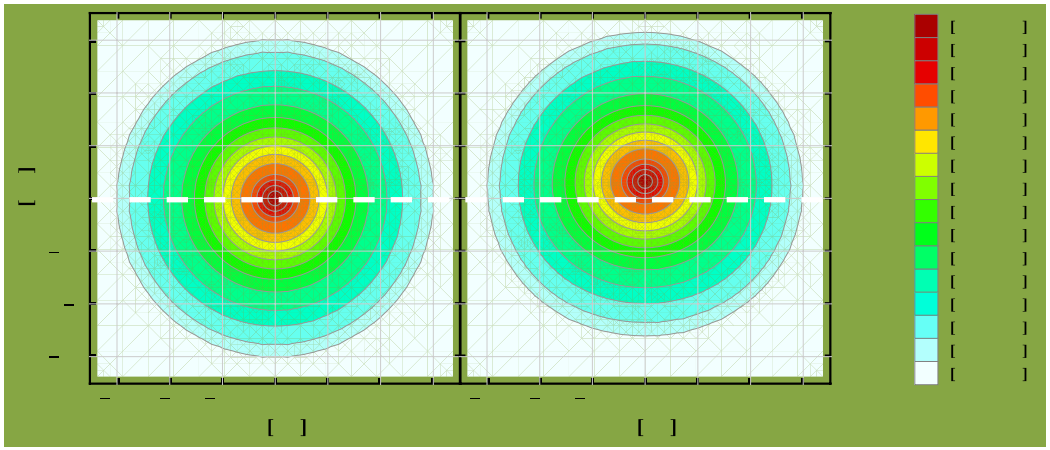

Accessing the Generalized Parton Distributions

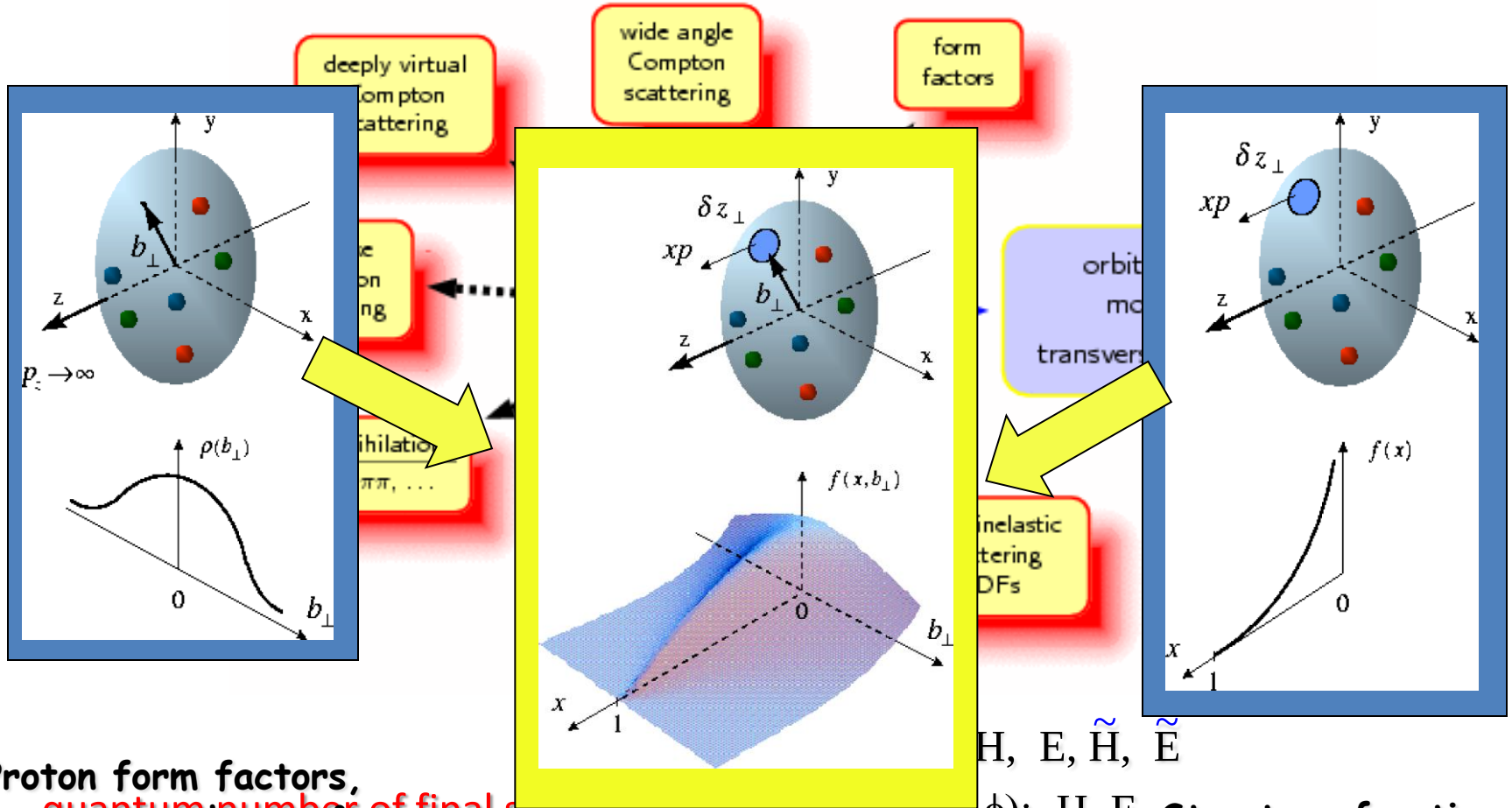

Proton form factors, transverse charge & current densities

quantum number of final state selects different GPDs:

H, E, $\tilde{H}$, $\tilde{E}$

✧ VM (ρ, ω, ϕ): H E

✧ Info on quark flavors via PS mesons (π, η): $\tilde{H}$ $\tilde{E}$

Structure functions, quark longitudinal momentum & helicity distributions

Accessing the GPDs

$$\frac{d\sigma}{dt} \sim A_0 \left[|H|^2(x,t,Q^2) - \frac{t}{4M_p^2} |E^2|(x,t,Q^2) \right]$$

Dominated by H
slightly dependent on E

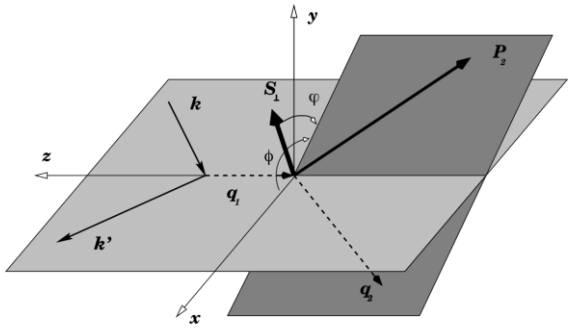

$$\phi = \phi_N - \phi_l$$

Angle btw the production and scattering planes

$$\varphi = \Phi_T - \phi_N$$

Angle btw the scattering plane and the transverse pol. vector

$$A_C = \frac{d\sigma^+ - d\sigma^-}{d\sigma^+ + d\sigma^-} \propto Re(A_{DVCS})$$

→ **Requires a positron beam at eRHIC**

$$A_{LU} \propto y \left[F_1(t) H(\xi,\xi,t,Q^2) - \frac{t}{4M^2} F_2(t) E(\xi,\xi,t,Q^2) + \ldots \right]$$

Dominated by H
slightly dependent on E

$$A_{UT} \propto \sqrt{\frac{-t}{4M^2}} \left[F_2(t) H(\xi,\xi,t,Q^2) - F_1(t) E(\xi,\xi,t,Q^2) + \ldots \right]$$

$\sin(\Phi_T - \phi_N)$
governed by E and H

Vector Meson Production

W & t dependences: probe transition from soft → hard regime

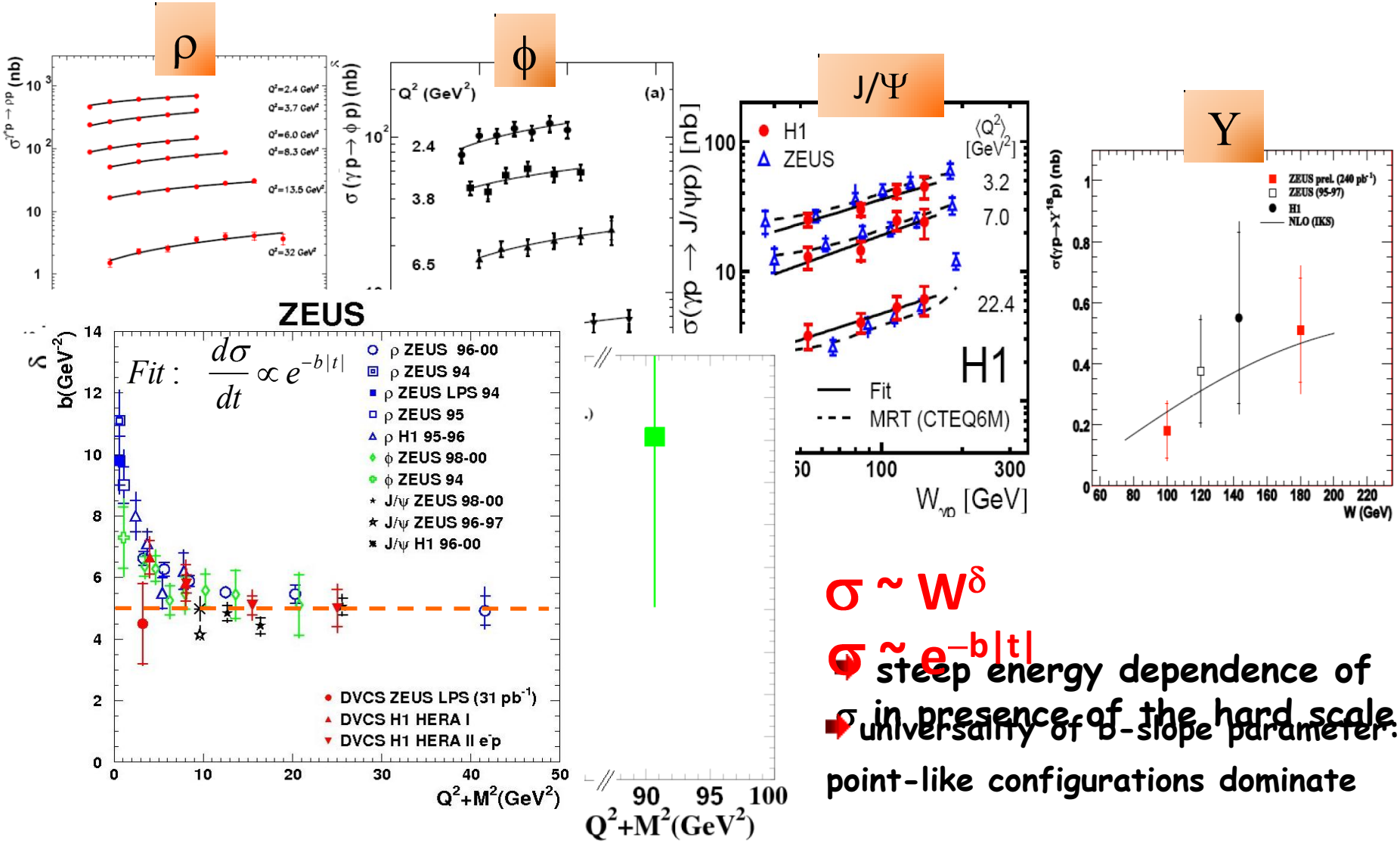

$\sigma \sim W^{\delta}$

$\sigma \sim e^{-b|t|}$

- steep energy dependence of σ in presence of the hard scale
- universality of b-slope parameter: point-like configurations dominate

Deeply Virtual Compton Scattering

VM (ρ, ω, φ, J/ψ, Υ)

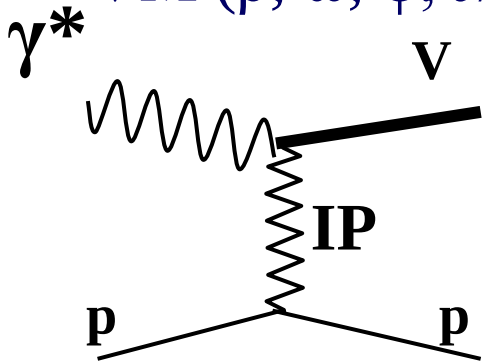

DVCS (γ)

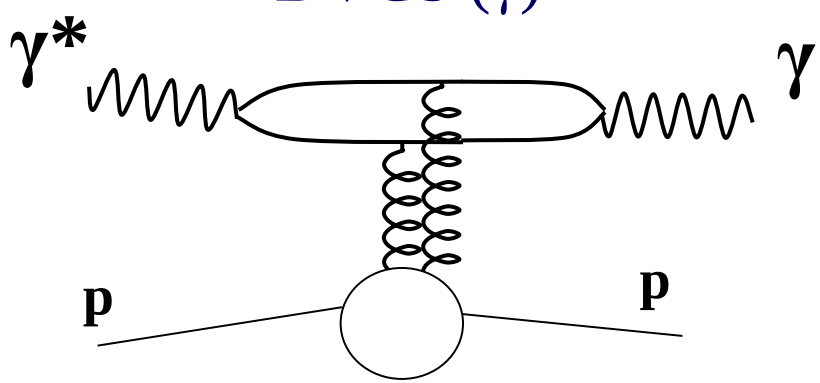

Scale: $Q^2 + M^2$ ⟷ Q^2

A GOLDEN MEASUREMENT!

DVCS properties:

- **Similar to VM production, but γ instead of VM in the final state**
- **Very clean experimental signature**
- **Not affected by VM wave-function uncertainty**
- **Hard scale provided by Q^2**
- **Sensitive to both quarks and gluons**

DVCS phase-space

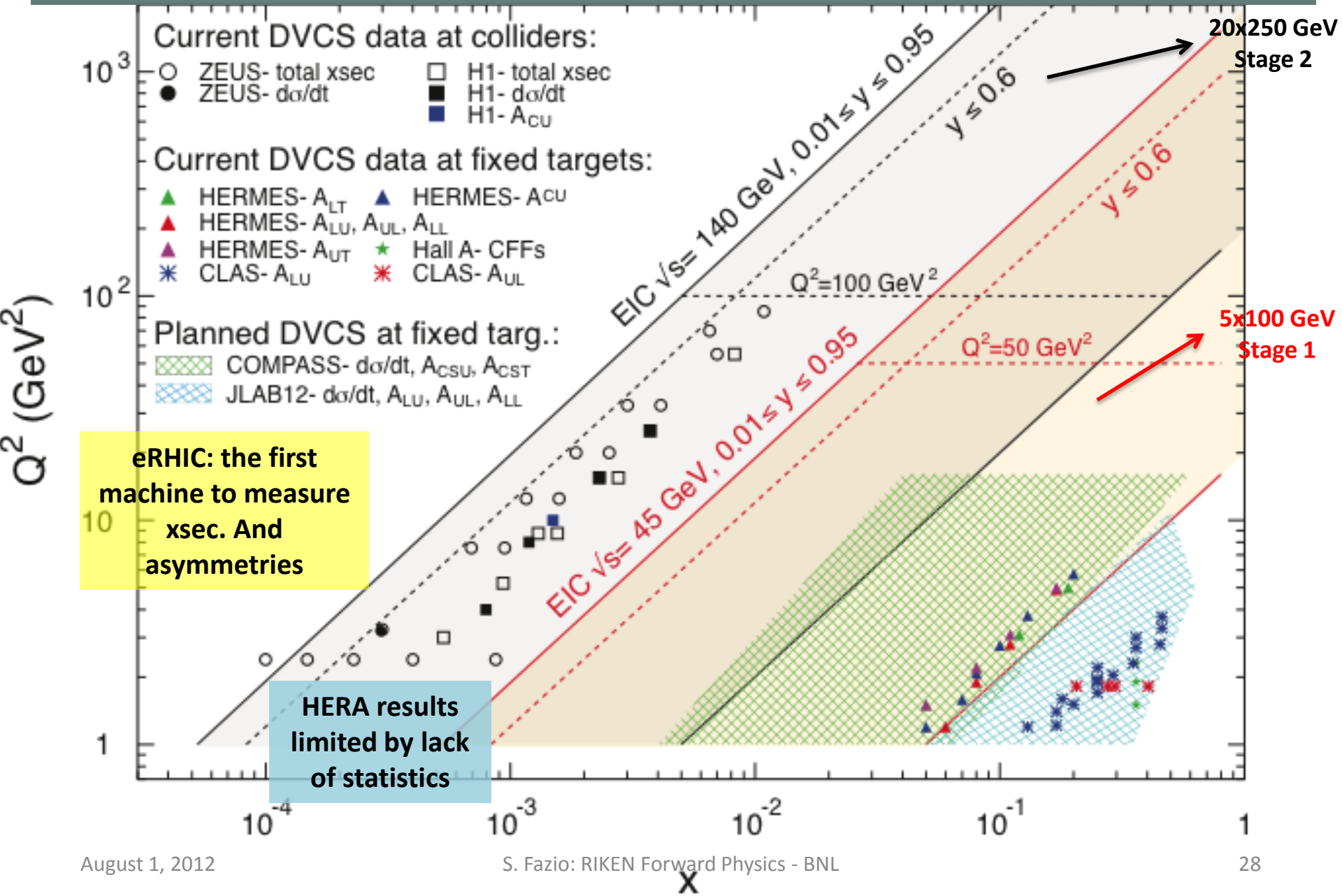

Scanning the phase space…

DVCS |t|-slope @ HERA

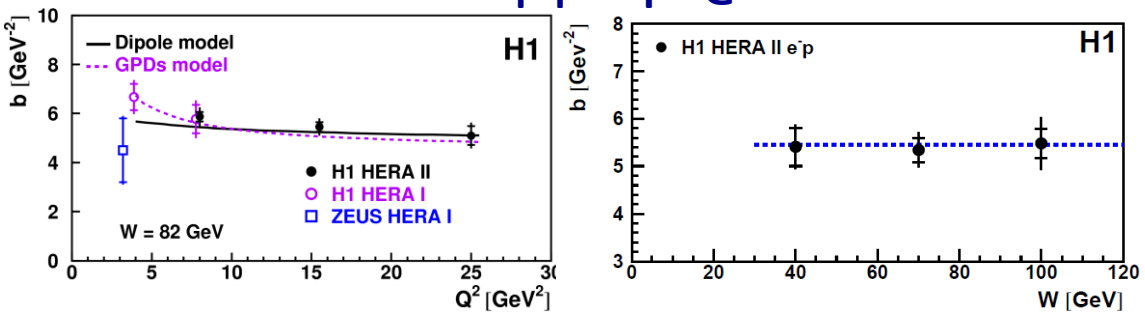

EIC lumi:
~10 fb^{-1}/year @ stage 1 – 5x100
~10 fb^{-1}/month @ stage 2 – 20x250

- **EIC will provide sufficient lumi to bin in multi-dimensions**
- **wide x and Q^2 range needed to extract GPDs**

20 X 250 – stage 2

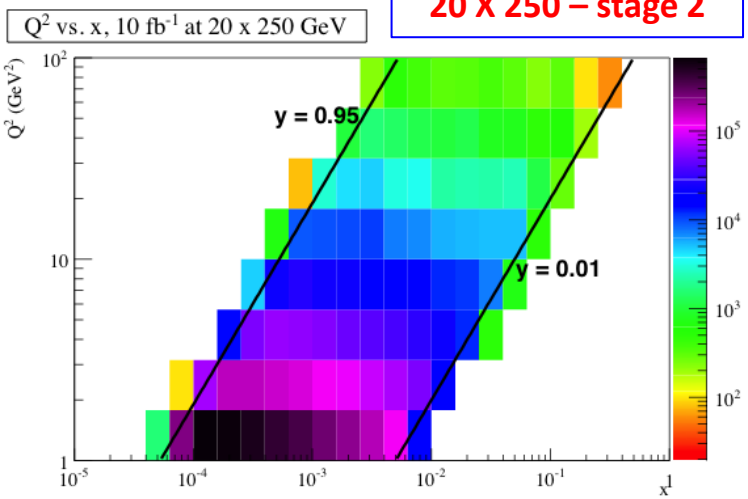

5 X 100 – stage 1

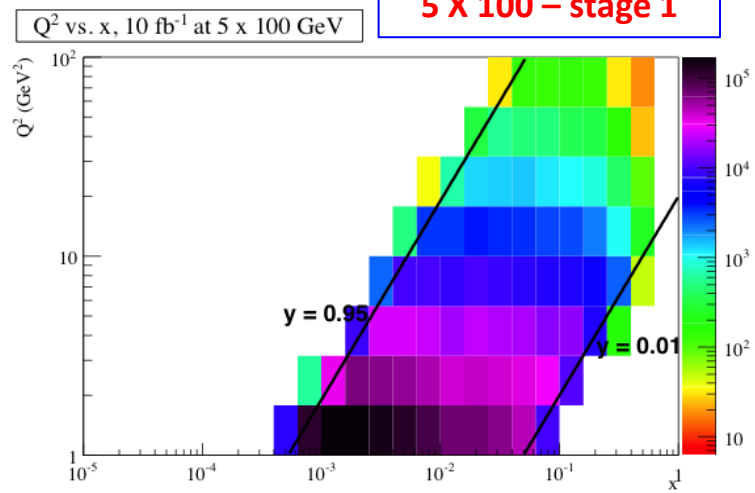

… we can do a fine binning in Q2 and W… and even in |t|

Direct |t| measurement @ eRHIC

Plots from J-H Lee

Accepted in"Roman Pot"(example) at s=20m

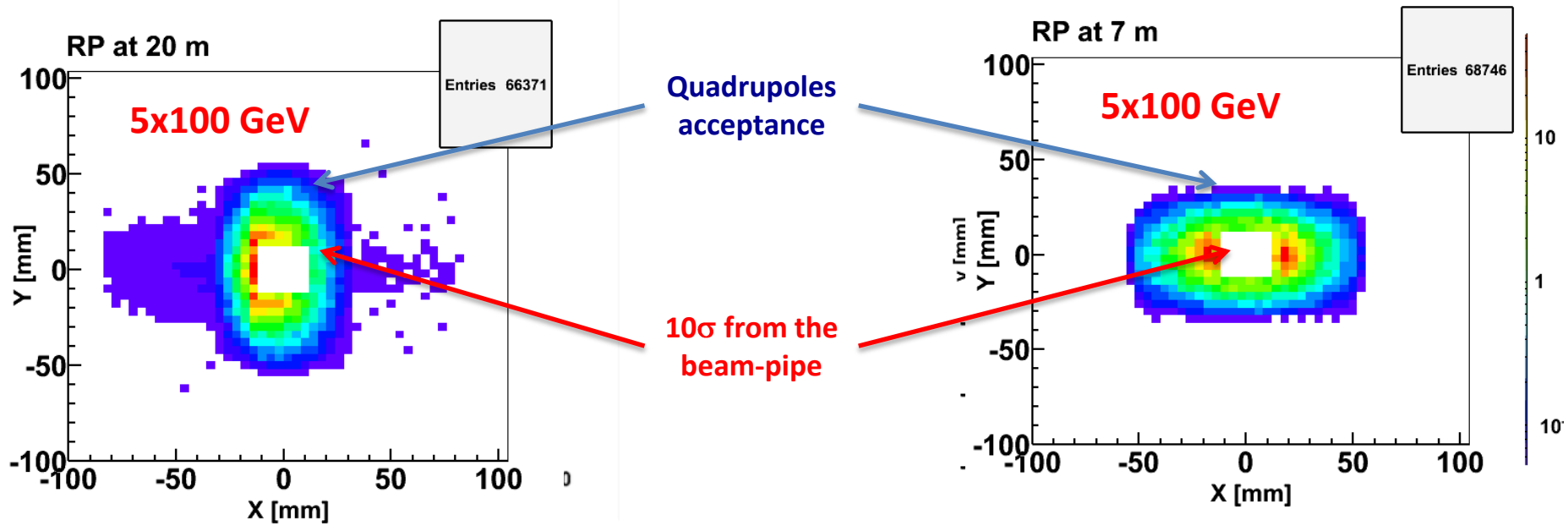

- high-t acceptance mainly limited by magnet aperture
- low-t acceptance limited by beam envelop (~10σ)
- t-resolution limited by
  - beam angular divergence ~100μrad for small t
  - uncertainties in vertex (x,y,z) and transport
  - ~<5-10% resolution in t (RP at STAR)

Roman Pots at HERA

ZEUS

$L = 27.77\ pb^{-1}$

55 events (DVCS + BH)

dσ/d|t|- Stage 1

$$\frac{d\sigma}{d|t|} = \frac{\#evt}{\Delta_{bin} \bullet A \bullet \mathcal{L}} \sim e^{-bt}$$

b=5.6

Specifications:

- **Statistical error down to 1%**
- **It uses smeared t values (5% momentum resol.)**
- **|t|-binning –> 3 * resolution (or higher)**

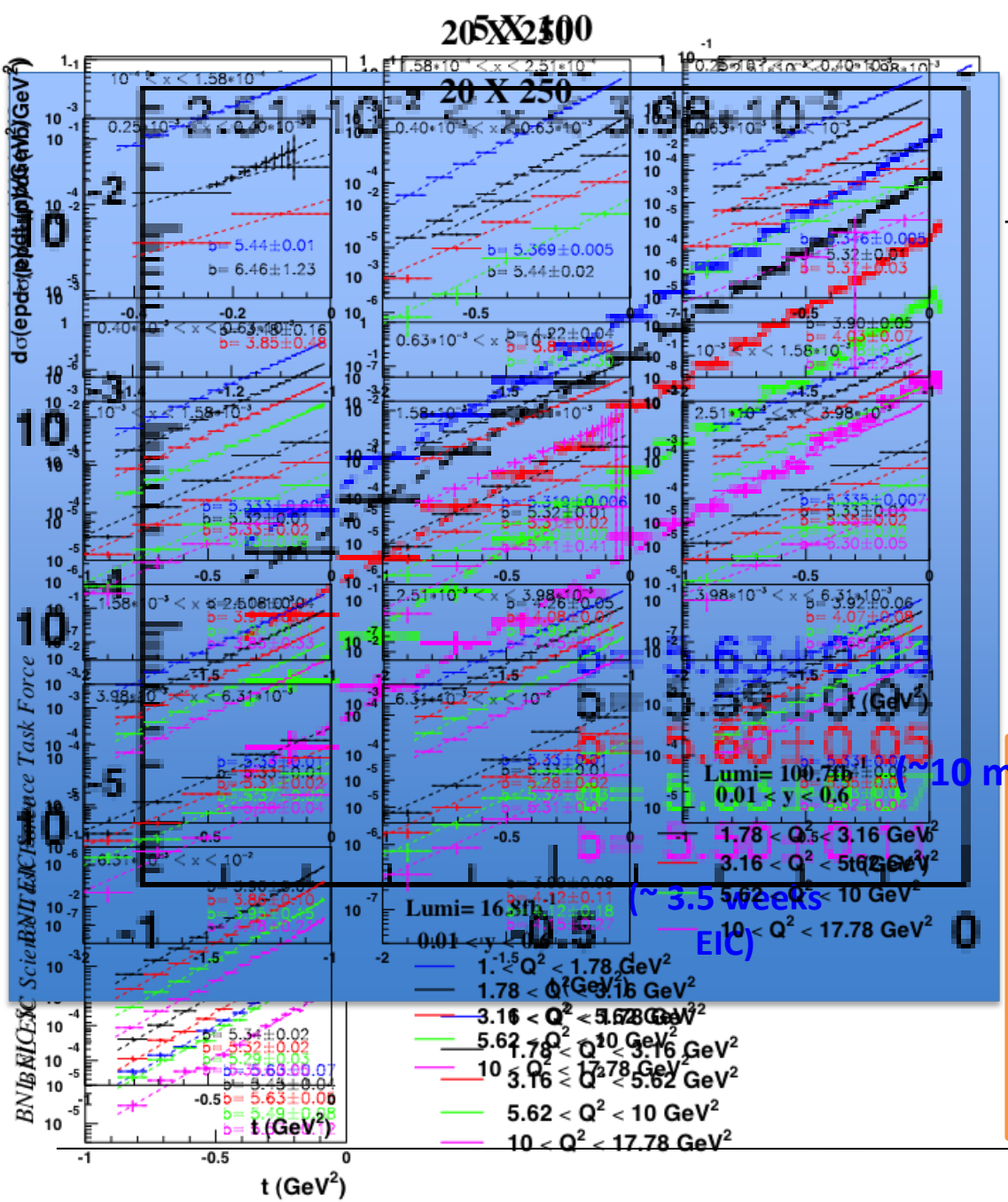

(~ 10 months)

(~ 3.5 weeks EIC)

DVCS |t|-slope @ HERA (15 years)

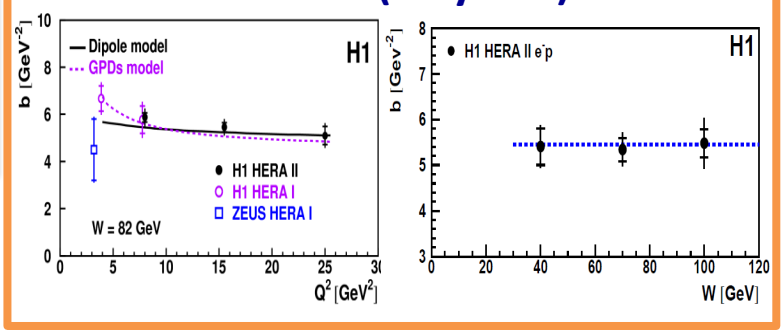

Asymmetries

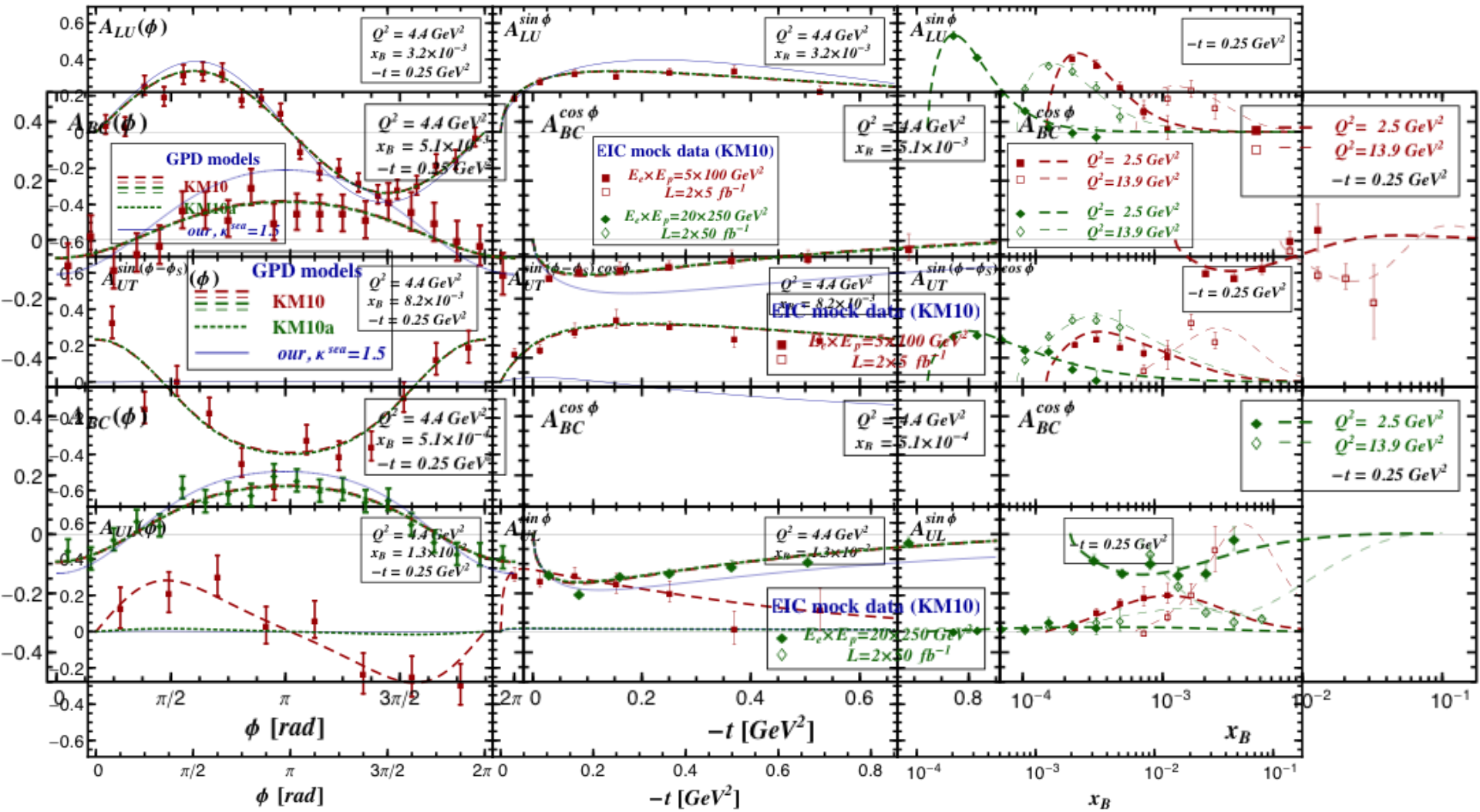

Plots from D. Mueller

Transverse target-spin asymmetry

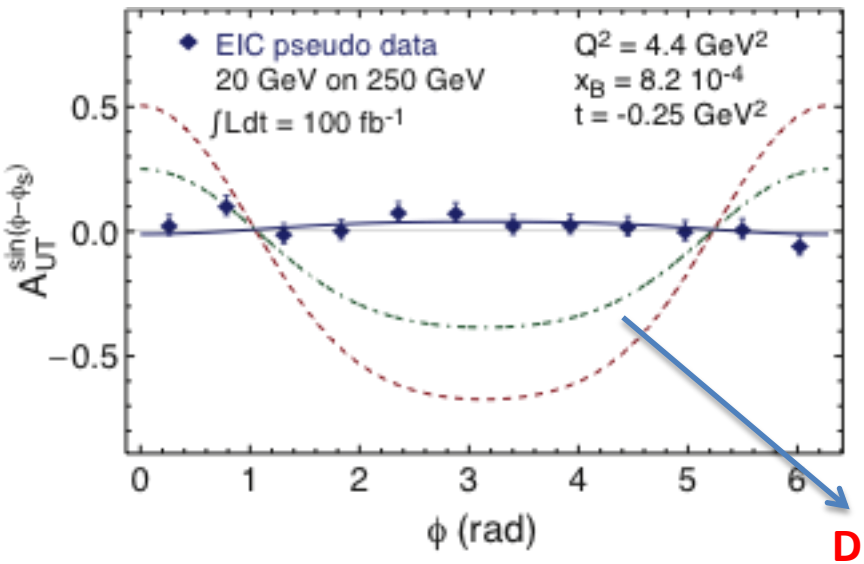

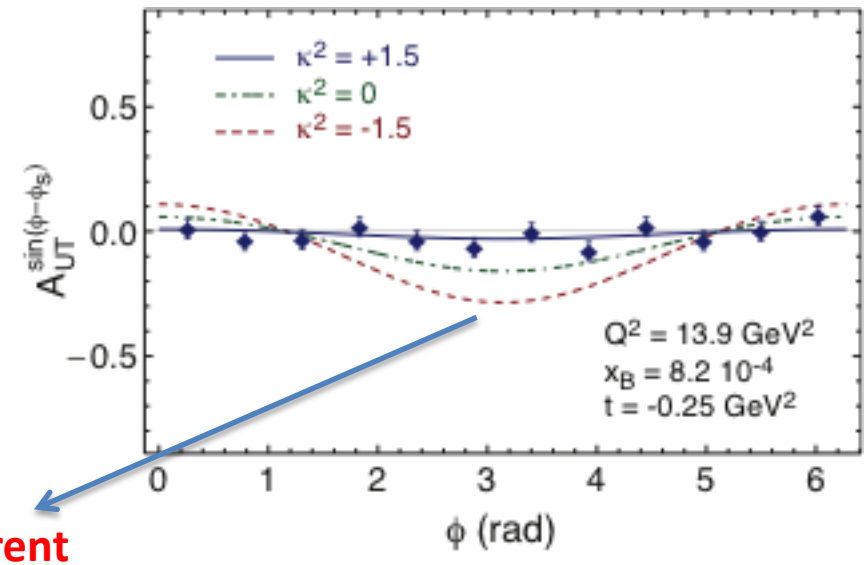

Different assumptions for E

$$A_{UT} \propto \sqrt{\frac{-t}{4M^2}}\left[F_2(t)H(\xi,\xi,t,Q^2) - F_1(t)E(\xi,\xi,t,Q^2) + \ldots\right]$$

$\sin(\Phi_T - \phi_N)$
governed by E and H

Gives access to GPD E

Imaging

Plots from D. Mueller

- Obtain the GPDs from global fits on present data and pseudo-data

...FIT...

- Fourier transform GPDs to obtain image in b-space

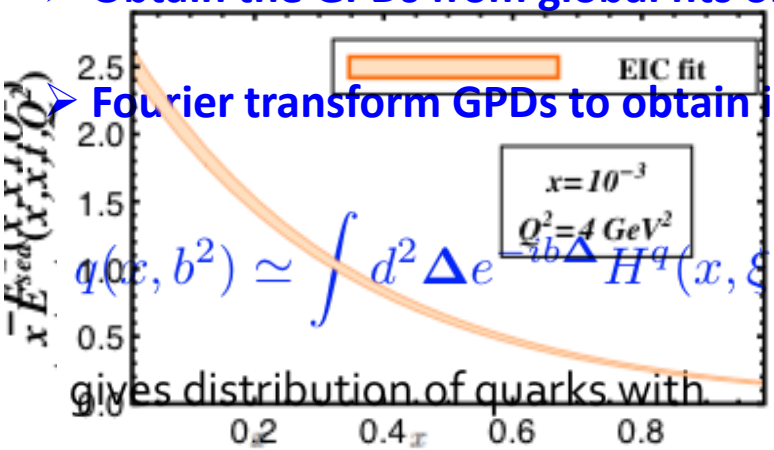

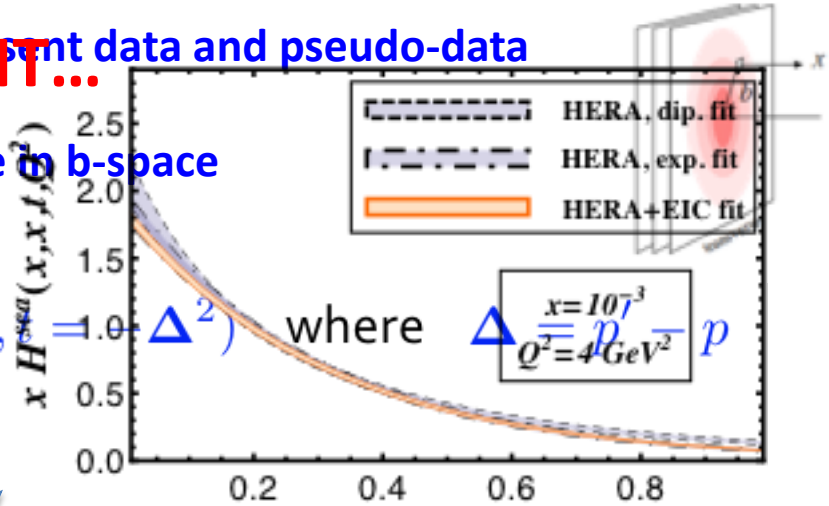

$$q(x,b^2) \simeq \int d^2\Delta\, e^{-ib\Delta} H^q(x,\xi=0,t=-\Delta^2)$$ where $\Delta = \bar{p} - p$

gives distribution of quarks with

- longitudinal momentum fraction x
- transverse distance b from proton center

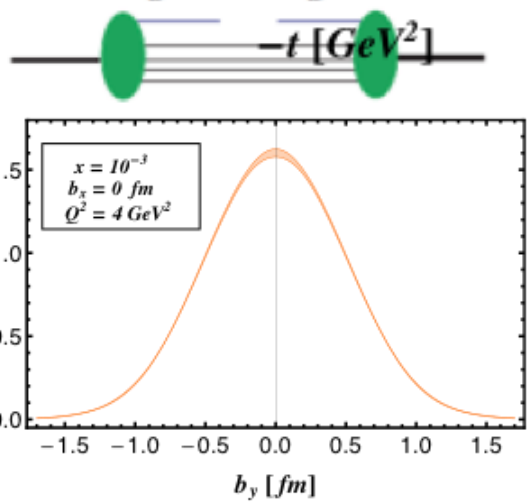

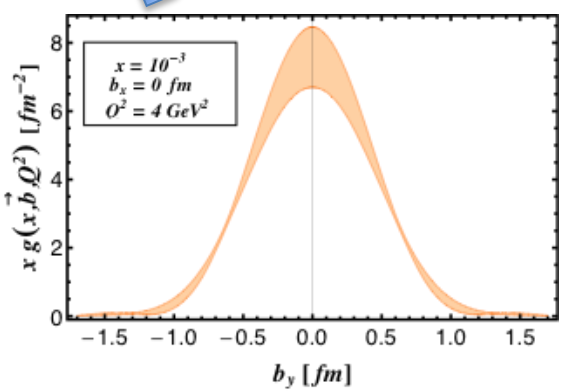

Errors are extrapolated for:
$|t| \rightarrow 0$; $|t| > 1.5$ GeV^2

$$q(x,\vec{b},\mu^2) = \frac{1}{4\pi}\int_0^\infty d|t|\, J_0\left(|\vec{b}|\sqrt{|t|}\right) H(x,\eta=0,t,\mu^2)$$

Imaging

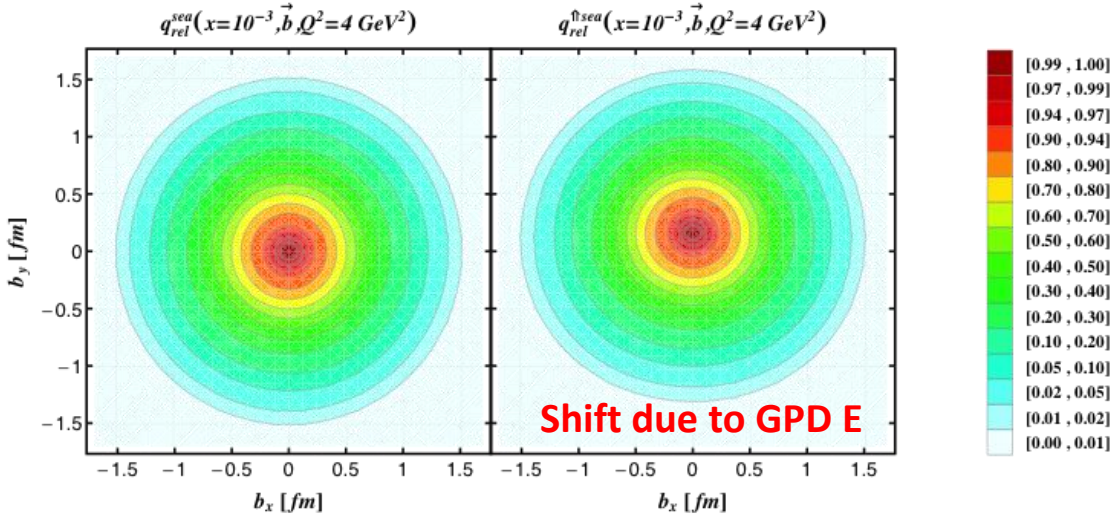

- A global fit over all mock data was done, based on the GPDs-based model:
  [K. Kumerički, D Müller, K. Passek-Kumerički 2007]
- Known values *q(x)*, *g(x)* are assumed for H^q, H^g (at t=0 forward limits E^q, E^g are unknown)
- Excellent reconstruction of H^{sea}, H^{sea} and good reconstruction of H^g (from $d\sigma/dt$)
- Reconstruction of GPD E (connection to the orbital momentum g-sum role)

Plots from D. Mueller

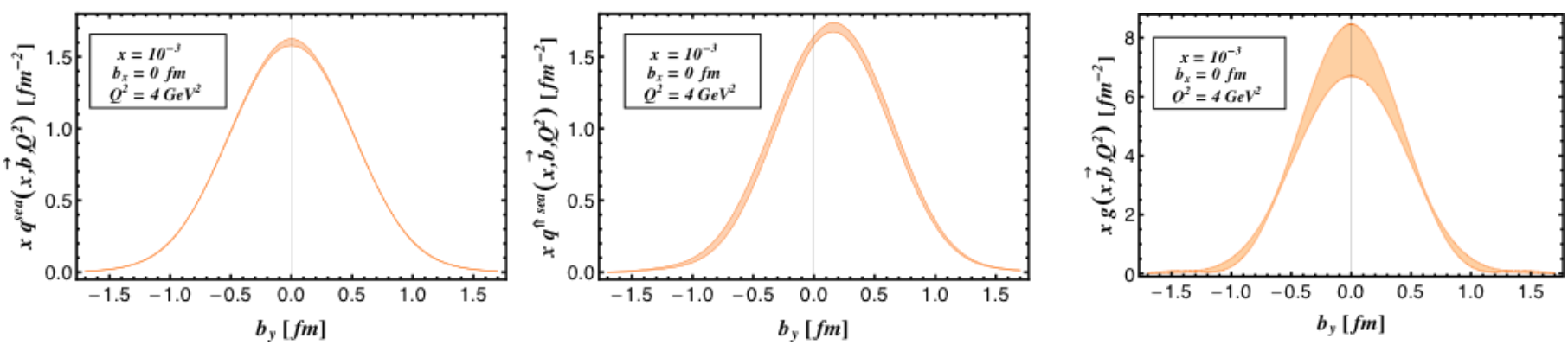

J/ψ

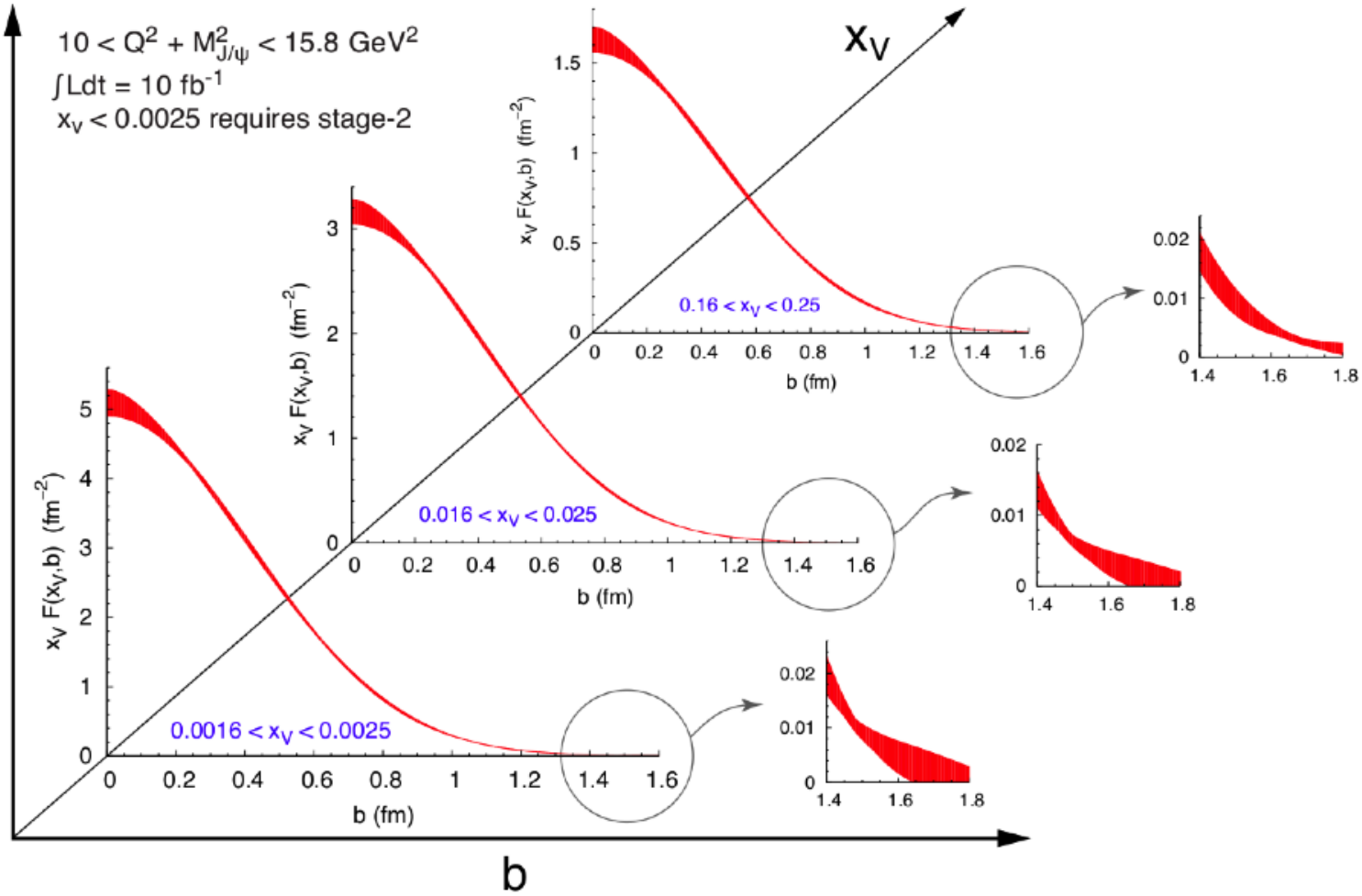

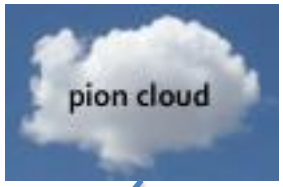

r and M. Diehl

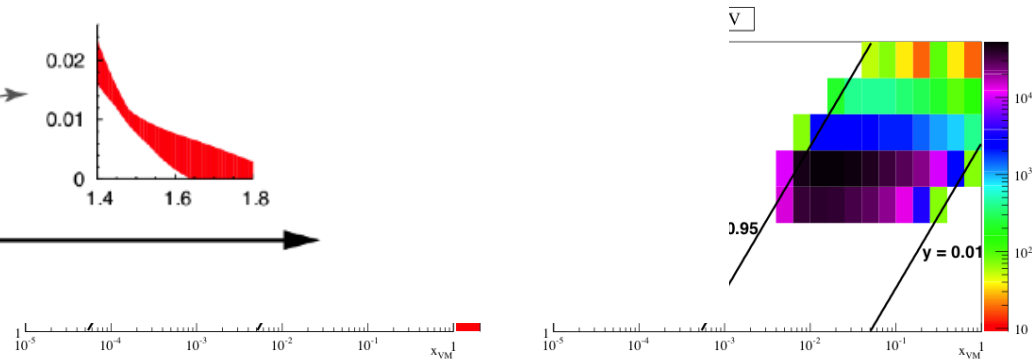

- Both photo- and electro-production can be computed

Summary

- **A lot of experience carried over from HERA**
- **eRHIC will be an ideal machine for precision measurements in QCD**
- **A lot of studies can be carried on with an high accuracy: PDFs, TMDs, GPDs**
- **Unique opportunity for understanding the gluon and sea quarks spin!**
- **Large potential for an accurate 2+1D imaging of the polarized and unpolarized quarks and gluons inside the hadrons**

Back up

- Electron and photon clusters are often very close!
- can affect the phi distribution reconstruction!

Crucial!

Our em cal must distinguish two clusters within the order of 1 deg

More studies on-going…

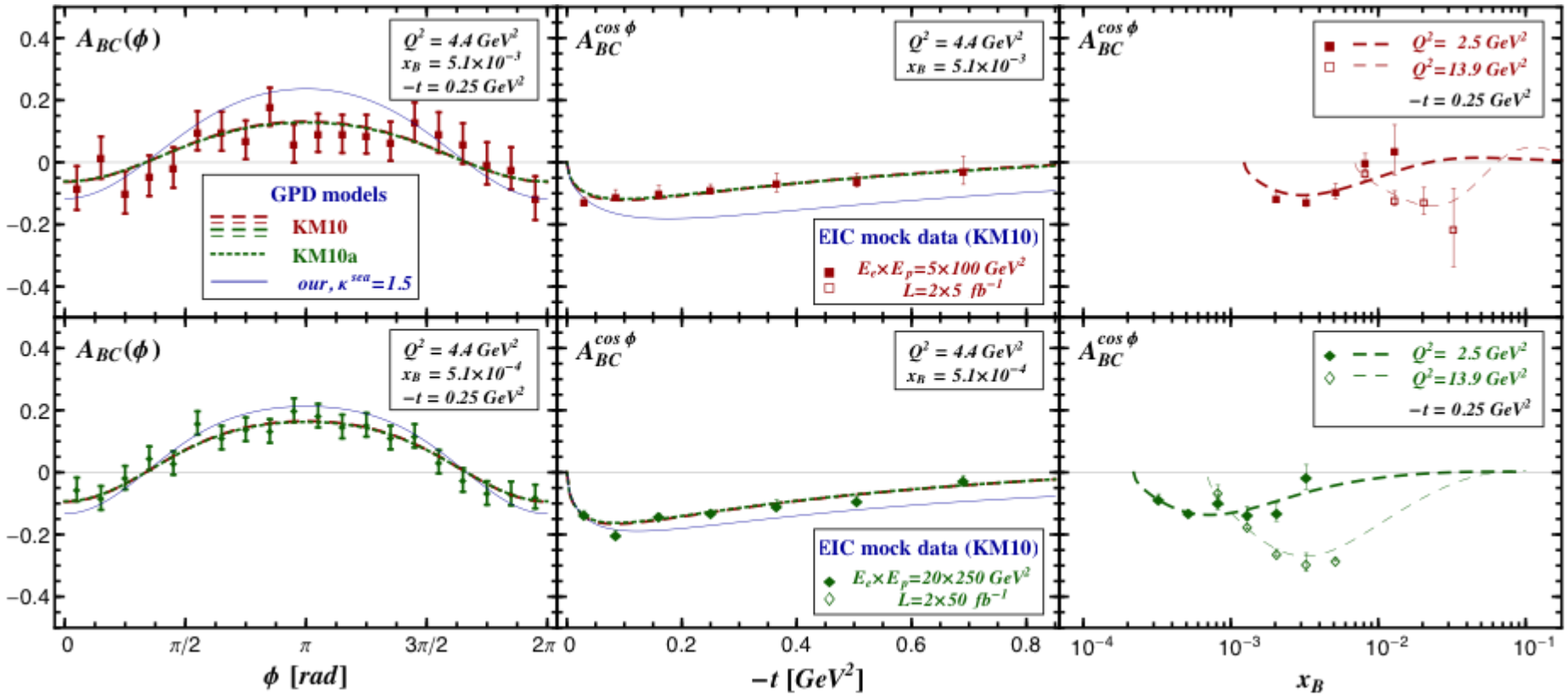

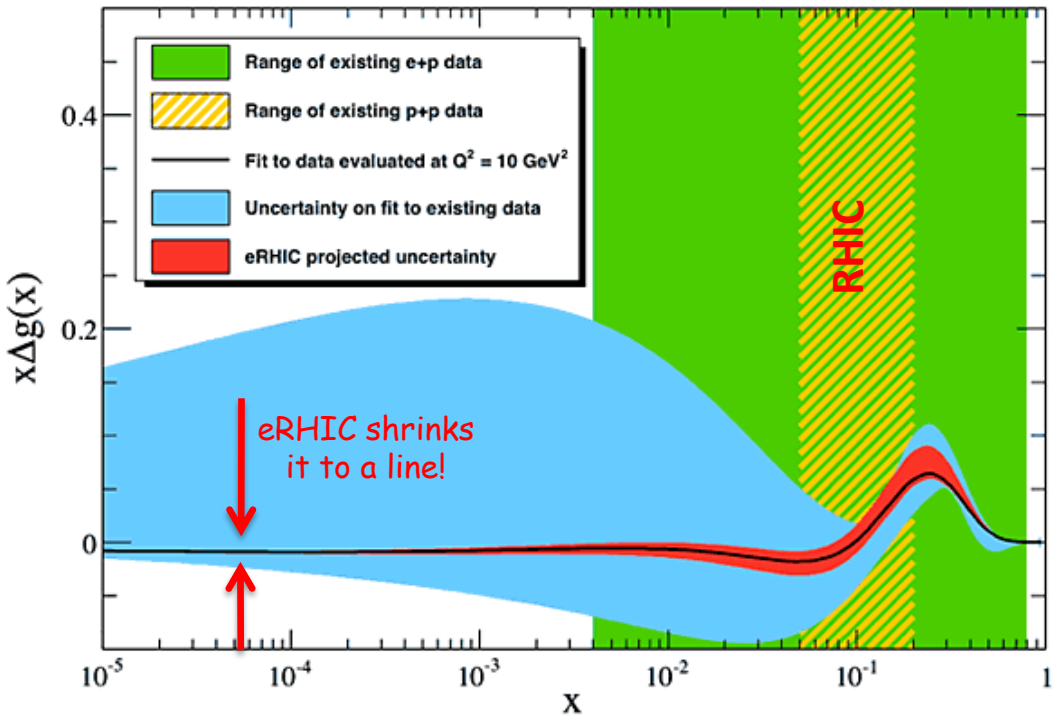
Range of existing e+p data
Range of existing p+p data
Fit to data evaluated at Q^2 = 10 GeV^2
Uncertainty on fit to existing data
eRHIC projected uncertainty
RHIC
eRHIC shrinks
it to a line!
$x\Delta g(x)$
0.4
0.2
0
10^{-5}
10^{-4}
10^{-3}
10^{-2}
10^{-1}
1
x

F_L extraction

$$\sigma_r(x,Q^2) = F_2(x,Q^2) - \frac{y^2}{Y^+} F_L(x,Q^2)$$

where: $Y^+ = 1 + (1-y)^2$

Strategy:

- Measure the reduced cross section
- Extract the y^2/Y^+ slope fir dufferebt s at fuxed x,Q^2

✓ **Plot based on eRHIC stage 1:**
- ✧ **5+100 GeV**
- ✧ **5+250 GeV**
- ✧ **5+325 GeV**

✓ **Statistical errors (included) are negligible**

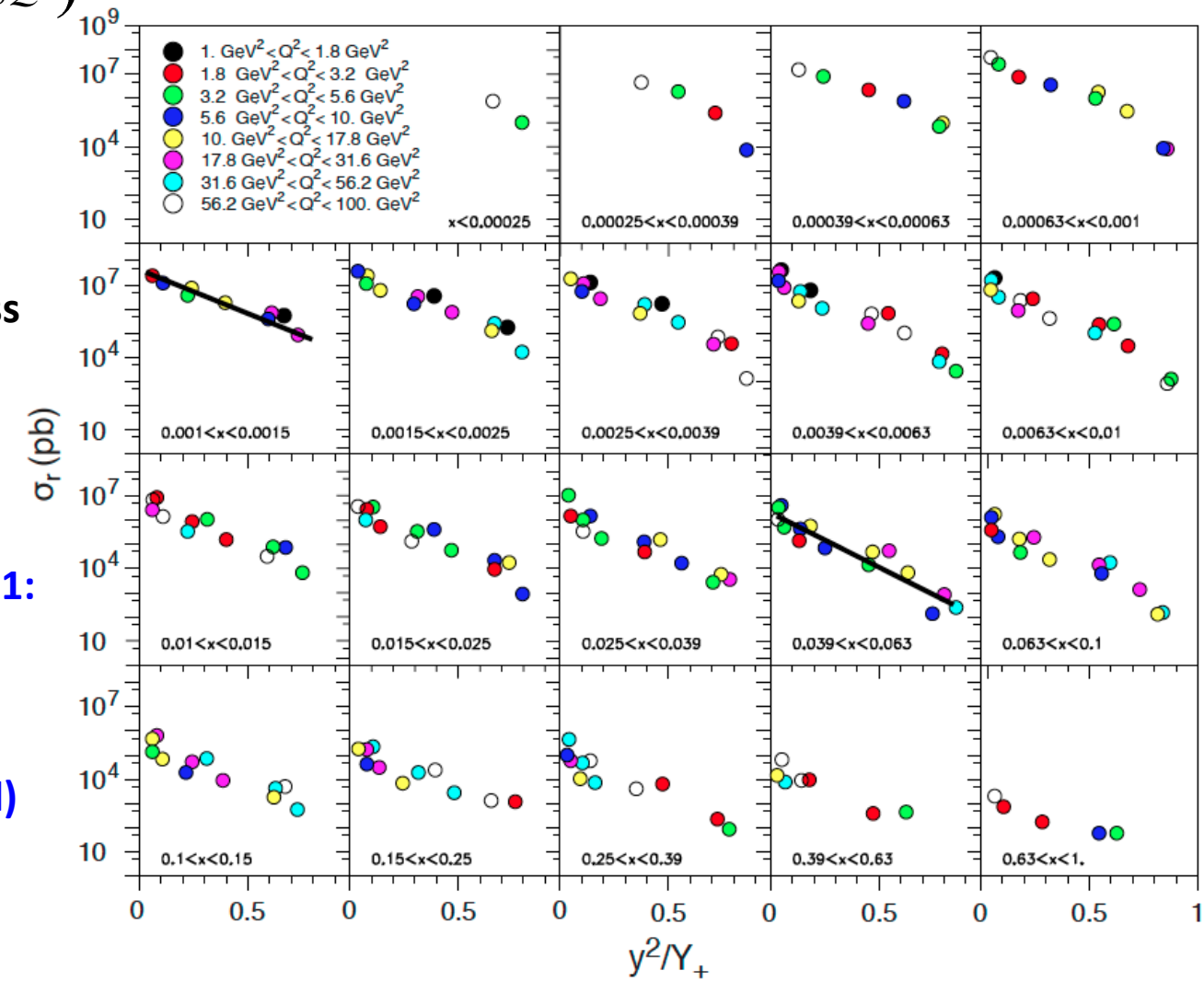

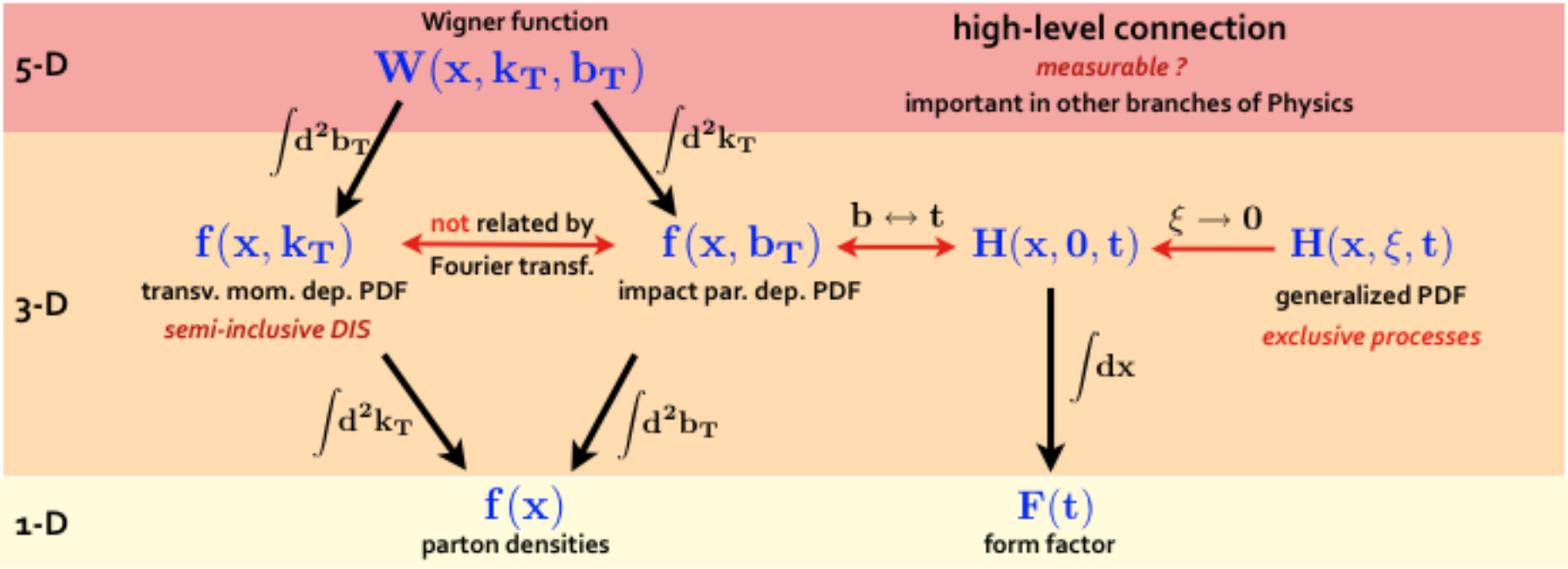
5-D
Wigner function
$W(x, k_T, b_T)$
high-level connection
measurable ?
important in other branches of Physics
$\int d^2b_T$
$\int d^2k_T$
3-D
$f(x, k_T)$
transv. mom. dep. PDF
semi-inclusive DIS
not related by
Fourier transf.
$f(x, b_T)$
impact par. dep. PDF
$b \leftrightarrow t$
$H(x, 0, t)$
$\xi \to 0$
$H(x, \xi, t)$
generalized PDF
exclusive processes
$\int dx$
$\int d^2k_T$
$\int d^2b_T$
1-D
$f(x)$
parton densities
$F(t)$
form factor

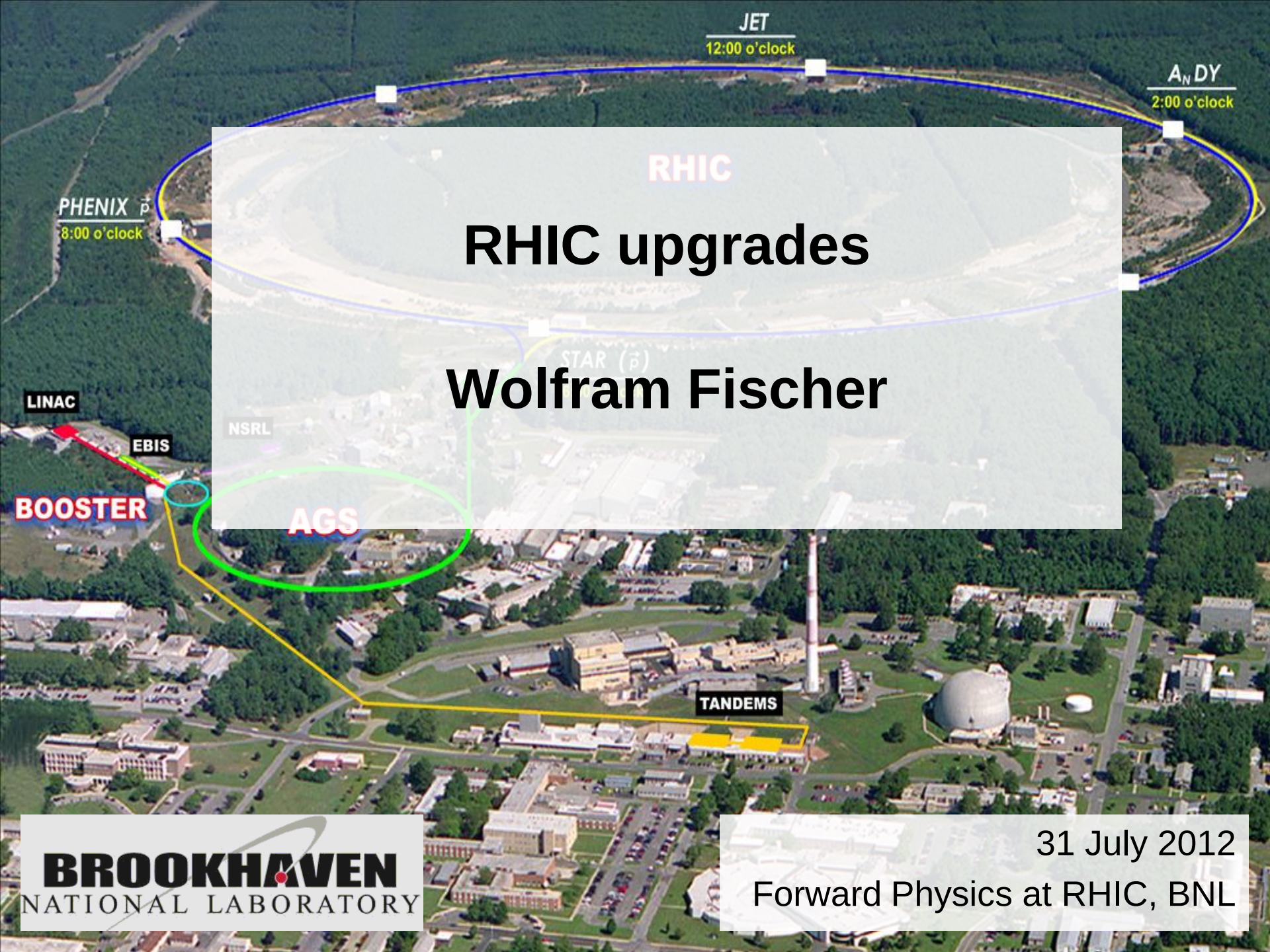

RHIC upgrades

Wolfram Fischer

BROOKHAVEN NATIONAL LABORATORY

31 July 2012

Forward Physics at RHIC, BNL

Relativistic Heavy Ion Collider

1 of 2 ion colliders (other is LHC), only polarized p-p collider

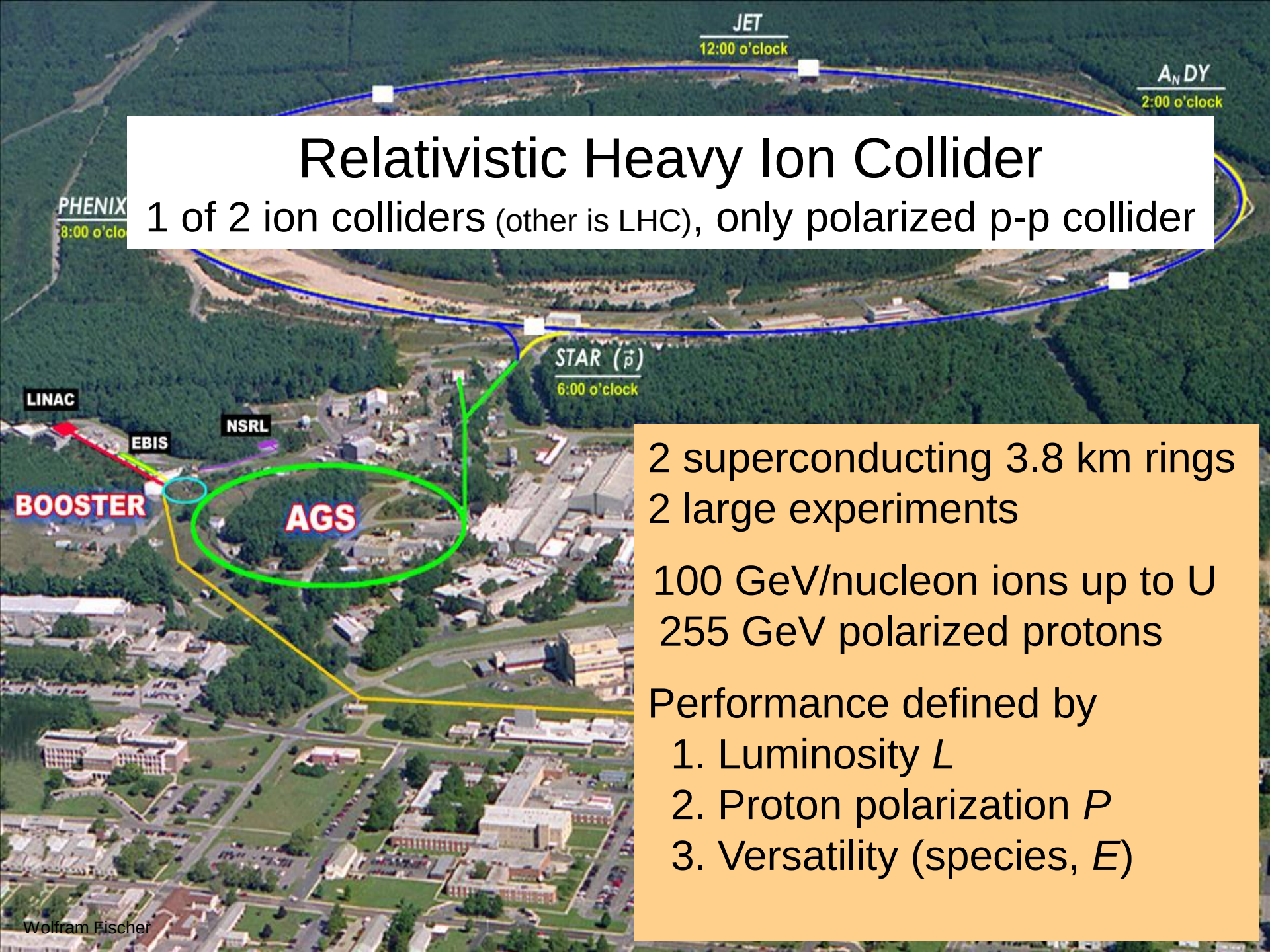

2 superconducting 3.8 km rings
2 large experiments

100 GeV/nucleon ions up to U
255 GeV polarized protons

Performance defined by

1. Luminosity *L*
2. Proton polarization *P*
3. Versatility (species, *E*)

Content

Run-12 overview (= status, operation in all modes possible)

- Polarized protons, $\sqrt{s}$ = 200, 510 GeV
- Uranium-uranium $\sqrt{s_{NN}}$ = 193 GeV, copper-gold $\sqrt{s_{NN}}$ = 200 GeV gold-gold $\sqrt{s_{NN}}$ = 5 GeV

Polarized proton upgrades

- Polarization and luminosity with source upgrade
- Luminosity with RHIC electron lenses
- R&D for polarized ^{3}He

Heavy upgrades

- Luminosity with stochastic cooling & 56 MHz SRF
- Low energy cooling
- **p-Au operation**

2012 RHIC Run (23.6 weeks of cryo ops) – most varied to date

100 GeV polarized protons

new records for L_{peak} (1), L_{avg} (2), P (3)

255 GeV polarized protons

highest energy polarized proton beam (4)

new records for L_{peak} (5), L_{avg} (6), P (7)

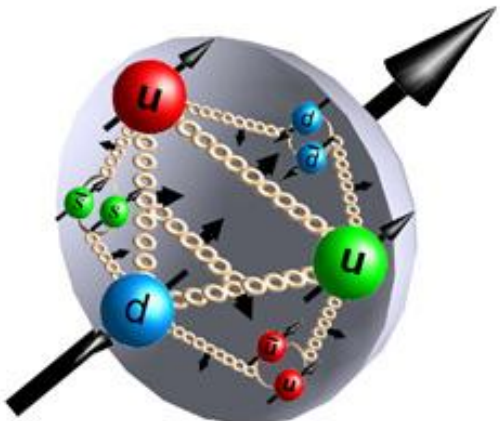

96.4 GeV/nucleon uranium-uranium

heaviest element in collider (8), shape

stochastic cooling: $L_{max} > L_0$ 1st time in hadron collider! (9)

all ions lost through burn-off 1st time in hadron collider! (10)

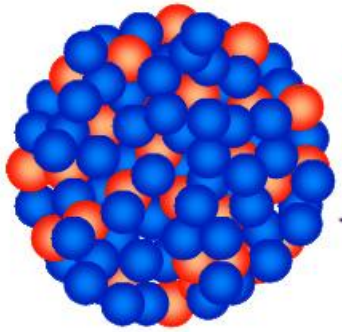

Uranium Nucleus

100 GeV/nucleon copper-gold

new species combination in collider (11)

highest ion charge/bunch (+8.5% rel. to Run-11) (12)

2.5 GeV/nucleon gold-gold collision test

lowest energy to date, 20% of nominal injection ($B\rho$) (13)

He-3 acceleration (unpolarized) in Booster and AGS

highest energy He-3 beam (14)

Run-12 – Polarized protons 100 GeV

Run Coordinator: V. Schoeffer

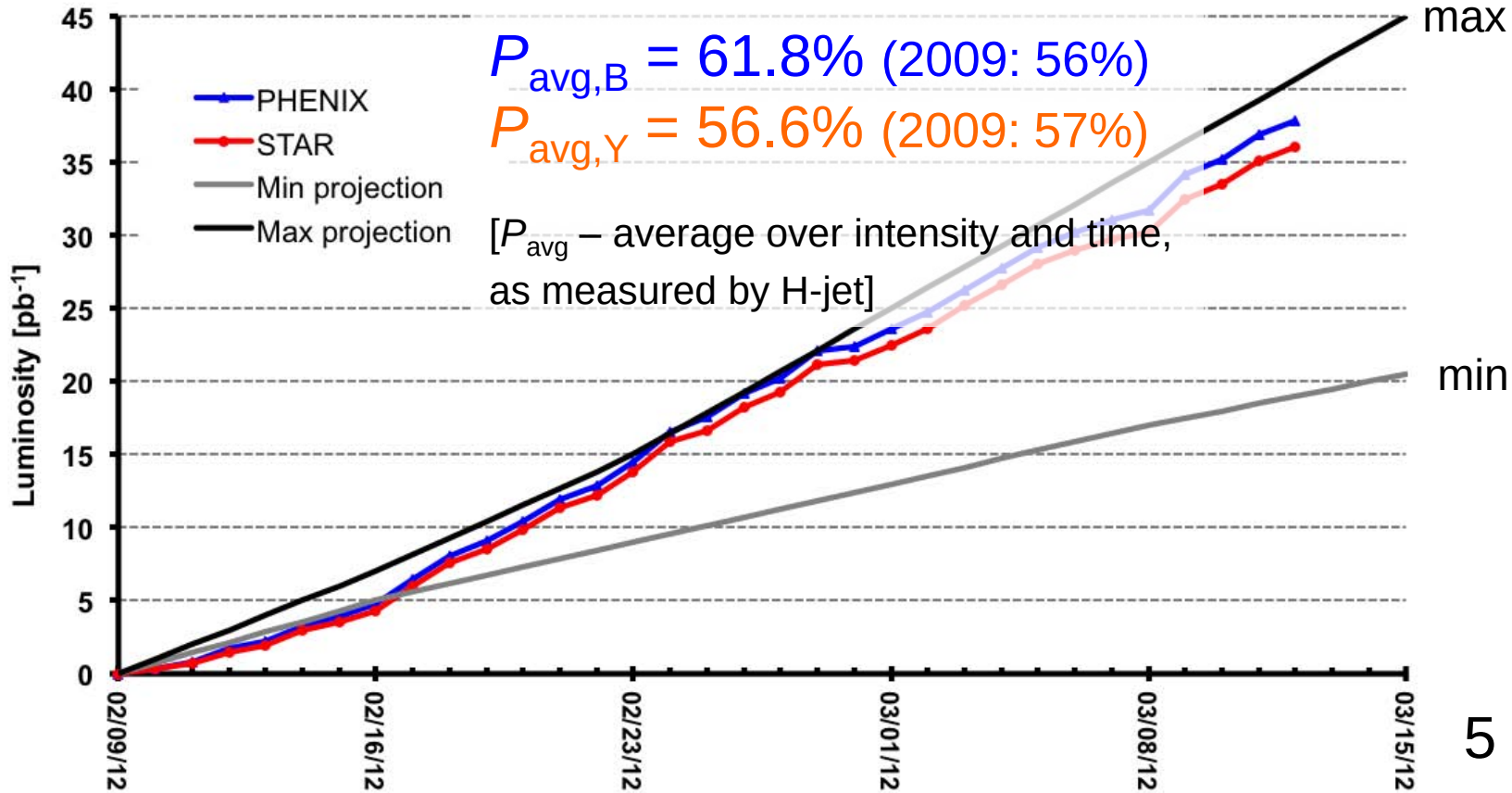

5 weeks

New: 2 new Landau cavities installed in RHIC; AGS horizontal alignment; 9 MHz system upgraded; AGS horizontal tune jump timing improved; operation from new Main Control Room; down ramp does not stop at injection any more, ramp from park to injection with 2x ramp speed compared to previous runs (saves 2.9 min per ramp)

Polarization details at www.phy.bnl.gov/cnipol (D. Smirnov)

Run-12 – Polarized protons 255 GeV

Run Coordinator: V. Schoeffer

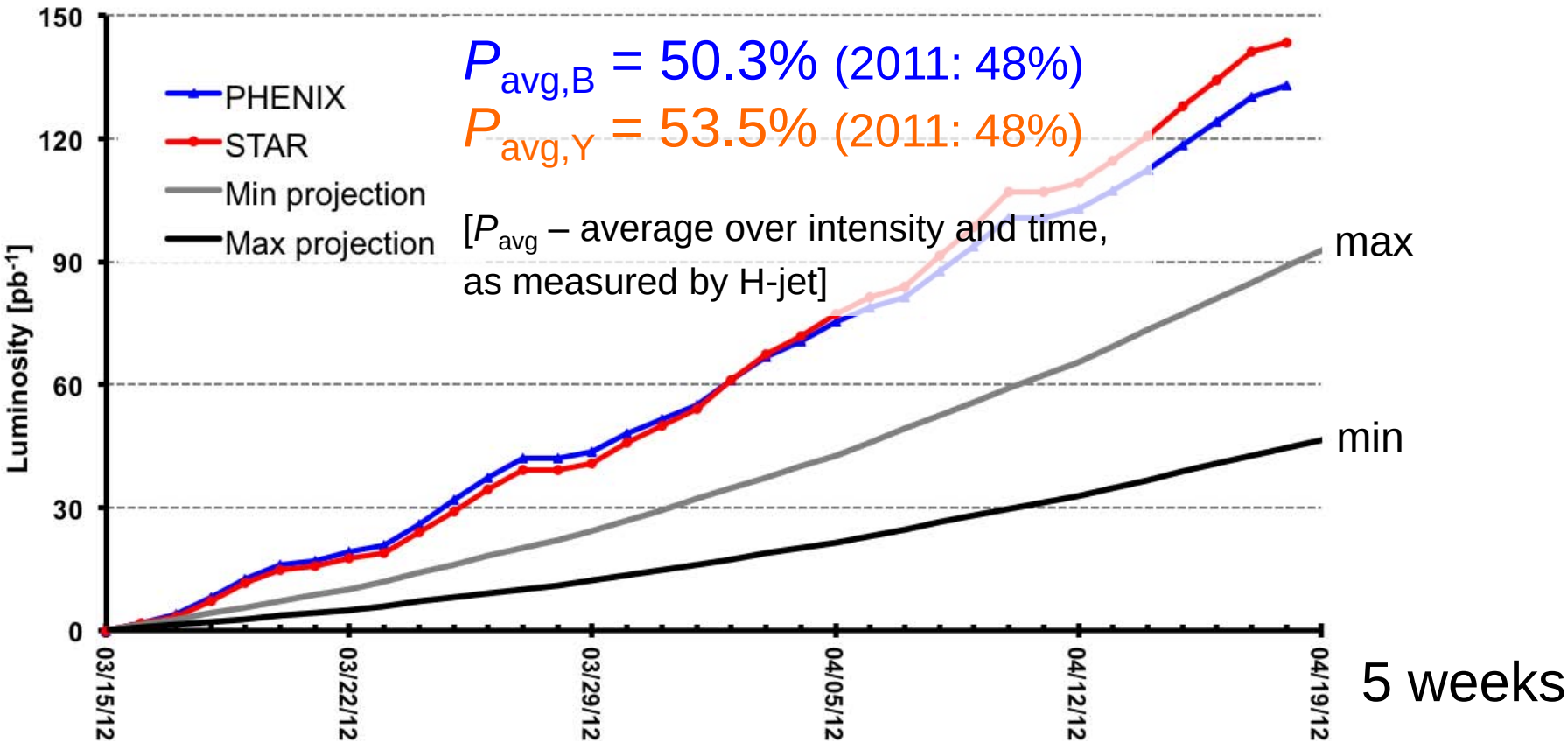

New: same as for 100 GeV; increased store energy to increase polarization lifetime; snakes ramp between 100 GeV and 255 GeV; scan of snake spin rotation axis angle and spin rotation angle; test of longitudinal injection damper; test of Landau phase error compensation (phase error from Booster) compensation

Polarization details at www.phy.bnl.gov/cnipol (D. Smirnov)

Polarization tests during Run-13 (M. Bai et al.)

Polarization lifetime at store (0.5-1.0%/h loss at 100 and 250 GeV)

- Energy change from 250 to 255 GeV => no difference
- Depolarization of non-colliding beam on/off the strongest snake resonance (=11/16) => no difference
- Spin tune change ±0.01=> no difference
- Snake spin rotation angle scan ±10 deg => small effect for –10 deg

Depolarization during energy and rotator ramps

- Orbit effect of last 2 strong intrinsic resonances
  => small effect for large orbit error
- Contribution of final β^*-squeeze => no difference
- Snake spin rotation angle => 5% (absolute) gain in Yellow
- Spin tune change ±0.01 => no difference

Absolute polarization at injection with H-jet

- 10 h for measurement in Yellow only (background minimization)
- P_{avg} = (63±4.4)%

=> Unlikely that large polarization gains can be made by further parameter changes, i.e. depolarization due to many small effects

Run-12 – Uranium-uranium 96.4 GeV/nucleon

Run Coordinator: Y. Luo

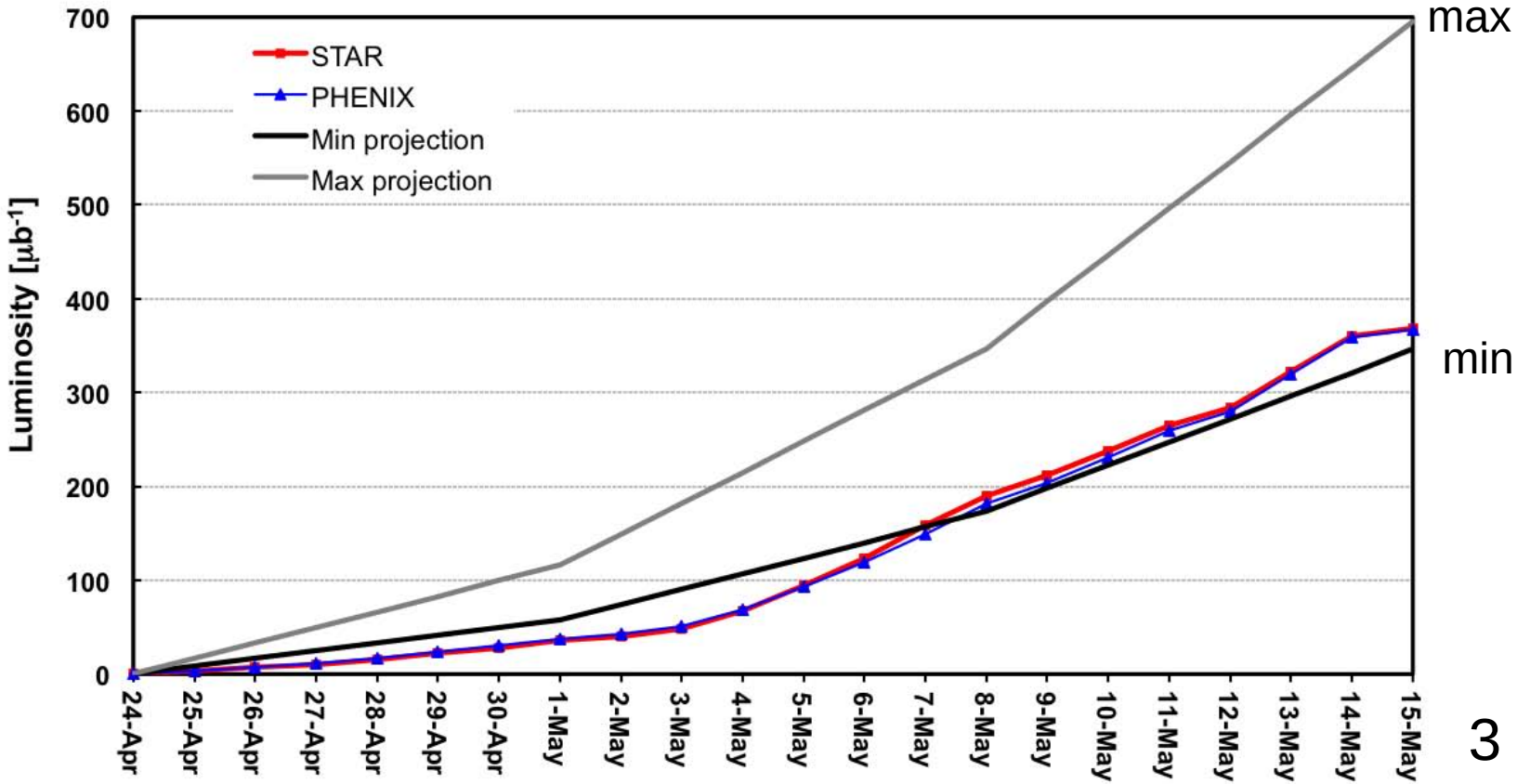

3 weeks

New: first use of EBIS for RHIC operation; first U-U operation in a collider; used standard lattice to increase off-momentum dynamic aperture; first use of Blue and Yellow horizontal stochastic cooling (resulting in 3D cooling in both rings); due to small beam size need micro-vernier scan every 1/2 h

Electron Beam Ion Source (EBIS)

- Inject single charge ion from primary source (e.g. hollow cathode source)
- 10 A electron beam creates desired charge state in trap (5 T sc solenoid)
- Source for high-charge state, high brightness ion beams
- Accelerated through RFQ and linac, injected into AGS Booster
- All ion species including noble gas, uranium and polarized ^{3}He

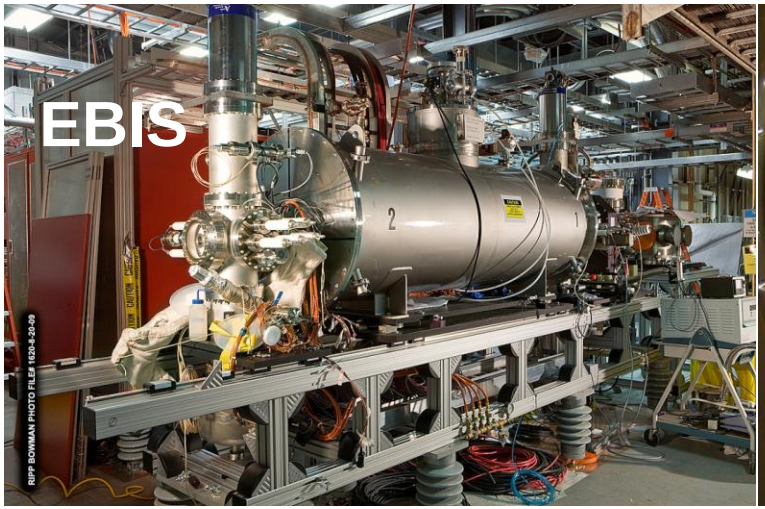

Operated for NASA Space Radiation Laboratory in 2011-12 with

- He^{+}, He^{2+}, Ne^{5+}, Ne^{8+}, Ar^{10+}, Kr^{18+}, Ti^{18+}, Fe^{20+}, Xe^{27+}, Ta^{33+}, Ta^{38+}

Operated for RHIC in 2012 with

- U^{39+} (not possible previously), Cu^{11+}, Au^{31+}

BROOKHAVEN NATIONAL LABORATORY

Preparation of U beams for RHIC

EBIS out: U^{39+}

AGS-to-RHIC transfer line

Stripping foil:

Al_2O_3 (5.2 mg/cm^2)

E_{kin} = 8.51 GeV/nucleon

U^{90+} ♋ U^{92+} (99.9% of intensity)

P. Thieberger, K. Zeno

Booster-to-AGS transfer line

Stripping foil:

Ni (4.4 mg/cm^2) + Al (9.0 mg/cm^2)

E_{kin} = 107 MeV/nucleon

U^{39+} ♋ U^{90+} (35% of intensity)

(had expected >50% based on GLOBAL)

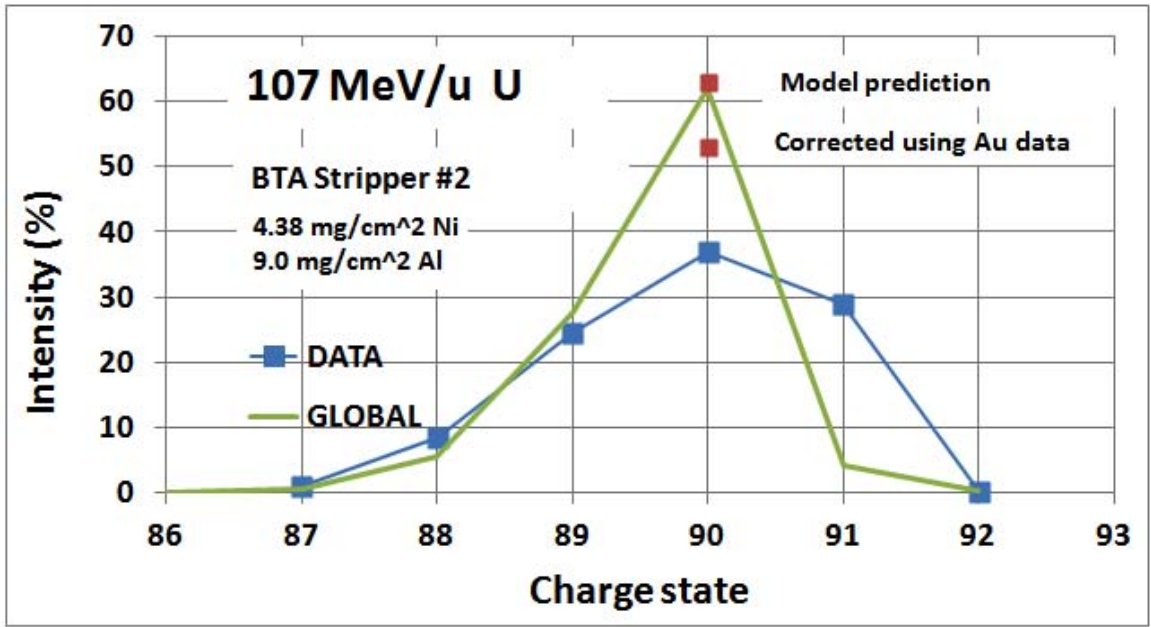

Now have full 3D stochastic cooling for heavy ions

longitudinal pickup

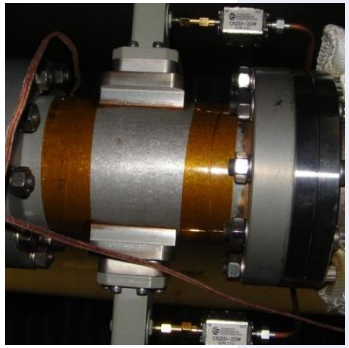

longitudinal kicker (closed)

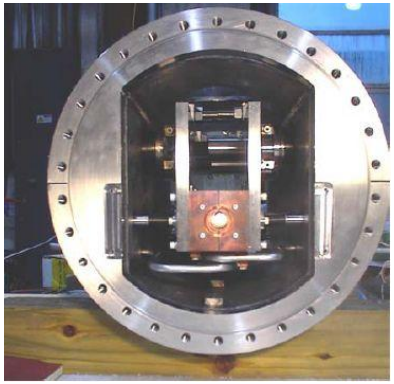

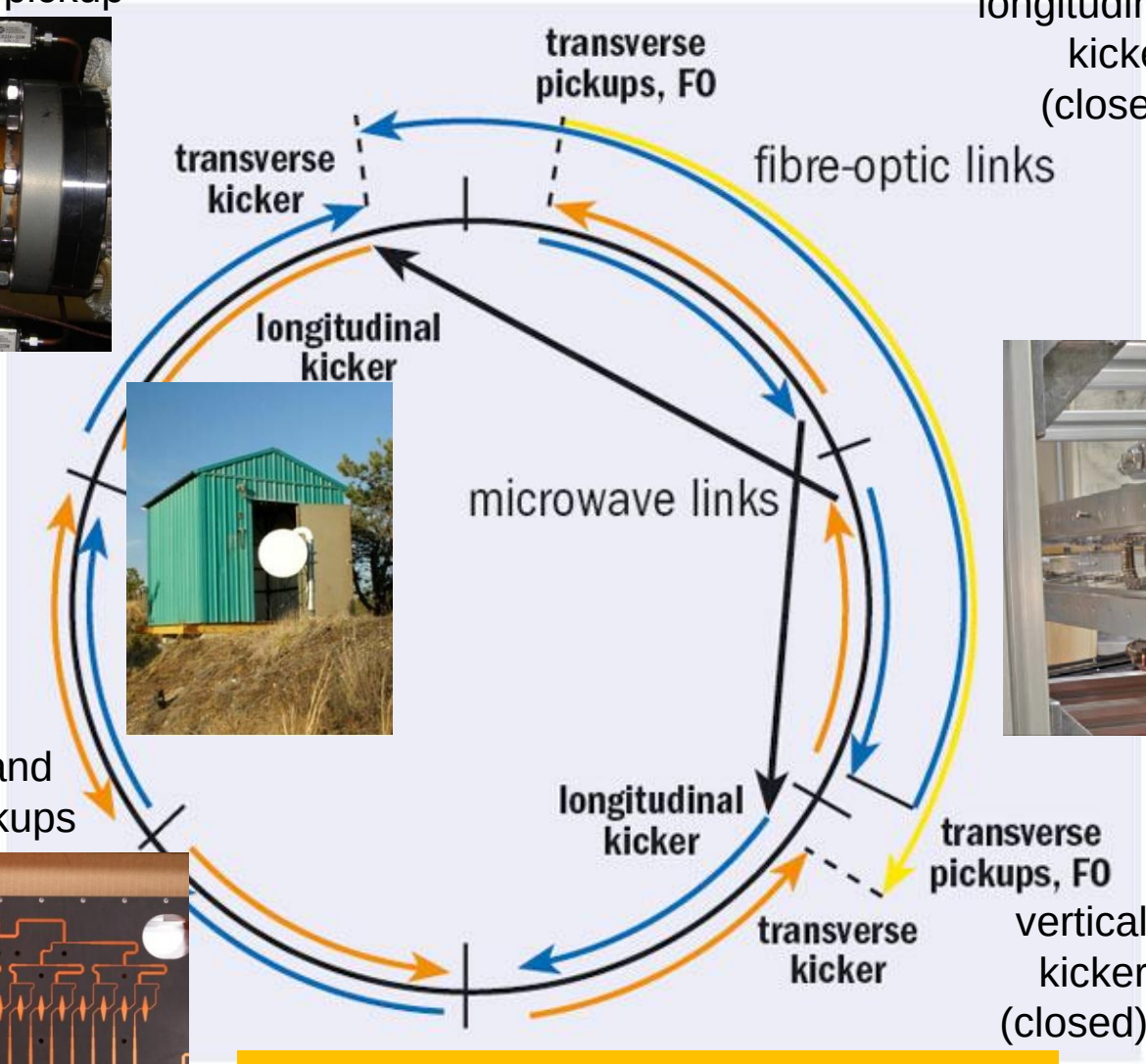

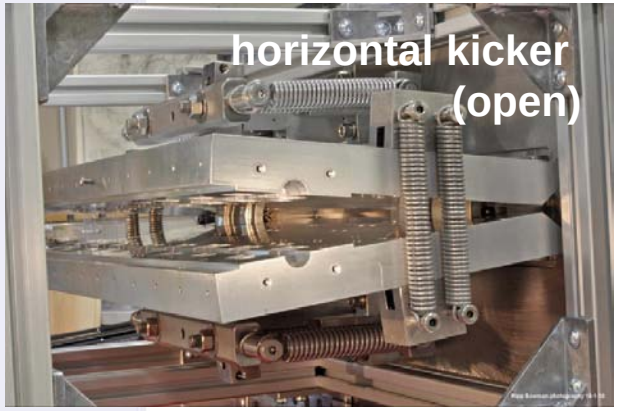

horizontal and vertical pickups

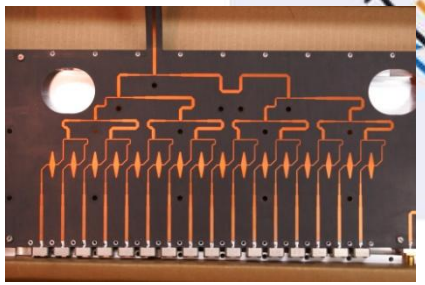

vertical kicker (closed)

5-9 GHz, cooling times ~1 h

M. Brennan, M. Blaskiewicz, F. Severino, PRL **100** 174803 (2008); PRSTAB, PAC, EPAC

U-U store – new mode in 2012

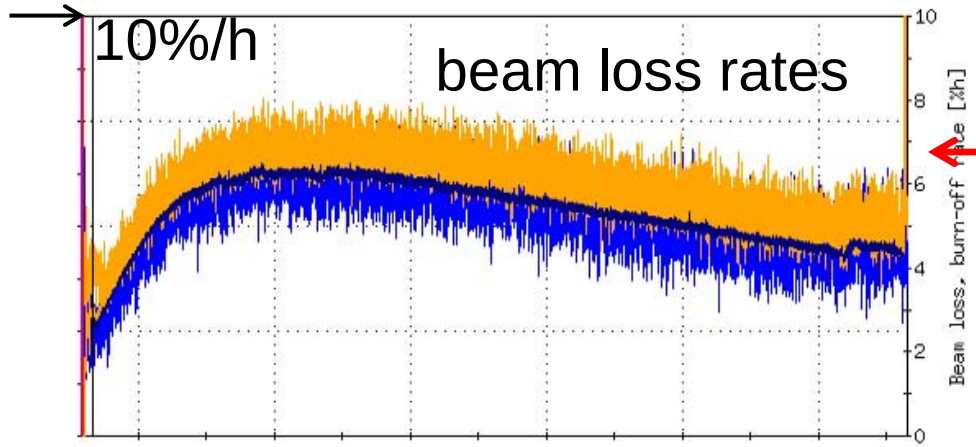

(1) Lattice optimized for large off-momentum dynamic aperture, not for smallest β* (Y. Luo)

$$L \propto \frac{N_b^2}{\beta^*} H\left(\frac{\beta^*}{\sigma_s}\right)$$

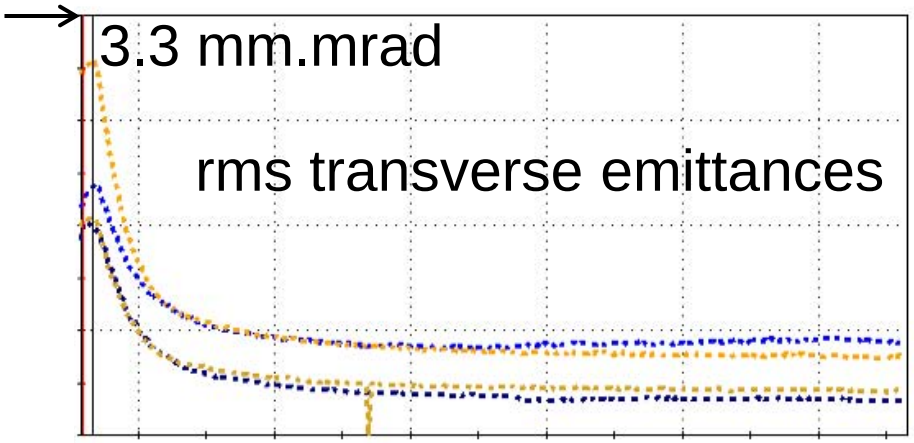

(2) Minimum loss rates given by total U-U cross sections, 2 largest contributions from BFPP and EMD:

	Au-Au	U-U
BFPP	117 b	329 b
EMD	99 b	160 b

$\sigma_{BFPP} \propto Z^7$

All beam loss though luminosity (burn-off)!

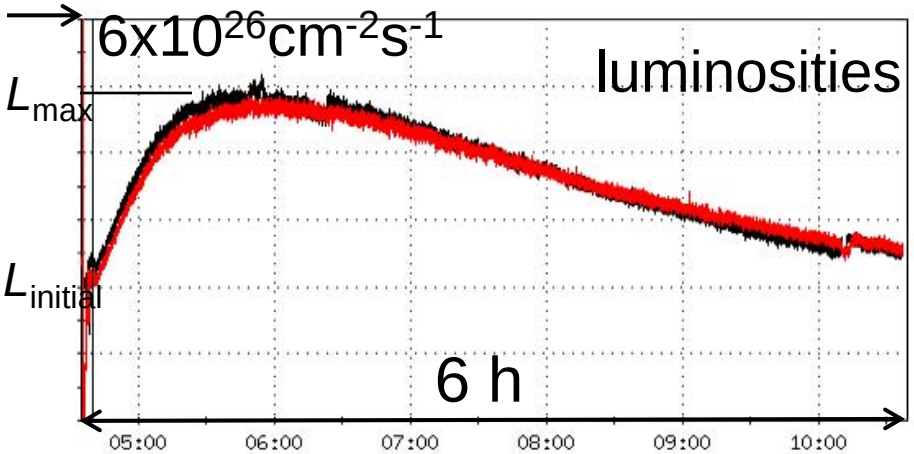

3D stochastic cooling leads to new feature in hadron collider:

$$L_{max} > L_{initial}$$

Run-12 – Copper-gold 100 GeV/nucleon

Run Coordinator: Y. Luo

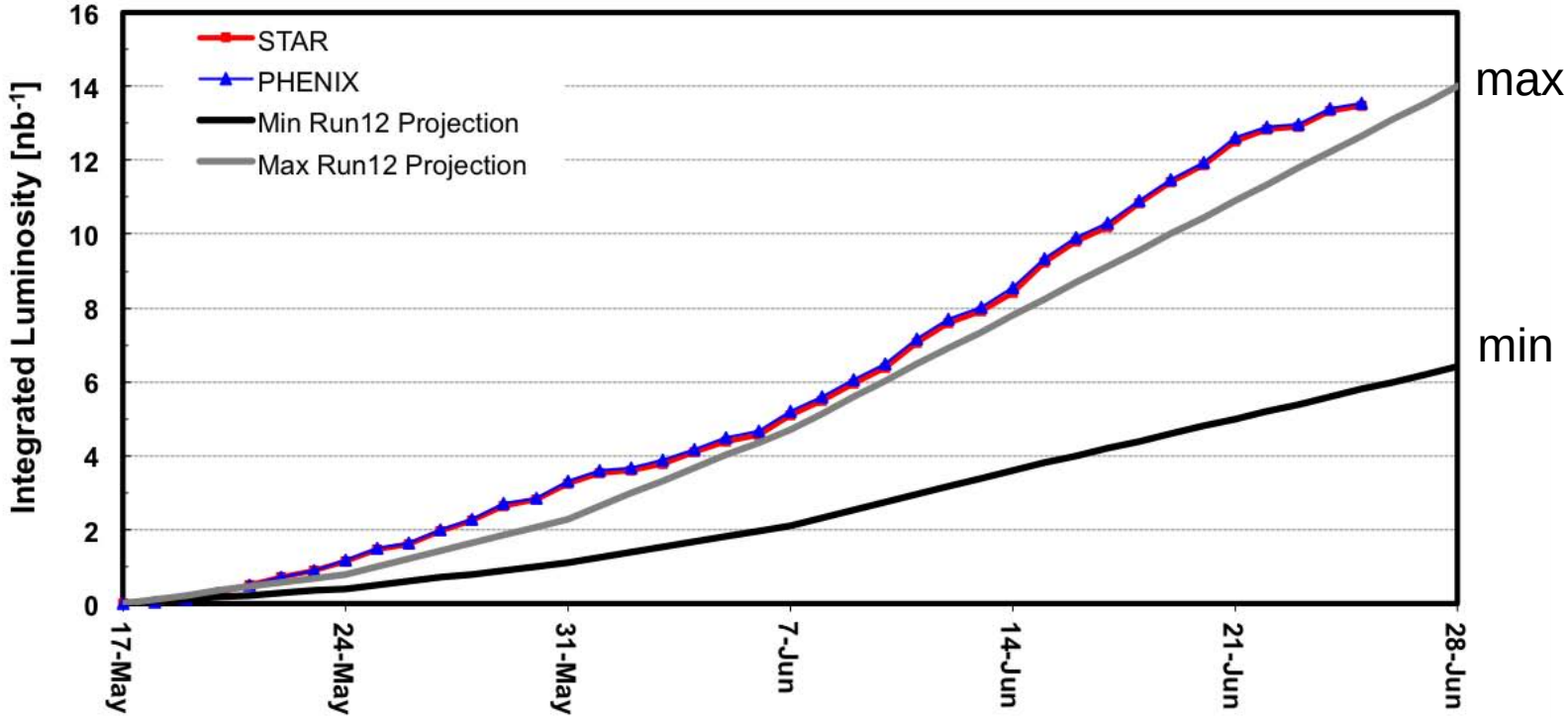

5.4 weeks

New: first Cu-Au operation in a collider; used standard lattice to increase off-momentum dynamic aperture; first use of Blue and Yellow horizontal stochastic cooling (resulting in 3D cooling in both rings)

Cu-Au store – new mode in 2012

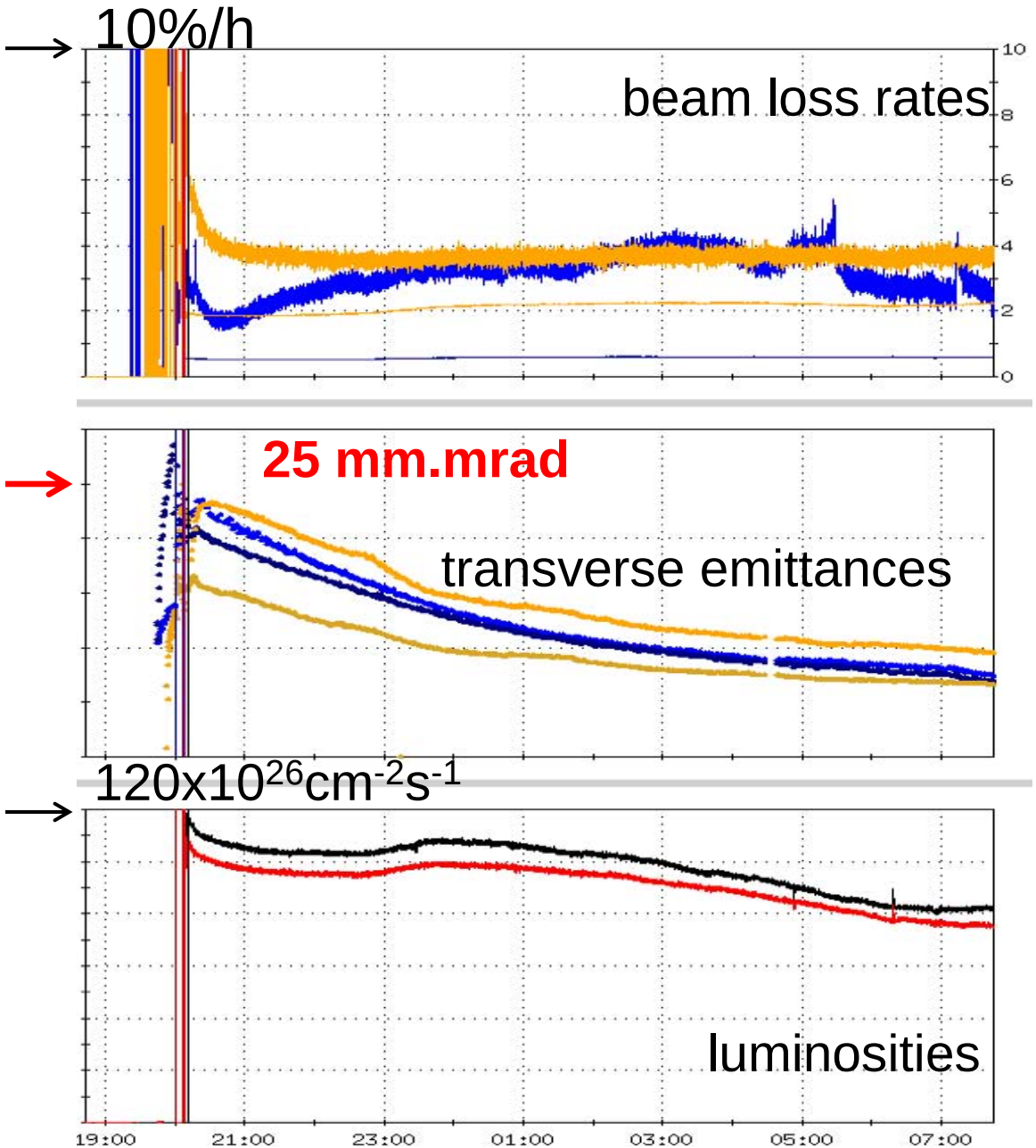

Cu and Au have different

- intrabeam scattering growth rates ($\sim Z^4 N_b/A^2$) $r_{IBS,Au} \approx 2x\ r_{IBS,Cu}$
- cooling rates ($\sim 1/N_b$) $r_{SC,Au} \approx 3x\ r_{SC,Cu}$

Stores start with large ε after undergoing instability at transition

Possible with stochastic cooling

Increase bunch intensity until loss at transition

Time-in-store as fraction of calendar time

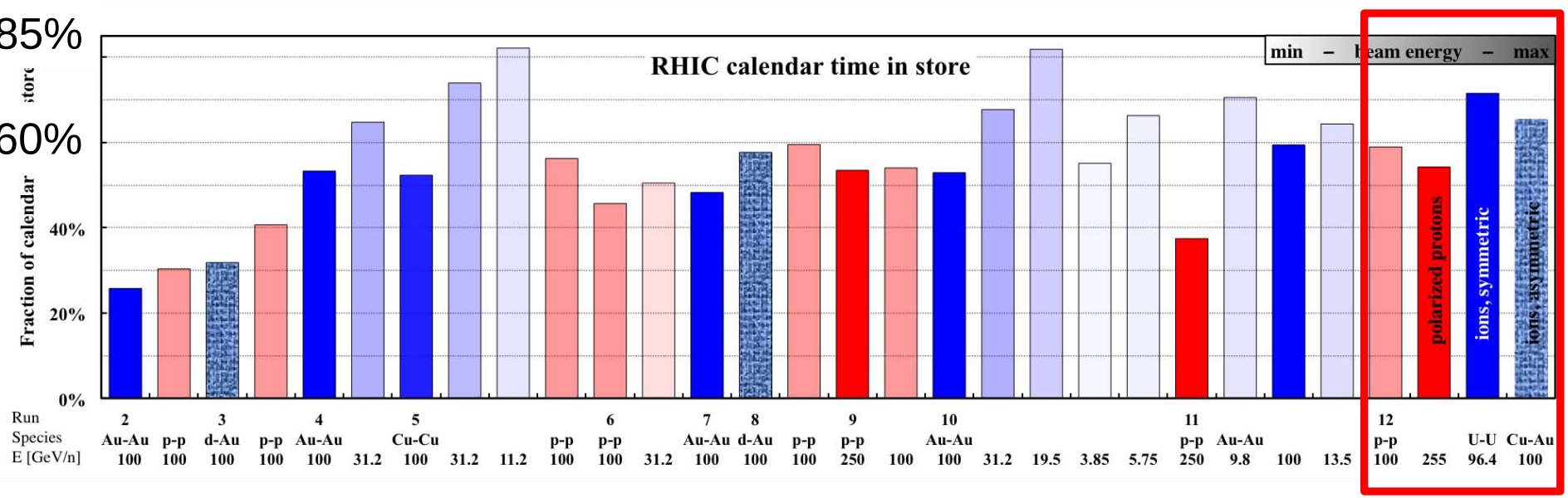

- Run-12 with low failure rates in all systems
- Highest time-in-store ratios to date
  even with increased APEX time during 255 GeV protons, and few weeks per species

RHIC ions – 6 species and 15 energies to date

$^{238}U^{92+}$–$^{238}U^{92+}$ ♑ first time in 2012, 3 weeks physics

96.4 GeV/nucleon

$^{197}Au^{79+}$–$^{197}Au^{79+}$

3.85, 4.6, 5.75, 9.8, 13.5, 19.5, 27.9, 31.2, 65.2, 100.0 GeV/nucleon

$^{63}Cu^{29+}$–$^{197}Au^{79+}$ ♑ first time in 2012, 5 weeks

99.9/100.0 GeV/nucleon

$^{63}Cu^{29+}$–$^{63}Cu^{29+}$

11.2, 31.2, 100.0 GeV/nucleon

d–$^{197}Au^{79+}$

100.7/100.0 GeV/nucleon

p≈–p≈

31.2, 100.2, 204.9, 249.9, 254.9 GeV

Can collide any species from protons (polarized) to uranium – with each other or with another species

RHIC heavy ions – luminosity evolution to date

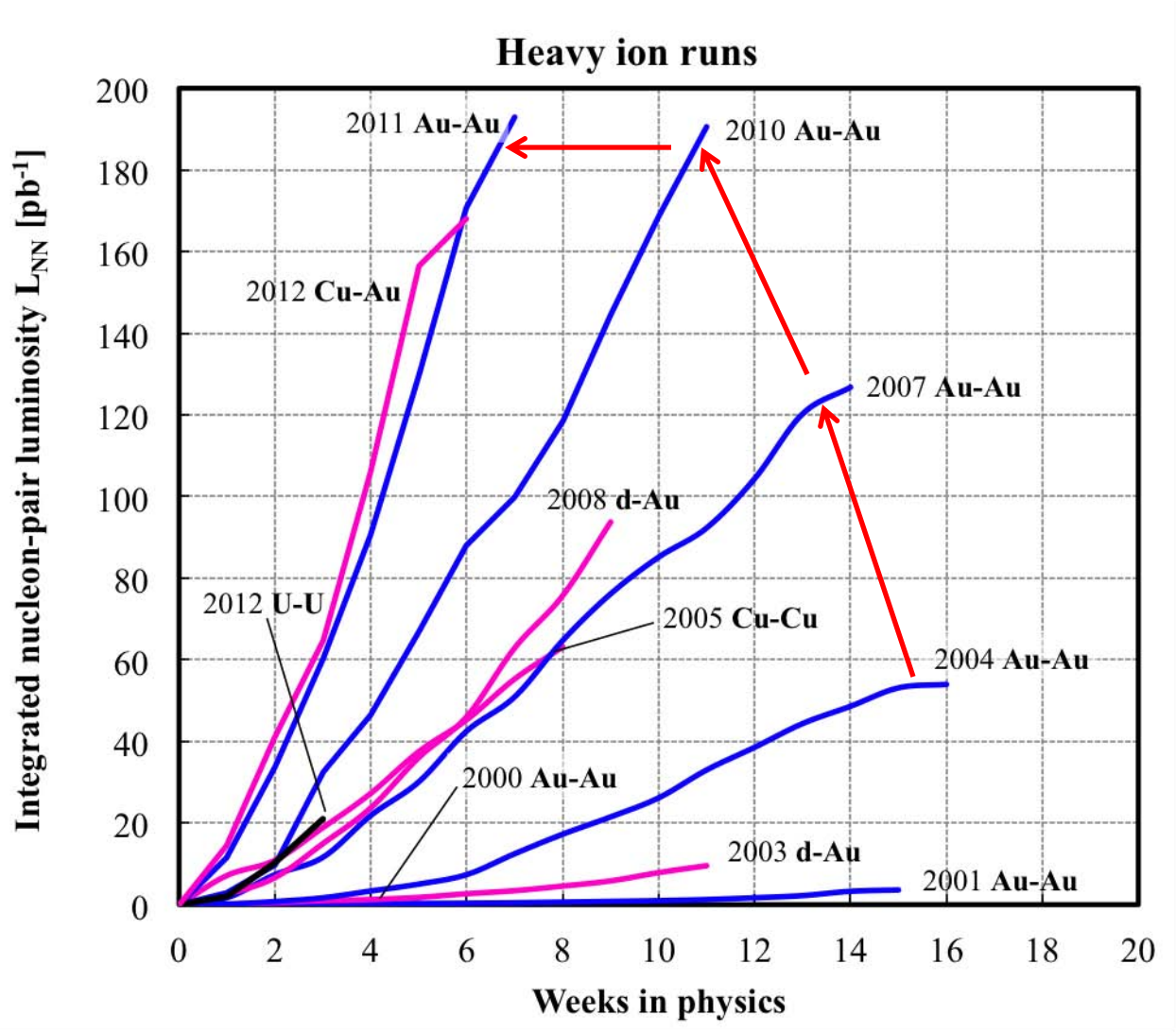

<L> = 15x design in 2011

About 2x increase in L_{int}/week each

- Run-4 to Run-7
- Run-7 to Run10
- Run-10 to Run-11

$\mathbf{L_{NN} = L\, N_1 N_2}$ (= luminosity for beam of nucleons, not ions)

RHIC polarized protons – luminosity and polarization

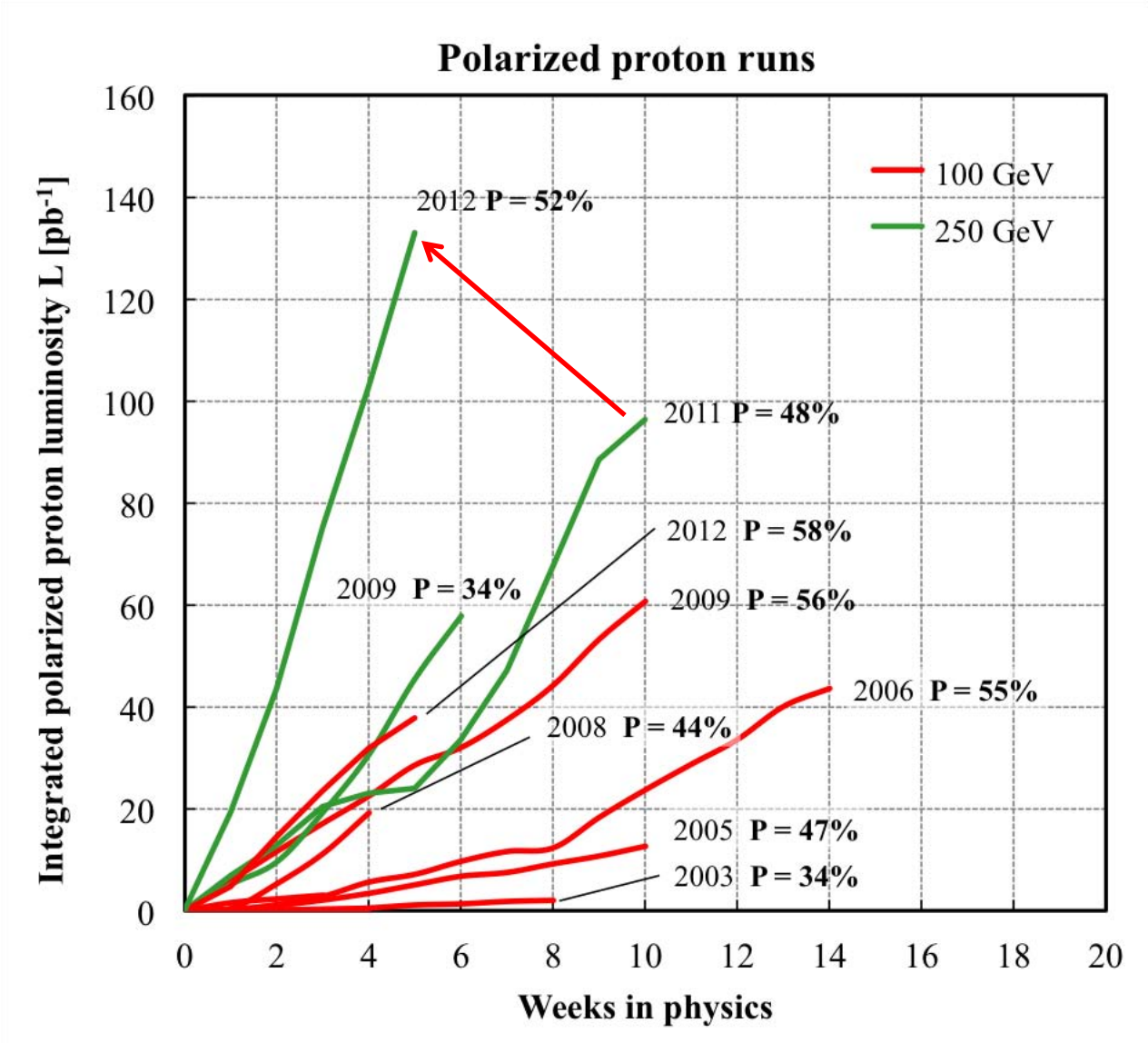

At 255 GeV in 2012

L_{avg} = 105x10^{30}cm^{-2}s^{-1}

P_{avg} = 52%

L_{avg} +15% relative to 2011

P_{avg} +8% relative to 2011

$FOM = LP^2$

(single spin experiments)

$FOM = LP^4$

(double spin experiments)

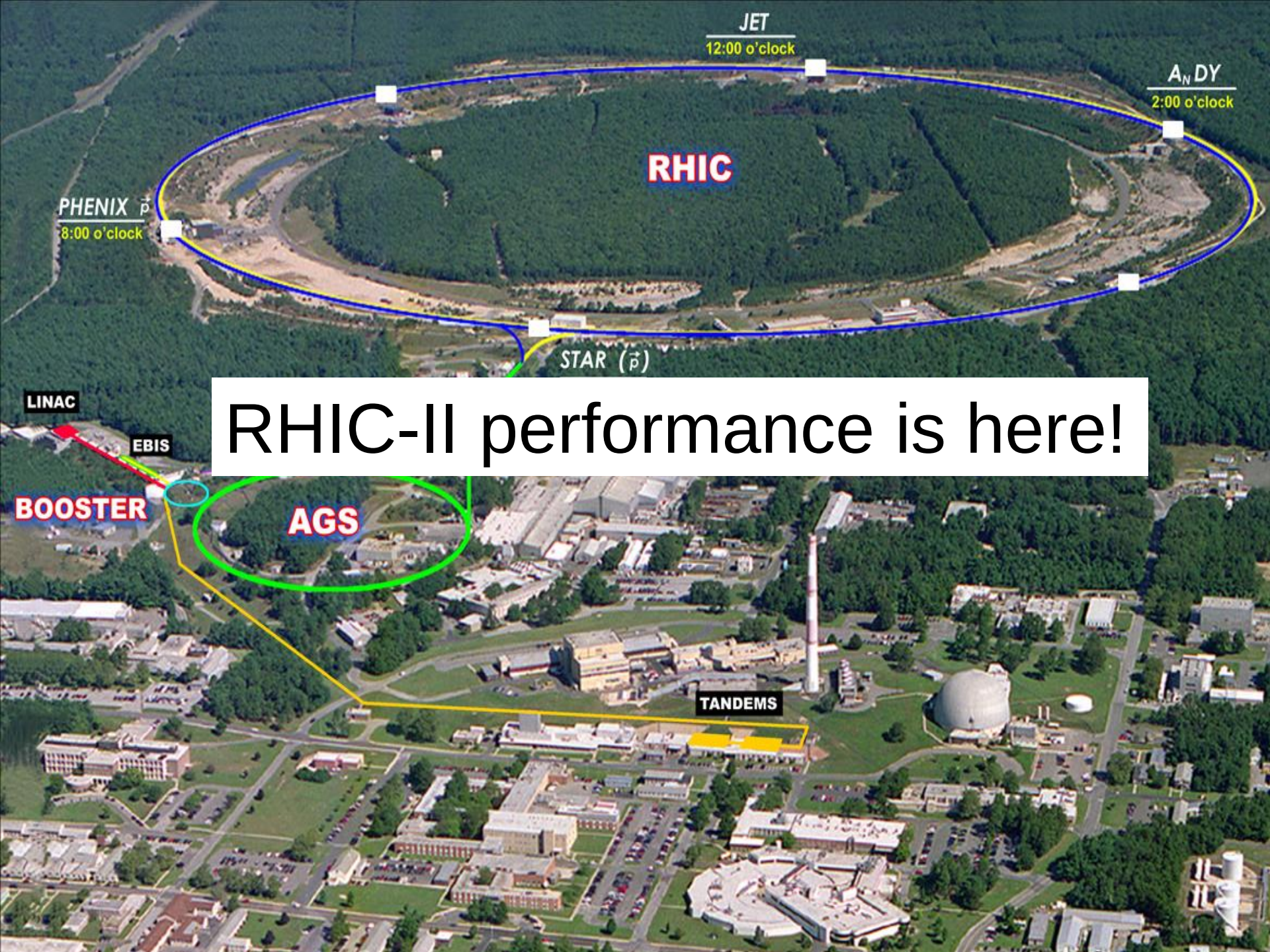

RHIC-II performance is here!

RHIC luminosity and polarization goals

parameter	unit	achieved		goals			
Au-Au operation		**2011**		**≥ 2014** 3D stochastic cooling + 56 MHz SRF			
energy	GeV/nucleon	100		100			
no colliding bunches	…	111		111			
bunch intensity	10^9	1.3		≥ 1.1			
avg. luminosity	$10^{26}\,cm^{-2}s^{-1}$	**30**		**40**			
p↑-p↑ operation		**2012**		**≥ 2013** source		**≥ 2014** source + e-lenses	
energy	GeV	100	255	100	250	100	250
no colliding bunches	…	– 107 –		– 107 –		– 107 –	
bunch intensity	10^{11}	1.6	1.7	1.6	2.0	1.8	2.5
avg. luminosity	$10^{30}\,cm^{-2}s^{-1}$	**33**	**105**	**30**	**150**	**60**	**300**
avg. polarization*	%	**59**	**52**	**– 60 –**		**– 65 –**	

*Intensity and time-averaged polarization as measured by the H-jet. Luminosity-averaged polarizations, relevant in single-spin colliding beam experiments, are higher. For example, for intensity-averaged P = 48% and $R_x = R_y$ = 0.2 (250 GeV, 2011), the luminosity-averaged polarization is P = 52%.

BROOKHAVEN NATIONAL LABORATORY

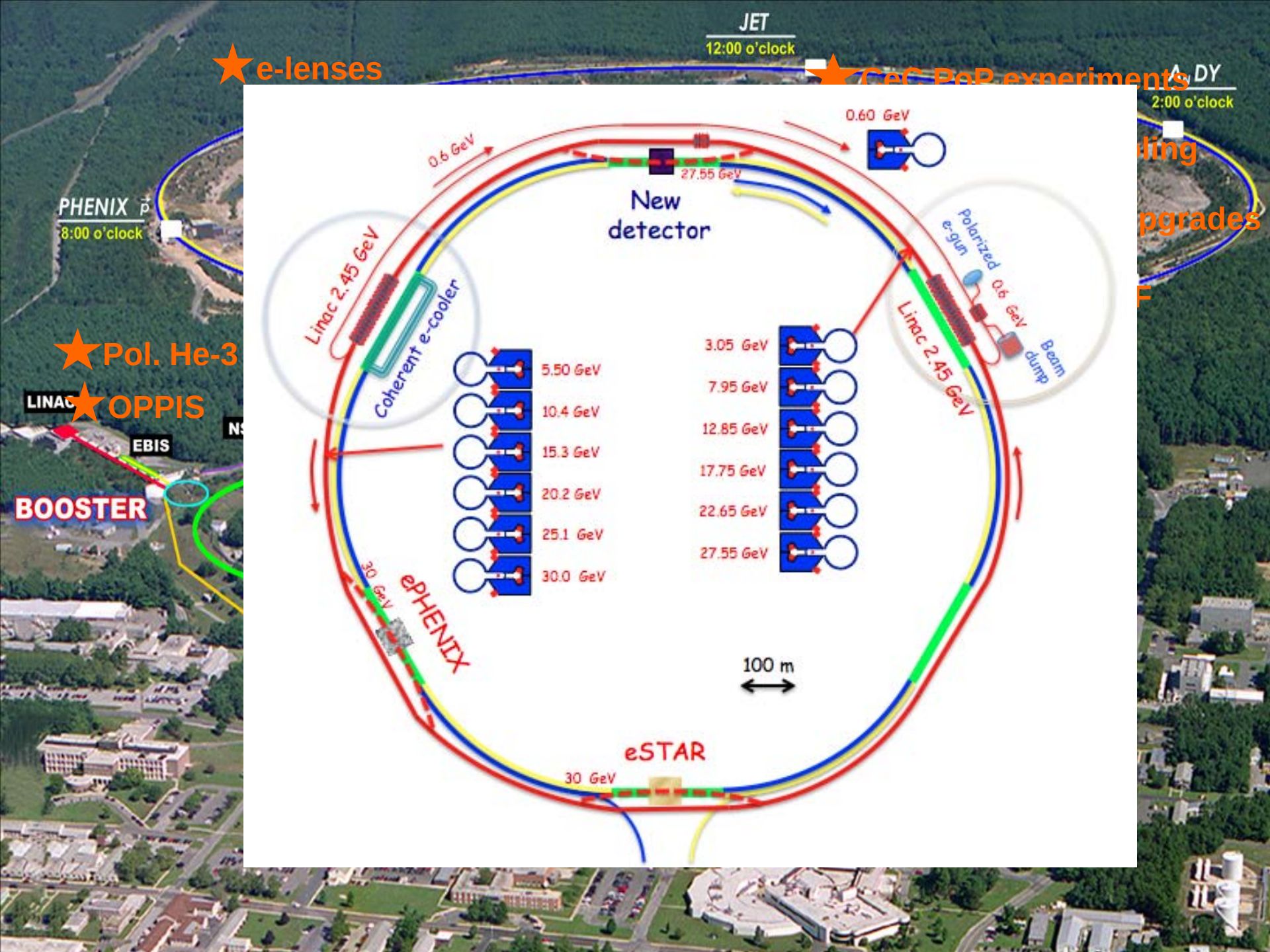
JET
12:00 o'clock
A DY
2:00 o'clock
PHENIX
8:00 o'clock
LINAC
EBIS
BOOSTER
★e-lenses
★CeC, PoP experiments
ling
pgrades
F
★Pol. He-3
★OPPIS
0.60 GeV
0.6 GeV
27.55 GeV
New detector
Linac 2.45 GeV
Coherent e-cooler
Polarized e-gun
0.6 GeV
Beam dump
Linac 2.45 GeV
5.50 GeV
10.4 GeV
15.3 GeV
20.2 GeV
25.1 GeV
30.0 GeV
3.05 GeV
7.95 GeV
12.85 GeV
17.75 GeV
22.65 GeV
27.55 GeV
30 GeV
ePHENIX
100 m
eSTAR
30 GeV

Polarized proton upgrades

- **New polarized source (OPPIS)**
  - 10x more intensity at source
  - +5% polarization
  - operation in Run-13 (full or partial)
- **Electron lenses**
  - mitigate head-on beam-beam effect
  - commissioning in Run-13
- **Polarized He-3 R&D**

Optically Pumped Polarized H⁻ source (OPPIS) – A. Zelenski

Upgraded OPPIS (2013)

Source
(H^+)

Goals:

n current
o 10mA
agnitude)
ation to 85-
increase)

nponents:

drogen
llaboration
ovosibirsk)
ducting
3 T)
gnostics
metry

=> 10x intensity from ABS was accelerated through Linac

Motivation

Bunch intensity in 2012 polarized proton physics store

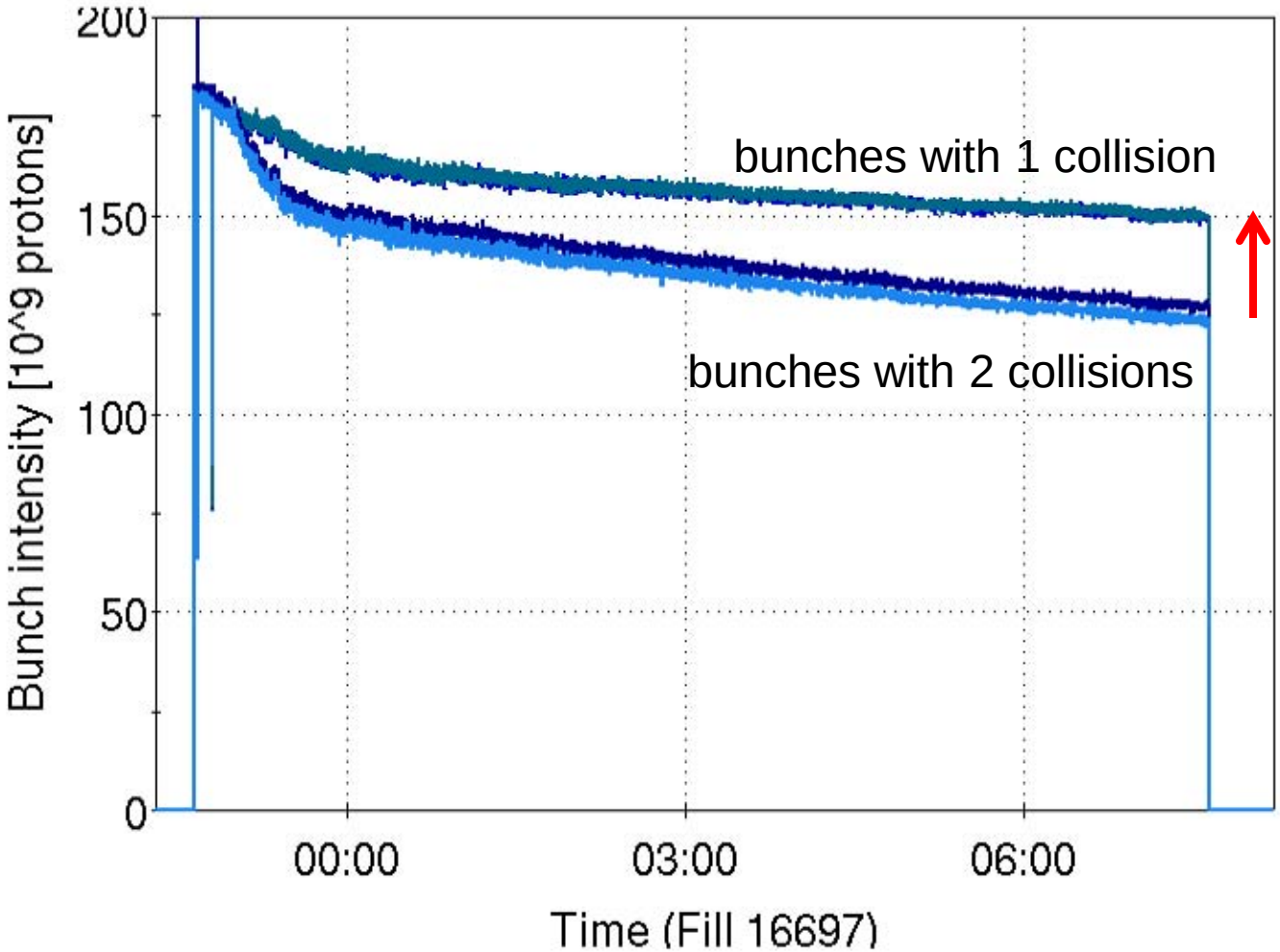

Goal:

Compensate for 1 of 2 beam-beam interactions with electron lenses

Then increase bunch intensity
$\Rightarrow$ up to 2× luminosity

Need new polarized proton source − under construction, A. Zelenski

$$L \mu N_b^2$$

Electron lenses – partial head-on beam-beam compensation

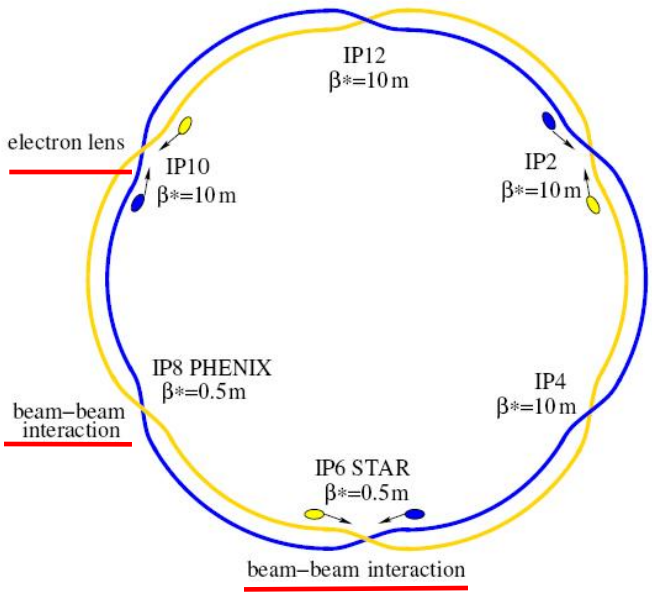

Basic idea:

- 2 beam-beam collisions with **positively** charged beam
- Add collision with a **negatively** charged beam – with matched intensity and same amplitude dependence

Compensation of nonlinear effects:

- e-beam current and shape
  => reduces tune spread
- $\Delta\psi_{x,y} = k\pi$ between p-p and p-e collision
  => reduces resonance driving terms

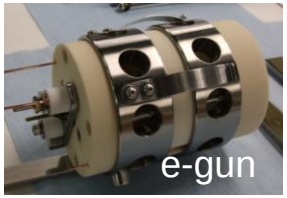

Installation in 2012
Expect up to 2x more luminosity

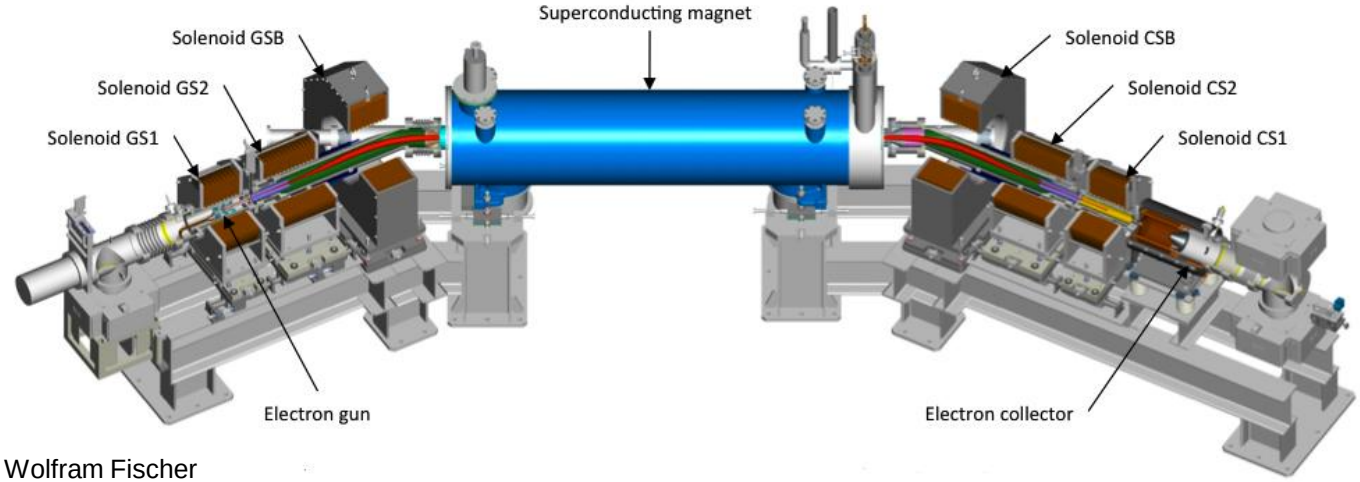

Polarized ^{3}He – Workshop 28-30 September 2011

Workshop on Opportunities for polarized He-3 in RHIC and EIC -- sponsored by the RIKEN BNL Research Center

28-30 September 2011
Universe
US/Eastern timezone

Workshop program

- ^{3}He⇝ source, ^{3}He⇝ beams from EBIS
- ^{3}He⇝ in Booster/AGS
- ^{3}He⇝ in RHIC and EIC
- Polarimetry (low and high energy)
- Physics with ^{3}He⇝ beams (theory and experiments)

Overview
Agenda
Call for Abstracts
View my abstracts
Submit a new abstract
Timetable
Contribution List
Book of abstracts
Registration

Timezone: US/Eastern
Room: Brookhaven Center, Bldg. 30
Dr. Aschenauer, Elke

Additional info: Guest Information System (GIS)

If you have a current BNL Appointment and a valid BNL Guest Number or you have a pending Guest Registration (GR) Number, it is not necessary to complete

Polarized ^{3}He in RHIC – plan under development

- Polarized ^{3}He source developed at MIT (R. Milner)
- Polarized ^{3}He beams from EBIS
- Polarimeter after EBIS linac at 2 MeV/nucleon (^{3}He, ^{4}He elastic scattering?)
- Un-polarized ^{3}He from EBIS:
  - Injection into Booster at low rigidity
  - Acceleration in Booster, AGS, RHIC?
  - Test carbon polarimeters
- Acceleration of polarized ^{3}He in Booster and transfer to AGS
  - Vertical tune in Booster < 4.19 !!
- Measure polarization at AGS injection energy, no depolarization?
- Accelerate ^{3}He in AGS and measure polarization on ramp and extraction
- Calibrate A_N of carbon polarimeter at extraction energy with up/down ramp?
- Transfer to RHIC and calibrate carbon polarimeter in RHIC (which ring?)
- Absolute polarization measurement at RHIC injection with pol. ^{3}He jet/cell
- Accelerate in RHIC and measure polarization on ramp and at store energy
  - May need 4 more snakes in Blue ring
- Calibrate A_N of carbon polarimeter at store energy with up/down ramp
- Absolute polarization measurement at RHIC store with pol. ^{3}He jet/cell

Development of Polarized ^{3}He Ion Source for RHIC

BNL-MIT Collaboration http://he3.xvm.mit.edu/

R. Milner, C. Epstein, MIT

- Spec.: deliver $^3He^{++}$ at ≈ 3 x 10^{12} atoms/sec with 70% polarization
- Concept: polarize ^{3}He gas in glass cell using MEOP in fringe field of ≈ 5 Tesla EBIS solenoid and feed into EBIS
- MEOP technology under development at MIT
  - two Keopsys 10 Watt lasers operational
  - data acquisition system operational
  - 20 liters of ^{3}He gas ordered
  - glass systems under construction
- Goal: to test principle of source using spare EBIS solenoid within the next year

Funded by DOE Office of Nuclear Physics R&D Program for Next Generation Nuclear Physics Accelerator Facilities

^{3}He accelerated in AGS in 2012 (H. Huang et al.)

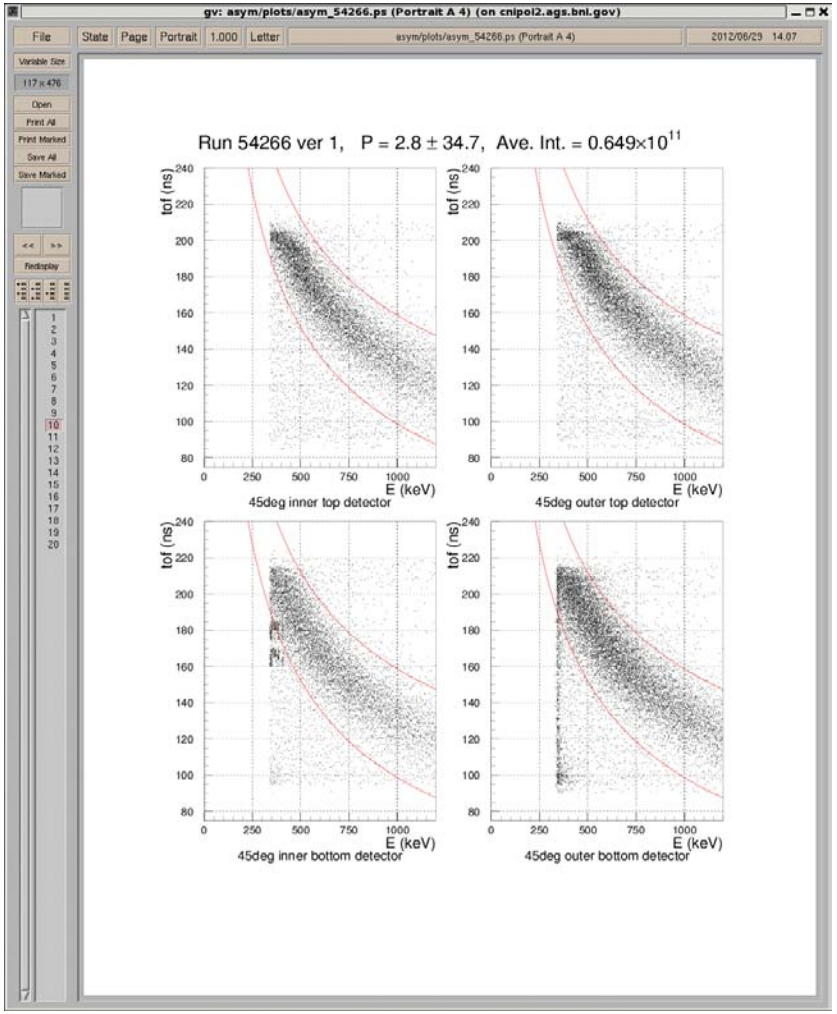

3×10^{10} ^{3}He accelerated in AGS

Carbon Bananas Seen in p-C polarimeters!

- Rate estimate: gain due to elastic cross section: $A^{2/3} = 3^{3/2} = 2.08$.
- O observed: ~2.
- A_N: estimated as 78% of p-C (Nigel Buttimore, Trinity College)

BROOKHAVEN NATIONAL LABORATORY

Heavy ion upgrades

- **56 MHz Superconducting RF system**

  stronger longitudinal focusing reduces migration into neighboring buckets

- **Low energy electron cooling**

  10x more luminosity for critical point search

- **Proton-gold collisions**

5(al.)
ng
14

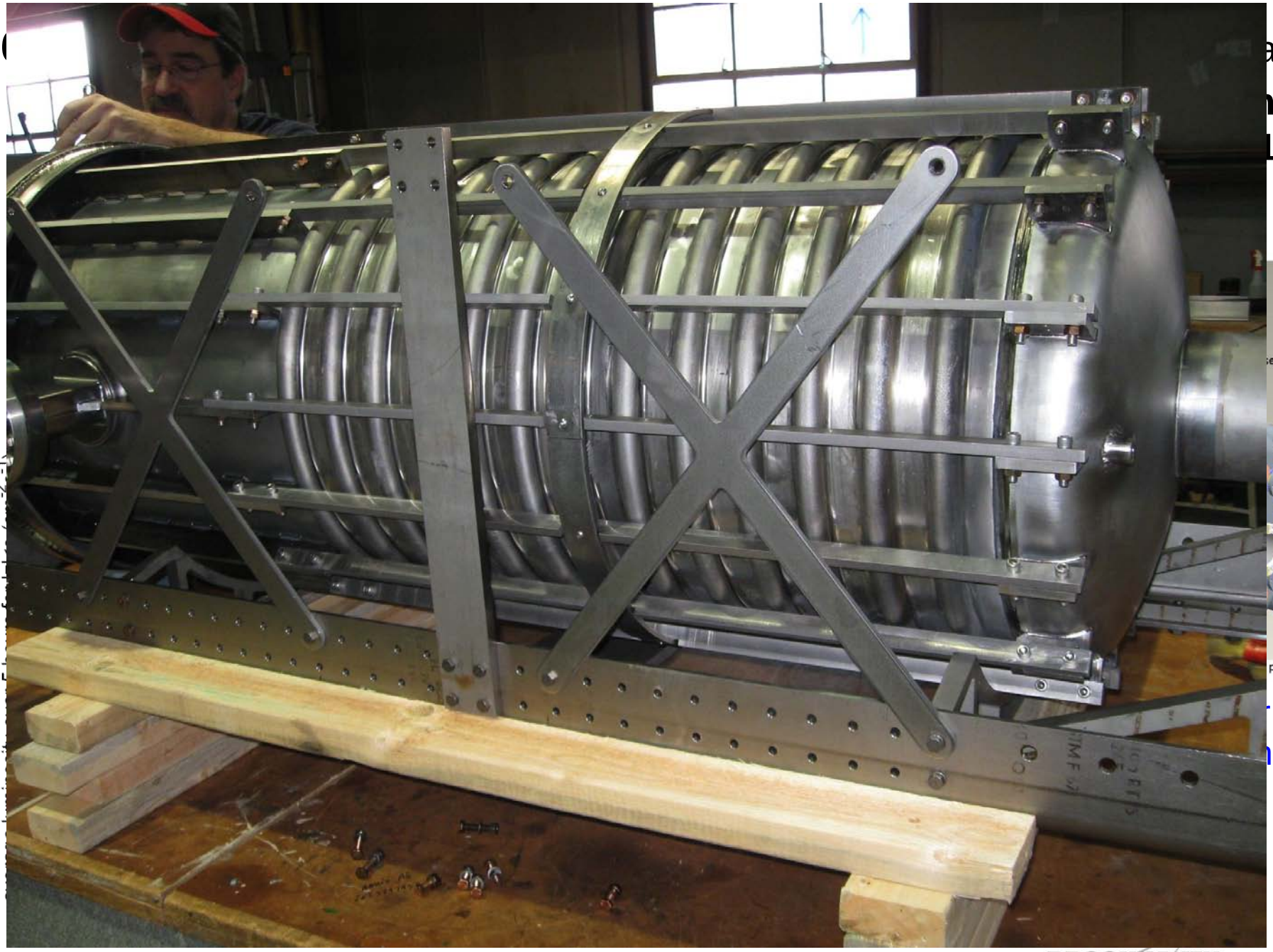

Calculation by M. Blaskiewicz

RHIC – Au-Au energy scan

US NSAC report 2007

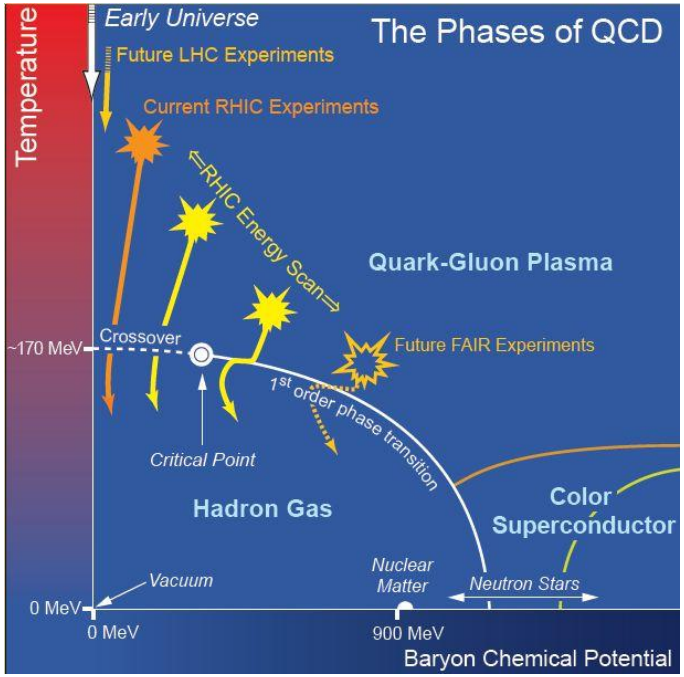

Energy scan – extends <u>below nominal injection energy</u> in search of critical point in QCD phase diagram

Effects to contend with (#s for 20% nominal ($B\rho$):

- Large beam sizes **(longitudinal and transverse) controlling losses becomes critical**
- Large magnetic field errors **(b_3 ~ 10, b_5 ~ 6 units from persistent currents in superconducting magnets)**
- Intrabeam scattering **(debunching ~min)**
- Space charge **($\Delta Q_{Laslett}$ ~ 0.1 – new regime for collider)**
- Beam-beam **(ξ/IP ~ 0.003)**
- Low event rates **(~ 1 Hz)**

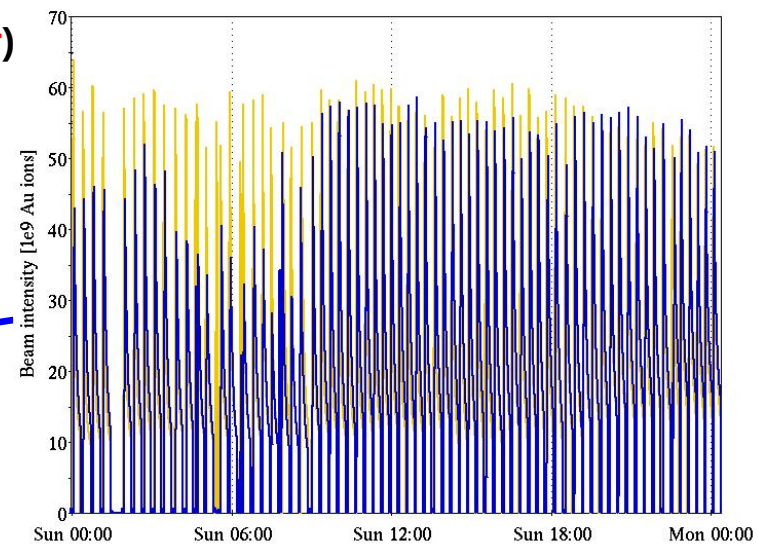

Full energy injection allows for short stores

- At 38% of nominal injection ($B\rho$)
- **May operate at 20% of nominal injection ($B\rho$)**

Au-Au energy scan to date

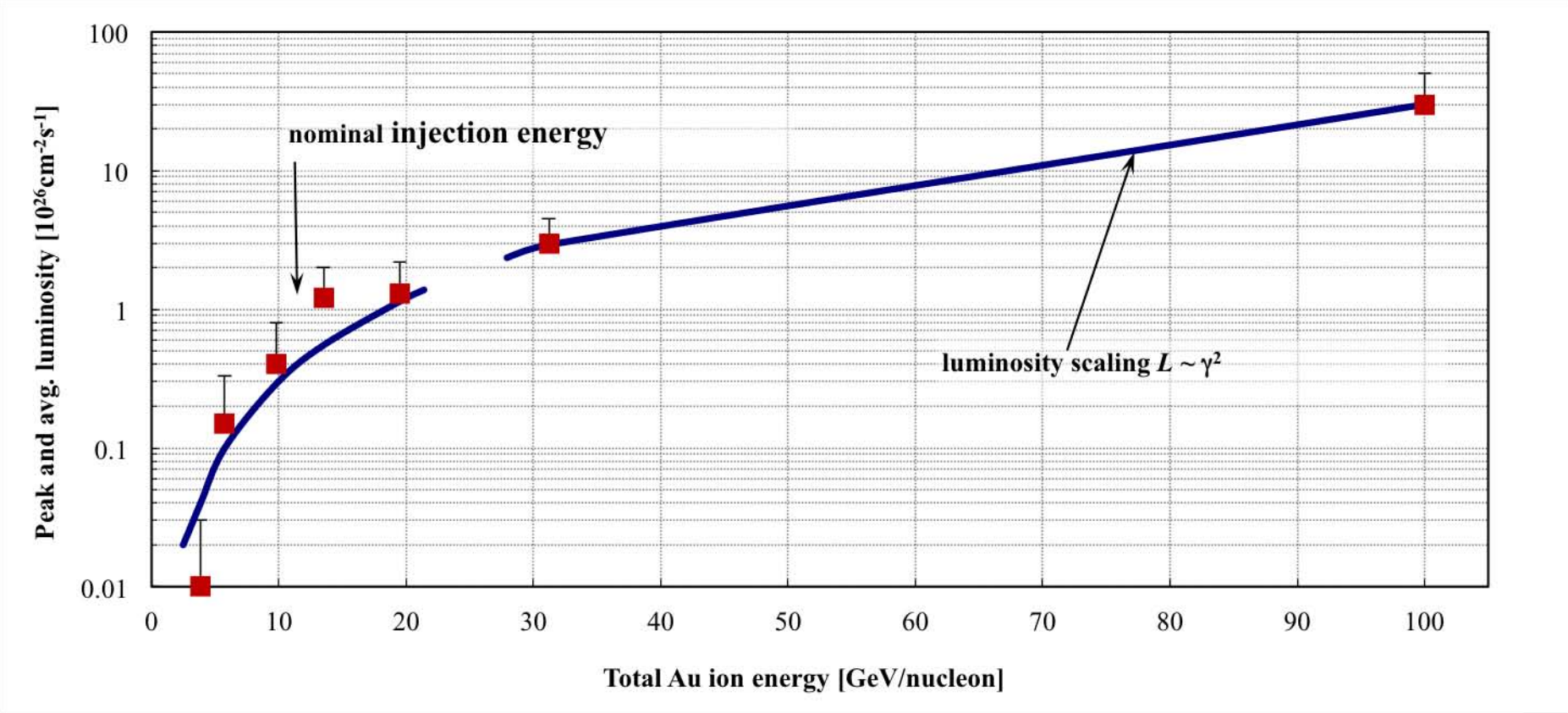

Peak and average luminosities fall faster than $1/\gamma^2$ at lowest energies
Need cooling at low energies to significantly increase luminosities

e-cooling for low energy RHIC operation

Will likely use high brightness SRF electron gun for bunched beam electron cooling; up to ~10x L; ready after 2017 (Fermilab Pelletron (cooled 8 GeV pbar for Tevatron use) is alternative option)

Can use CeC setup for bunched e-cooling test

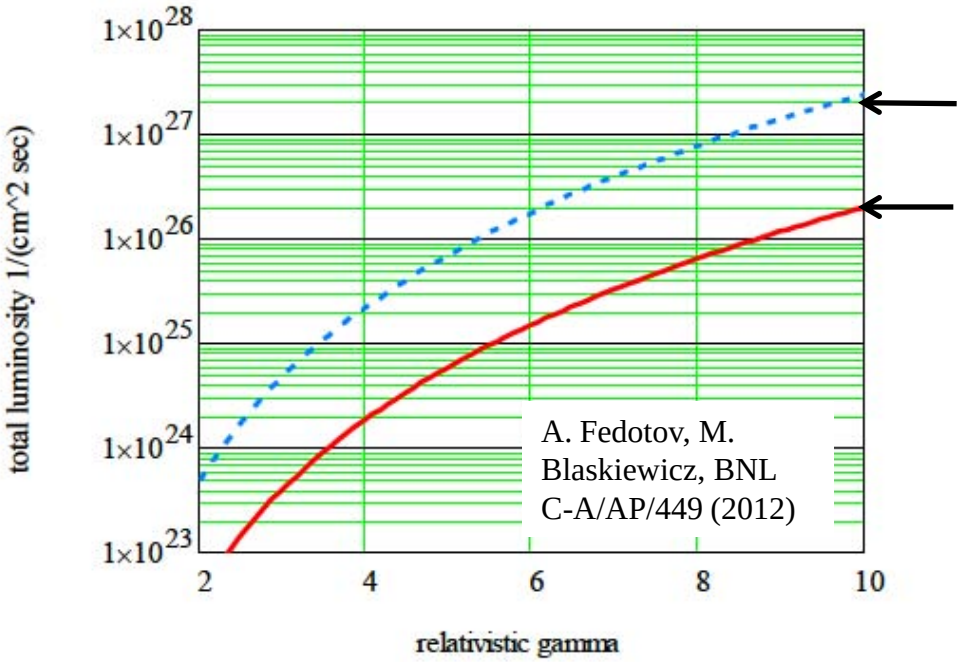

RHIC with cooling and long bunches (ΔQ_{sc} = 0.05, σ_s = 3m)

RHIC w/o cooling

Bunched e-cooling test layout, same as CeC layout

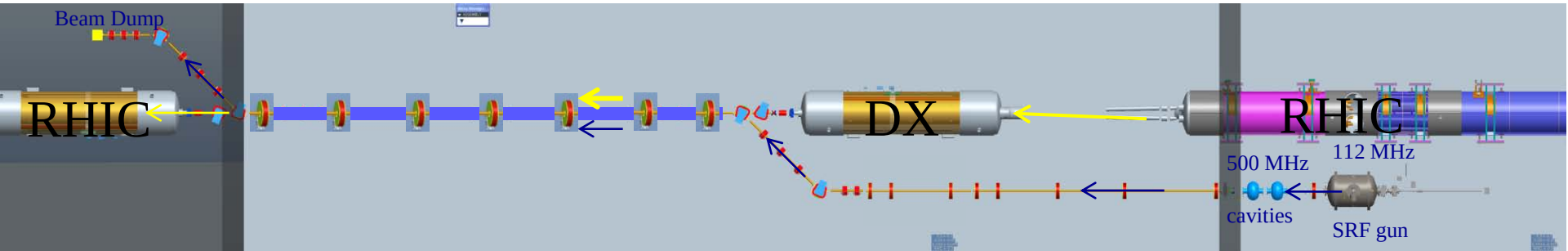

Proton-gold collisions in RHIC

now L_{avg} = 30 10^{26}cm^{-2}s^{-1}

Luminosity. The collider is designed for a Au-Au luminosity of about 2×10^{26} cm^{-2} sec^{-1} at top energy, while maintaining the potential for future upgrades by an order of magnitude. Operation with the heaviest ions imposes the most demanding requirements on the collider design, and gold-on-gold is taken as the prototypical example. The luminosity is energy dependent and decreases in first approximation propor **now L_{avg} = 10.5 10^{31}cm^{-2}s^{-1} (with P_{avg} = 53%)** will be higher, with ~1×10^{31} cm^{-2} sec^{-1} for pp collisions.

Range of ion masses. The expectations for interesting physics phenomena require a broad range of nuclei from the heaviest to the lightest, including protons. Asymmetric operation with heavy ions colliding on protons is considered to be crucial for the experimental program. The collider will allow collisions of beams of equal ion species from Au-Au all the way down to p-p. It will also allow operation of unequal species such as protons on gold ions.

Uranium is a viable species and can be considered as a future upgrade. However, at the present, an adequate source for uranium does not exist at Brookhaven and further R&D will be needed to achieve this goal.

Intersection Regions. The existing tunnel and the magnet lattice configuration provides for six experimental areas where the circulating beams cross. Three of the experimental areas presently

Asymmetric ion species under consideration in RHIC (to date)

proton-gold (p-Au)

- not yet done, part of the design
- requires moving IR6 and IR8 DX magnets horizontally by ~1 cm

deuteron-gold (d-Au)

- operated in 2003 and 2008

copper-gold (Cu-Au)

- operated in 2012

Polarized proton-polarized ^{3}He (p⇝-^{3}He⇝)

- likely request when ^{3}He⇝ is available
- RBRC Workshop on ^{3}He⇝ at BNL, 28-30 September 2011

RHIC Design Manual (July 1998)

IR design with beam splitting DX dipoles first

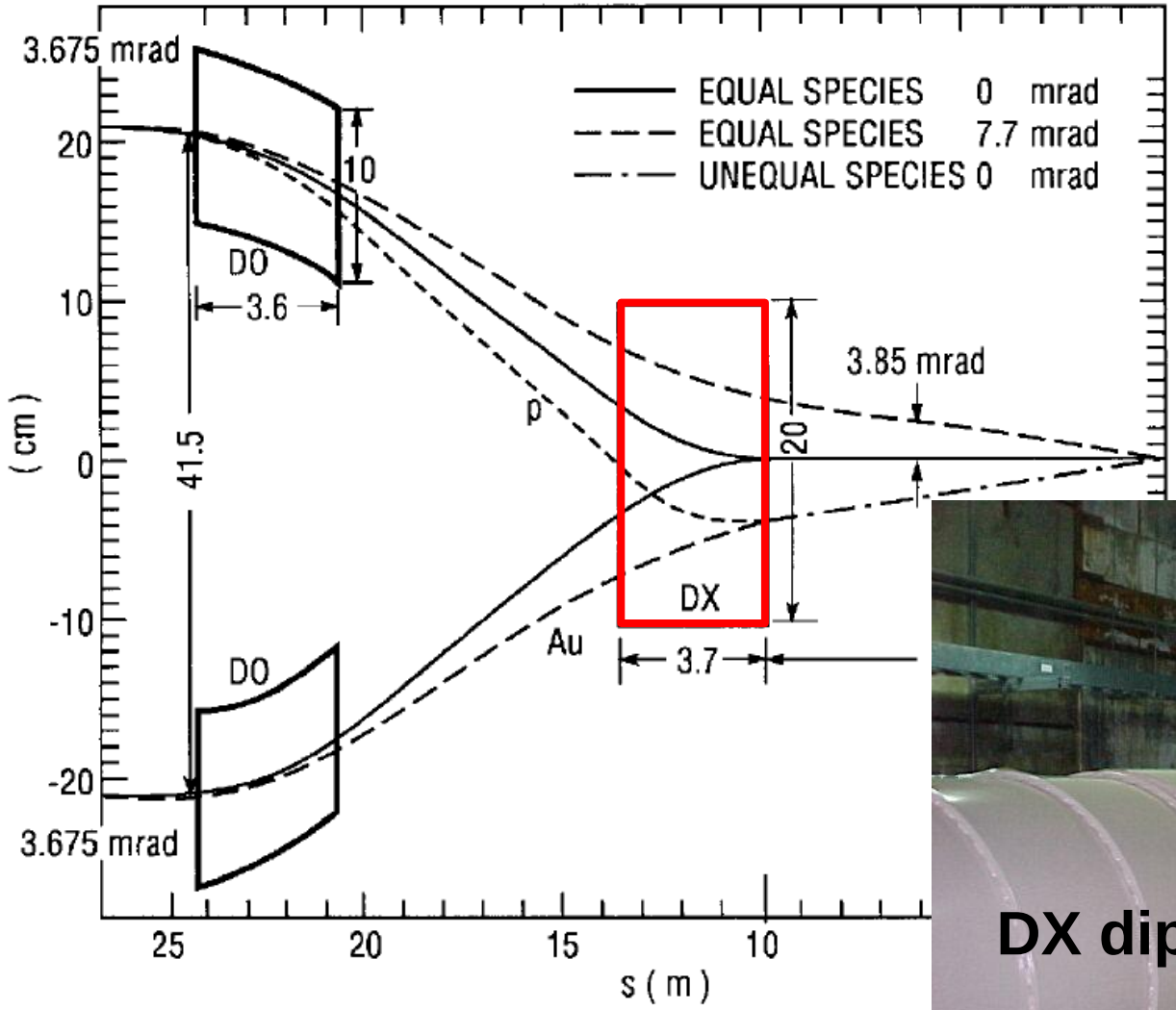

DX dipoles

- L_{mag} = 3.7 m, B_{max} = 4.3 T
- large aperture
  (18 cm coil ID)
- only magnets that need training
  (~5 for IR6/8 only)

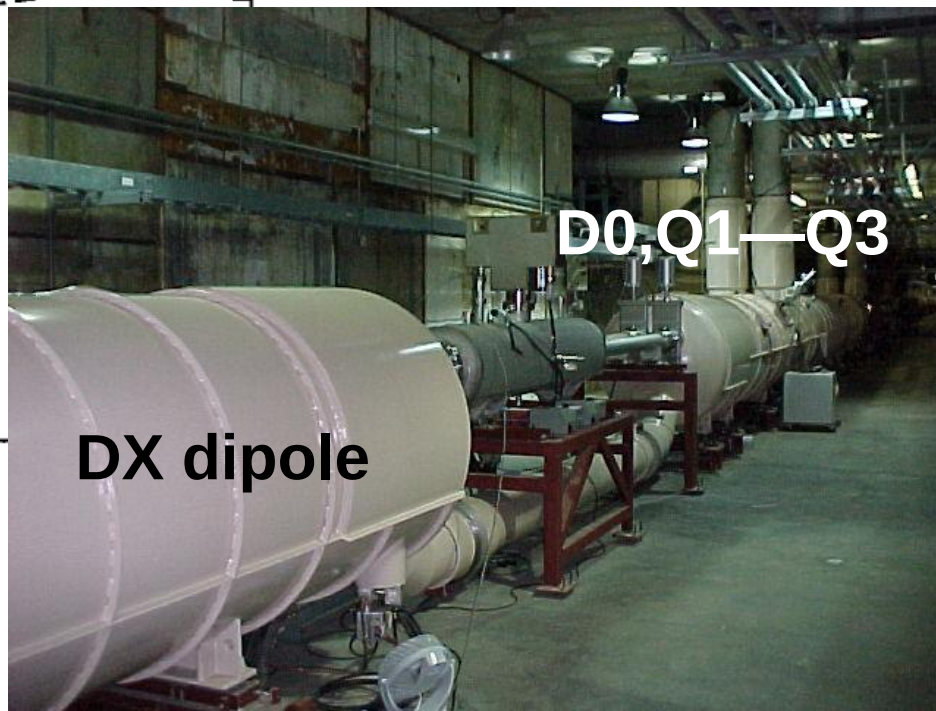

p-Au easier with stochastic cooling

- only need to accommodate initial Au emittances
- sufficient to move IR6 and IR8 DX magnets

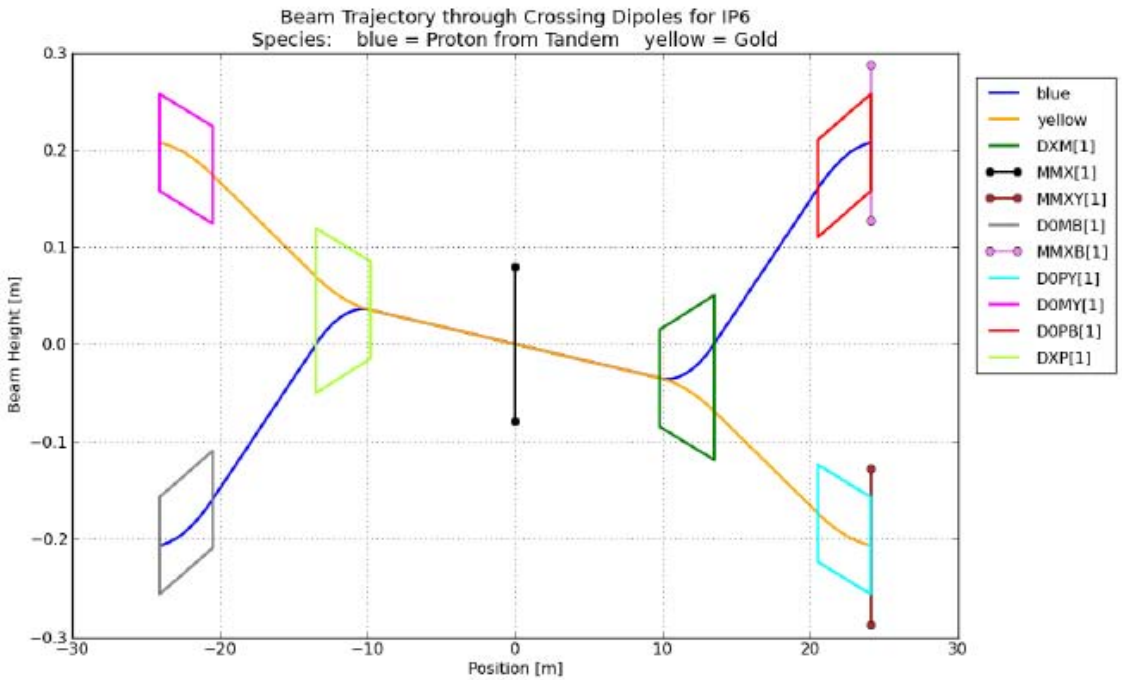

Figure 1. The beam trajectory through the crossing dipoles D0 and DX. The Au beam is 69.4mm from the central line in the DX magnet in the worst case. Additional room for beam size must also be taken into account.

colliding IR
move DX by 1cm

S. Tepikian, D. Trbojevic, C-A/AP/447 (Jan. 2012)

p-Au easier with stochastic cooling

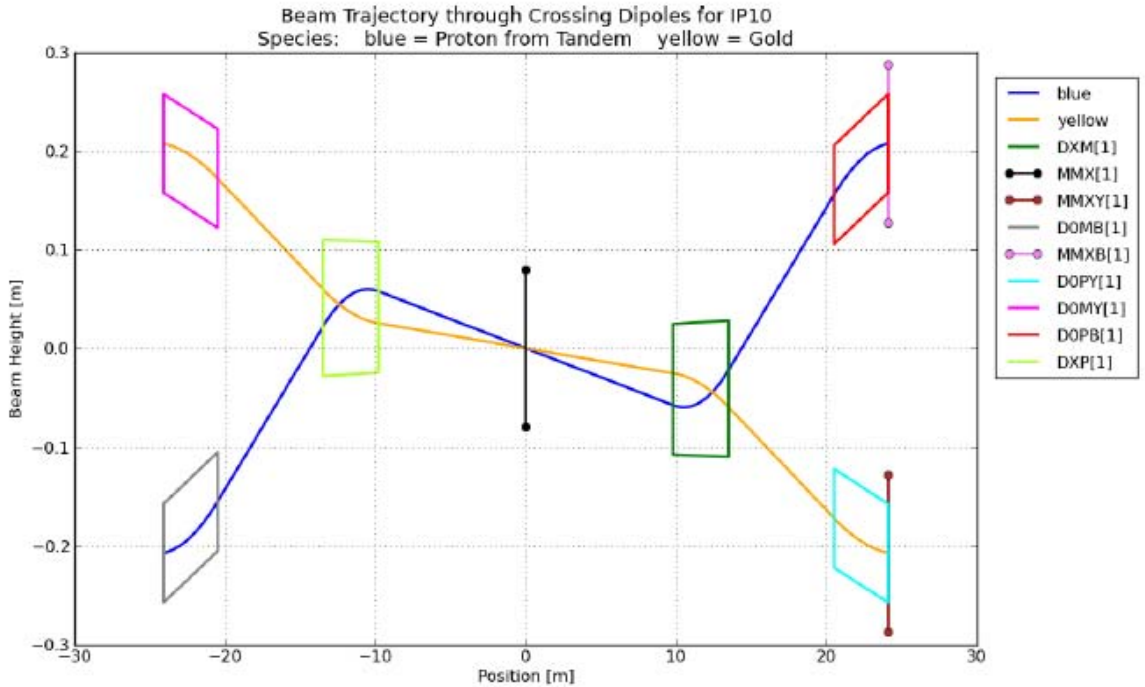

Figure 2. A non-colliding insertion. The crossing angle is -0.3305mrad. The beam trajectory is 59.8mm from the central axises for both beams in the DX magnet. The Blue beam reaches its peak at 10.5m from the IP, while the Yellow beam reaches its peak at 13.5m from the IP.

non-colliding IR
no DX move

S. Tepikian, D. Trbojevic, C-A/AP/447 (Jan. 2012)

Moving IR6 and IR8 DX magnets by 1cm

- Bellows allow for 1 cm movement
- Installed shielding creates tight spaces but acceptable
  "6:00 the bellows and ion pump stand were swapped to make space for the shielding, … cannot be moved because of the ion pump stand" (M. Mapes)
- Easier to do have p in Yellow, Au in Blue (different from d-Au!)

Can be done in ~ 2 shifts (i.e. during a run) when properly prepared in previous shut-down

Asymmetric collisions (p-Au)

- p-Au energies:

  100.8 GeV p on 100.0 GeV/nucleon Au ($\gamma_p = \gamma_{Au} = 107.4$)

- **Need to translate DX magnets horizontally by 1 cm**

  p are bent stronger than Au^{79+}

- For energy scan need to match Lorentz factor γ of both beams

Au-Au history and projections Parameter	unit	p 2013E	Au	p 2013E	Au
no of colliding bunches	…	111	111	111	111
ions/bunch, initial	10^9	140	1.0	180	1.4
charges per bunch	10^9e	140	79	180	107
average beam current/ring I_{avg}	mA	194	110	250	148
stored energy per beam	MJ	0.25	0.35	0.32	0.47
transverse rms emittance ε_{xy}	mm.mrad	2.9	2.9	2.8	2.8
rms bunch length σ_s	m	0.5	0.3	0.5	0.3
envelope function at IP β^*	m	0.9	0.9	0.7	0.7
beam-beam parameter ξ/IP	10^{-3}	4.3	2.4	5.9	3.1
initial luminosity L/IP	**10^{28} cm^{-2}s^{-1}**	**39**		**82**	
events per bunch-bunch crossing	…				
average / initial luminosity	%	60		70	
average store luminosity L_{avg}	**10^{28} cm^{-2}s^{-1}**	**24**		**57**	
time in store	%	55		55	
max luminosity/week	nb^{-1}			190	
min luminosity/week	nb^{-1}	78			

L_{pA}/week, min/max [pb^{-1}] 15 37

RHIC status and upgrades

Coming to the end of a major upgrade phase

- More than 10 firsts and records in Run-12

"RHIC-II performance without the RHIC-II upgrade project"

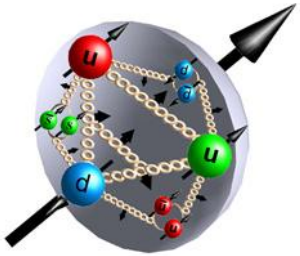

Near-term upgrades:

Run-13 – mainly for polarized protons

- Polarized source upgrade (partial or full) 10x source intensity, +5% P
- Electron lenses requires new lattice, commissioning in Run-13

Run-14 – mainly for heavy ions

- 56 MHz SRF, +30-50% *L*

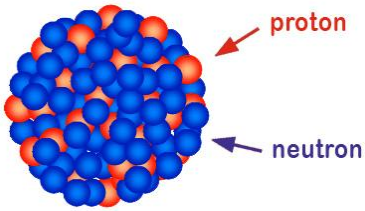

Uranium Nucleus

p-Au operation possible, ~2 shifts for DX move, E_{max} = 100 GeV/n (both p and Au)

Further upgrades possible

- Stochastic cooling upgrades
- Low-energy cooling for Au-Au up to ~10x *L*; ≥ 2017
- Polarized ^{3}He source, more snakes in Blue ring
- Beam pipe coating for intensity increases / shorter bunches
- Very high pp luminosity with CeC

eRHIC

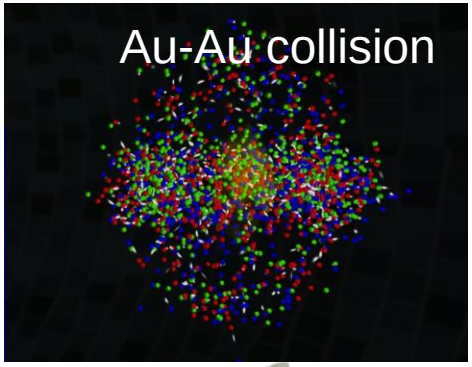

Process dependence Prompt Photon Production Sivers and Collins(?)

1 August 2012

Leonard Gamberg Penn State

Phys.Lett. B696 2011 w/ Zhongbo Kang ***BNL***
Phys.Lett. B704 2011 w/ U. D'Alesio, LG Zhong-Bo Kang, F. Murgia, C. Pisano
LG & Zhongbo Kang - in Prep

Outline

- **Transverse spin Effects - TSSAs**
- **Color Gauge Inv. & Gauge Links- "T-odd" TMDs**
- **T-odd PDFs & moments via ISI/FSIs ... QCD-Phases**
- Connection of twist 2 & twist 3 approach
- Generalizing the Generalized Parton Model (GPM) color gauge invariance CGI-GPM
- Contributions in Prompt γ
  - Direct & Fragmentation Sivers + Collins
- Some pheno results---(Collins is PRELIM!)

Comments Importance of TMDs in studying partonic content of the nucleon

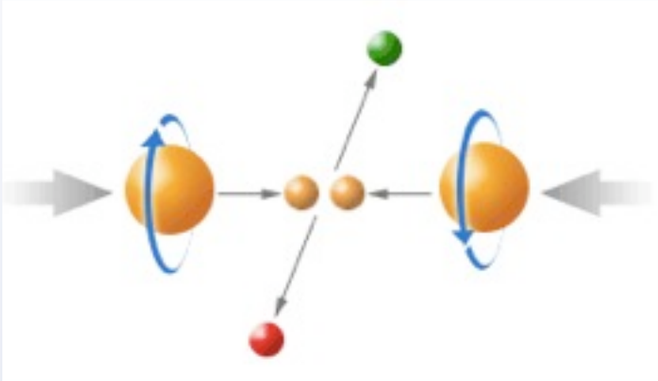

- Single inclusive hadron production in hadronic collisions largest/ oldest observed TSSAs
- From theory view notoriously challenging from partonic picture twist-3 power suppressed in hard scale (vs. w/ SIDIS, DY, e^+e^-)

Comments

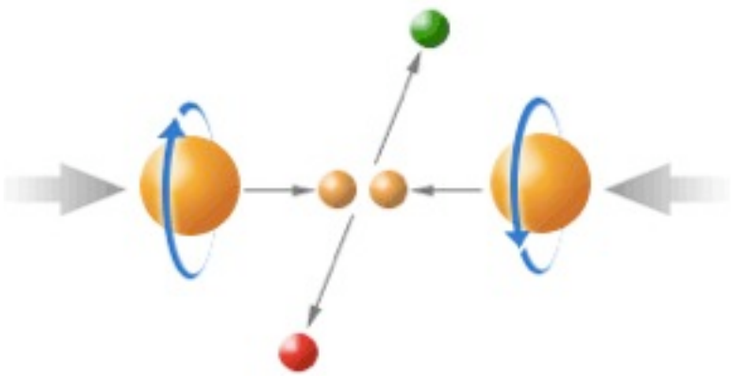

- Connection w/ twist 2 "TMD" approach
  - Operator level ETQS fnct 1st moment of Sivers

$$gT_F(x,x) = -\int d^2k_T \frac{|k_T^2|}{M} f_{1T}^{\perp}(x,k_T^2)$$ Boer Piljman Mulders NPB 2003

$$= -2M f_{1T}^{\perp(1)}(x) \quad + \quad \text{"UV" ...}$$

Kang, Qiu, Vogelsang, Yuan prd 2011
Kang & Prokudin prd 2012
"compatibility study"

$$f_{1T}^{\perp}(x,|\boldsymbol{b}_T|) = -2M \int d^2p_T \frac{|p_T|}{|\boldsymbol{b}_T|M} J_1(|\boldsymbol{b}_T||p_T|) f_{1T}^{\perp}(x,p_T^2)$$

Boer, LG, Musch, Prokudin to appear JHEP--arXiv:1107.529

Ingredients transverse SPIN Observable kinematics $P^{\uparrow}P \to \pi X$

- **Single Spin Asymmetry**

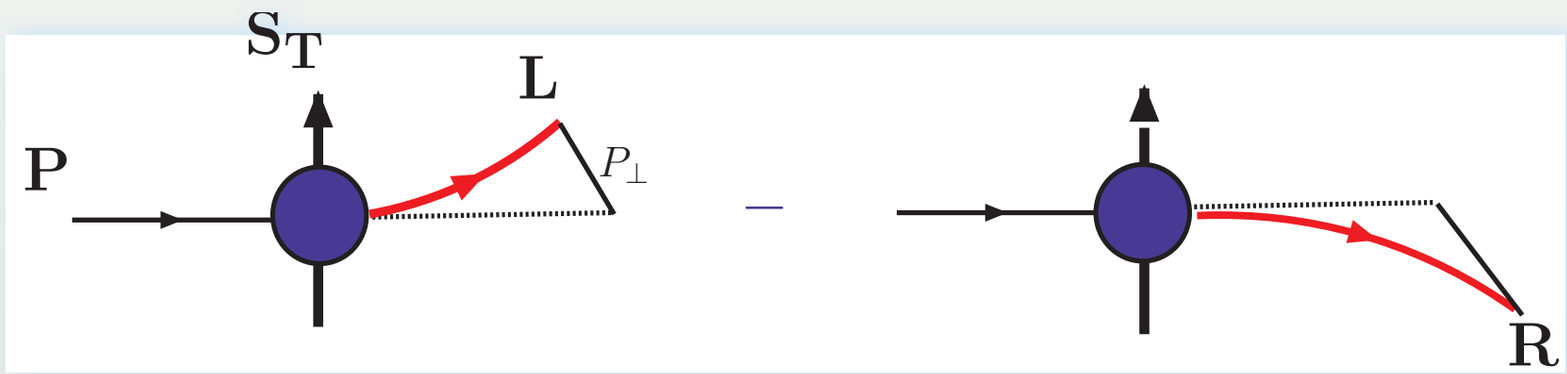

Parity Conserving interactions: SSAs Transverse Scattering plane

$$\Delta\sigma \sim iS_T \cdot (\mathbf{P} \times P_\perp^\pi)$$

- **Rotational invariance** $\sigma^{\downarrow}(x_F, \boldsymbol{p}_\perp) = \sigma^{\uparrow}(x_F, -\boldsymbol{p}_\perp)$

$\Rightarrow$ ***Left-Right Asymmetry***

$$\boldsymbol{A}_N = \frac{\sigma^{\uparrow}(x_F,\boldsymbol{p}_\perp) - \sigma^{\uparrow}(x_F,-\boldsymbol{p}_\perp)}{\sigma^{\uparrow}(x_F,\boldsymbol{p}_\perp) + \sigma^{\uparrow}(x_F,-\boldsymbol{p}_\perp)} \equiv \Delta\sigma$$

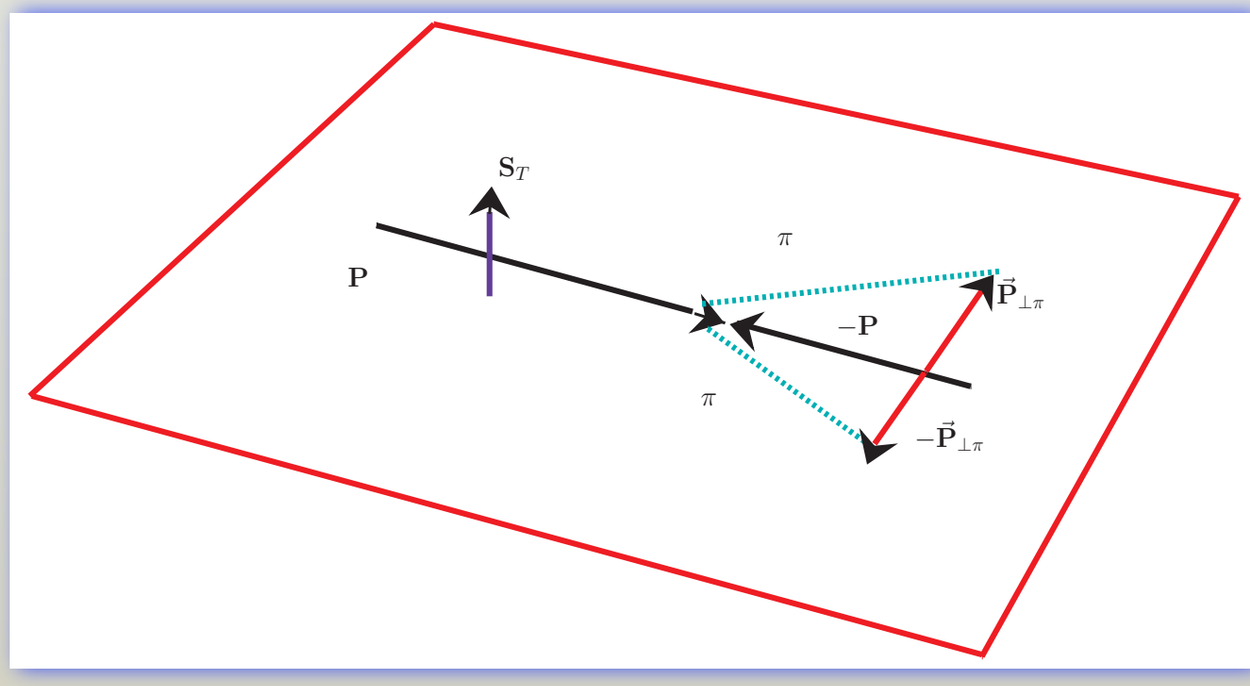

Reaction Mechanism w/ Partonic Description

Collinear factorized QCD parton dynamics

$$\Delta\sigma^{pp^\uparrow \to \pi X} \sim f_a \otimes f_b \otimes \Delta\hat{\sigma} \otimes D^{q\to\pi}$$

$$\Delta\hat{\sigma} \equiv \hat{\sigma}^\uparrow - \hat{\sigma}^\downarrow$$

$$|\uparrow / \downarrow\rangle = (|+\rangle \pm i|-\rangle)$$

$$\hat{a}_N = \frac{\hat{\sigma}^\uparrow - \hat{\sigma}^\downarrow}{\hat{\sigma}^\uparrow + \hat{\sigma}^\downarrow} \sim \frac{\mathrm{Im}\left(\mathcal{M}^{+*}\mathcal{M}^-\right)}{|\mathcal{M}^+|^2 + |\mathcal{M}^-|^2}$$

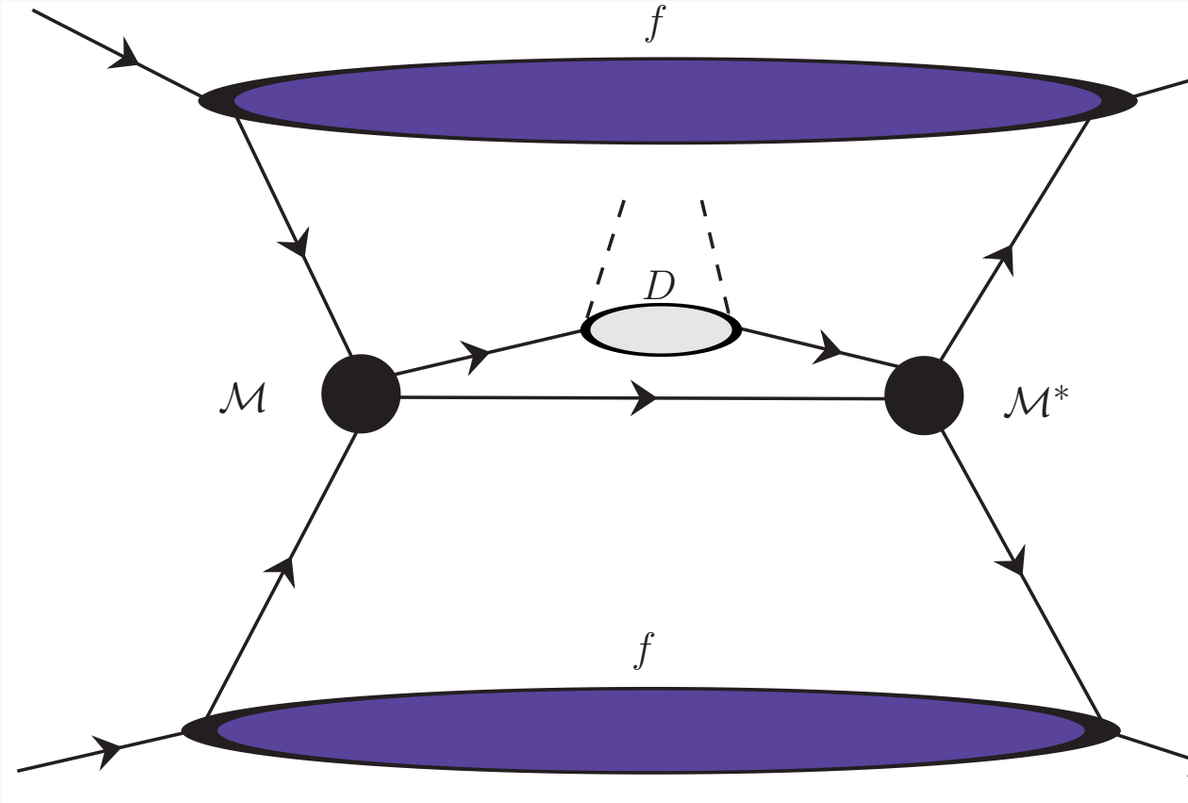

Transv. polarization cross section "interference" of helicity flip and non-flip amps.

Interference of helicity flip and non-flip amps
1) requires breaking of chiral symmetry m_q/E
2) relative phases require higher order corrections

Factorization Theorem at Partonic level

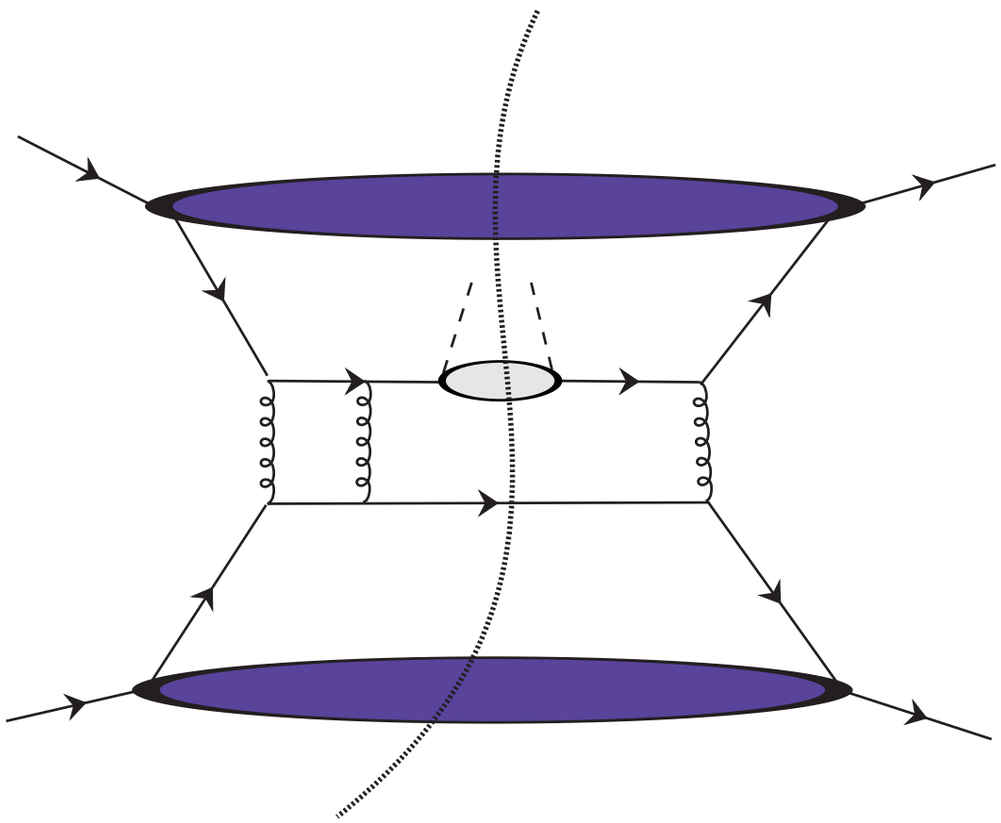

$$\Delta\hat{\sigma} \sim \mathcal{I}m[M^*{}_+ M_-]$$

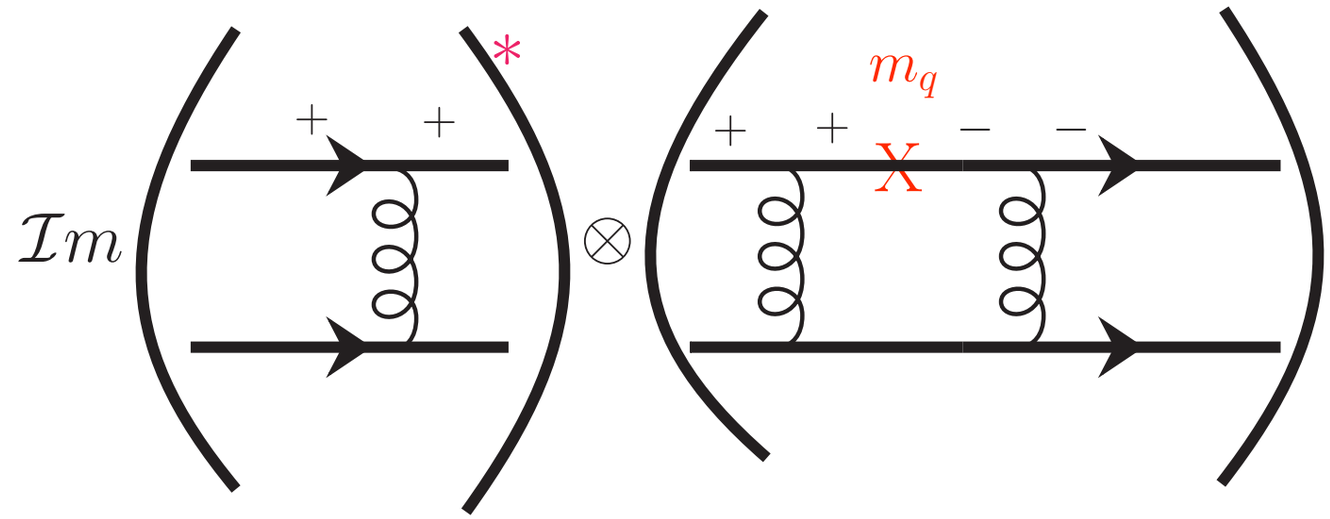

- **Born amps are real -- need "loops"----> phases**
- **QCD interactions conserve helicity up to corrections** $\mathcal{O}\left(\frac{m_q}{E_q}\right)$

Twist three and trivial in chiral limit

$$A_N \propto \frac{m_q}{E}\alpha_s$$

at the partonic level

Kane & Repko, PRL: 1978

Early theory in striking contrast exp.TSSAs in Inclusive Reactions

Transverse Single-Spin Asymmetries: From Low to High Energies!

p_{beam}=12 Gev/c	p_{beam}=22 Gev/c	p_{beam}=200 Gev/c	RHIC
ANL	BNL	FNAL	
$\sqrt{s}$=4.9 GeV	$\sqrt{s}$=6.6 GeV	$\sqrt{s}$=19.4 GeV	$\sqrt{s}$=62.4 GeV
← Fixed target →			Collider

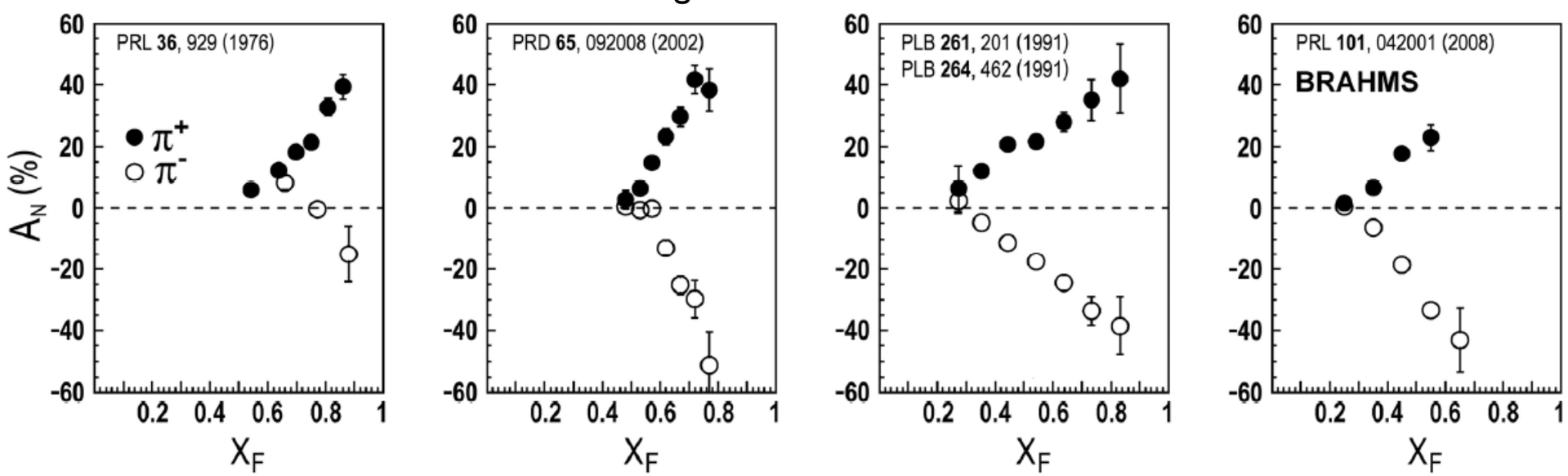

$$x_F = 2p_{long}/\sqrt{s}$$

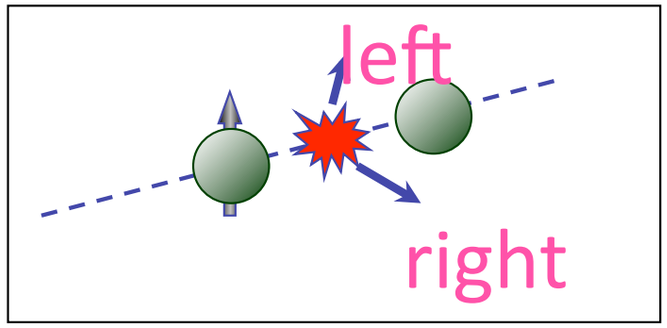

see talks of F. Giordono &T.Burton

Modern Era Transverse SSA's at $\sqrt{s}$ = 62.4 & 200 GeV at RHIC

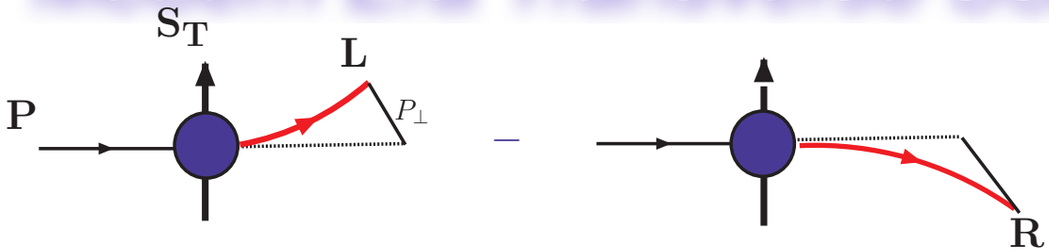

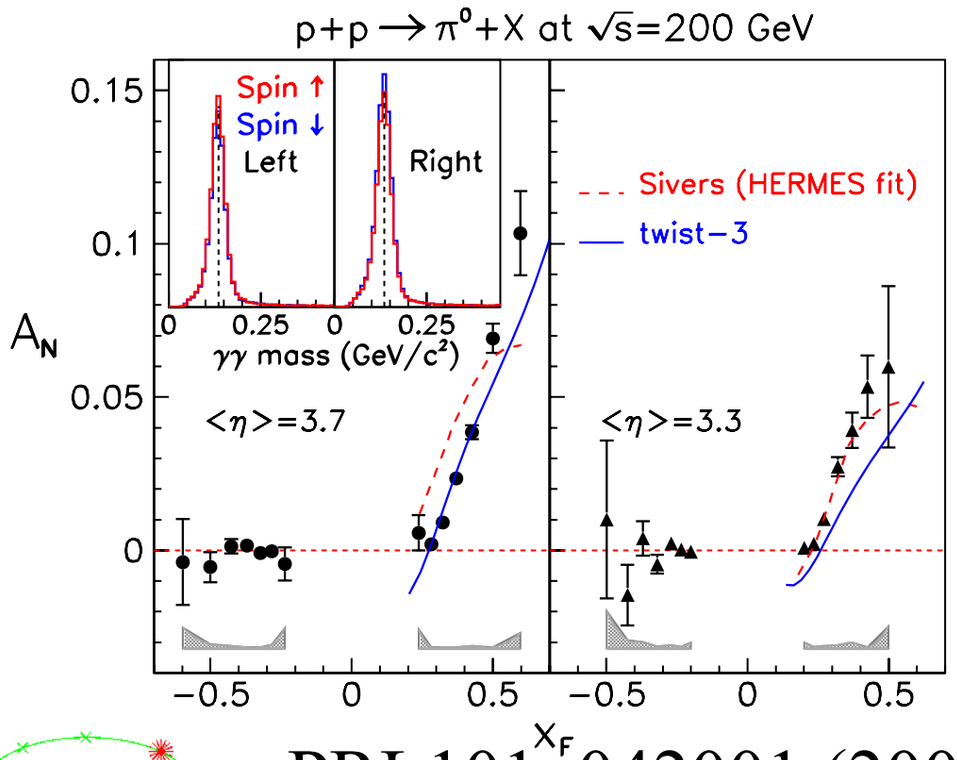

STAR

PHENIX

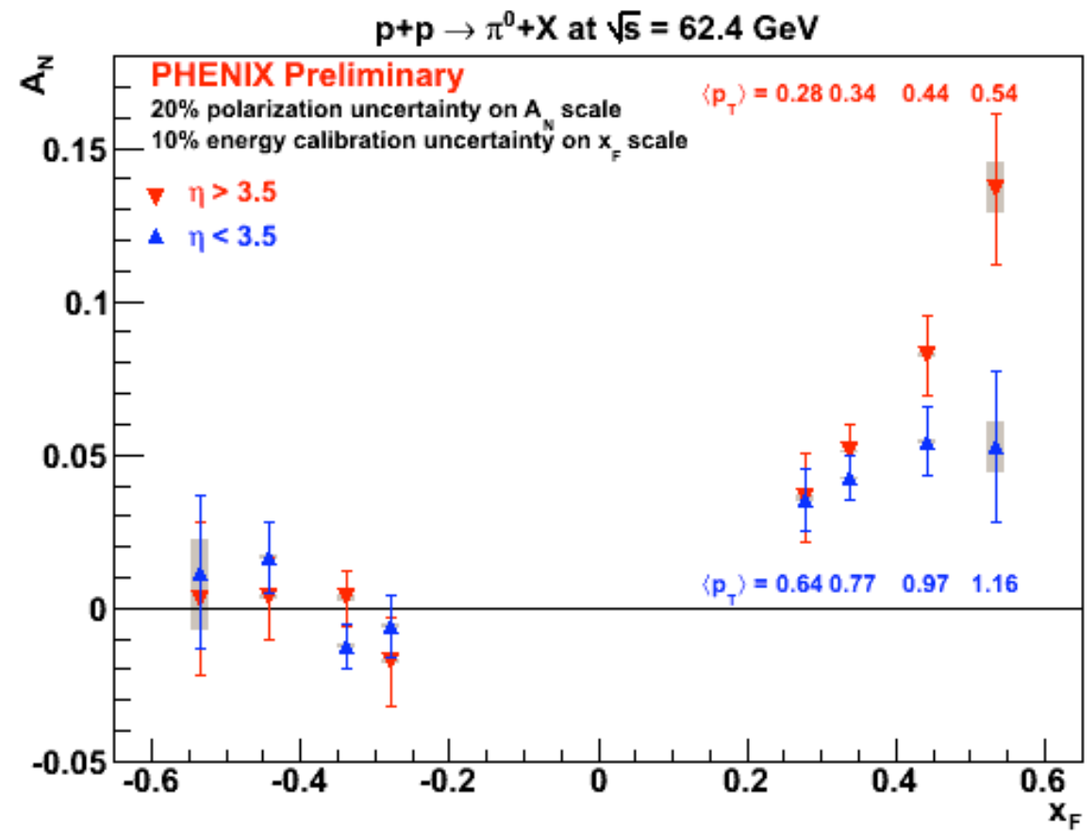

BRAHMS

PRL101, 042001 (2008)

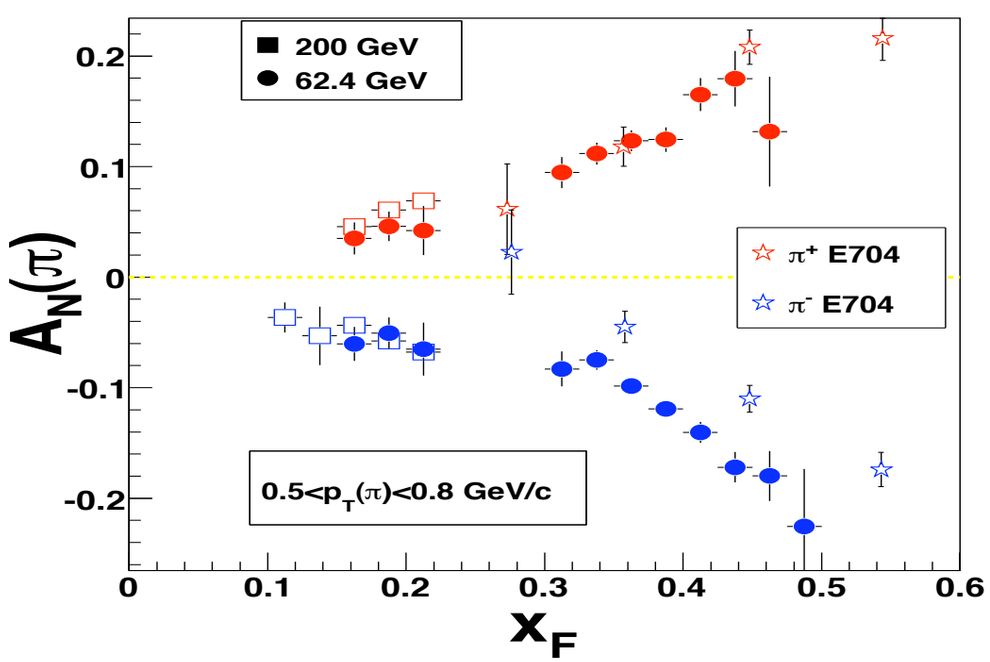

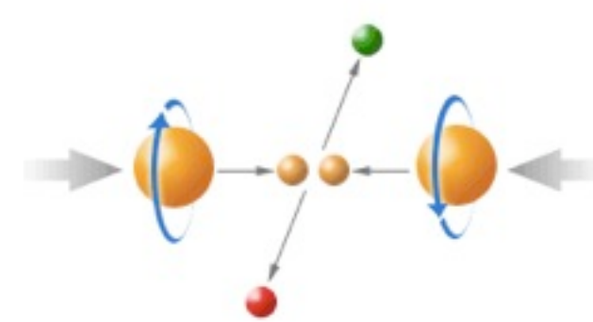

inclusive hadrons: $e\,p^{\uparrow} \rightarrow h\,X$

- scattered electron not detected (ignored) → Q2 ≈ 0 → huge statistics

  P_T, x_F w.r.t. **beam direction**

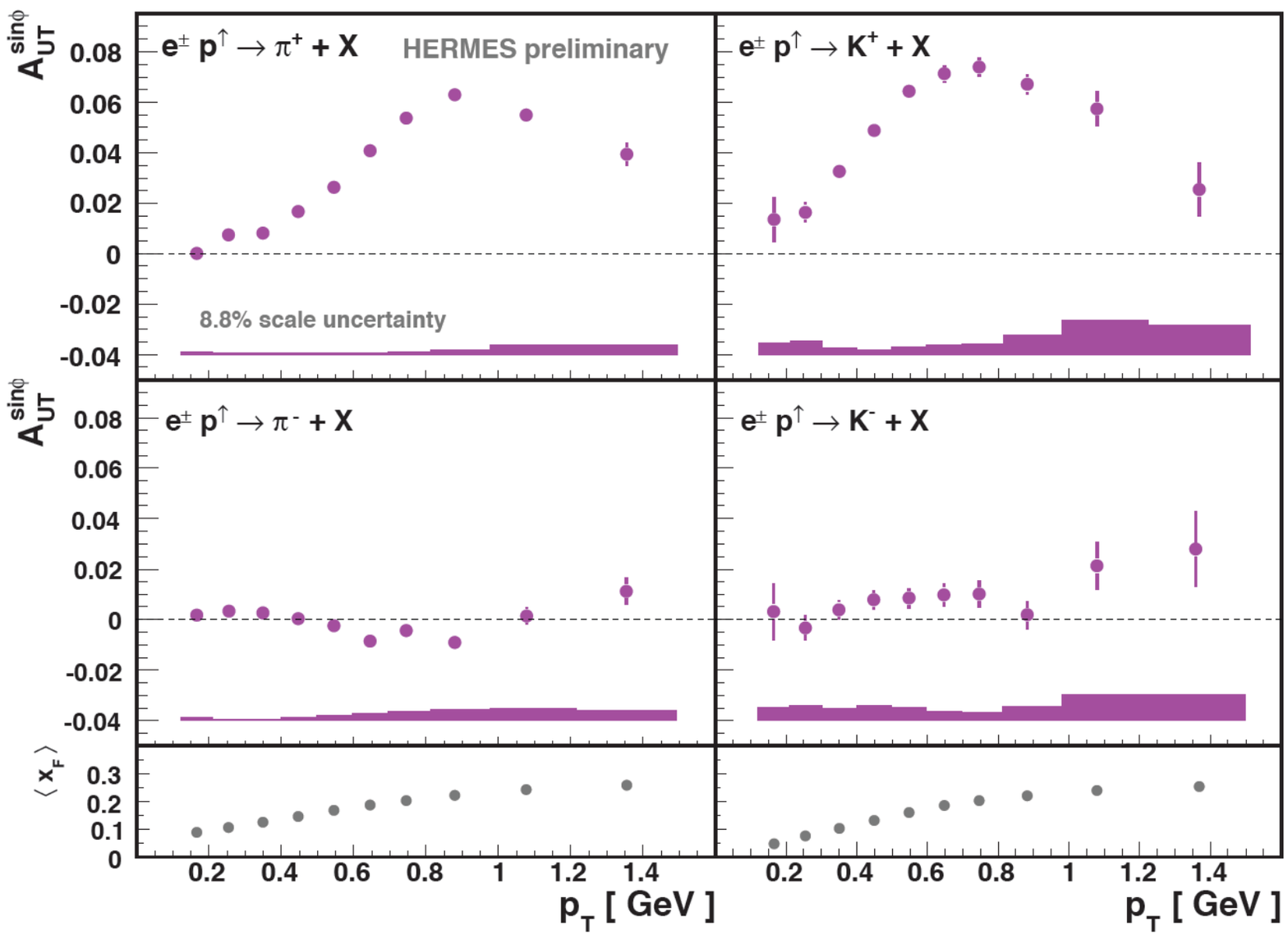

$$A_N = \frac{2}{\pi} A_{UT}^{\sin\varphi}$$

from D. Hasch

Not the full story @ Twist 3 approach ETQS approach

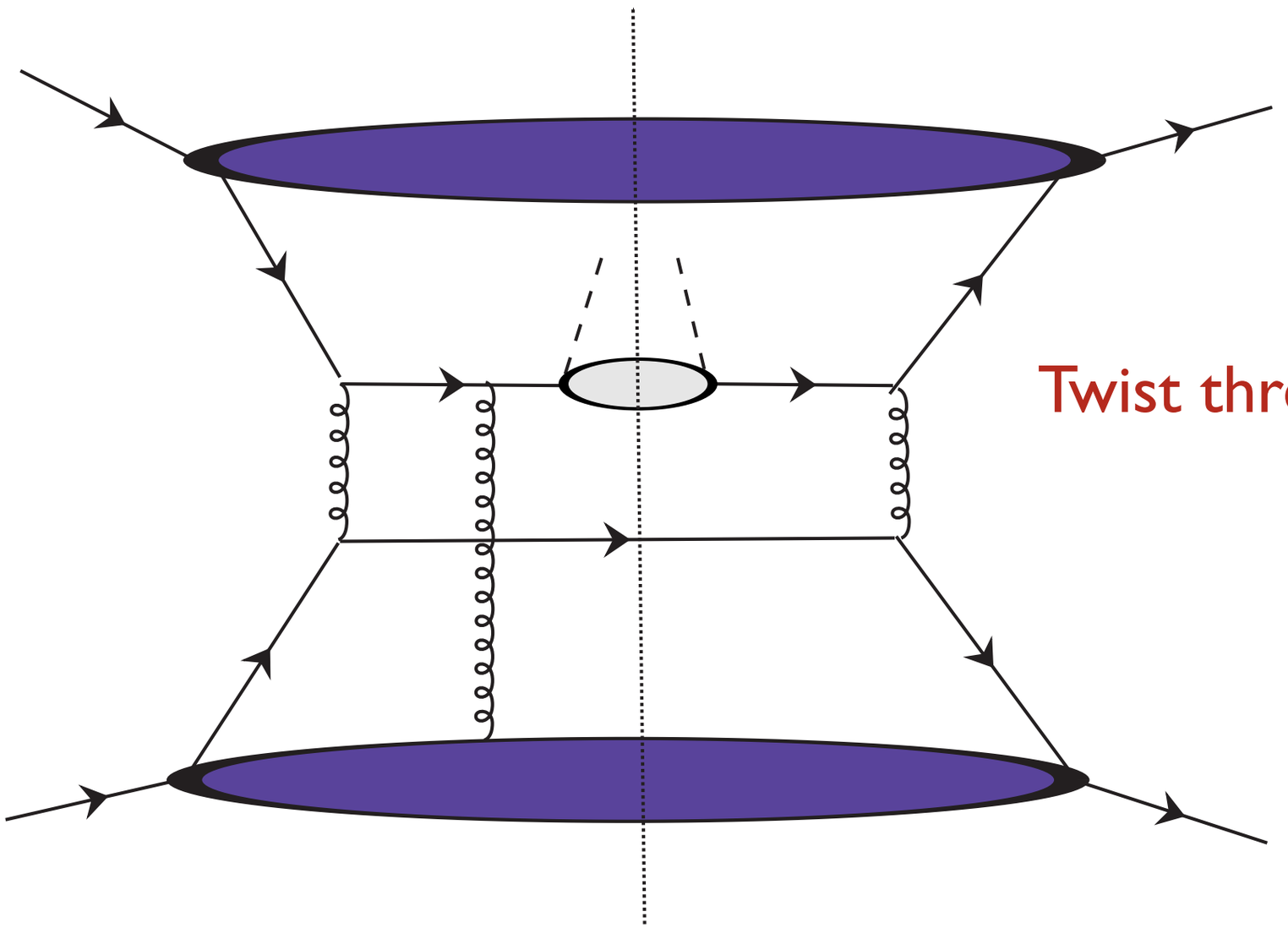

Twist three supressed by hard scale
but non-trival?!

Phases in soft poles of parton propagators in hard sub-process
Efremov & Teryaev PLB 1982 Qiu, Sterman 1991,1999

Factorization and Pheno: Qiu, Sterman 1991,1999..., Koike et al, 2000, ... 2011
Ji, Qiu, Vogelsang, Yuan, 2005 ... 2008 , Yuan, Zhou 2008, 2009, Kang, Qiu, 2008, 2009 ...
Vogelsang and Yuan 2007
Pheno studies, Kouvaris Ji, Qiu, Vogelsang! 2006

Twist 3 ETQS approach-"Partonic Picture"

$Q \sim P_T >> \Lambda_{\rm qcd}$ One scale Collinear fact Twist 3

Phases in soft poles of prop hard processes Efremov & Teryaev PLB 1982

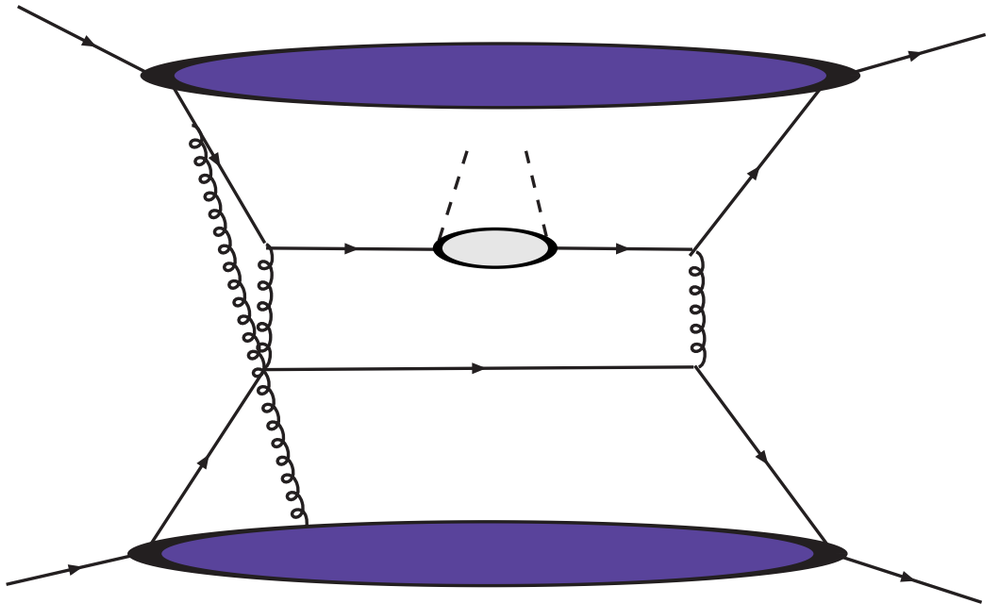

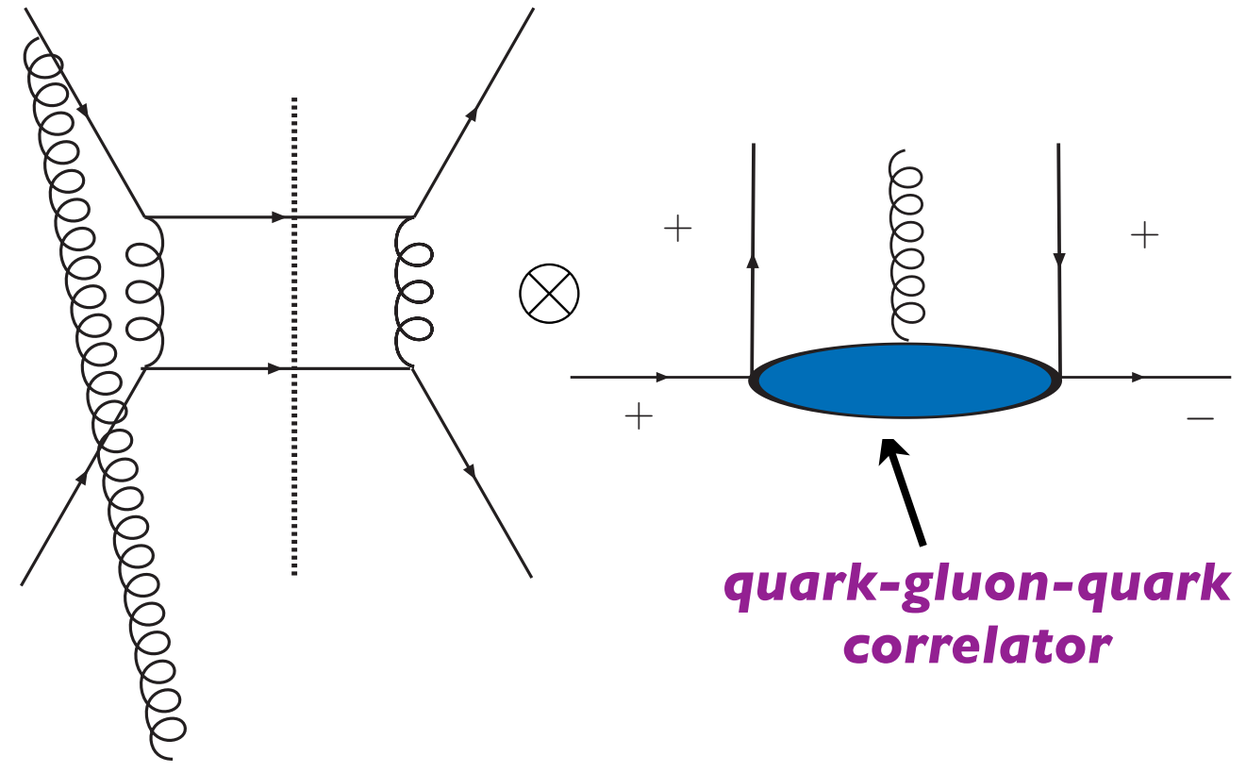

$$\Delta\sigma \sim f_a \otimes T_F \otimes H_{ETQS} \otimes D^{q\to h}$$

$$\frac{1}{xs + i\epsilon} = \mathcal{P}\left(\frac{1}{xs}\right) \pm i\pi\delta(xs)$$

- Phases from interference two parton three parton scattering amplitudes

- Factorization and Pheno: Qiu, Sterman 1991,1999..., Koike et al, 2000, ... 2010, Ji, Qiu, Vogelsang, Yuan, 2005 ... 2008 ..., Yuan, Zhou 2008, 2009, Kang, Qiu, 2008, 2009 ... Kouvaris Ji, Qiu, Vogelsang! 2006, Vogelsang and Yuan PRD 2007

Two methods to generate SSA in QCD

- Depends on momentum of probe $q^2 = -Q^2$ and momentum of produced hadron $\boldsymbol{P}_{h\perp}$ relative to hadronic scale $k_T^2 (\equiv k_\perp^2) \sim \Lambda_{\rm QCD}^2$

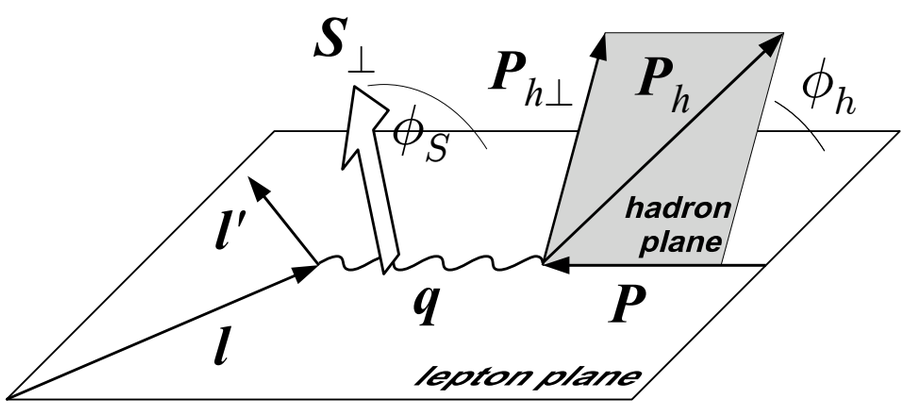

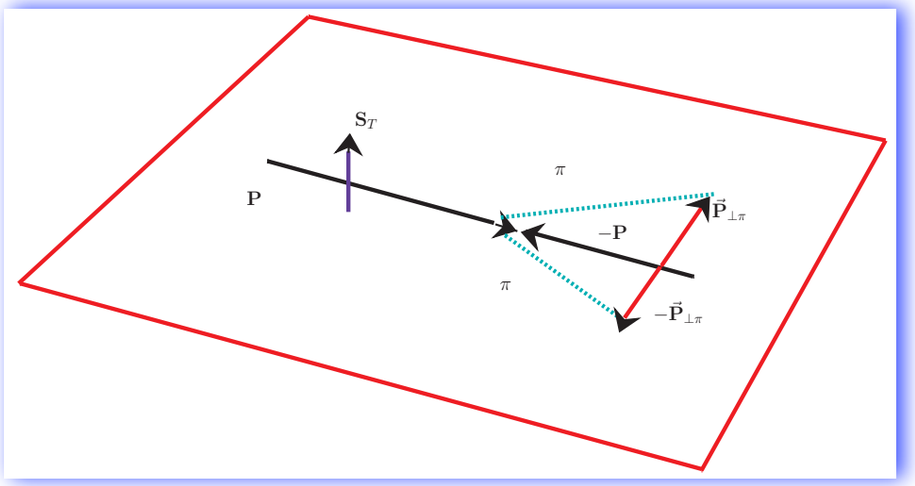

- $k_\perp^2 \sim P_{h\perp}^2 \ll Q^2$ two scales-TMDs

$$\Delta\sigma(P_h, S) \sim \Delta f_{a/A}^{\perp}(x, p_\perp) \otimes D_{h/c}(z, K_\perp) \otimes \hat{\sigma}_{\rm parton}$$

- $k_\perp^2 \ll P_{h\perp}^2 \sim Q^2$ twist 3 factorization-ETQSs

$$\Delta\sigma(P_h, S) \sim \frac{1}{Q} f_{a/A}^{\perp}(x) \otimes f_{b/B}(x) \otimes D_{h/c}(z) \otimes \hat{\sigma}_{\rm parton}$$

Connection of twist 3 and twist 2 approach "overlap regime"

Ji,Qiu,Vogelsang, Yuan PRL 2006 ...
Bacchetta, Boer, Diehl, Mulders JHEP 2008

see talks of Zhongo-Bo and Jian Wei

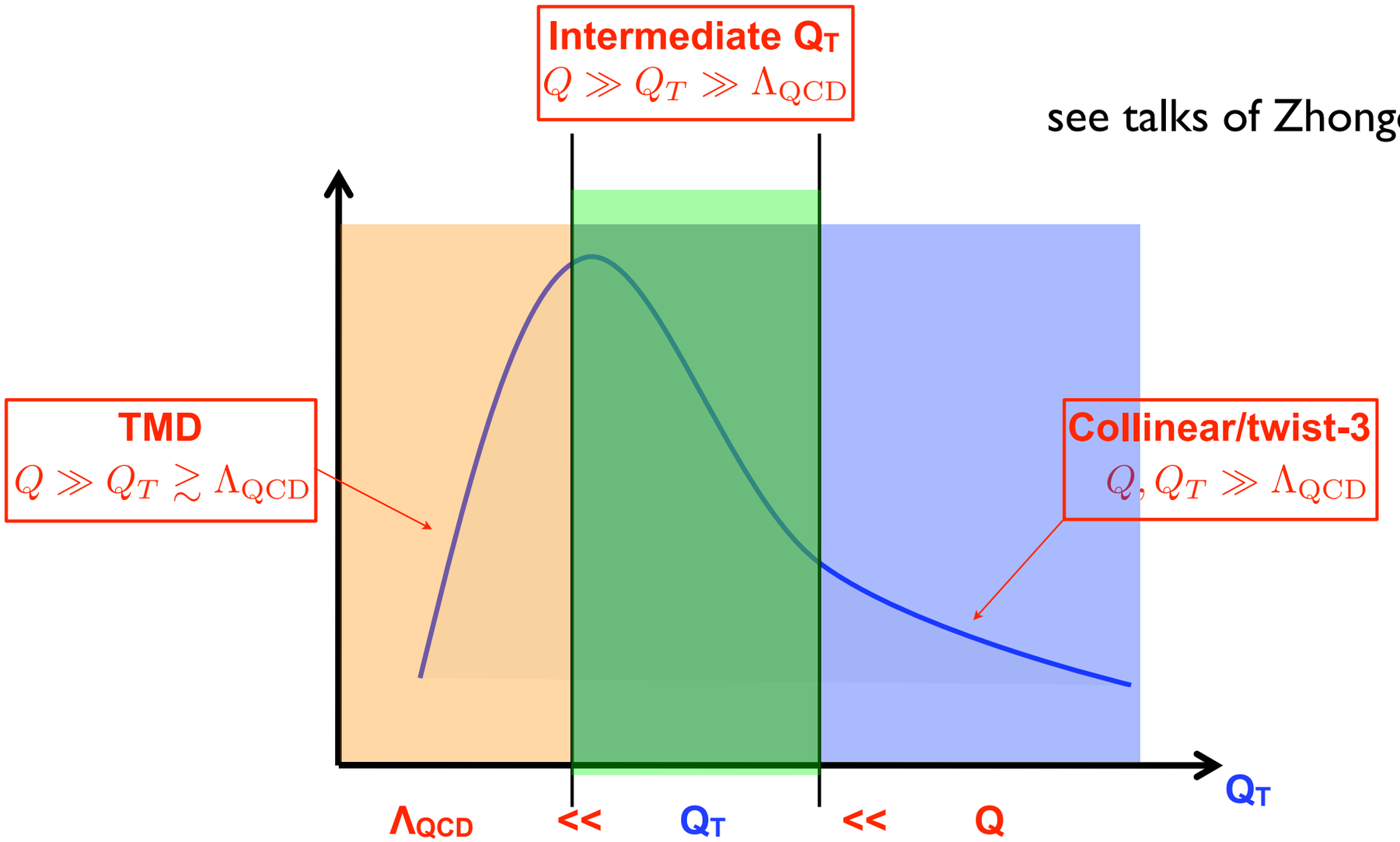

- Explore role parton model processes in twist-2&3 approaches
  LG & Z. Kang PLB 2011 & for Collins in prep, "exploring impact of Gauge Inv"

Motivation Study Process dependence using inclusive processes

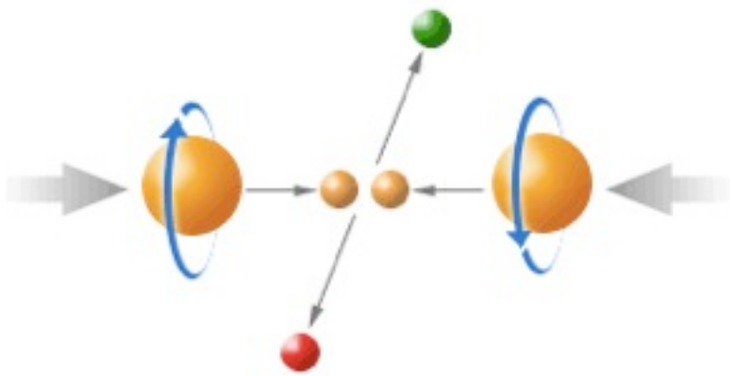

- Using btwn twist 2 "TMD" approach and twist 3 ETQS
  - Attempts to study process dependence in inclusive processes

$$gT_F(x,x) = -\int d^2k_T \frac{|k_T^2|}{M} f_{1T}^{\perp}(x,k_T^2)$$ Boer Piljman Mulders NPB 2003

$$= -2M f_{1T}^{\perp(1)}(x) \quad + \quad \text{"UV" ...}$$

Kang, Qiu, Vogelsang, Yuan prd 2011
Kang & Prokudin prd 2012
"compatibility study"

Generalizing the GPM CGI-GPM

- Feynman, Field, Fox (PRD 77 & 78)-incorporate intrinsic $\boldsymbol{k}_T$
- Include Transverse spin pol. w/ intrisic $\boldsymbol{k}_T$--Anselmino, Boglione, Murgia, ... et al. *PLB 95* & 98
- Pheno-Torino Cagliari group .... 1995-2012 inclusive processes
- Inclusive processes studied TW-3 formalism Kouvaris, Qiu, Vogelsang, Yuan PRD 2006, $pp \to \pi X$ & $pp \to \gamma X$
- What happens when you adopt ansatz of GPM including dynamical reaction mechanism of FSI/ISI in inclusive processes
- Take into account ISI/FSI process dependent Sivers function
- Since one scale, process-twist three is GPM connected w/twist 3 ? While we use $\boldsymbol{k}_T$ dependent TMDs we integrate over $\boldsymbol{k}_T$. Guides us to perform collinear expansion from GPM

TMD Factorization in Parton Model-"kinematics"

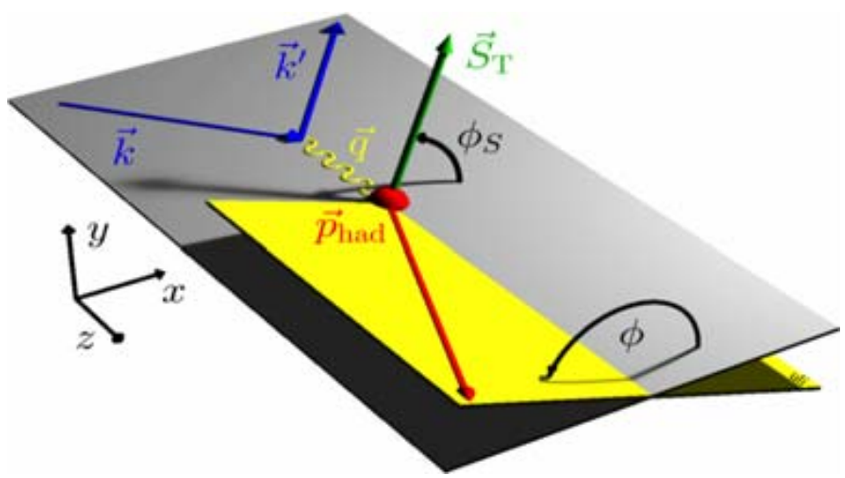

$$x_B = \frac{Q^2}{2P \cdot q}$$

$$z_h = \frac{P \cdot P_h}{P \cdot q} \approx \frac{P_h^-}{q^-}$$

Parton model & DIS kinematics

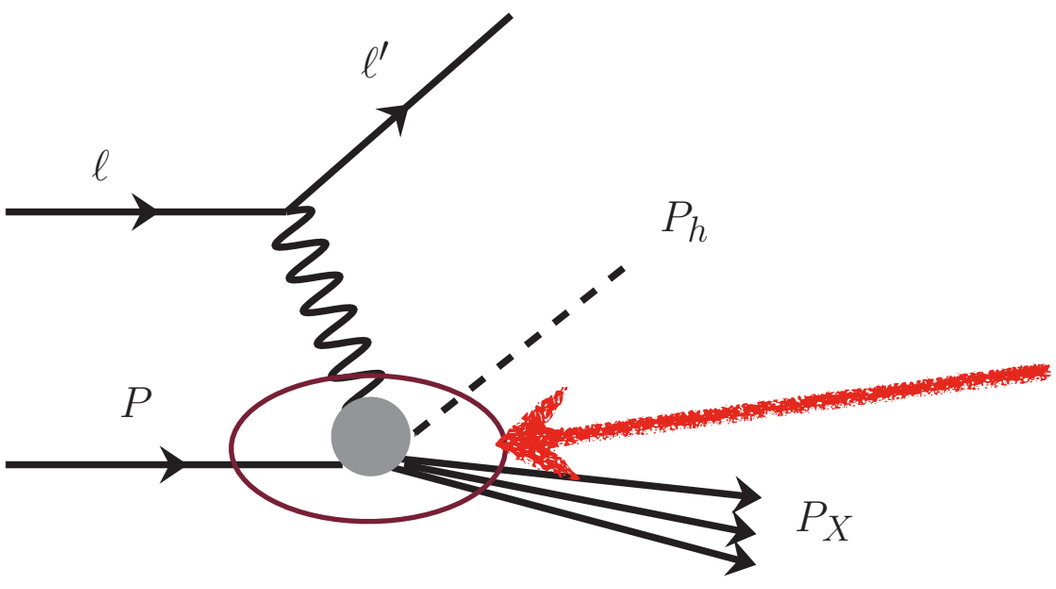

Factorize

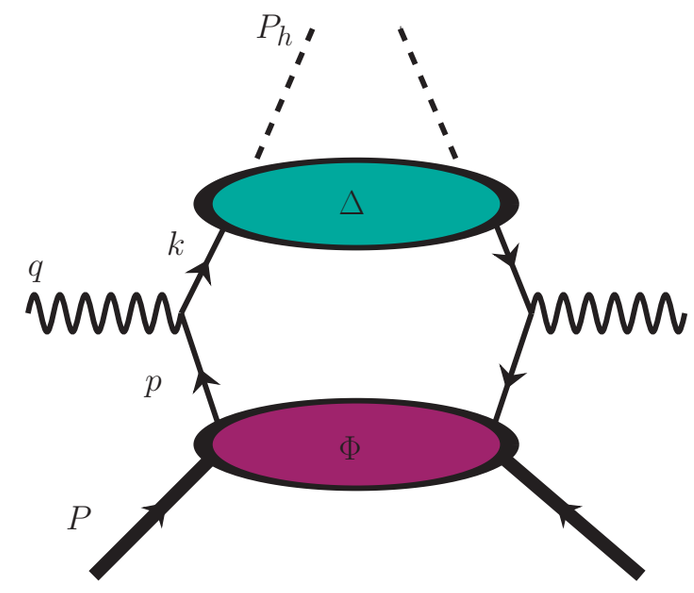

Factorization parton model P_T of hadron small sensitive to intrinsic transv. momentum of partons

$$W^{\mu\nu}(q,P,S,P_h) = \int \frac{d^2\mathbf{p}_T}{(2\pi)^4} \int \frac{d^2\mathbf{k}_T}{(2\pi)^4} \delta^2(\mathbf{p}_T - \frac{\mathbf{P}_{h\perp}}{z} - \mathbf{k}_T) \mathrm{Tr}\left[\left(\int dp^- \Phi\right)\gamma^\mu \left(\int dk^+ \Delta\right)\gamma^\nu\right]$$

Small transverse momentum !!!

$$\Phi(x,\mathbf{p}_T,S) \equiv \int dp^- \Phi(p,P,S)\Big|_{p^+=x_B P^+}, \qquad \Delta(z,\mathbf{k}_T) \equiv \int dk^+ \Delta(k,P_h)\Big|_{k^-=\frac{P^-}{z_h}}$$

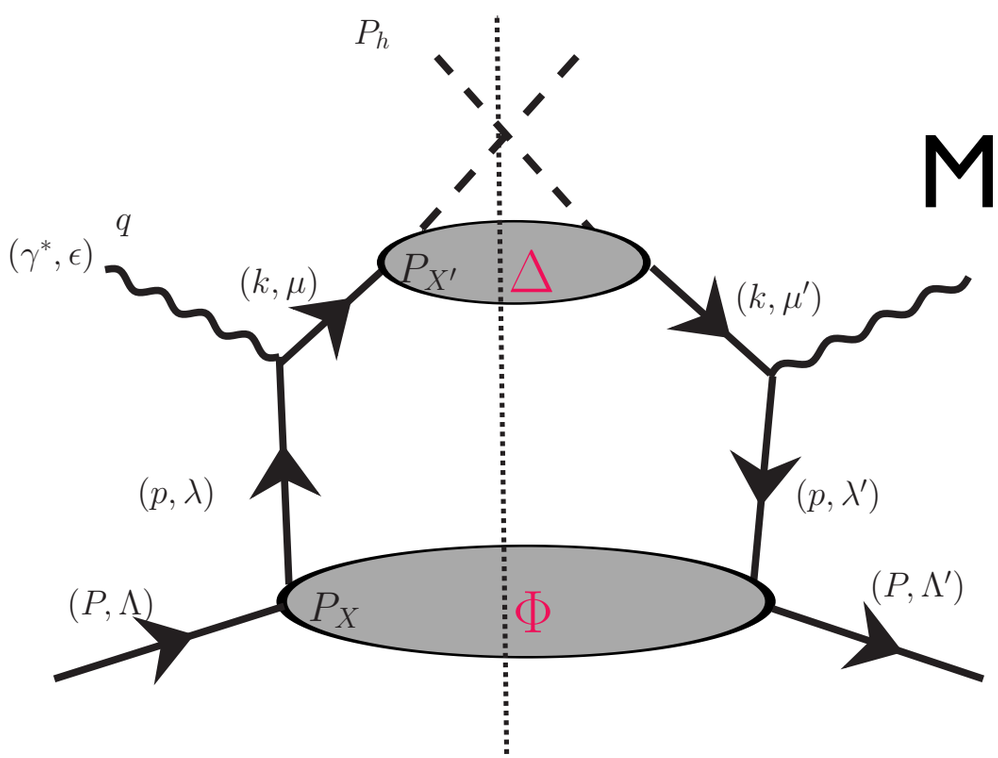

Minimal requirement satisfy color gauge invariance

Minimal Requirement Color Gauge Inv. Gauge links

Gauge link determined re-summing leading gluon interactions btwn soft and hard

Efremov,Radyushkin Theor. Math. Phys. 1981,Belitsky, Ji, Yuan NPB 2003,
Boer, Bomhof, Mulders Pijlman, et al. 2003 - 2008- NPB, PLB, PRD

$$\Phi^{[\mathcal{U}[\mathcal{C}]]}(x,p_T) = \int \frac{d\xi^- d^2\xi_T}{2(2\pi)^3} e^{ip\cdot\xi} \langle P|\overline{\psi}(0)\mathcal{U}^{[C]}_{[0,\xi]}\psi(\xi^-,\xi_T)|P\rangle|_{\xi^+=0}$$

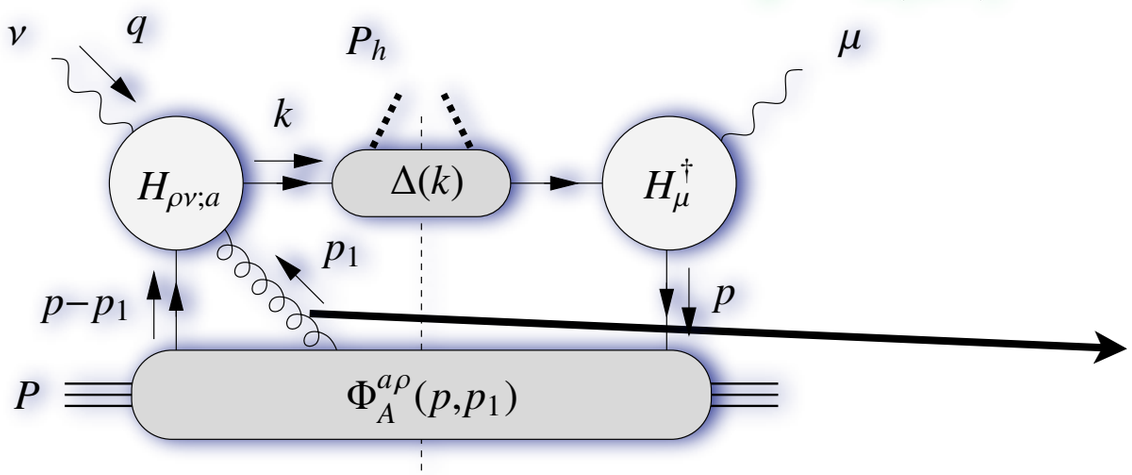

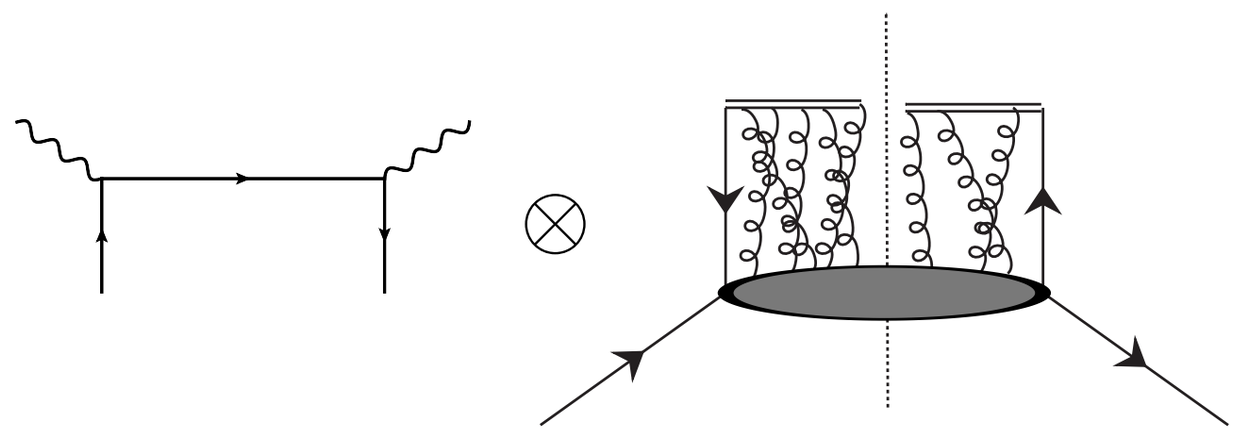

The path $[C]$ fixed by the hard subprocess in *factorization* procedure

$$W_{\mu\nu}(q,P,S,P_h) = \int d^4p d^4k \delta^4(p+q-k)\mathrm{Tr}\left[\Phi^{[U^C_{[\infty;\xi]}}(p)H^\dagger_\mu(p,k)\Delta(k)H_\nu(p,k)\right]$$

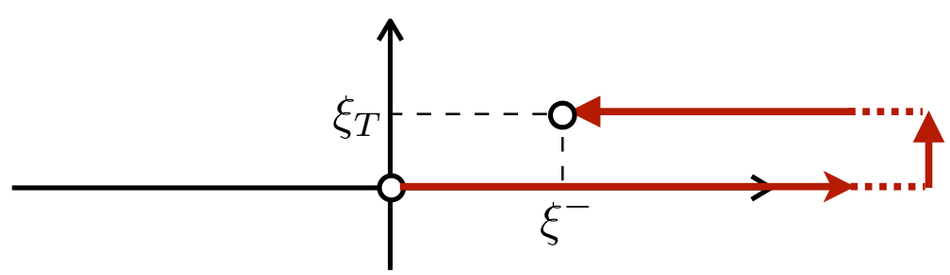

$U_{[+]}$

TSSAs thru "T-odd" non-pertb. **spin-orbit** *correlations....*

Sensitivity to $p_T \sim \mathbf{k}_T << \sqrt{Q^2}$

- Sivers PRD: 1990 **TSSA is associated w/ correlation** *transverse* **spin and momenta in initial state hadron**

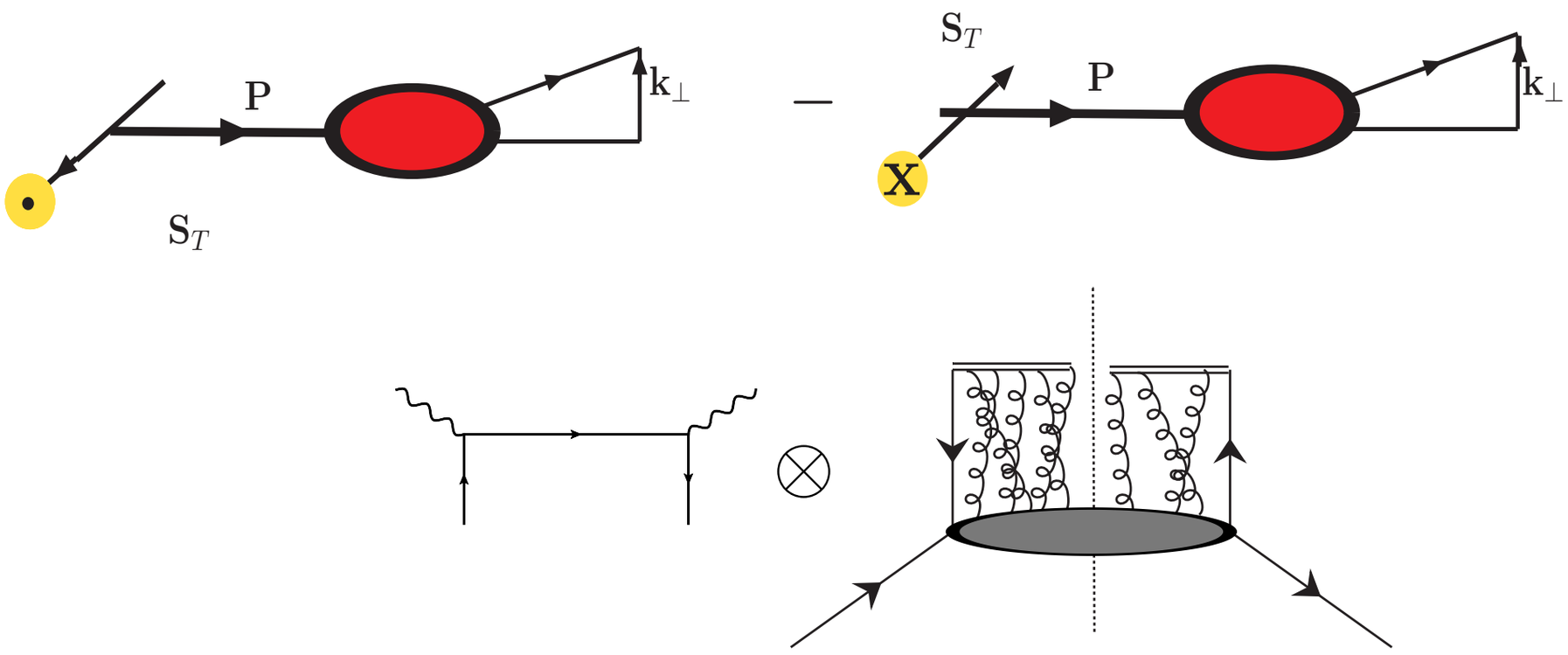

$$\Delta\sigma^{pp^\uparrow\to\pi X} \sim D \otimes f \otimes \Delta f^\perp \otimes \hat{\sigma}_{Born} \Longrightarrow \boldsymbol{\Delta f^\perp(x, k_\perp) = i S_T \cdot (P \times k_\perp)}\, f_{1T}^\perp(x, \boldsymbol{k}_\perp)$$

.... Fragmentation

- Collins NPB: 1993 **TSSA is associated with** $transverse$ **spin of fragmenting quark and transverse momentum of final state hadron**

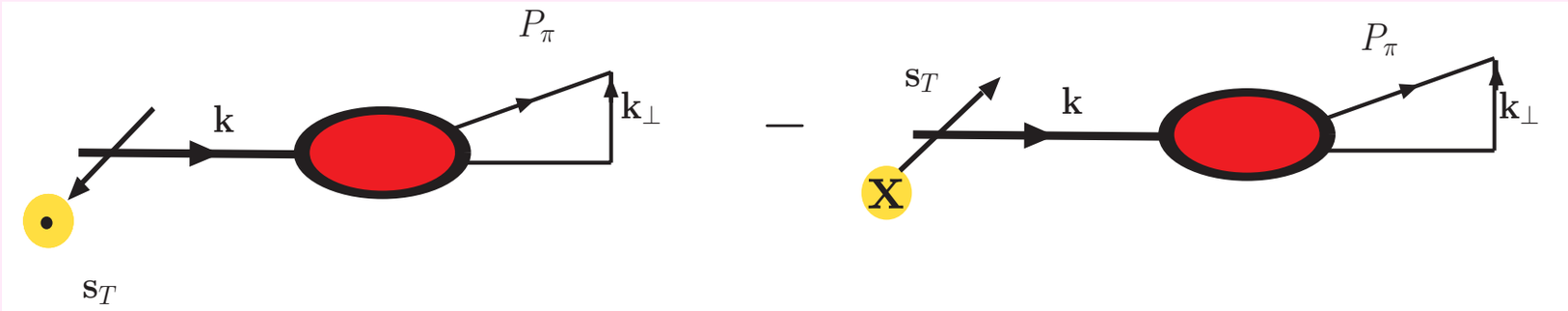

$$\Delta\sigma^{ep^\uparrow \to e\pi X} \sim \Delta D^\perp \otimes f \otimes \hat{\sigma}_{Born}$$

$$\boldsymbol{\Delta D^\perp(x, p_\perp) = i s_T \cdot (P \times p_\perp) H_1^\perp(x, p_\perp)}$$

Process Dependence break down of Universality

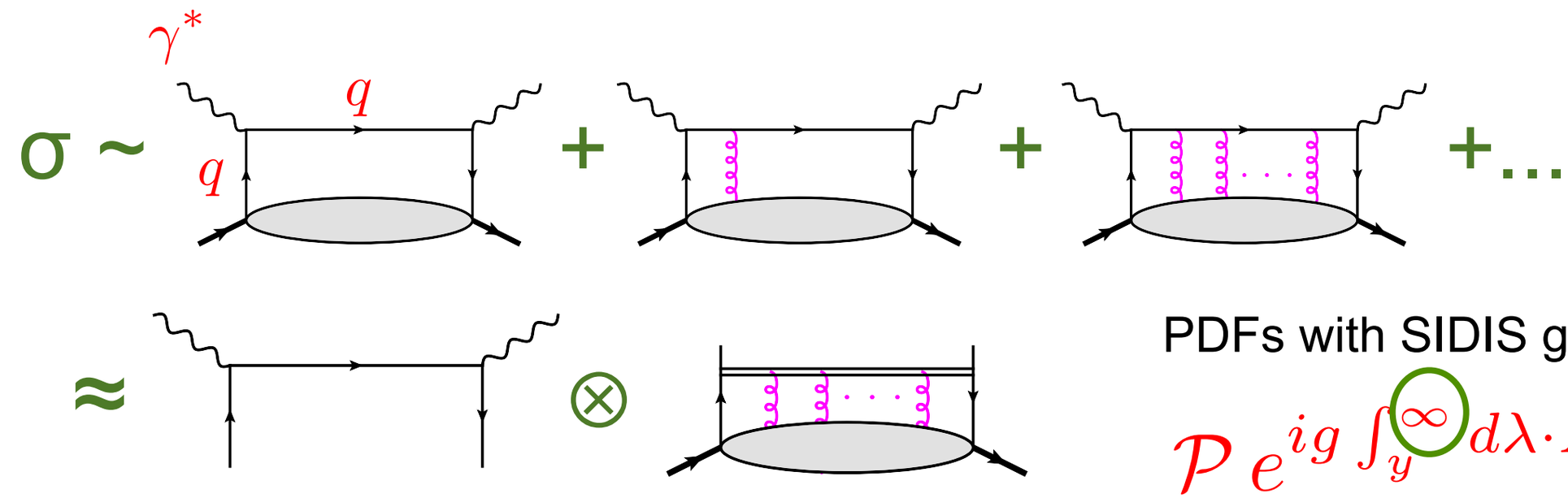

PDFs with SIDIS gauge link

$$\mathcal{P}\, e^{ig\int_y^{\infty} d\lambda\cdot A(\lambda)}$$

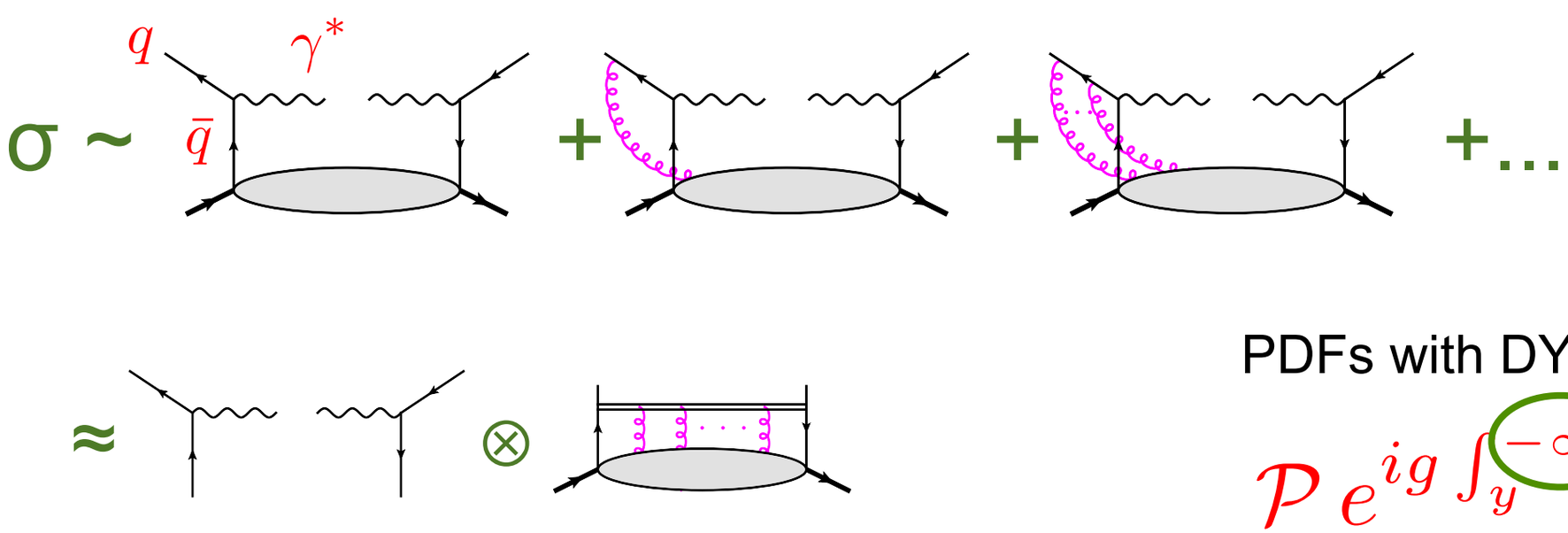

PDFs with DY gauge link

$$\mathcal{P}\, e^{ig\int_y^{-\infty} d\lambda\cdot A(\lambda)}$$

Classic example-same real pts opposite imaginary pts

Final-state interaction in SIDIS

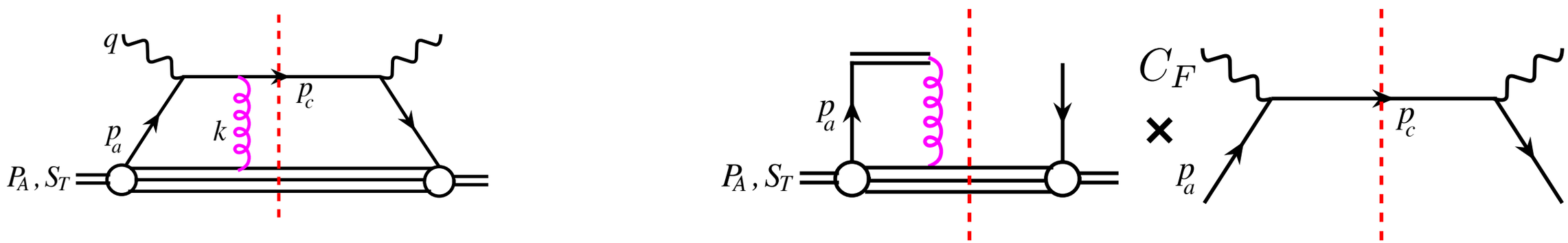

$$\bar{u}(p_c)(-ig)\gamma^- T^a \frac{i(\not{p}_c - \not{k})}{(p_c-k)^2+i\epsilon} \approx \bar{u}(p_c)\left[\frac{g}{-k^+ + i\epsilon}T^a\right] \quad \rightarrow -\bar{u}(p_c)T^a i\pi\delta(k^+)$$

and initial-state interaction in DY

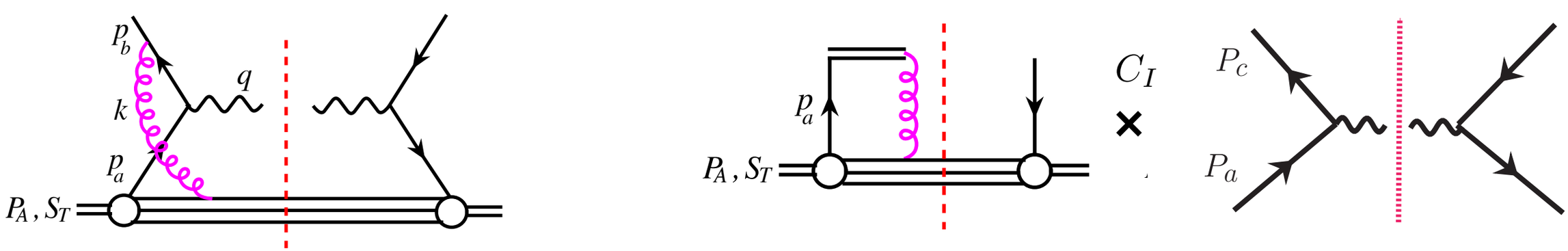

$$\bar{v}(p_b)(-ig)\gamma^- T^a \frac{-i(\not{p}_b + \not{k})}{(p_b+k)^2+i\epsilon} \approx \bar{v}(p_b)\left[\frac{g}{-k^+ - i\epsilon}T^a\right], \quad \rightarrow v(p_b)T^a i\pi\delta(k^+)$$

"Generalized Universality" Fund. Prediction of QCD Factorization

$$f_{1T\,sidis}^{\perp}(x,k_T) = -f_{1T\,DY}^{\perp}(x,k_T) \qquad p_T \sim \mathbf{k}_T << \sqrt{Q^2}$$

EIC conjunction with DY exp. E906-Fermi, RHIC II, Compass, JPARC

Process Dependence, Collins PLB 02, Brodsky et al. NPB 02, Boer Mulders Pijlman Bomhoff 03, 04 ...

$$d\sigma = L_{\mu\nu}\mathcal{W}^{\mu\nu} \Rightarrow$$

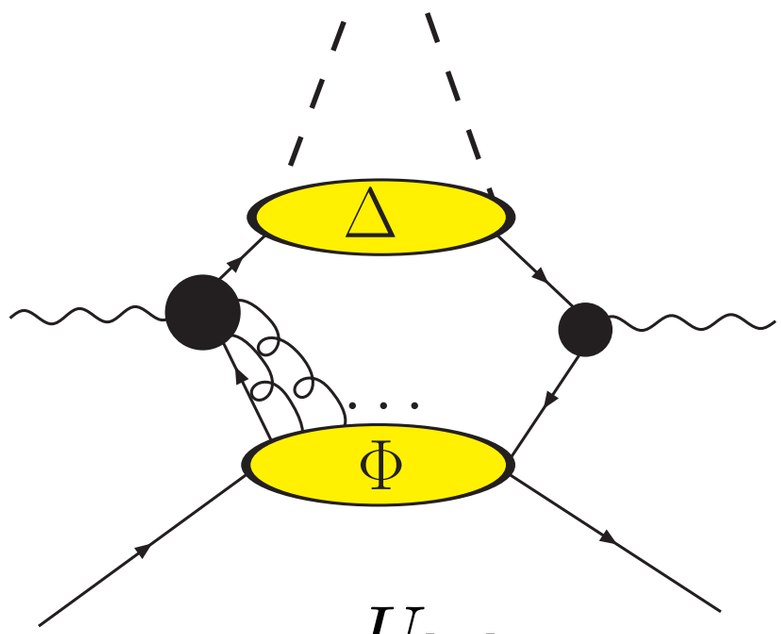

$U_{[+]}$

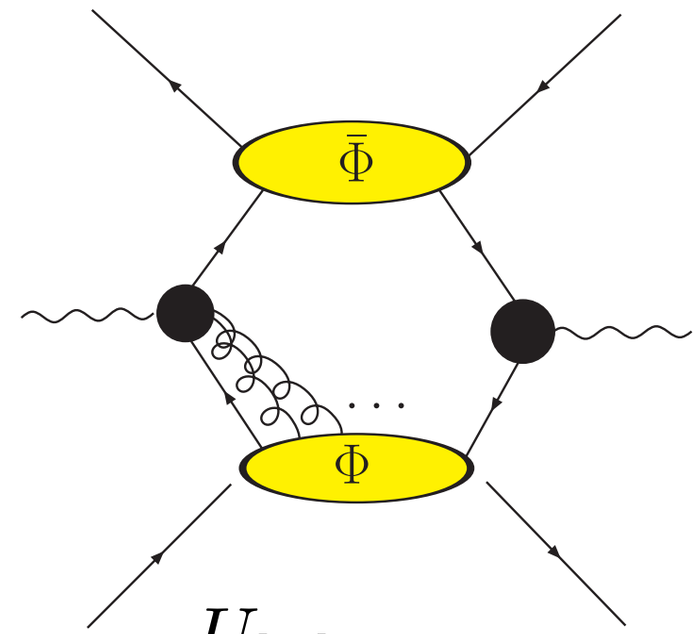

$U_{[-]}$

SIDIS

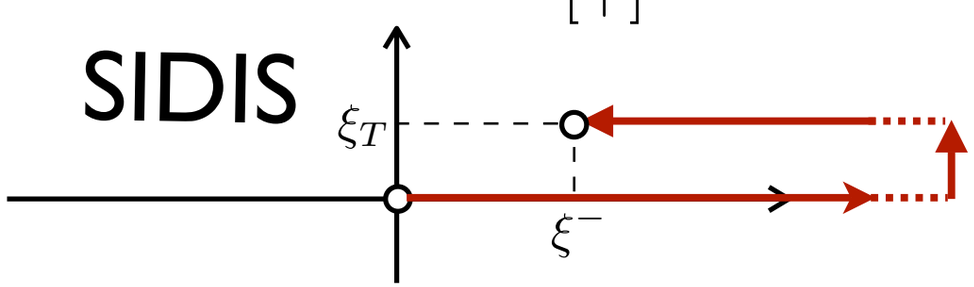

P&T

DY

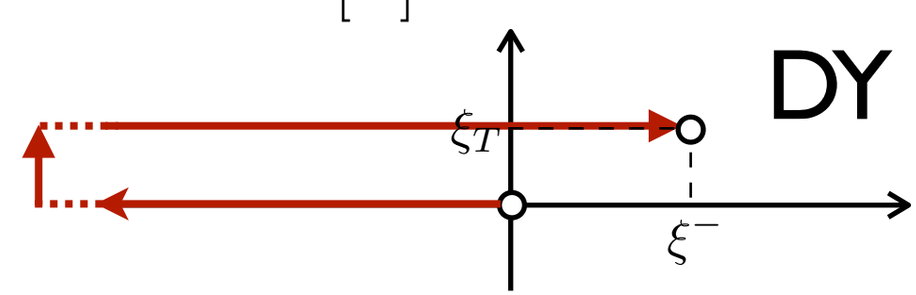

$$\Phi^{[+]*}(x,p_T) = i\gamma^1\gamma^3\Phi^{[-]}(x,p_T)i\gamma^1\gamma^3$$

{\em Model Assumptions}

- "WTIM" consider hadronic processes taking into account ISI/FSI in gen. parton model GPM
- Consider impact in three cases
  - Inclusive pion production at forward rapidity- Both Collins and Sivers can contribute
  - Direct photon - Sivers only, can be used to test sign change as in DY
  - Prompt Photon--?? Collins Contribution??

cont ...

Azimuthal asymmetric distribution of hadrons inside a high energy jet in transverse polarized nucleon-nucleon scattering

$$p^{\uparrow}\, p \longrightarrow h_1 \text{ jet } X$$

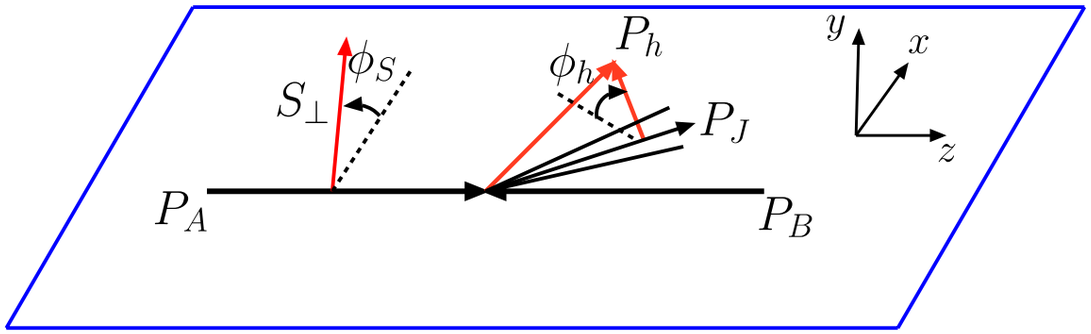

- Collins effect Yuan PRL 2008
- Pion about jet-Can disentangle Collins & Sivers
- w/o ISI/FSI- D'Alesio, Murgia, Pisano PRD10,
  w/ ISI/FSI- D'Alesio, LG, Kang, Murgia, Pisano w/ ISI/FSI-PLB 2011
  - Inclusive jet - Only Sivers, so can be used to test sign change as in DY

Caution !!! Comments

Similar studies performed for weighted k_T and unweighted

- photon Jet $p^{\uparrow}\, p \longrightarrow \gamma\, \mathrm{jet}\, X$ Bacchetta Bomhof, D'Alesio, Mulders, Murgia PRL 09
- 2-particle inclusive hadron production $p^{\uparrow}\, p \longrightarrow h_1\, h_2\, X$

Bacchetta Bomhof, Mulders, Piljman PRD05, Qiu Vogelsang Yuan PRD2007, Vogelsang Yuan PRD 2007

Merits "Pre-Collins Qiu Mulders Rogers" "PCQMR period"

1) two scale problem--TMD factorization

2) weighted submits to transverse moments leads to gluonic pole factors & gluonic pole matrix elements--connection to twist three formalism

Problems/Challenges-"post CQMR period"

Collins Qiu PRD 2007 & Mulders Rogers 2010

*) factorization violated cannot define even a generalized gauge link-color entangled

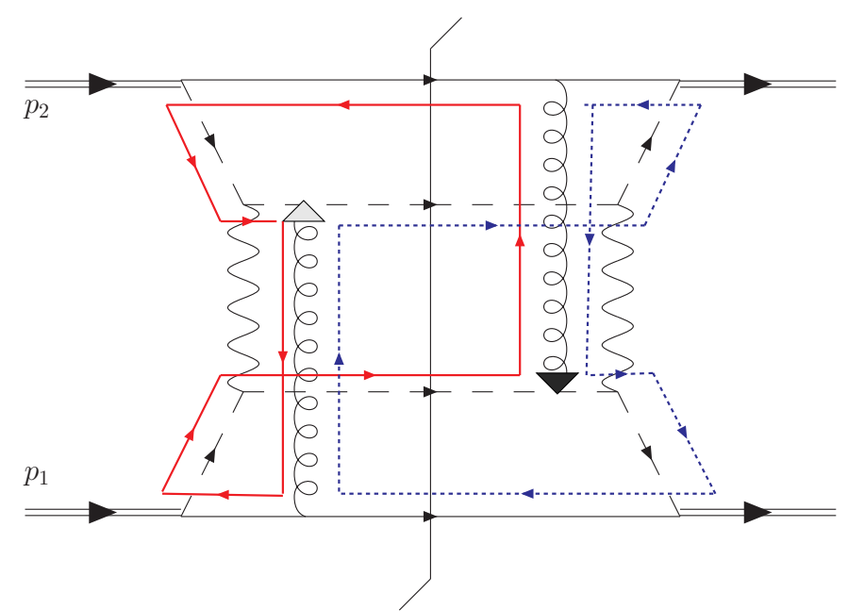

Generalizing the GPM CGI-GPM

- Feynman, Field, Fox (PRD 77 & 78)-incorporate intrinsic $\boldsymbol{k}_T$
- Include Transverse spin pol. w/ intrisic $\boldsymbol{k}_T$--Anselmino, Boglione, Murgia, ... et al. *PLB 95* & 98
- Pheno-Torino Cagliari group .... 1995-2012 inclusive processes
- Inclusive processes studied TW-3 formalism Kouvaris, Qiu, Vogelsang, Yuan PRD 2006, $pp \to \pi X$ & $pp \to \gamma X$
- What happens when you adopt ansatz of GPM including dynamical reaction mechanism of FSI/ISI in inclusive processes
- Take into account ISI/FSI process dependent Sivers function
- Since one scale, process-twist three is GPM connected w/twist 3 ? While we use $\boldsymbol{k}_T$ dependent TMDs we integrate over $\boldsymbol{k}_T$. Guides us to perform collinear expansion from GPM

Consider direct Photon in GPM

$$\Delta\sigma^{pp^{\uparrow}\to\gamma X} \sim \Delta f_a \otimes f_b \otimes \Delta\hat{\sigma}$$

Factorize w/ leading 1 gluon exchange get color phase

Vogelsang & Yuan PRD 2007 & agrees w/ "color flow" approach Bomhoff, Mulders, Pijlman 2006...

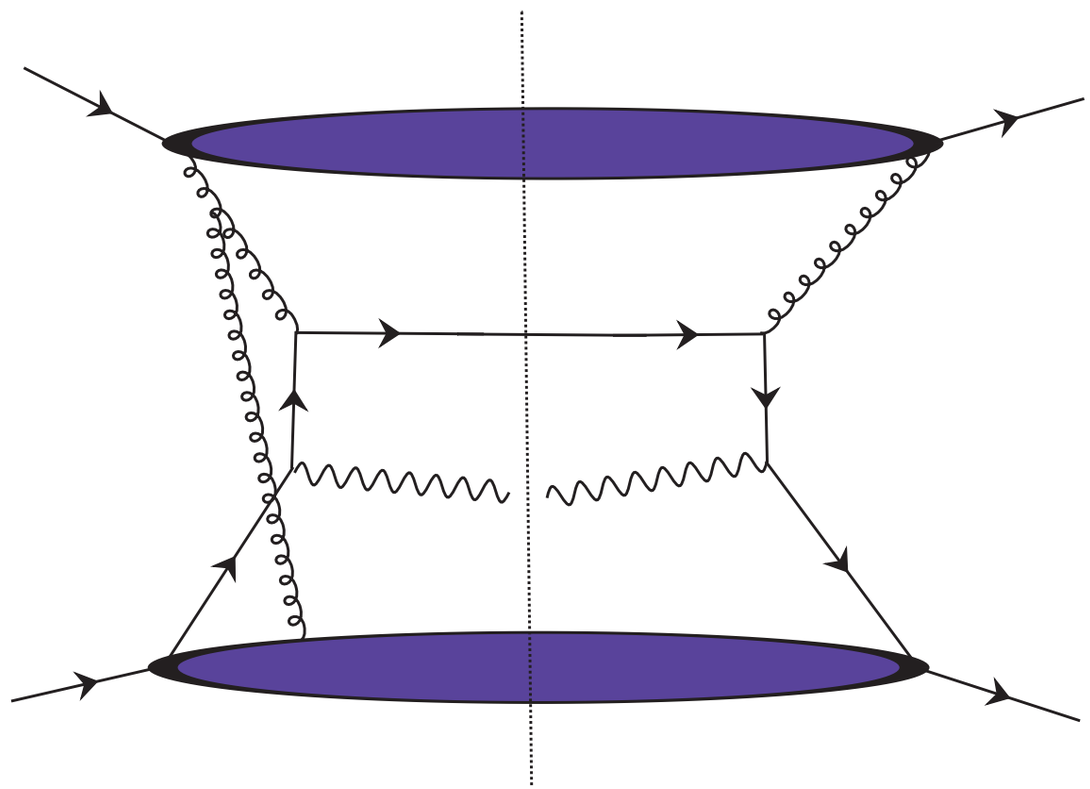

Method

- Use diagramatic rather than helicity approach
  Bacchetta Bomhoff Mulders Pijlman 2005 PRD
- Has advantage of directly connecting to matrix elements of quark and gluon fields
- Allows inclusion of effects of ISI/FSI to determine color structure

Spin Dependent Cross Section in GPM $pp \to \gamma X$

GPM Anselmino et al.

A_N is defined by the ratio $A_N = E_\gamma \frac{d\Delta\sigma}{d^3P_\gamma} \Big/ E_\gamma \frac{d\sigma}{d^3P_\gamma}.$

$$E_\gamma \frac{d\Delta\sigma}{d^3P_\gamma} = \frac{\alpha_{em}\alpha_s}{S} \sum_{a,b} \int \frac{dx_a}{x_a} d^2k_{aT} \Delta^N f^{\rm DIS}_{a/A}(x_a, k_{aT}) \frac{1}{2} S_A \cdot (\hat{P}_A \times \hat{k}_{aT})$$
$$\times \int \frac{dx_b}{x_b} d^2k_{bT} f_{b/B}(x_b, k_{bT}) H^U_{ab\to\gamma}(\hat{s}, \hat{t}, \hat{u}) \delta(\hat{s} + \hat{t} + \hat{u}).$$

$$f_{q/A^\uparrow}(x, \vec{k}_T) = f_{q/A}(x, k_T^2) + \tfrac{1}{2}\Delta^N f_{q/A^\uparrow}(x, k_T^2) \vec{S} \cdot (\hat{P} \times \vec{k}_T)$$

Observation

- Crucial point: Sivers function in inclusive single particle production contains both ISI and FSI
- Color factors entirely due to color structure of the partonic subprocess
- consider channel $qq' \to qq'$

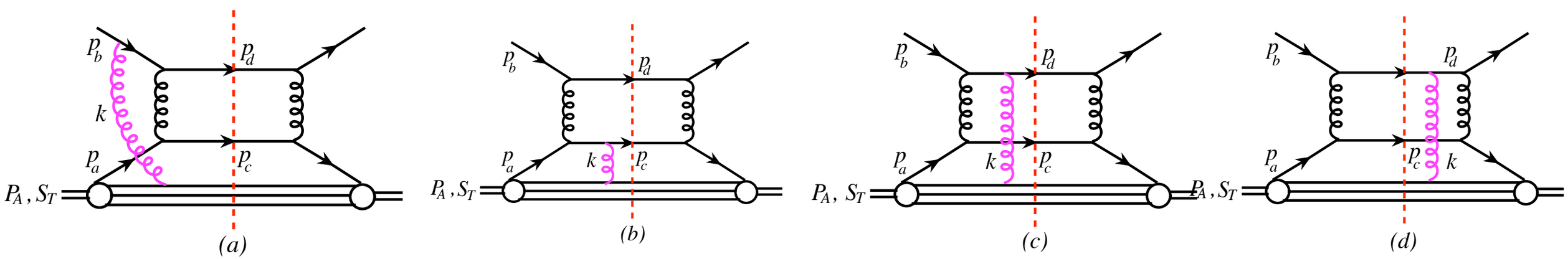

Consider direct Photon in GPM

GPM w/color
LG & Z. Kang
Phys.Lett. B696 2011

$$\Delta\sigma^{pp^\uparrow\to\gamma X} \sim \Delta f_a \otimes f_b \otimes \Delta\hat{\sigma}$$

Factorize w/ leading 1 gluon exchange get color phase

Vogelsang & Yuan PRD 2007 & agrees w/ "color flow" approach Bomhoff, Mulders, Pijlman

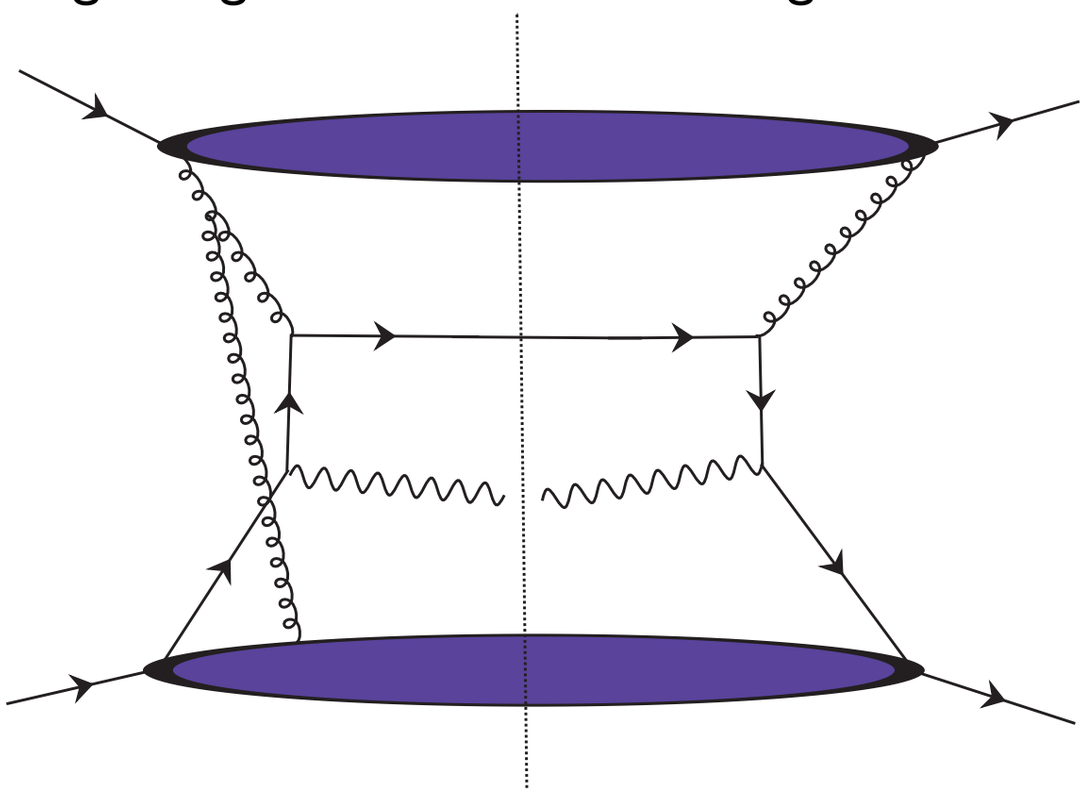

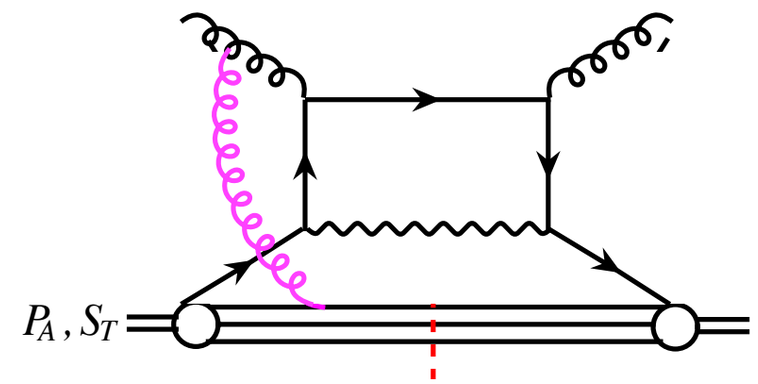

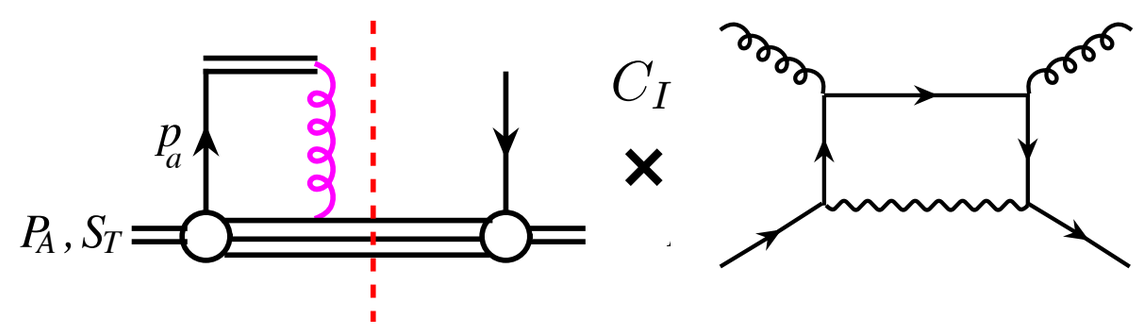

Get Sivers function for this process to use in GPM

Color modification of hard cross sections due to "phases"

$qg \to \gamma q$

t-channel

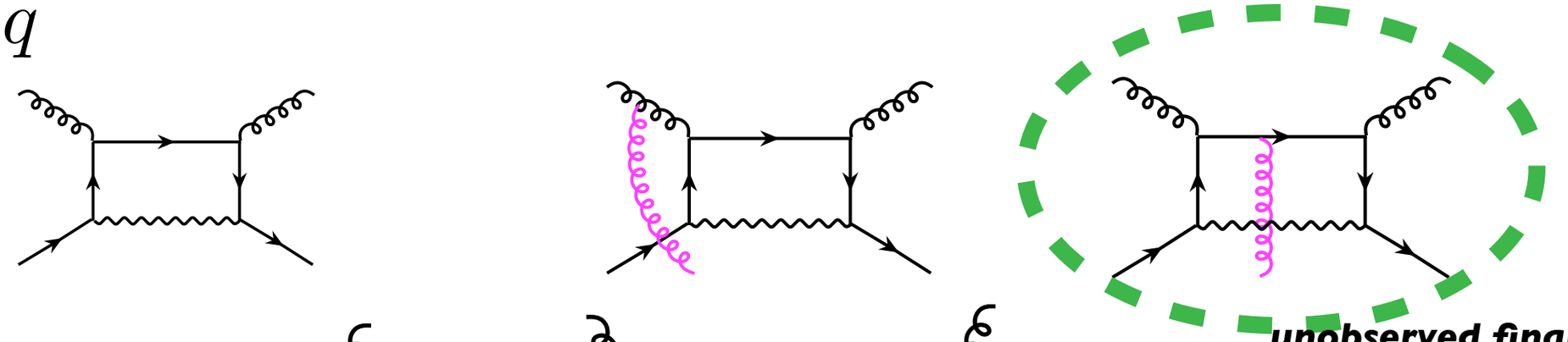

s-channel

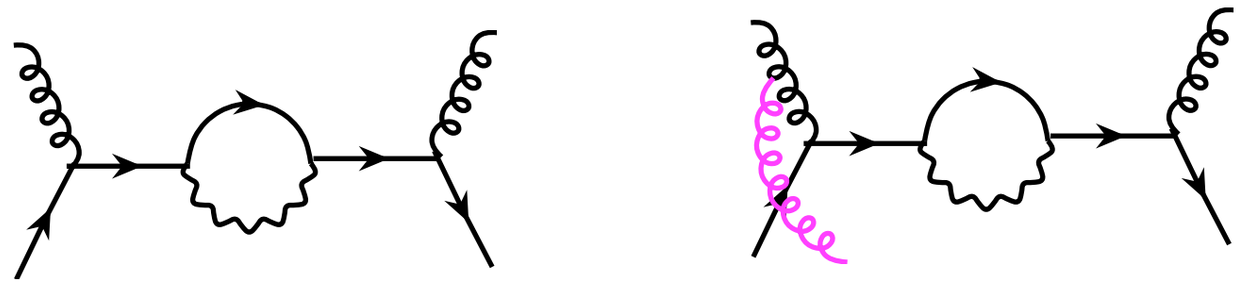

s-t interference

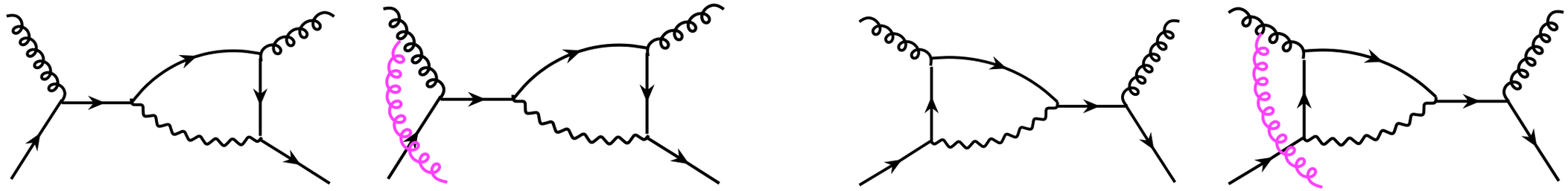

$\bar{q}q \to \gamma g$

t & u-channel

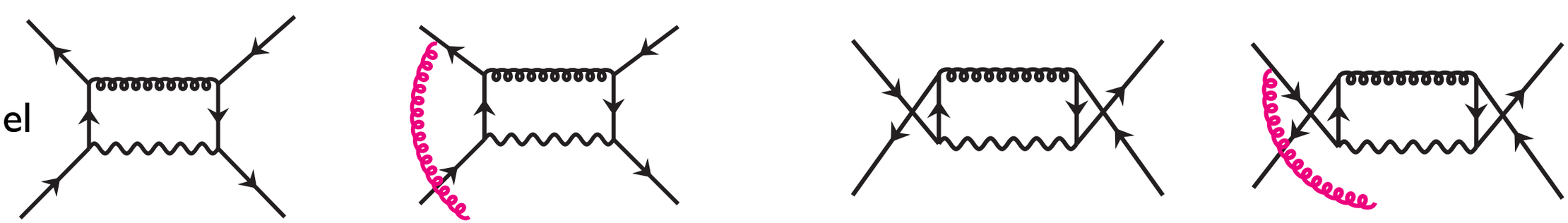

t-u interference

etc ....

Spin Dependent Cross Section in GPM $pp \to \gamma X$

$$f_{q/A^\uparrow}(x,\vec{k}_T) = f_{q/A}(x,k_T^2) + \frac{1}{2}\Delta^N f_{q/A^\uparrow}(x,k_T^2)\vec{S}\cdot(\hat{P}\times\vec{k}_T)$$

A_N is defined by the ratio $\quad A_N = E_\gamma \frac{d\Delta\sigma}{d^3P_\gamma}\Big/ E_\gamma \frac{d\sigma}{d^3P_\gamma}.$

$$E_\gamma \frac{d\Delta\sigma}{d^3P_\gamma} = \frac{\alpha_{em}\alpha_s}{S}\sum_{a,b}\int \frac{dx_a}{x_a} d^2k_{aT}\, \Delta^N f^{\rm DIS}_{a/A}(x_a,k_{aT})\frac{1}{2}S_A\cdot(\hat{P}_A\times\hat{k}_{aT})$$
$$\times \int \frac{dx_b}{x_b} d^2k_{bT} f_{b/B}(x_b,k_{bT}) H^U_{ab\to\gamma}(\hat{s},\hat{t},\hat{u})\delta(\hat{s}+\hat{t}+\hat{u}).$$

GPM Anselmino et al.

$$E_\gamma \frac{d\Delta\sigma}{d^3P_\gamma} = \frac{\alpha_{em}\alpha_s}{S}\sum_{a,b}\int \frac{dx_a}{x_a} d^2k_{aT}\, \Delta^N f^{ab\to\gamma}_{a/A}(x_a,k_{aT})\frac{1}{2}S_A\cdot(\hat{P}_A\times\hat{k}_{aT})$$
$$\times \int \frac{dx_b}{x_b} d^2k_{bT} f_{b/B}(x_b,k_{bT}) H_{ab\to\gamma}(\hat{s},\hat{t},\hat{u})\delta(\hat{s}+\hat{t}+\hat{u}),$$

GPM w/color
LG & Z. Kang
Phys.Lett. B696 2011

process-dependent Sivers function denoted as $\Delta^N f^{ab\to c}_{a/A}(x_a,k_{aT})$

Spin Dependent Cross Section in GPM $pp \to \pi X$

A_N is defined by the ratio $$A_N \equiv E_h \frac{d\Delta\sigma}{d^3P_h} \Big/ E_h \frac{d\sigma}{d^3P_h}.$$

$$E_h \frac{d\Delta\sigma}{d^3P_h} = \frac{\alpha_s^2}{S} \sum_{a,b,c} \int \frac{dx_a}{x_a} d^2k_{aT} \Delta^N f_{a/A}(x_a, k_{aT}) \frac{1}{2} S_A \cdot (\hat{P}_A \times \hat{k}_{aT}) \int \frac{dx_b}{x_b} d^2k_{bT} f_{b/B}(x_b, k_{bT})$$
$$\times \int \frac{dz_c}{z_c^2} D_{h/c}(z_c) H^U_{ab\to c}(\hat{s}, \hat{t}, \hat{u}) \delta(\hat{s} + \hat{t} + \hat{u}),$$

GPM Anselmino et al.

$$E_h \frac{d\Delta\sigma}{d^3P_h} = \frac{\alpha_s^2}{S} \sum_{a,b,c} \int \frac{dx_a}{x_a} d^2k_{aT} \Delta^N f^{ab\to c}_{a/A}(x_a, k_{aT}) \frac{1}{2} S_A \cdot (\hat{P}_A \times \hat{k}_{aT}) \int \frac{dx_b}{x_b} d^2k_{bT} f_{b/B}(x_b, k_{bT})$$
$$\times \int \frac{dz_c}{z_c^2} D_{h/c}(z_c) H^U_{ab\to c}(\hat{s}, \hat{t}, \hat{u}) \delta(\hat{s} + \hat{t} + \hat{u}),$$

process-dependent Sivers function denoted as $\Delta^N f^{ab\to c}_{a/A}(x_a, k_{aT})$

One gluon exchange approx for ISI and FSI

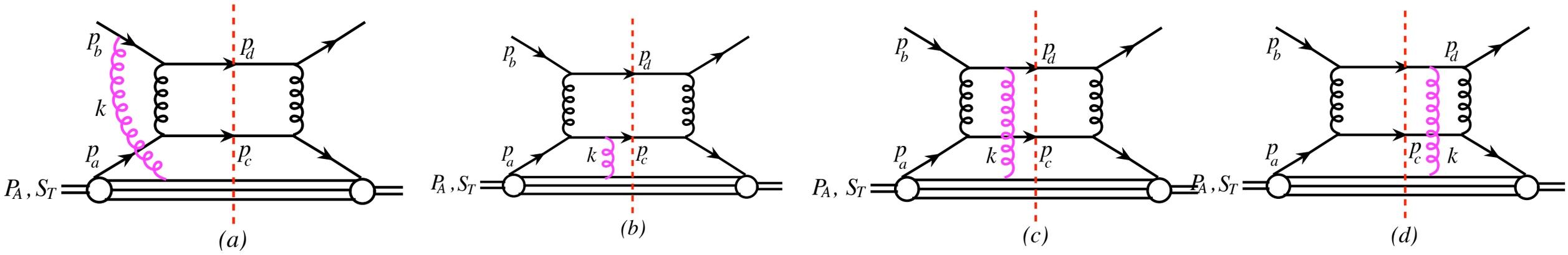

$$\left[\frac{-g}{-k^+ - i\epsilon}T^a\right] \qquad \left[\frac{g}{-k^+ + i\epsilon}T^a\right]$$

interaction w/unobserved particle "d" vanishes after summing over both cuts

$$\rightarrow C_I = -\frac{1}{2N_c^2}, \qquad \rightarrow C_{F_c} = -\frac{1}{4N_c^2},$$

calculate color factors

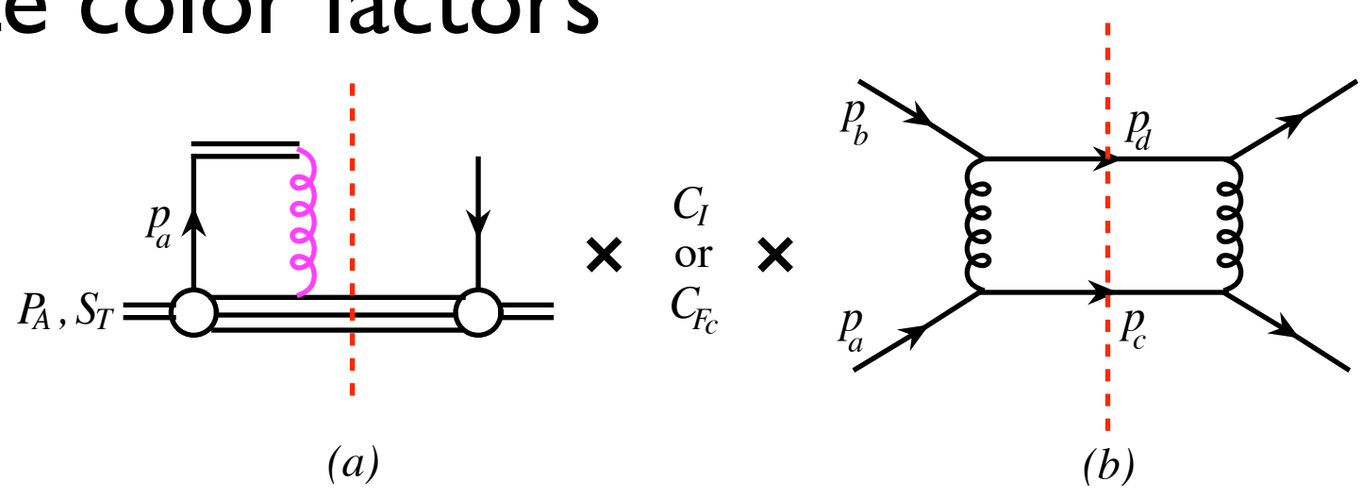

Note unpolarized color factor $$C_u = \frac{N_c^2 - 1}{4N_c^2}$$

Comparing imag. pt of eikonal propagators for subprocess in SIDIS and inclusive single particle production

Sivers function probed in $qq' \to qq'$ process is related to those in SIDIS

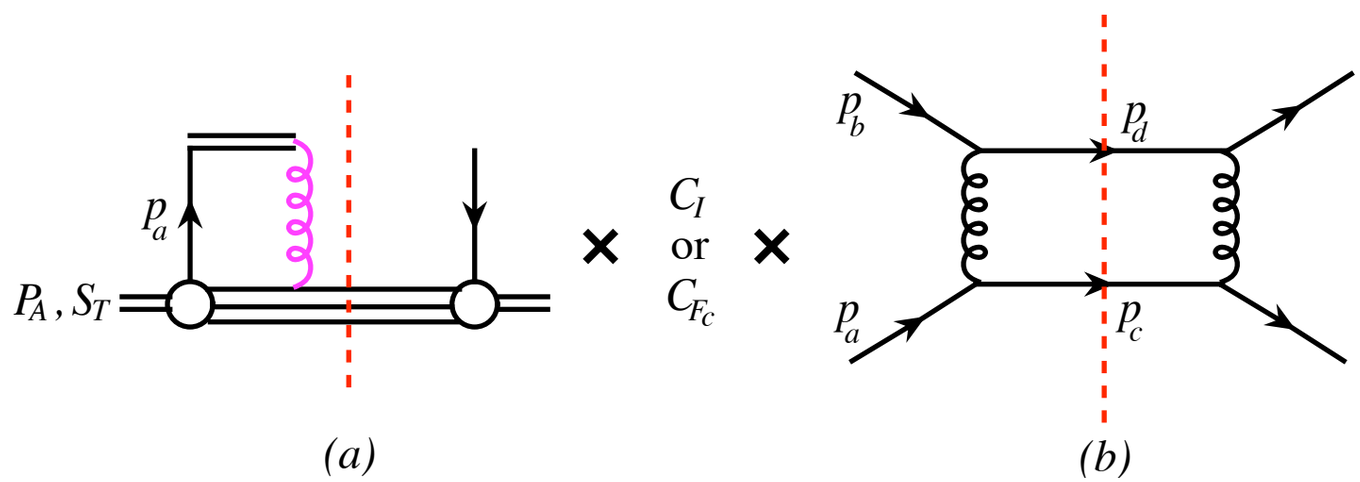

$$\Delta^N f_{a/A}^{qq' \to qq'} = \frac{C_I + C_{F_c}}{C_u} \Delta^N f_{a/A}^{\text{SIDIS}}.$$

Alternatively one can move color factors "process dependence" to hard parts

$$E_h \frac{d\Delta\sigma}{d^3P_h} = \frac{\alpha_s^2}{S} \sum_{a,b,c} \int \frac{dx_a}{x_a} d^2k_{aT} \Delta^N f_{a/A}^{ab\to c}(x_a, k_{aT}) \frac{1}{2} S_A \cdot (\hat{P}_A \times \hat{k}_{aT}) \int \frac{dx_b}{x_b} d^2k_{bT} f_{b/B}(x_b, k_{bT})$$
$$\times \int \frac{dz_c}{z_c^2} D_{h/c}(z_c) H_{ab\to c}^{U}(\hat{s}, \hat{t}, \hat{u}) \delta(\hat{s} + \hat{t} + \hat{u}),$$

$$E_h \frac{d\Delta\sigma}{d^3P_h} = \frac{\alpha_s^2}{S} \sum_{a,b,c} \int \frac{dx_a}{x_a} d^2k_{aT} \Delta^N f_{a/A}^{\mathrm{SIDIS}}(x_a, k_{aT}) \frac{1}{2} S_A \cdot (\hat{P}_A \times \hat{k}_{aT}) \int \frac{dx_b}{x_b} d^2k_{bT} f_{b/B}(x_b, k_{bT})$$
$$\times \int \frac{dz_c}{z_c^2} D_{h/c}(z_c) H_{ab\to c}^{\mathrm{Inc}}(\hat{s}, \hat{t}, \hat{u}) \delta(\hat{s} + \hat{t} + \hat{u}),$$

In spirit of twist 3 approach, color factors from hard part

In spirit of twist 3 approach

That is rearrange

$$\Delta^N f_{a/A}^{qq'\to qq'} H^U_{qq'\to qq'} = \frac{C_I + C_{F_c}}{C_u} \Delta^N f_{a/A}^{\rm SIDIS} H^U_{qq'\to qq'} = \Delta^N f_{a/A}^{\rm SIDIS} \left[C_I h_{qq'\to qq'} + C_{F_c} h_{qq'\to qq'} \right]$$

where hard partonic c.s. w/o color factors

$$h_{qq'\to qq'} = 2\frac{\hat{s}^2 + \hat{u}^2}{\hat{t}^2}.$$

Then "modified" GPM is

$$E_h \frac{d\Delta\sigma}{d^3P_h} = \frac{\alpha_s^2}{S} \sum_{a,b,c} \int \frac{dx_a}{x_a} d^2k_{aT} \Delta^N f_{a/A}^{\rm SIDIS}(x_a, k_{aT}) \frac{1}{2} S_A \cdot (\hat{P}_A \times \hat{k}_{aT}) \int \frac{dx_b}{x_b} d^2k_{bT} f_{b/B}(x_b, k_{bT})$$
$$\times \int \frac{dz_c}{z_c^2} D_{h/c}(z_c) H_{ab\to c}^{\rm Inc}(\hat{s}, \hat{t}, \hat{u}) \delta(\hat{s} + \hat{t} + \hat{u}),$$

$$H_{qq'\to qq'}^{\rm Inc} \equiv H_{qq'\to qq'}^{\rm Inc-I} + H_{qq'\to qq'}^{\rm Inc-F},$$

where,

$$H_{qq'\to qq'}^{\rm Inc-I} = C_I h_{qq'\to qq'}, \qquad H_{qq'\to qq'}^{\rm Inc-F} = C_{F_c} h_{qq'\to qq'}$$

The contributions for $pp \to \pi X$

the various contributing partonic subprocesses are given by

$$H^{\rm Inc-I}_{qq'\to qq'} = -H^{\rm Inc-I}_{\bar q\bar q'\to \bar q\bar q'} = -\frac{1}{N_c^2}\left[\frac{\hat s^2+\hat u^2}{\hat t^2}\right]$$

$$H^{\rm Inc-F}_{qq'\to qq'} = -H^{\rm Inc-F}_{\bar q\bar q'\to \bar q\bar q'} = -\frac{1}{2N_c^2}\left[\frac{\hat s^2+\hat u^2}{\hat t^2}\right]$$

$$H^{\rm Inc-I}_{q\bar q'\to q\bar q'} = -H^{\rm Inc-I}_{\bar q q'\to \bar q q'} = -\frac{N_c^2-2}{2N_c^2}\left[\frac{\hat s^2+\hat u^2}{\hat t^2}\right]$$

$$H^{\rm Inc-F}_{q\bar q'\to q\bar q'} = -H^{\rm Inc-F}_{\bar q q'\to \bar q q'} = -\frac{1}{2N_c^2}\left[\frac{\hat s^2+\hat u^2}{\hat t^2}\right]$$

$$H^{\rm Inc-I}_{qq'\to q'q} = -H^{\rm Inc-I}_{\bar q\bar q'\to \bar q'\bar q} = -\frac{1}{N_c^2}\left[\frac{\hat s^2+\hat t^2}{\hat u^2}\right]$$

$$H^{\rm Inc-F}_{qq'\to q'q} = -H^{\rm Inc-F}_{\bar q\bar q'\to \bar q'\bar q} = \frac{N_c^2-2}{2N_c^2}\left[\frac{\hat s^2+\hat t^2}{\hat u^2}\right]$$

$$H^{\rm Inc-I}_{q\bar q'\to \bar q' q} = -H^{\rm Inc-I}_{\bar q q'\to q'\bar q} = -\frac{N_c^2-2}{2N_c^2}\left[\frac{\hat s^2+\hat t^2}{\hat u^2}\right]$$

$$H^{\rm Inc-F}_{q\bar q'\to \bar q' q} = = -H^{\rm Inc-F}_{\bar q q'\to q'\bar q} = \frac{1}{N_c^2}\left[\frac{\hat s^2+\hat t^2}{\hat u^2}\right]$$

$$H^{\rm Inc-I}_{qq\to qq} = -H^{\rm Inc-I}_{\bar q\bar q\to \bar q\bar q} = -\frac{1}{N_c^2}\left[\frac{\hat s^2+\hat u^2}{\hat t^2}+\frac{\hat s^2+\hat t^2}{\hat u^2}\right]+\frac{N_c^2+1}{N_c^3}\frac{\hat s^2}{\hat t\hat u}$$

$$H^{\rm Inc-F}_{qq\to qq} = -H^{\rm Inc-F}_{\bar q\bar q\to \bar q\bar q} = -\frac{1}{2N_c^2}\left[\frac{\hat s^2+\hat u^2}{\hat t^2}\right]+\frac{N_c^2-2}{2N_c^2}\left[\frac{\hat s^2+\hat t^2}{\hat u^2}\right]+\frac{1}{N_c^3}\frac{\hat s^2}{\hat t\hat u}$$

$$H^{\rm Inc-I}_{q\bar q\to q'\bar q'} = -H^{\rm Inc-I}_{\bar q q\to \bar q' q'} = \frac{1}{2N_c^2}\left[\frac{\hat t^2+\hat u^2}{\hat s^2}\right]$$

$$H^{\rm Inc-F}_{q\bar q\to q'\bar q'} = -H^{\rm Inc-F}_{\bar q q\to \bar q' q'} = \frac{N_c^2-2}{2N_c^2}\left[\frac{\hat t^2+\hat u^2}{\hat s^2}\right]$$

$$H^{\rm Inc-I}_{q\bar q\to \bar q' q'} = -H^{\rm Inc-I}_{\bar q q\to q'\bar q'} = \frac{1}{2N_c^2}\left[\frac{\hat t^2+\hat u^2}{\hat s^2}\right]$$

$$H^{\rm Inc-F}_{q\bar q\to \bar q' q'} = -H^{\rm Inc-F}_{\bar q q\to q'\bar q'} = \frac{1}{N_c^2}\left[\frac{\hat t^2+\hat u^2}{\hat s^2}\right]$$

$$H^{\rm Inc-I}_{q\bar q\to q\bar q} = -H^{\rm Inc-I}_{\bar q q\to \bar q q} = -\frac{N_c^2-2}{2N_c^2}\left[\frac{\hat s^2+\hat u^2}{\hat t^2}\right]+\frac{1}{2N_c^2}\left[\frac{\hat t^2+\hat u^2}{\hat s^2}\right]-\frac{1}{N_c^3}\frac{\hat u^2}{\hat s\hat t}$$

$$H^{\rm Inc-F}_{q\bar q\to q\bar q} = -H^{\rm Inc-F}_{\bar q q\to \bar q q} = -\frac{1}{2N_c^2}\left[\frac{\hat s^2+\hat u^2}{\hat t^2}\right]+\frac{N_c^2-2}{2N_c^2}\left[\frac{\hat t^2+\hat u^2}{\hat s^2}\right]+\frac{1}{N_c^3}\frac{\hat u^2}{\hat s\hat t}$$

$$H^{\rm Inc-I}_{q\bar q\to \bar q q} = -H^{\rm Inc-I}_{\bar q q\to q\bar q} = -\frac{N_c^2-2}{2N_c^2}\left[\frac{\hat s^2+\hat t^2}{\hat u^2}\right]+\frac{1}{2N_c^2}\left[\frac{\hat t^2+\hat u^2}{\hat s^2}\right]-\frac{1}{N_c^3}\frac{\hat t^2}{\hat s\hat u}$$

$$H^{\rm Inc-F}_{q\bar q\to \bar q q} = -H^{\rm Inc-F}_{\bar q q\to q\bar q} = \frac{1}{N_c^2}\left[\frac{\hat s^2+\hat t^2}{\hat u^2}+\frac{\hat t^2+\hat u^2}{\hat s^2}\right]-\frac{N_c^2+1}{N_c^3}\frac{\hat t^2}{\hat s\hat u}$$

$$H^{\rm Inc-I}_{qg\to qg} = -H^{\rm Inc-I}_{\bar q g\to \bar q g} = \frac{1}{2(N_c^2-1)}\left[-\frac{\hat s}{\hat u}-\frac{\hat u}{\hat s}\right]+\frac{N_c^2}{2(N_c^2-1)}\left[\frac{\hat s^2+\hat u^2}{\hat t^2}\frac{\hat u}{\hat s}\right]$$

$$H^{\rm Inc-F}_{qg\to qg} = -H^{\rm Inc-F}_{\bar q g\to \bar q g} = \frac{1}{2N_c^2(N_c^2-1)}\left[-\frac{\hat s}{\hat u}-\frac{\hat u}{\hat s}\right]-\frac{1}{N_c^2-1}\left[\frac{\hat s^2+\hat u^2}{\hat t^2}\right]$$

$$H^{\rm Inc-I}_{qg\to gq} = -H^{\rm Inc-I}_{\bar q g\to g\bar q} = \frac{1}{2(N_c^2-1)}\left[-\frac{\hat s}{\hat t}-\frac{\hat t}{\hat s}\right]+\frac{N_c^2}{2(N_c^2-1)}\left[\frac{\hat s^2+\hat t^2}{\hat u^2}\frac{\hat t}{\hat s}\right]$$

$$H^{\rm Inc-F}_{qg\to gq} = -H^{\rm Inc-F}_{\bar q g\to g\bar q} = -\frac{1}{2(N_c^2-1)}\left[-\frac{\hat s}{\hat t}-\frac{\hat t}{\hat s}\right]-\frac{N_c^2}{2(N_c^2-1)}\left[\frac{\hat s^2+\hat t^2}{\hat u^2}\frac{\hat s}{\hat t}\right]$$

$$H^{\rm Inc-I}_{q\bar q\to gg} = -H^{\rm Inc-I}_{\bar q q\to gg} = -\frac{1}{2N_c^3}\left[\frac{\hat u}{\hat t}+\frac{\hat t}{\hat u}\right]-\frac{1}{N_c}\left[\frac{\hat t^2+\hat u^2}{\hat s^2}\right]$$

$$H^{\rm Inc-F}_{q\bar q\to gg} = -H^{\rm Inc-F}_{\bar q q\to gg} = -\frac{1}{2N_c}\left[\frac{\hat u}{\hat t}+\frac{\hat t}{\hat u}\right]+\frac{N_c}{2}\left[\frac{\hat t^2+\hat u^2}{\hat s^2}\frac{\hat u}{\hat t}\right]$$

Based on old parameterization

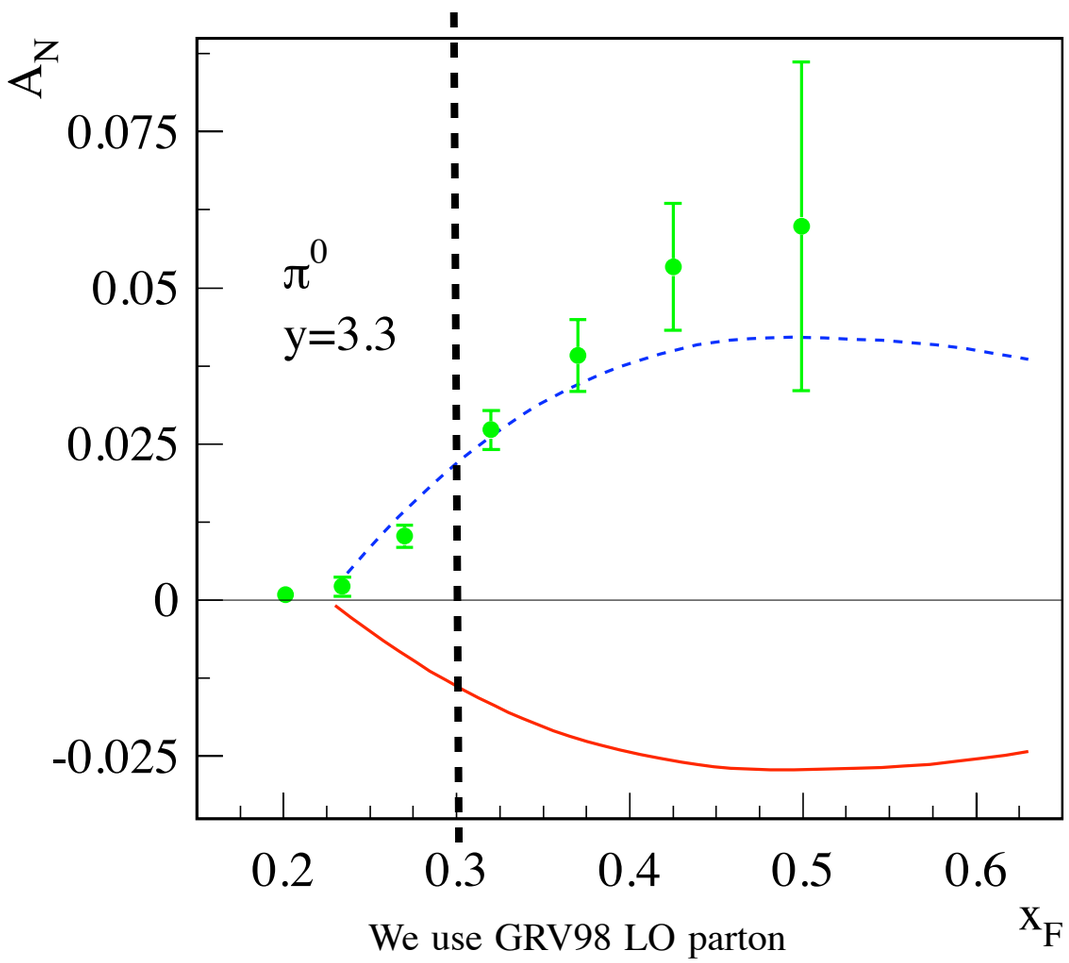

Sivers from Anselmino et al PRD72 (2005)
Fragmentation from Kretzer PRD62 (2000)

Based on new parameterization

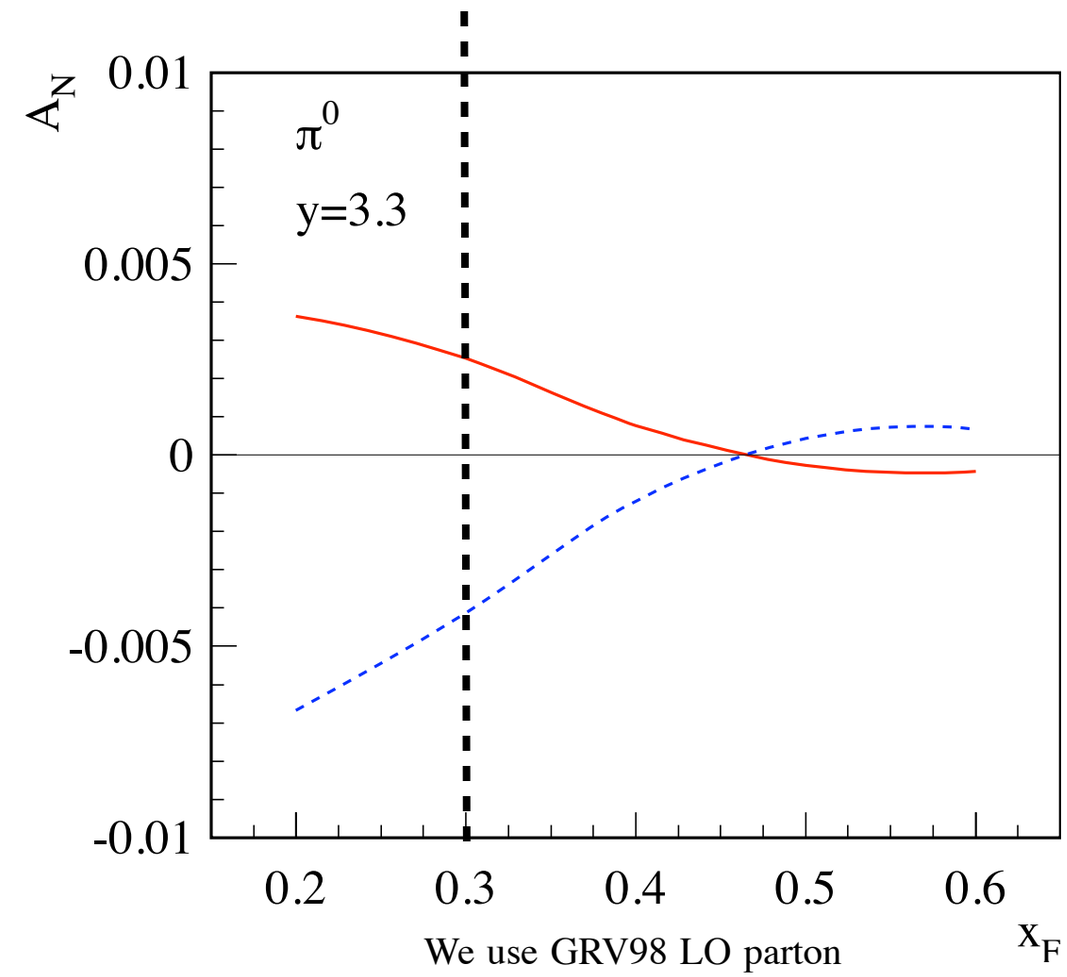

Sivers from Anselmino et al EPJA (2009)
Fragmentation from DSS PRD75 (2007)

$$H^{\rm Inc}_{qg\to qg} = H^{\rm Inc\text{-}I}_{qg\to qg} + H^{\rm Inc\text{-}F}_{qg\to qg} = -\frac{N_c^2+2}{N_c^2-1}\frac{\hat{s}^2}{\hat{t}^2},$$

vs.

forward direction, $\hat{t}$ is small, while $\hat{u} \sim -\hat{s}$,

$$H^{U}_{qg\to qg} = \frac{2\hat{s}^2}{\hat{t}^2}.$$

Model for PDFs

- unpolarized PDFs: $f_1^q(x, k_\perp^2) = f_1^q(x) g(k_\perp)$

- Sivers function: $\Delta^N f_{q/h^\uparrow}(x, k_\perp) = 2\mathcal{N}_q(x) f_1^q(x) h(k_\perp) g(k_\perp)$

$\mathcal{N}_q(x)$ is a fitted function

$$g(k_\perp) = \frac{1}{\pi \langle k_\perp^2 \rangle} e^{-k_\perp^2/\langle k_\perp^2 \rangle}$$

old Sivers: $$h(k_\perp) = \frac{2 k_\perp M_0}{k_\perp^2 + M_0^2}$$ Anselmino, et.al, 2005

new Sivers: $$h(k_\perp) = \sqrt{2e}\, \frac{k_\perp}{M_1} e^{-k_\perp^2/M_1^2}$$ Anselmino, et.al, 2009

Based on old parameterization

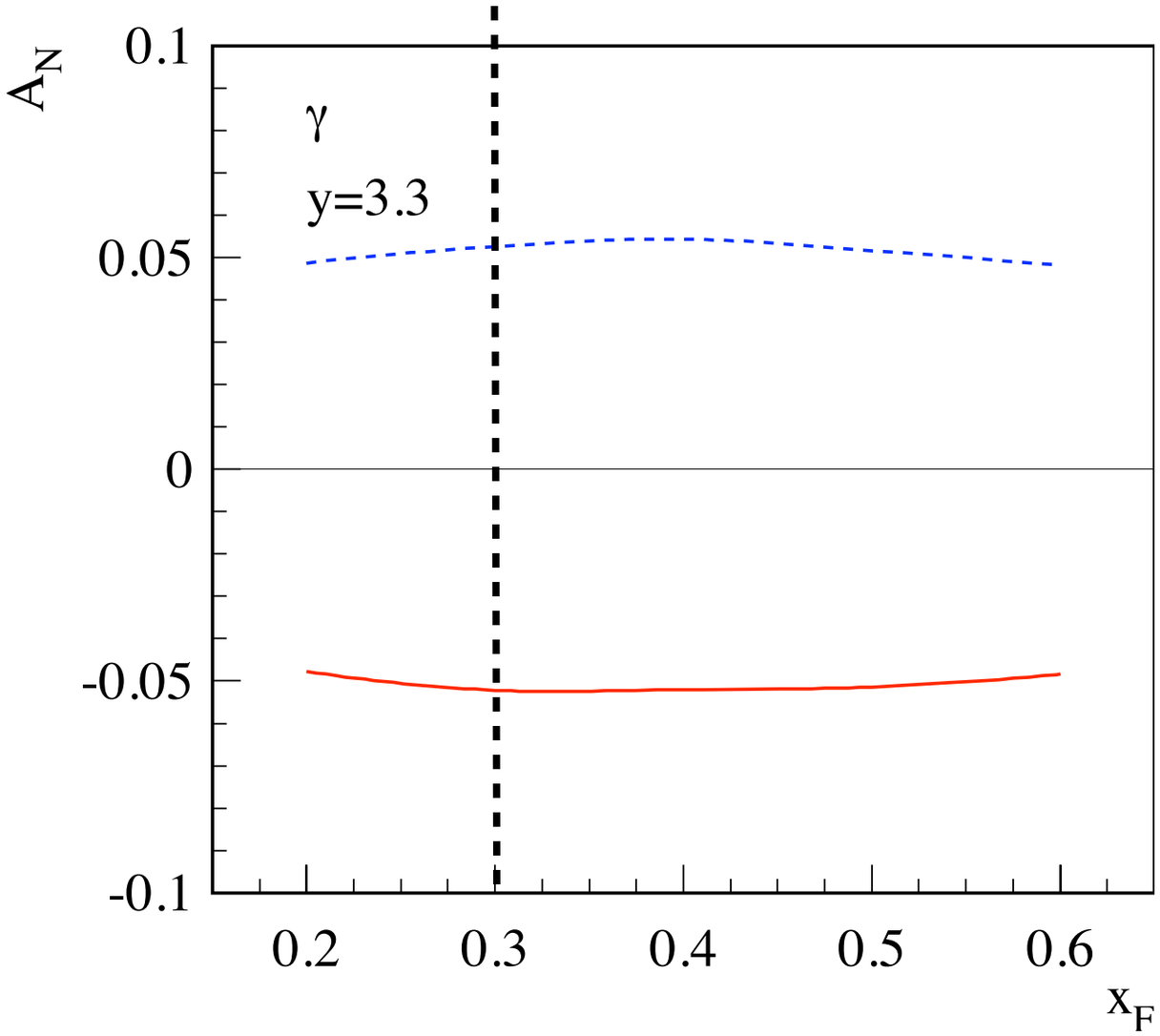

We use GRV98 LO parton

Sivers from Anselmino et al PRD72 (2005)
Fragmentation from Kretzer PRD62 (2000)

Based on new parameterization

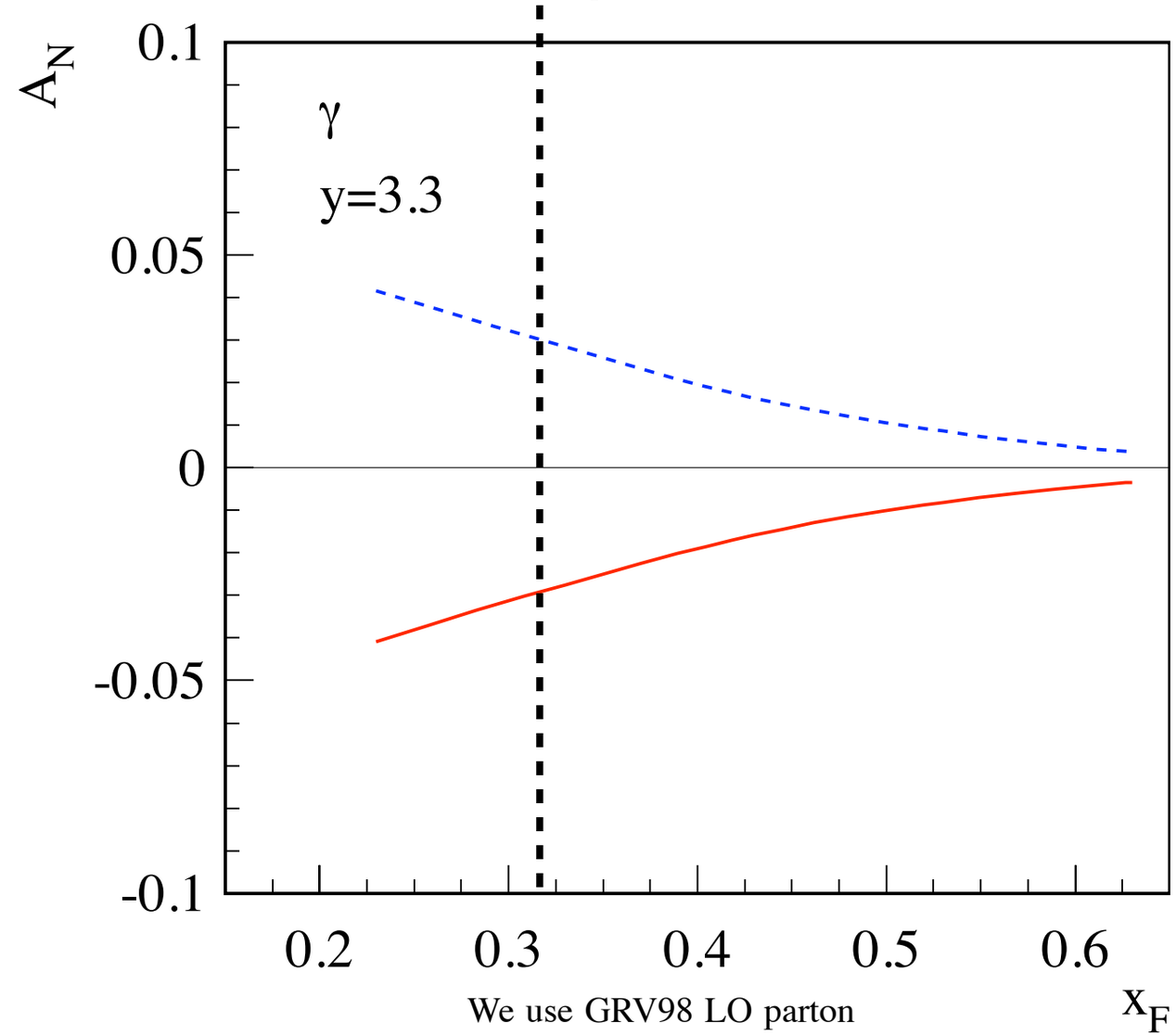

We use GRV98 LO parton

Sivers from Anselmino et al EPJA (2009)
Fragmentation from DSS PRD75 (2007)

$$H^U_{qg\to\gamma q} = \frac{1}{N_c} e_q^2 \left[-\frac{\hat{t}}{\hat{s}} - \frac{\hat{s}}{\hat{t}} \right]$$

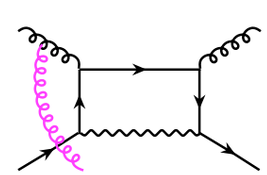

ISI drives result

$$H^{\rm Inc}_{qg\to\gamma q} = -\frac{N_c}{N_c^2-1} e_q^2 \left[-\frac{\hat{t}}{\hat{s}} - \frac{\hat{s}}{\hat{t}} \right]$$

Observations

- Hard amplitudes squared have same form in Mandelstam variables as twist-3 $\hat{s},\ \hat{t},\ \hat{u}$

  see Kouvaris, Qiu , Vogelsang, and Yuan PRD 2006

- However $\hat{s},\ \hat{t},\ \hat{u}$ depend on k_T in GPM whereas in twist-3 approach there has been collinear expansion on hard and soft factors

- We have shown that GPM expanded with respect to k_T results in twist-3 result {\em almost }

Collinear Expansion in GPM

- Here $\hat{s}, \hat{t}, \hat{u}$ depend on k_{aT}
- Delta function $\delta(\hat{s}+\hat{t}+\hat{u}) = \frac{1}{x_b S + T/z_c}\delta\left(x_a - x - \frac{2P_{hT}\cdot k_{aT}}{z_c x_b S + T}\right)$
- Expand in k_{aT} and study contribution from Sivers function and hard cross section

$$E_\gamma \frac{d\Delta\sigma}{d^3P_\gamma} = \frac{\alpha_{em}\alpha_s}{s}\sum_{abc}\int d^2k_{aT}\frac{\epsilon^{\alpha S_T n\hat{n}}}{M}k_{aT\alpha}\frac{1}{x_a}f_{1T}^{\perp\,\mathrm{SIDIS}}(x_a,k_{aT}^2)$$
$$\times\int\frac{dx_b}{x_b}f_{b/B}(x_b)\int\frac{dz_c}{z_c^2}H^{\mathrm{Inc}}_{ab\to c}(\hat{s},\hat{t},\hat{u})\frac{1}{x_b s + T/z_c}\Bigg|_{x_a = x + \frac{2P_{hT}\cdot k_{aT}}{z_c x_b S + T}}$$

Details: "collinear expansion" in GPM and keep linear in k_{aT}

$$\hat{s} = (p_a + p_b)^2 = x_a x_b S + \quad \mathcal{O}(k_T^2)$$

$$\hat{t} = (x_a P_A + k_{aT} - \frac{P_h}{z})^2 = \frac{x_a}{z} T - \frac{2P_{hT} \cdot k_{aT}}{z}$$

$$\hat{u} = (p_b - p_c)^2 = (x_b P_B - \frac{P_h}{z})^2 = \frac{x_b}{z} U$$

$$\delta(\hat{s} + \hat{t} + \hat{u}) = \frac{1}{x_b s + \frac{T}{z_c}} \delta(x_a - x - \frac{2P_{hT} \cdot k_{aT}}{x_b s + \frac{T}{z_c}})$$

$$x = -x_b U / (z_c x_b S + T)$$

Collinear twist three

$$E_h \frac{d\Delta\sigma^{(a)}}{d^3P_h} = \frac{\alpha_s^2}{S} \sum_{a,b,c} \int \frac{dz_c}{z_c^2} D_{h/c}(z_c) \frac{\epsilon^{P_{hT} S_A n \bar{n}}}{z_c \tilde{u}} \frac{1}{x} \left[T_{a,F}(x,x) - x \frac{d}{dx} T_{a,F}(x,x) \right] \int \frac{dx_b}{x_b} f_{b/B}(x_b) H^{\text{Inc}}_{ab\to c}(\tilde{s},\tilde{t},\tilde{u}) \frac{1}{x_b S + T/z_c}$$

Almost same as Kouvaris, Qiu, Vogelsang, and Yuan PRD 2006

$$H^{\text{Inc}}_{ab\to c}(\hat{s},\hat{t},\hat{u}) = H^{\text{Inc-I}}_{ab\to c}(\hat{s},\hat{t},\hat{u}) + H^{\text{Inc-F}}_{ab\to c}(\hat{s},\hat{t},\hat{u}), \qquad \text{CGI GPM}$$

$$H^{\text{twist-3}}_{ab\to c}(\hat{s},\hat{t},\hat{u}) = H^{\text{twist-3-I}}_{ab\to c}(\hat{s},\hat{t},\hat{u}) + H^{\text{twist-3-F}}_{ab\to c}(\hat{s},\hat{t},\hat{u}) \left(1 + \frac{\hat{u}}{\hat{t}}\right) \qquad \text{Kouvaris et al.}$$

N.B. *Difference here due to using eikonal approx. on for both ISI and FSI*

- Another term from k_{aT}-dependence from $H^{\rm Inc}_{ab\to c}(\hat{s},\hat{t},\hat{u})$

Thus to the leading order (linear in k_{aT} terms),

$$E_h\frac{d\Delta\sigma}{d^3P_h} = E_h\frac{d\Delta\sigma^{(a)}}{d^3P_h} + E_h\frac{\overset{\text{small}}{d\Delta\sigma^{(b)}}}{d^3P_h},$$

$$E_h\frac{d\Delta\sigma^{(a)}}{d^3P_h} = \frac{\alpha_s^2}{S}\sum_{a,b,c}\int\frac{dz_c}{z_c^2}D_{h/c}(z_c)\frac{\epsilon^{P_{hT}S_A n\bar{n}}}{z_c\tilde{u}}\frac{1}{x}\Big[\overset{\text{small}}{T_{a,F}(x,x)} - x\frac{d}{dx}T_{a,F}(x,x)\Big]\int\frac{dx_b}{x_b}f_{b/B}(x_b)H^{\rm Inc}_{ab\to c}(\tilde{s},\tilde{t},\tilde{u})\frac{1}{x_bS+T/z_c}$$

$$E_h\frac{d\Delta\sigma^{(b)}}{d^3P_h} = \frac{\alpha_s^2}{S}\sum_{a,b,c}\int\frac{dz_c}{z_c^2}D_{h/c}(z_c)\frac{\epsilon^{P_{hT}S_A n\bar{n}}}{z_c\tilde{u}}\frac{1}{x}\overset{\text{small}}{T_{a,F}(x,x)}\int\frac{dx_b}{x_b}f_{b/B}(x_b)\Big[-\tilde{s}\frac{\partial}{\partial\tilde{s}}H^{\rm Inc}_{ab\to c}(\tilde{s},-\tilde{s}-\tilde{u},\tilde{u})\Big]\frac{1}{x_bS+T/z_c}$$

Numerical Comparison of CGI-GPM and ETQS--Direct Photon

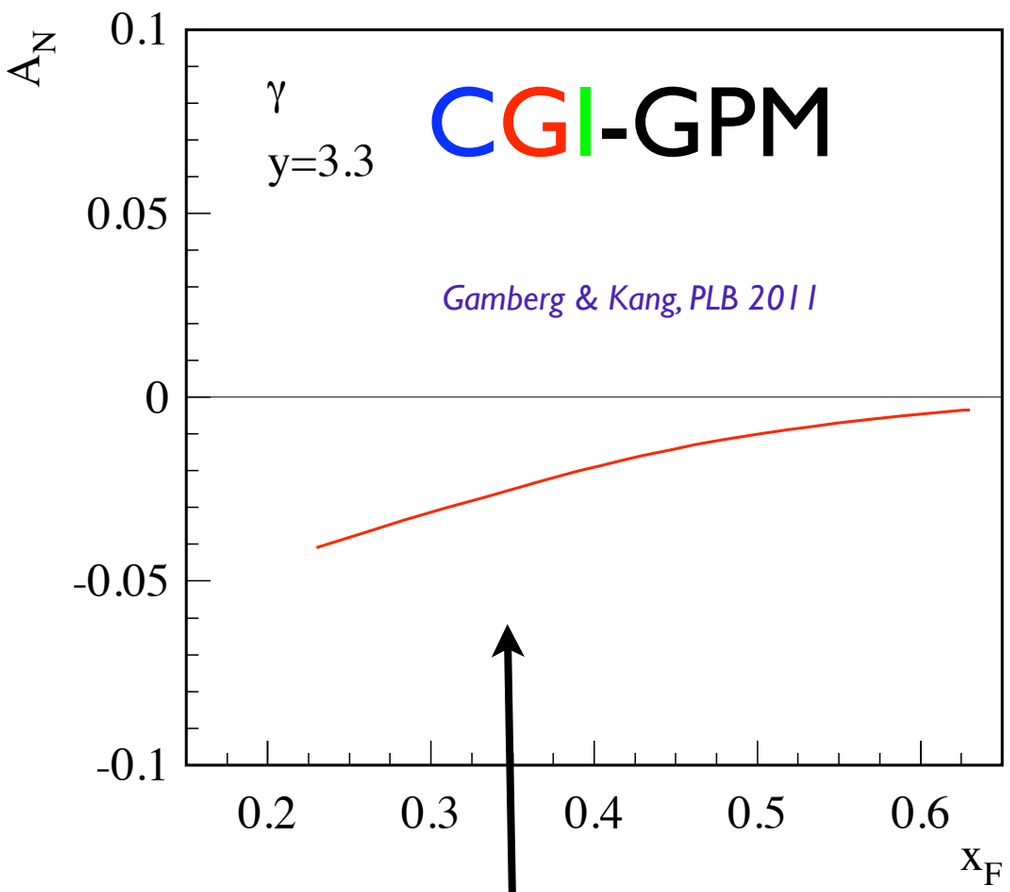

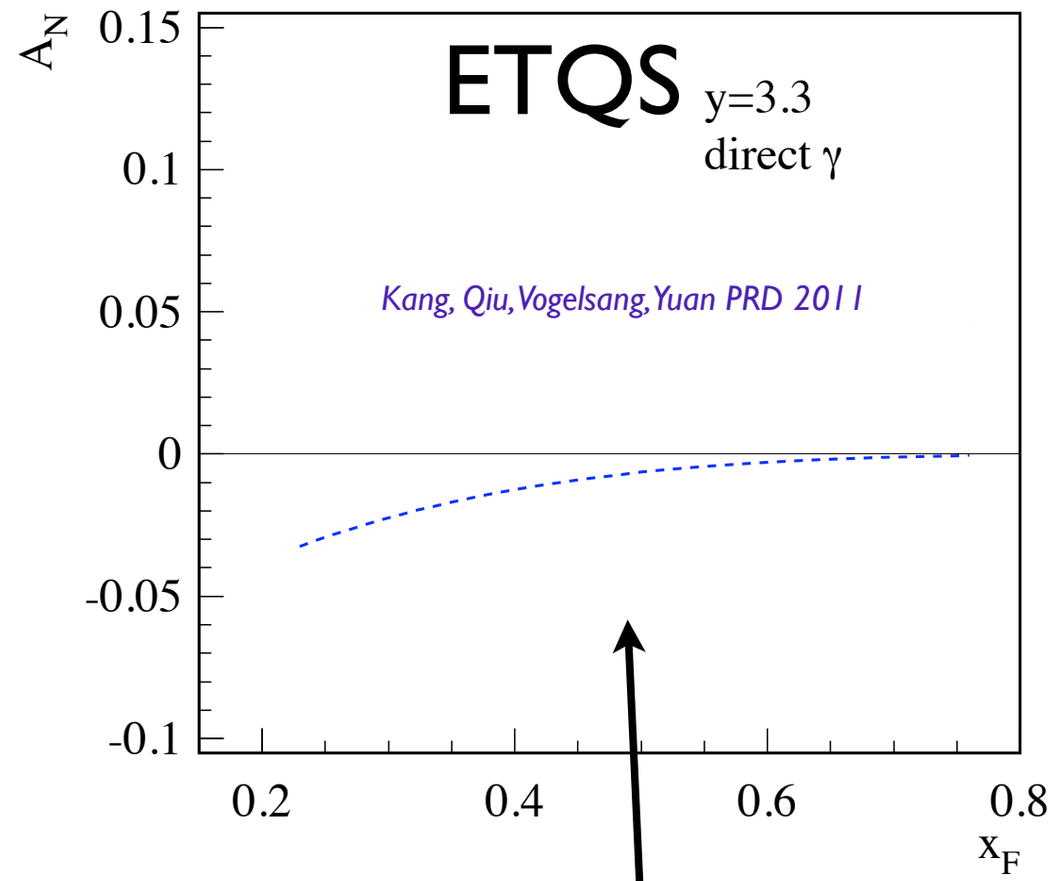

$$E_h \frac{d\Delta\sigma}{d^3P_h} = \frac{\alpha_s^2}{S} \sum_{a,b,c} \int \frac{dx_a}{x_a} d^2k_{aT} f_{1T}^{\perp a,\mathrm{SIDIS}}(x_a, k_{aT}^2) \frac{\epsilon^{k_{aT} S_A n\bar{n}}}{M} \int \frac{dx_b}{x_b} d^2k_{bT} f_{b/B}(x_b, k_{bT}^2)$$
$$\times \int \frac{dz_c}{z_c^2} D_{h/c}(z_c) H_{ab\to c}^{\mathrm{Inc}}(\hat{s}, \hat{t}, \hat{u}) \delta(\hat{s} + \hat{t} + \hat{u}),$$

$$E_h \frac{d\Delta\sigma(s_\perp)}{d^3P_h} = \frac{\alpha_s^2}{S} \sum_{a,b,c} \int \frac{dz}{z^2} D_{c\to h}(z) \int \frac{dx'}{x'} f_{b/B}(x') \int \frac{dx}{x} \sqrt{4\pi\alpha_s} \left(\frac{\epsilon^{P_{h\perp} s_\perp n\bar{n}}}{z\hat{u}} \right)$$
$$\times \left[T_{a,F}(x,x) - x \frac{d}{dx} T_{a,F}(x,x) \right] H_{ab\to c}(\hat{s}, \hat{t}, \hat{u}) \delta\left(\hat{s} + \hat{t} + \hat{u}\right),$$

Numerical Comparison of CGI-GPM and ETQS--Inclusive Pion

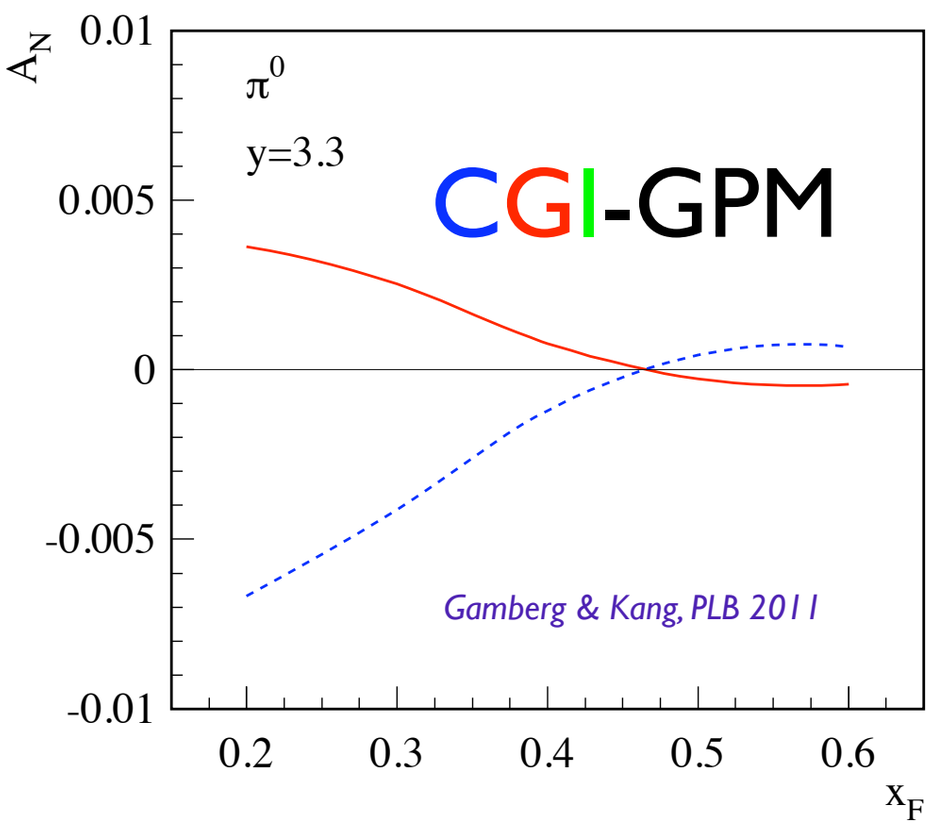

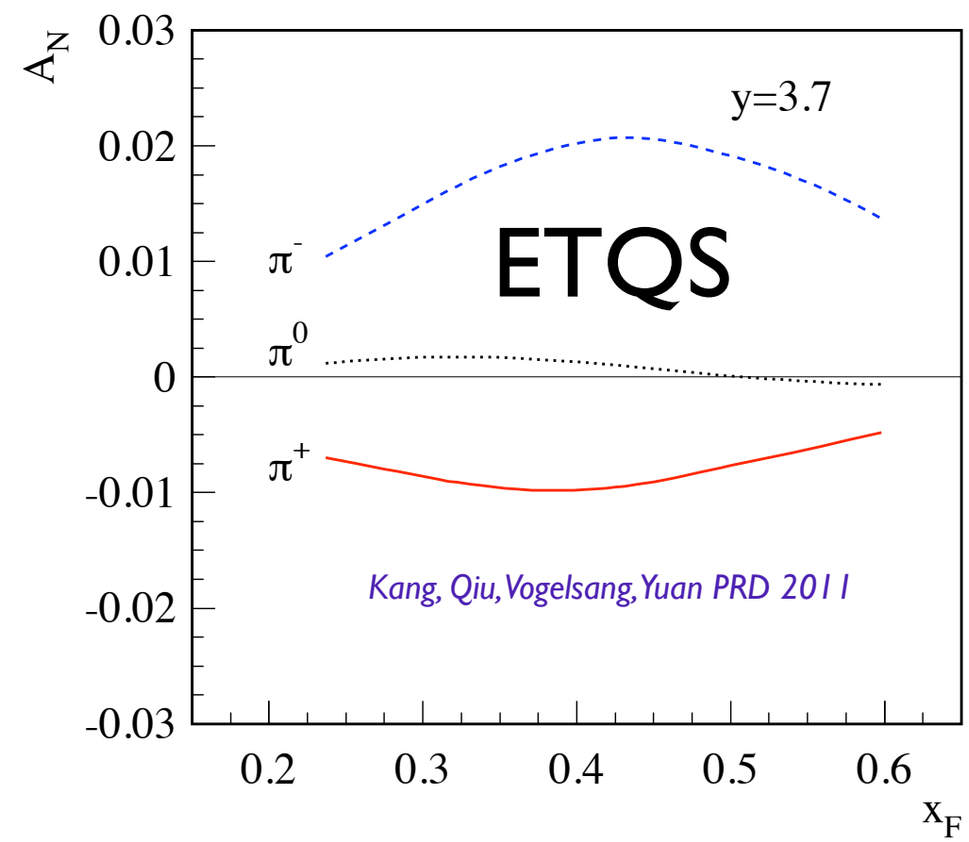

Compare red left w/ black dotted on right

Prompt photon production at RHIC

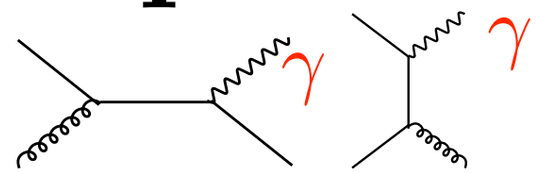

Leading order photon production, purely “direct” contribution.

A next-to-leading-order (NLO) calculation of prompt photon production is summarized by Vogelsang and Gordon from which one might know what is called direct and

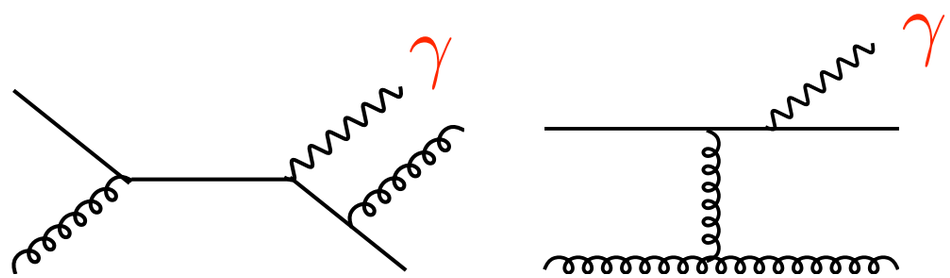

Photon production at NLO, which contains both “direct” and “fragmentation” contribution.

At NLO, we will have radiative corrections from 2 to 3 processes, such as qq to γ q g, see some sample diagrams .

These 2 to 3 processes have collinear divergence, one of which comes from the situation when the final-state quark is collinear to the outgoing photon.

Using factorization procedure, this part of collinear divergence is absorbed into the so-called photon fragmentation function in other words, when the photon is very close to the final-state quark, it is absorbed into quark-to-photon fragmentation function, this part is what we call ``fragmentation contribution''; while when they are well separated, this part belongs to the ``direct'' contribution at NLO. Exactly how much goes to ``direct'', how much goes to ``fragmentation'' depends on the factorization scale.

II. SPIN ASYMMETRY OF PROMPT PHOTON PRODUCTION

Similarly for the *spin-dependent* cross section, we could write

$$E\frac{d\Delta\sigma}{d^3P} = E\frac{d\Delta\sigma^{\rm dir}}{d^3P} + E\frac{d\Delta\sigma^{\rm frag}}{d^3P}.$$

Eventually the single transverse spin asymmetry is given by

$$A_N = E\frac{d\Delta\sigma}{d^3P}\Big/ E\frac{d\sigma}{d^3P}.$$

$$E\frac{d\Delta\sigma^{\rm frag}}{d^3P} = E\frac{d\Delta\sigma^{\rm frag}}{d^3P}\Big|_{\rm Sivers} + E\frac{d\Delta\sigma^{\rm frag}}{d^3P}\Big|_{\rm Collins},$$

ETQS formalism

$$T_{q,F}(x,x) = -\int d^2k_\perp \frac{|k_\perp|^2}{M} f_{1T}^{\perp q}(x,k_\perp^2)|_{\rm SIDIS}. \qquad \hat{H}_q(z) = -\frac{z^3}{M_h}\int d^2k_\perp |k_\perp|^2 H_1^{\perp q}(z, z^2k_\perp^2)$$

$$E\frac{d\Delta\sigma^{\rm frag}}{d^3P} = E\frac{d\Delta\sigma^{\rm frag}}{d^3P}\bigg|_{\rm Sivers} + E\frac{d\Delta\sigma^{\rm frag}}{d^3P}\bigg|_{\rm Collins},$$

where the first term is given by

$$E\frac{d\Delta\sigma^{\rm frag}}{d^3P}\bigg|_{\rm Sivers} = \epsilon_{\alpha\beta}s_\perp^\alpha P_{h\perp}^\beta \frac{\alpha_s^2}{S}\sum_{a,b,c}\int\frac{dz}{z^2}D_{c\to\gamma}(z)\int\frac{dx'}{x'}f_{b/B}(x')\int\frac{dx}{x}\left[\frac{1}{z\hat{u}}\right]$$
$$\times\left[T_{a,F}(x,x) - x\frac{d}{dx}T_{a,F}(x,x)\right]H_{ab\to c}^{\rm Sivers}(\hat{s},\hat{t},\hat{u})\delta\left(\hat{s}+\hat{t}+\hat{u}\right),$$

and the second term is given by

$$E\frac{d\Delta\sigma^{\rm frag}}{d^3P}\bigg|_{\rm Collins} = \epsilon_{\alpha\beta}s_\perp^\alpha P_{h\perp}^\beta \frac{\alpha_s^2}{S}\sum_{a,b,c}\int\frac{dx}{x}h_a(x)\int\frac{dx'}{x'}f_b(x')\int\frac{dz}{z}\left[-z\frac{\partial}{\partial z}\left(\frac{\hat{H}_c(z)}{z^2}\right)\right]$$
$$\times\left[\frac{1}{z}\frac{x-x'}{x(-\hat{u})+x'(-\hat{t})}\right]H_{ab\to c}^{\rm Collins}(\hat{s},\hat{t},\hat{u})\delta\left(\hat{s}+\hat{t}+\hat{u}\right)$$

Fragmentation

- In fragmentation the discussion slightly more complicated, since the gauge-links are not the only potential source of *T-odd effects*. As pointed out by Collins NPB93, also the *internal* final state interactions of the observed outgoing hadron with its accompanying jet, in matrix elements appearing as the one-particle inclusive out-state $\left| P_h \, X \right\rangle$ can produce T-odd

- Thus due to the explicit appearance of outstates, time-reversal symmetry does not constrain the parametrization of the fragmentation correlators (as does for pdfs)

- Hence *T-odd* fragmentation effects could arise from both FSI and gauge-links

Similarly unintegrated fragmentation there are in principle "two" types of gauge links
However more subtle!!! -Two types of T-odd effects
Reliability of Transversity Extraction Universality of Collins Fragmentation Function

$$\Delta_{\partial}^{\alpha\,[\mathcal{U}]}(z) \quad = \quad \int d^2k_T\; k_T^{\alpha}\Delta^{[\mathcal{U}]}(z,k_T) = \tilde{\Delta}_{\partial}^{\alpha}\left(\frac{1}{z}\right) + C_G^{[\mathcal{U}]}\,\pi\Delta_G^{\alpha}\left(\frac{1}{z},\frac{1}{z}\right)$$

$$\Delta^{[-]}(z,k_T) = \int \frac{d\xi^+ d^2\xi_T}{4z(2\pi)^3}\; e^{ik\cdot\xi}\,\langle 0\;|U^{[-]}_{[-\infty,0]}\psi(0)|x;P_h\rangle\langle x;P_h|\overline{\psi}(\xi^+,\xi_T)U^{[-]}_{[\xi,-\infty]}|0\rangle|_{\xi^-=0}$$

But no such constraint under time reversal

$$\cancel{\Delta^{[+]*}(x,p_T) \neq i\gamma^1\gamma^3\Delta^{[-]}(x,p_T)i\gamma^1\gamma^3}$$

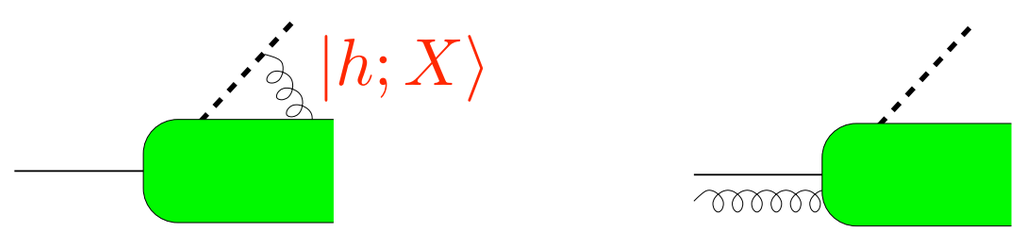

$$\Delta_{\partial}^{\alpha\,[C]}(z) \quad = \quad \tilde{\Delta}_{\partial}^{\alpha[\not{C}]}\left(\frac{1}{z}\right) + C_G^{[U(C)]}\,\pi\Delta_G^{\alpha[\not{C}]}\left(\frac{1}{z},\frac{1}{z}\right)$$

T-odd-FSI ***T-odd-Gauge link***

Reliability of Transversity Extraction Universality of Collins Fragmentation Function

- Collins NPB: 1993 **TSSA is associated with** $transverse$ **spin of fragmenting quark and transverse momentum of final state hadron**

$$\Delta_{\partial}^{\alpha\,[\mathcal{U}]}(z) \quad = \quad \int d^2k_T\; k_T^{\alpha}\Delta^{[\mathcal{U}]}(z,k_T) = \tilde{\Delta}_{\partial}^{\alpha}\left(\tfrac{1}{z}\right) + C_G^{[\mathcal{U}]}\,\pi\Delta_G^{\alpha}\left(\tfrac{1}{z},\tfrac{1}{z}\right)$$

$$D_{h/q^{\uparrow}}\left(z,K_T^2\right) = D_1^q\left(z,K_T^2\right) + H_1^{\perp q}\left(z,K_T^2\right)\frac{(\hat{\boldsymbol{k}}\times\boldsymbol{K}_T)\cdot\boldsymbol{s}_q}{zM_h},$$

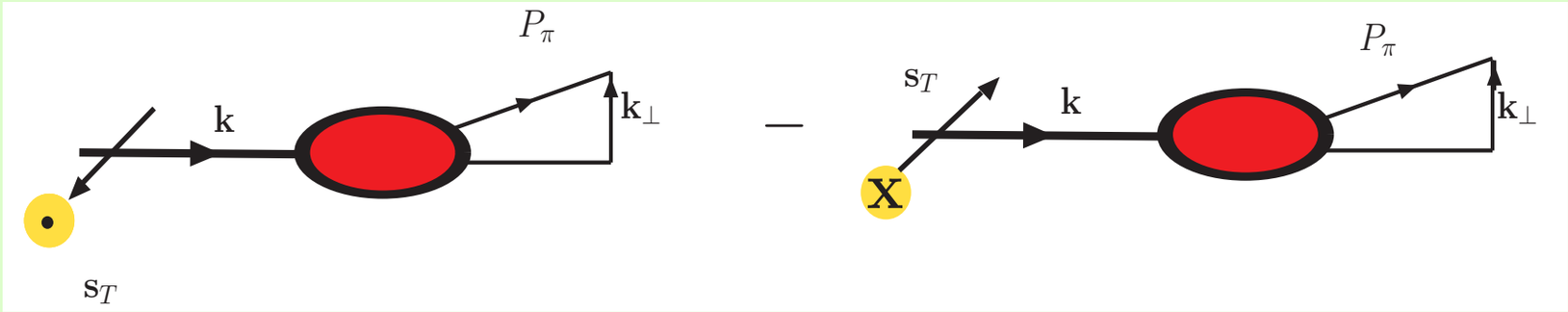

$$\frac{\epsilon_T^{ij}k_{Tj}}{M_h}H_1^{\perp}\left(z,k_T^2\right) = \frac{1}{2}\,\mathrm{Tr}\left[\Delta(z,k_T)i\sigma^{i-}\gamma_5\right].$$

Gluonic pole and higher moments Vanishes Collins Universal

LG, A. Mukherjee, P. Mulders PRD 2011

$$\lim_{x_1 \to 0} \quad \Delta_G(x, x - x_1) = \Delta_G(x, x) \to 0$$

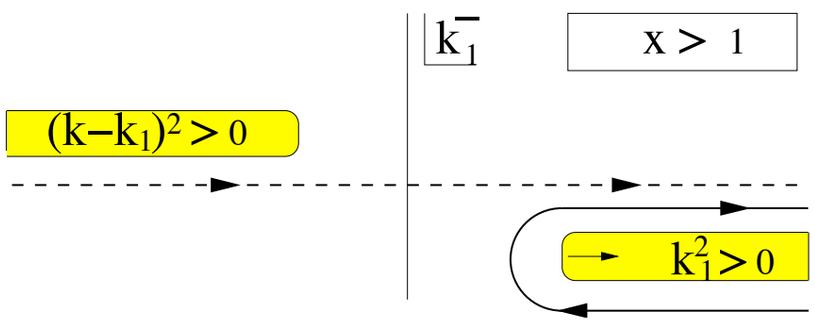

$$\Delta_G(x, x - x_1)$$

$$k_1^- = \frac{k_1^2 + k_{1T}^2 + i\epsilon}{2x_1}$$

For the case $x > 1$ the k_1^- integration can be wrapped around the cut k_1^2 which smoothly vanishes for $x_1 \to 0$ describes the by the arrow inside branch cut indicates that it harmlessly recedes to infinity

Agrees with earlier model analysis Collins, Metz PRL 2004
Agrees with earlier model analysis LG, A. Mukherjee, P. Mulders PRD 2008
Agrees with model independent spectral analysis A. Metz, S. Meissner PRL 2009
Agrees with 1 and 2 gluon exchange calculation from GL in hadron inside jet F. Yuan PRD 2009
Recent ppr. by Boer,Kang,Vogelsang,Yuan-predictions on Lambda polarization in SIDIS &

$e^+ e^-$

Collins *photon* fragmentation contribution

$$H_1^{\perp q}(z, z^2 k_\perp^2) = e_q^2 \frac{\alpha_{\rm em}}{2\pi^2} \alpha_s m_q C_F \, [\text{fig.a} + \text{fig.b} + \text{fig.c} + \text{fig.d}]$$

where

$$\text{fig.a} = \frac{1}{2zk^2(k^2 - m_q^2)} \left(3 - \frac{m_q^2}{k^2} \right)$$

$$\text{fig.b} = \frac{1}{(1-z)(k^2 - m_q^2)^2} \left[\frac{m_q^2}{k^2 - m_q^2} \ln\left(\frac{k^2}{m_q^2} \right) - \frac{1}{2z} \left(4 - 5z + 3(z-2)\frac{m_q^2}{k^2} + 2\left(\frac{m_q^2}{k^2} \right)^2 \right) \right]$$

$$\text{fig.c} = 0$$

$$\text{fig.d} = \frac{1}{((1-z)k^2(k^2 - m^2)} \left[1 + \frac{(1-z)k^2}{(1-z)k^2 - m_q^2} \ln\left(\frac{(1-z)k^2}{m_q^2} \right) \right]$$

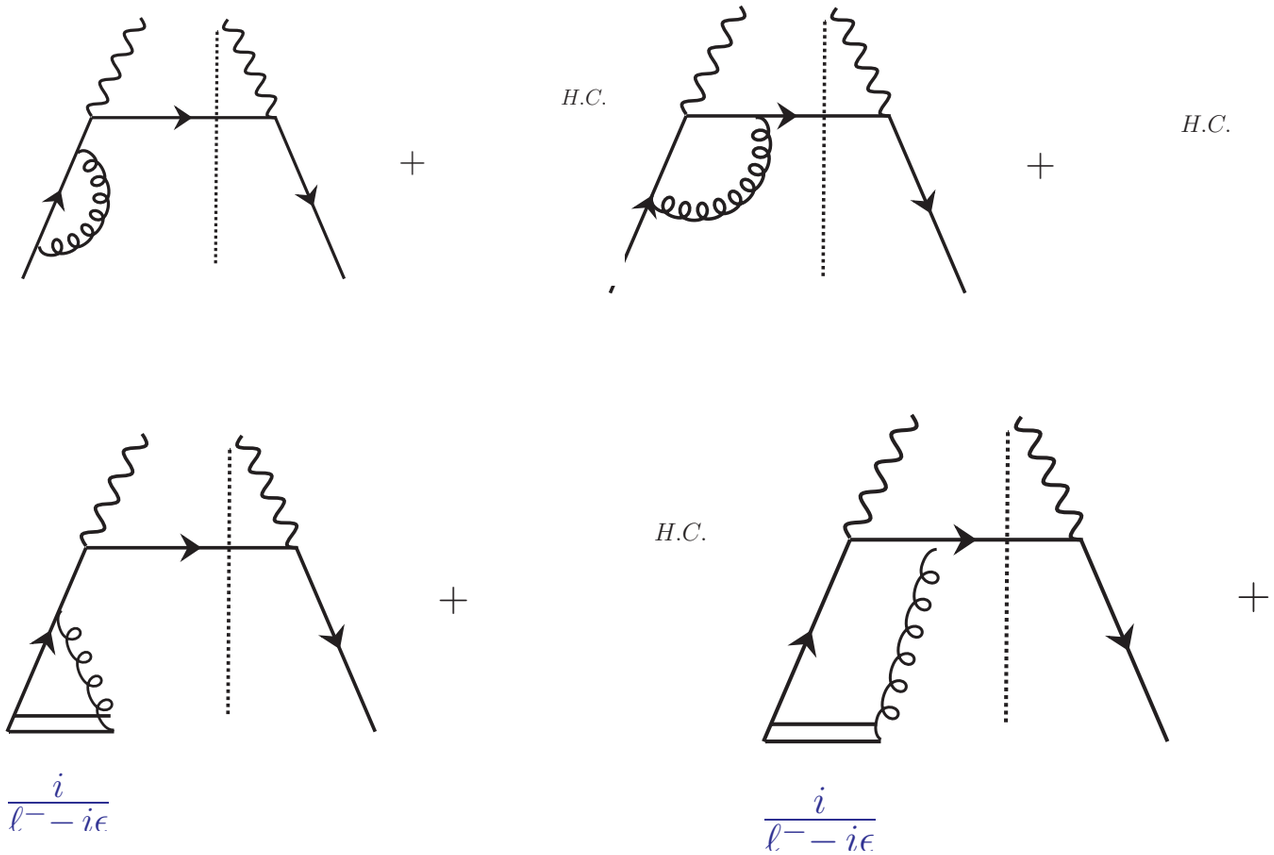

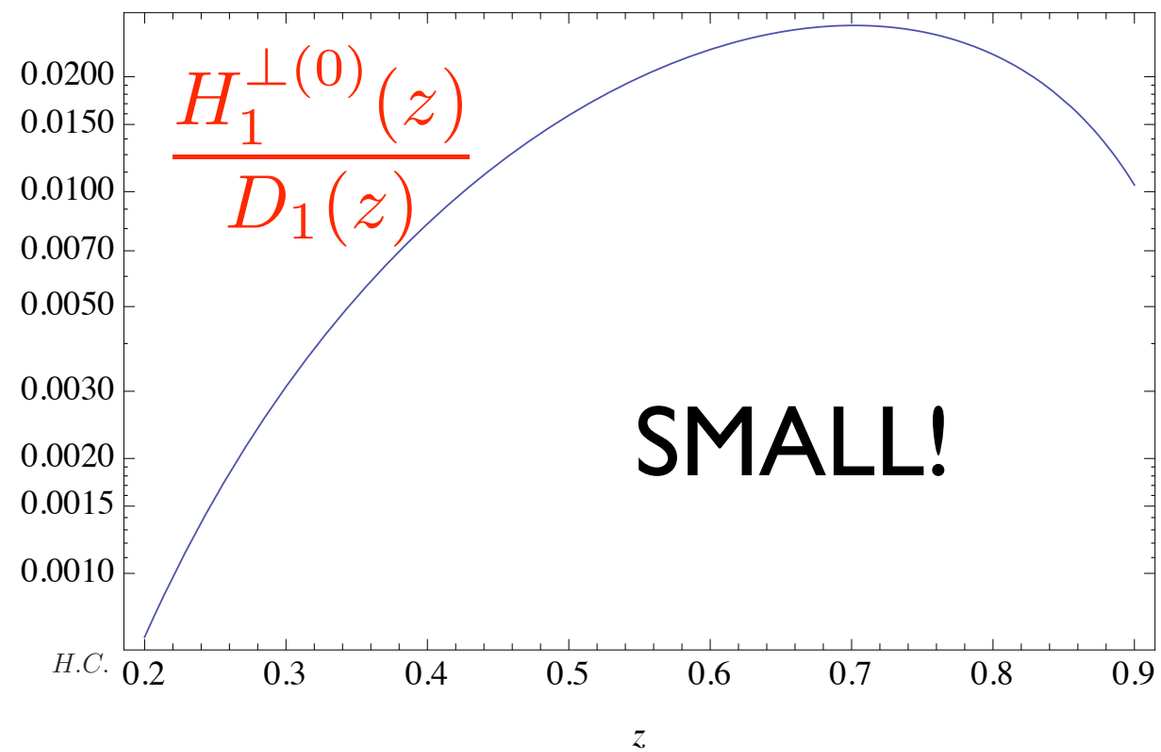

Direct & Fragmentation

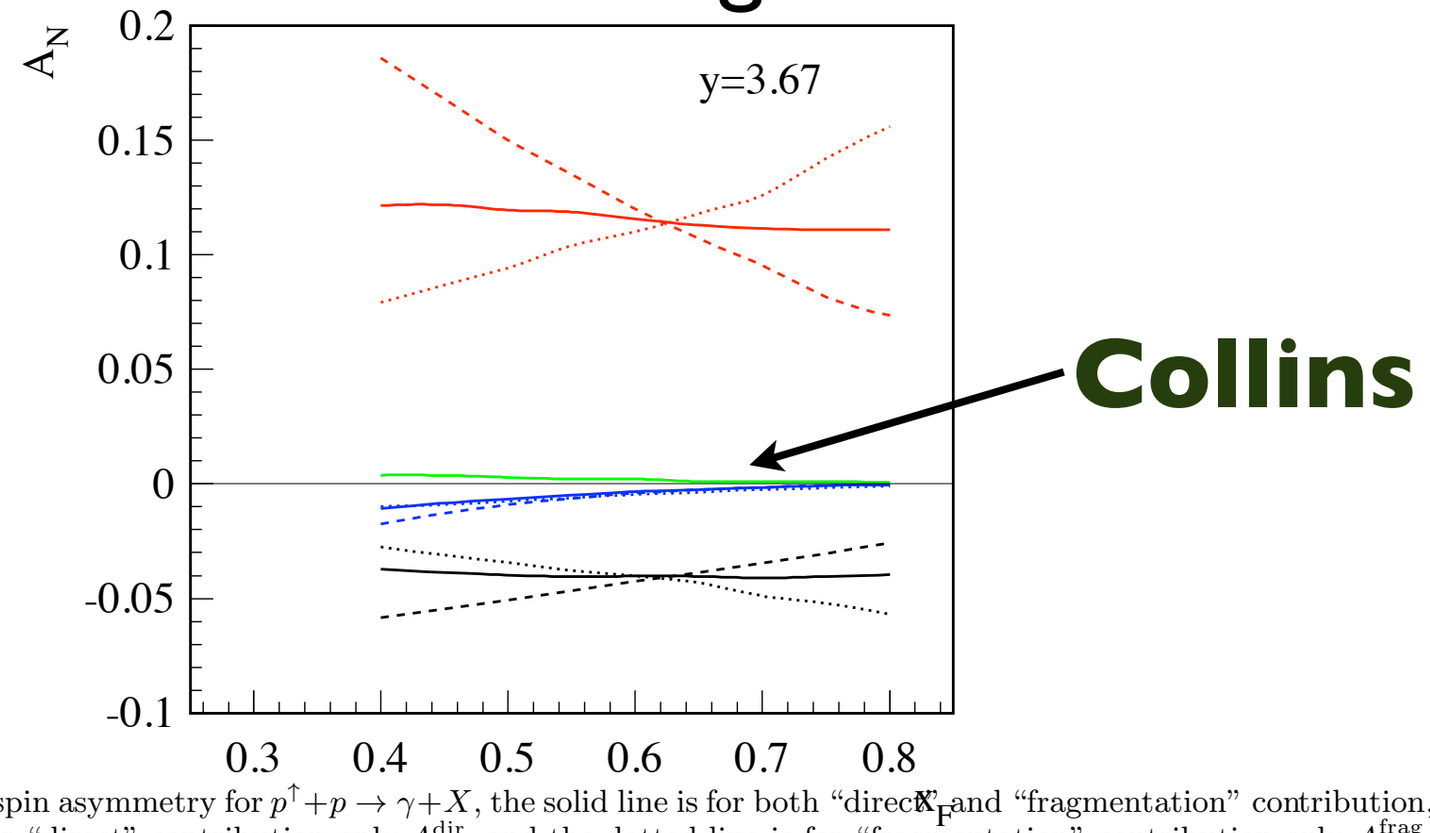

FIG. 4. Single transverse spin asymmetry for $p^{\uparrow}+p \to \gamma+X$, the solid line is for both "direct" and "fragmentation" contribution, while the dashed one is for "direct" contribution only $A_N^{\rm dir}$, and the dotted line is for "fragmentation" contribution only $A_N^{\rm frag}$. Green solid line is the Collins "fragmentation" asymmetry.

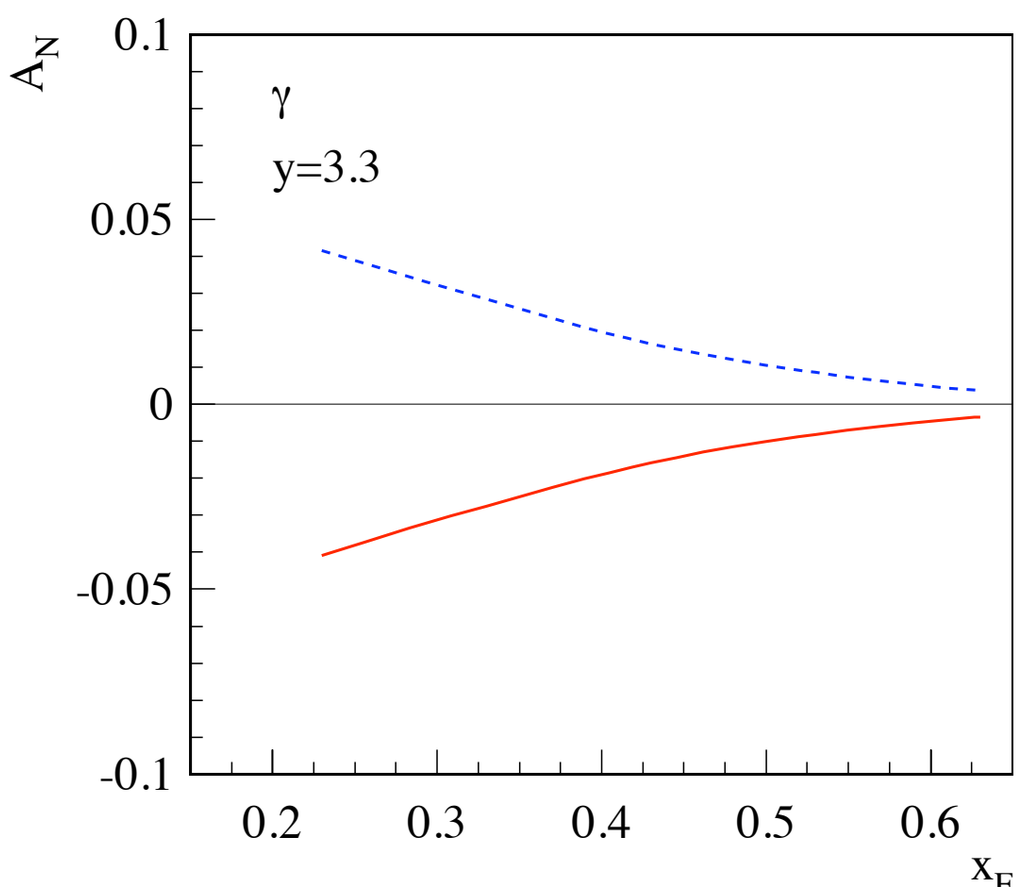

Sivers from Anselmino et al EPJA (2009)
Fragmentation from DSS PRD75 (2007)

Pion Collins--Bacchetta, Gamberg, Goldstein, Mukherjee PLB 08

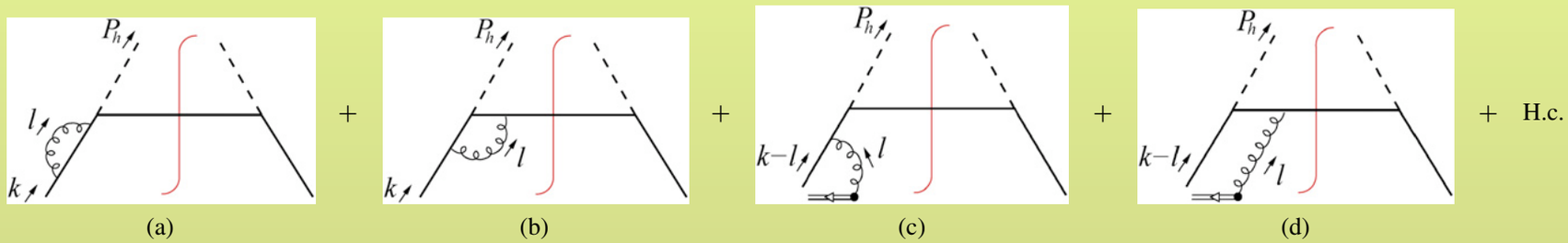

Fig. 3. Single gluon-loop corrections to the fragmentation of a quark into a pion contributing to the Collins function in the eikonal approximation. "H.c." stands for the Hermitian conjugate diagrams which are not shown.

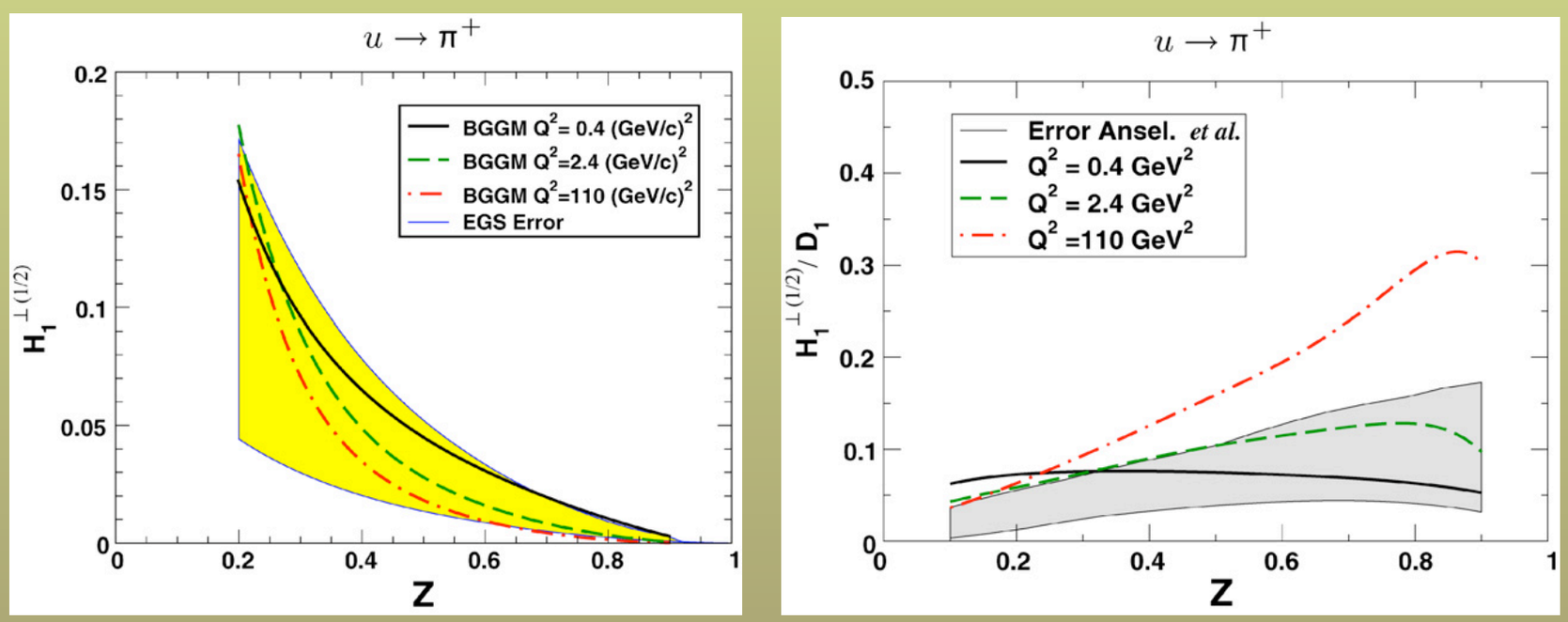

(a) (b)

Fig. 4. Half moment of the Collins function for $u \to \pi^+$ in our model. (a) $H_1^{\perp(1/2)}$ at the model scale (solid line) and at a different scale under the assumption in Eq. (37) (dot-dashed line), compared with the error band from the extraction of Ref. [6], (b) $H_1^{\perp(1/2)}/D_1$ at the model scale (solid line) and at two other scales (dashed and dot-dashed lines) under the assumption in Eq. (38). The error band from the extraction of Ref. [7] is shown for comparison.

Anselmino Prokudin et al. Ferrara Transversity 08

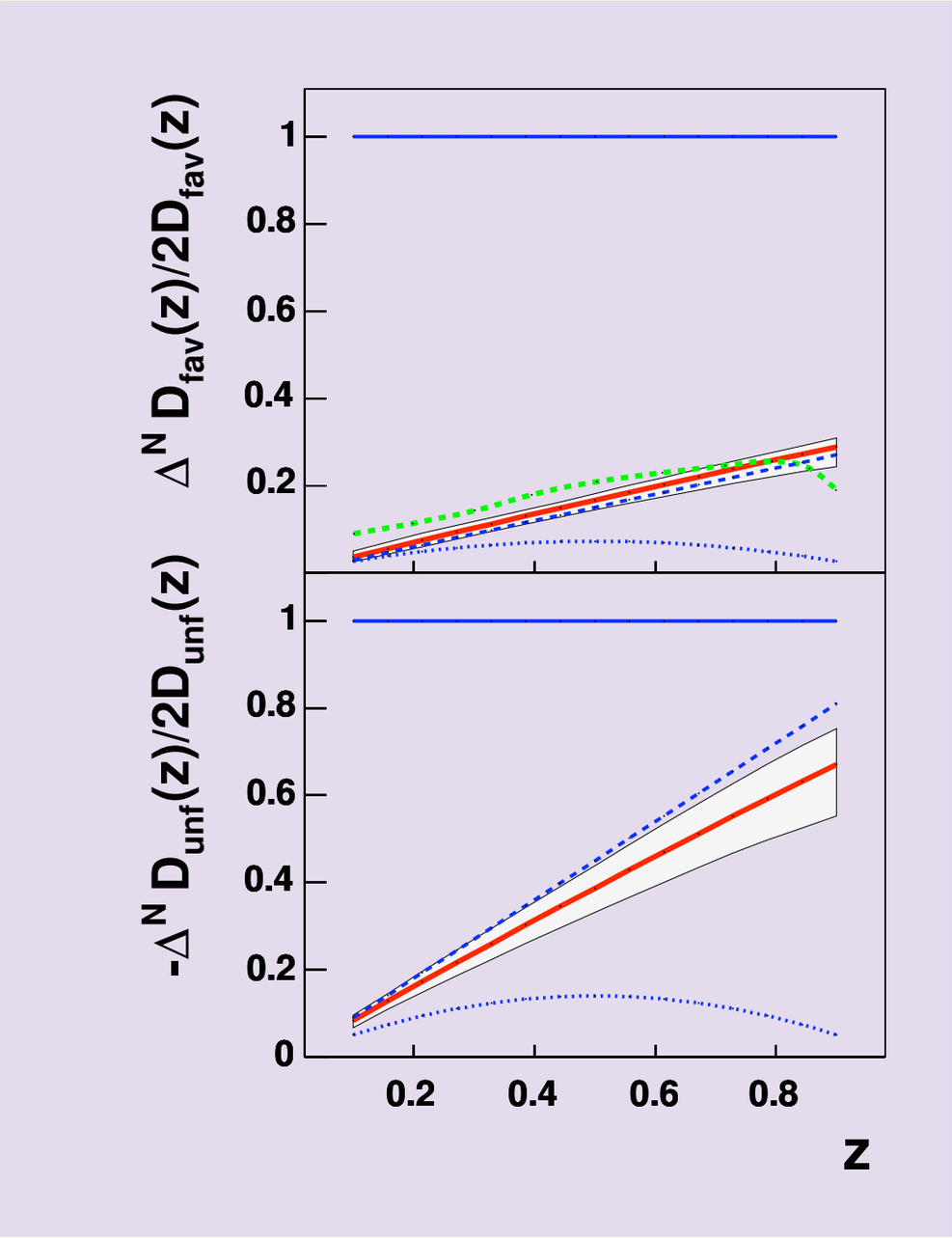

Bacchetta, Gamberg, Goldstein, Mukherjee PLB 08

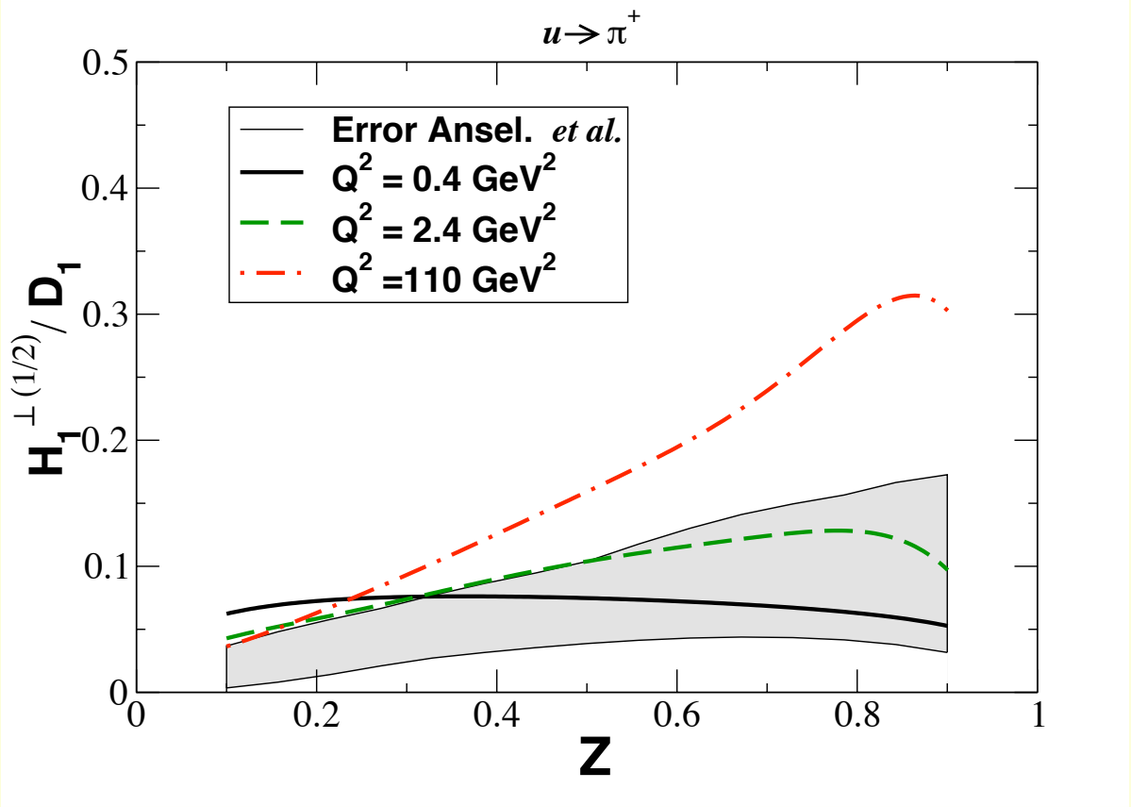

compared to Ref. [1] (dashed line), Ref. [2] (dotted line), and Ref. [3] (dashed green line)

[1] A. V. Efremov, K. Goeke, and P. Schweitzer, Phys. Rev. **D73**, 094025 (2006).

[2] W. Vogelsang and F. Yuan, Phys. Rev. **D72**, 054028 (2005).

[3] A. Bacchetta, L. Gamberg, G. R. Goldstein, A. Mukherjee PLB659:234-243,2008.

Conclusions

- Generalize GPM w/ color--can then perform global analysis
- Elephant in the room is break down of factorization for these processes
- Appears to be connection between generalized parton model at twist 3 and twist 3 approach
- Estimate mismatch-investigating LG Z. Kang
- TMD fact. is assumed in both GPM and GGPM is this a reasonable pheno. approximation?
- Direct photon driven by same ISI factor as in DY Collins is small!!!

Reliability of Transversity Extraction Universality of Collins Fragmentation Function

Belle KEKB measurement Collins Frag. Function PRL 2006 & PRD 2008

From talks of Ralf Seidl

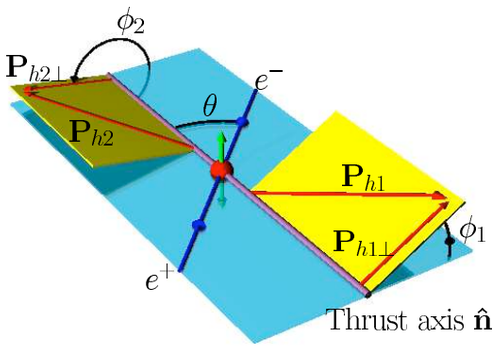

FIG. 2: Definition of the azimuthal angles ϕ_1 and ϕ_2 of the two hadrons, between the scattering plane and their transverse momenta $\mathbf{P}_{hi\perp}$ around the thrust axis $\hat{n}$. The angle θ is defined as the angle between the lepton axis and the thrust axis.

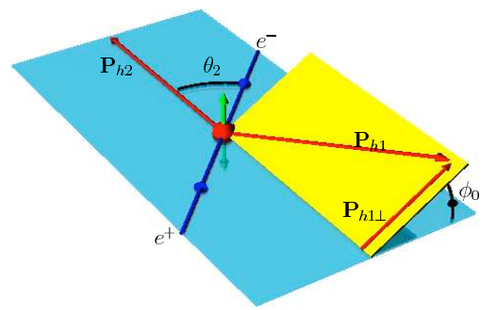

FIG. 3: Definition of the azimuthal angle ϕ_0 formed between the planes defined by the lepton momenta and that of one hadron and the second hadron's transverse momentum $P'_{h1\perp}$ relative to the first hadron.

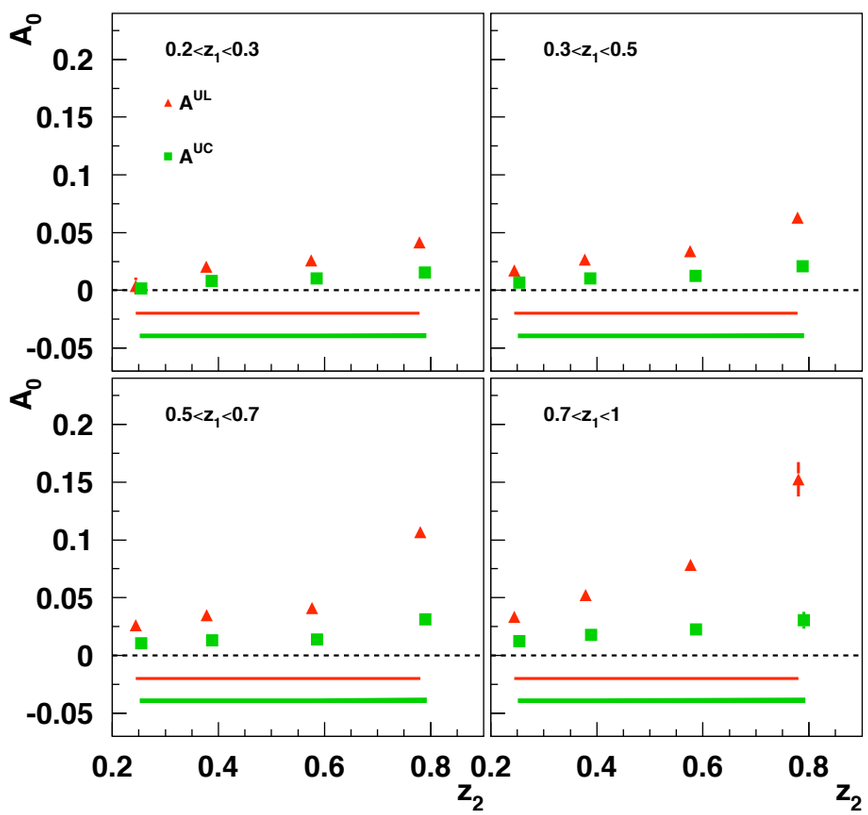

FIG. 17: Light quark (*uds*) A_0 asymmetry parameters as a function of z_2 for 4 z_1 bins. The UL data are represented by triangles and the systematic error by the upper error band. The UC data are described by the squares and their systematic uncertainty by the lower error band.

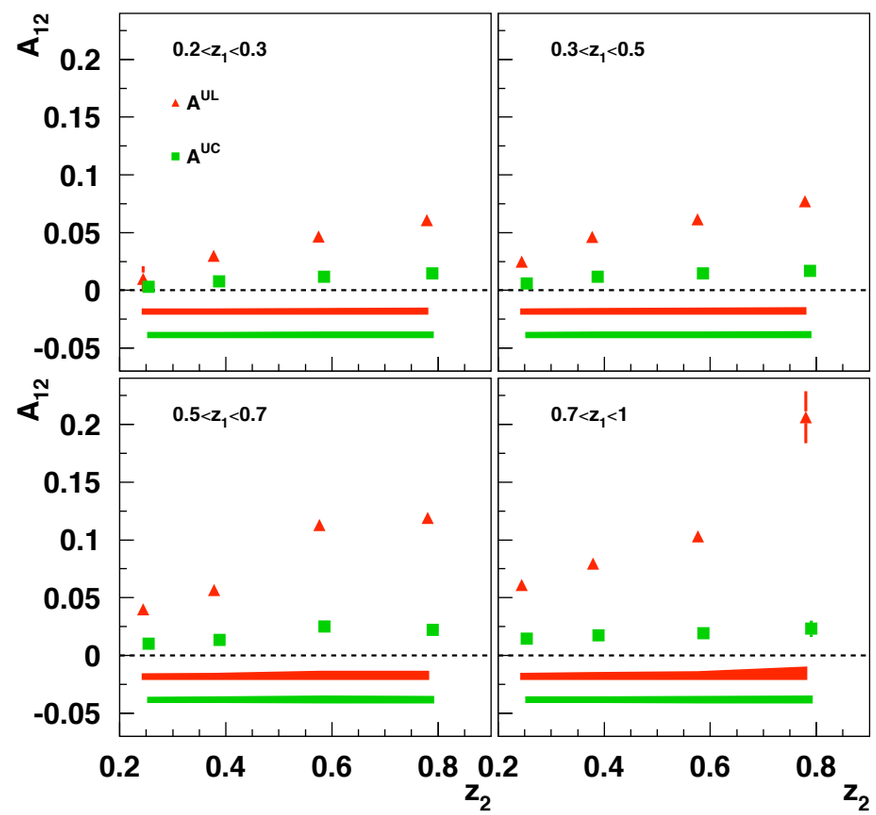

FIG. 18: Light quark (*uds*) A_{12} asymmetry parameters as a function of z_2 for 4 z_1 bins. The UL data are represented by triangles and the systematic error by the upper error band. The UC data are described by the squares and their systematic uncertainty by the lower error band.

Spin measurements at PHENIX and future plans

RBRC Workshop on Forward Physics at RHIC, BNL, July 2012

Francesca Giordano
for the PHENIX collaboration

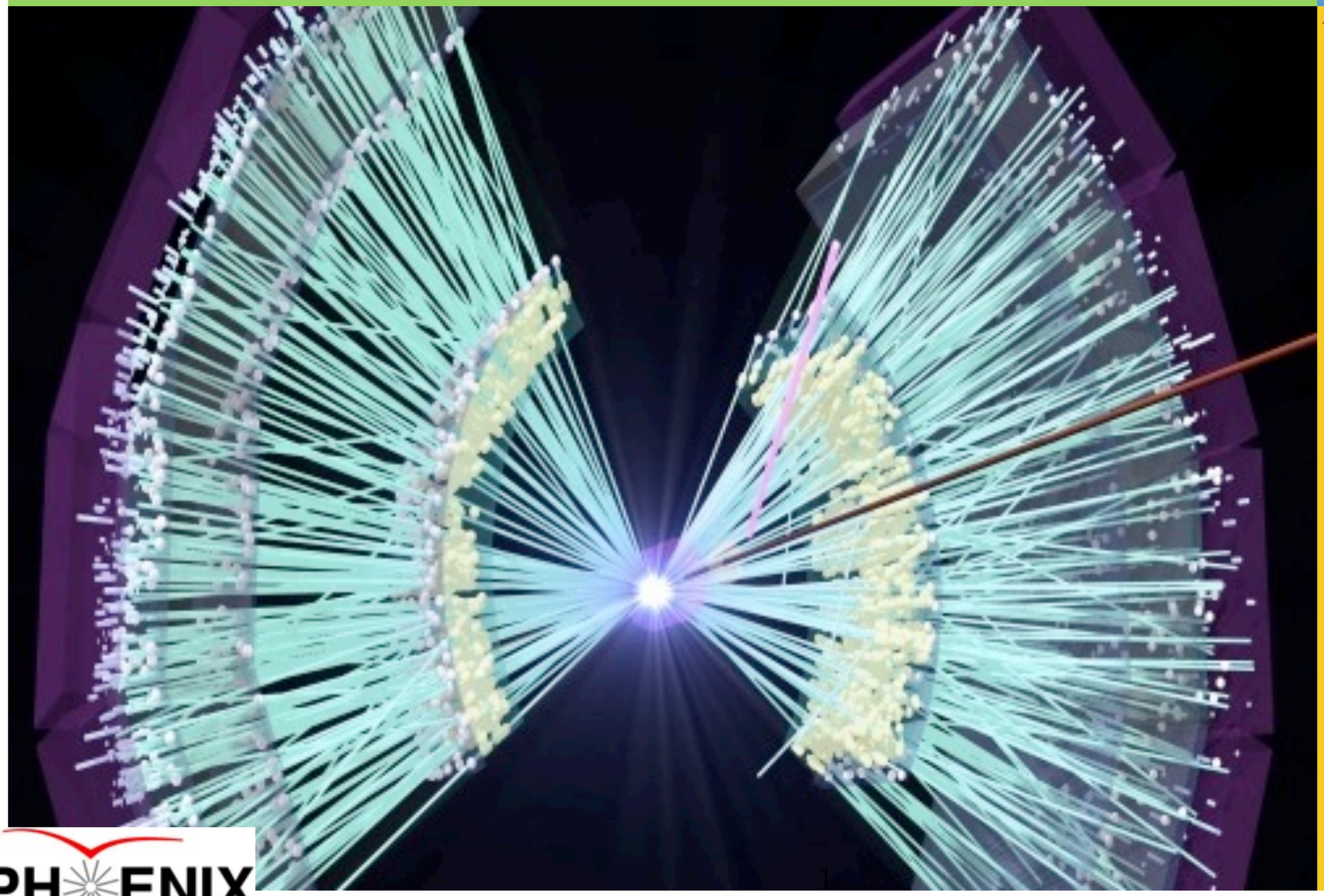

PHENIX

You think you understand something? Now add spin....

R. Jaffe

The proton structure:

where does the proton spin come from ?

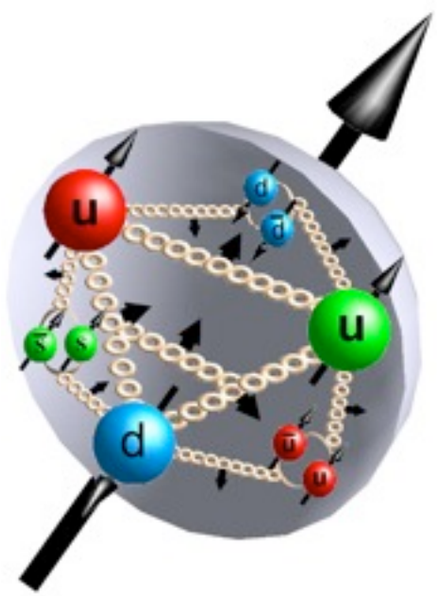

$$\frac{1}{2} = \frac{1}{2}\Delta\Sigma + \Delta G + L_z$$

quark spins — gluon spins — quark&gluon orbital motion

Δu_v Δd_v Δq_{sea}

valence flavors

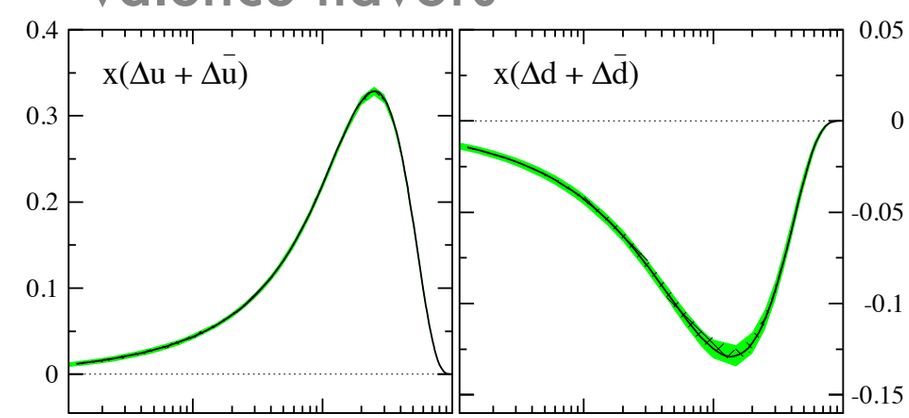

First *spin crisis:*

quarks only provide ≈ 30% of the proton spin

Where is the rest of the proton spin?

Gluon spin? Orbital motion?

The proton structure:

where does the proton spin come from ?

$$\frac{1}{2} = \frac{1}{2}\Delta\Sigma + \Delta G + L$$

quark spins — gluon spins — quark&gluon orbital motion

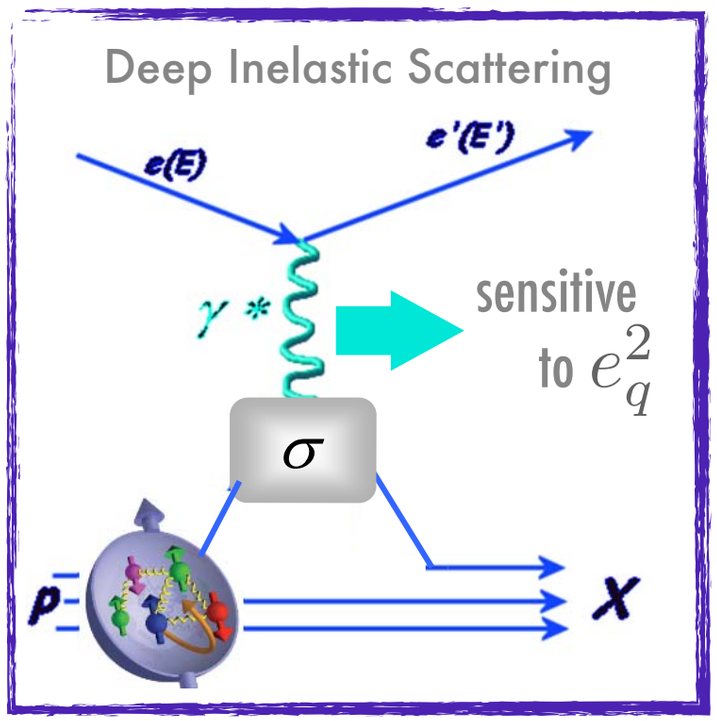

sea quarks & gluons

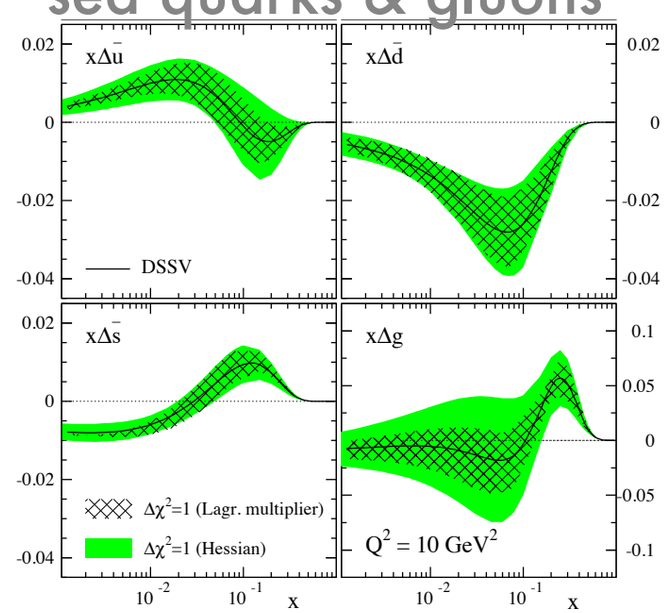

valence flavors

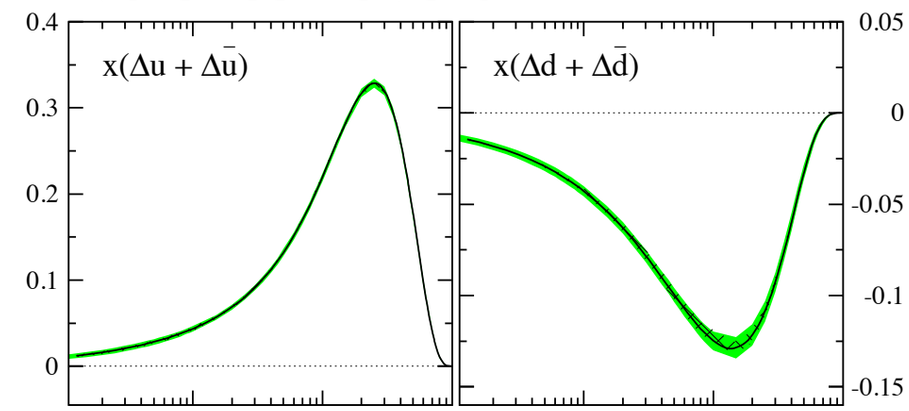

Most helicity results from Deep Inelastic scattering, but DIS can access gluons only indirectly, and sea quark distribution extractions are model-dependent

Polarized proton-proton collider

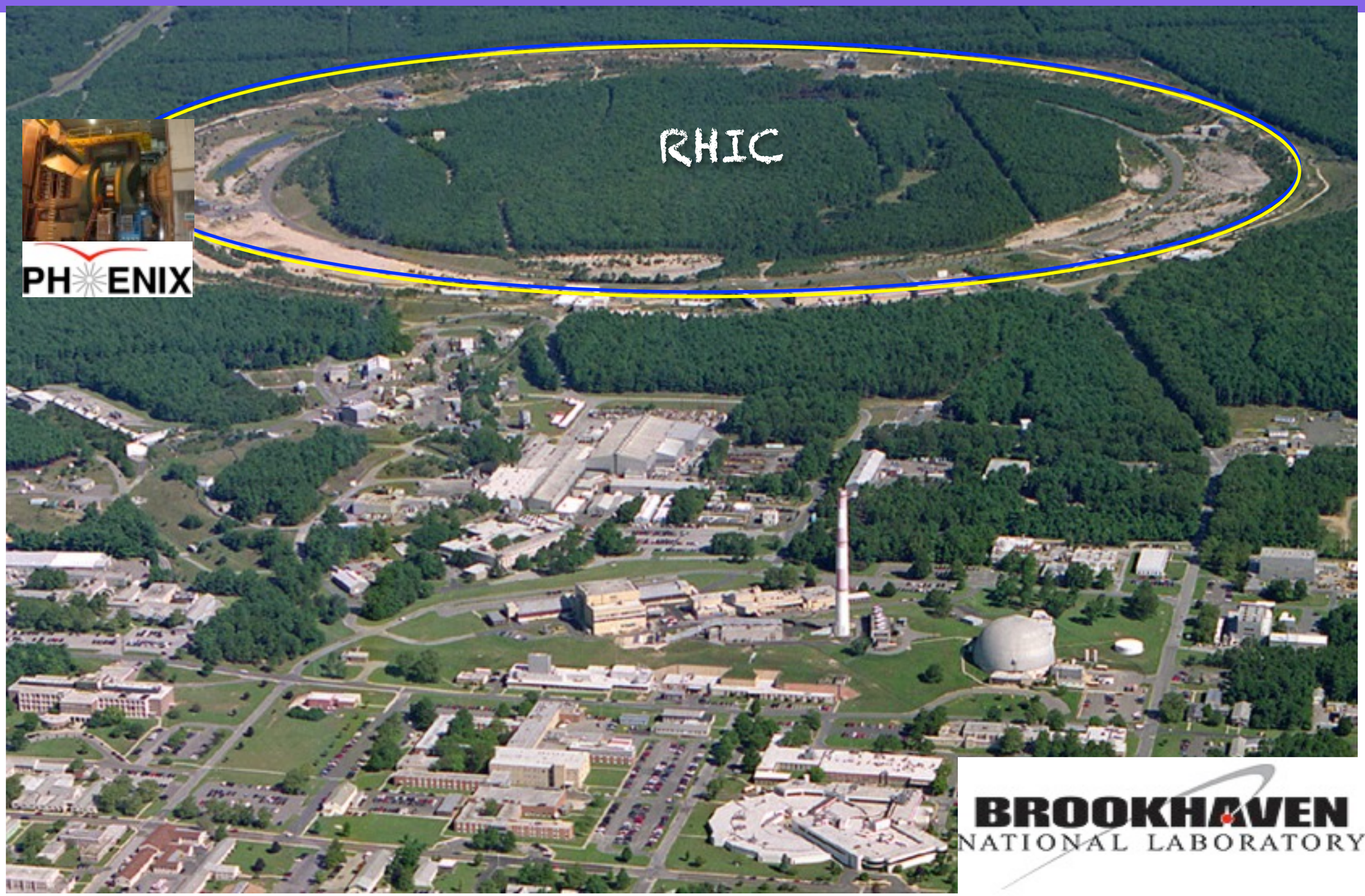

PHENIX

Central Arms:

$$|\eta| < 0.35$$

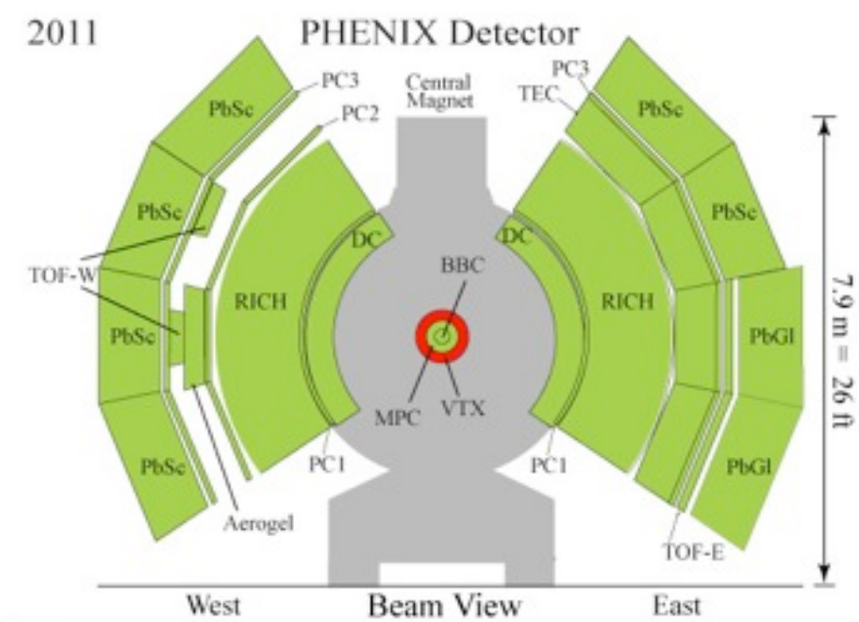

Tracking, Momentum and PID for:

- ☆charged and neutral hadrons
- ☆direct photons
- ☆e+e-

Forward Arms:

$$1.2 < |\eta| < 2.4$$

Tracking and Momentum for:

- ☆ $\mu^{\pm}$

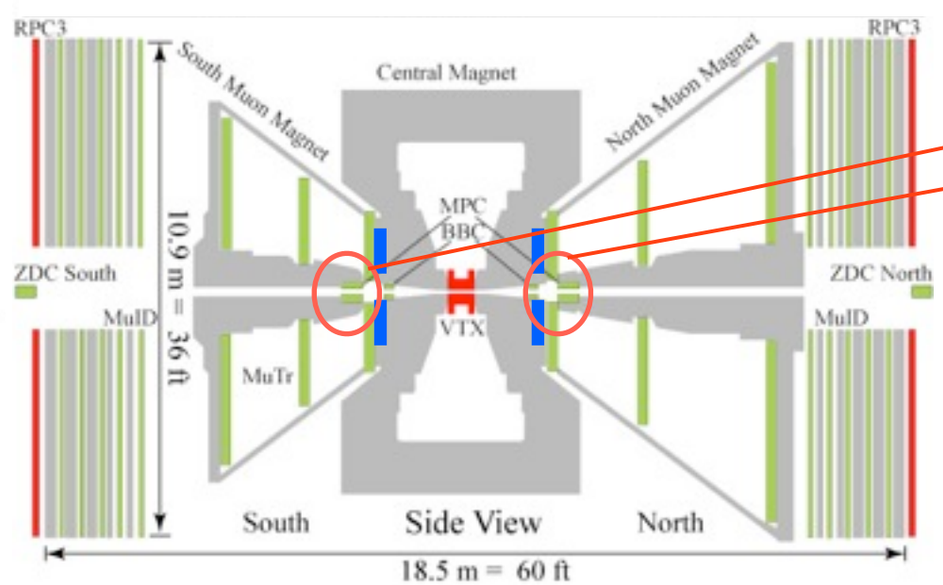

Even more forward: MPC

$$3.1 < |\eta| < 3.9$$

$$\pi^0 \to \gamma\gamma$$

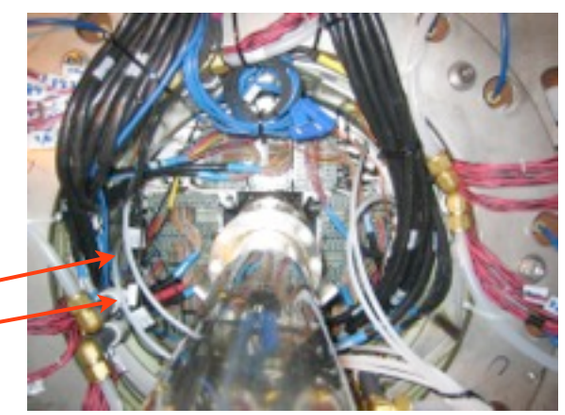

Gluon Helicity

Gluon polarization

$$\frac{1}{2} = \frac{1}{2}\Delta\Sigma + \Delta G + L$$

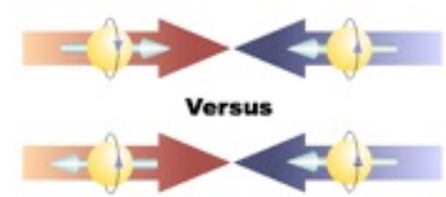

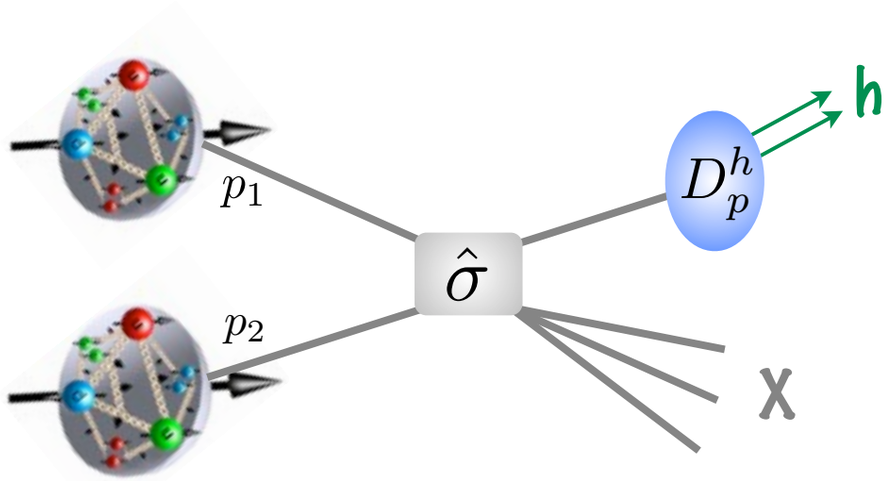

$$A_{LL} = \frac{\sigma^{++} - \sigma^{+-}}{\sigma^{++} + \sigma^{+-}}$$

$$\approx \frac{\Delta p_1 \times \Delta p_2 \times \hat{\sigma} \times D_p^h}{p_1 \times p_2 \times \hat{\sigma} \times D_p^h}$$

$$p_1,\, p_2 = q/g$$

$gg \to gg$

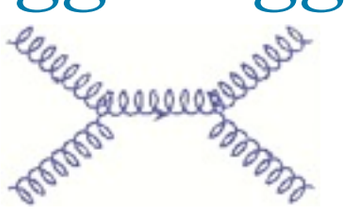

$$\propto \frac{\Delta g}{g}\frac{\Delta g}{g}$$

$gq \to gq$

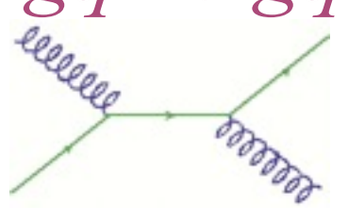

$$\propto \frac{\Delta q}{q}\frac{\Delta g}{g}$$

$qq \to qq$

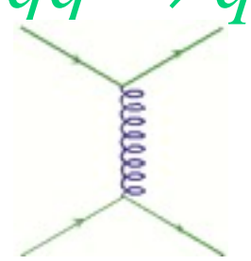

$$\propto \frac{\Delta q}{q}\frac{\Delta q}{q}$$

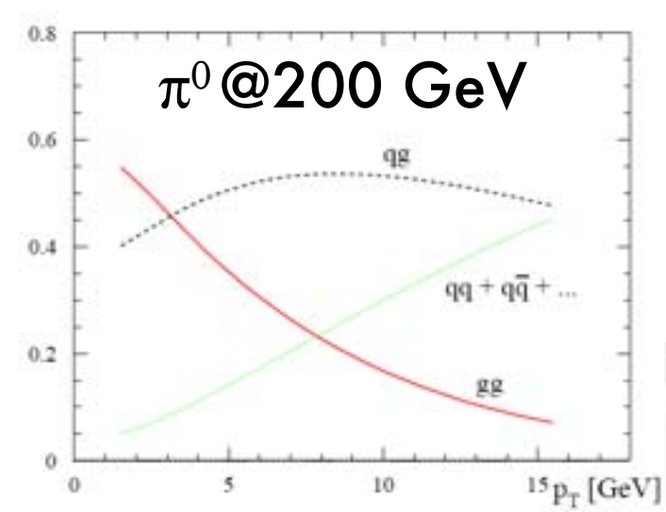

$\pi^0 A_{LL}$

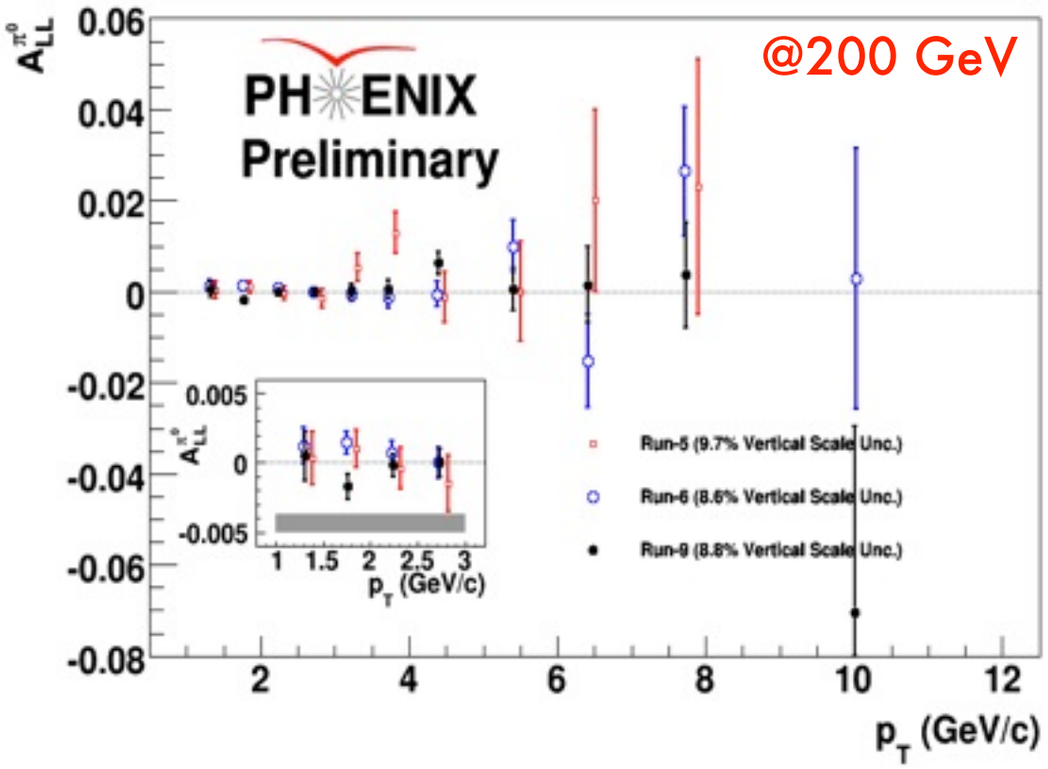

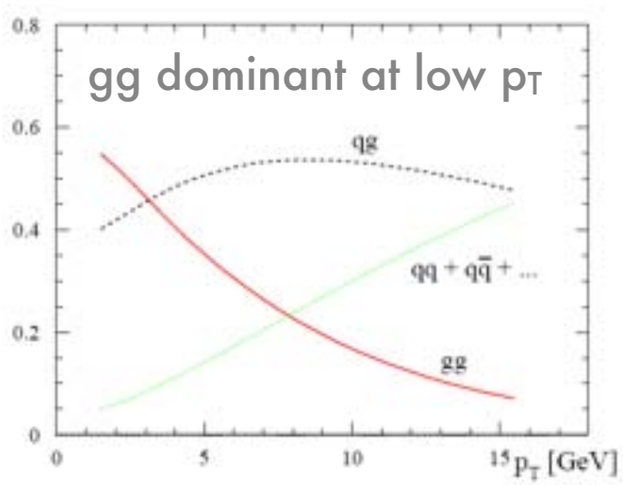

Swadhin Taneja

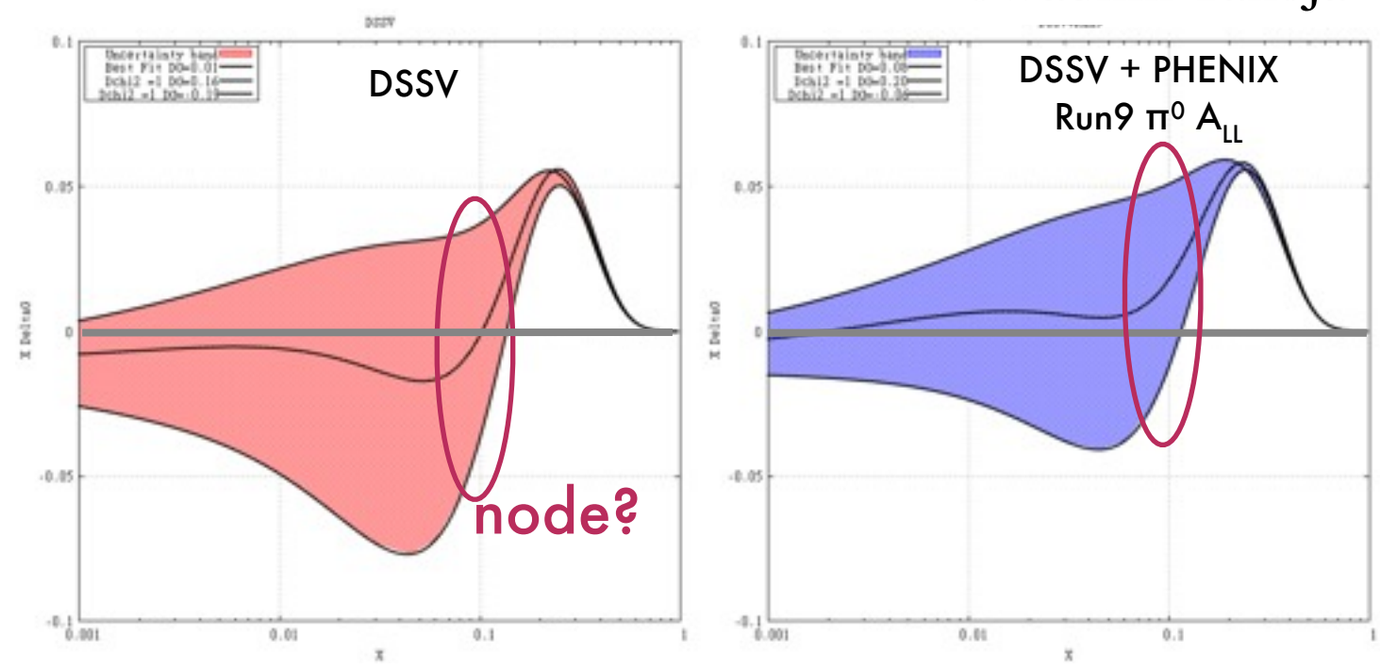

Mapping vs. x

PRL 101, (2008)072001 DSSV 08

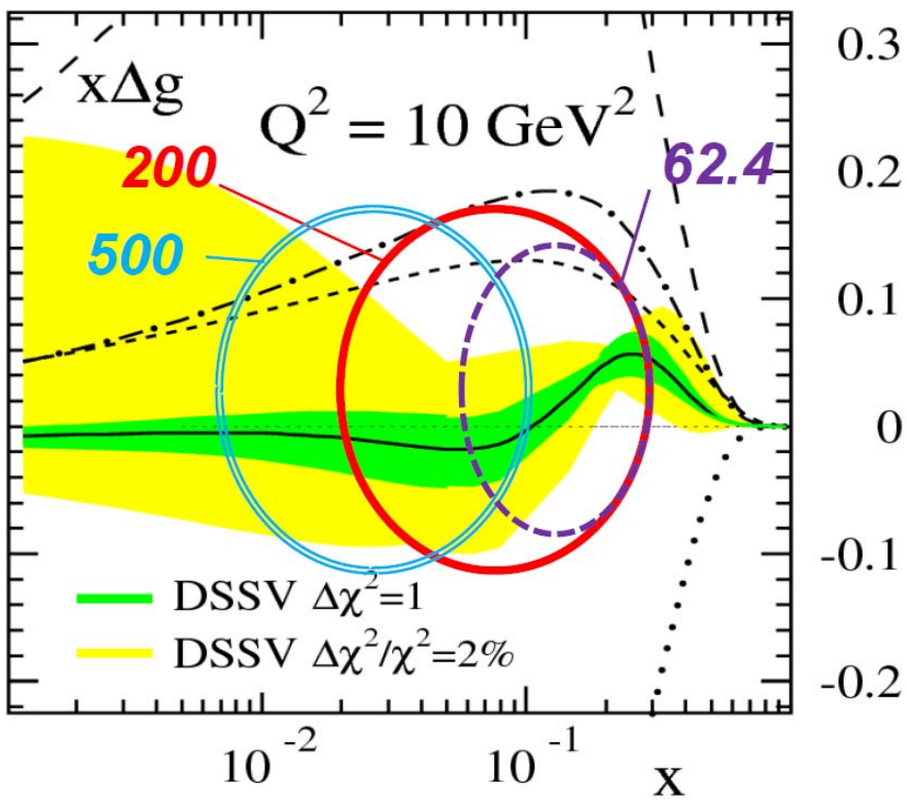

Different energy => different x

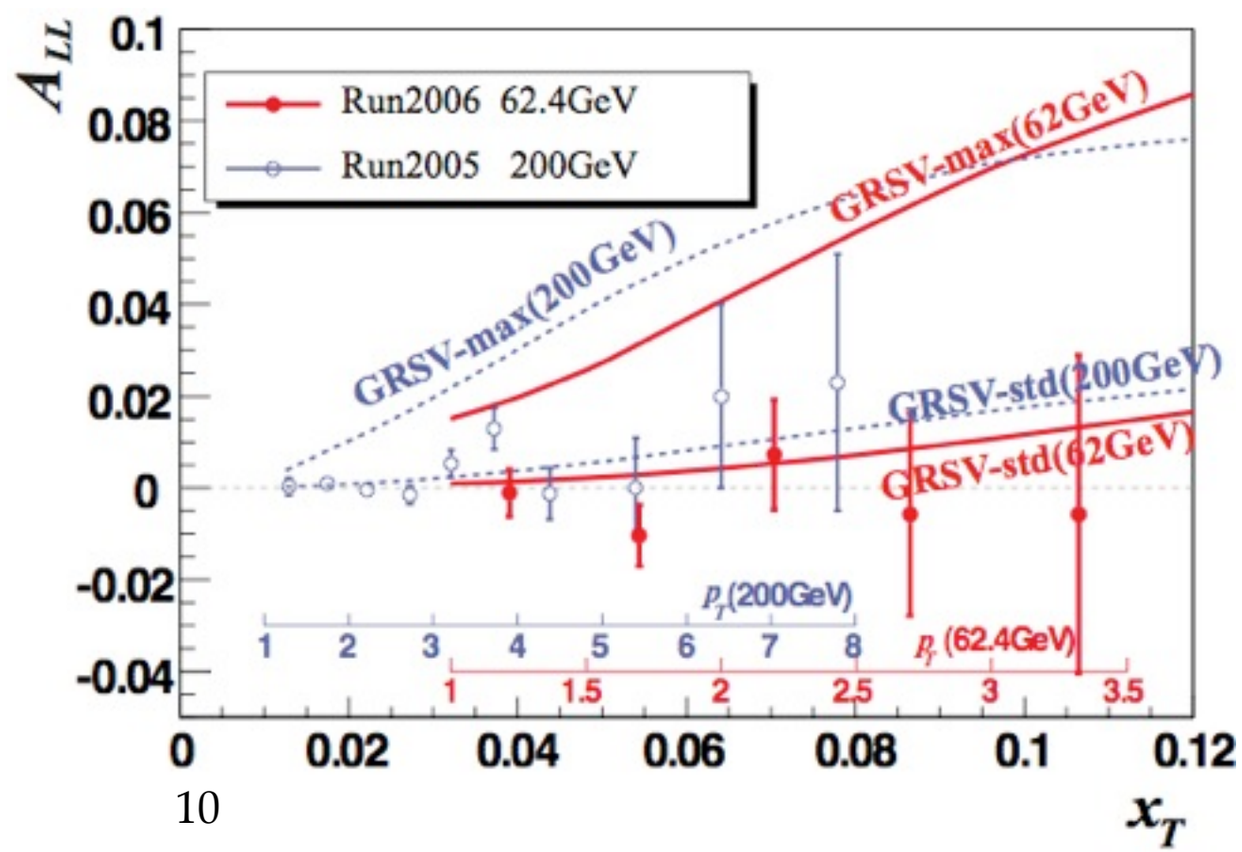

More probes @ midrapidity

π^0, π^+, π^-

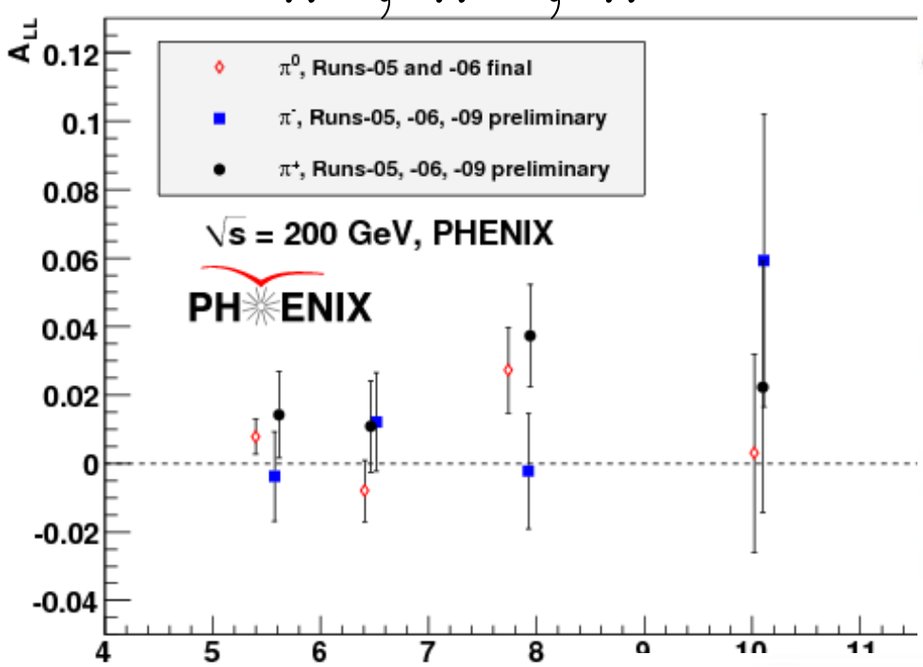

h^+

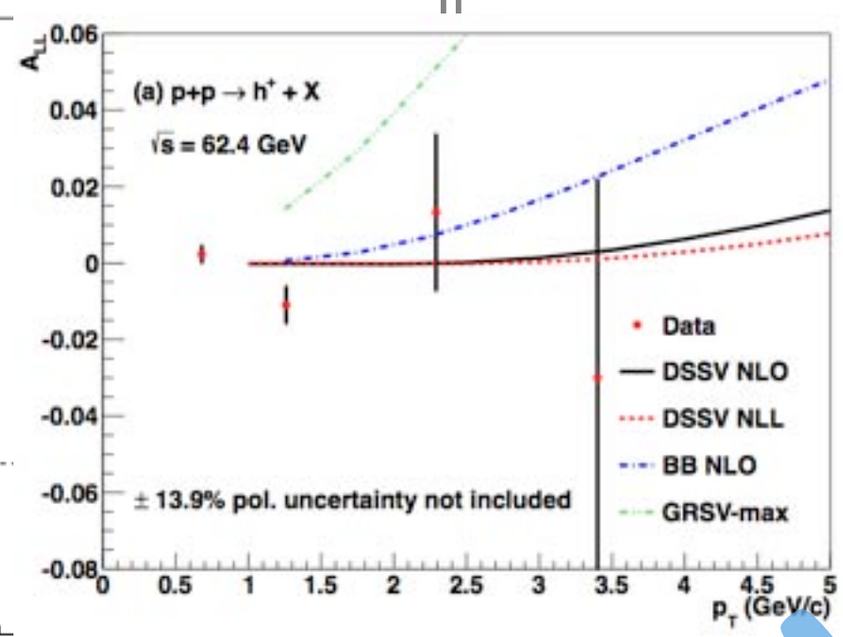

η

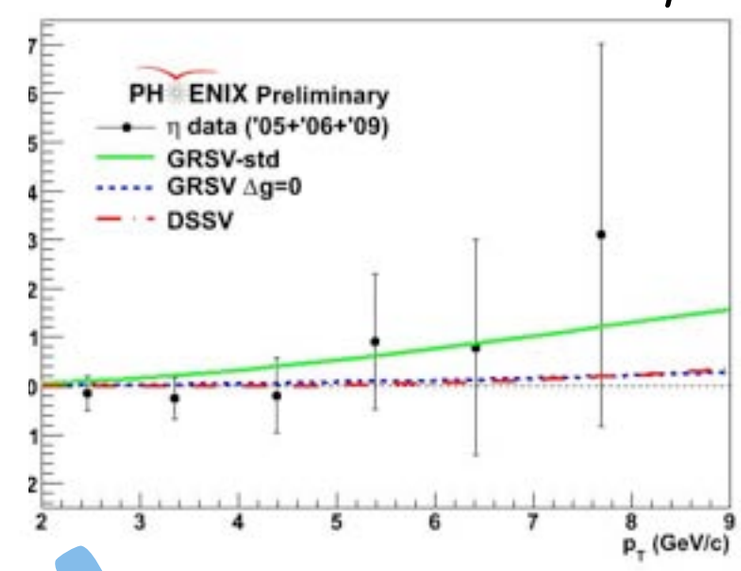

single electron

$D^+ \to \bar{K}^0 \nu_e e^+$
$D^0 \to \bar{K}^- \nu_e e^+$

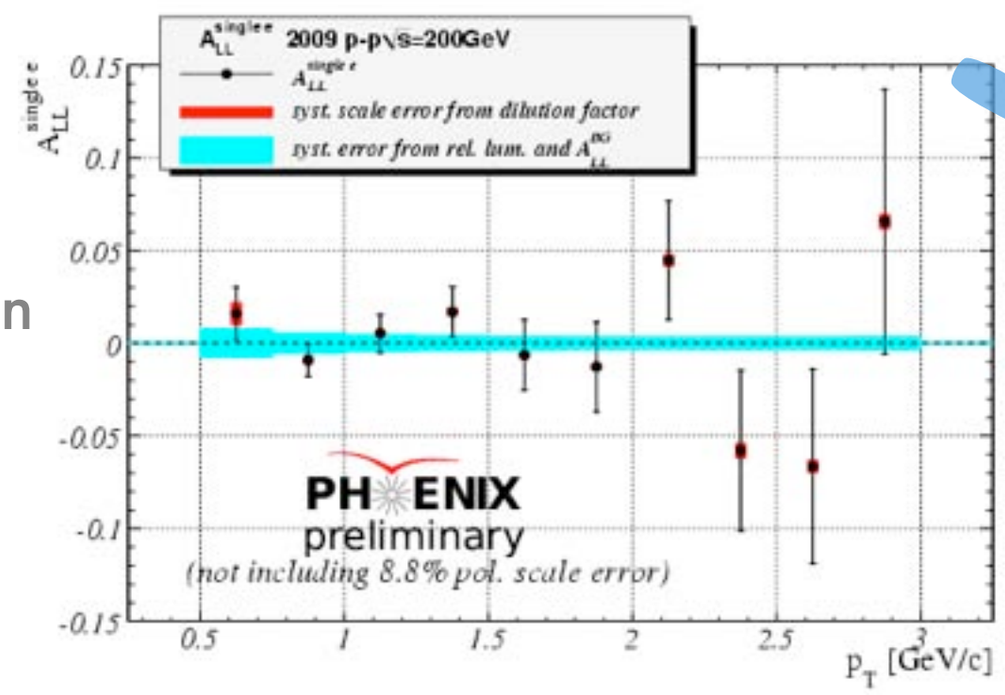

small gluon helicity
@ midrapidity

MPC: forward A_{LL}

Muon Piston Calorimeter:

$3.1 < |\eta| < 3.9$

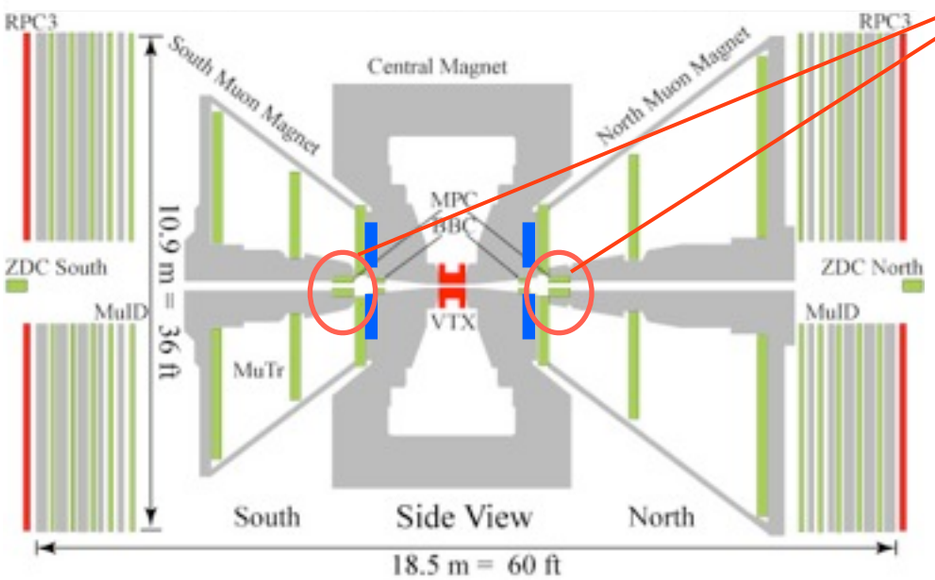

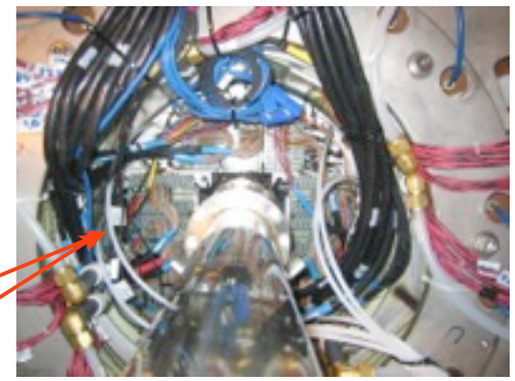

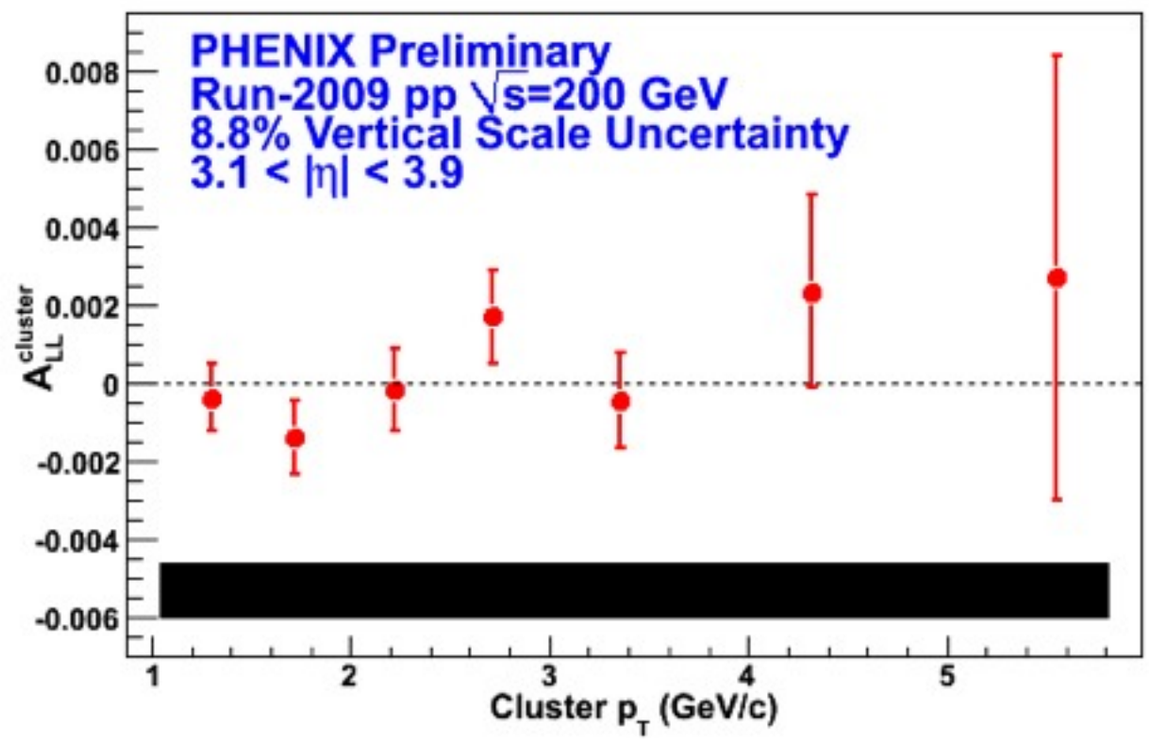

more data at 500 GeV in preparation...

Sea Quark Helicity

Sea quark helicity

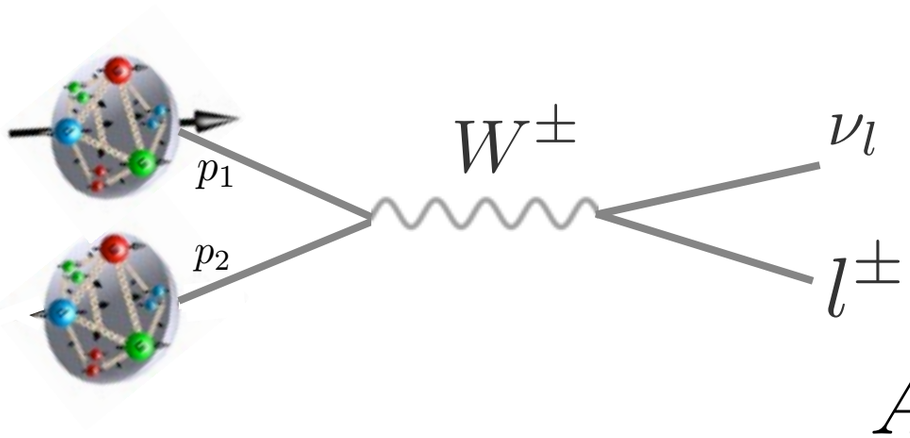

$$\frac{1}{2} = \frac{1}{2}\Delta\Sigma + \Delta G + L$$

$$A_L = \frac{\sigma^{\rightarrow} - \sigma^{\leftarrow}}{\sigma^{\rightarrow} + \sigma^{\leftarrow}}$$

$$\propto \Delta u_L \times \bar{d}_R + \Delta \bar{d}_R \times u_L$$

Accessing $W^{\pm}$

to "know" the quark (anti-quark) polarization state!

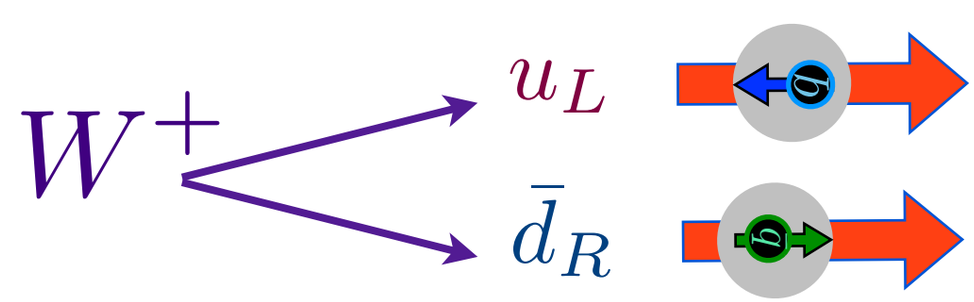

W central

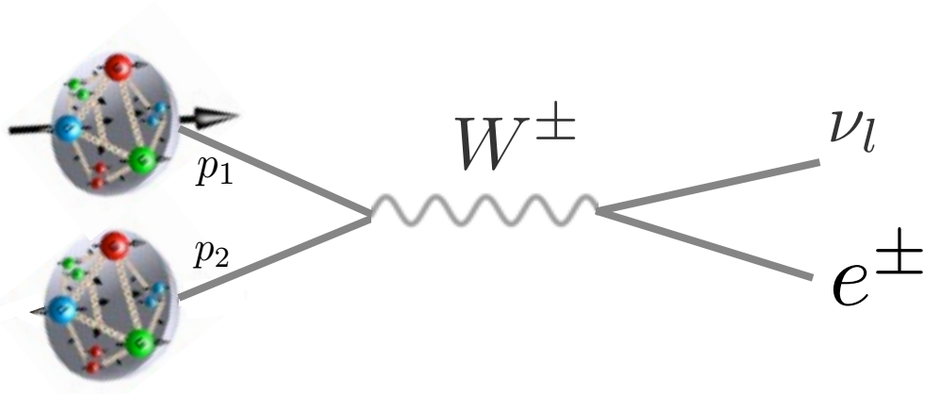

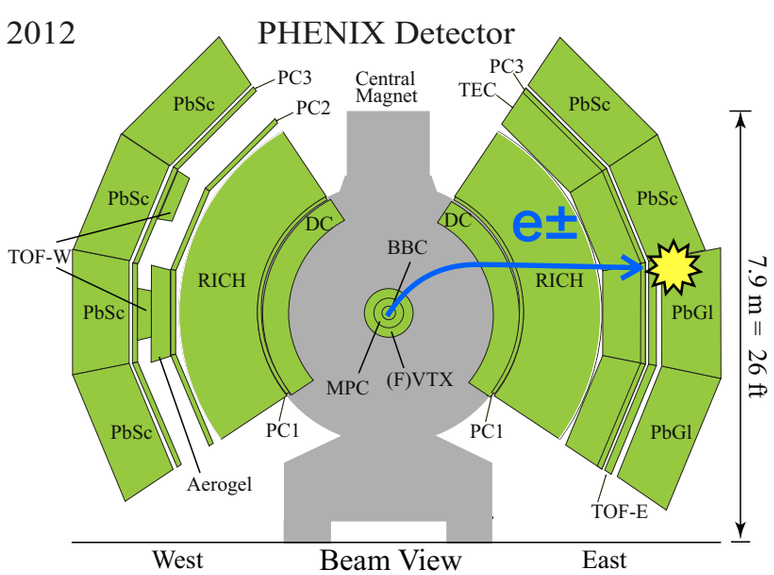

Non-zero asymmetry!

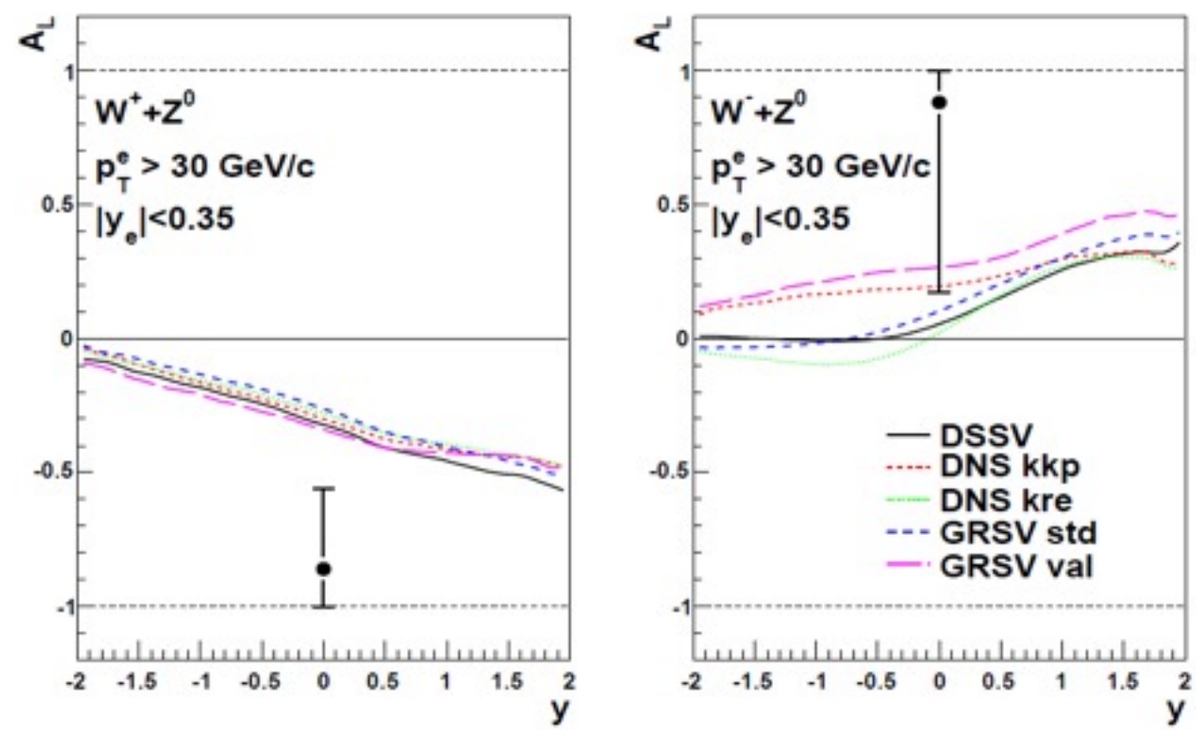

More data in progress...

W forward

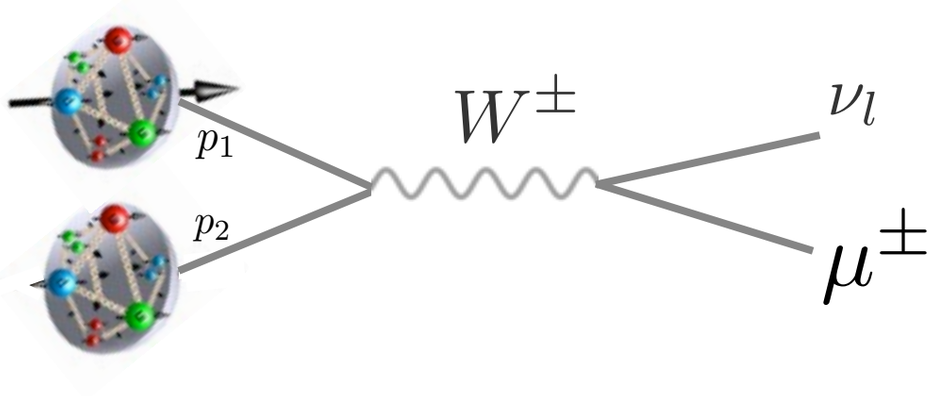

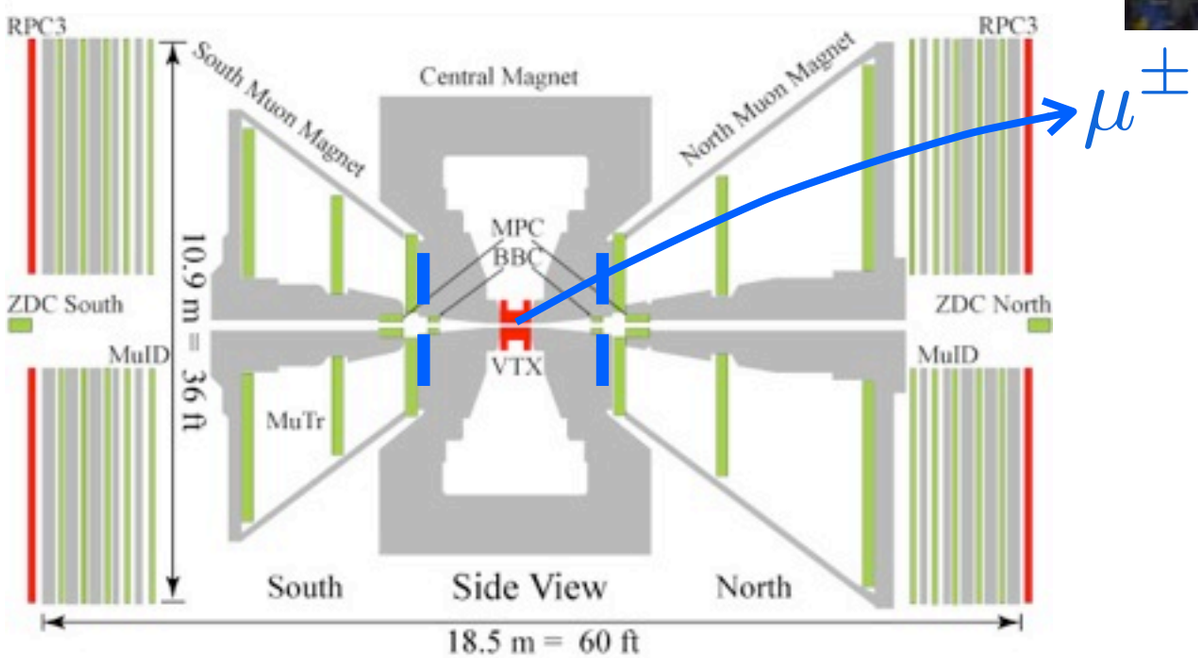

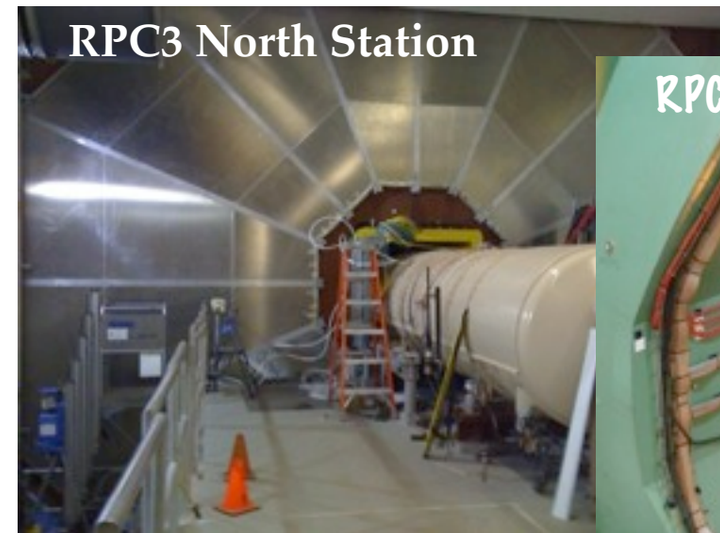

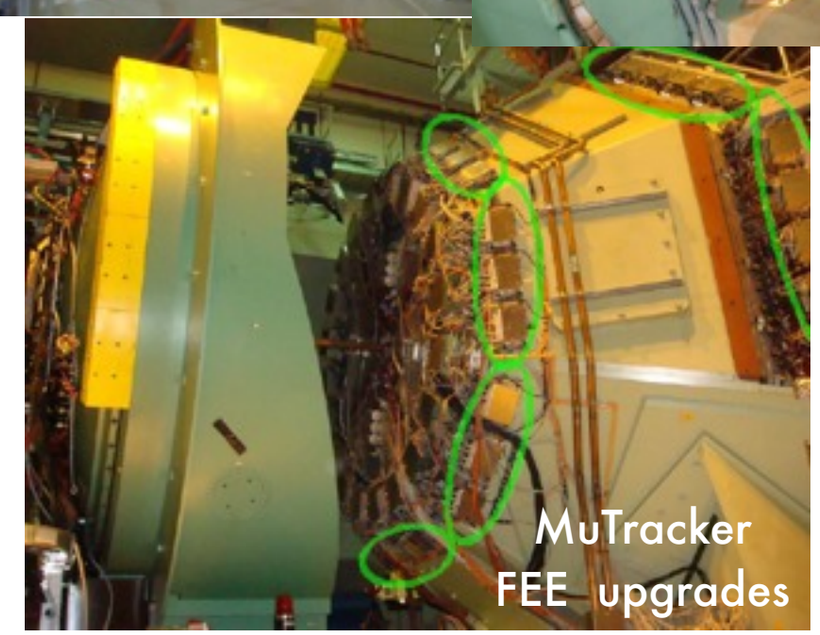

2012: Complete Forward Trigger upgrade

W forward

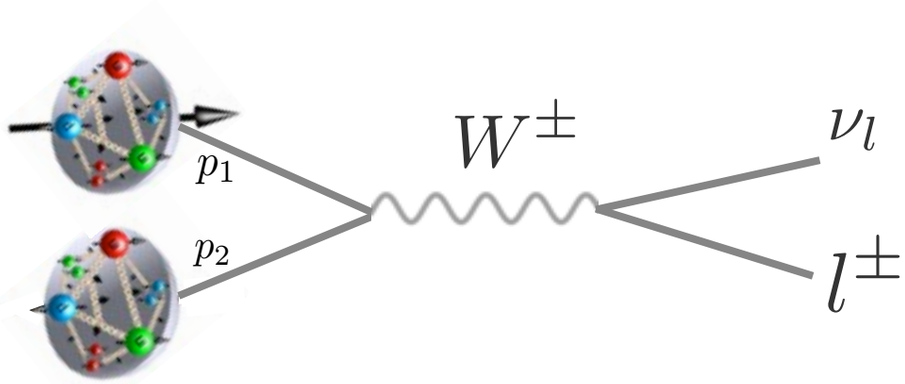

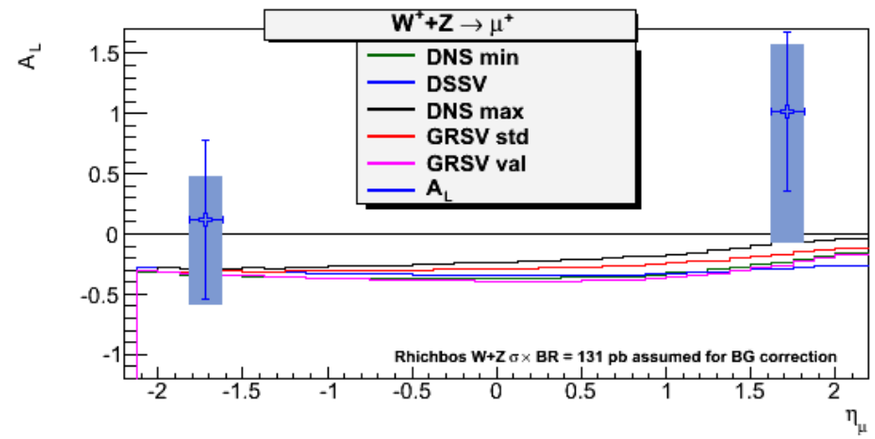

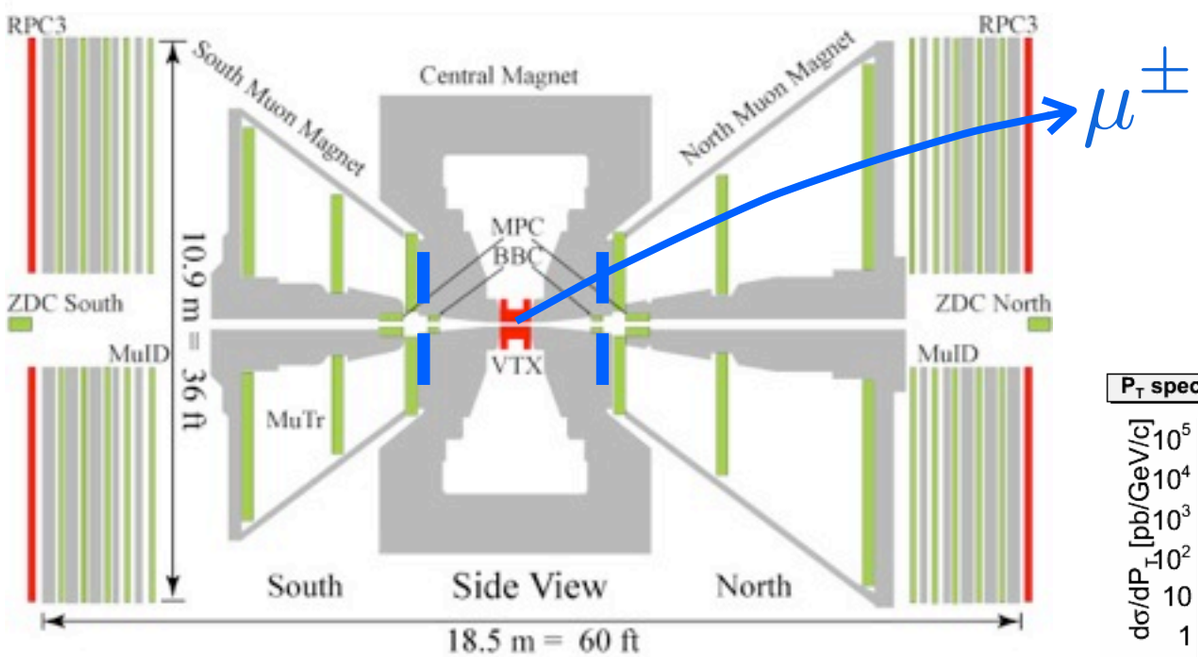

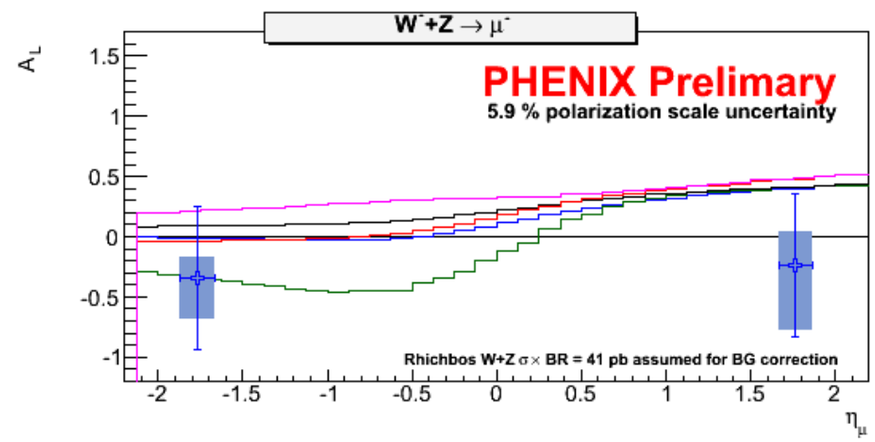

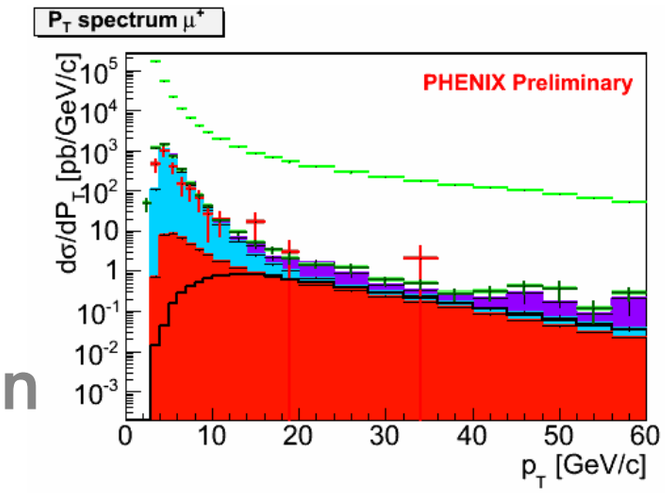

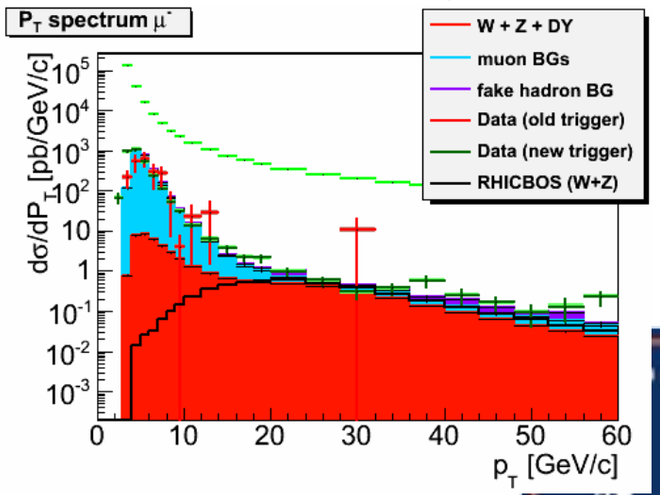

Additional background reduction with FVTX and RPC1

Transverse Spin

The proton structure:

where does the proton spin come from ?

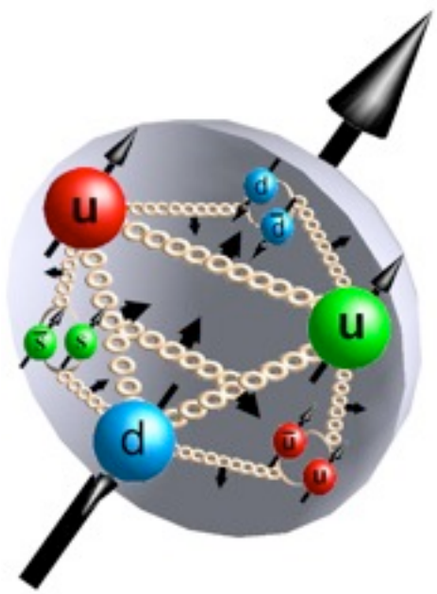

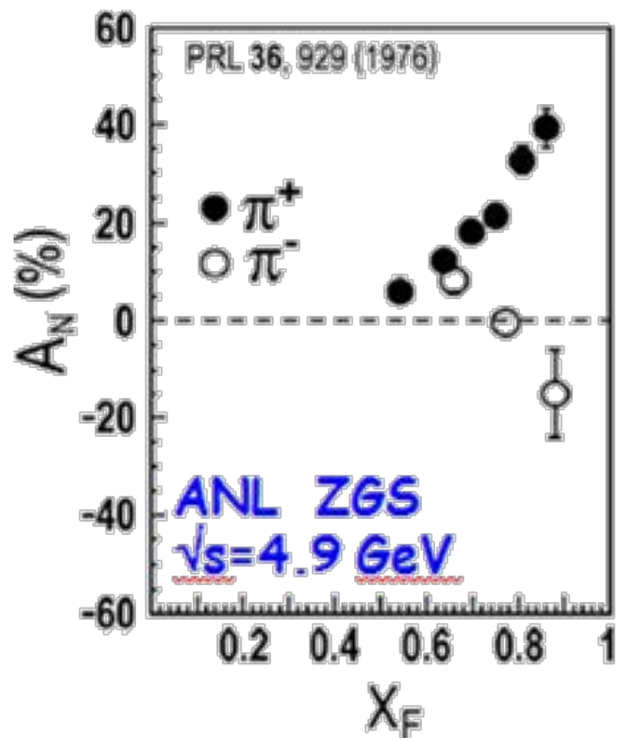

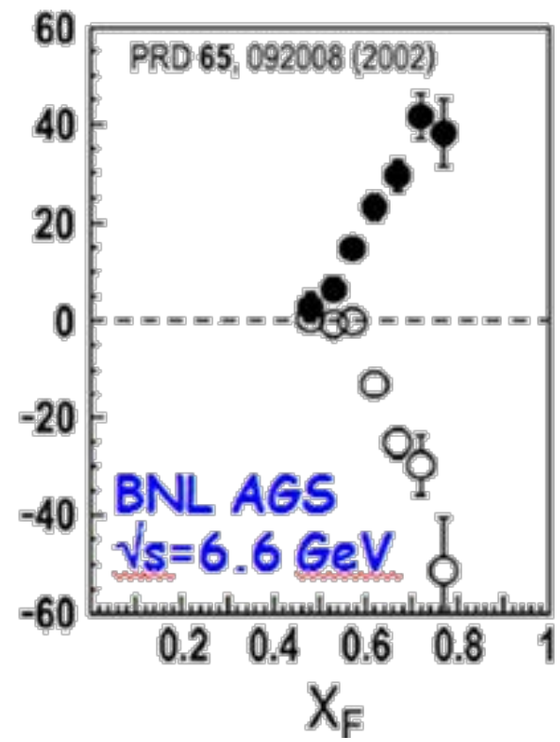

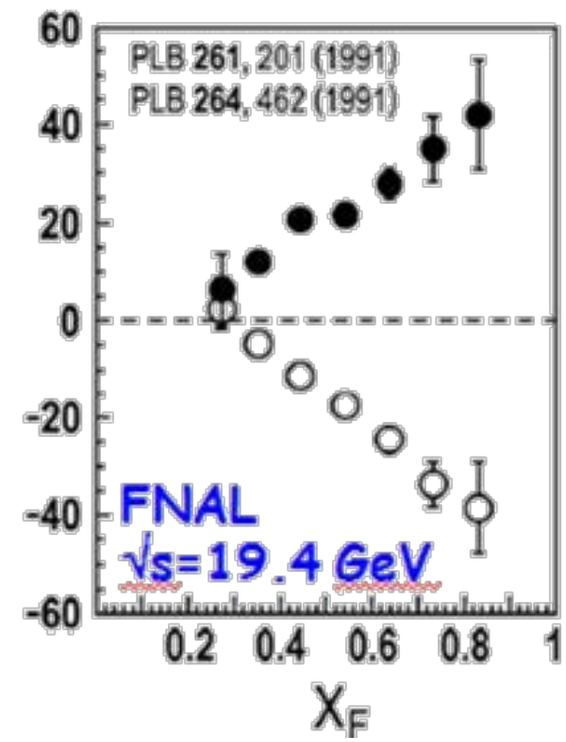

Second *spin crisis:*

transverse effect not small!

TMD Factorization

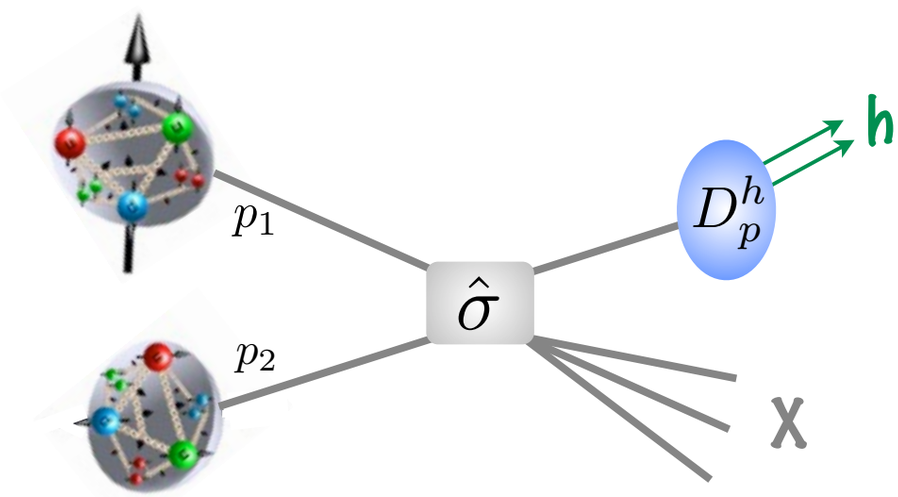

$$\sigma(pp \to hX) \propto DF \times DF \times \hat{\sigma}(qq \to qq) \times FF$$

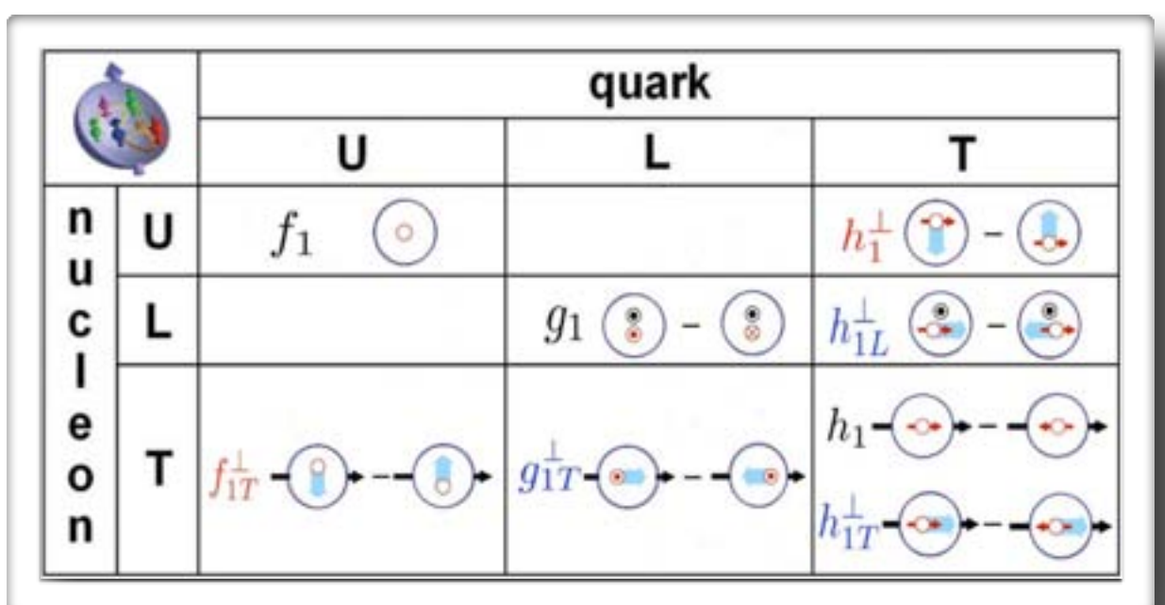

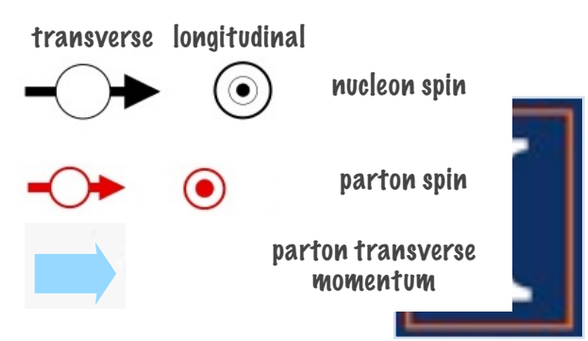

Transversity

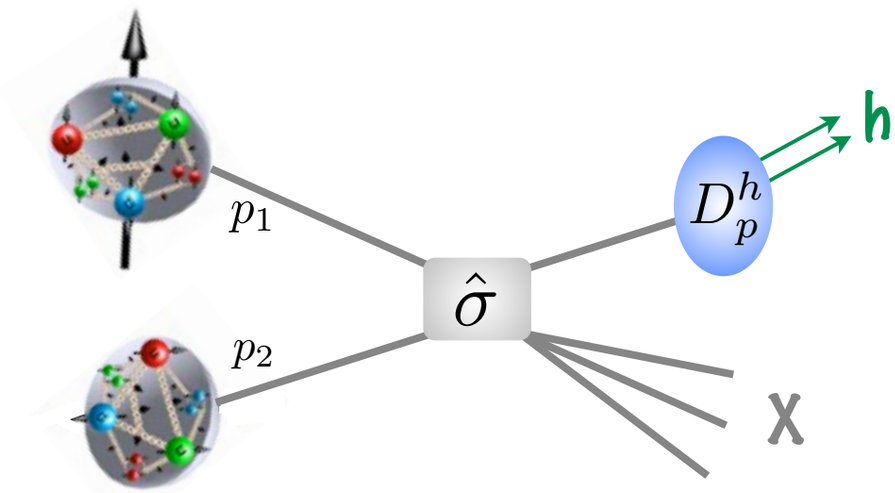

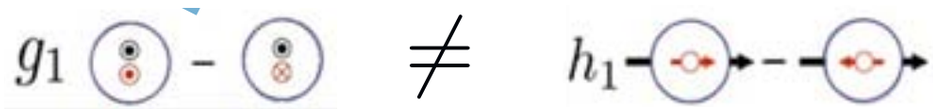

nucleon	quark: U	quark: L	quark: T
U	f_1		$h_1^\perp$
L		g_1	$h_{1L}^\perp$
T	$f_{1T}^\perp$	$g_{1T}^\perp$	h_1, $h_{1T}^\perp$

Accessible via the Collins mechanism:

left-right asymmetry from correlations between quark transverse spin and outgoing hadron direction

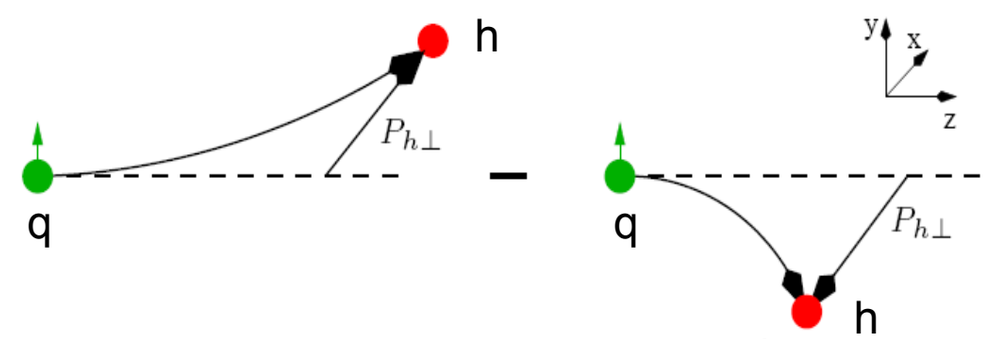

$$A_N \propto h_1 \times H_1^\perp$$

BUT!!

TMD factorization not valid in pp => hadron reaction!

A_N also generated by other effects:
- Higher twist effects
- Sivers effect

Sivers mechanism

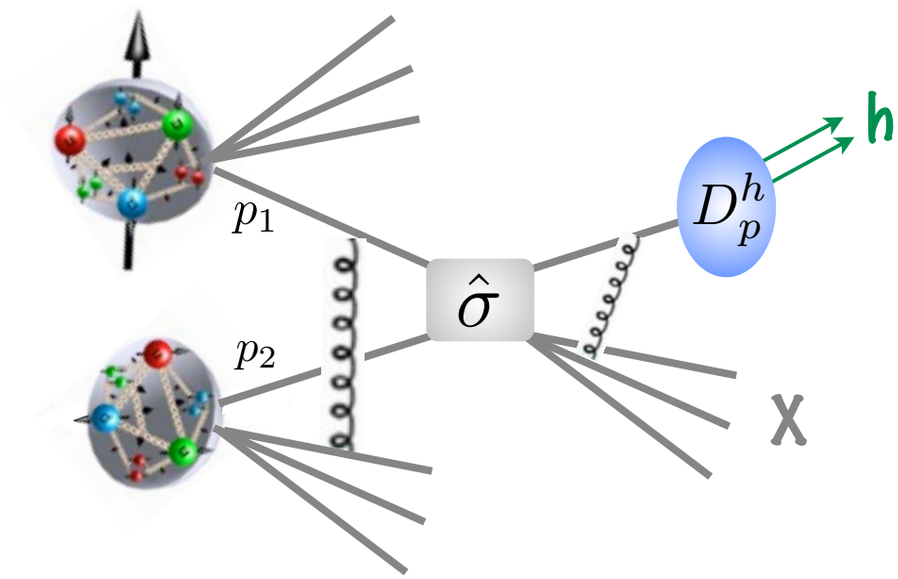

Azimuthal asymmetry generated by correlations between quark transverse momentum and the proton transverse spin

Spatial deformation due to spin-orbit correlations:
=> non zero Orbital Angular Momentum!

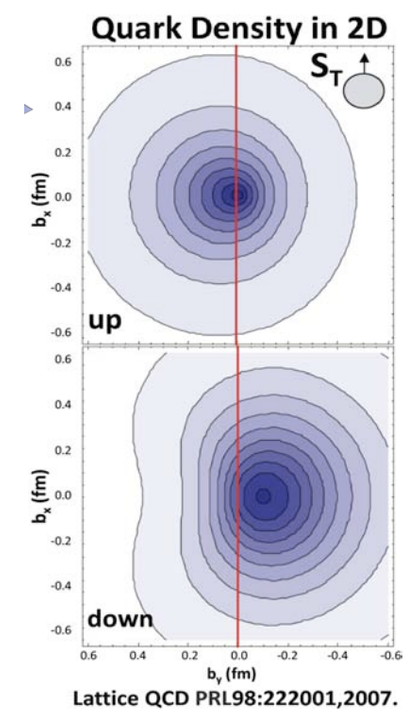

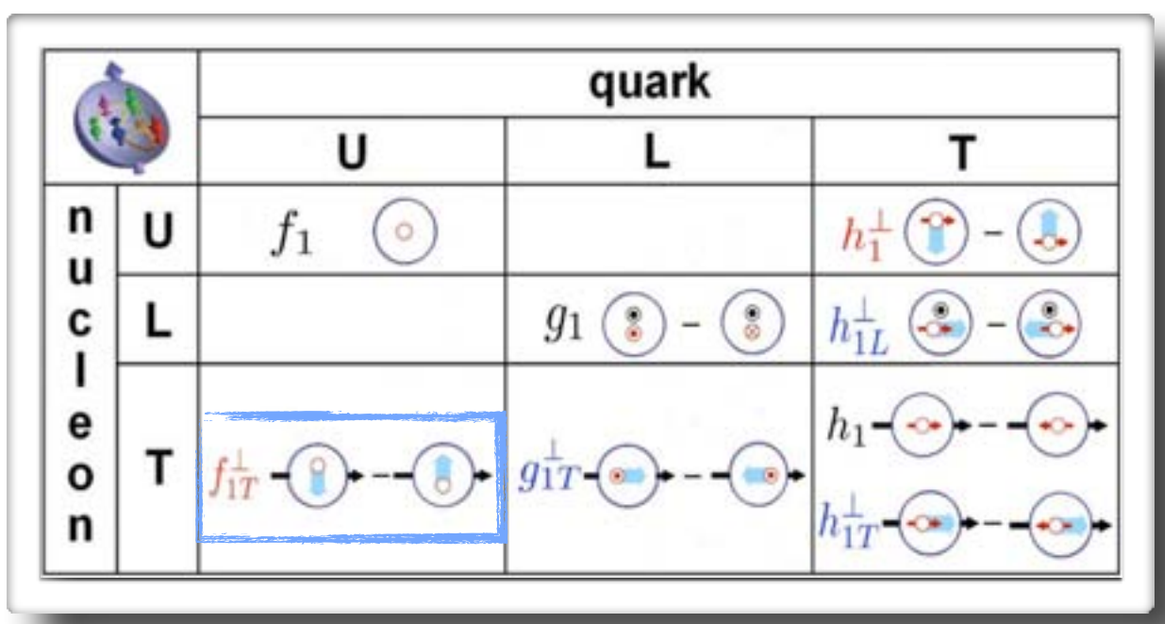

Which effect?

transversity

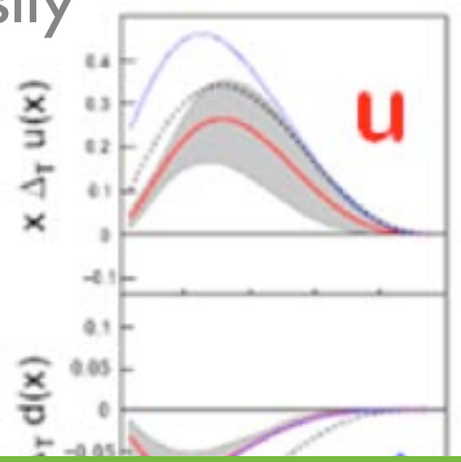

Sivers

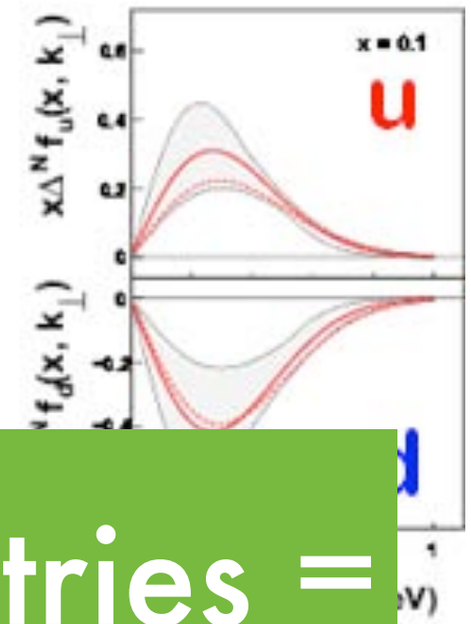

Single Spin Asymmetries = Collins + Sivers + ...

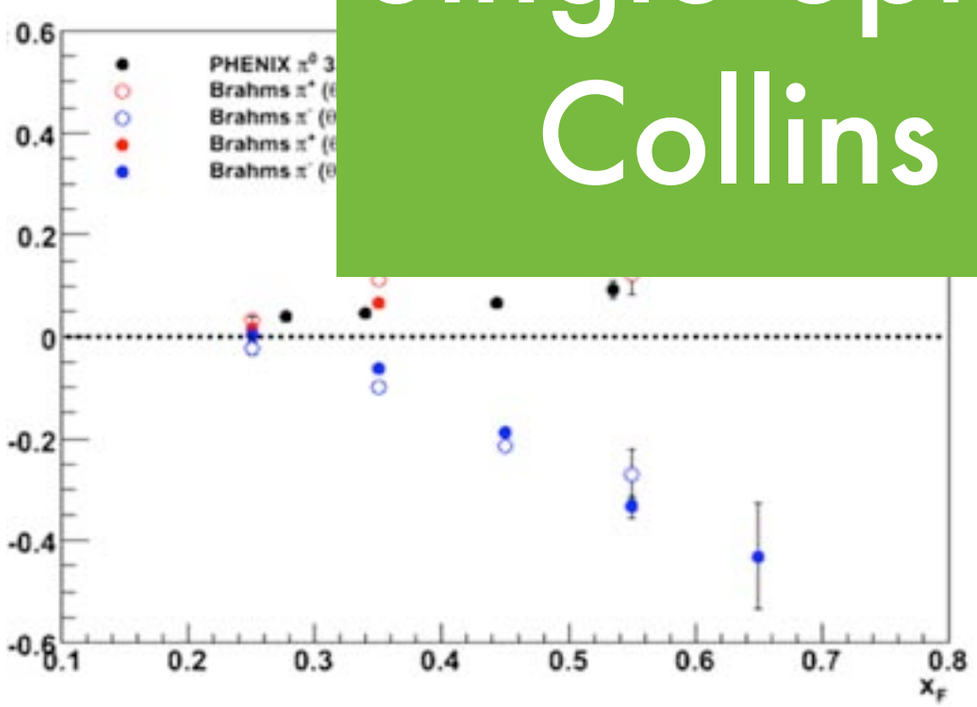

$1:0$

$\pi^0\,(u\bar{u}+d\bar{d})$ $\quad u:d\rightarrow\pi^0$ $\quad 2:1$

$\pi^-\,(\bar{u}d)$ $\quad u:d\rightarrow\pi^-$ $\quad 1:1$

A_N for π^0 @ midrapidity

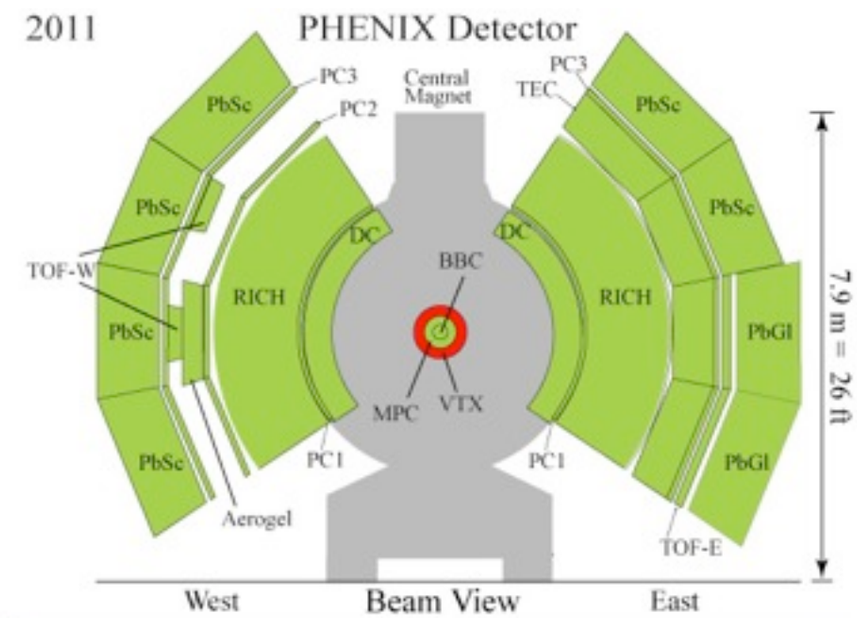

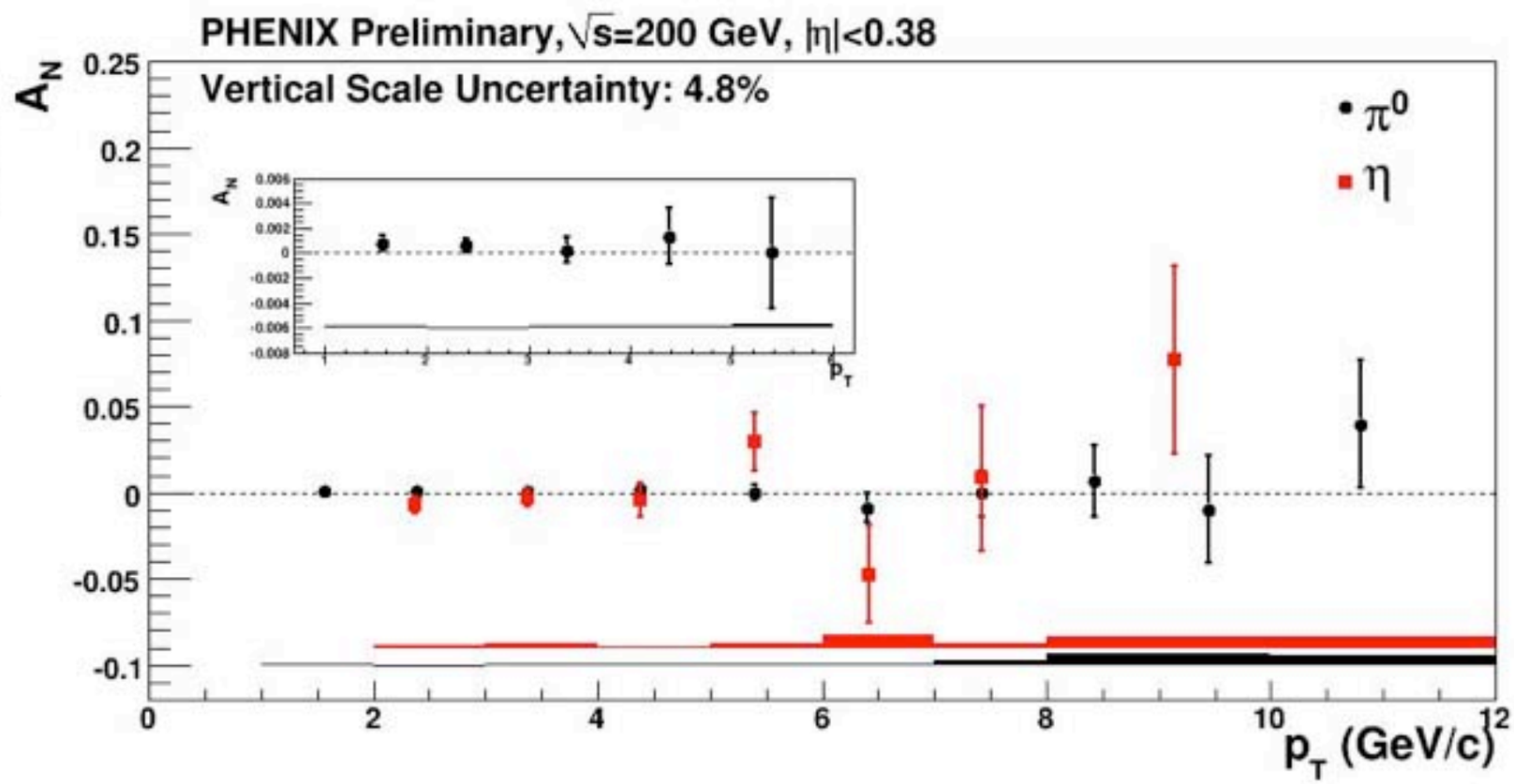

$A_N \approx 0$

A_N for π^0 forward

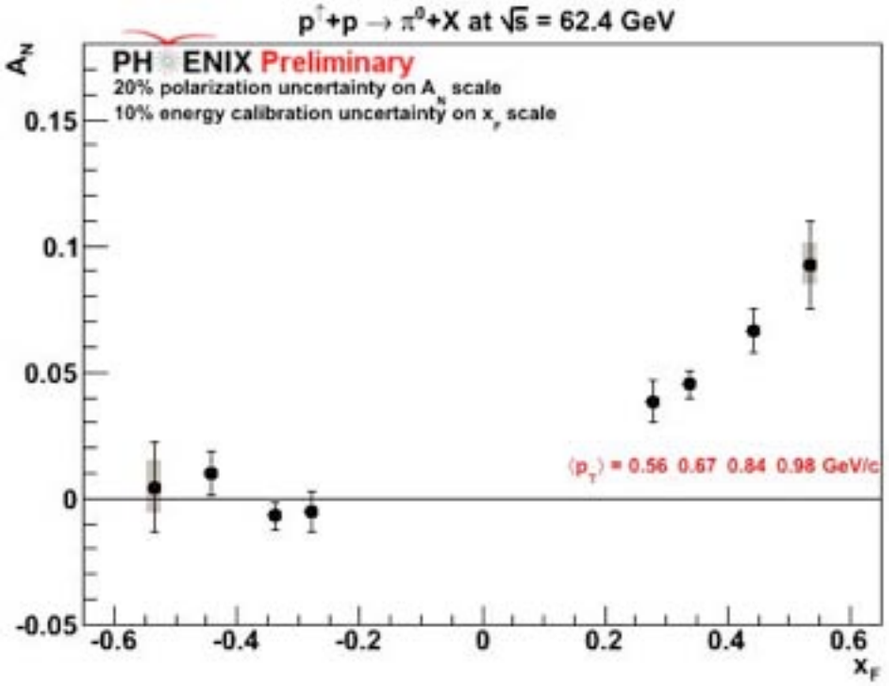

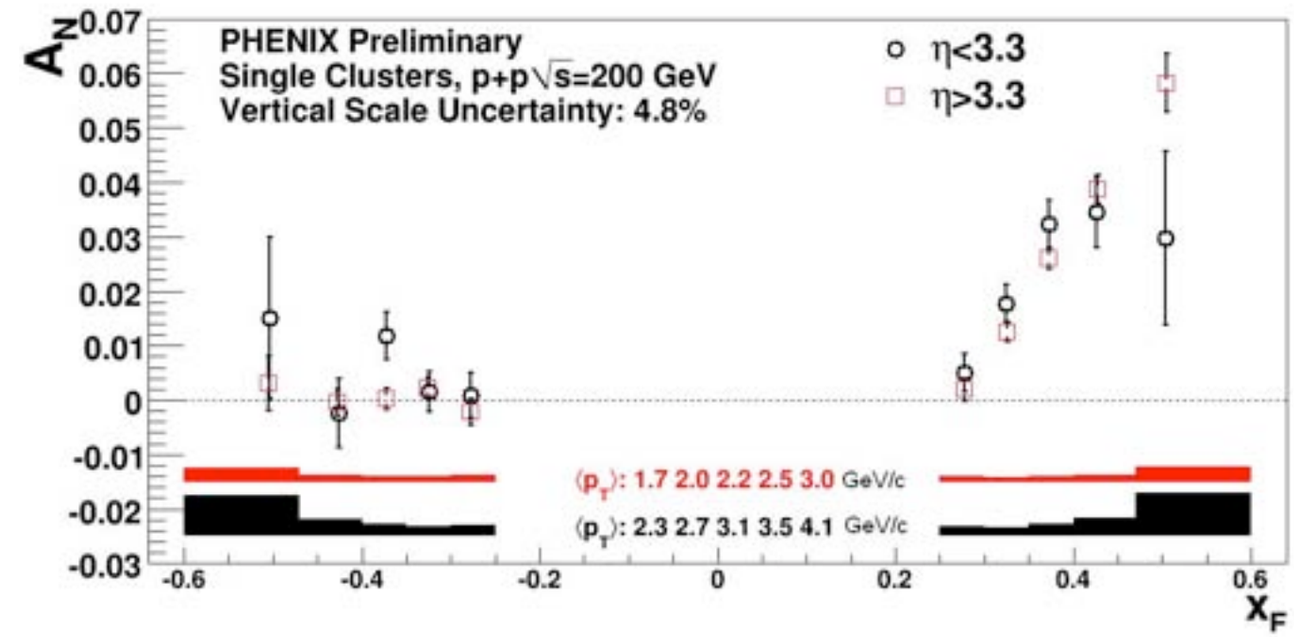

Fraction of clusters

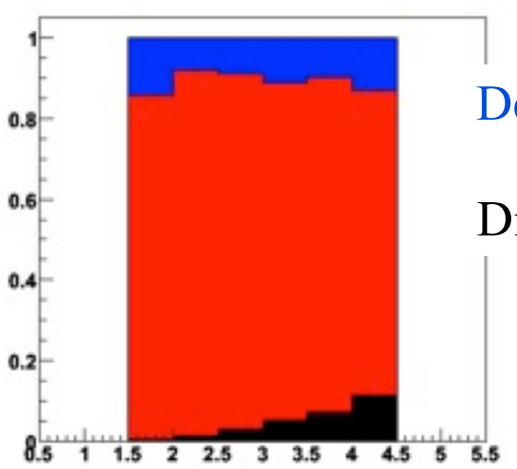

Decay photon

π^0

Direct photon

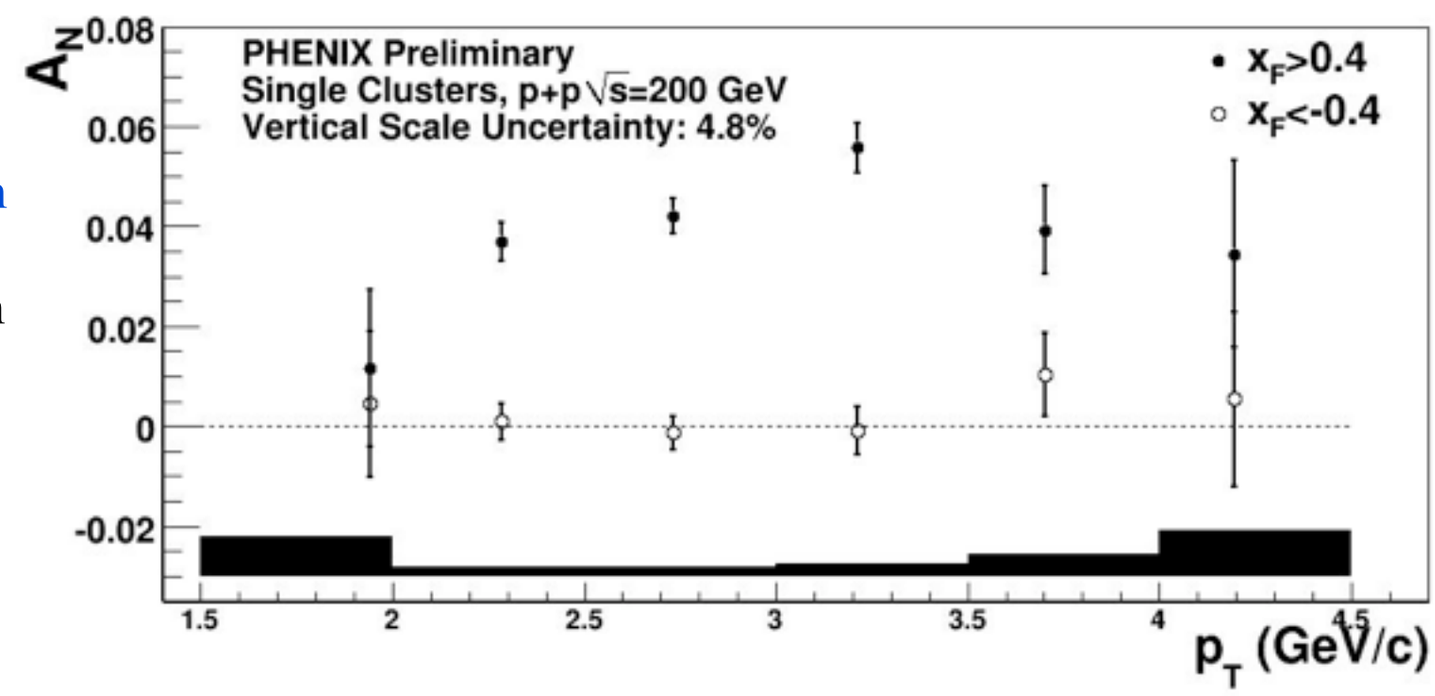

A_N η forward

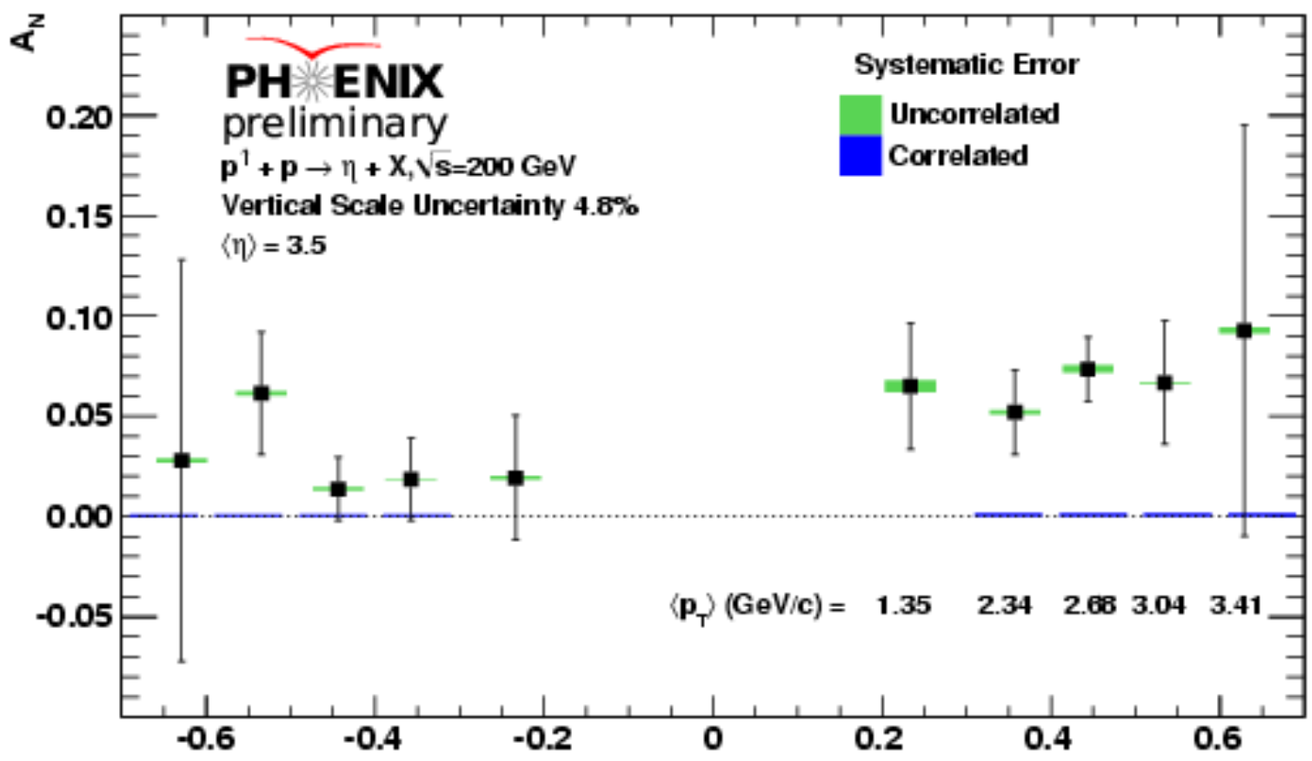

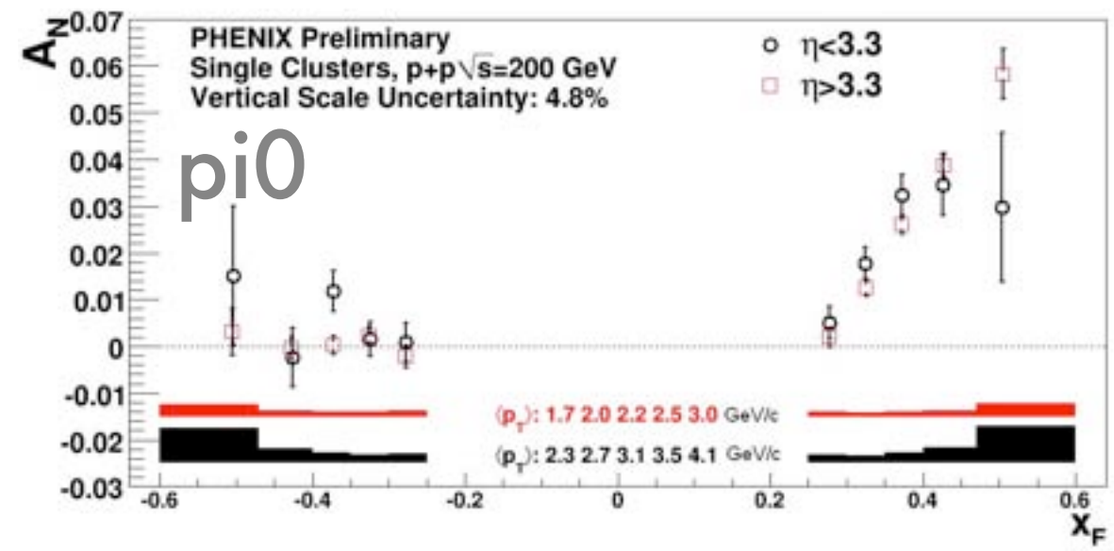

Larger asymmetry : strange contribution?

Transversity

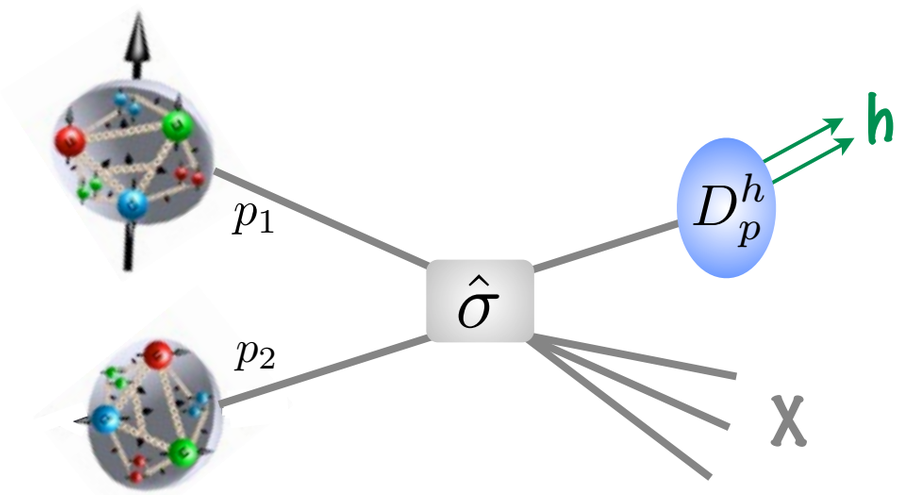

Accessible via the Collins mechanism:

left-right asymmetry from correlations between quark transverse spin and outgoing hadron direction

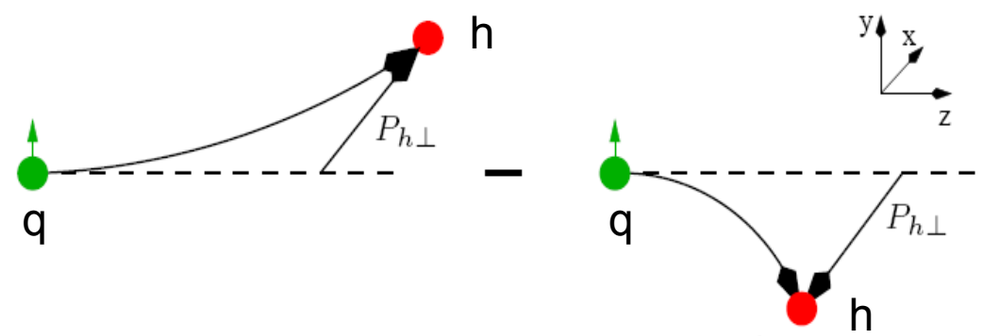

$$A_N \propto h_1 \times H_1^{\perp}$$

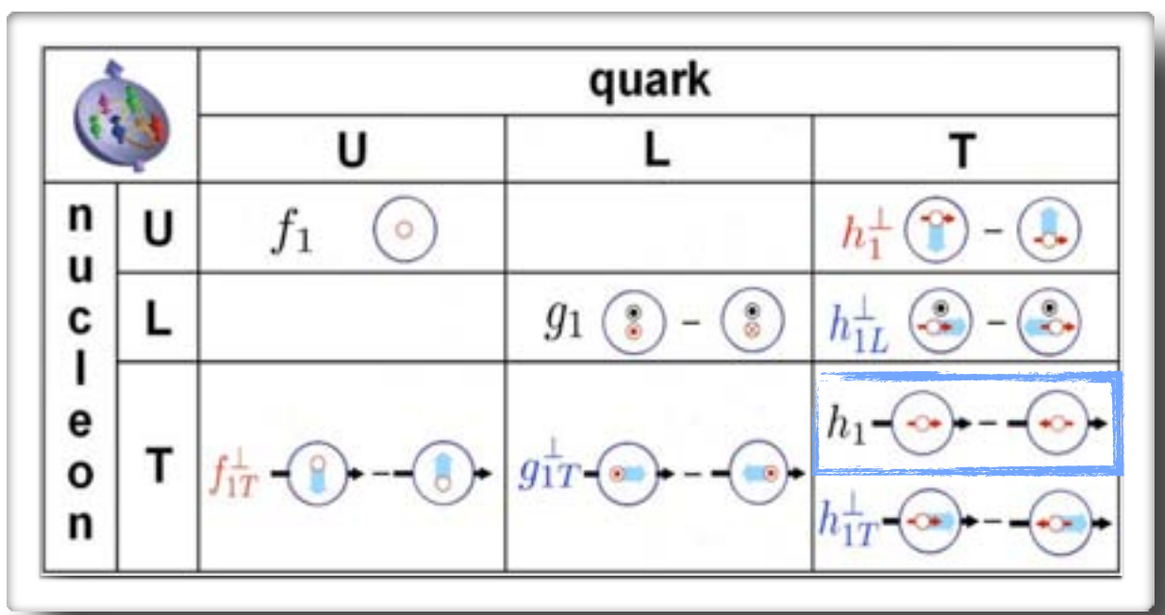

BUT!!

TMD factorization not valid in pp => hadron reaction!

A_N also generated by other effects:
- Higher twist effects
- Sivers effect

Transversity x IFF

Interference Fragmentation:
left-right asymmetry from correlations between quark transverse spin and relative orbital angular momentum of the hadron pair

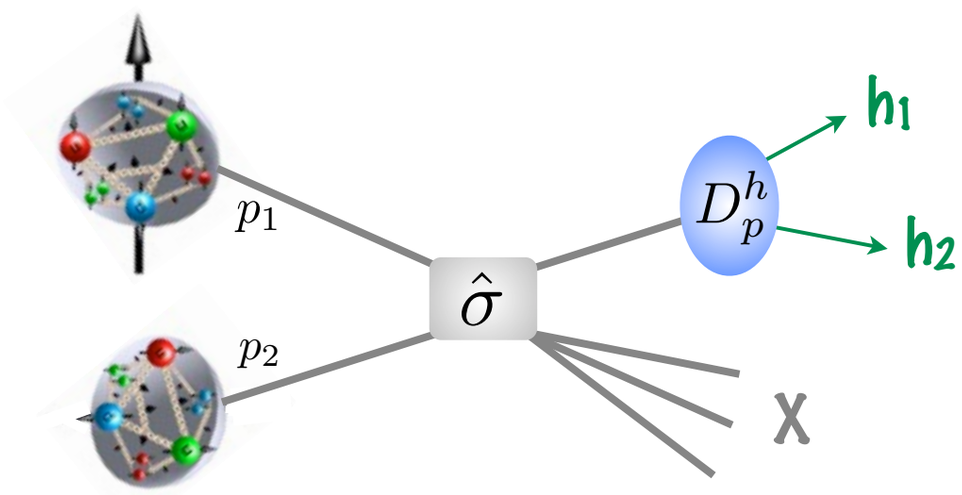

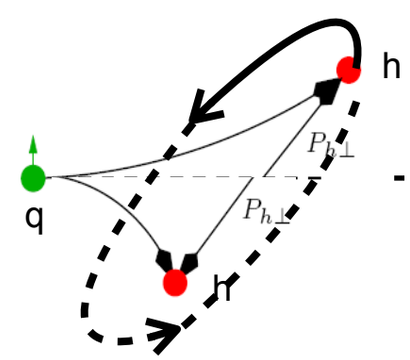

Collinear, no TMD!

Collinear factorization

Independent access to transversity

Measure of TMD factorization breaking in pp => hadrons reaction

Transversity x IFF @ midrapidity

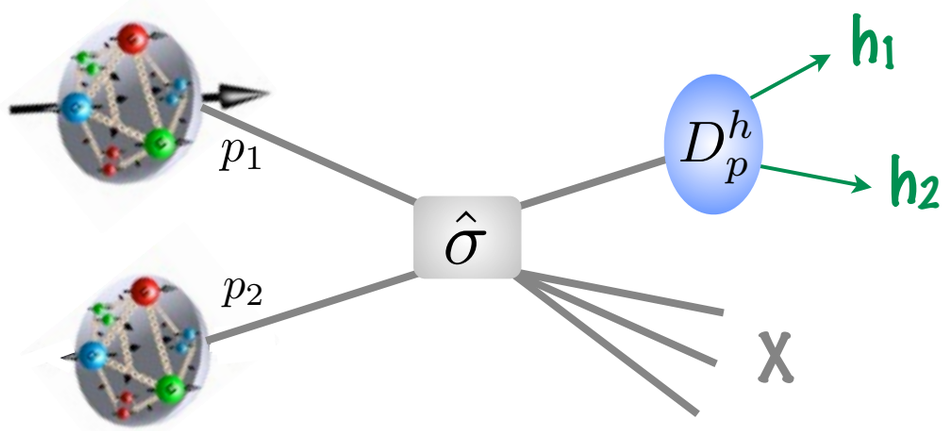

$$A_N \propto h_1 \times H_1^{\angle}$$

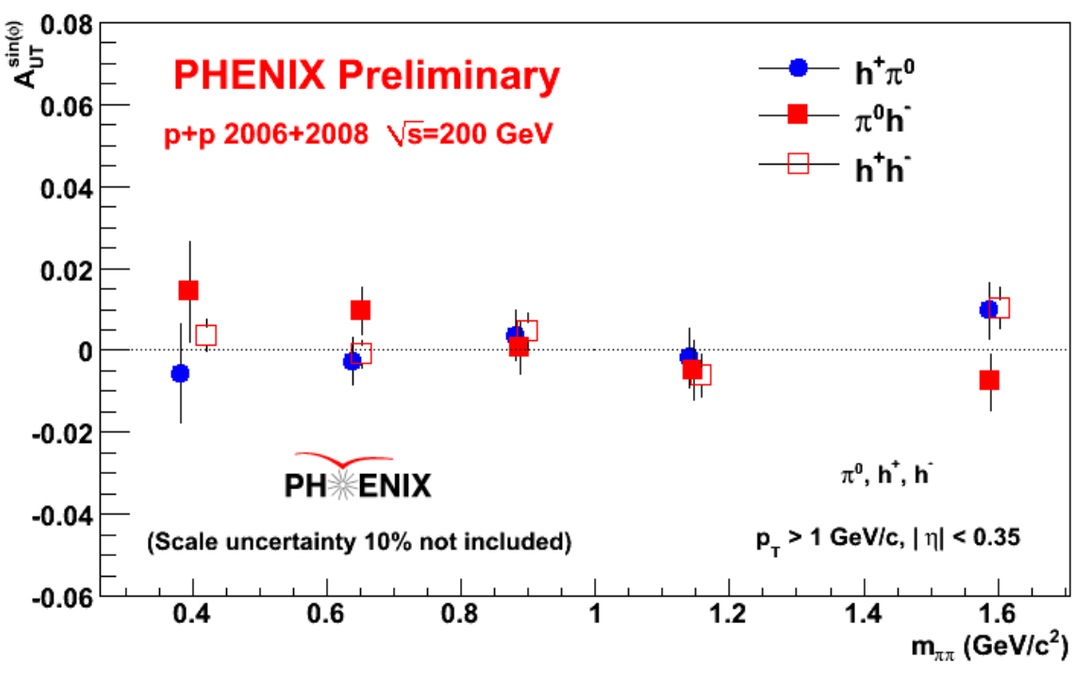

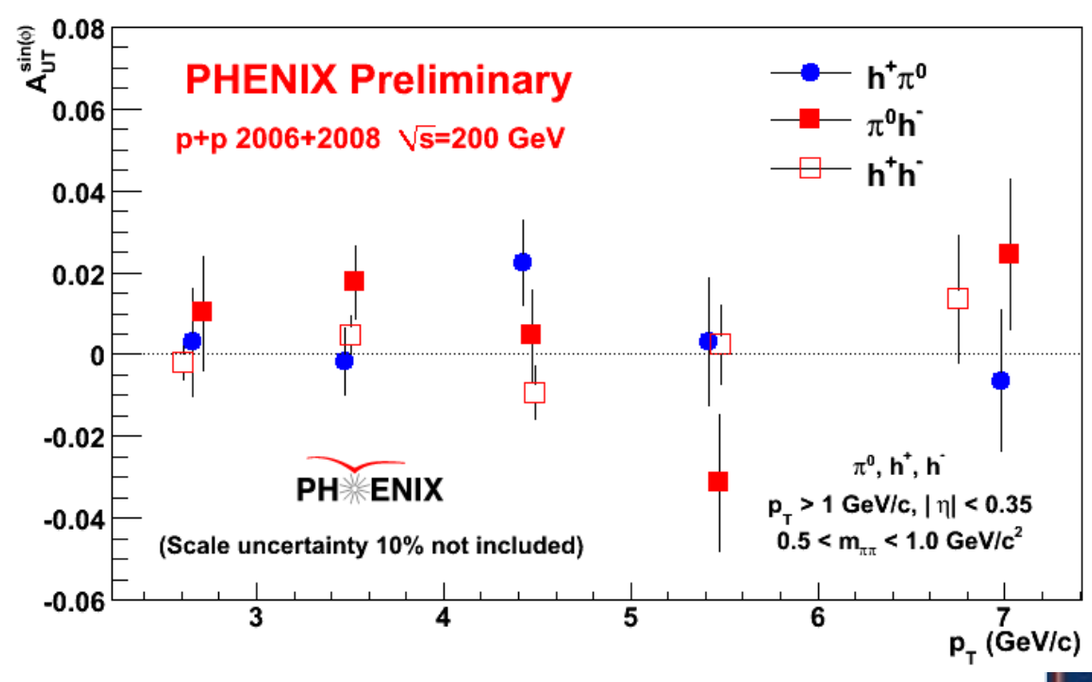

Near Future measurements

FVTX

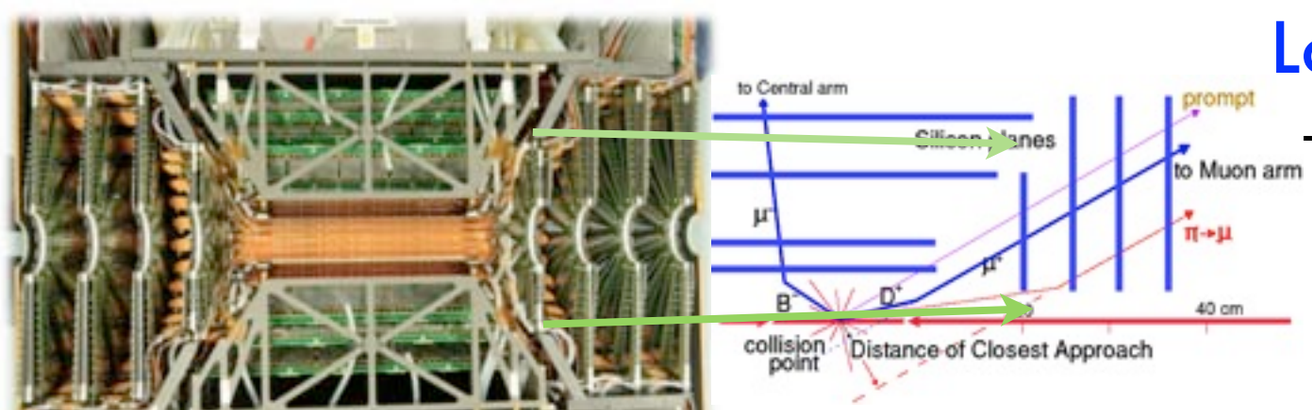

Longitudinal Spin program:

- Flavor dependent sea quark polarization:
  - S/B study for W - > muon
  - Drell-Yan for anti-u-quark polarization

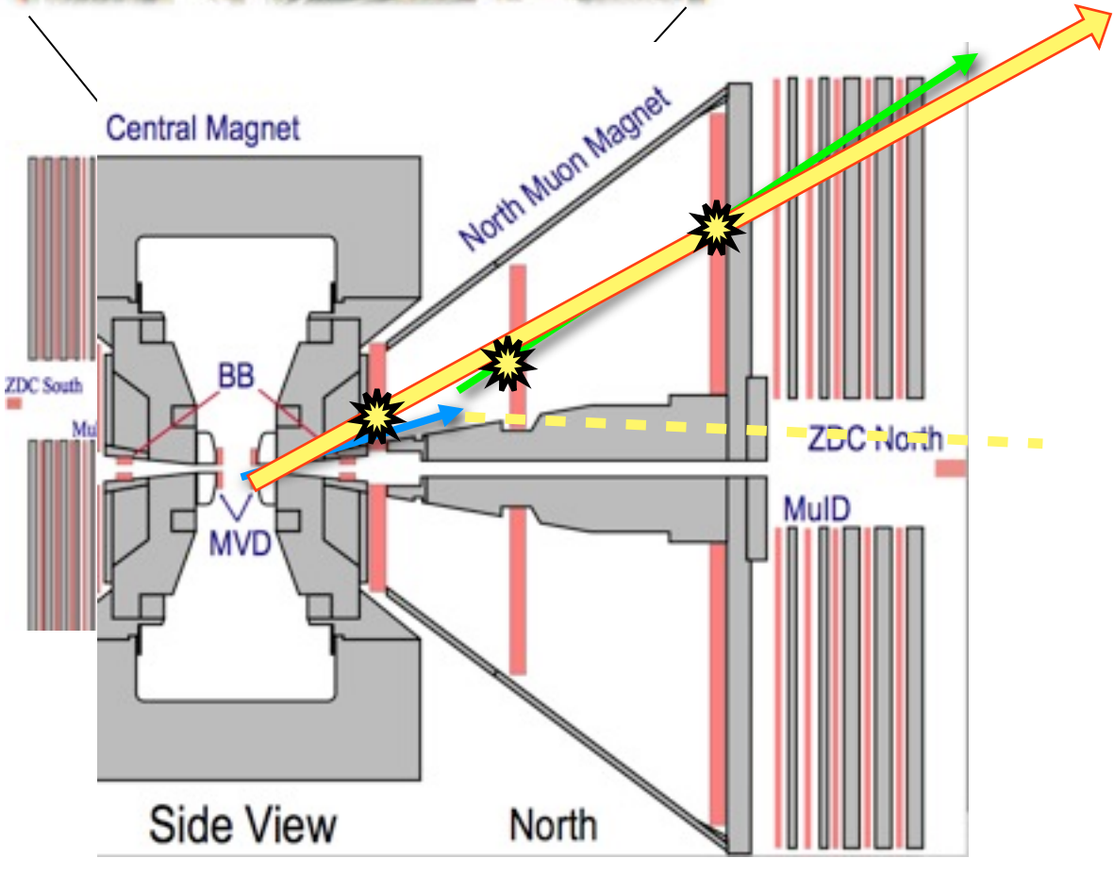

$\Delta\bar{u}/\bar{u}$ (L = 300 pb^{-1}) $\delta(A_{LL})\approx 1\%$

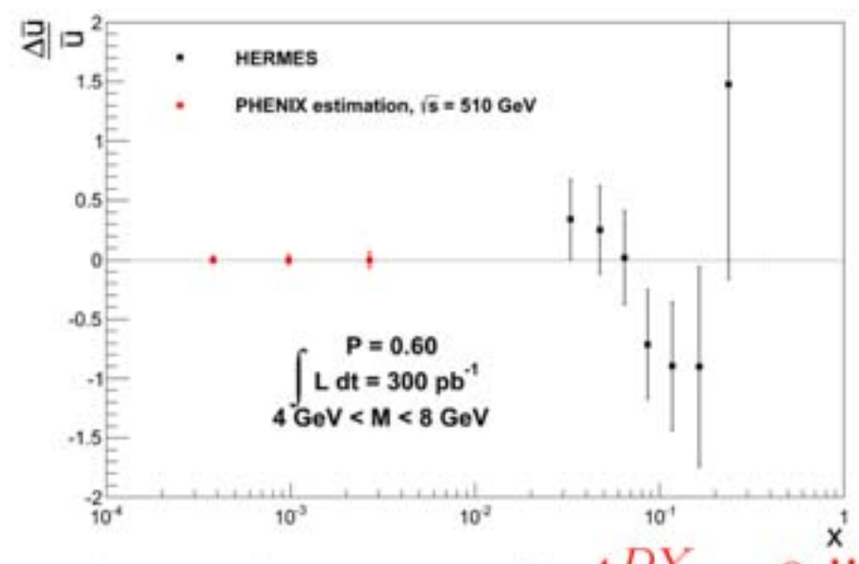

if anti-quarks carry no spin ➔ $A_{LL}^{DY} \equiv 0$!!!

FVTX

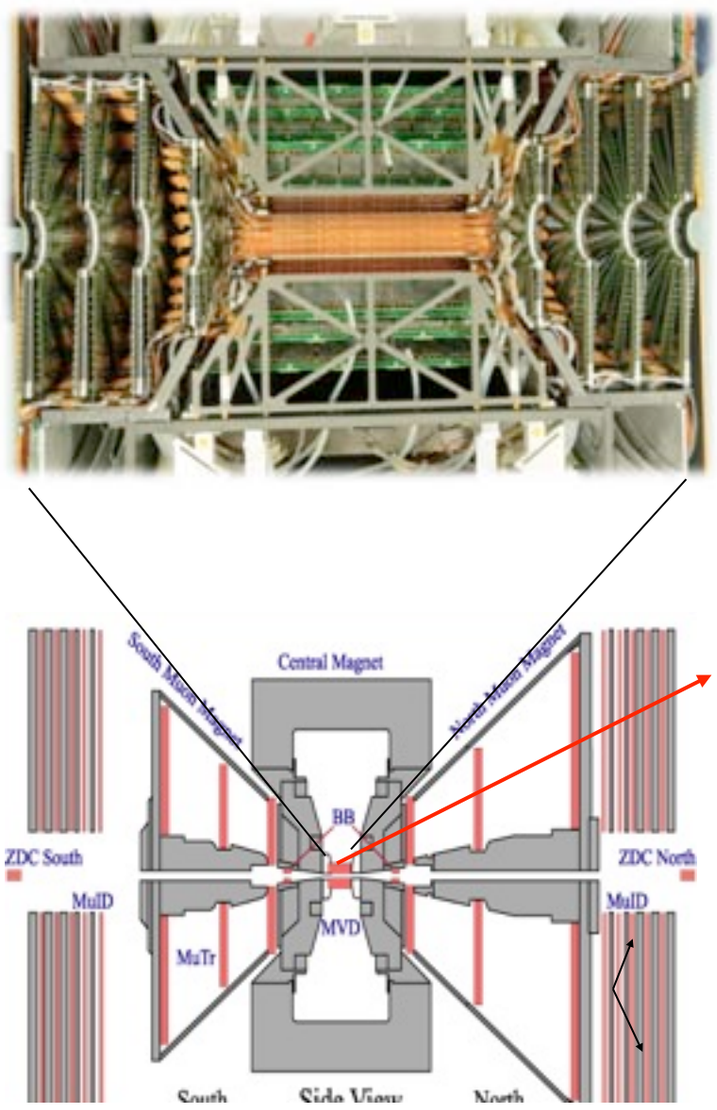

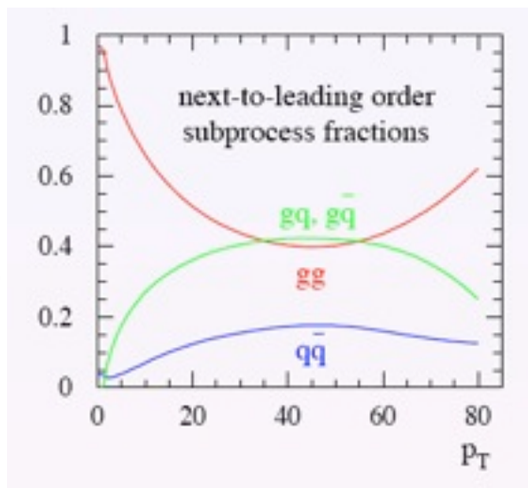

Longitudinal Spin program:

- Flavor dependent sea quark polarization:
  - S/B study for W - > muon
  - Drell-Yan for anti-u-quark polarization
- Gluon polarization at small-x (10^-3-10^-2):
  - Single high pT muon
  - Charm & Beauty measurements

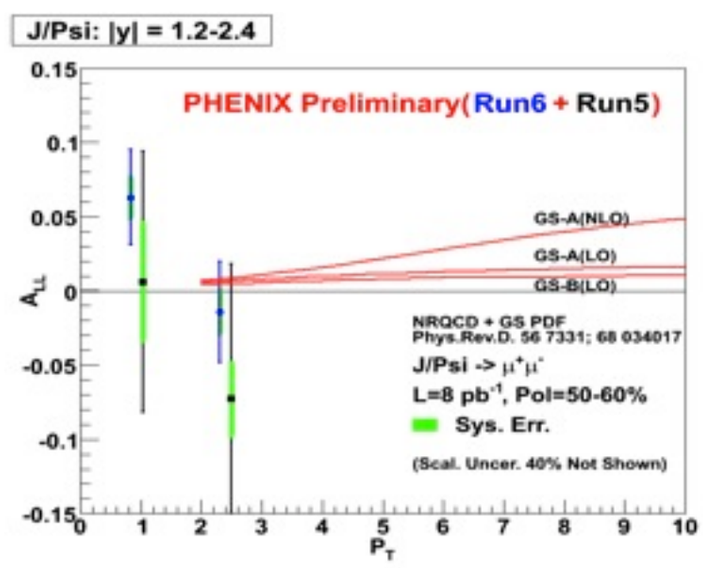

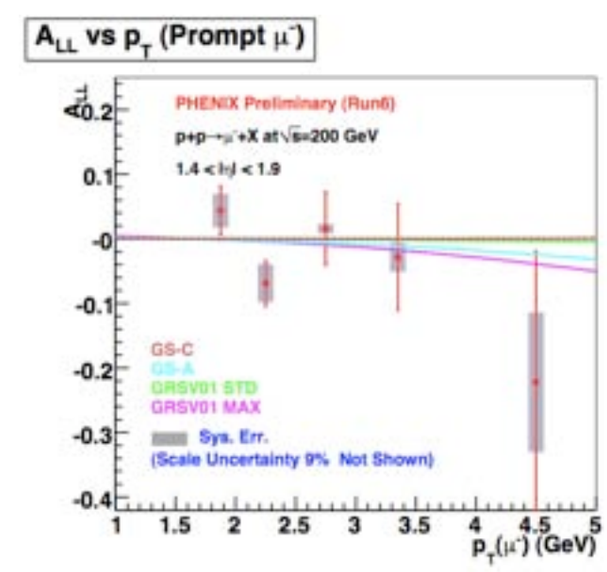

FVTX

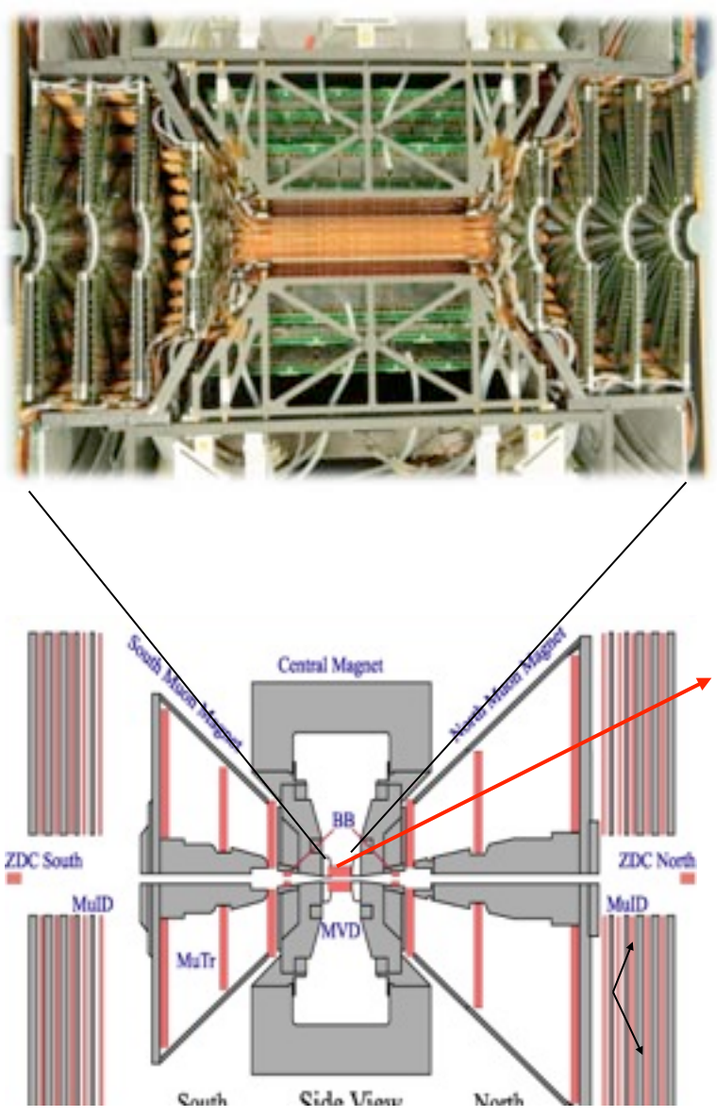

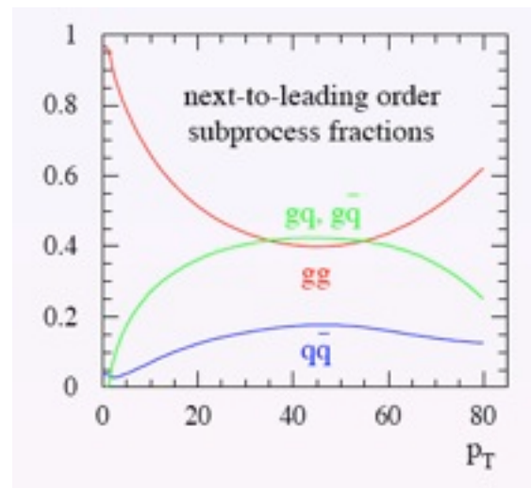

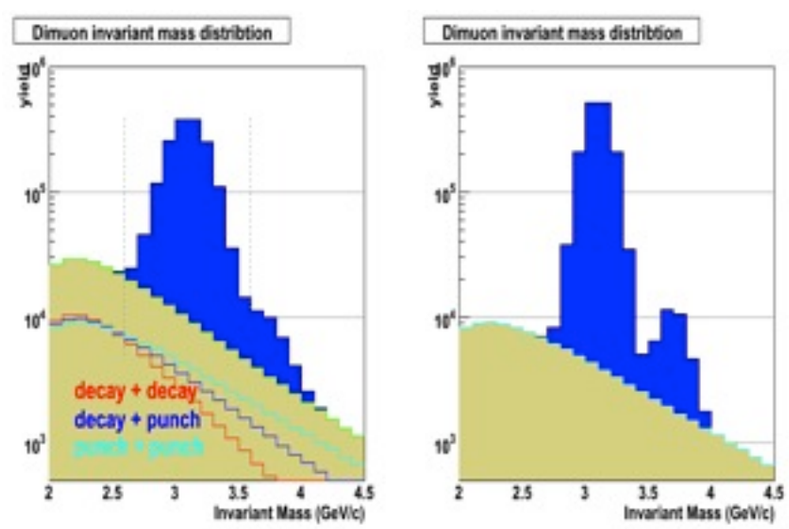

Transverse Spin program:

- Heavy flavors Transverse SSA
  - sensitive to gluon Sivers

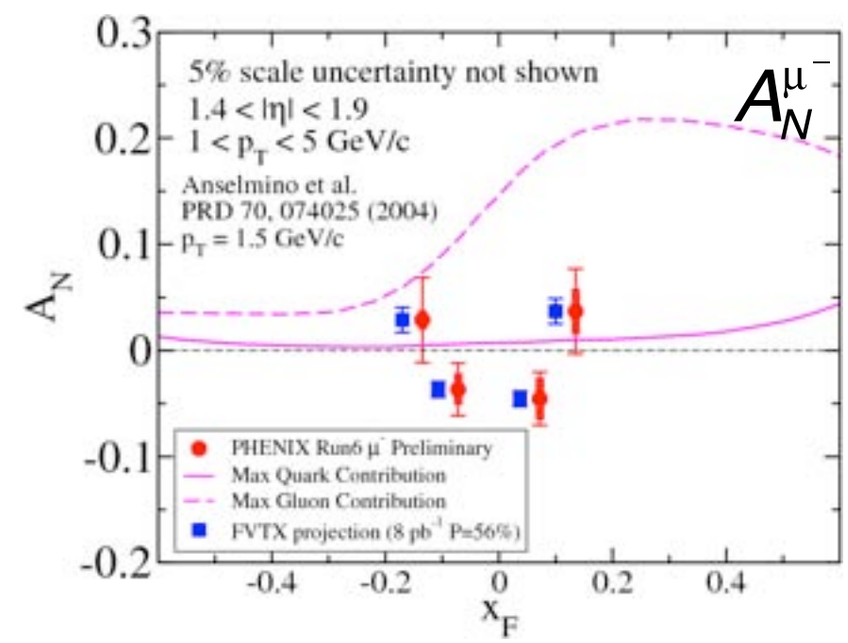

FVTX

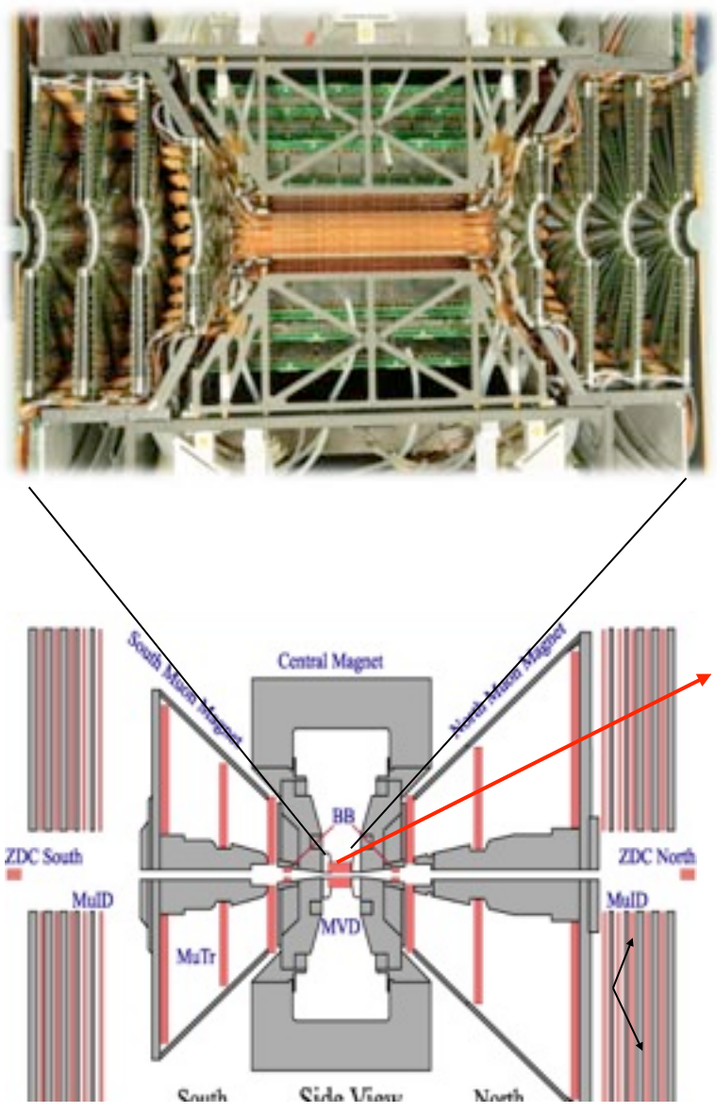

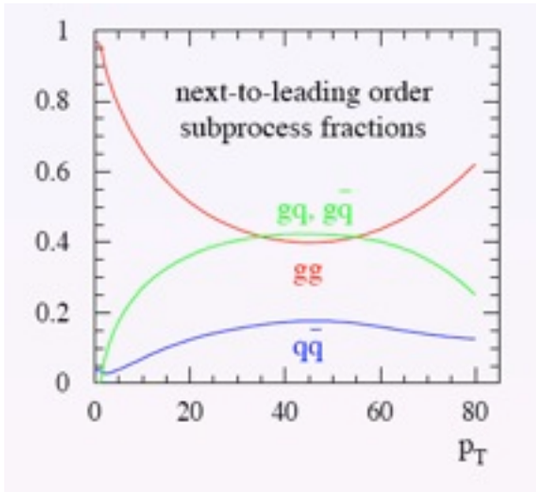

Transverse Spin program:

- Heavy flavors Transverse SSA
  - sensitive to gluon Sivers
- Drell-Yan Transverse SSA
  - sensitive to quark Sivers

PHENIX muon arms

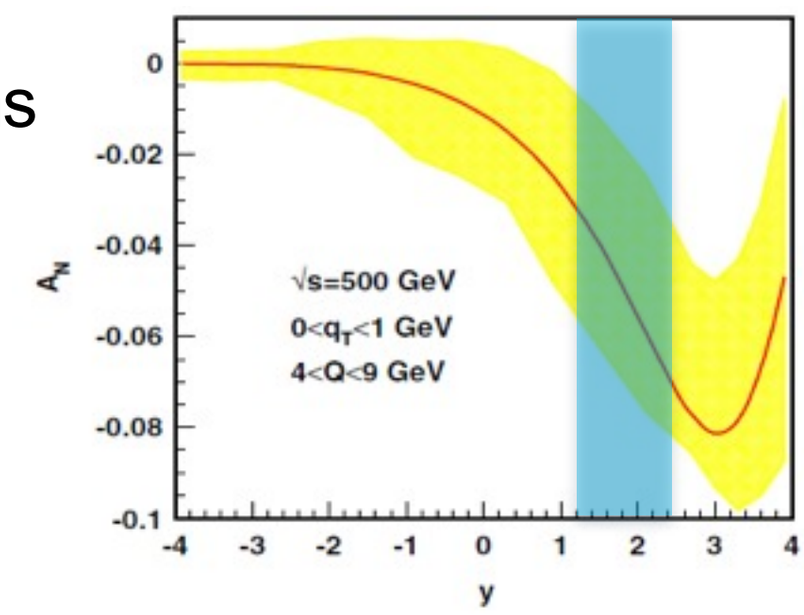

Sivers in Drell-Yan

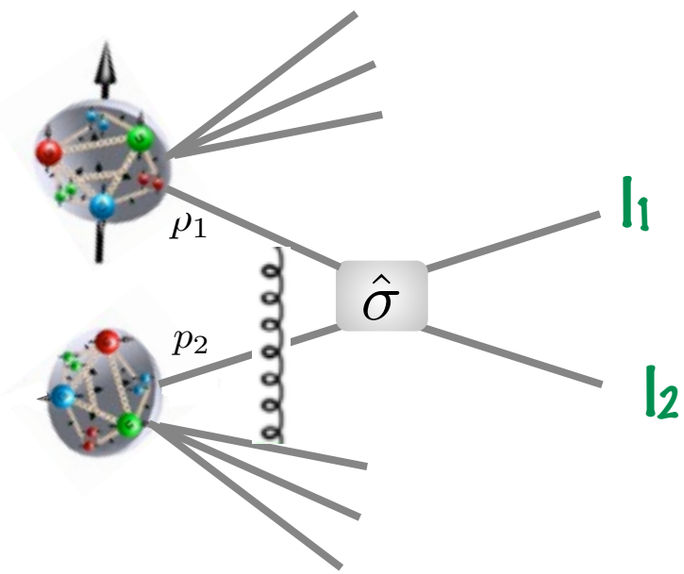

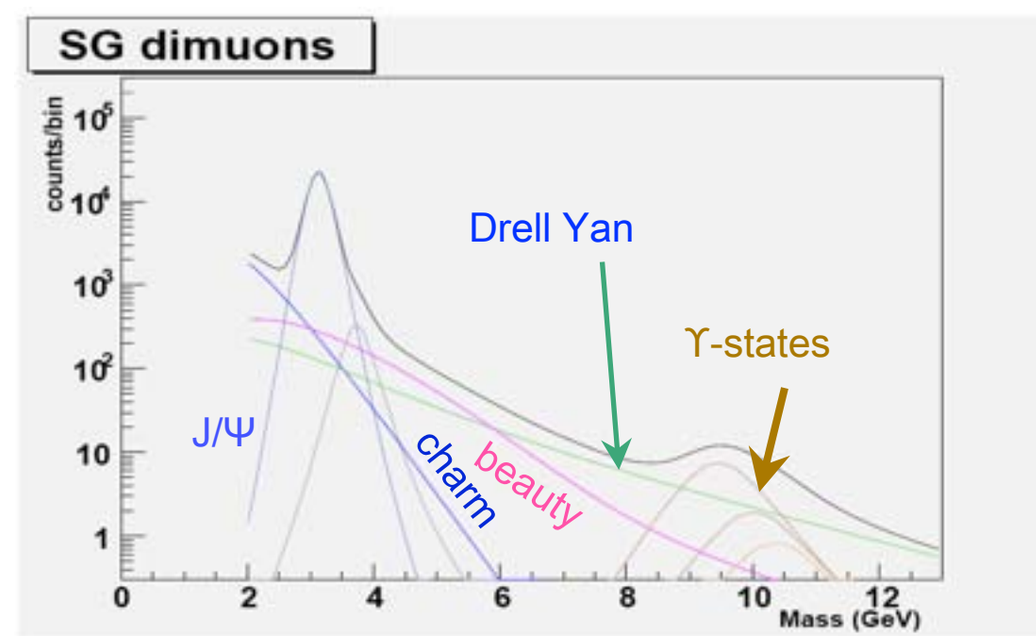

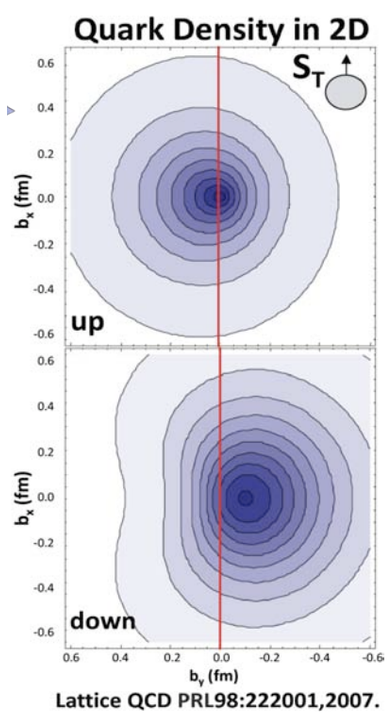

Lattice QCD PRL98:222001,2007.

Sivers effect gives access to the spatial quark distribution

$$TSSA^{DY}_{SIVERS} = - TSSA^{SIDIS}_{SIVERS}$$

SIDIS

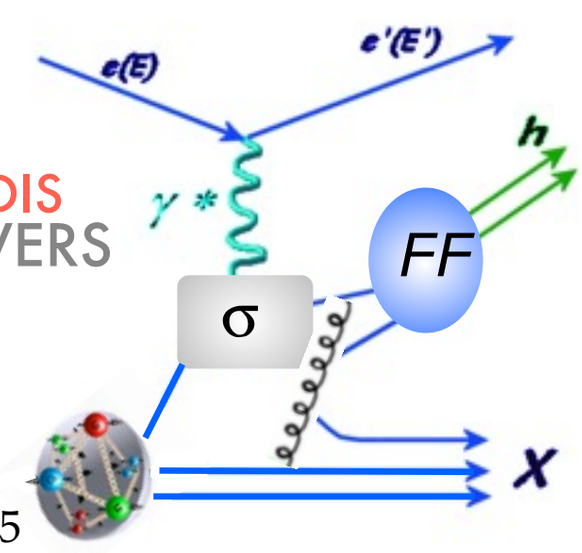

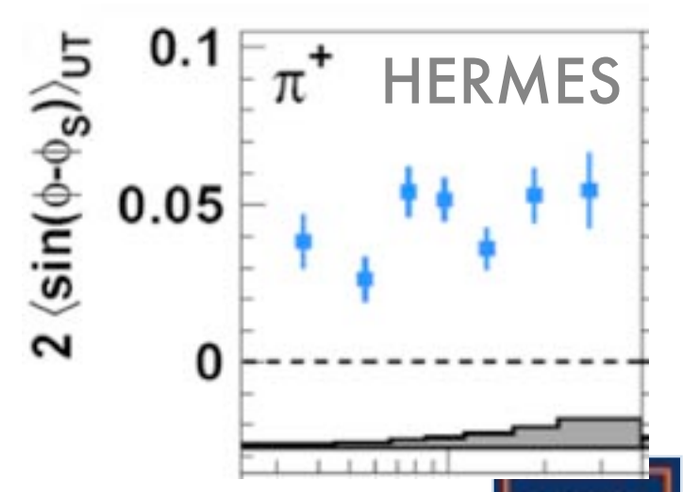

Forward

PHENIX

Physics program

Drell-Yan

Sivers Gluon Sivers

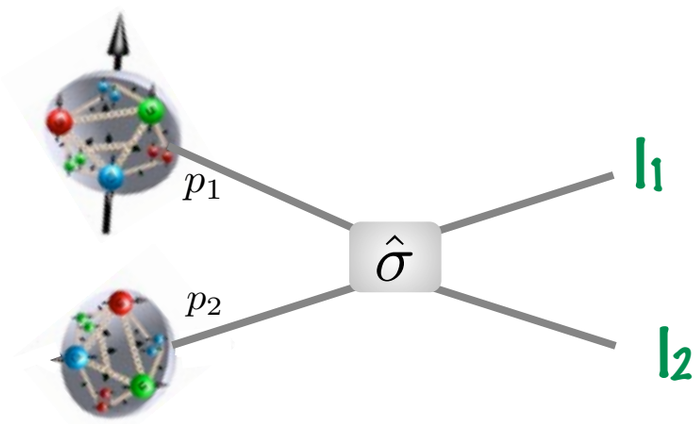

$pp \to$ jets

Collins

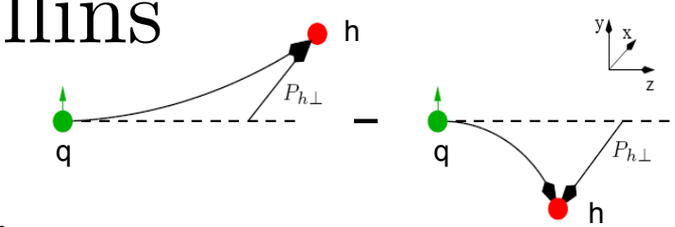

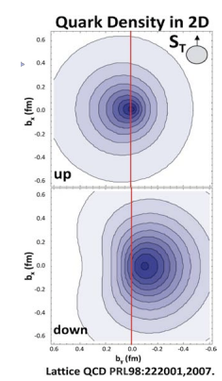

Sivers

Transversity $\times$ IFF

Heavy Flavors

e^+e^-, $\mu^+\mu^-$, $e\mu$, eX, μX

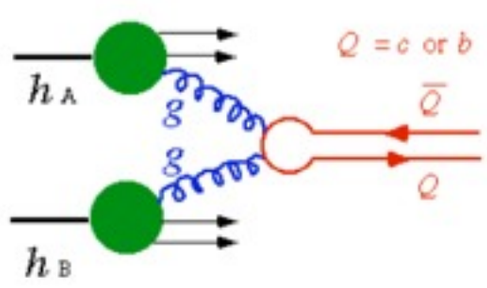

. . .

Boer-Mulders

Sea Transversity

$\bar{u}$ Helicity

Sivers in Drell-Yan

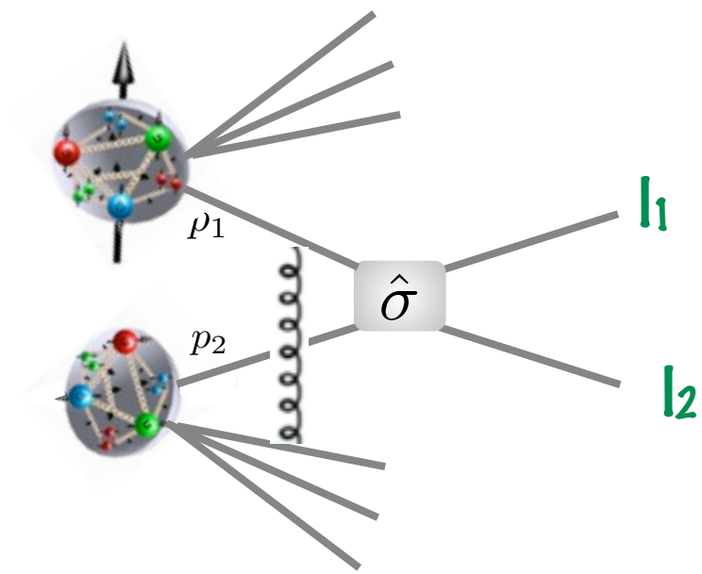

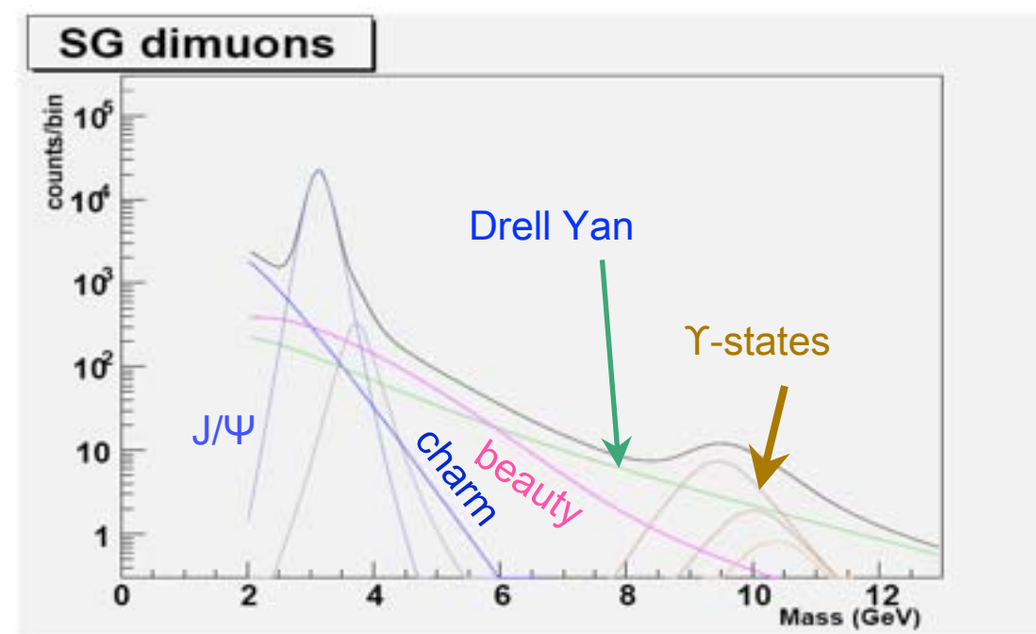

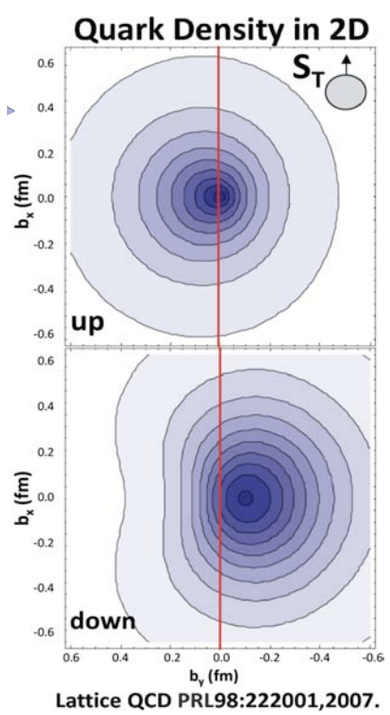

Lattice QCD PRL98:222001,2007.

Sivers effect gives access to the spatial quark distribution

$$TSSA^{DY}_{SIVERS} = - TSSA^{SIDIS}_{SIVERS}$$

SIDIS

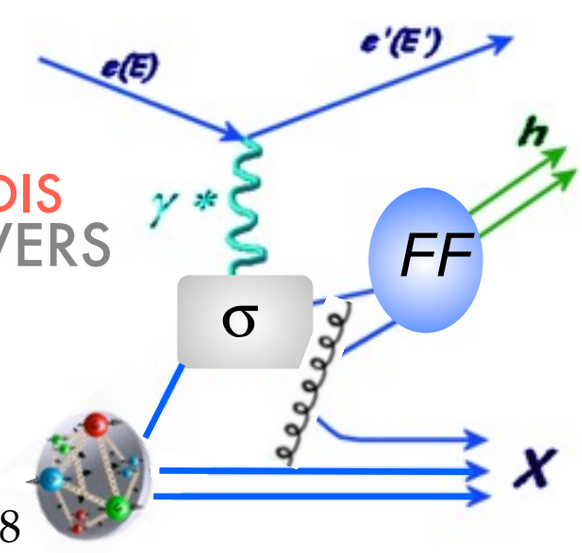

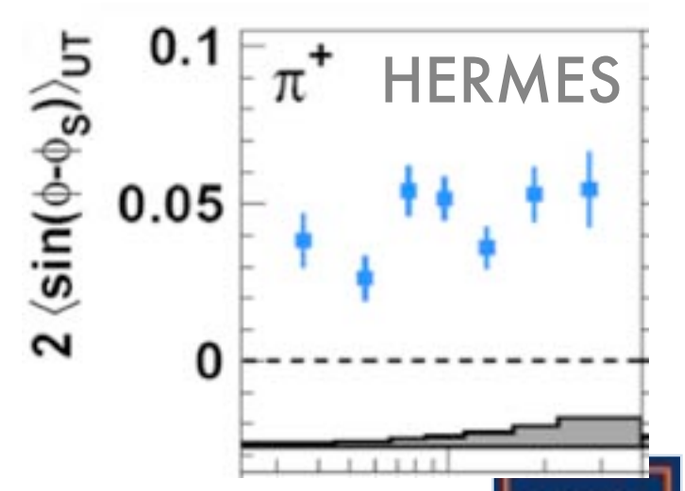

Mapping the Sivers mechanism

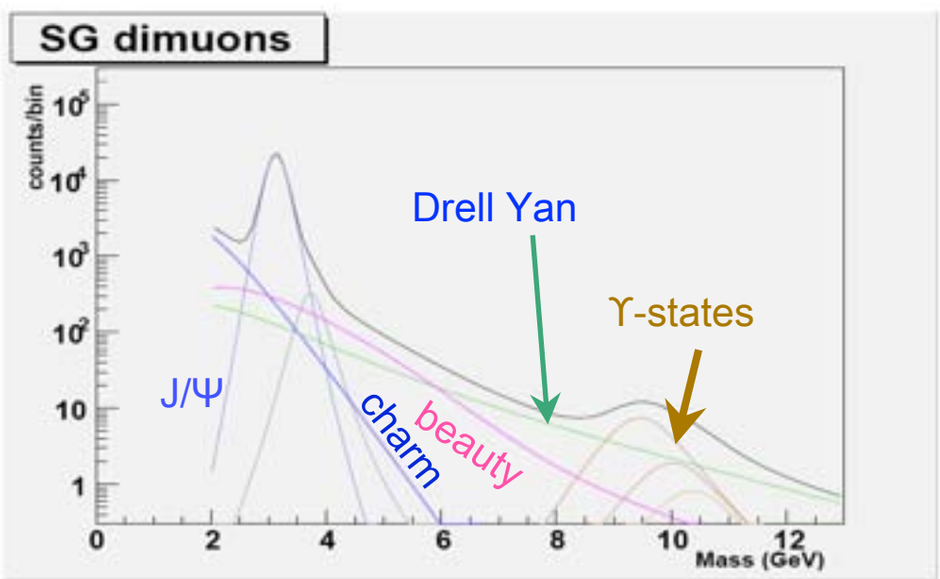

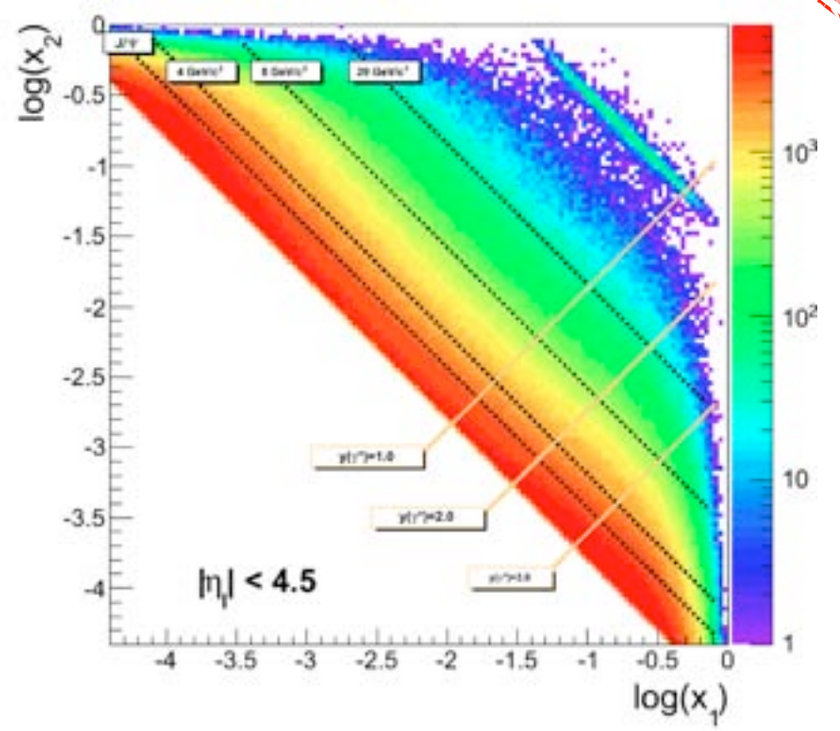

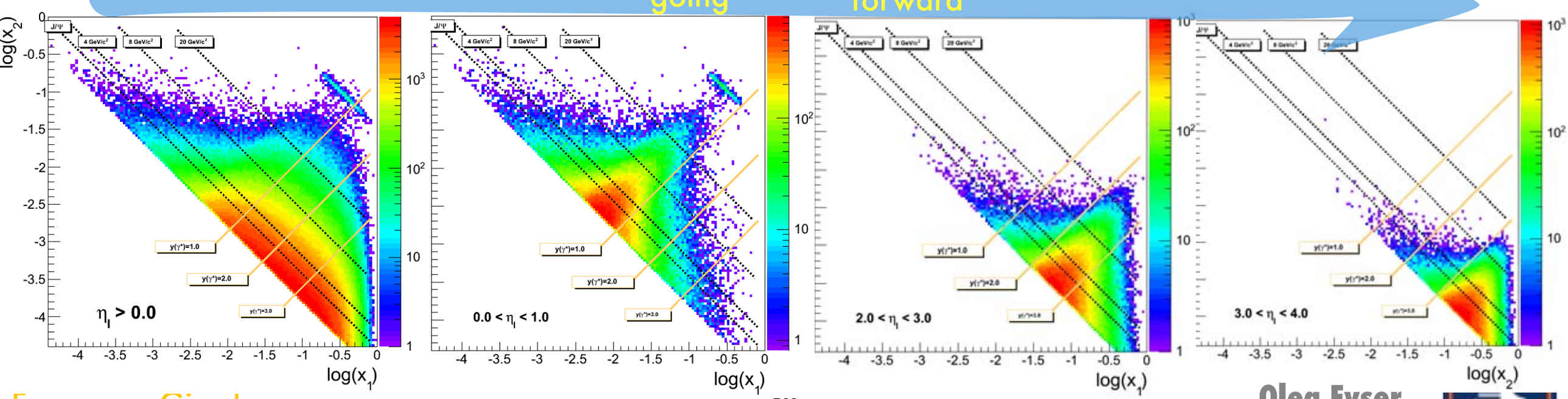

Francesca Giordano

Oleg Eyser

Sivers in Drell-Yan

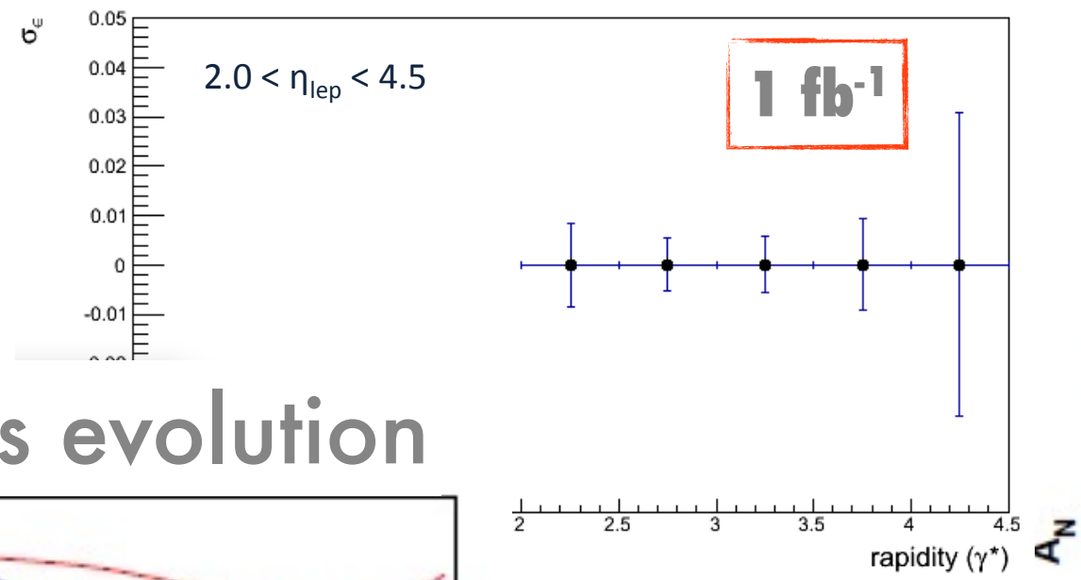

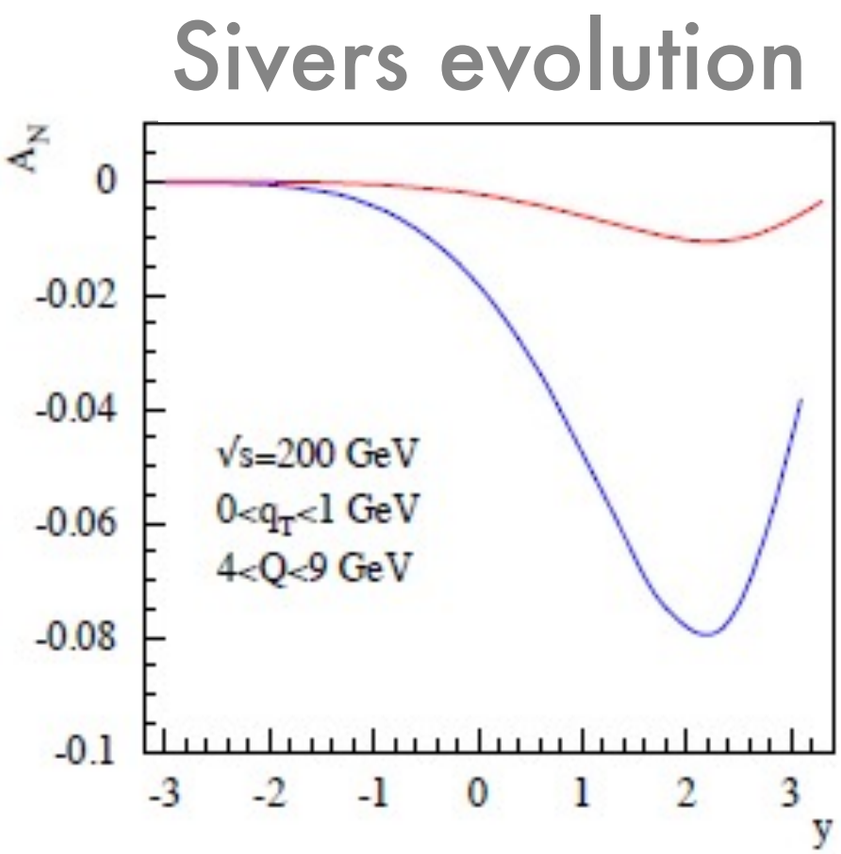

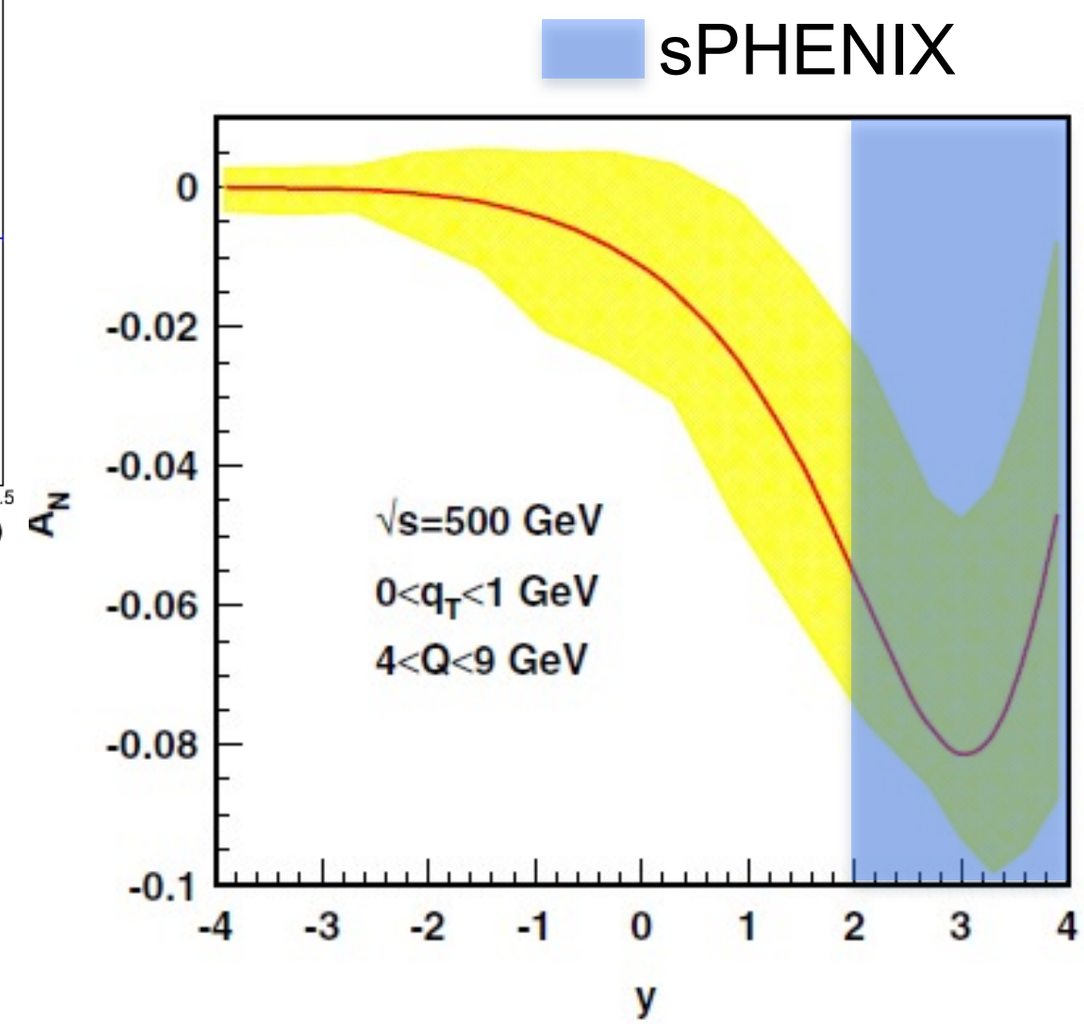

Sivers vs. Collins

Sivers mechanism

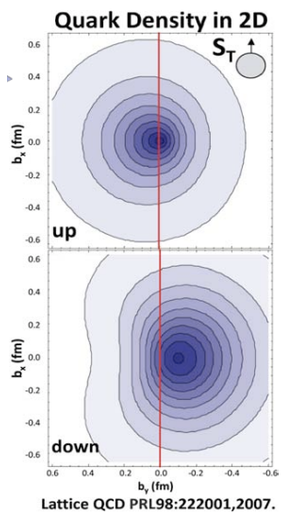

+ FSI + ISI

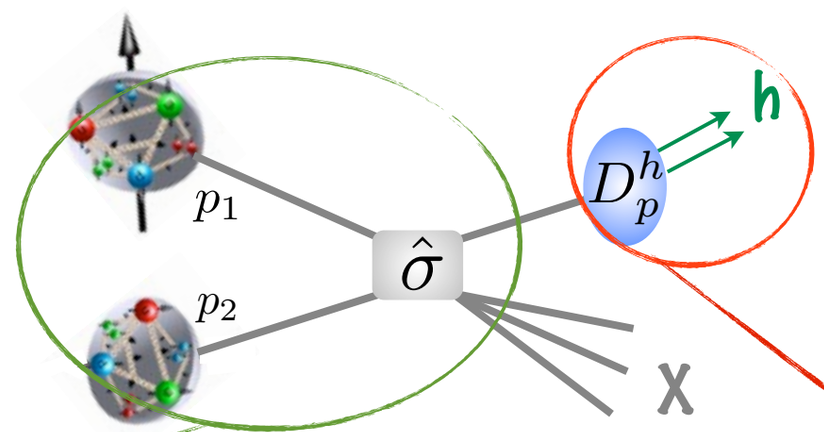

Collins mechanism

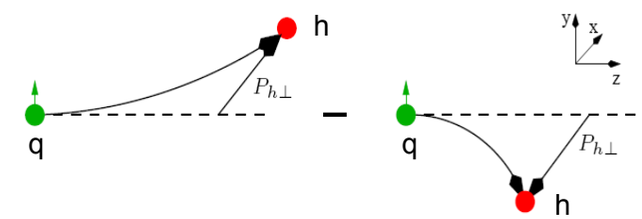

determines the
direction of the outgoing quark
>> the direction of the jet

determines the
hadron distribution within the jet

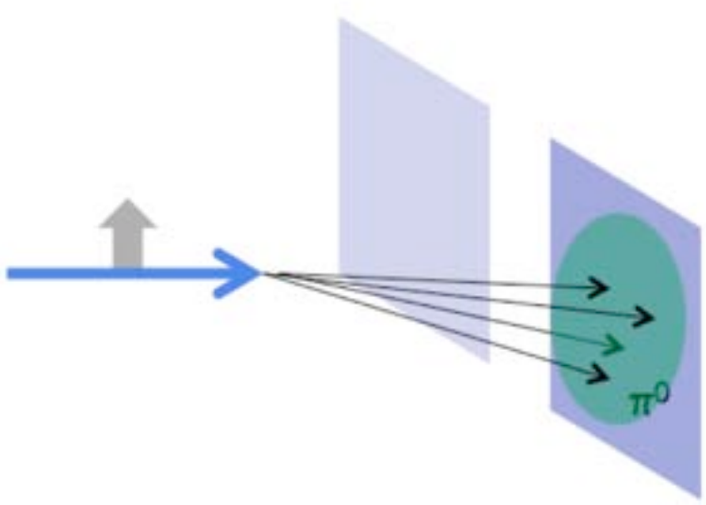

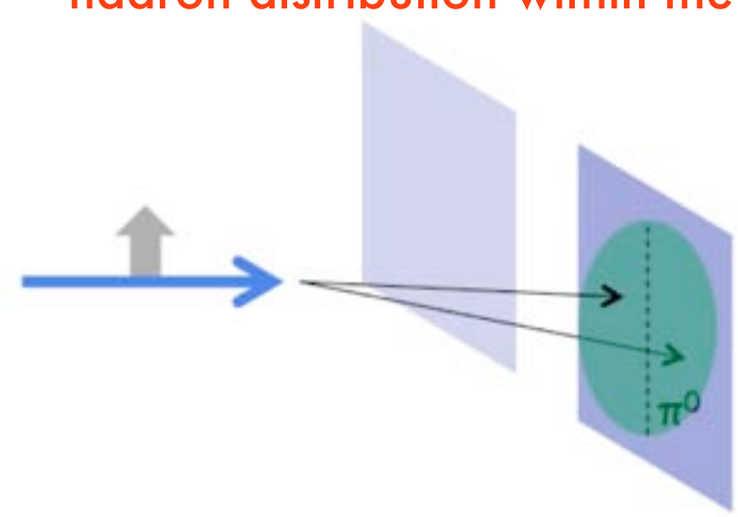

What's needed?

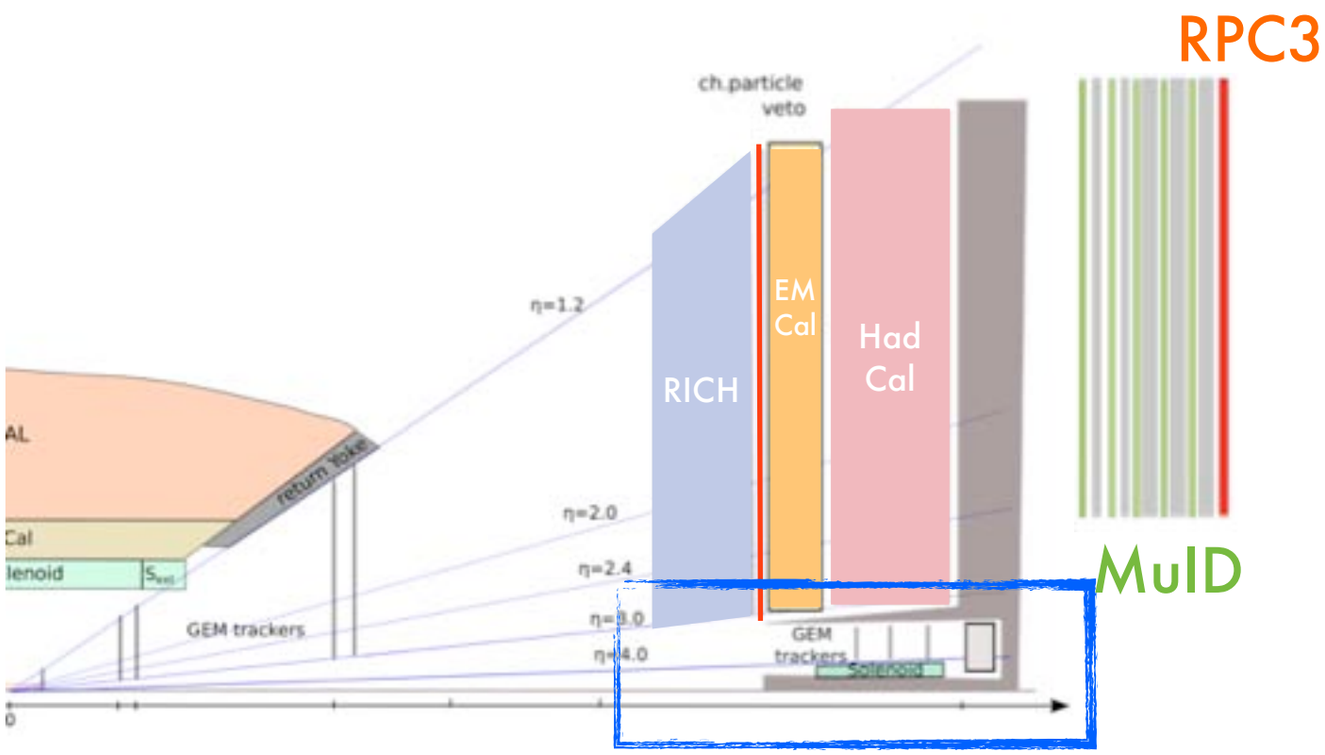

Good Tracking

Los Alamos, RBRC

Tracking chambers

Magnetic field

Los Alamos, RBRC, UCR

Good jet reconstruction

UIUC

Hadronic calorimeter

Lepton Identification

EM calorimeter + Preshower

RBRC, ISU

Hadron Identification

Ring Imaging Cherenkov

Stony Brook

Detector simulation in progress...

Summary

Broad spin program @ PHENIX

$$\frac{1}{2} = \frac{1}{2}\Delta\Sigma + \Delta G + L$$

Gluon polarization

$$\frac{1}{2} = \frac{1}{2}\Delta\Sigma + \Delta G + L$$

Flavor dependent quark polarization

A_N

Sivers + Collins

Forward

Boer-Mulders

Sea Transversity

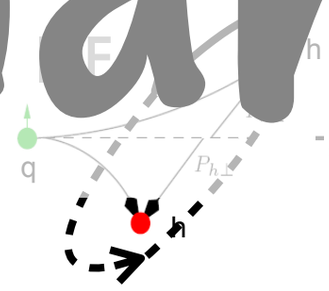

$$\frac{1}{2} = \frac{1}{2}\Delta\Sigma + \Delta G + L$$

Sivers

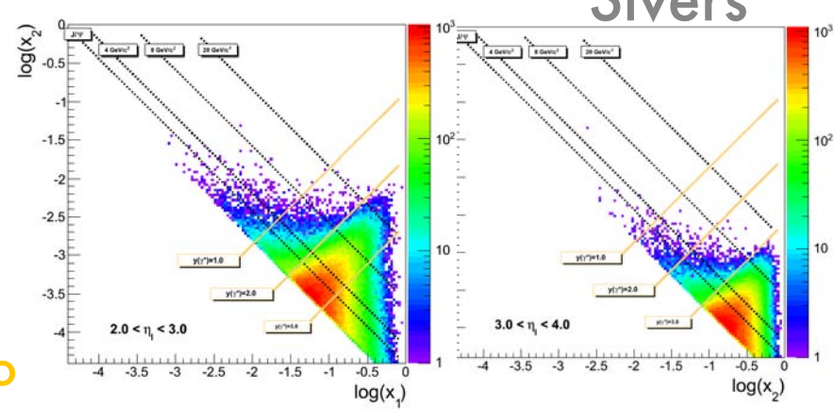

Sivers

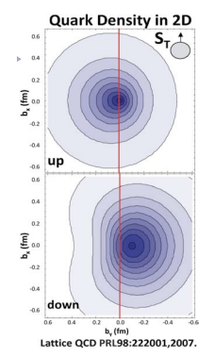

Collins

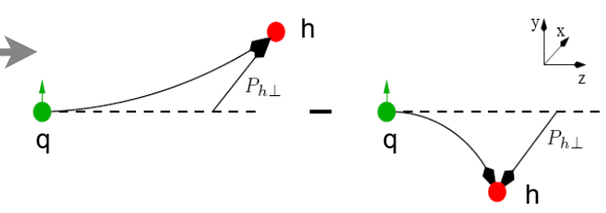

Thank you!

Low x Physics with a Future Forward Upgrade of sPHENIX

?

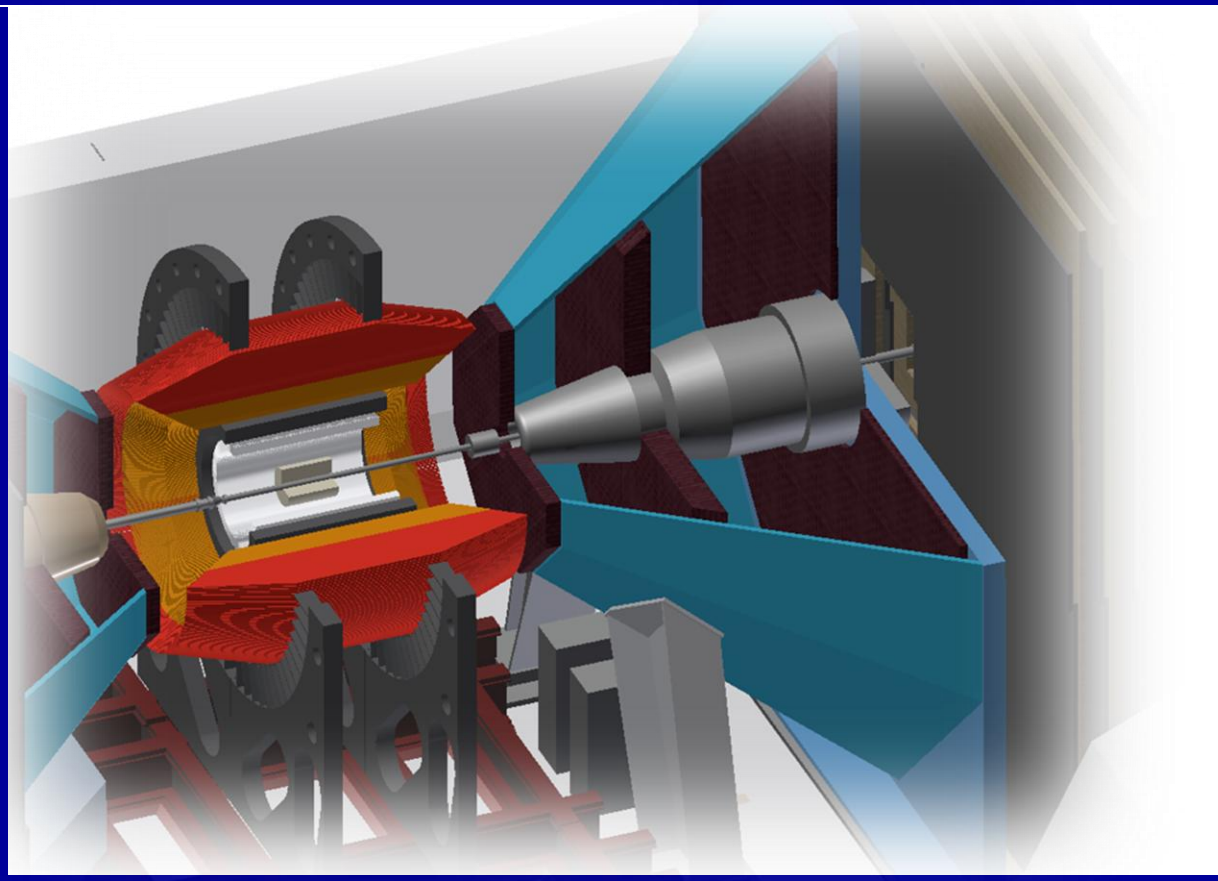

Matthias Grosse Perdekamp
University of Illinois

July 31, 2012

Content

- sPHENIX: Study Quark Parton Matter with Jets!
- A Unknown: The Initial State of Heavy Ion Collisions
- Forward Upgrade: Physics Goals
- Layout of the sPHENIX forward upgrade
- Next steps

The sPHENIX Detector Upgrade

PHENIX Collaboration arXiv:1207.6378v1
led by Jamie Nagle, David Morrison & John Haggerty

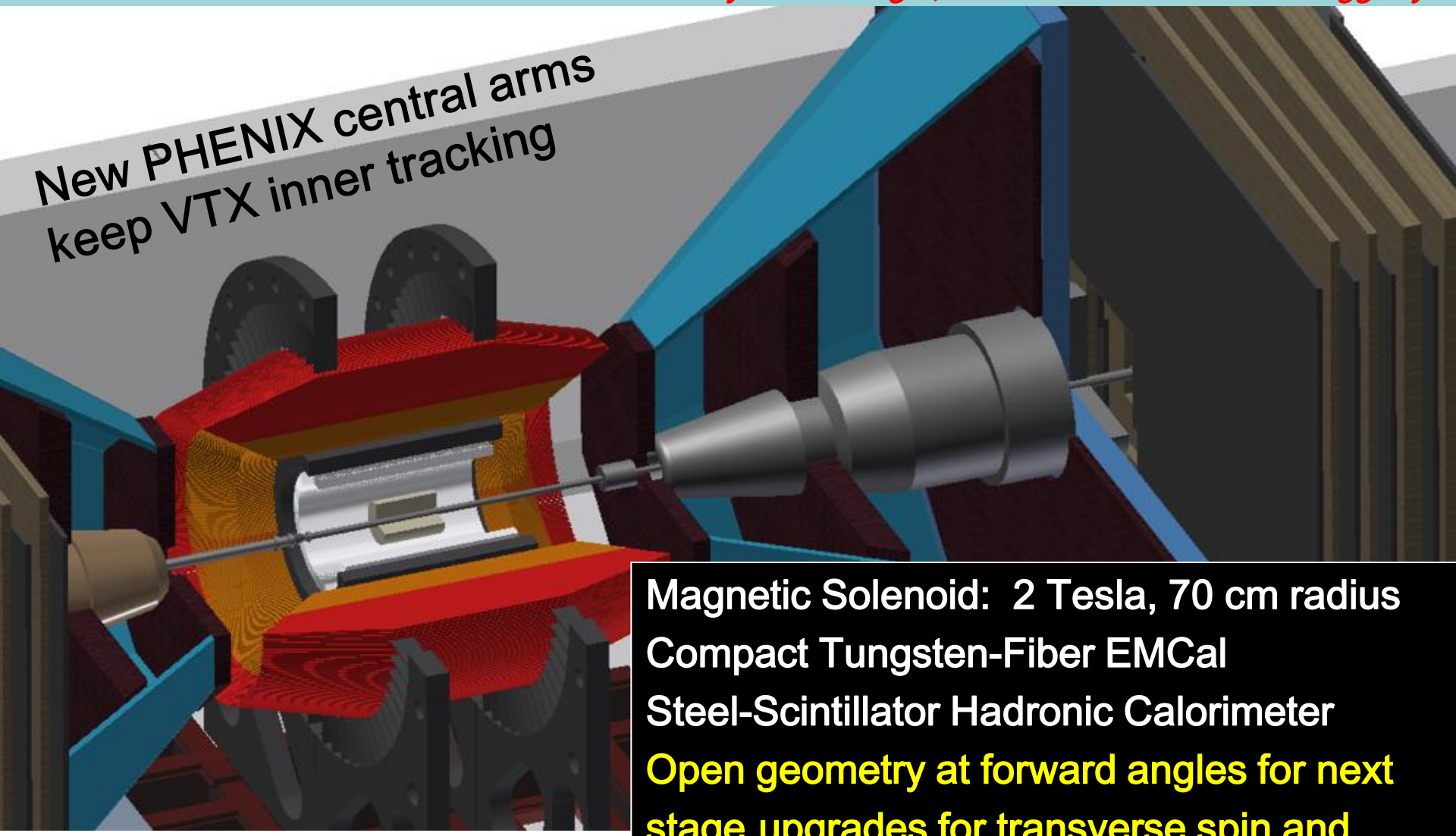

Magnetic Solenoid: 2 Tesla, 70 cm radius
Compact Tungsten-Fiber EMCal
Steel-Scintillator Hadronic Calorimeter
Open geometry at forward angles for next stage upgrades for transverse spin and eventual ePHENIX

sPHENIX: Large Acceptance & EMC & HCAL

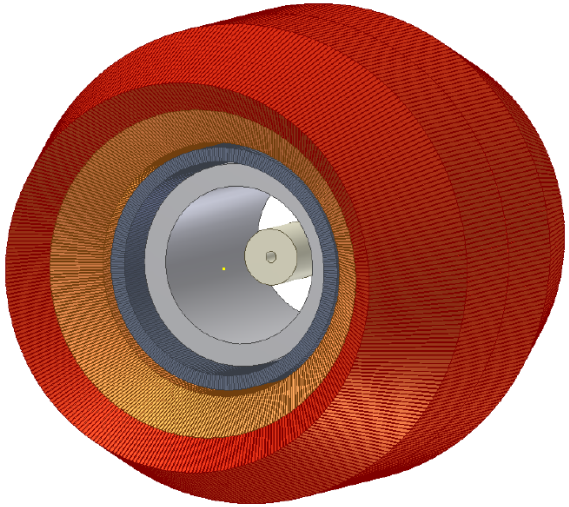

Accordion Tungsten-Fiber EMCal

- SBIR with Tungsten Heavy Powder
- Prototype being constructed
- 10 cm total thickness
- 14%/√E resolution
- Full GEANT-4 simulation results
- Silicon Photomultiplier readout

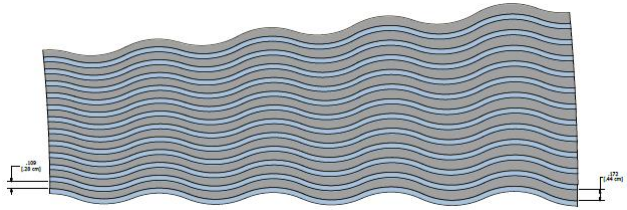

Steel-Scintillator Hadronic Calorimeter

- Also acts as flux return for magnetic field
- Prototype being constructed
- 1 meter total thickness
- 75%/ √E resolution
- Full GEANT-4 simulation results

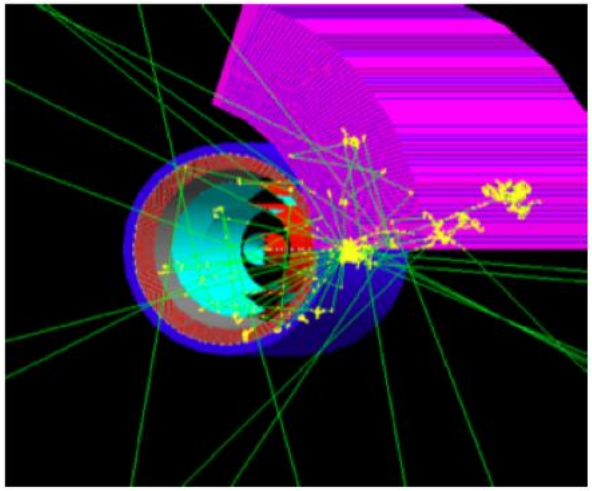

The Need for Hadronic Calorimetry

<u>All</u> heavy ion jet publications to date (i.e. ATLAS and CMS) come from hermetic calorimeter measurements !

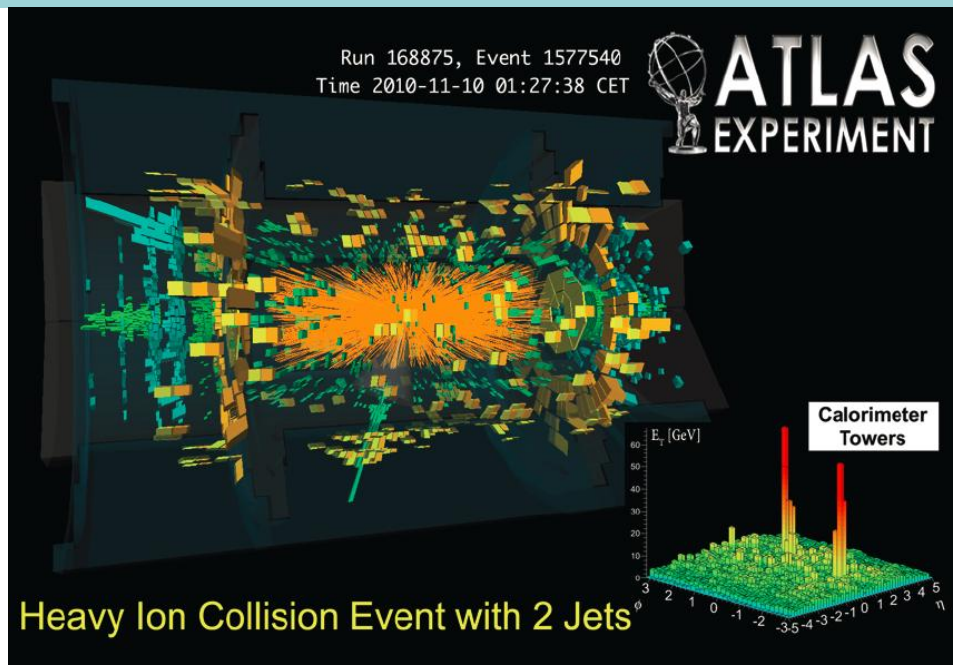

Critical to have EMCal + HCAL with hermetic coverage (no gaps, spokes, holes) with large coverage to see both jets and γ-jet and at very high rate. Then add in tracking information as key additional handle for systematic studies.

Study Strongly Interacting Quark – Parton Matter with Jet Probes !

Chris Coleman-Smith arXiv:1205.6781
Interaction of parton shower with medium

LHC

Good agreement with CMS
Dijet $A_J=(E_1-E_2)/(E_1+E_2)$
for $\alpha_s = 0.3$

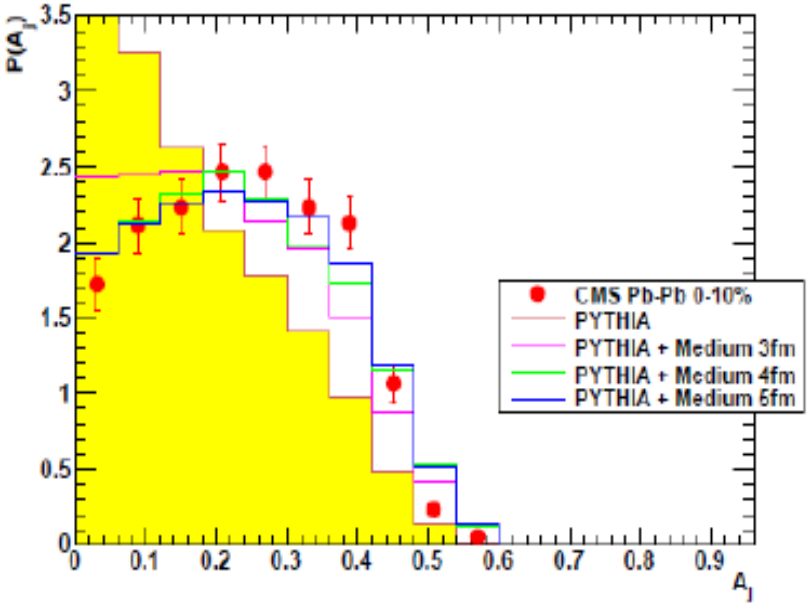

RHIC

sPHENIX dijets very sensitive to effective coupling

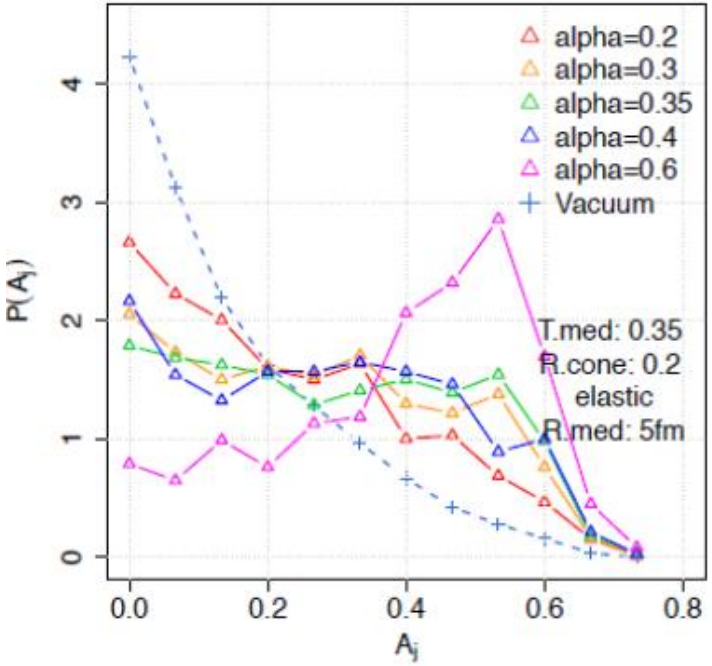

Jet Measurements at Different Scales and Temperatures at RHIC and the LHC will Explore the Dynamics of the Physical Properties of the QGP

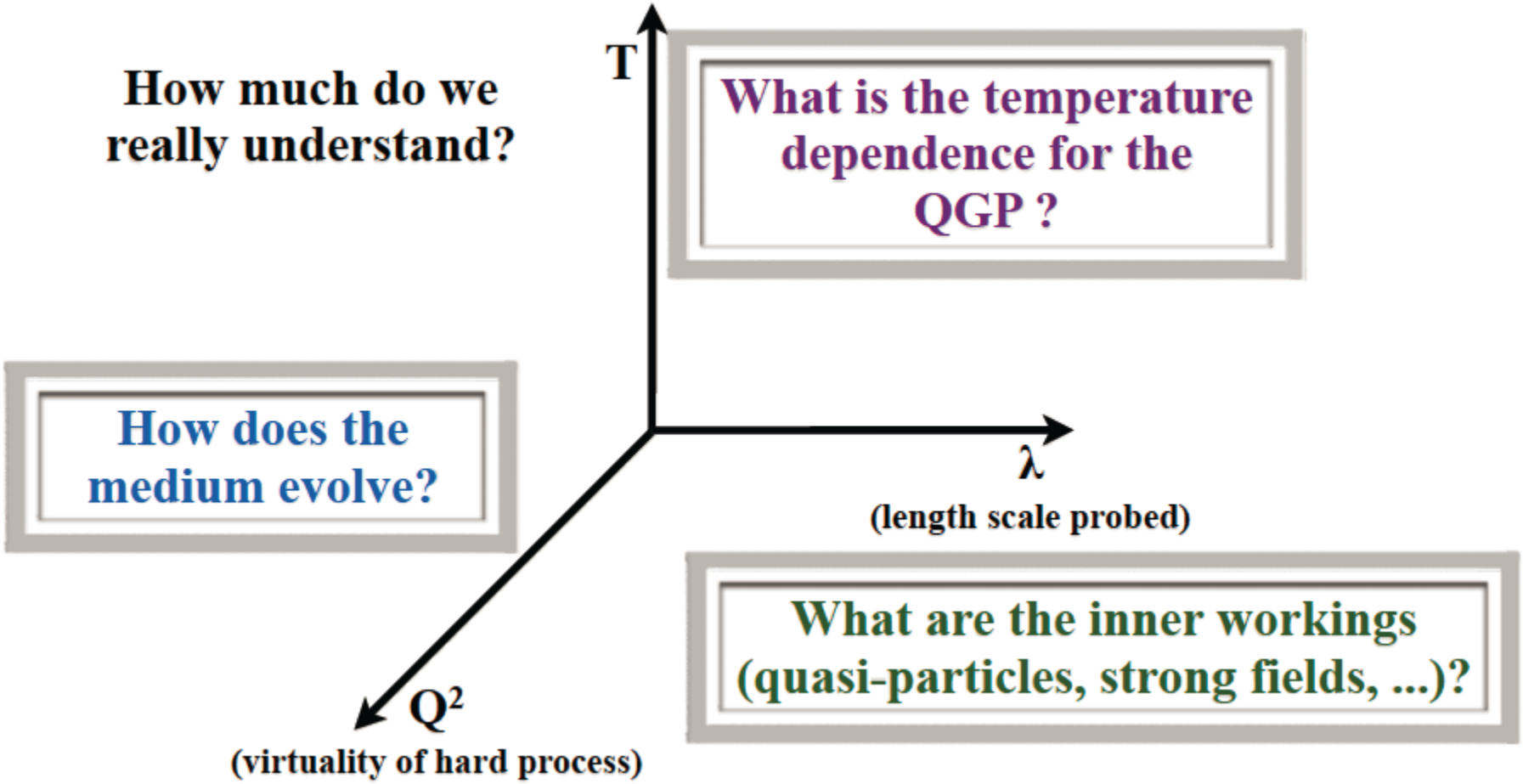

An Unknown:
The Initial State of Heavy Ion Collision

The Initial State of Nuclei in HI Collisions in particular the Nuclear Gluon Distribution $G_A(x)$

General interest:

- Extend Understanding of QCD into the non-perturbative regime of high field strengths and large gluon densities.
- Search for universal properties of nuclear matter at low x and high energies.

Heavy Ion Collisions:

- Understand the initial state to obtain quantitative description of the final state in HI-collisions.
- Establish theoretical framework to describe initial state of HI-collisions based on measurements of $G_A(x)$ in p/d-A or e-A.

Jet Quenching: Initial State Saturation of $G_A(x)$ or QGP Final State Effect ?

Quantify nuclear effects in hadron production ⇨ Nuclear modification factor:

$$R_{AA} = \frac{1}{\langle N_{coll} \rangle} \frac{d^2N^{A+A}/dp_T d\eta}{d^2N^{p+p}_{inel}/dp_T d\eta}$$

Two explanations for $R_{AuAu} < 1$

(I) suppression of nuclear $G_A(x)$
(II) final state effects of strongly interacting partonic matter

Control measurement of $R_{dAu} \sim 1$ ➔ final state effect!

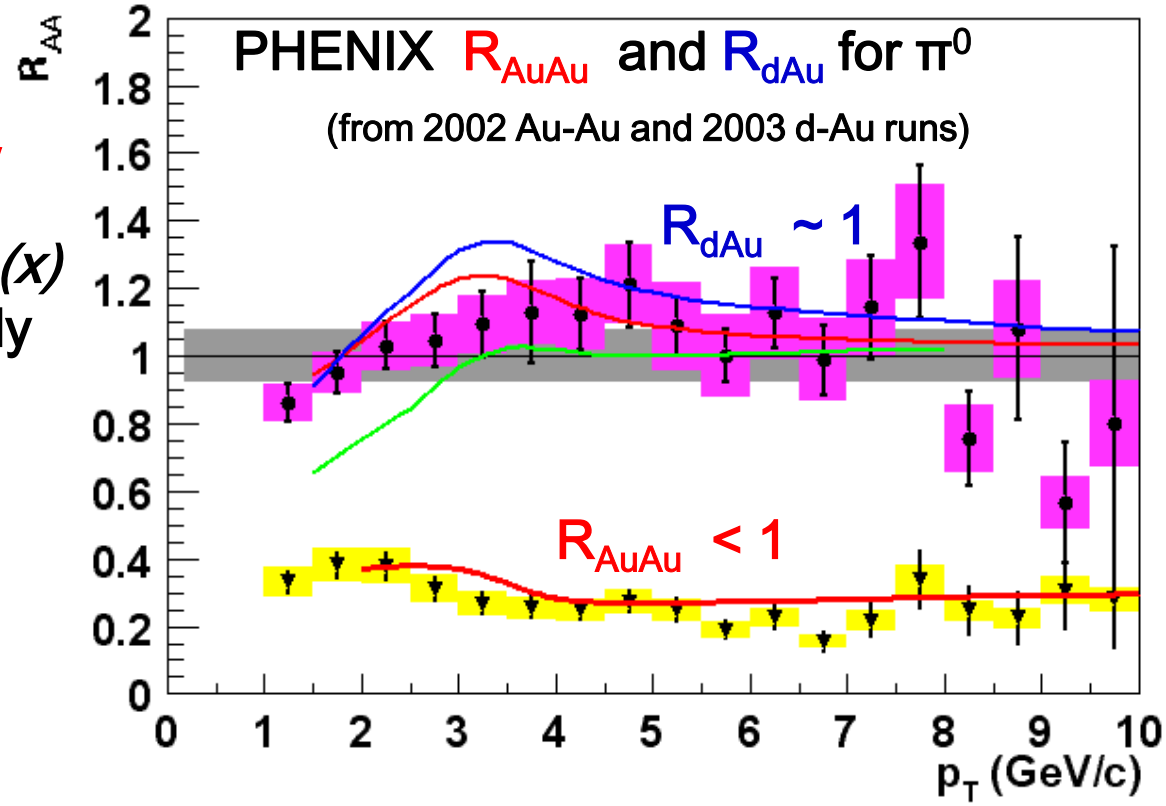

Elliptic Flow v_2 : Choice of Initial State $G_A(x)$ has Significant Impact on Hydro Calculations

PHOBOS v_2 vs Hydro Calculations

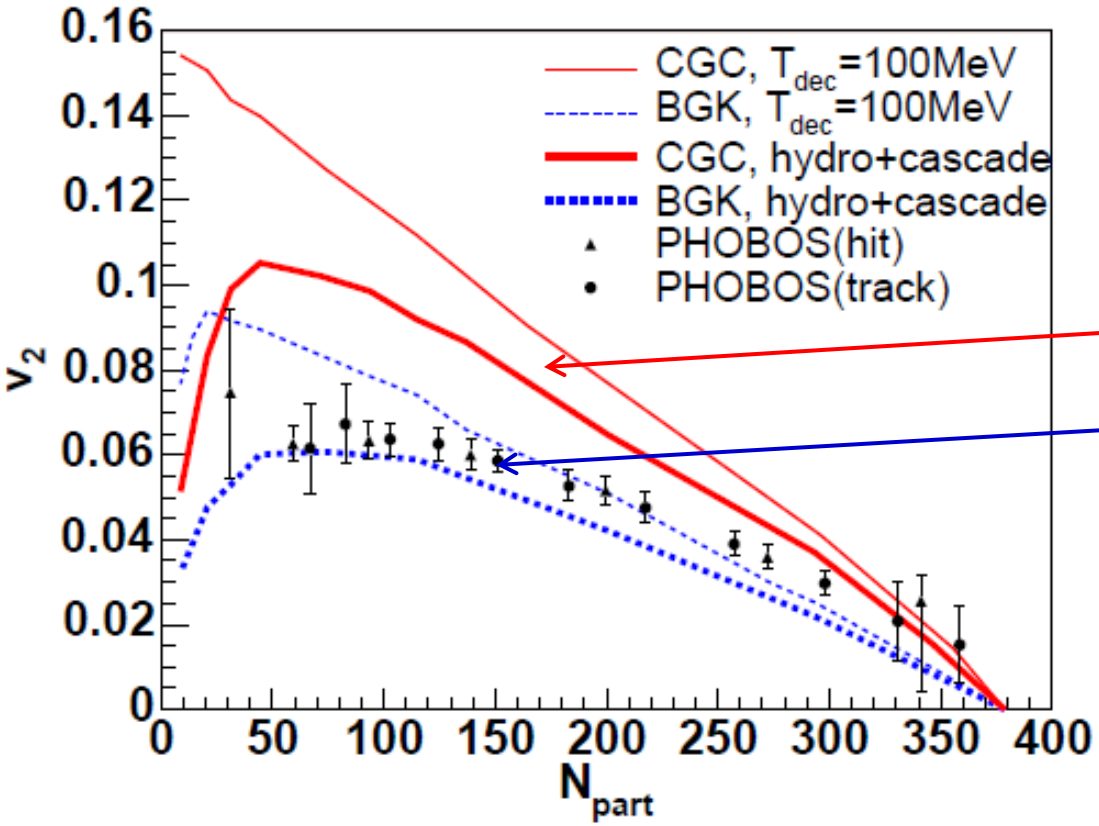

Color Glass Condensate

Brodsky-Gunion-Kuhn Model

Phys.Rev.Lett.39:1120

T. Hirano, U. Heinz, D. Kharzeev, R. Lacey, Y. Nara
Phys.Lett.B636:299-304,2006

➔ Knowledge of the initial state is important for the quantitative interpretation of experimental results in heavy ion collisions!

J/ψ Production: Some Relevant Cold Nuclear Matter Effects in the Initial State

(I) Shadowing (from fits to DIS data or model calculations)

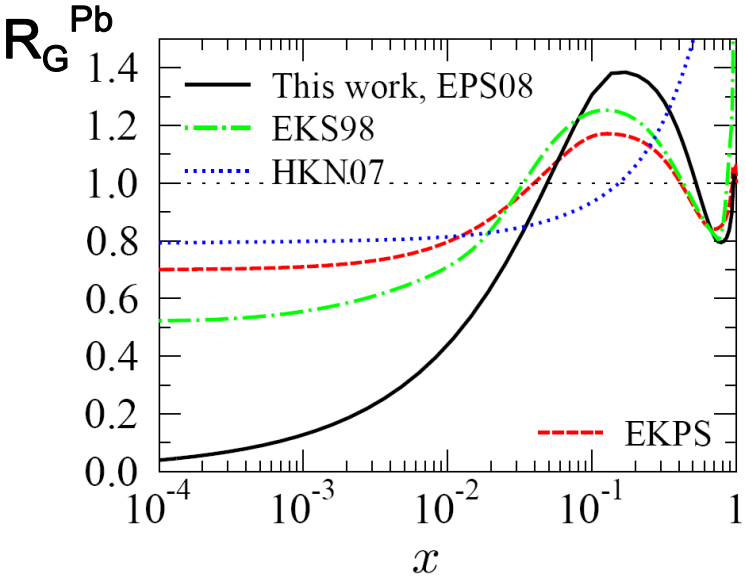

K. Eskola H. Paukkumen, C. Salgado JHEP 0807:102,2008

➔ DGLAP LO analysis of nuclear pdfs

$$G_{Pb}(x,Q^2)=R_G^{Pb}(x,Q^2)\, G_p(x,Q^2)$$

(II) Dissociation of $c\bar{c}$ into two D mesons by nucleus or co-movers

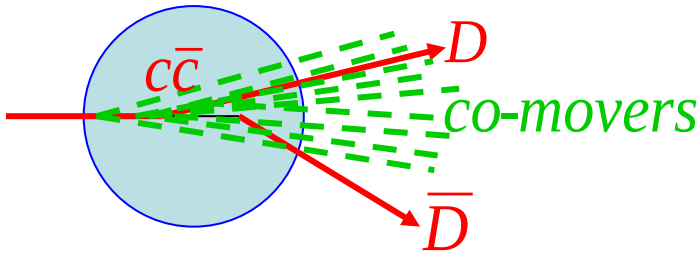

(III) Gluon saturation from non-linear gluon interactions for the high gluon densities at small x

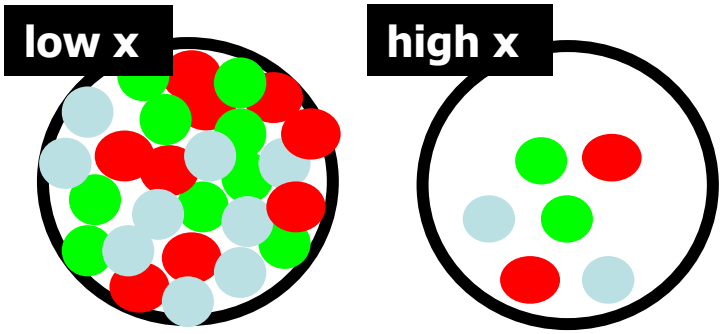

J/ψ : Some of the Suppression in A-A is from Cold Nuclear Matter Effects found in d-A Collisions

EKS shadowing + dissociation: use d-Au data to determine break-up cross section

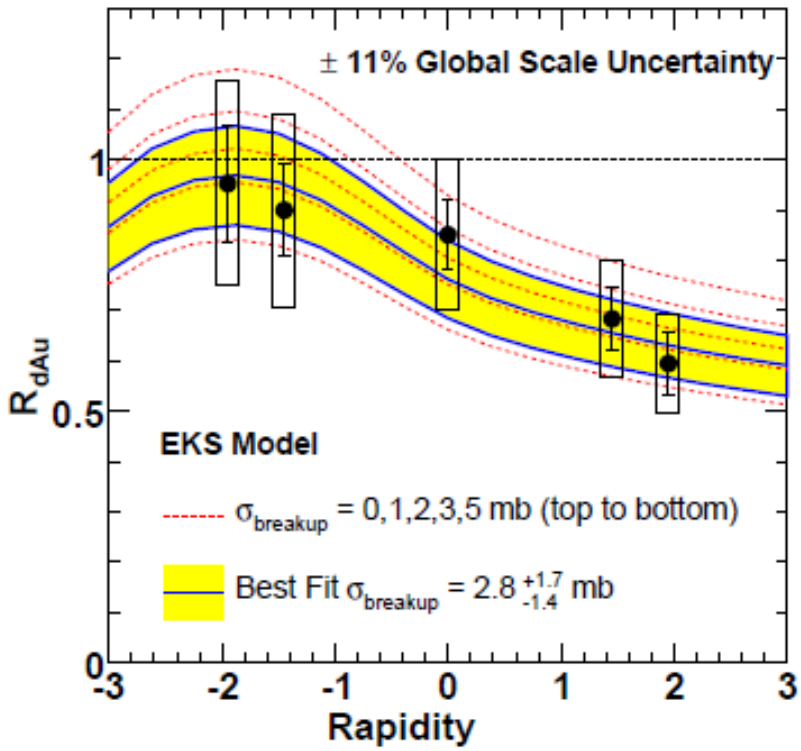

EKS shadowing + dissociation: from d-Au vs Au-Au data at forward-rapidity

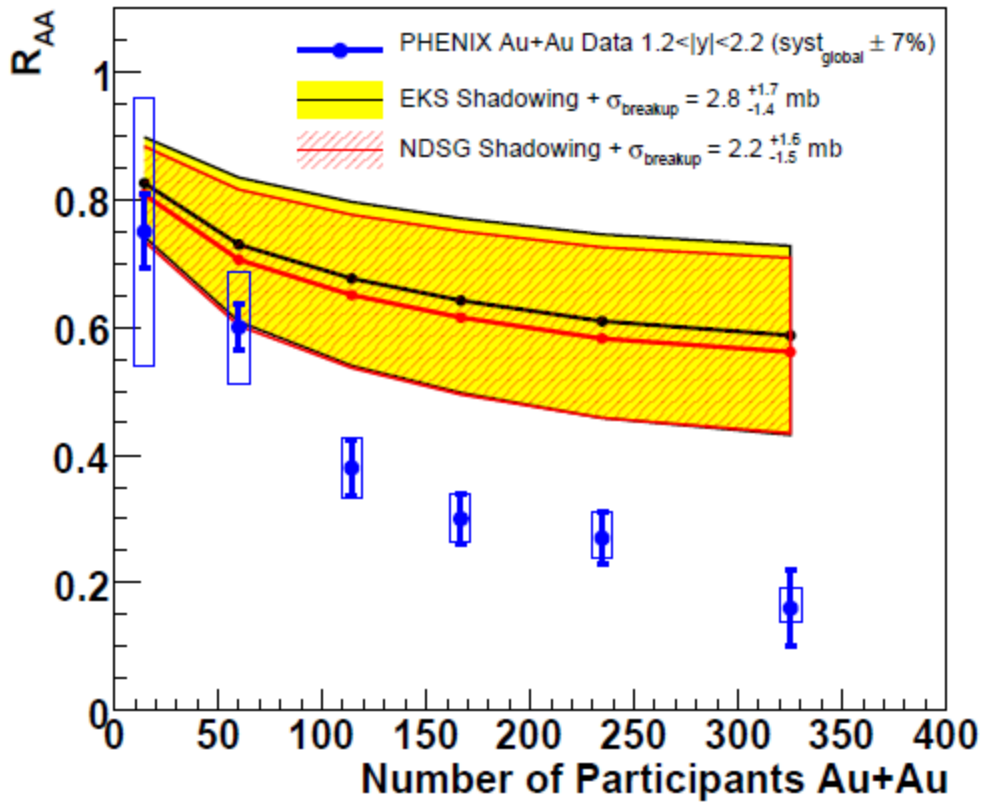

PRC 77,024912(2008)

(III) cont'd The Color Glass Condensate

see for example, F. Gelis, E. Iancu, J. Jalilian-Marian, R. Venugopalan, arXiv:1002.0333

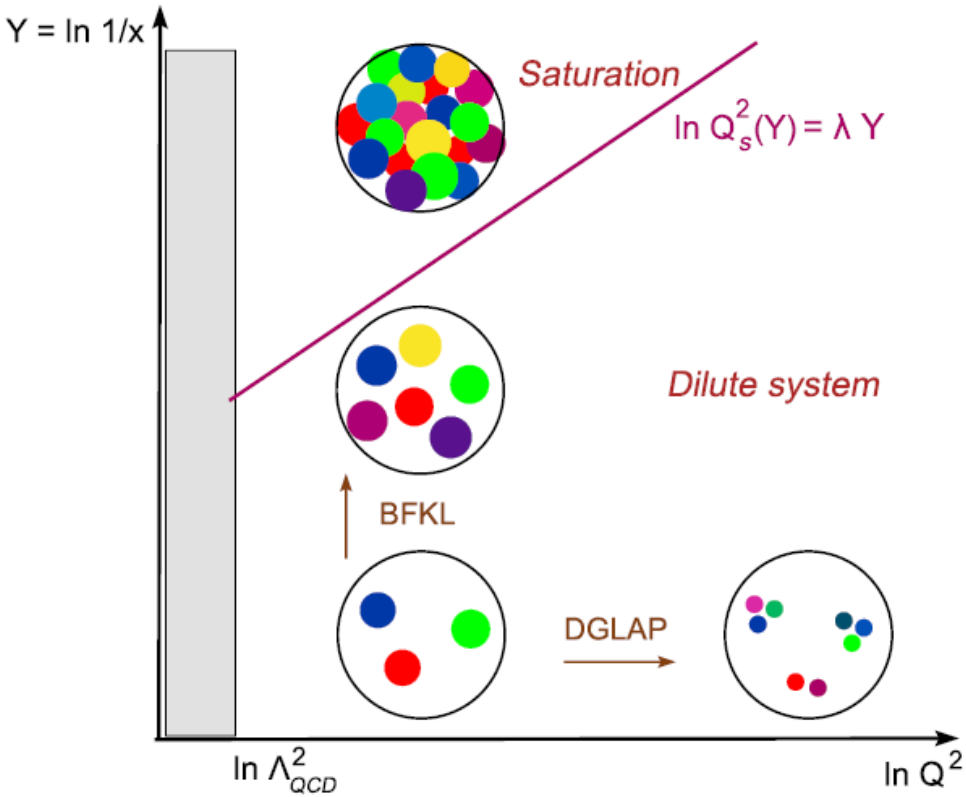

CGC: an effective field theory:

Small-x gluons are described as the <u>color fields</u> radiated by <u>fast color sources</u> at higher rapidity. This EFT describes the saturated gluons (slow partons) as a Color Glass Condensate.

The EFT provides a gauge invariant, universal distribution, $W(\rho)$:

> $W(\rho)$ ~ probability to find a configuration ρ of color sources in a nucleus.

The evolution of $W(\rho)$ is described by the JIMWLK equation.

A Possible Approach to Quantify the Initial State

(I) Measure $G_A(x)$ e.g. through direct photon or jet production in p-A or d-A at forward rapidity

and, possibly

(II) Search for onset of gluon saturation and verify CGC framework as an effective field theory at high field strengths in QCD.

Q: can we determine color configurations $w(\rho)$ and use the JIMWLK evolution to evolve them to scale needed, LHC & RHIC energies?

Suppression of Single of Di-Hadron Cross Sections in the Forward Direction:

Sufficient Evidence for Saturation Effects in the Gluon Field in the Initial State of d-Au Collisions at RHIC?

Theory vs Data ➔ CGC

J. Albacete and C. Marquet, PLB687, 184

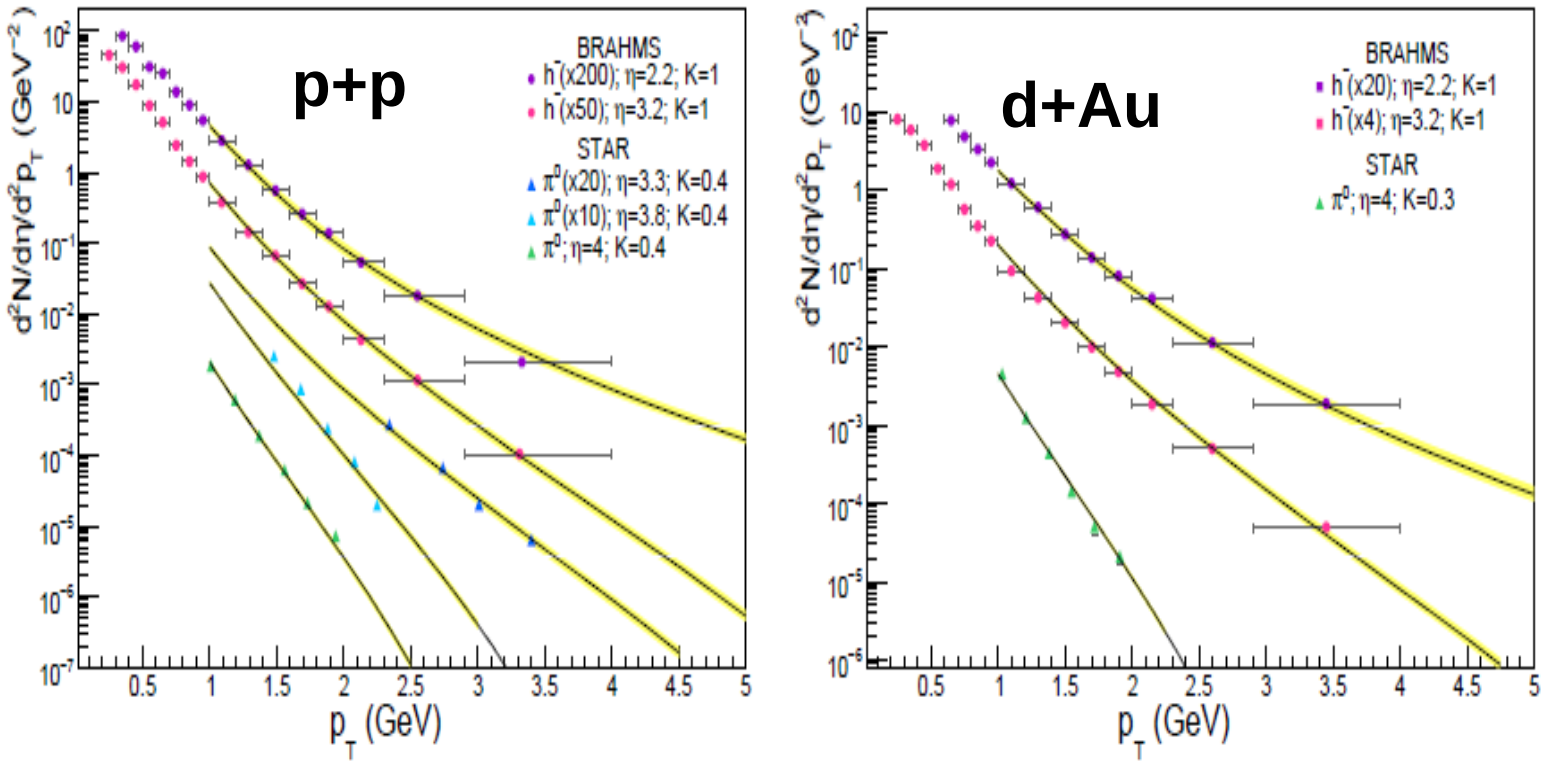

Not bad! However, different K factors for $h^{+,-}$ in BRAHMS and π^0 in STAR

Theory vs Data ➔ Cronin + Shadowing + E-loss

I.Vitev, T. Goldman, M.B. Johnson, JW. Qiu, Phys. Rev. D74 (2006)

Not bad either!

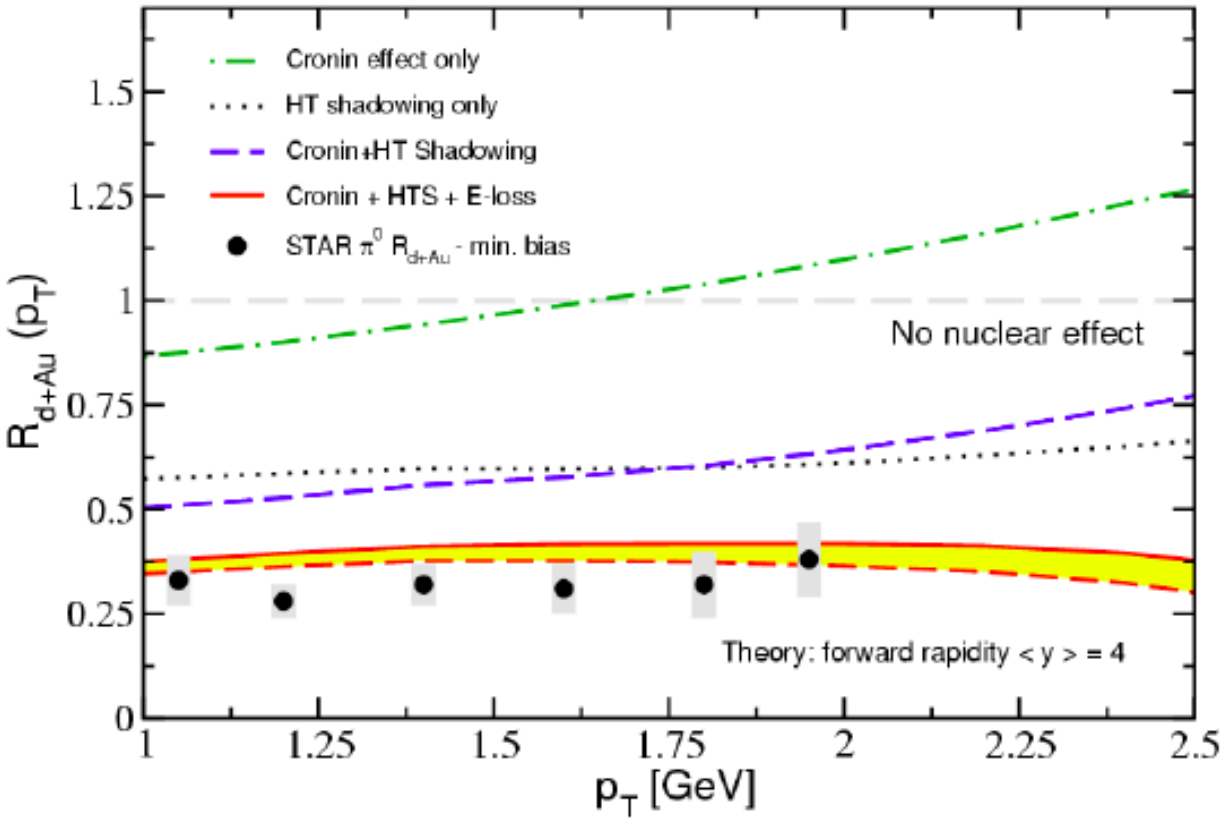

➔ R_{dA} results alone do not uniquely demonstrate gluon saturation. Competing explanations can account for observed hadron suppression in d-Au at forward rapidity !

Probing for Gluon Saturation Effects with Hadron-Hadron Correlations in d+Au

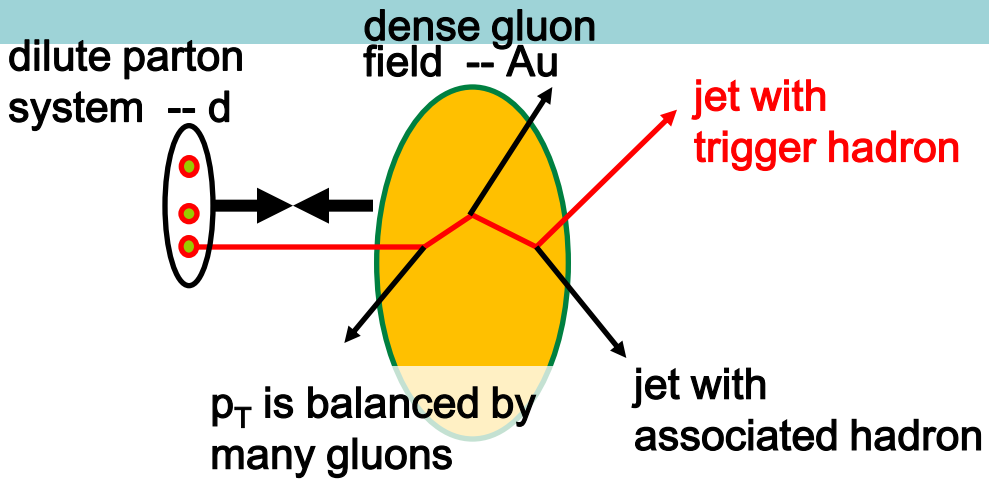

Idea:

Presence of dense gluon field in the Au nucleus leads to scattering of multiple gluons and parton can distribute its energy to many scattering centers

➔ **Mono-jet signature !**

D. Kharzeev, E. Levin, L. McLerran, Nucl.Phys.A748:627-640,2005

Experimental signature:

Angular correlation between hadrons in opposing hemispheres

➔ widening of correlation width of d-Au compared to pp

➔ reduction in associated yield of hadrons on the away site

Effects large at low x

➔ forward rapidity

➔ forward EMC upgrades in

STAR : $2 < \eta < 4$

PHENIX : $3.1 < |\eta| < 3.8$

Comparison to CGC Prediction

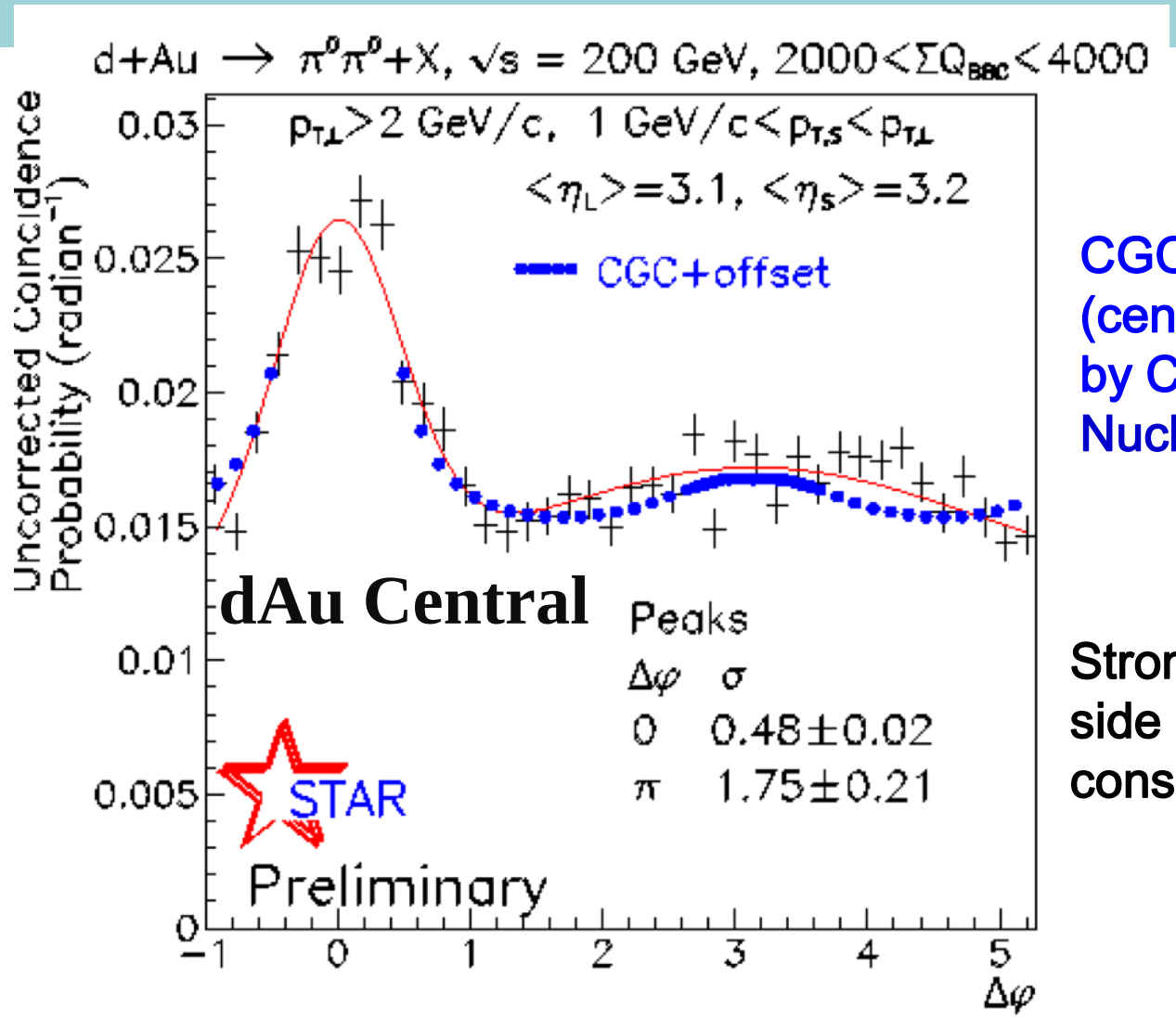

CGC prediction for b=0 (central collisions) by Cyrille Marquet Nucl.Phys.A796:41-60,2007

Strong suppression of away side peak in central dAu is consistent with CGC prediction

CGC Calculations K. Tuchin arXiv:09125479

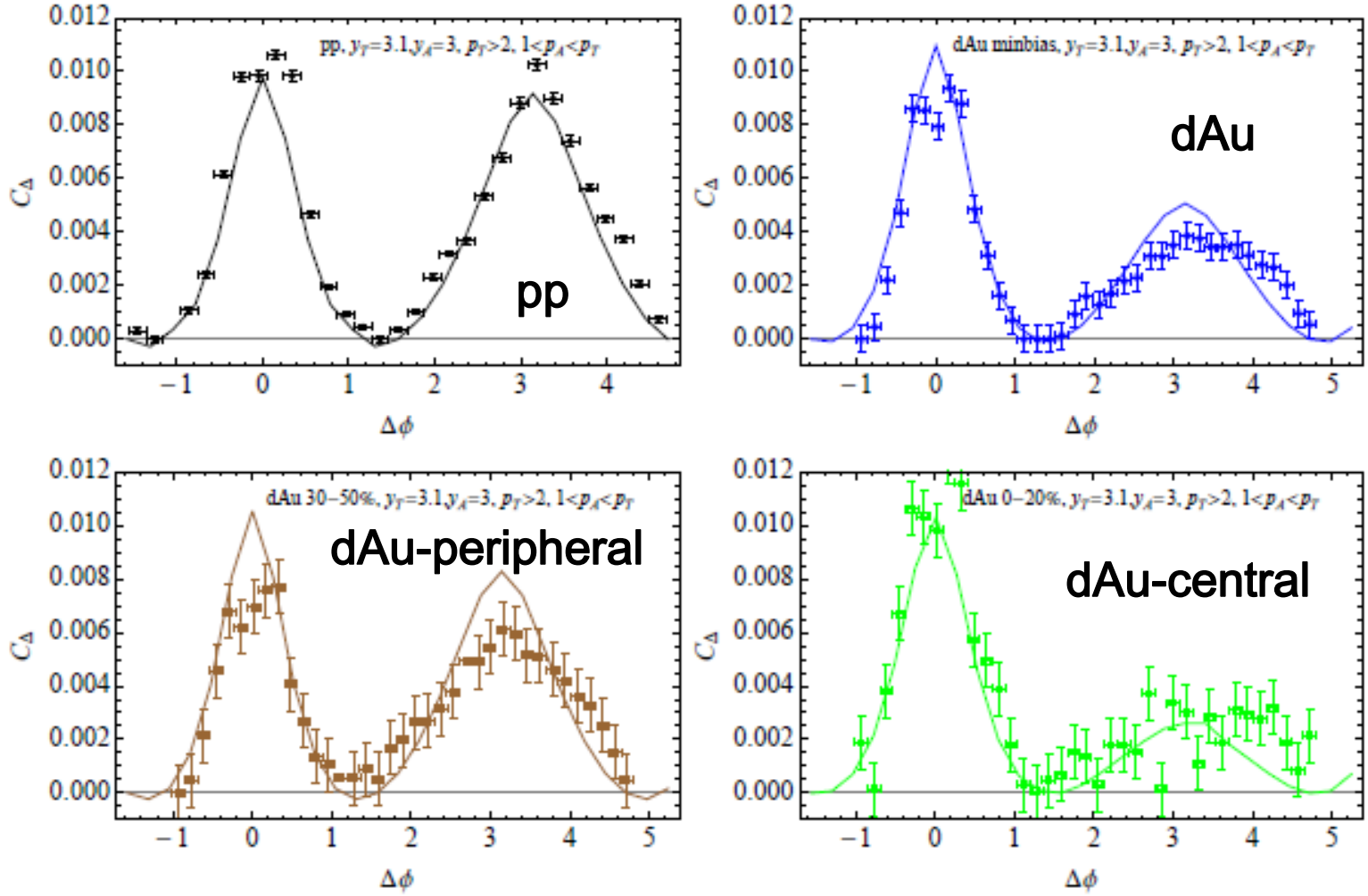

PHENIX J_{dA} vs x_{Au}^{frag}: Strong Suppression for Central Collisions at Low x_{Au}^{frag} !

No Suppression for Peripheral Collisions !

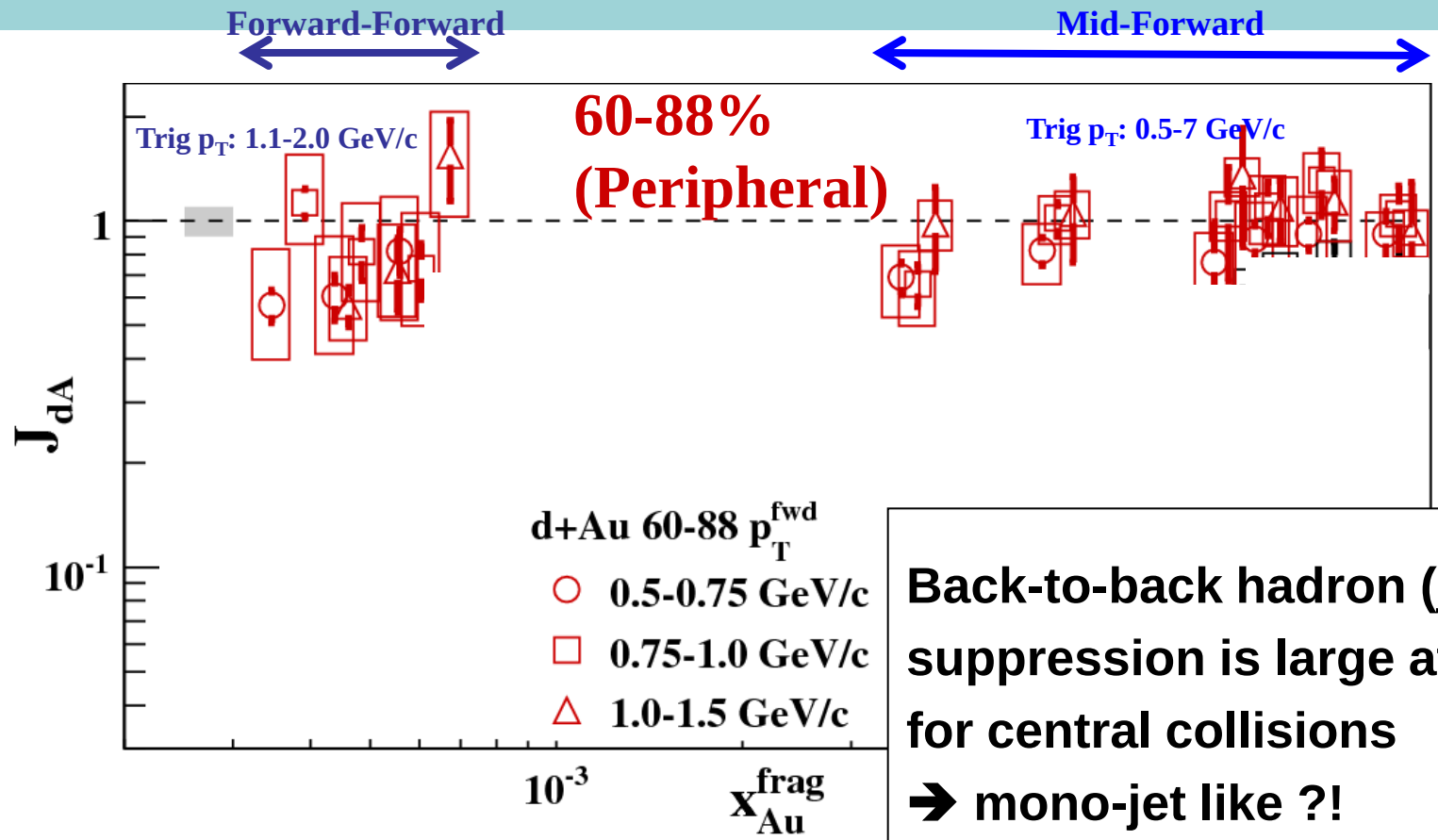

$$x_{Au}^{frag} \equiv \frac{\langle p_{T1}\rangle e^{-\langle \eta_1 \rangle} + \langle p_{T2}\rangle e^{-\langle \eta_2 \rangle}}{\sqrt{s}}$$

Back-to-back hadron (jet) suppression is large at low-x for central collisions

➔ mono-jet like ?!

➔ CGC ? Shadowing + E-loss?

PHENIX Phys.Rev.Lett. 107 (2011) 172301

Note: points for mid-fwd JdA are offset for visual clarity

Leading Order $J_{dA} \sim R_G^{AU}$

$$R_G^{Au}(x,Q^2) = \frac{xG_{Au}(x,Q^2)}{AxG_p(x,Q^2)}$$

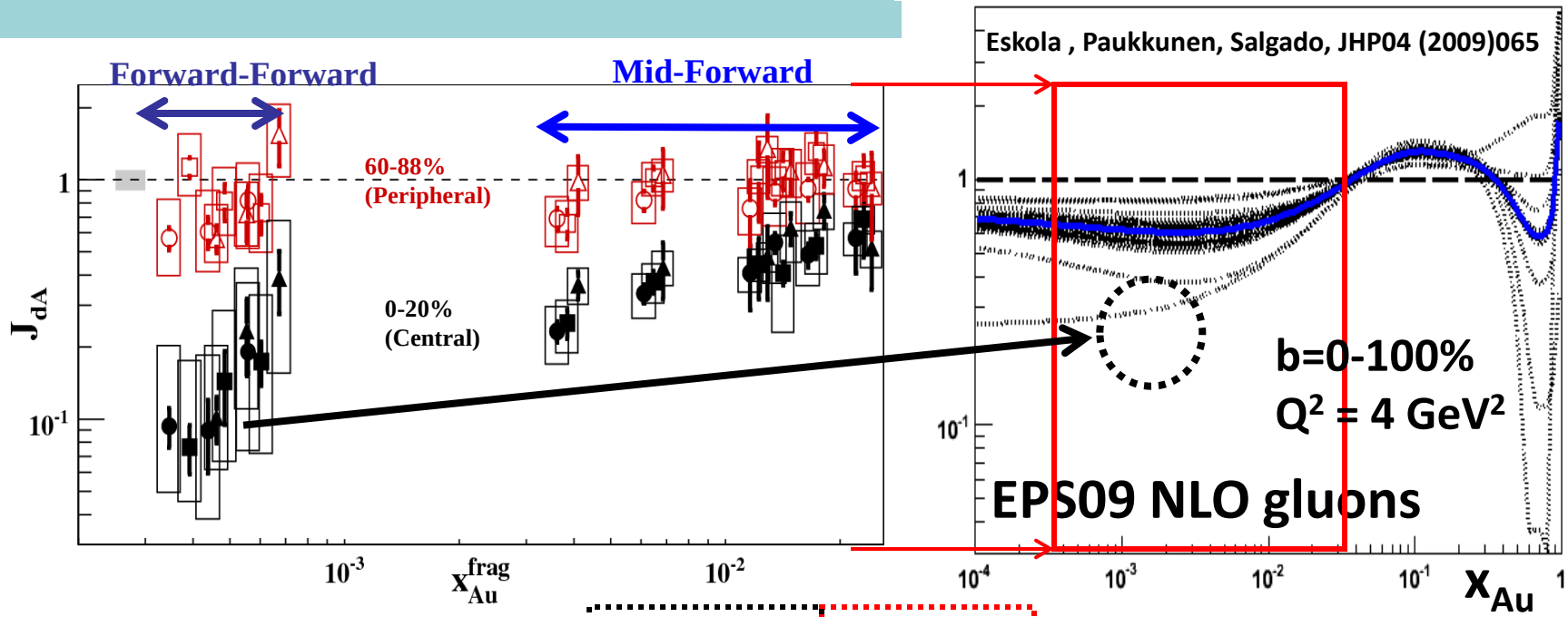

$$J_{dA} = \frac{\sigma_{dAu}^{pairs}/\sigma_{dAu}}{\langle N_{coll}\rangle \sigma_{pp}^{pairs}/\sigma_{pp}} \propto \frac{f_d^a(x_d) \otimes f_{Au}^b(x_{Au}) \otimes \hat{\sigma}^{ab\to cd} \otimes D(z_c, z_d)}{f_p^a(x_p) \otimes f_p^b(x_p) \otimes \hat{\sigma}^{ab\to cd} \otimes D(z_c, z_d)}$$

High x, mostly quarks
Weak effects expected

Low x, mostly gluons → $J_{dA} \sim R_G^{Au}$

courtesy Mickey Chiu

J_{dA} vs pQCD, Shadowing and Energy Loss

Z.-B.Kang, I. Vitev, H. Xing arXiv:1112.6021

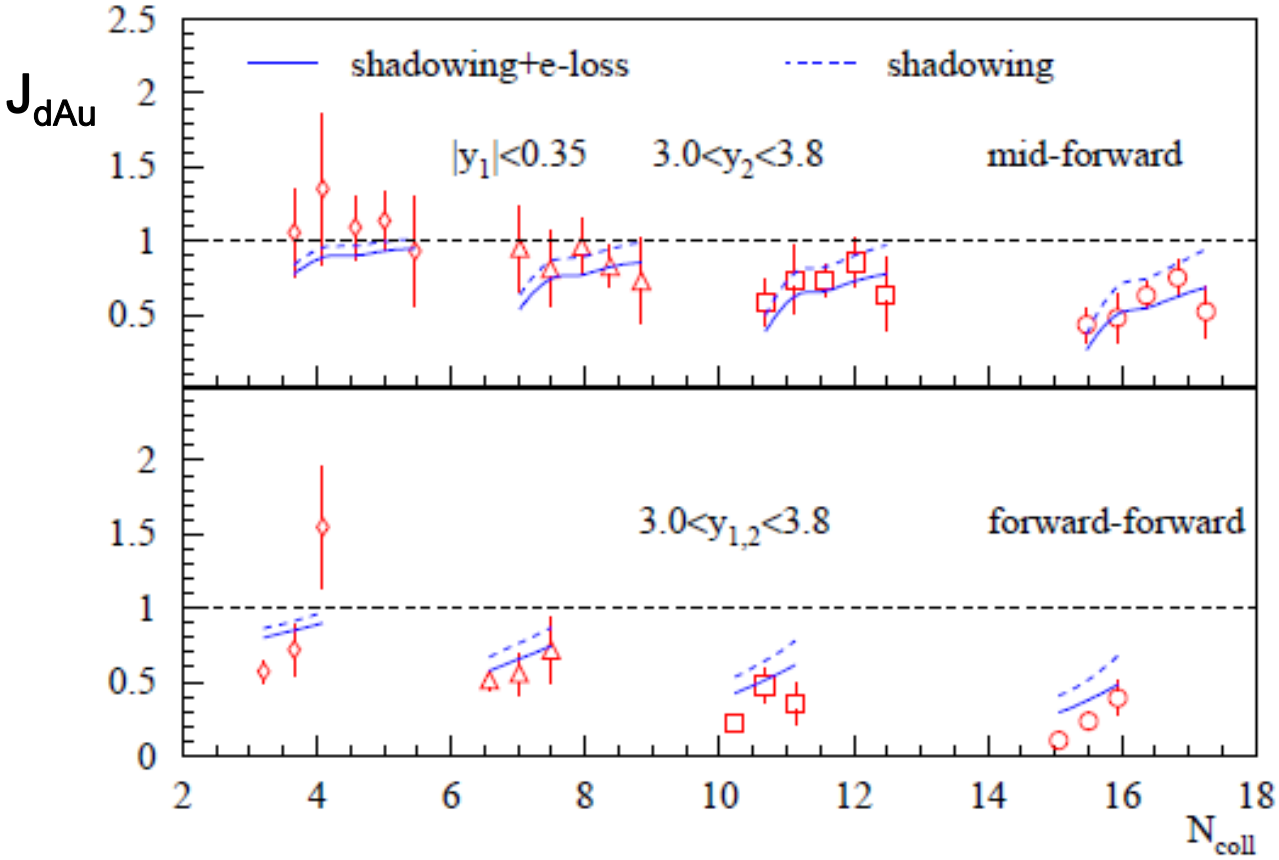

pQCD + shadowing + initial and final state energy loss

➔ $J_{dA} < 1$ is not a unique CGC signature

Will we be Able to Distinguish Between Different Theoretical Possibilities in the Future?

Uncertain!

One approach: measure cross sections for single and Back-to-back hadrons (including hadrons from heavy flavor production) + jets at different energies, for different rapidity intervals and for different nuclei and seek consistent description by competing model calculations.

Important input from theory: ability to carry out global analysis of different data sets including propagation of experimental errors .

Example, global CGC analysis between different data sets from p/dA at RHIC and LHC would test JIMWLK evolution of color configurations.

Additional challenge: quantitative understanding of background in back-to-back hadron or jet data

The d-Au Background in CY

M. Strikman and W. Vogelsang
arXiv:1009.6123

Model cross section for double parton-parton interaction as:

$$\frac{d^4\sigma_{\rm double}}{dp_{T,1}d\eta_1 dp_{T,2}d\eta_2} = \frac{1}{\pi R_{\rm int}^2}\sum_{abc\,a'b'c'}\int dx_a dx_b dz_c dx_{a'} dx_{b'} dz_{c'}\, f^p_{aa'}(x_a,x_{a'}) f^p_b(x_b) f^p_{b'}(x_{b'})$$
$$\times \frac{d^2\hat{\sigma}^{ab\to cX}}{dp_{T,1}d\eta_1}\frac{d^2\hat{\sigma}^{a'b'\to c'X'}}{dp_{T,2}d\eta_2} D_c^{\pi^0}(z_c)\, D_{c'}^{\pi^0}(z_{c'})\,.$$

Cross sections for di-hadron production have contributions from single and double parton interactions.

➔ (1) Double parton interactions found small at mid-rapidity and at moderately high p_T.
(2) Double parton interactions large for forward rapidity.
DPI contributions not negligble in p-p but greatly enhanced in d+Au!

➔DPI can give rise to large backgrounds observed in the d-Au correlation functions

Cross Sections for Single and Double Parton Interactions in pp

M. Strikman and W. Vogelsang
arXiv:1009.6123

Single Parton Int.

Double Parton Int.

Inserts:
r=DPI/SPI

For $\eta_1,\eta_2>3$

DPI dominates cross section for di-hadron production.

DPI further enhanced in d-Au ➔ CY Bckgd.

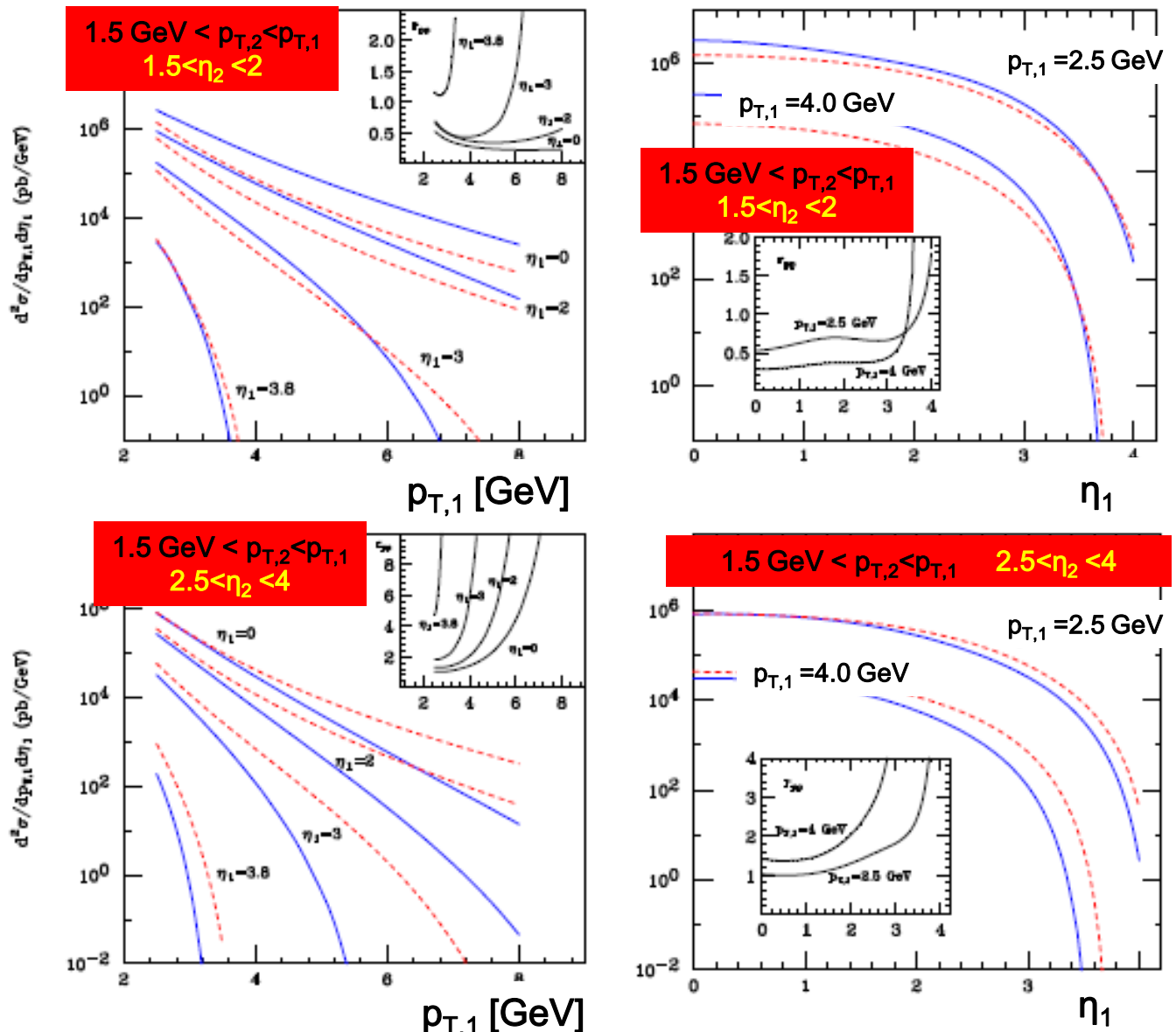

PYTHIA Study: Multi Parton Interactions Limit Ability to Tag low x with Di-Hadrons

Trigger forward ($3 < \eta_1 < 4$)

$p_{T,1} > 2$, $p_{T,2} > 1$

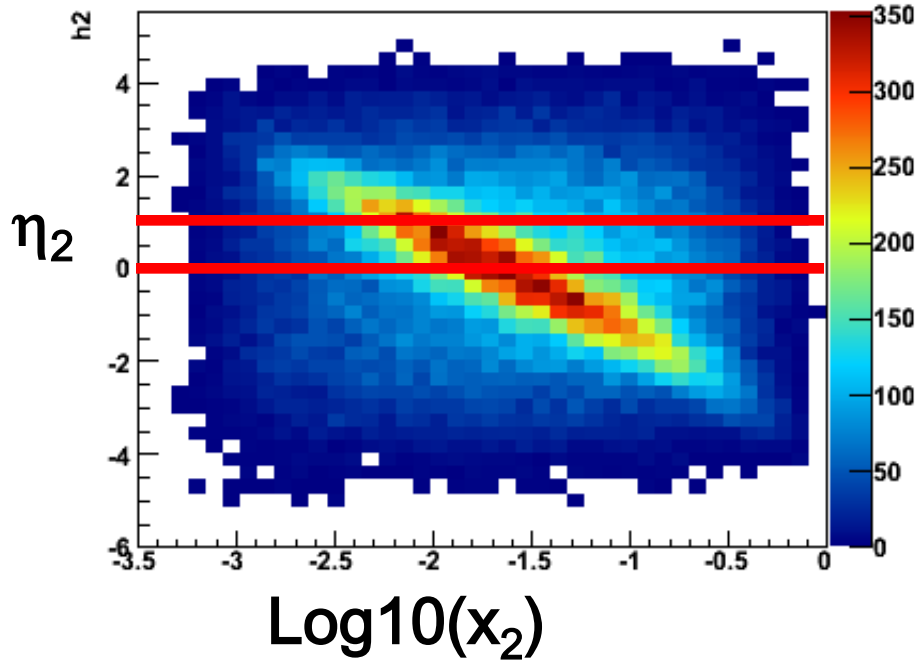

Next slide, show 1-D projections of x_2 distributions by taking η_2 slices

Trigger on away side in correlation function peaks

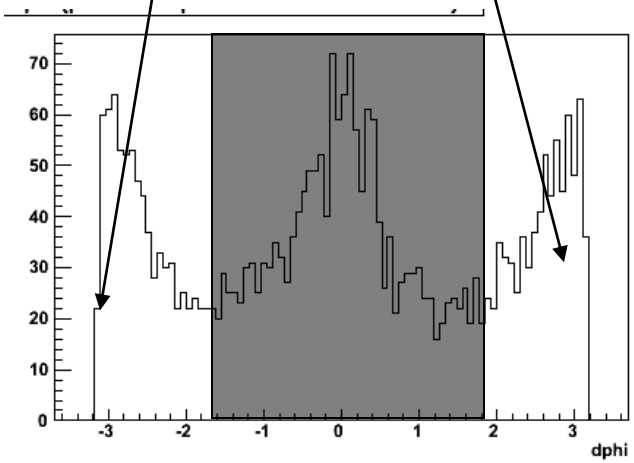

PYTHIA study including multi parton interactions.

(Beau Meredith)

Lowest $\langle x_2 \rangle$ for $1<\eta_2<2$ ➔ the Low x Needed for CGC Intepretation is not Reached

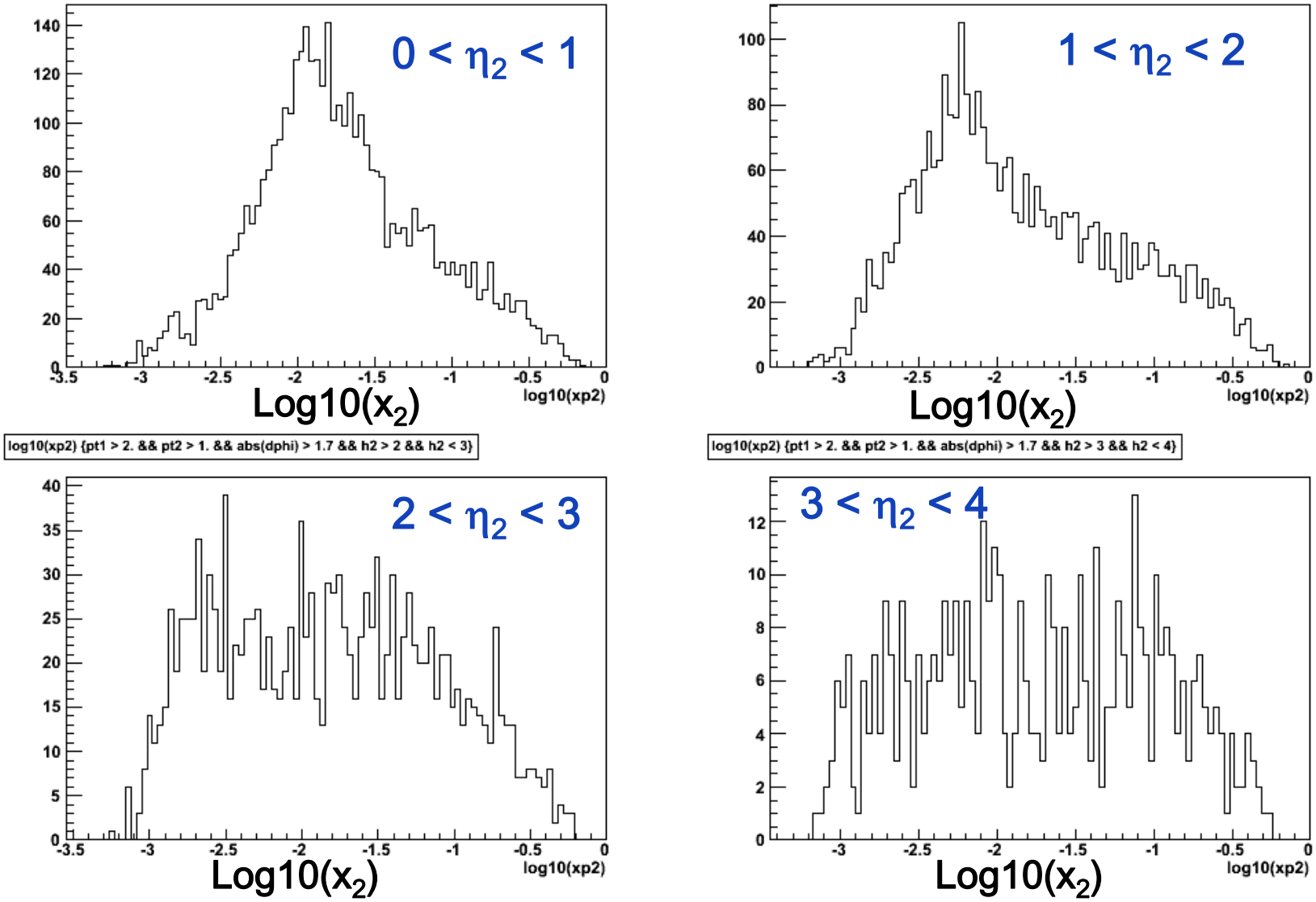

Parton/Jet η_2 for different Hadron η_2 Bins
➔ for η_2>2 Correlation Hadron-Jet is Lost (MPI!)

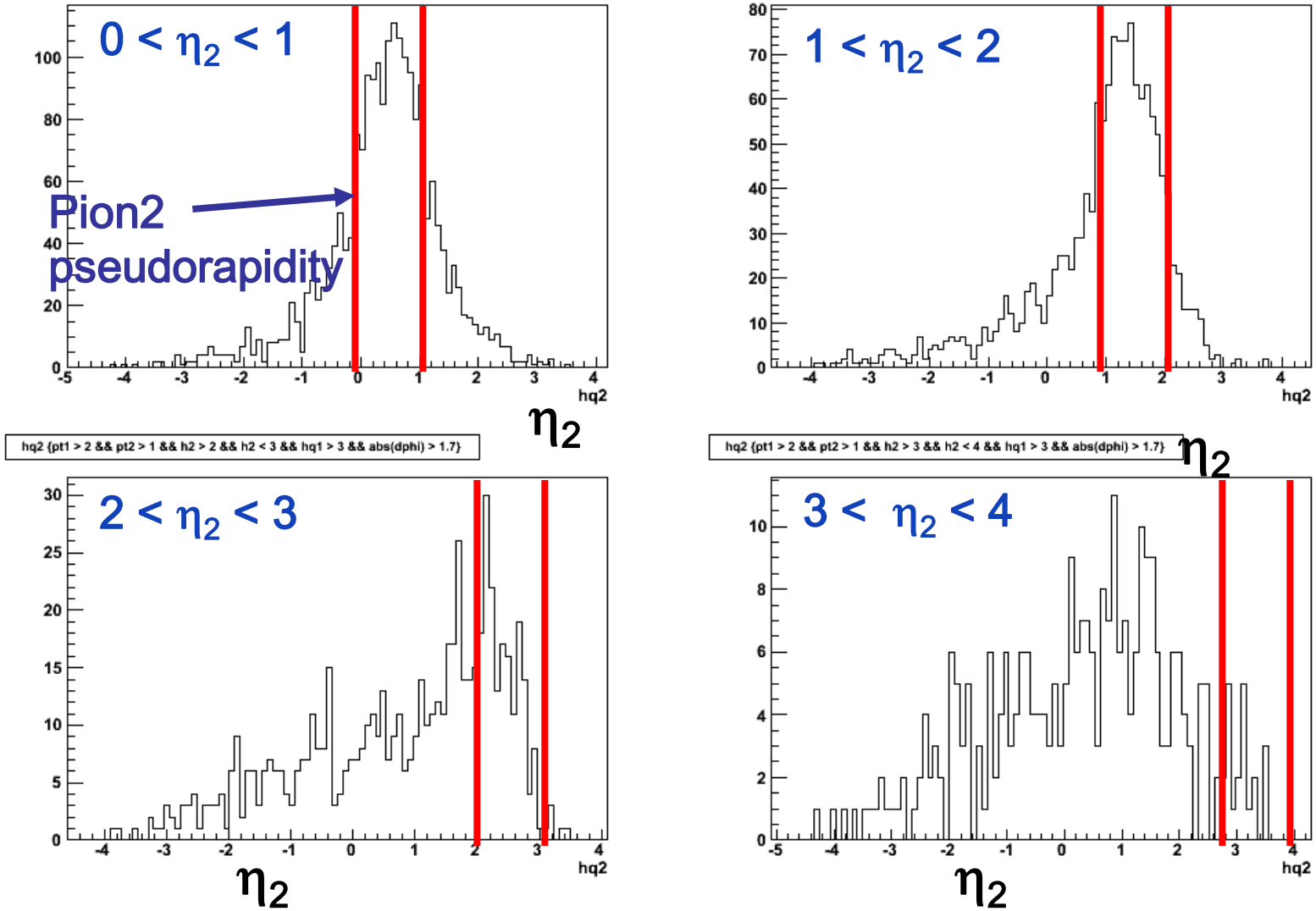

On the Interpretation of Forward-Forward Di-Hadron Correlations at RHIC

- Yields from multi parton interactions appear highest for forward-forward kinematics. This leads to a loss of the correlation between jet and hadron pseudo rapidity.
- In the presence of MPI "inclusive" forward di-hadron correlations in PHENIX and STAR seem to probe $<x_2>\sim 0.01$, to high for an interpretation within the CGC framework. Need to use background subtracted correlated yields.
- Future: p-A, higher luminosity and therefore higher p_T, for hadrons at RHIC jets and/or direct photons at LHC and with forward upgrades at RHIC .

History of PHENIX (Forward) Upgrades

2000	Central Arms	Initial installation
2002	South Muon Arm	Initial installation
2003	North Muon Arm	
2004	Aerogel	PID, hadron spectra
2005	TOF-West	PID, hadron spectra
2006	RXP	Reaction Plane
	MPC	d-A, A_N, A_{LL} di-hadron
2008	HBD	PID, low mass di-leptons
2011	VTX	c-, b-tagging, central tracking
2012	μ-Trigger	W-physics
	FVTX	c-, b-tagging
2014	*MPC-EX*	*π^0-photon separation*

Significant track record with staging instrumentation upgrades and attracting significant resources from outside DOE: NSF, funding sources in Japan, Russia, France, Germany, Israel, Korea, Brazil, China and institutional contributions

Forward Upgrades Completed for Run 2012

(I) Muon Trigger for W-physics in polarized p+p at √500 GeV

(II) Forward Vertex Tracker for heavy flavor physics in pp, pA, AA

FVTX

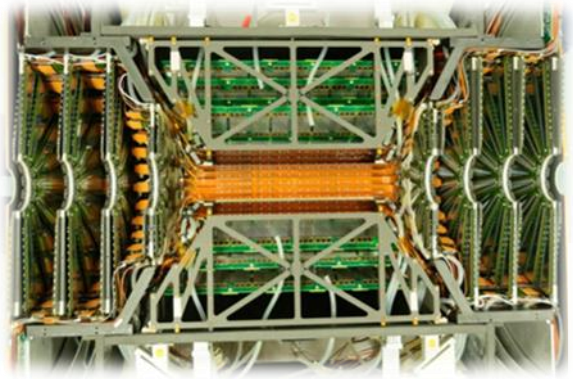

DOE, Los Alamos, BNL

(III) MPC FEE/Trigger Upgrade for forward spin measurements

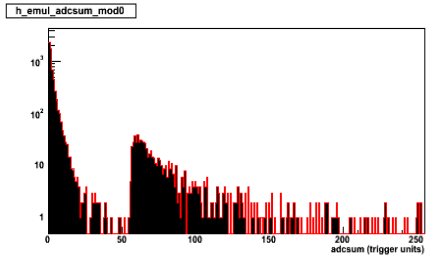

PHENIX-HBD, BNL

Forward Upgrades Completed for Run 2012 ➔ Selected Physics Channels

(I) Muon Trigger for W-physics

➔ quark and anti-quark helicity dis.

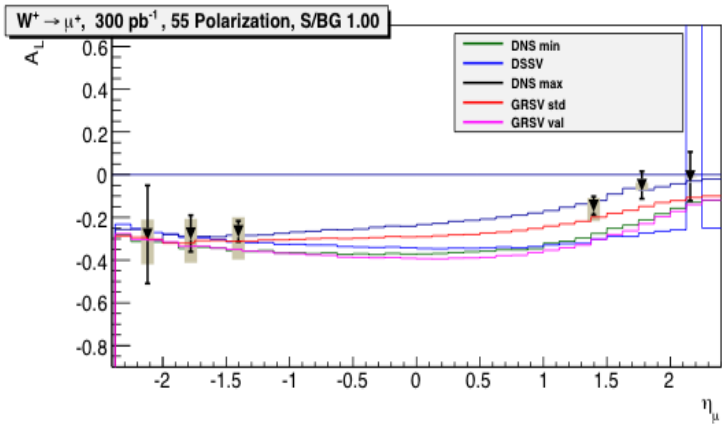

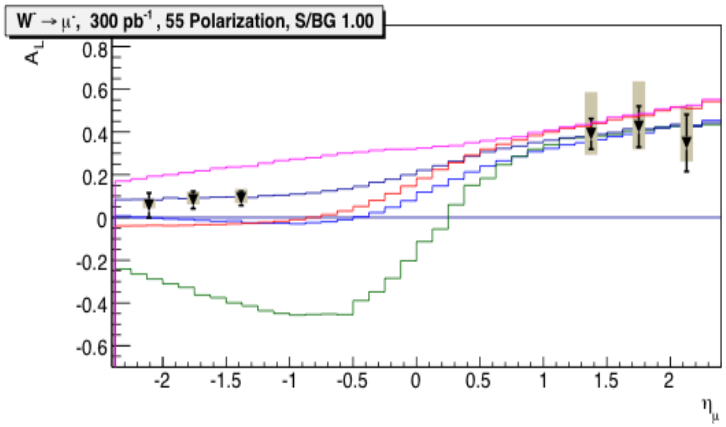

(II) Forward Vertex Tracker for

➔ spin asymmetries with flavor tag!

(a) Flavor tagging for heavy quark Physics in pp, pA and AA

(b) Background rejection for Drell-Yan and W-measurements.

(III) MPC FEE/Trigger Upgrade

➔ probe ΔG(x) at small x

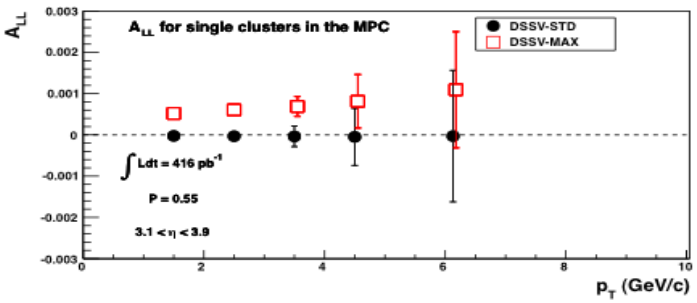

MPC-EX Upgrade aims for Run 2014

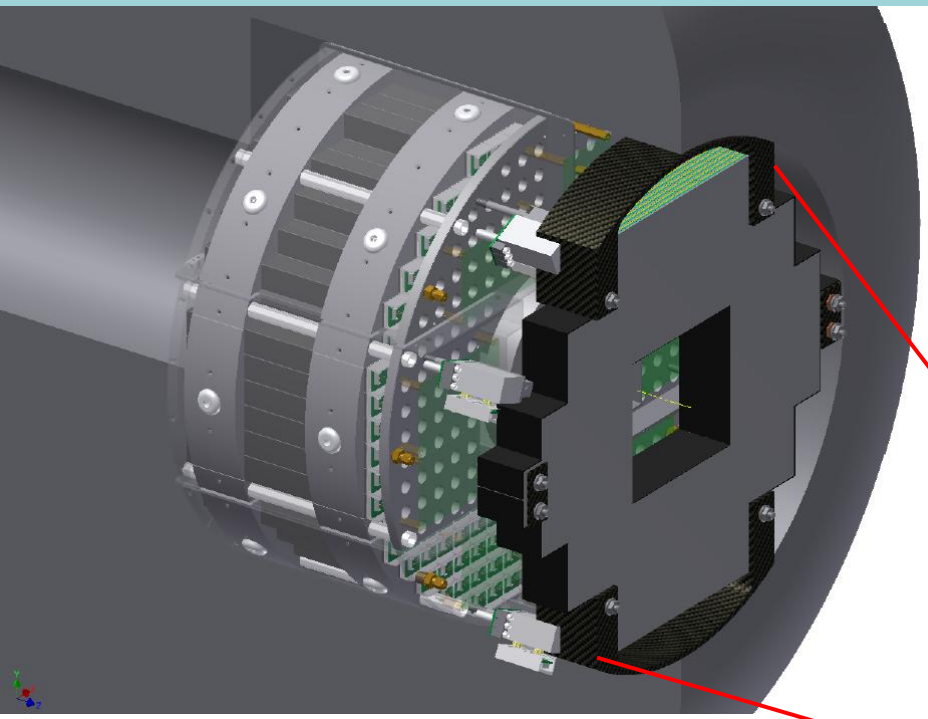

3.1<η<3.8

A combined charged particle tracker and EM pre-shower detector – dual gain readout allows sensitivity to MIPs and full energy EM showers.

- π^0 rejection → direct photons
- π^0 reconstruction out to >80GeV
- Charged track identification

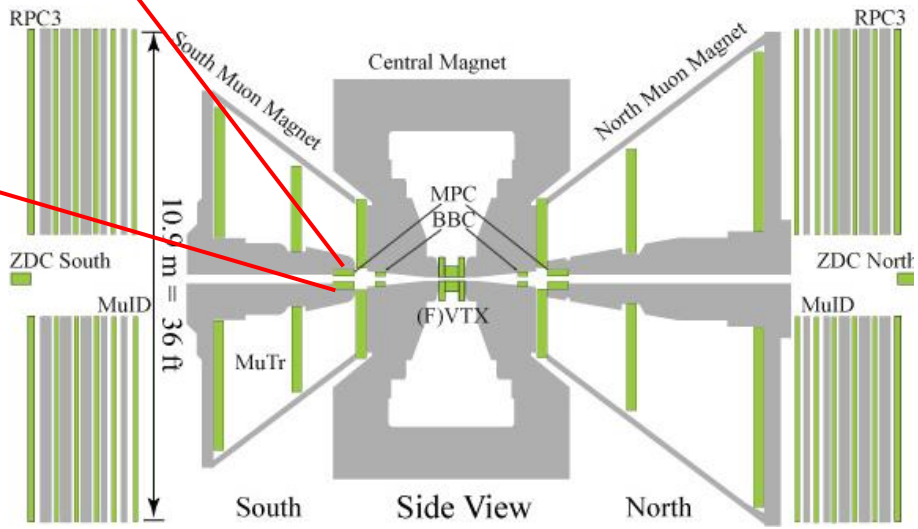

from John Lajoie, MPC-EX review – May 2012

MPC-EX Upgrade Physics Goals

(I) Measure nuclear gluon distribution from direct photon production in d+Au collisions

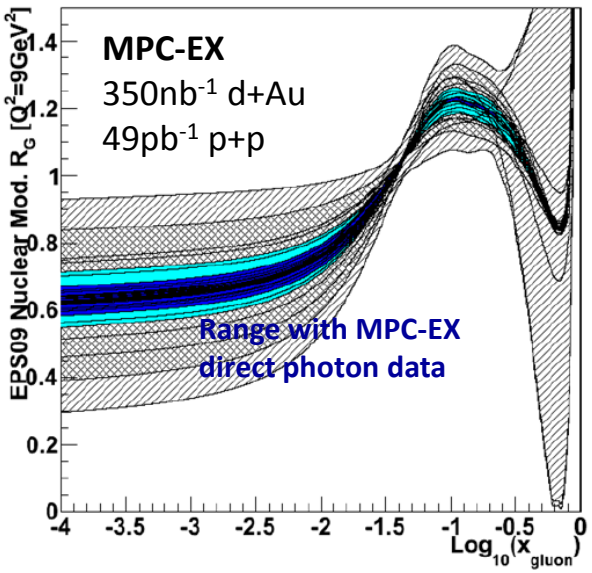

Central curve is

$$G_{Pb}(x,Q^2)=R_G^{Pb}(x,Q^2)\,G_p(x,Q^2)$$

with grey uncertainty bands from

K. Eskola H. Paukkumen, C. Salgado Nucl.Phys. A855 (2011)150 → EPS09

(II) Determine quark Transversity/Collins contribution to single transverse spin asymmetries A_N in polarized p+p collisions

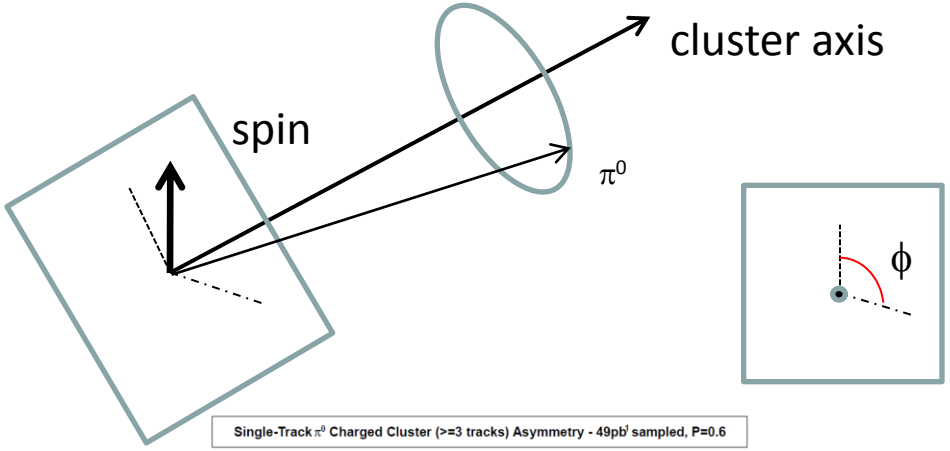

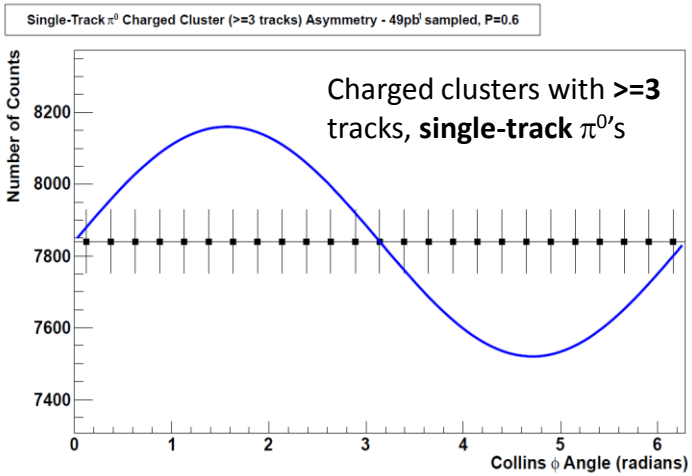

Scope of Possible Forward Upgrade of a Future sPHENIX Detector

Detector Layout for forward physics studies.
Use open sPHENIX geometry to introduce

- o tracking
- o charged particle identification
- o electromagnetic calorimeter
- o hadron calorimeter
- o muon detection

for measurements of jets, identified hadrons in jets, heavy flavor, Drell-Yan and direct photons inside large acceptance 1<η<4.

Use existing equipment where possible.

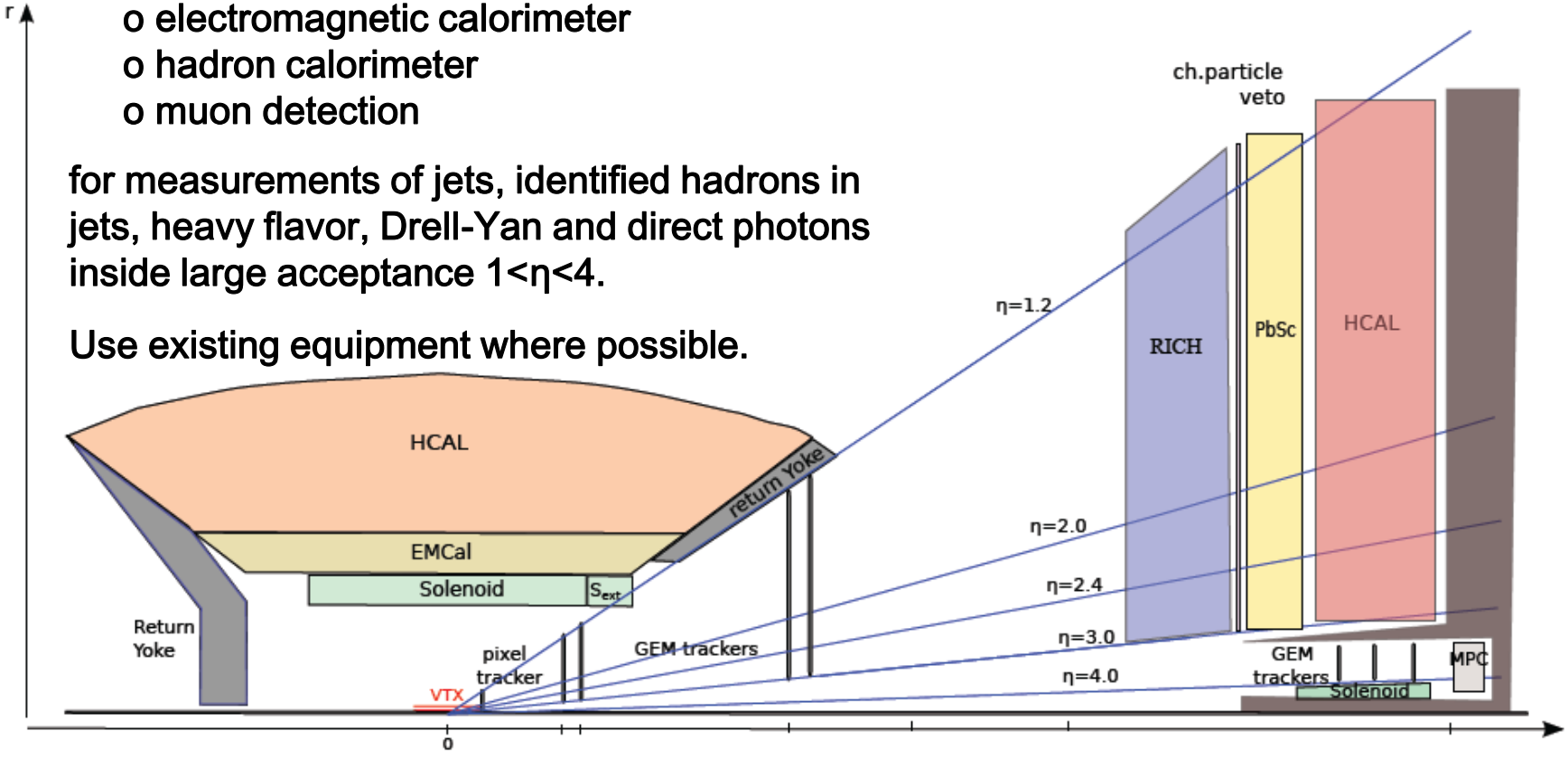

Forward Physics: What will be known ?

Cold Nuclear Matter Effects in Nucleon Structure:

(I) CNM effects at LHC energies will be firmly established through p+Pb collisions in inclusive hadron-, jet-, di-jet- and heavy flavor-channels.

(II) RHIC experiments will have measured the nuclear gluon distribution for one nucleus through direct photon production.

(III) RHIC has studied CNM effects (and will add more data) through inclusive hadron-production, di-hadron correlations and heavy flavor-channels.

Heavy Ion Physics:

(I) Forward RHIC data sets.

(II) Detailed studies at LHC energies will be available.

Forward Physics: What will we know ?

Nucleon Spin Physics:

(I) Measurements of quark and anti-quark helicity distributions in W-production further supported by new results from COMPASS and J-Lab12 → NSAC milestone for hadron physics HP8, 2013.

(II) Determination of the gluon spin contribution to the proton spin for $0.01 < x_{gluon} < 0.3$ from A_{LL} measurements for inclusive hadrons, jets and di-jets at RHIC → NSAC HP12, 2013.

(III) Precise measurements of single transverse spin asymmetries, A_N at RHIC. Collins and Sivers effects will be established separately in ep and pp (based on current and future results from RHIC, COMPASS & J-Lab12). COMPASS sign change observation likely in pion induced Drell-Yan → NSAC HP13, 2015.

sPHENIX Forward Physics

The study of transverse spin asymmetries has led to an advanced understanding of scattering processes involving the strong interaction:

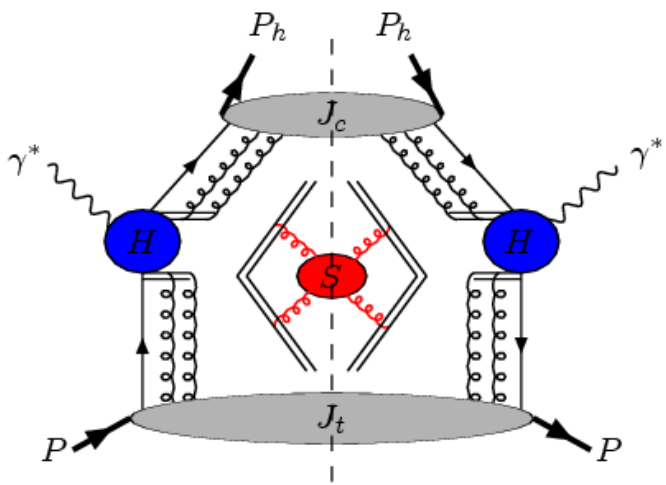

TMD framework: inclusion of final and initial state gluon radiation via gauge link integrals gives rise to large transverse spin effects and process dependence.

The PHENIX forward upgrade aims to

(1) quantitatively confirm TMD framework including decomposition of A_N observed in pp, process dependence and evolution.

(2) measure quark transversity dis. including large x → tensor charge !

(3) measure valence and sea-quark Sivers distributions
→ explore connection to L_z
(M. Burkhard arXiv: 1205.2916v1)

(4) Survey cold nuclear matter effects in the transition region to the saturation regime. Quantify the initial state for HI-Collisions.

Unique measurements at forward rapidity using jet observables and the Drell-Yan process!

Experimental Requirements Driven by p-p Goals

- Good Jet reconstruction to be able to measure Sivers cleanly
  - Electromagnetic and hadronic calorimetry
- Particle ID to measure Collins effect
  - Collins effect different for different hadrons →RICH
- B Field and tracker to determine charge sign of hadrons
- Vertex detector for heavy flavor tagging

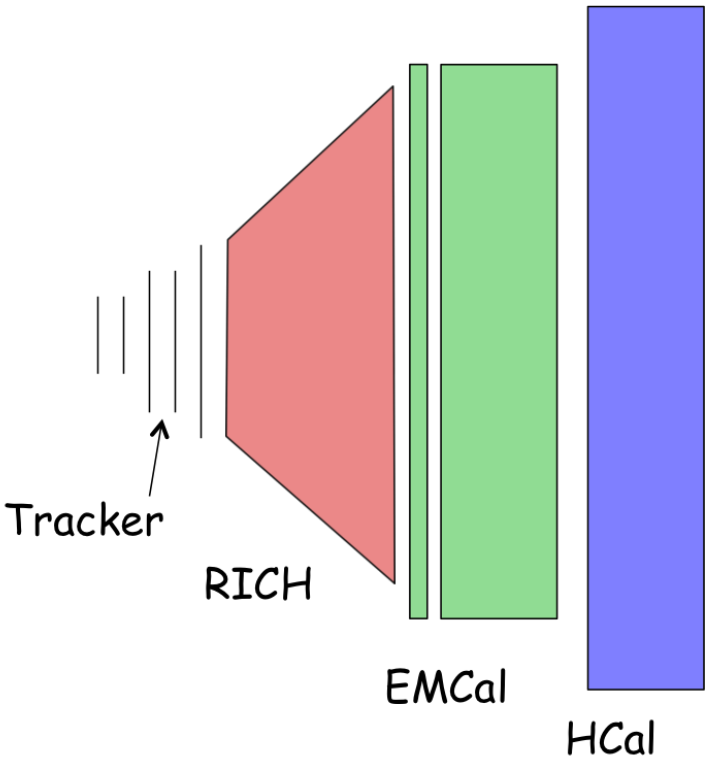

A-Dependence of Nucleon Structure ➔ Goals

p-A (I) Study the transition region near the saturation scale!

(II) **Measure $G_A(x)$ and quantify initial state for HI collisions at RHIC: heavy flavor, jets, jet-correlations, direct photon, Drell-Yan, different nuclei, beam energy.**

(III) Search for onset of gluon saturation and verify CGC framework as an effective field theory at high field strengths in QCD.

For example: can we determine color configurations $W(\rho)$ from RHIC data and use the JIMWLK evolution to evolve them to LHC energies?

(IV) Explore similarities between TMD and CGC formalisms.

Next Steps

- o Detector and sensitivity simulations in progress
- o RBRC workshop on "Forward Physics at RHIC"
  → July 30 to August 1st 2012
- o Initiate exploratory R&D
  - GEM-trackers at Los Alamos (LDRD)
  - EMC at RBRC (RIKEN)
  - HCAL at UIUC (NSF)
- o Report on Physics and Design Studies
  → November 2012
- o Explore funding possibilities: external funds, staging

Detector Layout for Physics Studies

Studies for detector components led by

GEM-trackers: Los Alamos, RBRC
RICH: Stony Brook
EMC: RBRC/RIKEN, ISU
HCAL: UIUC
Magnet: Los Alamos, RBRC, UCR

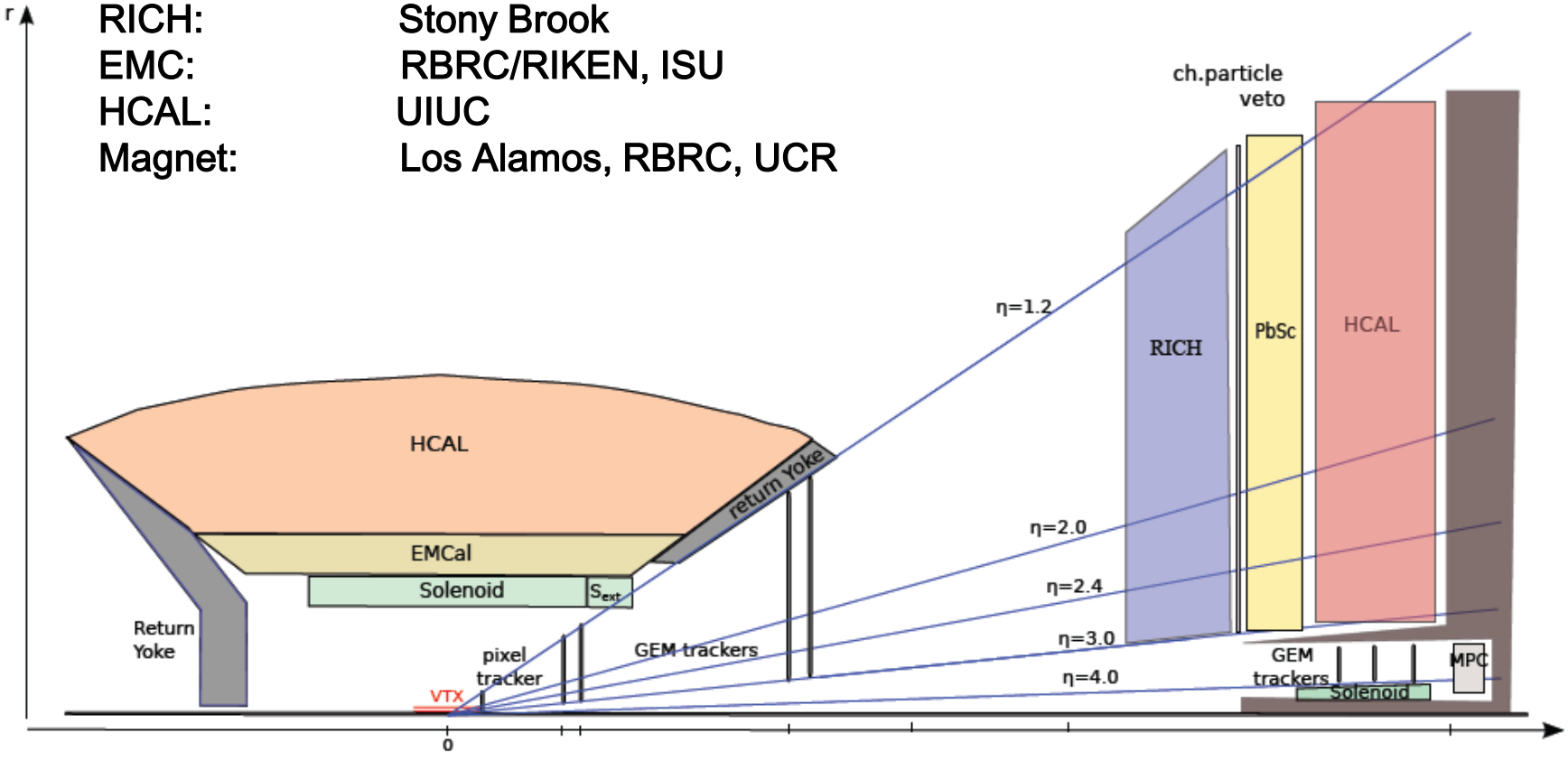

Summary

- PHENIX has started to evaluate the physics potential of a large acceptance sPHENIX forward detector for Drell-Yan and jet physics in polarized p-p, p-A and A-A collisions.
- Precision measurements with clean theoretical interpretation would become possible:

  Saturation physics, survey of the Sivers function, transversity distributions, tensor charge and tests of the evolution of transverse momentum dependent observables.
- Significant effort and care will be needed to meet the experimental and theoretical challenges: high luminosity + polarization, high performance detector, precision polarimetry, tools for the clean pdf extraction.
- We seek to utilize existing equipment as much as possible and to solicit substantial external funding sources.

Incomplete List of PHENIX Spin Collaborators who have Expressed Interest in the Forward Upgrade

Abilene Christian University, Abilene, TX 19973, USA
M. Daugherty, D. Isenhower R.Towell

Brookhaven National Laboratory, Upton, NY 11973, USA
S. Bazilevsky, M. Chiu

University of California, Riverside, Riverside, CA 92521, USA
K. Barish, R. Seto

CIAE, Beijing, China
X. Li

Georgia State University, Atlanta, GA 30303, USA
X. He, M. Sarsour

Hanyang University, Seoul 137-791, Korea
B. Kang, J. Kang, Y. Kim, B. Park

University of Illinois, Urbana, IL 61801, USA
M. Grosse Perdekamp

Iowa State University, Ames, IA 50011, USA
J. Hill, J. Lajoie

KEK, Tsukuba, Ibaraki,305-0801, Japan
N. Saito

Korea University, Seoul, 136-701, Korea
B. Hong, K. B. Lee, S. Park

Los Alamos National Laboratory, Los Alamos, NM 87545, USA
M. Brooks, M. Liu, X. Jiang, M. Leitch

Muhlenberg College, Allentown, PA 18104, USA
B. Fadem

New Mexico State University, NM 88003 USA
S. Pate

University of New Mexico, Albuquerque, NM 87131, USA
D. Fields

RIKEN Brookhaven Research Center, Upton, NY 11973, USA
J. Seele, K. Okada

RIKEN Institute, Hirosawa, Wako, 351-0198, Saitama, Japan
Y. Goto, I. Nakagawa, R. Seidl

Rikkyo University, Rikkyo, 3-34-1, Tokyo, 171-8501, Japan
K. Kurita and J. Murata

Seoul National University, Seoul, Korea
K. Tanida

Stony Brook University, Stony Brook, NY 11970, USA
A. Deshpande, K. Dehmelt, T. Hemmick

University of Michigan, Ann Arbor, MI 48109, USA
C. Aidala

20/14 institutions from the US, China, Korea and Japan

collaborators presently active in forward upgrade planning & studies, coordinators

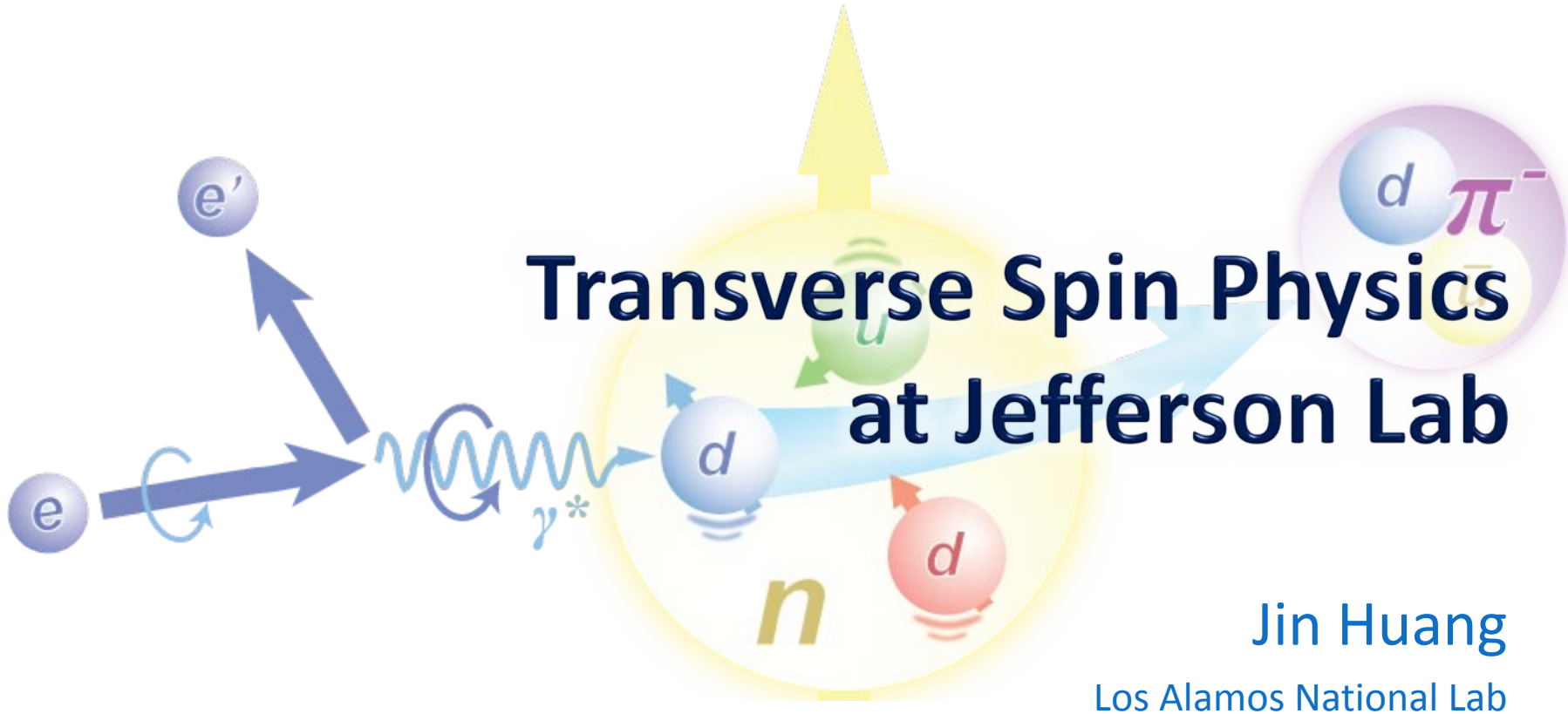

Transverse Spin Physics at Jefferson Lab

Jin Huang

Los Alamos National Lab

RBRC Forward Physics Workshop

Los Alamos NATIONAL LABORATORY EST. 1943

Jefferson Lab

Transverse Momentum Dependent (TMD) Parton Distributions

- TMD PDFs link
  - Intrinsic motion of partons
  - Parton spin
  - Spin of the nucleon
- Multi-Dimension structure
  - Imaging the 3D motion of the quark
  - Probes orbital motion of quarks
- A new phase of study, fast developing field
  - Great advance in theories (factorization, models, Lattice ...)
  - Experimentally, not systematically studied until recent years
  - Complementary study between CEBAF and RHIC

Leading-Twist TMD PDFs

Nucleon Spin

Quark Spin

Nucleon Polarization	Quark polarization: Unpolarized (U)	Quark polarization: Longitudinally Polarized (L)	Quark polarization: Transversely Polarized (T)
U	f_1 =		$h_1^{\perp}$ = – Boer-Mulders
L		g_1 = – Helicity	$h_{1L}^{\perp}$ = – Worm Gear (Kotzinian-Mulders)
T	$f_{1T}^{\perp}$ = – Sivers	g_{1T} = – Worm Gear (trans-helicity)	h_1 = – Transversity $h_{1T}^{\perp}$ = – Pretzelosity

: Survive trans. momentum integration

Access TMDs through Hard Processes

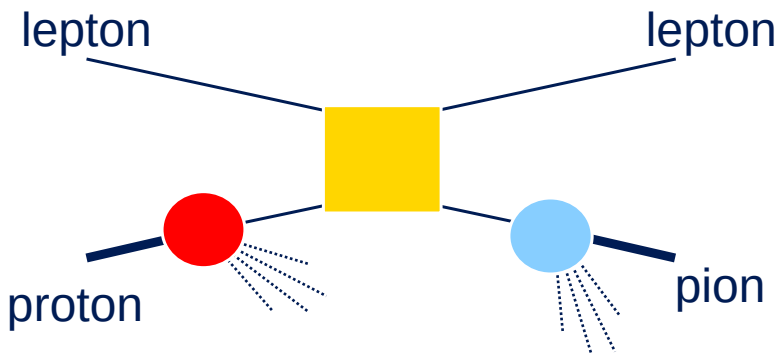

SIDIS

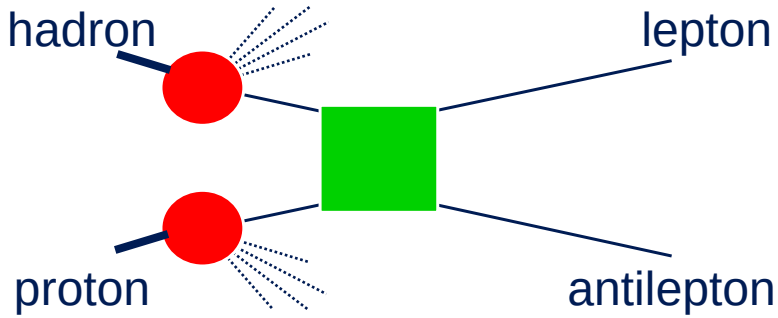

Drell-Yan, …

Partonic scattering amplitude

Fragmentation amplitude

Distribution amplitude

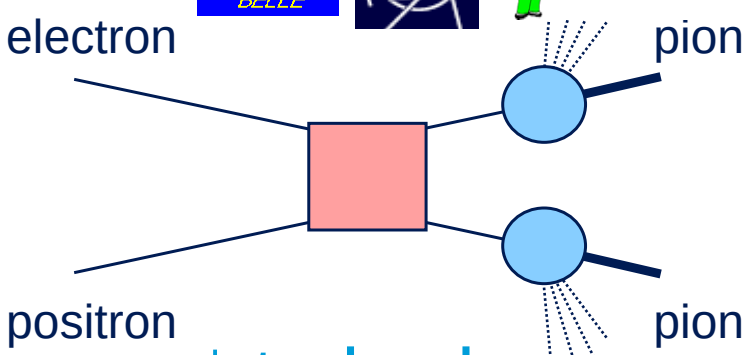

e^-e^+ to hadrons

Tool: Semi-inclusive DIS (SIDIS)

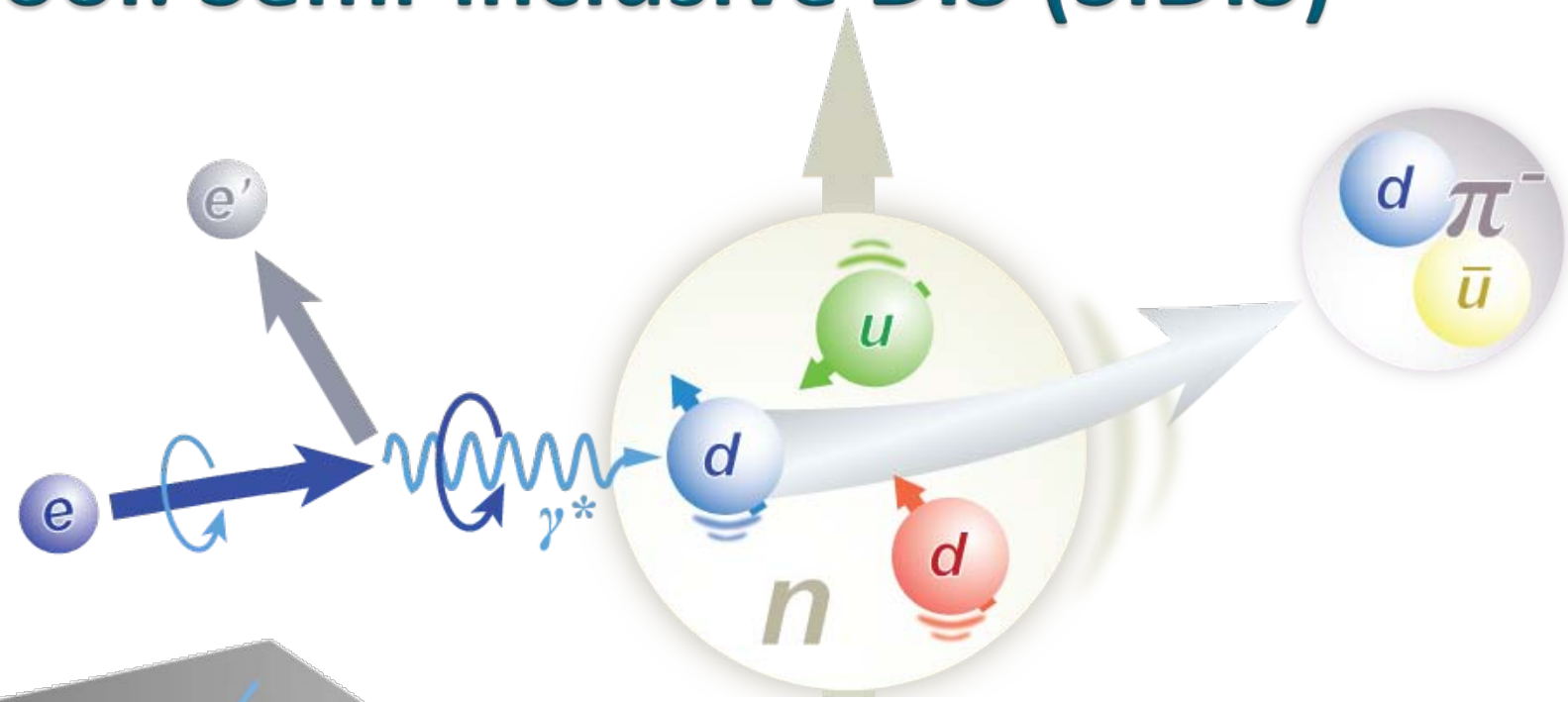

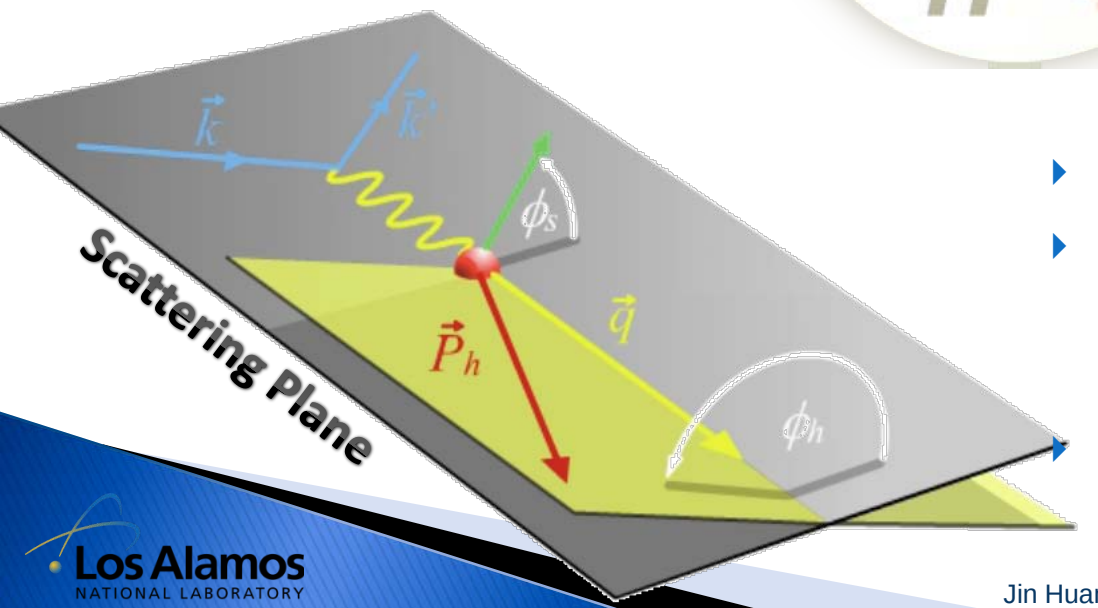

- Gold mine for TMDs
- Access all eight leading-twist TMDs through spin-comb. & azimuthal-modulations
- Tagging quark flavor/kinematics

TMDs in SIDIS Cross Section

$$\frac{d\sigma}{dx\,dy\,d\phi_S\,dz\,d\phi_h\,dP_{h\perp}^2} = \frac{\alpha^2}{xyQ^2}\frac{y^2}{2(1-\varepsilon)}\cdot$$

$$\{F_{UU,T} +$$

$$+\varepsilon\cos(2\phi_h)\cdot F_{UU}^{\cos(2\phi_h)} + \ldots$$

$$+ S_T\lambda_e[\sqrt{1-\varepsilon^2}\cos(\phi_h-\phi_S)\cdot F_{LT}^{\cos(\phi_h-\phi_S)} + \ldots]$$

$$+ S_L\lambda_e[\sqrt{1-\varepsilon^2}\cdot F_{LL} + \ldots]$$

$$+ S_L[\varepsilon\sin(2\phi_h)\cdot F_{UL}^{\sin(2\phi_h)} + \ldots]$$

$$+ S_T[\varepsilon\sin(\phi_h+\phi_S)\cdot F_{UT}^{\sin(\phi_h+\phi_S)}$$

$$+\sin(\phi_h-\phi_S)\cdot(F_{UT}^{\sin(\phi_h-\phi_S)} + \ldots)$$

$$+\varepsilon\sin(3\phi_h-\phi_S)\cdot F_{UT}^{\sin(3\phi_h-\phi_S)} + \ldots]\}$$

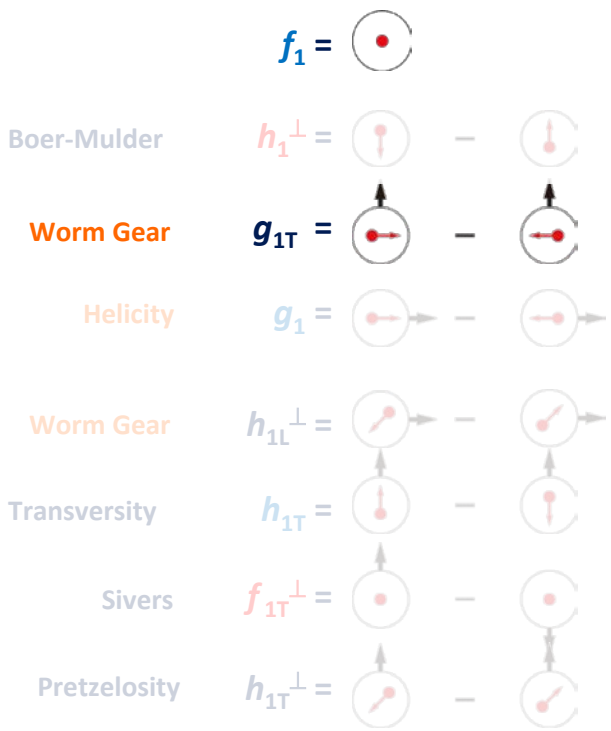

S_L, S_T: Target Polarization; λ_e: Beam Polarization

Accessing TMD through SIDIS e.g. experimental study of g_{1T}

- Double Beam-Target Spin Asymmetry (DSA) in SIDIS with transversely polarized target: A_{LT}

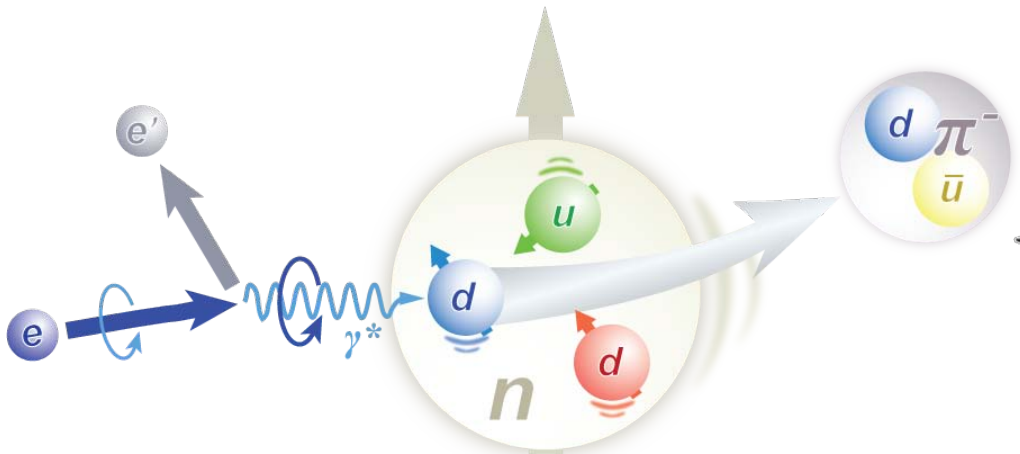

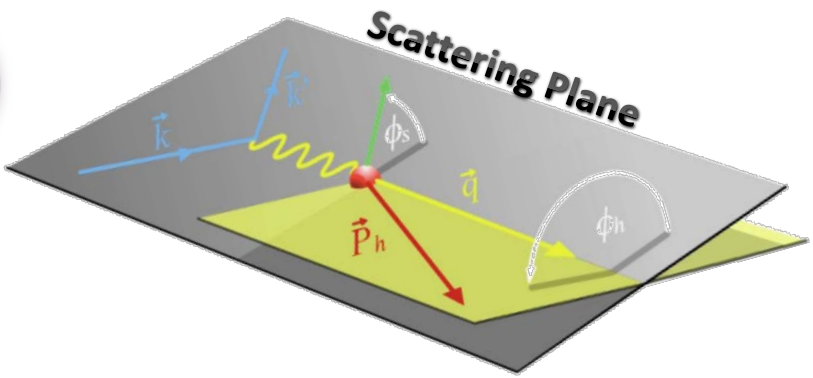

$$A_{LT}^{\cos(\phi_h-\phi_s)} \equiv 2\frac{\int d\phi_s^h\left(d\vec{\sigma}-d\overleftarrow{\sigma}\right)\cos(\phi_h-\phi_s)}{\int d\phi_s^h\left(d\vec{\sigma}+d\overleftarrow{\sigma}\right)}$$

$$\propto g_{1T}^q \otimes D_{1q}^h$$

- Technically, azimuthal amplitude in asymmetry extracted through methods considering acceptance and luminosity corrections, including
  - azimuthal asymmetry fits
  - Maximum likelihood analysis

Jefferson Lab Overview

- Newport News, Virginia
- Linear accelerator provides continuous polarized electron beam
  - $E_{\text{beam}} = 6\ \text{GeV}$
  - $P_{\text{beam}} = 85\%$
- 3 experimental halls A, B and C

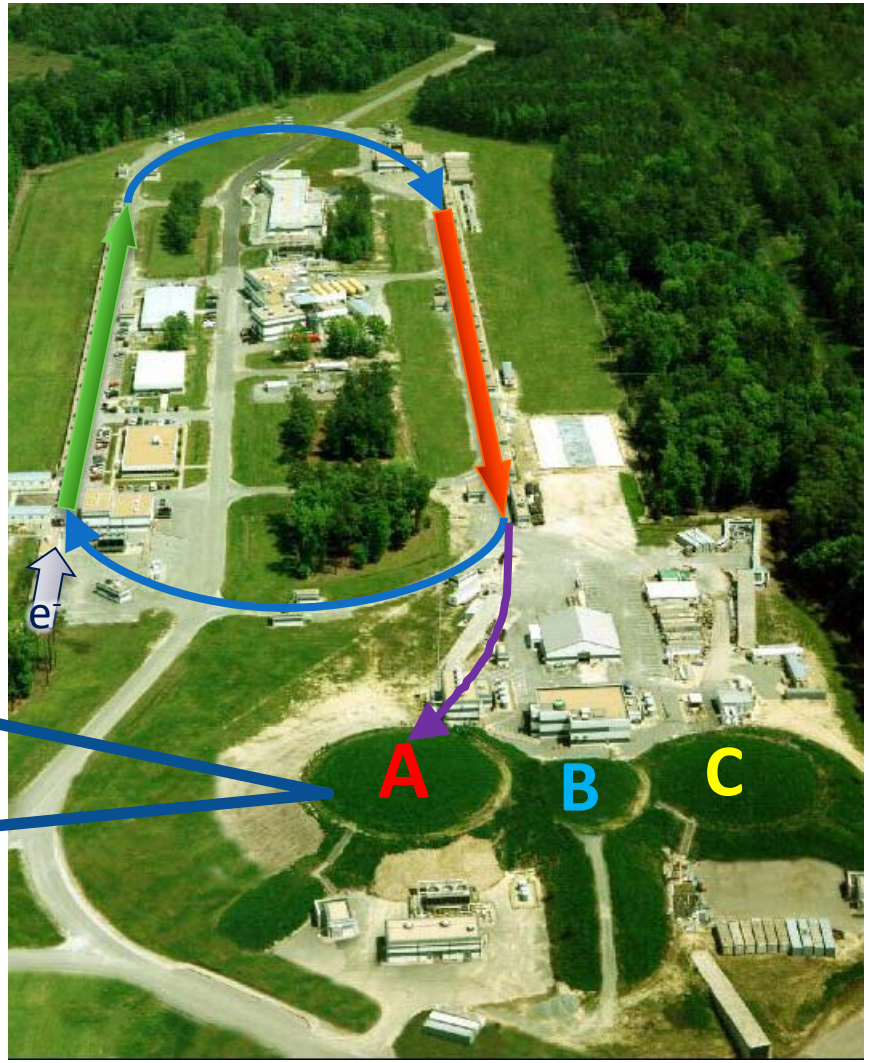

CEBAF @ JLab Today

- Superconducting recirculating electron accelerator
  - maximum energy 6 GeV
  - maximum current 200 uA
  - electron polarization 85%
- Equipment in 3 halls (simultaneous operation)

	L[$cm^{-2}s^{-1}$]	(pol.)
A: 2 High Resolution Spectrometers	10^{39}	(10^{36})
B: Large Acceptance Spectrometer	10^{34}	(10^{34})
C: 2 spectrometers and dedicated devices	10^{39}	(10^{35})

- JLab and User Community
  - ~600 JLab employees
  - ~2000 users from ~300 institutions, ~40 countries
  - ~ 1/4-1/3 of the nuclear physics PhDs in US
- Experiment scale: ~100 collaborators (10-20 core), ~run for few months

First exploring of TMD using polarized He3 Target

E06-010 6-GeV Transversity Experiment

- Successful data taking 2008-09
- Polarized electron beam
  - With 30 Hz helicity reversal
- Polarized ^{3}He target
- BigBite at 30º detect electron
  - Dipole magnet, P_e = 0.6 ~ 2.2 GeV/c
  - MWDC/shower-preshow/scitillator
- HRS_L at 16º detect hadron
  - QQDQ config, P_h = 2.35 GeV/c
  - Scintillator/drift chamber/Cherenkov

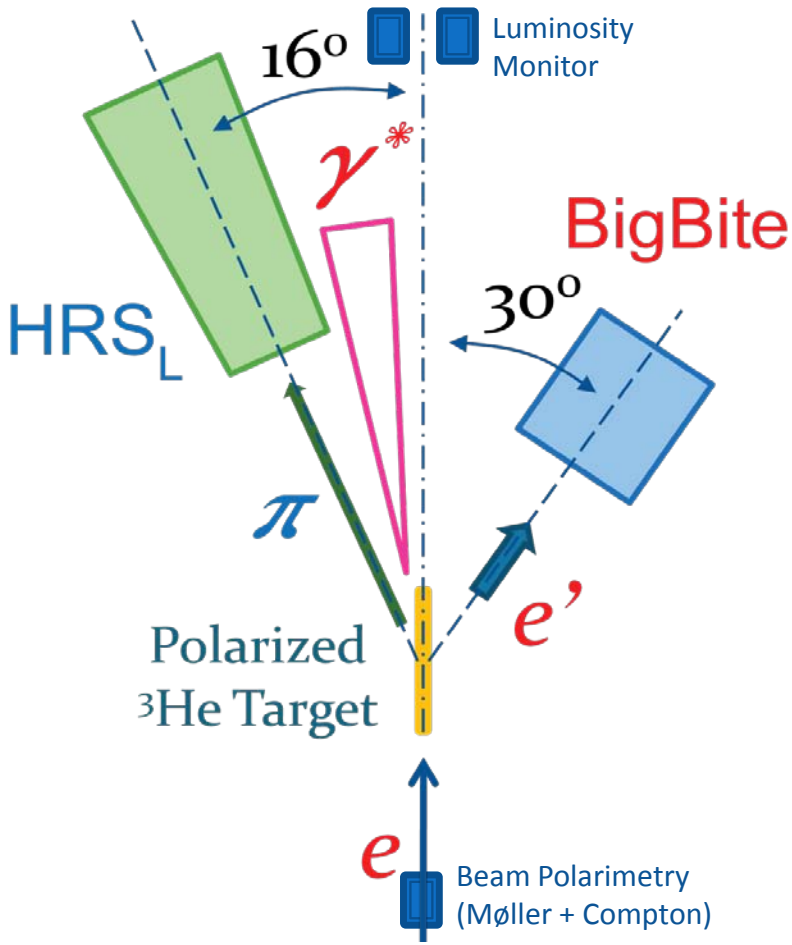

Rest of Left-HRS ~25 m

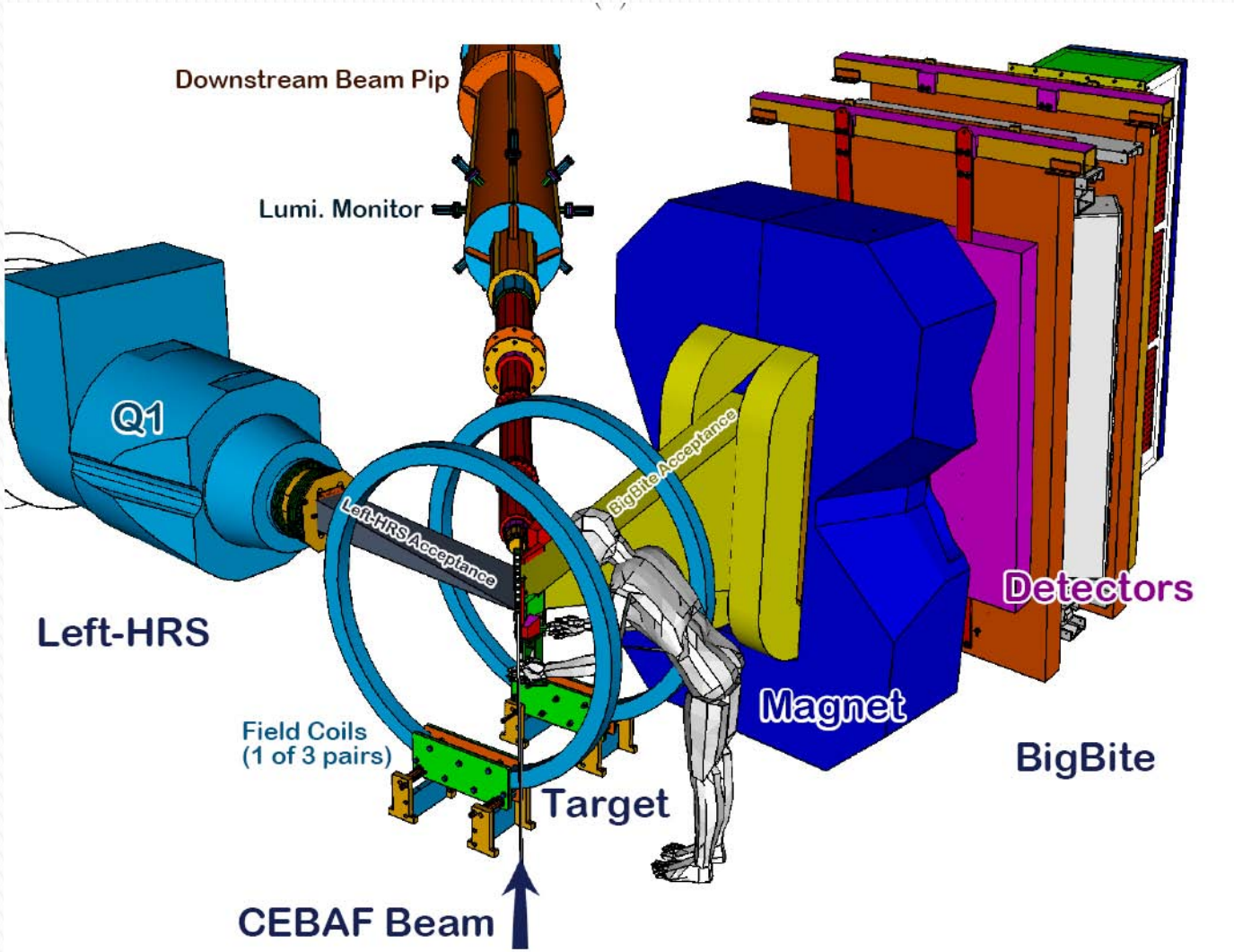

Experiment Setup

Only Small Part of Left-HRS and He-3 Target is Shown

Polarized Electron Beam

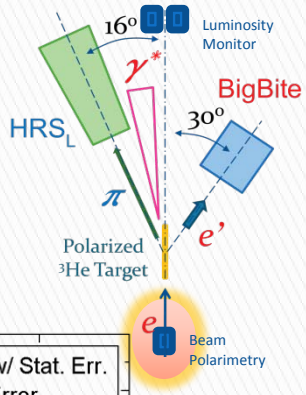

- Overall polarization
  <P>=76.8 +- 3.5%
- Fast beam helicity reversal at 30 Hz
- Beam charge balance between two helicity states

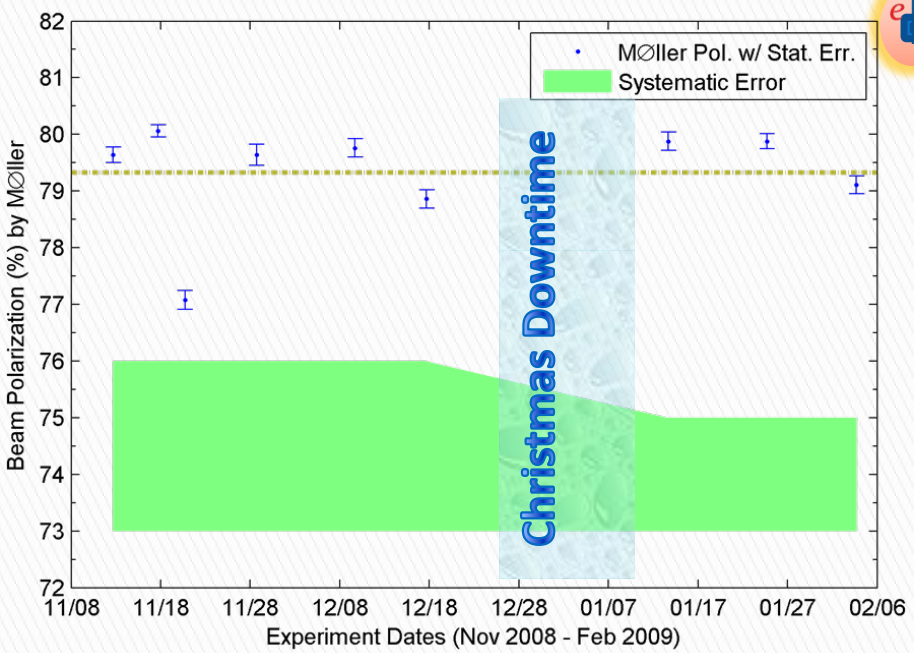

- Two method cross check
  - Moller polarimetry
  - Compton polarimetry

Polarized beam at Jefferson Lab is crucial

Polarimetery

Polarized ^{3}He Target

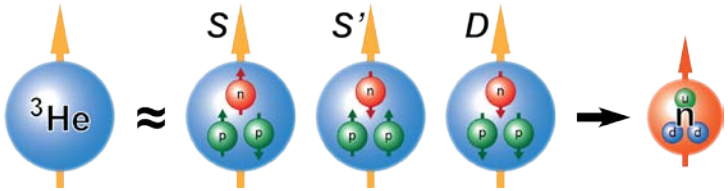

~90% ~1.5% ~8%

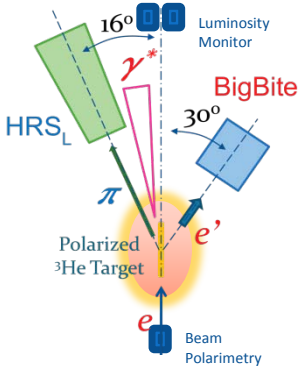

- High Luminosity polarize target: $L(n) = 10^{36}$ cm^{-2} s^{-1}(achieved), 10^{37} cm^{-2} s^{-1} (R&D)
- Compact size: No cryogenic support needed
- Proton dilution measured experimentally

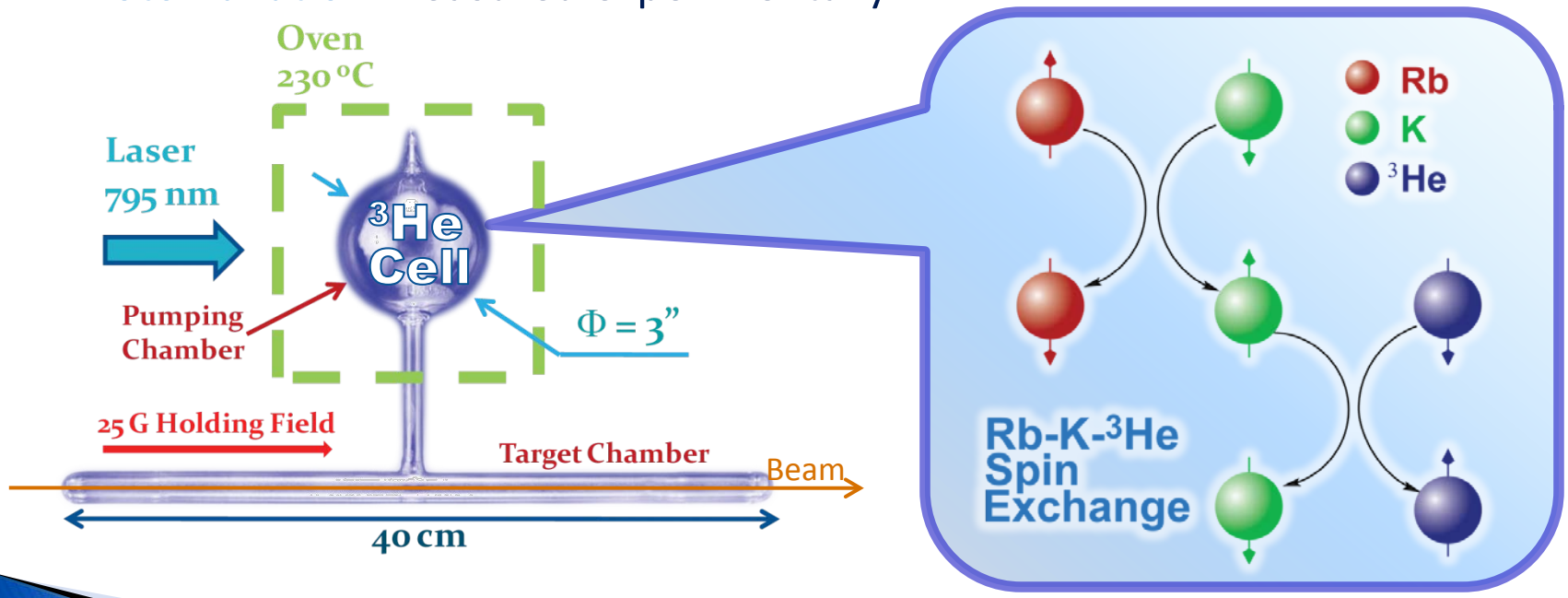

Highlights of Target Setup

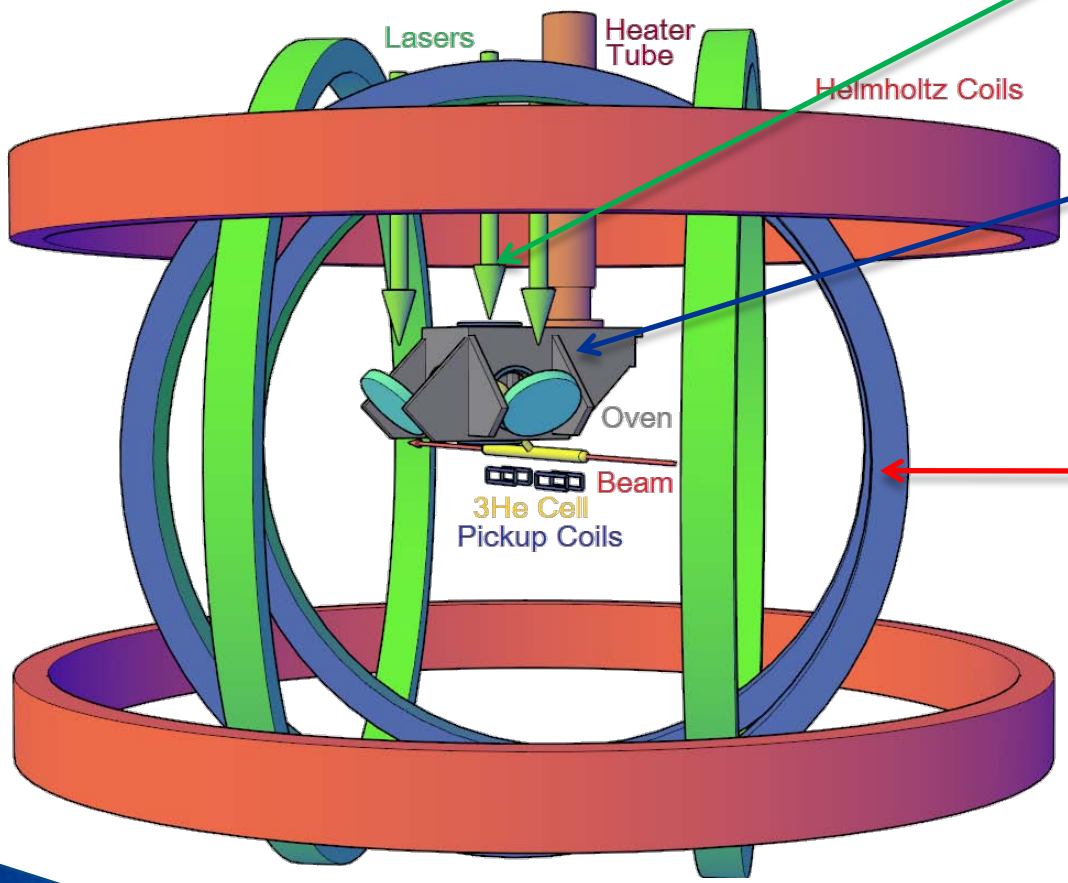

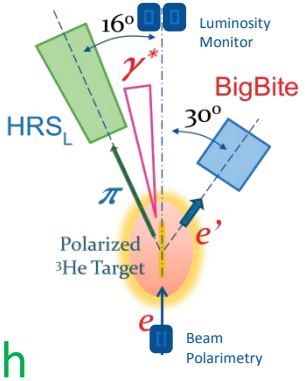

- New laser
  - Narrow line width
  - ^{3}He ↑P/P ~30%
- New optics and oven
  - Polarizing and polarimetery at 3 directions
- Holding magnet field
  - 3D field hold spin to any direction
- A smart target
  - Flip ^{3}He spin every 20min
  - $<10^{-3}$ failure rate
  - Auto analysis, log and early warnings

Performance of ^{3}He Target

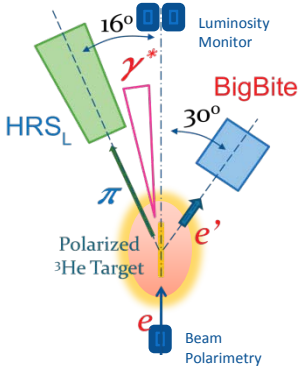

- High luminosity: $L(n) = 10^{36}$ cm^{-2} s^{-1}
- Record high 50-65% polarization in beam with automatic spin flip / 20min
- <P> = 55.4% ± 0.4% (stat. per spin state) ± 2.7 % (sys.)

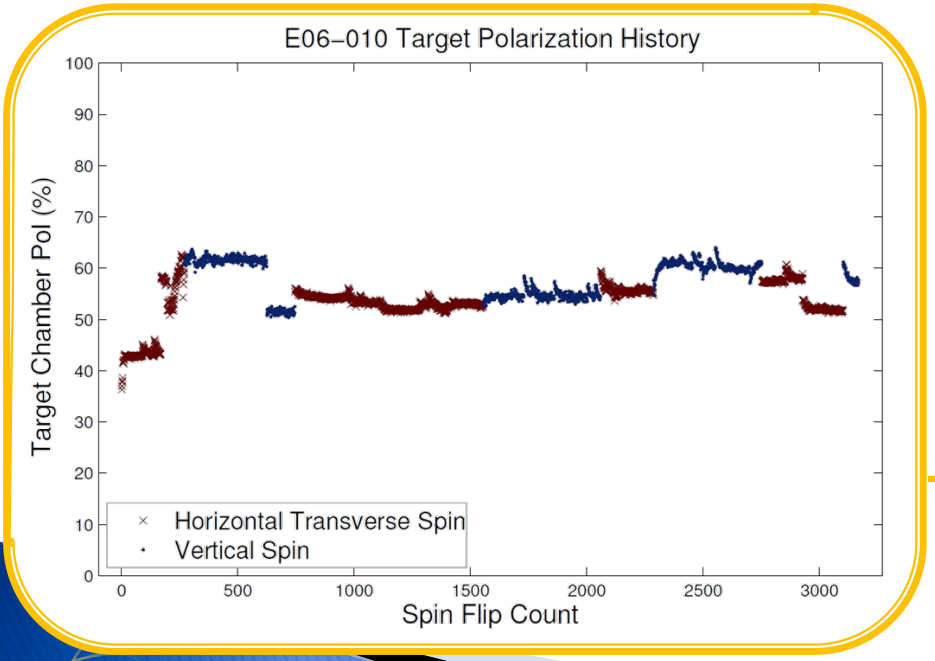

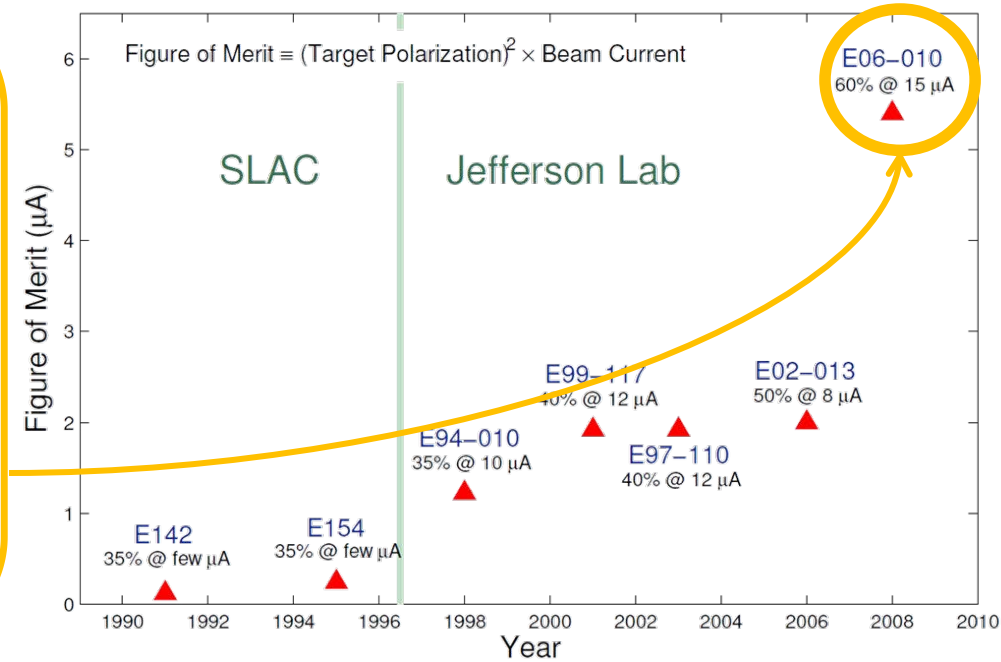

High Resolution Spectrometer (HRS)

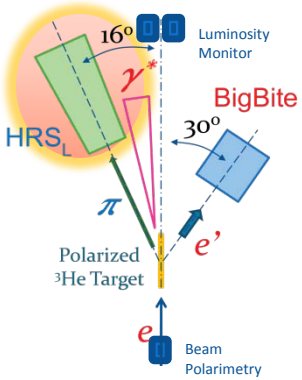

- HRS$_L$ to detect hadrons of p_h = 2.35 GeV
- QQDQ magnet configuration
  - Very high momentum resolution
- Drift chambers
  - Tracking
- Scintillator planes
  - Trigger & Timing, pi/p separation
- Gas Cherenkov & lead-glass shower detectors
  - e/hadron separation
- Aerogel Cherenkov & RICH
  - π/K separation

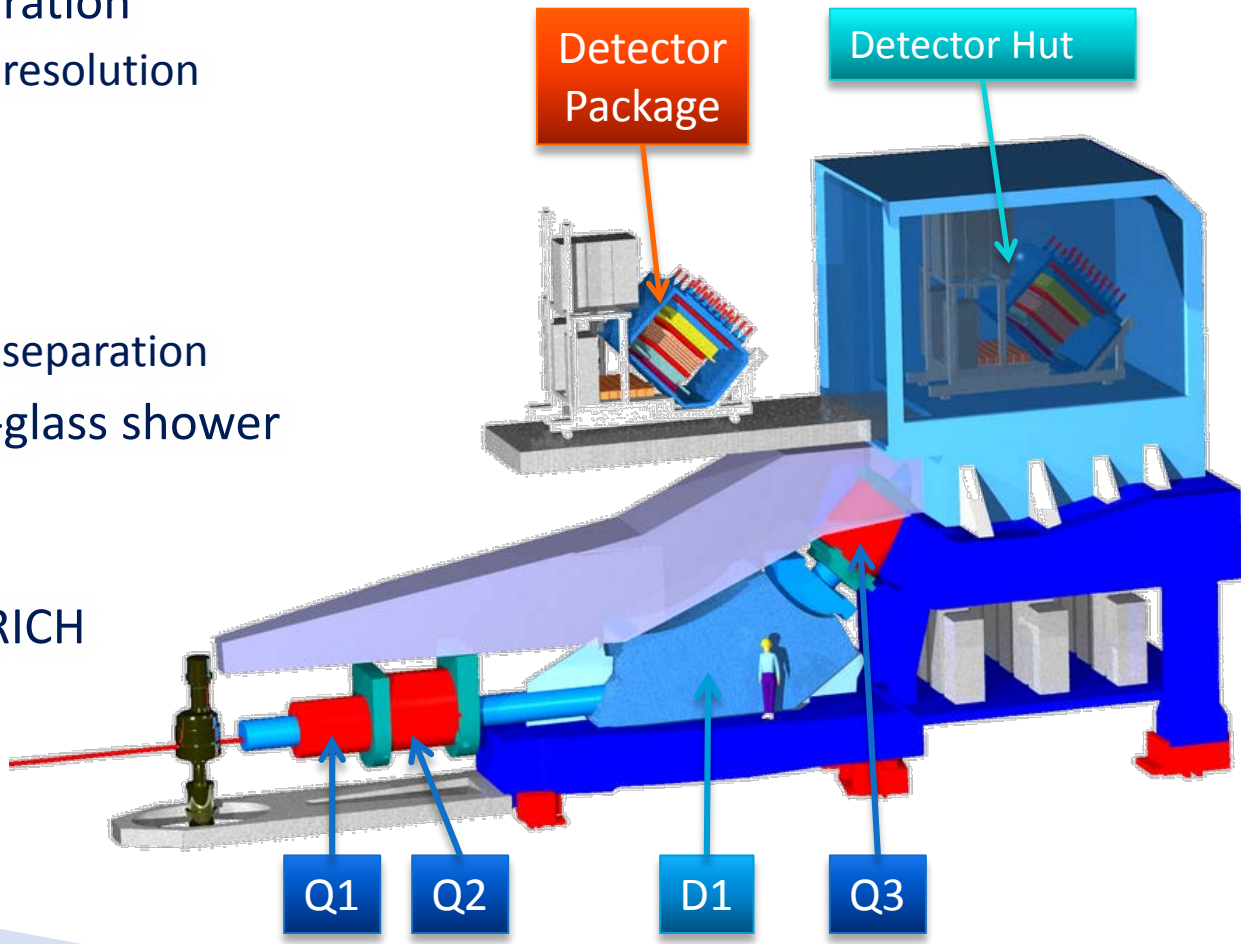

BigBite Spectrometer

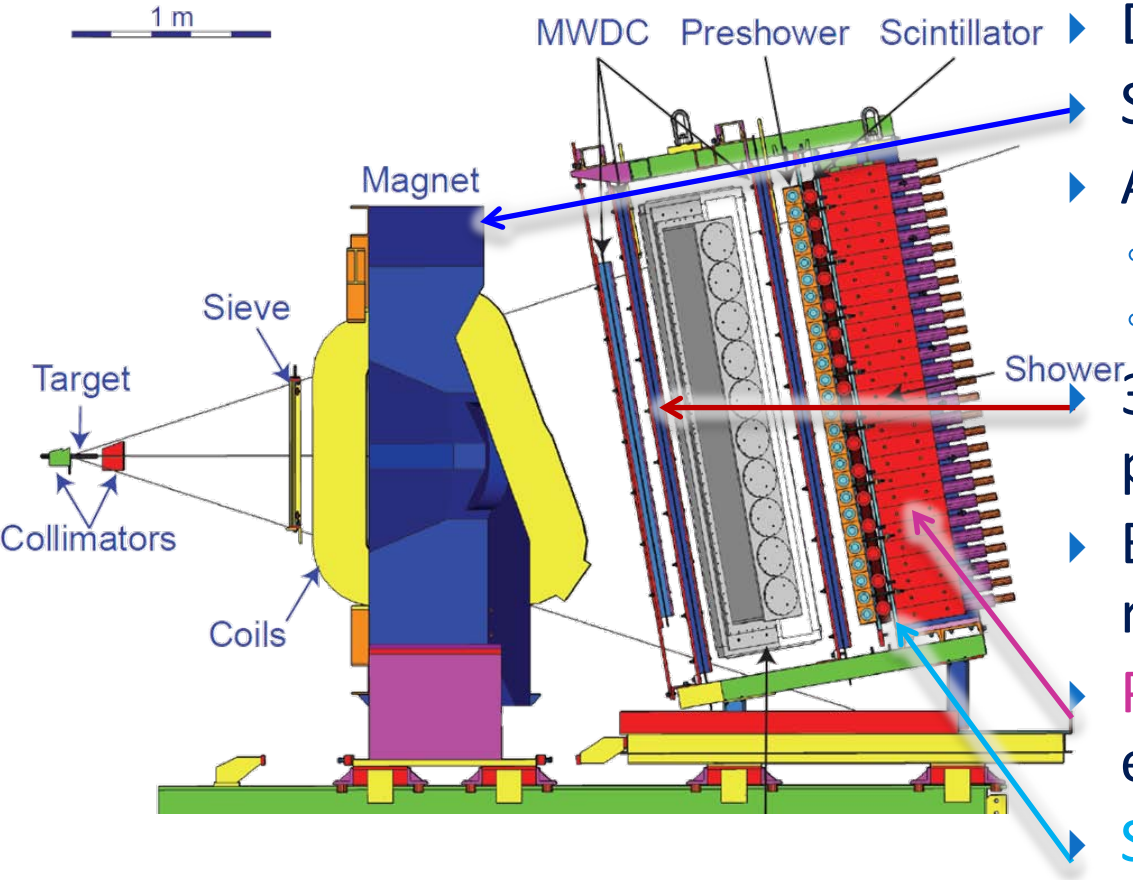

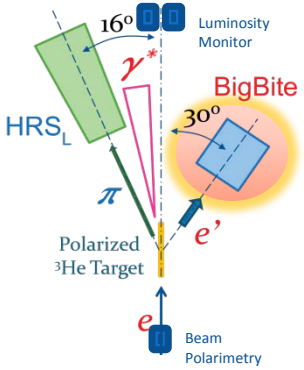

- Detects electrons
- Single dipole magnet
- A "big bite" of acceptance
  - $\Delta\Omega = 64$ msr
  - P : 0.6 ~ 2.2 GeV/c
- 3 wire chambers: 18 planes for precise tracking
- Bipolar momentum reconstruction
- Pre-shower and shower for electron PID
- Scintillator for coincidence with left HRS

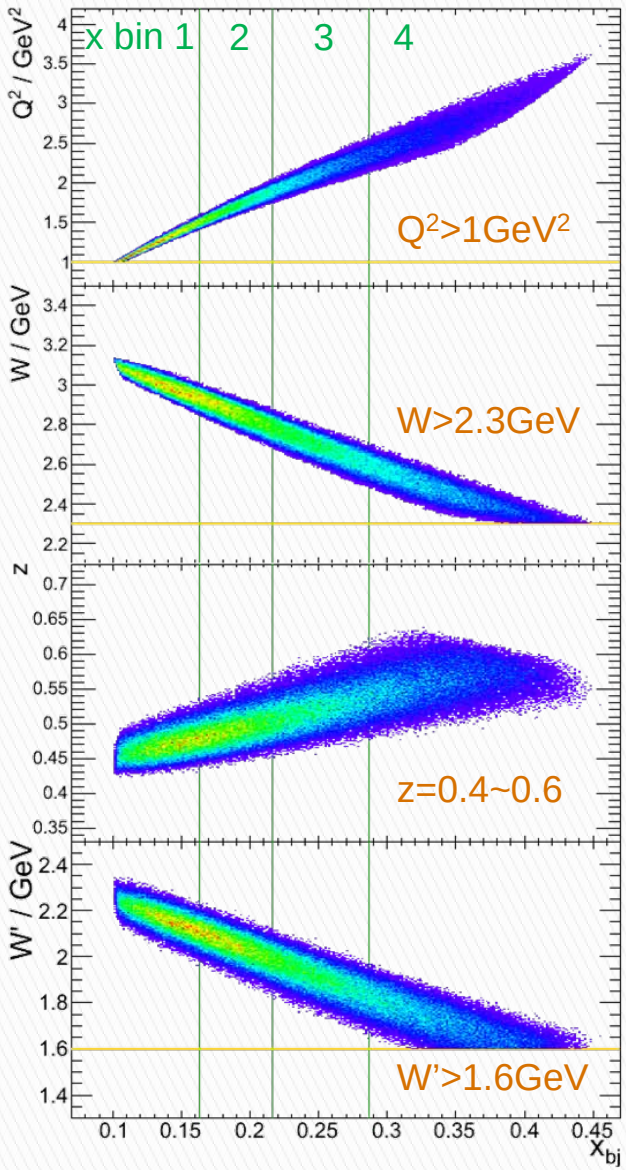

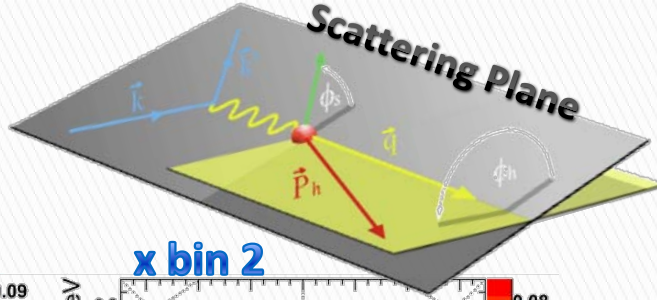

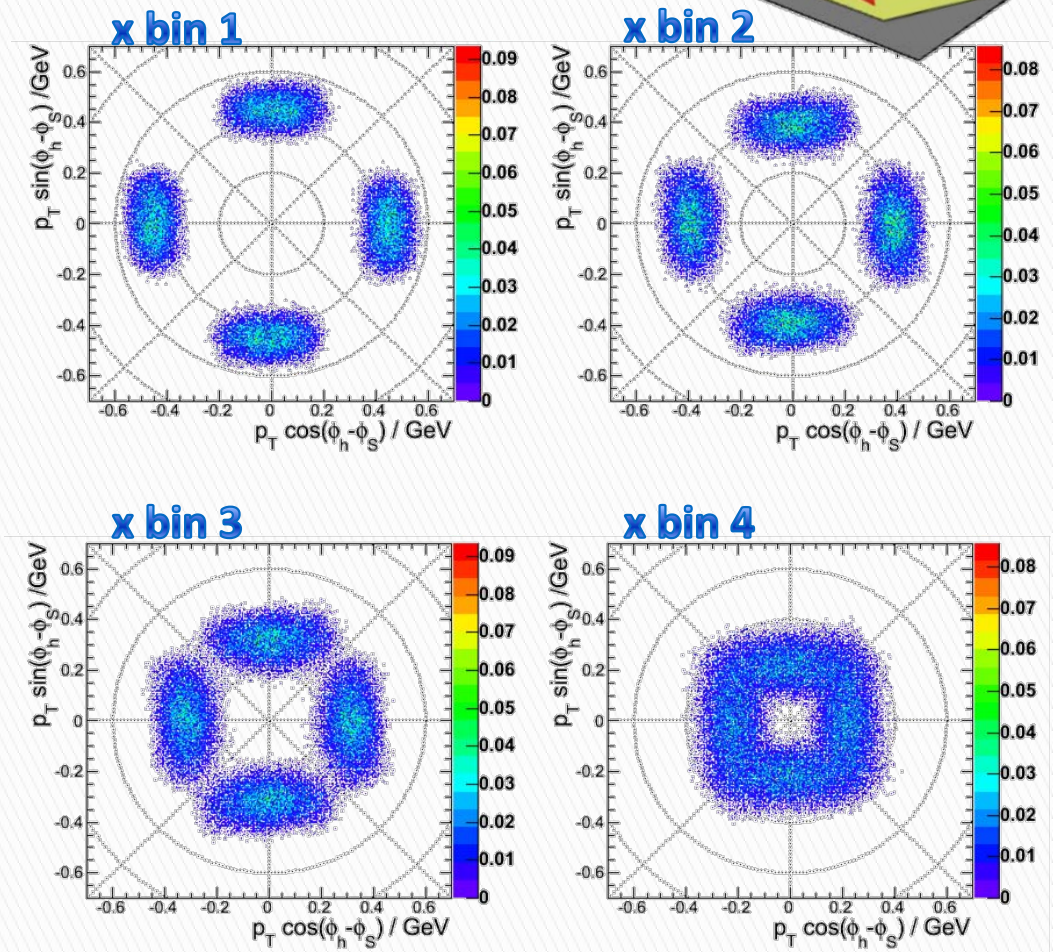

Kinematics coverage

p_T & ϕ_h- ϕ_S coverage

e ^{3}He → h X, Target SSA

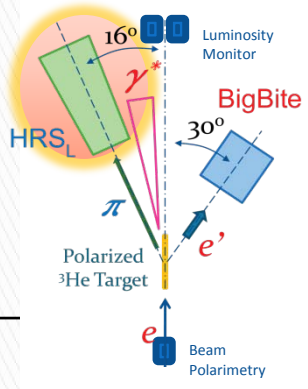

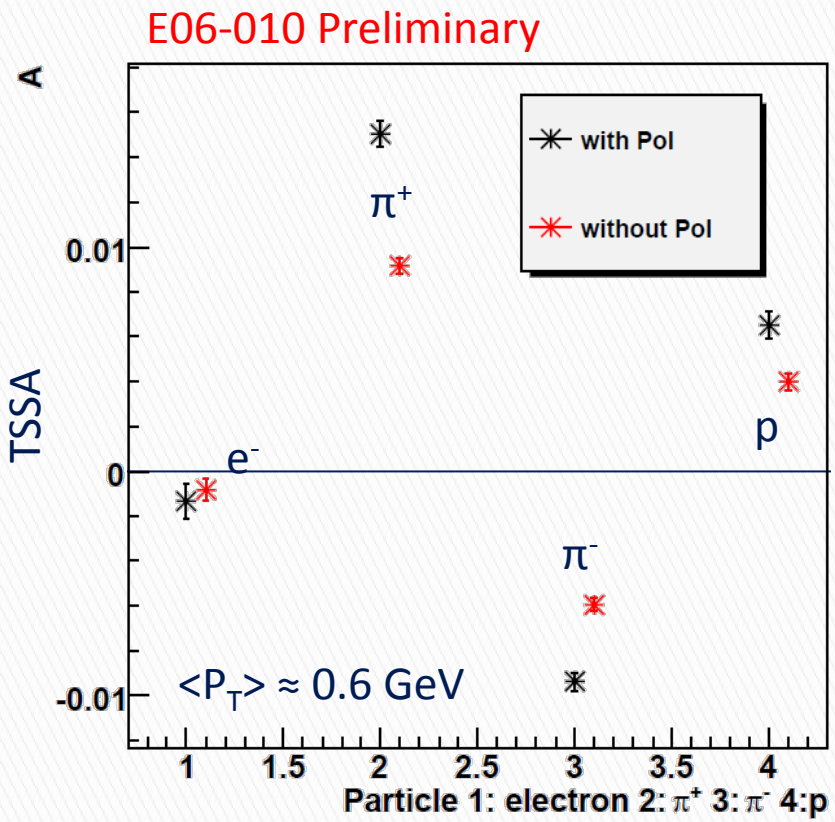

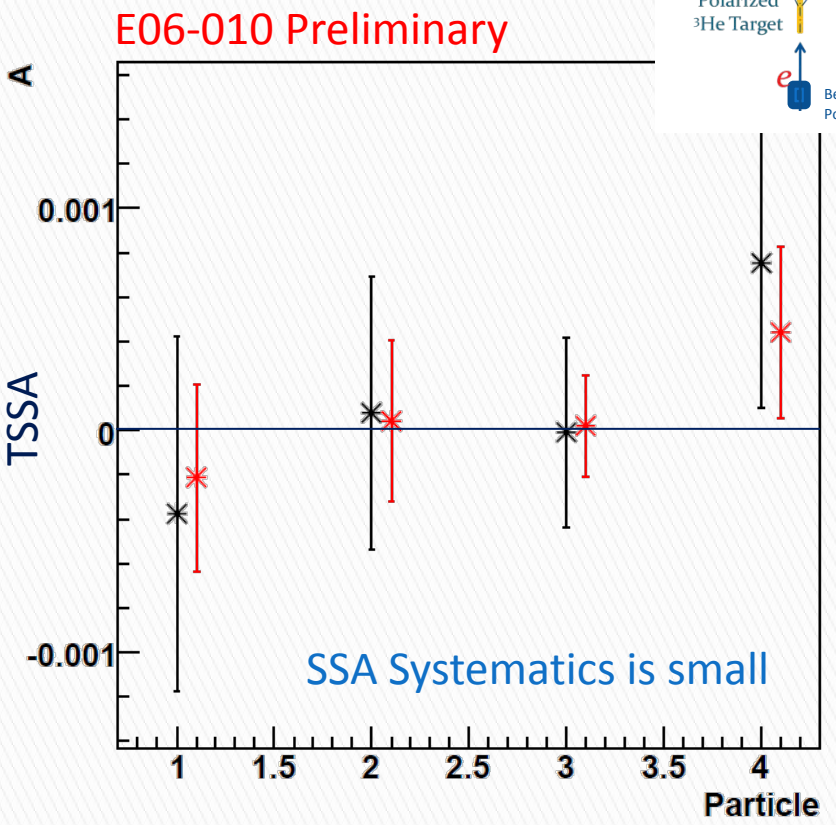

Left-right asymmetry

Spin parallel to P_h
(Sys. check, $A=S_T \times P_h=0$)

SSA Results on Neutron

- 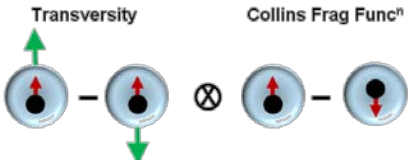

  Sizable Collins π^+ asymmetries at x=0.34?
  - Sign of violation of Soffer's inequality?
  - **Data are limited by stat. Needs more precise data!**

- 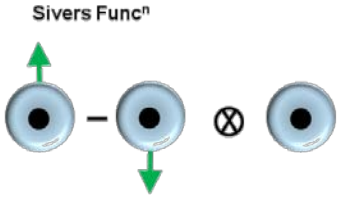

  Negative Sivers π^+ Asymmetry
  - Consistent with HERMES/COMPASS
  - **Independent demonstration of negative d quark Sivers function.**

X. Qian PRL 107 072003 (2011)

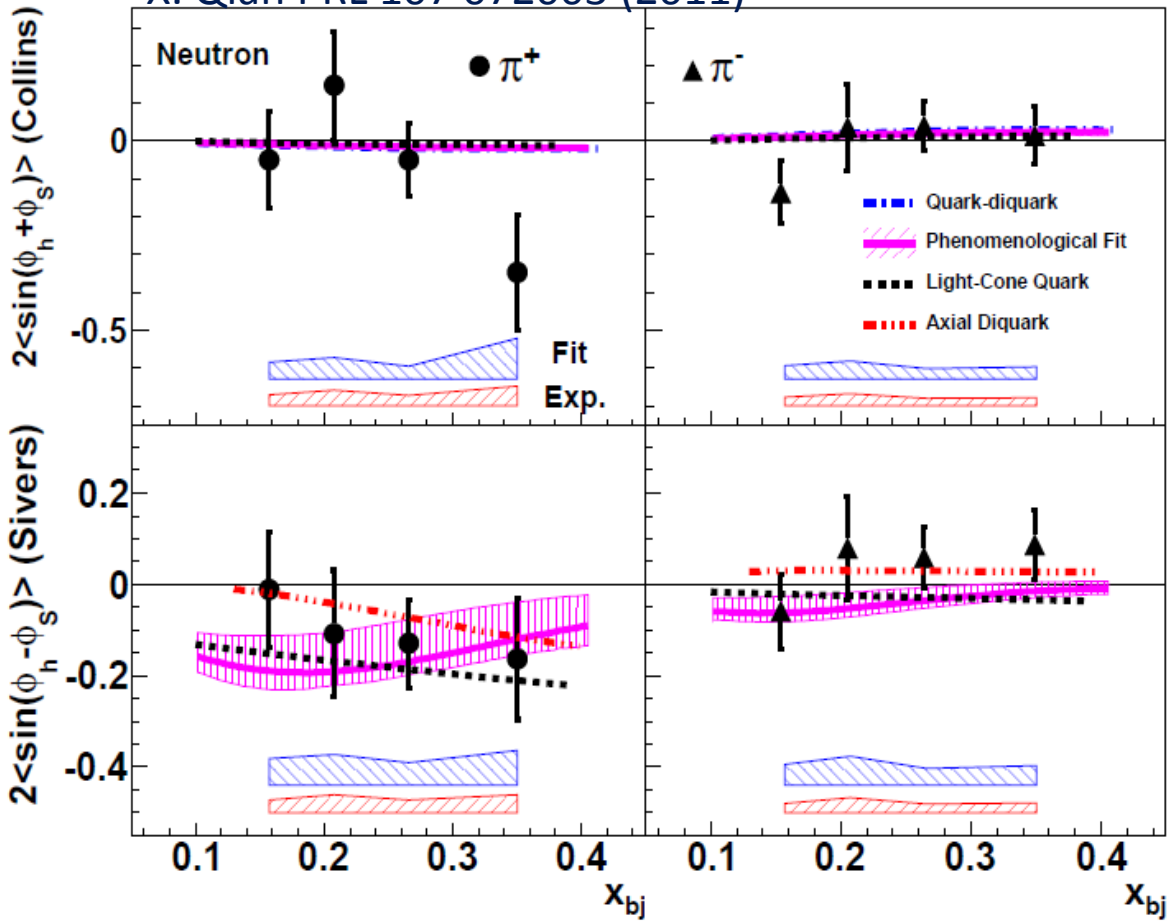

Model (fitting) uncertainties shown in blue band.

Best Measurements on Neutron at High x

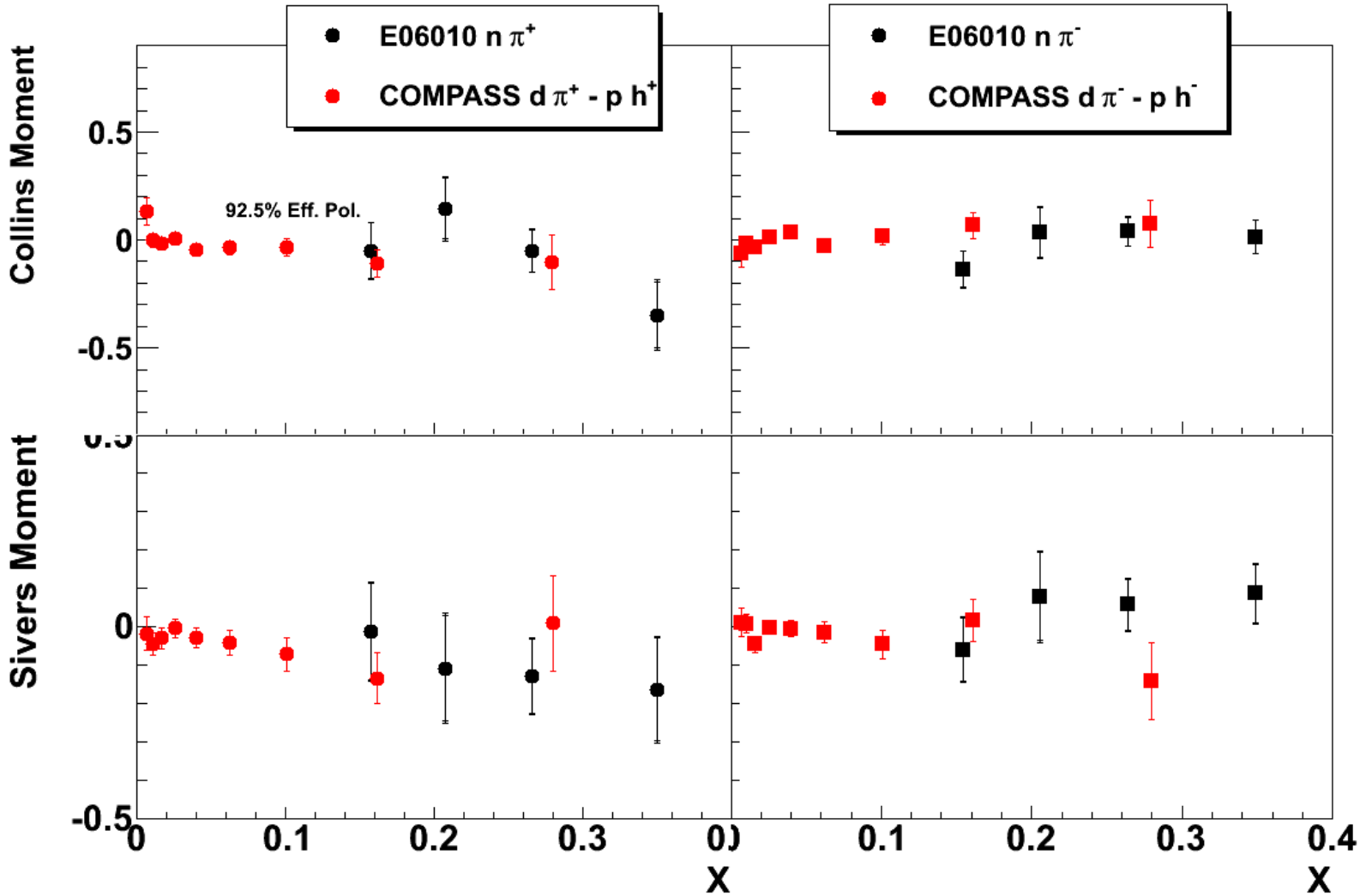

Neutron A_{LT}

- Access g_{1T} =
- Dominated by real part of interference between L=0 (S) and L=1 (P) states
  - Imaginary part -> Sivers effect
- No GPD correspondence

Huang, et. al. PRL. 108, 052001 (2012)

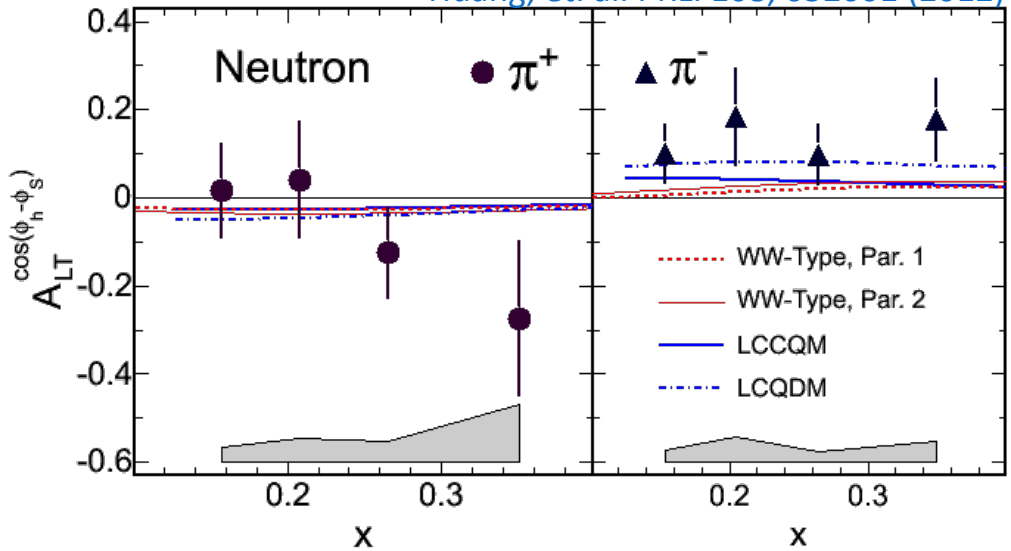

- Consistent with models in signs
- Suggest larger asymmetry, possible interpretations:
  - Larger quark spin-orbital interference
  - different P_T dependence
  - larger subleading-twist effects

JLab Polarized Proton/Deuteron Target

- Polarized NH_3/ND_3 targets also available at Jefferson Lab
  - Used in Hall B/CLAS SIDIS experiment
- New magnet with transverse opening (>25°) in design
  - Proposal approved for 12 GeV Era

- Dynamical Nuclear Polarization
- In-beam average polarization

  70-90% for p

  30-40% for d
- Luminosity up to
  - ~ 10^{35} (Hall C/A)
  - ~ 10^{34} (Hall B)

Hall C/A polarized p/D target

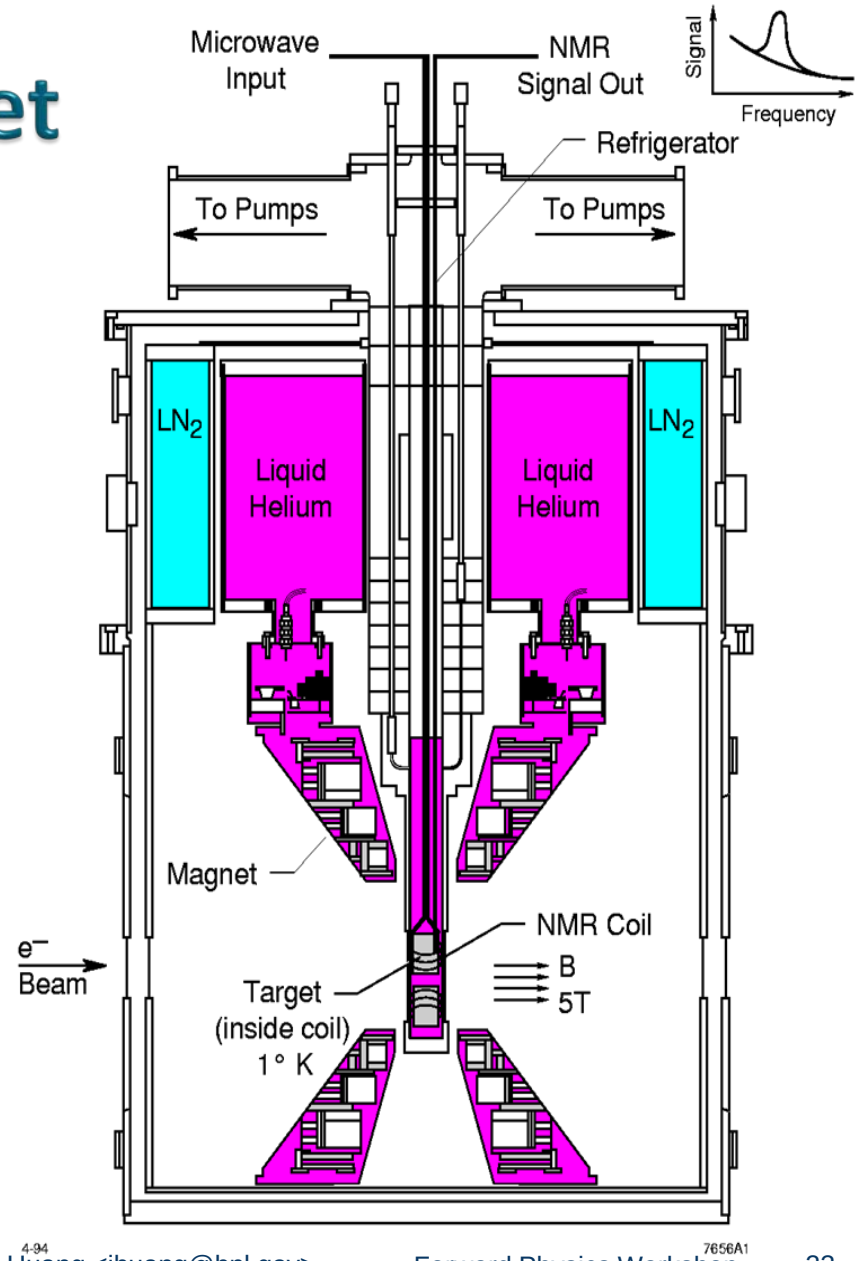

The other worm-gear function $h_{1L}^{\perp}$ studied in Hall B

$h_{1L}^{\perp} = -g_{1T}$ favored (naively)

d quark in neutron dominant $A_{LT}(n \to \pi^-)$

u in proton dominant $A_{LT}(n \to \pi^-)$

Huang, et. al. PRL. 108, 052001 (2012)

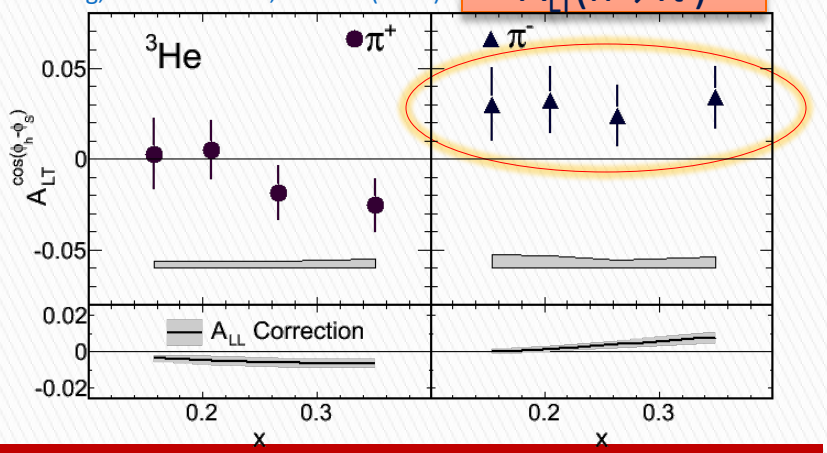

Avakian, et. al. PRL. 105.262002 (2010)

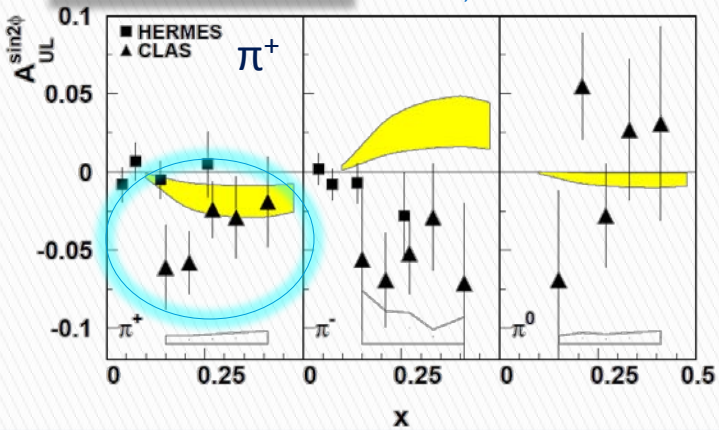

E06-010 A_{LT} on ^{3}He

CLAS A_{UL} on proton

Future is coming : 12 GeV Upgrade Project

Upgrade is designed to build on existing facility: vast majority of accelerator and experimental equipment have continued use

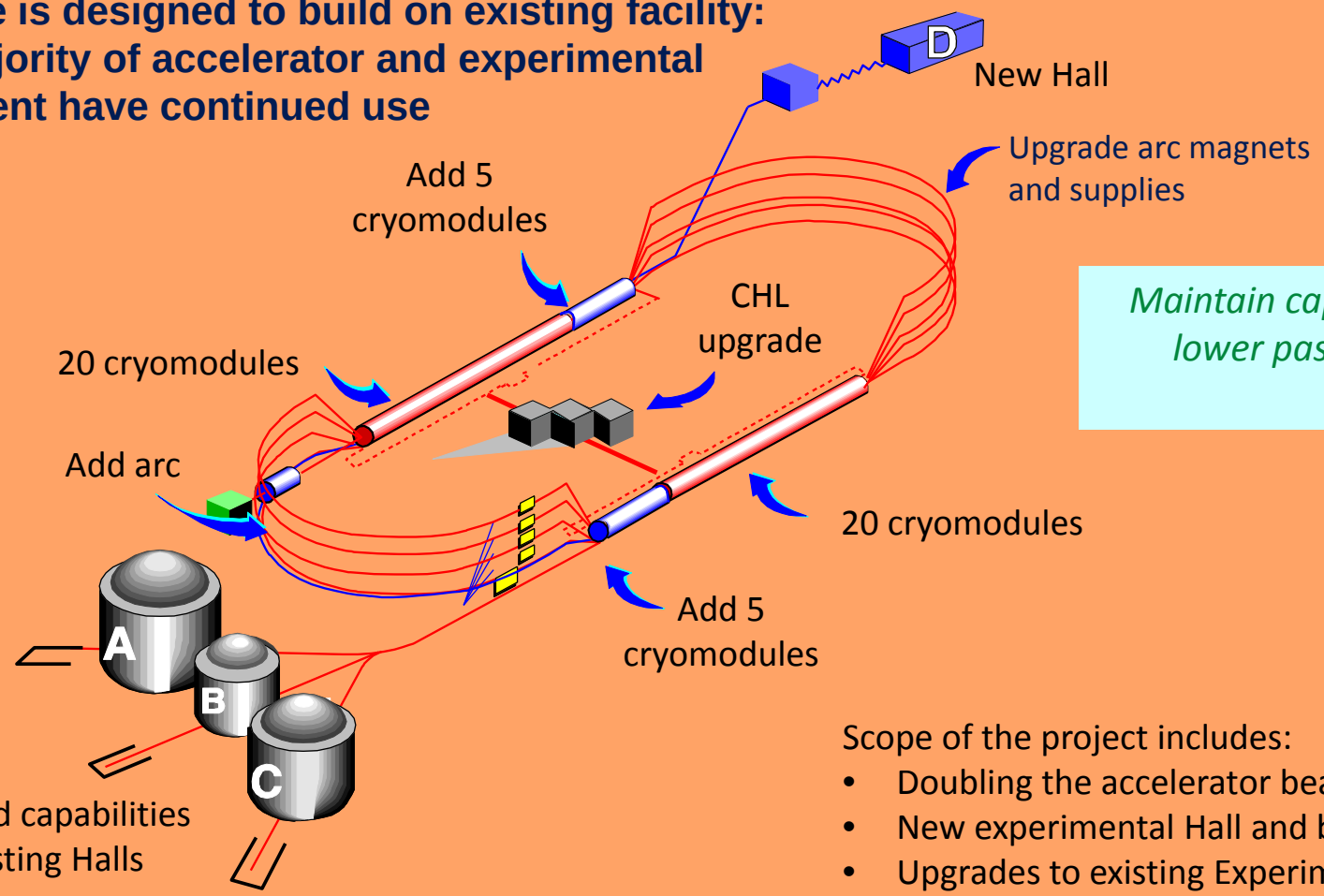

Maintain capability to deliver lower pass beam energies: 2.2, 4.4, 6.6….

Scope of the project includes:

- Doubling the accelerator beam energy
- New experimental Hall and beamline
- Upgrades to existing Experimental Halls

12 GeV Spin Physics Capabilities

Coherent programs on SIDIS / TMD physics planned

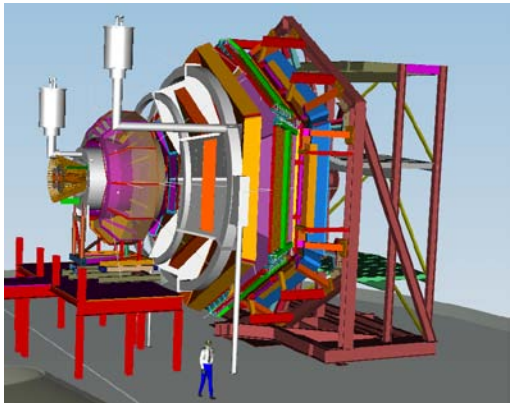

Hall B – understanding nucleon structure via GPDs and TMDs

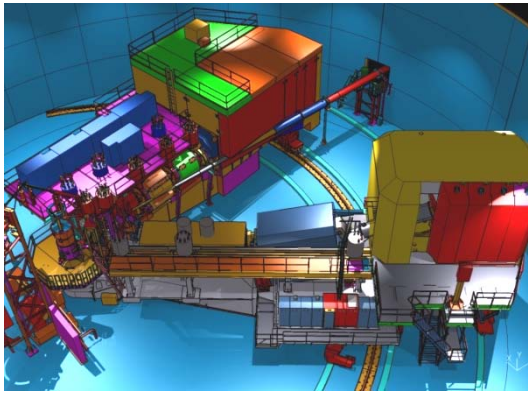

Hall C – precision determination of valence quark properties in nucleons and nuclei

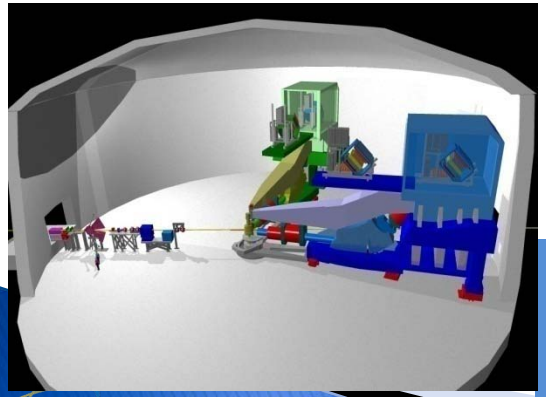

Hall A – future new experiments (e.g. SIDIS/PVDIS with SOLID, Super BigBite and Moller)

Rich spin programs, e.g.
Inclusive double spin asymmetries using 12 GeV

A_1^n at 11 GeV Hall C

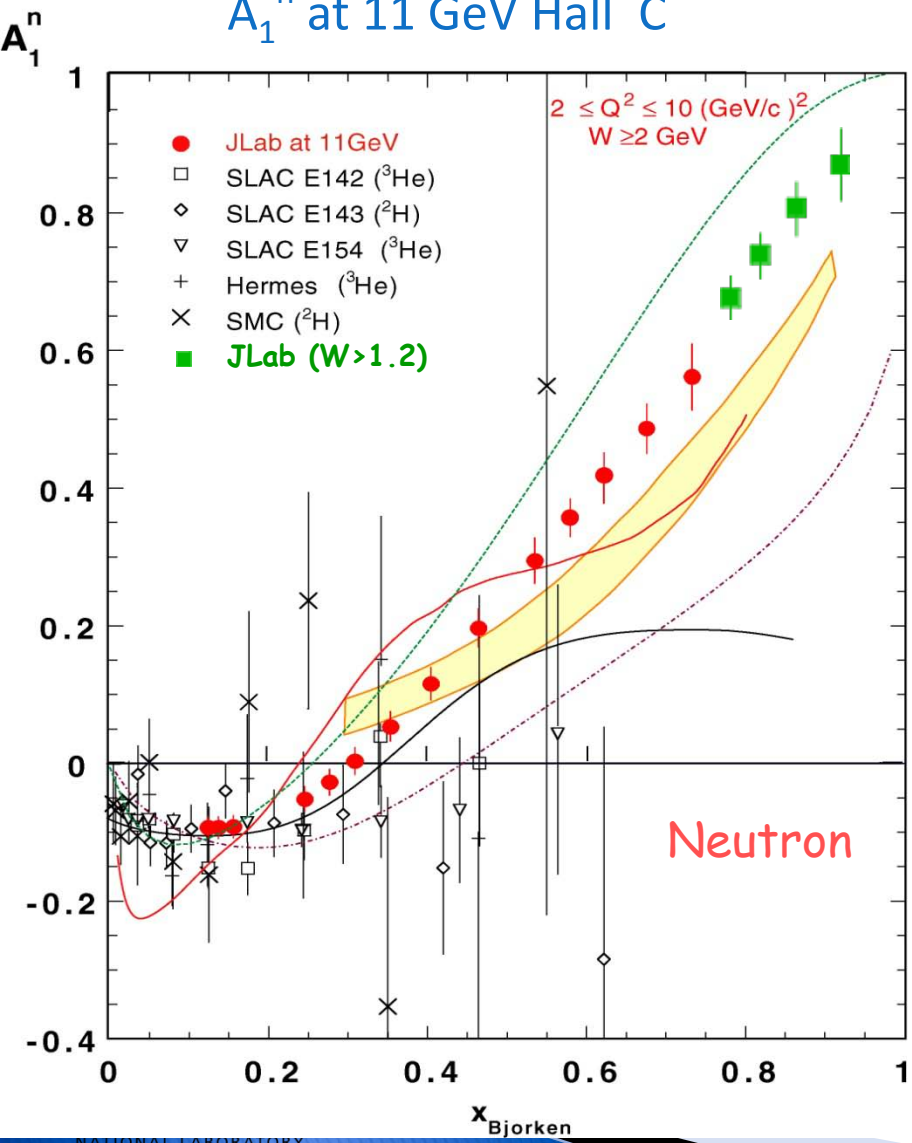

Hall B - CLAS 12

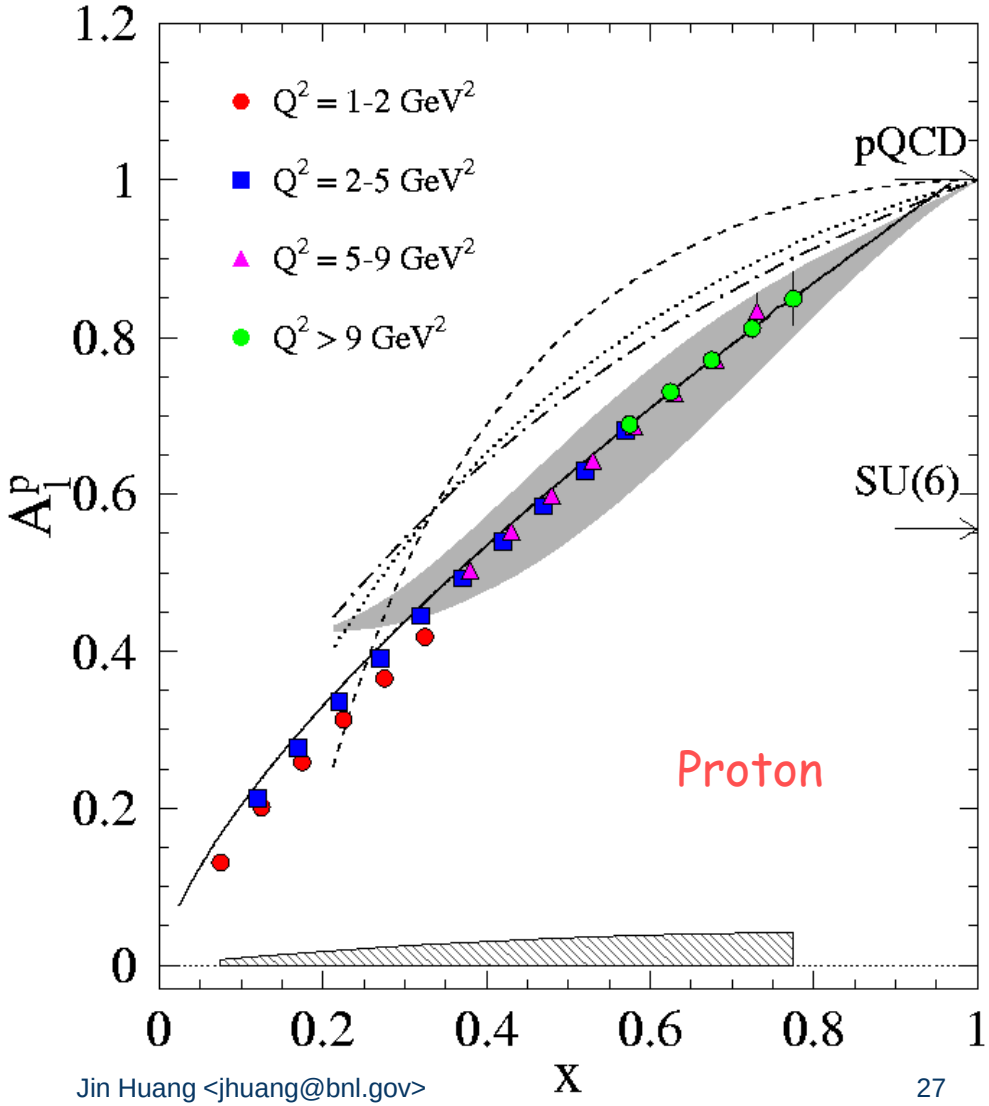

Key Device for High-Precision SIDIS measurement

The SoLID Spectrometer proposed for Hall A

- Key device to achieve high-precision mapping and minimizing systematics
- High Luminosity target and upgraded beam energy -> 12 GeV
- Large acceptance: enable 4D-mapping of asymmetries
- Full/symmetric azimuthal angular coverage: minimize systematics
- Device shared by three SIDIS experiment and a parity-violation DIS exp.
  - Budget: ~20M; early design stage; detector prototyping

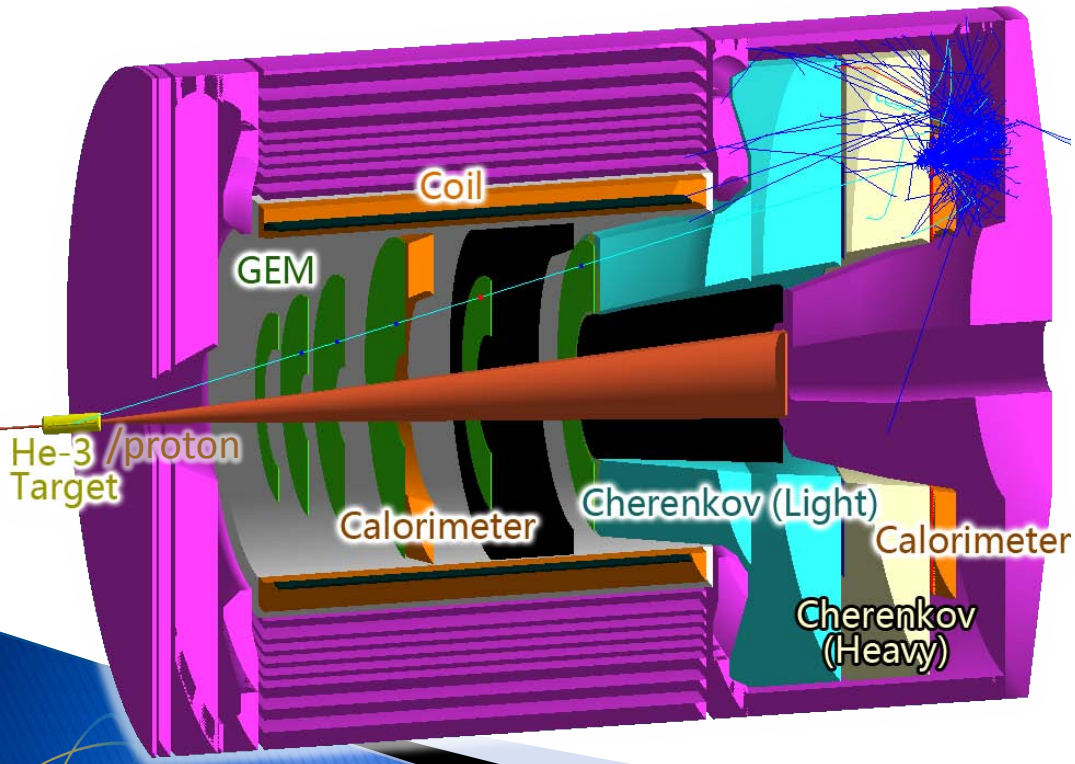

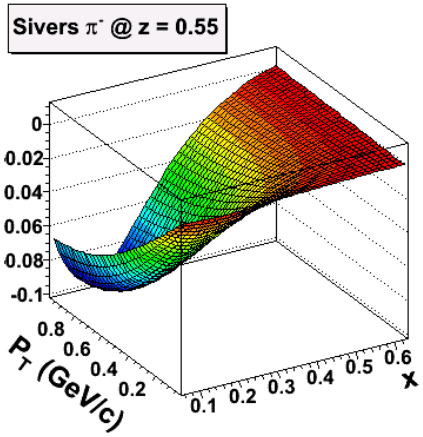

E12-10-006: 90 day
Single Spin Asymmetry on Transverse ^{3}He

E12-11-007: 30 day
Single and Double Spin Asymmetry on ^{3}He

E12-11-108: 120 day
Single and Double Spin Asymmetries on Transverse Proton

Phase space coverage

- Natural Extension of E06-010
- Much wider phase space
  - Also data at low and high z value to access target frag. and exclusive channels.
- Both transverse and longitudinal polarized target: 6/7 polarized leading twist TMDs Studied

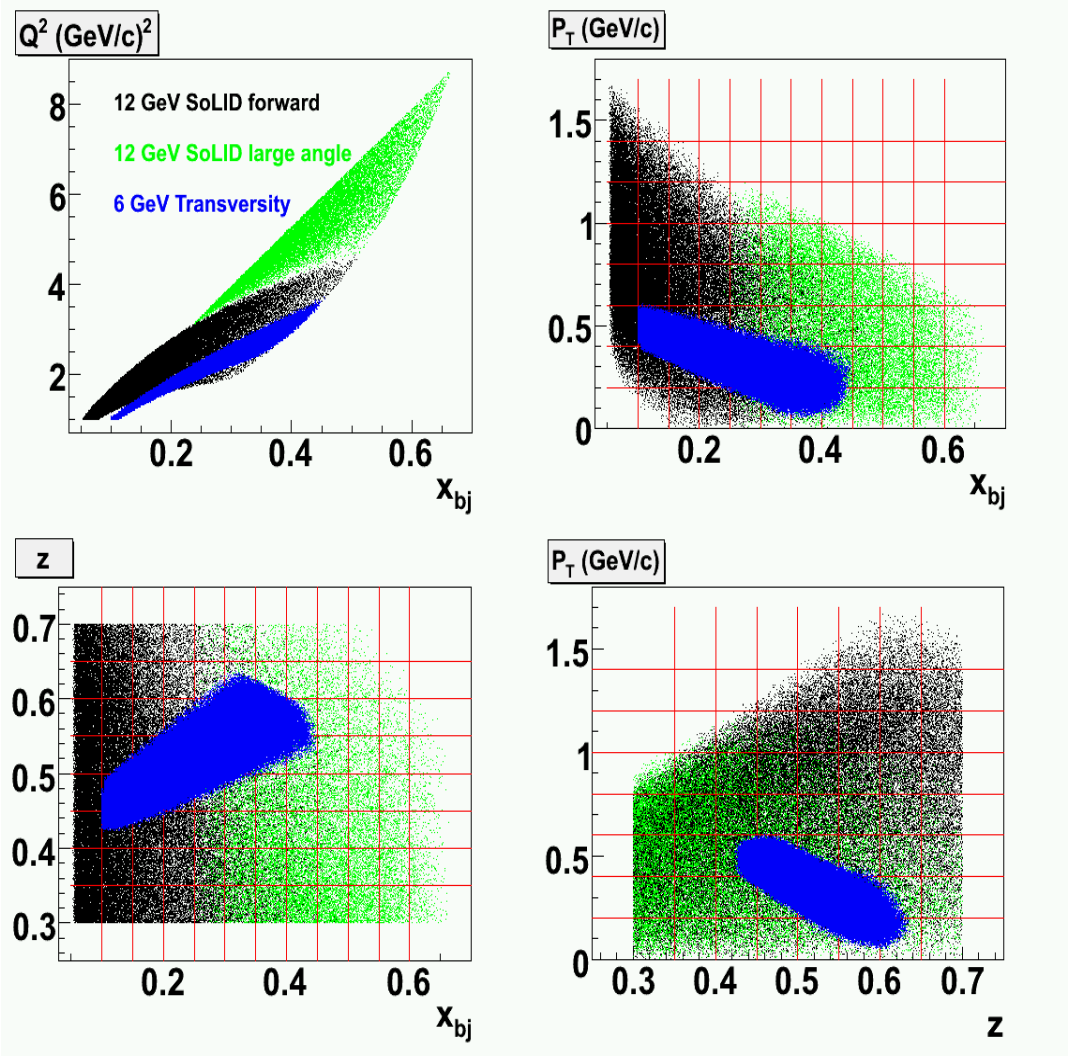

Transversity

h_{1T} =

- The third PDFs in addition to f_1 and g_{1L}
- 10% quark tensor charge (both u and d!) from both SSA data
  - Fundamental property, benchmark test of Lattice QCD

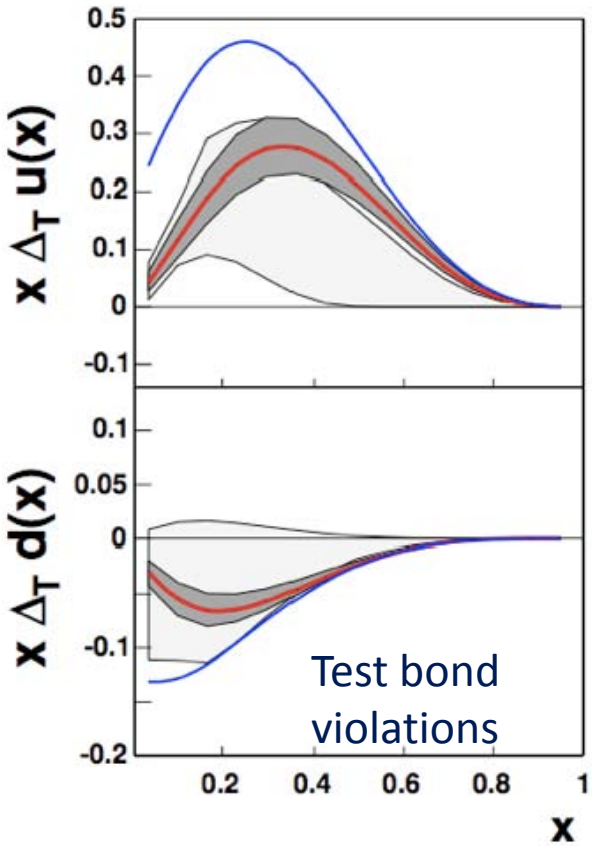

$$A_{UT}^{Collins} \propto \langle \sin(\phi_h + \phi_s) \rangle \propto h_{1T} \otimes H_1^{\perp}$$

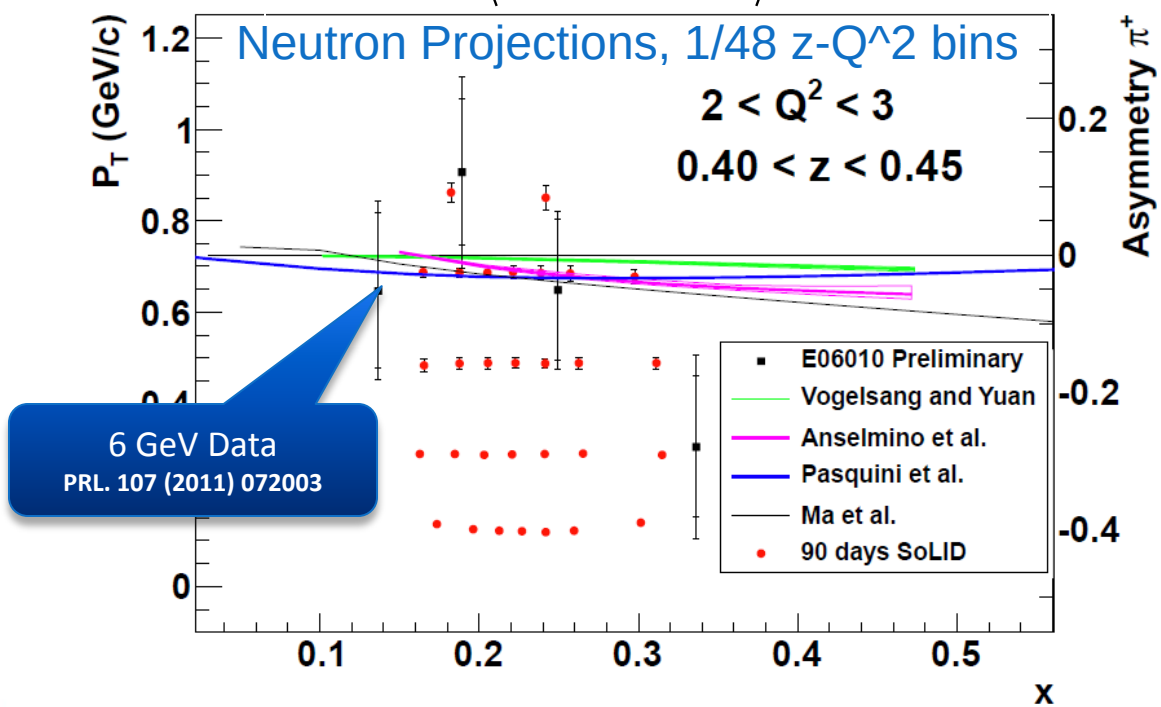

Proton data also planned

Sivers Effect

$$f_{1T}^{\perp q} =$$

$$f_{1T}^{\perp q}\Big|_{SIDIS} = -f_{1T}^{\perp q}\Big|_{D-Y}$$

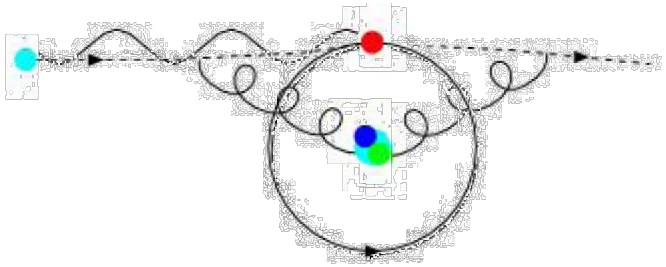

- Correlation between nucleon spin with quark angular momentum
- Important test for TMD factorization
- Relation with twist-3 quark-gluon corr. and RHIC measurements
- T-odd final state interaction -> Target SSA

$$gT_{q,F}(x,x) = -\int d^2k_\perp \frac{|k_\perp|^2}{M} f_{1T}^{\perp q}(x,k_\perp^2)|_{SIDIS}$$

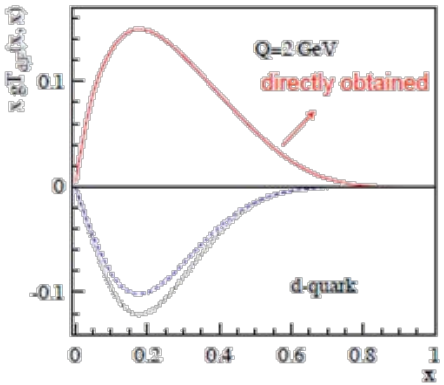

Neutron Projection , 1/48 z-Q^2 bins

$$A_{UT}^{Sivers} \propto \langle \sin(\phi_h - \phi_s) \rangle \propto f_{1T}^{\perp} \otimes D_1$$

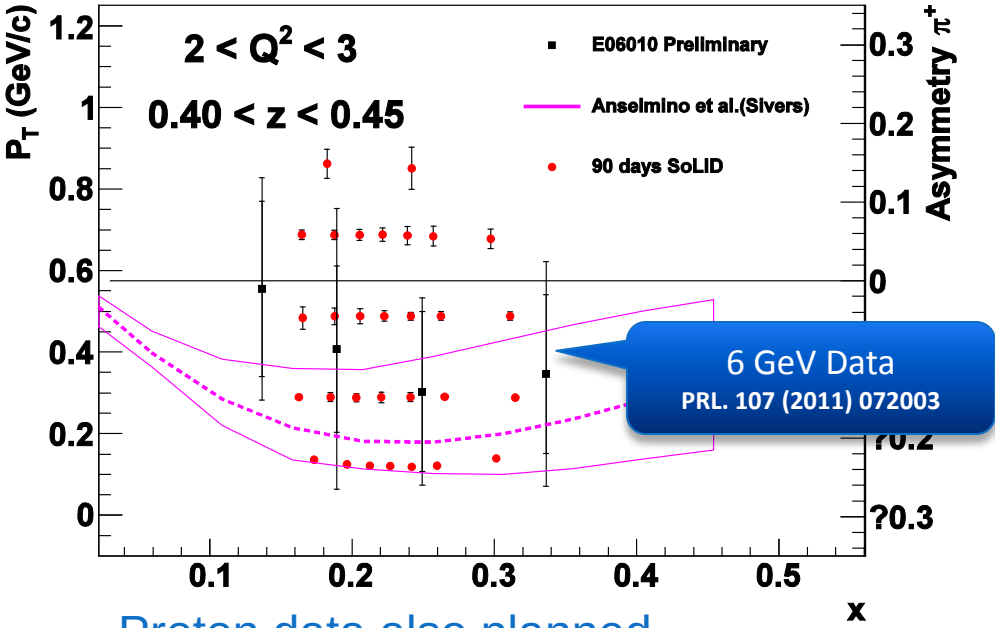

6 GeV Data
PRL. 107 (2011) 072003

Proton data also planned

Worm-gear functions

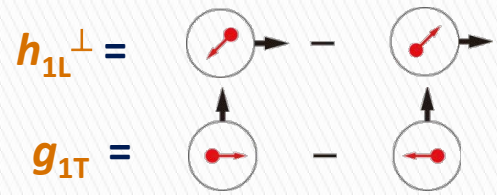

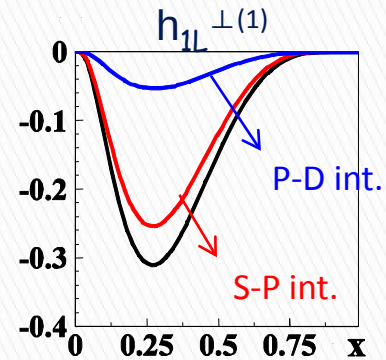

- Dominated by real part of interference between L=0 (S) and L=1 (P) states
- No GPD correspondence
- Lattice QCD -> Moments of worm-gear TMDs
- Model Calculations -> $h_{1L}^{\perp}$ =? $-g_{1T}$
- Connections with Collinear PDFs through WW approx. and LIR.

Neutron Projections, 1/48 z-Q^2 bins

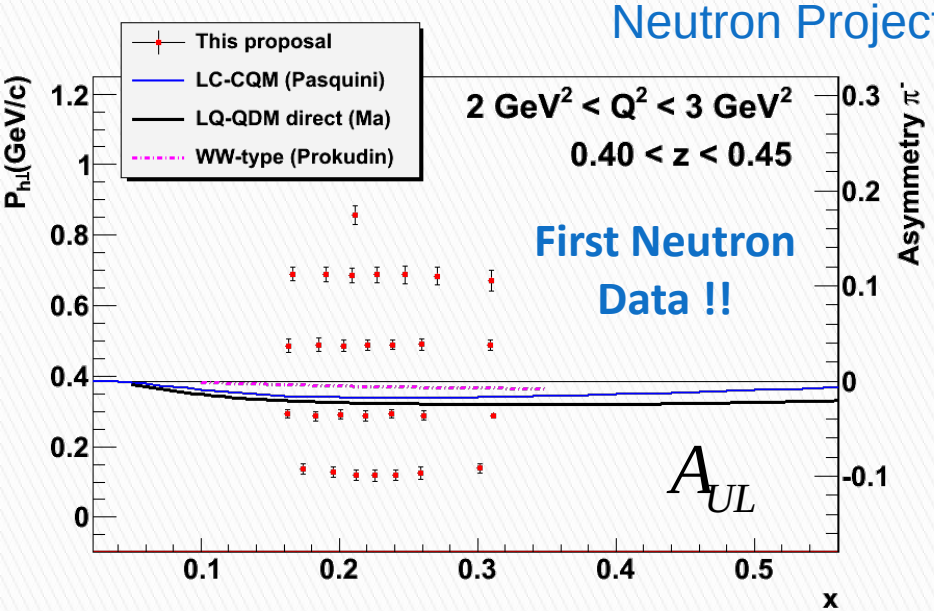

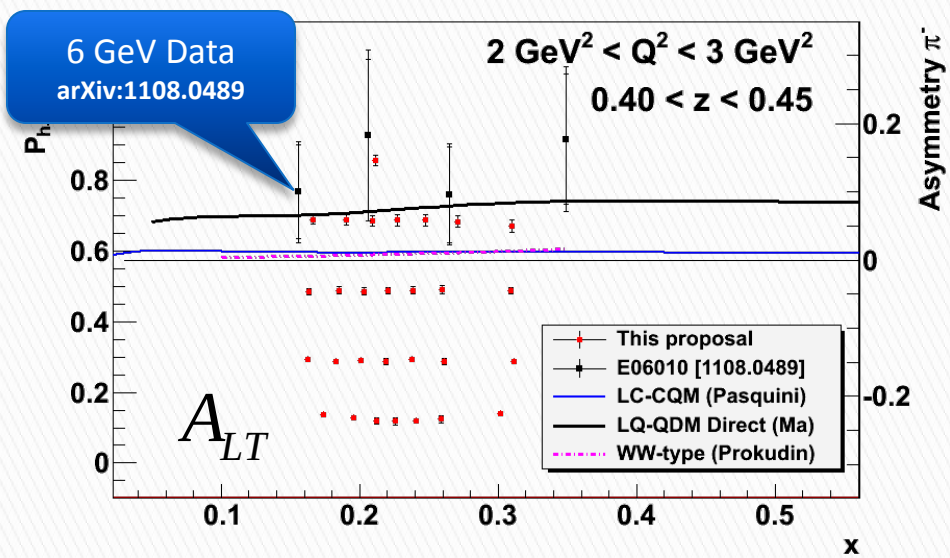

$$A_{UL} \sim h_{1L}^{\perp}(x) \otimes H^{\perp}{}_{1}(z)$$

$$A_{LT} \sim g_{1T}(x) \otimes D_1(z)$$

Pretzlosity: $h_{1T}^{\perp}$ =

- Relativistic effect of quark , PRD 78, 114024 (2008)
- (in models) direct measurement of OAM, PRD 58, 096008 (1998)
- Expect first non-zero Pretzelosity asymmetries

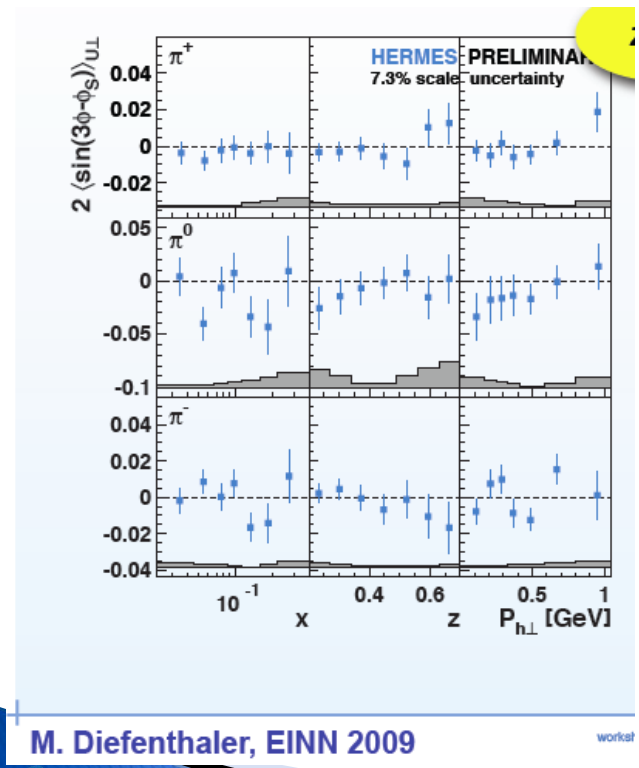

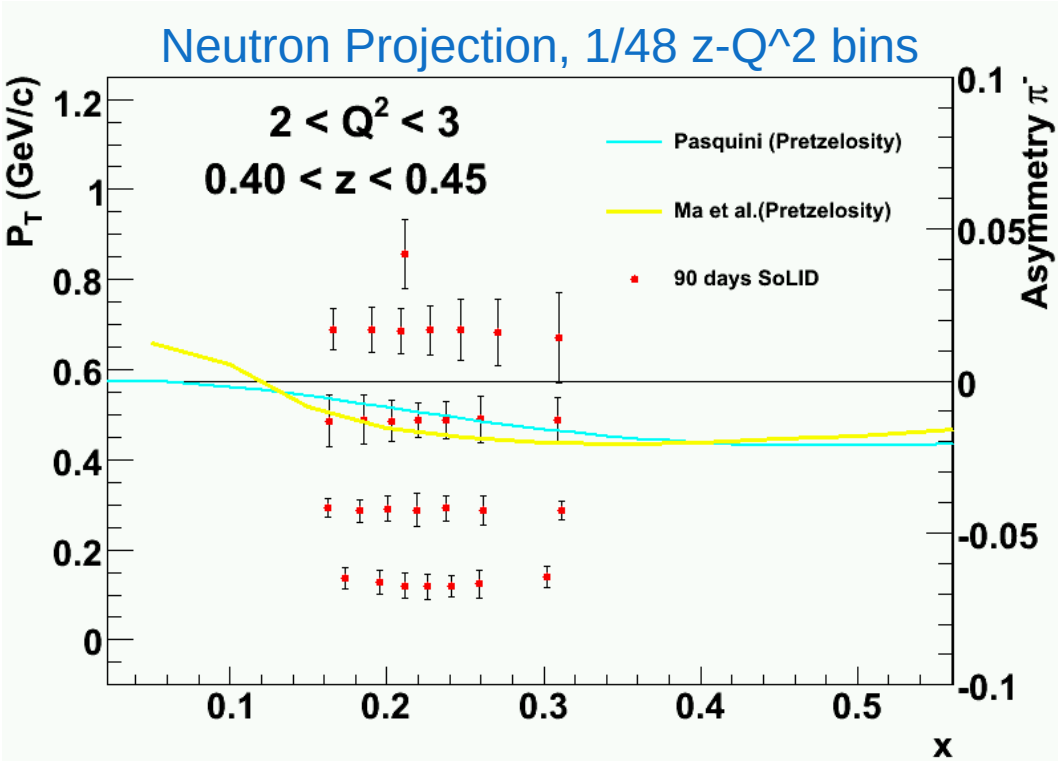

Proton data also planned

E12-11-007 Full projection, neutron A_{LT}

Satisfying the multi-D natural of this study

z= 0.3~0.7

x_{bj}

data point: Projection for neutron A_{LT} of π^-

Q^2 = 1~8 GeV^2

$P_{h\perp}$ (GeV/c)

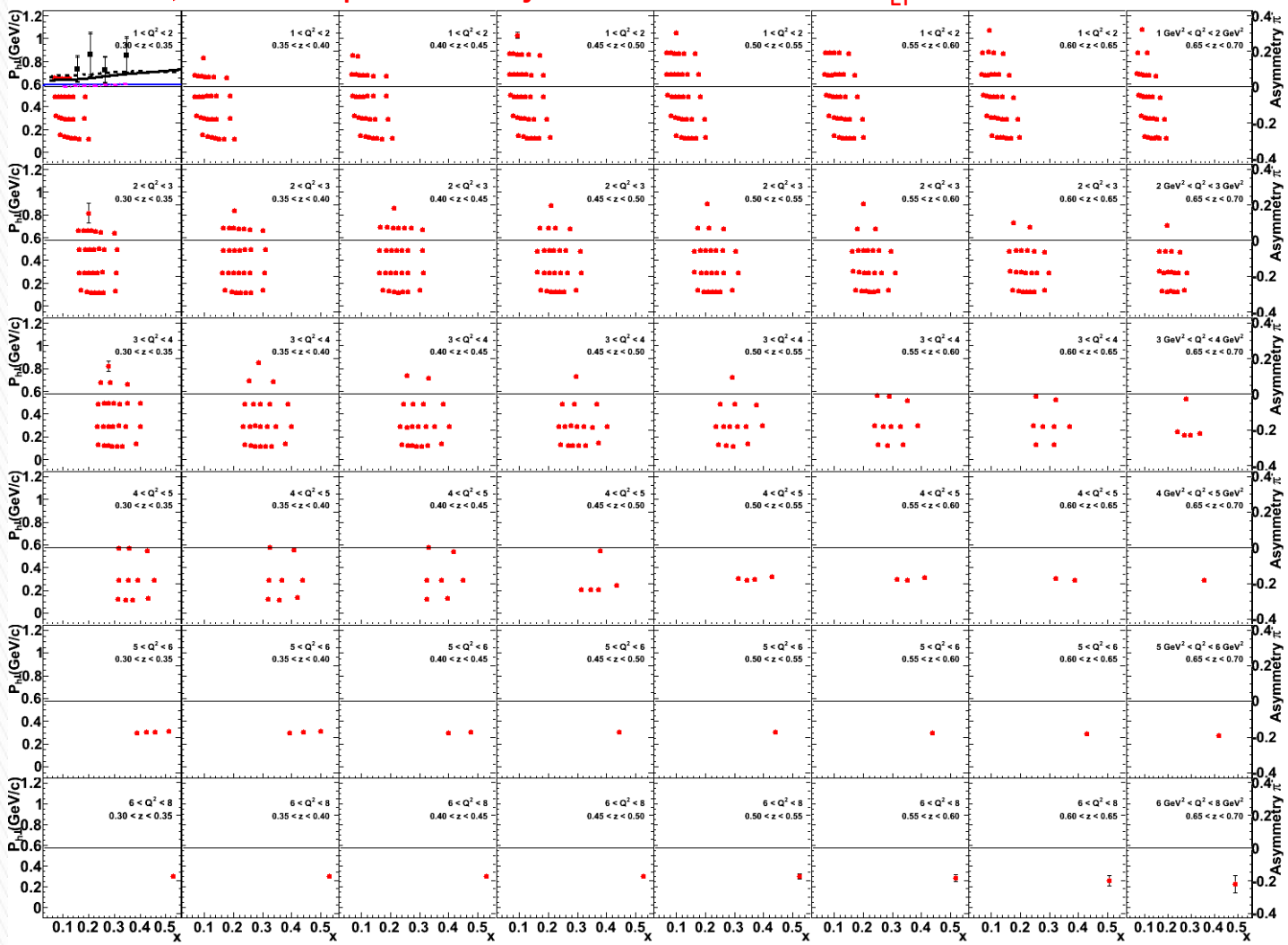

Illustration of precision: projection in 1-D (x)

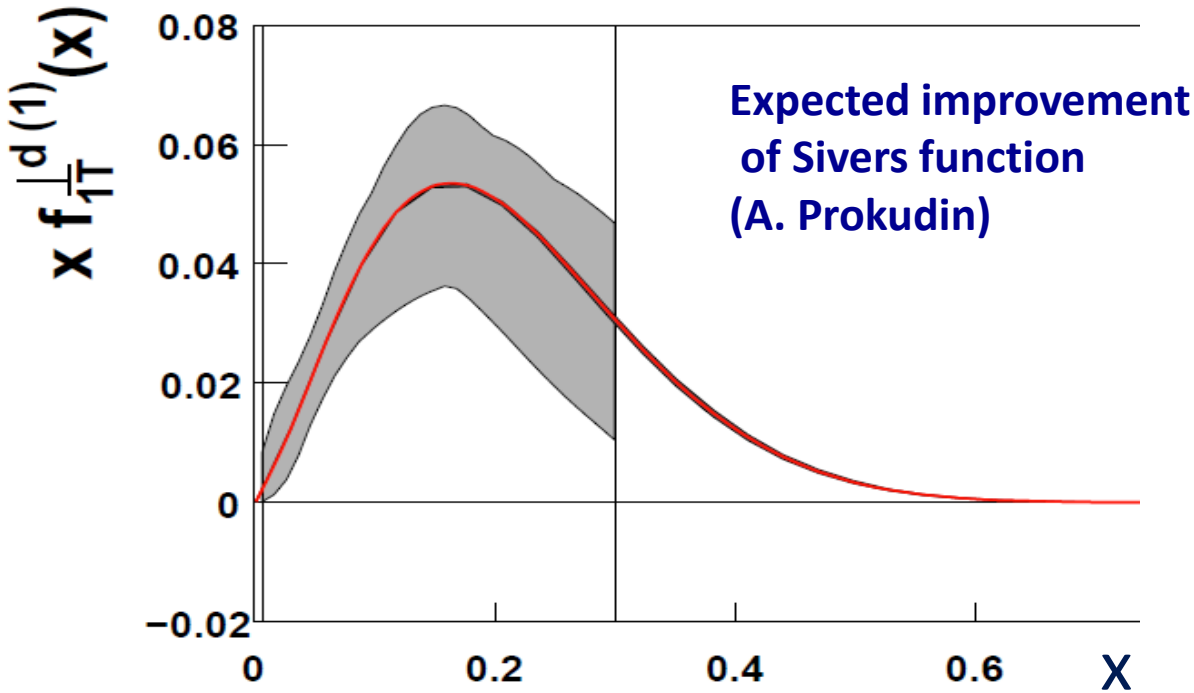

Assumption: We know the k_T dependence, Q^2 evolution of TMDs. Also knowledge on TMFF → project onto 1-D in x to illustrate the power of SoLID-^{3}He.

Polarized SIDIS programs in Hall B/CLAS12

- Toroidal spectrometer with ~2π azimuthal coverage
- Long. polarized p/D targets
- Transversely polarized HD ice target in tests

$A_{UL} \propto h_{1L}^{\perp} =$

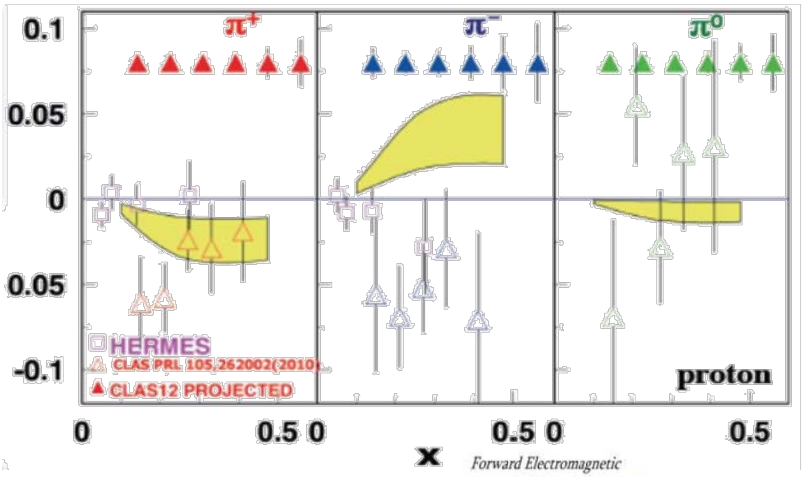

$A_1 \propto g_{1L} =$ 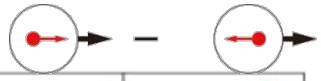

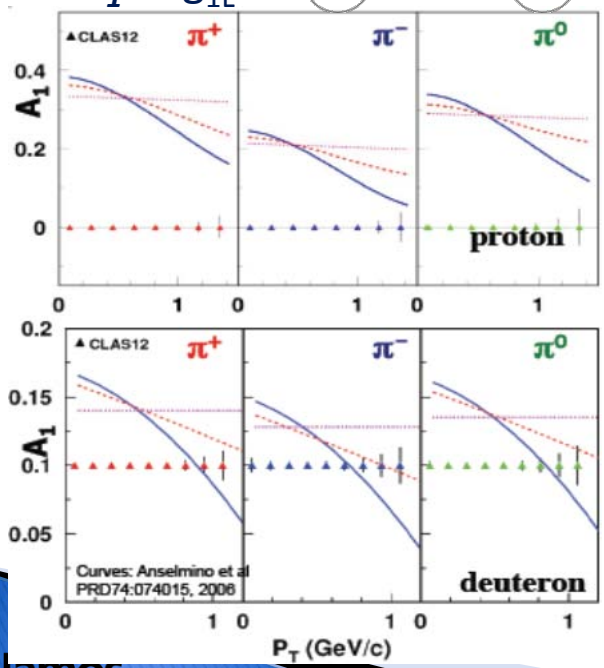

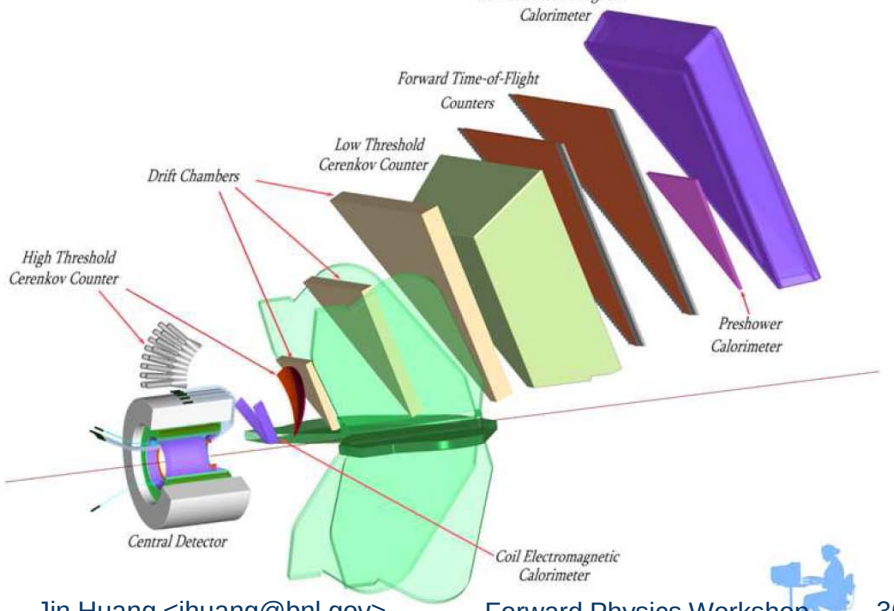

Summary

- Jefferson Lab probed TMD through SIDIS process
  - Hall A : transversely polarized ^{3}He target, first measurement on neutron SIDIS SSA and DSA
  - Hall B : SIDIS w/ long. polarized proton/deuteron target
  - Hall C : studied unpolarized SIDIS cross section using LH/LD targets

- Bright future for 12 GeV upgrade
  - Proposals to study all 8 leading-twist TMD functions
  - New instruments to map the SIDIS asymmetries in high precision
    - Hall A : polarized 3He/proton target with SoLID and Super BigBite spectrometer
    - Hall B : polarized proton/deuteron target with CLAS12
    - Hall C : study unpolarized SIDIS cross section

Probing high energy QCD via 2-particle correlations

Jamal Jalilian-Marian
Baruch College

Forward Physics at RHIC, BNL (2012)

Di-hadron correlations

Rapidity correlations

- ridge (near side)
  - nucleus-nucleus collisions
  - proton-proton collisions

Angular correlations (away side)

- large x (high p_t): pQCD
- small x: CGC
  - forward pA (dilute-dense) collisions

Di-jet correlations at large x (high p_t): pQCD

di-jets are back to back

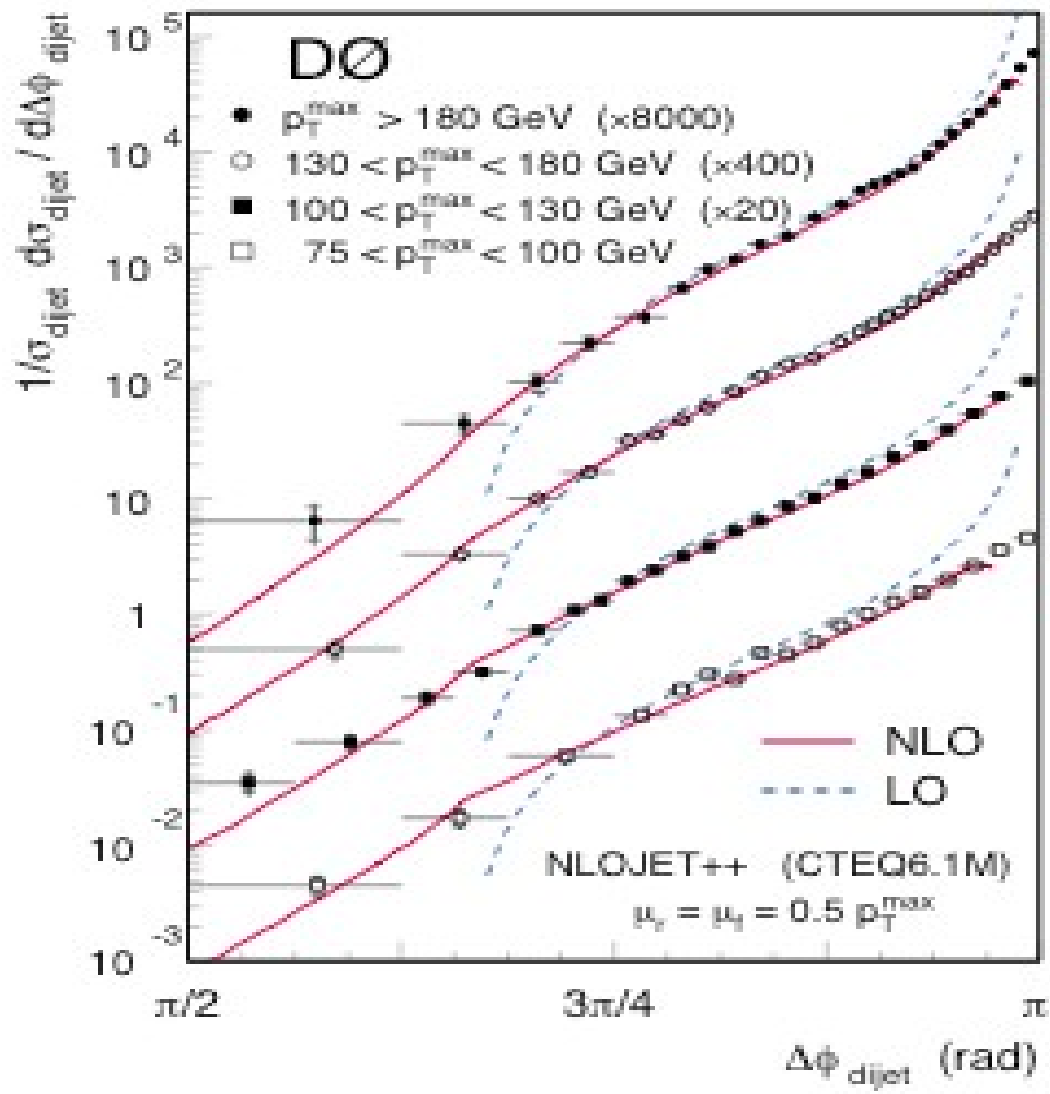

CGC: universal gluonic matter

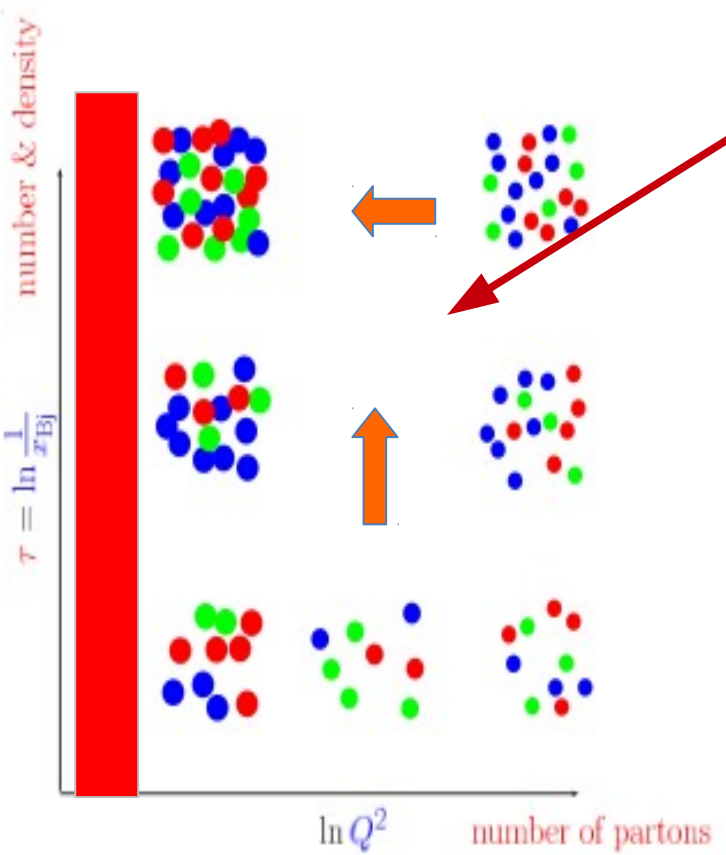

How does this happen ?

How do correlation functions of these evolve ?

Is there a universal fixed point for the RG evolution of d.o.f

How does the coupling run ?

How does saturation transition to chiral symmetry breaking and confinement

$$Q_s^2(x, b_t, A) \sim A^{1/3} \left(\frac{1}{x}\right)^{0.3}$$

QCD at low x: CGC

two main effects: *"multiple scatterings"*
evolution with ln (1/x)

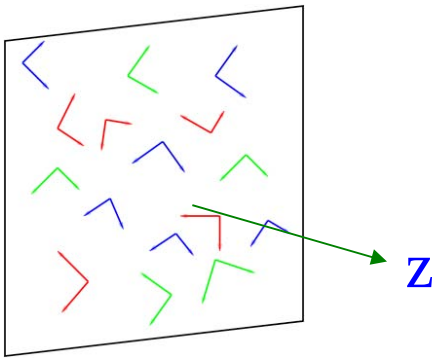

$$\mathbf{A}^{\mu}_{\mathbf{a}}(\mathbf{x_t}, \mathbf{x}^-) \sim \delta^{\mu +} \delta(\mathbf{x}^-)\, \alpha_{\mathbf{a}}(\mathbf{x_t})$$

$$\alpha^{\mathbf{a}}(\mathbf{k_t}) = \mathbf{g}\, \rho^{\mathbf{a}}(\mathbf{k_t})/\mathbf{k_t^2}$$

CGC observables: $< \mathrm{Tr}\, V \cdots\cdots V^\dagger >$ with

propagation of quarks and gluons in the background of the classical field

$$\mathbf{V}(\mathbf{x_t}) = \hat{\mathbf{P}}\mathbf{e}^{\mathbf{ig}\int \mathbf{dx}^-\, \mathbf{A}^+_{\mathbf{a}}\, \mathbf{t_a}}$$

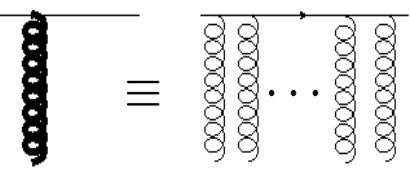

gluon distribution: $\sim \int^{\mathbf{Q}^2} \frac{\mathbf{d}^2\mathbf{k_t}}{\mathbf{k_t^2}}\, \phi(\mathbf{x}, \mathbf{k_t})$ with $\phi(\mathbf{k_t^2}) \sim < \rho^\star_{\mathbf{a}}(\mathbf{k_t})\, \rho_{\mathbf{a}}(\mathbf{k_t}) >$

<u>pQCD with collinear factorization:</u> *single scattering*
evolution with ln Q^2

JIMWLK evolution equation

re-sum ln (1/x)

$$\frac{d}{d\,ln 1/x}\langle O\rangle = \frac{1}{2}\left\langle \int d^2x\, d^2y\, \frac{\delta}{\delta\alpha_x^b}\, \eta_{xy}^{bd}\, \frac{\delta}{\delta\alpha_y^d}\, O \right\rangle$$

$$\eta_{xy}^{bd} = \frac{1}{\pi}\int \frac{d^2z}{(2\pi)^2}\frac{(x-z)\cdot(y-z)}{(x-z)^2(y-z)^2}\Big[\underbrace{1+U_x^\dagger U_y}_{\text{virtual}} - \underbrace{U_x^\dagger U_z - U_z^\dagger U_y}_{\text{real}}\Big]^{bd}$$

U is a Wilson line in adjoint representation

Color Glass Condensate

Advantages:

A systematic, first-principle approach to high energy scattering in QCD

Controlled approximations

Same formalism can describe a wide range of phenomena

Disadvantages:

Applicable at low x (high x, Q2 missing)

Observables

Talks by
J. Albacete, K. Dusling,
Y. Kovchegov, K. Tuchin

DIS:

structure functions
particle production

dilute-dense (pA, forward pp) collisions:

multiplicities

p_t spectra

di-hadron angular correlations

dense-dense (AA, pp) collisions:

multiplicities, spectra
long range rapidity correlations

Spin

2-particle kinematics in CGC

produced partons: k_1, y_1 k_2, y_2 $x_p = \frac{k_1 e^{y_1} + k_2 e^{y_2}}{\sqrt{s}}$ $x_A = \frac{k_1 e^{-y_1} + k_2 e^{-y_2}}{\sqrt{s}}$

scanning the wave-functions (RHIC) $k_1 \sim k_2 \sim k \sim 2\,GeV$

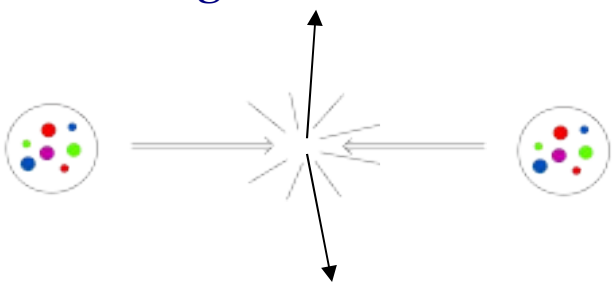

mid-mid correlations
probe moderate x

$$x_p \sim x_A \sim \frac{k}{\sqrt{S}} \sim 10^{-2}$$

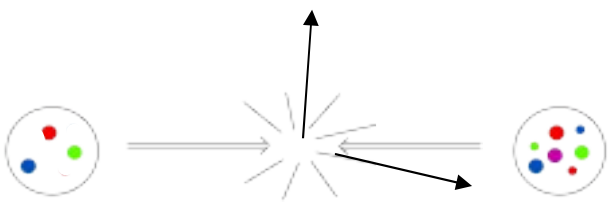

mid-forward

$$x_p \sim \frac{k}{\sqrt{S}} e^{y_1} \to 1 \quad x_A \sim \frac{k}{\sqrt{S}} \sim 10^{-2}$$

forward-forward

$$x_p \sim \frac{k}{\sqrt{S}} e^{y_1} \to 1 \quad x_A \sim \frac{k}{\sqrt{S}} e^{-y_2} \sim 10^{-4}$$

Di-jet production: pA

J. Jalilian-Marian, Y. Kovchegov
PRD70 (2004) 114017

$$\mathbf{q(p)\,T \to q(q)\,g(k)\,X}$$

LSZ reduction formalism

$$< q(q)\, g(k)_{out} | q(p)_{in} > = < 0_{out} | a_{out}(k) b_{out}(q) b^{\dagger}_{in}(p) | 0_{in} >$$

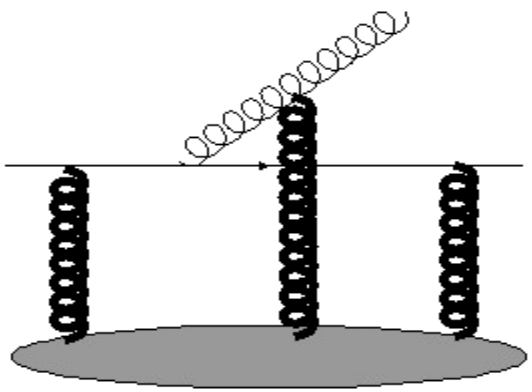

with

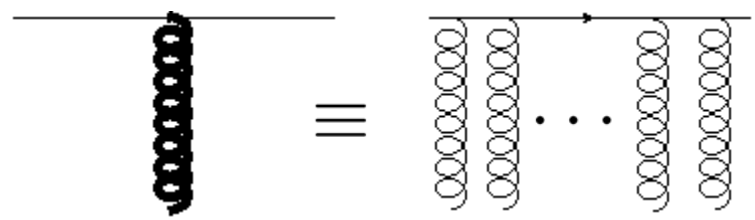

$$\mathcal{M}(q,k;p) \;=\; g \int d^4x\, d^4y\, d^4z\, d^4r\, d^4\bar{r}\, e^{i(q\cdot z + k\cdot r - p\cdot y)}$$

$$\bar{u}(q)[i\,\overrightarrow{\not\partial}_z] S_F(z,x) \gamma^{\nu} t^c S_F(x,y) [i\,\overleftarrow{\not\partial}_y] u(p)$$

$$G^{cb}_{\nu\rho}(x,\bar{r}) D^{\rho\mu}_{ba}(\bar{r},r)\, \epsilon_{\mu}(k)$$

Di-jet production: pA

$$\mathbf{q(p)\,T \to q(q)\,g(k)\,X}$$

$$\mathcal{M}(q,k;p) = g \int \frac{d^4k_1}{(2\pi)^4}\frac{d^4k_2}{(2\pi)^4}\frac{d^4k_3}{(2\pi)^4}$$

$$\bar{u}(q)\,\overrightarrow{\not{q}}\,S_F(q,k_1)\,\gamma^\nu\,t^c\,S_F(k_2,p)\,\overleftarrow{\not{p}}\,u(p)$$

$$G^{cb}_{\nu\rho}(k_2-k_1,k_3)\,D^{\rho\mu}_{ba}(k_3,k)\,\epsilon_\mu(k)$$

propagators

$$S_F(q,p) \equiv (2\pi)^4\delta^4(p-q)\,S^0_F(p) + S^0_F(q)\,\tau_f(q,p)\,S^0_F(p)$$

$$G^{\mu\nu}(q,p) \equiv (2\pi)^4\delta^4(p-q)\,G^{0\mu\nu}(p) + G^{0\mu}_\rho(q)\,\tau_g(q,p)\,G^{0\rho\nu}(p)$$

with

$$\tau_f(q,p) \equiv (2\pi)\delta(p^- - q^-)\,\gamma^- \int d^2x_t\,e^{i(q_t-p_t)\cdot x_t}\,[V(x_t)-1]$$

$$\tau_g(q,p) \equiv 2p^-\,(2\pi)\delta(p^- - q^-) \int d^2x_t\,e^{i(q_t-p_t)\cdot x_t}\,[U(x_t)-1]$$

Di-jet production: pA

$$\mathbf{q(p)\,T \to q(q)\,g(k)}$$

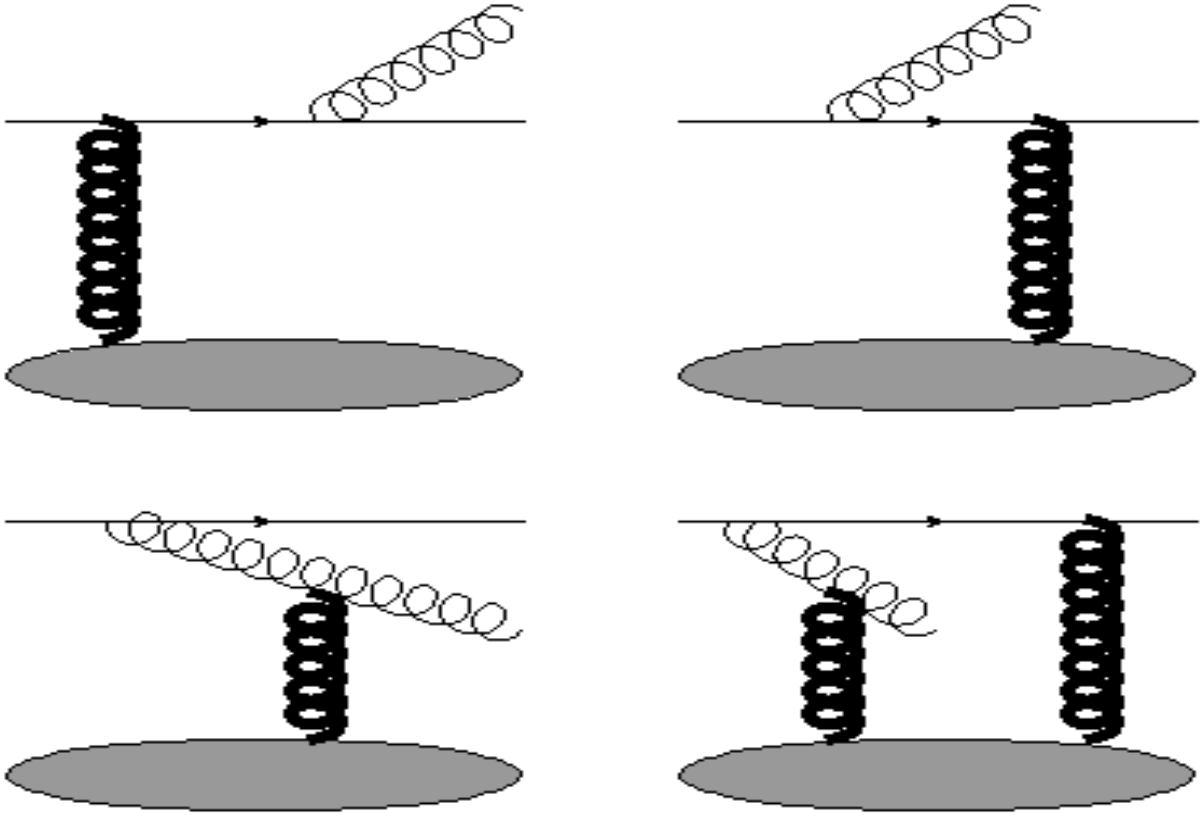

$$\mathbf{d\sigma \sim \int K \otimes \left[< TrV\,V^\dagger > + < TrV\,V^\dagger\,V\,V^\dagger > + \cdots \right]}$$

$\mathbf{V \equiv}$ 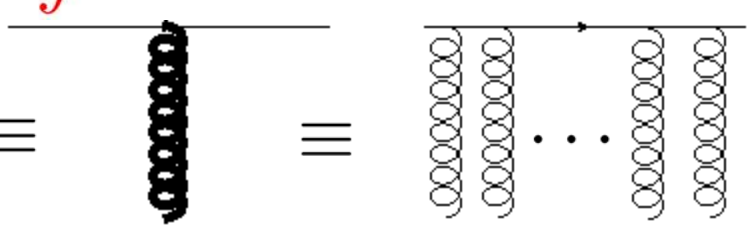 $\mathbf{\sim 1 + O(g\,\rho) + O(g^2\,\rho^2)}$

Di-jet production: pA

recall DIS, single inclusive production in pA probe ***dipoles***

$$< \mathrm{Tr}\, V\, V^\dagger >$$

di-jet production in pA (and DIS) probe ***quadrupoles***

This would be problematic in pQCD

$$< \mathrm{Tr}\, V\, V^\dagger\, V\, V^\dagger >$$

momentum space: J. Jalilian-Marian, Y. Kovchegov, PRD70 (2004) 114017

coordinate space: *C. Marquet, NPA796 (2007) 41*

including gluons in the projectile *F. Dominguez,C. Marquet, B-W. Xiao, F. Yuan, PRD83 (2011) 105005*

disappearance of back to back jets

Recent STAR measurement (arXiv:1008.3989v1):

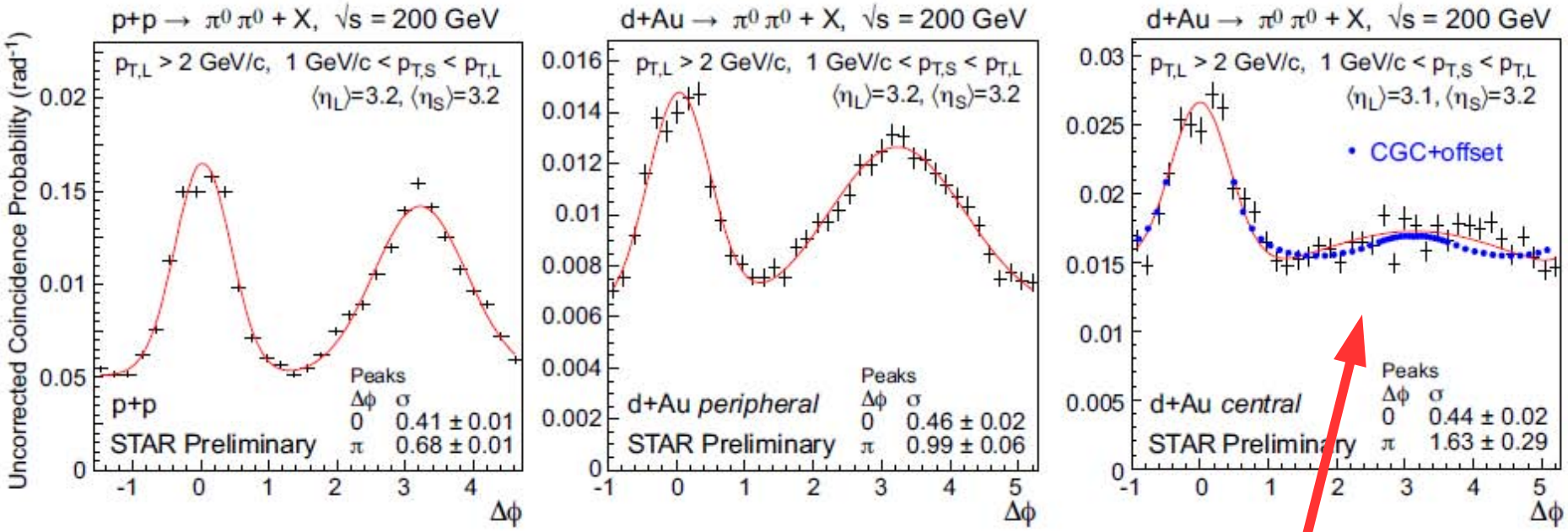

CGC fit from
Albacete + Marquet, PRL (2010)
using running coupling BK solution,
Also by Tuchin, NPA846 (2010)

multiple scatterings
de-correlate the hadrons

disappearance of back to back jets

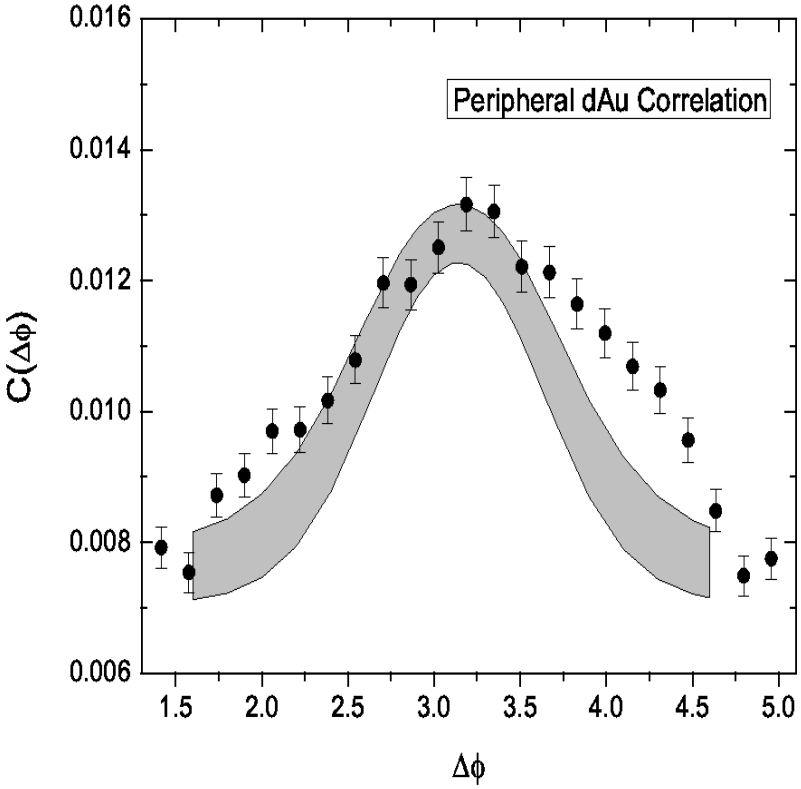

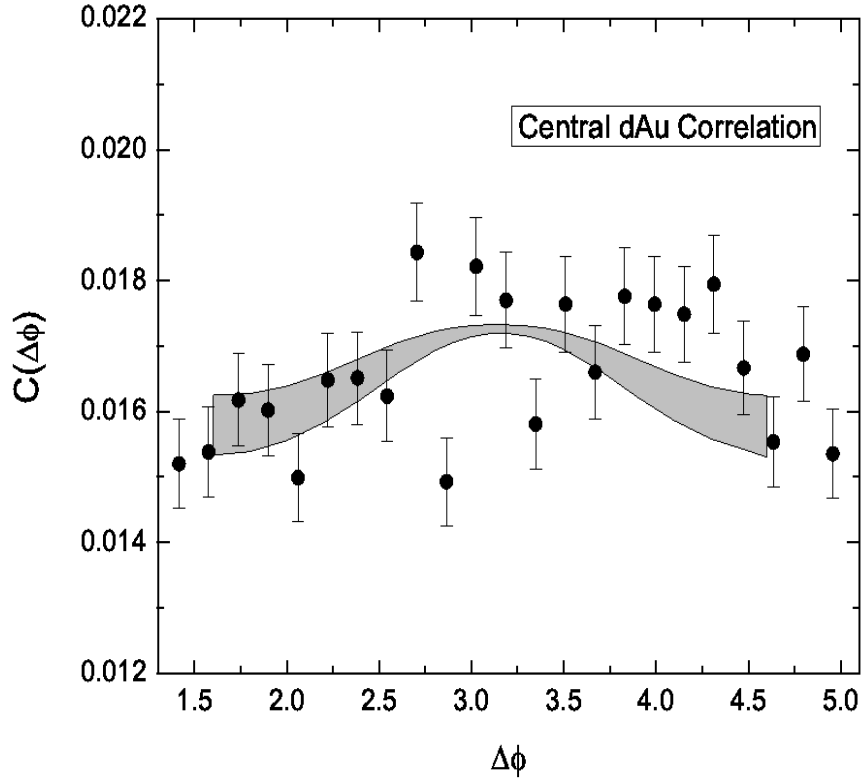

CGC fit from
A. Stasto, B-W. Xiao, F. Yuan, arXiv:1109.1817

alternative idea: shadowing + energy loss (M. Strikman et al.)
Z. Kang, I. Vitev and H. Xing, PRD85 (2012) 054024

Probing for Saturation Effects in Hadron-Hadron Correlations in d+Au with the Forward MPC

Beau Meredith, Phys.Rev.Lett. 107 (2011) 172301

Experimental signature:

- Broadening in the correlation of back-to-back jets or hadrons
- Suppression of away-side jets or hadrons

The MPC is an NSF funded UIUC built forward EMC based on $PbWO_4$ Crystals with APD readout.

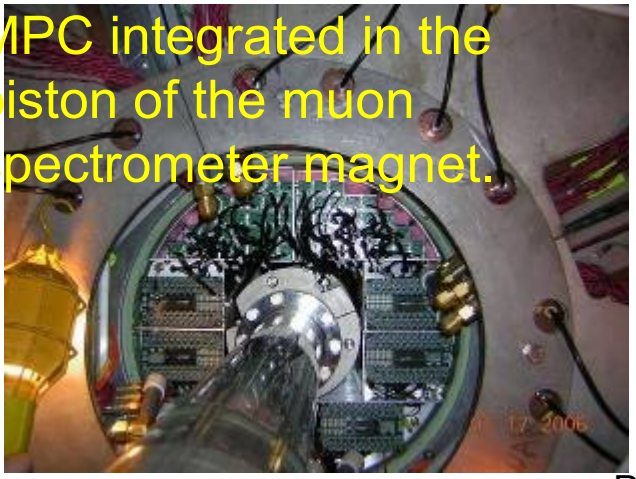

$$J_{dA} \sim \frac{N_{dAu}^{\text{back-to-back}} / N_{\text{N-N-collision}}}{N_{pp}^{\text{back-to-back}}}$$

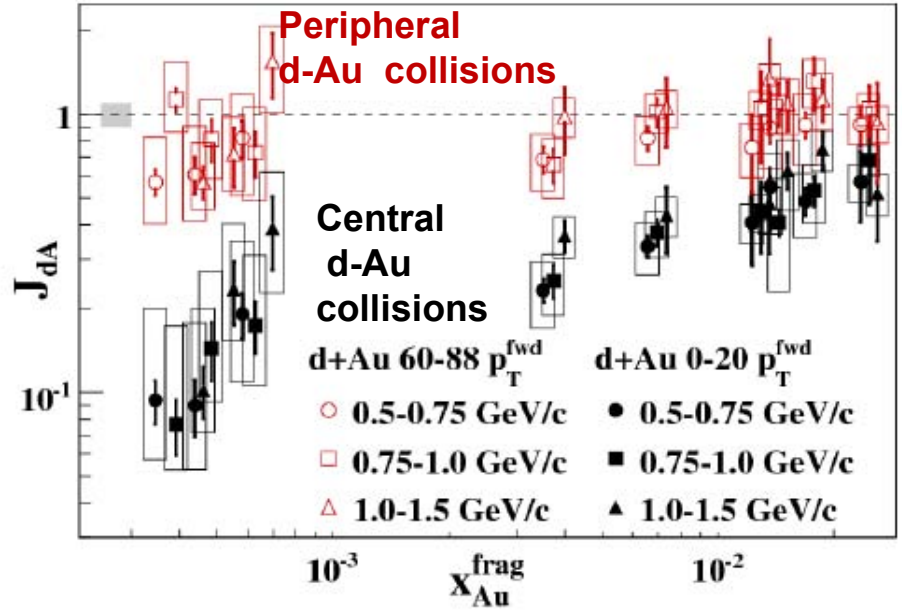

Away Side hadrons/jets in central d-Au suppressed by factor 5 at x~0.0005
Mono-jets !? CGC ?

Di-jet correlations in DIS

EIC

$$\gamma^\star\, \mathbf{p(A)} \to \mathbf{q\,\bar{q}\,X}$$

FG & JJM, PRD67 (2003)

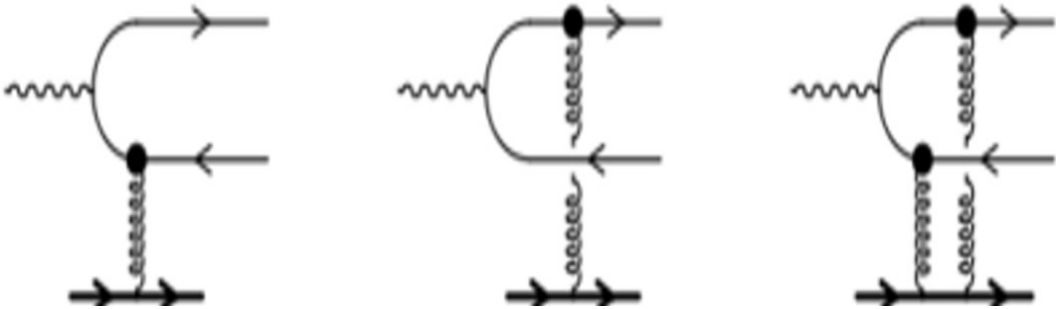

$$\gamma^\star\, \mathbf{p(A)} \to \mathbf{g\,g\,X}$$

JJM & YK, PRD70 (2004)
AK & ML, JHEP (2006)

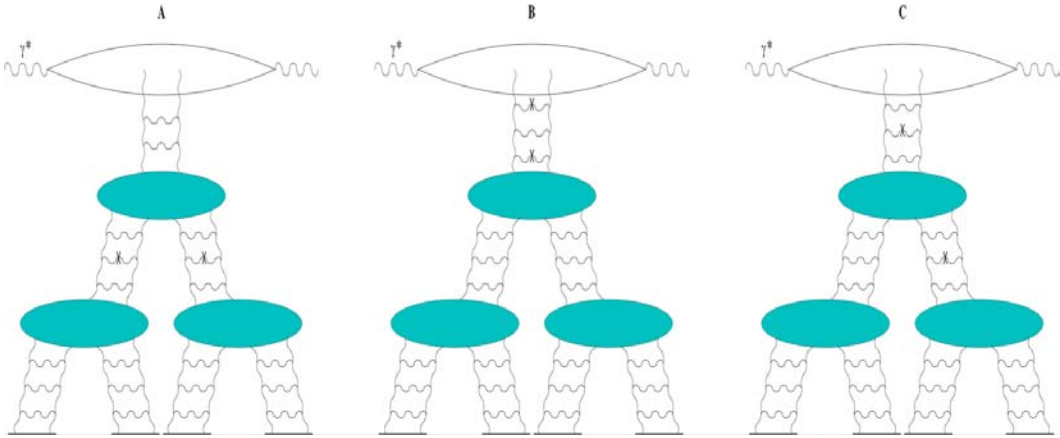

di-jet production in pA and DIS probes quadrupoles

di-jet production in pA

$$O_2(r,\bar{r}) \equiv Tr V_r\, V_{\bar{r}}^\dagger$$ **dipole** → **F2 in DIS, single hadron in pA**

$$O_4(r,\bar{r}:s) \equiv Tr V_r^\dagger\, t^a\, V_{\bar{r}}\, t^b\, [U_s]^{ab} = \frac{1}{2}\left[Tr V_r^\dagger\, V_s\;\; Tr V_{\bar{r}}\, V_s^\dagger - \frac{1}{N_c} Tr V_r^\dagger\, V_{\bar{r}}\right]$$

$$O_6(r,\bar{r}:s,\bar{s}) \equiv Tr V_r\, V_{\bar{r}}^\dagger\, t^a\, t^b\, [U_s\, U_{\bar{s}}^\dagger]^{ba} = \frac{1}{2}\left[Tr V_r\, V_{\bar{r}}^\dagger\, V_{\bar{s}}\, V_s^\dagger\, Tr V_s\, V_{\bar{s}}^\dagger - \frac{1}{N_c} Tr V_r\, V_{\bar{r}}^\dagger\right]$$

quadrupole

calculations: classical

how about quantum corrections (energy dependence) ?

energy (rapidity) dependence from JIMWLK evolution of O's

<u>evolution of a dipole is well known: BK eq.</u>

how does a quadrupole evolve?

Mean field + large N_c :Balitsky-Kovchegov eq.

$$\frac{d}{dy} S(r-\bar{r}) = \frac{\bar{\alpha}_s}{2\pi} \int d^2z \, \frac{(r-\bar{r})^2}{(r-z)^2(\bar{r}-z)^2} \left[S(r-z)\, S(\bar{r}-z) - S(r-\bar{r}) \right]$$

with $S(r-\bar{r}) \equiv \frac{1}{N_c} < \mathrm{Tr}\, V(r)\, V^\dagger(\bar{r}) >$ and

$$dP_{d \to d\, d} = \frac{\bar{\alpha}_s}{2\pi} \frac{(r-\bar{r})^2}{(r-z)^2(\bar{r}-z)^2} d^2z$$

dipole splitting probability

all n-point correlators are expressed in terms of the dipoles

NLO: Balitsky-Kovchegov-Weigert-Gardi-Chirilli (2007-2008)

Evolution of quadrupole from JIMWLK

$$\mathbf{Q}(\mathbf{r},\bar{\mathbf{r}},\bar{\mathbf{s}},\mathbf{s}) \equiv \frac{\mathbf{1}}{\mathbf{N_c}} < \mathbf{Tr}\,\mathbf{V}(\mathbf{r})\,\mathbf{V}^\dagger(\bar{\mathbf{r}})\,\mathbf{V}(\bar{\mathbf{s}})\,\mathbf{V}^\dagger(\mathbf{s}) >$$

radiation kernels
as in dipole

$$\frac{\mathbf{d}}{\mathbf{dy}}$$

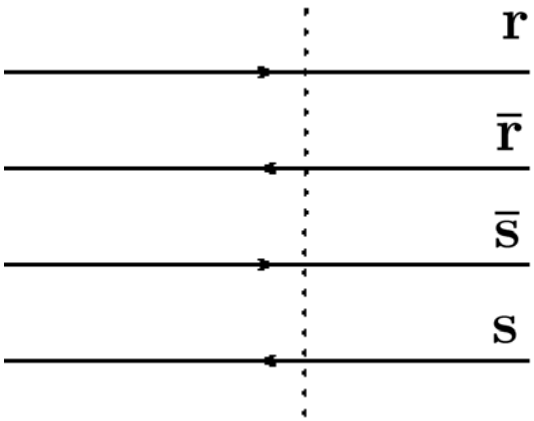

$=$

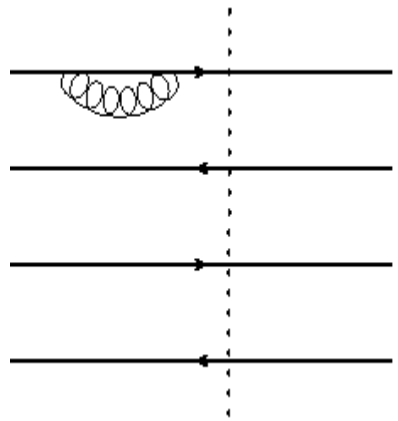

$+$

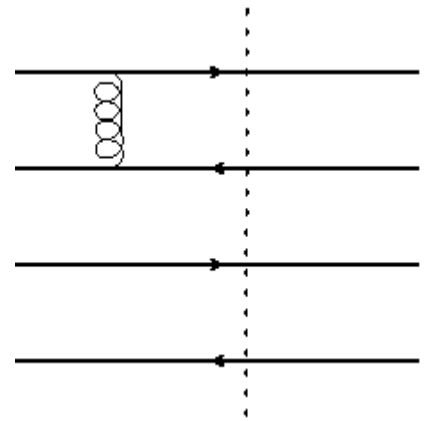

$$\frac{\mathbf{1}}{(\mathbf{r}-\mathbf{z})^2}$$

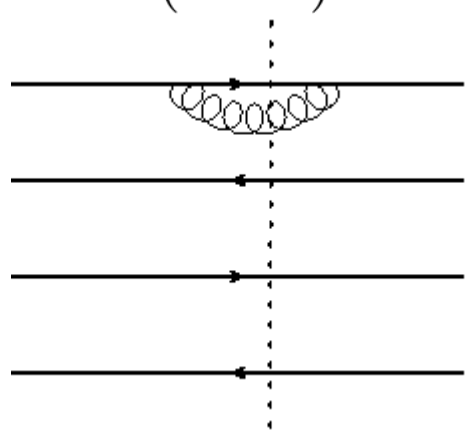

$$\frac{(\mathbf{r}-\mathbf{z})\cdot(\bar{\mathbf{r}}-\mathbf{z})}{(\mathbf{r}-\mathbf{z})^2(\bar{\mathbf{r}}-\mathbf{z})^2}$$

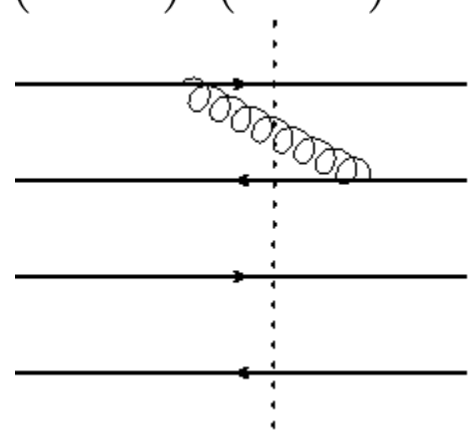

J. Jalilian-Marian, Y. Kovchegov (2004)
Dominguez, Mueller, Munier, Xiao (2011)
J. Jalilian-Marian (2011)
D. Triantafyllopoulos (2011)

$+ \cdots$

Evolution of quadrupole from JIMWLK

$$
\begin{aligned}
&\frac{d}{dy}\langle Q(r,\bar{r},\bar{s},s)\rangle \\
= \;& \frac{N_c\,\alpha_s}{(2\pi)^2}\int d^2z \Bigg\{ \Bigg\langle \left[\frac{(r-\bar{r})^2}{(r-z)^2(\bar{r}-z)^2}+\frac{(r-s)^2}{(r-z)^2(s-z)^2}-\frac{(\bar{r}-s)^2}{(\bar{r}-z)^2(s-z)^2}\right] Q(z,\bar{r},\bar{s},s)\,S(r,z) \\
+ \;& \left[\frac{(r-\bar{r})^2}{(r-z)^2(\bar{r}-z)^2}+\frac{(\bar{r}-\bar{s})^2}{(\bar{r}-z)^2(\bar{s}-z)^2}-\frac{(r-\bar{s})^2}{(r-z)^2(\bar{s}-z)^2}\right] Q(r,z,\bar{s},s)\,S(z,\bar{r}) \\
+ \;& \left[\frac{(\bar{r}-\bar{s})^2}{(\bar{r}-z)^2(\bar{s}-z)^2}+\frac{(s-\bar{s})^2}{(s-z)^2(\bar{s}-z)^2}-\frac{(\bar{r}-s)^2}{(s-z)^2(\bar{r}-z)^2}\right] Q(r,\bar{r},z,s)\,S(\bar{s},z) \\
+ \;& \left[\frac{(r-s)^2}{(r-z)^2(s-z)^2}+\frac{(s-\bar{s})^2}{(s-z)^2(\bar{s}-z)^2}-\frac{(r-\bar{s})^2}{(r-z)^2(\bar{s}-z)^2}\right] Q(r,\bar{r},\bar{s},z)\,S(z,s) \\
- \;& \left[\frac{(r-\bar{r})^2}{(r-z)^2(\bar{r}-z)^2}+\frac{(s-\bar{s})^2}{(s-z)^2(\bar{s}-z)^2}+\frac{(r-s)^2}{(r-z)^2(s-z)^2}+\frac{(\bar{r}-\bar{s})^2}{(\bar{r}-z)^2(\bar{s}-z)^2}\right] Q(r,\bar{r},\bar{s},s) \\
- \;& \left[\frac{(r-s)^2}{(r-z)^2(s-z)^2}+\frac{(\bar{r}-\bar{s})^2}{(\bar{r}-z)^2(\bar{s}-z)^2}-\frac{(\bar{r}-s)^2}{(\bar{r}-z)^2(s-z)^2}-\frac{(r-\bar{s})^2}{(r-z)^2(\bar{s}-z)^2}\right] S(r,s)\,S(\bar{r},\bar{s}) \\
- \;& \left[\frac{(r-\bar{r})^2}{(r-z)^2(\bar{r}-z)^2}+\frac{(s-\bar{s})^2}{(s-z)^2(\bar{s}-z)^2}-\frac{(r-\bar{s})^2}{(r-z)^2(\bar{s}-z)^2}-\frac{(\bar{r}-s)^2}{(\bar{r}-z)^2(s-z)^2}\right] S(r,\bar{r})\,S(\bar{s},s)\Bigg\rangle\Bigg\}
\end{aligned}
$$

$$\frac{d}{d\,y}Q = \int P_1\,[Q\,S] - P_2\,[Q] + P_3[S\,S]$$

with

$$P_1 - P_2 + P_3 = 0$$

"approximate solution": Iancu-Triantafyllopoulos, arXiv:1109.0302

quadrupole evolution in the linear regime

define $\mathbf{T}(\mathbf{r},\bar{\mathbf{r}}) \equiv \mathbf{1} - \mathbf{S}(\mathbf{r},\bar{\mathbf{r}})$ $\quad \mathbf{T_Q}(\mathbf{r},\bar{\mathbf{r}},\bar{\mathbf{s}},\mathbf{s}) \equiv \mathbf{1} - \mathbf{Q}(\mathbf{r},\bar{\mathbf{r}},\bar{\mathbf{s}},\mathbf{s})$

re-write the evolution eq. for T_Q rather than Q

expand in powers of gauge fields (or color charges)

ignore contribution of non-linear terms: T T and T_Q T

$\mathbf{O}(\alpha^{\mathbf{2}})$ $\quad \mathbf{T_Q}(\mathbf{r},\bar{\mathbf{r}},\bar{\mathbf{s}},\mathbf{s}) \to \mathbf{T}(\mathbf{r},\bar{\mathbf{r}}) + \mathbf{T}(\mathbf{r},\mathbf{s}) + \cdots$

with $\quad \mathbf{T}(\mathbf{r},\bar{\mathbf{r}}) \sim \alpha^{\mathbf{2}}(\mathbf{r},\bar{\mathbf{r}})$

quadrupole evolution reduces to a sum of BFKL evolution eqs

Dominguez, Mueller, Munier, Xiao (2011)
J. Jalilian-Marian (2011)
D. Triantafyllopoulos (2011)

di-hadron correlations in the high p_t limit

$\mathbf{O}(\alpha^2)$

Dominguez, Marquet, Xiao, Yuan (2011)
Dominguez, Xiao, Yuan (2011)

factorization of target distribution functions and hard scattering matrix element

$$\mathbf{d}\sigma \sim \mathbf{\Phi} \otimes \frac{\mathbf{d}\sigma^{\mathbf{2\to 2}}}{\mathbf{dt}}$$

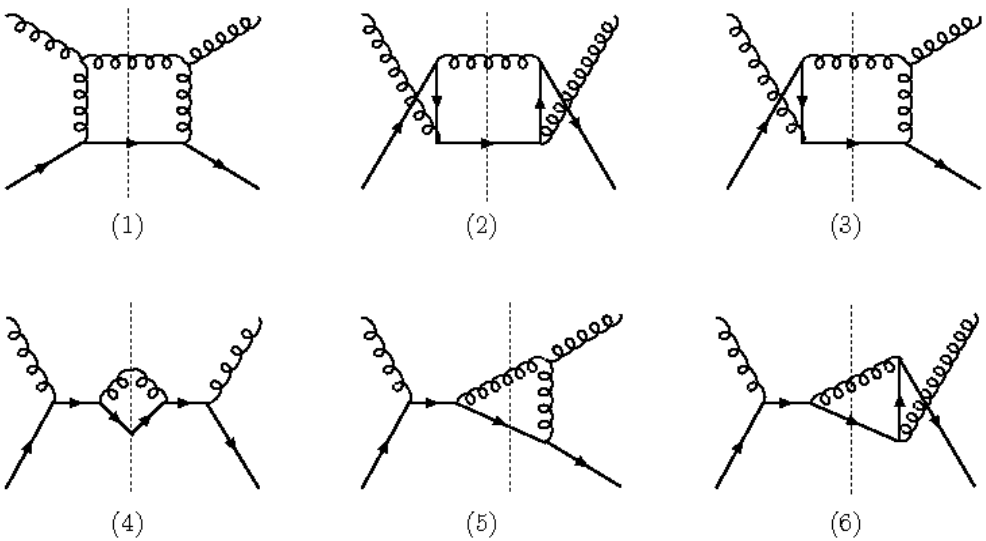

$$\frac{d\sigma^{q\,g\to q\,g}}{dt} \sim \frac{1}{s^2}\left[\frac{4}{9}\frac{s^2+u^2}{-s\,u} + \frac{s^2+u^2}{t^2}\right]$$

partons are back to back

quadrupole evolution in the linear regime

$\mathbf{O}(\alpha^4)$

momentum space

define $$\hat{\mathbf{T}}_4(\mathbf{l_1}, \mathbf{l_2}, \mathbf{l_3}, \mathbf{l_4}) \equiv \frac{\mathbf{1}}{\mathbf{N_c}} \mathbf{Tr}\, \rho(\mathbf{l_1})\, \rho(\mathbf{l_2})\, \rho(\mathbf{l_3})\, \rho(\mathbf{l_4})$$

assume $\mathbf{l_1} \neq \mathbf{l_2} \neq \mathbf{l_3} \neq \mathbf{l_4}$ subject to an overall delta function

contribution only from linear term in expansion of Wilson lines (except for the z-dependent ones)

quadrupole evolution eq. reduces to Bartels-Jaroszewicz-Kwiecinski-Praszalowicz (BJKP) eq. for evolution of 4-Reggeized gluons in a singlet state

quadrupole evolution in the linear regime

BJKP equation

$\mathbf{O}(\alpha^4)$: 4-gluon exchange

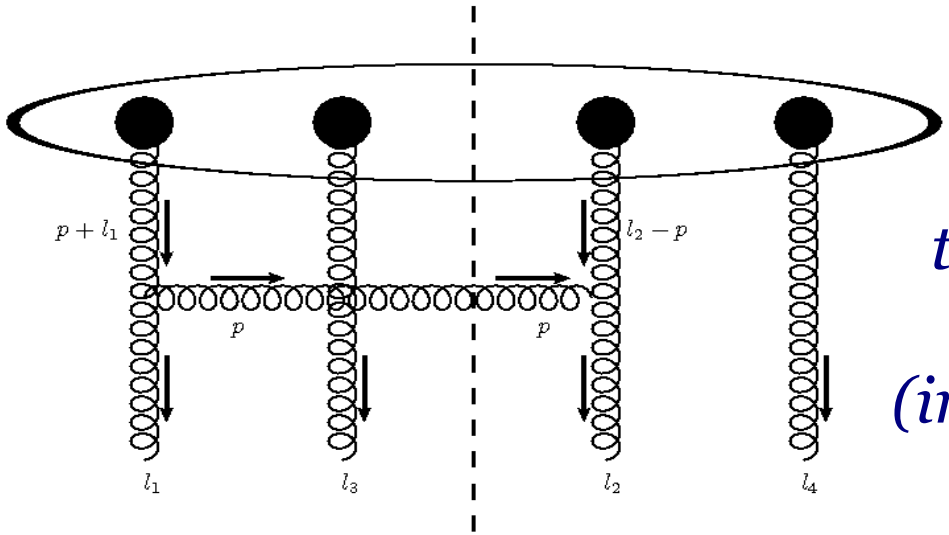

J. Jalilian-Marian, PRD85 (2012) 014037

the color structure is identical on both sides of this eq. (independent of color averaging)

$$\frac{d}{dy}\hat{T}_4(l_1,l_2,l_3,l_4) = \frac{N_c\,\alpha_s}{\pi^2}\int d^2p_t\left[\frac{p^i}{p_t^2}-\frac{(p^i-l_1^i)}{(p_t+l_1)^2}\right]\cdot\left[\frac{p^i}{p_t^2}-\frac{(p^i-l_2^i)}{(p_t+l_2)^2}\right]$$
$$\hat{T}_4(p_t+l_1,l_2-p_t,l_3,l_4)+\cdots$$
$$-\frac{N_c\,\alpha_s}{(2\pi)^2}\int d^2p_t\left[\frac{l_1^2}{p_t^2(l_1-p_t)^2}+\{l_1\to l_2,l_3,l_4\}\right]\hat{T}_4(l_1,l_2,l_3,l_4)$$

this will <u>de-correlate</u> the produced partons at high $p_t > Q_s$

color structure

$$\hat{\mathbf{T}}_4(\mathbf{l_1},\mathbf{l_2},\mathbf{l_3},\mathbf{l_4}) \equiv \frac{\mathbf{1}}{\mathbf{N_c}}\mathbf{Tr}\,\rho(\mathbf{l_1})\,\rho(\mathbf{l_2})\,\rho(\mathbf{l_3})\,\rho(\mathbf{l_4}) = \mathbf{Tr}\,(\mathbf{t^a}\,\mathbf{t^b}\,\mathbf{t^c}\,\mathbf{t^d})\,\rho^{\mathbf{a}}(\mathbf{l_1})\,\rho^{\mathbf{b}}(\mathbf{l_2})\,\rho^{\mathbf{c}}(\mathbf{l_3})\,\rho^{\mathbf{d}}(\mathbf{l_4})$$

$$\begin{aligned} Tr\,(t^a\,t^b\,t^c\,t^d) &= \frac{1}{4N_c}\left[\delta^{ab}\delta^{cd} - \delta^{ac}\delta^{bd} + \delta^{ad}\delta^{bc}\right] \\ &+ \frac{1}{8}\left[d^{abr}d^{cdr} - d^{acr}d^{bdr} + d^{adr}d^{bcr}\right] \\ &+ \frac{i}{8}\left[d^{abr}f^{cdr} - d^{acr}f^{bdr} + d^{adr}f^{bcr}\right] \end{aligned}$$

overall state is a singlet, how about pairwise?

for $N_c = 3$

$$\left[\delta^{\mathbf{ab}}\delta^{\mathbf{cd}} + \delta^{\mathbf{ac}}\delta^{\mathbf{bd}} + \delta^{\mathbf{ad}}\delta^{\mathbf{bc}}\right] = \mathbf{3}\left[\mathbf{d^{abr}d^{cdr}} + \mathbf{d^{acr}d^{bdr}} + \mathbf{d^{adr}d^{bcr}}\right]$$

can the exchanged pairs be in a bound state?

J. Bartels: YES!

the linear regime

$\mathbf{O}(\alpha^3)$: 3-gluon (odderon) exchange

$\mathbf{V}\,\mathbf{V}^\dagger\,\mathbf{V}$

Hatta, Iancu, Itakura, McLerran
Kovchegov et al.

BJKP equation

BJKP equation describes evolution of n-Reggeized gluons in a singlet state

JIMWLK (linear) and BJKP eqs. agree for n=2,3,4

non-linear interactions:

1) MV action with JIMWLK evolution

2) Triple (and more) pomeron vertices

Chirilli, Szymanowski, Wallon (2010)

QCD at high energy

Two distinct approaches:

1) CGC

McLerran-Venugopalan effective action
JIMWLK evolution

2) Reggeized-gluon exchange

BJKP equation
triple pomeron vertex

Conjecture: CGC contains BJKP + multi-pomeron vertices

quadrupole evolution: limits

$$< Q(r,\bar{r},\bar{s},s) > \equiv \frac{1}{N_c} < Tr\, V(r)\, V^\dagger(\bar{r})\, V(\bar{s})\, V^\dagger(s) >$$

can be calculated in a Gaussian model DMXY

line config.: $r = \bar{s},\ \bar{r} = s,\ z \equiv r - \bar{r}$

square config.: $r - \bar{s} = \bar{r} - s = r - \bar{r} = \cdots \equiv z$

"naive" Gaussian: $Q = S^2$

Gaussian $Q_|(z) \approx \frac{N_c+1}{2}[S(z)]^{2\frac{N_c+2}{N_c+1}} - \frac{N_c-1}{2}[S(z)]^{2\frac{N_c-2}{N_c-1}}$

Gaussian + large N_c $Q_|(z) \to S^2(z)[1 + 2\, log[S(z)]]$

quadrupole evolution: limits

$$< Q(r, \bar{r}, \bar{s}, s) > \equiv \frac{1}{N_c} < Tr\, V(r)\, V^\dagger(\bar{r})\, V(\bar{s})\, V^\dagger(s) >$$

Gaussian

$$Q_{sq}(z) = [S(z)]^2 \left[\frac{N_c+1}{2} \left(\frac{S(z)}{S(\sqrt{2}z)} \right)^{\frac{2}{N_c+1}} - \frac{N_c-1}{2} \left(\frac{S(\sqrt{2}z)}{S(z)} \right)^{\frac{2}{N_c-1}} \right]$$

Gaussian + large Nc

$$Q_{sq}(z) = \left[1 + 2 \ln \left(\frac{S(z)}{S(\sqrt{2}z)} \right) \right]$$

quadrupole evolution on lattice

a "random" (Gaussian) distribution of color charges (at initial rapidity y_0)

construct the Wilson line

evolve the Wilson line to a higher rapidity y

compute ensemble average of any number of Wilson lines at y

Dumitru-Jalilian-Marian-Lappi-Schenke-Venugopalan:PLB706 (2011) 219

Quadrupole evolution

comparing with "naive" Gaussian

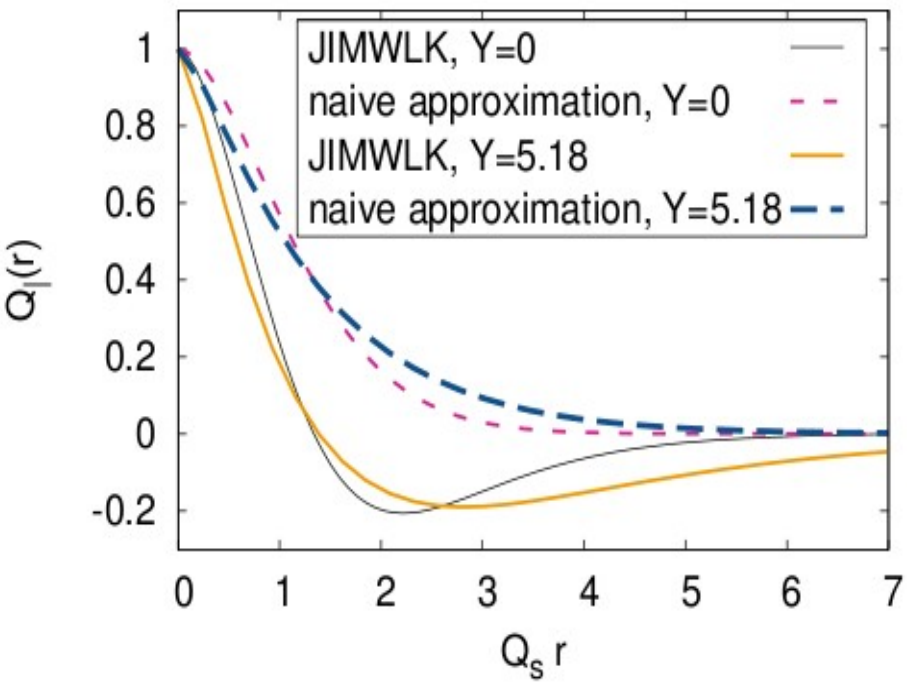

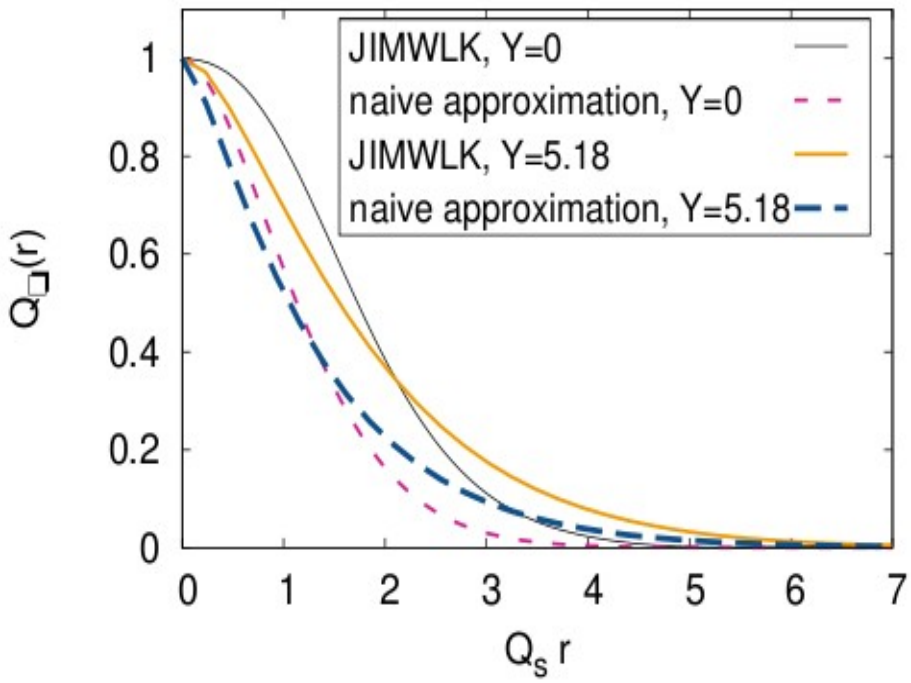

Quadrupole evolution

comparing with Gaussian + large N_c

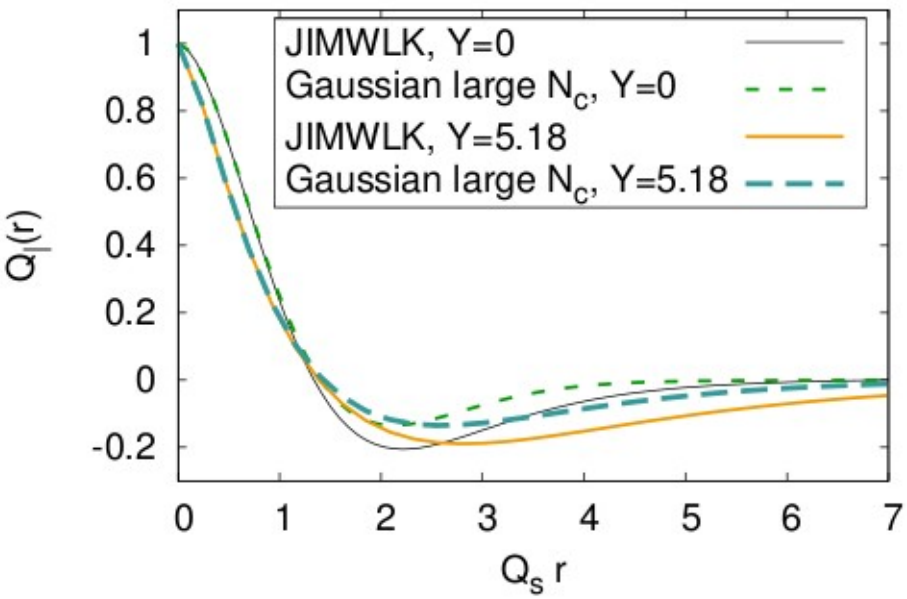

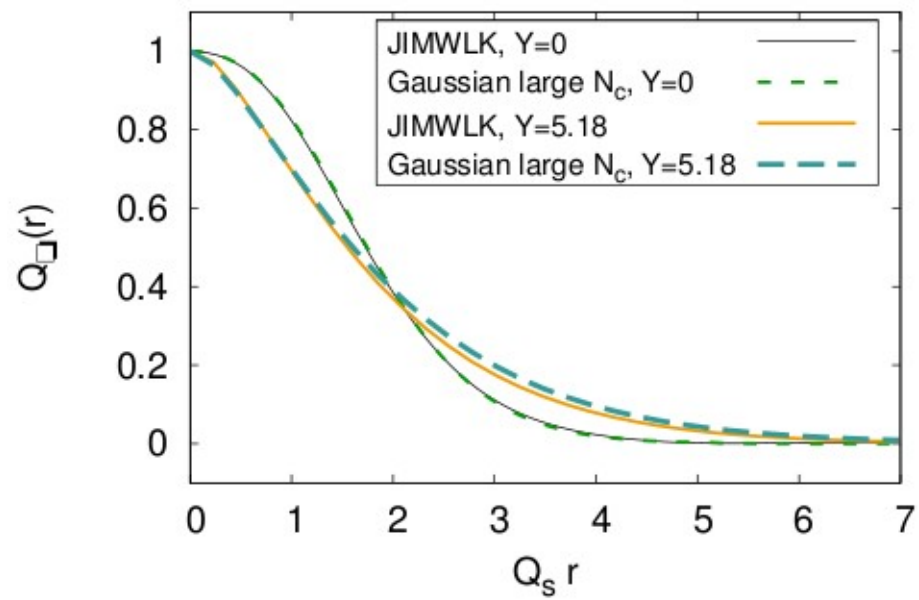

Quadrupole evolution

comparing with Gaussian

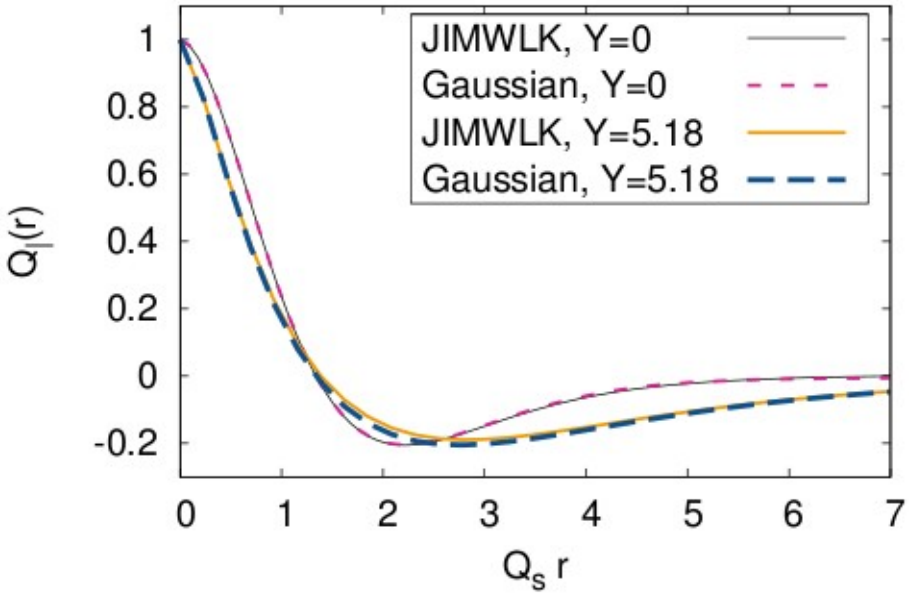

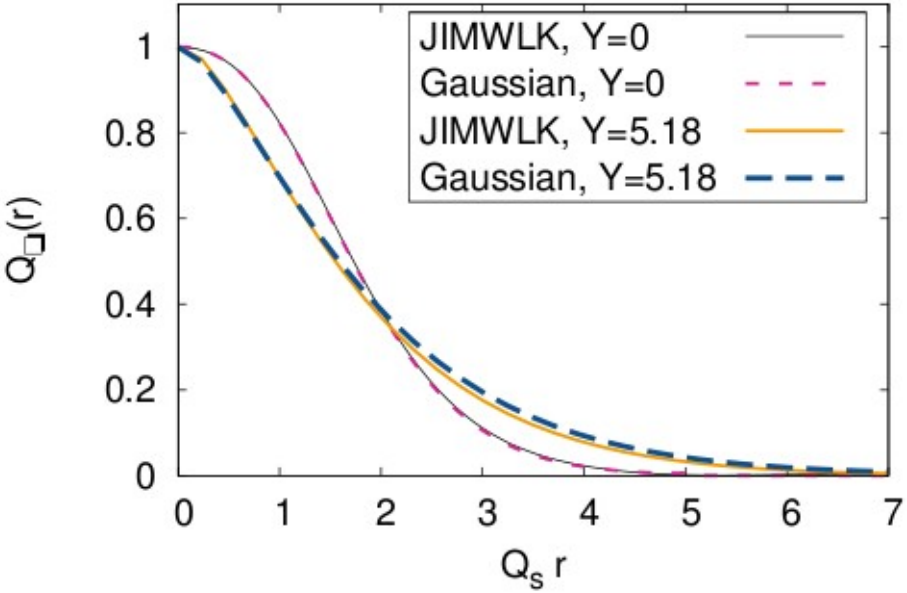

Quadrupole evolution

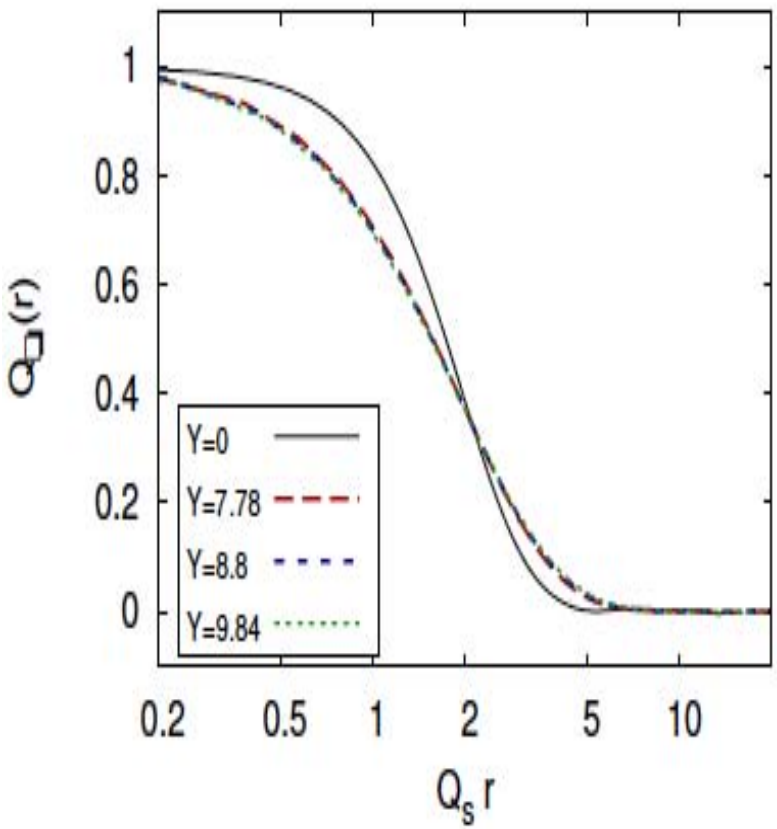

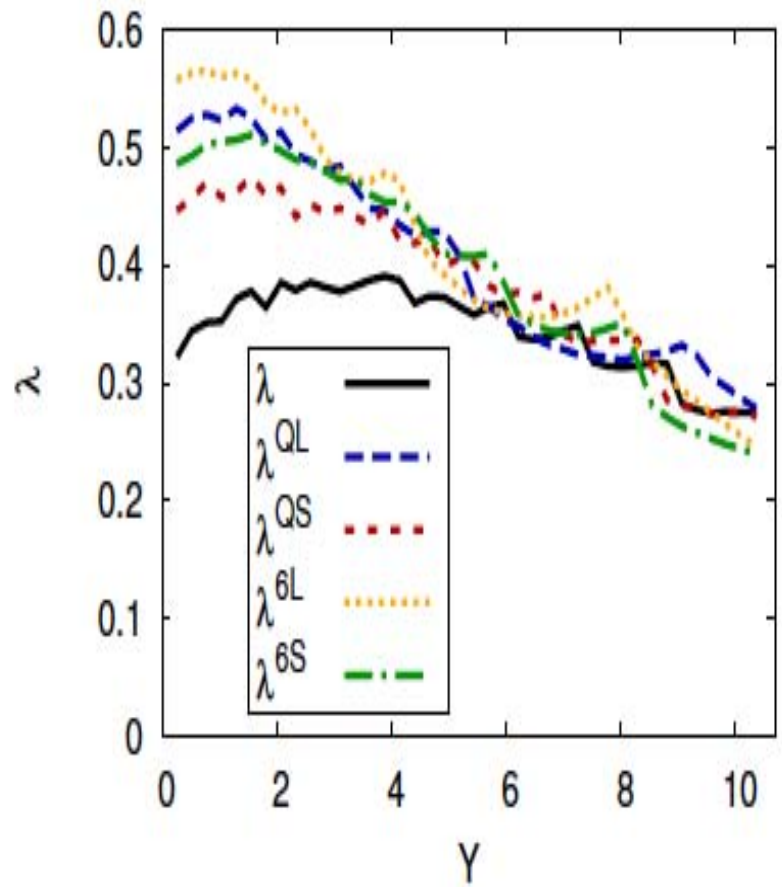

Geometric scaling also present in quadrupoles

Growth of the saturation scale

A simpler correlation to probe CGC: photon-hadron azimuthal correlation

based on arXiv:1204.1319

J. Jalilian-Marian and A. Rezaeian

photon-hadron azimuthal correlations

$$P(\Delta\theta) = \frac{d\sigma^{p(d)\,T\to h(q)\,\gamma(k)\,X}}{d^2\vec{b_t}\,dk_t^2\,dq_t^2\,dy_\gamma\,dy_l\,d\theta}[\Delta\theta] \Big/ \frac{d\sigma^{p(d)\,T\to h(q)\,\gamma(k)\,X}}{d^2\vec{b_t}\,dk_t^2\,dq_t^2\,dy_\gamma\,dy_l\,d\theta}[\theta = \theta_c]$$

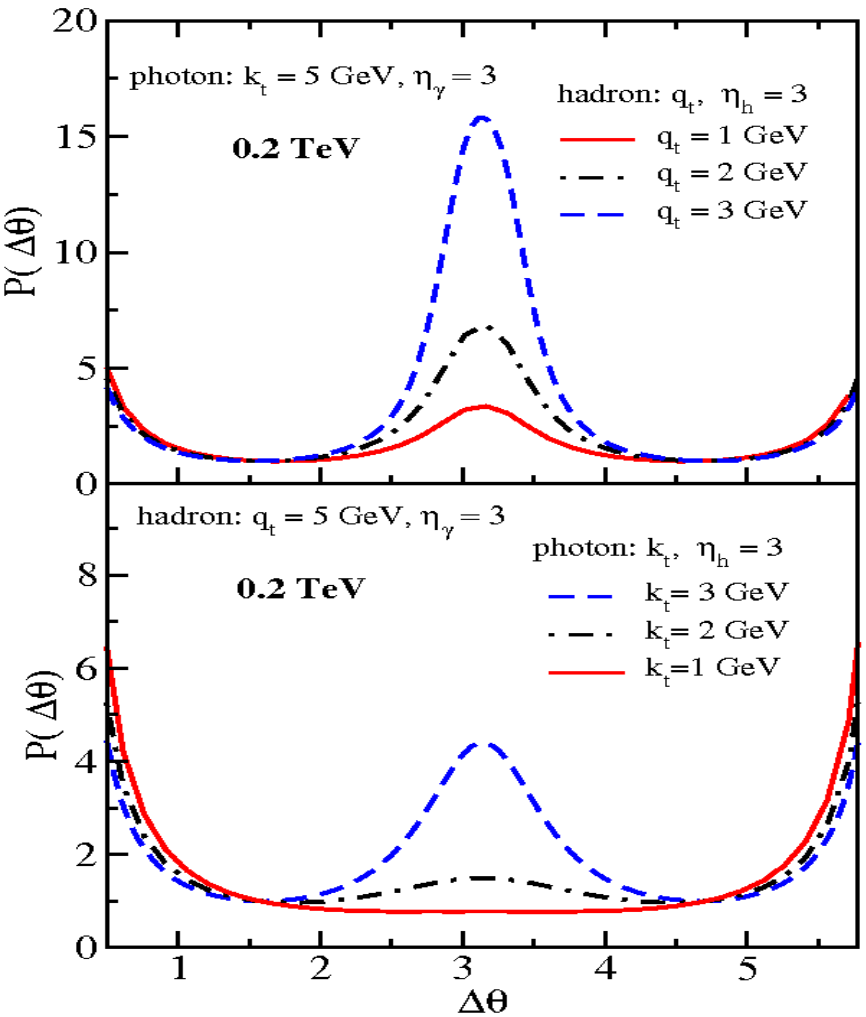

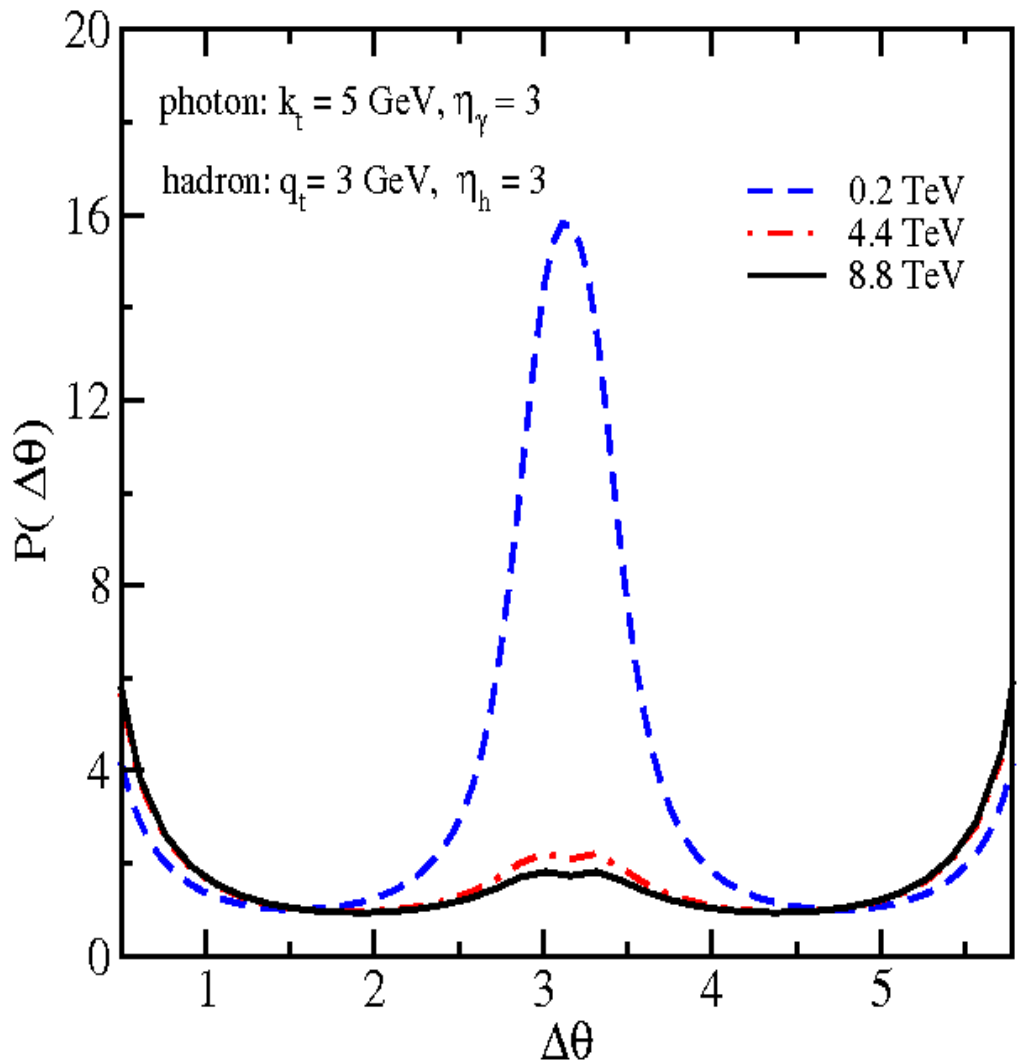

Centrality dependence

$$P(\Delta\theta) = \frac{d\sigma^{p(d)\,T\to h(q)\,\gamma(k)\,X}}{d^2\vec{b}_t\,dk_t^2\,dq_t^2\,dy_\gamma\,dy_l\,d\theta}[\Delta\theta] \Big/ \frac{d\sigma^{p(d)\,T\to h(q)\,\gamma(k)\,X}}{d^2\vec{b}_t\,dk_t^2\,dq_t^2\,dy_\gamma\,dy_l\,d\theta}[\theta=\theta_c]$$

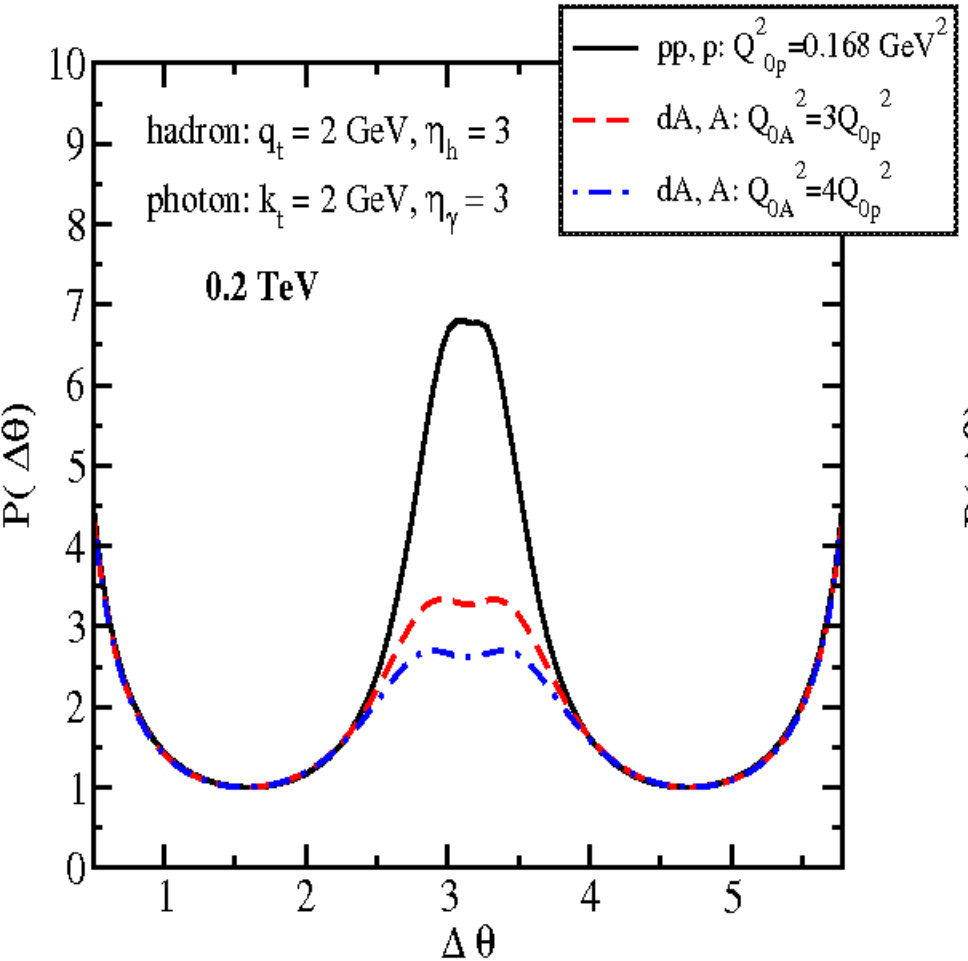

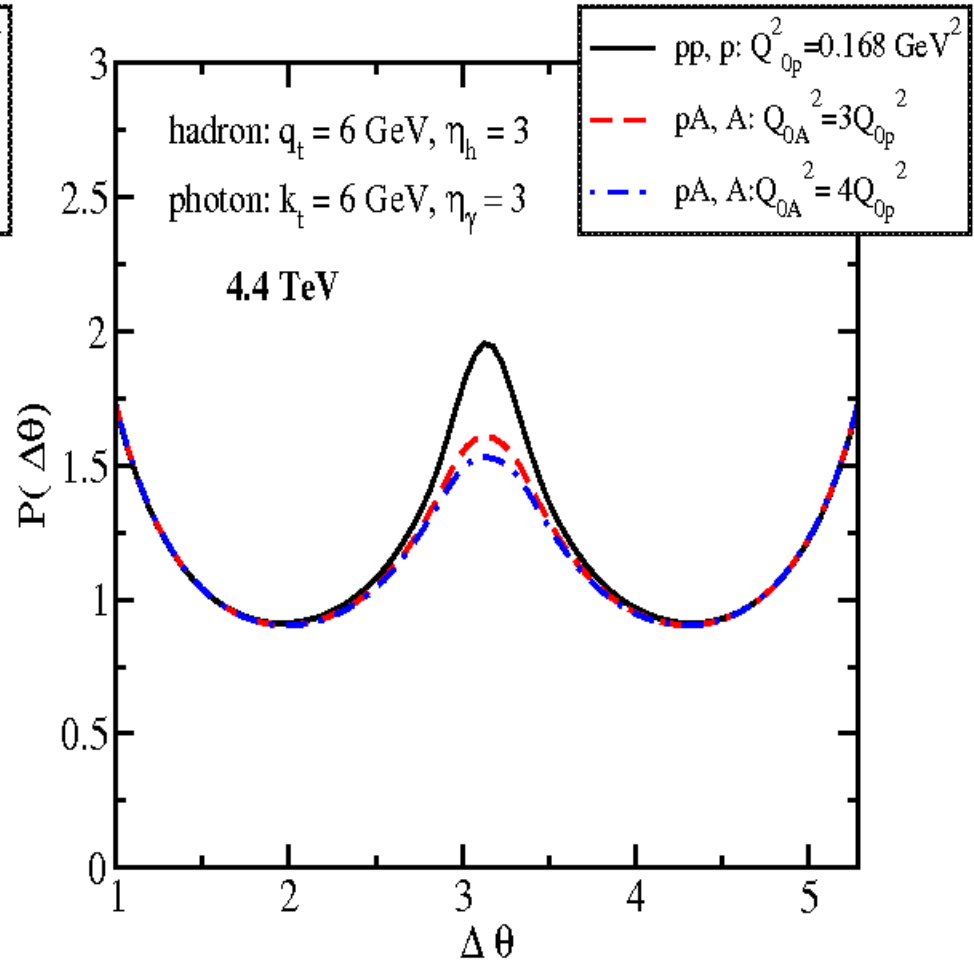

Photon production and photon-hadron correlations

new processes to probe the dynamics of high energy QCD

suppression of prompt photon spectrum in forward rapidity in p(d)A

disappearance of the away side peak in photon-hadron azimuthal correlations in p(d)A

need to measure these at RHIC/LHC

The role of initial conditions

McLerran-Venugopalan (93)

$$< \mathbf{O}(\rho) > \equiv \int \mathbf{D}[\rho]\, \mathbf{O}(\rho)\, \mathbf{W}[\rho]$$

$$\mathbf{W}[\rho] \simeq \mathbf{e}^{-\int \mathbf{d^2 x_t} \frac{\rho^{\mathbf{a}}(\mathbf{x_t})\rho^{\mathbf{a}}(\mathbf{x_t})}{\mathbf{2}\,\mu^{\mathbf{2}}}} \qquad \mu^{\mathbf{2}} \equiv \frac{\mathbf{g^2\, A}}{\mathbf{S_\perp}}$$

$$\mathbf{T(r_t)} \equiv \frac{\mathbf{1}}{\mathbf{N_c}} < \mathbf{Tr}\,[\mathbf{1} - \mathbf{V(r_t)}^\dagger\, \mathbf{V(0)}] > \sim \mathbf{1} - \mathbf{e}^{-[\mathbf{r_t^2\, Q_s^2}]^\gamma \log(\mathbf{e} + \frac{\mathbf{1}}{\mathbf{r_t\, \Lambda_{QCD}}})}$$

with $\gamma = \mathbf{1.119}$

how about higher order terms in ρ ?

$$\mathbf{W}[\rho] \simeq \mathbf{e}^{-\int \mathbf{d^2 x_t} \left[\frac{\rho^{\mathbf{a}}(\mathbf{x_t})\rho^{\mathbf{a}}(\mathbf{x_t})}{\mathbf{2}\,\mu^{\mathbf{2}}} - \frac{\mathbf{d^{abc}}\, \rho^{\mathbf{a}}(\mathbf{x_t})\rho^{\mathbf{b}}(\mathbf{x_t})\rho^{\mathbf{c}}(\mathbf{x_t})}{\kappa_{\mathbf{3}}} + \frac{\mathbf{F^{abcd}}\, \rho^{\mathbf{a}}(\mathbf{x_t})\rho^{\mathbf{b}}(\mathbf{x_t})\rho^{\mathbf{c}}(\mathbf{x_t})\rho^{\mathbf{d}}(\mathbf{x_t})}{\kappa_{\mathbf{4}}} \right]}$$

these higher order terms make the single inclusive spectra steeper and give <u>leading N_c</u> correlations (ridge)

Dumitru-Jalilian-Marian-Petreska, PRD84 (2011) 014018
Dumitru-Petreska,, arXiv:1112.4760 [hep-ph]

Two-hadron angular correlations

A unique window to dynamics of high energy QCD

We have just started to scratch the surface: there is much more to be understood

Sivers effect of Drell-Yan production in small-x regime

Zhong-Bo Kang

Theoretical Division, Group T-2
Los Alamos National Laboratory

Forward Physics at RHIC
RIKEN BNL Research Center Workshop
BNL, July 30-August 1, 2012

Outline

- Motivation
  - Why transverse spin and small-x could be probed at the same time?
- Single transverse spin asymmetry
  - Attempts to include small-x effect in the formalism for spin asymmetry
- Sivers effect of Drell-Yan production
  - Small-x formalism
  - Connection to TMD and collinear factorization
  - Numerical estimate
- Summary

Single transverse-spin asymmetry (SSA)

- Consider a transversely polarized proton scatter with an unpolarized proton

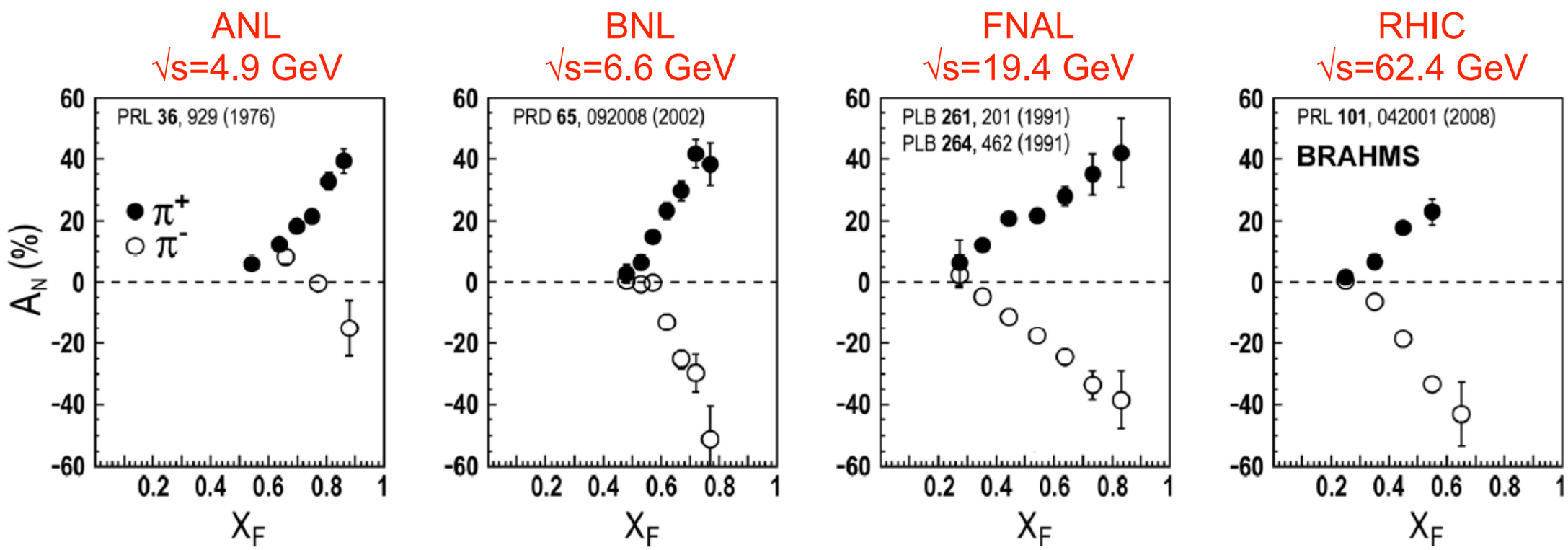

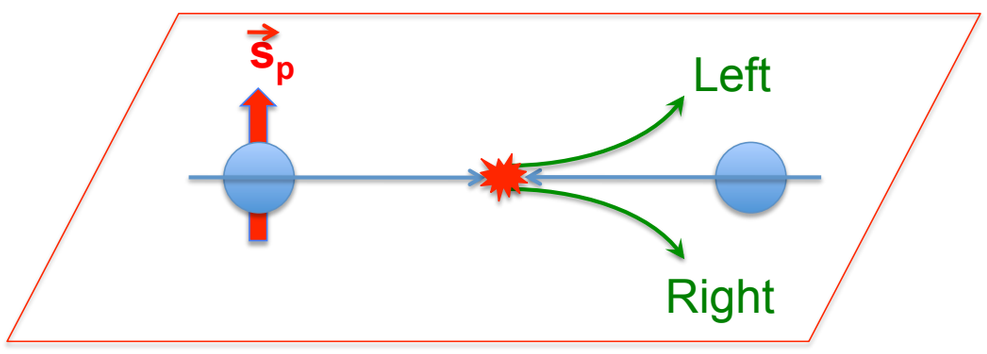

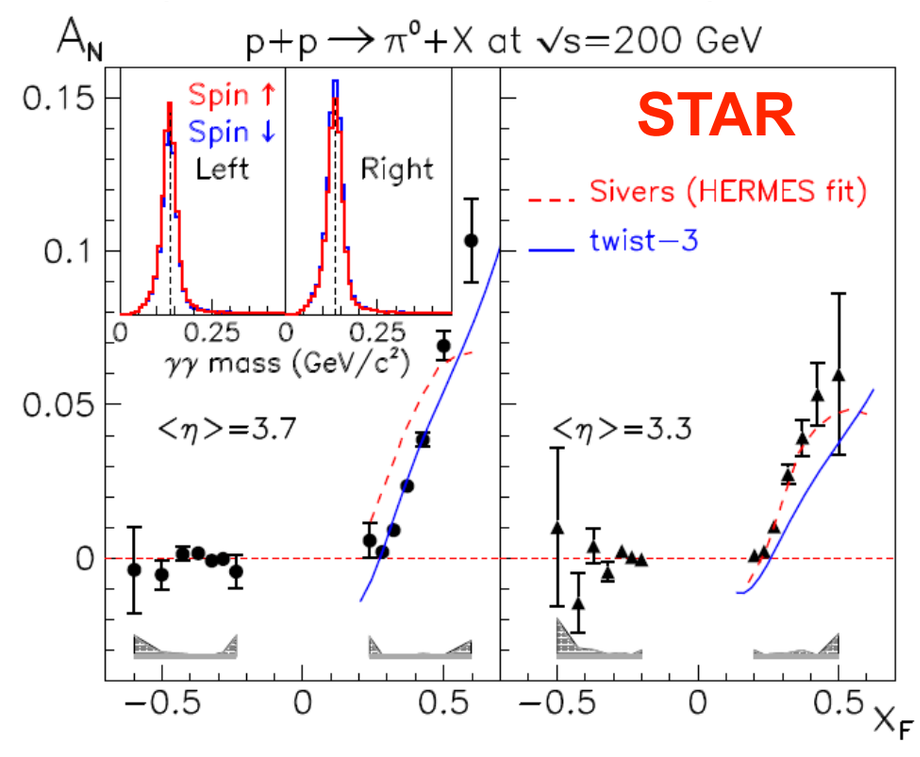

$$A_N \equiv \frac{\Delta\sigma(\ell,\vec{s})}{\sigma(\ell)} = \frac{\sigma(\ell,\vec{s}) - \sigma(\ell,-\vec{s})}{\sigma(\ell,\vec{s}) + \sigma(\ell,-\vec{s})}$$

Observation at high energy $\sqrt{s}$

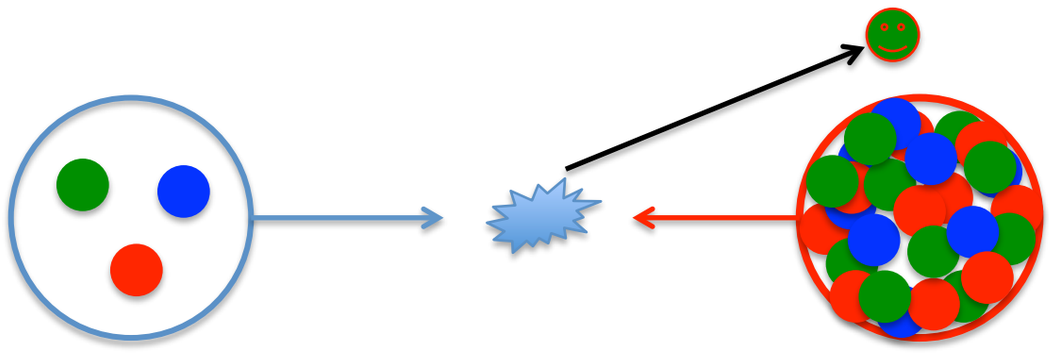

projectile: $x_1 \sim \frac{p_\perp}{\sqrt{s}} e^{+y} \sim 1$ valence

target: $x_2 \sim \frac{p_\perp}{\sqrt{s}} e^{-y} \ll 1$ gluon

- The spin asymmetry becomes the largest at forward rapidity region, corresponding to
  - The partons in the projectile (the polarized proton) have very large momentum fraction x: dominated by the valence quarks (spin effects are valence effects)
  - The partons in the target (the unpolarized proton or nucleus) have very small momentum fraction x: dominated by the small-x gluons
- Thus spin asymmetry in the forward region could probe both
  - The transverse spin effect from the valence quarks in the projectile: Sivers effect, and etc
  - The small-x gluon saturation physics in the target

Theoretical understanding in conventional factorization

- At leading twist formalism, assuming partons are collinear, the asymmetry is vanishing small

Kane-Pumplin-Repko, 1978

$\sigma(s_T) \sim$ 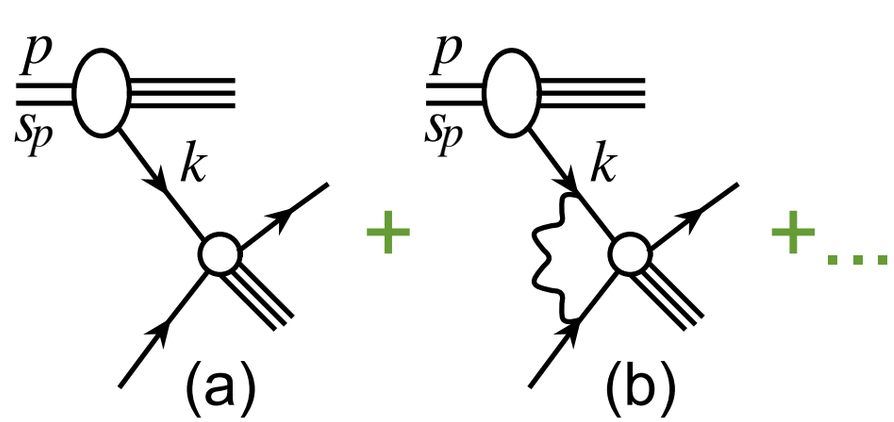

$+ \ldots \Big|^2$ ➡ $\Delta\sigma(s_T) \sim \mathrm{Re}[(a)]\cdot\mathrm{Im}[(b)]$

  - generate phase from loop diagrams, proportional to α_s
  - helicity is conserved for massless partons, helicity-flip is proportional to current quark mass m_q

Therefore we have

$$A_N \sim \alpha_s \frac{m_q}{\sqrt{s}} \frac{\delta q(x)}{\phi(x)}$$

$\delta q(x)$: tranversity

$\phi(x)$: unpolarized parton distribution

- $A_N \neq 0$: result of parton's transverse motion or correlations!

Understand SSA: related to parton transverse motion

- One could immediately think of two ways to include parton's transverse momentum into the formalism
  - Generalize the collinear distribution $f(x)$ to $f(x, k_\perp)$
  - Taylor expansion: $H(Q, k_\perp) = H(Q) + k_\perp H'(Q) + \cdots$, where $H'(Q) = dH(Q, k_\perp)/dk_\perp$ at $k_\perp = 0$, then ∫d²kt kt f(x,kt) = a higher-twist correlation
- The first one is called TMD approach (SIDIS, DY at low pt), the second one is called collinear twist-3 approach (pp→hX at high pt). They are closely related to each other.

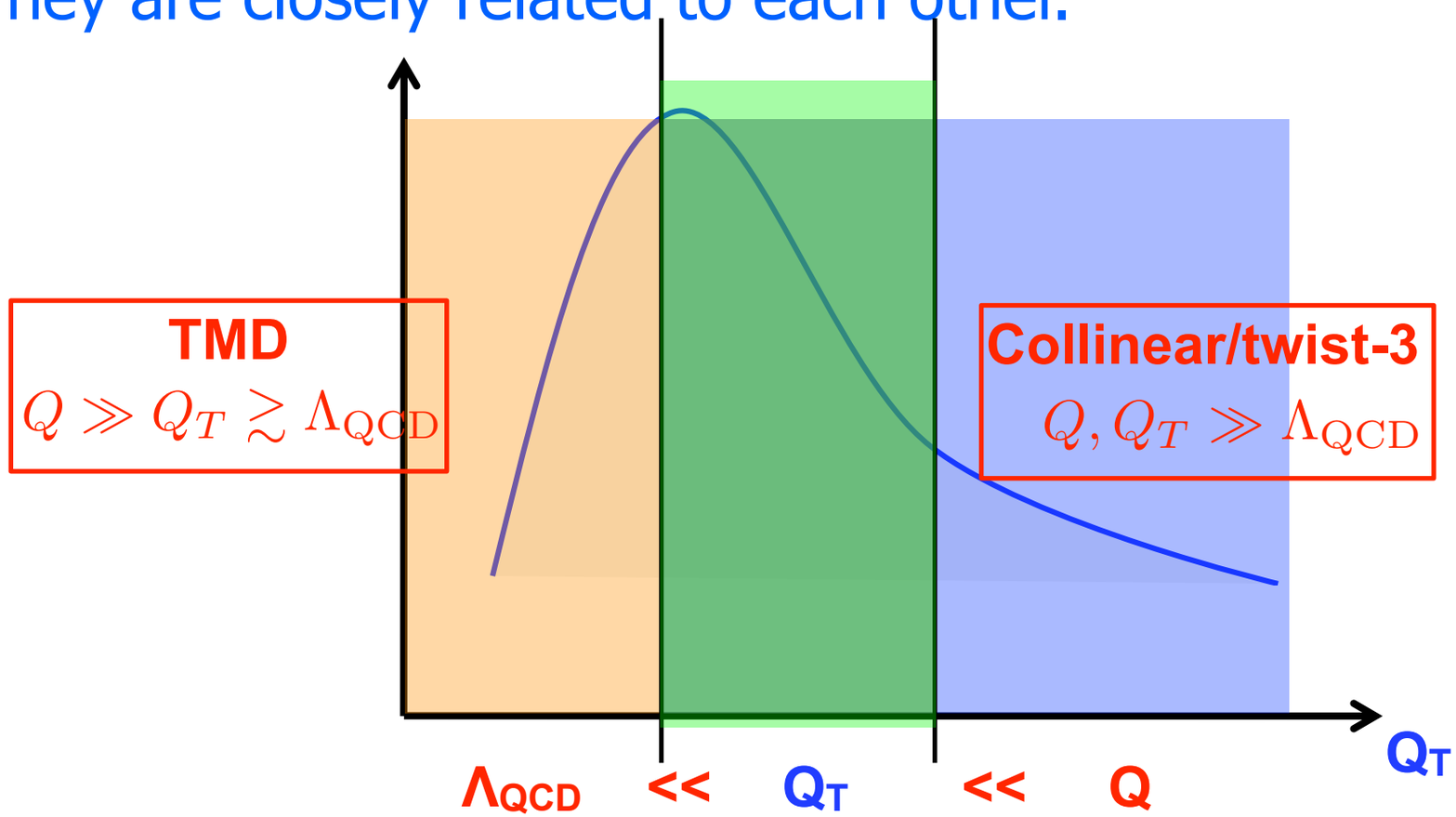

Inclusive hadron production at forward rapidity

- Gluon dipole distribution: numerical solution of BK equation

$$p + A \to h + X$$

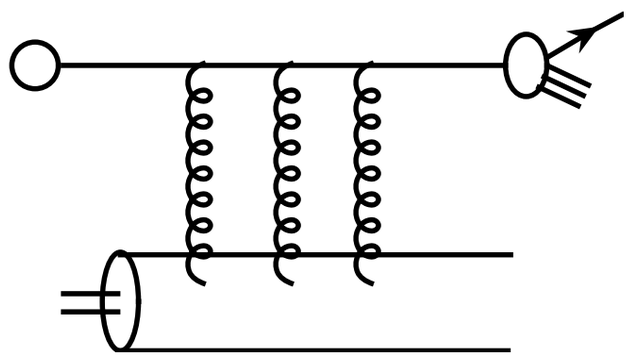

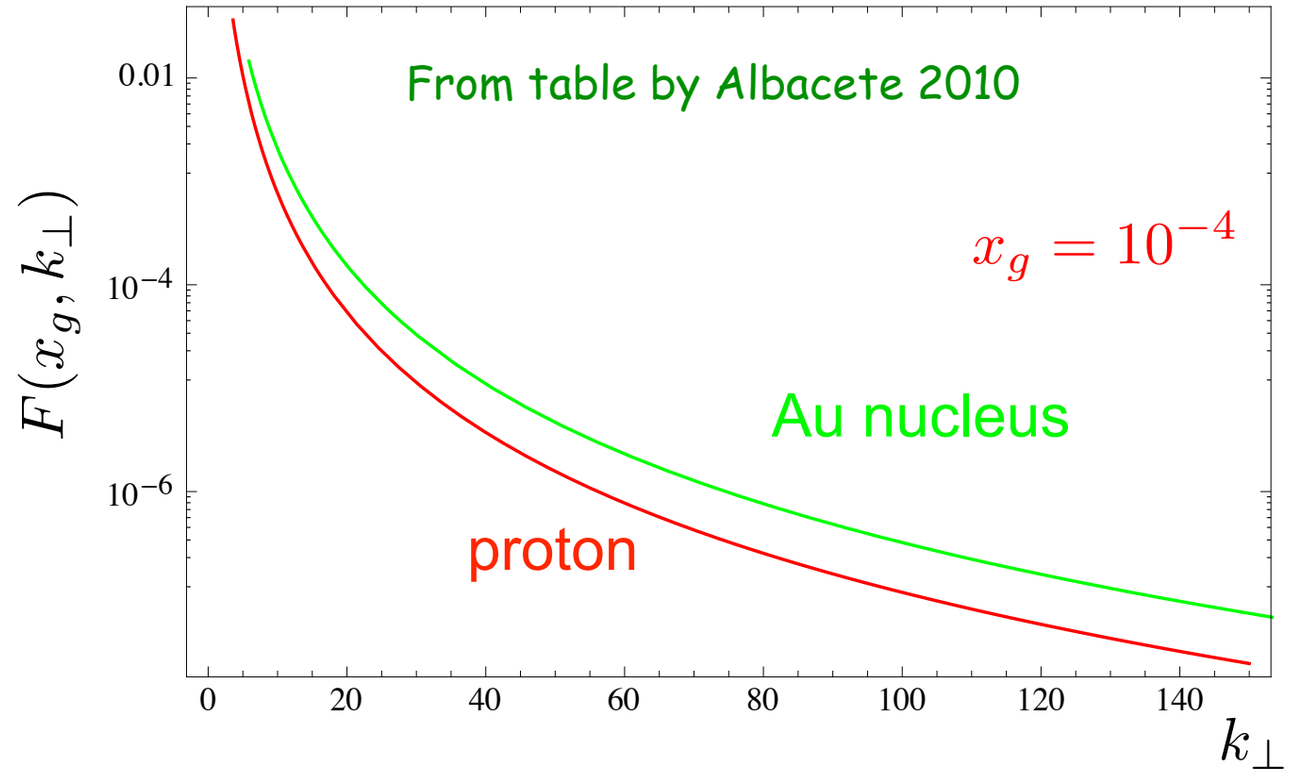

- Comparison with RHIC data

Albaete-Marquet, 2010

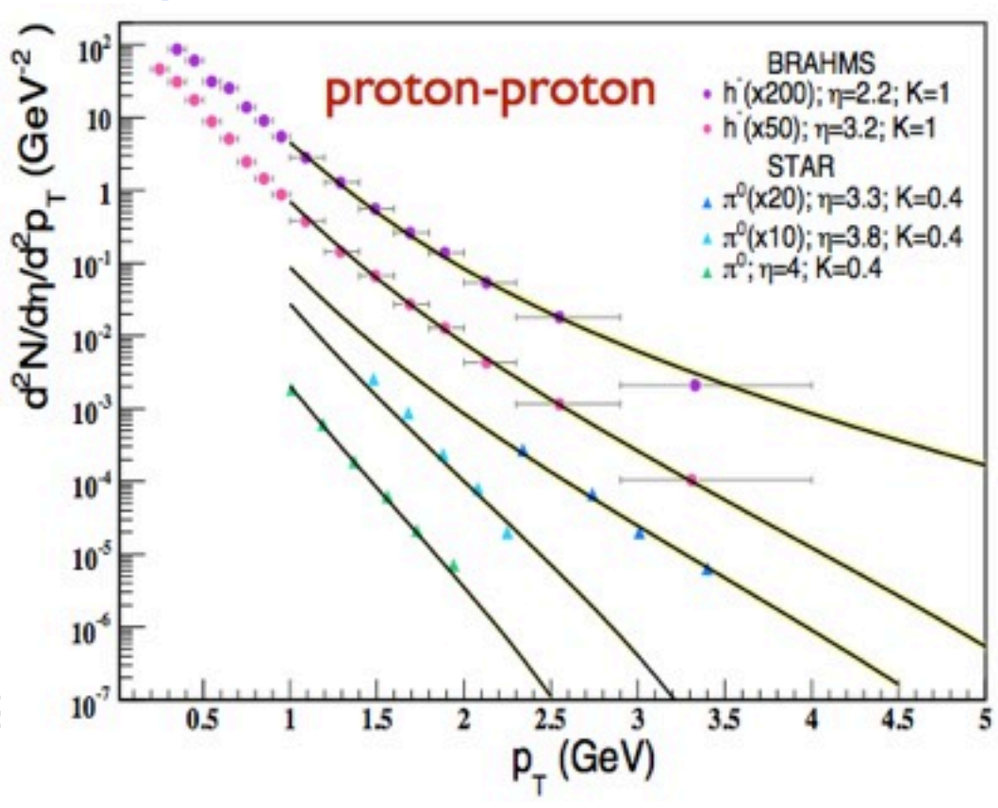

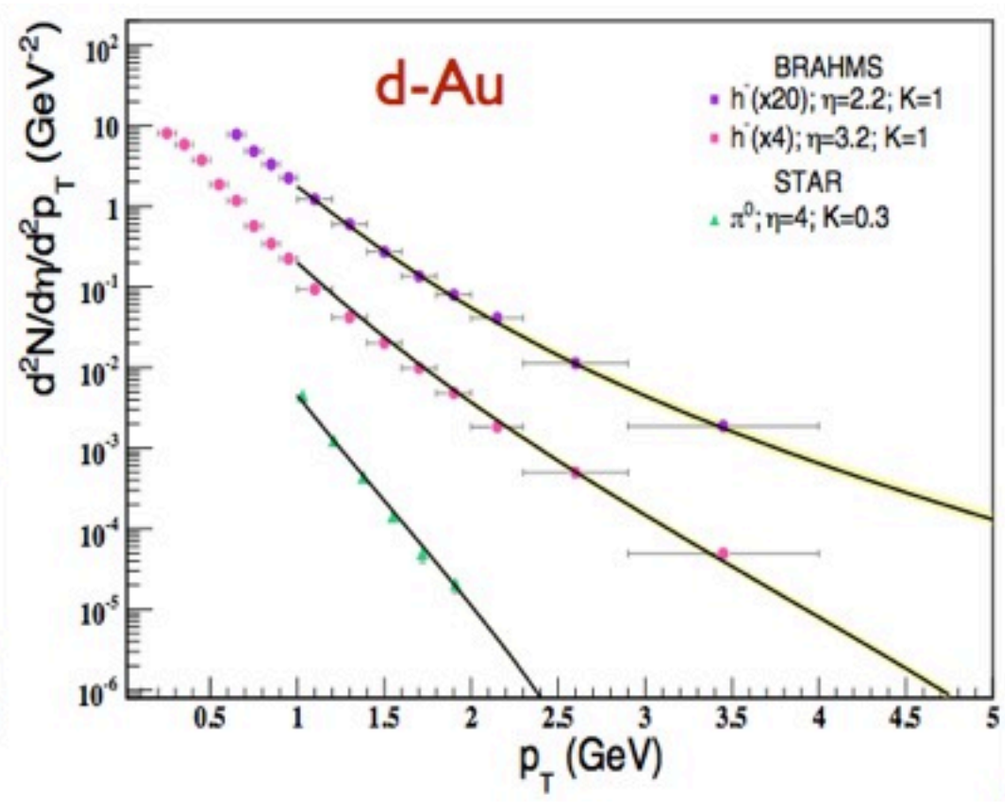

SSA of inclusive hadron production

- The source of single spin correlation for $A^{\uparrow} + B \to h(p_\perp) + X$

$$
\begin{aligned}
\Delta\sigma \quad = \quad & T_{a,F}(x,x) \otimes \phi_{b/B}(x') \otimes H_{ab\to c}(p_\perp, \vec{s}_T) \otimes D_{c\to h}(z) && \text{(I)} \\
+ \quad & \delta q_{a/A}(x) \otimes T^{(\sigma)}_{b,F}(x',x') \otimes H'_{ab\to c}(p_\perp, \vec{s}_T) \otimes D_{c\to h}(z) && \text{(II)} \\
+ \quad & \delta q_{a/A}(x) \otimes \phi_{b/B}(x') \otimes H''_{ab\to c}(p_\perp, \vec{s}_T) \otimes D^{(3)}_{c\to h}(z,z) && \text{(III)} \\
+ \quad & m_q \delta q_{a/A}(x) \otimes \phi_{b/B}(x') \otimes H'''_{ab\to c}(p_\perp, \vec{s}_T) \otimes D_{c\to h}(z) && \text{(IV)}
\end{aligned}
$$

Term	meaning	collinear	small-x	Remarks
(I)	Sivers $T_{q,F}(x,x)$	Qiu-Sterman 91, 98 hep-ph/9806356	Boer-Dumitru-Hayashigaki, 2006 hep-ph/0609083	process dependence of Sivers function
(II)	Boer-Mulders $T^{(\sigma)}_{q,F}(x',x')$	Kanazawa-Koike, 2000 hep-ph/000727		small in the collinear formalism
(III)	Collins $D^{(3)}_{c\to h}(z,z)$	Kang-Yuan-Zhou, 2010 1002.0399	Kang-Yuan, 2011 1106.1375	Collins function is universal
(IV)	Kane-Pumplin-Repko $m_q \delta q(x)$	Kane-Pumplin-Repko, 1978	(different from KPR) Kovchegov-Sievert 1201.5890	small?? (because of quark mass?)

Collins effect: include spin in the fragmentation process

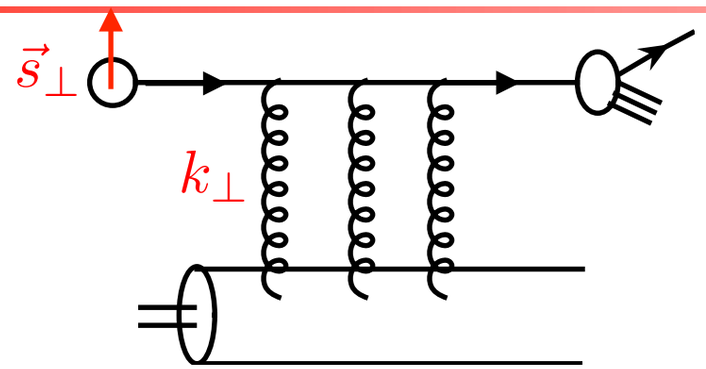

Kang-Yuan, arXiv: 1106.1375

$$P_{h\perp} = z\, k_\perp + P_{hT}$$

- Spin effect is always associated with the parton transverse momentum
  - generalized to include small transverse momentum in the fragmentation process

$$\frac{d\sigma}{dy_h d^2 P_{h\perp}} = \frac{K}{(2\pi)^2} \int_{x_F}^1 \frac{dz}{z^2} \int d^2 P_{hT} x_1 q(x_1) N_F(x_2, k_\perp) D_{h/q}(z, P_{hT})$$

  - Now we could introduce Collins function in the game

Collins function

$$\frac{d\Delta\sigma}{dy_h d^2 P_{h\perp}} = \frac{K}{(2\pi)^2} \int_{x_F}^1 \frac{dz}{z^2} \int d^2 P_{hT} I(S_\perp, P_{hT}) x_1 h(x_1) N_F(x_2, k_\perp) \delta\hat{q}(z, P_{hT})$$

$$I(S_\perp, P_{hT}) = \epsilon^{\alpha\beta} S_\perp^\alpha \left[P_{hT}^\beta - \frac{n \cdot P_{hT}}{n \cdot P_J} P_J^\beta \right] = |S_\perp||P_{hT}| \sin(\phi_h - \phi_s)$$

  - Nice thing: Collins function is universal, independent of gauge link

Data seems to support scaling analysis

- Scaling analysis for pt and xf dependence

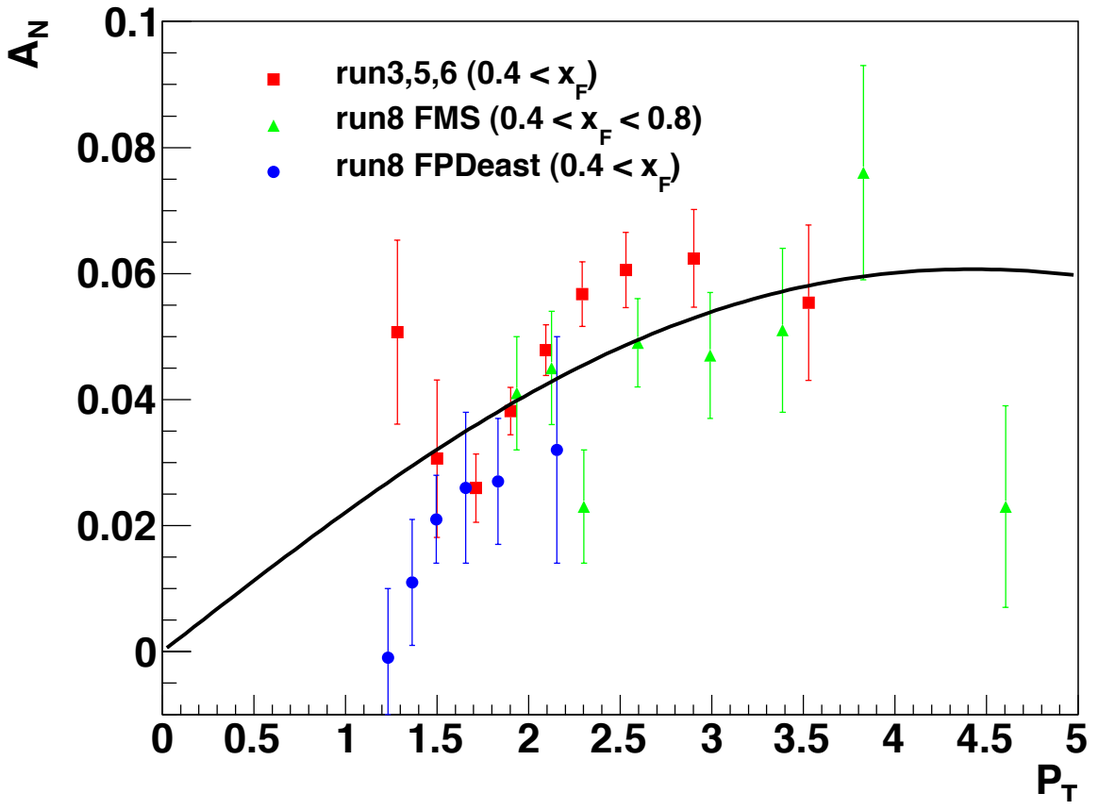

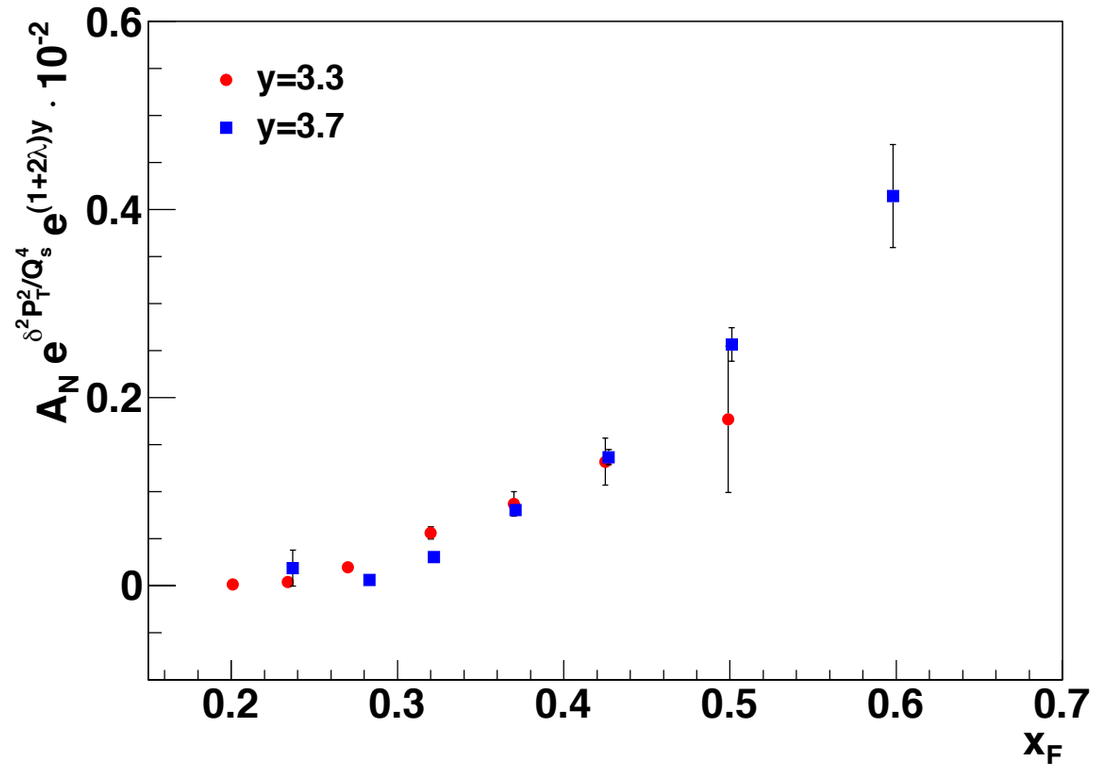

$$A_N \sim \frac{P_{h\perp}\Delta}{Q_s^2} e^{-\frac{\delta^2 P_{h\perp}^2}{(Q_s^2)^2}}$$

$$A_N e^{\delta^2 P_{h\perp}^2/Q_s^4} e^{(1+2\lambda)y_h} \sim x_F^{(1+\lambda)} \mathcal{F}(x_F)$$

- Compare pp and pA collisions

$$\frac{A_N^{pA\to h}}{A_N^{pp\to h}}\Big|_{P_{h\perp}\ll Q_s^2} \approx \frac{Q_{sp}^2}{Q_{sA}^2} e^{\frac{P_{h\perp}^2\delta^2}{Q_{sp}^4}} \qquad \frac{A_N^{pA\to h}}{A_N^{pp\to h}}\Big|_{P_{h\perp}\gg Q_s^2} \approx 1$$

Why Drell-Yan is so interesting: physics of gauge link

- Rescattering (gauge link) determined by hard process and its color flow

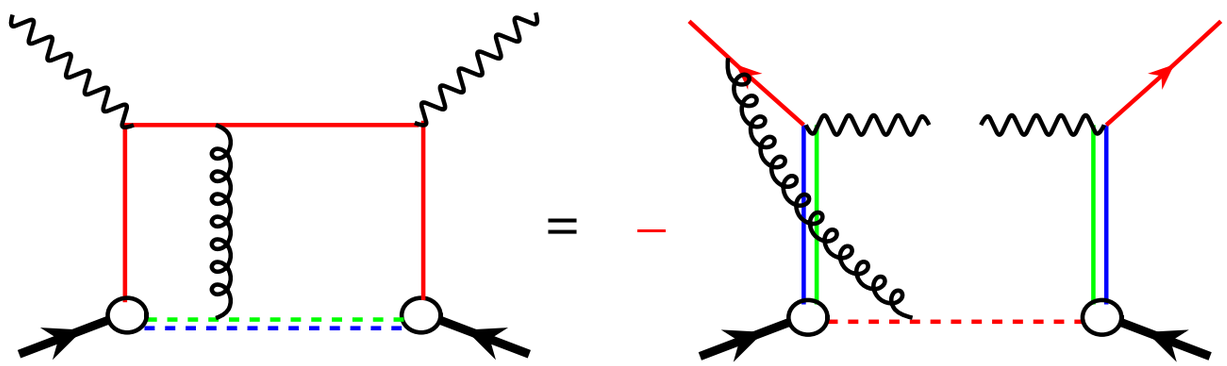

SIDIS = – DY

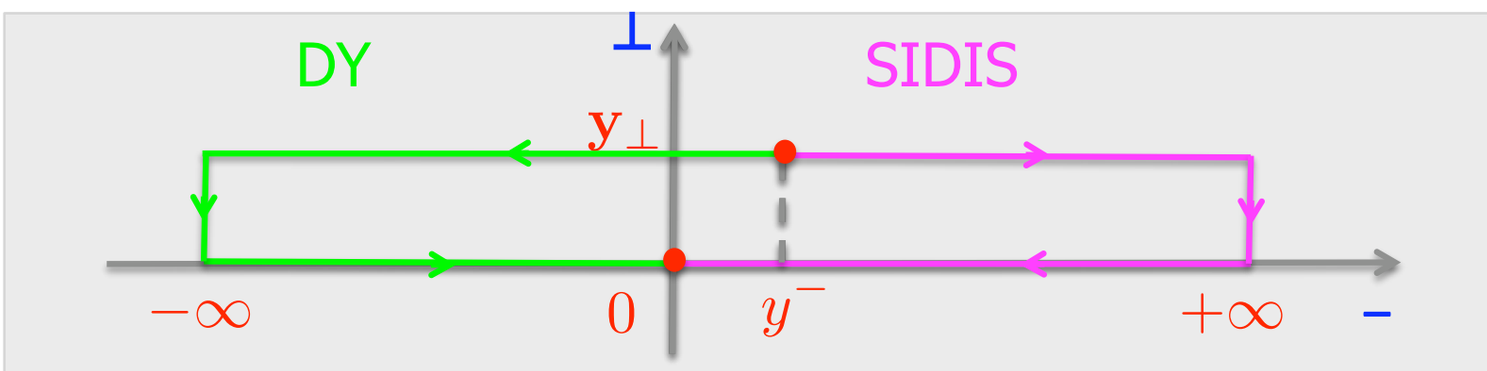

$$\Delta^N f^{\rm SIDIS}_{q/h^\uparrow}(x,k_\perp) = -\Delta^N f^{\rm DY}_{q/h^\uparrow}(x,k_\perp)$$

Central quest for the field at the moment

- Because gauge link is generated in the factorization procedure, for spin effect in small-x formalism, it is important to analyze the factorization properties

Sivers function from SIDIS $\ell + p^{\uparrow} \to \ell' + \pi(p_T) + X : \quad p_T \ll Q$

- Extract Sivers function from SIDIS (HERMES&COMPASS): a fit

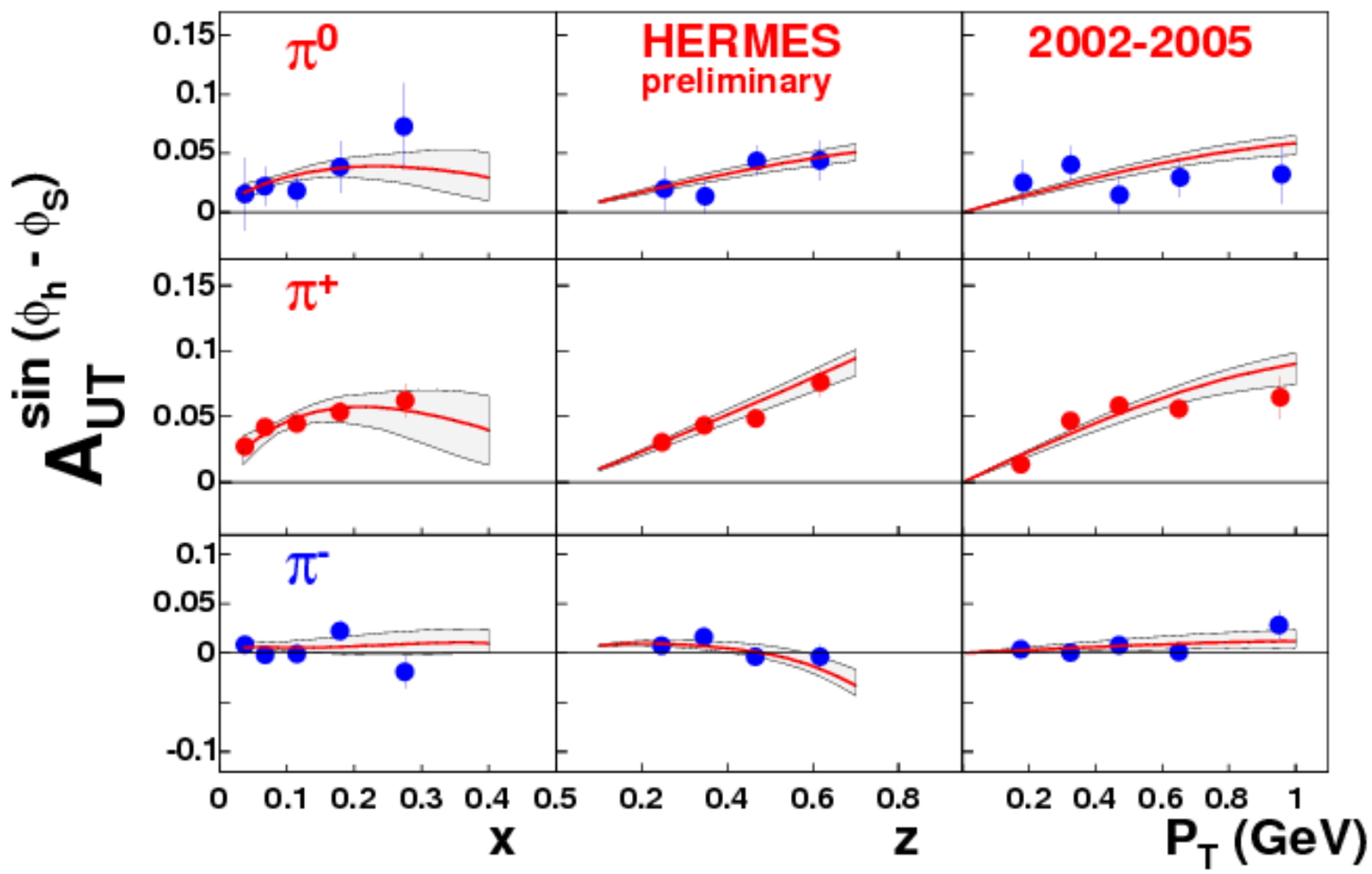

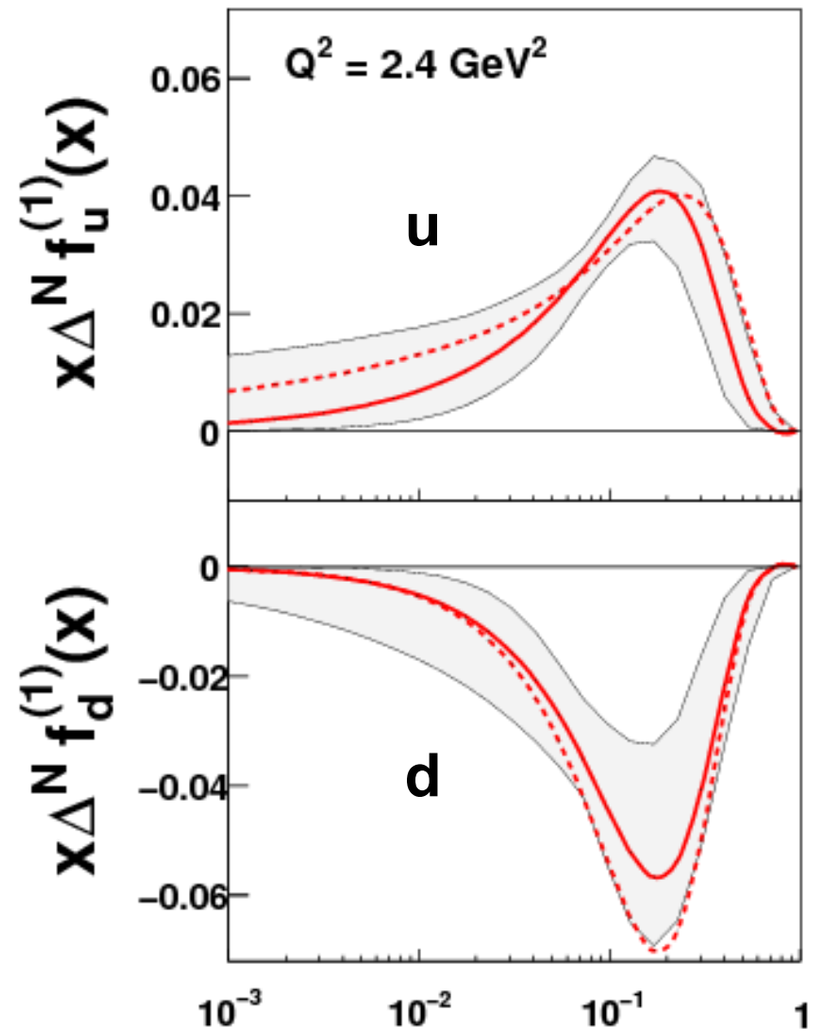

Anselmino, et.al., 2009

- u and d almost equal size, different sign
- d-Sivers is slightly larger

- Still needs DY results to verify the sign change, thus fully understand the mechanism of the SSAs

Drell-Yan production in small-x regime

- At leading order, Drell-Yan production is simple $p^{\uparrow} + A \to [\gamma^* \to]\ell^+\ell^- + X$
  - quark (from polarized proton) scatters off the classical gluon field to produce a virtual photon

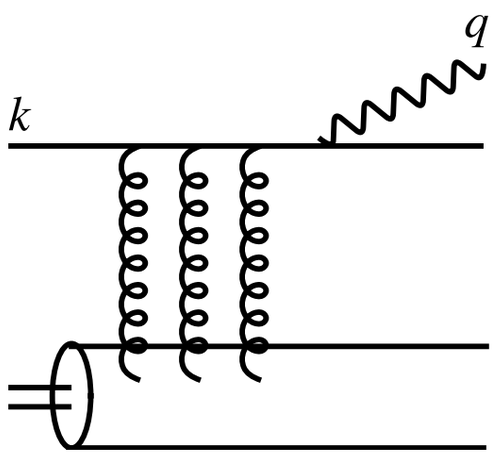

Kopeliovich-Raufeisen-Tarasov 01, Baier-Mueller-Schiff 04, Gelis-Jalilian-Marian 02, 03, Stasto-Xiao-Zaslavsky, 2012

- When high-energy partons scatter off the classic gluon field, the interaction is eikonal in that the projectile propagate through the target without changing their transverse position but picking up an eikonal phase

Bjorken-Kogut-Soper, 1971

$$\mathcal{S}|k^+, b, i\rangle \otimes |\mathcal{A}\rangle = U^{ij}[\mathcal{A}]|k^+, b, j\rangle \otimes |\mathcal{A}\rangle$$

$$U(x) = \mathcal{P}\exp\left\{ig_s \int_{-\infty}^{+\infty} dx^+ T^c A_c^-(x^+, x_\perp)\right\}$$

Quark splitting wave function: keep quark kt from proton

- Quark to photon splitting wave function in light-front perturbation theory $q \to q + \gamma^*$

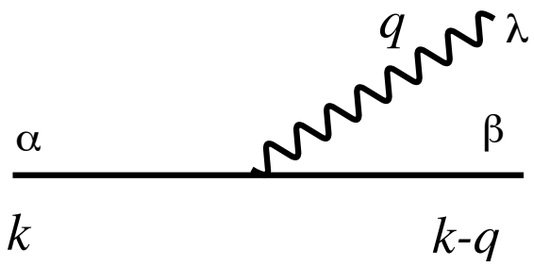

$$z = q^+/k^+ \qquad \epsilon_M^2 = (1-z)M^2$$

- In momentum space

$$\phi^\lambda_{\alpha\beta}(k,q) = \frac{1}{\sqrt{8(k-q)^+k^+q^+}} \frac{\bar{u}_\beta(k-q)\gamma_\mu \epsilon^\mu(q,\lambda)u_\alpha(k)}{(k-q)^- + q^- - k^-}$$

- In transverse coordinate space: $\psi^\lambda_{\alpha\beta}(k,q^+,r) = \int d^2q_\perp e^{iq_\perp\cdot r}\phi^\lambda_{\alpha\beta}(k,q)$

$$\psi^{T\lambda}_{\alpha\beta}(k,q^+,r) = 2\pi\sqrt{\frac{2}{q^+}} e^{izk_\perp\cdot r} i\epsilon_M K_1(\epsilon_M|r|) \begin{cases} \frac{r\cdot\epsilon_\perp^1}{|r|}\left[\delta_{\alpha-}\delta_{\beta-} + (1-z)\delta_{\alpha+}\delta_{\beta+}\right], & \lambda = 1, \\ \frac{r\cdot\epsilon_\perp^2}{|r|}\left[\delta_{\alpha+}\delta_{\beta+} + (1-z)\delta_{\alpha-}\delta_{\beta-}\right], & \lambda = 2. \end{cases}$$

$$\psi^L_{\alpha\beta}(k,q^+,r) = 2\pi\sqrt{\frac{2}{q^+}} e^{izk_\perp\cdot r}(1-z)MK_0(\epsilon_M|r|)\delta_{\alpha\beta}$$

The multiple scattering could happen before or after

- The interaction with the target could happen before or after the splitting of the virtual photon

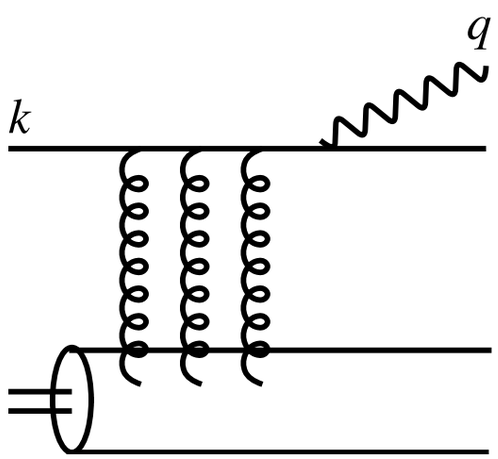

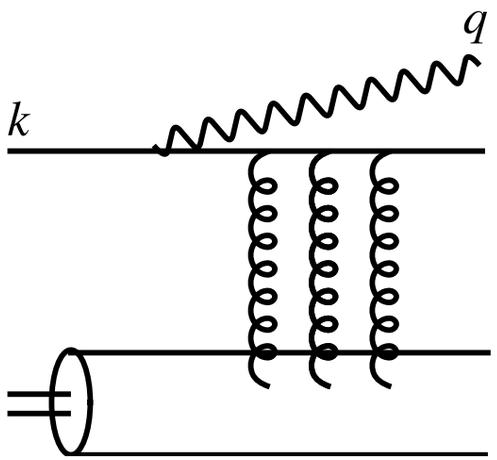

- The differential cross section for $q + A \to \gamma^* + X$

$$\frac{d\sigma(qA \to \gamma^* X)}{dq^+ d^2 q_\perp} = \alpha_{\rm em} e_q^2 \int \frac{d^2 b}{(2\pi)^2} \frac{d^2 r}{(2\pi)^2} \frac{d^2 r'}{(2\pi)^2} e^{-iq_\perp \cdot (r - r')} \sum_{\alpha\beta\lambda} \psi^{*\lambda}_{\alpha\beta}(k, q^+, r' - b) \psi^{\lambda}_{\alpha\beta}(k, q^+, r - b)$$
$$\times \left[1 + S^{(2)}_{x_A}(v, v') - S^{(2)}_{x_A}(b, v') - S^{(2)}_{x_A}(v, b) \right]$$

  - multiple scattering is taken care of by

$$S^{(2)}_{x_A}(x, y) = \frac{1}{N_c} \left\langle \mathrm{Tr}\left(U(x) U^\dagger(y) \right) \right\rangle_{x_A}$$

Transform to momentum space

- To better compare with TMD factorization, let's transform to momentum space

$$\frac{d\sigma(qA \to \gamma^* X)}{dy d^2 q_\perp} = \frac{\alpha_{\rm em}}{2\pi^2} e_q^2 \int d^2 b d^2 p_\perp F(x_A, p_\perp) \left[H_T(q_\perp, k_\perp, p_\perp, z) + H_L(q_\perp, k_\perp, p_\perp, z) \right]$$

  - Unintegrated gluon distribution (dipole gluon distribution)

$$F(x_A, p_\perp) = \int \frac{d^2 r_\perp}{(2\pi)^2} e^{i p_\perp \cdot r_\perp} \frac{1}{N_c} \left\langle \mathrm{Tr}\left(U(0) U^\dagger(r_\perp) \right) \right\rangle_{x_A}$$

  - Hard-part functions (transverse and longitudinal polarized photon)

$$\begin{aligned} H_T(q_\perp, k_\perp, p_\perp, z) &= \left[1 + (1-z)^2\right] \left[\frac{q_\perp - z k_\perp}{(q_\perp - z k_\perp)^2 + \epsilon_M^2} - \frac{q_\perp - z k_\perp - z p_\perp}{(q_\perp - z k_\perp - z p_\perp)^2 + \epsilon_M^2} \right]^2 \\ H_L(q_\perp, k_\perp, p_\perp, z) &= 2(1-z)^2 M^2 \left[\frac{1}{(q_\perp - z k_\perp)^2 + \epsilon_M^2} - \frac{1}{(q_\perp - z k_\perp - z p_\perp)^2 + \epsilon_M^2} \right]^2 \end{aligned}$$

Unpolarized quark distribution

- The probability to find unpolarized quark in transversely polarized proton
  - Spin-averaged quark distribution
  - Sivers function: an asymmetric parton distribution in a polarized hadron (kt correlated with the spin of the hadron)

Spin-dependent

$$f_{q/p^\uparrow}(x,k_\perp) = f_{q/p}(x,k_\perp^2) + \frac{\epsilon_{\alpha\beta} s_\perp^\alpha k_\perp^\beta}{M_p} f_{1T}^{\perp,q}(x,k_\perp^2)$$

Spin-independent

Differential cross section in pp and pA collisions

- Spin-averaged virtual photon cross section

$$\frac{d\sigma(p^\uparrow A \to \gamma^* X)}{dy d^2 q_\perp} = \frac{\alpha_{\rm em}}{2\pi^2}\sum_q e_q^2 \int_{x_p}^1 \frac{dz}{z} d^2k_\perp x f_{q/p}(x,k_\perp^2) \int d^2b d^2p_\perp F(x_A,p_\perp) \times \left[H_T(q_\perp,k_\perp,p_\perp,z) + H_L(q_\perp,k_\perp,p_\perp,z)\right]$$

- Spin-dependent virtual photon cross section

$$\frac{d\Delta\sigma(p^\uparrow A \to \gamma^* X)}{dy d^2 q_\perp} = \frac{\alpha_{\rm em}}{2\pi^2}\sum_q e_q^2 \int_{x_p}^1 \frac{dz}{z} d^2k_\perp \frac{\epsilon_{\alpha\beta} s_\perp^\alpha k_\perp^\beta}{M_p} x f_{1T}^{\perp,q}(x,k_\perp^2) \int d^2b d^2p_\perp F(x_A,p_\perp) \times \left[H_T(q_\perp,k_\perp,p_\perp,z) + H_L(q_\perp,k_\perp,p_\perp,z)\right]$$

- Virtual photon to DY lepton pair production

$$\frac{d\sigma(p^\uparrow A \to \ell^+\ell^- X)}{dM^2 dy d^2 q_\perp} = \frac{\alpha_{\rm em}}{3\pi M^2}\frac{d\sigma(p^\uparrow A \to \gamma^* X)}{dy d^2 q_\perp}$$

- Single transverse spin asymmetry

$$A_N = \frac{d\Delta\sigma(p^\uparrow A \to \ell^+\ell^- X)}{dM^2 dy d^2 q_\perp} \Big/ \frac{d\sigma(p^\uparrow A \to \ell^+\ell^- X)}{dM^2 dy d^2 q_\perp}$$

Compare to the usual TMD factorization formalism

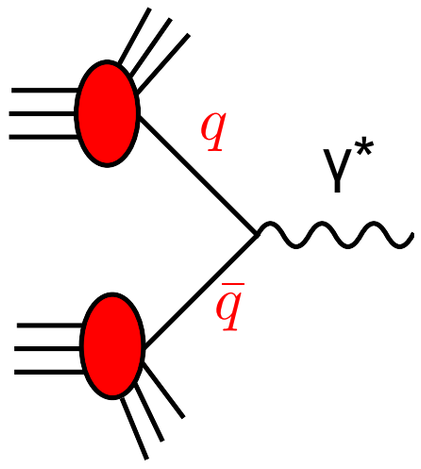

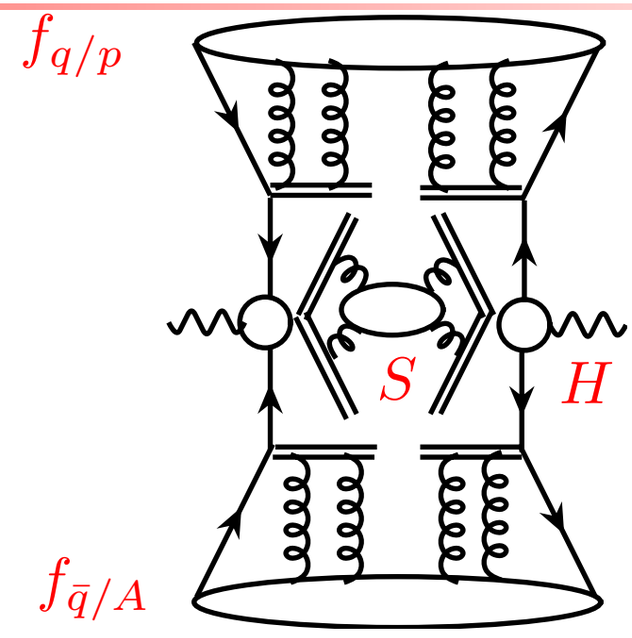

- The spin-averaged cross section in TMD factorization formalism

$$\frac{d\sigma(p^\uparrow A \to \ell^+\ell^- X)}{dM^2 dy d^2q_\perp} = \frac{4\pi\alpha_{\rm em}^2}{3N_c M^4}\sum_q e_q^2 \int d^2k_\perp d^2\ell_\perp d^2\lambda_\perp \delta^2\left(k_\perp+\ell_\perp+\lambda_\perp-q_\perp\right)$$
$$\times x_p f_{q/p}(x_p,k_\perp^2) x_A f_{\bar{q}/A}(x_A,\ell_\perp^2) H(M^2,x_p,x_A) S(\lambda_\perp)$$

- For spin-dependent cross section

$$\frac{d\Delta\sigma(p^\uparrow A \to \ell^+\ell^- X)}{dM^2 dy d^2q_\perp} = \frac{4\pi\alpha_{\rm em}^2}{3N_c M^4}\sum_q e_q^2 \int d^2k_\perp d^2\ell_\perp d^2\lambda_\perp \delta^2\left(k_\perp+\ell_\perp+\lambda_\perp-q_\perp\right)$$
$$\times \frac{\epsilon_{\alpha\beta} s_\perp^\alpha k_\perp^\beta}{M_p} x_p f_{1T}^{\perp,q}(x_p,k_\perp^2) x_A f_{\bar{q}/A}(x_A,\ell_\perp^2) H(M^2,x_p,x_A) S(\lambda_\perp)$$

- How could the gluon distribution come in the game?

Quark distribution can be generated from the UGD

- Anti-quark distribution is generated from unintegrated gluon distribution

Marquet-Xiao-Yuan, 2009

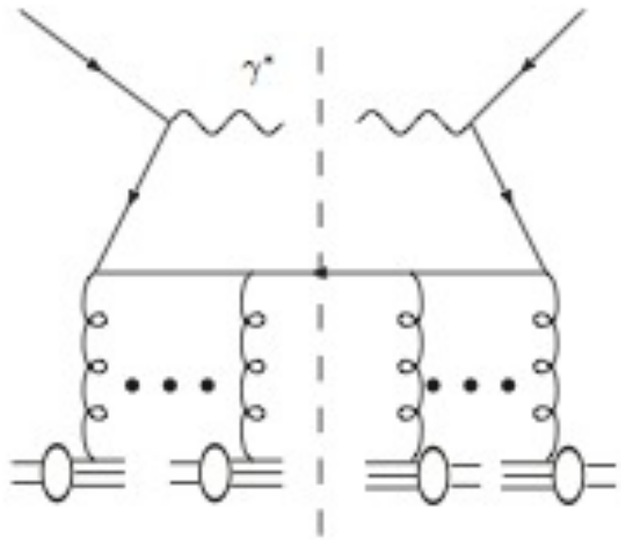

- This generation in the perturbative region can be easily computed

$$f_{\bar{q}/A}(x_A, \ell_\perp^2) = \frac{N_c}{8\pi^4} \int \frac{d\hat{z}}{x_A} \int d^2b d^2p_\perp F(x_A, p_\perp) A(p_\perp, \ell_\perp, \hat{z})$$

$$A(p_\perp, \ell_\perp, \hat{z}) = \left[\frac{\ell_\perp |\ell_\perp - p_\perp|}{(1-\hat{z})\ell_\perp^2 + \hat{z}(\ell_\perp - p_\perp)^2} - \frac{\ell_\perp - p_\perp}{|\ell_\perp - p_\perp|} \right]^2$$

TMD factorization in terms of dipole gluon distribution

- Since anti-quark distribution is expanded to NLO, we keep the LO for hard and soft factor

$$H(M^2, x_p, x_A) = 1 \qquad S(\lambda_\perp) = \delta^2(\lambda_\perp)$$

- Differential cross section in terms of dipole gluon distribution

$$\frac{d\sigma(p^\uparrow A \to \ell^+\ell^- X)}{dM^2 dy d^2q_\perp} = \frac{\alpha_{\rm em}^2}{6\pi^3 M^4}\sum_q e_q^2 \int d^2k_\perp x_p f_{q/p}(x_p, k_\perp^2)\int d\hat{z}\int d^2b d^2p_\perp F(x_A, p_\perp) A(p_\perp, q_\perp - k_\perp, \hat{z})$$

$$\frac{d\Delta\sigma(p^\uparrow A \to \ell^+\ell^- X)}{dM^2 dy d^2q_\perp} = \frac{\alpha_{\rm em}^2}{6\pi^3 M^4}\sum_q e_q^2 \int d^2k_\perp \frac{\epsilon_{\alpha\beta} s_\perp^\alpha k_\perp^\beta}{M_p} x_p f_{1T}^{\perp,q}(x_p, k_\perp^2)$$
$$\times \int d\hat{z}\int d^2b d^2p_\perp F(x_A, p_\perp) A(p_\perp, q_\perp - k_\perp, \hat{z})$$

Find the leading term in small-x formalism

- One could also find the leading term in the small-x formalism we have just derived (leading: $M \gg q_\perp \sim k_\perp \sim p_\perp(Q_s)$)

$$\frac{d\sigma(p^\uparrow A \to \gamma^* X)}{dy d^2 q_\perp} = \frac{\alpha_{\rm em}}{2\pi^2}\sum_q e_q^2 \int_{x_p}^1 \frac{dz}{z} d^2k_\perp x f_{q/p}(x,k_\perp^2)\int d^2b d^2p_\perp F(x_A,p_\perp)$$
$$\times\left[H_T(q_\perp,k_\perp,p_\perp,z)+H_L(q_\perp,k_\perp,p_\perp,z)\right]$$

- Dominated by the large z-->1 region: introduce a delta-function, integrate out z first

$$\int d\hat{z}\delta(\hat{z}-1/(1+\Lambda^2/\epsilon_M^2))=1 \qquad \Lambda^2=(1-z)(q_\perp-k_\perp)^2+z(q_\perp-k_\perp-p_\perp)^2$$

- At qt<<M, they are consistent with TMD factorization

$$\frac{d\sigma(p^\uparrow A \to \ell^+\ell^- X)}{dM^2 dy d^2 q_\perp} = \frac{\alpha_{\rm em}^2}{6\pi^3 M^4}\sum_q e_q^2 \int d^2k_\perp x_p f_{q/p}(x_p,k_\perp^2)\int d\hat{z}\int d^2b d^2p_\perp F(x_A,p_\perp)A(p_\perp,q_\perp-k_\perp,\hat{z})$$

$$\frac{d\Delta\sigma(p^\uparrow A \to \ell^+\ell^- X)}{dM^2 dy d^2 q_\perp} = \frac{\alpha_{\rm em}^2}{6\pi^3 M^4}\sum_q e_q^2 \int d^2k_\perp \frac{\epsilon_{\alpha\beta}s_\perp^\alpha k_\perp^\beta}{M_p} x_p f_{1T}^{\perp,q}(x_p,k_\perp^2)$$
$$\times\int d\hat{z}\int d^2b d^2p_\perp F(x_A,p_\perp)A(p_\perp,q_\perp-k_\perp,\hat{z})$$

Connection to collinear factorization approach - I

- When $M \sim q_\perp \gg Q_s(p_\perp)$, the usual collinear factorization should work (dilute region)
  - We should treat kt and pt (parton intrinsic transverse momenta) as small compared with the Drell-Yan pair's momentum qt

$$H_T(q_\perp, k_\perp, p_\perp, z) = \left[1 + (1-z)^2\right] \left[\frac{q_\perp - zk_\perp}{(q_\perp - zk_\perp)^2 + \epsilon_M^2} - \frac{q_\perp - zk_\perp - zp_\perp}{(q_\perp - zk_\perp - zp_\perp)^2 + \epsilon_M^2}\right]^2$$

$$H_L(q_\perp, k_\perp, p_\perp, z) = 2(1-z)^2 M^2 \left[\frac{1}{(q_\perp - zk_\perp)^2 + \epsilon_M^2} - \frac{1}{(q_\perp - zk_\perp - zp_\perp)^2 + \epsilon_M^2}\right]^2$$

  - Drop kt, we could have

$$\int d^2k_\perp f_{q/p}(x, k_\perp^2) = f_{q/p}(x)$$

  - Drop pt, the hard-part function vanish, thus need to expand to higher order

Connection to collinear factorization approach - II

- In the dilute parton region, we have the relation between the UGD and collinear gluon distribution

$$\int d^2b\, d^2p_\perp p_\perp^2 F(x_A, p_\perp) = \frac{2\pi^2\alpha_s}{N_c} x_A f_{g/A}(x_A)$$

Baier-Mueller-Schiff 04

- Thus expand the hard-part function to the 2nd order

$$\int d^2b \int d^2p_\perp F(x_A, p_\perp) p_\perp^\rho p_\perp^\sigma \frac{1}{2}\frac{\partial}{\partial p_\perp^\rho \partial p_\perp^\sigma}\left[H_T(q_\perp, k_\perp = 0, p_\perp, z) + H_L(q_\perp, k_\perp = 0, p_\perp, z)\right]_{p_\perp \to 0}$$

- Eventually the spin-averaged cross section can be written as

$$\frac{d\sigma(p^\uparrow A \to \ell^+\ell^- X)}{dM^2 dy d^2q_\perp} = \frac{\alpha_{\rm em}^2 \alpha_s}{3\pi N_c M^2}\sum_q e_q^2 \int_{x_p}^1 \frac{dz}{z}\, x f_{q/p}(x) x_A f_{g/A}(x_A) H(q_\perp, z)$$

$$H(q_\perp, z) = \frac{1}{4} g_\perp^{\rho\sigma} \frac{\partial}{\partial p_\perp^\rho \partial p_\perp^\sigma}\left[H_T(q_\perp, k_\perp = 0, p_\perp, z) + H_L(q_\perp, k_\perp = 0, p_\perp, z)\right]_{p_\perp \to 0}$$

$$= \frac{z^2}{(q_\perp^2 + \epsilon_M^2)^2}\left\{\left[1 + (1-z)^2\right] - \frac{2z^2 q_\perp^2 \epsilon_M^2}{(q_\perp^2 + \epsilon_M^2)^2}\right\}.$$

Connection to collinear factorization approach - III

- DY production (q+g channel) in collinear factorization approach

$$\frac{d\sigma(p^\uparrow A \to \ell^+\ell^- X)}{dM^2 dy d^2q_\perp} = \sigma_0 \frac{\alpha_s}{4\pi^2} \sum_q e_q^2 \int \frac{dx}{x}\frac{dx_A}{x_A} f_{q/p}(x) f_{g/A}(x_A) \hat{\sigma}_{qg}(\hat{s},\hat{t},\hat{u}) \delta\left(\hat{s}+\hat{t}+\hat{u}-M^2\right)$$

- Partonic cross section

$$\hat{\sigma}_{qg}(\hat{s},\hat{t},\hat{u}) = 2\,T_R\left[-\frac{\hat{s}}{\hat{t}} - \frac{\hat{t}}{\hat{s}} - \frac{2M^2\hat{u}}{\hat{s}\hat{t}}\right]$$

- Using the relations: $\hat{s} = \frac{q_\perp^2+\epsilon_M^2}{z(1-z)}, \qquad \hat{t} = -\frac{q_\perp^2+\epsilon_M^2}{z}, \qquad \hat{u} = -\frac{q_\perp^2}{1-z},$

- We have

$$\hat{\sigma}_{qg}(\hat{s},\hat{t},\hat{u}) = \frac{1}{1-z}\left\{\left[1+(1-z)^2\right] - \frac{2z^2 q_\perp^2 \epsilon_M^2}{\left(q_\perp^2+\epsilon_M^2\right)^2}\right\}$$

- The small-x cross section is consistent with the above formalism
- Remaining issue: what happens to the spin-dependent cross section

Spin asymmetry at RHIC 510 GeV - I

- Transverse momentum dependence

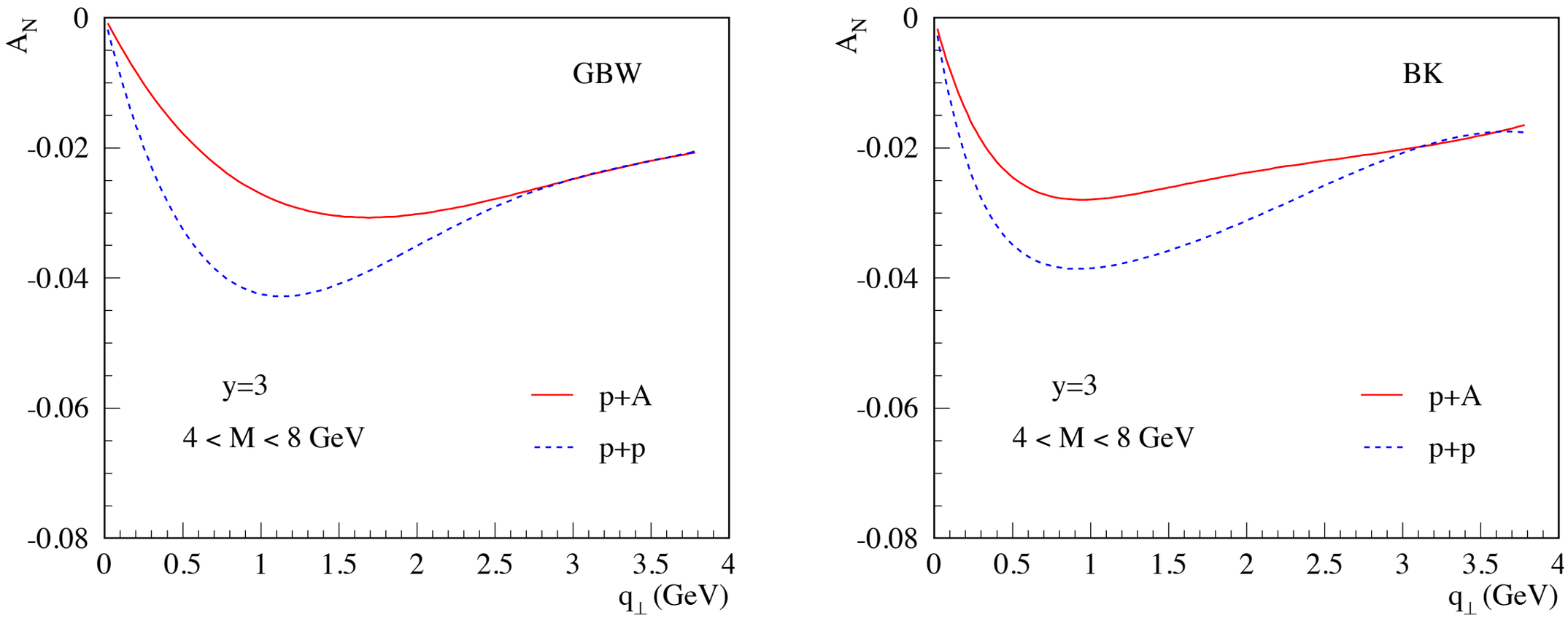

- Spin asymmetry is smaller in pA compared to pp, due to larger saturation scale

Spin asymmetry at RHIC 510 GeV - II

- Rapidity dependence

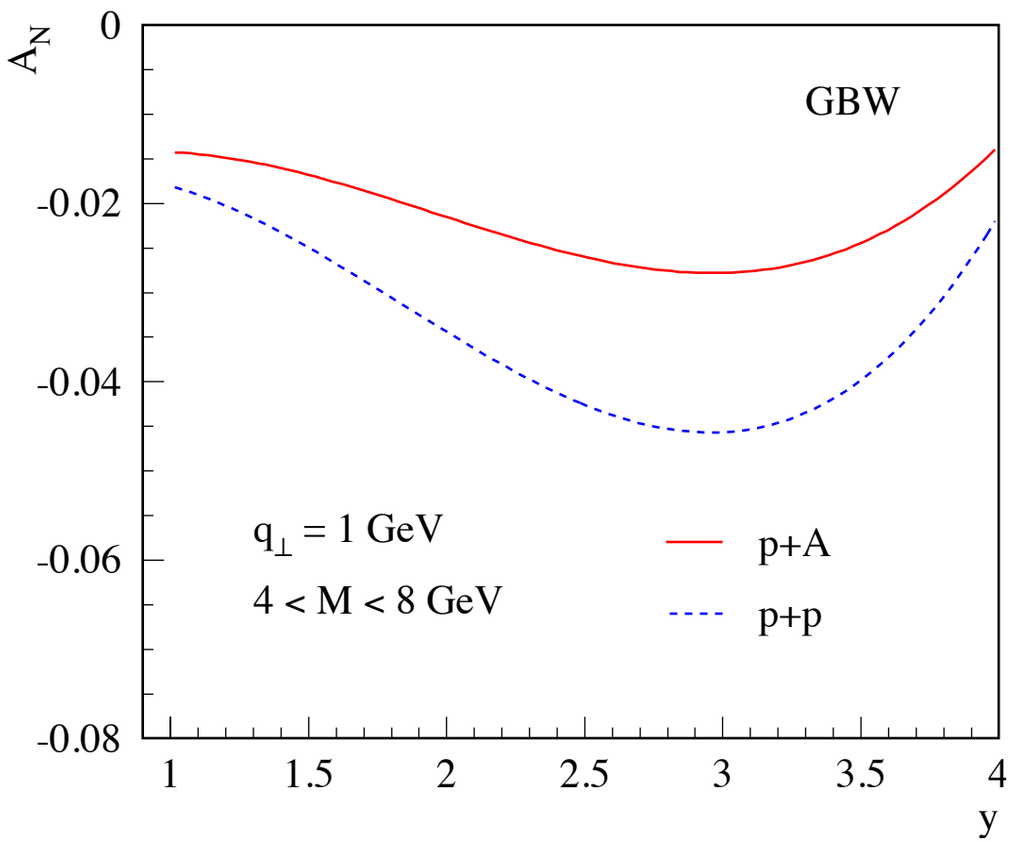

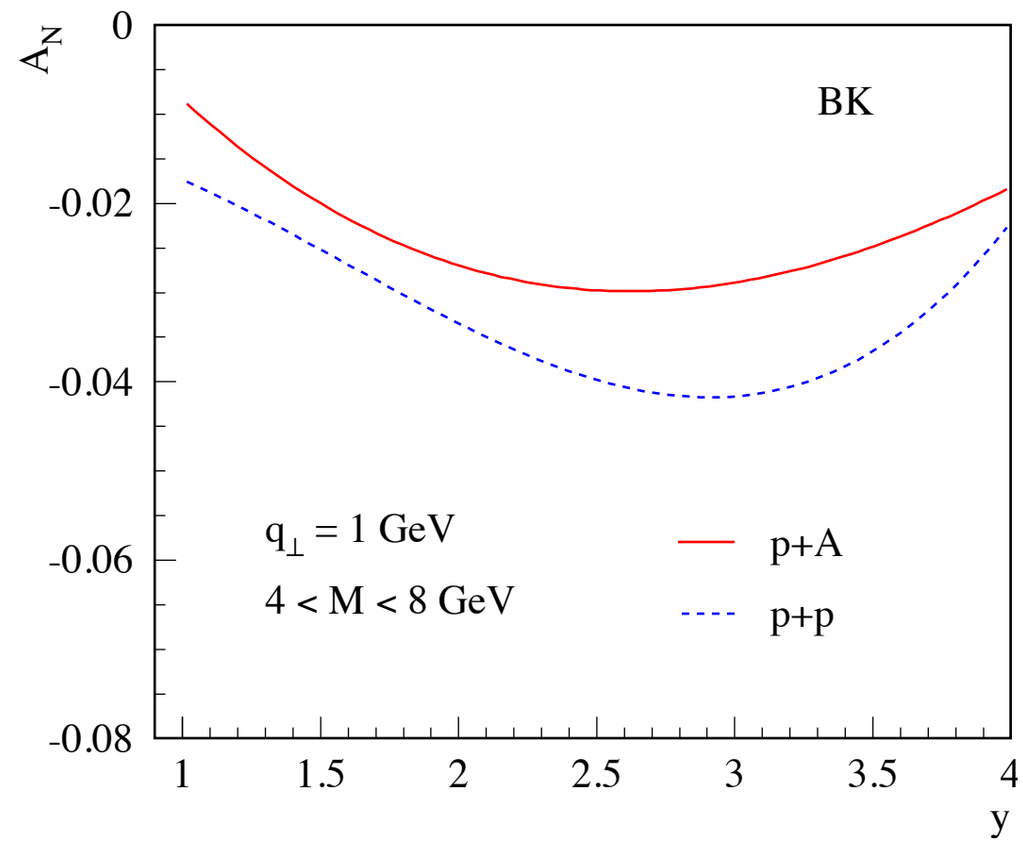

- The maximum happens at y~3, which corresponds to xp ~ 0.2 in the polarized proton (the Sivers function is largest at around this point)

Summary

- Forward region is a good place to study both the transverse spin physics and small-x gluon saturation
- Both effects become important in this region, we might find some advantages to study both of them in the same framework
- There are more to understand
  - Factorization properties for small-x formalism
  - What is the advantage to study polarized pp and pA

Single transverse-spin asymmetry in the forward and backward directions at RHIC

Yuji Koike (Niigata Univ.)

Riken-BNL Research Center Workshop on
“Forward Physics at RHIC (2012)”,
BNL, July 30 - Aug.1, 2012

Contents:

1. Introduction

2. Twist-3 analysis/predition for SSA at RHIC based on the quark-gluon correlation functions

   -A_N for $p^\uparrow p \to \{\pi, K, \eta, \text{jet}, \gamma\}X$

3. Multi-gluon contribution to SSA

   -Impact of 3-gluon correlation functions to $p^\uparrow p \to \{D, \gamma, \pi\}X$

4. Summary

1. Introduction

⋆ Single spin asymmetry (SSA)

- $p^{\uparrow}p \to \pi X$ $\qquad A_N = \dfrac{\sigma^{\uparrow} - \sigma^{\downarrow}}{\sigma^{\uparrow} + \sigma^{\downarrow}}$

- FNAL-E704('91)($\sqrt{s} = 20$ GeV), RHIC($\sqrt{s} = 200$, 62 GeV):
  $A_N \sim 0.3$ at large $x_F = 2p_{||}/\sqrt{s}$.

$x_F > 0$

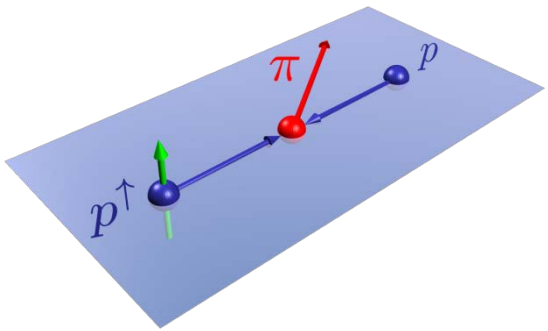

FNAL-E704

$\sqrt{s} = 20$ GeV

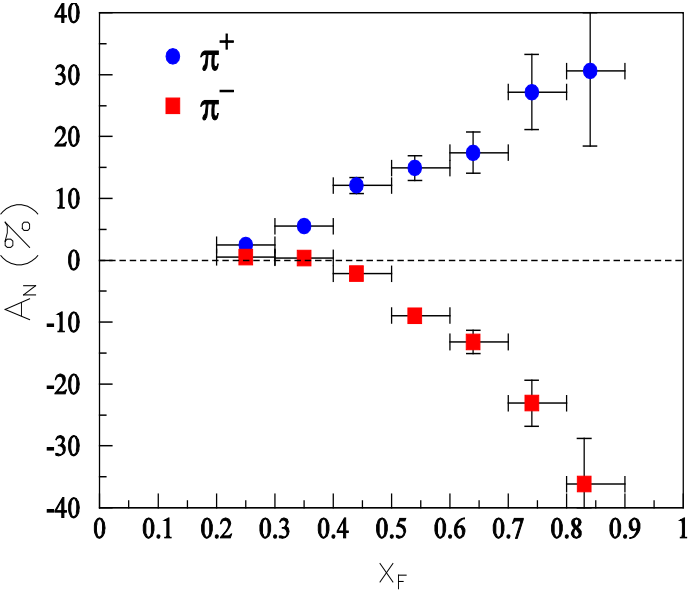

P.L. B264 ('91) 462
P.L. B261 ('91) 201

RHIC-STAR, PRL92('04)
hep-ex/0801.2990, PRL 101(2008)
$\sqrt{s} = 200$ GeV

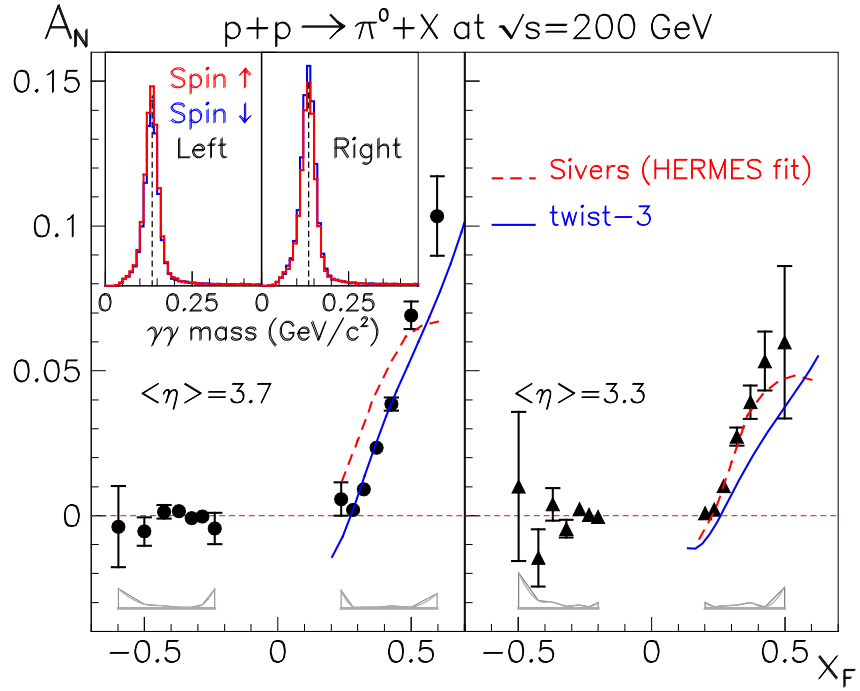

⋆ QCD-mechanisms for SSA in the two regions of P_T

- Naively "T-odd" distribution/fragmentation functions (Sivers, Collins *etc*)

  · Describes SSA in the region of $\Lambda_{\rm QCD} \leq q_\perp \ll Q$ in the framework of TMD factorization.

  · TMD distributions are process dependent!

- Multi-parton correlation functions (quark-gluon, purely gluonic *etc*)
  (Efremov-Teryaev, Qiu-Sterman, Eguchi-YK-Tanaka,..)

  · Describes SSA in the region of $q_\perp \sim Q \gg \Lambda_{\rm QCD}$ as a twist-3 observable in the framework of collinear factorization.

  · Multi-parton correlation functions are process-independent!

⋆ Inclusive cross section for $pp \to hX$

$$\sigma(p^{\uparrow}p \to hX) =$$

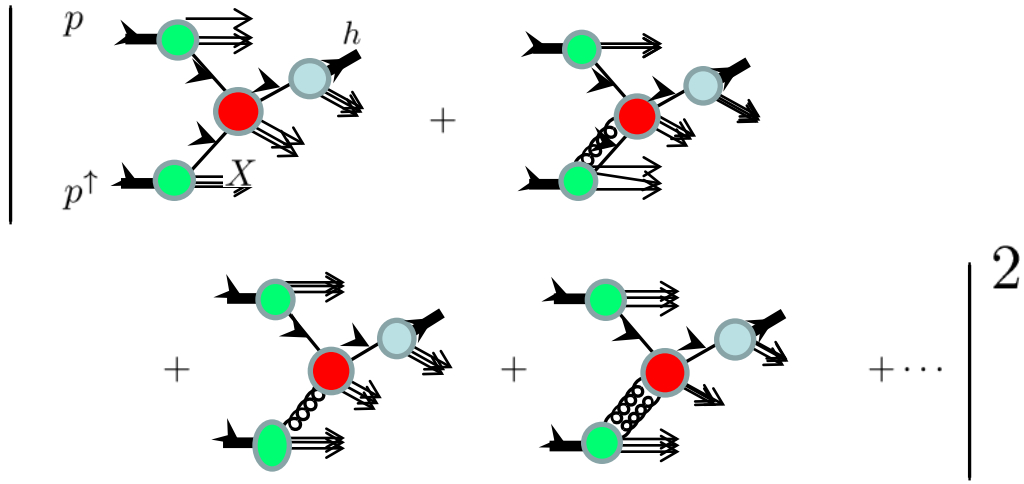

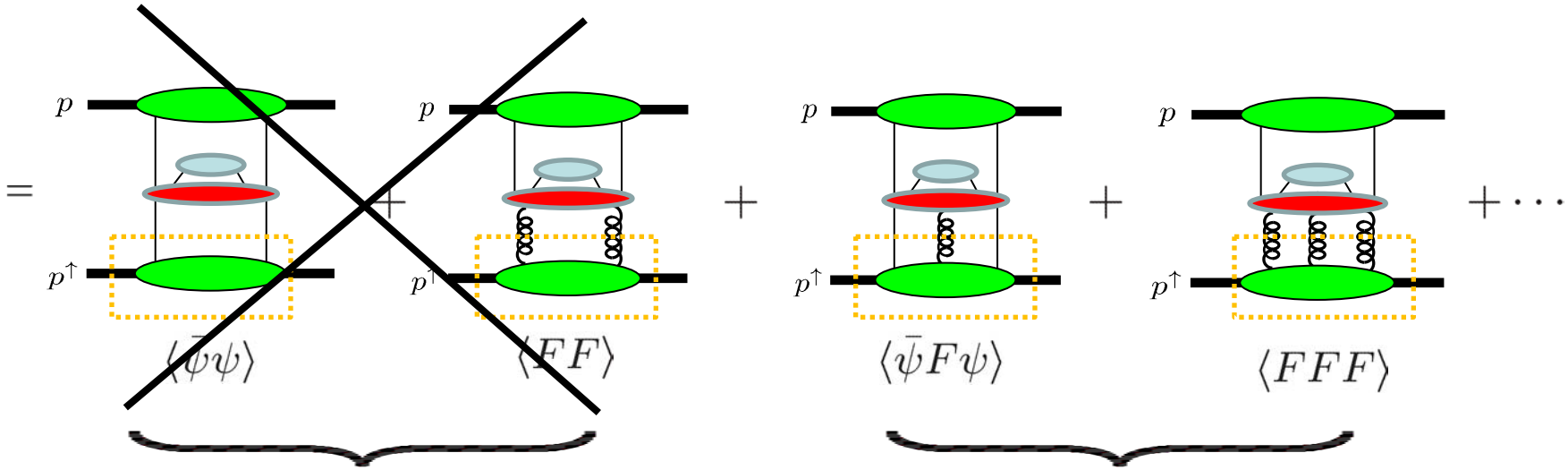

NO SSA

SSA

2. Twist-3 analysis/predition for SSA at RHIC based on the quark-gluon correlation functions

· Present the prediction/outcome for $p^{\uparrow}p \to (\eta, \gamma, \text{jet})X$, using our previous twist-3 analysis of the RHIC data on $p^{\uparrow}p \to (\pi, K)X$.

K. Kanazawa and YK, PRD82,034009 (2010), PRD83,114024 (2011), and in preparation.

· Unpolarized cross section can be well-described by NLO QCD in the collinear factorization at $P_T \geq 1$ GeV for RHIC data.

★ RHIC-STAR ('04)

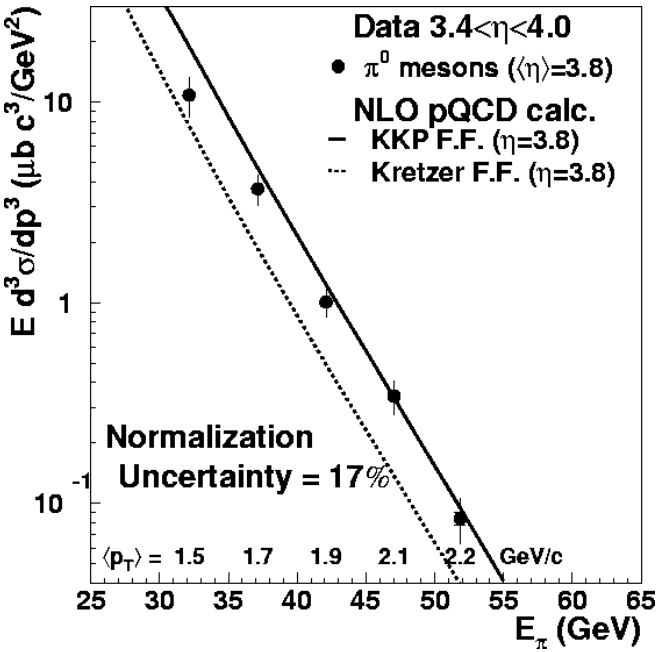

★ RHIC-BRAHMS ('07)

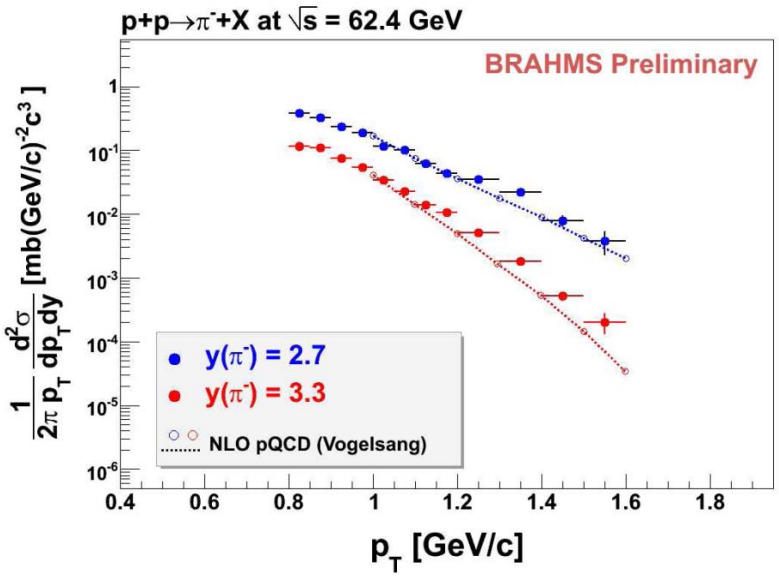

Theory calculation: Jäger, Schäfer, Stratmann, Vogelsang, PRD67,054005('03)

· RHIC + EIC (eRHIC) provides us with a good opportunity to understand SSA in terms of the twist-3 mechanism.

⋆ Quark-gluon correlation functions in the ⊥ polarized nucleon.

$$\int \frac{d\lambda}{2\pi} \int \frac{d\mu}{2\pi} e^{i\lambda x_1} e^{i\mu(x_2-x_1)} \langle PS|\bar{\psi}_j(0) g F^{\alpha\beta}(\mu n) n_\beta \psi_i(\lambda n)|PS\rangle$$
$$= \frac{M_N}{4} (\not{p})_{ij}\, \epsilon^{\alpha p n S_\perp} G_F(x_1,x_2) + i\frac{M_N}{4} (\gamma_5 \not{p})_{ij}\, S_\perp^\alpha \widetilde{G}_F(x_1,x_2) + \cdots$$

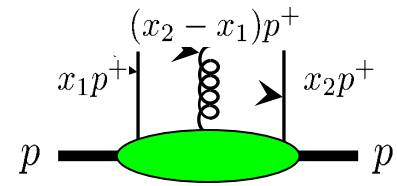

M_N: Nucleon mass.

$p^2 = n^2 = 0,\ p \cdot n = 1$

- Symmetry property from P- and T- invariance.

$$G_F(x_1,x_2) = G_F(x_2,x_1), \qquad \widetilde{G}_F(x_1,x_2) = -\widetilde{G}_F(x_2,x_1)$$

⋆ The twist-3 contribution to SSA can be expressed in terms of $\left\{ G_F(x_1,x_2), \widetilde{G}_F(x_1,x_2) \right\}$.

(Factorization and Gauge invariance proved in LO QCD.)

(Eguchi, YK, Tanaka, NPB763('07)198.)

· Cross section from the twist-3 distributions occurs as pole contributions in the hard part.

"Complex phase" is given by this imaginary part!

$p^\uparrow p \to \pi X$

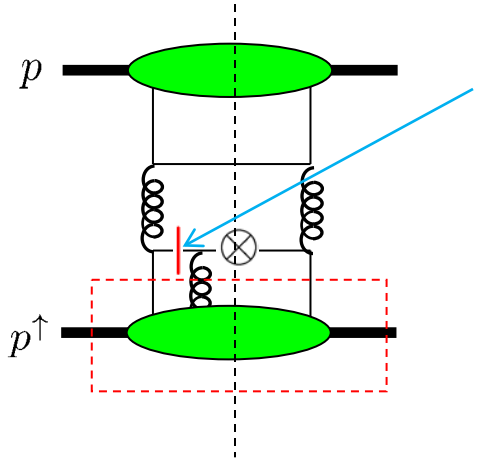

The pole of this propagator sets $x_1 = x_2$

$\to$soft-gluon-pole (SGP)

$\to G_F(x,x)$ (Note: $\widetilde{G}_F(x,x) \equiv 0$)

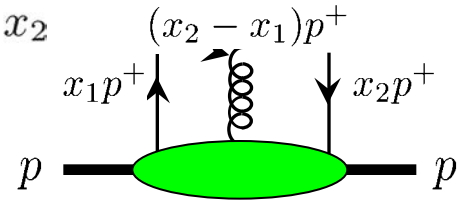

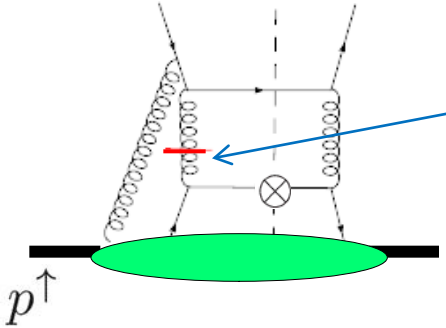

This pole sets $x_1 = 0$.

$\to$ Soft-fermion-pole (SFP).

$\to G_F(x,0)$ and $\widetilde{G}_F(x,0)$

⋆ Description of RHIC data

K. Kanazawa and YK, PRD82,034009 (2010), PRD83,114024 (2011)

- Inclusion of all contributions from the quark-gluon correlation functions.

$$\Delta\sigma \sim \{\hat{\sigma}_{\mathsf{SGP}} \otimes \left(G_F(x,x) - x\frac{dG_F(x,x)}{dx}\right) + \hat{\sigma}_{\mathsf{SFP}} \otimes \left(G_F(0,x) + \tilde{G}_F(0,x)\right)\} \otimes f(x') \otimes D(z)$$

Kouvaris-Qiu-Vogelsang-Yuan (2006) Koike-Tomita (2009)

- Reasonable description of SSA for pions and kaons with this formula:

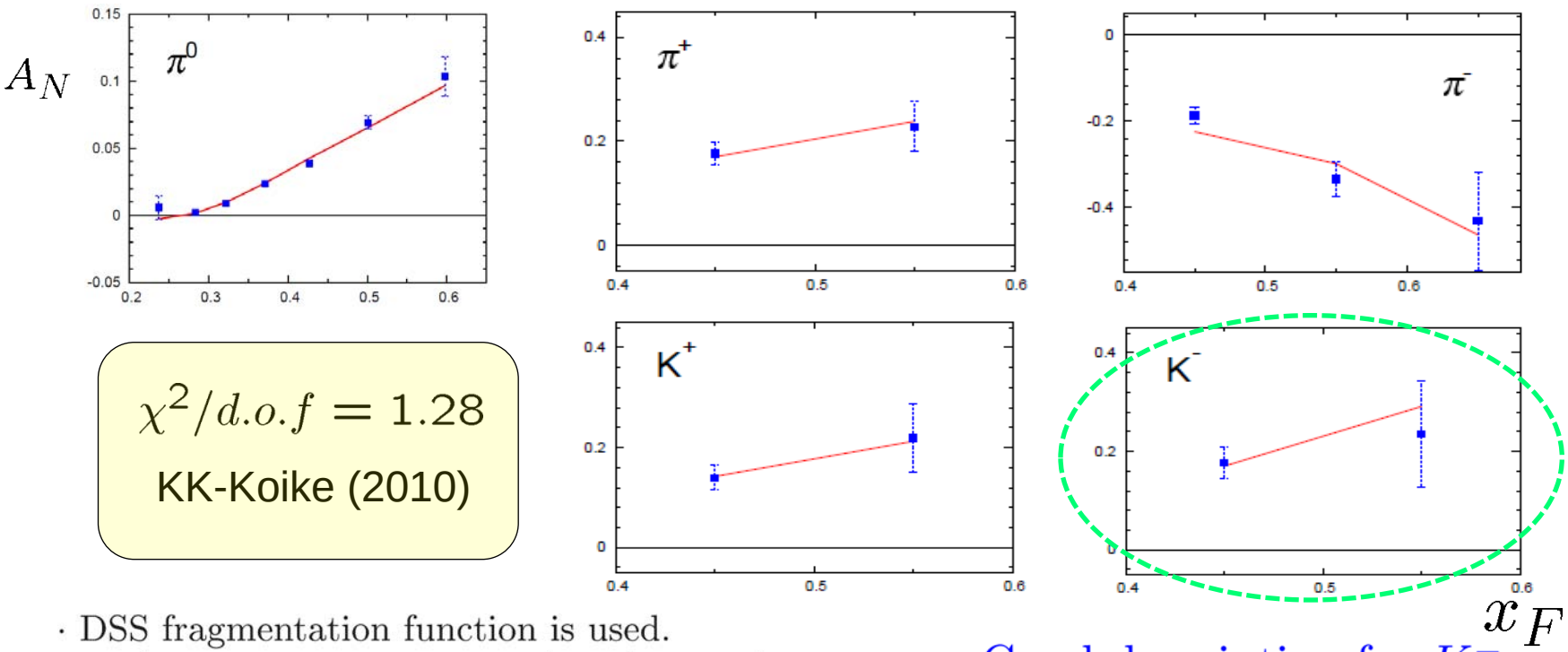

$\chi^2/d.o.f = 1.28$

KK-Koike (2010)

· DSS fragmentation function is used.
(de Florian *el al*, PRD75(2007)114010)

Good description for K^-

SFP is also important!

⋆ Comparison of P_T-dependence with the STAR result.

$A_N(\pi^0)$

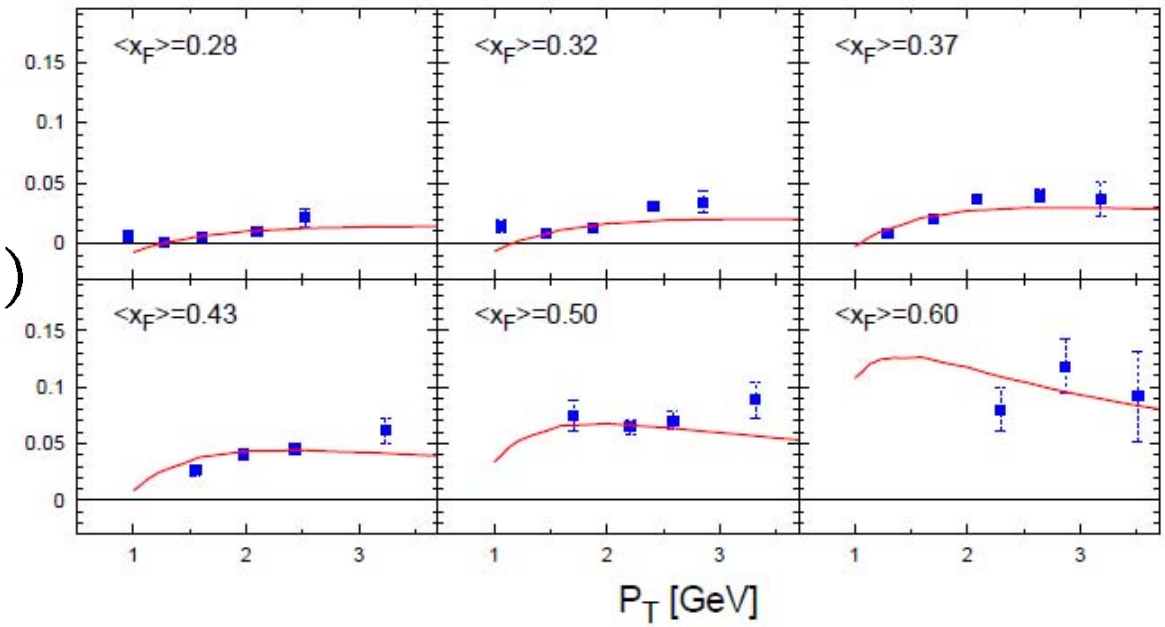

★ STAR (2008)

PT dependence is well reproduced :

$$A_N^{\text{tw3}} = \frac{\Delta\sigma^{\text{tw3}}}{\sigma^{\text{unp}}} \sim \mathcal{O}\left(\frac{M_N}{Q}\right) \otimes \frac{N_q(P_T^2) - N_g(P_T^2)}{D_q(P_T^2) + D_g(P_T^2)}$$

rapid decrease of $N_g(P_T^2)$ and $D_g(P_T^2)$ is crucial. (DSS FF)

$D_q,\ N_q(>0)$ from quark-frag. channel
$D_g,\ N_g(>0)$ from gluon-frag. channel

at low P_T, $\begin{cases} \Delta\sigma^{\text{tw3}} \text{ decrease } \textit{slowly} \\ \sigma^{\text{unp}} \text{ decrease } \textit{rapidly} \end{cases}$ as a function of $P_T(=Q)$.

$\Rightarrow$ A_N slightly increase at low P_T.

⋆ P_T-dependence of $A_N^{\pi^0}$ at large P_T region for various x_F.

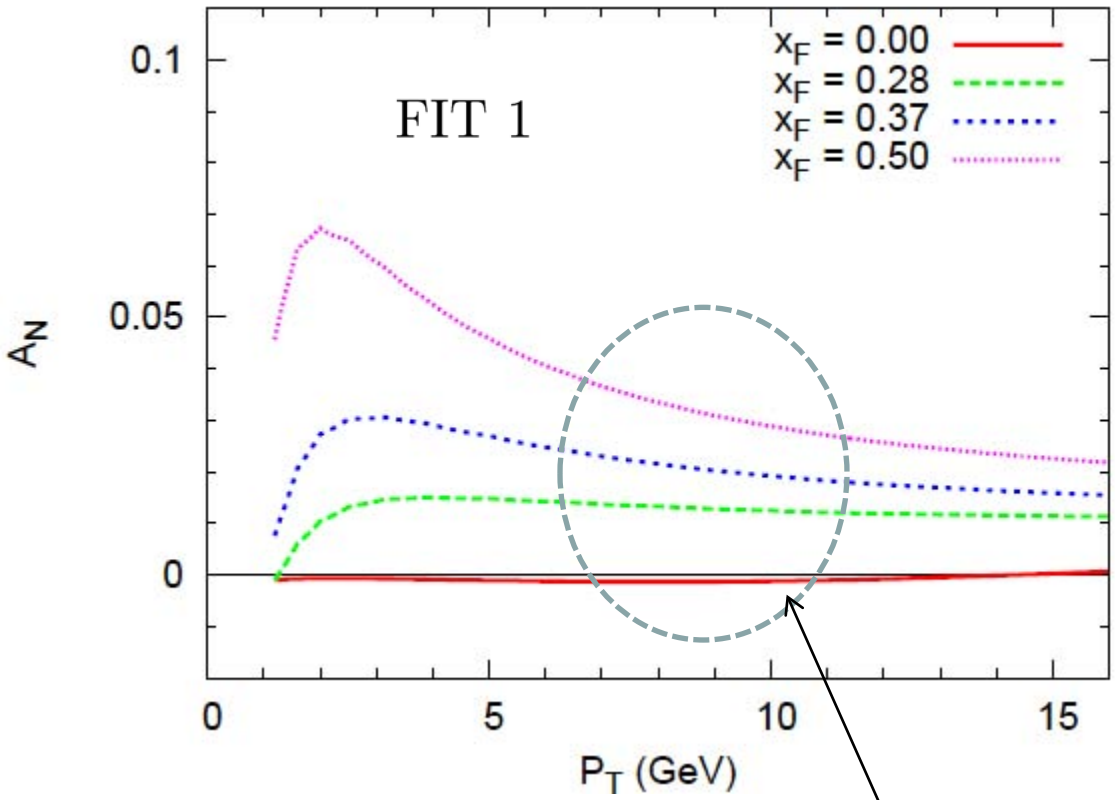

$$A_N \sim O\left(\frac{M_N P_T}{-T}\right) + O\left(\frac{M_N P_T}{-U}\right)$$

$$T = -\frac{S}{2}\left(\sqrt{x_T^2 + x_F^2} - x_F\right)$$

$$U = -\frac{S}{2}\left(\sqrt{x_T^2 + x_F^2} + x_F\right)$$

At $x_F \gg x_T$:

$$-T \to P_T^2/x_F$$

$$-U \to x_F S$$

Does not fall off as fast as $1/P_T$
by the coexistence of two terms.

⋆ Prediction of A_N for the η-meson production.

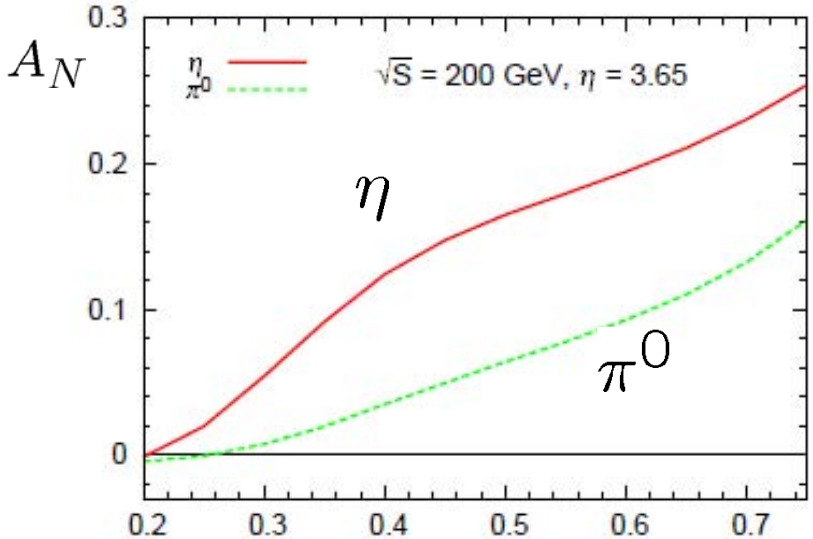

STAR, arXiv:1205.6826[nucl-ex]

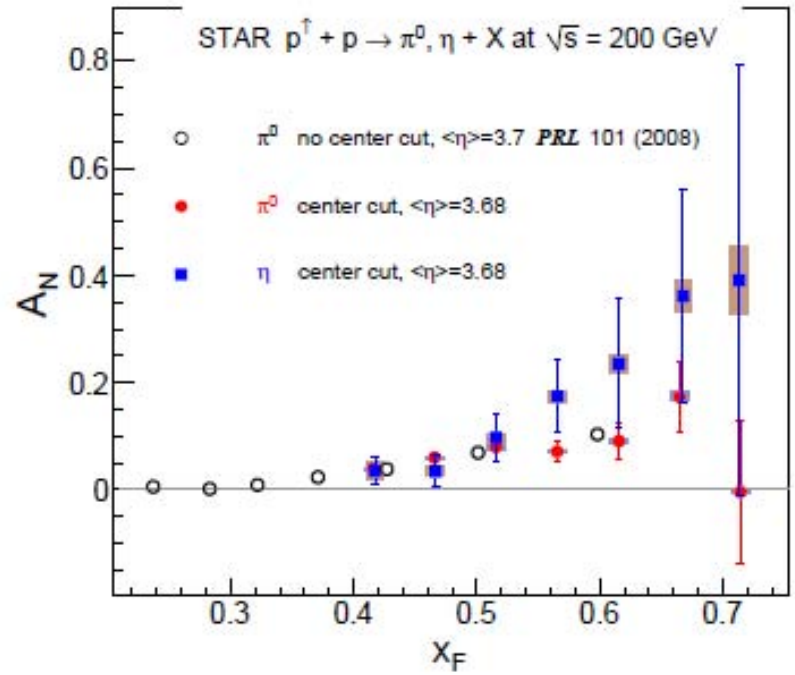

- Calculated A_N^η is consistent with the STAR data.

  - $A_N^\eta > A_N^{\pi^0}$ is due to the $\langle \bar{s} F^{+\perp} s \rangle$ in $p^\uparrow$ and the larger strangeness component in the η fragmentation function (Aidala *et al.*,PRD83,034002(2011).

- Caveat: Our analysis does not include the contribution from the 3-gluon correlation functions and the twist-3 fragmentation function.

⋆ Origin of the difference between π and η

★ Decomposition of the asymmetries into *each fragmentation channel*

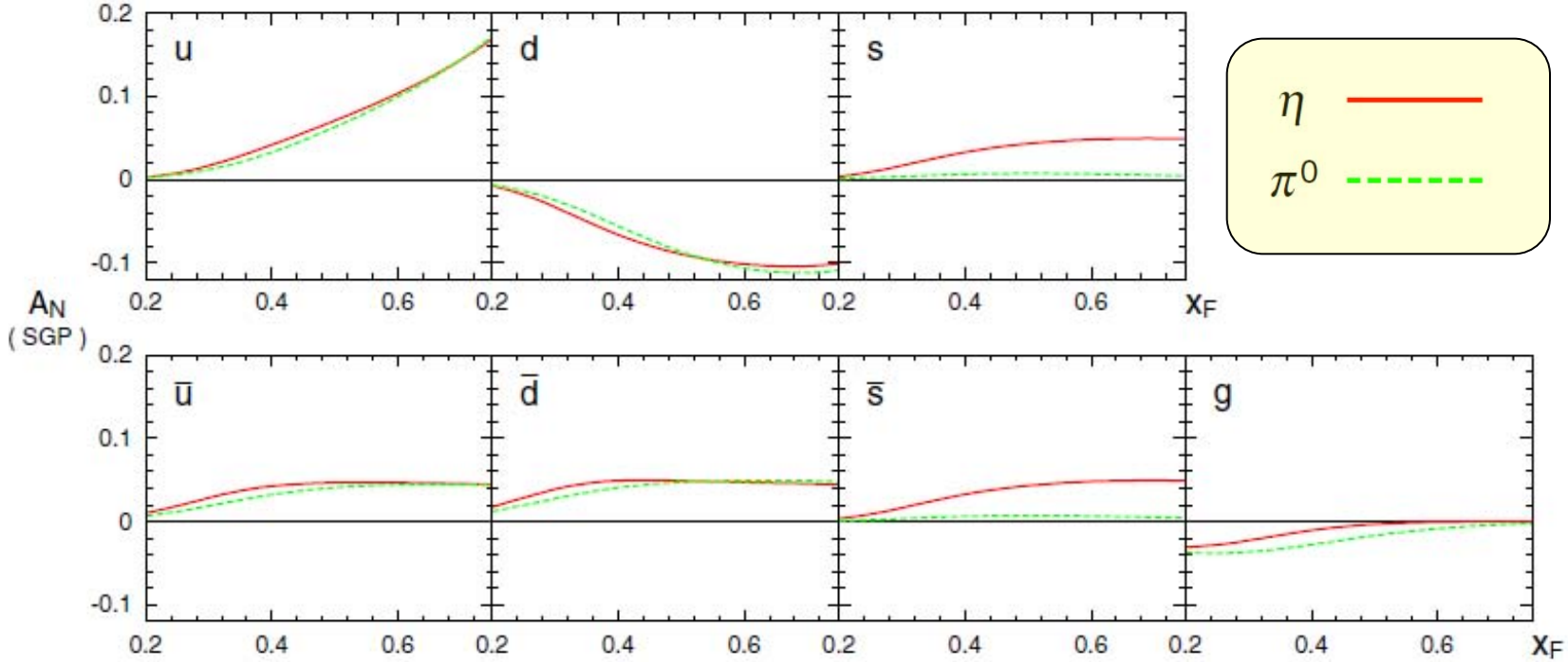

- The difference comes from the strange components.

⋆ A_N for $p^\uparrow p \to \gamma X$ and $p^\uparrow p \to \text{jet}X$.

No contribution from the twist-3 fragmentation function!

(Kang, Qiu, Vogelsang, Yuan, Phys. Rev. D **83** (2011) 094001)

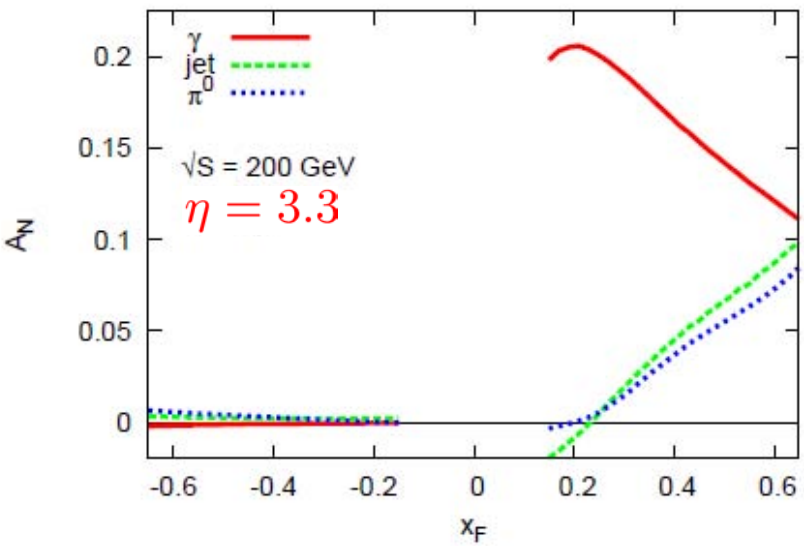

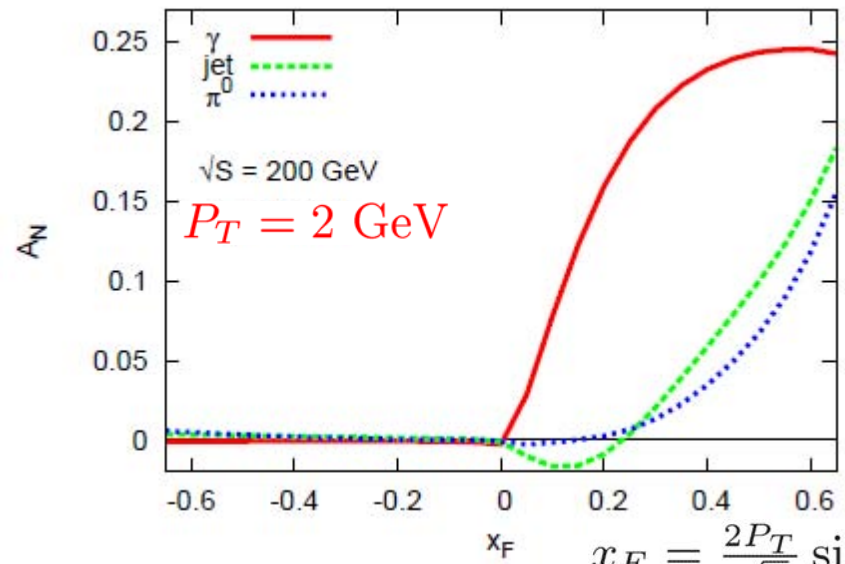

$x_F = \frac{2P_T}{\sqrt{S}} \sinh \eta$

· SGP contributions dominate for all these processes.

· Color factors for the polarized $\Delta\hat{\sigma}$ are much smaller for $\Delta\hat{\sigma}^{\pi,\text{jet}}$ compared with $\Delta\hat{\sigma}^{\gamma}$ relative to the unpolarized $\hat{\sigma}$.

· In $\Delta\hat{\sigma}^{\pi,\text{jet}}$, FSI dominates at large x_F due to the kinematic factor $\hat{s}/\hat{t}$.

$\leftrightarrow$ Only ISI exists in $\Delta\hat{\sigma}^{\gamma}$.

· A_N^{γ} is caused through $\Delta\hat{\sigma}^{qg\to q\gamma}$, while $A_N^{\pi,\text{jet}}$ is caused through $\Delta\hat{\sigma}^{qg\to qg}$ and $\Delta\hat{\sigma}^{qg\to gq}$.

$\Rightarrow$ Different behaviors for A_N^{γ} and $A_N^{\text{jet},\pi}$.

· Quark-gluon correlations give $A_N^{\gamma,\text{jet},\pi} \simeq 0$ at $x_F < 0$.

$\Rightarrow$ 3-gluon correlation can be the only source of $A_N^{\text{jet},\gamma}$ at $x_F < 0$. (See next)

⋆ P_T-dependence of $A_N^{\mathrm{jet},\gamma}$ (η-integrated)

RHIC-STAR, arXiv:1205.2735[nucl-ex]

A_N^{jet}

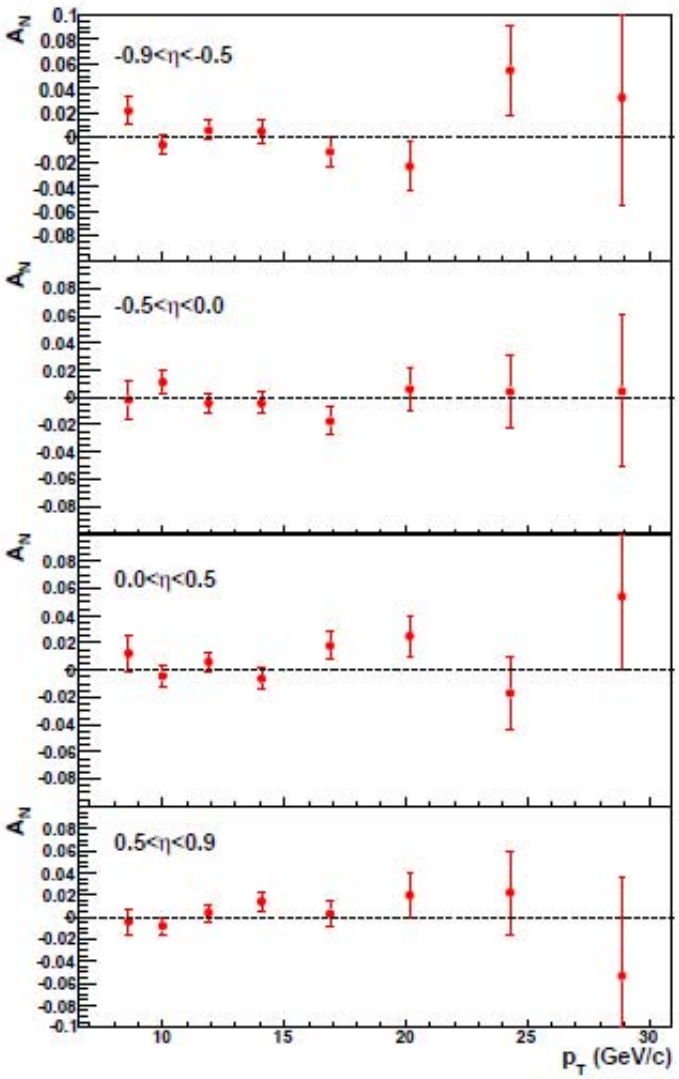

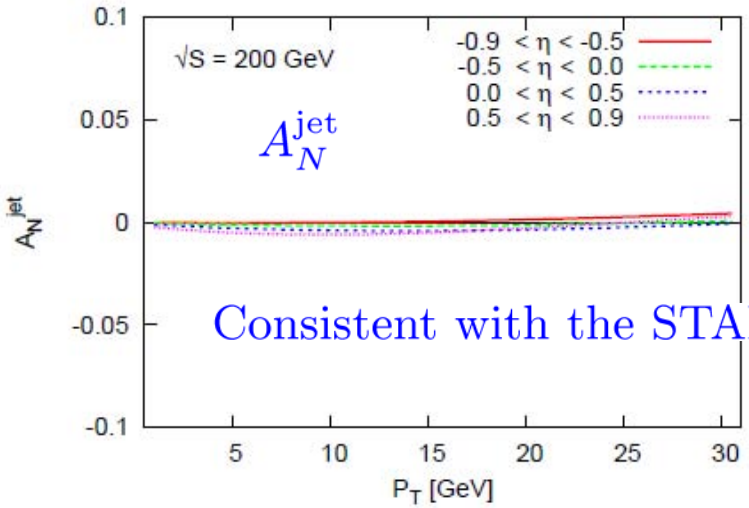

Consistent with the STAR data!

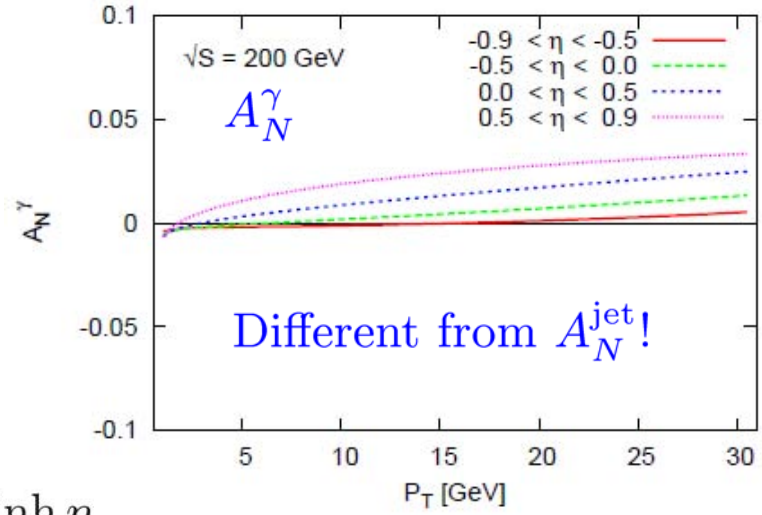

Different from A_N^{jet}!

$$x_F = \frac{2P_T}{\sqrt{S}} \sinh \eta$$

$\star$ A_N for $\sqrt{S} = 500$ GeV vs. $\sqrt{S} = 200$ GeV $\quad A_N(500\,\text{GeV}) \simeq 0.5 A_N(200\,\text{GeV})$

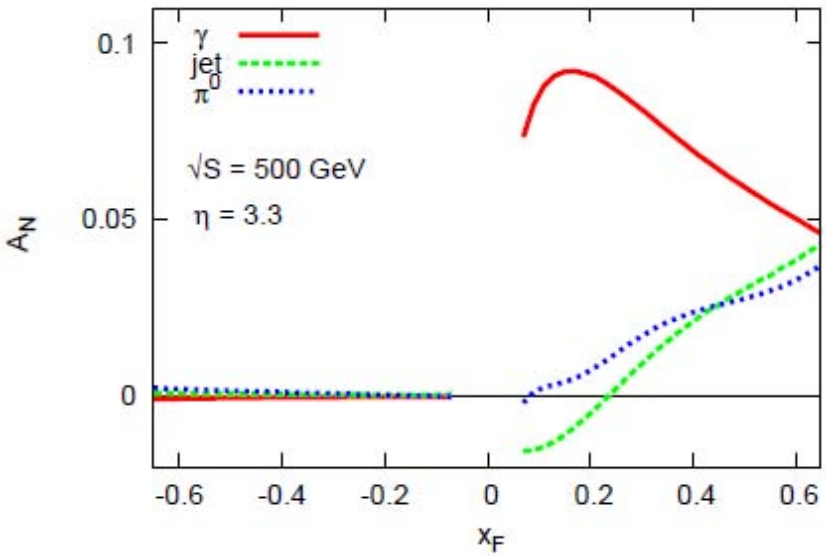

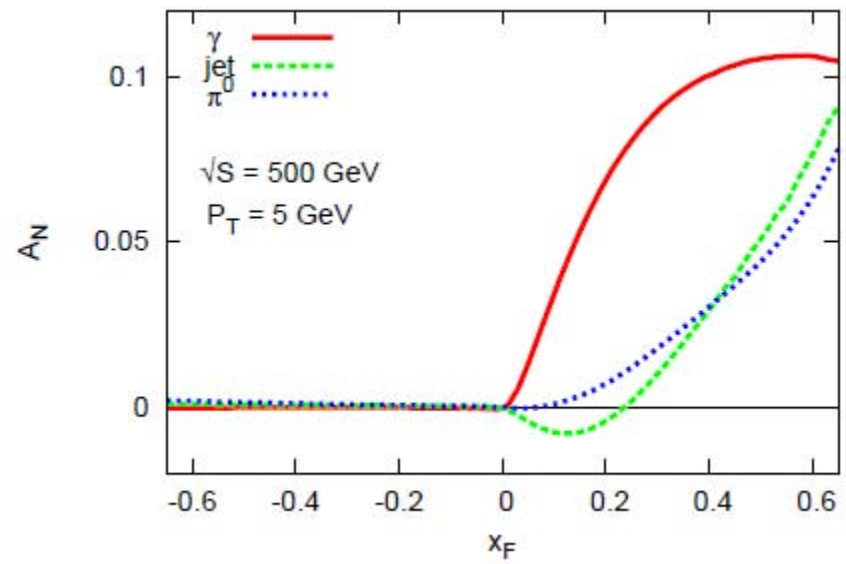

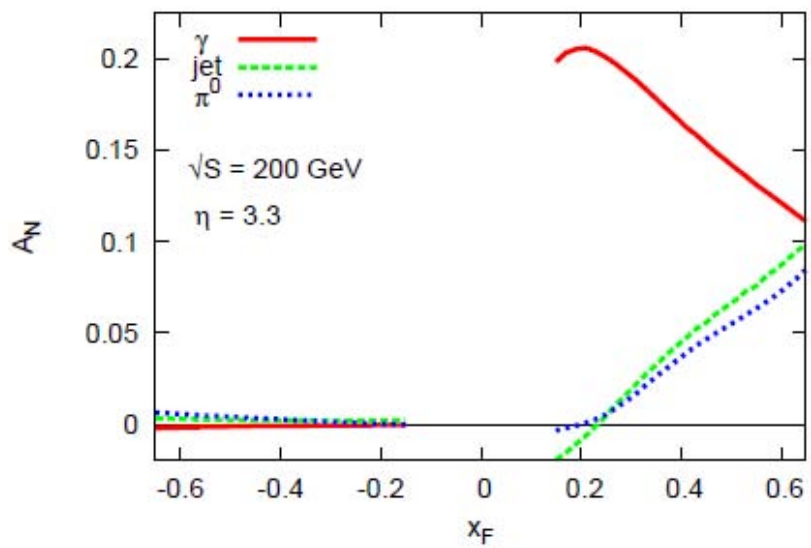

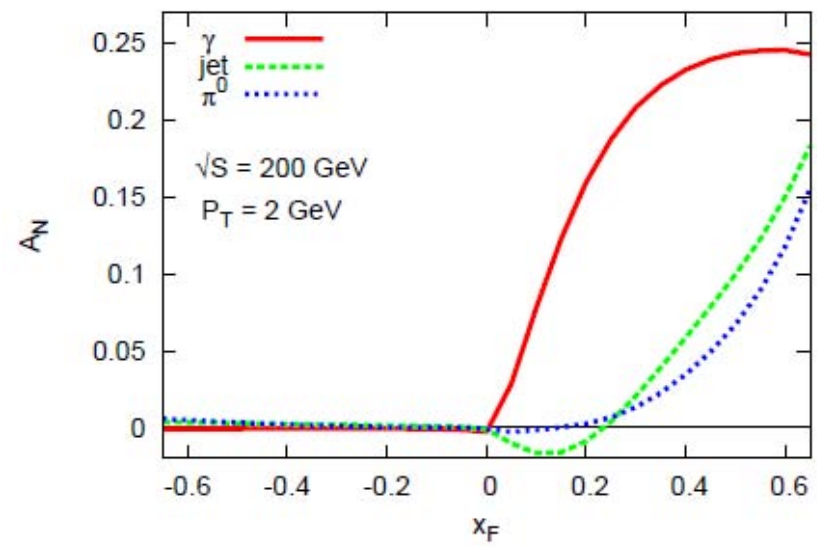

3. Multi-gluon contribution to SSA.

· See the impact of the 3-gluon correlation function on $p^{\uparrow}p \to (\gamma, \pi)X$ using the parametrization for $p^{\uparrow}p \to DX$.

For the formalism, see (for $ep^{\uparrow} \to eDX$):
H.Beppu, YK, T. Tanaka, S. Yoshida, PRD 82(2010)054005,(arXiv:1007.2034)
YK, T. Tanaka, S.Yoshida, PRD 83(2011)114014 (arXiv:1104.0798) .

For earlier works, see

Kang-Qiu (PRD 78('08)034005), Kang-Qiu-Vogelsang-Yuan (PRD 78('08)114013)

⋆ Twist-3 "three-gluon" correlation functions

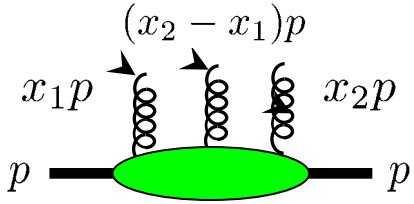

Beppu-Koike-Tanaka-Yoshida (PRD 82('10)054005)

See also, Belitsky-Ji-Lu-Osborne, PRD63,094012(2001)
Braun-Manashov-Pirnay, PRD80,114002(2009).

-Two independent correlation functions $O(x_1, x_2)$ and $N(x_1, x_2)$ due to Hermiticity, PT-invariance and Permutation symmetry

$$O^{\alpha\beta\gamma}(x_1, x_2) = -gi^3 \int \frac{d\lambda}{2\pi} \int \frac{d\mu}{2\pi} e^{i\lambda x_1} e^{i\mu(x_2 - x_1)} \langle pS | d^{bca} F_b^{\beta n}(0) F_c^{\gamma n}(\mu n) F_a^{\alpha n}(\lambda n) | pS \rangle$$

$$= 2iM_N \left[O(x_1, x_2) g^{\alpha\beta} \epsilon^{\gamma pnS} + O(x_2, x_2 - x_1) g^{\beta\gamma} \epsilon^{\alpha pnS} + O(x_1, x_1 - x_2) g^{\gamma\alpha} \epsilon^{\beta pnS} \right]$$

$$N^{\alpha\beta\gamma}(x_1, x_2) = -gi^3 \int \frac{d\lambda}{2\pi} \int \frac{d\mu}{2\pi} e^{i\lambda x_1} e^{i\mu(x_2 - x_1)} \langle pS | i f^{bca} F_b^{\beta n}(0) F_c^{\gamma n}(\mu n) F_a^{\alpha n}(\lambda n) | pS \rangle$$

$$= 2iM_N \left[N(x_1, x_2) g^{\alpha\beta} \epsilon^{\gamma pnS} - N(x_2, x_2 - x_1) g^{\beta\gamma} \epsilon^{\alpha pnS} - N(x_1, x_1 - x_2) g^{\gamma\alpha} \epsilon^{\beta pnS} \right].$$

$F_a^{\alpha n} \equiv F_a^{\alpha\mu} n_\mu$ $\quad$ n: lightlike vector satisfying $p \cdot n = 1$.

$\epsilon^{\gamma pnS} \equiv \epsilon^{\gamma\mu\nu\lambda} p_\mu n_\nu S_\lambda$ etc. $\quad$ Gauge-links suppressed above.

$p^{\uparrow}p \to DX$

YK, S.Yoshida, PRD84(2011)014026 (arXiv:1104.3943 [hep-ph]).

$\star$ Three-gluon contribution to $p^{\uparrow}(p) + p(p') \to D(P_h) + X$

$$P_h^0 \frac{d\sigma^{3\text{gluon}}}{d^3 P_h} = \frac{\alpha_s^2 M_N \pi}{S} \epsilon^{P_h p n S_\perp} \sum_{f=c\bar{c}} \int \frac{dx'}{x'} G(x') \int \frac{dz}{z^3} D_a(z) \int \frac{dx}{x} \delta\left(\tilde{s} + \tilde{t} + \tilde{u}\right) \frac{1}{\tilde{u}}$$

$$\times \Bigg[\delta_f \Bigg\{ \left(\frac{d}{dx} O(x,x) - \frac{2O(x,x)}{x} \right) \hat{\sigma}^{O1} + \left(\frac{d}{dx} O(x,0) - \frac{2O(x,0)}{x} \right) \hat{\sigma}^{O2} + \frac{O(x,x)}{x} \hat{\sigma}^{O3} + \frac{O(x,0)}{x} \hat{\sigma}^{O4} \Bigg\}$$

$$+ \Bigg\{ \left(\frac{d}{dx} N(x,x) - \frac{2N(x,x)}{x} \right) \hat{\sigma}^{N1} + \left(\frac{d}{dx} N(x,0) - \frac{2N(x,0)}{x} \right) \hat{\sigma}^{N2} + \frac{N(x,x)}{x} \hat{\sigma}^{N3} + \frac{N(x,0)}{x} \hat{\sigma}^{N4} \Bigg\} \Bigg].$$

$$\tilde{s} = (xp + x'p')^2 \qquad \tilde{t} = (p_c - xp)^2 - m_c^2 \qquad \tilde{u} = (p_c - x'p')^2 - m_c^2,$$

$\delta_c = 1$ (D-meson) and $\delta_{\bar{c}} = -1$ ($\bar{D}$-meson) $\qquad p_c = \frac{P_h}{z}$

· Receives derivative contributions from $O(x,x), O(x,0), N(x,x), N(x,0)$.

· O-function contributes to D and $\bar{D}$ with opposite signs.

· 4 hard cross sections for the derivative terms are dominant and have similar magnitude (at RHIC energy): $\hat{\sigma}^{O1} \simeq \hat{\sigma}^{O2} \sim \hat{\sigma}^{N1} \simeq -\hat{\sigma}^{N2}$ ($\gg \hat{\sigma}^{O3}, \hat{\sigma}^{N3}, \hat{\sigma}^{O4}, \hat{\sigma}^{N4}$).

· At $m_c \to 0$, one has $\hat{\sigma}^{O1} = \hat{\sigma}^{O2}$ and $\hat{\sigma}^{N1} = -\hat{\sigma}^{N2}$ and $\hat{\sigma}^{O3,O4,N3,N4} = 0$.

At the RHIC energy the cross section can be approximated as

$$P_h^0 \frac{d\sigma^{3\text{gluon}}}{d^3 P_h} \simeq \frac{\alpha_s^2 M_N \pi}{S} \epsilon^{P_h p n S_\perp} \sum_{f=c\bar{c}} \int \frac{dx'}{x'} G(x') \int \frac{dz}{z^3} D_a(z) \int \frac{dx}{x} \delta\left(\tilde{s}+\tilde{t}+\tilde{u}\right) \frac{1}{\tilde{u}}$$
$$\times \left[\delta_f \left(\frac{d}{dx} O(x) - \frac{2O(x)}{x} \right) \hat{\sigma}^{O1} + \left(\frac{d}{dx} N(x) - \frac{2N(x)}{x} \right) \hat{\sigma}^{N1} \right].$$

where $O(x) \equiv O(x,x) + O(x,0)$, $N(x) \equiv N(x,x) - N(x,0)$.

NB. For Drell-Yan and SIDIS (with large Q^2), the results are not simplied like this.

⋆ Model calculation of A_N^D

Ansatz: $O(x) = \pm N(x)$

Two models for the functions with constant K_G, K'_G.

$$\begin{cases} \text{Model 1: } O(x) = K_G \times x\,G(x) \\ \text{Model 2: } O(x) = K'_G \times \sqrt{x}\,G(x) \end{cases}$$

· $G(x)$:unpolarized gluon distribution function
Gluck, Jimenez-Delgado, Reya Eur.phys.J.C53(2008)

· D-meson fragmentation function by
KKKS (Kneesh *et al.* NPB799('08)34)

⋆ We determine K_G, K'_G so that A_N is consistent with the RHIC preliminary data.

A_N for $p^{\uparrow}p \to \bar{D}X$

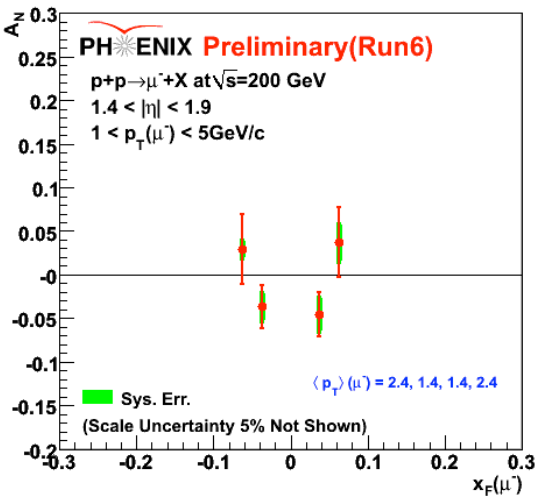

$\star$ $O(x) = -N(x)$ case @ $\sqrt{S} = 200$ GeV, $P_T = 2$ GeV

Cancellation between $O(x)$ and $N(x)$ for D!

Model 1:
$O(x) = 0.004xG(x)$

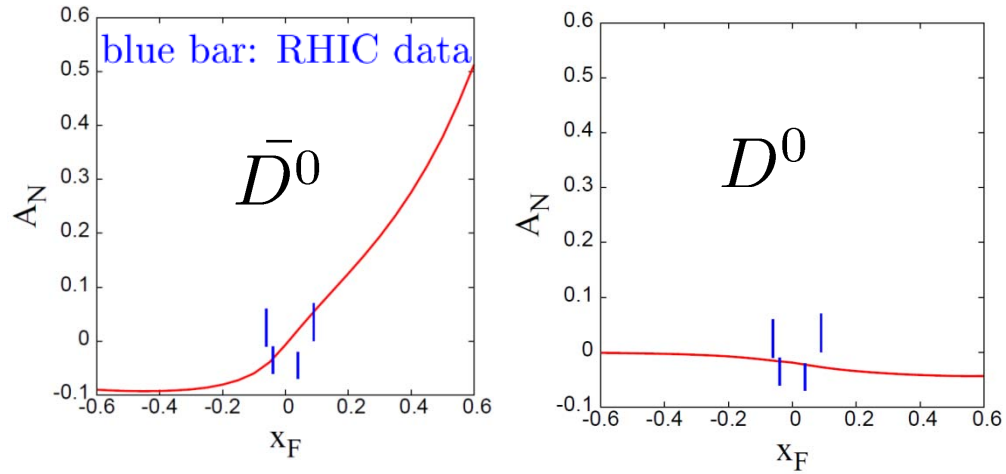

Model 2:
$O(x) = 0.001\sqrt{x}G(x)$

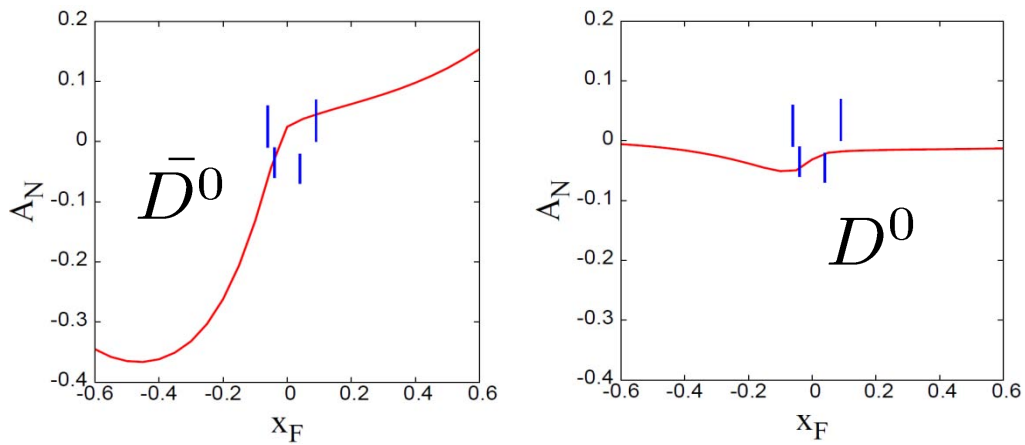

· If $O(x)$ and $N(x)$ do not cancel, A_N rises at large x_F by the derivative contribution.

· A_N at $x_F < 0$ strongly depends on the small-x behavior of 3-gluon correlation function.

Direct photon production: $p^{\uparrow}p \to \gamma X$

YK and Yoshida, Phys. Rev. D **85** (2012) 034030

⋆ LO diagrams for $p^{\uparrow}(p,S) + p(p') \to \gamma(q) + X$

Twist-2(unpolarized cross section)

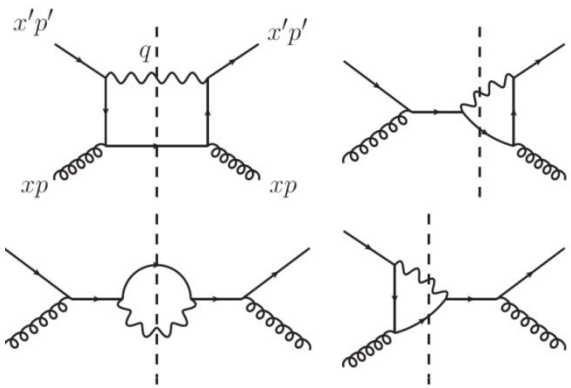

$gq \to \gamma q$

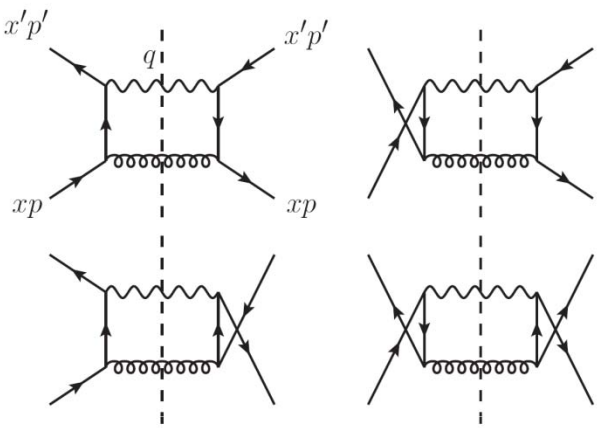

$q\bar{q} \to \gamma g$

Twist-3(polarized cross section)

initial state interaction

pole at $x_1 = x_2$

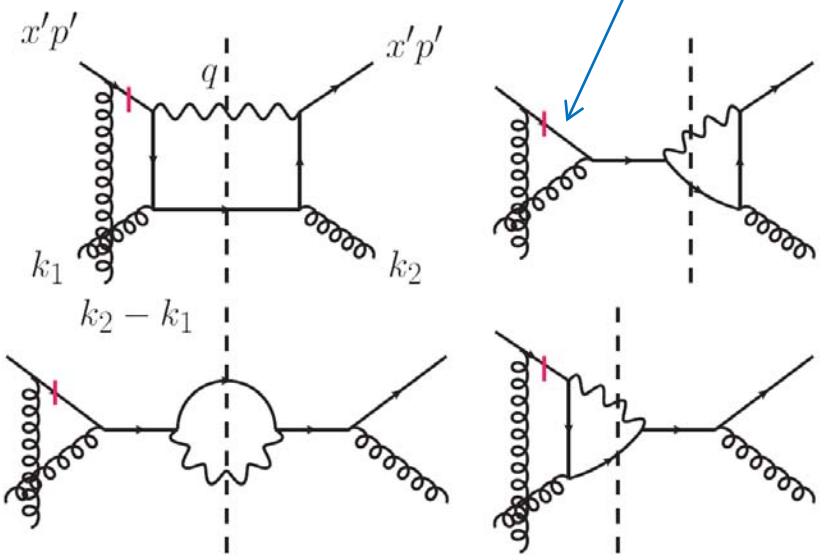

+ mirrors

⋆ Three-gluon contribution to $p^{\uparrow}(p) + p(p') \to \gamma(q) + X$.

$\hat{s} = (xp + x'p')^2$,
$\hat{t} = (xp - q)^2$,
$\hat{u} = (x'p' - q)^2$

$$E_\gamma \frac{d\sigma}{d^3q} = \frac{4\alpha_{em}\alpha_s M_N \pi}{S} \sum_a e_a^2 \int \frac{dx'}{x'} f_a(x') \int \frac{dx}{x} \delta(\hat{s} + \hat{t} + \hat{u}) \epsilon^{qpnS_\perp} \frac{1}{\hat{u}}$$

$$\times \left[\delta_a \left(\frac{d}{dx} O(x) - \frac{2O(x)}{x} \right) - \left(\frac{d}{dx} N(x) - \frac{2N(x)}{x} \right) \right] \left(\frac{1}{N} \left(\frac{\hat{s}}{\hat{u}} + \frac{\hat{u}}{\hat{s}} \right) \right)$$

$$O(x) \equiv O(x,x) + O(x,0)$$
$$N(x) \equiv N(x,x) - N(x,0)$$

The same as twist-2 cross section
(also from master formula!)
(YK,Tanaka,Yoshida,('11))

$\delta_a = 1$ for a =quark, $\delta_a = -1$ for a =anti-quark.

$\hat{s} = (xp + x'p')^2$, $\hat{t} = (xp - q)^2$, $\hat{u} = (x'p' - q)^2$

· This differs from the previous study (X. Ji, Phys.lett.B289 ('92)137).

· If $O(x) \simeq N(x)$, quarks in the unpolarized nucleon are NOT active. $\to$ Small A_N^γ.

· If $O(x) \simeq -N(x)$, quarks in the unpolarized nucleon are active. $\to$ Large A_N^γ.

⋆ Estimate of A_N for $p^\uparrow p \to \gamma X$ by the models determined from $p^\uparrow p \to DX$.

(i) Case 1: $O(x) = N(x)$

· Only anti-quark contribution from the unpolarized nucleon are active for the polarized cross section.

@ $\sqrt{S} = 200$ GeV, $P_T = 2$ GeV

Model 1: $O(x) = 0.004 \times xG(x)$

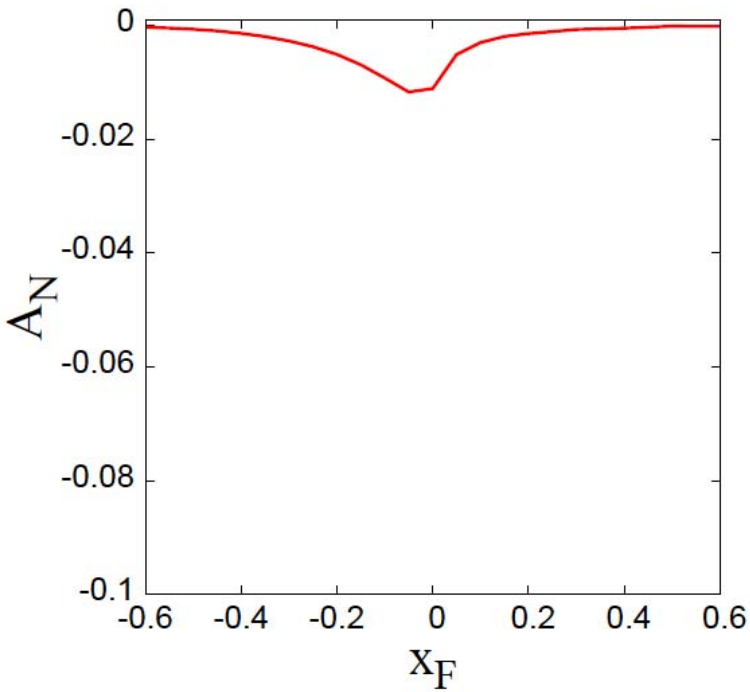

Model 2: $O(x) = 0.001\sqrt{x}G(x)$

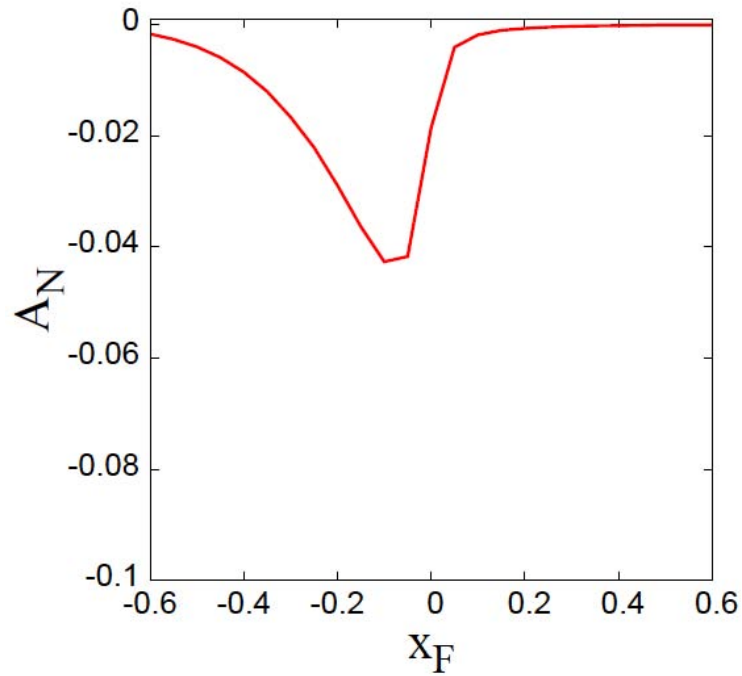

(ii) Case 2: $O(x) = -N(x)$

$\rightarrow$ Quark contribution from the unpolarized nucleon is active, while anti-quark contribution is cancelled.

Model 1: $O(x) = 0.004 \times xG(x)$

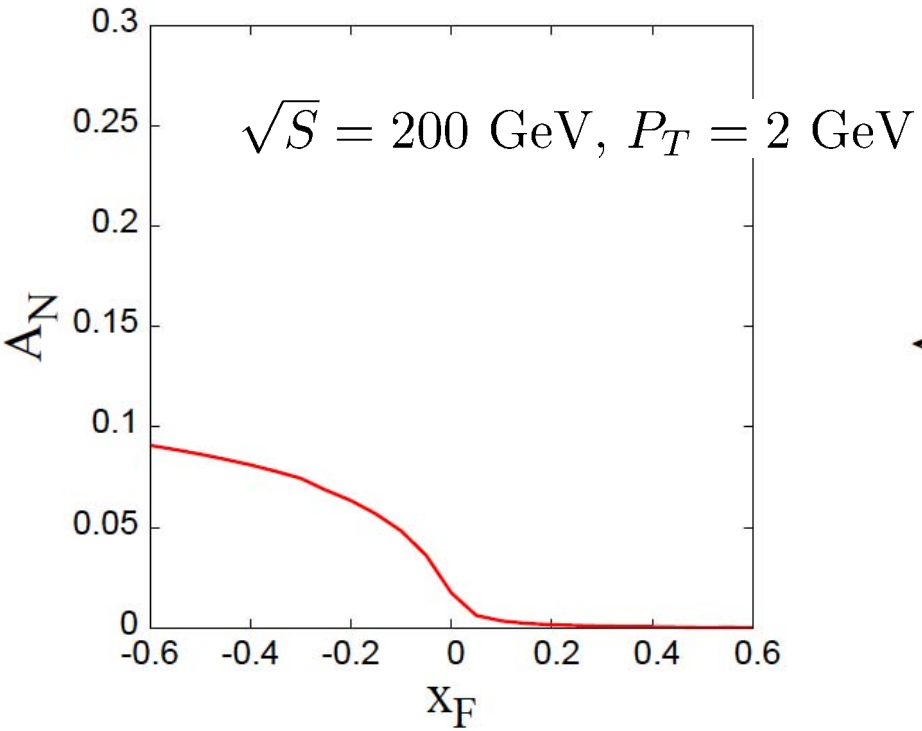

Model 2: $O(x) = 0.001\sqrt{x}G(x)$

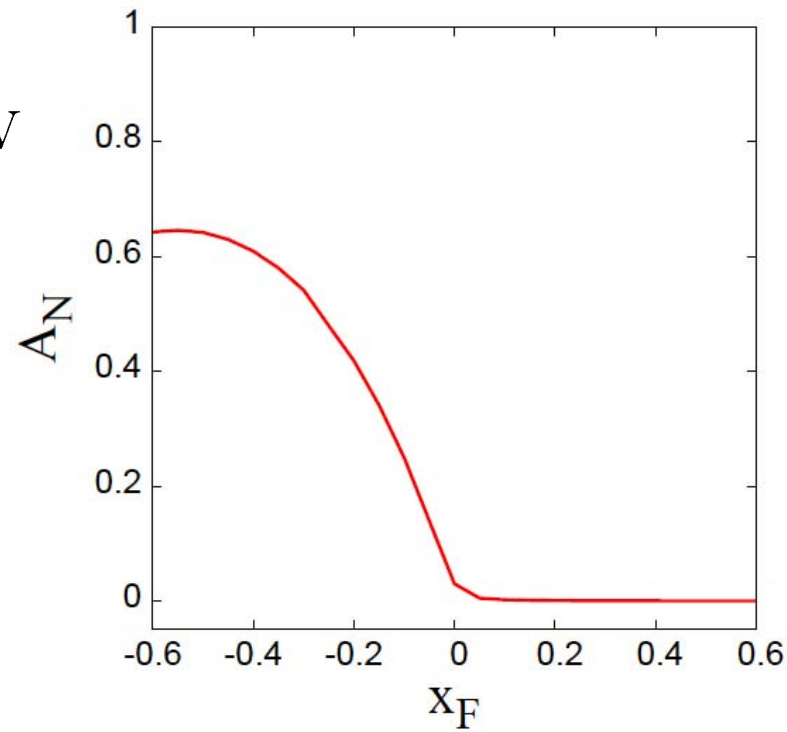

· $A_N \sim 0$ at $x_F > 0$ regardless of magnitude of the 3-gluon correlation functions.

· Behavior at $x_F < 0$ is sensitive to small x behavior similarly to $pp \rightarrow DX$.

Impact of the 3-gluon correlation functions on $p^{\uparrow}p \to \pi X$

(Beppu, YK, Kanazawa, Yoshida, in preparation.)

⋆ 3-gluon contribution to $p^{\uparrow}p \to \pi X$

Ex. Purely gluonic contributions

pole at $x_1 = x_2$

FSI

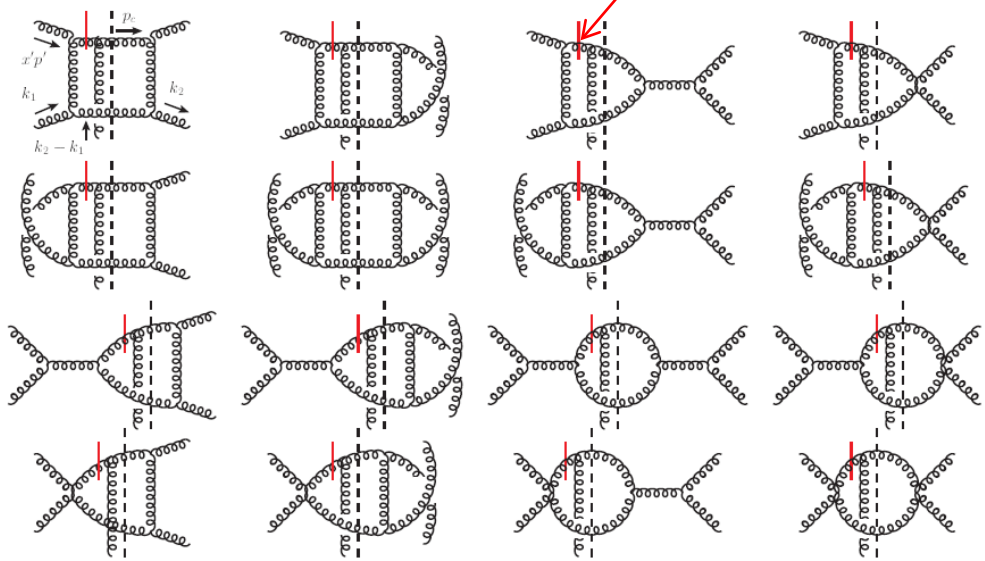

$+ \cdots$

ISI

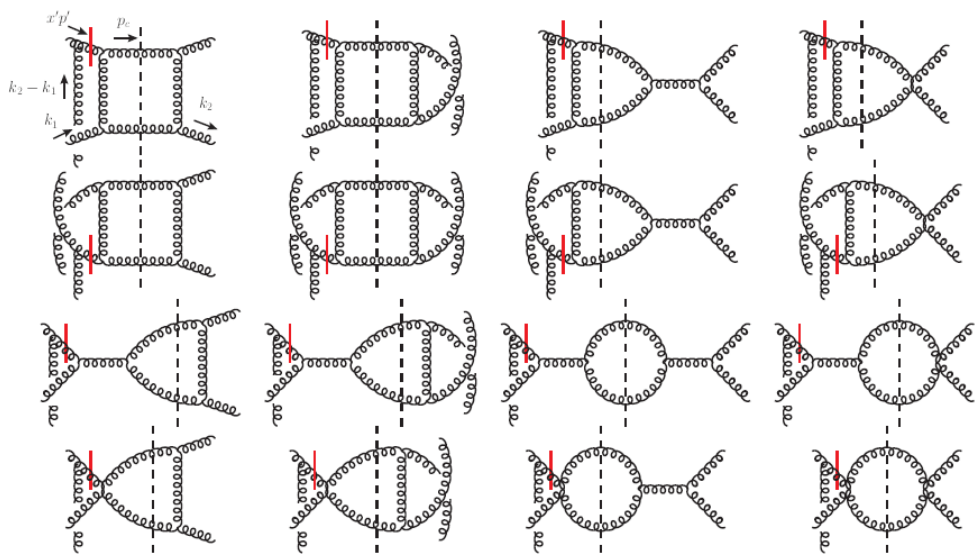

$+ \cdots$

$\star$ 3-gluon contribution to the cross section for $p^{\uparrow}(p,S)+p(p')\to\pi(P_h)+X$

$$P_h^0\frac{d^3\Delta\sigma}{d^3P_h} = \frac{2\pi M_N\alpha_s^2}{S}\sum_{b=q,g}\sum_{c=q,g}\int\frac{dx}{x}\int\frac{dx'}{x'}f_b(x')\int\frac{dz}{z^2}D_c(z)\delta(\hat{s}+\hat{t}+\hat{u})\epsilon^{P_h pnS_\perp}\frac{1}{z\hat{u}}$$
$$\times\left[\delta_b\left(\frac{d}{dx}O(x)-\frac{2O(x)}{x}\right)\hat{\sigma}^{(O)}_{gb\to c}+\left(\frac{d}{dx}N(x)-\frac{2N(x)}{x}\right)\hat{\sigma}^{(N)}_{gb\to c}\right]$$

$$O(x)\equiv O(x,x)+O(x,0) \qquad \hat{\sigma}^{(O,N)}_{gb\to c}=\hat{\sigma}^{(O,N)I}_{gb\to c}-\frac{\hat{s}}{\hat{t}}\hat{\sigma}^{(O,N)F}_{gb\to c}$$
$$N(x)\equiv N(x,x)-N(x,0)$$

$$\hat{s}=(xp+x'p')^2,\quad \hat{t}=(xp-P_h/z)^2,\quad \hat{u}=(x'p'-P_h/z)^2.$$

(i) Case 1: $O(x) = N(x)$

Model 1: $O(x) = 0.004 \times xG(x)$

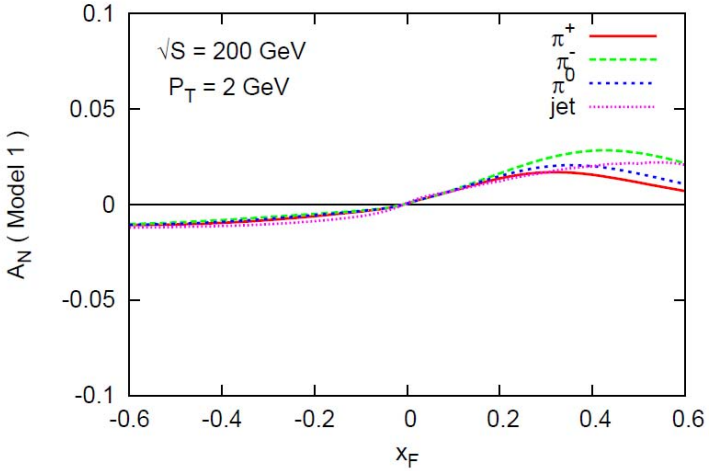

Model 2: $O(x) = 0.001\sqrt{x}G(x)$

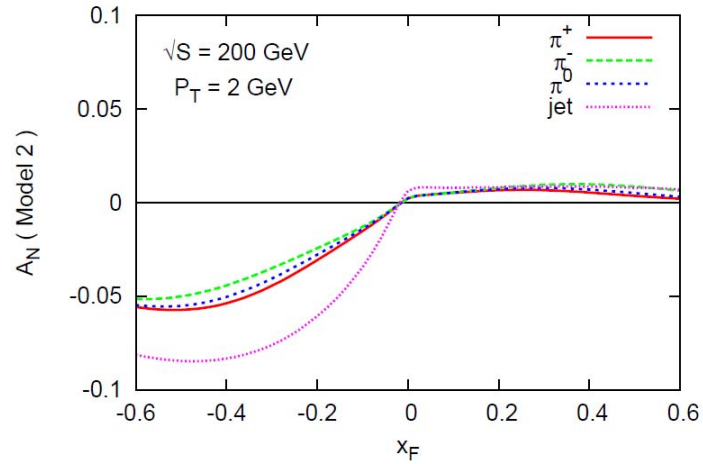

(ii) Case 2: $O(x) = -N(x)$

Model 1: $O(x) = 0.004 \times xG(x)$

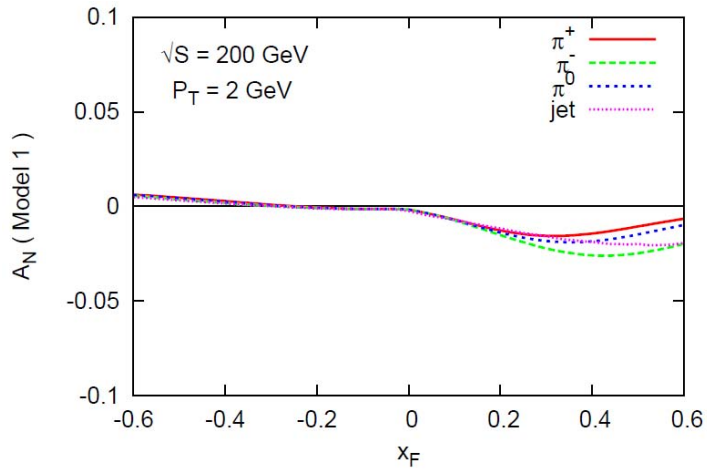

Model 2: $O(x) = 0.001\sqrt{x}G(x)$

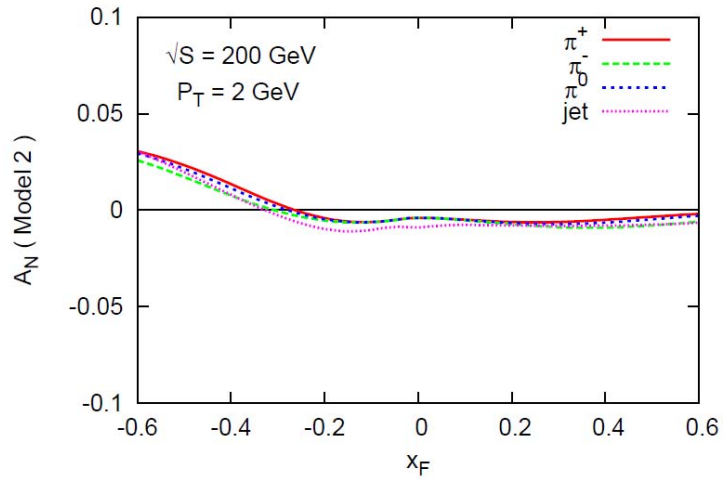

Model 2 gives too large A_N at $x_F < 0$. $\Rightarrow$ Unlikely!

⋆ 3-gluon contribution to $A_N^{\pi^0}$ vs. STAR data.

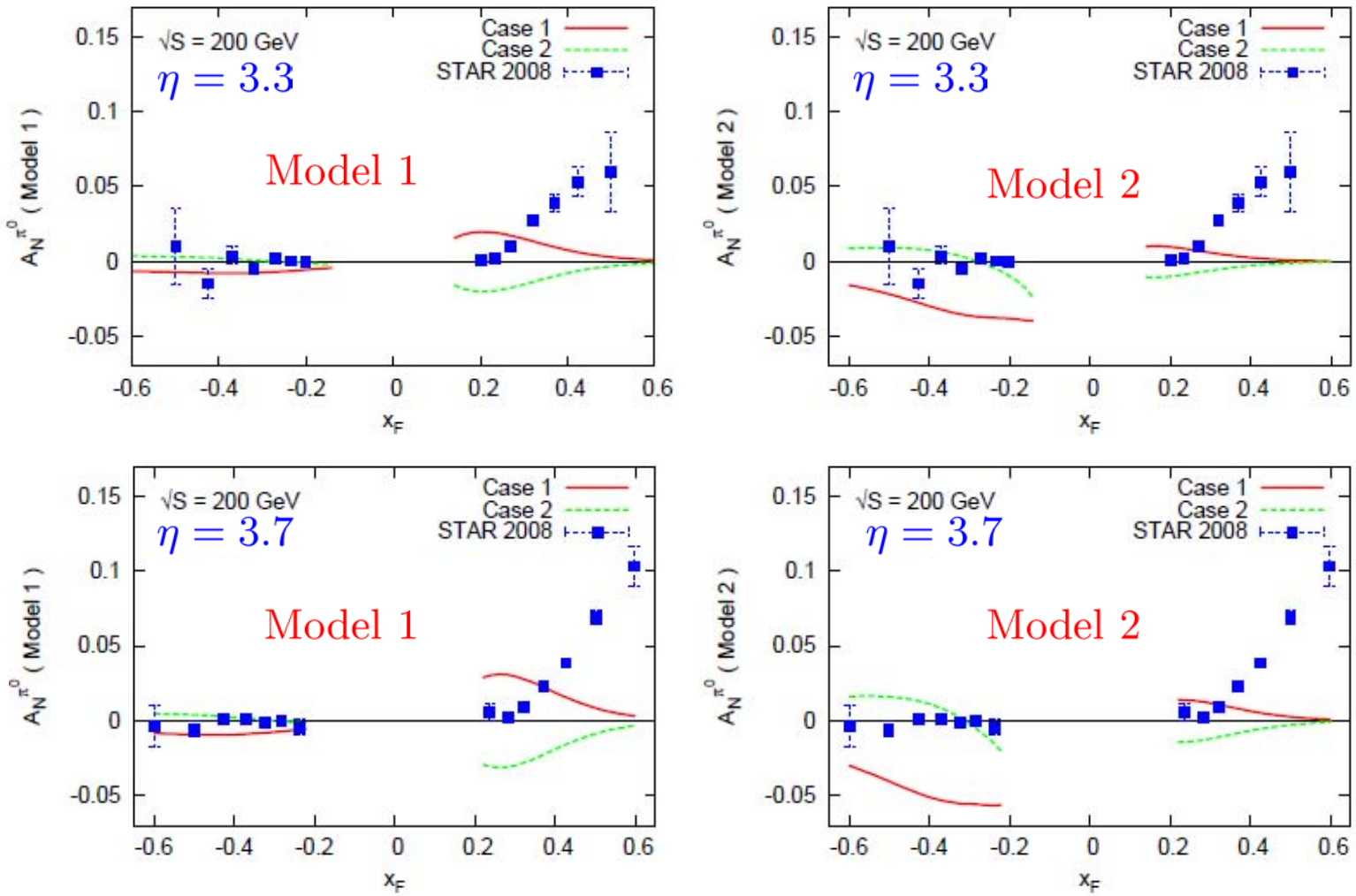

· Model 1 disturbes the fitting of A_N at $x_F > 0$.

· Model 2 disturbes the fitting of A_N at $x_F < 0$.

⇒ A good constraint for the 3-gluon correlation function.

4. Summary

⋆ Characteristics of the twist-3 analysis based the quark-gluon correlation functions

· Fitting of the STAR and BRAHMS data reproduces A_N of π and K by the combination of SGP and SFP contributions.

· This analysis also reproduces the observed peculiar pattern of the P_T-dependence of $A_N^{\pi^0}$.

· Our prediction for A_N^η is approximately consistent with the STAR data. The origin of $A_N^\eta \sim 2A_N^{\pi^0}$ is the strangeness content in the η fragmentation function and the strangeness-gluon correlation in the nucleon.

· $A_N^{\mathrm{jet},\gamma} = 0$ at $x_F < 0$ in the present analysis implies that the nonzero $A_N^{\mathrm{jet},\gamma}$ at $x_F < 0$ can be ascribed to the 3-gluon correlation function.

· Peculiar pattern of the P_T-dependence of A_N^γ can be used as a test for the twist-3 mechanism.

⋆ Characteristics of the 3-gluon contribution to A_N

· Complete LO twist-3 cross section formula have been derived for $p^{\uparrow}p \to \{D, \ell^+\ell^-, \gamma, \pi, \text{jet}\}X$.

· $A_N^{\gamma} \simeq 0$ at $x_F > 0$, which is model-independent.
⇒ The roles of the quark-gluon correlation and the 3-gluon correlation are clearly separated.

· The upper bound for the 3-gluon correlations extracted from the RHIC A_N^D data already disturbes the observed A_N^{π}.
⇒ A better constraint for the 3-gluon correlations.

Putting Spin on Color Glass

Yuri Kovchegov
The Ohio State University

based on arXiv:1201.5890 [hep-ph] with Matthew Sievert

(special thanks to Michael Lisa)

Outline

- Introduction (STSAs, saturation/CGC)
- Calculation of STSA in CGC
- Properties of the obtained result
- Conclusions and outlook

Introduction

Single Transverse Spin Asymmetry

- Consider polarized proton scattering on an unpolarized proton or nucleus.

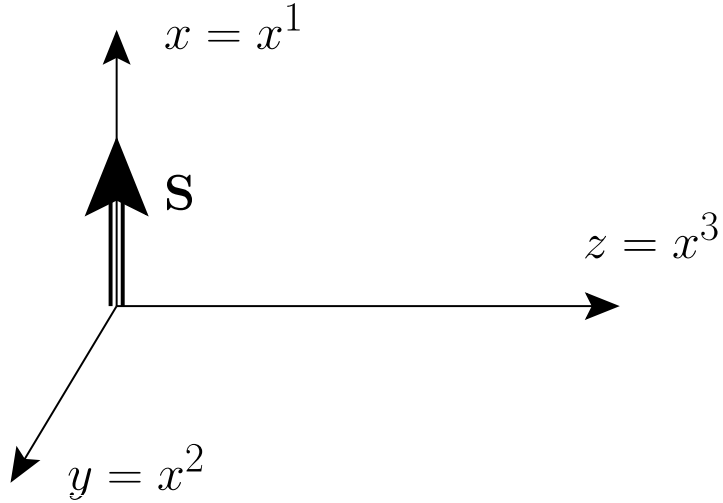

- Single Transverse Spin Asymmetry (STSA) is defined by

$$A_N(\mathbf{k}) \equiv \frac{\frac{d\sigma^{\uparrow}}{d^2k\,dy} - \frac{d\sigma^{\downarrow}}{d^2k\,dy}}{\frac{d\sigma^{\uparrow}}{d^2k\,dy} + \frac{d\sigma^{\downarrow}}{d^2k\,dy}} = \frac{\frac{d\sigma^{\uparrow}}{d^2k\,dy}(\mathbf{k}) - \frac{\mathbf{d}\sigma^{\uparrow}}{\mathbf{d^2k\,dy}}(-\mathbf{k})}{\frac{d\sigma^{\uparrow}}{d^2k\,dy}(\mathbf{k}) + \frac{\mathbf{d}\sigma^{\uparrow}}{\mathbf{d^2k\,dy}}(-\mathbf{k})} \equiv \frac{d(\Delta\sigma)}{2\,d\sigma_{unp}}$$

STSA: the data

- The asymmetry is non-zero, and is an increasing function of Feynman-x of the polarized proton:

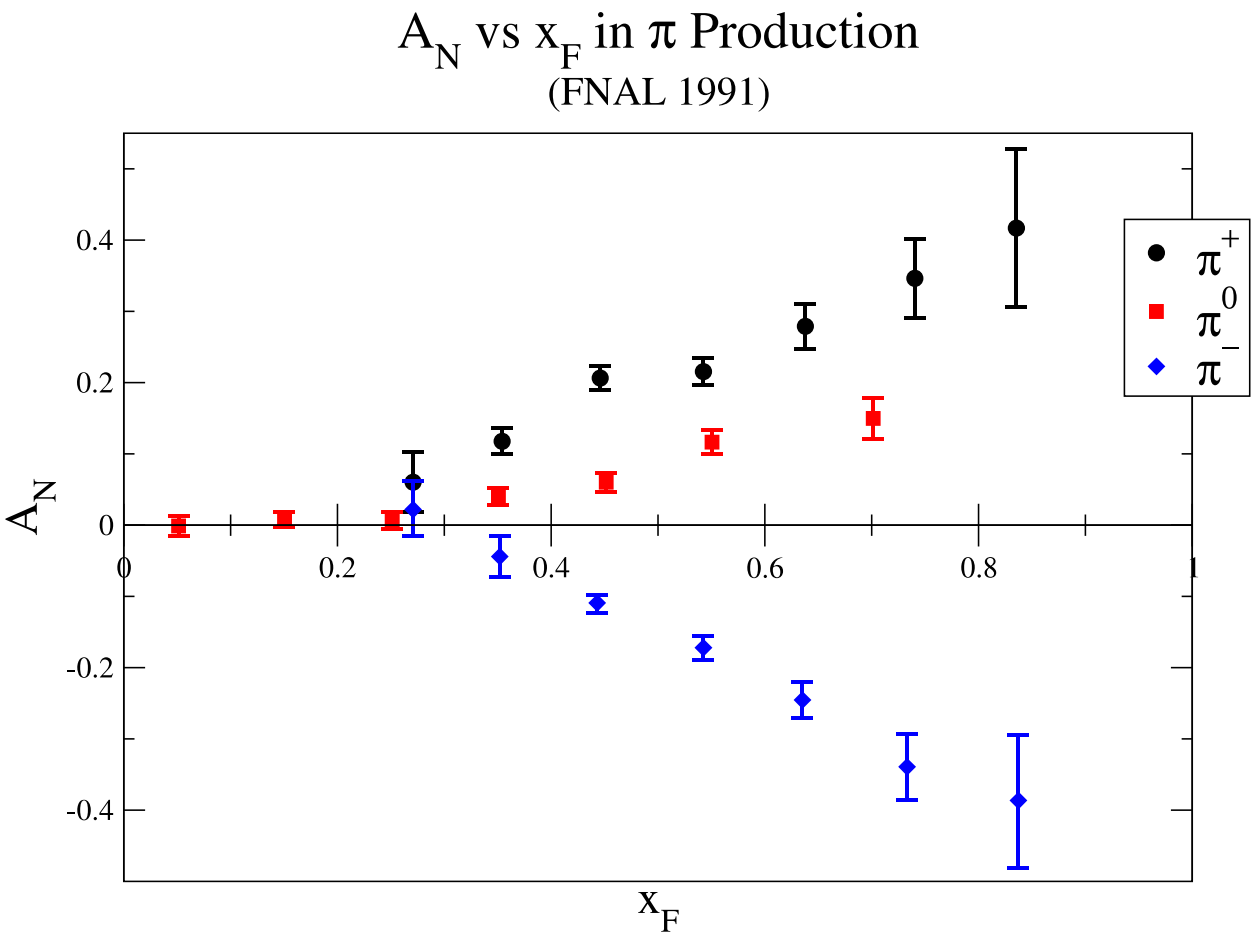

Fermilab
E581 & E704
collaborations
1991

STSA: a more recent data

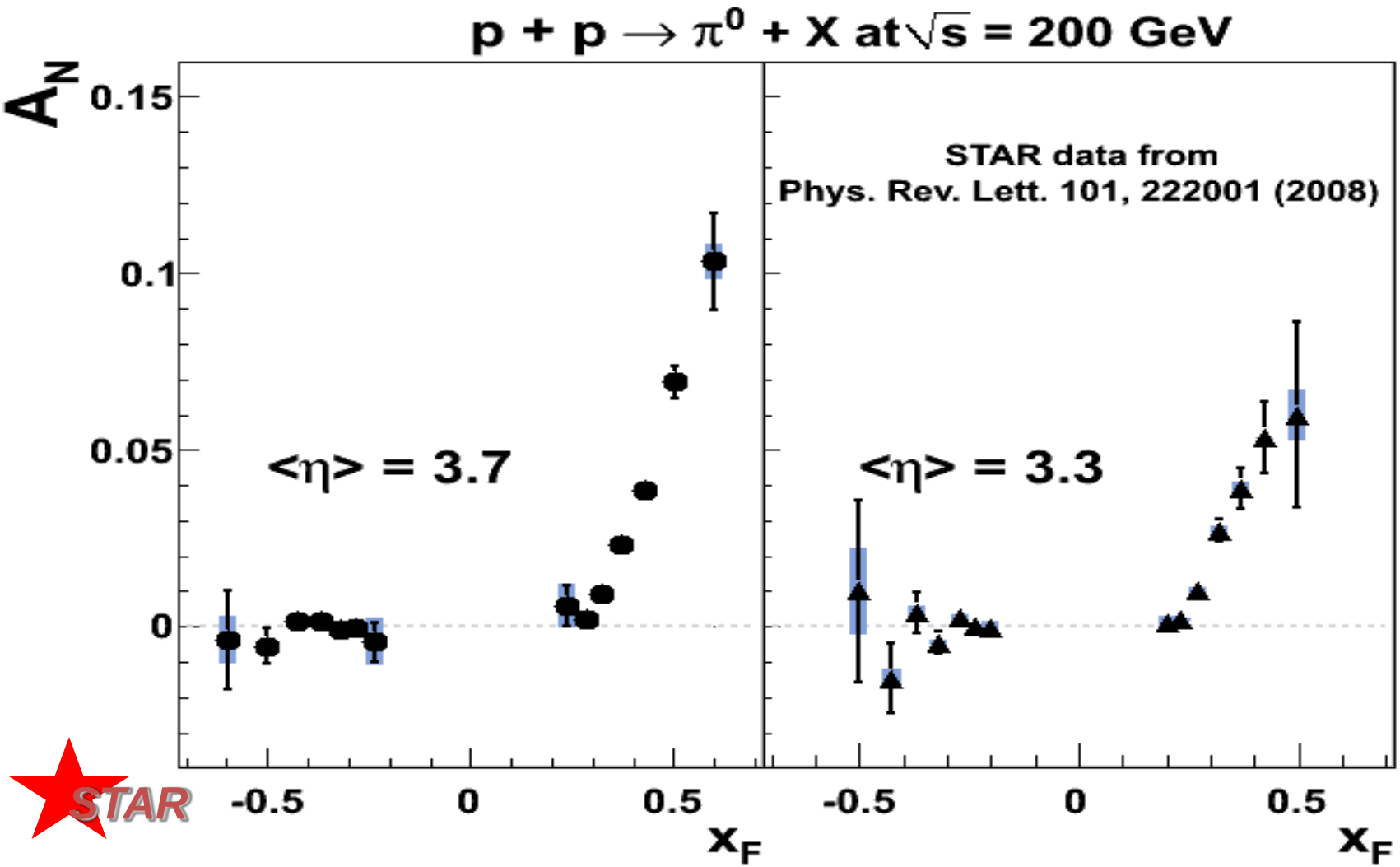

STSA: the data

- STSA is also a non-monotonic function of transverse momentum p_T, which has zeroes (nodes), where its sign changes:

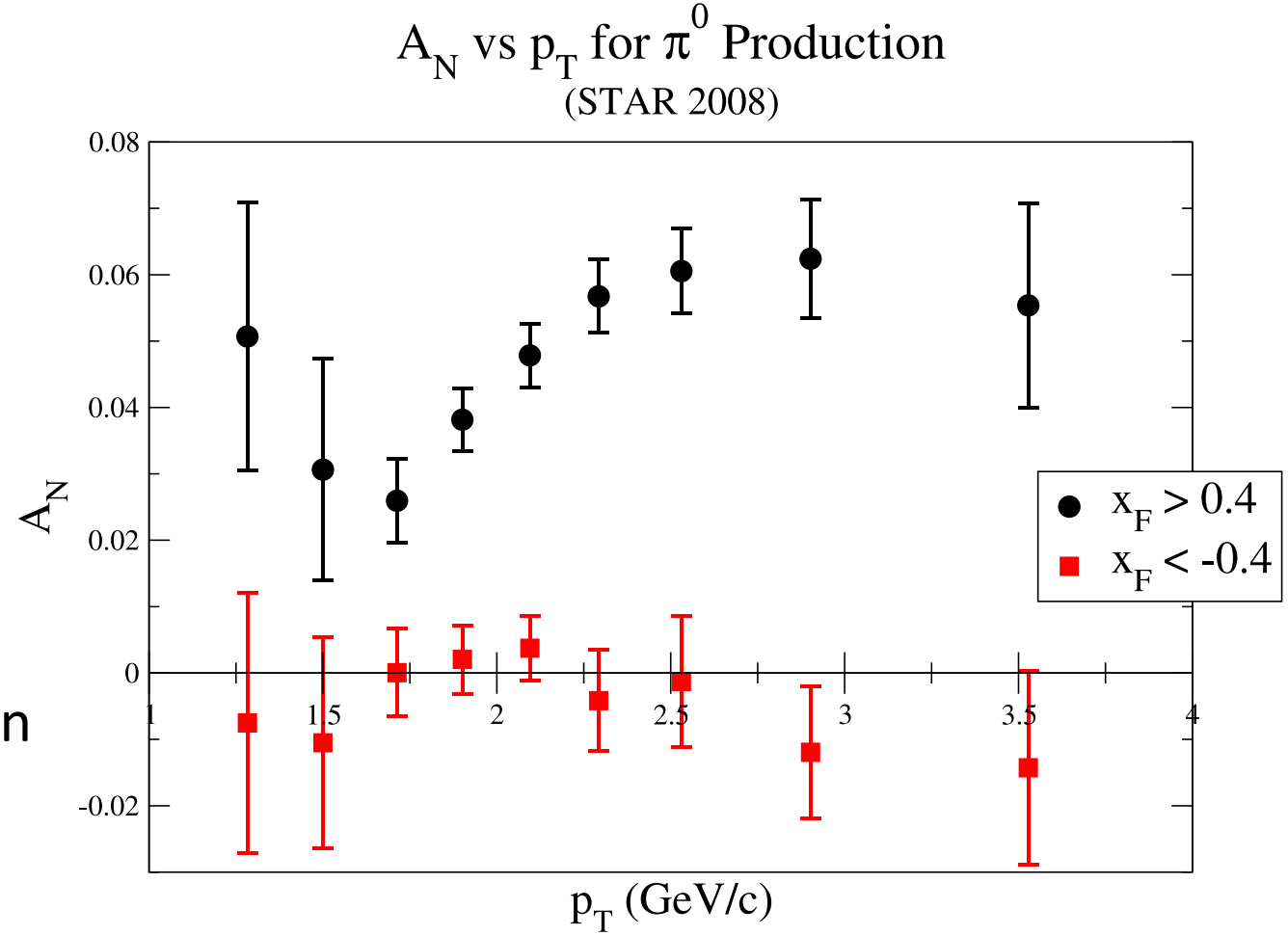

RHIC,
STAR collaboration
2008

STSA: a more recent data

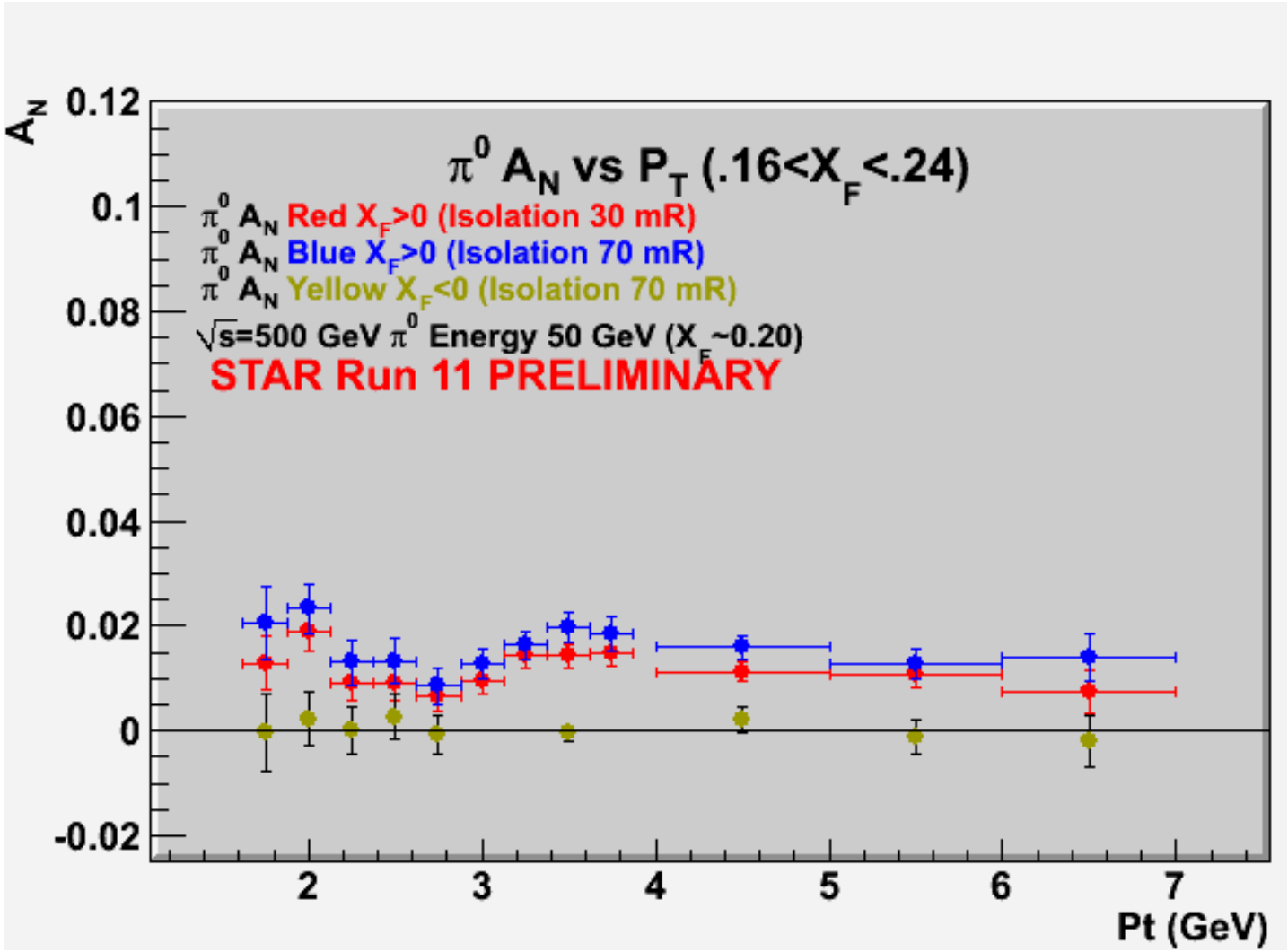

Theoretical Explanations

The origin of STSA (in the collinear factorization framework) is in

- polarized PDF (Sivers effect)
- polarized fragmentation (Collins effect)
- hard scattering

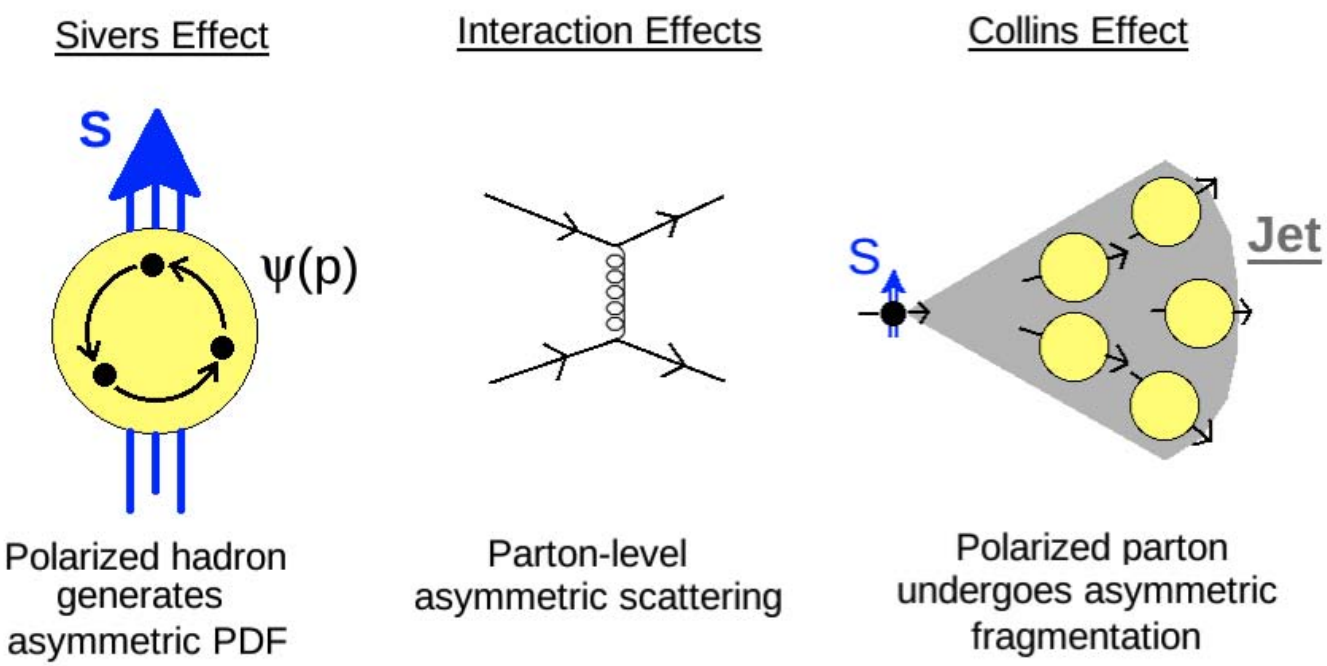

High Energy QCD: saturation physics

- Saturation physics is based on the existence of a large internal momentum scale Q_S which grows with both energy s and nuclear atomic number A

$$Q_S^2 \sim A^{1/3}\, s^{\lambda}$$

such that

$$\alpha_S = \alpha_S(Q_S) << 1$$

and we can calculate total cross sections, particle spectra and multiplicities, etc, from <u>first principles</u>.

- Bottom line: everything is considered perturbative.

Map of High Energy QCD

Saturation physics allows us to study regions of high parton density in the small coupling regime, where calculations are still under control!

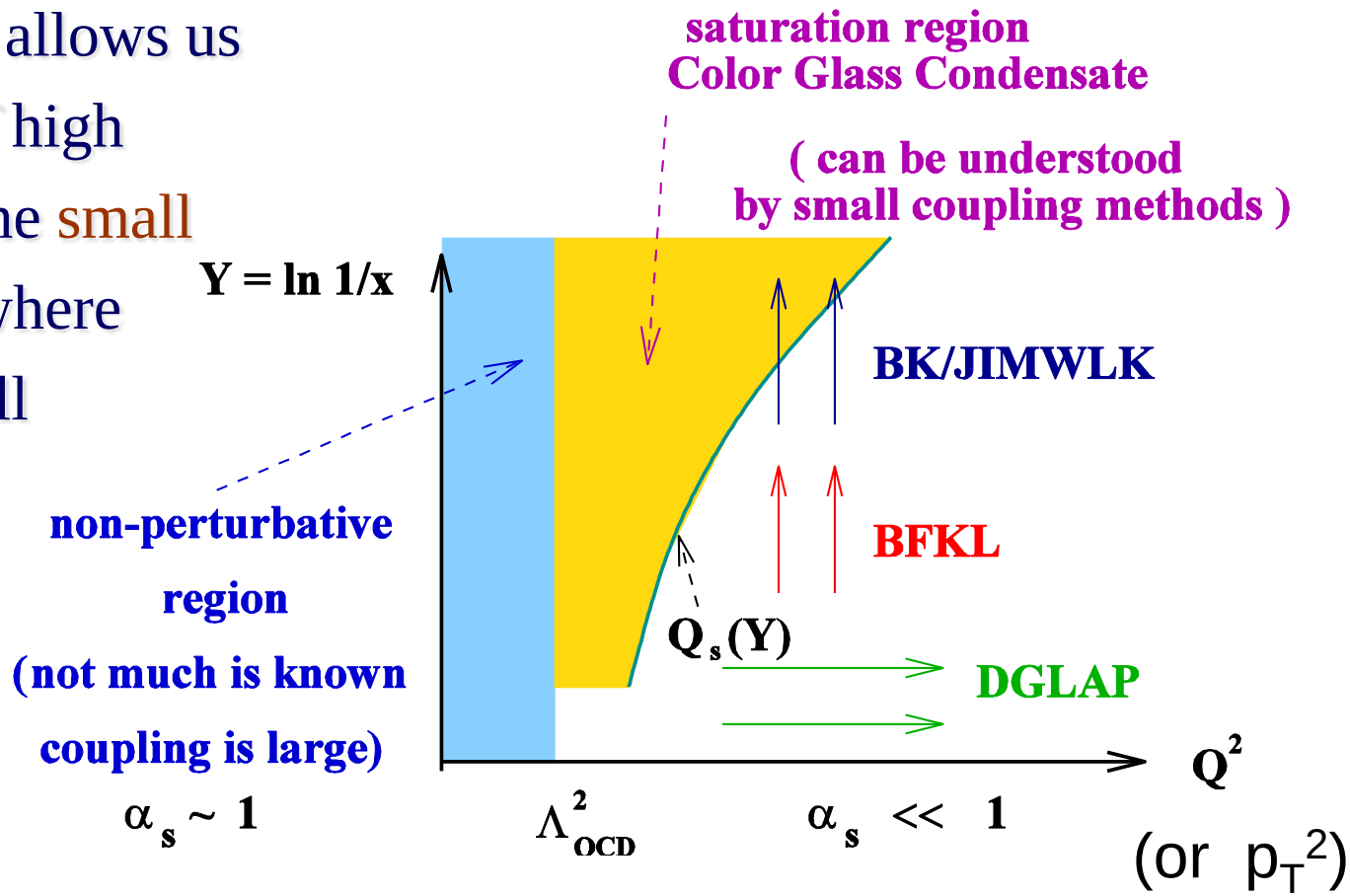

Transition to saturation region is characterized by the <u>saturation scale</u>

$$Q_S^2 \sim A^{1/3}\left(\frac{1}{x}\right)^{\lambda}$$

A reference

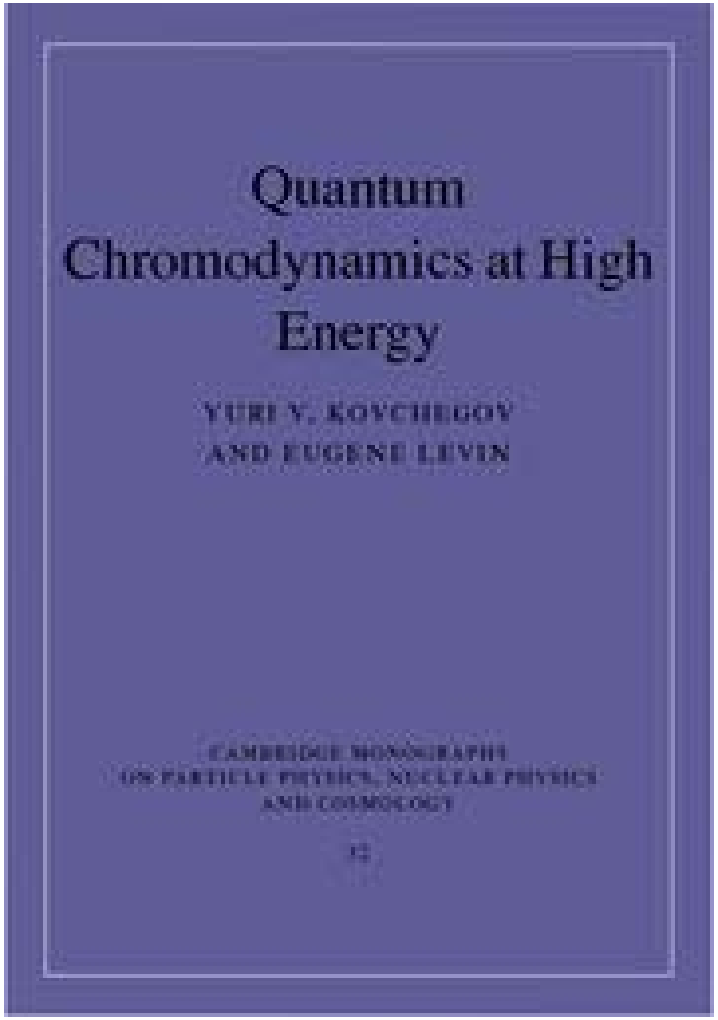

Coming in August 2012
from Cambridge U Press

Calculation of STSA in CGC

Forward quark production

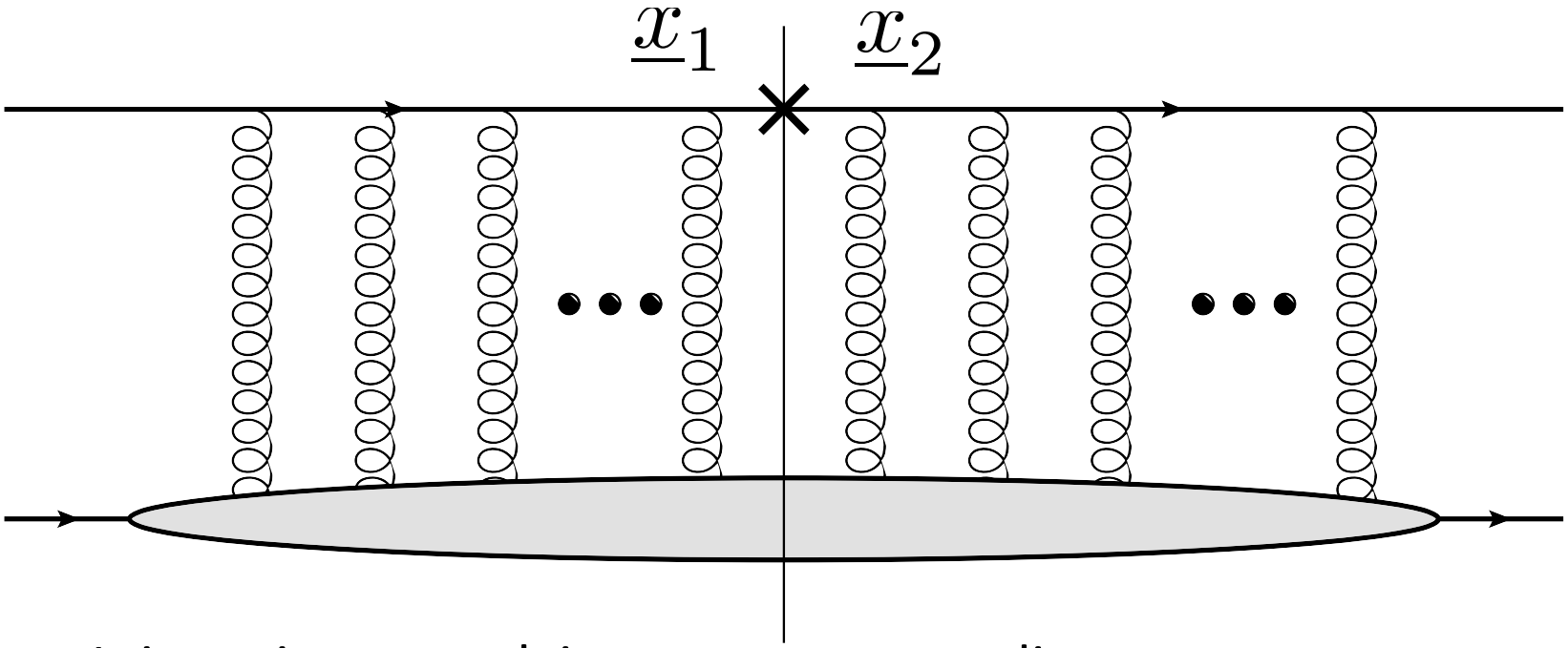

- It is easier to work in transverse coordinate space:

$$\frac{d\sigma}{d^2k\,dy} \propto |M(\underline{k})|^2 = \int d^2x_1\, d^2x_2\, M(\underline{x}_1)\, M(\underline{x}_2)^*\, e^{-i\,\underline{k}\cdot(\underline{x}_1-\underline{x}_2)}$$

- The quark (transverse) coordinates are different on two sides of the cut!

Forward quark production

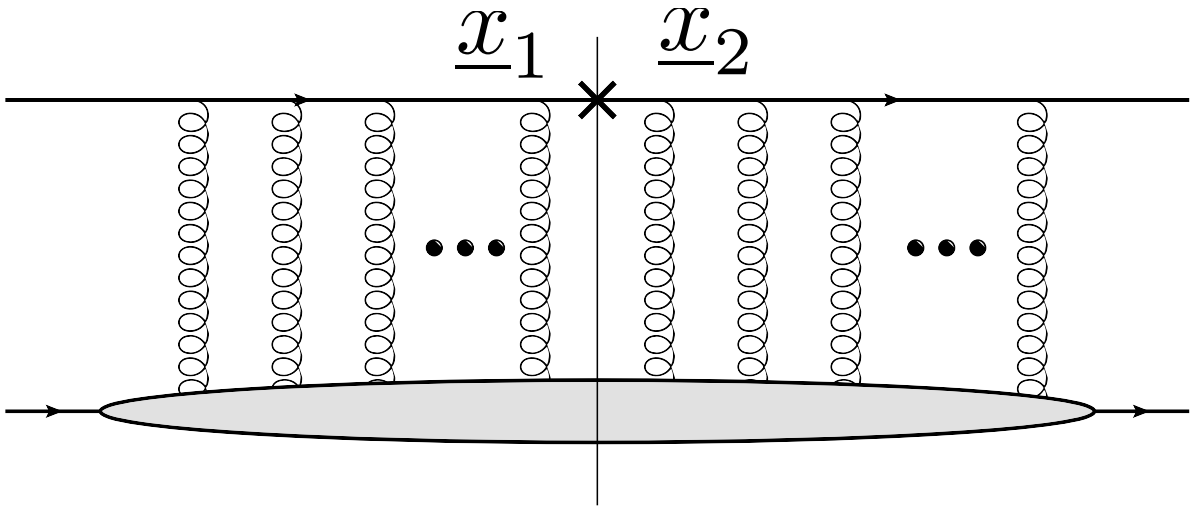

- The eikonal quark propagator is given by the Wilson line

$$V(\underline{x}) = \mathrm{P}\exp\left[i\,g\int_{-\infty}^{\infty} dx^+\,A^-(x^+, x^- = 0, \underline{x})\right]$$

with the light cone coordinates $x^\pm = \dfrac{t \pm z}{\sqrt{2}}$

Forward quark production

Dumitru, Jalilian '02

- The amplitude squared is

$$\frac{1}{N_c}\left\langle \mathrm{tr}\left\{\left[V(\underline{x}_1)-1\right]\left[V^\dagger(\underline{x}_2)-1\right]\right\}\right\rangle = 1+\frac{1}{N_c}\left\langle \mathrm{tr}\left[V(\underline{x}_1)\,V^\dagger(\underline{x}_2)\right]\right\rangle$$

- The quark dipole scattering amplitude is

$$N(\underline{x}_1,\underline{x}_2) = 1-\frac{1}{N_c}\left\langle \mathrm{tr}\left[V(\underline{x}_1)\,V^\dagger(\underline{x}_2)\right]\right\rangle$$

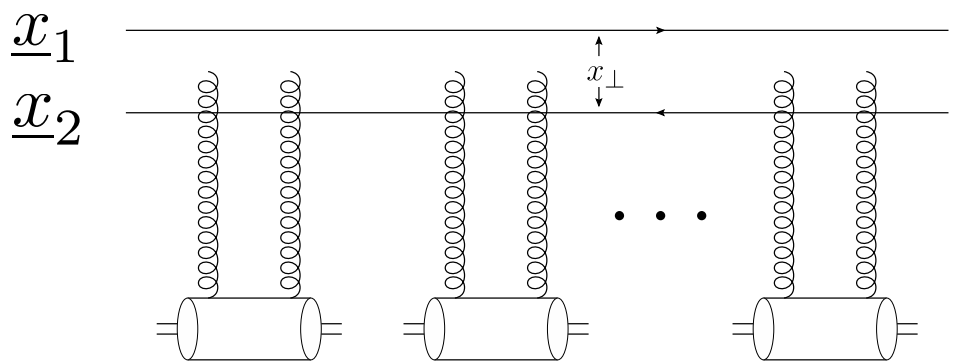

- Hence quark production is related to the dipole amplitude! Valid both in the quasi-classical Glauber-Mueller/McLerran-Venugopalan multiple-rescattering approximation and for the LLA small-x evolution (BFKL/BK/JIMWLK).

Dipole Amplitude

- Dipole scattering amplitude is a universal degree of freedom in CGC.
- It describes the DIS cross section and structure functions:

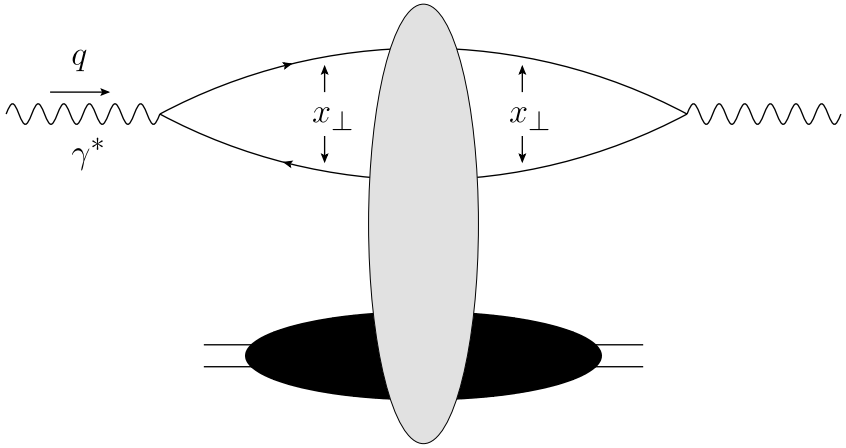

- It also describes single inclusive quark (shown above) and gluon production cross section in DIS and in pA.
- Even works for diffraction in DIS and pA.
- For correlations need also qudrupoles. (J.Jalilian-Marian, Yu.K. ‘04)

Spin-dependent quark production

- The eikonal quark production is indeed spin-independent, and hence can not generate STSA.

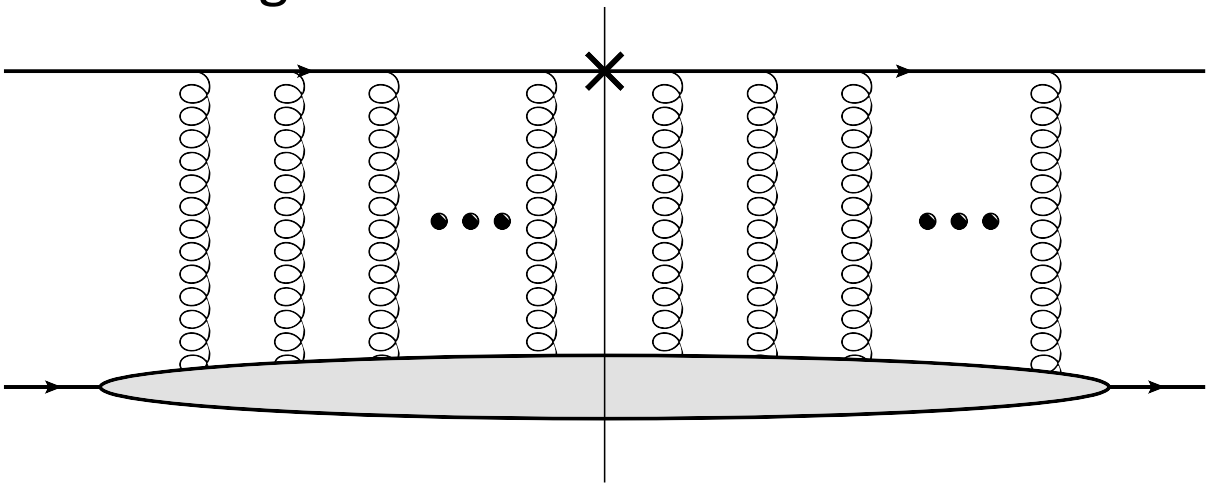

- Simple recoil, while spin-dependent, is suppressed by 1/s:

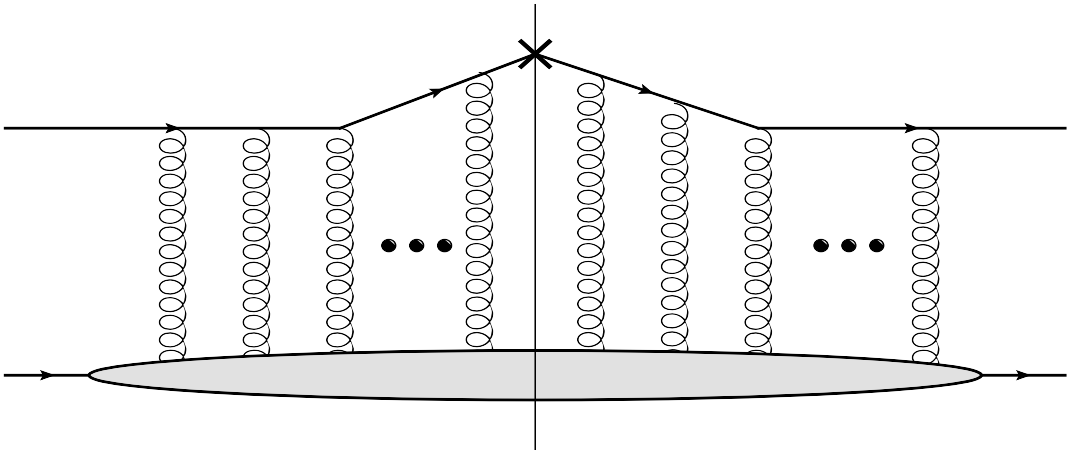

Spin-dependent quark production

The only way to include spin dependence without 1/s suppression is through the splitting in the projectile before or after the collision with the target:

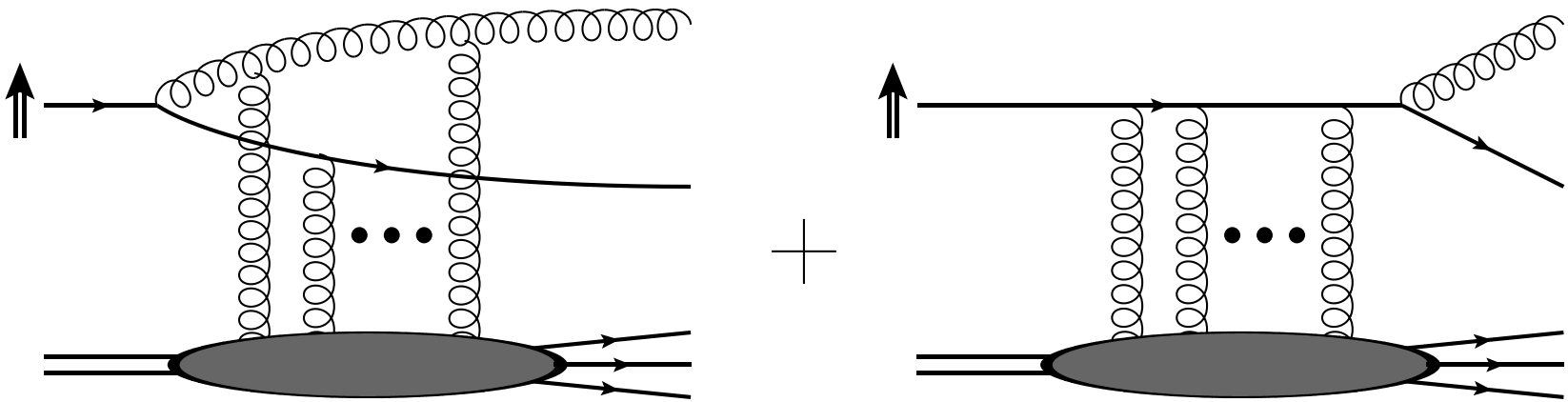

Let's calculate the corresponding quark production cross section, find its spin-dependent part, and see if it gives an STSA.

Production Cross Section

Squaring the amplitude we get the following diagrams contributing to the production cross section:

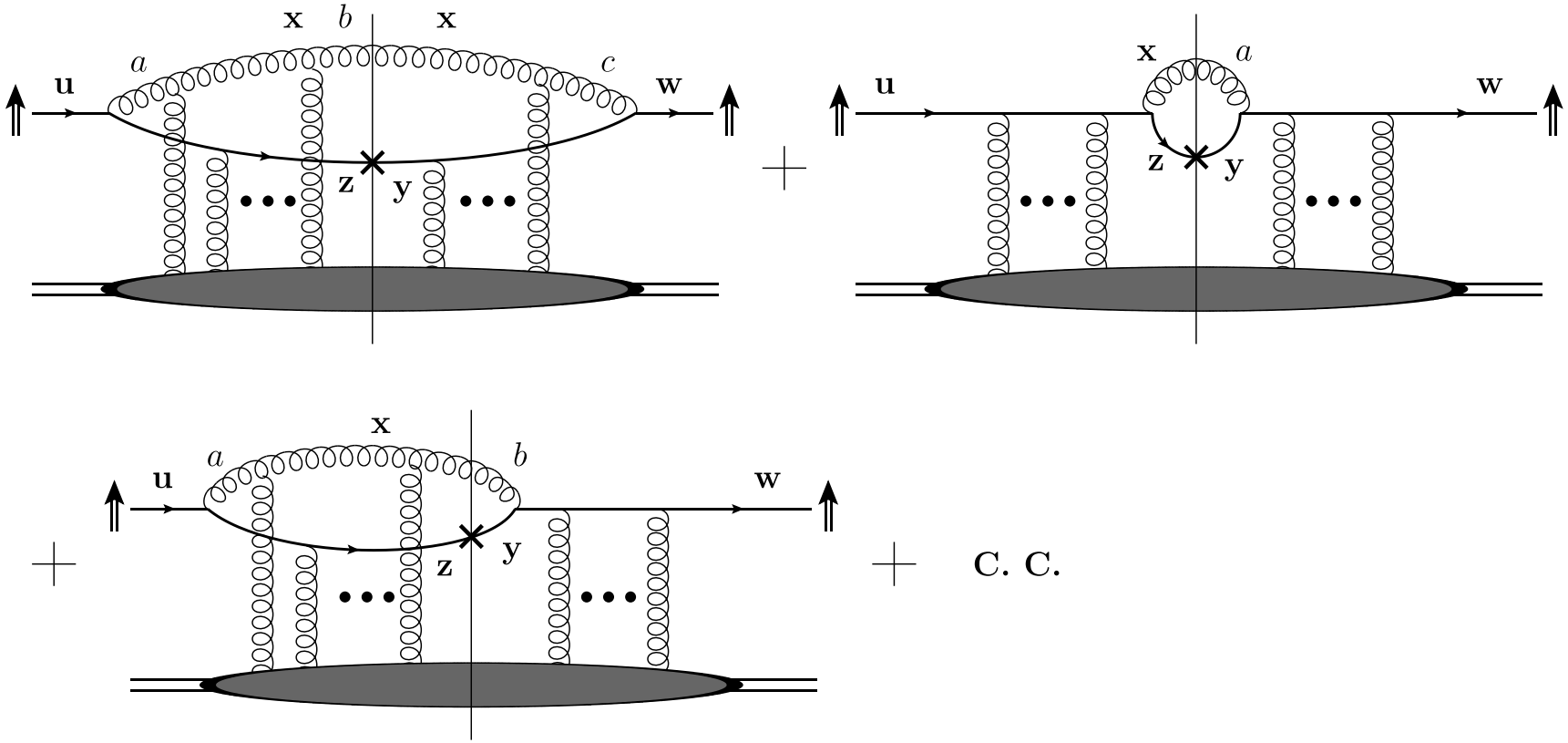

Extracting STSA

- STSA can be thought of as the term proportional to

$$(\vec{S} \times \vec{p}) \cdot \vec{k}$$

- To get a k_T-odd part of the cross section

$$\frac{d\sigma^{(q)}}{d^2k\, dy_q} = \frac{C_F}{2\,(2\pi)^3}\,\frac{\alpha}{1-\alpha}\int d^2x\, d^2y\, d^2z\, e^{-i\mathbf{k}\cdot(\mathbf{z}-\mathbf{y})}\,\Phi_\chi(\mathbf{z}-\mathbf{x}\,,\,\mathbf{y}-\mathbf{x})\,\mathcal{I}^{(\mathbf{q})}(\mathbf{x}\,,\,\mathbf{y}\,,\,\mathbf{z})$$

  we need the $\mathbf{y} \leftrightarrow \mathbf{z}$ anti-symmetric part of the integrand.

- This may either come from the wave function squared or from the interaction with the target.
- Our LO wave function is symmetric: need to find the anti-symmetric interaction!

C-even and C-odd dipoles

- To find the anti-symmetric interaction we decompose the dipole amplitude into real symmetric (C-even) and imaginary anti-symmetric (C-odd) parts:

$$\frac{1}{N_c}\,\langle \mathrm{tr}\left[V_{\mathbf{x}}\,V_{\mathbf{y}}^{\dagger}\right]\rangle = S_{\mathbf{x}\,\mathbf{y}} + i\,O_{\mathbf{x}\,\mathbf{y}}$$

- The symmetric part is

$$S_{\mathbf{x}\,\mathbf{y}} = \frac{1}{2}\left\{\frac{1}{N_c}\,\langle \mathrm{tr}\left[V_{\mathbf{x}}\,V_{\mathbf{y}}^{\dagger}\right]\rangle + \frac{1}{N_c}\,\langle \mathrm{tr}\left[V_{\mathbf{y}}\,V_{\mathbf{x}}^{\dagger}\right]\rangle\right\}$$

- The anti-symmetric part is

$$O_{\mathbf{x}\,\mathbf{y}} = \frac{1}{2\,i}\left\{\frac{1}{N_c}\,\langle \mathrm{tr}\left[V_{\mathbf{x}}\,V_{\mathbf{y}}^{\dagger}\right]\rangle - \frac{1}{N_c}\,\langle \mathrm{tr}\left[V_{\mathbf{y}}\,V_{\mathbf{x}}^{\dagger}\right]\rangle\right\}$$

- As $\mathbf{x} \leftrightarrow \mathbf{y}$ interchanges quark and antiquark, it is C-parity!

C-even and C-odd dipoles

- S_{xy} is the usual C-even dipole amplitude, to be found from the BK/JIMWLK equations: describes DIS, unpolarized quark and gluon production
- O_{xy} is the C-odd odderon exchange amplitude, obeying a different evolution equation (Yu.K., Szymanowski, Wallon '03)
- At LO the odderon is a 3-gluon exchange:

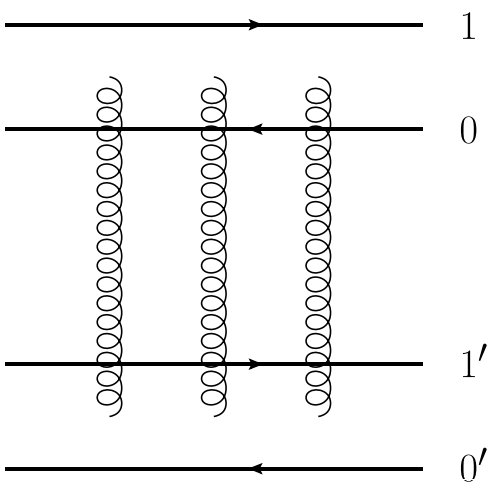

- The intercept of the odderon is zero (Bartels, Lipatov, Vacca '99):

$$\sigma_{odd} \sim s^0 \sim const$$

- In our setup, odderon naturally generates STSA.

STSA in high energy QCD

- When the dust settles, the spin-dependent part of the production cross section is

$$d(\Delta\sigma^{(q)}) = \frac{C_F}{(2\pi)^3}\,\frac{\alpha}{1-\alpha}\int d^2x\, d^2y\, d^2z\, e^{-i\mathbf{k}\cdot(\mathbf{z}-\mathbf{y})}\,\Phi_{pol}(\mathbf{z}-\mathbf{x}\,,\,\mathbf{y}-\mathbf{x})\,\mathcal{I}^{(\mathbf{q})}_{\mathbf{anti}}(\mathbf{x}\,,\,\mathbf{y}\,,\,\mathbf{z})$$

with the C-odd interaction with the target

$$\mathcal{I}^{(q)}_{anti}\Big|_{\mathrm{large}-N_c} = i\,[O_{\mathbf{z}\,\mathbf{y}} + O_{\mathbf{u}\,\mathbf{w}} - O_{\mathbf{z}\,\mathbf{x}}\,S_{\mathbf{x}\,\mathbf{w}} - O_{\mathbf{u}\,\mathbf{x}}\,S_{\mathbf{x}\,\mathbf{y}} - S_{\mathbf{z}\,\mathbf{x}}\,O_{\mathbf{x}\,\mathbf{w}} - S_{\mathbf{u}\,\mathbf{x}}\,O_{\mathbf{x}\,\mathbf{y}}]$$

- Note that the interaction contains nonlinear terms: only those survive in the end.
- The expression for the interaction at any N_c is known.

Properties of the obtained STSA contribution

Odderon STSA properties

Our odderon STSA is a non-monotonic function of transverse momentum and an increasing function of Feynman-x:

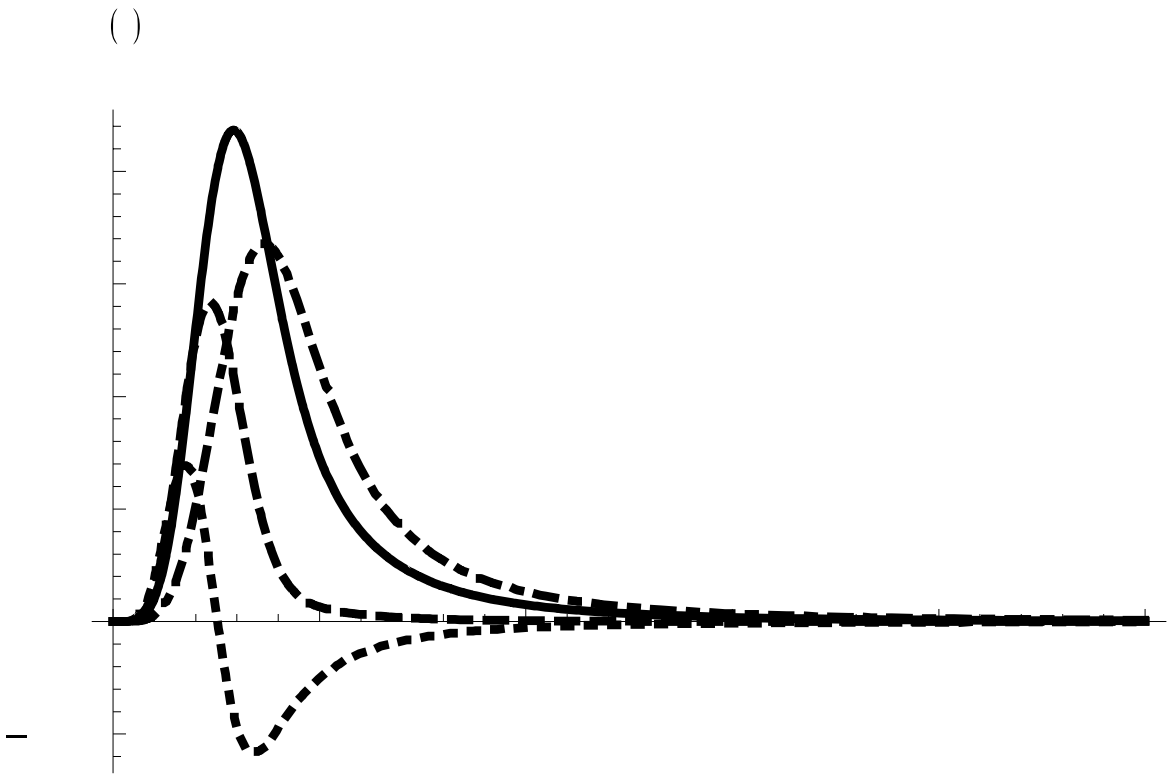

Warning: very crude approximation of the formula. (Q_s=1 GeV)
Curves are for (Feynman-x) α =0.9 (dash-dotted), 0.7 (solid), 0.6 (dashed), 0.5 (dotted).

Dependence on density gradient

- Our STSA is proportional to the square of the gradient of the nuclear profile function T(b):

$$A_N \sim \int d^2b \, [\nabla \mathbf{T}(\mathbf{b})]^2 \ldots$$

- The asymmetry is larger for peripheral collisions, and is dominated by edge effects.

- It is also smaller for nuclei (pA) than for the proton target (pp).

Odderon STSA properties

To illustrate this we plot A_N with a different large-b (IR) cutoff:

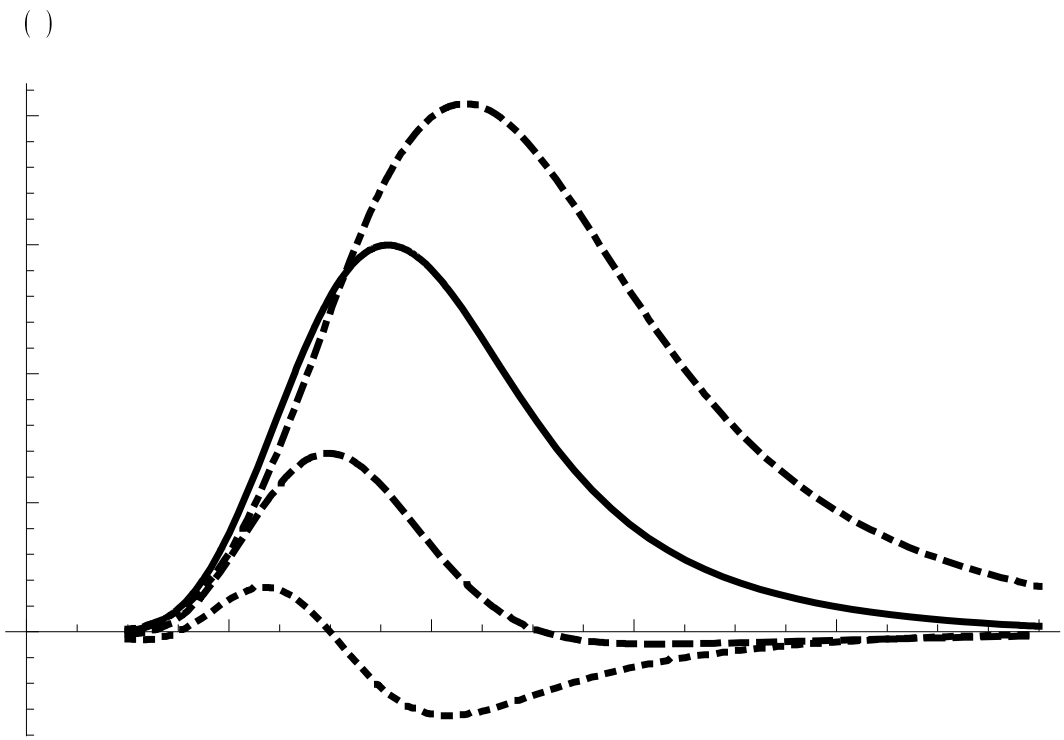

Warning: very crude approximation of the formula. (Q_s=1 GeV)
Curves are for (Feynman-x) α =0.9 (dash-dotted), 0.7 (solid), 0.6 (dashed), 0.5 (dotted).

Odderon STSA at high-p_T

- The odderon STSA is a steeply-falling function of p_T:

$$d(\Delta\sigma^{(q)})\Big|_{k_T \gg Q_s} \propto \frac{k^2}{k_T^{10}}$$

(our spin is in x^1-direction).

- However, the suppression at high transverse momentum is gone for $k_T \sim Q_s$ (from one to a few GeV).

Nuclear (unpolarized) target

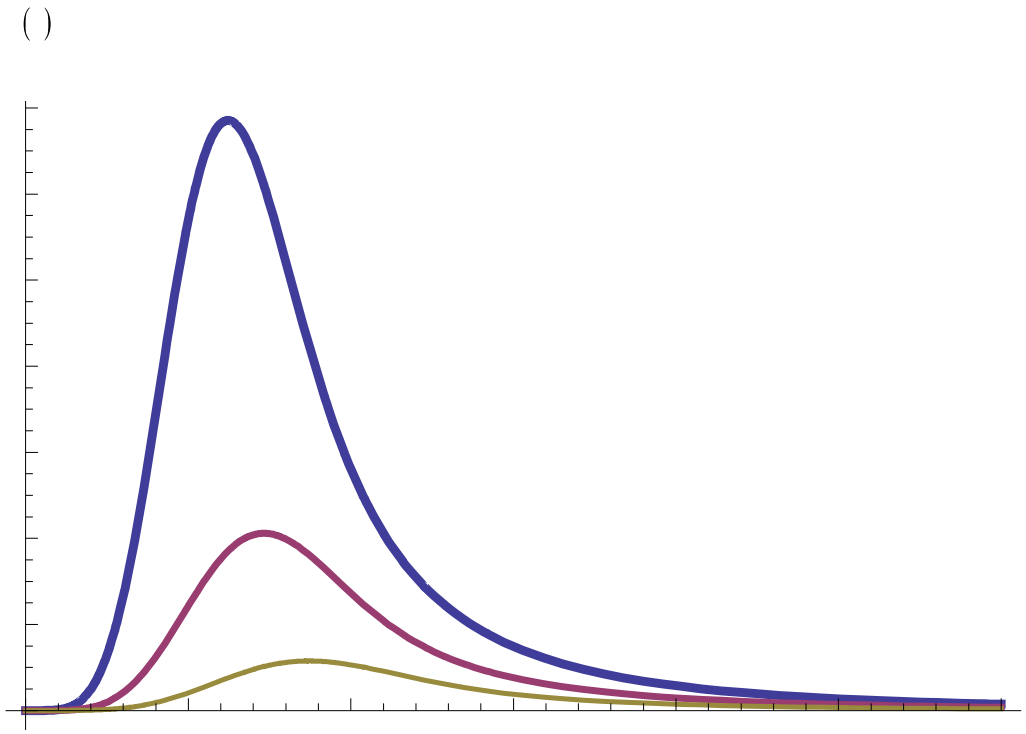

Target radius is R=1 fm (top curve), R=1.4 fm (middle curve), R=2 fm (bottom curve): strong suppression of odderon STSA in nuclei. Warning: crude approximation of the exact formula!

Gluon STSA

- is also found along the same lines:

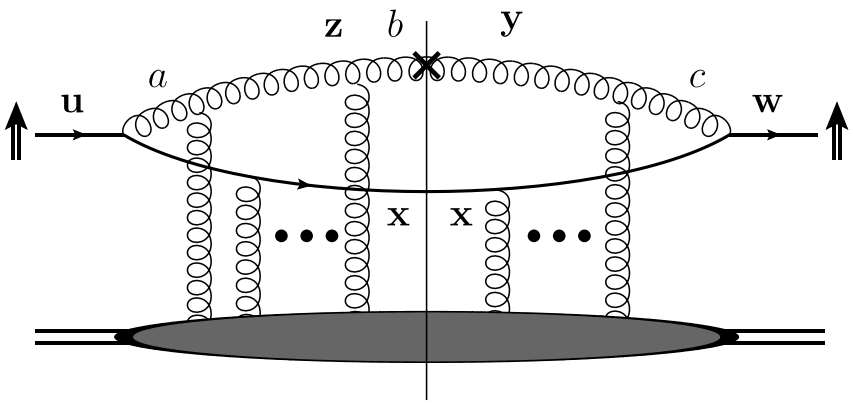

+

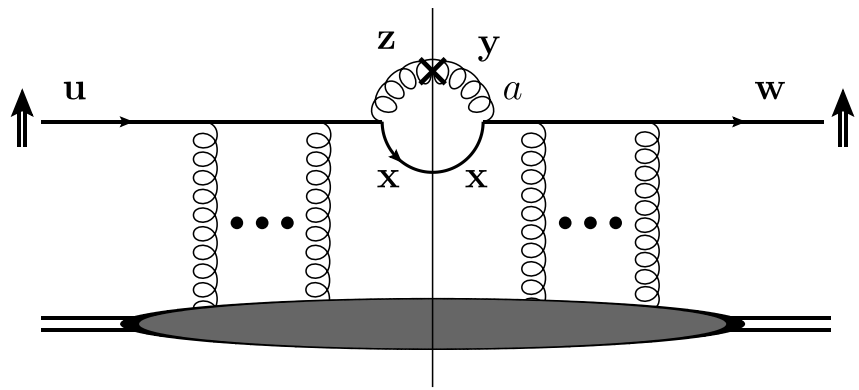

+

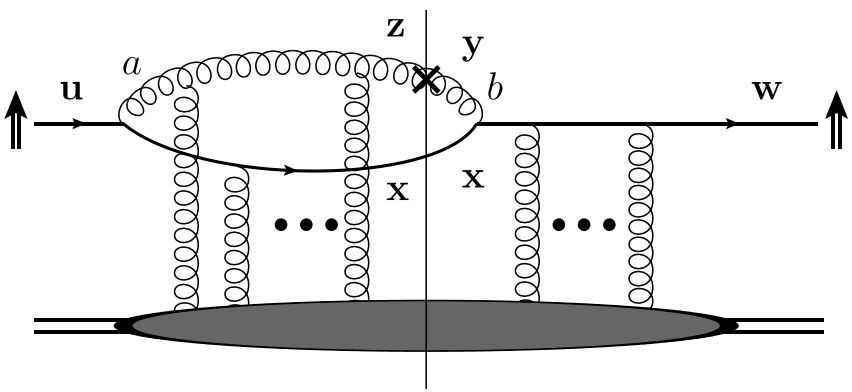

+ c. c.

Properties TBD, likely similar to quark STSA

Prompt photon STSA

- is zero (in this mechanism).
- The photon asymmetry originated in the following spin-dependent production cross-section

$$d(\Delta\sigma^{(\gamma)}) = \frac{1}{(2\pi)^3} \int d^2x\, d^2y\, d^2z\, e^{-i\mathbf{k}\cdot(\mathbf{z}-\mathbf{y})}\, \Phi_{pol}(\mathbf{x}-\mathbf{z}\,,\, \mathbf{x}-\mathbf{y}, \alpha)\, \mathcal{I}^{(\gamma)}_{\mathbf{anti}}(\mathbf{x}\,,\, \mathbf{y}\,,\, \mathbf{z})$$

with the interaction with the target linear in the odderon exchange

$$\mathcal{I}^{(\gamma)}_{anti} = i\,[O_{\mathbf{u}\,\mathbf{w}} - O_{\mathbf{x}\,\mathbf{w}} - O_{\mathbf{u}\,\mathbf{x}}]$$

- This cross section is zero since

$$\int d^2x\, O_{\mathbf{x},\,\mathbf{x}+\mathbf{y}} = 0$$

for any odd function

$$O_{\mathbf{x},\,\mathbf{y}} = -O_{\mathbf{y},\,\mathbf{x}}$$

Conclusions

- We have found a new mechanism for STSA generation within the high-energy QCD approach, due to the odderon exchange.
- The STSA found appears to have correct qualitative features: it is non-monotonic in p_T and increases with increasing Feynman-x.
- Predicts zero prompt photon STSA.
- Our STSA is proportional to density gradient squared: dominated by peripheral collisions.
- For polarized proton-nucleus scattering our STSA would be smaller than in polarized proton-proton scattering, like in many other approaches, going back to pp values for peripheral collisions.
- More studies of the results are needed and are under way to determine its properties.

Outlook

- We have explored the case of C-even wave function squared and C-odd interactions.
- One also needs to look into the case of C-odd wave function squared and C-even interaction with the target:

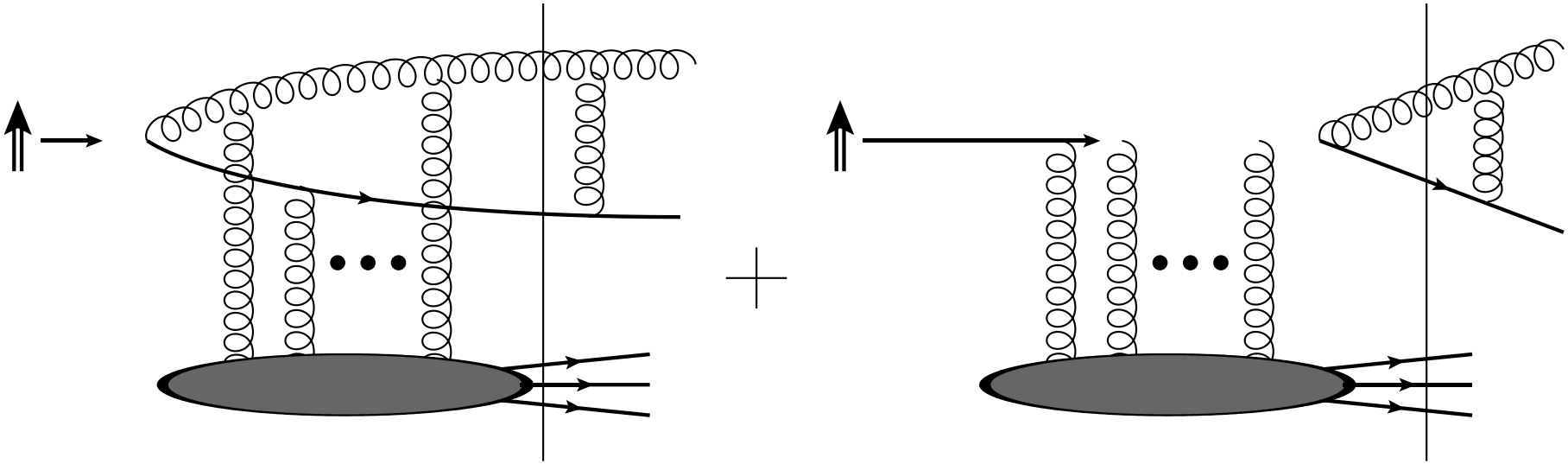

- This is the analogue of the works by Brodsky, Hwang, Schmidt ’02 and Collins ’02 in our saturation language.
- As $O_{xy} \sim \alpha_S S_{xy}$ this is of the same order as the odderon STSA.

Outlook

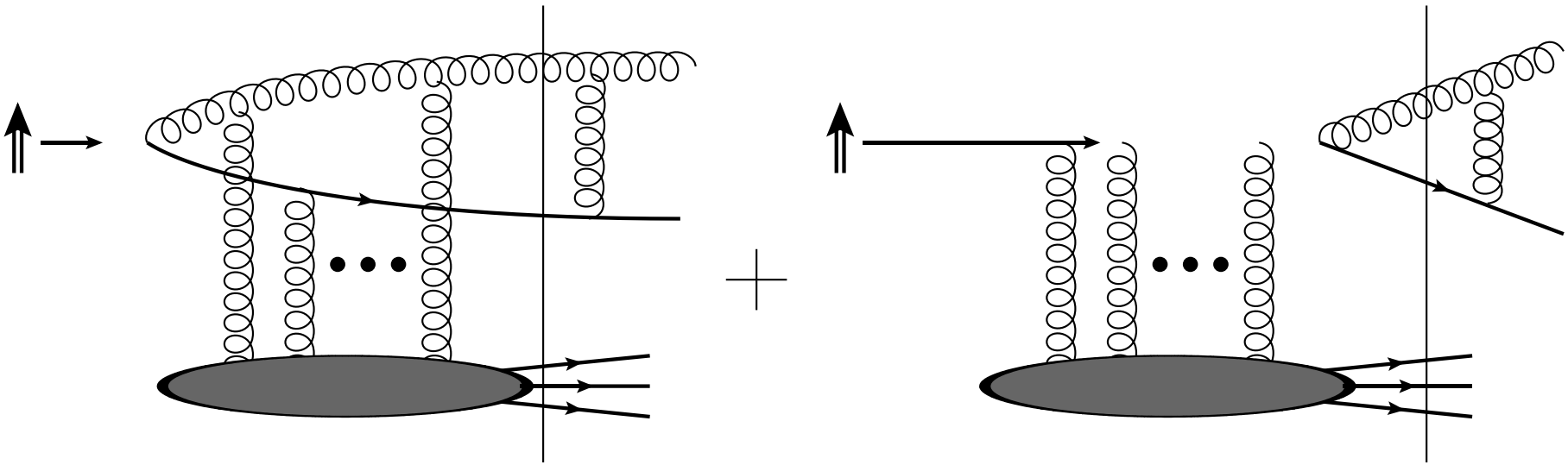

- May be lower-twist than the odderon STSA, but the two may be comparable for $k_T \sim Q_s$.
- Would lead to non-zero STSA for prompt photons.
- Looks like a final-state interaction, though represents Sivers effect.

EIC e+A science programme

Matthew A. C. Lamont
Brookhaven National Lab

BROOKHAVEN
NATIONAL LABORATORY

10 week INT programme - Fall 2010

Organizers:
Daniel Boer
KVI, University of Groningen
D.Boer@rug.nl

Markus Diehl
DESY
markus.diehl@desy.de

Richard Milner
MIT
milner@mit.edu

Raju Venugopalan
Brookhaven National Laboratory
raju@quark.phy.bnl.gov

Werner Vogelsang
University of Tübingen
werner.vogelsang@uni-tuebingen.de

Program Coordinator:
Inge Dolan
inge@phys.washington.edu
(206) 685-4286

Talks online

Application form

Exit report

Friends of the INT

Obtain an INT preprint number

INT homepage

Gluons and the quark sea at high energies: distributions, polarization, tomography

September 13 to November 19, 2010

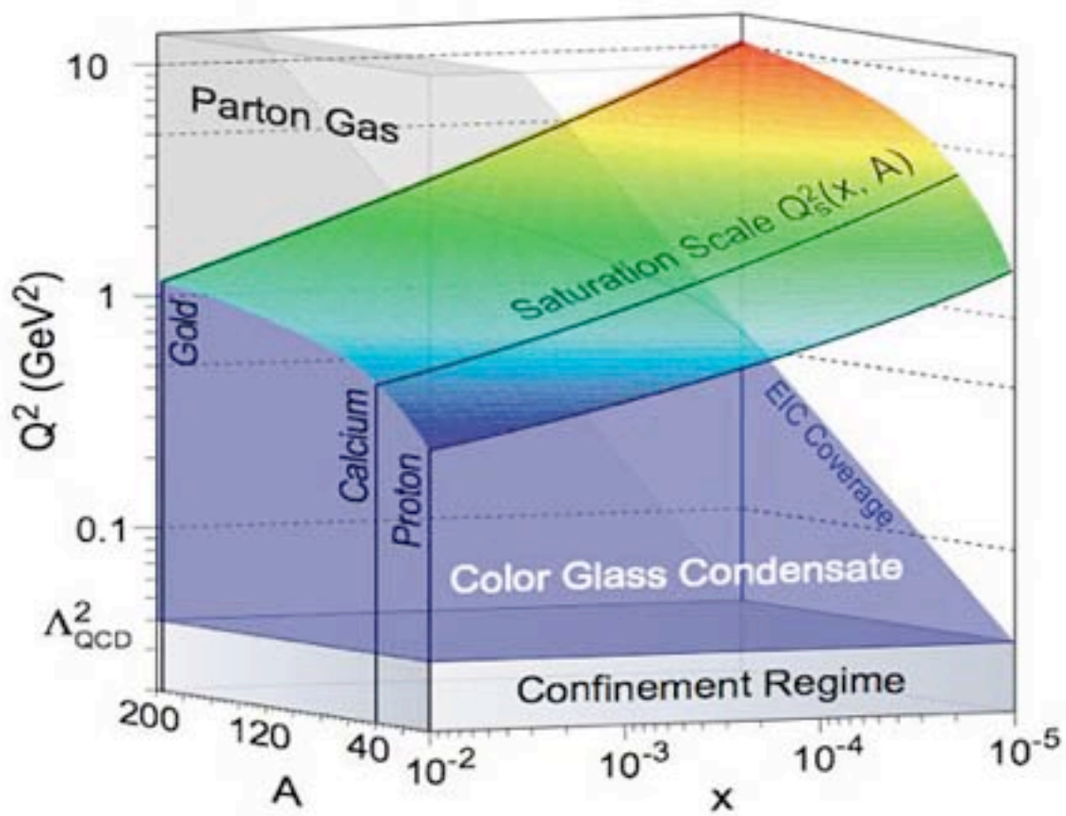

This INT program will address open questions about the dynamics of gluons and sea quarks in the nucleon and in nuclei. Answers to these questions are crucial for a deeper understanding of hadron and nuclear structure in QCD at high energies. Many of them are relevant for understanding QCD final states at the LHC, which often provide a background for physics beyond the standard model. The topics addressed in this program have important ramifications for understanding the matter produced in heavy-ion collisions at RHIC and the LHC.

http://www.int.washington.edu/PROGRAMS/10-3/

10 week INT programme - Fall 2010

week	dates	topics
1	13–17 Sept	**Workshop** on "Perturbative and Non-Perturbative Aspects of QCD at Collider Energies" Agenda
2	20–24 Sept	open conceptual issues: factorization and universality, spin and flavor structure, distributions and correlations Agenda
3–5	27 Sept – 15 Oct	small x, saturation, diffraction, nuclear effects; connections to p+A and A+A physics; fragmentation/hadronization in vacuum and in medium Agenda for week 3 Agenda for week 4 Agenda for week 5
6–7	18–29 Oct	parton densities (unpolarized and polarized), fragmentation functions, electroweak physics Agenda for week 6 Agenda for week 7
8–9	1–12 Nov	longitudinal and transverse nucleon structure; spin and orbital effects (GPDs, TMDs, and all that) Agenda for week 8 Agenda for week 9
10	16–19 Nov	**Workshop** on "The Science Case for an EIC" Agenda for week 10

http://www.int.washington.edu/PROGRAMS/10-3/

INT Writeup….

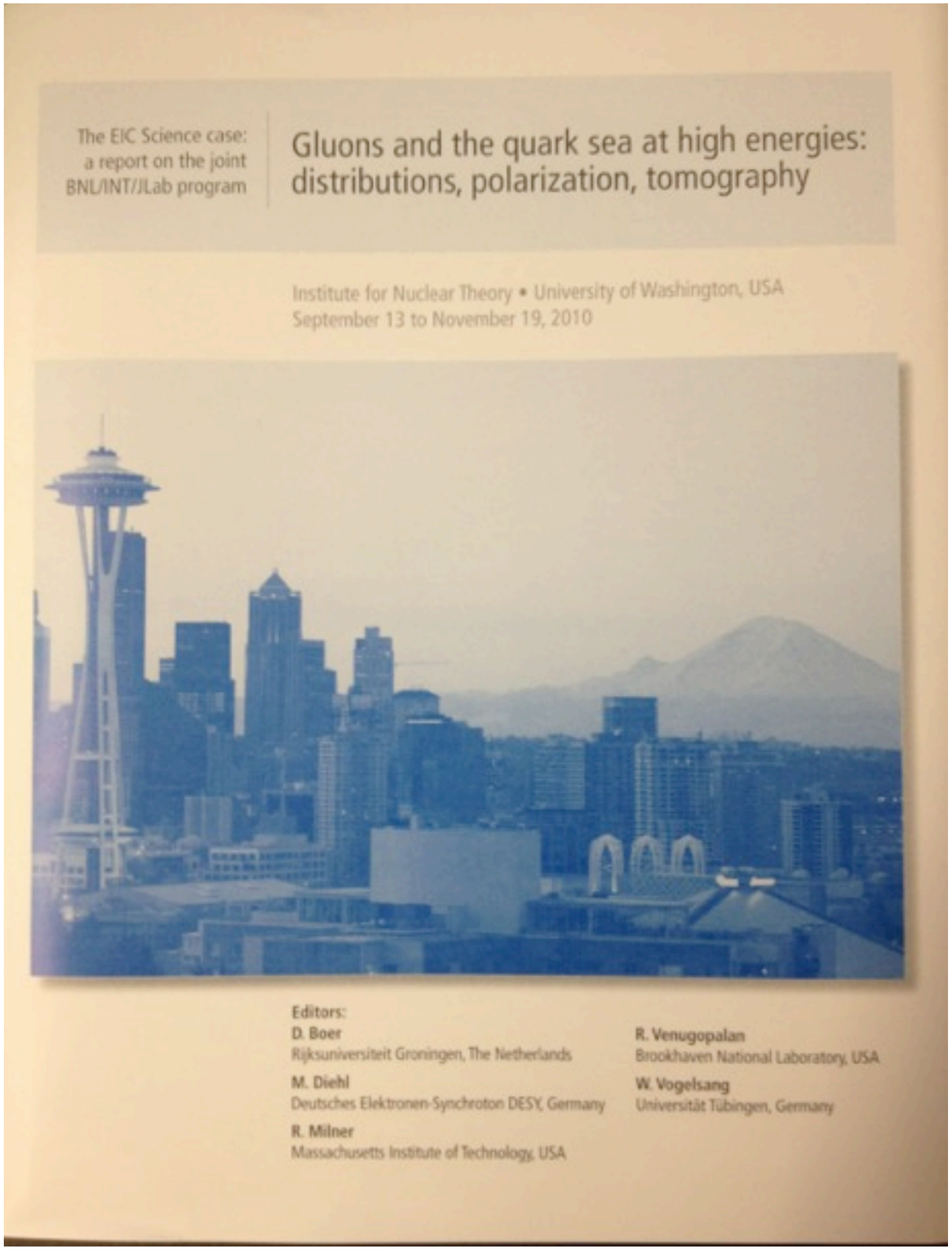

The EIC Science case: a report on the joint BNL/INT/JLab program

Gluons and the quark sea at high energies: distributions, polarization, tomography

Institute for Nuclear Theory • University of Washington, USA
September 13 to November 19, 2010

Editors:
D. Boer
Rijksuniversiteit Groningen, The Netherlands
M. Diehl
Deutsches Elektronen-Synchroton DESY, Germany
R. Milner
Massachusetts Institute of Technology, USA
R. Venugopalan
Brookhaven National Laboratory, USA
W. Vogelsang
Universität Tübingen, Germany

- ~ 6 months to write
  - ➡ 189 authors
  - ➡ 7 chapters, 550 pages
- arXiv:1108.1713

INT Writeup….

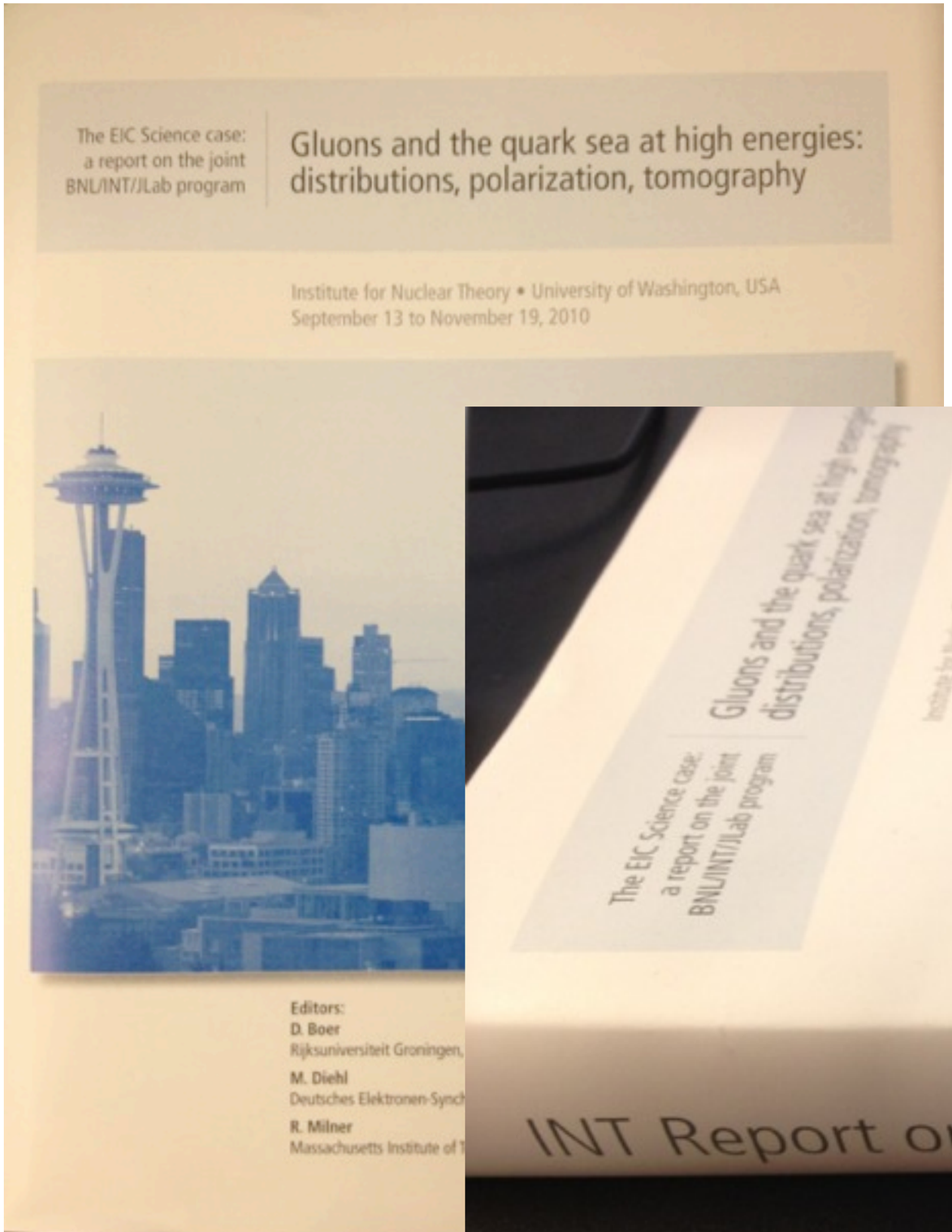

- ~ 6 months to write
  - ➡ 189 authors
  - ➡ 7 chapters, 550 pages
- arXiv:1108.1713

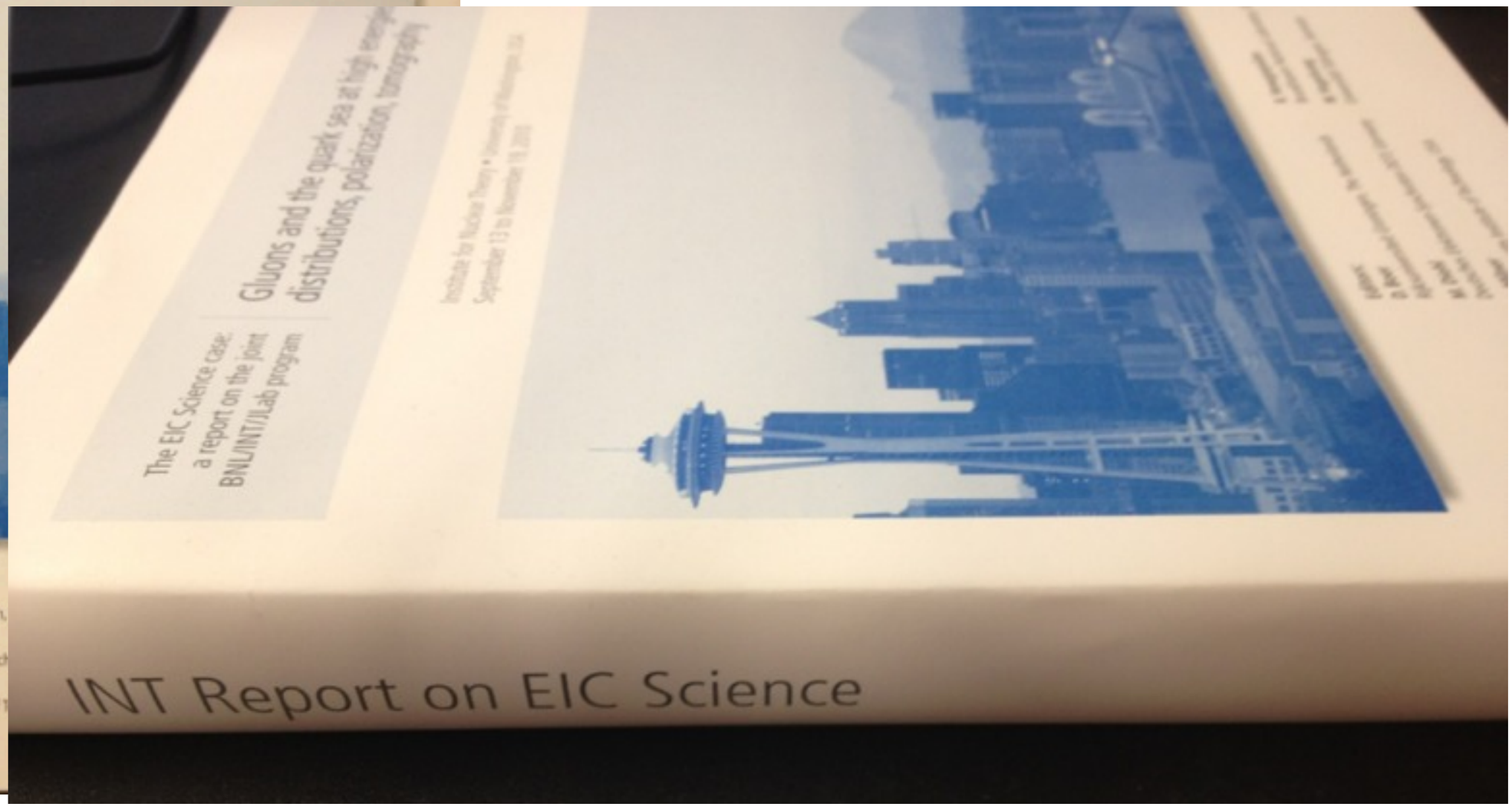

White Paper (almost complete?)

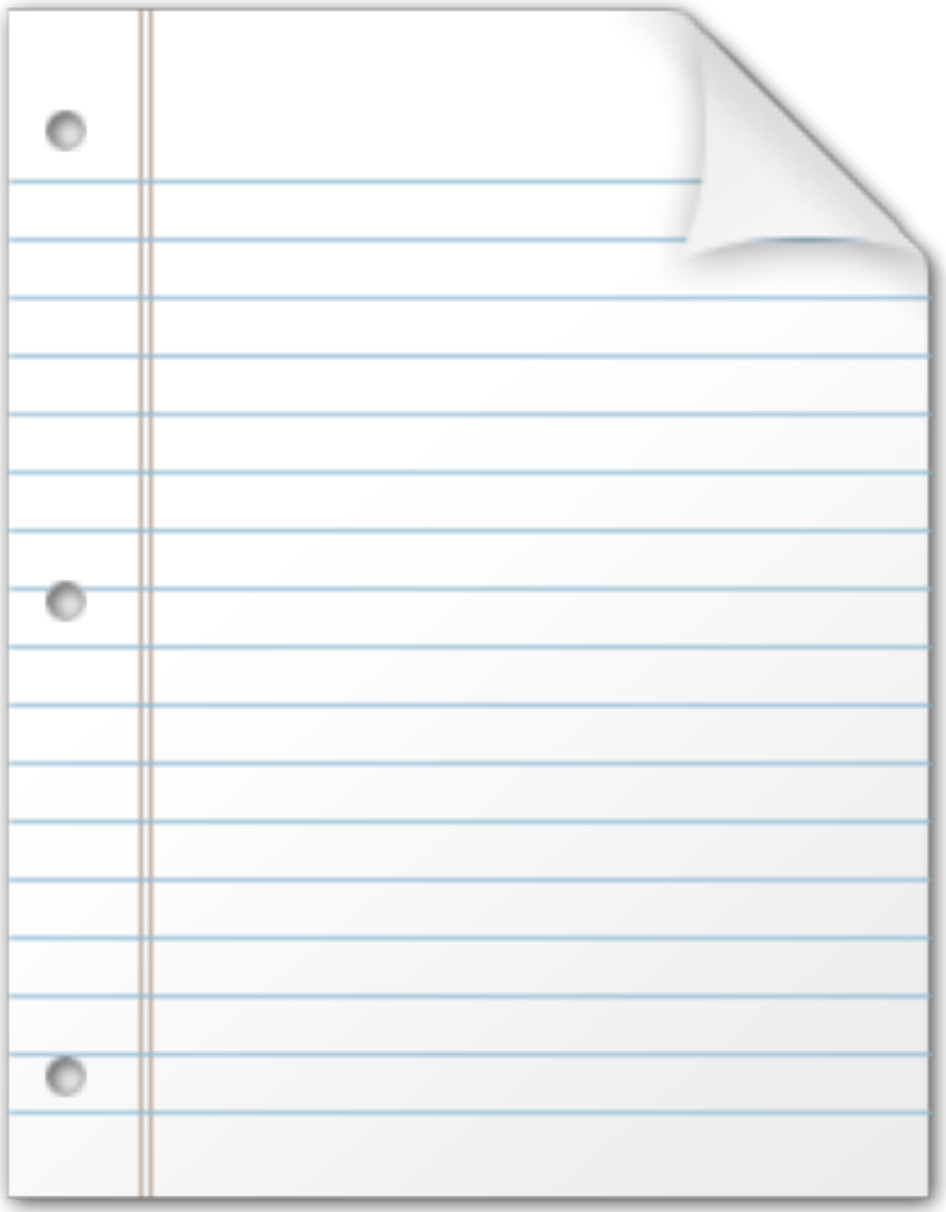

White Paper (almost complete?)

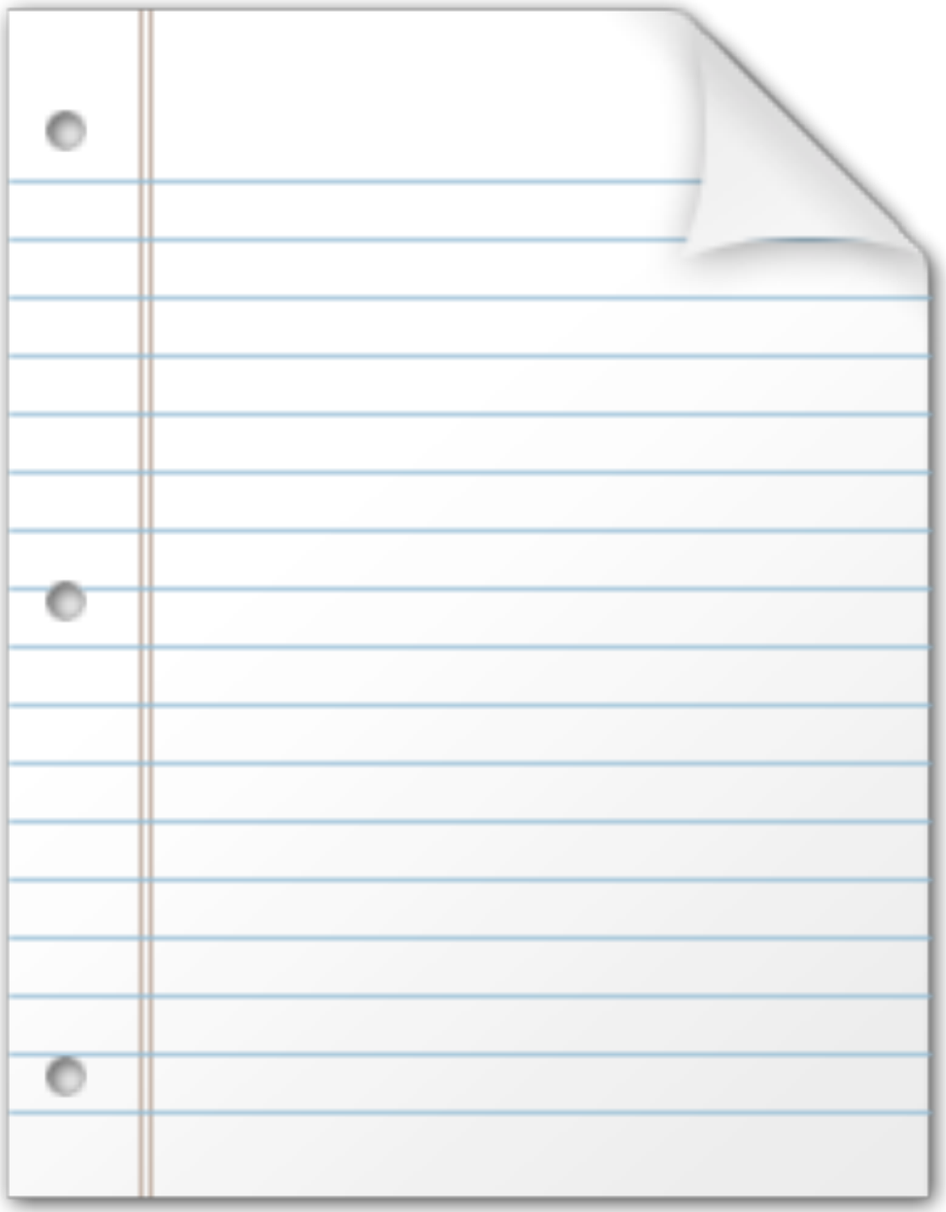

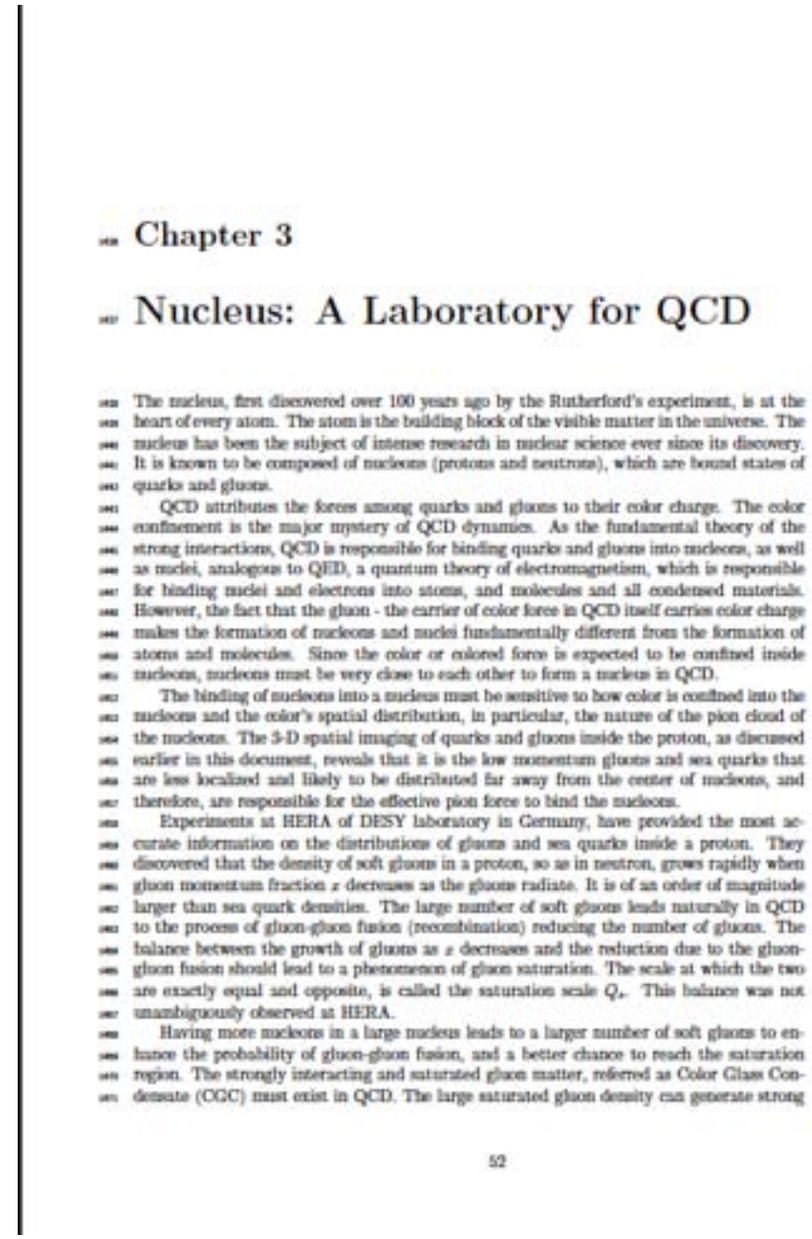

Chapter 3

Nucleus: A Laboratory for QCD

The nucleus, first discovered over 100 years ago by the Rutherford's experiment, is at the heart of every atom. The atom is the building block of the visible matter in the universe. The nucleus has been the subject of intense research in nuclear science ever since its discovery. It is known to be composed of nucleons (protons and neutrons), which are bound states of quarks and gluons.

QCD attributes the forces among quarks and gluons to their color charge. The color confinement is the major mystery of QCD dynamics. As the fundamental theory of the strong interactions, QCD is responsible for binding quarks and gluons into nucleons, as well as nuclei, analogous to QED, a quantum theory of electromagnetism, which is responsible for binding nuclei and electrons into atoms, and molecules and all condensed materials. However, the fact that the gluon - the carrier of color force in QCD itself carries color charge makes the formation of nucleons and nuclei fundamentally different from the formation of atoms and molecules. Since the color or colored force is expected to be confined inside nucleons, nucleons must be very close to each other to form a nucleus in QCD.

The binding of nucleons into a nucleus must be sensitive to how color is confined into the nucleons and the color's spatial distribution, in particular, the nature of the pion cloud of the nucleons. The 3-D spatial imaging of quarks and gluons inside the proton, as discussed earlier in this document, reveals that it is the low momentum gluons and sea quarks that are less localized and likely to be distributed far away from the center of nucleons, and therefore, are responsible for the effective pion force to bind the nucleons.

Experiments at HERA of DESY laboratory in Germany, have provided the most accurate information on the distributions of gluons and sea quarks inside a proton. They discovered that the density of soft gluons in a proton, so as in neutron, grows rapidly when gluon momentum fraction x decreases as the gluons radiate. It is of an order of magnitude larger than sea quark densities. The large number of soft gluons leads naturally in QCD to the process of gluon-gluon fusion (recombination) reducing the number of gluons. The balance between the growth of gluons as x decreases and the reduction due to the gluon-gluon fusion should lead to a phenomenon of gluon saturation. The scale at which the two are exactly equal and opposite, is called the saturation scale Q_s. This balance was not unambiguously observed at HERA.

Having more nucleons in a large nucleus leads to a larger number of soft gluons to enhance the probability of gluon-gluon fusion, and a better chance to reach the saturation region. The strongly interacting and saturated gluon matter, referred as Color Glass Condensate (CGC) must exist in QCD. The large saturated gluon density can generate strong

52

- Soon to be made public…
- ~ 120 pages

Big Thanks!!

- Y Kovchegov, T Ullrich
  - ➡ (White Paper editors)

- J Albacete, V Guzey, T Lappi, C Marquet, M Stratmann, G Watt
  - ➡ Friendly theorists who have put up with me for months asking for data in different forms

- EIC Science Task Force
  - ➡ Especially L Zheng and T Toll for plots in this talk

Measuring the glue via Structure Functions

$$\sigma_r(x, Q^2) = F_2^A(x, Q^2) - \frac{y^2}{Y+} F_L^A(x, Q^2)$$

quark+anti-quark momentum distributions

gluon momentum distribution

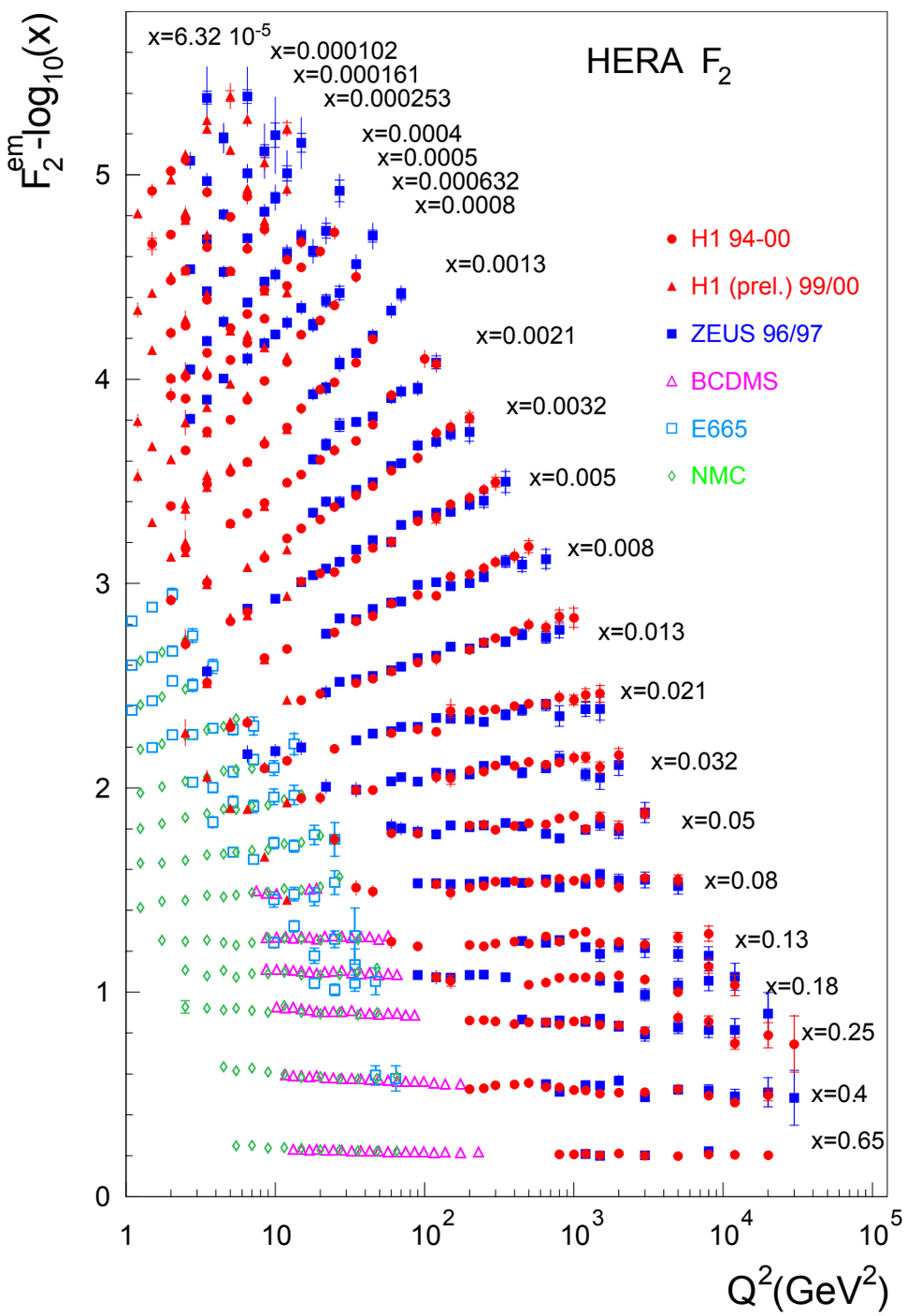

Measuring the glue via Structure Functions

$$\sigma_r(x,Q^2) = F_2^A(x,Q^2) - \frac{y^2}{Y+} F_L^A(x,Q^2)$$

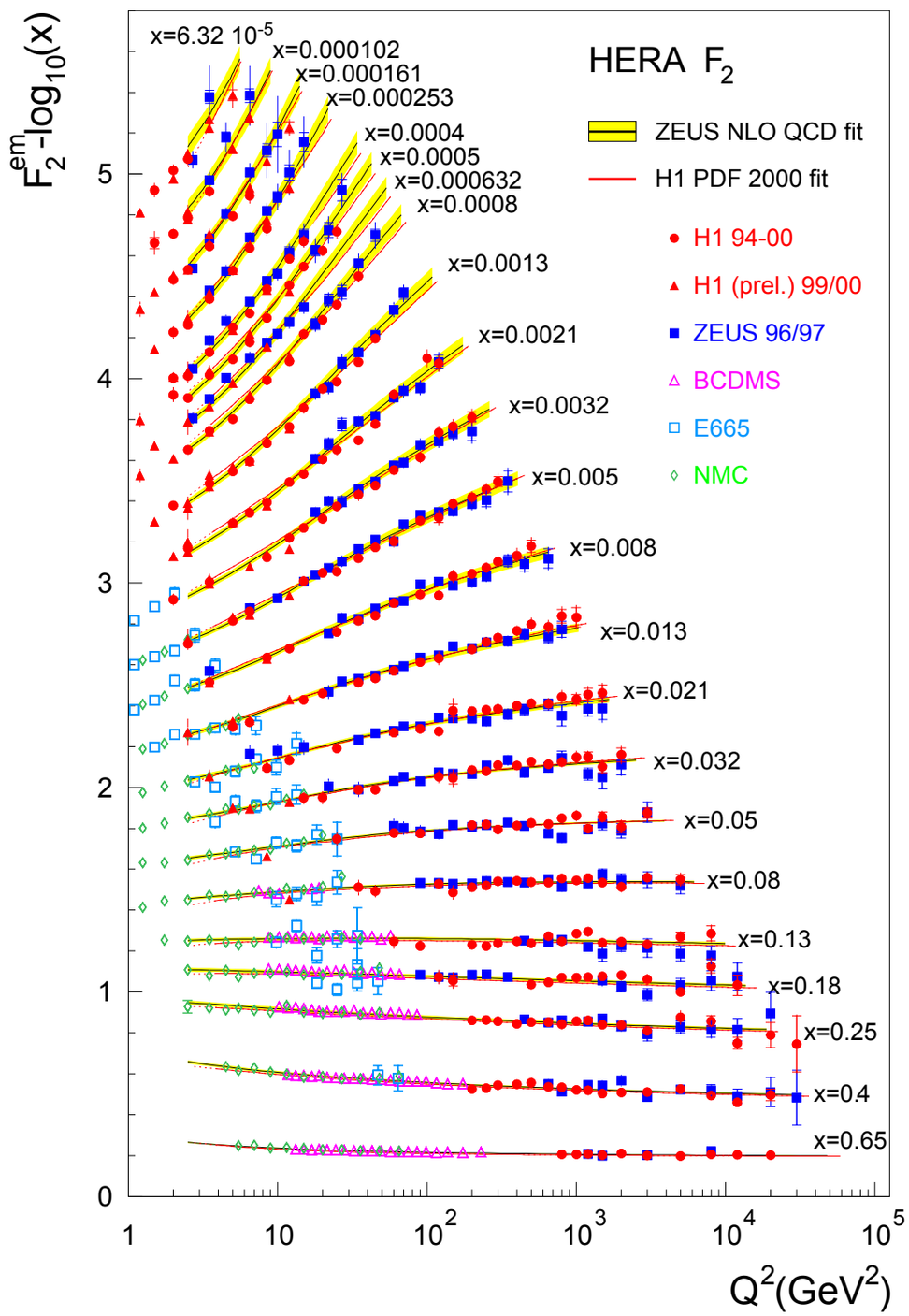

Scaling violation: $dF_2/d\ln Q^2$ and linear DGLAP Evolution $\Rightarrow G(x,Q^2)$

Measuring the glue via Structure Functions

$$\sigma_r(x,Q^2) = F_2^A(x,Q^2) - \frac{y^2}{Y+} F_L^A(x,Q^2)$$

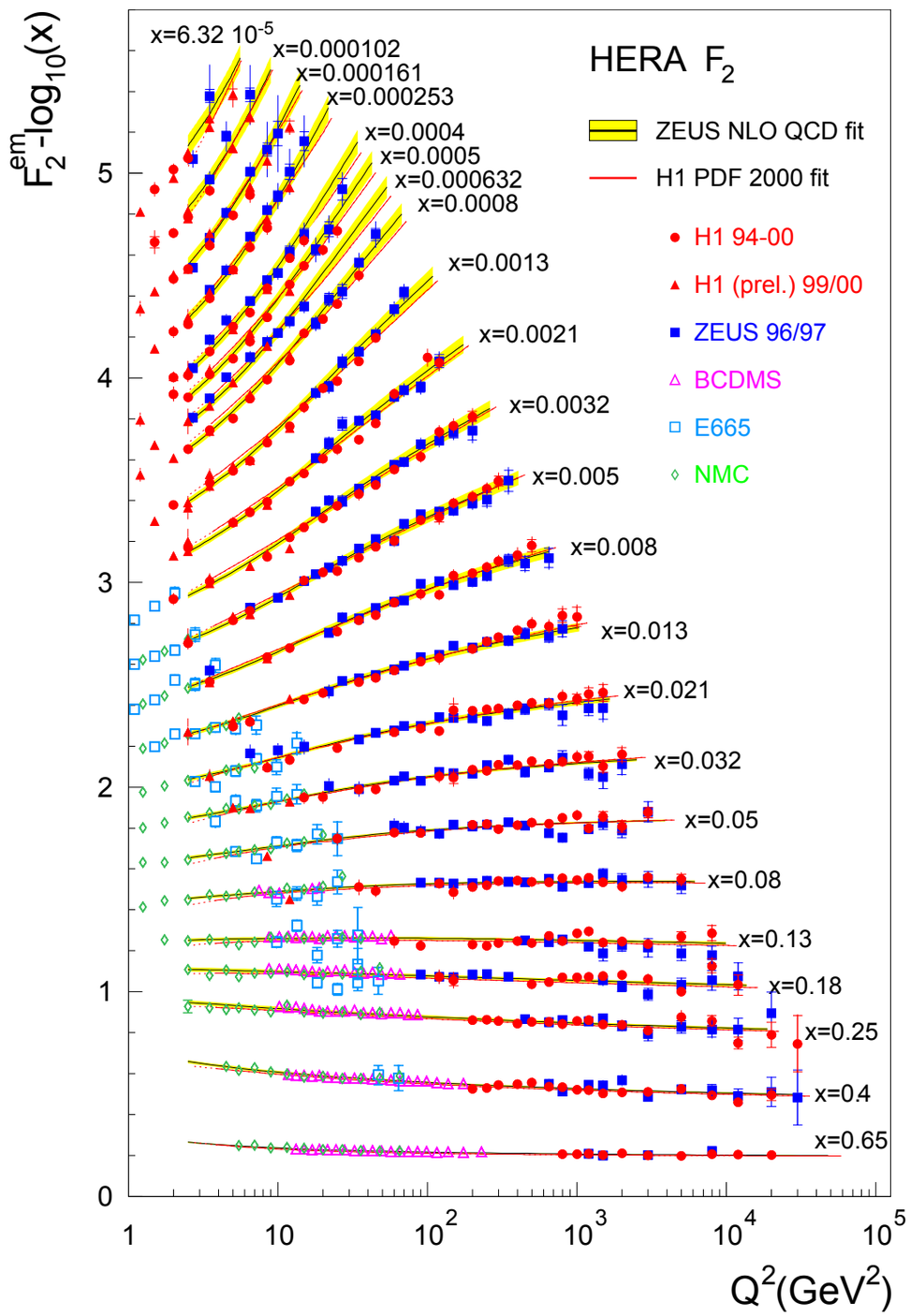

Scaling violation: $dF_2/d\ln Q^2$ and linear DGLAP Evolution $\Rightarrow G(x,Q^2)$

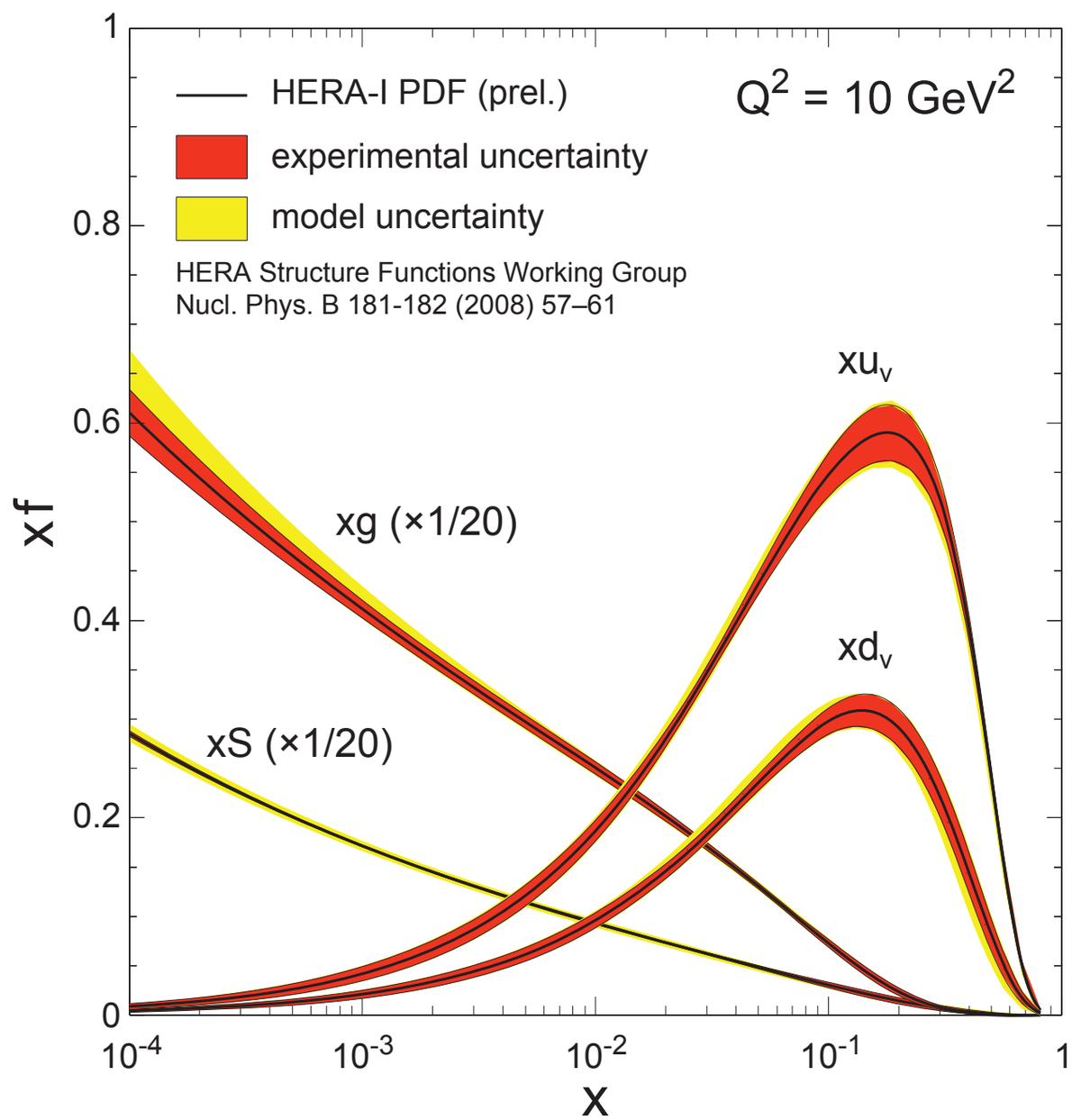

Measuring the glue via Structure Functions

$$\sigma_r(x,Q^2) = F_2^A(x,Q^2) - \frac{y^2}{Y+} F_L^A(x,Q^2)$$

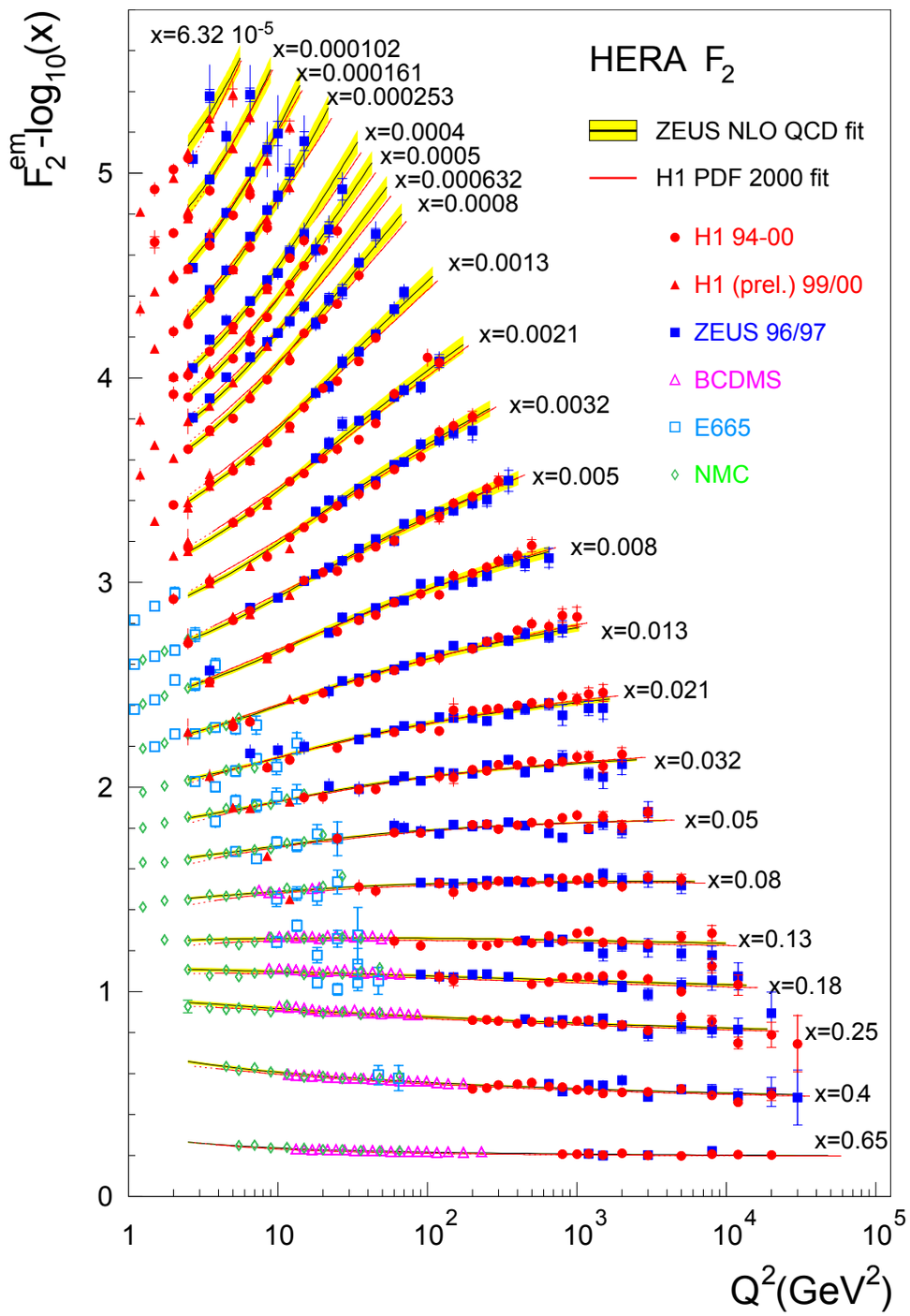

Scaling violation: $dF_2/d\ln Q^2$ and linear DGLAP Evolution $\Rightarrow G(x,Q^2)$

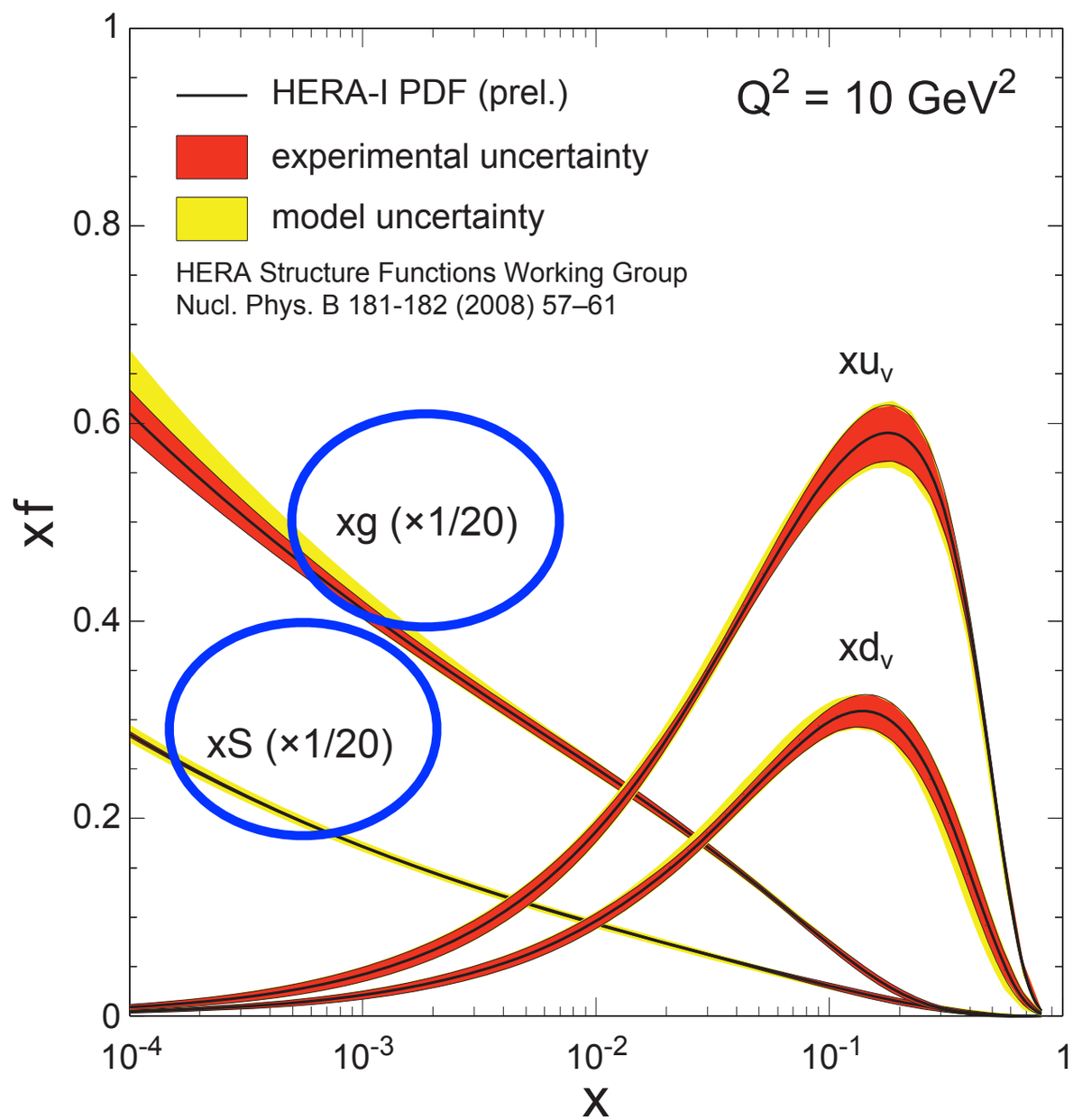

Measuring the glue via Structure Functions

$$\sigma_r(x,Q^2) = F_2^A(x,Q^2) - \frac{y^2}{Y+} F_L^A(x,Q^2)$$

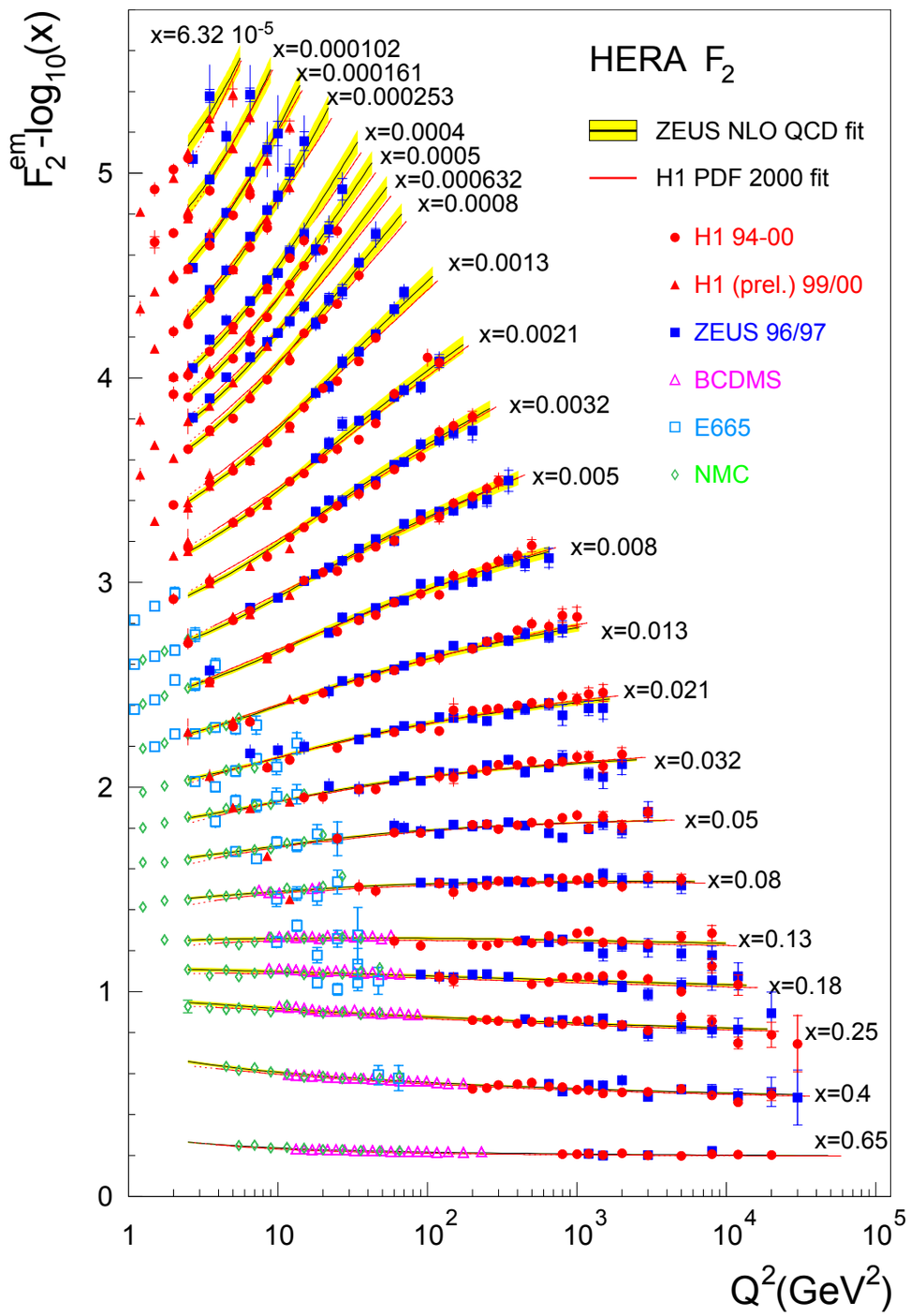

Scaling violation: $dF_2/d\ln Q^2$ and linear DGLAP

Evolution $\Rightarrow G(x,Q^2)$

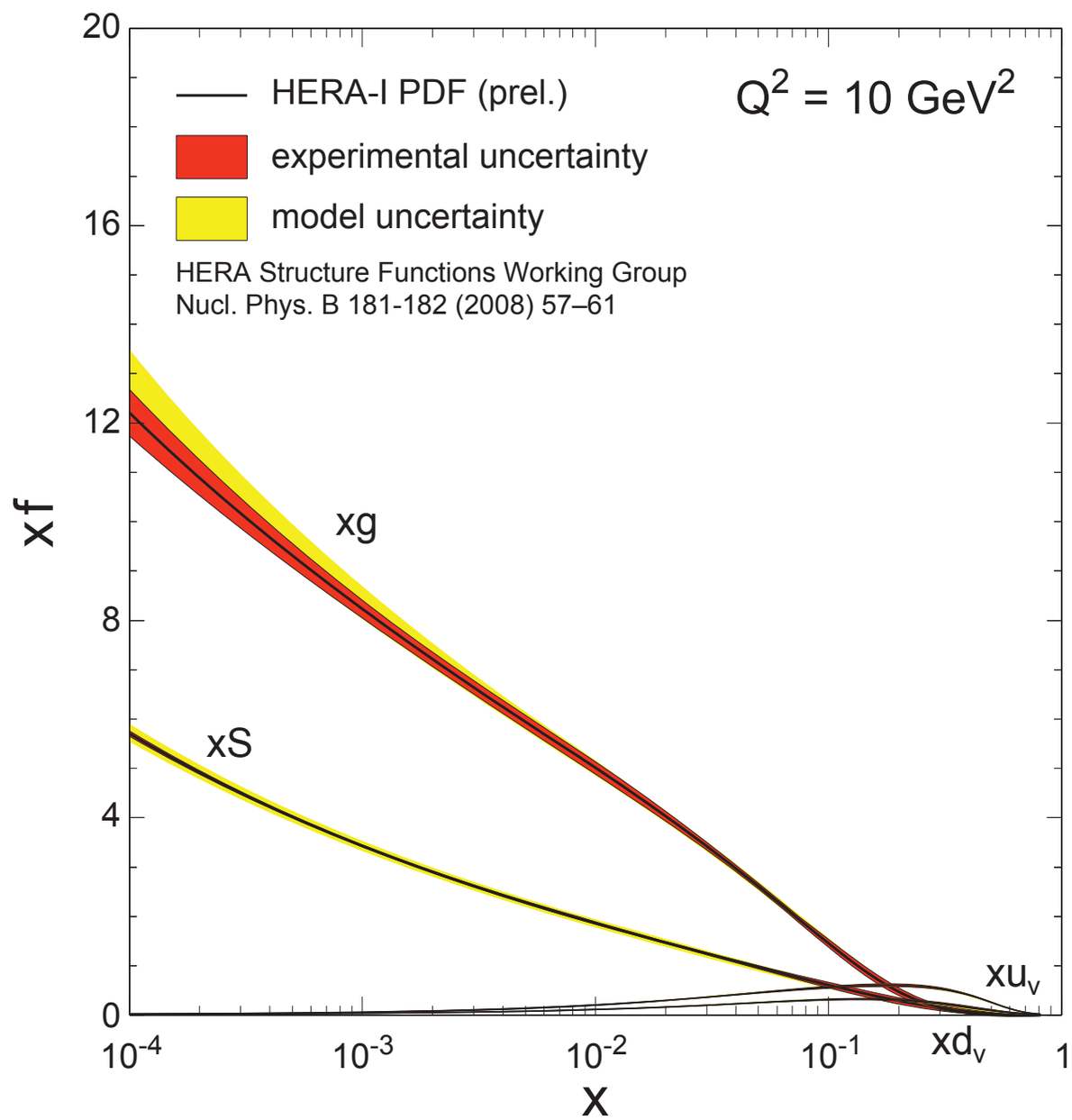

Saturation Scale, Q_s

- As we go higher in energy (larger values of 1/x) we move away from the *linear BFKL* regime to the *non-linear BK/JIMWLK* realm
- Take advantage of the fact that gluons are self-interacting

➡ Not only can we have gluon splitting, but also recombination

- Tame the explosive growth of the gluon density in the nucleon observed from fitting HERA data

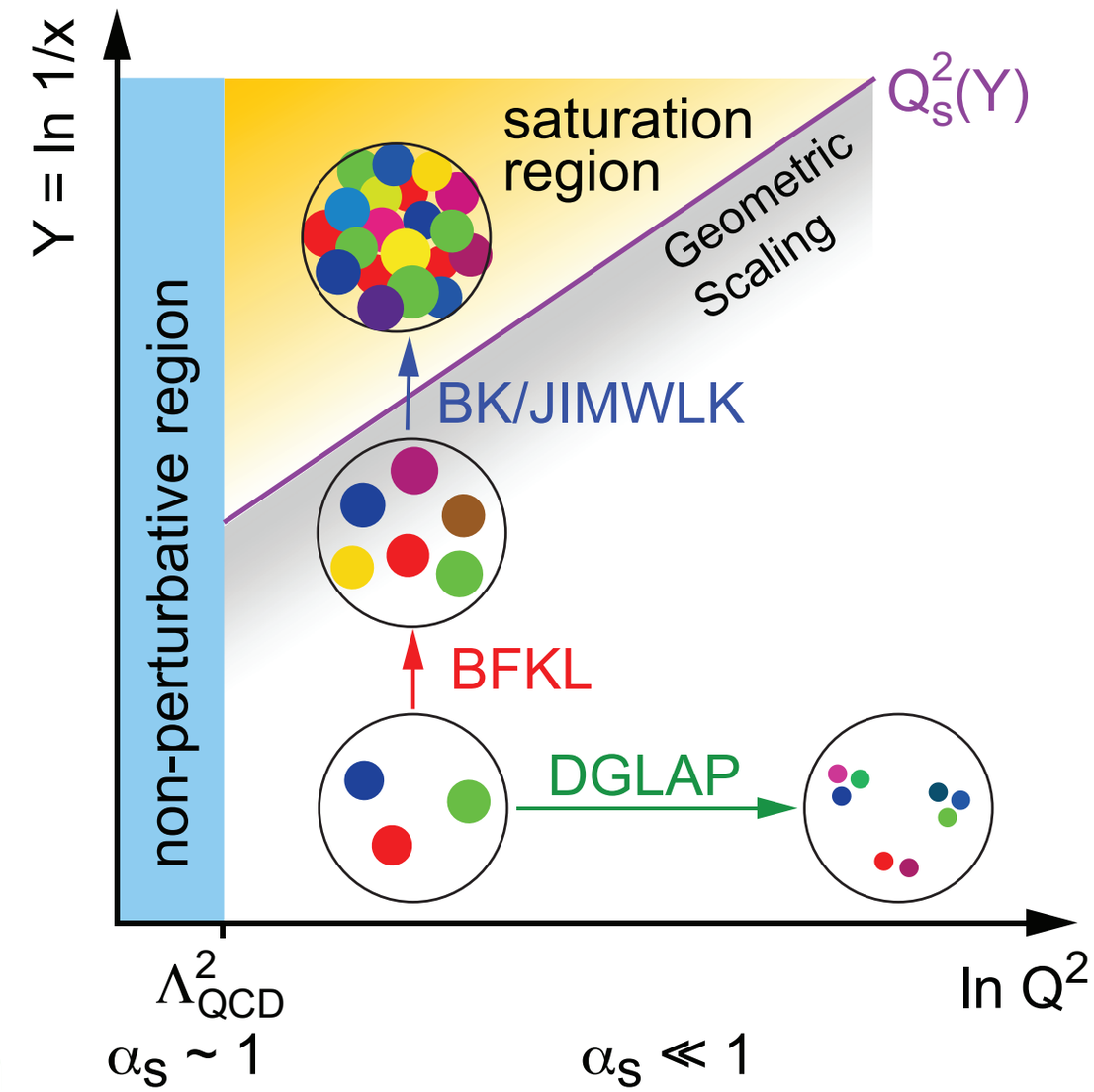

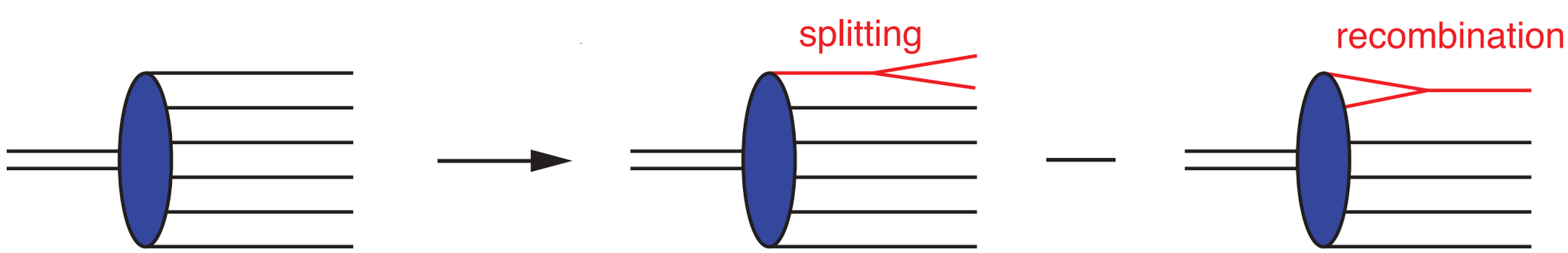

Nuclear “oomph” effect

- When we accelerate the nucleus to high energy, we give it a Lorentz boost

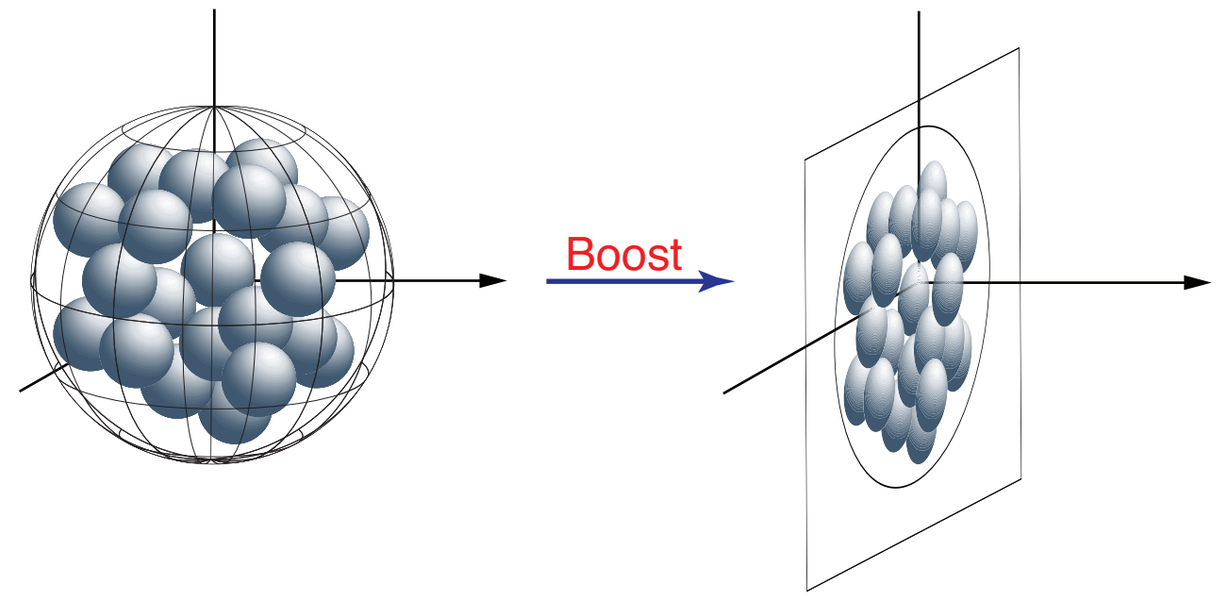

- Incoming probe interacts coherently with all of the nucleons in the nucleus

➡ Qs is given a boost simply by the geometry of the collision system

$$Q_s^2(x) \sim A^{1/3} \left(\frac{1}{x}\right)^{\lambda}$$

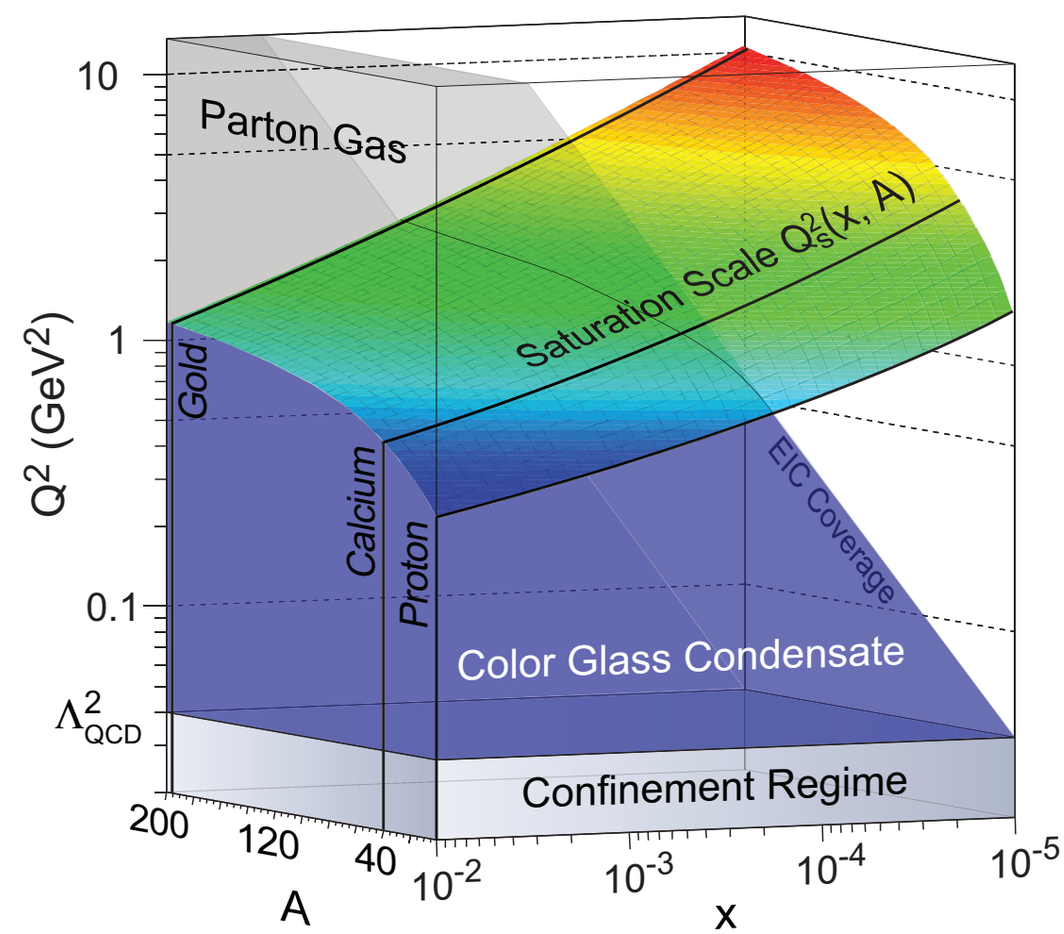

Nuclear "oomph" effect

Pocket formula: $Q_s^2(x) \sim A^{1/3}\left(\frac{1}{x}\right)^{\lambda} \sim \left(\frac{A}{x}\right)^{1/3}$

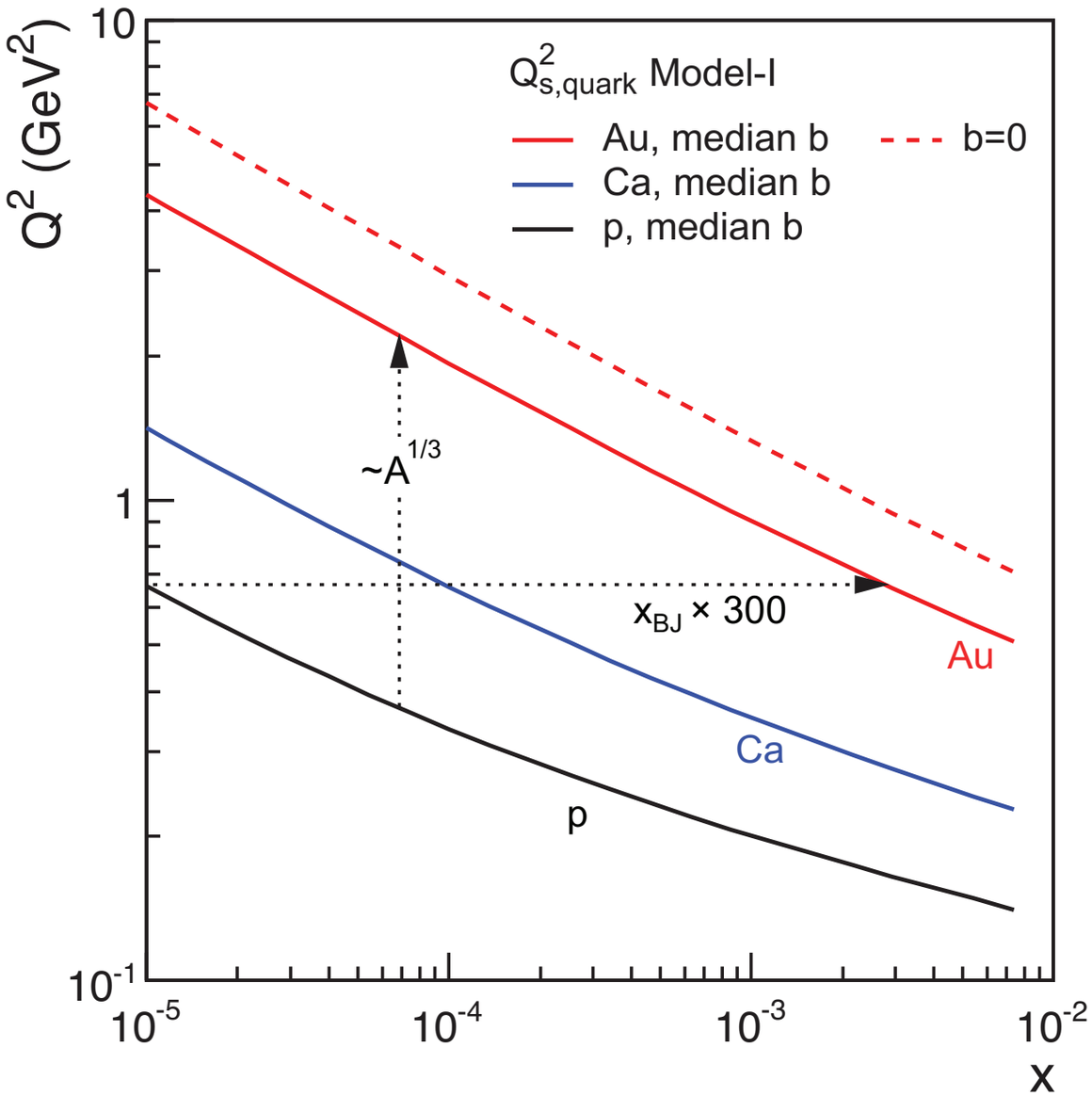

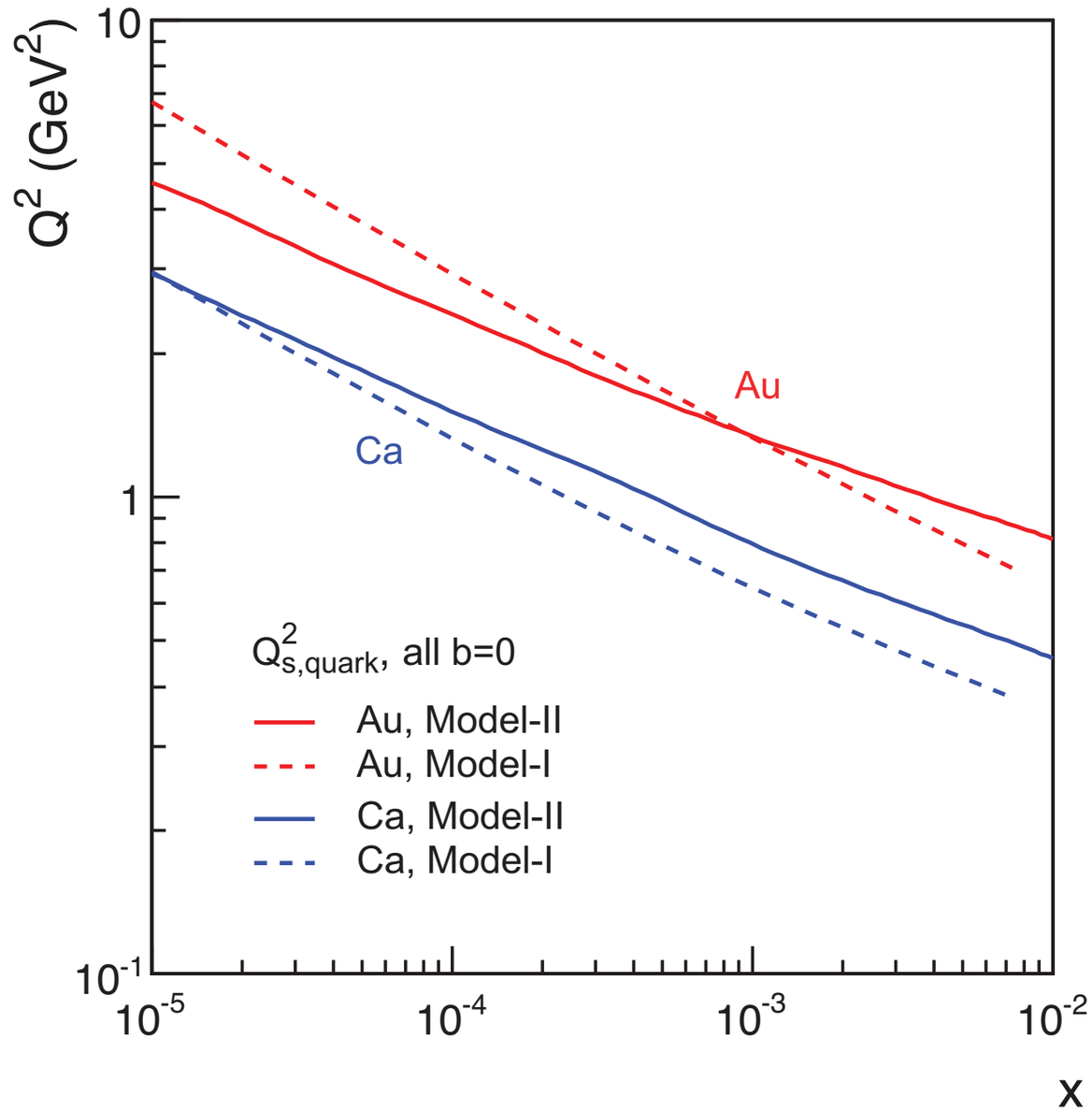

Fundamental questions which arise:

- What is the role of strong gluon fields, parton saturation effects and collective gluon excitations in scattering off nuclei?

  ➡ tantalising hints of a saturated/CGC regime have been observed at HERA/RHIC/LHC

- Can we experimentally find the evidence of non-linear QCD evolution in high-energy scattering off nuclei?

  ➡ x-dependence of DIS cross-sections and structure functions

  ➡ The discovery of the saturation regime would not be complete without unambiguous evidence in favour of these non-linear equations

Fundamental questions which arise:

- What is the momentum and spatial distribution of gluons and sea quarks in nuclei?

  ➡ Large-x: the physics of multiple scatterings at allows us to reconstruct the momentum and impact parameter distributions of gluons and sea quarks in nuclei

  ➡ Small-x: momentum distribution may allow us to identify the saturation scale, Q_s

- Are there strong colour (quark and gluon density) fluctuations inside of a large nucleus? How does the nucleus respond to the propagation of a colour charge through it?

  ➡ Need to understand fluctuations in order to fully understand the spatial and momentum distributions of sea quarks and gluons

Golden Measurements

Deliverables	Observables	What we learn	Stage-1	Stage-II
integrated gluon distributions	$F_{2,L}$	nuclear wave function; saturation, Q_s	gluons at $10^{-3} < x < 1$	saturation regime
k_T dependent gluons; gluon correlations	di-hadron correlations	non-linear QCD evolution / universality	onset of saturation	measure Q_s
transport coefficients in cold matter	large-x SIDIS; jets	parton energy loss, shower evolution; energy loss mechanisms	light flavours and charm; jets	rare probes and bottom; large-x gluons

Silver Measurements

Deliverables	Observables	What we learn	Stage-I	Stage-II
integrated gluon distributions	$F^c_{2,L}$, $F^D_{2,L}$	nuclear wave function; saturation, Q_s	difficult measurement / interpretation	saturation regime
flavour separated nuclear PDFs	charged current and γZ structure functions	EMC effect origin	full flavour separation for $10^{-2} < x < 1$	measure Q_s
k_T dependent gluons	SIDIS at small x	non-linear QCD evolution / universality	onset of saturation	rare probes and bottom; large-x gluons
b-dependent gluons; gluon correlations	DVCS; diffractive vector mesons	interplay between small-x evolution and confinement	moderate x with light, heavy nuclei	smaller x, saturation

How do we try to answer these questions?

- Need to undertake nuclear DIS measurements at a new facility

  ➡ Existing measurements with heavy ions are very sparse

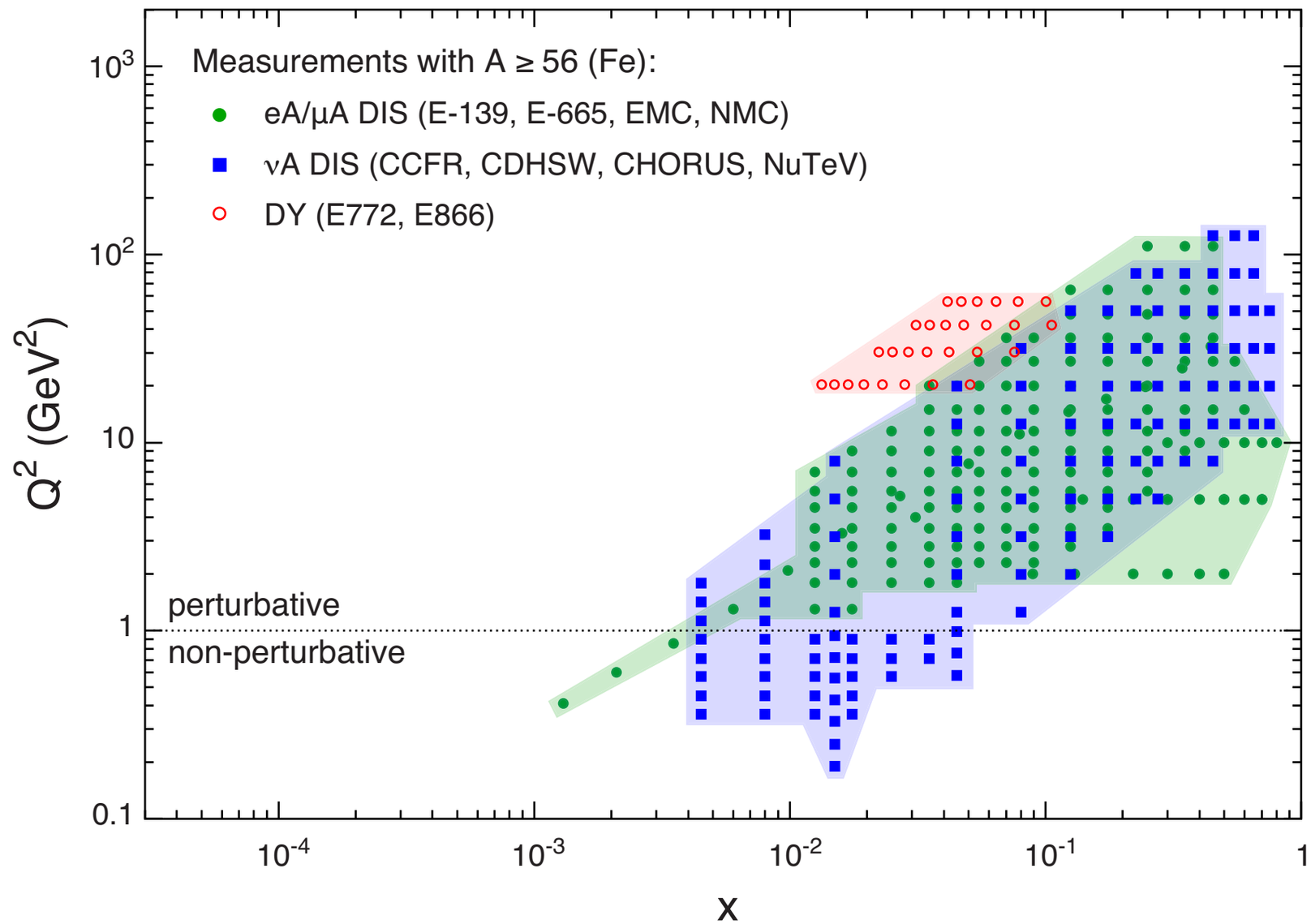

How do we try to answer these questions?

- Need to undertake nuclear DIS measurements at a new facility
  - ➡ Existing measurements with heavy ions are very sparse
  - ➡ A new accelerator (eRHIC) with a staged approach would address these questions in a new phase space

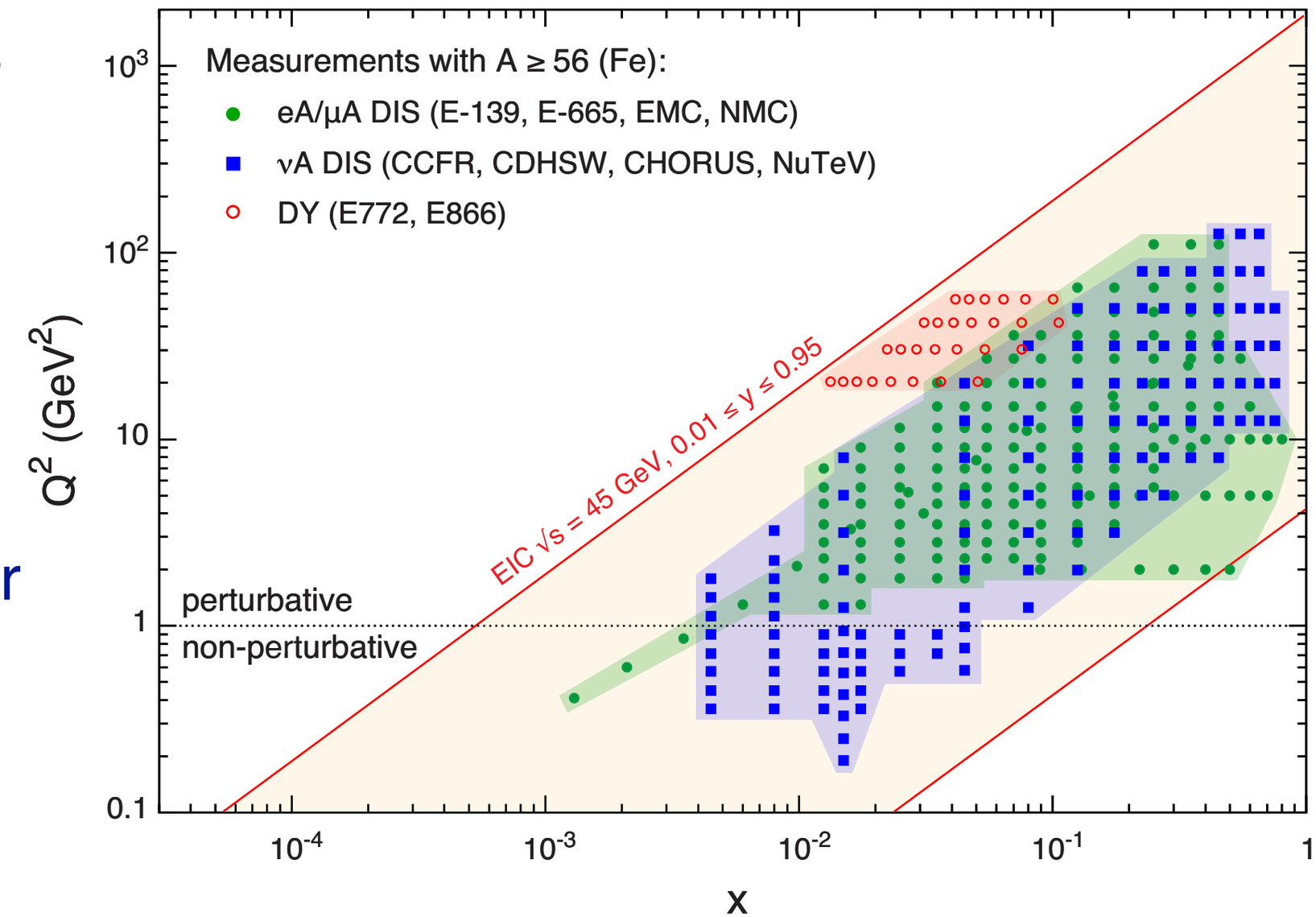

How do we try to answer these questions?

- Need to undertake nuclear DIS measurements at a new facility
  - ➡ Existing measurements with heavy ions are very sparse
  - ➡ A new accelerator (eRHIC) with a staged approach would address these questions in a new phase space

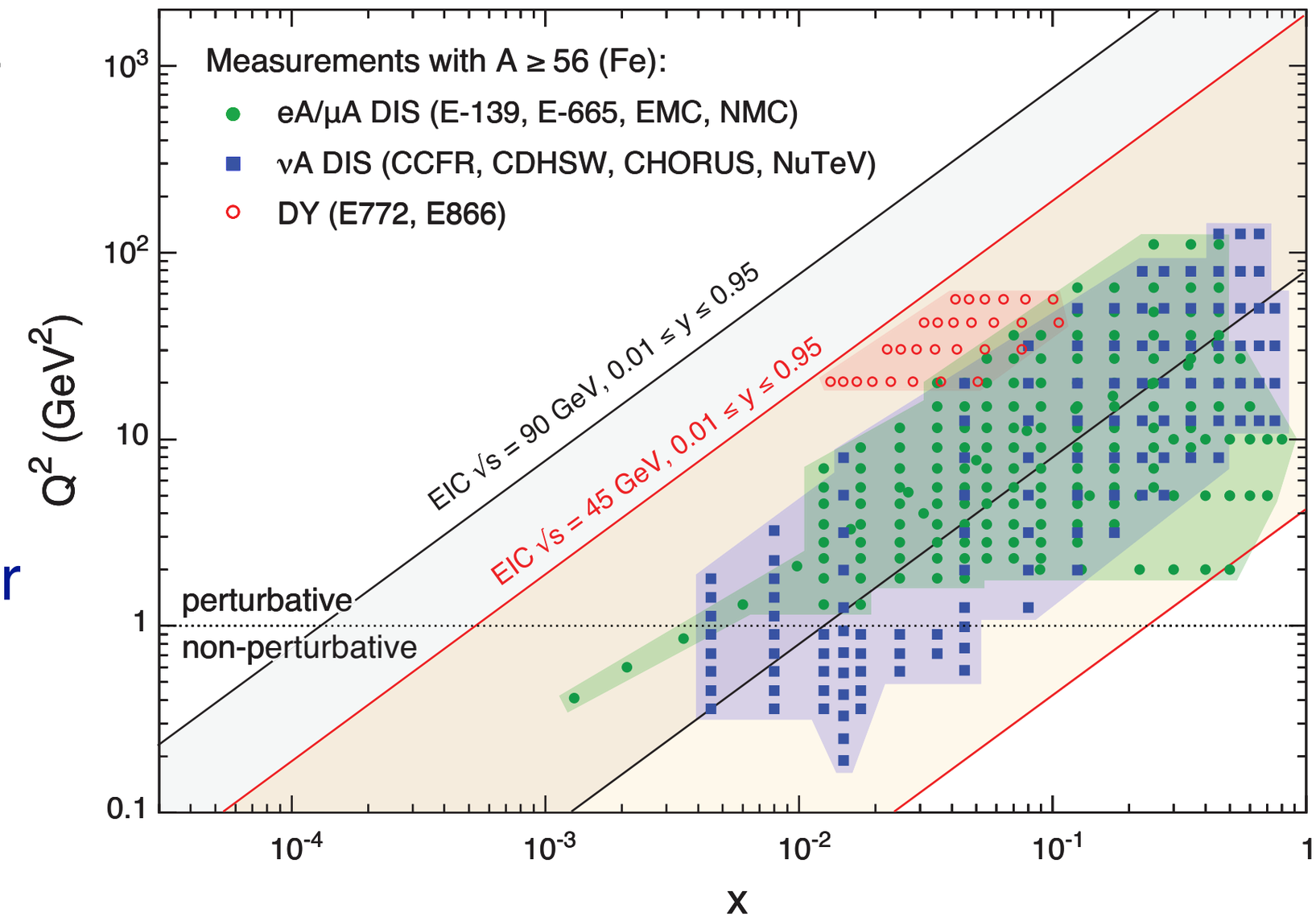

How do we try to answer these questions?

- Need to undertake nuclear DIS measurements at a new facility
  - ➡ Existing measurements with heavy ions are very sparse
  - ➡ A new accelerator (eRHIC) with a staged approach would address these questions in a new phase space

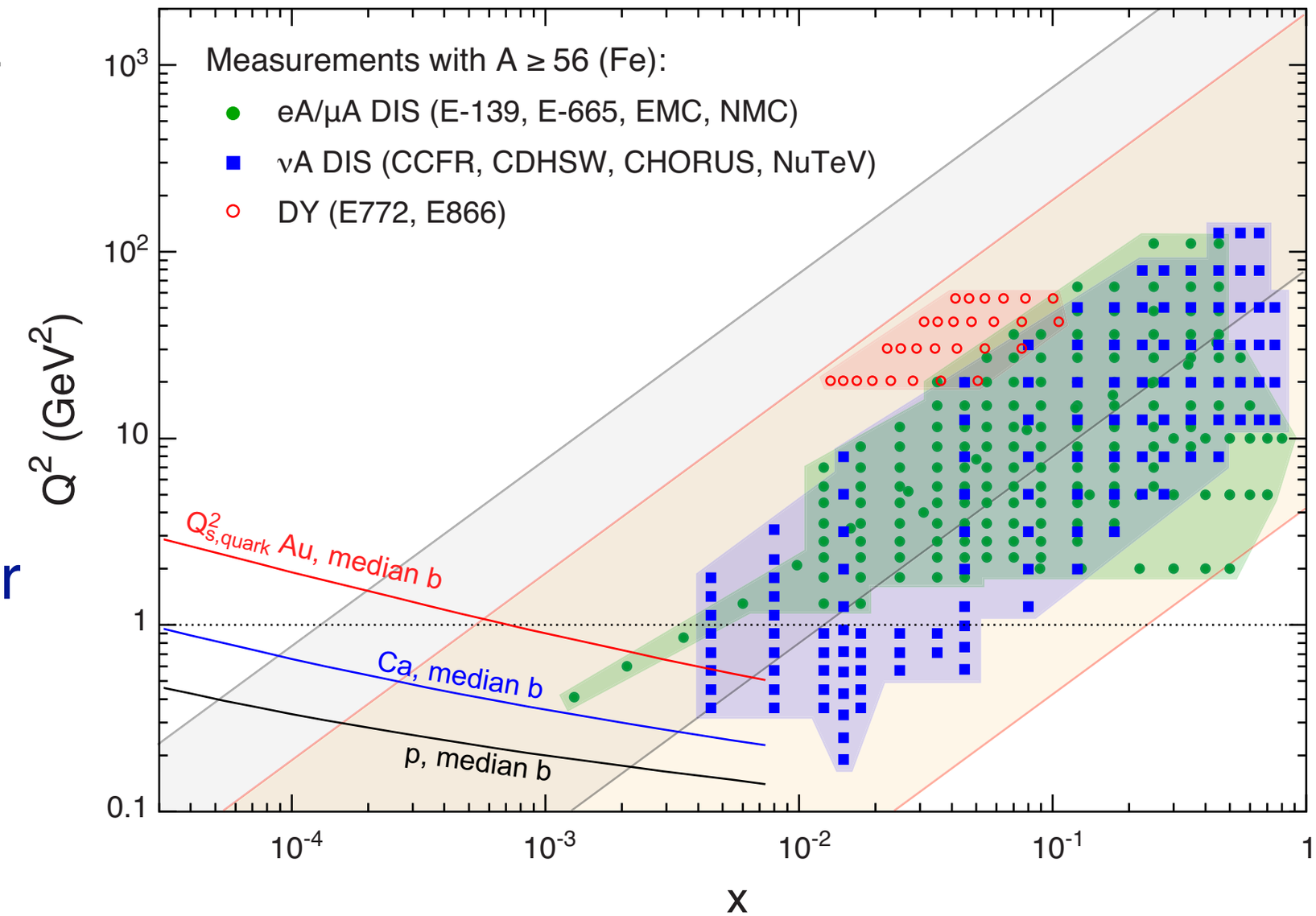

Integrated gluon distributions from inclusive structure functions

Integrated gluon distributions from inclusive structure functions

Deliverables	Observables	What we learn	Stage-I	Stage-II
integrated gluon distributions	$F_{2,L}$	nuclear wave function; saturation, Q_s	gluons at $10^{-3} < x < 1$	saturation regime

integrated gluon distributions	$F^c_{2,L}$, $F^D_{2,L}$	nuclear wave function; saturation, Q_s	difficult measurement / interpretation	saturation regime

charm diffractive

The effects of higher-twist corrections on F_L

$$\frac{F_L - F_L^{leading\ twist}}{F_L}$$

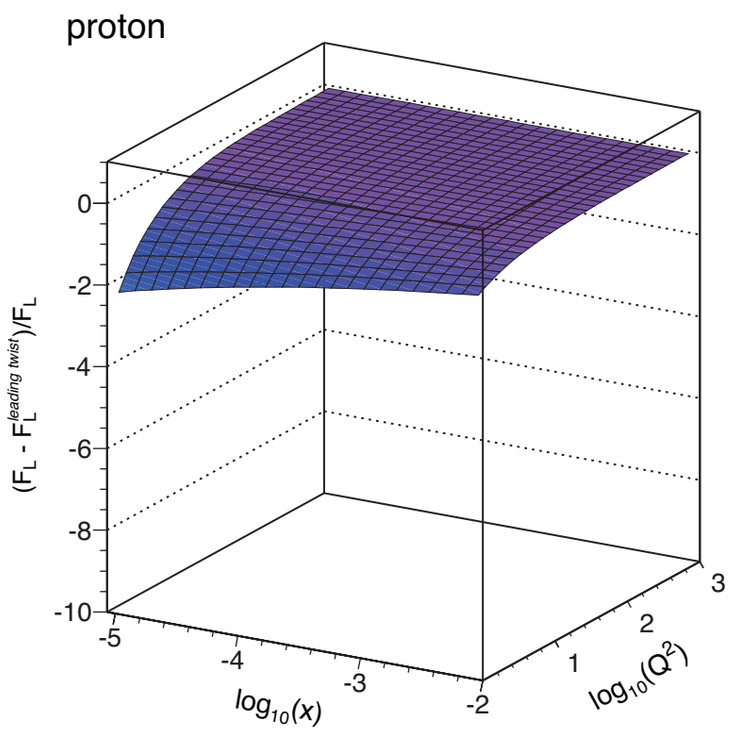

- Plotting F_L-$F_L^{\text{leading twist}}/F_L$ coming out of saturation inspired GBW model

  ➡ protons: little effect of leading twist corrections, only starting to come in at small-x and small Q2

The effects of higher-twist corrections on F_L

$$\frac{F_L - F_L^{leading\ twist}}{F_L}$$

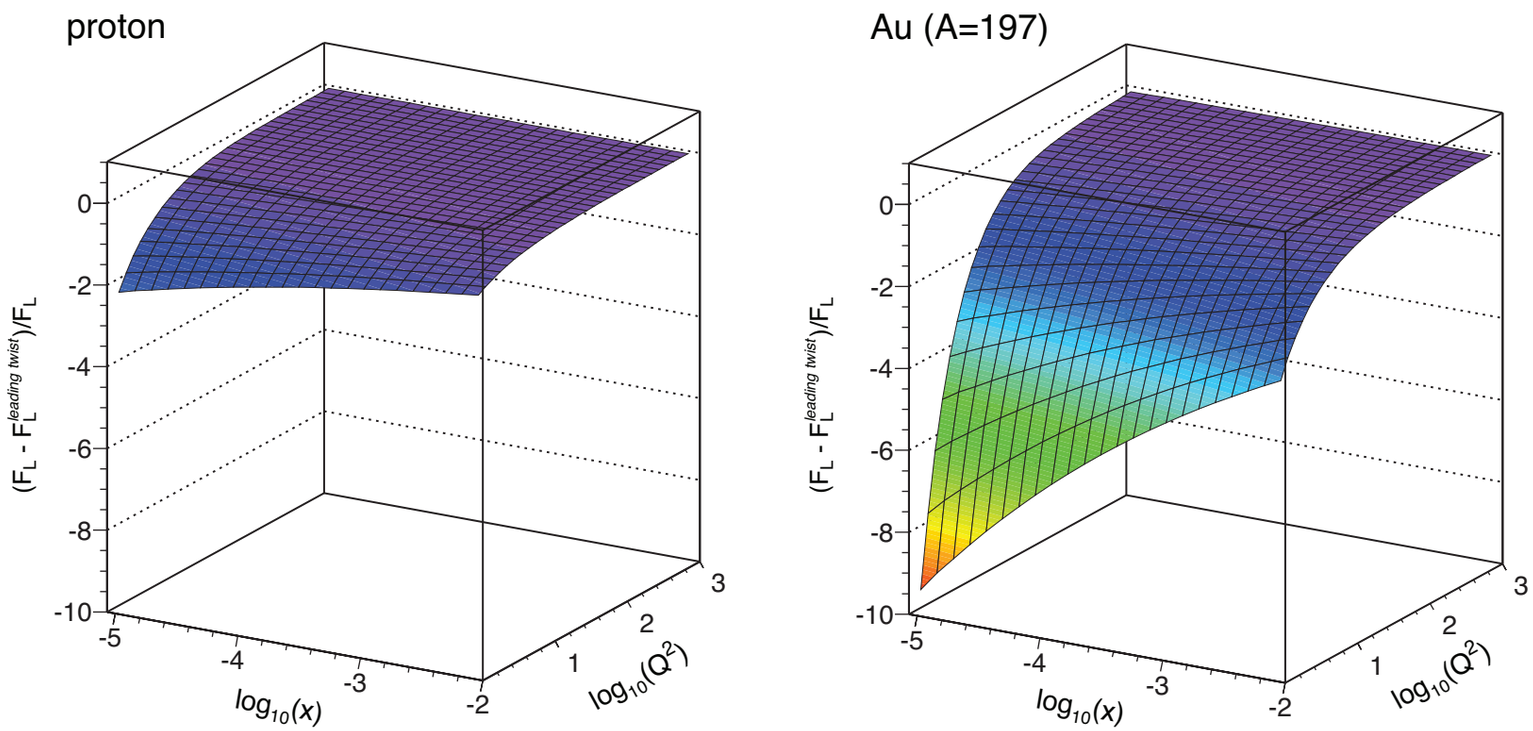

- Plotting F_L-$F_L^{leading\ twist}/F_L$ coming out of saturation inspired GBW model
  - ➡ protons: little effect of leading twist corrections, only starting to come in at small-x and small Q2
  - ➡ Au: much larger corrections coming from leading twist contributions
    - nuclear “oomph” effects well manifested in the F_L structure function

Measuring the gluons: extracting F_L

$$\sigma_r(x, Q^2) = F_2^A(x, Q^2) - \frac{y^2}{Y+} F_L^A(x, Q^2)$$

Measuring the gluons: extracting F_L

$$\sigma_r(x, Q^2) = F_2^A(x, Q^2) - \frac{y^2}{Y+} F_L^A(x, Q^2)$$

- $F_L \sim \alpha_s \, xG(x,Q^2)$
  - ➡ $y = Q^2/xs$
  - ➡ require an energy scan to extract F_L

Measuring the gluons: extracting F_L

$$\sigma_r(x,Q^2) = F_2^A(x,Q^2) - \frac{y^2}{Y+} F_L^A(x,Q^2)$$

- $F_L \sim \alpha_s \, xG(x,Q^2)$
  - ➡ $y = Q^2/xs$
  - ➡ require an energy scan to extract F_L
- 3 different proton energies run at HERA
  - ➡ 2 low-statistics runs
  - ➡ bad for F_L extraction

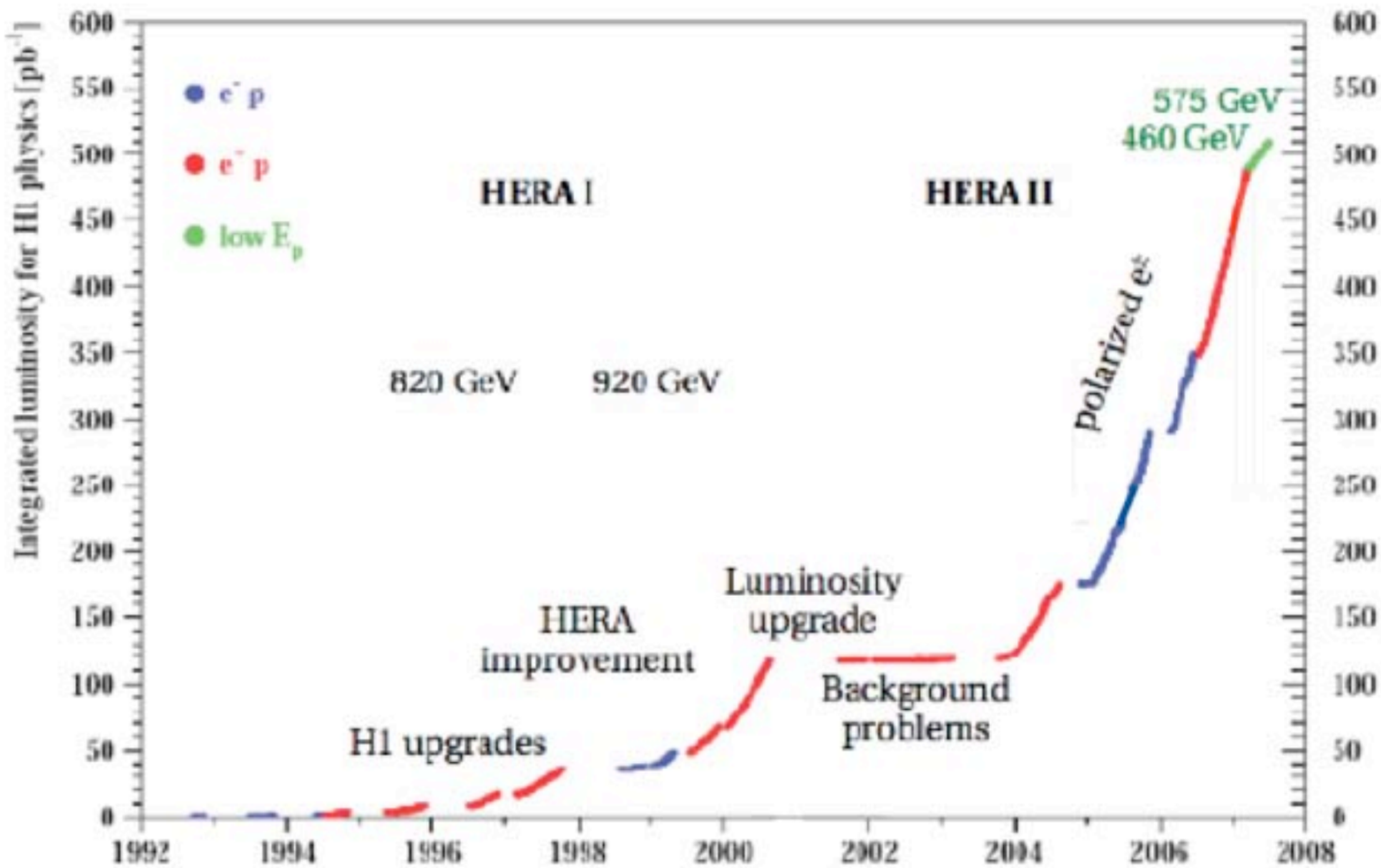

Measuring the gluons: extracting F_L

$$\sigma_r(x,Q^2) = F_2^A(x,Q^2) - \frac{y^2}{Y+} F_L^A(x,Q^2)$$

- $F_L \sim \alpha_s\, xG(x,Q^2)$
  - ➡ $y = Q^2/xs$
  - ➡ require an energy scan to extract F_L
- 3 different proton energies run at HERA
  - ➡ 2 low-statistics runs
  - ➡ bad for F_L extraction

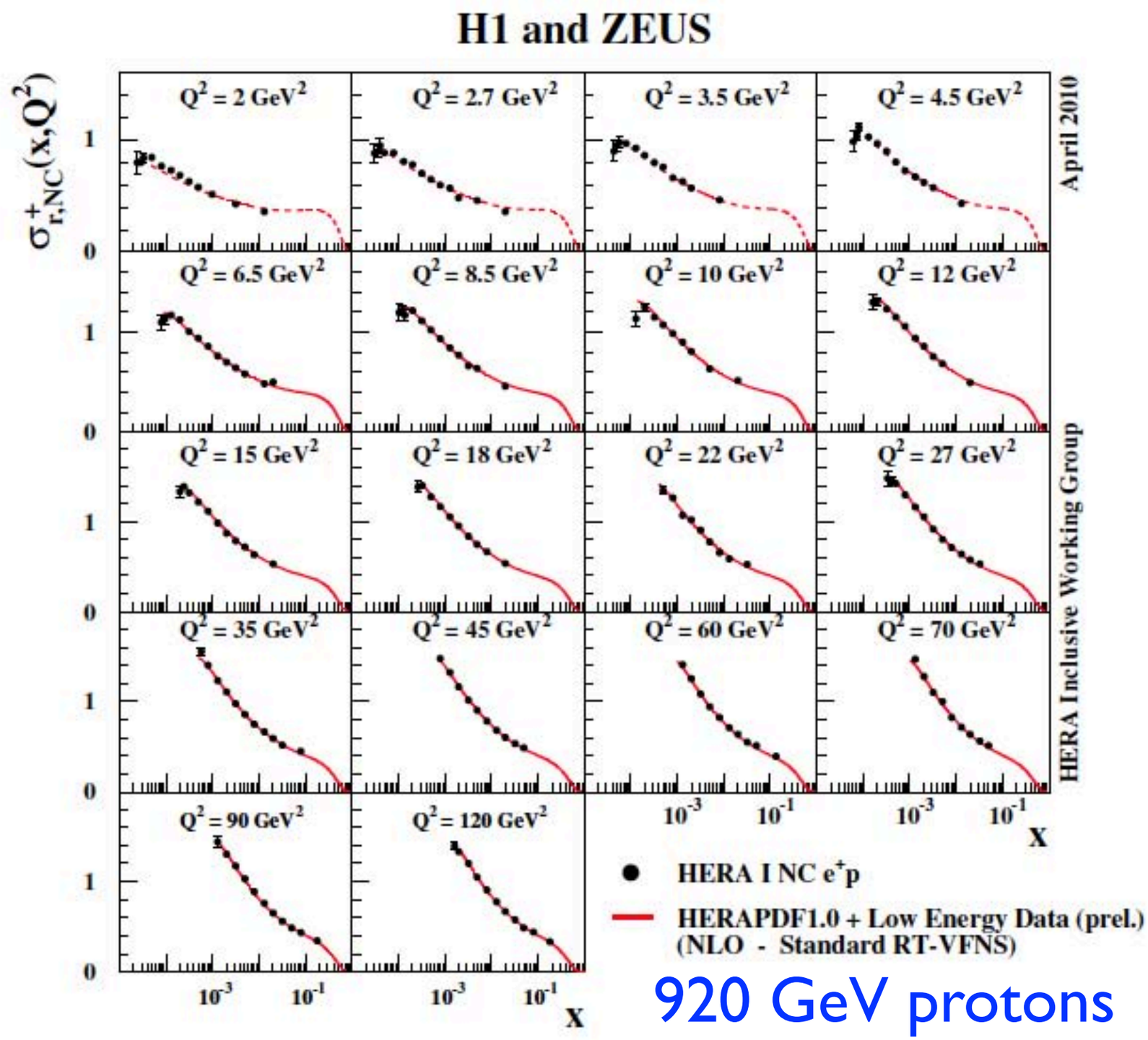

920 GeV protons

Measuring the gluons: extracting F_L

$$\sigma_r(x,Q^2) = F_2^A(x,Q^2) - \frac{y^2}{Y+} F_L^A(x,Q^2)$$

- $F_L \sim \alpha_s\, xG(x,Q^2)$
  - ➡ $y = Q^2/xs$
  - ➡ require an energy scan to extract F_L
- 3 different proton energies run at HERA
  - ➡ 2 low-statistics runs
  - ➡ bad for F_L extraction

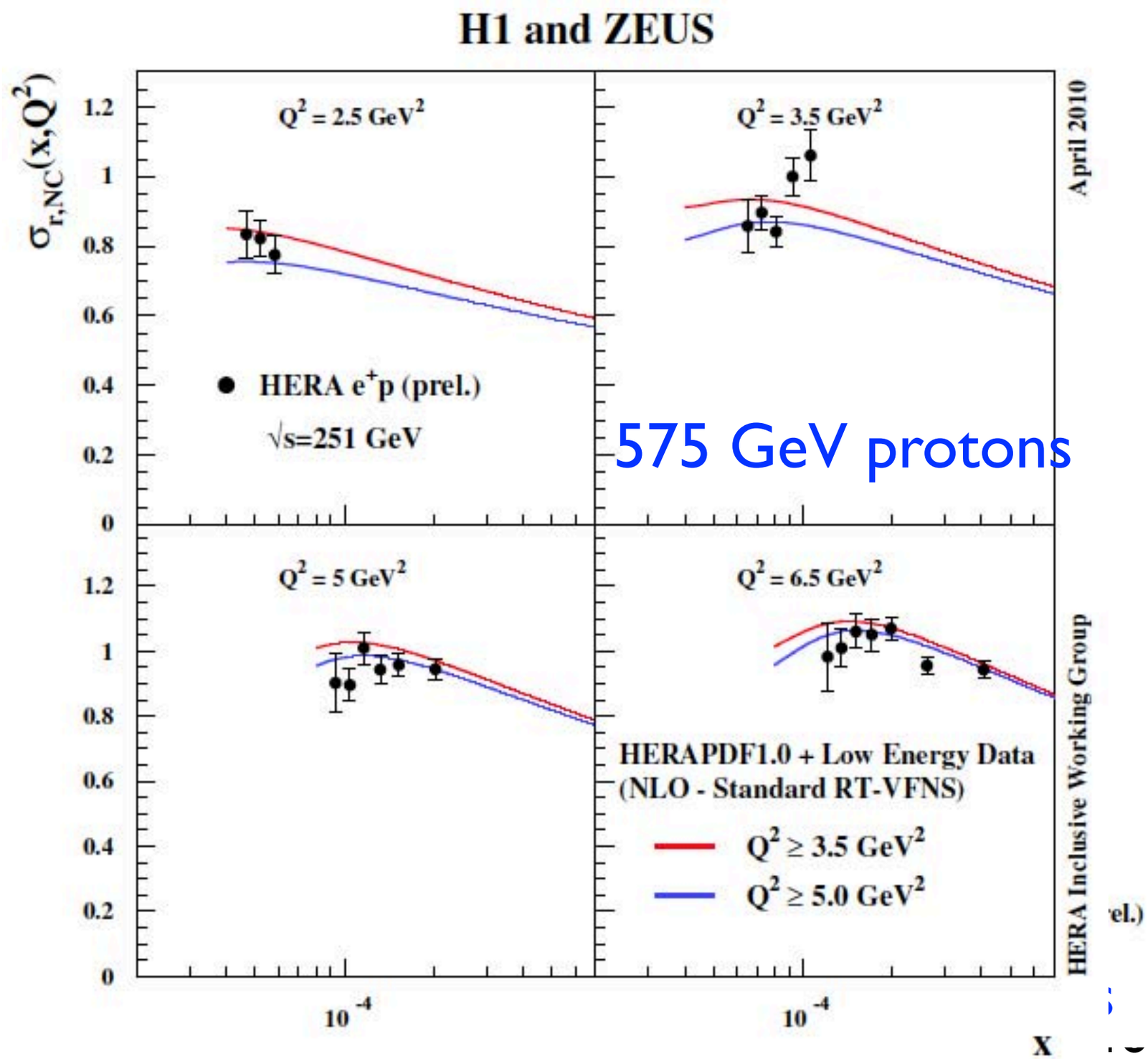

Measuring the gluons: extracting F_L

$$\sigma_r(x,Q^2) = F_2^A(x,Q^2) - \frac{y^2}{Y+} F_L^A(x,Q^2)$$

- $F_L \sim \alpha_s\, xG(x,Q^2)$
  - ➡ $y = Q^2/xs$
  - ➡ require an energy scan to extract F_L
- 3 different proton energies run at HERA
  - ➡ 2 low-statistics runs
  - ➡ bad for F_L extraction

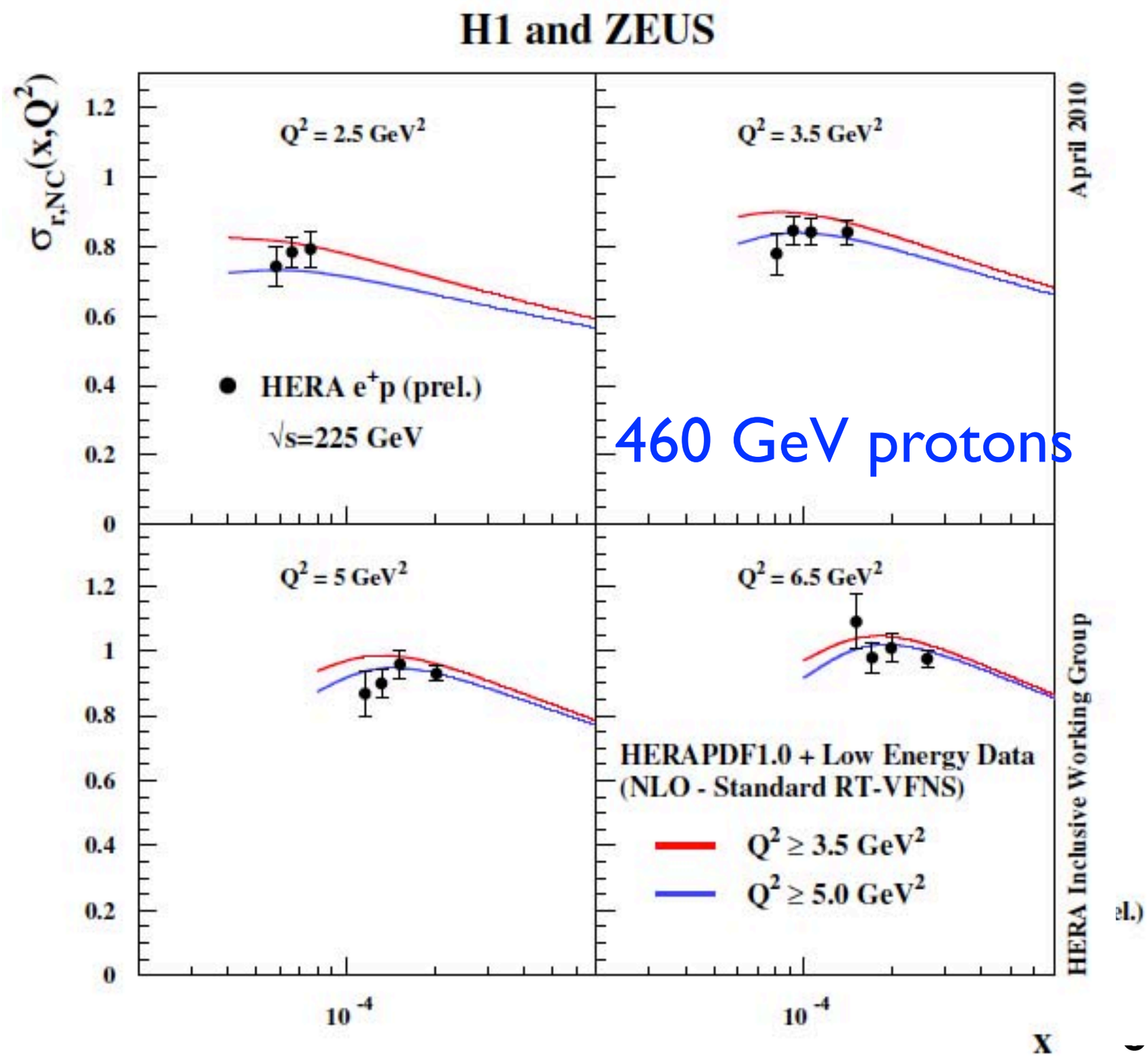

Measuring the gluons: extracting F_L

$$\sigma_r(x,Q^2) = F_2^A(x,Q^2) - \frac{y^2}{Y+} F_L^A(x,Q^2)$$

- $F_L \sim \alpha_s\, xG(x,Q^2)$
  - ➡ $y = Q^2/xs$
  - ➡ require an energy scan to extract F_L
- 3 different proton energies run at HERA
  - ➡ 2 low-statistics runs
  - ➡ bad for F_L extraction

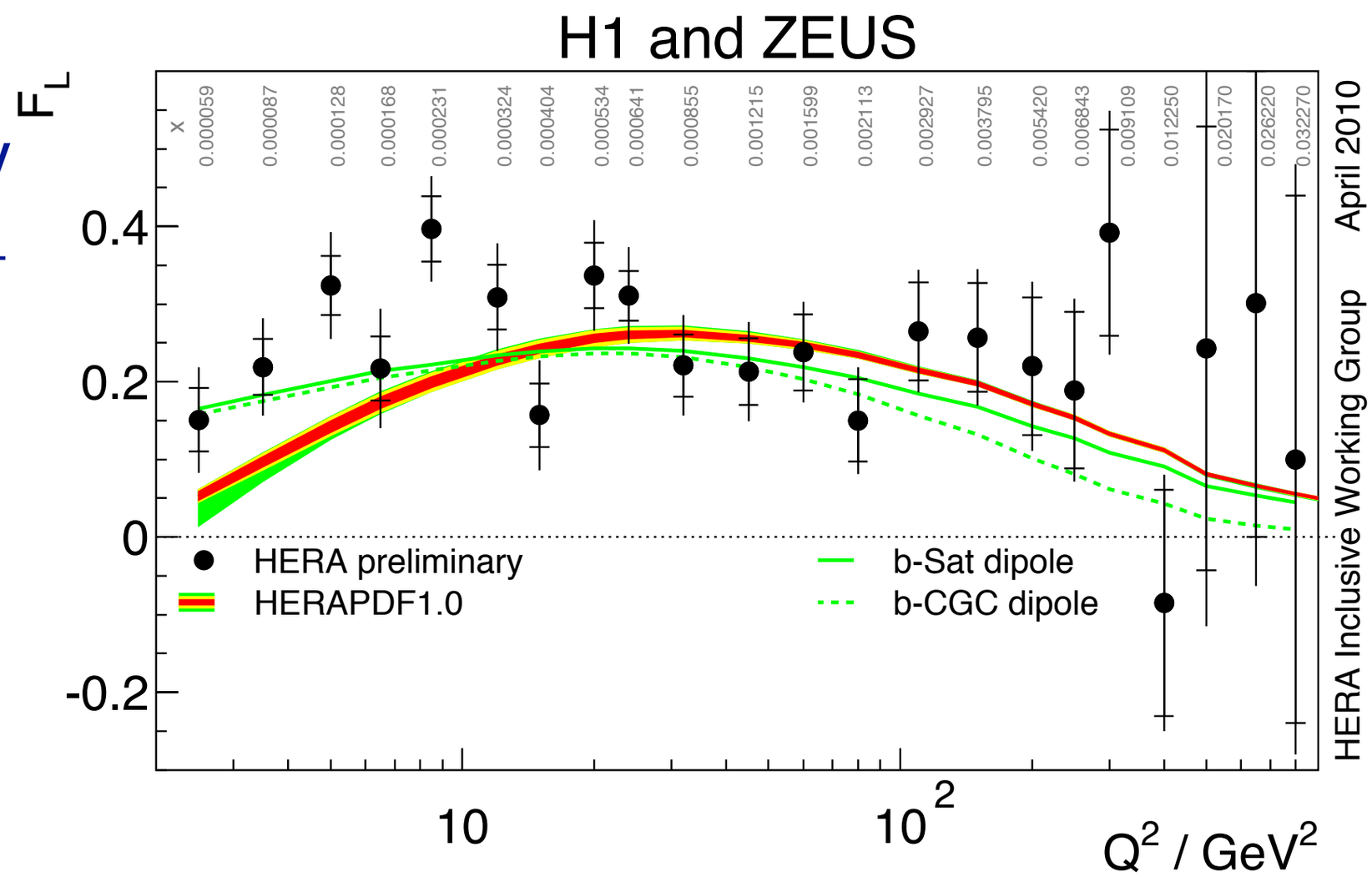

Feasibility study: $\sigma_r(x,Q^2) = F_2^A(x,Q^2) - \frac{y^2}{Y^+} F_L^A(x,Q^2)$

Strategies:

slope of y^2/Y_+ for different s at fixed x & Q^2

e+p: 1st stage

5x50 - 5x325 running combined 4 weeks/each (50% eff)

stat. error shown and negligible

To Do:

refine method & test how well we can extract F_L in e+A collisions

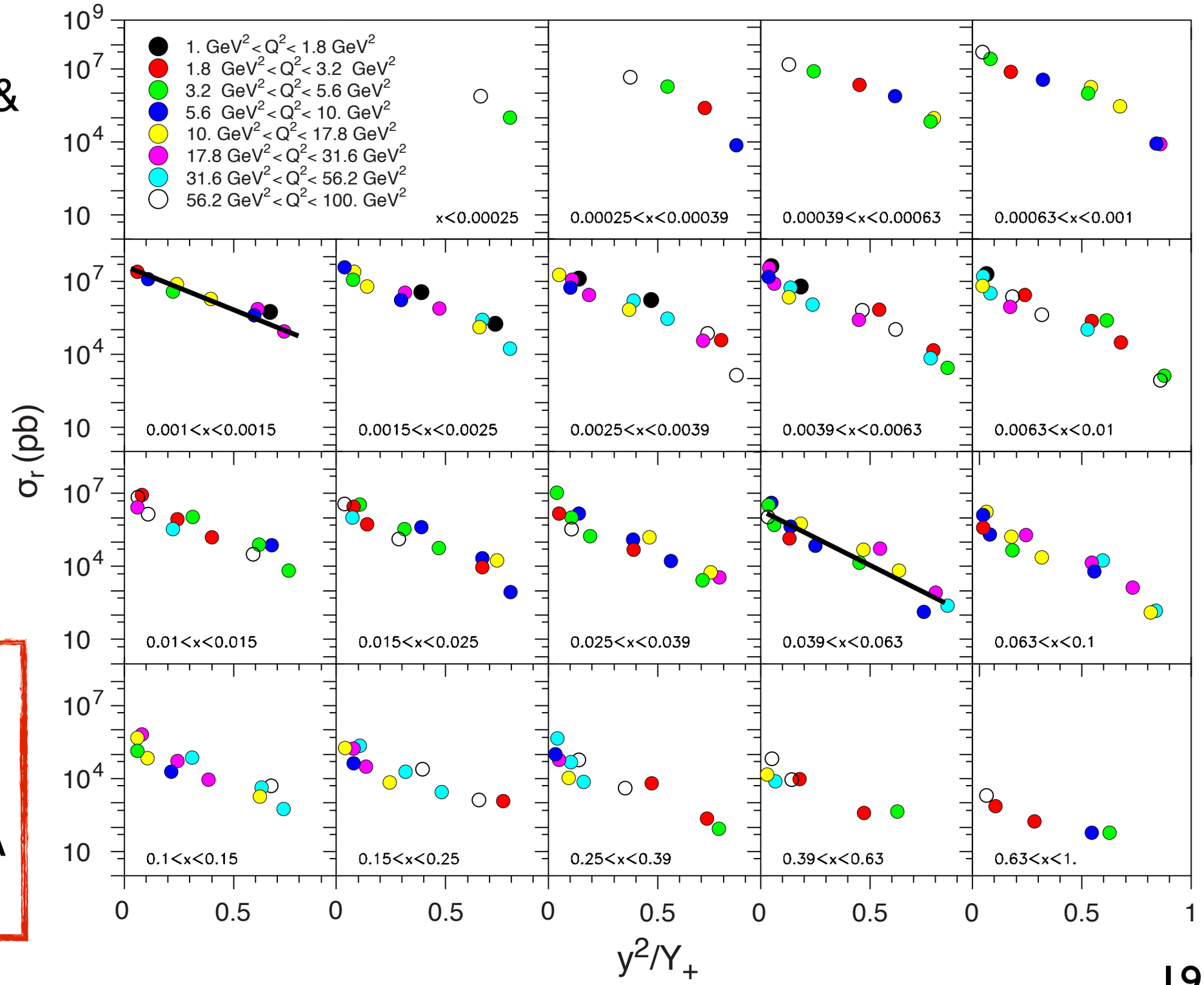

Feasibility study: $\sigma_r(x,Q^2) = F_2^A(x,Q^2) - \frac{y^2}{Y^+} F_L^A(x,Q^2)$

Strategies:
slope of y^2/Y_+ for different s at fixed x & Q^2

e+Au: 1st stage
5x50 - $A\int Ldt = 2\ fb^{-1}$
5x75 - $A\int Ldt = 4\ fb^{-1}$
5x100 - $A\int Ldt = 4\ fb^{-1}$
running combined
4 weeks/each
(50% eff)

statistical errors only are shown

Will be dominated by systematics, but would need a full detector simulation in order to estimate them

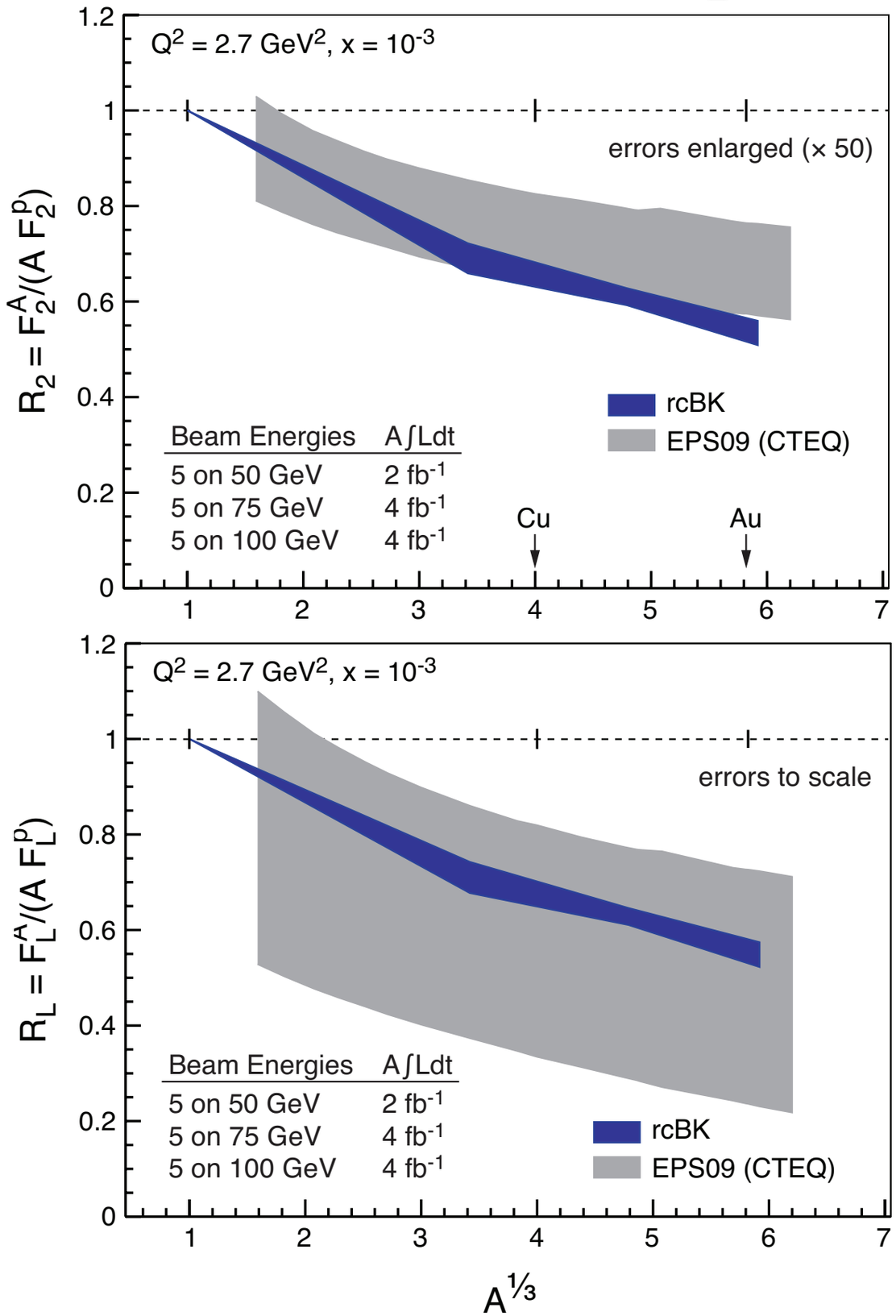

Charm and diffractive structure functions, $F^{D}_{2,L}$, $F^{c}_{2,L}$

Charm and diffractive structure functions, $F^D_{2,L}$, $F^c_{2,L}$

- $F^c_{2,L}$ give more direct access to the gluon distribution than the inclusive F_2 structure function
  - ➡ Due to the high charm mass, they probe higher values of x
    - Less sensitive to non-linear effects
  - ➡ QCD calculations with non-zero m_c are scheme dependent
    - Can absorb non-linear signals if not handled correctly

Charm and diffractive structure functions, $F^D_{2,L}$, $F^c_{2,L}$

- $F^c_{2,L}$ give more direct access to the gluon distribution than the inclusive F_2 structure function
  - ➡ Due to the high charm mass, they probe higher values of x
    - Less sensitive to non-linear effects
  - ➡ QCD calculations with non-zero m_c are scheme dependent
    - Can absorb non-linear signals if not handled correctly
- $F^D_{2,L}$ is also sensitive to the gluon distribution
  - ➡ Differences between linear and non-linear models appear at higher Q^2 than for F_2 (8 GeV^2 vs 2 GeV^2)
    - More experimentally challenging measurement than F_2

$$x_{\mathbb{P}} = 10^{-3}$$

$$Q^2 = 5GeV^2$$

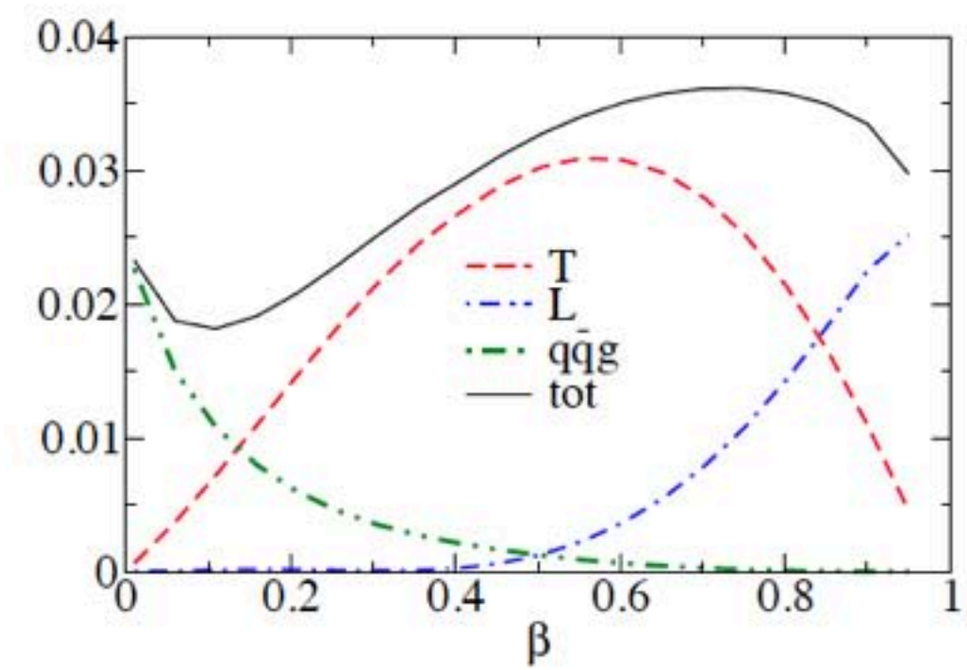

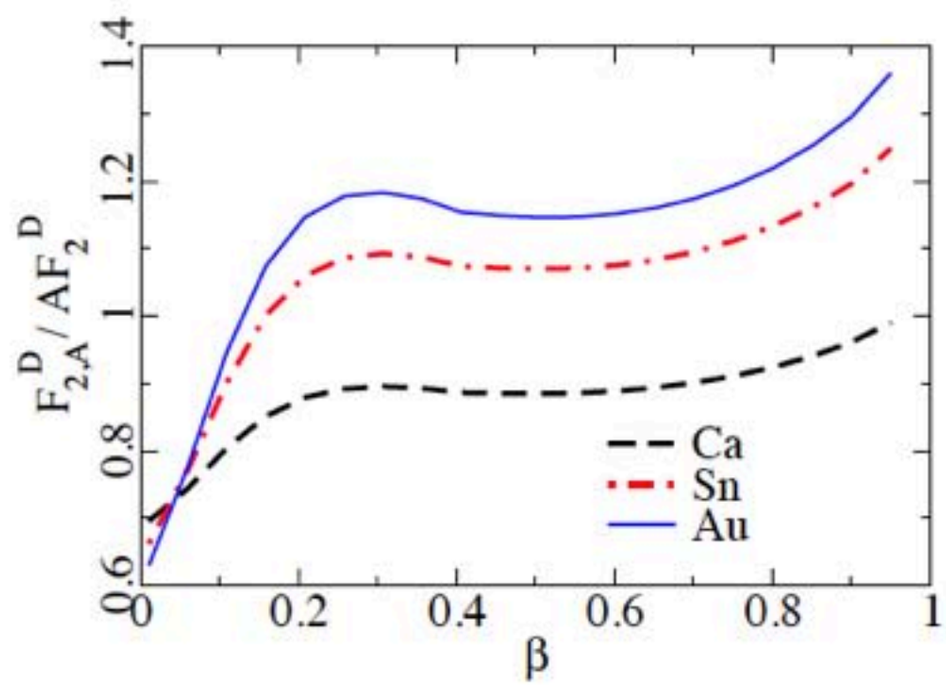

k_T dependent gluons, gluon correlations from di-hadron correlations, SIDIS (semi-inclusive DIS)

k_T dependent gluons, gluon correlations from di-hadron correlations, SIDIS (semi-inclusive DIS)

Deliverables	Observables	What we learn	Stage-I	Stage-II

Direct link between p_T of produced hadron and that of the small-x gluon

$$e + A \rightarrow e + h + X$$

k_T dependent gluons	SIDIS at small x	non-linear QCD evolution / universality	onset of saturation	rare probes and bottom; large-x gluons

k_T dependent gluons, gluon correlations from di-hadron correlations, SIDIS (semi-inclusive DIS)

$$e+A \rightarrow e + h_1 + h_2 + X$$

Deliverables	Observables	What we learn	Stage-I	Stage-II
k_T dependent gluons; gluon correlations	di-hadron correlations	non-linear QCD evolution / universality	onset of saturation	measure Q_s

$$e+A \rightarrow e + h + X$$

k_T dependent gluons	SIDIS at small x	non-linear QCD evolution / universality	onset of saturation	rare probes and bottom; large-x gluons

di-hadron Correlations

- For details of these measurements, please refer to Liang Zheng's talk yesterday morning
- Plots come from his MC development as discussed yesterday

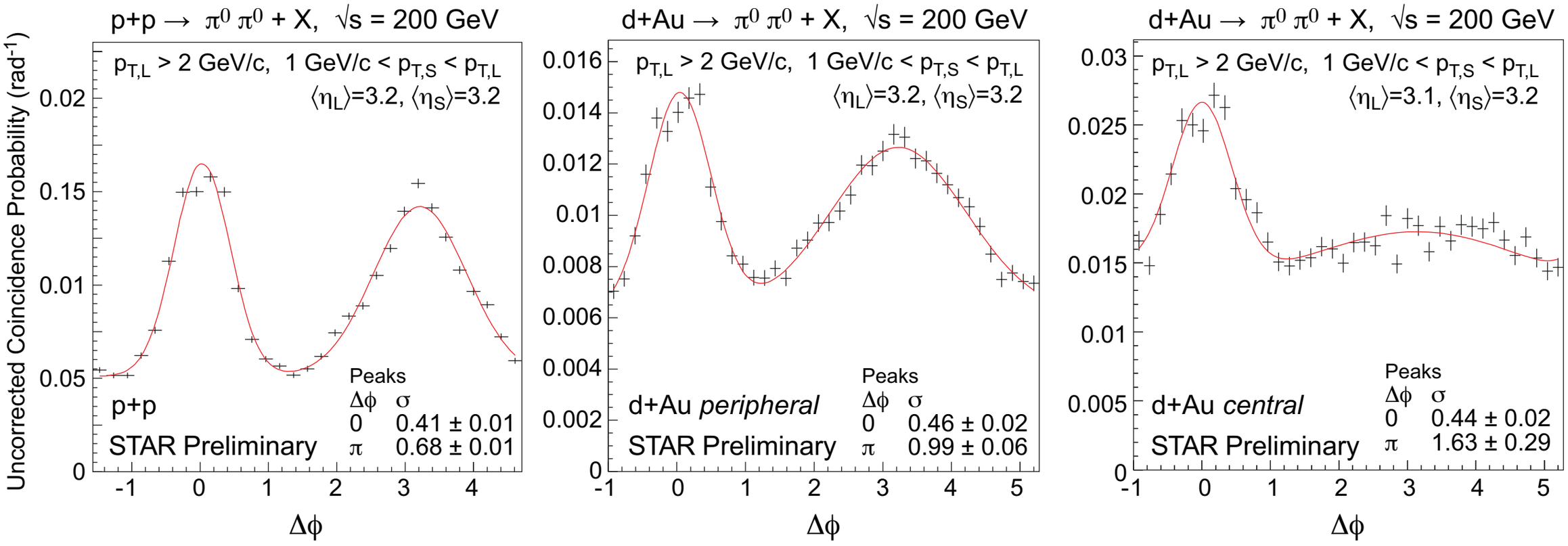

di-hadron Correlations

- For details of these measurements, please refer to Liang Zheng's talk yesterday morning
- Plots come from his MC development as discussed yesterday

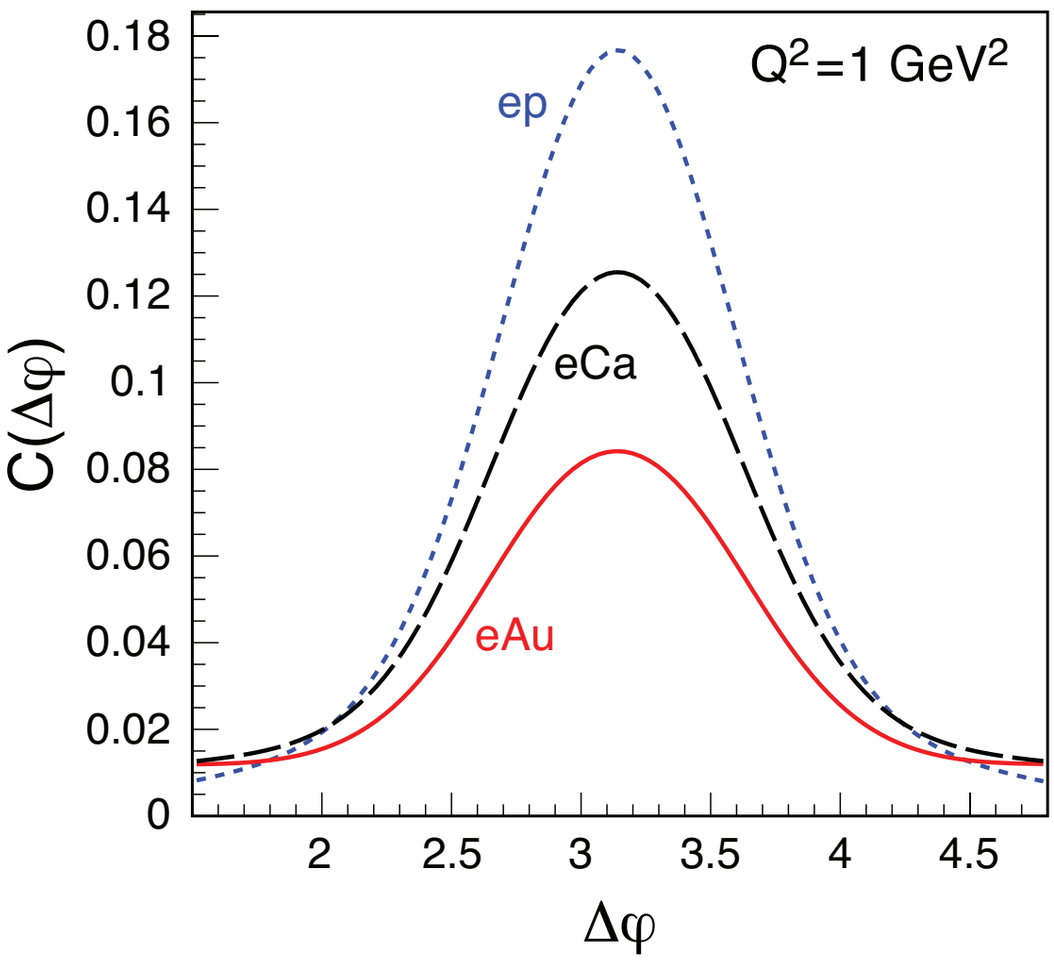

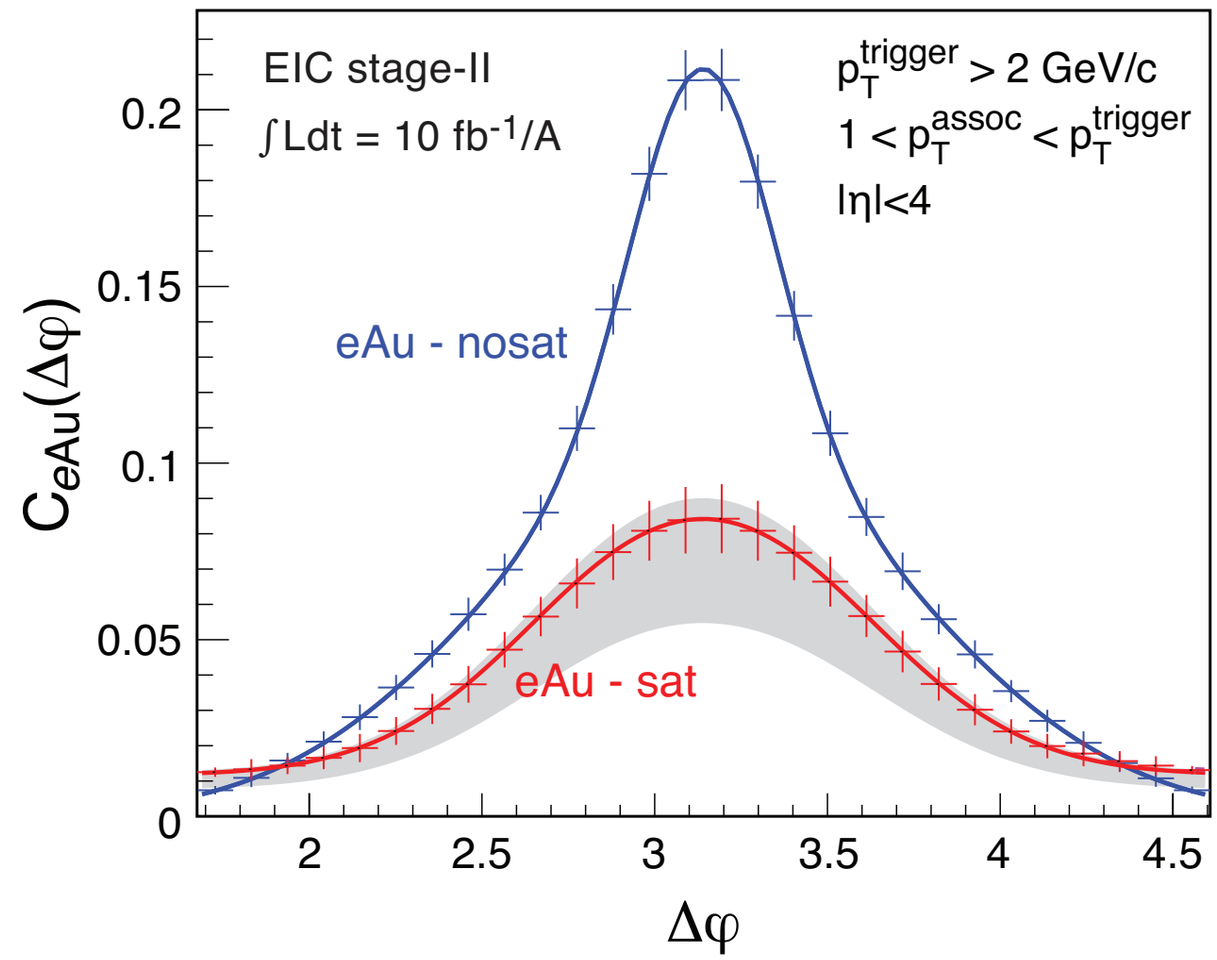

Saturation model prediction courtesy of Bo-wen, Feng ...

di-hadron Correlations

- For details of these measurements, please refer to Liang Zheng's talk yesterday morning
- Plots come from his MC development as discussed yesterday

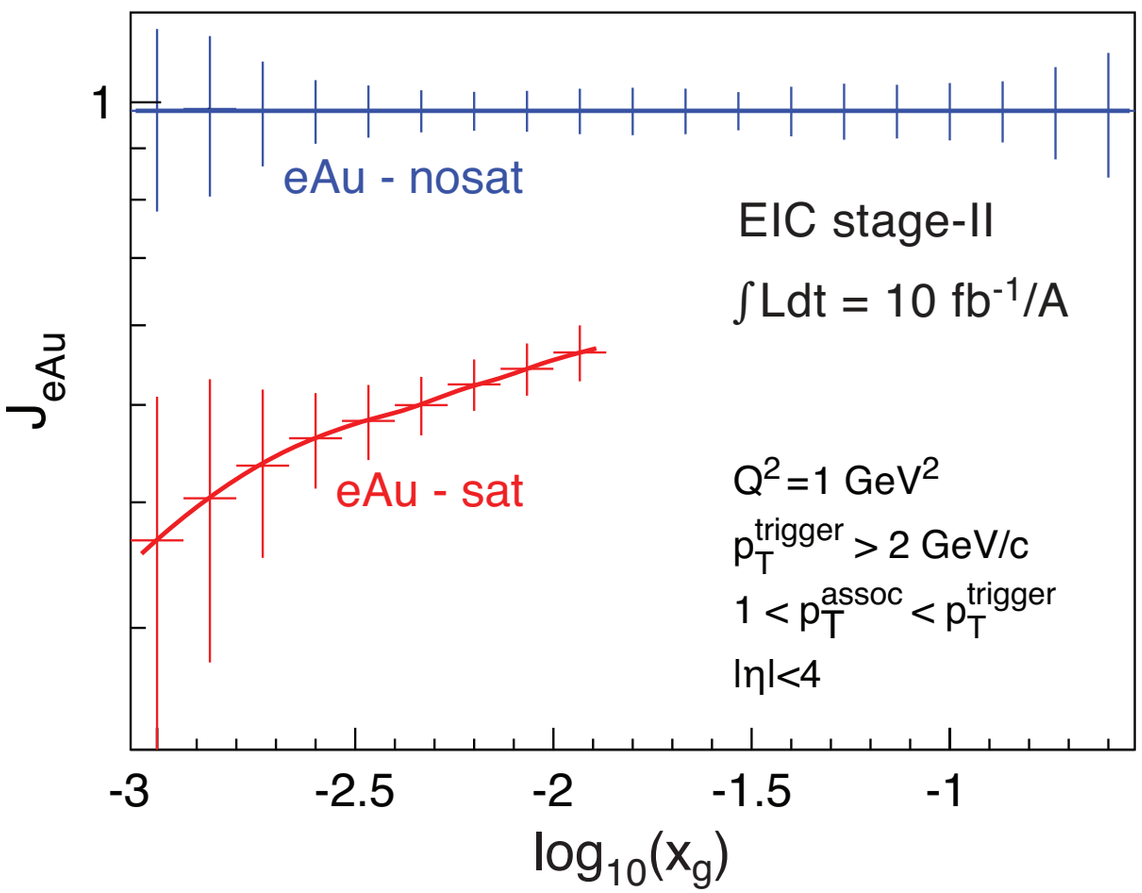

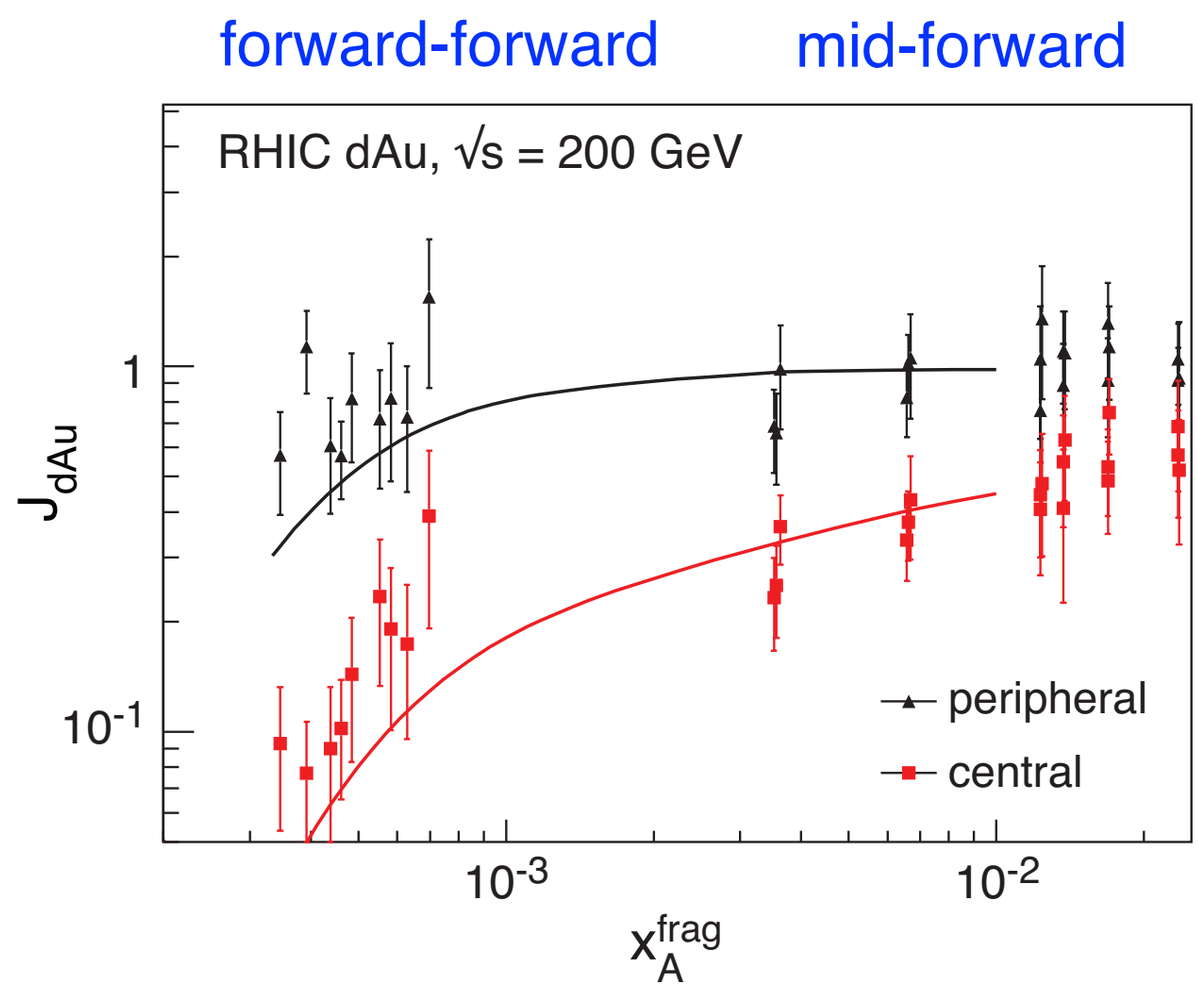

J_{eAu} - relative yield of di-hadrons produced in *e*Au compared to *ep* collisions

Note that x_A^{frag} is not an exact value - curves come from saturation model

b dependent gluons, gluon correlations from DVCS and diffractive vector meson production

Diffractive Vector Meson Production

Deliverables	Observables	What we learn	Stage-I	Stage-II
b-dependent gluons; gluon correlations	DVCS; diffractive vector mesons	interplay between small-x evolution and confinement	moderate x with light, heavy nuclei	smaller x, saturation

b-dependent gluons from DVCS and DVMP

- Transverse position distribution of gluons can be determined from Deeply Virtual Compton Scattering (DVCS: $e+A \rightarrow e+\gamma+A$) and Diffractive Vector Meson Production (DVMP: $e+A \rightarrow e+VM+A$)

  ➡ Proportional to the square of the gluon distribution!!

- Coherent diffraction (intact nuclear target)

  ➡ transverse distribution of gluon density

- Incoherent diffraction (dissociated nuclear target)

  ➡ transverse gluon correlations in addition

b-dependent gluons from DVCS and DVMP

- Transverse position distribution of gluons can be determined from Deeply Virtual Compton Scattering (DVCS: e+A → e+γ+A) and Diffractive Vector Meson Production (DVMP: e+A → e+VM+A)

  ➡ Proportional to the square of the gluon distribution!!

- Coherent diffraction (intact nuclear target)

  ➡ transverse distribution of gluon density

- Incoherent diffraction (dissociated nuclear target)

  ➡ transverse gluon correlations in addition

DVMP

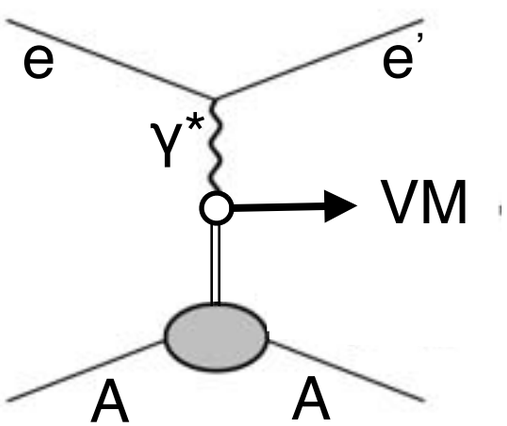

b-dependent gluons from DVCS and DVMP

- Transverse position distribution of gluons can be determined from Deeply Virtual Compton Scattering (DVCS: e+A → e+γ+A) and Diffractive Vector Meson Production (DVMP: e+A → e+VM+A)

  ➡ Proportional to the square of the gluon distribution!!

- Coherent diffraction (intact nuclear target)

  ➡ transverse distribution of gluon density

- Incoherent diffraction (dissociated nuclear target)

  ➡ transverse gluon correlations in addition

DVMP

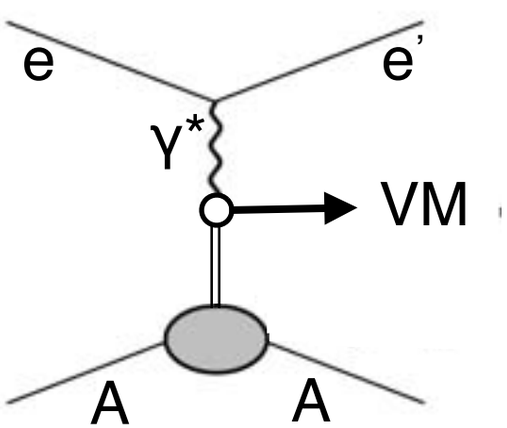

DVCS

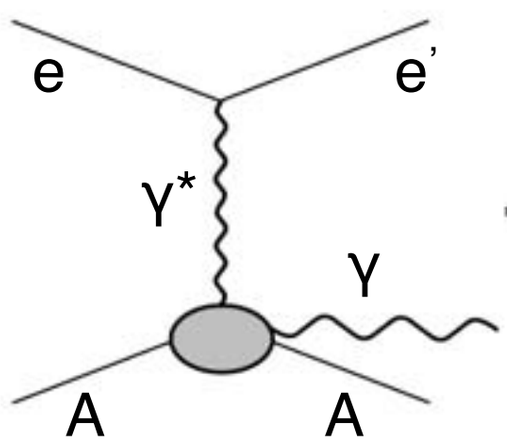

b-dependent gluons from DVCS and DVMP

- Transverse position distribution of gluons can be determined from Deeply Virtual Compton Scattering (DVCS: e+A → e+γ+A) and Diffractive Vector Meson Production (DVMP: e+A → e+VM+A)

  ➡ Proportional to the square of the gluon distribution!!

- Coherent diffraction (intact nuclear target)

  ➡ transverse distribution of gluon density

- Incoherent diffraction (dissociated nuclear target)

  ➡ transverse gluon correlations in addition

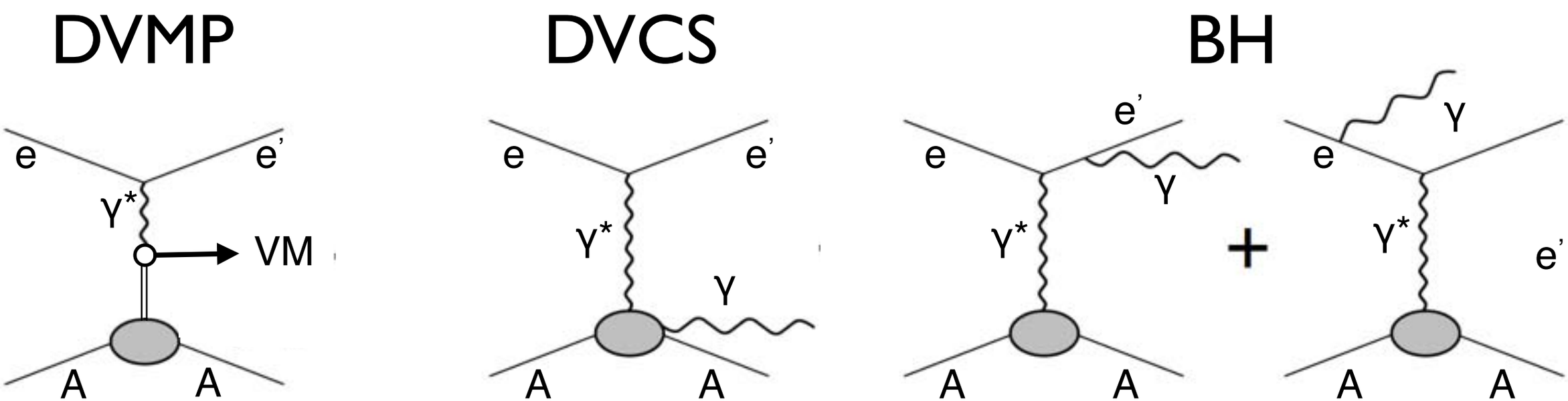

DVCS and Bethe-Heitler interference terms become difficult to distinguish experimentally

Hard Diffraction

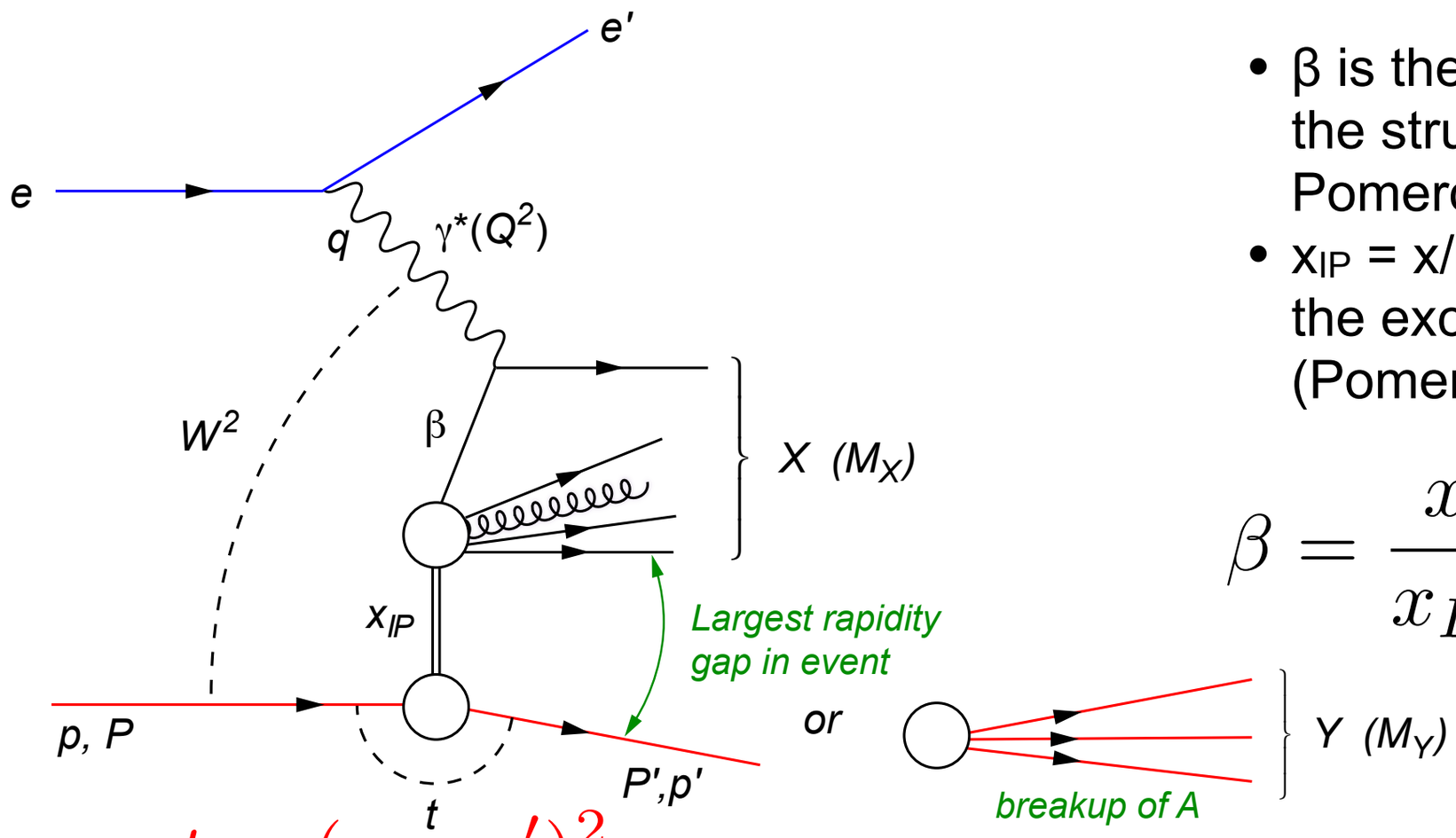

$$t = (p - p')^2$$

- β is the momentum fraction of the struck parton w.r.t. the Pomeron
- $x_{IP} = x/\beta$: momentum fraction of the exchanged object (Pomeron) w.r.t. the hadron

$$\beta = \frac{x}{x_{I\!P}} = \frac{Q^2}{Q^2 + M_X^2 - t}$$

- Diffraction in e+p:
  - HERA: 15% of all events are diffractive

- Diffraction in e+A:
  - Predictions: $\sigma_{diff}/\sigma_{tot}$ in e+A ~25-40%
  - Coherent diffraction (nuclei intact)
  - Incoherent diffraction: breakup into nucleons (nucleons intact)

Visualising Diffractive events

A DIS event (experimental view)

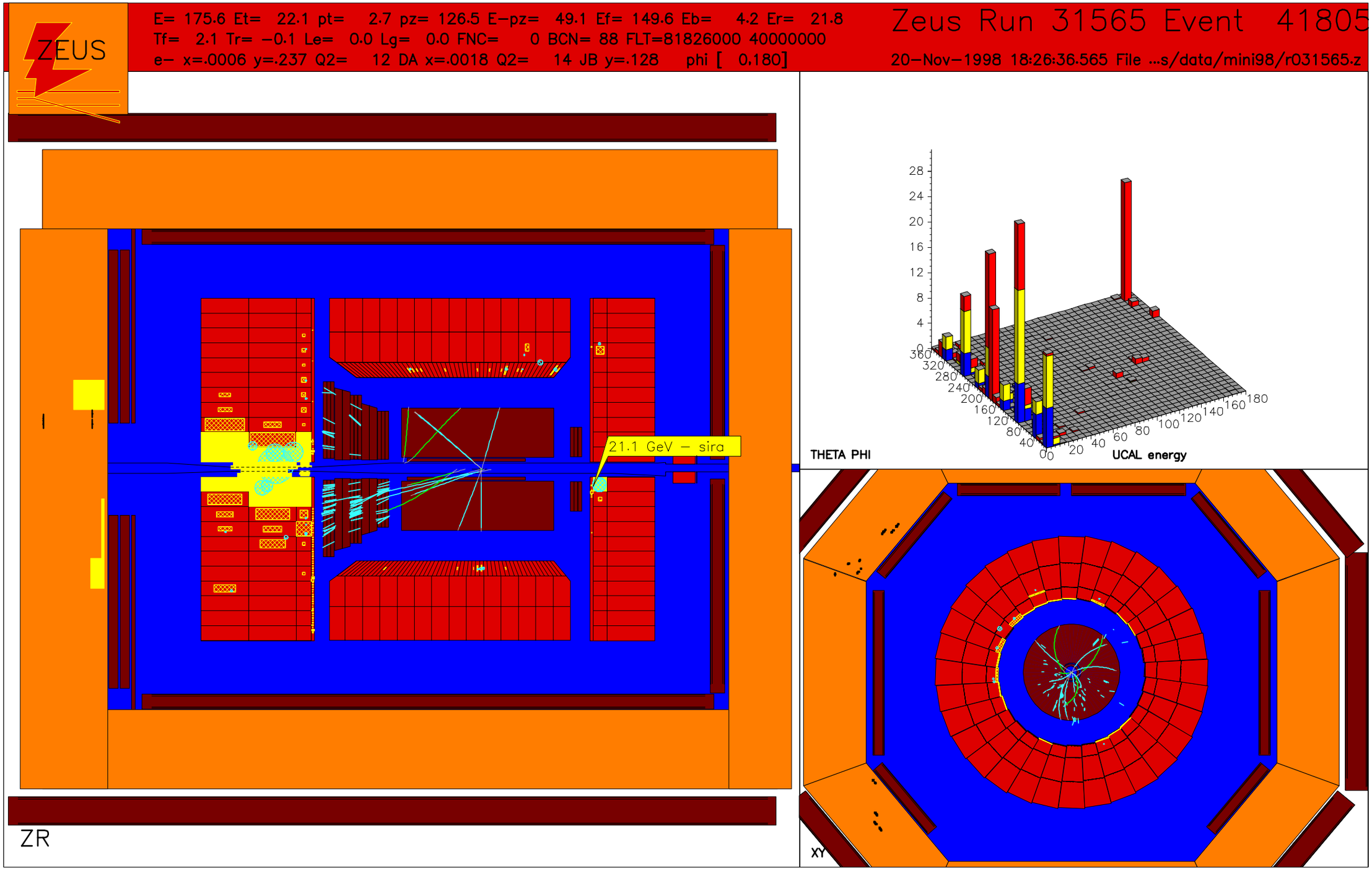

Visualising Diffractive events

A DIS event (experimental view)

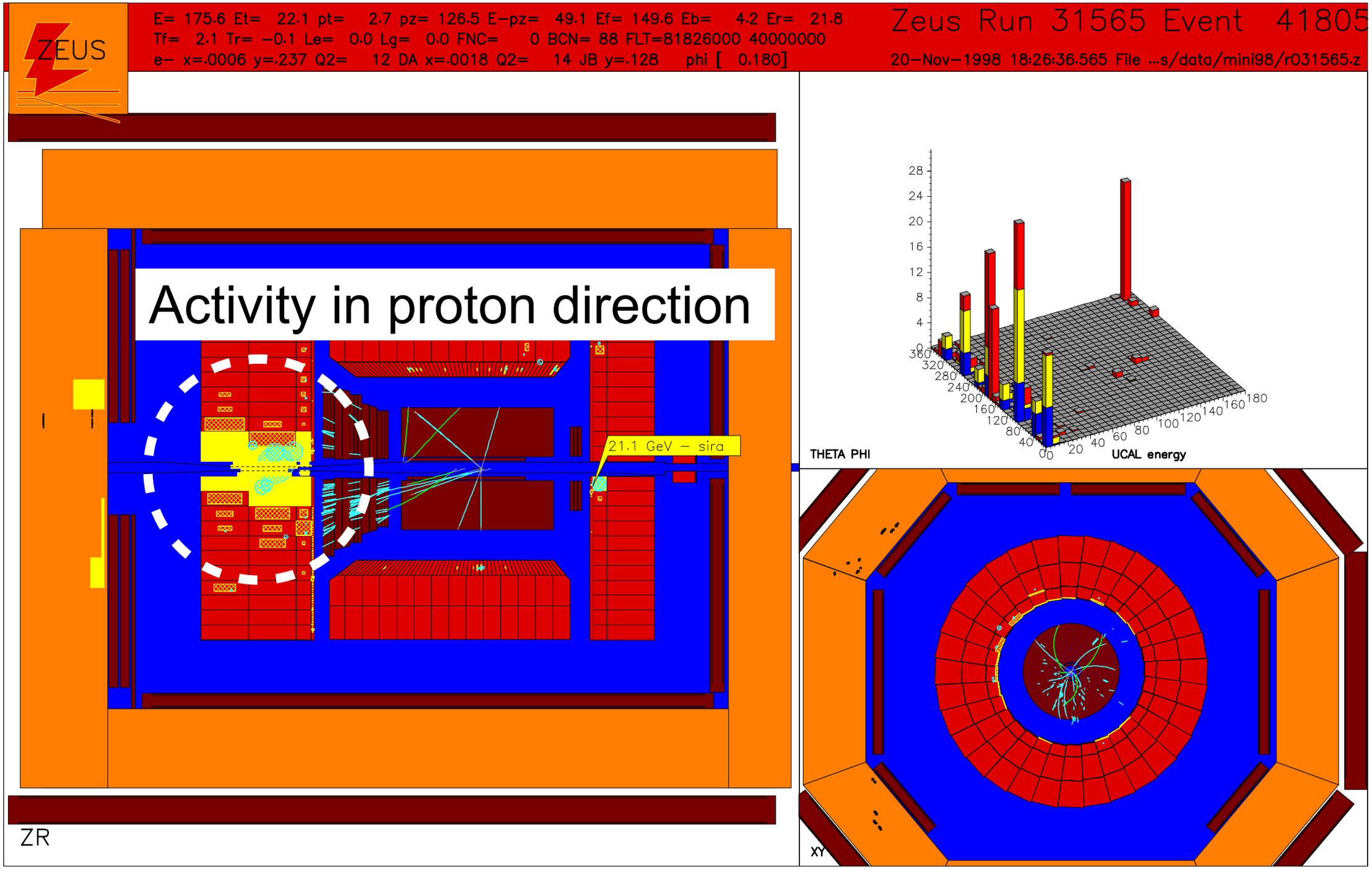

Visualising Diffractive events

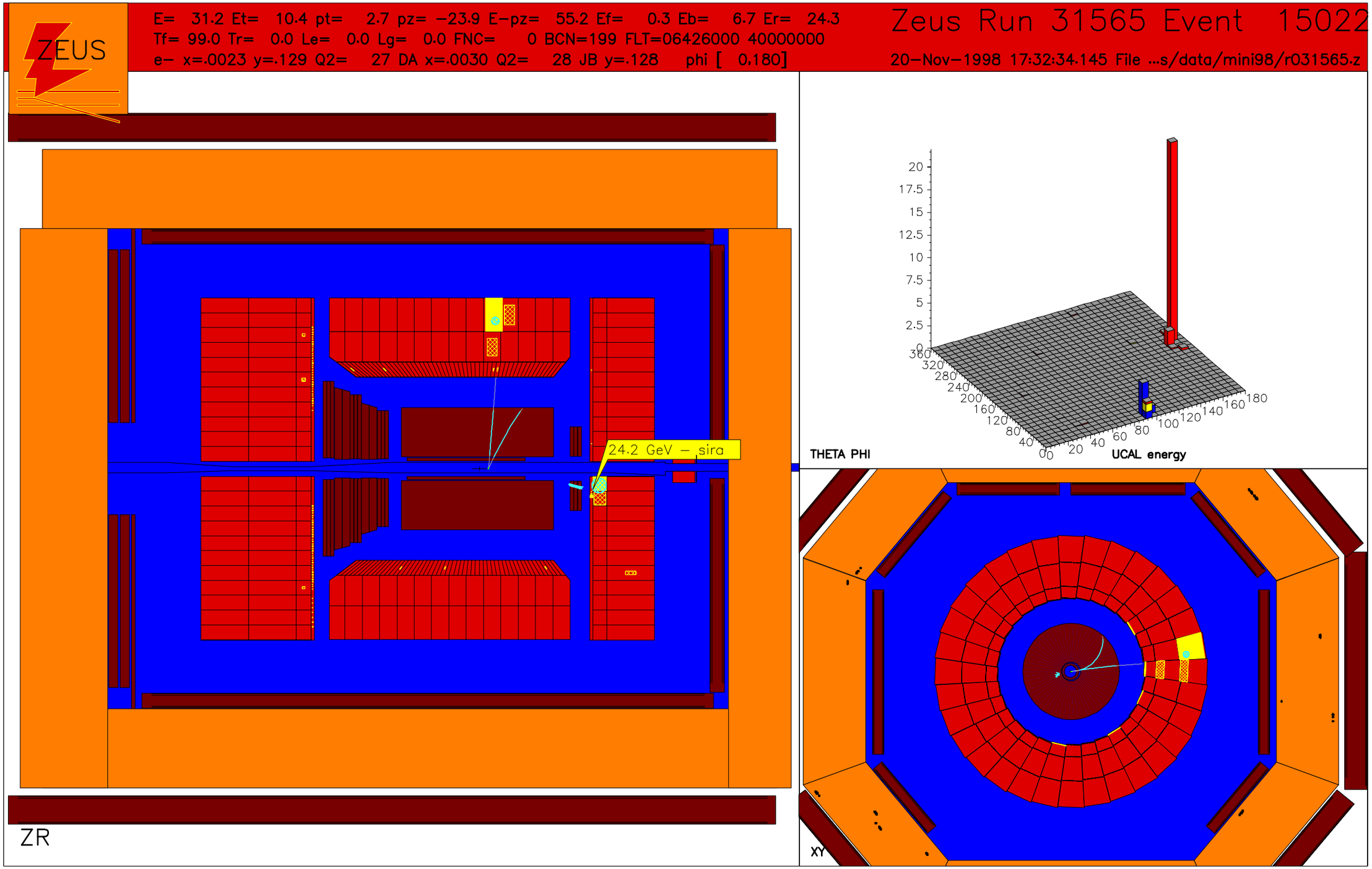

Visualising Diffractive events

A diffractive event (experimental view)

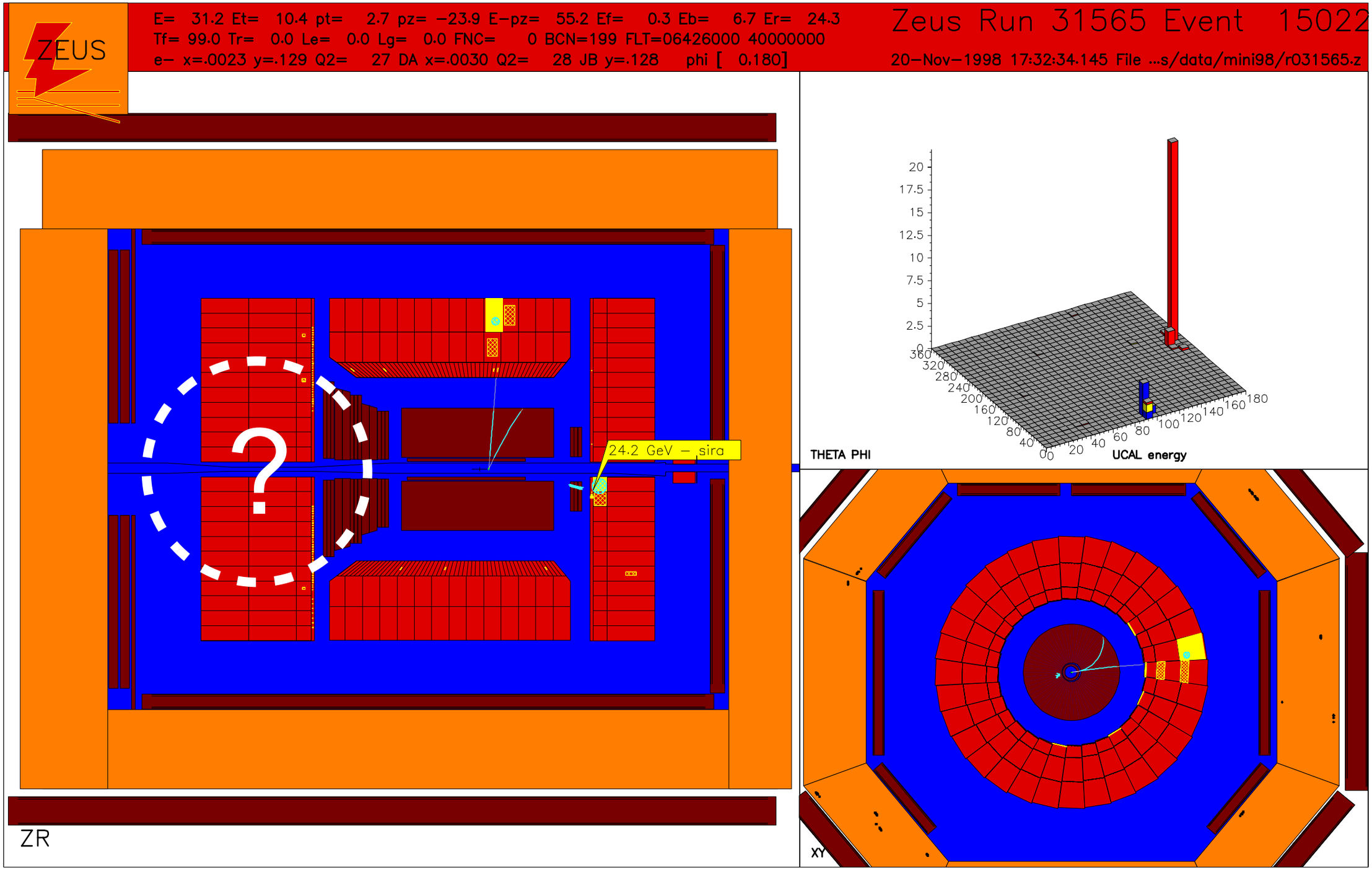

Diffractive cross-sections: Saturation vs Non-Sat

- Ratio of diffractive to total cross-sections between saturation model (Marquet) and Leading-Twist Shadowing (Guzey, Strickman).
  - ➡ Very little difference for LTS between e+p and e+Au, independent of Q^2
  - ➡ For saturation model, e+Au ~ 2*e+p, again independent of Q^2
  - ➡ Simulated error bars (10 fb^{-1}) can easily distinguish between these two scenarios
    - Note that the statistical errors are scaled on the plot so they are visible!

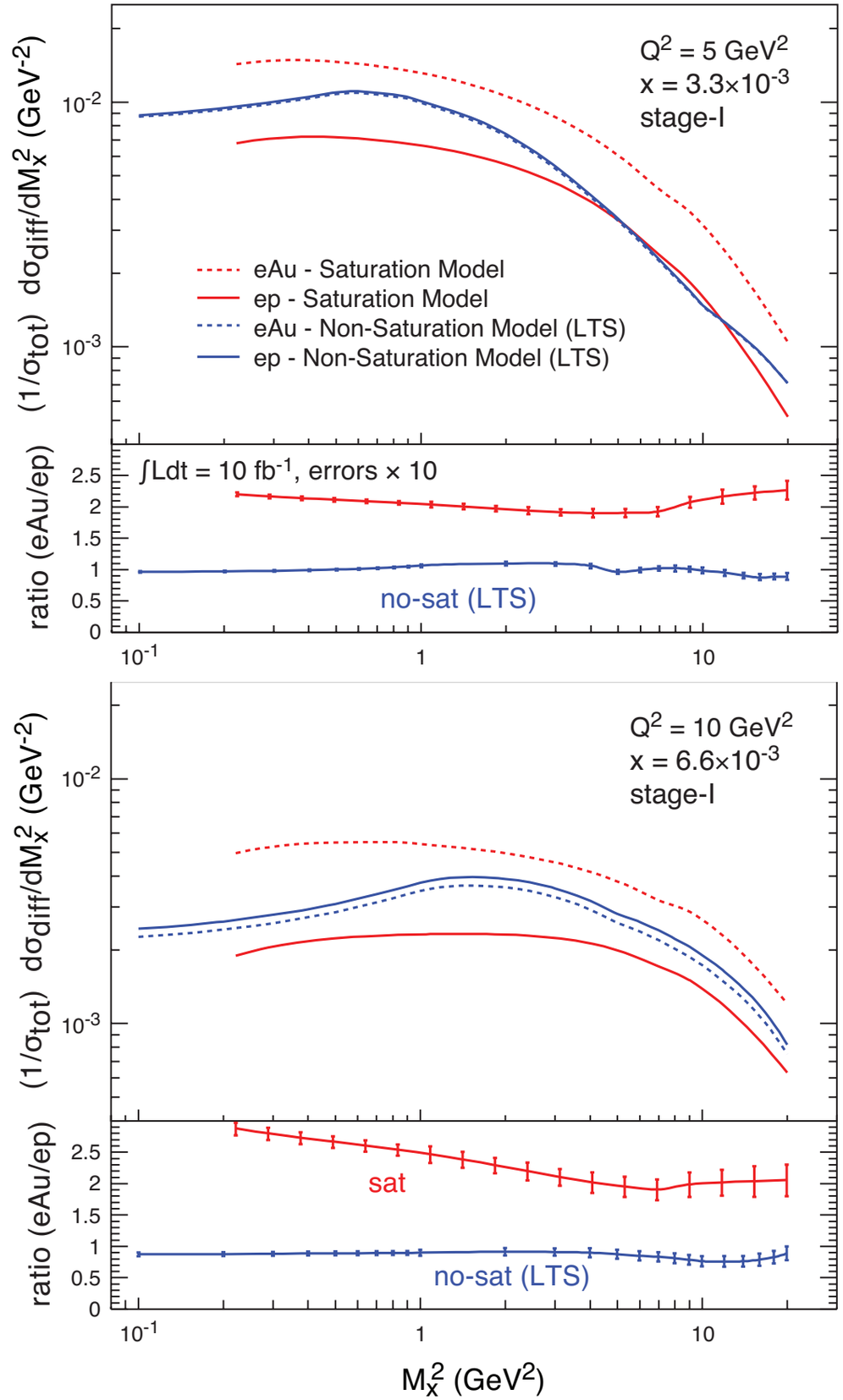

Exclusive Vector Meson Production in e+A

- Many event generators exist for e+p collisions
  - ➡ Pythia (v6), LEPTO, PEPSI, RAPGAP….
- Dearth of event generators for e+A collisions
  - ➡ DPMJET-III
- Work at BNL (T. Toll, T. Ullrich) to write an e+A generator (SARTRE)
  - ➡ Comparison of saturation vs non-saturation scenarios
  - ➡ First case study is that of exclusive diffractive J/ψ production

Exclusive Vector Meson Production in e+A

e+A → e+J/ψ+A'

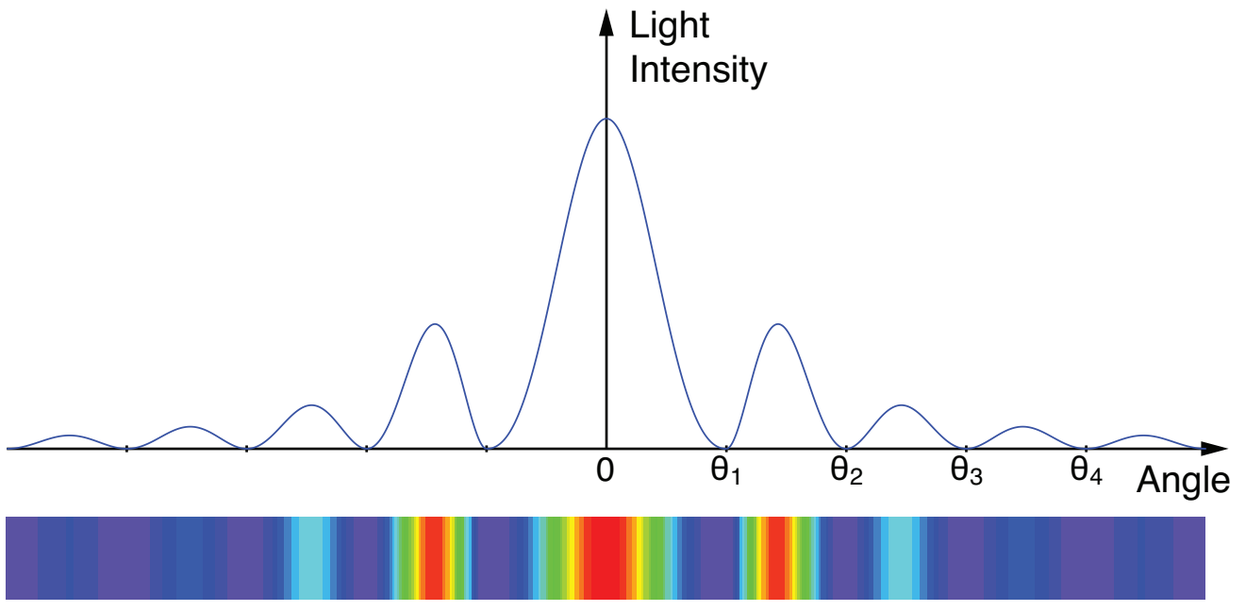

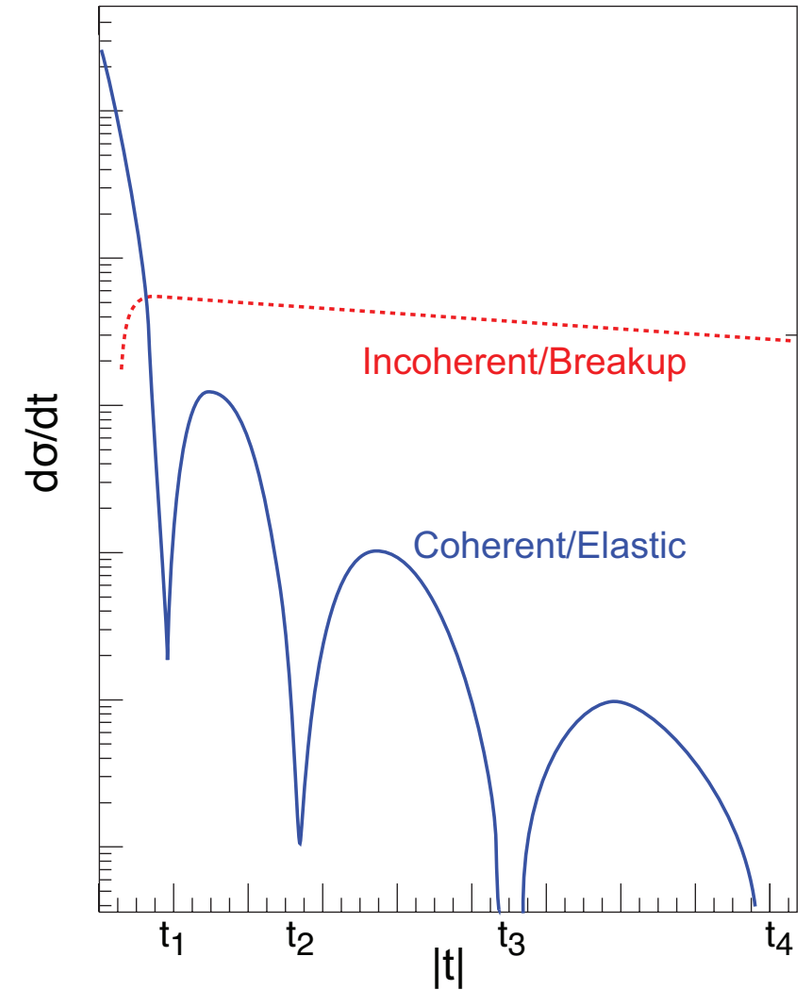

- Low-t: coherent diffraction dominates - gluon density
- High-t: incoherent diffraction dominates - gluon correlations
- Just like in optics - the positions of the diffractive minima are related to the size of the obstacle

➡ $\theta_i \sim 1/(kR)$

Exclusive Vector Meson Production in e+A

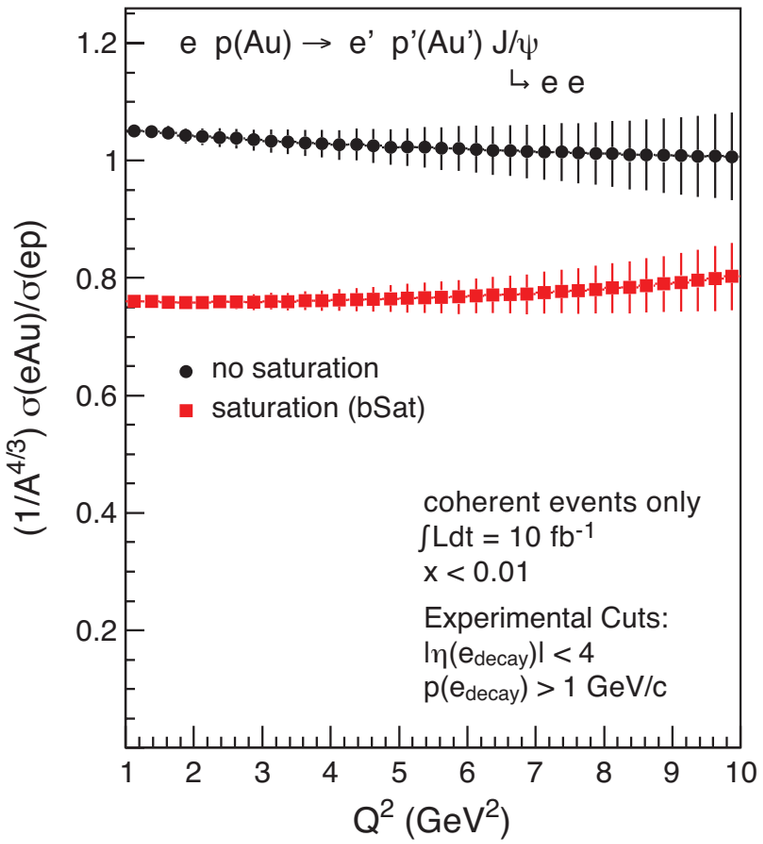

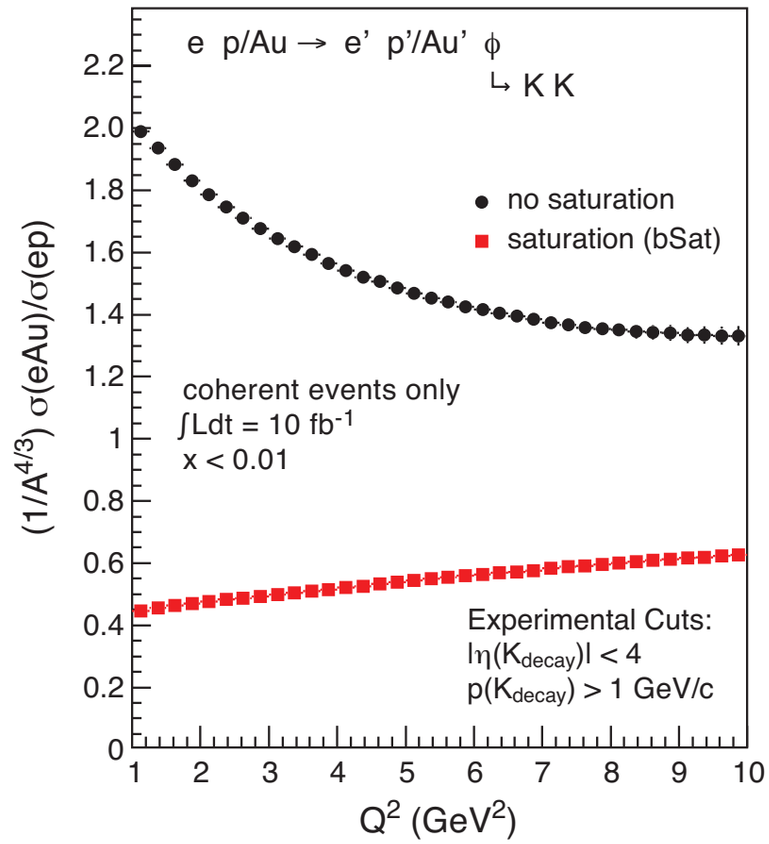

- Diffraction with final state VM - plots from Sartre event generator
  - ➡ Clean - only one new final state particle generated
  - ➡ Unambiguously identified via the presence of a rapidity gap
  - ➡ J/ψ less sensitive to saturation effects that phi
    - expected as ϕ has larger wave function

Exclusive Vector Meson Production in e+A

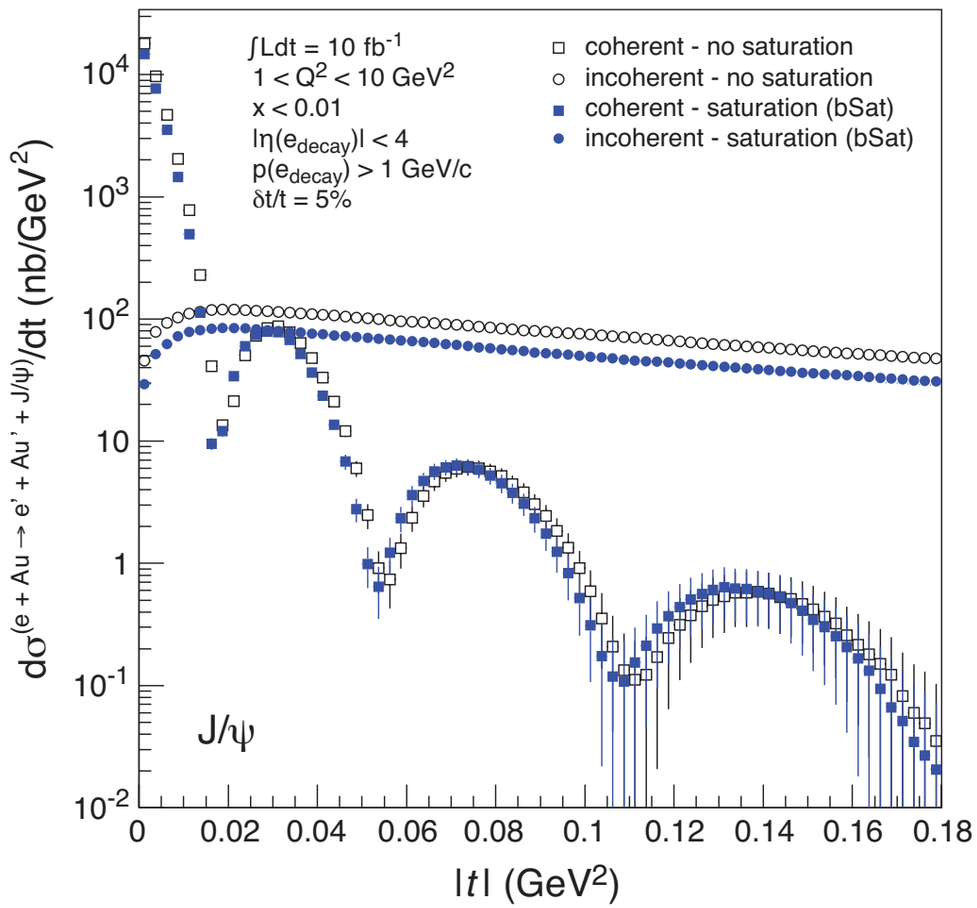

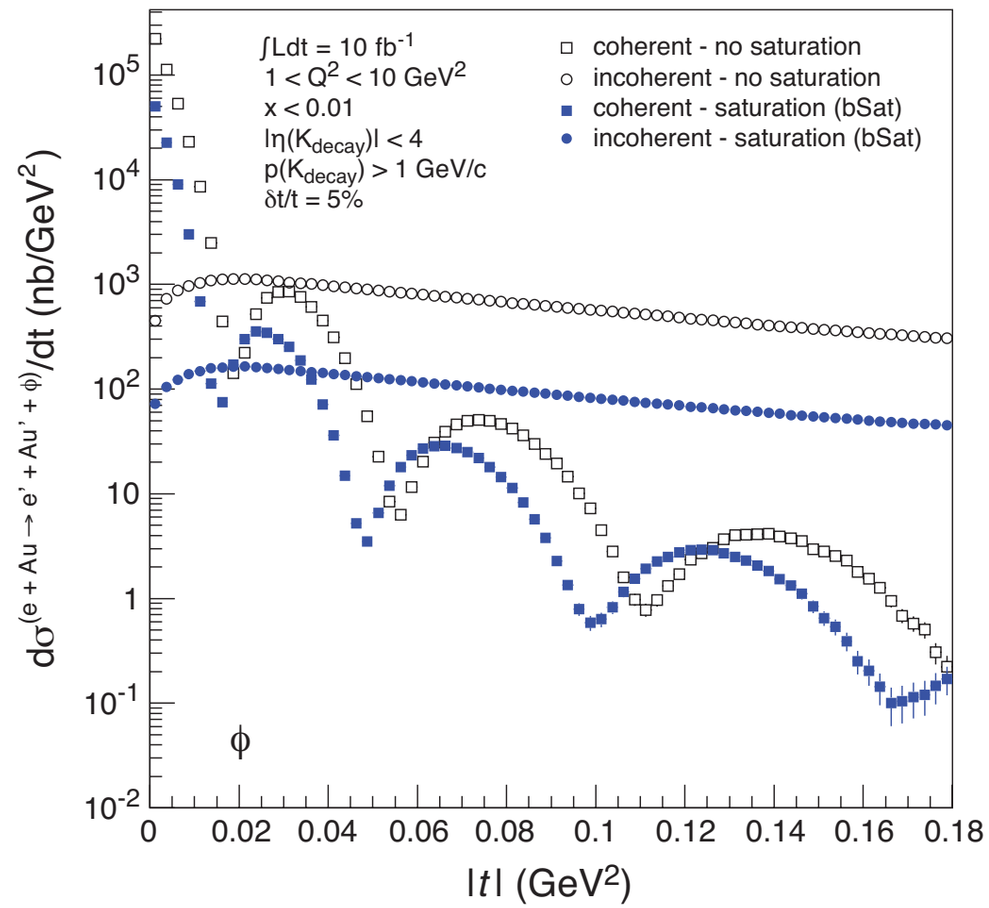

- Low-t: coherent diffraction dominates - gluon density
- High-t: incoherent diffraction dominates - gluon correlations

➡ Need good breakup detection efficiency to discriminate between the two scenarios

- unlike protons, forward spectrometer won't work for heavy ions
  - measure emitted neutrons in a ZDC
- rapidity gap with absence of break-up fragments sufficient to identify coherent events

Comparison of Sartre to preliminary STAR UPC data

Coherent Diffraction (γ^*+IP) in UPC at RHIC

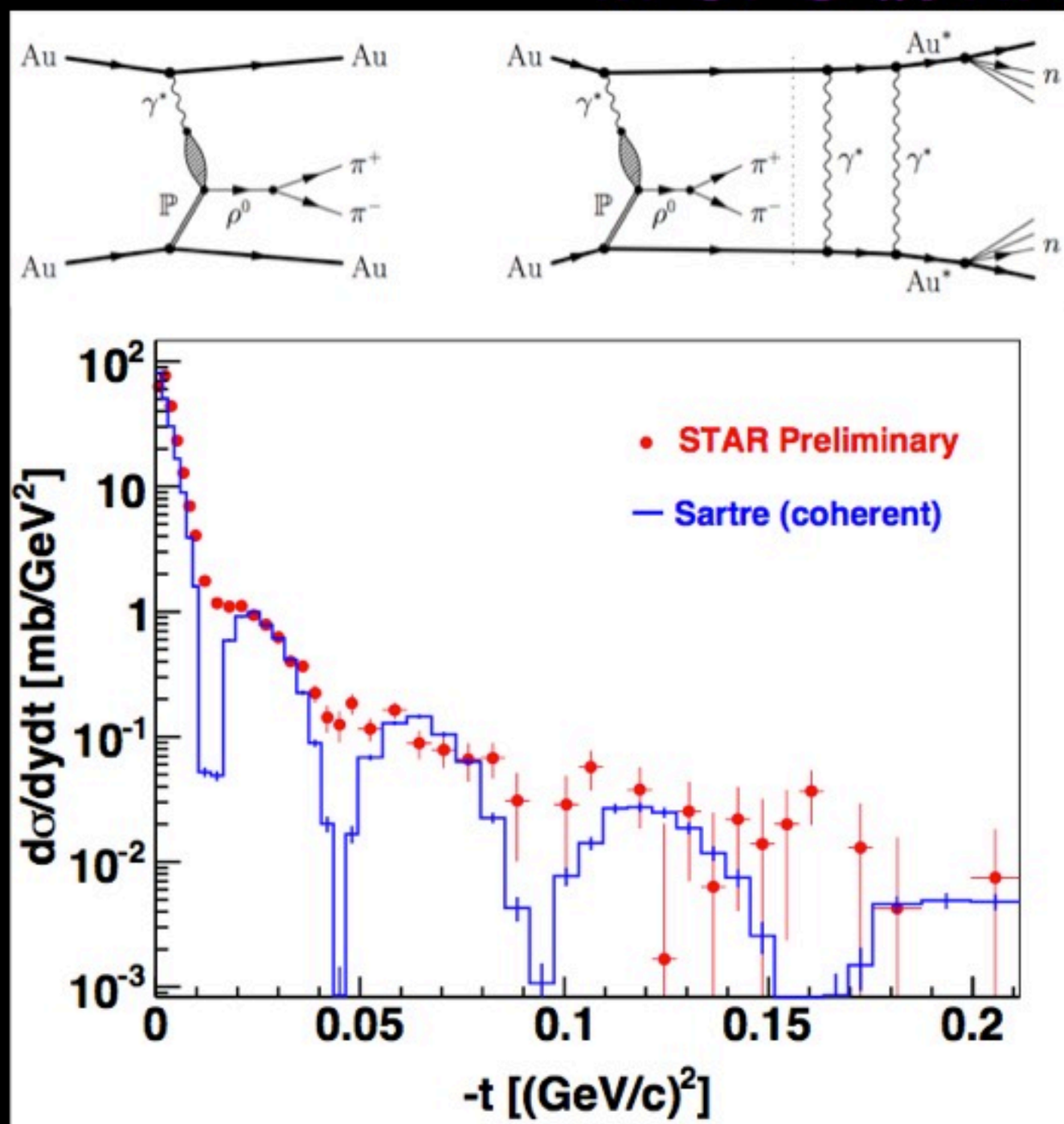

- Coherent diffractive ρ production in Au +Au at $\sqrt{s_{NN}}$=200 GeV
- Data: STAR/RHIC Ultra-peripheral AuAu Collision
- Simulation: Sartre

15

transport coefficients in cold nuclear matter from large-x semi-inclusive DIS and jets

Transport coefficients in cold nuclear matter

Deliverables	Observables	What we learn	Stage-I	Stage-II
transport coefficients in cold matter	large-x SIDIS; jets	parton energy loss, shower evolution; energy loss mechanisms	light flavours and charm; jets	rare probes and bottom; large-x gluons

Jets and hadronization

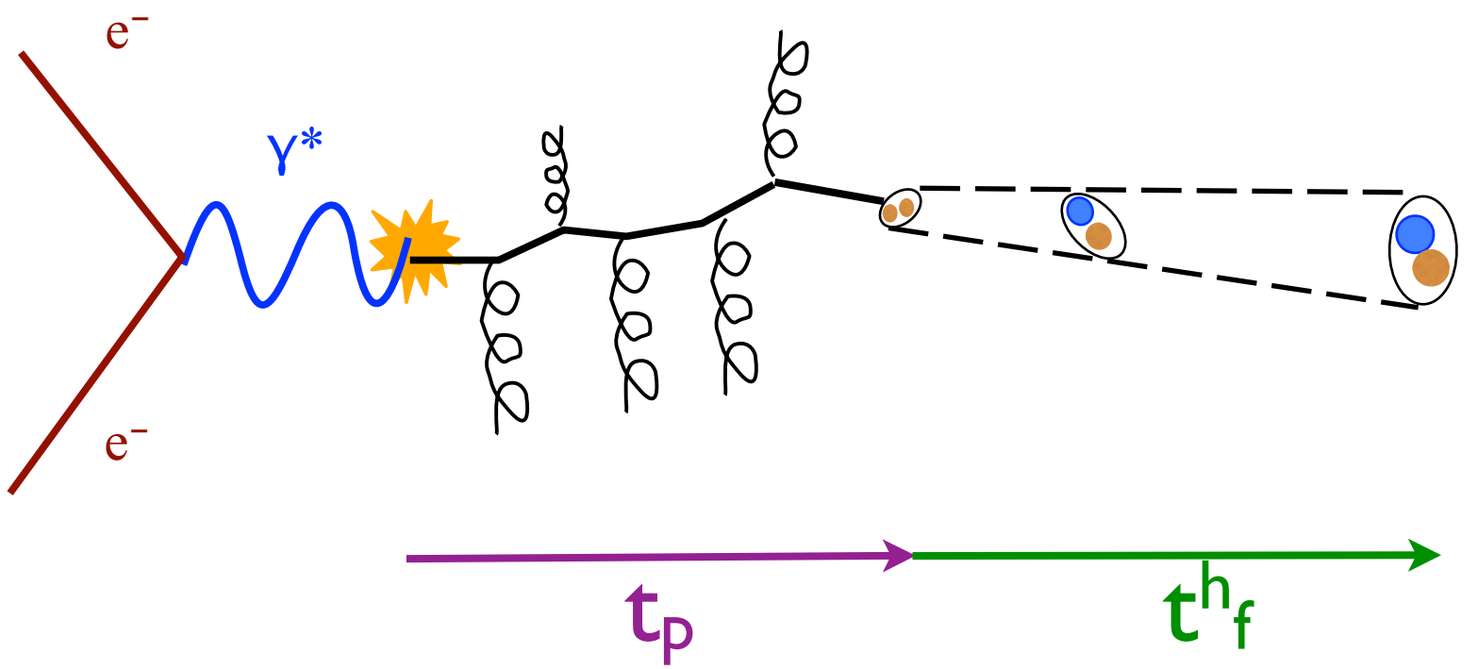

- t_p - production time of propagating quark
- t^h_f - hadron formation time

Jets and hadronization

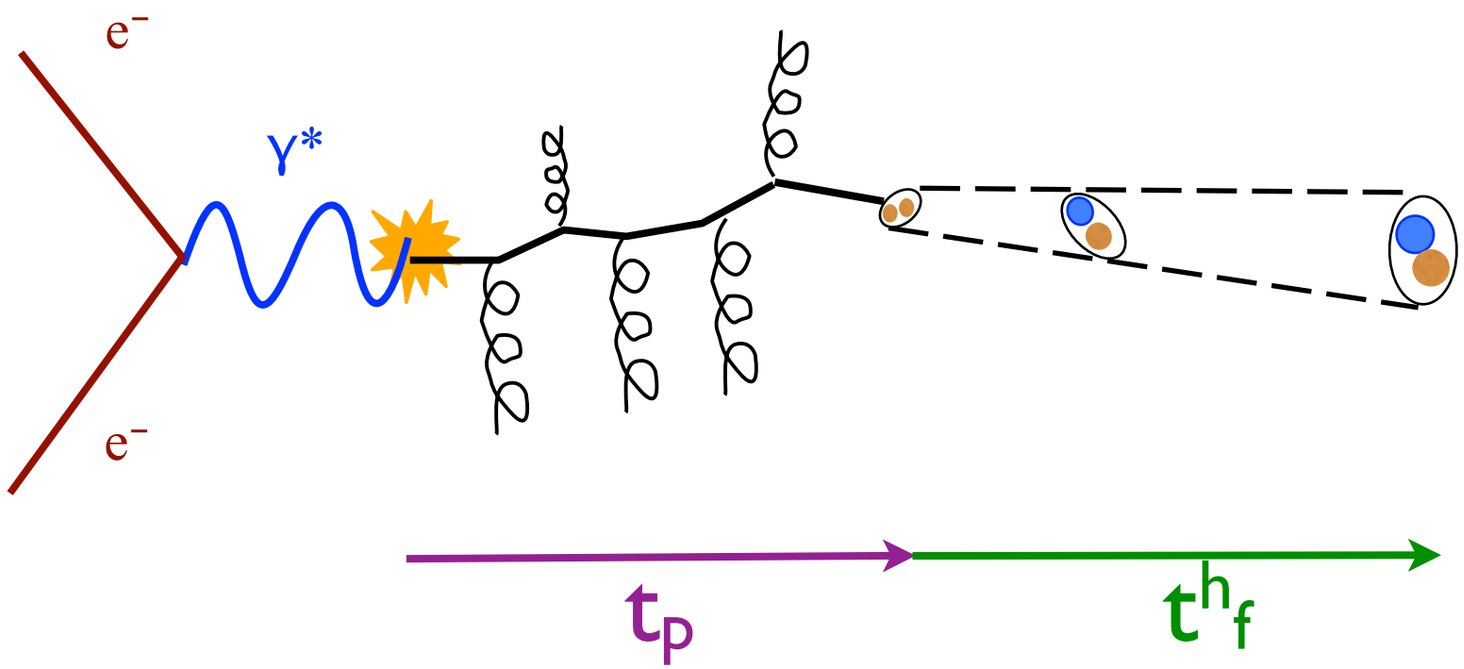

What happens if we add a nuclear medium?

- t_p - production time of propagating quark
- t^h_f - hadron formation time

Jets and hadronization

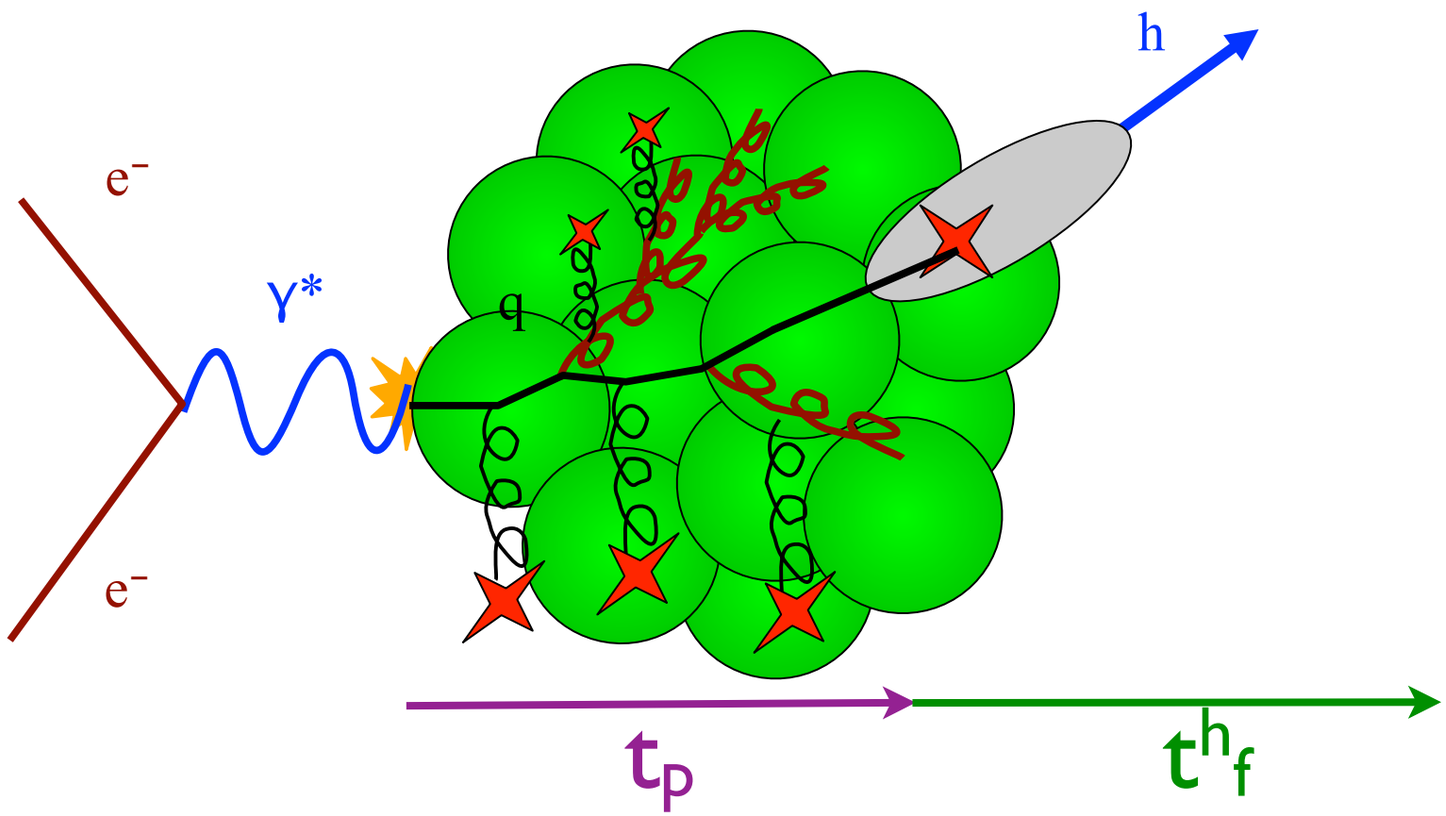

What happens if we add a nuclear medium?

- t_p - production time of propagating quark
- t^h_f - hadron formation time

Jets and hadronization

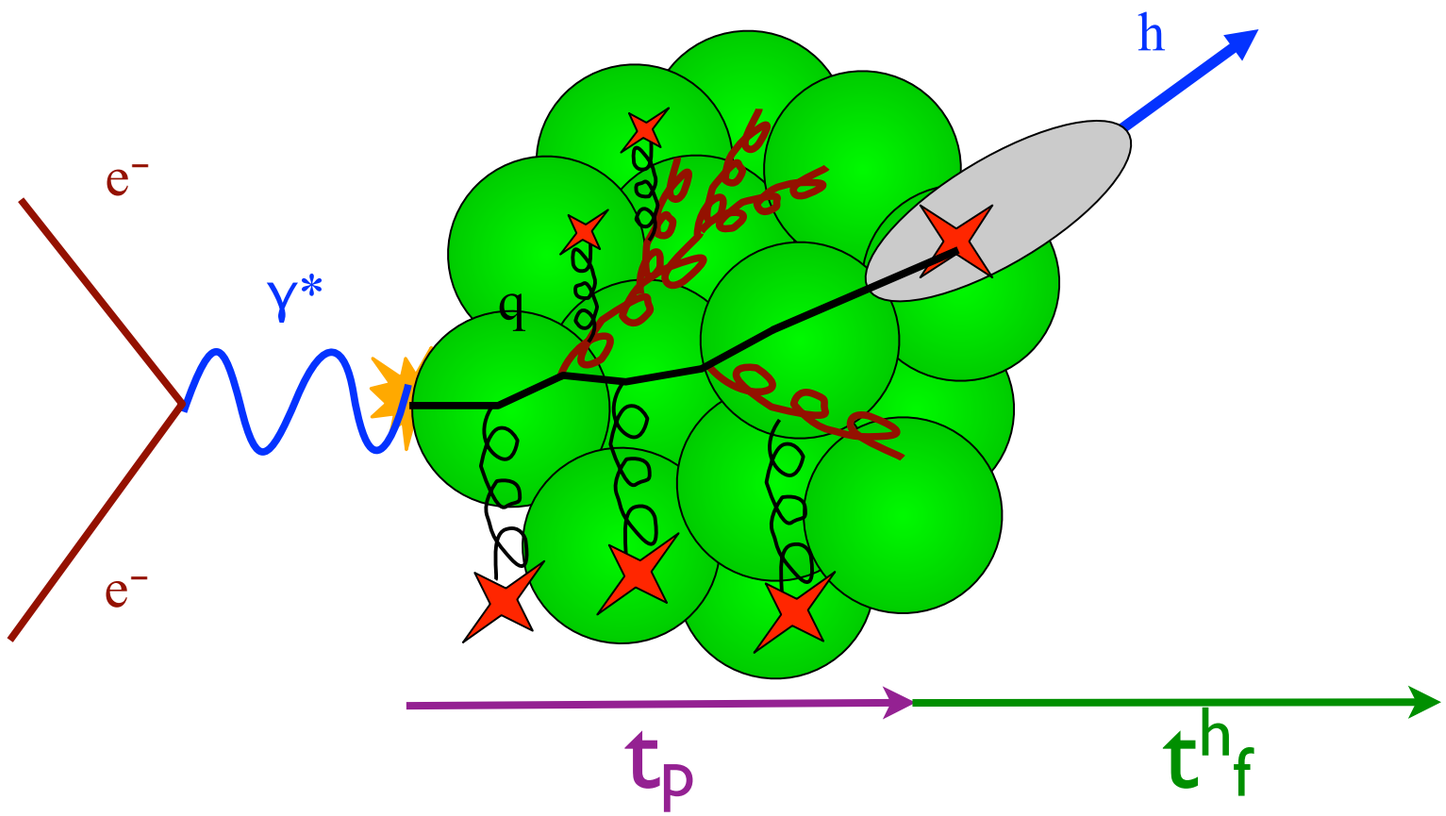

What happens if we add a nuclear medium?

- t_p - production time of propagating quark
- t^h_f - hadron formation time

Observables:

Broadening: $\Delta p_T^2 = \langle p_T^2 \rangle_A - \langle p_T^2 \rangle_p$: direct link to saturation scale

Jets and hadronization

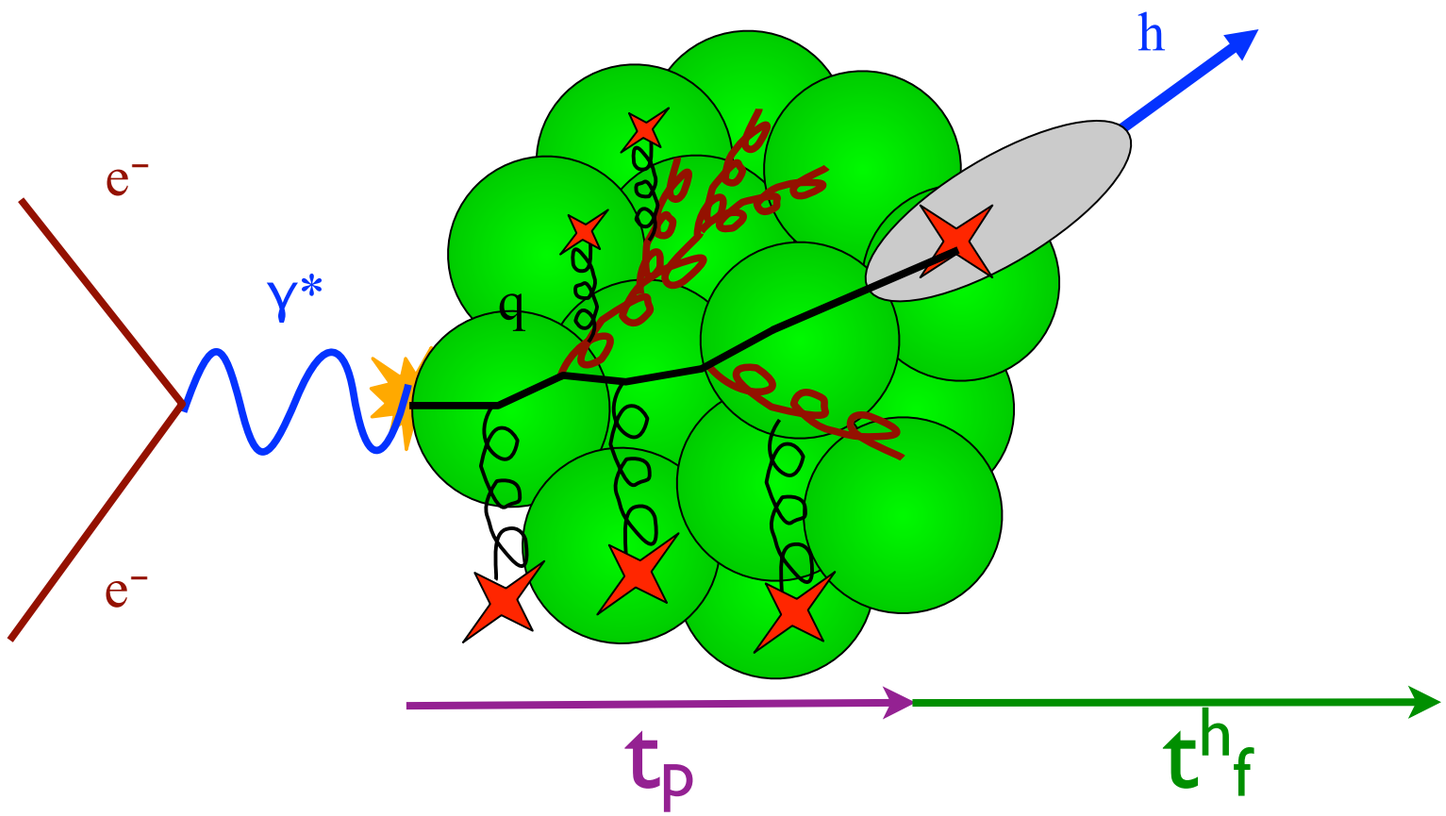

What happens if we add a nuclear medium?

- t_p - production time of propagating quark
- t^h_f - hadron formation time

Observables:

Broadening: $\Delta p_T^2 = \langle p_T^2 \rangle_A - \langle p_T^2 \rangle_p$: direct link to saturation scale

Attenuation: $R_A^h(Q^2, \nu, z_h, p_T^2)$: ratio of hadron production in A to D, modifications of nPDFs cancel out

Jets and hadronization

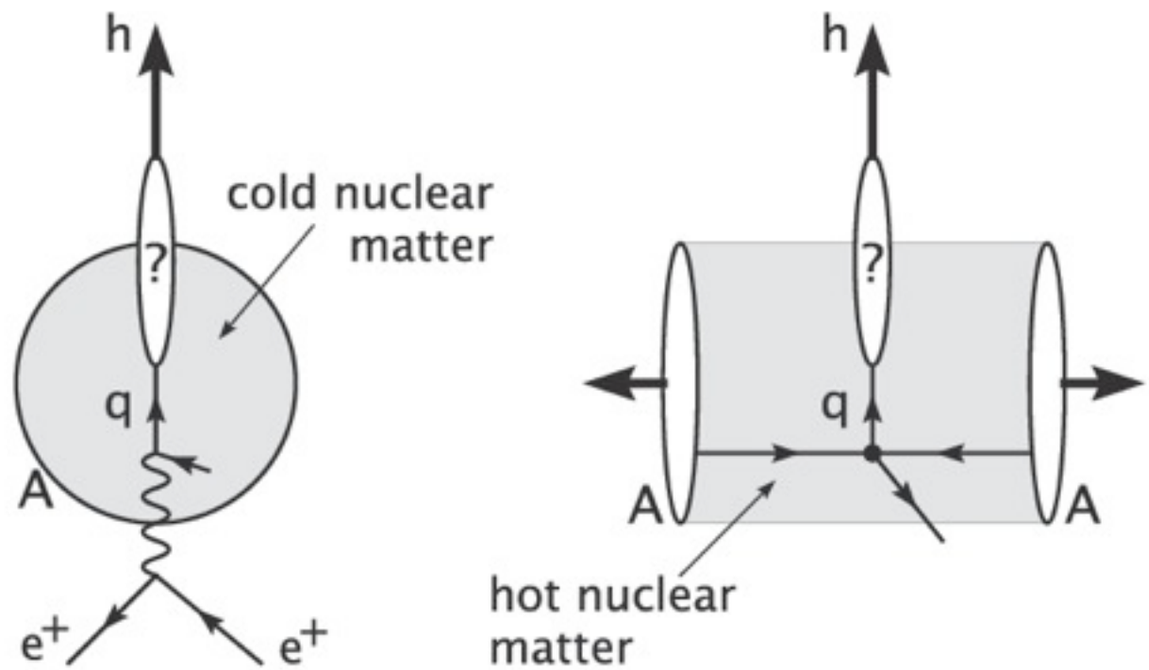

- t_p - production time of propagating quark
- t^h_f - hadron formation time

Observables:

Broadening: $\Delta p_T^2 = \langle p_T^2 \rangle_A - \langle p_T^2 \rangle_p$: direct link to saturation scale

Attenuation: $R_A^h(Q^2, \nu, z_h, p_T^2)$: ratio of hadron production in A to D, modifications of nPDFs cancel out

How can the EIC contribute?

HERMES:

E_e = 27 GeV → $\sqrt{s}$ = 7.2 GeV

E_h = 2-15 GeV

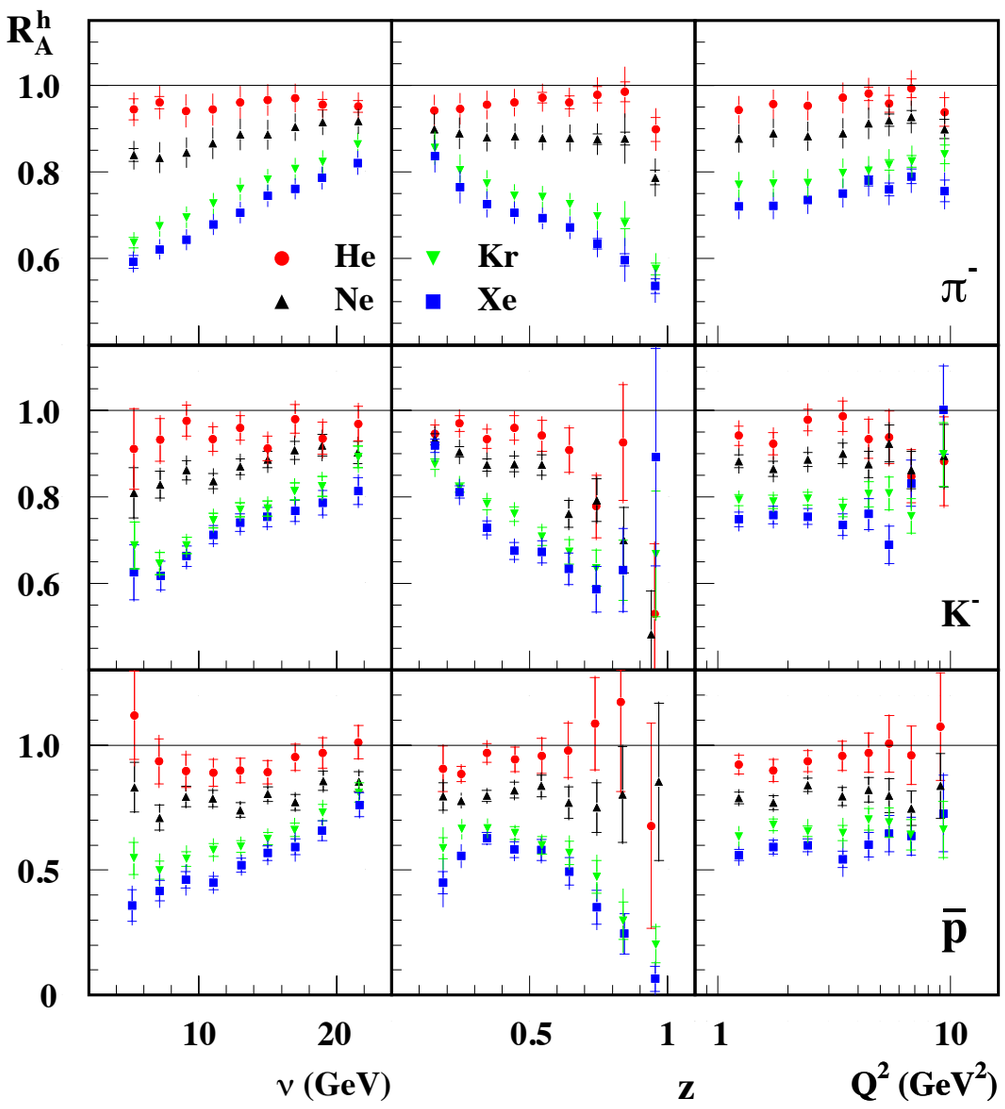

ν = virtual photon energy

$Z_h = E_h/\nu$

How can the EIC contribute?

HERMES:

E_e = 27 GeV → $\sqrt{s}$ = 7.2 GeV

E_h = 2-15 GeV

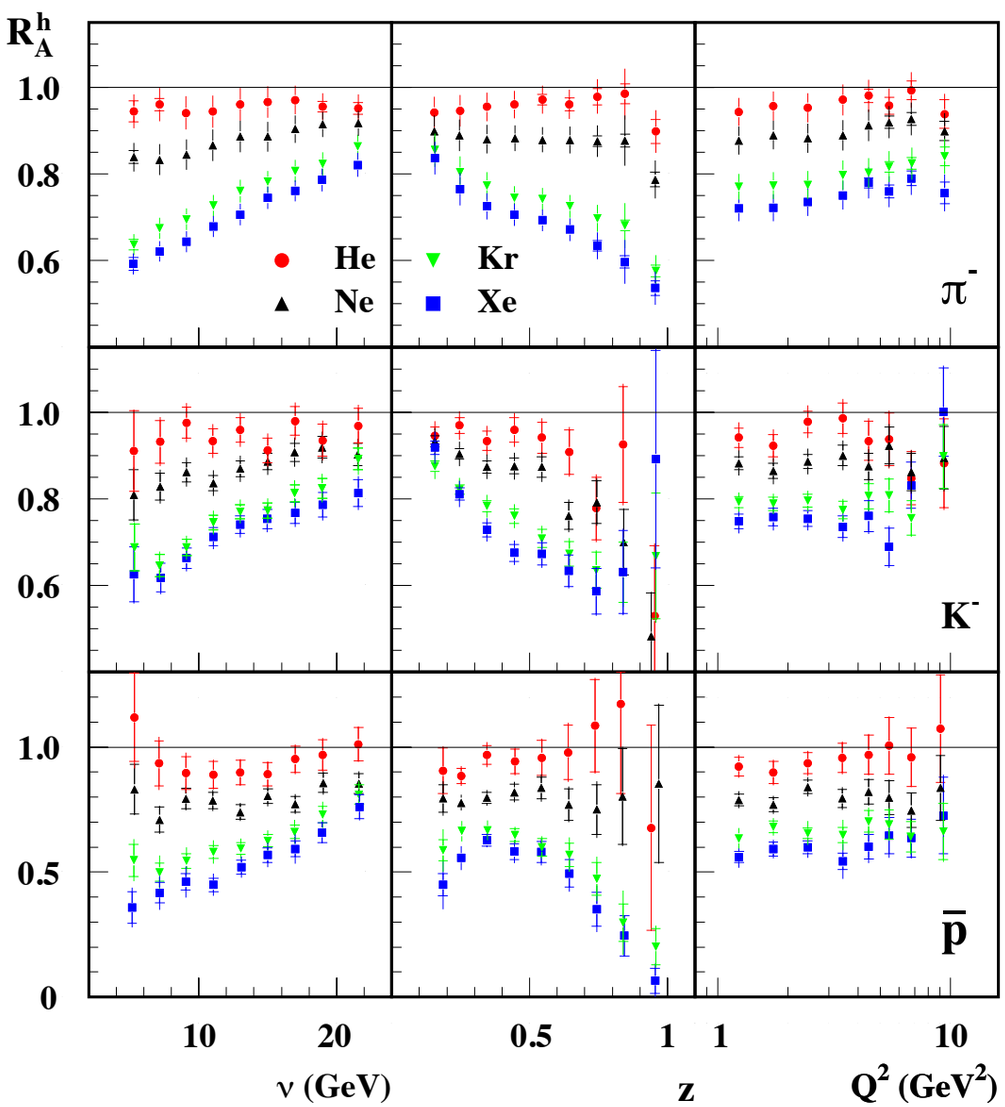

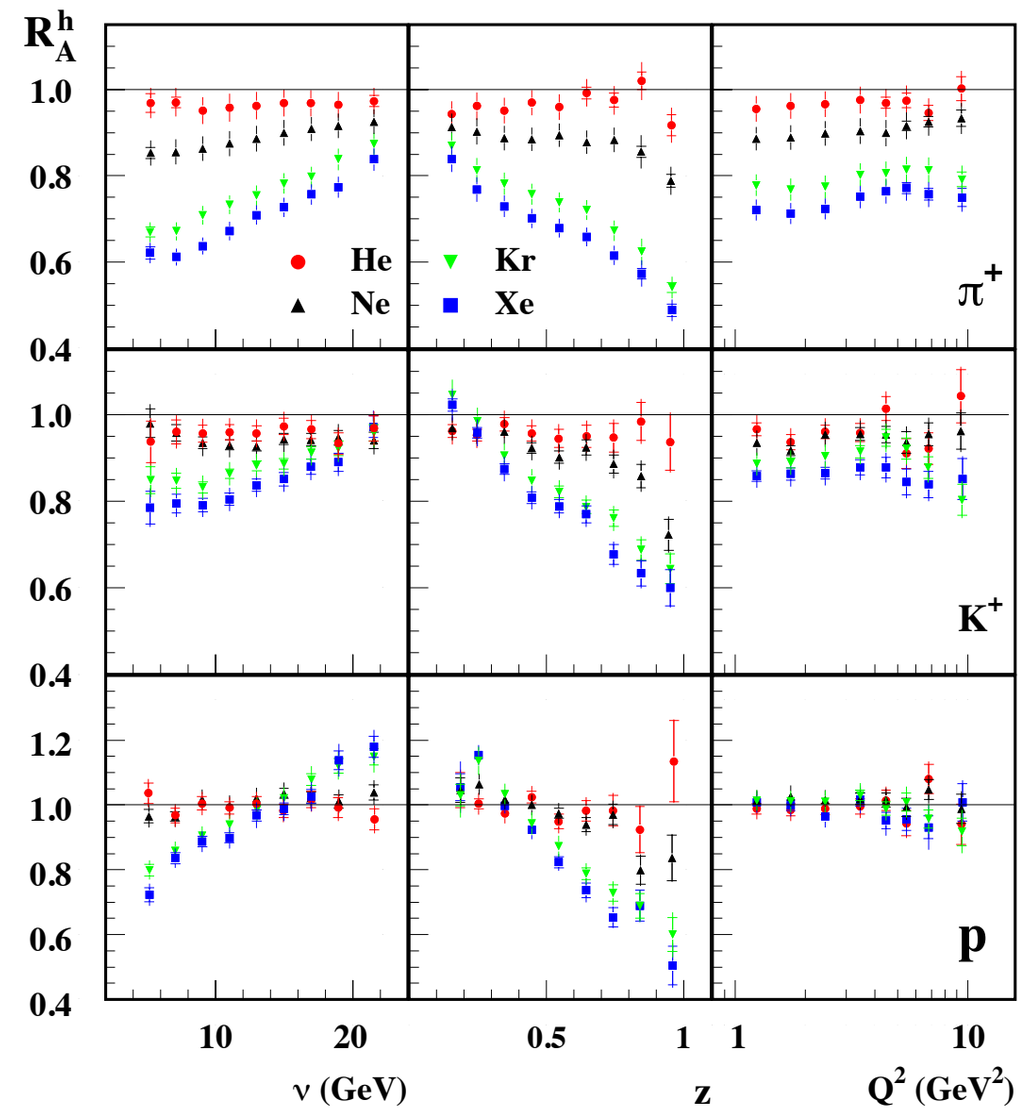

ν = virtual photon energy

$Z_h = E_h/\nu$

How can the EIC contribute?

HERMES:

E_e = 27 GeV → $\sqrt{s}$ = 7.2 GeV

E_h = 2-15 GeV

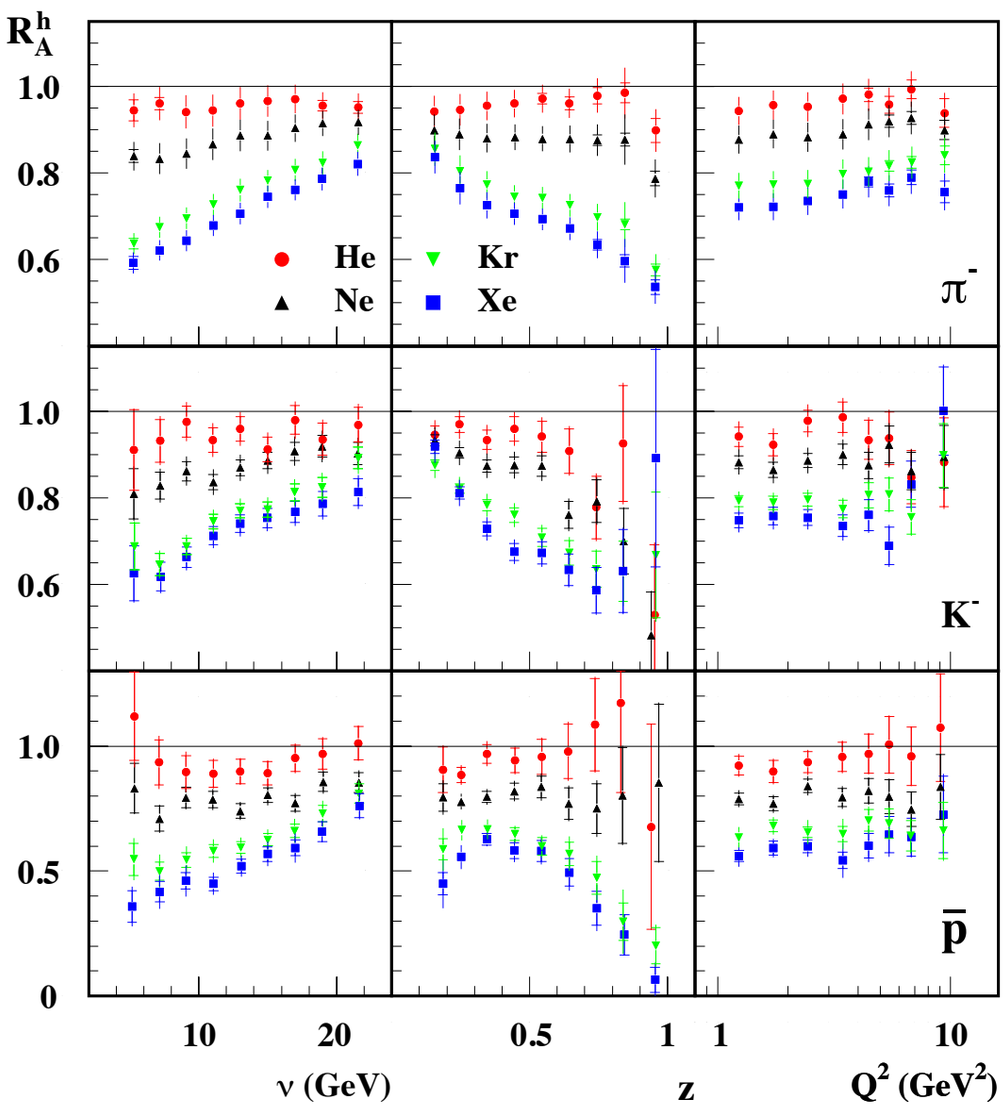

EIC:

light hadrons:

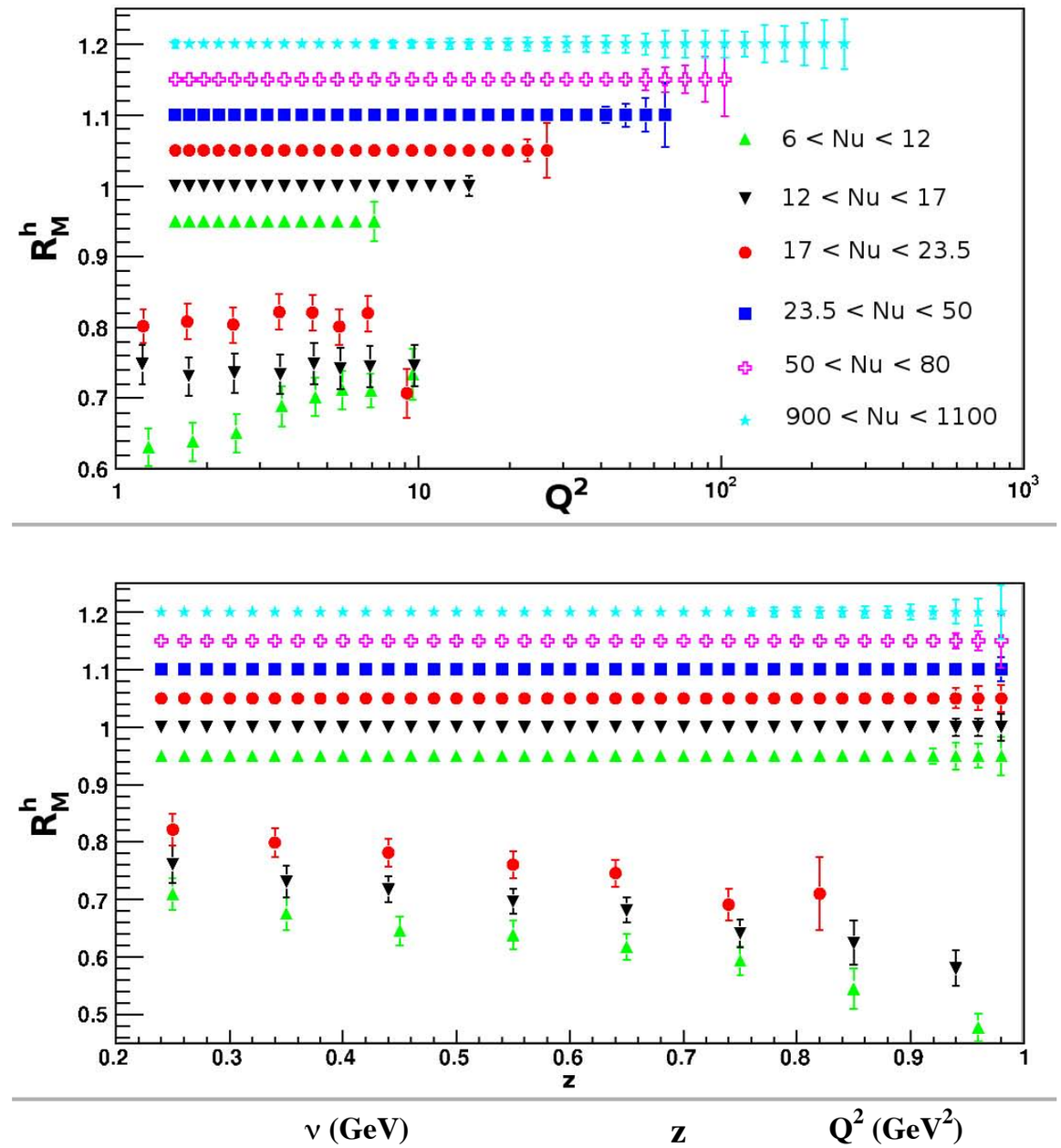

ν = virtual photon energy

$Z_h = E_h/\nu$

large ν range → boost

hadronization in and out of nucleus

How can the EIC contribute?

HERMES:

E_e = 27 GeV → $\sqrt{s}$ = 7.2 GeV

E_h = 2-15 GeV

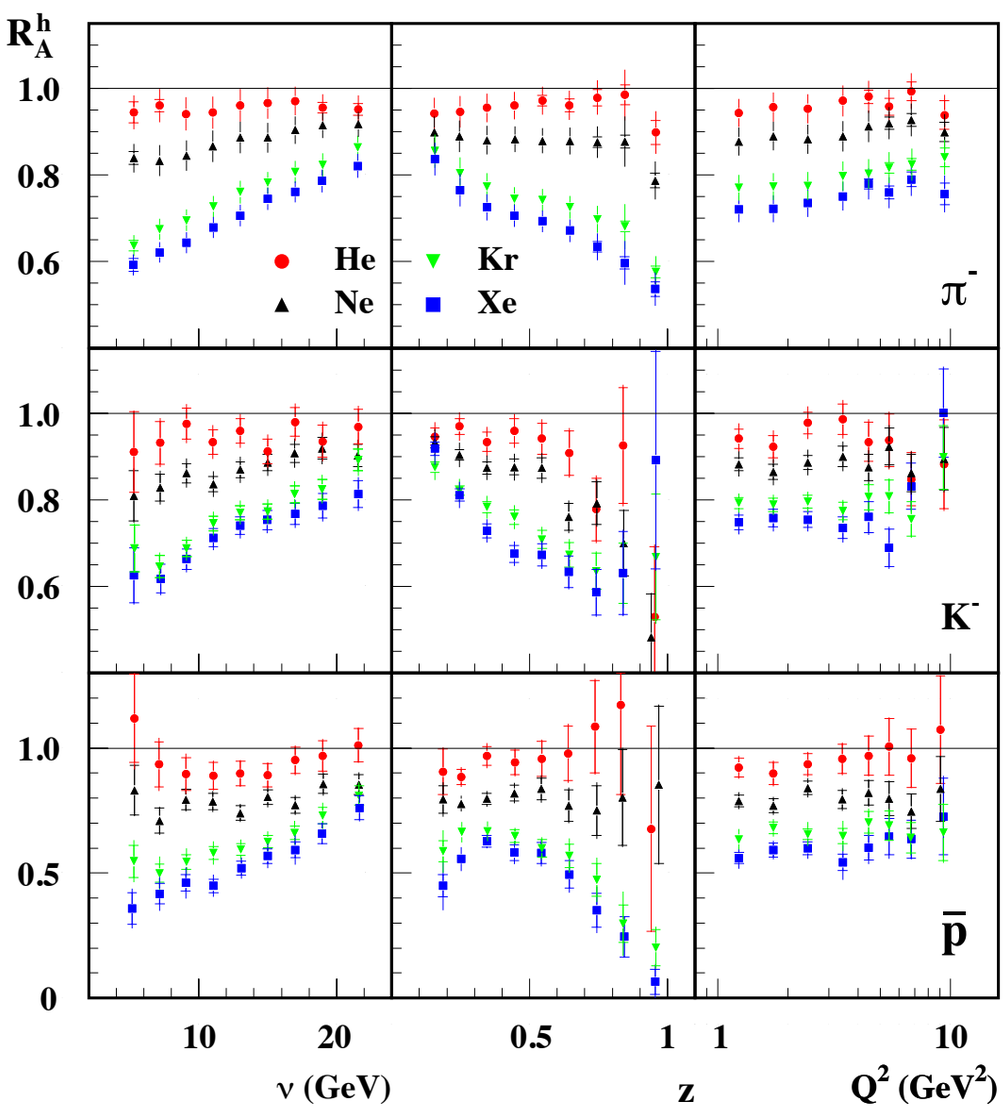

EIC:

charm hadrons:

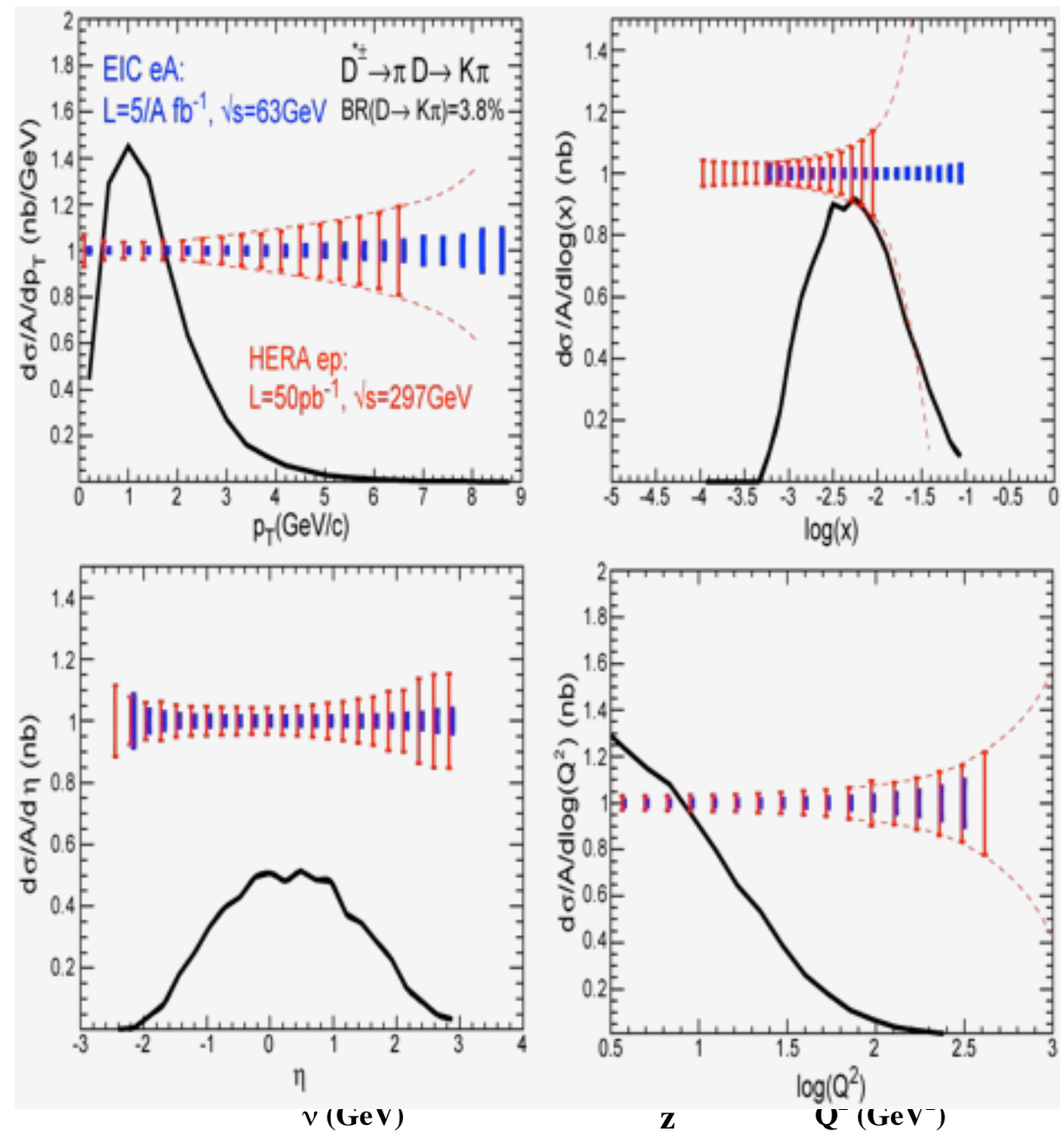

ν = virtual photon energy

$Z_h = E_h/\nu$

large ν range → boost hadronization in and out of nucleus

How can the EIC contribute?

HERMES:

E_e = 27 GeV → $\sqrt{s}$ = 7.2 GeV

E_h = 2-15 GeV

EIC:

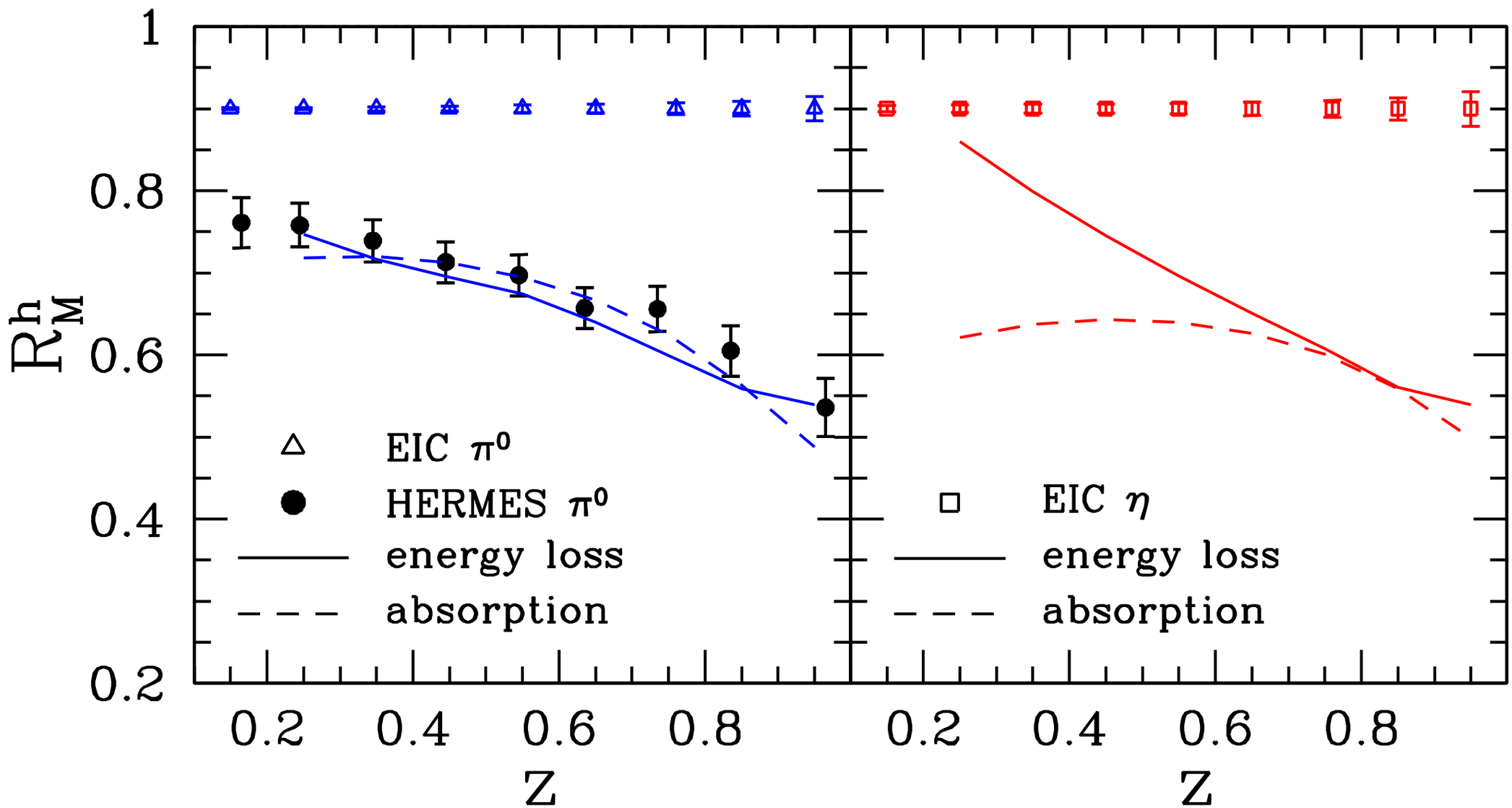

ν = virtual photon energy

$Z_h = E_h/\nu$

large ν range → boost hadronization in and out of nucleus

Jets at an EIC

- E665 at FNAL have measured jets in μ+A at $\sqrt{s} \sim 30$ GeV
  - ➡ Feasible to start a jet programme in phase 1
  - ➡ caveat that collider kinematics are different to fixed target

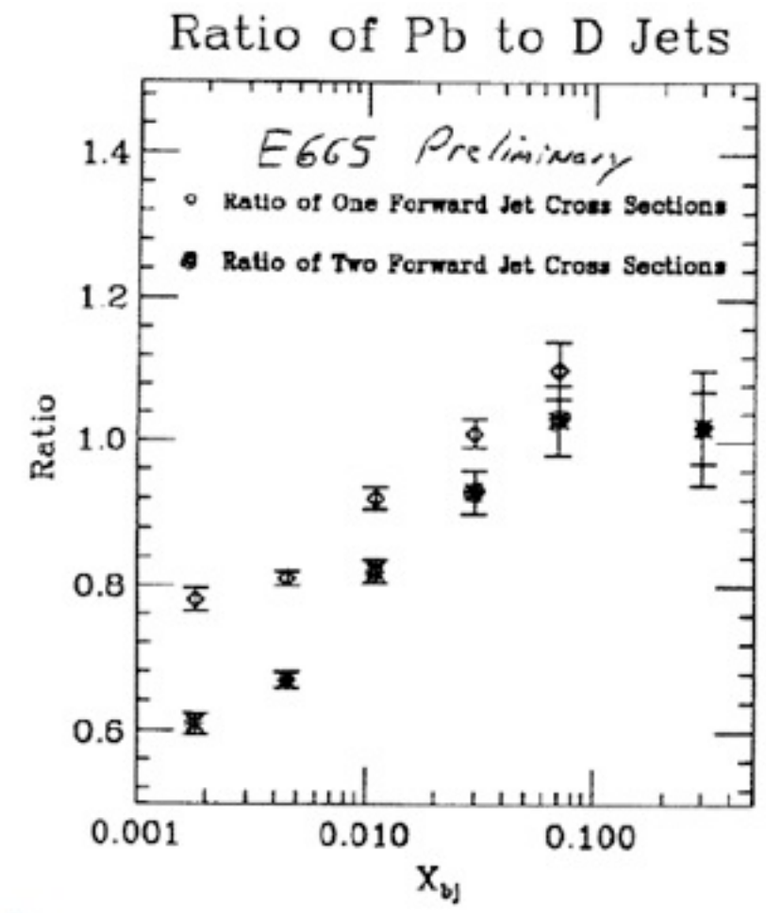

Jets at an EIC

- E665 at FNAL have measured jets in μ+A at $\sqrt{s} \sim 30$ GeV
  - ➡ Feasible to start a jet programme in phase 1
  - ➡ caveat that collider kinematics are different to fixed target

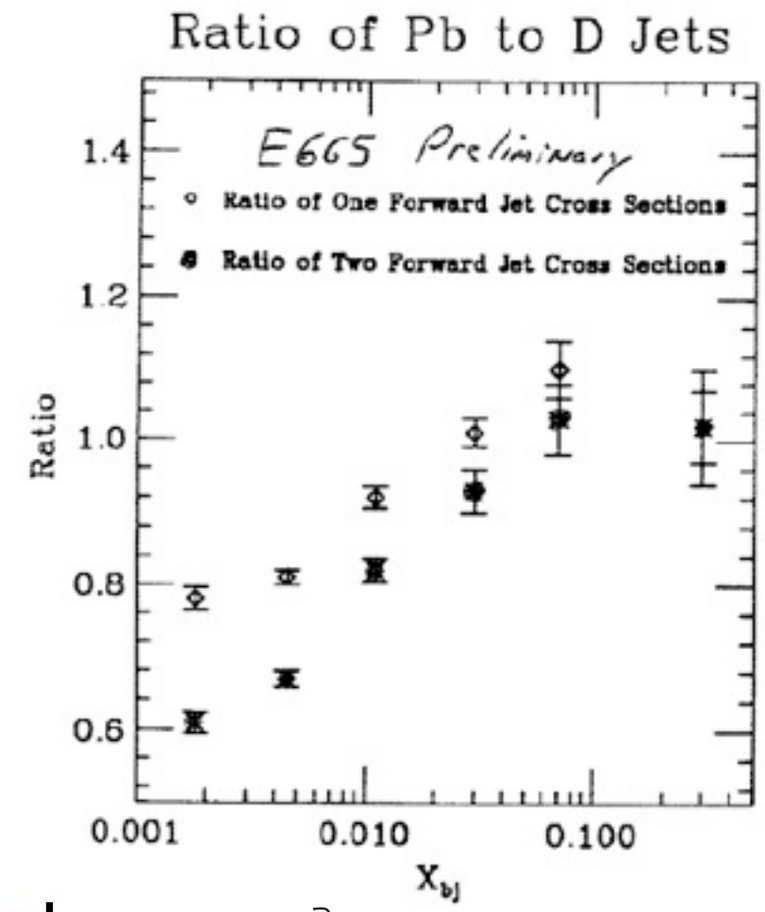

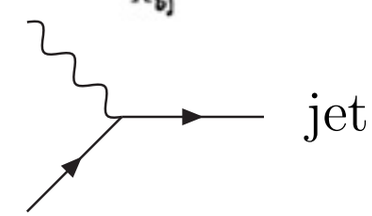

1+1 jets, dominated by q processes → allow study of parton propagation through cold nuclear matter

Jets at an EIC

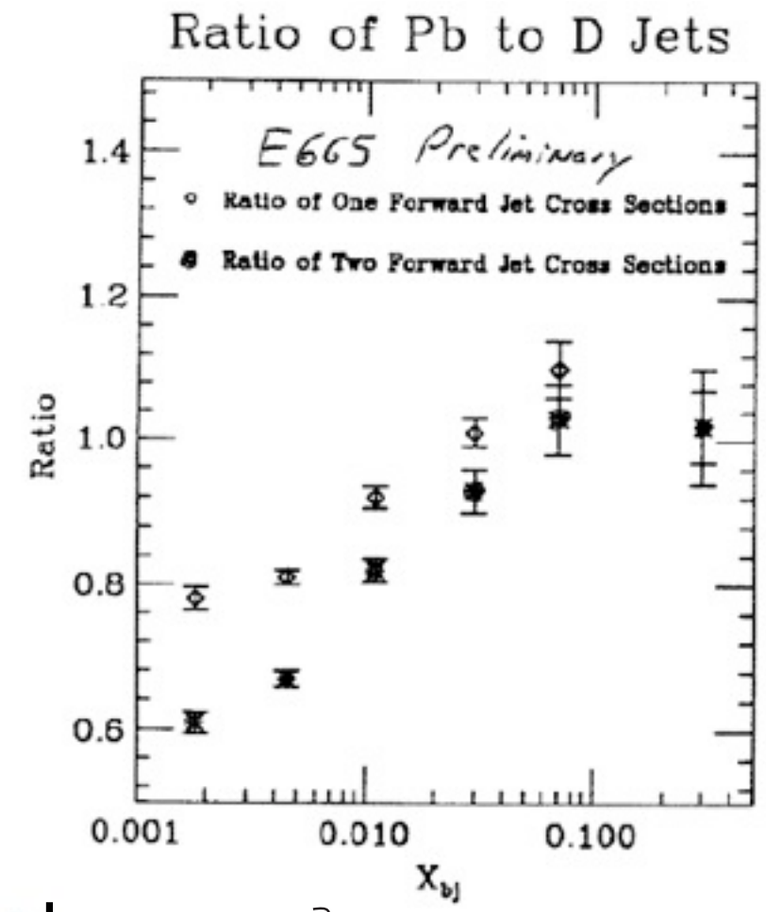

- E665 at FNAL have measured jets in μ+A at $\sqrt{s} \sim 30$ GeV
  - ➡ Feasible to start a jet programme in phase 1
  - ➡ caveat that collider kinematics are different to fixed target

1+1 jets, dominated by q processes → allow study of parton propagation through cold nuclear matter

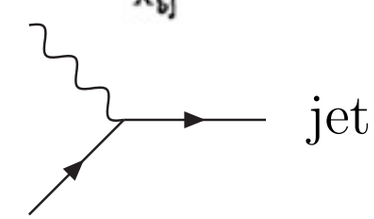

$$\frac{d^2\sigma_{2+1}}{dx dQ^2} = A_q(x,Q^2)q^A(x,Q^2) + A_g(x,Q^2)g_A(x,Q^2)$$

2+1 jets→ sensitive to nuclear gluons

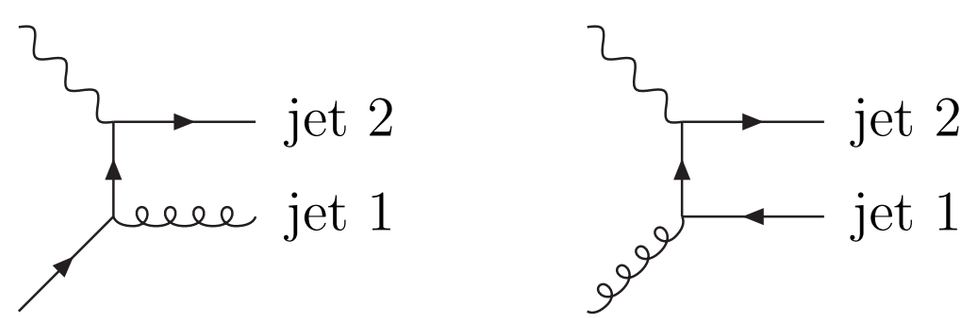

By measuring 1+1 jets, can extract information on gluons

Jets at an EIC

1+1 jets, dominated by q processes → allow study of parton propagation through cold nuclear matter

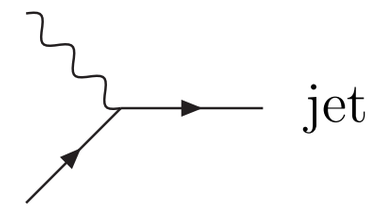

$$\frac{d^2\sigma_{2+1}}{dx dQ^2} = A_q(x,Q^2)q^A(x,Q^2) + A_g(x,Q^2)g_A(x,Q^2)$$

2+1 jets→ sensitive to nuclear gluons

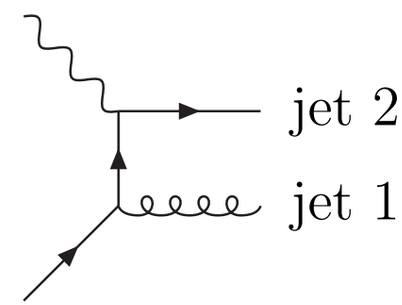

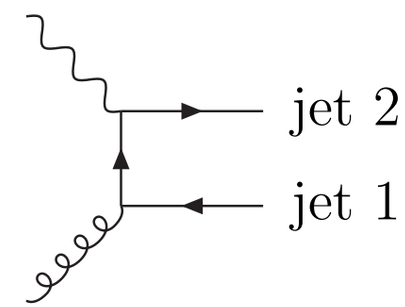

By measuring 1+1 jets, can extract information on gluons

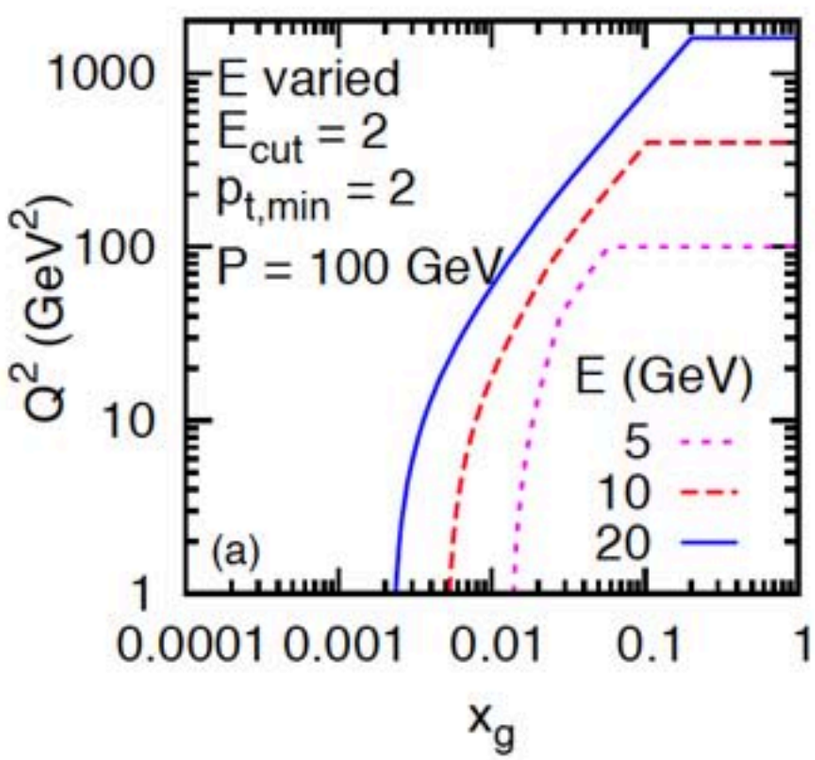

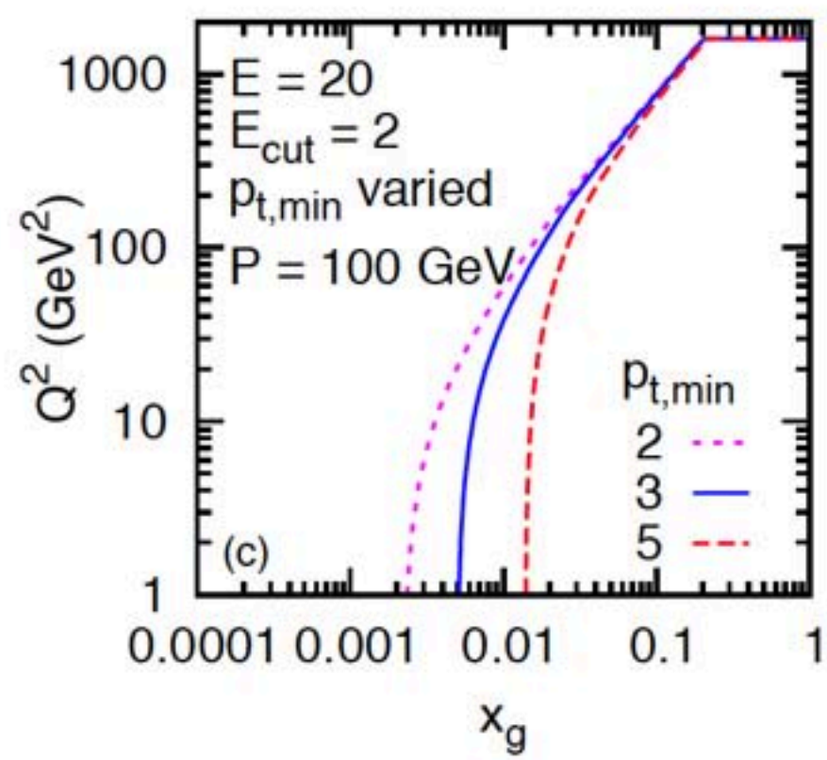

Summary and Conclusions

- The e+A physics programme at an EIC will give us an unprecedented opportunity to study gluons in nuclei
- Low-x: Measure the properties of gluons where saturation is the dominant governing phenomena
- Higher-x: Understand how fast partons interact as they traverse nuclear matter and provide new insight into hadronization
- Understanding the role of gluons in nuclei is crucial to understanding RHIC (and LHC) heavy-ion results

Good headway can be made on these measurements already with a stage-I eRHIC (E_e = 5 GeV)

- The INT programme in the Fall of 2010 allowed us to formulate the observables in terms of golden and silver measurements
  - ➡ A detailed write-up of the whole programme is on the ArXiV
  - ➡ An EIC White Paper (not just e+A) will be released to the community shortly

BACKUP

DIS Kinematics

$e(k) + p(p) \rightarrow e(k') + X(p_X)$

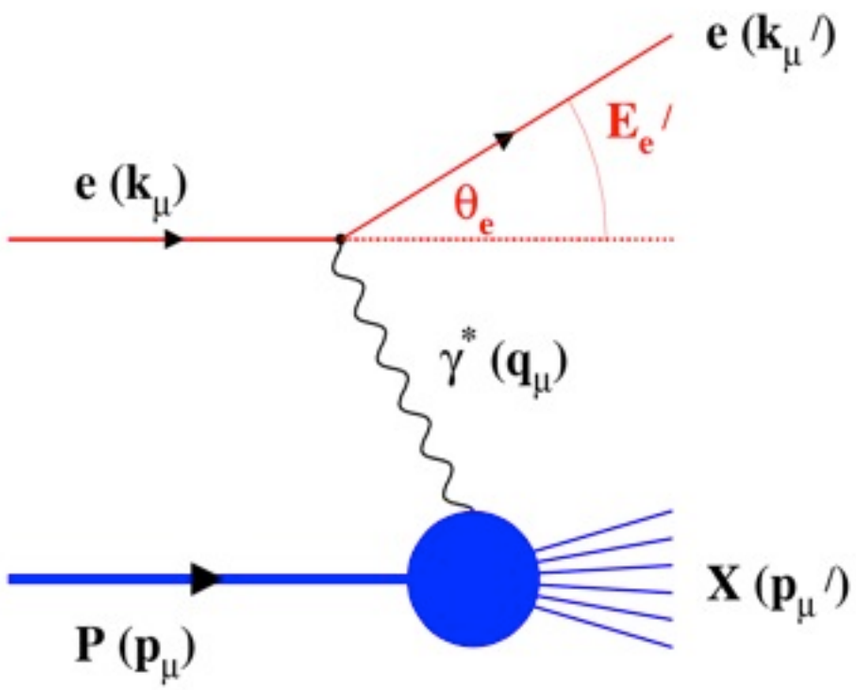

DIS Kinematics

e(k) + p(p) → e(k') +X(px)

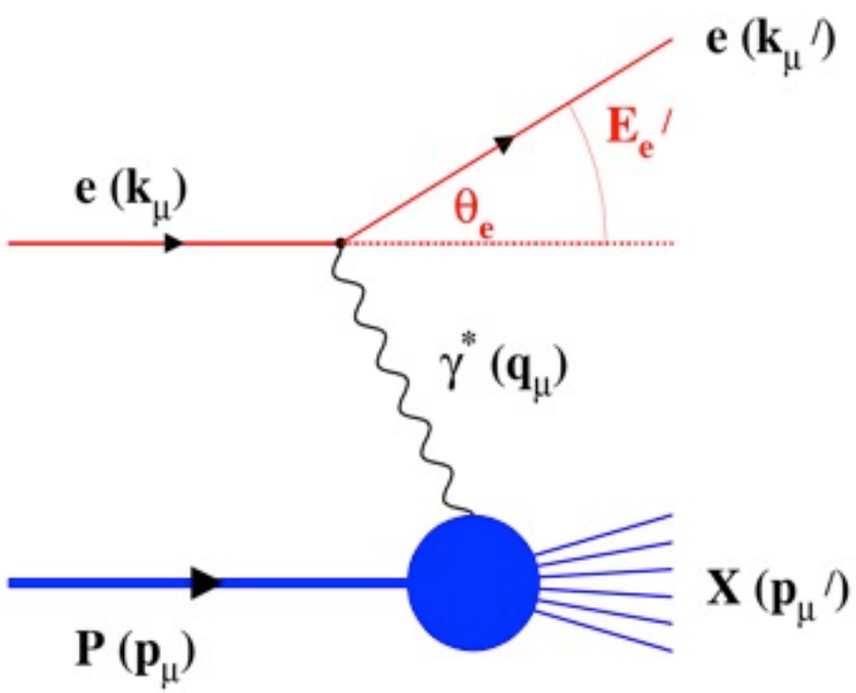

$$Q^2 = -q^2 = -(k_\mu - k'_\mu)^2$$

$$Q^2 = 4E_e E'_e sin^2(\frac{\theta'_e}{2})$$

Measure of resolution power or "Virtuality"

DIS Kinematics

e(k) + p(p) → e(k') +X(px)

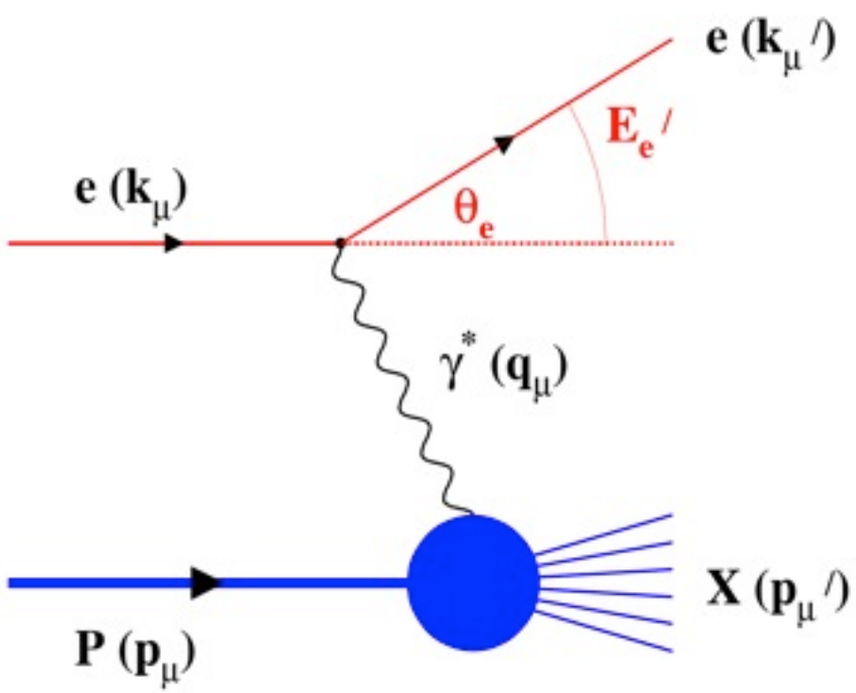

$$Q^2 = -q^2 = -(k_\mu - k'_\mu)^2$$

$$Q^2 = 4E_e E'_e sin^2(\frac{\theta'_e}{2})$$

Measure of resolution power or "Virtuality"

$$y = \frac{pq}{pk} = 1 - \frac{E_{e'}}{E_e} cos^2(\frac{\theta'_e}{2})$$

Measure of inelasticity

DIS Kinematics

e(k) + p(p) → e(k') +X(px)

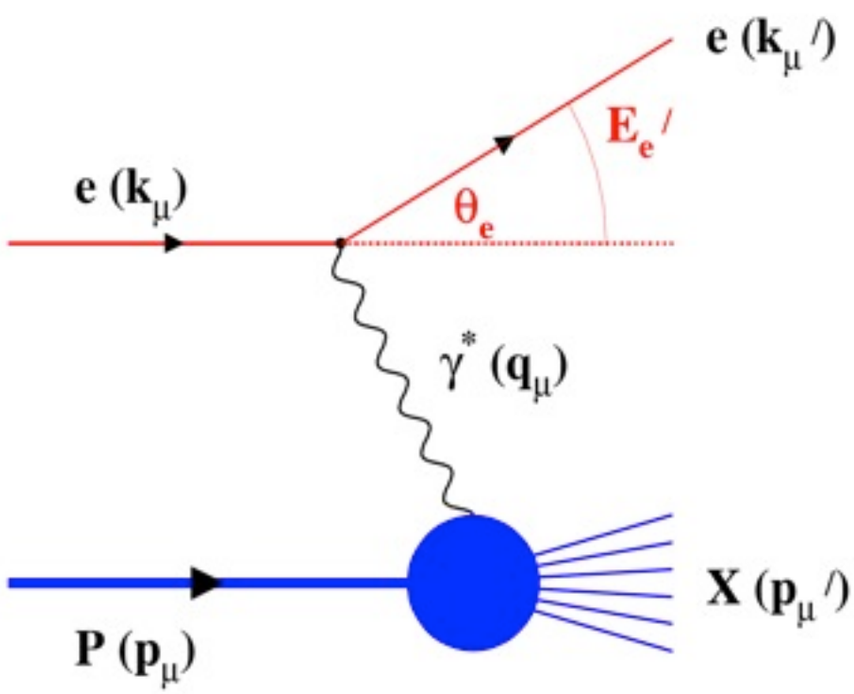

$$Q^2 = -q^2 = -(k_\mu - k'_\mu)^2$$

$$Q^2 = 4E_e E'_e sin^2(\frac{\theta'_e}{2})$$

Measure of resolution power or "Virtuality"

$$y = \frac{pq}{pk} = 1 - \frac{E_{e'}}{E_e} cos^2(\frac{\theta'_e}{2})$$

Measure of inelasticity

$$x = \frac{Q^2}{2pq} = \frac{Q^2}{sy}$$

Measure of momentum fraction of struck quark

DIS Kinematics

e(k) + p(p) → e(k') +X(px)

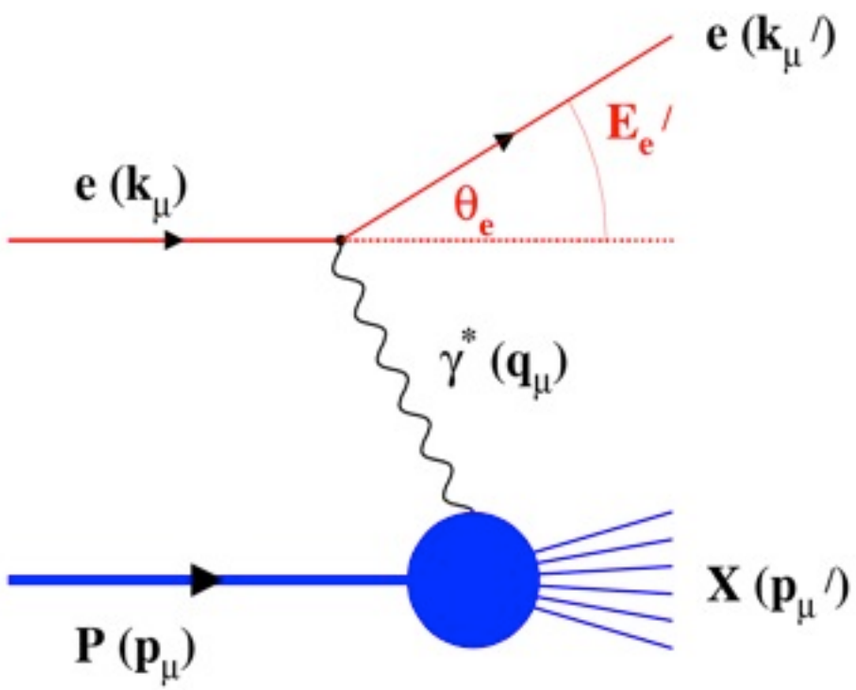

$$Q^2 = -q^2 = -(k_\mu - k'_\mu)^2$$

$$Q^2 = 4E_e E'_e sin^2(\frac{\theta'_e}{2})$$

Measure of resolution power or "Virtuality"

$$y = \frac{pq}{pk} = 1 - \frac{E_{e'}}{E_e} cos^2(\frac{\theta'_e}{2})$$

Measure of inelasticity

$$x = \frac{Q^2}{2pq} = \frac{Q^2}{sy}$$

Measure of momentum fraction of struck quark

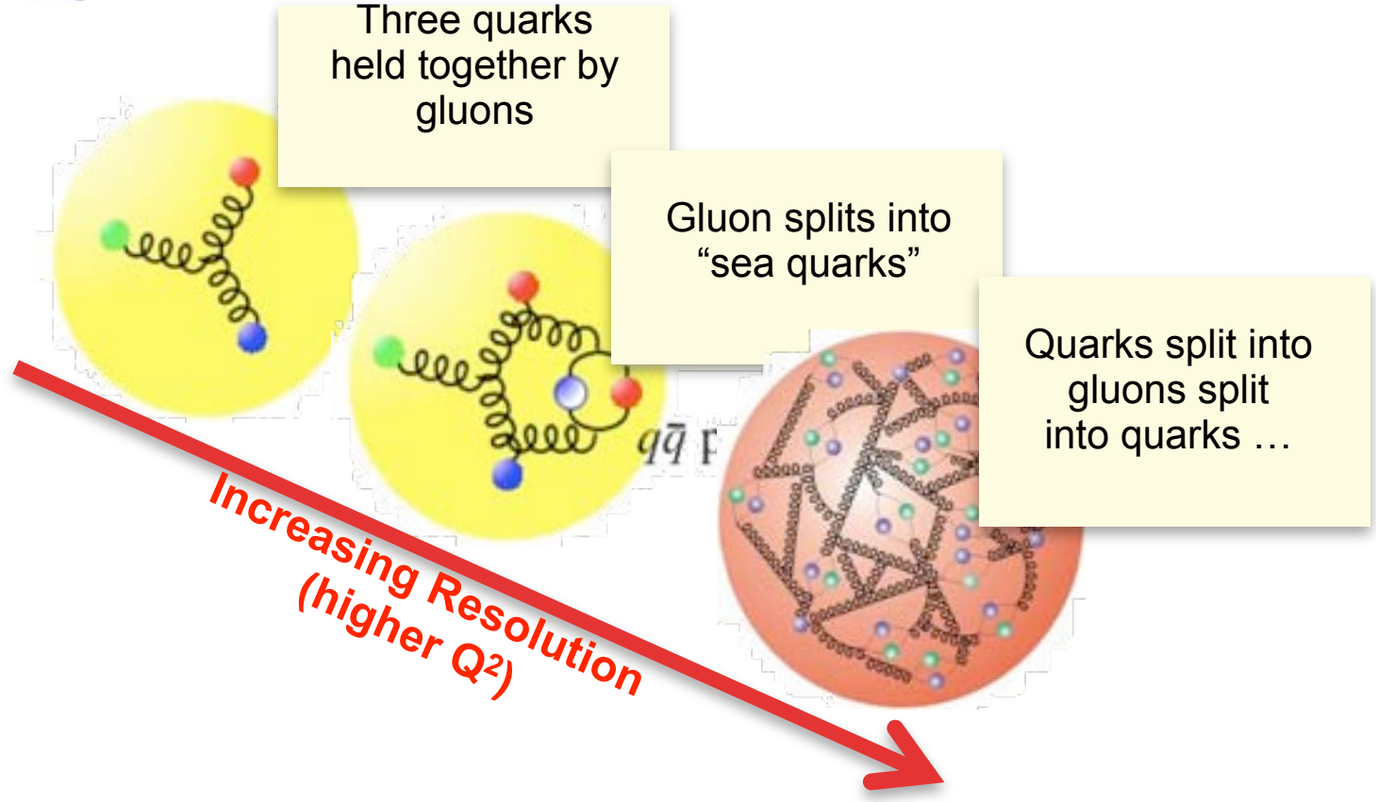

Getting a "Feel" for Non-Linear QCD

Dipole Model: $\frac{d\sigma_{q\bar{q}}}{d^2b} = 2\mathcal{N}(x, r, b)$

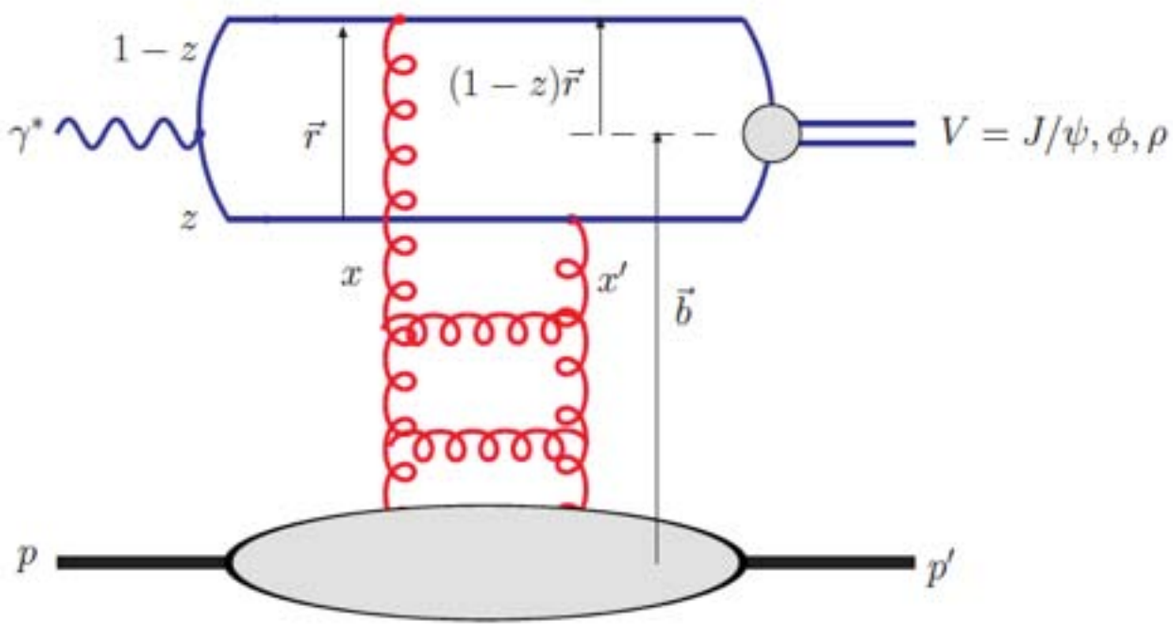

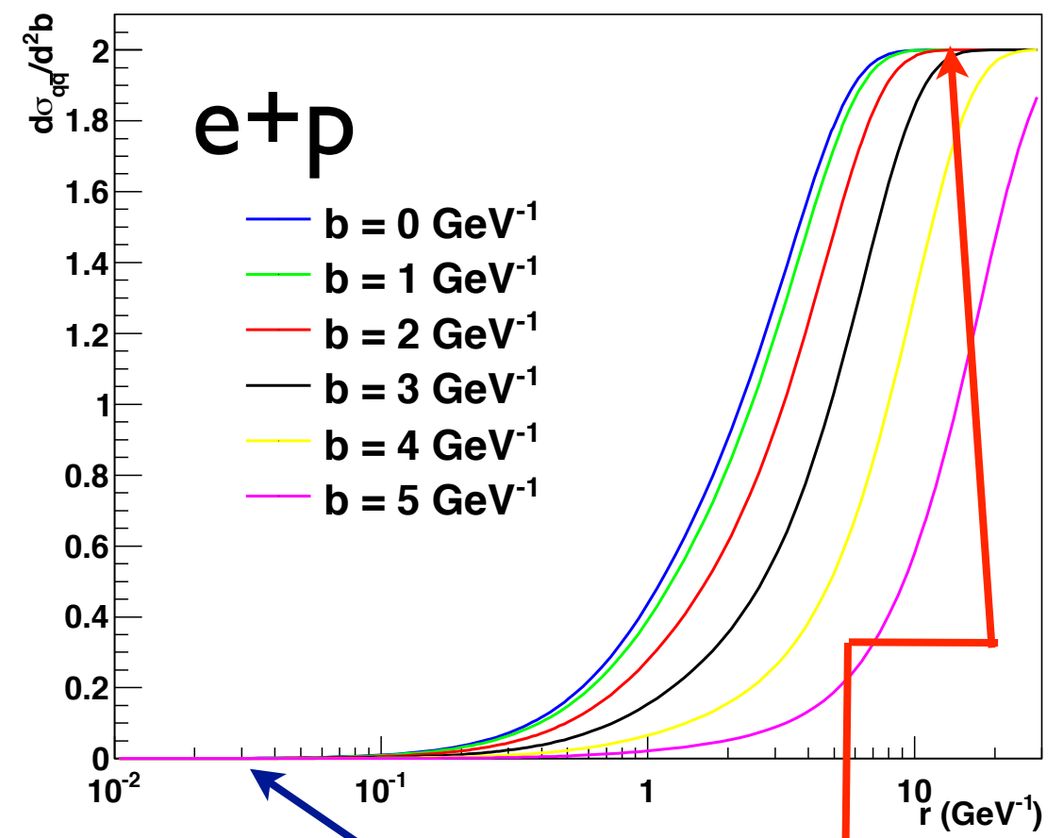

$$\mathcal{N}(x, r, b) = 1 - \exp\left(-r^2 \frac{\pi^2}{2N_c} \alpha_s(\mu^2) x G(x, \mu^2) T(b)\right)$$

$\mathcal{N} =$ Dipole Scattering Amplitude

0 dilute system, linear QCD

1 saturated, non-linear regime

Getting a "Feel" for Non-Linear QCD

Dipole Model: $\frac{d\sigma_{q\bar{q}}}{d^2b} = 2\mathcal{N}(x, r, b)$

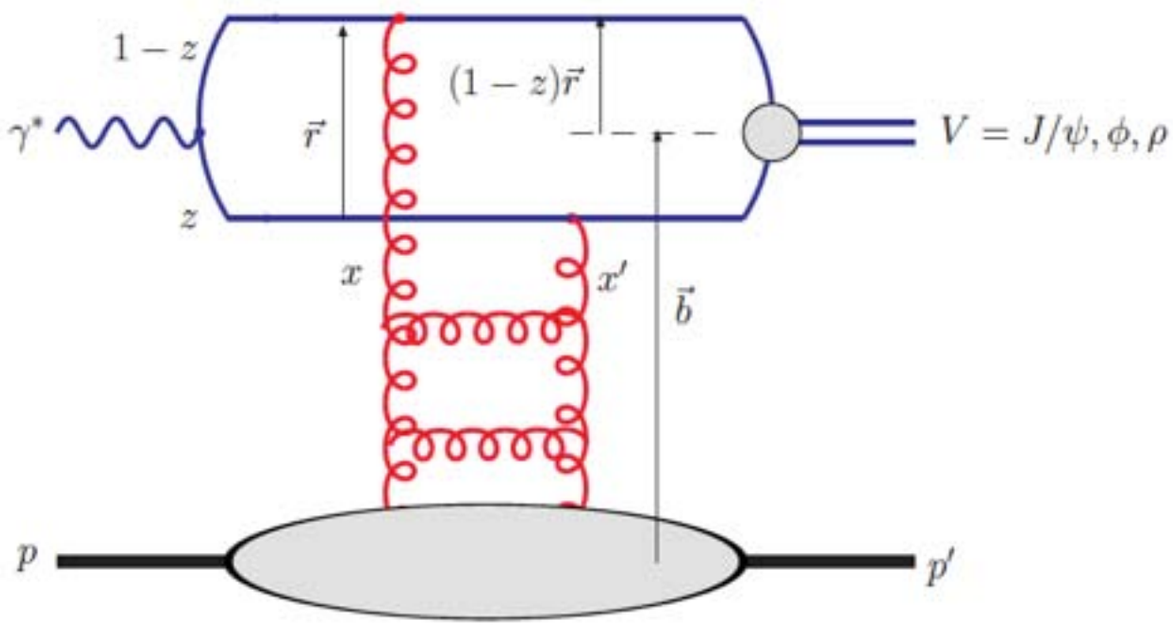

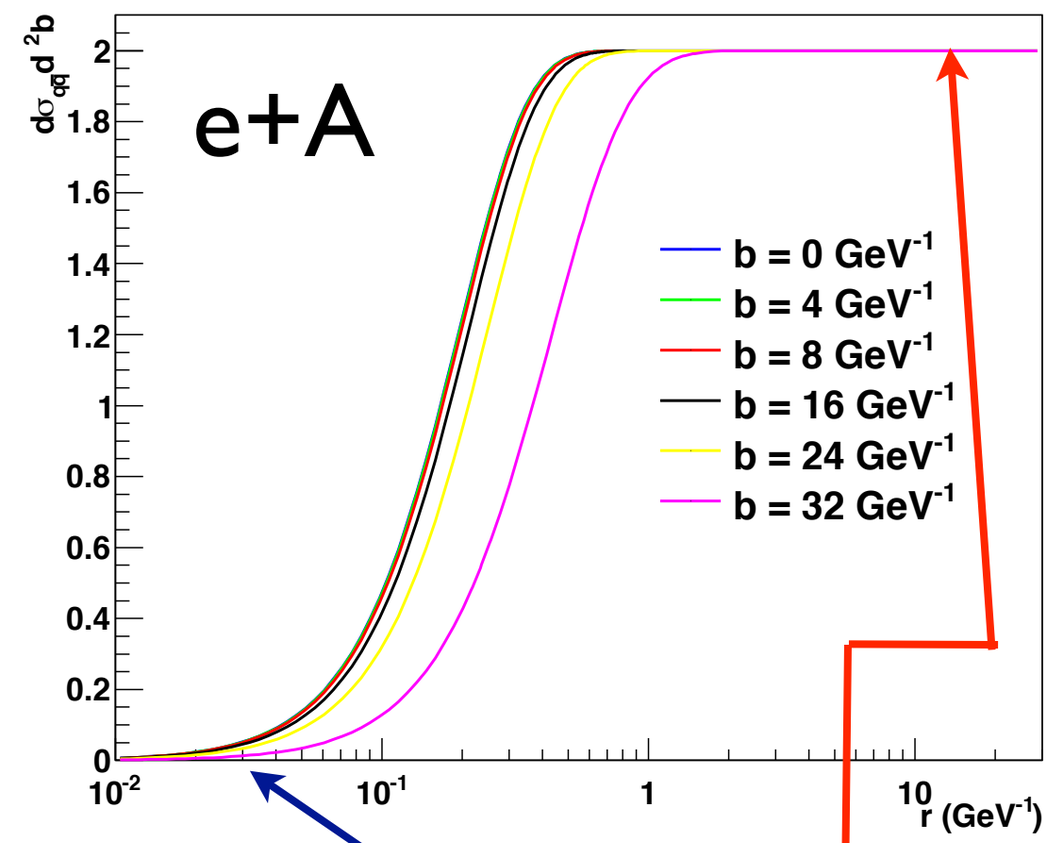

$$\mathcal{N}(x, r, b) = 1 - \exp\left(-r^2 \frac{\pi^2}{2N_c} \alpha_s(\mu^2) x G(x, \mu^2) T(b)\right)$$

$\mathcal{N} =$ Dipole Scattering Amplitude

0 dilute system, linear QCD

1 saturated, non-linear regime

Getting a "Feel" for Non-Linear QCD

To assess typical values of $\mathcal{N}$ calculate average:

$$\langle \mathcal{N} \rangle_{2,L} = \frac{\int d^2b\, d^2r\, dz\, [\psi^* \psi]_{2,L}\, \mathcal{N}^2}{\int d^2b\, d^2r\, dz\, [\psi^* \psi]_{2,L}\, \mathcal{N}}$$

$\langle \mathcal{N} \rangle_2 \longrightarrow F_2$

$\langle \mathcal{N} \rangle_L \longrightarrow F_L$

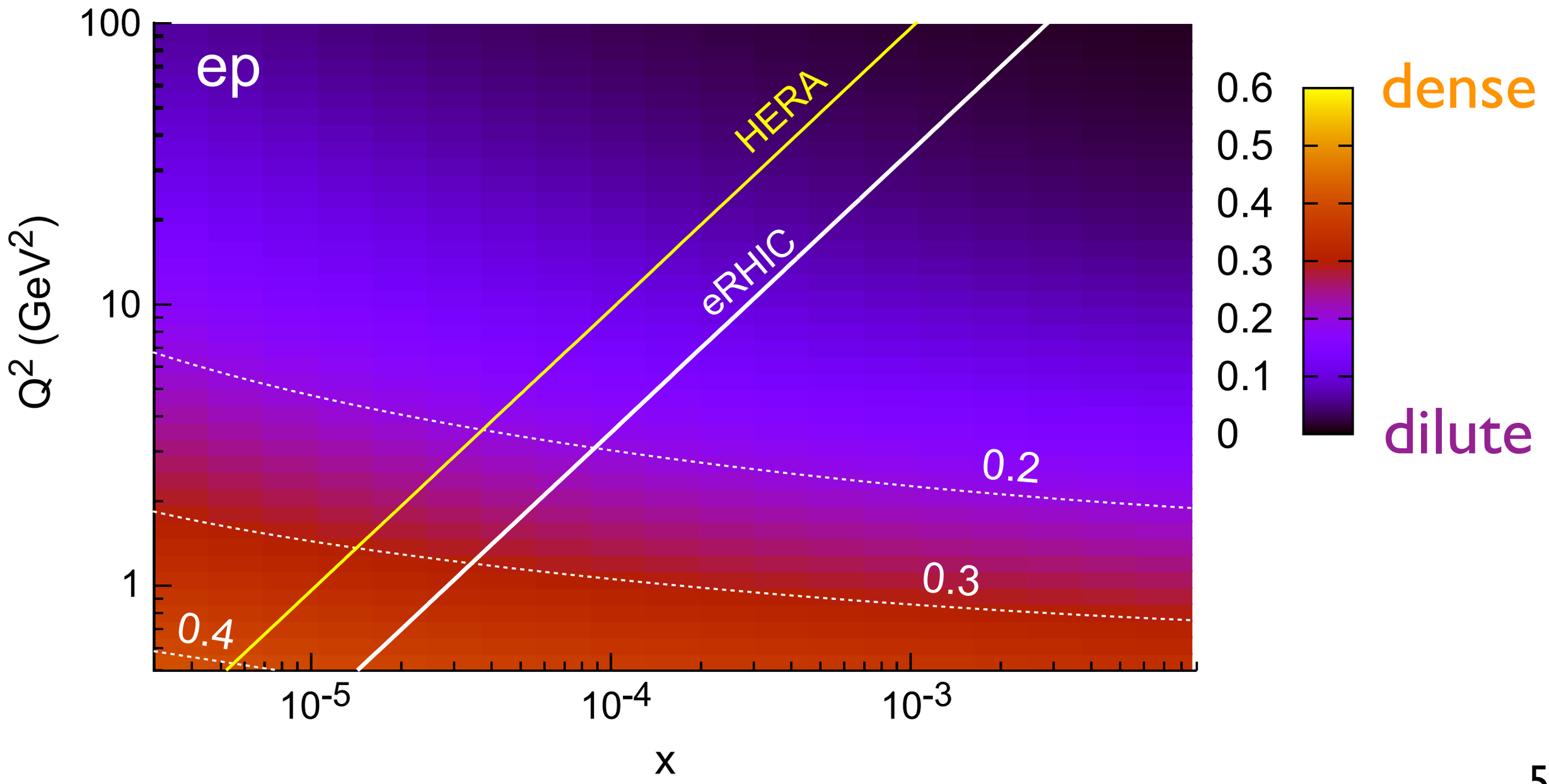

Getting a "Feel" for Non-Linear QCD

To assess typical values of $\mathcal{N}$ calculate average:

$$\langle \mathcal{N} \rangle_{2,L} = \frac{\int d^2b\, d^2r\, dz\, [\psi^* \psi]_{2,L}\, \mathcal{N}^2}{\int d^2b\, d^2r\, dz\, [\psi^* \psi]_{2,L}\, \mathcal{N}}$$

$\langle \mathcal{N} \rangle_2 \longrightarrow F_2$

$\langle \mathcal{N} \rangle_L \longrightarrow F_L$

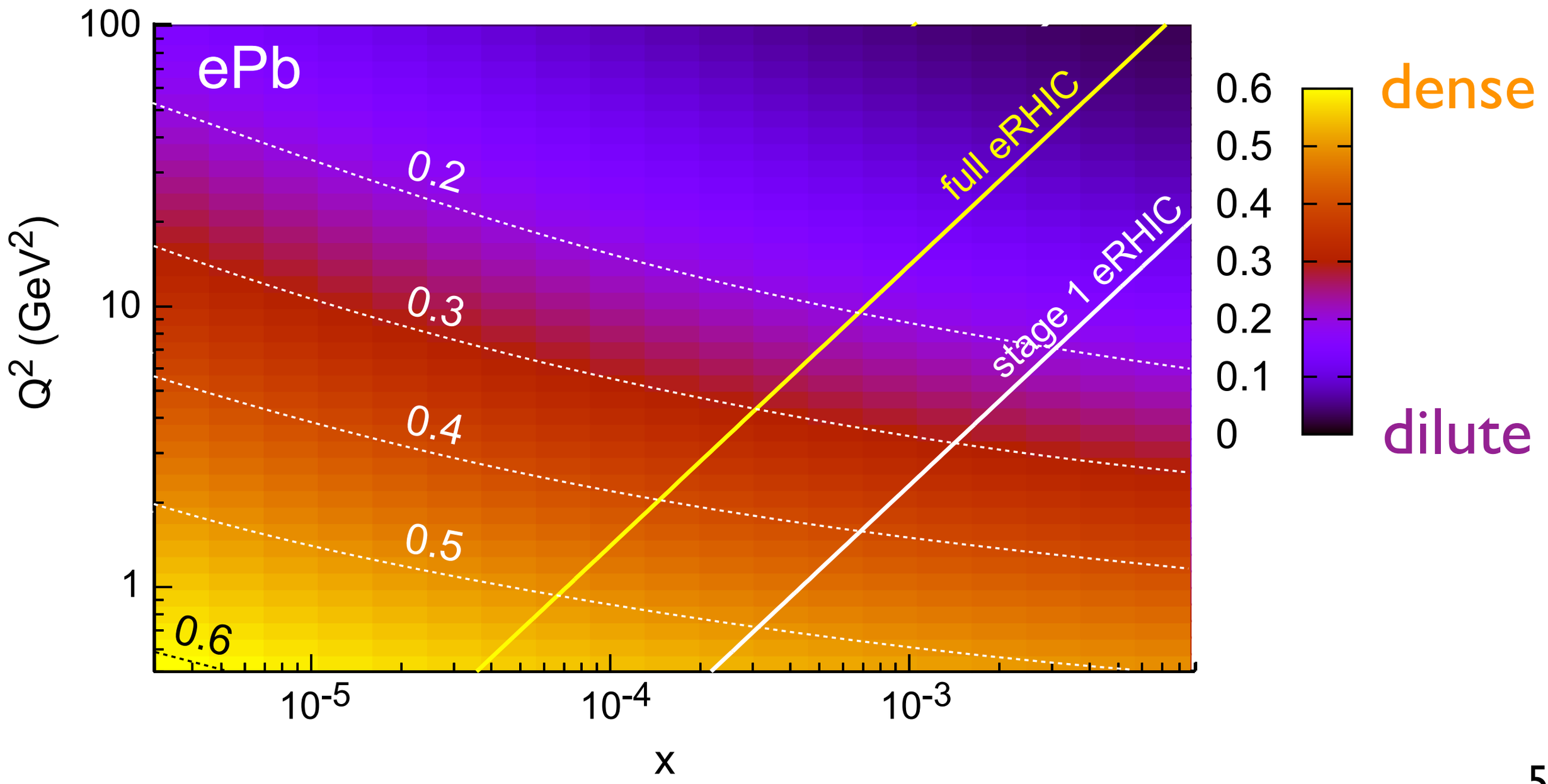

Forward di-hadron correlations at STAR

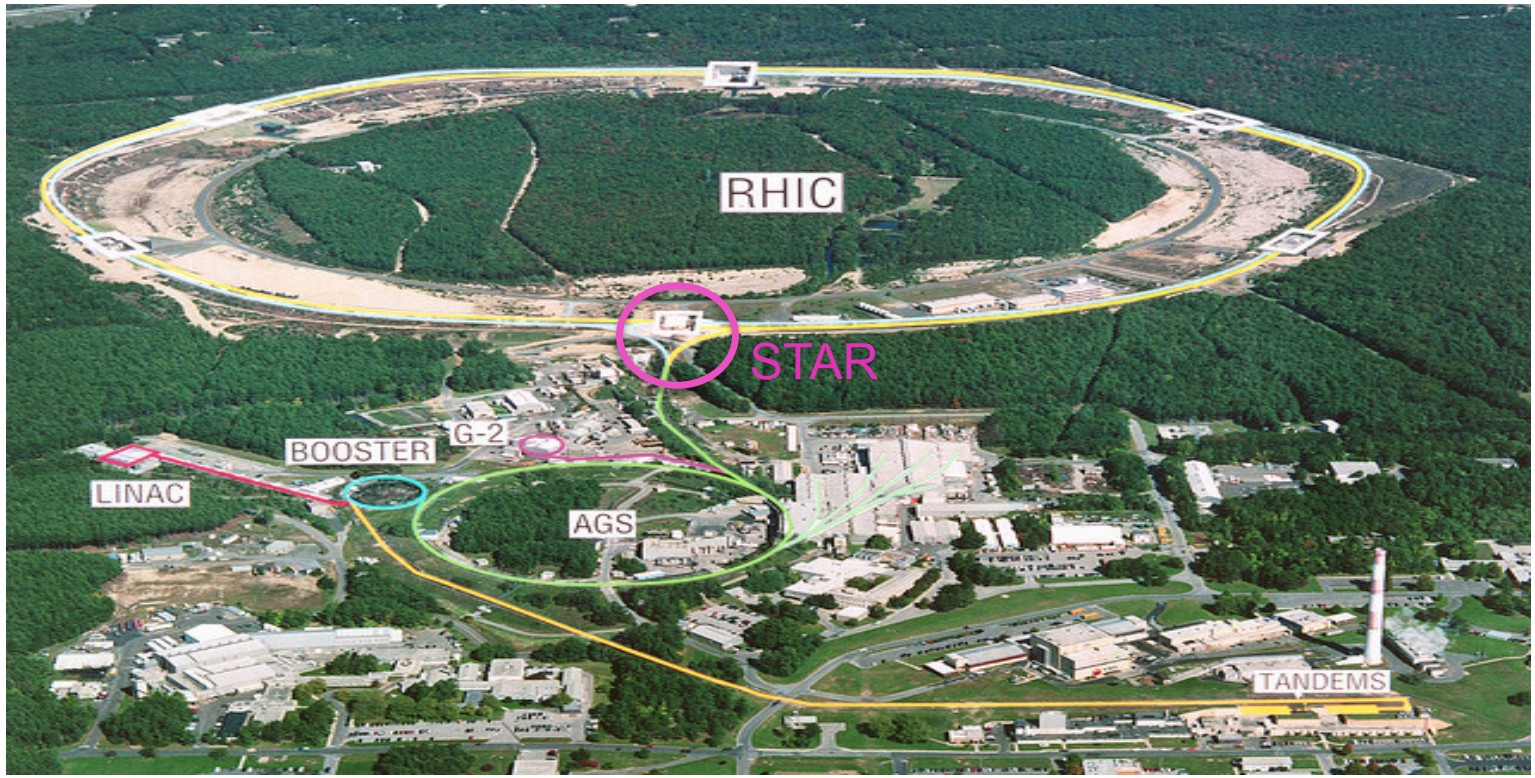

Forward physics at RHIC workshop

July 30th, 2012

Xuan Li, Temple University

Outline

- Introduction
  - Motivation
- Are there differences between gluon distribution functions inside the proton and a larger nucleus?
- Low x physics studies at STAR through measurements of forward di-hadron correlations.
  - Forward π^0 + mid-rapidity π^0 or h.
  - Forward π^0 + forward π^0
  - Forward π^0 + near-forward jet-like cluster.
- Summary & Outlook

What does the nucleon parton distribution look like?

- The nucleon quark distribution is well known.

- Rapid rise of the gluon density at low-x evident from $\partial F_2(x,Q^2)/\partial \ln Q^2$.
- $xg(x) \approx \partial F_2(x,Q^2)/\partial \ln Q^2$
- $F_2(x,Q^2)$ is the structure function at fixed x.

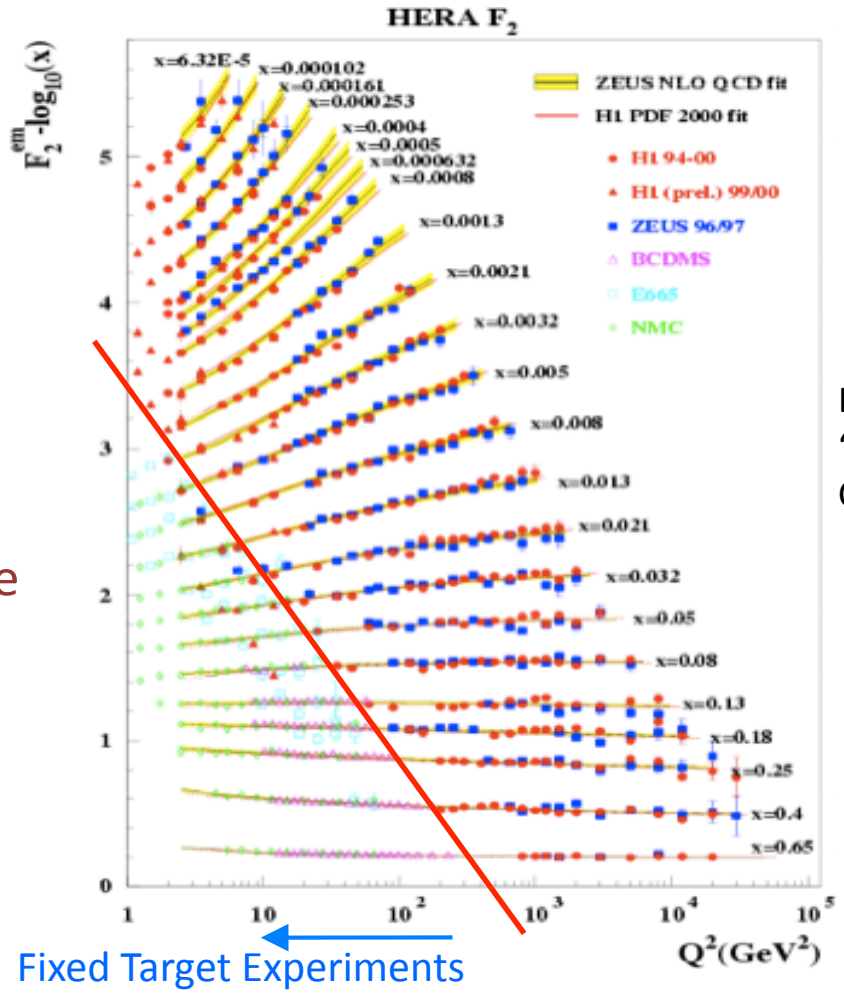

E. Rizvi, talk presented at the "International Euro Physics Conference on High Energy Physics", July 2003

- The nucleon gluon density is derived from the structure function (x, Q^2) and is well known in the 0.0001<x<0.3.

What does the nucleon parton distribution look like?

- The nucleon quark distribution is well known.

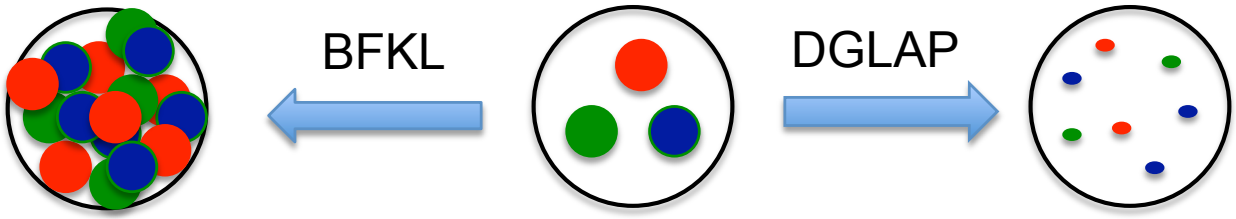

DGLAP

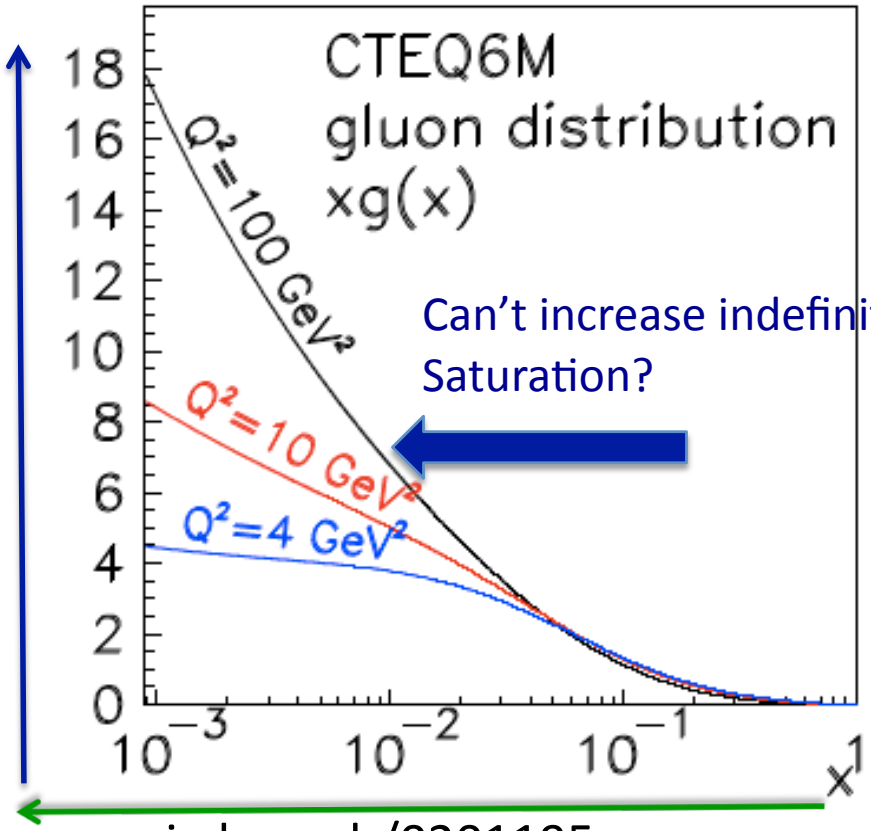

Can't increase indefinitely.
Saturation?

arxiv:hep-ph/0201195

BFKL

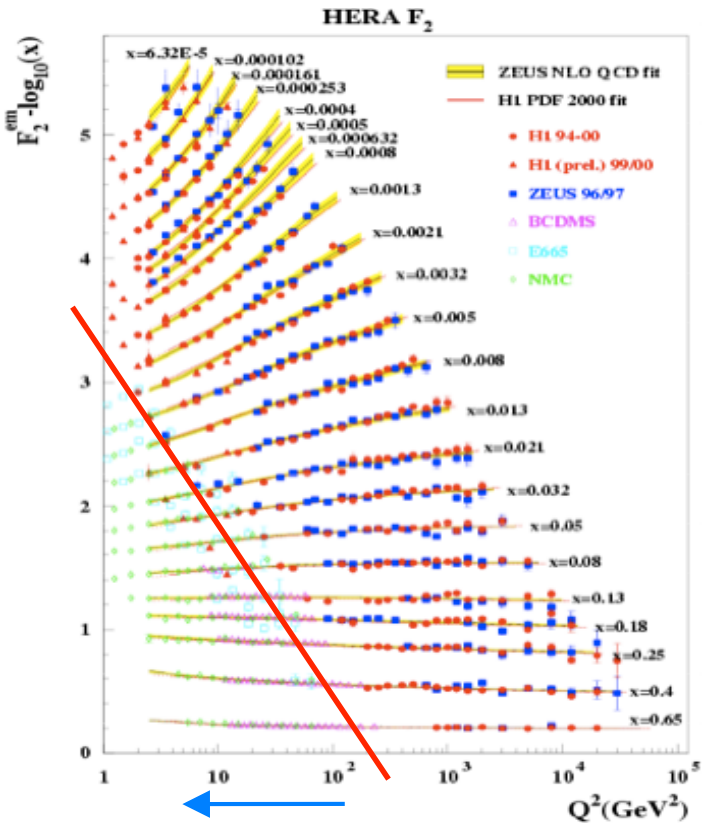

Fixed Target Experiments

What is the saturation state?

- When gluon recombination balances gluon splitting, saturation is realized.

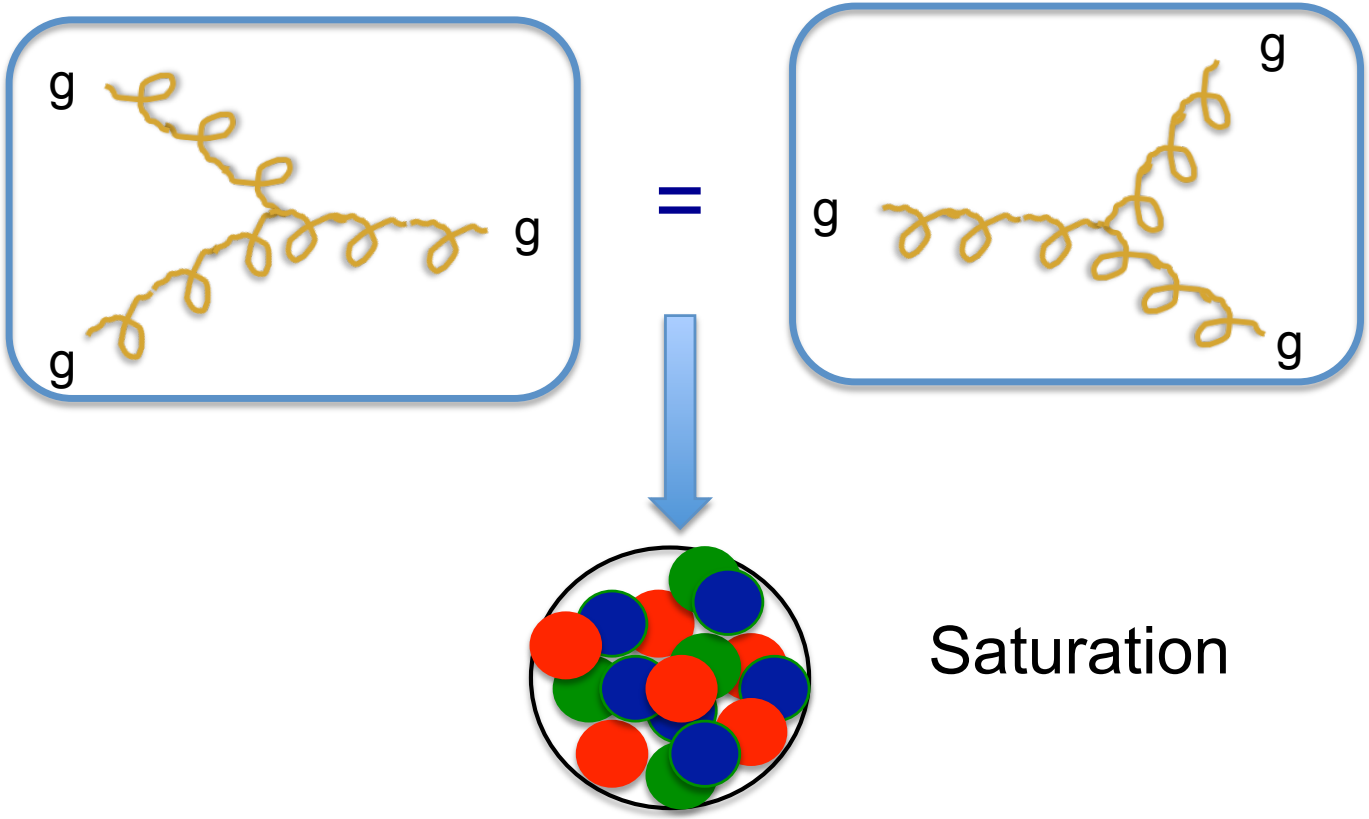

- The nucleon gluon saturation is expected to be at x<0.0001 region.

What is the saturation state?

- When gluon recombination balances gluon splitting, saturation is realized.

$$x \sim \frac{2p_T}{\sqrt{s}} e^{-y}$$

Q_s is saturation scale

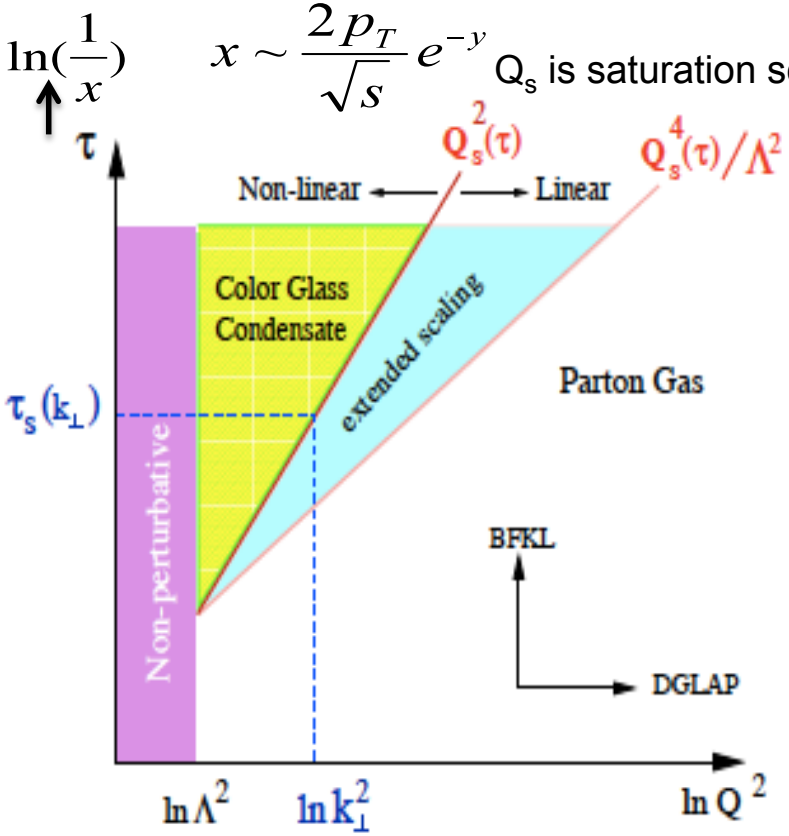

The Color Glass Condensate (CGC) describes the saturation state,

Color: gluons carry color charge.

Glass: fast source (larger x) has a normal time scale $1/Q_s$, they emitted slow parton (lower x) with a dilation time scale.

Condensate: high gluon density.

Iancu and Venugopalan,

hep-ph/0303204

How about a larger nucleus?

- Fixed target experiments derived the nuclear gluon density only at 0.02<x<0.3.

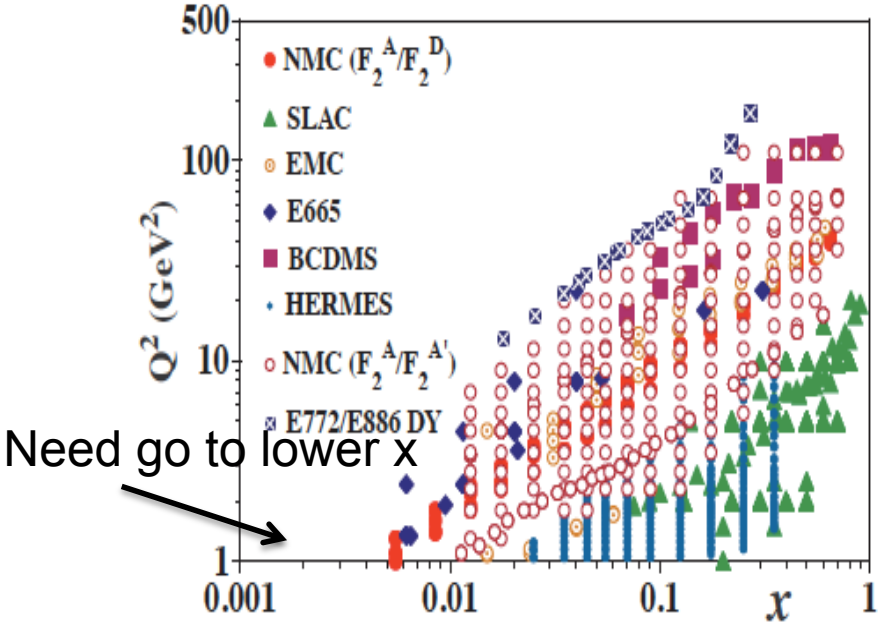

Current fixed target results
[Phys. Rev. C70 (2004)044905]

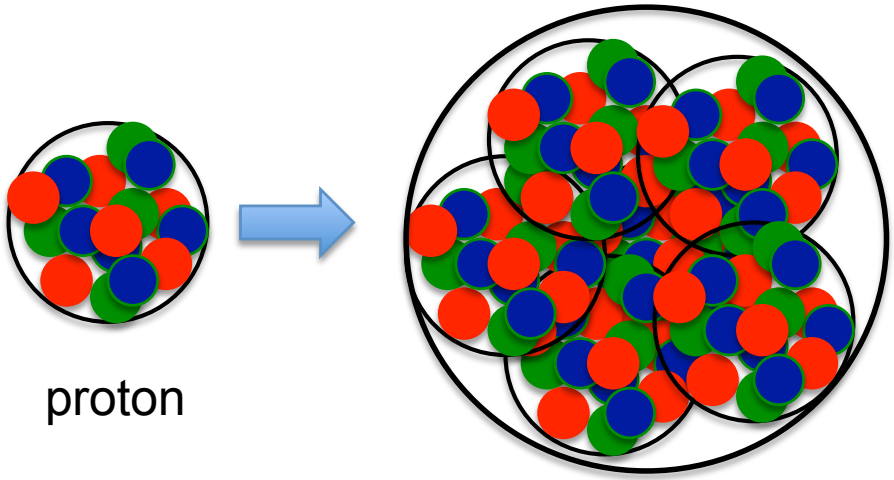

- Nuclear (mass number A) gluon density ≈ $A^{1/3}$ × nucleon gluon density at a given x, leading to the expectation $Q_s^2 \approx A^{1/3} x^{\beta}$. [hep-ph/0304189]
  For example, for Au nucleus, the saturation is expected at x≈0.001.

How to probe low x gluons

- Forward inclusive production.

RHIC is a hadron collider including p+p and d+Au collisions.

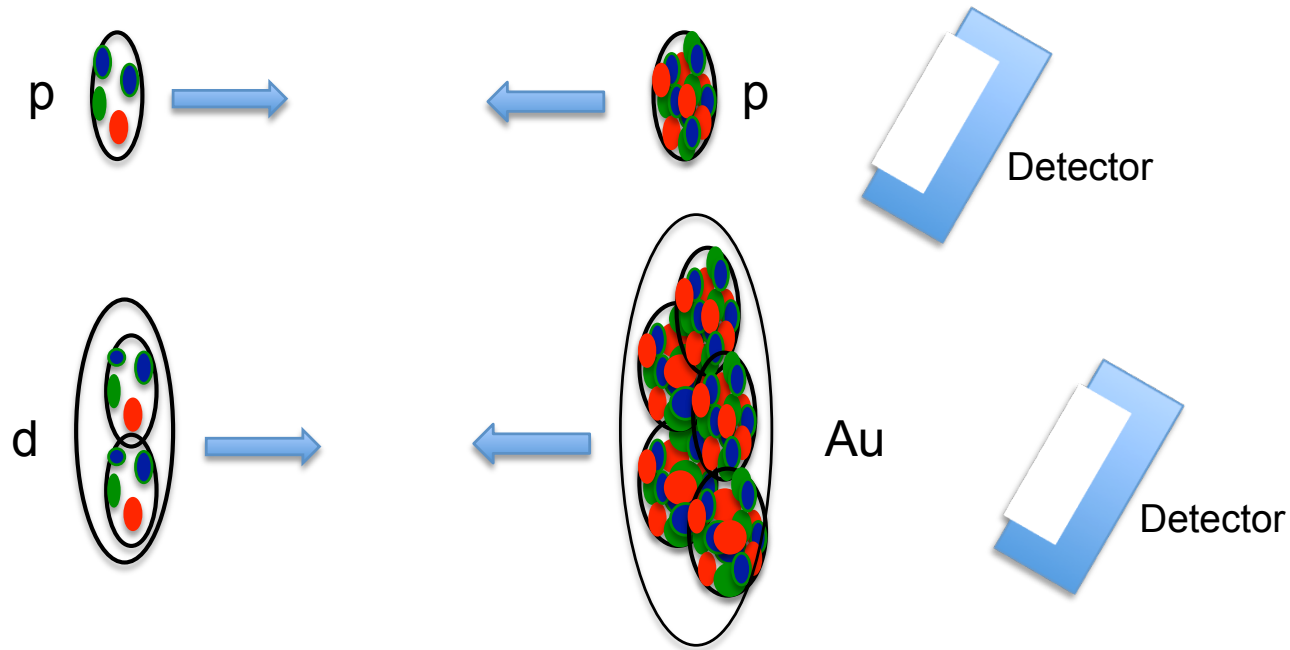

How to probe low x gluons

- Forward inclusive production.

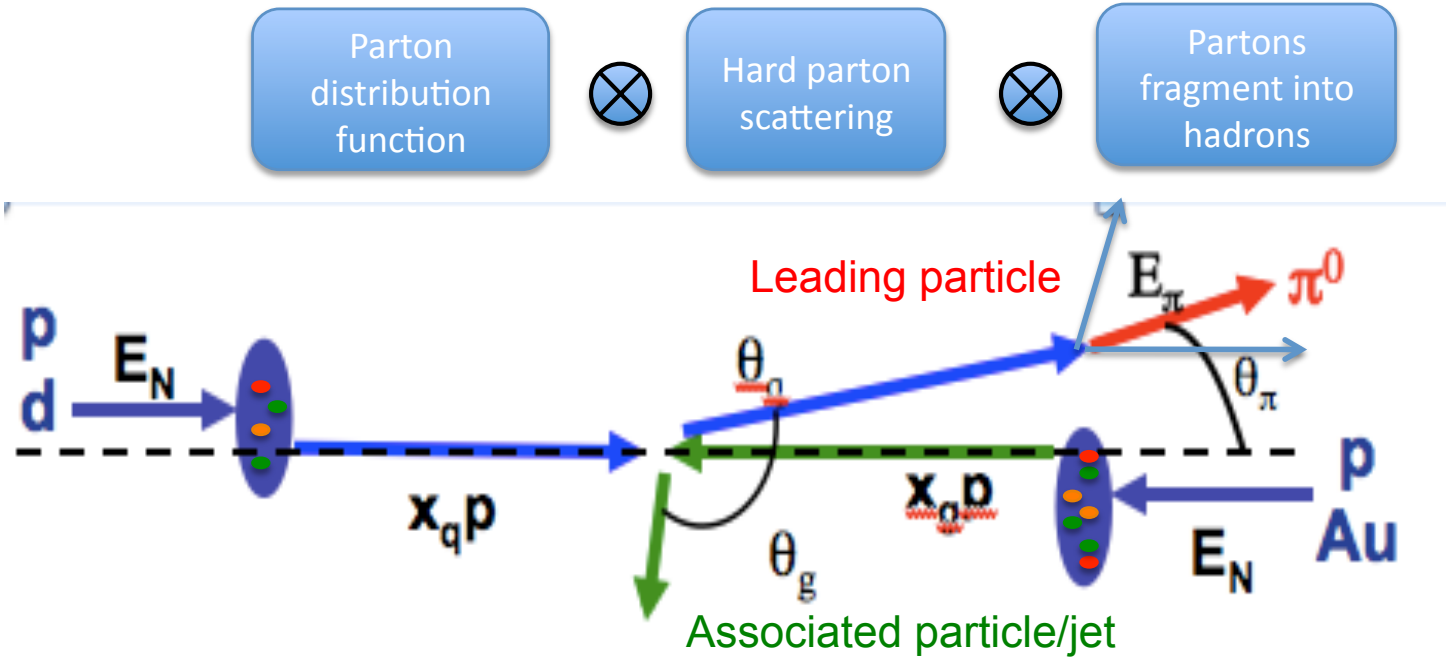

$x_q = p_q/p_N$,
$x_g = p_g/p_N$,
$\eta_\pi = -\ln(\tan\theta_\pi/2)$
$p_T \approx E_\pi \sin(\theta_\pi)$

- The factorization mechanism is taken as universal and applied in nucleon (nucleus)+ nucleon (nucleus) collisions.
- Large rapidity (η_π~4) inclusive π production and correlations **probes asymmetric partonic collisions.**
- Mostly **high-x_q valence quark (x>0.2)** + **low-x_g gluon (x<0.01).**

How to probe low x gluons

- Forward inclusive π^0 production measurements.

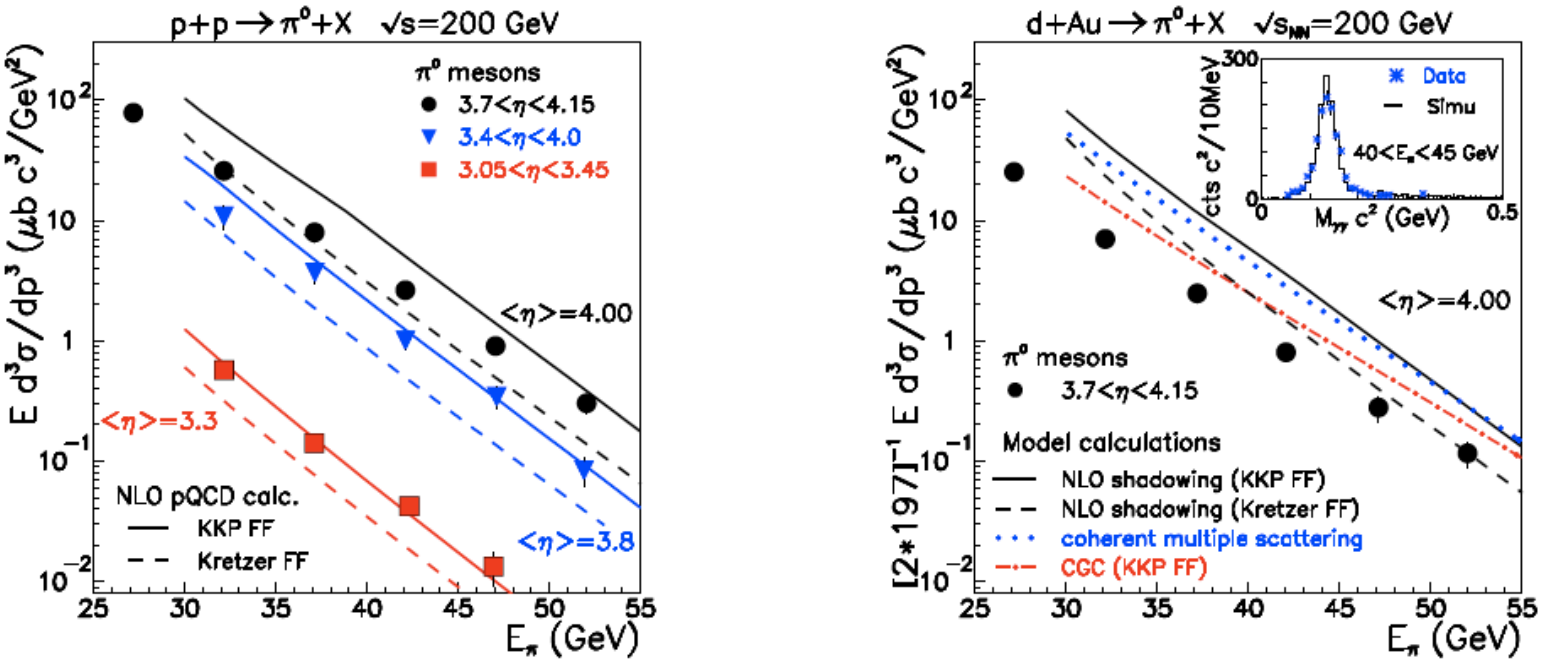

Phys. Rev. Lett. 97.152302

- pp data is in agreement with perturbative QCD.
- Suppression of forward inclusive particle in dAu data is better described by the Color Glass Condensate (CGC).
- But …

How to probe low x gluons

- Inclusive π^0 to correlated π^0-π^0.

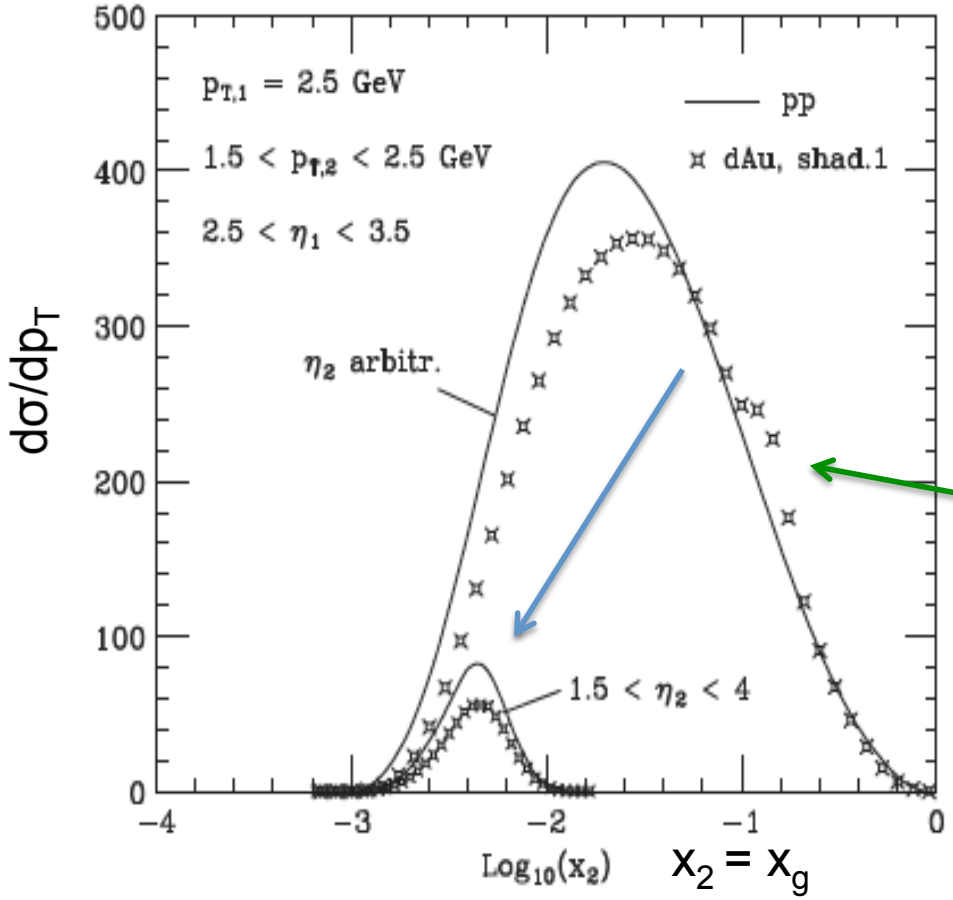

- From inclusive π^0 to π^0-π^0 correlations.
- Inclusive π^0 integrated x.
- Correlated π^0-π^0 allows us selection x.

Anti-shadowing related with the EMC effect.

Phys. Lett. B603 (2004) 173

Forward π^0-forward π^0 are more sensitive to low x gluon than inclusive production.

The soft gluon x is related to associated particle in correlations

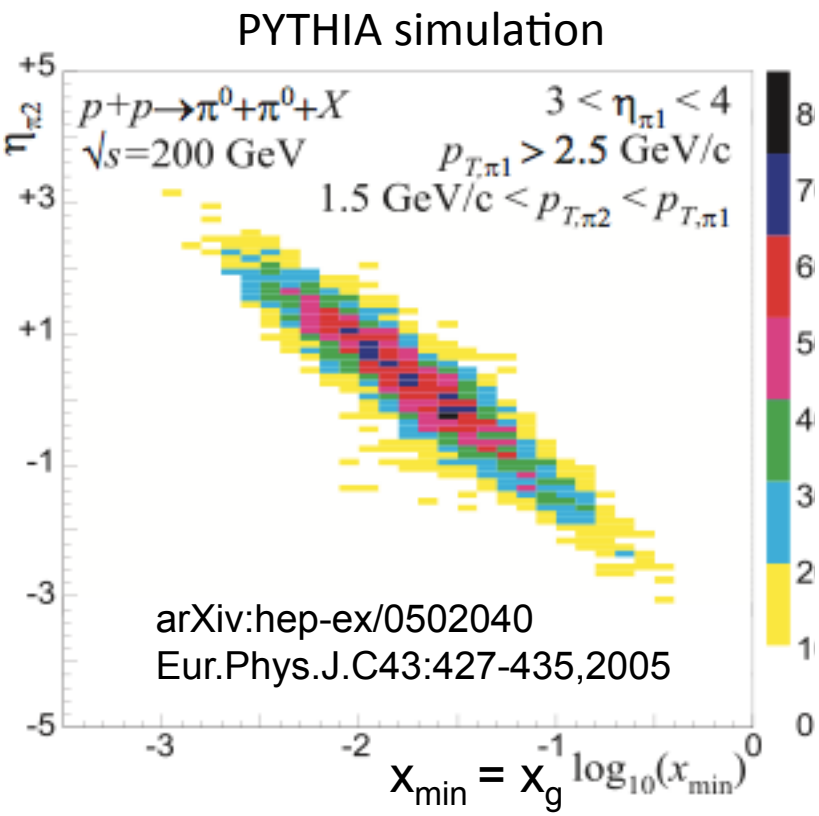

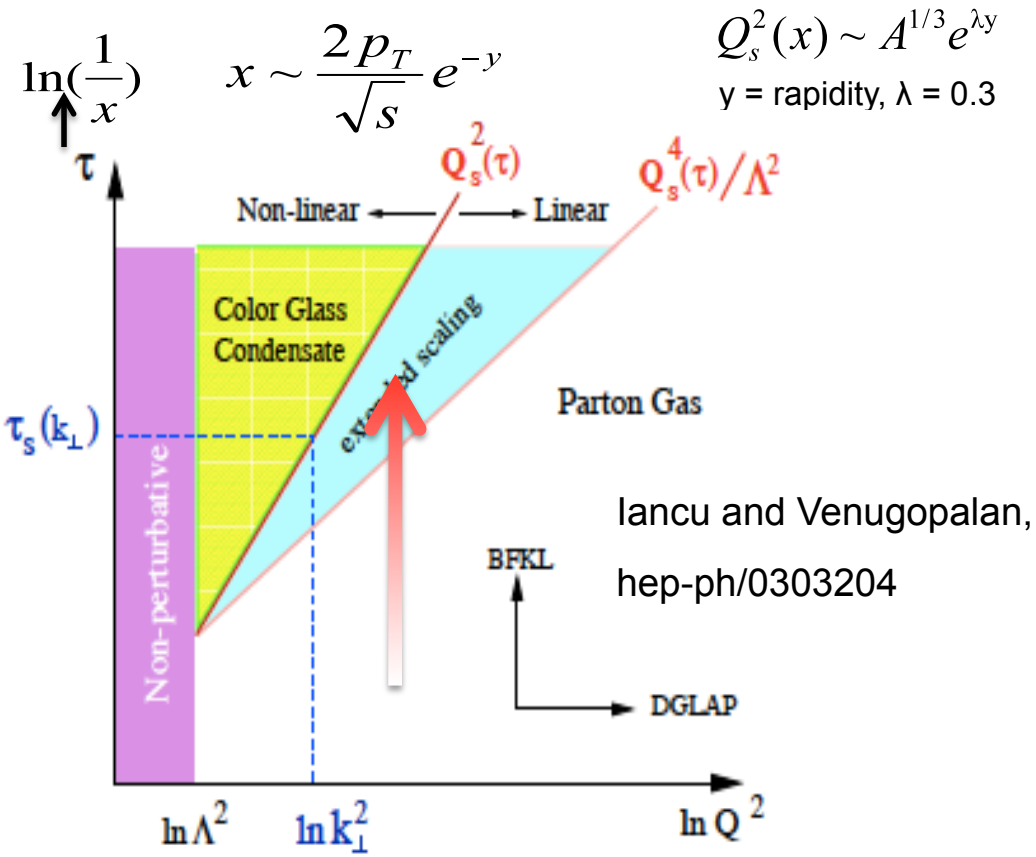

- At fixed low Q^2 ($>\Lambda^2$), the gluon density increases rapidly as x decreases. The state transfers from dilute parton gas to Color Glass Condensate (CGC).

Back to back correlations

- pQCD 2➔2 process =back-to-back di-jet (Works well for p+p)

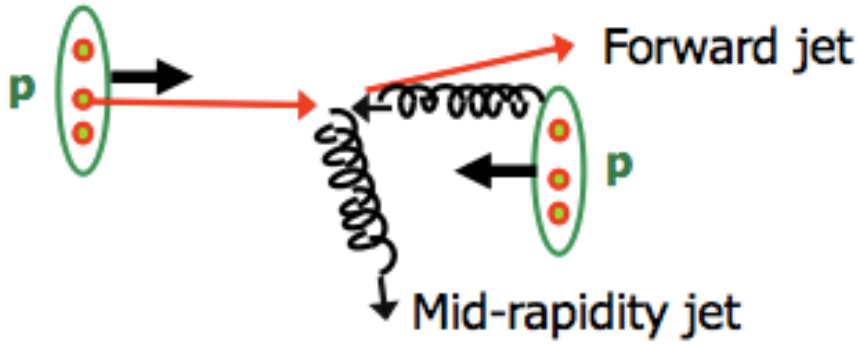

- With high gluon density, 2➔1 (or 2➔many) process = Mono-jet ?

With high gluon density
2➔1 (or 2➔many) process = Mono-jet ?

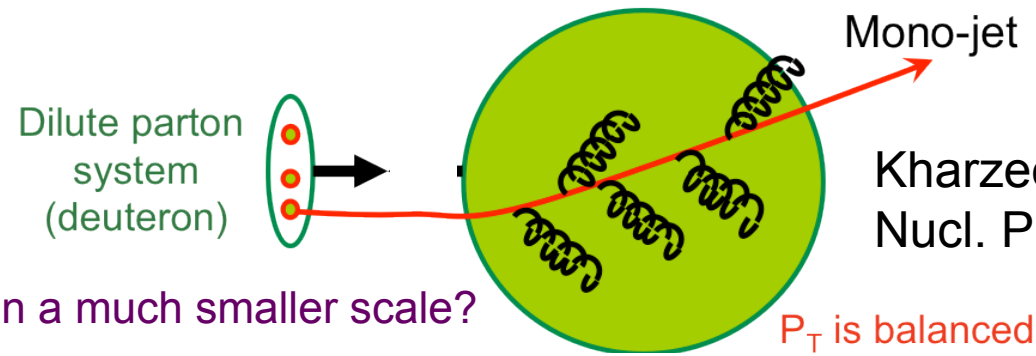

Kharzeev, Levin, McLerran
Nucl. Phys. A748 (2005) 627

Mossbauer effect on a much smaller scale?

P_T is balanced by many gluons

Dense gluon field (Au)

CGC predicts suppression of back-to-back correlation.

What we use to probe low x gluons

- The Solenoid Tracker at RHIC (STAR) is located at the 6 o'clock position of RHIC.

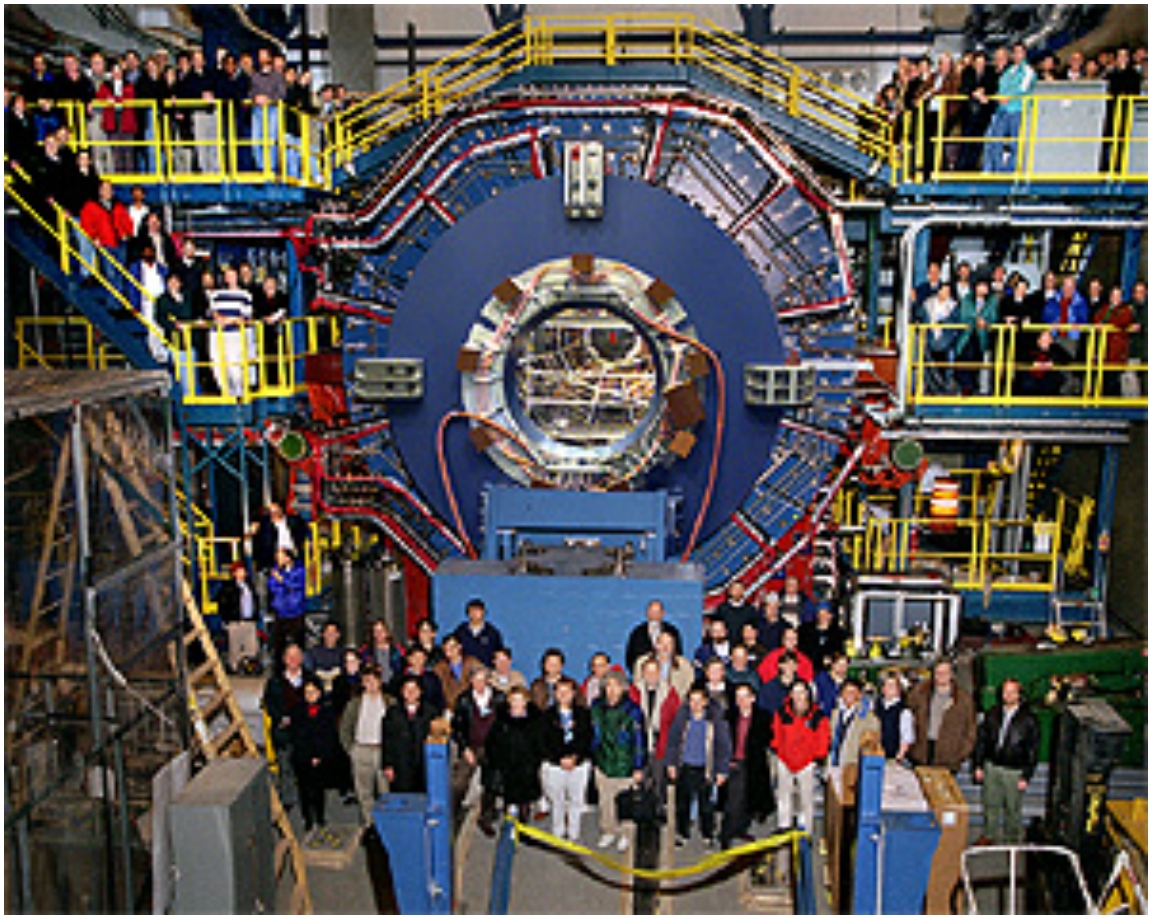

Beam view

STAR Detectors

- The schematics of STAR in RHIC run8.

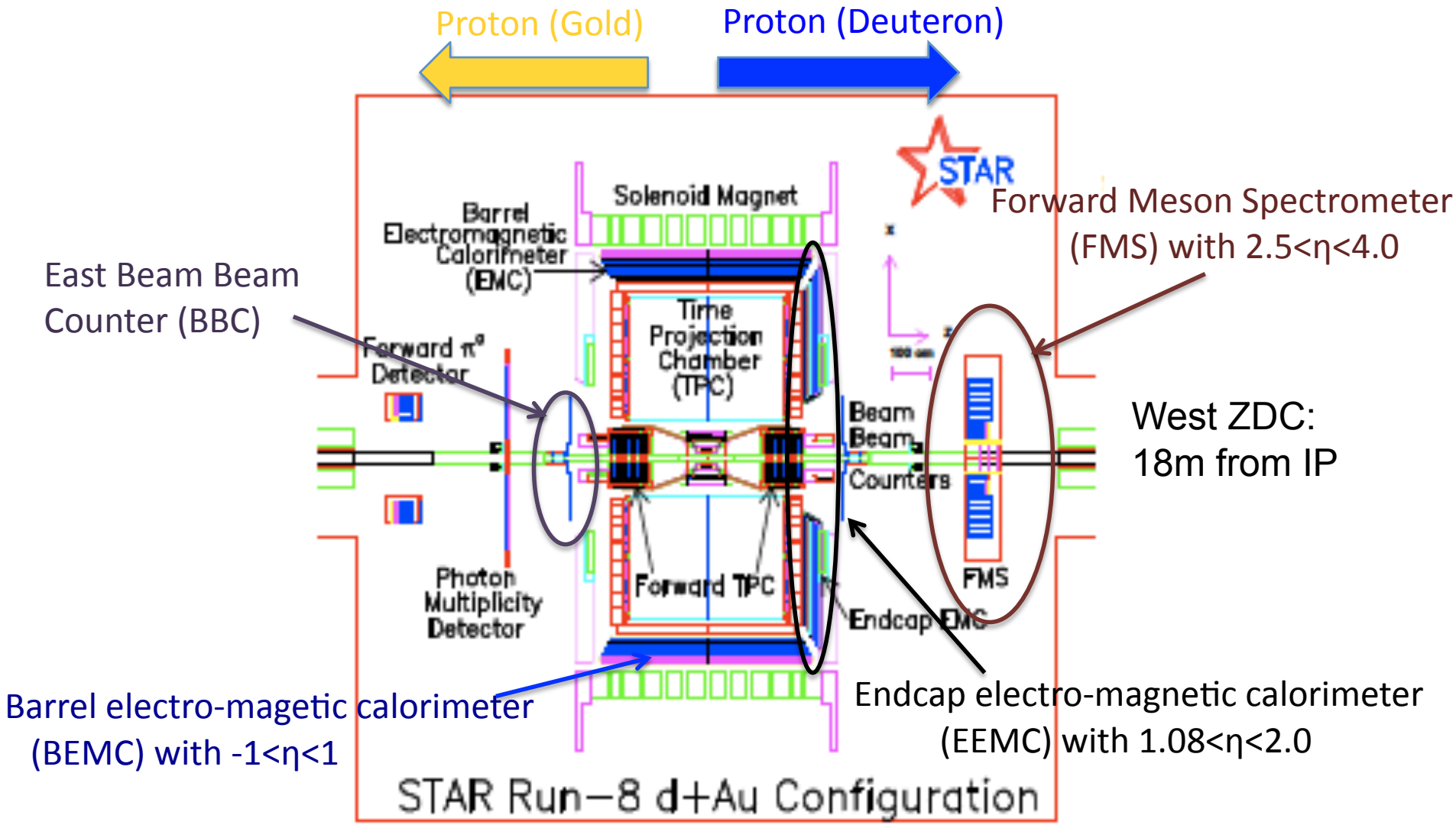

- We use the data of run8 p+p and d+Au collision at $\sqrt{s} = 200\text{GeV}$.

STAR Detectors

- The detectors of STAR used for correlations.

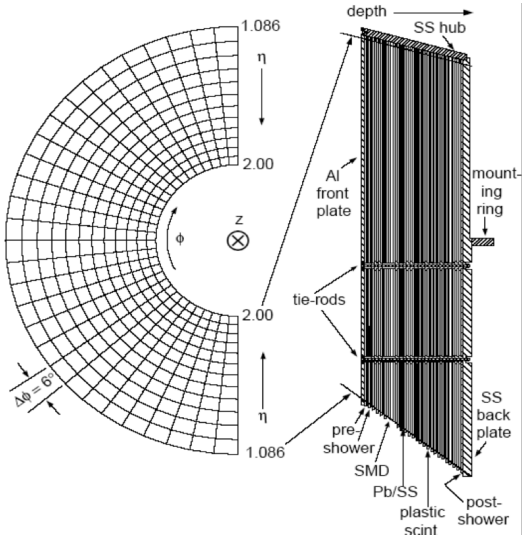

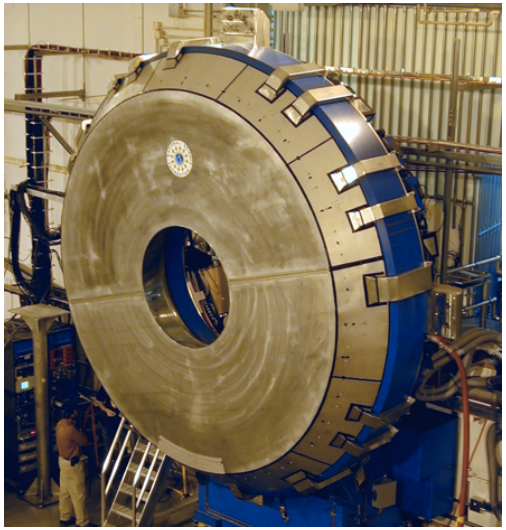

EEMC measuring range 1<η<2
Tower range Δϕ=0.1, Δη=0.057-0.099

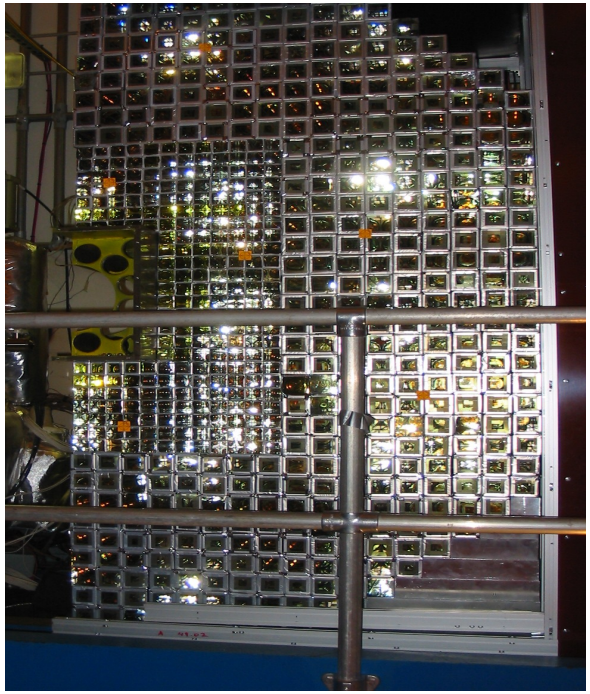

Front view of north half of FMS.
FMS measuring range 2.5<η<4.
Δϕ=0.058, Δη=0.1 for large cells.

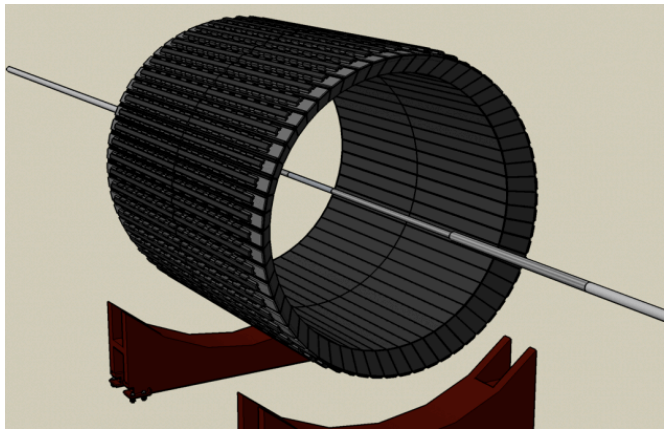

BEMC measuring range -1<η<1. Tower range Δϕ=0.05, Δη=0.05.

Rapidity dependence of azimuthal correlations

- At fixed low Q^2 ($>\Lambda^2$), the gluon density increases rapidly as x decreases.

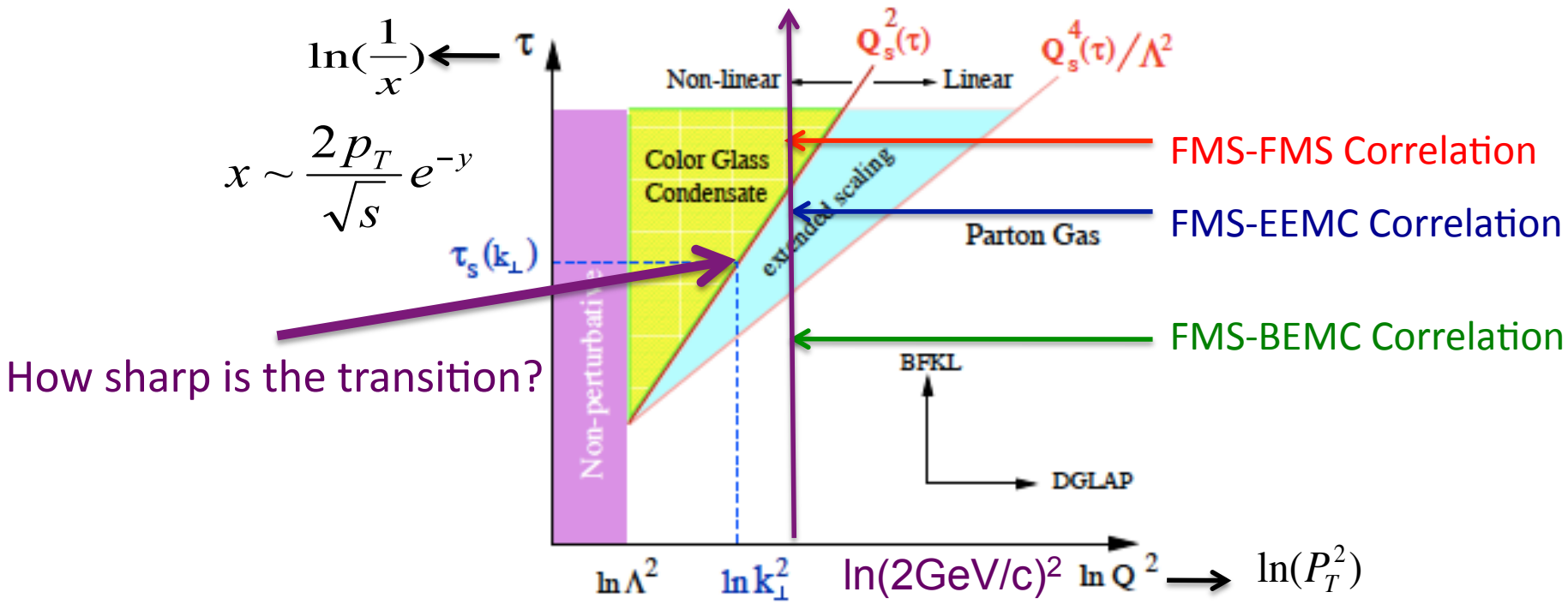

Iancu and Venugopalan, hep-ph/0303204

- Nearly continuous EM system (spans $-1<\eta<4$) at STAR provides acceptance for azimuthal correlations at different pseudo-rapidity.

π^0 reconstruction in the FMS

- The triggered particle is π^0 reconstructed in the most forward detector — FMS.

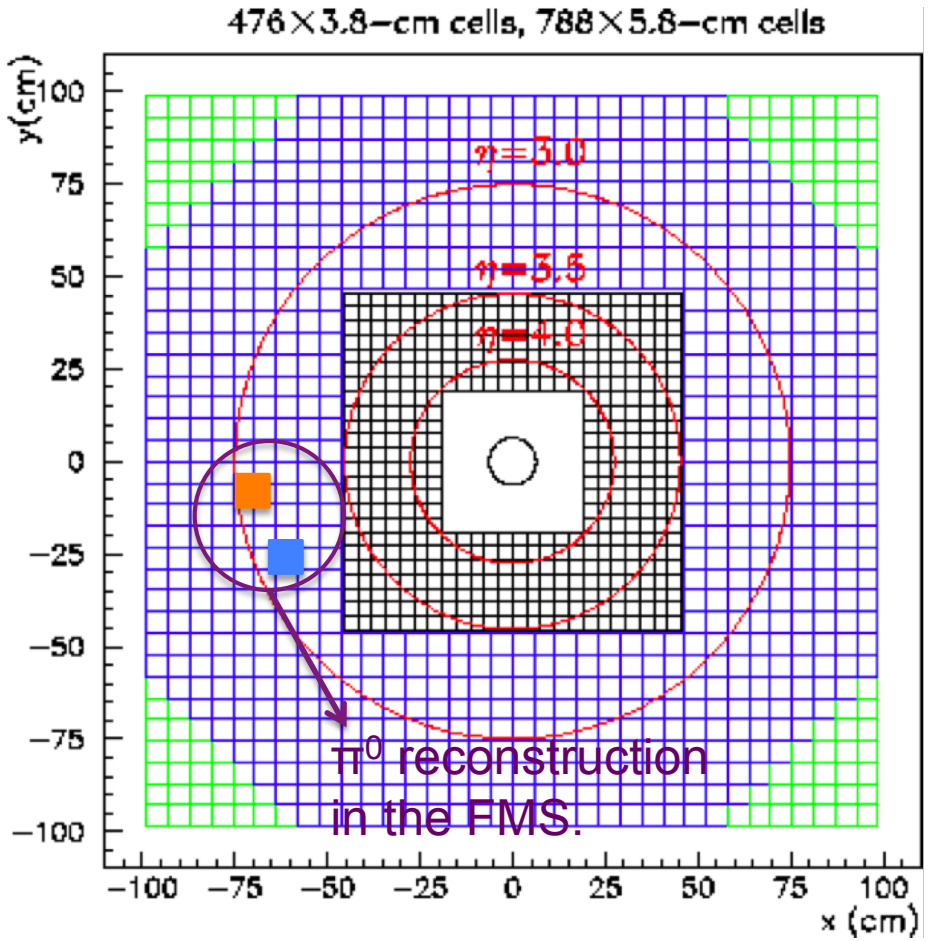

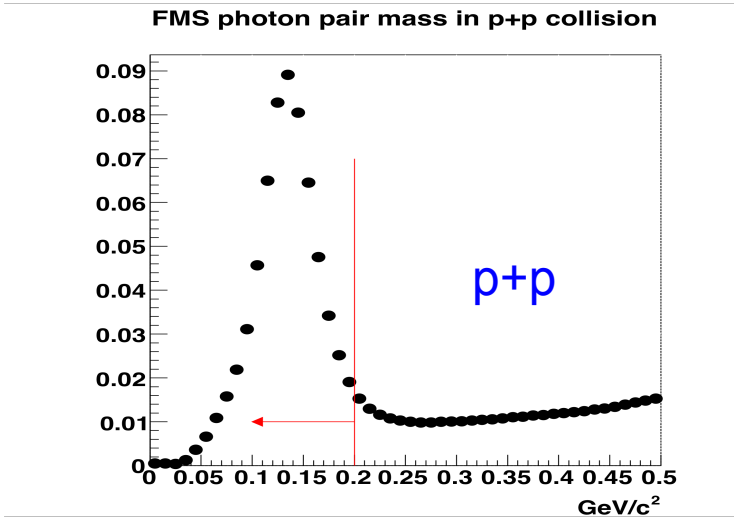

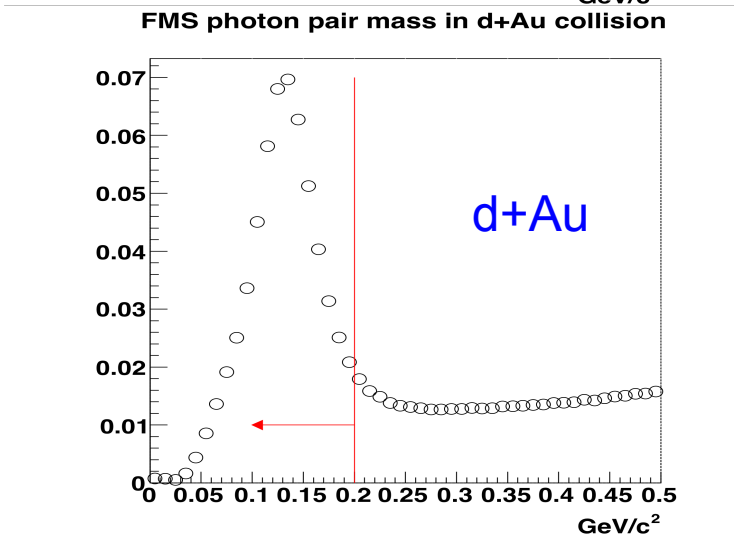

- There are clear π^0 peaks in the FMS during p+p and d+Au collisions.

Forward-mid rapidity correlations

- FMS-BEMC(TPC) azimuthal correlations probe nuclei gluon density at $0.008 < x_{BJ} < 0.07$.

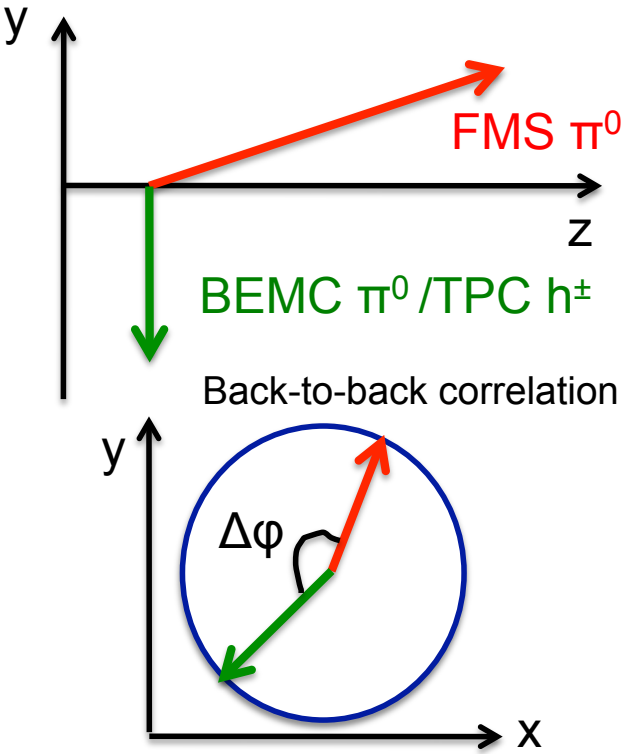

E. Braidot (arXiv:1102.0931)

P_T(FMS) > 2.0 GeV/c ; 1.0 GeV/c < P_T(BEMC/TPC) < P_T(FMS)

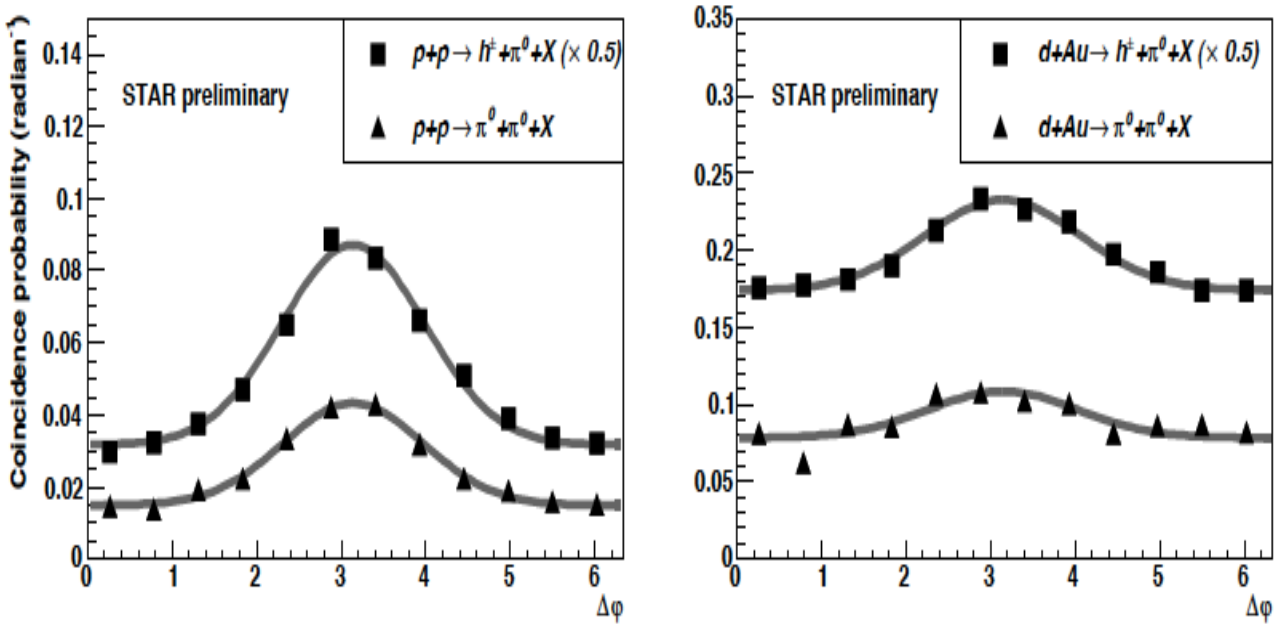

σ_{up}=0.846±0.025,b_{up}=0.063±0.001
σ_{low}=0.829±0.045,b_{low}=0.015±0.001

σ_{up}=0.915±0.025,b_{up}=0.348±0.002
σ_{low}=0.880±0.111,b_{low}=0.078±0.002

- Higher pedestal in d+Au than in p+p.
- No significant broadening from p+p to d+Au.
- Similar away-side correlation strength.

Forward-forward rapidity correlation

- FMS-FMS azimuthal correlations probe gluon density at $0.0009 < x < 0.005$.

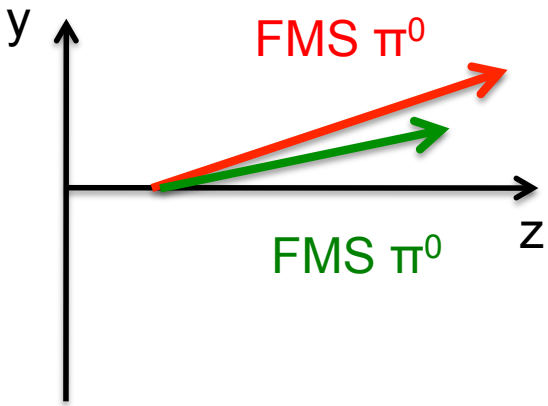

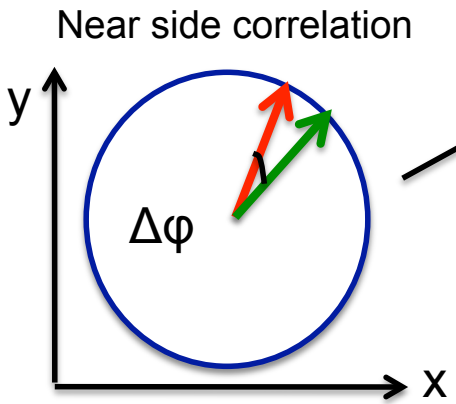

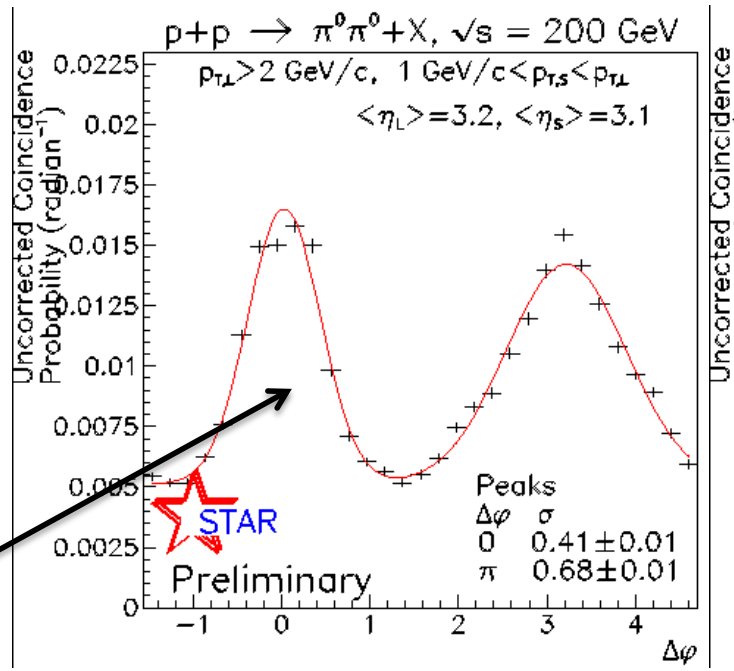

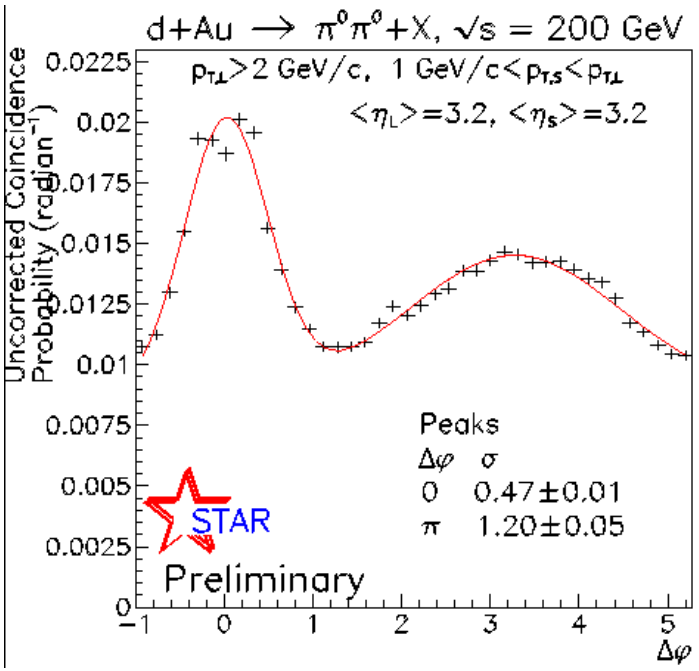

arXiv:hep-ex/1005.2378

- Similarity of near side peak in pp and dAu data.
- There is significant broadening from pp to dAu in forward-forward rapidity azimuthal correlations in the away side peak.

Forward-forward rapidity correlation

- FMS-FMS azimuthal correlations probe gluon density at $0.0009 < x < 0.005$.

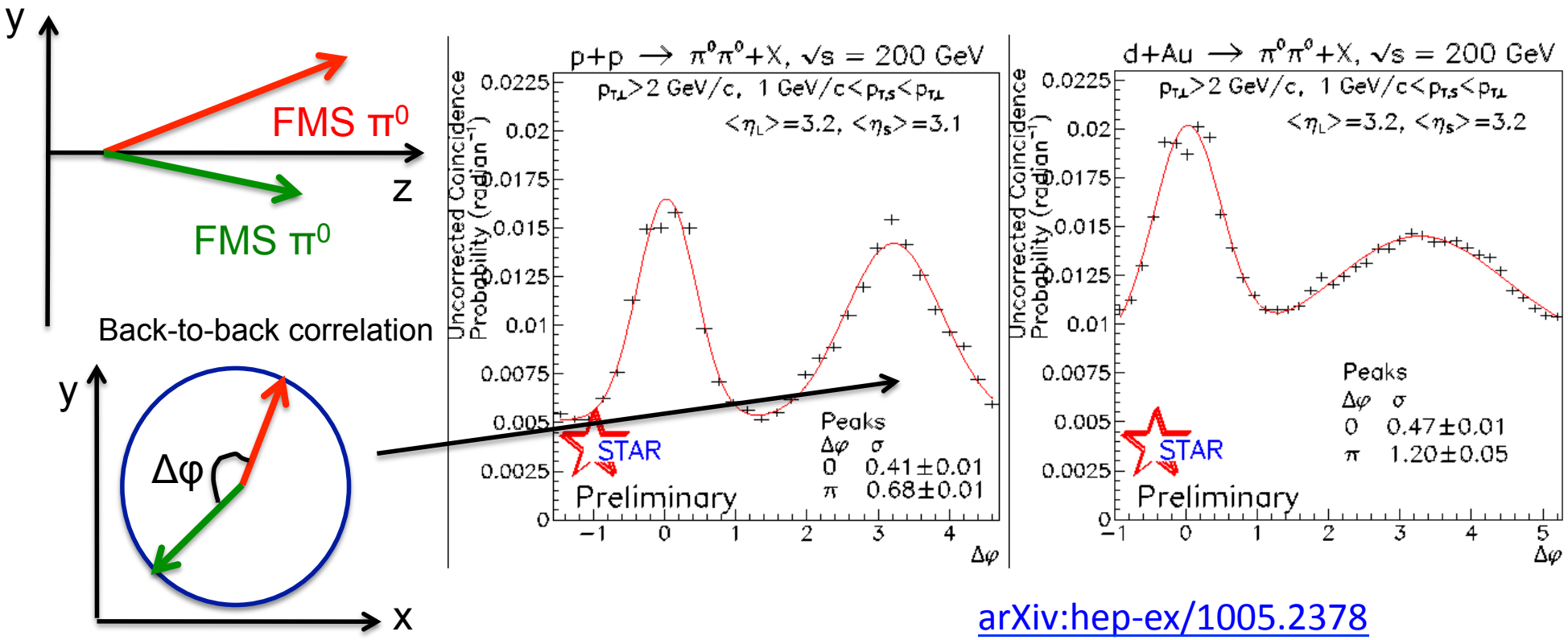

arXiv:hep-ex/1005.2378

- Similarity of near side peak in pp and dAu data.
- There is significant broadening from pp to dAu in forward-forward rapidity azimuthal correlations in the away side peak.

Forward-forward rapidity correlation

- Centrality cut on the dAu data.

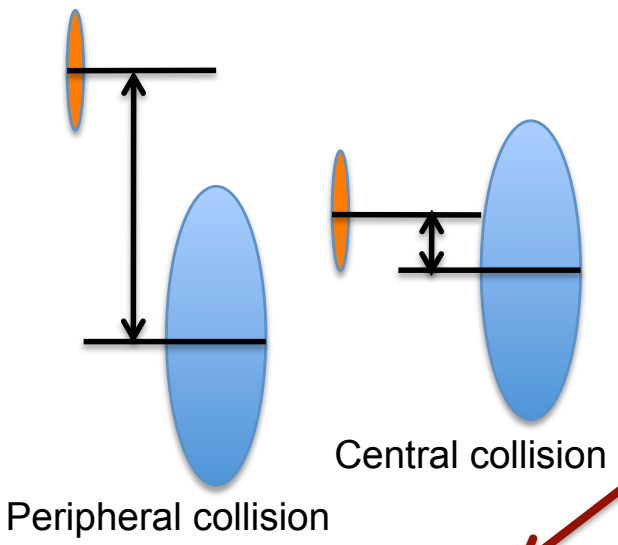

dAu centrality averaged

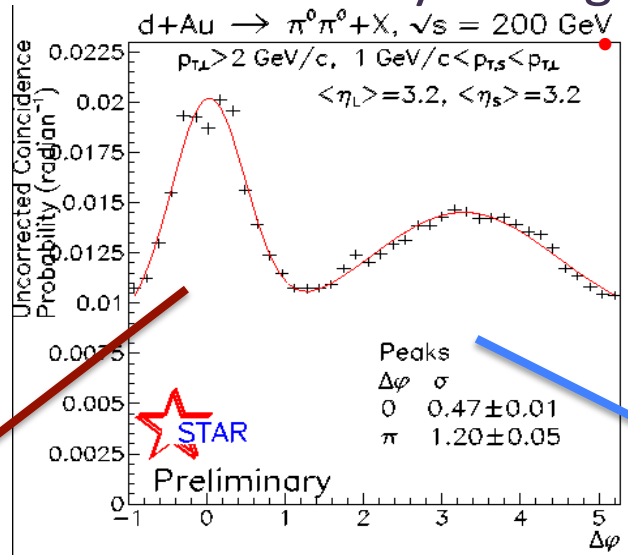

The suppression of the height of the away side peak in the central dAu collisions suggests forward-forward correlations at low x are consistent with gluon saturation in nuclei at RHIC.

dAu peripheral

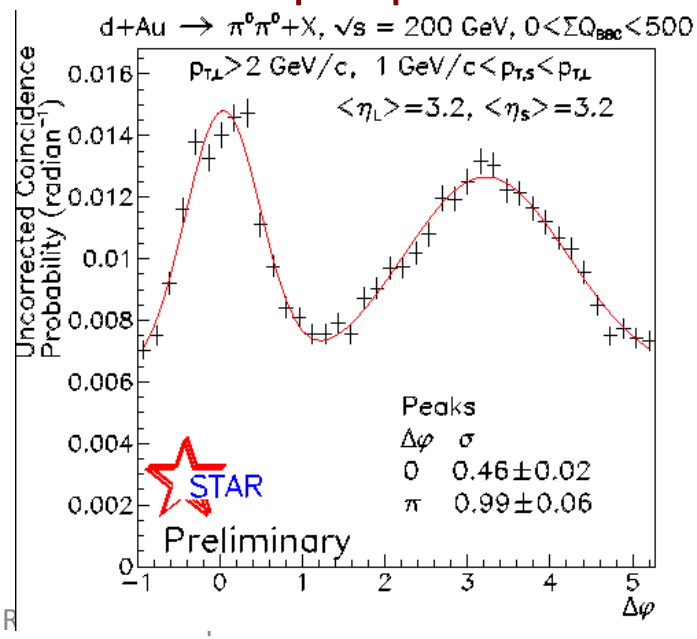

dAu central

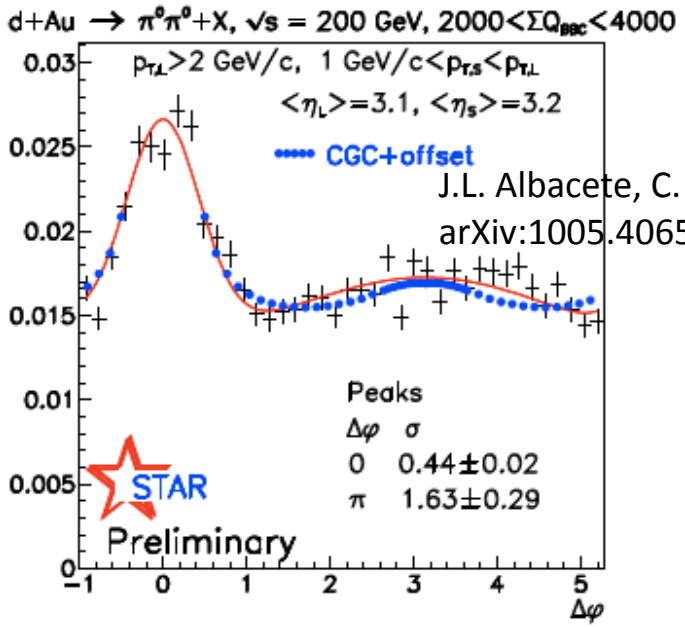

J.L. Albacete, C. Marquet
arXiv:1005.4065

The event reconstruction in the EEMC

- The event is reconstructed based on the energy deposition in the EEMC.

One event of the energy deposition in the EEMC with FMS π^0 trigger (p_t>2.0GeV/c) in p+p collision at $\sqrt{s}$ = 200GeV.

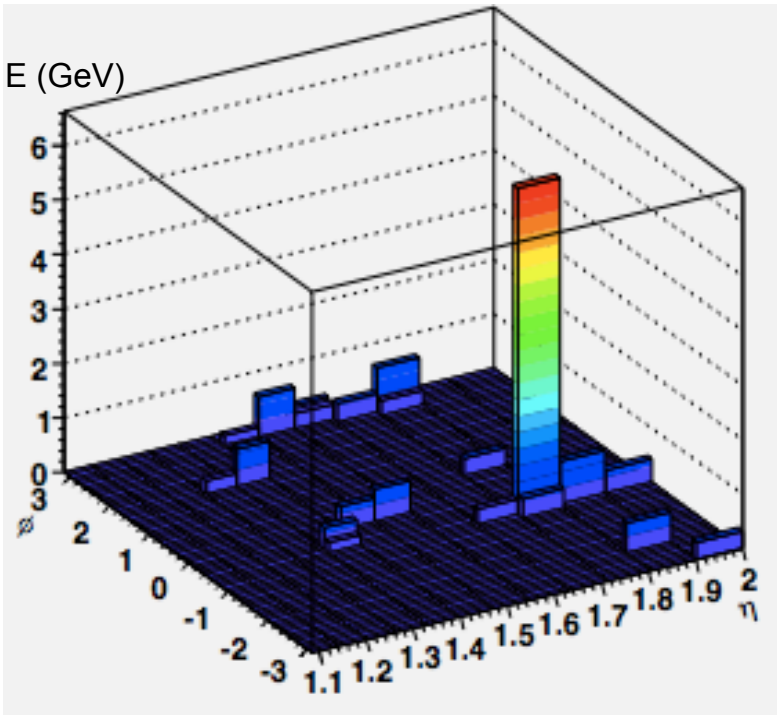

- The π^0 usually is the leading particle inside a jet measured in the EM calorimeter.
- The initial gluon state is independent of the final fragmentation process. Jet-like clusters can be surrogates of fragment partons.

Jet-like cluster are reconstructed with cone algorithm

- Energy E_{jet}: $E_{jet} = \Sigma E_{Ti}$, E_{Ti} is the energy of tower i.
- Mass M_{jet}: (1) Assuming hits of towers are zero mass. Projecting T_i energy to its center to get the momentum vector of the tower p_{Ti}.
- (2) The jet-like momentum vector $p_{jet} = \Sigma p_{Ti}$.
- (3) M_{jet} =sqrt($E_{jet}^2 - P_{jet}^2$).

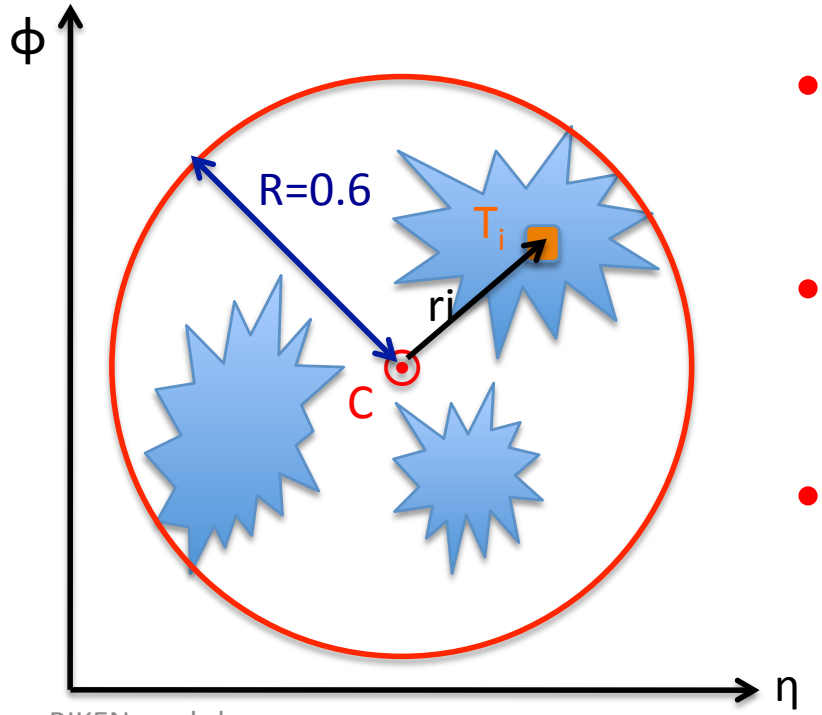

- Jet-like cluster pseudo-rapidity η: based on the jet-cluster center.
- Jet-like cluster polar angle ϕ: based on the jet-like cluster center.
- P_t of jet-like cluster: based on the jet-like cluster center.

Data & simulation comparison for EEMC jet-like cluster mass

- Cuts: EEMC tower threshold 600MeV. p_t^{FMS}>2.0GeV/c, 1.0GeV/c<p_t^{EEMC}<p_t^{FMS} (Data & simulation)

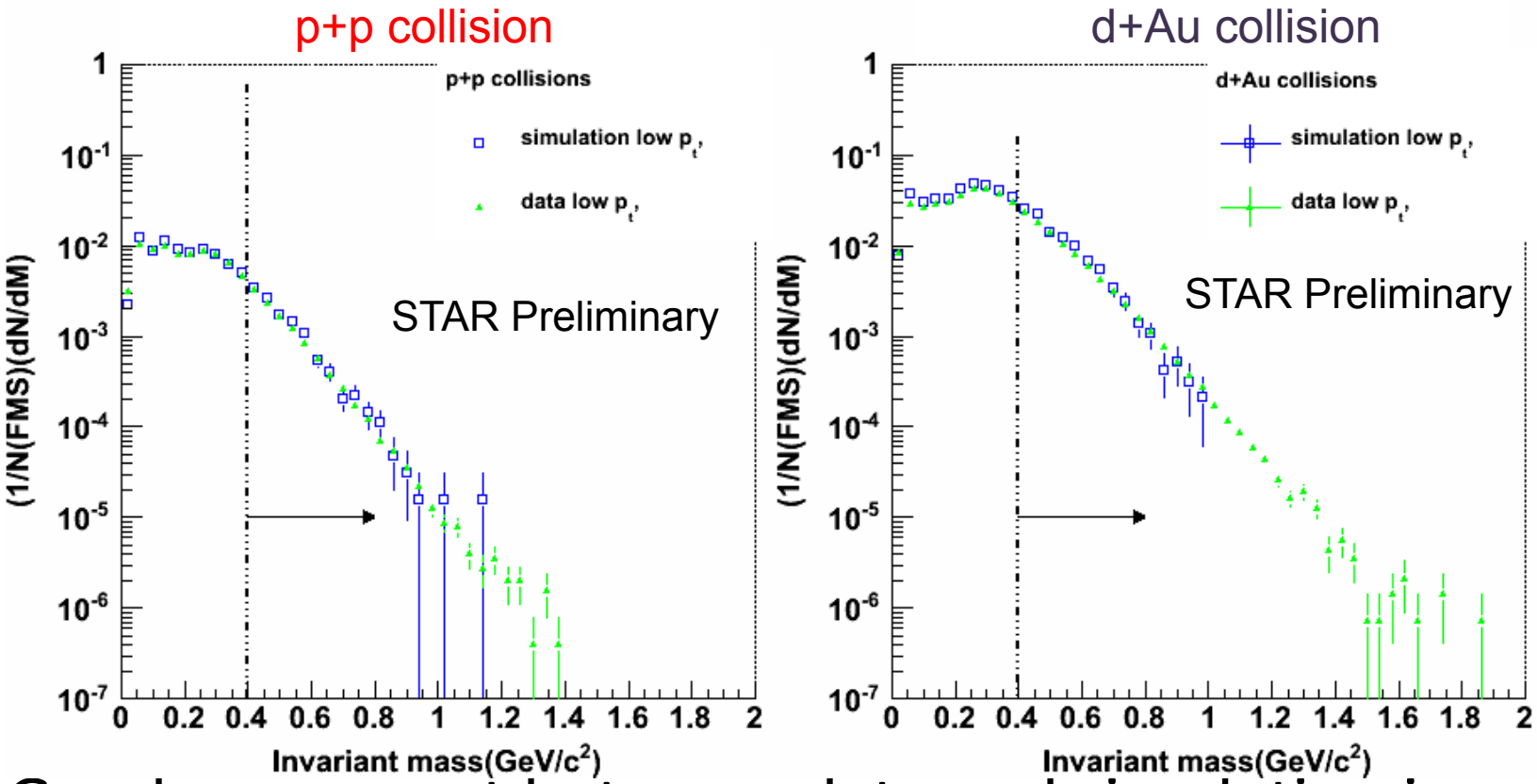

- Good agreement between data and simulation in both p+p and d+Au collisions.

Data & simulation comparison for EEMC jet-like cluster energy

- Cuts: EEMC tower threshold 600MeV. p_t^{FMS}>2.0GeV/c, 1.0GeV/c<p_t^{EEMC}<p_t^{FMS} (Data & simulation)

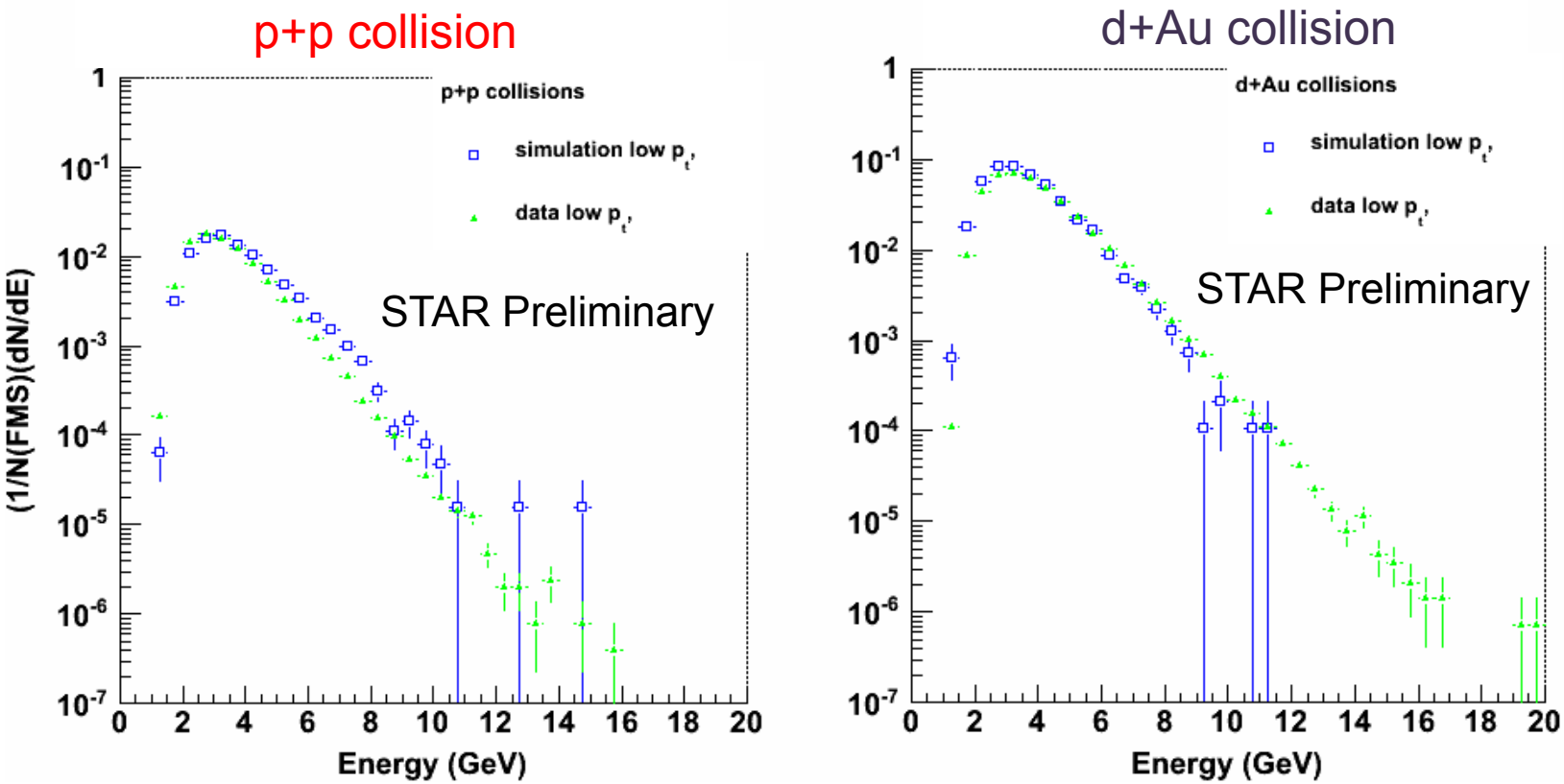

- Good agreement between data and simulation in both p+p and d+Au collisions.

FMS (π^0)-EEMC (jet-like cluster) correlations

P_T(FMS) > 2.0 GeV/c ; 1.0 GeV/c < P_T(EEMC) < P_T(FMS)

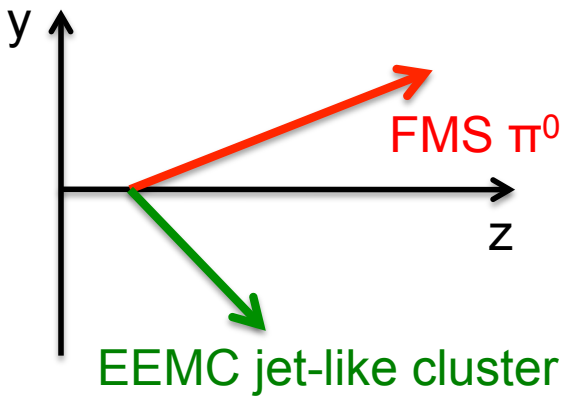

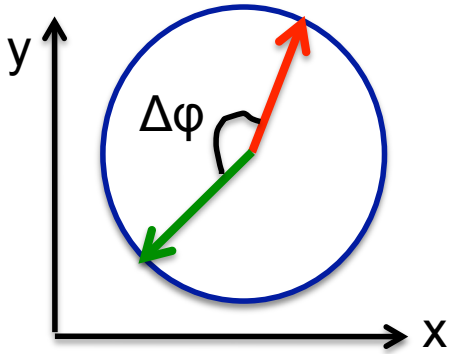

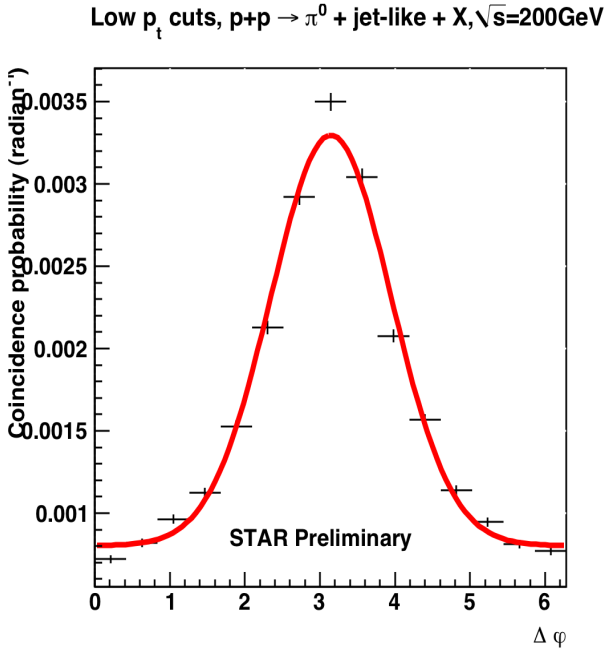

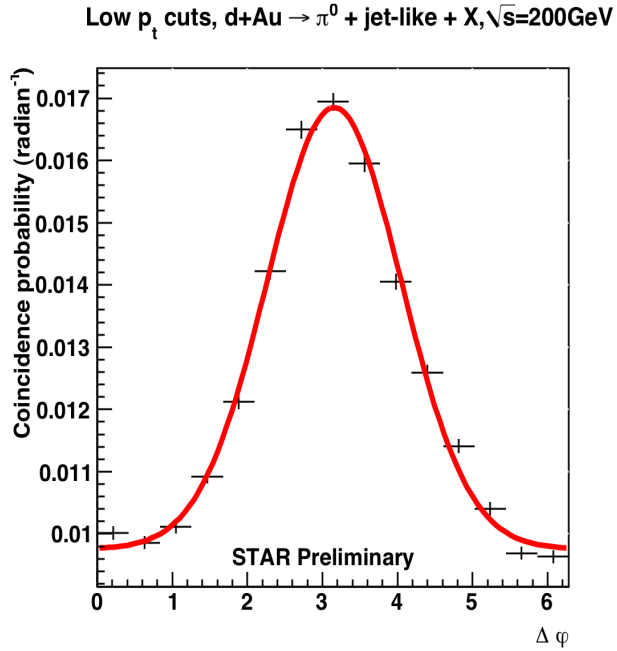

Fit function: $G(x) = b + \frac{A_1}{\sqrt{2\pi}\sigma}\exp(\frac{1}{2}(\frac{x - A_2}{\sigma})^2)$

- EEMC tower threshold 600MeV, EEMC jet-like cluster M>0.4GeV/c^2.
- σ_{pp} = 0.7978 ± 0.0120, σ_{dAu}= 0.8935± 0.0157
- b_{pp}= 0.00080 and b_{dAu}= 0.00970

- σ_{dAu}-σ_{pp} = 0.0957 ± 0.0200. There is significant broadening from p+p to d+Au collisions for the correlation peak width.

Theory predictions on the pedestal

- From leading twist to double parton scattering.

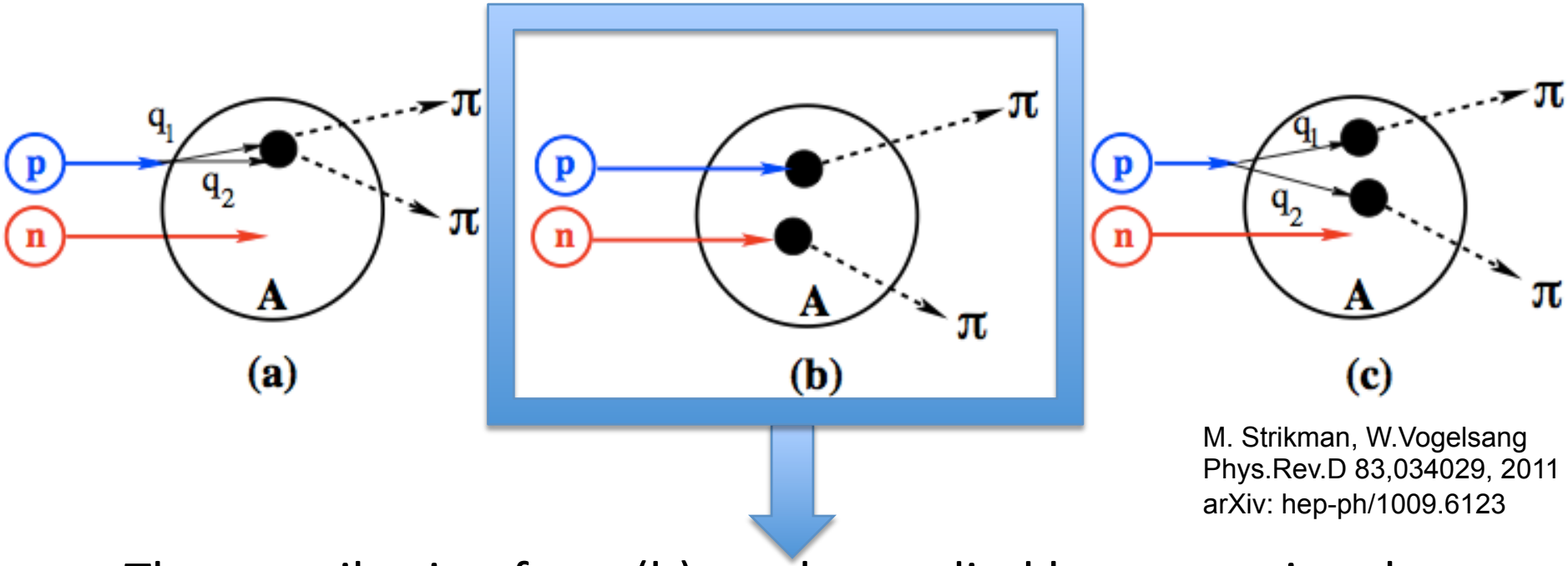

M. Strikman, W.Vogelsang
Phys.Rev.D 83,034029, 2011
arXiv: hep-ph/1009.6123

- The contribution from (b) can be studied by comparing the pedestal (uncorrelated part) of the correlations in d+Au and p +Au collisions.
- A deuteron beam facing neutron tag is used in d+Au collisions as a p+Au approach.

Tagging Spectator Neutrons from Deuteron Beam

- It may also be useful to distinguish between p+Au and d+Au collisions by looking for events where the neutron in the deuteron remains intact

Deuteron-facing (West) ZDC Response

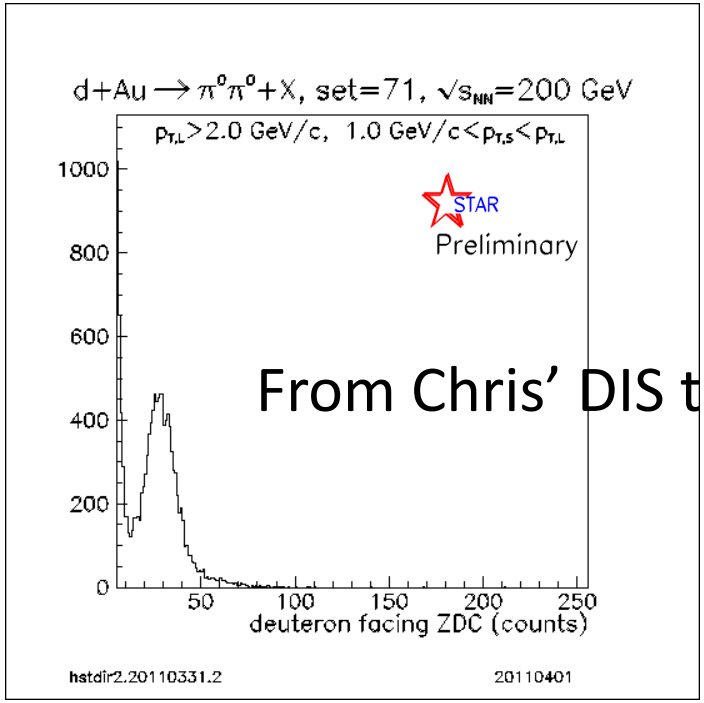

From Chris' DIS talk

Gold-facing (East) BBC Charge Sum

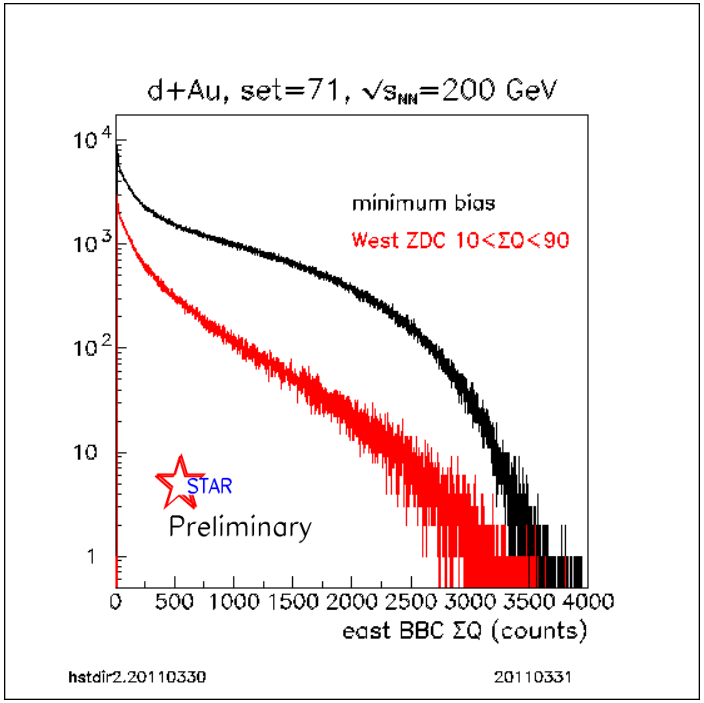

- Minimum Bias Run 8 d+Au Data
- Tag spectator neutrons using deuteron-facing (West) ZDC
- Clear single-neutron peak
- Cutting on single-neutron peak biases towards peripheral collisions

What has been done in FMS-FMS correlations

- FMS-FMS π^0-π^0 correlations.

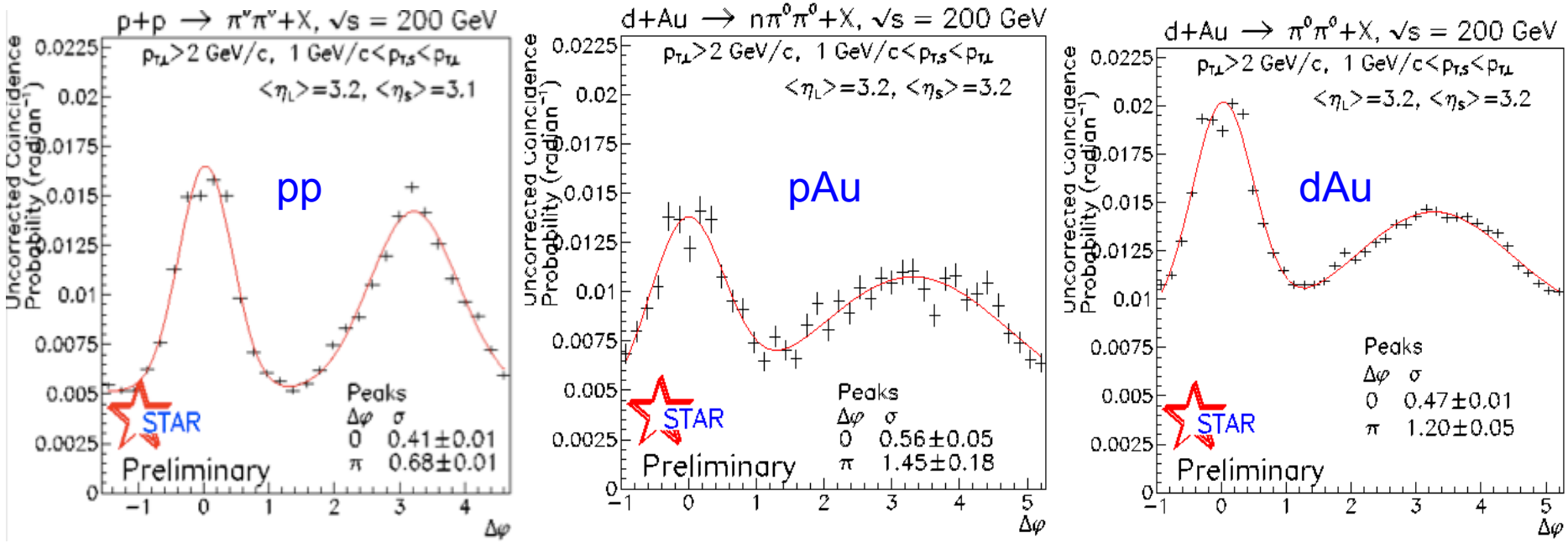

ArXiv:1109.0649

- Multi-parton interactions appear to contribute to the pedestal in d+Au collisions but less significantly to p+Au collisions.

ZDC west neutron tag in deuteron beam

- dAu FMS π^0 and EEMC jet-like coincidence.

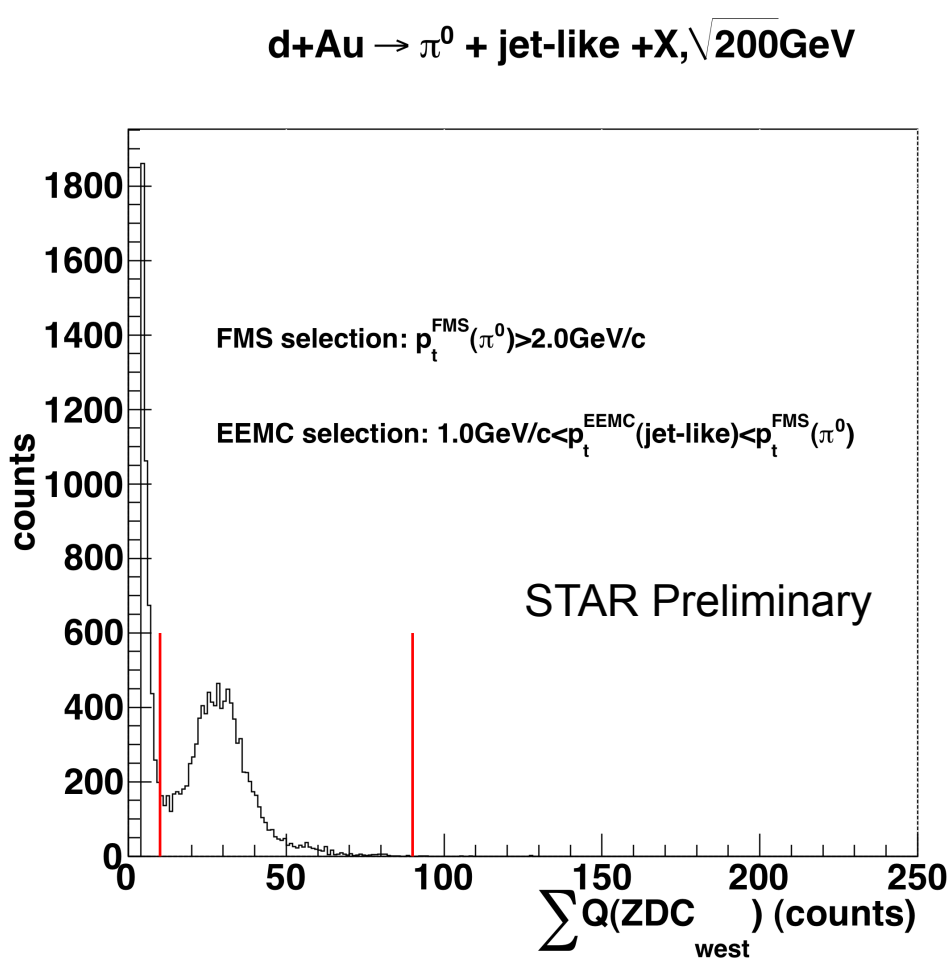

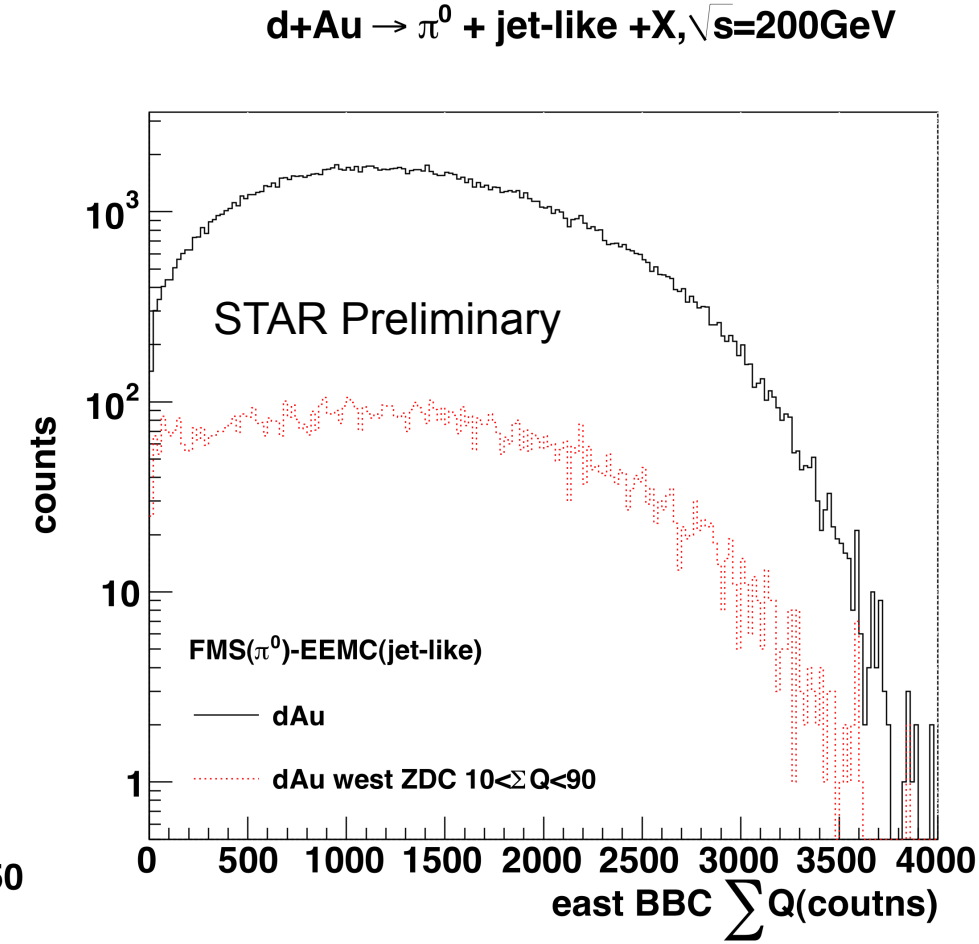

The ZDC west charge sum in forward π^0 triggered dAu looks similar like forward-forward data.

FMS-EEMC correlations in p+Au approach

- The coincidence probability of azimuthal correlation.
- P_t^{FMS}>2.0GeV/c and 1.0GeV/c<p_t^{EEMC}<p_t^{FMS} (M^{EEMC}>0.4GeV/c^2)

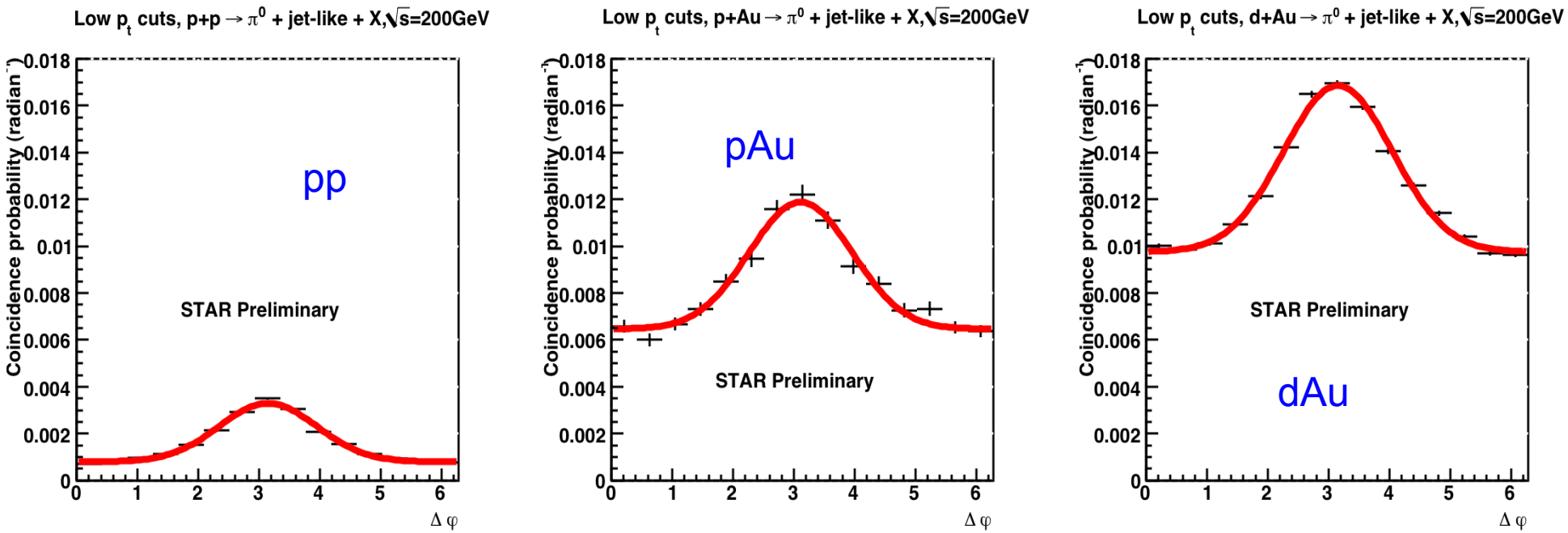

- The p+Au approach only impacts on the pedestal, the other qualities like the width of the correlation peak are analogous like in d+Au collisions.
- The independent double parton scattering contributes to FMS π^0 + EEMC jet-like cluster correlations in d+Au collisions as well.

Summary

- Forward studies at RHIC provide opportunities to explore the initial state of the proton and the nuclei.
- Comparison of p+Au to d+Au suggest independent double parton scattering is present in d+Au, affecting only the azimuthal correlation pedestal.
- The rapidity dependences of the correlations suggest a smooth transition process from dilute parton gas to dense CGC state.

Outlook of nucleus gluon saturation study

The final state π^0s or jet-like clusters are complex objects that can include not only color interactions from initial states but also from final states.

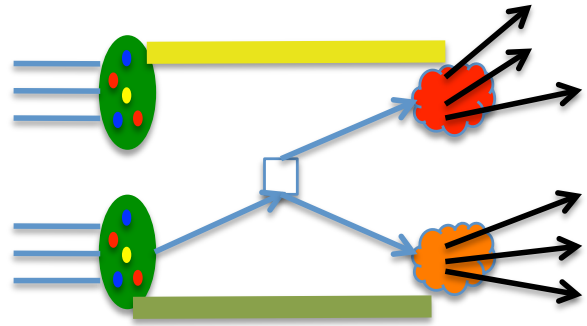

- A Electron Ion Collider (EIC)?

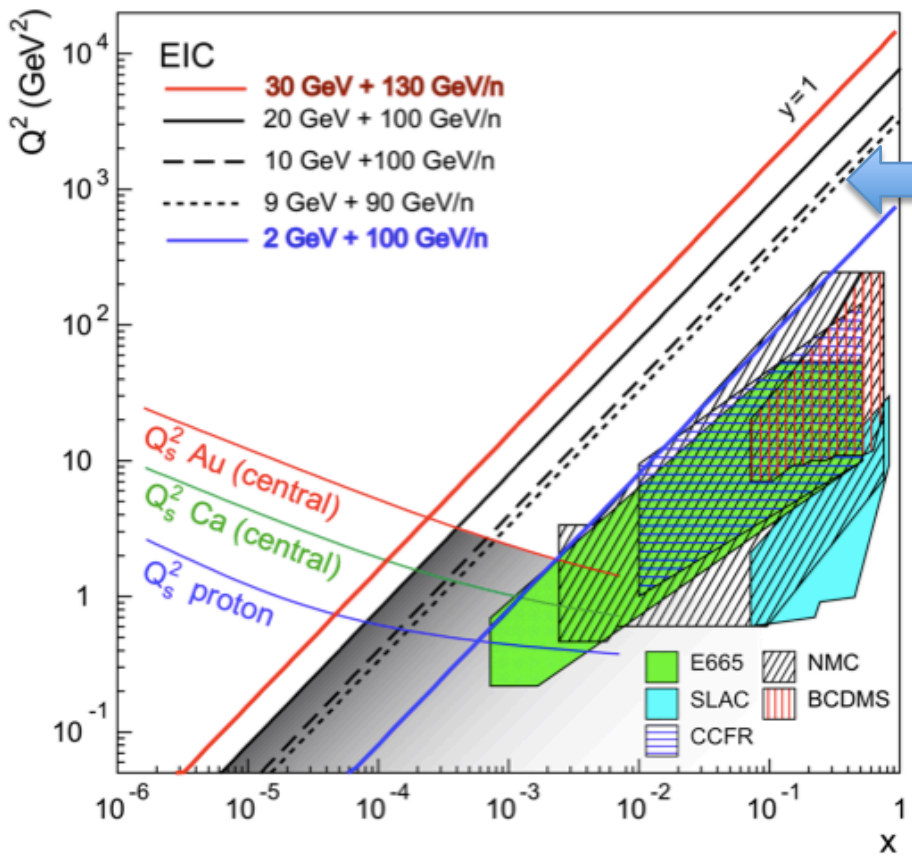

- Go to lower x than fixed target experiment.
- DIS process is much cleaner than the hadron-hadron interaction.

Transverse Single Spin Asymmetries in Proton-Nucleus collisions

Jianwei Qiu

Brookhaven National Laboratory

Based on works done with Arbat, Collins, Kang, Rogers, Vitev, Sterman, Zhang, …

RBRC Workshop on "Forward Physics at RHIC (2012)"
Riken/BNL Research Center, BNL, July 30 – August 1, 2012

Outline

- ❑ Transverse single spin asymmetry (SSA)
- ❑ Do we understand it?
  - ✧ TMD factorization
  - ✧ Collinear factorization
- ❑ SSA of single hadron production in hadronic collisions
- ❑ SSA in the forward region of pA collisions
- ❑ Summary

Transverse single-spin asymmetry (SSA)

❑ Consistently observed for over 35 years!

ANL – 4.9 GeV | BNL – 6.6 GeV | FNAL – 20 GeV | BNL – 62.4 GeV

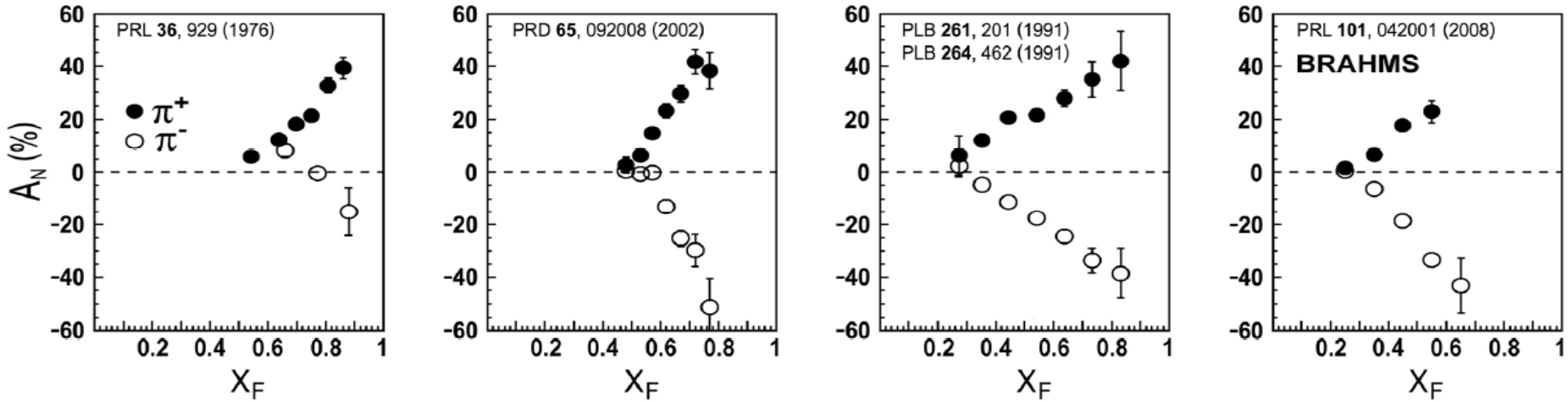

❑ Definition:

$$p(\vec{s}_\perp) + p \to h(\pi^\pm, \pi^0, ...) + X$$

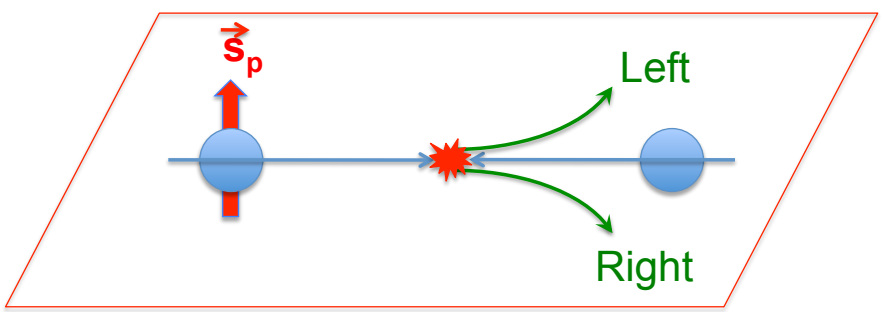

$$A_N \equiv \frac{\Delta\sigma(\ell, \vec{s})}{\sigma(\ell)} = \frac{\sigma(\ell, \vec{s}) - \sigma(\ell, -\vec{s})}{\sigma(\ell, \vec{s}) + \sigma(\ell, -\vec{s})}$$

BNL – 200 GeV

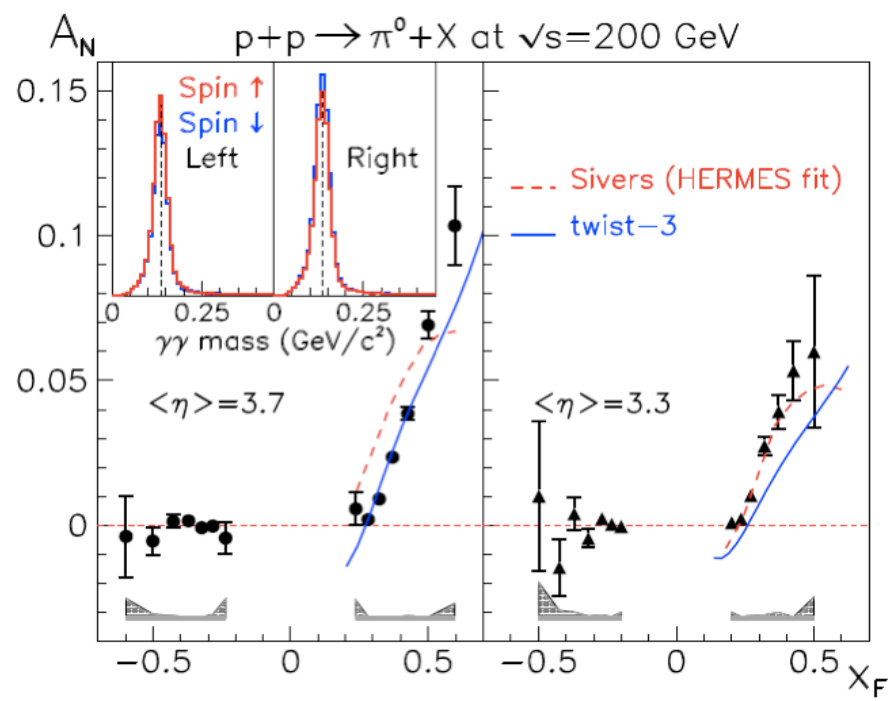

Do we understand it?

Kane, Pumplin, Repko, PRL, 1978

❑ Early attempt:

Cross section: $\sigma_{AB}(p_T, \vec{s}) \propto$

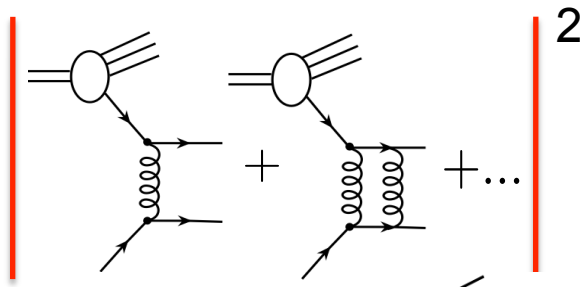

Asymmetry: $\sigma_{AB}(p_T, \vec{s}) - \sigma_{AB}(p_T, -\vec{s}) =$

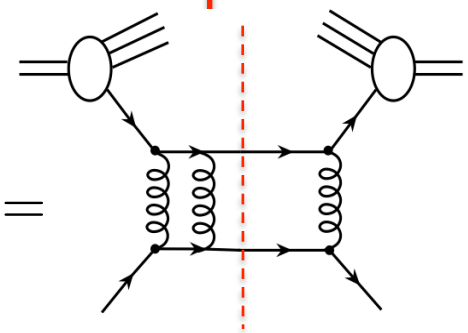

$\propto \alpha_s \dfrac{m_q}{p_T}$

Too small to explain available data!

❑ What do we need?

$$A_N \propto i\vec{s}_p \cdot (\vec{p}_h \times \vec{p}_T) \Rightarrow i\epsilon^{\mu\nu\alpha\beta} p_{h\mu} s_\nu p_\alpha p'_{h\beta}$$

Need a phase, a spin flip, enough vectors

❑ Vanish without parton's transverse motion:

➡ **A direct probe for parton's transverse motion,**

Spin-orbital correlation, QCD quantum interference

Current understanding of SSAs

- Two scales observables – $Q_1 >> Q_2 \sim \Lambda_{QCD}$:

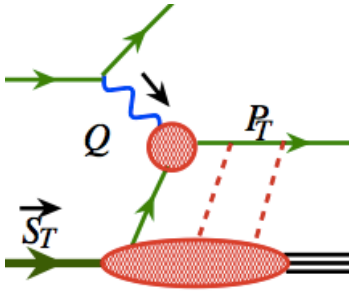

SIDIS: $Q >> P_T$

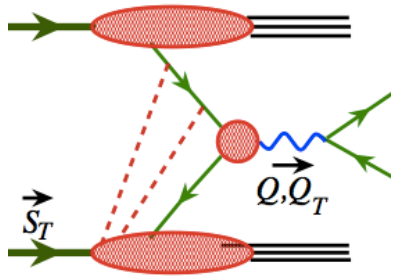

DY: $Q >> Q_T$

→ TMD factorization
TMD distributions

Talks by Mulders, Yuan, …

- One scale observables – $Q >> \Lambda_{QCD}$:

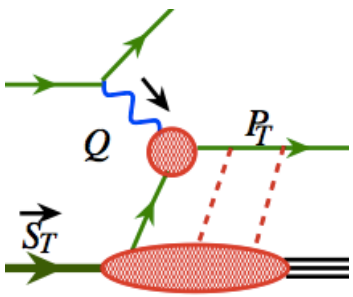

SIDIS: $Q \sim P_T$

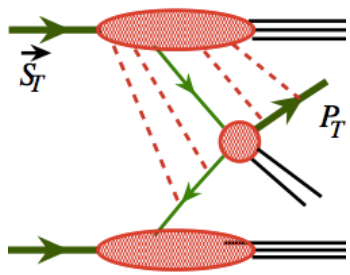

Jet, Particle: P_T

→ Collinear factorization
Twist-3 distributions

- Symmetry plays important role:

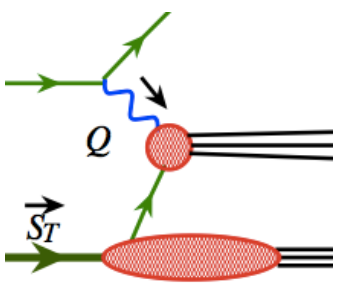

Inclusive DIS
Single scale
Q

Parity
Time-reversal

→ $A_N = 0$

How TMDs generate spin asymmetry?

❑ Sivers' effect – Sivers' function:

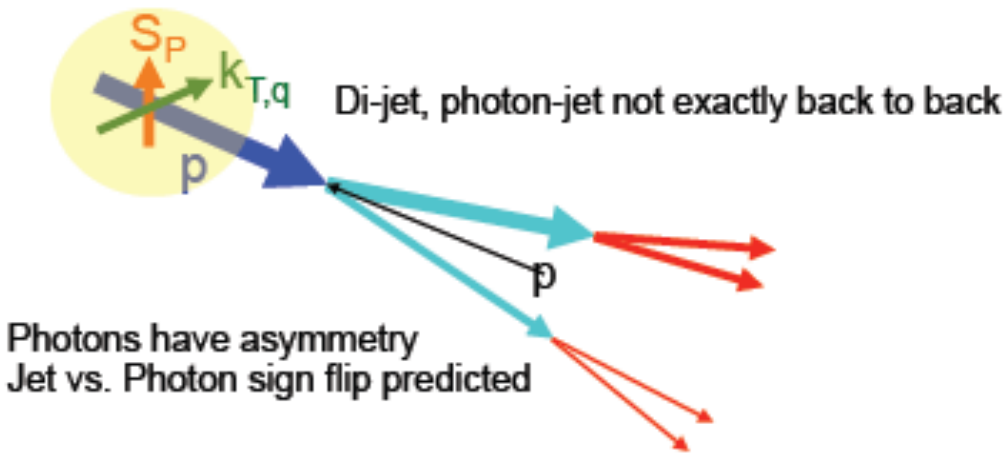

Hadron spin influences parton's transverse motion

❑ Collin's effect – Collin's function:

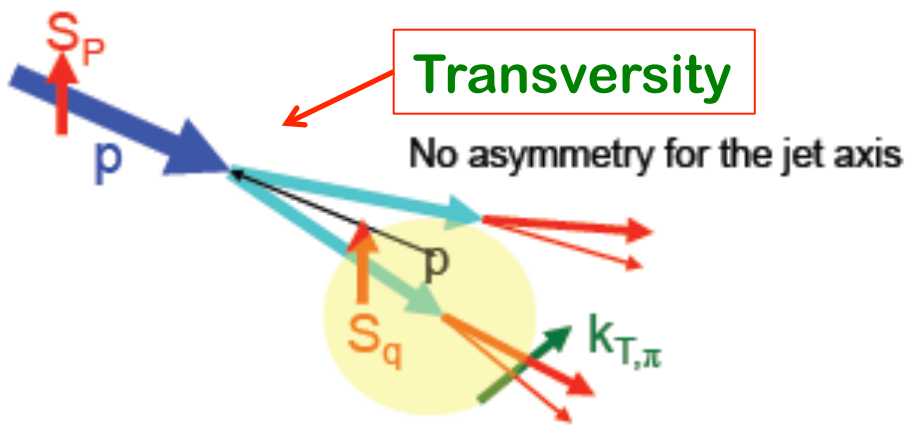

Parton's transverse spin affects its hadronization

❑ Separation of different effects?

Best in SIDIS, at EIC

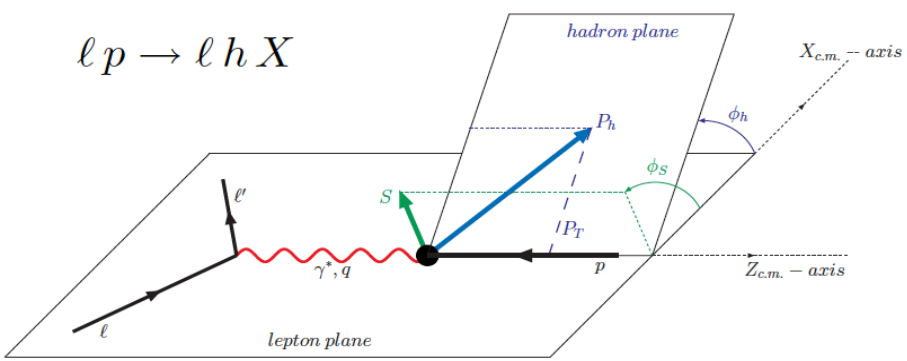

Our knowledge of TMDs

- Sivers function from low energy SIDIS:

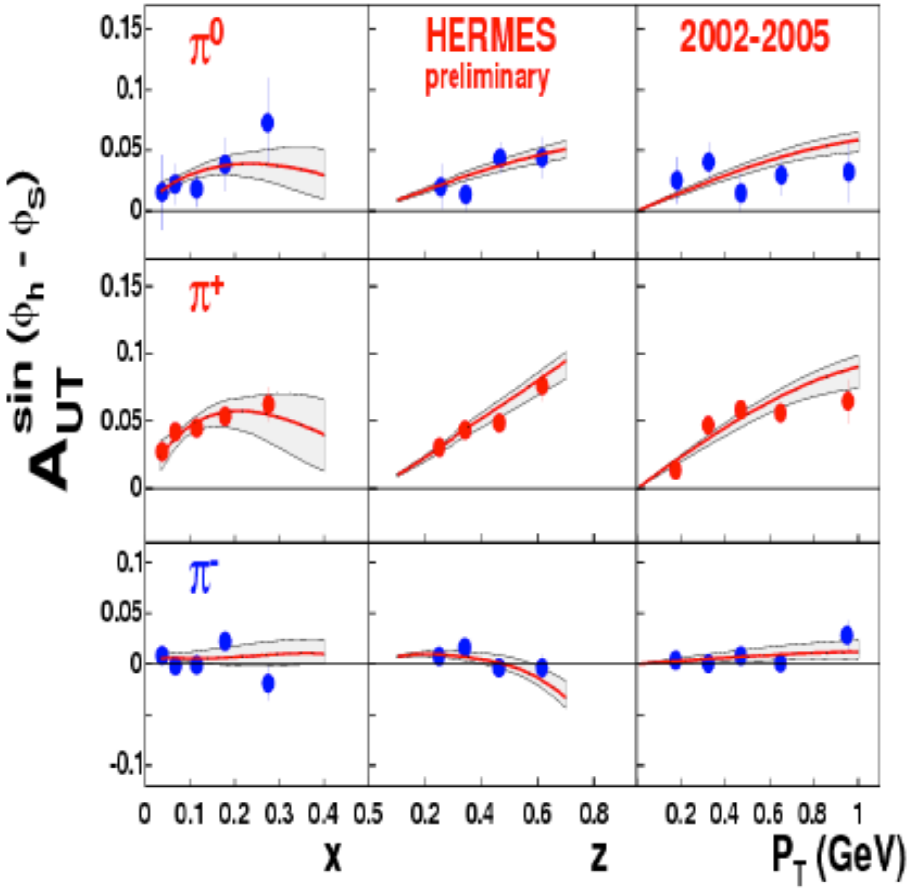

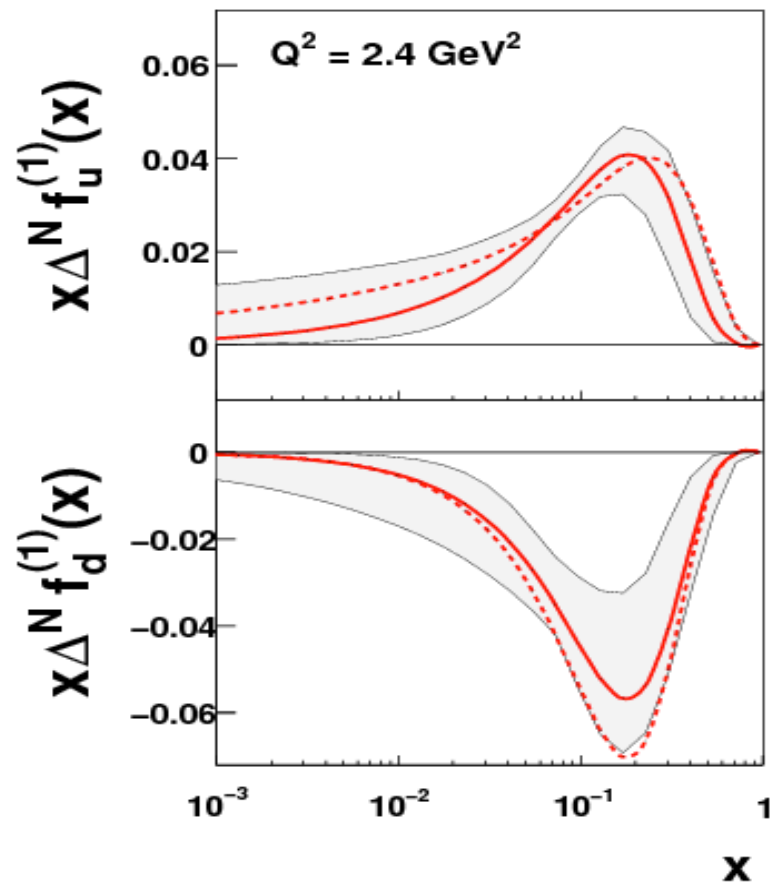

EIC can do much better job in extracting TMDs

- NO TMD factorization for hadron production in p+p collisions!

Collins and Qiu, 2007, Vogelsang and Yuan, 2007, Mulders and Rogers, 2010, …

Critical test of TMD factorization

❑ TMD distributions with non-local gauge links:

$$f_{q/h^\uparrow}(x,\mathbf{k}_\perp,\vec{S}) = \int \frac{dy^- d^2y_\perp}{(2\pi)^3} e^{ixp^+y^- - i\mathbf{k}_\perp\cdot\mathbf{y}_\perp} \langle p,\vec{S}|\overline{\psi}(0^-,\mathbf{0}_\perp)\,\boxed{\text{Gauge link}}\,\frac{\gamma^+}{2}\psi(y^-,\mathbf{y}_\perp)|p,\vec{S}\rangle$$

SIDIS:

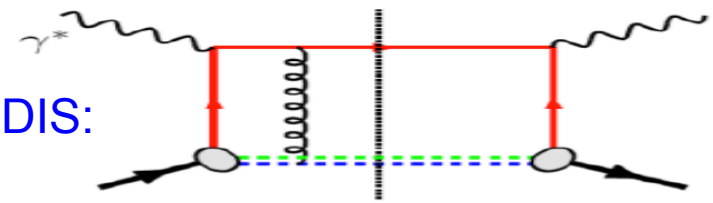

DY:

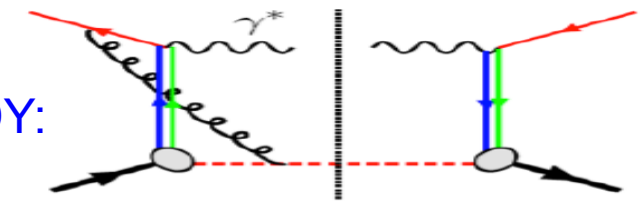

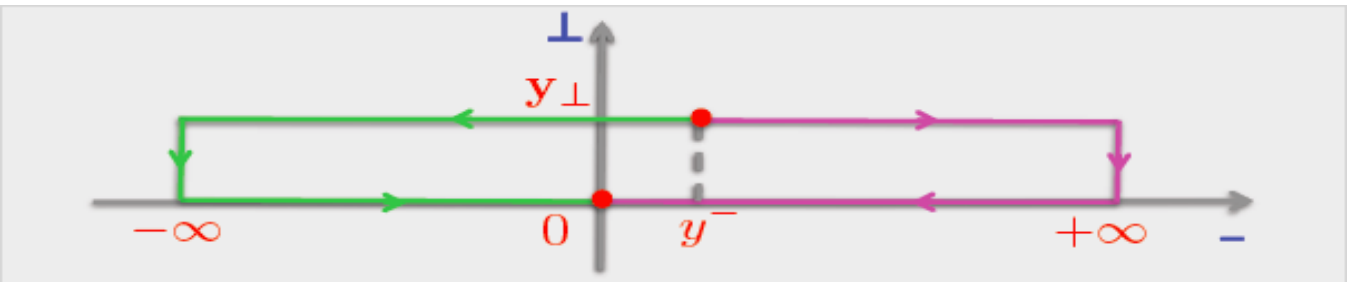

- For a fixed spin state:

$$f^{\text{SIDIS}}_{q/h^\uparrow}(x,\mathbf{k}_\perp,\vec{S}) \neq f^{\text{DY}}_{q/h^\uparrow}(x,\mathbf{k}_\perp,\vec{S})$$

❑ Parity + Time-reversal invariance:

$$\Rightarrow \quad f^{\text{Sivers}}_{q/h^\uparrow}(x,k_\perp)^{\text{SIDIS}} = -f^{\text{Sivers}}_{q/h^\uparrow}(x,k_\perp)^{\text{DY}}$$

The sign change is a critical test of TMD factorization approach

Another critical test of TMD factorization

❑ Predictive power of QCD factorization:

- ✧ Infrared safety of short-distance hard parts
- ✧ Universality of the long-distance matrix elements
- ✧ QCD evolution or scale dependence of the matrix elements

❑ QCD evolution:

If there is a factorization/invariance, there is an evolution equation

❑ Collinear factorization – DGLAP evolution:

$$\sigma_{\rm phy}(Q,\Lambda_{\rm QCD}) \approx \sum_f \hat{\sigma}_f(Q,\mu) \otimes \phi_f(\mu,\Lambda_{\rm QCD}) \quad \rightarrow \quad \frac{d}{d\mu}\sigma_{\rm phy}(Q,\Lambda_{\rm QCD}) = 0$$

Scaling violation of nonperturbative functions

Evolution kernels are perturbative – a test of QCD

Evolution equations for TMDs

Boer, 2001, 2009, Idilbi, et al, 2004
Aybat, Rogers, 2010
Kang, Xiao, Yuan, 2011
Aybat, Collins, Qiu, Rogers, 2011

❑ Collins-Soper equation:

– b-space quark TMD with γ^+

$$\frac{\partial \tilde{F}_{f/P^\uparrow}(x, \mathbf{b}_\mathrm{T}, S; \mu; \zeta_F)}{\partial \ln \sqrt{\zeta_F}} = \tilde{K}(b_T; \mu) \tilde{F}_{f/P^\uparrow}(x, \mathbf{b}_\mathrm{T}, S; \mu; \zeta_F) \qquad \tilde{K}(b_T; \mu) = \frac{1}{2} \frac{\partial}{\partial y_s} \ln \left(\frac{\tilde{S}(b_T; y_s, -\infty)}{\tilde{S}(b_T; +\infty, y_s)} \right)$$

❑ RG equations:

$$\frac{d\tilde{K}(b_T; \mu)}{d \ln \mu} = -\gamma_K(g(\mu)) \qquad \frac{d\tilde{F}_{f/P^\uparrow}(x, \mathbf{b}_\mathrm{T}, S; \mu; \zeta_F)}{d \ln \mu} = \gamma_F(g(\mu); \zeta_F/\mu^2) \tilde{F}_{f/P^\uparrow}(x, \mathbf{b}_\mathrm{T}, S; \mu; \zeta_F).$$

❑ Evolution equations for Sivers function:

$$F_{f/P^\uparrow}(x, k_T, S; \mu, \zeta_F) = F_{f/P}(x, k_T; \mu, \zeta_F) - F_{1T}^{\perp f}(x, k_T; \mu, \zeta_F) \frac{\epsilon_{ij} k_T^i S^j}{M_p}$$

CS: $$\frac{\partial \ln \tilde{F}_{1T}'^{\perp f}(x, b_T; \mu, \zeta_F)}{\partial \ln \sqrt{\zeta_F}} = \tilde{K}(b_T; \mu) \qquad \tilde{F}_{1T}'^{\perp f}(x, b_T; \mu, \zeta_F) \equiv \frac{\partial \tilde{F}_{1T}^{\perp f}(x, b_T; \mu, \zeta_F)}{\partial b_T}$$

RGs: $$\frac{d\tilde{F}_{1T}'^{\perp f}(x, b_T; \mu, \zeta_F)}{d \ln \mu} = \gamma_F(g(\mu); \zeta_F/\mu^2) \tilde{F}_{1T}'^{\perp f}(x, b_T; \mu, \zeta_F)$$

$$\frac{d\tilde{K}(b_T; \mu)}{d \ln \mu} = -\gamma_K(g(\mu)) \quad \Rightarrow \quad \frac{\partial \gamma_F(g(\mu); \zeta_F/\mu^2)}{\partial \ln \sqrt{\zeta_F}} = -\gamma_K(g(\mu)),$$

Scale dependence of Sivers function

Aybat, Collins, Qiu, Rogers, 2011

- Up quark Sivers function:

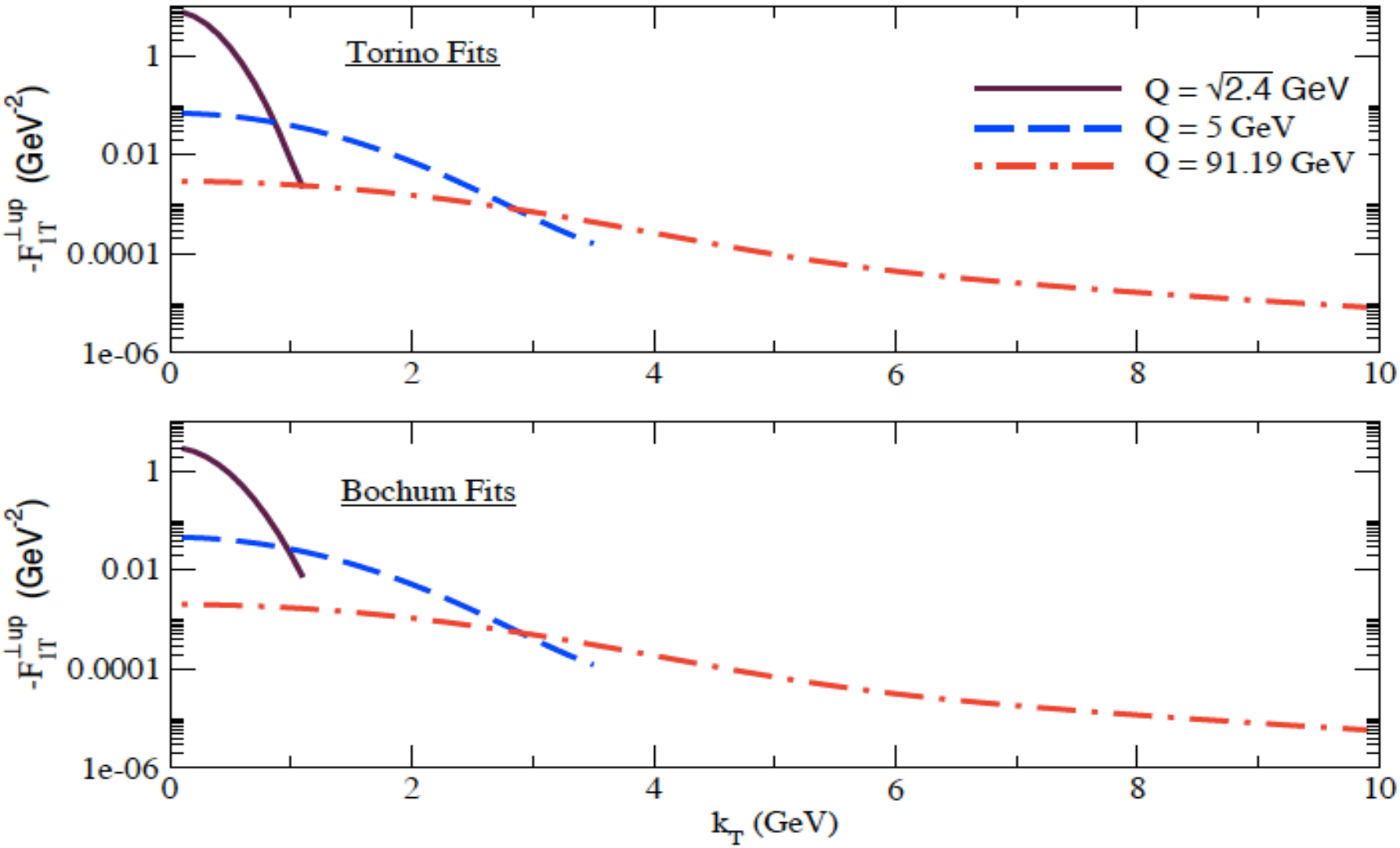

Very significant growth in the width of transverse momentum

Importance of the evolution

Aybat, Rogers, 2012

- SSAs – Sivers function:

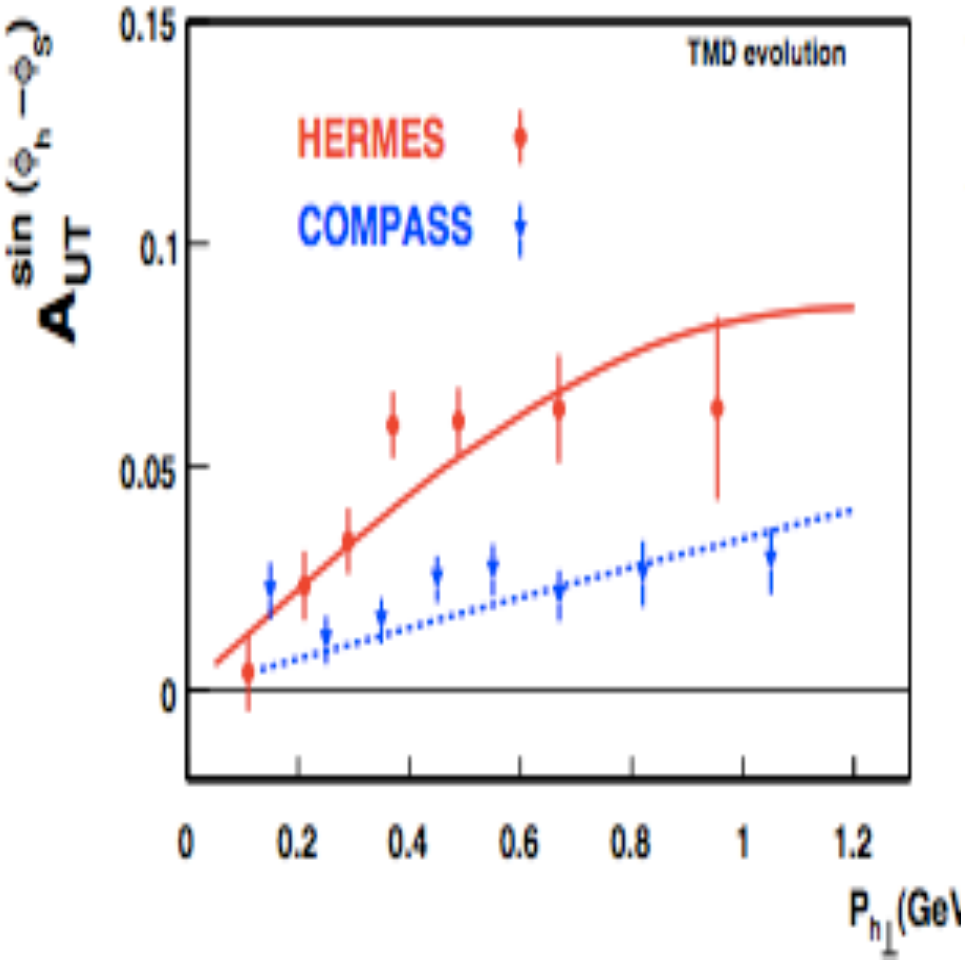

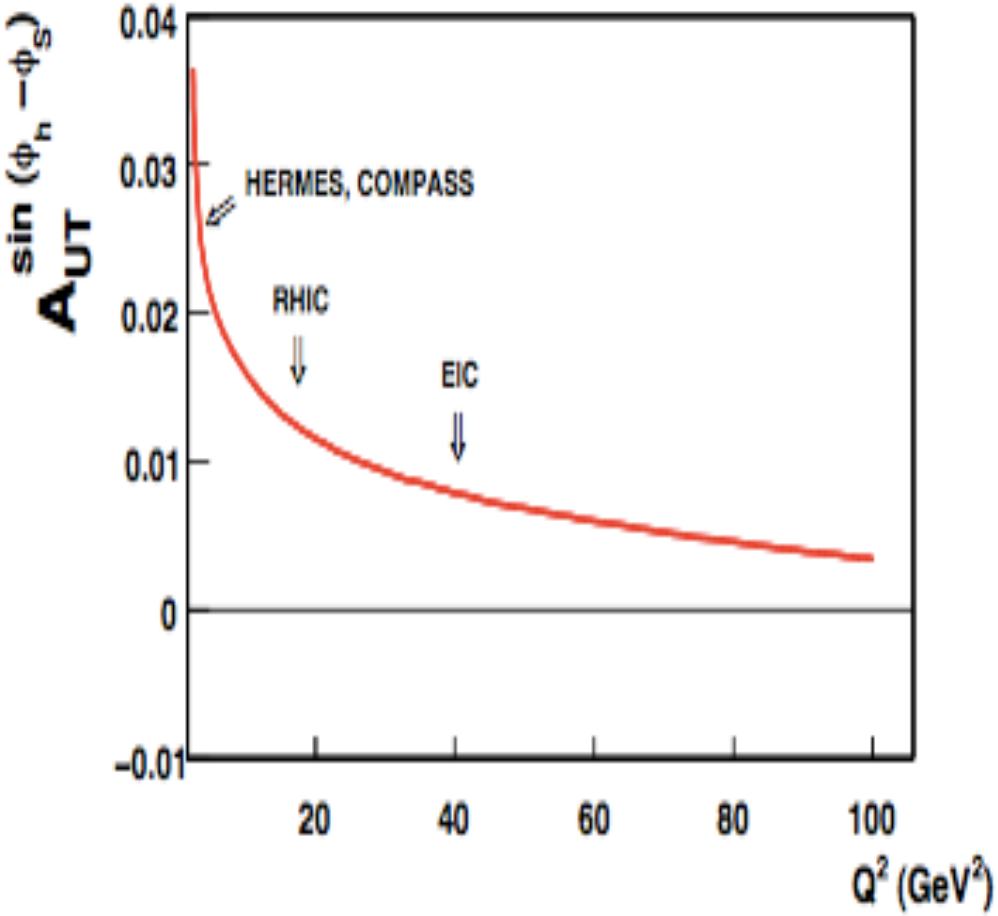

Q^2 dependence – effectiveness of the probe?

How collinear factorization generates SSA?

❑ Collinear factorization beyond leading power:

$\sigma(Q,\vec{s}) \propto$ 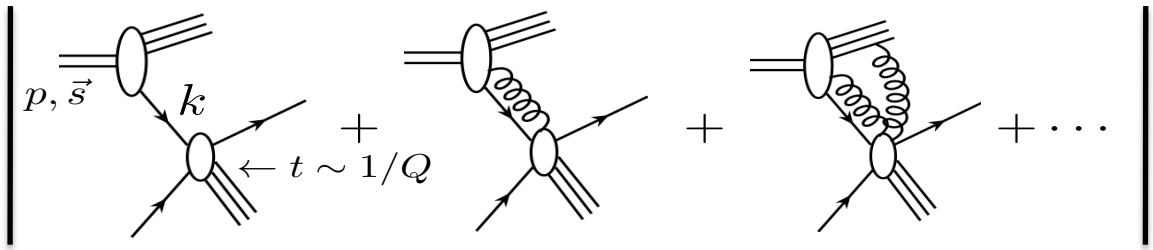

$^2 \left(\frac{\langle k_\perp \rangle}{Q}\right)^n$ – Expansion

$$\sigma(Q, s_T) = H_0 \otimes f_2 \otimes f_2 + (1/Q)\, H_1 \otimes f_2 \otimes f_3 + \mathcal{O}(1/Q^2)$$

Too large to compete!

Three-parton correlation

❑ Single transverse spin asymmetry:

Efremov, Teryaev, 82;
Qiu, Sterman, 91, etc.

$$\Delta\sigma(s_T) \propto T^{(3)}(x,x) \otimes \hat{\sigma}_T \otimes D(z) + \delta q(x) \otimes \hat{\sigma}_D \otimes D^{(3)}(z,z) + \ldots$$

$T^{(3)}(x,x) \propto$ 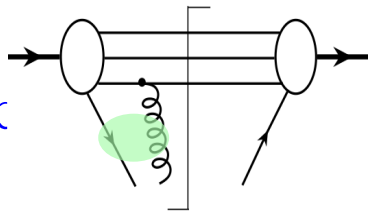

Qiu, Sterman, 1991, …

$D^{(3)}(z,z) \propto$ 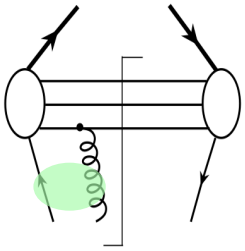

Kang, Yuan, Zhou, 2010

$T^{(3\sigma)}(x,x) \propto$ 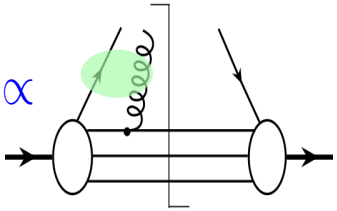

Kanazawa, Koike, 2000

Integrated information on parton's transverse motion!

Twist-3 distributions relevant to A_N

❑ Two-sets Twist-3 correlation functions:

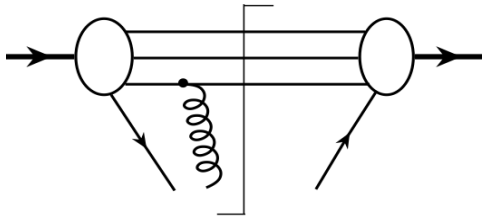

No probability interpretation!

$$\widetilde{\mathcal{T}}_{q,F} = \int \frac{dy_1^- dy_2^-}{(2\pi)^2} e^{ixP^+y_1^-} e^{ix_2P^+y_2^-} \langle P, s_T|\overline{\psi}_q(0)\frac{\gamma^+}{2}\left[\epsilon^{s_T\sigma n\bar{n}}F_\sigma{}^+(y_2^-)\right]\psi_q(y_1^-)|P, s_T\rangle$$

Kang, Qiu, 2009

$$\widetilde{\mathcal{T}}^{(f,d)}_{G,F} = \int \frac{dy_1^- dy_2^-}{(2\pi)^2} e^{ixP^+y_1^-} e^{ix_2P^+y_2^-} \frac{1}{P^+}\langle P, s_T|F^{+\rho}(0)\left[\epsilon^{s_T\sigma n\bar{n}}F_\sigma{}^+(y_2^-)\right]F^{+\lambda}(y_1^-)|P, s_T\rangle(-g_{\rho\lambda})$$

$$\widetilde{\mathcal{T}}_{\Delta q,F} = \int \frac{dy_1^- dy_2^-}{(2\pi)^2} e^{ixP^+y_1^-} e^{ix_2P^+y_2^-} \langle P, s_T|\overline{\psi}_q(0)\frac{\gamma^+\gamma^5}{2}\left[i\, s_T^\sigma\, F_\sigma{}^+(y_2^-)\right]\psi_q(y_1^-)|P, s_T\rangle$$

$$\widetilde{\mathcal{T}}^{(f,d)}_{\Delta G,F} = \int \frac{dy_1^- dy_2^-}{(2\pi)^2} e^{ixP^+y_1^-} e^{ix_2P^+y_2^-} \frac{1}{P^+}\langle P, s_T|F^{+\rho}(0)\left[i\, s_T^\sigma\, F_\sigma{}^+(y_2^-)\right]F^{+\lambda}(y_1^-)|P, s_T\rangle\,(i\epsilon_{\perp\rho\lambda})$$

Role of color magnetic force!

❑ Twist-2 distributions:

- Unpolarized PDFs:

$$q(x) \propto \langle P|\overline{\psi}_q(0)\frac{\gamma^+}{2}\psi_q(y)|P\rangle$$
$$G(x) \propto \langle P|F^{+\mu}(0)F^{+\nu}(y)|P\rangle(-g_{\mu\nu})$$

- Polarized PDFs:

$$\Delta q(x) \propto \langle P, S_\parallel|\overline{\psi}_q(0)\frac{\gamma^+\gamma^5}{2}\psi_q(y)|P, S_\parallel\rangle$$
$$\Delta G(x) \propto \langle P, S_\parallel|F^{+\mu}(0)F^{+\nu}(y)|P, S_\parallel\rangle(i\epsilon_{\perp\mu\nu})$$

❑ Twist-3 fragmentation functions:

See Kang, Yuan, Zhou, 2010, Kang 2010

Test QCD at twist-3 level

❑ Scaling violation – "DGLAP" evolution:

Kang, Qiu, 2009; Yuan, Zhou, 2009
Vogelsang, Yuan, 2009, Braun et al, 2009

$$\mu_F^2 \frac{\partial}{\partial \mu_F^2} \begin{pmatrix} \widetilde{\mathcal{T}}_{q,F} \\ \widetilde{\mathcal{T}}_{\Delta q,F} \\ \widetilde{\mathcal{T}}^{(f)}_{G,F} \\ \widetilde{\mathcal{T}}^{(d)}_{G,F} \\ \widetilde{\mathcal{T}}^{(f)}_{\Delta G,F} \\ \widetilde{\mathcal{T}}^{(d)}_{\Delta G,F} \end{pmatrix} = \begin{pmatrix} K_{qq} & K_{q\Delta q} & K^{(f)}_{qG} & K^{(d)}_{qG} & K^{(f)}_{q\Delta G} & K^{(d)}_{q\Delta G} \\ K_{\Delta qq} & K_{\Delta q\Delta q} & K^{(f)}_{\Delta qG} & K^{(d)}_{\Delta qG} & K^{(f)}_{\Delta q\Delta G} & K^{(d)}_{\Delta q\Delta G} \\ K^{(f)}_{Gq} & K^{(f)}_{G\Delta q} & K^{(ff)}_{GG} & K^{(fd)}_{GG} & K^{(ff)}_{G\Delta G} & K^{(fd)}_{G\Delta G} \\ K^{(d)}_{Gq} & K^{(d)}_{G\Delta q} & K^{(df)}_{GG} & K^{(dd)}_{GG} & K^{(df)}_{G\Delta G} & K^{(dd)}_{G\Delta G} \\ K^{(f)}_{\Delta Gq} & K^{(f)}_{\Delta G\Delta q} & K^{(ff)}_{\Delta GG} & K^{(fd)}_{\Delta GG} & K^{(ff)}_{\Delta G\Delta G} & K^{(fd)}_{\Delta G\Delta G} \\ K^{(d)}_{\Delta Gq} & K^{(d)}_{\Delta G\Delta q} & K^{(df)}_{\Delta GG} & K^{(dd)}_{\Delta GG} & K^{(df)}_{\Delta G\Delta G} & K^{(dd)}_{\Delta G\Delta G} \end{pmatrix} \otimes \begin{pmatrix} \widetilde{\mathcal{T}}_{q,F} \\ \widetilde{\mathcal{T}}_{\Delta q,F} \\ \widetilde{\mathcal{T}}^{(f)}_{G,F} \\ \widetilde{\mathcal{T}}^{(d)}_{G,F} \\ \widetilde{\mathcal{T}}^{(f)}_{\Delta G,F} \\ \widetilde{\mathcal{T}}^{(d)}_{\Delta G,F} \end{pmatrix}$$

$$(x, x+x_2, \mu, s_T) \qquad (\xi, \xi+\xi_2; x, x+x_2, \alpha_s) \qquad \int d\xi \int d\xi_2$$

❑ Evolution equation – consequence of factorization:

Factorization: $\Delta\sigma(Q, s_T) = (1/Q) H_1(Q/\mu_F, \alpha_s) \otimes f_2(\mu_F) \otimes f_3(\mu_F)$

DGLAP for f_2: $\dfrac{\partial}{\partial \ln(\mu_F)} f_2(\mu_F) = P_2 \otimes f_2(\mu_F)$

Evolution for f_3: $\dfrac{\partial}{\partial \ln(\mu_F)} f_3 = \left(\dfrac{\partial}{\partial \ln(\mu_F)} H_1^{(1)} - P_2^{(1)} \right) \otimes f_3$

"Interpretation" of twist-3 correlation functions

❑ Measurement of direct QCD quantum interference:

Qiu, Sterman, 1991, …

$T^{(3)}(x, x, S_\perp) \;\propto$

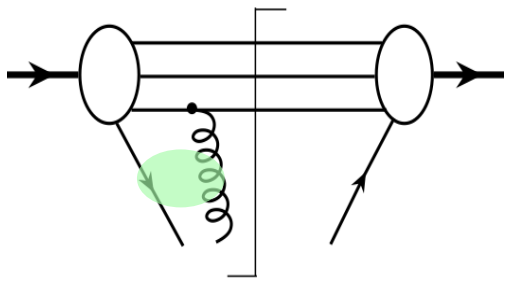

Interference between a single active parton state and an active two-parton composite state

❑ "Expectation value" of QCD operators:

$$\langle P, s|\overline{\psi}(0)\gamma^+\psi(y^-)|P, s\rangle \longrightarrow \langle P, s|\overline{\psi}(0)\gamma^+\left[\epsilon_\perp^{\alpha\beta} s_{T\alpha}\int dy_2^- F_\beta{}^+(y_2^-)\right]\psi(y^-)|P, s\rangle$$

$$\langle P, s|\overline{\psi}(0)\gamma^+\gamma_5\psi(y^-)|P, s\rangle \longrightarrow \langle P, s|\overline{\psi}(0)\gamma^+\left[i\, g_\perp^{\alpha\beta} s_{T\alpha}\int dy_2^- F_\beta{}^+(y_2^-)\right]\psi(y^-)|P, s\rangle$$

How to interpret the "expectation value" of the operators in RED?

A simple example

- The operator in Red – a classical Abelian case:

Qiu, Sterman, 1998

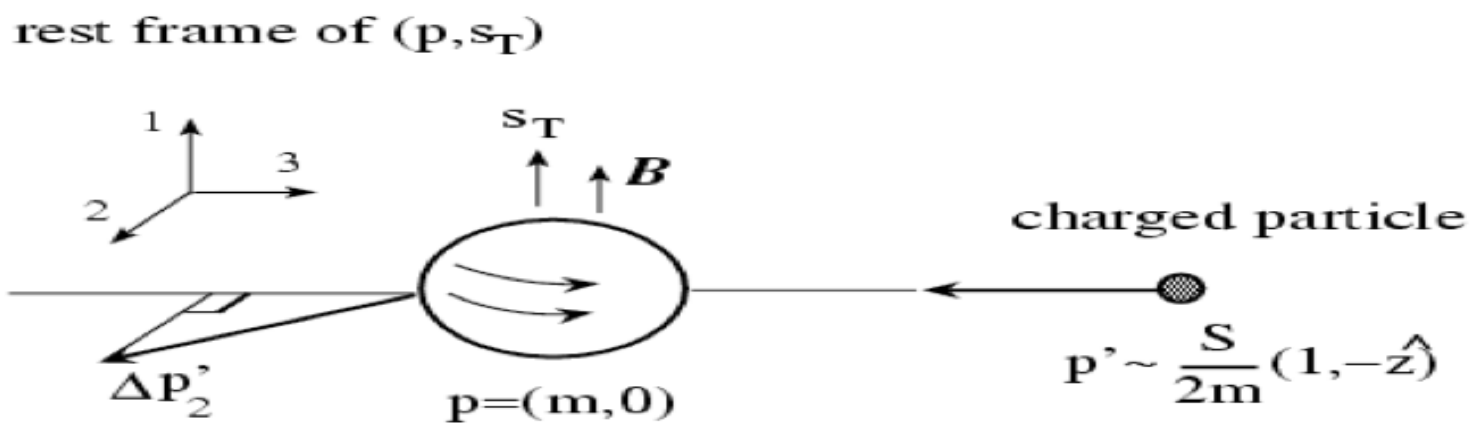

- Change of transverse momentum:

$$\frac{d}{dt}p_2' = e(\vec{v}' \times \vec{B})_2 = -ev_3B_1 = ev_3F_{23}$$

- In the c.m. frame:

$$(m,\vec{0}) \to \bar{n} = (1,0,0_T), \quad (1,-\hat{z}) \to n = (0,1,0_T)$$

$$\Longrightarrow \quad \frac{d}{dt}p_2' = e\,\epsilon^{s_T\sigma n\bar{n}}\,F_\sigma{}^+$$

- The total change:

$$\Delta p_2' = e\int dy^-\,\epsilon^{s_T\sigma n\bar{n}}\,F_\sigma{}^+(y^-)$$

Net quark transverse momentum imbalance caused by color Lorentz force inside a transversely polarized proton

Transition from low p_T to high p_T

- Two-scale becomes one-scale:

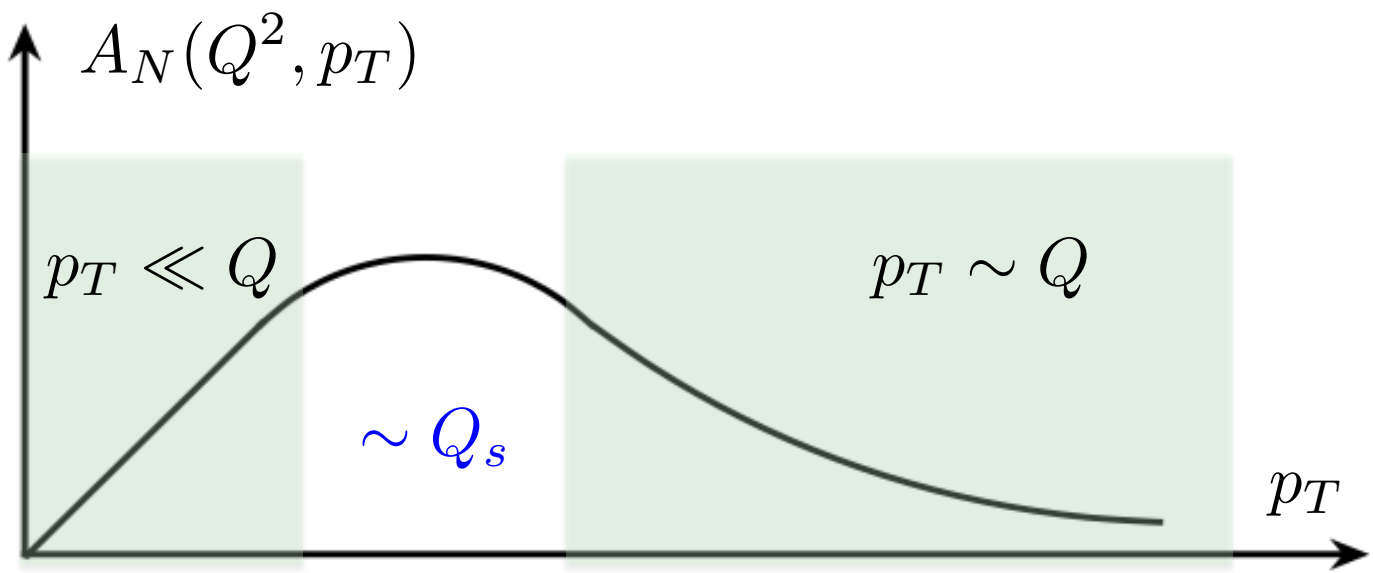

TMD Collinear Factorization

- TMD factorization to collinear factorization:

Ji,Qiu,Vogelsang,Yuan,
Koike, Vogelsang, Yuan

Two factorization are consistent in the overlap region: $\Lambda_{\rm QCD} \ll p_T \ll Q$

A_N finite – requires correlation of multiple collinear partons

No probability interpretation! New opportunities!

Single hadron production in hadronic collisions

❑ Process:

$$p(\vec{s}_\perp) + p \to h(\pi^\pm, \pi^0, ...) + X$$

$$A_N \equiv \frac{\Delta\sigma(\ell, \vec{s})}{\sigma(\ell)} = \frac{\sigma(\ell, \vec{s}) - \sigma(\ell, -\vec{s})}{\sigma(\ell, \vec{s}) + \sigma(\ell, -\vec{s})}$$

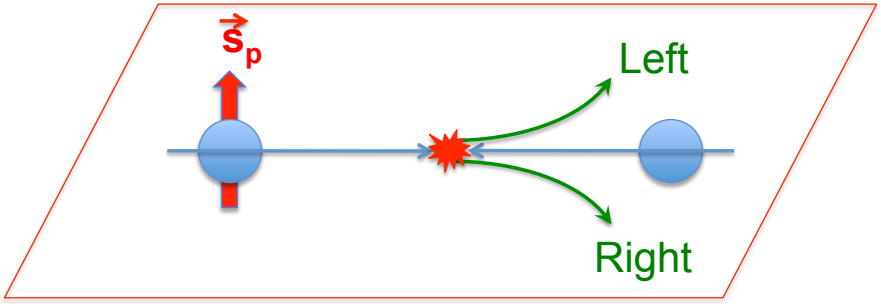

❑ Single hard scale – collinear factorization:

Qiu, Sterman, 1991, 1998

$$A_N \propto \sigma(p_T, S_\perp) - \sigma(p_T, -S_\perp)$$

$$= T^{(3)}_{a/A}(x, x, S_\perp) \otimes \phi_{b/B}(x') \otimes \hat{\sigma}^T_{ab\to c} \otimes D_{h/c}(z)$$

Efremov, Teryaev, Qiu, Sterman, ...

$$+ \delta q_{a/A}(x, S_\perp) \otimes T^{(3\sigma)}_{b/B}(x', x') \otimes \hat{\sigma}^\phi_{ab\to c} \otimes D_{h/c}(z)$$

Kanazawa, Koike, ...

$$+ \delta q_{a/A}(x, S_\perp) \otimes \phi_{b/B}(x', x') \otimes \hat{\sigma}^D_{ab\to c} \otimes D^{(3)}_{h/c}(z, z)$$

Kang, Yuan, Zhou, ...

$$+ \text{ power corrections}$$

Leading power contribution to cross section cancels!

Only one twist-3 distribution at each term!

Valid when $p_T^2 \gg Q_s^2$, **Corrections:** $\propto \left(\frac{Q_2^2}{p_T^2}\right)^n$

SSAs generated by twist-3 PDFs

- First non-vanish contribution – interference:

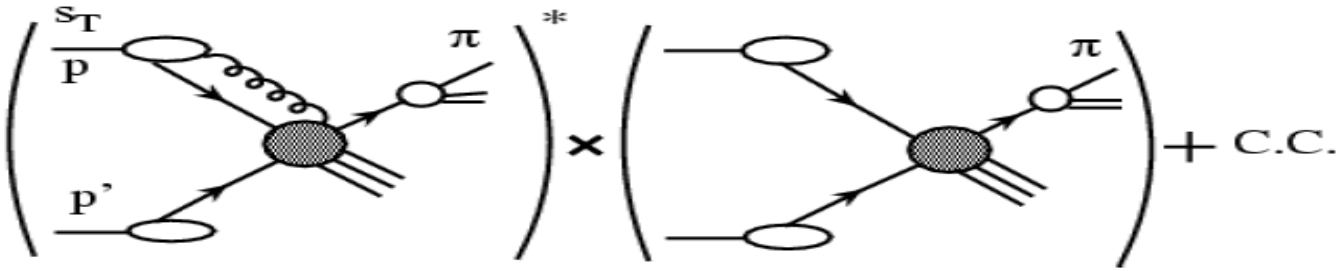

- Dominated by the derivative term – forward region:

$$E\frac{d\Delta\sigma}{d^3\ell} \propto \epsilon^{\ell_T s_T n \bar{n}}\, D_{c\to\pi}(z) \otimes \left[-x\frac{\partial}{\partial x}T_F(x,x)\right]$$

$$\otimes \frac{1}{-\hat{u}}\left[G(x')\otimes\Delta\hat{\sigma}_{qg\to c} + \sum_{q'} q'(x')\otimes\Delta\hat{\sigma}_{qq'\to c}\right]$$

Qiu, Sterman, 1998, …

$$A_N \propto \left(\frac{\ell_\perp}{-\hat{u}}\right)\frac{n}{1-x} \quad \text{if } T_F(x,x)\propto q(x)\propto(1-x)^n$$

Kouvaris, Qiu, Vogelsang, Yuan, 2006

- Complete leading order contribution:

$$E_\ell\frac{d^3\Delta\sigma(\vec{s}_T)}{d^3\ell} = \frac{\alpha_s^2}{S}\sum_{a,b,c}\int_{z_{\min}}^1\frac{dz}{z^2}D_{c\to h}(z)\int_{x'_{\min}}^1\frac{dx'}{x'}\frac{1}{x'S+T/z}\phi_{b/B}(x')\sqrt{4\pi\alpha_s}\left(\frac{\epsilon^{\ell s_T n\bar{n}}}{z\hat{u}}\right)$$

$$\times\frac{1}{x}\left[T_{a,F}(x,x) - x\left(\frac{d}{dx}T_{a,F}(x,x)\right)\right]H_{ab\to c}(\hat{s},\hat{t},\hat{u})$$

Unpolarized single hadron production

- **PHENIX:**

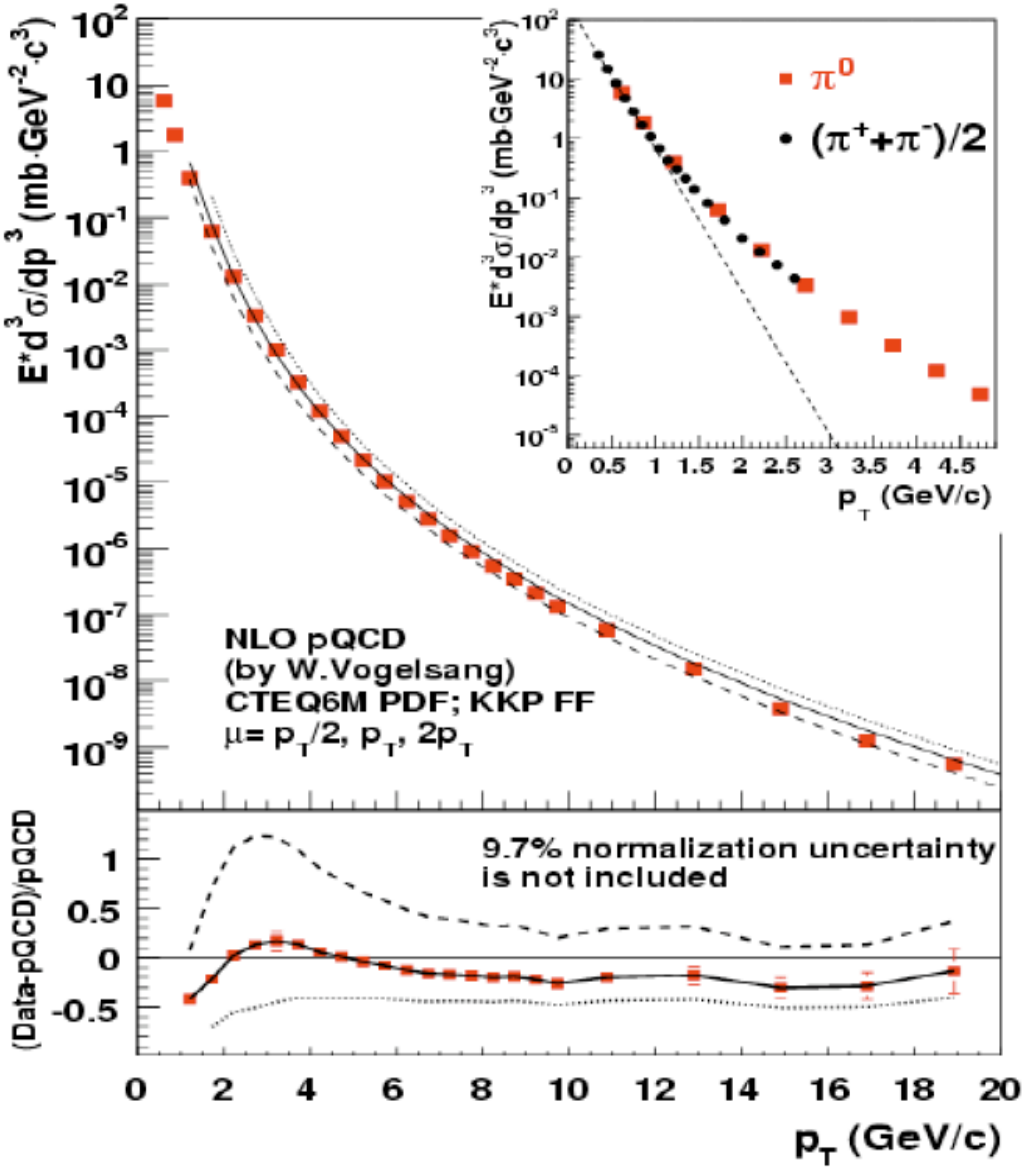

PRD76, 051106 (2007)

QCD factorization/calculation works at RHIC energies!

Extending x coverage and particle type

- **BRAHMS:** Large rapidity p,K,p cross sections for p+p, √s=200 GeV

PRL98, 252001 (2007)

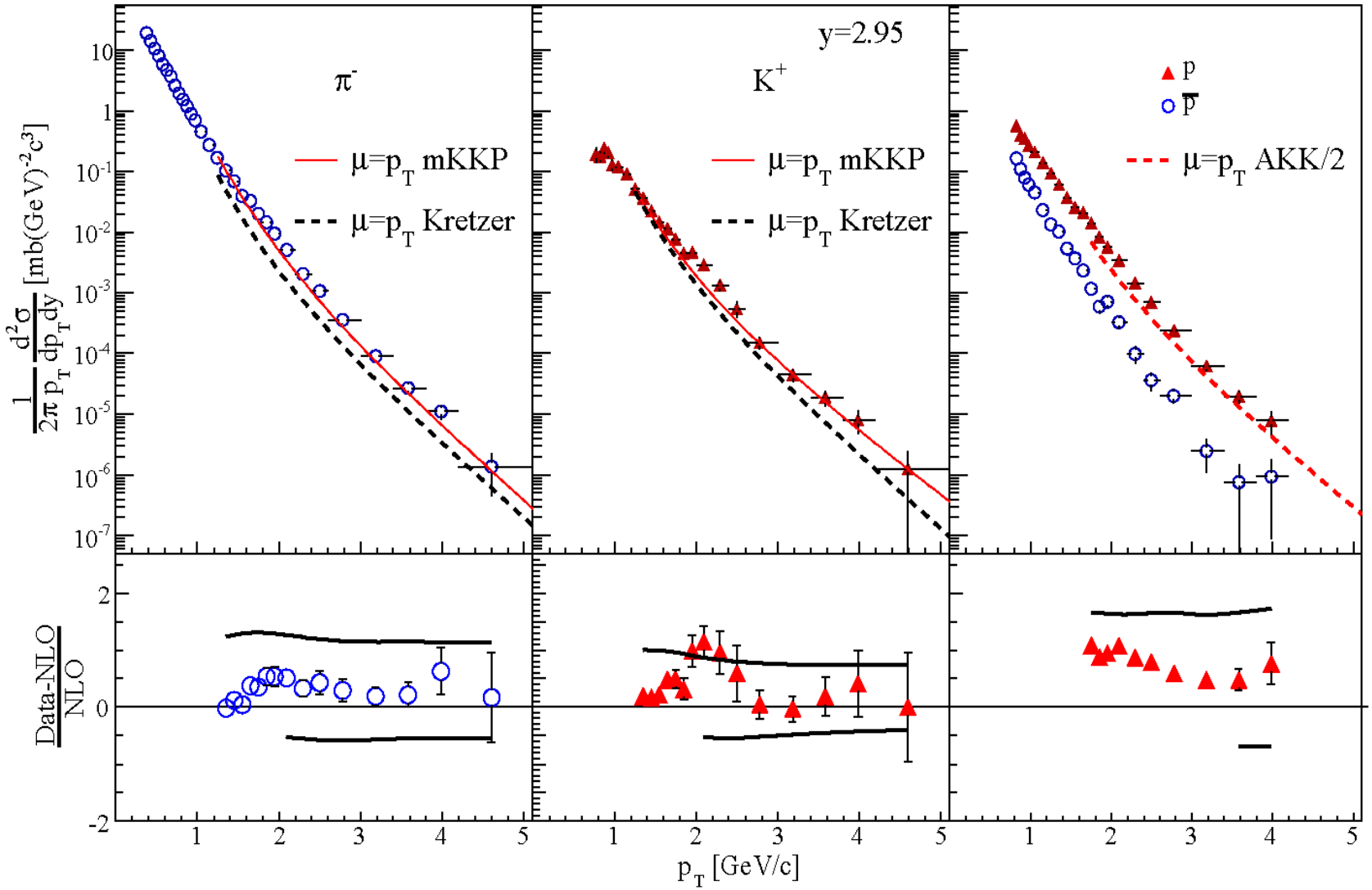

QCD factorization/calculation works at RHIC energies!

Asymmetries from the $T_F(x,x)$

- Lowest order tree-level contribution: Kouvaris, Qiu, Vogelsang, Yuan, 2006

(FermiLab E704)

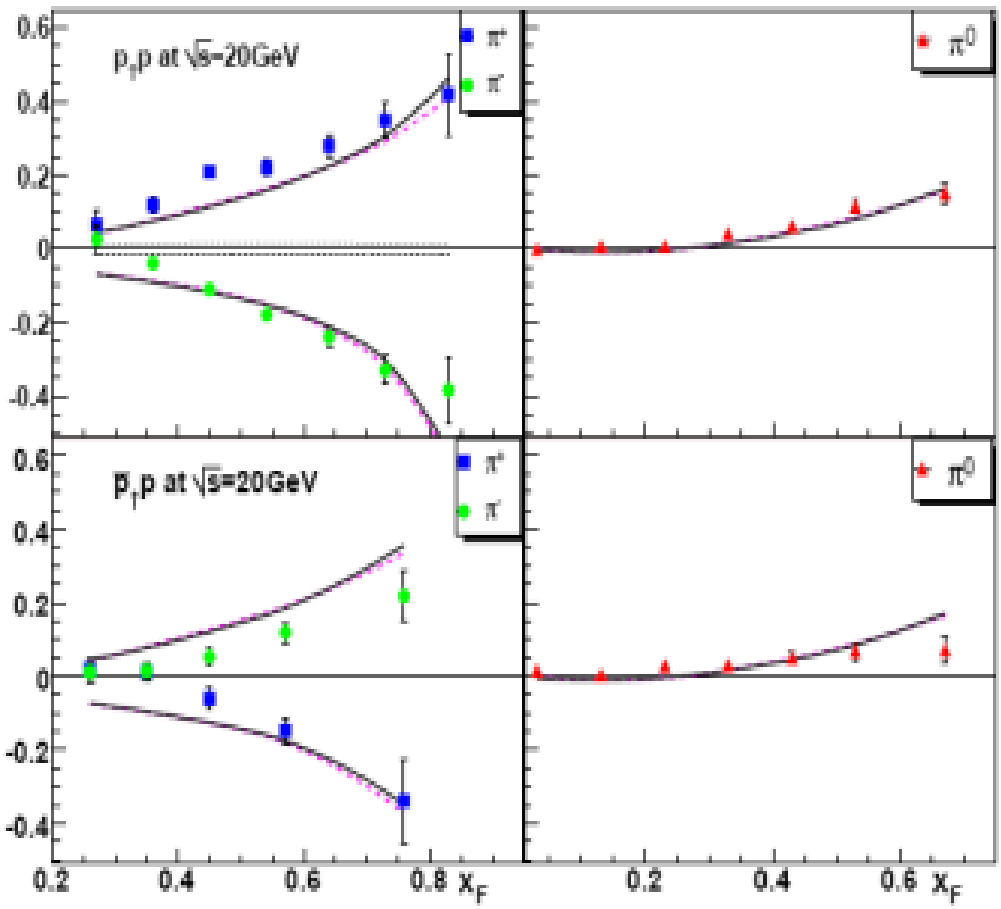

(RHIC STAR)

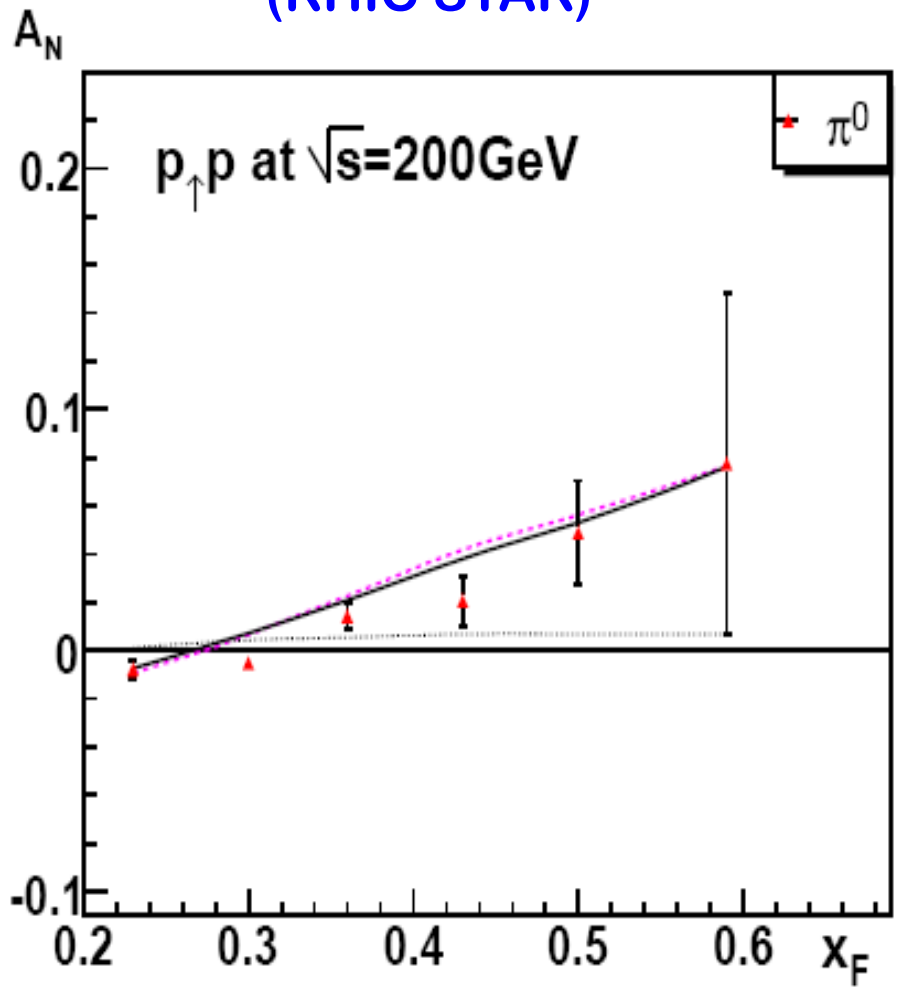

- A_N for jet, D, … production at RHIC and EIC, …

Nonvanish twist-3 function → Nonvanish transverse motion

SSA in the forward region of pA collisions

Excellent probe for distinguishing various contributions to SSA

Excellent probe for studying small-x Physics

SSA increases as x_F (or y) increases

Ideal kinematics for SSA and small-x

Large xF (or y) ⟷ Large SSA ⟷ Small-x

❑ Leading power predictions – single scale:

$$p(\vec{s}_\perp) + p \to h(\pi^\pm, \pi^0, ...) + X$$

$$A_N \equiv \frac{\Delta\sigma(\ell, \vec{s})}{\sigma(\ell)} = \frac{\sigma(\ell, \vec{s}) - \sigma(\ell, -\vec{s})}{\sigma(\ell, \vec{s}) + \sigma(\ell, -\vec{s})}$$

$$\begin{aligned} A_N &\propto \sigma(p_T, S_\perp) - \sigma(p_T, -S_\perp) \\ &= T^{(3)}_{a/A}(x, x, S_\perp) \otimes \phi_{b/B}(x') \otimes \hat{\sigma}^T_{ab\to c} \otimes D_{h/c}(z) \\ &+ \delta q_{a/A}(x, S_\perp) \otimes T^{(3\sigma)}_{b/B}(x', x') \otimes \hat{\sigma}^\phi_{ab\to c} \otimes D_{h/c}(z) \\ &+ \delta q_{a/A}(x, S_\perp) \otimes \phi_{b/B}(x', x') \otimes \hat{\sigma}^D_{ab\to c} \otimes D^{(3)}_{h/c}(z, z) \end{aligned}$$

"Sivers effect" + "Collins effect"

➡ nuclear gluon distribution at $G^A(x)$

Contribution from the 2nd term seems to be small!

Kanazawa, Koike, …

Power corrections

❑ Power corrections:

To both numerator and denominator: $A_N \equiv \frac{\Delta\sigma(\ell,\vec{s})}{\sigma(\ell)} = \frac{\sigma(\ell,\vec{s})-\sigma(\ell,-\vec{s})}{\sigma(\ell,\vec{s})+\sigma(\ell,-\vec{s})}$

❑ Inclusive cross section in the forward region:

Coherent multiple scattering – dominated by t-channel

Qiu, Vitev, 2006

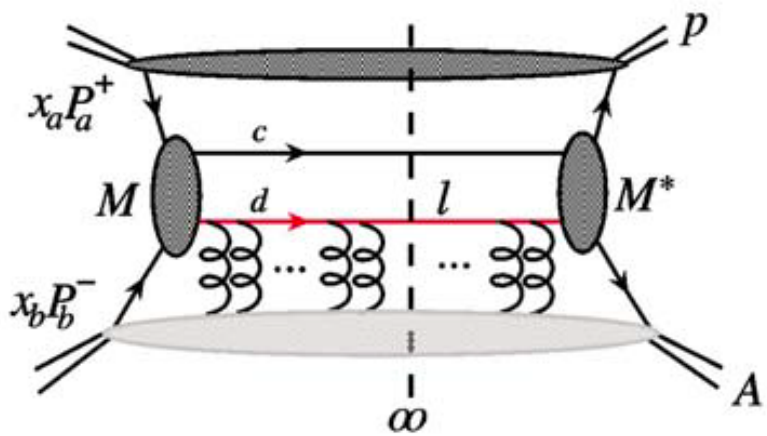

$$\sigma(\ell) = \sigma^{(2)}(\ell) + \left(\frac{Q_s^2}{\ell_T^2}\right)\sigma^{(4)}(\ell) + \left(\frac{Q_s^2}{\ell_T^2}\right)^2 \sigma^{(6)}(\ell) + \ldots$$

Size of power correction: $\alpha_s \frac{1/\ell_T^2}{R_N^2} \langle F^{+\perp} F^{+\perp} \rangle A^{1/3}$

Coherence at small-x

- Similarity to DIS:

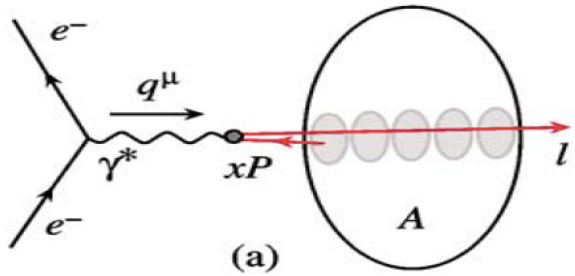

DIS

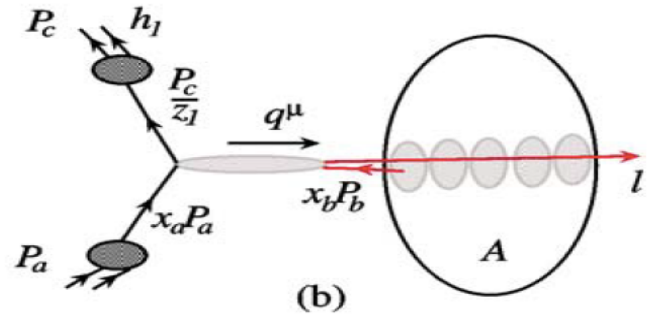

T-channel of pA

- "Snapshot" does not have a "sharp" depth at small x_B

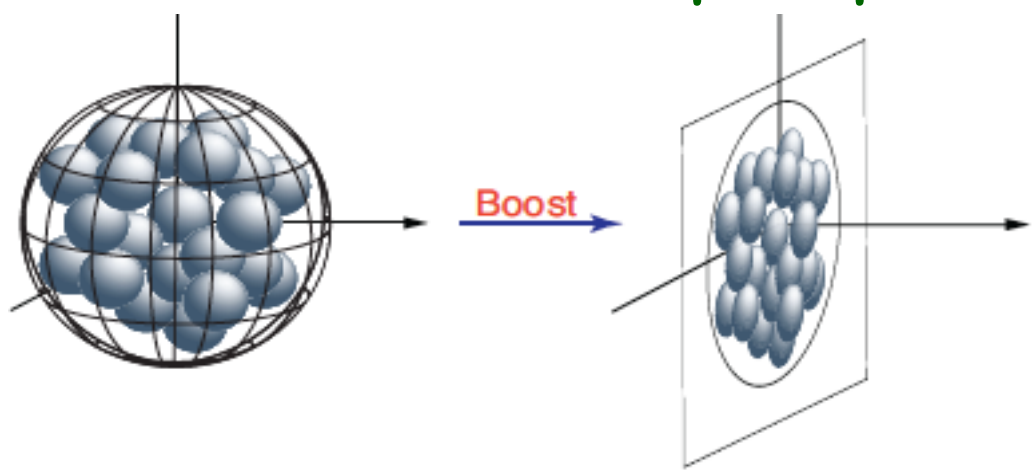

Probe size: transverse - $\frac{1}{Q} \ll 1\ \mathrm{fm}$, longitudinal size - $\frac{1}{xp} \sim \frac{1}{Q} \ll 1\ \mathrm{fm}$

Longitudinal size > Lorentz contracted nucleon: $\frac{1}{xp} > 2R\frac{m}{p}$

$$x < x_c = \frac{1}{2mR} \sim 0.1$$

Coherent multiple scattering

- **LO contribution to DIS cross section:**

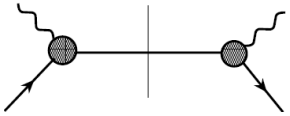

$\delta(x - x_B)$

- **NLO contribution:**

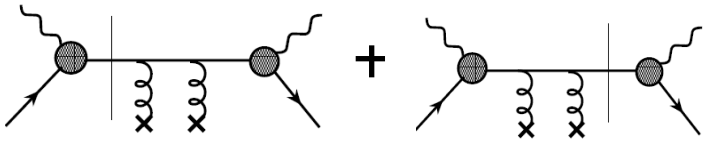

$$\frac{g^2}{Q^2}\left(\frac{1}{2N_c}\right)\left[2\pi^2\tilde{F}^2(0)\right] x_B \lim_{x_1\to x}\left[\frac{1}{x-x_1}\delta(x_1-x_B)+\frac{1}{x_1-x}\delta(x-x_B)\right]$$

$$\int \frac{dy_2^- dy_1^-}{(2\pi)^2}\left[F^{+\alpha}(y_2^-)F_\alpha{}^+(y_1^-)\right]\theta(y_2^-) \qquad x_B\left[-\frac{d}{dx}\delta(x-x_B)\right]$$

- **Nth order contribution:**

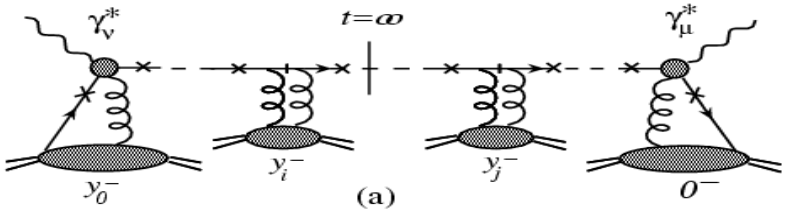

$$\left[\frac{g^2}{Q^2}\left(\frac{1}{2N_c}\right)\left[2\pi^2\tilde{F}^2(0)\right]\right]^N x_B^N \lim_{x_i\to x}\sum_{m=0}^{N}\delta(x_m-x_B)\left[\prod_{i=1}^{m}\left(\frac{1}{x_{i-1}-x_m}\right)\right]\left[\prod_{j=1}^{N-m}\left(\frac{1}{x_{m+j}-x_m}\right)\right]$$

Infrared safe!

$$x_B^N\left[(-1)^N\frac{1}{N!}\frac{d^N}{dx^N}\delta(x-x_B)\right]$$

Resummation of power corrections

Qiu and Vitev, PRL (2004)

❑ Transverse structure function:

$$F_T(x_B, Q^2) = \sum_{n=0}^{N} \frac{1}{n!} \left[\frac{\xi^2}{Q^2} \left(A^{1/3} - 1 \right) \right]^n x_B^n \frac{d^n}{dx_B^n} F_T^{(0)}(x_B, Q^2)$$

$$\approx F_T^{(0)}(x_B(1+\Delta), Q^2)$$

$$\Delta \equiv \frac{\xi^2}{Q^2} \left(A^{1/3} - 1 \right)$$

$$\xi^2 = \frac{3\pi\alpha_s}{8R^2} \langle F^{+\alpha} F_\alpha{}^{+} \rangle$$

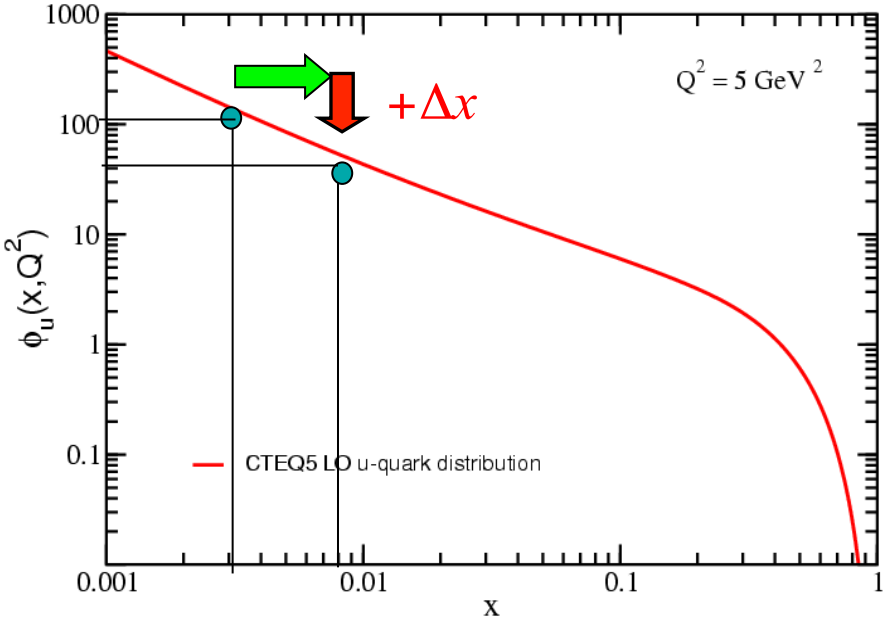

Single parameter for the power correction, and is proportional to the same characteristic scale

❑ Similar result for longitudinal structure function:

Power corrections to the shadowing

- **Largest power corrections:**

ξ^2 : 0.09 - 0.12 GeV^2

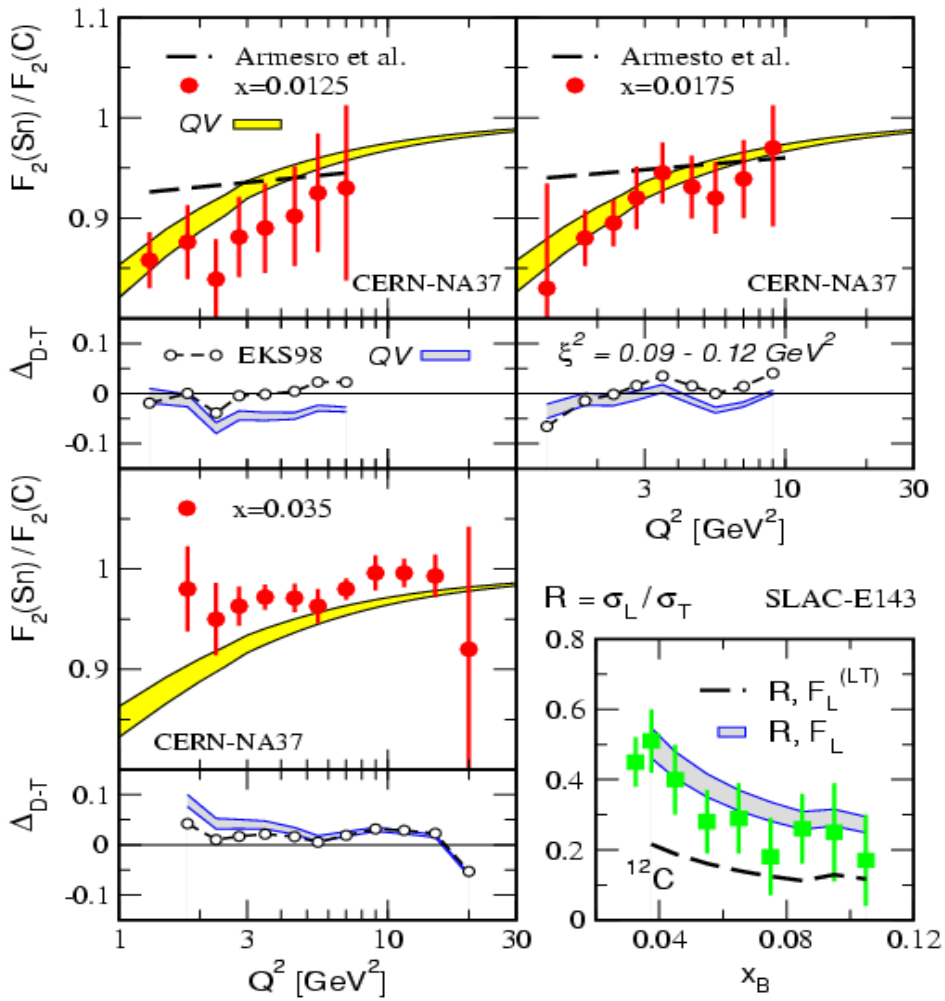

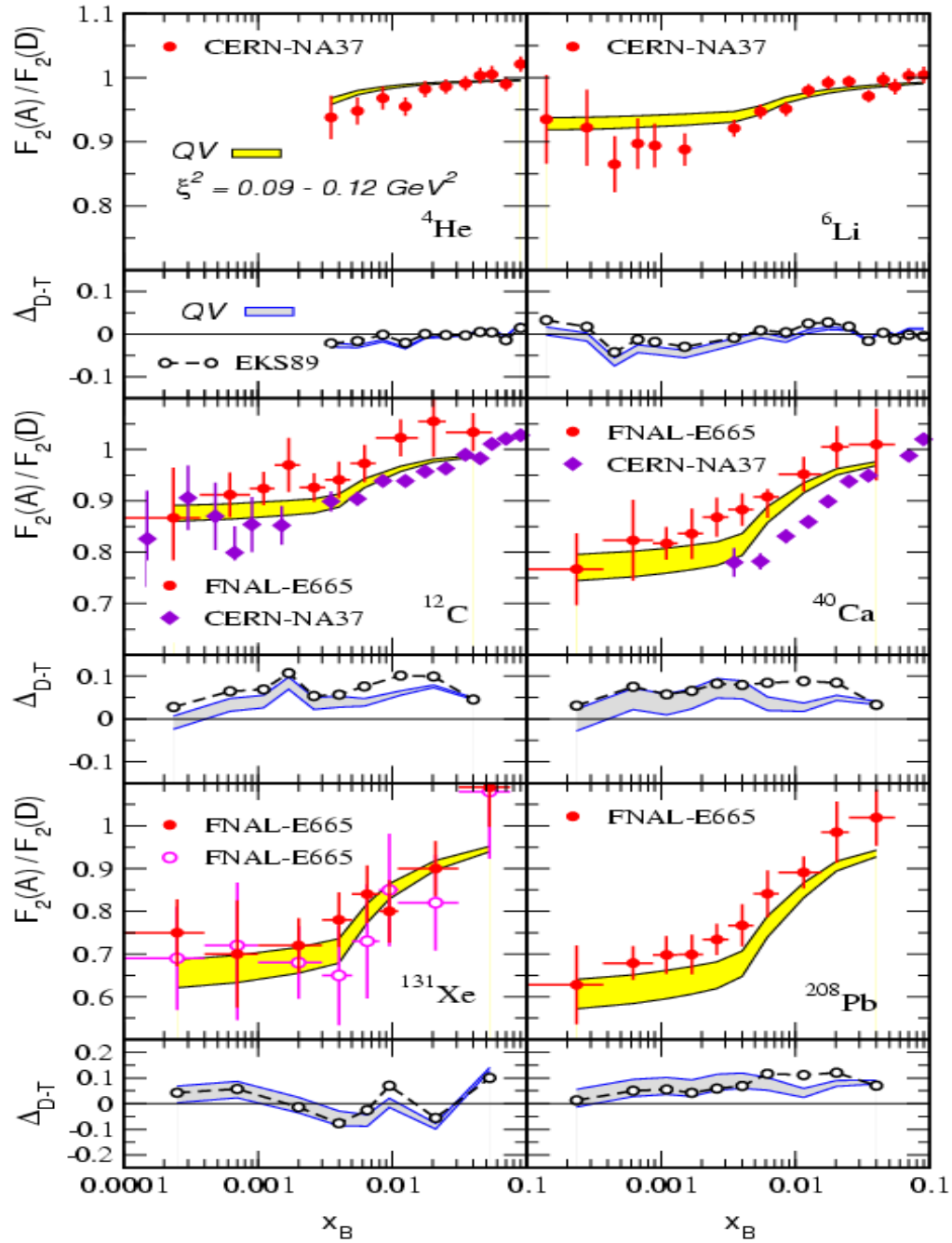

Qiu, Vitev, 2004

Leading power corrections in forward pA

- **Factorized formula:**

$$\frac{d\sigma_{NN}^{h_1}}{dy_1\, d^2 p_{T_1}} = \sum_{abcd} \int \frac{dz_1}{z_1^2} D_{h_1/c}(z_1) \int dx_a \frac{\phi_{a/N}(x_a)}{x_a} \left[\frac{1}{x_a S + U/z_1}\right] \frac{\alpha_s^2}{S} \int dx_b\, \delta(x_b - \bar{x}_b) F_{ab\to cd}(x_b)$$

- **LO proton-proton scattering:**

$$F_{ab\to cd}(x_b) \equiv \frac{\phi_{b/N}(x_b)}{x_b} |\bar{M}_{ab\to cd}|^2$$

- **Resummation for pA collisions:**

$$\int dx_b \frac{(-1)^N}{N!} \left[C_d \frac{\bar{x}_b \xi^2}{-t}(A^{1/3}-1)\right]^N \frac{d^N \delta(x_b - \bar{x}_b)}{dx_b^N} F_{ab\to cd}(x_b)$$

$$= F_{ab\to cd}\left(x_b\left[1 + C_d \frac{\xi^2}{-t}(A^{1/3}-1)\right]\right).$$

In principle, no free parameter!

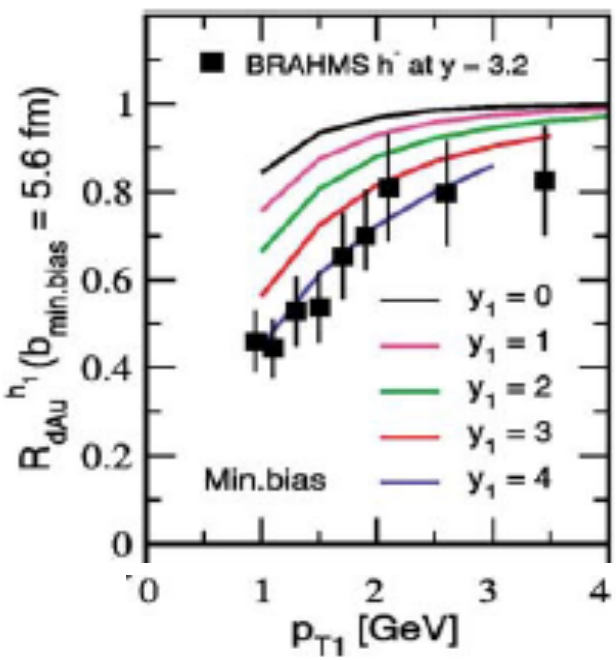

Di-hadron in d-A collisions

Kang, Vitev, Xing, 2012

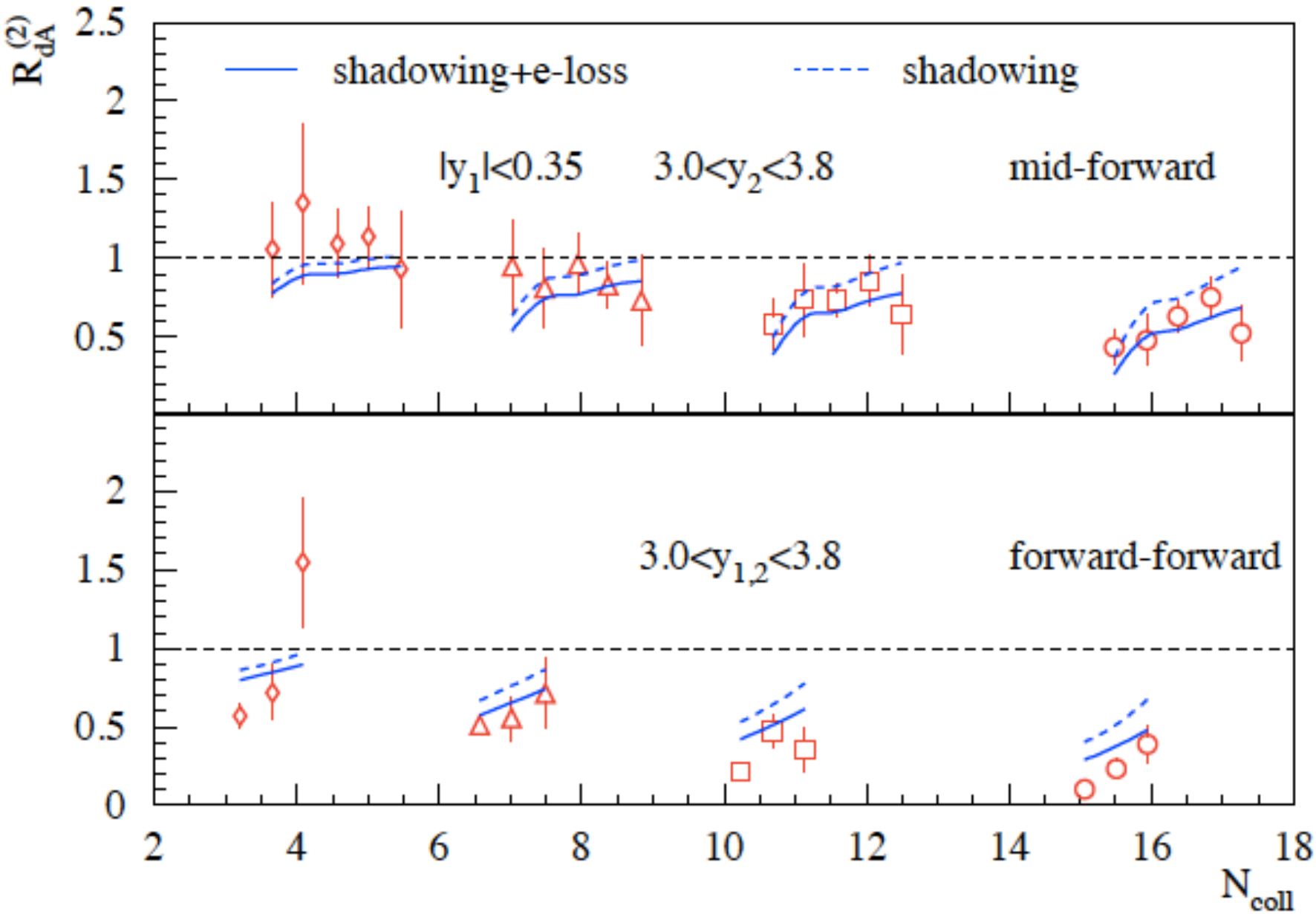

SSA in pA collisions

- To numerator:

$$A_N \equiv \frac{\Delta\sigma(\ell,\vec{s})}{\sigma(\ell)} = \frac{\sigma(\ell,\vec{s}) - \sigma(\ell,-\vec{s})}{\sigma(\ell,\vec{s}) + \sigma(\ell,-\vec{s})}$$

- Leading power approximation:

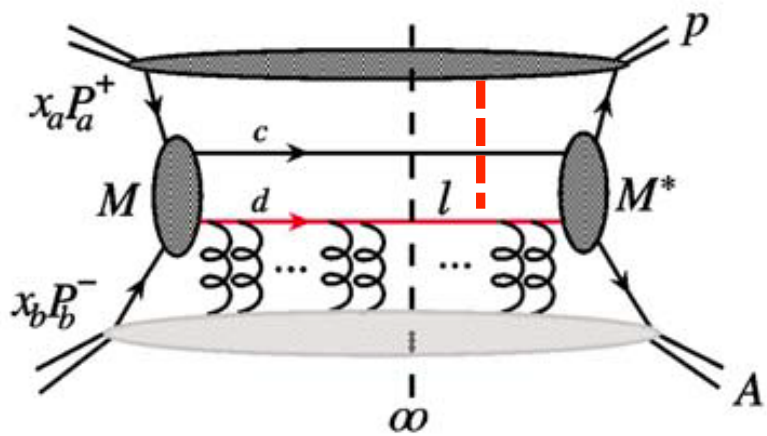

The momenta of all additional scatterings are fixed by the unpinched poles!

- Same shift from the coherent multiple scattering:

$$A_N(pp) \sim A_N(pA) \qquad \text{When} \qquad \ell_T^2 \gg Q_s^2$$

Only small difference due to the convolution over $T_F(x,x)$ vs. $q(x)$

Note: A_N(photon) =\= 0!

TMD-type approach

- **TMD or small-x approach:**

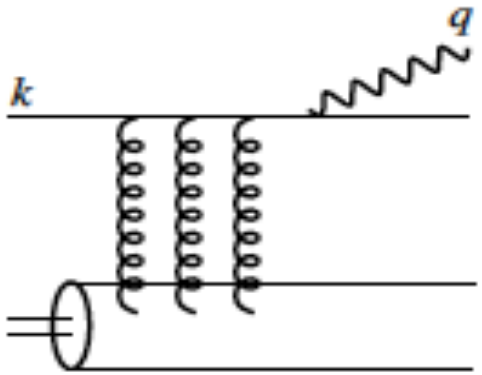

No TMD factorization for single hadron production

Relevant when $\ell_T^2 \leq Q_s^2$

- **Matching:**

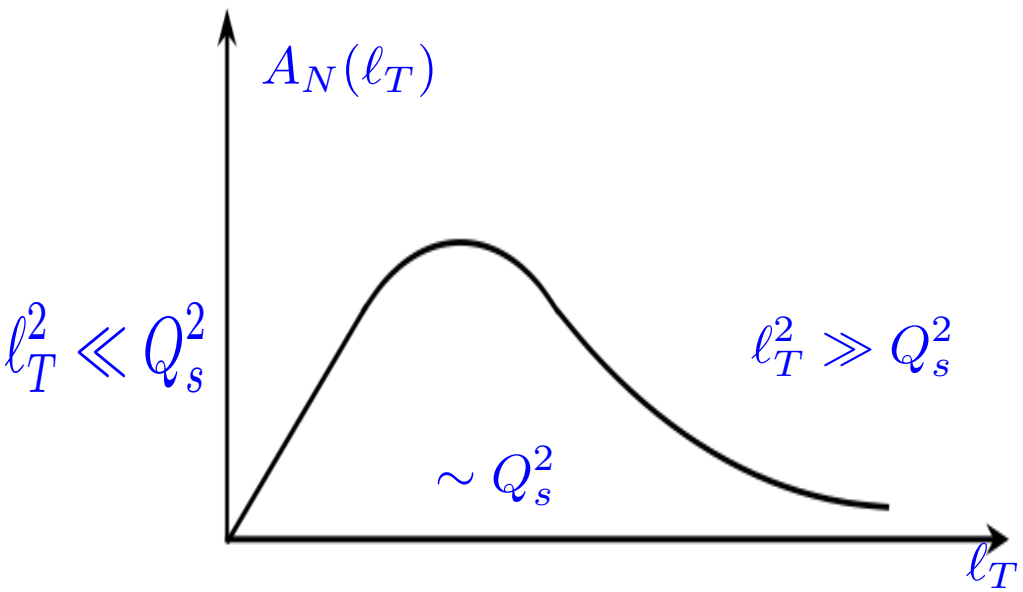

Recall:

Single hadron spectrum

$$\frac{d\sigma}{d\ell_T^2} \propto \left(\frac{1}{\ell_T^2 + a}\right)^{\alpha}$$

$\Rightarrow$ $a \propto Q_s^2$

Summary

- QCD factorization/calculation have been very successful in interpreting HEP scattering data

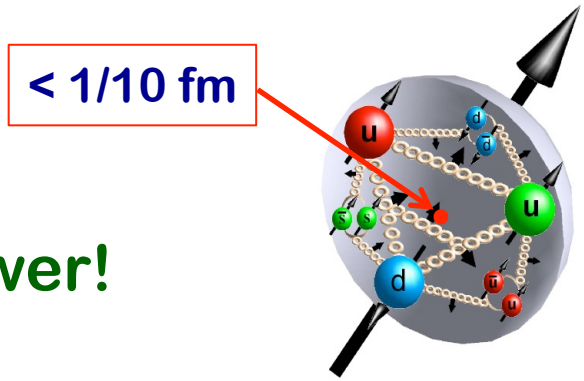

- QCD is much richer than the leading power!

- Transverse spin opens a new domain to test QCD dynamics and new observables for parton correlations

- SSA in pA is an excellent observable to study small-x physics in a nucleus

Thank you!

Backup slices

Scale dependence of Sivers function

Aybat, Collins, Qiu, Rogers, 2011

❑ Kernel is not perturbative for all b:

CSS prescription:
(not unique)

$$\mathbf{b}_* = \frac{\mathbf{b}_T}{\sqrt{1+b_T^2/b_{\max}^2}} \qquad \mu_b = \frac{C_1}{b_*}$$

$$\tilde{K}(b_T;\mu) = \tilde{K}(b_*;\mu_b) - \int_{\mu_b}^{\mu} \frac{d\mu'}{\mu'}\gamma_K(g(\mu')) - g_K(b_T)$$

❑ Q^2-dependence of Sivers function:

$$\tilde{F}'^{\perp\, f}_{1T}(x,b_T;\mu,\zeta_F) = \tilde{F}'^{\perp\, f}_{1T}(x,b_T;\mu_0,Q_0^2)\exp\left\{\ln\frac{\sqrt{\zeta_F}}{Q_0}\tilde{K}(b_*;\mu_b) + \int_{\mu_0}^{\mu}\frac{d\mu'}{\mu'}\left[\gamma_F(g(\mu');1) - \ln\frac{\sqrt{\zeta_F}}{\mu'}\gamma_K(g(\mu'))\right]\right.$$
$$\left. + \int_{\mu_0}^{\mu_b}\frac{d\mu'}{\mu'}\ln\frac{\sqrt{\zeta_F}}{Q_0}\gamma_K(g(\mu')) - g_K(b_T)\ln\frac{\sqrt{\zeta_F}}{Q_0}\right\}$$

$$F^{\perp\, f}_{1T}(x,k_T;\mu,\zeta_F) = \frac{-1}{2\pi k_T}\int_0^\infty db_T\, b_T J_1(k_T b_T)\tilde{F}'^{\perp\, f}_{1T}(x,b_T;\mu,\zeta_F)$$ – Evolved Sivers function

❑ Small-b perturbative contribution – match to twist-3:

$$\tilde{F}'^{\perp\, f}_{1T}(x,b_T;\mu,\zeta_F) = \sum_j \frac{M_p b_T}{2}\int_x^1 \frac{d\hat{x}_1\, d\hat{x}_2}{\hat{x}_1\,\hat{x}_2}\tilde{C}^{\rm Sivers}_{f/j}(\hat{x}_1,\hat{x}_2,b_*;\mu_b^2,\mu_b,g(\mu_b))\, T_{F\, j/P}(\hat{x}_1,\hat{x}_2,\mu_b)$$
$$\times\exp\left\{\ln\frac{\sqrt{\zeta_F}}{\mu_b}\tilde{K}(b_*;\mu_b) + \int_{\mu_b}^{\mu}\frac{d\mu'}{\mu'}\left[\gamma_F(g(\mu');1) - \ln\frac{\sqrt{\zeta_F}}{\mu'}\gamma_K(g(\mu'))\right]\right\}\times\exp\left\{-g^{\rm Sivers}_{j/P}(x,b_T) - g_K(b_T)\ln\frac{\sqrt{\zeta_F}}{Q_0}\right\}$$

Kang, Xiao, Yuan, 2011

TMD-Factorization with Evolution

T. C. Rogers

C.N. Yang Institute for Theoretical Physics, SUNY Stony Brook

- What is needed.
- Summary of TMD-factorization.
- Recent results.
- Summary of work in progress.

Workshop on Forward Physics at RHIC – July 31, 2012

Example:

- Drell-Yan q_T distribution.

Get $\dfrac{d\sigma}{d\mathbf{q}_T \cdots}$

For <u>all</u> q_T.

$$q^2 = Q^2 \gg \Lambda^2_{QCD}$$

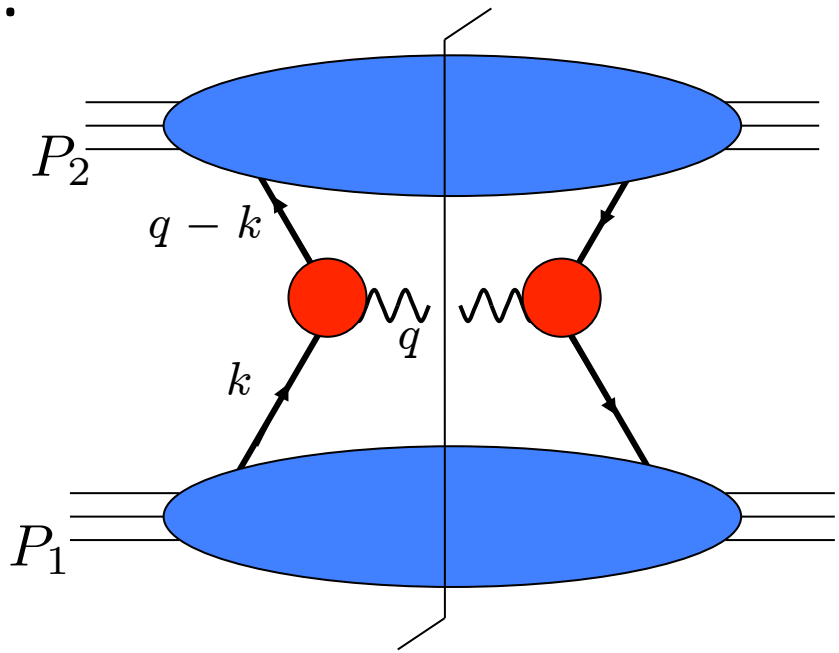

$$k_1 = k$$

$$k_2 = q - k$$

$$\mathbf{k}_{1T} + \mathbf{k}_{2T} = \mathbf{q}_T$$

Regions of Transverse Momentum:

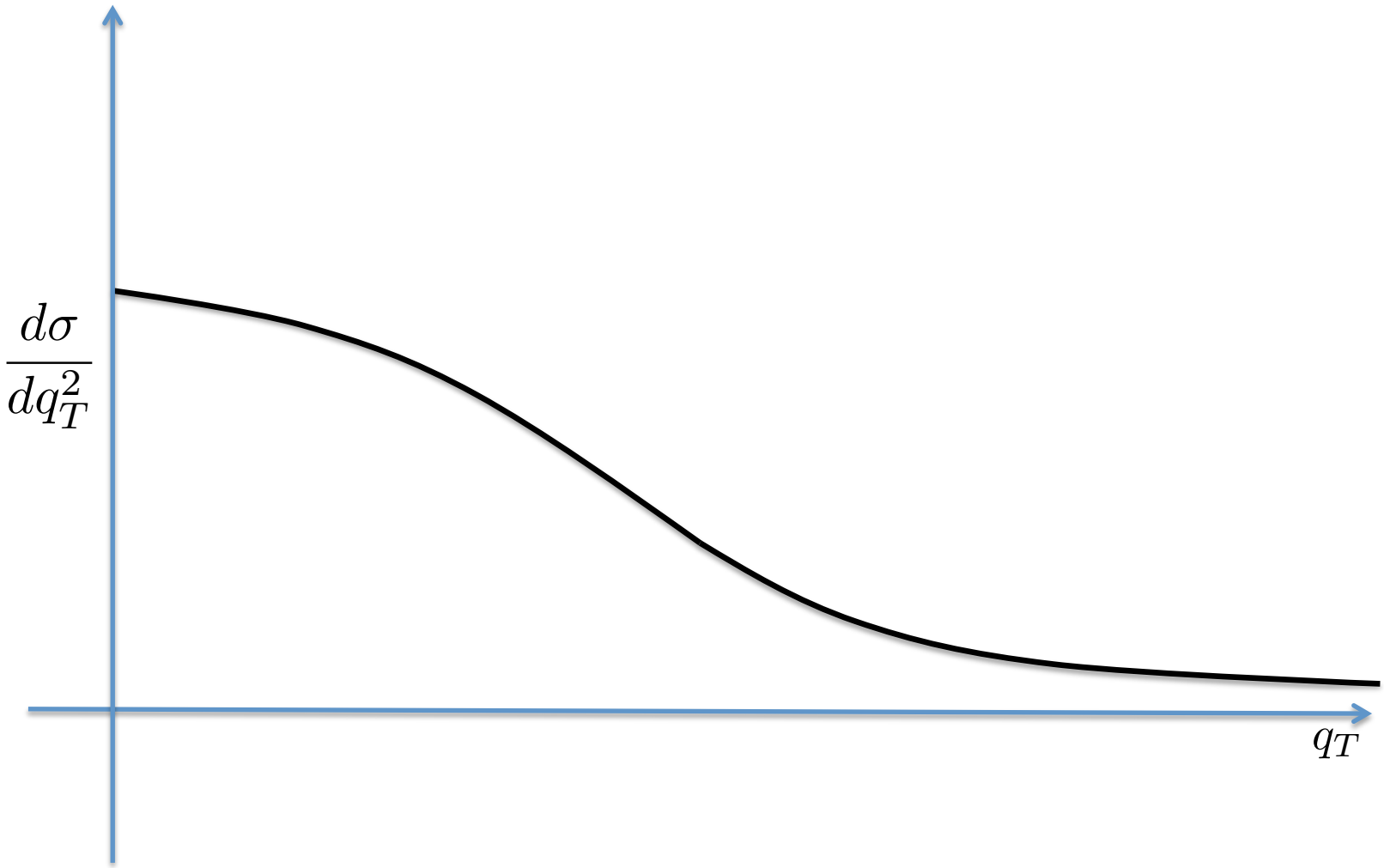

Regions of Transverse Momentum:

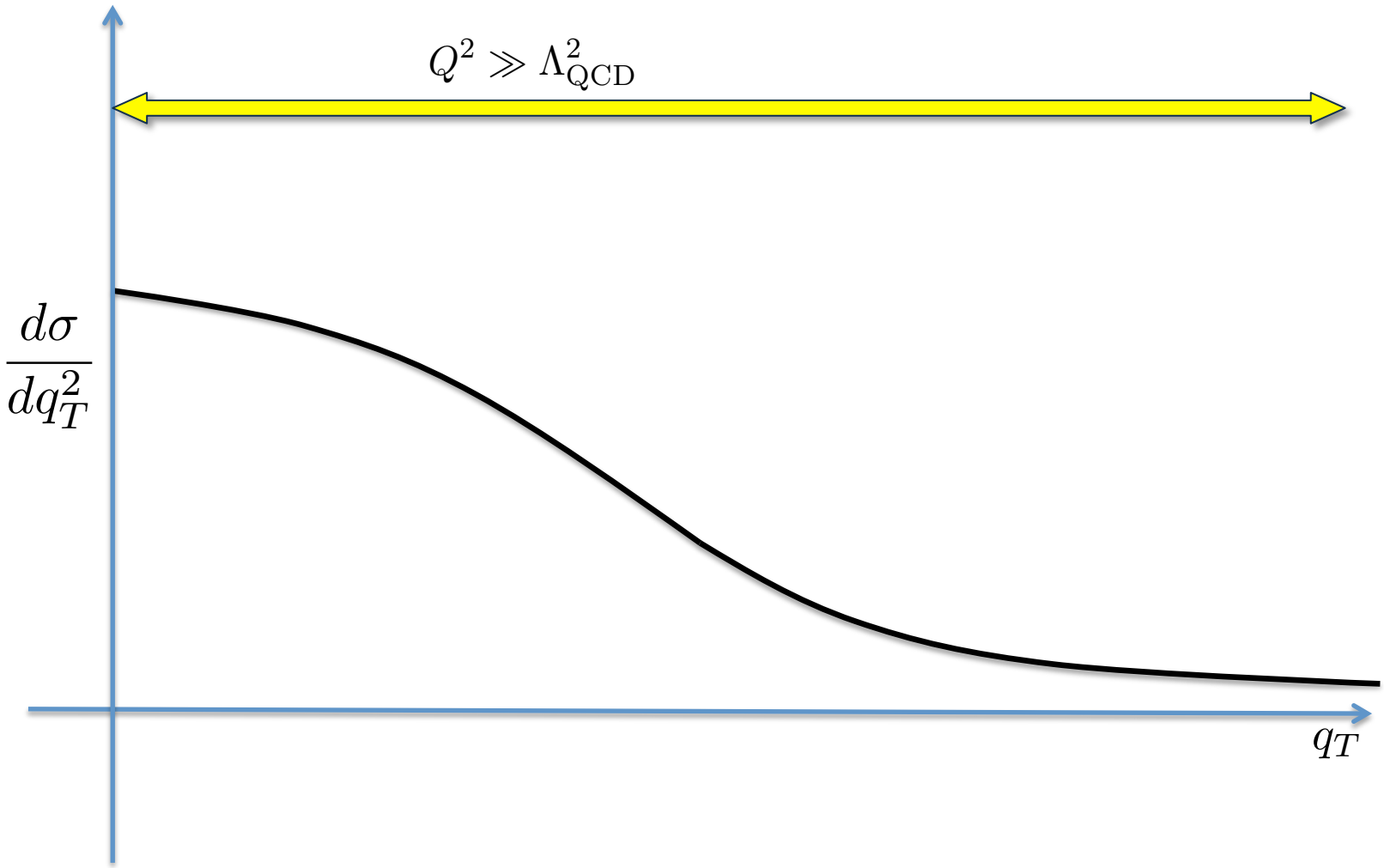

Regions of Transverse Momentum:

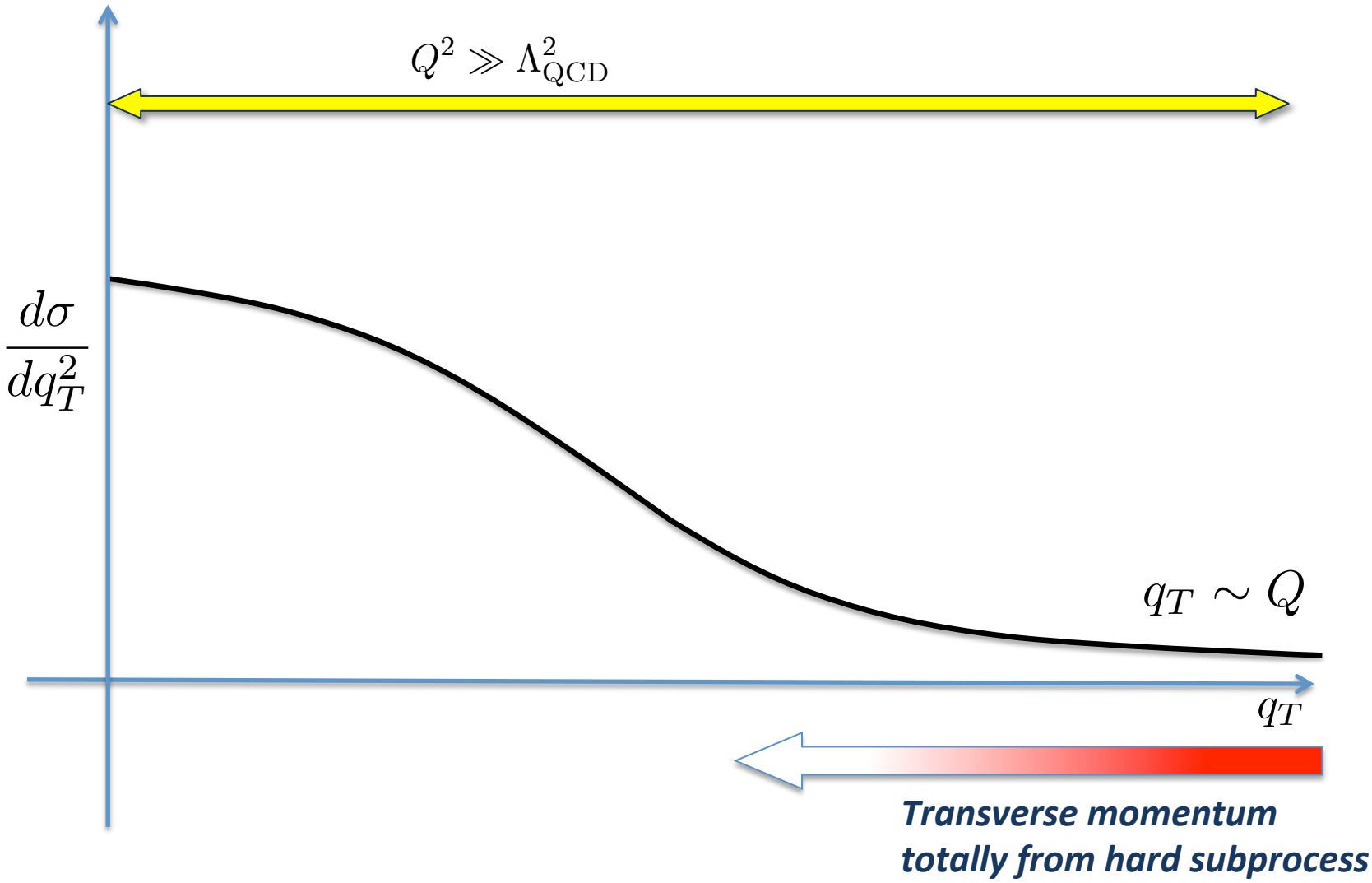

Regions of Transverse Momentum:

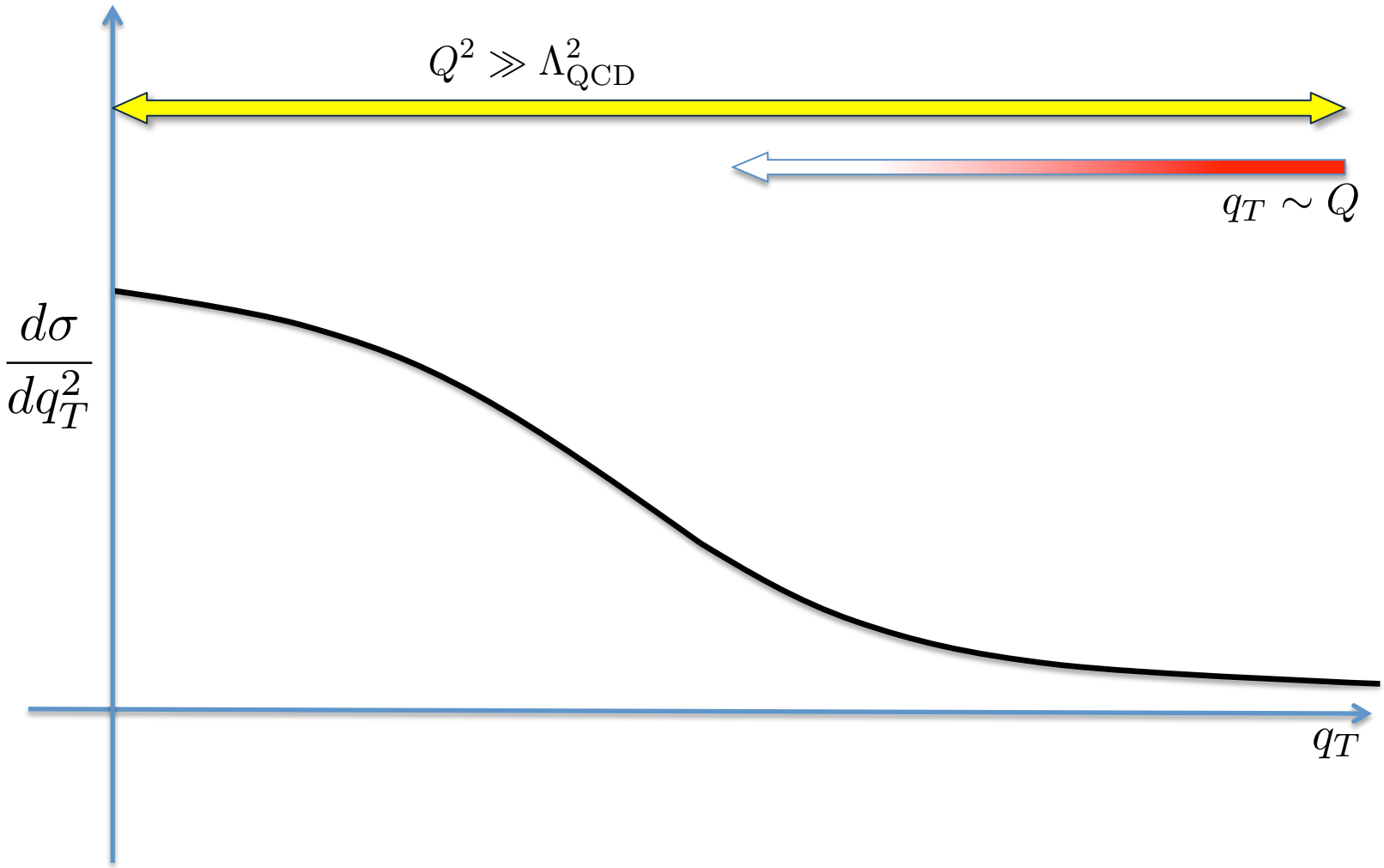

Regions of Transverse Momentum:

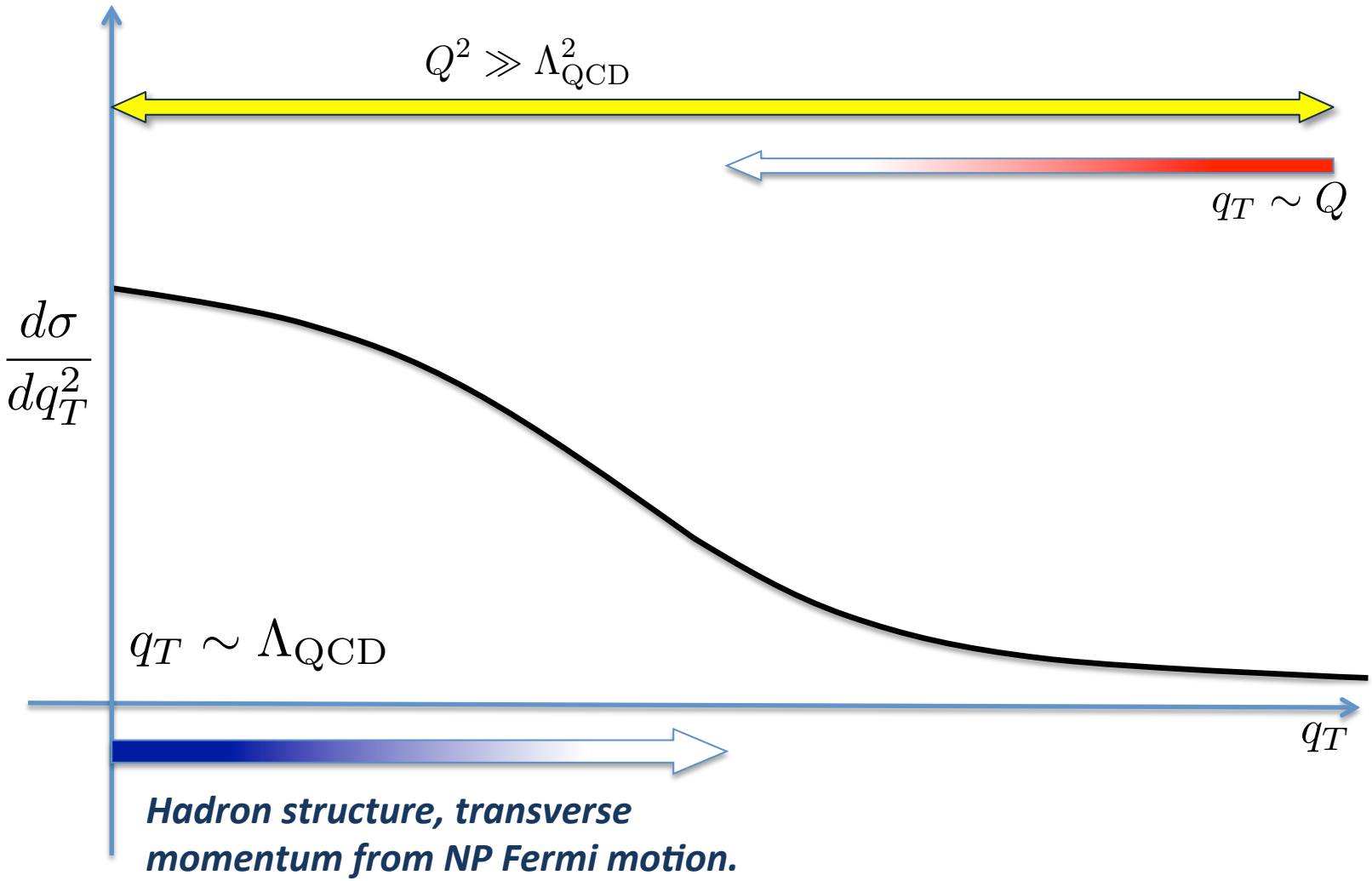

Regions of Transverse Momentum:

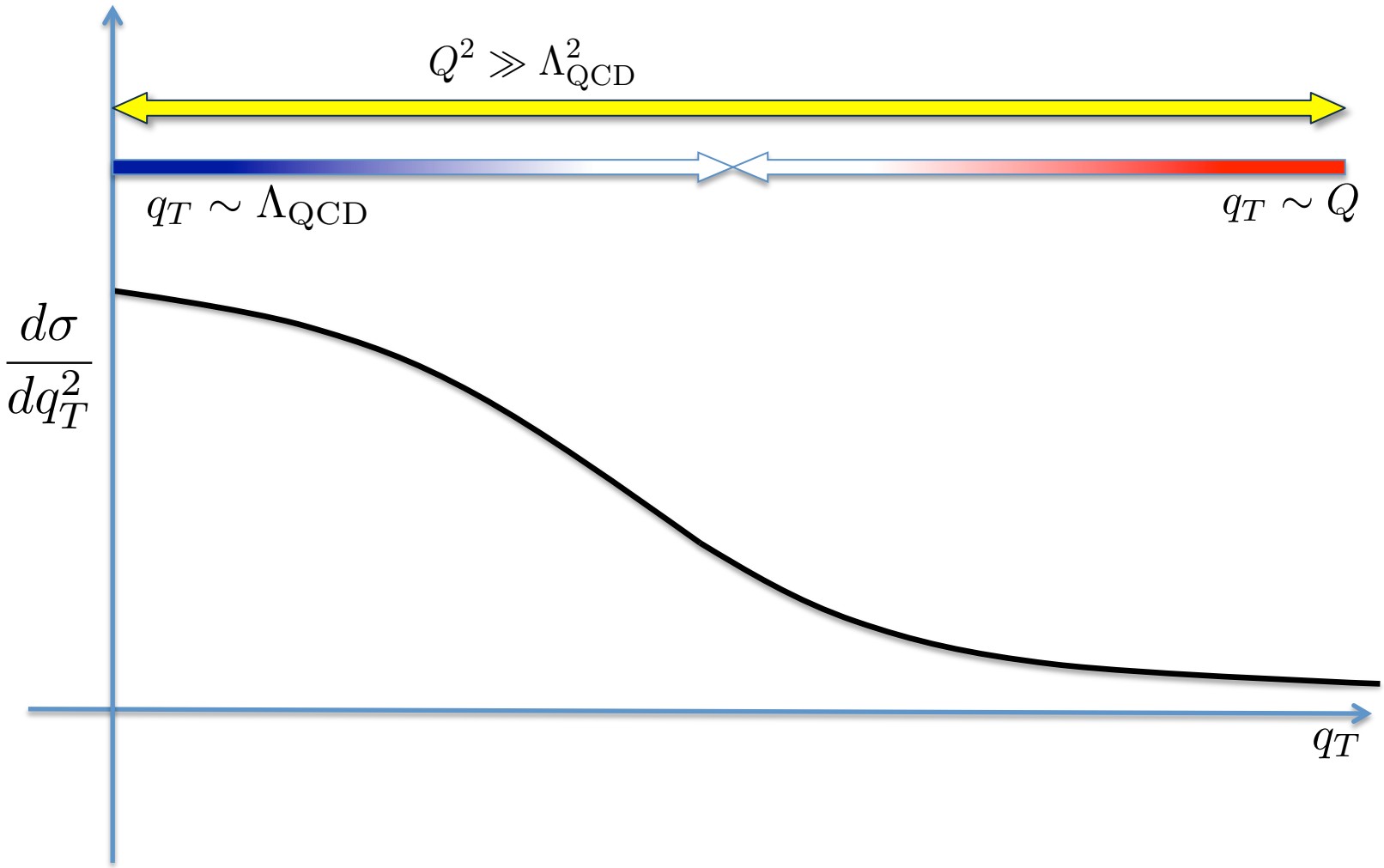

Regions of Transverse Momentum:

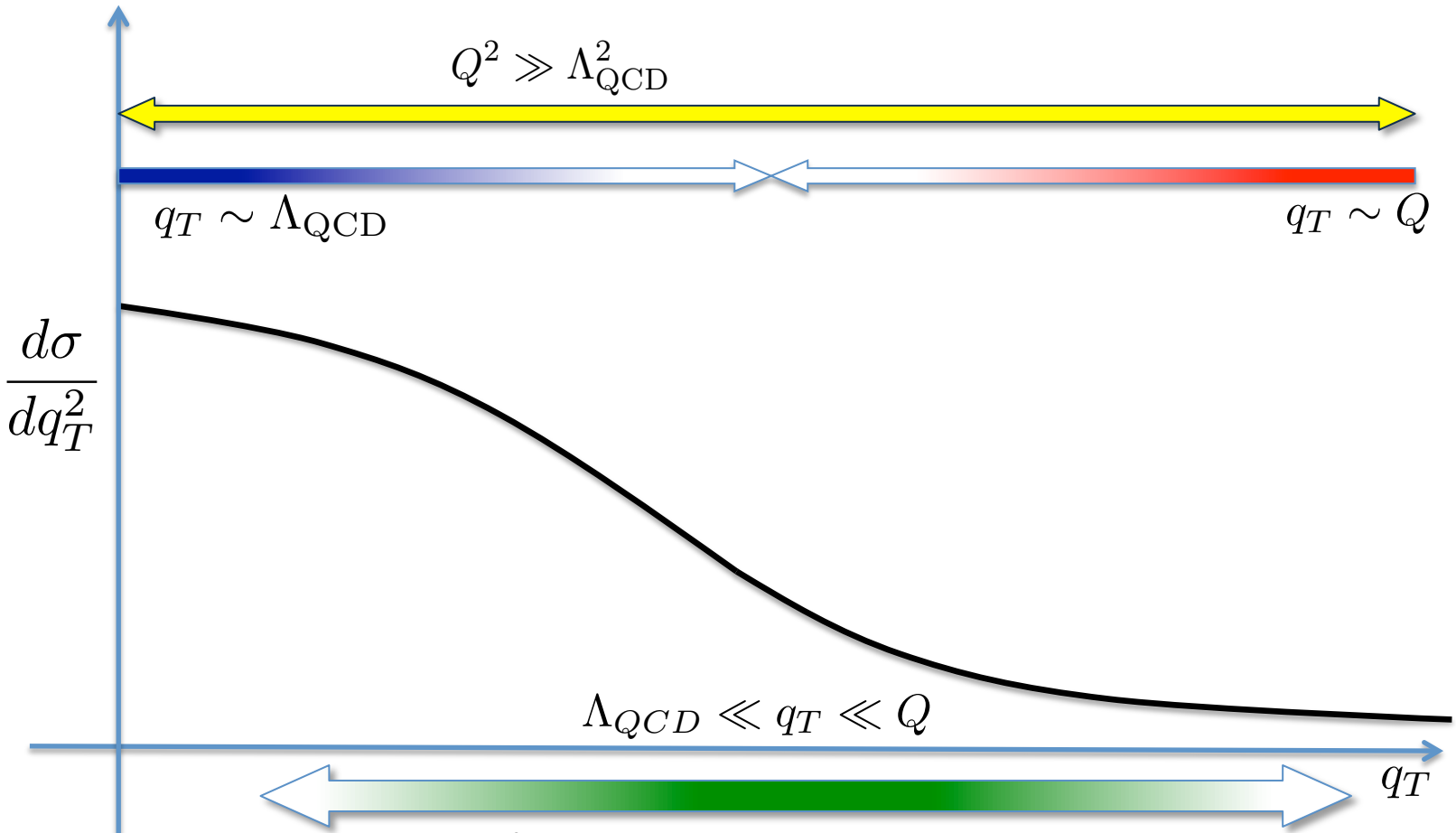

<u>Intermediate transverse momentum:</u>

- Transverse momentum dependence calculable from collinear fact. using hard scale q_T.
- Transverse momentum resummation.

Regions of Transverse Momentum:

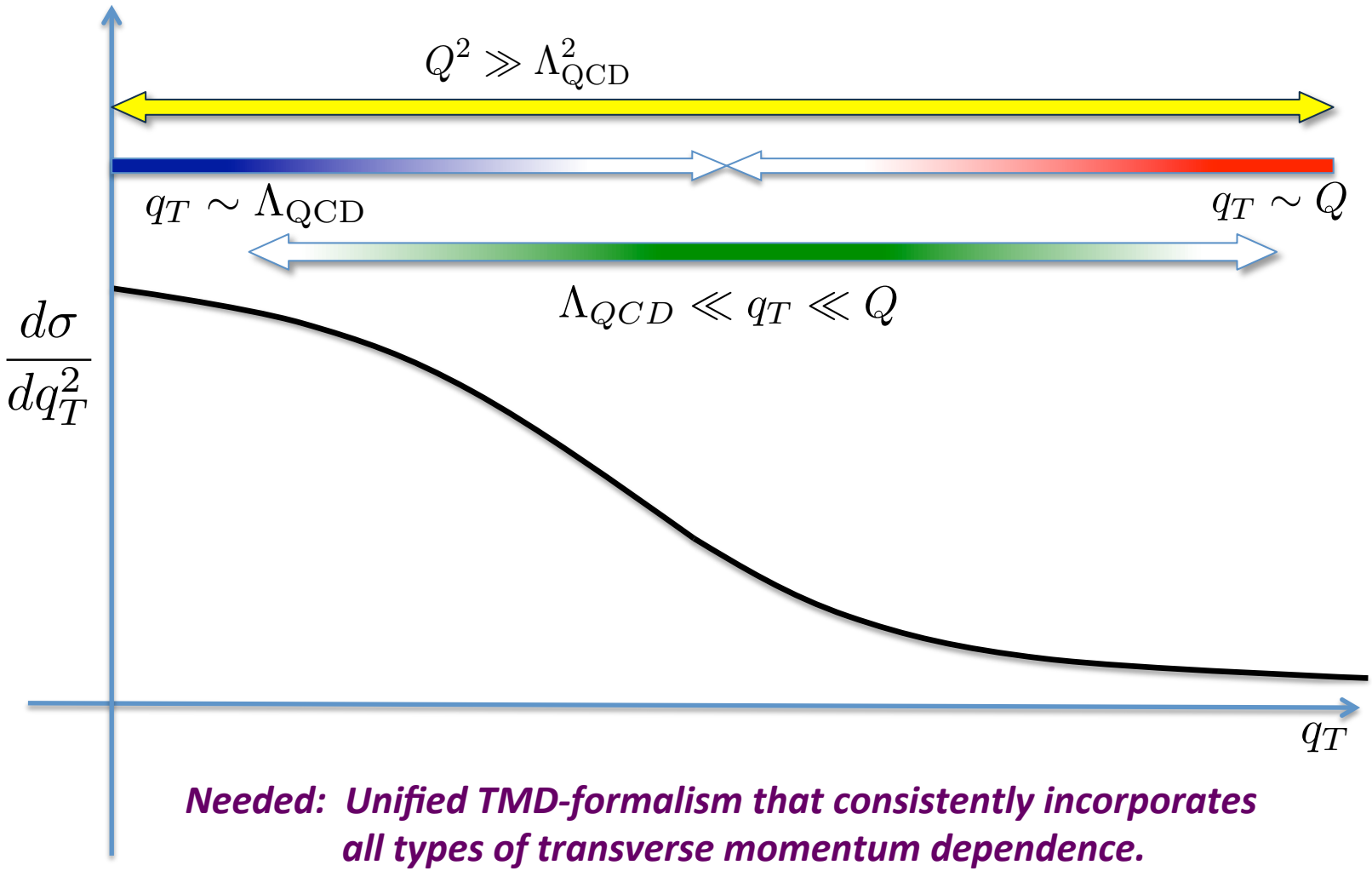

Needed: Unified TMD-formalism that consistently incorporates all types of transverse momentum dependence.

What is Needed from TMD-Factorization?

- q_T-distribution calculable in pQCD (small coupling and finite coefficients) for all q_T.

- TMD PDFs describing intrinsic properties of hadrons at low q_T.
  - Hard part calculable at $q_T \longrightarrow 0$.

- TMD PDFs separately well-defined with:
  - Universality (akin to collinear PDFs) or,
  - Non-Universality predicted by factorization derivation (e.g., Sivers sign flip) &,
  - Calculable Non-Universality from Evolution (evolution equations).

- Maximum perturbative input:
  - Transverse momentum dependence calculable using collinear factorization at intermediate q_T.
  - Match to totally collinear factorization description at large q_T.

- Error is Λ/Q suppressed point-by-point over full range of q_T.

TMD-Factorization

$$W_{DY}^{\mu\nu} = \sum_f |\mathcal{H}_f(Q;\mu/Q)|^{\mu\nu}$$

Each point and each term to be discussed in turn in rest of talk…

$$\times \int d^2\mathbf{k}_{1T}\, d^2\mathbf{k}_{2T}\, F_{f/P_1}(x_1, \mathbf{k}_{1T}; \mu; \zeta_1)\; F_{f/P_2}(x_2, \mathbf{k}_{2T}; \mu; \zeta_2)\, \delta^{(2)}(\mathbf{k}_{1T} + \mathbf{k}_{2T} - \mathbf{q}_T)$$

$$+ Y(q_T, Q)$$

$$+ \mathcal{O}\left(\left(\frac{\Lambda}{Q}\right)^a\right)$$

(Collins (2011) Chapters 10,13,14)

(Collins, Soper, Sterman (1982,1983))
(Ji, Ma, Yuan (2004))
…

What is Needed from TMD-Factorization?

- q_T-distribution calculable in pQCD (small coupling and finite coefficients) for all q_T.

Regions of Transverse Momentum:

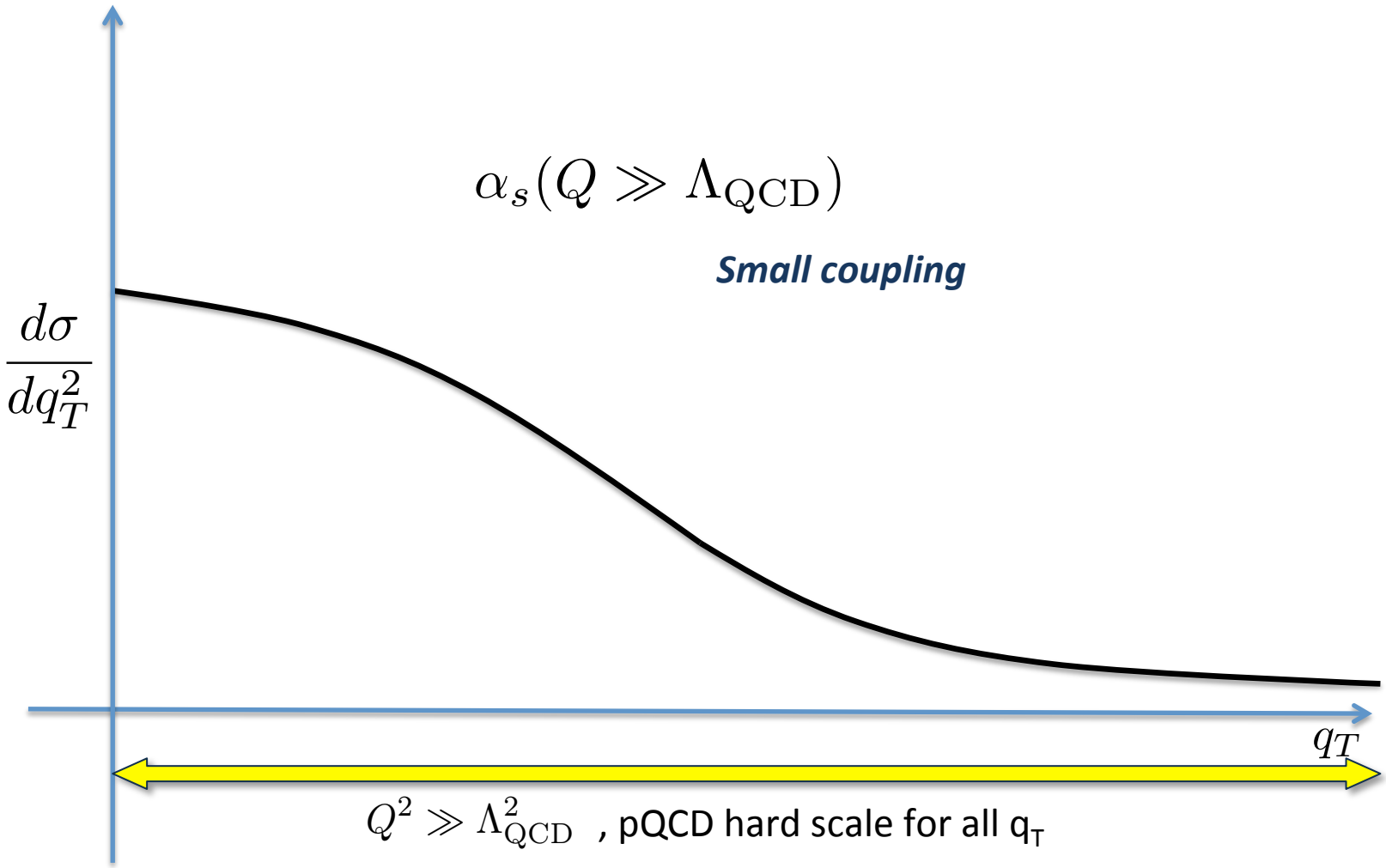

What is Needed from TMD-Factorization?

- q_T-distribution calculable in pQCD (small coupling and finite coefficients) for all q_T.

- TMD PDFs describing intrinsic properties of hadrons at low q_T.
  - Hard part calculable at $q_T \longrightarrow 0$.

TMD-Factorization

$$W_{DY}^{\mu\nu} = \sum_f |\mathcal{H}_f(Q;\mu/Q)|^{\mu\nu}$$

$$\times \int d^2\mathbf{k}_{1T}\, d^2\mathbf{k}_{2T}\, F_{f/P_1}(x_1, \mathbf{k}_{1T}; \mu; \zeta_1)\; F_{f/P_2}(x_2, \mathbf{k}_{2T}; \mu; \zeta_2)\, \delta^{(2)}(\mathbf{k}_{1T} + \mathbf{k}_{2T} - \mathbf{q}_T)$$

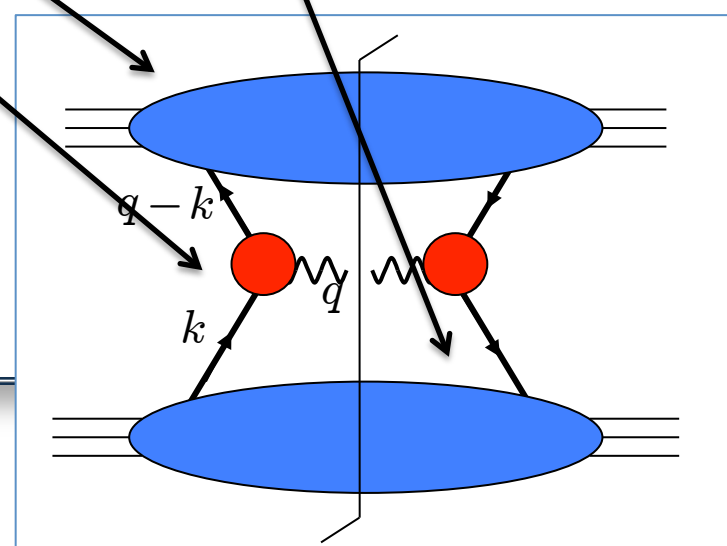

What is Needed from TMD-Factorization?

- q_T-distribution calculable in pQCD (small coupling and finite coefficients) for all q_T.

- TMD PDFs describing intrinsic properties of hadrons at low q_T.
  - Hard part calculable at $q_T \longrightarrow 0$.

What is Needed from TMD-Factorization?

- q_T-distribution calculable in pQCD (small coupling and finite coefficients) for all q_T.

- TMD PDFs describing intrinsic properties of hadrons at low q_T.
  - Hard part calculable at $q_T \longrightarrow 0$.

- TMD PDFs separately well-defined with:
  - Universality (akin to collinear PDFs) or,
  - Non-Universality predicted by factorization derivation (e.g., Sivers sign flip) &,
  - Calculable Non-Universality from Evolution (evolution equations).

TMD-Factorization

$$W_{DY}^{\mu\nu} = \sum_f |\mathcal{H}_f(Q;\mu/Q)|^{\mu\nu}$$

Similar to generalized TMD parton model

$$\times \int d^2\mathbf{k}_{1T}\, d^2\mathbf{k}_{2T}\, \underbrace{F_{f/P_1}(x_1, \mathbf{k}_{1T}; \mu; \zeta_1)}_{\text{TMD PDF for hadron 1.}}\, \underbrace{F_{f/P_2}(x_2, \mathbf{k}_{2T}; \mu; \zeta_2)}_{\text{TMD PDF for hadron 2.}}\, \delta^{(2)}(\mathbf{k}_{1T} + \mathbf{k}_{2T} - \mathbf{q}_T)$$

TMD part: $q_T \ll Q$

What is Needed from TMD-Factorization?

- q_T-distribution calculable in pQCD (small coupling and finite coefficients) for all q_T.

- TMD PDFs describing intrinsic properties of hadrons at low q_T.
  - Hard part calculable at $q_T \longrightarrow 0$.

- TMD PDFs separately well-defined with:
  - Universality (akin to collinear PDFs) or,
  - Non-Universality predicted by factorization derivation (e.g., Sivers sign flip) &,
  - Calculable Non-Universality from Evolution (evolution equations).

- Maximum perturbative input:
  - Transverse momentum dependence calculable using collinear factorization at intermediate q_T.

TMD-Factorization

$$W_{DY}^{\mu\nu} = \sum_f |\mathcal{H}_f(Q;\mu/Q)|^{\mu\nu}$$

$$\times \int d^2\mathbf{k}_{1T}\, d^2\mathbf{k}_{2T}\, F_{f/P_1}(x_1, \mathbf{k}_{1T}; \mu; \zeta_1)\; F_{f/P_2}(x_2, \mathbf{k}_{2T}; \mu; \zeta_2)\, \delta^{(2)}(\mathbf{k}_{1T} + \mathbf{k}_{2T} - \mathbf{q}_T)$$

$$F_{f/P_1}(x_1, \mathbf{k}_{1T}; \mu; \zeta_1) = \underbrace{\mathcal{C}_{f/f'}(x/x', \mathbf{k}_{1T}, \zeta_1, \mu, \alpha_s(\mu))}_{\textit{Perturbatively calculable coefficient functions}} \otimes \underbrace{f_{f'/P_1}(x'; \mu)}_{\textit{Collinear PDFs}} + \underbrace{\mathcal{O}\left(\frac{\Lambda_{QCD}}{k_{1T}}\right)}_{\textit{Error}}$$

TMD part

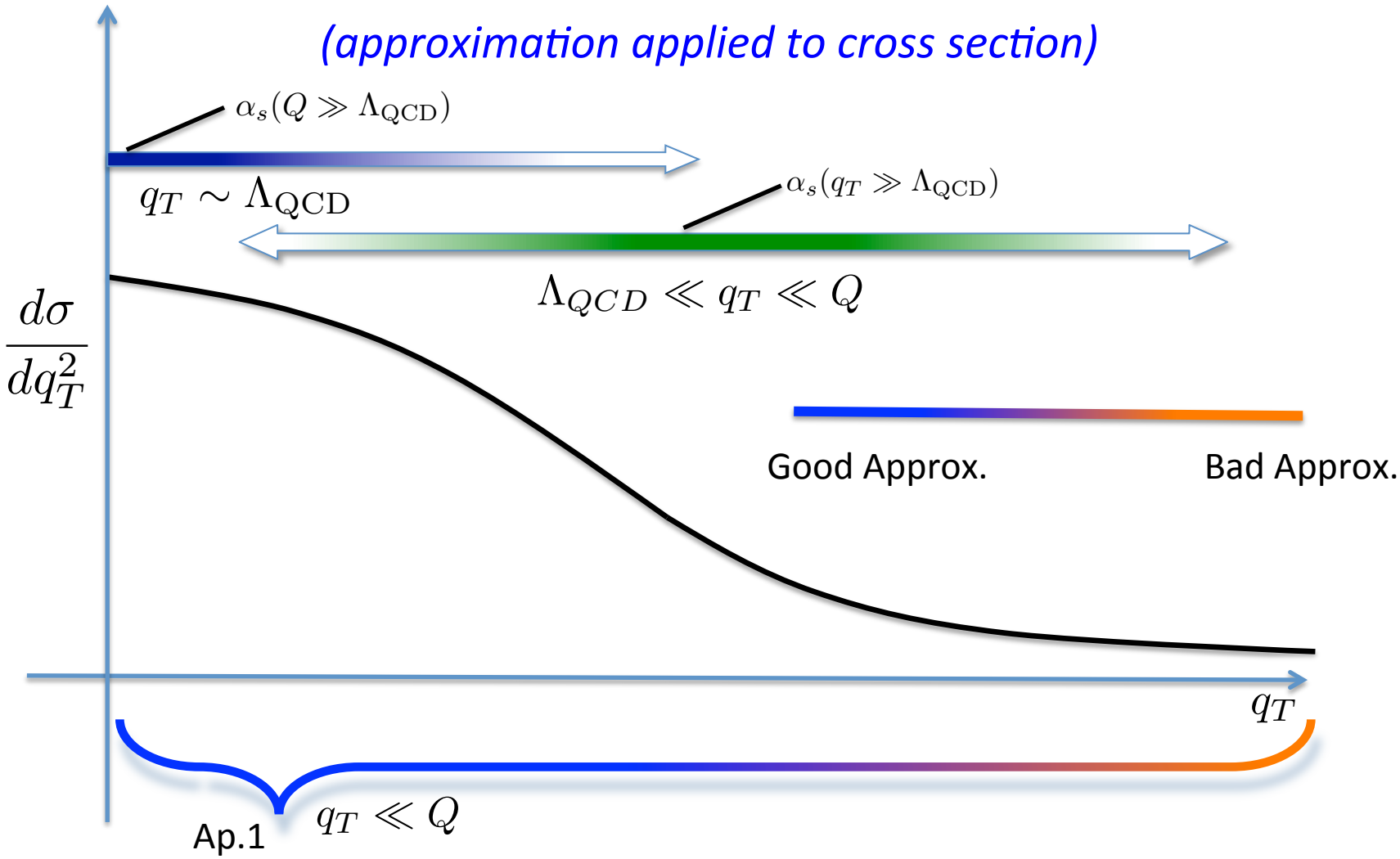
(approximation applied to cross section)
$\alpha_s(Q \gg \Lambda_{\rm QCD})$
$q_T \sim \Lambda_{\rm QCD}$
$\alpha_s(q_T \gg \Lambda_{\rm QCD})$
$\Lambda_{QCD} \ll q_T \ll Q$
$\frac{d\sigma}{dq_T^2}$
Good Approx.
Bad Approx.
q_T
Ap.1
$q_T \ll Q$

q_T regions:

- TMD part: **(q_T << Q)**

$$\frac{d\sigma}{dq_T} - \mathrm{Ap.1}\left(\frac{d\sigma}{dq_T}\right) = \mathcal{O}\left(\frac{q_T}{Q}\right) \times \frac{d\sigma}{dq_T}$$

What is Needed from TMD-Factorization?

- q_T-distribution calculable in pQCD (small coupling and finite coefficients) for all q_T.

- TMD PDFs describing intrinsic properties of hadrons at low q_T.
  - Hard part calculable at $q_T \longrightarrow 0$.

- TMD PDFs separately well-defined with:
  - Universality (akin to collinear PDFs) or,
  - Non-Universality predicted by factorization derivation (e.g., Sivers sign flip) &,
  - Calculable Non-Universality from Evolution (evolution equations).

- Maximum perturbative input:
  - Transverse momentum dependence calculable using collinear factorization at intermediate q_T.
  - Match to totally collinear factorization description at large q_T.

TMD-Factorization

$$W_{DY}^{\mu\nu} = \sum_f |\mathcal{H}_f(Q;\mu/Q)|^{\mu\nu}$$

$$\times \int d^2\mathbf{k}_{1T}\, d^2\mathbf{k}_{2T}\, F_{f/P_1}(x_1, \mathbf{k}_{1T}; \mu; \zeta_1)\; F_{f/P_2}(x_2, \mathbf{k}_{2T}; \mu; \zeta_2)\, \delta^{(2)}(\mathbf{k}_{1T} + \mathbf{k}_{2T} - \mathbf{q}_T)$$

$$+ Y(q_T, Q)$$

Largest q_T:

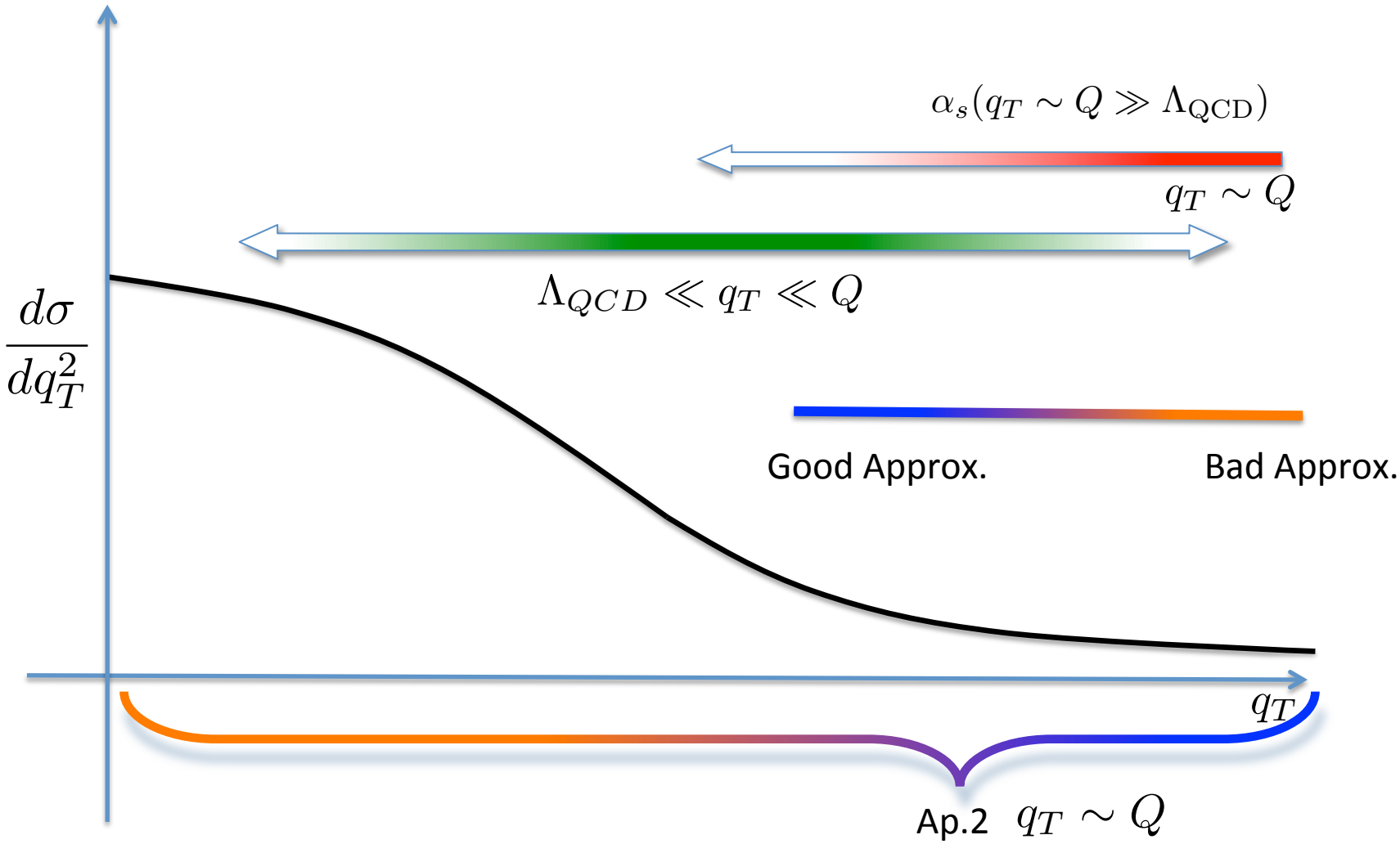
$\alpha_s(q_T \sim Q \gg \Lambda_{\rm QCD})$
$q_T \sim Q$
$\Lambda_{QCD} \ll q_T \ll Q$
$\frac{d\sigma}{dq_T^2}$
Good Approx.
Bad Approx.
q_T
Ap.2 $q_T \sim Q$

Approximations:

- TMD part: **(q_T << Q)**

$$\frac{d\sigma}{dq_T} - \mathrm{Ap.1}\left(\frac{d\sigma}{dq_T}\right) = \mathcal{O}\left(\frac{q_T}{Q}\right) \times \frac{d\sigma}{dq_T}$$

- Y-term: **(Remainder)**

$$\begin{aligned}
&\mathrm{Ap.2}\left(\frac{d\sigma}{dq_T} - \mathrm{Ap.1}\left(\frac{d\sigma}{dq_T}\right)\right) \\
&\qquad = \left(\frac{d\sigma}{dq_T} - \mathrm{Ap.1}\left(\frac{d\sigma}{dq_T}\right)\right) + \mathcal{O}\left(\frac{\Lambda_{\mathrm{QCD}}}{q_T}\right) \times \left(\frac{d\sigma}{dq_T} - \mathrm{Ap.1}\left(\frac{d\sigma}{dq_T}\right)\right) \\
&\qquad = \left(\frac{d\sigma}{dq_T} - \mathrm{Ap.1}\left(\frac{d\sigma}{dq_T}\right)\right) + \mathcal{O}\left(\frac{\Lambda_{\mathrm{QCD}}}{\cancel{q_T}}\right) \times \mathcal{O}\left(\frac{\cancel{q_T}}{Q}\right) \times \frac{d\sigma}{dq_T}
\end{aligned}$$

Approximations:

- TMD part: **(q_T << Q)**

$$\frac{d\sigma}{dq_T} - \mathrm{Ap.1}\left(\frac{d\sigma}{dq_T}\right) = \mathcal{O}\left(\frac{q_T}{Q}\right) \times \frac{d\sigma}{dq_T}$$

- Y-term: **(Remainder)**

$$\mathrm{Ap.2}\left(\frac{d\sigma}{dq_T} - \mathrm{Ap.1}\left(\frac{d\sigma}{dq_T}\right)\right)$$
$$= \left(\frac{d\sigma}{dq_T} - \mathrm{Ap.1}\left(\frac{d\sigma}{dq_T}\right)\right) + \mathcal{O}\left(\frac{\Lambda_{\mathrm{QCD}}}{q_T}\right) \times \left(\frac{d\sigma}{dq_T} - \mathrm{Ap.1}\left(\frac{d\sigma}{dq_T}\right)\right)$$
$$= \left(\frac{d\sigma}{dq_T} - \mathrm{Ap.1}\left(\frac{d\sigma}{dq_T}\right)\right) + \mathcal{O}\left(\frac{\Lambda_{\mathrm{QCD}}}{\cancel{q_T}}\right) \times \mathcal{O}\left(\frac{\cancel{q_T}}{Q}\right) \times \frac{d\sigma}{dq_T}$$

- Total:

$$\frac{d\sigma}{dq_T} = \mathrm{Ap.1}\left(\frac{d\sigma}{dq_T}\right) + \left(\frac{d\sigma}{dq_T} - \mathrm{Ap.1}\left(\frac{d\sigma}{dq_T}\right)\right)$$
$$= \underbrace{\mathrm{Ap.1}\left(\frac{d\sigma}{dq_T}\right)}_{\textit{TMD part}} + \underbrace{\mathrm{Ap.2}\left(\frac{d\sigma}{dq_T} - \mathrm{Ap.1}\left(\frac{d\sigma}{dq_T}\right)\right)}_{\textit{Y-term}} + \underbrace{\mathcal{O}\left(\frac{\Lambda_{\mathrm{QCD}}}{Q}\right) \times \frac{d\sigma}{dq_T}}_{\textit{Error}}$$

Regions of Transverse Momentum:

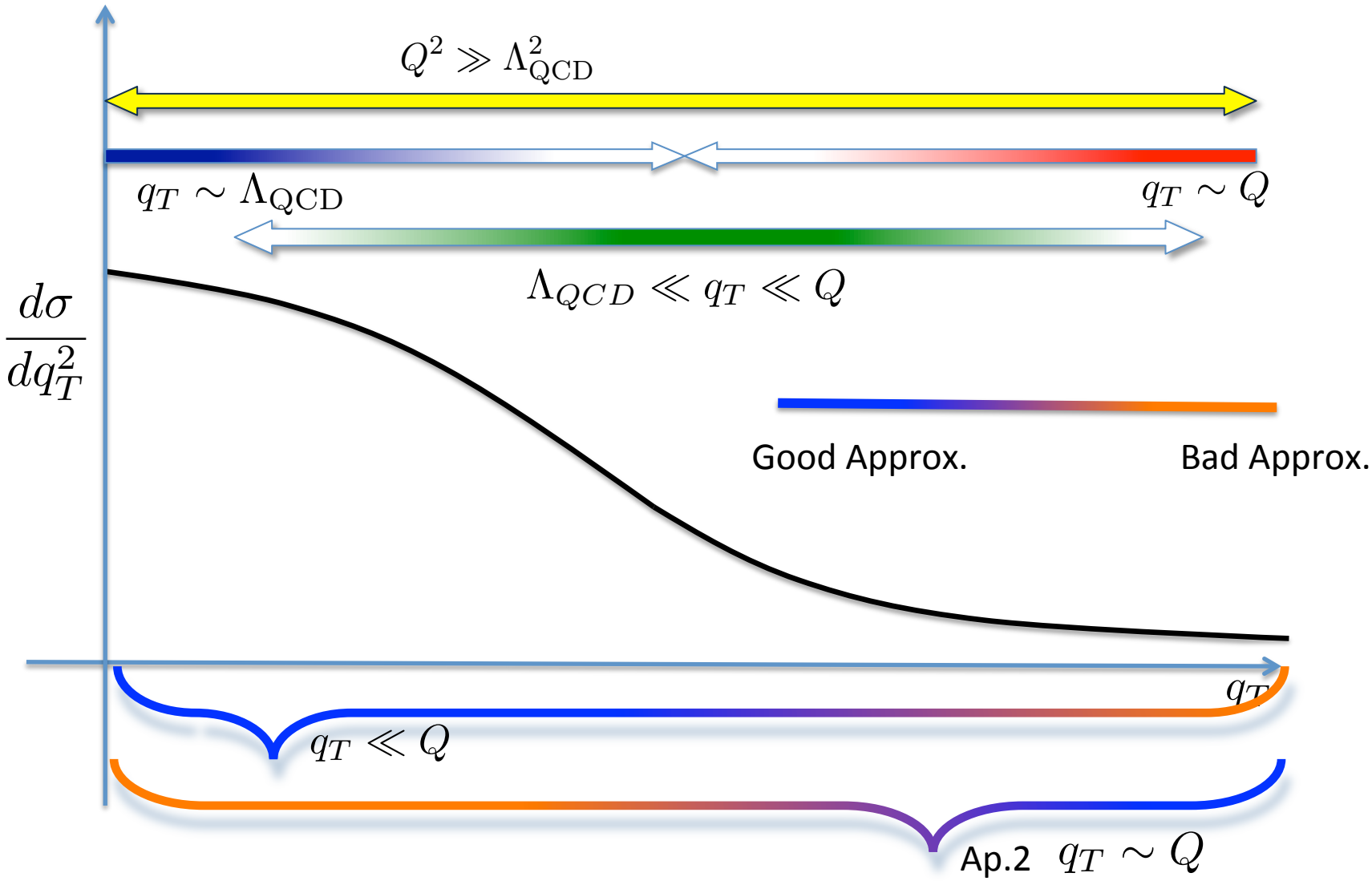

TMD-factorization

$$W_{DY}^{\mu\nu} = \sum_f |\mathcal{H}_f(Q;\mu/Q)|^{\mu\nu}$$

$$\times \int d^2\mathbf{k}_{1T}\, d^2\mathbf{k}_{2T}\, F_{f/P_1}(x_1, \mathbf{k}_{1T}; \mu; \zeta_1)\; F_{f/P_2}(x_2, \mathbf{k}_{2T}; \mu; \zeta_2)\, \delta^{(2)}(\mathbf{k}_{1T} + \mathbf{k}_{2T} - \mathbf{q}_T)$$

$$+ Y(q_T, Q)$$

$$\boxed{+ \mathcal{O}\left(\left(\frac{\Lambda}{Q}\right)^a\right)}$$

What is Needed from TMD-Factorization?

- q_T-distribution calculable in pQCD (small coupling and finite coefficients) for all q_T.

- TMD PDFs describing intrinsic properties of hadrons at low q_T.
  - Hard part calculable at $q_T \longrightarrow 0$.

- TMD PDFs separately well-defined with:
  - Universality (akin to collinear PDFs) or,
  - Non-Universality predicted by factorization derivation (e.g., Sivers sign flip) &,
  - Calculable Non-Universality from Evolution (evolution equations).

- Maximum perturbative input:
  - Transverse momentum dependence calculable using collinear factorization at intermediate q_T.
  - Match to totally collinear factorization description at large q_T.

- Error is Λ/Q suppressed point-by-point over full range of q_T.

Focus: TMD part

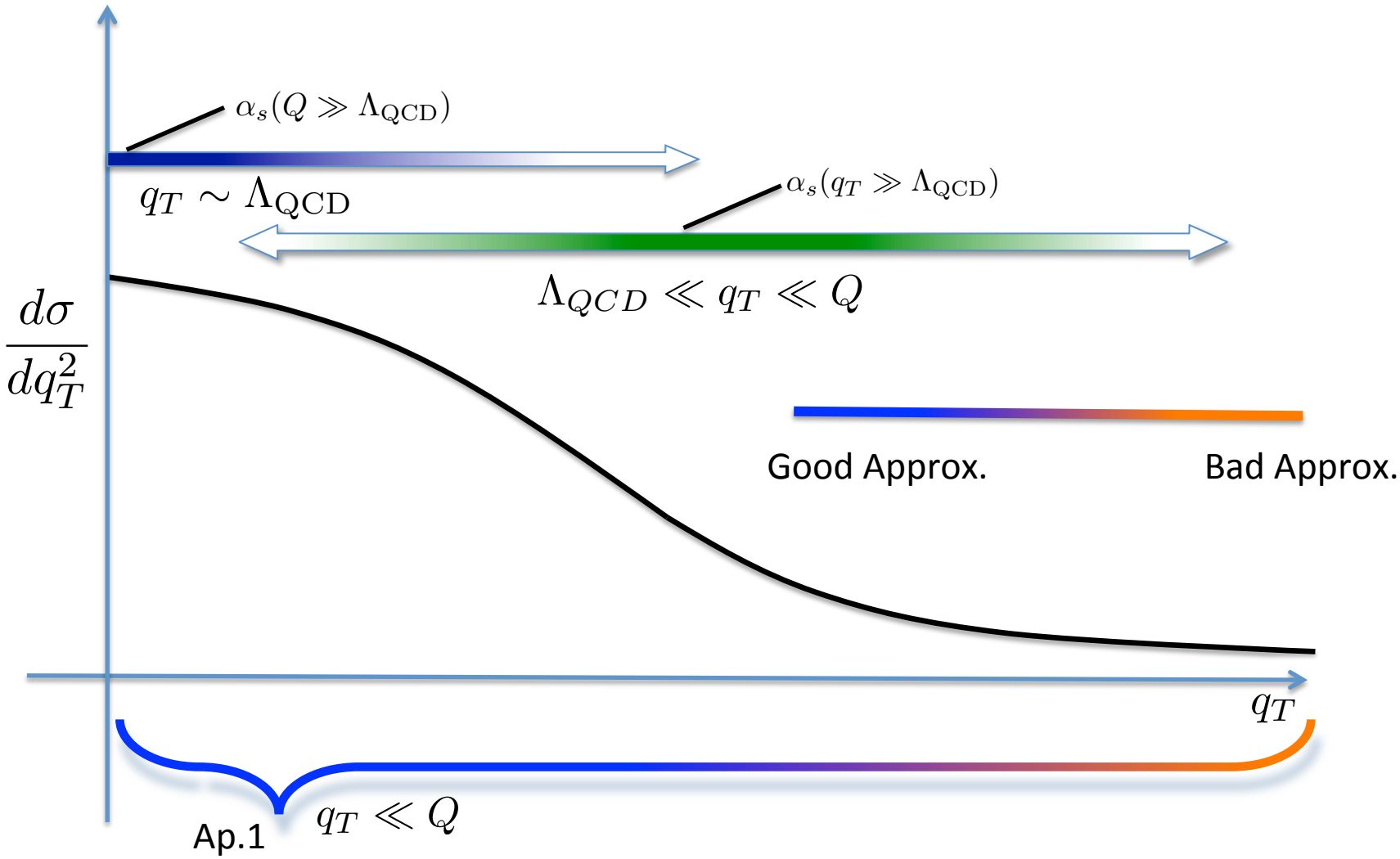

What is Needed from TMD-Factorization?

- q_T-distribution calculable in pQCD (small coupling and finite coefficients) for all q_T.

- TMD PDFs describing intrinsic properties of hadrons at low q_T.
  - Hard part calculable at $q_T \longrightarrow 0$.

- TMD PDFs separately well-defined with:
  - Universality (akin to collinear PDFs) or,
  - Non-Universality predicted by factorization derivation (e.g., Sivers sign flip) &,
  - Calculable Non-Universality from Evolution (evolution equations).

- Maximum perturbative input:
  - Transverse momentum dependence calculable using collinear factorization at intermediate q_T.
  - Match to totally collinear factorization description at large q_T.

- Error is Λ/Q suppressed point-by-point over full range of q_T.

Definitions:

- Integrated PDF:

$$f(x) = \text{F.T.}\, \langle p|\, \bar{\psi}(0, w^-, \mathbf{0}_t) \underline{V_w^\dagger(u_\text{J})} \gamma^+ \underline{V_0(u_\text{J})} \psi(0) |p\rangle$$

$$u_\text{J} = (0, 1, \mathbf{0}_t)$$

- TMD PDF:

$$F_{f/P_1}(x_1, \mathbf{k}_{1T}) = \quad \text{F.T.}\, \langle p|\, \bar{\psi}(0, w^-, \mathbf{w}_t) \quad \underline{??} \quad \psi(0)\, |p\rangle$$

Definitions:

- Paths of Wilson lines in <u>coordinate space</u>:

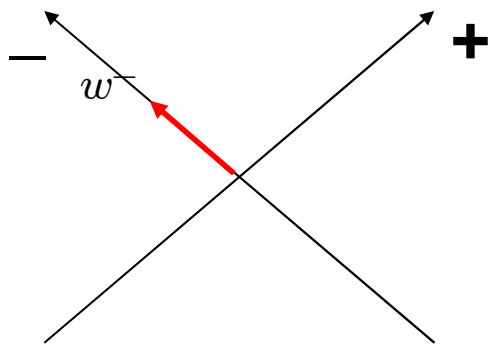

Standard (Integrated)

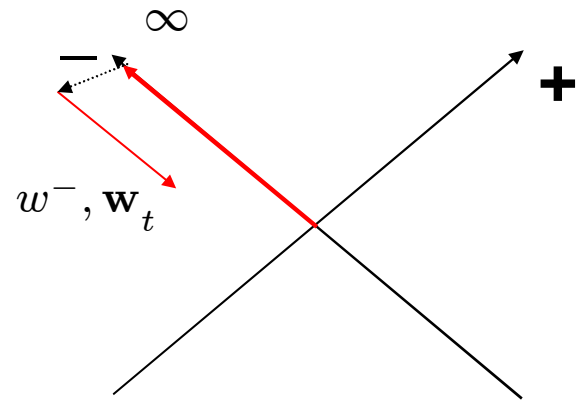

Unintegrated First Try

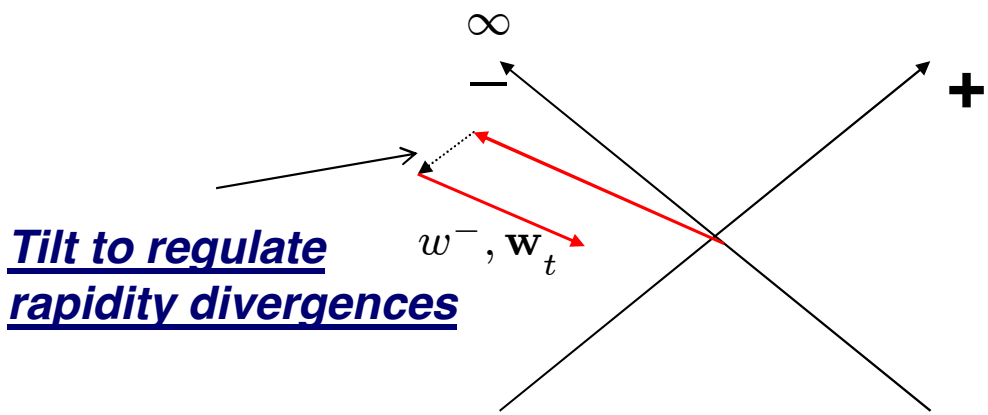

<u>Tilt to regulate rapidity divergences</u>

Unintegrated "tilted" Wilson lines

Definitions:

- "Unsubtracted" TMD PDF:

$$\tilde{F}^{\text{unsub}}_{f/P}(x, \mathbf{b}; \mu; y_P - y_B) \sim \text{F.T.}$$

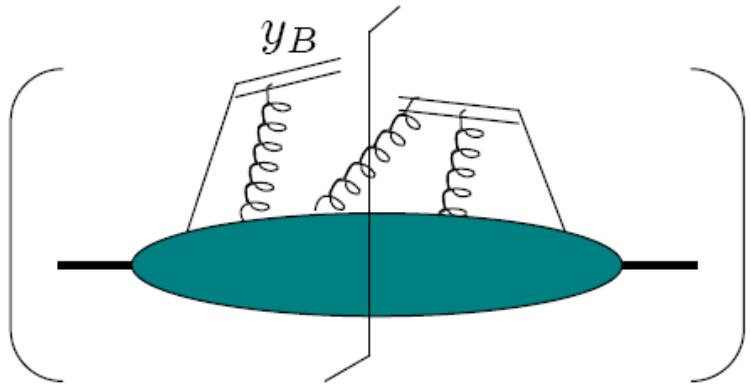

- Soft Factor:

$$\tilde{S}(\mathbf{b}; y_A, y_B) \sim \text{F.T.}$$

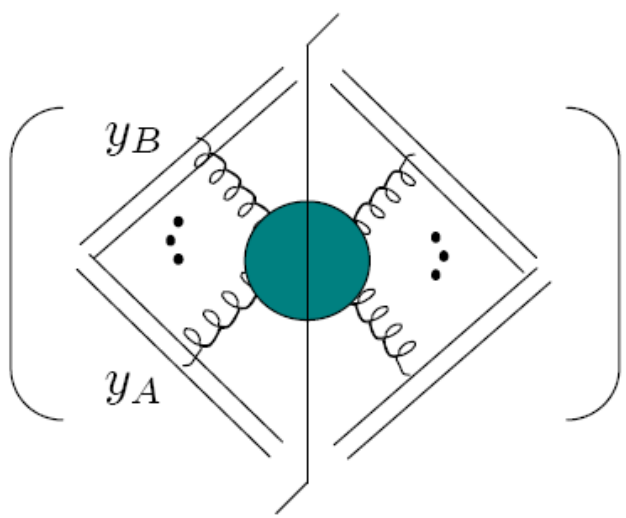

Definitions:

(Dictated by factorization requirements)

$$F_{f/P}(x, b; \mu; \zeta_F) = \sqrt{\frac{\quad}{\quad}}$$

$$\zeta_F = 2M_p^2 x^2 e^{2(y_P - y_s)}$$

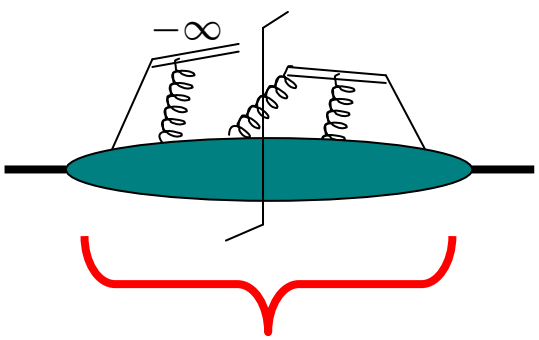

"Unsubtracted"

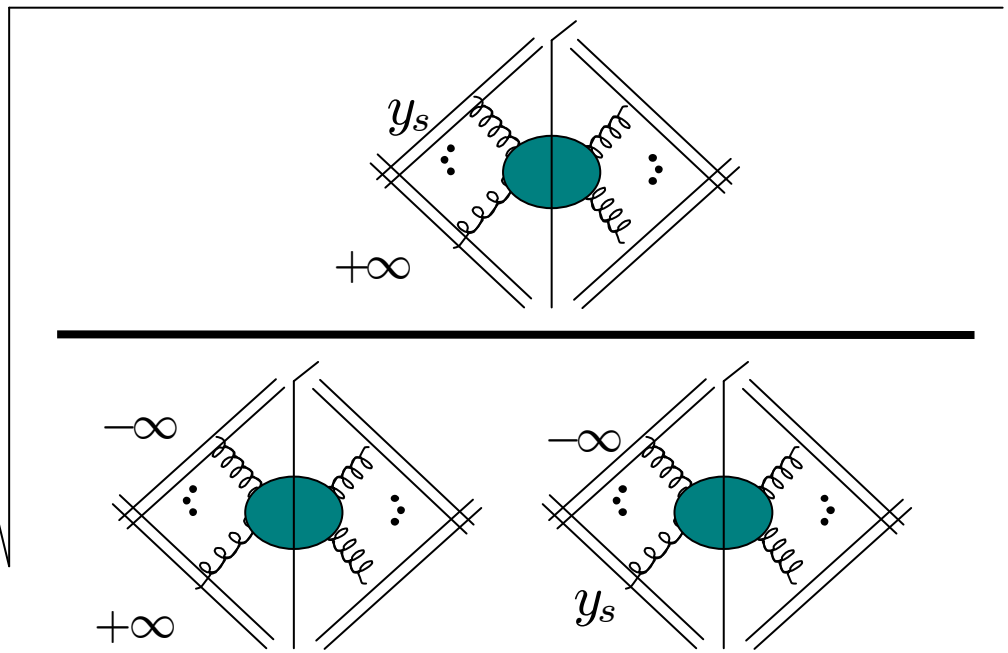

(UV and rapidity renormalization needed)

Implements Subtractions/Cancellations

(Collins (2011), chapt. 13)

Example:

- Drell-Yan q_T distribution.

Get $\dfrac{d\sigma}{d\mathbf{q}_T \cdots}$

For <u>all</u> q_T.

$$q^2 = Q^2 \gg \Lambda^2_{QCD}$$

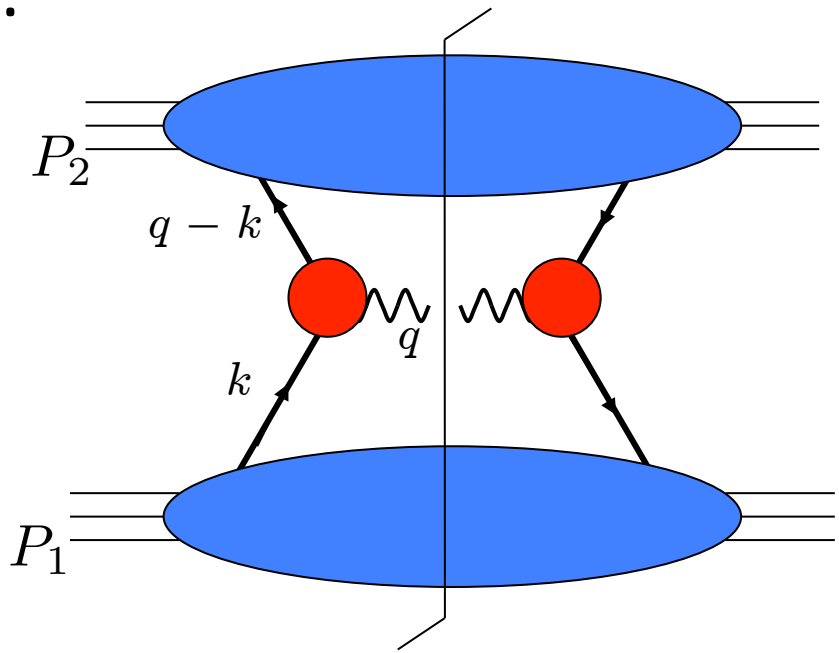

$$k_1 = k$$

$$k_2 = q - k$$

$$\mathbf{k}_{1T} + \mathbf{k}_{2T} = \mathbf{q}_T$$

Definitions:

(Dictated by factorization requirements)

$$\zeta_1\zeta_2 \sim Q^4$$

$$F_{f/P}(x, b; \mu; \zeta_F) = \qquad \zeta_F = 2M_p^2 x^2 e^{2(y_P - y_s)}$$

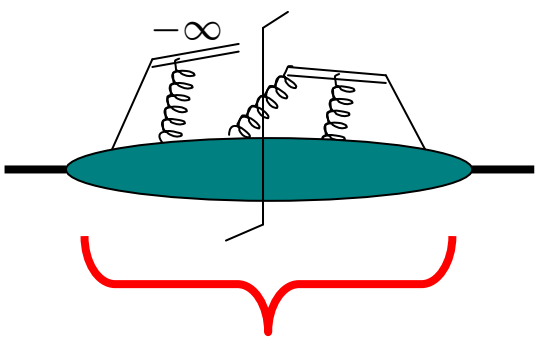

"Unsubtracted"

$\times$

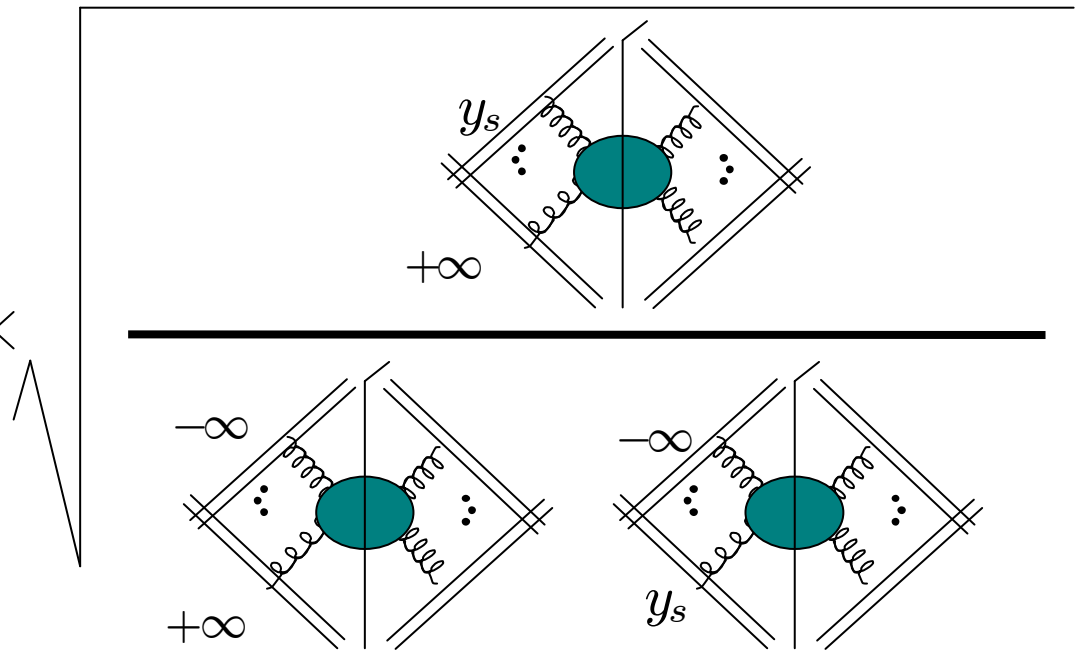

(UV and rapidity renormalization needed)

Implements Subtractions/Cancellations

(Collins (2011), chapt. 13)

Origin of Square Root

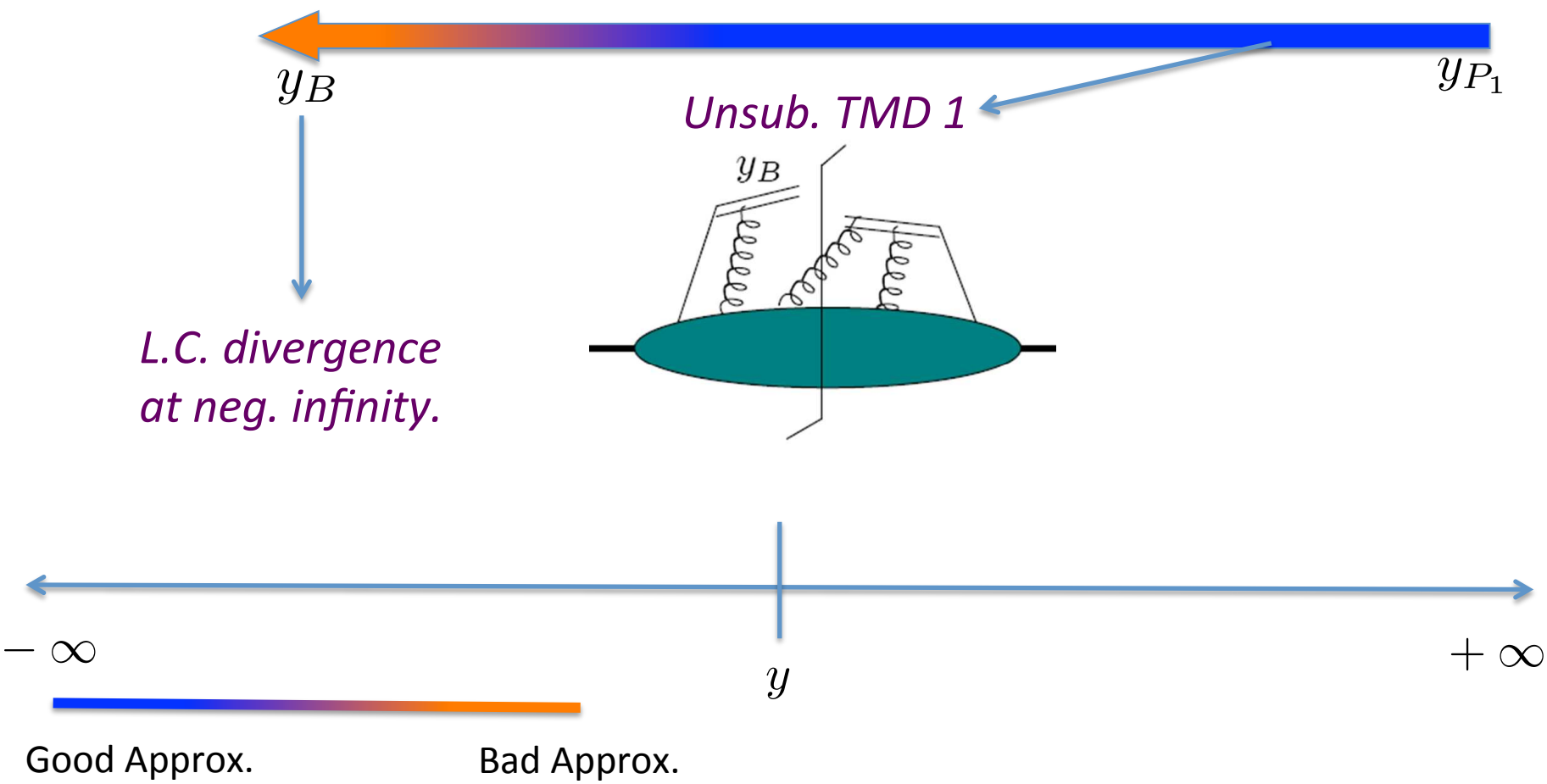

Origin of Square Root

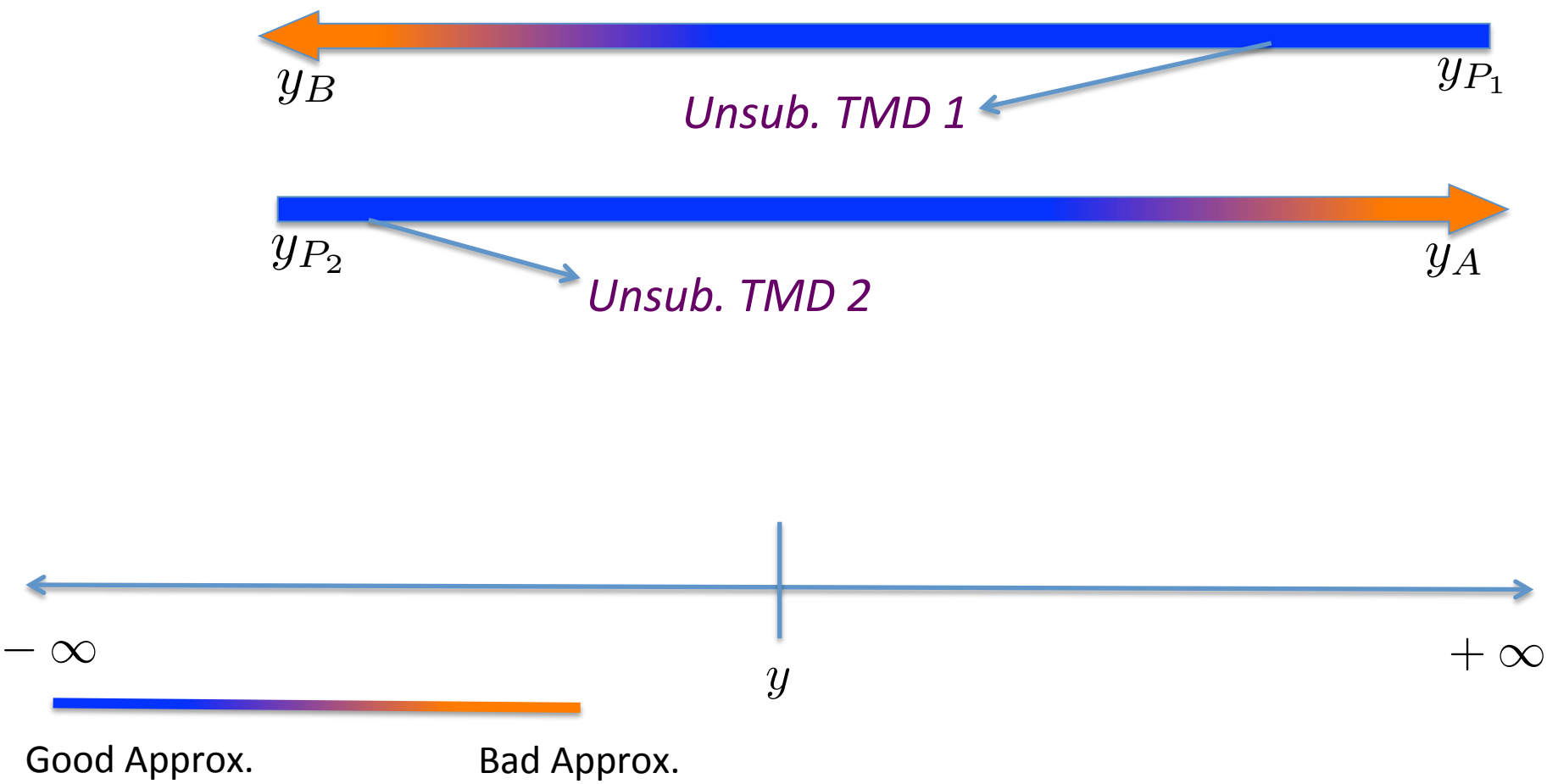

Origin of Square Root

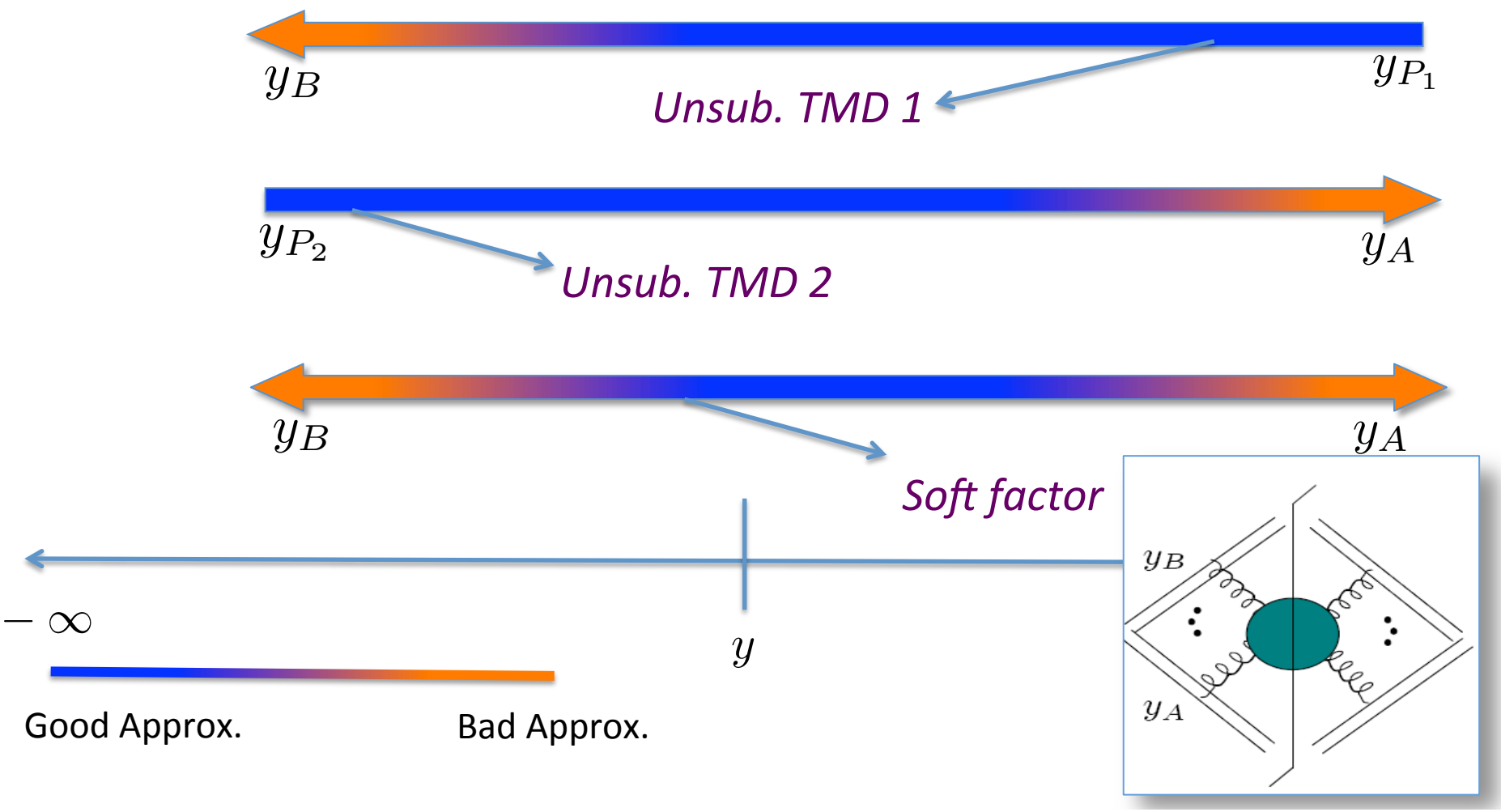

Origin of Square Root

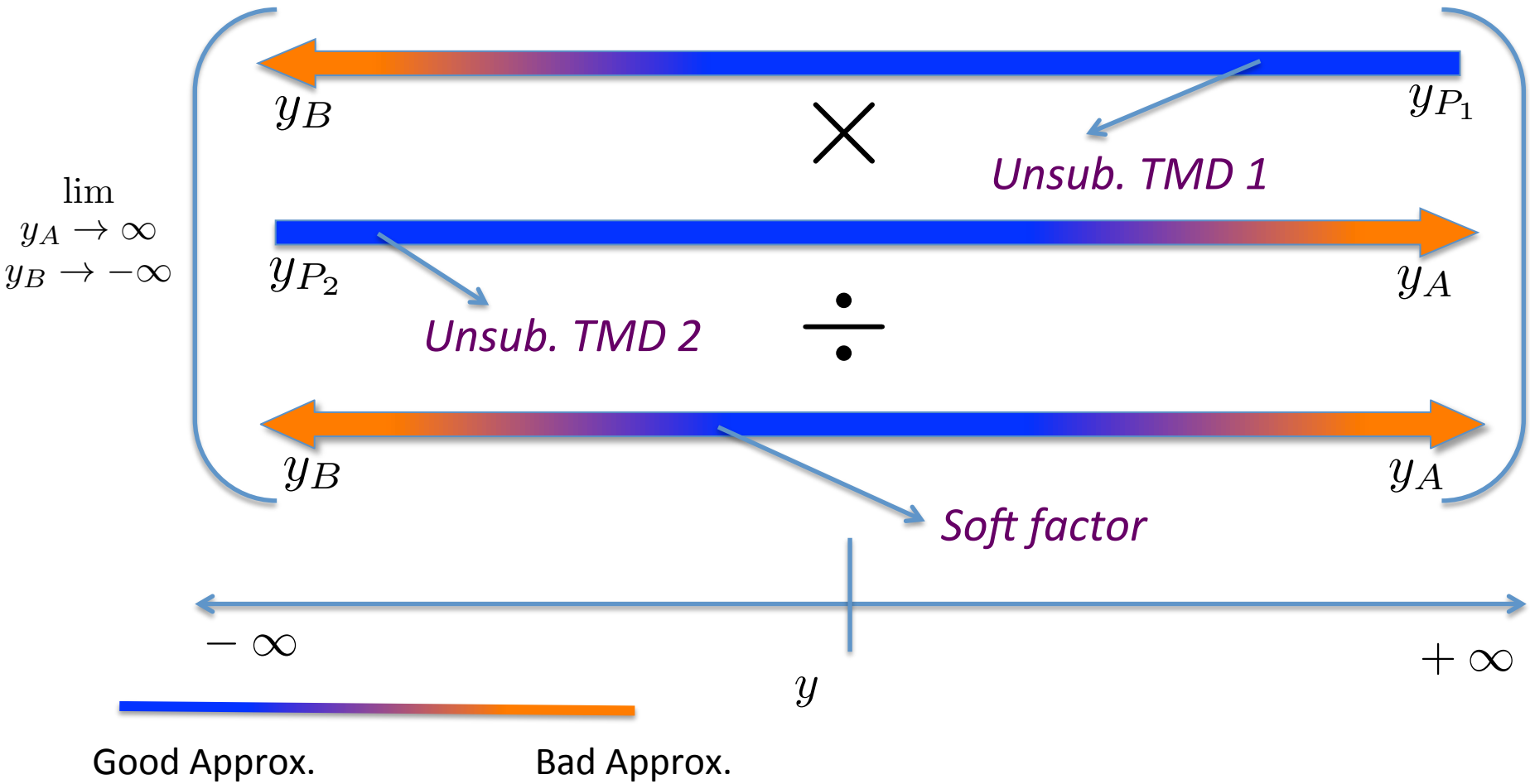

Origin of Square Root

- Start with only the hard part factorized:

$$d\sigma = |\mathcal{H}|^2 \, \frac{\tilde{F}_1^{\text{unsub}}(y_1 - (-\infty)) \times \tilde{F}_2^{\text{unsub}}(+\infty - y_2)}{\tilde{S}(+\infty, -\infty)}.$$

Origin of Square Root

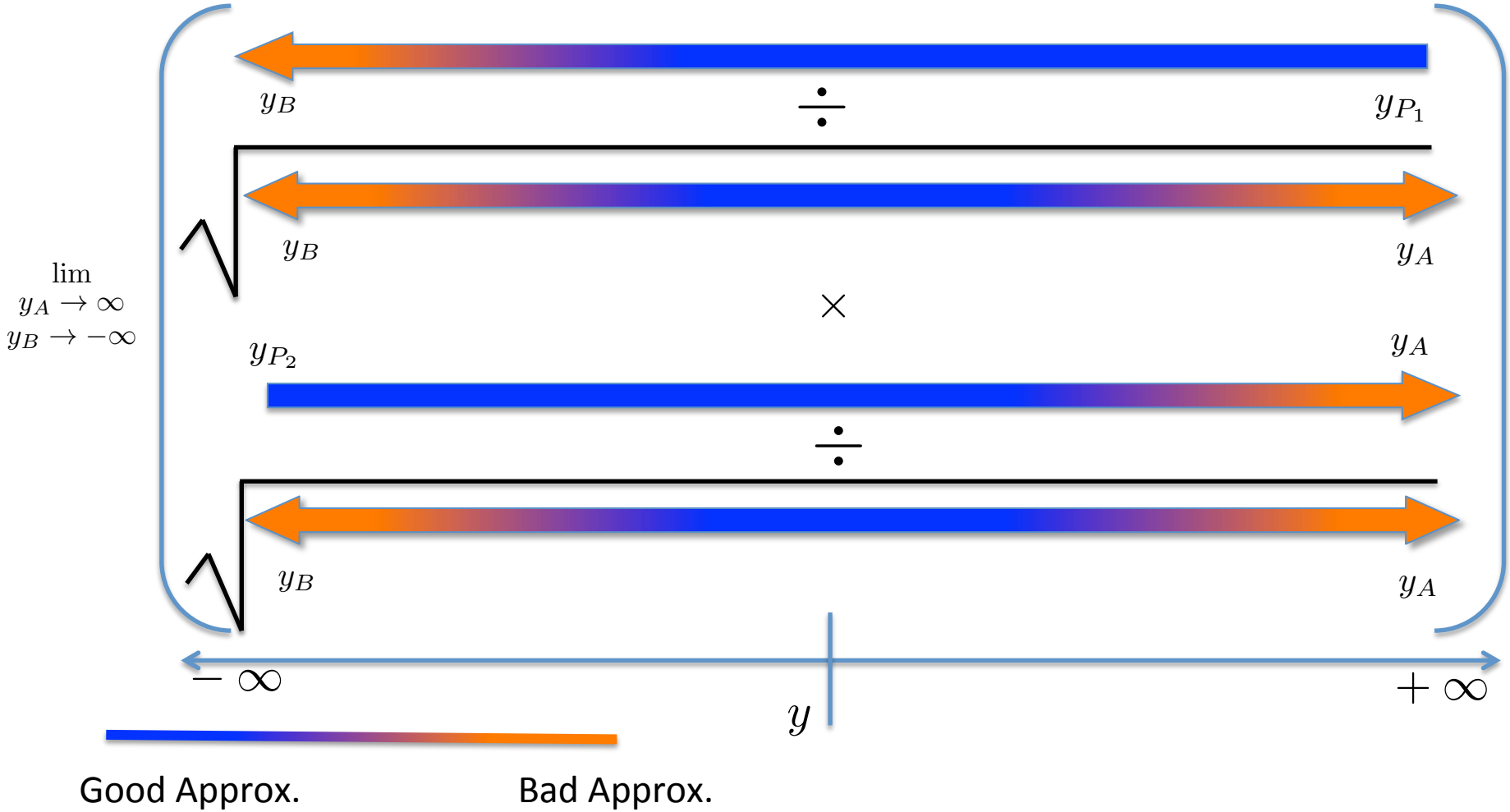

Good Approx. Bad Approx.

Origin of Square Root

- Start with only the hard part factorized:

$$d\sigma = |\mathcal{H}|^2 \, \frac{\tilde{F}_1^{\text{unsub}}(y_1 - (-\infty)) \times \tilde{F}_2^{\text{unsub}}(+\infty - y_2)}{\tilde{S}(+\infty, -\infty)}.$$

- Separate soft part:

$$d\sigma = |\mathcal{H}|^2 \, \frac{F_1^{\text{unsub}}(y_1 - (-\infty))}{\sqrt{\tilde{S}(+\infty, -\infty)}} \times \frac{\tilde{F}_2^{\text{unsub}}(+\infty - y_2)}{\sqrt{\tilde{S}(+\infty, -\infty)}}.$$

Origin of Square Root

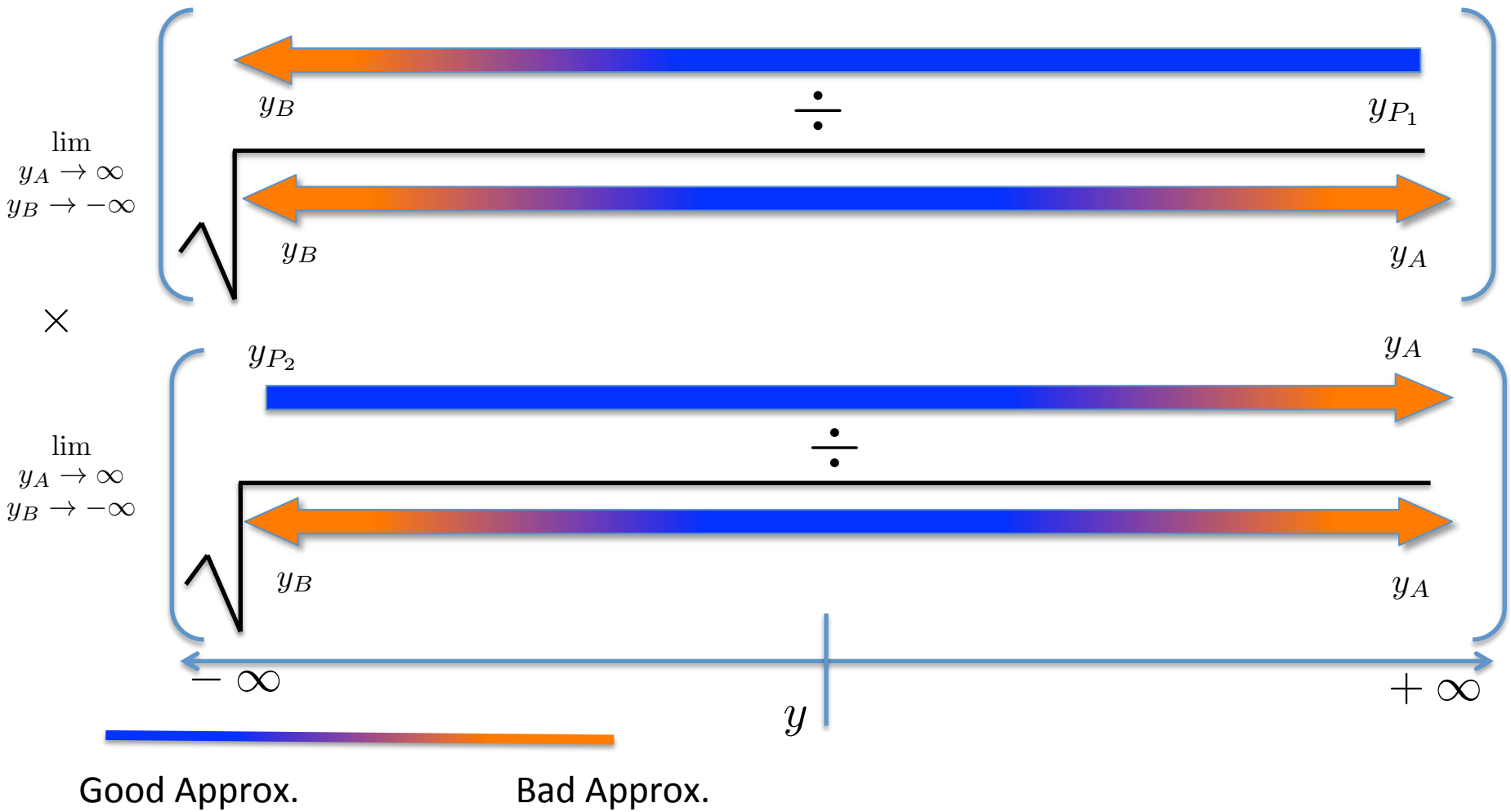

Origin of Square Root

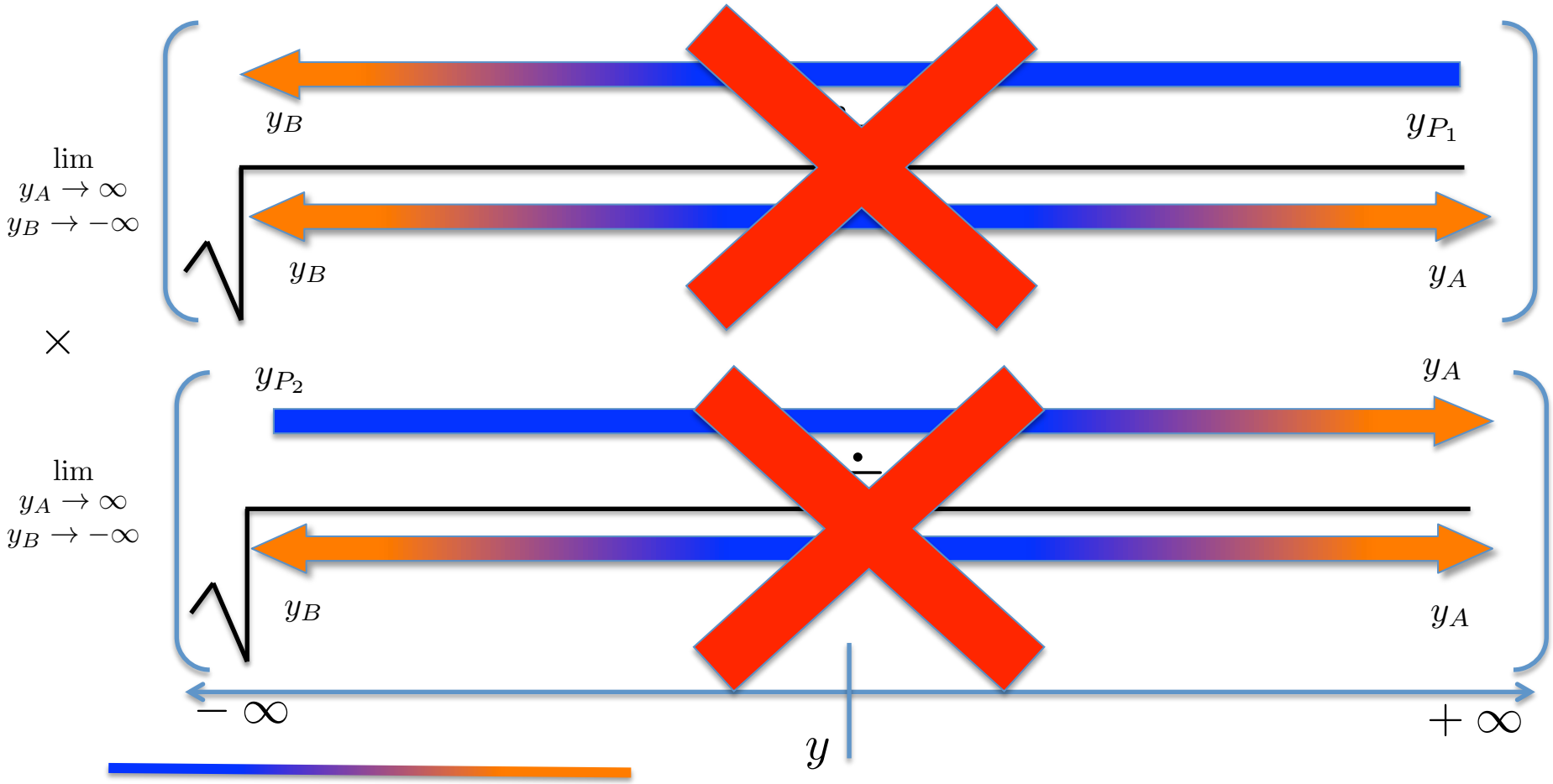

Good Approx. Bad Approx.

Origin of Square Root

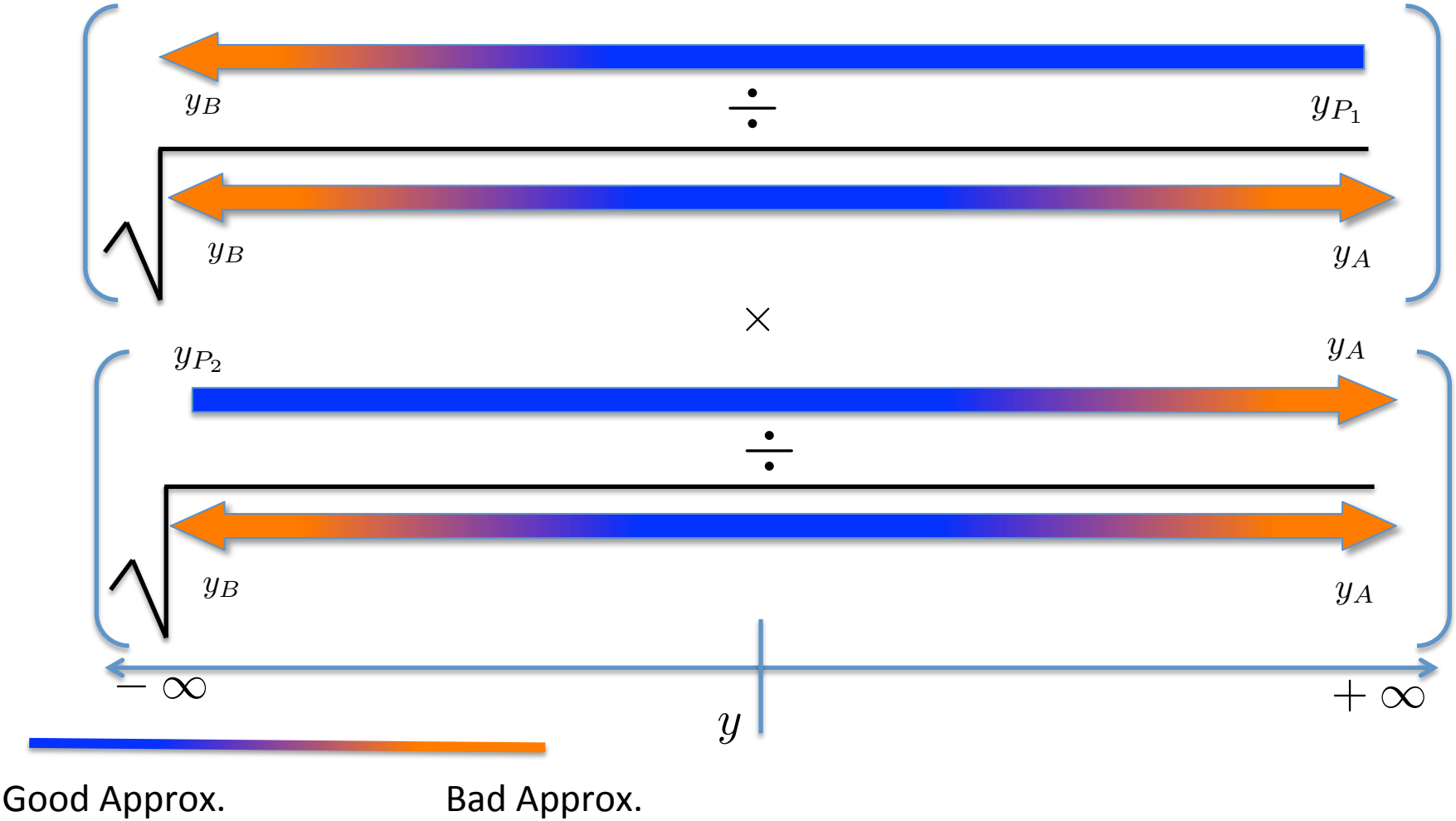

Good Approx. Bad Approx.

Origin of Square Root

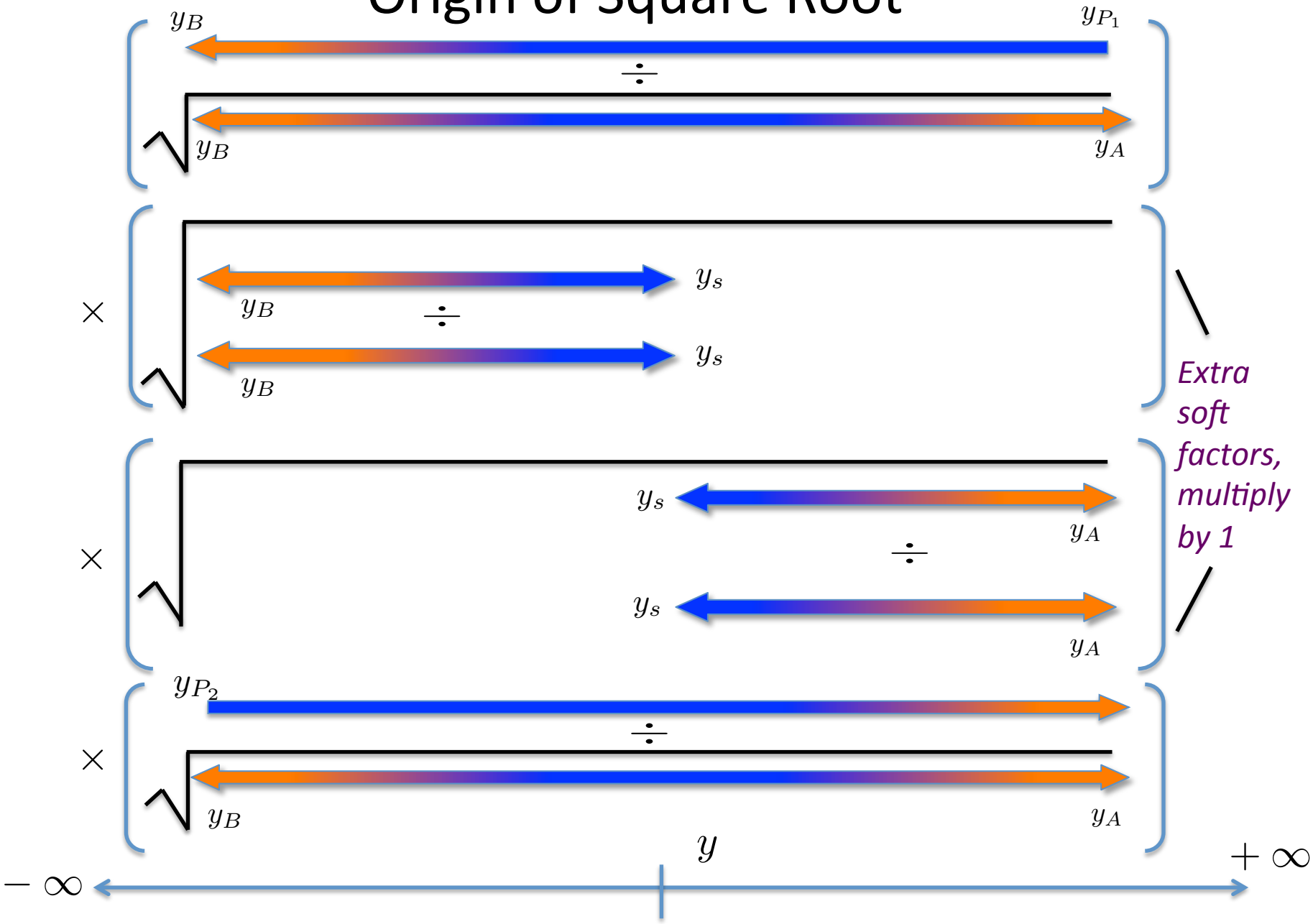

Origin of Square Root

- Start with only the hard part factorized:

$$d\sigma = |\mathcal{H}|^2 \, \frac{\tilde{F}_1^{\text{unsub}}(y_1 - (-\infty)) \times \tilde{F}_2^{\text{unsub}}(+\infty - y_2)}{\tilde{S}(+\infty, -\infty)}.$$

- Separate soft part:

$$d\sigma = |\mathcal{H}|^2 \, \frac{F_1^{\text{unsub}}(y_1 - (-\infty))}{\sqrt{\tilde{S}(+\infty, -\infty)}} \times \frac{\tilde{F}_2^{\text{unsub}}(+\infty - y_2)}{\sqrt{\tilde{S}(+\infty, -\infty)}}.$$

- Multiply by: $\dfrac{\sqrt{\tilde{S}(+\infty, y_s)\, \tilde{S}(y_s, -\infty)}}{\sqrt{\tilde{S}(+\infty, y_s)\, \tilde{S}(y_s, -\infty)}}$

Origin of Square Root

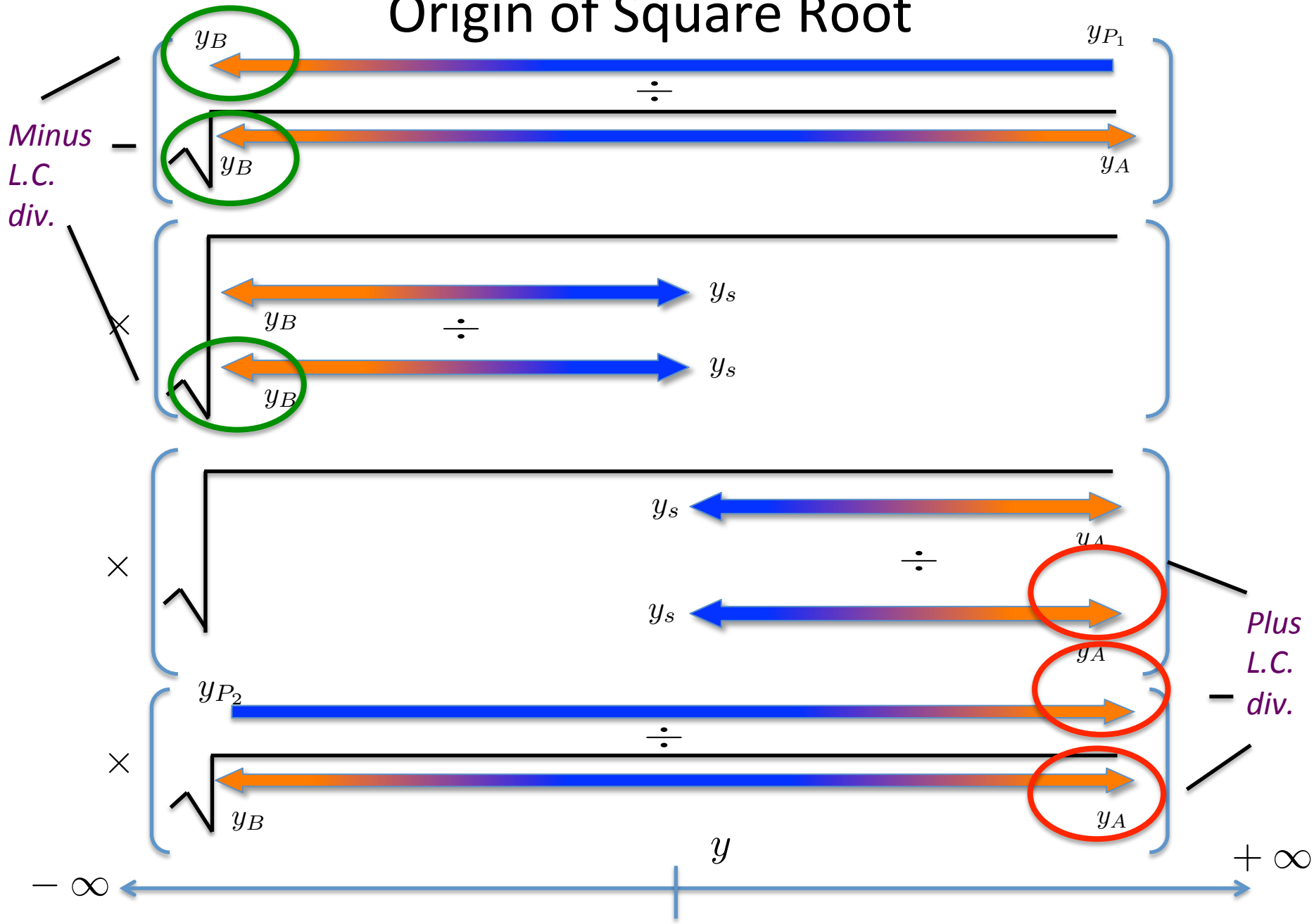

Origin of Square Root

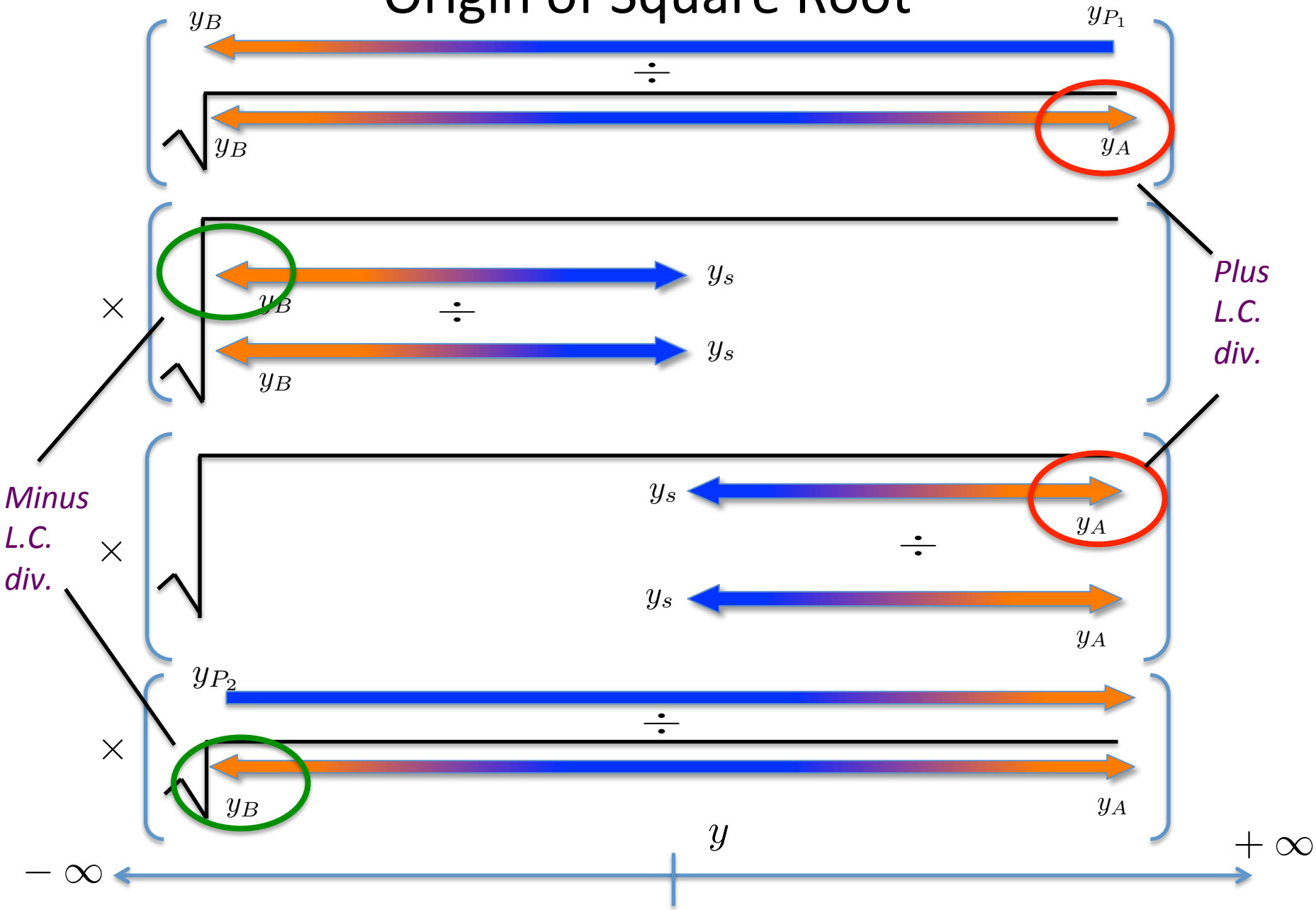

Origin of Square Root

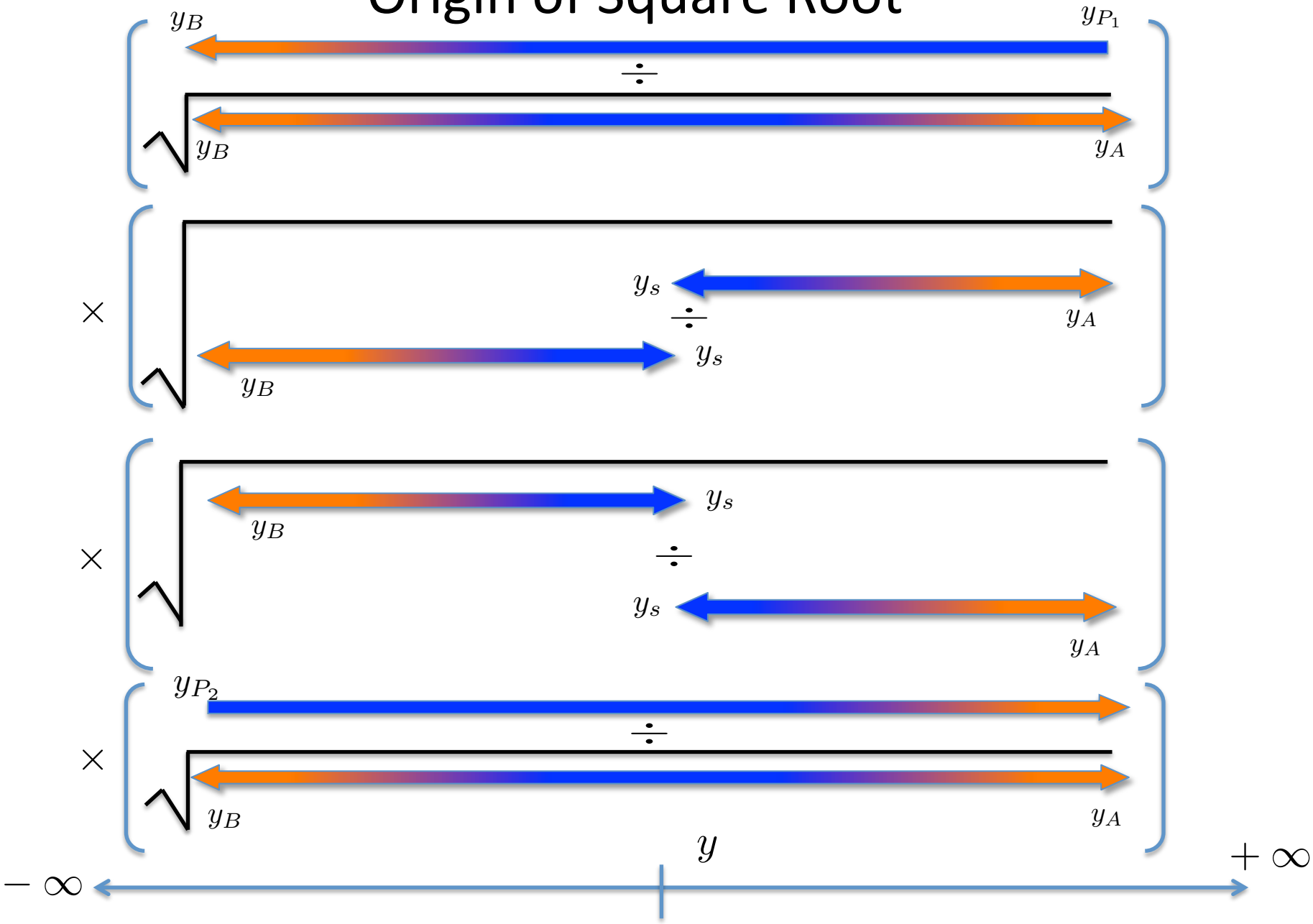

Origin of Square Root

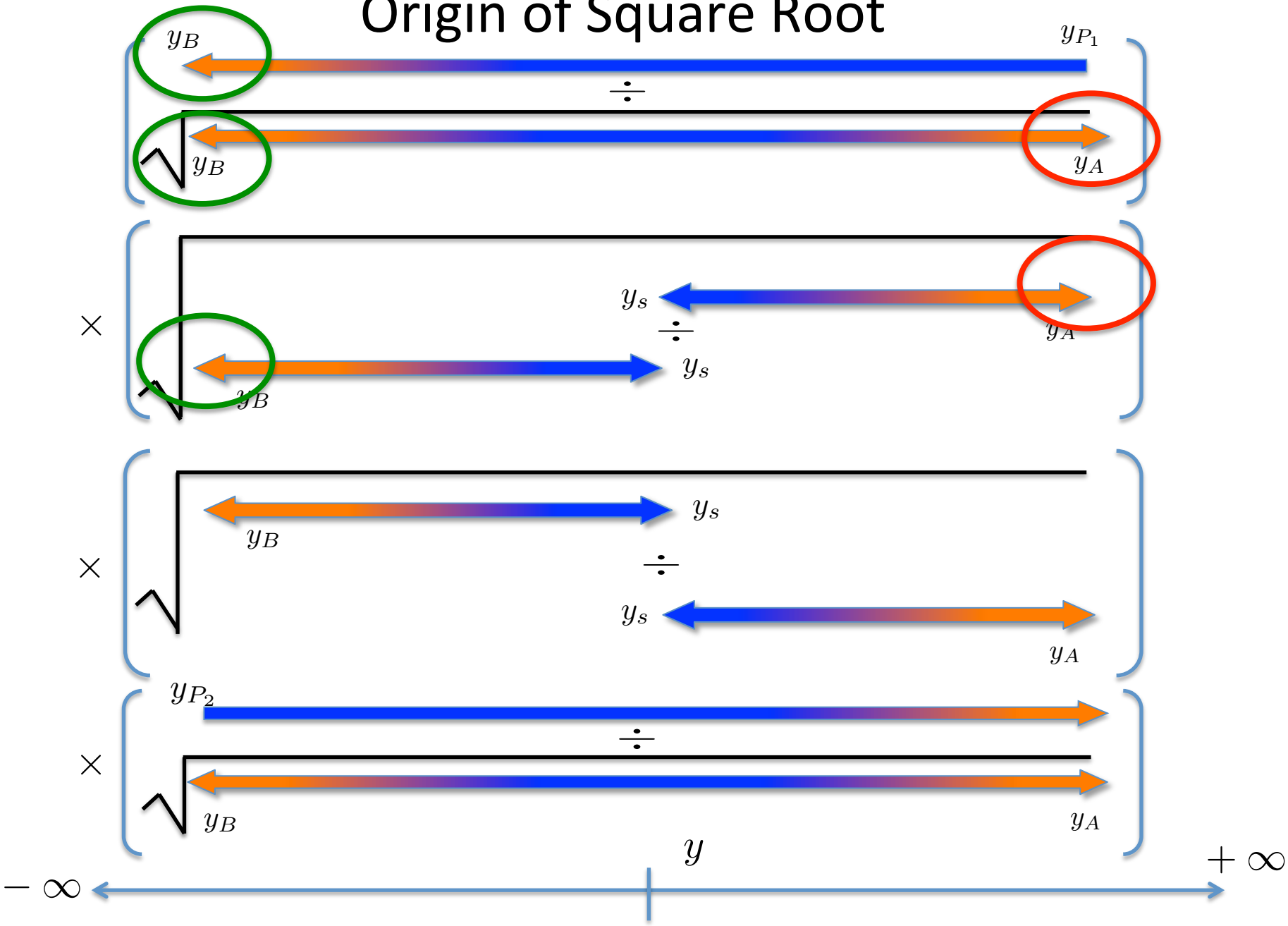

Origin of Square Root

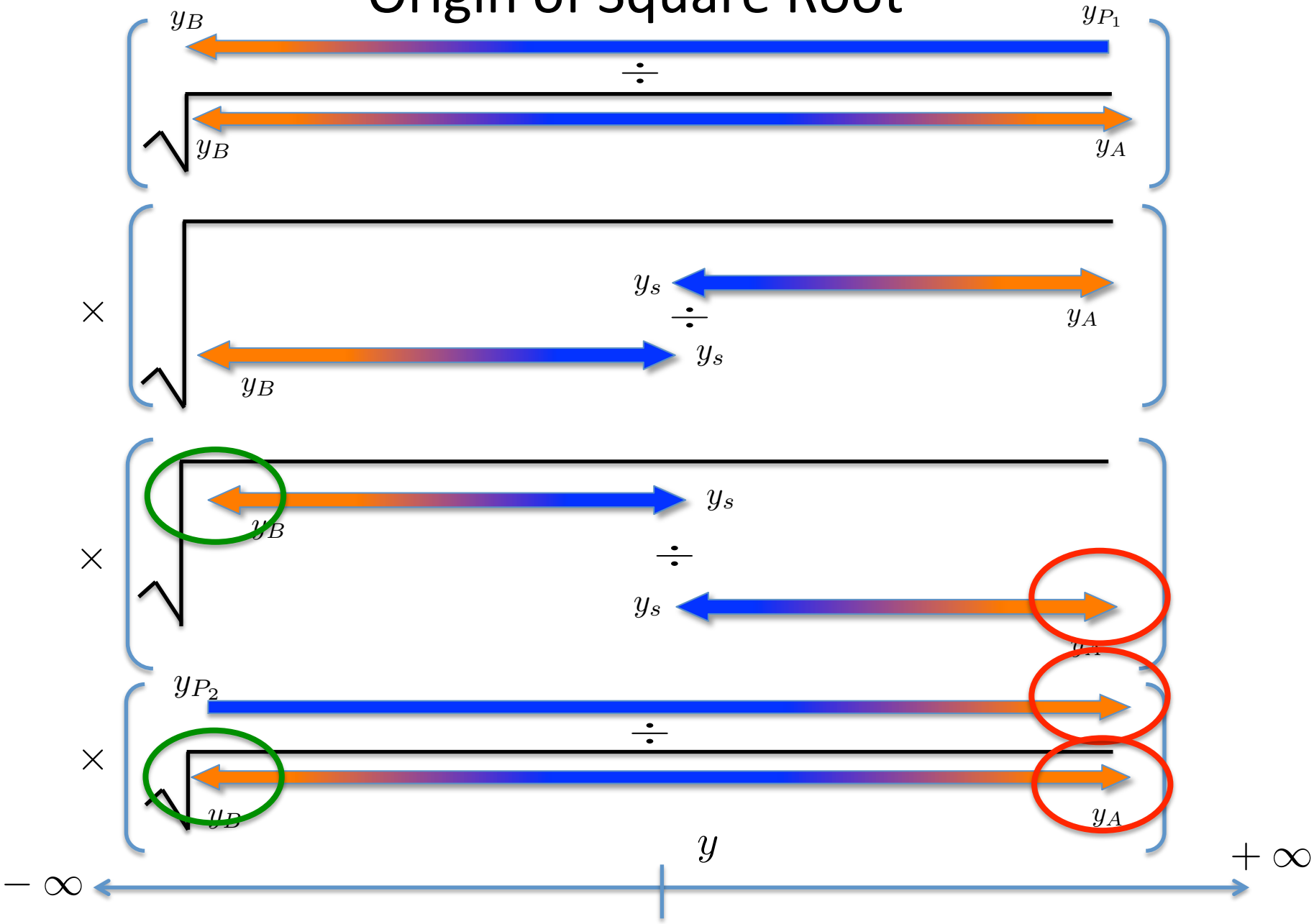

Origin of Square Root

- Start with only the hard part factorized:

$$d\sigma = |\mathcal{H}|^2 \, \frac{\tilde{F}_1^{\rm unsub}(y_1 - (-\infty)) \times \tilde{F}_2^{\rm unsub}(+\infty - y_2)}{\tilde{S}(+\infty, -\infty)}.$$

- Separate soft part:

$$d\sigma = |\mathcal{H}|^2 \, \frac{F_1^{\rm unsub}(y_1 - (-\infty))}{\sqrt{\tilde{S}(+\infty, -\infty)}} \times \frac{\tilde{F}_2^{\rm unsub}(+\infty - y_2)}{\sqrt{\tilde{S}(+\infty, -\infty)}}.$$

- Multiply by: $\dfrac{\sqrt{\tilde{S}(+\infty, y_s)\,\tilde{S}(y_s, -\infty)}}{\sqrt{\tilde{S}(+\infty, y_s)\,\tilde{S}(y_s, -\infty)}}$

- Rearrange factors: $d\sigma = |\mathcal{H}|^2 \left\{ F_1^{\rm unsub}(y_1 - (-\infty)) \sqrt{\dfrac{\tilde{S}(+\infty, y_s)}{\tilde{S}(+\infty, -\infty)\tilde{S}(y_s, -\infty)}} \right\}$

$$\times \left\{ \tilde{F}_2^{\rm unsub}(+\infty - y_2) \sqrt{\frac{\tilde{S}(y_s, -\infty)}{\tilde{S}(+\infty, -\infty)\tilde{S}(+\infty, y_s)}} \right\}$$

Origin of Square Root

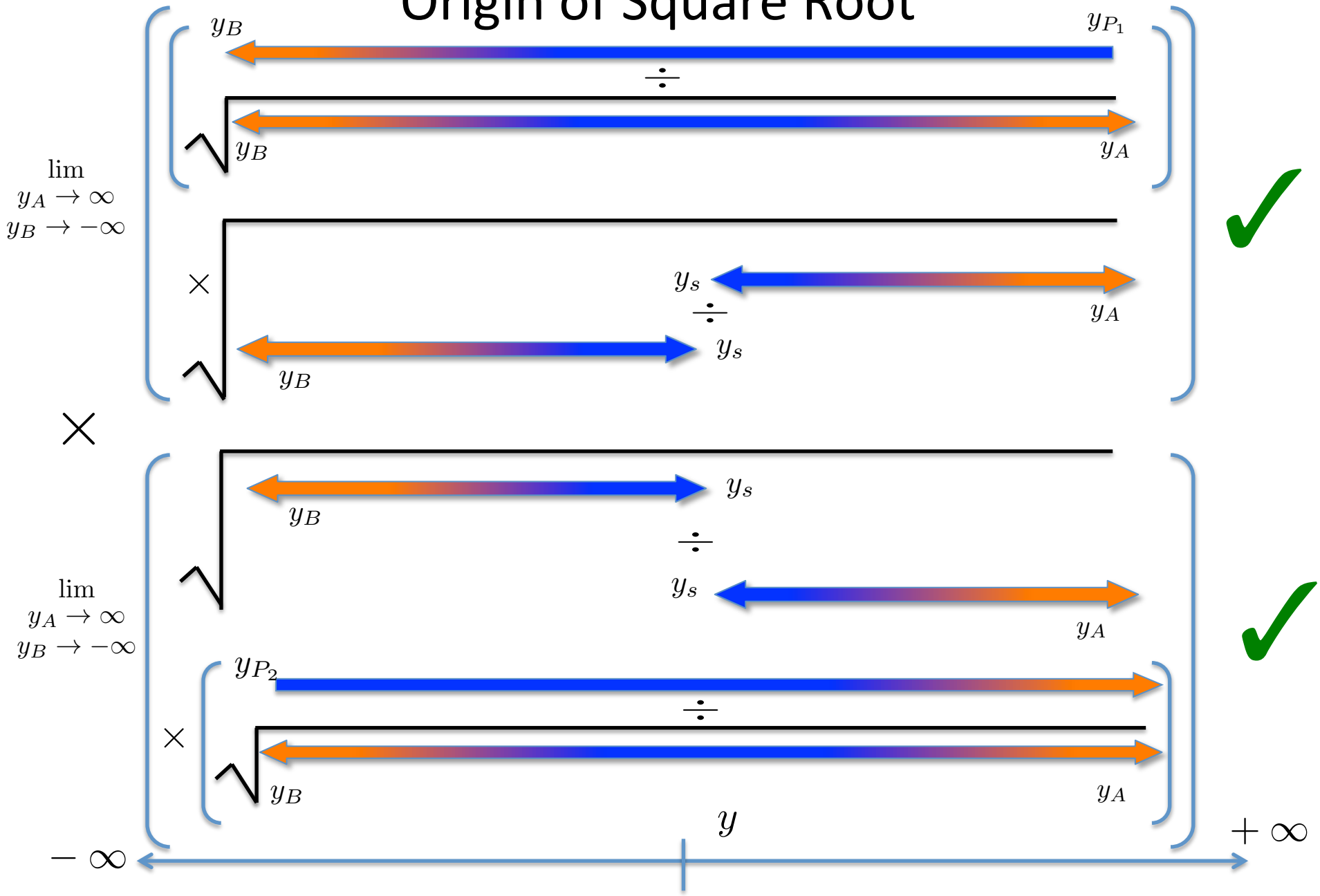

Origin of Square Root

- Start with only the hard part factorized:

$$d\sigma = |\mathcal{H}|^2 \, \frac{\tilde{F}_1^{\text{unsub}}(y_1 - (-\infty)) \times \tilde{F}_2^{\text{unsub}}(+\infty - y_2)}{\tilde{S}(+\infty, -\infty)}.$$

- Separate soft part:

$$d\sigma = |\mathcal{H}|^2 \, \frac{F_1^{\text{unsub}}(y_1 - (-\infty))}{\sqrt{\tilde{S}(+\infty, -\infty)}} \times \frac{\tilde{F}_2^{\text{unsub}}(+\infty - y_2)}{\sqrt{\tilde{S}(+\infty, -\infty)}}.$$

- Multiply by: $\dfrac{\sqrt{\tilde{S}(+\infty, y_s)\,\tilde{S}(y_s, -\infty)}}{\sqrt{\tilde{S}(+\infty, y_s)\,\tilde{S}(y_s, -\infty)}}$

- Rearrange factors: $d\sigma = |\mathcal{H}|^2 \left\{ F_1^{\text{unsub}}(y_1 - (-\infty)) \sqrt{\dfrac{\tilde{S}(+\infty, y_s)}{\tilde{S}(+\infty, -\infty)\tilde{S}(y_s, -\infty)}} \right\}$

$$\times \left\{ \tilde{F}_2^{\text{unsub}}(+\infty - y_2) \sqrt{\frac{\tilde{S}(y_s, -\infty)}{\tilde{S}(+\infty, -\infty)\tilde{S}(+\infty, y_s)}} \right\}$$

Separately well-defined

Definitions:

(Dictated by factorization requirements)

$$\zeta_1\zeta_2 \sim Q^4$$

$$F_{f/P}(x, b; \mu; \zeta_F) = \qquad \zeta_F = 2M_p^2 x^2 e^{2(y_P - y_s)}$$

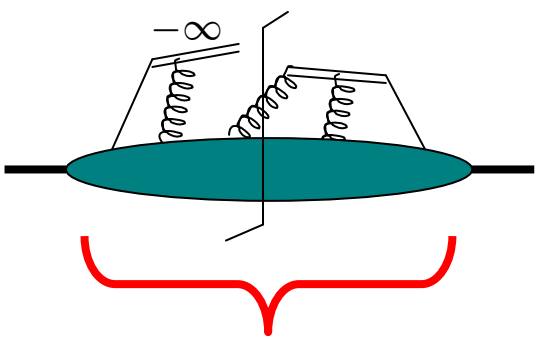

"Unsubtracted"

$\times$

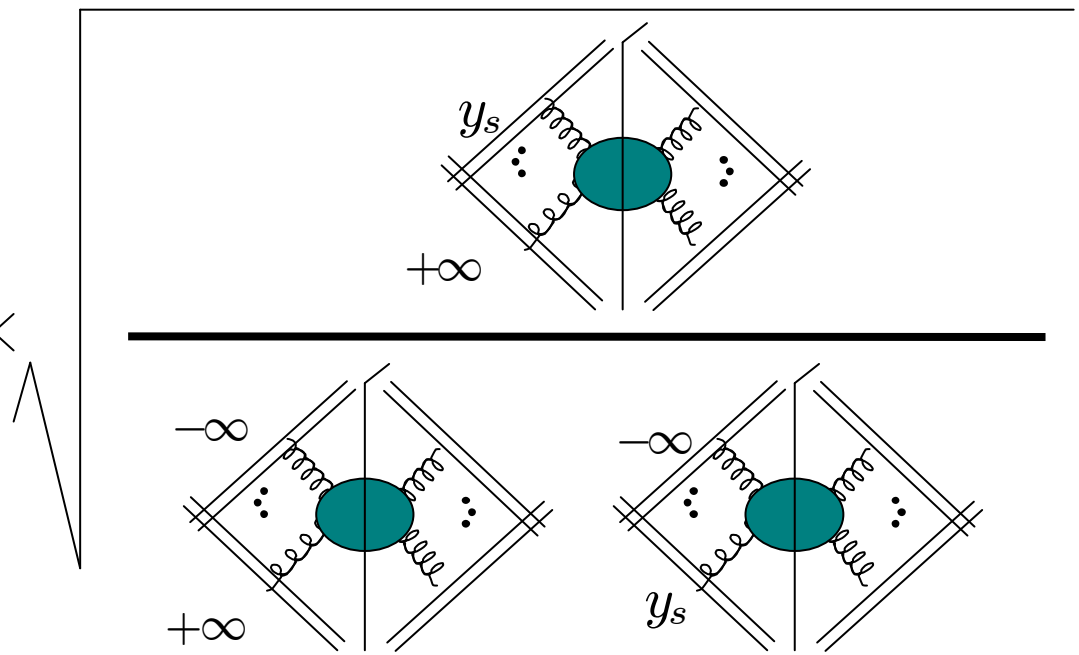

(UV and rapidity renormalization needed)

Implements Subtractions/Cancellations

(Collins (2011), chapt. 13)

TMD-Factorization

$$W_{DY}^{\mu\nu} = \sum_f |\mathcal{H}_f(Q;\mu/Q)|^{\mu\nu}$$

$$\times \int d^2\mathbf{k}_{1T}\, d^2\mathbf{k}_{2T}\, \underline{F_{f/P_1}(x_1, \mathbf{k}_{1T}; \mu; \zeta_1)}\ \underline{F_{f/P_2}(x_2, \mathbf{k}_{2T}; \mu; \zeta_2)}\, \delta^{(2)}(\mathbf{k}_{1T} + \mathbf{k}_{2T} - \mathbf{q}_T)$$

$$+ Y(q_T, Q)$$

$$+ \mathcal{O}\left(\left(\frac{\Lambda}{Q}\right)^a\right)$$

Evolution

- Collins-Soper Equation:
  - $$\frac{\partial \ln \tilde{F}(x, b_T, \mu, \zeta)}{\partial \ln \sqrt{\zeta}} = \tilde{K}(b_T; \mu)$$

Perturbatively calculable from definition at small b.

$$\tilde{K}(b_T; \mu) = \frac{1}{2} \frac{\partial}{\partial y_n} \ln \frac{\tilde{S}(b_T; y_n, -\infty)}{\tilde{S}(b_T; +\infty, y_n)}$$

- RG:
  - $$\frac{d\tilde{K}}{d \ln \mu} = -\gamma_K(g(\mu))$$
  - $$\frac{d \ln \tilde{F}(x, b_T; \mu, \zeta)}{d \ln \mu} = -\gamma_F(g(\mu); \zeta/\mu^2)$$

Perturbatively calculable, from definitions

Scales

- UV divergences:

$$\frac{d\tilde{K}}{d\ln\mu} = -\gamma_K(g(\mu))$$

$$\frac{d\ln\tilde{F}(x, b_T; \mu, \zeta)}{d\ln\mu} = -\gamma_F(g(\mu); \zeta/\mu^2)$$

Scales

- UV divergences:

Hard

$$|\mathcal{H}_f(Q;\mu/Q)^2|^{\mu\nu} = e_f^2 |H_0^2|^{\mu\nu}\left(1+\frac{C_F\alpha_s}{\pi}\left[\frac{3}{2}\ln\left(Q^2/\mu^2\right)-\frac{1}{2}\ln^2\left(Q^2/\mu^2\right)-4+\frac{\pi^2}{2}\right]\right)+\mathcal{O}(\alpha_s^2)$$

- No y_s in hard part.
- Pert. theory with: $\mu \sim Q$

Non-Hard

Scales

- UV divergences:

$$\frac{d\tilde{K}}{d\ln\mu} = -\gamma_K(g(\mu))$$

$$\frac{d\ln\tilde{F}(x,b_T;\mu,\zeta)}{d\ln\mu} = -\gamma_F(g(\mu);\zeta/\mu^2)$$

- Light-cone divergences:

$$\frac{\partial\ln\tilde{F}(x,b_T,\mu,\zeta)}{\partial\ln\sqrt{\zeta}} = \tilde{K}(b_T;\mu)$$

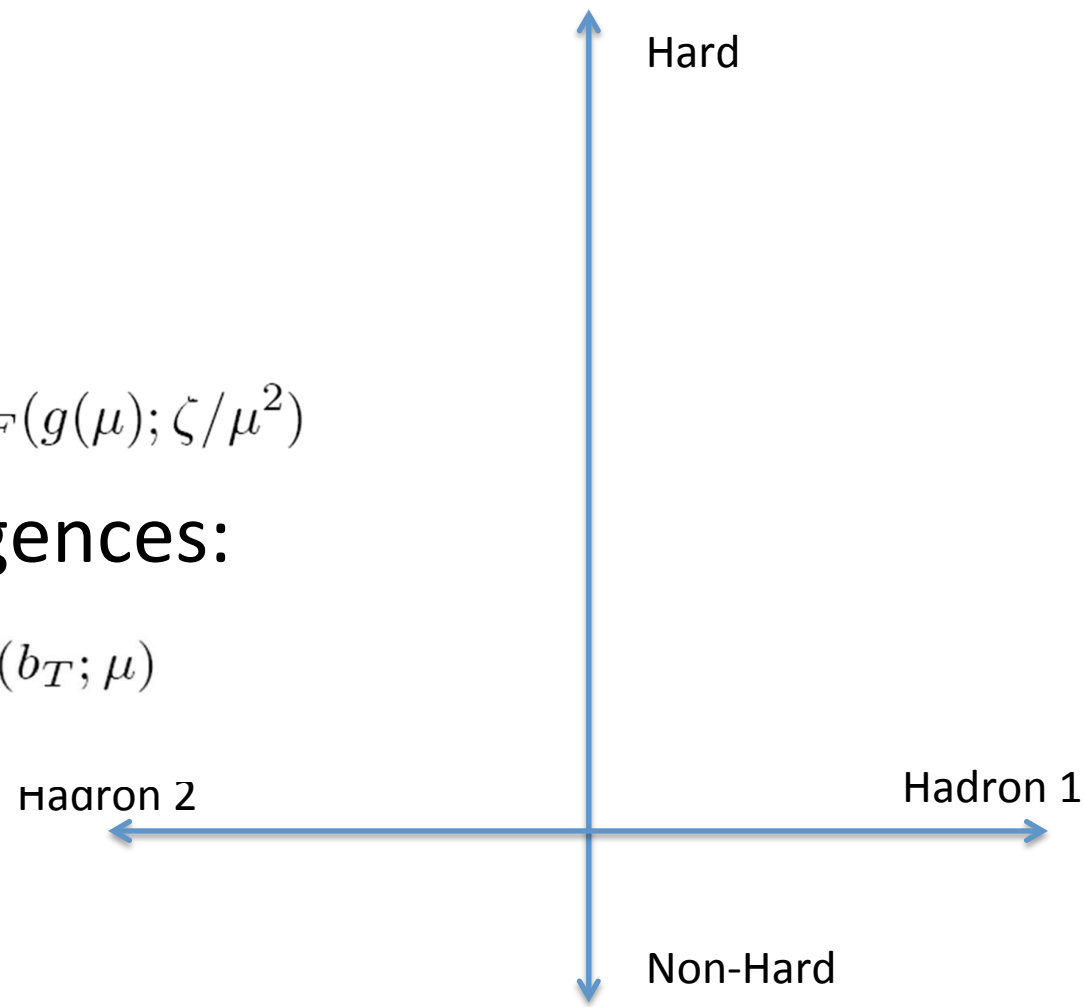

Recall: Origin of Square Root

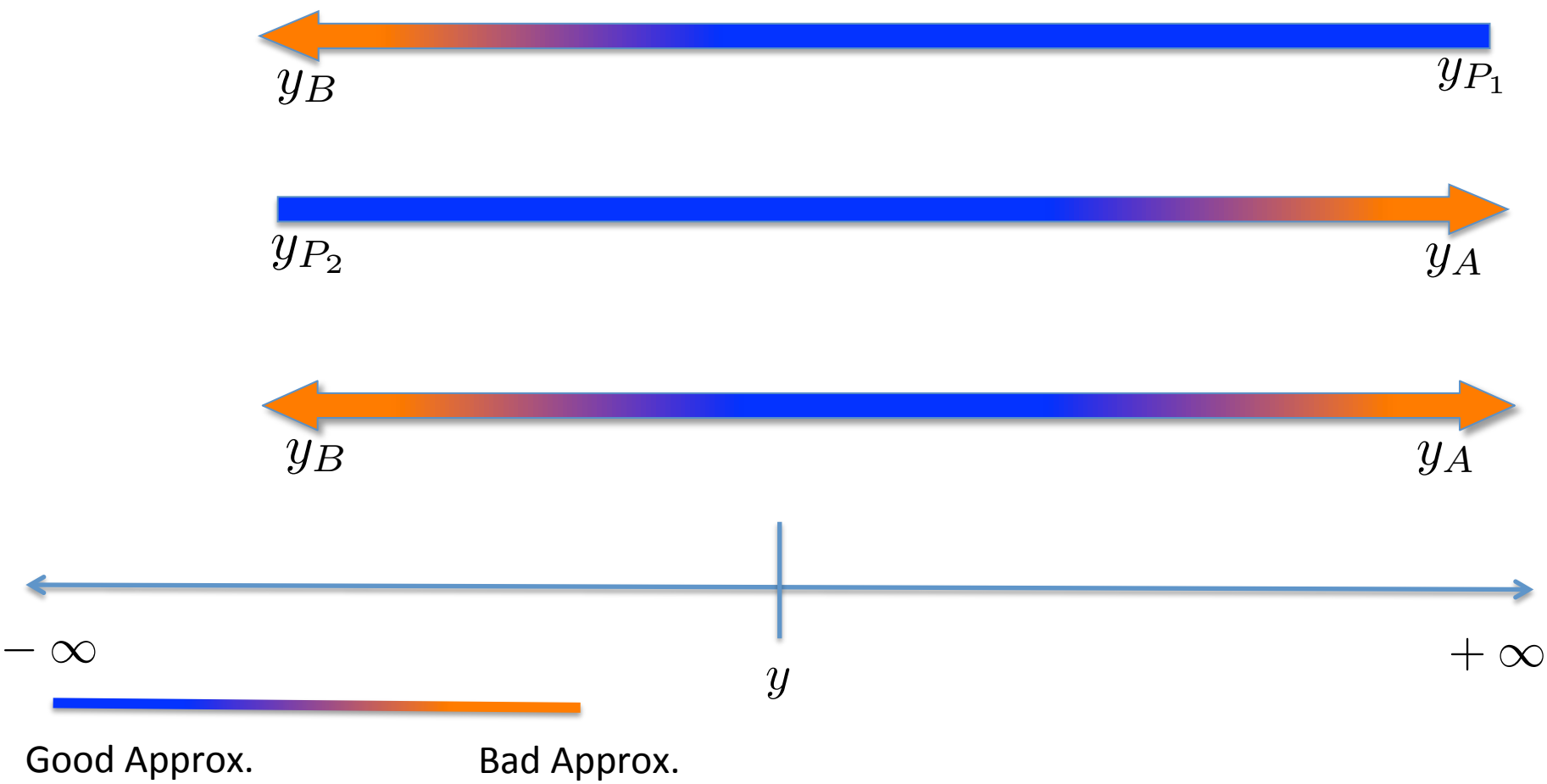

Scales

- UV divergences:

$$\frac{d\tilde{K}}{d\ln\mu} = -\gamma_K(g(\mu))$$

$$\frac{d\ln\tilde{F}(x,b_T;\mu,\zeta)}{d\ln\mu} = -\gamma_F(g(\mu);\zeta/\mu^2)$$

- Light-cone divergences:

$$\frac{\partial\ln\tilde{F}(x,b_T,\mu,\zeta)}{\partial\ln\sqrt{\zeta}} = \tilde{K}(b_T;\mu)$$

  - Pert. theory requires:

$$\zeta \sim \mu^2$$

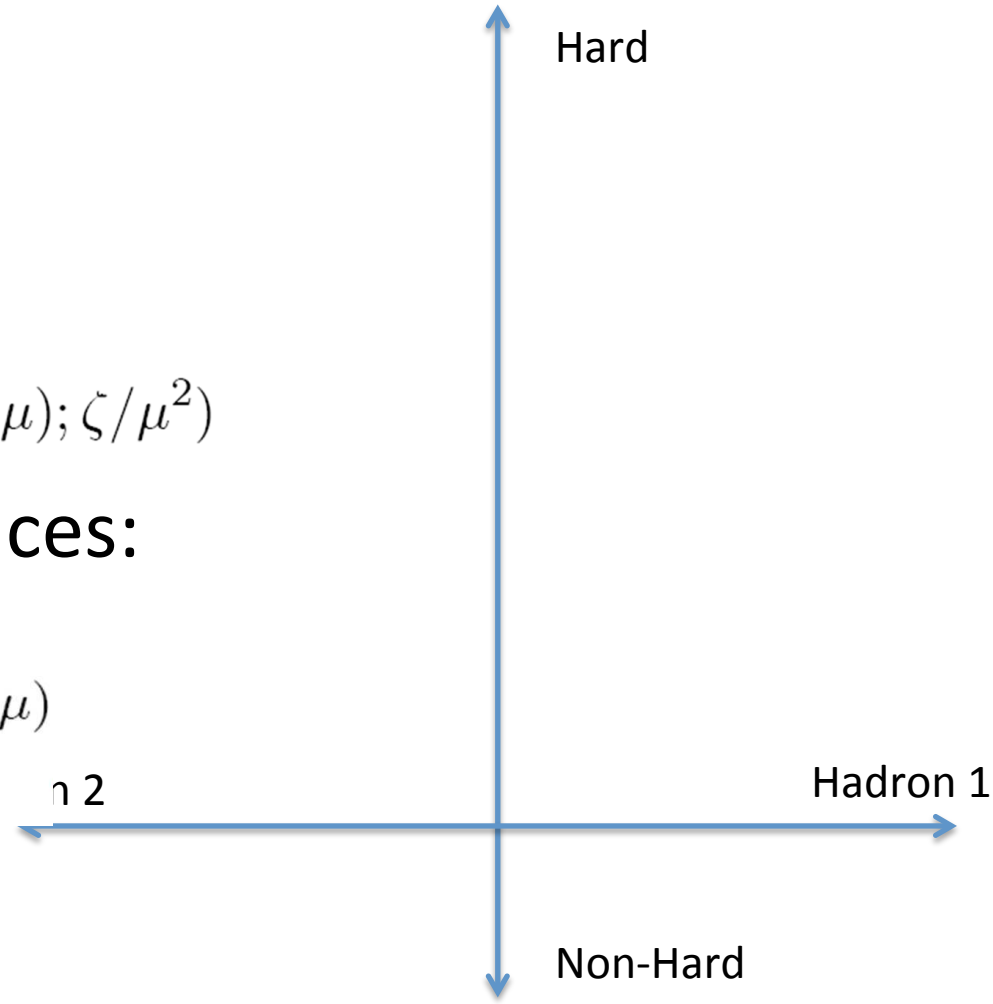

Scales

- UV divergences:
- Light-Cone divergences:
- Maximize perturbative input.

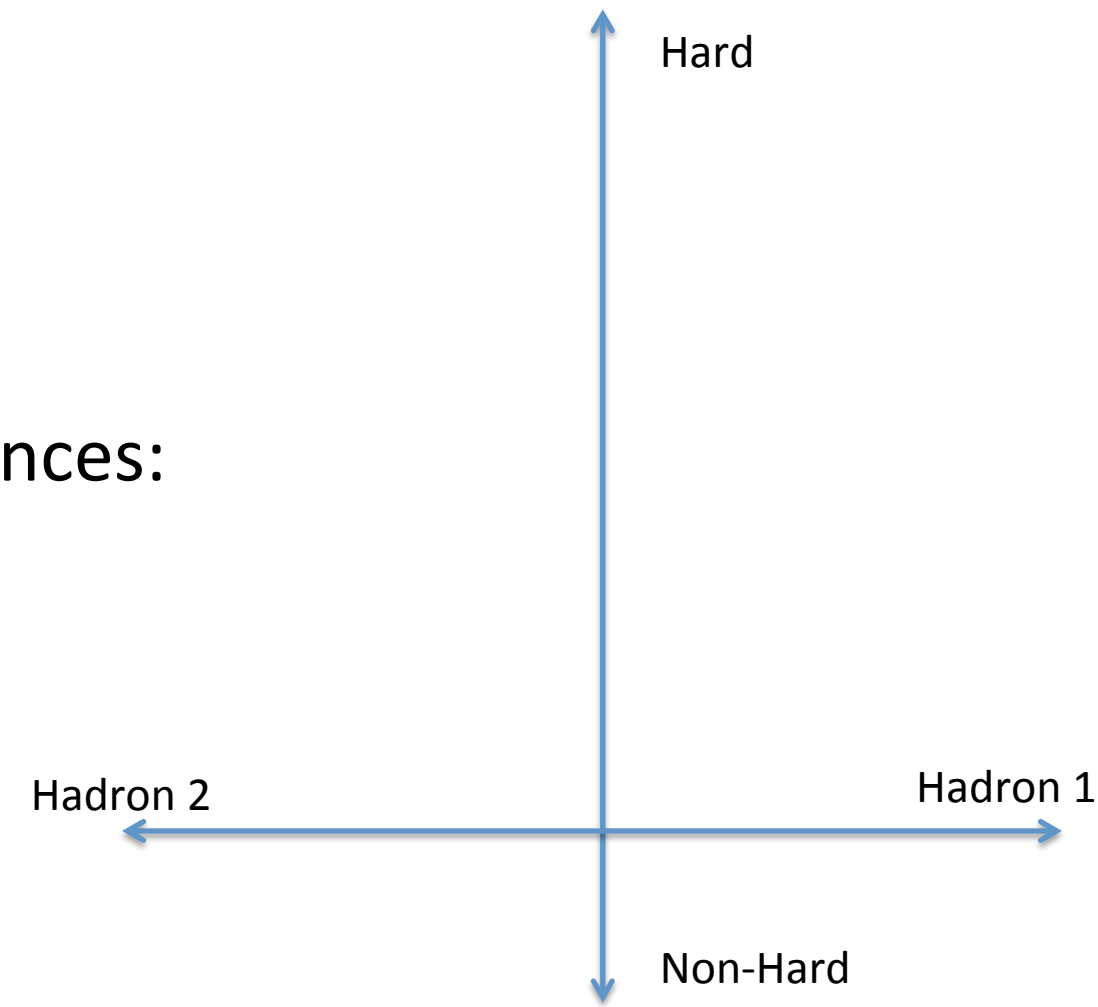

Recap

Regions of Transverse Momentum:

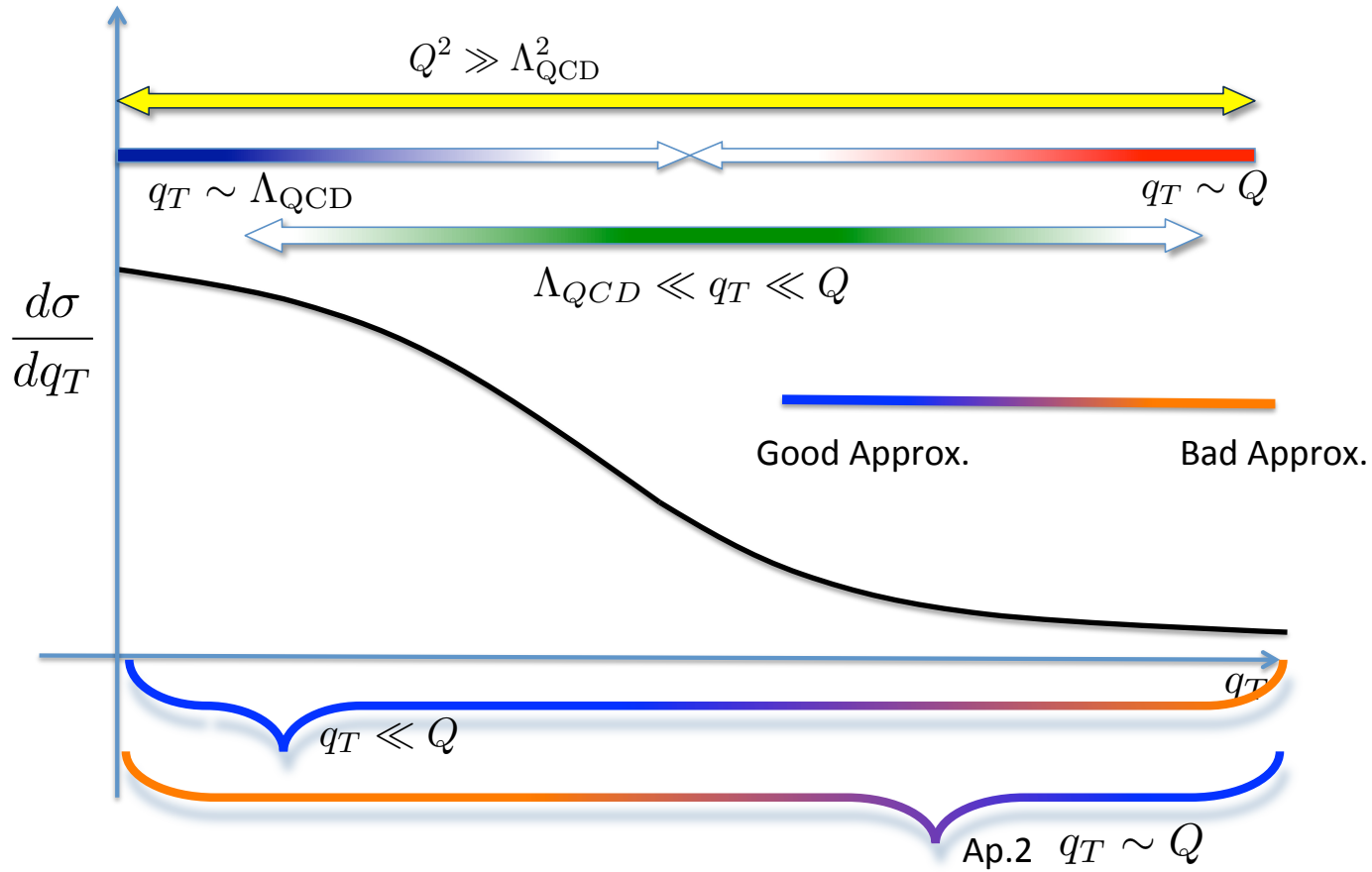

Recap

Regions of Transverse Momentum:

$$W_{DY}^{\mu\nu} = \sum_f |\mathcal{H}_f(Q;\mu/Q)|^{\mu\nu}$$

Similar to generalized TMD parton model

$$\times \int d^2\mathbf{k}_{1T}\, d^2\mathbf{k}_{2T}\, F_{f/P_1}(x_1, \mathbf{k}_{1T}; \mu; \zeta_1)\; F_{f/P_2}(x_2, \mathbf{k}_{2T}; \mu; \zeta_2)\, \delta^{(2)}(\mathbf{k}_{1T} + \mathbf{k}_{2T} - \mathbf{q}_T)$$

TMD PDF for hadron 1.

TMD PDF for hadron 2.

TMD part: $q_T \ll Q$

Ap.2 $q_T \sim Q$

Recap

Regions of Transverse Momentum:

$$W_{DY}^{\mu\nu} = \sum_f |\mathcal{H}_f(Q;\mu/Q)|^{\mu\nu}$$

Similar to generalized TMD parton model

$$\times \int d^2\mathbf{k}_{1T}\, d^2\mathbf{k}_{2T}\, F_{f/P_1}(x_1,\mathbf{k}_{1T};\mu;\zeta_1)\; F_{f/P_2}(x_2,\mathbf{k}_{2T};\mu;\zeta_2)\, \delta^{(2)}(\mathbf{k}_{1T}+\mathbf{k}_{2T}-\mathbf{q}_T)$$

TMD PDF ***TMD PDF***

$$F_{f/P_1}(x_1,\mathbf{k}_{1T};\mu;\zeta_1) = \underbrace{\mathcal{C}_{f/f'}(x/x',\mathbf{k}_{1T},\zeta_1,\mu,\alpha_s(\mu))}_{\text{Perturbatively calculable coefficient functions}} \otimes \underbrace{f_{f'/P_1}(x';\mu)}_{\text{Collinear PDFs}} + \underbrace{\mathcal{O}\left(\frac{\Lambda_{QCD}}{k_{1T}}\right)}_{\text{Error}}$$

Perturbatively calculable coefficient functions ***Collinear PDFs*** ***Error***

Ap.2 $q_T \sim Q$

Recap

Regions of Transverse Momentum: Evolution

- Collins-Soper Equation:
  - $$\frac{\partial \ln \tilde{F}(x, b_T, \mu, \zeta)}{\partial \ln \sqrt{\zeta}} = \tilde{K}(b_T; \mu)$$

    Perturbatively calculable from definition at small b.

$$\tilde{K}(b_T; \mu) = \frac{1}{2} \frac{\partial}{\partial y_n} \ln \frac{\tilde{S}(b_T; y_n, -\infty)}{\tilde{S}(b_T; +\infty, y_n)}$$

- RG:
  - $$\frac{d\tilde{K}}{d \ln \mu} = -\gamma_K(g(\mu))$$
  - $$\frac{d \ln \tilde{F}(x, b_T; \mu, \zeta)}{d \ln \mu} = -\gamma_F(g(\mu); \zeta/\mu^2)$$

Perturbatively calculable, from definitions

Implementation (b_T-space)

One physical scale for evolution, dictated by requirements of PT:

$$\boxed{\mu \sim \sqrt{\zeta_1} \sim \sqrt{\zeta_2} \sim Q}$$

$$\tilde{F}_{f/H}(x, b_T, \mu, \zeta) = \sum_j \int_x^1 \frac{d\hat{x}}{\hat{x}} \tilde{C}_{f/j}(x/\hat{x}, b_*; \mu_b, g(\mu_b)) f_{j/H}(x, \mu_b) \times \quad \text{A}$$

$$\times \exp\left\{ \ln \frac{\sqrt{\zeta}}{\mu_b} \tilde{K}(b_*; \mu_b) + \int_{\mu_b}^{\mu} \frac{d\mu'}{\mu'} \left[\gamma_F(g(\mu'); 1) - \ln \frac{\sqrt{\zeta}}{\mu'} \gamma_K(g(\mu')) \right] \right\} \times \quad \text{B}$$

$$\times \exp\left\{ g_{j/H}(x, b_T) + g_K(b_T) \ln \frac{\sqrt{\zeta}}{Q_0} \right\} \quad \text{C}$$

$$\boxed{b_*(b_T) \equiv \frac{b_T}{\sqrt{1 + b_T^2/b_{max}^2}} \qquad \mu_b(b_T) \sim 1/b_*}$$

(CS matching)

Evolved TMD PDFs constructed from old fits:

(CSS formalism.)

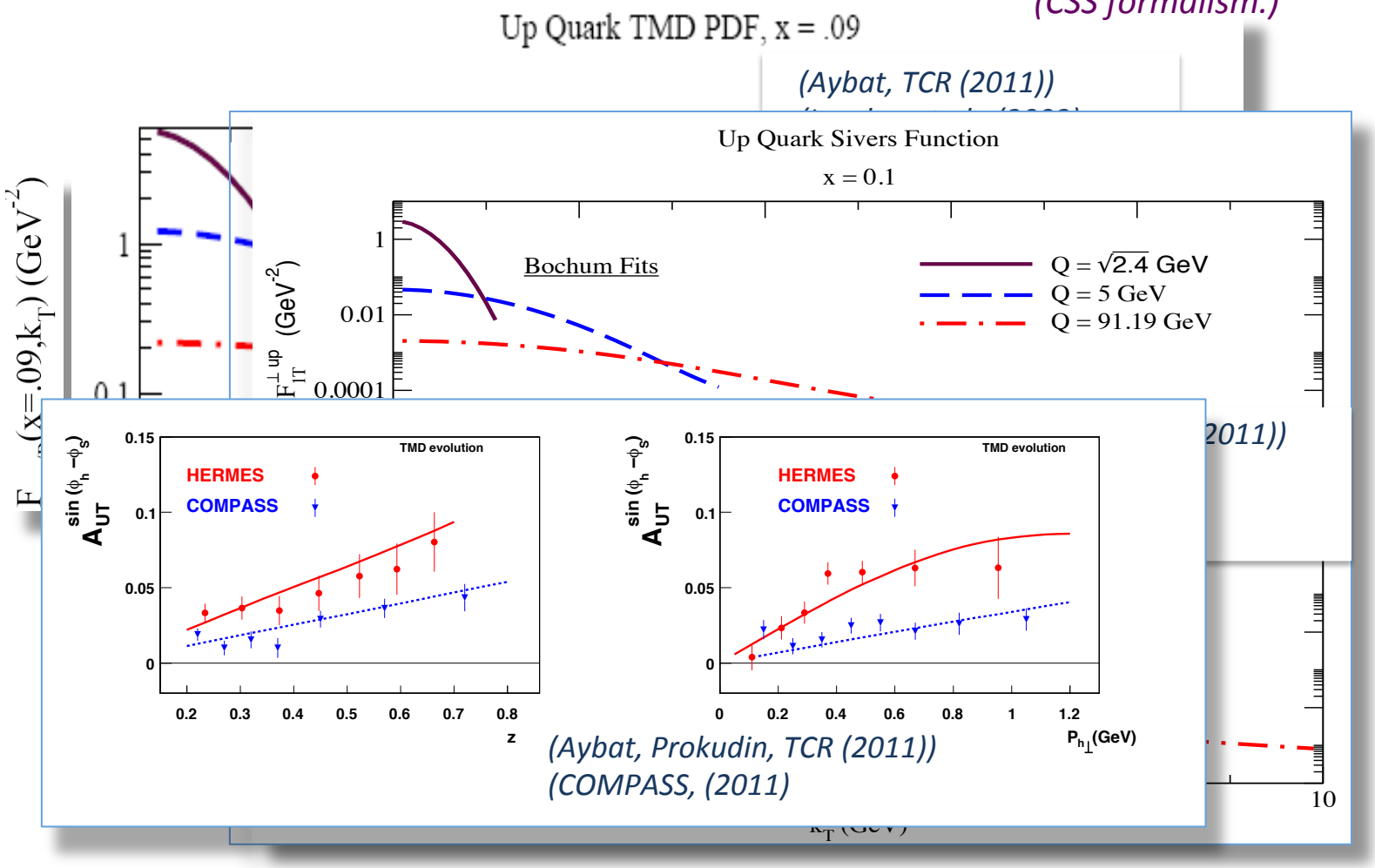

(Aybat, TCR (2011))

(Aybat, Prokudin, TCR (2011))
(COMPASS, (2011)

https://projects.hepforge.org/tmd/

More recent fitting

- Fixed scale. Sum rules.
  (A. Bacchetta, M. Radici (2012))

- Lowest order evolution:
  (M. Anselmino, M. Boglione, S. Melis (2012))

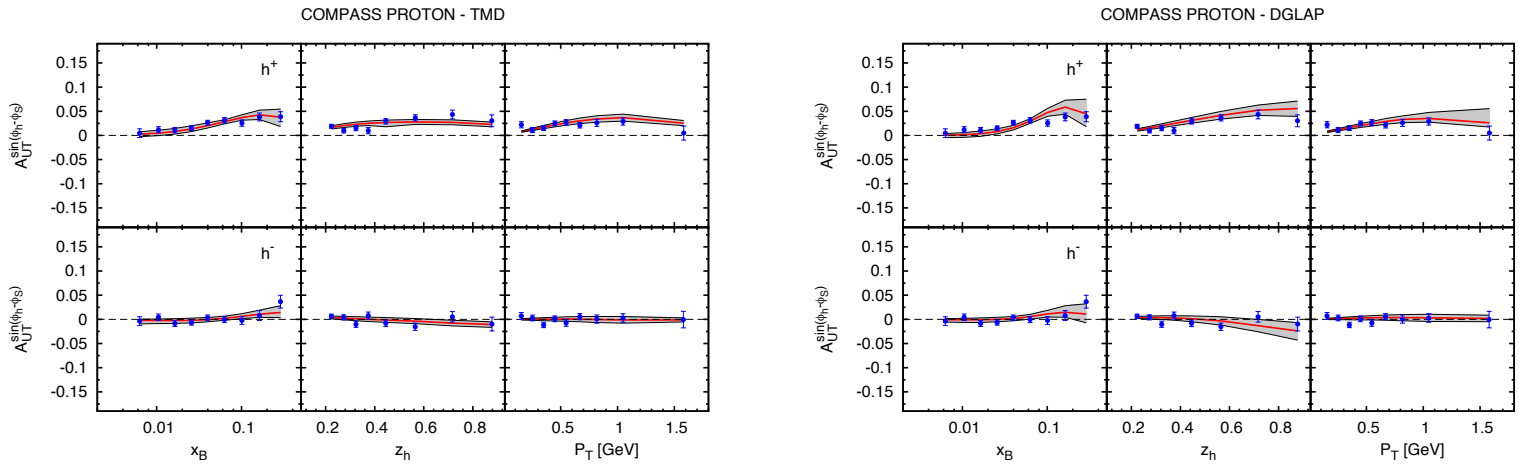

- Spin dep.
  (Z.-B. Kang,J.-W. Qiu (2012))

- Direct fitting in coordinate space.
  (Boer,Gamberg,Musch,Prokudin (2011))

- Other current fitting activity:
  (Torino-JLab group: A. Prokudin, S. Melis,…)

Testing/Using TMD-Factorization

- New fitting projects, analogous to collinear case.

- Key issue: Maximum amount of data, maximum variety of processes.
  - Cyclic process of fitting and predicting. Analogous to collinear factorization.
    - Much already available:
      - DY, Z/W in pp, pA
      - DY,Z/W in $p\bar{p}$
      - SIDIS
      - e+ e- to back-to-back hadrons.

- Isolate interesting non-perturbative contributions.
  - E.g., compare intrinsic transverse momentum of sea and valence quarks.

    (E.g., Compare unpolarized pp and $p\bar{p}$.)

  - Extraction of model parameters.

- Comparing alternative TMD formalisms (e.g. SCET, small-x, etc.)
  - What are the distinctive different phenomenological predictions?
  - What is predicted to be universal vs. non-universal?

Implementation

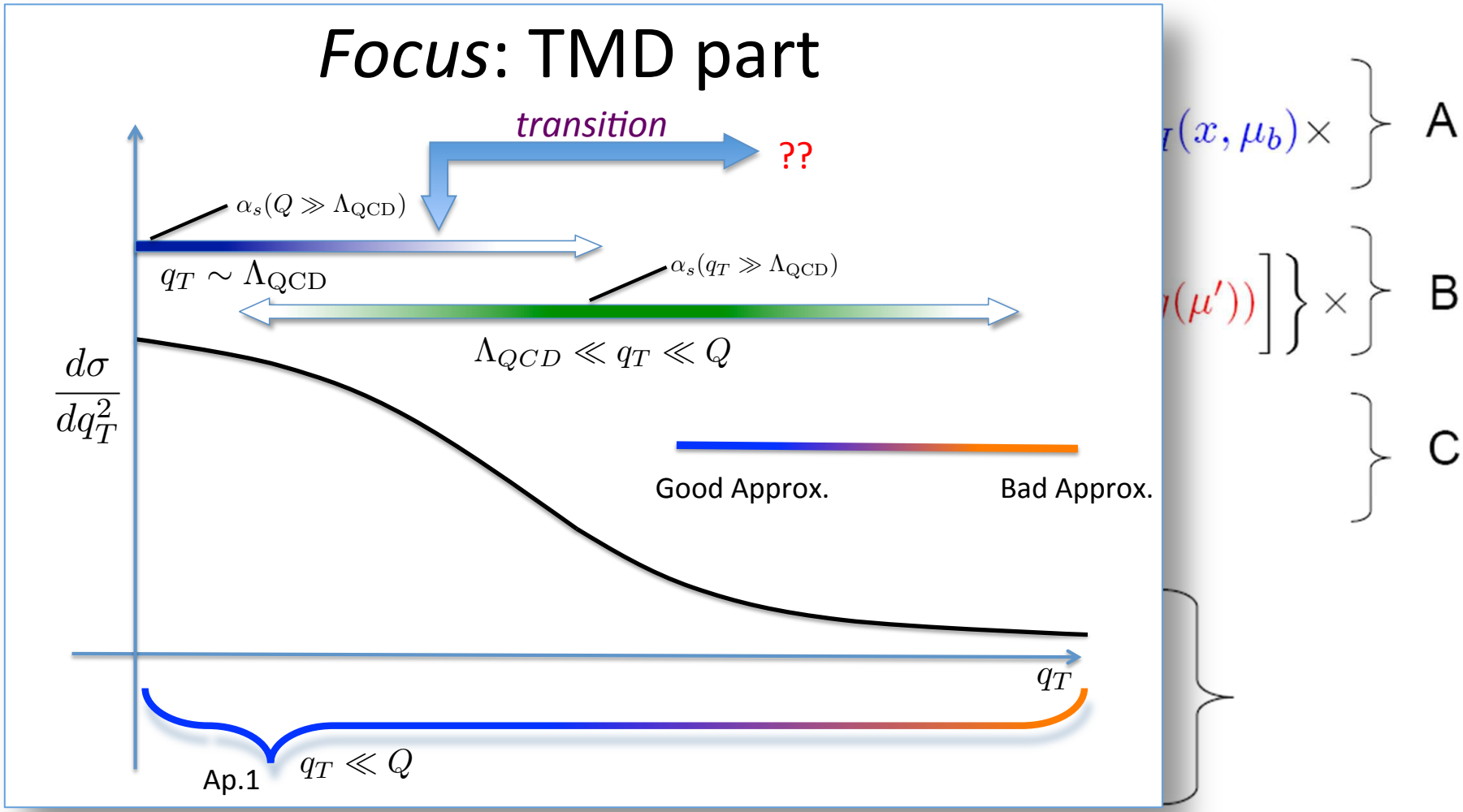

Momentum Space Evolution

(Coll. with C. Aidala, work in progress)

- Perform all fitting directly in momentum space, with evolution formulated in momentum space.

- Isolate non-perturbative transverse momentum dependent contributions at small q_T.
  - Intrinsic transverse momentum of sea and valence quarks in DY.

(Compare unpolarized pp and $p\bar{p}$.)

Momentum Space Evolution

(Coll. with C. Aidala, work in progress)

$$\tilde{F}_{f/P_1}(x_1, \mathbf{b}_T; \mu, \zeta_1) = \int d^2\mathbf{k}_T \, e^{-i\mathbf{k}_T \cdot \mathbf{b}_T} \, F_{f/P_1}(x_1, \mathbf{k}_T; \mu, \zeta_F)$$

$$\tilde{K}(\mathbf{b}_T; \mu) = \int d^2\mathbf{k}_T \, e^{-i\mathbf{k}_T \cdot \mathbf{b}_T} \, K(\mathbf{k}_T; \mu)$$

$$\frac{\partial}{\partial \ln \sqrt{\zeta_F}} F(x, \mathbf{k}_T; \mu, \zeta_F) = \int d^2\mathbf{q}_T \, K(\mathbf{q}_T; \mu) \, F_{f/P_1}(x_1, \mathbf{k}_T - \mathbf{q}_T; \mu, \zeta_F)$$

$$\frac{d}{d \ln \mu} K(k_T; \mu) = -\gamma_K(g(\mu)) \, \delta(\mathbf{k}_T)$$

$$\frac{d}{d \ln \mu} F_{f/P_1}(x, \mathbf{k}_T; \mu, \zeta_F) = \gamma_F(g(\mu); \zeta_F/\mu^2) \, F_{f/P_1}(x, \mathbf{k}_T; \mu, \zeta_F)$$

Momentum Space Evolution

(Coll. with C. Aidala, work in progress)

- General solutions constructed with a matching defined in k_T space:

$$\mathbf{b}_*(\mathbf{b}_\mathrm{T}) \equiv \frac{\mathbf{b}_\mathrm{T}}{\sqrt{1 + b_T^2/b_\mathrm{max}^2}}$$

$$\mu_*(b_T) = C_1/b_*$$

$$\alpha_s(\mu_*(b_T)) \overset{b_T \to \infty}{=} \alpha_s(C_1/b_{max})$$

(Transverse coord. space)

$$\mathbf{k}_*(\mathbf{k}_T) \equiv \hat{\mathbf{k}}_T \sqrt{k_{min}^2 + k_T^2}$$

$$\mu_*(k_T) \equiv C_1 k_*$$

$$\alpha_s(\mu_*(k_T)) \overset{k_T \to 0}{=} \alpha_s(C_1 k_{min})$$

(Transverse mom. space)

(A. Kulesza, J. Stirling (2001), R. Ellis, S. Veseli (1997))

Momentum Space Evolution

(Coll. with C. Aidala, work in progress)

- General solutions constructed with a matching defined in k_T space:

$$\mathbf{b}_*(\mathbf{b}_\mathrm{T}) \equiv \frac{\mathbf{b}_\mathrm{T}}{\sqrt{1 + b_T^2/b_\mathrm{max}^2}}$$

$$\mu_*(b_T) = C_1/b_*$$

$$\alpha_s(\mu_*(b_T)) \overset{b_T \to \infty}{=} \alpha_s(C_1/b_{max})$$

(Transverse coord. space)

$$\mathbf{k}_*(\mathbf{k}_T) \equiv \hat{\mathbf{k}}_T \sqrt{k_{min}^2 + k_T^2}$$

$$\mu_*(k_T) \equiv C_1 k_*$$

$$\alpha_s(\mu_*(k_T)) \overset{k_T \to 0}{=} \alpha_s(C_1 k_{min})$$

(Transverse mom. space)

(A. Kulesza, J. Stirling (2001), R. Ellis, S. Veseli (1997))

(Study evolution of different transverse momentum regions.)

$$F_{f/p_1}(x_1, \mathbf{k}_t; \mu, \zeta_F) \equiv F_{f/p_1}^{\mathrm{Tail}}(x_1, \mathbf{k}_t; \mu, \zeta_F) + F_{f/p_1}^{\mathrm{Core}}(x_1, \mathbf{k}_t; \mu, \zeta_F)$$

Momentum Space Evolution

(Coll. with C. Aidala, work in progress)

- General solution
  defined in k_T spa

$$\mathbf{b}_*(\mathbf{b}_\mathrm{T}) \equiv \frac{\mathbf{b}_\mathrm{T}}{\sqrt{1+b_T^2/}}$$

$$\mu_*(b_T) = C_1/b_*$$

$$\alpha_s(\mu_*(b_T)) \overset{b_T\to\infty}{=} \alpha_s \qquad in)$$

(Transverse coord. spa

2001),

(Study evolution of differe

)

$$F_{f/p_1}(x_1, \mathbf{k}_t; \mu, \zeta_F) \equiv$$

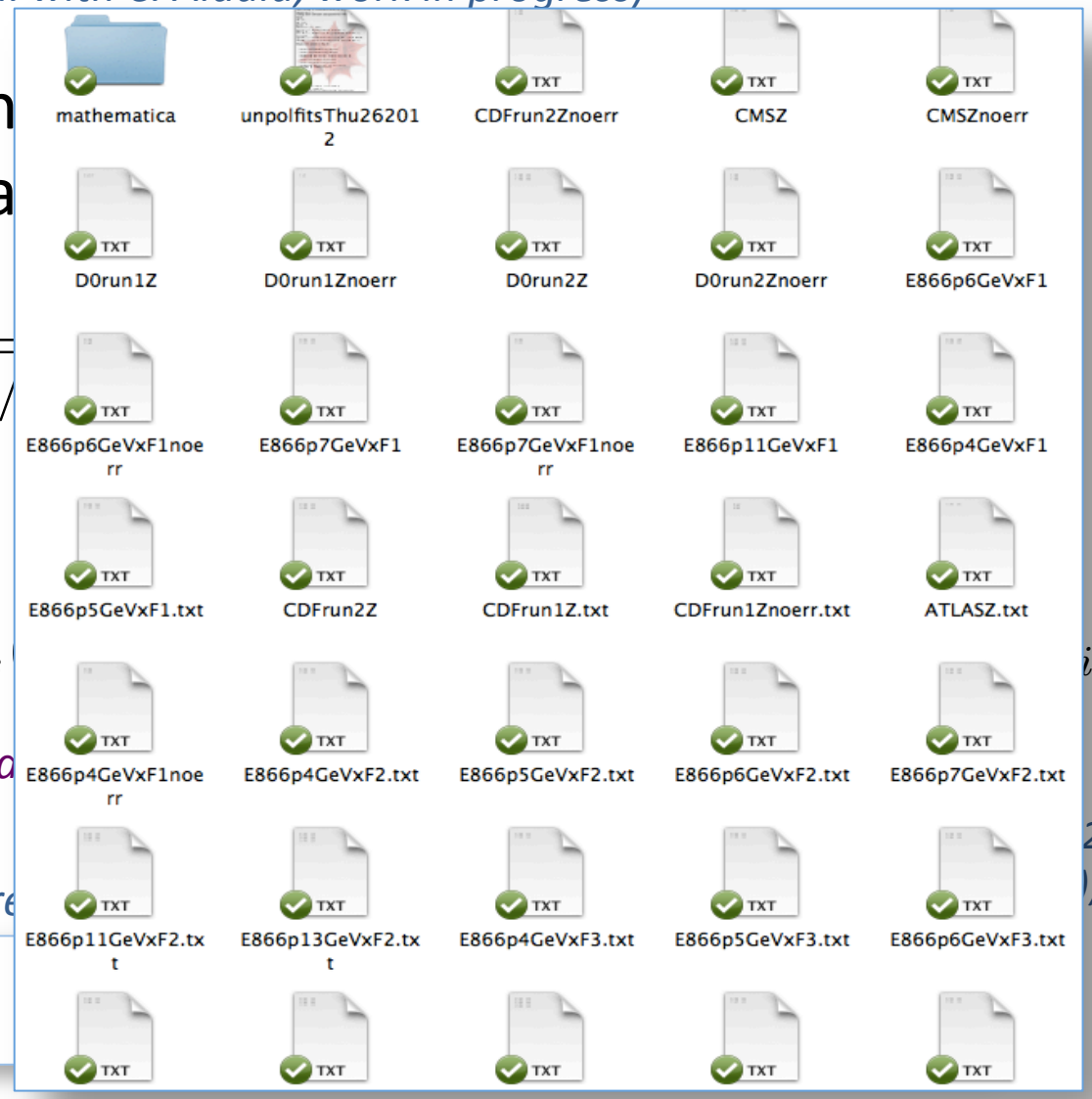

Thanks!

COMPASS transverse spin physics program and plans for GPD measurements

Andrzej Sandacz

National Centre for Nuclear Research, Warsaw

on behalf of the COMPASS Collaboration

August 1, 2012

Outline

- COMPASS experiment
- New results with transversely polarised protons and deuterons
- Planned GPD measurements and results from DVCS test runs
- Conclusions

♠ Planned DY measurements at COMPASS → talk by IhnJea Choi

COmmon
Muon and
Proton
Apparatus for
Structure and
Spectroscopy

wide physics program carried on using both muon and hadron beam

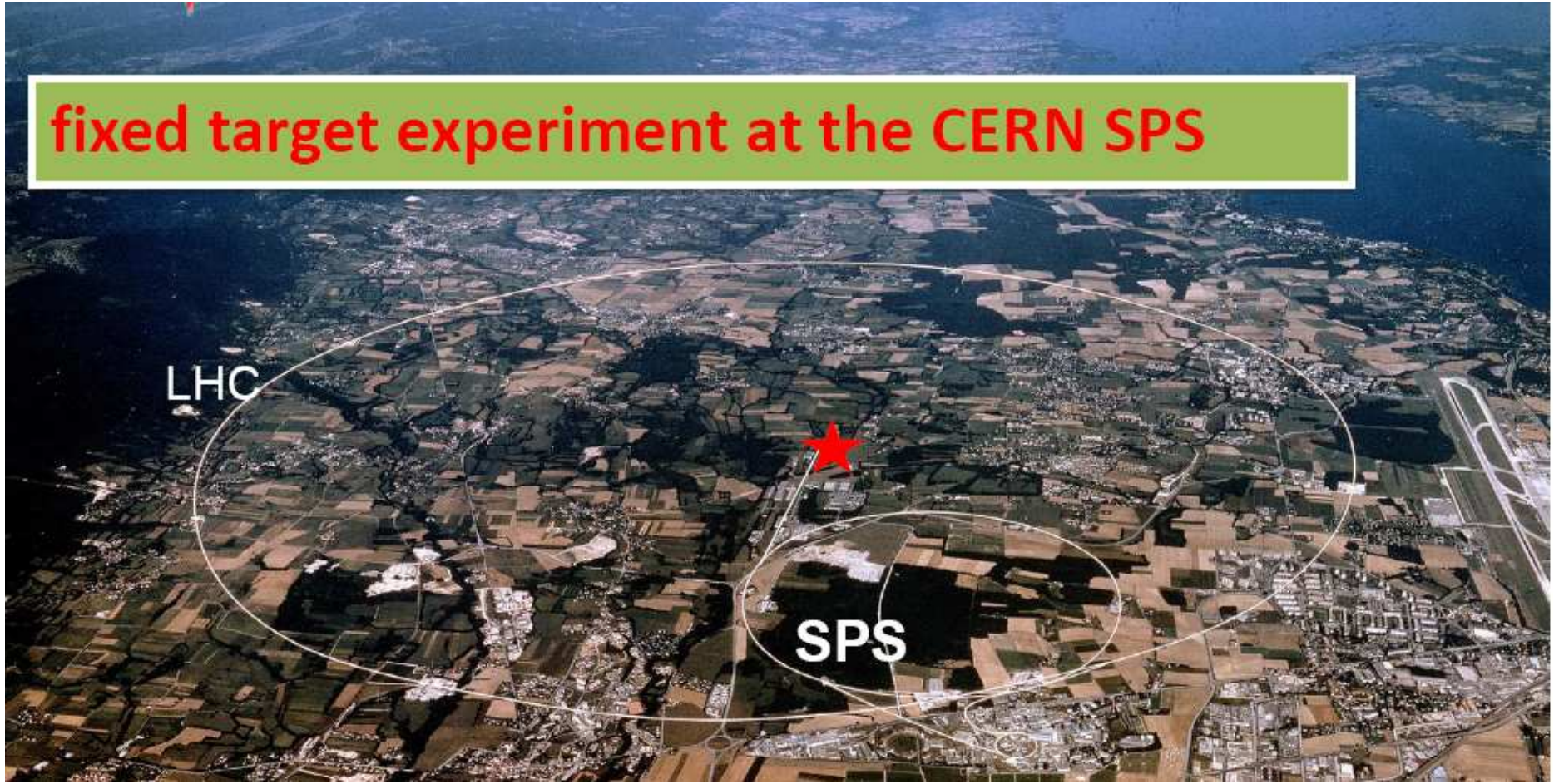

COMPASS spectrometer

NIM A 577 (2007) 455

- **high energy beams**
- **large angular acceptance**
- **broad kinematical range**

two stages spectrometer

Large Angle Spectrometer (SM1)

Small Angle Spectrometer (SM2)

variety of tracking detectors

SciFi	*Straws*
Silicon	*DC*
Micromega	*MWPC*
(P)GEM	*LDC*

to cope with different particle flux
from $\theta = 0$ to $\theta \approx 200$ mrad
with a good azimuthal acceptance

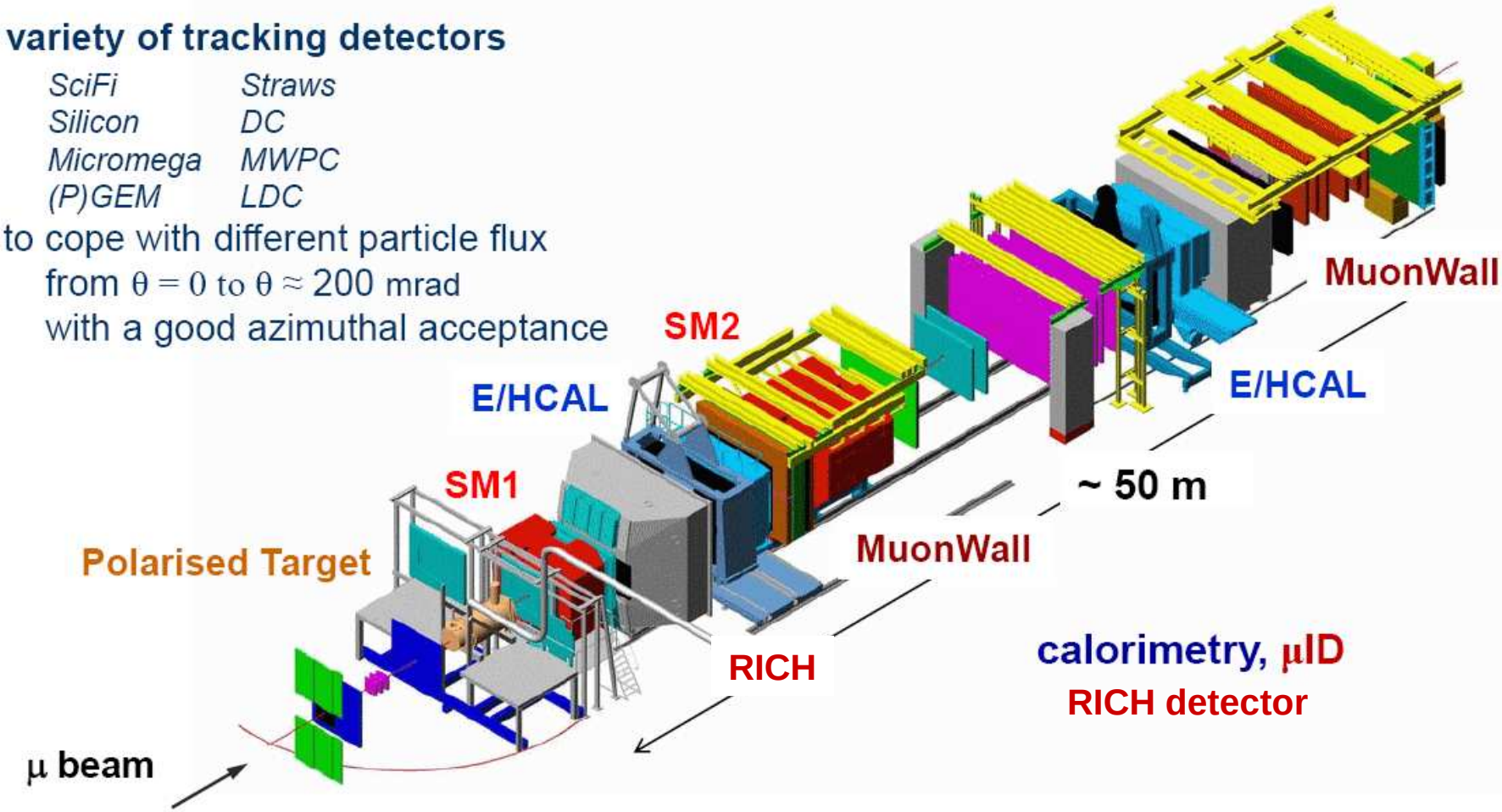

COMPASS polarised target

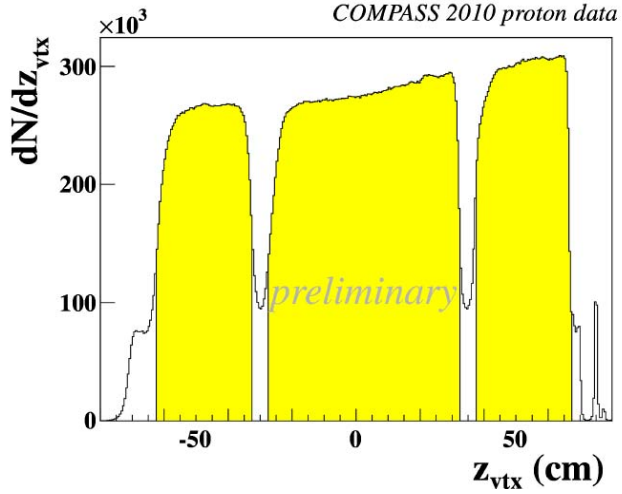

^{3}He – ^{4}He dilution refrigerator (T~50mK)

solenoid 2.5T
dipole magnet 0.6T

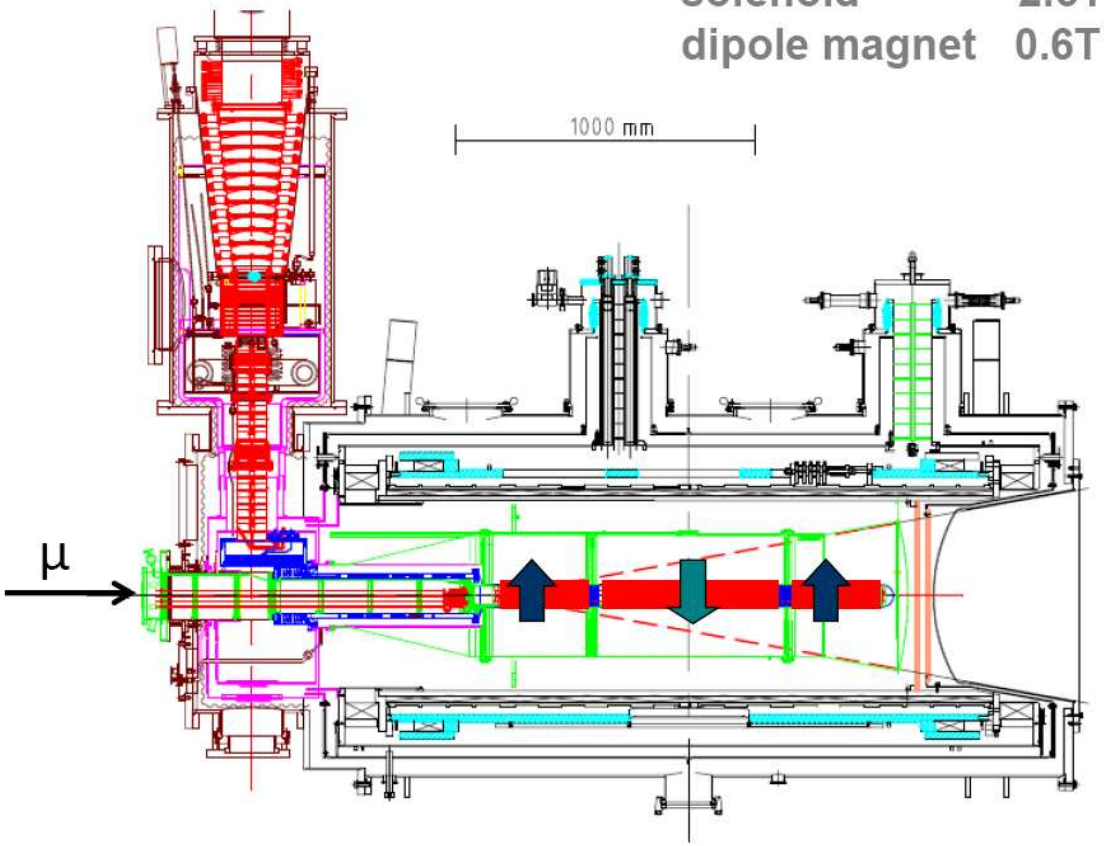

acceptance > ± 180 mrad

3 target cells
30, 60, and 30 cm long

opposite polarisation

	d (^{6}LiD)	p (NH_3)
polarization	50%	90%
diliution factor	40%	16%

transverse spin reversed every several days

COMPASS data taking

2002
2003 — 160 GeV μ L & T polarised deuteron target (^{6}LiD)
2004

2005 CERN shutdown, new large apperture PT magnet, 2 => 3 PT cells

2006 — 160 GeV μ L polarised deuteron target (^{6}LiD)

2007 — 160 GeV μ L & T polarised proton target (NH_3)

2008 — 190 GeV hadron beams LH_2 and nuclear targets
2009 — hadron spectroscopy & Primakoff reactions

2010 — 160 GeV μ T polarised proton target (NH_3)

2011 — 200 GeV μ L polarised proton target (NH_3)

2012 — Primakoff (taking data now) + DVCS run (since October)

New results with transversely polarised protons and deuterons

- Sivers asymmetry — p (2010)

  Sivers TMD, related to quarks OAM — subm. to PL B, hep-ex/1205,5122

- Collins asymmetry — p (2010)

  sensitive to transversity — subm. to PL B, hep-ex/1205,5121

- Two-hadron azimuthal asymmetry — d (2002 – 04), p (2007, 2010)

  sensitive to transversity — PL B 713 (2012) 10; prel.

- Azimuthal asymmetry for exclusive ρ^0 — d (2003 – 04), p (2007, 2010)

  sensitve to GPDs E => Ji sum rule — accepted by Nucl. Phys. B

Quark structure of the nucleon

when intrinsic parton transverse momentum not neglected

8 TMD PDFs needed for complete description of the nucleon structure

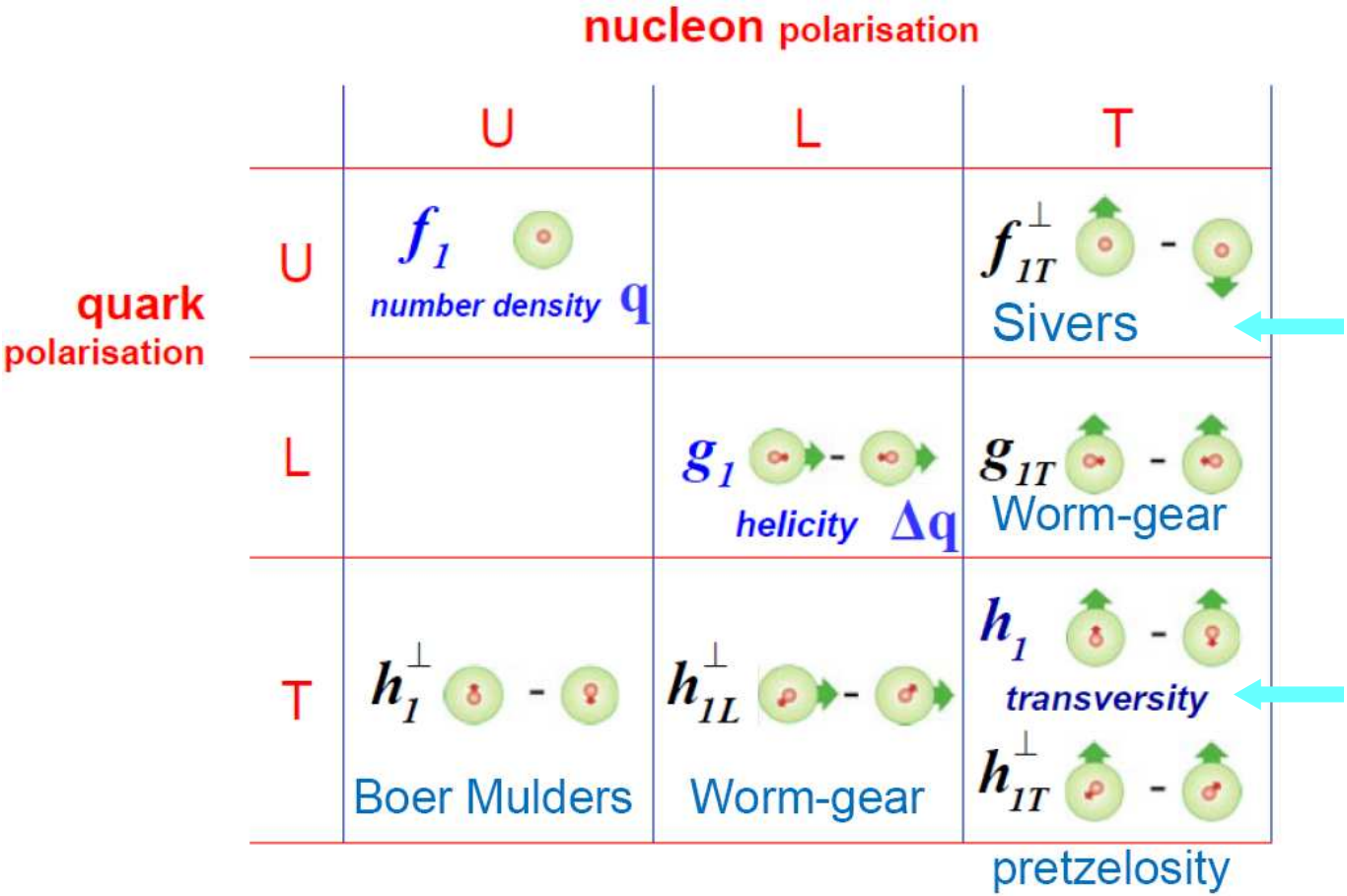

upon integration over transverse momentum only f_1, g_1 and h_1 survive

transversity (h_1) is chiral-odd => in contrast to f_1 and g_1 cannot be measured in inclusive DIS

possible in SIDIS, if coupled to a non-zero chiral-odd fragmentation function

SIDIS cross section

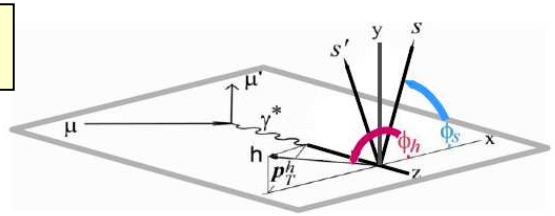

$$
\begin{aligned}
\frac{d\sigma}{dx\,dy\,d\psi\,dz\,d\phi_h\,dP_{h\perp}^2} = \\
&\frac{\alpha^2}{xyQ^2}\,\frac{y^2}{2\,(1-\varepsilon)}\left(1+\frac{\gamma^2}{2x}\right)\Bigg\{F_{UU,T}+\varepsilon\,F_{UU,L}+\sqrt{2\,\varepsilon(1+\varepsilon)}\,\cos\phi_h\,F_{UU}^{\cos\phi_h} \\
&+\varepsilon\,\underbrace{\cos(2\phi_h)}_{h_1^\perp H_1^\perp}\,F_{UU}^{\cos 2\phi_h}+\lambda_e\,\sqrt{2\,\varepsilon(1-\varepsilon)}\,\sin\phi_h\,F_{LU}^{\sin\phi_h} \\
&+S_\parallel\left[\sqrt{2\,\varepsilon(1+\varepsilon)}\,\sin\phi_h\,F_{UL}^{\sin\phi_h}+\varepsilon\,\underbrace{\sin(2\phi_h)}_{h_{1L}^\perp H_1^\perp}\,F_{UL}^{\sin 2\phi_h}\right]+S_\parallel\lambda_e\left[\sqrt{1-\varepsilon^2}\,F_{LL}+\sqrt{2\,\varepsilon(1-\varepsilon)}\,\cos\phi_h\,F_{LL}^{\cos\phi_h}\right] \\
&+|\boldsymbol{S}_\perp|\Bigg[\underbrace{\sin(\phi_h-\phi_S)}_{f_{1T}^\perp D_1}\left(F_{UT,T}^{\sin(\phi_h-\phi_S)}+\varepsilon\,F_{UT,L}^{\sin(\phi_h-\phi_S)}\right) \\
&\quad+\varepsilon\,\underbrace{\sin(\phi_h+\phi_S)}_{h_{1T}^\perp H_1^\perp}\,F_{UT}^{\sin(\phi_h+\phi_S)}+\varepsilon\,\underbrace{\sin(3\phi_h-\phi_S)}_{h_1\,H_1^\perp}\,F_{UT}^{\sin(3\phi_h-\phi_S)} \\
&\quad+\sqrt{2\,\varepsilon(1+\varepsilon)}\,\sin\phi_S\,F_{UT}^{\sin\phi_S}+\sqrt{2\,\varepsilon(1+\varepsilon)}\,\sin(2\phi_h-\phi_S)\,F_{UT}^{\sin(2\phi_h-\phi_S)}\Bigg] \\
&+|\boldsymbol{S}_\perp|\lambda_e\Bigg[\sqrt{1-\varepsilon^2}\,\underbrace{\cos(\phi_h-\phi_S)}_{g_{1T}D_1}\,F_{LT}^{\cos(\phi_h-\phi_S)}+\sqrt{2\,\varepsilon(1-\varepsilon)}\,\cos\phi_S\,F_{LT}^{\cos\phi_S} \\
&\quad+\sqrt{2\,\varepsilon(1-\varepsilon)}\,\cos(2\phi_h-\phi_S)\,F_{LT}^{\cos(2\phi_h-\phi_S)}\Bigg]\Bigg\},
\end{aligned}
$$

18 structure functions
14 azimuthal modulations
all measured in COMPASS

A Bacchetta et al., 2006

Sivers asymmetries from 2010 run

$$N_h^{\pm}(\Phi_S) = N_h^0(1 \pm A_S^h \sin(\Phi_S))$$

with $\Phi_S = \phi_h - \phi_s$

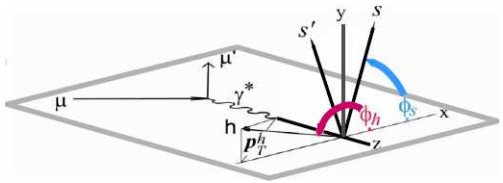

$$A_{Siv} = \frac{A_S^h}{f \cdot P_T} = \frac{\sum_q e_q^2 f_{1T}^q(x, k_\perp^2) \otimes D_{1,q}(z, p_\perp^2)}{\sum_q e_q^2 f_1^q(x, k_\perp^2) \otimes D_{1,q}(z, p_\perp^2)}$$

P_T – target polarisation, f – dilution factor

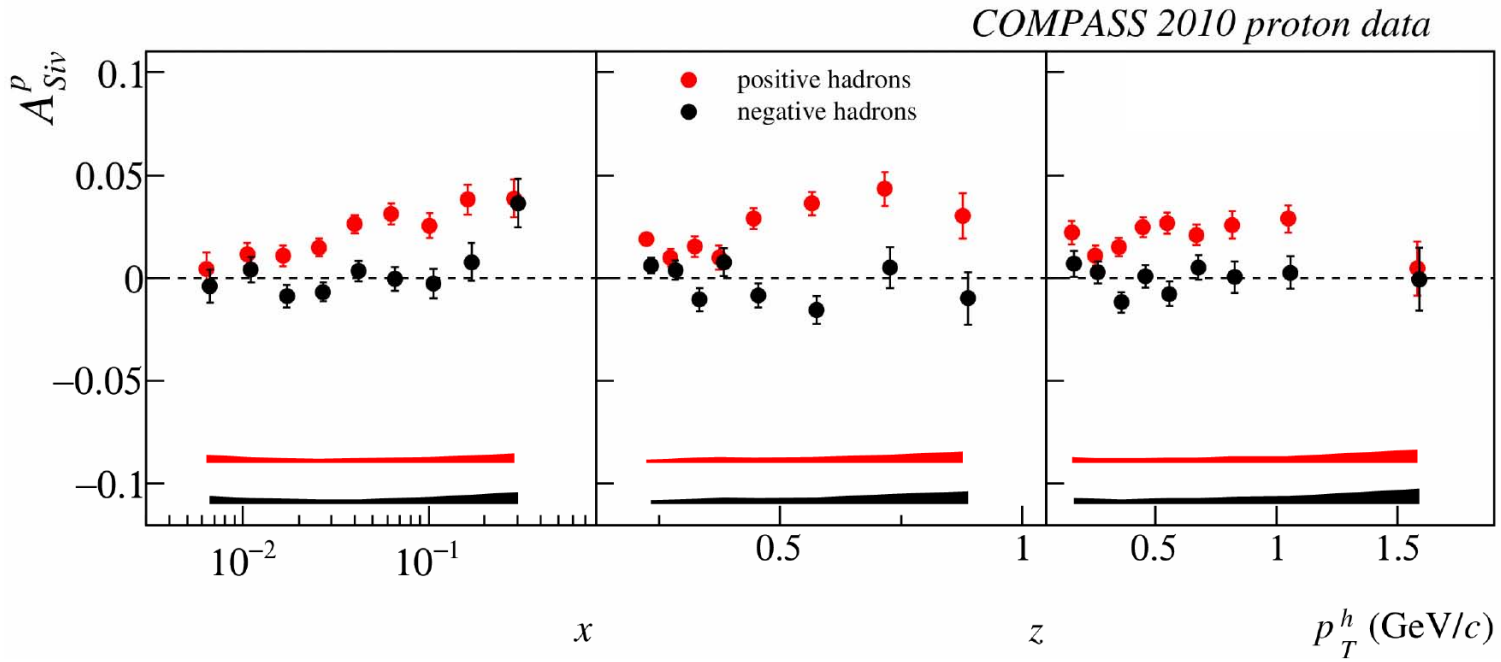

- positive asymmetry for h+ , stays positive well below the valence region (down to $x \approx 10^{-2}$)
- for h^- the asymmetry compatible with zero
- good agreement with 2007 published results, significant reduction of statistical uncertainty

More on kinematic dependence of Sivers asymmetry

comparison to HERMES

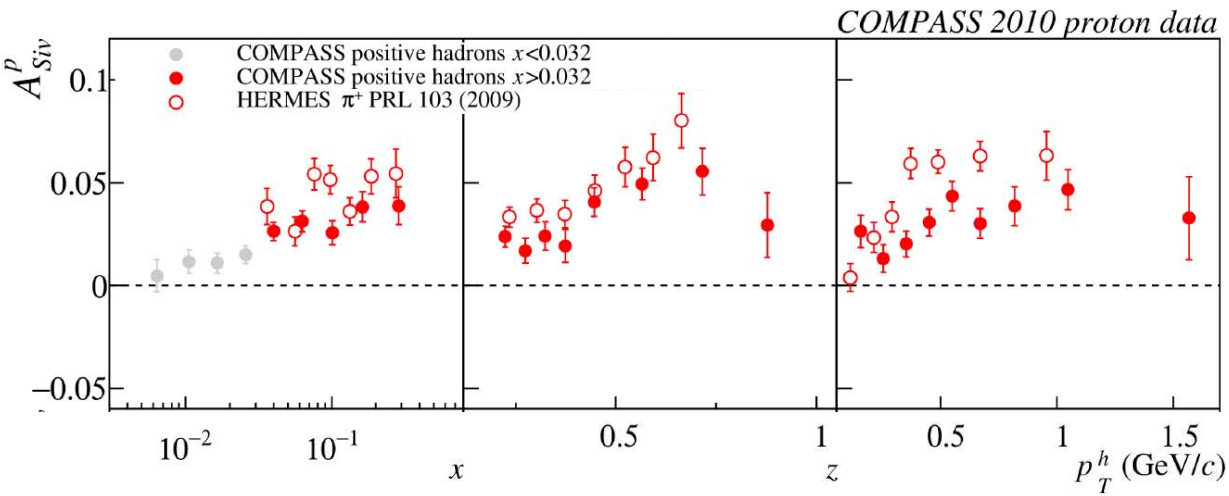

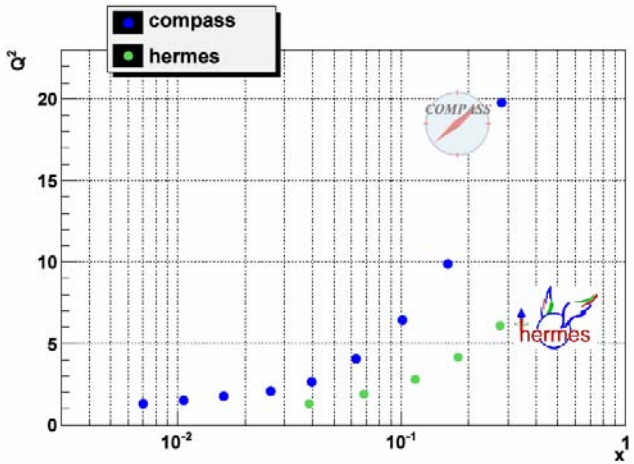

asymmetries in different *y* ranges

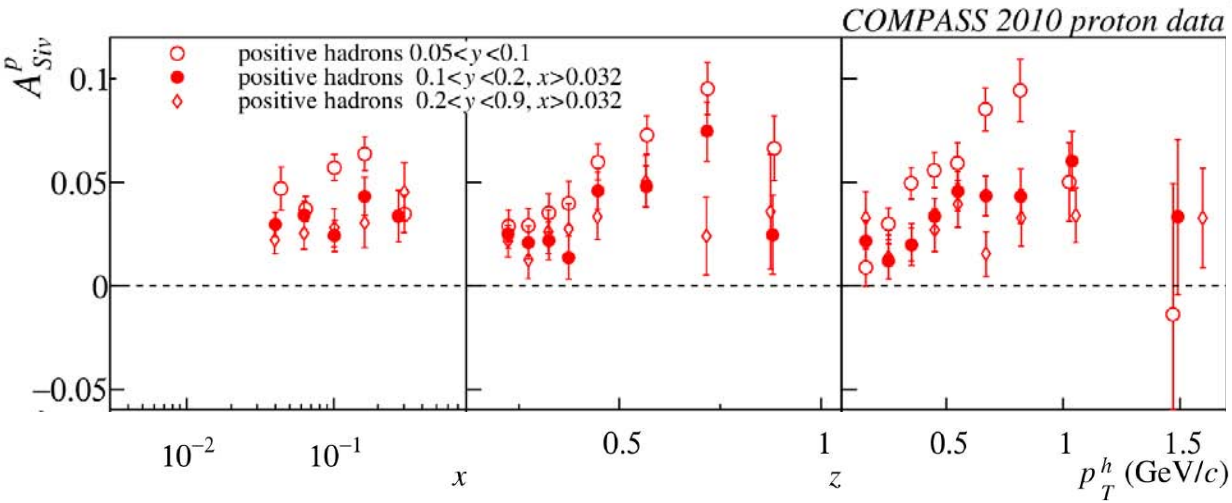

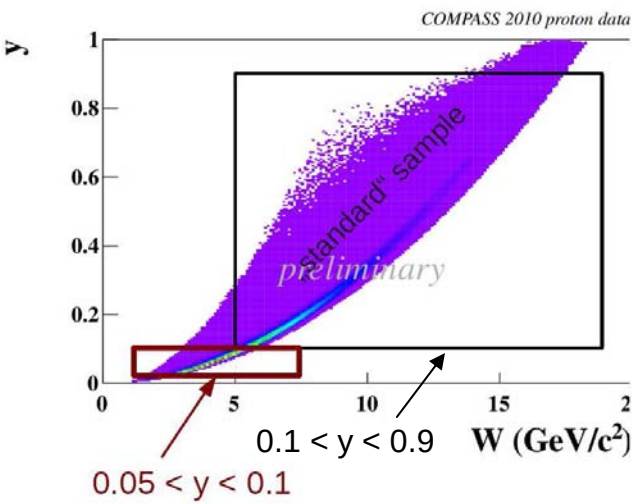

clear increase of Sivers asymmetry for h^+ at low Q^2 and y (or W)

not shown are asymmetries for h^-, no significant dependence and compatible with zero

Comparison to model predictions

predictions from S.M. Aybat, A. Prokhudin and T.C. Rogers (arXiv:1112.4423)

Sievers asymmetry evaluated for HERMES range using Sievers function of M. Anselmino et al. (arXiv:1107.4446)

and then evolved to COMPASS kinematic region

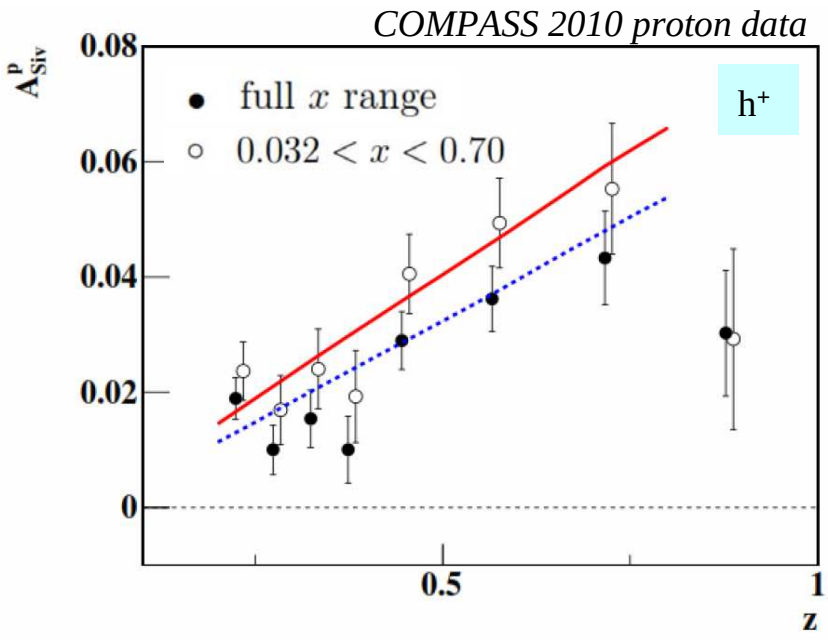

good agreement (apart of highest z ?)

current TMD approach foresees a strong Q^2-dependence of the Sievers function

M. Anselmino, M. Boglione and S. Melis (arXiv:1204.1239) Q^2-dependent global fit to HERMES, COMPASS deuteron and COMPASS 2007 proton data reproduces them well

high precision of COMPASS 2010 proton results
expected to improve significantly future global fits of Sivers function

Collins asymmetries from 2010 run

$$N_h^{\pm}(\Phi_C) = N_h^0(1 \pm A_C^h \sin(\Phi_C))$$

with $\Phi_C = \phi_h - \phi_{s'} = \phi_h + \phi_S - \pi$

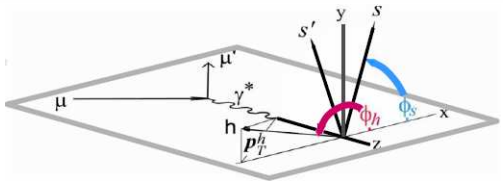

$$A_{Coll} = \frac{A_C^h}{f \cdot P_T \cdot D_{nn}} = \frac{\sum_q e_q^2 h_1^q(x,k_\perp^2) \otimes H_{1,q}^{\perp}(z,p_\perp^2)}{\sum_q e_q^2 f_1^q(x,k_\perp^2) \otimes D_{1,q}(z,p_\perp^2)}$$

Collins FF

P_T – target polarisation, f – dilution factor

D_{nn} – spin transfer coeff. from initial to struck quark

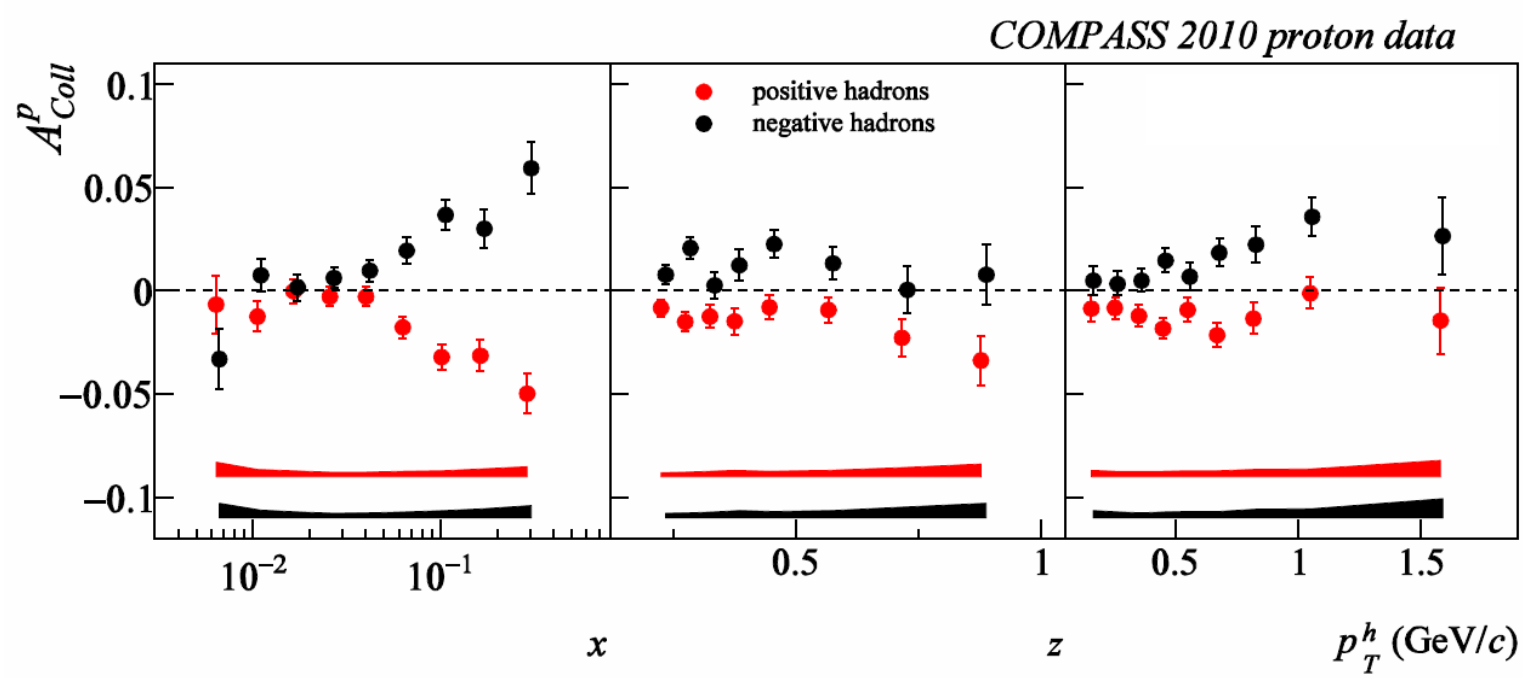

- in valence region mirror symmetry wrt hadron charge => $H^{\perp}_{1,fav} \approx - H^{\perp}_{1,unf}$ (Collins FF)
- at small-x range (< 0.03), not covered by HERMES, asymmetries compatible with zero
- confirm published results from 2007 with statistical uncertainties improved by factor ~ 2

Comparison to HERMES and Q^2 dependence

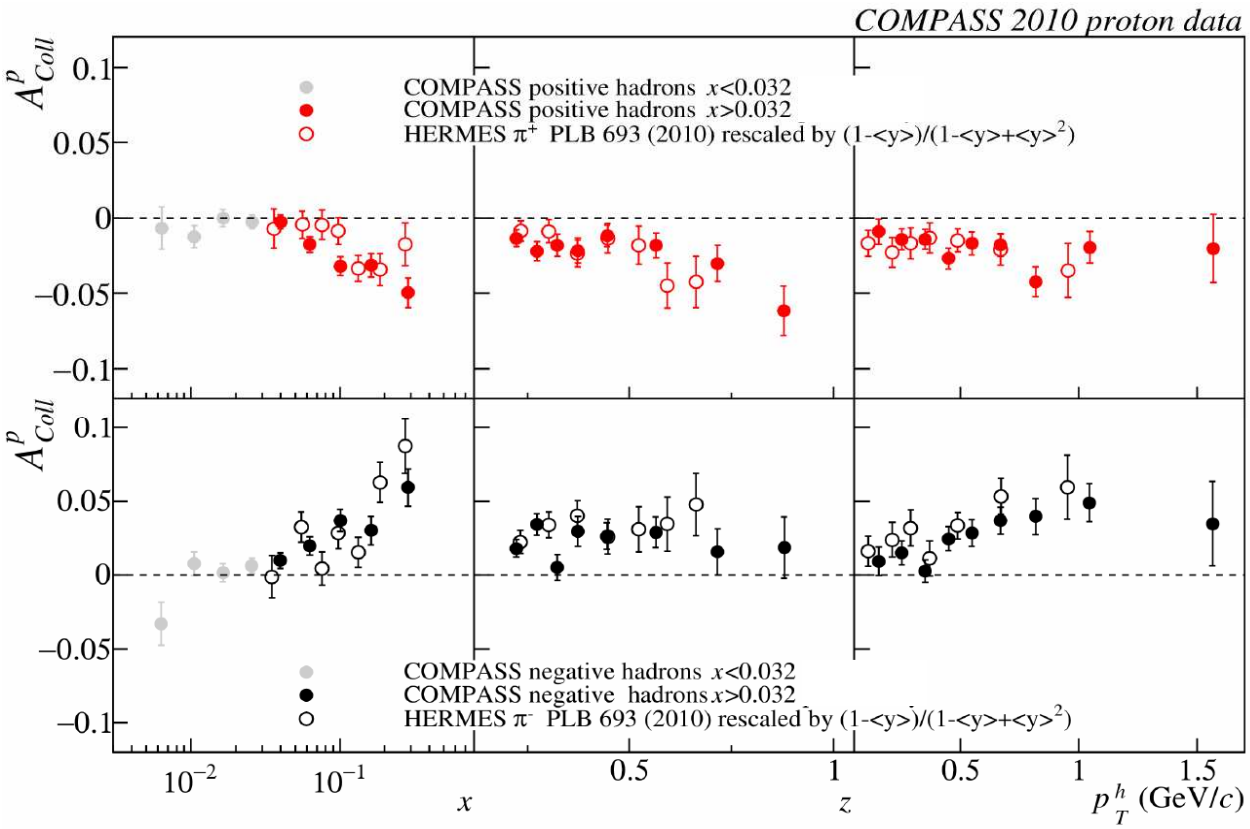

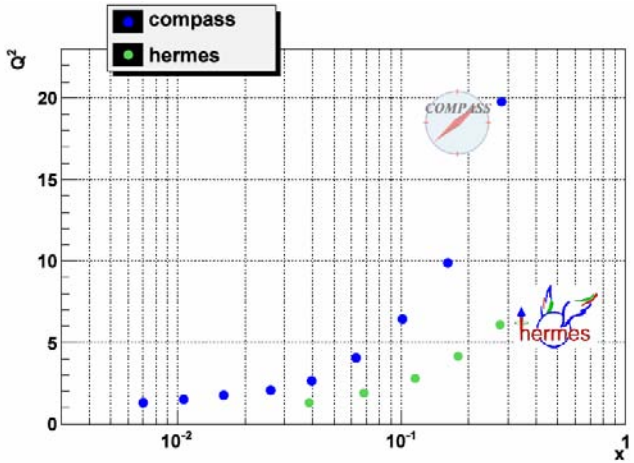

- in overlap region good agreement with HERMES
- non-trivial result; at COMPASS <Q^2> larger by a factor 2-3

→ weak Q^2> dependence of the Collins asymmetry

Comparison to model predictions

predictions from the fit (Anselmino at al.) to HERMES p, COMPASS d and Bell e^+e^- data

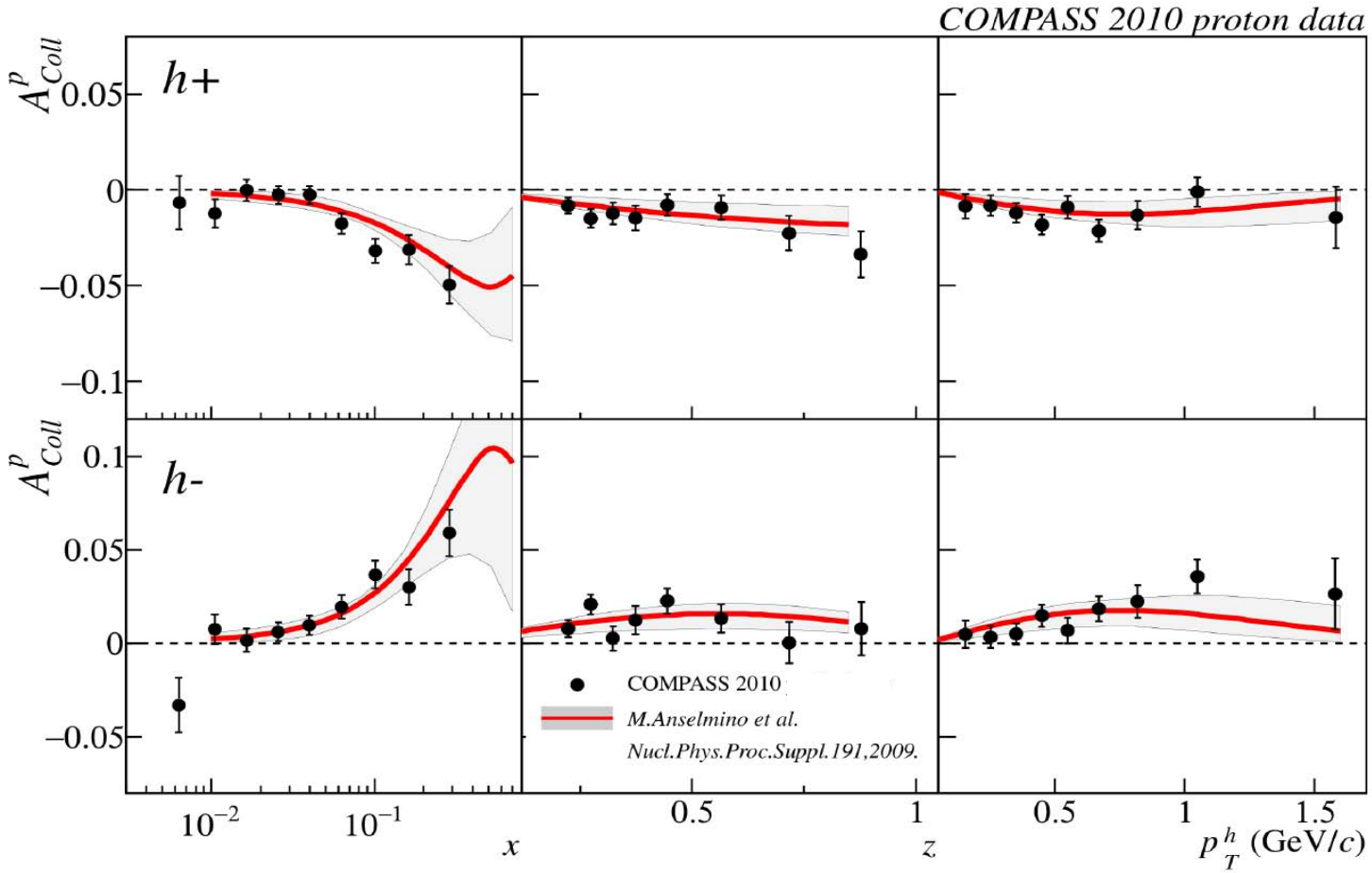

observed agreement supports the weak Q^2 dependence of the Collins FF assumed in the model

Two-hadron asymmetries

$l\ p^{\uparrow} \rightarrow l\ h_1\ h_2\ X$

alternative method to access transversity, valid within framework of collinear factorization

fragmentation of transversely polarised quark into two unpolarised hadrons

$$N^{\pm}_{2h}(x,z,y,M_h^2,\cos\theta,\Phi_{RS}) = N^0_{2h}(1 \pm f\ P_T\ D_{nn}\ A_{UT}^{\sin\Phi_{RS}}\ \sin\theta\ \sin\Phi_{RS})$$

with $\Phi_{RS} = \Phi_R + \Phi_S - \pi$

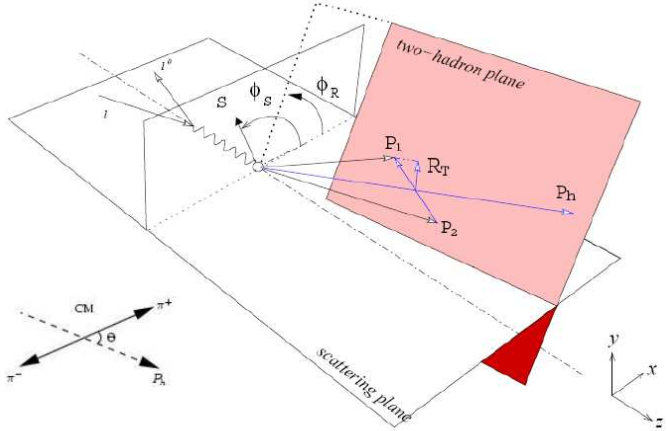

P_T – target polarisation, f – dilution factor

D_{nn} – transverse spin transfer coeff.

Interference FF

$$A_{UT}^{\sin\Phi_{RS}} = \frac{|\mathbf{p_1}-\mathbf{p_2}|}{2M_h} \frac{\sum_q e_q^2 \cdot h_1^q(x) \cdot H_{1,q}^{\sphericalangle}(z,M_h^2,\cos\theta)}{\sum_q e_q^2 \cdot f_1^q(x) \cdot D_{1,q}(z,M_h^2,\cos\theta)}$$

Selection of events (for 2010)

DIS cuts common with single hadron analysis

- $Q^2 > 1\ (\mathrm{GeV}/c)^2$
- $0.1 < y < 0.9$
- $W > 5\ \mathrm{GeV}/c^2$
- spectrometer acceptance: $0.003 < x_{bj} < 0.7$

cuts specific for 2-hadron analysis

- Vertex with at least **3** outgoing tracks. $\hookrightarrow$ All h^+h^- pair combinations are taken into account
- $z > 0.1$ for each hadron
- $x_F > 0.1$ for each hadron
- $E_{miss} > 3$ GeV for each pair
- $\mathbf{R_T} > 0.07\ \mathrm{GeV}/c$ for each pair

Results for two-hadron asymmetries

PLB 713 (2012) 10

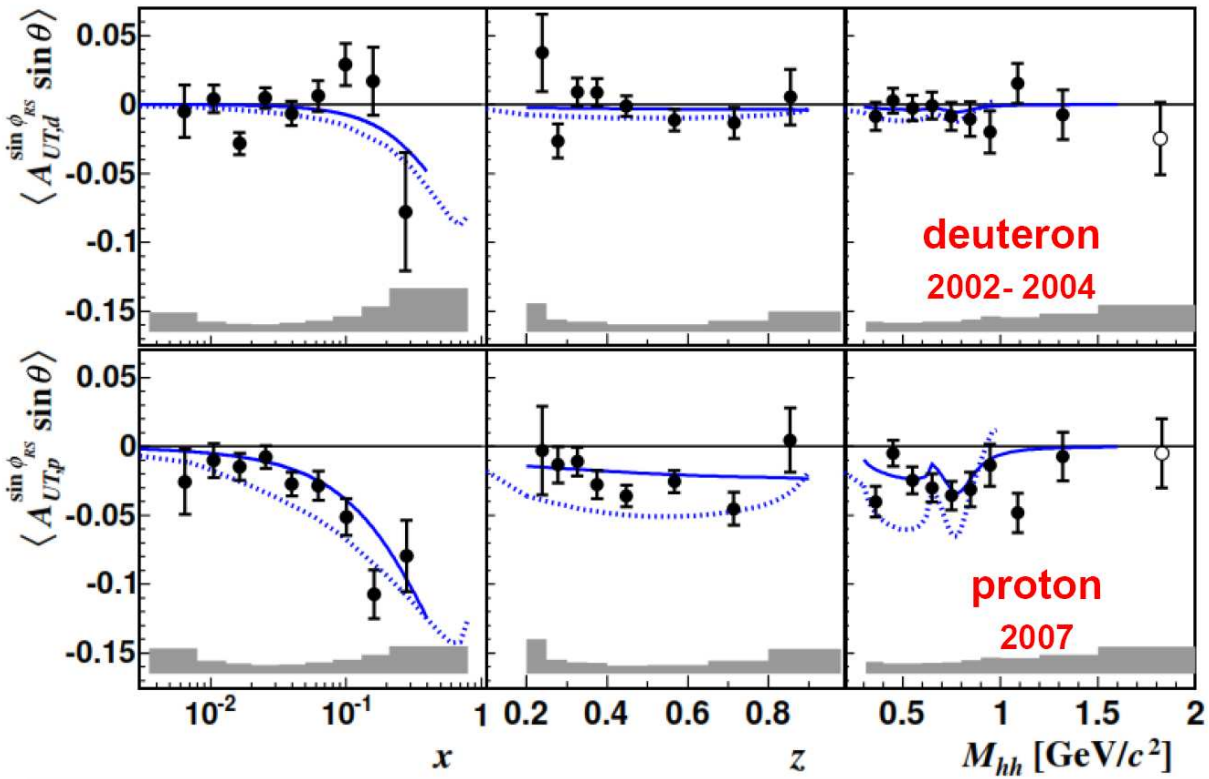

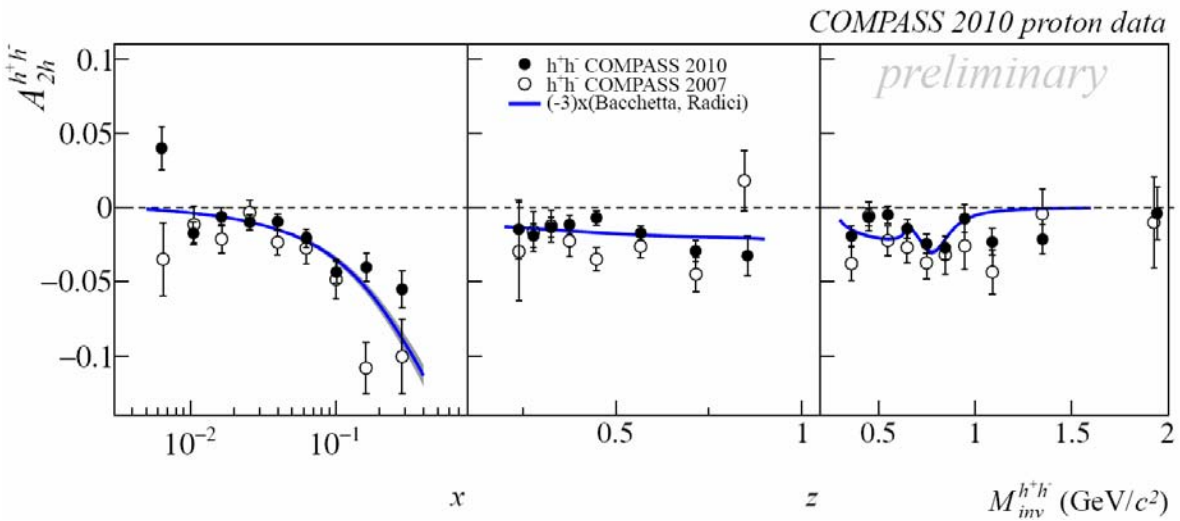

Bacchetta et al. hep-ph/0708037

Ma et al. PR D77 (2008) 14035

- for deuteron compatible with 0
- for proton large negative asymmetries in valence region

  compatible with 0 at $x < 0.03$
- no strong dependence on z and M_{hh}
- good agreement between 2007 and 2010 data

  in 2010 data significantly reduced uncertainties
- good agreement with HERMES in common kinematic region

  wider kinematic range in x, z and M_{hh} at COMPASS
- reasonable agreement with models of Bacchetta and Ma

Extraction of valence quarks transversity from two-hadron asymmetries

using Interference FF from Belle and following approach of Bacchetta, Courtoy and Radici

PRL 107:012001,2001

transversity of u_v and d_v extracted from COMPASS deuteron and 2010 proton data

C. Elia, PhD thesis, Trieste 2011

COMPASS 2010 proton data

$xh_1^{u_v}(x) - \frac{1}{4}xh_1^{d_v}(x)$

COMPASS deuteron data

$xh_1^{u_v}(x) + xh_1^{d_v}(x)$

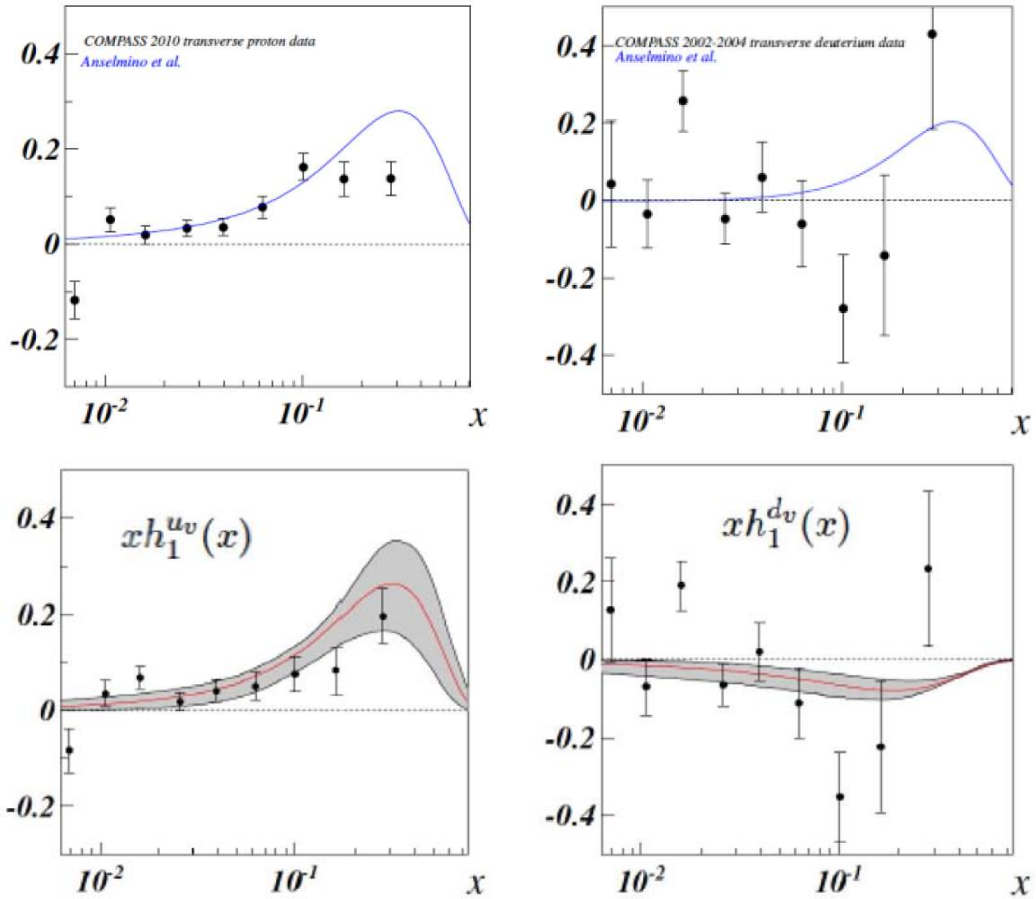

Hard Exclusive Meson Production and GPDs

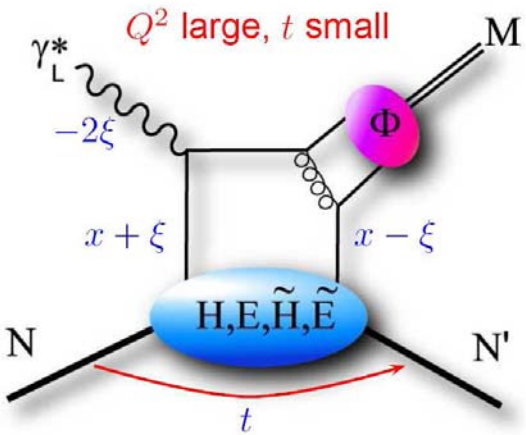

- 4 Generalised Parton Distributions (GPDs)
  for each quark flavour and for gluons
  GPDs depend on 3 variables: x, ξ, t
- collinear factorisation proven only for σ_L
  σ_T suppressed by $1/Q^2$
- quarks and gluons enter at the same order of α_S
- for vector mesons (ρ, ω, φ): H, E
  H: non-flip; E: nucleon helicity flip

separation wrt quark flavours and gluons

ρ^0	2/3 u + 1/3 d + 3/8 g
ω	2/3 u – 1/3 d + 3/8 g
ϕ	s, g
ρ^+	u–d
J/ψ	g

LT observables in VM exclusive meson production relevant for GPDs

for longitudinal γ*

unpolarised cross section $(\sigma_{00}^{++} \equiv \sigma_L)$

$$\frac{d\sigma_{00}^{++}}{dt} = (1-\xi^2)\,|\,\underline{H_M}\,|^2 - (\xi^2 + \frac{t}{4M_p^2})\,|\,E_M\,|^2 - 2\xi^2\,\mathrm{Re}(E_M^* H_M)$$

transverse target spin dependent cross section

$$\frac{1}{2}(\frac{d\sigma_{00}^{\uparrow\uparrow}}{dt} - \frac{d\sigma_{00}^{\downarrow\downarrow}}{dt}) = -\mathrm{Im}\frac{d\sigma_{00}^{+-}}{dt} = \Gamma'\sqrt{1-\xi^2}\,\frac{\sqrt{t_0 - t}}{M_p}\,\mathrm{Im}(\underline{E_M^* H_M})$$

access to GPD E related to orbital momentum

H_M, E_M are weighted sums of convolutions of the GPDs $H^{q,g}$, $E^{q,g}$ with hard scattering kernel and meson DA

weights depend on contributions of various quark flavours and of gluons to the production of meson M

$$\Gamma' = \frac{\alpha_{\mathrm{em}}}{Q^6}\,\frac{x_B^2}{1-x_B} \qquad \xi = \frac{x_B}{2-x_B}, \qquad -t_0 = \frac{4\xi^2 M_p^2}{1-\xi^2}$$

(large Q^2 approximation)

Give access to the orbital angular momentum of quarks

$$\boxed{\frac{1}{2}\int_{-1}^{1} dx\; x\;[H_q(x,\xi,t) + E_q(x,\xi,t)] \overset{t\to 0}{=} J_q = \frac{1}{2}\Delta\Sigma + L_q}$$

Ji's sum rule

So far GPD E poorly constrained by data (mostly by Pauli form factors)

Exclusive ρ^0 production on $p^\uparrow$ and $d^\uparrow$ at COMPASS

$\mu N \rightarrow \mu \rho^0 N$

i.e. incoherent process

Transversely polarised proton target (NH_3), 2007, 2010
Transversely polarised deuteron target (^{6}LiD), 2003-2004

note: there was no RPD for these data

only two tracks of opposite charge associated to the primary vertex

DIS cuts

$1 < Q^2 < 10$ GeV^2
$0.1 < y < 0.9$
$W > 5$ GeV

cuts specific for exclusive ρ^0 analysis

$0.5 < M_{\pi\pi} < 1.1$ GeV
$-2.5 < E_{miss} < 2.5$ GeV
$E_{\rho 0} > 15$ GeV
$0.05 < p_T^2 < 0.5$ GeV^2 [NH_3]
$0.1 < p_T^2 < 0.5$ GeV^2 [^{6}LiD]

$E_{miss} = (M_X^2 - M_p^2)/(2M_p)$

proton data (797 000 evts)
deuteron data (97 000 evts)

dominant non-excusive bkg.

dominant coherent contrib.

dominant non-exclusive bkg.

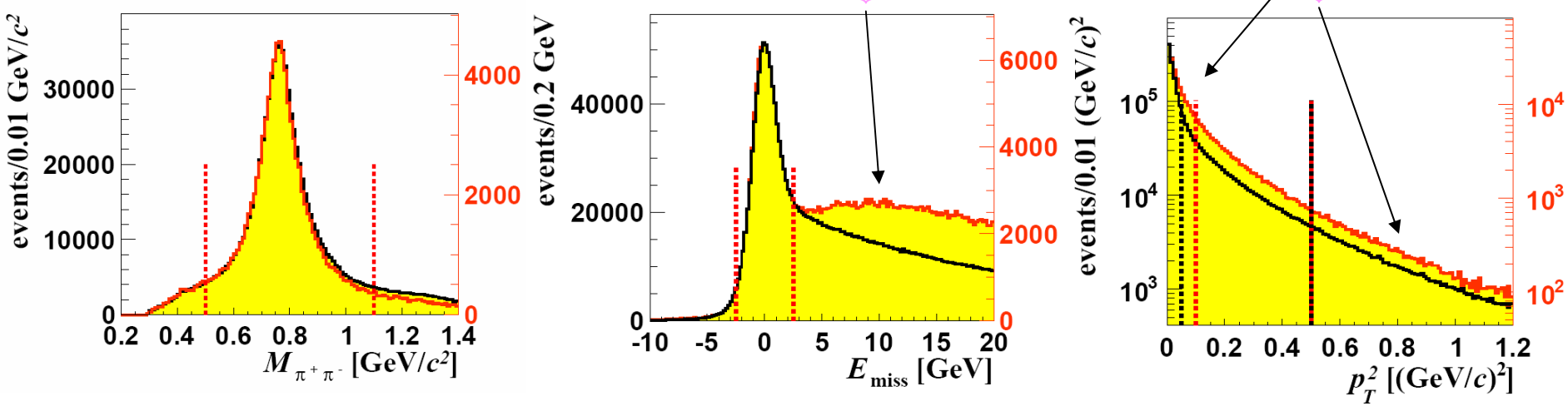

TTS asymmetry $A_{UT}^{\sin(\phi-\phi_s)}$ for exlusive ρ^0 production from COMPASS

$\mu\, N \rightarrow \mu\, \rho^0\, N$

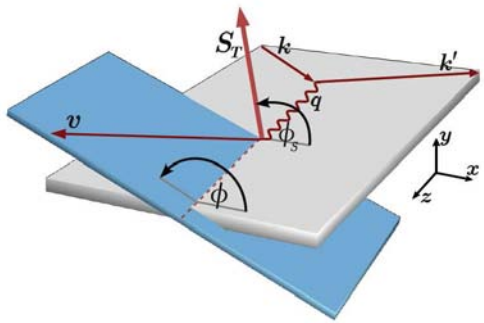

$$\left[\frac{\alpha_{em}}{8\pi^3}\frac{y^2}{1-\epsilon}\frac{1-x_{Bj}}{x_{Bj}}\frac{1}{Q^2}\right]^{-1}\frac{\mathrm{d}\sigma}{\mathrm{d}x_{Bj}\mathrm{d}Q^2\mathrm{d}t\mathrm{d}\phi\mathrm{d}\phi_s} \simeq$$

$$\underbrace{\frac{1}{2}\left(\sigma_{++}^{++}+\sigma_{++}^{--}\right)+\epsilon\sigma_{00}^{++}}_{\text{unpolarised cross section}} - S_T\sin\left(\phi-\phi_s\right)\mathrm{Im}\left(\sigma_{++}^{+-}+\epsilon\sigma_{00}^{+-}\right)+\ldots$$

$$A_{UT}^{\sin(\phi-\phi_s)} = -\frac{\mathrm{Im}(\sigma_{++}^{+-}+\epsilon\,\sigma_{00}^{+-})}{\frac{1}{2}(\sigma_{++}^{++}+\sigma_{++}^{--})+\epsilon\,\sigma_{00}^{++}}$$

number of exclusive events

after bin-by-bin correction for SIDIS background

$$N(\phi-\phi_S) = F\,n\,a\,\sigma_0\left(1\pm f\,|P_T|\,A_{UT}^{\sin(\phi-\phi_S)}\sin(\phi-\phi_S)\right)$$

F – flux, n – number of nucleons, a – acceptance, σ_0 – unpolarised cross section

f – dilution factor, P_T – target transverse polarisation

asymmetry extracted form a fit of the number of events in 12 bins of ϕ - ϕ_s for each of the two(*) target cells and polarisation state (+,-)

(*) for 3-cell target used for proton data (2007, 2010) upstream and downstream ones were combined

Results on $A_{UT}^{\sin(\phi-\phi s)}$ for exlusive ρ^0 production from COMPASS

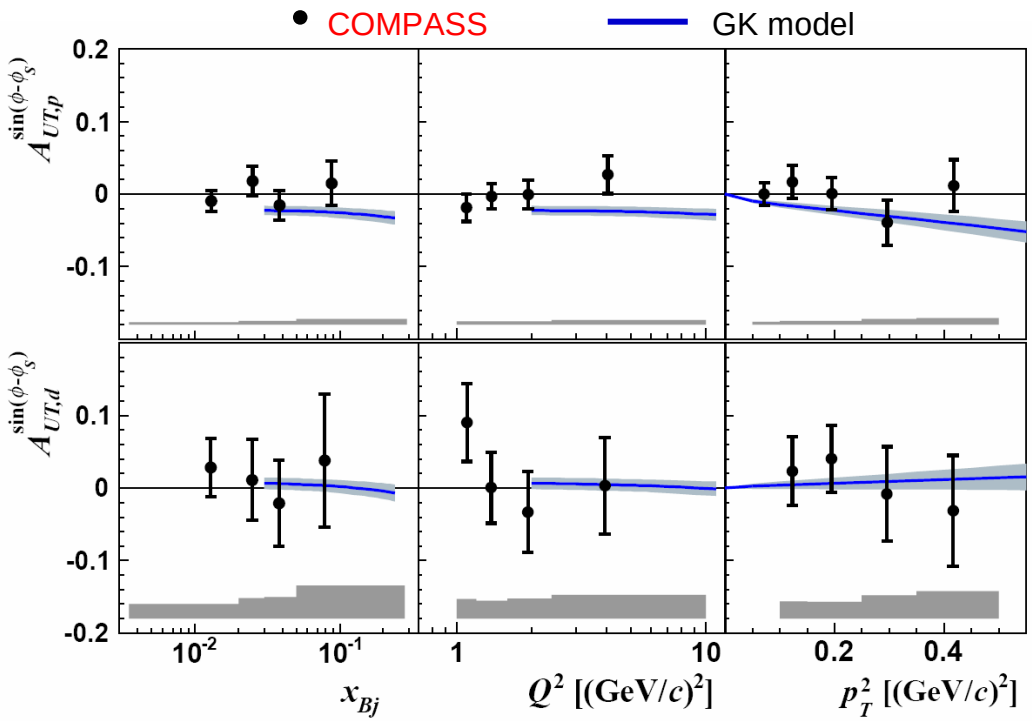

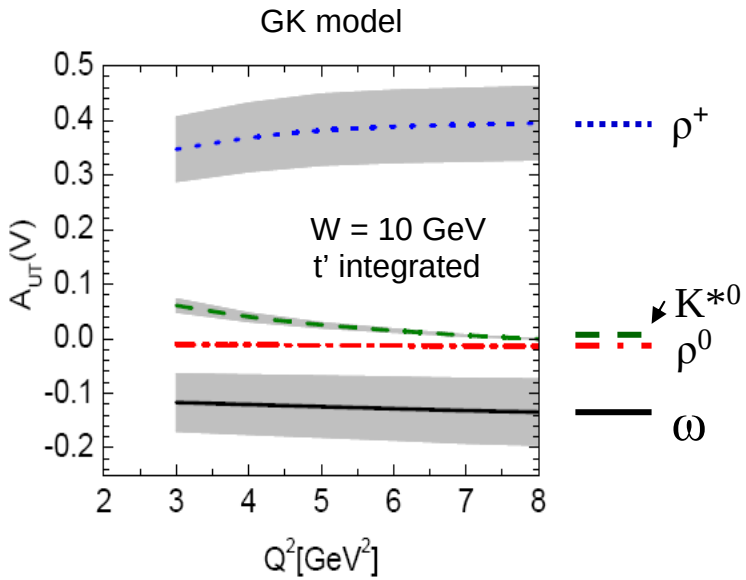

- $A_{UT}^{\sin(\phi-\phi s)}$ for transversely polarised protons and deuterons compatible with 0
- for the proton agreement with HERMEs results
  COMPASS results with statistical errors improved by factor 3 and extended kinematic range
- for the deuteron the first measurement
- reasonable agreement with predictions of the GPD model of Goloskokov - Kroll

[EPJ C59 (2009) 809]

small values expected due to approximate cancellation of contributions from E^u and E^d, $E^u \approx -E^d$

$E^p_{\rho 0} \sim \frac{2}{3} E^u + \frac{1}{3} E^d + \frac{3}{8} E^g$ vs. $E^p_{\omega} \sim \frac{2}{3} E^u - \frac{1}{3} E^d + \frac{3}{8} E^g$ (cf. upper-right plot)

COMPASS-II

EUROPEAN ORGANIZATION FOR NUCLEAR RESEARCH

CERN–SPSC–2010–014
SPSC-P-340
May 17, 2010

- Generalized Parton Distributions (GPD)
- Drell-Yan
- Pion (and kaon) Polarizabilities

COMPASS-II Proposal

Approved December 2010, first measurements 2012

The COMPASS Collaboration

wwwcompass.cern.ch/compass/proposal/compass-II_proposal/compass-II_proposal.pdf

Future GPD program in context of COMPASS-II time lines

Part of the COMPASS-II proposal scheduled presently by CERN

- 2012: pion and kaon polarisabilities (Primakoff) + comissioning and test run for DVCS
- 2013: long SPS shutdown
- 2014: Drell-Yann measurements with transversely polarised protons (NH_3 target)
- 2015-2016: stage 1 of GPD program and in parallel SIDIS (LH target)

Further subjects to be pursued at COMPASS-II > 2016

- ✓ additional year of Drell-Yann measurements
- ✓ stage 2 of GPD program (transversely polarised target and RPD)
- ✓ hadron program (spectroscopy in diffractive and central production)

The GPDs in the next several years

- **H1, ZEUS, HERMES, JLab 6 GeV** provided/providing first results

- The **energy upgrade** of the **CEBAF** accelerator will allow access to the **high x_B** region which requires **large luminosity**.

- The **GPD** project at **COMPASS** will explore **intermediate x_B** (0.01-0.10) and **large Q^2** (up to ~8(16) GeV^2) range

  COMPASS will be **the only experiment in this range** before availability of new colliders

  for several years COMPASS **unique** due to availability of lepton **beams of both charges**

Generalized Parton Distributions and DVCS

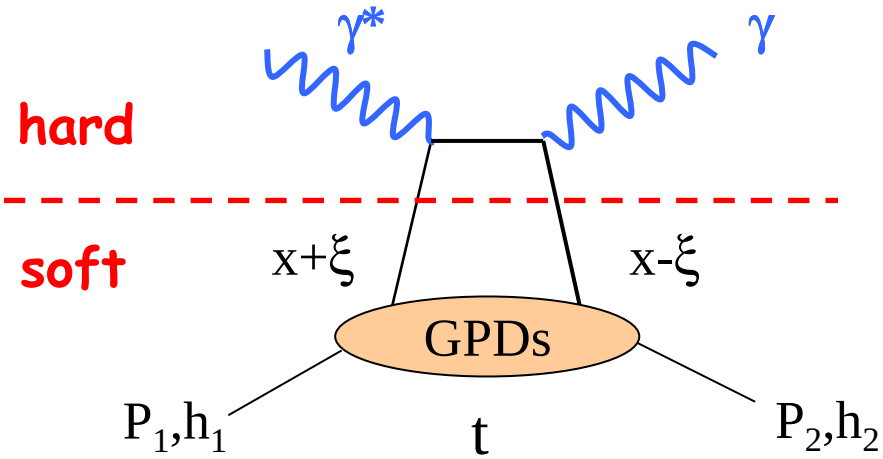

Factorisation:
Q^2 large, $-t<1$ GeV^2

$$\xi = \frac{x_B}{2 - x_B}$$

P_i, h_i – proton momentum and helicity

4 Generalised Parton Distributions : $H, E, \tilde{H}, \tilde{E}$ depending on 3 variables: x, ξ, t

for each quark flavour and for gluons

for DVCS gluons contribute at higher orders in α_s

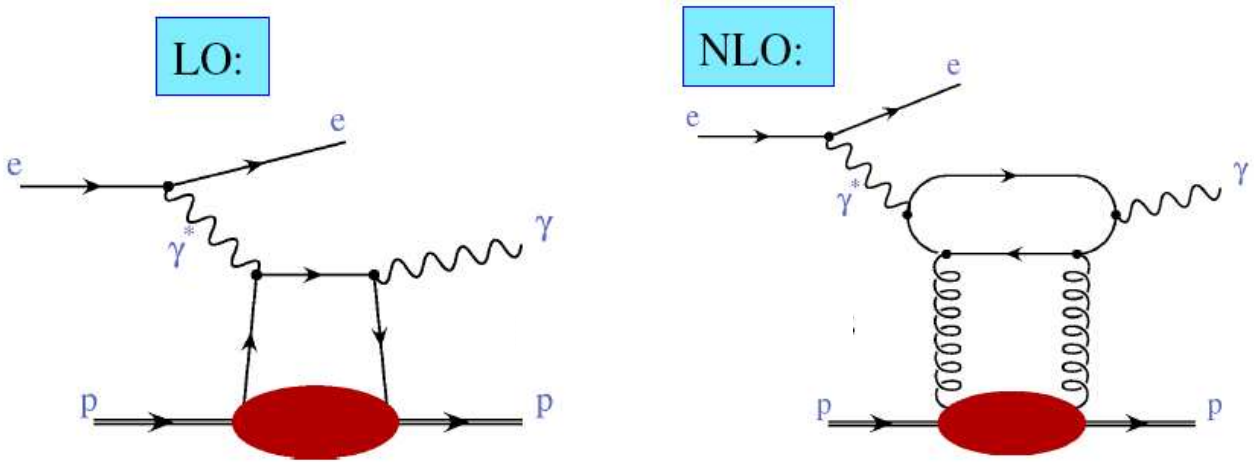

COMPASS kinematical coverage for DVCS

CERN SPS high energy polarised muon beam 100/190 GeV

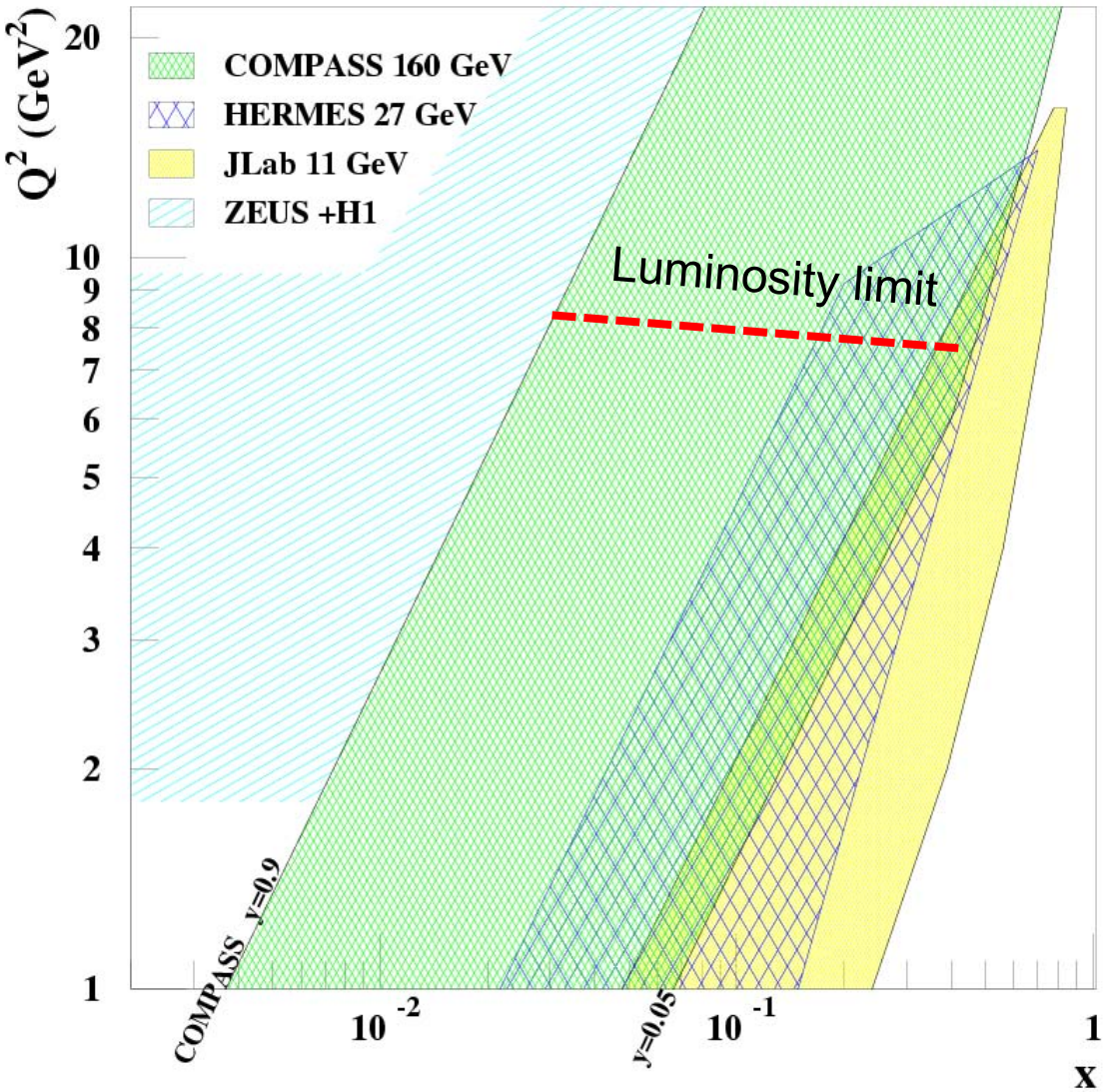

with a 2.5m long LH_2 target
$L = 10^{32}\ cm^{-2}\ s^{-1}$

$Q^2 \rightarrow 8\ GeV^2$

$\rightarrow 16\ GeV^2$ if luminosity increased by factor 4

$\sim 10^{-2} < x < \sim 10^{-1}$

$x \rightarrow 0.20$ with extension of present calorimetry

Interplay of DVCS and BH at 160 GeV

DVCS :

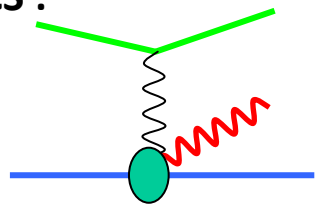

Bethe-Heitler :

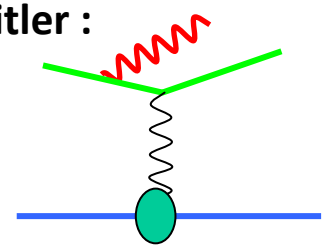

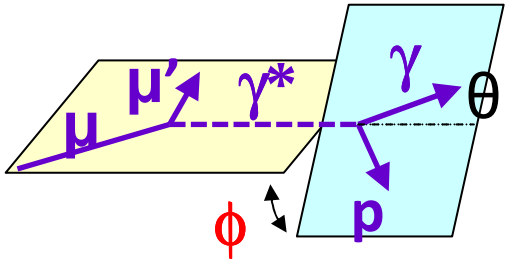

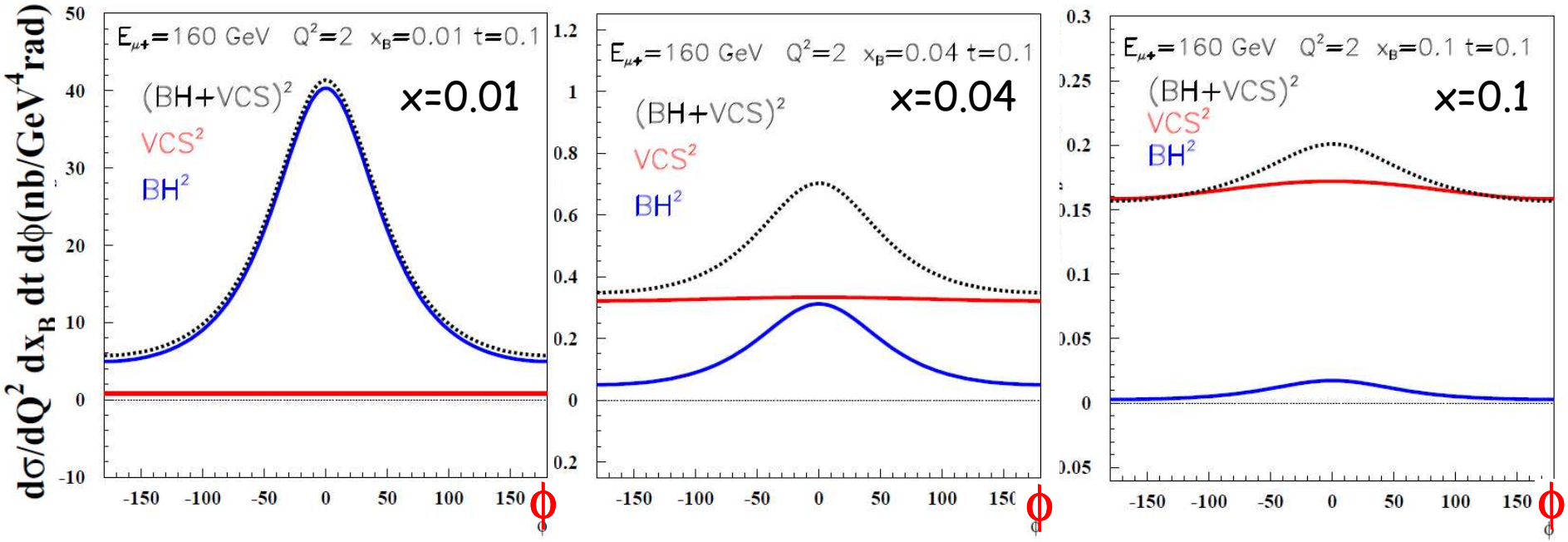

BH dominates

excellent reference yield

BH and DVCS at the same level

access to DVCS amplitude through the interference

DVCS dominates

study of $d\sigma^{DVCS}/dt$

‘Stage 1’ of COMPASS GPD program

DVCS and HEMP with unpolarised proton target

to constrain GPD H

- GPD - 3-dimensional picture of the partonic nucleon structure or spatial parton distribution in the transverse plane

$$H(x, \xi=0, t) \rightarrow H(x, r_{x,y})$$

probability interpretation
Burkardt

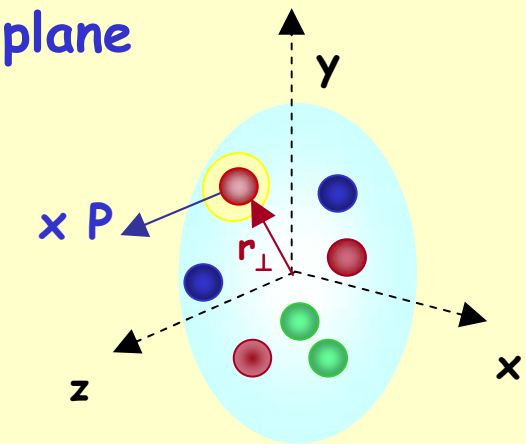

Nucleon tomography from fits to elastic form factors

from GPD fits to $F_{1,2}^{p,n}$ Diehl, Feldmann, Jakob, Kroll – (2005)

valence quarks unpolarized proton

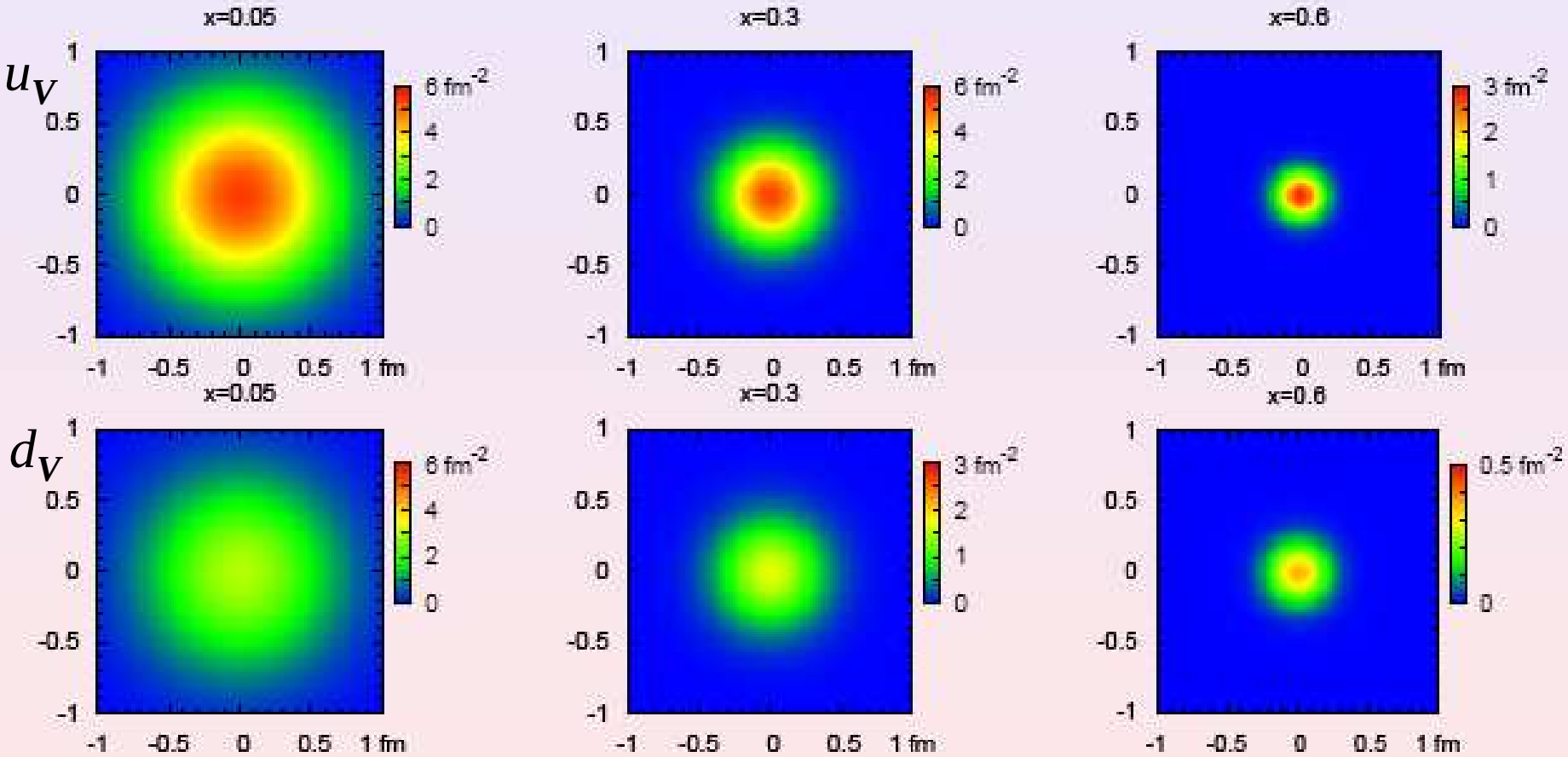

DVCS + BH with $\mu+\downarrow$ and $\mu-\uparrow$ beams
and unpolarized proton target

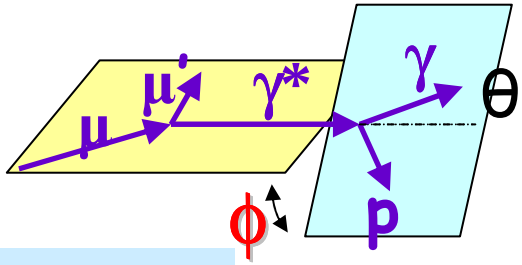

$$d\sigma_{(\mu p\to\mu p\gamma)} = d\sigma^{BH} + d\sigma^{DVCS}_{unpol} + P_\mu\, d\sigma^{DVCS}_{pol}$$
$$+ e_\mu\, a^{BH}\, \mathcal{R}e T^{DVCS} + e_\mu P_\mu\, a^{BH}\, Im T^{DVCS}$$

Beam Charge & Spin Difference

$$\mathcal{D}_{CS,U} \equiv d\sigma(\mu^{+\downarrow}) - d\sigma(\mu^{-\uparrow}) = 2(e_\mu\, a^{BH}\, \mathcal{R}e T^{DVCS} + P_\mu\, d\sigma^{DVCS}_{pol})$$

$$c_0^{Int} + c_1^{Int}\cos\phi + c_2^{Int}\cos 2\phi + c_3^{Int}\cos 3\phi$$

$$s_1^{DVCS}\sin\phi$$

Beam Charge & Spin Sum

$$\mathcal{S}_{CS,U} \equiv d\sigma(\mu^{+\downarrow}) + d\sigma(\mu^{-\uparrow}) = 2(\underline{d\sigma^{BH}} + d\sigma^{DVCS}_{unpol} + e_\mu P_\mu\, a^{BH}\, Im T^{DVCS})$$

$$c_0^{DVCS} + c_1^{DVCS}\cos\phi + c_2^{DVCS}\cos 2\phi$$

$$s_1^{Int}\sin\phi + s_2^{Int}\sin 2\phi$$

t-slope measurement for DVCS; relevant for nucleon 'tomography'

Using $\mathcal{S}_{CS,U}$, integrating over ϕ and subtracting BH $\longrightarrow$ $d\sigma_{DVCS}/dt \sim \exp(-B|t|)$

'tomography': $B(x) \Leftrightarrow \langle r_T^2 \rangle(x)$

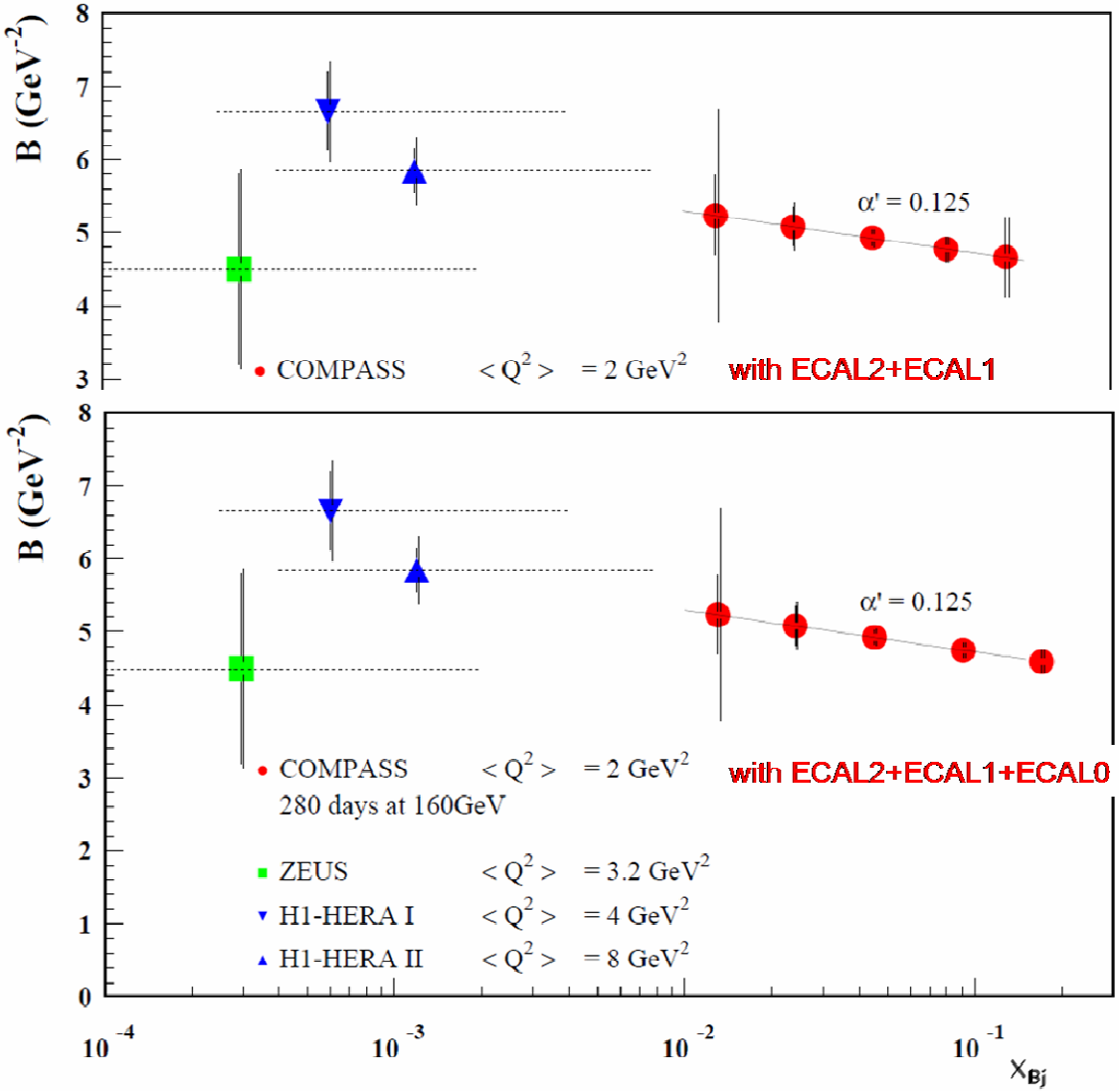

FFS model

adapted for COMPASS (by AS)

assumed

$$B(x) = b_0 + 2\,\alpha'\,\ln(x_0/x)$$

with $\alpha' = 0.125\ \mathrm{GeV}^{-2}$

160 GeV muon beam
2.5m LH_2 target
ε_{global} = 10%, 280 days
L = 1222pb^{-1}

$0.06 < |t| < 0.64\ \mathrm{GeV}^2$

assumed 3% systematic error on extracted DVCS c.s.

t-slope measurement for exclusive ρ^0 production

$$d\sigma_{\gamma N \to \rho N}/dt \sim \exp(-B|t|)$$

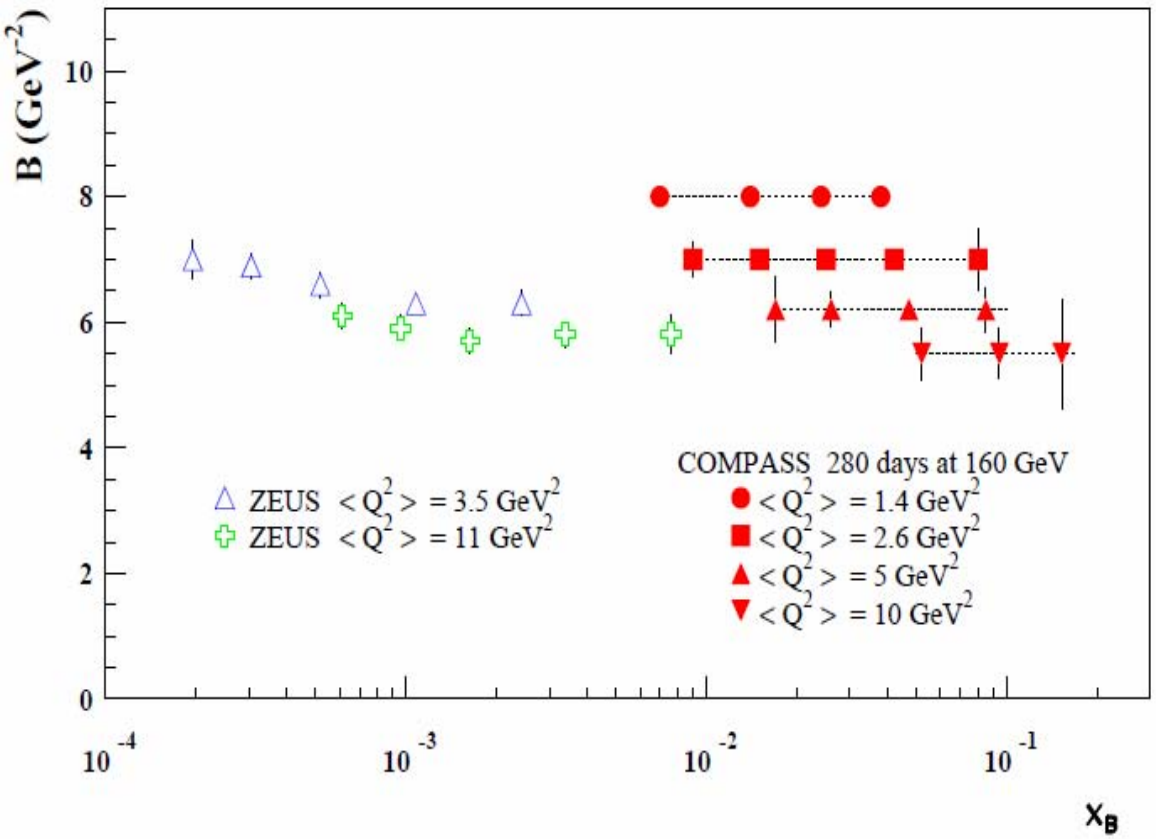

At large Q^2 slope B sensitive mostly to the nucleon size

model by AS with normalisation to Goloskokov and Kroll

160 GeV muon beam
2.5m LH_2 target
ε_{global} = 10%, 280 days
L = 1222pb^{-1}

$0.06 < |t| < 0.64$ GeV^2

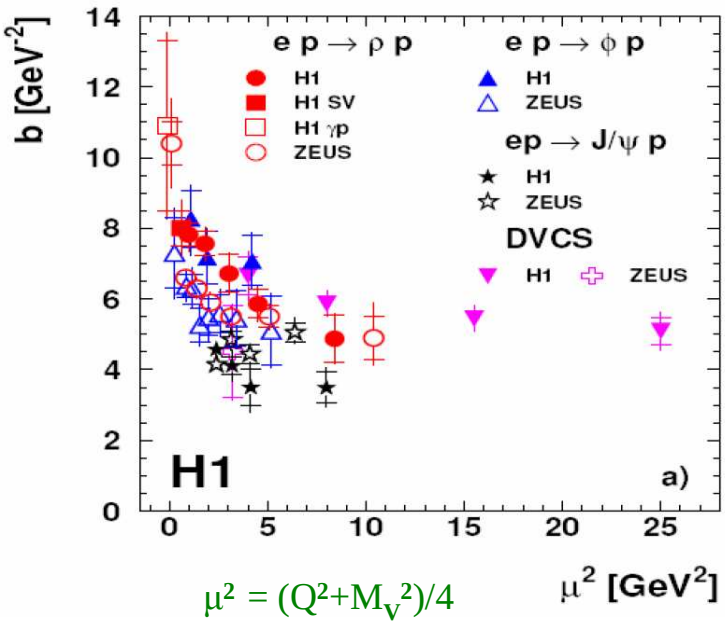

$\mu^2 = (Q^2+M_V^2)/4$
(= Q^2 for DVCS)

Beam Charge&Spin Difference of cross sections

$$\mathcal{D}_{CS,U} \equiv d\sigma(\mu^{+\downarrow}) - d\sigma(\mu^{-\uparrow}) = 2(e_\mu\, a^{BH}\, \mathcal{R}e T^{DVCS} + P_\mu\, d\sigma^{DVCS}_{pol})$$

$$c_0^{Int} + c_1^{Int}\cos\phi + c_2^{Int}\cos 2\phi + c_3^{Int}\cos 3\phi$$

$$s_1^{DVCS}\sin\phi$$

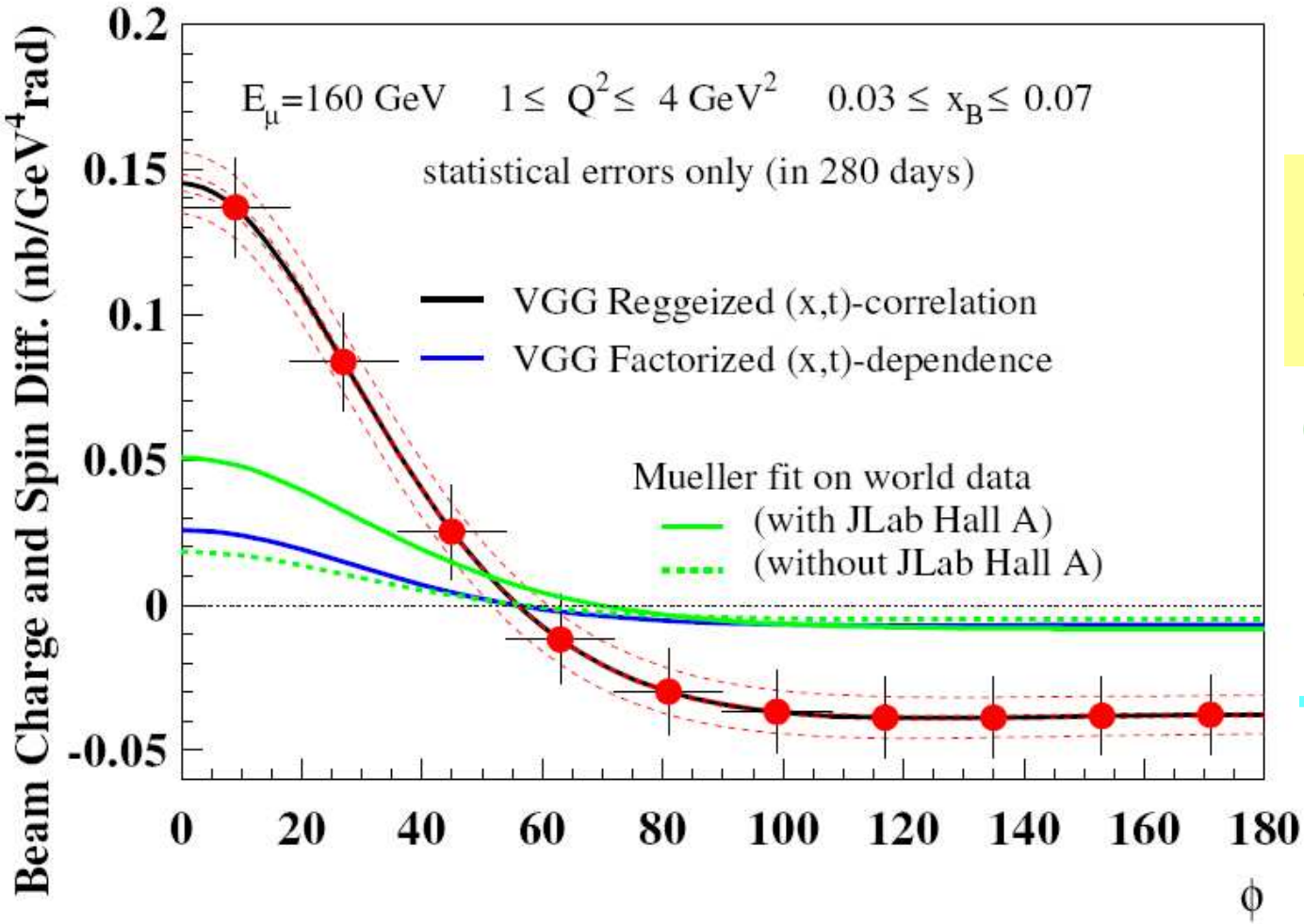

160 GeV muon beam
2.5m LH_2 target
ε_{global} = 10%, 280 days
L = 1222pb^{-1}

0.06 < |t| < 0.64 GeV^2

$$\ldots + c_1^{Int}\cos\varphi + \ldots$$

$\Rightarrow \mathcal{R}e(F_1\mathcal{H})$

Sensitivity of COMPASS; cosϕ modulation

$$BCSA = \mathcal{D}_{CS,U} / \mathcal{S}_{CS,U} = A_0 + A^{\cos\phi}_{CS,U} \cos\phi + A_2 \cos 2\phi$$

$A^{\cos\phi}_{CS,U}$ => c_1^{Int} $\boxed{=> \mathcal{R}e(F_1\mathcal{H})}$

Mueller's fits to world data

VGG

$\mathcal{R}e(F_1\mathcal{H})$ > 0 at H1

< 0 at HERMES/JLab

Value of x_B for the node?

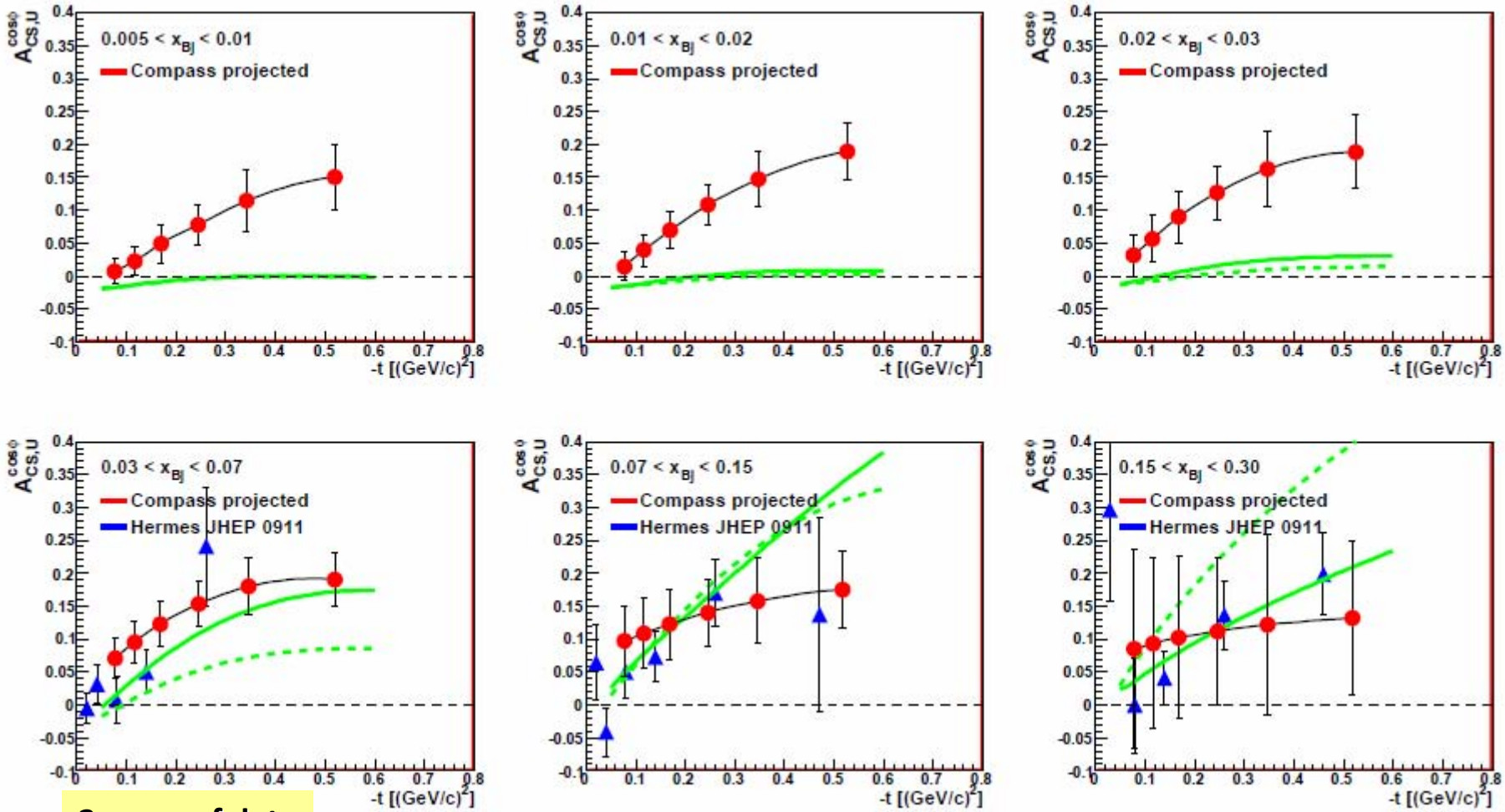

2 years of data

with ECAL2 + ECAL1 + ECAL0

‘Stage 2’ of COMPASS GPD program

DVCS and HEMP with transversely polarised proton target (NH_3)

to constrain GPD E

- **Contribution to the nucleon spin puzzle**

  E related to the orbital angular momentum

$$J_q = \frac{1}{2} \int x \left(H^q(x,\xi,0) + E^q(x,\xi,0) \right) dx$$

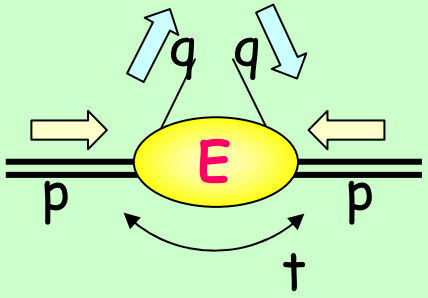

Sensitivity to GPD E

the most promissing Transverse Target Spin asymmetry

$$A^{D}_{CS,T}\,(\text{ or } A_{UT})\ \sin(\phi\text{-}\phi s)\cos\phi \rightarrow c_{1,\mathrm{T}\text{-}}^{Int}$$

COMPASS HERMES

$$c_{1,T-}^{Int} \propto -\frac{M}{Q}\mathrm{Im}\left\{\frac{t}{4M^2}\left[(2-x_B)F_1\mathcal{E} - 4\frac{1-x_B}{2-x_B}F_2\mathcal{H}\right] + x_B\xi\left[F_1(\mathcal{H}+\mathcal{E}) - (F_1+F_2)(\widetilde{\mathcal{H}} + \frac{t}{4M^2}\widetilde{\mathcal{E}})\right]\right\}$$

Study of azimuthal asymmetries from transversely polarized NH_3 target is a part of Phase 2 of COMPASS GPD program

example: COMPASS projections for

$$A^{D}_{CS,T} \sin(\phi-\phi s)\cos\phi$$

FFS model

adapted for COMPASS (by AS)

160 GeV muon beam
1.2m NH_3 target
ε_{global} = 10%, 280 days
ECAL1+ECAL2 only

for $\mu\, p^{\uparrow} \rightarrow \mu\, \gamma\, p$
dilution factor f=0.26

0.10 (0.14) < |t| < 0.64 GeV²

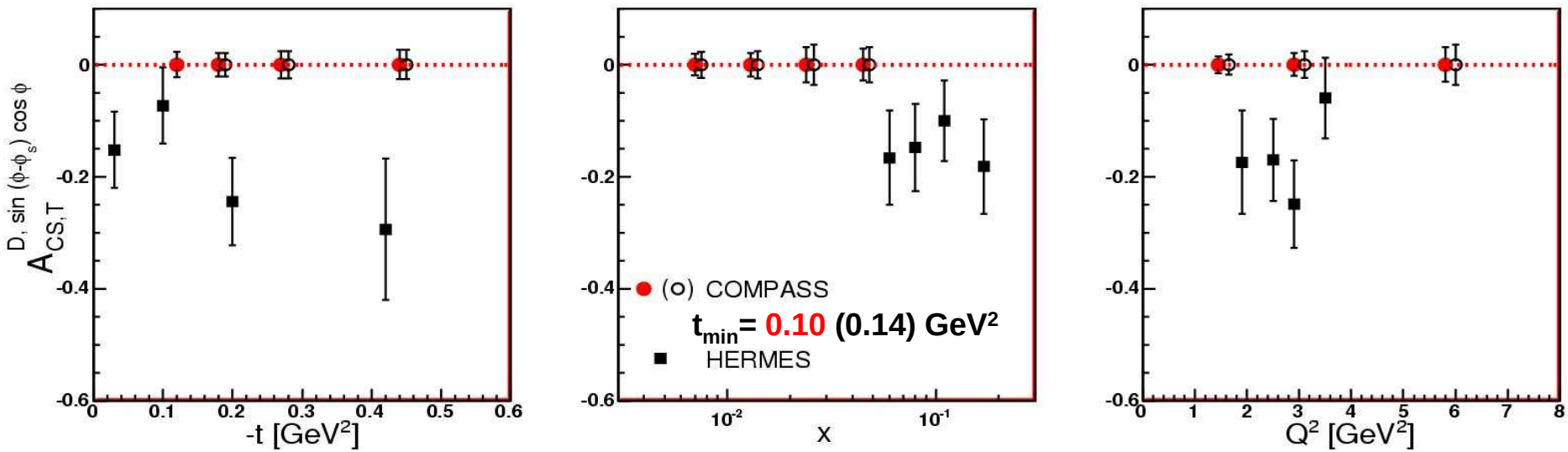

Typical statistical errors of TTS azimuthal asymmetries:

projections for COMPASS ≈ 0.03

for HERMES ≈ 0.08

DVCS test runs in 2008-2009

with COMPASS 'hadron' set-up

Goal: evaluate feasibility to detect DVCS/BH in the COMPASS setup

$$\mu\, p \rightarrow \mu\, p\, \gamma$$

LH 40 cm

in the small RPD

in EMCals

target region

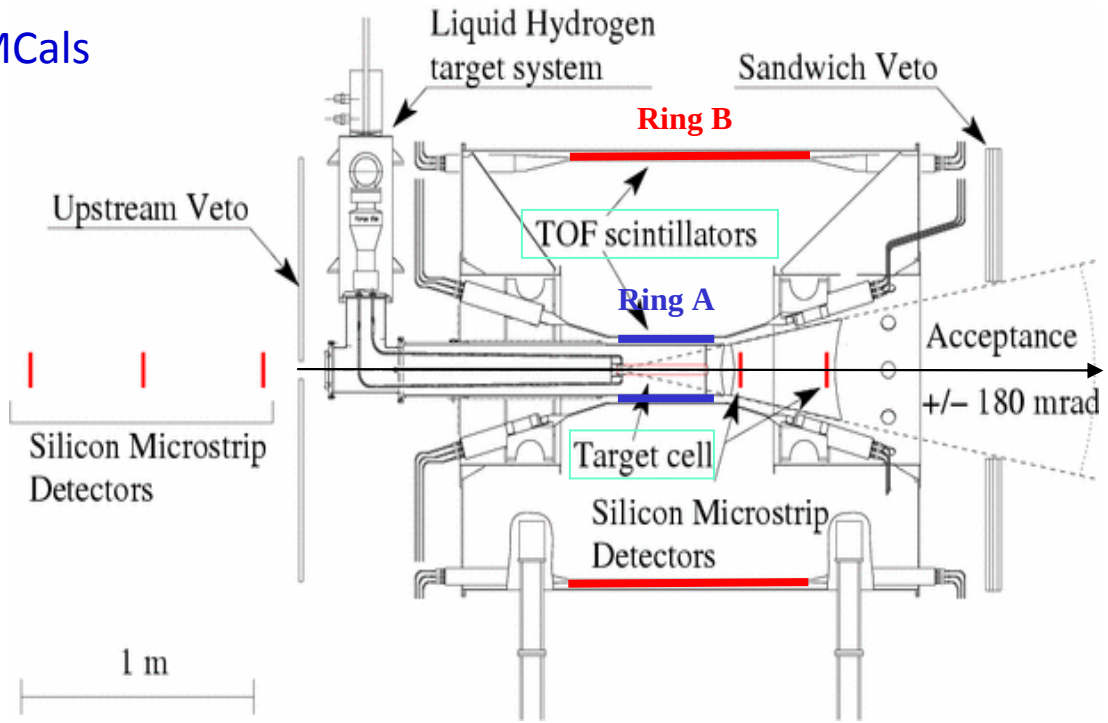

- Target: 40 cm LH_2
- Recoil Detector (1 m long)
- ECAL1 & ECAL2

Short: 1.5 day in 2008 and 10 days in 2009 of 160 GeV muon beam (μ^+ and μ^-)

Exclusive γ production from 2009 DVCS test run

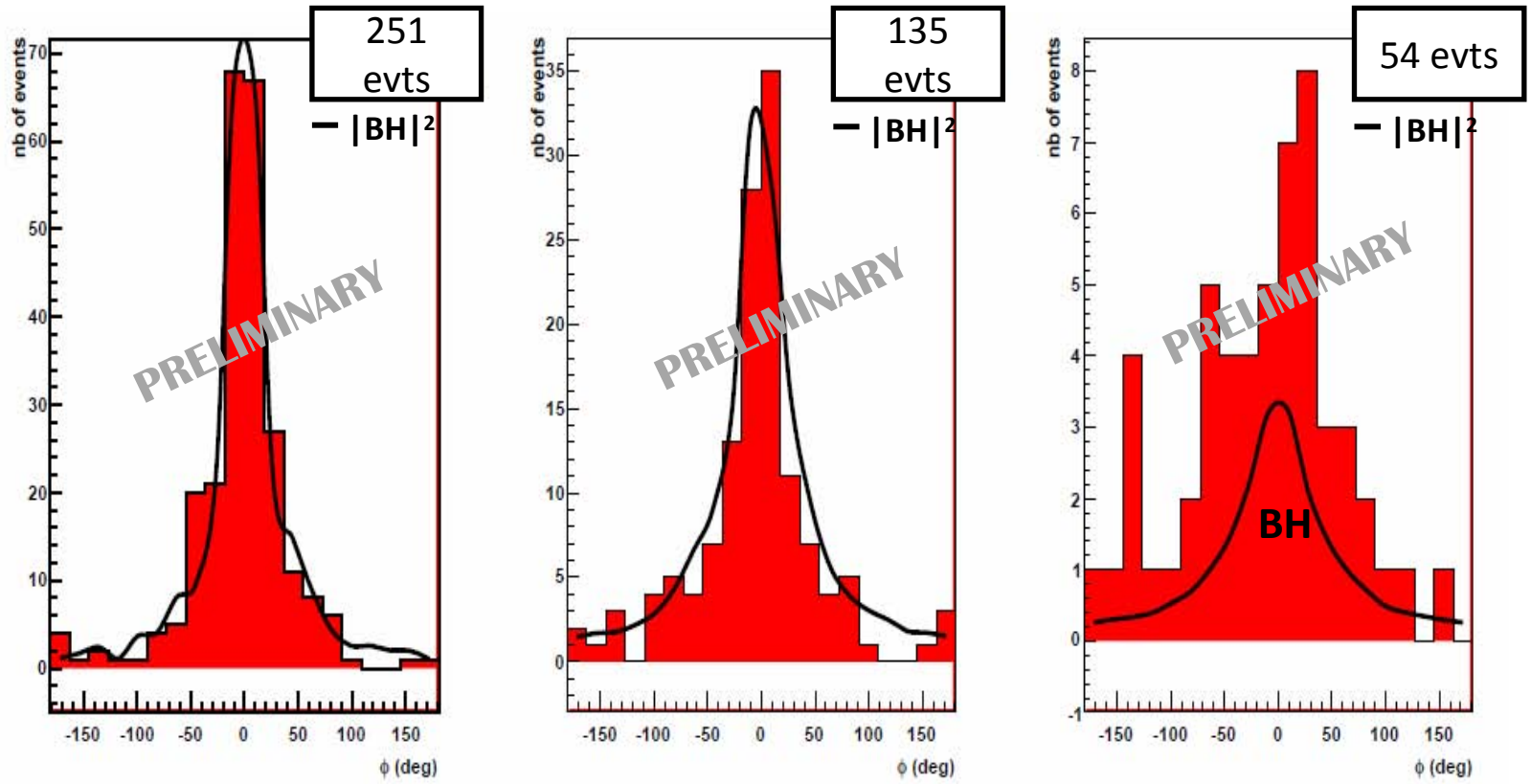

$0.005 < x_B < 0.01$ | $0.01 < x_B < 0.03$ | $x_B > 0.03$

$\epsilon_{\mu p \to \mu' \gamma p} \approx 35\%$

$\times (0.8)^4$ for SPS + COMPASS avail. + trigger eff + dead time

$\varepsilon_{global} \approx 0.14$ confirmed $\varepsilon_{global} = 0.1$ assumed for COMPASS-II projections

54 evts ≈ 20 BH
+ 22 DVCS
+ about 12 γ from π^0

upper limit

New developments - target and recoil detector

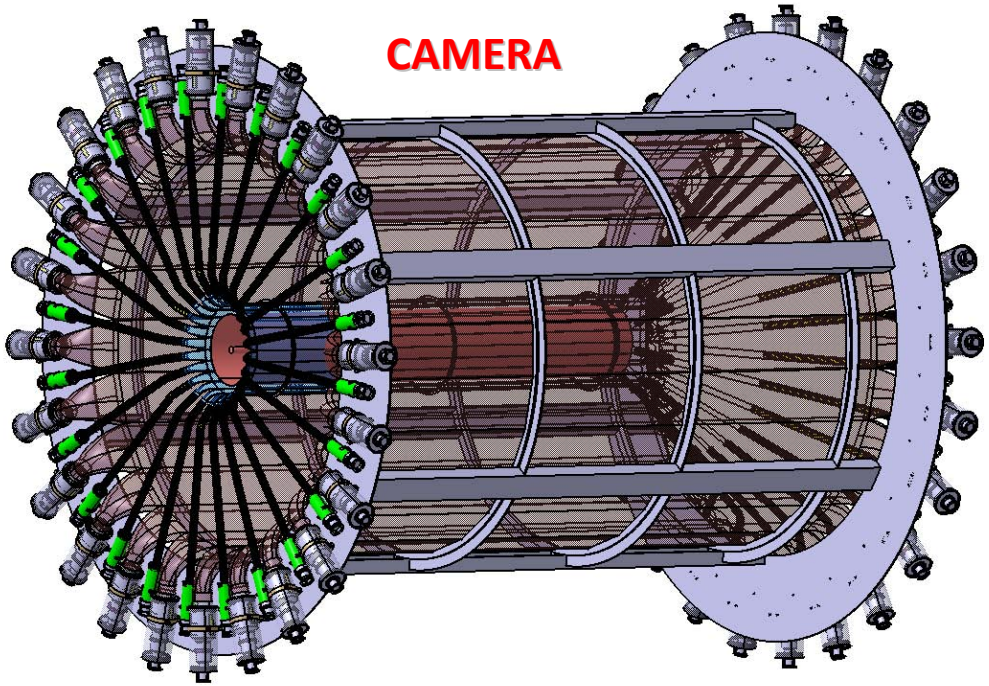

- 2.5m long LH target
- 4m long ToF barrel
  of 2 scintillator layers
- recoil proton ID by ToF and ΔE
- ≈ 300 ps time resolution
- full scale prototype tested

high occupancy due to δ rays

GANDALF project:

- 1 GHz digitsation of PMT signal to cope with high rate
- resolution > 10 ENOB
- self triggered

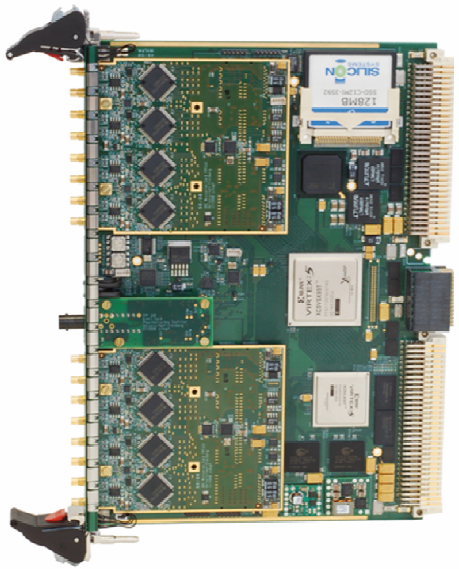

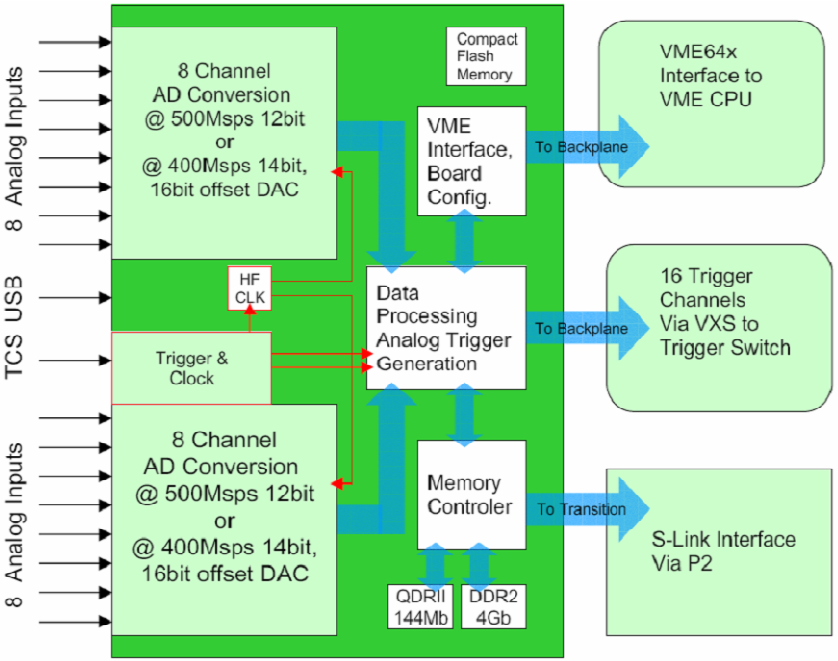

New developments - large-angle electromagnetic calorimeter ECAL0

existing
ECAL1&2

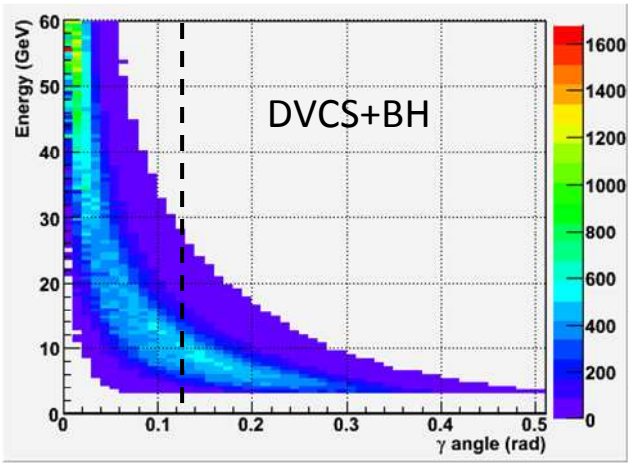

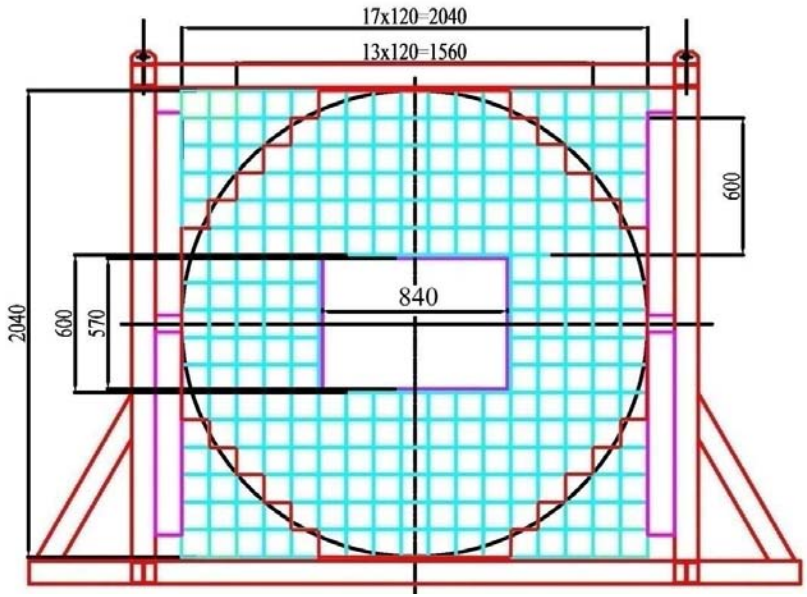

ECAL0 location and specifications

ECAL0 located downstream of CAMERA

- transverse size 204x204 cm^2 (approx.)
  modules arranged in a circular array of 1.02 m radius
- hole size 84x60 cm^2
- granularity 4x4 cm^2
- energy range 0.1 - 30 GeV
- polar angle range 0.15-0.5 rad.
- energy resolution ~ (5-7)%/sqrt(E)
- time resolution 0.5-0.6 ns
- thickness $\lesssim$ 50 cm
- insensitive to magnetic field

Total:	194	9-cell modules
	1746	MAPDs and read out channels
	the weight about 6 tons	

ECAL0 module

Module:

- size is 12x12 cm^2
- 9 cells, size is 4x4 cm^2
- 9 light collection systems
- 9 MAPDs
- 9 MSADC channels
- Temperature stabilization system (Peltier element, electronics)
- 9 Amplifiers
- Control system (LED, Laser)
- Power supply

ECAL0 cell

252mm or 15 radiation length

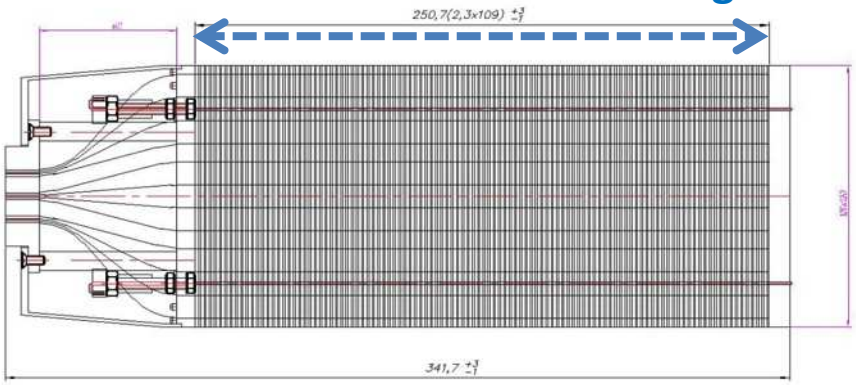

shashlyk technology
109 plates made of Sc 1.5 mm /Pb 0.8 mm

Micropixel Avalanche Photo Diodes
3 x 3 mm², number of pixels ~ 135 000

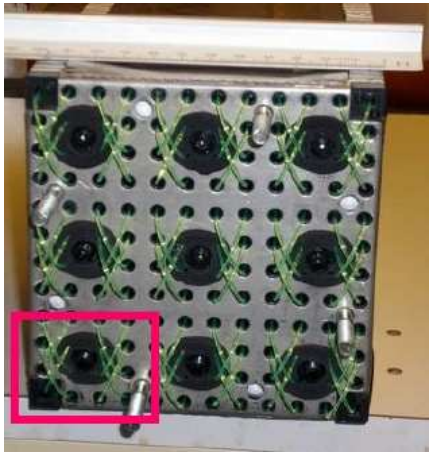

module for tests in 2011

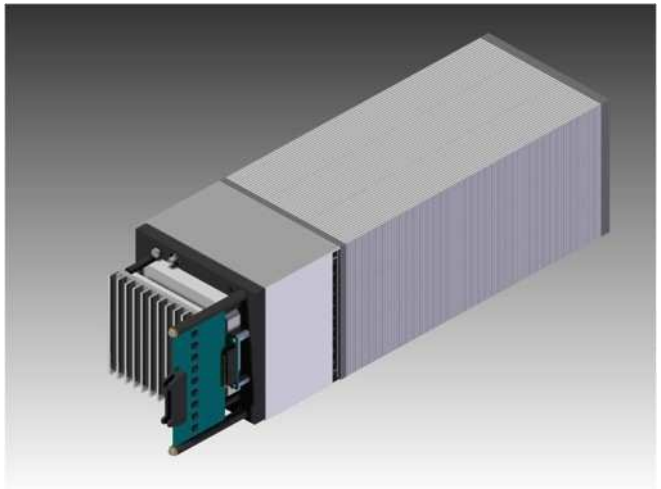

Start of GPD program of COMPASS-II in 2012 - ‘dress rehearsal’

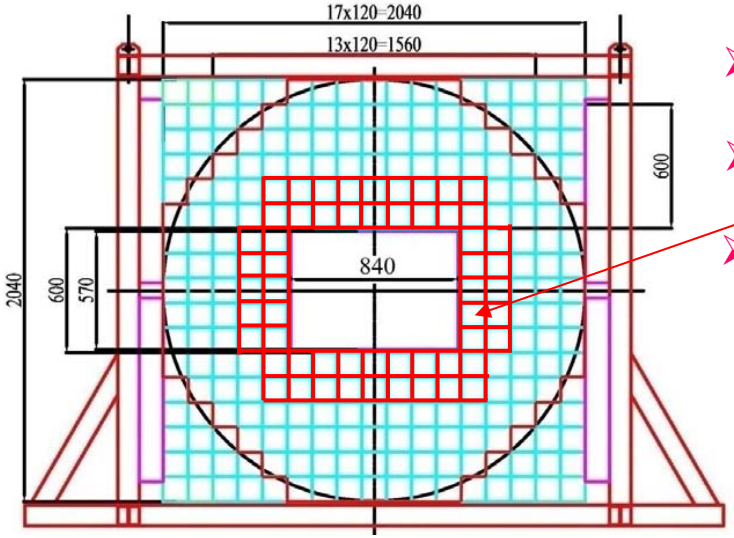

- 2.5m LH target and CAMERA ready by September 2012
- reduced ECAL0 (56 modules) ready in September 2012
- 6 weeks of comissioning and DVCS data taking

  after 18 weeks of Primakoff measurements
  which is the main goal in 2012

- projection for a physics result

  from 1 week of DVCS test in 2012
  1/40 of the complete statistics

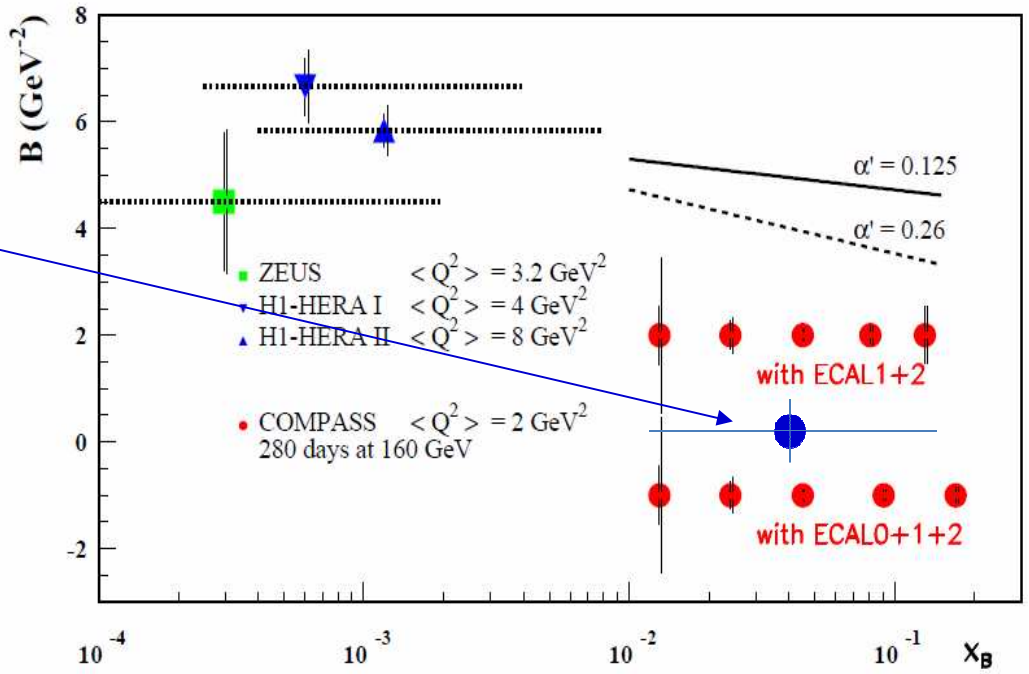

Complete GPD program of Stage 1 with complete ECAL0 is scheduled for 2015-2016

Summary-I , new results on transverse spin asymmetries

- COMPASS full set of data for transversely polarised targets available
  - ✓ polarised deuterons, ^{6}LiD target, 2002-2004
  - ✓ polarised protons, NH3 target 2007 and 2010
- All azimuthal spin asymmetries for deuteron compatible with zero
  - ✓ approximate cancellation of u- and d-quark contributions
  - ✓ important for global fits to disentangle different flavour contributions
- Collins and two-hadron asymmetries for proton
  - ✓ h^+ and h^- Collins asymmetries in valence region large and of opposite sign

    no strong dependence on Q^2 / y (LT)
  - ✓ two-hadron asymmetry large in valence region, no strong dependence on M_{hh}
- Sivers asymmetries for proton
  - ✓ large asymmetry for h^+ dependence on Q^2 / y (Q^2 evolution ?)
- Transverse Target Spin Asymmetry for exclusive ρ^0 production
  - ✓ both asymmetries for proton and deuteron compatible with zero

    approximate cancellation of contributions of GPD E^u and E^d

Summary-II , on GPD program

- COMPASS has a great potential for GPD physics
  - ✓ unique polarised μ^+ and μ^- beams
  - ✓ favourable kinematic domain (x_{Bj})
- Large projects for new apparatus
  - ✓ 4m RPD + large angle ECAL0 (phase 1)
  - ✓ recoil proton detector incorporated into a large polarised target (phase 2)
- Investigation of GPDs with both DVCS and HEMP on unpolarised nucleons
  - ✓ t-slope of DVCS and HEMP cross section

    → transverse distribution of partons
  - ✓ Beam Charge&Spin sum and difference of DVCS cross sections

    → $\mathcal{R}e\, T^{DVCS}$ and $\mathcal{I}m\, T^{DVCS}$ for the GPD H determination
  - ✓ Production of vector mesons ρ^0, ω, φ … → flavour separation for GPD H
  - ✓ Production of π^0 → sensitivity to GPDs $\tilde{E}$ and $\bar{E}_T$ ($\equiv 2\tilde{H}_T + E_T$)
- Transverse Target Spin Asymmetries for DVCS and hard exclusive VM production

  → GPD E and angular momentum of partons

Backup

cosϕ and cos2ϕ modulations ^{6}LiD

$$N(\phi_h) \propto N_0 \cdot (1 + \varepsilon_1 A^{UU}_{\cos\phi_h} \cos\phi_h + \varepsilon_2 A^{UU}_{\cos 2\phi_h} \cos 2\phi_h)$$

$$\langle \cos\phi_h \rangle = \frac{1}{Q}\,\mathrm{Cahn} + \frac{1}{Q}\,\mathrm{BM}$$

$$\langle \cos 2\phi_h \rangle = \mathrm{BM} + \frac{1}{Q^2}\,\mathrm{Cahn}$$

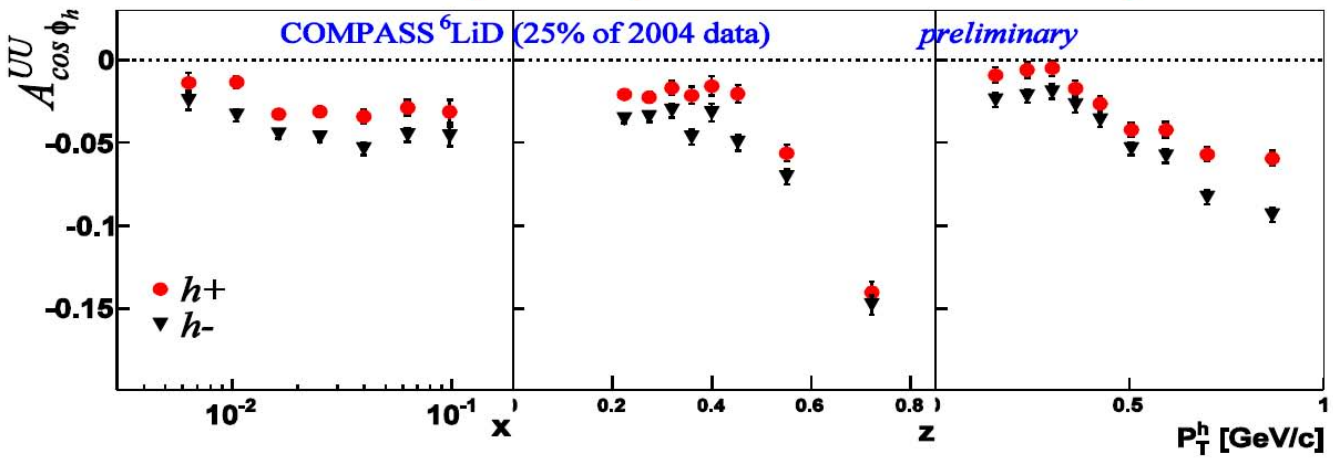

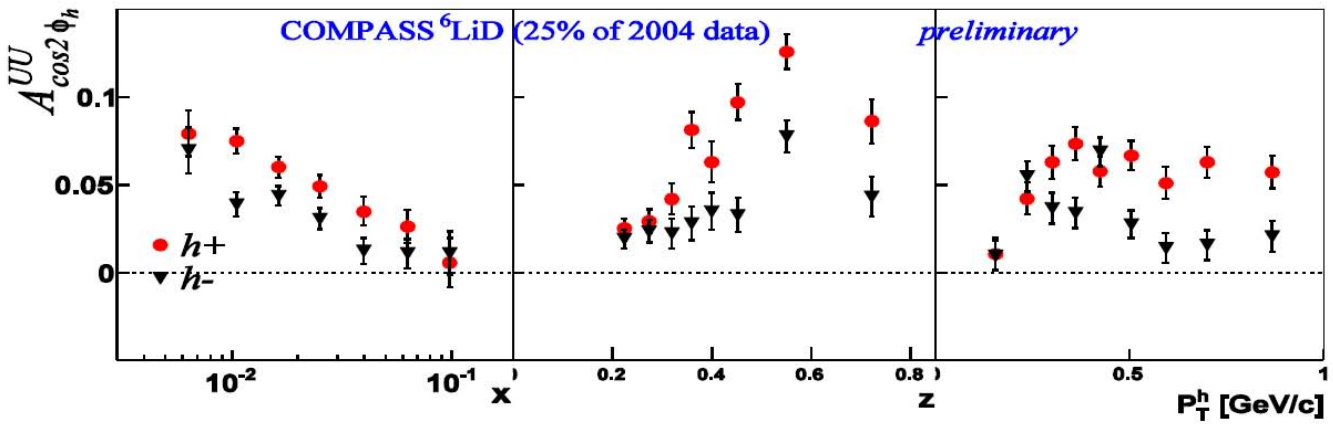

GPDs properties, links to DIS and form factors

$H^q, \tilde{H}^q \leftrightarrow h_1 = h_2$ for $\boldsymbol{P_1} = \boldsymbol{P_2}$ recover usual parton densities

$$H^q(x,0,0) = \quad q(x), \qquad \tilde{H}^q(x,0,0) = \Delta q(x) \qquad for\ x > 0$$
$$H^q(x,0,0) = -\bar{q}(-x), \quad \tilde{H}^q(x,0,0) = \Delta\bar{q}(-x) \qquad for\ x < 0$$

$E^q, \tilde{E}^q \leftrightarrow h_1 \neq h_2$ no similar relations; these GPDs decouple for $\boldsymbol{P_1} = \boldsymbol{P_2}$

$E^q, \tilde{E}^q \neq 0$ **needs** orbital angular momentum between partons

$$\int dx H^q(x,\xi,t) = F_1^q(t) \quad \textbf{Dirac} \qquad \int dx \tilde{H}^q(x,\xi,t) = g_A^q(t) \quad \textbf{axial}$$

$$\int dx E^q(x,\xi,t) = F_2^q(t) \quad \textbf{Pauli} \qquad \int dx \tilde{E}^q(x,\xi,t) = g_P^q(t) \quad \textbf{pseudoscalar}$$

Ji's sum rule $\quad \frac{1}{2}\int dx\, x\,(H^q + E^q) = J^q(t)$

$J^q(0)$ **total** angular momentum carried by quark flavour *q*
(helicity and **orbital** part)

Observables and their relationship to GPDs

(at leading order:)

$$T^{DVCS} \sim \int_{-1}^{+1} \frac{H(x,\xi,t)}{x \pm \xi + i\varepsilon} dx + \ldots \sim \quad P\int_{-1}^{+1} \frac{H(x,\xi,t)}{x \pm \xi} dx - i\pi H(\pm\xi,\xi,t) + \ldots$$

Beam charge asymmetry contains Re*T*, integrated GPDs over *x*

Beam or target spin asymmetry contains Im*T*, therefore GPDs at $x = \xi$ and $-\xi$

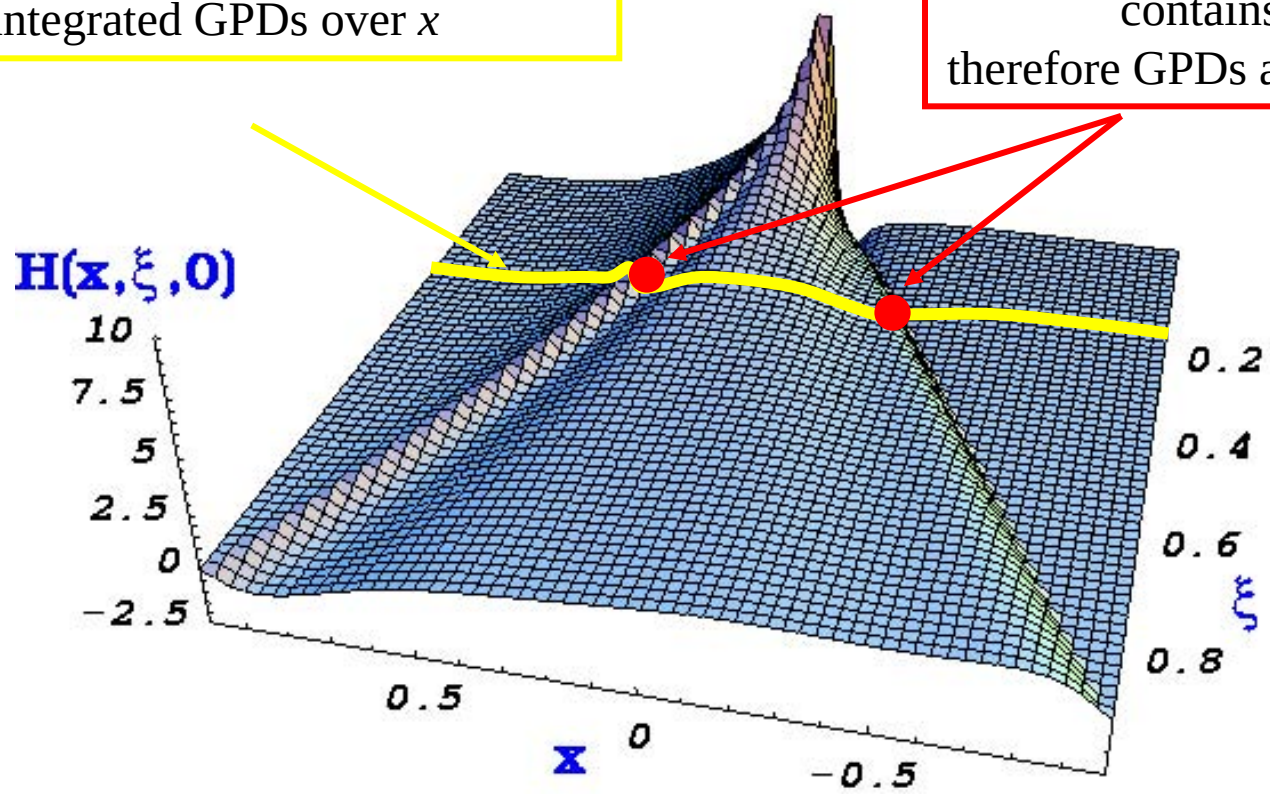

Assumptions for the proposal projections

- polarised muon beam with 160 GeV energy
- 48 s SPS period with 9.6 s spill duration
- μ^+ beam intensity 4.6 x 10^8 muons / spill
- 3 times smaller intensity for μ^- beam
- running time 280 days (70 days with μ^+, 210 days with μ^-)
- a) 2.5 m LH target => $\mathcal{L}$ = 1. x 10^{32} $cm^{-2}s^{-1}$ for μ^+ beam
  b) 1.2 m NH_3 target => $\mathcal{L}$ = 3.4 x 10^{32} $cm^{-2}s^{-1}$ for μ^+ beam
- a new recoil proton detector(s) (RPD) surrounding the target(s)
- two existing electromagnetic calorimeters (ECAL1, ECAL2)
  + additional new large angle calorimeter (ECAL0)
- an overall global efficiency ε_{global} = 0.1

2 generators for single photon production (BH+DVCS) used:

a) VGG code b) FFS model adapted for COMPASS (by AS)

Recoil proton detector for hadron program

Small 1 m long Recoil Proton Detector and a 40cm LH target in 2008/2009

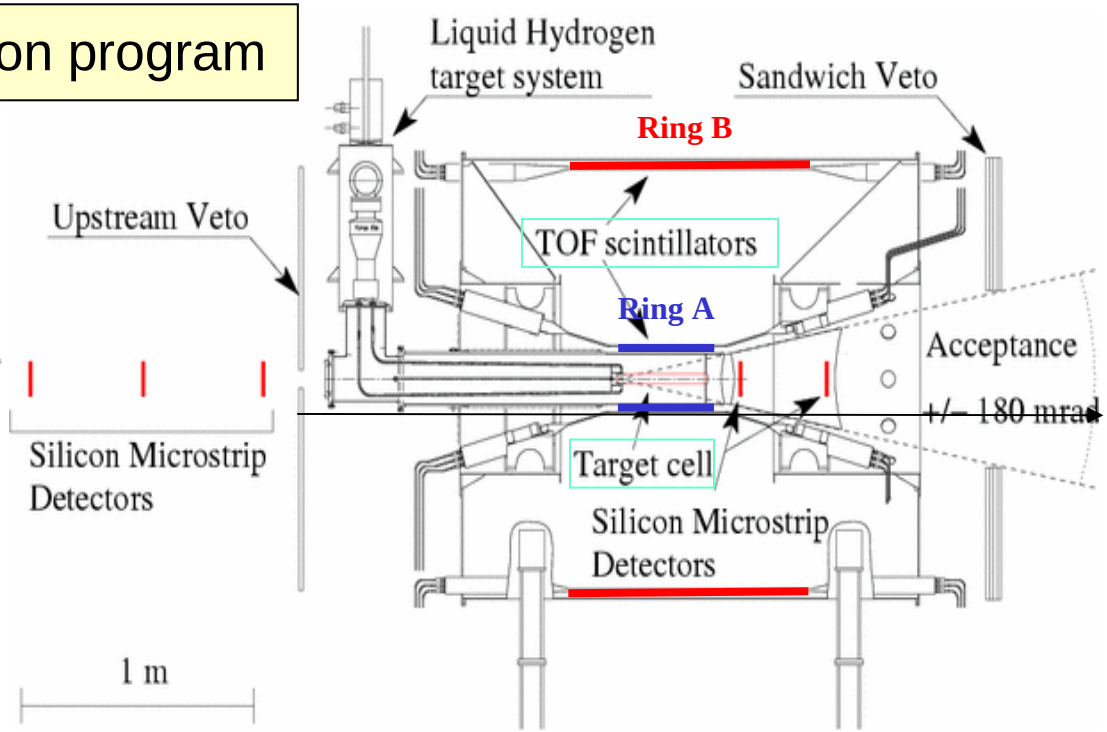

Proton identification in RPD

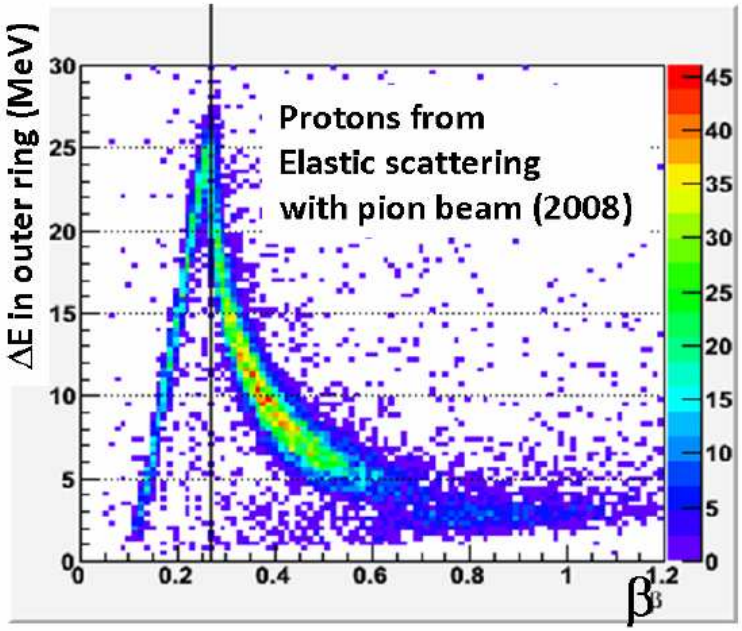

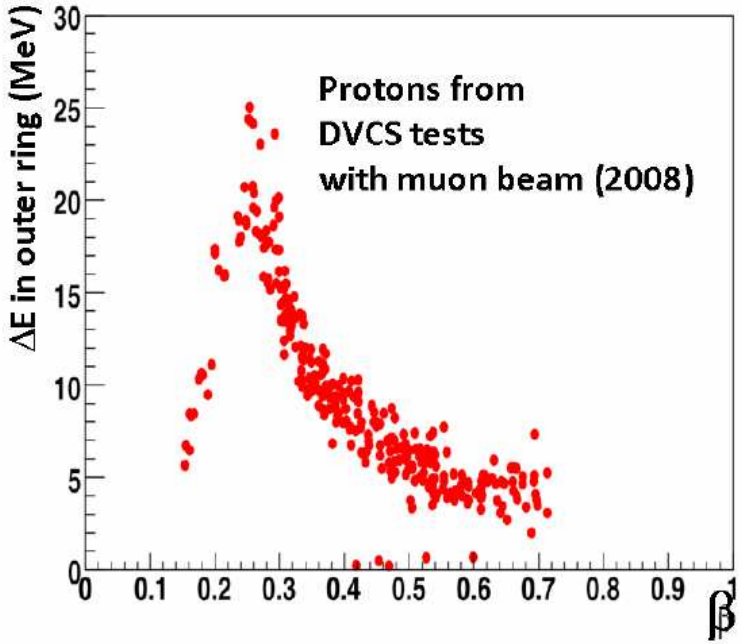

Selection of single γ events

$$\vec{p}_{miss} = \vec{p}_{\mu} - \vec{p}_{\mu'} - \vec{p}_{\gamma}$$

- one vertex with μ and μ'
- no other charged tracks
- only 1 high energy photon
- 1 proton in RPD with p < 1 GeV/c
- exclusivity cuts in transverse plane

  $|\Delta p_{\perp}| < 0.2$ GeV

  $|\Delta\phi| < 41$ deg

- exclusivity cut on energy ballance (E_{miss})

  $E_{miss} = E_{\mu} + M_p - (E_{\mu'} + E_{p'} + E_{\gamma})$

  $|E_{miss}| < 20$ GeV

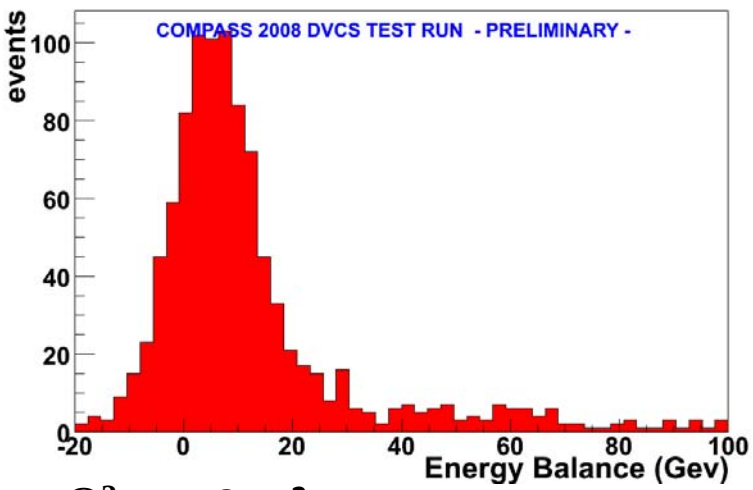

- $1 < Q^2 < 4$ GeV²

$\Delta p_{\perp} = |P^{\perp}_{miss}| - |P^{\perp}_{RPD}|$

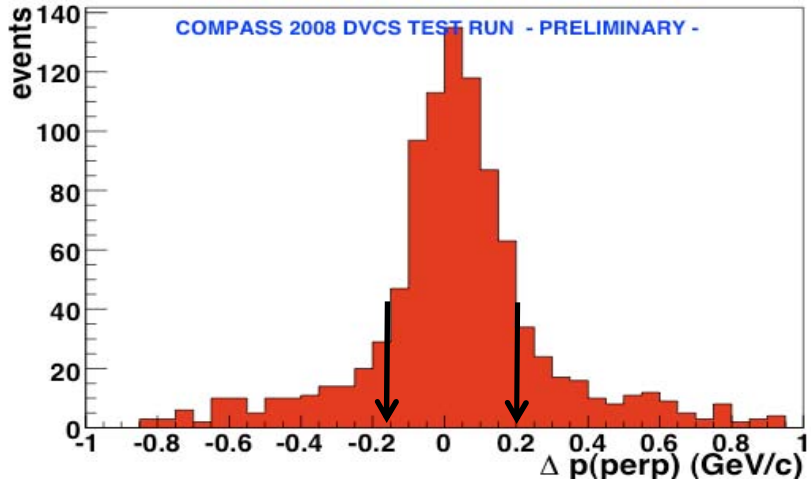

$\Delta\phi = \phi_{miss} - \phi_{RPD}$

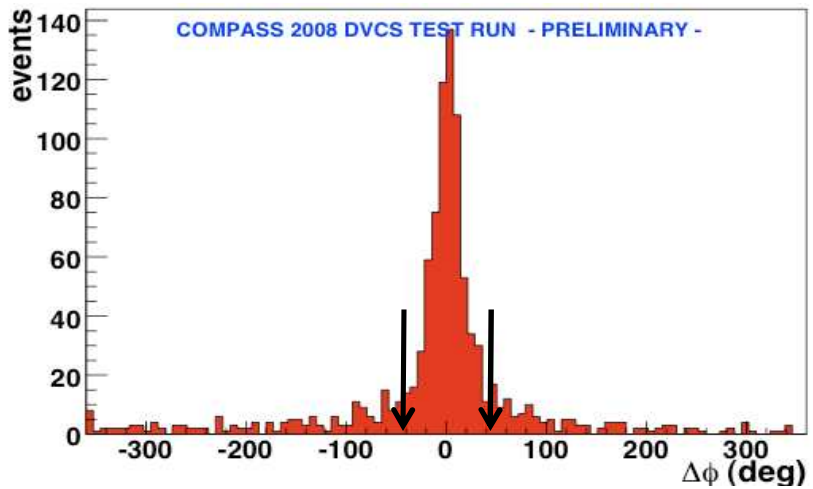

Nuclear Parton Densities

status & future avenues

Marco Stratmann

BROOKHAVEN NATIONAL LABORATORY

marco@bnl.gov

work done in collaboration with D. de Florian, R. Sassot, and P. Zurita: PRD85 (2012) 074028
(arXiv:1112.6324)

Outline

- **Nuclear PDFs 101**
  framework, experimental input, main features of nPDFs
- **strategies to parametrize nPDFs**
  overview of existing analyses, issues
- **results of our new global QCD analysis**
  what is new, some technical aspects, comparison to data & other fits
- **future avenues in dA (pA) collisions at RHIC (LHC)**
  prompt photons, Drell Yan

foundation: pQCD & factorization

QCD improved parton model - a success story ever since

- describes quantitatively a large variety of hard processes in e^+e^-, ep, pp, ...
- **key assumption**: factorization of long- and short-distance physics

  corrections: inverse powers of large scale

$$\frac{d\sigma}{dp_T} = \sum_{ab} \underbrace{f_a(x_a,\mu) \otimes f_b(x_b,\mu)}_{\text{from experiment}} \otimes \underbrace{d\hat{\sigma}_{ab}(\mu)}_{\text{calculable}} + \mathcal{O}\left(\frac{1}{p_T^n}\right)$$

- predictive power
- **systematic framework** to compute higher order corrections

  NLO standard; NNLO known or on the horizon

foundation: pQCD & factorization

QCD improved parton model - a success story ever since

- describes quantitatively a large variety of hard processes in e^+e^-, ep, pp, ...
- **key assumption**: factorization of long- and short-distance physics

  corrections: inverse powers of large scale

$$\frac{d\sigma}{dp_T} = \sum_{ab} \underbrace{f_a(x_a,\mu) \otimes f_b(x_b,\mu)}_{\text{from experiment}} \otimes \underbrace{d\hat{\sigma}_{ab}(\mu)}_{\text{calculable}} + \mathcal{O}\left(\frac{1}{p_T^n}\right)$$

- predictive power
- **systematic framework** to compute higher order corrections

  NLO standard; NNLO known or on the horizon
- small amount of phenomenological parameters to be determined from data

  parton densities, masses, α_s, fragmentation fcts.

parton content of **free** protons
rather well known by now in broad x, Q^2 range
some fine details are missing though

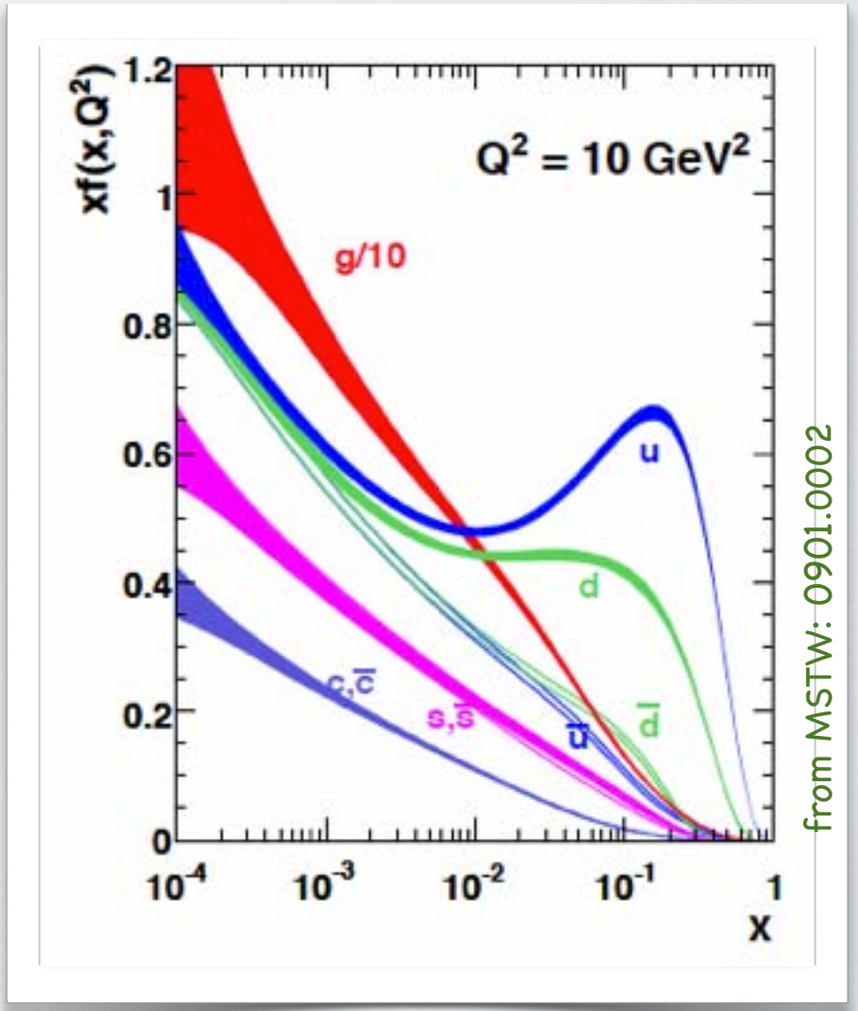

PDFs for bound nucleons

main idea:

- keep standard pQCD framework and **assume factorization** also for nuclei

$$\frac{d\sigma}{dp_T} = \sum_{ab} f_a(x_a, \mu) \otimes f_b(x_b, \mu) \otimes d\hat{\sigma}_{ab}(\mu) + \mathcal{O}(\frac{1}{p_T^n})$$

PDFs for bound nucleons

main idea:

- keep standard pQCD framework and **assume factorization** also for nuclei

pp -> pA collisions

$$\frac{d\sigma}{dp_T} = \sum_{ab} f_a(x_a,\mu) \otimes f_b^A(x_b,\mu) \otimes d\hat{\sigma}_{ab}(\mu) + \mathcal{O}(\frac{1}{p_T^n})$$

introduce universal nuclear PDF

PDFs for bound nucleons

main idea:

- keep standard pQCD framework and **assume factorization** also for nuclei

pp -> pA collisions

$$\frac{d\sigma}{dp_T} = \sum_{ab} f_a(x_a,\mu) \otimes f_b^A(x_b,\mu) \otimes d\hat{\sigma}_{ab}(\mu) + \mathcal{O}(\frac{1}{p_T^n})$$

introduce universal nuclear PDF

dictates use of same

- DGLAP scale evolution
- hard scattering cross sections

as for free proton PDFs

PDFs for bound nucleons

main idea:

- keep standard pQCD framework and **assume factorization** also for nuclei

pp -> pA collisions

$$\frac{d\sigma}{dp_T} = \sum_{ab} f_a(x_a,\mu) \otimes f_b^A(x_b,\mu) \otimes d\hat{\sigma}_{ab}(\mu) + \mathcal{O}(\frac{1}{p_T^n})$$

introduce universal nuclear PDF

dictates use of same
- DGLAP scale evolution
- hard scattering cross sections

as for free proton PDFs

all nuclear effects are universally absorbed into a set of non-perturbative nPDFs independent of the hard probe

PDFs for bound nucleons

main idea:

- keep standard pQCD framework and **assume factorization** also for nuclei

pp -> pA collisions

$$\frac{d\sigma}{dp_T} = \sum_{ab} f_a(x_a,\mu) \otimes f_b^A(x_b,\mu) \otimes d\hat{\sigma}_{ab}(\mu) + \mathcal{O}(\frac{1}{p_T^n})$$

introduce universal nuclear PDF

dictates use of same
- DGLAP scale evolution
- hard scattering cross sections

as for free proton PDFs

all nuclear effects are universally absorbed into a set of non-perturbative nPDFs independent of the hard probe

- very restrictive framework which makes testable predictions for a slew of hard probes

PDFs for bound nucleons

main idea:

- keep standard pQCD framework and **assume factorization** also for nuclei

pp -> pA collisions

$$\frac{d\sigma}{dp_T} = \sum_{ab} f_a(x_a,\mu) \otimes f_b^A(x_b,\mu) \otimes d\hat{\sigma}_{ab}(\mu) + \mathcal{O}(\frac{1}{p_T^n})$$

introduce universal nuclear PDF

dictates use of same
- DGLAP scale evolution
- hard scattering cross sections

as for free proton PDFs

all nuclear effects are universally absorbed into a set of non-perturbative nPDFs independent of the hard probe

- very restrictive framework which makes testable predictions for a slew of hard probes
- **complication** (often happily ignored): nuclear modifications of final-state hadrons

  hard to accommodate (modified fragmentation?)

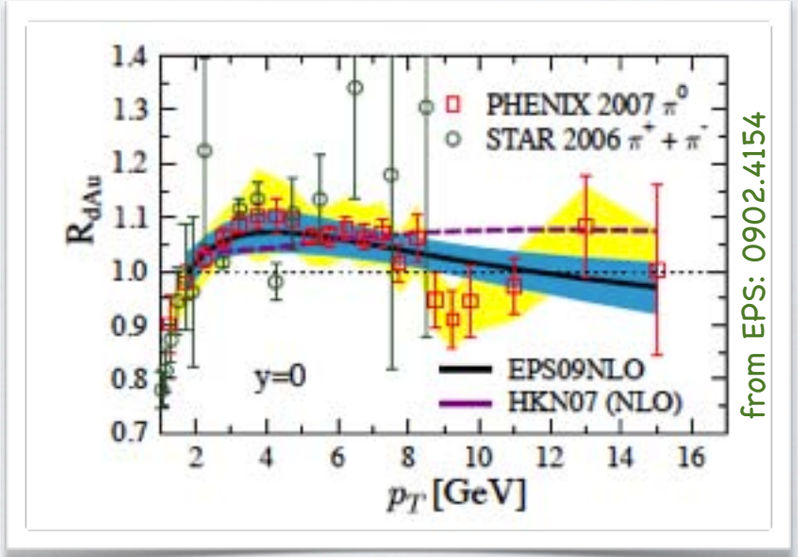

nuclear PDFs: what do we expect to learn ?

factorization and/or DGLAP evolution will eventually break down - **so what?**

nuclear PDFs: what do we expect to learn ?

factorization and/or DGLAP evolution will eventually break down - **so what?**

- nPDFs can parametrize nuclear effects with little bias and without assuming certain "mechanisms" to model the observed modifications/effects
  link to models of nucleon structure at low scales and proposed nuclear modifications
- a global QCD analysis of many hard probes will reveal tensions due to the assumed framework (linear DGLAP / factorization)

nuclear PDFs: what do we expect to learn ?

factorization and/or DGLAP evolution will eventually break down - **so what?**

- nPDFs can parametrize nuclear effects with little bias and without assuming certain "mechanisms" to model the observed modifications/effects
  link to models of nucleon structure at low scales and proposed nuclear modifications
- a global QCD analysis of many hard probes will reveal tensions due to the assumed framework (linear DGLAP / factorization)
- map out kinematic regime where nPDF framework applies and study transition to saturation region
  - transition often characterized by "saturation scale" $Q_s(x,A)$
  - non-linear effects (recombination) demanded by unitarity

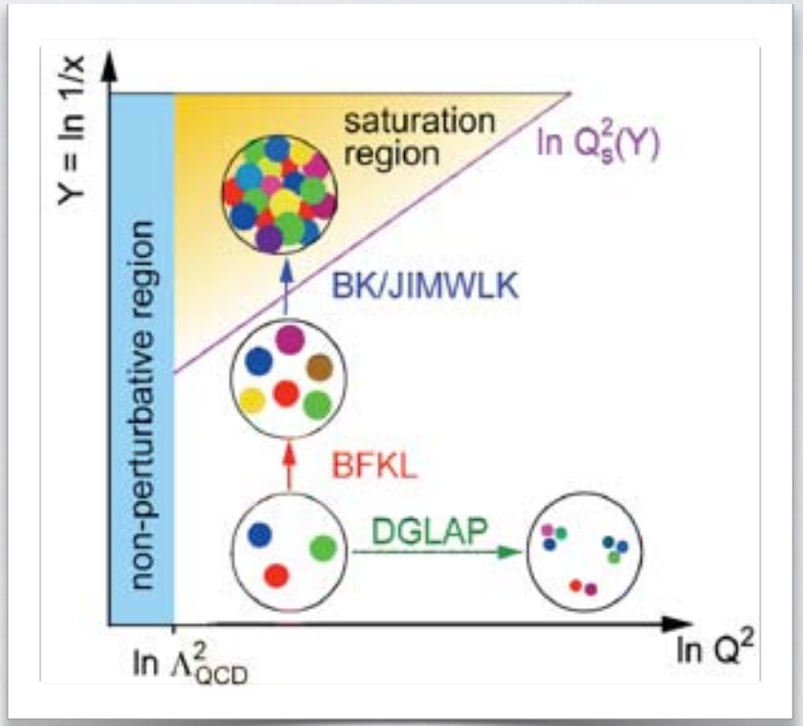

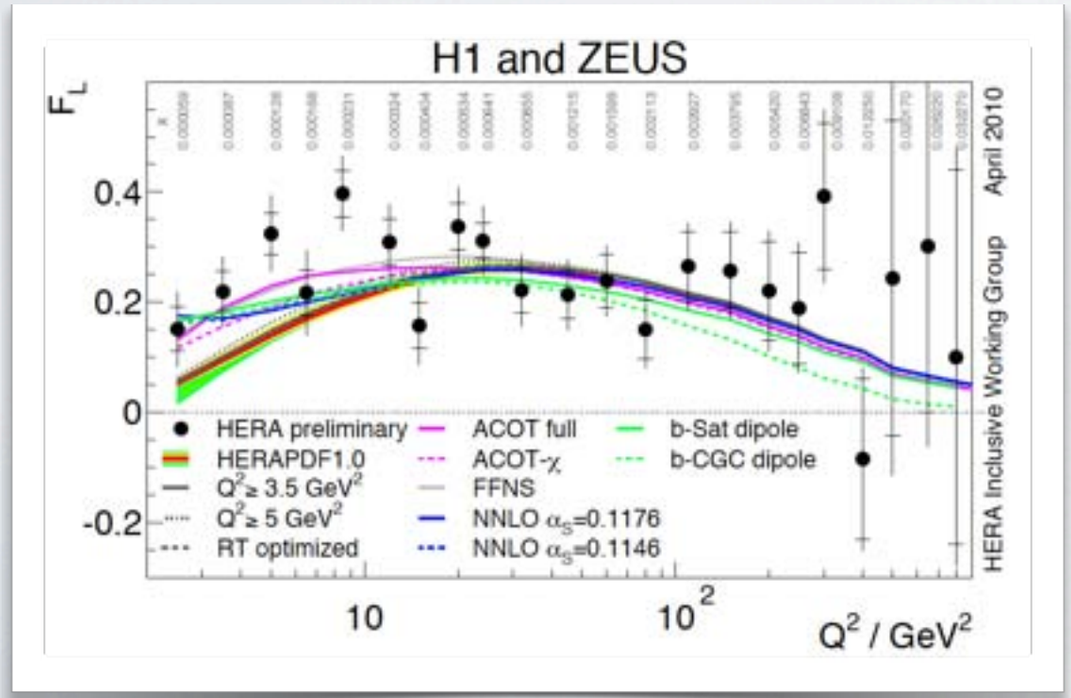

- no unambiguous hints for saturation in ep down to $x = 10^{-5}$
- most promising so far: RHIC hadron yields in dAu collisions
- effects amplified in eA/pA collisions; "nuclear oompf" $\propto A^{1/3}$

experimental input

thriving experimental programs since the early seventies

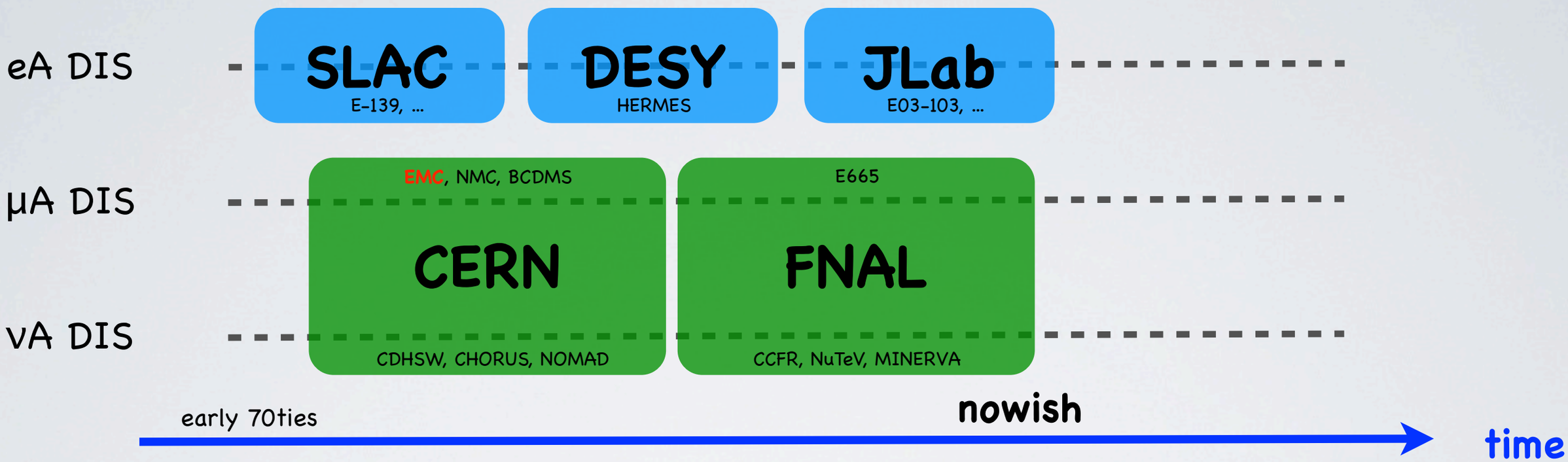

experimental input

thriving experimental programs since the early seventies

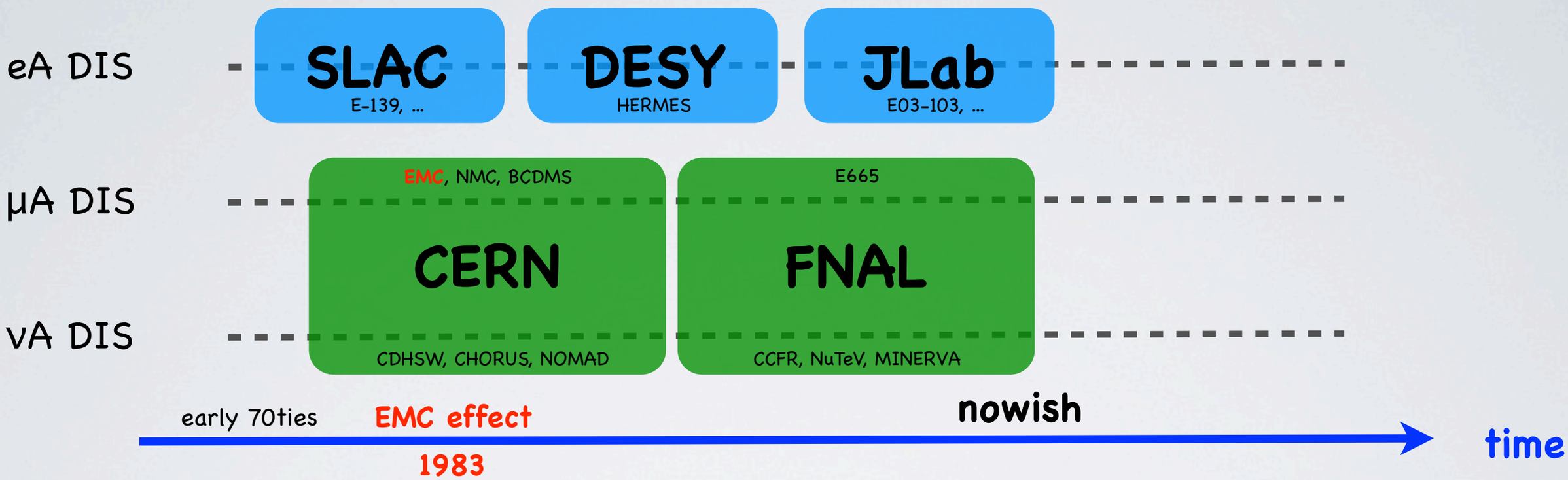

experimental input

thriving experimental programs since the early seventies

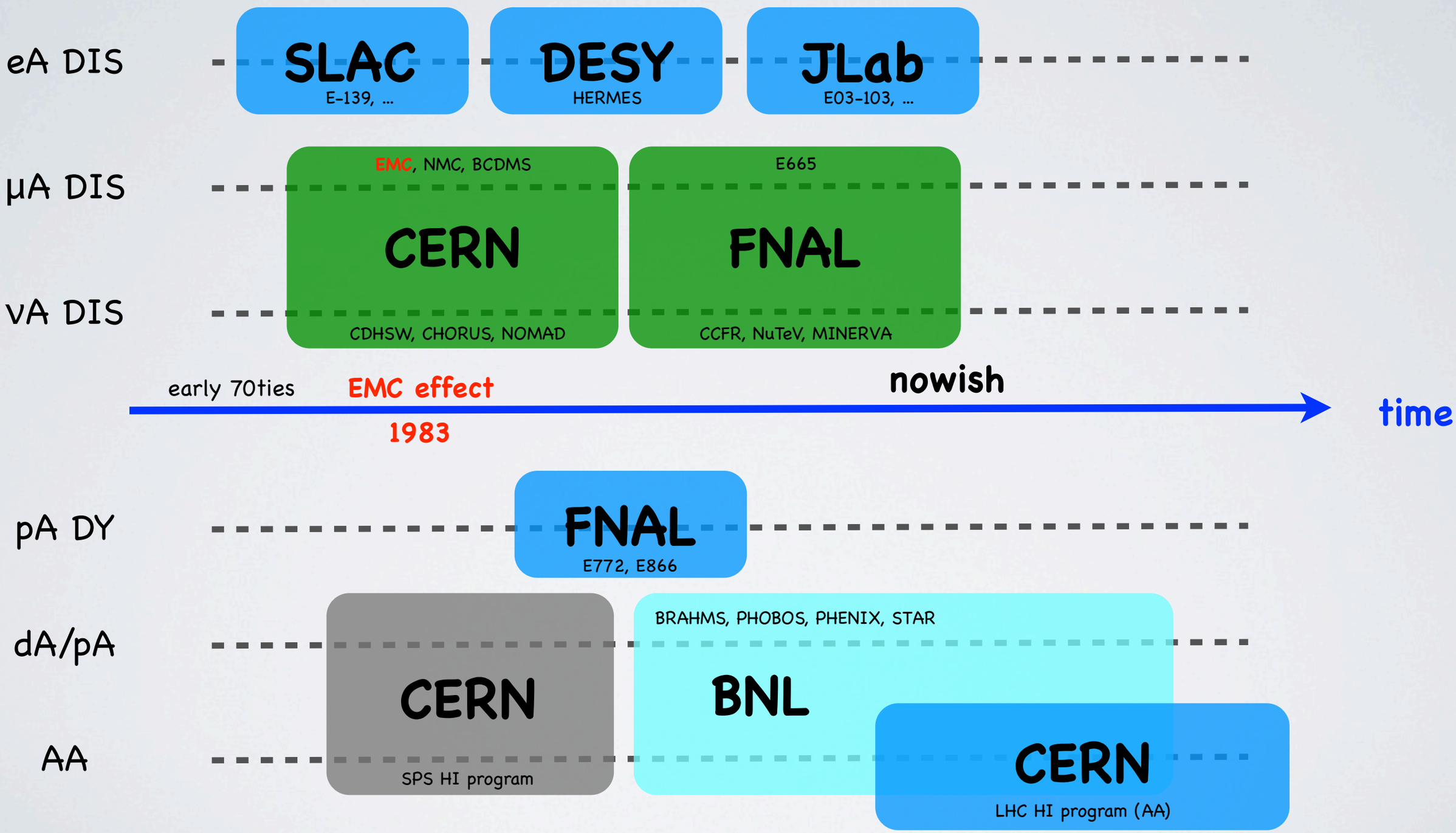

experimental input

thriving experimental programs since the early seventies

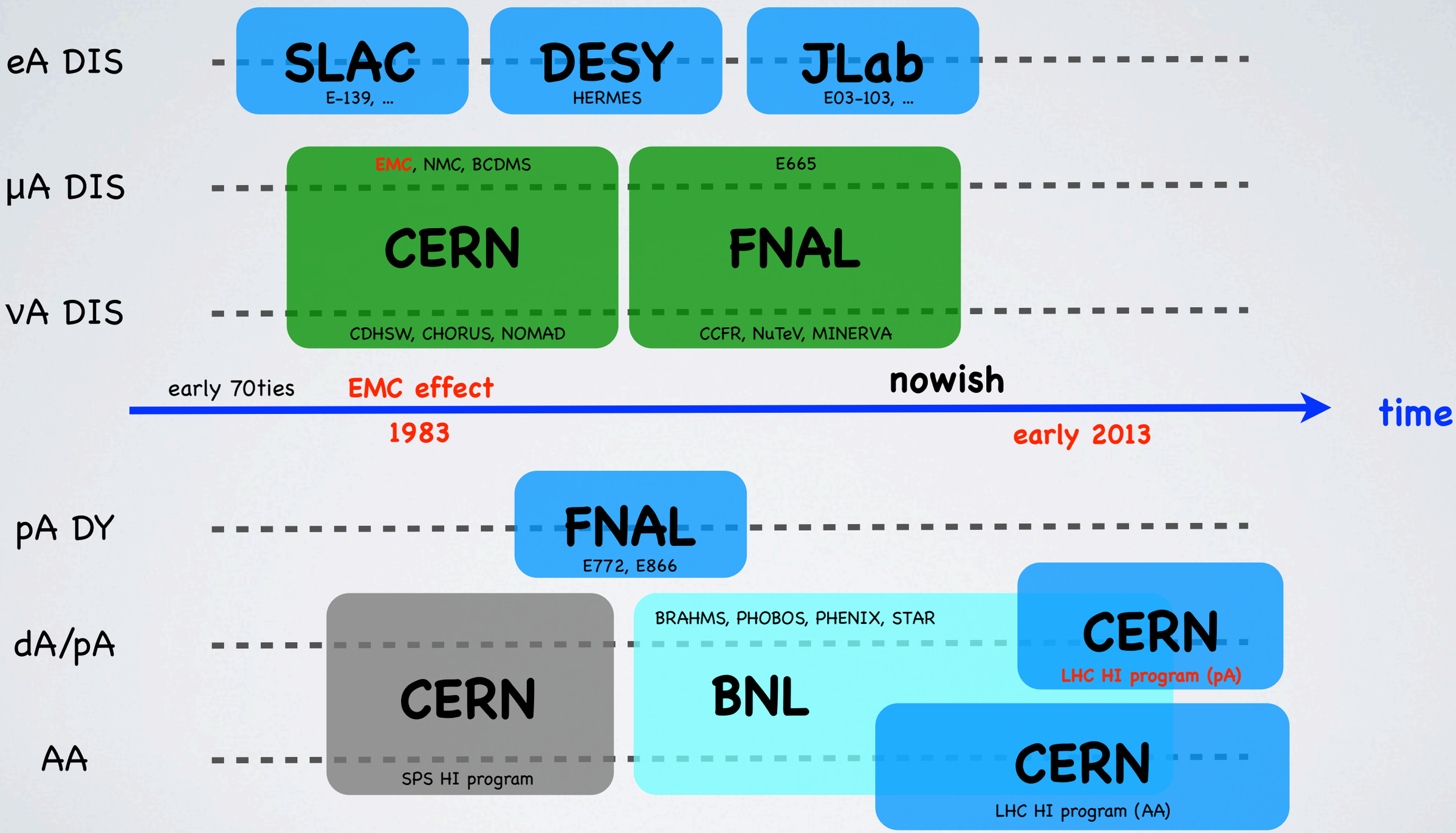

experimental input

thriving experimental programs since the early seventies

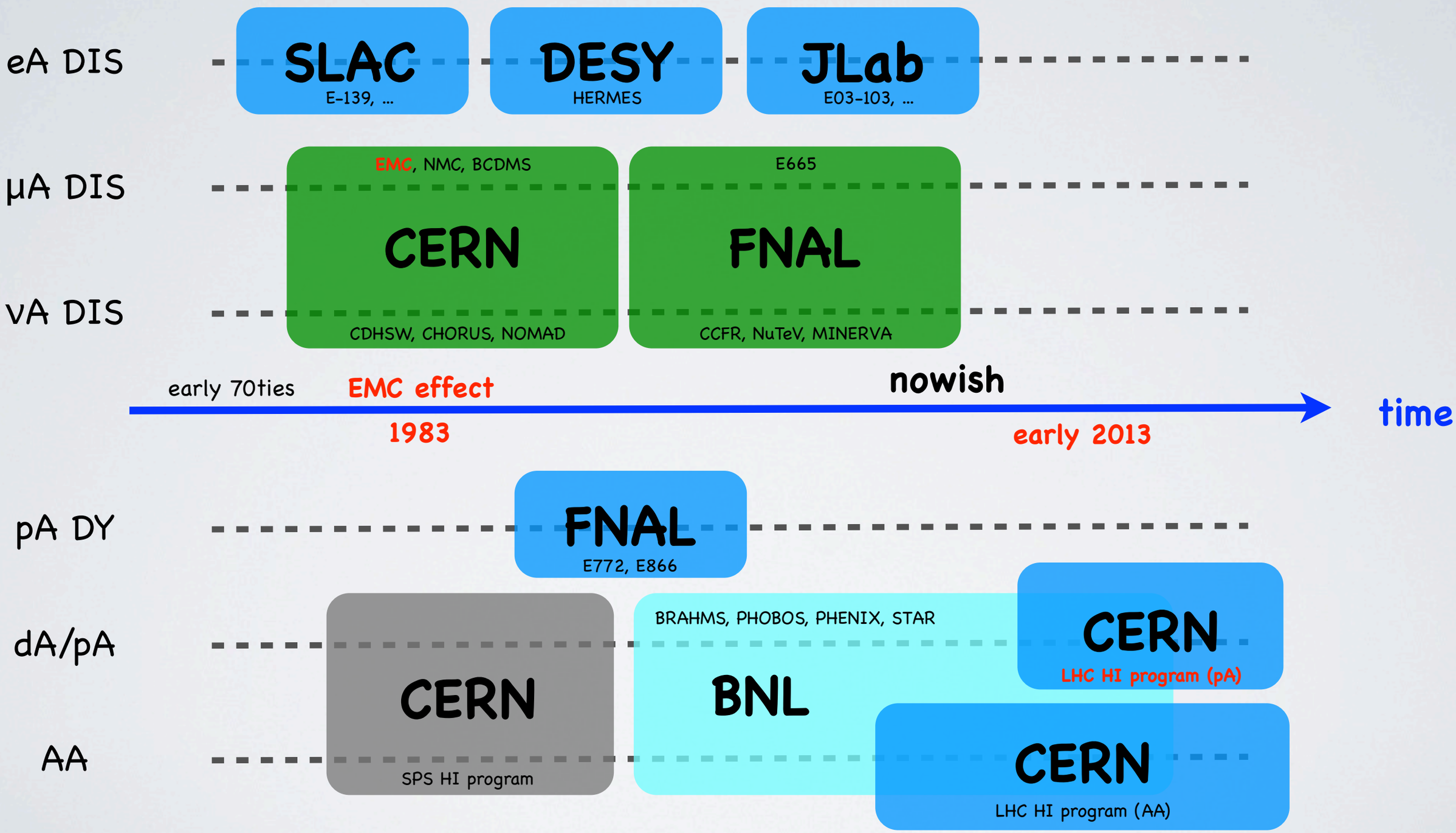

biggest obstacle for nPDF analysis: no eA collider yet

experimental input

thriving experimental programs since the early seventies

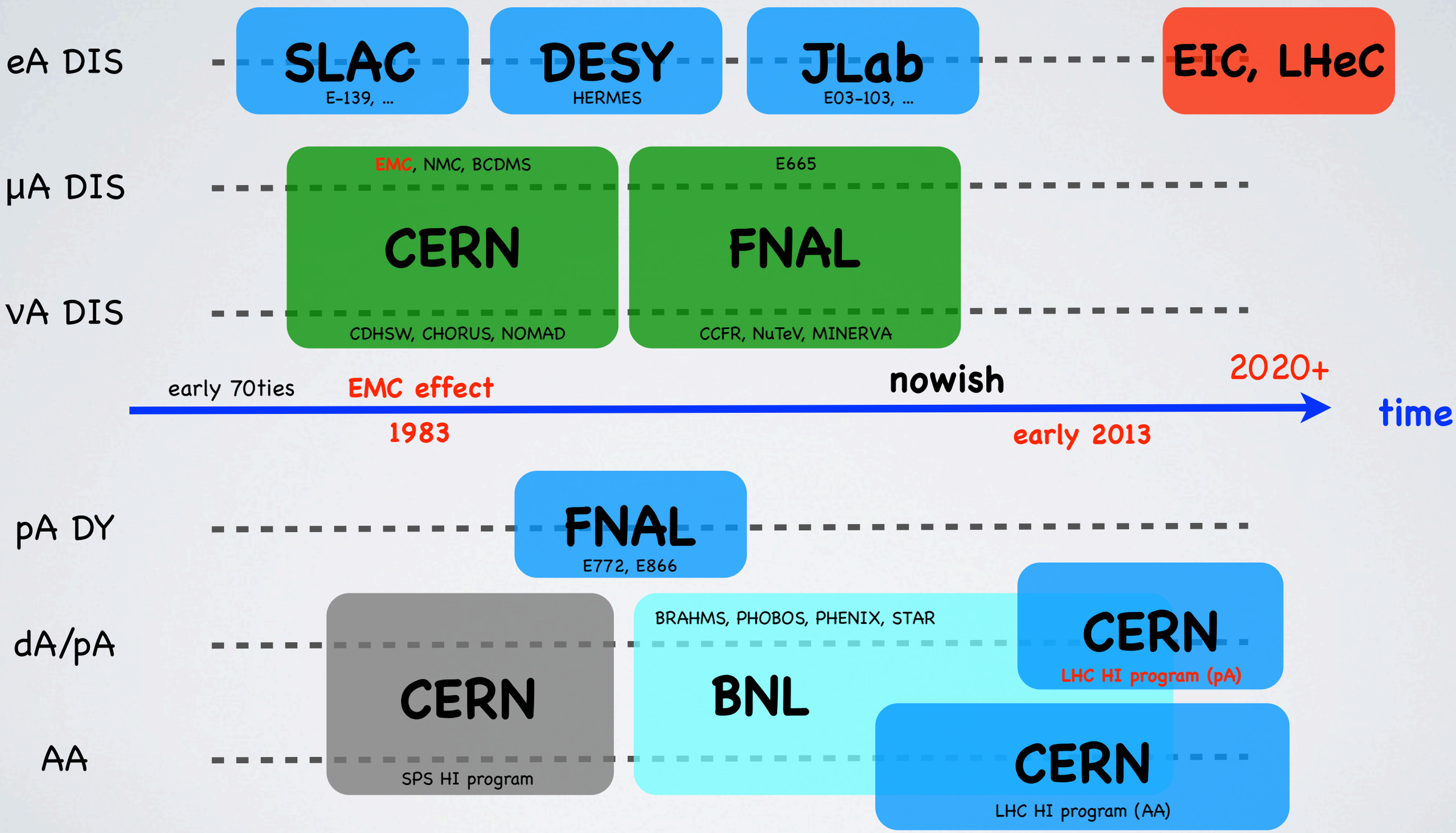

biggest obstacle for nPDF analysis: no eA collider yet

experimental input: x,Q^2 plane

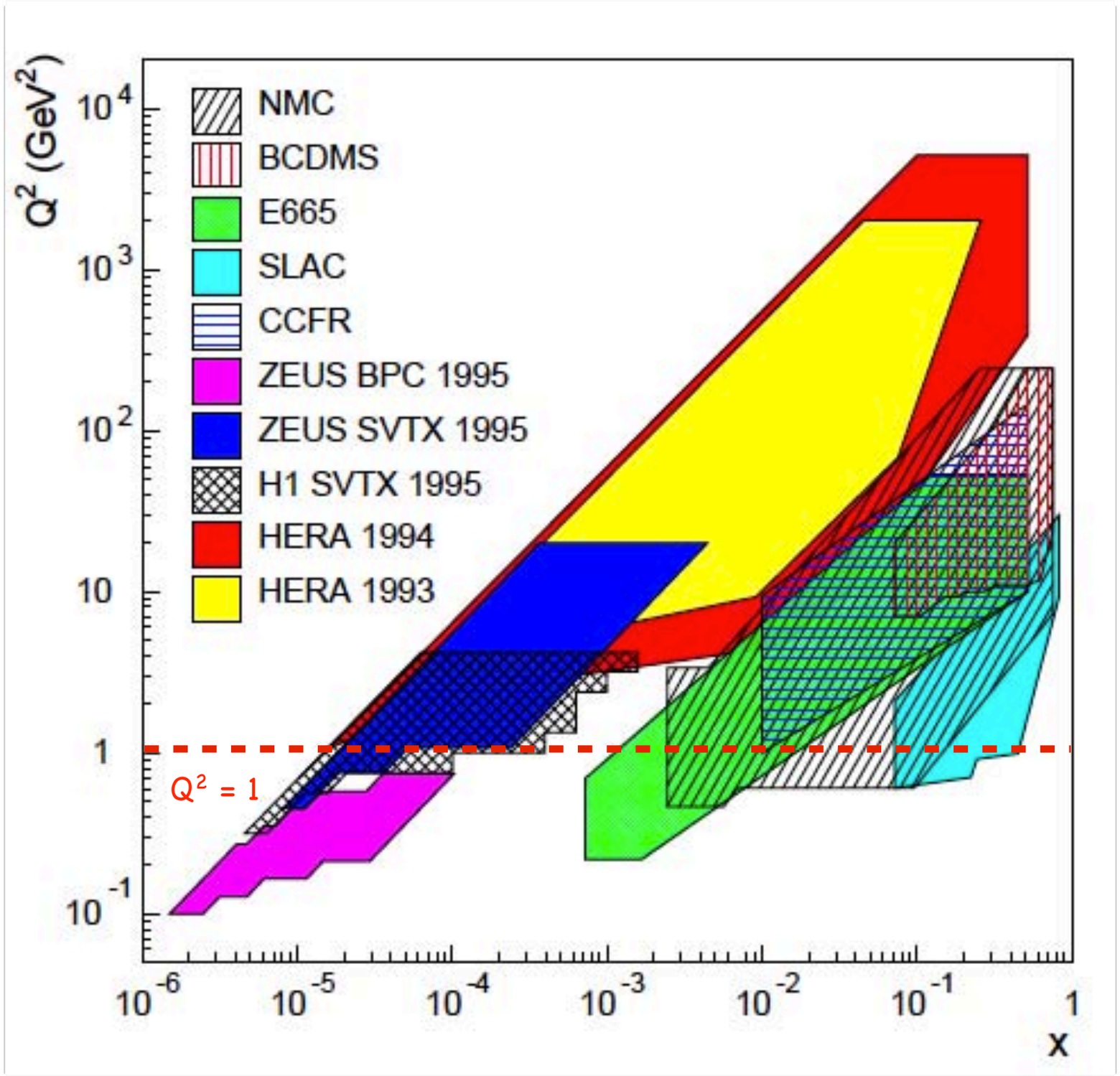

current kinematic coverage
for electron-proton DIS

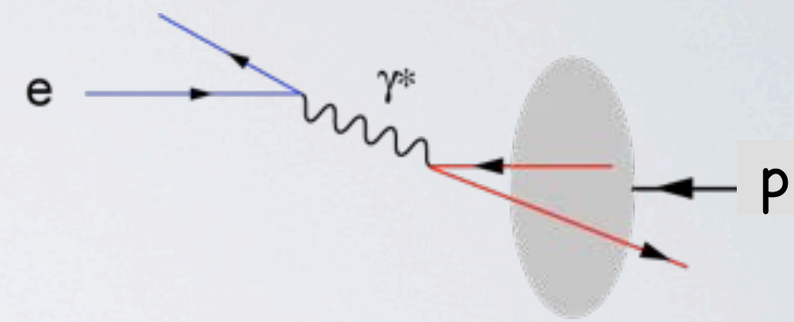

determines small-x behaviour
of quarks and gluons in
all analyses of proton PDFs

experimental input: x,Q^2 plane

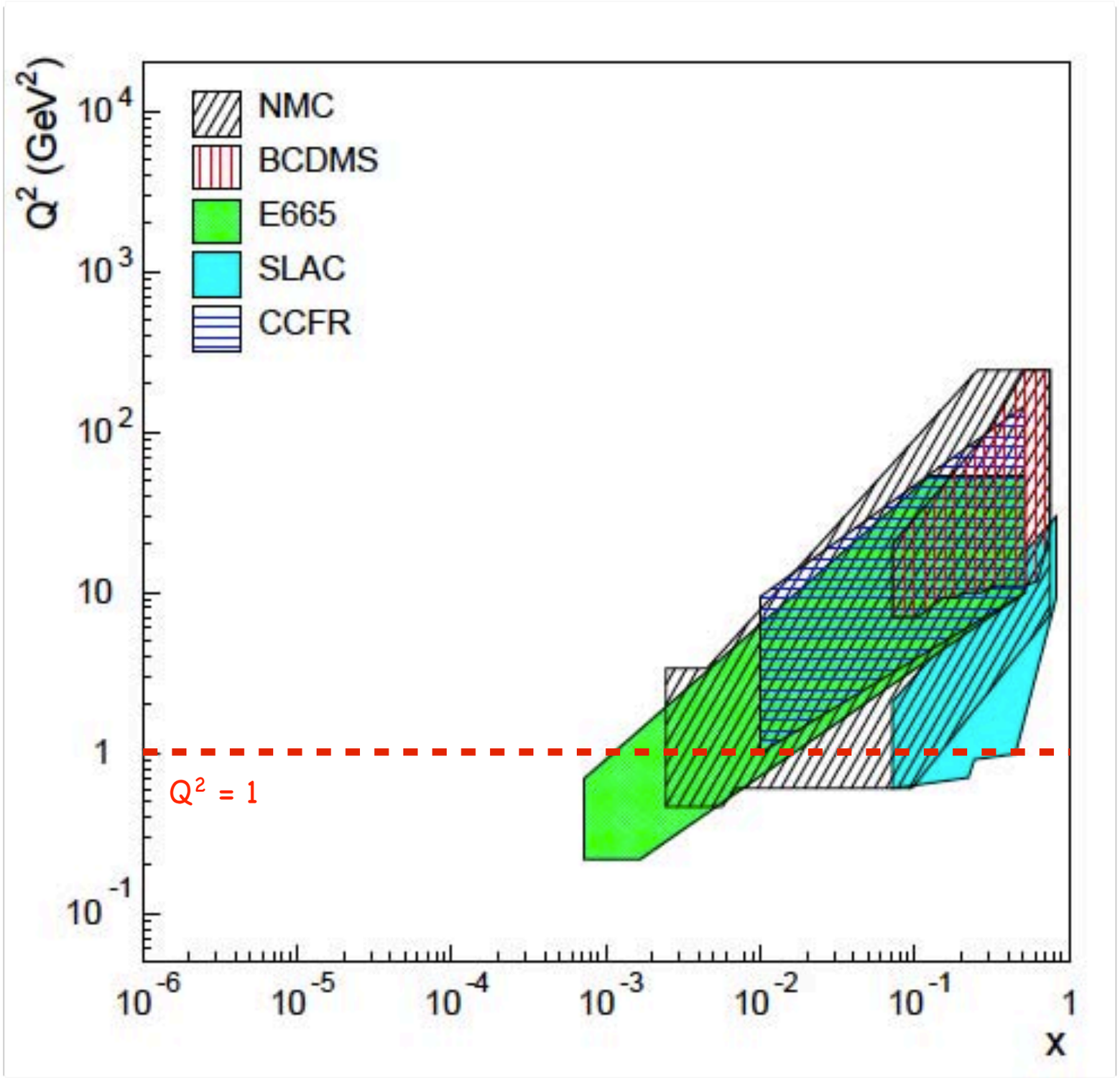

much more limited coverage in eA DIS

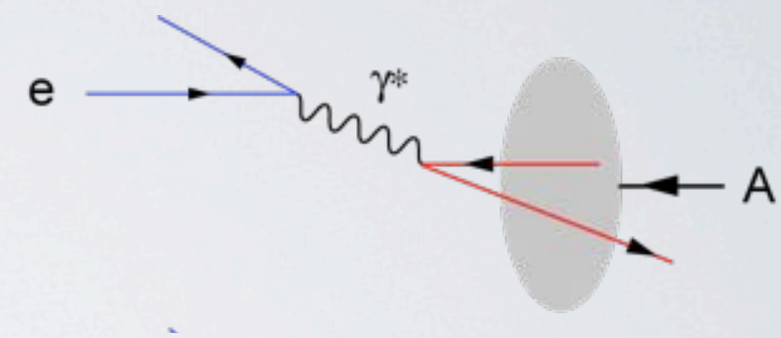

yet, the best constraint for nPDFs

experimental input: x,Q^2 plane

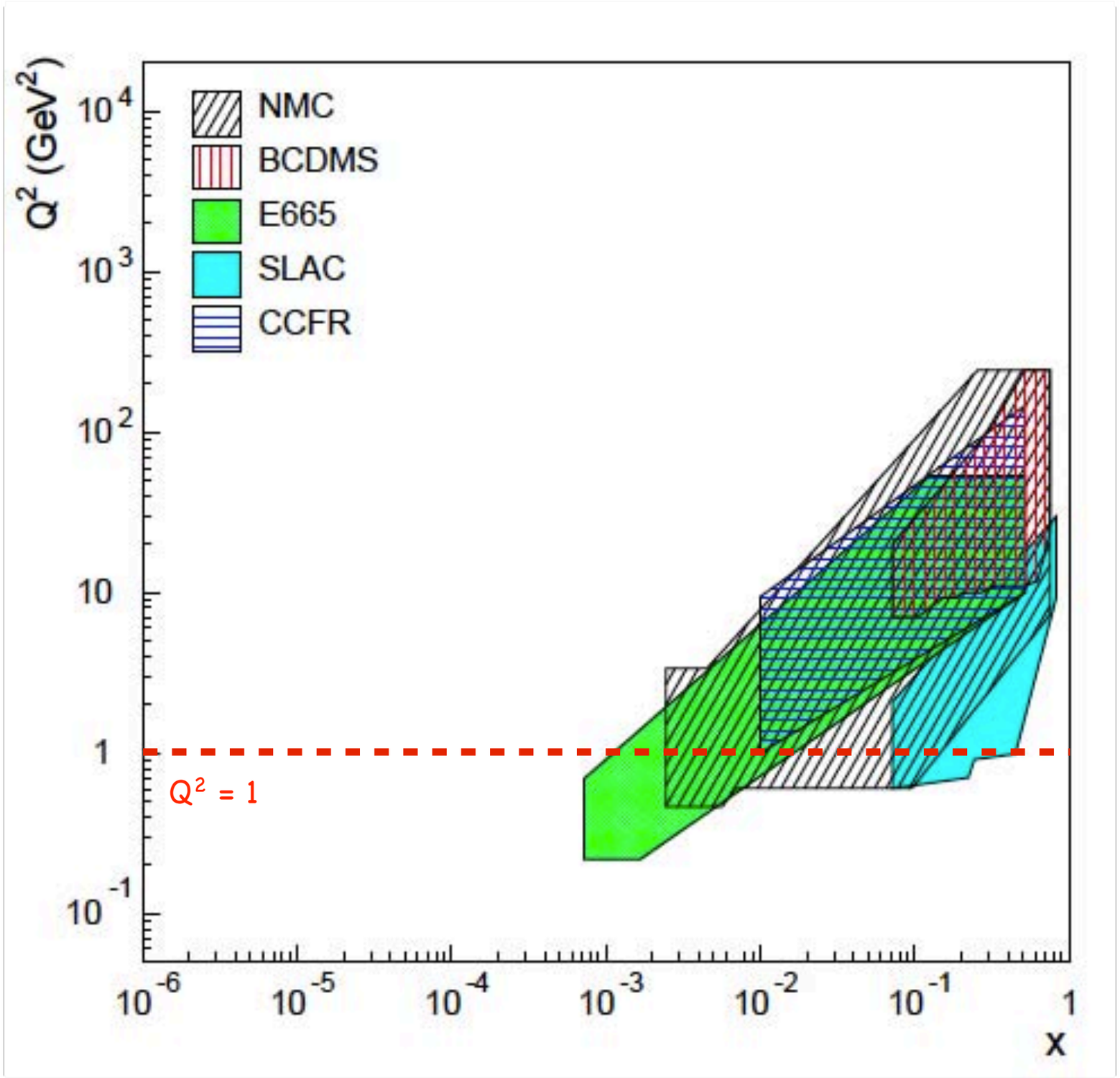

much more limited coverage in eA DIS

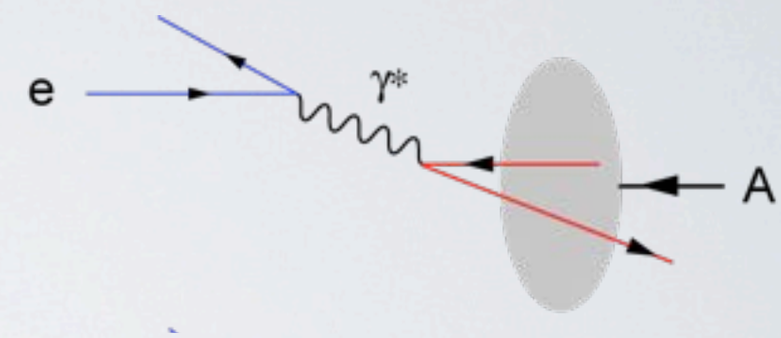

yet, the best constraint for nPDFs

- low x, low Q^2
  where saturation is relevant
- high Q^2
  to test scale evolution

an electron-ion collider
(EIC, LHeC projects)
is in high demand

the many facets of nPDFs

nuclei behave rather differently than a simple incoherent superposition of protons and neutrons → quarks and gluons in bound nucleons exhibit highly non-trivial momentum distributions

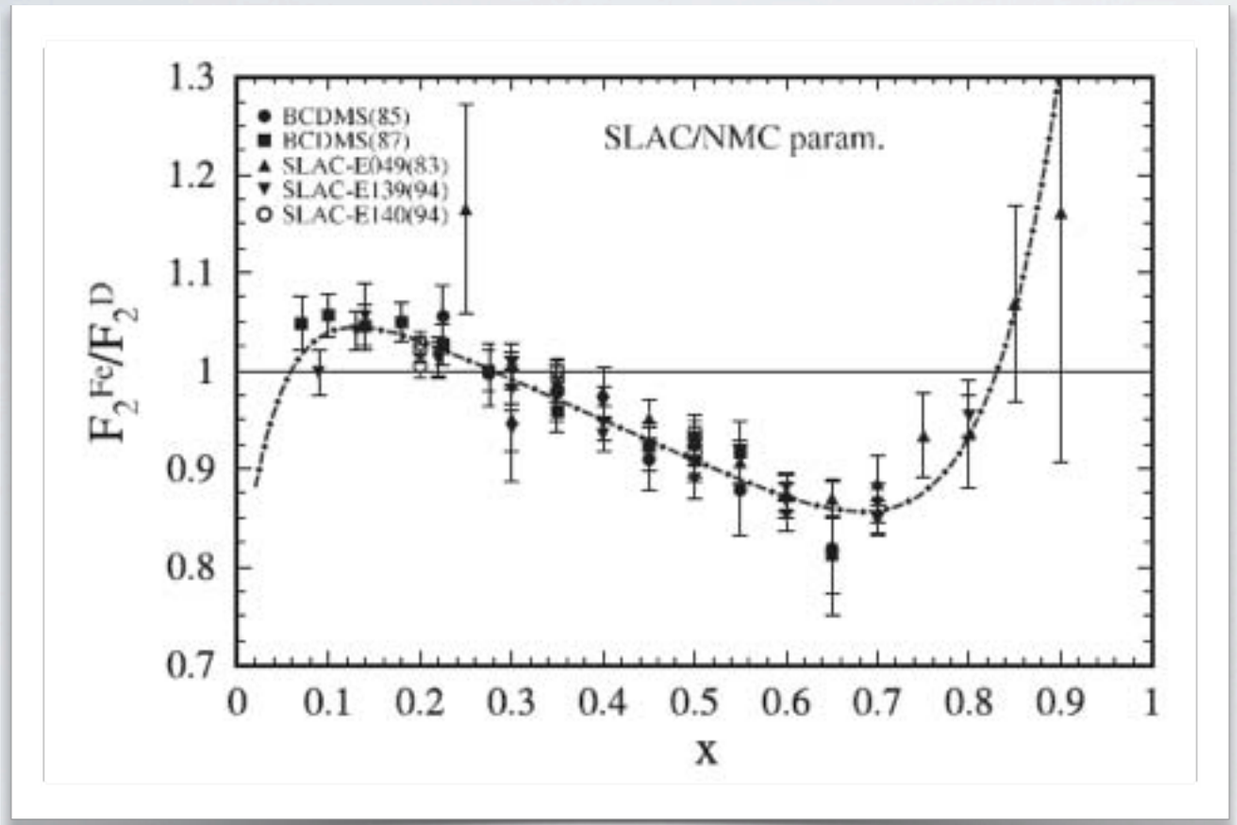

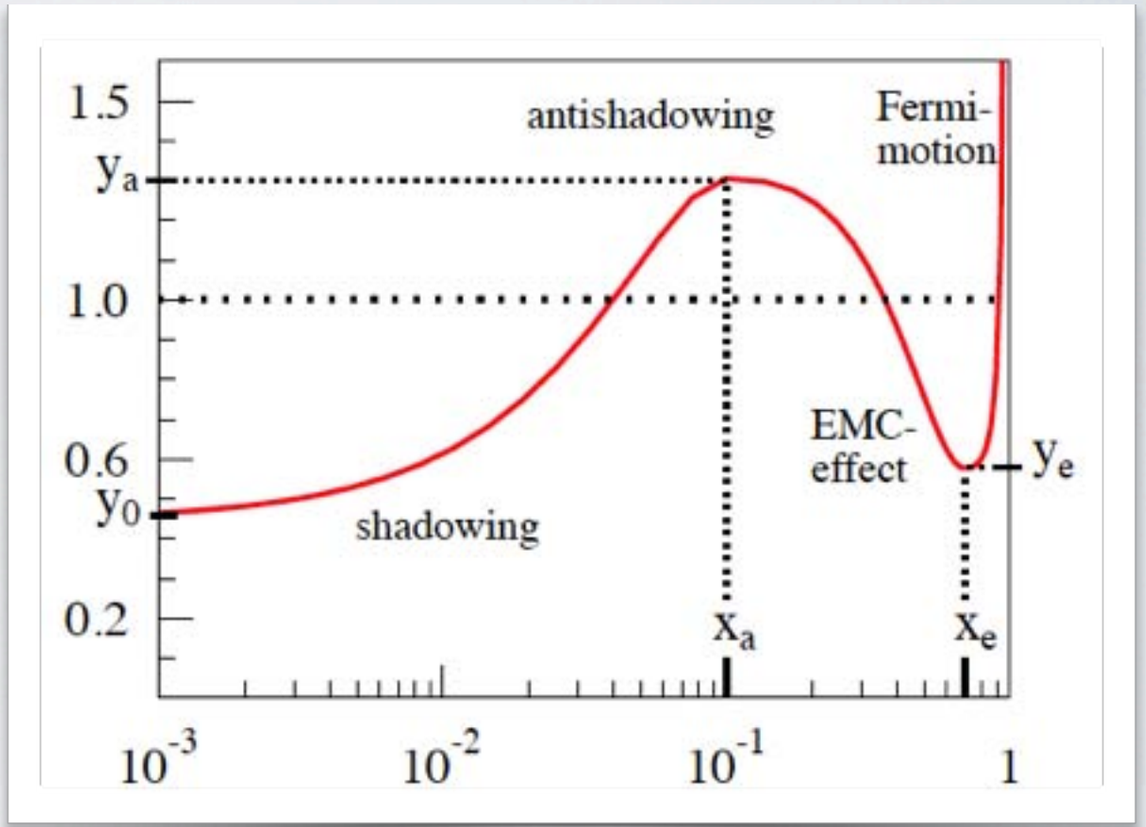

nuclear modifications traditionally parametrized as ratios

$$f_i^A(x_N, Q_0) = R_i^A(x_N, Q_0) \times f_i^p(x_N, Q_0)$$

scaling variable (per nucleon) $p_N = p_A/A$

$$x_N = \frac{Q^2}{2p_N \cdot q} \qquad 0 < x_N < A$$

strategies to parametrize nPDFs

all **measurements** usually given in terms of ratios w.r.t. some light nucleus

e.g. $$R_A(x_N, Q^2) = \frac{F_2^A(x_N, Q^2)}{F_2^D(x_N, Q^2)}$$

where $$F_2^A = \frac{1}{A}\left[Z\,F_2^{p/A} + (A - Z)\,F_2^{n/A}\right]$$

- nPDFs give distributions in bound proton $f_i^{p/A}(x_N, Q^2)$
- ... assume isospin invariance for $f_i^{n/A}(x_N, Q^2)$

strategies to parametrize nPDFs

all **measurements** usually given in terms of ratios w.r.t. some light nucleus

e.g. $$R_A(x_N, Q^2) = \frac{F_2^A(x_N, Q^2)}{F_2^D(x_N, Q^2)}$$

where $$F_2^A = \frac{1}{A}\left[Z\,F_2^{p/A} + (A - Z)\,F_2^{n/A}\right]$$

- nPDFs give distributions in bound proton $f_i^{p/A}(x_N, Q^2)$
- ... assume isospin invariance for $f_i^{n/A}(x_N, Q^2)$

conventional ansatz

input scale of O(1 GeV)

free proton densities

multiplicative nuclear correction factor $$f_i^{p/A}(x_N, Q_0) = R_i^A(x_N, Q_0) \times f_i^p(x_N, Q_0)$$

choose ansatz and determine from data

used in
Hirai, Kumano, Nagai (HKN) arXiv:0709.3038
Eskola, Paukkunen, Salgado (EPS) arXiv:0902.4154
de Florian, Sassot, MS, Zurita (DSSZ) arXiv:1112.6324

- works well with small amount of parameters
- cannot account for $x_N > 1$ region [as free proton PDFs limited to $0 < x_N < 1$]

strategies to parametrize nPDFs

all **measurements** usually given in terms of ratios w.r.t. some light nucleus

e.g. $$R_A(x_N, Q^2) = \frac{F_2^A(x_N, Q^2)}{F_2^D(x_N, Q^2)}$$

where $$F_2^A = \frac{1}{A}\left[Z\,F_2^{p/A} + (A-Z)\,F_2^{n/A}\right]$$

- nPDFs give distributions in bound proton $f_i^{p/A}(x_N, Q^2)$
- ... assume isospin invariance for $f_i^{n/A}(x_N, Q^2)$

conventional ansatz

multiplicative nuclear correction factor

input scale of O(1 GeV)

free proton densities

$$f_i^{p/A}(x_N, Q_0) = R_i^A(x_N, Q_0) \times f_i^p(x_N, Q_0)$$

choose ansatz and determine from data

used in
Hirai, Kumano, Nagai (HKN) arXiv:0709.3038
Eskola, Paukkunen, Salgado (EPS) arXiv:0902.4154
de Florian, Sassot, MS, Zurita (DSSZ) arXiv:1112.6324

- works well with small amount of parameters
- cannot account for $x_N > 1$ region [as free proton PDFs limited to $0 < x_N < 1$]

direct ansatz

parametrize nPDFs directly $f_i^{p/A}(x_N, Q_0)$

used in Keppel, Kovarik, Olness, ... (nCTEQ) arXiv:0907.2357

- still dependent on some free proton PDF to compute ratios
- natural to choose same functional form as for proton PDF

convolutional approach

define nPDF through a weight function

choose ansatz and determine from data

$$f_i^{p/A}(x_N, Q_0) = \int_{x_N}^{A} \frac{dy}{y}\, W_i^A(y, Q_0)\, f_i^p\left(\frac{x_N}{y}, Q_0\right)$$

used in de Florian, Sassot (nDS) hep-ph/0311227

- W can be viewed as an effective nucleon momentum density in a nucleus

a brief history of selected nPDF fits

nDS de Florian, Sassot - hep-ph/0311227

- **first NLO analysis** $\chi^2/\mathrm{d.o.f.} = \mathbf{0.74}$
- only SLAC & NMC DIS sets and some DY data
- convolutional approach in Mellin N-space
- no error analysis

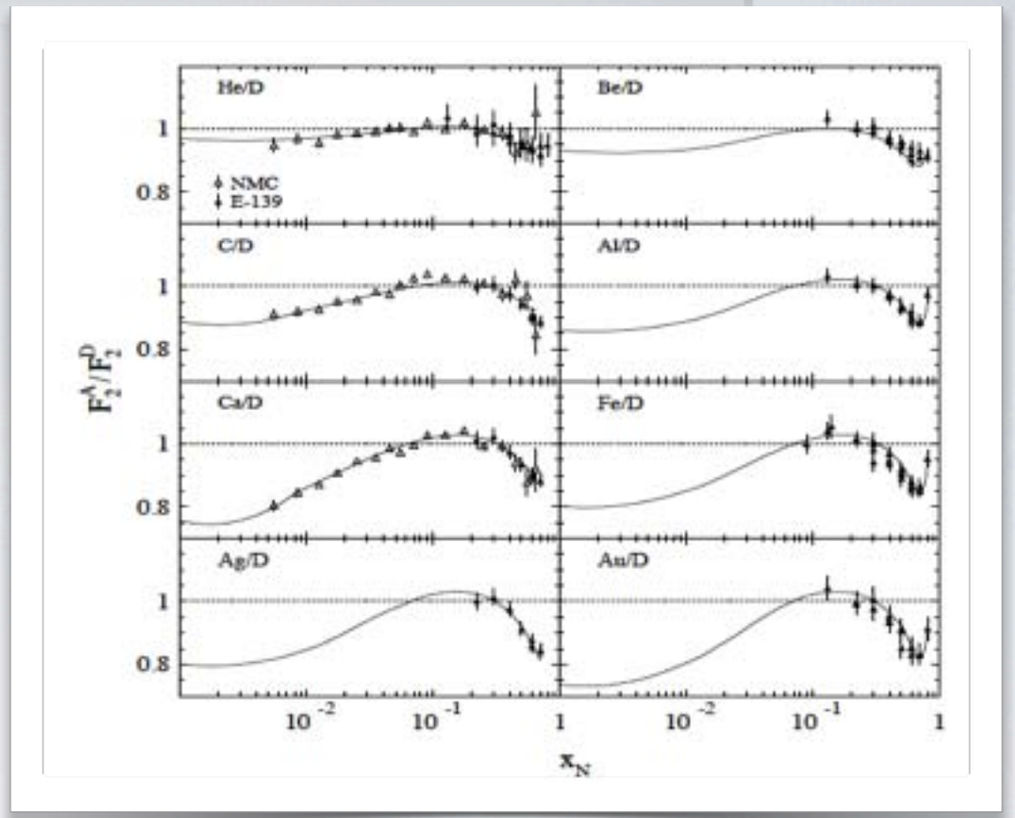

a brief history of selected nPDF fits

nDS de Florian, Sassot - hep-ph/0311227

- **first NLO analysis** $\chi^2/\mathrm{d.o.f.} = \mathbf{0.74}$
- only SLAC & NMC DIS sets and some DY data
- convolutional approach in Mellin N-space
- no error analysis

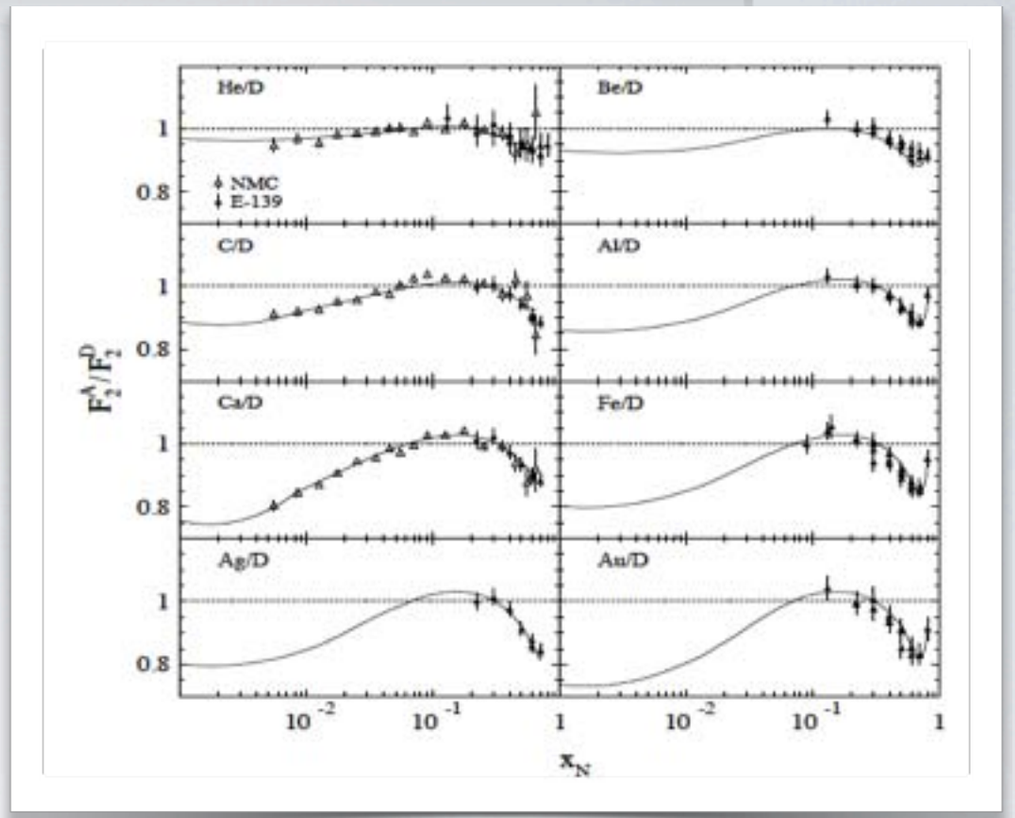

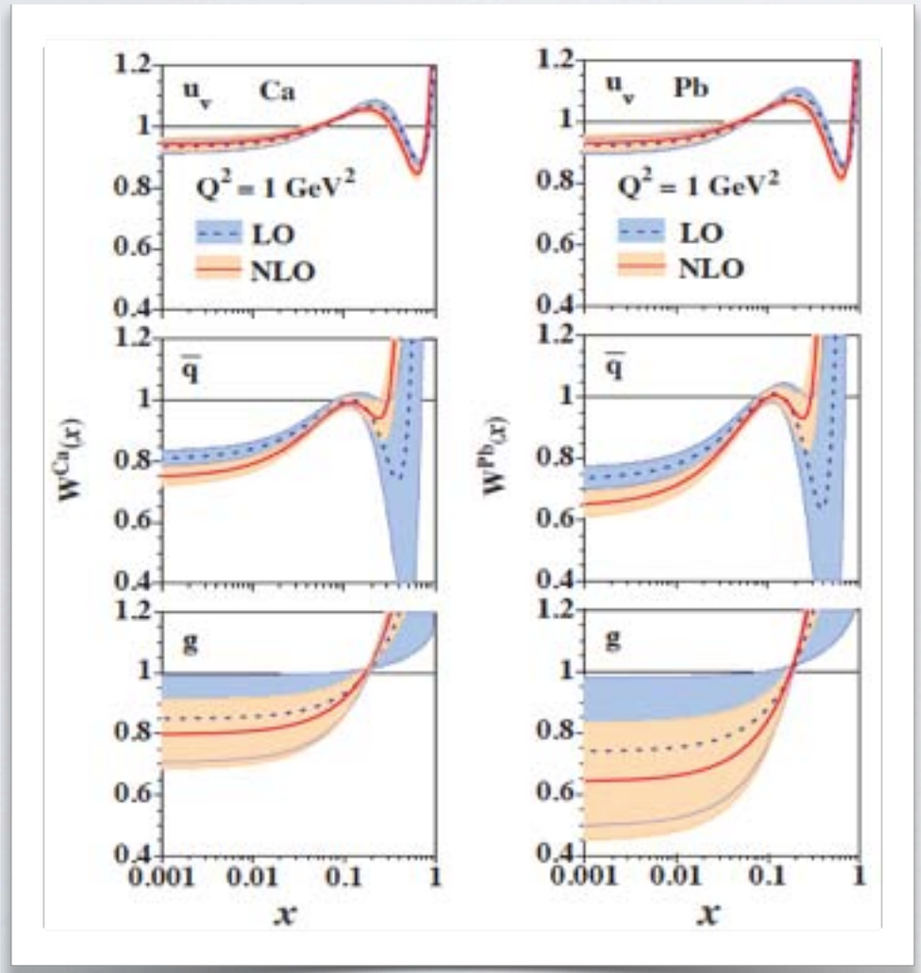

HKN Hirai, Kumano, Nagai - arXiv:0709.3038

- LO and NLO analyses $\chi^2/\mathrm{d.o.f.} = \mathbf{1.2}$
- standard DIS and DY data sets
- standard multiplicative ansatz
- **first error analysis** (Hessian method)

a brief history of selected nPDF fits

nDS de Florian, Sassot - hep-ph/0311227

- **first NLO analysis** $\chi^2/\mathrm{d.o.f.} = \mathbf{0.74}$
- only SLAC & NMC DIS sets and some DY data
- convolutional approach in Mellin N-space
- no error analysis

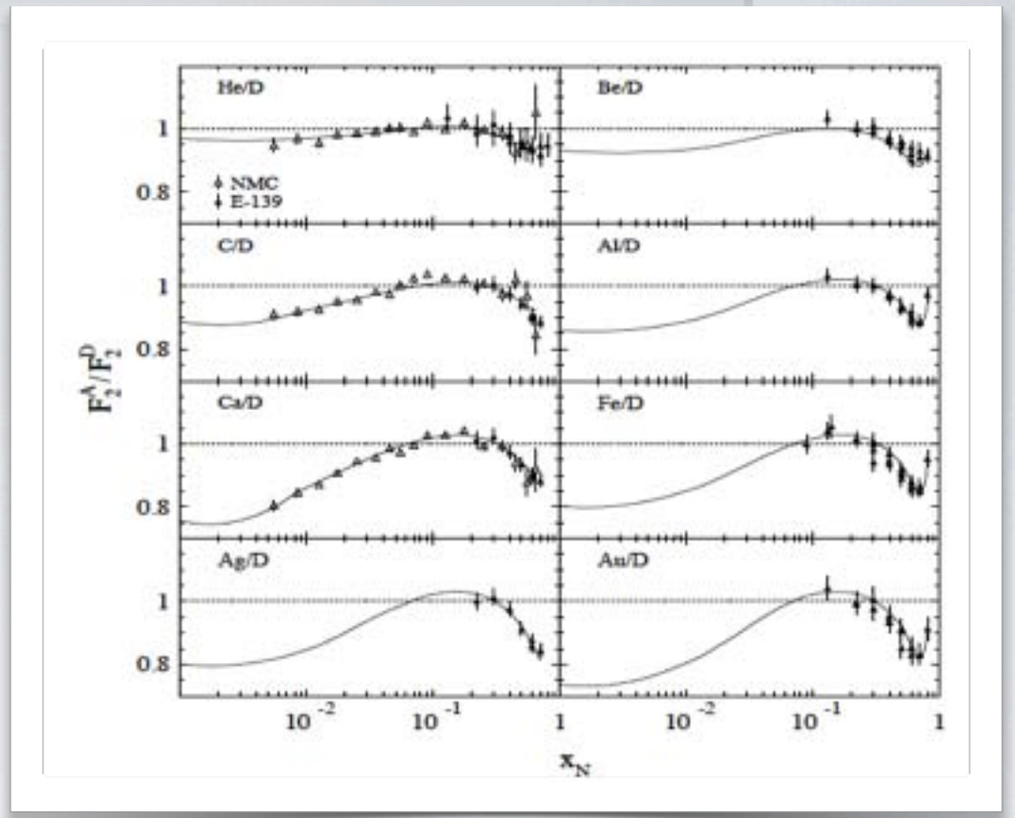

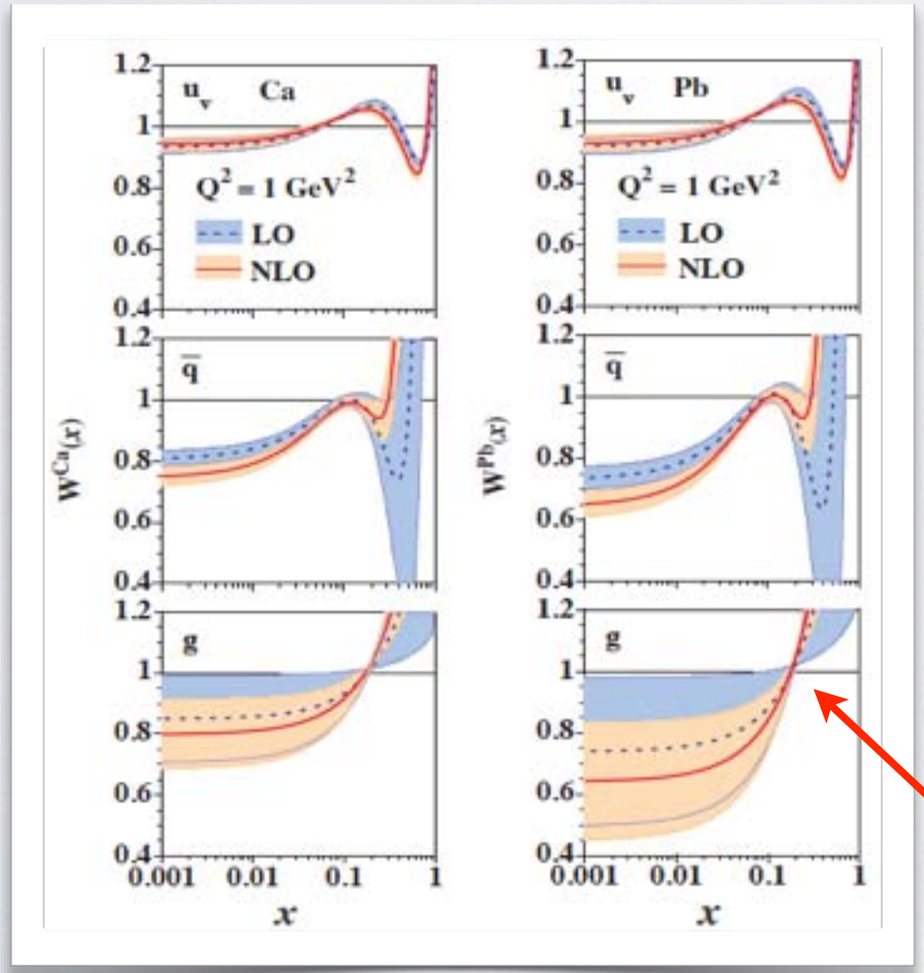

HKN Hirai, Kumano, Nagai - arXiv:0709.3038

- LO and NLO analyses $\chi^2/\mathrm{d.o.f.} = \mathbf{1.2}$
- standard DIS and DY data sets
- standard multiplicative ansatz
- **first error analysis** (Hessian method)
- rather "unusual" gluon distribution at large x

selected nPDF fits (cont'd)

EPS Eskola, Paukkunen, Salgado - arXiv:0902.4154

- NLO analysis $\chi^2/\mathrm{d.o.f.} = \mathbf{0.8}$
- usual DIS & DY data
- **RHIC dAu data to constrain gluon better**
- complicated piecewise multipl. ansatz
- Hessian error analysis

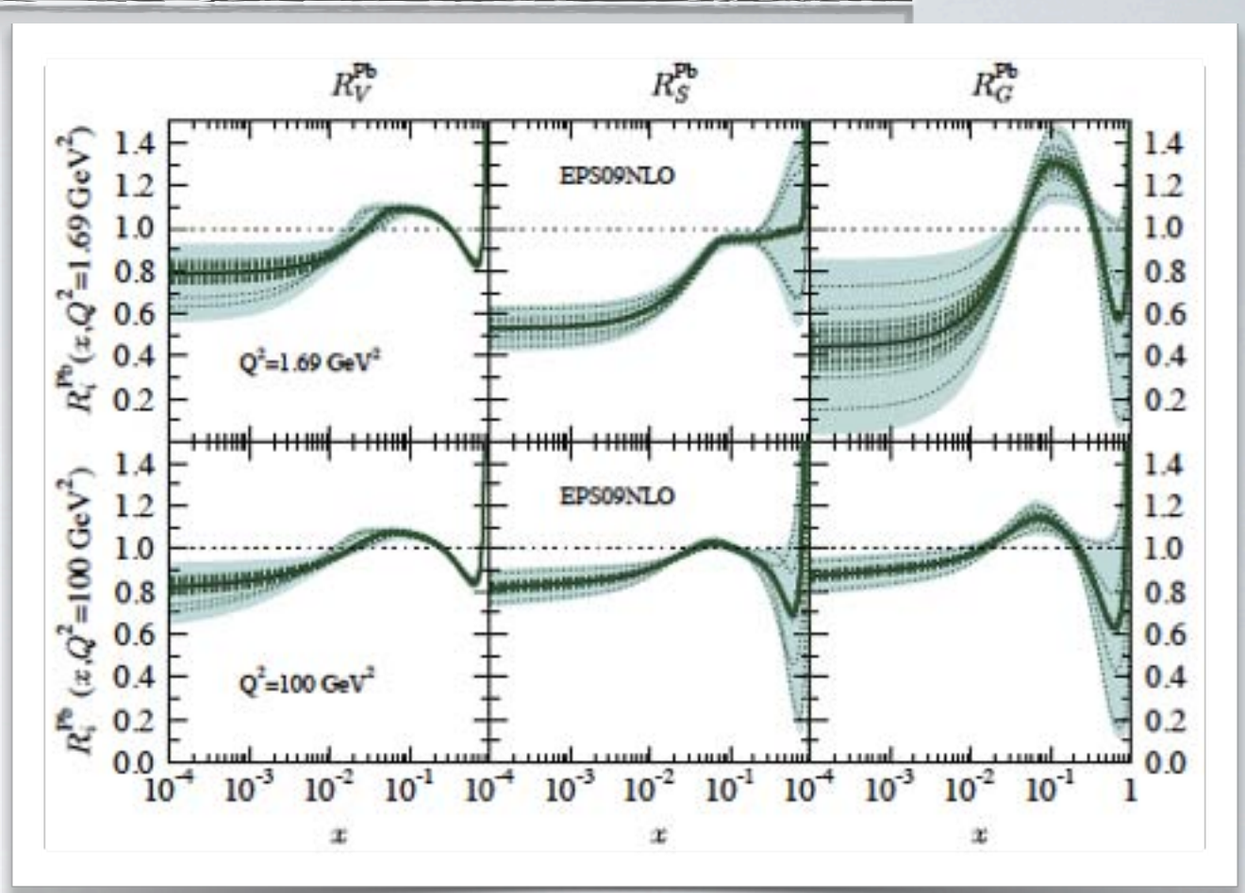

selected nPDF fits (cont'd)

EPS Eskola, Paukkunen, Salgado - arXiv:0902.4154

- NLO analysis $\chi^2/\mathrm{d.o.f.} = \mathbf{0.8}$
- usual DIS & DY data
- **RHIC dAu data to constrain gluon better**
- complicated piecewise multipl. ansatz
- Hessian error analysis
- huge anti-shadowing/EMC effect for gluon

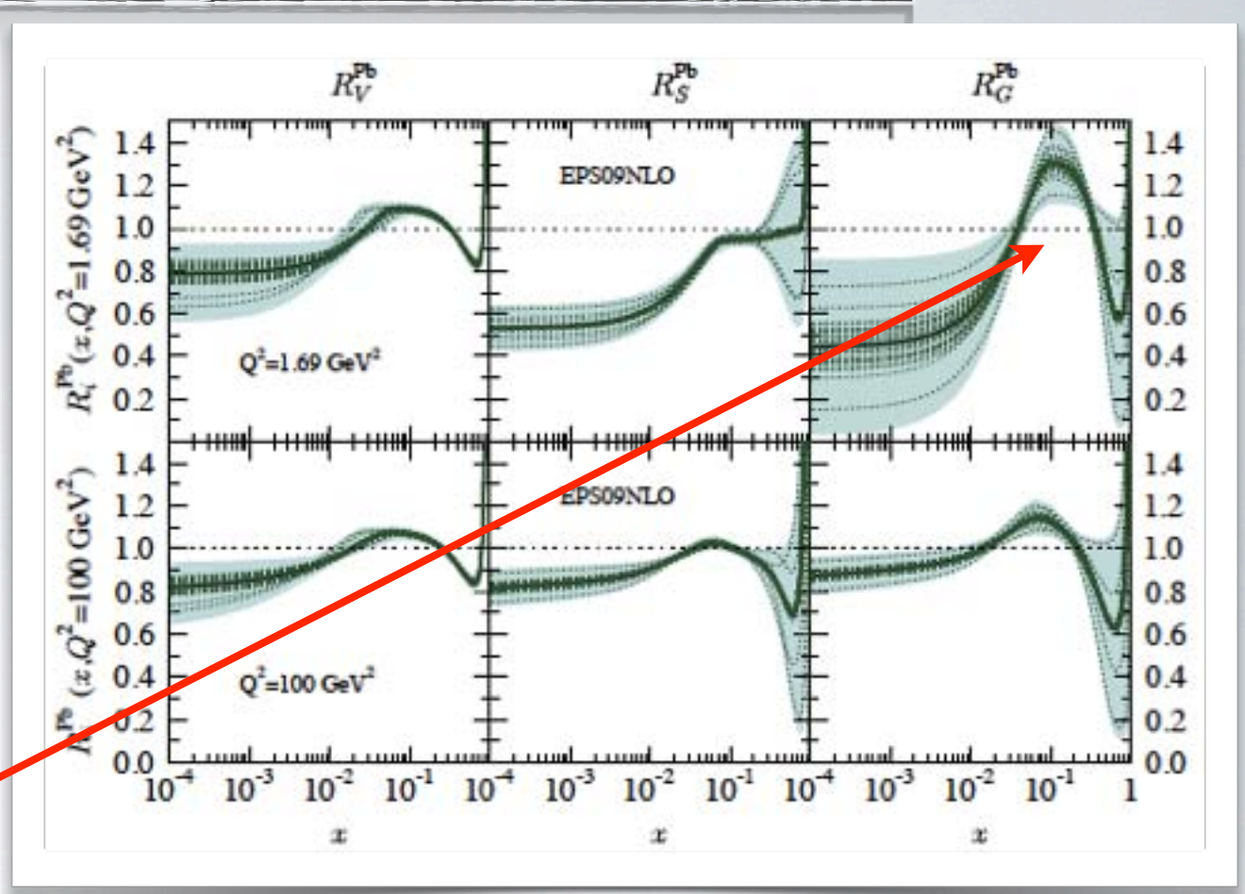

selected nPDF fits (cont'd)

EPS Eskola, Paukkunen, Salgado - arXiv:0902.4154

- NLO analysis $\chi^2/\mathrm{d.o.f.} = 0.8$
- usual DIS & DY data
- **RHIC dAu data to constrain gluon better**
- complicated piecewise multipl. ansatz
- Hessian error analysis
- huge anti-shadowing/EMC effect for gluon

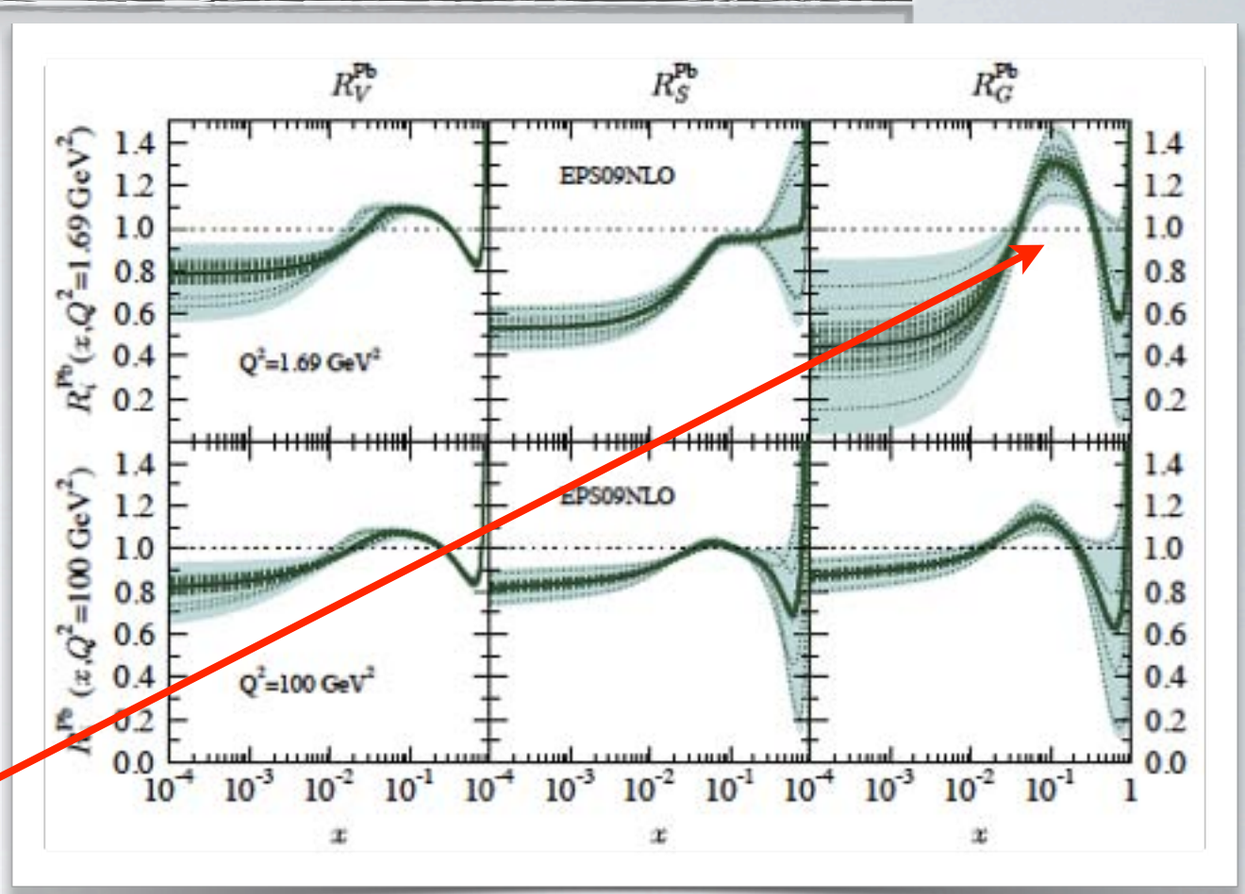

nCTEQ Keppel, Kovarik, ... - arXiv:0907.2357

- direct ansatz a la CTEQ
- DIS & DY plus **CC neutrino DIS data**

selected nPDF fits (cont'd)

EPS Eskola, Paukkunen, Salgado - arXiv:0902.4154

- NLO analysis $\chi^2/\mathrm{d.o.f.} = 0.8$
- usual DIS & DY data
- **RHIC dAu data to constrain gluon better**
- complicated piecewise multipl. ansatz
- Hessian error analysis
- huge anti-shadowing/EMC effect for gluon

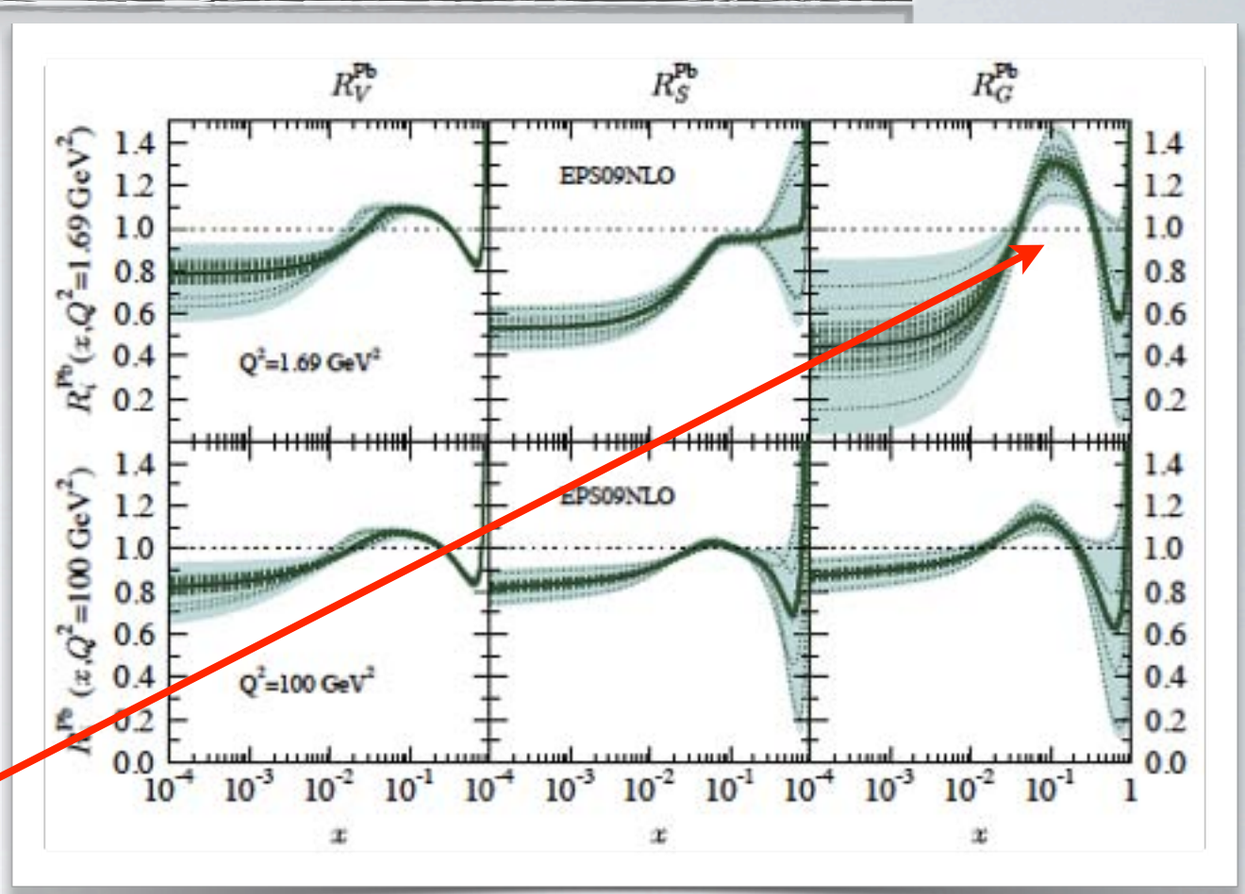

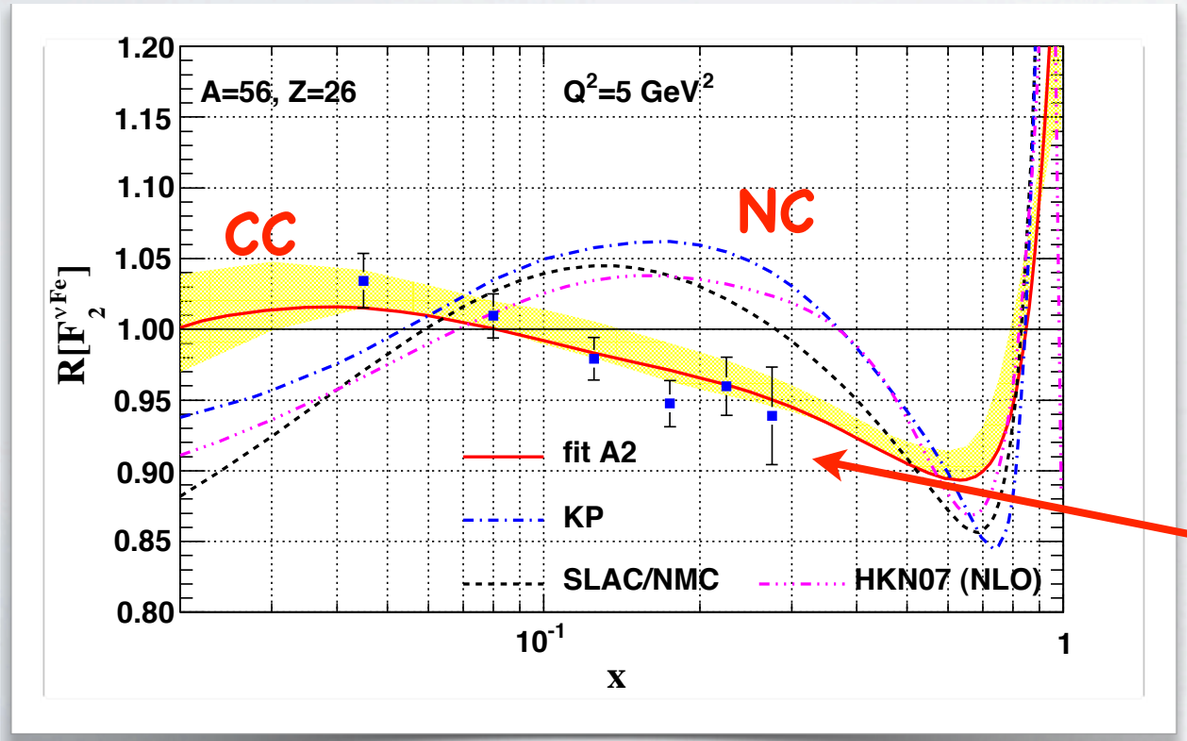

nCTEQ Keppel, Kovarik, ... - arXiv:0907.2357

- direct ansatz a la CTEQ
- DIS & DY plus **CC neutrino DIS data**
- find tension between NC and CC DIS data

breakdown of factorization

DSSZ global analysis

de Florian, Sassot, MS, Zurita - arXiv:1112.6324

why do we need yet another set of nPDFs ?

DSSZ global analysis

de Florian, Sassot, MS, Zurita - arXiv:1112.6324

why do we need yet another set of nPDFs ?

- no truly global analysis yet
  - include charged lepton DIS, Drell-Yan, CC neutrino DIS, and RHIC dAu data

DSSZ global analysis

de Florian, Sassot, MS, Zurita - arXiv:1112.6324

why do we need yet another set of nPDFs ?

- no truly global analysis yet
  - include charged lepton DIS, Drell-Yan, CC neutrino DIS, and RHIC dAu data
- use up-to-date proton PDFs as reference set
  - many different sets to choose from - take MSTW

Martin, Stirling, Thorne, Watt - arXiv:0901.0002

DSSZ global analysis

de Florian, Sassot, MS, Zurita - arXiv:1112.6324

why do we need yet another set of nPDFs ?

- no truly global analysis yet
  - include charged lepton DIS, Drell-Yan, CC neutrino DIS, and RHIC dAu data
- use up-to-date proton PDFs as reference set
  - many different sets to choose from - take MSTW

    Martin, Stirling, Thorne, Watt - arXiv:0901.0002
- improve on the treatment of heavy flavors
  - e.g. NLO massive Wilson coefficients for CC DIS

    Blumlein, Hasselhuhn, Kovacikova, Moch - arXiv:1104.3449
- provide some estimate of nPDF uncertainties

DSSZ global analysis

de Florian, Sassot, MS, Zurita - arXiv:1112.6324

why do we need yet another set of nPDFs ?

- no truly global analysis yet
  - include charged lepton DIS, Drell-Yan, CC neutrino DIS, and RHIC dAu data
- use up-to-date proton PDFs as reference set
  - many different sets to choose from - take MSTW

    Martin, Stirling, Thorne, Watt - arXiv:0901.0002
- improve on the treatment of heavy flavors
  - e.g. NLO massive Wilson coefficients for CC DIS

    Blumlein, Hasselhuhn, Kovacikova, Moch - arXiv:1104.3449
- provide some estimate of nPDF uncertainties

main questions to address

- do we really see a tension between charged lepton and neutrino DIS data
- do RHIC dAu data imply strong modifications of the nuclear gluon distribution

DSSZ global analysis - preliminaries

- use multiplicative nuclear modification factor $\mathbf{f_i^A(x, Q_0) = R_i^A(x, Q_0) \times f_i^p(x, Q_0)}$
- initial scale **Q_0 = 1 GeV**, NLO DGLAP evolution to all other scales Q > Q_0
- parametrize both valence distributions as

needs to be flexible enough to accommodate (anti-)shadowing, EMC effect, Fermi motion

$$\mathbf{R_v^A(x, Q_0) = \epsilon_1\, x^{\alpha_v}(1-x)^{\beta_1} \times [1 + \epsilon_2(1-x)^{\beta_2}] \times [1 + a_v(1-x)^{\beta_3}]}$$

DSSZ global analysis - preliminaries

- use multiplicative nuclear modification factor $\mathbf{f_i^A(x, Q_0) = R_i^A(x, Q_0) \times f_i^p(x, Q_0)}$
- initial scale **Q_0 = 1 GeV**, NLO DGLAP evolution to all other scales Q > Q_0
- parametrize both valence distributions as

needs to be flexible enough to accommodate (anti-)shadowing, EMC effect, Fermi motion

$$\mathbf{R_v^A(x, Q_0) = \epsilon_1\, x^{\alpha_v}(1-x)^{\beta_1} \times [1 + \epsilon_2(1-x)^{\beta_2}] \times [1 + a_v(1-x)^{\beta_3}]}$$

- data do not allow to discriminate different sea quark flavors (tried in analysis)

$$\mathbf{R_s^A(x, Q_0) = R_v^A(x, Q_0)\, \frac{\epsilon_s}{\epsilon_1} \frac{1 + a_s x^{\alpha_s}}{a_s + 1}}$$

- need another modification factor for gluons

$$\mathbf{R_g^A(x, Q_0) = R_v^A(x, Q_0)\, \frac{\epsilon_g}{\epsilon_1} \frac{1 + a_g x^{\alpha_g}}{a_g + 1}}$$

DSSZ global analysis - preliminaries

- use multiplicative nuclear modification factor $\mathbf{f_i^A(x, Q_0) = R_i^A(x, Q_0) \times f_i^p(x, Q_0)}$
- initial scale **Q_0 = 1 GeV**, NLO DGLAP evolution to all other scales Q > Q_0
- parametrize both valence distributions as

needs to be flexible enough to accommodate (anti-)shadowing, EMC effect, Fermi motion

$$\mathbf{R_v^A(x, Q_0) = \epsilon_1\, x^{\alpha_v}(1-x)^{\beta_1} \times [1 + \epsilon_2(1-x)^{\beta_2}] \times [1 + a_v(1-x)^{\beta_3}]}$$

- data do not allow to discriminate different sea quark flavors (tried in analysis)

$$\mathbf{R_s^A(x, Q_0) = R_v^A(x, Q_0)\, \frac{\epsilon_s}{\epsilon_1} \frac{1 + a_s x^{\alpha_s}}{a_s + 1}}$$

- need another modification factor for gluons

$$\mathbf{R_g^A(x, Q_0) = R_v^A(x, Q_0)\, \frac{\epsilon_g}{\epsilon_1} \frac{1 + a_g x^{\alpha_g}}{a_g + 1}}$$

quality of the fit unchanged by relating $R_{s,g}$ to common R_V

but need different normalization and small-x behavior

DSSZ global analysis - preliminaries

- use multiplicative nuclear modification factor $\mathbf{f_i^A(x, Q_0) = R_i^A(x, Q_0) \times f_i^p(x, Q_0)}$
- initial scale **Q_0 = 1 GeV**, NLO DGLAP evolution to all other scales Q > Q_0
- parametrize both valence distributions as

needs to be flexible enough to accommodate (anti-)shadowing, EMC effect, Fermi motion

$$\mathbf{R_v^A(x, Q_0) = \epsilon_1\, x^{\alpha_v}(1-x)^{\beta_1} \times [1 + \epsilon_2(1-x)^{\beta_2}] \times [1 + a_v(1-x)^{\beta_3}]}$$

- data do not allow to discriminate different sea quark flavors (tried in analysis)

$$\mathbf{R_s^A(x, Q_0) = R_v^A(x, Q_0)\, \frac{\epsilon_s}{\epsilon_1}\, \frac{1 + a_s x^{\alpha_s}}{a_s + 1}}$$

- need another modification factor for gluons

$$\mathbf{R_g^A(x, Q_0) = R_v^A(x, Q_0)\, \frac{\epsilon_g}{\epsilon_1}\, \frac{1 + a_g x^{\alpha_g}}{a_g + 1}}$$

quality of the fit unchanged by relating $R_{s,g}$ to common R_V

but need different normalization and small-x behavior

resulting "EMC effect" and "Fermi motion" for sea and gluons not constrained by data

DSSZ global analysis - preliminaries

- use multiplicative nuclear modification factor $\mathbf{f_i^A(x, Q_0) = R_i^A(x, Q_0) \times f_i^p(x, Q_0)}$
- initial scale **Q_0 = 1 GeV**, NLO DGLAP evolution to all other scales Q > Q_0
- parametrize both valence distributions as

needs to be flexible enough to accommodate (anti-)shadowing, EMC effect, Fermi motion

$$\mathbf{R_v^A(x, Q_0) = \epsilon_1 x^{\alpha_v}(1-x)^{\beta_1} \times [1 + \epsilon_2 (1-x)^{\beta_2}] \times [1 + a_v (1-x)^{\beta_3}]}$$

- data do not allow to discriminate different sea quark flavors (tried in analysis)

$$\mathbf{R_s^A(x, Q_0) = R_v^A(x, Q_0) \frac{\epsilon_s}{\epsilon_1} \frac{1 + a_s x^{\alpha_s}}{a_s + 1}}$$

- need another modification factor for gluons

$$\mathbf{R_g^A(x, Q_0) = R_v^A(x, Q_0) \frac{\epsilon_g}{\epsilon_1} \frac{1 + a_g x^{\alpha_g}}{a_g + 1}}$$

quality of the fit unchanged by relating $R_{s,g}$ to common R_V

but need different normalization and small-x behavior

resulting "EMC effect" and "Fermi motion" for sea and gluons not constrained by data

- 3 parameters constrained by charge & momentum conservation

also, fit unchanged if $\epsilon_g = \epsilon_s$

DSSZ global analysis - preliminaries

- use multiplicative nuclear modification factor $\mathbf{f_i^A(x, Q_0) = R_i^A(x, Q_0) \times f_i^p(x, Q_0)}$
- initial scale **Q_0 = 1 GeV**, NLO DGLAP evolution to all other scales Q > Q_0
- parametrize both valence distributions as

needs to be flexible enough to accommodate (anti-)shadowing, EMC effect, Fermi motion

$$\mathbf{R_v^A(x, Q_0) = \epsilon_1 x^{\alpha_v}(1-x)^{\beta_1} \times [1 + \epsilon_2 (1-x)^{\beta_2}] \times [1 + a_v (1-x)^{\beta_3}]}$$

- data do not allow to discriminate different sea quark flavors (tried in analysis)

$$\mathbf{R_s^A(x, Q_0) = R_v^A(x, Q_0) \frac{\epsilon_s}{\epsilon_1} \frac{1 + a_s x^{\alpha_s}}{a_s + 1}}$$

- need another modification factor for gluons

$$\mathbf{R_g^A(x, Q_0) = R_v^A(x, Q_0) \frac{\epsilon_g}{\epsilon_1} \frac{1 + a_g x^{\alpha_g}}{a_g + 1}}$$

quality of the fit unchanged by relating $R_{s,g}$ to common R_V

but need different normalization and small-x behavior

resulting "EMC effect" and "Fermi motion" for sea and gluons not constrained by data

- 3 parameters constrained by charge & momentum conservation

also, fit unchanged if $\epsilon_g = \epsilon_s$

total of 9 parameters per nucleus

$$\xi \in \{\alpha_v, \alpha_s, \alpha_g, \beta_1, \beta_2, \beta_3, a_v, a_s, a_g\}$$

parametrizing the A dependence

total of 9 parameters per nucleus

$\xi \in \{\alpha_{\mathbf{v}}, \alpha_{\mathbf{s}}, \alpha_{\mathbf{g}}, \beta_{\mathbf{1}}, \beta_{\mathbf{2}}, \beta_{\mathbf{3}}, \mathbf{a_v}, \mathbf{a_s}, \mathbf{a_g}\}$

- A dependence implemented as

$$\xi = \gamma_\xi + \lambda_\xi \mathbf{A}^{\delta_\xi}$$

- fit does not fix all parameters, assume

$$\delta_{\mathbf{a_g}} = \delta_{\mathbf{a_s}} \qquad \delta_{\alpha_{\mathbf{g}}} = \delta_{\alpha_{\mathbf{s}}}$$

parametrizing the A dependence

total of 9 parameters per nucleus

$$\xi \in \{\alpha_\mathbf{v}, \alpha_\mathbf{s}, \alpha_\mathbf{g}, \beta_\mathbf{1}, \beta_\mathbf{2}, \beta_\mathbf{3}, \mathbf{a_v}, \mathbf{a_s}, \mathbf{a_g}\}$$

- A dependence implemented as

$$\xi = \gamma_\xi + \lambda_\xi \mathbf{A}^{\delta_\xi}$$

- fit does not fix all parameters, assume

$$\delta_{\mathbf{a_g}} = \delta_{\mathbf{a_s}} \qquad \delta_{\alpha_\mathbf{g}} = \delta_{\alpha_\mathbf{s}}$$

25 free parameters in total

parameter	γ	λ	δ
α_v	-0.256	0.252	-0.017
α_s	0.001	-6.89×10^{-4}	0.286
α_g	1.994	-0.401	0.286
β_1	-5.564	5.36	0.0042
β_2	-59.62	69.01	0.0407
β_3	2.099	-1.878	-0.436
a_v	-0.622	1.302	-0.062
a_s	-0.980	2.33×10^{-6}	1.505
a_g	0.0018	2.35×10^{-4}	1.505

optimum NLO parameters at the input scale

A dependence of fit parameters

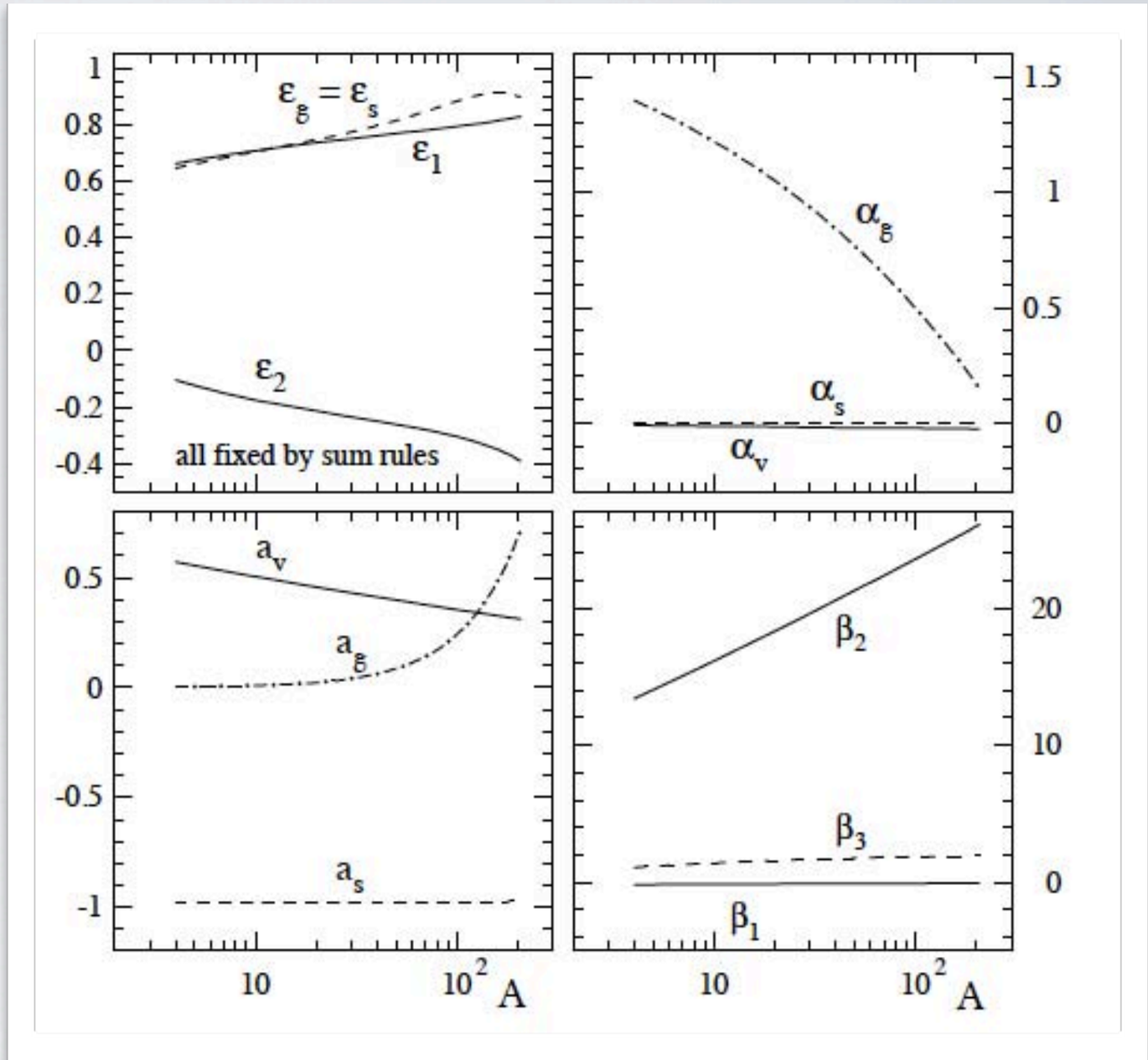

aside: A dependence of F_2^A/F_2^p @ eRHIC

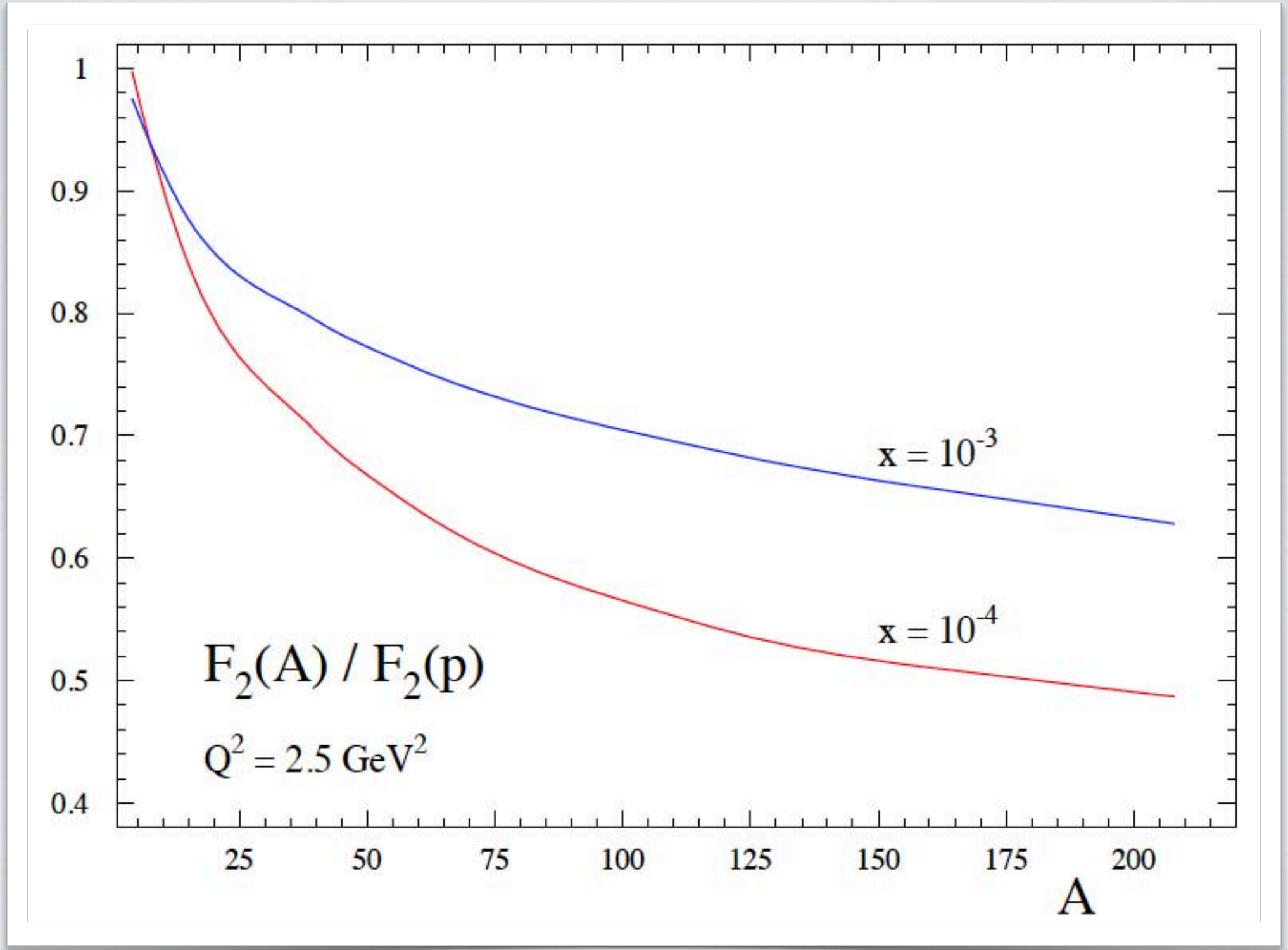

aside: A dependence of F_2^A/F_2^p @ eRHIC

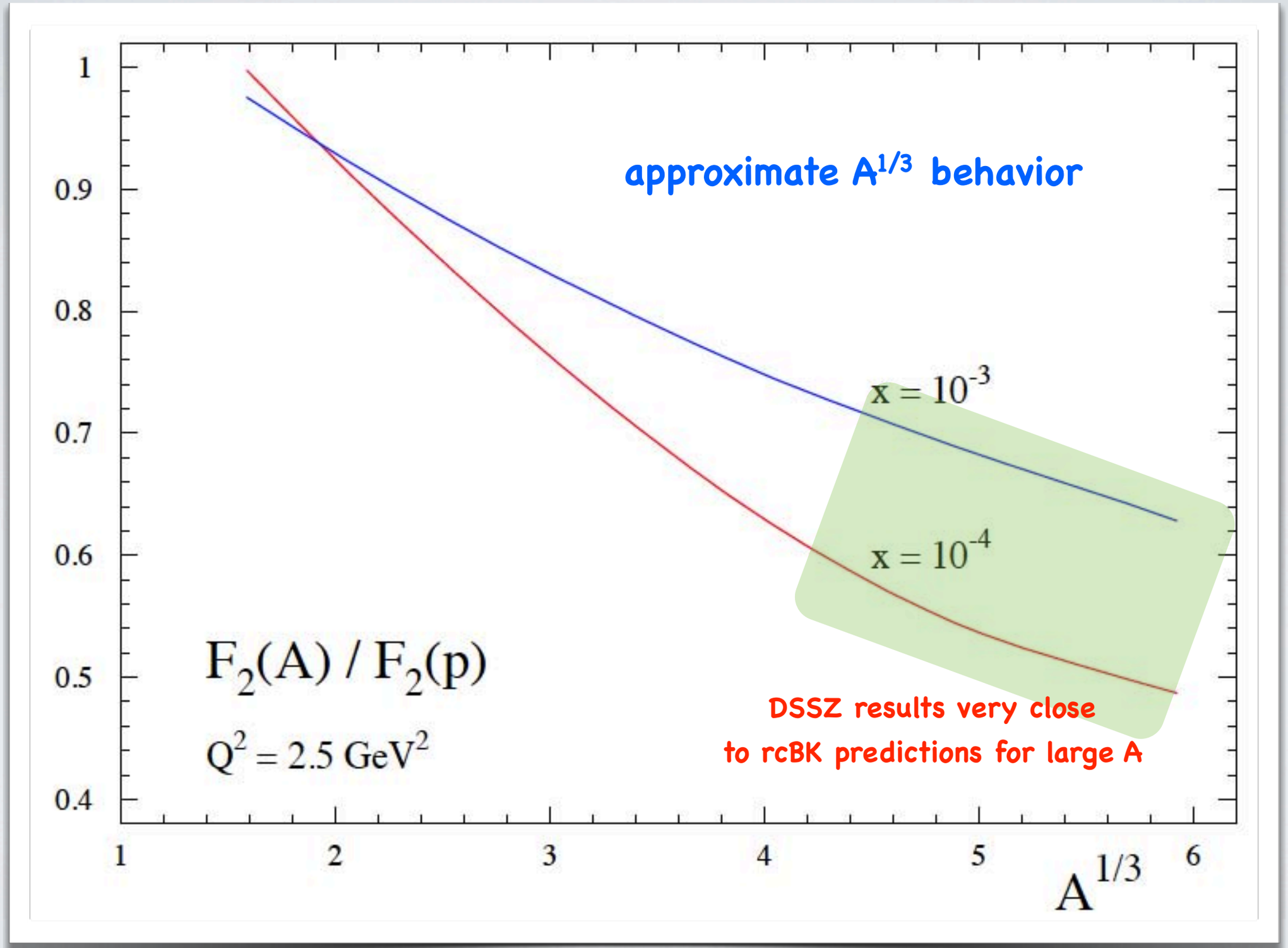

aside: A dependence of F_2^A/F_2^p @ eRHIC

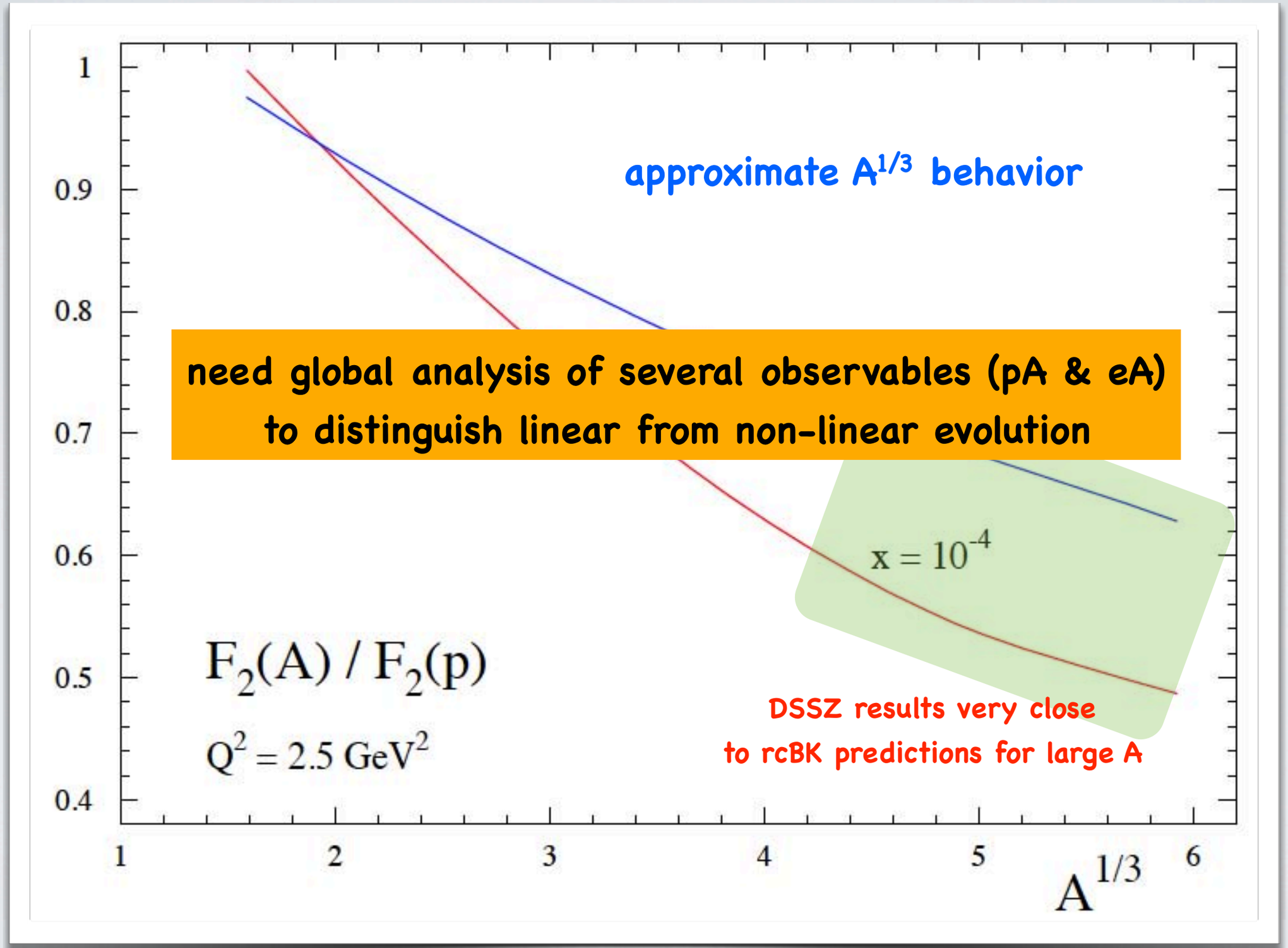

overall quality of the fit

- optimum parameters determined from standard chi-squared optimization

relative normalization or artificial weights for certain data sets

not needed/used in DSSZ analysis

$$\chi^2 \equiv \sum_i \omega_i \frac{(d\sigma_i^{exp} - d\sigma_i^{th})^2}{\Delta_i^2}$$

uncertainty for each point

DSSZ: add sys + stat in quadrature [+ theor. unc.]

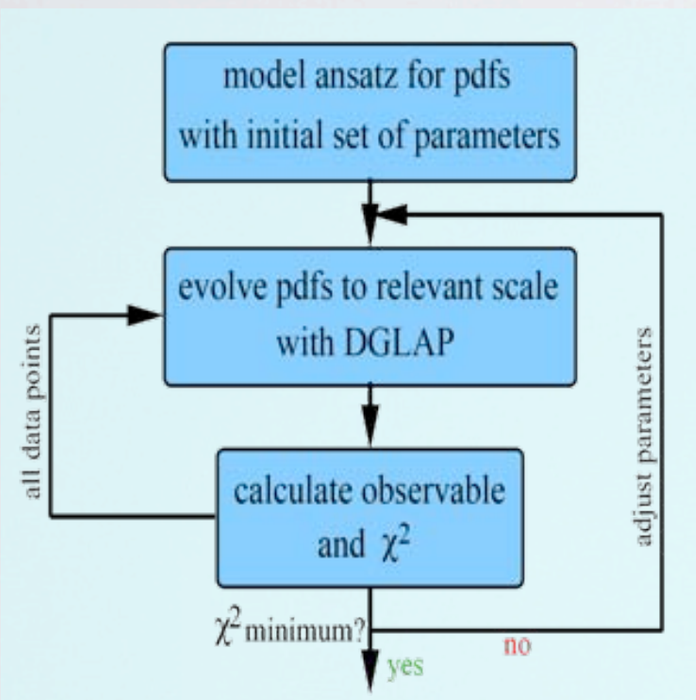

optimum set of parameters

total $\chi^2 : 1544.7/1579$pts.
$\chi^2/\text{d.o.f} : 0.994$

measurement	collaboration	# points	χ^2
F_2^{He}/F_2^D	NMC	17	18.18
	E139	18	2.71
F_2^{Li}/F_2^D	NMC	17	17.35
F_2^{Li}/F_2^D Q^2 dep.	NMC	179	197.36
F_2^{Be}/F_2^D	E139	17	44.17
F_2^{C}/F_2^D	NMC	17	27.85
	E139	7	9.66
	EMC	9	6.41
F_2^{C}/F_2^D Q^2 dep.	NMC	191	201.63
F_2^{Al}/F_2^D	E139	17	13.22
F_2^{Ca}/F_2^D	NMC	16	18.60
	E139	7	12.13
F_2^{Cu}/F_2^D	EMC	19	18.62
F_2^{Fe}/F_2^D	E139	23	34.95
F_2^{Ag}/F_2^D	E139	7	9.71
F_2^{Sn}/F_2^D	EMC	8	16.59
F_2^{Au}/F_2^D	E139	18	10.46
F_2^{C}/F_2^{Li}	NMC	24	33.17
F_2^{Ca}/F_2^{Li}	NMC	24	25.31
F_2^{Be}/F_2^{C}	NMC	15	11.76
F_2^{Al}/F_2^{C}	NMC	15	6.93
F_2^{Ca}/F_2^{C}	NMC	15	7.71
F_2^{Ca}/F_2^{C}	NMC	24	26.09
F_2^{Fe}/F_2^{C}	NMC	15	10.38
F_2^{Sn}/F_2^{C}	NMC	15	4.69
F_2^{Sn}/F_2^{C} Q^2 dep.	NMC	145	102.31
F_2^{Pb}/F_2^{C}	NMC	15	9.57
$F_2^{\nu Fe}$	NuTeV	78	109.65
$F_3^{\nu Fe}$	NuTeV	75	79.78
$F_2^{\nu Fe}$	CDHSW	120	108.20
$F_3^{\nu Fe}$	CDHSW	133	90.57
$F_2^{\nu Pb}$	CHORUS	63	20.42
$F_3^{\nu Pb}$	CHORUS	63	79.58
$d\sigma_{DY}^{C}/d\sigma_{DY}^{D}$	E772	9	9.87
$d\sigma_{DY}^{Ca}/d\sigma_{DY}^{D}$	E772	9	5.38
$d\sigma_{DY}^{Fe}/d\sigma_{DY}^{D}$	E772	9	9.77
$d\sigma_{DY}^{W}/d\sigma_{DY}^{D}$	E772	9	19.29
$d\sigma_{DY}^{Fe}/d\sigma_{DY}^{Be}$	E866	28	20.34
$d\sigma_{DY}^{W}/d\sigma_{DY}^{Be}$	E866	28	26.07
$d\sigma_{\pi^0}^{dAu}/d\sigma_{\pi^0}^{pp}$	PHENIX	20	27.71
$d\sigma_{\pi^0}^{dAu}/d\sigma_{\pi^0}^{pp}$	STAR	11	3.92
$d\sigma_{\pi^\pm}^{dAu}/d\sigma_{\pi^\pm}^{pp}$	STAR	30	36.63
Total		1579	1544.70

NC DIS
897.5/894

CC DIS
488.2/532

Drell Yan
90.7/92

dAu->piX 68.3/61

overall quality of the fit

- optimum parameters determined from standard chi-squared optimization

relative normalization or artificial weights for certain data sets

not needed/used in DSSZ analysis

$$\chi^2 \equiv \sum_i \omega_i \frac{(d\sigma_i^{exp} - d\sigma_i^{th})^2}{\Delta_i^2}$$

uncertainty for each point

DSSZ: add sys + stat in quadrature [+ theor. unc.]

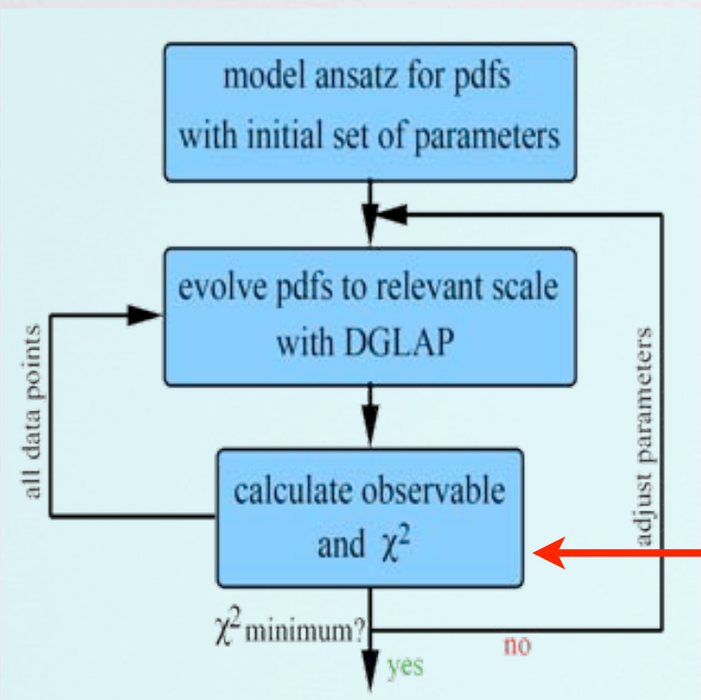

NLO analysis: potential bottleneck

optimum set of parameters

total χ^2 : 1544.7/1579pts.
χ^2/d.o.f : 0.994

measurement	collaboration	# points	χ^2
F_2^{He}/F_2^D	NMC	17	18.18
	E139	18	2.71
F_2^{Li}/F_2^D	NMC	17	17.35
F_2^{Li}/F_2^D Q^2 dep.	NMC	179	197.36
F_2^{Be}/F_2^D	E139	17	44.17
F_2^{C}/F_2^D	NMC	17	27.85
	E139	7	9.66
	EMC	9	6.41
F_2^{C}/F_2^D Q^2 dep.	NMC	191	201.63
F_2^{Al}/F_2^D	E139	17	13.22
F_2^{Ca}/F_2^D	NMC	16	18.60
	E139	7	12.13
F_2^{Cu}/F_2^D	EMC	19	18.62
F_2^{Fe}/F_2^D	E139	23	34.95
F_2^{Ag}/F_2^D	E139	7	9.71
F_2^{Sn}/F_2^D	EMC	8	16.59
F_2^{Au}/F_2^D	E139	18	10.46
F_2^{C}/F_2^{Li}	NMC	24	33.17
F_2^{Ca}/F_2^{Li}	NMC	24	25.31
F_2^{Be}/F_2^{C}	NMC	15	11.76
F_2^{Al}/F_2^{C}	NMC	15	6.93
F_2^{Ca}/F_2^{C}	NMC	15	7.71
F_2^{Ca}/F_2^{C}	NMC	24	26.09
F_2^{Fe}/F_2^{C}	NMC	15	10.38
F_2^{Sn}/F_2^{C}	NMC	15	4.69
F_2^{Sn}/F_2^{C} Q^2 dep.	NMC	145	102.31
F_2^{Pb}/F_2^{C}	NMC	15	9.57
$F_2^{\nu Fe}$	NuTeV	78	109.65
$F_3^{\nu Fe}$	NuTeV	75	79.78
$F_2^{\nu Fe}$	CDHSW	120	108.20
$F_3^{\nu Fe}$	CDHSW	133	90.57
$F_2^{\nu Pb}$	CHORUS	63	20.42
$F_3^{\nu Pb}$	CHORUS	63	79.58
$d\sigma_{DY}^{C}/d\sigma_{DY}^{D}$	E772	9	9.87
$d\sigma_{DY}^{Ca}/d\sigma_{DY}^{D}$	E772	9	5.38
$d\sigma_{DY}^{Fe}/d\sigma_{DY}^{D}$	E772	9	9.77
$d\sigma_{DY}^{W}/d\sigma_{DY}^{D}$	E772	9	19.29
$d\sigma_{DY}^{Fe}/d\sigma_{DY}^{Be}$	E866	28	20.34
$d\sigma_{DY}^{W}/d\sigma_{DY}^{Be}$	E866	28	26.07
$d\sigma_{\pi^0}^{dAu}/d\sigma_{\pi^0}^{pp}$	PHENIX	20	27.71
$d\sigma_{\pi^0}^{dAu}/d\sigma_{\pi^0}^{pp}$	STAR	11	3.92
$d\sigma_{\pi^\pm}^{dAu}/d\sigma_{\pi^\pm}^{pp}$	STAR	30	36.63
Total		1579	1544.70

NC DIS 897.5/894

CC DIS 488.2/532

Drell Yan 90.7/92

dAu->piX 68.3/61

technical aspects: Mellin technique

source of trouble: ubiquitous convolutions

$$\otimes: \quad g(x) = \int_x^1 \frac{dy}{y}\, f(y)\, P\left(\frac{x}{y}\right)$$

$$d\sigma^A_{DIS} = \sum_i f_i^A \otimes d\hat{\sigma}_{i\gamma^* \to X}$$

$$d\sigma^A_{DY} = \sum_{ij} f_i^p \otimes f_j^A \otimes d\hat{\sigma}_{ij \to l\bar{l}X}$$

$$d\sigma^A_{dA \to \pi X} = \sum_{ijk} f_i^d \otimes f_j^A \otimes d\hat{\sigma}_{ij \to kX} \otimes D_k^{A,\pi}$$

increasing level of painfulness

technical aspects: Mellin technique

source of trouble: ubiquitous convolutions

$$\otimes: \quad g(x) = \int_x^1 \frac{dy}{y}\, f(y)\, P(\frac{x}{y})$$

$$d\sigma^A_{DIS} = \sum_i f^A_i \otimes d\hat{\sigma}_{i\gamma^* \to X}$$

increasing level of painfulness

$$d\sigma^A_{DY} = \sum_{ij} f^p_i \otimes f^A_j \otimes d\hat{\sigma}_{ij \to l\bar{l}X}$$

$$d\sigma^A_{dA \to \pi X} = \sum_{ijk} f^d_i \otimes f^A_j \otimes d\hat{\sigma}_{ij \to kX} \otimes D^{A,\pi}_k$$

"natural language" for pQCD calculations: **Mellin moments**

$$\phi(N) \equiv \int_0^1 dx\, x^{N-1}\, \phi(x)$$

integral transformation
complex Mellin N space

$$\phi(x) \equiv \frac{1}{2\pi i} \int_{C_N} dN\, x^{-N}\, \phi(N)$$

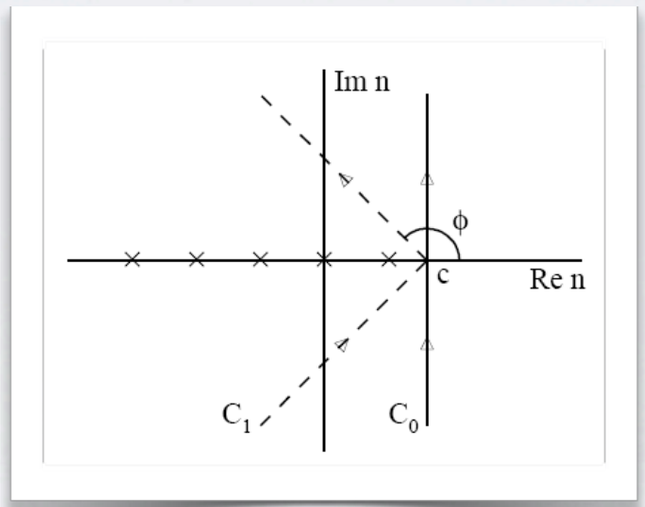

R.H. Mellin
Finnish mathematician
1854 - 1933

technical aspects: Mellin technique

source of trouble: ubiquitous convolutions

$$\otimes: \quad g(x) = \int_x^1 \frac{dy}{y}\, f(y)\, P(\frac{x}{y})$$

$$d\sigma^A_{DIS} = \sum_i f_i^A \otimes d\hat{\sigma}_{i\gamma^* \to X}$$

increasing level of painfulness

$$d\sigma^A_{DY} = \sum_{ij} f_i^p \otimes f_j^A \otimes d\hat{\sigma}_{ij \to l\bar{l}X}$$

$$d\sigma^A_{dA \to \pi X} = \sum_{ijk} f_i^d \otimes f_j^A \otimes d\hat{\sigma}_{ij \to kX} \otimes D_k^{A,\pi}$$

"natural language" for pQCD calculations: **Mellin moments**

$$\phi(N) \equiv \int_0^1 dx\, x^{N-1}\, \phi(x)$$

integral transformation
complex Mellin N space

$$\phi(x) \equiv \frac{1}{2\pi i} \int_{C_N} dN\, x^{-N}\, \phi(N)$$

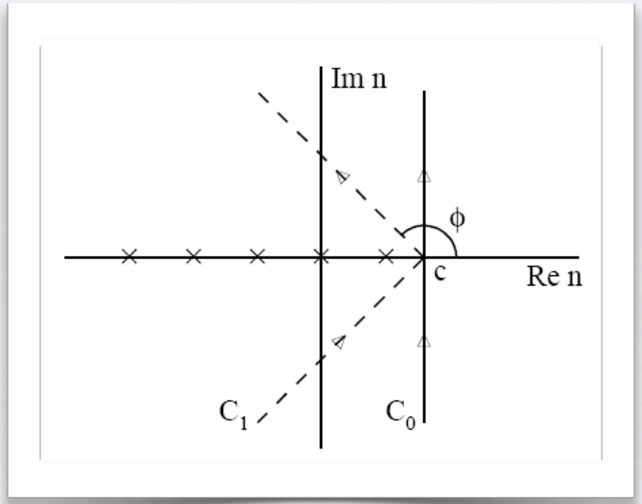

R.H. Mellin
Finnish mathematician
1854 - 1933

well-known property: convolutions factorize into simple products $\quad g(n) = f(n) \times P(n)$

- ✓ analytic solution to DGLAP evolution equations in Mellin space — numerically very efficient
- ✓ analytic expressions for DIS coefficient functions in Mellin space — no K factor approximations needed
- ✓ efficient numerical way to deal with complicated pp/pA cross sections

MS, Vogelsang - hep-ph/0108241

technical aspects: heavy flavors in CC DIS

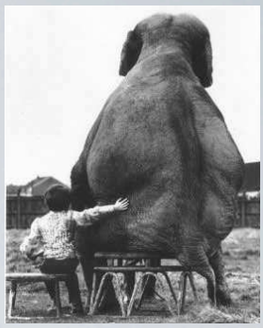

charm production in CC DIS is of particular interest

idea: at LO $\mathbf{W^+ s' \to c}$ $\mathbf{s' \equiv |V_{cs}|^2 s + |V_{cd}|^2 d}$

- important to include charm mass through slow rescaling prescription $\xi = x(1 + m^2/Q^2)$ Barnett '76
- prescription also needed for consistent factorization of collinear singularities in NLO Gottschalk '81

technical aspects: heavy flavors in CC DIS

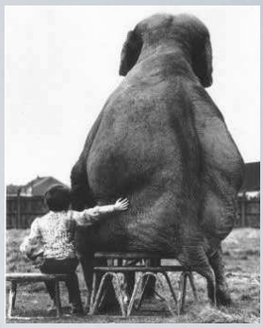

charm production in CC DIS is of particular interest

idea: at LO $\mathbf{W^+ s' \to c}$ $\mathbf{s' \equiv |V_{cs}|^2 s + |V_{cd}|^2 d}$

- important to include charm mass through slow rescaling prescription $\xi = x(1 + m^2/Q^2)$ Barnett '76
- prescription also needed for consistent factorization of collinear singularities in NLO Gottschalk '81

used to extract strangeness from CC neutrino data in proton PDF fits

need to control nuclear corrections for Fe and Pb targets

technical aspects: heavy flavors in CC DIS

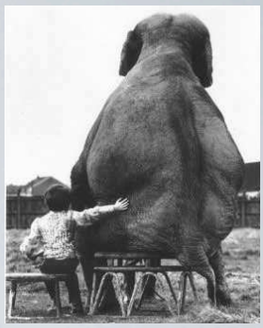

charm production in CC DIS is of particular interest

idea: at LO $\mathbf{W^+ s' \to c}$ $\mathbf{s' \equiv |V_{cs}|^2 s + |V_{cd}|^2 d}$

- important to include charm mass through slow rescaling prescription $\xi = x(1 + m^2/Q^2)$ Barnett '76
- prescription also needed for consistent factorization of collinear singularities in NLO Gottschalk '81

used to extract strangeness from CC neutrino data in proton PDF fits

need to control nuclear corrections for Fe and Pb targets

complication: gluonic contributions in NLO Gottschalk '81; Gluck, Kretzer, Reya '96; Kretzer, MS '99

- dilute sensitivity to strangeness $\mathbf{W\, g \to c\, \bar{s}'}$
- keeping charm mass gets more complicated

$$\mathcal{F}_i^c(x) = s'(\xi) + \frac{\alpha_s}{2\pi} \int_\xi^1 \frac{d\zeta}{\zeta} \left[H_i^{(1),q}(\zeta)\, s'(\frac{\xi}{\zeta}) + H_i^{(1),g}(\zeta)\, g(\frac{\xi}{\zeta}) \right]$$

- make use of recently obtained expressions in Mellin space Blumlein, Hasselhuhn, Kovacikova, Moch

$$\mathcal{F}_i^c(N) = s'(N) + \frac{\alpha_s}{2\pi} \left[H_i^{(1),q}(N)\, s'(N) + H_i^{(1),g}(N)\, g(N) \right]$$

technical aspects: heavy flavors in CC DIS

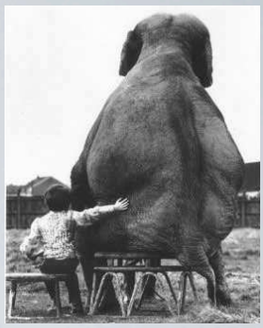

charm production in CC DIS is of particular interest

idea: at LO $\mathbf{W^+ s' \to c}$ $\quad \mathbf{s' \equiv |V_{cs}|^2 s + |V_{cd}|^2 d}$

- important to include charm mass through slow rescaling prescription $\xi = x(1 + m^2/Q^2)$ Barnett '76
- prescription also needed for consistent factorization of collinear singularities in NLO Gottschalk '81

used to extract strangeness from CC neutrino data in proton PDF fits

need to control nuclear corrections for Fe and Pb targets

complication: gluonic contributions in NLO Gottschalk '81; Gluck, Kretzer, Reya '96; Kretzer, MS '99

- dilute sensitivity to strangeness $\mathbf{W\, g \to c\, \bar{s}'}$
- keeping charm mass gets more complicated

$$\mathcal{F}_i^c(x) = s'(\xi) + \frac{\alpha_s}{2\pi} \int_\xi^1 \frac{d\zeta}{\zeta} \left[H_i^{(1),q}(\zeta)\, s'\!\left(\frac{\xi}{\zeta}\right) + H_i^{(1),g}(\zeta)\, g\!\left(\frac{\xi}{\zeta}\right) \right]$$

- make use of recently obtained expressions in Mellin space Blumlein, Hasselhuhn, Kovacikova, Moch

$$\mathcal{F}_i^c(N) = s'(N) + \frac{\alpha_s}{2\pi} \left[H_i^{(1),q}(N)\, s'(N) + H_i^{(1),g}(N)\, g(N) \right]$$

positive impact on quality of our fit to CC DIS data: 26% gain in χ^2

review of charged lepton DIS data

fit all "classic" EMC, NMC, and E-139 DIS data

- impose cut $\mathbf{Q^2 > 1\,GeV^2}$
- $\chi^2 = 857.5/894\text{pts.}$
- neglect, as usual, nuclear effects in deuterium

  found to be small in Hirai, Kumano, Nagai

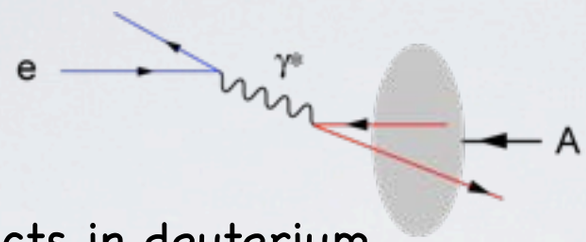

recall

main constraint from DIS data

$0.01 \lesssim x \lesssim 0.8$

$$F_2^A(N) = x \sum_q e_q^2 \Big[(q^A(N) + \bar{q}^A(N))(1 + \frac{\alpha_s}{2\pi} C_2^q(N)) + \frac{\alpha_s}{2\pi} C_2^g(N) g^A(N) \Big]$$

weak indirect constraint from scale evolution

review of charged lepton DIS data

fit all "classic" EMC, NMC, and E-139 DIS data

- impose cut $Q^2 > 1\,\mathrm{GeV}^2$
- $\chi^2 = 857.5/894\mathrm{pts.}$
- neglect, as usual, nuclear effects in deuterium
  found to be small in Hirai, Kumano, Nagai

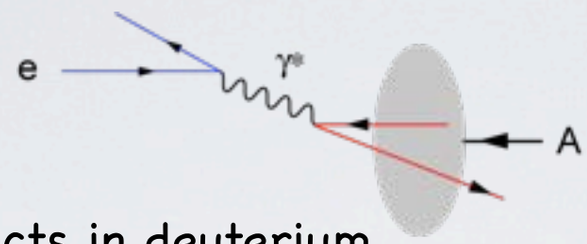

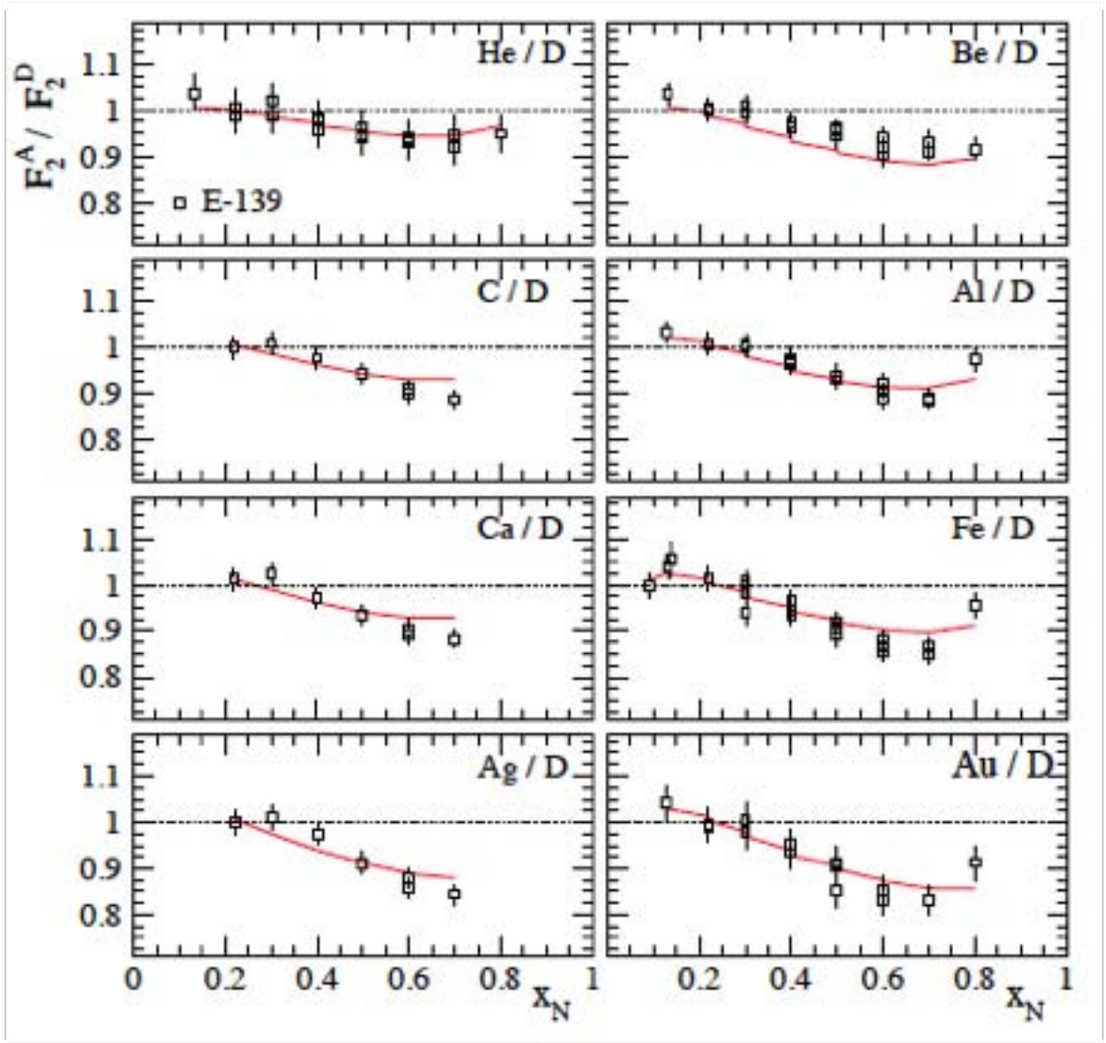

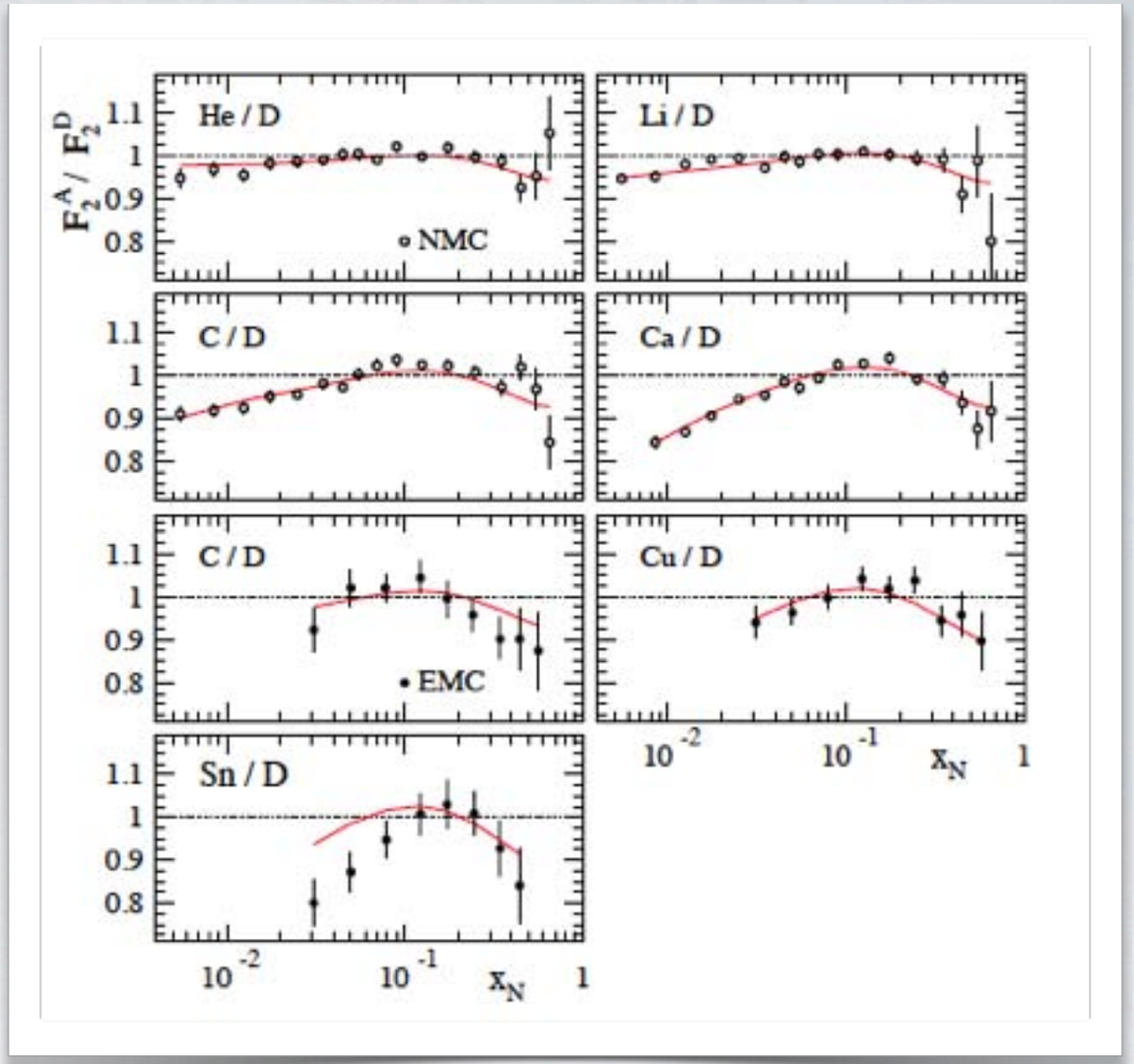

recall

main constraint from DIS data $0.01 \lesssim x \lesssim 0.8$

$$F_2^A(N) = x \sum_q e_q^2 \Big[(q^A(N) + \bar{q}^A(N))(1 + \frac{\alpha_s}{2\pi} C_2^q(N)) + \frac{\alpha_s}{2\pi} C_2^g(N) g^A(N) \Big]$$

weak indirect constraint from scale evolution

Drell Yan di-muon data

fit all E772 and E866 DY pA data

- di-muons have inv. mass M > 4 GeV (sets scale)
- $\chi^2 = 90.7/92\text{pts.}$

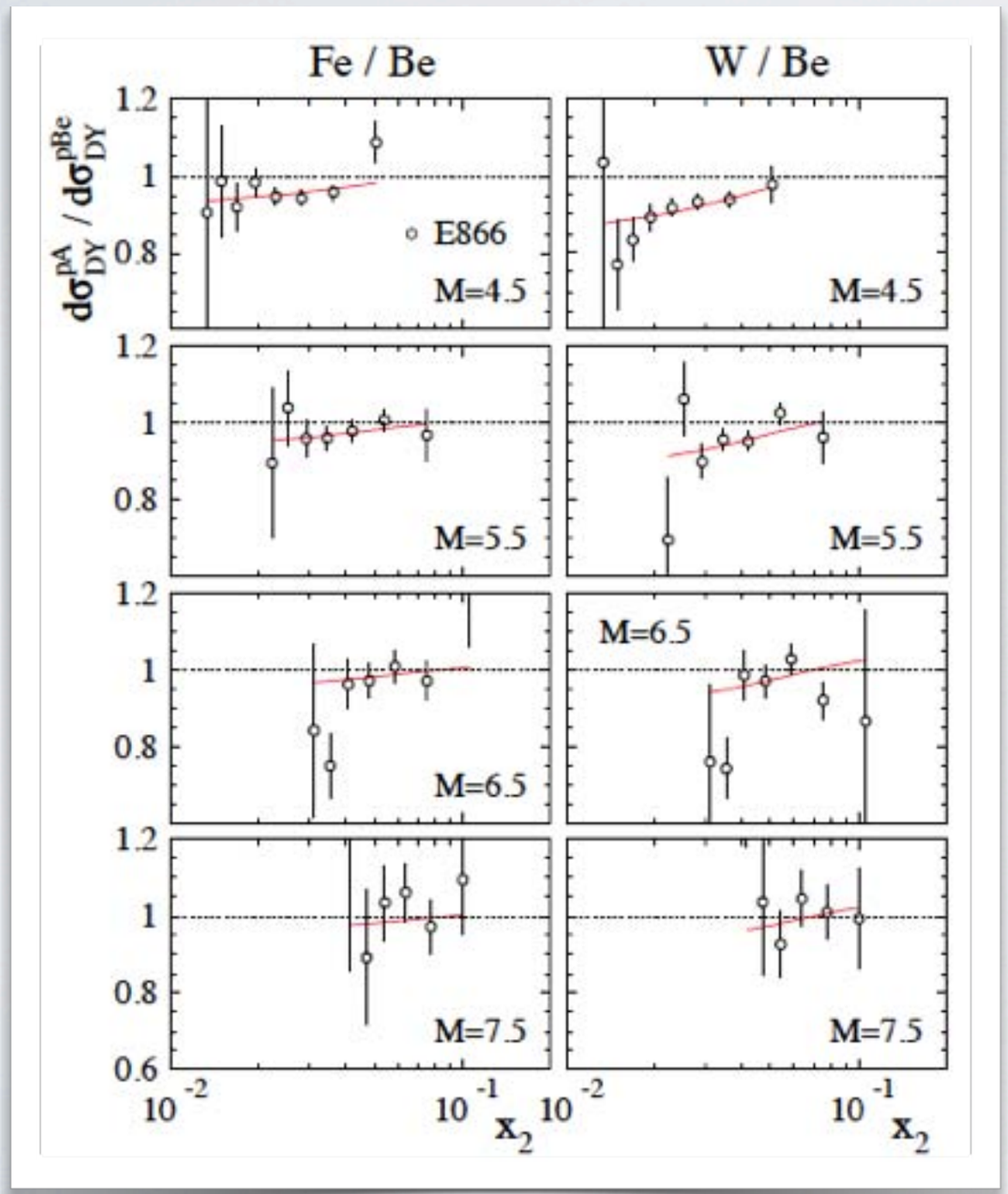

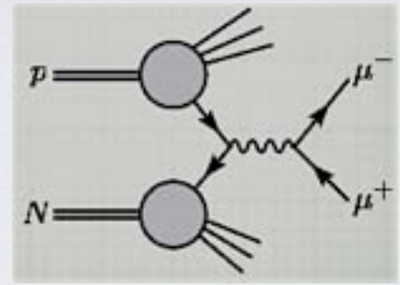

$$x_{1,2} = \sqrt{M^2/s}\, e^{\pm y}$$

$$\frac{d^2\sigma}{dMdy} = \frac{4\pi\alpha^2}{9M^3} \sum_{ij} \int dx_1 dx_2\, f_i^p(x_1)\, f_j^A(x_2)\, \frac{d\hat{\sigma}_{ij}}{dMdy}$$

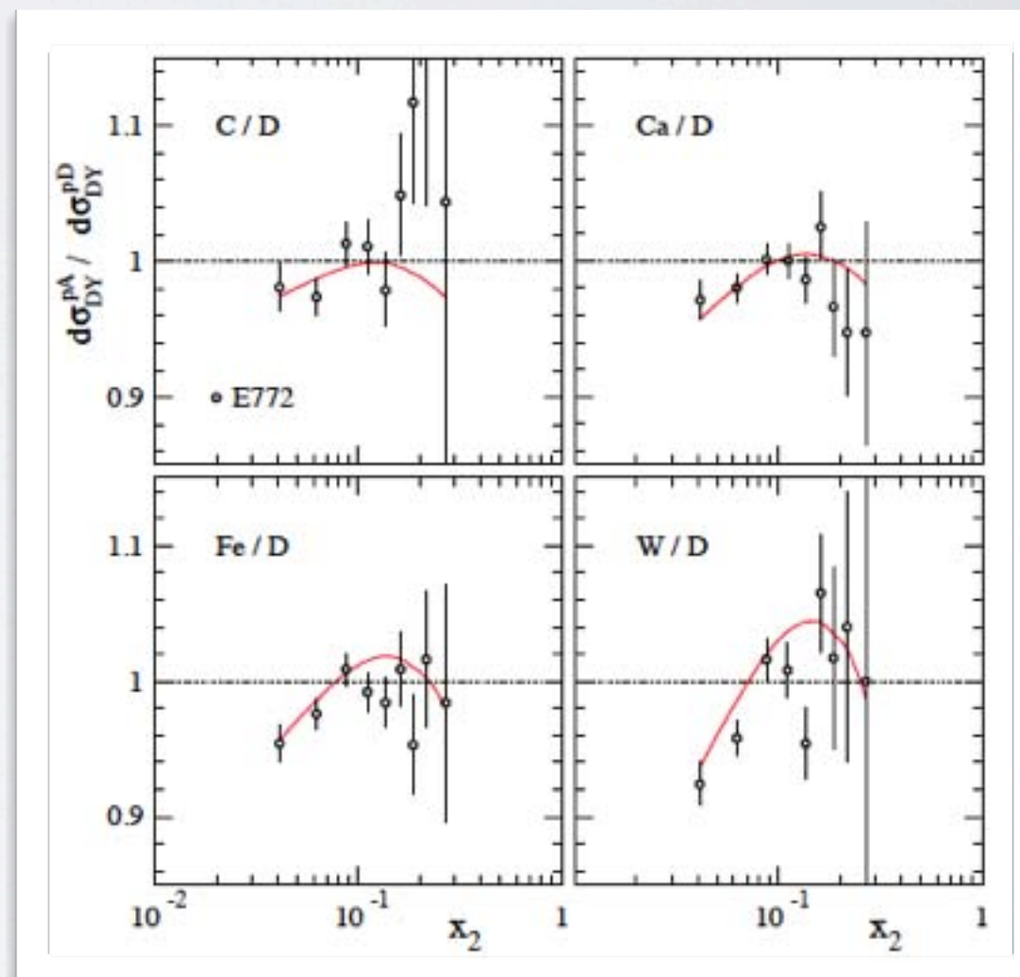

Drell Yan di-muon data

fit all E772 and E866 DY pA data

- di-muons have inv. mass M > 4 GeV (sets scale)
- $\chi^2 = 90.7/92\text{pts.}$

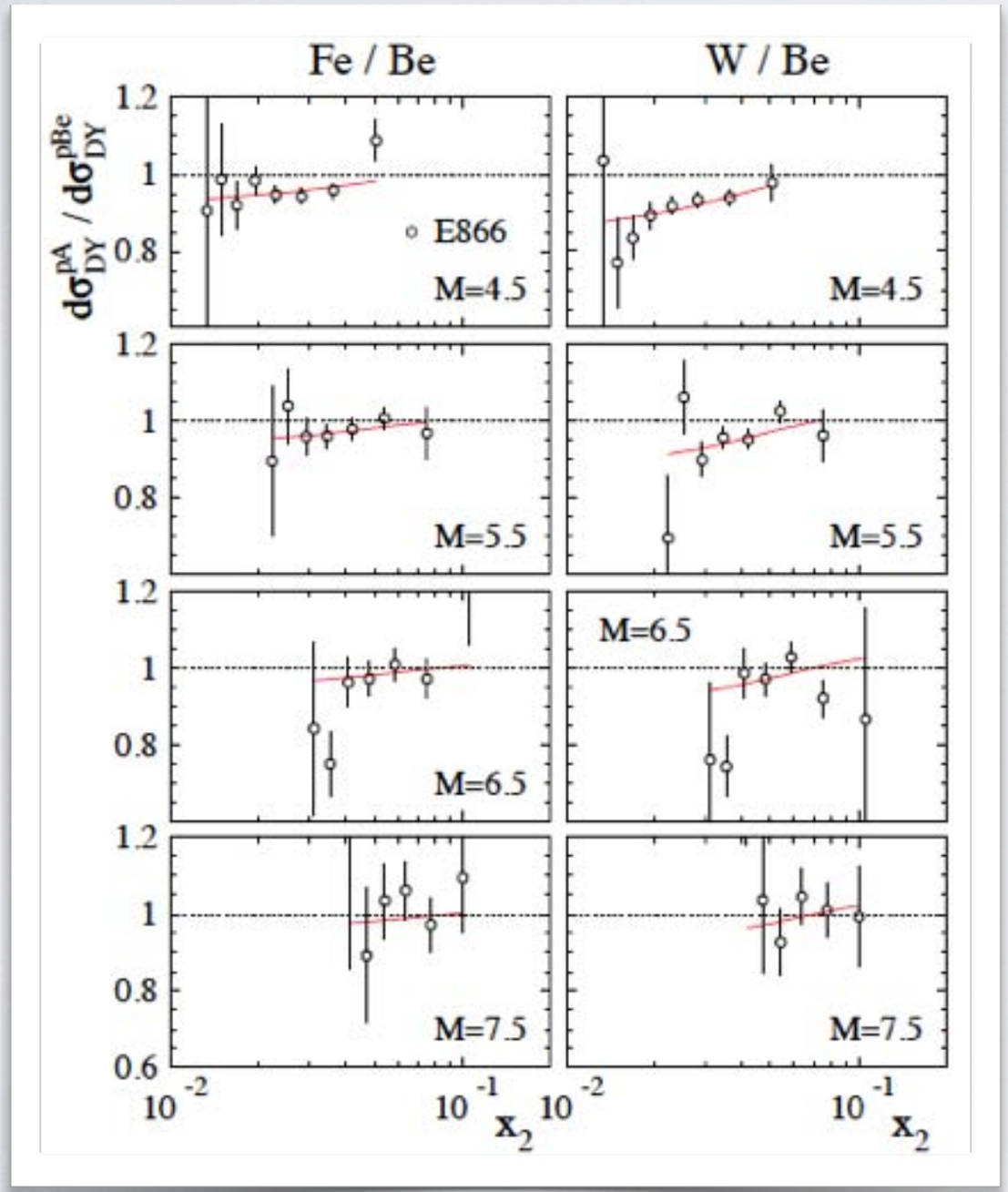

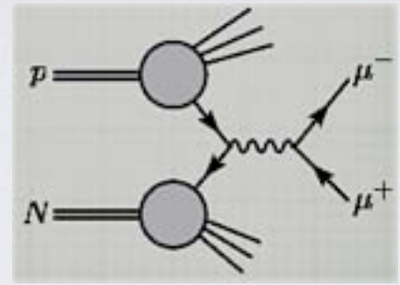

$$x_{1,2} = \sqrt{M^2/s}\, e^{\pm y}$$

DY data mainly help to disentangle val/sea quarks gluons through evolution

$$\frac{d^2\sigma}{dMdy} = \frac{4\pi\alpha^2}{9M^3} \sum_{ij} \int dx_1 dx_2\, f_i^p(x_1)\, f_j^A(x_2)\, \frac{d\hat{\sigma}_{ij}}{dMdy}$$

$x_2 \in [0.01, 0.2]$

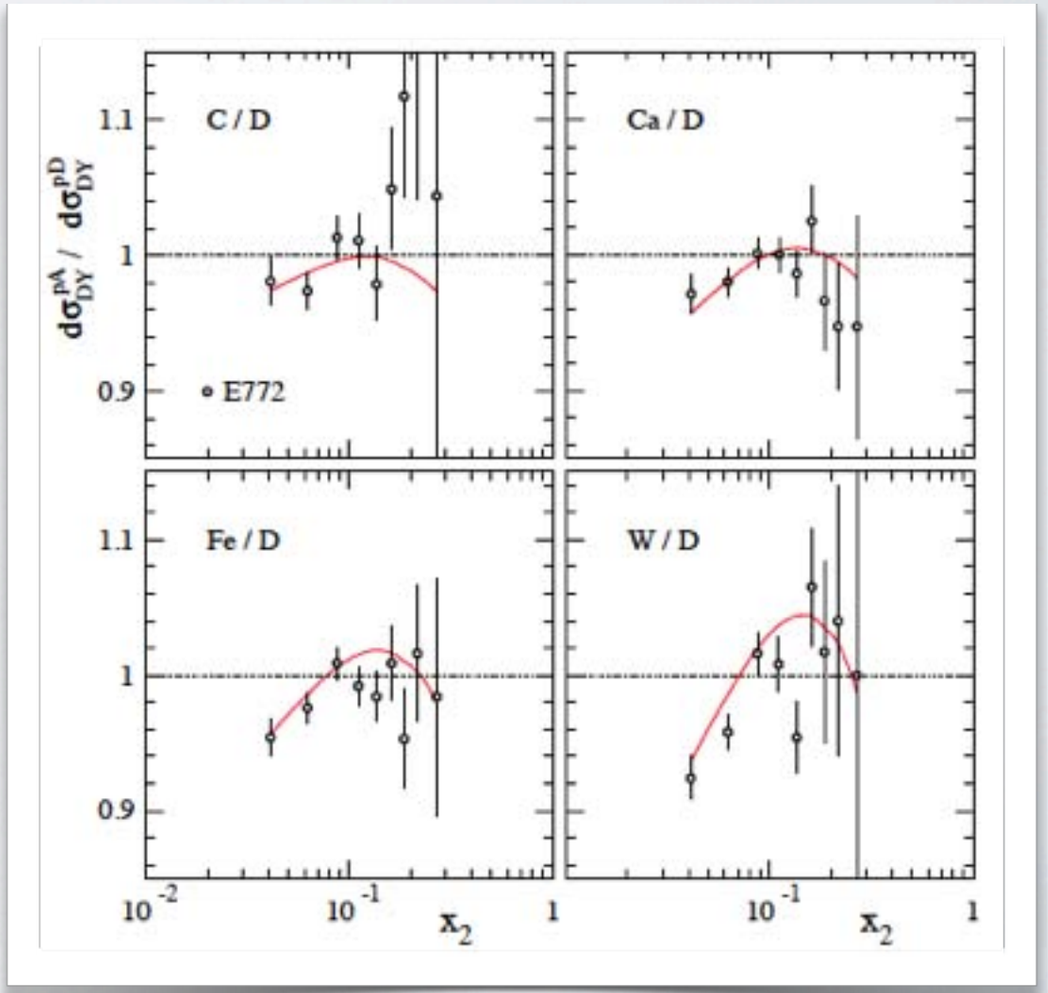

Drell Yan di-muon data

fit all E772 and E866 DY pA data

- di-muons have inv. mass M > 4 GeV (sets scale)
- $\chi^2 = 90.7/92\text{pts.}$

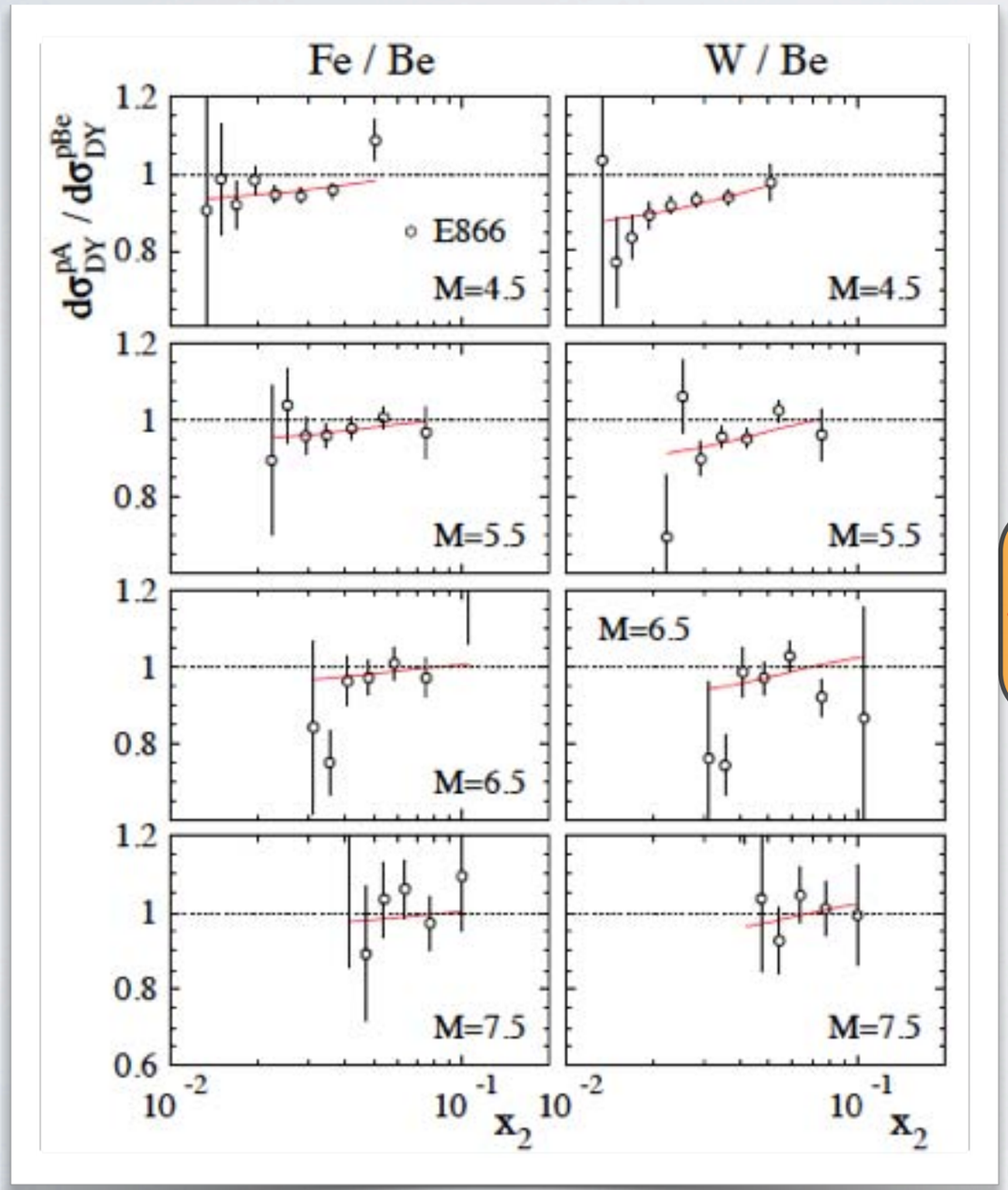

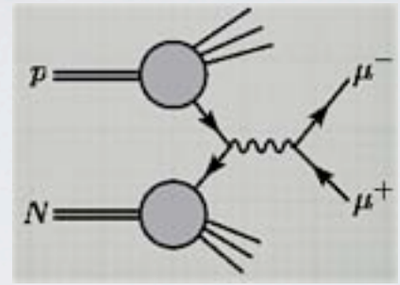

$$x_{1,2} = \sqrt{M^2/s}\, e^{\pm y}$$

DY data mainly help to disentangle val/sea quarks gluons through evolution

$$\frac{d^2\sigma}{dMdy} = \frac{4\pi\alpha^2}{9M^3} \sum_{ij} \int dx_1 dx_2\, f_i^p(x_1)\, f_j^A(x_2)\, \frac{d\hat{\sigma}_{ij}}{dMdy}$$

$x_2 \in [0.01, 0.2]$

"evidence" for shadowing of sea quarks

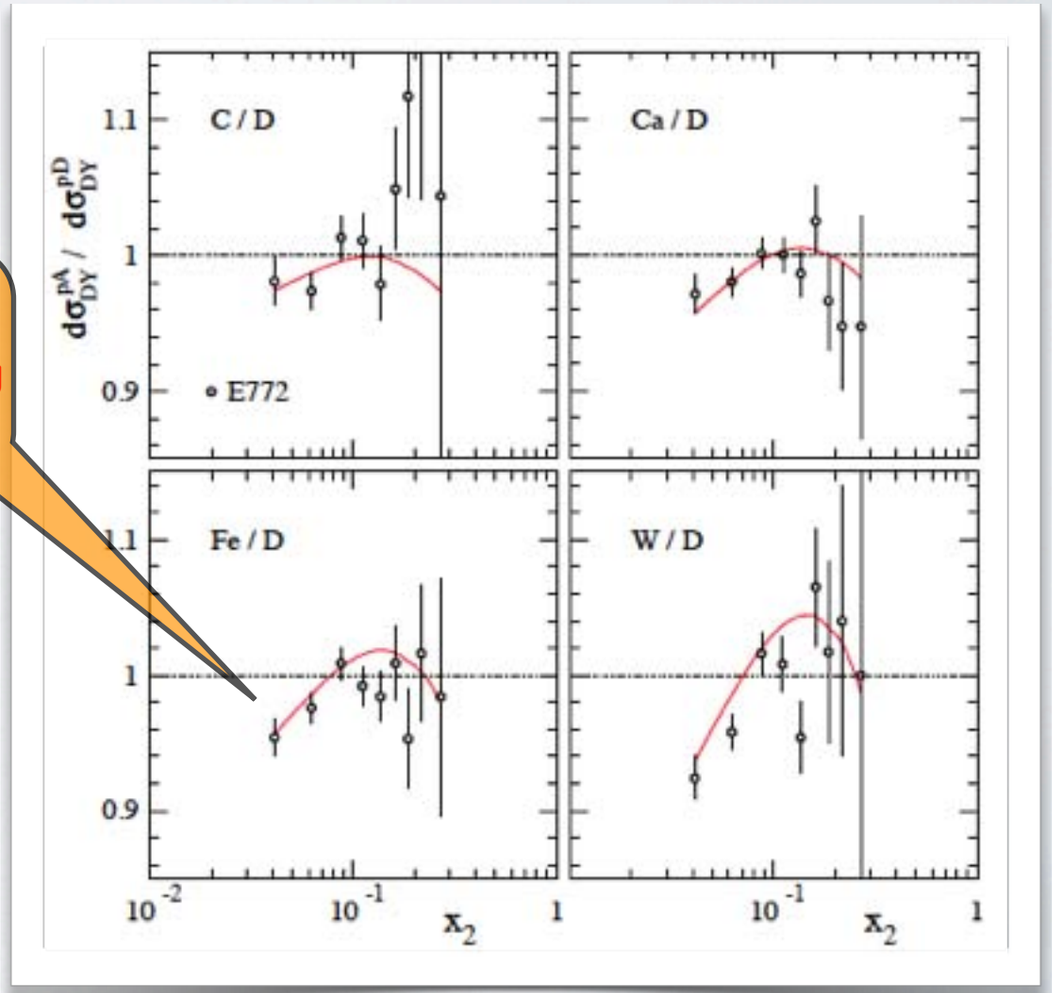

CC neutrino DIS data

fit CDHSW, NuTeV, and CHORUS str. fct. data

substantial interest:

- nCTEQ claim of "**factorization breaking**" for nPDFs
- neutrino data are a vital constraint on strangeness (and help to separate quark flavors) in proton PDF fits

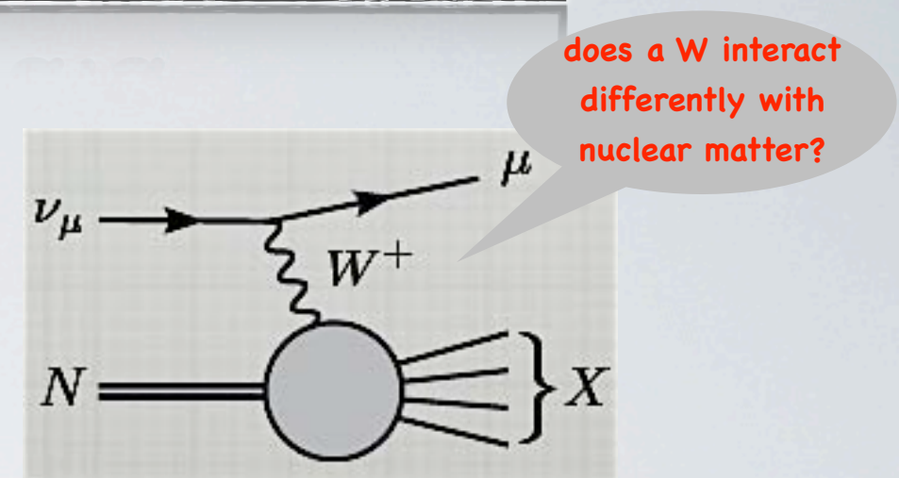

$$\frac{d^2\sigma^{\nu A,\bar{\nu}A}}{dxdy} \simeq xy^2 F_1^{\nu A,\bar{\nu}A} + (1-y)F_2^{\nu A,\bar{\nu}A} \pm xy(1-\frac{y}{2})F_3^{\nu A,\bar{\nu}A}$$

CC neutrino DIS data

fit CDHSW, NuTeV, and CHORUS str. fct. data

substantial interest:

- nCTEQ claim of "**factorization breaking**" for nPDFs
- neutrino data are a vital constraint on strangeness (and help to separate quark flavors) in proton PDF fits

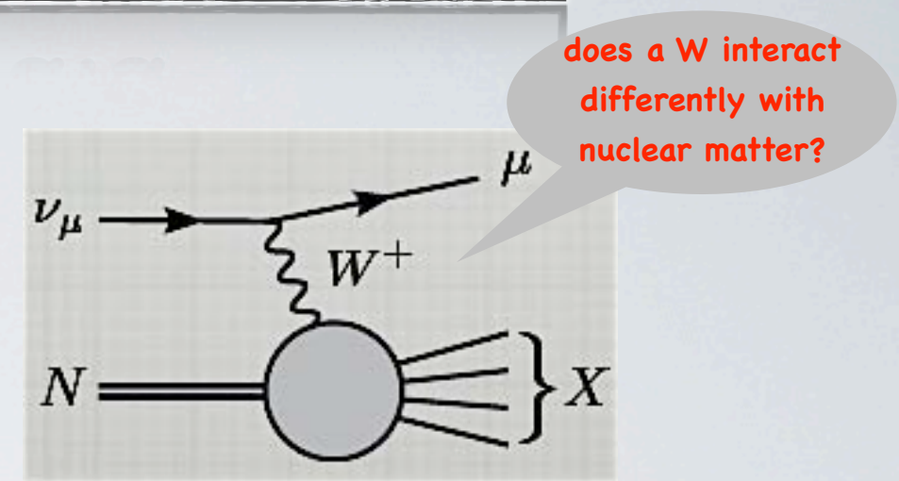

$$\frac{d^2\sigma^{\nu A,\bar{\nu}A}}{dxdy} \simeq xy^2 F_1^{\nu A,\bar{\nu}A} + (1-y)F_2^{\nu A,\bar{\nu}A} \pm xy(1-\frac{y}{2})F_3^{\nu A,\bar{\nu}A}$$

here is how the "tension" story goes

- CC DIS data probe different combinations of up-/down-type quarks than charged-lepton DIS
- neutrino and antineutrino beams probe 4 different structure functions

$$F_2^{\nu A}(x_N) \simeq x_N[\bar{u}^A + \bar{c}^A + d^A + s^A](x_N)$$

$$F_2^{\bar{\nu} A}(x_N) \simeq x_N[u^A + c^A + \bar{d}^A + \bar{s}^A](x_N)$$

$$F_3^{\nu A}(x_N) \simeq [-(\bar{u}^A + \bar{c}^A) + d^A + s^A](x_N)$$

$$F_3^{\bar{\nu} A}(x_N) \simeq [u^A + c^A - (\bar{d}^A + \bar{s}^A)](x_N)$$

CC neutrino DIS data

fit CDHSW, NuTeV, and CHORUS str. fct. data

substantial interest:

- nCTEQ claim of "**factorization breaking**" for nPDFs
- neutrino data are a vital constraint on strangeness (and help to separate quark flavors) in proton PDF fits

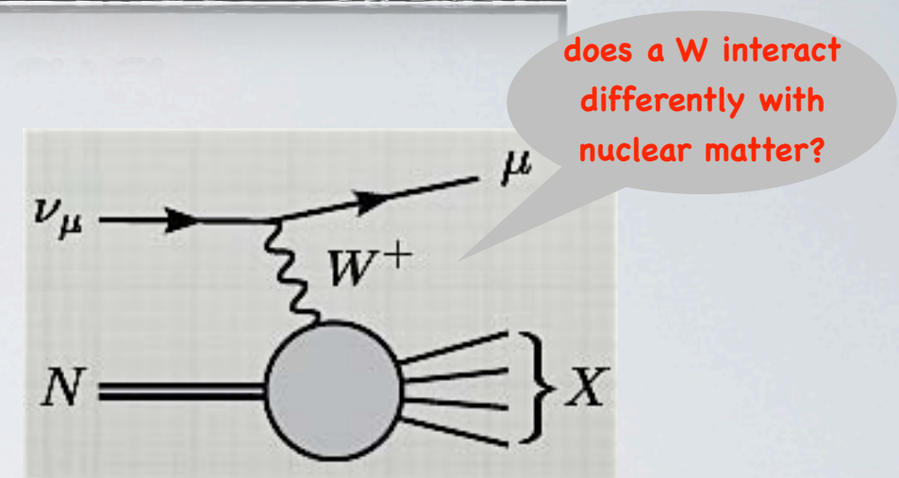

$$\frac{d^2\sigma^{\nu A,\bar{\nu}A}}{dxdy} \simeq xy^2 F_1^{\nu A,\bar{\nu}A} + (1-y)F_2^{\nu A,\bar{\nu}A} \pm xy(1-\frac{y}{2})F_3^{\nu A,\bar{\nu}A}$$

here is how the "tension" story goes

- CC DIS data probe different combinations of up-/down-type quarks than charged-lepton DIS
- neutrino and antineutrino beams probe 4 different structure functions

$$F_2^{\nu A}(x_N) \simeq x_N[\bar{u}^A + \bar{c}^A + d^A + s^A](x_N)$$

$$F_2^{\bar{\nu} A}(x_N) \simeq x_N[u^A + c^A + \bar{d}^A + \bar{s}^A](x_N)$$

$$F_3^{\nu A}(x_N) \simeq [-(\bar{u}^A + \bar{c}^A) + d^A + s^A](x_N)$$

$$F_3^{\bar{\nu} A}(x_N) \simeq [u^A + c^A - (\bar{d}^A + \bar{s}^A)](x_N)$$

- experiments extract (under certain assumptions)

$$F_{2,3} \equiv (F_{2,3}^{\nu A} + F_{2,3}^{\bar{\nu} A})/2 \longrightarrow$$

- F_2 probes total quark singlet
- F_3 probes sum of valence PDFs

CC neutrino DIS data

fit CDHSW, NuTeV, and CHORUS str. fct. data

substantial interest:

- nCTEQ claim of "**factorization breaking**" for nPDFs
- neutrino data are a vital constraint on strangeness (and help to separate quark flavors) in proton PDF fits

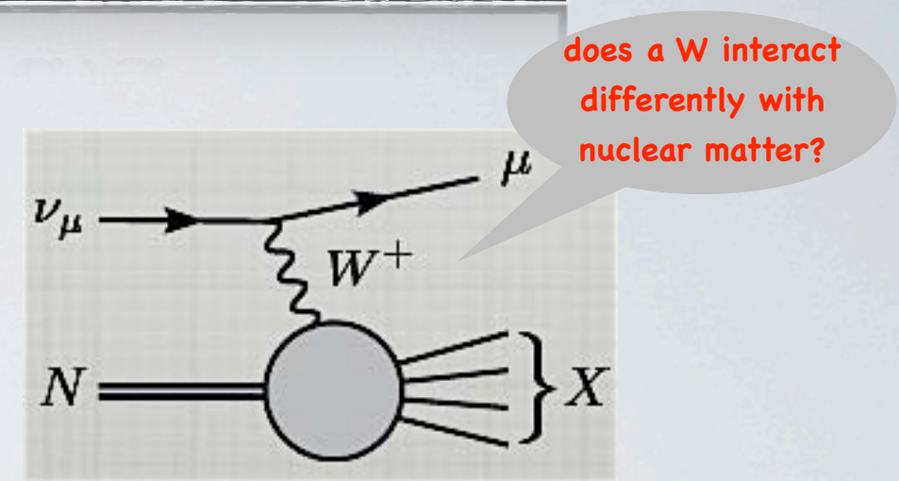

$$\frac{d^2\sigma^{\nu A,\bar{\nu}A}}{dxdy} \simeq xy^2 F_1^{\nu A,\bar{\nu}A} + (1-y)F_2^{\nu A,\bar{\nu}A} \pm xy(1-\frac{y}{2})F_3^{\nu A,\bar{\nu}A}$$

here is how the "tension" story goes

- CC DIS data probe different combinations of up-/down-type quarks than charged-lepton DIS
- neutrino and antineutrino beams probe 4 different structure functions

$$F_2^{\nu A}(x_N) \simeq x_N[\bar{u}^A + \bar{c}^A + d^A + s^A](x_N)$$

$$F_2^{\bar{\nu} A}(x_N) \simeq x_N[u^A + c^A + \bar{d}^A + \bar{s}^A](x_N)$$

$$F_3^{\nu A}(x_N) \simeq [-(\bar{u}^A + \bar{c}^A) + d^A + s^A](x_N)$$

$$F_3^{\bar{\nu} A}(x_N) \simeq [u^A + c^A - (\bar{d}^A + \bar{s}^A)](x_N)$$

- experiments extract (under certain assumptions)

$$F_{2,3} \equiv (F_{2,3}^{\nu A} + F_{2,3}^{\bar{\nu} A})/2 \longrightarrow$$

- F_2 probes total quark singlet
- F_3 probes sum of valence PDFs

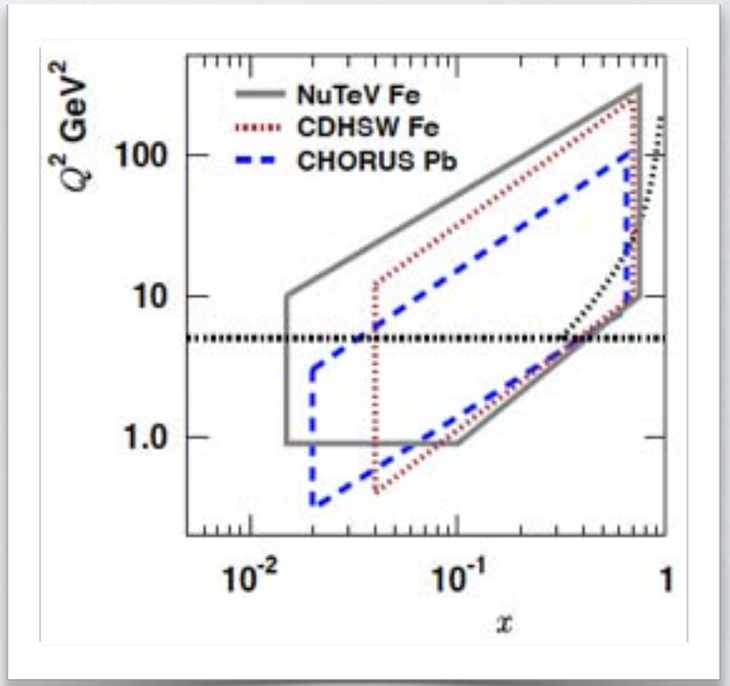

kinematics overlaps with charged lepton DIS data

CC neutrino DIS data

fit CDHSW, NuTeV, and CHORUS str. fct. data

substantial interest:

- nCTEQ claim of "**factorization breaking**" for nPDFs
- neutrino data are a vital constraint on strangeness (and help to separate quark flavors) in proton PDF fits

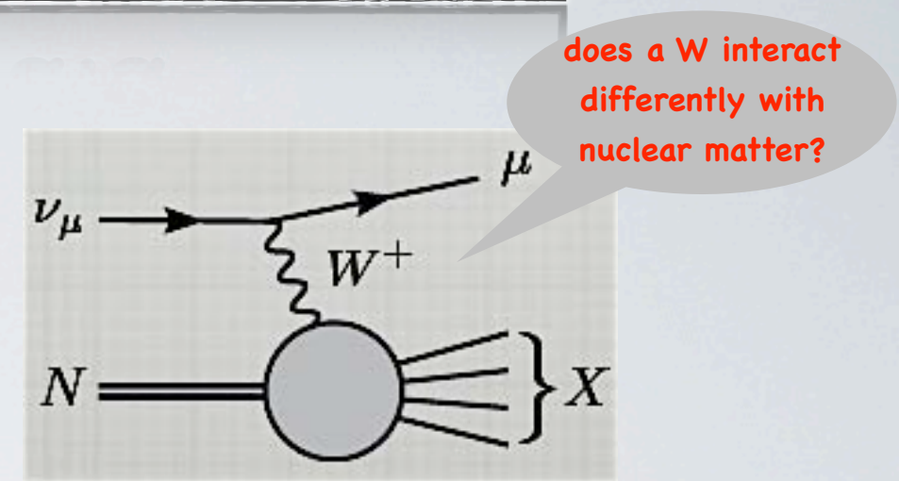

$$\frac{d^2\sigma^{\nu A,\bar{\nu}A}}{dxdy} \simeq xy^2 F_1^{\nu A,\bar{\nu}A} + (1-y)F_2^{\nu A,\bar{\nu}A} \pm xy(1-\frac{y}{2})F_3^{\nu A,\bar{\nu}A}$$

here is how the "tension" story goes

- CC DIS data probe different combinations of up-/down-type quarks than charged-lepton DIS
- neutrino and antineutrino beams probe 4 different structure functions

$$F_2^{\nu A}(x_N) \simeq x_N[\bar{u}^A + \bar{c}^A + d^A + s^A](x_N)$$

$$F_2^{\bar{\nu} A}(x_N) \simeq x_N[u^A + c^A + \bar{d}^A + \bar{s}^A](x_N)$$

$$F_3^{\nu A}(x_N) \simeq [-(\bar{u}^A + \bar{c}^A) + d^A + s^A](x_N)$$

$$F_3^{\bar{\nu} A}(x_N) \simeq [u^A + c^A - (\bar{d}^A + \bar{s}^A)](x_N)$$

potential tension with what we have learned from NC DIS

- experiments extract (under certain assumptions)

$$F_{2,3} \equiv (F_{2,3}^{\nu A} + F_{2,3}^{\bar{\nu} A})/2 \longrightarrow$$

- F_2 probes total quark singlet
- F_3 probes sum of valence PDFs

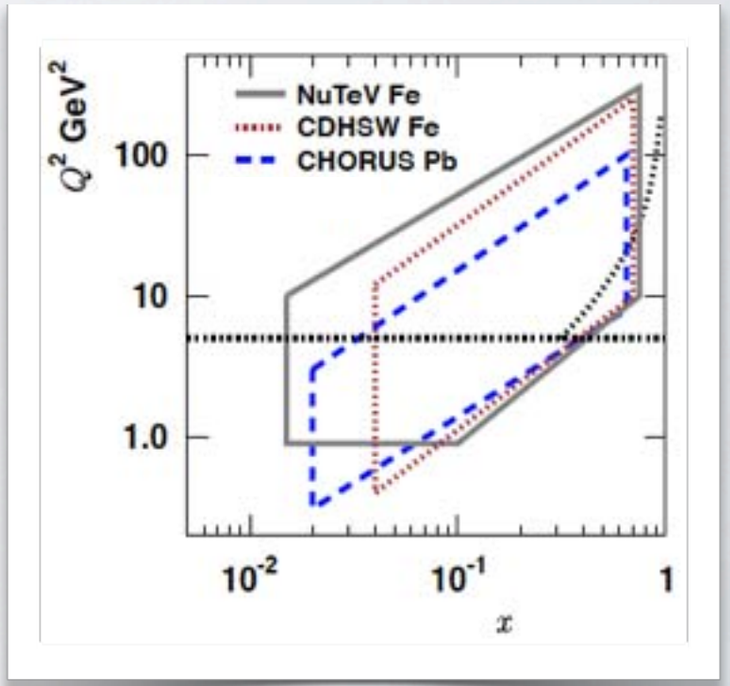

kinematics overlaps with charged lepton DIS data

CC neutrino DIS data (cont'd)

find: data remarkably well reproduced by fit $\chi^2 = 488.2/532$pts.

$\mathbf{F_2(x, Q^2)}$

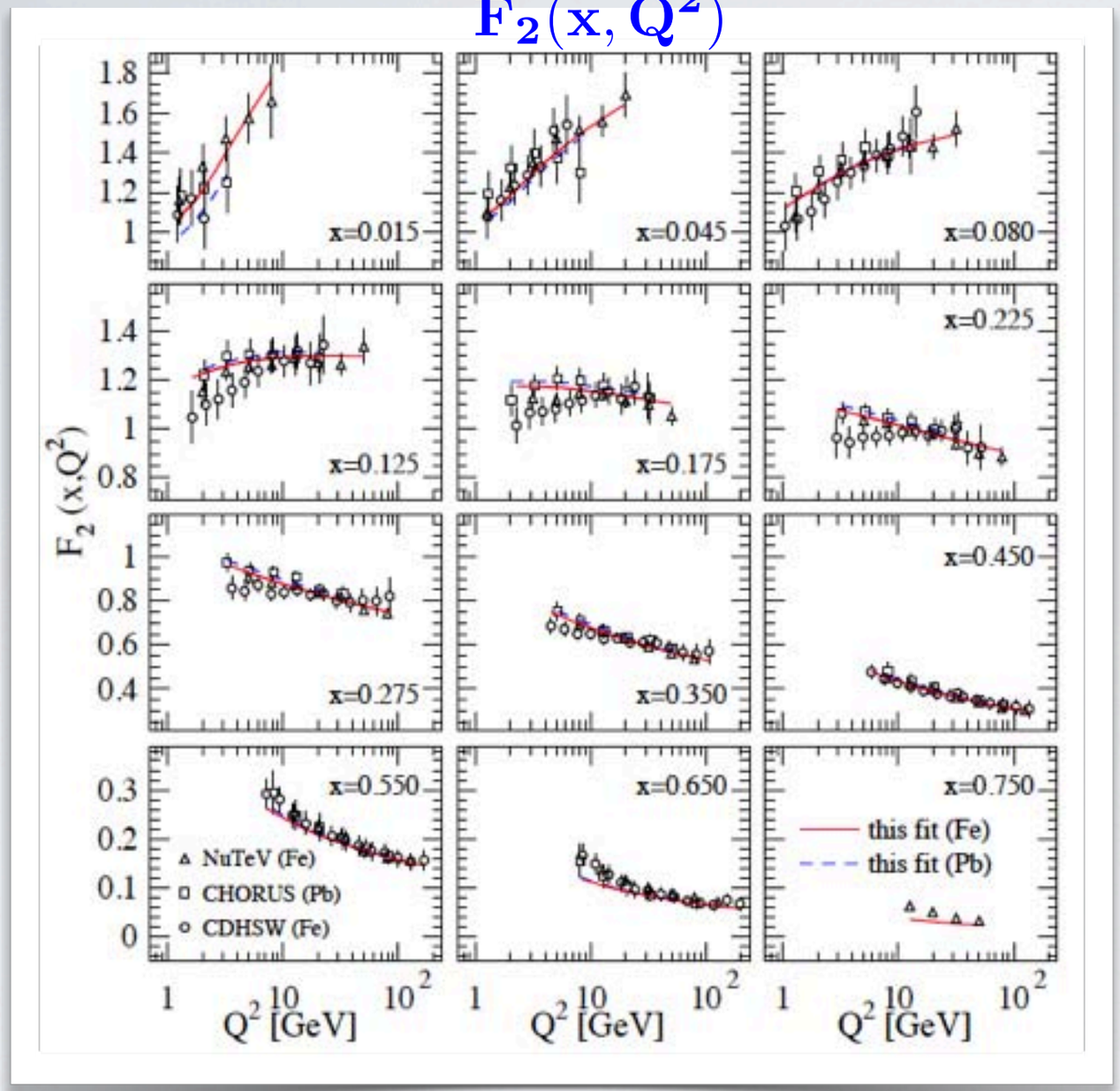

$\mathbf{xF_3(x, Q^2)}$

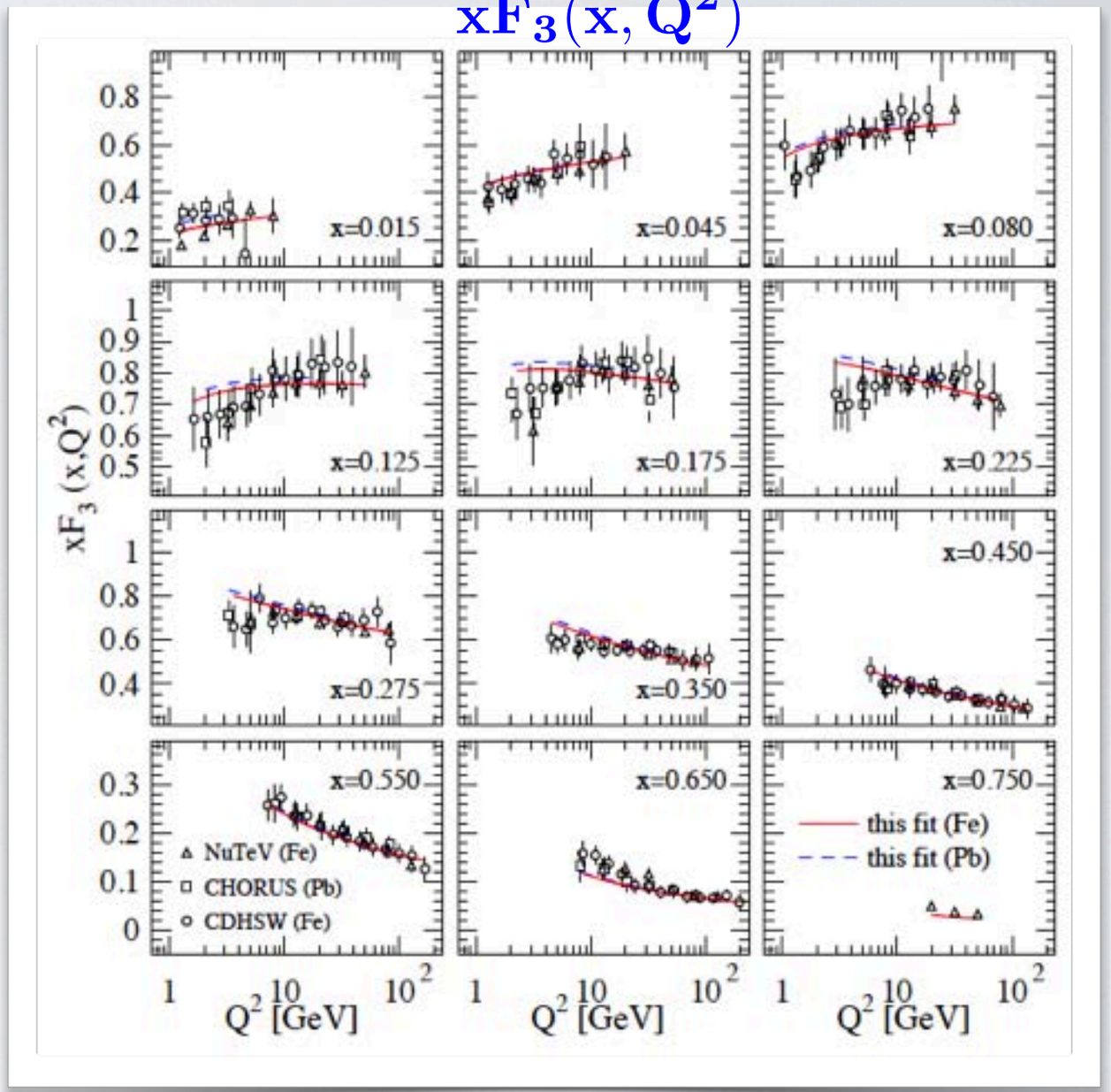

- absolute cross sections rather than ratios -> more sensitive to set of proton PDF in R_i^A (incl. as theor. uncertainty)

CC neutrino DIS data (cont'd)

find: data remarkably well reproduced by fit $\chi^2 = 488.2/532$pts.

$\mathbf{F_2(x, Q^2)}$

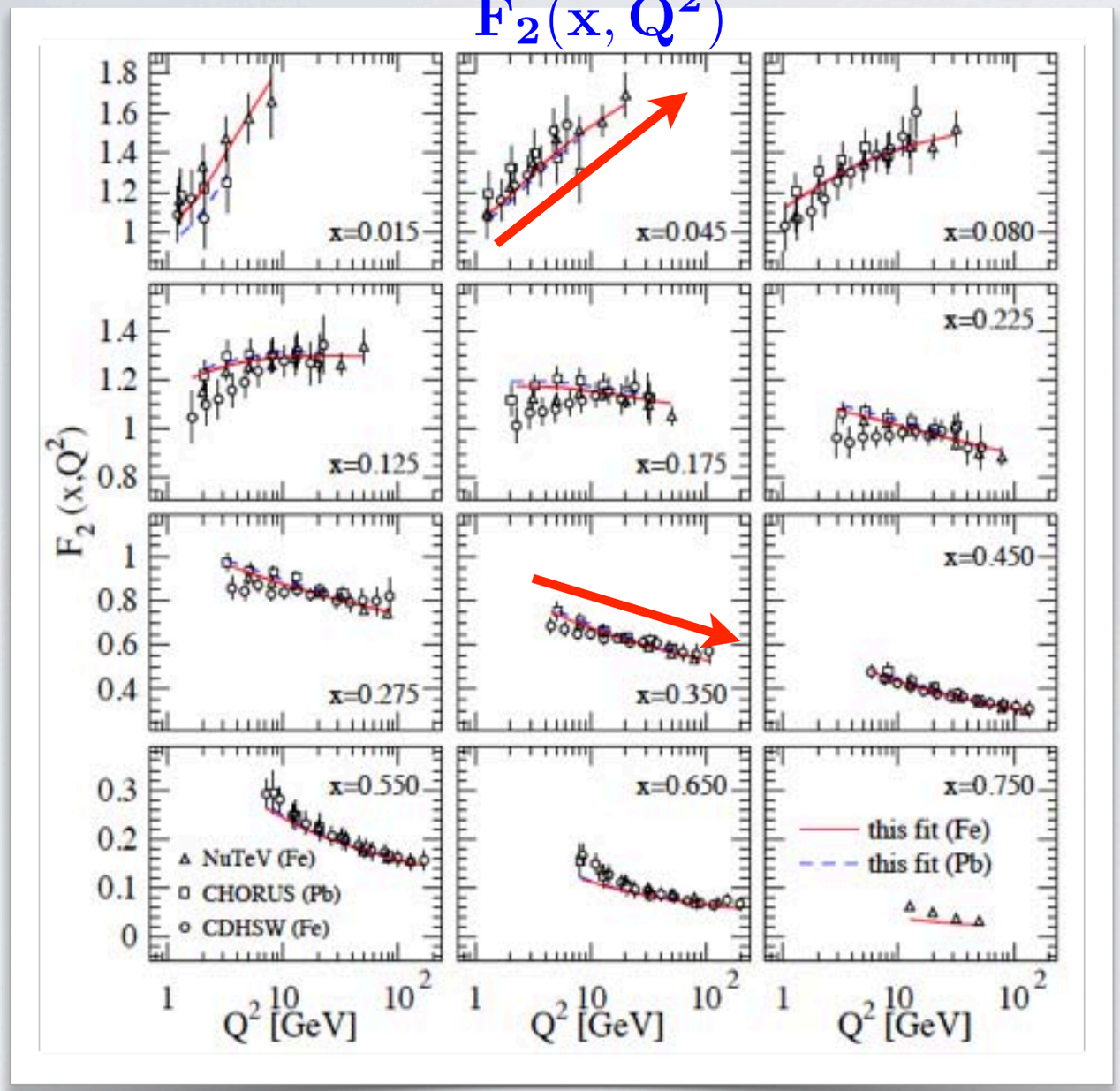

$\mathbf{xF_3(x, Q^2)}$

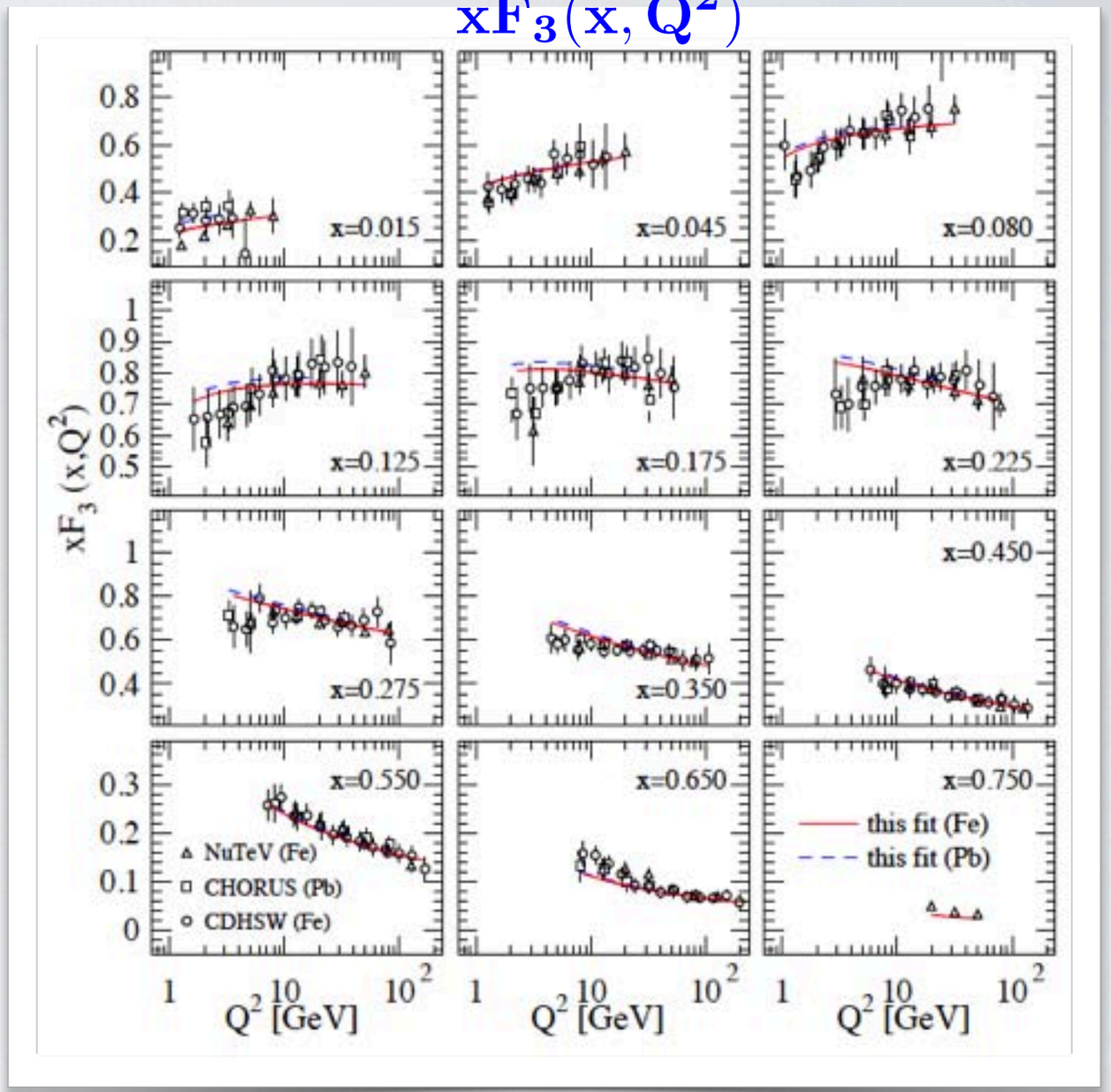

- absolute cross sections rather than ratios -> more sensitive to set of proton PDF in R_i^A (incl. as theor. uncertainty)
- data feature typical pattern of scaling violations

CC neutrino DIS data (cont'd)

find: data remarkably well reproduced by fit $\chi^2 = 488.2/532$pts.

$\mathbf{F_2(x, Q^2)}$

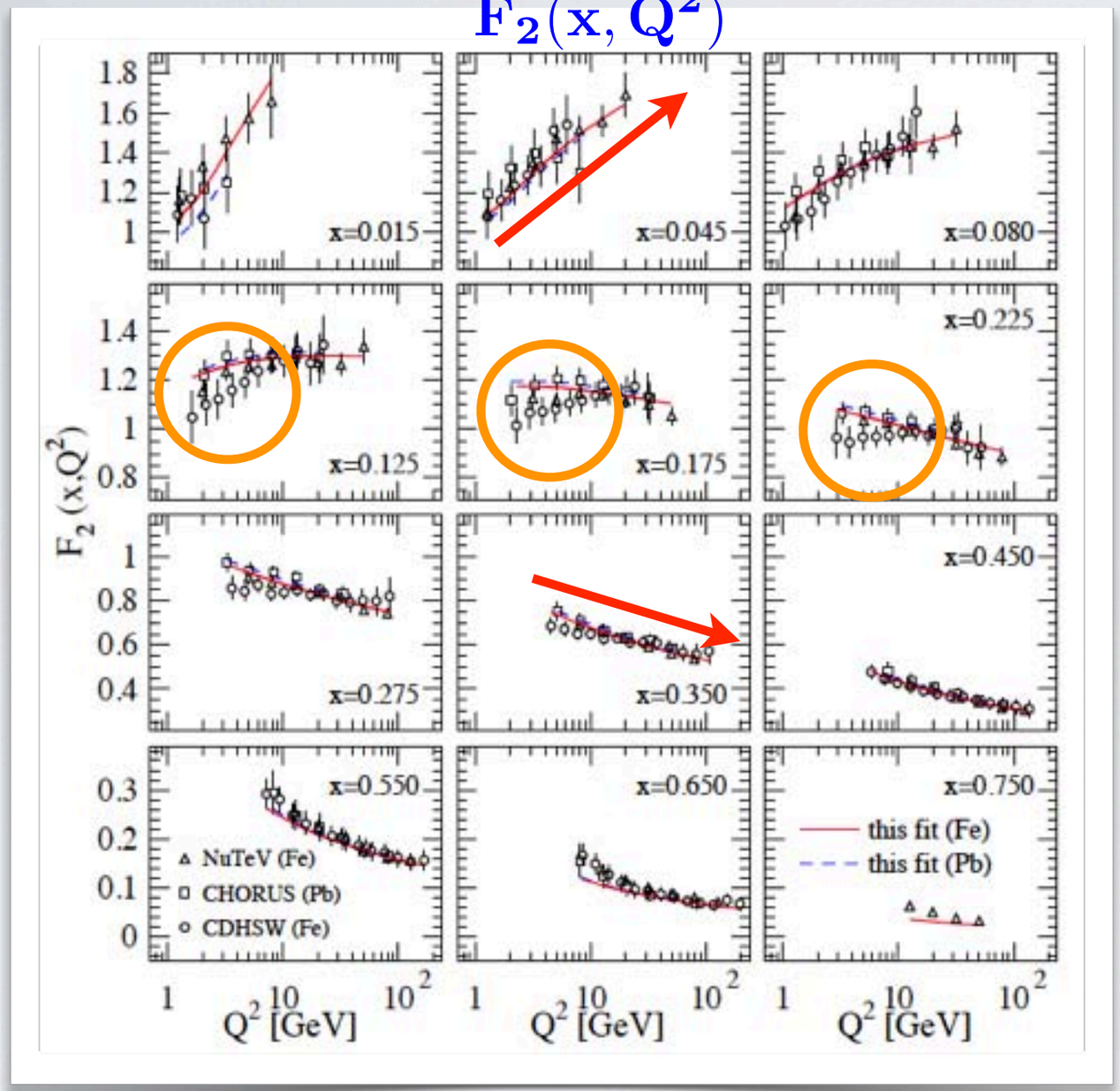

$\mathbf{xF_3(x, Q^2)}$

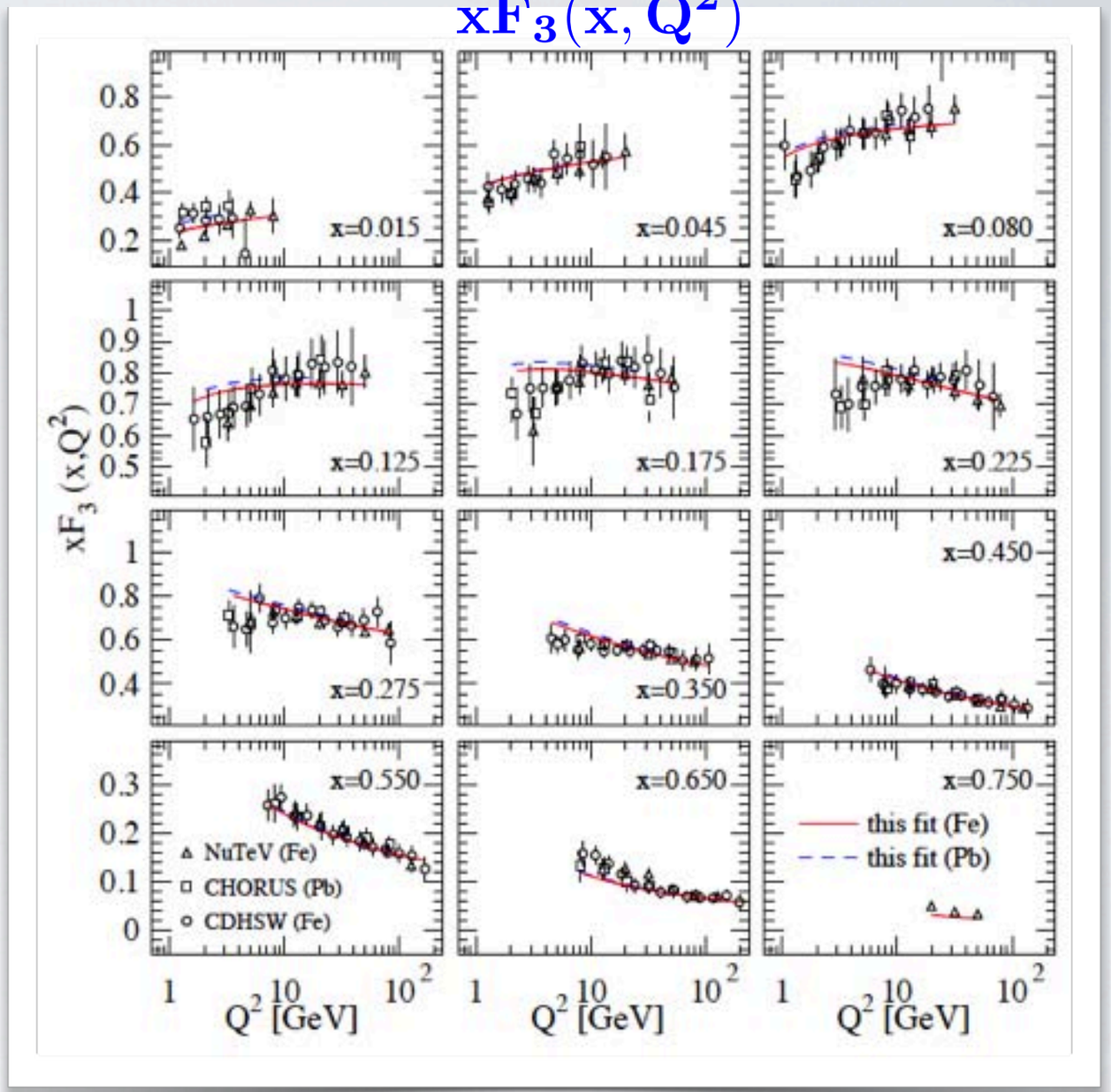

- absolute cross sections rather than ratios -> more sensitive to set of proton PDF in R_i^A (incl. as theor. uncertainty)
- data feature typical pattern of scaling violations
- slope of CDHSW data does not match with other data

CC neutrino DIS data (cont'd)

find: data remarkably well reproduced by fit $\chi^2 = 488.2/532$pts.

$\mathbf{F_2(x, Q^2)}$

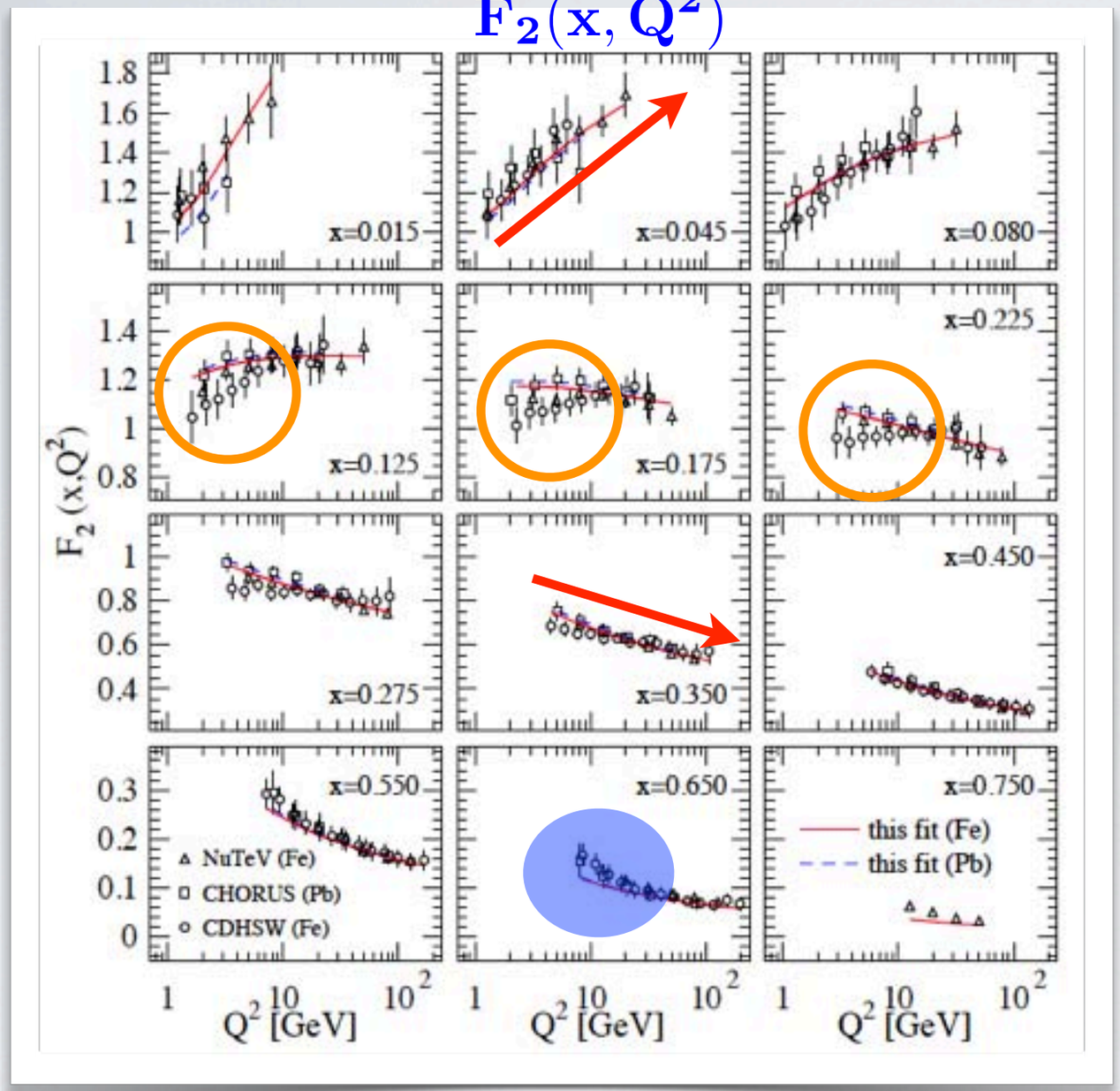

$\mathbf{xF_3(x, Q^2)}$

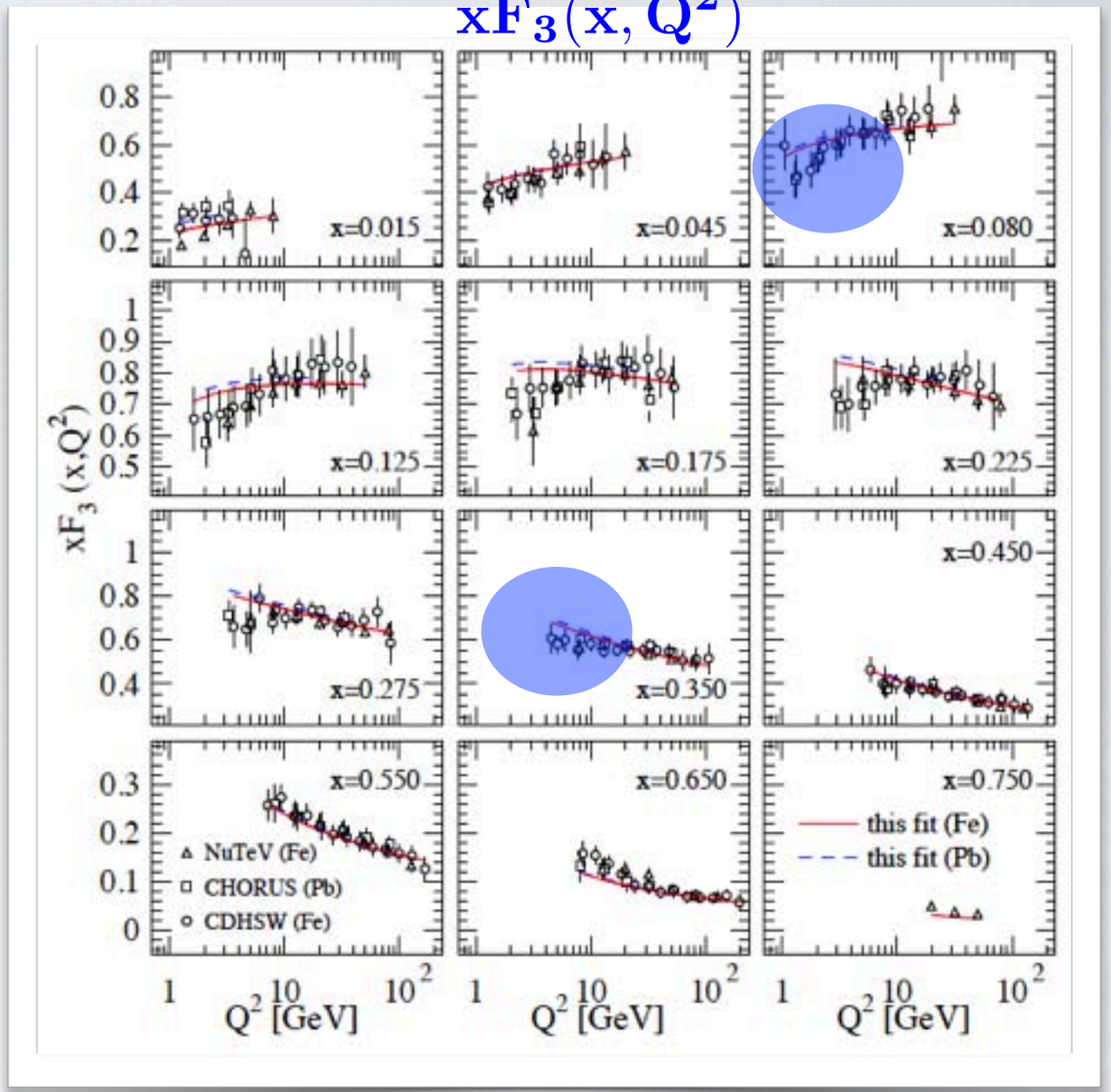

- absolute cross sections rather than ratios -> more sensitive to set of proton PDF in R_i^A (incl. as theor. uncertainty)
- data feature typical pattern of scaling violations
- slope of CDHSW data does not match with other data

some mild tensions

often with CDHSW data

CC neutrino DIS data (cont'd)

no indication for factorization breaking

find same pattern of nuclear effects for CC and NC DIS

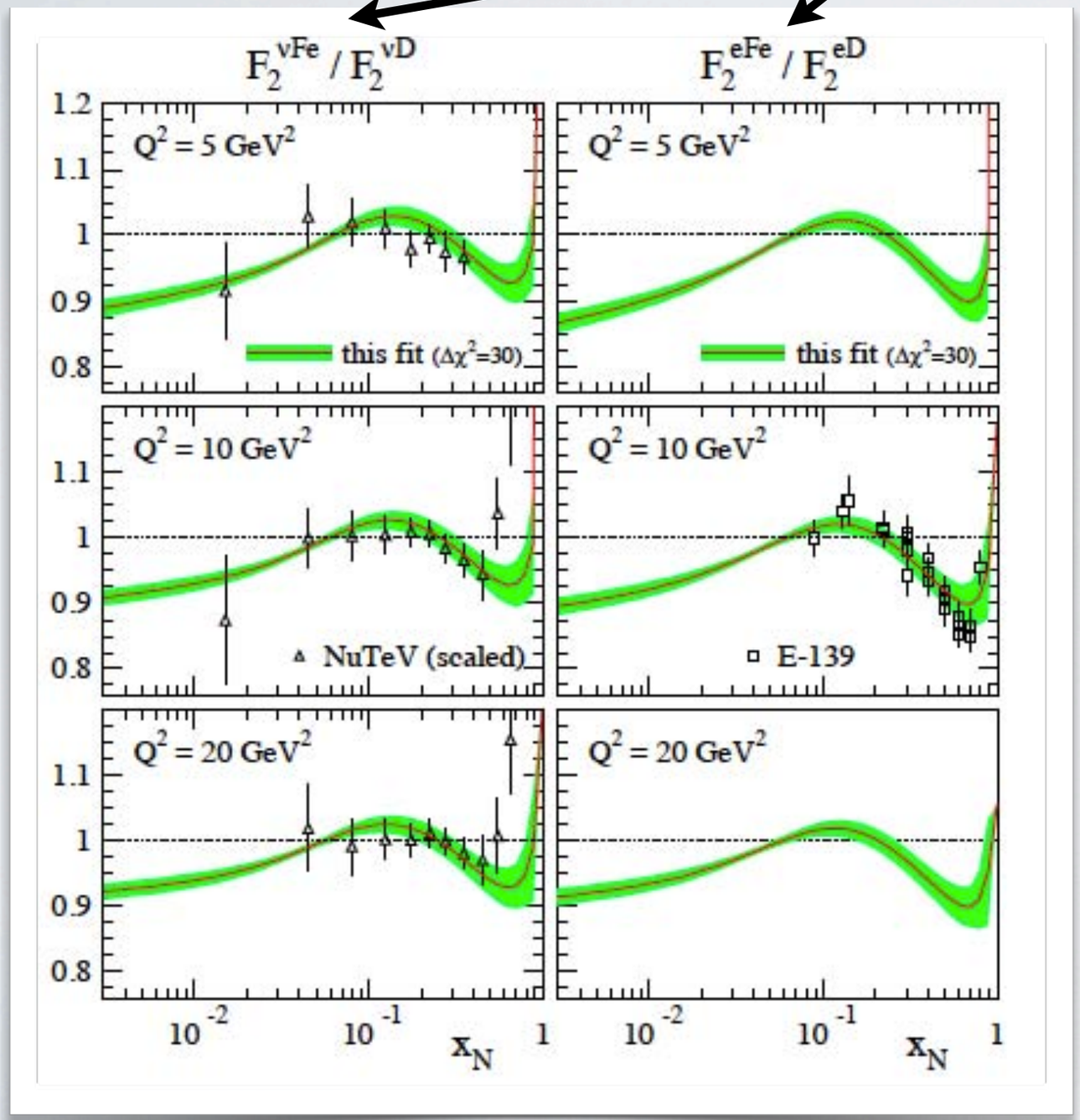

at variance with nCTEQ result

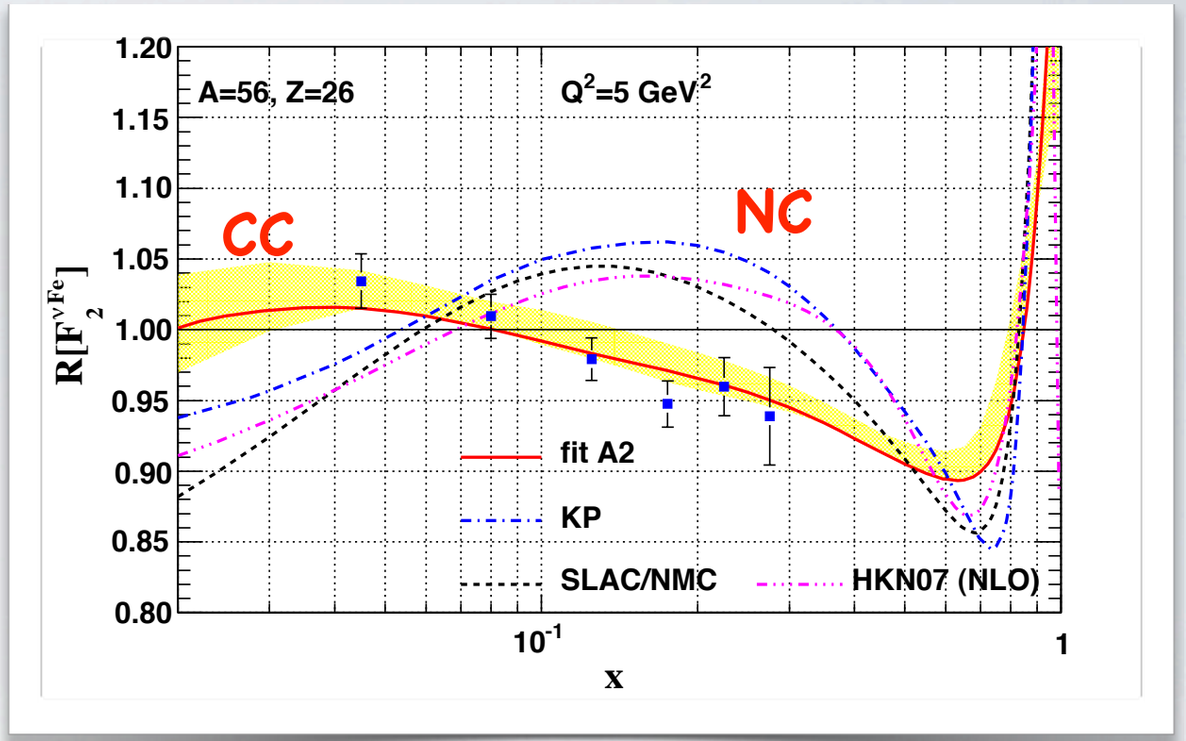

CC neutrino DIS data (cont'd)

no indication for factorization breaking

find same pattern of nuclear effects for CC and NC DIS

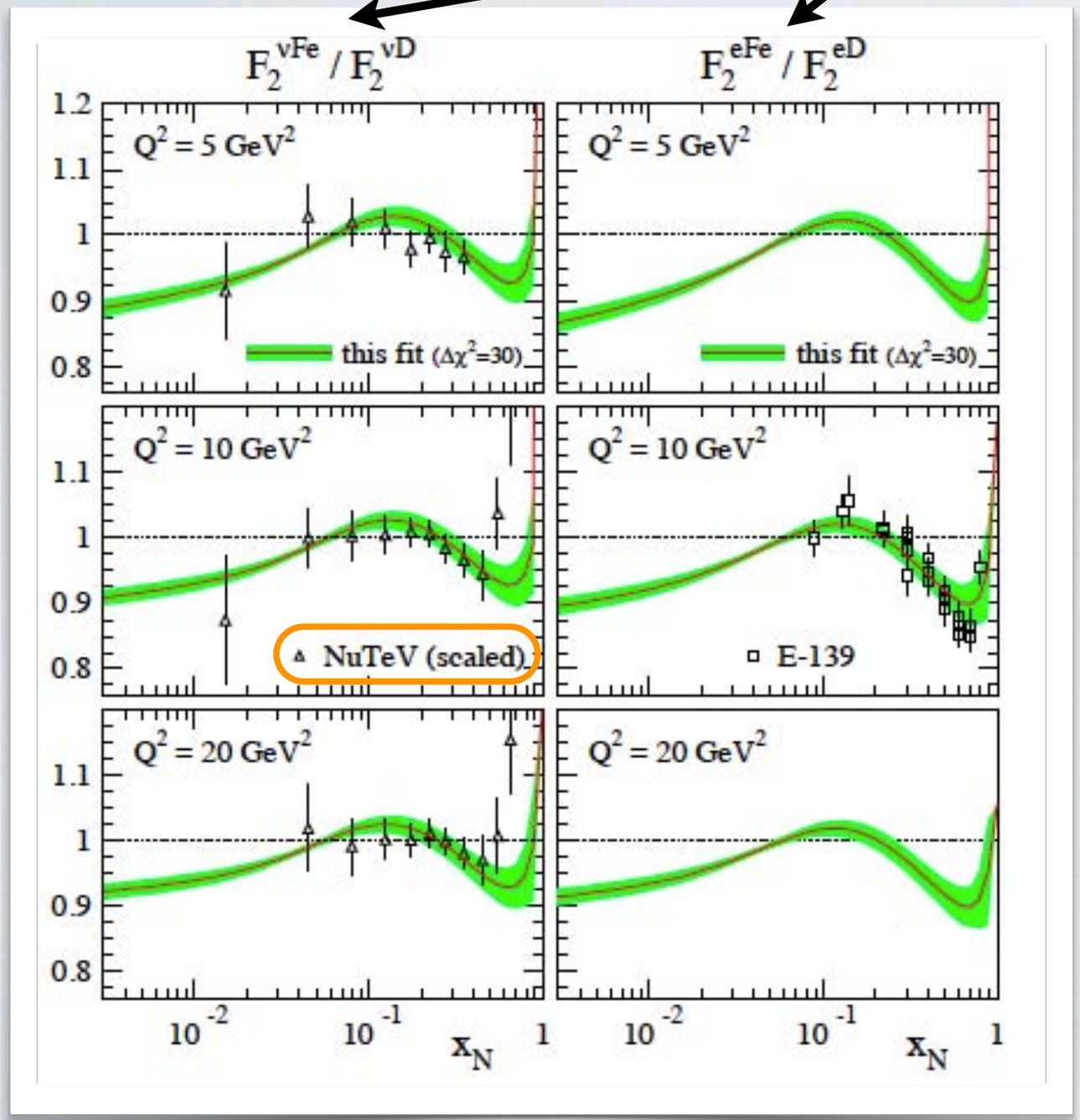

at variance with nCTEQ result

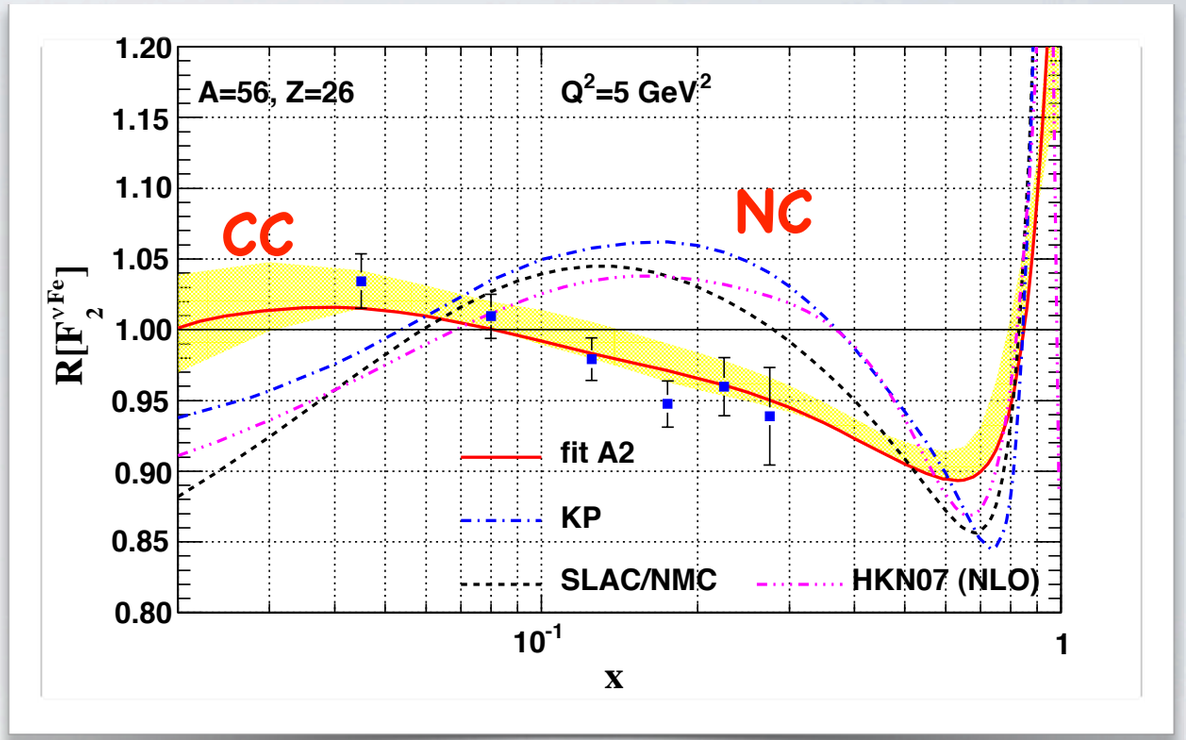

- "theoretical data": $\mathbf{F_2^{\nu D}}$ not measured

CC neutrino DIS data (cont'd)

no indication for factorization breaking

find same pattern of nuclear effects for CC and NC DIS

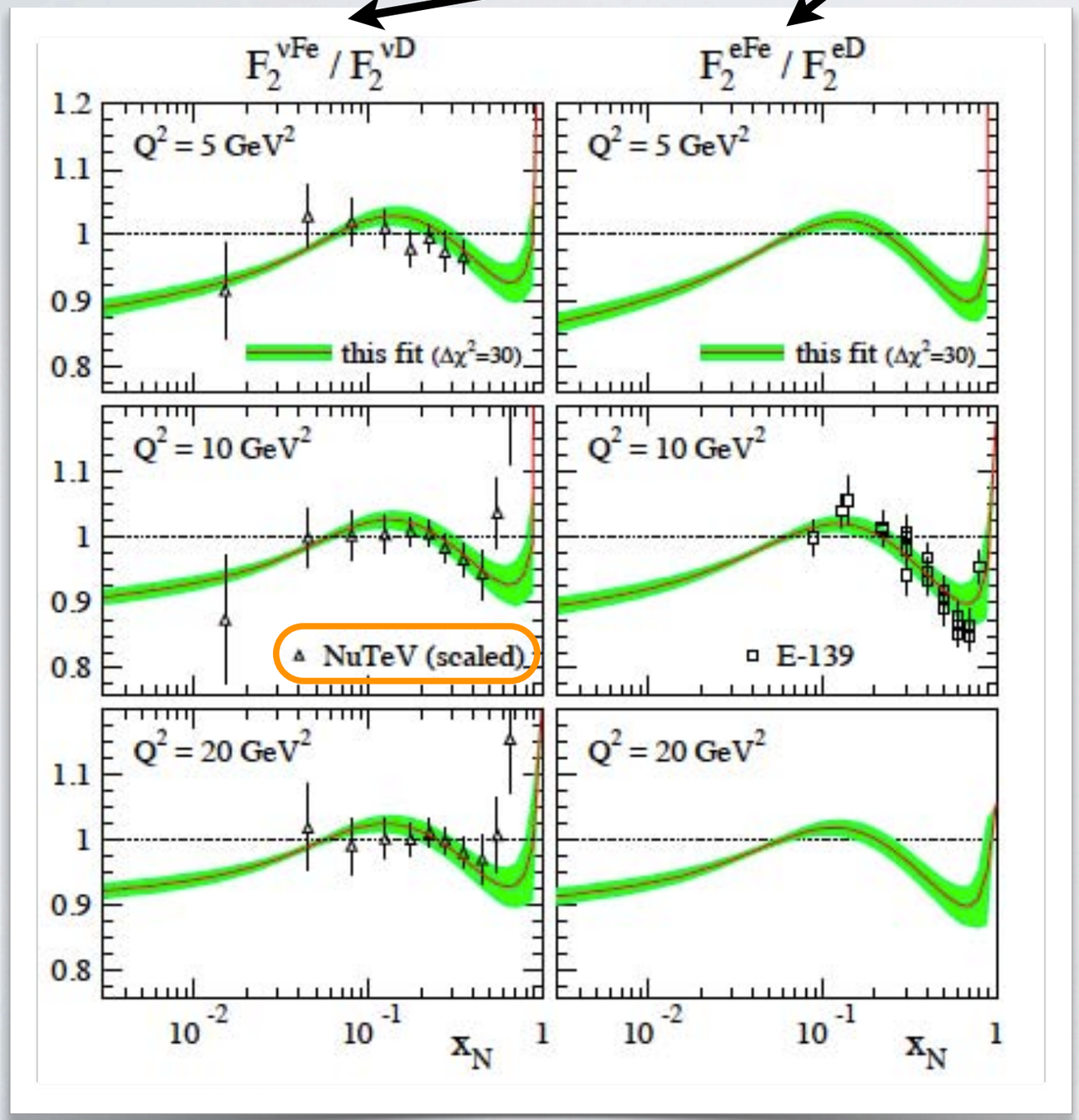

at variance with nCTEQ result

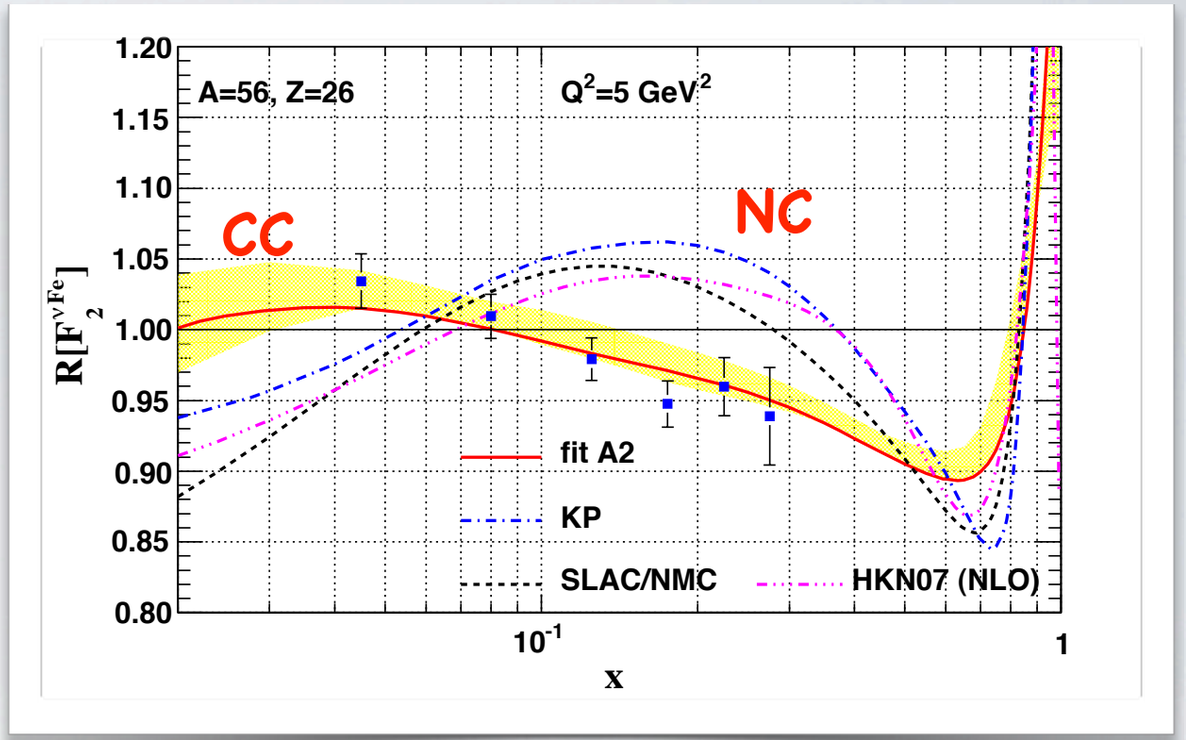

- "theoretical data": $\mathbf{F_2^{\nu D}}$ not measured
- nCTEQ fits to cross sections not str. fcts.

CC neutrino DIS data (cont'd)

no indication for factorization breaking

find same pattern of nuclear effects for CC and NC DIS

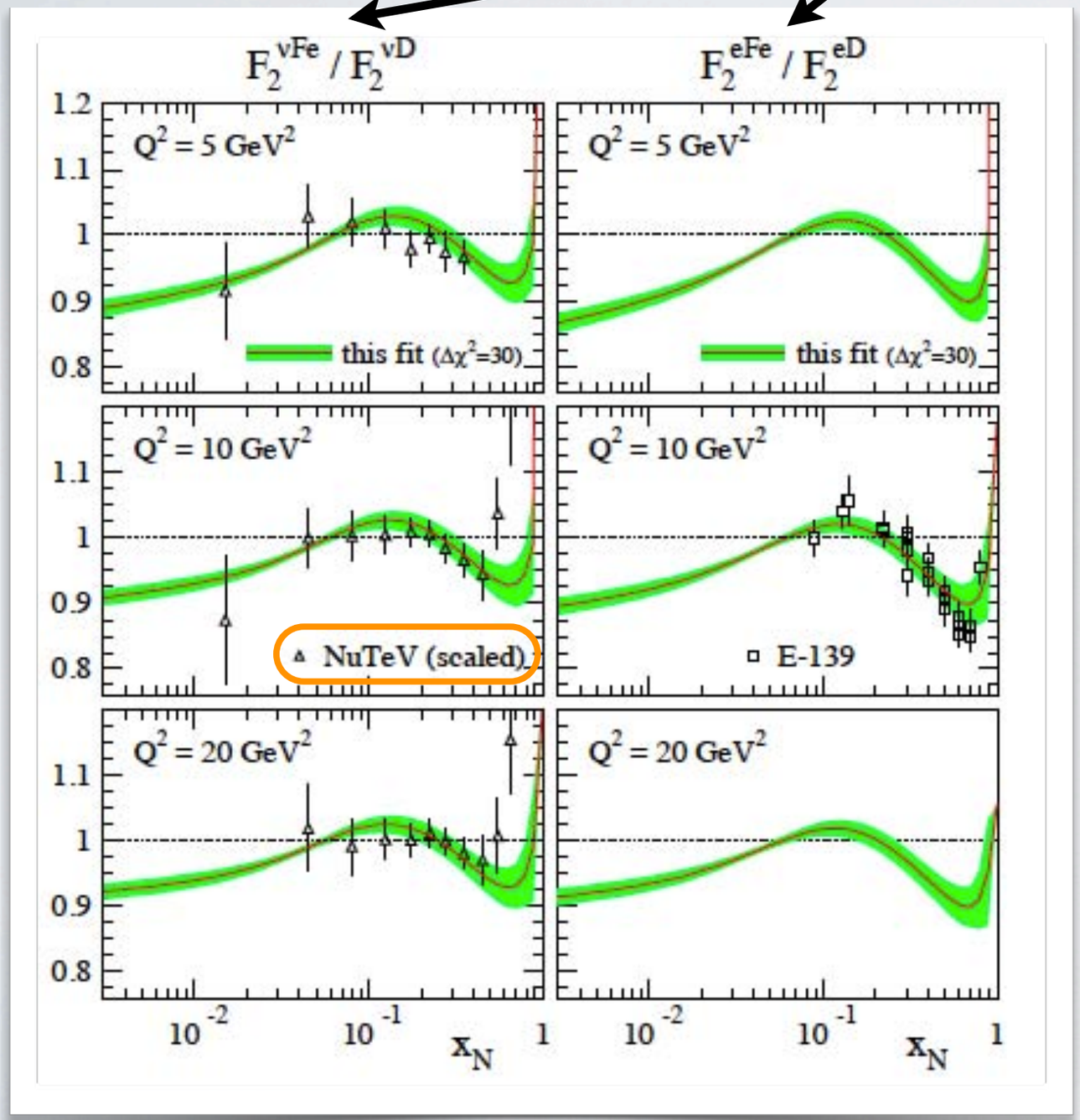

at variance with nCTEQ result

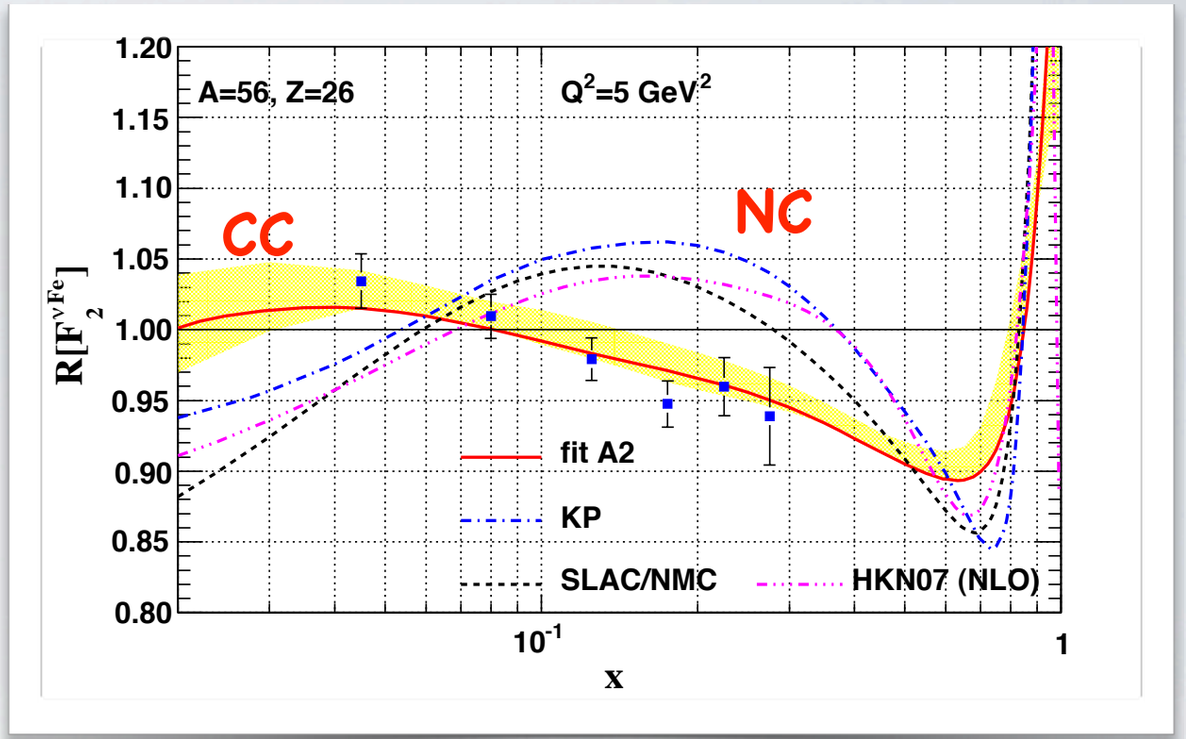

- "theoretical data": $\mathbf{F_2^{\nu D}}$ not measured
- nCTEQ fits to cross sections not str. fcts.
- also EPS finds compatible nuclear effects
  (no re-fit including CC DIS yet)

pion production in dA

most difficult probe to analyze (yet, perhaps one of the most interesting ones)

$$\mathbf{d\sigma^{A}_{dA\to\pi X} = \sum_{ijk} f^{d}_{i} \otimes f^{A}_{j} \otimes d\hat{\sigma}_{ij\to kX} \otimes D^{A,\pi}_{k}}$$

wanted

pion production in dA

most difficult probe to analyze (yet, perhaps one of the most interesting ones)

$$d\sigma^{A}_{dA\to\pi X} = \sum_{ijk} f_i^d \otimes f_j^A \otimes d\hat{\sigma}_{ij\to kX} \otimes D_k^{A,\pi}$$

wanted

free proton PDF
"known"

known to NLO
[plus certain all-order resummations]
many contributing subprocesses

fragmentation functions
fairly well known for pions
but what about possible nuclear modifications?
can have an impact even if small

pion production in dA

most difficult probe to analyze (yet, perhaps one of the most interesting ones)

$$d\sigma^{A}_{dA\to\pi X} = \sum_{ijk} f_i^d \otimes f_j^A \otimes d\hat{\sigma}_{ij\to kX} \otimes D_k^{A,\pi}$$

wanted

free proton PDF
"known"

known to NLO
[plus certain all-order resummations]
many contributing subprocesses

fragmentation functions
fairly well known for pions
but what about possible nuclear modifications?
can have an impact even if small

mid-rapidity neutral pion data from PHENIX and STAR first analyzed in EPS fit

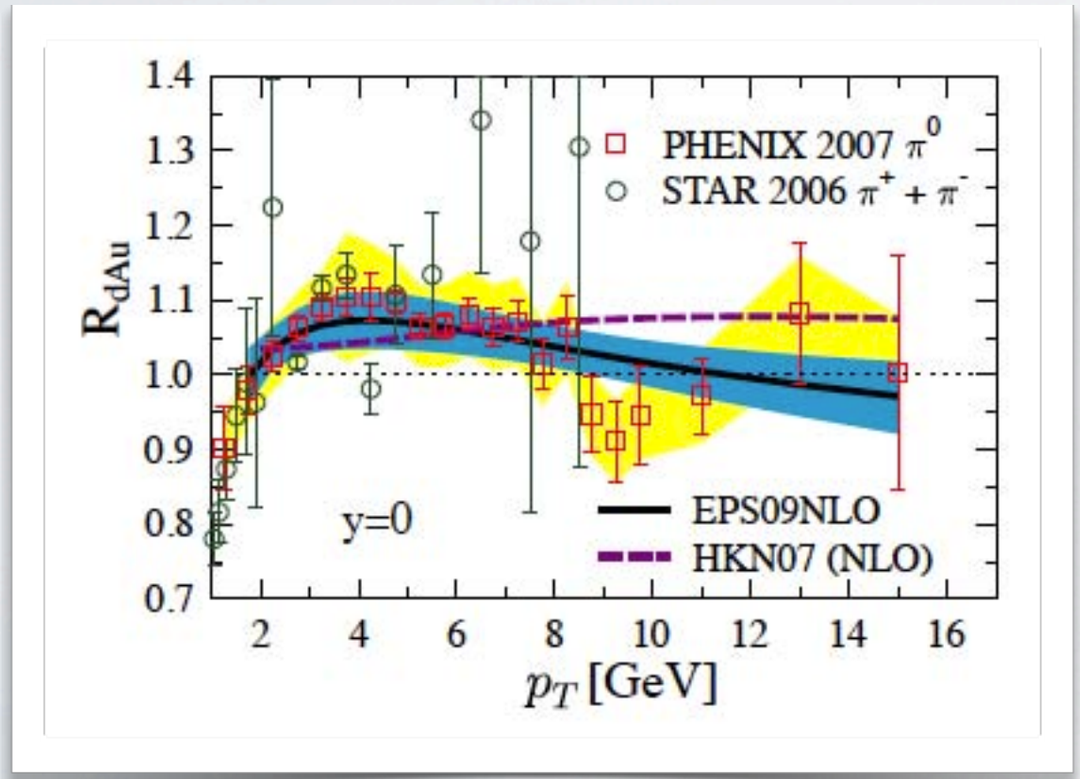

- fit to min. bias ratio $R^{\pi}_{dAu} = \frac{\frac{1}{2A} d^2\sigma_{dAu}/dp_T dy}{d^2\sigma_{pp}/dp_T/dy}$
- use up-to-date vacuum fragmentation functions
  DSS: de Florian, Sassot, MS - include RHIC pp data

pion production in dA

most difficult probe to analyze (yet, perhaps one of the most interesting ones)

$$d\sigma^{A}_{dA\to\pi X} = \sum_{ijk} f_i^d \otimes f_j^A \otimes d\hat{\sigma}_{ij\to kX} \otimes D_k^{A,\pi}$$

wanted

free proton PDF
"known"

known to NLO
[plus certain all-order resummations]
many contributing subprocesses

fragmentation functions
fairly well known for pions
but what about possible nuclear modifications?
can have an impact even if small

mid-rapidity neutral pion data from PHENIX and STAR first analyzed in EPS fit

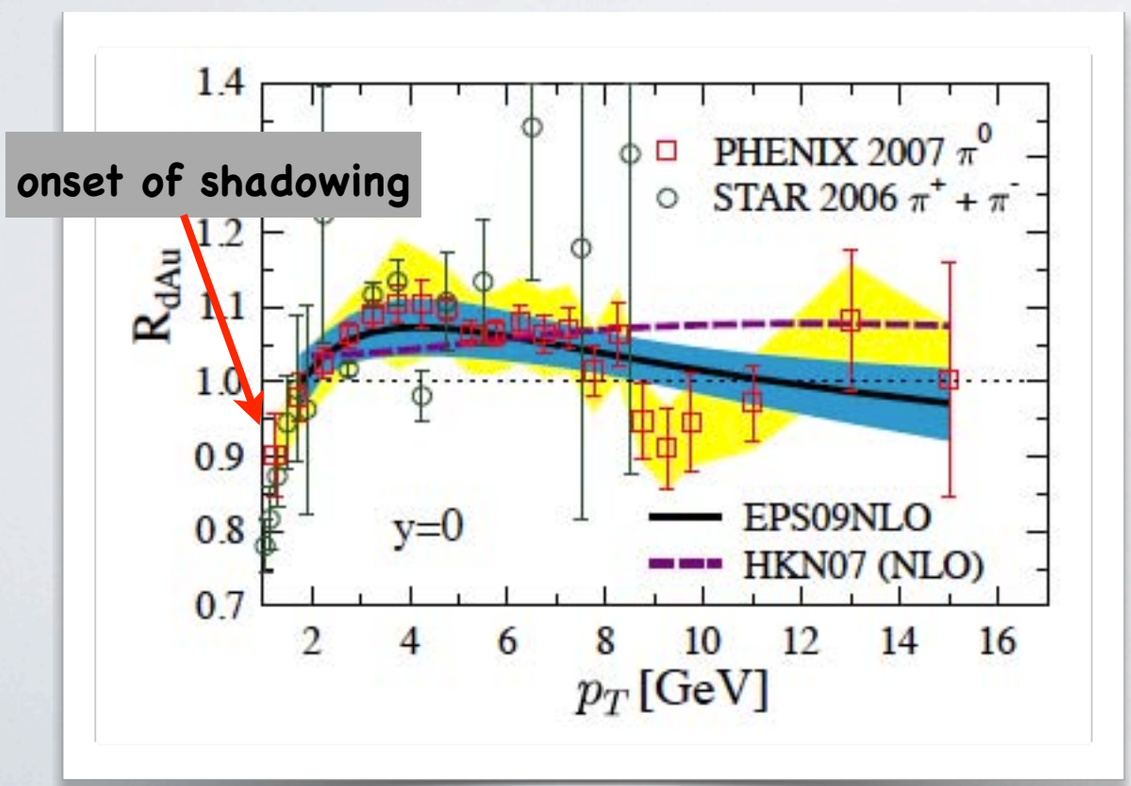

- fit to min. bias ratio $R^{\pi}_{dAu} = \frac{\frac{1}{2A} d^2\sigma_{dAu}/dp_T dy}{d^2\sigma_{pp}/dp_T/dy}$
- use up-to-date vacuum fragmentation functions
  DSS: de Florian, Sassot, MS - include RHIC pp data
- find BIG impact on gluon nPDF

pion production in dA

most difficult probe to analyze (yet, perhaps one of the most interesting ones)

$$d\sigma^{A}_{dA\to\pi X} = \sum_{ijk} f_i^d \otimes f_j^A \otimes d\hat{\sigma}_{ij\to kX} \otimes D_k^{A,\pi}$$

wanted

free proton PDF
"known"

known to NLO
[plus certain all-order resummations]
many contributing subprocesses

fragmentation functions
fairly well known for pions
but what about possible nuclear modifications?
can have an impact even if small

mid-rapidity neutral pion data from PHENIX and STAR first analyzed in EPS fit

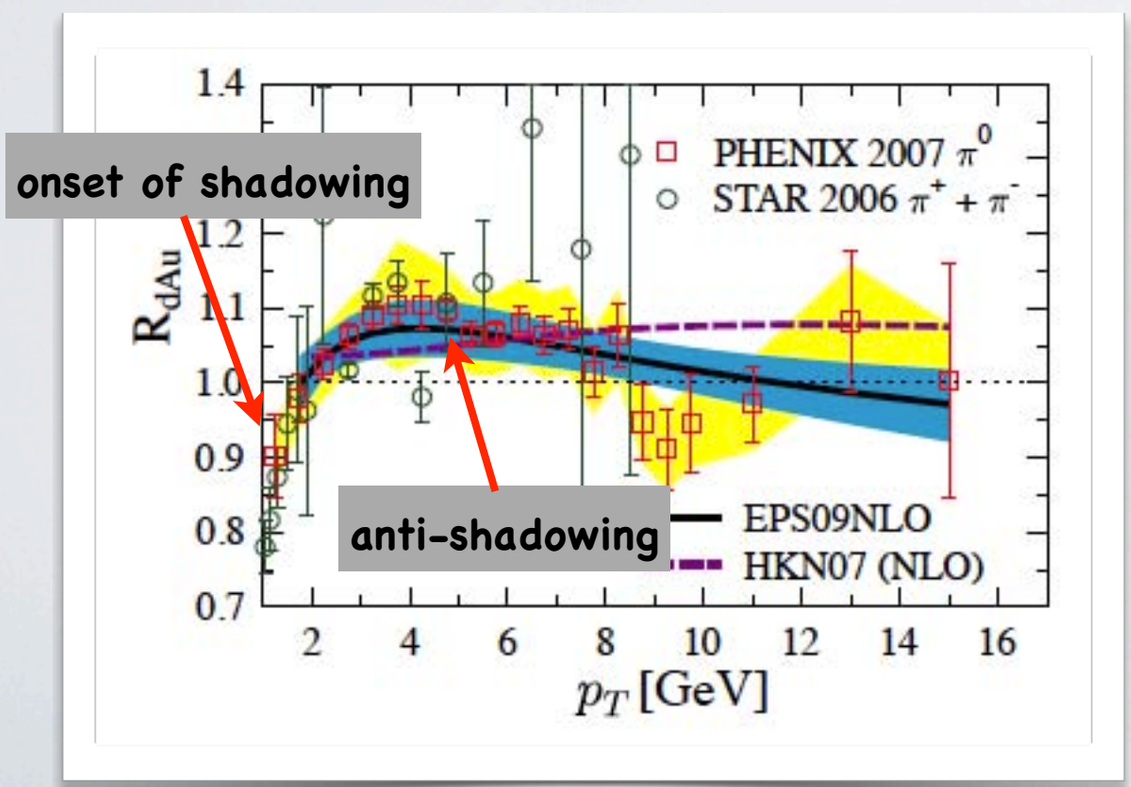

- fit to min. bias ratio $R^{\pi}_{dAu} = \frac{\frac{1}{2A} d^2\sigma_{dAu}/dp_T dy}{d^2\sigma_{pp}/dp_T/dy}$
- use up-to-date vacuum fragmentation functions
  DSS: de Florian, Sassot, MS - include RHIC pp data
- find BIG impact on gluon nPDF

pion production in dA

most difficult probe to analyze (yet, perhaps one of the most interesting ones)

$$d\sigma^{A}_{dA\to\pi X} = \sum_{ijk} f_i^d \otimes f_j^A \otimes d\hat{\sigma}_{ij\to kX} \otimes D_k^{A,\pi}$$

wanted

free proton PDF
"known"

known to NLO
[plus certain all-order resummations]
many contributing subprocesses

fragmentation functions
fairly well known for pions
but what about possible nuclear modifications?
can have an impact even if small

mid-rapidity neutral pion data from PHENIX and STAR first analyzed in EPS fit

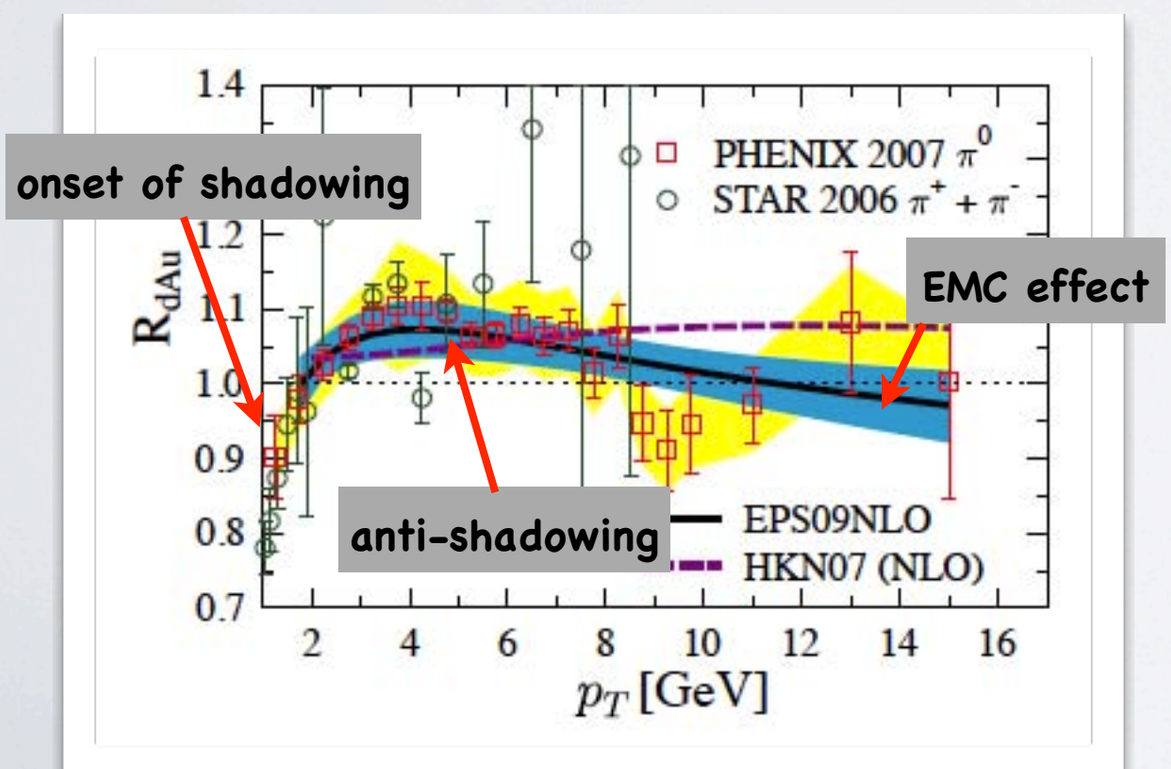

- fit to min. bias ratio $R^{\pi}_{dAu} = \frac{\frac{1}{2A} d^2\sigma_{dAu}/dp_T dy}{d^2\sigma_{pp}/dp_T/dy}$
- use up-to-date vacuum fragmentation functions
  DSS: de Florian, Sassot, MS - include RHIC pp data
- find BIG impact on gluon nPDF

pion production in dA

most difficult probe to analyze (yet, perhaps one of the most interesting ones)

$$d\sigma^{A}_{dA\to\pi X} = \sum_{ijk} f_i^d \otimes f_j^A \otimes d\hat{\sigma}_{ij\to kX} \otimes D_k^{A,\pi}$$

wanted

free proton PDF
"known"

known to NLO
[plus certain all-order resummations]
many contributing subprocesses

fragmentation functions
fairly well known for pions
but what about possible nuclear modifications?
can have an impact even if small

mid-rapidity neutral pion data from PHENIX and STAR first analyzed in EPS fit

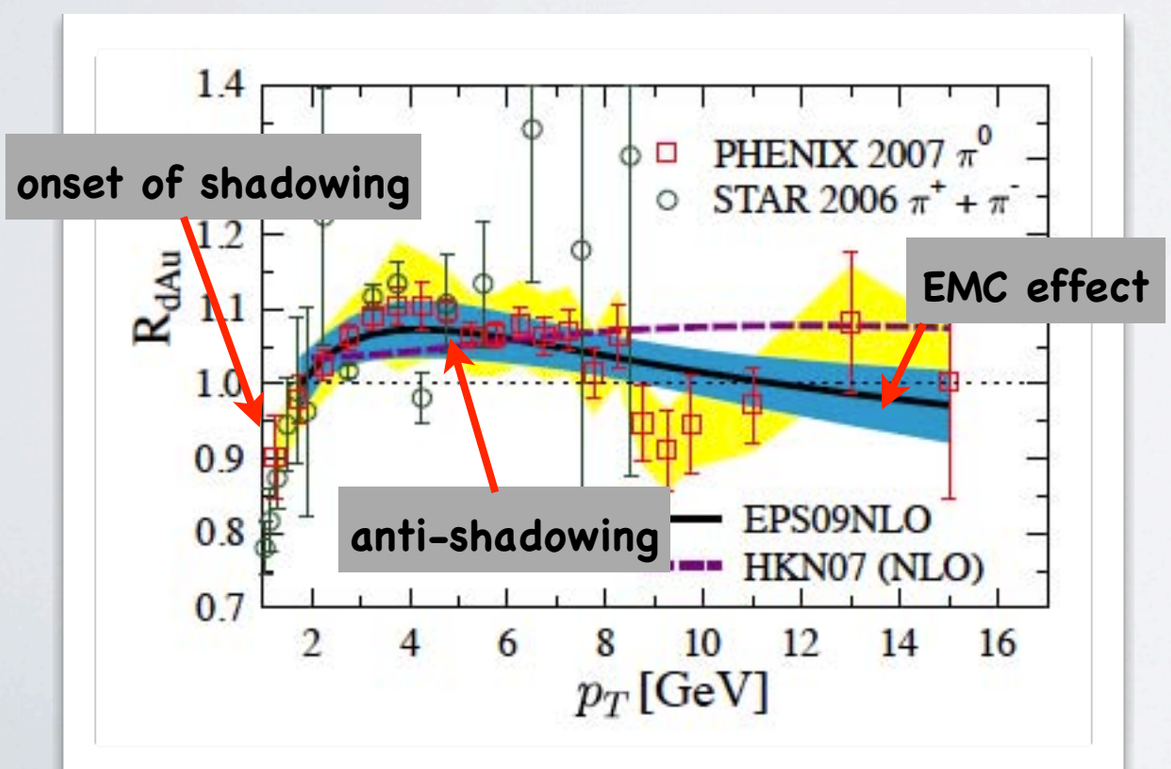

- fit to min. bias ratio $R^{\pi}_{dAu} = \frac{\frac{1}{2A} d^2\sigma_{dAu}/dp_T dy}{d^2\sigma_{pp}/dp_T/dy}$
- use up-to-date vacuum fragmentation functions
  DSS: de Florian, Sassot, MS - include RHIC pp data
- find BIG impact on gluon nPDF

potential caveat: need to assign large weight to dAu data in fit

pion production in dA - cont'd

what is different in DSSZ analysis

- ✓ more data, including also charged pions from STAR
- ✓ no artificially large weight w.r.t. other data sets
- ✓ try to estimate impact of modifications in hadronization

pion production in dA - cont'd

what is different in DSSZ analysis

- ✓ more data, including also charged pions from STAR
- ✓ no artificially large weight w.r.t. other data sets
- ✓ try to estimate impact of modifications in hadronization

fragmentation in a medium - what is known ?

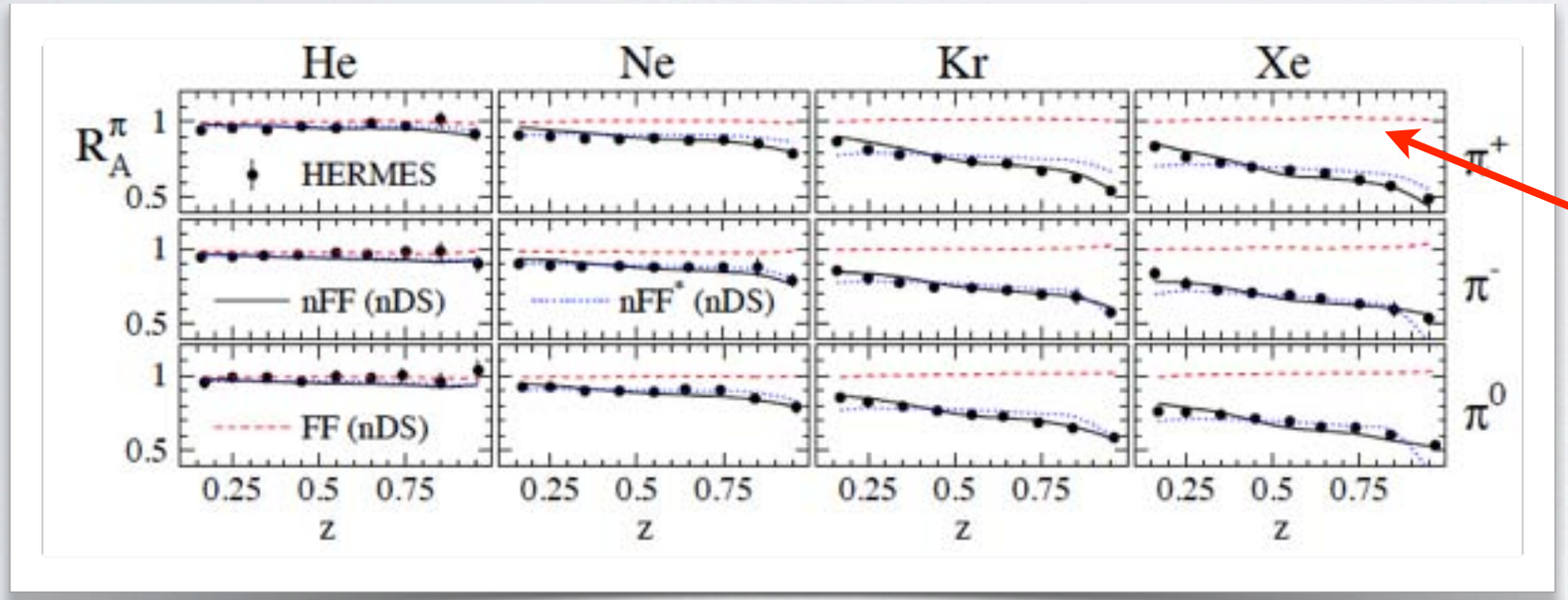

- effects known to be large in eA
- cannot be described as an initial-state effect (= nPDFs)
- hadron attenuation increases with A and z (rather flat in x and Q^2)

HERMES

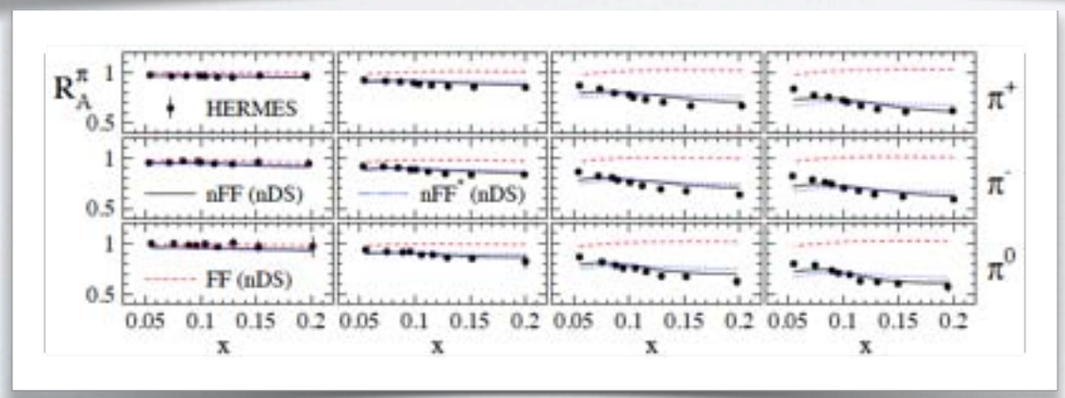

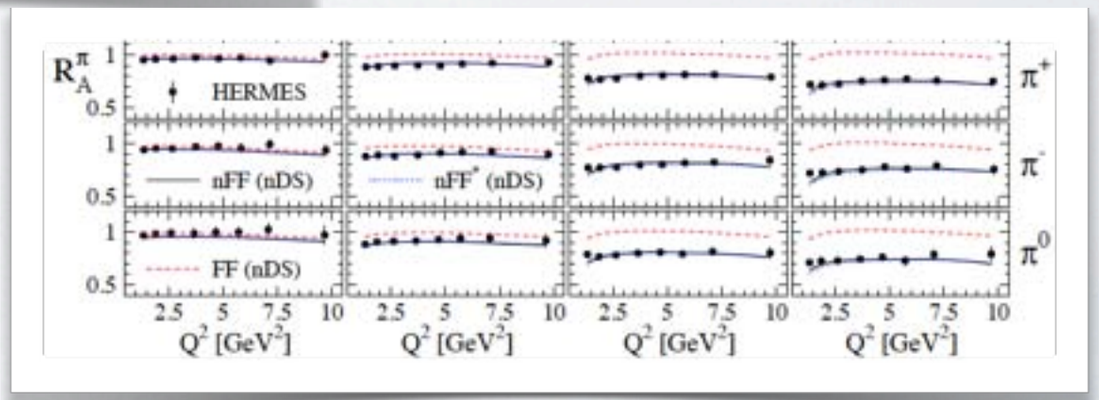

medium modified fragmentation

how to model fragmentation in a medium ?

medium modified fragmentation

how to model fragmentation in a medium ?

bold attempt: extend FFs to medium modified FFs ("in the background of a nucleus A") Sassot, MS, Zurita 0912.1311

choose convolution ansatz to modify vacuum FFs

DSS vacuum FFs

$$\mathbf{D^H_{i/A}(z, Q_0) = \int_z^1 \frac{dy}{y} W_i(y, A)\, D^H_i\left(\frac{z}{y}, Q_0\right)}$$

from fit to HERMES and RHIC dAu pion data

medium modified fragmentation

how to model fragmentation in a medium ?

bold attempt: extend FFs to medium modified FFs ("in the background of a nucleus A") Sassot, MS, Zurita 0912.1311

choose convolution ansatz to modify vacuum FFs

DSS vacuum FFs

$$D^{H}_{i/A}(z, Q_0) = \int_z^1 \frac{dy}{y} W_i(y, A)\, D^{H}_{i}\left(\frac{z}{y}, Q_0\right)$$

from fit to HERMES and RHIC dAu pion data

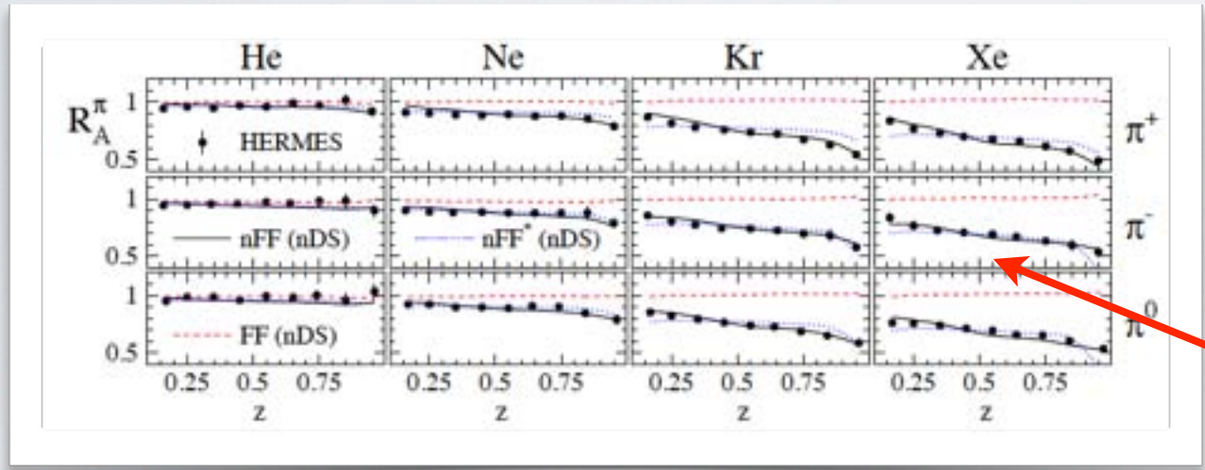

works well

Experiment	A	H	Data type	Data points	χ^2
HERMES [6]	He,Ne,Kr,Xe	π^+	z	36	39.3
		π^-	z	36	23.0
		π^0	z	36	27.4
		π^+	x	36	69.4
		π^-	x	36	55.4
		π^0	x	36	49.7
		π^+	Q^2	32	21.0
		π^-	Q^2	32	27.1
		π^0	Q^2	32	34.7
PHENIX [14]	Au	π^0	p_T	22	13.7
STAR (prel.) [16]	Au	π^0	p_T	13	12.8
STAR [15]	Au	$\pi^\pm$	p_T	34	22.5
Total				381	396.0

medium modified fragmentation

how to model fragmentation in a medium ?

bold attempt: extend FFs to medium modified FFs ("in the background of a nucleus A") Sassot, MS, Zurita 0912.1311

choose convolution ansatz to modify vacuum FFs

DSS vacuum FFs

$$D^{H}_{i/A}(z, Q_0) = \int_z^1 \frac{dy}{y} W_i(y, A)\, D^{H}_{i}\left(\frac{z}{y}, Q_0\right)$$

from fit to HERMES and RHIC dAu pion data

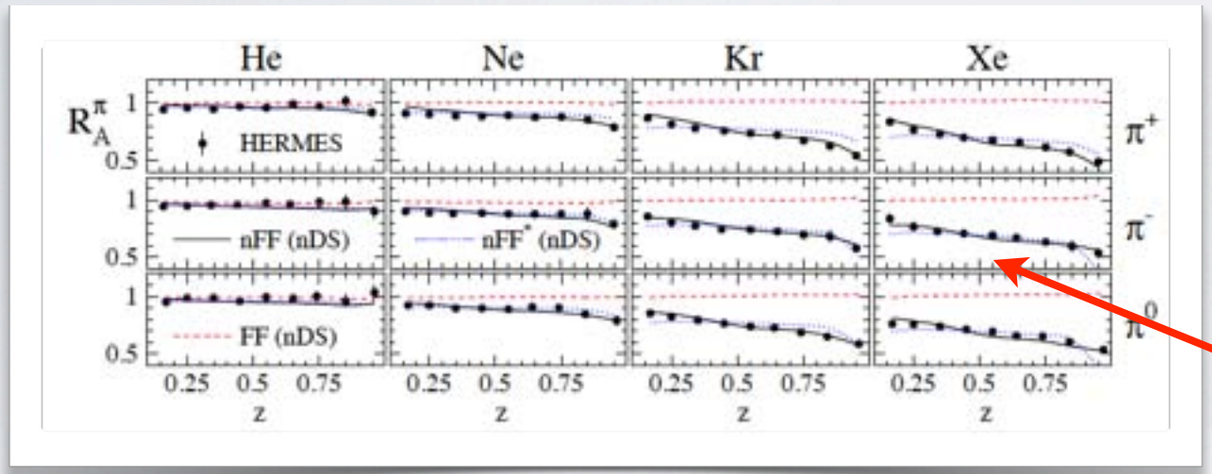

works well

Experiment	A	H	Data type	Data points	χ^2
HERMES [6]	He,Ne,Kr,Xe	π^+	z	36	39.3
		π^-	z	36	23.0
		π^0	z	36	27.4
		π^+	x	36	69.4
		π^-	x	36	55.4
		π^0	x	36	49.7
		π^+	Q^2	32	21.0
		π^-	Q^2	32	27.1
		π^0	Q^2	32	34.7
PHENIX [14]	Au	π^0	p_T	22	13.7
STAR (prel.) [16]	Au	π^0	p_T	13	12.8
STAR [15]	Au	$\pi^\pm$	p_T	34	22.5
Total				381	396.0

find:

- suppressed quark -> pion fragmentation (incr. with A)
- mildly enhanced gluon fragmentation around z=0.5

medium modified fragmentation

how to model fragmentation in a medium ?

bold attempt: extend FFs to medium modified FFs ("in the background of a nucleus A") Sassot, MS, Zurita 0912.1311

choose convolution ansatz to modify vacuum FFs

DSS vacuum FFs

$$\mathbf{D^H_{i/A}(z, Q_0) = \int_z^1 \frac{dy}{y} W_i(y, A)\, D^H_i\left(\frac{z}{y}, Q_0\right)}$$

from fit to HERMES and RHIC dAu pion data

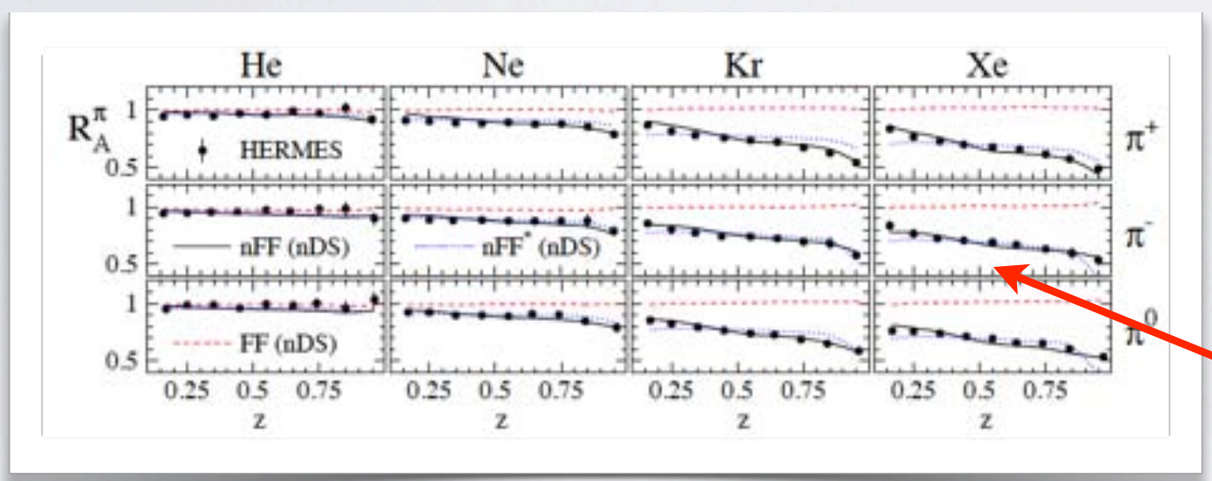

works well

Experiment	A	H	Data type	Data points	χ^2
HERMES [6]	He,Ne,Kr,Xe	π^+	z	36	39.3
		π^-	z	36	23.0
		π^0	z	36	27.4
		π^+	x	36	69.4
		π^-	x	36	55.4
		π^0	x	36	49.7
		π^+	Q^2	32	21.0
		π^-	Q^2	32	27.1
		π^0	Q^2	32	34.7
PHENIX [14]	Au	π^0	p_T	22	13.7
STAR (prel.) [16]	Au	π^0	p_T	13	12.8
STAR [15]	Au	$\pi^\pm$	p_T	34	22.5
Total				381	396.0

find:

- suppressed quark -> pion fragmentation (incr. with A)
- mildly enhanced gluon fragmentation around z=0.5

use both DSS vacuum and effective nuclear FFs in DSSZ nPDF analysis

more on mid rapidity pions

at RHIC (mid rapidity) we probe large z
and mostly pions from gluons

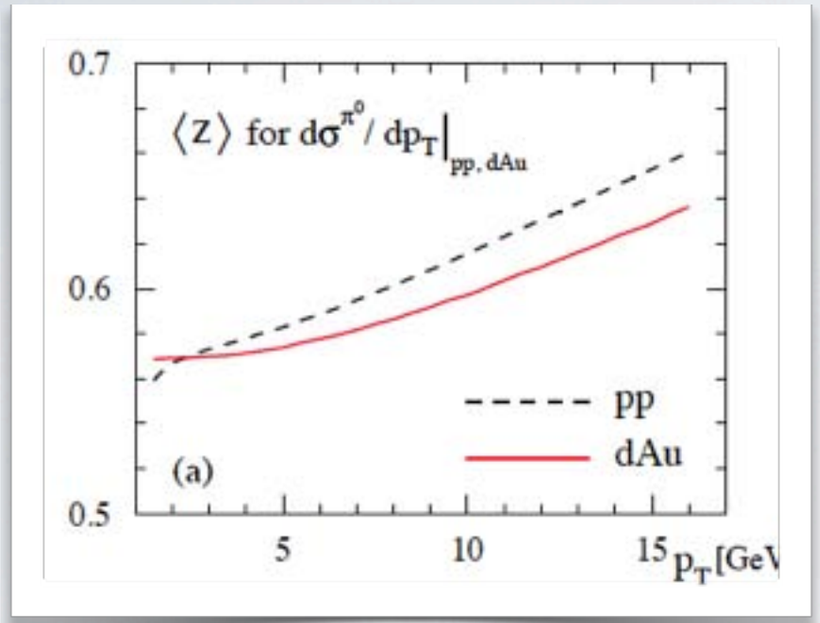

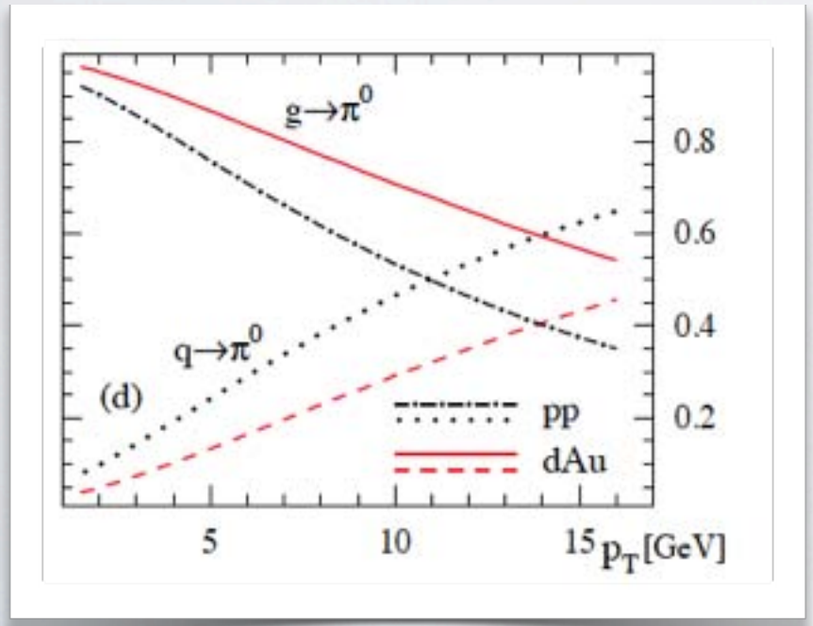

Sassot, MS, Zurita 0912.1311

more on mid rapidity pions

at RHIC (mid rapidity) we probe large z and mostly pions from gluons

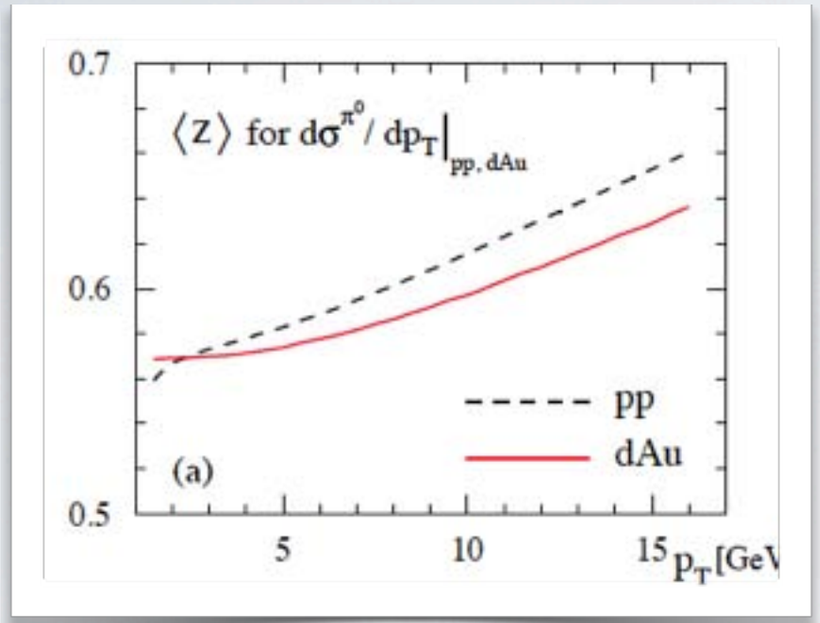

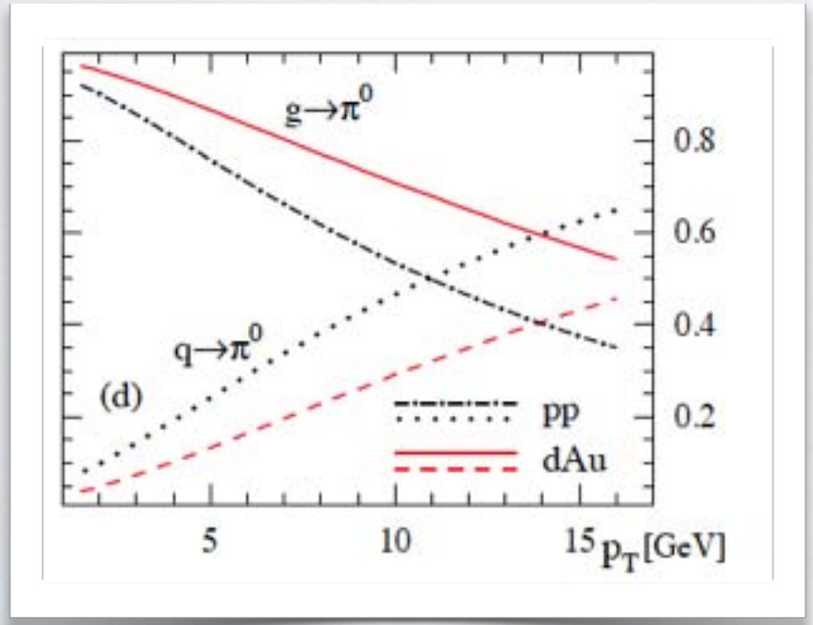

Sassot, MS, Zurita 0912.1311

result of our nPDF fit

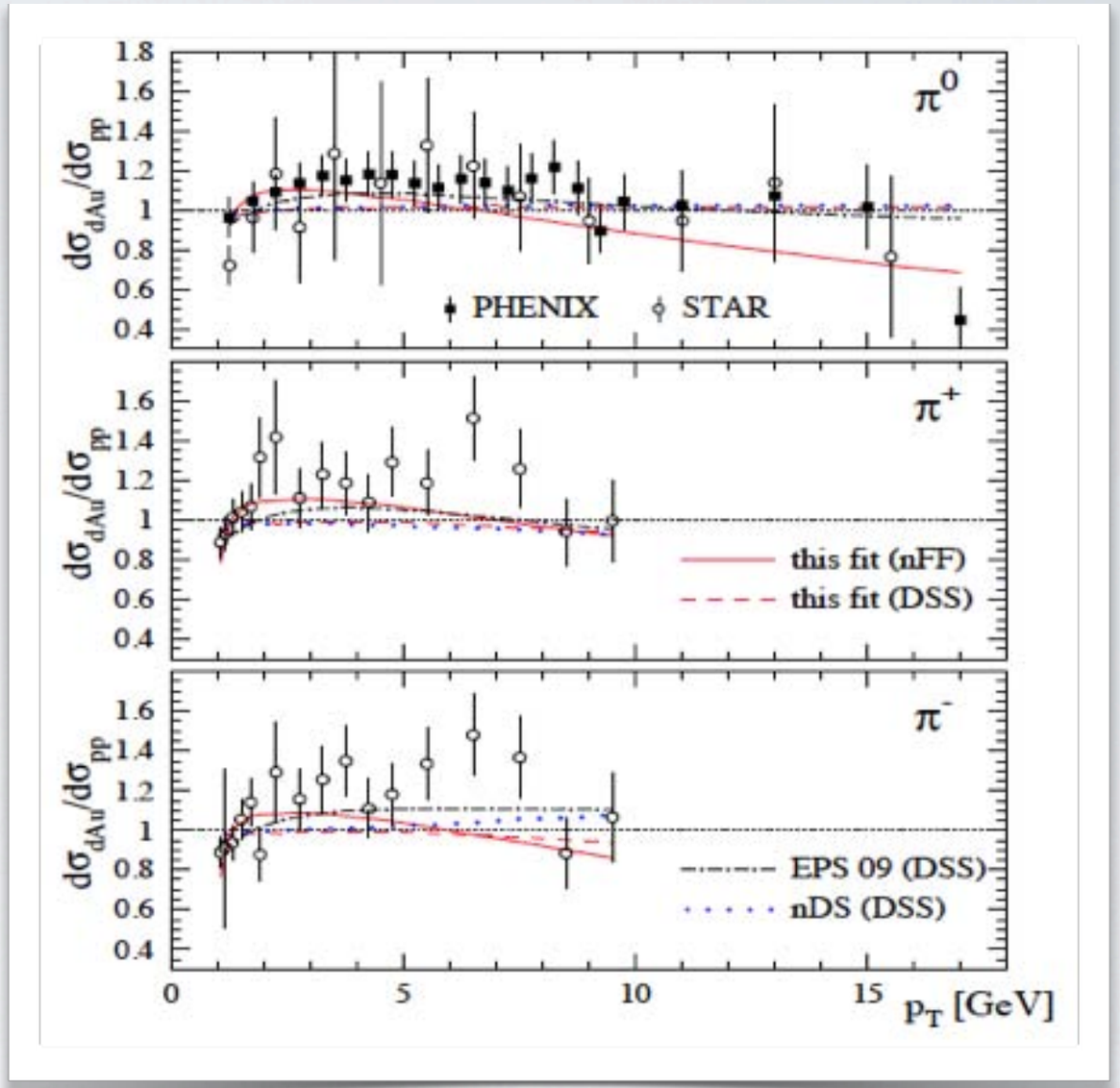

- good fit within large exp. uncertainties
- choice of FF has some impact (but not too much)

$$\chi^2 : \mathbf{68.3}\,(\mathrm{nFF}) \rightarrow \mathbf{83.6}\,(\mathrm{DSS})$$

more on mid rapidity pions

at RHIC (mid rapidity) we probe large z and mostly pions from gluons

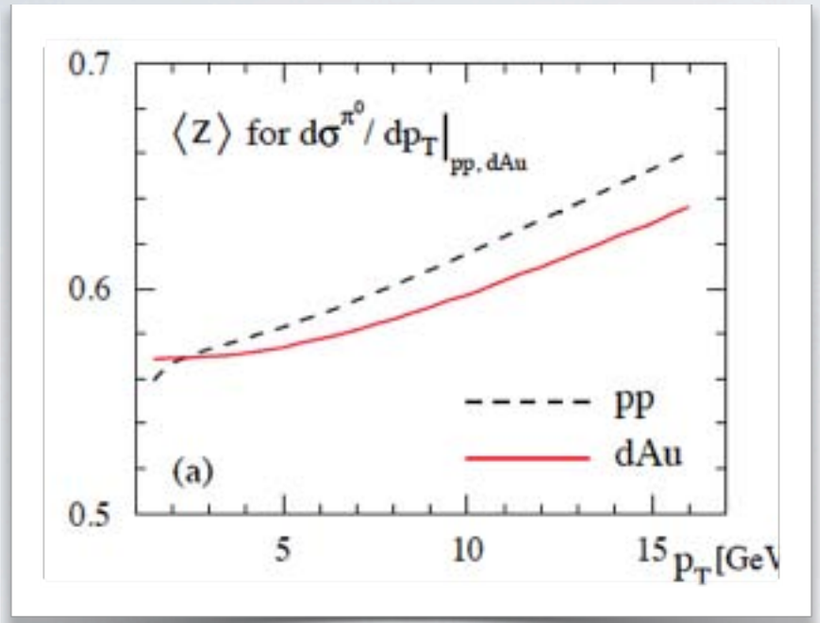

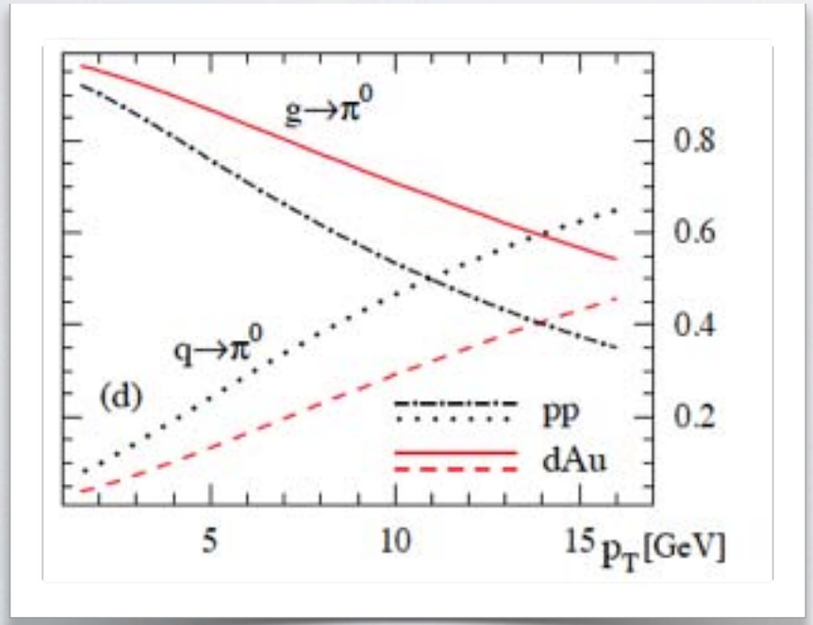

Sassot, MS, Zurita 0912.1311

result of our nPDF fit

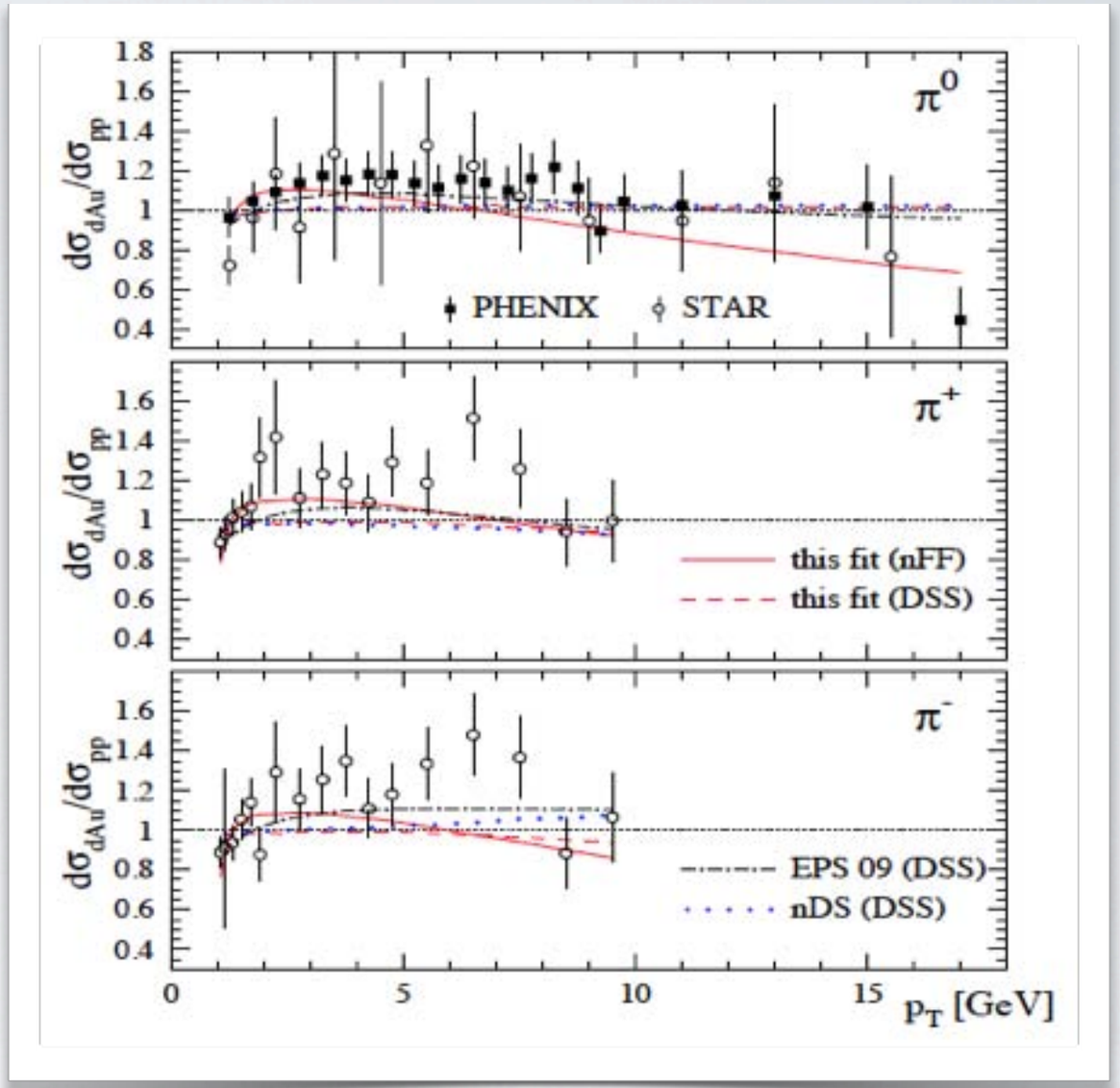

- good fit within large exp. uncertainties
- choice of FF has some impact (but not too much)

$$\chi^2 : \mathbf{68.3}\,(\mathrm{nFF}) \rightarrow \mathbf{83.6}\,(\mathrm{DSS})$$

- unlike EPS fit, limited impact on gluon (no weight factor)

more on mid rapidity pions

at RHIC (mid rapidity) we probe large z and mostly pions from gluons

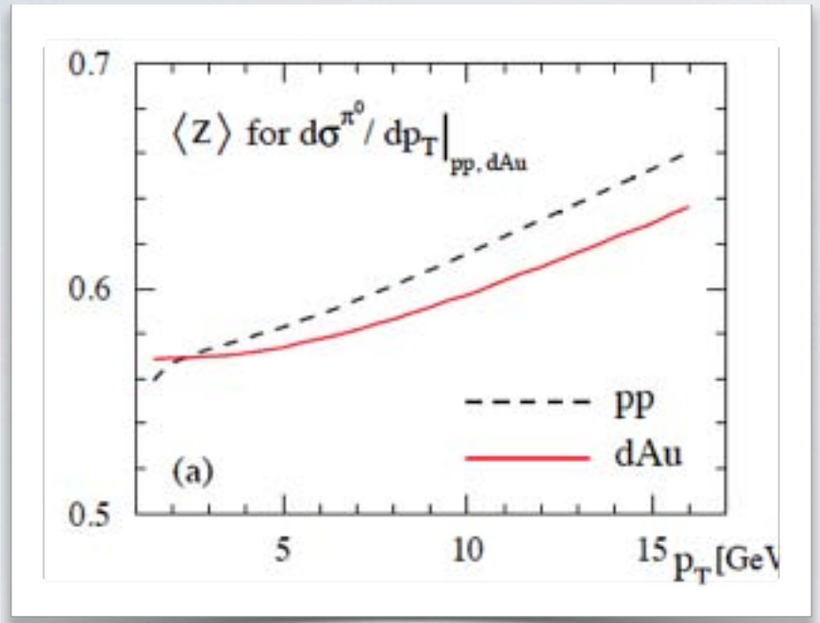

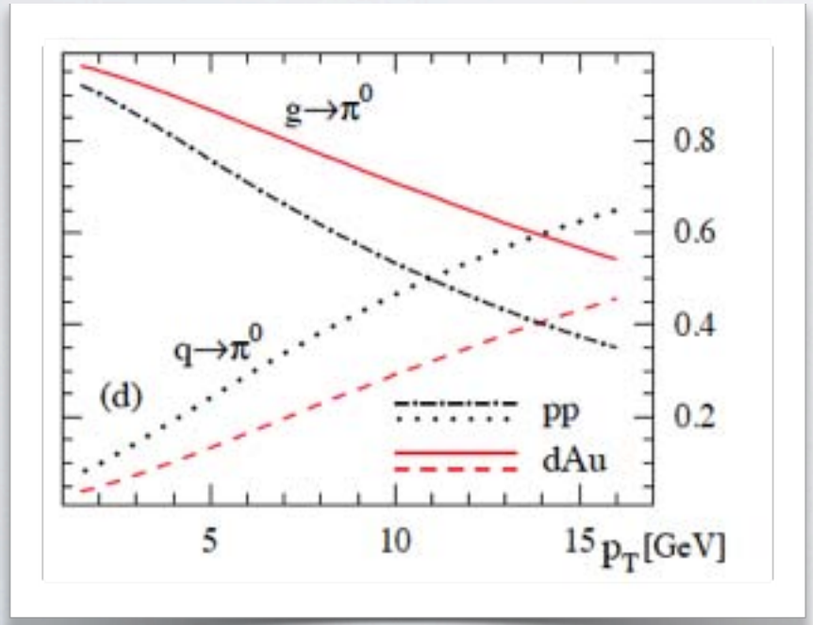

Sassot, MS, Zurita 0912.1311

result of our nPDF fit

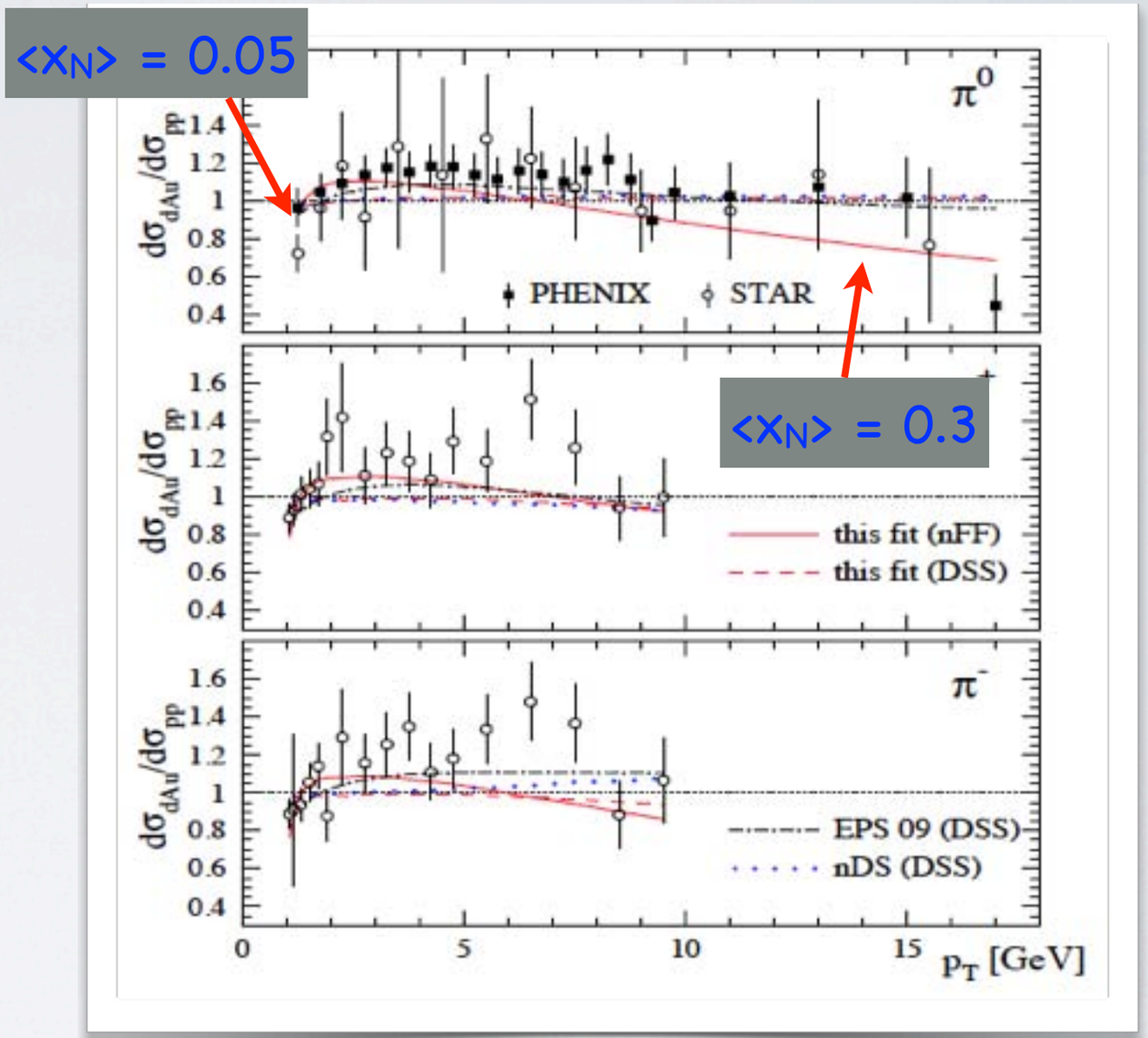

- good fit within large exp. uncertainties
- choice of FF has some impact (but not too much)

$$\chi^2 : \mathbf{68.3}\,(\mathrm{nFF}) \rightarrow \mathbf{83.6}\,(\mathrm{DSS})$$

- unlike EPS fit, limited impact on gluon (no weight factor)

more on mid rapidity pions

at RHIC (mid rapidity) we probe large z and mostly pions from gluons

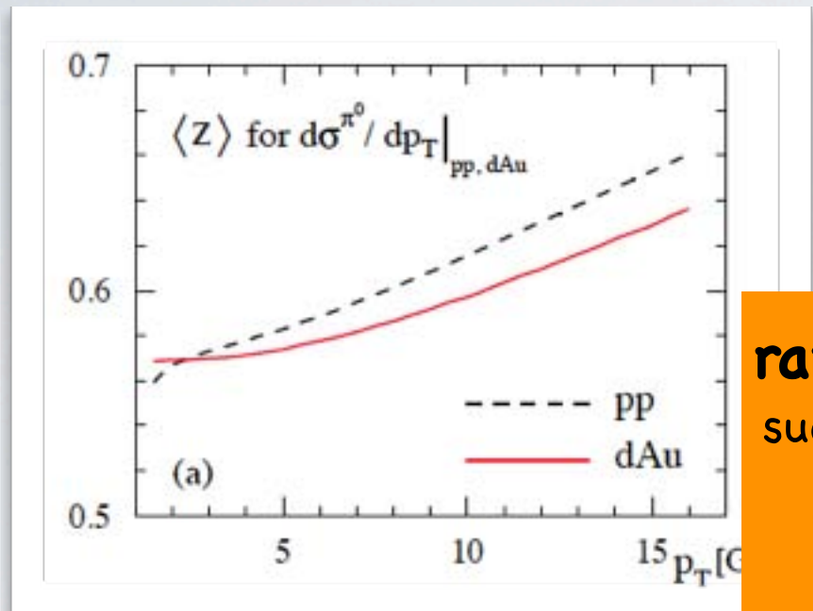

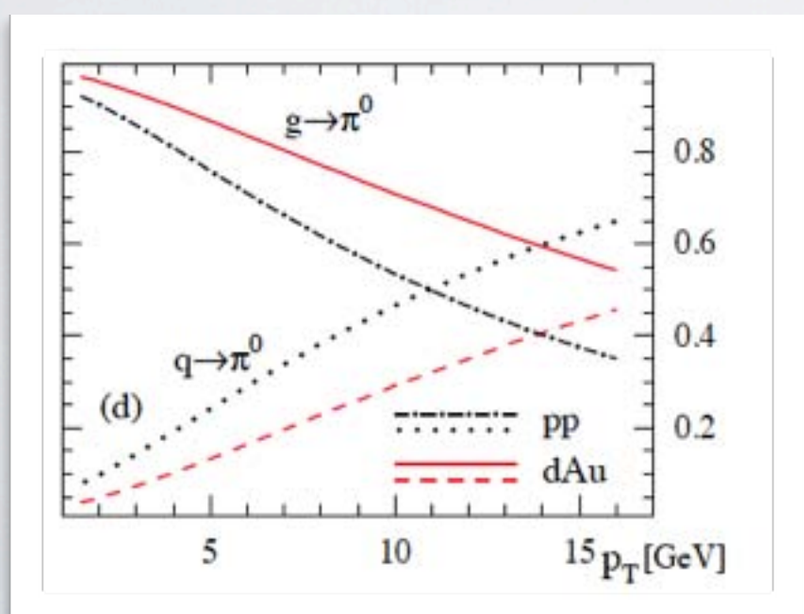

result of our nPDF fit

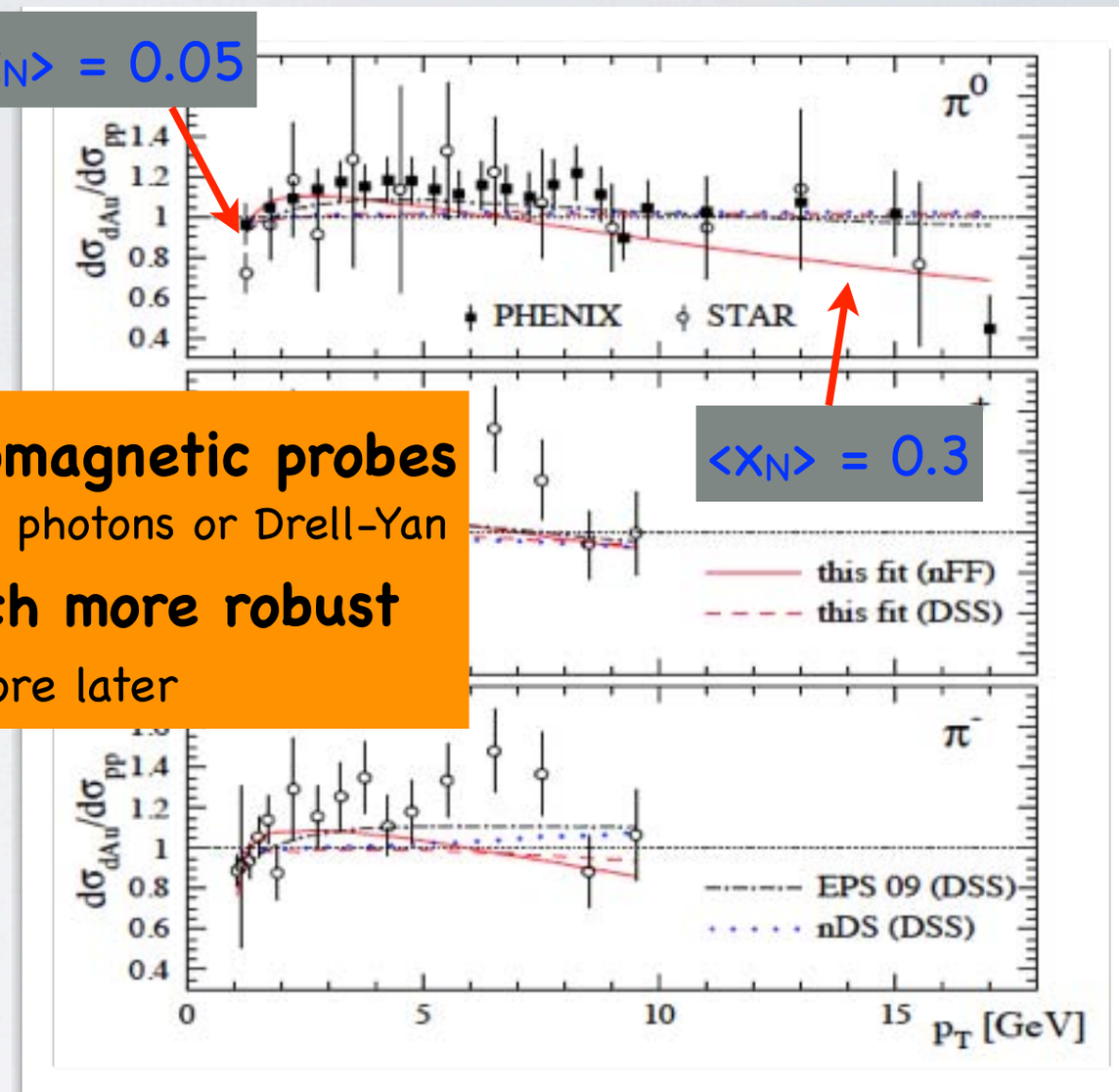

rare electromagnetic probes
such as prompt photons or Drell-Yan
are a much more robust
more later

- good fit within large exp. uncertainties
- choice of FF has some impact (but not too much)

$$\chi^2 : \mathbf{68.3}\,(\mathrm{nFF}) \rightarrow \mathbf{83.6}\,(\mathrm{DSS})$$

- unlike EPS fit, limited impact on gluon (no weight factor)

Sassot, MS, Zurita 0912.1311

pions in dAu at forward rapidity

why interesting

- allows to access smaller x in nucleus
- gets one closer to the region where one expects saturation effects

$$x_{1,2} \simeq \frac{p_T}{\sqrt{s}} e^{\pm y}$$

pions in dAu at forward rapidity

why interesting

- allows to access smaller x in nucleus
- gets one closer to the region where one expects saturation effects

$$x_{1,2} \simeq \frac{p_T}{\sqrt{s}} e^{\pm y}$$

data indicate strong suppression of gluons at small x and low scales

forward suppression well described within **non-linear rcBK evolution** (CGC)

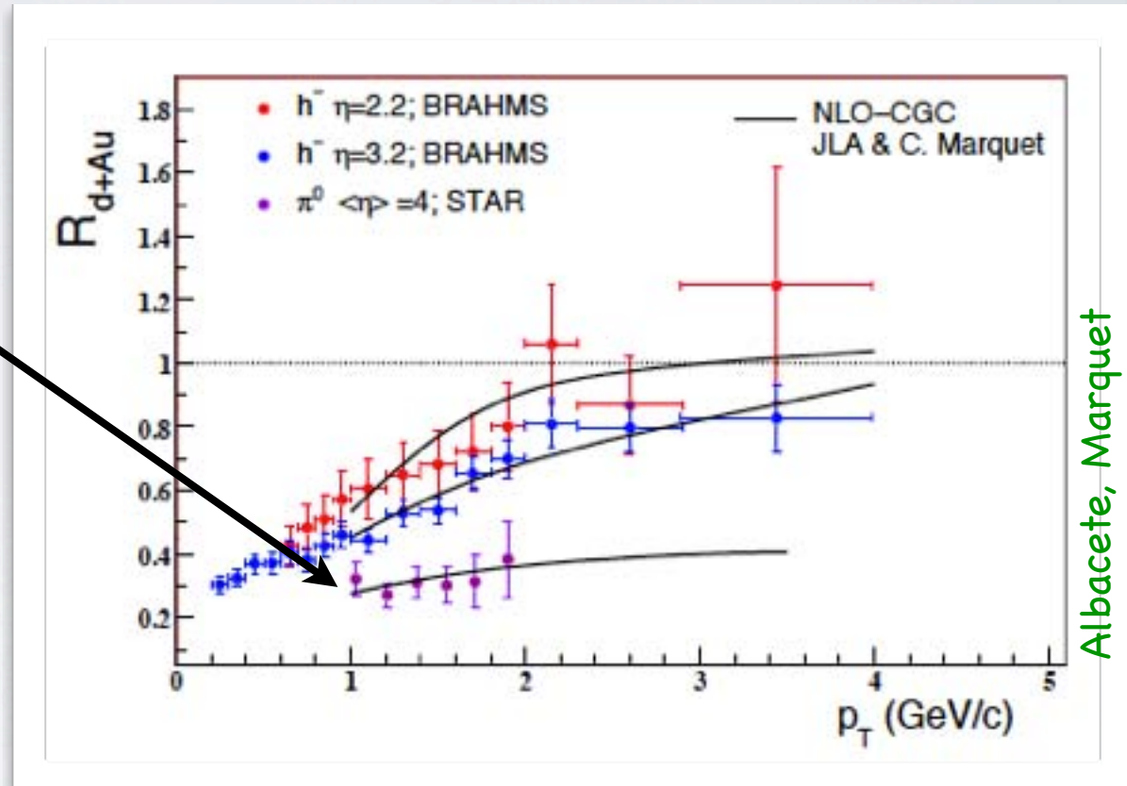

pions in dAu at forward rapidity

why interesting

- allows to access smaller x in nucleus
- gets one closer to the region where one expects saturation effects

$$x_{1,2} \simeq \frac{p_T}{\sqrt{s}} e^{\pm y}$$

data indicate strong suppression of gluons at small x and low scales

forward suppression well described within **non-linear rcBK evolution** (CGC)

what does it take to describe it with nPDFs

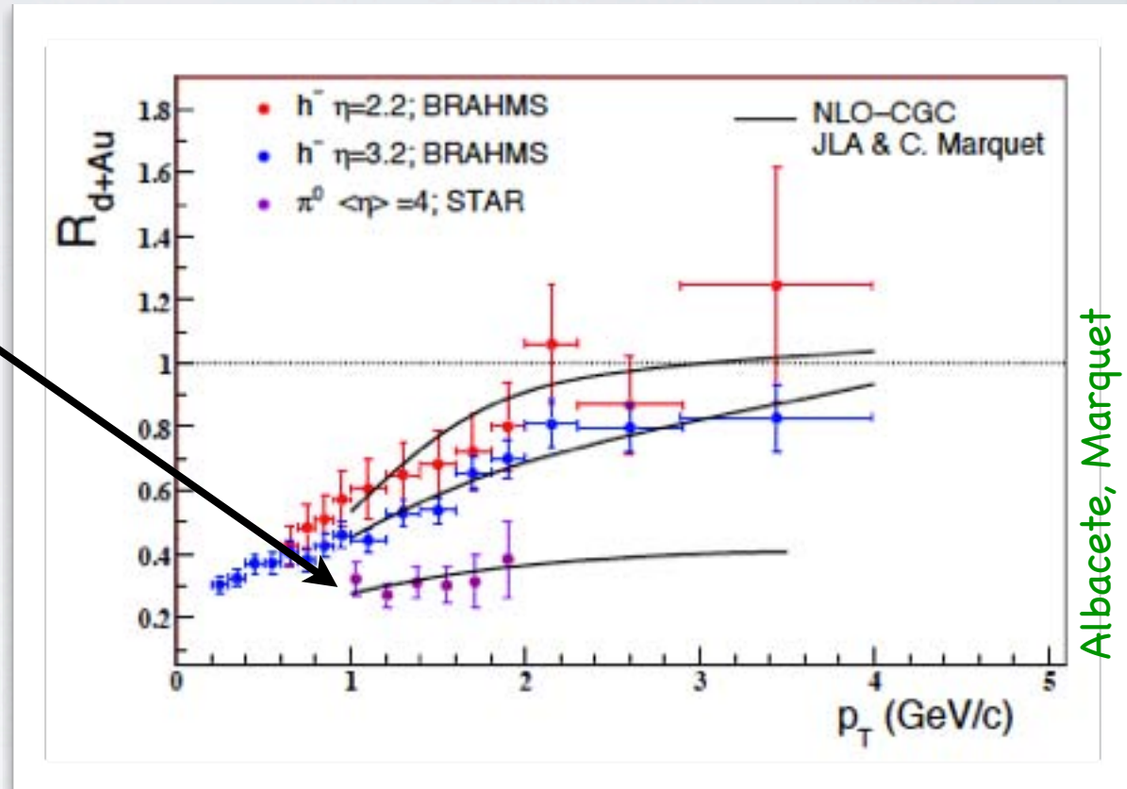

pions in dAu at forward rapidity

why interesting

- allows to access smaller x in nucleus
- gets one closer to the region where one expects saturation effects

$$x_{1,2} \simeq \frac{p_T}{\sqrt{s}} e^{\pm y}$$

data indicate strong suppression of gluons at small x and low scales

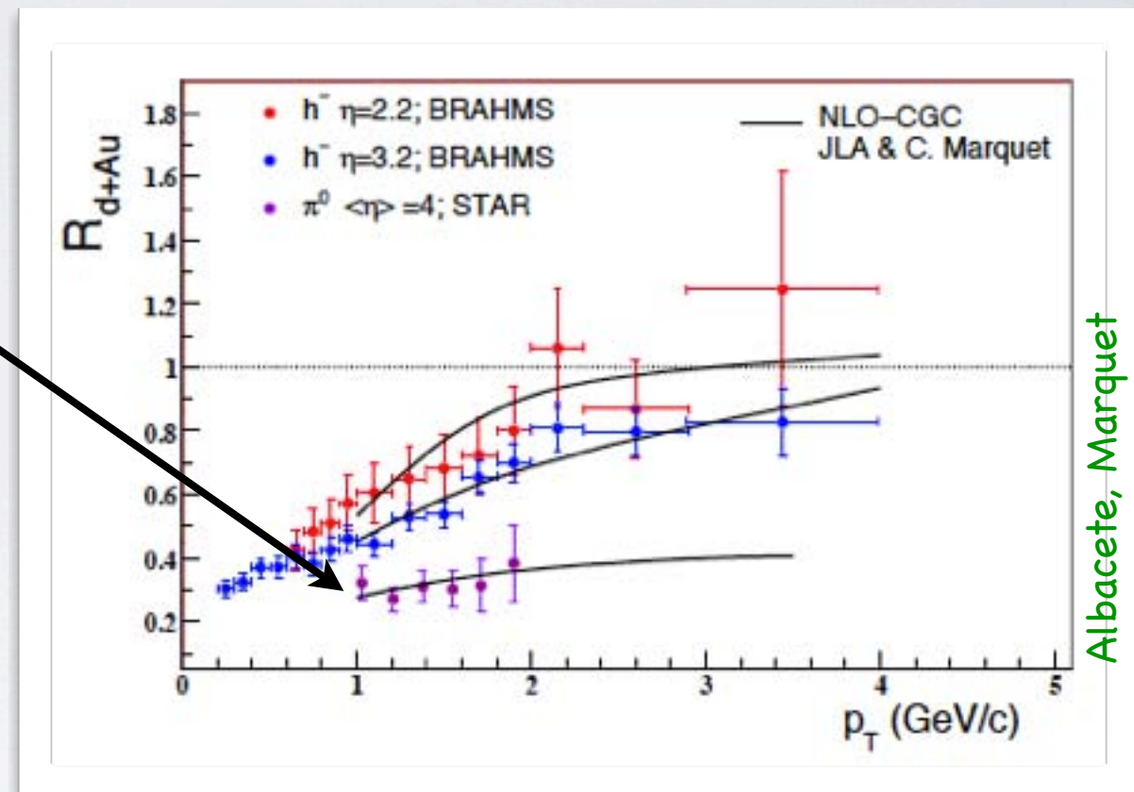

forward suppression well described within **non-linear rcBK evolution** (CGC)

what does it take to describe it with nPDFs

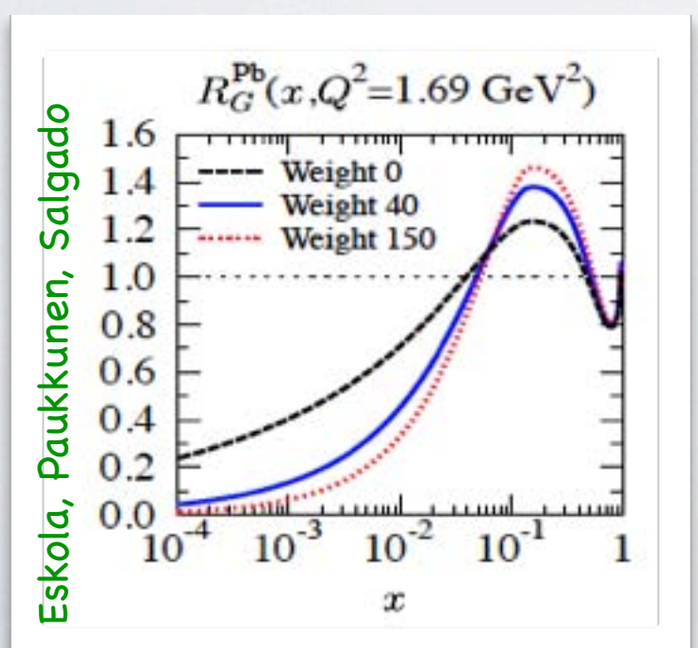

- need humongous shadowing at a scale of about 1 GeV

pions in dAu at forward rapidity

why interesting

- allows to access smaller x in nucleus
- gets one closer to the region where one expects saturation effects

$$x_{1,2} \simeq \frac{p_T}{\sqrt{s}} e^{\pm y}$$

data indicate strong suppression of gluons at small x and low scales

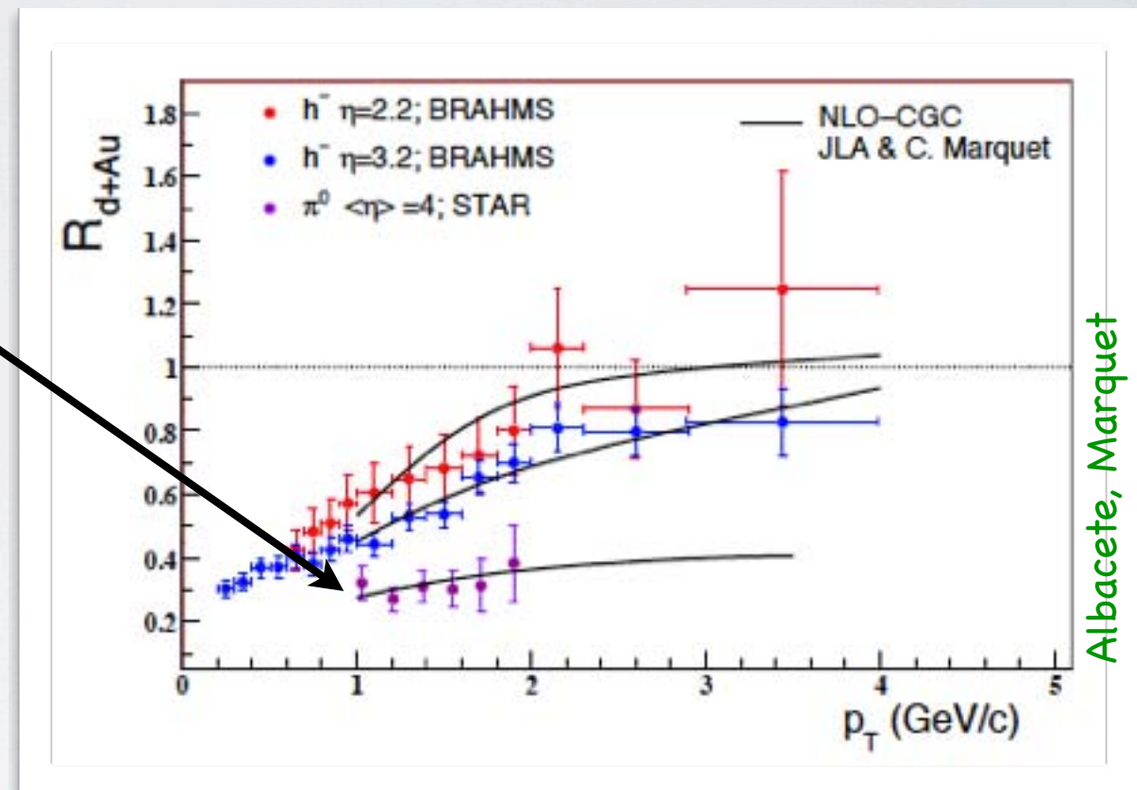

forward suppression well described within **non-linear rcBK evolution** (CGC)

what does it take to describe it with nPDFs

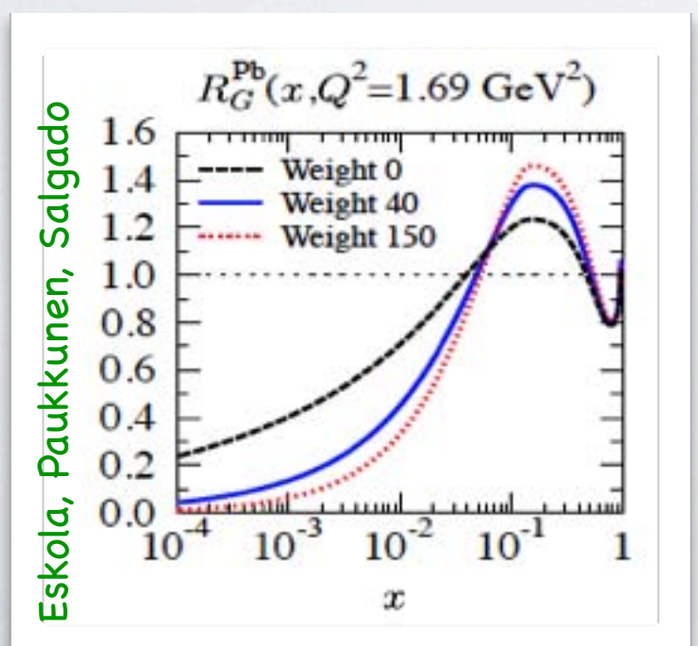

- need humongous shadowing at a scale of about 1 GeV

⚠ could be much less if final-state effects are relevant

advocated by Frankfurt, Strikman; Kopeliovich; ...

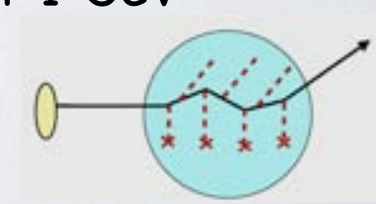

pions in dAu at forward rapidity

why interesting

- allows to access smaller
- gets one closer to the re
  one expects saturation e

$$x_{1,2} \simeq \frac{p_T}{\sqrt{s}} e^{\pm y}$$

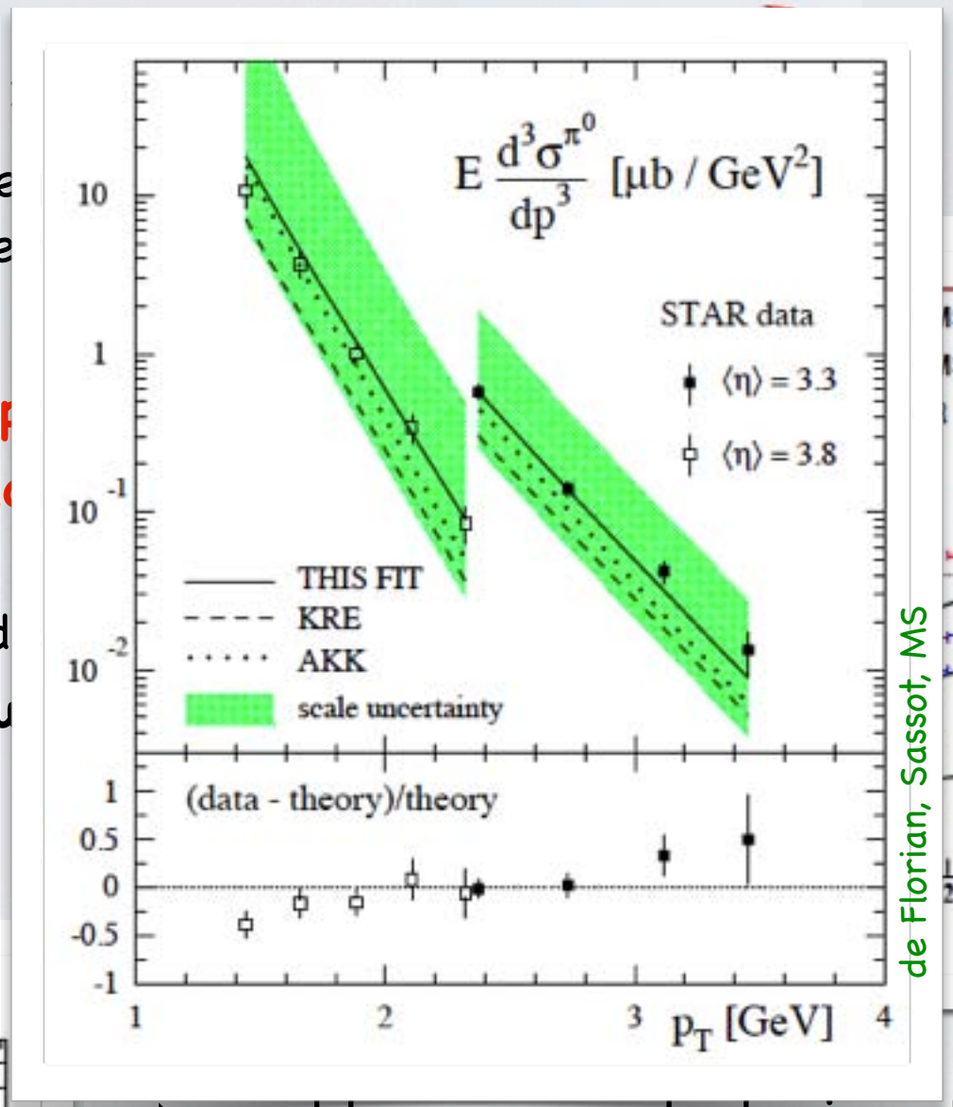

de Florian, Sassot, MS

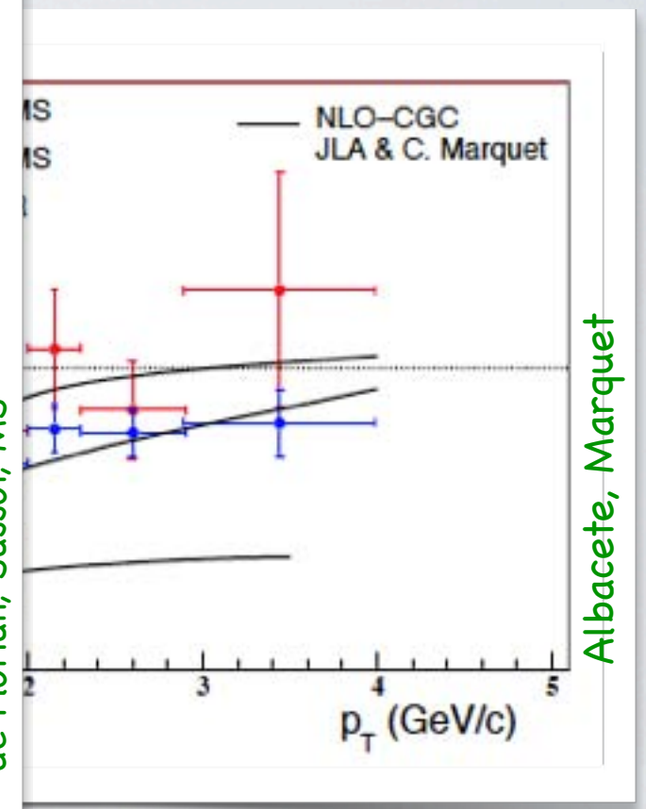

Albacete, Marquet

data indicate strong supp
of gluons at small x and l

forward suppression well d
within **non-linear rcBK evolu**

what does it take to describe

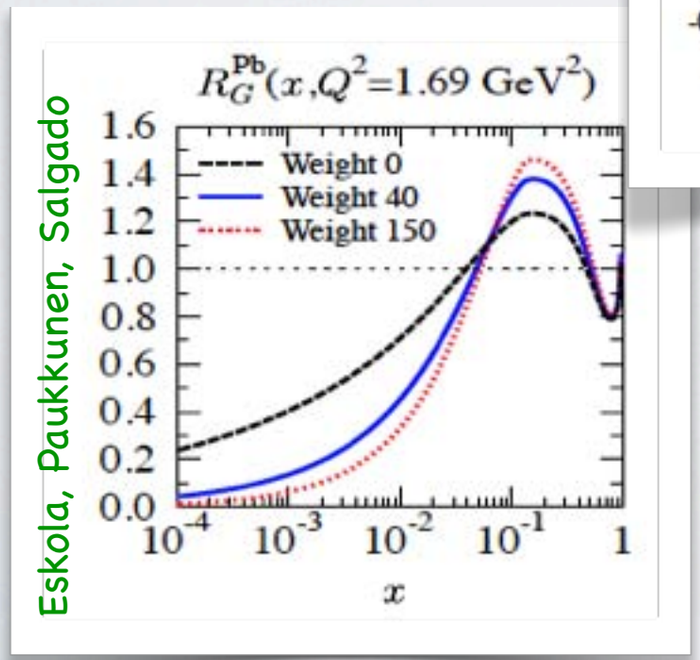

Eskola, Paukkunen, Salgado

- need humongous shadowing at a scale of about 1 GeV

⚠ could be much less if final-state effects are relevant
advocated by Frankfurt, Strikman; Kopeliovich; ...

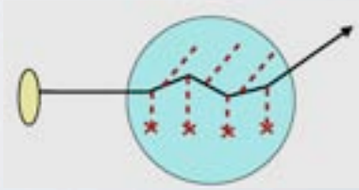

⚠ pQCD does not work well at small p_T and large y
corrections become excessive; pp data for y=4 not used in any fit

general issue with pQCD and forward physics at RHIC
recall: CGC has Q_S as additional semi-hard scale

how "bad" are extreme initial conditions?

we refrain from using the forward dAu data in our analysis ...

... however, there is enough freedom at small x to enforce a good description at the expense of strong shadowing

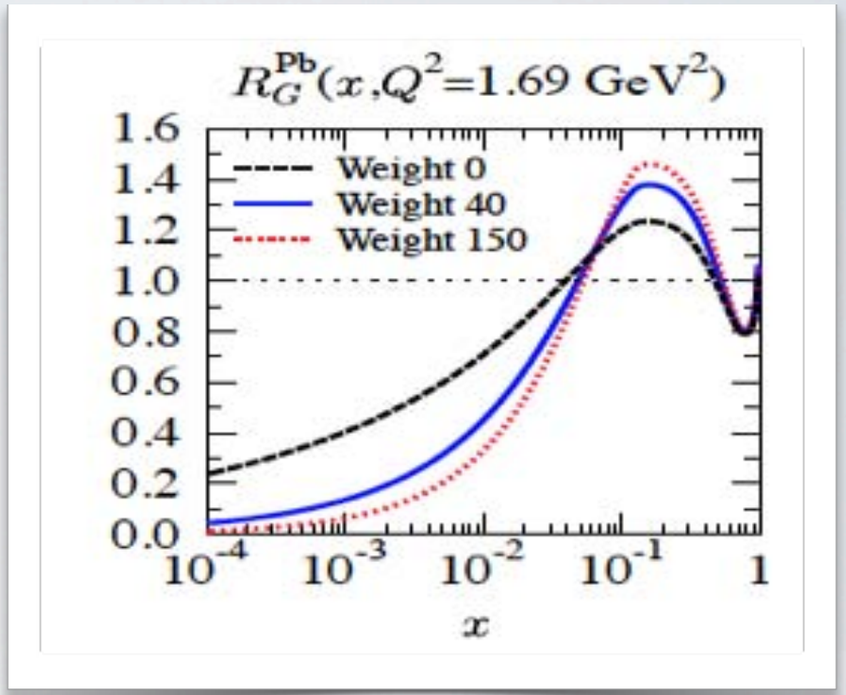

how "bad" are extreme initial conditions?

we refrain from using the forward dAu data in our analysis ...

... however, there is enough freedom at small x to enforce a good description at the expense of strong shadowing

an evil choice of initial conditions ?

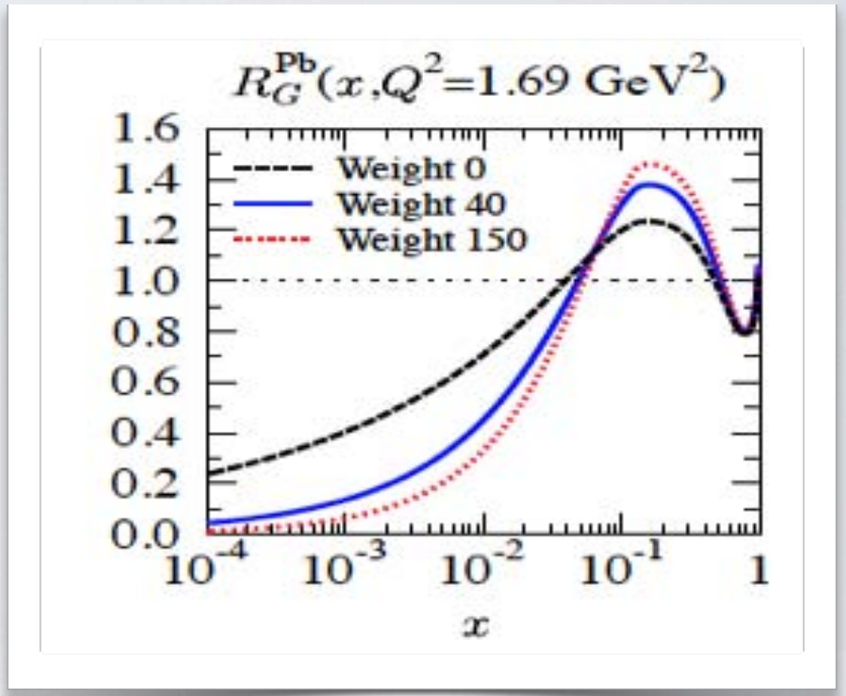

how "bad" are extreme initial conditions?

we refrain from using the forward dAu data in our analysis ...

... however, there is enough freedom at small x to enforce a good description at the expense of strong shadowing

an evil choice of initial conditions ?

well, ...

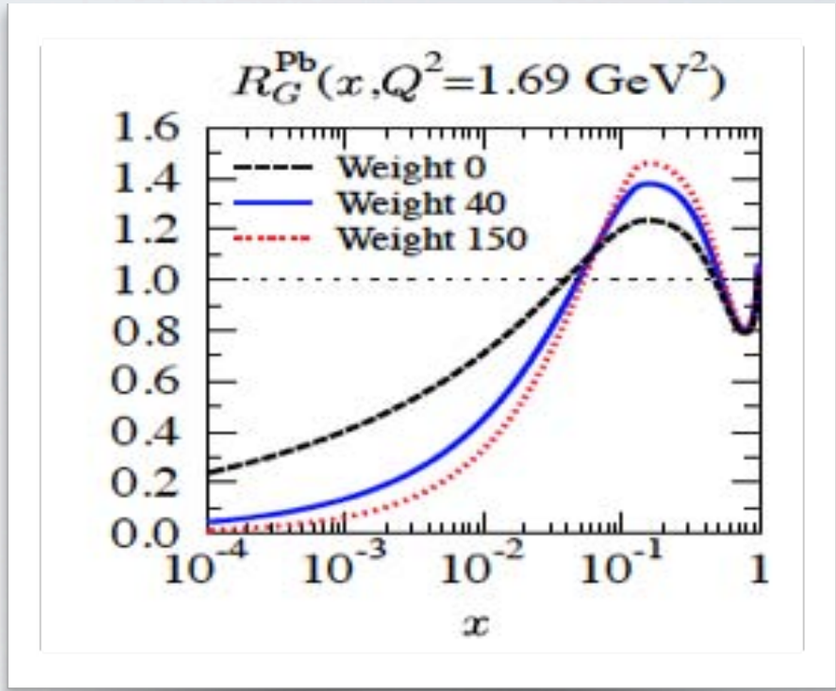

- DGLAP only predicts the scale evolution
- input usually quickly washed out

how "bad" are extreme initial conditions?

we refrain from using the forward dAu data in our analysis ...

... however, there is enough freedom at small x to enforce a good description at the expense of strong shadowing

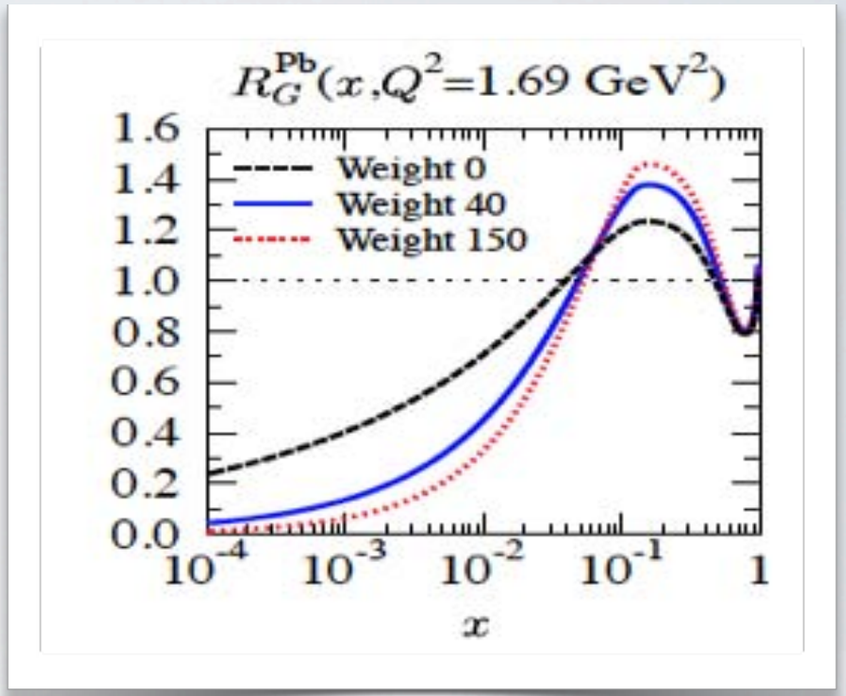

an evil choice of initial conditions ?

well, ...

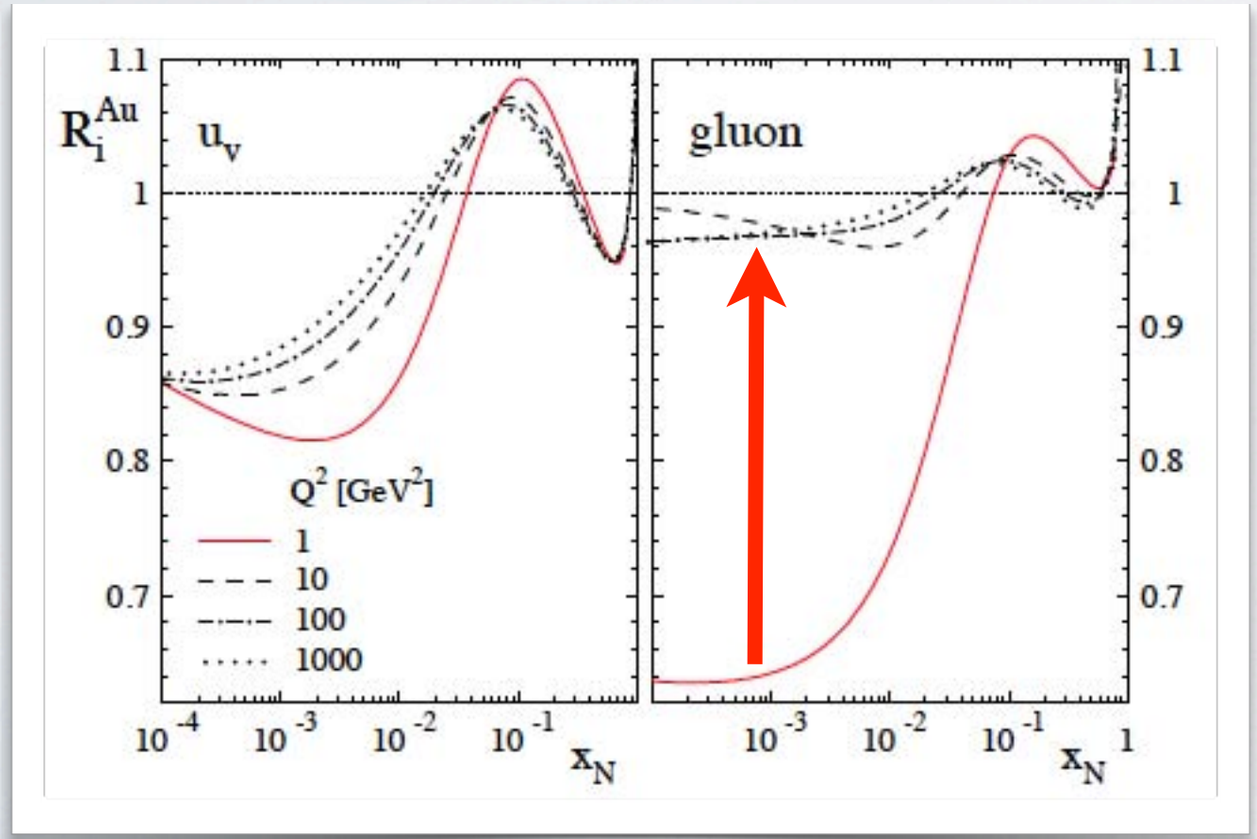

- DGLAP only predicts the scale evolution
- input usually quickly washed out

a strong shadowing of the gluon would quickly evolve away

how about using nPDFs in AA collisions ?

many observables of interest involve

small p_T, global properties, centrality dependence, ...

how about using nPDFs in AA collisions ?

many observables of interest involve

small p_T, global properties, centrality dependence, ...

- **nPDFs are collinear objects**
  there is no impact parameter or other geometrical dependence

  recently: EPS nPDFs decorated with some b dependence
  Helenius, Eskola, Honkanen, Salgado arXiv:1205.5359

- **many observables in AA have no "hard scale"**
  not amenable to pQCD calculations in standard factorizations

- **assuming factorization in AA is a stretch**
  there might be some hard probes where things work out though

how about using nPDFs in AA collisions ?

many observables of interest involve

small p_T, global properties, centrality dependence, ...

- **nPDFs are collinear objects**
  there is no impact parameter or other geometrical dependence
  recently: EPS nPDFs decorated with some b dependence
  Helenius, Eskola, Honkanen, Salgado arXiv:1205.5359

- **many observables in AA have no "hard scale"**
  not amenable to pQCD calculations in standard factorizations

- **assuming factorization in AA is a stretch**
  there might be some hard probes where things work out though

we do not touch AA data for the time being
nPDFs should be determined from probes in eA or pA
preferentially electromagnetic ones (free of hadronization issues)

DSSZ nPDFs and their uncertainties

uncertainties at input scale of 1 GeV (for gold nucleus)

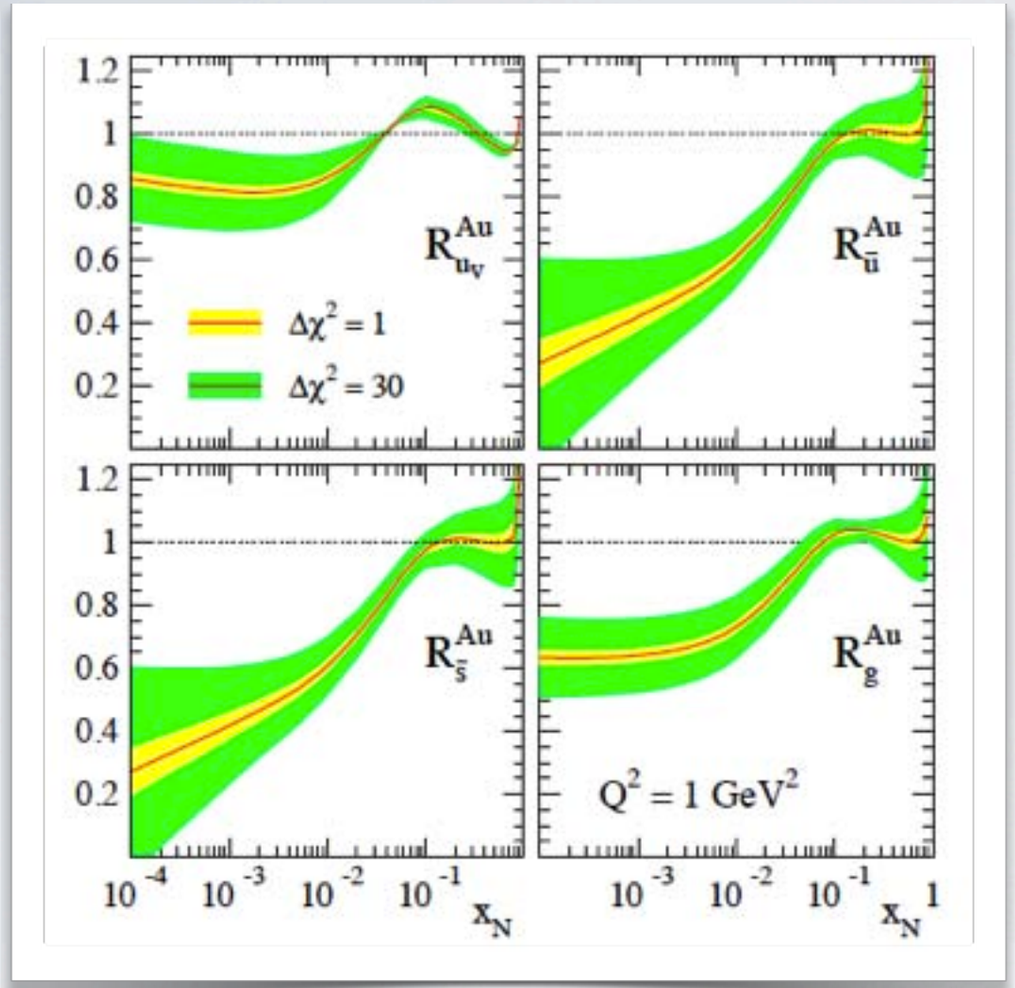

DSSZ nPDFs and their uncertainties

uncertainties at input scale of 1 GeV (for gold nucleus)

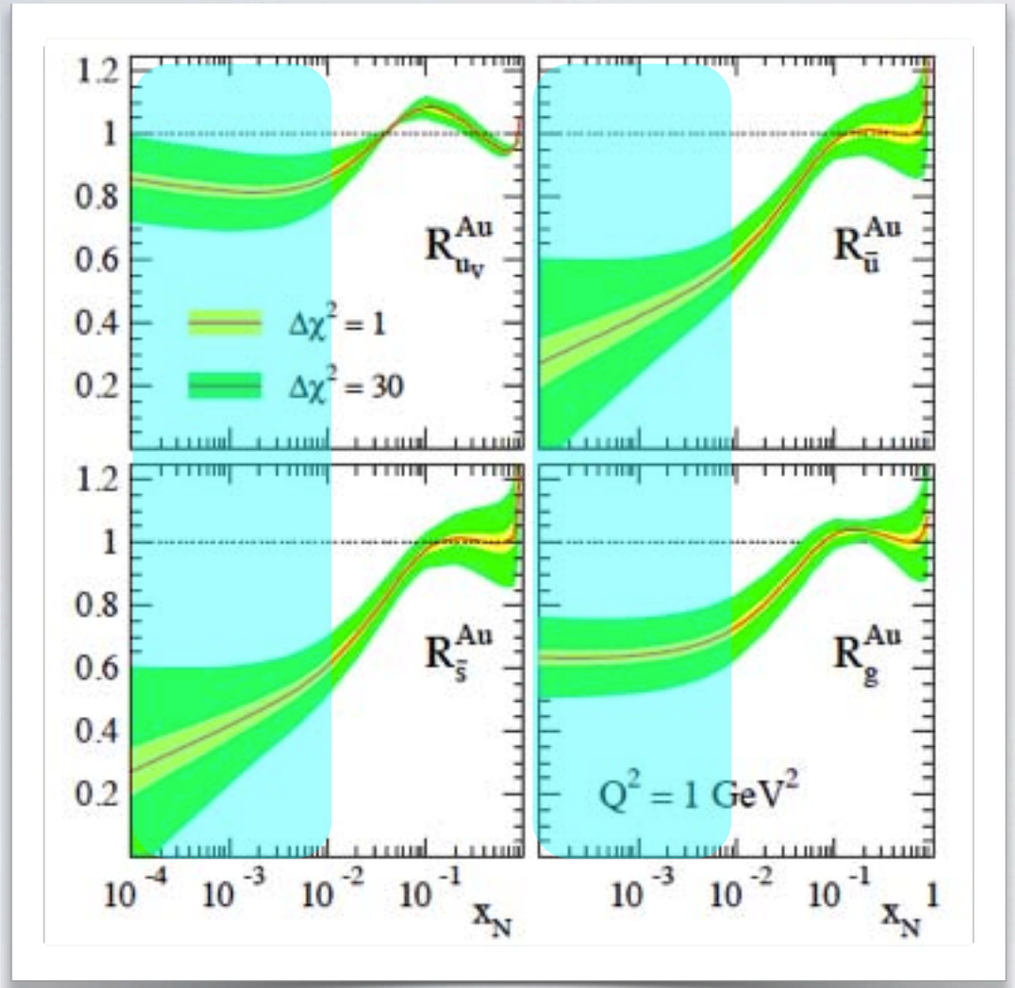

- **uncertainties below 0.01** merely reflect extrapolation of chosen functional form
  not constrained by any data

DSSZ nPDFs and their uncertainties

uncertainties at input scale of 1 GeV (for gold nucleus)

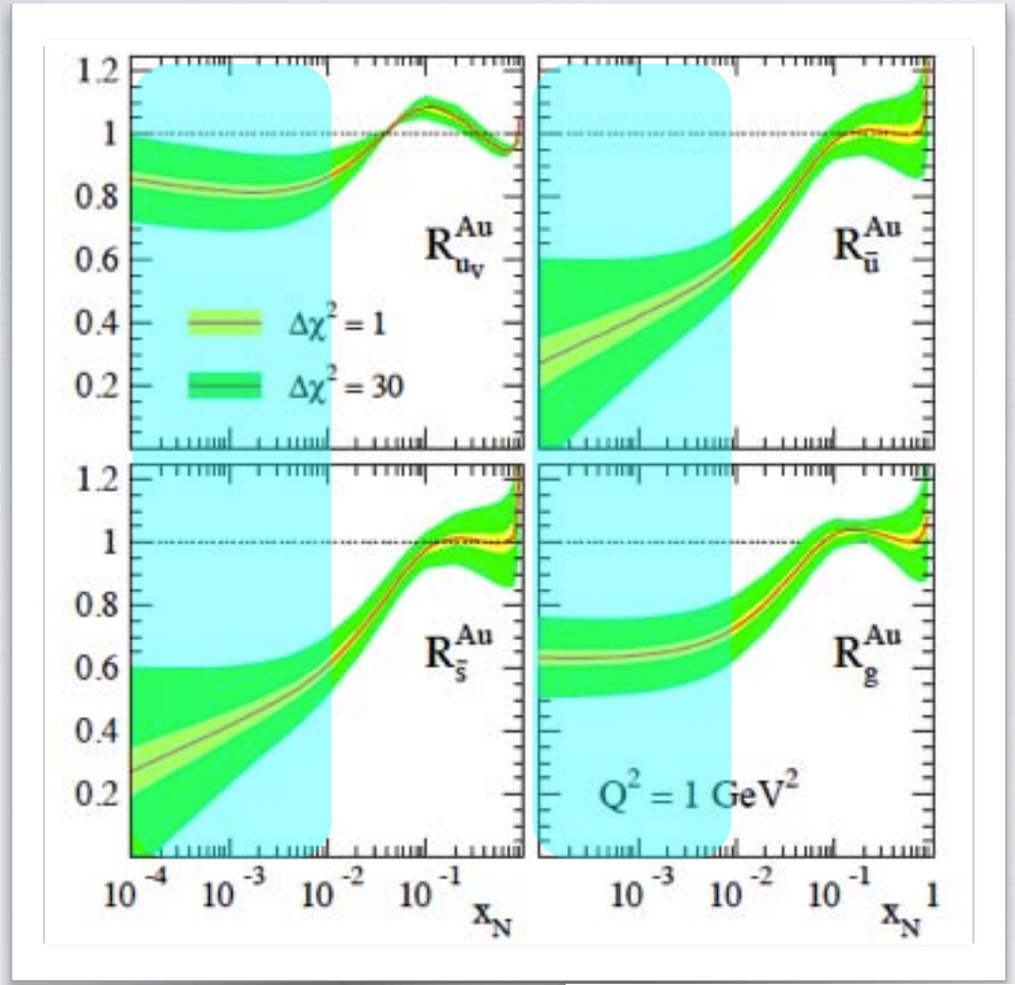

- **uncertainties below 0.01** merely reflect extrapolation of chosen functional form
  not constrained by any data

- nuclear modifications quickly diminish under evolution

evolve to 10 GeV²

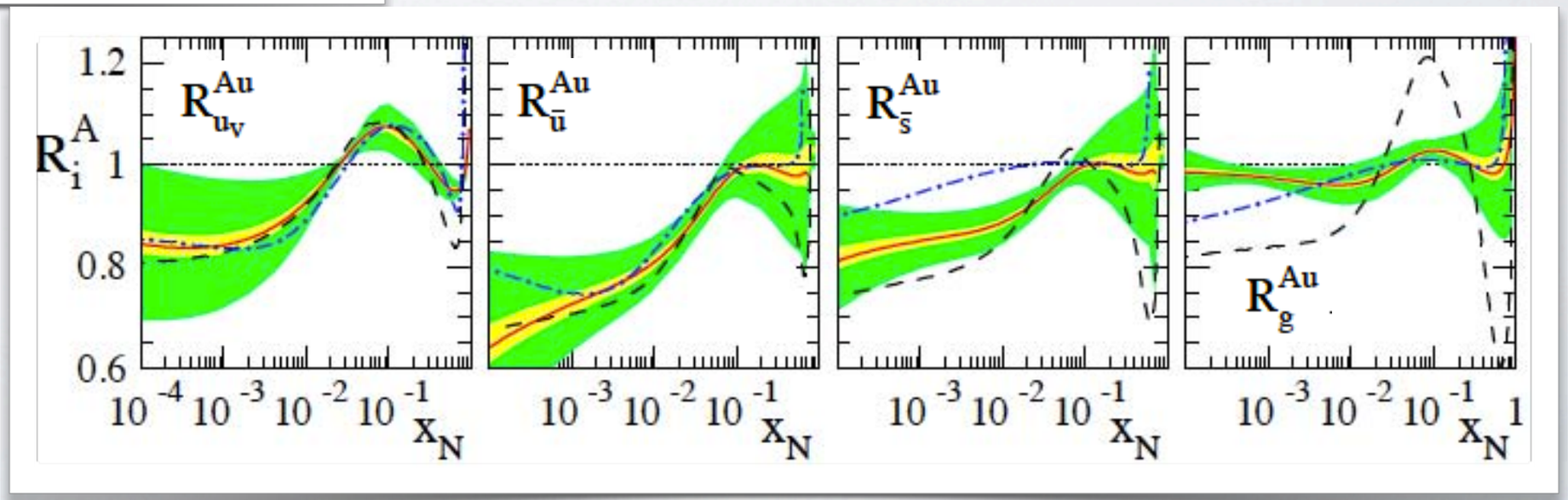

DSSZ nPDFs and their uncertainties

uncertainties at input scale of 1 GeV (for gold nucleus)

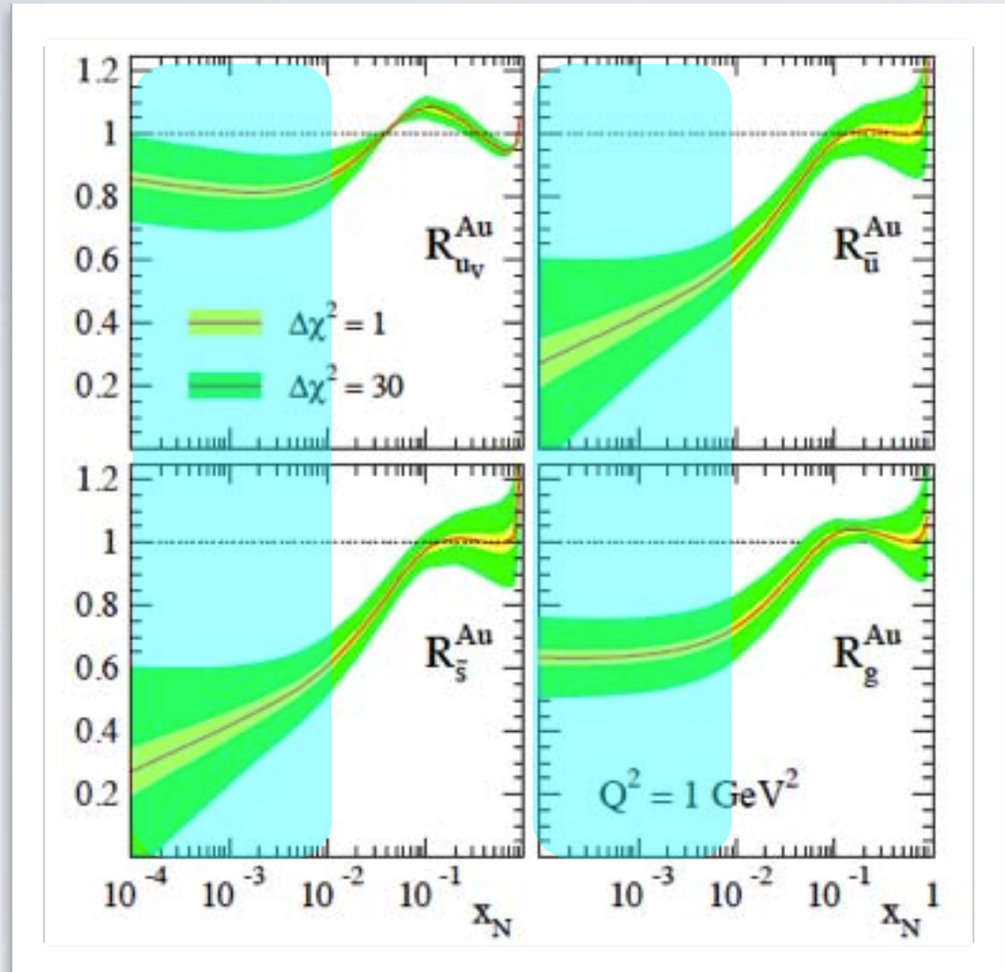

- **uncertainties below 0.01** merely reflect extrapolation of chosen functional form
  not constrained by any data

- nuclear modifications quickly diminish under evolution
- evolution imprints different nuclear effects on individual quark flavors
  recall: we start with $R^A_{\bar{u}} = R^A_{\bar{d}} = R^A_{\bar{s}}$

evolve to 10 GeV²

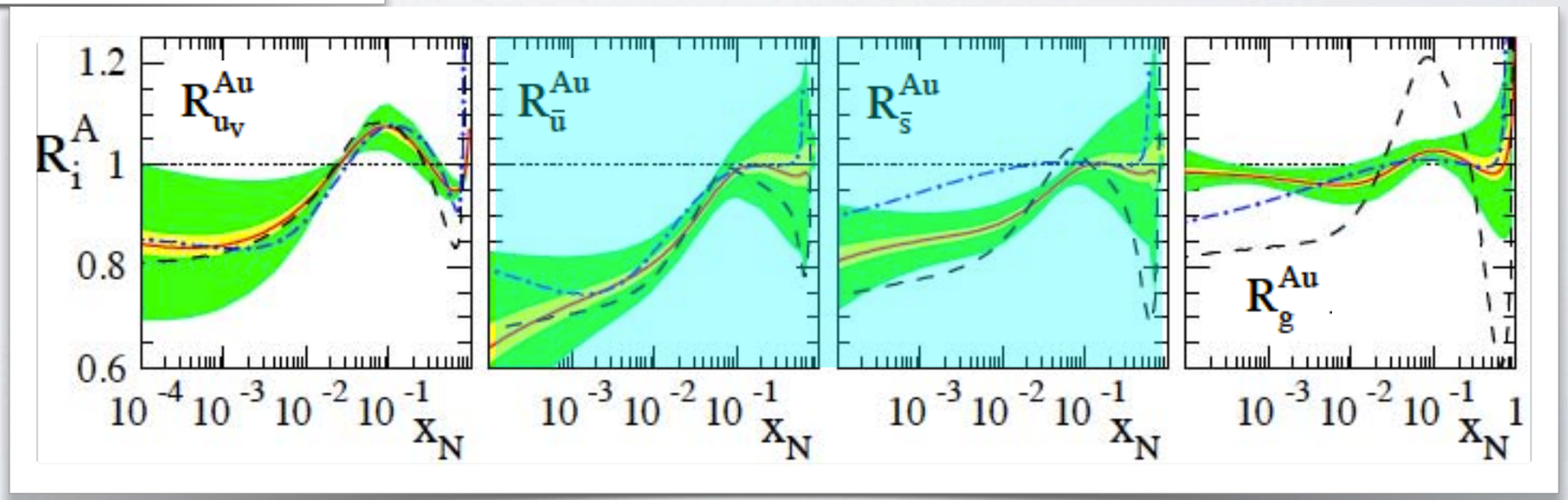

DSSZ nPDFs and their uncertainties

uncertainties at input scale of 1 GeV (for gold nucleus)

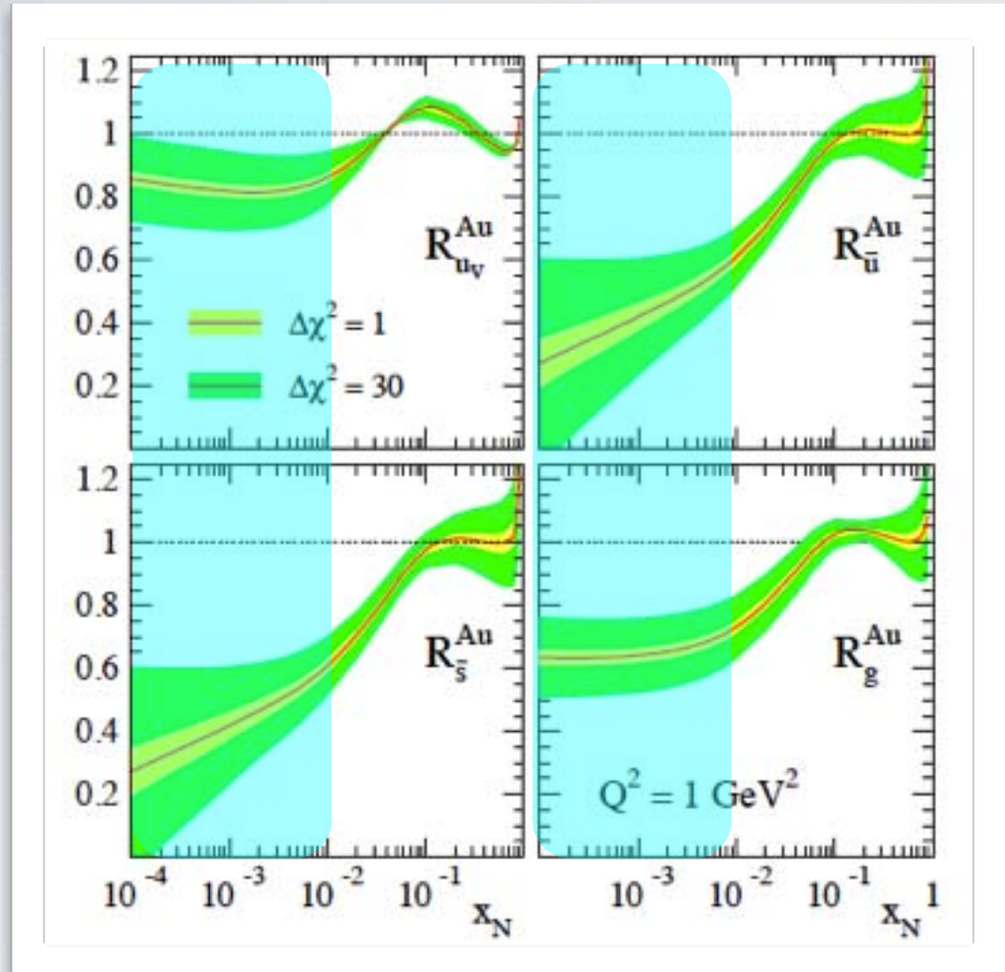

- **uncertainties below 0.01** merely reflect extrapolation of chosen functional form
  not constrained by any data

- nuclear modifications quickly diminish under evolution
- evolution imprints different nuclear effects on individual quark flavors
  recall: we start with $R^A_{\bar{u}} = R^A_{\bar{d}} = R^A_{\bar{s}}$
- $R^A_{u_V}$ exhibits textbook-like behavior

evolve to 10 GeV²

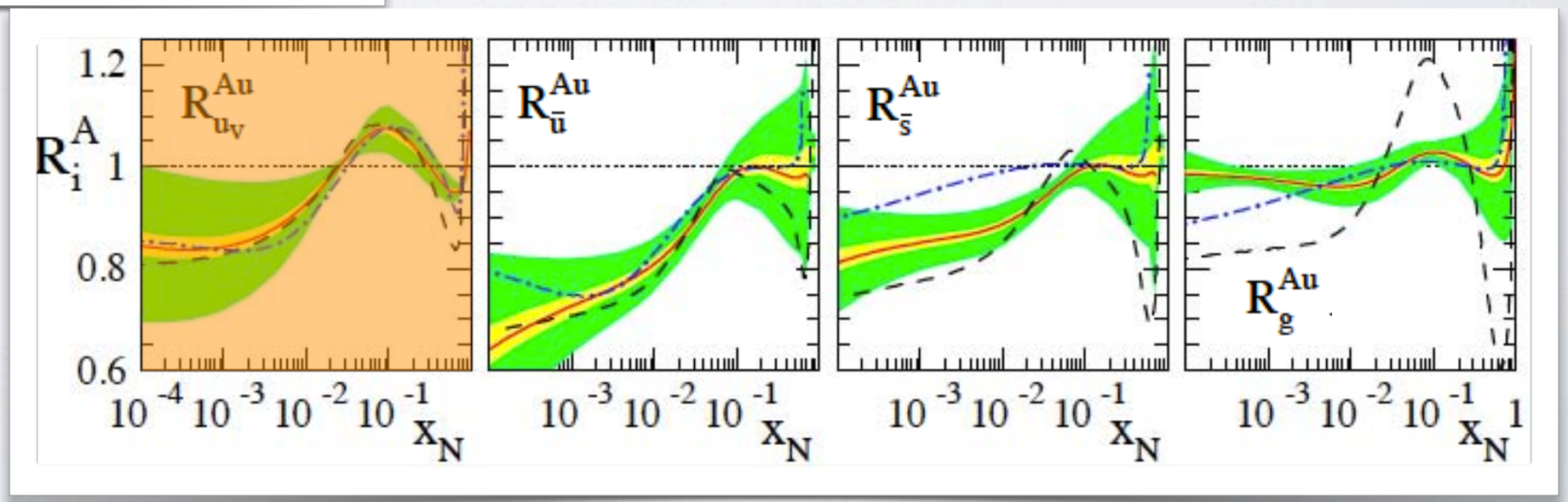

DSSZ nPDFs and their uncertainties

uncertainties at input scale of 1 GeV (for gold nucleus)

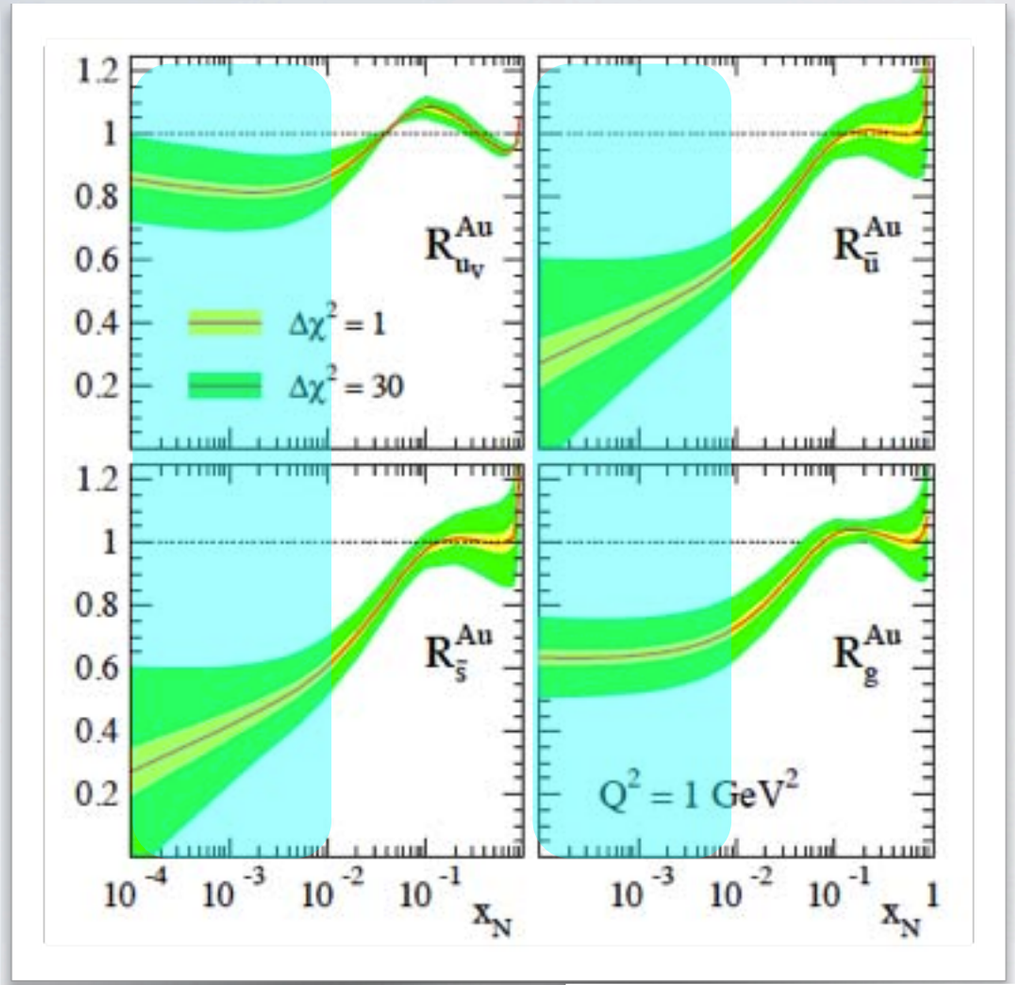

- **uncertainties below 0.01** merely reflect extrapolation of chosen functional form
  not constrained by any data

- nuclear modifications quickly diminish under evolution
- evolution imprints different nuclear effects on individual quark flavors
  recall: we start with $R^A_{\bar{u}} = R^A_{\bar{d}} = R^A_{\bar{s}}$
- $R^A_{u_V}$ exhibits textbook-like behavior
- little evidence for anti-shadowing in sea (and gluon)

evolve to 10 GeV²

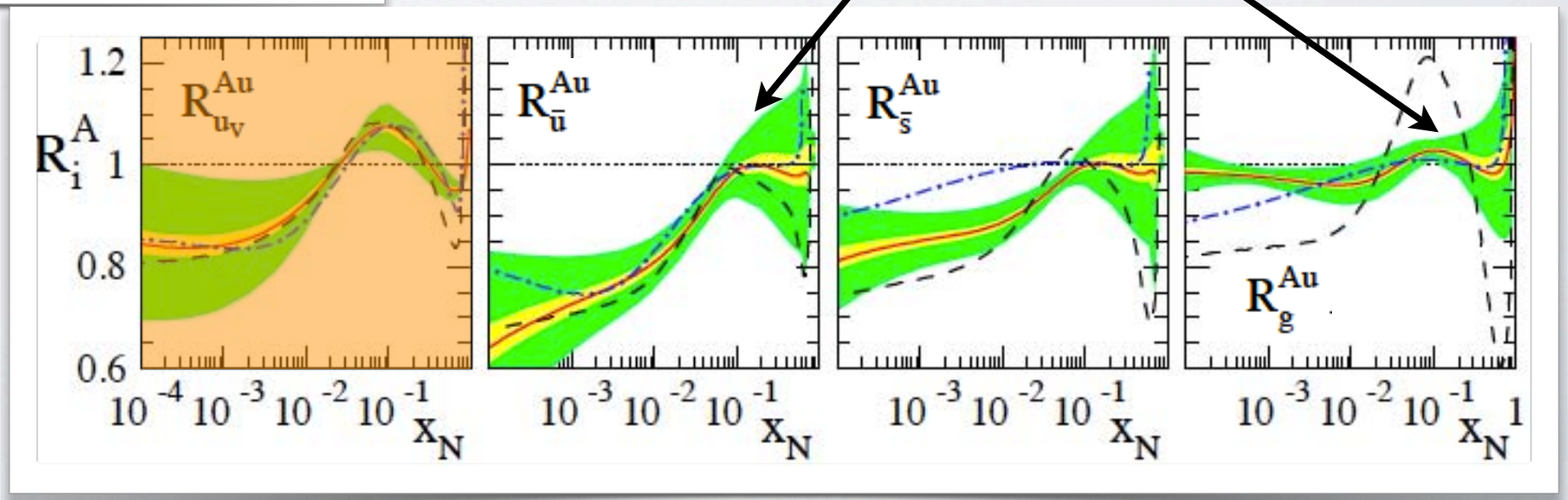

DSSZ nPDFs and their uncertainties

A dependence at $Q^2 = 10\ GeV^2$

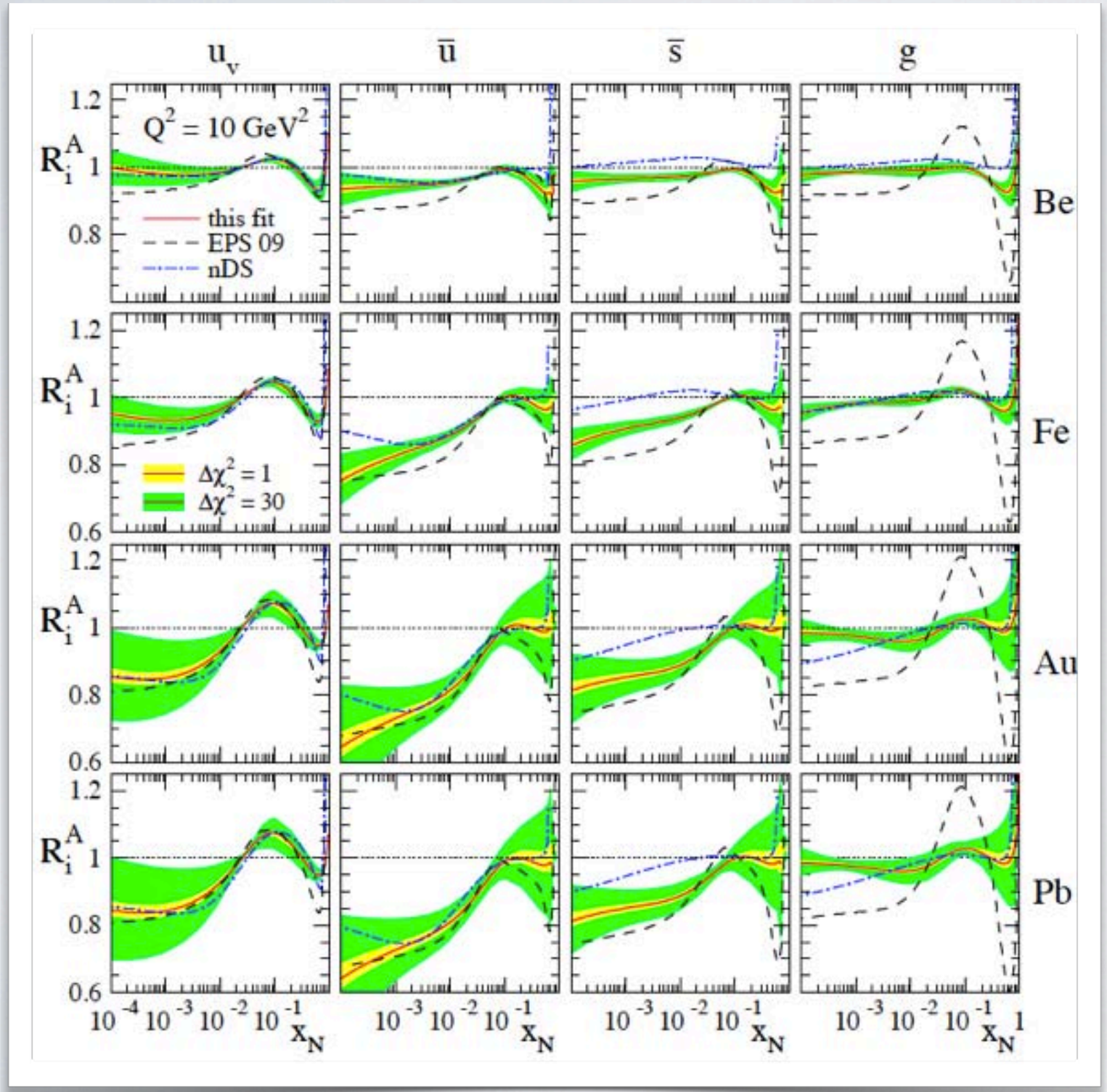

DSSZ nPDFs and their uncertainties

A dependence at $Q^2 = 10\ GeV^2$

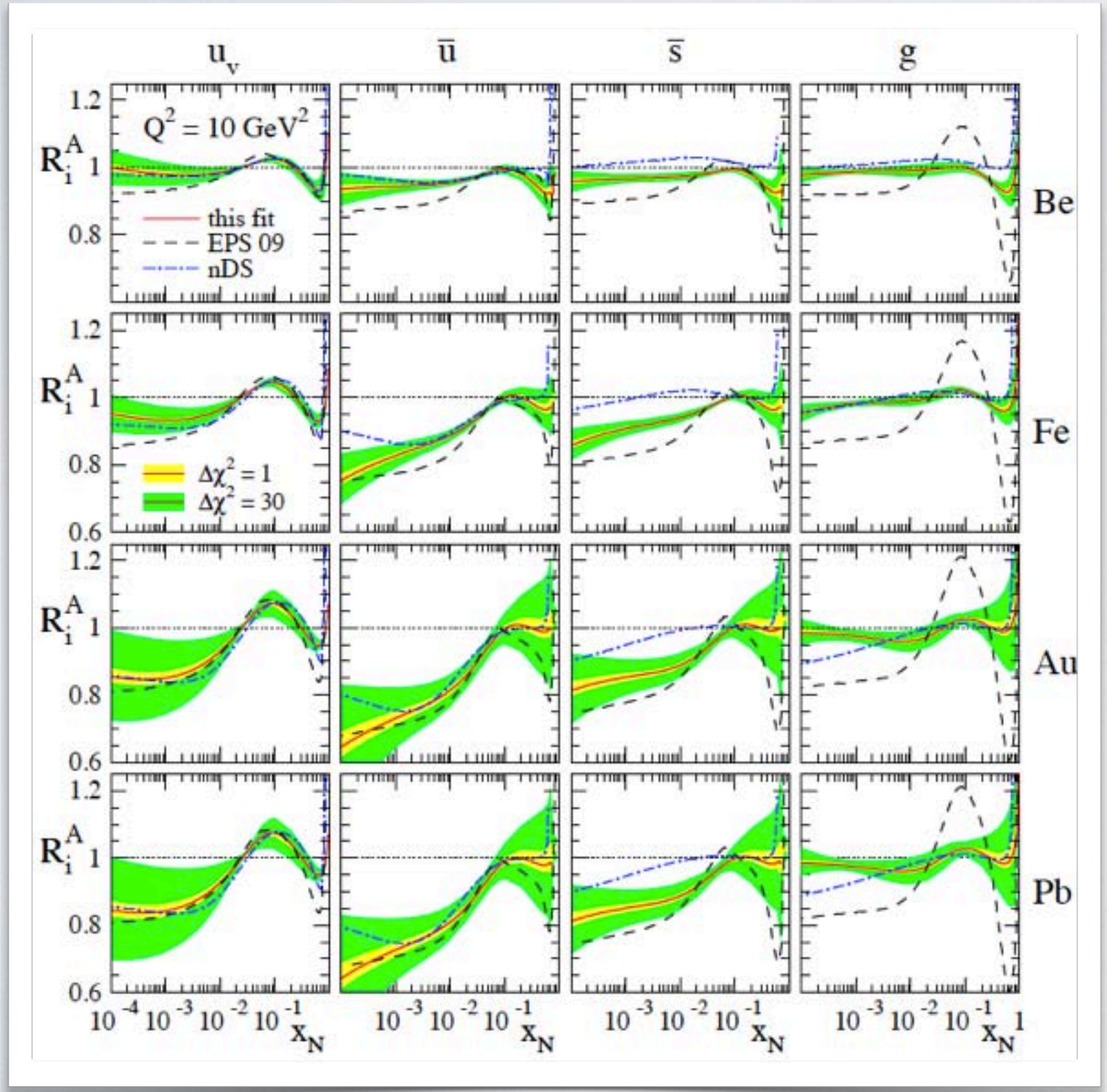

- nuclear modifications increase with A

DSSZ nPDFs and their uncertainties

A dependence at $Q^2 = 10\ \mathrm{GeV}^2$

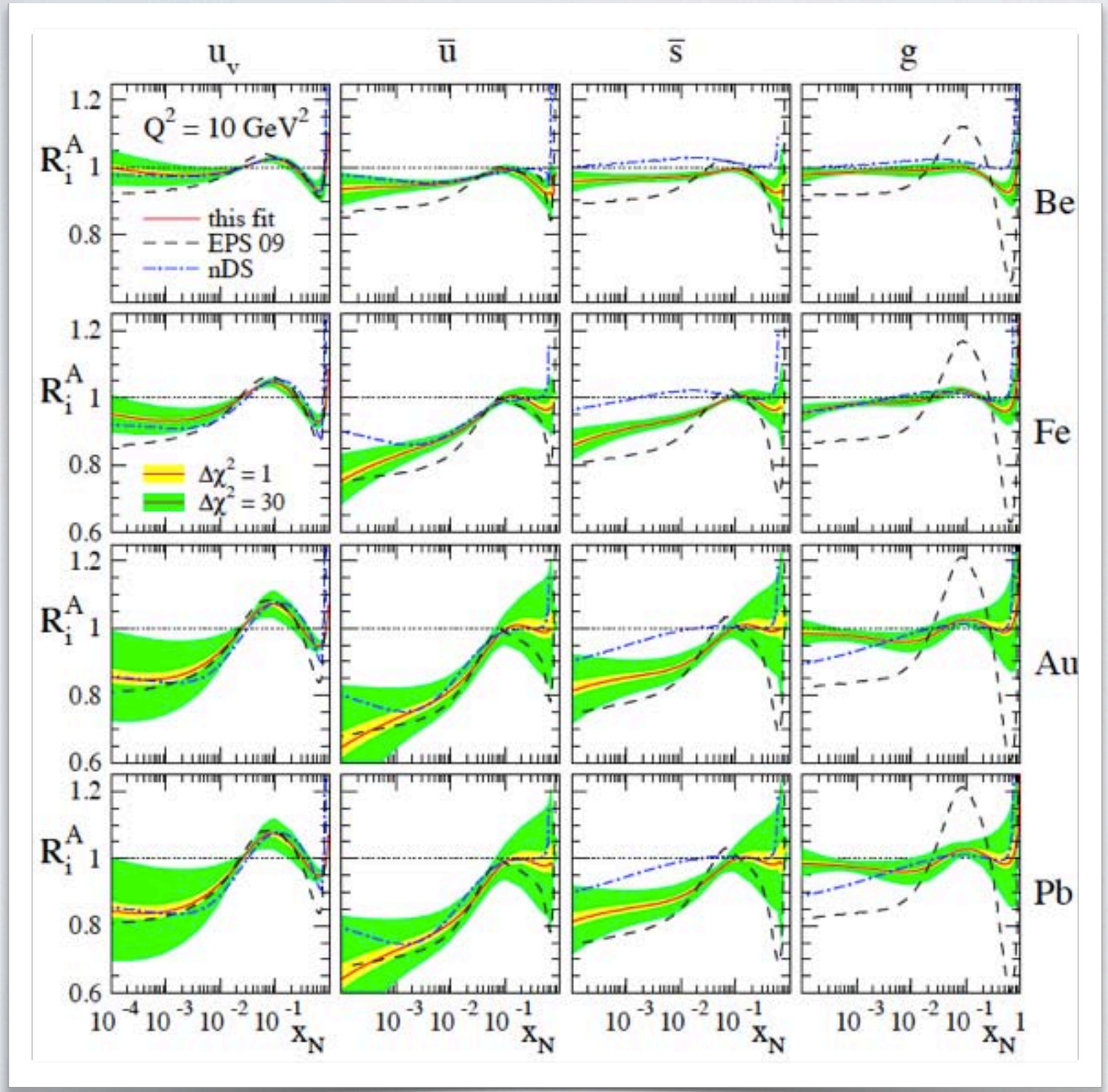

- nuclear modifications increase with A
- good agreement with previous fits for $R^A_{u_V}$ and $R^A_{\bar{u}}$

DSSZ nPDFs and their uncertainties

A dependence at $Q^2 = 10$ GeV^2

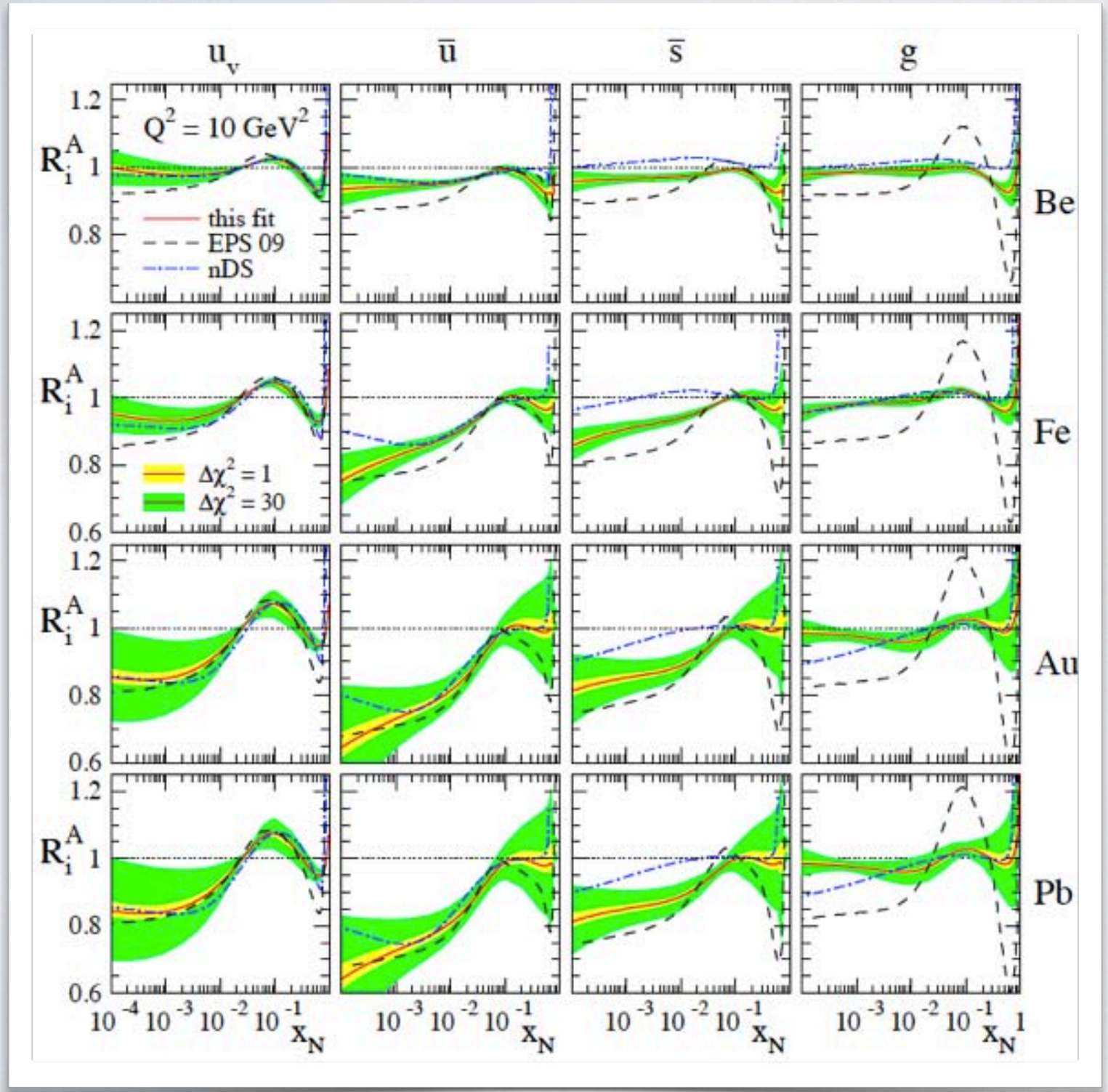

- nuclear modifications increase with A
- good agreement with previous fits for $R^A_{u_V}$ and $R^A_{\bar{u}}$
- less so for $R^A_{\bar{s}}$

due to recent changes in free proton PDFs

DSSZ nPDFs and their uncertainties

A dependence at Q^2 = 10 GeV^2

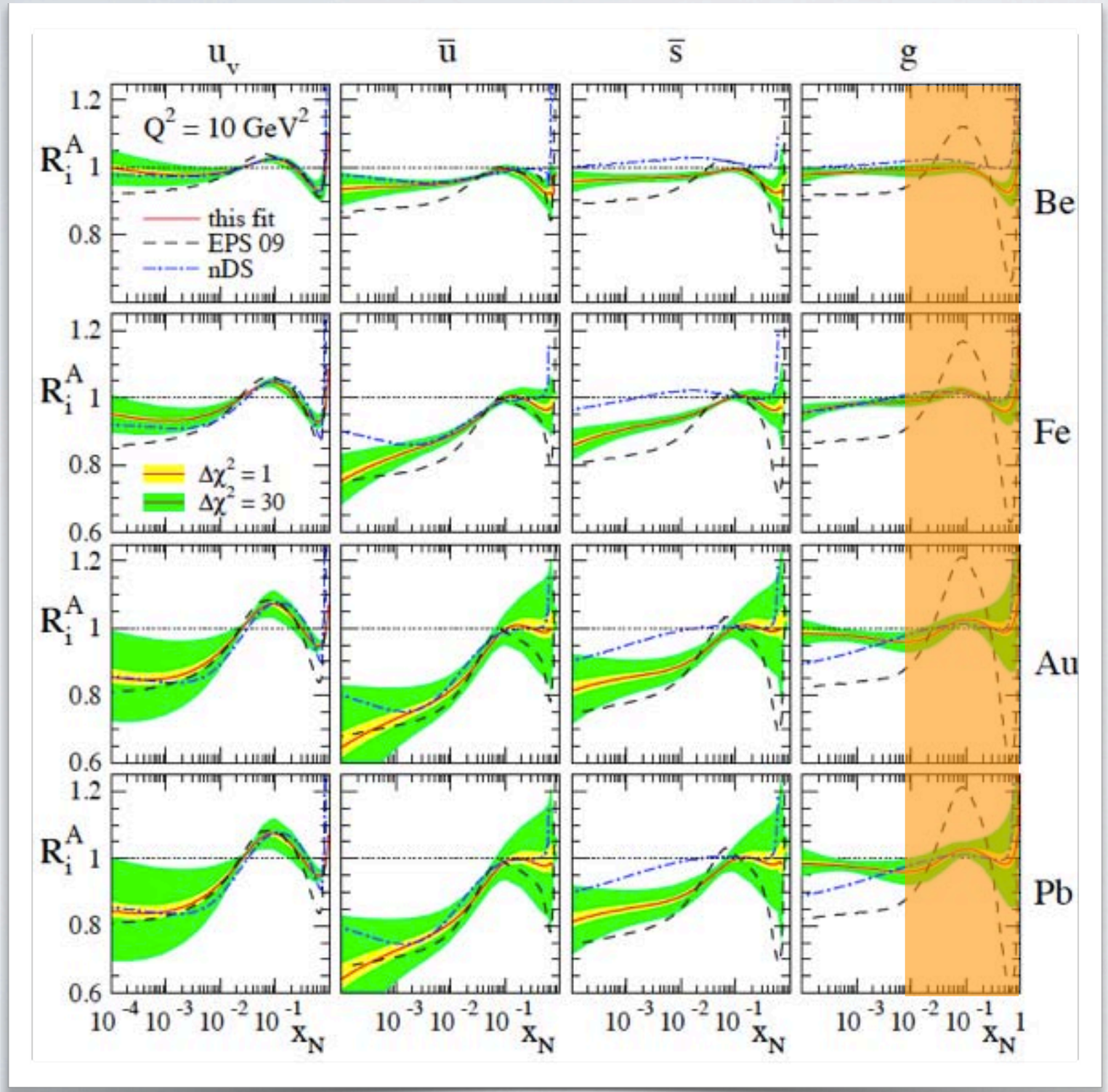

- nuclear modifications increase with A
- good agreement with previous fits for $R^A_{u_V}$ and $R^A_{\bar{u}}$
- less so for $R^A_{\bar{s}}$

  due to recent changes in free proton PDFs
- **MUCH less anti-shadowing and EMC effect than for EPS gluon**

  driven by the way dAu data are analyzed

DSSZ nPDFs: peculiarities

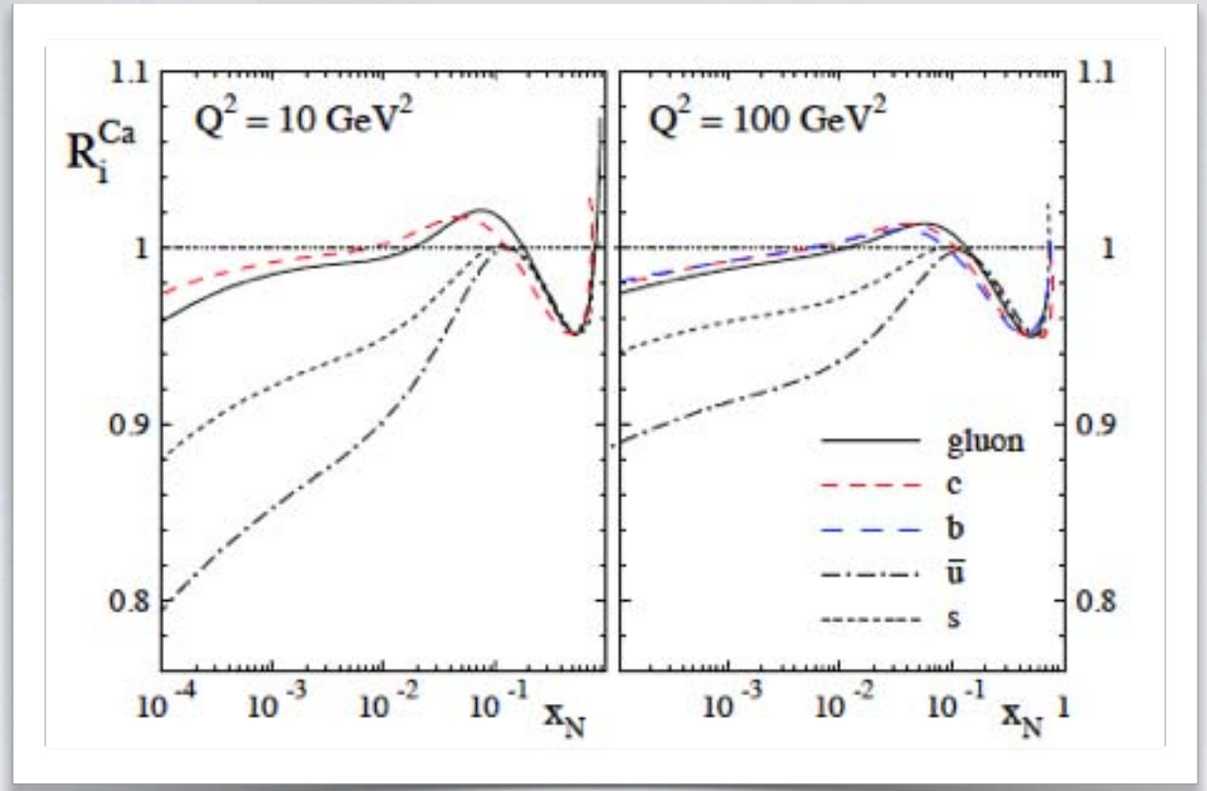

perturbatively generated charm and bottom nPDFs

DSSZ nPDFs: peculiarities

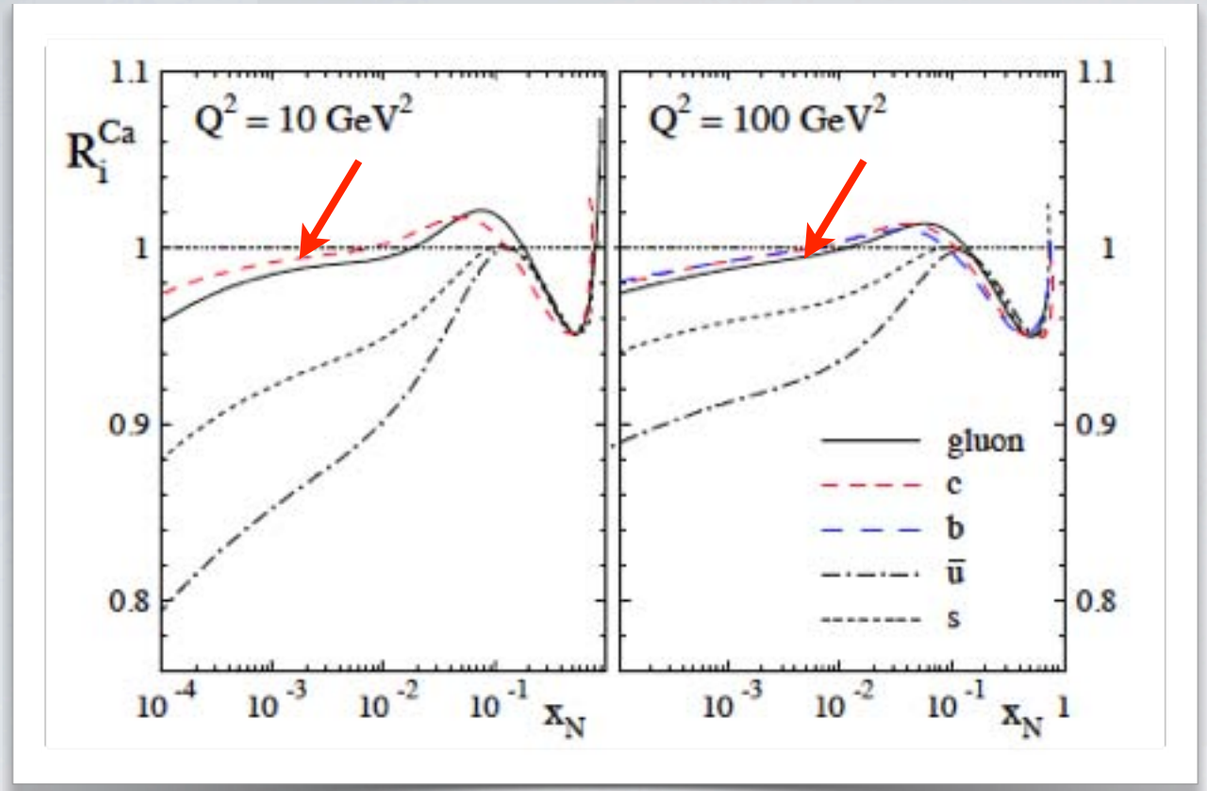

perturbatively generated charm and bottom nPDFs

- modifications for c,b follow closely the gluon

  no surprise, as they are generated from gluon splitting

DSSZ nPDFs: peculiarities

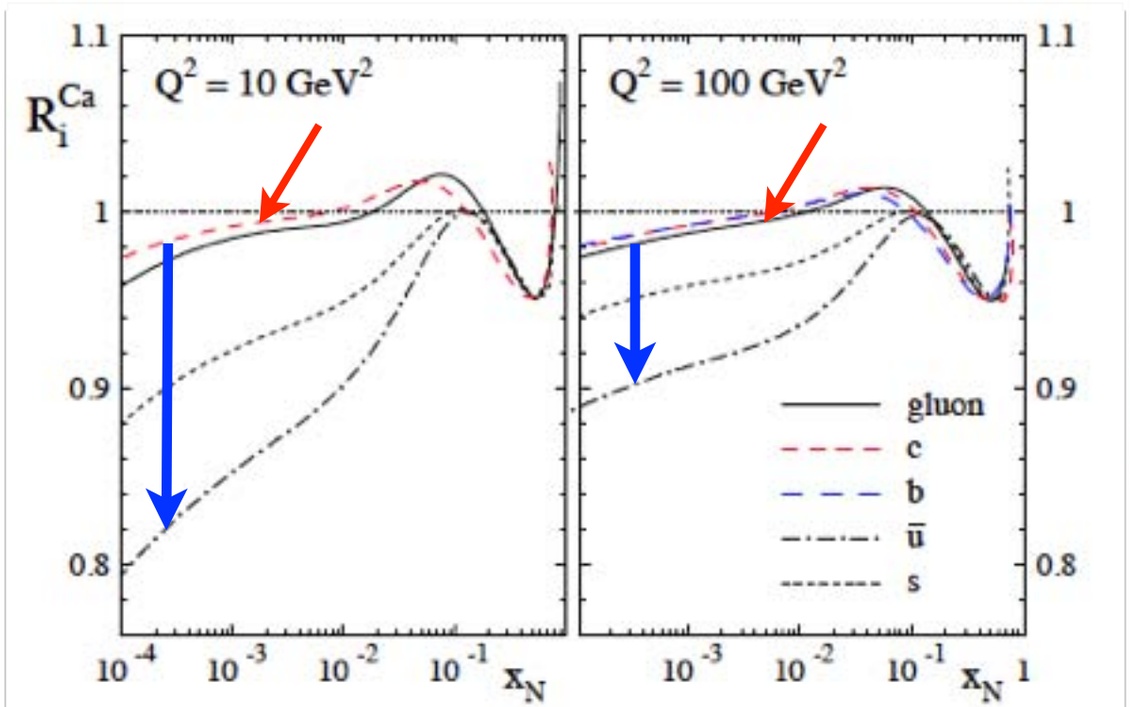

perturbatively generated charm and bottom nPDFs

- modifications for c,b follow closely the gluon
  no surprise, as they are generated from gluon splitting
- hierarchy in amount of low-x suppression:
  the stronger, the lighter the quark

DSSZ nPDFs: peculiarities

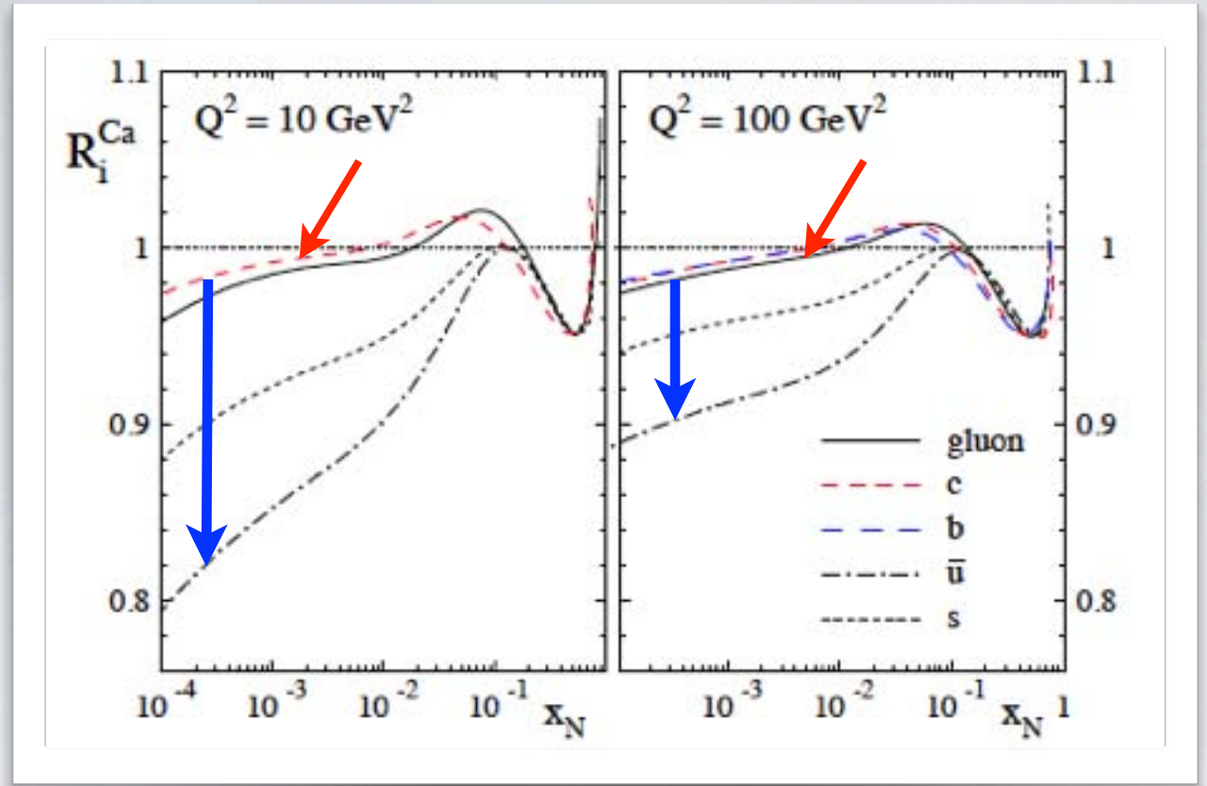

perturbatively generated charm and bottom nPDFs

- modifications for c,b follow closely the gluon
  no surprise, as they are generated from gluon splitting
- hierarchy in amount of low-x suppression:
  the stronger, the lighter the quark

the issue of "negative gluons"

- MSTW exercises the possibility of **negative gluons** at small x and low scales [improves their fit of HERA data]
  not a problem since PDFs are not observables but F_L should stay positive

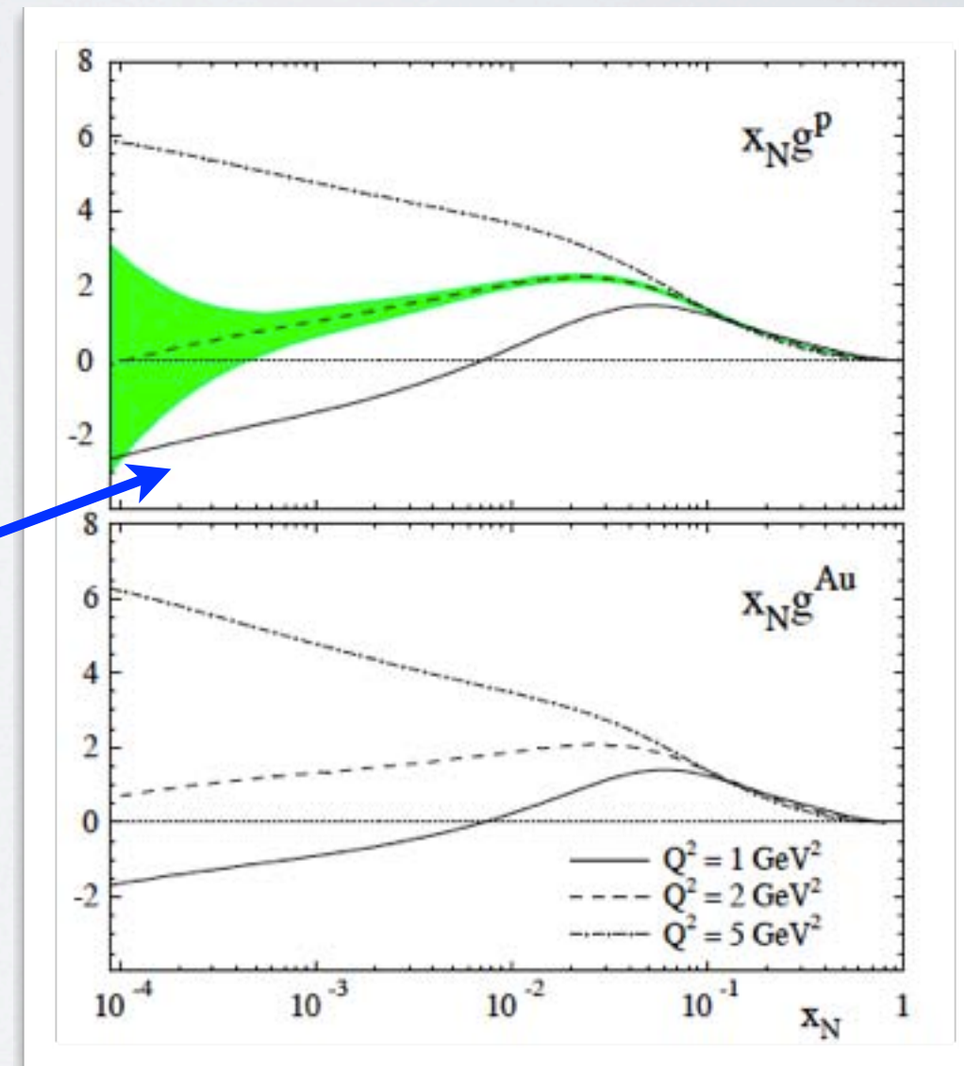

DSSZ nPDFs: peculiarities

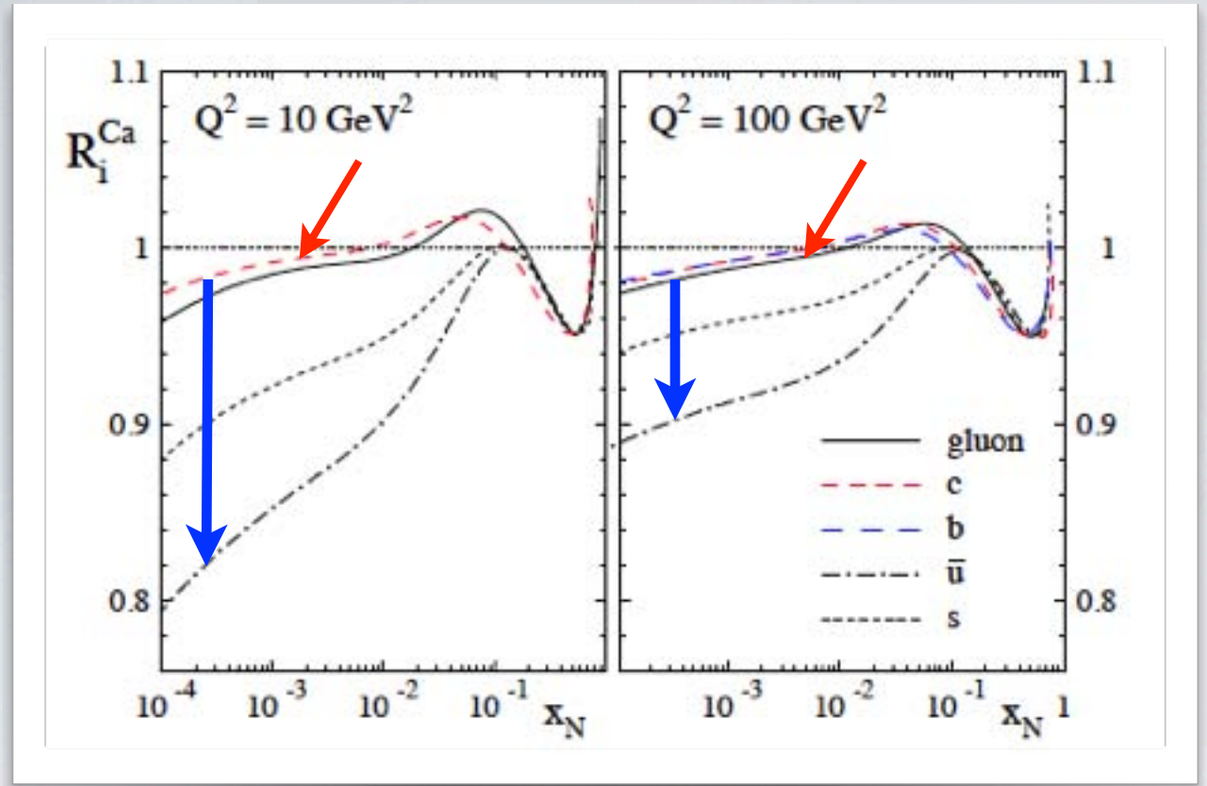

perturbatively generated charm and bottom nPDFs

- modifications for c,b follow closely the gluon
  no surprise, as they are generated from gluon splitting
- hierarchy in amount of low-x suppression:
  the stronger, the lighter the quark

the issue of "negative gluons"

- MSTW exercises the possibility of **negative gluons** at small x and low scales [improves their fit of HERA data]
  not a problem since PDFs are not observables but F_L should stay positive
- evolution quickly pushes the gluon up

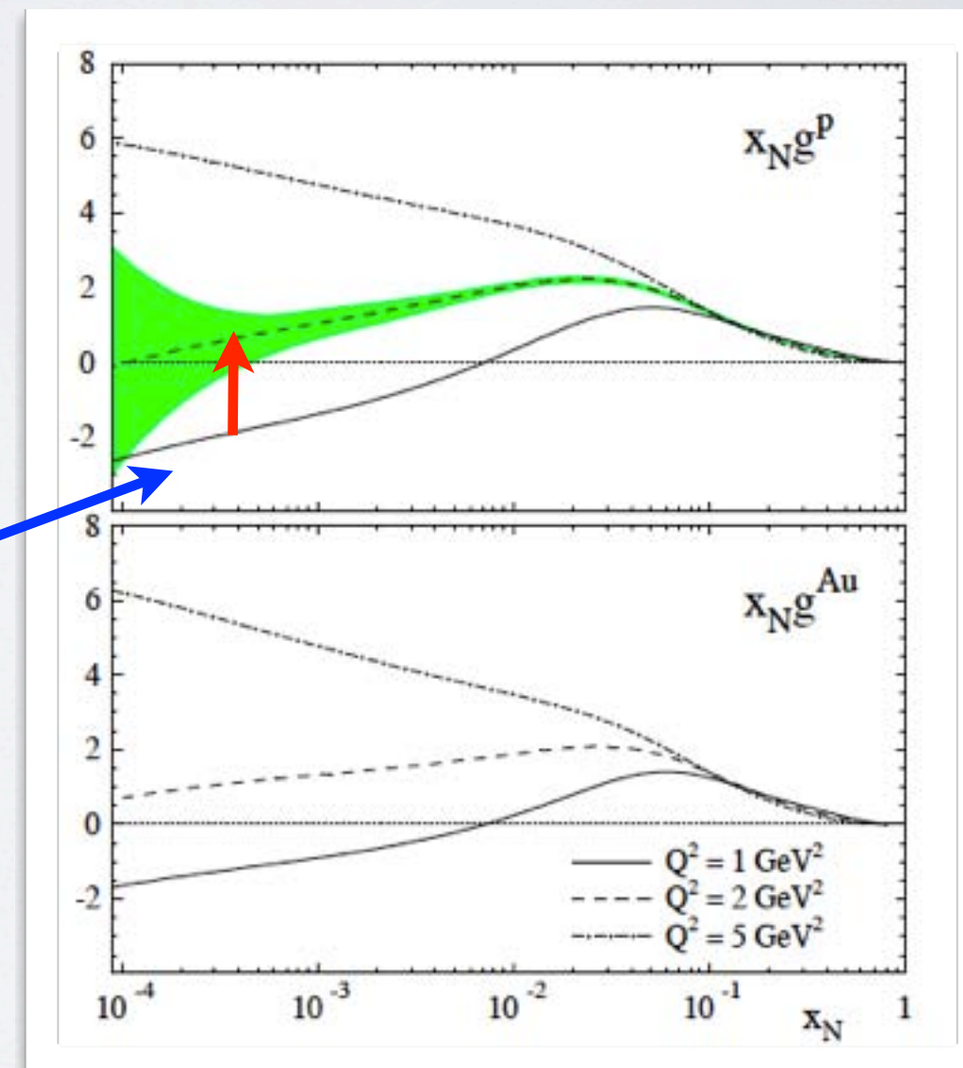

DSSZ nPDFs: peculiarities

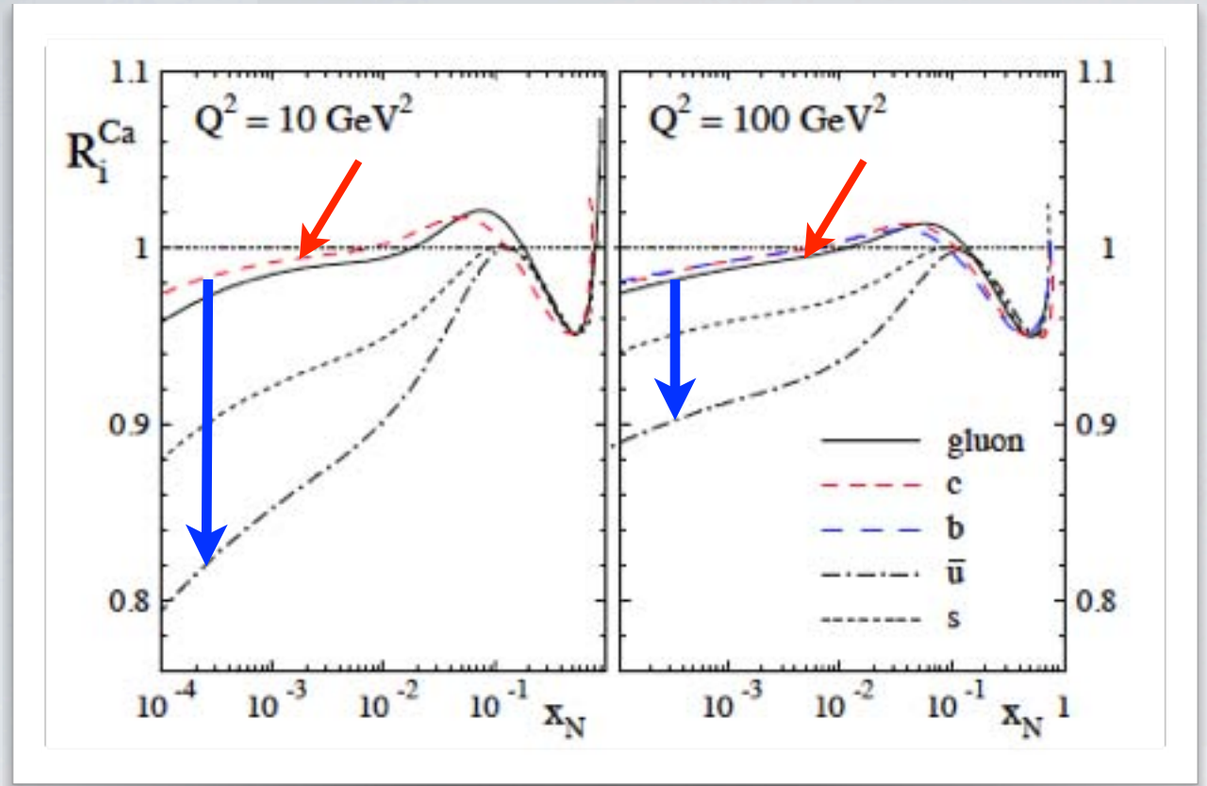

perturbatively generated charm and bottom nPDFs

- modifications for c,b follow closely the gluon
  no surprise, as they are generated from gluon splitting
- hierarchy in amount of low-x suppression:
  the stronger, the lighter the quark

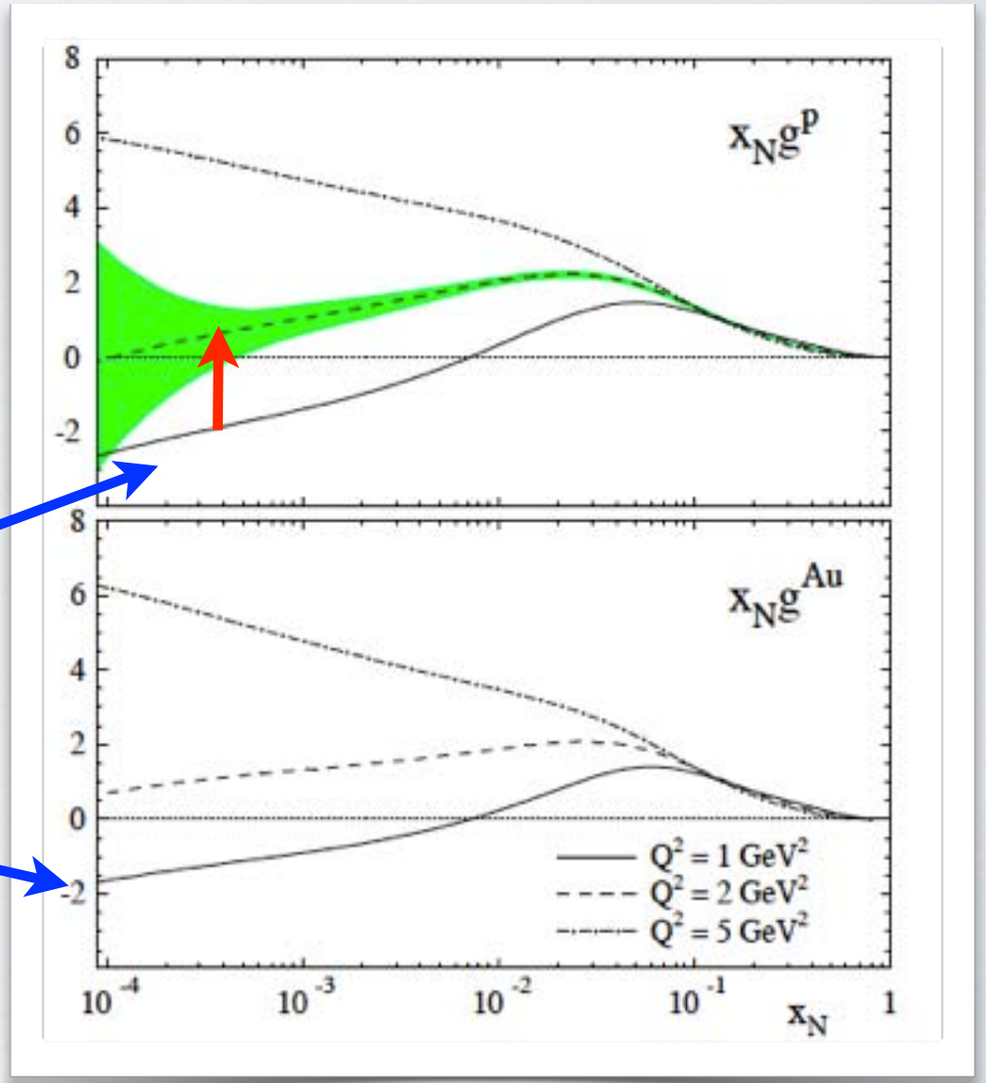

the issue of "negative gluons"

- MSTW exercises the possibility of **negative gluons** at small x and low scales [improves their fit of HERA data]
  not a problem since PDFs are not observables but F_L should stay positive
- evolution quickly pushes the gluon up
- our nPDF gluon is tied to the MSTW through R_g^A
  and gets negative too -> R_g^A ill defined at low scales (nodes)

DSSZ nPDFs: peculiarities

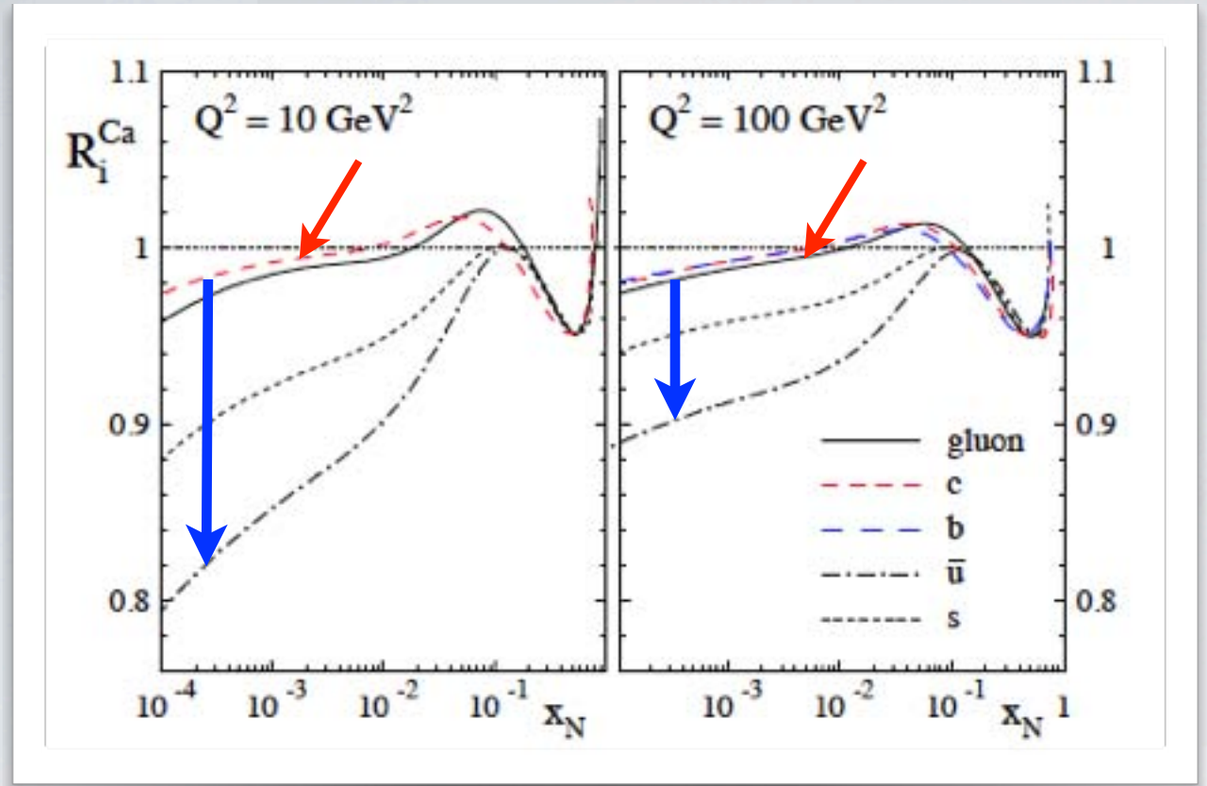

perturbatively generated charm and bottom nPDFs

- modifications for c,b follow closely the gluon
  no surprise, as they are generated from gluon splitting
- hierarchy in amount of low-x suppression:
  the stronger, the lighter the quark

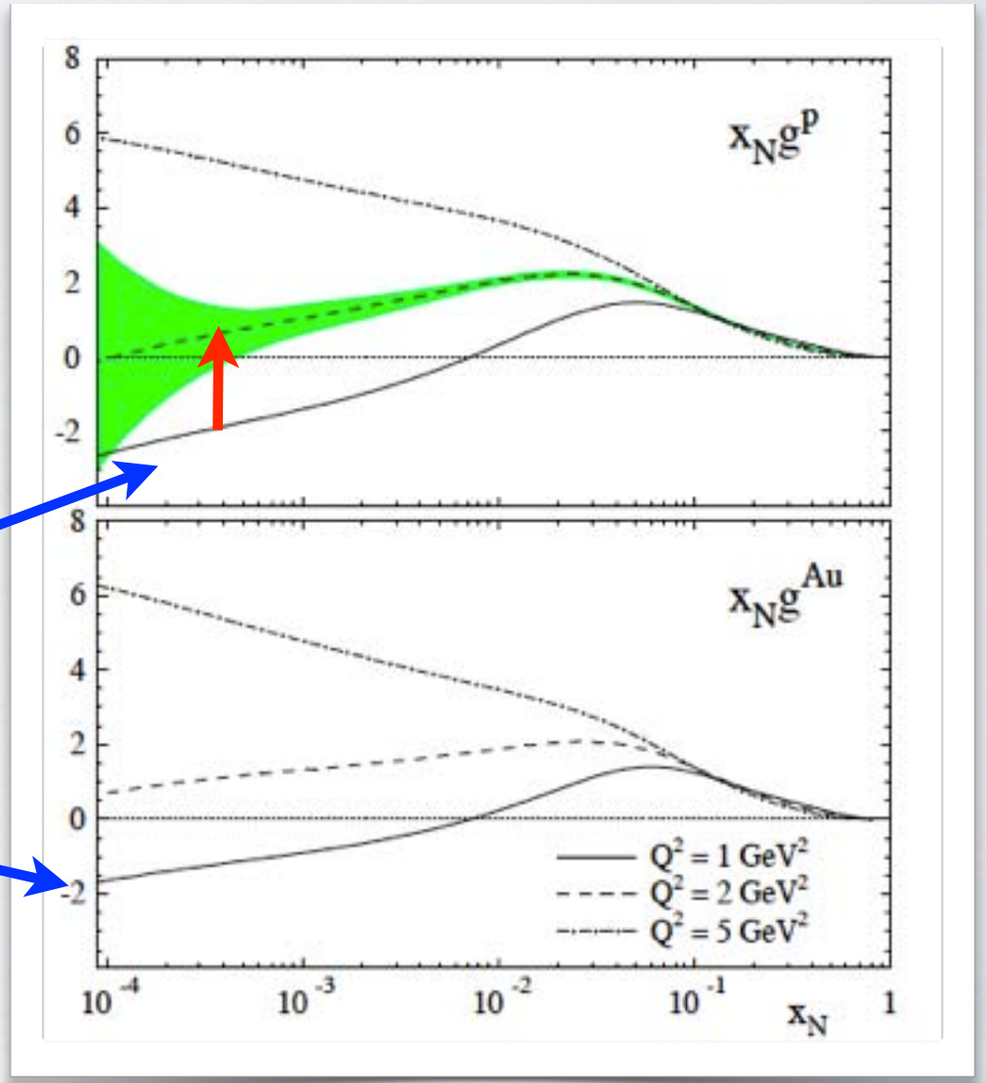

the issue of "negative gluons"

- MSTW exercises the possibility of **negative gluons** at small x and low scales [improves their fit of HERA data]
  not a problem since PDFs are not observables but F_L should stay positive
- evolution quickly pushes the gluon up
- our nPDF gluon is tied to the MSTW through R_g^A
  and gets negative too -> R_g^A ill defined at low scales (nodes)

one must take trad. ratios R_i^A with a pinch of salt in NLO

some future avenues for nPDF fits
RHIC & LHC

prompt photons in dAu / pPb

complication: "isospin effects" = dilution of u-quark density from neutrons $\mathbf{u^A(x) < u^p(x)}$

→ ratio dAu/pp not unity even w/o nuclear modifications

see also Arleo et al, 1103.1471

prompt photons in dAu / pPb

complication: "isospin effects" = dilution of u-quark density from neutrons $u^A(x) < u^P(x)$

→ ratio dAu/pp not unity even w/o nuclear modifications

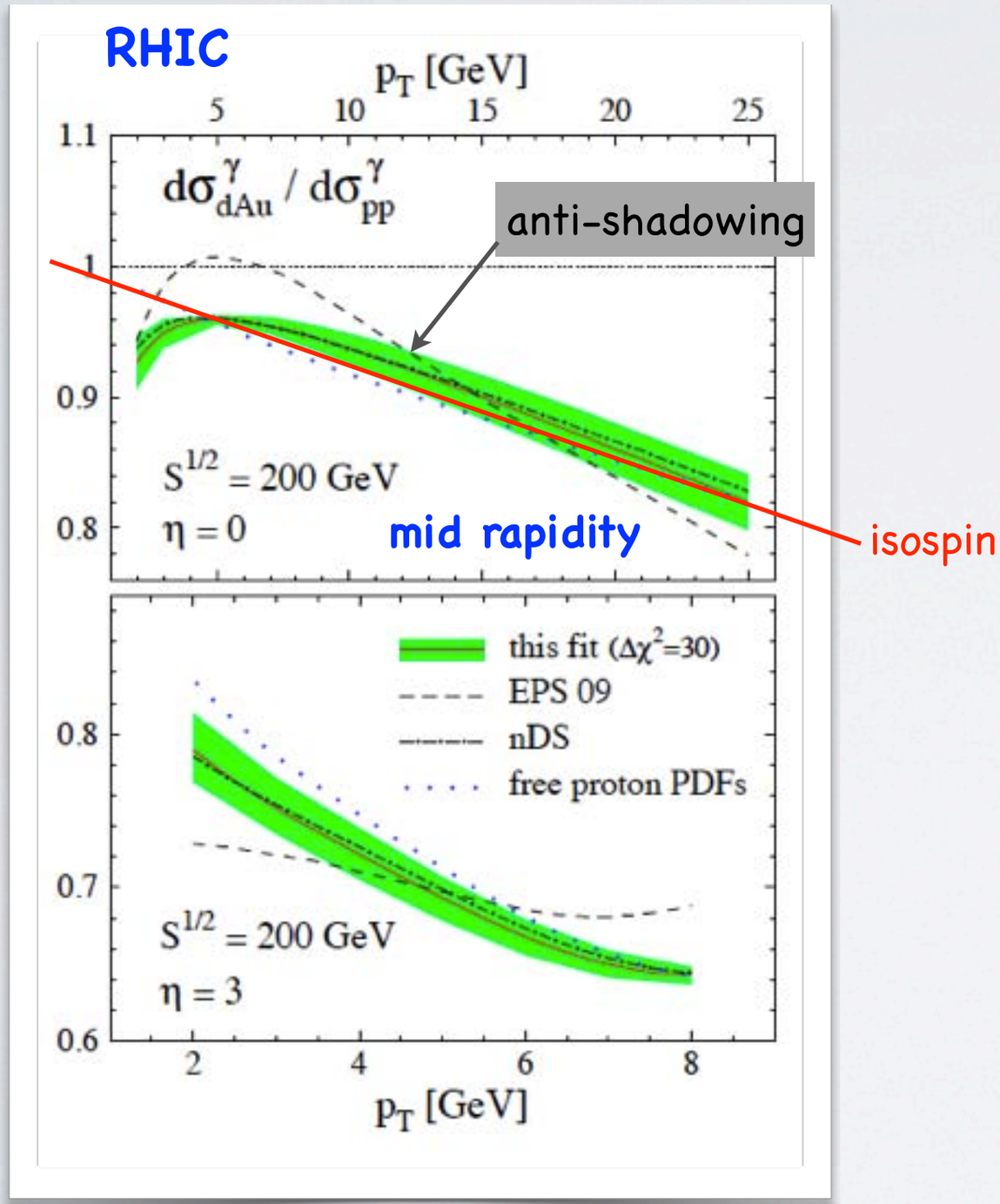

see also Arleo et al, 1103.1471

prompt photons in dAu / pPb

complication: "isospin effects" = dilution of u-quark density from neutrons $u^A(x) < u^P(x)$

→ ratio dAu/pp not unity even w/o nuclear modifications

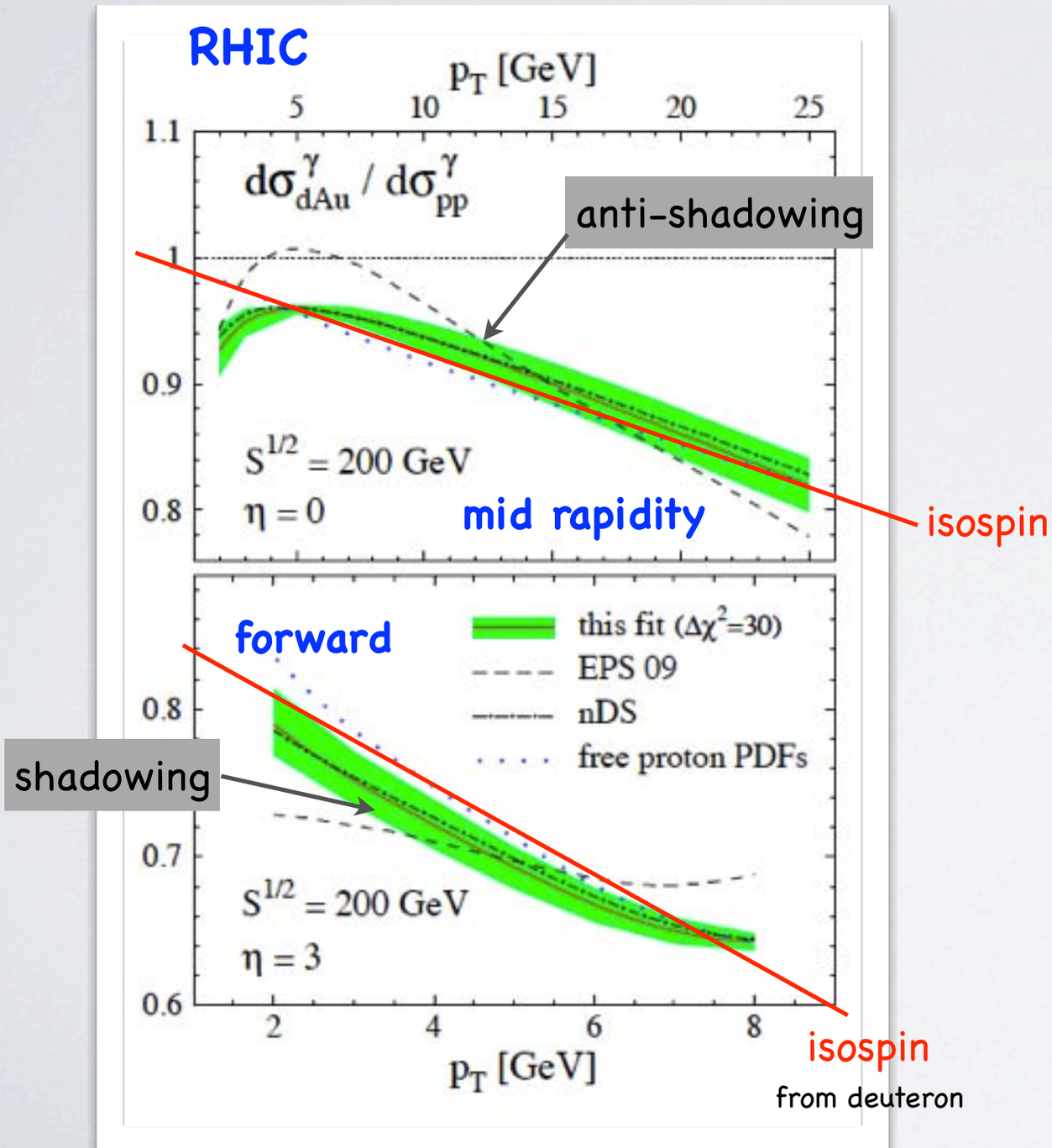

see also Arleo et al, 1103.1471

prompt photons in dAu / pPb

complication: "isospin effects" = dilution of u-quark density from neutrons $u^A(x) < u^P(x)$

→ ratio dAu/pp not unity even w/o nuclear modifications

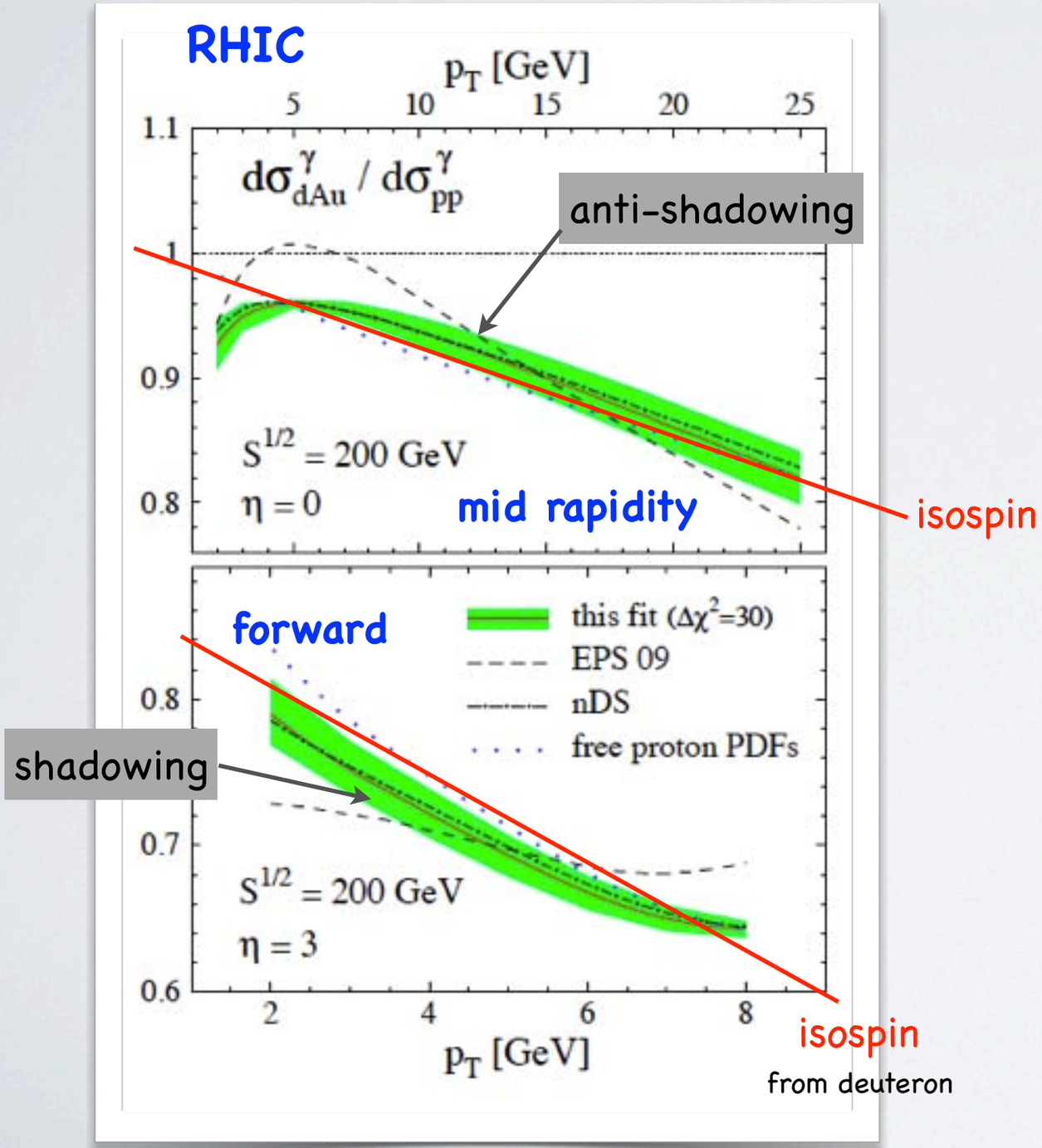

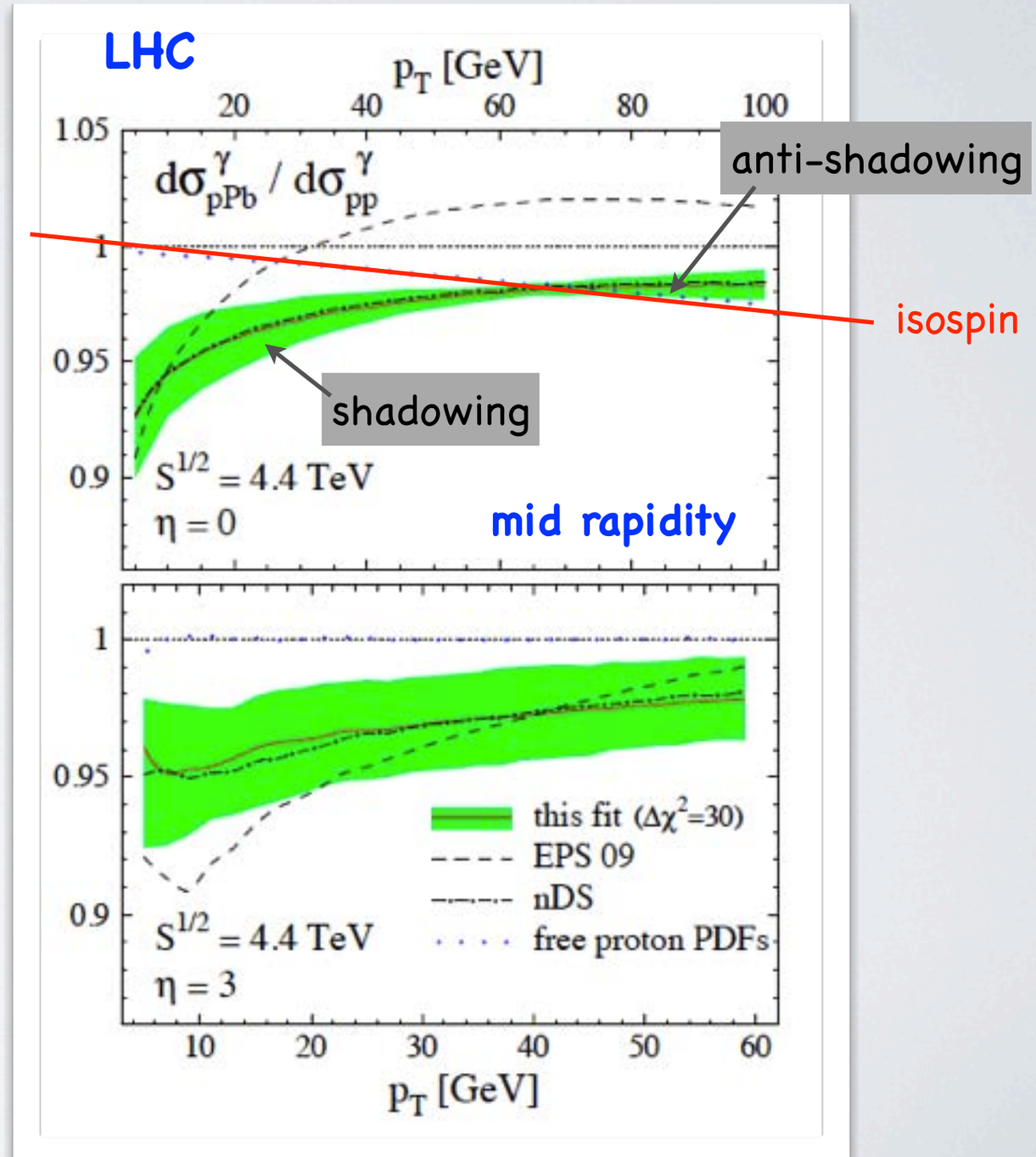

see also Arleo et al, 1103.1471

prompt photons in dAu / pPb

complication: "isospin effects" = dilution of u-quark density from neutrons $u^A(x) < u^P(x)$

→ ratio dAu/pp not unity even w/o nuclear modifications

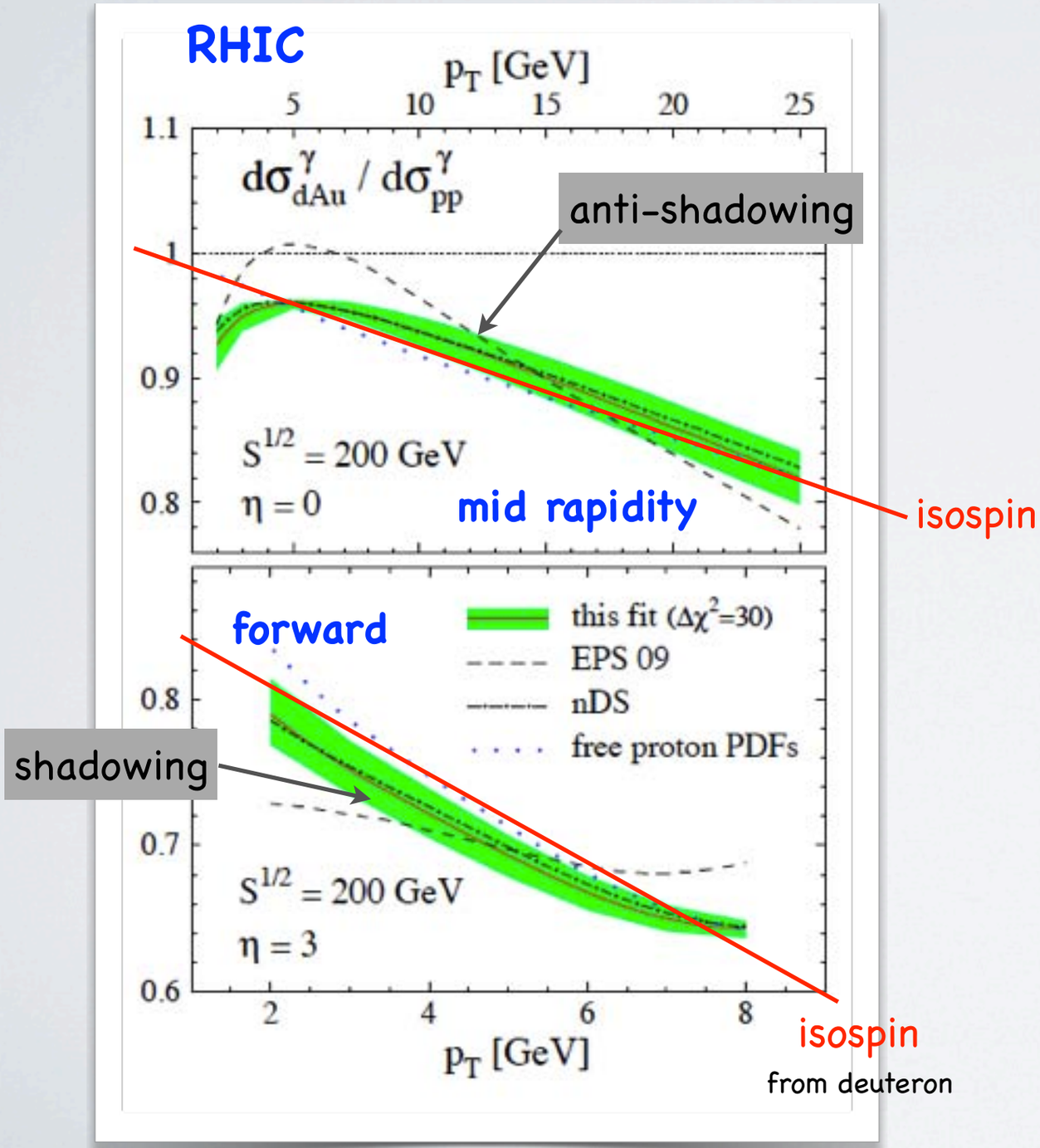

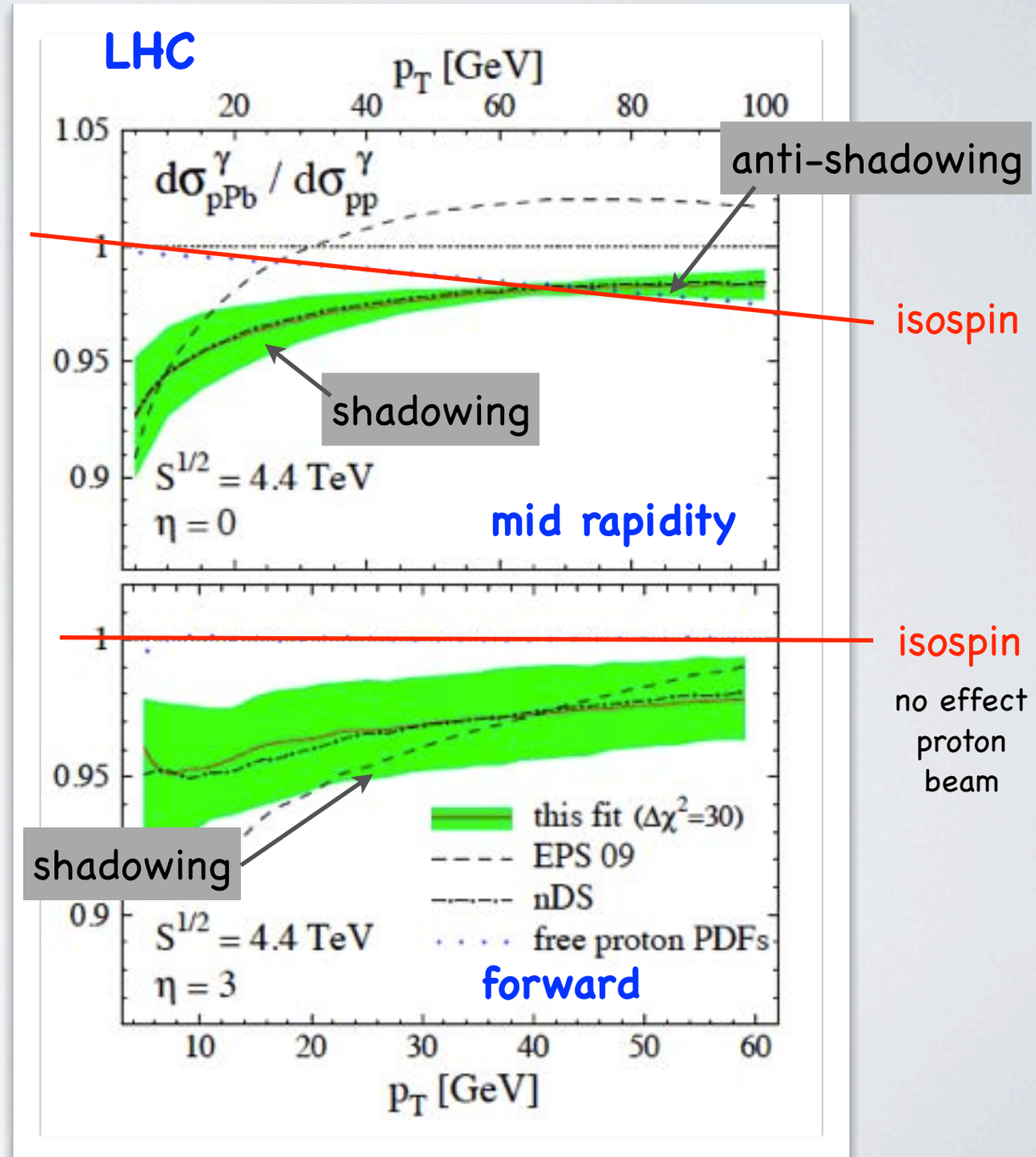

see also Arleo et al, 1103.1471

prompt photons - impact

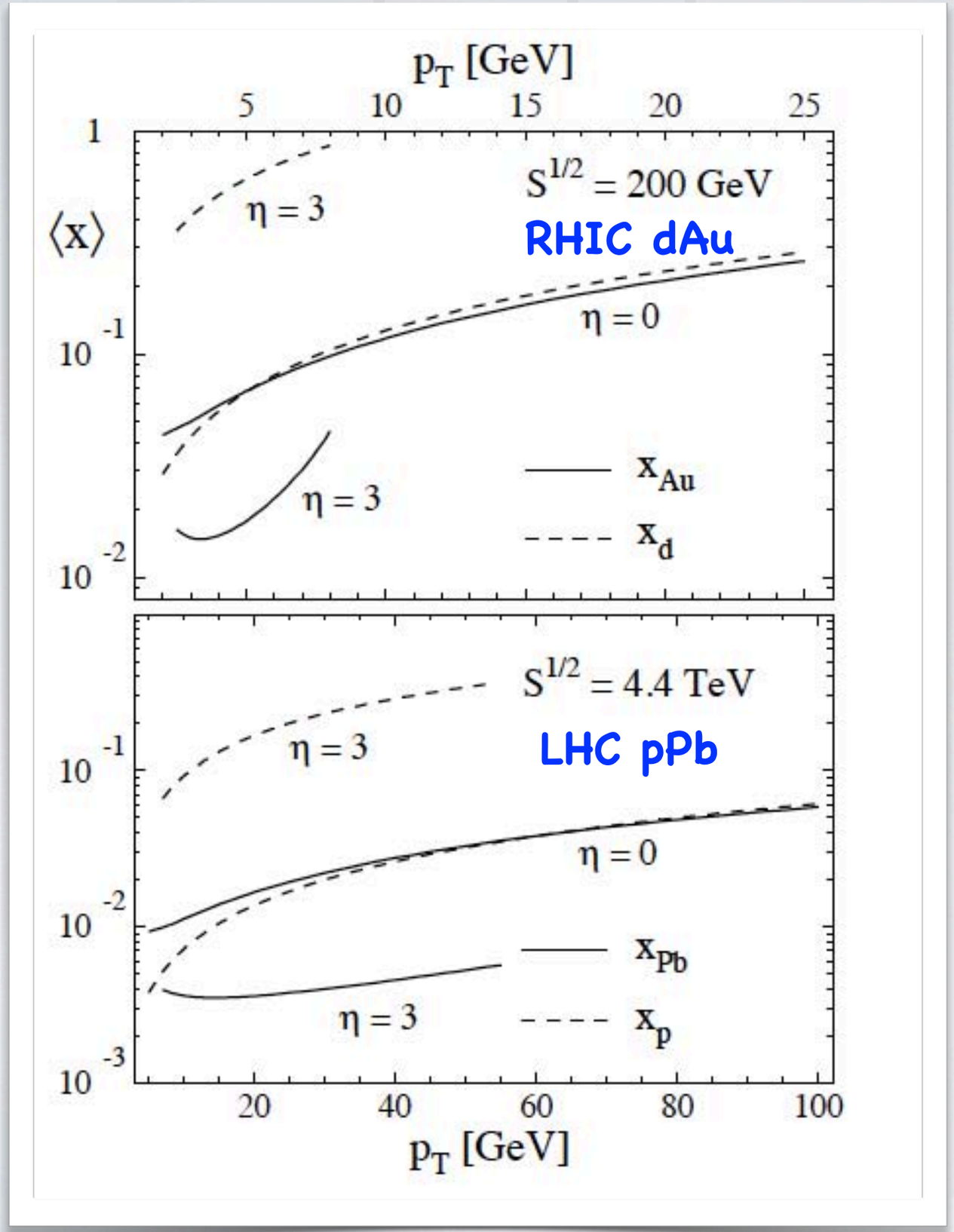

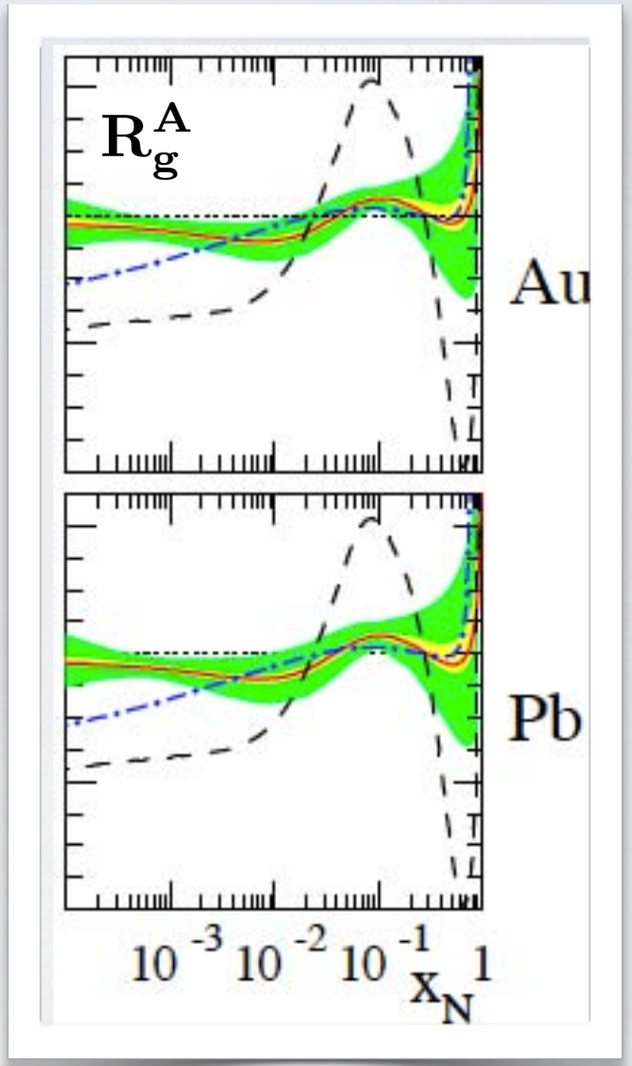

prompt photons - impact

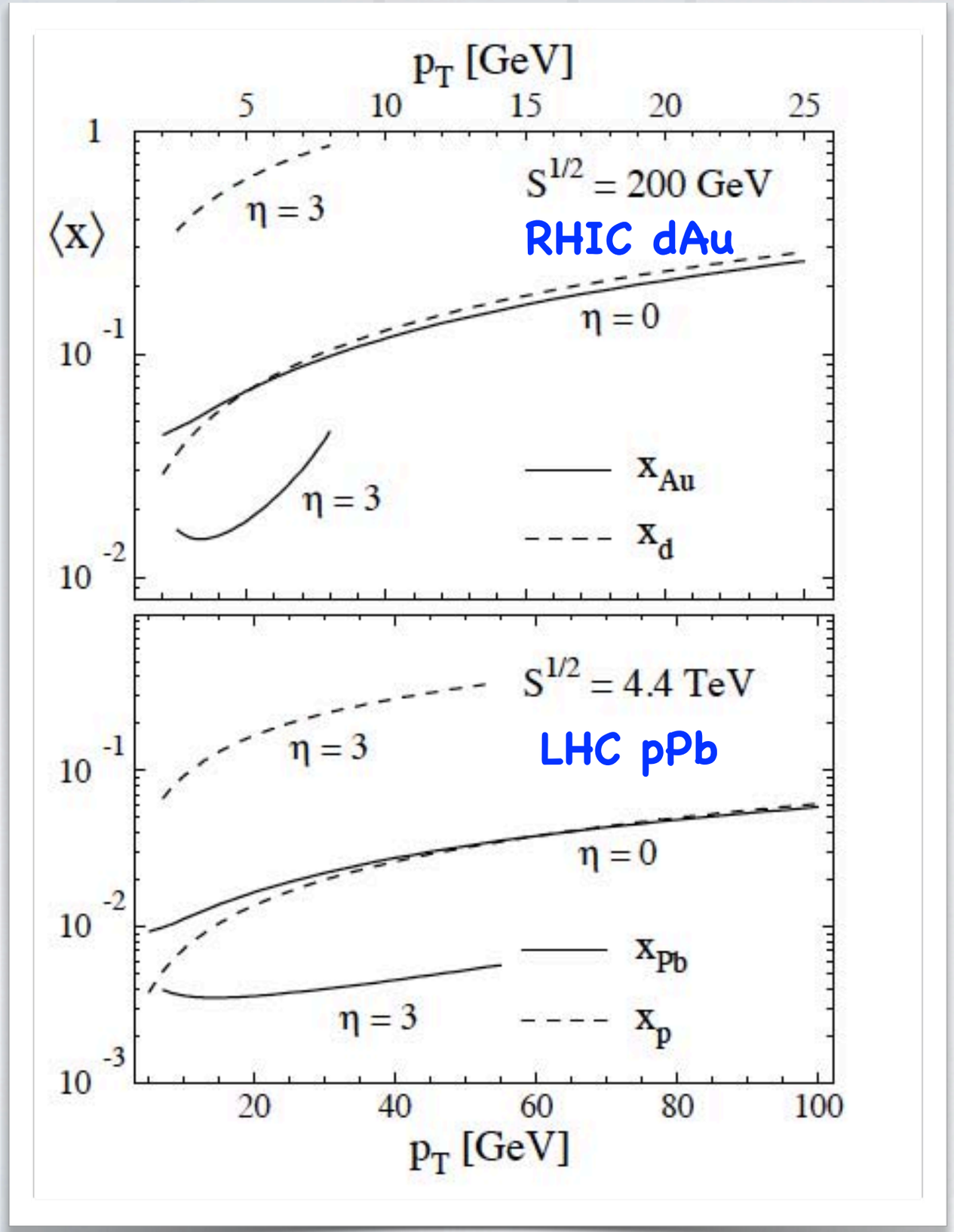

- can resolve characteristic differences between EPS and DSSZ gluons in anti-shadowing [and EMC] region

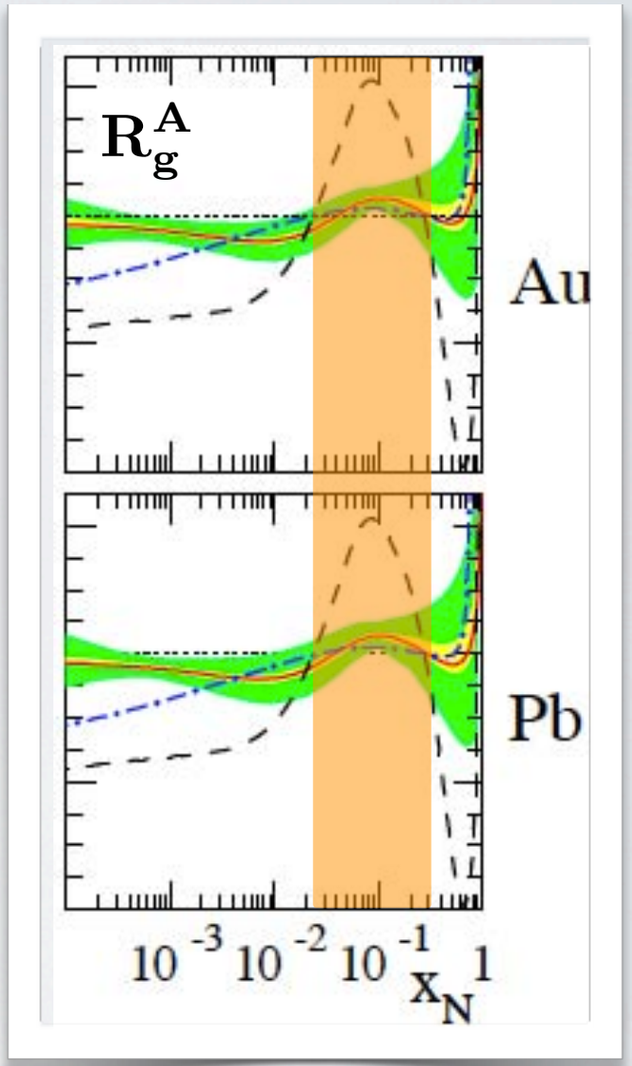

prompt photons - impact

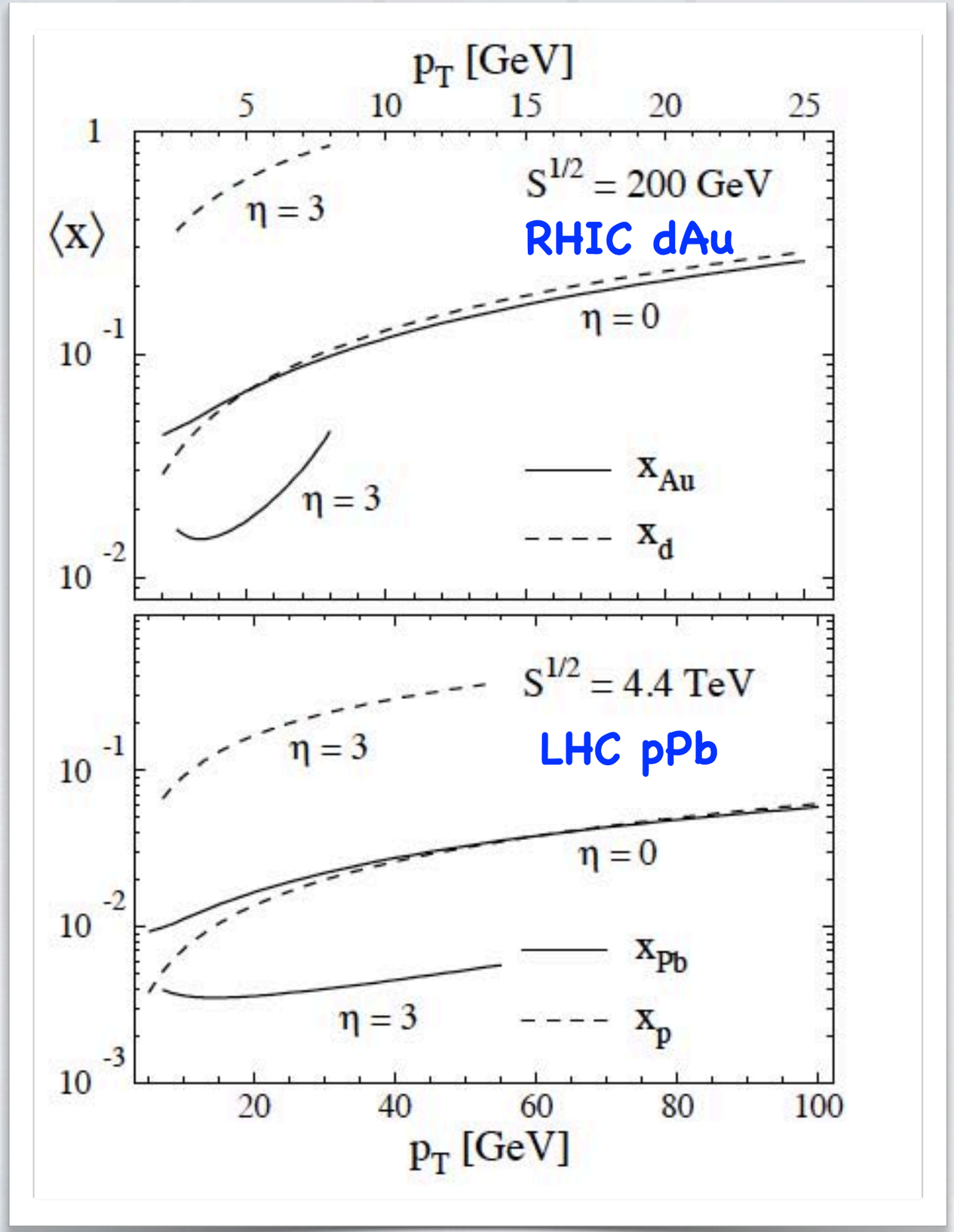

- can resolve characteristic differences between EPS and DSSZ gluons in anti-shadowing [and EMC] region

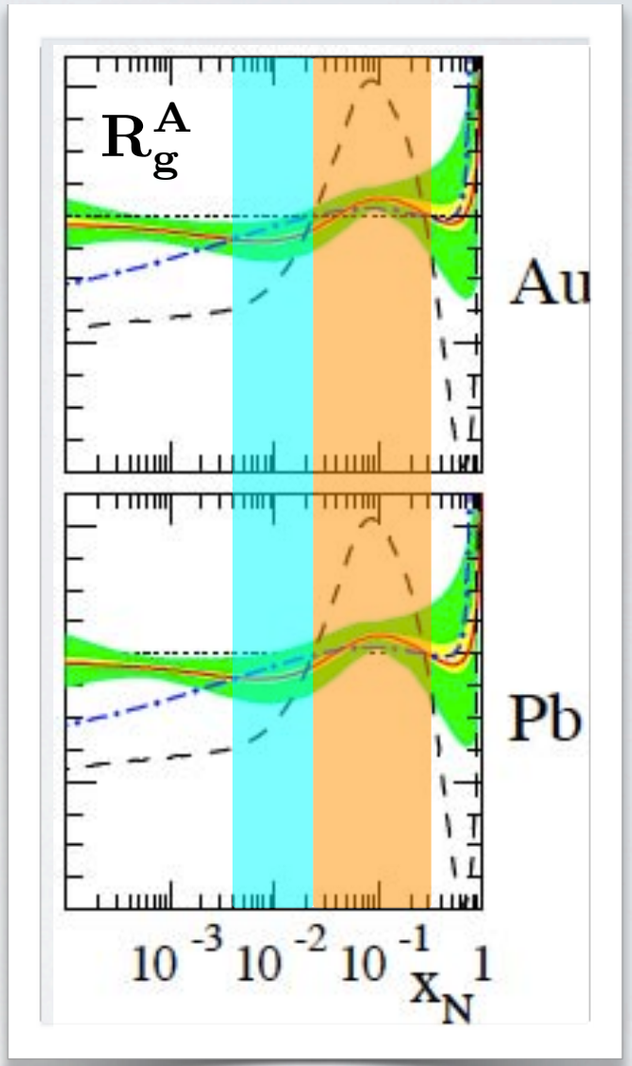

- can probe into shadowing region

prompt photons - impact

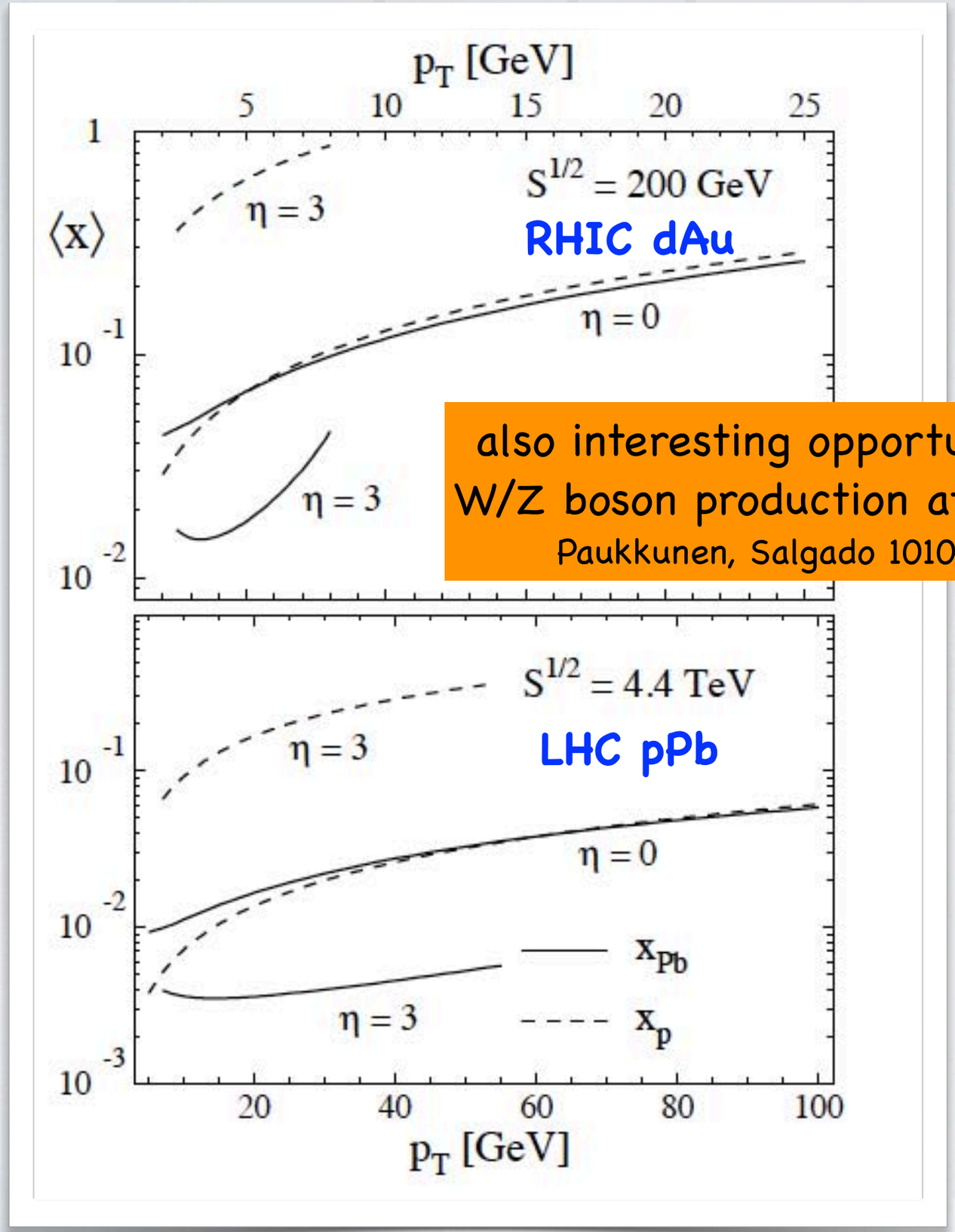

also interesting opportunities in W/Z boson production at the LHC
Paukkunen, Salgado 1010.5392

- can resolve characteristic differences between EPS and DSSZ gluons in anti-shadowing [and EMC] region

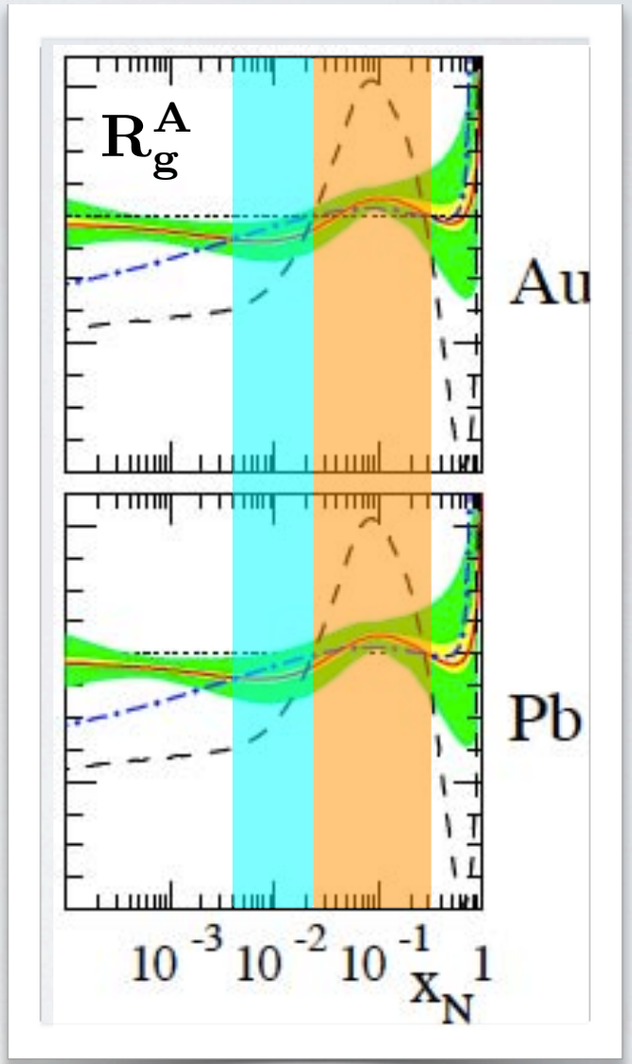

- can probe into shadowing region

Drell Yan lepton pairs in dAu/pPb

LO $$d\sigma_{DY}^{pA} \propto e_u^2 \left[u(x_1)\bar{u}^A(x_2) + \bar{u}(x_1)u^A(x_2)\right] + e_d^2 \left[d(x_1)\bar{d}^A(x_2) + \bar{d}(x_1)d^A(x_2)\right]$$

$$x_{1,2} = \sqrt{M^2/s}\, e^{\pm y}$$

Drell Yan lepton pairs in dAu/pPb

LO $$d\sigma_{DY}^{pA} \propto e_u^2 \left[u(x_1)\bar{u}^A(x_2) + \bar{u}(x_1)u^A(x_2)\right] + e_d^2 \left[d(x_1)\bar{d}^A(x_2) + \bar{d}(x_1)d^A(x_2)\right]$$

large positive y

$$x_{1,2} = \sqrt{M^2/s}\, e^{\pm y}$$

Drell Yan lepton pairs in dAu/pPb

LO $$d\sigma_{DY}^{pA} \propto e_u^2 \left[u(x_1)\bar{u}^A(x_2) + \bar{u}(x_1)u^A(x_2)\right] + e_d^2 \left[d(x_1)\bar{d}^A(x_2) + \bar{d}(x_1)d^A(x_2)\right]$$

large positive y

large negative y

$$x_{1,2} = \sqrt{M^2/s}\, e^{\pm y}$$

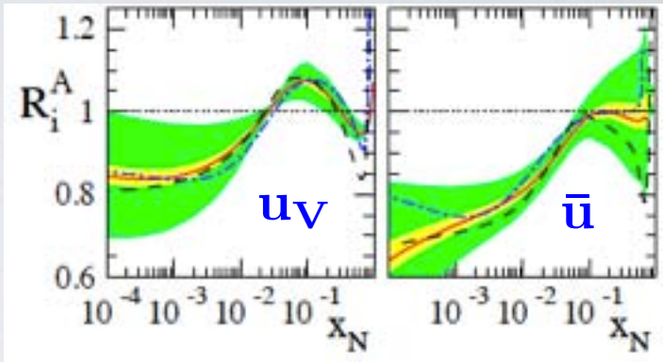

Drell Yan lepton pairs in dAu/pPb

LO $$d\sigma_{DY}^{pA} \propto e_u^2 \left[u(x_1)\bar{u}^A(x_2) + \bar{u}(x_1)u^A(x_2)\right] + e_d^2 \left[d(x_1)\bar{d}^A(x_2) + \bar{d}(x_1)d^A(x_2)\right]$$

large positive y

large negative y

$$x_{1,2} = \sqrt{M^2/s}\, e^{\pm y}$$

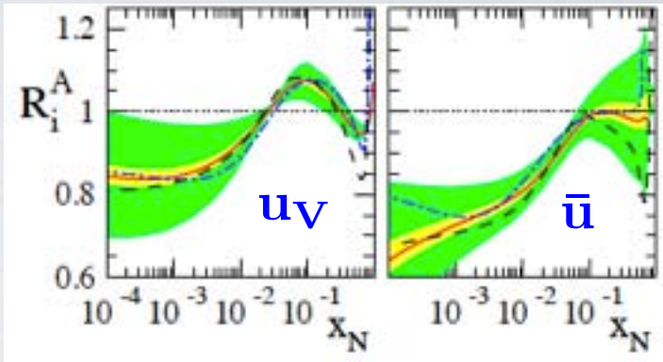

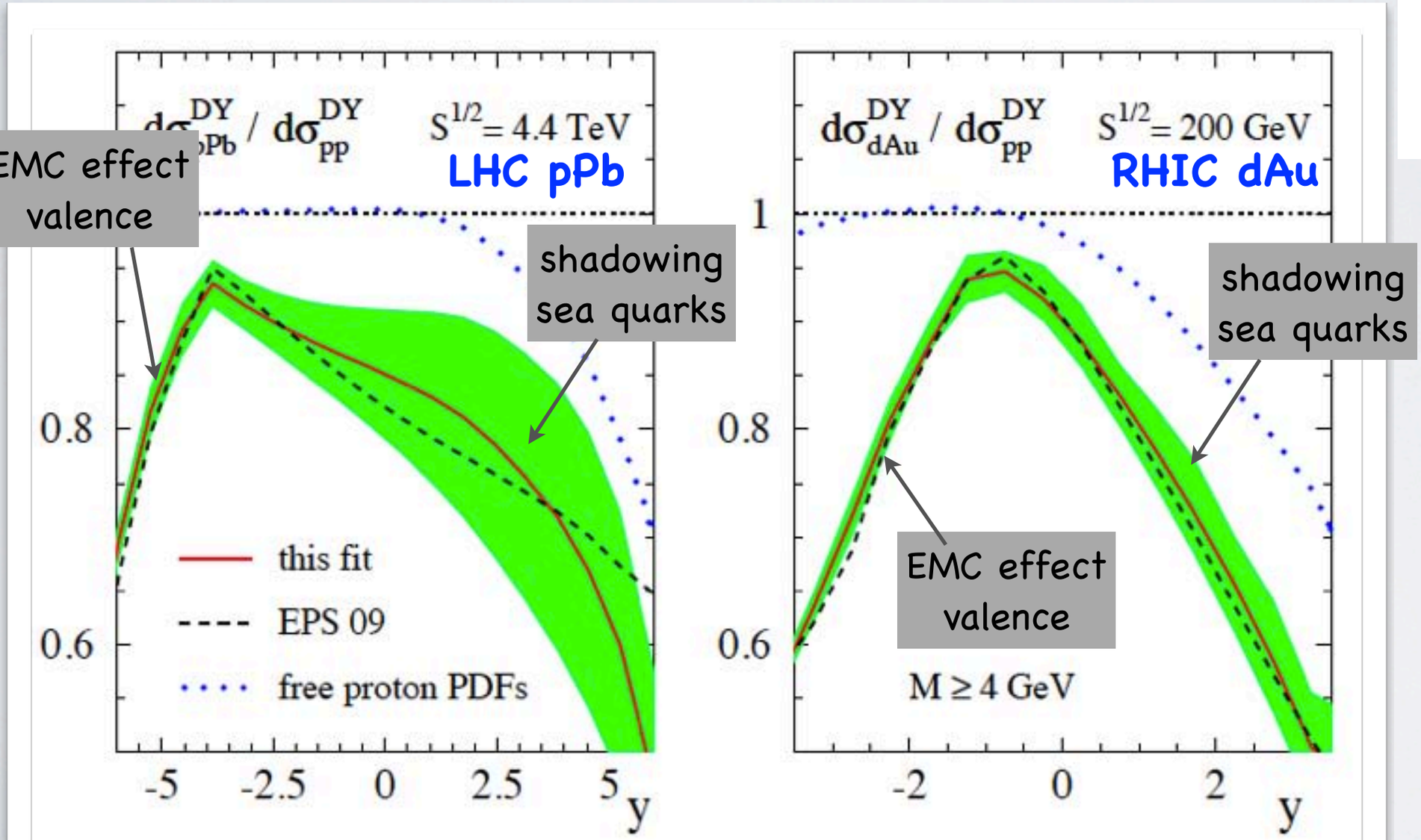

Drell Yan lepton pairs in dAu/pPb

LO $$d\sigma_{DY}^{pA} \propto e_u^2 \left[u(x_1)\bar{u}^A(x_2) + \bar{u}(x_1)u^A(x_2)\right] + e_d^2 \left[d(x_1)\bar{d}^A(x_2) + \bar{d}(x_1)d^A(x_2)\right]$$

large positive y

large negative y

$$x_{1,2} = \sqrt{M^2/s}\, e^{\pm y}$$

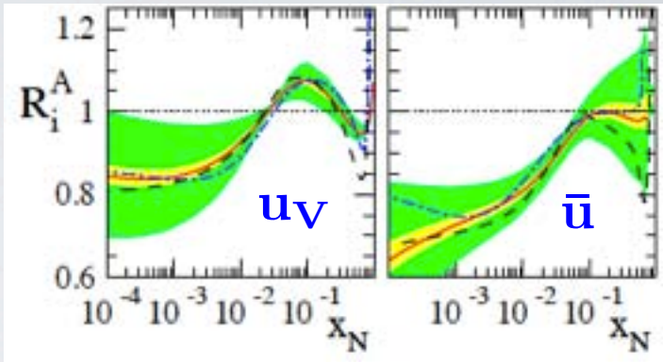

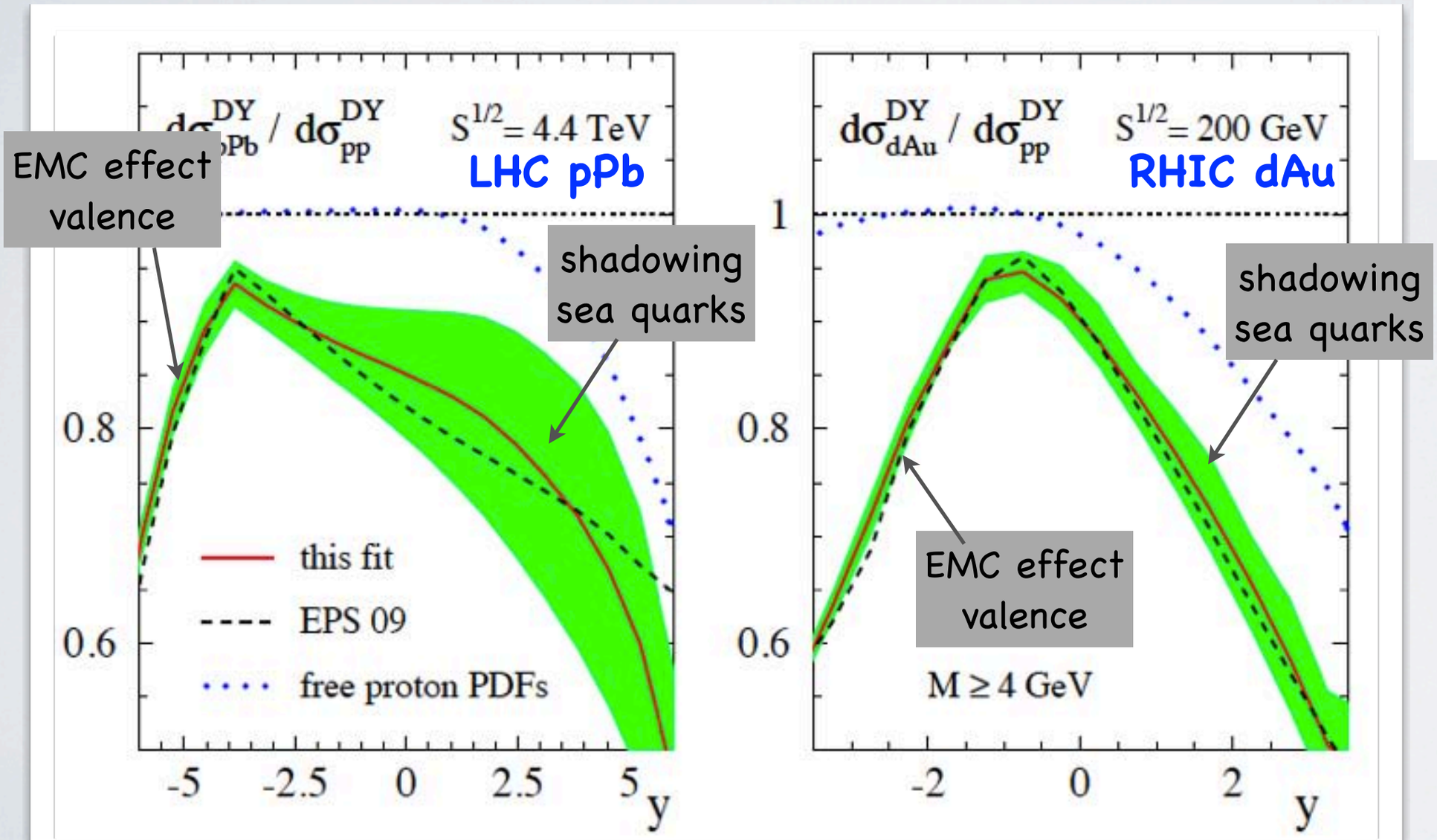

x reach at y=3

RHIC: $x_2 \simeq 10^{-3}$

LHC: $x_2 \simeq 5 \times 10^{-5}$

potential of pPb @ LHC

first run scheduled for early 2013

see Salgado et al., 1105.3919

kinematic reach

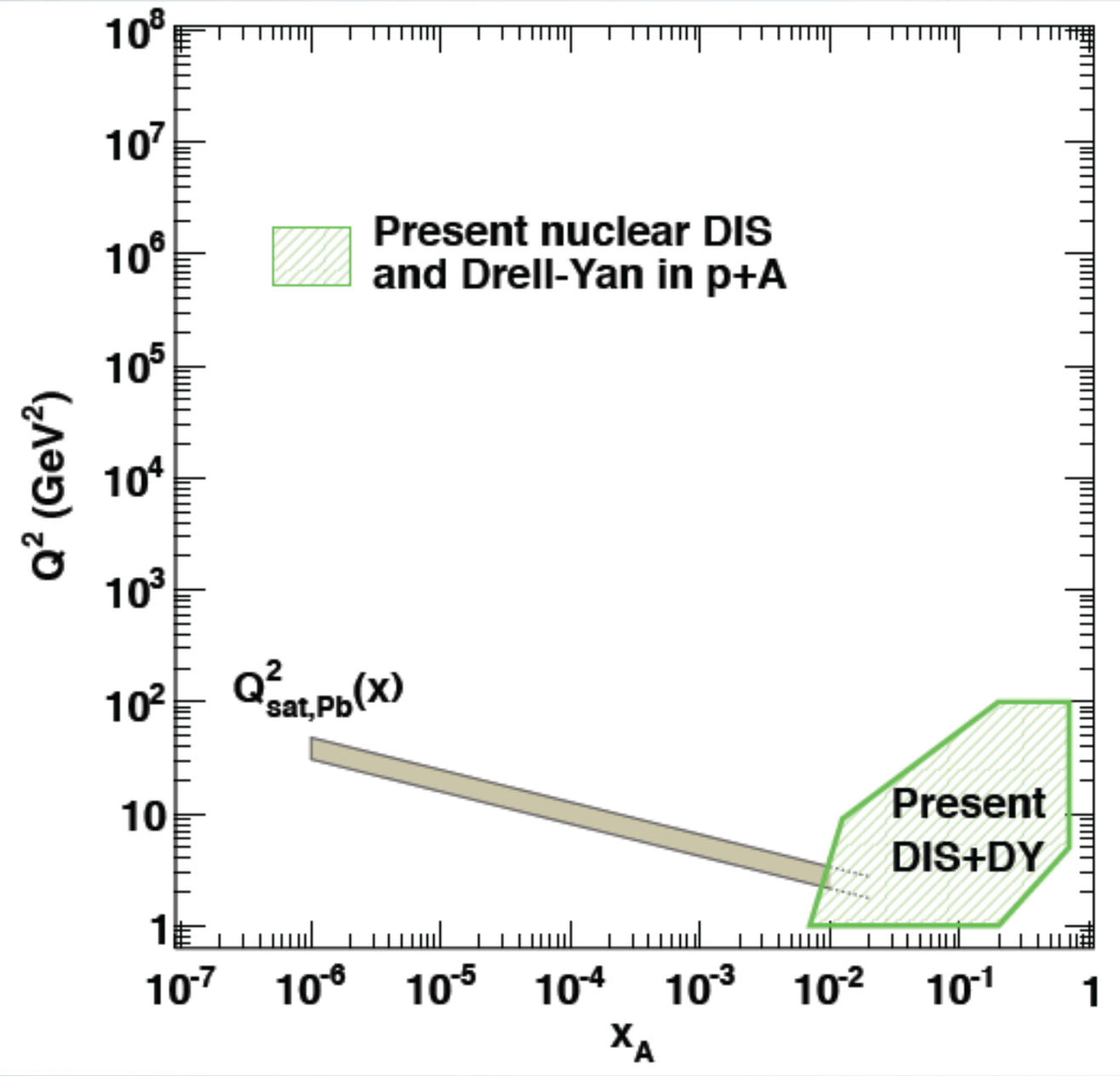

potential of pPb @ LHC

first run scheduled for early 2013

see Salgado et al., 1105.3919

kinematic reach

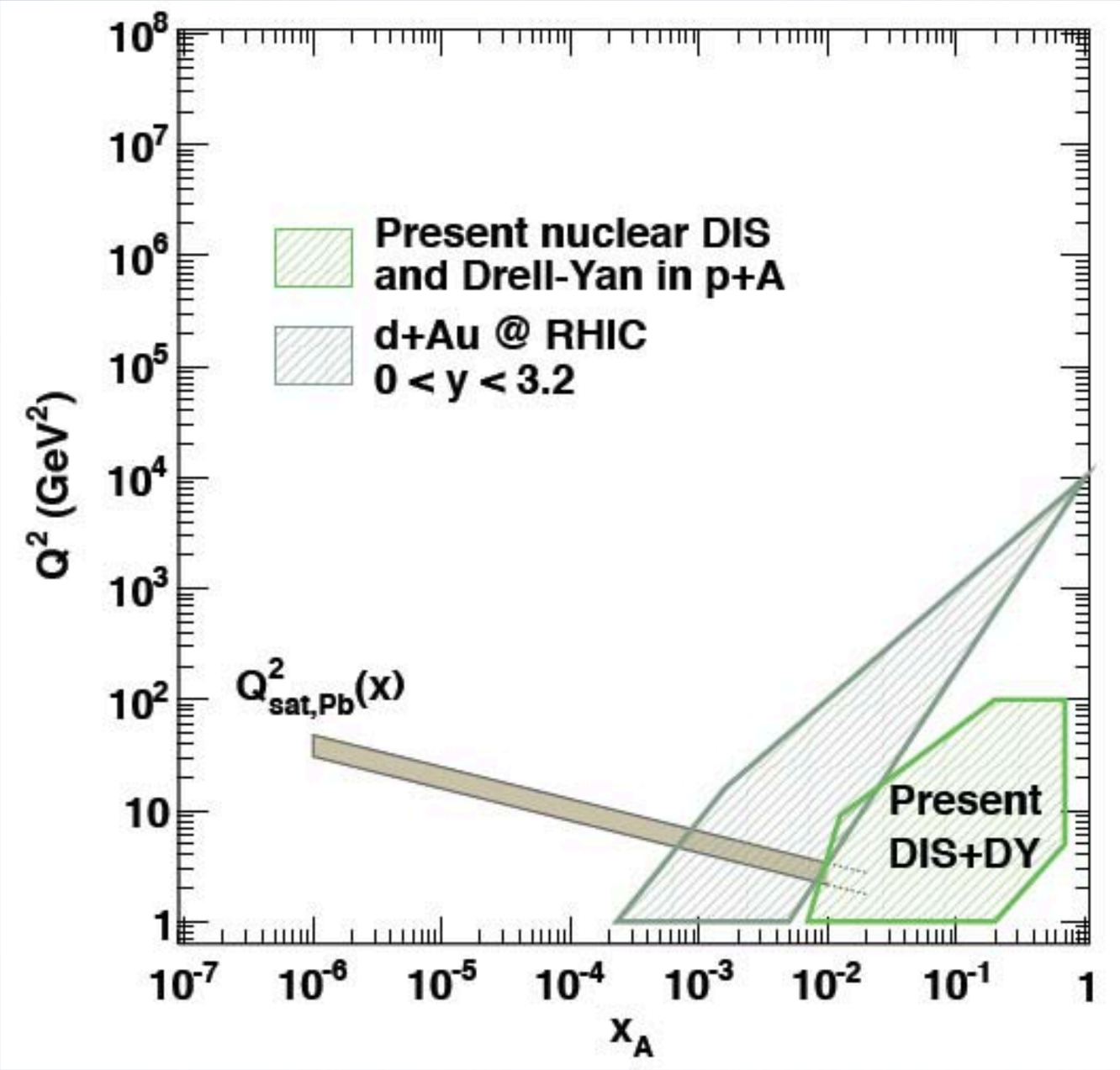

potential of pPb @ LHC

first run scheduled for early 2013

see Salgado et al., 1105.3919

kinematic reach

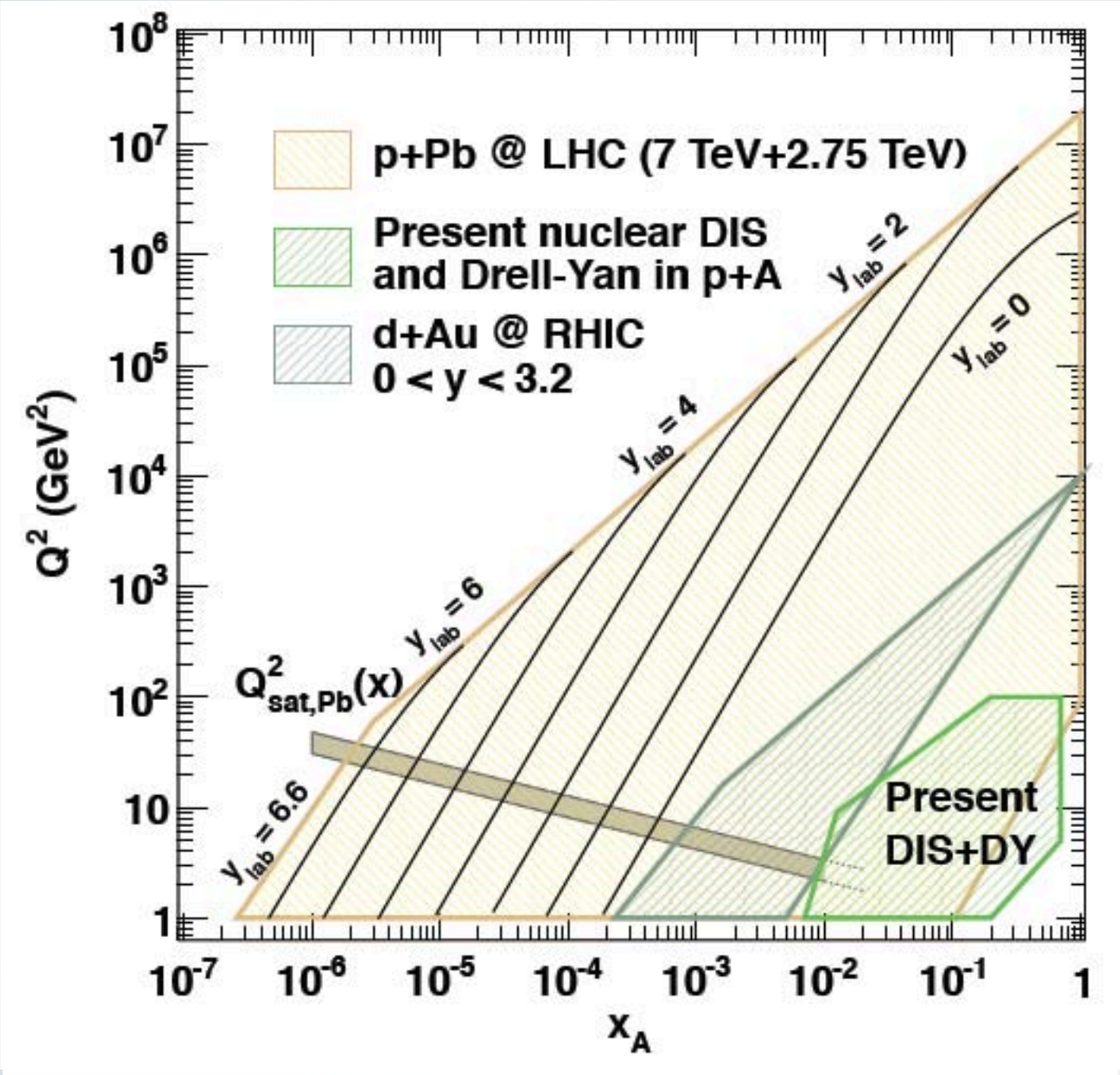

potential of pPb @ LHC

first run scheduled for early 2013

see Salgado et al., 1105.3919

kinematic reach

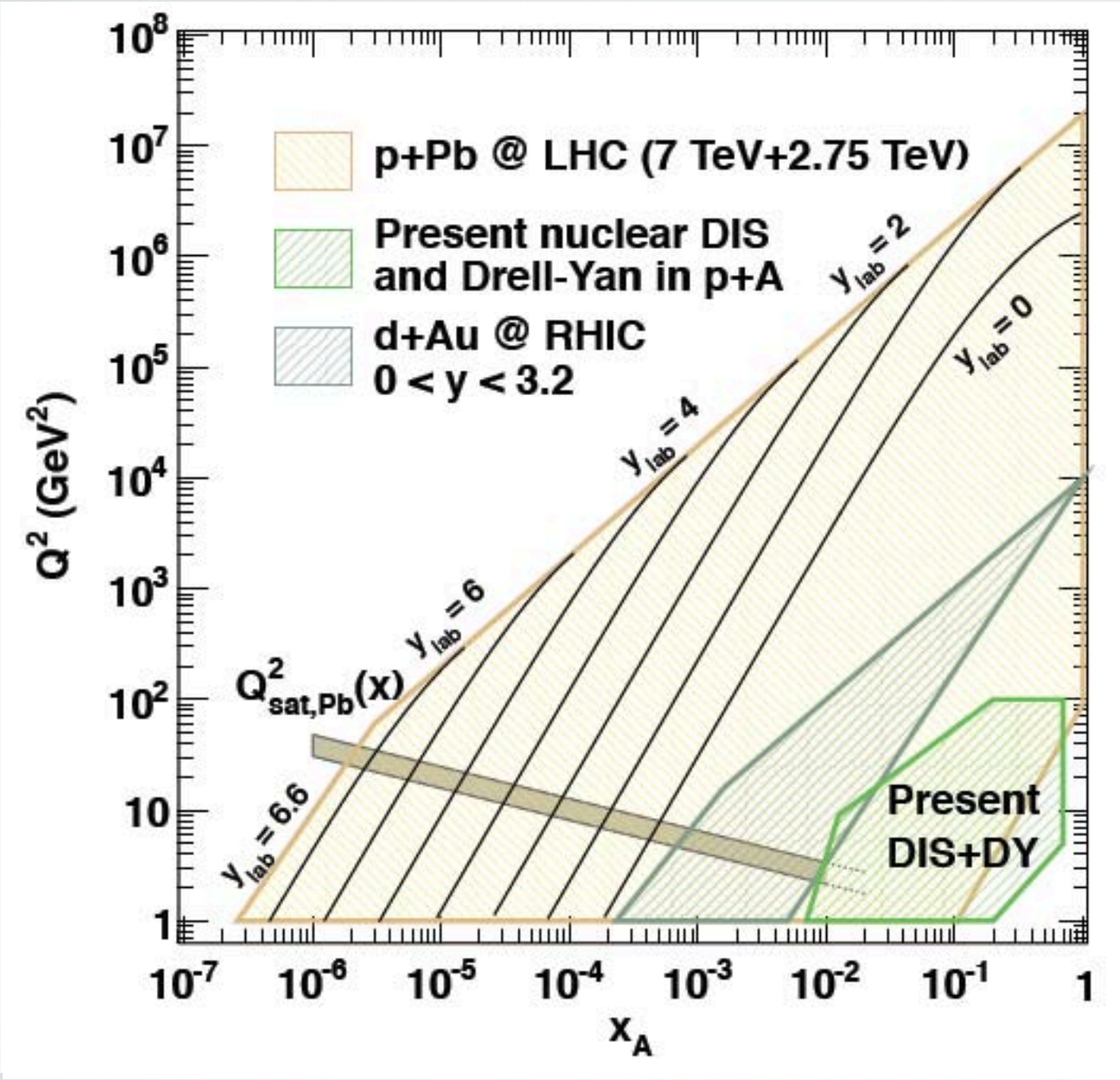

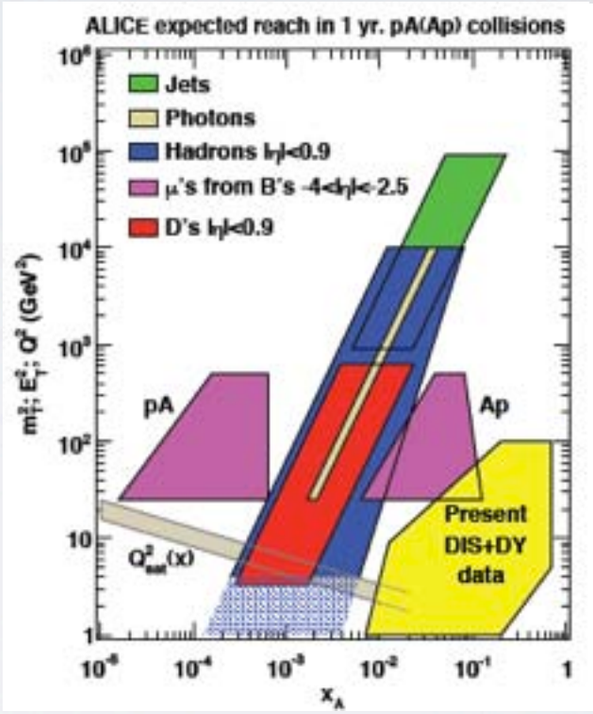

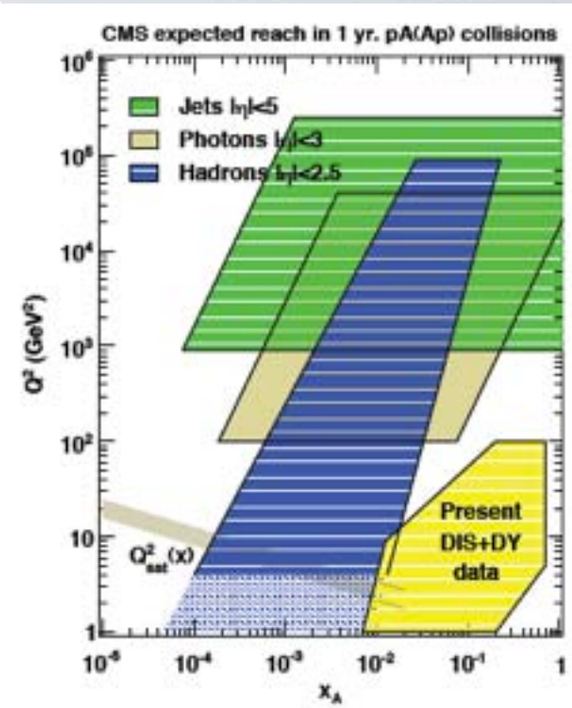

- small x already accessible at mid rapidity
- many conceivable probes

potential of pPb @ LHC

first run scheduled for early 2013

see Salgado et al., 1105.3919

kinematic reach

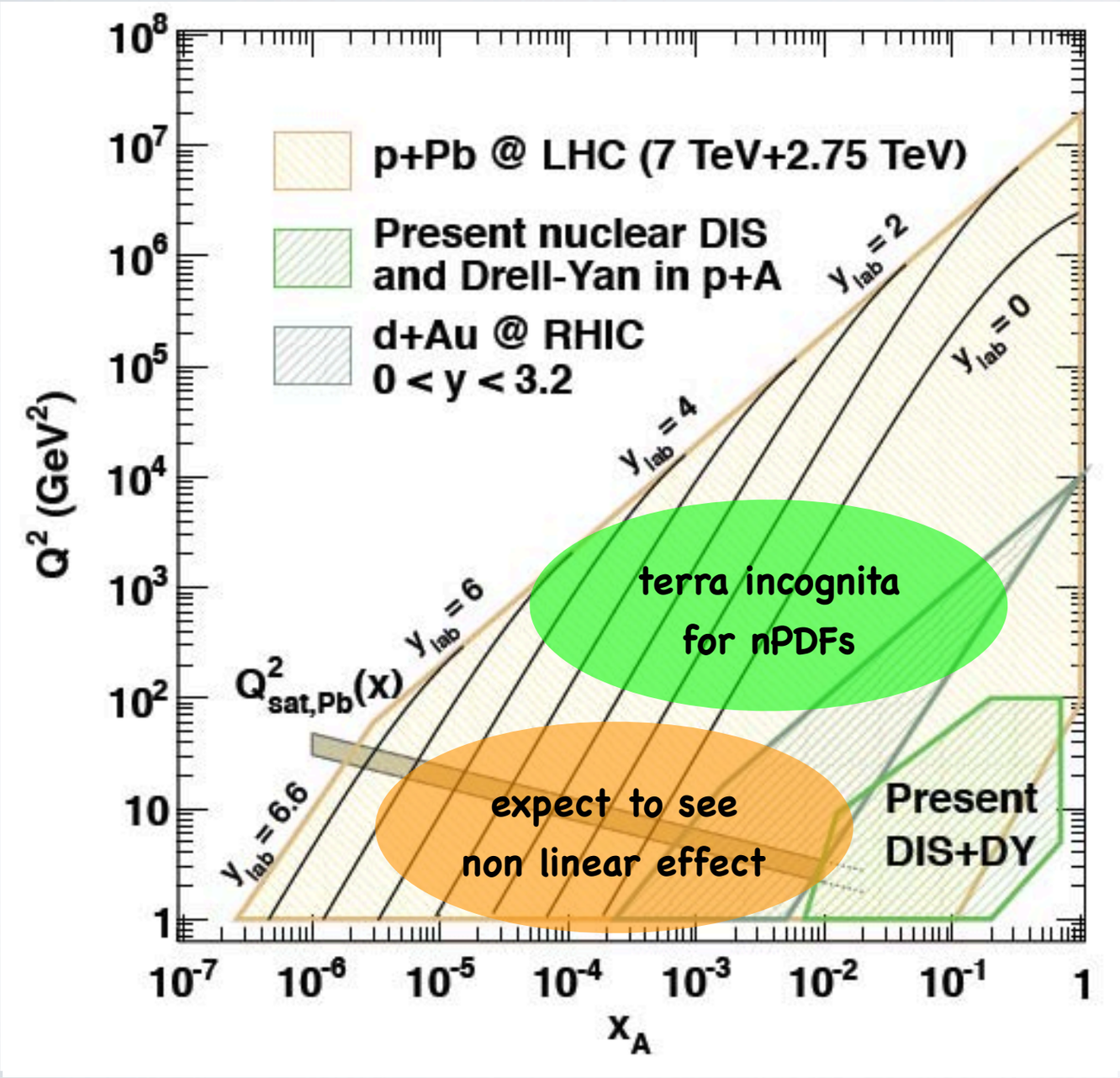

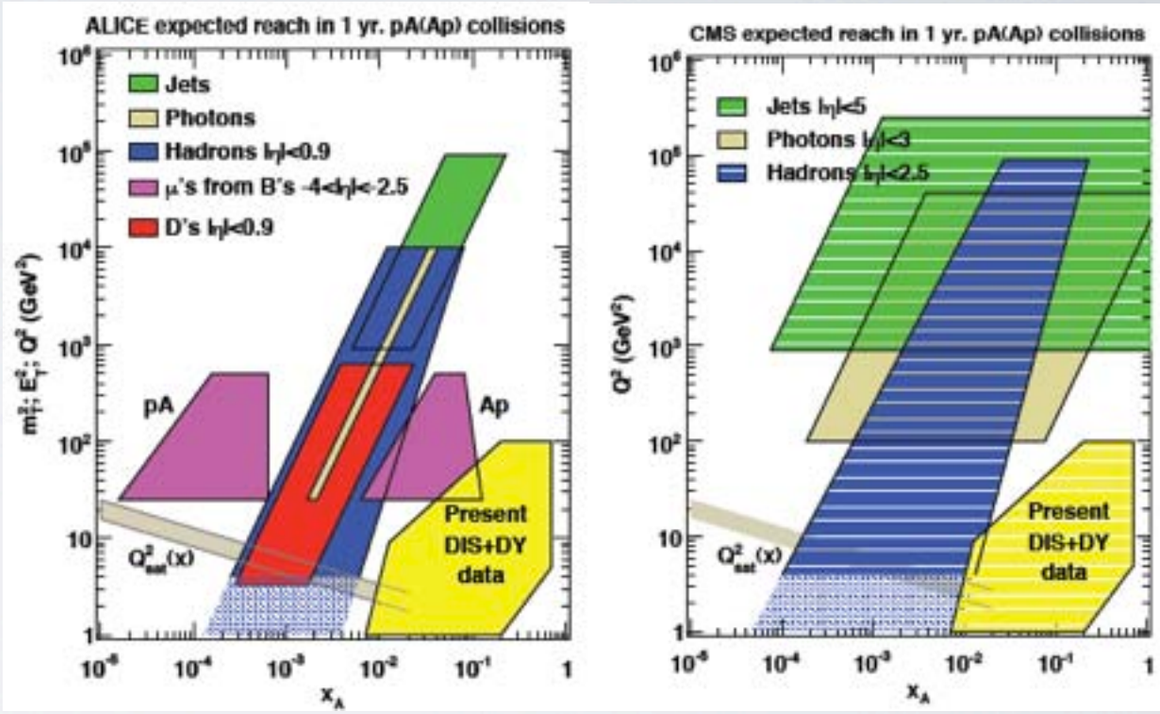

- small x already accessible at mid rapidity
- many conceivable probes

expect great impact on nPDF fits

take away message

- **first fully global QCD analysis of nuclear PDFs at NLO**
  includes charged lepton DIS, neutrino DIS, Drell Yan, and dAu pion data

- **main observations**
  no tension with neutrino DIS data (unlike in nCTEQ fit)
  much more moderate modifications of gluon from RHIC data (unlike in EPS fit)

- **technical advances**
  treatment of heavy quark mass effects
  use of numerical efficient Mellin technique throughout
  uncertainty estimates with improved Hessian method (eigenvector/error sets)

- **exciting prospects for upcoming LHC pPb and future RHIC runs**
  impact of electromagnetic probes (prompt photons and Drell Yan)

more distant future: electron-ion collider (EIC/LHeC)

to study nPDFs, universality, factorization, and the transition to saturation with precision

Looking forward in pA@LHC

Mark Strikman, PSU

Forward physics at RHIC,
July 30, 2012

Summary of some of the discussions at the workshop pA@LHC, CERN, June 4 - 7

Main emphasize: Forward physics - LHC vs RHIC

what issues can be best studied at LHC

what issues can be best studied at RHIC

where one can gain from coordinated studies

will talk little on the results presented at pA@LHC by speakers who will also speak at this meeting.

will not talk about benchmark measurements which are mostly for central rapidities.

MACHINE

Collision energy:

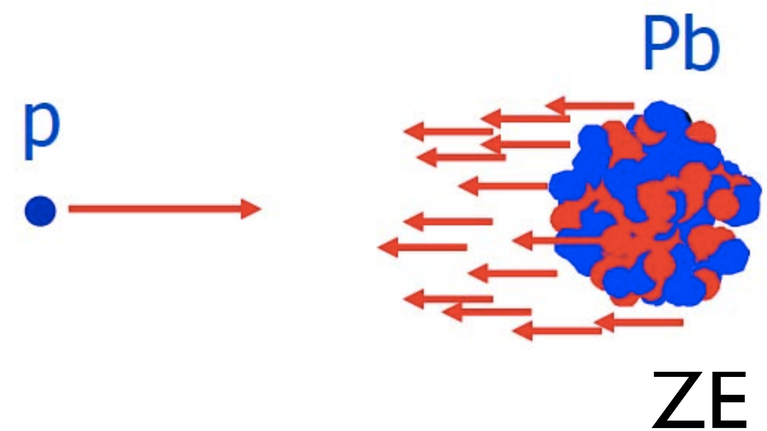

Beam energy at LHC: E_p=3.5 TeV (or 4 TeV)
E_A=1.38 TeV

$$\sqrt{s_{pN}} = 4.4\,TeV$$

SCHEDULE

- Feasibility Run - I : (2011-Oct 31)
  Stored Pb bunches in presence of many proton bunches – OK
- Feasibility Run – II: 2012 (Aug/Sep)
- 1st Physics Run: March 2013

Target p-Pb performance in 2012 (ATLAS/CMS)

Main choice:	**Units**	**200 ns**		**100 ns**	
Beam energy/(Z TeV)	Z TeV	3.5	4	3.5	4
Colliding bunches		356	356	550	550
β^*	m	0.7	0.6	0.7	0.6
Emittance protons	μm	3.75	3.75	3.75	3.75
Emittance Pb	μm	1.5	1.5	1.5	1.5
Pb/bunch	10^8	1.2	1.2	0.8	0.8
p/bunch	10^{10}	1.15	1.15	1.15	1.15
Initial Luminosity L_0	10^{28} cm^{-2} s^{-1}	**6.2**	**8.3**	**6.4**	**8.5**
Operating days		**22**	**24**	**22**	**24**
Difficulty (subjective)		**0.9**	**1**	**0.9**	**1**
Integrated luminosity	nb^{-1}	**15.4**	**22.4**	**15.9**	**23.1**
Nucleon-nucleon	pb^{-1}	**3.2**	**4.7**	**3.3**	**4.8**

Integrated luminosity by scaling from 2011 (c.f. ~7 pb^{-1} NN in Pb-Pb)
Average Pb bunch intensities from best 2011 experience.
Proton bunch intensities conservative, another factor 10 **???**
Proton emittance conservative, another factor 1.37 **?**
Untested moving encounter effects, possible reduction factor 0.1 **??**

All 6 detectors plan to take pA data

only ALICE , ATLAS, CMS took AA data

LHCb, LHCf, TOTEM

acceptance at larger rapidities than ATLAS and CMS
important for forward physics

aim to exchange event information with

ATLAS CMS

Details on detectors - David D'Entrria talk - just one slide

Comparison of Angular Coverage

Michael Schmelling

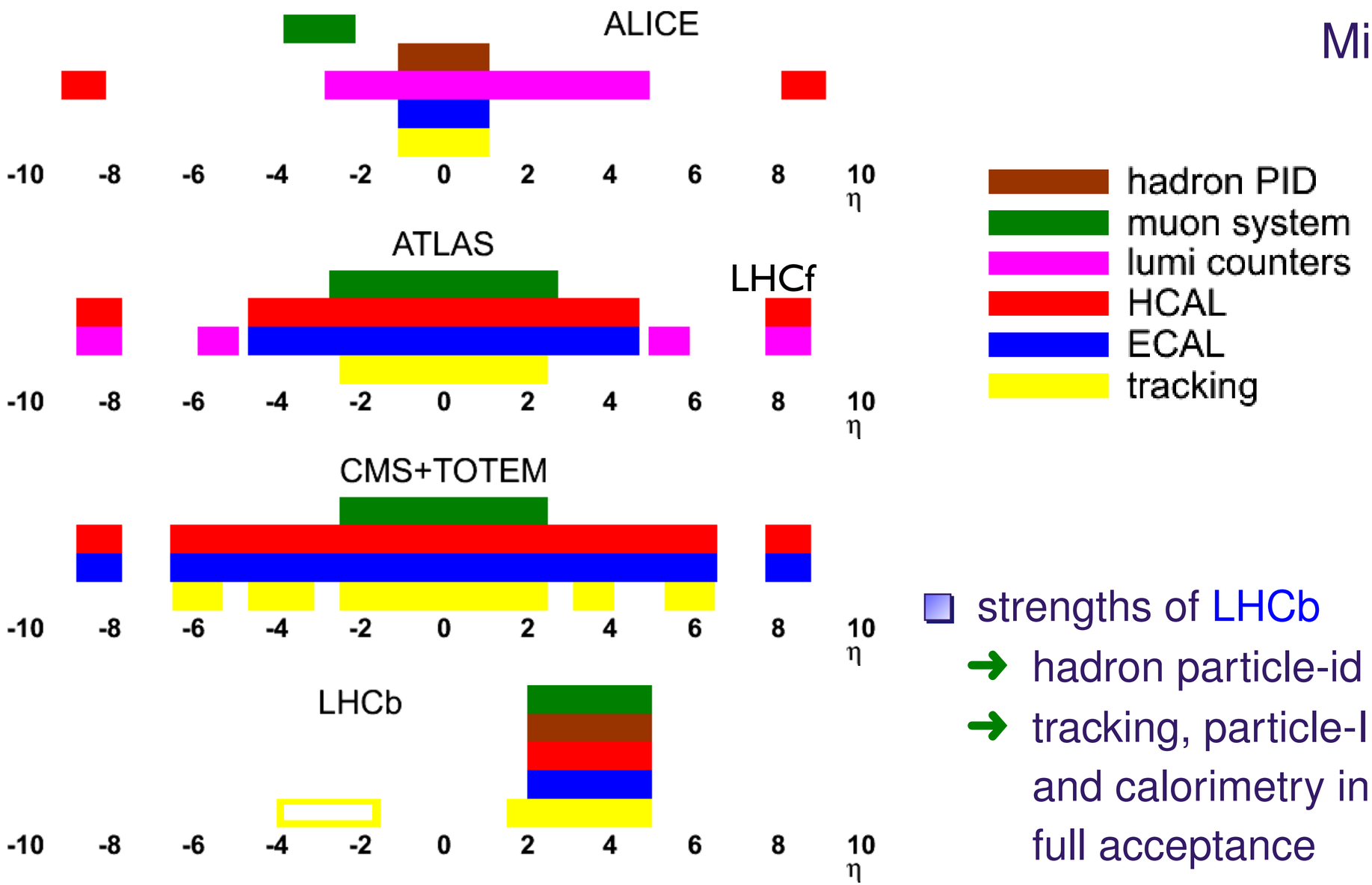

- strengths of LHCb
  - ➜ hadron particle-id
  - ➜ tracking, particle-ID and calorimetry in full acceptance

Nuclear pdfs

Juan Rojo descibed plans to perform extraction of nuclear pdfs using only LHC data (dijets, Z,W, γ') from AA and pA. Similar to pp program.

Problems - no corresponding data base for eA as for ep

Main interest: the ratios nuclear pdf/nucleon pdf at moderate Q^2.
Expected very small (few %) deviations from one for $Q^2 \sim 10^4$ GeV^2.
Instability of backward evolution.

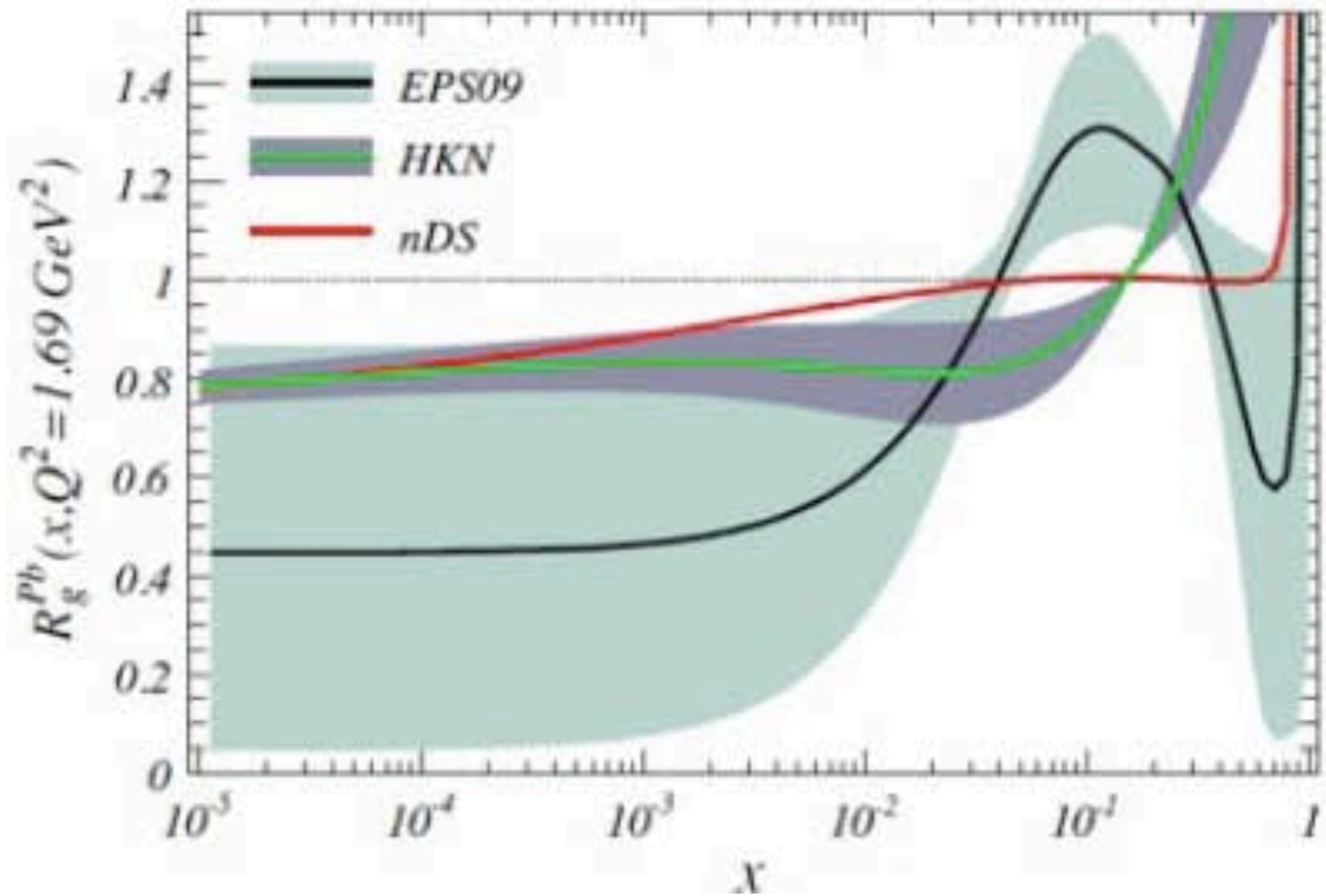

No data on $F_{2A}(x < 10^{-2})$ for $Q^2 \geq 4$ GeV^2. Gluons for x<0.05.

RHIC forward data are not in the LT kinematics

Parametrizations based on fitting the data with no theory input - uncertainty at normalization point even begger than in the plot.

Prediction of the LT theory of nuclear shadowing based on factorization theorem for diffraction and AGK

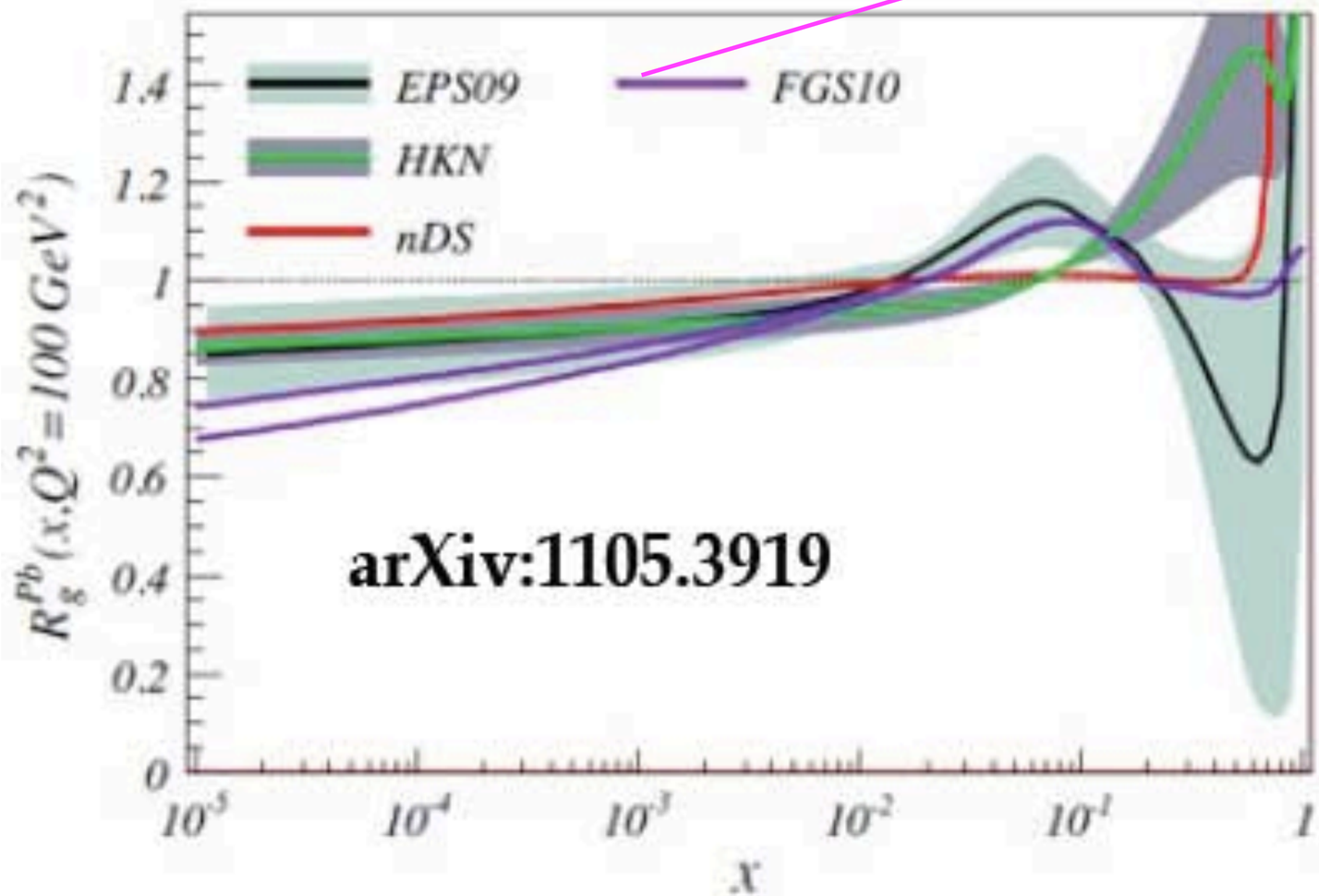

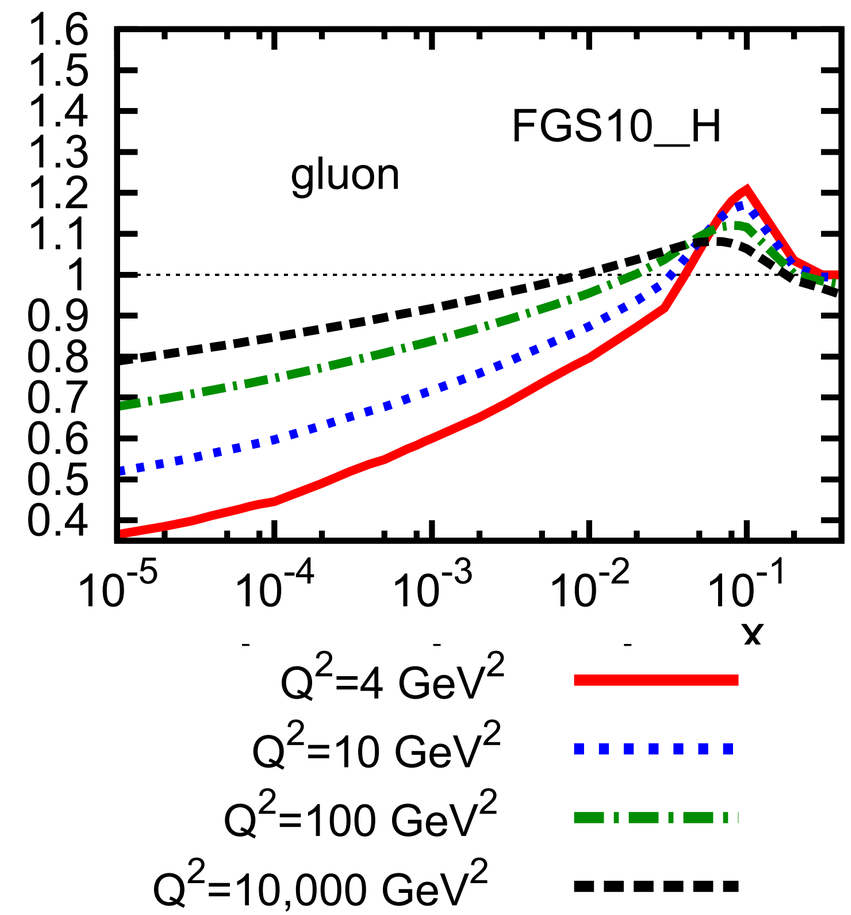

Strong reduction of nuclear shadowing at fixed x due to the DGLAP flow of partons from larger x

Another challenge:determine nuclear diagonal generalized parton distributions ≡ b dependent npdfs

Ilkka Helenius
In collaboration with
Kari J. Eskola, Heli Honkanen, and Carlos A. Salgado

Nuclear modifications with spatial dependence

- We replace
$$R_i^A(x,Q^2) \to r_i^A(x,Q^2,\mathbf{s}),$$
where $\mathbf{s}$ = the transverse position of the nucleon
- Definition
$$R_i^A(x,Q^2) \equiv \frac{1}{A}\int \mathrm{d}^2\mathbf{s}\, T_A(\mathbf{s}) r_i^A(x,Q^2,\mathbf{s}),$$
where $R_i^A(x,Q^2)$ from EKS98 or EPS09 (= data!)
- Assumption: spatial dependence related to $T_A(\mathbf{s})$
$$r_A(x,Q^2,\mathbf{s}) = 1 + c_1(x,Q^2)[T_A(\mathbf{s})] + c_2(x,Q^2)[T_A(\mathbf{s})]^2 + c_3(x,Q^2)[T_A(\mathbf{s})]^3 + c_4(x,Q^2)[T_A(\mathbf{s})]^4$$

Important: No A dependence in the fit parameters $c_j(x,Q^2)$
(unlike some earlier analyses with only one fit parameter)

Series in powers of T is reasonably strength of interaction is small - otherwise convergence is poor. - example
1-exp(-1) -ok
1-exp(-2.5) -bad

expression not valid for x >10^{-2}-due to finite coherence length, EMC effect, etc

Spatial Dependence of Nuclear Modifications

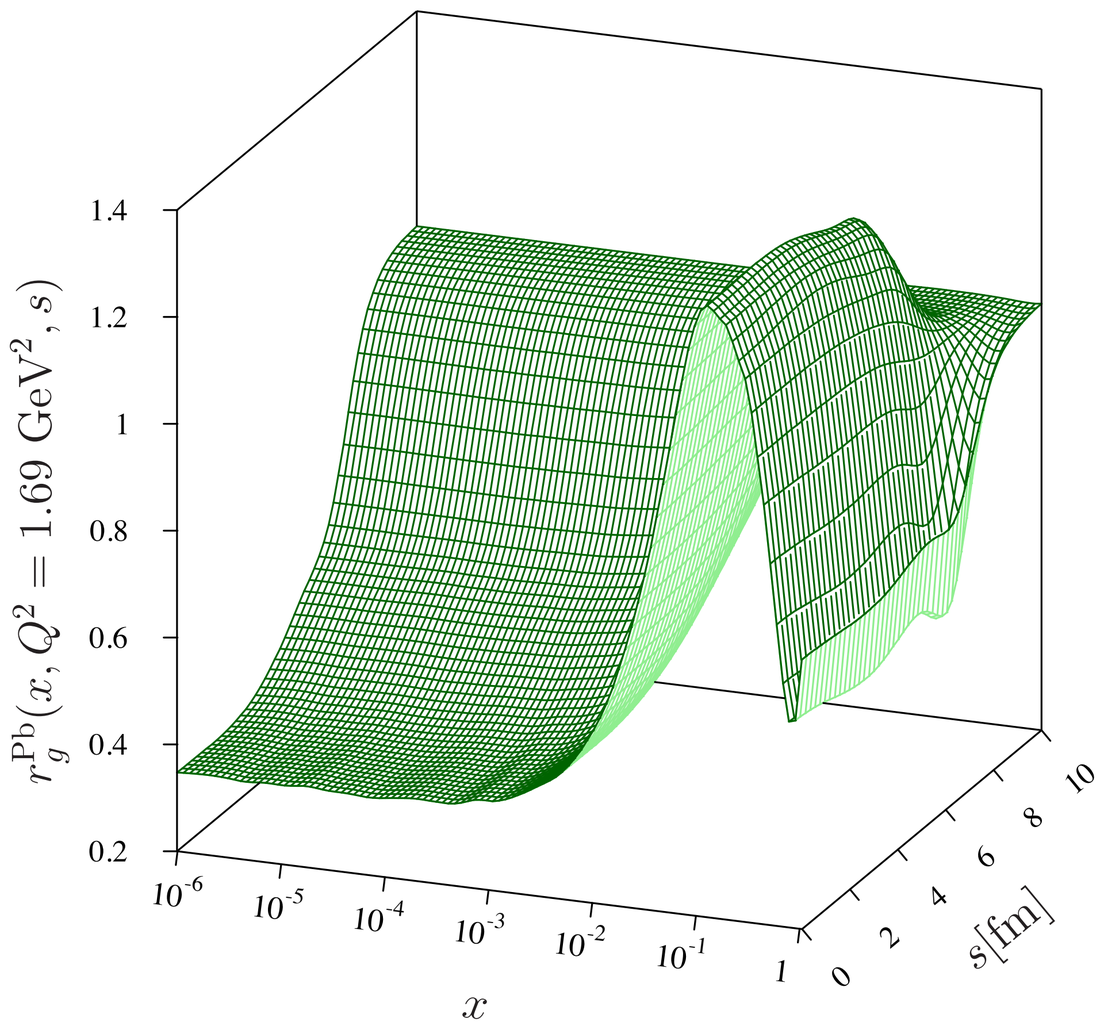

Helenius et al fit to EKS09

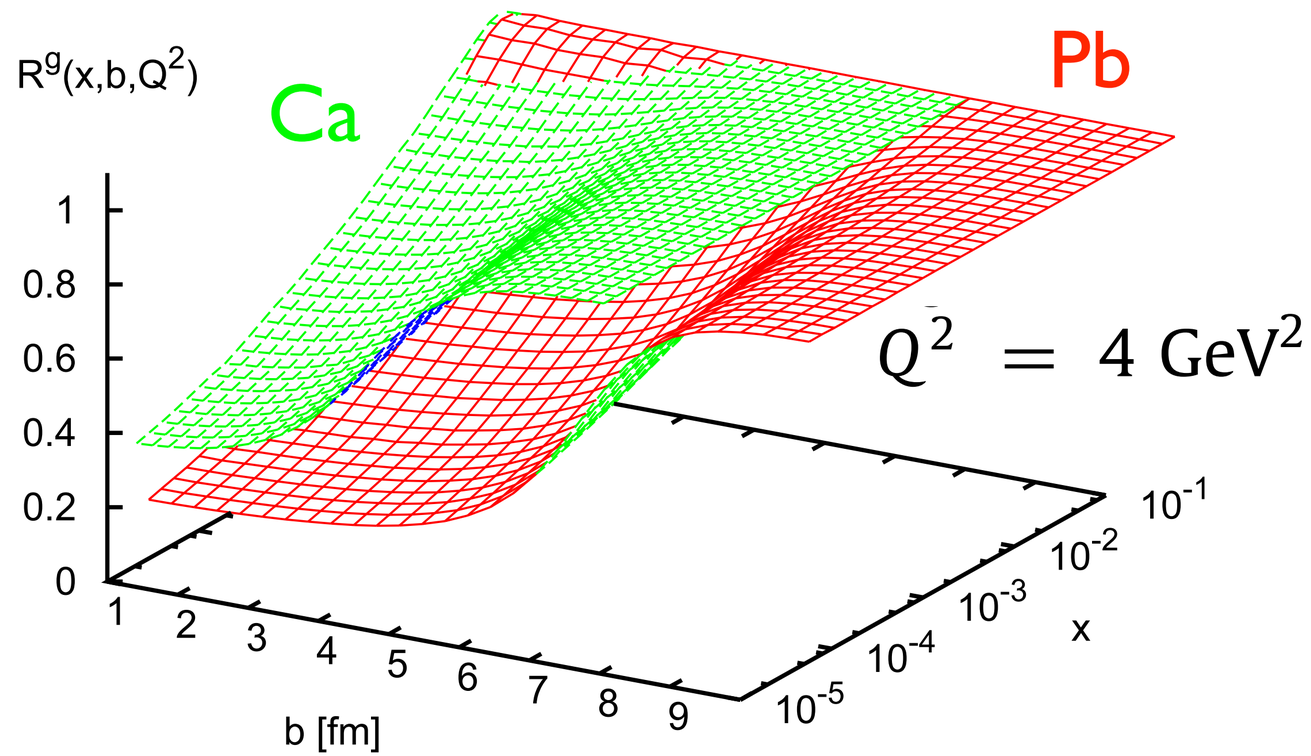

Frankfurt, Guzey, MS - calculation in LT theory

Several features similar

Measurement of npdfs

Most interesting - small x: LT shadowing, new physics at very small x, etc

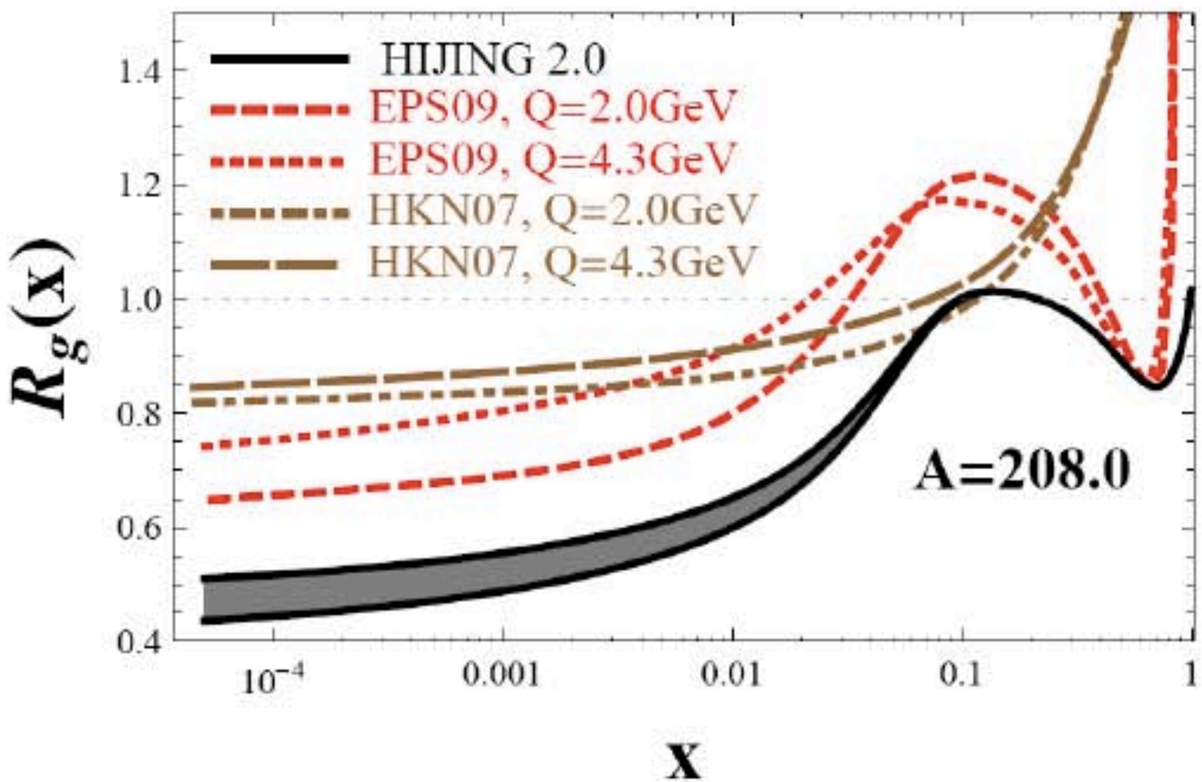

Relevant for MC models of generic AA collisions. HIJING uses gluon shadowing to fit RHIC data (X.N.Wang). No scaling violation & violation of the momentum sum rule

Main challenge for measurements is not the counting rate but angular acceptance (plus for jets dealing with pedestal and other backgrounds)

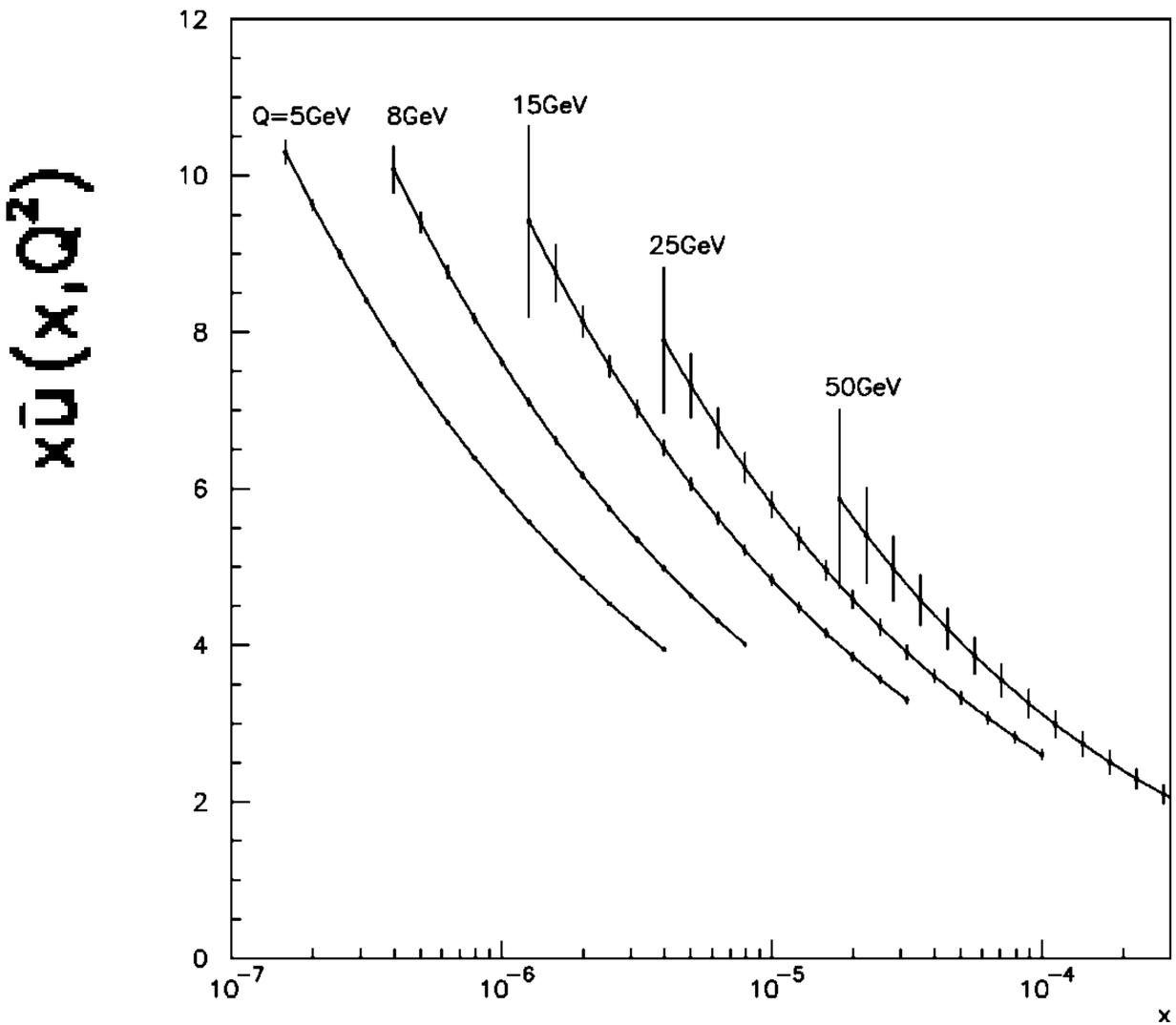

Full acceptance detector FELIX.

The u antiquark momentum distribution with error bars calculated from the Drell-Yan cross section and a data sample corresponding to an integrated luminosity of 100 pb^{-1}

Alvero, Collins, MS, Whitmore 94

for minimal lumi of the pA run errors are 4 times larger

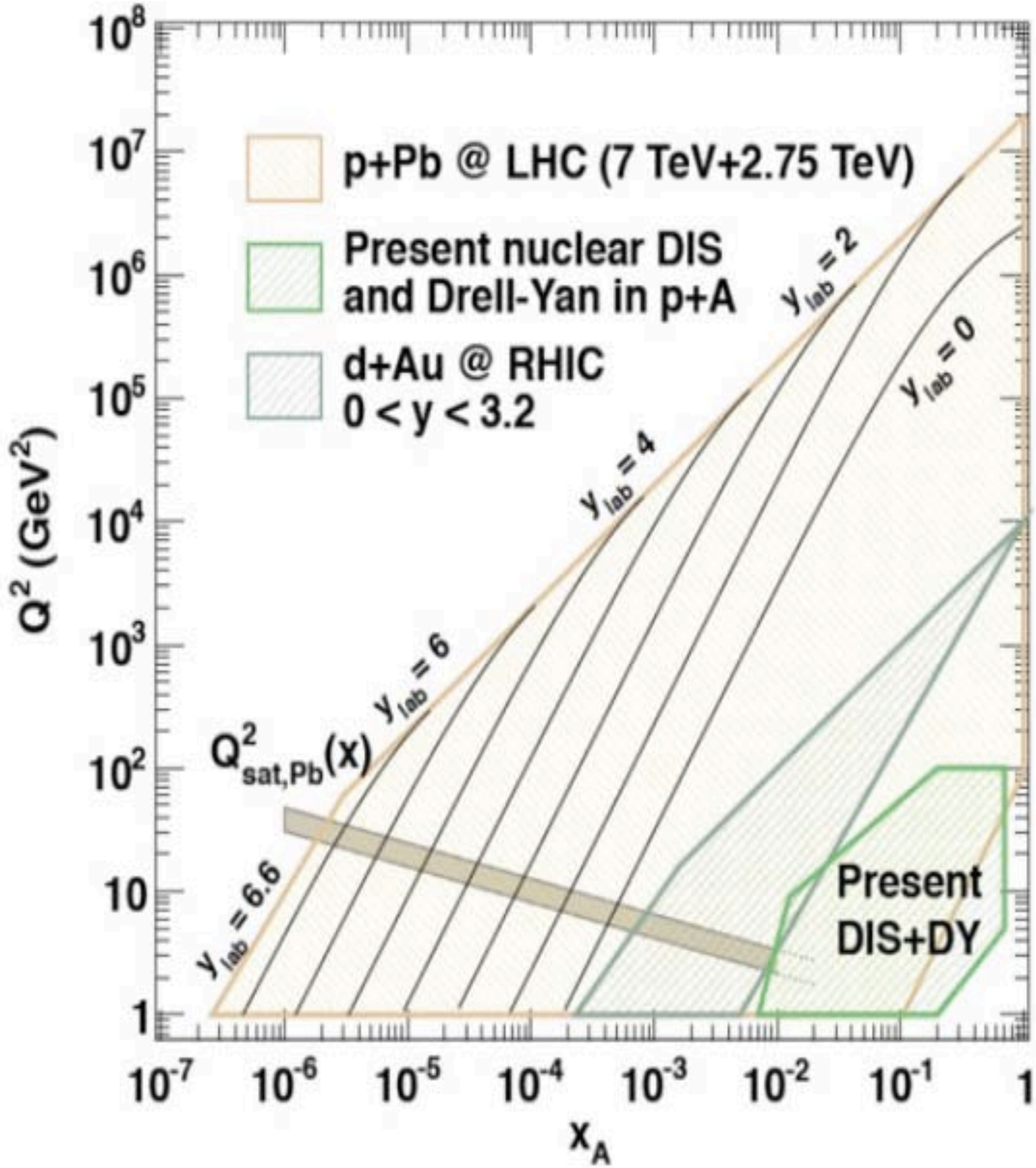
p+Pb @ LHC (7 TeV+2.75 TeV)
Present nuclear DIS and Drell-Yan in p+A
d+Au @ RHIC 0 < y < 3.2
$y_{lab} = 2$
$y_{lab} = 0$
$y_{lab} = 4$
$y_{lab} = 6$
$y_{lab} = 6.6$
$Q^2_{sat,Pb}(x)$
Present DIS+DY
Q^2 (GeV^2)
x_A
10^8
10^7
10^6
10^5
10^4
10^3
10^2
10
1
10^{-7}
10^{-6}
10^{-5}
10^{-4}
10^{-3}
10^{-2}
10^{-1}
1

LHCb is sensitive to
low-x and a high-x parton collisions.

Two different regions are probed
→ inputs for PDF fits

- W/Z measurements probe

  $Q^2 = 10'000\ GeV^2$, $x = 1.7 \cdot 10^{-4}$

- Low mass Drell-Yan (γ^*)

  $Q^2 = 25\ GeV^2$, $x = 8 \cdot 10^{-6}$

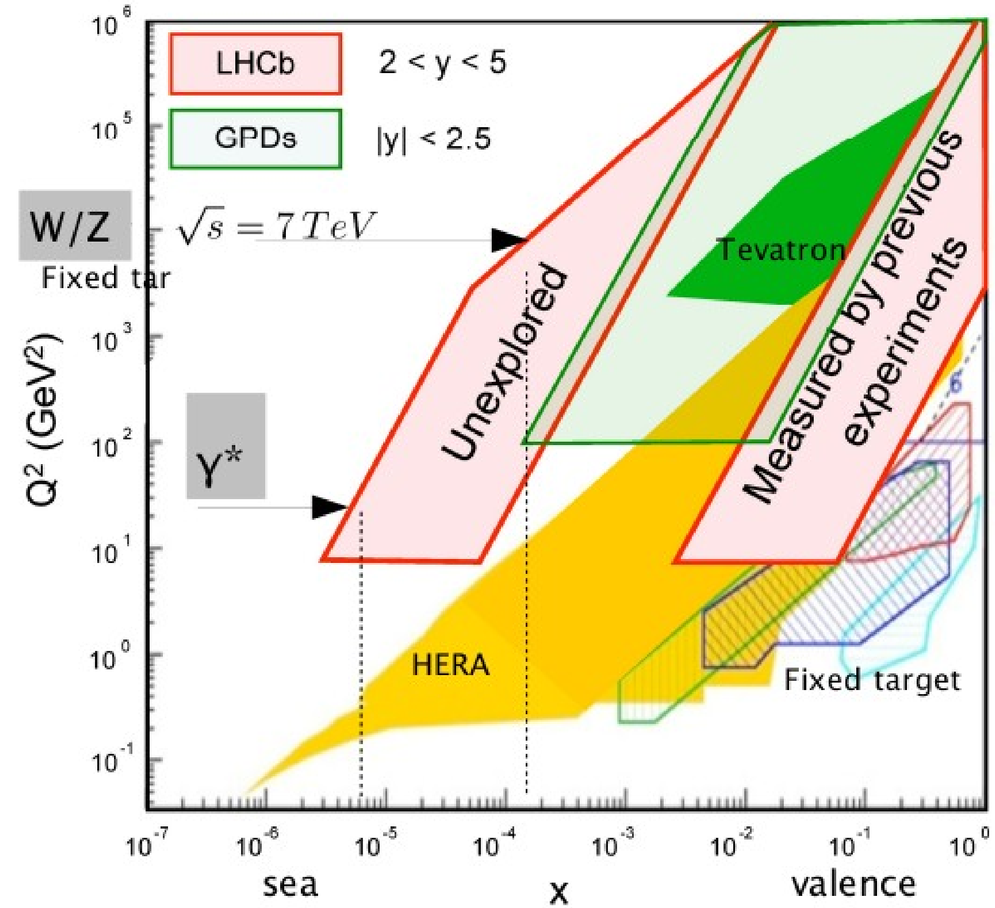

Strength of LHCb - ability to measure c-quark and b-quark contributions to dileptons at forward rapidities and separate them from DY. Hence measure DY as well as gluon pdf for similar x.

Low-x WS - 27-30 June

M. Rangel

Low Mass Drell-Yan Production

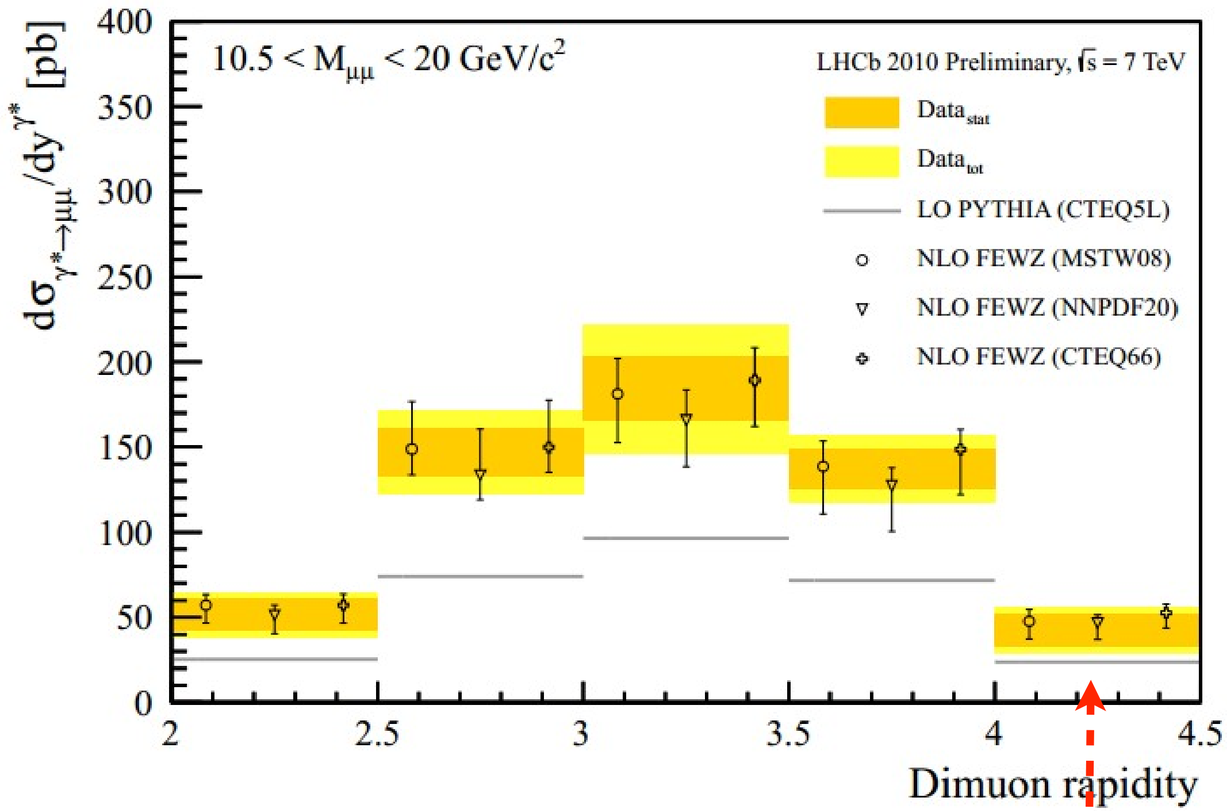

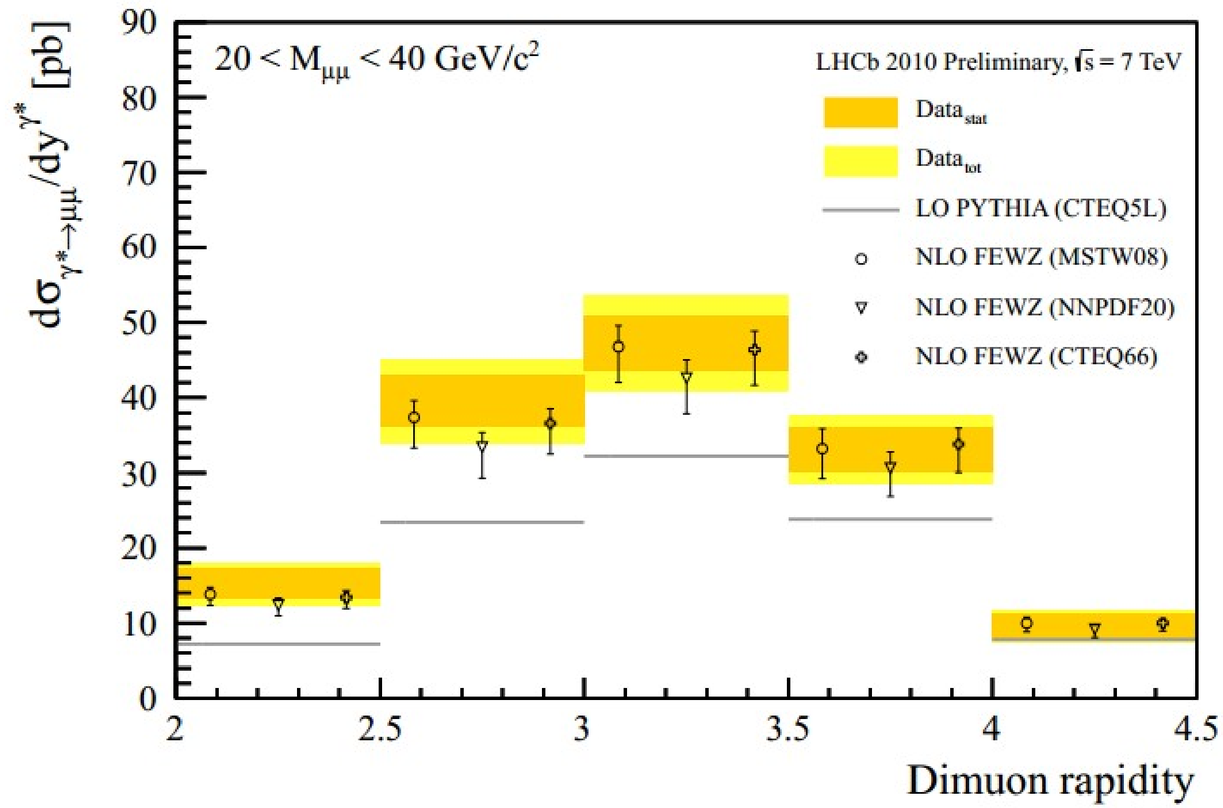

$$x = 3 \cdot 10^{-5}$$

Reaching small x at modest virtualities to observe nonlinear effects

- Use of differential cross sections -- DY
- Ultraperipheral AA collisions

DY: In the leading log approximation $\dfrac{d\sigma^{l^+l^-}}{dy\,dM^2\,dp_t^2}$

differential cross section at $p_t \sim 0$ is suppressed by the DDT form factor - a minimum

However exponentiating soft gluon radiation *in the impact parameter* space results in *flattening* of the spectrum in the $p_t \sim 0$ limit. Plateau for $p_t < p_0$

$$p_0^2 \propto \Lambda_{QCD}^2 \left(\frac{Q^2}{\Lambda_{QCD}^2}\right)^{\gamma}, \quad \gamma = \left(1 + \frac{\beta_2}{2\Sigma_C}\right)^{-1} \qquad \gamma_{q\bar{q}} = 0.372$$

Much smaller virtualities than $M^2(l^+l^-)$ can be probed in DY process !!

Predictions – pA @ LHC

J-W. Qiu

- "Cronin" effect for Z^0 production?

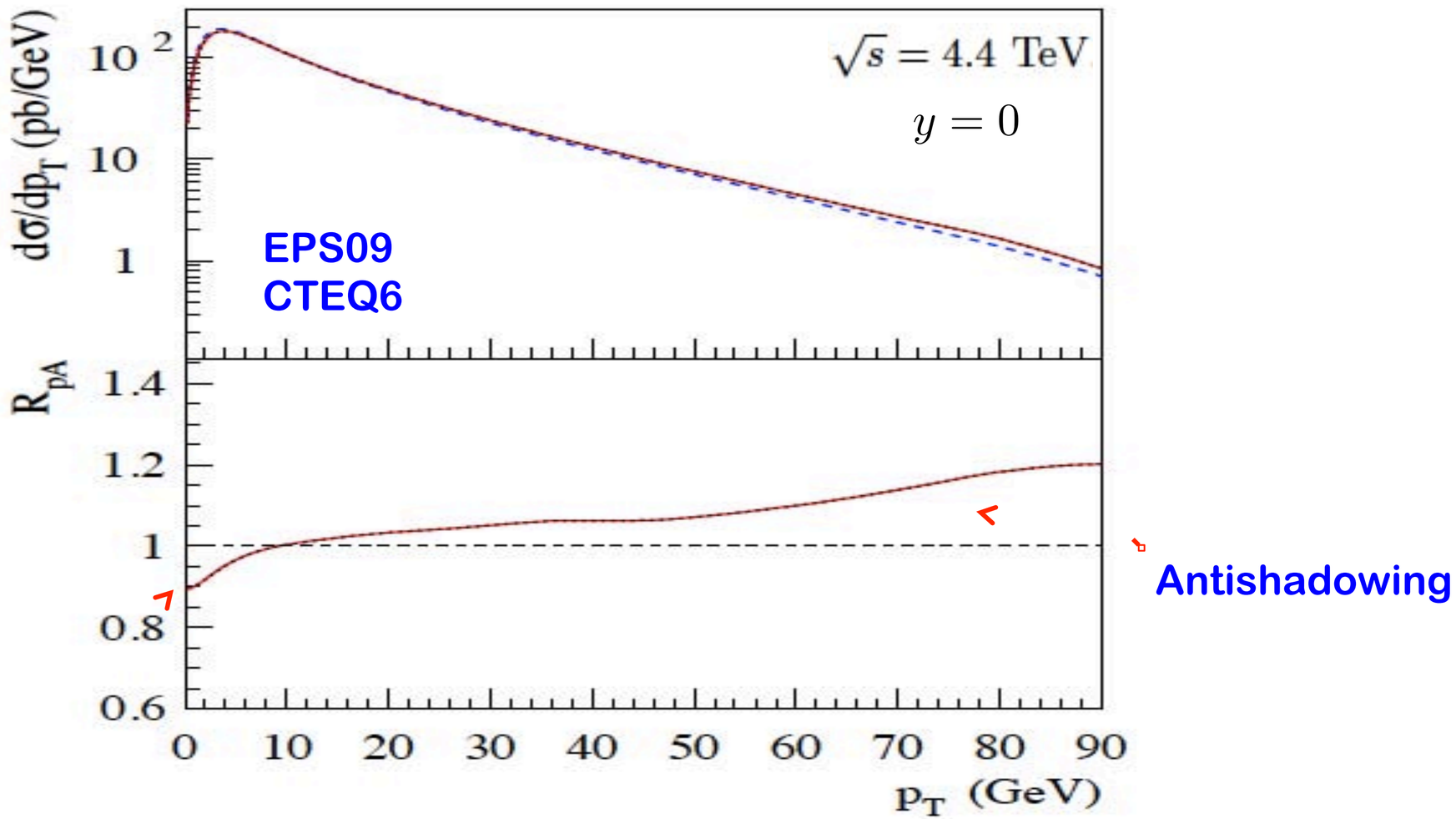

A factor of ~2 larger effect at moderate p_t with FGS10

$A^{1/3}$-type power correction has "no" effect!

Ultraperipheral Collisions ≡ UPC

Based on our study

ELSEVIER

Available online at www.sciencedirect.com

ScienceDirect

Physics Reports 458 (2008) 1–171

PHYSICS REPORTS

www.elsevier.com/locate/physrep

The physics of ultraperipheral collisions at the LHC

A.J. Baltz[a], G. Baur[b], D. d'Enterria[c], L. Frankfurt[d], F. Gelis[e], V. Guzey[f,w], K. Hencken[g,h,1], Yu. Kharlov[i], M. Klasen[j], S.R. Klein[k], V. Nikulin[l], J. Nystrand[m], I.A. Pshenichnov[n,o], S. Sadovsky[i], E. Scapparone[p], J. Seger[q], M. Strikman[r,*,1], M. Tverskoy[l], R. Vogt[k,s,t,1], S.N. White[a], U.A. Wiedemann[u], P. Yepes[v,1], M. Zhalov[l]

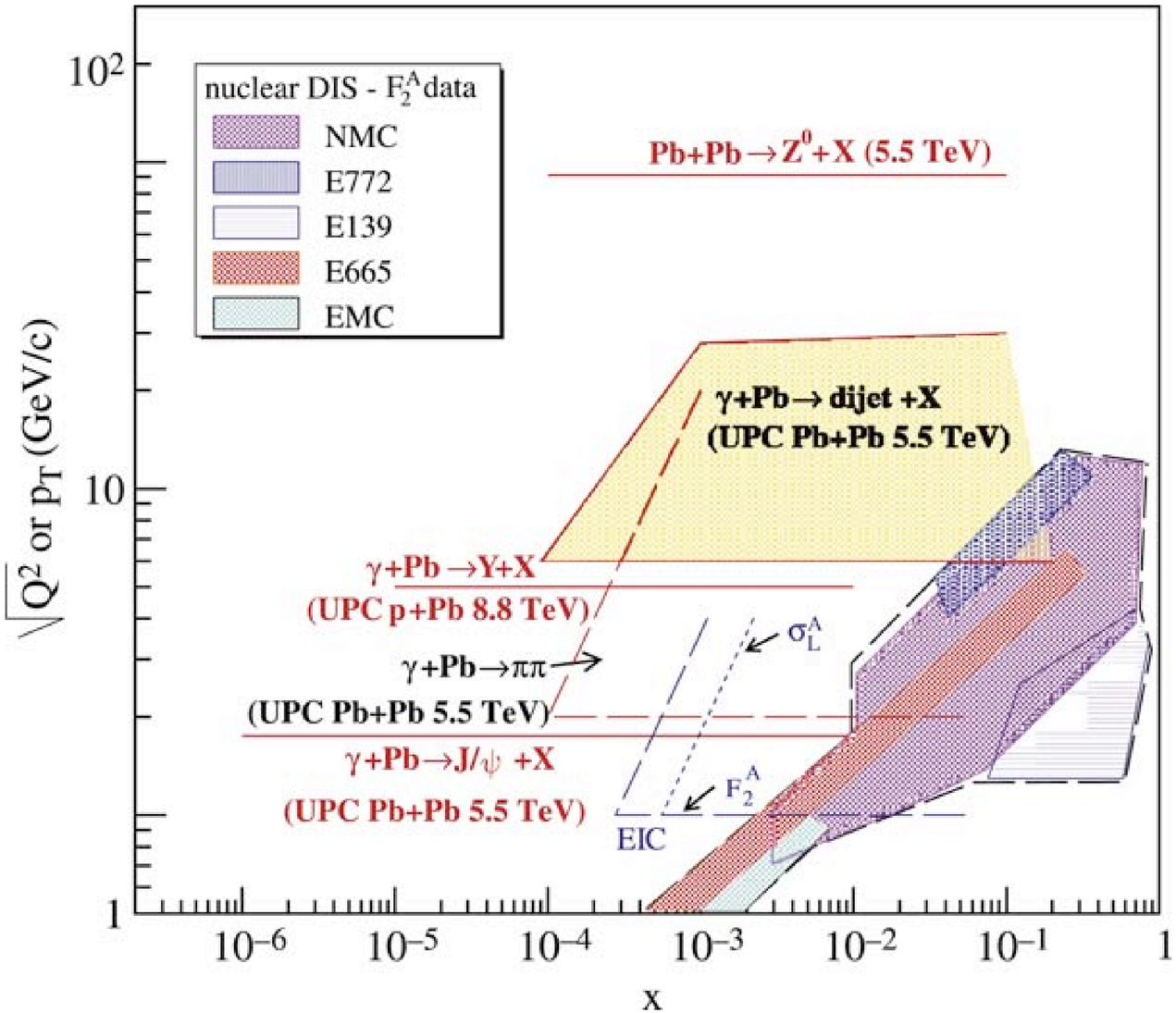

The kinematic range in which UPCs at the LHC can probe gluons in protons and nuclei in quarkonium production, dijet and dihadron production. The Q value for typical gluon virtuality in exclusive quarkonium photoproduction is shown for J /ψ and ϒ . The transverse momentum of the jet or leading pion sets the scale for dijet and π π production respectively. For comparison, the kinematic ranges for J /ψ at RHIC, F_{2A} ,$\sigma_L{}^A$ and Z^0 hadroproduction at the LHC are also shown.

Warning - in case of exclusive processes with J /ψ - connection between nuclear shadowing in diagonal and off diagonal kinematics needs further theoretical investigation

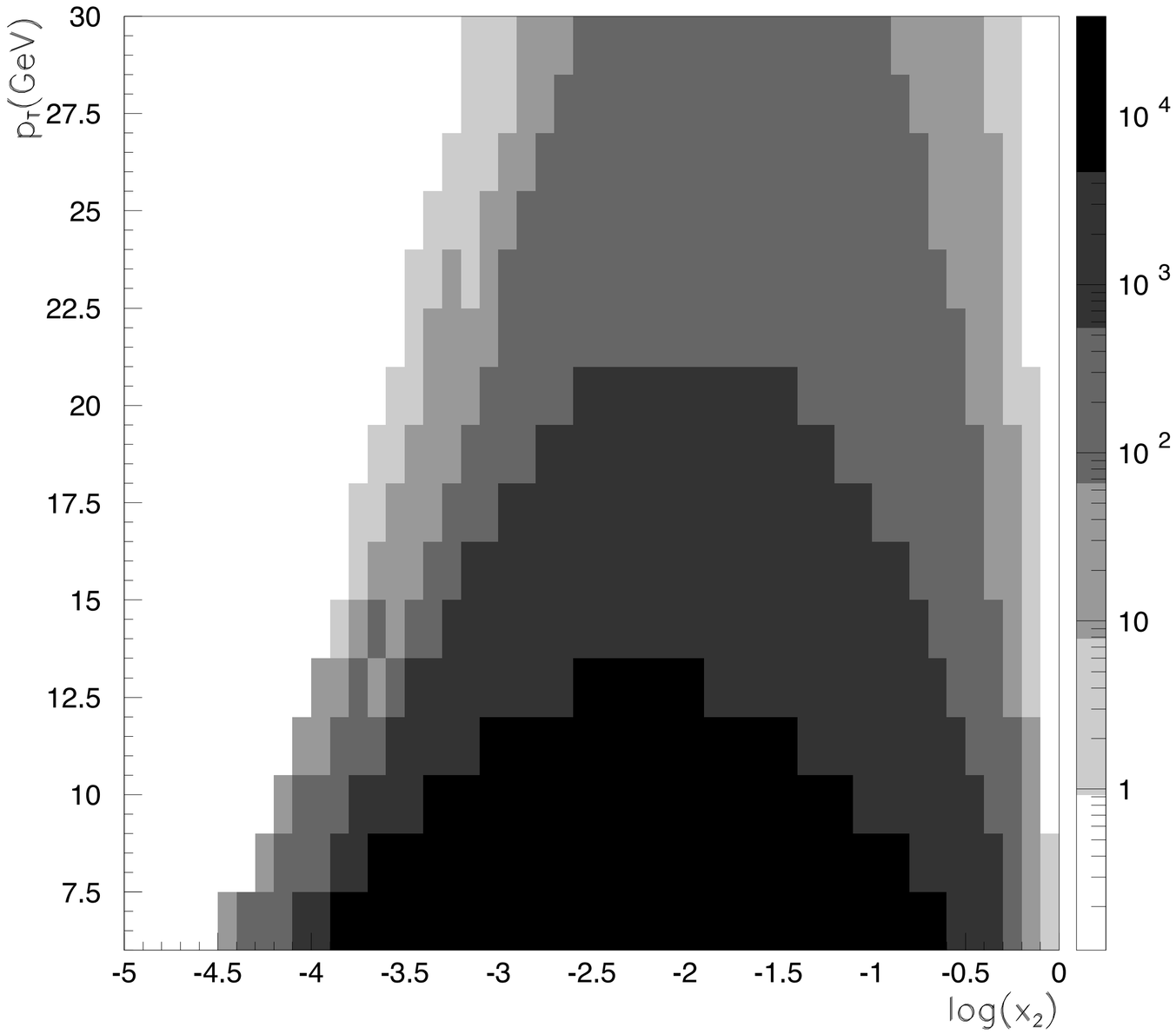

Expected rate of b-jet photoproduction for a 1 month LHC Pb+Pb run at 7.4×10^{29} $cm^{-2}s^{-1}$. including acceptance of ATLAS

Many more interesting questions to study - like inclusive leading pion A-dependence as a function of p_t, associated multiplicity at different rapidities,...

R. Vogt, S. White, MS

Parton propagation through cold media.

RHIC - suppression of forward pion & dipion production:
definitely breakdown of pQCD in the kinematics where it works for pp

Explanations:

$2 \rightarrow 2$ mechanism with fractional energy losses near black regime and small effect of p_t broadening effect

$2 \rightarrow 1$ mechanism with p_t broadening and A-dependent splitting of "1"

For single forward pion production $2 \rightarrow 2$ appears to dominate (correlation data)

For forward double pion production double parton scattering complicates interpretation.
Additional complications: soft and hard color fluctuations (will discuss later)

LHC pA: acceptance for reasonably large p_t only for rapidities corresponding to rather small x in the proton

➠ sensitivity only to relatively large energy losses, large sensitivity to gluon shadowing, and to p_t broadening.

Acceptance over large range of y (CMS & ATLAS)

➠ Ability to look for correlation of forward hadron with $y = -4 \div 0$ hadrons / minijets corresponding to $x_A > 0.01$ where nuclear shadowing is absent (allows to distinguish $2 \rightarrow 1$ and $2 \rightarrow 2$)

➠ UPC (γA) forward pion production (within tracking acceptance of CMS& ATLAS) about the same kinematics as at RHIC for $y \sim 4$ - high sensitivity to fractional energy losses.

Very forward hadron production (x_F > 0.3 moderate p_t)

First data on pp →π^0+X from LHCf

Data on pp →n+X are coming from LHCf and other LHC experiments

Currently no forward low p_t production is available from RHIC,

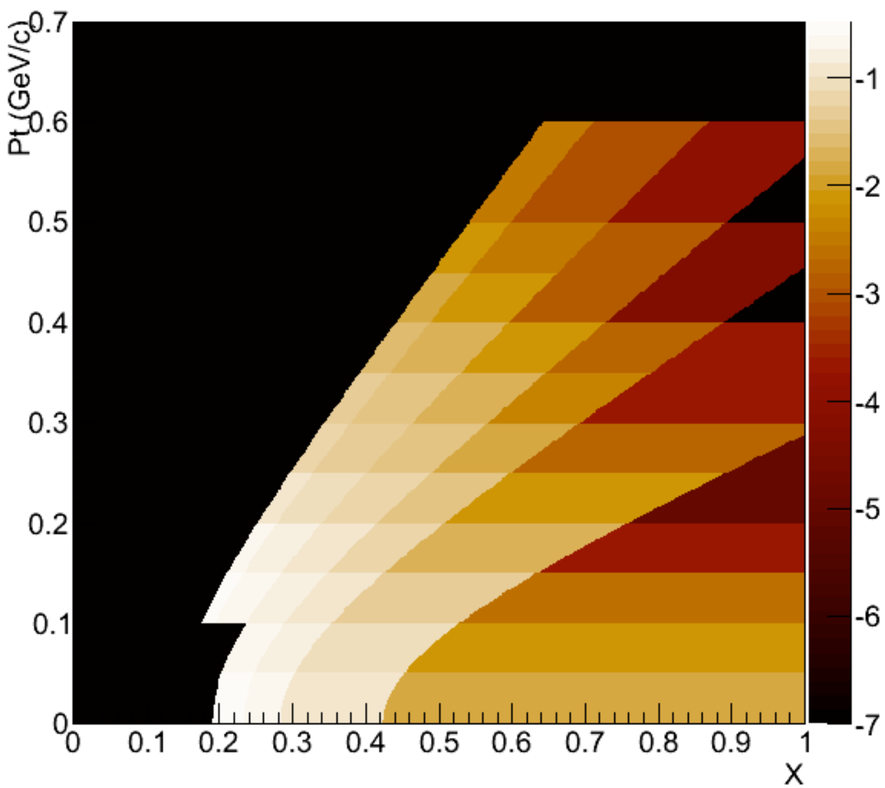

LHCf range

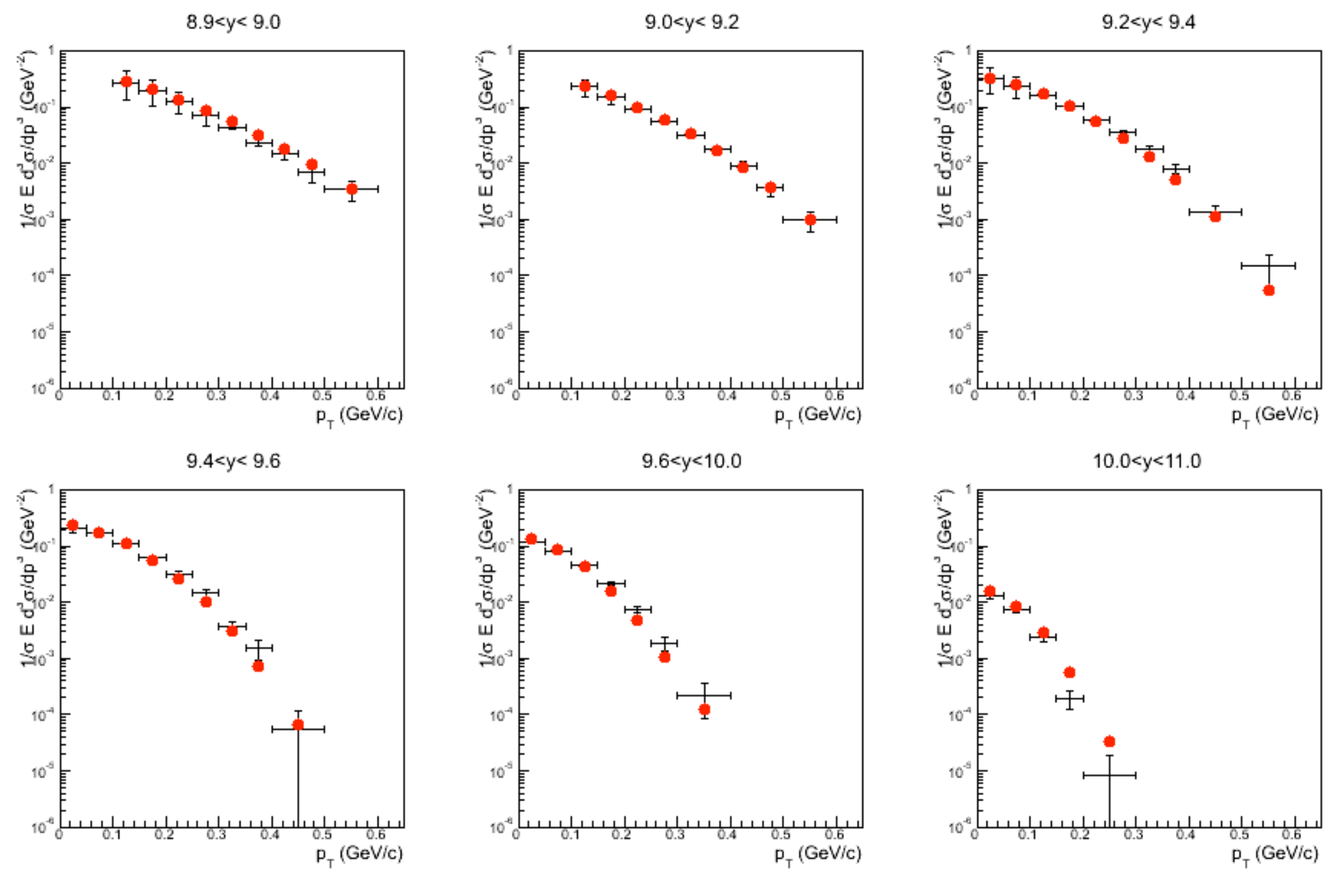

LHCf pp →π^0+X data

Leading hadron production in the central pA(pp) collisions

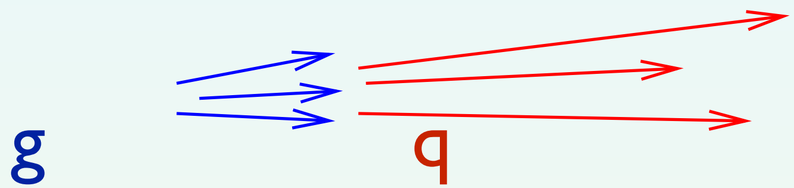

fast partons in a nucleon before collisions

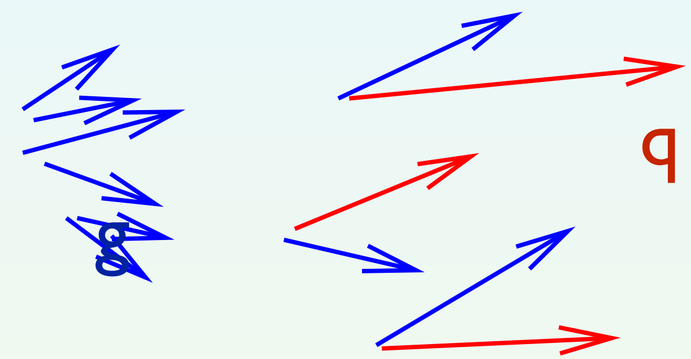

fast partons in a nucleon after central collisions:
large p_t (determined by black limit) and splitting

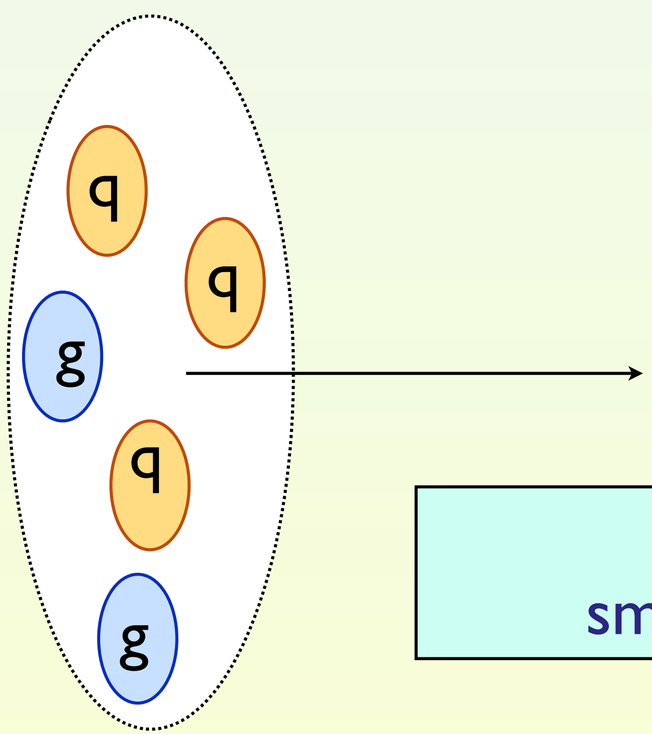

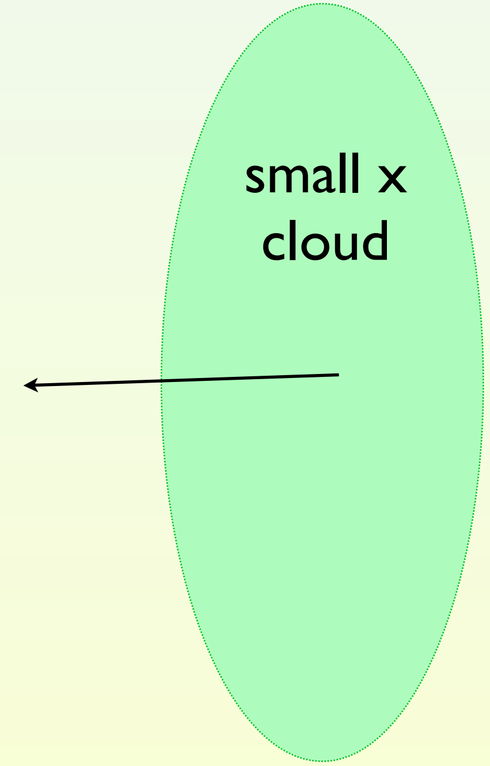

Large x partons burn
small holes in the small x cloud

Expectation: The leading particle spectrum should be strongly suppressed in the central pA collisions as compared to minimal bias pp collisions since each leading parton gets large transverse momentum and hence fragments independently and may also split into a couple of partons with comparable energies. The especially pronounced suppression for nucleons: for $z \geq 0.1$ the differential multiplicity of pions should exceed that of nucleons. This model neglects additional suppression due to finite fractional energy losses in BDR

$$\frac{1}{N}\left(\frac{dN}{dz}\right)^{pA\to h+X} = \sum_{a=q,g}\int dx\, x f_a^{(p)}(x, Q^2_{\rm eff}) D_{h/a}(z/x, Q^2_{\rm eff})$$

The limiting curve of leading particles from hadron-nucleus collisions at infinite A

A. Berera [a,1], M. Strikman [a], W.S. Toothacker [b], W.D. Walker [c], J.J. Whitmore [a]

Physics Letters B 403 (1997) 1–7

Simple model of p_t broadening - eikonal rescattering model with saturation (Boer, Dumitru 2003), effective energy losses (mentioned before) are neglected

$$C(k_t) \sim \frac{1}{Q_s^2 \log \frac{Q_s}{\Lambda_{QCD}}} \exp\left(-\frac{\pi k_t^2}{Q_s^2 \log \frac{Q_s}{\Lambda_{QCD}}}\right).$$

Quark gets a transverse momentum of the order Q_s but does not loose significant energy. Use of the convolution formula for fixed transverse momentum of the produced hadron using $C(k_t)$ - Dumitru, Gerland, MS -PRL03. Other calculations with similar logic -Gelis, Stasto, Venugopalan (06)

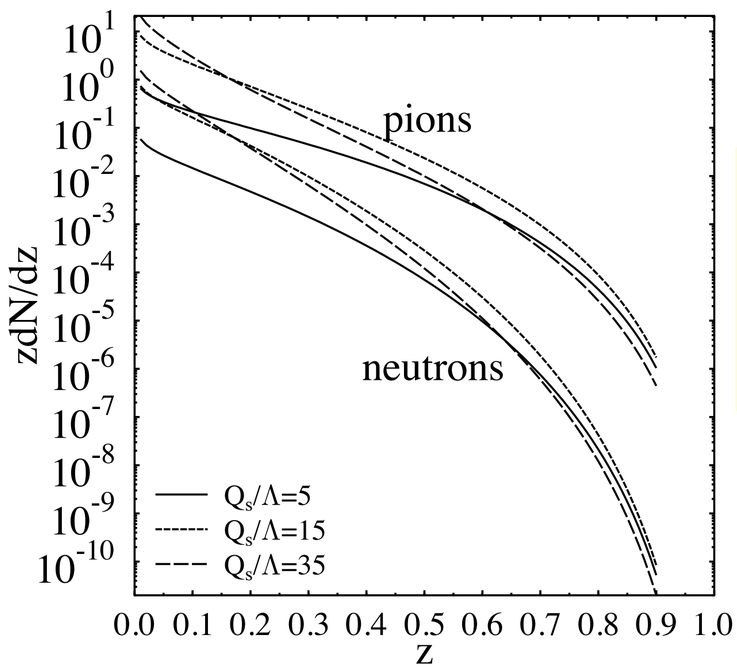

Steep fall with z, strong E_{inc} dependence

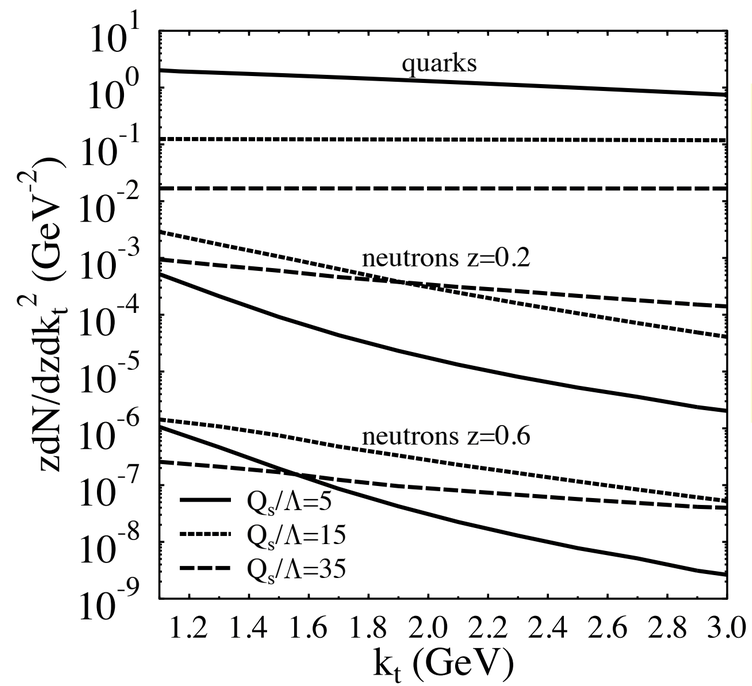

Weak p_t dependence, becomes weaker with increase of E_{inc}

Longitudinal (integrated over p_t) and transverse distributions in Color Glass Condensate (CGC) model for central pA collisions. Spectra for central pp - the same trends.

Very few forward baryons in central collisions!!!

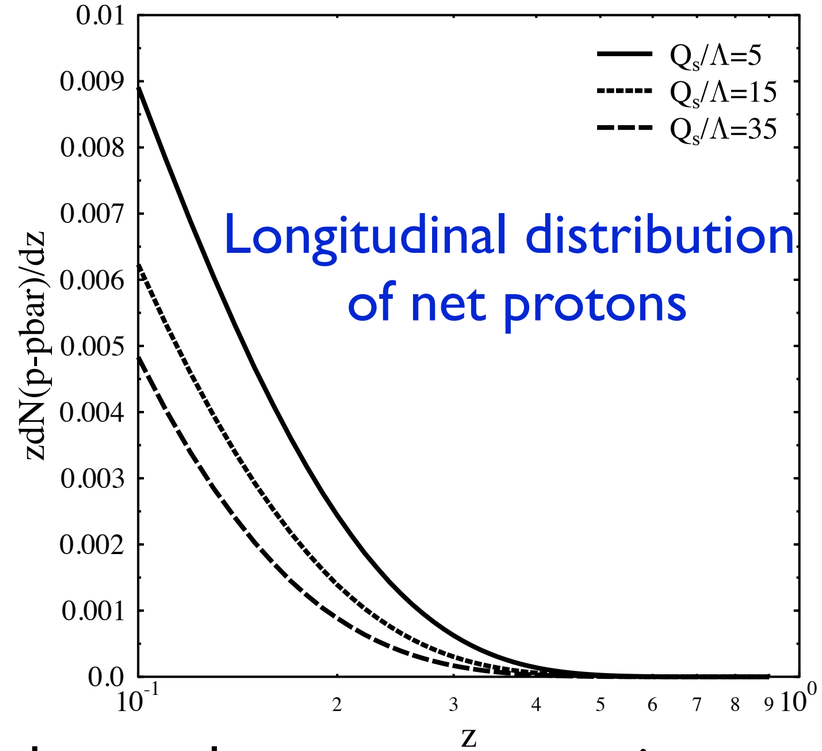

Large flow of energy to central rapidities
- obvious implications for AA

Warnings: Parton carrying a fraction y of the quark momentum carries $y\ p_t$ part of the quark's transverse momentum. Condition for independent fragmentation $y\ p_t > 1/r_N \sim .3 - 0.5$ GeV/c

For RHIC (LHC) independent fragmentation is probably safe for $z > 0.2$ (0.1)

➠ Photon - proton contribution has to be subtracted!!! Very large - discuss later

Experimental prospects:

TOTEM: $x_F \geq 0.8$ broad range of p_t can check both suppression and p_t broadening

neutrons from ZDC (CMS, ALICE, LHCf); π^0+ (LHCf) -large z , moderate p_t

RHIC: need pA run preferably at different energies and for several nuclei to avoid model dependent procedure for determining centrality of collision.

Warning: Color fluctuations in nucleon and nucleon density in nucleus may reduce the suppression

How to determine centrality of pA collisions (discussion session)

Number of neutrons in ZDC - very different geometry of nucleus heating in pA and AA collisions, sensitivity to the contribution of low energy cascades? !

Central hadron multiplicity ∝ number of collisions in Glauber model - how reliable is the model? Role of hard contributions?

Jet production in the region where LT works and shadowing is small — Low rate

need for
- cross calibration of different methods,
- tests of Glauber approximation — Gribov - Glauber color fluctuations

Space time picture of soft high energy hA scattering (Gribov - Glauber model) is qualitatively different Glauber QM model

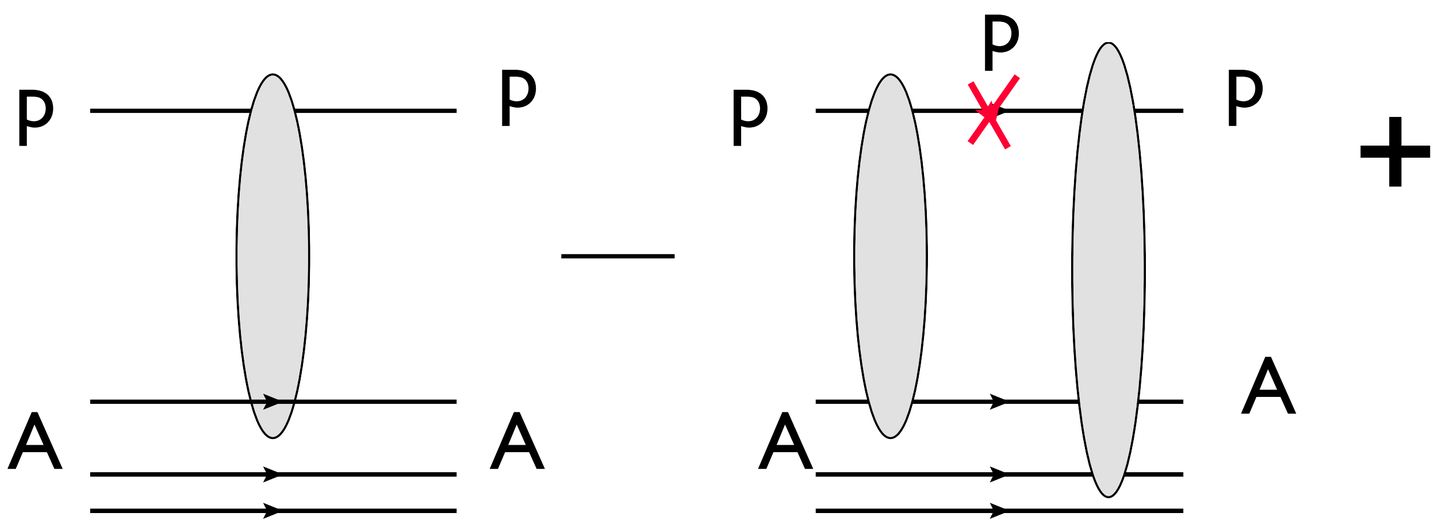

Glauber model

in rescattering diagrams proton in intermediate state - zero at high energy

- cancelation of AFS diagrams (Mandelstam & Gribov)- no time for a proton to come together between collisions with two nucleons

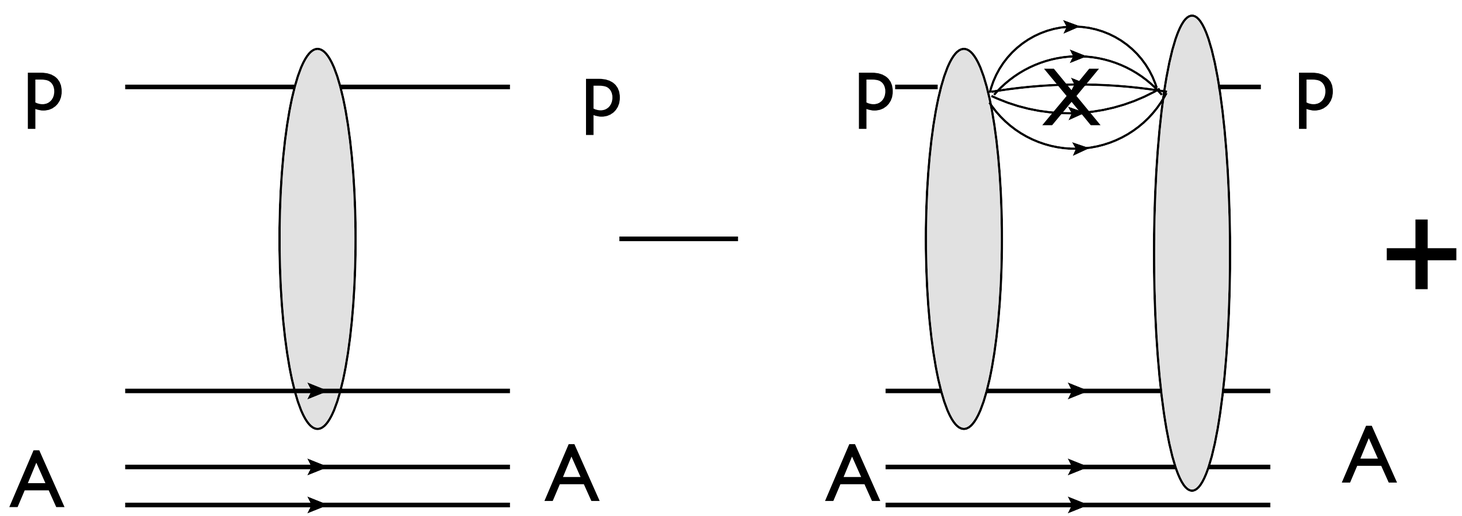

High energies = Gribov -Glauber model

X= set of intermediate states the same as in pN diffraction

$$\sigma_2 \propto \int dt F_A^2(t) \frac{d\sigma(p+p \to p + X(p + \ inel \ diff))}{dt}$$

Potential problem for Gribov- Glauber approximation:
average impact factor <b> at LHC for inelastic collisions ~ 1.3 fm

$\Rightarrow \quad 2\langle b\rangle > r_{NN} \sim 1.7$ fm $\Rightarrow$

projectile proton can hit two nucleons at the same light-cone time.

Convenient picture of diffraction -

Good - Walker scattering eigen state formalism $\sigma_n |n\rangle = T |n\rangle$

Allows a probabilistic formulation of inelastic shadowing in the Gribov-Glauber model, calculation of total, elastic, diffractive cross pA cross sections

Useful quantity - $P(\sigma)$ -probability that nucleon interacts with cross section σ

If there were no fluctuations of strength - there will be no inelastic diffraction at t=0:

$$\left.\frac{\frac{d\sigma(pp\to X+p)}{dt}}{\frac{d\sigma(pp\to p+p)}{dt}}\right|_{t=0} = \frac{\int(\sigma-\sigma_{tot})^2 P(\sigma)d\sigma}{\sigma_{tot}^2} \equiv \omega_\sigma$$

variance

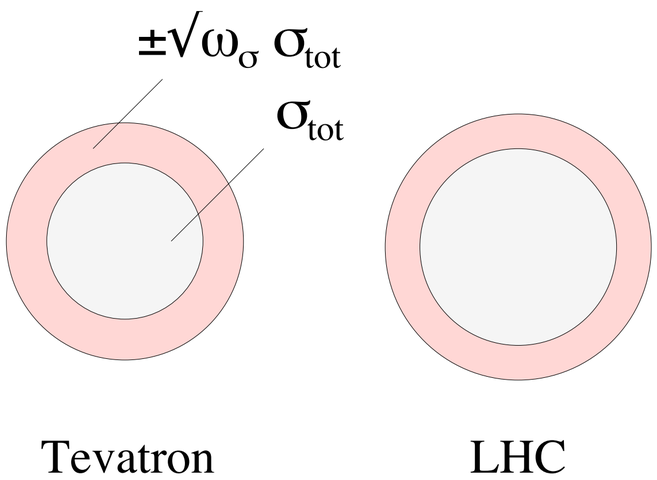

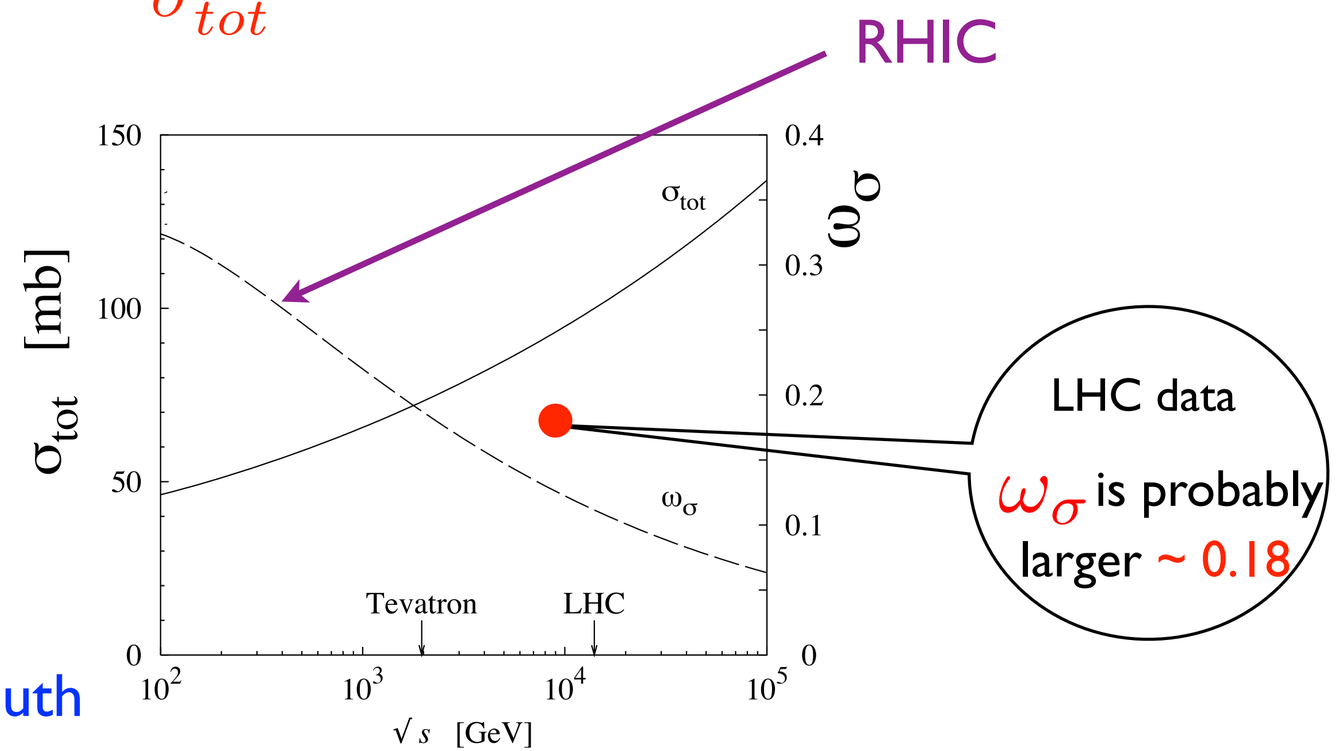

Both small and large configurations lead to grouth of periphery - still there is a correlation between σ and parton distributions -smaller σ, harder quark and gluon distributions

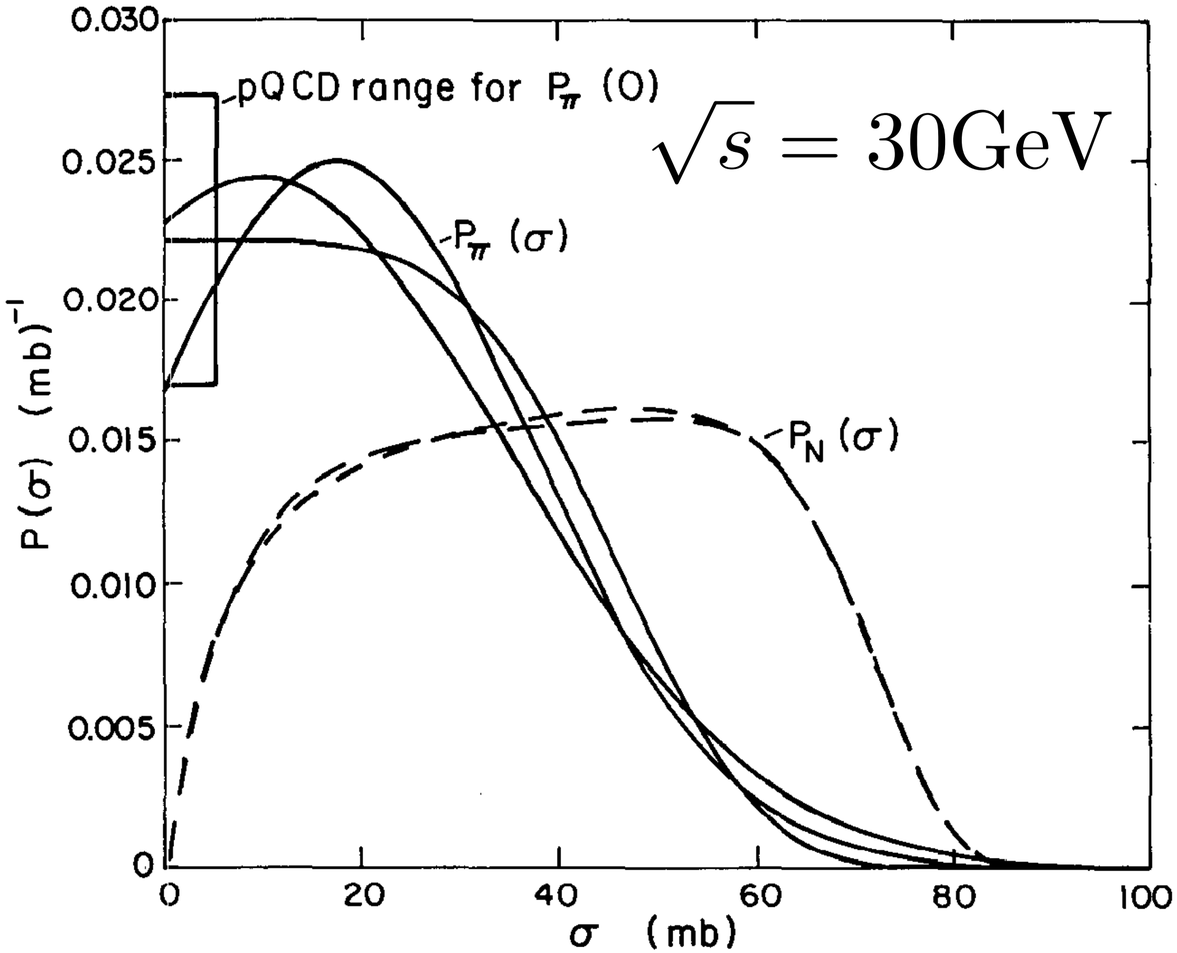

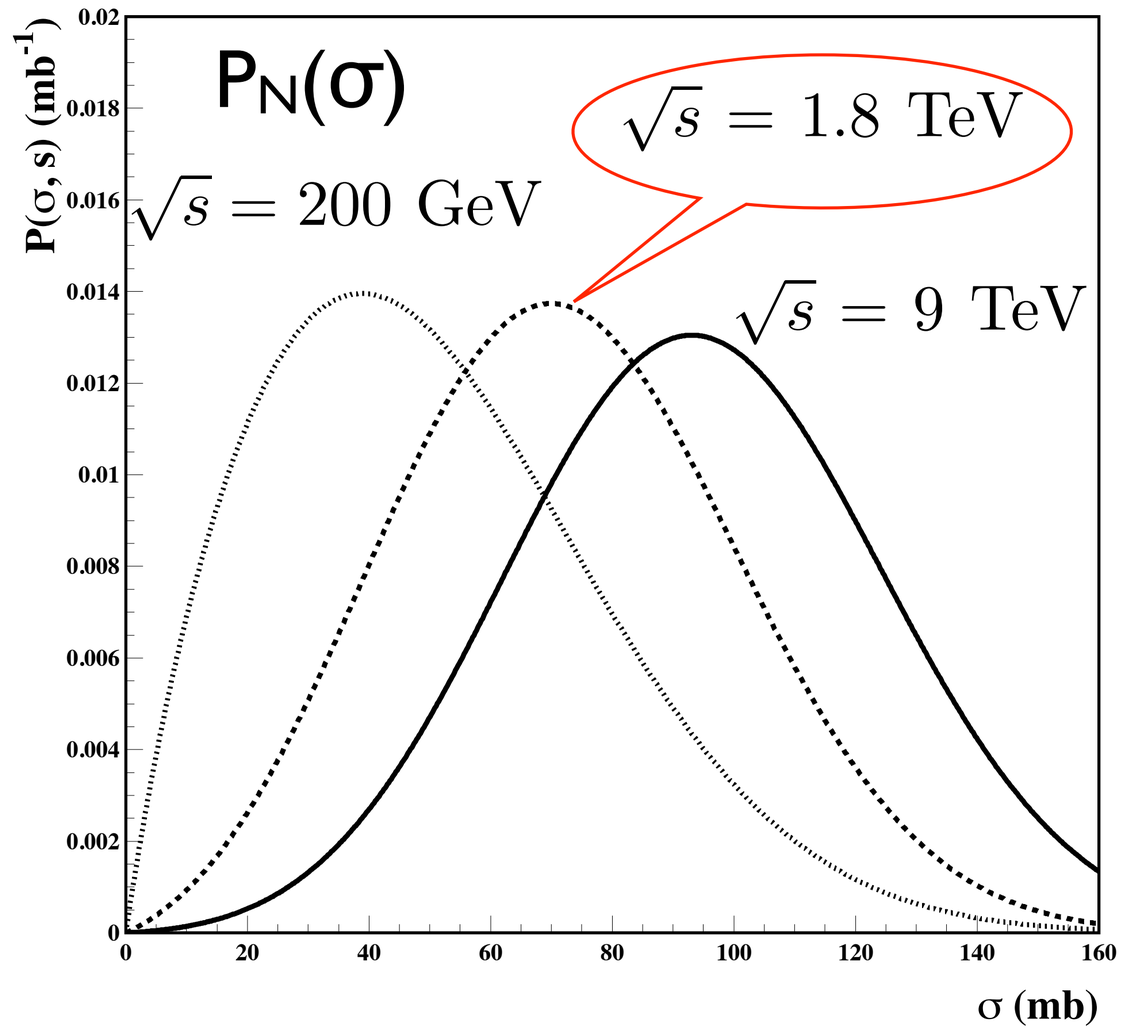

$P_N(\sigma)$ extracted from pp,pd diffraction Baym et al 93.

$P_\pi(\sigma)$ is also shown

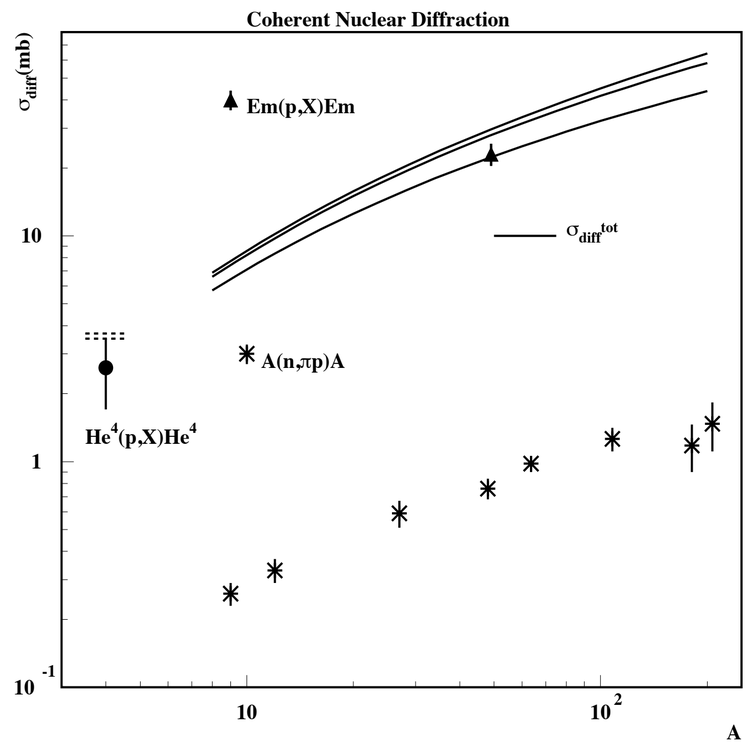

The inelastic small t coherent diffraction off nuclei provides one of the most stringent tests of the presence of the fluctuations of the strength of the interaction in NN interactions. The answer is expressed through $P(\sigma)$ - probability distribution for interaction with the strength σ. (Miller &FS 93)

$$\sigma_{diff}^{hA} = \int d^2b \left(\int d\sigma P_h(\sigma) |\langle h|F^2(\sigma,b)|h\rangle| - \left(\int d\sigma P(\sigma) |\langle h|F(\sigma,b)|h\rangle| \right)^2 \right) .$$

Here $F(\sigma,b) = 1 - e^{-\sigma T(b)/2}$, $T(b) = \int_{-\infty}^{\infty} \rho_A(b,z) dz$, and $\rho_A(b,z)$ is the nuclear density.

Color fluctuations/inelastic shadowing

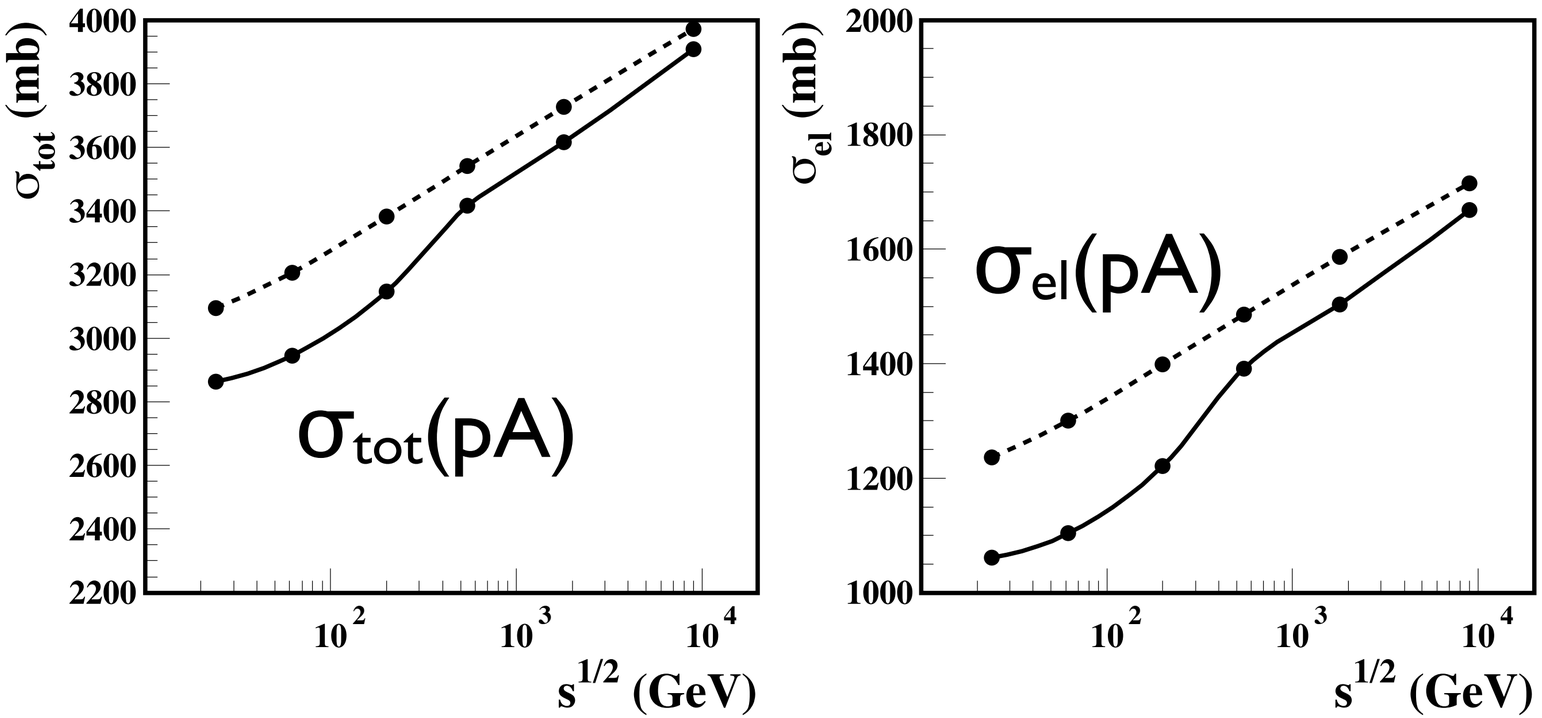

Guzey & MS

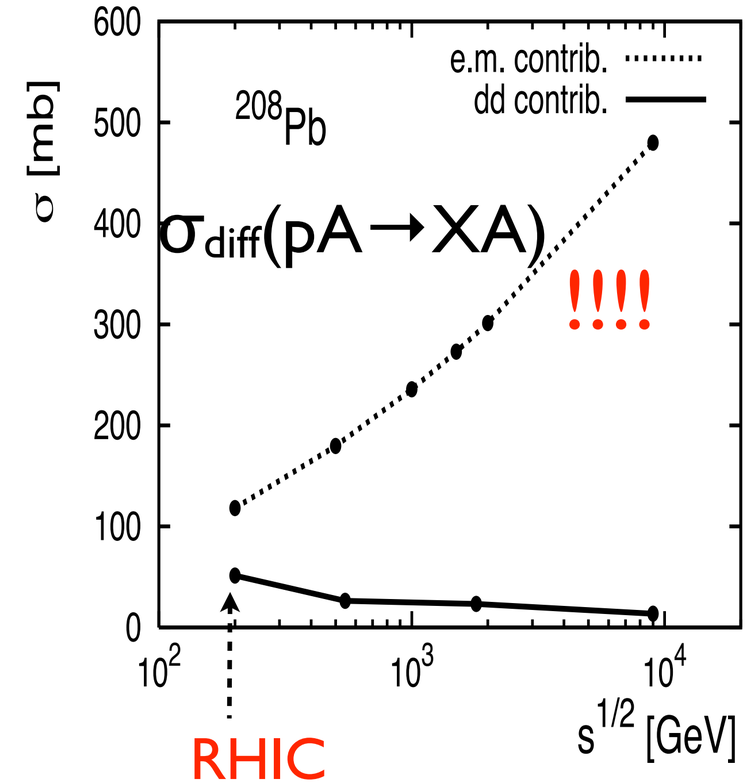

⇒ E.M. interaction dominates by far in diffraction at LHC- huge cross section
true for hard diffraction as well (Guzey, MS)

⇒ inelastic diffraction can be measured at RHIC - important check of the picture

⇒ Many interesting γp processes can be studies in UPC pA at LHC

Fluctuations in the number of interactions even at small b given by variance of P(σ).

Simple illustration - two component model ≡ quasieikonal approximation:

$$P(\sigma) = \frac{1}{2}\delta(\sigma - \sigma_{tot}(1-\sqrt{\omega_\sigma})) + \frac{1}{2}\delta(\sigma - \sigma_{tot}(1-\sqrt{\omega_\sigma}))$$

RHIC $\sigma_1 = 25\,mb,\ \sigma_2 = 75\,mb$

number of wounded nucleons at small b differs for two components by a factor of ≥3 !!!

LHC $\sigma_1 = 60\,mb,\ \sigma_2 = 140\,mb$

color fluctuations lead to addition dispersion as compared to geometrical model

$\Delta\omega = \omega_\sigma$ in pA

$\Delta\omega = 2\ \omega_\sigma$ in AA

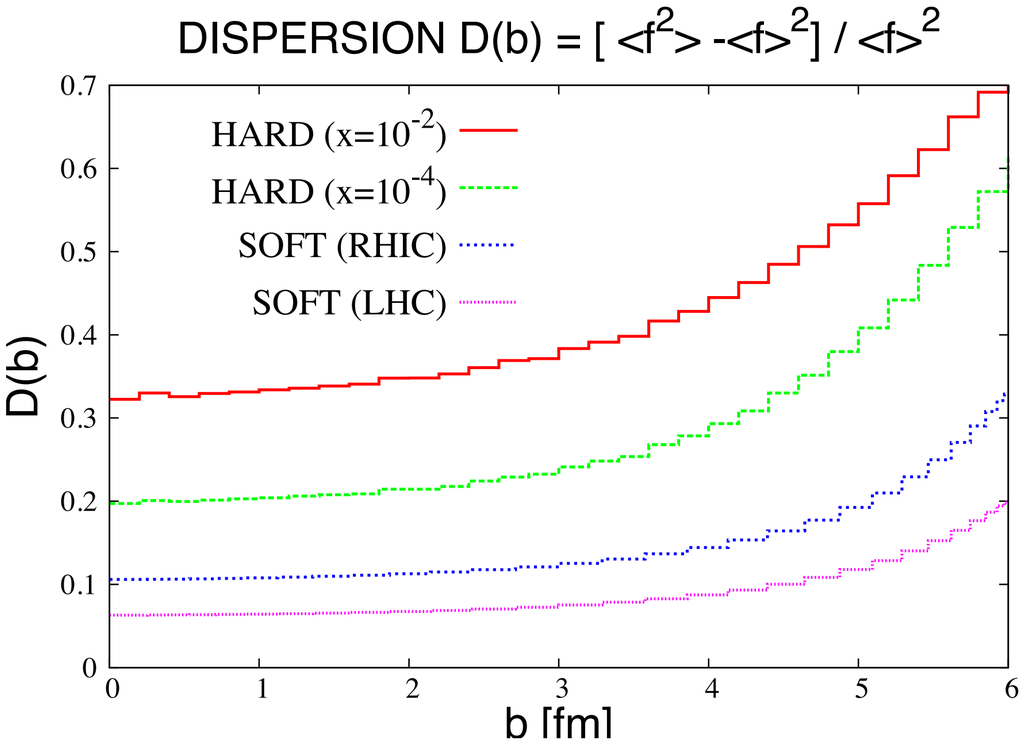

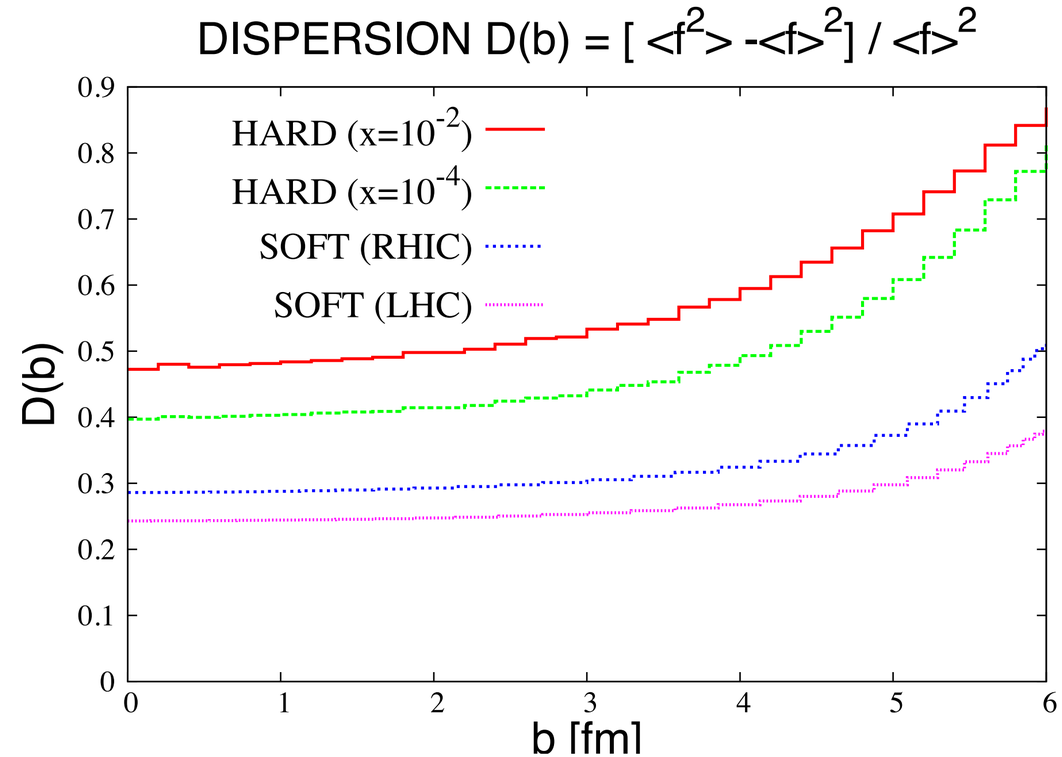

effect of fluctuations of the number of nucleons

nucleon color fluctuations + fluctuations of the number of nucleons

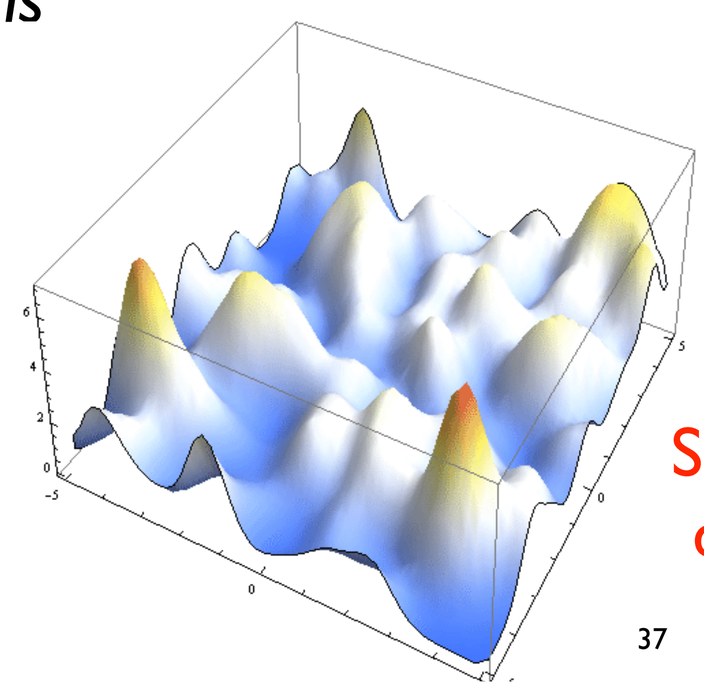

Snapshot of transverse distribution of gluons

Alvioli & MS

Expectation: configurations with larger σ □ softer x distribution

configurations with smaller σ □ harder x distribution

The presence of a parton with large $x>0.6$ requires three quarks to exchange rather large momenta, one may expect that these configurations have a smaller transverse size (+ few gluons & sea quarks at low Q scale) and hence interact with the target with a smaller effective cross section: $\sigma < \sigma^{inel}(NN)$

RHIC: tests are difficult as one needs a process which has inclusive cross section linear in A at large x: Single pion production at very large p_t?

For current dA runs the color fluctuation effect would lead to additional suppression of pion yield for central collisions due to adopted procedure of definition of centrality.

At smaller x, or for photon trigger study of correlation between hard and soft components of pA interaction is promising way to probe nucleon structure FS83

LHC - jets with large p_t - -- no nuclear shadowing effects

Inclusive jet/dijet cross section measurements

Using full 2010 dataset (**37 pb^{-1}**)
$\rightarrow$ probe perturbative QCD in new kinematic regime

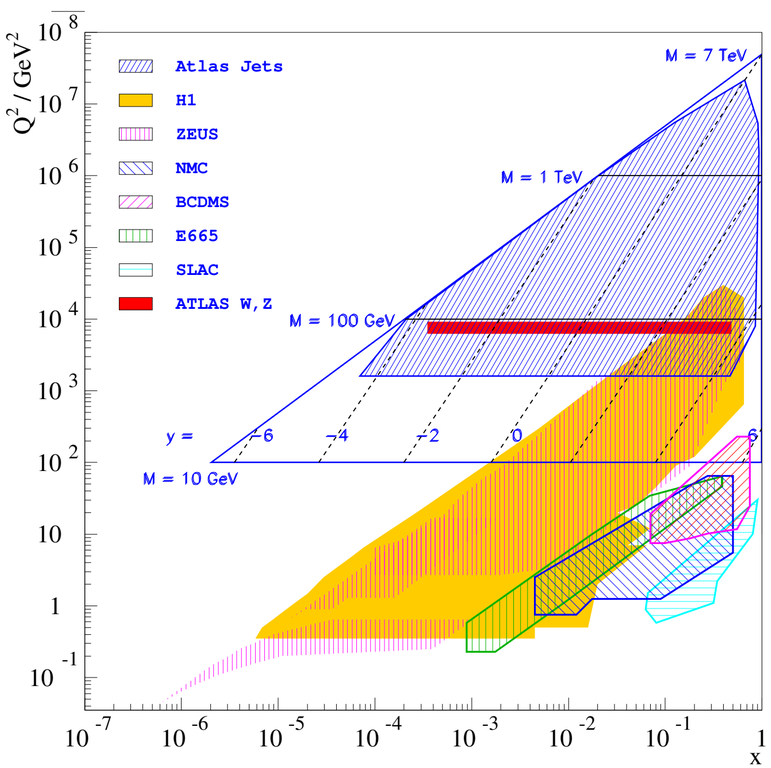

$7 \cdot 10^{-5} < x < 0.9$
$Q^2 > 2 \cdot 10^7$ GeV^2

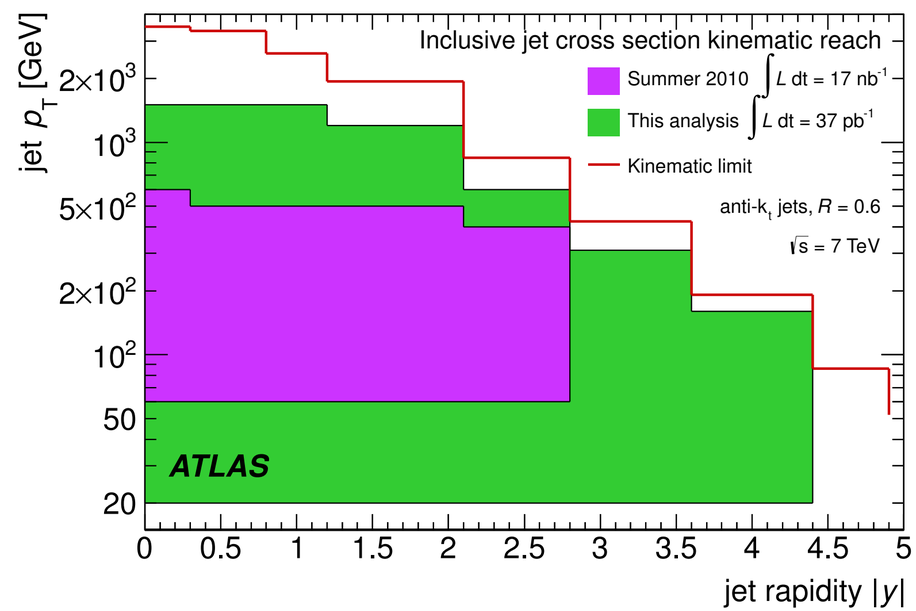

A lot of events at x> 0.6 at large p_t !!!

20 GeV$<p_T^{jet}<$1.5 TeV
70 GeV $< m_{12} <$ 5 TeV
$|y|$ <4.4

C. Doglioni - 29/05/2012

$$\nu(x,A) = 1 + \sigma_{eff}(x)\frac{A-1}{A^2}\int T^2(b)\ d^2b$$

number of wounded nucleons > ν(A)

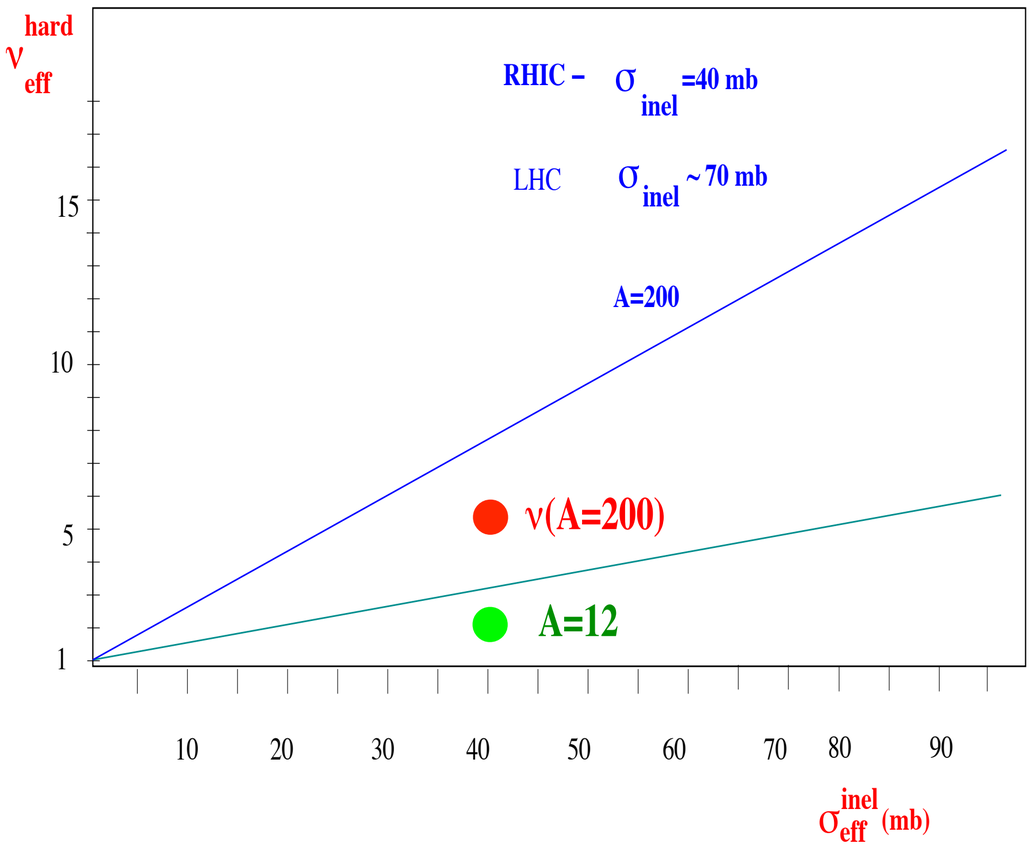

Dependence of the number of inelastic interactions with the target on the transverse size of the probed configuration for a hard trigger like p +A→jet$_1$ (forward x) + (jet$_2$) + X reaction

Significant reduction of ν(x,A) for x≳0.6(based on suppression of the sea at large x and also the analysis of the EMC effect)

Expectation:

σ_{incl} (pA) = A σ_{incl} (pN)

σ_{cental} (pA) <<T_A(b=0) σ_{incl} (pN)

mimics absorption for p_t ≳ 100 GeV/c

Small x trigger - $\sigma_{eff} > \sigma_{inel}$???

Multiparton interactions in pA.--- probing parton correlations in nucleons - maybe feasible at LHC (4 jets) . Two forward pions at RHIC (Vogelsang, MS)

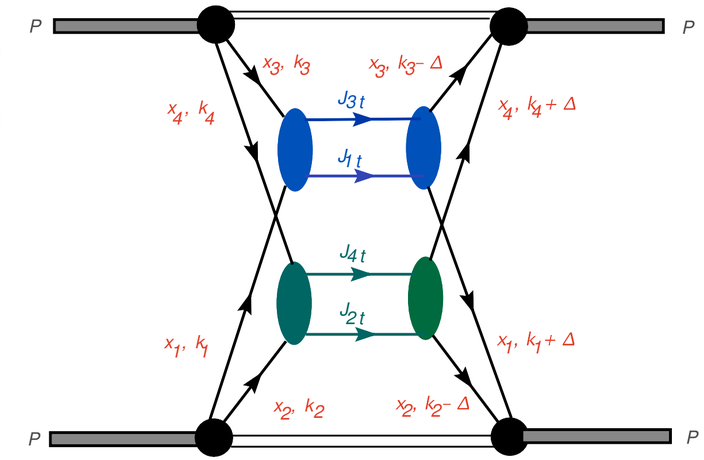

Experimentally one measures the ratio

$$\frac{\frac{d\sigma(p+\bar{p}\to jet_1+jet_2+jet_3+\gamma)}{d\Omega_{1,2,3,4}}}{\frac{d\sigma(p+\bar{p}\to jet_1+jet_2)}{d\Omega_{1,2}}\cdot\frac{d\sigma(p+\bar{p}\to jet_3+\gamma)}{d\Omega_{3,4}}} = \frac{f(x_1,x_3)f(x_2,x_4)}{Sf(x_1)f(x_2)f(x_3)f(x_4)}$$

where $f(x_1,x_3), f(x_2,x_4)$ longitudinal light-cone double parton densities and

S is ``transverse correlation area". One selects kinematics where 2 →4 contribution is small

CDF observed the effect in a restricted x-range: two balanced jets, and jet + photon and found

$$S = 14.5 \pm 1.7^{+\ 1.7}_{-\ 2.3}\ mb$$

No dependence of S on x_i was observed.

A naive expectation (based on r_N=0.8 fm) is S~ 55 mb. Gluon radius is smaller --- S~ 35 mb. So S~ 15mb indicate presence of significant correlations between partons in the nucleon. Is it transverse plane correlation or correlation of x's ?

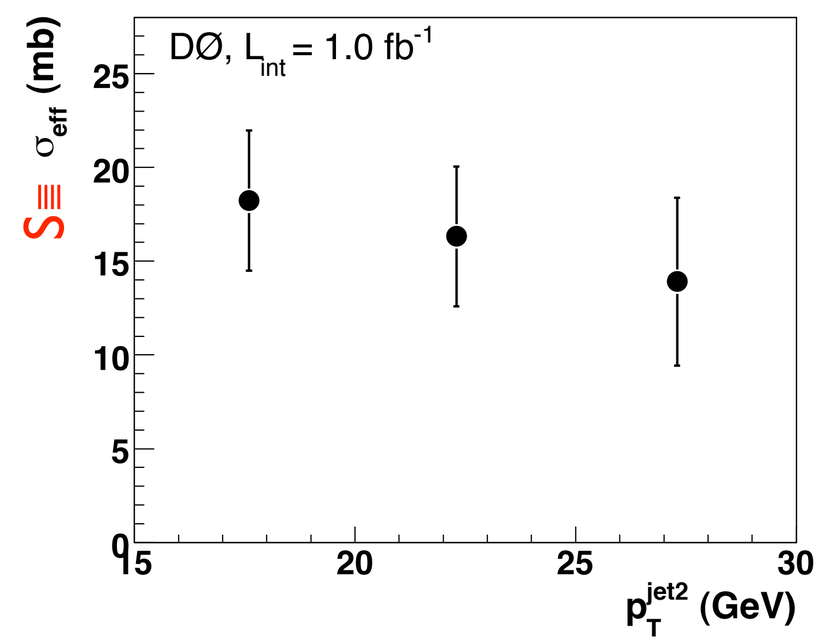

Similar results from D0.

Multiparton interactions in proton - nucleus collisions

MS & Treleani 95 - PRL 2002

$$\sigma = \sigma_1 \cdot A + \sigma_2$$

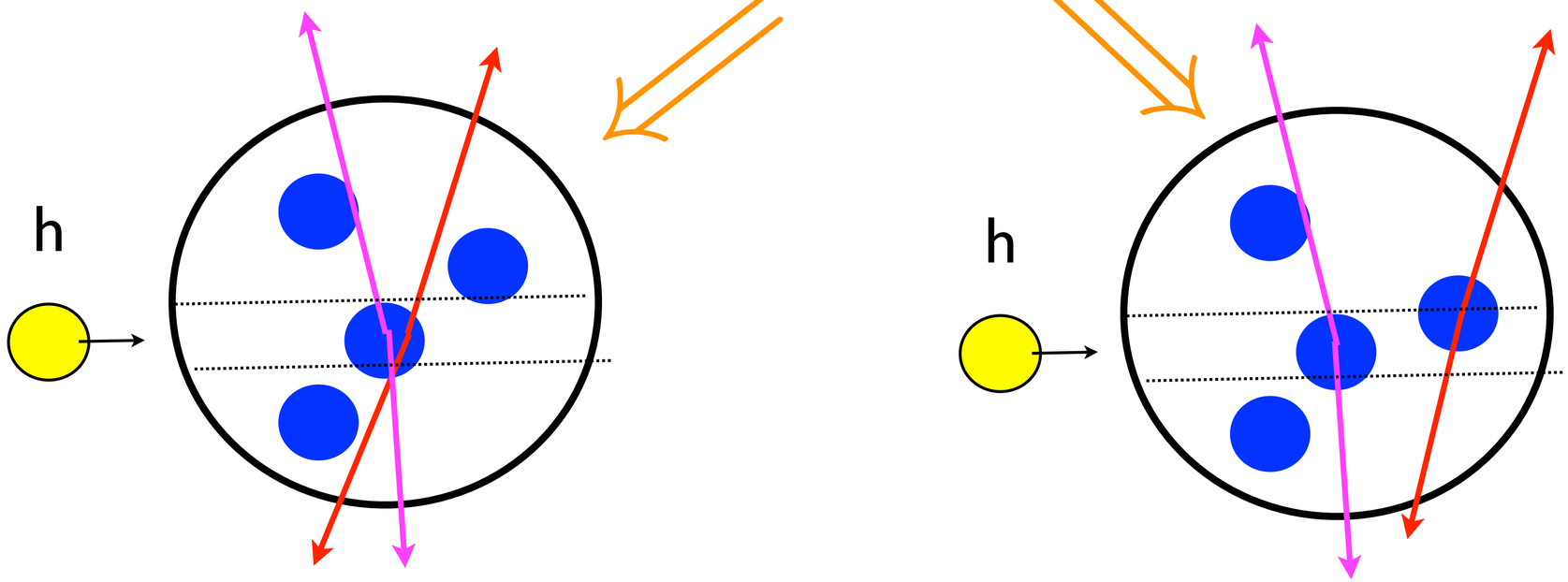

$$R \equiv \frac{\sigma_2}{\sigma_1 \cdot A} \approx \frac{(A-1)}{A^2} \cdot \sigma_{eff} \int T^2(b)\, d^2b \approx 0.68 \cdot \left(\frac{A}{12}\right)^{0.39} \quad |A \geq 12, \sigma_{eff} \sim 14mb$$

$$T(b) = \int_{-\infty}^{\infty} dz \rho_A(z,b), \int T(b) d^2b = A.$$

"Antishadowing effect": For A=200, and σ_{eff}=14 mb $\quad \frac{\sigma_{pA}}{\sigma_{pp}} \approx 3$ $\quad$ linear in σ_{eff} !!

Measurement of R allows to separate longitudinal and transverse correlations of partons as it measures $R=f(x_1,x_2)/f(x_1)f(x_2)$ - Blok, Dokshitzer, Frankfurt, MS R-1.2

Conclusions

pA@LHC will provide important information on high density small x physics in variety of pA channels complementary to

$\gamma A/\gamma p$. Clear path to probing nonlinear effects at moderate p_t and x at least down to 10^{-4}

Forward region -- critical tests of p_t broadening, energy losses, looking for $2 \to 1$ mechanism of pion/jet production.

Very forward region -- critical tests of the onset of black regime
Very important to have pA RHIC vs LHC comparison

Effects of color fluctuations can be studied with large x_p trigger

Multiparton interactions - need for high lumi

Cold nuclear matter effects on heavy quark production

Kirill Tuchin

IOWA STATE UNIVERSITY
OF SCIENCE AND TECHNOLOGY

Forward Physics at RHIC workshop, BNL, July-August 2012

Heavy quarks: motivation

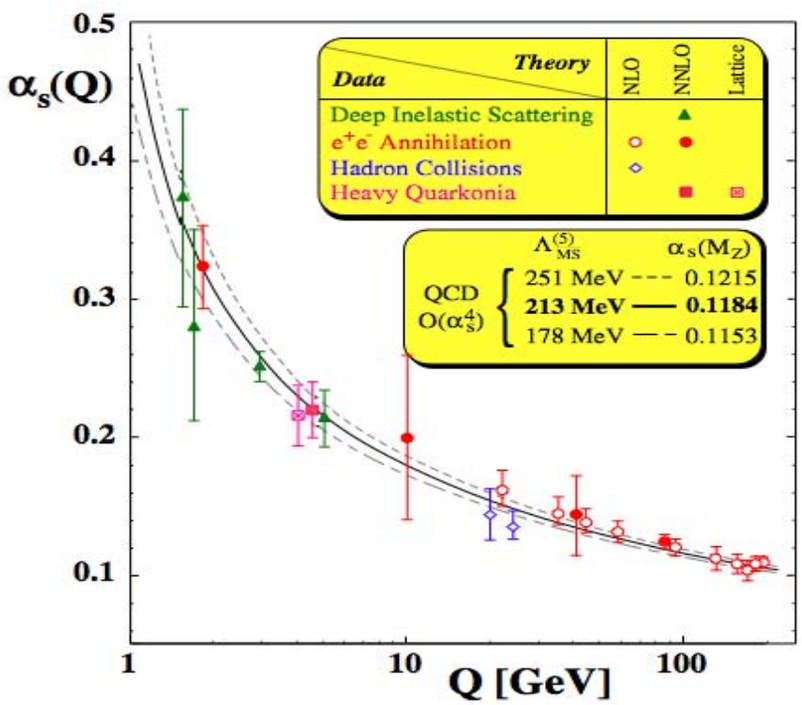

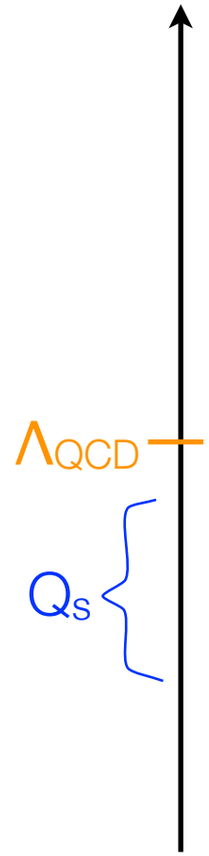

Flavor	Mass
u	$1.5 - 4.5$ MeV
d	$5.0 - 8.5$ MeV
s	$80 - 155$ MeV
c	$1.0 - 1.4$ GeV
b	$4.0 - 4.5$ GeV
t	174.3 ± 5.1 GeV

Light quarks

Heavy quarks

Heavy quarks have masses that are much larger than the typical QCD scale Λ_{QCD}

Asymptotic freedom: $\alpha_s(m^2) \ll 1$ Perturbation theory is applicable!

Higher twist effects ~ $\dfrac{\langle \alpha_s G^2 \rangle}{m^4} \ll 1$ $\dfrac{Q_s^2}{m^2}$

J/ψ in hot medium

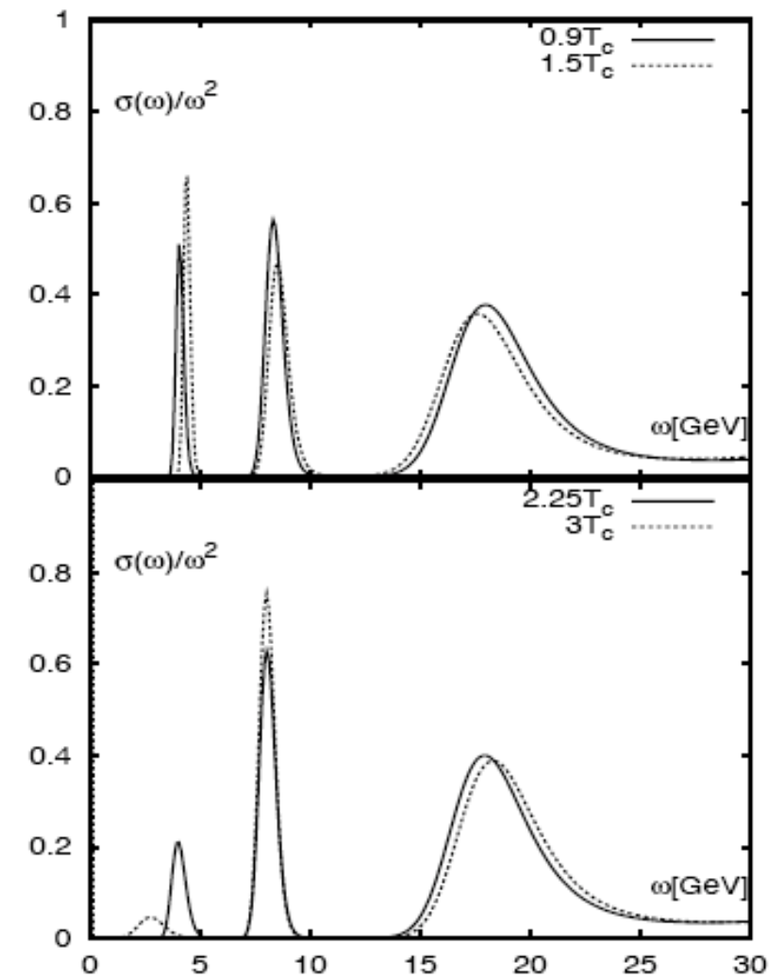

Immersing J/ψ in quark-gluon plasma modifies

- J/ψ binding potential V(r,T)
- J/ψ wave function Φ(r,T),
- J/ψ formation rate $\propto |\Phi(r,T)|^2$,

and turns on new production mechanisms such as recombination etc.

If we have a good theoretical control of these processes we will be able to extract medium properties from the J/ψ production cross sections.

First, we need to understand J/ψ production in pp and in pA collisions.

Factorization ?

Hard pQCD:

Factorization → Universal pdf's → Phenomenology

- Factorization is broken if the hard amplitude involves *simultaneous* interactions with more than two partons at a time.

- Coherent scattering: $l_c >> R_A$ (coherence effects start at $l_c \sim R_p$)

CGC/saturation = implementing the coherence.

Assuming factorization...

The effective absorption cross sections from fits of Ramona's calculations to PHENIX d+Au R_{CP} data are shown for each shadowing model. 3

This is **not** an attempt to extract physics from the d+Au R_{CP}! This is just a parameterization of the data that is independent at each rapidity.

The red points are the averages at y = -1.7 and +1.7.

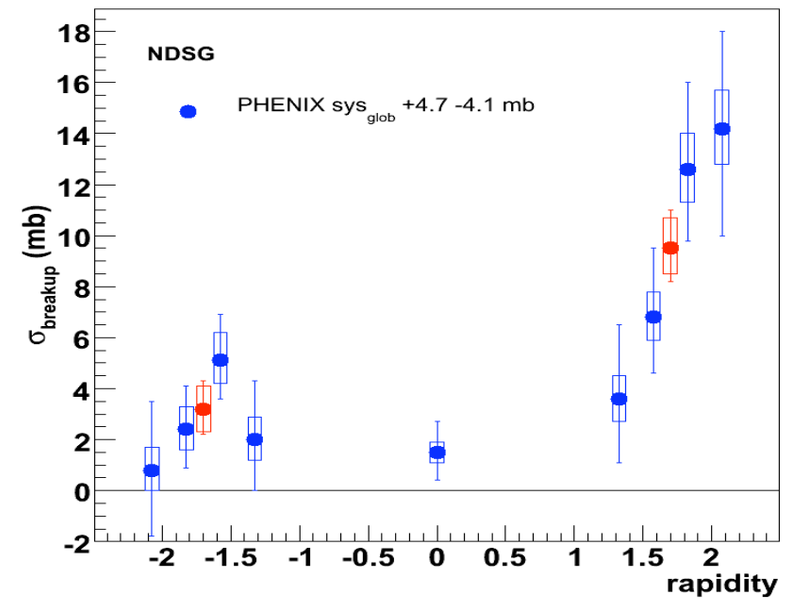

Slide stolen from T. Frawley

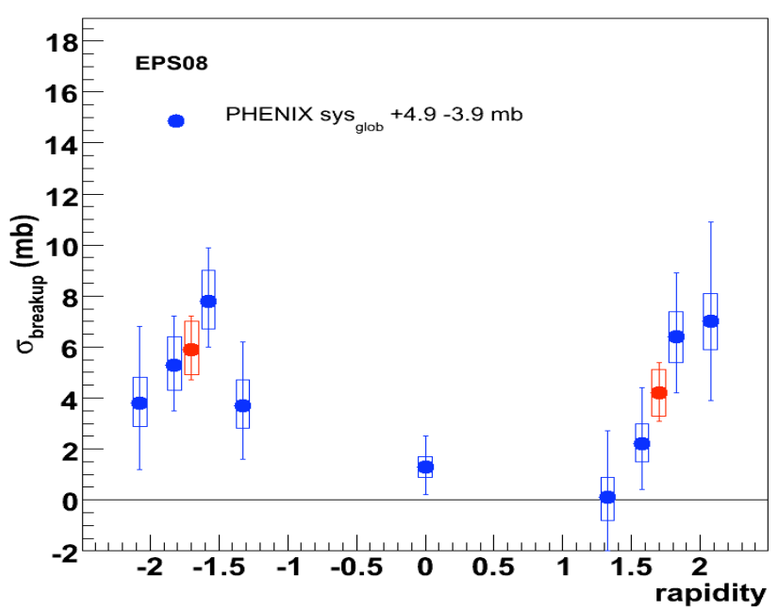

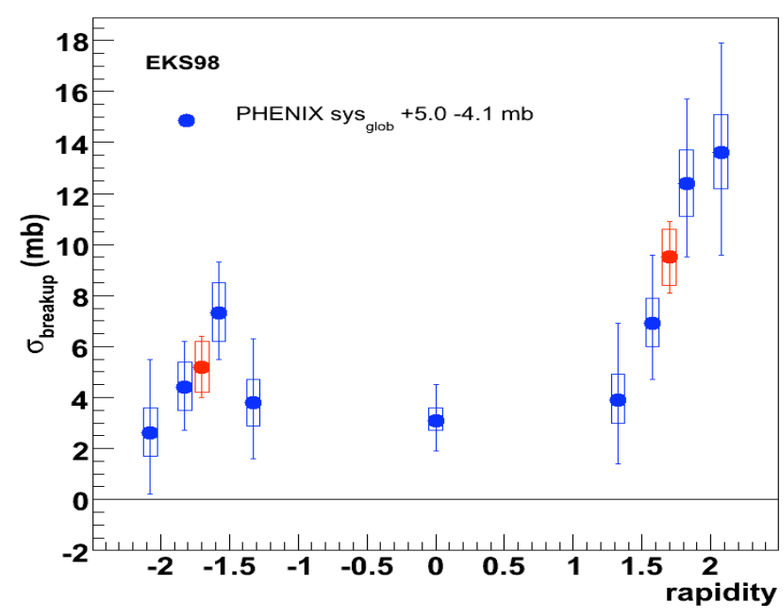

This does not look like a reasonable behavior.

Coherence

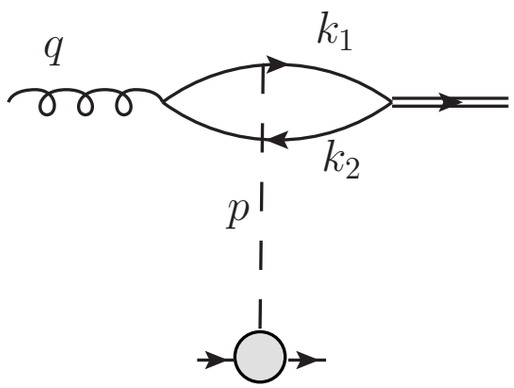

Longitudinal momentum transfer

$$p_z = q_z - k_{1z} - k_{2z} \approx \frac{\boldsymbol{k}_1^2 + m^2}{2z\omega} + \frac{(\boldsymbol{p} - \boldsymbol{k}_1)^2 + m^2}{2(1-z)\omega}$$

$$|\boldsymbol{k}_1 - \boldsymbol{k}_2| \sim \alpha_s m \ll p_\perp \qquad z \approx 1/2$$

$$p_z = \frac{1}{\omega}\left[p_\perp^2 + (2m)^2\right] = \frac{2}{\sqrt{s}} e^{-y}\left[p_\perp^2 + (2m)^2\right]$$

The *longitudinal form factor* is a measure of the coherence of high energy process

$$\mathcal{F}_L(p_z) = \frac{1}{A}\int d^2b \int_{-\infty}^{\infty} d\xi\, \rho(\boldsymbol{b}, \xi)\, e^{ip_z\xi}$$

Coherent scattering: $l_c \sim \dfrac{1}{p_z} > R_A$ ☞ $\mathcal{F}_L \approx 1$

The longitudinal form factor

For the "hard sphere" nucleus

$$\mathcal{F}_L = \frac{3}{(p_z R_A)^3}\left[\sin(p_z R_A) - p_z R_A \cos(p_z R_A)\right]$$

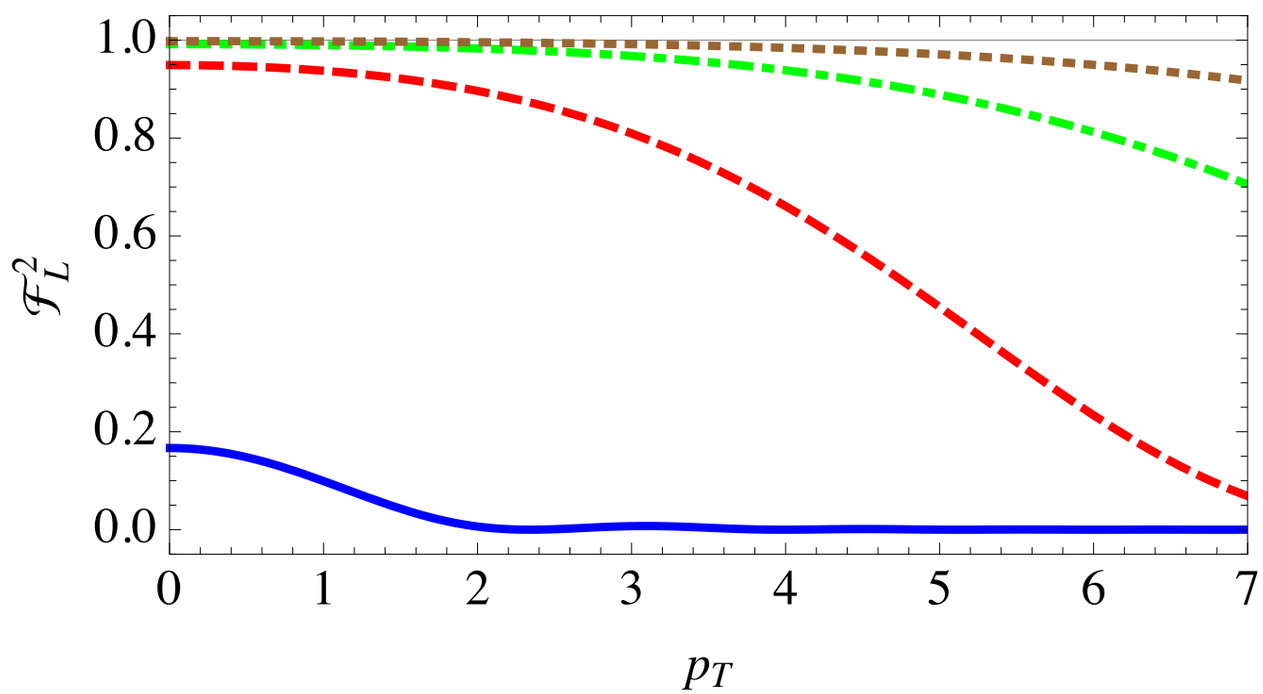

FIG. 8: (Color online). Square of the longitudinal form factor as a function of transverse momentum of J/ψ in GeV's. Lines from bottom to top: $\sqrt{s} = 0.2$ TeV, $y = 0$ (blue, solid), $\sqrt{s} = 0.2$ TeV, $y = 1.7$ (red, dashed), $\sqrt{s} = 2.76$ TeV, $y = 0$ (green, dot-dashed), $\sqrt{s} = 5.5$ TeV, $y = 0$ (brown dashed).

The time scales

A pre-hadron cc pair is produced over time

$$\tau_P = l_c/c = 7\, e^y \,\mathrm{fm}$$

J/ψ wave function is formed over time

$$\tau_F = \frac{2\, M_\psi}{M_{\psi'} - M_\psi} l_c = 42\, e^y \,\mathrm{fm}$$

Hierarchy of scales required for the dipole model: $\tau_F \gg \tau_P \gg \tau_{INT}$

J/ψ production mechanisms in pp

Baier Ruckl, 1981

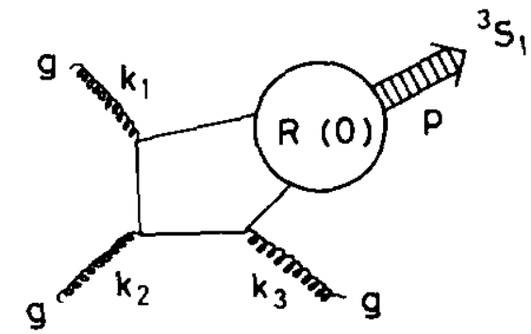

- Color singlet model

$q\bar{q}$ must have the same quantum numbers as the final quarkonia.

The wave function parameter ψ(0) is uniquely fixed using the J/ψ decay rate.

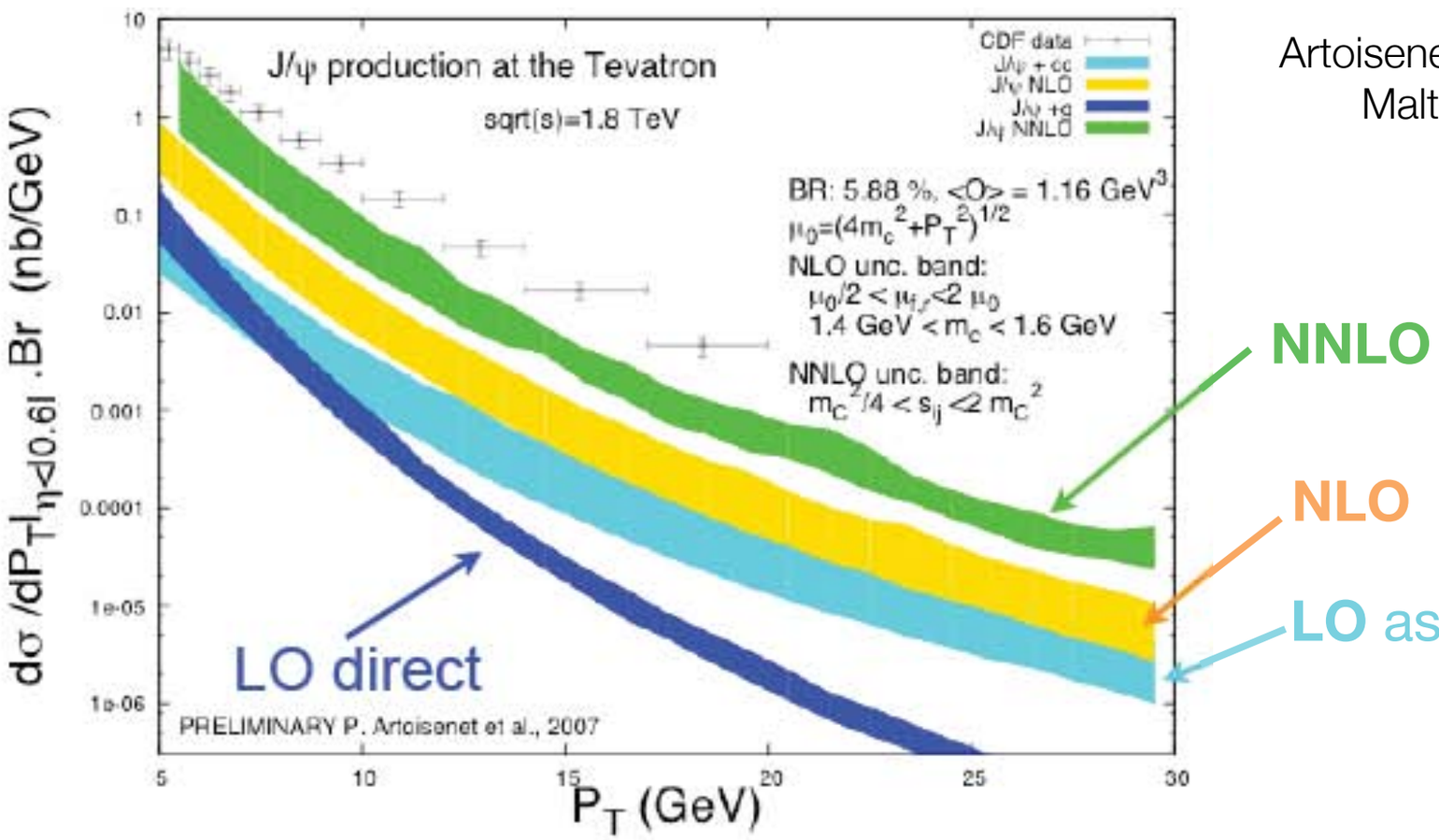

Artoisenet, Landsberg, Maltoni, 2007

- Far from data
- Strong scale dependance
- Poor convergence

J/ψ production mechanisms in pp (cont.)

- Non-relativistic QCD model

Gives the best fit to Tevatron p_T spectra, but has a lot of free parameters (non-perturbative matrix elements).

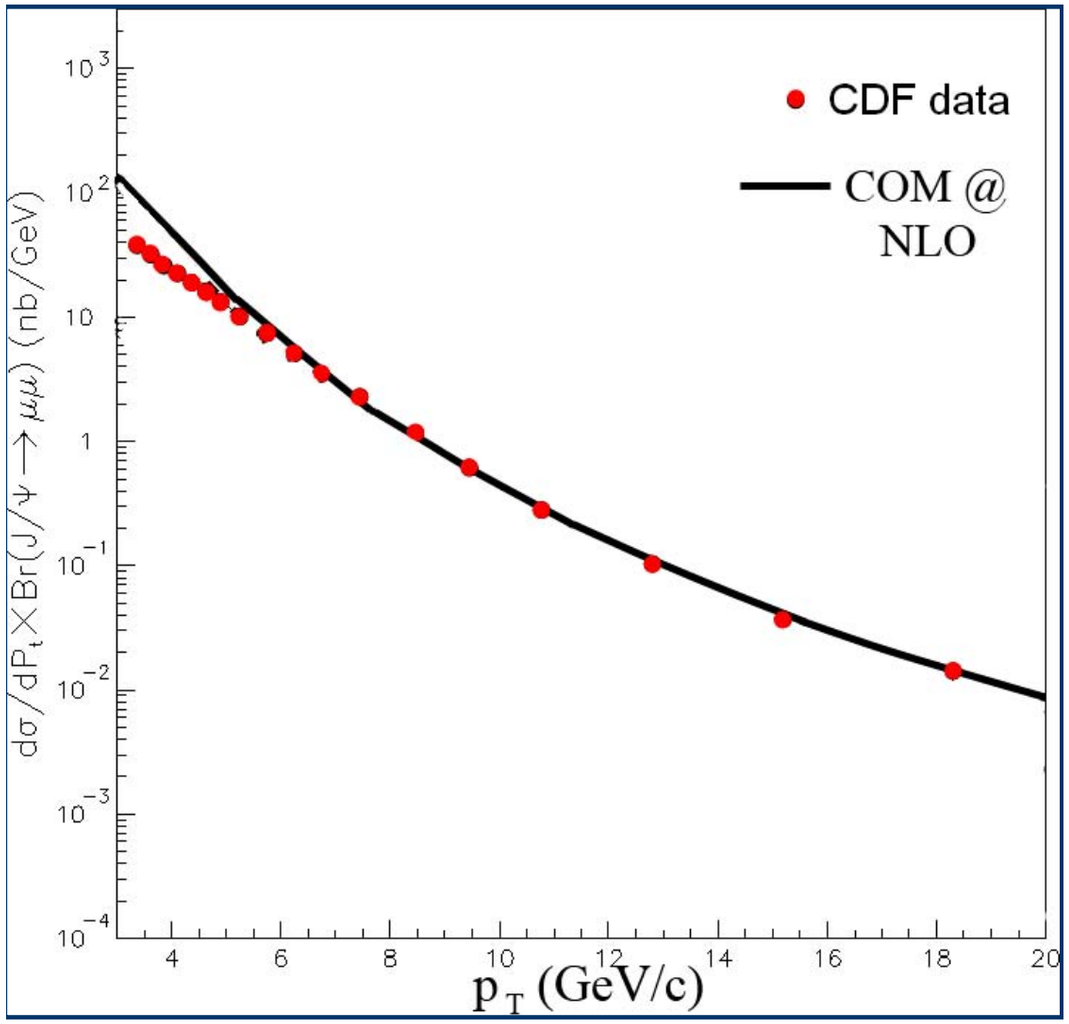

- Misses polarization.
- Fails for associated production

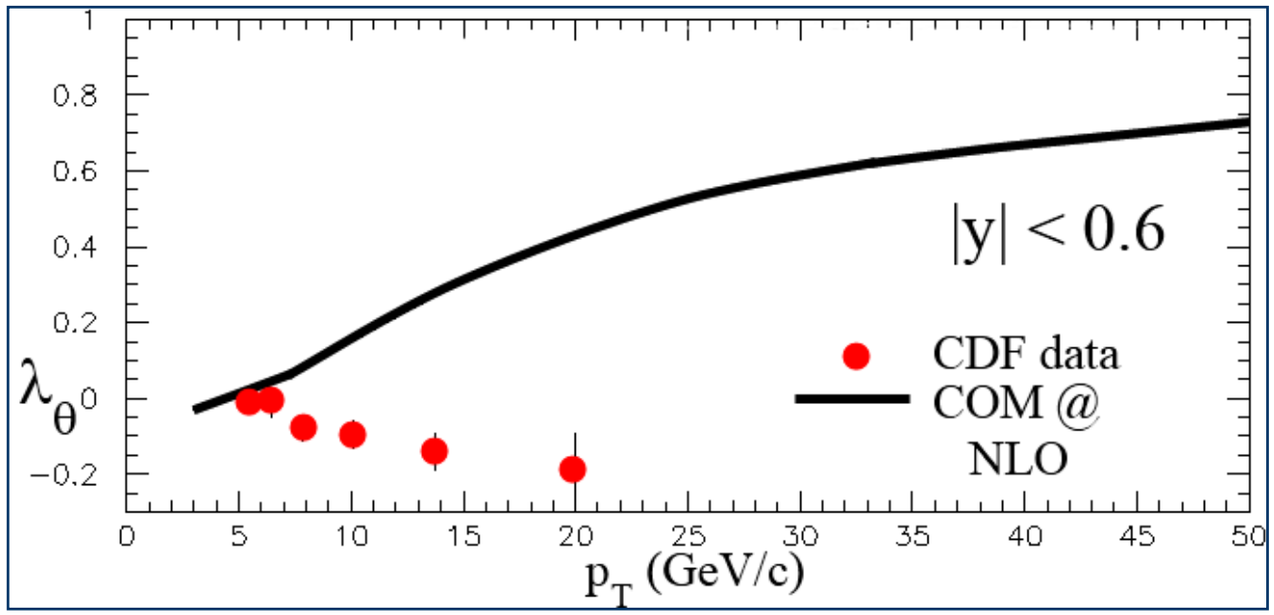

J/ψ production mechanisms (cont.)

Higher twist effects must be properly taken into account

Qiu, Sterman

Do we have a chance to understand the J/ψ production in pA and AA if we don't fully understand it in pp?

Possibly yes, because we have an additional parameter A>>1 that allows to re-sum parametrically large higher twists contributions.

Production of J/ψ: pp vs pA

Kharzeev, KT (2005)
Kharzeev, Levin, KT (2008)

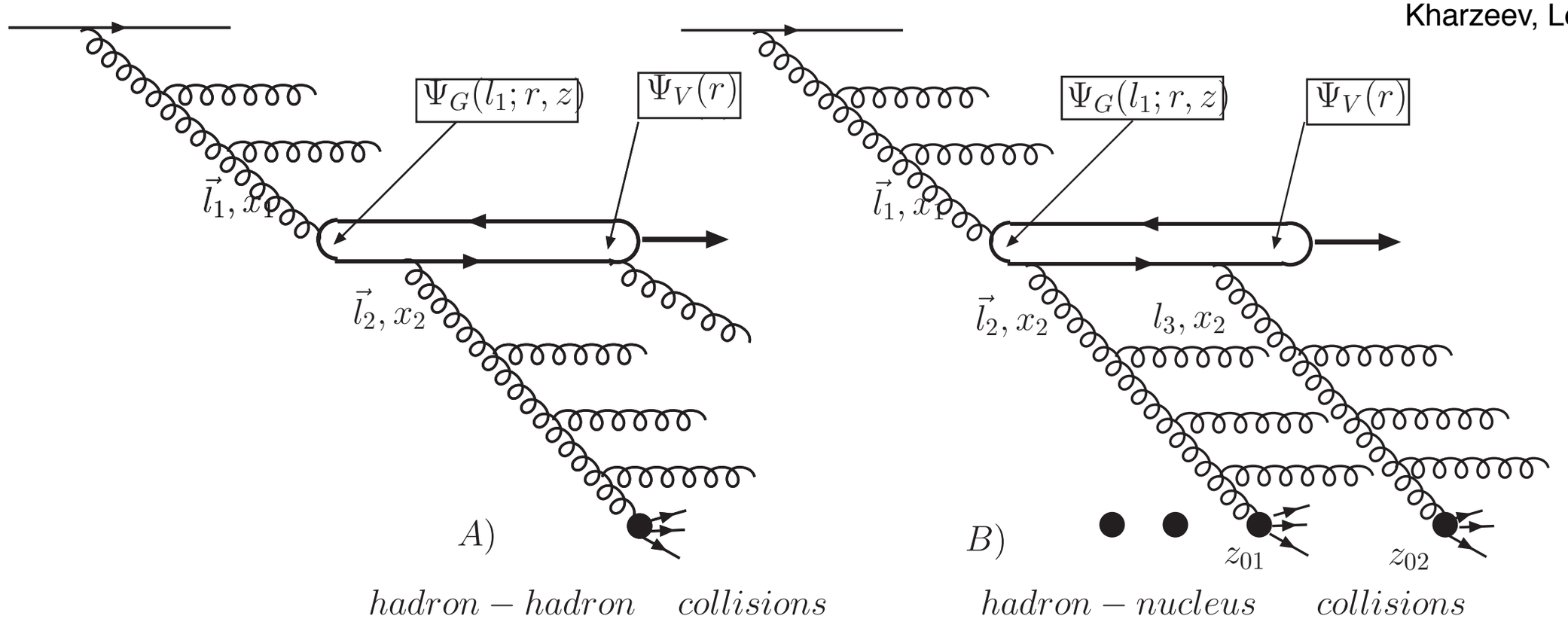

$$\alpha_s^3 A^{1/3} = \alpha_s \underbrace{(\alpha_s^2 A^{1/3})}_{\alpha_s^2 A^{1/3} \sim 1} \sim \alpha_s$$

$$\alpha_s^4 A^{2/3} = (\alpha_s^2 A^{1/3})^2 \sim 1$$

This diagram breaks factorization.

Quasi-classical approximation

Dominguez, Kharzeev, Levin, Mueller, KT (2011)

Kharzeev, Levin, KT (2012)

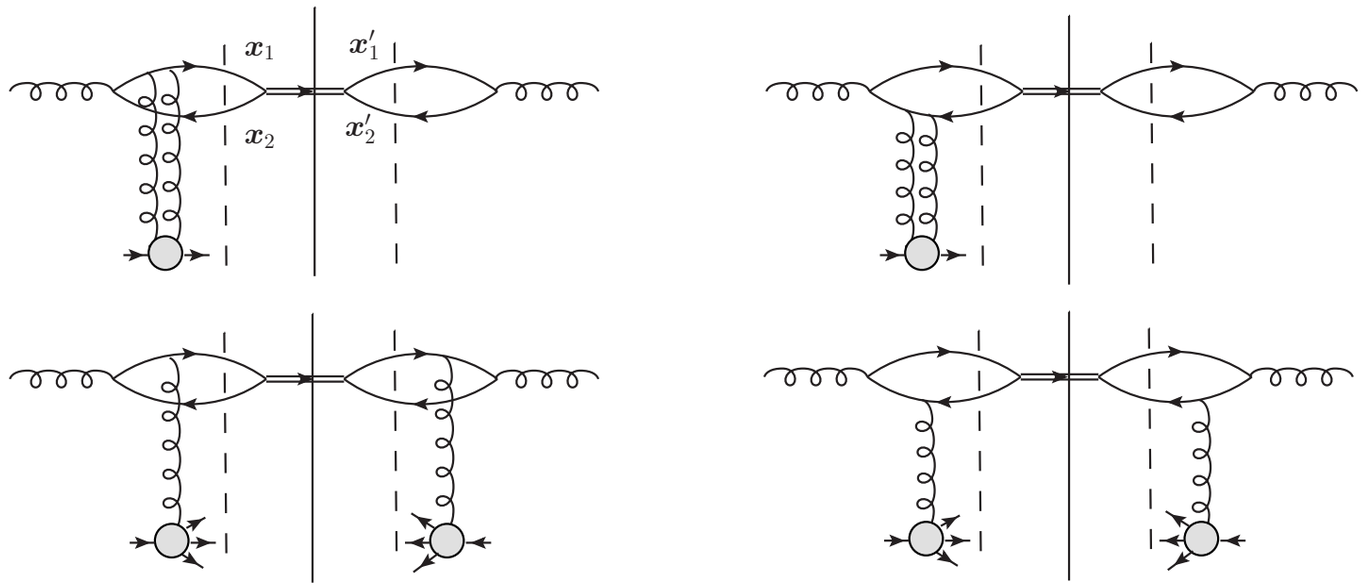

$$\boldsymbol{x}_1 = \boldsymbol{b} + \frac{1}{2}\boldsymbol{r}\,, \quad \boldsymbol{x}_2 = \boldsymbol{b} - \frac{1}{2}\boldsymbol{r}\,,$$

$$\boldsymbol{x}_1' = \boldsymbol{b}' + \frac{1}{2}\boldsymbol{r}'\,, \quad \boldsymbol{x}_2' = \boldsymbol{b}' - \frac{1}{2}\boldsymbol{r}'\,,$$

$$\boldsymbol{\Delta} = \boldsymbol{b} - \boldsymbol{b}'\,, \quad \boldsymbol{B} = \frac{1}{2}(\boldsymbol{b} + \boldsymbol{b}')$$

FIG. 1: One of the interactions before the last inelastic scattering. The diagrams that are complex conjugate to the first row of diagrams are not shown. The vertical dashed line denotes the last inelastic interaction when the $c\bar{c}$ pair is converted into the color-singlet state. The vertical solid line is the cut corresponding to the final state.

$$-\frac{1}{8}Q_s^2(B)\left[(\boldsymbol{x}_1 - \boldsymbol{x}_1')^2 + (\boldsymbol{x}_2 - \boldsymbol{x}_2')^2\right] = -\frac{1}{4}Q_s^2(B)\left(\Delta^2 + \frac{1}{4}(\boldsymbol{r} - \boldsymbol{r}')^2\right)$$

modulo log's (dropping logs: GBW model/geometric scaling)

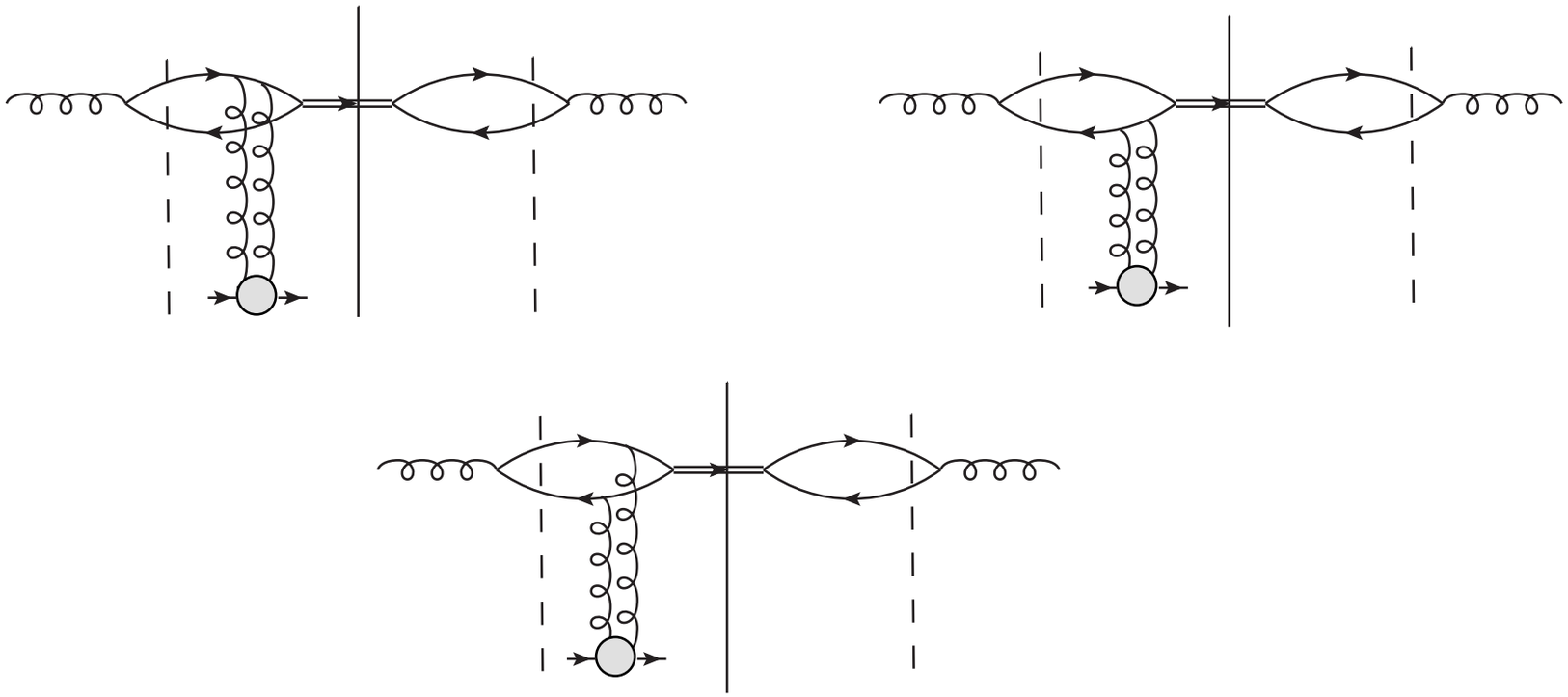

FIG. 2: One of the interactions after the last inelastic interactions. Complex conjugate diagrams are not shown.

$$-\frac{1}{8}Q_s^2(B)\left[(\boldsymbol{x}_1-\boldsymbol{x}_2)^2+(\boldsymbol{x}_1'-\boldsymbol{x}_2')^2\right]=-\frac{1}{8}Q_s^2(B)(r^2+r'^2)$$

modulo log's

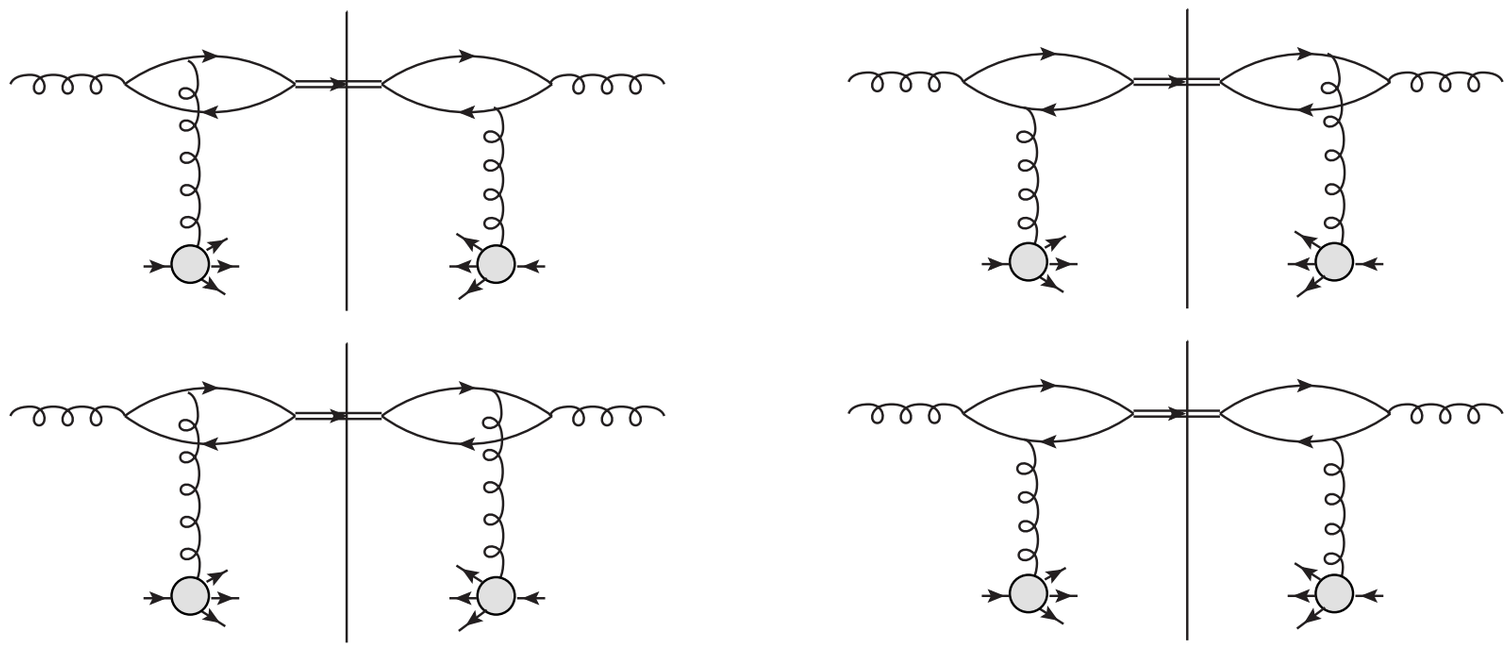

FIG. 3: The last inelastic interaction.

$$-\frac{1}{8}Q_s^2(B)\left[(\boldsymbol{x}_2-\boldsymbol{x}_1')^2+(\boldsymbol{x}_1-\boldsymbol{x}_2')^2-(\boldsymbol{x}_1-\boldsymbol{x}_1')^2-(\boldsymbol{x}_2-\boldsymbol{x}_2')^2\right]=-\frac{1}{4}Q_s^2(B)\,\boldsymbol{r}\cdot\boldsymbol{r}'$$

modulo log's

Amplitude for J/ψ production $\quad A(p_\perp) = \frac{1}{p_\perp^2}\mathcal{F}(p_\perp)$ with the form-factor:

$$\mathcal{F}(p_\perp) = \int \frac{d^3k}{(2\pi)^3}\Psi_G(k)\,\Psi_V(k-p) = 2\pi\alpha_s \int_0^1 dz \int \frac{d^2r}{4\pi}\Phi(r,z)\left(e^{-i\frac{1}{2}\boldsymbol{r}\cdot\boldsymbol{p}} - e^{i\frac{1}{2}\boldsymbol{r}\cdot\boldsymbol{p}}\right)$$

g→J/ψ transition amplitude squared

$$\Phi(\boldsymbol{r},z) = \frac{g}{\pi\sqrt{2N_c}}\left\{m_c^2 K_0(m_c r)\phi_T(r,z) - \left[z^2 + (1-z)^2\right] m_c K_1(m_c r)\partial_r\phi_T(r,z)\right\}$$

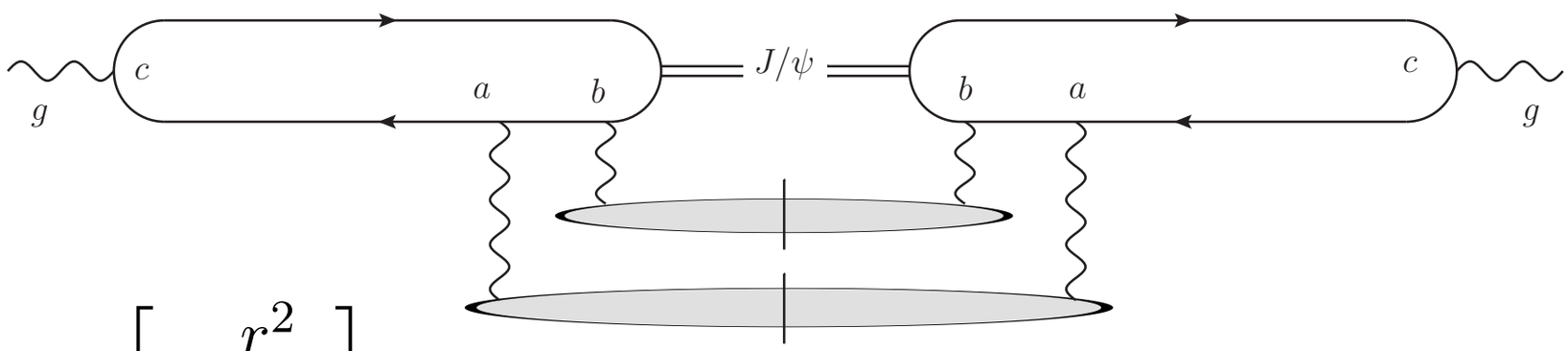

J/ψ wave function

$$\phi_T(r,z) = N_T z(1-z)\exp\left[-\frac{r^2}{2R_T^2}\right]$$

N_T, R_T are fixed from DIS

Total inclusive cross section

Sum over multiple scatterings, integrate over p_T and over the longitudinal coordinate of the last inelastic interaction ξ

$$\frac{d\sigma_{gA\to J/\psi X}}{d^2b} = \int_0^1 dz \int \frac{d^2r}{4\pi}\Phi(\boldsymbol{r},z)\int_0^1 dz' \int \frac{d^2r'}{4\pi}\Phi^*(\boldsymbol{r'},z')$$
$$\times \int_0^{T(b)} d\xi\, \frac{\boldsymbol{r}\cdot\boldsymbol{r'}Q_s^2}{4T(b)} \exp\left\{-\frac{1}{16}Q_s^2(\boldsymbol{r}-\boldsymbol{r'})^2\frac{\xi}{T(b)} - \frac{1}{8}Q_s^2(r^2+r'^2)\left(1-\frac{\xi}{T(b)}\right)\right\}$$

☞ $$\frac{d\sigma_{pA\to J/\psi X}}{dyd^2b} = x_1 G(x_1,m_c^2)\int_0^1 dz \int \frac{d^2r}{4\pi}\Phi(\boldsymbol{r},z)\int_0^1 dz' \int \frac{d^2r'}{4\pi}\Phi^*(\boldsymbol{r'},z')$$
$$\times \frac{4\boldsymbol{r}\cdot\boldsymbol{r'}}{(\boldsymbol{r}+\boldsymbol{r'})^2}\left(e^{-\frac{Q_s^2}{16}(\boldsymbol{r}-\boldsymbol{r'})^2} - e^{-\frac{Q_s^2}{8}(r^2+r'^2)}\right)$$

From pA to AA

Now c-dipole can scatter in both nuclei ⇒ need to account for the nuclear matter distribution in another nucleus

$$\frac{\alpha_s \pi^2}{4C_F} x_1 G(x_1, a^2) = \int d^2 b_1 \, \frac{Q_{s1}^2}{8}$$

Kovchegov (2001)

$$\frac{d\sigma_{A_1 A_2 \to J/\psi X}}{dy \, d^2 b \, d^2 B} = \int_0^1 dz \int \frac{d^2 \boldsymbol{r}}{4\pi} \int_0^1 dz' \int \frac{d^2 \boldsymbol{r}'}{4\pi} \, \Phi(\boldsymbol{r}, z) \, \Phi^*(\boldsymbol{r}', z') \, 2T_{A_1 A_2 \to JX}(\boldsymbol{r}, \boldsymbol{r}')$$

$$T_{A_1 A_2 \to JX}(\boldsymbol{r}, \boldsymbol{r}') = \frac{C_F}{2\alpha_s \pi^2} \frac{Q_{s1}^2 Q_{s2}^2}{Q_{s1}^2 + Q_{s2}^2} \frac{4\boldsymbol{r} \cdot \boldsymbol{r}'}{(\boldsymbol{r} + \boldsymbol{r}')^2} \left(e^{-\frac{1}{16}(Q_{s1}^2 + Q_{s2}^2)(\boldsymbol{r} - \boldsymbol{r}')^2} - e^{-\frac{1}{8}(Q_{s1}^2 + Q_{s2}^2)(r^2 + r'^2)} \right)$$

At small r: $$T_{A_1 A_2 \to JX}(\boldsymbol{r}, \boldsymbol{r}') \approx \frac{C_F}{2\alpha_s \pi^2} Q_{s1}^2 Q_{s2}^2 \, 4\boldsymbol{r} \cdot \boldsymbol{r}' \left(\frac{1}{16} - \frac{1}{512} (Q_{s1}^2 + Q_{s2}^2)(3r^2 + 3r'^2 - 2\boldsymbol{r} \cdot \boldsymbol{r}') \right)$$

Averaging over angles: $$\left\langle T_{A_1 A_2 \to JX}(\boldsymbol{r}, \boldsymbol{r}') \right\rangle \approx \frac{C_F}{\alpha_s \pi^2} \frac{r^2 r'^2}{16^2} \underbrace{(Q_{s1}^2 Q_{s2}^4 + Q_{s1}^4 Q_{s2}^2)}_{\text{3 scatterings}}$$

Low x evolution

The low x evolution gives energy/rapidity dependence

Glauber-Mueller formula for quark dipole scattering is the initial condition

$$N_F(\boldsymbol{r}, \boldsymbol{b}, y_0) = 1 - e^{-\frac{1}{8}\boldsymbol{r}^2 Q_s^2(y_0)}$$

Amplitude for gluon (adjoint) dipole:

$$N_A(\boldsymbol{r}, \boldsymbol{b}, y) = 2N_F(\boldsymbol{r}, \boldsymbol{b}, y) - N_F^2(\boldsymbol{r}, \boldsymbol{b}, y)$$

$$\Rightarrow \quad N_A(\boldsymbol{r}, \boldsymbol{b}, y_0) = 1 - e^{-\frac{1}{4}\boldsymbol{r}^2 Q_s^2(y_0)}$$

Replacing $N_F(y_0)$ by $N_F(y)$ accounts for the low-x evolution of the cross section.

$N_F(y)$ satisfies the BK equation.

Numerical calculations

$$R_{A_1 A_2} = \frac{\int_{\mathcal{S}} d^2b \frac{d\sigma_{A_1 A_2 \to J/\psi X}}{dy\, d^2b}}{A_1\, A_2\, \frac{d\sigma_{pp \to J/\psi X}}{dy}}$$

The production mechanism in pp is not known, so consider the simplest one-parameter model:

$$\frac{d\sigma_{pp \to J/\psi X}}{dy} = C\, \frac{d\sigma_{AA \to J/\psi X}}{dy}\bigg|_{A=1}$$

N_F is parameterized with DHJ or bCGC models.

DHJ model

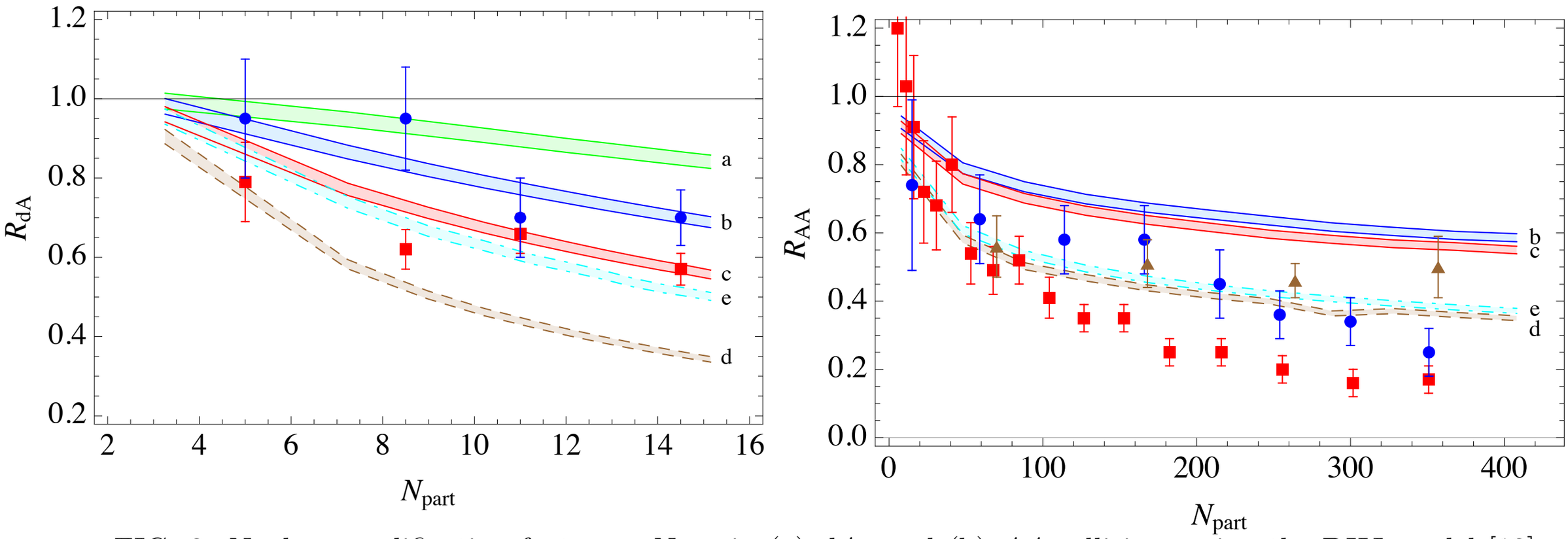

FIG. 3: Nuclear modification factor vs $N_{\rm part}$ in (a) dAu and (b) AA collisions using the DHJ model [13]. Band 'a' (green) represents rapidity $y = -1.7$ at $\sqrt{s} = 200$ GeV, 'b' (blue): $y = 0$, $\sqrt{s} = 200$ GeV, 'c' (red): $y = 1.7$, $\sqrt{s} = 200$ GeV, 'd' (brown): $y = 3.25$, $\sqrt{s} = 2.76$ TeV, 'e' (cyan): $y = 0$, $\sqrt{s} = 5.5$ TeV. $m = 1.5$ GeV, $C = 1$. Experimental data [16–19] is represented by (blue) circles in 'b', by (red) squares in 'c' and by (brown) triangles in 'd'. (Color online).

Reasonable agreement with dA and AA at LHC, undershooting of AA at RHIC

bCGC model

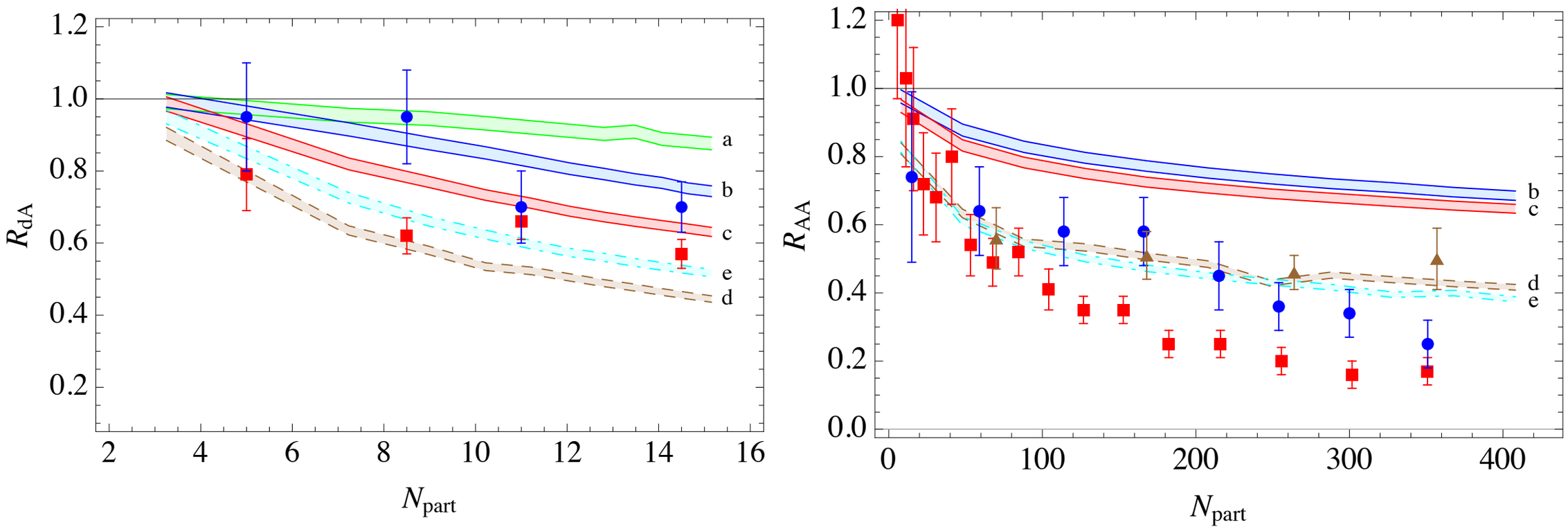

FIG. 3: Nuclear modification factor vs $N_{\rm part}$ in (a) dAu and (b) AA collisions using the DHJ model [13]. Band 'a' (green) represents rapidity $y = -1.7$ at $\sqrt{s} = 200$ GeV, 'b' (blue): $y = 0$, $\sqrt{s} = 200$ GeV, 'c' (red): $y = 1.7$, $\sqrt{s} = 200$ GeV, 'd' (brown): $y = 3.25$, $\sqrt{s} = 2.76$ TeV, 'e' (cyan): $y = 0$, $\sqrt{s} = 5.5$ TeV. $m = 1.5$ GeV, $C = 1$. Experimental data [16–19] is represented by (blue) circles in 'b', by (red) squares in 'c' and by (brown) triangles in 'd'. (Color online).

Reasonable agreement with dA and AA at LHC, undershooting of AA at RHIC

Conclusions I

•The cold nuclear matter effects alone cannot provide neither quantitative nor even a qualitative description of the AA data. Additional mechanisms beyond the initial state effects are required to explain the experimental data.

- NMF is well described with C=1 ⇒

evidence that J/ψ production mechanism in pp collisions is similar to that in pA implying that it is perhaps dominated by the higher twist effects.

pT - spectrum

To obtain the p_T spectrum we have to keep the logarithms that were neglected in the GBW model, e.g. instead of $\boldsymbol{r}\cdot\boldsymbol{r}'$ we have

$$
\begin{aligned}
J(\boldsymbol{r},\boldsymbol{r}',\boldsymbol{\Delta}) &= \int \frac{d\ell^2}{\ell^4} e^{-i\boldsymbol{\Delta}\cdot\boldsymbol{\ell}} \left(e^{i\frac{1}{2}(\boldsymbol{r}-\boldsymbol{r}')\cdot\boldsymbol{\ell}} + e^{-i\frac{1}{2}(\boldsymbol{r}-\boldsymbol{r}')\cdot\boldsymbol{\ell}} - e^{-i\frac{1}{2}(\boldsymbol{r}+\boldsymbol{r}')\cdot\boldsymbol{\ell}} - e^{i\frac{1}{2}(\boldsymbol{r}+\boldsymbol{r}')\cdot\boldsymbol{\ell}} \right) \\
&= \frac{2\pi}{4} \Bigg[-\left(\frac{1}{2}(\boldsymbol{r}-\boldsymbol{r}')-\boldsymbol{\Delta}\right)^2 \ln \frac{1}{\mu|\frac{1}{2}(\boldsymbol{r}-\boldsymbol{r}')-\boldsymbol{\Delta}|} \\
&\quad - \left(\frac{1}{2}(\boldsymbol{r}-\boldsymbol{r}')+\boldsymbol{\Delta}\right)^2 \ln \frac{1}{\mu|\frac{1}{2}(\boldsymbol{r}-\boldsymbol{r}')+\boldsymbol{\Delta}|} \\
&\quad + \left(\frac{1}{2}(\boldsymbol{r}+\boldsymbol{r}')+\boldsymbol{\Delta}\right)^2 \ln \frac{1}{\mu|\frac{1}{2}(\boldsymbol{r}+\boldsymbol{r}')+\boldsymbol{\Delta}|} \\
&\quad + \left(\frac{1}{2}(\boldsymbol{r}+\boldsymbol{r}')-\boldsymbol{\Delta}\right)^2 \ln \frac{1}{\mu|\frac{1}{2}(\boldsymbol{r}+\boldsymbol{r}')-\boldsymbol{\Delta}|} \Bigg] .
\end{aligned}
$$

We assume that the short distance effects can be approximately factored out:

$$J(\boldsymbol{r},\boldsymbol{r}',\boldsymbol{\Delta}) \approx \underbrace{\boldsymbol{r}\cdot\boldsymbol{r}'}_{\text{projects onto } 1^{--} \text{ state}} \underbrace{F(\Delta)}_{\text{from pp}}$$

We are interested to calculate the nuclear modification of p_T spectrum in pA collisions. So we use the pp spectrum as input.

$$F(\Delta) = \frac{1}{\sigma_{pp\to J/\psi X}} \int \frac{d\sigma_{pp\to J/\psi X}(p_\perp)}{d^2 p_\perp} e^{-i\boldsymbol{p}\cdot\boldsymbol{\Delta}} d^2 p_\perp$$

Fit of experimental data: $$\frac{d\sigma_{pp\to J/\psi X}}{\sigma_{pp}\, d^2 p_\perp} = \mathcal{N}\left(1 + \frac{p_\perp^2}{p_0^2}\right)^{-6}$$

Its Fourier image: $$F(\Delta) = \frac{(p_0\Delta)^5}{384} K_5(p_0\Delta)$$

Going through the same steps as for the total cross section we got the final expression for the spectrum:

$$\frac{d\sigma_{A_1A_2\to J/\psi X}}{d^2p_\perp dy d^2B_1 d^2B_2} = \frac{d\sigma_{A_1A_2\to J/\psi X}}{dy d^2B_1 d^2B_2} \frac{1}{Q_{s1}^2 + Q_{s2}^2} \int \frac{d^2\Delta}{(2\pi)^2} e^{i\boldsymbol{\Delta}\cdot\boldsymbol{p}} F(\Delta) \frac{4}{\Delta^2} \left(1 - e^{-\frac{1}{4}(Q_{s1}^2+Q_{s2}^2)\Delta^2}\right)$$

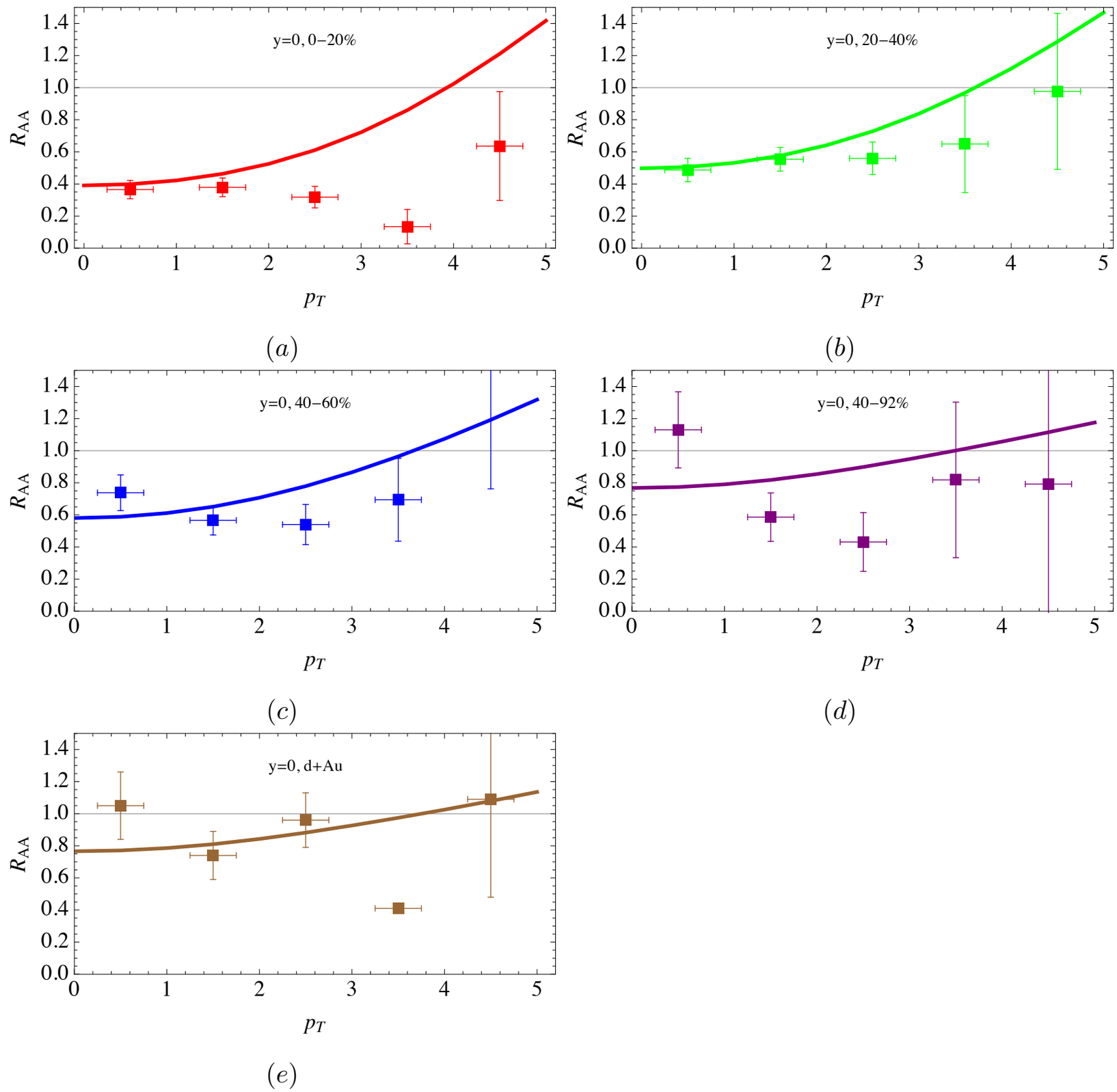

FIG. 4: (Color online). Nuclear modification factor for J/ψ's vs $p_\perp$ in GeV at $\sqrt{s} = 200$ GeV, $y = 0$ in $AuAu$ for centralities (a) 0-20%, (b) 20-40%, (c) 40-60%, (d) 60-92% and in (e) minbias dAu. Data is from [32, 33].

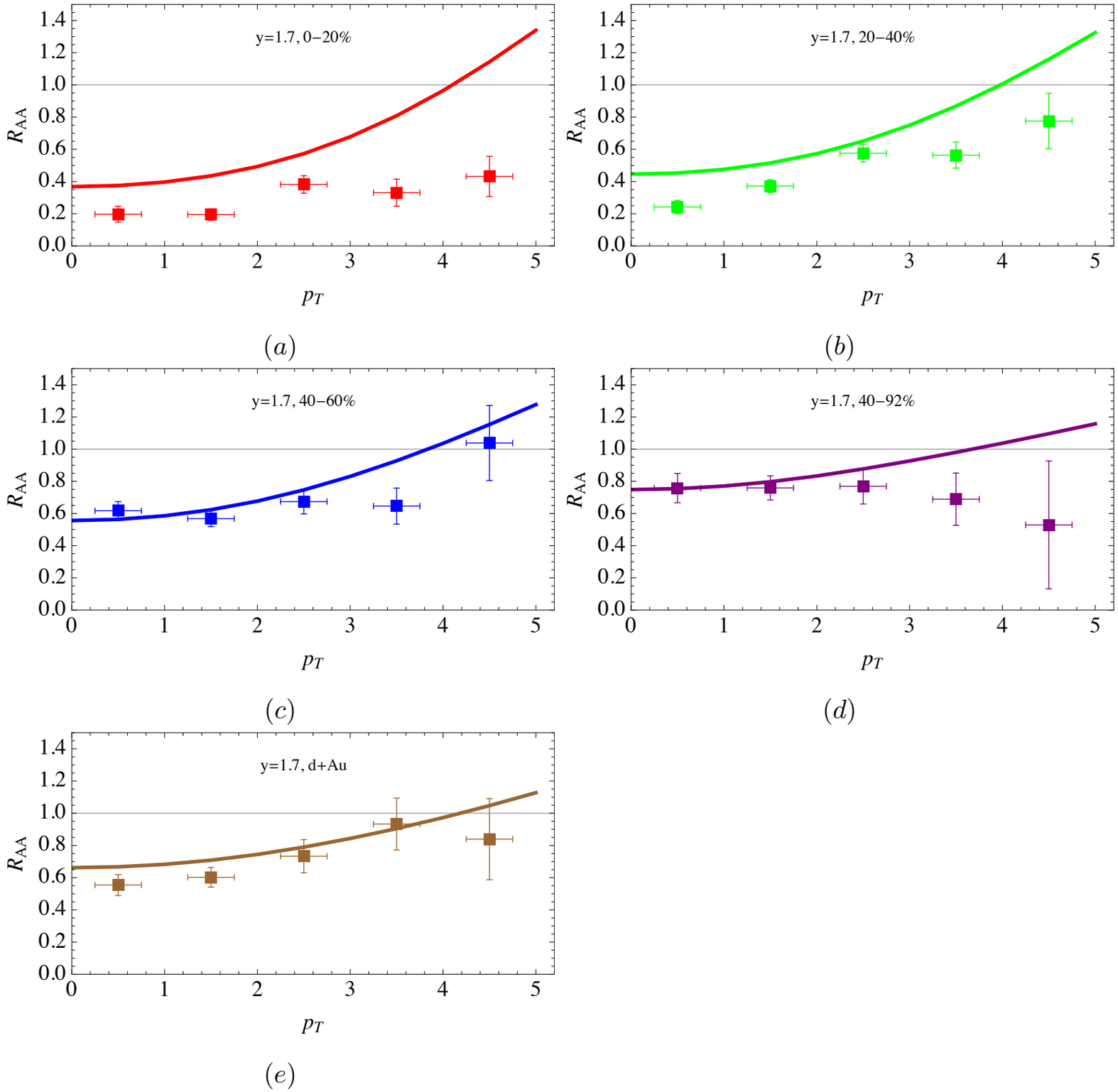

FIG. 5: (Color online). Nuclear modification factor for J/ψ's vs $p_\perp$ in GeV at $\sqrt{s} = 200$ GeV, $y = 1.7$ in $AuAu$ for centralities (a) 0-20%, (b) 20-40%, (c) 40-60%, (d) 60-92% and in (e) minbias dAu. Data is from [32, 33].

Preliminary PHENIX

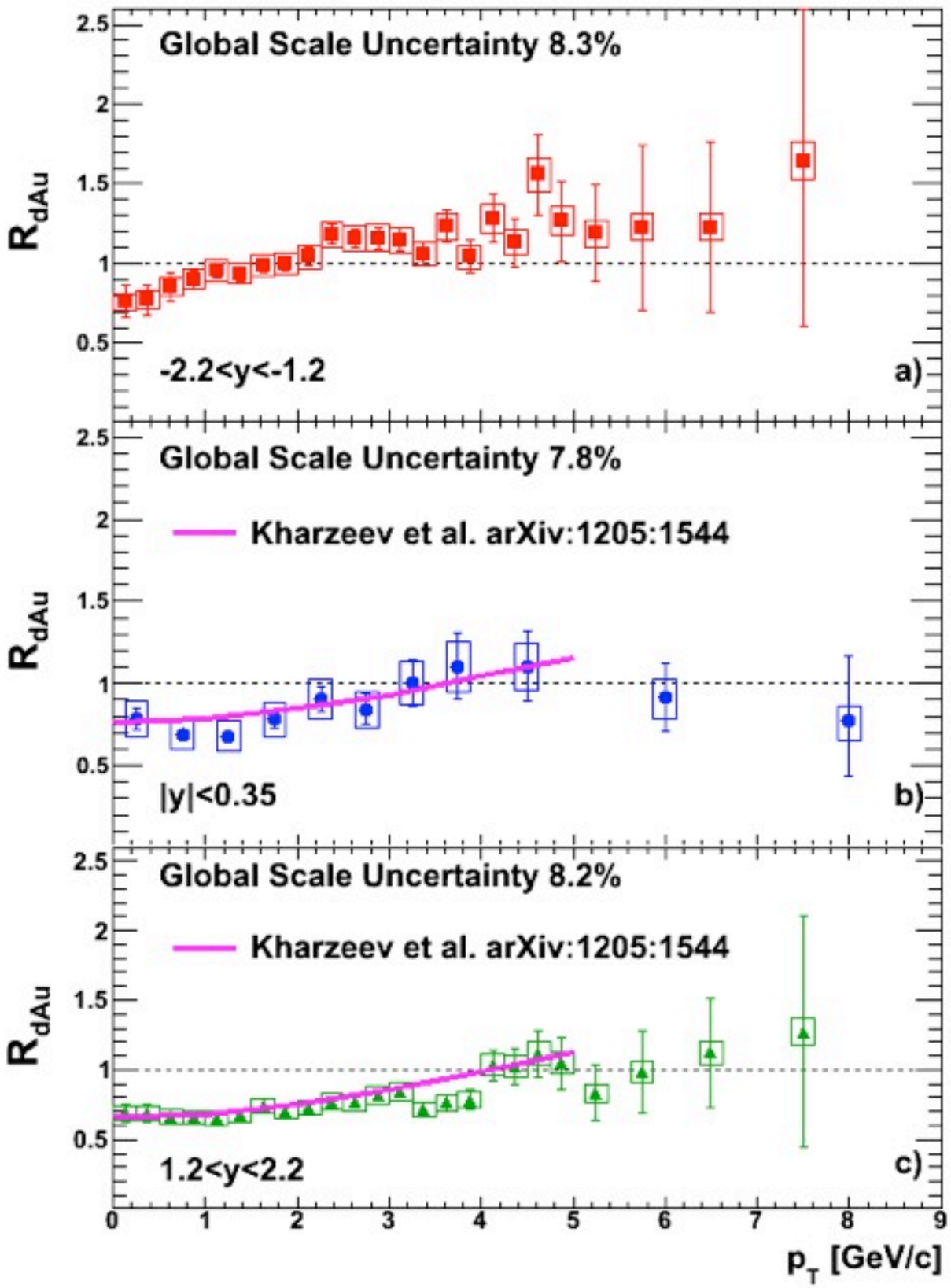

Predictions for LHC

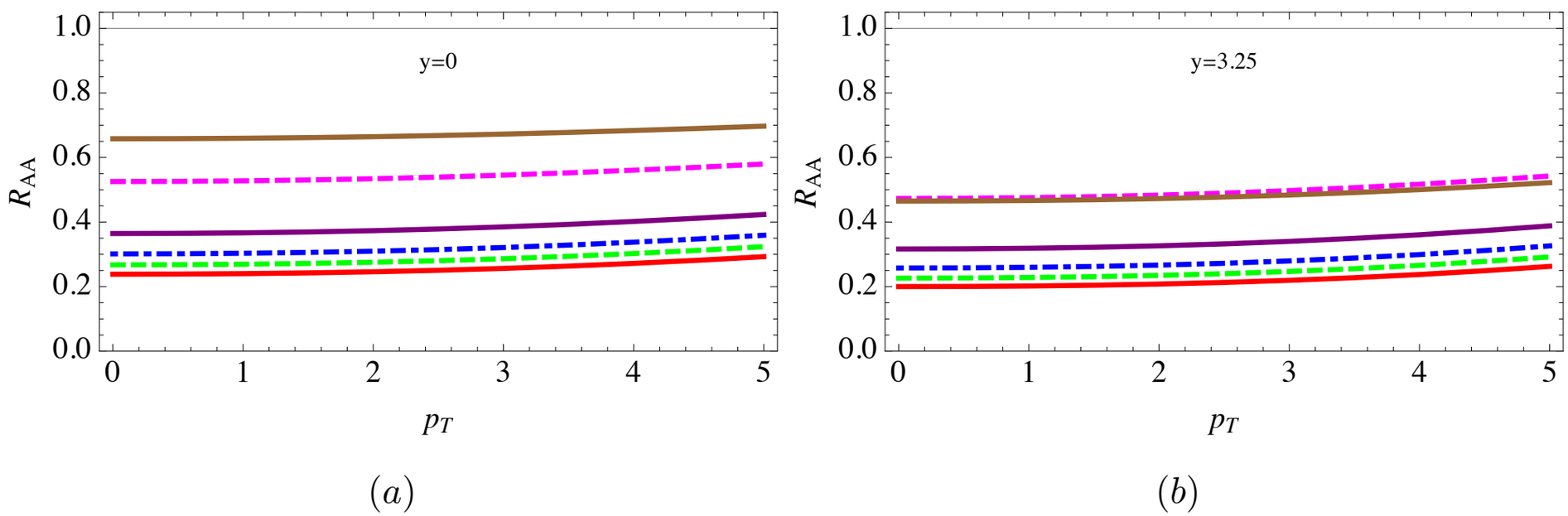

FIG. 6: (Color online). Nuclear modification factor for J/ψ's vs $p_\perp$ in GeV at $\sqrt{s} = 7$ TeV in $PbPb$ for rapidities (a) $y = 0$ and (b) $y = 3.25$. Each line corresponds to a different centrality bin; from bottom to top: 0-10% (solid red), 10-20% (dashed green), 20-30% (dash-dotted blue), 30-50% (solid purple), 50-80% (dashed magenta) and in minbias pPb (solid brown).

Conclusions II

- J/ψ suppression that originates from the initial state (cold nuclear matter) effects increases at the LHC energies compared to RHIC. Meanwhile, the experimental data on AA collisions indicate that J/ψ's are suppressed less at LHC than at RHIC.

- The hot (or any other) non-CGC effect increases with p_T :

✓ Possible explanation: dissociation of J/ψ in magnetic field.

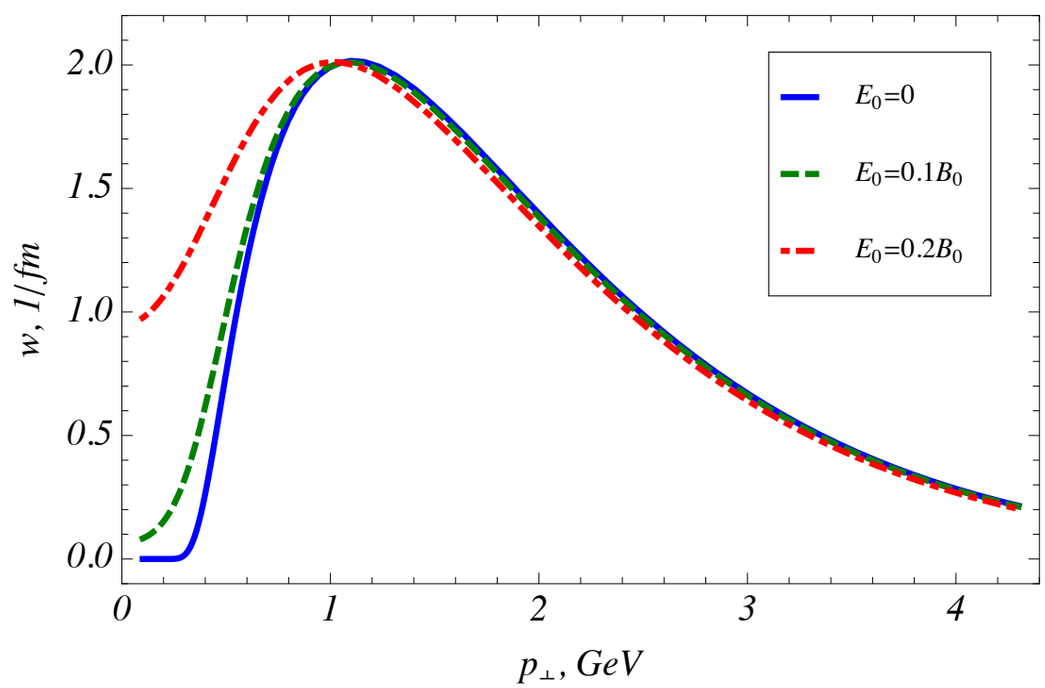

KT (2010)

Open charm

Kovchegov, KT (2006)

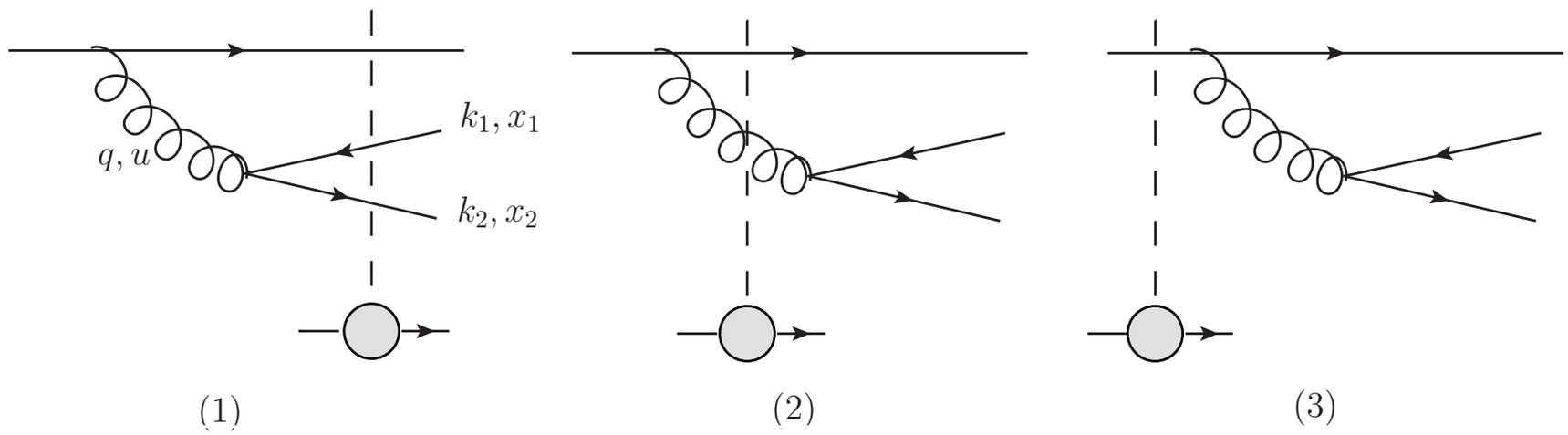

Usual approximation is to neglect the contribution of valence quark, which is true if $q \ll 2m$

KT (2005,2007)

$$\frac{d\sigma^{q_v \to q\bar{q}X}_{\rm fact}}{d^2\ell\, d^2q\, dy\, dz\, d^2b} = \frac{1}{(2\pi)^4} C_F \left(\frac{\alpha_s}{\pi}\right)^2 \frac{m^2}{q^2} \int d^2r d^2r'\, e^{-i\boldsymbol{\ell}\cdot(\boldsymbol{r}-\boldsymbol{r}')}$$
$$\times \left\{ K_1(rm) K_1(r'm) \frac{\boldsymbol{r}\cdot\boldsymbol{r}'}{rr'} [(1-z)^2 + z^2] + K_0(rm) K_0(r'm) \right\}$$
$$\times \left\{ S_F\big((1-z)(\boldsymbol{r}-\boldsymbol{r}')\big) S_F\big(z(\boldsymbol{r}-\boldsymbol{r}')\big) + 1 \right.$$
$$\left. - S_F\big((1-z)\boldsymbol{r}\big) S_F(z\boldsymbol{r}) - S_F\big((1-z)\boldsymbol{r}'\big) S_F(z\boldsymbol{r}') \right\}.$$

$$S_F = 1 - N$$

Proton factorization limit

Kopeliovich, Tarasov (2002)

KT (2005)

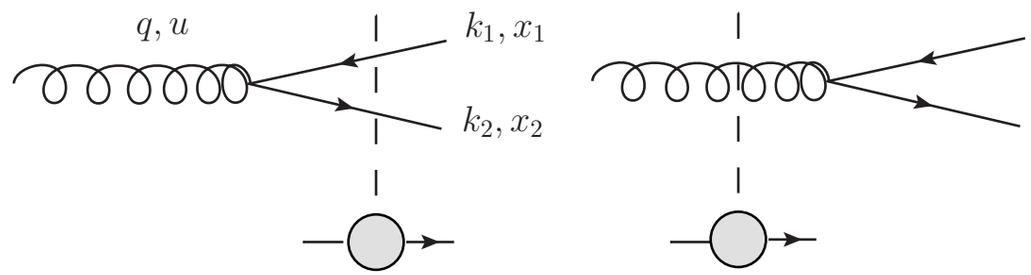

$$x_p G(x_p, Q^2) = \int^{Q^2} \varphi(x_p, q^2)\, dq^2 \qquad \varphi(x_p, q^2) = \frac{\alpha_s C_F}{\pi\, q^2}$$

Unintegrated gluon distribution factors out ☞

collinear factorization on the proton side.

In the chiral limit $\phi^{g\to q\bar{q}}(\boldsymbol{r}, \boldsymbol{r}', z) = \frac{2g^2}{(2\pi)^2}\delta(\boldsymbol{u})\delta(\boldsymbol{u}')\frac{\boldsymbol{r}\cdot\boldsymbol{r}'}{r^2 r'^2} P_{qg}(z)$

$$P_{qg}(z) = \frac{1}{2}[(1-z)^2 + z^2]$$

Open charm

It is important to know the cold-nuclear matter effects on open charm!

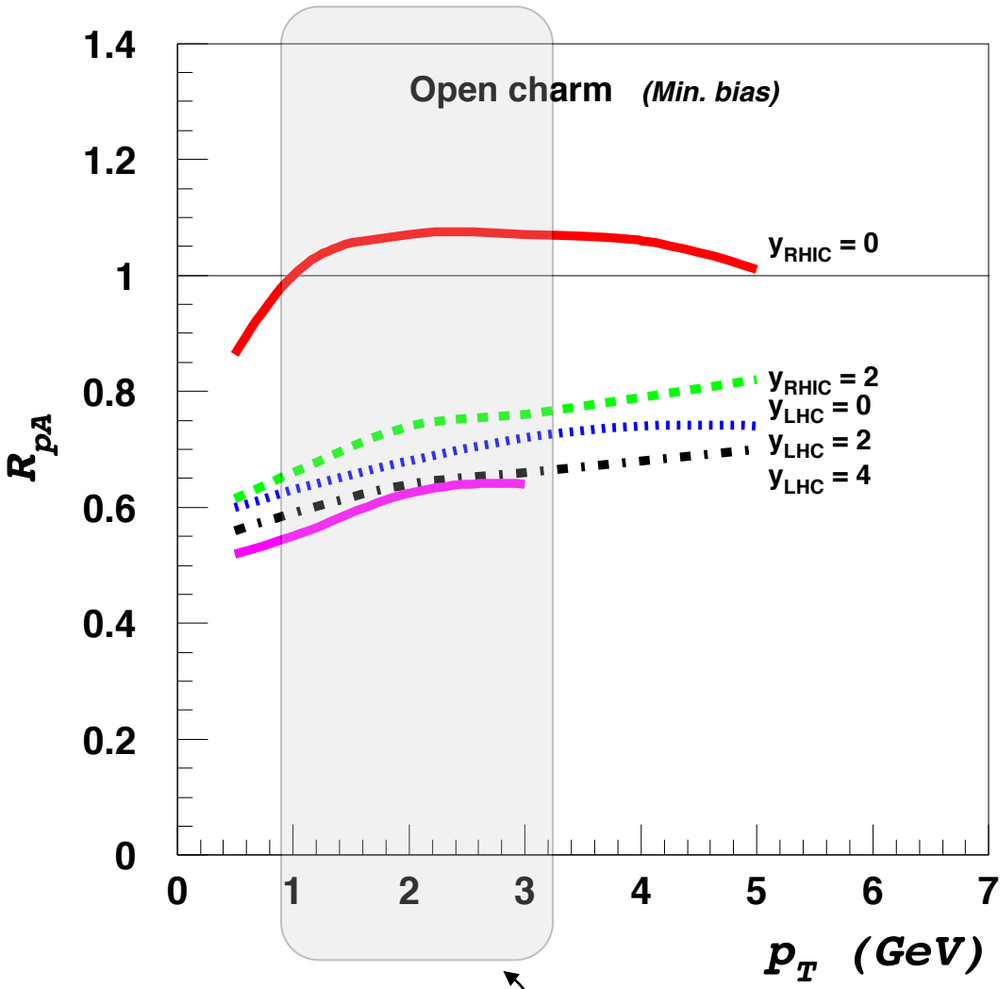

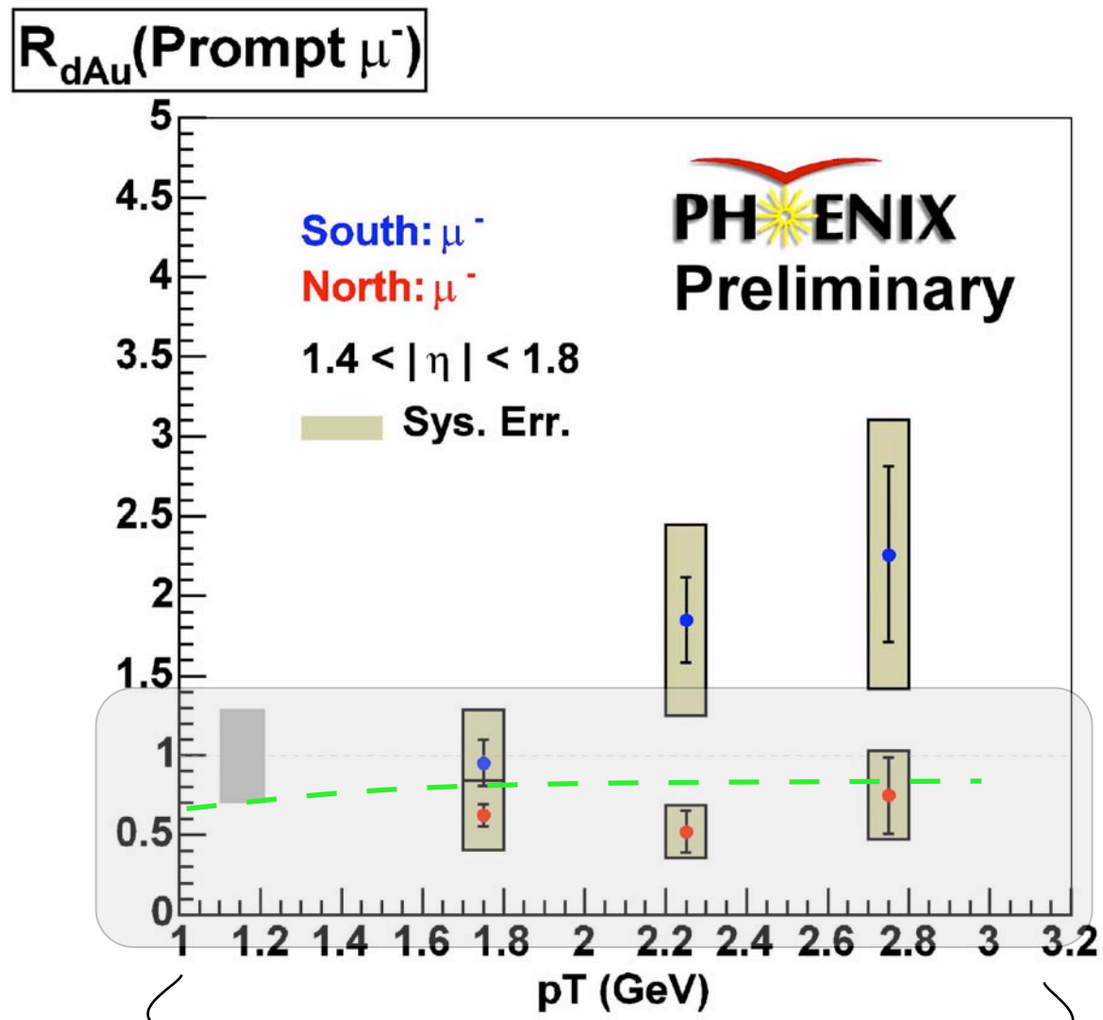

KT, 2007

Suppression of heavy quarks in forward direction

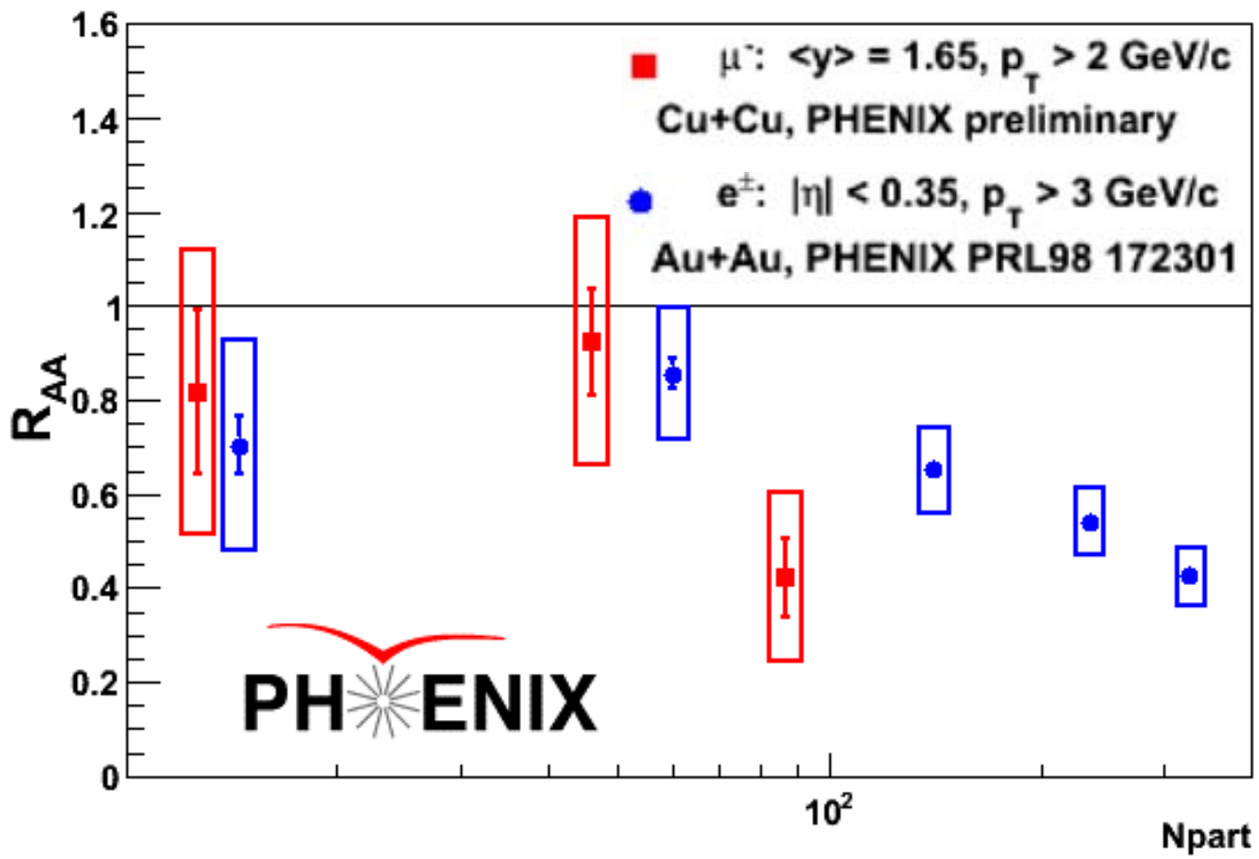

Similar effect for heavy-ion collisions. The overall suppression is a combination of cold and hot nuclear matter effects.

c-quark: proton factorization

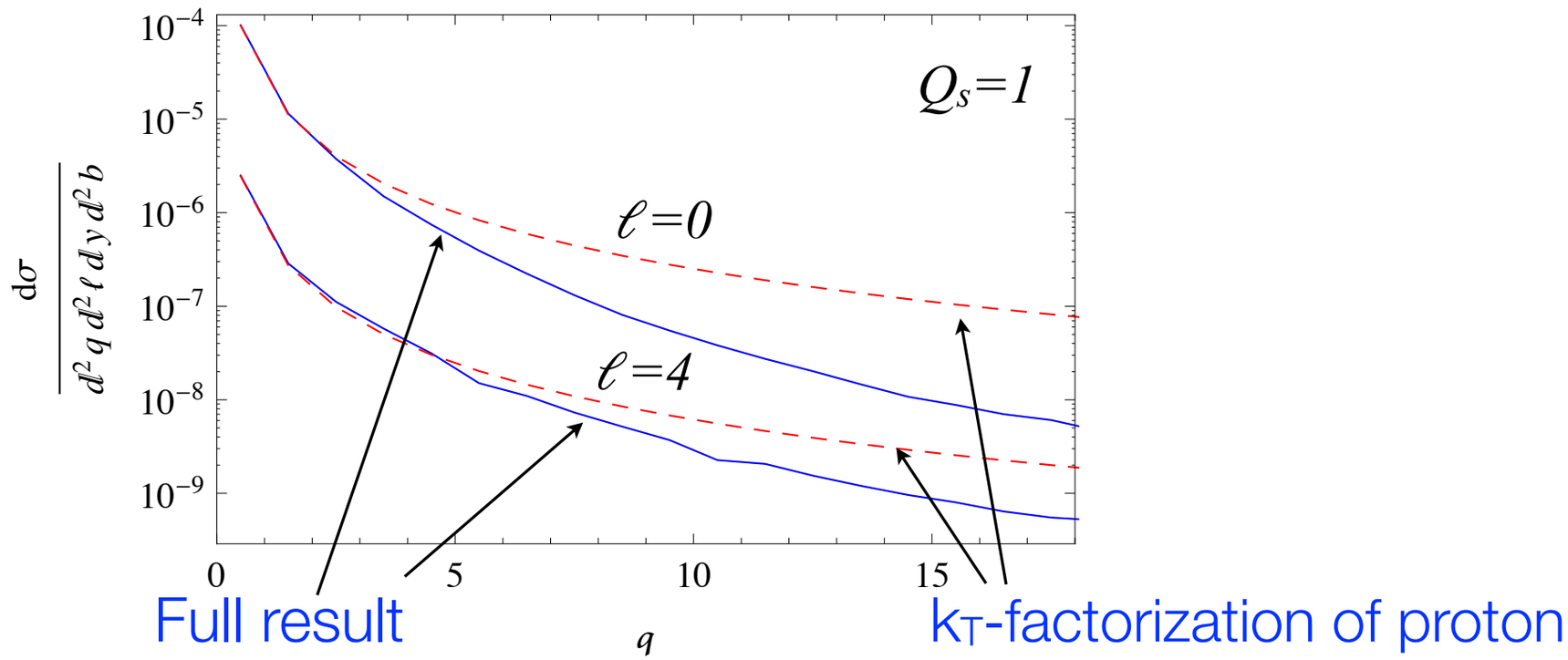

$\ell=4, Q_s=1$

c-quark: nucleus factorization

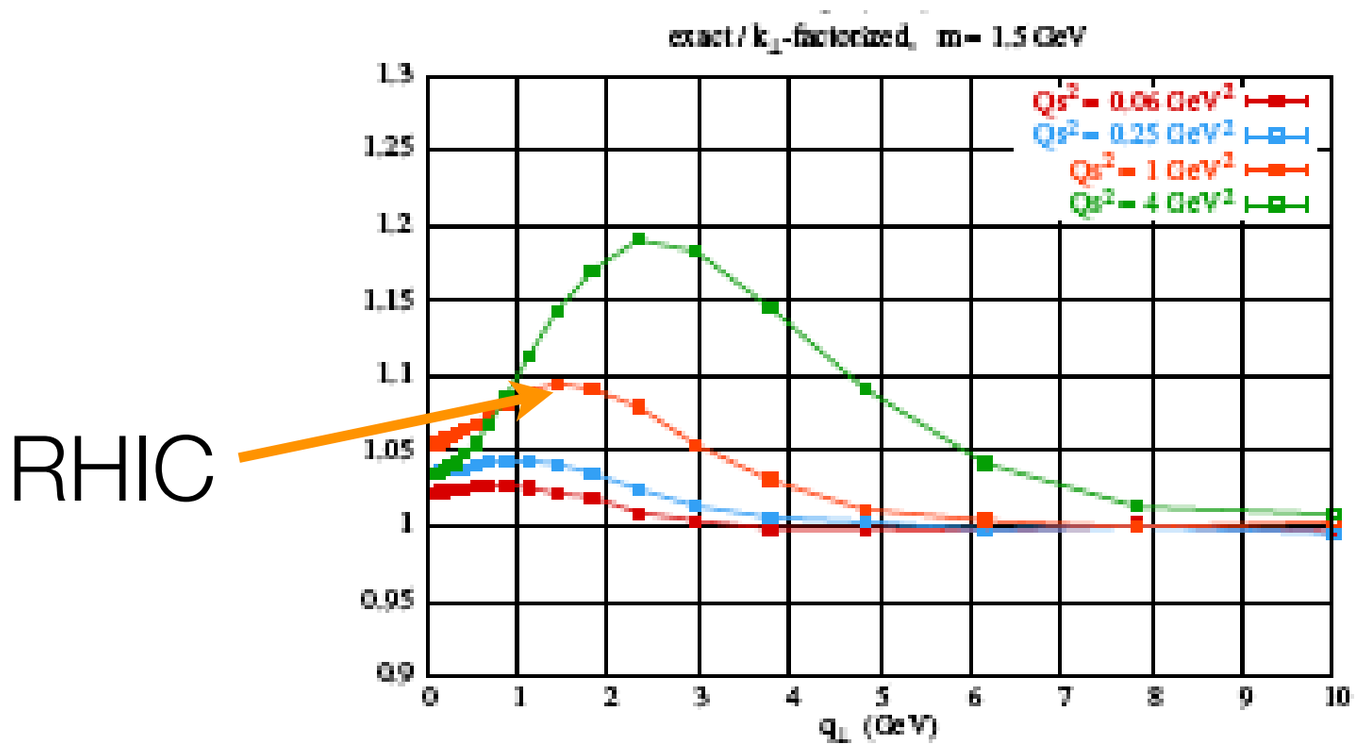

Fujii, Gelis, Venugopalan

Where is transition to hard pQCD?

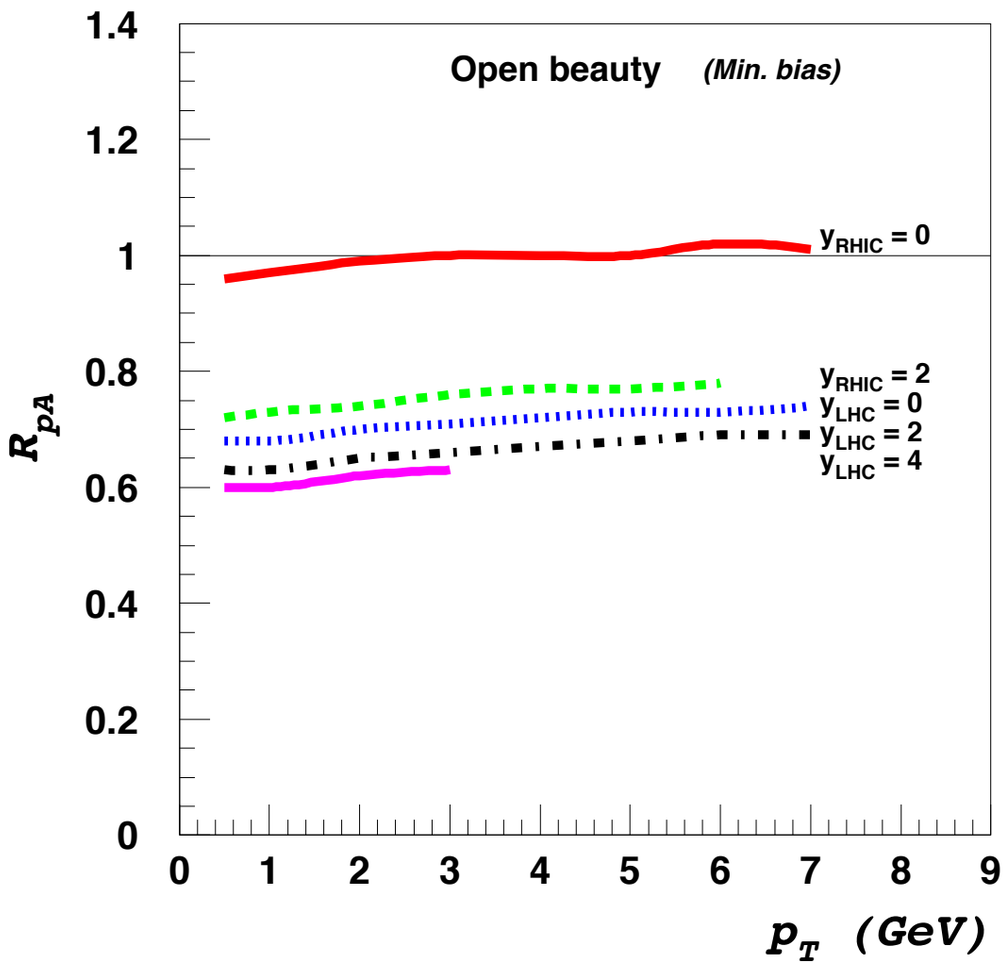

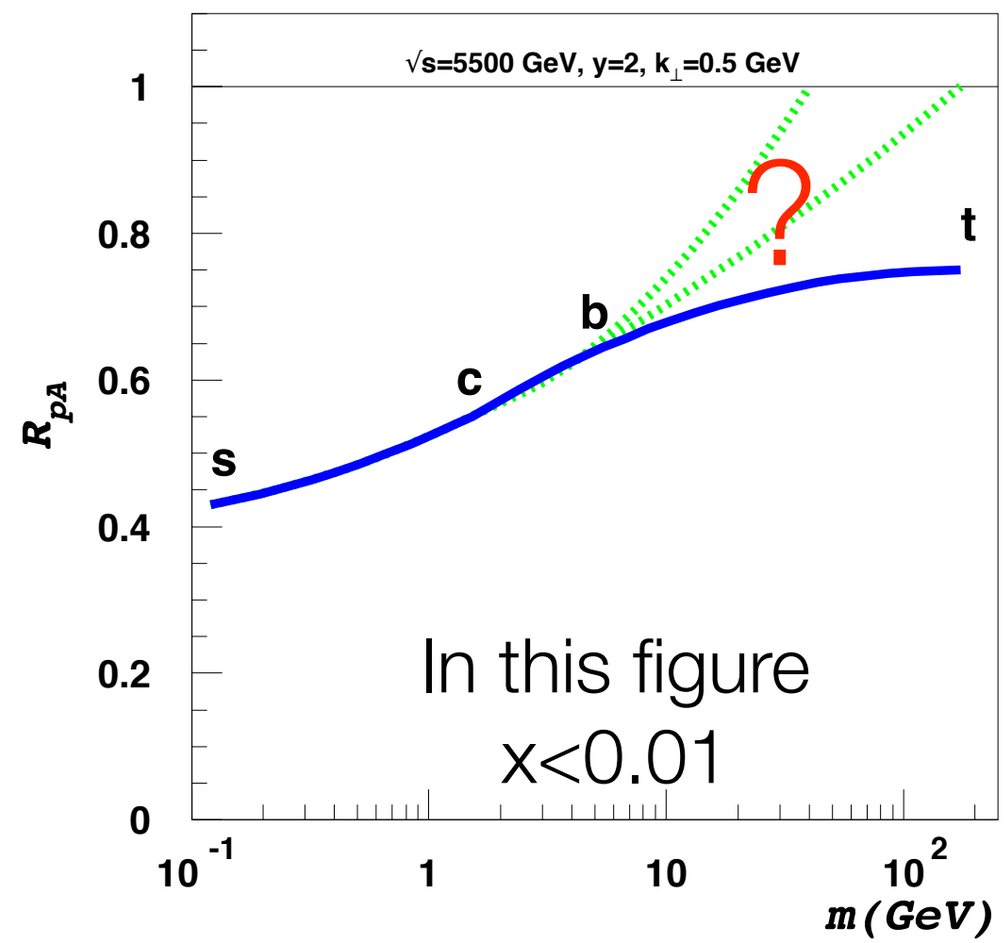

$$\alpha_s \log \frac{Q_s^2}{\Lambda_{\rm QCD}} \overset{?}{\Leftrightarrow} \alpha_s \log \frac{Q^2}{Q_s^2}$$

Summary

- Cold nuclear matter (CNM) effects on J/ψ are now under a good theoretical control, especially at LHC energies.

- CNM effects increase with energy and rapidity and decrease with p_T.

- The difference between the NMF due to CNM and the one experimentally observed may be due to QGP or magnetic field. Its energy and p_T dependence is puzzling.

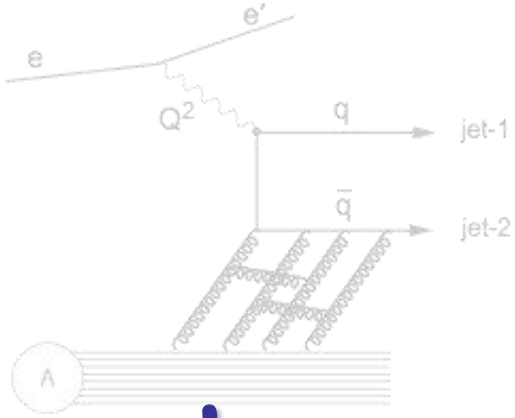

Dihadron correlations at eRHIC and Monte Carlo development

Liang Zheng

BNL/IOPP,CCNU

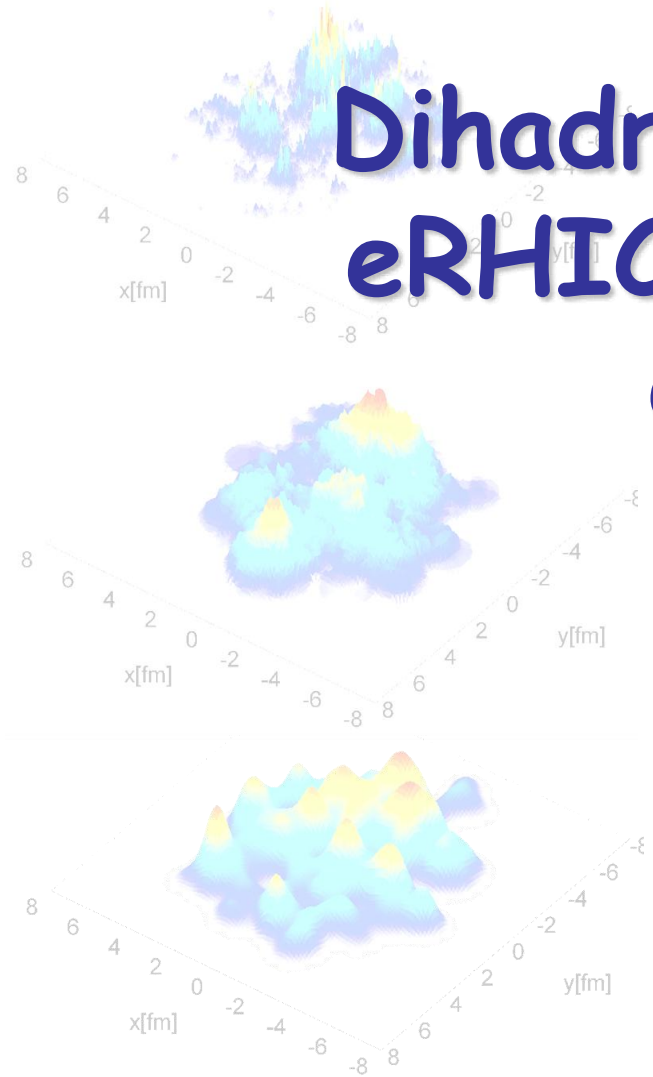

BROOKHAVEN NATIONAL LABORATORY

HUAZHONG UNIVERSITY

Outline

- Motivation
- RHIC forward dAu program
- Dihadron correlation at future eRHIC
  - Monte Carlo results
  - Compared with CGC prediction
  - The power of Monte Carlo
- Summary and Prospects

Motivation

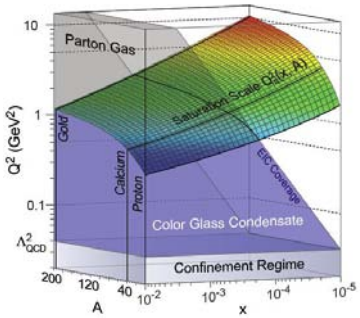

- eA program will investigate the nuclei structure with great precision
  - Probing gluon dynamics, establish the existence of the saturation regime.
  - Study cold nuclear medium effect with parton propagation and hadronization in nuclear matter.
  - Image nuclear gluon structure.
- dihadron correlation is a key measurement in the eA program to help us explore the saturation physics.

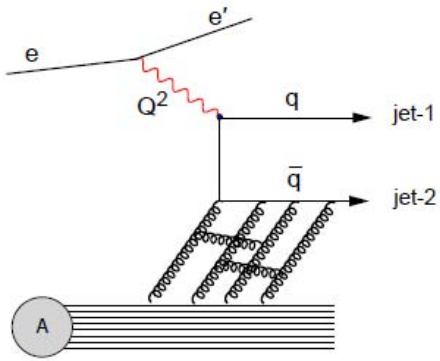

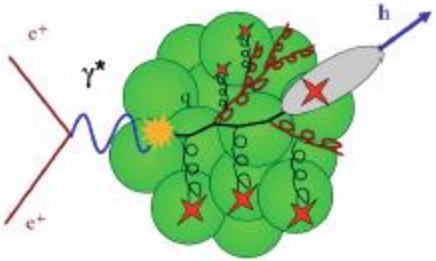

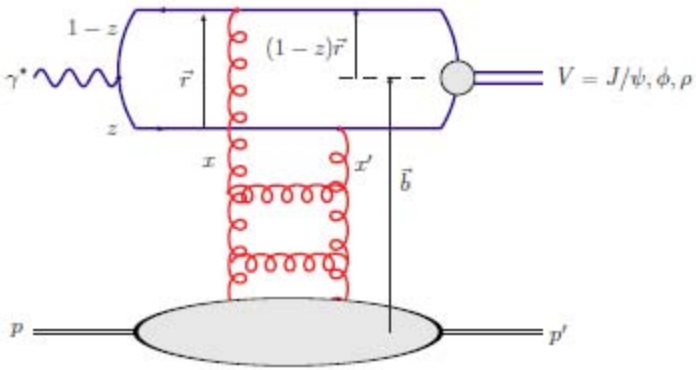

RHIC forward dAu program

Nuclear modification factor

$$R_{dAu} \equiv \frac{1}{\langle N_{coll} \rangle} \frac{d^2N^{d+Au}/dp_T d\eta}{d^2N^{p+p}_{inel}/dp_T d\eta}$$

PHENIX $|\eta| < 0.35$

PRL 98 (2007), 172302

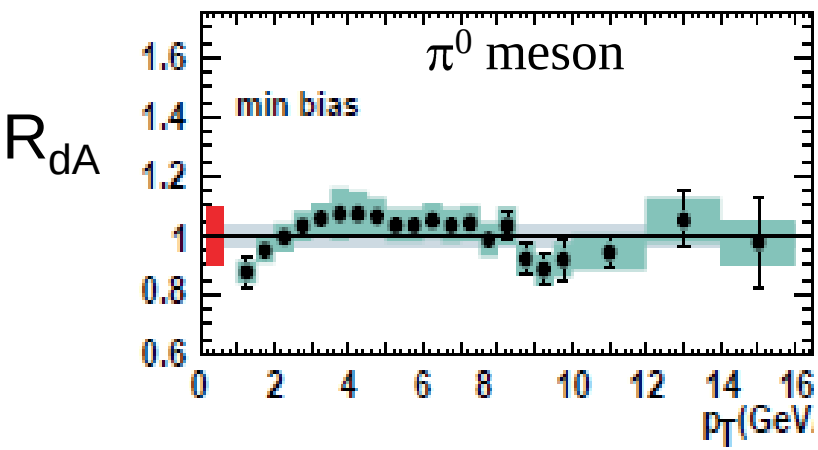

R_{dA} ~ 1 at mid rapidity

STAR, BRAHMS

Forward η

PRL 97 (2006), 152302

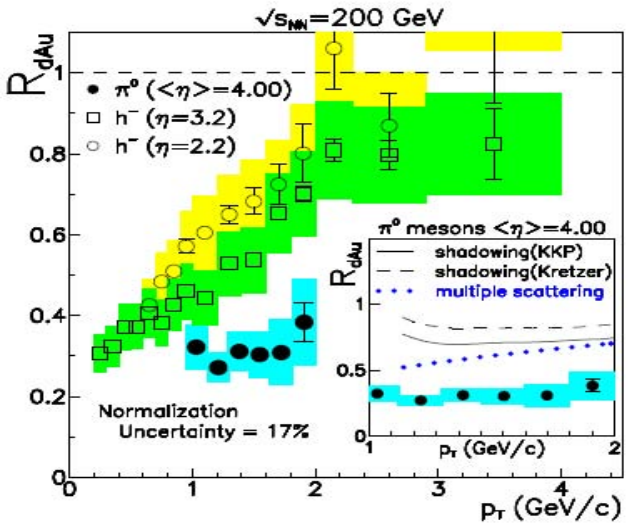

R_{dA}<1, Single hadron production suppressed at forward rapidity.

Cold Nuclear Matter (CNM) effect.

Probing small x region. $x_2 = \frac{M_T}{\sqrt{S}} e^{-y}$

Dihadron correlation at RHIC forward dAu program

Guzey, Strikman, Vogelsang, PL B603, 173

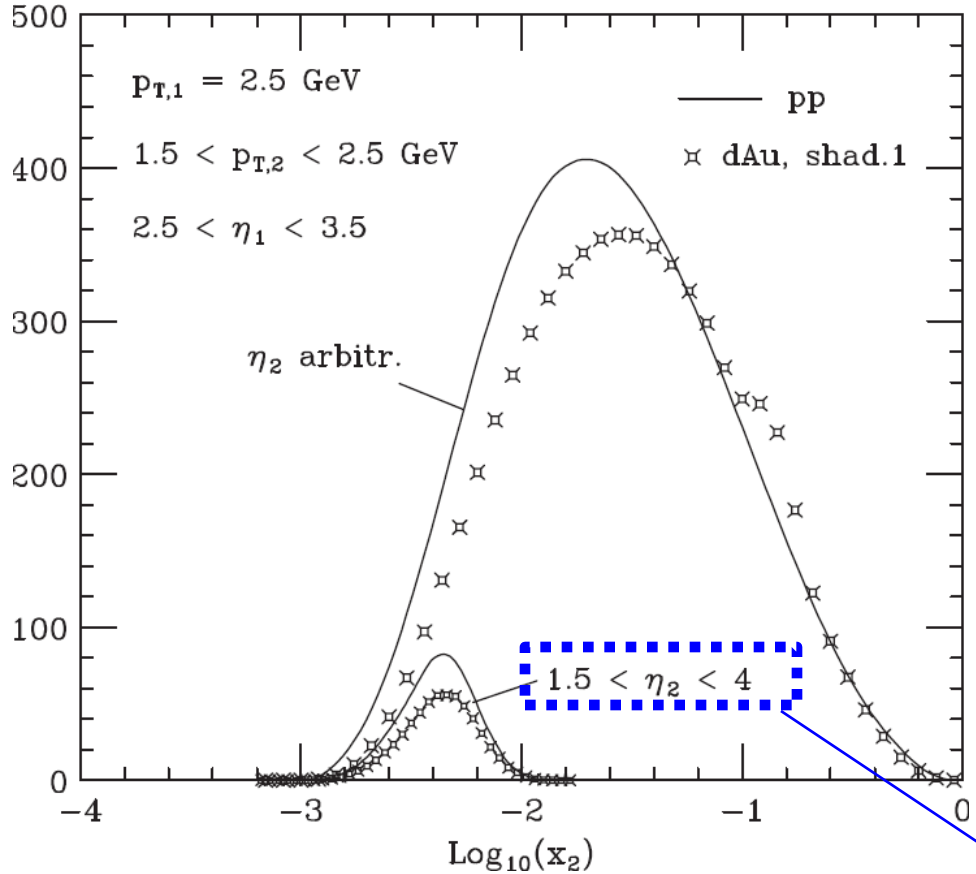

Eur.Phys.J.C43:427-435,2005

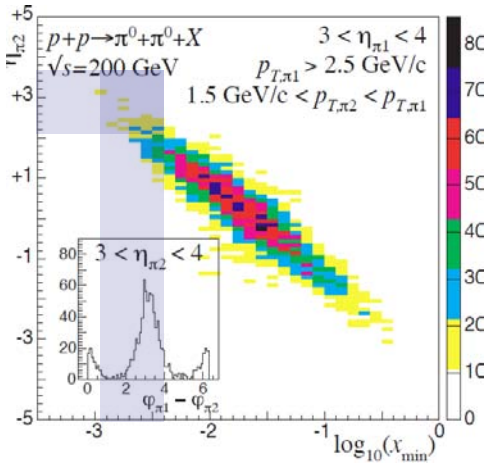

The rapidity of associate particle correlated with the x of struck gluon.

From the Pythia 2->2 process

Probably onset of saturation.

Constrain x range.

Approach to smaller mean x

Dihadron correlation measurement

CY (Conditional Yield)

$$CY = \frac{1}{N_{trig}} \frac{dN^{assoc}}{d\Delta\varphi}$$

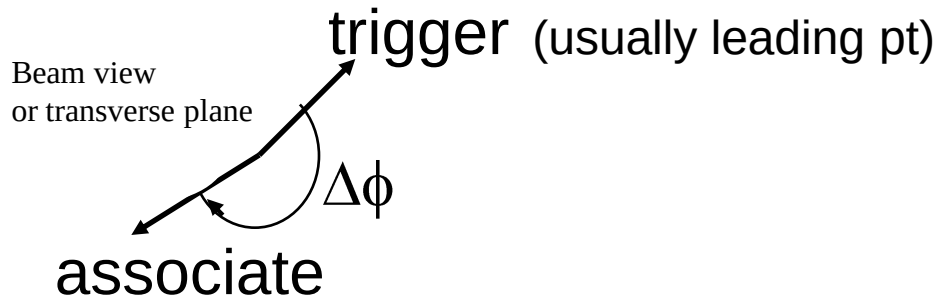

Phys. Rev. Lett. 91 072304

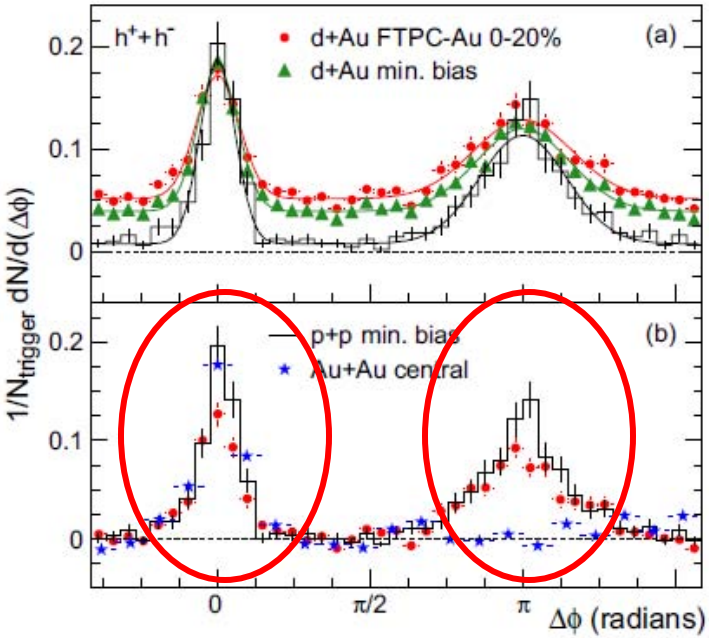

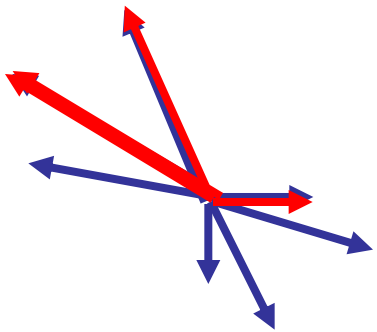

Nearside peak: delivers jet fragmentation information

Awayside peak: medium k_T kick both from initial and final state

pp dAu dihadron correlation are similar at mid rapidity, suppression in AuAu collision is dominated by final state interaction

Dihadron correlation measurement

$$J_{dA} = \frac{\sigma_{dA}^{pair}/\sigma_{dA}}{\langle N_{coll}\rangle\, \sigma_{pp}^{pair}/\sigma_{pp}}$$

Dihadron pair nuclear modification factor

$$J_{dA} = R_{dA}^{trig} \times I_{dA}$$

$$I_{dA} = \frac{CY_{dA}}{CY_{pp}}$$

PHENIX arXiv:1109.2133v1

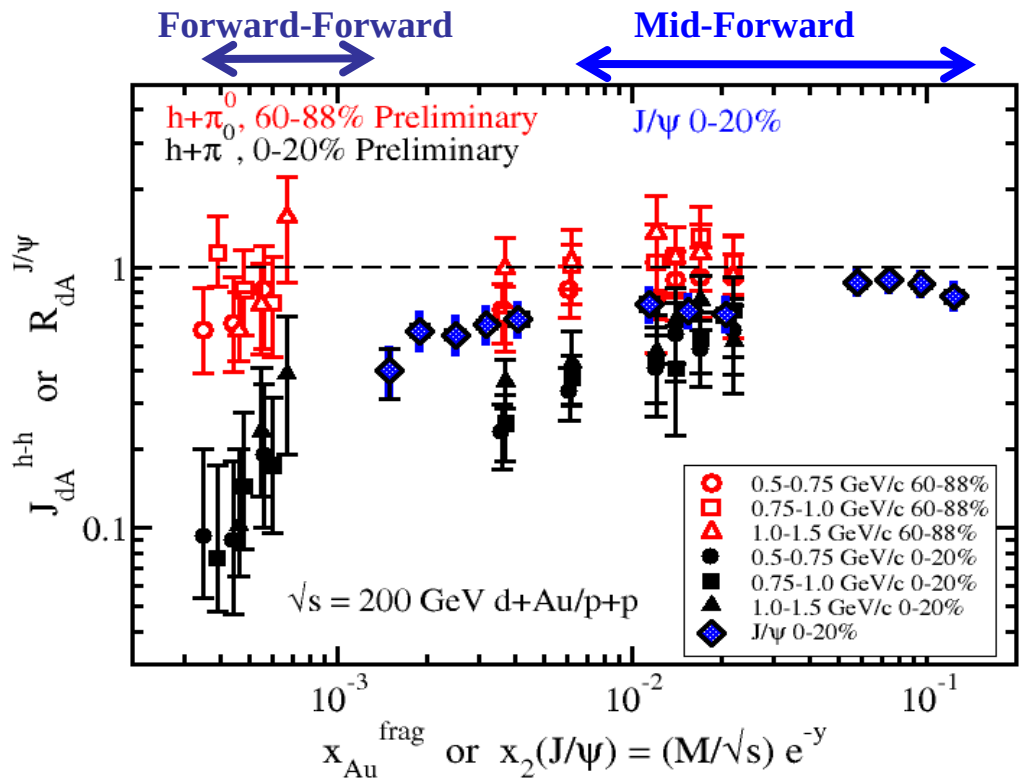

Dihadron correlation at RHIC forward dAu program

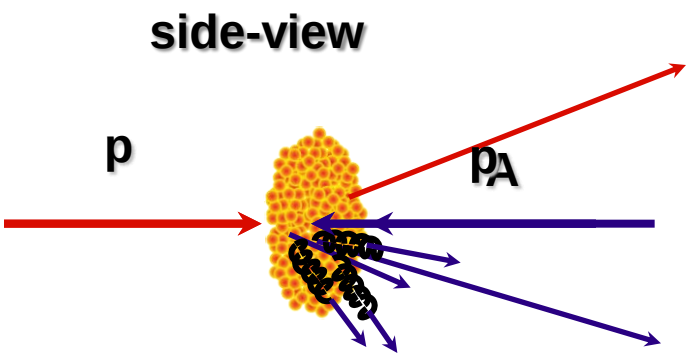

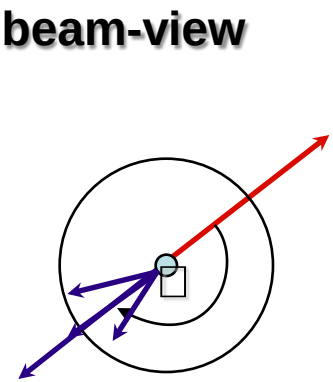

arXiv:1008.3989v1

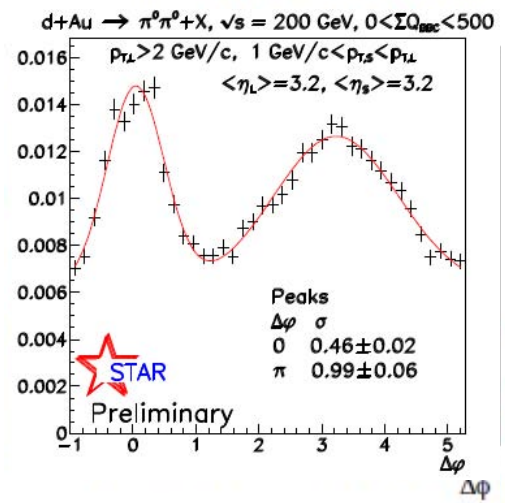

Low gluon density (pp):
pQCD predicts 2→2 process
⇒ back-to-back di-jet

High gluon density (pA):
2 → many process
⇒ expect broadening of away-side

Multiple emissions de-correlate the away side peak for forward-forward di-pion correlation.

Gluon densities saturate first in the center of the nucleus.

Dihadron correlation at RHIC forward dAu program

CGC model

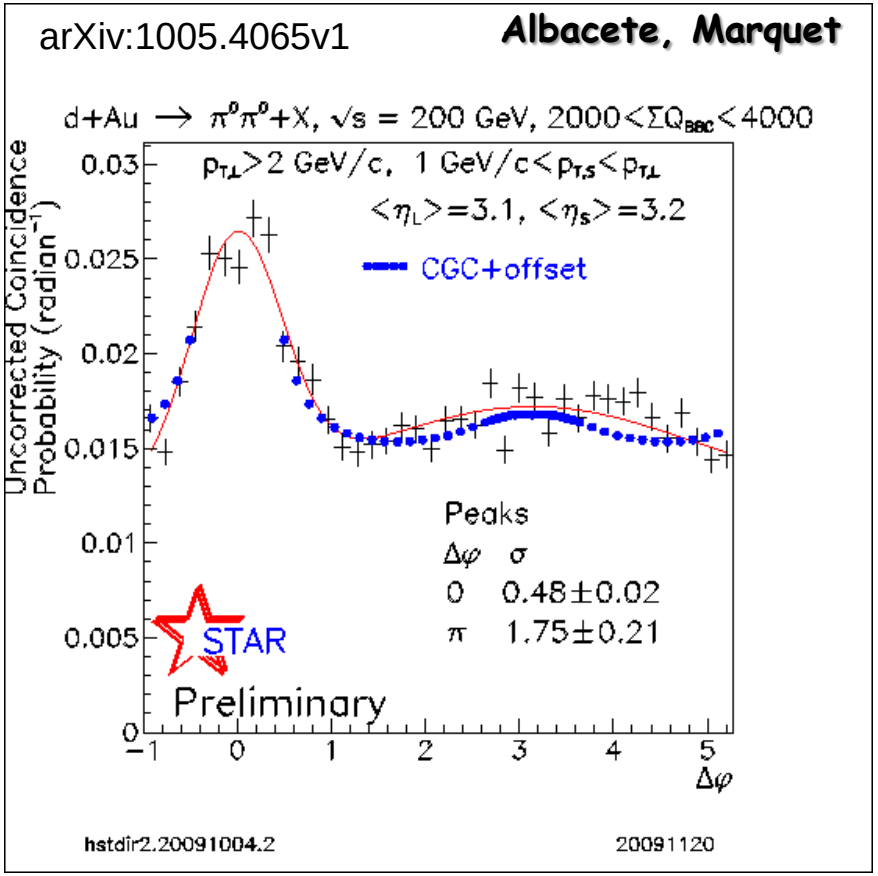

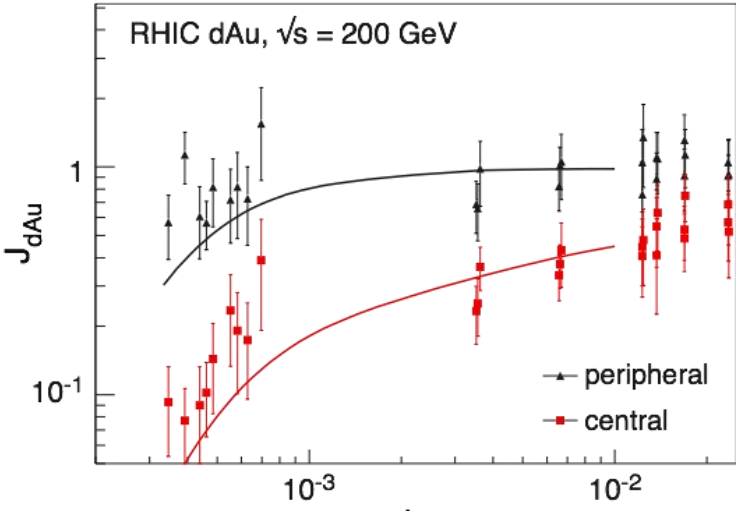

Bowen et al. 2012

Dihadron correlation at RHIC forward dAu program

Multiple parton interaction (Non CGC formalism)

Kang,Vitev,Xing, arXiv:1112.6021v1

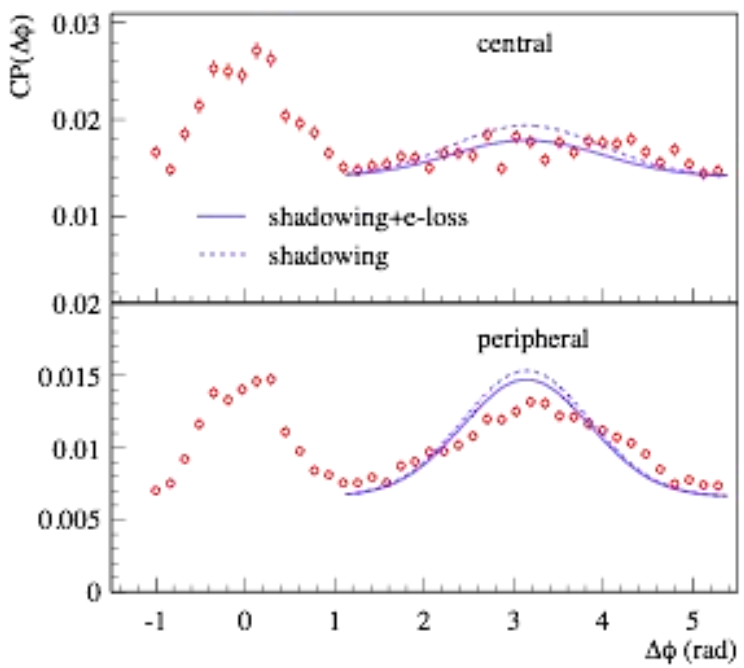

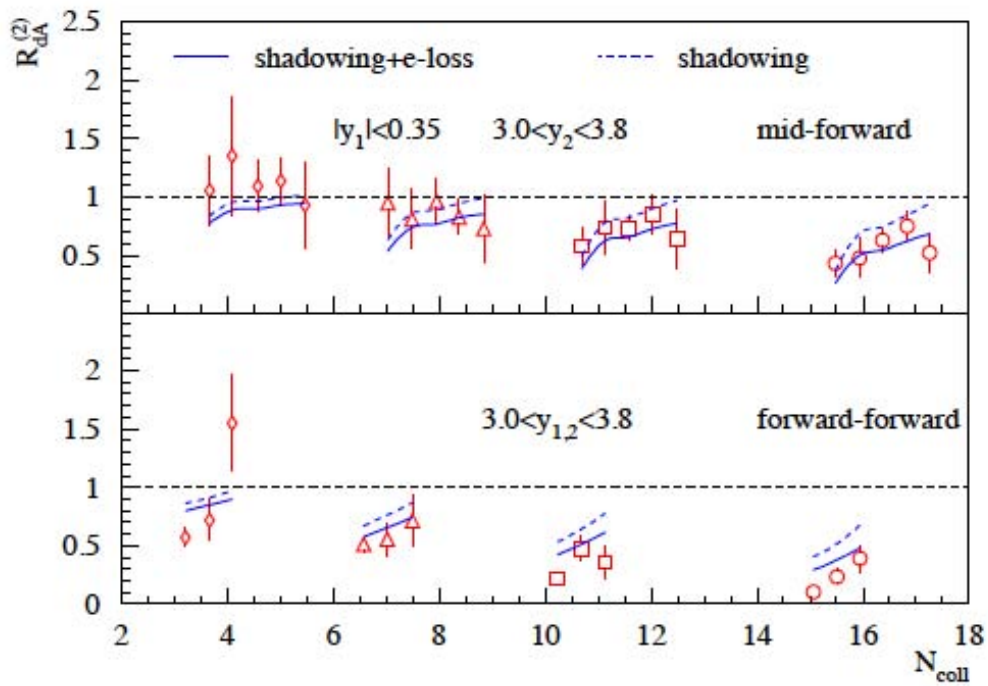

Dihadron correlation at eRHIC

EIC:

– Extract the spatial multi-gluon correlations and study their non-linear evolution

– Control final state

- essential for understanding the transition from a deconfined into a confined state.(in AA)

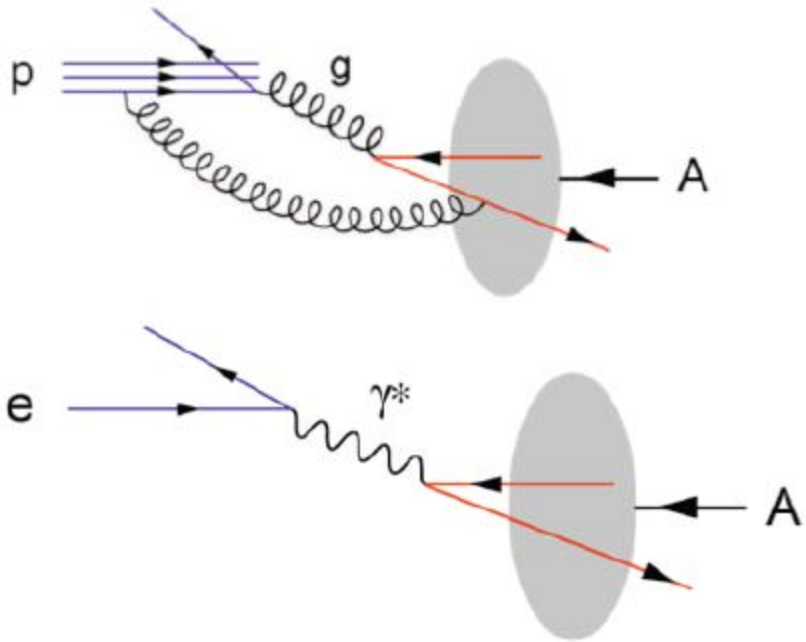

Advantage over p(d)A:

– eA experimentally much cleaner

- no “spectator” background to subtract

- Access to the exact kinematics of the DIS process (x, Q^2)

DIS kinematics

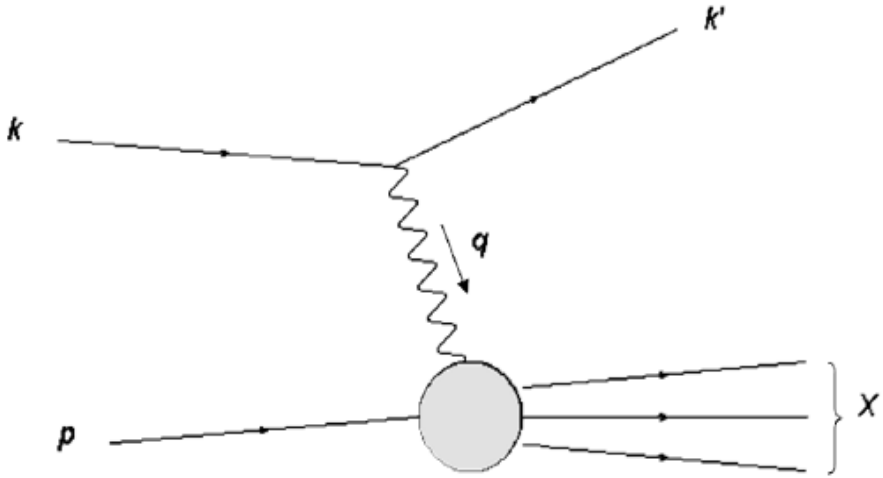

Event wise variables:

$$
\begin{aligned}
s &= (p+k)^2, \\
W^2 &= (p+q)^2, \\
Q^2 &= -q^2, \\
x &= \frac{Q^2}{2p\cdot q} = \frac{Q^2}{W^2+Q^2}, \\
y &= \frac{p\cdot q}{p\cdot k} = \frac{Q^2}{sx}, \\
\nu &= p\cdot q/M_p
\end{aligned}
$$

Particle wise variables:

p_T is defined with respect to virtual photon

$$z_h = \frac{p_h \cdot p}{q \cdot p}$$

theoretical prediction from CGC

Pocket formula: $Q_s^2(x) \sim A^{1/3}\left(\frac{1}{x}\right)^{\lambda} \sim \left(\frac{A}{x}\right)^{1/3}$

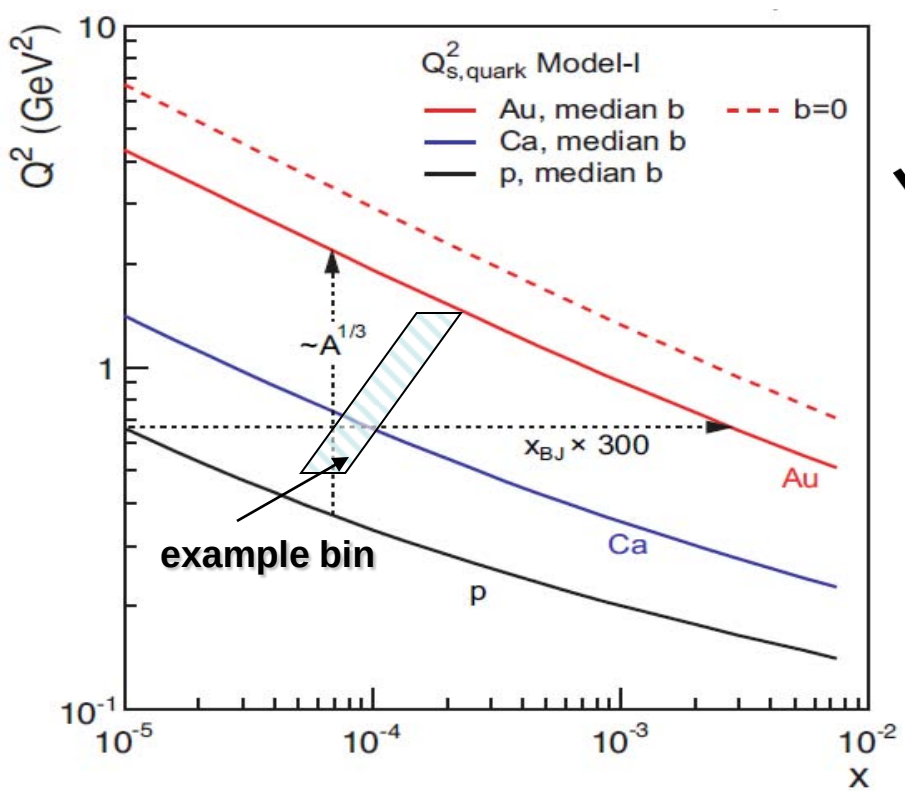

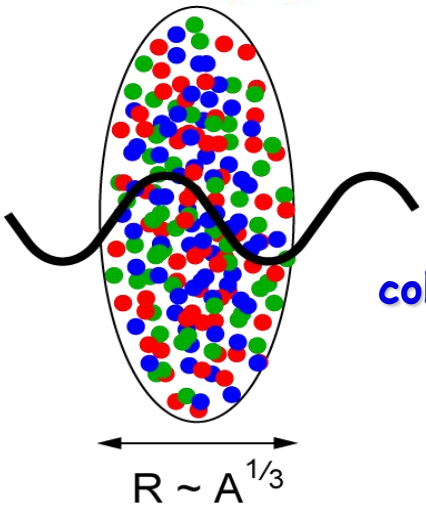

L ~ A$^{1/3}$

Probe interacts coherently with all nucleons

Bin:0.5<Q^2<1.5GeV^2, 0.6<y<0.8

<x>=1.01x10^{-4},

<y>=0.69,

<Q^2>=0.84GeV^2,

<W^2>=8322GeV^2,

<nu>=4434GeV

theoretical prediction from CGC

Bowen, Dominguez, Yuan 2011/2012

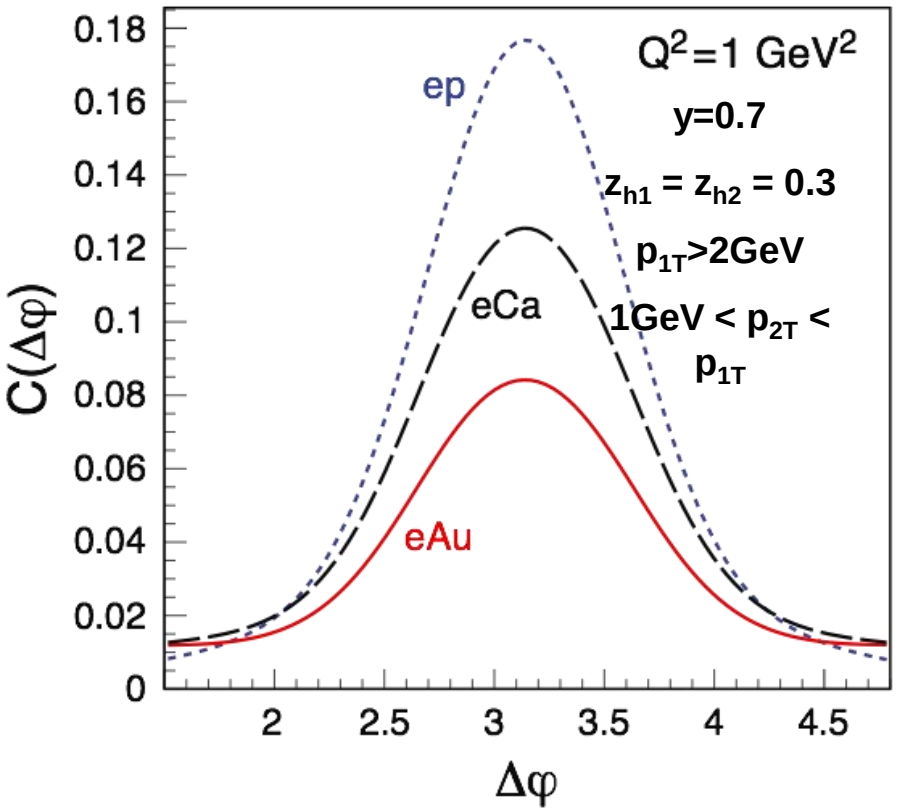

ep: $Q^2 > Q_s^2$, dilute system.

eAu: $Q^2 < Q_s^2$, dense system.

A factor ~ 2 suppression from ep to eAu at EIC energy.

Probing x range as low as 10^{-4}

Our Monte Carlo approach for the eA simulation

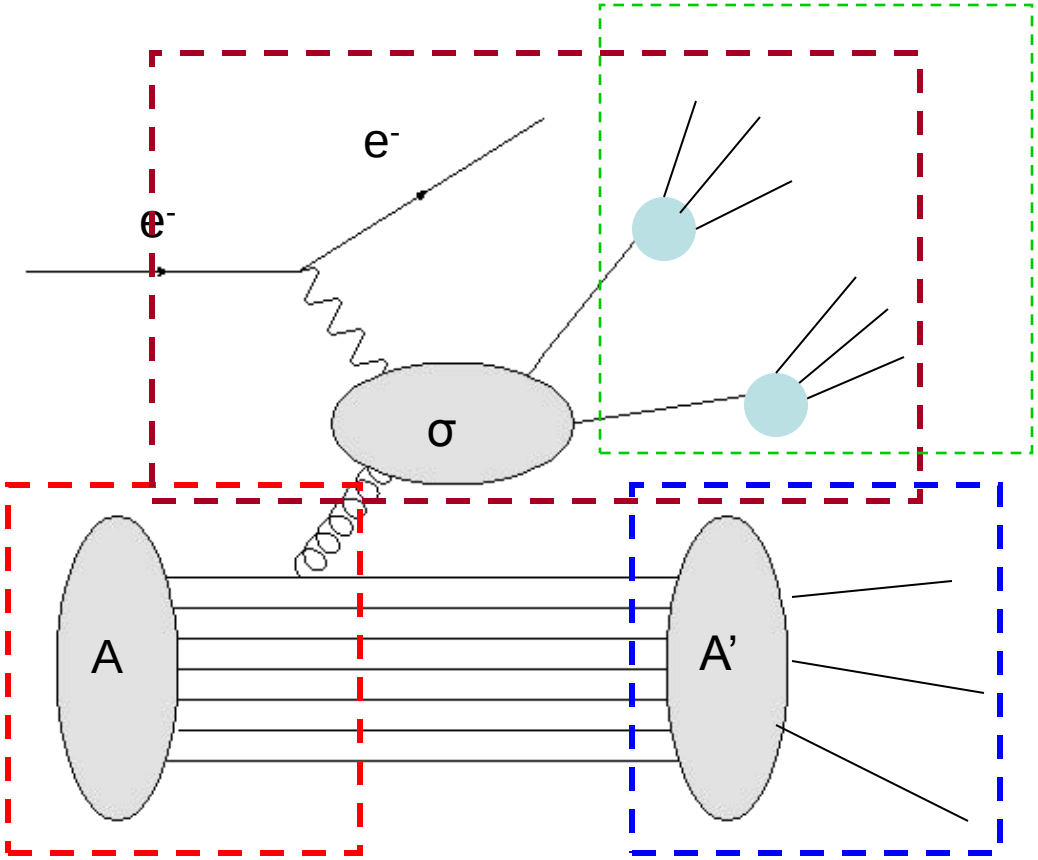

A hybrid model consisting of DPMJet and PYTHIA with nPDF EPS09.

Nuclear geometry by DPMJet and nPDF provided by EPS09.

Parton level interaction and jet fragmentation completed in PYTHIA.

Nuclear evaporation (gamma dexcitation/nuclear fission/fermi break up) treated by DPMJet

Energy loss effect from routine by Salgado&Wiedemann to simulate the nuclear fragmentation effect in cold nuclear matter (under development).

Dihadron correlation at eRHIC

PGF

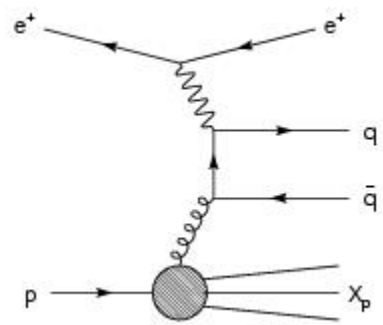

Resolved

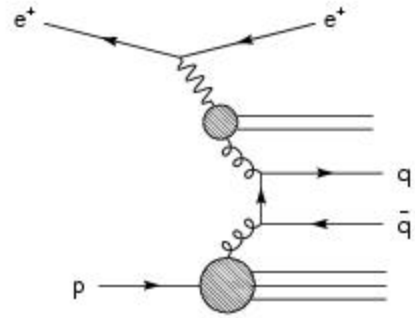

Dominant process: Photon Gluon Fusion (PGF), sensitive to the property of strong gluon field.

QCDC

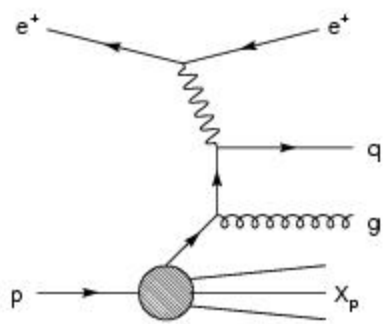

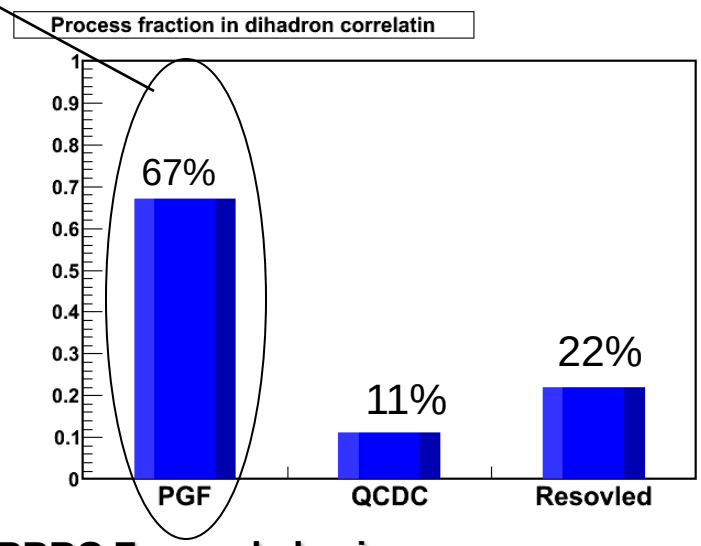

$Q^2=4GeV^2$

from PYTHIA simulation

Results for Q^2=1 GeV^2

Scattered electron pseudo-rapidity

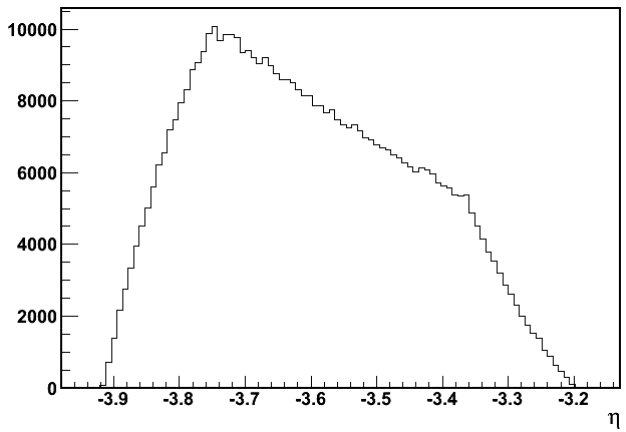

Leading particle span

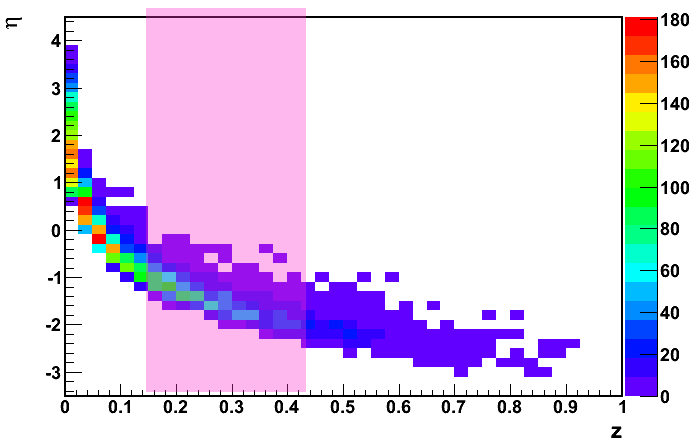

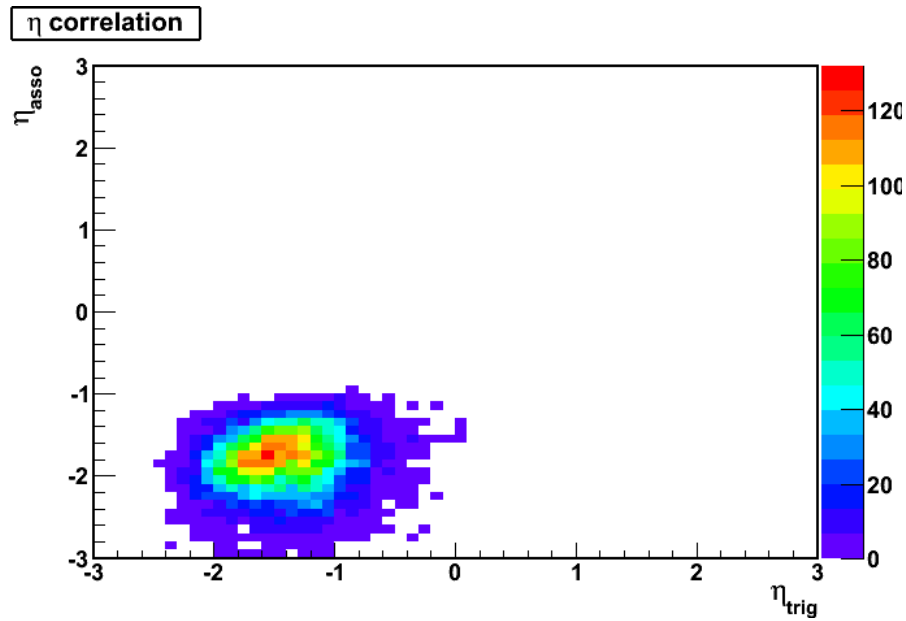

Trigger/associate particle cut:

$|\eta|<4$ ($2<\theta<178$ deg),

$p_T^{Trig}>2$, $1<p_T^{Asso}<2$

$0.15<z^{Trig,Asso}<0.45$

Results for Q^2=1 GeV^2

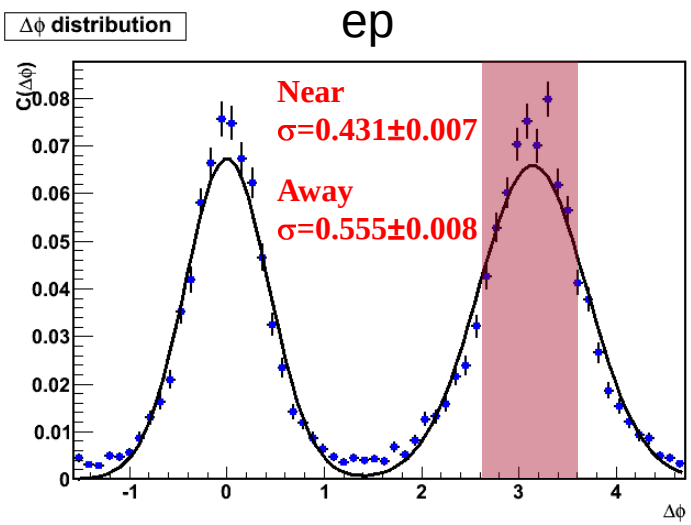

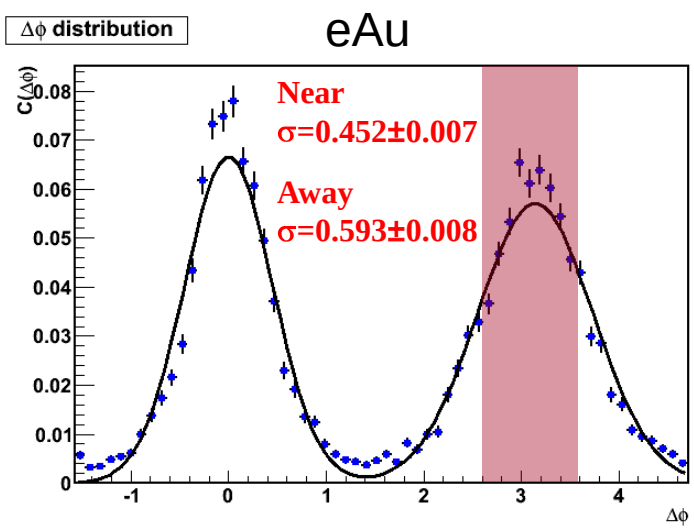

30+100 GeV 10M events

0.5<Q2<1.5, 0.6<y<0.8

|η|<4 (2<θ<178 deg),

p_T^{Trig}>2, 1<p_T^{Asso}<2

0.15<$z^{Trig,Asso}$<0.45

Nuclear PDF gives no strong suppression effect

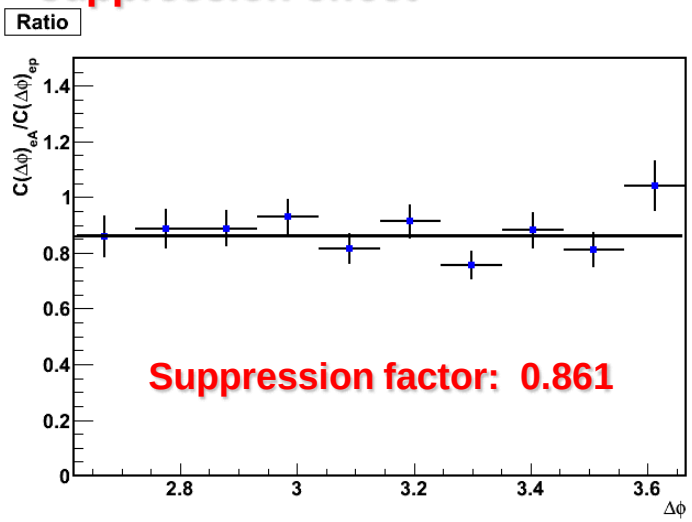

Compare with CGC prediction

EIC white paper

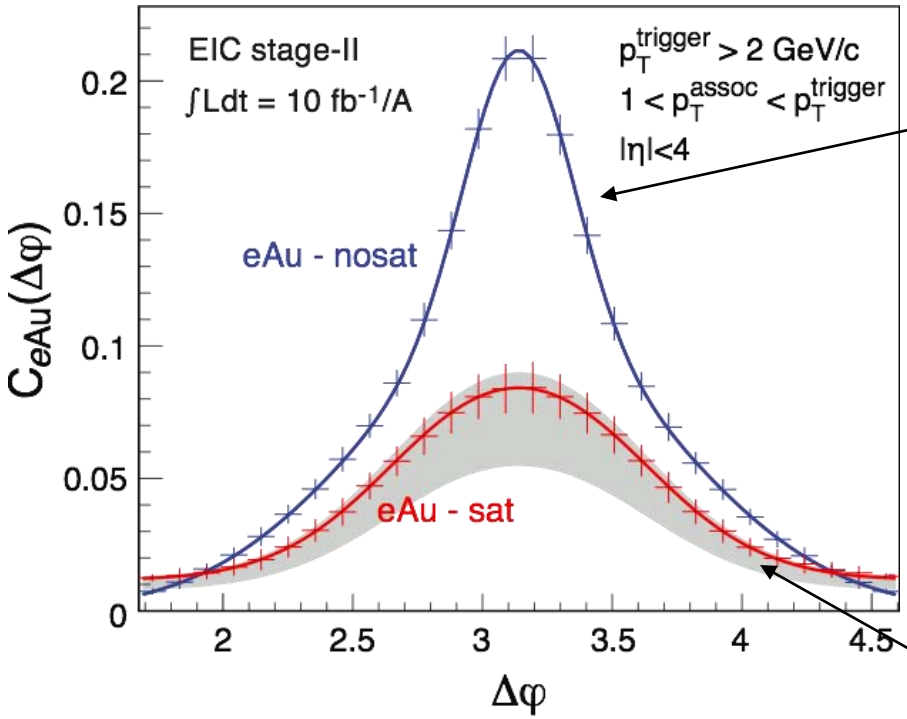

Results from our Monte Carlo, no saturation included.

A good discrimination of different models with a few months running.

Prediction from CGC calculation.

Compare with CGC prediction

Theoretical results from Bowen

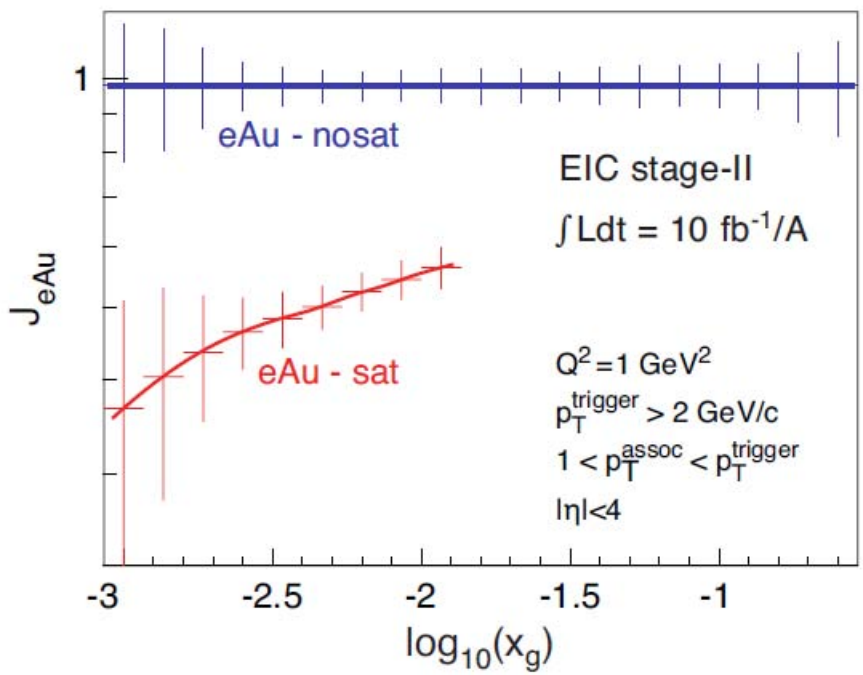

Similar to JdA we can define a JeA here.

$$J_{eA} = \frac{1}{A^{1/3}} \frac{\sigma_{eA}^{pair}/\sigma_{eA}}{\sigma_{ep}^{pair}/\sigma_{ep}}$$

The absence of nuclear effect would correspond to J_{eA}=1.

J_{eA} <1 would signify suppression of dihadron correlation.

Well controlled kinematics, pronounced signal between sat and non-sat.

The power of Monte Carlo

2 →2 back to back parton

Intrinsic k_T smears parton back to back correlation
Fragmentation p_T introduce p_T with respect to jet axis for hadrons.
Parton shower affects the parton p_T imbalance and the jet profile.
Medium energy loss effect

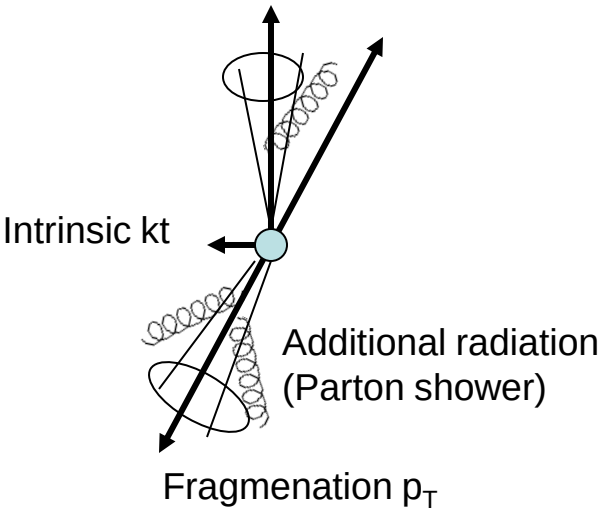

ep 30x100GeV	MC approach	Theoretical model
Intrinsic k_T	PARP(91)=0.4	$0.4<Q_s^2<0.6$ GeV^2
Fragmentation p_T	PARJ(21)=0.4	$<p_T^2>=0.2$ GeV^2
Parton shower	IS/FS	Not available

The power of Monte Carlo

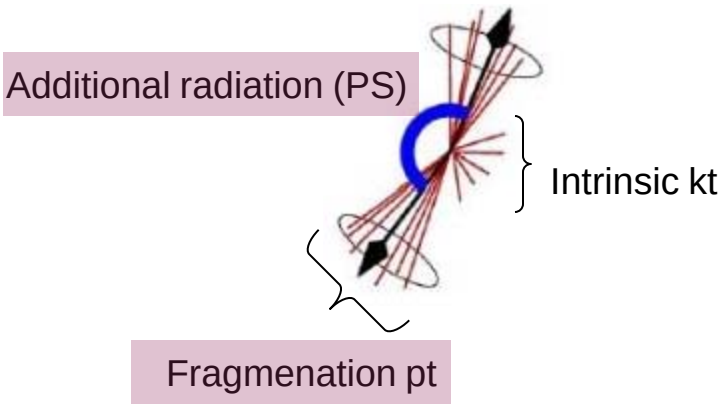

With only intrinsic kt, no fragmentation pt, no Parton Shower

MC side	Theory side
Intrinsic k_T = 0.4 GeV	**$0.4<Qs^2<0.6$ GeV^2**

ep 30x100GeV

MC cuts:

$3.5<Q^2<4.5$

$0.65<y<0.75$

pt trig>2GeV

$1<p_T$ asso$<p_T$ trig

$0.25<z1,z2<0.35$

Theoretical input:

$Q^2=4$

$y=0.7$

p_T trig>2GeV

$1<p_T$ asso$<p_T$ trig

$z1=z2=0.3$

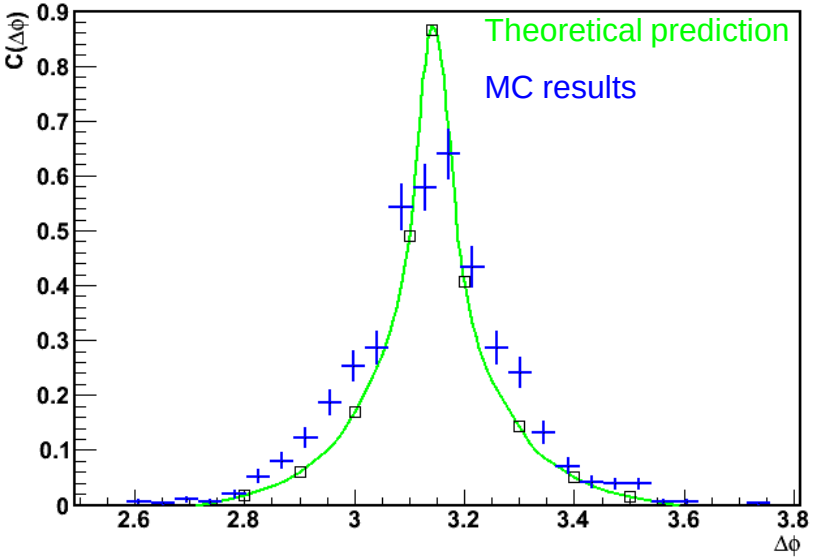

Theoretical curves from B.W.Xiao

The power of Monte Carlo

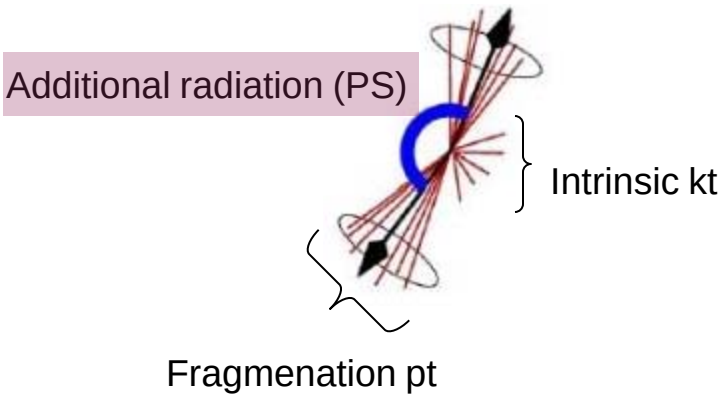

Intrinsic kt + fragmentation pt, no Parton Shower

MC side	Theory side
Intrinsic k_T = 0.4 GeV	**$0.4<Qs^2<0.6$ GeV^2**
Frag p_T = 0.4 GeV	**$<p_T^2>$ = 0.2 GeV^2**

Seeing the fact that we have different treatment to PDF and fragmentation process, we have come to an agreement in ep for these two approaches.

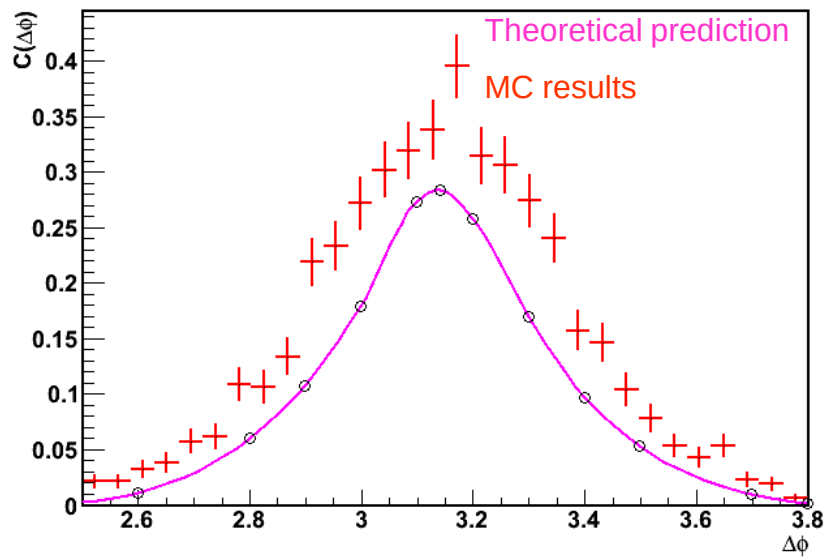

Theoretical curves from B.W.Xiao

The power of Monte Carlo

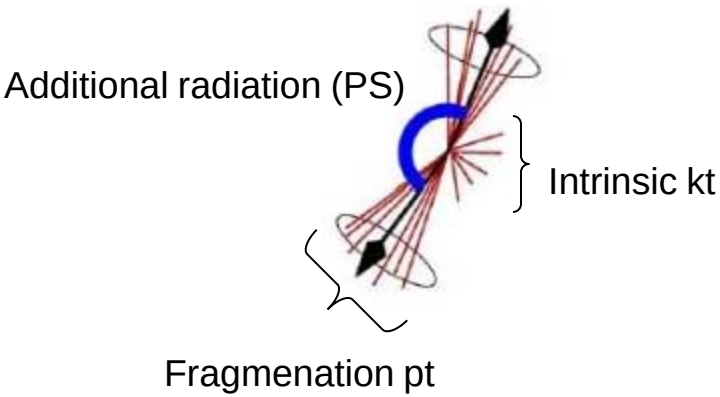

Intrinsic kt + fragmentation pt, with Parton Shower on

MC side	Theory side
Intrinsic k_T = 0.4 GeV **Frag p_T = 0.4 GeV** **Parton shower on**	**$0.4<Qs^2<0.6$ GeV^2** **$<p_T^2>$ = 0.2 GeV^2**

As parton shower in MC can be used as a good way to compensate the theory results.
Stretch the theoretical curve of eAu based on the PS effect on ep.

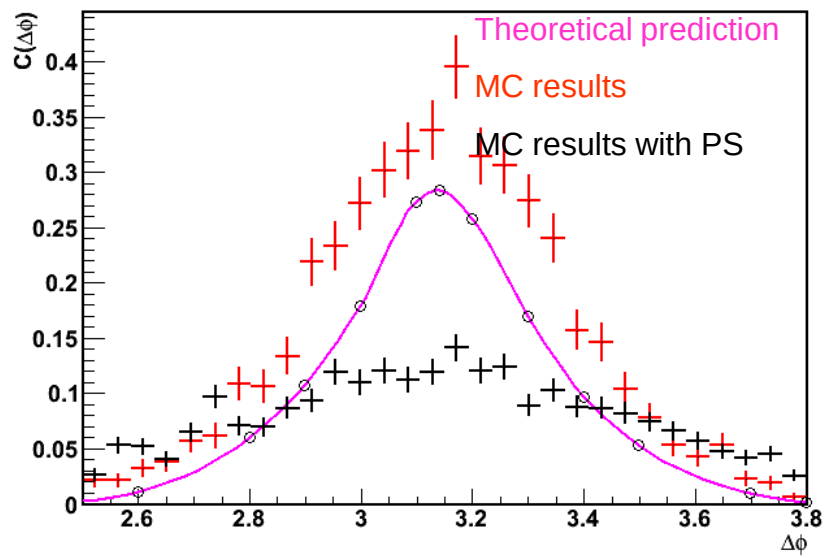

Theoretical curves from B.W.Xiao

Energy loss effect under development

Possible to include some final energy loss effect.
According to PyQM developed by Raphael.
The probability for a parton to loose energy ΔE is given by

$$P(\Delta E) = \sum_{n=0}^{\infty} \frac{1}{n!} \left[\prod_{i=1}^{n} \int d\omega_i \frac{dI(\omega_i)}{d\omega} \right] \times \left(\Delta E - \sum_{i=1}^{n} \omega_i \right) \exp\left[-\int d\omega \frac{dI}{d\omega} \right]$$

$$= p_0\, \delta(\Delta E) + p(\Delta E)$$

Salgado & Wiedemann PRD 68, 014008 (2003)

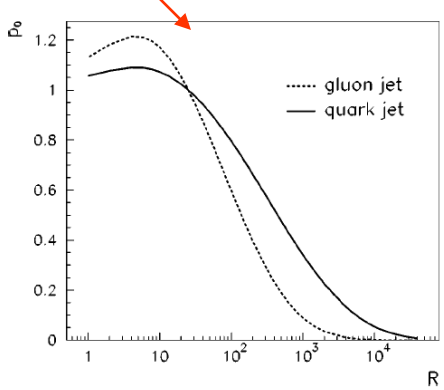

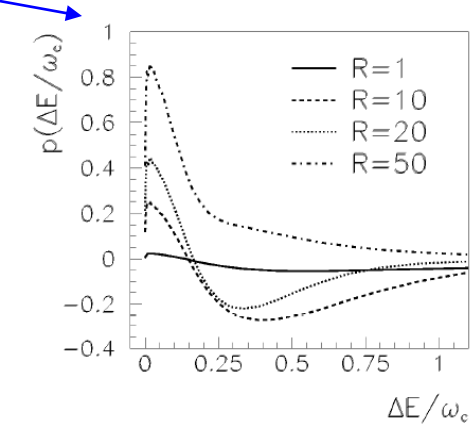

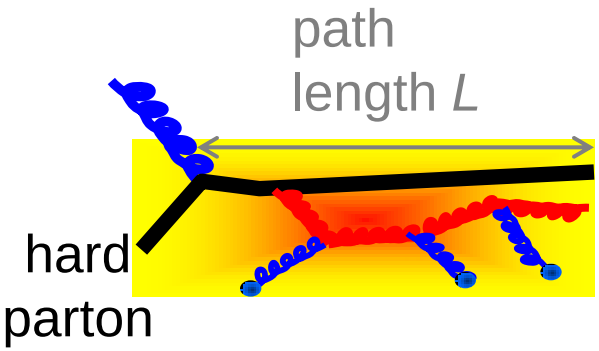

This radiation spectrum usually depends on the length of medium L, and the transport coefficient

$$\hat{q} = \langle k_t^2 \rangle_{\text{medium}} / \lambda$$

Energy loss effect under development

Comparison with Hermes data
27.6 GeV eXe vs eD

$$R_A^h(Q^2,\nu,z_h,P_\perp^2) = \frac{N_A^h(Q^2,\nu,z_h,P_\perp^2)/N_A^e(Q^2,\nu)}{N_D^h(Q^2,\nu,z_h,P_\perp^2)/N_D^e(Q^2,\nu)}$$

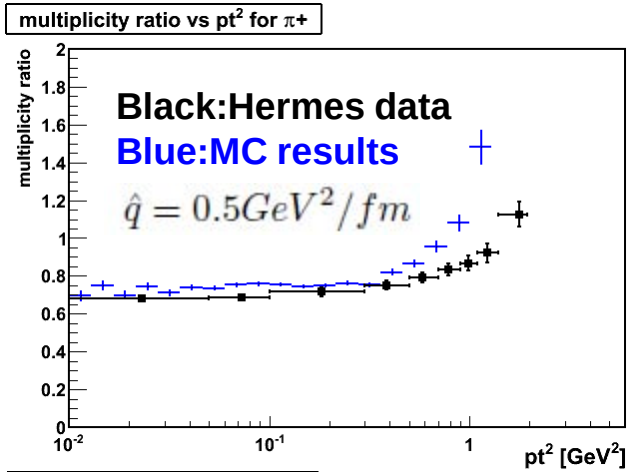

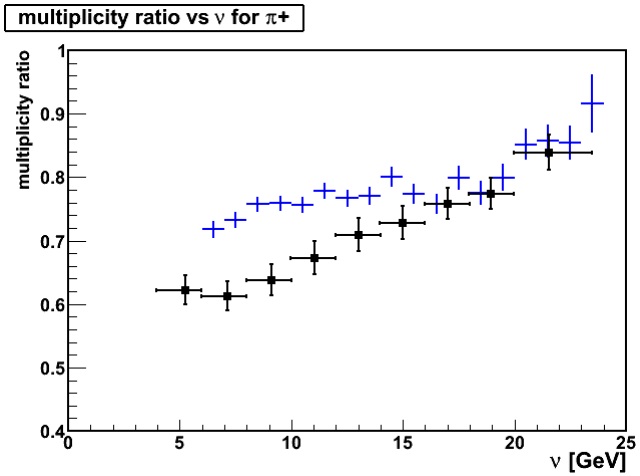

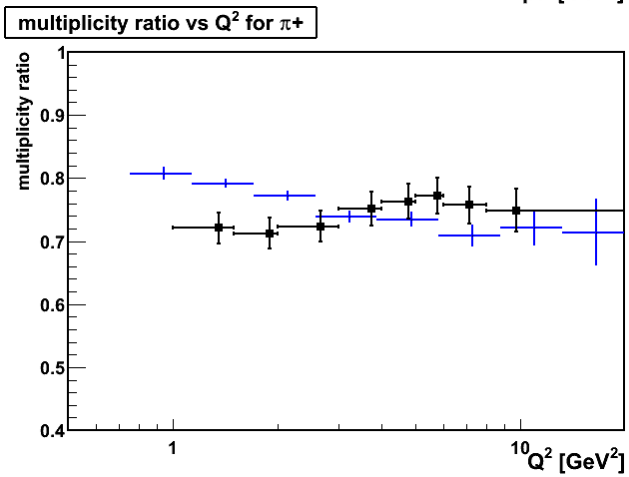

Summary & Prospects

- Dihadron correlation is a very important measurement in the future eRHIC eA program.
- A generic Monte Carlo generator design based on pQCD calculation in the vacuum with flexible nuclear effects added on.
- Energy loss effect in cold nuclear medium to be included in this Monte Carlo.
- Can be utilized to understand dA or pA data and extract the model parameters as an input in our eAu simulation.

Thank you for your attention

Forward Physics at RHIC

July 30 – August 1, 2012
Small Seminar Room, Physics Department

Monday July 30

08:30 - 09:00		*Registration*
09:00 - 09:45	Mark Strikman	Looking Forward in pA@ LHC
09:45 - 10:30	Javier Albacete	Testing the CGC with RHIC Forward Data
10:30 - 11:00		*Coffee Break*
11:00 - 11:45	Yuri Kovchegov	Putting Spin on Color Glass
11:45 - 12:30	Zhongbo Kang	Sivers Effect of Drell-Yan Production in Small-x Regime
12:30 - 01:30		*Lunch Break*
01:30 - 02:15	Kevin Dusling	Long Range Rapidity Correlations in pp, pA and AA Collisions
02:15 - 03:00	Xuan Li	Forward Di-hadron Correlations at STAR
03:00 - 03:30		*Coffee Break*
03:30 - 04:15	Jamal Jalilian-Marian	Probing High Energy QCD via Di-hadron Correlations
04:15 - 05:00	Kirill Tuchin	Cold Nuclear Matter Effects on Heavy Quark Production

Tuesday July 31

09:00 - 09:45	Wolfram Fischer	RHIC Upgrades
09:45 - 10:30	David d'Enterria	Forward Physics at the LHC
10:30 - 11:00		*Coffee Break*
11:00 - 11:45	Matthias Grosse-Perdekamp	Low x Physics with a Future Forward Upgrade of sPHENIX
11:45 - 12:30	Liang Zheng	Dihadron Correlations at eRHIC and Monte Carlo Development
12:30 - 01:30		*Lunch Break*
01:30 - 02:15	Francesca Giordano	Spin Measurements at PHENIX and Future Plans
02:15 - 03:00	Ted Rogers	QCD Evolution of TMD PDFs
03:00 - 03:30		*Coffee Break*
03:30 - 04:15	Tom Burton	The STAR Transverse Spin Programme: Present and Future
04:15 - 05:00	Jianwei Qiu	Transverse Single-spin Asymmetry in pA Collisions

Wednesday August 1

09:00 - 09:45	Marco Stratmann	Nuclear Parton Densities - Status & Future Avenues
09:45 - 10:30	Yuji Koike	Single Transverse Spin Asymmetry in the Forward and Backward Directions
10:30 - 11:00		*Coffee Break*
11:00 - 11:45	Matt Lamont	EIC e+A Science Programme
11:45 - 12:30	Leonard Gamberg	Sivers and Collins Effect: Single Spin Asymmetries in Photon Production
12:30 - 01:30		*Lunch Break*
01:30 - 02:15	IhnJea Choi	Sivers Asymmetries in Polarized Drell-Yan Production of Muon Pairs at COMPASS
02:15 - 03:00	Jin Huang	Transverse Spin Physics at Jefferson Lab
03:00 - 03:30		*Coffee Break*
03:30 - 04:15	Salvatore Fazio	Opportunities for ep Physics at an eRHIC
04:15 - 05:00	Andrzej Sandacz	COMPASS Transverse Spin Physics Program and Plans for GPD Measurements

Back to Contents

Forward Physics at RHIC

July 30 – August 1, 2012

List of Registered Participants

Name	Affiliation	E-Mail Address
Javier (Lopez) Albacete	IPN IN2P3 CNRS	javier.lopez-albacete@cea.fr
Yasuyuki Akiba	RIKEN	akiba@bnl.gov
Kenneth Barish	UC Riverside	Kenneth.Barish@ucr.edu
Stefan Bathe	Baruch / BNL	stefan.bathe@baruch.cuny.edu
Kieran Boyle	BNL	kboyle@bnl.gov
Thomas Burton	BNL	tpb@bnl.gov
IhnJea Choi	University of Illinois	ijchoi@illinois.edu
William Christie	BNL	christie@bnl.gov
Cesar DaSilva	LANL	slash@rcf.rhic.bnl.gov
David d'Enterria	CERN	dde@cern.ch
Kevin Dusling	North Carolina State University	kein_dusling@ncsu.edu
Oleg Eyser	BNL	keyser@bnl.gov
Salvatore Fazio	BNL	sfazio@bnl.gov
Wolfram Fischer	BNL	wfischer@bnl.gov
Leonard Gamberg	Penn State University	lpg10@psu.edu
Francesca Giordano	University of Illinois	fgiord@illinois.edu
Yuji Goto	RIKEN	goto@bnl.gov
Matthias Grosse Perdekamp	University of Illinois	mgp@illinois.edu
Wlodek Guryn	BNL	guryn@bnl.gov
Martin Hentschinski	BNL	hentsch@bnl.gov
Jin Huang	LANL	jhuang@bnl.gov
Jamal Jalilian-Marian	Baruch College	jamal.jalilian-marian@baruch.cuny.edu
Zhongbo Kang	LANL	zkang@quark.phy.bnl.gov
Yuji Koike	Niigata University	koike@nt.sc.niigata-u.ac.jp
Yuri Kovchegov	The Ohio State University	kovchegov.1@asc.ohio-state.edu
Matt Lamont	BNL	macl@bnl.gov
Kwangbok Lee	LANL	kwangboklee1@gmail.com
Angela Leroux-Lindsey	NYU	all13@nyu.edu
Xuan Li	Temple University	xuanli@bnl.gov
Ming Liu	LANL	ming@bnl.gov
Yan-Qing Ma	BNL	yqma@bnl.gov
Andrew Manion	Stony Brook University	Andrew.Manion@stonybrook.edu
Mriganka Mouli Mondal	Texas A&M University	mriganka@rcf.rhic.bnl.gov
Itaru Nakagawa	RIKEN	itaru@bnl.gov
Akio Ogawa	BNL	akio@bnl.gov
Kensuke Okada	RBRC	okada@bnl.gov
Jianwei Qiu	BNL	jqiu@bnl.gov
Ted Rogers	Stony Brook University	tedconantrogers@gmail.com
Takao Sakaguchi	BNL	takao@bnl.gov

Back to Contents

Forward Physics at RHIC

July 30 – August 1, 2012

List of Registered Participants

Name	Affiliation	E-Mail Address
Andrzej Sandacz	Natn'l Centre for Nuclear Res, Warsaw	sandacz@fuw.edu.pl
Joseph Seele	RBRC	seele@bnl.gov
Ralf Seidl	RIKEN	rseidl@riken.jp
Richard Seto	UC Riverside	richard.seto@ucr.edu
Prashanth Shanmuganathan	Kent State University	sprashan@kent.edu
Ernst Sichtermann	Lawrence Berkeley National Lab	EPSichtermann@lbl.gov
Paul Stankus	Oak Ridge National Laboratory	paul.w.stankus@gmail.com
Marco Stratmann	BNL	marco@bnl.gov
Mark Strikman	Penn State University	strikman@phys.psu.edu
Bernd Surrow	Temple University	surrow@temple.edu
Rusty Towell	Abilene Christian University	rusty.towell@acu.edu
Larry Trueman	BNL (Retired)	trueman@bnl.gov
Kirill Tuchin	Iowa State University	tuchink@gmail.com
Raju Venugopalan	BNL	raju@bnl.gov
Flemming Videbaek	BNL	videbaek@bnl.gov
Anselm Vossen	Indiana University/CEEM	agvossen@gmail.com
Jiang Xiaodong	Los Alamos National Laboratory	xjiang@bnl.gov
Liang Zheng	BNL	liangzhphy@gmail.com

Back to Contents

RBRC Workshop Proceedings

Volume 110 – P- and CP-odd Effects in Hot and Dense Matter, June 25-27, 2012 – BNL-98398-2012
Volume 109 – New Horizons for Lattice Computations with Chiral Fermions, May 14-18, 2012 – BNL-98392-2012
Volume 108 – Hyperon-Hyperon Interactions and Searches for Exotic Di-Hyperons in Nuclear Collisions, February 29 – March 2, 2012 – BNL-97035-2012
Volume 107 – Future Directions in High Energy QCD, October 20-22, 2011 – BNL-98119-2011
Volume 106 – Fluctuations, Correlations and RHIC Low Energy Runs, October 3-5, 2011 – BNL-96514-2011
Volume 105 – Opportunities for Polarized He-3 in RHIC and EIC, September 28-30, 2011 – BNL-96418-2011
Volume 104 – Brookhaven Summer Program on Quarkonium Production in Elementary and Heavy Ion Collisions, June 6-18, 2011 – BNL-96171-2011
Volume 103 – Opportunities for Drell-Yan Physics at RHIC, May 11-13, 2011 – BNL-95236-2011-2011
Volume 102 – Initial State Fluctuations and Final-State Particle Correlations, February 2-4, 2011 – BNL-94704-2011
Volume 101 – RBRC Scientific Review Committee Meeting, October 27-29, 2010 – BNL-94589-2011
Volume 100 – Summer Program on Nucleon Spin Physics, July 14-27, 2010 – BNL-96163-2011
Volume 99 – The Physics of W and Z Bosons, June 24-25, 2010 – BNL-94287-2010
Volume 98 – Saturation, the Color Glass Condensate and the Glasma: What Have we Learned from RHIC? – May 10-12, 2010 – BNL-94271-2010
Volume 97 – RBRC Scientific Review Committee Meeting, October 21-22, 2009 – BNL-90674-2009
Volume 96 – P- and CP-Odd Effects in Hot and Dense Matter, April 26-30, 2010 – BNL-94237-2010
Volume 95 – Progress in High-pT Physics at RHIC, March 17-19, 2010 – BNL-94214-2010
Volume 94 – Summer Program on Nucleon Spin Physics at LBL, June 1-12, 2009
Volume 93 – PHENIX Spinfest School 2009 at BNL - July 1-31, 2009. BNL-90343-2009
Link: PHENIXSpinfestSchool2009@BNL
Volume 92 – PKU-RBRC Workshop on Transverse Spin Physics, June 30 - July 4, 2008, Beijing, China – BNL-81685-2008
Volume 91 – RBRC Scientific Review Committee Meeting, November 17-18, 2008 – BNL-81556-2008
Volume 90 – PHENIX Spinfest School 2008 at BNL, August 4-8, 2008 – BNL-81478-2008
Volume 89 – Understanding QGP through Spectral Functions and Euclidean Correlators, April 23-25, 2008 – BNL-81318-2008
Volume 88 – Hydrodynamics in Heavy Ion Collisions and QCD Equation of State, April 21-22, 2008 – BNL-81307-2008
Volume 87 – RBRC Scientific Review Committee Meeting, November 5-6, 2007 – BNL-79570-2007
Volume 86 – Global Analysis of Polarized Parton Distributions in the RHIC Era, October 8, 2007 – BNL-79457-2007
Volume 85 – Parity-Violating Spin Asymmetries at RHIC-BNL, April 26-27, 2007 – BNL-79146-2007
Volume 84 – Domain Wall Fermions at Ten Years, March 15-17, 2007 – BNL 77857-2007
Volume 83 – QCD in Extreme Conditions, July 31 - August 2, 2006 – BNL-76933-2006
Volume 82 – RHIC Physics in the Context of the Standard Model, June 18-23, 2006 – BNL-76863-2006
Volume 81 – Parton Orbital Angular Momentum (Joint RBRC/University of New Mexico Workshop) February 24-26, 2006 – BNL-75937-2006
Volume 80 – Can We Discover the QCD Critical Point at RHIC?, March 9-10, 2006 – BNL-75692-2006
Volume 79 – Strangeness in Collisions, February 16-17, 2006 – BNL-79763-2008
Volume 78 – Heavy Flavor Productions and Hot/Dense Quark Matter, December 12-14, 2005 – BNL-76915-2006
Volume 77 – RBRC Scientific Review Committee Meeting, October 10-12, 2005 – BNL-52649-2005
Volume 76 – Odderon Searches at RHIC, September 27-29, 2005 – BNL-75092-2005
Volume 75 – Single Spin Asymmetries, June 1-3, 2005 – BNL-74717-2005
Volume 74 – RBRC QCDOC Computer Dedication and Symposium on RBRC QCDOC, May 26, 2005 – BNL-74813-2005
Volume 73 – Jet Correlations at RHIC, March 10-11, 2005 – BNL-73910-2005
Volume 72 – RHIC Spin Collaboration Meetings XXXI (January 14, 2005), XXXII (February 10, 2005), XXXIII (March 11, 2005) – BNL-73866-2005
Volume 71 – Classical and Quantum Aspects of the Color Glass Condensate – BNL-73793-2005
Volume 70 – Strongly Coupled Plasmas: Electromagnetic, Nuclear & Atomic – BNL-73867-2005
Volume 69 – RBRC Scientific Review Committee – BNL-73546-2004
Volume 68 – Workshop on the Physics Programme of the RBRC and UKQCD QCDOC Machines – BNL-73604-2004
Volume 67 – High Performance Computing with BlueGene/L and QCDOC Architectures
Volume 66 – RHIC Spin Collaboration Meeting XXIX, October 8-9, 2004, Torino Italy – BNL-73534-2004
Volume 65 – RHIC Spin Collaboration Meetings XXVII (July 22, 2004), XXVIII (September 2, 2004), XXX (December 6, 2004) – BNL-73506-2004

Back to Contents

Volume 64 – Theory Summer Program on RHIC Physics – BNL-73263-2004
Volume 63 – RHIC Spin Collaboration Meetings XXIV (May 21, 2004), XXV (May 27, 2004), XXVI (June 1, 2004) – BNL-72397-2004
Volume 62 – New Discoveries at RHIC, May 14-15, 2004 – BNL- 72391-2004
Volume 61 – RIKEN-TODAI Mini Workshop on "Topics in Hadron Physics at RHIC", March 23-24, 2004 – BNL-72336-2004
Volume 60 – Lattice QCD at Finite Temperature and Density – BNL–72083-2004
Volume 59 – RHIC Spin Collaboration Meeting XXI (January 22, 2004), XXII (February 27, 2004), XXIII (March 19, 2004)– BNL-72382-2004
Volume 58 – RHIC Spin Collaboration Meeting XX – BNL-71900-2004
Volume 57 – High pt Physics at RHIC, December 2-6, 2003 – BNL-72069-2004
Volume 56 – RBRC Scientific Review Committee Meeting – BNL-71899-2003
Volume 55 – Collective Flow and QGP Properties – BNL-71898-2003
Volume 54 – RHIC Spin Collaboration Meetings XVII, XVIII, XIX – BNL-71751-2003
Volume 53 – Theory Studies for Polarized pp Scattering – BNL-71747-2003
Volume 52 – RIKEN School on QCD "Topics on the Proton" – BNL-71694-2003
Volume 51 – RHIC Spin Collaboration Meetings XV, XVI – BNL-71539-2003
Volume 50 – High Performance Computing with QCDOC and BlueGene – BNL-71147-2003
Volume 49 – RBRC Scientific Review Committee Meeting – BNL-52679
Volume 48 – RHIC Spin Collaboration Meeting XIV – BNL-71300-2003
Volume 47 – RHIC Spin Collaboration Meetings XII, XIII – BNL-71118-2003
Volume 46 – Large-Scale Computations in Nuclear Physics using the QCDOC – BNL-52678
Volume 45 – Summer Program: Current and Future Directions at RHIC – BNL-71035
Volume 44 – RHIC Spin Collaboration Meetings VIII, IX, X, XI – BNL-71117-2003
Volume 43 – RIKEN Winter School – Quark-Gluon Structure of the Nucleon and QCD – BNL-52672
Volume 42 – Baryon Dynamics at RHIC – BNL-52669
Volume 41 – Hadron Structure from Lattice QCD – BNL-52674
Volume 40 – Theory Studies for RHIC-Spin – BNL-52662
Volume 39 – RHIC Spin Collaboration Meeting VII – BNL-52659
Volume 38 – RBRC Scientific Review Committee Meeting – BNL-52649
Volume 37 – RHIC Spin Collaboration Meeting VI (Part 2) – BNL-52660
Volume 36 – RHIC Spin Collaboration Meeting VI – BNL-52642
Volume 35 – RIKEN Winter School – Quarks, Hadrons and Nuclei – QCD Hard Processes and the Nucleon Spin – BNL-52643
Volume 34 – High Energy QCD: Beyond the Pomeron – BNL-52641
Volume 33 – Spin Physics at RHIC in Year-1 and Beyond – BNL-52635
Volume 32 – RHIC Spin Physics V – BNL-52628
Volume 31 – RHIC Spin Physics III & IV Polarized Partons at High Q^2 Region – BNL-52617
Volume 30 – RBRC Scientific Review Committee Meeting – BNL-52603
Volume 29 – Future Transversity Measurements – BNL-52612
Volume 28 – Equilibrium & Non-Equilibrium Aspects of Hot, Dense QCD – BNL-52613
Volume 27 – Predictions and Uncertainties for RHIC Spin Physics & Event Generator for RHIC Spin Physics III – Towards Precision Spin Physics at RHIC – BNL-52596
Volume 26 – Circum-Pan-Pacific RIKEN Symposium on High Energy Spin Physics – BNL-52588
Volume 25 – RHIC Spin – BNL-52581
Volume 24 – Physics Society of Japan Biannual Meeting Symposium on QCD Physics at RIKEN BNL Research Center – BNL-52578
Volume 23 – Coulomb and Pion-Asymmetry Polarimetry and Hadronic Spin Dependence at RHIC Energies – BNL-52589
Volume 22 – OSCAR II: Predictions for RHIC – BNL-52591
Volume 21 – RBRC Scientific Review Committee Meeting – BNL-52568
Volume 20 – Gauge-Invariant Variables in Gauge Theories – BNL-52590
Volume 19 – Numerical Algorithms at Non-Zero Chemical Potential – BNL-52573
Volume 18 – Event Generator for RHIC Spin Physics – BNL-52571
Volume 17 – Hard Parton Physics in High-Energy Nuclear Collisions – BNL-52574
Volume 16 – RIKEN Winter School - Structure of Hadrons - Introduction to QCD Hard Processes – BNL-52569
Volume 15 – QCD Phase Transitions – BNL-52561
Volume 14 – Quantum Fields In and Out of Equilibrium – BNL-52560
Volume 13 – Physics of the 1 Teraflop RIKEN-BNL-Columbia QCD Project First Anniversary Celebration – BNL-66299

Back to Contents

Volume 12 – Quarkonium Production in Relativistic Nuclear Collisions – BNL-52559
Volume 11 – Event Generator for RHIC Spin Physics – BNL-66116
Volume 10 – Physics of Polarimetry at RHIC – BNL-65926
Volume 9 – High Density Matter in AGS, SPS and RHIC Collisions – BNL-65762
Volume 8 – Fermion Frontiers in Vector Lattice Gauge Theories – BNL-65634
Volume 7 – RHIC Spin Physics – BNL-65615
Volume 6 – Quarks and Gluons in the Nucleon – BNL-65234
Volume 5 – Color Superconductivity, Instantons and Parity (Non?)-Conservation at High Baryon Density – BNL-65105
Volume 4 – Inauguration Ceremony and Non-Equilibrium Many Body Dynamics – BNL-64912
Volume 3 – Hadron Spin-Flip at RHIC Energies – BNL-64724
Volume 2 – Perturbative QCD as a Probe of Hadron Structure – BNL-64723
Volume 1 – Open Standards for Cascade Models for RHIC – BNL-64722

Back to Contents

Li Keran

Nuclei as heavy as bulls
Through collision
Generate new states of matter.
T.D. Lee

©CCASTA

Organizers

Yuji Goto (RIKEN)
Matthias Grosse-Perdekamp (Illinois)
Cesar Luiz da Silva (LANL)
Akio Ogawa (BNL)
Joe Seele (RBRC)
Ralf Seidl (RIKEN)
Raju Venugopalan (BNL)
Werner Vogelsang (Tuebingen)
Anselm Vossen (Indiana)

RIKEN BNL Research Center
Bldg. 510A, Brookhaven National Laboratory
Upton, NY 11973-5000, USA

August 2012